Acc
[illegible]

Cuk-H03520-7-P024433

AJR

⑦

American
Journal of
Roentgenology

July 1977

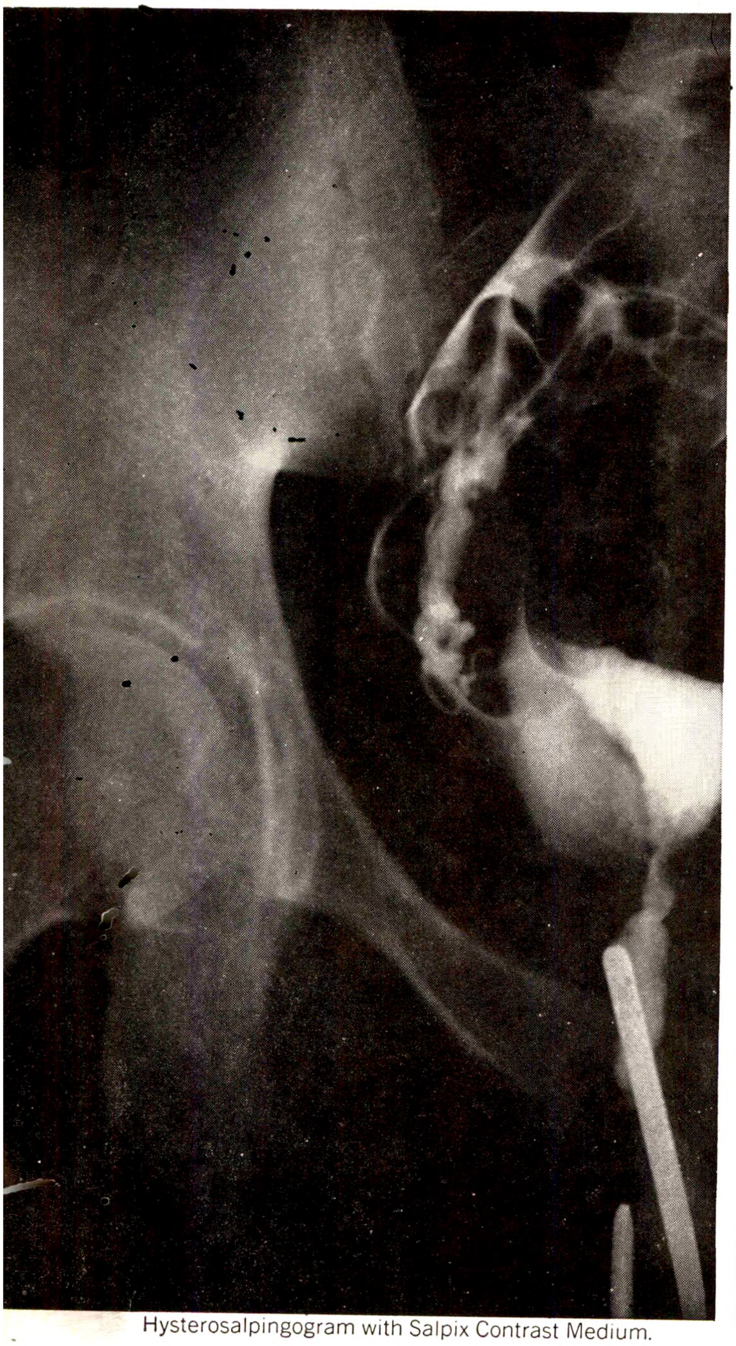

Hysterosalpingogram with Salpix Contrast Medium.

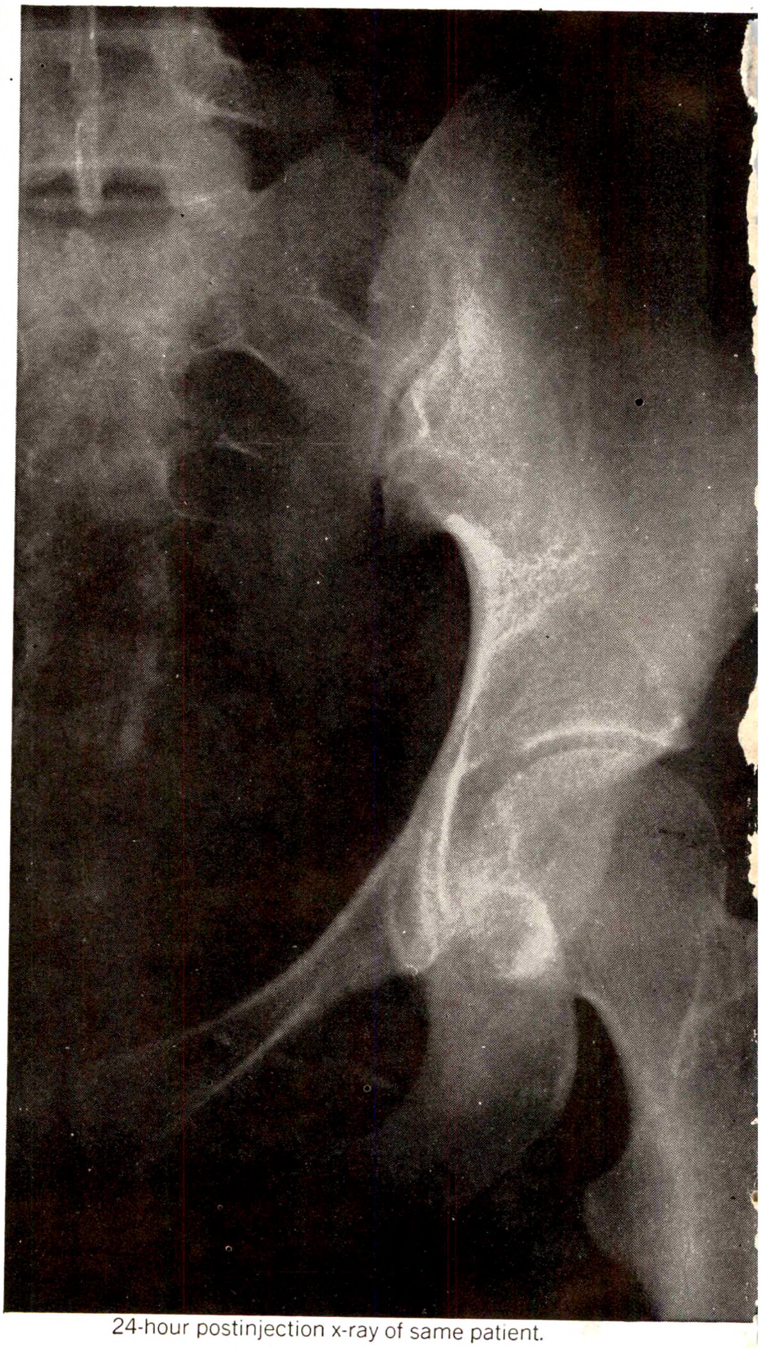

24-hour postinjection x-ray of same patient.

now you see it **now you don't**

With Salpix as your contrast medium, your gynecologic patient needn't undergo the 24-hour postinjection x-ray usually required with iodized oils. Water-soluble Salpix leaves virtually no irritating radiopaque residue to produce foreign-body reactions, yet it provides the viscosity needed for adequate visualization.

Contraindications: Contraindications to hysterosalpingography include the presence of severe vaginal or cervical infections, existing or recent pelvic infection, marked cervical erosion or endocervicitis, and pregnancy. The procedure is contraindicated during the immediate pre- or post-menstrual phase.

Sensitivity Test: If indicated in the patient's history, an intracutaneous skin test or sublingual absorption observation may be done with 0.1 cc Salpix.

Warning: Not for intravenous use.

© ORTHO PHARMACEUTICAL CORPORATION 1970

CONTRAST MEDIUM

Salpix

TRADEMARK

EACH CC CONTAINS:

sodium acetrizoate 0.53 g and polyvinylpyrrolidone 0.23 g

Ortho

ORTHO PHARMACEUTICAL CORPORATION • RARITAN, NEW JERSEY 08869

P. 24433

Official Journal
American Roentgen Ray Society
American Radium Society

AJR

Including Diagnostic Radiology • Radiation Oncology • Nuclear Medicine
Ultrasonography • Related Sciences

Editor Melvin M. Figley

Assistant Editor Rosalind H. Troupin

Editor Emeritus Traian Leucutia

Associate Editors Luther W. Brady • Kenneth L. Krabbenhoft • E. Frederick Lang • Russell H. Morgan

Consulting Editorial Board Kent Ellis • E. Robert Heitzman • Donald L. King • John A. Kirkpatrick, Jr. Eugene C. Klatte • John G. McAfee • Thomas H. Newton Robert G. Parker • Stewart R. Reuter • William B. Seaman • Robert J. Shalek • John Storer • Michel M. Ter-Pogossian • Joseph P. Whalen • David M. Witten

Editorial Staff K. A. Murray, manager • M. B. Wieckowicz, manuscript editor • M. J. Leonard, assistant manuscript editor • C. P. Kaiser, secretary

Published monthly by Charles C Thomas, 301–327 East Lawrence Avenue, Springfield, Illinois 62717. All correspondence, except editorial office business, should be addressed to the publisher. Annual subscription prices: United States and possessions, $40; others, $50; residents in training in U.S., $20 (letter from department required with dates of residency); single copies, $5. Foreign subscription delivery not guaranteed. Undelivered or damaged copies replaced within 60 days of publication; 90 days for foreign subscribers. Allow 90 days for address changes. © 1977 by American Roentgen Ray Society. Second-class postage paid at Springfield, Illinois, and at additional mailing offices (no. 020240). Printed in U.S. at George Banta Company.

American Roentgen Ray Society

OFFICERS 1976–1977

President: Seymour F. Ochsner
President Elect: Harry Z. Mellins
1st Vice-president: E. Frederick Lang
2nd Vice-president: Richard G. Lester
Secretary: James F. Martin
Treasurer: Joseph D. Calhoun

COMMITTEES 1976–1977

Executive Council: S. F. Ochsner, H. Z. Mellins, E. F. Lang, R. G. Lester, J. F. Martin, J. D. Calhoun, M. M. Figley, T. Leucutia, H. C. Carlson, R. A. Alfidi, R. A. Gagliardi, A. E. James, E. Gedgaudas, G. A. Kling, T. F. Leigh, C. B. Holman, R. Buenger, E. C. Klatte, J. P. Tampas, J. L. Gwinn, C. E. Bickham, Jr., chairman

Finance and Budget: R. G. Evens, J. P. Tampas, R. McLelland, J. L. Gwinn, H. G. Carlson

Publications: K. Ellis, F. F. Ruzicka, Jr., E. R. Heitzman, J. V. Rogers, Jr., R. A. Gagliardi, chairman

Editorial Policy: M. M. Figley, E. F. Lang, L. Brady, K. Krabbenhoft, R. Morgan, E. R. Heitzman, J. V. Rogers, K. Ellis, F. F. Ruzicka, Jr., R. A. Gagliardi, chairman

Advisory Committee on Education and Research: G. Wilson, G. W. Hartman, L. F. Rogers, E. Gedgaudas, A. E. James, chairman

Scientific Exhibits: G. Dodd, B. G. Brogdon, R. A. Alfidi, chairman

Constitution and Bylaws: J. H. Walker, W. M. Whitehouse, J. P. Tampas, chairman

American Board of Radiology Representatives: J. F. Roach, R. W. McConnell, S. W. Nelson

Program Committee: S. F. Ochsner, J. F. Martin, C. E. Bickham, Jr., M. M. Figley, R. A. Gagliardi, R. A. Alfidi, E. Gedgaudas, G. A. Kling, A. E. James, H. Z. Mellins, chairman

Instruction Courses: E. Gedgaudas, director; H. O. Peterson, associate director

American College of Radiology Board of Chancellors Representative: W. B. Seaman

Annual Meeting: September 27–30, 1977, Sheraton Hotel, Boston, Massachusetts

Scientific Program: Harry Z. Mellins, president-elect, Peter Bent Brigham Hospital, Boston, Massachusetts

Manager Annual Meeting: George A. Kling, Harper Hospital, Detroit, Michigan

Membership: Charles E. Bickham, Jr., Suburban Hospital, 8600 Old Georgetown Road, Bethesda, Maryland 20014

Business Office: Keith W. Gundlach, comptroller, American College of Radiology, 20 North Wacker Drive, Chicago, Illinois 60606

American Radium Society

OFFICERS 1977–1978

President: Richard H. Jesse
President Elect: Frederick W. George
1st Vice-president: Ivor Fix
2d Vice-president: John Durant
Secretary: Alfred S. Ketcham
Treasurer: Simon Kramer

COMMITTEES 1977–1978

Executive: F. Rutledge, L. W. Brady, R. H. Jesse, F. W. George, I. Fix, J. Durant, S. Kramer, A. S. Ketcham, V. Marcial, chairman

Public Relations: C. Honaker, R. H. Jesse, chairman

Publication: K. L. Krabbenhoft, A. F. Schroeder, G. Seydel, D. Hussey, A. Raventos, L. W. Brady, chairman

Scientific Program: F. George, D. Johnson, M. Boone, P. Chretien, P. J. DiSaia, D. Hussey, R. C. Landgren, C. Perez, S. T. Cantril, R. H. Jesse, chairman

Local Arrangements: J. Helsper, J. J. Romagosa, J. M. Thomson, Jr., A. J. Ballantyne, S. Kramer, S. Ochsner, chairman

Nominating: M. Kligerman, G. Lewis, J. Vaeth, chairman

Constitution and By-Laws: A. S. Glicksman, P. J. DiSaia, K. L. Krabbenhoft, chairman

Janeway Lecture: S. Levitt, L. Davis, A. S. Ketcham, chairman

Audiovisual: C. R. Bogardus, J. Helsper, B. Herrington, L. Bloebaum, C. Honaker, F. George, chairman

Resident Essay: J. T. Phillips, J. Curry, R. Schweitzer, J. T. Wharton, chairman

American Board of Radiology, Representatives: J. J. Stein, R. E. King, N. duV Tapley

American College of Radiology Board of Chancellors Representative: L. W. Brady

American College of Radiology Council Representative: J. del Regato

Editorial Board of AFCOS Newsletter Representative: J. Vaeth

National Council on Radiation Protection and Measurements Liason Representative: L. W. Davis

Annual Meeting: April 26–30, 1978, Marriott Hotel, New Orleans, Louisiana

Scientific Program: R. H. Jesse, M. D. Anderson Hospital, 6723 Bertner Drive, Houston, TX 77030

Local Arrangements: S. Ochsner, 1514 Jefferson Highway, New Orleans, LA 70121

Membership: A. S. Ketcham, secretary, University of Miami School of Medicine, P.O. Box 520875 Biscayne Annex, Miami, Florida 33152

Business Office: N. V. Jordan, c/o R. H. Jesse, M. D. Anderson Hospital and Tumor Institute, 6723 Bertner Avenue, Houston, Texas 77030

Calonje Products Corporation is a full-service professional organization whose products encompass the most trusted names in the medical industry.

But is that enough?

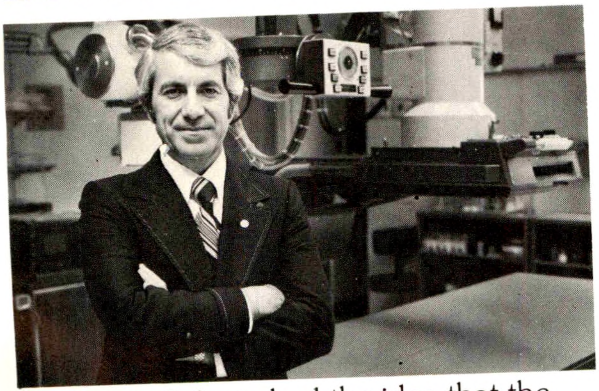

No. Steve Calonje had the idea that the finest equipment and accessories—plus personal service—were the essential considerations in satisfying his customers.

Calonje Products Corporation has established effective systems to support these ideals—prompt, dependable, individualized service of the products offered. "We represent the top manufacturers in the field, but that's not what I call *full* service," says Calonje. "Making products available—even the best on the market—is not enough."

Drawing from a catalog of established, trusted names in the medical industry, Calonje Products Corporation stands ready to equip *and service* x-ray facilities for a full range of capabilities. XONICS-STANDARD, EXDA, BURDICK, DUPONT, KODAK AND PAKO are among the lines available to you through Calonje Products Corporation. Calonje holds the franchise for these products in the Louisiana and southern Mississippi area.

Calonje products and services fulfill the electronics requirements of all phases of the medical profession, offering the complete line of Abbott Heart Monitoring Equipment, including Telemetry. In addition, Calonje carries the Burdick EKG, Diathermy and Ultrasound systems.

Calonje Products Corporation is the name to remember when your needs demand the finest in x-ray equipment, consultant services, film, accessories, sales and service.

May we send you our catalog?

Calonje Products Corporation

4440 Earhart Blvd./New Orleans, La. 70125/(504) 822-8011

Fleet® Barium Enema Prep Kits: Make us your first choice for fewer retakes.

The greatest defect in colon examinations is in the preparation of the colon.[1]

Fleet® Barium Enema Prep Kits systematize and improve colon prepping because they conform to the recommended method which provides a combination of diet, hydration and proven laxation which stimulates the large and small intestines.[2] The result? Cleaner colons, clearer x-rays and fewer retakes.

All Fleet Prep Kits offer three laxative steps: 1½ oz. of Fleet® Phospho®-Soda followed by four Fleet® Bisacodyl tablets, plus a final cleansing step. Prep Kit 1 offers Fleet® Bisacodyl suppository. Prep Kit 2 offers a large-volume disposable Fleet® Bagenema. And Prep Kit 3 offers our new Fleet® Bisacodyl enema. And all three Prep Kits have easy-to-follow instructions with a choice of flexible time-tables to fit your schedule.

With Fleet Barium Enema Prep Kits, you'll be sure of convenient, dependable, effective colon prepping every time. And that's reason enough to make Fleet Prep Kits your first choice for fewer retakes.

NDC 0132-0211-01
Fleet. Barium Enema Prep Kit 1
CONTENTS: FLEET® PHOSPHO-SODA BUFFERED SALINE LAXATIVE, 1½ FL. OZ. (45 ML); FLEET® BISACODYL, NF CONTACT LAXATIVE, 4 ENTERIC-COATED TABLETS, 5 MG EA.; FLEET® BISACODYL, NF CONTACT LAXATIVE, 1 SUPPOSITORY, 10 MG.
Fleet. Phospho-soda buffered saline laxative flavored
NDC 0132-0210-01
Fleet Barium Enema Prep Kit 2
CONTENTS: FLEET® PHOSPHO-SODA BUFFERED SALINE LAXATIVE, 1½ FL. OZ. (45 ML); FLEET® BISACODYL, NF CONTACT LAXATIVE, 4 ENTERIC-COATED TABLETS, 5 MG EA; FLEET® BAGENEMA, 1 UNIT; SOAPSUDS PACKET (1)
NDC 0132-0212-01
Fleet. Barium Enema Prep Kit 3
CONTENTS: FLEET® PHOSPHO-SODA BUFFERED SALINE LAXATIVE, 1½ FL. OZ. (45 ML); FLEET® BISACODYL, NF CONTACT LAXATIVE, 4 ENTERIC-COATED TABLETS, 5 MG EA.; FLEET® READY-TO-USE BISACODYL ENEMA, 10 MG BISACODYL, U.S.P.
Fleet. ready-to-use bisacodyl enema
10 mg Rectal Contact Laxative
Comfortip.
1¼ Fluid Ounces (37 ml)

Fleet Barium Enema Prep Kits
for cleaner colons, clearer x-rays and fewer retakes.

Fleet pharmaceuticals
C.B. Fleet Co., Inc.
Lynchburg, Va. 24505

[1] Dr. R.E. Miller, Ad Hoc Committee on Detection of Cancer of the Colon, Detection of Colon Lesions, American College of Radiology, (Chicago, Ill., 1973) p. 76.

[2] Dr. W.R. Eyler, Ibid. pp. 203, 204.

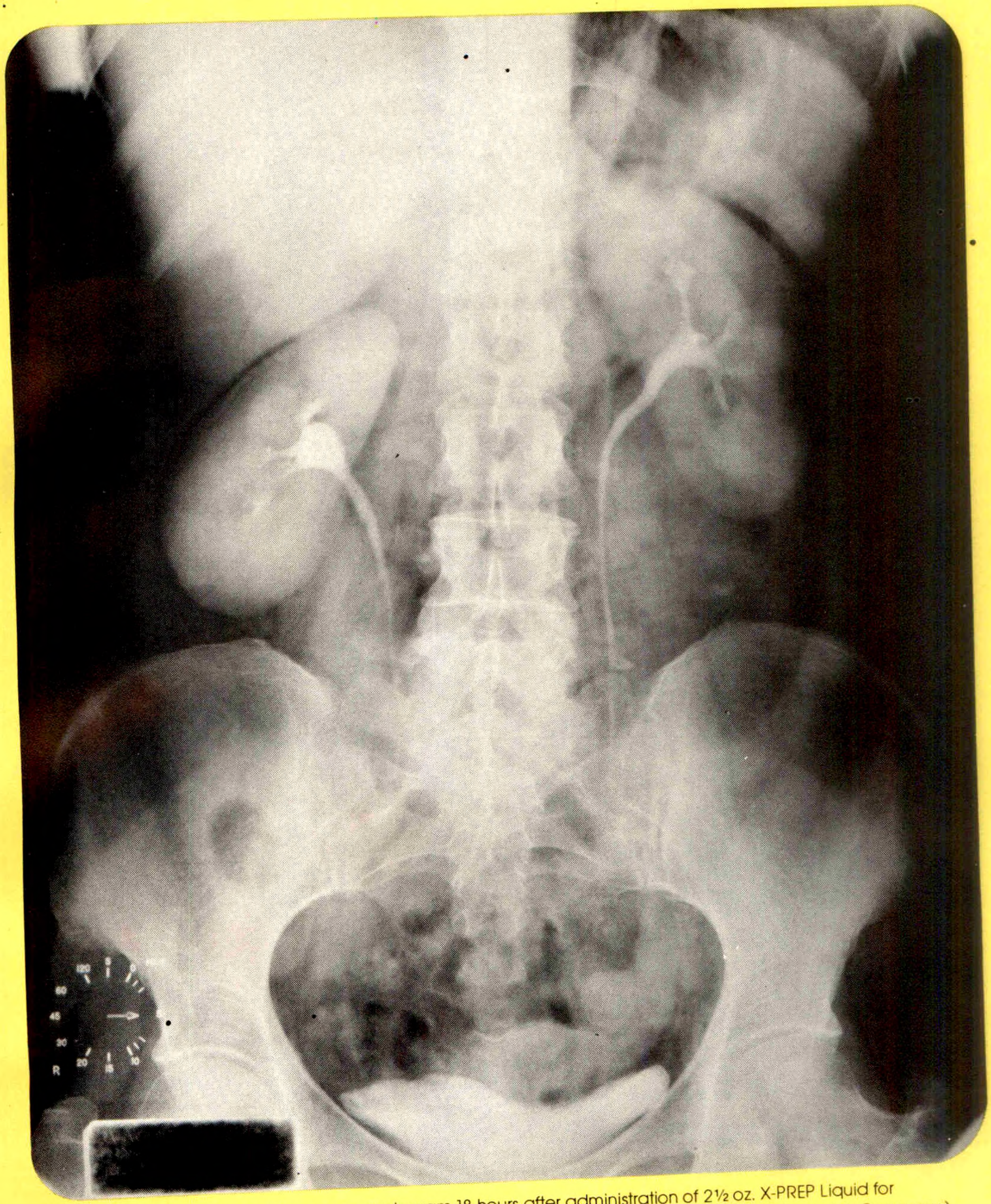

[redacted]

Excellent visualization in intravenous pyelogram 18 hours after administration of 2½ oz. X-PREP Liquid for preradiographic bowel cleansing. (In the files of the Medical Department of The Purdue Frederick Company.)

To prep the bowel for intravenous pyelography

X-PREP® Liquid

(standardized extract of senna fruit)

One step • One dose • One bottle

☐ X-PREP Liquid is designed specifically for preradiographic bowel cleansing—without enemas, suppositories or overhydration.

☐ A single 2½ oz. oral dose is usually all that is required. No residual oil droplets (such as may occur with castor oil).

☐ Pleasant taste meets with high patient acceptance. Ease of administration is appreciated by the patient and nursing staff.

Gray Pharmaceutical Co., Affiliate
The Purdue Frederick Company

© COPYRIGHT 1975, GRAY PHARMACEUTICAL CO./NORWALK, CONN. 06856 A7901 160875

TONY
RAG

KODAK'S RARE EARTH IMAGING. IT CAN BE COMMON PRACTICE.

The rare earth phosphors in Kodak Lanex screens absorb more x-rays—more energy—to achieve twice the speed of fast calcium tungstate screens. Image quality is similar, but exposure time, milliamperage, or kilovoltage can be reduced. As a result, you can handle both your regular and special examinations routinely. And you can get more efficient use from your present exposure equipment.

Specifically, Kodak Lanex screens absorb about 60% of the x-ray quanta that exit from a patient. Whereas, fast calcium tungstate screens absorb about 40%.

While Lanex screens absorb more x-rays, they also convert more of the absorbed energy into usable light. This dual efficiency enables Lanex screens, with Kodak ortho G film, to provide image quality similar to fast calcium tungstate screens, with Kodak X-Omat RP film, but at twice the speed.

And that means you can use shorter exposure times to minimize the effects of voluntary or involuntary motion in geriatric or pediatric patients.

Or you can reduce kilovoltage to obtain increased subject contrast in angiographic or tomographic examinations.

Or you can use lower milliamperage settings for a smaller focal spot for improved geometric sharpness.

Or you can distribute your work load to utilize low-powered or portable units.

With Kodak rare earth imaging products, the opportunities are many.

Ask your Kodak Technical Sales Representative about them. Or contact your medical x-ray products dealer. Or write:

Eastman Kodak Company,
Department 740-B, Rochester,
New York 14650.

TURNING ENERGY INTO IMAGES

Kodak

RADIOGRAPHY • COMPUTERIZED TOMOGRAPHY
ULTRASOUND • NUCLEAR MEDICINE • THERMOGRAPHY

the reason is clear™

- Excellent image quality
- Rapid visualization of renal pelvis, ureters, and bladder...maximal opacification of renal passages may begin as early as 5 minutes after injection
- 8 indications*

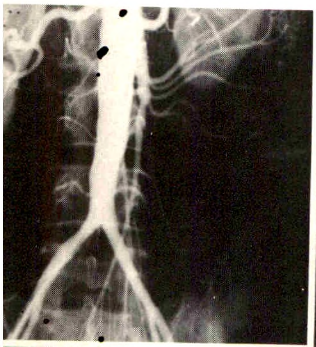
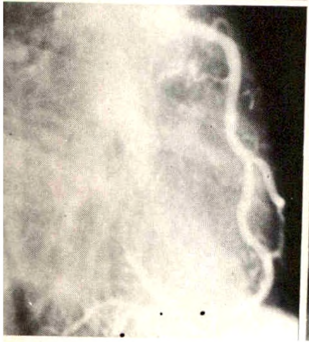

Aortography

Selective coronary arteriography

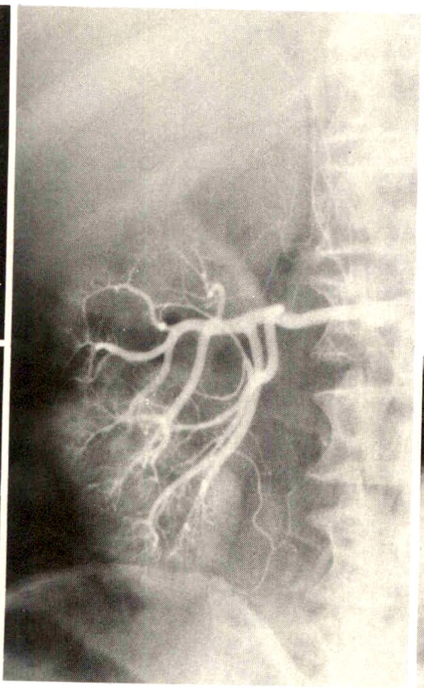

Selective renal arteriography

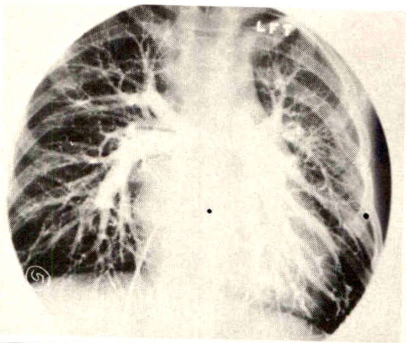
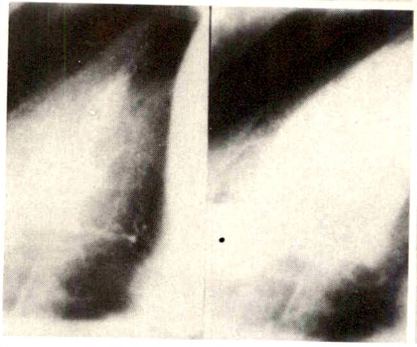

Pediatric angiocardiography

Left ventriculography performed following coronary arteriography

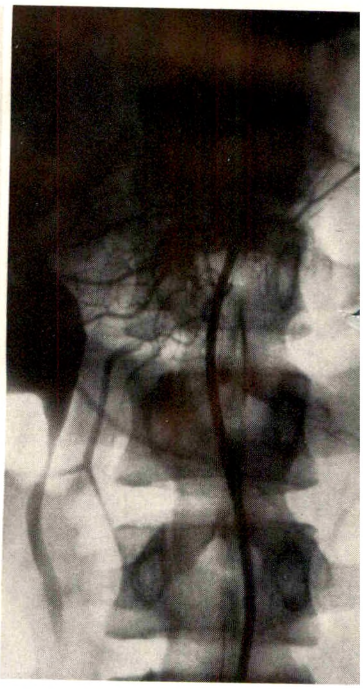

Selective visceral arteriography

Renografin®-76

Diatrizoate Meglumine and
Diatrizoate Sodium Injection U.S.P.

Squibb™
contrast media

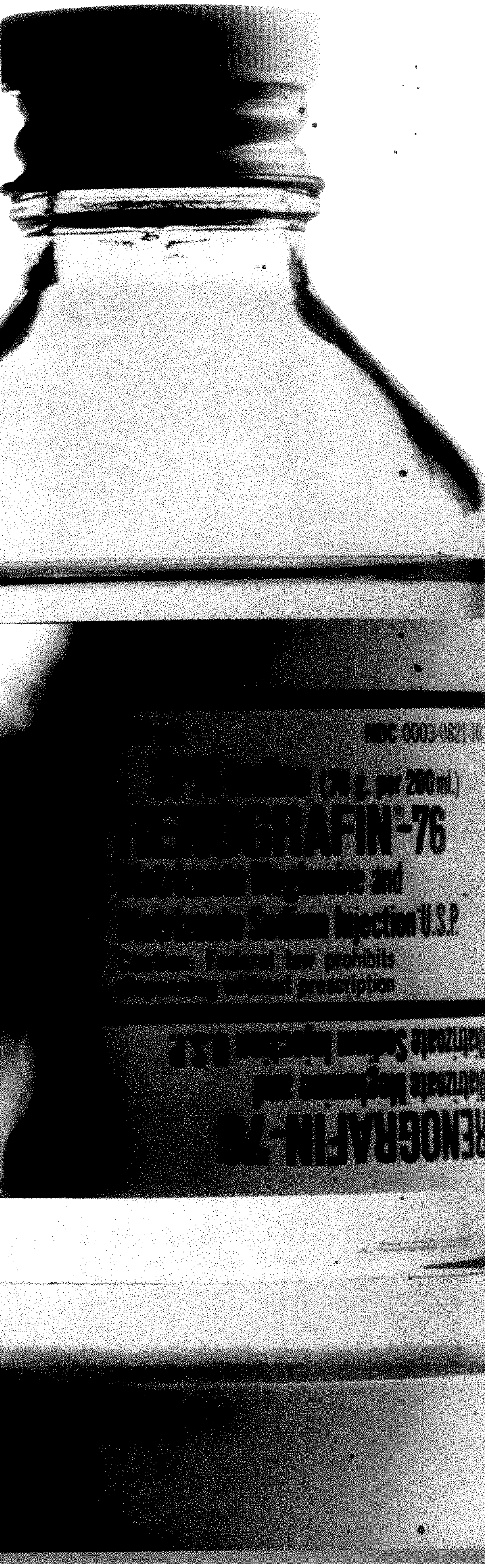
NDC 0003-0821-10
(76 g. per 200 ml.)
RENOGRAFIN®-76
Diatrizoate Meglumine and
Diatrizoate Sodium Injection U.S.P.
Caution: Federal law prohibits
dispensing without prescription

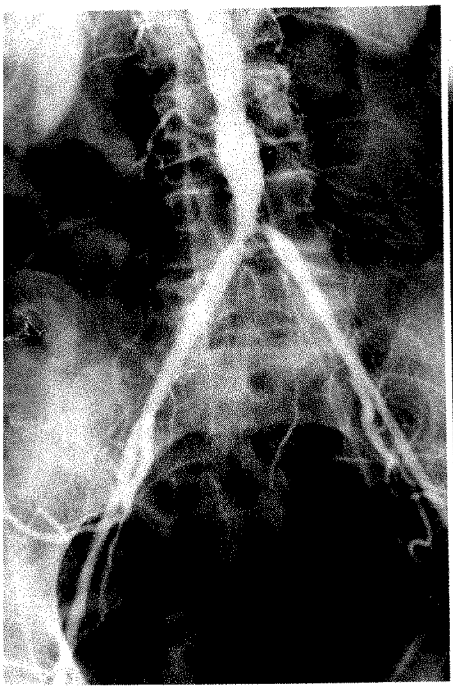

Peripheral arteriography

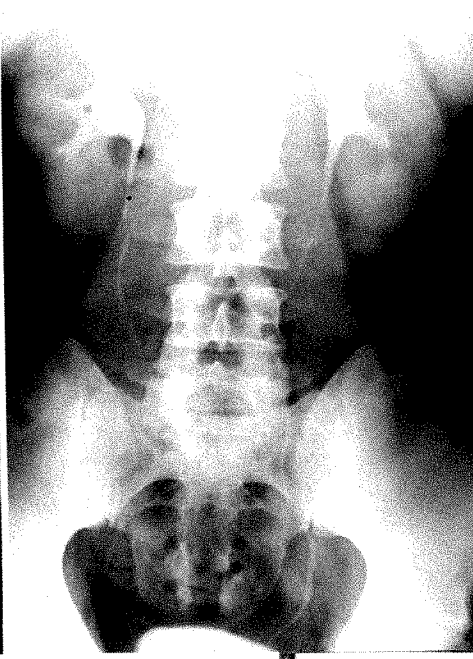

Excretion urography

*For dosage and administration recommendations, see package insert.

Please see following page for brief summary.

RENOGRAFIN®-76
Diatrizoate Meglumine and Diatrizoate Sodium Injection U.S.P.

Renografin-76 (Diatrizoate Meglumine and Diatrizoate Sodium Injection U.S.P.) is supplied as a sterile, aqueous solution providing 66% diatrizoate meglumine and 10% diatrizoate sodium with 0.32% sodium citrate as a buffer and 0.04% edetate disodium as a sequestering agent. The solution contains approximately 37% (370 mg./ml.) bound iodine and *approximately 4.48 mg. (0.19 mEq.) sodium per ml.*

CONTRAINDICATIONS: In patients with a hypersensitivity to salts of diatrizoic acid. Urography contraindicated in patients with anuria.

WARNINGS: A definite risk exists with the use of contrast agents in excretion urography in patients with multiple myeloma. There has been anuria with progressive uremia, renal failure and death. This risk of the procedure in these patients is not a contraindication; however, partial dehydration in preparation for study is not recommended since it may predispose for precipitation of myeloma protein in renal tubules. No therapy, including dialysis, has been successful in reversing this effect. Myeloma should be considered in persons over 40 before undertaking urographic procedures.

In cases of known or suspected pheochromocytoma, if the physician feels that the possible benefits outweigh the considered risks, radiopaque materials should be administered with extreme caution; however, an absolute minimum of material should be injected, the blood pressure should be assessed throughout the procedure, and measures for treating a hypertensive crisis should be available.

Contrast media may promote sickling in homozygous individuals when injected I.V. or intra-arterially. Although a history of sensitivity to iodine *per se* or to other contrast media is not an absolute contraindication, administration of diatrizoate requires extreme caution in such cases. Perform thyroid function tests prior to administration of Renografin-76 (Diatrizoate Meglumine and Diatrizoate Sodium Injection U.S.P.) since iodine-containing contrast agents may alter the test results.

Weigh the inherent risks against necessity for performing *angiocardiography* in cyanotic infants and patients with chronic pulmonary emphysema. In *pediatric angiocardiography*, a dose of 10 to 20 ml. may be particularly hazardous in infants weighing less than 7 kg.; this risk is probably significantly increased if these infants have preexisting right heart "strain," right heart failure, and effectively decreased or obliterated pulmonary vascular beds. Perform *urography* with extreme caution in persons with severe concomitant hepatic and renal disease. Perform *selective coronary arteriography* only in selected patients and those in whom expected benefits outweigh the procedural risk. Perform *selective visceral arteriography* with extreme caution in presence of severe generalized atherosclerosis, specifically with plaques or aneurysms at level of iliac or femoral arteries.

Usage in Pregnancy: Use Renografin-76 (Diatrizoate Meglumine and Diatrizoate Sodium Injection U.S.P.) in pregnant patients only when the physician deems its use essential to the welfare of the patient since safe use during pregnancy has not been established.

PRECAUTIONS: Diagnostic procedures involving use of contrast agents should be performed under the direction of personnel with prerequisite training and a thorough knowledge of the particular procedure. Appropriate facilities should be available for coping with situations which may arise as a result of the procedure and for emergency treatment of severe reactions to the contrast agent itself; competent personnel and emergency facilities should be available for at least 30 to 60 minutes after I.V. administration since delayed reactions have been known to occur. These severe life-threatening reactions suggest hypersensitivity to the contrast agent. A personal or family history of asthma or allergy or a history of a previous reaction to a contrast agent warrants special attention and may predict more accurately than pretesting the likelihood of a reaction although not the type nor severity of the reaction in the individual. The value of any pretest is questionable. The pretest most performed is the slow I.V. injection of 0.5 to 1.0 ml. of the preparation prior to injection of the full dose; however, the absence of a reaction to the test dose does not preclude the possibility of reaction to the full diagnostic dose. Should the test dose produce an untoward response, the necessity for continuing the examination should be re-evaluated. If deemed essential, examination should proceed with all possible caution. In rare instances, reaction to the test dose may be extremely severe; therefore, close observation and facilities for emergency treatment are indicated.

Renal toxicity has been reported in a few patients with liver dysfunction who were given oral cholecystographic agents followed by urographic agents; therefore, if known or suspected hepatic or biliary disorder exists, administration of Renografin-76 (Diatrizoate Meglumine and Diatrizoate Sodium Injection U.S.P.) should be postponed following the ingestion of cholecystographic agents. Consider the functional ability of the kidneys before injecting the contrast agent. Use cautiously in severely debilitated patients and in those with marked hypertension. Bear in mind the possibility of thrombosis when using percutaneous techniques. Since contrast agents may interfere with some chemical determinations made on urine specimens, collect urine before or two or more days after administration of the contrast agent.

In *excretion urography*, adequate visualization may be difficult or impossible in uremic patients or others with severely impaired renal function (see Contraindications). In *aortography* repeated intra-aortic injections may be hazardous; this also applies to *pediatric angiocardiography* particularly in infants weighing less than 7 kg. (see Warnings). In *peripheral arteriography*, hypotension or moderate decreases in blood pressure seem to occur frequently with intra-arterial (brachial) injections; this is transient and usually requires no treatment. Monitor blood pressure during the immediate 10 minutes after injection. It is recommended that *selective coronary arteriography* not be performed for about 4 weeks after diagnosis of myocardial infarction; mandatory prerequisites to this procedure are experienced personnel, ECG monitoring apparatus, and adequate facilities for immediate resuscitation and cardioversion.

ADVERSE REACTIONS: Nausea, vomiting, flushing, or a generalized feeling of warmth are the reactions seen most frequently with intravascular injection. Symptoms which may occur are chills, fever, sweating, headache, dizziness, pallor, weakness, severe retching and choking, wheezing, a rise or fall in blood pressure, facial or conjunctival petechiae, urticaria, pruritus, rash, and other eruptions, edema, cramps, tremors, itching, sneezing, lacrimation, etc. Antihistaminic agents may be of benefit; rarely, such reactions may be severe enough to require discontinuation of dosage. There have been a few reports of a burning or stinging sensation or numbness, of venospasm or venous pain, and of partial collapse of the injected vein. Neutropenia or thrombophlebitis may occur. Severe reactions which may require emergency measures (see Precautions) are a possibility and include cardiovascular reaction characterized by peripheral vasodilatation with hypotension and reflex tachycardia, dyspnea, agitation, confusion, and cyanosis progressing to unconsciousness. An allergic-like reaction ranging from rhinitis or angioneurotic edema to laryngeal or bronchial spasm or anaphylactoid shock may occur. Temporary renal shutdown or other nephropathy may occur.

Adverse reactions as a consequence of *excretion urography* include cardiac arrest, ventricular fibrillation, anaphylaxis with severe asthmatic reaction, and flushing due to generalized vasodilatation. Risks of *aortography* procedures include injury to aorta and neighboring organs, pleural puncture, renal damage (including infarction and acute tubular necrosis with oliguria and anuria), accidental selective filling of right renal artery during translumbar procedure in presence of preexistent renal disease, retroperitoneal hemorrhage from translumbar approach, spinal cord injury and pathology associated with syndrome of transverse myelitis, generalized petechiae, and death following hypotension, arrhythmia, and anaphylactoid reactions. In *pediatric angiocardiography*, arrhythmia and death have occurred. During *peripheral arteriography*, hemorrhage from puncture site, thrombosis of the vessel, and brachial plexus palsy (following axillary artery injection) have occurred. During *selective coronary arteriography* and *selective coronary arteriography with left ventriculography*, transient ECG changes (most patients); transient arrhythmias (infrequent); ventricular fibrillation (from manipulation of catheter or administration of medium); hypotension; chest pain; myocardial infarction; transient elevation of creatinine phosphokinase (occurred in about 30% of patients tested); fatalities have been reported; hemorrhage, thrombosis, pseudoaneurysms at puncture site, dislodgment of arteriosclerotic plaques, dissection of coronary vessels, and transient sinus arrest have occurred due to the procedure. Adverse reactions in *selective renal arteriography* include nausea, vomiting, hypotension, hypertension, and post-arteriographic transient elevations in BUN, serum creatinine and glucose. Complications of *selective visceral arteriography* include hematomas, thrombosis, pseudoaneurysms at injection site, dislodgment of arteriosclerotic plaques; other reactions may include urticaria, hypotension, hypertension, and insignificant changes in renal function and liver chemistry tests.

For full prescribing information, consult package insert.

HOW SUPPLIED: Available in 20 ml. and 50 ml. single-dose vials and in 100 ml. and 200 ml. single-dose bottles.

SQUIBB HOSPITAL DIVISION
E. R. Squibb & Sons, Inc.

SQUIBB®
the reason
is clear™
contrast media™

©1976 E. R. SQUIBB & SONS, INC. H626-502

Machlett
For neuroradiography

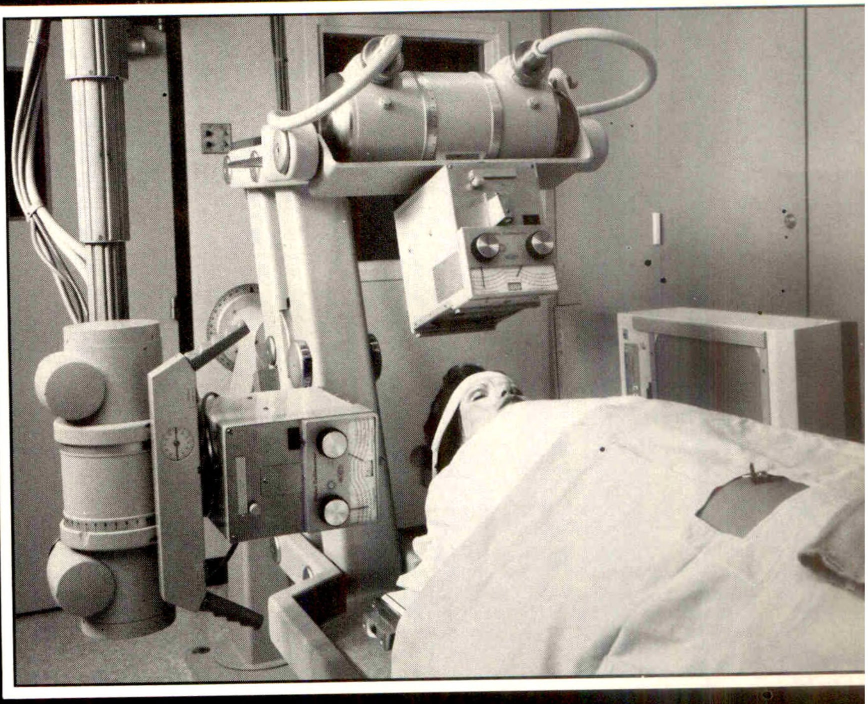

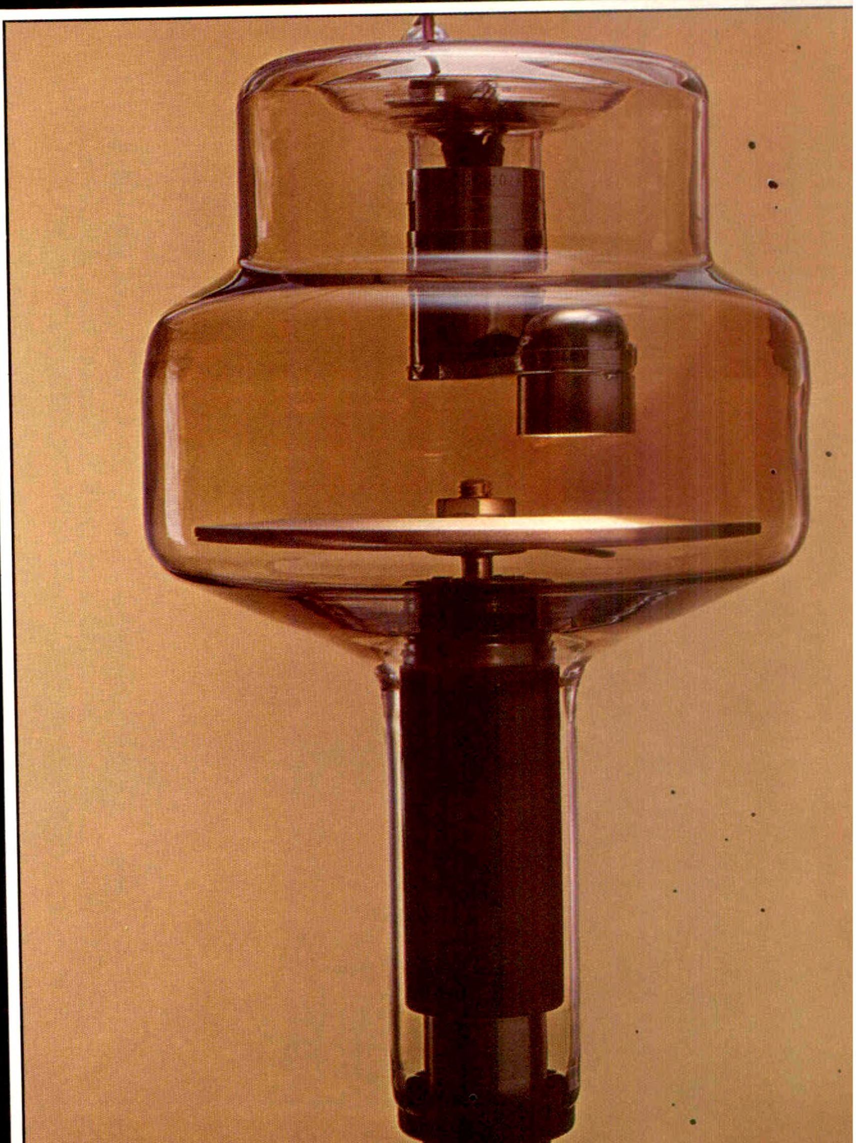

dynamax 68E
dynamax 78E
procedure-designed x-ray tubes

Designed for the exacting techniques of neuroradiography Machlett's Dynamax 78E and Dynamax 68E inserts feature a large focus to permit the use of heavy-duty angiographic procedures with conventional films and screens.

Dynamax 78E 10/57 inserts biased for small focus will resolve 7 1/2 lines per millimeter at 3-power magnification at 100 mA and 70 kVp.

Dynamax 68E 13/87 inserts biased for small focus will resolve 5 lines per millimeter at 2-power magnification at 140 mA and 70 kVp.

For complete information contact your x-ray dealer or

MACHLETT

The Machlett Laboratories, Incorporated
1063 Hope Street
Stamford, Connecticut 06907
(203) 348-7511

A Raytheon Company

KODAK:
HELPING TURN
ENERGY
INTO IMAGES.

RADIOGRAPHY · COMPUTERIZED TOMOGRAPHY
ULTRASOUND · NUCLEAR MEDICINE · THERMOGRAPHY

Kodak products. For the constant imaging needs of today's radiography.

Kodak's role in diagnostic imaging stems from almost a century of expertise in photography—out of which Kodak has built a background of expertise in radiography.

And this translates into Kodak products: quality medical x-ray films and intensifying screens that interact with energy to help create diagnostic images.

For general radiography: Kodak X-Omat RP film—a high-contrast, fast film, providing excellent detail; Kodak X-Omat L film—a wide-latitude film that can record a wide range of tissue densities; Kodak X-Omat G film—a high-contrast film, providing excellent sharpness of detail with a low quantum mottle graininess. And many others… plus Kodak Lanex screens which, when used with Kodak ortho G film, provide increased speed and reduced patient exposure.

For special imaging technics: Kodak X-Omat subtraction masking film, as well as Kodak films for radiation therapy monitoring, for duplicating, for cinefluorography, for spot filming, and for photofluorography, and Kodak Min-R screen and film for mammography.

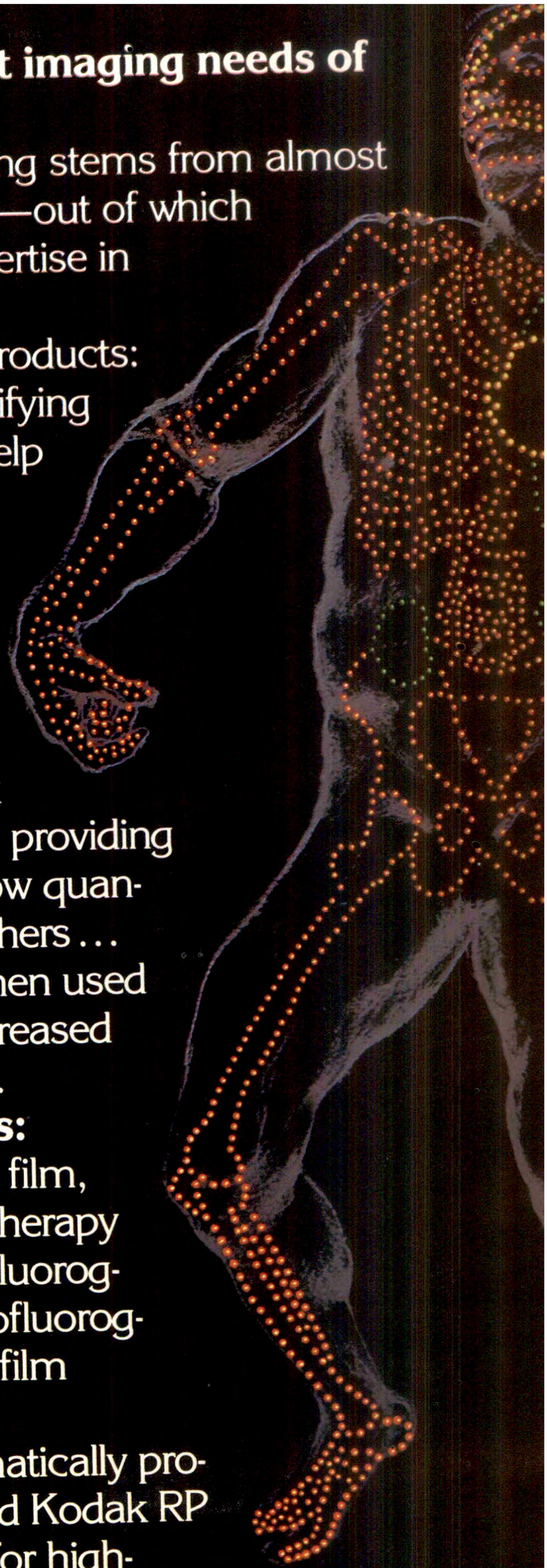

All of these films can be automatically processed in the dependable, 90-second Kodak RP X-Omat processor, model M6A-N—for high-volume radiography; or the smaller, compact, 150-second Kodak RP X-Omat processor, model M7A—for satellite areas. The model

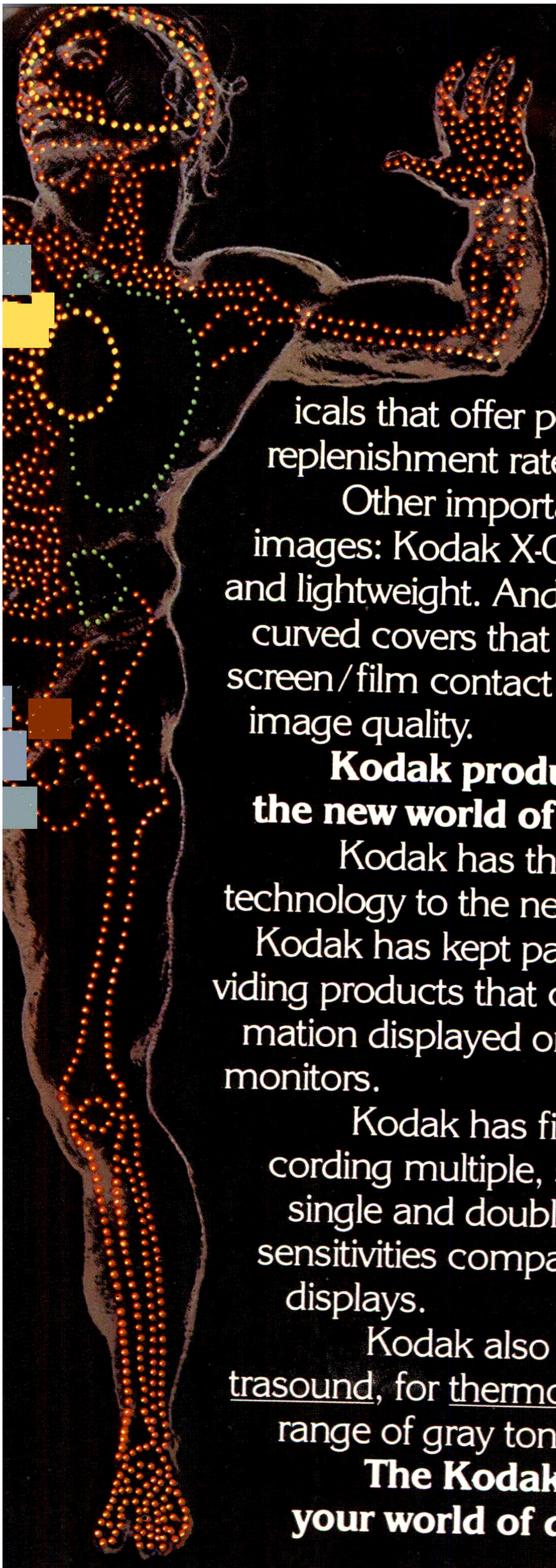

M7A processor uses tap water to wash films, saves on water heating costs. The model M7A processor also offers an energy-saving, standby-control unit that conserves power when the processor is not in use. Both processors can use our carefully formulated chemicals that offer potential economies through lower replenishment rates.

Other important tools for turning energy into images: Kodak X-Omatic cassettes. They're durable and lightweight. And they have specially designed curved covers that roll out air to create an intimate screen/film contact when closed, for consistently high image quality.

Kodak products. For the changing needs of the new world of diagnostic imaging.

Kodak has the expertise in how to apply imaging technology to the new diagnostic modalities. And Kodak has kept pace with the growing needs by providing products that can accurately record the information displayed on cathode-ray tubes or video monitors.

Kodak has films for nuclear medicine; for recording multiple, single, or dynamic images. Both single and double emulsion films. With spectral sensitivities compatible with cathode-ray tube displays.

Kodak also has films for CT scanning, for ultrasound, for thermography that can capture a wide range of gray tones.

The Kodak TSR: The logical link with your world of diagnostic imaging.

Your needs direct the extent of Kodak's help to you and your staff—through the services of your Kodak Technical Sales Representative whose qualifications are based on extensive training and experience in diagnostic imaging. Your Kodak TSR offers personal service and technical expertise directed to producing quality results on the view box. Your TSR can also arrange for seminars, lectures, special training courses for technologists, maintenance training for personnel involved with processors . . . or provide manuals, product brochures, technical

publications, technical aid materials, slide lectures, medical charts and audiovisual presentations. Contact your TSR to help you get the most out of your Kodak products and to help you get the most out of your x-ray department. Or consult your medical x-ray products dealer. Or write:
Eastman Kodak Company, Dept. 740-B,
Rochester, New York 14650.

TURNING ENERGY
INTO IMAGES

Kodak

RADIOGRAPHY • COMPUTERIZED TOMOGRAPHY
ULTRASOUND • NUCLEAR MEDICINE • THERMOGRAPHY

Boston City Hospital rate by 18% with Du Pont

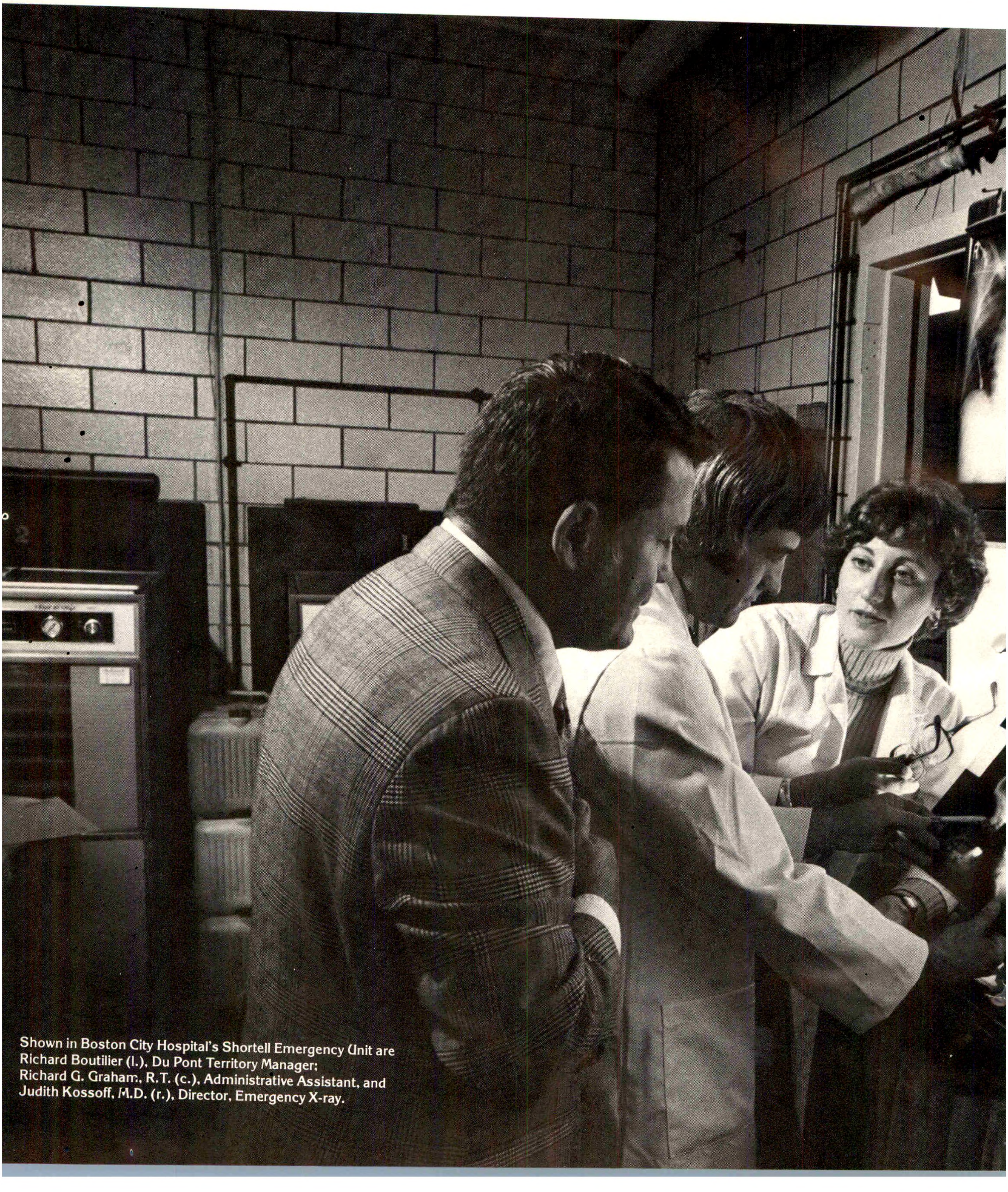

Shown in Boston City Hospital's Shortell Emergency Unit are Richard Boutilier (l.), Du Pont Territory Manager; Richard G. Graham, R.T. (c.), Administrative Assistant, and Judith Kossoff, M.D. (r.), Director, Emergency X-ray.

reduces its X-ray repeat Quality Control Program.

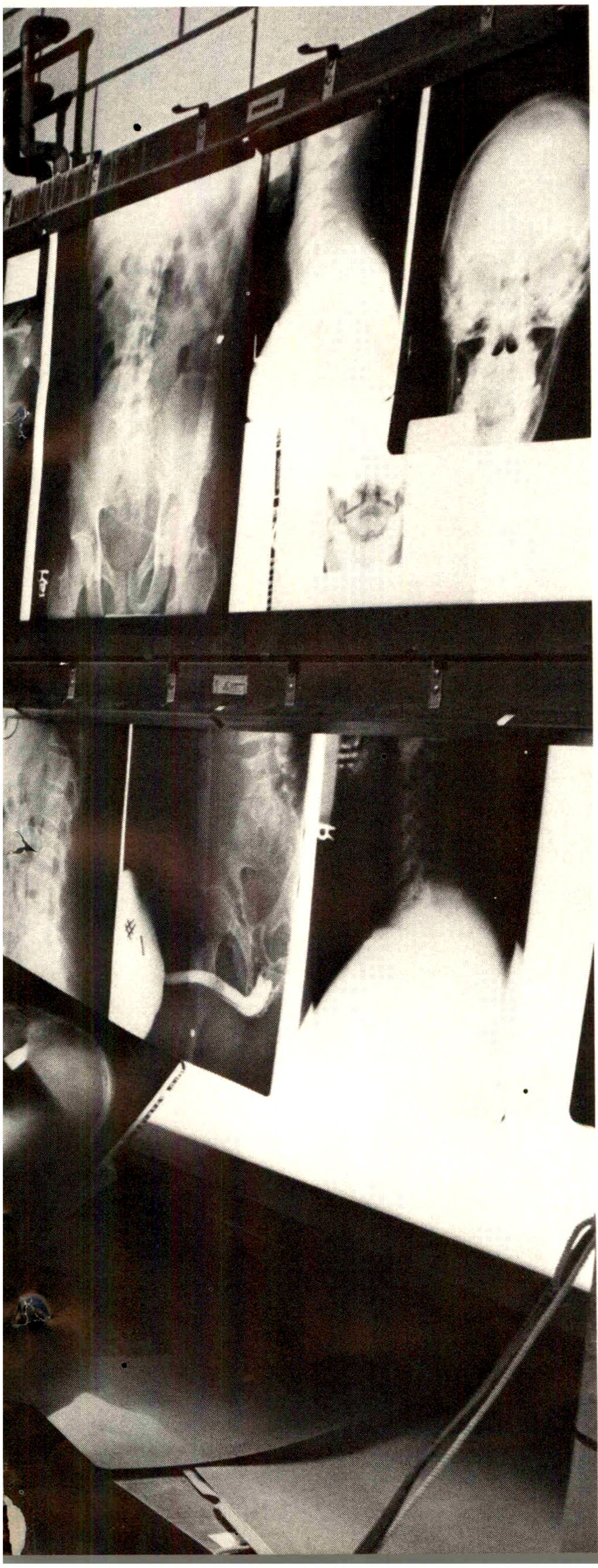

Annual film costs are cut by $7,500 in Shortell Emergency Unit. Department achieves increase in quality radiographs.

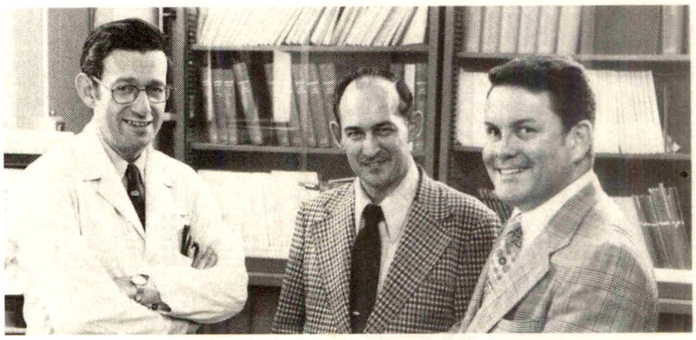

Jerome H. Shapiro, M.D. (l.), Director, Department of Radiology; Walter Stanton (c.), Du Pont Sales Service Representative, and Richard Boutilier (r.), Du Pont Territory Manager.

"Cost effectiveness has become crucial in today's environment," says Jerome H. Shapiro, M.D., Director of Boston City Hospital's Radiology Department. "Du Pont services have helped us realize a decrease in the spoilage of film, an increase in film quality and improved department efficiency."

Du Pont Quality Control services—the cost control analysis, repeat analysis, and other controls, calibrations and inspections done by the Du Pont team for a year—had an estimated value of over $10,000. Yet they didn't cost the hospital one additional dollar. In fact, the Radiology Department's cost of repeats decreased 18%.

Savings like these are typical of the results that can be achieved when Du Pont works with a radiology department. As Dick Graham, R.T., Administrative Assistant, says, "The Du Pont team gives the staff extra confidence in programs that can achieve high quality radiographs yet help us reduce costs."

It's all part of Du Pont's commitment—personal involvement and quality in everything we do and sell to provide reduced operating costs and better patient care.

Personal Involvement: The key to extra quality radiologic systems.

DU PONT

REG. U.S. PAT & TM OFF

a significant advance in postevacuation cholecystography

Kinevac®

Sincalide for Injection

- a convenient alternative to the fatty meal
- optimal gallbladder contraction in 5 to 15 minutes
- complete physician control

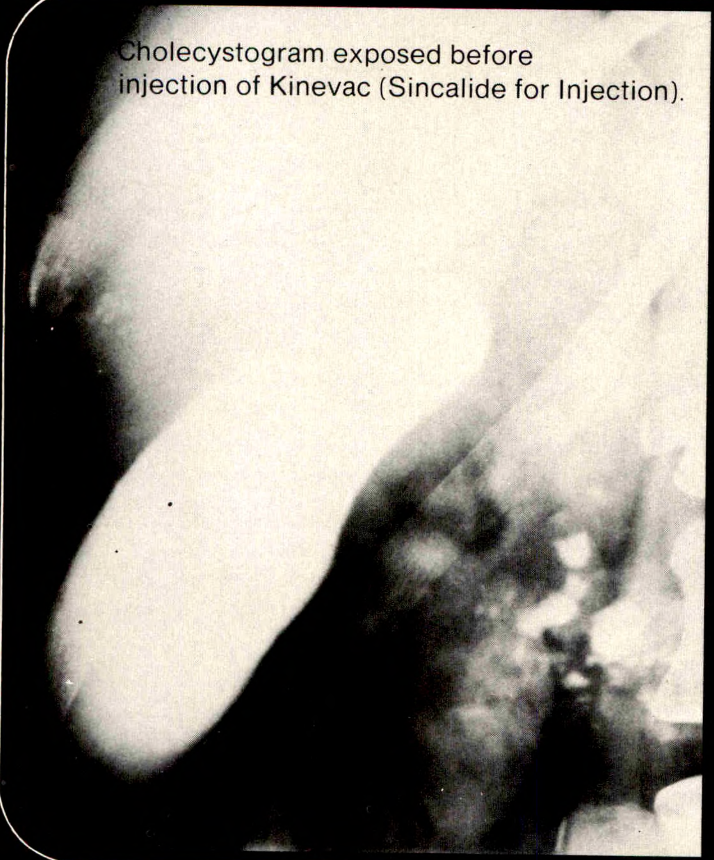

Cholecystogram exposed before injection of Kinevac (Sincalide for Injection).

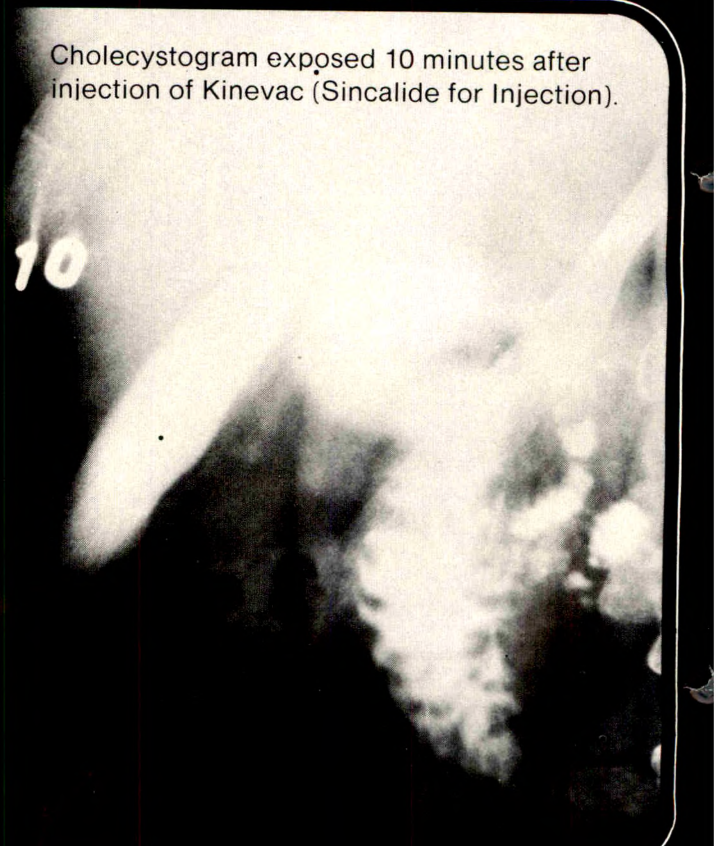

Cholecystogram exposed 10 minutes after injection of Kinevac (Sincalide for Injection).

Rapid, predictable gallbladder contraction

In cholecystography, Kinevac produces diagnostically satisfactory gallbladder contraction in 5 to 15 minutes.

A convenience to physician and patient

Provides the physician with an alternative to the fatty meal or fatty meal substitute when such a choice is desirable, gives greater control, permits a barium meal examination immediately following cholecystography, and results in an economy of time and personnel.

Valuable adjunct in diagnosis of diseases

Kinevac provides a sample of gallbladder bile that may be aspirated from the duodenum for analysis. In conjunction with secretin, it stimulates pancreatic secretion for analysis of its composition and examination of its cytology.

A significant scientific achievement

Sincalide, the C-terminal octapeptide of cholecystokinin synthesized in The Squibb Institute for Medical Research, reproduces all the known biological activity of the intact cholecystokinin molecule.

Kinevac®

Sincalide for Injection

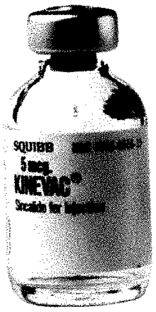

KINEVAC (Sincalide for Injection)

DESCRIPTION: Kinevac (Sincalide for Injection) is a sterile, lyophilized, white powder of the synthetic C-terminal octapeptide of cholecystokinin. Each vial provides 5 mcg. sincalide with 45 mg. sodium chloride as a carrier; sodium hydroxide or hydrochloric acid may be added during manufacture to adjust the pH to 5.5 to 6.5. When reconstituted with 5 ml. of Sterile Water for Injection U.S.P., each ml. contains 1 mcg. sincalide and 9 mg. sodium chloride.

CONTRAINDICATIONS: Contraindicated in patients sensitive to sincalide.

WARNINGS: Usage in Pregnancy—Although no teratogenic or antifertility effects were seen in animal studies, data are inadequate to determine the safety of sincalide in human pregnancy. Accordingly, sincalide should be used in pregnant women only when, in the judgment of the physician, the benefits outweigh the possible risk to the fetus.

Usage in Children—The safety of sincalide for use in children has not been established.

PRECAUTIONS: The possibility exists that stimulation of gallbladder contraction in patients with small gallbladder stones could lead to the evacuation of the stones from the gallbladder, resulting in their lodging in the cystic duct or in the common bile duct. The risk of such an event is considered to be minimal because sincalide, when given as directed, does not ordinarily cause complete contraction of the gallbladder.

ADVERSE REACTIONS: G.I. symptoms such as abdominal discomfort or pain, and an urge to defecate, frequently accompany the injection of sincalide. These phenomena are usually manifestations of the physiologic action of the drug, which include delayed gastric emptying and increased intestinal motility, and are not to be construed as necessarily indicating an abnormality of the biliary tract unless there is other clinical or radiologic evidence of disease. Nausea, dizziness, and flushing occur occasionally.

For full prescribing information, consult package insert.

HOW SUPPLIED: Kinevac (Sincalide for Injection) is supplied in cartons of 10 vials each vial containing 5 mcg. of sincalide.

SQUIBB®

contrast media™

The leader in
radiologic
diagnostics

© 1977 E. R. Squibb & Sons, Inc. H637-501

American Journal of Roentgenology
Guidelines for Authors

The *American Journal of Roentgenology* publishes original and timely contributions to the advancement of radiologic diagnoses and treatment. Although the content is predominantly clinical in origin, laboratory investigations are accepted when their relevance to clinical practice is demonstrable. Material published elsewhere, in substance or illustration, will not be considered. Prior publication of abstracts, however, will not prejudice publication of the complete study. Contributions are reviewed by two outside consultants and are accepted on condition that they are submitted only to this Journal and that they will not be reprinted or translated without consent of the Editor. Statements within an article are the responsibility of the authors and not the Journal or its publisher.

Address all manuscripts and correspondence to the Editor, Dr. Melvin M. Figley, 403 Pacific National Bank Building, 4545 15th Avenue N.E., Seattle, Washington 98105.

Manuscript Form

Manuscripts should be typed double-spaced throughout, including references, tables, and footnotes. Tables, footnotes, and figure legends should be on separate sheets, and a separate title page should be provided. In addition to the original typewritten copy, a duplicate copy complete with figures, tables, and references is required. Authors' names should be on title page only and should not be on figures so that author anonymity can be maintained during the review process.

Figures should be submitted as 13 X 18 cm glossy prints, untrimmed and unmounted. Each should be numbered to correspond with figure legends, and the top should be indicated. Written permission is required for reproduction of previously published figures, and such material must be clearly noted and credited in the manuscript. Specific permission for publication of facial photographs of patients is required. Line illustrations and graphs should be drawn in black ink on white background. Labels on all figures should be of professional quality and sufficiently large to be easily read when reduced in size.

References should be cited in the text by number (e.g., [3, 4]). The bibliography should be arranged in the numerical order that references are cited in the text and typed double-spaced throughout. Data for each reference should be arranged according to the uniform style on bibliographic citations adopted by many biomedical journals. Provide all authors' names and inclusive pages. Abbreviations for titles of medical periodicals should conform to those published in *Index Medicus*. Examples:

1. Miller RE, Chernish SM, Skucas J, Rosenak BD, Rodda BE: Hypotonic roentgenography with glucagon. *Am J Roentgenol* 121:264–274, 1974
2. Boijsen E: Superior mesenteric angiography, in *Angiography*, edited by Abrams H, Boston, Little, Brown, 1971, pp 1091–1119

Organization

Title page. Titles should be brief and specific. Include full names and addresses of all authors and acknowledgment of grant support when appropriate.

Abstract. A description of the purpose, methods, results, and conclusions of the study is required. It should be informative to a reader who has not read the text of the article.

Introduction. Clearly state the purpose of the investigation including necessary background facts.

Materials and methods. Describe the protocol clearly so that an experienced worker can understand what was done. Use standard abbreviations as presented in the *Council of Biology Editors Style Manual*, 3d ed. Metric measurements should be used throughout.

Results. Present results in logical sequence.

Discussion. Interpret the results to lend meaning and importance to the observations. If hypotheses and speculation are included, they must be labeled as such. When results differ from those of previous investigators, an attempt should be made to explain the discrepancy.

References. Only include those references which provide adequate background and present fairly any opposing evidence and concepts. Accuracy of reference data is the responsibility of the author.

Legends. Legends should be brief but should provide sufficient description to interpret the figure.

Special Communications

Case Reports. Concise case reports are accepted if they present unusual experiences that are medically important and educational. Clarity and brevity are essential.

Technical notes. Brief descriptions of new techniques or significant modifications of older ones which are directly applicable to clinical practice will be accepted.

Letters to the Editor. Letters are subject to editing and condensation. Criticism of published articles should be objective and constructive. Letters may also discuss matters of general interest to radiologists.

Proofs and Reprints

Galley proofs will be sent to authors for correction of errors and approval of illustrations. The corrected proof, copy-edited manuscript, and reprint order should be returned to the editorial office within 48 hr of receipt. Failure to adhere to this schedule may mean publication without the author's approval.

Impact of Computed Tomography on Utilization of Cerebral Angiograms

ERIC B. LARSON,[1] GILBERT S. OMENN,[1] M. THEODORE MARGOLIS,[2] AND JOHN W. LOOP[3]

In order to assess the effects of computed tomography (CT) of the brain on utilization of cerebral angiography, a retrospective analysis of three cohorts of patients was undertaken. Each cohort consisted of 50 consecutive patients receiving angiography either before a CT scanner was available, after installation of CT, or 1 year after CT. Since availability of CT, a progressive decrease in the proportion of angiograms that are normal has occurred (from 36% to 16%). Patients being evaluated for mass lesions account for the decrease. We conclude that CT is making neurodiagnostic evaluation more efficient and less invasive for patients with suspected mass lesions.

Introduction

Computed tomography (CT) of the brain is an important technologic advance in diagnostic radiology [1, 2], an advance which could result in decreased utilization of other neurodiagnostic procedures, especially invasive procedures [2–4]. The number of pneumoencephalograms has decreased since introduction of CT at the Mayo Clinic [5, 6]. The impact of CT on utilization of cerebral angiography is more complex. At the Mayo Clinic angiography was performed at about equal rates before and after installation of CT [6], suggesting that CT does not replace cerebral angiography. However, CT may have affected selection of patients receiving angiography.

The study reported here was designed to determine whether the proportion of patients with normal cerebral angiograms changed following installation of CT at our institution. The study is a comparison of cohorts of patients receiving angiography at a time before CT was available, shortly after CT became available, and more than 1 year after installation of CT. From our results, we conclude that CT has reduced the proportion of normal angiograms, primarily in patients being evaluated for suspected mass lesions.

Subjects and Methods

The study site, the Mason Clinic and Virginia Mason Hospital, is a multispecialty clinic with a 300 bed general and referral hospital which serves patients with the full range of neurological diseases. The hospital has an active division of neuroradiology; in September 1974, an EMI CT 1000 brain scanner became operational. While CT is performed on inpatients and outpatients, cerebral angiograms are performed exclusively on inpatients. These angiograms are generally requested by one of the four neurologists or two neurosurgeons on the medical staff. All angiograms were performed, interpreted, or reviewed by one neuroradiologist. There was no staff turnover among neurological specialists during the study period.

Three cohorts of 50 patients each were formed to represent patients before CT, after CT, and 1 year after CT. The cohorts were formed by selecting 50 consecutive patients receiving angiograms beginning November 1973 (before CT), November 1974 (after CT), and November 1975 (1 year after CT). Data were gathered from the angiogram reports, CT reports, and medical records and included patient age and sex, clinical impression before angiography, results of angiography, and results of CT scan if performed.

The clinical impression before angiography was classified as suspected mass lesion or suspected cerebrovascular disease. This classification was complicated in three cases in each cohort because the clinical impression before angiography specified both vascular and mass lesions as likely possibilities. These cases were designated unclassified. Of the patients with suspected mass lesions, primary or metastatic brain tumor was specifically stated as a possibility in 93% of cases.

Angiographic results were classified as normal (negative) or abnormal (positive). A normal study was defined to include those few examinations with vascular abnormalities described as insignificant or minimal. Abnormal angiograms were further divided into those showing significant vascular abnormalities and those with mass lesions, primarily tumors. Vascular abnormalities included intracranial and extracranial atherosclerotic changes, arteriovenous malformations, aneurysms, and parenchymal abnormalities associated with vascular disorders (infarction, hemorrhage, or mass effect). CT results were accepted only when CT was performed less than 1 month before angiography and were classified as either normal or abnormal.

Initially, an 80 X 80 CT image matrix was used. In February 1975, a 160 X 160 image matrix was installed. The larger matrix was used for patients in the 1 year after CT cohort. Conray® contrast enhancement was used on 36% of patients in the after CT cohort and 70% of patients in the 1 year after CT cohort. All statistical comparisons were made using Fisher's two-tailed *t* test or χ^2 analysis [7].

Results

The before and after CT cohorts were comparable in mean age and sex ratio (table 1). However, the 1 year after CT cohort contained significantly fewer males and was younger ($P < .05$). Successive cohorts contained increasing percentages of patients for whom the clinical impression was suspected cerebrovascular disease, but these differences were not statistically significant.

Received January 10, 1977; accepted after revision April 4, 1977.

These data have been reported in the *Bulletin of the Mason Clinic* (30:131–138, 1976), a nonspecialty journal of primarily regional circulation.

[1] Robert Wood Johnson Clinical Scholars Program and Department of Medicine, University of Washington School of Medicine, Seattle, Washington 98195. Address reprint requests to E. B. Larson.

[2] Department of Radiology, Mason Clinic, Seattle, Washington 98101.

[3] Department of Radiology, Harvorview Medical Center, Seattle, Washington 98204.

TABLE 1

Age, Sex Ratio, and Clinical Impression

	Before CT	After CT	1 Year After CT
Age (yr):			
Mean ± SD	55.6 ± 13.1	54.6 ± 11.2	49.6 ± 16.0
Range	24–81	17–83	15–78
Sex:			
Male	28(56)	30(60)	18(36)
Female	22(44)	20(40)	32(64)
Clinical impression:			
Suspected vascular disease	14(28)	18(36)	21(42)
Suspected mass lesions	33(66)	29(58)	26(52)
Unclassified	3(6)	3(6)	3(6)

Note.—Numbers in parentheses are percentages.

TABLE 2

Results of Angiograms

Finding	Before CT		After CT		1 Year After CT	
	No.	%	No.	%	No.	%
Normal	18*	36	10	20	8*	16
Vascular abnormality	20	40	25	50	26	52
Brain tumor	10	20	10	20	12	24
Enlarged ventricles/atrophy	1	2	2	4	3	6
Subdural hematoma	1	2	3	6	1	2

* $P < .05$ by χ^2 analysis.

The number of normal angiograms in the before CT, after CT, and 1 year after CT cohorts was 18, 10, and eight, respectively. The difference between the before CT group and 1 year after CT group is statistically significant. The types of abnormalities demonstrated by angiography were similar for the three cohorts (table 2).

In table 3 the angiographic results are classified in relation to the clinical impressions before angiography. All but two of the normal angiographic examinations involved patients examined for suspected mass lesions. Among patients with suspected mass lesions, the proportion of normal angiograms decreased, accounting for the overall decrease in normal angiograms in the two after CT cohorts. The proportion of patients who had suspected mass lesions confirmed at angiography increased from 12/33 (36%) to 14/29 (48%) to 15/26 (58%) across the three cohorts.

CT and angiographic results are compared in table 4. Of the 10 patients with normal angiograms in the after CT cohort, all eight who had CT scans had normal scans and all scans were done to rule out suspected mass lesions. There were no patients with suspected mass lesions who had normal CT scans and abnormal angiograms or vice versa, whereas 12 patients with suspected mass lesions had both abnormal angiograms and abnormal CT scans.

The results in the 1 year after CT cohort are similar but less uniform. One patient with a suspected pituitary tumor had a normal CT scan which was then followed by an angiogram demonstrating the suspected tumor (a false negative CT). There were two patients who had normal angiograms and abnormal CT scans. In one patient, a 78-year-old female evaluated for onset of headaches, the CT abnormality may represent an artifact, since the patient's symptoms have resolved, all other studies have been normal, and she remains asymptomatic after 8 months follow-up. The second patient, a 15-year-old boy with a chronic pyschomotor seizure disorder, was evaluated for the onset of tonic-clonic seizures. CT showed a small area of diminished density in the right posterotemporal area which corresponded to the location of focal electroencephalographic abnormalities. Following the normal angiogram, the patient was discharged on phenytoin and has remained free of seizures after 9 months follow-up. The underlying abnormality is unknown and may represent an old cyst. The first case represents a false positive CT. The second may represent a true positive CT, although CT artifact cannot be excluded.

Table 4 also shows that CT scanning did not detect all vascular abnormalities noted at angiography. Of the 24 patients in the two cohorts with vascular abnormalities noted angiographically who had CT scans, 11 (46%) had normal CT scans. The normal CT scans occurred in nine patients with intravascular changes of atherosclerosis and two with arteritis. One patient had only extracranial vascular disease; the other 10 patients had intracranial disease. Abnormalities detected by CT included seven infarctions, five mass effects, and one case of ventricular dilatation.

Discussion

In this study, we have examined the indications for and results of cerebral angiograms before and after CT in order to see whether the availability of CT has decreased the frequency of negative angiograms. The results show that such a reduction has occurred. They confirm the impression of neurologists at this institution that CT enables them to utilize angiography to evaluate patients with known lesions, rather than using it to exclude possible lesions in the differential diagnosis. The results also confirm a report from the Mayo Clinic documenting a steady decrease in the frequency of negative angiograms since the advent of CT [6].

Our conclusions are qualified by the fact that the study is a retrospective cohort analysis of patients selected by their physicians for angiography. Prospective random allocation of patients to CT was not and, to our knowledge, has not been done. The study also did not evaluate patient outcome; in fact, we do not know of a study which convincingly demonstrates improved patient outcome as a result of CT.

However, a decreased proportion of normal angiograms occurred in two separate after CT cohorts compared to a control before CT cohort. Therefore, the observation is

TABLE 3

Distribution of Patients by Clinical Impression and Angiographic Results

Clinical Impression before Angiogram	Angiographic Diagnosis	Cohort		
		Before CT	After CT	1 Year After CT
Mass lesion	Normal	17(34)*	10(20)	7(14)*
	Mass lesion	12(24)	14(28)	15(30)
	Vascular abnormality	4(8)	5(10)	4(8)
Vascular abnormality	Normal	1(2)	0	1(2)
	Vascular abnormality	13(26)	18(36)	20(40)
	Mass lesion	0	0	0
Unclassified	Vascular abnormality	3(6)	2(4)	2(4)
	Mass lesion	0	1(2)	1(2)

Note.—Numbers in parentheses are percentages.
* $P < .05$ by χ^2 analysis.

TABLE 4

Comparison of Angiographic and CT Results

Angiographic Result	CT Result		No. CT*	Total
	Normal	Abnormal		
After CT cohort:				
Normal	8	0	2	10†
Vascular abnormality	4	8	13	25
Mass lesion	0	12	3	15
Total	12	20	18	50
1 year after CT cohort:				
Normal	3	2	3	8†
Vascular abnormality	7	5	14	26
Mass lesion	1	14	1	16
Total	11	21	18	50

* Includes one CT study which could not be interpreted due to artifact and two CT studies performed more than 1 month before angiogram.
† All were clinically suspected of mass lesions.

reproducible over time and has also been noted at another institution [6]. These results suggest that certain patients with suspected mass lesions were spared an uncomfortable invasive procedure because of CT.

The observed reduction in proportion of normal angiograms presumably occurred because physicians are stopping negative diagnostic workups short of invasive studies (angiography or pneumoencephalography). In increasing numbers of cases, a negative CT scan provides physicians with enough diagnostic assurance that further evaluation is unnecessary. A similar observation has been made in groups of patients being managed for head injuries; a regional neurosurgical center reported that frequency of both invasive radiologic procedures and exploratory operations fell after availability of CT. However, there was no change in overall mortality [8].

The impact of the availability of CT must be analyzed separately for groups of patients with different categories of neurological disorders. Thus CT has been associated with an increased cost of neurodiagnostic evaluation without a significant decrease in use of angiography and without any apparent improvement in measurable components of patient care for cohorts of patients with cerebrovascular disease [9]. By contrast, we have observed after installation of CT a reduced proportion of normal angiograms among inpatients suspected of having brain tumors [10]. Furthermore, CT substituted for other neurodiagnostic procedures to such an extent that the average cost of the neurodiagnostic workup was not increased by the addition of CT [10]. We conclude that CT scanning, at least for patients with suspected mass lesions, has helped make neurodiagnostic evaluations more efficient, less hazardous, and less uncomfortable, a distinct improvement in one component of medical care.

REFERENCES

1. Hounsfield GN: Computerized transverse axial scanning (tomography): I Description of a system. *Br J Radiol* 46: 1016–1022, 1973
2. Ambrose J: Computerized transverse axial scanning (tomography): II Clinical application. *Br J Radiol* 46:1023–1047, 1973
3. Baker HL Jr, Campbell JK, Houser OW, Reese DF, Sheedy PF, Holman CB, Kurland RL: Computer assisted tomography of the head: an early evaluation. *Mayo Clin Proc* 49:17–27, 1974
4. New PFJ, Scott WR, Schnur JA, Davis KR, Taveras JM: Computerized axial tomography with the EMI scanner. *Radiology* 110:109–123, 1974
5. Baker HL Jr: The impact of computed tomography on neuroradiologic practice. *Radiology* 116:637–640, 1975
6. Baker HL Jr: Computed tomography and neuroradiology: a fortunate primary union. *Am J Roentgenol* 127:101–110, 1976
7. Armitage P: *Statistical Methods in Medical Research*. New York, Wiley 1971
8. Ambrose J, Gooding MR, Uttley D: EMI scan in the management of head injuries. *Lancet* 2:847–848, 1976
9. Larson EB, Omenn GS, Loop JW, Margolis MT: Computed tomography of the brain in patients with cerebrovascular disease. Submitted for publication
10. Larson EB, Omenn GS: The impact of CT on the care of patients with suspected brain tumor. *Med Care* In press, 1977

Note

The July issue was mailed out of sequence because of a prolonged strike at the journal's former printer.

Computed Tomography in Cerebral Hemiatrophy

CHARLES G. JACOBY,[1] RAYMUNDO T. GO, AND FRANCIS J. HAHN

The clinical and radiographic findings in four cases of cerebral hemiatrophy are presented. CT findings reflect the underlying gross pathologic changes and are in agreement with those seen on plain skull radiography and pneumoencephalography. The most impressive finding was unilateral loss of cerebral volume with ipsilateral displacement of the midline structures. The differential diagnosis primarily includes Sturge-Weber syndrome and linear sebaceous nevus syndrome. The recognition of compensatory calvarial changes should indicate that the cerebral abnormalities are the result of an atrophic or hypoplastic process that began in early life.

Introduction

The combination of radiographic findings commonly referred to as cerebral hemiatrophy represents the end stage of a number of etiologies resulting in atrophy or hypoplasia of one cerebral hemisphere. The clinical presentation of these patients is hemiplegia and a convulsive disorder. Mental retardation may or may not be present, and there may be shortening of the extremities on the affected side. Unilateral hypoplasia of the face and flattening of the curvature of the calvarium may be noted on physical examination [1].

In reviewing the pathologic findings, Alpers and Dear [2] found two general patterns. In one, there was absence of brain tissue with replacement by a cystlike structure with fibrous walls. The second pattern showed a generalized shrinkage of the hemisphere with all lobes involved. The gyri were smaller than normal, and the sulci were widened. In a large number of cases, the opposite cerebellar hemisphere was also atrophied. The meninges were thick and adherent to the hemisphere.

When the insult to the brain occurs in early life (usually before 2 years) a spectrum of compensatory changes may occur in the skull which correlate roughly with the amount of underlying brain atrophy and early onset of symptoms [3]. These changes can be recognized on plain film examination of the skull; they include thickening of the calvarium with loss of the convolutional markings of the inner table. On frontal view, the curvature of the calvarium is flattened. There is enlargement of the air cells of the frontal, ethmoid, and sphenoid sinuses; overpneumatization of the mastoid air cells leads to elevation of the petrous ridge. Two of our cases also demonstrated a diminished size of the middle cranial fossa.

Pneumoencephalography shows dilatation of the affected lateral ventricle with displacement of the midline structures toward this side. Some cases show no filling of the subarachnoid space over the affected hemisphere, and others show enlargement of the subarachnoid space with coarse sulci [1]. Taveras and Wood [4] also described large abnormal collections over the surface of the hemisphere due to external porencephaly.

This report describes four cases of cerebral hemiatrophy in which computed tomography was performed and correlates findings with those of plain skull radiography and pneumoencephalography.

Case Reports

Case 1

E. B., a 16-year-old male with a seizure disorder, right hemiparesis, and mental retardation, was first seen at 4 months of age when he sustained head trauma with a linear skull fracture and subdural hematoma. Dark blood (3–4 ml) was evacuated from the subdural space in the left parietal region.

Pneumoencephalography was performed when the patient was about 2½ years old. While the examination was not available for review, the report indicated presence of an enlarged left lateral ventricle with shift of the septum pellucidum to the left. Right lateral, third, and fourth ventricles were considered normal, and the impression was left cerebral atrophy.

The most recent admission (patient age, 16 years) was to evaluate an apparent decline in intelligence quotient. Physical examination showed a spastic hemiparesis on the right with the right arm flexed. There was weakness of the right extremities, and deep tendon reflexes were hyperactive on the right.

Plain skull radiographs showed thickening of the left calvarium with loss of convolutional markings on the same side. Elevation of the left petrous ridge with increased volume of the left mastoid air cells was present. Left ethmoid cells were enlarged and extended into the orbital roof. The volume of the left hemicranium and in particular, the left middle fossa was decreased. There was a lateral extension of the sphenoid air cell on the left.

CT examination showed left calvarial thickening with enlargement of the ethmoidal and mastoid air cells (fig. 1). The left middle cranial fossa and left cerebral hemisphere were of diminished size, and midline structures were displaced to the left. The left lateral ventricle was dilated, especially in the occipital region.

Comment. The typical findings of unilateral cerebral atrophy and compensatory skull changes were present in this patient. The cause is presumed to have been head trauma in infancy.

Case 2

M. F., a 17-year-old female, was evaluated for increase in frequency of seizures. Her gestational period was marked only by first trimester bleeding; the delivery was uneventful. A right hemiplegia was noted shortly after birth, and the first grand mal seizure occurred at age 3 years.

Physical examination at age 17 showed hyperreflexia of the right upper and lower extremities and a spastic gait. The right upper extremity was held in flexion at the elbow, wrist, and finger

---

Received October 26, 1976; accepted after revision March 25, 1977.

[1] All authors: Department of Radiology, University of Iowa Hospitals and Clinics, Iowa City, Iowa 52242. Address reprint requests to C. G. Jacoby.

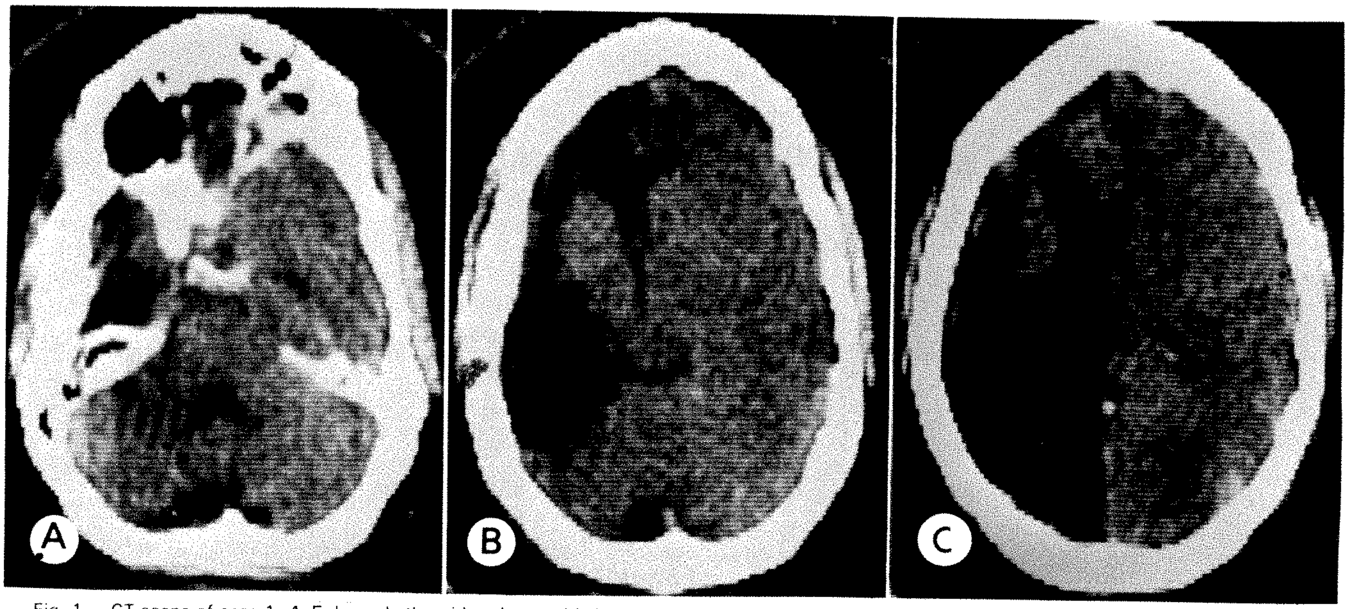

Fig. 1.—CT scans of case 1. *A*, Enlarged ethmoid and mastoid air cells on left and diminished volume of left middle fossa. *B*, Dilatation of frontal horn of left lateral ventricle with ipsilateral midline displacement, and widening of left sylvian fissure. *C*, Large area of low absorption continuous with body of lateral ventricle, most likely representing dilated occipital horn. Left calvarial thickening seen on all views.

joints. No skin lesions were present, and mental status was normal.

Plain skull radiographs showed left calvarial thickening with loss of the convolutional markings. The petrous ridge was elevated, and left frontal and mastoid air cells were enlarged.

CT showed enlargement of the left frontal and mastoid air cells in addition to left calvarial thickening (fig. 2). The left middle cranial fossa was smaller than the right. Although there seemed to be a slight difference in the level of the section on both sides, we did not feel it was enough to explain the asymmetry of the air cells and the size of the middle fossae. There was a generalized diminution in size of the left hemisphere with dilatation of the lateral ventricle. Increased lucency lateral to the left temporal lobe was present. Both the midline cerebral structures and the bony ridge at the attachment of the falx cerebri were displaced to the left.

Comment. The coexistent bony changes imply a developmental process rather than an acquired abnormality.

Case 3

E. S., a 16-year-old male, was evaluated for cerebral palsy with left spastic hemiplegia and convulsions beginning at age 7. His mental status was normal. No early childhood history was available.

Plain skull radiographs showed thickening of the right temporal and parietal calvarium with loss of the convolutional markings and diminished volume of the right middle fossa. The mastoid air cells, petrous pyramids, and paranasal sinuses were bilaterally symmetrical.

CT showed thickening of the right calvarium and dilatation of the right lateral ventricle. A large area of diminished absorption, most likely representing subarachnoid fluid, replaced brain tissue of the temporal lobe.

Comment. Childhood onset of hemiplegia and convulsions were present without mental retardation. CT demonstrated both the soft tissue and bone abnormalities.

Case 4

L. S., a 6-year-old male, has been followed in our neurology clinic for left hemiparesis and seizure disorder. At the onset of symptoms, the patient was 1 year old and beginning to walk. Physical examination showed no skin lesions. There was a left central facial nerve paralysis and left hemiparesis without spasticity.

Plain skull radiographs performed at the age of 3 years showed mild thickening of the right calvarium with loss of convolutional markings on this side. Paranasal sinus and mastoid pneumatization appeared equal bilaterally. Pneumoencephalography was also performed at age 3 and showed a uniformly dilated right lateral ventricle. Left lateral, third, and fourth ventricles were of normal size but displaced to the right. There was better filling of the sulci on the left than on the right.

CT examination performed at age 5 years 10 months showed dilatation of the right lateral ventricle (fig. 3). Left lateral, third, and fourth ventricles were of normal size and displaced to the right. No abnormal low absorption areas were seen and the sulci were not visualized. Increased thickness of the calvarium was accompanied by slight flattening of the curvature of the calvarium on the right. No frontal or sphenoid air cells were seen. The mastoid pneumatization was more prominent on the left (not illustrated).

Comment. This case showed only minor right hemiatrophy and skull thickening.

Discussion

Most findings seen pathologically, on plain film examination, or on pneumoencephalography were identifiable on CT studies on our patients. The most impressive finding was unilateral loss of cerebral volume with ipsilateral displacement of the midline structures (table 1). In one case (case 2) the falx attachment was also displaced, indicating that the process began before or during the time of greatest growth of the calvarium, thus excluding a contra-

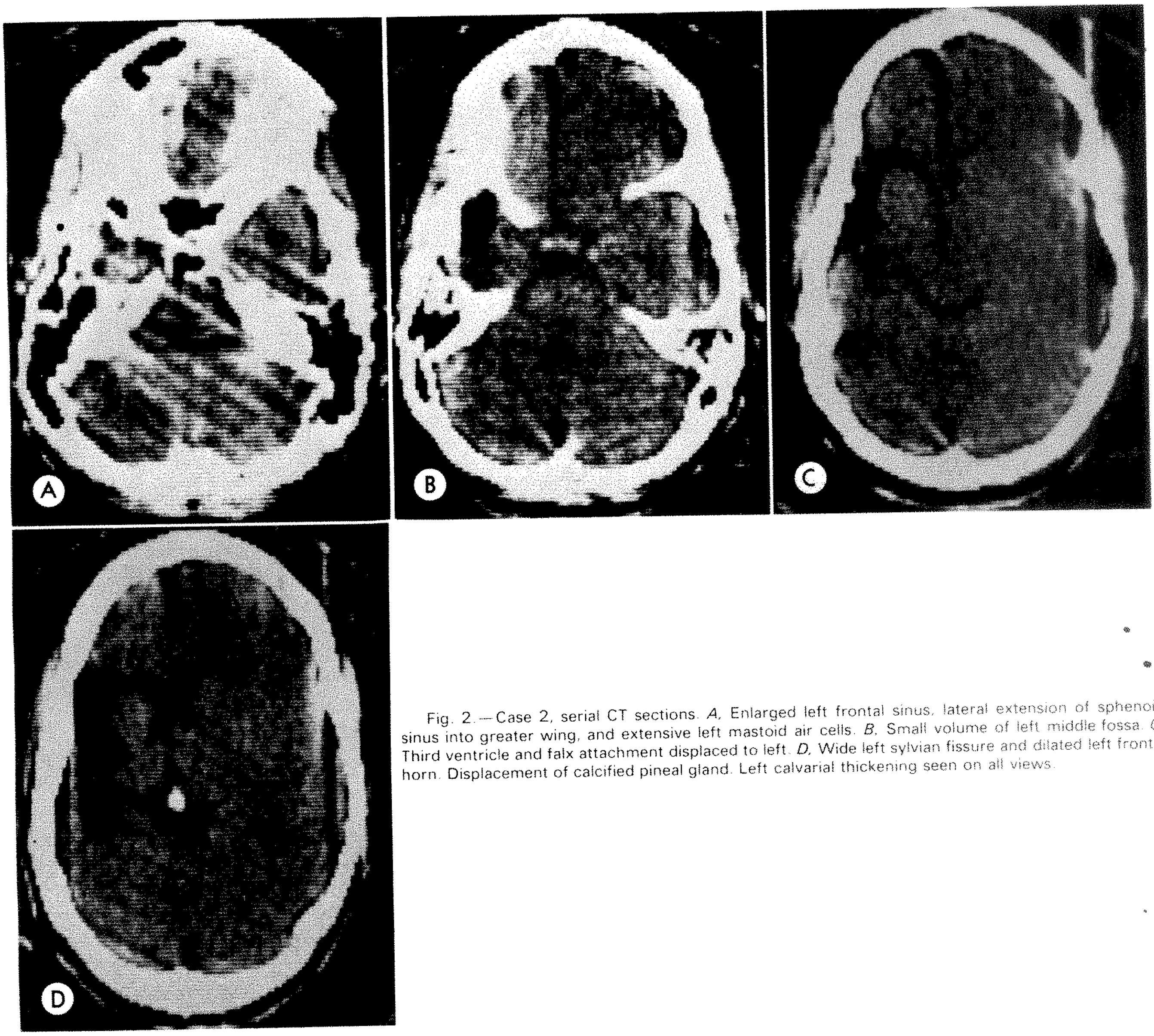

Fig. 2.—Case 2, serial CT sections. *A*, Enlarged left frontal sinus, lateral extension of sphenoid sinus into greater wing, and extensive left mastoid air cells. *B*, Small volume of left middle fossa. *C*, Third ventricle and falx attachment displaced to left. *D*, Wide left sylvian fissure and dilated left frontal horn. Displacement of calcified pineal gland. Left calvarial thickening seen on all views.

lateral lesion acquired later in life. The affected lateral ventricle was enlarged, and the third ventricle was of normal size but displaced position. Abnormal areas of diminished absorption may be seen overlying the cortical regions, most likely representing widening of the subarachnoid space or external porencephaly. In some cases, these areas of diminished absorption may indicate gliosis.

The compensatory skull changes were also recognizable. Unilateral thickening of the calvarium was present in each case. Diminished volume of the affected middle fossa was seen in cases 1 and 3 and confirmed by plain film examination. This finding was also suggested on CT examination of case 2, but a submental vertex view was not available for confirmation. Overdevelopment of paranasal sinuses and mastoid air cells was recognizable in the two cases that showed asymmetry of pneumatization on plain film examination (cases 1 and 2). However, this finding should be interpreted cautiously because if the plane of the section is at a different level on the two sides, a factitious asymmetry may result. We believe that this explains the asymmetric mastoid air cells of case 4, since skull radiographs showed symmetrical pneumatization bilaterally.

Differential Diagnosis

Sturge-Weber syndrome (encephalotrigeminal angiomatosis) shows similarities to our cases both clinically and radiographically. This is to be expected, since this condition represents cerebral atrophy associated with leptomeningeal angiomas. Mental retardation, convulsions, and hemiparesis are present but a clinically distinguishing feature is the port-wine facial nevus. Asymmetry of the skull is present, and unilateral ventricular dilatation and

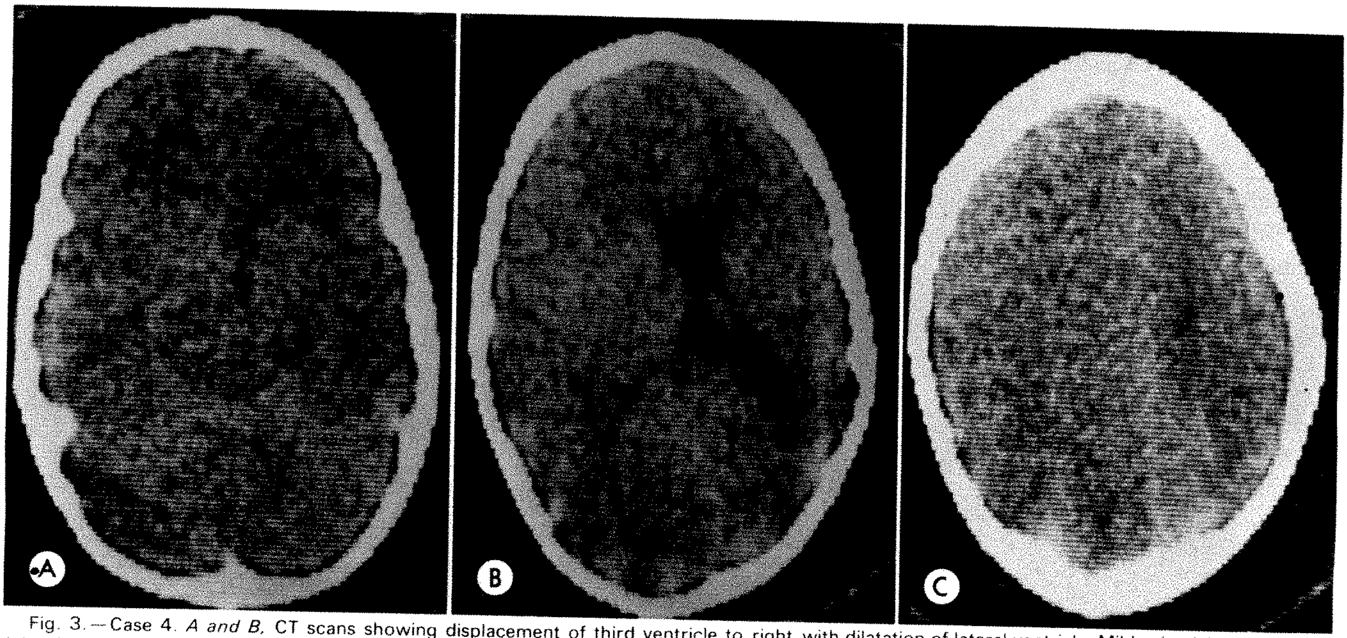

Fig. 3.—Case 4. *A and B,* CT scans showing displacement of third ventricle to right with dilatation of lateral ventricle. Mild calvarial thickening on right. *C,* CT scan at higher level showing right calvarial thickening.

TABLE 1

Summary of CT Findings

CT Finding	Case 1	Case 2	Case 3	Case 4
Unilateral calvarial thickening	+	+	+	+
Asymmetry of paranasal sinuses	+	+	–	–
Diminished volume of middle cranial fossa	+	+	–	–
Displaced midline structures	+	+	+	+
Dilatation of lateral ventricle	+	+	+	+
Low absorption areas	+	+	+	–

enlarged subarachnoid spaces may be seen [5]. Intracranial calcification is present on skull radiographs in 50%–60% of cases [6], but is present histologically in all cases [5]. Thus it is to be expected that calcification should be present in most, if not all, cases on CT examination. Indeed, Boltshauser et al. [7] described nine cases studied by CT and noted that the area of calcification appeared more extensive by this method than by radiographs. They also described bilateral calcification in this disorder and estimated that it occurred in up to 15% of cases. CT scans are included for three of their cases and asymmetrical skull thickening (although not mentioned in the text) can be seen in each case. In these cases of bilateral calcification, the skull thickening is on the side of the more extensive calcification. Harwood-Nash [8] also illustrated two cases; his figure 22*A* suggested slight calvarial thickening and flattening adjacent to the occipital region.

Linear sebaceous nevus syndrome is a neurocutaneous syndrome similar to tuberous sclerosis with mental retardation, convulsions, and characteristic linear nevus of the face. Marden et al. [9] described a case with enlargement of the left lateral ventricle and normal right lateral, third, and fourth ventricles. Skull radiographs showed elevation of the left petrous ridge and extensive erosion of the sella turcica and body of sphenoid bone. Unfortunately, presence of skull asymmetry could not be determined from the published photograph. Lansky et al. [10] described three additional cases of this syndrome. In two, the skull radiographs were reported as normal at ages 5 and 9 months, respectively. In one of these cases, pneumoencephalography demonstrated lack of filling of the subarachnoid space over one cerebral hemisphere and ventricles of normal size. The third case had asymmetry of the skull clinically with flattening over the left parietal area. No radiographs of this case were reported. It is to be expected that the skull asymmetry and unilateral ventricular dilatation in this syndrome would be recognized on CT examination and may resemble hemiatrophy.

An important diagnostic feature of cerebral hemiatrophy on CT is the ipsilateral midline shift. The concomitant displacement of the falx attachment (case 2) indicates that the midline displacement is developmental rather than acquired. Midline shift in the late atrophic stage of progressive multifocal leukoencephalopathy has been described [11], but the absence of unilateral calvarial changes and decrease in brain size helps to differentiate this condition. When a midline shift is due to mass effect, such as acute cerebral infarction, brain tumor, abscess, or subdural hematoma, the midline shift is away from the mass effect and unilateral calvarial changes are not seen.

The presence of a large localized area of diminished absorption representing replacement of brain tissue by subarachnoid fluid is also seen in arachnoid cysts [12]. Similar changes may be seen as the end stage of massive cerebral infarction. However, midline displacement in this condition is unusual [4], and calvarial changes would not be expected.

CT findings in cerebral hemiatrophy reflect the underlying gross pathologic changes and are in agreement with findings on plain skull radiography and pneumoencephalography. The recognition of compensatory calvarial changes should indicate that the observed cerebral abnormalities are the result of an atrophic or hypoplastic process that began in early life.

ACKNOWLEDGMENTS

We thank Dr. Kenneth D. Dolan for helpful suggestions in reviewing the manuscript, Dr. Steven H. Cornell for providing material on case 3, and Mrs. Carole Hoffman for typing the manuscript.

REFERENCES

1. Dyke CG, Davidoff LM, Masson CB: Cerebral hemiatrophy with homolateral hypertrophy of the skull and sinuses. *Surg Gynecol Obstet* 57:588-600, 1933
2. Alpers BJ, Dear RB: Hemiatrophy of the brain. *J Nerv Ment Dis* 89:653-669, 1939
3. Ross AT: Cerebral hemiatrophy with compensatory homolateral hypertrophy of the skull and sinuses and diminution of cranial volume. *Am J Roentgenol* 45:332-341, 1941
4. Taveras JM, Wood EH: *Diagnostic Neuroradiology*, 2d ed, vol 1. Baltimore, Williams & Wilkins, 1976
5. DiChiro G, Lindgren E: Radiographic findings in 14 cases of Sturge-Weber syndrome. *Acta Radiol* (Stockh) 35:387-399, 1951
6. Coulam CM, Brown LR, Reese DF: Sturge-Weber syndrome. *Semin Roentgenol* 11:55-60, 1976
7. Boltshauser E, Wilson J, Hoare RD: Sturge-Weber syndrome with bilateral intracranial calcification. *J Neurol Neurosurg Psychiatry* 39:429-435, 1976
8. Harwood-Nash DC: Congenital craniocerebral abnormalities and computed tomography. *Semin Roentgenol* 12:39-51, 1977
9. Marden TM, Venters HD: A new neurocutaneous syndrome. *Am J Dis Child* 112:79-81, 1966
10. Lansky LL, Funderburk S, Cuppage FE, Schimke RN, Diehl AM: Linear sebaceous nevus syndrome. A hamartoma variant. *Am J Dis Child* 123:587-590, 1972
11. Carroll BA, Lane B, Norman D, Enzmann D: Diagnosis of progressive multifocal leukoencephalopathy by computed tomography. *Radiology* 122:137-141, 1977
12. Banna M: Arachnoid cysts on computed tomography. *Am J Roentgenol* 127:979-982, 1976

Refinements in Chiba Needle Transhepatic Cholangiography

JOSEPH T. FERRUCCI, JR.,[1] AND JACK WITTENBERG[1]

The recent wide acceptance of Chiba needle transhepatic cholangiography prompted this elaboration of present techniques, intraprocedure observations, and special interpretive considerations based on a series of 100 consecutive examinations. The established safety margin of this technique now permits up to 15 needle passes to obtain a cholangiogram; thus success rates of duct opacification presently approach 100%. Special phenomena related to the small caliber of the needle include duct filling from "invisible" radicles, perivenous or periductal dissection of contrast, and pseudolesions in an incompletely decompressed stagnant bile column. The role of fine needle cholangiography in light of other present day technology for evaluating obstructive jaundice (ultrasonography, computed tomography, and endoscopic retrograde cholangiography) is discussed.

Percutaneous transhepatic cholangiography with the fine caliber (23 gauge; OD, 0.7 mm) thin-walled "Chiba" needle has become rapidly accepted as the preferred approach for direct opacification of the biliary ducts in the evaluation of cholestatic jaundice [1–5]. Safer and more successful than conventional sheathed needle transhepatic cholangiography, it has also proved more successful, easier to perform, and less costly than endoscopic retrograde cholangiography [3–4].

The standard techniques outlined in prior reports by us [4] and others [1, 5] emphasize bile duct opacification by an injection-withdrawal maneuver utilizing fluoroscopic control. In view of the increasing popularity of the method and the critical role of fluoroscopic observations during intrahepatic contrast deposition, further elaboration of indications, techniques, and special interpretive considerations appears warranted.

This review is based on a series of 100 consecutive fine-needle cholangiograms performed at the Massachusetts General Hospital since June 1975. The overall success rate of bile duct opacification was 94/100 (94%), with 71/72 (99%) successful studies obtained when duct dilatation was present. When ducts were normal in caliber or sclerosed, duct opacification was achieved in 23/28 (82%) of cases.

Complications were infrequent and included pneumothorax in two of 100 and sepsis (fever and hypotension) in four of 100 patients, all of whom had obstructed ducts. Low grade febrile reactions were observed in seven of 100 cases, often within 2–3 hr, but only when dilated ducts were shown. No bleeding or bile extravasation was encountered.

Technical Considerations

Details of technique have been outlined in previous reports [1, 4, 5]. Important factors include use of the lateral approach, the injection-withdrawal maneuver, and avoidance of undue duct distension. Use of a short 30° noncutting beveled needle obviates bleeding.

With increasing confidence in the safety of the procedure, prior technical restrictions have been relaxed; we now perform up to 15 needle passes to obtain a cholangiogram. Some workers set no limit on the number of needle passes [6]. Thus the overall success rate of duct opacification presently approaches 100%; only one failure has occurred in the last 41 consecutive cases. By the same token when ducts were dilated, successful puncture occurred on the first or second pass in 48/72 (67%) of the entire series. Following an unsuccessful needle pass on subsequent attempts, the direction of the needle is altered through a series of 10° fanlike steps superiorly and inferiorly, and then dorsally and ventrally, until a duct is entered.

Aspiration of bile is usually not successful, often prolongs the procedure, and is not an essential safety measure provided undue duct filling is avoided. If high grade ductal obstruction is disclosed and bile can be aspirated, contrast is replaced volume for volume to obtain a cholangiogram. Injection of the least volume of contrast necessary to establish the diagnosis will minimize septic complications. Preprocedure prophylactic antibiotics are not routine but are administered if the patient is clinically icteric or has a history of cholangitis. A history of biliary sepsis is not considered an absolute contraindication to the procedure since patients with recent attacks of cholangitis can be safely studied under appropriate antibiotic coverage, provided undue duct distension is avoided. If a surgical lesion of the biliary ducts has been displayed, immediate laparotomy is not mandatory, but parenteral antibiotics are administered while awaiting surgery.

Fluoroscopic Observations

Transparenchymal Needle Track

Following initial thrust of the needle to the appropriate depth within the hepatic substance, gradual incremental withdrawal with intermittent injections of small amounts of contrast is carried out under fluoroscopic control. Because the needle passes in and out of the hepatic parenchyma along the same path, a distinct track is created which appears as a persistent linear streak of contrast

---

Received January 24, 1977; accepted after revision April 4, 1977.

[1] Department of Radiology, Massachusetts General Hospital and Harvard Medical School, Boston, Massachusetts 02114. Address reprint requests to J. T. Ferrucci, Jr., at Massachusetts General Hospital.

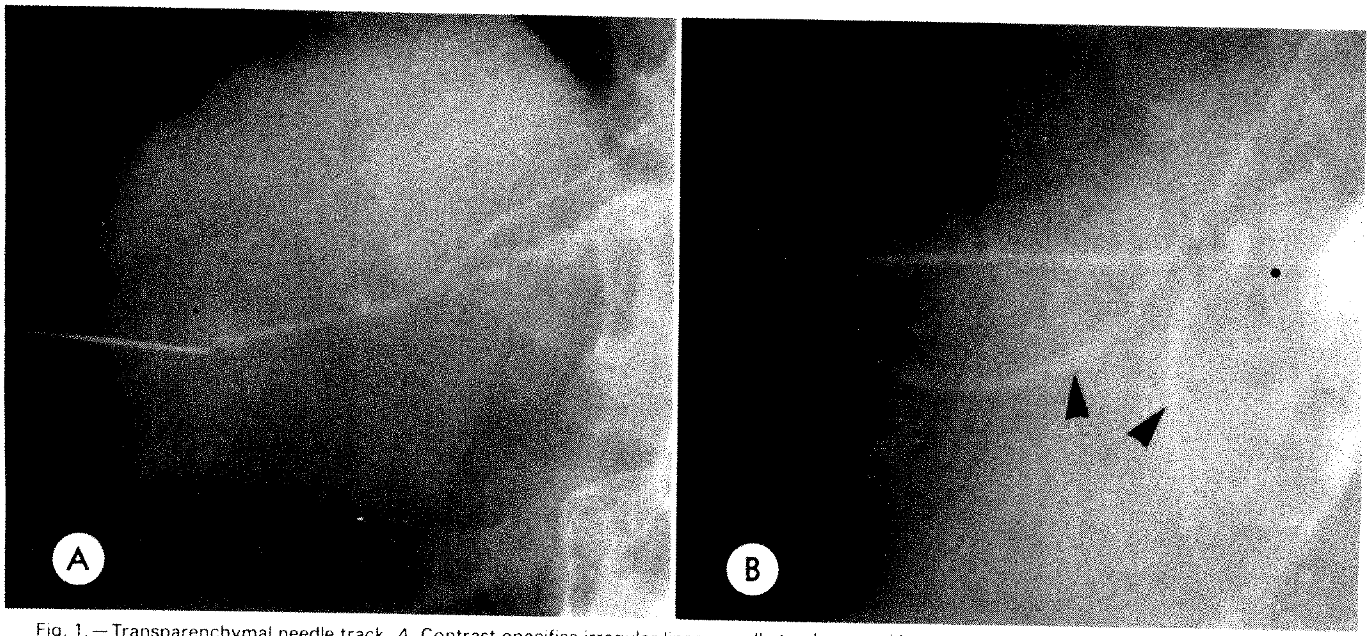

Fig. 1.—Transparenchymal needle track. *A*, Contrast opacifies irregular linear needle track created by entry-withdrawal needle motion. *B*, Preferential contrast flow via track into venous channels (*arrows*) may divert contrast from small biliary radicles.

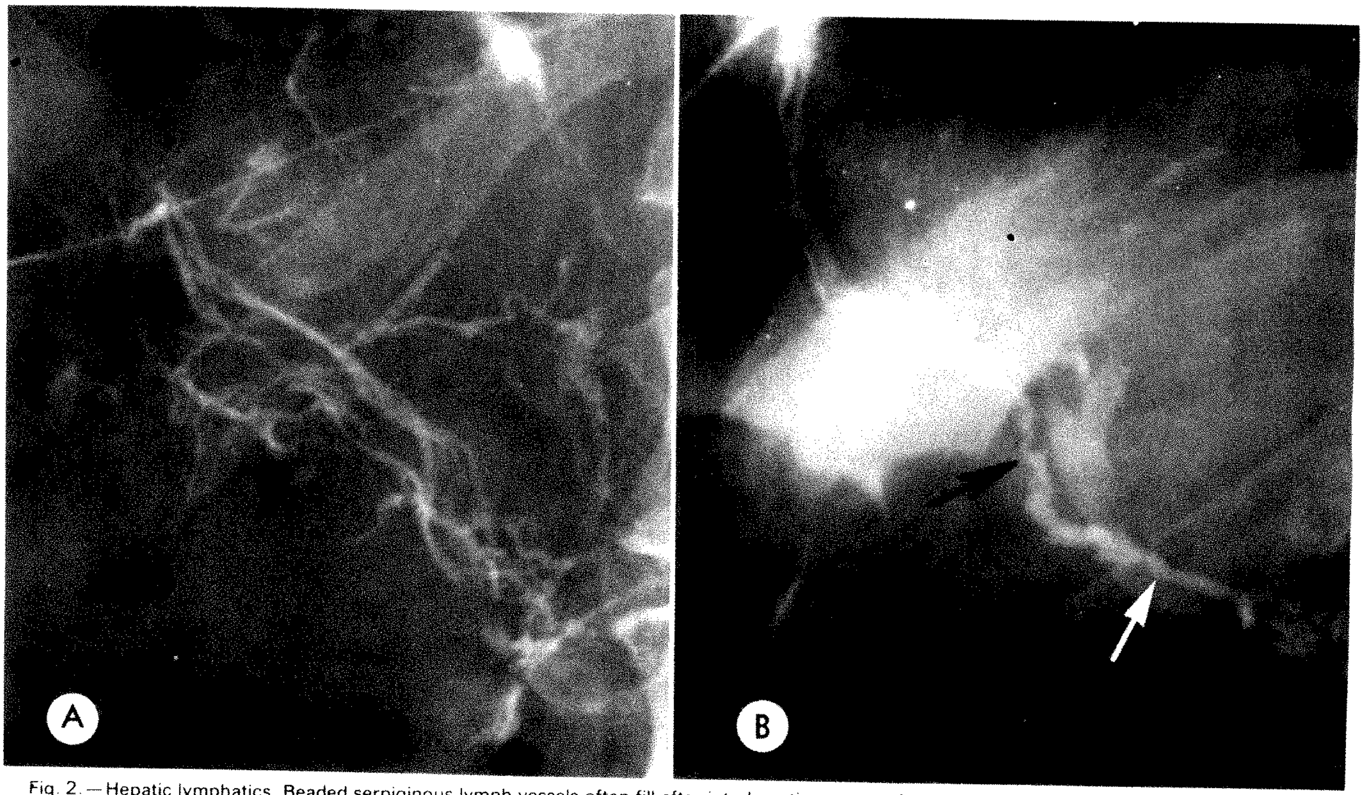

Fig. 2.—Hepatic lymphatics. Beaded serpiginous lymph vessels often fill after intrahepatic contrast deposition and course medially and inferiorly from porta hepatis. They may appear as branching multichannel network (*A*) or as single trunk (*B*, *arrows*) which could be misinterpreted as irregular or sclerosed biliary radicle.

medium, often reaching several centimeters in length (fig. 1*A*). This may act as a conduit for the preferential flow of contrast material into venous structures originally punctured deep within the liver substance, even though the needle has been withdrawn peripherally (fig. 1*B*). The net effect of this preferential flow of contrast from the needle tip into previously punctured venous branches is that contrast tends to be diverted from small biliary radicles which may be entered as the needle is being withdrawn further, and negative passes result. There is no ready corrective maneuver for this situation, and further punctures in another plane will usually be required.

Hepatic Lymphatics

Serpiginous beaded lymph vessels are frequently opacified following deposition of contrast medium in the hepatic parenchyma. These rarely exceed 2–3 mm in diameter and may appear as a single or branching multichannel network extending inferiorly and medially from the area of the porta hepatis (fig. 2*A*). When single lymphatic channels are identified, the appearance may initially be confused with a small caliber or sclerosed intrahepatic biliary radicle (fig. 2*B*). Fluoroscopically, the rate of contrast flow in both structures is similar, but the anatomic course of the lymph vessels permits ready recognition [7, 8]. The diagnostic significance of hepatic lymph channel filling following transparenchymal contrast injection otherwise appears minimal. Although lymphatic dilatation has been reported in hepatic cirrhosis, Okuda et al. [7] found no correlation between opacified lymphatics and the presence of hepatobiliary disease in 125 cases observed during transhepatic contrast injections. Increasing use of fine needle biliary duct puncture should provide more in vivo data on this question.

Filling From "Invisible" Radicles

Because of its small caliber (23 gauge; OD, 0.7 mm), the fine needle will occasionally puncture tiny intrahepatic radicles of insufficient size to be recognized during fluoroscopy (invisible), yet large enough to carry contrast distally into the common duct itself (fig. 3). In such cases, fluoroscopic screening confined to the intraparenchymal locus of the needle tip will yield the false impression that a negative pass has been made. Hence brief fluoroscopic scanning over the region of the distal common duct is recommended at the conclusion of each "negative" withdrawal to detect serendipitous duct opacification from tiny unrecognized intrahepatic radicles.

Interpretive Problems

Adventitial Dissection

The small diameter of the Chiba needle often permits contrast to be deposited within rather tightly confined anatomic spaces such as the adventitial planes surrounding the major vascular structures and biliary ducts entering the porta hepatis (fig. 4). Dissection of opaque material along the adventitial planes of these large tubular structures may occur and result in misleading radiographic appearances. In two cases adventitial dissection has simulated the appearance of intraluminal contrast within the biliary system and in one case resulted in a false positive diagnosis of biliary duct obstruction. Fluoroscopically, the slower flow of contrast in adventitial compartments permits differentiation from contrast material within the lumen of the biliary system where centrifugal flow is more rapid.

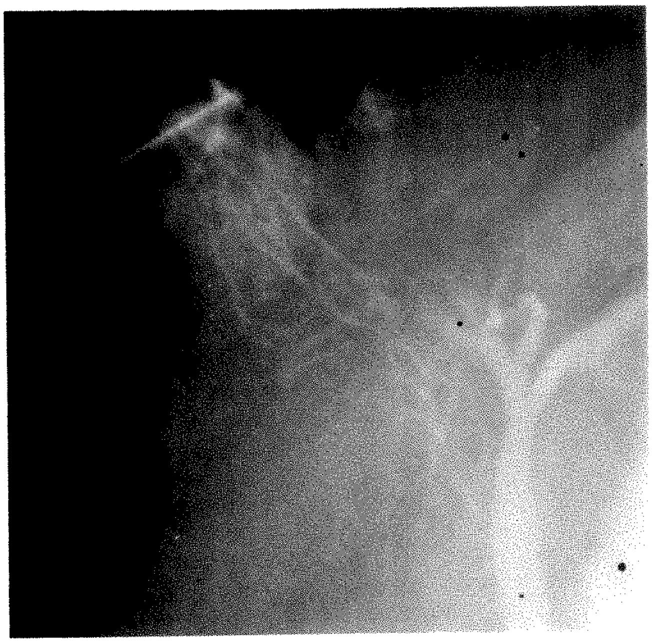

Fig. 3.—Common duct filling from tiny "invisible" biliary radicle. Despite excellent local parenchymal stain, opacification of lymph channels, and filling of common duct proper, actual site of entry into biliary tree (minute peripheral radicle) is not evident.

Stagnant Bile Column

In the presence of obstructing lesions of the common bile duct, elevated intraluminal pressure and increased viscosity of stagnant bile may cause poor distal flow of the opaque medium and prevent adequate mixing of injected contrast and bile. Resulting interpretive problems include *false proximal localization of the site obstruction* and *admixture pseudodefects.*

Kittredge and Baer [9] recently drew attention to the phenomenon of false proximal localization of the site of common bile duct obstruction due to inspissated bile in the presence of high grade surgical obstruction distally. This occurred despite the use of conventional large caliber 18–20 gauge sheathed needles. Since the small caliber of the Chiba needle is much more likely to inhibit free aspiration of bile, particularly when excessive viscosity is present, false localization of the site of obstruction at a more proximal level in the biliary tree is not unexpected with this technique and has occurred in four patients in the present series, all of whom also had high grade distal obstruction. As illustrated in figures 5 and 6, initial fluoroscopy and radiographs may suggest an obstructing process in the proximal extrahepatic ducts because of incomplete mixing of contrast and bile within the distal portion of the obstructed system. Although all of our cases were correctly interpreted, potential diagnostic errors could be expected to include undetected distal common duct calculi and false positive diagnoses of high periportal neoplastic infiltration when only a localized obstructing periampullary

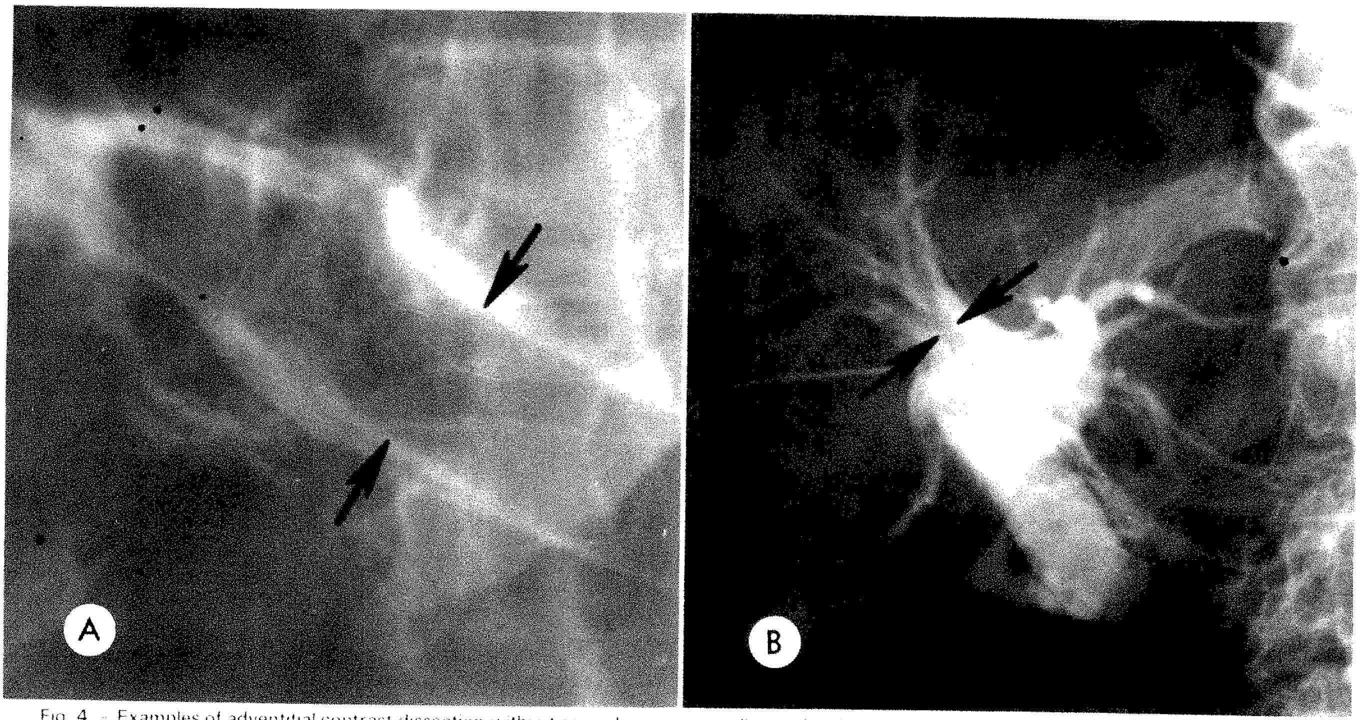

Fig. 4.—Examples of adventitial contrast dissection within tissue planes surrounding major ducts and vessels of porta hepatis. *A*, Splenoportal venous junction. *B*, Periportal dissection disclosing negative outline of hepatic arterial branches (*arrows*) and opacification of several normal biliary radicles.

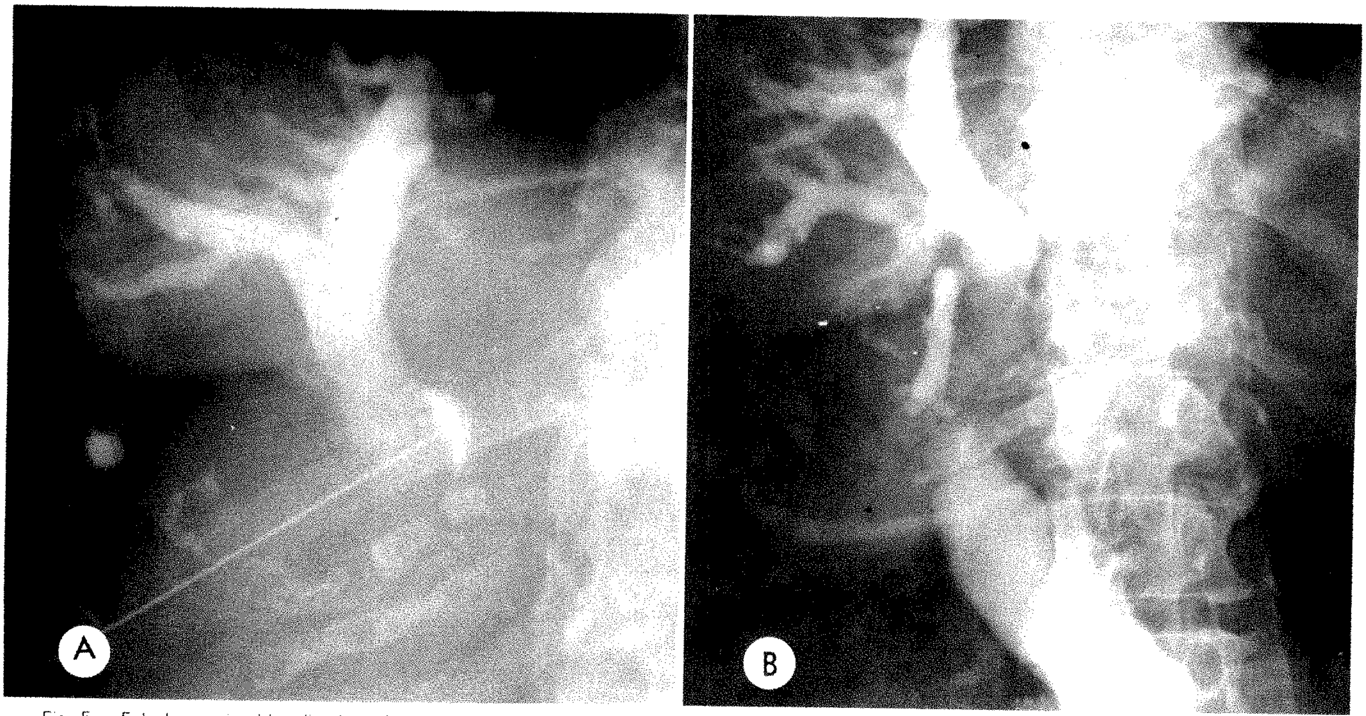

Fig. 5.—Falsely proximal localization of level of obstruction due to obstructive inspissation and stagnation of bile column. *A*, Initial film showing apparent block at level of common hepatic duct in porta hepatis. *B*, Delayed semierect film permiting better mixing with opacification of entire length of dilated distal common duct. Diagnosis, carcinoma of head of pancreas.

tumor is present. Kittredge and Baer [9] also commented on a hazy, poorly defined interface of the contrast column as suggestive of this effect. However, in our experience accurate interpretation in such cases usually requires a combination of semierect, delayed, or prone films (after removing the needle) to assure complete opacification of

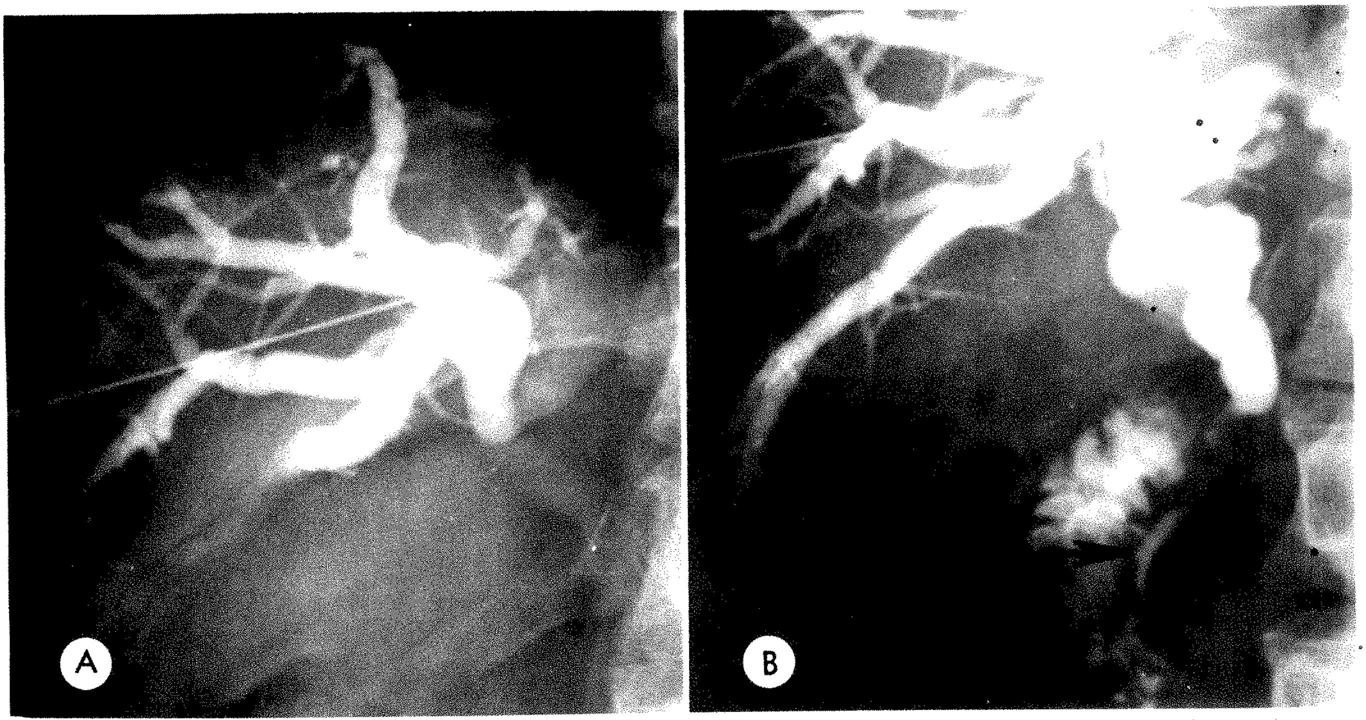

Fig. 6.—Another example of falsely proximal level of block due to distal lesion. 56-year-old man with bronchogenic carcinoma and obstructive jaundice. *A,* Initial film indicating obstruction at level of porta hepatis. Termination of contrast column is hazy and indistinct. *B,* Delayed upright film showing improved filling for several centimeters distally and delineation of short irregular stricture. Distal common duct is of normal caliber (*arrows*). Diagnosis, peripancreatic lymph node metastases.

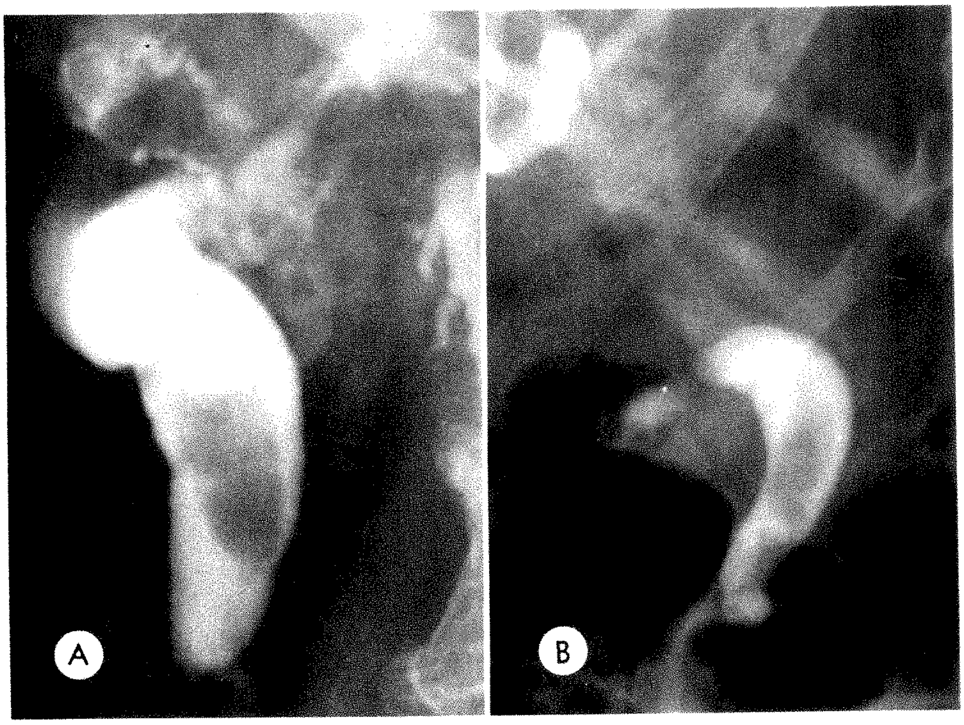

Fig. 7.—Two cases illustrating elongated admixture pseudodefects simulating calculi as result of local incomplete contrast-bile mixing. At surgery, both patients found to have benign periampullary strictures with no stone or other discrete lesion.

the entire length of the extrahepatic biliary tree.

Admixture pseudodefects may occur in a stagnant bile column when there is incomplete local mixing of bile with injected contrast. In the present series this produced a single elongated filling defect simulating a large oval calculus in two patients with benign periampullary strictures (fig. 7). In both cases the defect was seen in the mid-portion of the common duct above the strictured area

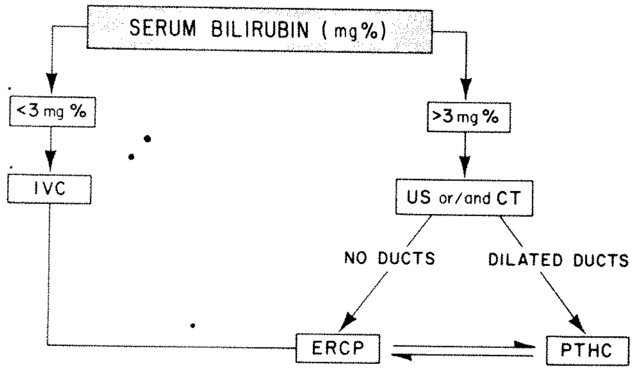

Fig. 8.—Schema relating role of percutaneous transhepatic cholangiography to other techniques for evaluation of obstructive jaundice.

at the choledochoduodenal junction, yet no corresponding lesion was found at subsequent common duct exploration. Subsequently identical pseudodefects have been recognized in this segment of the duct during routine postoperative cholangiography with normal results on careful follow-up studies. The effect is considered analagous to spurious filling defects occasionally observed as a result of contrast layering within the fundus of an intact gallbladder during intravenous cholangiography. Familiarity with this appearance in the setting of common duct stasis and the use of positional maneuvers such as semierect views should aid the differential diagnosis.

"Chiba" Needle versus Endoscopic Retrograde Cholangiography

While the fine needle has largely superceded the conventional sheathed needle assembly for percutaneous cholangiography, many investigators agree it is also rapidly replacing endoscopic retrograde cholangiography as the procedure of initial choice for direct biliary duct opacification in investigation of obstructive jaundice [3–5]. When duct dilatation is present, fine needle puncture more consistently produces successful cholangiograms (100% compared to 70% for ERCP) [1, 2, 4, 5], and is generally quicker, less expensive, and more widely available at smaller institutions where reliable endoscopic capabilities may be lacking. On the contrary, ERCP affords a broader diagnostic approach including opportunity for endoscopic diagnosis and biopsy in addition to cholangiography and pancreatography. It is thus more effectively utilized for evaluation of a subset of clinical problems other than obstructive jaundice, namely, undiagnosed abdominal pain with or without laboratory abnormalities suggestive of pancreatobiliary disease.

On the basis of the foregoing, a logical approach to the investigation of patients with suspected biliary obstruction has been developed (fig. 8). This schema utilizes either intravenous cholangiography or gray scale ultrasonography (and/or computed tomography) as the initial noninvasive study as indicated by the serum bilirubin level. The probability of duct opacification by intravenous cholangiography diminishes rapidly above total bilirubin levels of 3 mg/100 ml, and thus cross-sectional imaging studies should be substituted as the primary screening techniques when more severe cholestasis is evident. Barium studies, radionuclide examinations, and angiography play only a secondary role.

It is to be noted that even though dilated ducts are disclosed by ultrasound (and/or CT), direct needle cholangiography is still recommended for precise delineation of the level and nature of the obstructing lesion prior to surgery. In this regard, evolving medicolegal considerations may reinforce the desire of the abdominal surgeon for thorough preoperative visualization of the biliary tree when surgical manipulation is imminent.

If either fine needle cholangiography or ERCP fails, the alternate procedure is employed. With this approach, rapid accurate diagnosis of biliary obstruction can be achieved with a wide margin of safety and cost effectiveness.

REFERENCES

1. Okuda K, Tanikawa K, Emura T, Kuratomi S, Jinnouchi S, Urabe K, Sumikoshi T, Kanda Y, Fukuyama Y, Musha H, Mori H, Shimokawa Y, Yakushiji F, Matsuura Y: Nonsurgical percutaneous transhepatic cholangiography—diagnostic significance in medical problems of the liver. *Am J Dig Dis* 19: 21–36, 1974
2. Redeker AG, Karvountzis GG, Richman RH, Horisawa M: Percutaneous transhepatic cholangiography: an improved technique. *JAMA* 231:386–387, 1975
3. Elias E, Hamlyn AN, Jain S, Long RG, Summerfield JA, Dick R, Sherlock S: A randomized trial of percutaneous transhepatic cholangiography versus endoscopic retrograde cholangiography for bile duct visualization in obstructive jaundice. *Gastroenterology* 71:439–443, 1976
4. Ferrucci JT Jr, Wittenberg J, Sarno RA, Dreyfuss JR: Fine needle transhepatic cholangiography: a new approach to obstructive jaundice. *Am J Roentgenol* 127:403–407, 1976
5. Pereiras R, White P, Dusol M Jr, Irvin G III, Hutson D, Lieberman B, Schiff E: Percutaneous transhepatic cholangiography utilizing the Chiba University needle. *Radiology* 121:219–221, 1976
6. Pereiras R Jr, Chiprut RO, Greenwald RA, Schiff ER: The "skinny" needle: a rapid, simple and accurate method in the diagnosis of cholestasis. *Ann Intern Med* 86:562–568, 1977
7. Okuda K, Sumikoshi T, Kanda Y, Fukuyama Y, Koen Y, Musha H, Koji S, Yukio N, Yukihiro T, Kazuro K: Hepatic lymphatics as opacified by percutaneous injection of contrast medium. *Radiology* 120:321–326, 1976
8. Goldberg HI, Dodds WJ, Lawson TL, Stewart ET, Moss AA: Hepatic lymphatics demonstrated by percutaneous transhepatic cholangiography. *Am J Roentgenol* 123:415–419, 1976
9. Kittredge RD, Baer JW: Percutaneous transhepatic cholangiography: Problems in interpretation. *Am J Roentgenol* 125: 35–46, 1975

CT Demonstration of the Splenic Vein–Pancreatic Relationship: The Pseudodilated Pancreatic Duct

FRANK E. SEIDELMANN,[1] WILLIAM N. COHEN, PATRICK J. BRYAN, AND JERRY BROWN

Cross-sectional anatomy of the splenic vein-pancreatic relationship is reviewed and correlated with findings on computed tomography. A layer of fat which is normally present between the splenic vein and the pancreas may simulate a dilated pancreatic duct. Distinct demonstration of the splenic vein as a structure separate from the pancreas was possible in 43 of 86 patients studied. An additional 25% of the patients had partial or indistinct demonstration of the splenic vein. Appreciation of this normal relationship on CT is imperative to avoid misinterpretation of the fat layer as a dilated pancreatic duct. In addition, the measured size of the pancreas may be falsely overestimated by addition of the splenic vein width if the intervening fat is not identified.

Introduction

CT scanning of the body has permitted clear in vivo visualization of soft tissue anatomic structures in a cross-sectional dimension. Lack of precise familiarity with normal anatomic relationships in this display can result in erroneous CT interpretations.

This study was prompted by an earlier experience in which we erroneosuly thought CT findings showed mild pancreatic enlargement and a dilated pancreatic duct (figs. 1*A* and 1*B*). Because the patient had normal pancreatic enzymes, endoscopic retrograde cholangiopancreatography was performed which delineated a normal-sized pancreatic duct and demonstrated choledocholithiasis (fig. 1*C*). At surgery a normal-sized pancreas was confirmed. The low density linear structure believed to be a dilated pancreatic duct was actually the layer of normal fat between the pancreas and the splenic vein. Pancreatic size was overestimated by inclusion of the splenic vein diameter in the measurement.

The splenic vein-pancreatic relationship as demonstrated by ultrasonography has been previously reviewed [1, 2]. This report reviews the normal anatomic relationships of these structures as demonstrated by CT, emphasizing their cross-sectional depiction. The frequency of CT identification of the splenic vein as a structure separate from the pancreas is also presented.

Cross-Sectional Anatomy

The splenic vein is formed by the union of five or six tributary veins returning blood from the spleen. It lies inferior to the splenic artery and is usually located at the T12–L1 level (fig 2). The splenic vein is less tortuous than the splenic artery. After formation, the vein traverses the lienorenal ligament, passes anterior to the left kidney or the left adrenal gland, and continues via a groove in the posterosuperior surface of the pancreas [3,4]. The splenic vein is separated from the abdominal aorta by the superior mesenteric artery (fig 2). Tributaries of the splenic vein include the short gastric, left gastroepiploic, pancreatic, and inferior mesenteric veins. Upon reaching the right paraspinal area, the splenic vein unites with the superior mesenteric vein at a right angle to form the portal vein (figs. 3 and 4). The portal vein lies immediately anterior to the inferior vena cava.

Case Material and Findings

A random retrospective study of 86 patients who had CT scanning of the abdomen, including the area of the pancreas (without known or suspected pathology of this organ), was undertaken to determine the splenic vein–pancreatic relationship. A Delta body scanner (Ohio Nuclear, Solon, Ohio) was employed with a scan time of 2 min 43 sec.

Distinct identification of the splenic vein was possible in 43 (50%) patients (fig 4). In an additional 21 (24.4%), partial or indistinct visualization of the splenic vein was established (fig 5). Incomplete visualization can be partly explained by the splenic vein passing out of the scanning slice in its cephalad course to its termination in the portal vein (fig 3). It is in this group that the intervening fat may produce the appearance of a dilated pancreatic duct.

In the remaining 22 cases (25.6%), the splenic vein could not be identified as a distinct structure separate from the pancreas. In nine (10% of the total group), the cause could be attributed to lack of adequate adipose tissue; in 12 others the cause was image degradation by motion or clip artifact (nine cases and three cases, respectively). The final case of nonvisualization was due to artifacts from dense ingested contrast in the stomach.

Discussion

Distinct visualization of the splenic vein as a structure separated by intervening fat from the pancreas was possible in 50% of those studied. Partial or indistinct demonstration occurred in 25% of patients. In this latter group, failure to recognize the splenic vein may result in a false impression of a dilated pancreatic duct. Caution must also be exercised so that splenic vein width is not included in the measurement of the pancreatic body and tail; otherwise the size of the pancreas may be overestimated. Splenic vein dilatation

---

Received January 24, 1977; accepted March 18, 1977.

[1] All authors: Department of Radiology, Upstate Medical Center, Syracuse, New York 13210.

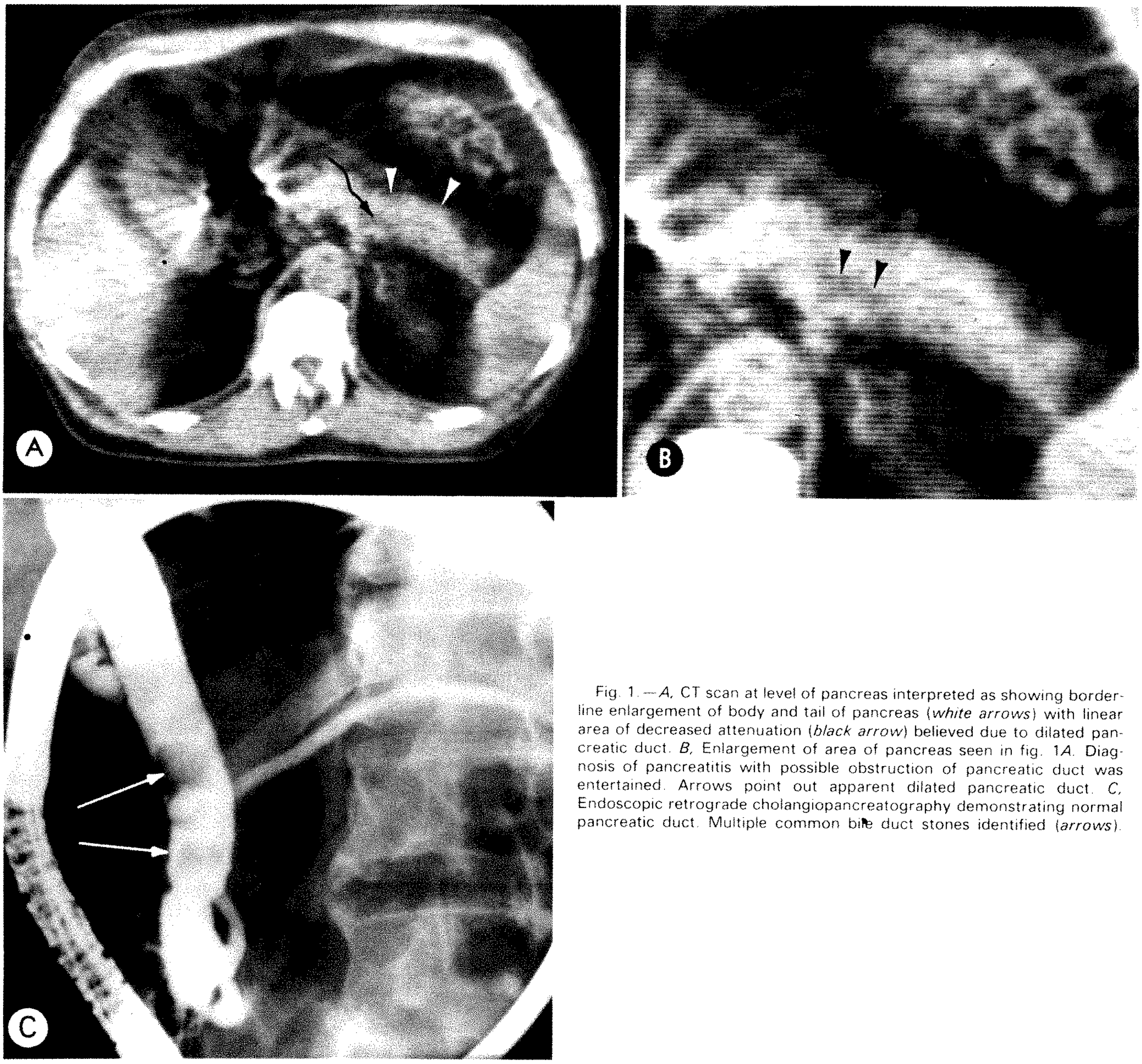

Fig. 1.—*A,* CT scan at level of pancreas interpreted as showing borderline enlargement of body and tail of pancreas (*white arrows*) with linear area of decreased attenuation (*black arrow*) believed due to dilated pancreatic duct. *B,* Enlargement of area of pancreas seen in fig. 1*A*. Diagnosis of pancreatitis with possible obstruction of pancreatic duct was entertained. Arrows point out apparent dilated pancreatic duct. *C,* Endoscopic retrograde cholangiopancreatography demonstrating normal pancreatic duct. Multiple common bile duct stones identified (*arrows*).

due to portal hypertension (as in hepatic cirrhosis) is one clinical situation in which appreciation of this relationship is necessary in measuring the pancreas (fig. 5).

In patients with normal pancreatic enzymes, the splenic vein-pancreatic relationship should be kept in mind to avoid erroneous diagnosis of an enlarged pancreas with a dilated pancreatic duct. The faster CT scanners (less than 20 sec scan time) may improve demonstration of the splenic vein by as much as 10% by eliminating motion artifacts.

REFERENCES

1. Leopold GR: Gray scale ultrasonic angiography of the upper abdomen. *Radiology* 117:665–672, 1975
2. Filly RA, Carlsen EN: Newer ultrasonographic anatomy in the upper abdomen II. The major systemic veins and arteries with a special note on localization of the pancreas. *J Clin Ultrasound* 4:91–96, 1976
3. Gray H: *Anatomy of the Human Body*, edited by Goss CM 28th ed. Phildelphia, Lea & Febiger, 1966
4. Warwick R, Williams PL: *Gray's Anatomy*, 35th British ed. Philadelphia, Saunders, 1973

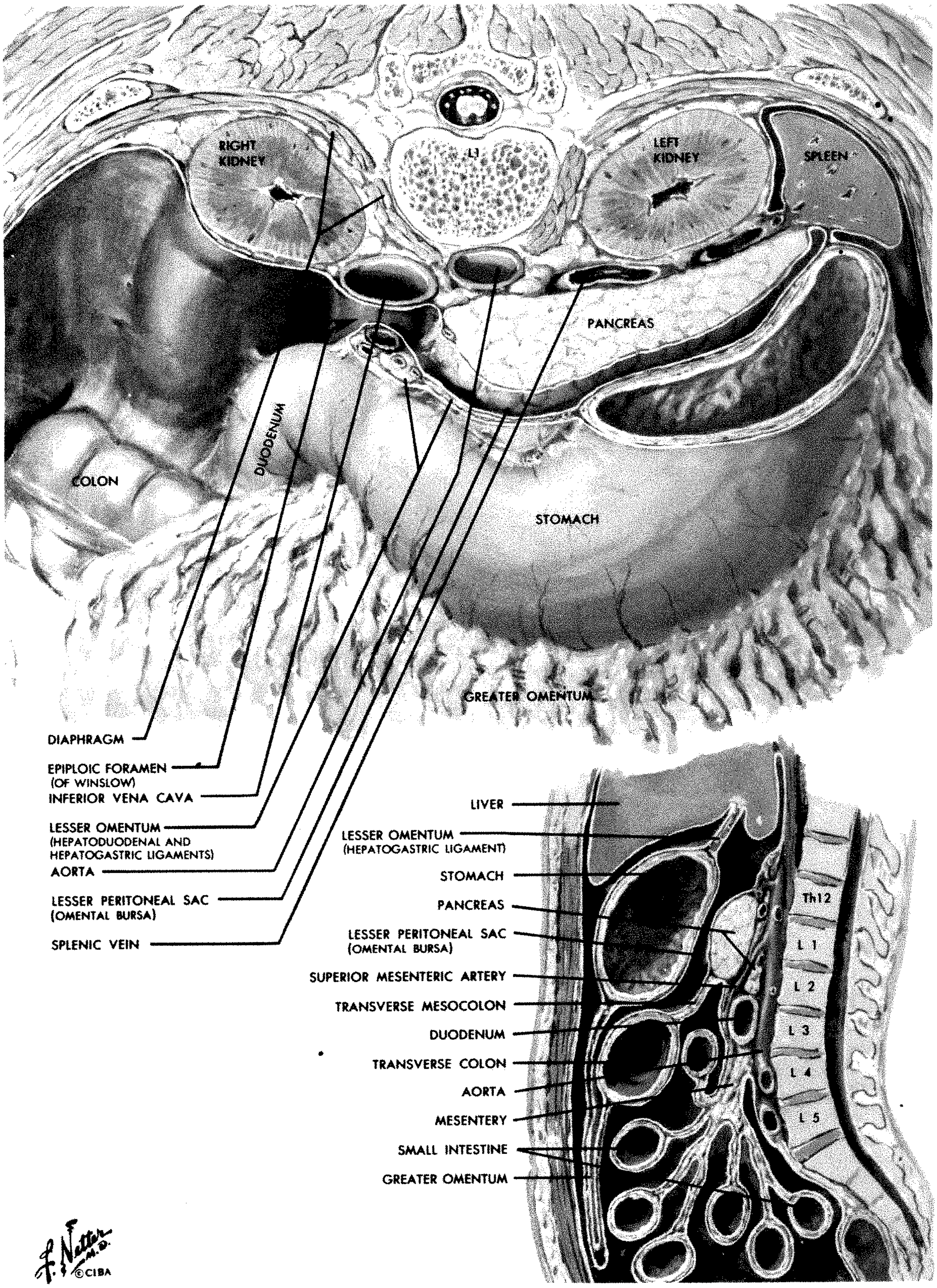

Fig. 2. – Cross-sectional gross anatomic demonstration of splenic vein–pancreatic relationship (*upper*) and sagittal section (*lower*). Note that superior mesenteric artery arises posterior and inferior to splenic vein. (© 1957, 1964 CIBA Pharmaceutical Co., Division of CIBA-GEIGY Corp. Reprinted with permission from Netter FH: *CIBA Collection of Medical Illustrations*)

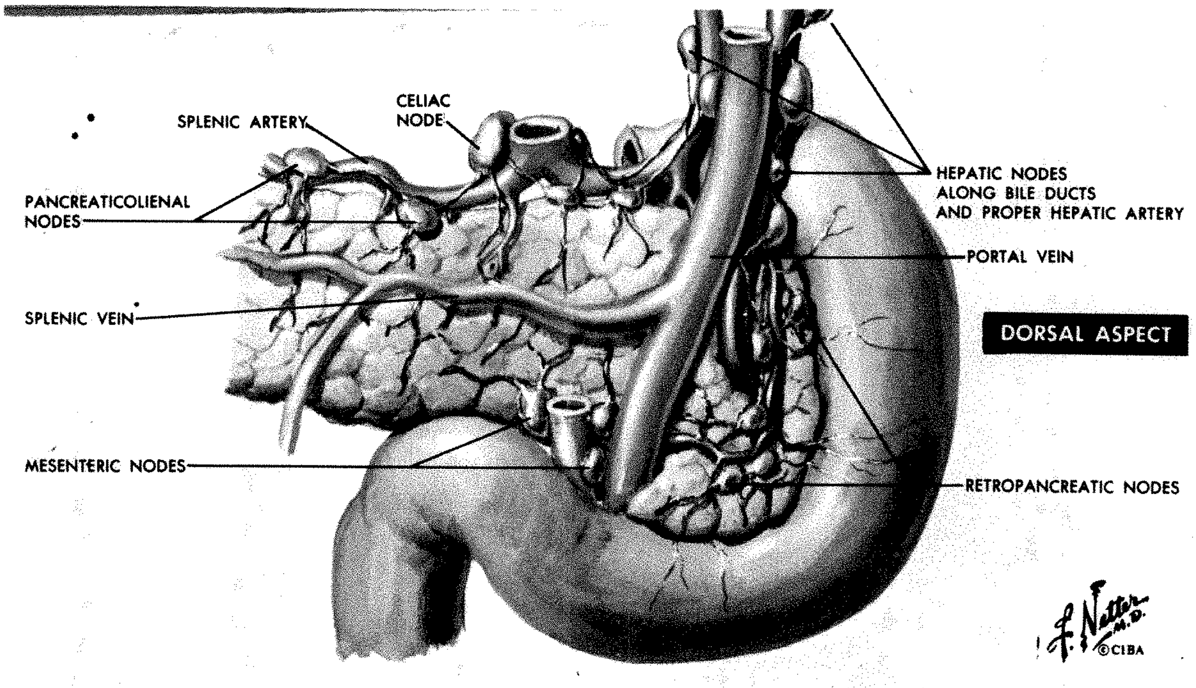

Fig. 3.—Splenic vein pancreatic relationship viewed from dorsal aspect. Note cephalic course of splenic vein near its termination in portal vein. Entire splenic vein may not be included in single CT scan slice, accounting for occasional incomplete demonstration. (© 1957, 1964 CIBA Pharmaceutical Co., Division of CIBA-GEIGY Corp. Reprinted with permission from Netter FH: *CIBA Collection of Medical Illustrations*)

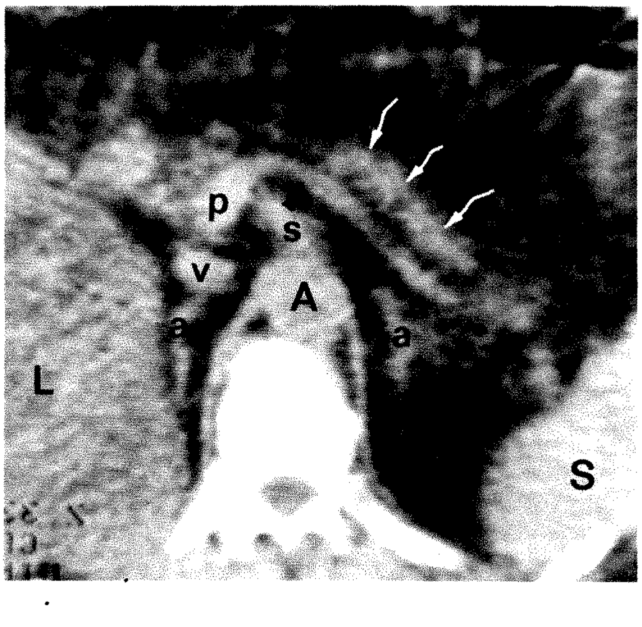

Fig. 4.—CT scan showing entire splenic vein (*black arrows*) as separate structure distinct from pancreas (*white arrows*). Area of decreased attenuation between splenic vein and pancreas represents intervening fat. Splenic vein courses anterior to left adrenal (a) and is separated from aorta (A) by superior mesenteric artery (s). Splenic vein can be followed to its termination in portal vein (p) anterior to inferior vena cava (v) and right adrenal (a). L = liver, S = spleen.

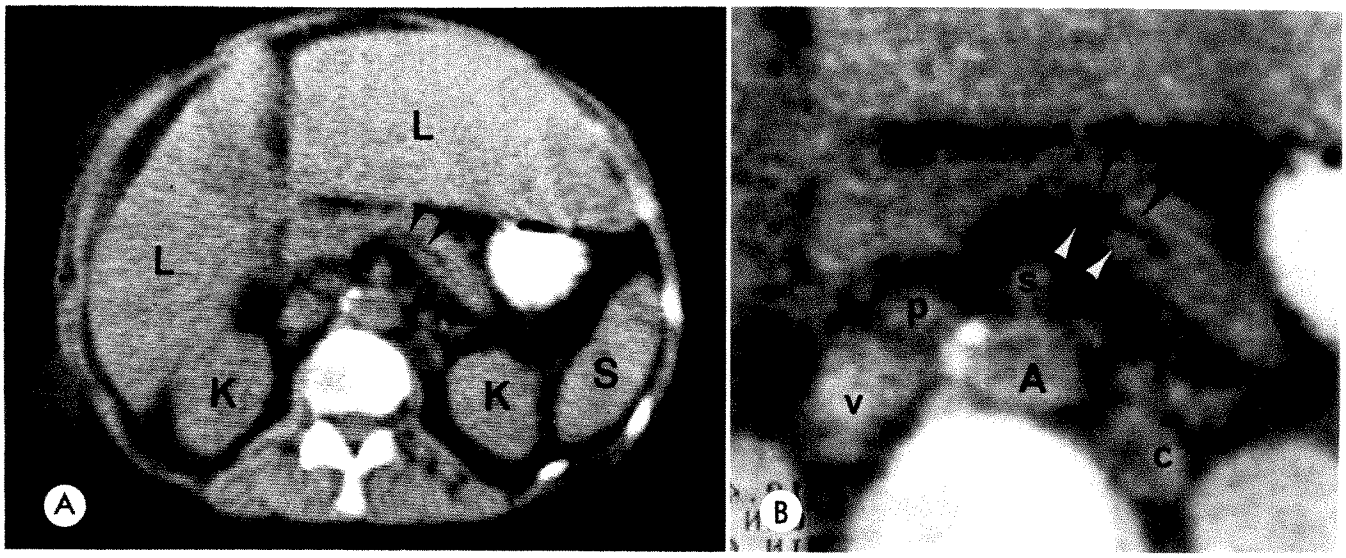

Fig. 5.—CT scan showing partial visualization of splenic vein. Patient had cirrhosis, hepatosplenomegaly, and portal hypertension. Intervening fat (*arrows*) separates body of pancreas from splenic vein, producing appearance of dilated pancreatic duct. K = kidney, L = liver, S = spleen. *B*, Enlargement of area of pancreas seen in fig. 5*A* showing separation of pancreas from splenic vein (*white arrows*) by intervening fat (*black arrows*). A = aorta, c = collateral venous structures, most likely hemiazygos vein, secondary to patient's portal hypertension; p = portal vein; s = superior mesenteric artery; v = inferior vena cava.

P 24,433

UNIVERSITY COLLEGE OF MEDICINE
LIBRARY

Retrospective Comparison of Radionuclide Scans and Computed Tomography of the Liver and Pancreas

ROBERT L. MacCARTY,[1] HEINZ W. WAHNER,[2] DAVID H. STEPHENS,[1]
PATRICK F. SHEEDY,[1] AND ROBERT R. HATTERY[1]

Computed tomography (CT) and radionuclide examinations of the liver and pancreas in 50 patients were compared retrospectively to evaluate their value as diagnostic tests. CT was superior to ^{75}Se-selenomethionine in evaluating pancreatic disease. Both ^{99m}Tc-sulfur colloid scans and CT scans were sensitive detectors of liver masses; however, there were more false positive ^{99m}Tc-sulfur colloid scans (16% compared to 4%). CT was superior in detecting biliary obstruction and ascites, in assessing diseases that involved the liver extrinsically, and in evaluating the status of adjacent organs. ^{99m}Tc-sulfur colloid scans were more sensitive in detection of diffuse nonneoplastic liver diseases (cirrhosis, hepatitis, and cholangitis). Simultaneous interpretation of CT and radionuclide scans was often more helpful than independent interpretation, and the two techniques are therefore complementary.

Computed tomography (CT) head scanning is firmly established, and its impact on medical practice has been profound and well recognized [1]. CT body scanning is a newer adaptation of the same technique in which the relationship to other diagnostic methods is less well established. The value of CT body scans compared with that of other imaging methods is being increasingly discussed in relation to cost-benefit analyses.

Early experience with CT body scanning offered considerable promise for improved diagnosis of diseases of the liver and pancreas [2-7], two organs that continue to present frequent diagnostic challenges despite recent advances. To compare the information provided by CT scans of the liver and pancreas with the information provided by radionuclide scans of the same organs, we studied retrospectively a group of Mayo Clinic patients.

Subjects and Methods

Of the first 400 patients examined on the EMI 5000 prototype body scanner at the Mayo Clinic, 120 also had nuclear medicine examinations. There was no defined selective process in choosing patients for CT scans, other than an initial preference for patients with known or suspected malignancies. Radionuclide procedures were requested by the patients' physicians as a part of the clinical work-up. An inherent bias toward diagnostically difficult problems may have been present in the selection of patients.

Patients were included in this study if they had both CT and radionuclide scans of the liver or pancreas (or both) and if both types of scans were technically satisfactory and temporally close. Two patients with normal livers had scans several months apart; all others had CT and radionuclide scans within 2 months of each other. Only patients whose final diagnoses were established beyond reasonable doubt by surgical exploration, tissue diagnosis, specific tests, or follow-up were included in the final study group. Tissue was available for histologic diagnosis in almost all the abnormal as well as in many of the normal cases. There were 54 cases, 46 involving the liver and eight involving the pancreas.

The original scan interpretations were used in most cases, and these were made without knowledge of the final diagnosis. In an attempt to eliminate observer error, all the scans were reviewed; changes in interpretation were made in less than 10% of cases. For final tabulation, the interpretation on review was used.

All scans were performed according to routine procedures prevailing in the departments of nuclear medicine and diagnostic radiology. CT scans were performed using the EMI 5000 prototype body scanner with 18 sec scan time. Contrast medium was used in some cases at the discretion of the radiologists in charge at the time of the original examination. Multiple cross-sectional views were obtained at 1.5 cm intervals through the area of interest, as judged from a preliminary radiograph of the abdomen. Each section was examined with multiple window settings.

The radioisotope examinations were conducted as follows. For the pancreas, examinations were performed after an overnight fast and a Lund test meal in the morning. Images were obtained in one projection. The patient was positioned with the left side elevated about 10° in order to separate the liver from the pancreas. The camera head with a 1,000 parallel hole collimator was angled toward the right kidney or right costal margin. Dual nuclide organ scanning technique was used; the liver was first labeled with ^{99m}Tc-sulfur colloid, and a Medical Data System on-line computer was used for data storage and subtraction technique. Image storage was started at the time of injection and extended over 1 hr. The dose was 3.5 μCi/kg of ^{75}Se-selenomethionine (Squibb, Princeton, N.J.).

For the liver and spleen, four views (anterior, posterior, right lateral, and left lateral) were obtained on all patients (1 million counts each for three liver views and an equal time, as used for the liver images, for the spleen) using a large field of view (LFOV) or high performance (HP) gamma camera (Searle Radiographics Inc., Schiller Park, Ill.) and using the technitium energy peak and a 20% window. Examinations were performed 5 min after intravenous injection of sulfur colloid labeled with 4 mCi of ^{99m}Tc. Sulfur colloid and the ^{99m}Tc generator were from commercial sources (Squibb, Princeton, N.J.).

For gallium scans, anterior and lateral views were obtained using a dual 12.7 cm rectilinear scanner (Maxiscanner, General Electric, Medical, Milwaukee, Wisc.) with a high energy collimator (NISE) with 12.7 cm focal length. Examinations were performed 24, 48, and 72 hr after the intravenous injection of

---

Received November 18, 1976; accepted after revision March 31, 1977.

[1] Department of Diagnostic Roentgenology, Mayo Clinic and Mayo Foundation, Rochester, Minnesota 55901. Address reprint requests to R. L. MacCarty.

[2] Section of Diagnostic Nuclear Medicine, Mayo Clinic and Mayo Foundation, Rochester, Minnesota 55901.

TABLE 1

Comparison of CT and Radioisotope Scans of Pancreas

Diagnosis	No. Cases	CT	Radioisotope
Normal	5	3(2)	1(4)
Carcinoma	3	3	1*(2)
Total	8	6(2)	2(6)

Note.—Numbers in parentheses indicate equivocal results.

* Positive gallium scan, 12 cm islet cell carcinoma.

TABLE 3

Comparison of Scans of Liver Masses

Diagnosis	No. Cases	CT Positive	^{99m}Tc Positive
Metastasis	7	6	6
Hepatoma	2	1	2
Hemangioma	1	1	1
Nodular hyperplasia	1	1	0
Abscess	1	1	1
Hematoma	1	1	1
Total	13	11	11

3–5 mCi of ^{67}Ga-gallium citrate (Diagnostic Isotopes Inc., Upper Saddle River, N. J.). There were seven gallium scans—six in the liver group and one in the pancreas group.

Results

Pancreas

Eight pancreases, three with carcinomas and five normal, were scanned (table 1). The CT scans were correctly positive for all three carcinomas and correctly negative for three of the five normal cases (two were equivocal). Pancreatic radionuclide scans were correctly normal in one case (four without uptake) and correctly positive in one case (two equivocal). The single positive radionuclide scan involved a 12 cm islet cell carcinoma which took up gallium.

Liver

The CT scans of 25 normal livers were correctly negative in 22 cases (two equivocal), and ^{99m}Tc-sulfur colloid scans were correctly negative in 18 cases (three equivocal). There were four false positive radionuclide scans and one false positive CT scan (table 2).

Liver masses. Thirteen patients had liver masses, including seven with metastases, two with hepatomas, and one each with hematoma, hemangioma, abscess, and nodular hyperplasia (table 3). CT scans were correctly positive in six of the seven cases of metastases; the false negative scan involved a carcinoma of the pancreas. The primary lesion was correctly diagnosed by CT, but at surgery, several metastatic nodules 1–2 cm in diameter, not seen on CT, were present in the right lobe of the liver. The ^{99m}Tc-sulfur colloid scan also failed to show these lesions; this was the only false negative ^{99m}Tc-sulfur colloid liver scan in the group of patients with metastases.

Both patients with hepatomas had grossly positive radionuclide scans, but only one had an unequivocally positive CT scan. The patient with the hemangioma also had a strongly positive ^{99m}Tc-sulfur colloid scan, but the CT scan was obviously positive only after the intravenous injection of contrast medium. In the patient with nodular hyperplasia, the CT scan was positive, whereas the ^{99m}Tc-sulfur colloid scan showed normal uptake in the involved area. The abscess and the hematoma were both readily apparent on CT and ^{99m}Tc-sulfur colloid scans, and the abscess produced a strongly positive gallium scan.

Diffuse liver disease (nonneoplastic). Of eight patients with diffuse nonneoplastic liver diseases, four had cirrhosis, three had cholangitis, and one had hepatitis. The CT scans were positive in three (two with cirrhosis and one with cholangitis), gave false negative results in two, and gave equivocal results in three. The ^{99m}Tc-sulfur colloid scans were positive in all eight cases (table 4).

Discussion

Even though the number of patients who had pancreas scans for comparative study was small, the CT scans were superior both in sensitivity and specificity to the ^{75}Se-selenomethionine scans. Because normal glands frequently are not visualized, particularly in sick patients, and because of the nonspecific nature of the information they provide,

TABLE 2

Comparison of CT and Radionuclide Scans of Normal Liver

Result	CT	^{99m}Tc-Sulfur Colloid
Correct (negative)	22	18
False positive	1	4
Equivocal	2	3
Total	25	25

TABLE 4

Comparison of Scans of Diffuse Nonneoplastic Liver Diseases

Diagnosis	No. Cases	CT Positive	CT Negative	^{99m}Tc Positive
Cirrhosis	4	2(1)	1	4
Hepatitis	1	0(1)	0	1
Cholangitis	3	1(1)	1	3
Total	8	3(3)	2	8

Note.—Numbers in parentheses indicate equivocal results.

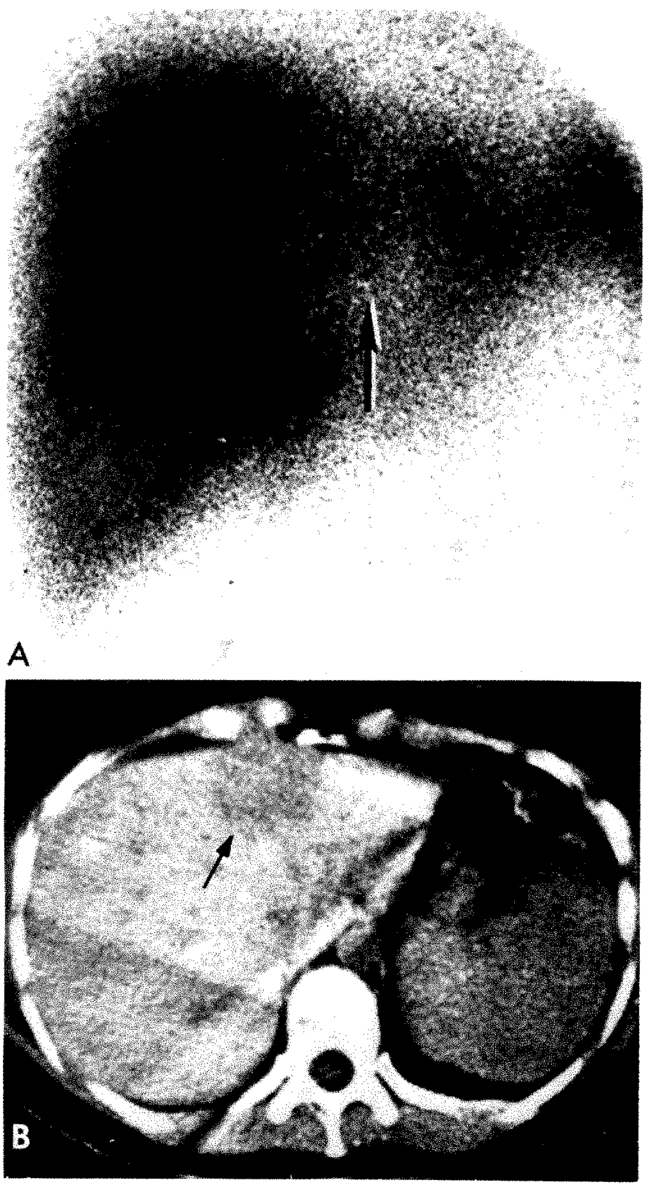

Fig. 1.—*A*, ^{99m}Tc-sulfur colloid scan showing poorly defined area of diminished uptake in region of porta hepatis (*arrow*). *B*, CT scan on same patient showing lesion as discrete 6 cm mass at junction of right and left lobes of liver (*dark arrow*). At surgery this proved to be metastatic lesion from islet cell carcinoma of pancreas. (Reprinted from [4])

←

^{75}Se-selenomethionine scans have not gained wide clinical application. CT scans more consistently demonstrate the pancreas, are capable of showing localized or diffuse enlargement of the organ, and may even demonstrate dilatation of the pancreatic duct [4]. They also provide important additional information about the surrounding tissues (e.g., bile ducts, gallbladder, and lymph nodes) that is not available on the selenomethionine scans.

^{99m}Tc-sulfur colloid and CT liver scans are both very sensitive in detecting liver masses [2]. However, because of their greater contrast resolution capability, and because images are composed of relatively thin sections of tissue (13 mm), CT scans are more likely to show mass lesions as discrete defects. Liver masses sometimes produce nonspecific poorly defined abnormalities on ^{99m}Tc-sulfur colloid scans, particularly if the lesions are confluent or if they are outside the plane of focus of the collimator (fig. 1).

However, lesions whose attenuation coefficients approximate that of the surrounding tissue may not be apparent on CT but may be grossly obvious on ^{99m}Tc-sulfur colloid scans (fig. 2). Thus, CT liver scans should be done with and without intravenous contrast medium when mass lesions are suspected [7, 8]. Presumably because of differences in vascularity and differential accumulation of iodinated medium, small differences in the attenuation coefficients of masses and surrounding parenchyma can be enhanced with the intravenous injection of contrast medium (iodinated diatrizoate or iothalamate) (fig. 3). Even so, an occasional mass in the liver may escape detection by CT (fig. 2).

CT has significant advantages over ^{99m}Tc-sulfur colloid in defining the nature and extent of lesions that arise outside the liver and involve it extrinsically (fig. 4), because

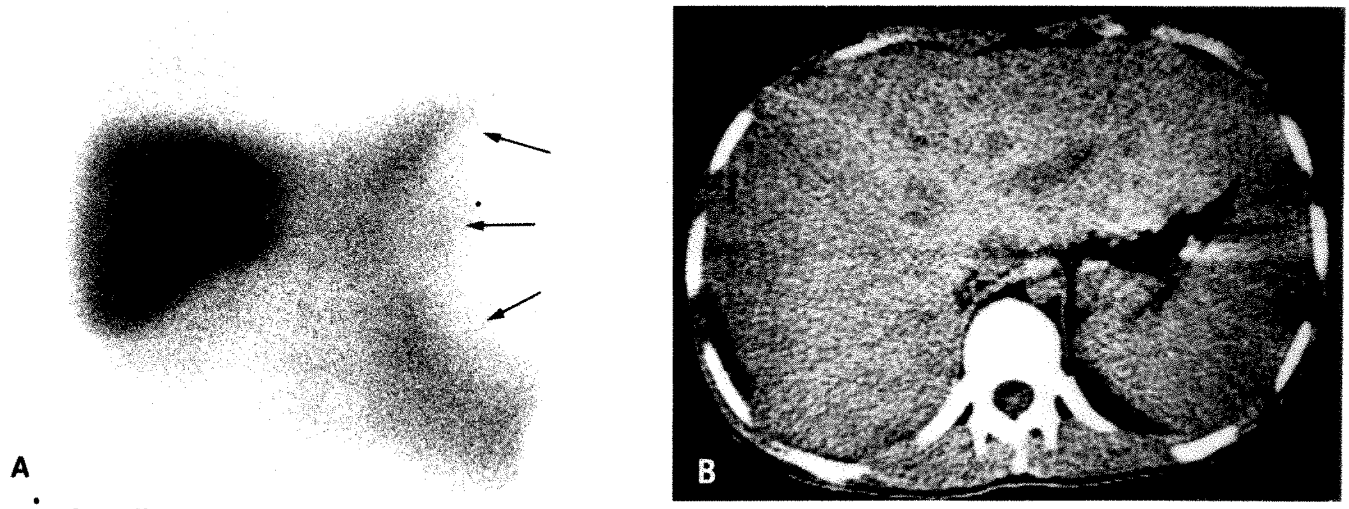

Fig. 2.—*A*, ^{99m}Tc-sulfur colloid scan, posterior view, showing large lesion occupying much of lateral portion of right lobe of liver (*arrows*). Hepatoma proved by biopsy. (Reprinted from [4]) *B*, CT scan of same patient showing almost undetectable lesion because attenuation coefficient of hepatoma is similar to that of hepatic parenchyma.

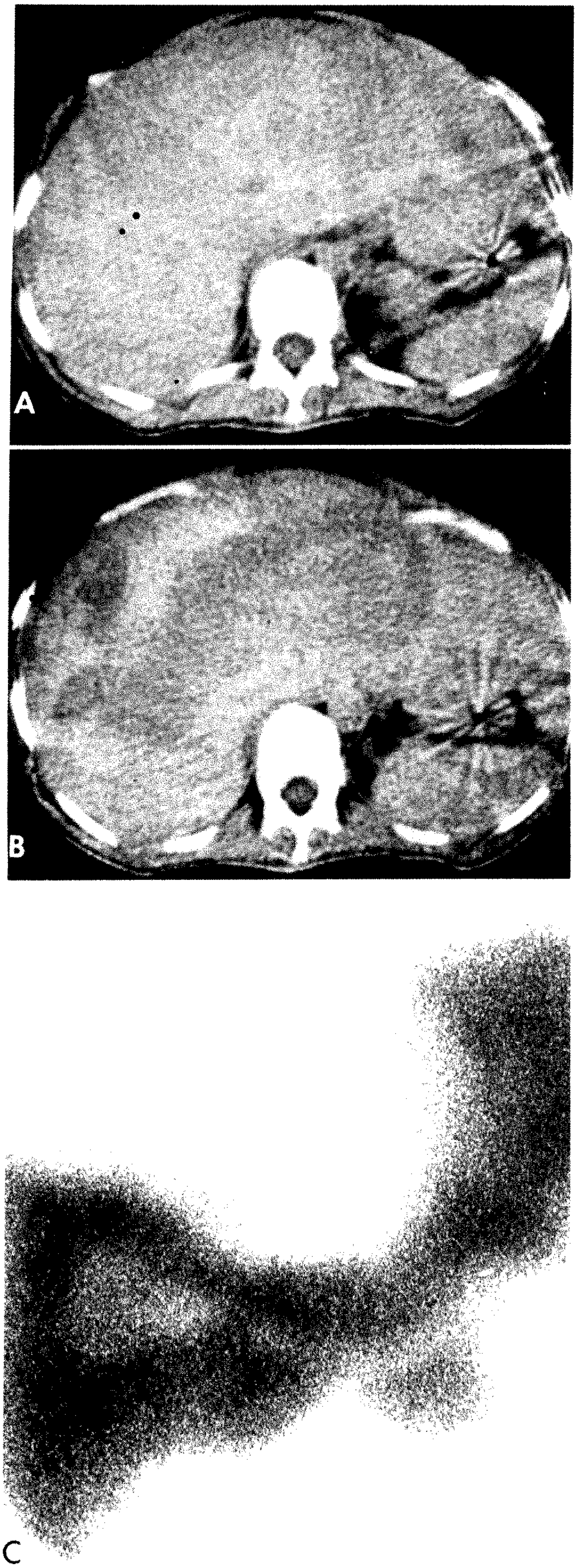

Fig. 3.—*A*, CT scan before injection of contrast medium showing only hepatomegaly. *B*, CT scan after injection showing large areas of low density where liver is involved by diffuse hemangioma. *C*, Anterior view of ^{99m}Tc-sulfur colloid scan of same patient also showing extensive liver involvement.

←

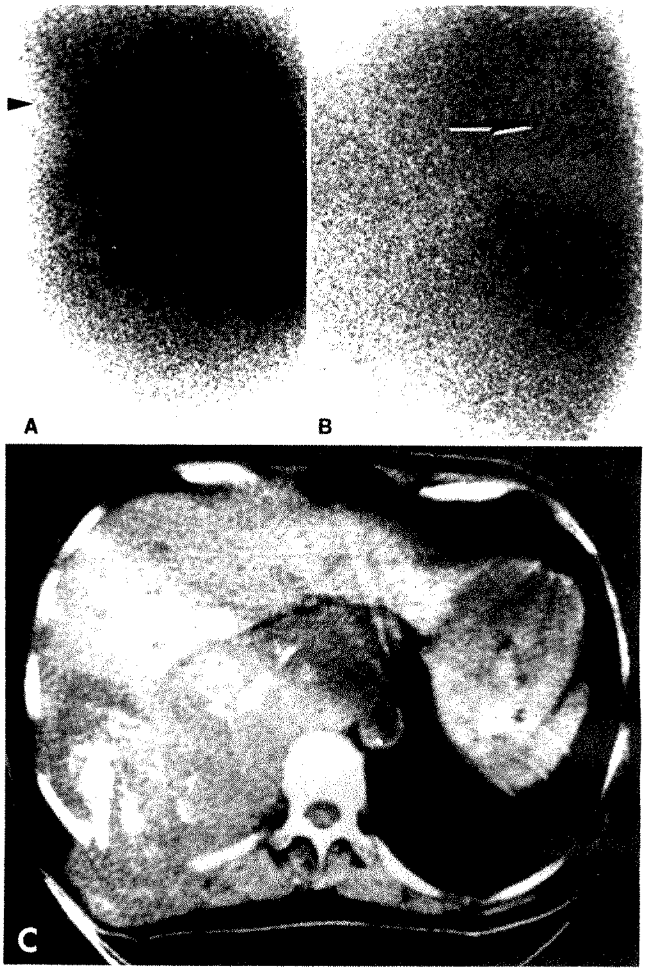

Fig. 4.—*A*, ^{99m}Tc-sulfur colloid scan, right lateral view, showing subtle marginal defect posteriorly and superiorly (*arrowhead*). *B*, ^{99m}Tc-sulfur colloid scan, posterior view, showing very equivocal area of diminished uptake in dome of right lobe of liver (*arrow*). *C*, CT scan of same patient showing large malignant retroperitoneal histiocytoma displacing the liver anteriorly, invading posterior aspect of right lobe of liver, and extending through chest wall posteriorly into subcutaneous tissues. Note areas of increased density within tumor. Plain film showed calcification.

CT provides an image that includes all tissues in the section rather than an image of only those organs that have accumulated the radioisotope (fig. 5).

^{99m}Tc-sulfur colloid liver scans are much more sensitive indicators of the presence of diffuse nonneoplastic disease than is CT [2, 8]. Hepatitis, cirrhosis, and cholangitis may produce alterations in phagocytic activity of Kupffer cells before gross alterations in parenchymal morphology have occurred. In such cases, the pattern of uptake of ^{99m}Tc-sulfur colloid may be distinctly abnormal, whereas CT shows no alteration in attenuation of x-ray photons and no alteration of internal architecture (fig. 6).

CT may be helpful if there is predominantly fatty change in the liver [2, 8]. In such cases the density relationship between the portal structures and the hepatic parenchyma

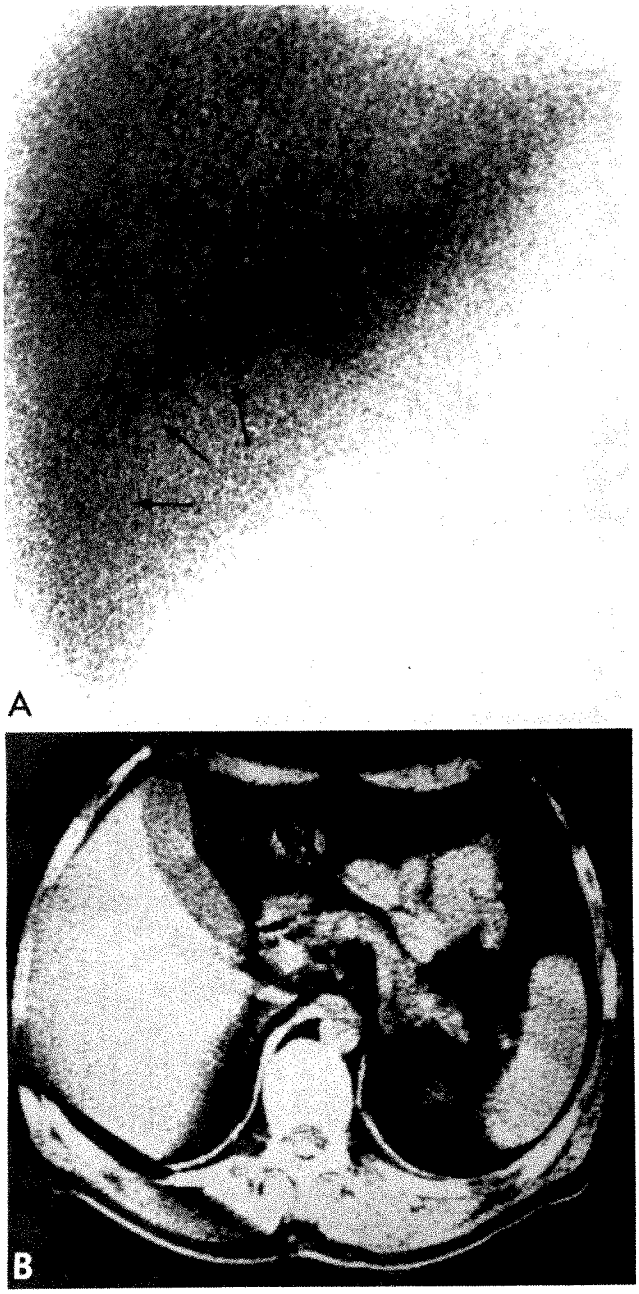

Fig. 5.—*A*, ^{99m}Tc-sulfur colloid scan, anterior view, showing large marginal defect at inferior aspect of right lobe of liver (*arrows*). False positive examination. *B*, CT scan of same patient showing defect as prominent gallbladder fossa.

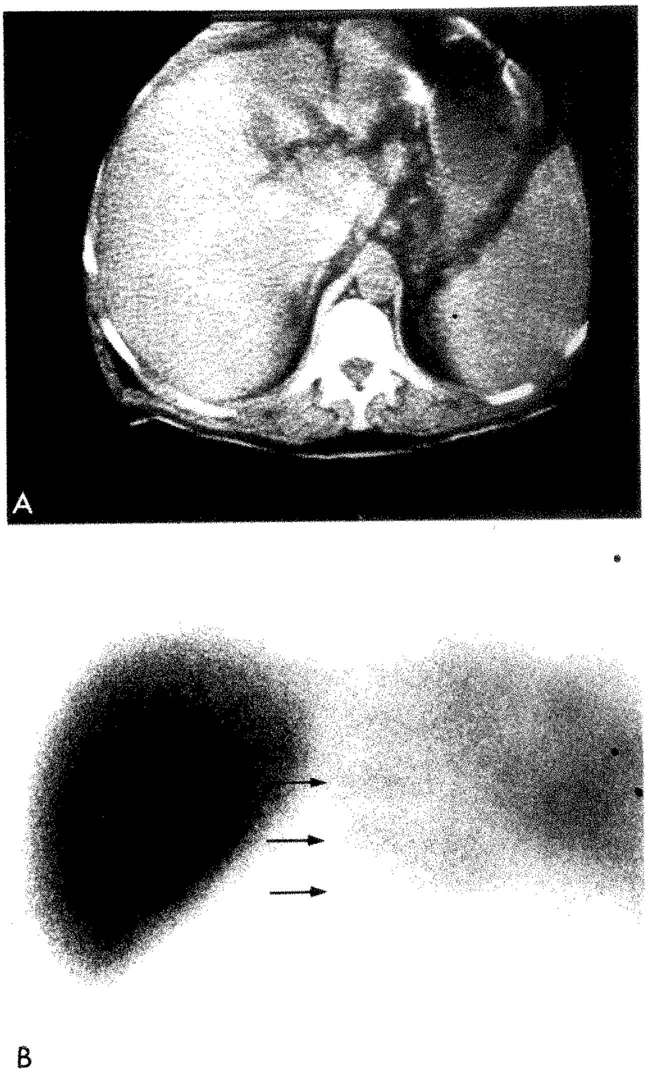

Fig. 6.—*A*, CT scan showing no definite evidence of liver disease; questionable splenomegaly. *B*, ^{99m}Tc-sulfur colloid scan, posterior view, of the same patient showing patchy decreased uptake in small right lobe of liver; splenomegaly with increased uptake of sulfur colloid by spleen as compared with liver; and uptake of sulfur colloid by reticuloendothelial cells in vertebral bodies (*arrows*) and lung bases. Findings due to cirrhosis.

is reversed. Normally, portal structures, which contain bile or blood, are of lower density than the parenchyma, but with sufficient fatty replacement the parenchyma becomes less dense than the portal structures (fig. 7).

In advanced cirrhosis, CT may show exaggerations in the lobular architecture of the liver (fig. 8). Regenerative nodules may be visible as low density areas (fig. 9). CT is also sensitive to the presence of ascites (fig. 8), information that may be inferred with difficulty from a ^{99m}Tc-sulfur colloid scan (so-called halo sign).

^{99m}Tc-sulfur colloid liver scans provide two other important pieces of information in patients with diffuse liver disease: (1) increased uptake of colloid by the spleen relative to the liver and (2) uptake of colloid by reticuloendothelial cells in the lungs and vertebral column. These findings are not features of neoplastic liver disease and are helpful in the differential diagnosis (fig. 6*B*). This is information of a physiologic nature that is not available on CT scans.

Evaluation of the overall size and shape of the liver is somewhat easier with ^{99m}Tc-sulfur colloid scans than with CT because the scans provide profiles of the entire organ rather than cross sections.

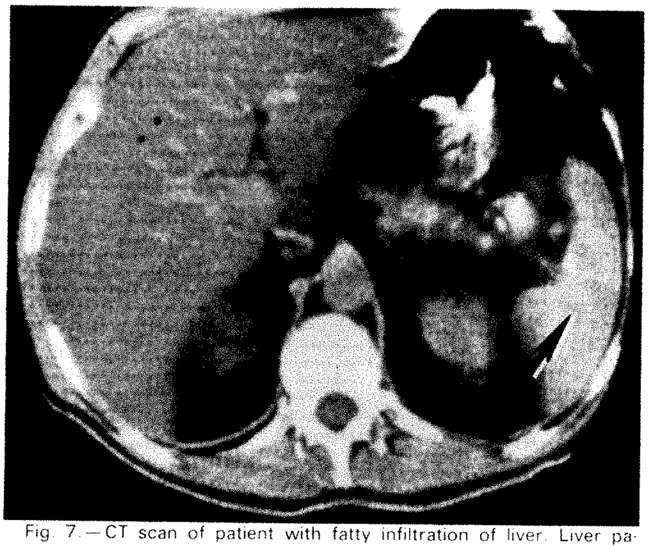

Fig. 7.—CT scan of patient with fatty infiltration of liver. Liver parenchyma less dense than spleen (*arrow*) and less dense than portal structures, which appear as linear branching structures of relatively increased density within liver.

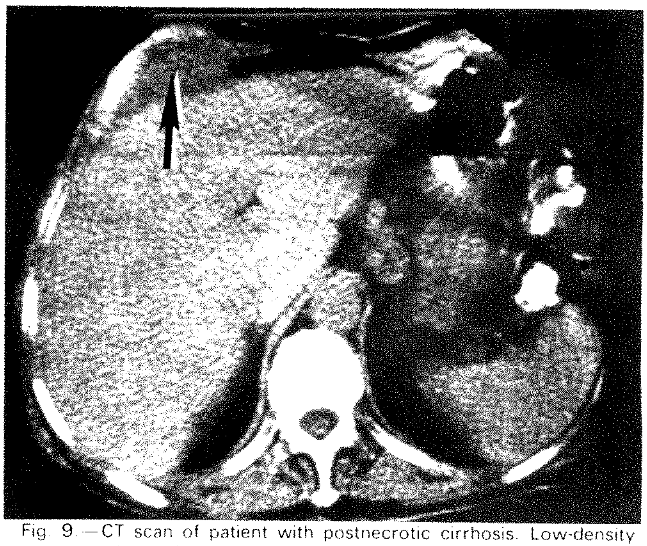

Fig. 9.—CT scan of patient with postnecrotic cirrhosis. Low-density area on anterior surface of right lobe of liver considered (but not proven) to represent regenerative nodule (*arrow*).

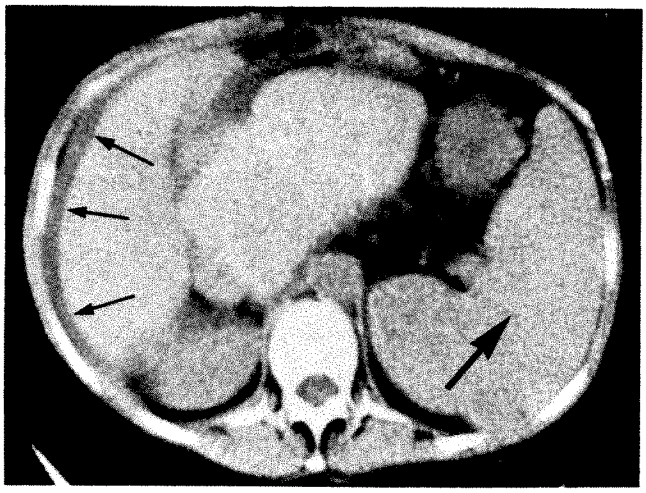

Fig. 8.—CT scan of patient with advanced cirrhosis showing splenomegaly (*large arrow*), exaggerated lobular architecture of liver due to scarring and regeneration, and curvilinear collection of ascitic fluid around right lateral margin of liver (*small arrows*).

Conclusions

In this series, CT was superior to ^{75}Se-selenomethionine in evaluating pancreatic disease. Both the ^{99m}Tc-sulfur colloid scans and the CT scans were sensitive detectors of liver masses; however, there were more false positive ^{99m}Tc-sulfur colloid scans (16% compared to 4%). CT scans showed masses more discretely and showed whether peripheral masses were intrinsic or extrinsic better than ^{99m}Tc-sulfur colloid scans did. CT was superior in detecting biliary obstruction and ascites and in assessing the status of adjacent organs. In some cases, masses with attenuation coefficients similar to the surrounding parenchyma were difficult to distinguish on CT; these masses were more obvious on ^{99m}Tc-sulfur colloid scans. ^{99m}Tc-sulfur colloid scans were more sensitive in the detection of diffuse nonneoplastic liver diseases. The information obtained from simultaneous interpretation of CT and ^{99m}Tc-sulfur colloid scans was often more valuable than the information obtained from either one alone, and in this sense, the two techniques are complementary.

REFERENCES

1. Baker HL Jr: The impact of computed tomography on neuroradiologic practice. *Radiology* 116:637–640, 1975
2. Alfidi RJ, Haaga JR, Havrilla TR, Pepe RG, Cook SA: Computed tomography of the liver. *Am J Roentgenol* 127: 69–74, 1976
3. Philips RL, Stephens DH: Computed tomography of liver specimens. *Radiology* 115:43–46, 1975
4. Sheedy PF II, Stephens DH, Hattery RR, Muhm JR, Hartman GW: Computed tomography of the body: initial clinical trial with the EMI prototype. *Am J Roentgenol* 127:23–51, 1976
5. Stanley RJ, Sagel SS, Levitt RG: Computed tomography of the body: early trends in application and accuracy of the method. *Am J Roentgenol* 127:53–67, 1976
6. Stephens DH, Hattery RR, Sheedy PF II: Computed tomography of the abdomen: early experience with the EMI body scanner. *Radiology* 119:331–335, 1976
7. Stephens DH, Sheedy PF II, Hattery RR, Hartman GW: Initial clinical experience with computerized tomography of the body. *Radiol Clin North Am* 14:149–158, 1976
8. Stephens DH, Sheedy PF II, Hattery RR, MacCarty RL: Computed tomography of the liver. *Am J Roentgenol* 128: 579–590, 1977

Calcitonin Treatment in Hereditary Bone Dysplasia with Hyperphosphatasemia: A Radiographic and Histologic Study of Bone

J. P. WHALEN,[1] M. HORWITH,[2] L. KROOK,[1,3] I. MacINTYRE,[4] E. MENA,[5]
F. VITERI,[6] B. TORUN,[6] AND E. A. NUNEZ[7]

Two children with bone dysplasia with hyperphosphatasemia (juvenile Paget's disease) were treated with synthetic human calcitonin. The progress of bone disease was monitored radiographically and histologically. Pretreatment radiographs showed markedly abnormal bone, characterized by lack of discrete cortex and absence of normal modeling. During treatment a discrete cortex was formed composed of compact bone, and more normal modeling occurred. This coincided with a histologic change from woven bone before treatment to a more lamellar type during treatment.

Introduction

Hereditary bone dysplasia with hyperphosphatasemia is a rare bone disease, first described in 1956 by Bakwin and Elger [1]. It is clinically detected in early childhood because of the abnormal modeling of bone which results in marked deformities of the skeleton. These result in enlargement of the head and bowing and thickening of the long bones. On radiographic analysis, virtually all bones are affected. The most significant biochemical findings are sustained marked elevation of the serum alkaline phosphatase level and increased urinary excretion of hydroxyproline. Immature woven bone is seen microscopically where mature lamellar bone is normally found [2–6].

Four patients with this disease are currently under treatment with human synthetic calcitonin. After 4½ months of therapy, all four demonstrated a marked improvement. The clinical and biochemical response to the hormone treatment has been reported [7]. We describe here the radiographic and histologic response of bone of two of these patients.

Subjects and Methods

Three siblings, two affected with the disease and a third (CA-32) presumably normal, were studied. The two affected siblings, a 4-year-old male (MG-31) and a 7-year-old female (BL-30), were hospitalized in the metabolic unit of the Institute of Nutrition of Central America and Panama. They were maintained on a low proline diet, calorically adequate for their height and weight. The two patients were treated with 0.5 mg human synthetic calcitonin (CIBA-Geigy) twice a day.

Radiographs of the entire skeleton were obtained prior to treatment. At 4½ months, 6 months, and 1 year radiographs were obtained for comparison with pretreatment radiographs. The upper extremities, skull, spine, and chest were omitted. Standardization of radiographs of the hips and lower extremities regarding positioning, film distance, and centering was attempted, so total diameter and characteristics of the medullary cavity and cortex could be precisely compared.

Open iliac crest biopsies were initially carried out on all three siblings. Repeat biopsies were obtained on the two affected children after 4½ months of treatment. The biopsies included the cartilaginous cap, the trabeculae immediately beneath (primary trabeculae), and the deeper trabeculae (secondary trabeculae). This allowed histologic comparison of the bones of the affected children and the normal child at each of these sites. Furthermore, it allowed comparison of these same areas before and during treatment.

For light microscopy, small pieces of tissue were fixed in buffered formalin. The tissues were demineralized under water pump vacuum in 10% formic acid buffered to pH 4.5 with sodium citrate. After paraffin embedding and sectioning at 4–6 μm, bone tissue sections were stained with hematoxylin and eosin, and with toluidine blue.

Results

Clinical and Biochemical Responses

Clinical and biochemical data have been reported in a previous publication [7]. Briefly, both patients showed marked decrease in pain and improvement in mobility. Prior to treatment, the affected girl could only assume the supine position; after 4½ months of treatment, she was able to sit unassisted. The serum alkaline phosphatase and urinary hydroxyproline diminished significantly. The boy also was able to assume only the supine position at onset of therapy; after 4½ months of treatment, he could stand with support of rails.

Radiographic Findings

The radiographs of both patients before therapy were highly abnormal. The bone lacked a distinct separation of a cortex and medullary cavity. Moreover, the diaphysis was often as wide or wider than the metaphysis, reflecting

---

Received December 9, 1976; accepted after revision March 11, 1977.
This study was supported by a grant from CIBA-Geigy and by grant AM 12957 and training grant T01 AM 5350 from the National Institutes of Health.

[1] Department of Radiology, New York Hospital–Cornell Medical Center, 525 East 68th Street, New York, New York 10021.
[2] Department of Medicine, New York Hospital–Cornell Medical Center, 525 East 68th Street, New York, New York 10021.
[3] Department of Pathology, New York State Veterinary College, Ithaca, New York 14850.
[4] Wellcome Unit of Endocrinology, Royal Postgraduate Medical School, London, England.
[5] Roosevelt Hospital, Guatemala City, Guatemala.
[6] Institute of Nutrition of Central America and Panama, Guatemala City, Guatemala.
[7] Department of Anatomy, Columbia University Medical College, New York, New York 10027.

Am J Roentgenol 129:29–35, July 1977

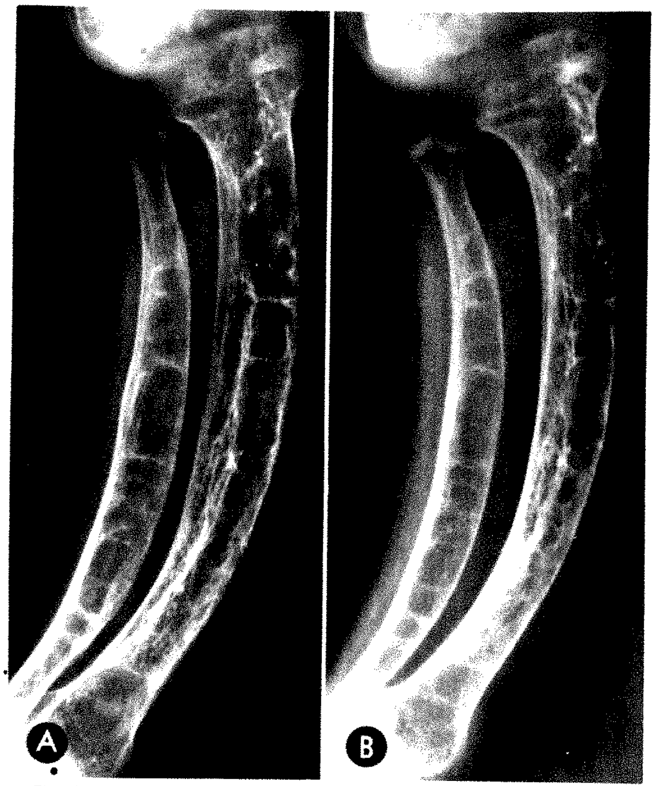

Fig. 1.—Affected girl (BL-30). *A*, Radiograph of tibia and fibula prior to treatment. *B*, Radiograph after 4½ months of treatment showing improved modeling of bone. Diameter of tibia decreased by about 25%. Note descrete cortex of lateral portion of tibia.

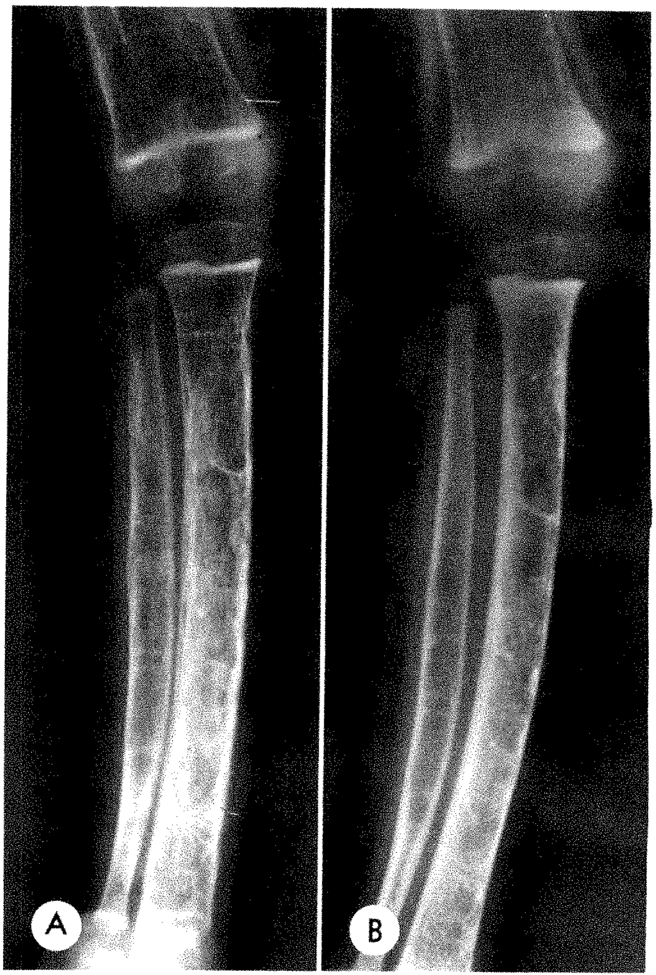

Fig. 2.—Affected boy (MG-31). Radiographs of lower extremities before treatment (*A*) and after 4½ months of treatment (*B*).

a failure in the normal modeling process. Pretreatment radiographs typically appeared as meshed radiolucent bone (figs. 1*A*, 2*A*, and 3*A*). Radiographs taken at all intervals after beginning of therapy showed dramatic improvement in modeling. This was demonstrated by progressive diaphyseal narrowing and formation of a discrete compact cortex, with progressive disappearance of the meshlike cortex. Figures 1*B*, 2*B*, and 3*B* illustrate these changes after 4½ months of therapy, and figures 3*C* and 3*D* illustrate the progressive improvement at 6 months and 1 year.

Histologic Findings

Normal sibling. The histologic appearance of primary and secondary trabeculae of metaphyseal bone is shown in figure 4. Many remnants of the cartilaginous core were found throughout the trabeculae, especially in primary trabeculae (fig. 4*A*). On the other hand, osteoclasts and Howship's lacunae were rarely encountered. The trabecular surfaces typically were smooth and lined by osteoblasts. Superficially situated osteocytes were fairly inactive. They were elongated and rather small, and there was no basophilia of the lacunar rim. However, the more deeply located osteocytes were more active and were typically enlarged and rounded (fig. 4*A*). It should be noted that the cartilaginous core is subjected to the resorptive activity of these active osteocytes. When exposed to polarized light, the collagen fibers are uniformly birefringent (fig. 4*C*). Cementing lines occurred very rarely, and osteoid seams were inconspicuous (figs. 4*A* and 4*B*).

Affected siblings. Before treatment, the histologic appearance of trabecular bone of both affected children was distinctly different from that of the normal child. One of the major differences was the complete absence of cartilaginous core in both primary and secondary trabeculae (figs. 5*A* and 6*A*). Also, the trabeculae were more slender and the lining osteoblasts were large compared to those of the normal child. Thick osteoid seams covered the trabeculae (fig. 5*A*). Another major difference between the normal and affected children was the intense osteocytic osteolysis in trabeculae of the latter. Practically all osteocytes and their lacunae were enlarged. Also, the lacunar rims stained basophilically or metachromatically, and numerous cementing lines were present to give a mosaic pattern to the trabeculae (figs. 5*A* and 6*A*). The cementing lines sometimes merged from diffuse areas of basophilia or metachromasia. There was a moderate

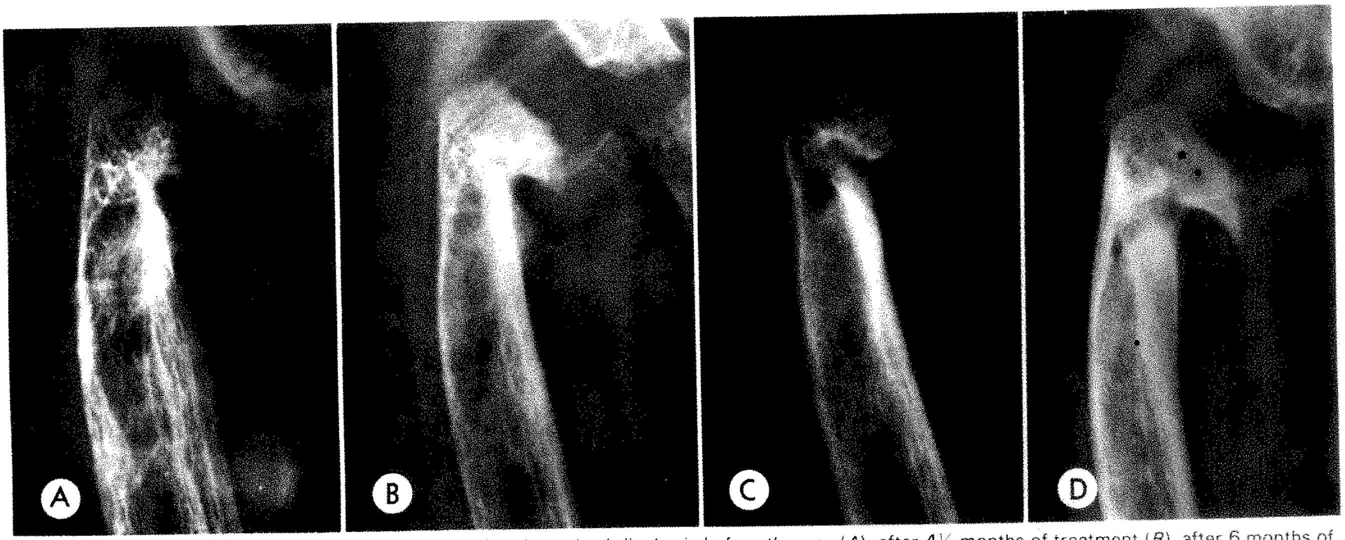

Fig. 3.—Affected boy. Radiographs of femoral head and proximal diaphysis before therapy (*A*), after 4½ months of treatment (*B*), after 6 months of treatment (*C*), and after 1 year of treatment (*D*). Note that diameter of diaphysis narrowed with treatment reflecting improved modeling. Discrete cortex which formed shows progressive thickening. Compact lamellar bone replaced pretreatment meshlike cortex. (*A* and *B* reprinted with permission from [7])

fibroplasia between the trabeculae. Multinucleated osteoclasts were rarely found on the surfaces of trabeculae. When found, the deeper regions of the trabeculae were also typically characterized by intense osteolysis (fig. 5*B*). Examination of histologic sections with polarized light revealed poorly organized collagen fibrils (fig. 6*B*).

Administration of synthetic human calcitonin for 4½ months caused marked histologic changes in bony trabeculae of both patients. The most striking change was the inhibition of osteocytic osteolysis. The osteocytes were small, elongated, and without basophilia of the lacunar rim; cementing lines were also markedly reduced (fig. 6*C*). When the sections were studied with polarized light, the collagen fraction of the matrix was almost uniformly birefringent. A lamellar pattern of trabecular bone was then evident in most histologic sections, although some areas of woven bone were still found (figs. 6*C* and 6*D*). No osteoclasts were found on the surfaces of trabeculae, and the osteoblasts appeared smaller than those observed before hormone therapy. Conspicuous osteoid seams were not seen.

Discussion

Although it has been firmly established that calcitonin inhibits bone resorption [8–10], the physiologic role of calcitonin is still unclear. Recent studies indicate that calcitonin might be important in the regulation of bone modeling during growth and development. For example, calcitonin excess in growing rats and turtles causes a modeling error which can be detected both radiographically and histologically [11, 12]. The human disease, familial bone dysplasia with hyperphosphatasemia, is characterized by excessive bone resorption resulting in altered bone modeling [4, 5, 13]. Although it has not yet been established that this disease is a calcitonin deficiency state, calcitonin administration seemed a logical treatment since it inhibits bone resorption.

Clinical improvement in a 5-year-old child treated with human synthetic calcitonin has been reported [6, 14]. This plus the dramatic regression of familial bone dysplasia in our patients after 4½ months of calcitonin administration [7] present clear evidence of the beneficial effect of calcitonin on the progress of this disease. In the four siblings we studied, calcitonin treatment reduced bone pain and tenderness while increasing patient mobility. Serum alkaline phosphatase and urinary hydroxyproline levels were also decreased significantly.

The present radiographic and histologic observations before and during treatment of this disease add to the knowledge of the pathogenesis of this disease and to the possible mechanisms of action of calcitonin on bone.

The histologic appearance of bone before calcitonin treatment clearly manifested excessive resorption, primarily due to osteocytic osteolysis. Osteoclasts were rarely encountered. The sparsity of osteoclasts suggests that surface osteoclasia, unlike in Paget's disease in adults [15], plays little or no role in the pathogenesis of this disease. The absence of cartilaginous cores in the bony trabeculae of the diseased tissue, in contrast to the bone of the healthy sibling, is another manifestation of accelerated osteocytic resorption, in this case, of cartilage. Studies in normal animals have demonstrated that the cartilaginous cores within the range of osteocytes are removed by them. Such resorption of the cartilaginous core mediated by deep-seated osteocytes has been termed osteocytic chondrolysis [12]. Thus the absence of remnants of cartilage in trabeculae of patients with familial bone dysplasia could be due to its removal by the hyperactive osteocytes that we found in patients with this disease.

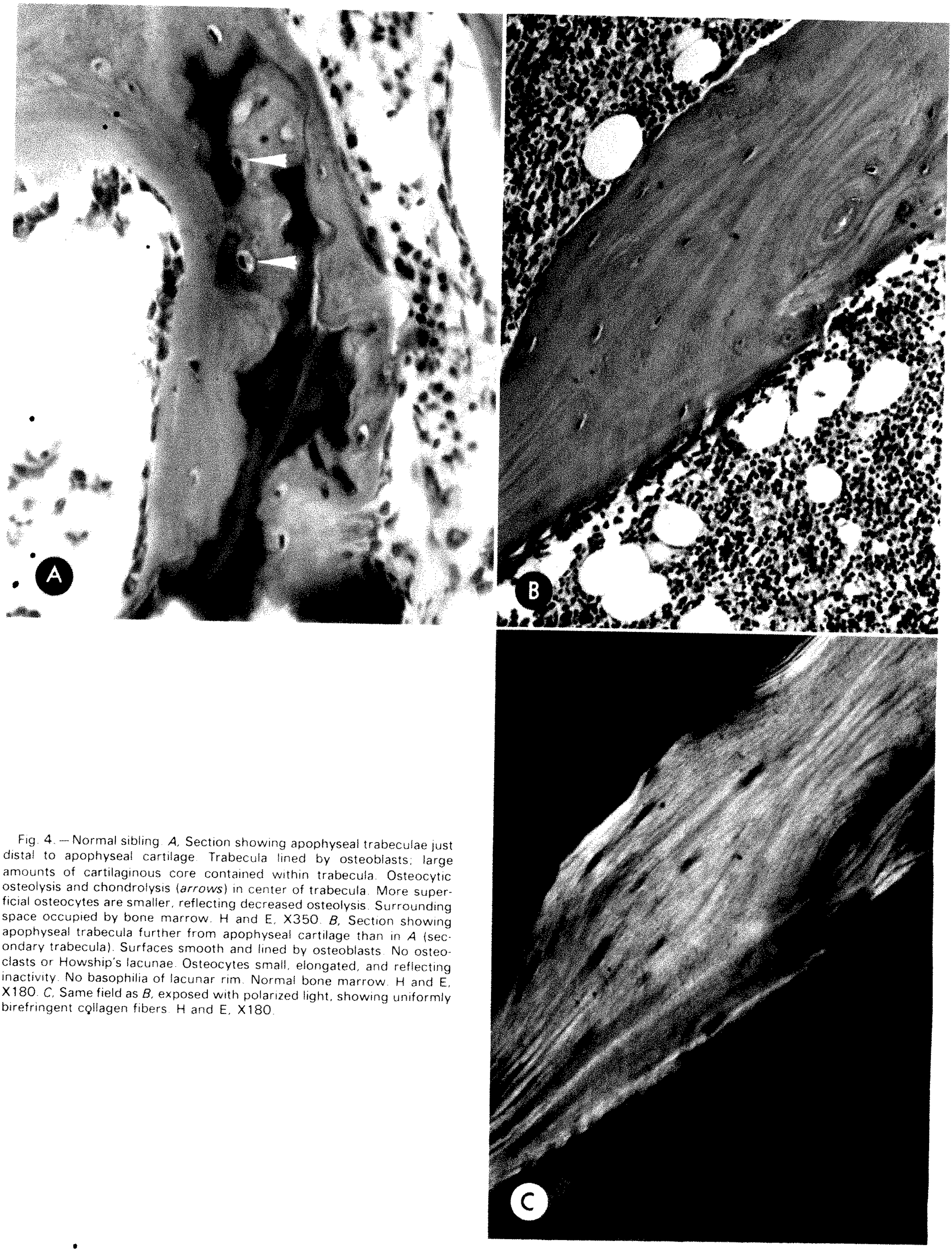

Fig. 4.—Normal sibling. *A,* Section showing apophyseal trabeculae just distal to apophyseal cartilage. Trabecula lined by osteoblasts; large amounts of cartilaginous core contained within trabecula. Osteocytic osteolysis and chondrolysis (*arrows*) in center of trabecula. More superficial osteocytes are smaller, reflecting decreased osteolysis. Surrounding space occupied by bone marrow. H and E, X350. *B,* Section showing apophyseal trabecula further from apophyseal cartilage than in *A* (secondary trabecula). Surfaces smooth and lined by osteoblasts. No osteoclasts or Howship's lacunae. Osteocytes small, elongated, and reflecting inactivity. No basophilia of lacunar rim. Normal bone marrow. H and E, X180. *C,* Same field as *B,* exposed with polarized light, showing uniformly birefringent collagen fibers. H and E, X180.

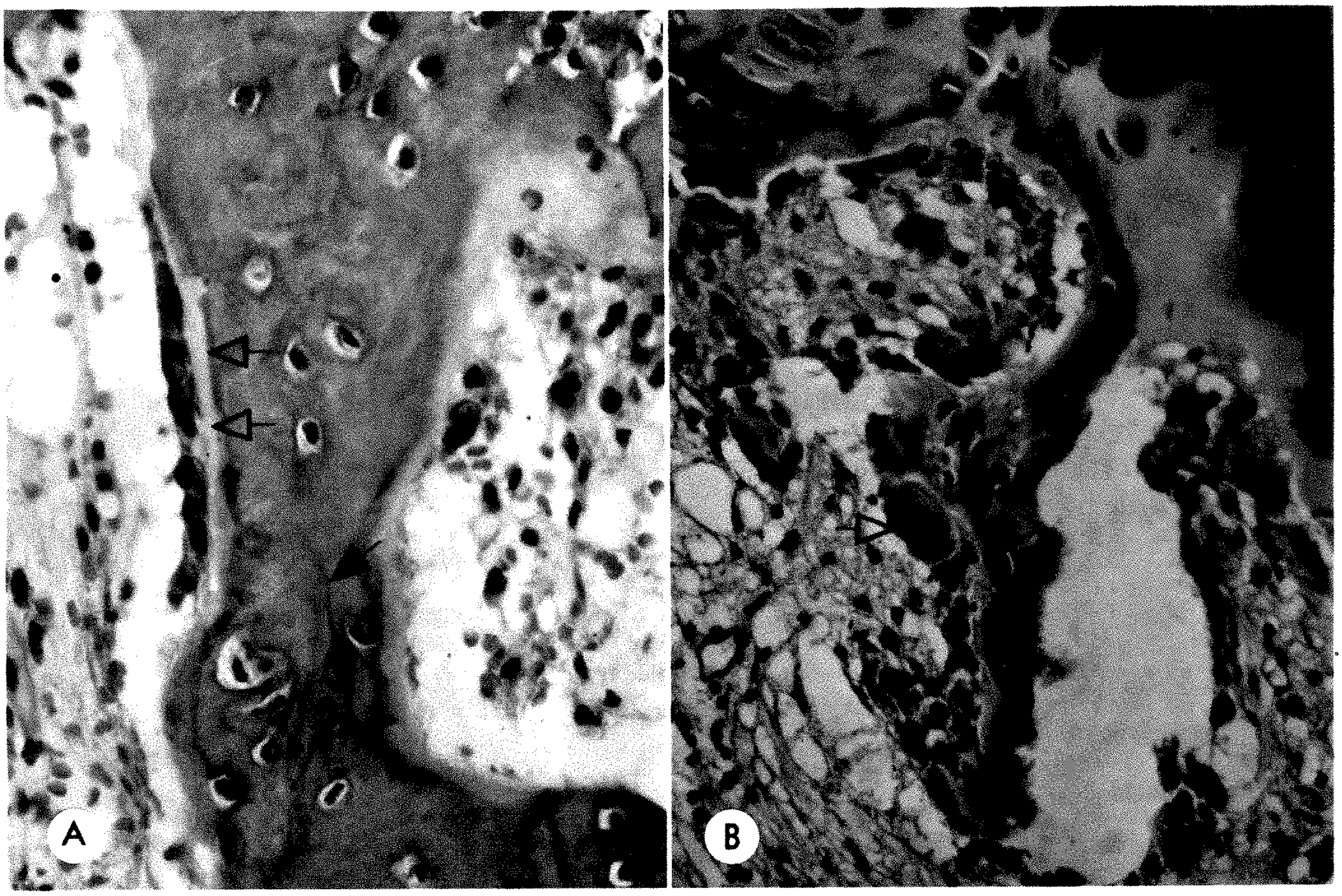

Fig. 5.—Affected boy. *A*, Section showing apophyseal trabecula just distal to apophyseal cartilage. Surfaces lined by large osteoblasts, wide osteiod seams present (*open arrows*). Osteocytic osteolysis very intense throughout (both centrally and superficially); cementing lines (*solid arrow*) present. Pronounced marrow fibroplasia. Note absence of cartilaginous core. H and E, X350. *B*, Section showing apophyseal trabecula (primary). Surface osteoclasia (*open arrow*) shown. Bone altered by intense osteocytic osteolysis (*solid arrow*). H and E, X450.

The presence of large numbers of cementing lines in the diseased bone probably reflects intermittent accelerated rate of osteocytic resorption. They are produced, for instance, by calcitonin inhibition of bone resorption occurring with bone modeling in growth [12]. In a study by Belanger et al. [16] of adult Paget's disease, a condition characterized by excessive bone resorption and pain, the presence of numerous cementing lines was considered to be due to a shrinking of the metachromatic areas where osteocytic osteolysis had taken place into thin bands. It was also suggested that the accumulation of these lines in a tissue where the replacement of lysed matrix lags, as in Paget's disease, or, as in the present disease state, leads to a mosaic pattern which characterizes the bone of these disease processes.

We propose that excessive internal resorption of bone by osteocytes plays a major role in the pathophysiology of familial bone dysplasia with hyperphosphatasemia. Osteocytic resorption leads to a decrease in total compact bone. Although production of bone may be increased, excessive resorption is increased to a greater extent. This leads to the thinning of bony trabeculae. As a result of such bone loss, the intertrabecular spaces become progressively and irregularly enlarged and eventually become filled with loose connective tissue and fat cells. Such bone appears radiographically as a meshwork of radiolucency, lacking a distinct separation between a cortex and medullary cavity.

As stated earlier, calcitonin treatment had strikingly beneficial clinical effects; this improvement is clearly evident in the changes seen in bone. After calcitonin administration, there was histologic evidence that osteocytic osteolysis was almost entirely inhibited, returning osteocytes to near normal activity. Accompanying the inhibition of internal resorption was the replacement of immature woven bone by a normal lamellar bone and the disappearance of prominent osteiod seams. Cementing lines were also fewer following calcitonin treatment. This improvement in the morphology of bone was clearly evident radiographically. For the first time a definite cortex and medullary cavity were visible in radiographs.

In the past, the role of osteocytic osteolysis in bone modeling has been uncertain [17]. This study demonstrates that accelerated osteocytic osteolysis and chondrolysis is inhibited during calcitonin therapy. This change coincides with the replacement of immature woven bone by normal lamellar bone.

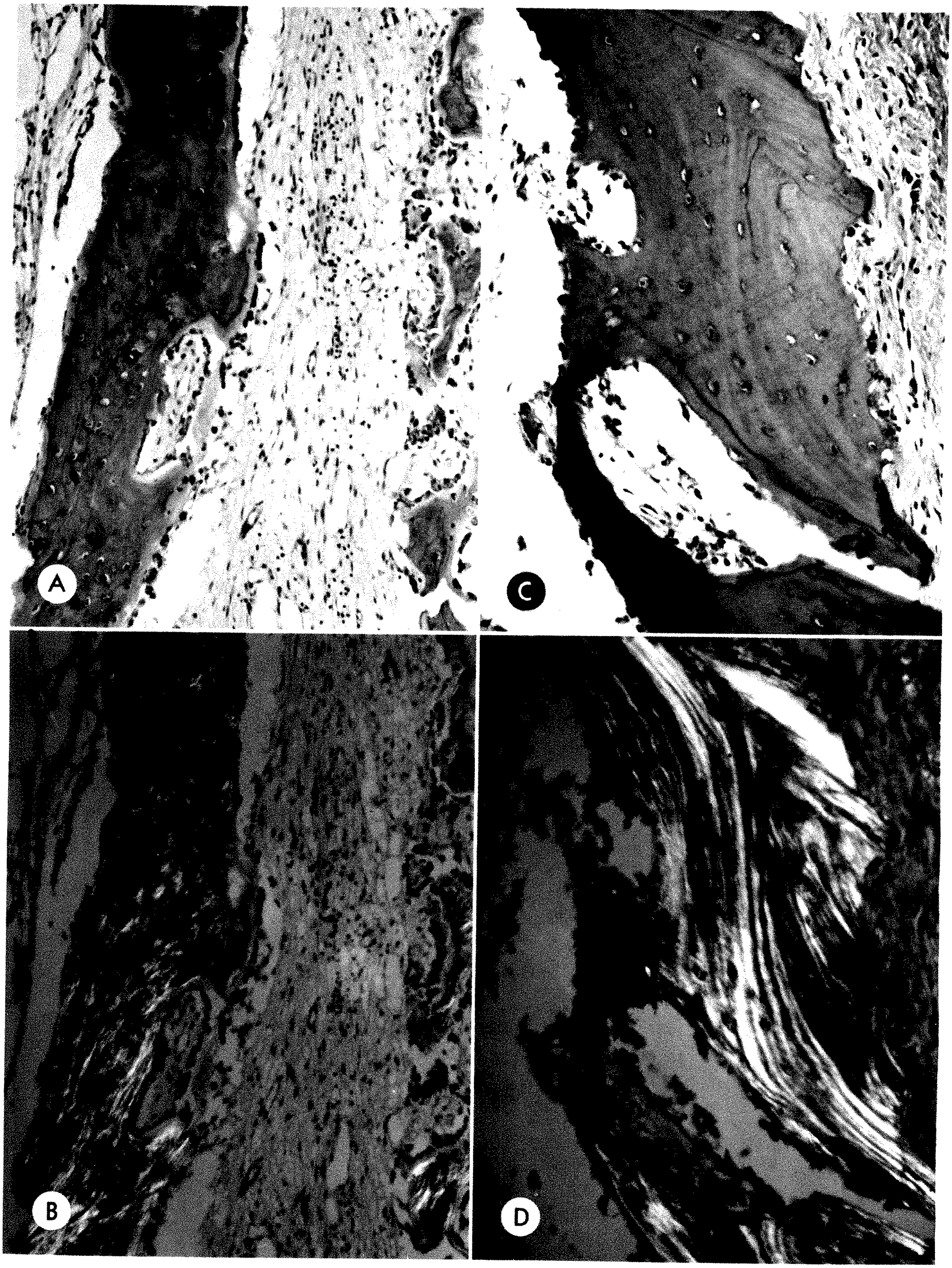
A
C
B
D

REFERENCES

1. Bakwin H, Eiger MS: Fragile bones with macrocranium. *J Pediatr* 49:558–564, 1956
2. Stemmermann GN: An histologic and histochemical study of familial osteoectasia (chronic idiopathic hyperphosphatasia). *Am J Pathol* 48:641–652, 1966
3. Choremis C, Yannakos D, Papadatos C, Baroutsou E: Osteitis deformans (Paget's disease) in an 11-year-old boy. *Helv Paediatr Acta* 13:185–188, 1958
4. Caffey J: Familial hyperphosphatasemia with atelia and hypermetabolism of growing membranous bone: review of the clinical, radiographic and chemical features, in *Progress in Pediatric Radiology: Intrinsic Diseases of Bones,* edited by Kaufmann HJ, New York, S. Karger, 1973, pp 438–468
5. Eyring EJ, Eisenberg E: Congenital hyperphosphatasia: a clinical, pathological and biochemical study of two cases. *J Bone Joint Surg* [*Am*] 50:1099–1117, 1968
6. Wodehouse NJY, Fisher MJ, Siguardsson G, Joplin GE, MacIntyre I: Paget's disease in a 5-year-old: acute response to human calcitonin. *Br Med J* 4:267–268, 1972
7. Horwith M, Nunez EA, Krook L, Viteri F, Torun B, Mena E, Suh SM, Eisenberg E, MacIntyre I, Whalen JP: Hereditary bone dysplasia with hyperphosphatasemia: response to synthetic human calcitonin. *Clin Endocrinol* (Oxf) 5, suppl.: 341s–352s, 1976
8. MacIntyre I, Parsons JA, Robinson CJ: The effects of thyrocalcitonin on the blood-bone calcium equilibrium in the perfused tibia of the cat. *J Physiol* 191:393–405, 1967
9. Raisz LG, Au WJW, Friedman J, Nieman I: Thyrocalcitonin and bone resorption. *Am J Med* 43:684–690, 1967
10. Munson PL, Gray TK: Function of thyrocalcitonin in normal physiology. *Fed Proc* 29:1206–1209, 1970
11. Belanger LF, Diamond MT, Copp DH: Histological observations on bone and cartilage of growing turtles treated with calcitonin. *Gen Comp Endocrinol* 20:297–304, 1973
12. Whalen JP, Krook L, MacIntyre I, Nunez EA: Calcitonin, parathyroidectomy, and modeling of bones in the growing rat. *J Endocrinol* 66:207–212, 1975
13. Thompson RC Jr, Gaull GE, Horwitz S, Schenk RK: Hereditary hyperphosphatasia. Studies of three siblings. *Am J Med* 47:209–219, 1969
14. Doyle FH, Woodhouse NJY, Glen CA, Joplin GF, MacIntyre I: Healing of the bones in juvenile Paget's disease treated by human calcitonin. *Br J Radiol* 47:9–15, 1974
15. Mihaud G: Calcitonin. *Biomedicine* 24:159–162, 1975
16. Belanger LF, Jarry L, Uhthoff HK: Osteocytic osteolysis in Paget's disease. *Rev Can Biol* 27:37–44, 1968
17. Cameron DA: The ultrastructure of bone, in *The Biochemistry and Physiology of Bone,* vol 1, edited by Bourne GH, New York, Academic Press, 1972, pp 191–236

John Caffey was invited to comment. His editorial appears in this issue.

←

Fig. 6.—Affected girl. *A,* Section showing apophyseal trabecula. Intense osteocytic osteolysis, no cartilaginous core, and wide osteoid seams. Immature woven bone; loose connective tissue between trabeculae. H and E, X180. *B,* Same field as *A,* exposed with polarized light, showing very poor birefringency of immature collagen. H and E, X180. *C,* Section after 4½ months of treatment showing that trabecula contain small elongated osteocytes without basophilia of lacunar rims. Fewer cementing lines. H and E, X200. *D,* Same field as *C,* exposed with polarized light, showing collagen fraction of matrix with more normal birefringency. Primarily lamellar type bone compared to pretreatment biopsy. H and E, X200.

Neonatal Mucolipidosis II (I-Cell Disease): Clinical and Radiologic Features in Three Cases

HEIDI B. PATRIQUIN,[1] PAIGE KAPLAN,[2] HANS PETER KIND,[2] AND ANDRES GIEDION[3]

Three unrelated southern Italian children manifested I-cell disease within the first month of life, but it was not recognized initially. Radiologic findings of osteopenia, subperiosteal new bone formation and resorption, and irregular metaphyses suggested systemic bone disease. Premature suture synostosis was evident at age 2–4 weeks. Review of the literature and experience with these cases establish these findings as a valuable and specific clue to the diagnosis of I-cell disease. By 6–10 months of age, the clinical and radiologic features were similar to those in Hurler syndrome. Cardiorespiratory death occurred in two cases.

Introduction

Mucolipidosis II (I-cell disease, inclusion-cell disease, or Leroy syndrome) usually becomes apparent in an affected child within the first year of life, but is rarely diagnosed at birth. Linear growth is retarded, starting either in utero or after birth, and usually stops by the second year. Psychomotor development is impaired: the child may learn to sit but rarely to walk or talk. The facies, which is gargoyle-like due to the periorbital puffiness, flat broad nasal bridge, anteverted nares, prominent maxilla and gums, wide mouth, and large tongue, becomes progressively coarser. The skin is thick and doughy. Joint contractures slowly worsen. A clubfoot, dislocated hip, or immobile thumb are often the first causes for parental concern. The Hurler-like radiologic features after the age of 6–12 months were described by Taber et al. [1].

I-cell disease gets its name from inclusion bodies found in skin fibroblasts, I cells. In tissue culture, fibroblasts contain cytoplasmic granular inclusions which are lysosomes containing heterogeneous material. These accumulations are due to the deficient or absent activity of most lysosomal acid hydrolases in these cells.

This report describes three affected infants whose clinical and radiologic features differ from the classical description but are typical for this age group; two of them are followed through the evolution of their disease.

Case Reports

Detailed clinical and laboratory findings and a summary of the enzyme studies on cases 1–3 have been deposited with a documentation service.*

Case 1

S. P. (Kinderspital, Zurich), a boy, was small for gestational age; a chest film shortly after birth showed skeletal disease suggestive of congenital hyperparathyroidism. He was a small floppy infant with a flat occiput, bushy eyebrows, long eyelashes, prominent maxilla, flat nose, and high arched palate. He had hepatomegaly and umbilical and inguinal hernias. Splenomegaly was noted at 3 months. Heart and lungs were normal.

The diagnosis of I-cell disease was made on the basis of inclusion granules, markedly reduced lysosome hydrolase activities, and elevated serum activities. The radiologic findings are shown in figure 1 and table 1. The baby had recurrent pneumonia, but it has not been possible to follow his progress after the age of 3 months.

Case 2

M. T. (Montreal Children's Hospital 469012), a girl, was examined at 2 weeks of age because of head asymmetry. She had premature synostoses of the coronal and anterior sagittal sutures, as well as generalized skeletal abnormalities (fig. 2 and table 1).

At age 2½ months the patient was still small and had the characteristic facial deformities (fig. 2*E*). She also had long fingers and toes, hyperconvex nails, and a right simian crease. There were calcaneovalgus deformities; bowing of the forearms and legs; generalized flexion contractures of joints; hemangiomata on the left wrist, scalp, and neck; and a sacral dimple. The labia majora were flat, resembling an empty scrotum. Although a coronal craniectomy was performed, there was no further skull growth.

During the next 4 months the patient's features coarsened and her growth was slow. She did not progress mentally. At age 7 months, she developed pneumonia which was complicated by disseminated intravascular coagulation and intractable heart failure leading to death. Permission for an autopsy was refused.

Case 3

A. C. (Montreal Children's Hospital 431992), a girl, appeared normal at birth. At age 1 month congestive heart failure developed, presumably due to endocardial fibroelastosis diagnosed by cardiac catheterization. Synostosis of sutures as well as other skeletal abnormalities were noted radiologically (fig. 3 and table 1).

At age 10 months the patient was evaluated because of a tower-shaped skull with a very flat occiput and closed anterior fontanelle. Her face was coarse; findings included telecanthus, periorbital bagginess, prominent maxilla, long philtrum, wide

---

Received November 3, 1976; accepted after revision March 14, 1977.
Presented at the annual meeting of the Society for Pediatric Radiology, Washington, D.C., September 1976.

[1] Department of Radiology, Centre Hospitalier Universitaire, Sherbrooke, Quebec, Canada.
[2] Department of Genetics, Montreal Children's Hospital, Montreal, Quebec, Canada.
[3] Kinderspital, University of Zurich, Zurich, Switzerland.

* See NAPS document no. 03016 for three pages of tabular data on clinical and laboratory findings and enzyme studies. Order from ASIS/NAPS, c/o Microfiche Publications, P.O. Box 3513, Grand Central Station, New York, New York 10017.

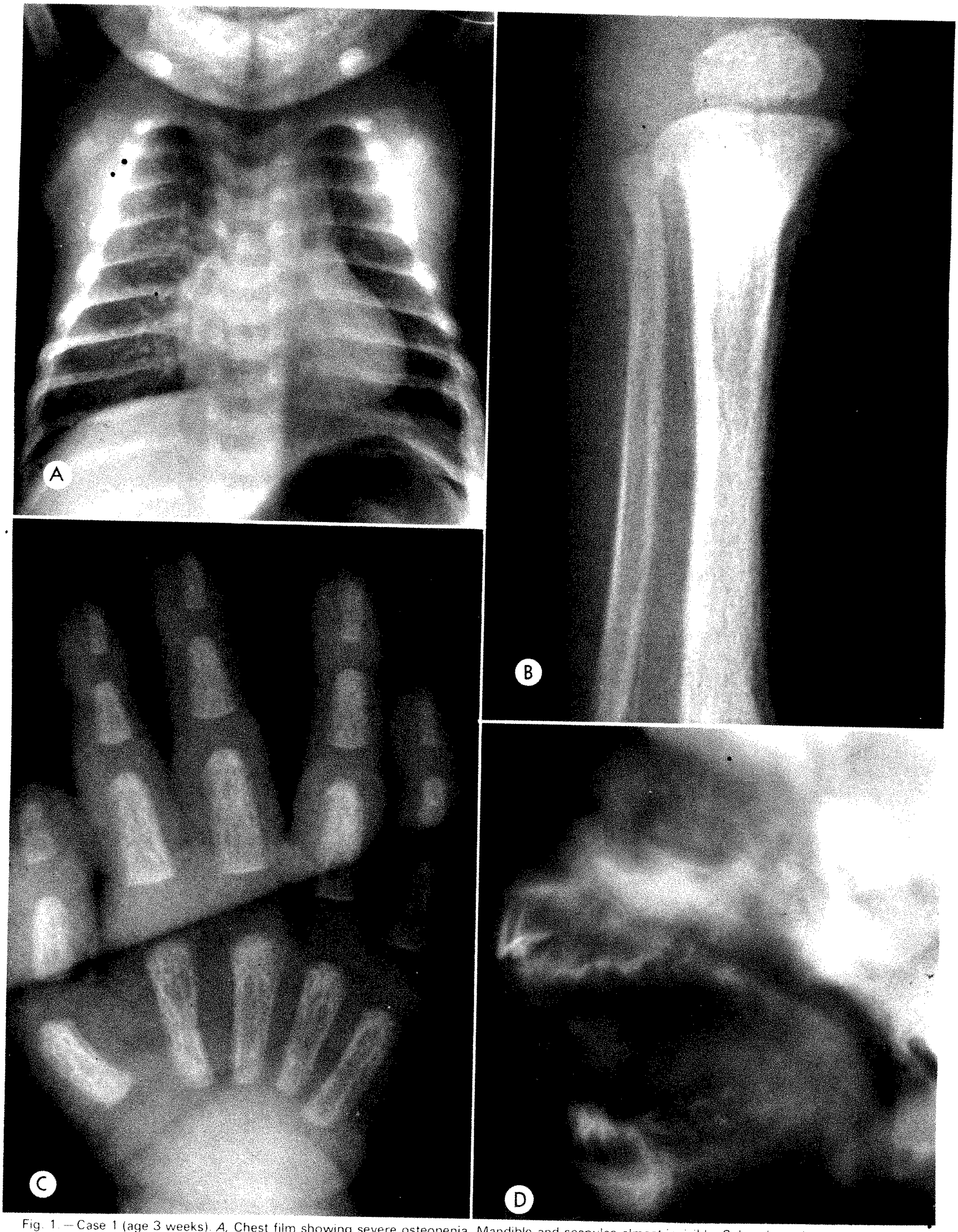

Fig. 1.—Case 1 (age 3 weeks). *A,* Chest film showing severe osteopenia. Mandible and scapulae almost invisible. Subperiosteal resorption and periosteal reaction present in ribs and upper humeri. Lamina dura absent. *B and C,* Leg and hand showing fragmented metaphyses. Subperiosteal resorption and new bone are combined in long bones. Cortex of phalanges invisible. *D,* Mandible.

TABLE 1

Summary of Radiologic Findings

Findings	Case 1	Case 2	Case 3	References to Cases with Some Similar Findings
General skeletal	Profound osteopenia; periosteal new bone formation; subperiosteal bone resorption; coarse trabeculae	At age 2–6 weeks, same as case 1; progression to thick cortices at age 6 months	Periosteal cloaking at age 2 months	[2–4]
Skull	Flat occiput; absent lamina dura of tooth buds; small mandible	Premature synostosis of coronal and anterior sagittal sutures; arrested skull growth despite craniectomy at age 2½ months; absent lamina dura of tooth buds; small mandible	Premature synostosis of coronal and metopic lambdoid sutures; arrested skull growth despite craniectomy at age 10 months; lamina dura present; small mandible	[1]
Vertebral column	Normal	Normal at age 1 month; scoliosis, gibbus (L1) at age 6 months; decreased anteroposterior diameter of vertebral bodies	Bone-in-bone appearance at age 2 months	[1]
Pelvis	Normal	Narrow ischium at age 1 month; flared iliac wings, coxa vara at age 6 months	Same as case 2; coxa vara at age 14 months	[1]
Thorax:				
Ribs	Thin; periosteal cloaking	Wide; periosteal cloaking; costochondral junctions at age 1 month; at age 6 months, thick	Thick at age 14 months	[1–4]
Lungs	Normal	Terminal pneumonia (age 7 months)	Recurrent pneumonia after surgery (age 10 months) and until death (age 16 months)	[5]
Heart	Normal	Terminal congestive heart failure	Cardiomegaly (left atrium and ventricle); congestive heart failure at age 1 month	[6]
Long bones	Metaphyseal fragmentation, irregularity	Periosteal new bone formation and resorption at age 1 month; proximal femoral, humeral erosions at age 6 months; metaphyseal fragmentation and irregularity (more severe than case 1 at age 1 month) progressing to wide regular metaphyses at age 6 months	Periosteal new bone, proximal femoral erosions at age 2 months	[2, 4, 6]
Hands	Carpal maturation normal, knee advanced	Knee advanced at age 1 month; delayed disharmonious carpal maturation, Hurler-like metacarpals at 6 months; stippled tarsal epiphyses at age 1 month	Carpal maturation greatly delayed at age 14 months; Hurler-like metacarpals at at age 1 year	[3, 4, 7]

alveolar ridge, high arched palate, low-set ears, and a short broad neck. The hands were square, the fingers thick, and there was a right simian crease. She was hypotonic and could not sit, lift her head, or bear weight. Hip and thumb movements were reduced. A grade 3/6 systolic murmur was heard maximally over the mitral area. Radiography showed marked cardiomegaly, and mitral insufficiency was suspected.

Linear growth rate declined and stopped at the third percentile at age 14 months. Skull growth also stopped, and bilateral lambdoid and posterior parasagittal craniectomy were performed without subsequent growth. The patient was barely aware of her environment and did not speak. She had several upper respiratory infections and died at age 16½ months.

The autopsy findings suggested that death was due to coronary insufficiency accompained by mitral insufficiency. The mitral valve, left ventricle (endocardium, myocardium, papillary muscle), and main coronary arteries were thickened, with elastosis and deposition of "clear" foam cells. The clear cells were also seen in the kidney epithelium and in paramucous gland areas of the epiglottis. Microscopy of the ribs showed narrow zones of poliferating cartilage and a thick cambium layer containing collagen and large clear osteoblasts. The resting zone contained swollen vacuolated cartilage cells and areas of mucinous degeneration.

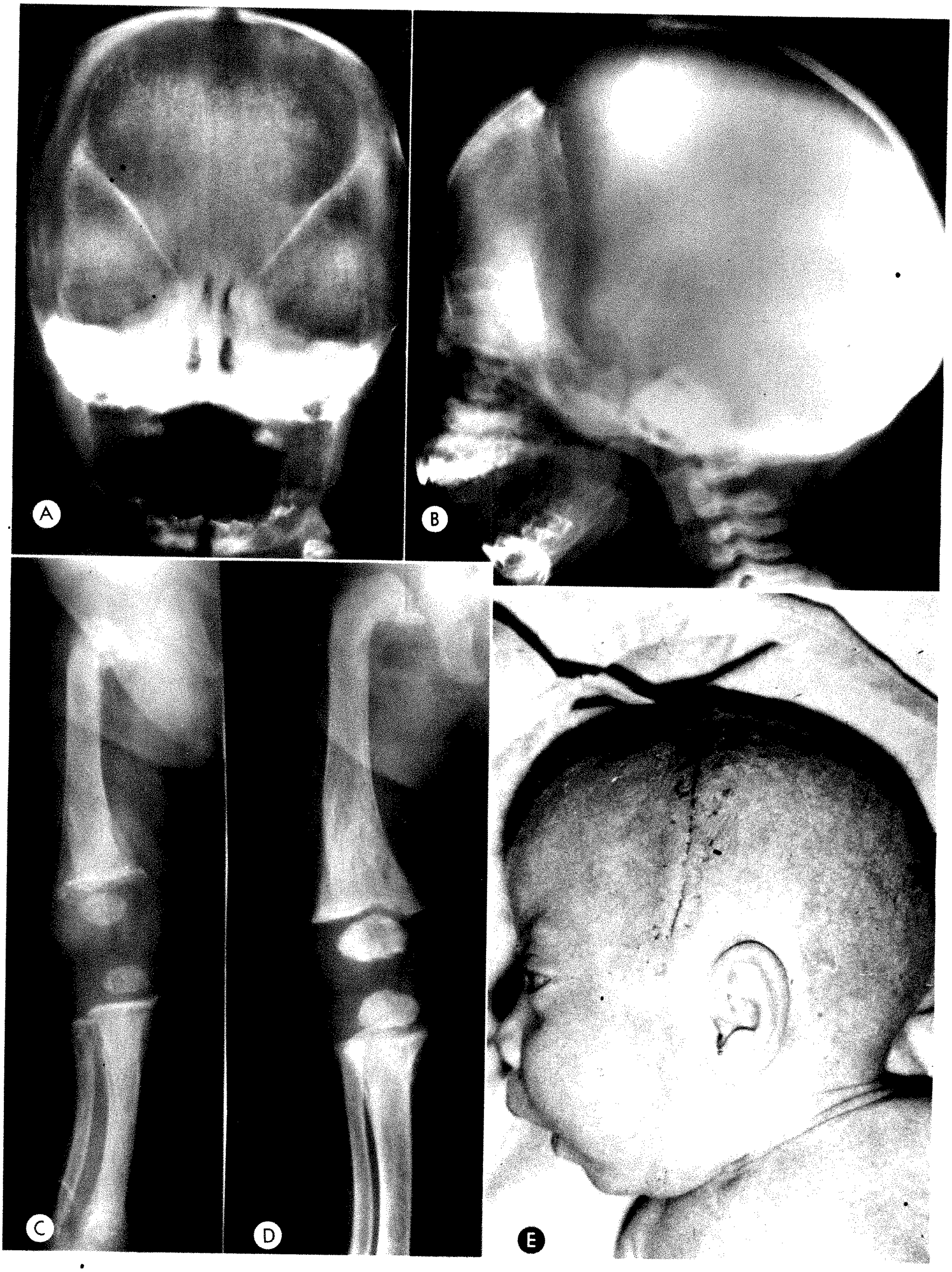
A
B
C
D
E

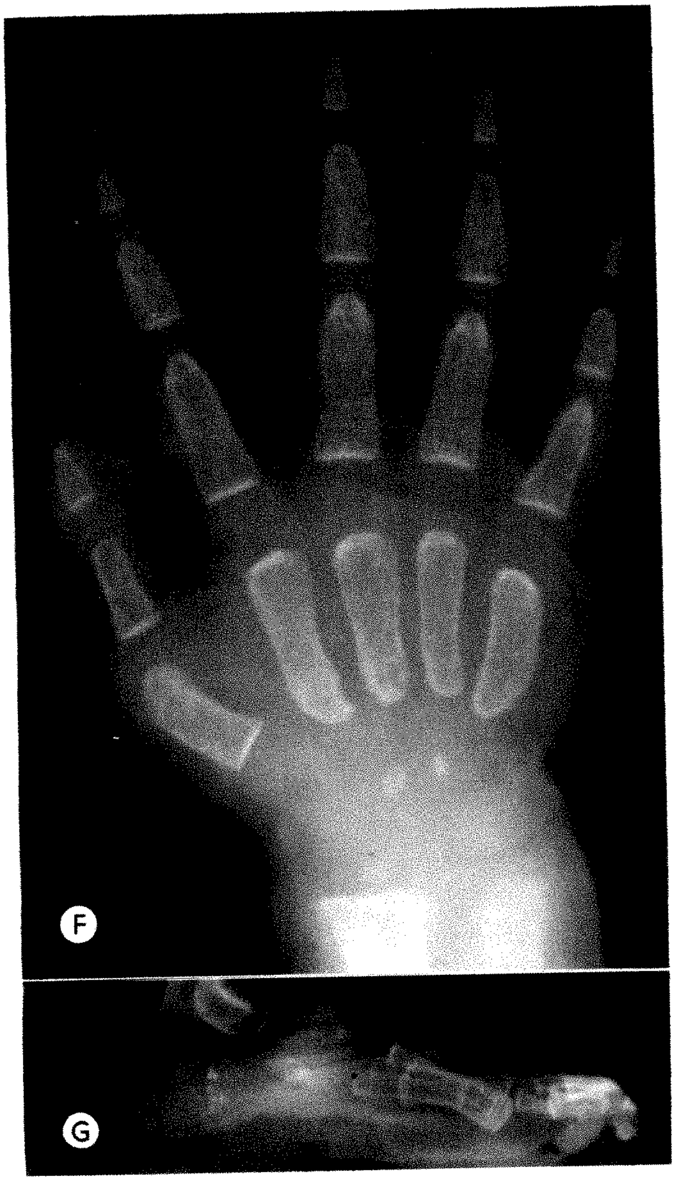

Fig. 2.—Case 2. *A*, Anteroposterior skull film (age 2 weeks) showing premature synostosis of coronal suture and osteopenia. *B*, Lateral skull film (age 4 months) after coronal craniectomy showing vault has thickened, other sutures closed. Lamina dura still absent. *C and D*, Extremities at ages 2 weeks and 3 months, respectively. Fragmented, poorly defined metaphyses heal and become widened and smooth; subperiosteal resorption along shaft of all bones and at upper femora and tibia heals, but leaves coxa vara deformity. *E*, Profile (age 2½ months) after craniectomy showing low-set ears, small mandible, long philtrum, and tower-shaped skull. *F*, Hand showing signs resembling Hurler syndrome. *G*, Foot (age 1 month) showing stippled calcaneal ossification.

Discussion

The diagnosis in our three patients was established according to the presently accepted criteria described by Wiesmann et al. [8, 9]: (1) decreased acid hydrolase activity in cultured fibroblasts, and increased activity of these enzymes in the culture medium; (2) increased acid hydrolase activity in body fluids (serum) (case 1); and (3) acidophilic inclusions in skin fibroblasts (I cells).

Clinical Findings

The three families reported here came from the same region of Italy but were not related to each other. Most affected children have been European. In two of the families there was parental consanguinity, as was reported in four families by Walbaum et al. [2]. The disease occurs in both sexes and in siblings. The parents are phenotypically normal and may have inclusions in their fibroblasts. All these factors suggest autosomal recessive inheritance.

When our patients were first examined, I-cell disease was not recognized. It was only at the ages of 6–10 months that the Hurler-like features of the disease became obvious in two patients: psychomotor retardation, coarse facies, thick tight skin, and joint contractures. Growth had decelerated or stopped. Corneal clouding is said to be present in Hurler syndrome and absent in I-cell disease. Perhaps serial slit lamp examination allowed its early detection in two of our patients. While hemangiomas are not regarded as typical of the disease, they were seen in two of our patients as well as in two patients reported by Leroy and Martin [7].

Death was due to cardiorespiratory failure in two of our patients. This seems to be the most common cause of death, which usually occurs in early childhood [7]. Unlike other reported cases [10], the cardiac lesions were on the left side exclusively in our one patient who had an autopsy.

Biochemical Data

The fibroblasts in I-cell disease show reduced activities of acid hydrolases, while their culture media and extracellular fluids contain an excess. The fibroblasts of our three patients showed these enzymatic abnormalities. In one patient tested, there were raised levels of hydrolases in the serum. There are several theories about the lysosomopathy [11]. One suggests that the lysosome "leaks" its enzymes; a second theory is that the enzymes are immunologically inhibited; a third is that the hydrolases are defective and cannot enter the lysosome [12]. Lymphocytes in peripheral blood may have vacuoles and granular inclusions. This occurred in one patient.

The appearance of children with I-cell disease is similar to that in Hurler syndrome, generalized gangliosidosis, and the other mucolipidoses (I and III). In both the Hurler syndrome and I-cell disease there is dwarfism; progressively coarsening facies with a flat nasal bridge, epicanthic folds, anteverted nostrils, and a short neck; joint immobility with claw hands; and kyphoscoliosis. The thick tight skin, thick gums, normal urinary polysaccharides, and fibroblast enzyme studies distinguish mucolipidosis II from the Hurler syndrome.

I-cell disease is differentiated from generalized gangliosidosis by the presence of I cells, absence of abnormal gangliosides, and normal or low activity of galactosidase in liver [6]. In mucolipidoses I and III, inclusions may occur in cultured cells [10]; however, the degree of physical, mental, and skeletal involvement is milder and easily distinguished.

Radiologic Findings

Our patients were examined radiologically because of head deformity (cases 2 and 3) and low birth weight (case 1). The initial diagnosis in each was active systemic bone disease. Subperiosteal bone resorption strongly suggested

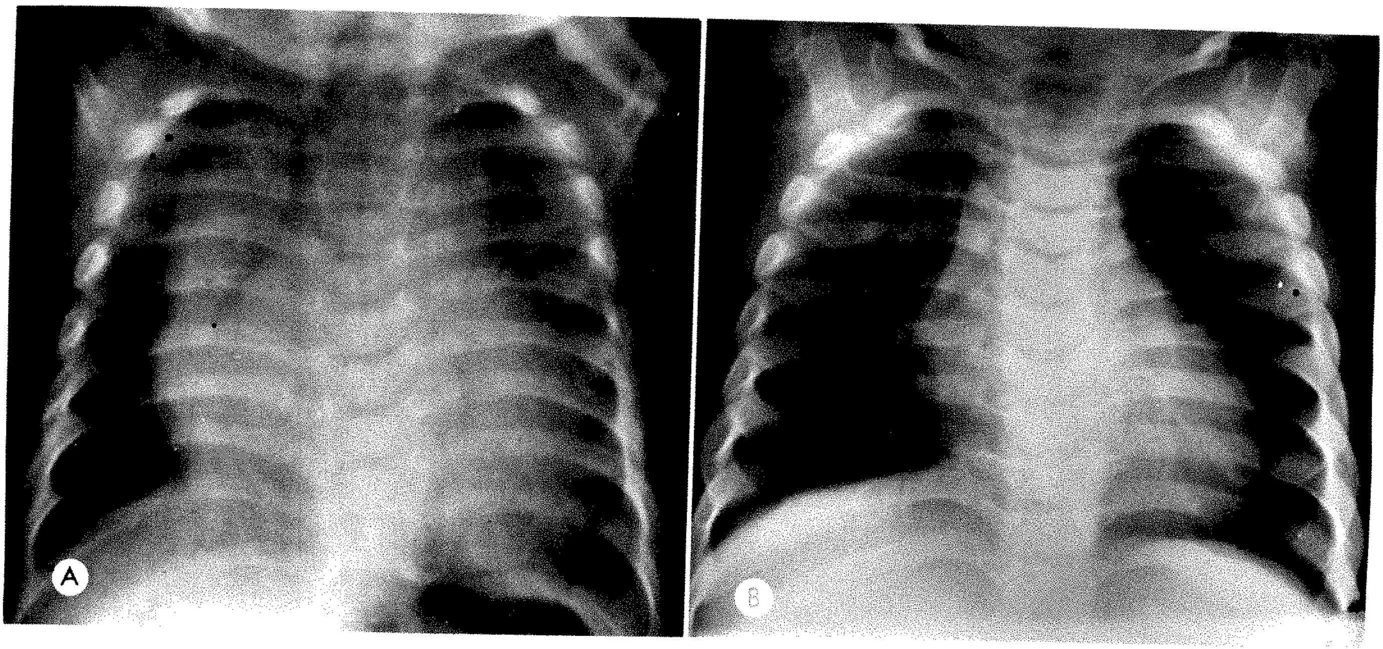

Fig. 3.—Case 3. *A*, Chest film (age 1 month) showing cardiomegaly and osteopenia of thoracic cage; thin ribs. *B*, Chest film (age 14 months) showing widened ribs.

hyperparathyroidism; this diagnosis was made by three experienced pediatric radiologists in case 1. Normal serum calcium in the newborn does not exclude this diagnosis. The periosteal new bone and the metaphyseal irregularities were reminiscent of a systemic infection such as syphilis or osteomyelitis. The fragmented metaphyses mimicked the corner fractures seen in the abused child, syphilis, or scurvy. The fuzzy metaphyses and the premature suture synostosis slightly resembled rickets, unusual at such an early age.

The striking radiologic resemblance to congenital hyperparathyroidism is unexplained. There was no such stimulation in at least one of our cases, who had normal calcium, phosphorus, and parathormone assays (case 1).

The stippled tarsal bone at age 2 months in one patient suggested bone dysplasia; it resembled three cases of I-cell disease described by Leroy and Martin [7] and a case of GM$_1$gangliosidosis described by Taybi [13]. In the two patients who had serial radiology the metaphyses became smoother, the cortex thicker, and the skeleton developed the Hurler-like radiologic features described by Taber et al. [1] in older children.

Suture synostosis of such early onset and severity has not been reported in I-cell disease [6, 7]. It is probably initially a manifestation of dysostosis rather than of microencephalia, judging by the compensatory asymmetric skull growth. As the disease progresses, brain and skull growth stop altogether.

There has been little description of the radiologic features of I-cell disease in neonates. Maroteux et al. [14] and Leroy et al. [5] noted periosteal cloaking in a 4-day-old and a 1½-month-old child. Leroy wondered if this could represent an exaggerated form of the normal neonatal cloaking described by Shopfner [15]. Since then Walbaum et al. [2] described a newborn with periosteal newborn formation and irregular metaphyses, and initially suspected syphilis. Joannard et al. [3] noted osteomalcia, fractures, and periosteal new bone in a 24-hr-old child. Iannaccone and Capotorti [4] also described severe osteoporosis in a 1-day-old child. Taybi [13] described a case of neonatal GM$_1$gangliosidosis with periosteal cloaking and cupped epiphyses, but the long bones were already severely deformed.

On the basis of our experience and a review of the literature, we believe that the radiologic findings of severe osteopenia, absent lamina dura, metaphyseal irregularities, and subperiosteal bone resorption in a neonate strongly suggest hyperparathyroidism or mucolipidosis II (I-cell disease). The latter diagnosis is confirmed by skin fibroblast culture and acid hydrolase assay.

ACKNOWLEDGMENTS

We thank the following physicians and surgeons who referred the patients and conducted clinical and laboratory investigations: N. Herschkowitz and U. Wiesmann (Bern); D. Koziol (Schwenningen); B. J. Reilly (Toronto); E. Delvin and S. Joshi (Montreal); P. Macleod (Vancouver); and J. S. Dunbar (Cincinnati). We also thank Drs. S. Jequier and A. Poznanski for reviewing the manuscript, G. Raymond for photography, and J. Turgeon for typing the manuscript.

REFERENCES

1. Taber P, Gyepes MT, Philippart M, Ling S: Roentgenographic manifestations of Leroy's I-cell disease. *Am J Roentgenol* 118:213–221, 1973
2. Walbaum R, Dehaene PH, Scharfman W, Farriaux JP, Tondeur M, Vamos-Hurwitz E, Kint JA, Van Hoof F: La mucolipidose de type II (I-cell disease). *Arch Fr Pediatr* 30:577–N593, 1973

3. Joannard A, Bost M, Pont J, Dieterlen M, Frappat P, Beaudoing A: La mucolipidose type II. *Pediatrie* 24:825–841, 1974
4. Iannaccone G, Capotorti L: A contribution to the so-called pseudo-Hurler syndrome: reports of two siblings with unusually severe bone alterations. *Ann Radiol* 12:355–364, 1969
5. Leroy JG, Spranger JW, Feingold M, Opitz JM, Croher AC: I-cell disease: a clinical picture. *J Pediatr* 79:360–365, 1971
6. Blank E, Linder D: I-cell disease (mucolipidosis II): a lysosomopathy. *Pediatrics* 54:797–805, 1974
7. Leroy JG, Martin JJ: Mucolipidosis II, I-cell disease: present status of knowledge. *Birth Defects: Orig Art Ser* 11(6): 283–293, 1975
8. Wiesmann UL, Vasselia F, Herschkowitz NN: Mucolipidosis II (I-cell disease). *Acta Paediatr Scand* 63:9–16, 1974
9. Wiesmann UL, Herschkowitz NN: Studies on the pathogenetic mechanism of I-cell disease in cultured fibroblasts. *Pediatr Res* 8:865–870, 1974
10. Glaser JH, McAlister WH, Sly WS: Genetic heterogeneity in multiple lysosomal hydrolase deficiency. *J Pediatr* 85: 192–198, 1974
11. McKusick VA: *Heritable Disorders of Connective Tissue*, 4th ed. St. Louis, Mosby, 1972
12. Hickman S, Neufeld EF: A hypothesis for I-cell disease: defective hydrolases that do not enter lysosomes. *Biochem Biophys Res Commun* 49:992, 1972
13. Taybi H: *The Radiology of Syndromes*. Chicago, Year Book Medical Publishers, 1975
14. Maroteux P, Hors-Cayla MC, Pont J: La mucolipidose de type II. *Presse Med* 78:179–181, 1970
15. Shopfner C: Periosteal bone growth in normal infants. *Am J Roentgenol* 97:154–163, 1966

Unilateral Locked Facet in Cervical Spine Injuries

A. T. SCHER[1]

Among 525 patients who sustained trauma to the cervical spinal cord, 86 (16%) had unilateral locking of facets. If the diagnosis is not promptly made, neurological recovery of root deficit will be impaired and orthopedic deformity will result. Since there is often only minimal forward displacement at the site of dislocation, it is possible not only to miss the locking of facets but even to erroneously conclude that no fracture or dislocation is present. Rotation of the cervical spine above the level of dislocation results in a diagnostic appearance on the lateral view. Rotation of the spinous processes was seen in the anteroposterior view in only one-third of the cases. The necessity of obtaining x-rays which adequately demonstrate the lower cervical spine is emphasized and the technique briefly described.

Introduction

Flexion-rotation injuries are the most frequent cause of the fractures and dislocations of the cervical spine associated with spinal cord injury. The most common orthopedic injury occuring after flexion-rotation trauma to the cervical spine is dislocation with unilateral locking of facets [1]. It has been our experience that the diagnosis of this condition is usually not made on initial radiographic examination. Instead, patients are often referred with a diagnosis of "subluxation or dislocation" of the cervical spine. In a series of patients who had sustained unilateral interlocking of facets, Braakman and Vinken [2] found that 16 of 33 were diagnosed incorrectly. If the correct diagnosis is not promptly made, reduction becomes extremely difficult. In the presence of an unreduced locked facet, root recovery is impaired and persistent orthopedic deformity will occur.

There are two primary reasons for incorrect diagnosis: (1) inadequate demonstration of the lower cervical spine (C6–T1) on the lateral view; and (2) failure to recognize the condition radiographically. This paper reviews the diagnostic radiologic features and the radiographic techniques necessary for correct diagnosis.

Case Material and Findings

From 1963 to 1973, 525 patients who sustained trauma to the cervical spinal cord were seen in our spinal injuries unit. Most of the injuries were sustained in motor vehicle accidents and falls; the remainder were due to industrial accidents, assaults, and sports injuries.

Dislocation with unilateral facet interlocking was present in 86 of the 525 cases (16%). In 68 of the 86 (79%), the injury involved the C4–C5 and C5–C6 regions. The anteroposterior view was helpful in the specific diagnosis in only one-third of the cases. Associated fractures were present in 30 cases (35%). The most common fractures involved the vertebral bodies and spinous processes, and were usually evident on the lateral view. Less common were fractures of the neural arches and the lateral masses, often only recognized on the anteroposterior view. The oblique views sometimes demonstrated inconspicuous fractures of the articular facets and pedicles.

Discussion

Anatomy of Apophyseal Joints

The superior and inferior articular facets form an articular pillar which projects laterally at the junction of the pedicle and lamina of the vertebral body. The rounded articular facets have smooth joint surfaces lined with cartilage and synovial membrane. The joint itself is bound together by a loose capsule which allows a wide excursion on movement. In flexion there may be as much as 5 mm of anterior displacement of the inferior articular facet of the upper vertebral body in relation to the lower [4].

The plane of each joint surface forms an angle of about 45° with the long axis of the spinal canal. The largest angle is formed by the C4–C5 joint spaces, and caudally and cranially the angle decreases gradually. Because the joint planes are perpendicular to the sagittal plane, they are easily visible on the lateral view of the cervical spine. Exceptions are the C2–C3 joints which slope laterally by 10–20° and as a result are not clearly seen. This may give rise to diagnostic errors [5].

Mechanism of Injury

Experimental studies have shown that in order to produce dislocation with unilateral interlocking a rotational element as well as forward displacement are necessary [6]. In forced combined cervical flexion and rotation injuries, the inferior articular facet of the upper vertebra is displaced forward, overrides the superior articular facet of the lower vertebra, and becomes locked in the dislocated position. The dislocation is illustrated in figure 1. The term locked is appropriate in that the dislocated facet cannot return to its normal position unless reduction of the dislocation is obtained by traction, manipulation, or surgery. It has also been shown experimentally that the joint capsule and interspinous ligament must be completely ruptured for dislocation to take place. The posterior longitudinal ligament and the annulus fibrosus on the affected side are usually only slightly damaged [7].

Received May 14, 1976; accepted after revision April 4, 1977.

[1] Spinal Injuries Unit, Conradie Hospital, Cape Town, South Africa.

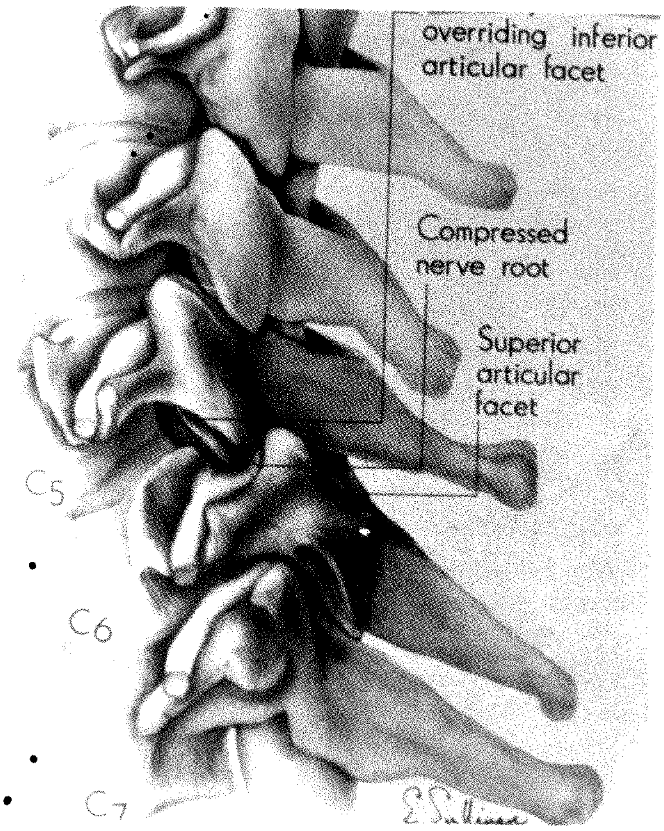

Fig. 1.—Illustration of unilateral interlocking of facets in cervical spine. (Reprinted with permission from Schneider RC: *Head and Neck Injuries in Football.* Baltimore, Williams & Wilkins, 1971.)
←

Radiographic Technique

In patients with acute injury to the cervical spinal cord, the radiographic projections must provide optimal visualization of the *entire* cervical spine, while avoiding unnecessary manipulation of the patient's head and neck. We have found that the "pulled lateral view" or, if unsuccessful, the "swimmer's view" will in most cases demonstrate the lower cervical and first thoracic vertebrae adequately.

In the pulled lateral view the patient is supine with the film placed on the lateral aspect of the shoulder. The shoulders are pulled down by two assistants who stand on either side of the patient. Grasping the arms above the elbow, they then pull the arms across the chest and downward toward the feet. Light countertraction to the head is applied using radiotranslucent halter or tongbar if the patient is undergoing skull traction. This countertraction serves to maintain the position of the head against the pull on the shoulder. There should be close supervision by a physician to ensure that the neck is not inadvertently flexed or extended.

In the so-called swimmers view the patient is supine with the cassette placed on the lateral aspect of the shoulder. The arm on the same side as the cassette is raised above the head while the opposite arm is pulled down toward the

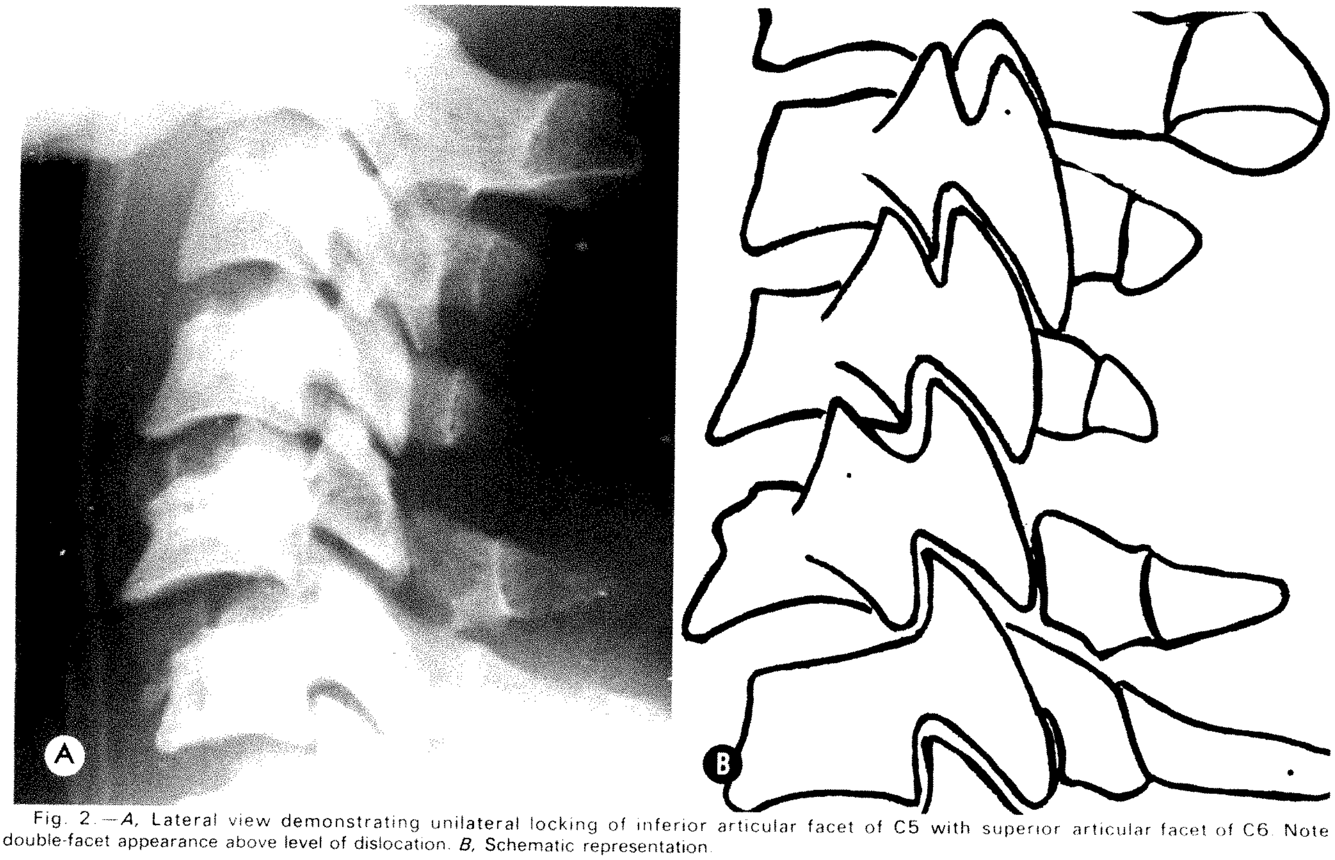

Fig. 2.—*A,* Lateral view demonstrating unilateral locking of inferior articular facet of C5 with superior articular facet of C6. Note double-facet appearance above level of dislocation. *B,* Schematic representation.

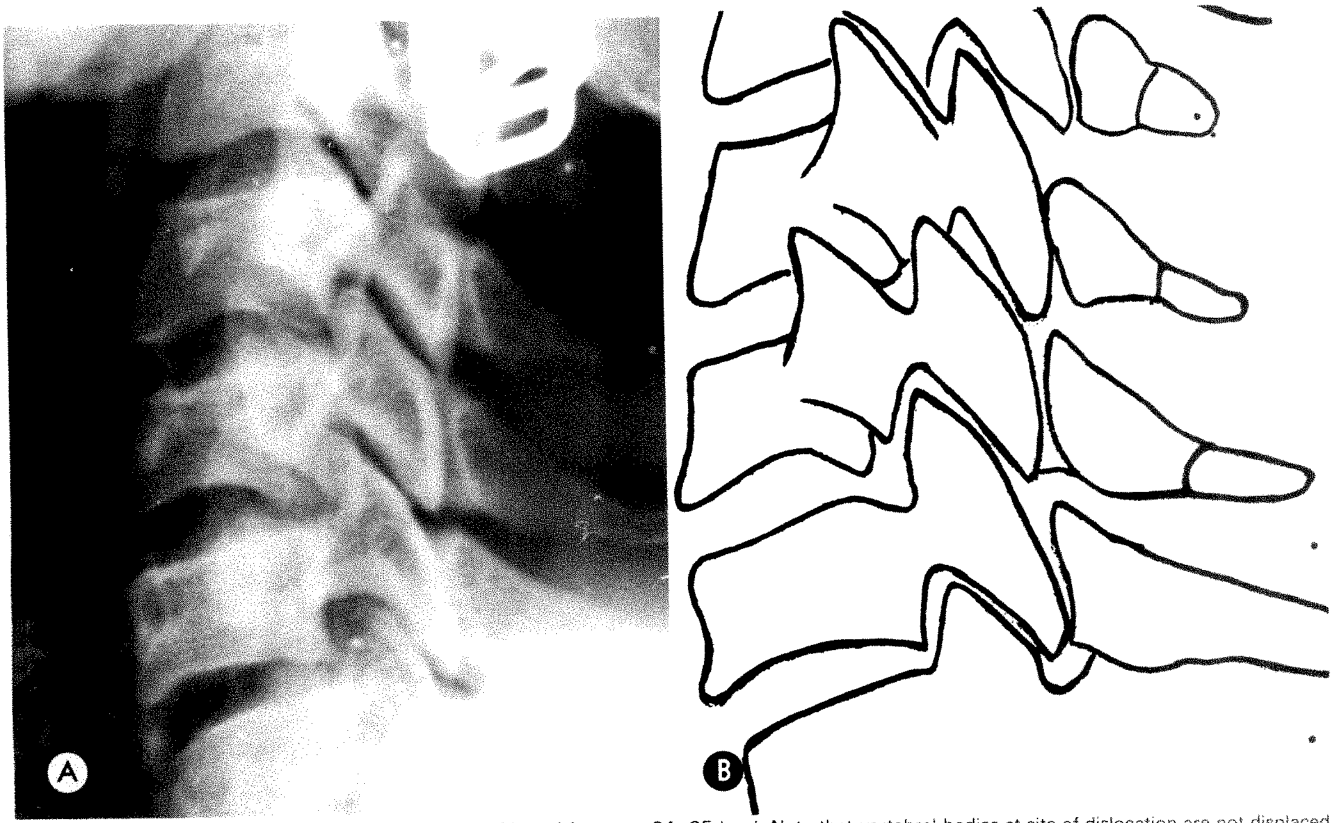

Fig. 3.—*A*, Lateral view demonstrating unilateral locking of facets at C4–C5 level. Note that vertebral bodies at site of dislocation are not displaced. *B*, Schematic representation.

feet to depress the shoulder. The tube is centered on the head of the humerus at the level of the acromion process. Care must be taken that the film and tube are parallel.

While the anteroposterior view may be helpful, the diagnosis is usually made on the lateral view. Once the diagnosis is made, it is still necessary to determine the side of the lesion. Standard 45° oblique views do not provide good visualization of the apophyseal joints. We have found that 20° oblique views, as described by Lodge and Higginbottom [3], are most useful in demonstrating this and in providing further visualization of the apophyseal joints. Often fractures of the pedicles of tips of the articular facets are demonstrated.

Diagnostic Appearance

Use of the correct radiographic technique will ensure adequate demonstration of the entire cervical spine and prevent diagnostic errors due to failure of visualization of the traumatized region. However, lack of familiarity with the diagnostic appearance on the lateral and anteroposterior views can often lead to incorrect diagnosis, even when adequate x-rays are available.

Lateral view. Rotation of the cervical spine above the level of dislocation results in a diagnostic appearance on the lateral view. The articular facets of the vertebrae below the level of dislocation lie symmetrically parallel to each other in a true lateral position, so that only one set (a superior and inferior articular facet) of articular facets per vertebra is visible. Above the level of dislocation a double set of articular facets for each vertebra will be present. This is because of the rotation of the vertebrae which now effectively lie in an oblique position in relation to x-ray beam (fig. 2).

This appearance may not be immediately obvious but should be sought routinely in cases of cervical spine trauma. The diagnosis is often missed because too much attention is given to the shift of the vertebral bodies in relation to one another; thus the essential lesion, the interlocking, is overlooked. In nine of our cases the forward displacement of the vertebral body was minimal and was initially thought to be the only finding. An illustrative case is shown in figure 3.

Other features demonstrated on the lateral view include fractures of the spinous processes and divergence of the spinous processes at the level of dislocation. The latter is due to rupture of the posterior ligamentous complex which must occur before dislocation will take place.

Anteroposterior view. Several investigators have stressed that in the anteroposterior view, the spinous processes above the level of the facet locking will be rotated toward the locked side. This is expected due to the rotational component necessary to produce the dislocation [6] (fig. 4). When present, this appearance serves to confirm the diagnosis made on the lateral view and also indicates the

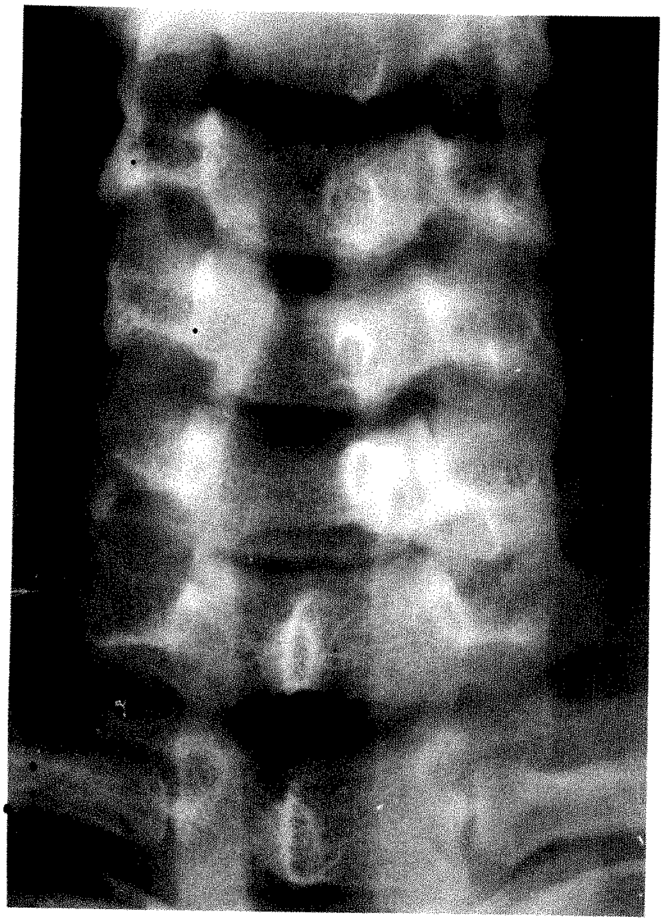

Fig. 4.—Anteroposterior view demonstrating rotation of spinous process of C6 to left indicating presence of unilateral interlocking of facets at C6–C7 level on left side.

side of dislocation. However, this appearance was seen in only one-third of our cases, in agreement with the findings of Braakman and Vinken [2]. The anteroposterior view is of considerable value in demonstrating fractures of the neural arches or lateral masses; in fact it is often only on this view that these features are visualized.

REFERENCES

1. Cheshire DJE: The stability of the cervical spine following conservative treatment of fracture and dislocation. *Int J Paraplegia* 7:193–203, 1970
2. Braakman R, Vinken PJ: Old luxations of the lower cervical spine. *J Bone Joint Surg* [*Br*] 50:52–60, 1968
3. Lodge T, Higgenbottom E: Fractures and dislocations of the cervical spine. *X-ray Focus* 7:1–6, 1966
4. Penning L: Diagnostic clues by x-ray: injuries of the lower cervical spine. *Acta Neurochir* (Wien) 22:234–244, 1970
5. Braakman R, Penning L: *Injuries of the cervical spine*. Amsterdam, Execerpta Medica, 1971
6. Roaf R: A study of the mechanics of spinal injuries. *J Bone and Joint Surg* [*Br*] 42:810–823, 1960
7. Beatson RT: Fractures and dislocations of the cervical spine. *J Bone Joint Surg* [*Br*] 45:21–35, 1963

Injuries of the Medial Epicondylar Ossification Center of the Humerus

JOSEPH W. CHESSARE,[1] LEE F. ROGERS,[1] HARVEY WHITE,[2] AND MIHRAN O. TACHDJIAN[3]

The complex nature of the ossification centers makes elbow injuries in a child or adolescent difficult to evaluate. The medial epicondylar ossification center is involved in a significant proportion. Injuries vary from simple avulsions to wide displacement with entrapment in the elbow. When entrapment occurs, it may be mistaken for the trochlear ossification center and the true nature of the injury overlooked. Radiographic findings are presented. The anteroposterior view was found to be diagnostic in minimal or marked avulsions of the medial epicondyle because of the characteristic inferior displacement. The anteroposterior view may not always be diagnostic in cases of entrapment of the medial epicondyle; the lateral view is usually diagnostic. In elbow dislocation, the presence and position of the medial epicondyle must be ascertained. Comparison and oblique views are often of value.

Introduction

The elbow is a common site of injury in children. The complex nature of the ossification centers makes these injuries difficult to evaluate. Knowledge of the developmental anatomy of the distal humerus is necessary for correct radiographic interpretation.

The distal humerus has four centers of ossification (fig. 1). The capitellum is the first center to appear at 6–12 months of age. The medial epicondylar ossification center appears next at 5–7 years. The trochlear ossification center is usually demonstrated by age 10 years but may appear as early as age 7. The lateral epicondyle appears last at 12–14 years.

The medial epicondyle is involved in a significant proportion of childhood or adolescent elbow injuries. In a study of 400 consecutive elbow fractures in children, medial epicondylar fracture comprised 10% of the cases, and was the third most common fracture after supracondylar (58%) and lateral condylar fractures (13%) [1].

The medial epicondyle does not contribute to the longitudinal growth of the humerus and therefore is not really an epiphysis, but an apophysis. It unites with the distal humeral metaphysis at age 18–20 years. The medial epicondyle has several important anatomic relationships. The common tendon of the flexorpronator group of muscles originates on the anterior aspect of the medial epicondyle. The ulnar collateral ligament extends from the coronoid and olecronon processes of the ulna to the medial epicondyle. The ulnar nerve runs in a groove behind the medial epicondyle. This accounts for the occasional association of ulnar nerve injury with medial epicondylar fracture.

Fractures of the medial epicondyle are usually caused by a valgus stress producing traction on the flexorpronator tendon and subsequently on the medial epicondyle itself (fig. 2A). The valgus stress may be produced by a fall on the outstretched hand or by a fall on the elbow. Direct trauma is a less common cause of medial epicondylar injury.

Case Materials

The records of Childrens Memorial Hospital between 1963–1976 were searched for medial epicondylar injuries. A preliminary series of 42 cases was found. Radiographs were not available for five cases, and two were excluded when they were found to be supracondylar fractures. Thus, 35 consecutive cases are included in this study: 25 males and 10 females. We reviewed and analyzed all cases. The frequency of injury was approximately equal on the right and the left; 16 and 19 injuries, respectively. Ages ranged from 3 years 9 months to 17 years (average, 11.3 years). This is similar to Smith's series [2]. Almost three-fourths of the patients (25 of 35) were between 9 and 14 years.

Findings

We have classified injuries of the medial epicondyle into five groups on the basis of radiographic findings. This grouping has both diagnostic and therapeutic significance (table 1).

Minimal Avulsion

Twelve patients in this series sustained a minimally displaced (< 1 cm) fracture of the medial epicondyle. When radiographically identifiable displacement occurs, the medial epicondyle is virtually always displaced inferiorly. Some anterior or posterior displacement may occur as well. Inferior displacement, caused by the pull of the flexorpronator tendon, is best identified on the anteroposterior view. The lateral view proved to be of little benefit in this injury. Subtle displacement may be overlooked without comparison views of the uninjured elbow. Another characteristic radiographic finding is localized soft tissue swelling about the medial epicondyle with obliteration of adjacent

---

Received October 8, 1976; accepted after revision March 4, 1977.
Presented at the annual meeting of the American Roentgen Ray Society, Washington, D.C., September 1976.

[1] Department of Radiology, McGaw Medical Center of Northwestern University, Chicago, Illinois 60611.

[2] Department of Radiology, Childrens Memorial Hospital, Chicago, Illinois 60614.

[3] Department of Orthopedic Surgery, Childrens Memorial Hospital, Chicago, Illinois 60614.

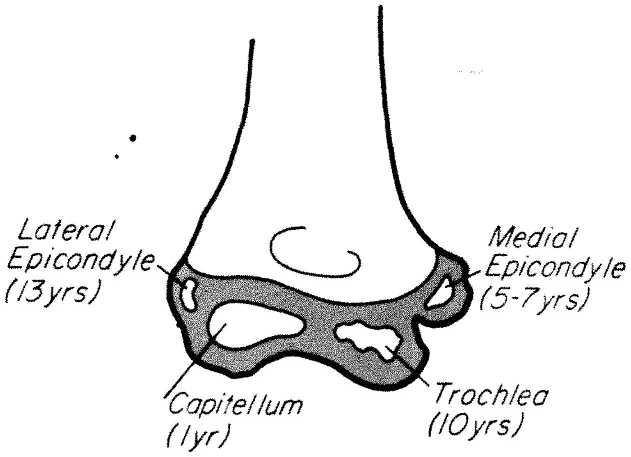

Fig. 1.—Average time of appearance of ossification centers at distal humerus.

TABLE 1
Injuries of the Medial Epicondyle

Classification	No. Cases
Simple avulsion of medial epicondyle:	
Minimally displaced	12
Moderately or severely displaced	6
Little League elbow:	
Acute avulsion of medial epicondyle	1
Chronic injury	1
Isolated entrapment of medial epicondyle	3
Medial epicondylar injury associated with elbow dislocation:	
Without entrapment in joint	7
With entrapment in joint	4
Fracture of medial humeral condyle	1
Total	35

fascial planes (fig. 2*B*). This injury is usually treated with closed reduction and immobilization.

Moderate to Severe Avulsion

Separation of more than 1 cm occurred in six patients. While both anteroposterior and lateral views of the elbow were obtained, the anteroposterior view was the most helpful in demonstrating the degree of separation and the position of the medial epicondyle. Marked regional soft tissue swelling is characteristic (figs. 2*C* and 2*D*). Treatment of this injury varies and may consist of simple immobilization or open reduction and internal fixation.

Little League Elbow

One case of acute injury and one case of chronic injury are included in this series. Little League elbow, an avulsion fracture of the medial epicondyle occuring in child or adolescent baseball pitchers, has been described by Brogden and Crow [3]. It is produced by violent contraction of the flexorpronator groups of muscles during the acceleration phase of throwing. The injury may occur acutely with sudden pain over the medial aspect of the elbow while pitching. Radiographically, there is separation of the medial epicondyle with associated soft tissue swelling. Treatment usually consists of closed reduction and immobilization.

The injury may develop more chronically and insidiously with separation, fragmentation, enlargement, and roughening of the medial epicondyle [4]. These patients have pain, tenderness, and swelling aggravated by pitching and improved by rest. One patient in our series presented with a chronic sports-related injury of the medial epicondyle (figs. 3*A*, 3*B*). Chronic pitching injuries of the medial epicondyle are treated simply with rest of the elbow and cessation of pitching.

Isolated Entrapment

Isolated entrapment of the medial epicondyle occurred in three patients. It is caused by a valgus stress with temporary opening of the elbow joint space medially. The epicondyle is avulsed and then drawn into the joint by traction from the attached flexor pronator muscle group and the ulnar collateral ligament. When the force is released, the joint closes entrapping the medial epicondyle (fig. 4*A*).

The entrapped medial epicondyle is commonly overlooked [5]. Knowledge of the developmental anatomy of the elbow is essential for correct diagnosis because the radiographic appearance will vary with patient age (fig. 4*B*). When entrapment occurs before ossification of the trochlear center, the entrapped medial epicondyle may be mistaken for the "normal" trochlea. The key to the correct diagnosis is the absence of the medial epicondyle from its normal location; the trochlear center should never ossify before the medial epicondylar center (fig. 5).

After trochlear ossification, the entrapped medial epicondyle is usually seen between the trochlea and the coronoid process of the ulna in the anteroposterior projection (fig. 6*B*). If it lies slightly posterior to the trochlea and thereby overlaps it, identification may be possible only on the lateral view. In the older adolescent, the site from which an intraarticular bony fragment originated may be obscure. A subtle sign of entrapment on the anteroposterior view is widening of the elbow joint space medially. The entrapped medial epicondyle is usually readily identified on the lateral view.

Careful evaluation of ulnar nerve function is important. Although ulnar nerve paralysis is uncommon with medial epicondylar fracture, it is most likely to be found with entrapment of the medial epicondyle [1, 6, 7]. Good results are obtained with early recognition of this injury and removal of the entrapped epicondyle from the joint [2, 6, 8].

Avulsion Associated with Dislocation

In children and adolescents, avulsion of the medial epicondyle is commonly associated with posterolateral elbow dislocation due to tight attachment of the ulnar

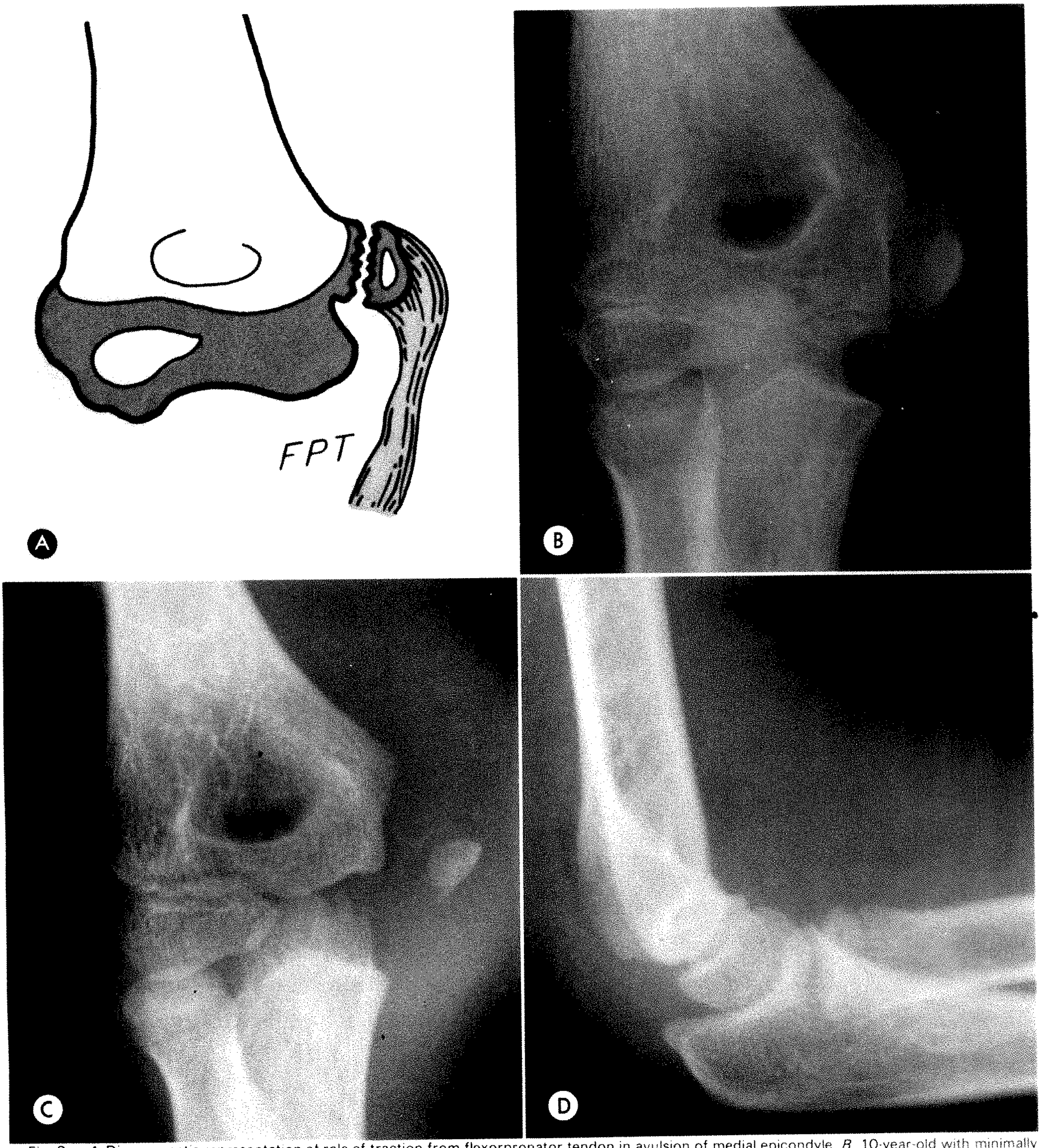

Fig. 2. – *A,* Diagrammatic representation of role of traction from flexorpronator tendon in avulsion of medial epicondyle. *B,* 10-year-old with minimally displaced avulsion. Anteroposterior view showing inferior displacement and localized soft tissue swelling. *C and D,* Anteroposterior and lateral views of another 10-year-old with widely displaced avulsion. Note marked soft tissue swelling. At surgery, no injury to trochlear center was found although metaphyseal flake was attached to medial epicondyle (*C*).

collateral ligament both to the medial epicondyle and the ulna. As the ulna is displaced posterolaterally, the ulnar collateral ligament produces traction on the medial epicondyle. In other series, medial epicondyle separation has been associated with elbow dislocation in up to 50% of cases [1, 2]. In this series, 11 of 35 cases (31%) had posterolateral elbow dislocation. When elbow dislocation occurs, the medial epicondyle may remain in normal position, be avulsed but not entrapped, or be avulsed and entrapped.

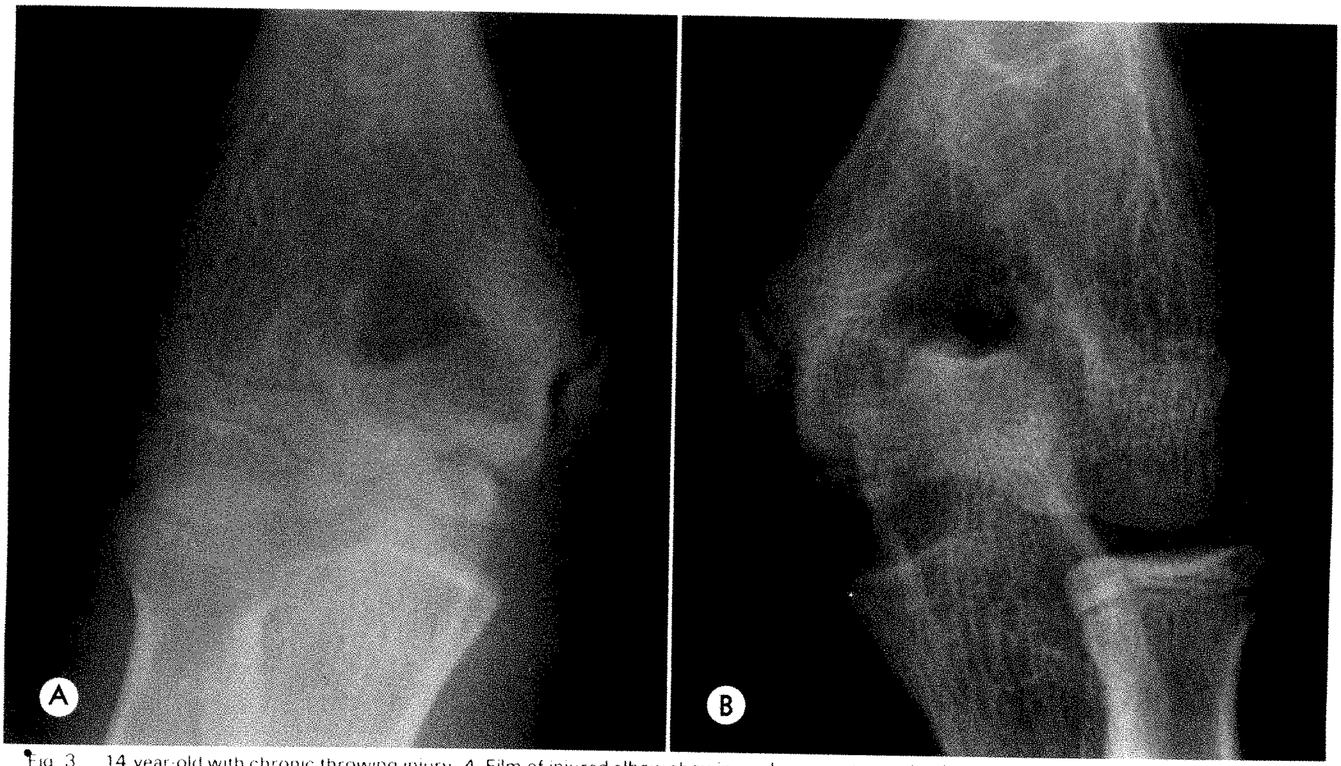

Fig 3 14 year-old with chronic throwing injury. *A*, Film of injured elbow showing enlargement, roughening, and fragmentation of medial epicondyle. *B*, Opposite elbow

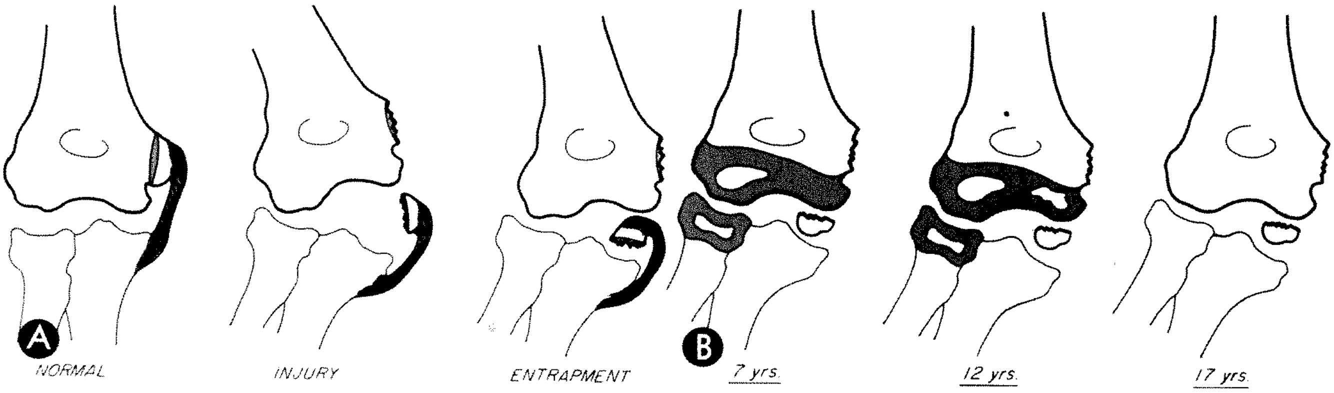

Fig. 4.—*A*, Diagram of entrapment mechanism with role of ulnar collateral ligament depicted. *B*, Anatomy of entrapment before and after trochlear ossification and in older adolescent.

In elbow dislocation, it must be determined whether the medial epicondyle is ossified and, if so, its position. Because entrapment does not occur until reduction of the dislocation, postreduction films must be carefully analyzed (fig. 6) [9]. Comparison films also may be helpful.

When elbow dislocation occurs and the medial epicondyle remains in place, only the dislocation is treated. We found two such cases, but they were not included in the series since no medial epicondylar injury occurred.

Seven cases (20%) had dislocation and avulsion without entrapment of the medial epicondyle. In this injury, the avulsed medial epicondyle can be treated like an isolated avulsion after elbow reduction. Four patients (11%) sustained elbow dislocation with entrapment of the medial epicondyle at the time of reduction. The importance of careful study of the postreduction radiographs has already been emphasized. Radiographic features are similar to those in isolated entrapment.

Clinically, entrapment may be suspected when, after reduction of an elbow dislocation, there is limited flexion and extension and lack of free motion. Unrecognized entrapment has serious consequences, since the incarcerated medial epicondyle will damage the articular cartilage with subsequent early development of degenerative arthritis. The entrapped epicondyle must be removed from the joint.

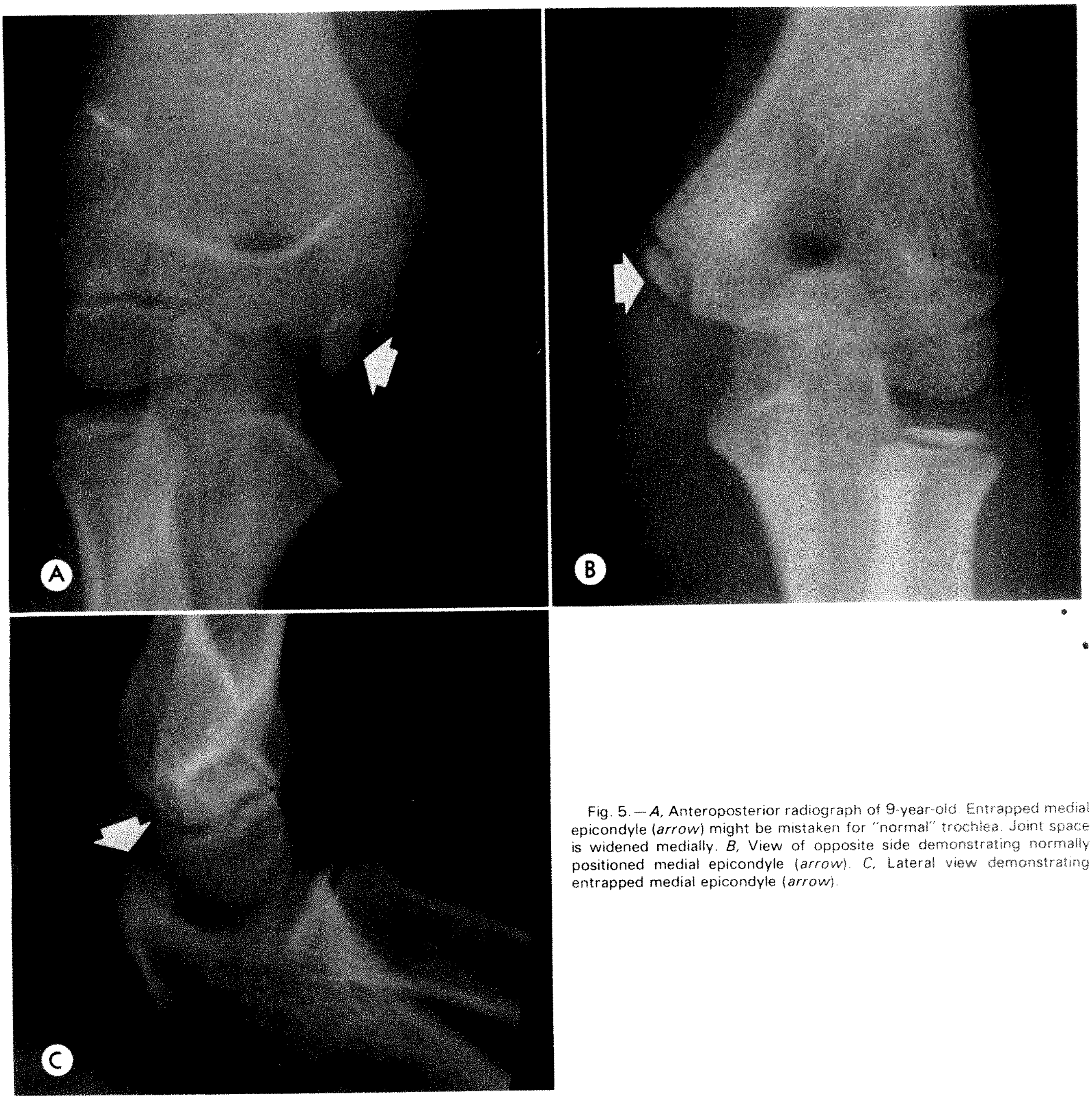

Fig. 5.—*A*, Anteroposterior radiograph of 9-year-old. Entrapped medial epicondyle (*arrow*) might be mistaken for "normal" trochlea. Joint space is widened medially. *B*, View of opposite side demonstrating normally positioned medial epicondyle (*arrow*). *C*, Lateral view demonstrating entrapped medial epicondyle (*arrow*).

Fracture of Medial Humeral Condyle

A Salter-Harris type IV fracture of the medial humeral condyle was found in one patient. In such injuries the fracture line extends obliquely from the capitellotrochlear groove to the medial supracondylar ridge just above the medial epicondyle (fig. 7*A*) and involves both the articular surface and growth plate. The fracture fragment consists of a portion or the whole trochlea, a metaphyseal flake, and the medial epicondyle. This is a rare injury with only 25 cases reported up to July 1975 [10]. This injury poses a diagnostic challenge in the young child before ossification of the trochlea. It has been stated that a clue to the diagnosis may be the radiographic detection of a metaphyseal humeral fragment attached to the medial epicondyle [11].

In this series, three children with avulsion fractures of the medial epicondyle had radiographically detectable metaphyseal flakes but did not have a type IV medial humeral condylar fracture (fig. 2*C*). The presence of a metaphyseal flake is not diagnostic of this injury. The diagnosis may be suspected clinically by virtue of elbow instability and lack of free motion.

One patient in our series had been treated elsewhere for

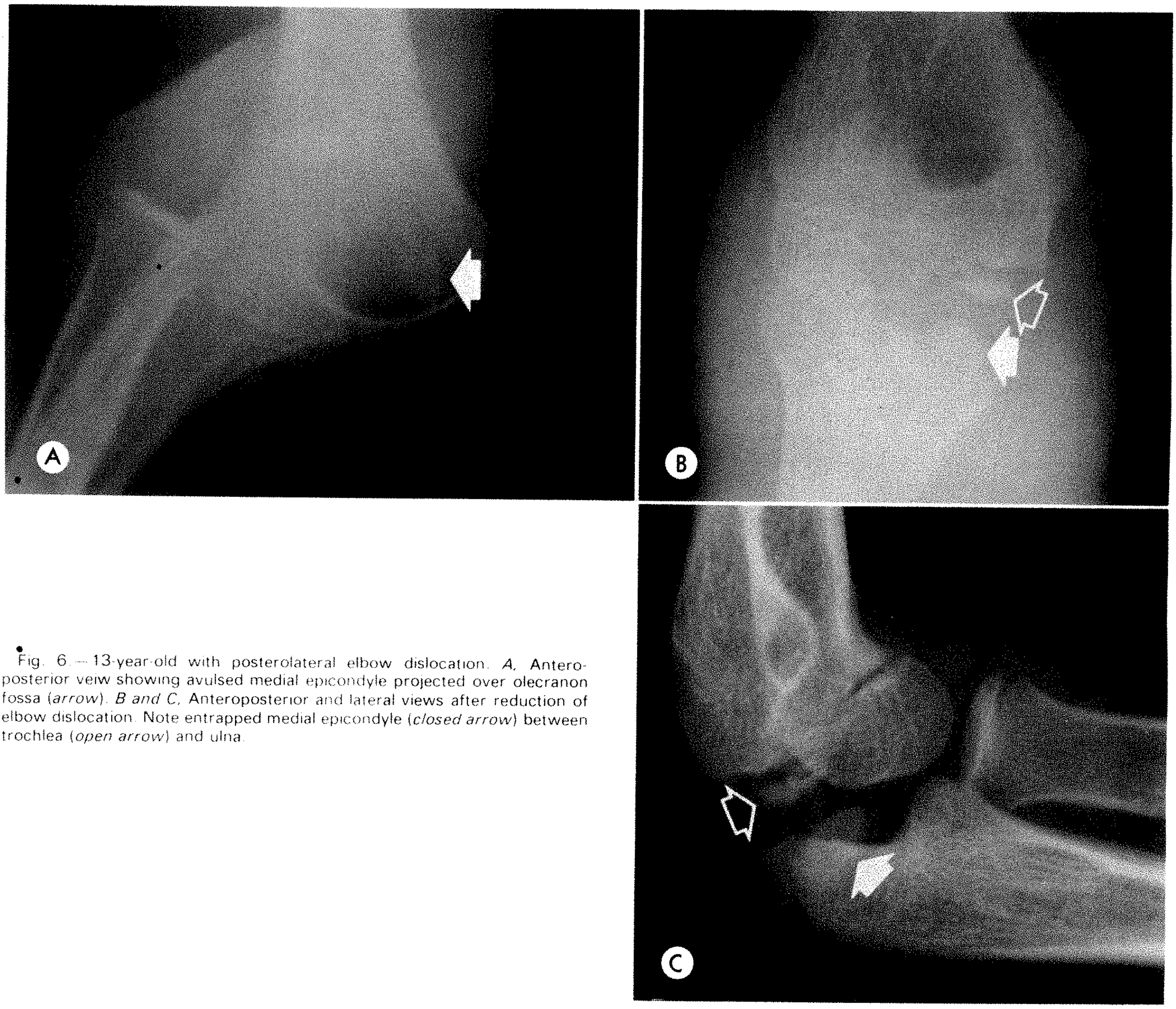

Fig. 6.—13-year-old with posterolateral elbow dislocation. *A*, Anteroposterior veiw showing avulsed medial epicondyle projected over olecranon fossa (*arrow*). *B and C*, Anteroposterior and lateral views after reduction of elbow dislocation. Note entrapped medial epicondyle (*closed arrow*) between trochlea (*open arrow*) and ulna.

1 month in a cast for "medial epicondylar avulsion." When referred, the child had persistent swelling, pain, and loss of full extension and flexion. Radiographs revealed a widely separated flake of bone with associated soft tissue deformity (fig. 7*B*). The flake of bone appeared to represent the just ossifying medial epicondyle and a metaphyseal fragment. At surgery, the fracture fragment consisted of the medial epicondyle, a metaphyseal fragment, and the cartilaginous trochlear center. Cothay [12] reported a similar case.

The distinction between this complex injury and simple medial epicondylar avulsion has great clinical consequence since the former is unstable, carries a definite risk of nonunion, and may result in growth disturbance of the medial aspect of the humerus. If the diagnosis is not made and the injury is treated conservatively, a poor functional result can be expected [11]. Ulnar nerve injury may occur and long term loss of flexion and extension are the rule [10]. Anatomic reduction is essential, usually requiring open reduction and internal fixation [10, 11].

REFERENCES

1. Fahey JJ: *Fracture of the Elbow in Children,* Instructional Course Lectures, St. Louis, Mosby, 1960, pp 13–45
2. Smith FM: Medial epicondyle injuries. *JAMA* 142:396–402, 1950
3. Brogdon BG, Crow NE: Little Leaguer's elbow. *Am J Roentgenol* 83:671–675, 1960
4. Torg JS, Pollack H, Sweterlitsch P: The effect of competitive pitching on the shoulders and elbows of preadolescent baseball players. *Pediatrics* 49:267–272, 1972
5. Keon-Cohen BT: Fractures at the elbow. *J Bone Joint Surg [Am]* 48:1623–1639, 1966
6. Collins R, Lavine SA: Fractures of the medial epicondyle of the humerus with ulnar nerve paralysis. *Clin Proc Child Hosp DC* 20:274–277, 1964
7. Patrick J: Fracture of medial epicondyle with displacement

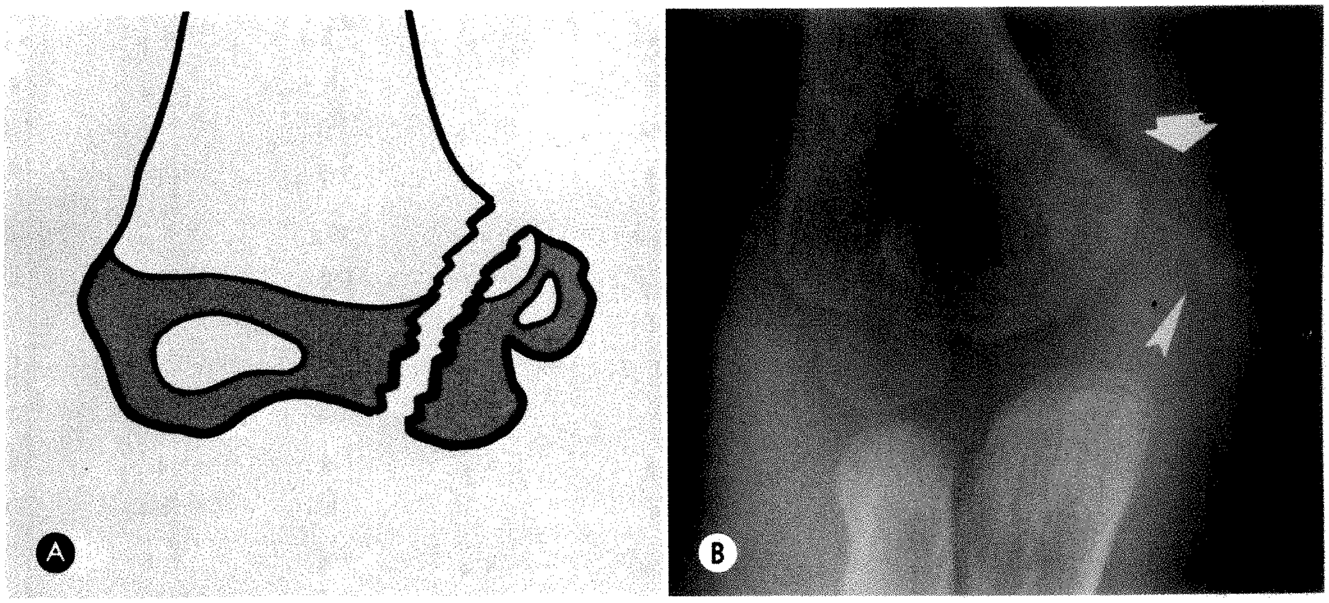

Fig. 7.—3.8-year-old with medial humeral condylar fracture. *A,* Line drawing of fracture and fracture fragment. *B,* Pretreatment radiograph showing avulsion of faintly ossified medial epicondyle (*arrow*) and humeral metaphyseal flake (*arrowhead*).

into elbow joint. *J Bone Joint Surg* 28:143, 1946

8. Tachdjian MO: *Pediatric Orthopedics,* Philadelphia, Saunders, 1972
9. Harris JH, Harris WH: *The Radiology of Emergency Medicine.* Baltimore, Williams & Wilkins, 1975
10. El Ghawabi MH: Fracture of the medial condyle of the humerus. *J Bone Joint Surg* [*Am*] 57:677–680, 1975
11. Fahey JF, O'Brien ET: Fracture separation of the medial humeral condyle in a child confused with fracture of the medial epicondyle. *J Bone Joint Surg* [*Am*] 53:1102–1104, 1971
12. Cothay DM: Injury to the lower medial epiphysis of the humerus before development of the ossific center. *J Bone Joint Surg* [*Br*] 49:766–767, 1967

Laminar Avulsion in a Cervical Vertebra

CHRISTIAN V. CIMMINO[1] AND DAVID W. SCOTT, III[1]

An unusual avulsion fracture involving the lamina of a cervical vertebra, most likely due to tear of a ligamentum flavum, is described. Its radiographic features may be quite subtle. Simulation of this fracture on dried skeleton allowed a better understanding of its appearance on the standard projections, its mechanism of occurrence, and its delayed recognition on the patient's anteroposterior view. Only awareness of the existence of this type of fracture and special efforts directed toward its detection will determine its true frequency.

A fracture of the cervical spine is described which we have not recognized before and have not found noted in recent orthopedic or radiologic literature. It's radiographic features may be quite subtle. When knowledge of its existence is more widely disseminated, it may be found that this fracture is not as unusual as now believed.

Schmorl [1] mentions isolated injuries to the ligamenta flava (yellow ligaments) as an association of subluxations. He believes these injuries are constantly present in most forms of vertebral body and arch fractures.

The ligamenta flava connect the laminae of adjacent vertebrae, extending from the articular capsules to the point where the laminae fuse to form the spinous process. The ligaments are made up chiefly of yellow elastic tissue (hence, the name). They allow separation of the laminae during flexion, but permit the gradual approach to the endpoint of normal flexion. With a violent stress of flexion, the endpoint is reached and exceeded, and the ligament is torn with or without avulsion of a piece of its bony attachment.

Case Report

A 15-year-old girl injured in an automobile accident was seen in the emergency room with neck pain. Physical examination was normal except for pain on motion of the neck. Radiographs were interpreted as normal. She was treated with a collar and analgesics. Because of continued neck pain, repeat studies were made 9 days later, and again were called normal. Symptomatic treatment continued for several months until the pain eventually disappeared. The avulsion fracture was finally recognized on the studies made 1 year later, prior to her discharge from medical follow-up. Review of the previous films showed indisputable evidence of the fracture. Laminography would probably have been of great aid in defining this fracture.

Discussion

The rationality of our diagnosis of avulsion of the lamina due to tear of a yellow ligament was supported by our studies on a dried skeleton. We cut out a piece of bone from the caudal surface of the right lamina of the third cervical vertebra and ressecured it to the lamina after separating it several millimeters therefrom with radiolucent plastic (fig. 1) to better see the "fracture" after radiography. We then made radiographs in anteroposterior, lateral, and two oblique projections, comparing these with the patient's studies (figs. 2–5).

It is evident that the patient's fracture was practically identical to the simulated fracture in the dried bone. Remarkably, only after we did the in vitro studies did we recognize the patient's fracture on the anteroposterior study. The laminae are usually radiographically silent on the frontal studies because their bone mass is so slight in relation to the superimposed vertebral bodies. Close observation of the area between the pedicle and the bulbous or bifid tip of the spinous process will often allow recognition of the normal laminae. The oblique views confirm their delicate nature, where they appear as biconcave lenslike structures.

There are primarily three differential diagnoses. One is avulsion from the spinous process associated with overflexion of the interspinous ligament (the familiar clay-shoveler's fracture of the seventh cervical vertebra). This fracture is more dorsal, involving the spinous process rather than the lamina. The basic mechanism of the two fractures, overflexion, must be similar. In the case of the spinous process avulsion, the interspinous ligament is involved; in the case of the laminar fracture, the ligamentum

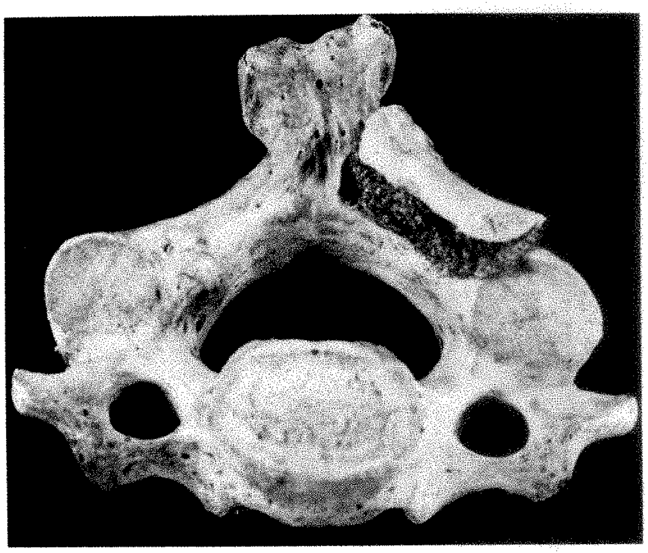

Fig. 1.—Slightly oblique caudal aspect of third cervical vertebra showing simulated fracture of right lamina. Fragment is separated by radiolucent plastic.

Received October 28, 1976; accepted after revision April 11, 1977.

[1] Radiologic Associates of Fredericksburg, Ltd., 1701 Fall Hill Avenue, Fredericksburg, Virginia 22401. Address reprint requests to D. W. Scott, III.

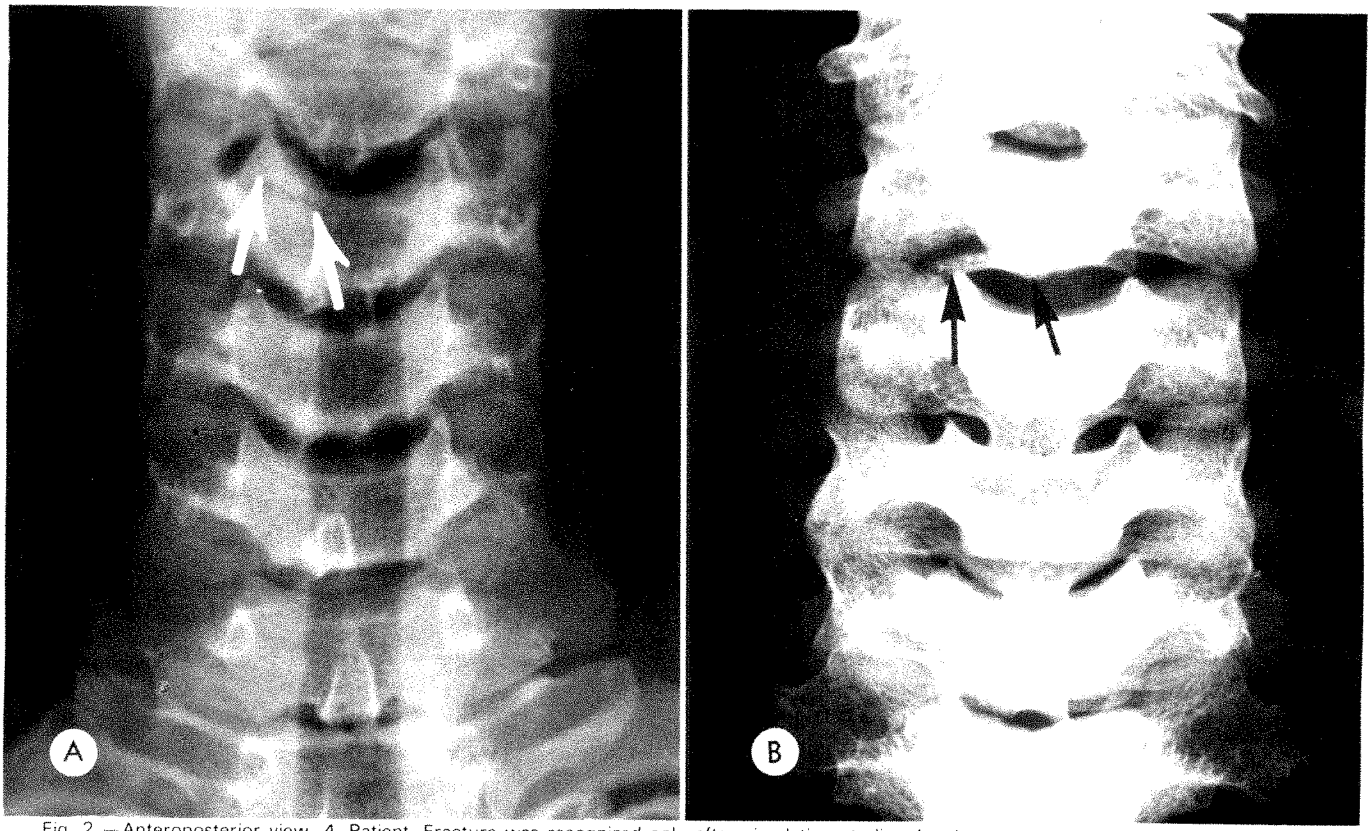

Fig. 2.—Anteroposterior view. *A*, Patient. Fracture was recognized only after simulation studies. Laminae are not recognized even on scrutiny of area between pedicle and bifid spinous process. *B*, Simulation.

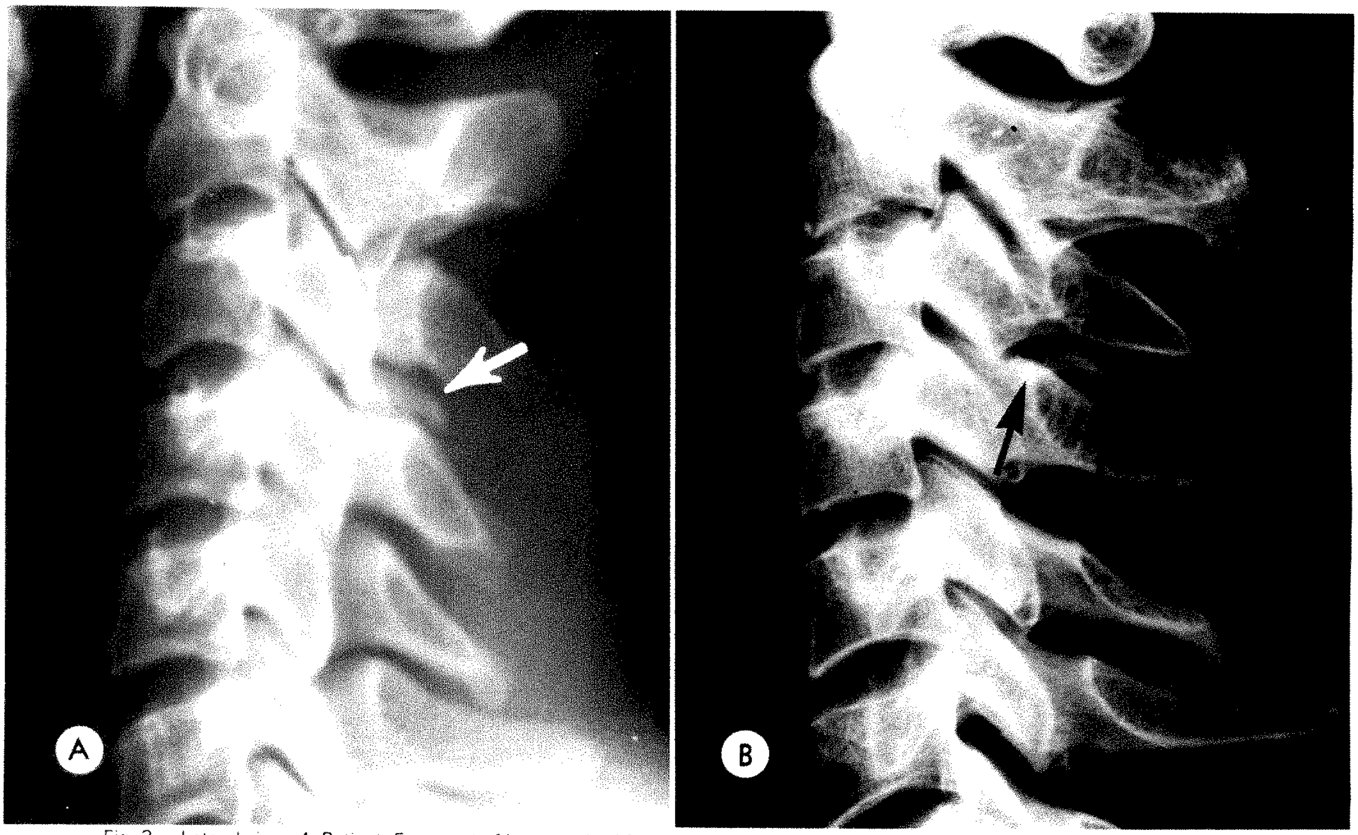

Fig. 3.—Lateral view. *A*, Patient. Fragment of bone avulsed from caudal surface of lamina of third cervical vertebra. *B*, Simulation.

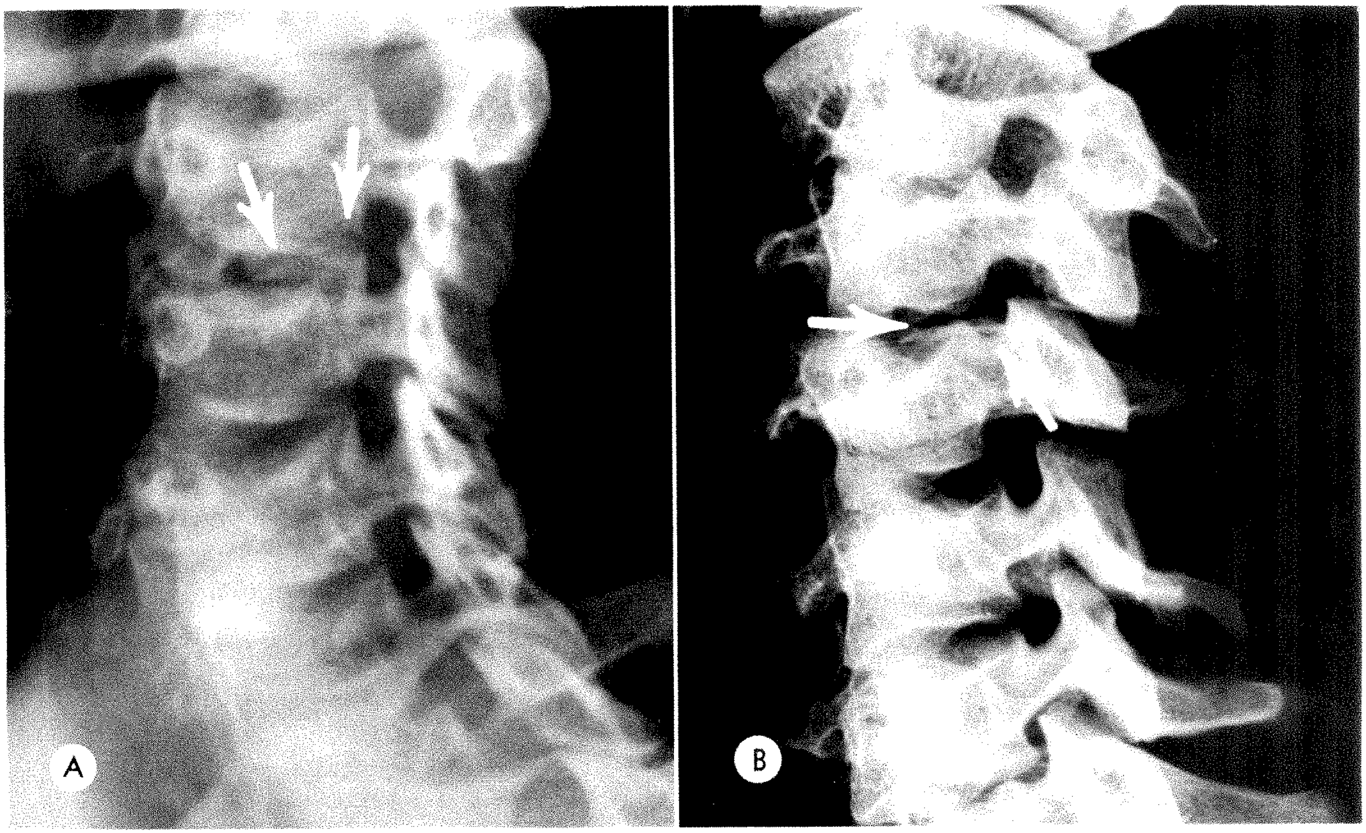

Fig. 4.—Left anterior oblique view. *A*, Patient. Arrows indicate fragment off right lamina which is now largely superimposed on vertebral body. Left normal laminae (biconcave lenslike structures) are clearly seen. *B*, Simulation.

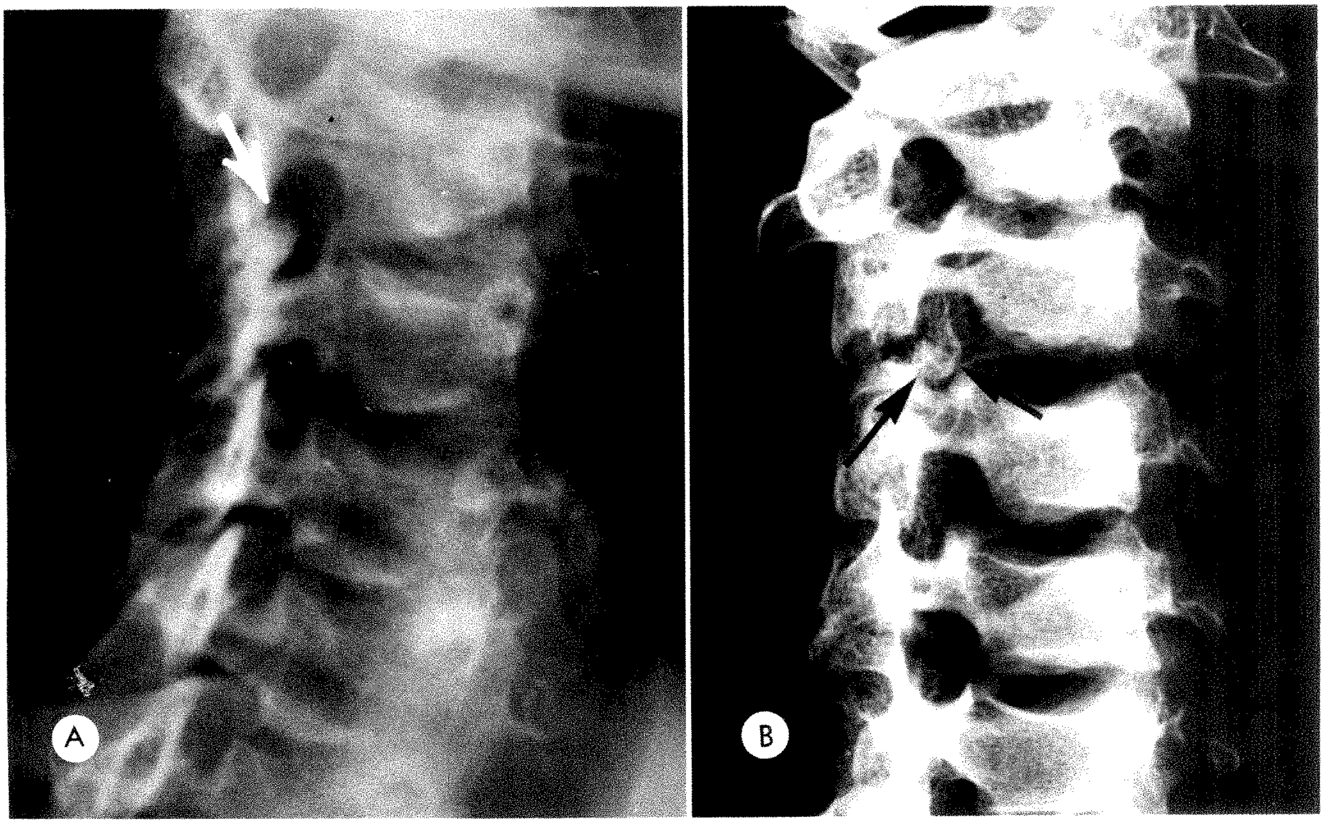

Fig. 5.—Right anterior oblique view. *A*, Patient. Fragment of bone between fine biconcave lenslike structures of right lamina of third and fourth vertebrae. *B*, Simulation.

flavum is involved. Second, prominent osteophytoses about a degenerated apophyseal joint, if large enough, may mimic a laminar fracture. Careful inspection will permit the diagnosis of osteoarthritis. Finally, overlapping of the right and left laminae can produce a Mach effect. Identification of the two intact structures will exclude a laminar fracture.

REFERENCE

1. Schmorl G: *The Human Spine in Health and Disease.* New York, Grune & Stratton, 1971

Radiographic Manifestations of Bone Metastases from Renal Carcinoma

GLENN S. FORBES,[1] RICHARD A. McLEOD, AND ROBERT R. HATTERY

From 1964 to 1974, 1,668 patients with renal carcinoma were seen at the Mayo Clinic. Bone metastases were present in 167 of these patients (only lung metastatic involvement ranked higher in frequency). More than one-third of the patients with bone metastasis from renal carcinoma had this as a presenting lesion of occult renal tumor. This group constituted 4% of all patients with renal carcinoma evaluated during the study period. While most bone lesions were in the pelvis and lower lumbar spine, any bone may be involved. All patients with bone metastases from renal carcinoma have a poor prognosis. However, some bone lesions appeared as long as 10 or more years after the initial tumor.

The most common radiographic features are a lytic destructive process with indistinct margins, erosion of the cortex, and frequent expansion into the soft tissues. Pathologic fractures are common in the long bones, and calcifications are occasionally seen. The synovial joints are not affected. A well defined sclerotic margin is a common finding after radiation treatment, although it is not a reliable indicator of the stability of the lesion.

Renal carcinoma is one of the more unusual metastatic tumors. Numerous reports describe the wide spectrum of occurrence and behavior of various metastases from renal carcinoma [1–6]. In one series 10% of patients presented because of symptoms secondary to metastatic disease, but almost 25% of patients actually had radiographic or clinical evidence of metastases when first seen for therapy [7].

Postmortem studies reveal that as many as 25%–32% of patients with renal carcinoma have metastases to the skeleton, although the percentage detected clinically during the course of disease may be lower [8]. Bone metastases from renal carcinoma are difficult to classify radiographically, and the radiographic appearance of the metastasis is a poor indicator of prognosis. In addition, there is occasional difficulty in establishing the correct diagnosis because the bone lesion may mimic other entities in its radiographic appearance. This may be of considerable importance, since some studies have indicated that one-fourth to one-third of patients with renal carcinoma have no symptoms directly referable to the primary tumor [1, 2]. Although metastatic bone lesions are a common concern for radiologists, there is scant reference in the literature to the spectrum of the radiographic appearance and the clinical implications of bone metastases from renal carcinoma [9–11].

Clinical Material

From 1964 to 1974, 1,668 patients who had renal carcinoma were seen at the Mayo Clinic. Evaluation of the primary tumor or of specific clinical complaints revealed involvement of the skeletal system in 167 patients (10%). The frequency of bone involvement was second only to lung involvement with metastases from renal carcinoma. This included both bone lesions in early stages and late metastatic development.

The ages of the patients ranged from 34 to 80 years, with an average age at onset of bone metastases of 58 years. Nine patients were in their 30s. There were 102 men and 65 women (table 1).

The patients were divided into three groups. The first group (63 patients) had bone lesions as the first sign of disease and no evidence of renal tumors. The second group (24 patients) had bone metastases at the time of diagnosis of the renal tumor, but the metastases themselves were not the basis for the presenting signs and symptoms. The third group (80 patients) developed bone metastases during the course of the disease after the initial primary tumor diagnosis. Although this was usually within 1–2 years, in seven of these 80 patients metastases developed after a latent period of 10 or more years after treatment for the initial renal tumor, during which time no recurrent disease was evident.

Radiographic Features

Location

Although any bone in the skeleton may be affected, metastases predominantly involved the pelvis, sacrum, and lumbar spine; 58 of 167 patients had lesions in the pelvis or sacrum. In four patients, the small bones of the hands or feet were involved (fig. 1*A*).

Of all bone lesions, 63 were solitary metastases of unsuspected renal carcinomas (fig. 1*B*). Three of the four lesions in the small bones of the extremities were solitary lesions, and the patients had no overt evidence of the underlying renal carcinoma (fig. 2). Most of the lesions in the long bones developed in the metaphysis; 12 of 47 extended into the epiphyseal region (fig. 3) or involved secondary epiphyseal ossification centers. Nine lesions developed in the diaphysis (table 2).

Types of Changes

Matrix. In all patients who had radiographs taken before radiation therapy was begun, a destructive process—

• Received October 5, 1976; accepted after revision April 4, 1977.
Presented at the annual meeting of the American Roentgen Ray Society, Washington, D.C., September, 1976.

[1] All authors: Department of Diagnostic Roentgenology, Mayo Clinic and Mayo Foundation, Rochester, Minnesota 55901. Address reprint requests to G. S. Forbes.

TABLE 1

Summary of Clinical Features

Feature	No.	%
Sex:		
Male	102	61
Female	65	39
Survival after appearance of bone metastasis (years):		
0–2	147	88
2–5	19	11
>5	1	1
Primary renal tumor:		
Right side	79	47
Left side	88	53
Renal vein involvement:		
Yes	58	35
No	44	26
Unknown	65	39

TABLE 2

Radiographic Features of Lesions in Long Bones

Feature	No.	%
Location:		
Metaphyseal	26	55
Extension into other region:		
Diaphyseal	9	19
Epiphyseal	12	26
Types of changes:		
Margin:		
Well defined	7	15
Indistinct or poorly defined	40	85
Sclerotic (before treatment)	0	0
Cortical destruction	40	85
Intramedullary or endosteal erosion	7	15
Lytic matrix	47	100
Soft tissue mass	14	30
Pathologic fracture	20	43

Note.—Data on 47 lesions; no synovial effusions or joint involvement seen.

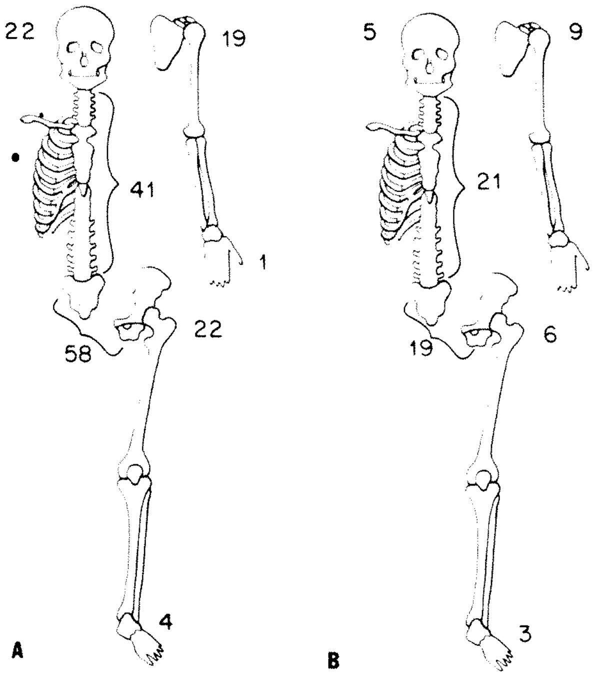

Fig. 1.—*A*, Distribution of all bone metastases from renal carcinoma. Most lesions occur in lower spine and pelvis. *B*, Distribution of solitary metastases that were presenting complaint of patients with renal carcinoma (note similarity to *A*). Lesions in small bones of extremities can be initial manifestation of occult renal carcinoma.

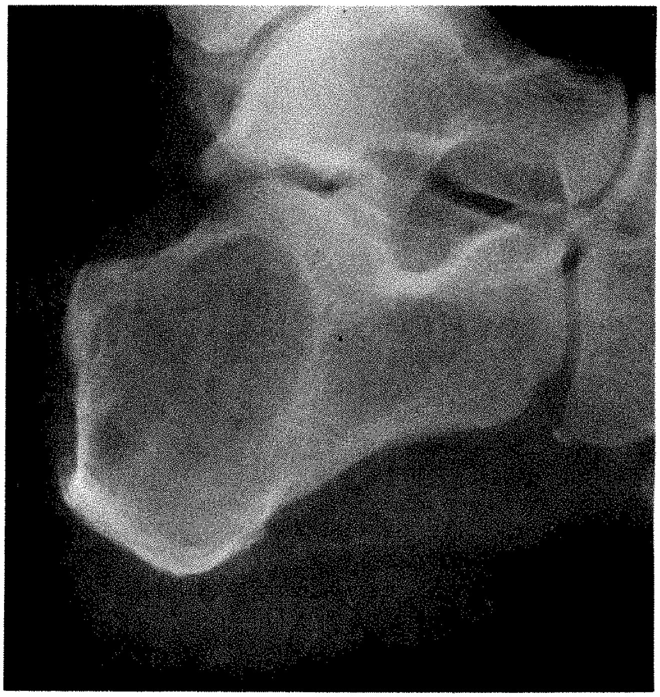

Fig. 2.—Solitary lesion in calcaneus of patient whose only complaint was foot pain. Biopsy suggested adenocarcinoma, and primary renal tumor was detected on urogram. Patient died of disseminated disease after 14 months.

predominantly lysis, with various degrees of mottling and trabeculation—was demonstrated in the bone. No patient had a confirmed blastic bone response or sclerosis before the institution of therapy.

Cortex. A predominant feature in most lesions was erosion or gross destruction of the bone cortex. This occurred in 40 of 47 lesions of the long bones. Most lesions destroy cortical bone locally and then extend into the soft tissues. Less commonly, the tumor will extend throughout the medullary portion of the shaft, with widening and endosteal scalloping, before breaking through the cortex (fig. 4). Seven lesions were primarily intramedullary, with minimal or no cortical changes at the time of diagnosis.

Boundary. Before radiation therapy, all lesions had an indistinct margin between metastatic and normal bone. A more well defined margin may appear after radiation treatment to the lesion; however, this does not necessarily

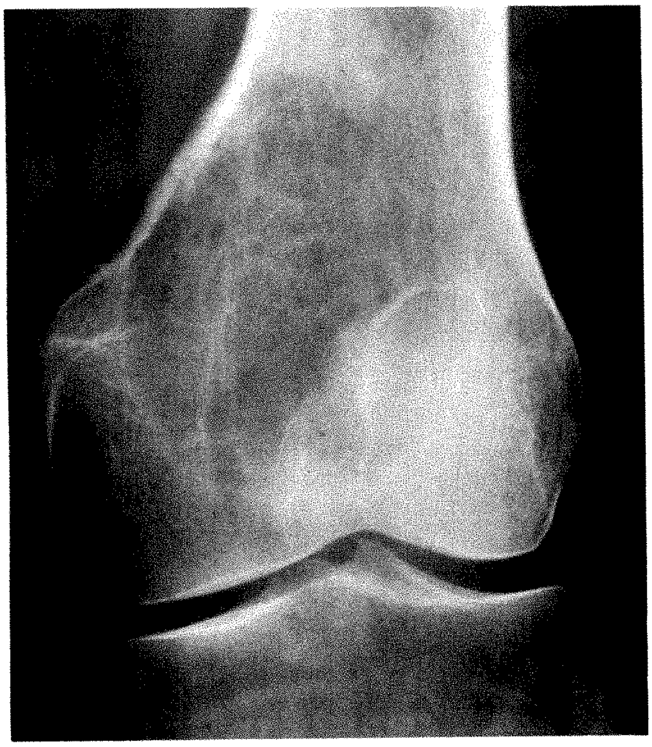

Fig. 3.—Solitary bone lesion extending into epiphyseal portion of long bone. Biopsy confirmed metastatic renal carcinoma.

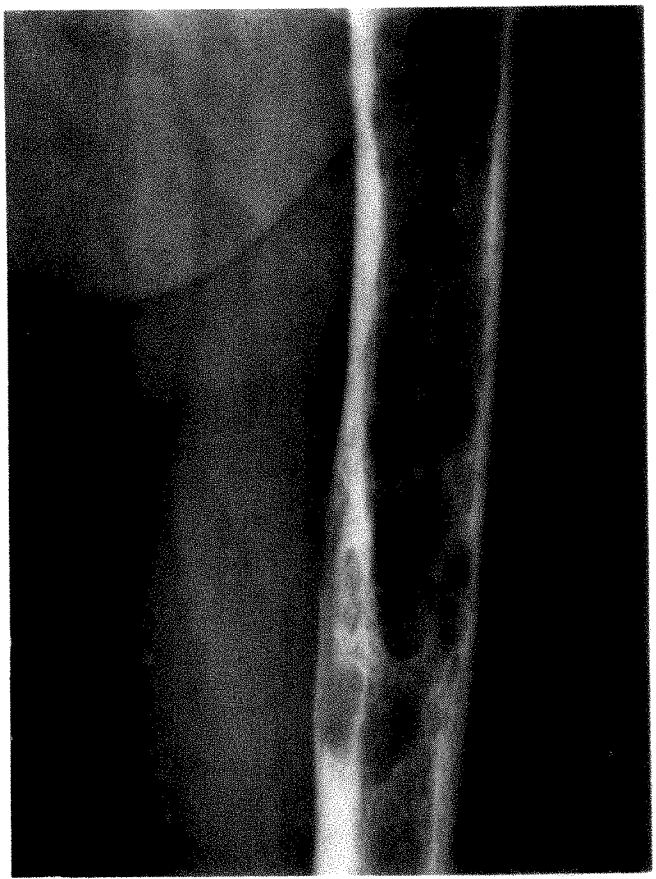

Fig. 4.—Unusual metastatic lesion from renal carcinoma, with extension throughout medullary portion of bone shaft without transcortical destruction.

indicate a better prognosis. Further rapid bone destruction may occur despite the development of more distinct margination after treatment (fig. 5). A thin sclerotic rim at the margin between metastasis and normal bone was evident in 14 patients after radiation therapy.

Soft Tissue. In 14 lesions, a soft tissue mass adjacent to the region of bone destruction was apparent radiographically.

Calcification. Before radiation therapy, calcification either in adjacent soft tissues (fig. 6) or within the bone lesion was seen in three patients. After radiation treatment, bony fragments and calcification that might be interpreted as sclerosis or soft tissue calcification are frequently seen.

Pathologic Fracture. There were 20 pathologic fractures through metastases in long bones; 15 (75%) occurred in the upper humerus or proximal femur.

Joint. There was no evidence of articular destruction or of involvement of a synovial-lined joint in any patient. However, three lesions in the pelvis or sacrum extended across the sacroiliac joint (fig. 7).

Discussion

The most common bone metastasis from renal carcinoma is a lytic destructive lesion in the pelvis or sacrum. More than one-third of our patients had lesions involving the pelvis. This has been attributed to the frequent anastomoses between renal veins and the paravertebral plexus of veins about the pelvis and lower spine, and the hematogenous spread of metastatic deposits through these systems [12]. However, osseous metastases may occur anywhere and may be seen frequently in the extraaxial skeleton, including the small bones of the hands and feet. Gall et al. [13] recently noted that metastases to the feet often are secondary to kidney carcinomas. If the primary tumor has already been identified, any lytic destructive lesion may be a metastasis.

More than one-third of the patients with renal carcinoma bone metastases presented with the bone metastasis as the first sign of disease (figs. 8 and 9). Because 4% of all our patients with renal carcinoma were in this group, occult renal carcinoma should be included in the differential diagnosis of solitary bone tumors. In particular, the small bones of the extremities were occasionally the site of a presenting lesion; thus the appearance of a lytic destructive lesion in the foot without other signs of disease might alert the physician to the possibility of a metastasis from an occult renal carcinoma.

Most of the metastases were aggressive lytic lesions, usually with cortical erosion or destruction. Several lesions had an expansile appearance (fig. 5); this should suggest the possibility of a metastasis from renal carcinoma. Although most metastases were in the metaphysis, tumors also involved the diaphysis or extended into the epiphysis. Thus neither skeletal location nor location within a long bone should deter recognition of such a lytic process as

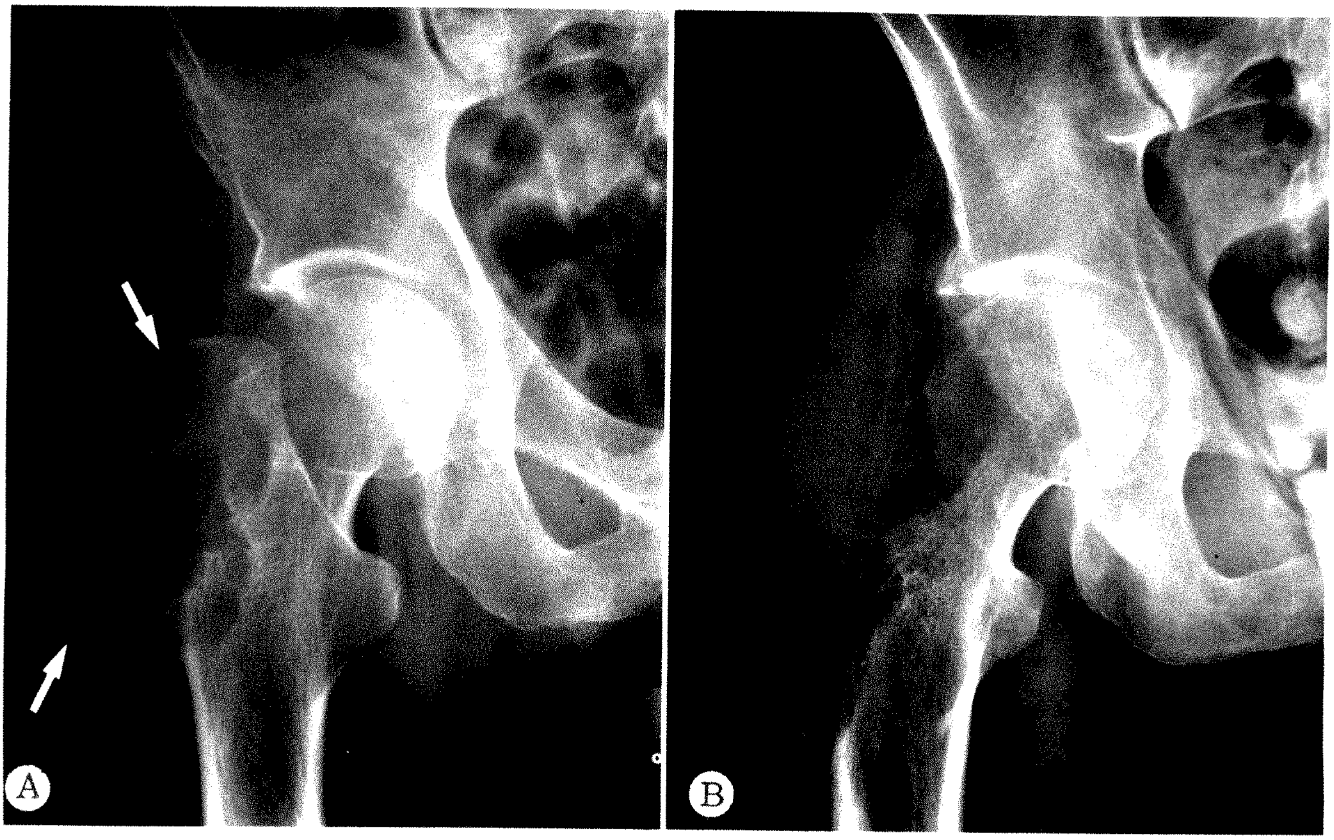

Fig. 5 — *A*, Rapidly expanding destructive lesion with extension into soft tissue, often characteristic of bone metastasis from renal carcinoma. Bone margins fairly well defined, but tumor extends into soft tissue (*arrows*). *B*, More advanced destruction only 5 months later.

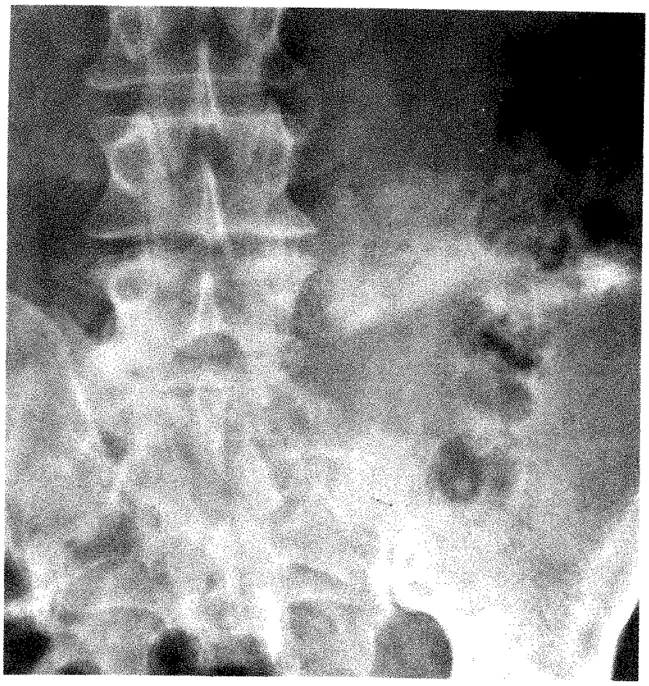

Fig. 6. — Iliac bone lesion showing marked destruction, extension into soft tissues, and soft tissue calcification. No other lesion apparent when patient presented with back pain, and diagnosis of primary bone tumor was entertained.

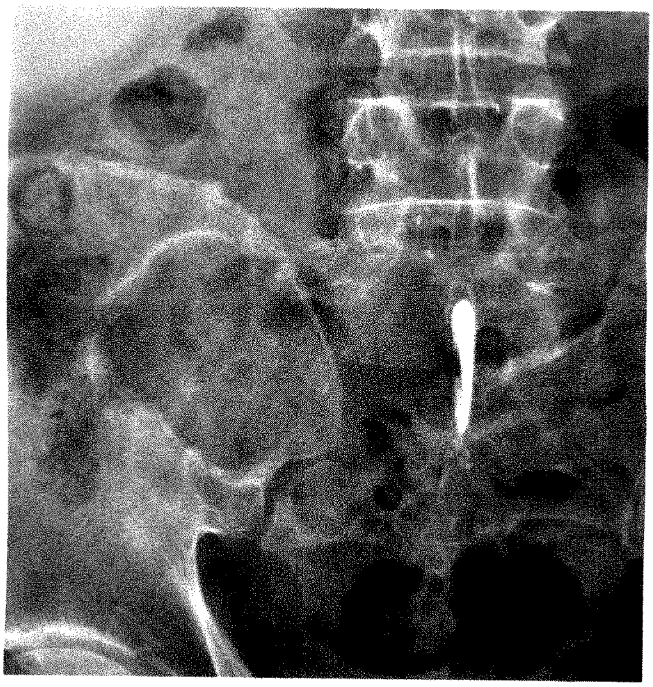

Fig. 7. — Marginal sclerosis after radiation treatment. Note extension across sacroiliac joint and involvement of sacrum and posterior portion of L5.

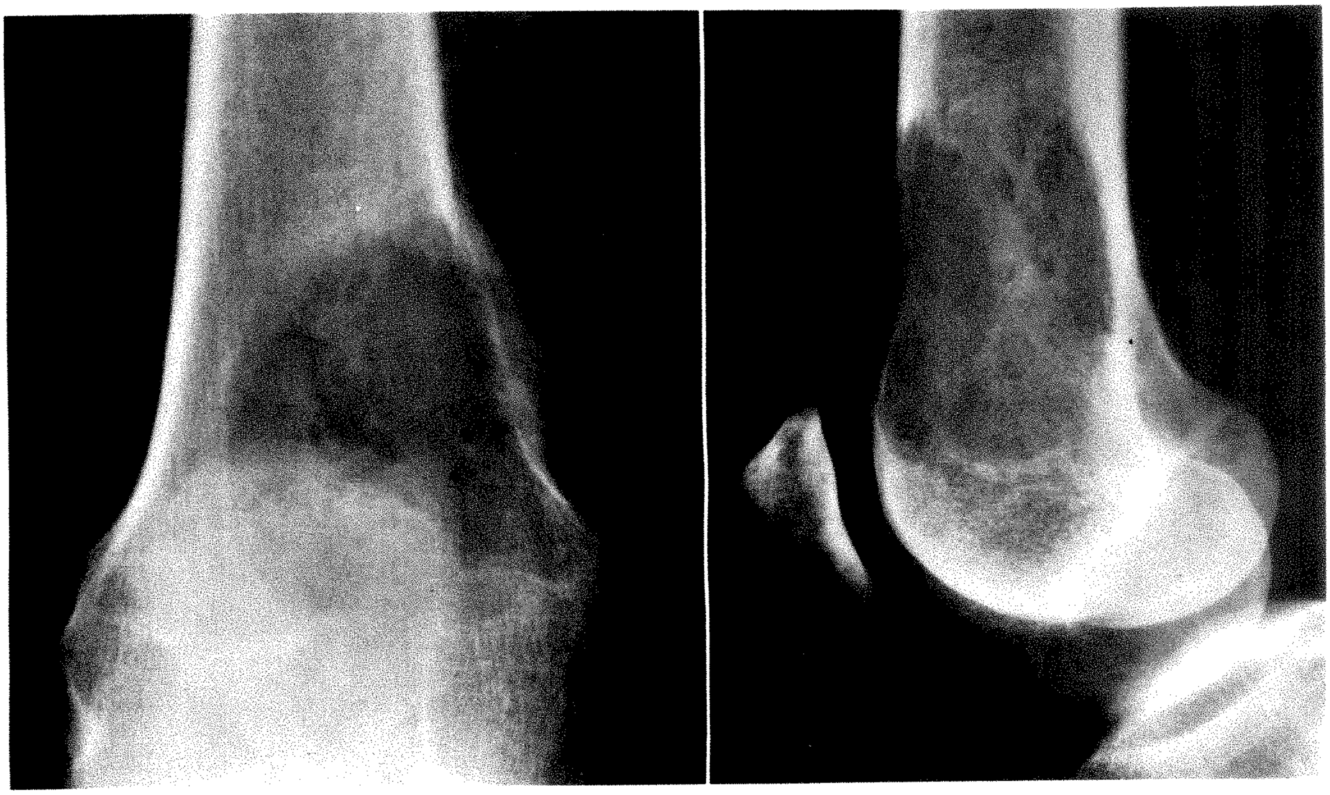

Fig. 8.—Solitary lesion which caused knee pain in 39-year-old man with no genitourinary symptoms. Note cortical destruction, soft tissue extension, and periosteal reaction which simulate appearance of primary bone tumor.

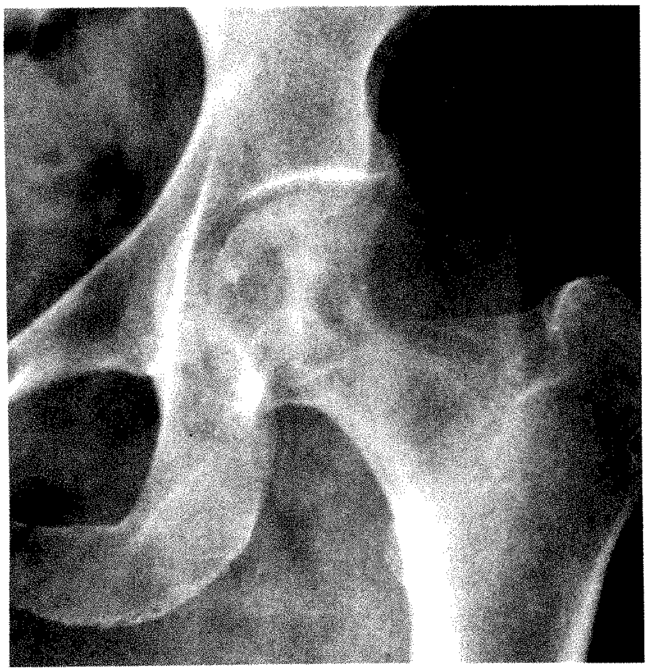

Fig. 9.—Solitary presenting lesion in left hip of 42-year-old woman with no symptoms referable to genitourinary system. Proximity to joint space and cystic nature suggested other diagnoses. Biopsy demonstrated metastasis from renal carcinoma; 3 cm primary tumor found in kidney.

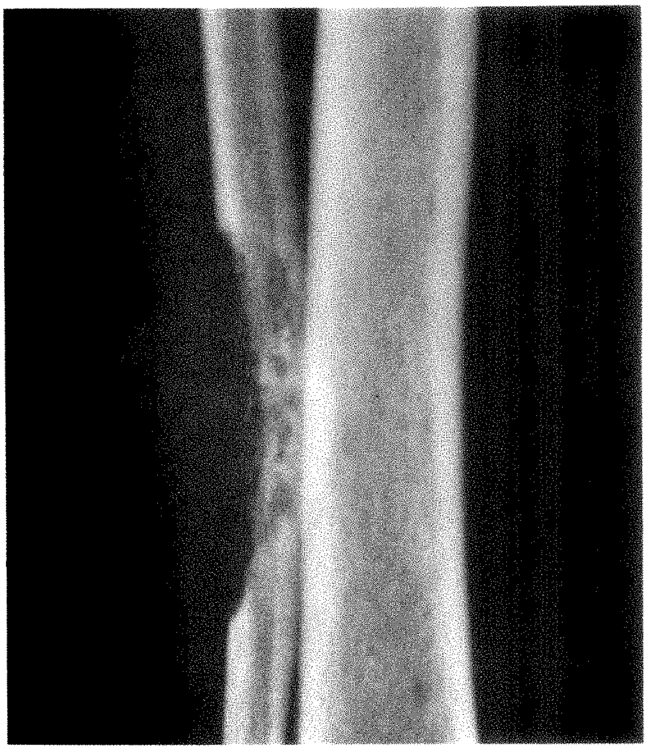

Fig. 10.—Single metastatic lesion of fibula which developed 24 years after original renal carcinoma. Patient had been free of disease in interim.

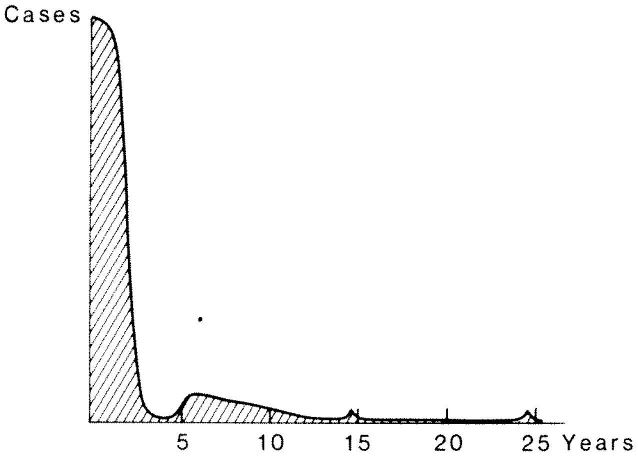

Fig. 11.—Time between occurrence of renal carcinoma bone metastases and initial tumor for 167 cases.

a metastasis.

One of the least understood aspects of renal carcinoma is the long quiescent period that may occur, followed by the sudden appearance of metastases from an almost forgotten tumor. One of our patients had a nephrectomy for renal carcinoma at our institution in 1944 and subsequent radiation therapy. She was lost to follow-up for 24 years. Then, with the onset of leg pain, she returned. No disease referable to the original renal tumor had been apparent in the interim. The remaining kidney was normal on urography. Biopsy of the fibula revealed a metastatic lesion from the renal carcinoma (fig. 10). Thus, although most lesions appear within 1–2 years, bone metastases have developed 10, 20, or more years after removal of the primary renal tumor with no apparent disease in the interim (fig. 11). Whether this relates to an underlying tumor-host interaction or an immune response is not known [14, 15]. Once a bone metastasis occurs, however, a rapid downhill course seems inevitable regardless of the length of the quiescent period. Of 123 patients who died, only one lived 5 years after bone metastasis appeared.

REFERENCES

1. Weigensberg IJ: Metastatic renal carcinoma: unusual and deceptive presenting features. *South Med J* 65:611–616, 1972
2. Weigensberg IJ: The many faces of metastatic renal carcinoma. *Radiology* 98:353–358, 1971
3. Chute R, Ireland EF Jr, Houghton JD: Solitary distant metastases from unsuspected renal carcinomas. *J Urol* 80:420–424, 1958
4. Bradham RR, Wannamaker CC, Pratt-Thomas HR: Renal cell carcinoma metastases 25 years after nephrectomy (letter to the editor). *JAMA* 223:921–922, 1973
5. Johnson RM, Lindskog GE: 100 Cases of tumor metastatic to lung and mediastinum: treatment and results. *JAMA* 202: 94–98, 1967
6. Arkless R: Renal carcinoma: how it metastasizes. *Radiology* 84:496–501, 1965
7. Skinner DG, Colvin RB, Vermillion CD, Pfister RC, Leadbetter WF: Diagnosis and management of renal cell carcinoma: a clinical and pathologic study of 309 cases. *Cancer* 28: 1165–1177, 1971
8. Johnston AD: Pathology of metastatic tumors in bone. *Clin Orthop* 73:8–32, 1970
9. Gooding CA, O'Connor JF, Dealy JB Jr: Angiographic manifestations of osseous metastases from renal cell carcinoma. *Vasc Dis* 3:208–220, 1966
10. Sherman RS, Pearson TA: The roentgenographic appearance of renal cancer metastasis in bone. *Cancer* 1:276–285, 1948
11. Cook SA, Tarar RA, Lalli AF: Bony metastasis in renal cell carcinoma. *Cleve Clin Q* 42:263–265, 1975
12. Anson BJ, Cauldwell EW: The pararenal vascular system: a study of 425 anatomical specimens. *Q Bull Northwestern Univ Med School* 21:320–328, 1947
13. Gall RJ, Sim FH, Pritchard DJ: Metastatic tumors to the bones of the foot. *Cancer* 37:1492–1495, 1976
14. Hrushesky WJ, Murphy GP: Investigation of a new renal tumor model. *J Surg Res* 15:327–336, 1973
15. Varkarakis MJ, Bhanalaph T, Moore RH, Murphy GP: Prognostic criteria of renal cell carcinoma. *J Surg Oncol* 6:97–107, 1974

Testicular Venography for Undescended Testes

MORTON G. GLICKMAN,[1] ROBERT M. WEISS,[2] AND YACOV ITZCHAK[1]

Retrograde venography of the internal spermatic vein was performed for testicular localization in 15 children and young adults with undescended testes. Six of the patients had bilateral studies. In 15 of the 21 venograms attempted, the internal spermatic vein was present; in the other six the testis and the internal spermatic vein were congenitally absent. The testis was accurately localized by venography in 13 of the 15 patients. In one of the two failures a competent valve prevented retrograde injection, but techniques were subsequently devised that permitted retrograde injection beyond competent valves. In the other venographic failure the left kidney was absent and no internal spermatic vein could be identified arising from the left renal vein, although at surgery the testis and the internal spermatic vein were present. Presumably the internal spermatic vein arose from the inferior vena cava, which was not explored venographically. In each of the surgically verified cases of testicular agenesis the internal spermatic vein was also absent.

The anatomy of the left and right internal spermatic veins is reviewed and catheterization techniques are described. Internal spermatic venography appears to be reliable and clinically useful. Preoperative testicular localization often reduces the extent of the surgical exploration and the anesthesia time. With further experience this technique may permit accurate prediction of congenital absence of a testis.

The standard therapy for an undescended testis consists of an initial inguinal exploration with the aim of transposing the testis into the scrotum. If the testis is not found at or below the internal inguinal ring, the exploration must be extended to the level of the renal pedicle before the diagnosis of congenital absence can be established. If the location of the undescended testis can be identified preoperatively, the extent of exploration and the anesthesia time can be reduced. If congenital absence of the testis can be accurately predicted, surgery may be avoided.

Jacobs [1] described two patients with undescended testes in whom gonadal venography localized testicular tissue preoperatively. The ages of these patients were not reported. Vitale et al. [2] reported successful testicular localization in four adult patients using gonadal arteriography and venography. In a prior report [3] we described successful localization of undescended testes in nine pediatric patients by testicular venography. This communication enlarges upon our previously reported series, reviews the anatomy of the testicular veins, and describes techniques of catheterization that we consider simpler and more reliable in children than those previously described.

Patient Population

We attempted catheterization of testicular veins in 15 patients: on the left side in five, on the right side in four, and bilaterally in six. The patients ranged in age from 5 to 17 years. In each instance of bilateral nonpalpable undescended testes, a human chorionic gonadotropin stimulation test had previously demonstrated the presence of functioning testicular tissue [4, 5]. This test can identify the rare case of anorchia.

Anatomy

The testis is immediately drained by a surrounding network of tortuous veins, the pampiniform plexus. The veins of the pampiniform plexus unite to form the origin of the internal spermatic vein immediately above the testis. The left internal spermatic vein terminates in the inferior surface of the left renal vein. In the presence of duplicated left renal veins, the internal spermatic vein terminates in the inferior of the two renal veins. The right internal spermatic vein terminates in the inferior vena cava in over 90% of patients and in the right renal vein in 10% or less [6].

In all cases in this series in which a left internal spermatic vein was identified, its orifice was located within a few millimeters of the left lateral border of the vertebral column in the frontal projection. Once the catheter tip had entered the left renal vein, the left lateral boder of the spine provided an excellent reference point for beginning the search for the orifice of the left testicular vein. The right internal spermatic veins in this series branched from the anterolateral wall of the vena cava in five patients. In all of these the orifice was at the same level as the right renal vein or within 1 cm below it. In one patient the right internal spermatic vein branched from the inferior surface of the right renal vein near its origin.

Occasionally the internal spermatic veins are solitary, but more often two or three parallel internal spermatic veins are present [7]. Free communications exist between these veins, and catheterization and injection of any one permits opacification of all.

The internal spermatic vein receives branches from retroperitoneal structures other than the testis. A relatively constant branch drains the inferolateral portion of the renal capsule. The inferior renal capsular vein was opacified in half of our patients in whom the internal spermatic vein was injected. Connections between the internal spermatic vein and the pelvic veins that terminate in the internal iliac

---

Received February 14, 1977; accepted after revision April 13, 1977.

[1] Department of Radiology, Yale University School of Medicine, New Haven, Connecticut 06510. Address reprint requests to M. G. Glickman.

[2] Department of Surgery (Urology), Yale University School of Medicine, New Haven, Connecticut 06510.

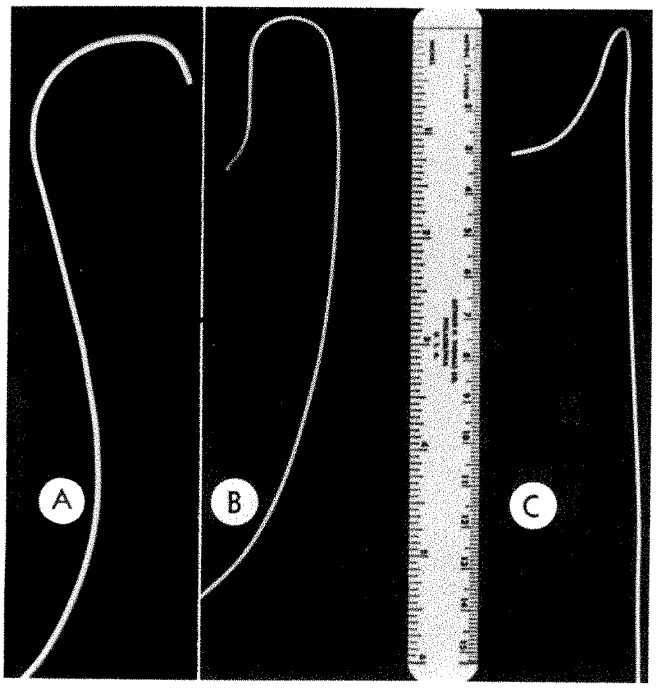

Fig. 1.—*A*, Catheter configuration for left spermatic venography. *B and C*, Catheter configuration for right internal spermatic venography (patient supine). *B*, Catheter tip points toward right and horizontal segment stabilizes catheter across lateral diameter of vena cava. *C*, Catheter rotated 90° to demonstrate anterior deflection of tip, permitting cannulation of internal spermatic vein orifice on anterolateral wall of vena cava.

vein have been described [7]. Connections between the internal spermatic vein and the ureteral vein and between the internal spermatic and the azygos or hemiazygos system are also present anatomically [7]. These veins were opacified infrequently in this series. In patients in whom connections between the internal spermatic vein and other venous systems were opacified, injection of a higher volume of contrast medium was required to opacify the pampiniform plexus. However, in no case, was more than 10 ml required for injection.

The left ureteral vein enters the inferior surface of the left renal vein and can be mistaken for the internal spermatic vein. The size and course of both the left and right ureteral veins are similar to that of the internal spermatic veins [1]. The testicular vein is usually found medial to the ureteral vein, but in two cases in this series it was found lateral to the ureteral vein. The ureteral vein can be accurately distinguished from the testicular vein because the ureteral vein is in close proximity to the ureter throughout its course.

Ahlberg et al. [7] have observed right gonadal veins that branched from the left renal vein. In patients in whom the right testicular vein does not branch from the vena cava or the right renal vein, the inferior surface of the left renal vein should be probed before absence of the right testicular vein can be established.

Catheterization Technique

Thin-walled polyethylene catheters were used: no. 4 French in infants and young children and no. 5 French in those over 12 years of age. To catheterize the left internal spermatic vein, two curves each forming an angle of approximately 90° with the shaft of the catheter were formed (fig. 1*A*). The distance between the two curves was about 1.5 times the anticipated lateral diameter of the vena cava. Using a catheter with this shape, the left renal vein could easily be catheterized from the vena cava. Once the catheter tip had entered the left renal vein, the proximal curve on the catheter served to advance the tip toward the left and the distal curve to point the tip inferiorly. The tip of the catheter was then advanced along the inferior surface of the left renal vein until it engaged the orifice of the internal spermatic vein. When the internal spermatic vein could not be easily cannulated, the curves were not sharp enough or the distance between the two curves was not optimal, usually too small. A new catheter was shaped according to the anatomic information provided during manipulation of the first catheter.

In occasional cases the left internal spermatic vein could be entered, but the catheter was not sufficiently stable for injection. The catheter tip was then advanced down the testicular vein using a tip deflector guide wire system. The tip deflector wire was placed at the orifice of the renal vein at its junction with the vena cava, and a 90° angle was formed in the guide wire. With the tip deflector maintained in this position, the catheter was gradually advanced until the tip was in a stable position within the internal spermatic vein.

The right internal spermatic vein was more difficult to catheterize because of the position of the orifice on the anterolateral wall of the vena cava. The vena cava is ovoid in shape with the lateral diameter larger than the anteroposterior diameter. A curve was designed containing a horizontal segment with length approximately equal to the lateral diameter of the vena cava. This segment spans the widest lumen of the vena cava and stabilizes the catheter. Distal to this segment the catheter tip is curved so that it points anterolaterally and inferiorly (figs. 1*B* and 1*C*). After insertion over a guide wire, the curve is formed in the right atrium and moved down to the level of the renal veins. This catheter configuration permits probing of the anterolateral wall of the vena cava with the tip parallel to the course of the right internal spermatic vein.

Using this catheter, the orifice of the right internal spermatic vein was readily engaged. The tip was advanced into the vein by slowly withdrawing the catheter at the puncture site. If the orifice of the right internal spermatic vein was not found in its expected position, an aberrant internal spermatic vein was sought by probing the inferior surfaces of the right and the left renal vein using a catheter shaped as described for the left testicular vein.

Once the catheter tip was firmly seated within the appropriate internal spermatic vein, 4–5 ml of contrast medium was injected by hand at a rate of about 1 ml/sec. A single film exposed near the end of injection was usually sufficient to demonstrate the entire length of the internal spermatic vein and the pampiniform plexus.

TABLE 1

Summary of Findings

Case No.	Age	Side	Location by Venography	Location by Surgery
1......	12	L, R	Both inguinal	Both inguinal
2......	22	R	Unsuccessful	Abdominal
3......	9	L	Inguinal	Inguinal
4......	5	R	Inguinal	Inguinal
5......	6	R	Absent	Absent
6......	5	L, R	Abdominal, absent	Abdominal, absent
7......	17	L, R	Inguinal, absent	Inguinal, absent
8......	5	L, R	Both inguinal	Both inguinal
9......	17	L	Inguinal	Inguinal
10......	16	L	Abdominal	Abdominal
11......	12	L	Inguinal	Inguinal
12......	5	L	Abdominal	Abdominal
13......	8	L, R	Both absent	No surgery
14......	13	R	Abdominal	Awaiting surgery
15......	10	L, R	Inguinal, absent	Both inguinal

Competent valves may interfere with retrograde injection of the internal spermatic vein and make localization of the testis more difficult [1]. In a series of 84 elderly men whose gonadal veins were examined at autopsy, valves were present in the left internal spermatic vein in 60% and in the right internal spermatic vein in 77% [6]. Valves that were present were incompetent in 36% of the men. The frequency of valvular incompetence in children, however, is probably much less.

In about half of our cases valves were present in the internal spermatic veins and were competent. They were most often located close enough to the orifice of the vein to permit advancement of the catheter through the valve. In four cases the catheter could not be advanced through the valve. By using a very slow injection with the patient in a semierect position, contrast medium passed retrograde through the valve in two patients. In the other two a small guide wire (0.045 cm) was advanced through the catheter tip, down the testicular vein, and through the valve, and injection was made with the wire in place. This maneuver was successful in one of the two patients.

In several patients early in the series we attempted to identify the right internal spermatic vein by venacavography and by injection of the left or right renal vein during a Valsalva maneuver with the patient in both the upright and prone position. None of these attempts proved successful.

Findings

The results are summarized in table 1. Of the 21 internal spermatic venograms attempted, the vein was identified and catheterized in 14, eight on the left and six on the right. In 13 of these the venogram was technically adequate to localize the testis. In the other (case 2) a competent valve prevented opacification of the caudal end of the internal spermatic vein. The presence of the vein suggested that the testis was not congenitally absent, and opacification down to the lower abdomen indicated that the testis was located in the lower abdomen, in the pelvis, or in the inguinal canal. At surgery, a grossly normal testis was found in the lower abdomen.

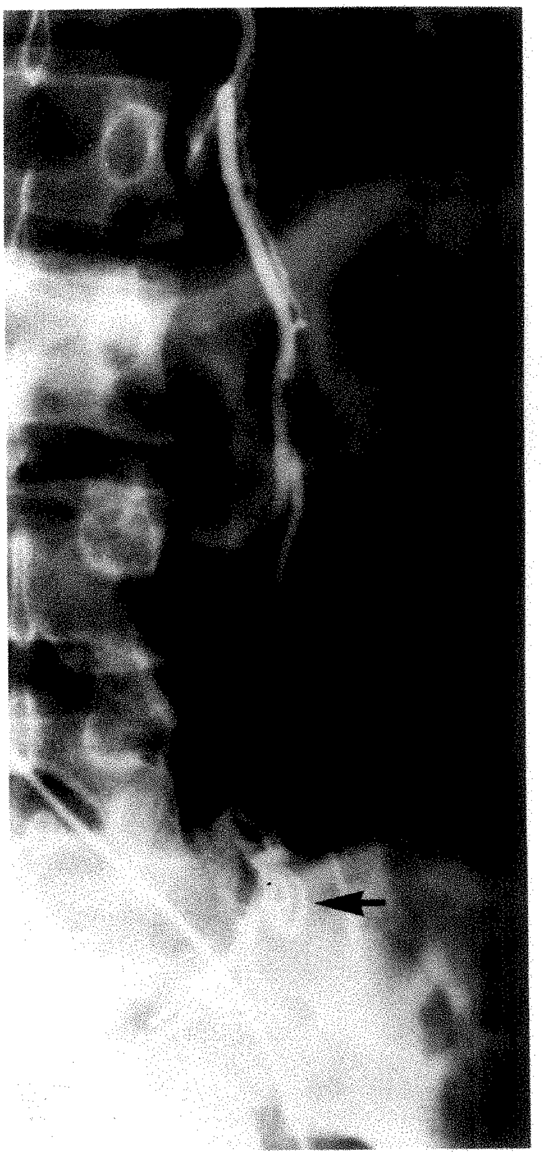

Fig. 2.—16-year-old boy with undescended left testis. Left internal spermatic venogram shows normal pampiniform plexus just above pelvic inlet (*arrow*). Anastomoses between internal spermatic vein and pelvic vein are opacified below pampiniform plexus. At surgery, normal testis was found in predicted location. Internal spermatic vein was not sufficiently redundant to permit relocation of testis, and it was removed.

In all cases in which the internal spermatic vein was present, a testis was found at surgery. In two of these the testis was dysgenic. Agenesis of the testis was uniformly associated with absence of the internal spermatic vein. Exploration has been performed in 12 of the 13 with complete internal spermatic vein opacification. In 10, the testis was venographically localized to the inguinal canal (seven left, three right). In three the venogram indicated an intraabdominal localization (two left, one right). The testis was found in the predicted location in all 12.

The internal spermatic vein was not indentified in seven instances, two involving the left side and five the right side. Exploration has been carried out in six of these, two on the left and four on the right side. In five no internal spermatic vein and no testis was found. In the sixth instance (case 15), a patient with an absent left kidney, a testis and internal spermatic vein were found in the inguinal canal. At the time of venography, the left renal vein which received only adrenal and muscular vein branches was carefully examined, but the anterolateral wall of the vena cava was not.

The position of the testis was identified venographically by opacification of the pampiniform plexus. The pampiniform plexus in most cases consisted of a network of tortuous veins, most of which were larger in caliber than the internal spermatic vein (fig. 2). Occasionally little tortuosity was present, and the pampiniform plexus consisted only of two or three veins arced around the ovoid testis. On 11 venograms the pampiniform plexus was opacified and was sufficiently characteristic for confident localization.

On two venograms the internal spermatic vein was opacified down to the level of the internal inguinal ring, which is sufficient to localize the testis to the inguinal canal, but the pampiniform plexus could not be opacified. In one of these cases a competent valve obviated optimal opacification of the internal spermatic vein. In the other, exploration revealed a rudimentary undifferentiated testis within the inguinal canal. In this case the pampiniform plexus was anatomically absent.

Most of these examinations were performed on an outpatient basis. Mild sedation was used in patients under six years of age and in mentally retarded patients. The only complication was extravasation of contrast medium from the proximal portion of the internal spermatic vein near the tip of the catheter in one patient. This undoubtedly resulted from too forceful an injection. The patient experienced mild pain during the injection, but no analgesic therapy was required. The patient's vital signs remained stable and there was no clinical evidence of sequela. In spite of the extravasation, the entire length of the spermatic vein and the pampiniform plexus were opacified. Surgery 2 weeks after the venogram verified the presence of a normal testis within the inguinal canal, and the venous drainage at the level of the testis appeared unimpaired.

Discussion

In all but one case both the left and right internal spermatic veins were sucessfully catheterized in children and young adults in whom a testis was present at surgery. The internal spermatic vein which was proved to be present but which was not indentified by venography might have been indentified if the vena cava had been examined. Two patients, one with unilateral and one with bilateral undescended testes, have not yet had surgery.

In patients with a normal pampiniform plexus by venography, the location of the testis was evident preoperatively and the extent of exploration could be minimized. Although the presence of competent valves increased the technical difficulty of the procedure, successful retrograde opacification was often accomplished. As experience with internal spermatic venography increases, it may be possible to accurately predict congenital absence of the testis if venographic examination is thorough and no internal spermatic vein is identified.

Some investigators use selective arteriography instead of or in addition to venography for localization of undescended testes [2, 8]. In our hands the right spermatic artery can be successfully catheterized using the same catheter shape described here for the right internal spermatic vein. For the left spermatic artery we use the same shape with the curves in the opposite direction. However, we have found that the venous approach is technically simpler, more comfortable for the patient, and probably safer, especially in children. The spermatic arteries are smaller than the veins, and spasm frequently occurs at the catheter tip, obstructing the lumen until the catheter is withdrawn.

We believe that the likelihood of complications is greater with arteriography than with venography. Venography produces no discomfort other than during the injection of local anesthetic. Venography can be safely performed on an outpatient basis, while for arteriographic procedures we prefer that patients be hospitalized. Perhaps selective arteriography should be suggested if venography fails, but we believe that with the techniques described herein the frequency of unsuccessful venography should be very low.

REFERENCES

1. Jacobs JB: Selective gonadal venography. *Radiology* 92: 885–888, 1969
2. Vitale PJ, Mansour K, Seebode JJ: Selective gonadal angiography for testicular localization in patients with crytorchism. *Surg Forum* 25:538, 1974
3. Weiss RM, Glickman MG, Lytton B: Veongraphic localization of the nonpalpable undescended testis in children. *J Urol* In press, 1977
4. Goldberg LM, Skaist LB, Morrow MW: Congenital absence of testes: anorchism and monorchism. *J Urol* 111:840–845, 1974
5. Levitt SB, Schneider K, Kogan SJ, Sobel E, Fleisher N, Becker J: In palpable undescended testes vs. anorchia—Role of endocrine studies in therapy. Read at Amer. Acad. Ped., Washington, D.C., 1975 (Oct).
6. Ahlberg NE, Bartley O, Chidekel N: Right and left gonadal veins: an anatomical and statistical study. *Acta Radiol [Diagn]* (Stockh) 4:593–600, 1966
7. Ahlberg NE, Bartley O, Chidekel N, Fritjofsson A: Phlebography in varicocele scroti *Acta Radiol [Diagn]* 4:517–528, 1966
8. Ben-Menachem Y, de Berardinis MC, Salinas R: Localization of intraabdominal testes by selective testicular arteriography: a case report. *J Urol* 112:493–494, 1074

Testicular Venography in the Nonpalpable Testis

ARTHUR B. DIAMOND,[1] CHIEN-HSING MENG,[2] MICHAEL KODROFF,[3] AND STANFORD M. GOLDMAN[4]

Localization and identification of a nonpalpable testis can be done accurately by testicular venography. The identification of the pampiniform plexus is essential to the localization of the testis by this method. We evaluated 15 patients 3–39 years of age with 21 nonpalpable testes. Fourteen successful testicular venograms were performed showing four retroperitoneal testes, four testes within the inguinal canal, and two testes located in the superficial inguinal pouch. Three nonpalpable testes were thought to be due to true agenesis, and one venogram was performed after prior surgical removal of the testis. Catheterization of the left testicular vein was accomplished with greater ease and accuracy (79%) to the right side (42%).

The finding of a nonpalpable testis on physical examination may represent agenesis of the testis, incomplete descent of the testis, or an ectopic location of the testis. Because of the increased risk of carcinoma, the surgical approach to the nonpalpable testis is complete exploration from inguinal canal to the hilum of the kidney. By the use of angiography, the nonpalpable testis can usually be localized and identified preoperatively. Furthermore, the amount of testicular tissue can often be evaluated.

Our experience with 15 patients who underwent testicular venography is reported. The value of this technique in the management of the nonpalpable testis is emphasized.

Subjects and Methods

The series included 15 patients from 3 to 39 years old with a total of 21 nonpalpable testes. Seven radiologists, including residents with varying years of training, and one full-time angiographer performed these studies.

The right testicular vein was catheterized using a J-shaped end-hole catheter. The right lateral and anterolateral wall of the inferior vena cava was probed until the catheter engaged the right testicular vein. Occasionally the right testicular vein entered the right renal vein, so this also had to be catheterized.

For the left testicular vein, a wider secondary curve was used to enable the catheter to first engage the left renal vein and then be advanced into the left testicular vein. The latter enters the inferior margin of the left renal vein usually just left of the lumbar spine. This constant relationship was used to full advantage during catheterization. Two other smaller veins were frequently encountered in this location, and these were distinguished by small hand injections of radiopaque contrast.

Renografin 60 (5–10 ml) was injected at a rate of 2–3 ml/sec. One film every other second for six films (12 sec) was used. The supine or appropriate oblique position best demonstrated the course of the spermatic vein. Care was taken to shield the normal testis during fluoroscopy and filming.

Representative Case Reports

Case 1: Retroperitoneal Testis

E. C., a 3-year-old normal white male, was admitted for evaluation of bilateral nonpalpable testicles. Empty scrotal sacs were noticed since birth. On physical examination, the scrotal sac was small with multiple rugal folds. No testicular tissue was palpable either within the scrotal sac, the inguinal canals, the superpubic area, or the thigh. A left testicular venogram showed that the testicular vein ended above the iliac crest in a cluster of veins thought to represent the pampiniform plexus (fig. 1). Right testicular vein catheterization was unsuccessful. At surgery, a left testicle was found within the peritoneum at the site demonstrated on the venogram and was mobilized and repositioned in the scrotal sac. The right testicle was visualized through the peritoneal cavity at exactly the same level and was also mobilized and repositioned in the scrotal sac.

Comment. The very well demonstrated pampiniform plexus marks the exact site of the intraabdominal testis. This preoperative localization allowed the performance of a very precise and definitive surgical procedure. The testicle was thought to be normal at angiography, and this was confirmed at surgery. Our experience has shown that undescended testicles are often at the same level bilaterally. This point can be used to advantage by the surgeon when only one vein can be angiographically located.

Case 2: Inguinal Canal Testis

M. P., a 29-year-old male from India, was admitted for evaluation of a nonpalpable testicle on the left. The testicular venogram showed the pampiniform plexus to be located in the inguinal canal (fig. 2). A left orchiopexy was performed.

Comment. The multiple parallel veins identify the characteristic appearance of the normal pampiniform plexus. The position of the testis can accurately be determined from this study.

Case 3: Superficial Inguinal Pouch Testis

A. H., a 28-year-old male, was admitted for investigation of oligiospermia and bilateral nonpalpable testes. No testicles were palpable within the scrotum or inguinal canals. The hair distribution was feminine and the patient was obese. Buccal smear showed a normal karyotype. Left testicular venography showed an atrophic pampiniform plexus in the left scrotum (fig. 3). Right testicular venography was unsuccessful. Prone abdominal aortography showed a left spermatic artery but did not demonstrate the right spermatic artery.

At surgery, a left orchiectomy was performed after finding a rudimentary testis in the superficial inguinal pouch. The testicle measured 1.0 X 0.8 cm and showed degenerated seminiferous tubules on histologic examination. After exploration of the right scrotum and inguinal canal, an atrophic testis was identified. The right testis was larger than the left testis and was not removed.

Received November 15, 1976; accepted after revision March 25, 1977.

[1] Department of Radiology, Montgomery General Hospital, Olney, Maryland 20832. Address reprint requests to A. B. Diamond.
[2] Deceased. Formerly Department of Radiology, Albert Einstein College of Medicine, Bronx, New York 10461.
[3] Department of Radiology, Virginia Commonwealth University, Medical College of Virginia, Richmond, Virginia 23219.
[4] Department of Radiology, Sinai Hospital of Baltimore, Inc., Belvedere at Greenspring Avenues, Baltimore, Maryland 21215.

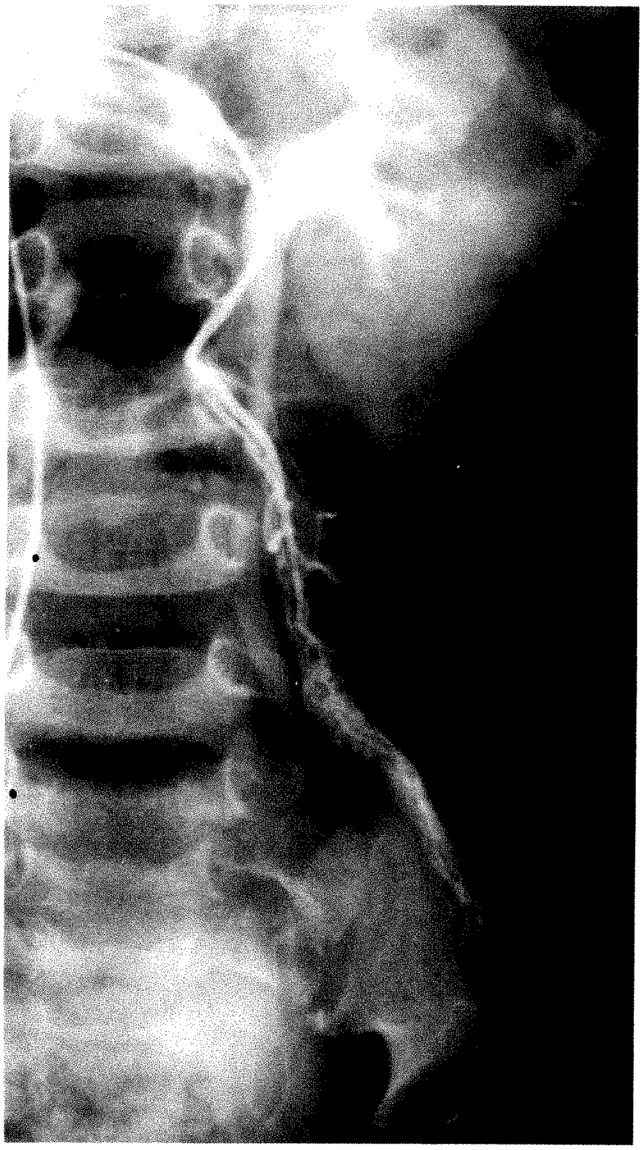

Fig. 1.—Case 1: retroperitoneal testis. Left testicular venogram shows characteristic appearance of pampiniform plexus. Multiple parallel veins of pampiniform plexus marks location of testis.

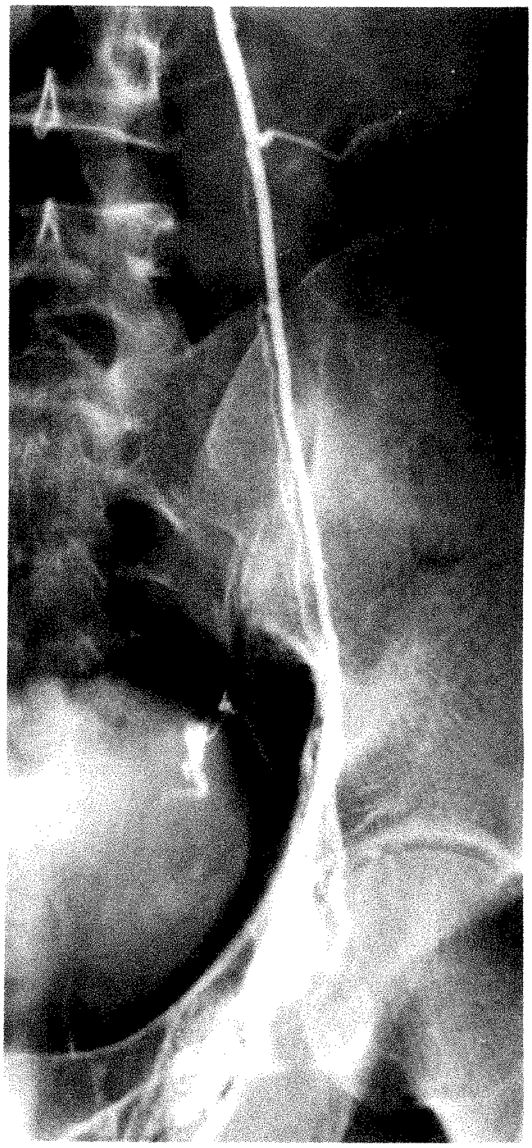

Fig. 2.—Case 2: inguinal canal testis. Left testicle at level of inguinal canal. Pampiniform plexus is average size. Collateral vessel partially fills left hypogastric vein.

Bilateral silastic testicular protheses were anchored into the scrotum.

Case 4: Agenesis of Testis

R. M., a 5-year-old white male, was admitted for evaluation of bilateral nonpalpable testes since birth. Two years before admission he was explored elsewhere in the right inguinal region and retroperitoneum with no demonstrable evidence of testicular tissue. The patient was admitted at this time for left-sided exploration. On physical examination, the scrotum was hypoplastic with no palpable testes in the scrotum or inguinal canals. The buccal smear was chromatin negative. Left testicular venography showed an atrophic vein that tapered off halfway between the renal vein and the iliac crest (fig. 4). A few small venous channels were seen, but no real pampiniform plexus was demonstrated. A diagnosis of testicular atrophy or agenesis was made.

A left inguinal and retroperitoneal dissection as well as an intraabdominal exploration was carried out up to the level of the lower pole of the kidney with no testicular tissue found. The vein described at the time of venography was visualized with only a wisp of tissue in this location. On microscopic examination, no testicular tissue was identified.

Comment. Radiographic absence of the pampiniform plexus coincides in this case with the surgical impression of agenesis of the testicle. However, faulty radiographic technique with incomplete filling of the vein or prior surgical resection may cause the same appearance.

Developmental Anatomy

Detailed discussions have been published on the embryology of the testis [1] and the internal spermatic vein [1–3]. Pertinent embryologic and anatomic points will be summarized here.

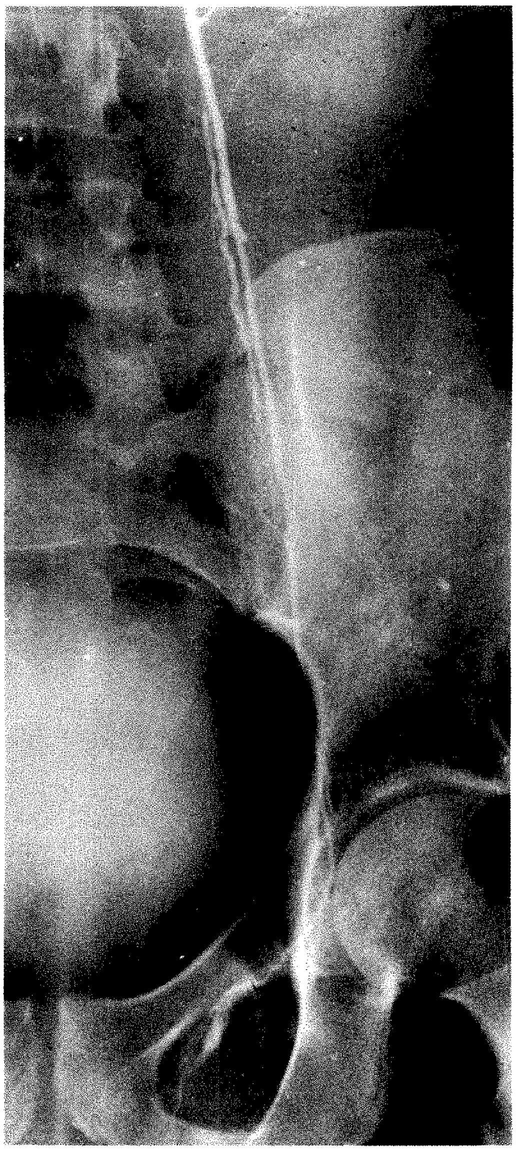

Fig. 3.—Case 3: superficial inguinal pouch testis. Note markedly hypoplastic pampiniform plexus. Testis is located below level of external inguinal ring at superficial inguinal pouch.

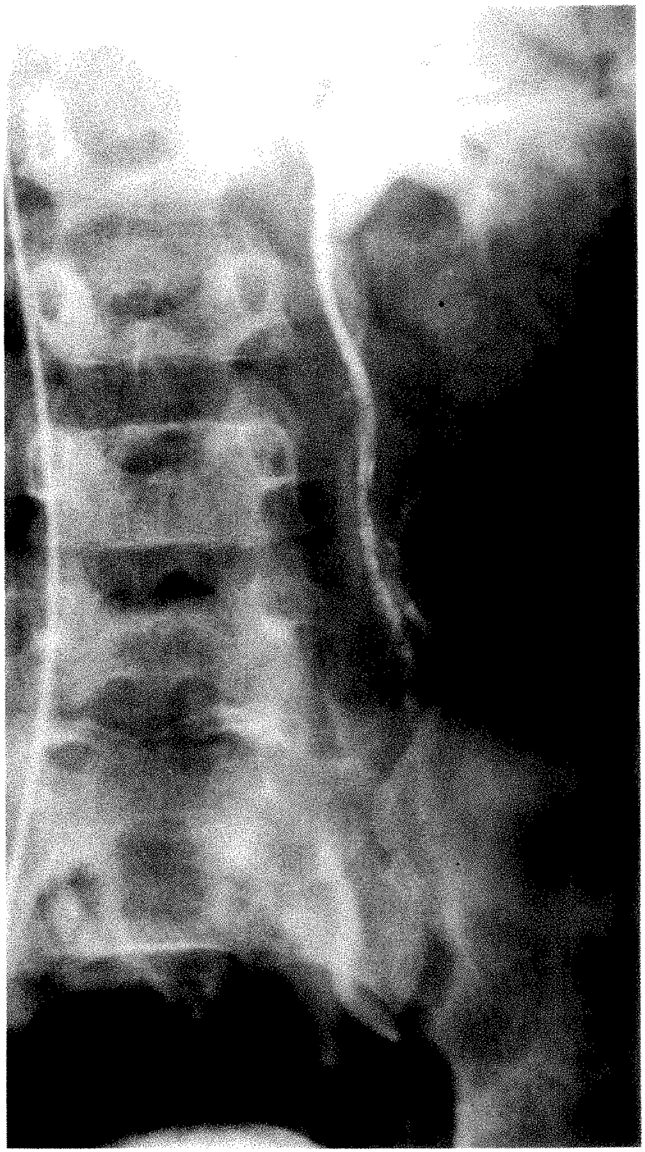

Fig. 4.—Case 4: testicular agenesis. Atrophic left testicular vein is seen without definite identification of pampiniform plexus.

Testis

As the testis descends from its embryonic retroperitoneal abdominal position to its adult position, it passes through the abdominal wall (inguinal canal) bringing its blood, nerve supply, and ductal connections with it. Initially the testis arises from the ventral aspect of the mesonephric ridge extending caudad from the diaphragm. With faster development and elongation of the trunk, it assumes a more caudad position. The testis is always covered by peritoneum and, therefore, is always outside the peritoneal tube. At the end of 6 months the internal descent is complete and the testis lies at the site of the future internal inguinal ring [1]. The external descent then begins with the migration through the inguinal canal into the scrotum. This process is usually complete at birth in the full term infant (97.3%), but 21% of premature male newborns have an empty scrotum [4].

Testicular Vein

The internal testicular veins begin as small veins draining the testis and epididymis. They coalesce and proceed cranially to form the pampiniform plexus which consists of a network of 8–10 veins. At the level of the external inguinal ring these join to form the internal testicular vein. Frequently it is duplicated along all or part of its cephalic course. Ascending slightly medially, they lie just behind the peritoneum anterior to the psoas muscle. The testicular artery travels with the veins.

The internal testicular veins are remnants of the paired subcardinal veins below the level of the kidney. The final

TABLE 1

Location of Nonpalpable Testis

Location	No. Cases	Successful Venographic Localization
Retroperitoneum	6	4
Inguinal canal	5	4
Superficial inguinal canal	4	2
Agenesis	4	3
Prior surgical resection (retroperitoneum)	1	1
Unknown	1	...
Total	21	14

Note. – Seven of the 21 studies were unsuccessful.

attachments remain the same despite the shift to segments of different venous origin than originally present. The right subcardinal vein is incorporated into the anterolateral wall of the inferior vena cava at or near the level of the right renal vein. Drainage into the right renal vein occurs in 10% of the population [2]. Occasionally there is a double entry of the right testicular vein into the inferior vena cava [5] or a simultaneous entry into the renal vein and the inferior vena cava [2]. The left subcardinal vein drains into the inferior border of the great subcardinal anastamosis which becomes the stem of the left renal vein. Occasionally the left vein divides as it approaches the renal vein, with both divisions entering the renal vein. Rarely, one division enters the suprarenal vein, second lumbar vein, or a bifid renal vein [6]. Communicating veins connect the middle and upper portions of the vein with veins of the lumbar plexus, renal capsule, ureter, and surrounding connective tissue [5, 7].

Valves may be seen near the orifice of both testicular veins. However, in an autopsy study, Ahlberg et al [7] found that 40% of left veins and 23% of right veins lacked valves. In addition, incompetent valves occurred on the left in 10% of cases and on the right in 16%. Therefore, absent or incompetent valves in the cranial portion of the vein were present in approximately one-half of the cases. More detailed anatomic studies of the testicular veins have been reported [7, 8].

Results and Discussion

Testicular venography has been used in the evaluation of varicocele [3, 7, 9, 10] and abdominal malignancies [5]. It has been used in a few smaller series for the diagnosis and localization of hypoplastic and nonpalpable testis [5, 11]. This series represents the largest group of patients with nonpalpable testis evaluated by venography.

Table 1 shows the anatomic location of 21 nonpalpable testes in this series. (We prefer the term nonpalpable testis to undescended testis until the status of the testis is known.) Fourteen successful testicular venograms were performed showing four retroperitoneal testes, four inguinal canal testis, and two superficial inguinal pouch testes. Three cases of testicular agenesis were demonstrated. One testicular venogram was performed in a patient who, unknown to himself, had a retroperitoneal testis removed years earlier. This venogram showed the blind-ending testicular vein in the retroperitoneum. Sixteen of the 21 cases have been proven surgically.

As expected, catheterization of the testicular vein was accomplished with greater ease and greater accuracy on the left side where the anatomy is most constant and predictable. Of 13 left testicular vein catheterizations, 11 (79%) were successful; the success rate for right testicular vein studies was 42% (three of eight). One attempted right testicular venogram which we labeled unsuccessful did yield important surgical information. In this study the testicular vein was identifed to the level of the internal inguinal ring, thus obviating a retroperitoneal exploration. Valves, which are frequently located along the course of the testicular vein, did not interfere with the performance of these examinations. This supports the previous observation of Jacobs [5].

The presence of a testicular vein does not indicate the presence of a testicle since the testicular vein drains other structures besides the testis. In addition, other veins drain into the testicular vein as a source of collateral circulation. The localization of the testes by venography therefore rests with the positive identification of the pampiniform plexus.

In our series, the retroperitoneum is the most common location of the nonpalpable testes (table 1). Venography denotes the location and gives a rough estimate of testicular size (e.g., cases 2 and 3) but in no way indicates the function of the testes. Before orchiectomy or orchiopexy, a biopsy should be done to determine the status of the testicular tissue.

Six cases of bilateral cryptorchidism were studied. In four of the six the nonpalpable testes were at the same level. This suggests that in patients with bilateral nonpalpable testes, if there is technical difficulty and only one testis can be localized by venography, the contralateral testis is frequently in an identical position. This point may be of value in the surgical management of these patients.

In our hands the most accurate diagnosis of testicular agenesis is made when the vein is identified but the pampiniform plexus is absent (case 4) provided that the radiographic technique is not faulty. This supports the previous experience of Jacobs [5] who reported two surgically confirmed anorchid patients with blind-ending testicular veins. We have also observed a blind-ending testicular vein after prior surgical removal of the testis. Direct magnification radiography may be useful in establishing the presence of a pampiniform plexus in cases of extreme hypoplasia.

In addition to testicular venography, prone aortography was performed in nine patients. In seven patients, the testicular artery in question was identified. However, in only two cases could the entire course of the artery be traced. The termination of the artery coincided with the venographic site of localization in both of these cases.

Selective catheterization of the testicular arteries, rather than prone aortography, is needed for definitive localization of the undescended testes. Vitale et al. [12], in a single case report, has shown that testicular localization can be accurately done by selective arteriography. It is not our intention to compare selective testicular venography with arteriography. However, in our hands, the latter has been of limited value because of the difficulty in its performance. Notkovich [13] describes three basic gonadal arterial patterns with 16.9% of patients having double gonadal arteries (sometimes bilateral). In addition to the anatomic variations, the procedure itself may be uncomfortable. In one report, it was necessary to use spinal anesthesia and then a "light" general anesthesia to accomplish the study [14].

We have been impressed with the ability of venography to localize the nonpalpable testes. We feel that the examination allows the surgeon to plan his surgical approach and decide on the proper management of the patient.

DEDICATION

To Dr. Chien-Hsing Meng who was an inspiration to everyone with whom he worked. Many radiologists are forever in his debt, and his influence will be long felt.

REFERENCES

1. Arey LB: *Developmental Anatomy*. Philadelphia, Saunders, 1974
2. Ahlberg NE, Bartley O, Chidekel N: Occurrence of valves in the main trunk of the renal vein. *Acta Radiol* [*Diagn*] (Stockh) 7:431–437, 1968
3. Ferris EJ, Hipona FA, Kahn PC, Philipps E, Shapiro JH: *Venography of the Inferior Vena Cava and Its Branches*. Baltimore, Williams & Wilkins, 1969
4. Scorer CG: The descent of the testis. *Arch Dis Child* 39: 605–609, 1964
5. Jacobs JB: Selective gonadal venography. *Radiology* 92: 885–888, 1969
6. Anson BJ, Kurth LE: Common variations in the renal blood supply. *Surg Gynecol Obstet* 100:157–162, 1955
7. Ahlberg NE, Bartley O, Chidekel N, Fritjofsson A: Phlebography in varicocele scroti. *Acta Radiol* [*Diagn*] (Stockh) 4: 517–528, 1966
8. Ahlberg NE, Bartley O, Chidekel N: Right and left gonadal veins: an anatomical and statistical study. *Acta Radiol* [*Diagn*] (Stockh) 4:593–601, 1966
9. Charny CW, Baum S: Varicocele and infertility. *JAMA* 204: 75–78, 1968
10. Diamond A, Ravitz G: Venographic demonstration of a varicocele in a boy. *J Urol* 114:640–641, 1975
11. Amin M, Wheeler CS: Selective venography in abdominal cryptorchidism. *J Urol* 115:760–761, 1976
12. Vitale PJ, Khademi M, Seebode JJ: Selective gonadal angiography for testicular localization in patients with cryptorchism. *Surg Forum* 25:538–540, 1974
13. Notkovich H: Variations of the testicular and ovarian arteries in relation to the renal pedicle. *Surg Gynecol Obstet* 103: 487–495, 1956
14. Ben Menachem Y, de Berardinis MC, Salinas R: Localization of intra-abdominal testis by selective testicular arteriography: a case report. *J Urol* 112:493–494, 1974

Polyarteritis Nodosa and Hepatitis-B Surface Antigen: Role of Angiography in Diagnosis

RICHARD G. FISHER,[1] DAVID Y. GRAHAM,[2] MASOOD GRANMAYEH,[1] AND J. GUILLERMO TRABANINO[2]

Two patients with polyarteritis nodosa who presented with vague constitutional systems and hepatitis-B antigenemia are reported. Angiography was used as the primary diagnostic procedure and confirmed the diagnosis in each case. Angiography is a relatively simple and direct means for establishing the diagnosis of polyarteritis nodosa. In these patients, the typical finding of aneurysm formation in multiple organs was observed. Arterial narrowing was also widespread. Multiple renal infarcts are shown in one case, and bronchial arteriography revealed aneurysms and narrowing in bronchial and intercostal arteries in one patient who had a recent pulmonary infarction and a normal pulmonary arteriogram. The relationship of the hepatitis-B antigen and polyarteritis is also emphasized.

Introduction

Polyarteritis nodosa is a life-threatening disease of unknown cause. The pathogenesis is unclear, but most evidence implicates an autoimmune or hypersensitivity reaction which leads to necrotizing inflammation of segments of medium and small arteries. Polyarteritis was first noted to be associated with hepatitis by Paull [1]; he reported four patients who developed polyarteritis after vaccination for yellow fever. Three of the patients also developed hepatitis. Subsequent reports [2, 3] confirmed the association between hepatitis and polyarteritis and, more recently, between hepatitis-B surface antigen and polyarteritis [4, 5].

The clinical manifestations of polyarteritis are protean and the diagnosis, even when considered, is difficult to confirm because of the patchy nature of the disease. Tissue biopsy, taken at random, often fails to confirm the suspected diagnosis [6]. However, angiography is a potentially useful tool because it allows a large number of vessels in a variety of organs to be surveyed rapidly.

This report describes two cases and reemphasizes the value of angiography in confirming the diagnosis of polyarteritis nodosa. The two patients had vague constitutional symptoms and liver disease. Serologic studies revealed circulating hepatitis-B surface antigen in each. Angiography was used as the primary diagnostic procedure and was successful in confirming the clinical suspicion of polyarteritis in each case. A standard angiographic procedure was used, with catheter aortography and selective visceral and renal arteriography accomplished by percutaneous technique.

Case Reports

Case 1

A 32-year-old white man noted the sudden onset of progressively severe left back and flank pain 4 weeks before admission. The next day he developed generalized malaise, muscle aches, polyarthralgia, and fever. The pain remained constant, was not exacerbated by changes in position, and was unrelated to meals. He was admitted to an outlying hospital, where laboratory evaluation was normal except for the following: SGOT, 320 IU; SGPT, 560 IU; and total bilirubin, 1.5 mg/dl. Liver and pancreatic scans as well as radiologic studies of the gallbladder, upper gastrointestinal tract, and small bowel were normal. Subsequent abdominal radiographs revealed that much of the barium administered to the patient from the upper gastrointestinal and small bowel series remained localized in the transverse colon. At Ben Taub General Hospital, exploratory laparotomy failed to reveal evidence of mechanical intestinal obstruction; redundant loops of sigmoid colon were plicated to the abdominal wall.

Laboratory evaluation revealed SGOT, 260 IU; SGPT, 329 IU; and positive hepatitis-B surface antigen. Percutaneous liver biopsy revealed nonspecific reactive hepatitis. Abdominal angiography was requested in an attempt to prove the clinical suspicion of polyarteritis nodosa. Arteriography (selective celiac arteriography, bilateral selective renal arteriography) revealed the classic changes of periarteritis nodosa along with widespread aneurysm formation, vascular narrowing, and renal infarction (fig. 1).

After angiography, prednisone (60 mg/day) was administered. The patient subsequently developed hypertension, and Aldomet and Inderal were added to his medication. He suffered a bout of prolonged chest pain, bradycardia, and a cardiac arrest 2 weeks after laparotomy. Electrocardiographic changes revealed a diaphragmatic myocardial infarction. He was resuscitated and recovered and is undergoing therapy for polyarteritis nodosa.

Case 2

A 34-year-old white man was admitted complaining of 4 weeks of constant nonradiating epigastric pain. He also complained of malaise, fatigue, anorexia, and weight loss of 9 kg over the previous 6 weeks. He had noticed numbness on the sole and dorsum of the left foot.

Physical examination was unremarkable, except for jaundice and slight tenderness and swelling of the left testicle. Laboratory evaluation included SGOT, 320 IU; SGPT, 472 IU; serum albumin, 3.1 g/dl; total protein, 6.0 g/dl; alkaline phosphatase, 181 IU; and total bilirubin, 2.5 mg/dl. The sedimentation rate was 46 mm/hr. Antinuclear antibody was negative. The hepatitis-B associated antigen was positive. A percutaneous liver biopsy revealed chronic active hepatitis, and prednisone was adminis-

---

Received December 13, 1976; accepted after revision March 25, 1977.

[1] Department of Radiology, Ben Taub General Hospital, Houston, Texas 77030. Address reprint requests to R. G. Fisher.

[2] Department of Medicine, Ben Taub General Hospital, Houston, Texas 77030.

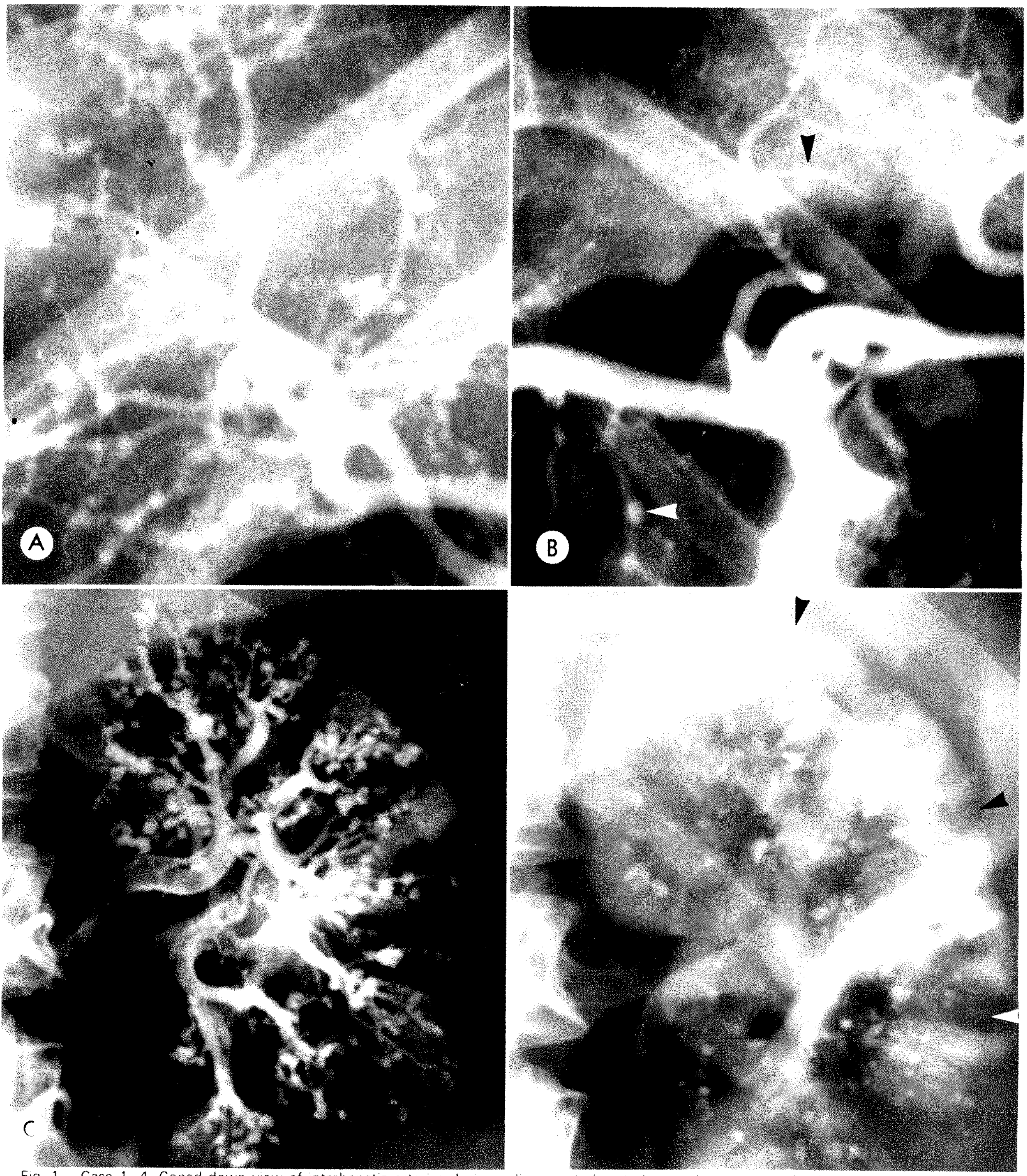

Fig. 1.—Case 1. *A,* Coned down view of intrahepatic arteries during celiomesenteric arteriogram (common trunk) showing multiple aneurysms involving virtually all medium and small arteries. *B,* Coned down view of splenic artery from same injection showing aneurysm in pancreatic artery (*white arrow*) and in smaller intrasplenic arteries (*black arrow*). *C,* Selective left renal arteriogram showing multiple aneurysms arising from medium and small arteries, typical of polyarteritis nodosa. Right kidney contained identical aneurysms. *D,* Nephrographic phase of left renal arteriogram showing contrast media lingering in aneurysms. Multiple sharply marginated defects in cortex (*arrows*) represent multiple renal infarcts resulting from fibrotic occlusion of small arteries.

tered at a rate of 60 mg/day. The patient subsequently developed hypertension and continued to complain of abdominal pain. Because polyarteritis was suspected, abdominal angiography was performed. Selected celiac arteriography and aortography revealed wide distribution of aneurysms throughout the liver and several subtle aneurysms in the kidneys (figs. 2*A* and 2*B*).

Prednisone therapy was continued. The patient was admitted 3 months later for complaints of shortness of breath. Chest radiography revealed a right middle lobe infiltrate; lung scan revealed a perfusion-ventilation defect on the right side. Pulmonary angiography was normal. However, selective bronchial arteriography revealed changes of vascular narrowing and aneurysm formation in one of the left bronchial arteries and several of the intercostal arteries (fig. 2*C*).

Cytoxin therapy was begun. The patient was readmitted 1 month later with increased pulmonary symptoms, and a diagnosis of pulmonary noncardiosis was established. Gantrisin (6 g/day) was administered, and there was resolution of the pulmonary infiltrates.

Discussion

The angiographic findings in polyarteritis nodosa include microaneurysms, stenosis, and occlusion of vessels in multiple organs [7]. Microaneurysms form as a result of necrosis of the vascular walls with destruction of the internal lamina. Although virtually every organ can be involved, the kidneys (85% of cases) and the liver (66%) are the intraabdominal organs most frequently involved [8].

Case 1 had extensive involvement of the intrahepatic vessels as well as the pancreatic vessels (figs. 1*A* and 1*B*) and arteries in both kidneys (figs. 1*C* and 1*D*). Case 2 also exhibited extensive involvement of the intrahepatic arteries, subtle changes in the renal arteries, and aneurysms and narrowing in the left bronchial and several intercostal arteries (fig. 2). To the best of our knowledge, arteriographic demonstration of bronchial artery involvement has not been reported previously.

Clinical Considerations

Hepatitis-B infections have been associated with a variety of hypersensitivitylike phenomena, including skin rashes, arthritis, and renal glomerular changes [9]. Many of these features are thought to be manifestations of antigen-antibody complex diseases, although conclusive evidence is lacking. Circulating hepatitis-B surface antigen (HBsAg)-antibody complexes have been demonstrated in some patients, and HBsAg-IgM-B_1C alone and in combination has been demonstrated in arterial lesions of several patients with polyarteritis [10, 11]. Glomerular lesions, typical of immune complex disease, have also been described in some patients with hepatitis-B surface antigen and polyarteritis. The association between hepatitis-B antigenemia and polyarteritis is now well established, being detected in 40%–54% of cases examined [12].

Studies attempting to prove that this association bears a causal relationship have yielded conflicting results. An attractive but unproven hypothesis is that hepatitis-B antigen-associated polyarteritis nodosa is an immune complex disease involving antigen-antibody circulating complexes. It is interesting that in one recent series [12], antibodies of the hepatitis-B core antigen were detected in the sera of 38 of 39 subjects with polyarteritis nodosa.

Traditionally, the diagnosis of polyarteritis nodosa is suspected in patients with multisystemic complaints and is confirmed by biopsy of affected tissue. The incidence of positive biopsy is low, although the probability of obtaining successful biopsy can be improved slightly by testing clinically involved areas.

The kidneys have been reported to be involved in 85% of cases. Although renal biopsy usually provides useful tissue, the complications of renal biopsy are increased in patients with polyarteritis nodosa. Therefore, the procedure probably cannot be undertaken without increased risk [13].

Angiography

The angiographic findings of polyarteritis were first described in 1965 by Fleming and Stern [14] when they demonstrated multiple intrarenal aneurysms in a patient with polyarteritis. Later that year, Bron et al. [7] described similar angiographic findings in multiple visceral organs. Angiography has subsequently been used as part of the diagnostic evaluation of many patients suspected of having polyarteritis nodosa [15–22].

The radiographic findings correlate well with the different stages of the disease; aneurysms are seen in the acute stage, and narrowing and thrombosis of arteries with scar formation in chronic or healing phases. Usually there is simultaneous involvement of multiple organs, although all stages of the disease may be seen in a single organ or in a single vessel simultaneously. While follow-up arteriography has revealed a regression of the aneurysms, there is no apparent direct correlation between their disappearance and the clinical course of the disease process [22]. The angiographic findings of polyarteritis nodosa are not specific and may be seen in any form of necrotizing angiitis, including hypersensitivity angiitis [20], angiitis associated with drug abuse [23, 24], and the arterial necrosis of malignant hypertension [20].

Since patients with polyarteritis often have hypertension, differentiation between the arteriographic changes of malignant hypertension and those of polyarteritis is important. In malignant hypertension, microaneurysms are absent, and segmental arterial narrowing and irregularity with a reduction in the number of arteries is seen. Prominent dilated proximal extrarenal arteries in hypertensive patients is more helpful than most other findings. Differentiation occasionally can be difficult, and the intraarterial use of vasodilators may be helpful [20].

Although the angiographic appearance of periarteritis nodosa is not absolutely pathognomonic, when it is combined with the clinical picture the diagnosis can be considered firmly established. The frequency with which angiographic studies fail to confirm the diagnosis of polyarteritis is unknown, since angiographic evaluation of a

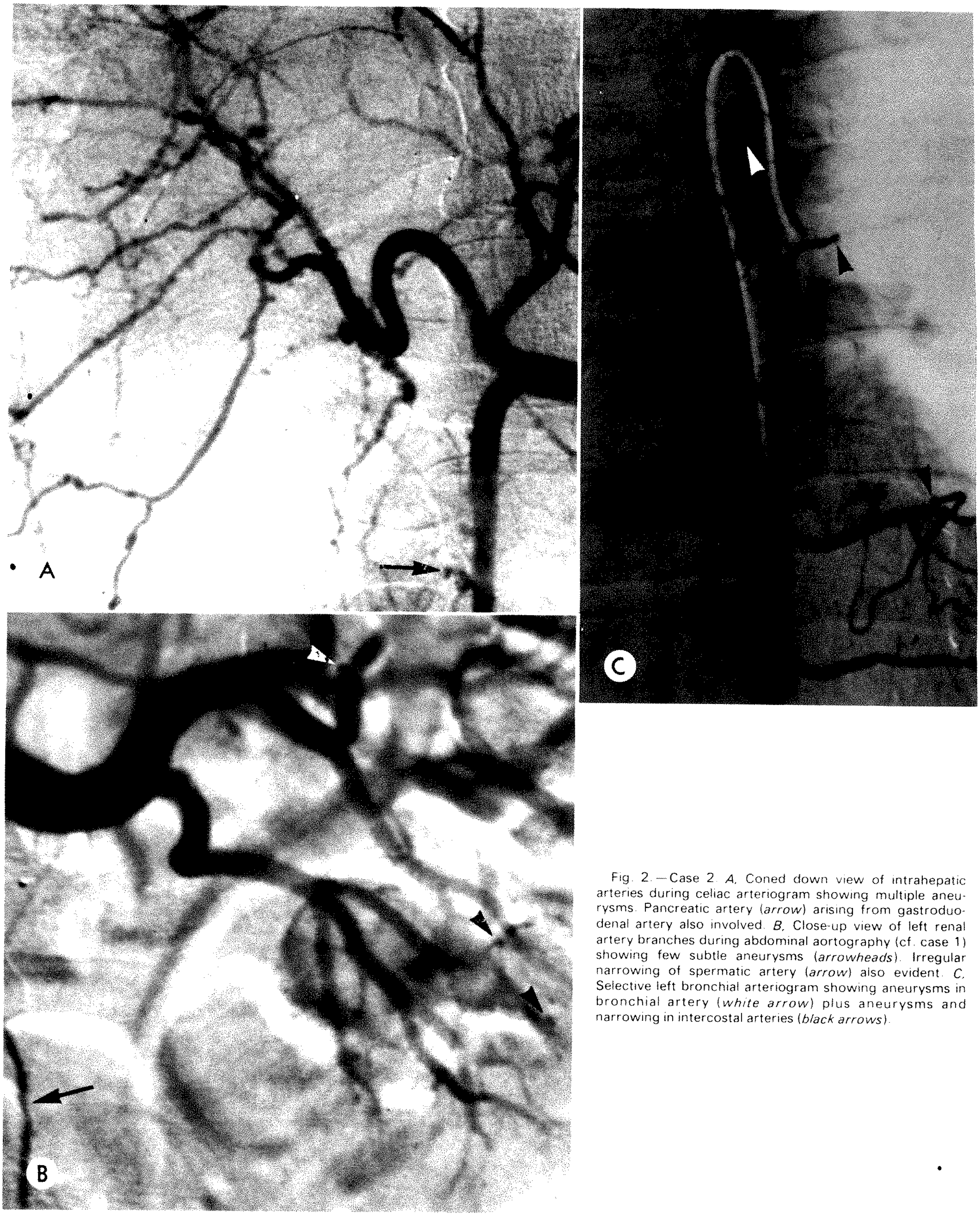

Fig. 2.—Case 2. *A*, Coned down view of intrahepatic arteries during celiac arteriogram showing multiple aneurysms. Pancreatic artery (*arrow*) arising from gastroduodenal artery also involved. *B*, Close-up view of left renal artery branches during abdominal aortography (cf. case 1) showing few subtle aneurysms (*arrowheads*). Irregular narrowing of spermatic artery (*arrow*) also evident. *C*, Selective left bronchial arteriogram showing aneurysms in bronchial artery (*white arrow*) plus aneurysms and narrowing in intercostal arteries (*black arrows*).

large series of patients has not yet been reported [22]. Studies of this type could establish the incidence of false negative and false positive angiographic findings and define the studies required to exclude the diagnosis. Since renal angiography alone may fail to diagnose polyarteritis, evaluation of the splanchnic vasculature should be a standard part of the angiographic evaluation of patients suspected of having polyarteritis nodosa.

REFERENCES

1. Paull R: Periarteritis nodosa (panarteritis nodosa) with report of four proven cases. *Calif Med* 67:309–314, 1947
2. Mowrey FH, Lundberg EA: The clinical manifestations of essential polyangiitis (periarteritis nodosa) with emphasis on the hepatic manifestations. *Ann Intern Med* 40:1145–1164, 1954
3. Rose GA: The natural history of polyarteritis. *Br Med J* 2:1148–1152, 1957
4. Gocke DJ, Hsu K, Morgan C, Bombardieri S, Lockshin M, Christian CL: Association between polyarteritis and Australia antigen. *Lancet* 2:1149–1153, 1970
5. Prince AM, Trepo C: Role of immune complexes involving SH antigen in pathogenesis of chronic active hepatitis and polyarteritis nodosa. *Lancet* 1:1309–1312, 1971
6. Harrison TR: *Harrison's Principles of Internal Medicine.* New York, McGraw-Hill, 1974
7. Bron KM, Strott CA, Shapiro AP: The diagnostic value of angiographic observations in polyarteritis nodosa. *Arch Intern Med* 116:450–454, 1965
8. Kohn BJ, Stulberg JH: Angiographic diagnosis of polyarteritis nodosa. *Calif Med* 114:40–42, 1971
9. Duffy J, Lidsky MD, Sharp JT, Davis JS, Person DA, Hollinger FB, Min K: Polyarthritis, polyarteritis and hepatitis B. *Medicine* 55:19–37, 1976
10. Gocke D, Hsu K, Morgan C, Bombardieri S, Lockshin M, Christian CL: Vasculitis in association with Australian antigen. *J Exp Med* 134:330S, 1971
11. Gerber MA, Brodin A, Steinberg D, Vernace S, Yang CH, Paronetto F: Periarteritis nodosa, Australian antigen and lymphatic leukemia. *N Engl J Med* 286:14–17, 1972
12. Trepo CG, Zuckerman AJ, Bird RC, Prince AM: The role of circulating hepatic B antigen/antibody immune complexes in the pathogenesis of vascular and hepatic manifestations of polyarteritis nodosa. *J Clin Pathol* 27:863–868, 1974
13. Anderson R: Arteriography in polyarteritis nodosa. *Br J Urol* 40:556–559, 1968
14. Fleming RJ, Stern LS: Multiple intraparenchymal renal aneurysms in periarteritis nodosa. *Radiology* 84:100–103, 1965
15. Chudáček Z: Angiographic diagnosis of polyarteritis nodosa in the liver, kidney and mesentery. *Br J Radiol* 40:864–865, 1967
16. Efsen F, Lorenzen U: Nephronangiography in periarteritis nodosa. *Acta Radiol* [*Diagn*] (Stockh) 7:225–229, 1968
17. Herschman A, Blum R, Lee CL: Angiographic findings in polyarteritis nodosa. *Radiology* 94:147–148, 1970
18. Capps JH, Klein RM: Polyarteritis nodosa as a cause of perirenal and retroperitoneal hemorrhage. *Radiology* 94:143–146, 1970
19. Bron KM, Gajaraj A: Demonstration of hepatic aneurysms in polyarteritis nodosa by arteriography. *N Engl J Med* 282:1024–1025, 1970
20. Bron KM, Stilley JW, Shapiro AP: Renal arteriography enhanced by tolazoline: value in the diagnosis of polyarteritis nodosa complicated by perinephric hematoma. *Radiology* 99:295–301, 1971
21. McLain LG, Bookstein JJ, Kelsch RC: Polyarteritis nodosa diagnosed by renal arteriography. *J Pediatr* 80:1032–1035, 1972
22. Robins JM, Bookstein JJ: Regressing aneurysms in periarteritis nodosa:a report of three cases. *Radiology* 104:39–42, 1972
23. Halpern M, Citron BP: Necrotizing angiitis associated with drug abuse. *Am J Roentgenol* 3:663–671, 1971
24. Koff RS, Widrich WC, Robbins AH: Necrotizing angiitis in a methaphetamine user with hepatitis-B angiographic diagnosis: five month follow-up results and localization of bleeding site. *N Engl J Med* 288:946–947, 1973

Computed Tomography in the Diagnosis of Subcapsular and Perirenal Hematoma

EVERETT G. SCHANER,[1] JAMES E. BALOW,[2] AND JOHN L. DOPPMAN[1]

Six patients are described in whom subcapsular and perirenal hematomas were demonstrated by computed tomography. This new diagnostic tool provided a rapid noninvasive means of visualizing the hematoma, its extent, location, and relationship to renal parenchyma. Serial examinations were used to follow progress of the hematomas toward resolution. Correlation is made with conventional radiography, angiography, and gray scale ultrasound.

Introduction

Since the development of whole body computed tomography (CT), preliminary reports have emphasized its usefulness in the diagnosis of renal pathology. CT examination of the excised kidnay [1] as well as in vivo studies have demonstrated a spectrum of renal pathology including benign cysts, tumor, hydronephrosis, atrophy, and cortical scarring [1-6]. The kidneys are particularly suited to evaluation by CT since they are surrounded by retroperitoneal and perinephric fat whose absorption coefficient or μ (-5 to -15 old Hounsfield units or HU) is considerably lower than that of normal renal parenchyma ($+25$ to $+30$ HU). This difference is further enhanced by the intravenous infusion of contrast material.

The identification and localization of intrarenal, subcapsular, and perirenal hematomas, whether secondary to trauma, spontaneous hemorrhage, or percutaneous renal biopsy, is difficult using conventional radiography. Urography with tomography may demonstrate loss of the normal renal contour and adjacent psoas margin, renal enlargement, nonfunction, and calyceal compression [7, 8]. Occasionally, the elevated renal capsule can be identified tomographically, indicating a subcapsular collection. However, its distinction from the perirenal fascial layers is often not possible [8]. Selective renal angiography may be of value in differential diagnosis by demonstrating stretched capsular vessels and compression of renal parenchyma, indicating a subcapsular process. It should be noted, however, that capsular vessels may be displaced from the renal parenchyma in both subcapsular and perirenal hematomas. Thus opacification of capsular vessels does not unequivocally define the location of the hematoma [8-11].

We describe two patients who developed symptomatic subcapsular and perirenal hematomas following percutaneous renal biopsy and a third in whom a symptomatic perirenal hematoma developed after minor trauma. Each patient was examined by CT. An EMI CT 5000 scanner with a 20 sec scan time and 320 × 320 matrix display was employed. CT scans were also performed in three asymptomatic patients following percutaneous renal biopsy.

Case Reports

Case 1

A. A., a 42-year-old white male, was referred to the National Institutes of Health for evaluation of fever of unknown origin. Febrile episodes had been recurrent, but previous extensive clinical and laboratory evaluation was unrevealing. Routine urinalysis on admission revealed microscopic hematuria. Percutaneous renal biopsy, which the patient tolerated without incident, was performed with a modified Vim-Silverman needle using intravenous pyelography and ultrasound localization. The platelet count, prothrombin time, and partial thromboplastin time were normal. Seven days after the biopsy, the patient developed left flank pain, nausea, and vomiting. A tender left upper quadrant mass was present on physical examination.

Urography revealed lack of contrast excretion and enlargement of the left kidney. Tomography demonstrated elevated capsular and perirenal fascia (fig. 1*A*). Gray scale ultrasonography confirmed the presence of left renal enlargement. Increased echoes were noted in the lower pole of the kidney, and a crescentic relatively sonolucent mass was defined behind and below the kidney (figs. 1*B* and 1*C*).

A CT scan during the infusion of contrast media revealed an enlarged, poorly visualized left kidney with a faint contrast blush noted anteriorly and medially. The renal capsule and a subcapsular mass were directly visualized, as was a lenticular mass lying posterior to the left kidney and confirmed by the perirenal fascia (fig. 2*A*). A repeat CT scan 5 days later revealed a decrease from $+40$ to $+18$ HU of the subcapsular hematoma with excellent visualization of the thickened capsular rind (fig. 2*B*). Angiography performed at this time revealed compression of renal parenchyma, elevation of a renal capsular artery, and a thickened capsular rind indicating a subcapsular collection. The posterior perirenal hematoma was not appreciated angiographically (fig. 3). A third CT scan performed 20 days after the bleed demonstrated a slight decrease in size of both the subcapsular and perirenal collections (fig. 2*C*). The patient made an uneventful recovery without specific treatment.

Case 2

B. L., a 26-year-old white female, was admitted with a diagnosis of lupus erythematosis. Routine urinalysis demonstrated white blood cell, granular, and red blood cell casts. A percutaneous renal biopsy, performed under fluoroscopic control without complication, revealed diffuse proliferative glomerulonephritis.

Received November 10, 1976; accepted after revision March 23, 1977.

[1] Diagnostic Radiology Department, Building 10, Room 6S211, Clinical Center, National Institutes of Health, Bethesda, Maryland 20014. Address reprint requests to E. G. Schaner.

[2] Division of Cancer Treatment, National Cancer Institute, National Institutes of Health, Bethesda, Maryland 20014.

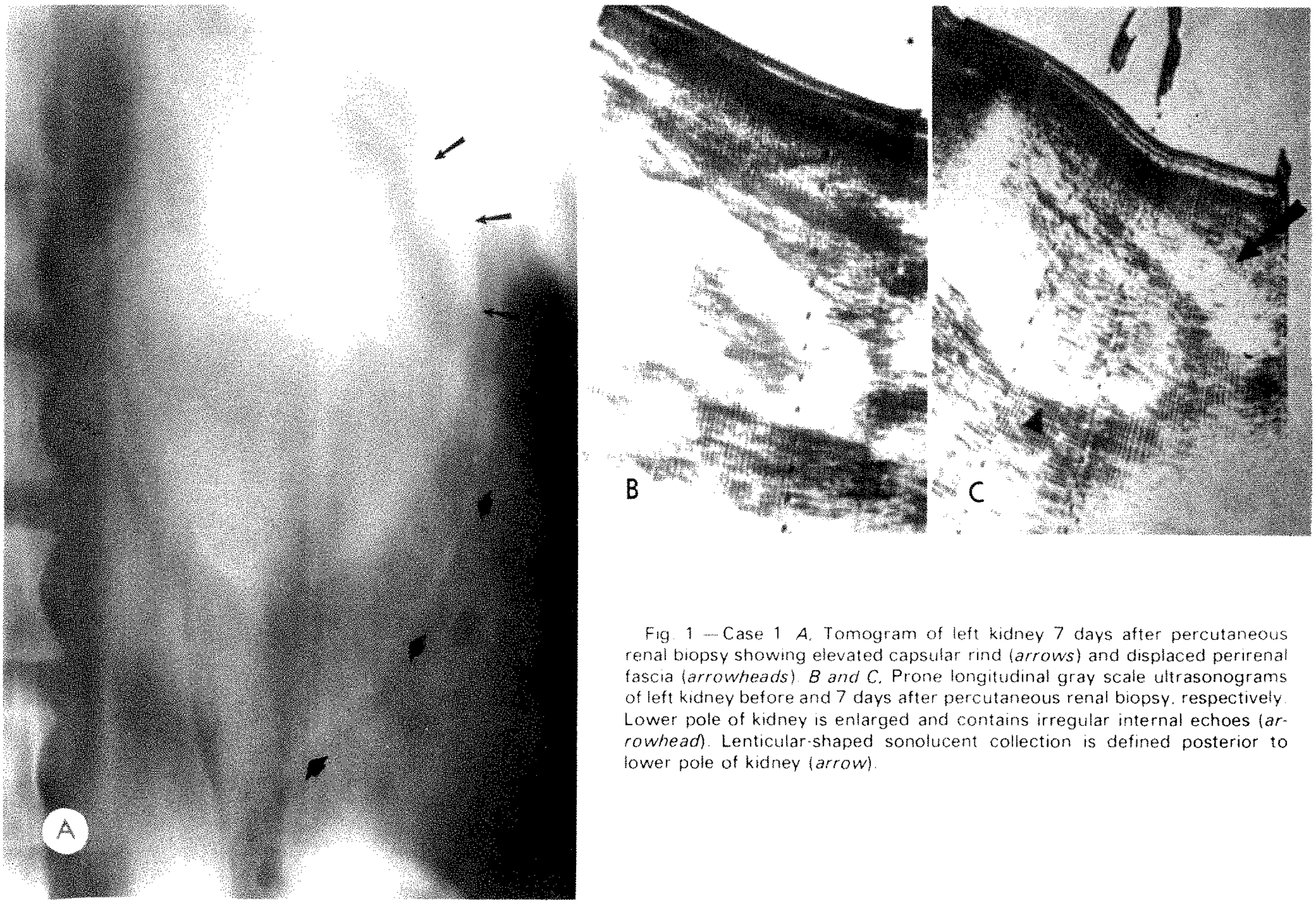

Fig. 1.—Case 1. *A,* Tomogram of left kidney 7 days after percutaneous renal biopsy showing elevated capsular rind (*arrows*) and displaced perirenal fascia (*arrowheads*). *B and C,* Prone longitudinal gray scale ultrasonograms of left kidney before and 7 days after percutaneous renal biopsy, respectively. Lower pole of kidney is enlarged and contains irregular internal echoes (*arrowhead*). Lenticular-shaped sonolucent collection is defined posterior to lower pole of kidney (*arrow*).

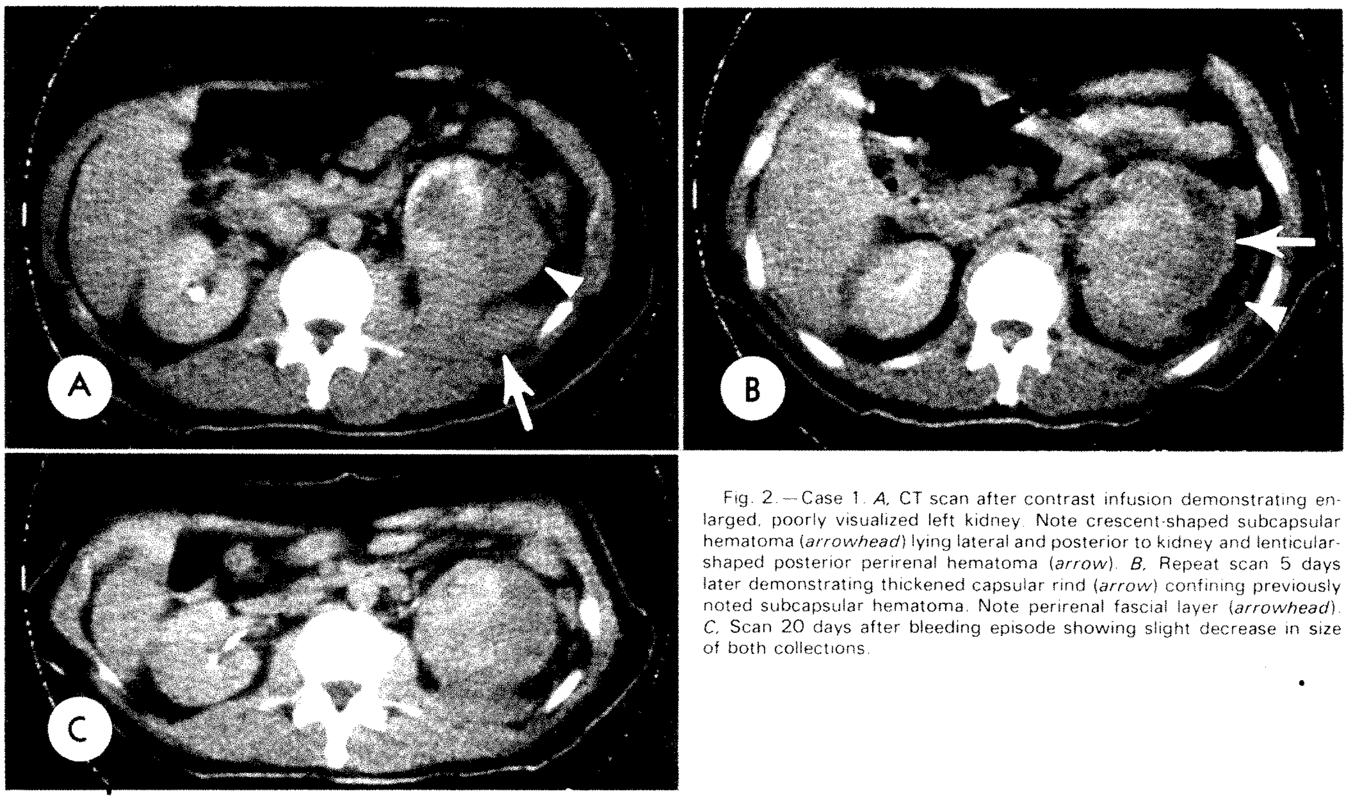

Fig. 2.—Case 1. *A,* CT scan after contrast infusion demonstrating enlarged, poorly visualized left kidney. Note crescent-shaped subcapsular hematoma (*arrowhead*) lying lateral and posterior to kidney and lenticular-shaped posterior perirenal hematoma (*arrow*). *B,* Repeat scan 5 days later demonstrating thickened capsular rind (*arrow*) confining previously noted subcapsular hematoma. Note perirenal fascial layer (*arrowhead*). *C,* Scan 20 days after bleeding episode showing slight decrease in size of both collections.

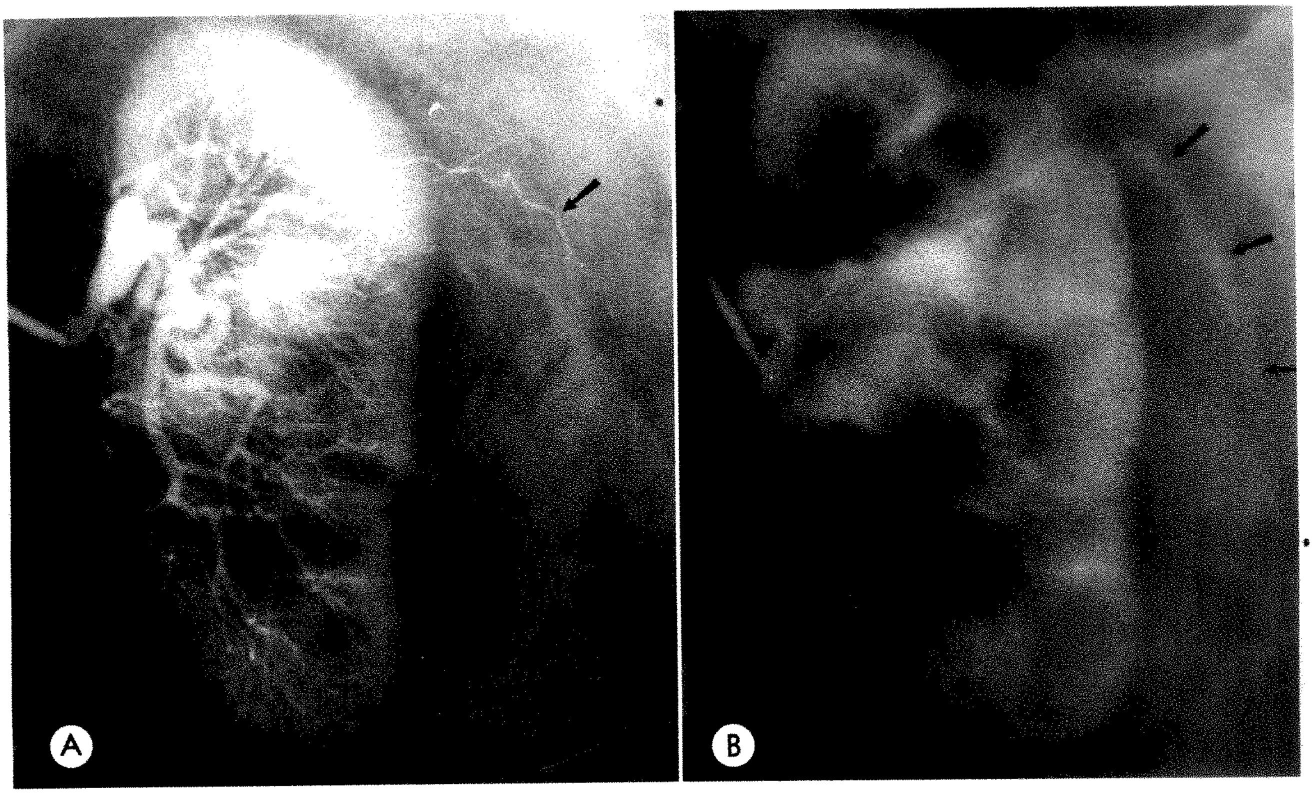

Fig. 3.—Case 1. Selective left renal arteriogram 5 days after development of subcapsular and perirenal hematomas. *A*, Arterial phase showing elevated capsular artery (*arrow*). *B*, Capillary phase showing opacification of thickened renal capsule (*arrows*). Perirenal hematoma not appreciated angiographically.

At the time of biopsy, hematocrit was 23% and platelet count, 99,000; prothrombin and partial thromboplastin times were normal. One week after the biopsy she developed left leg deep venous thromboplebitis and pulmonary embolus as documented by venography and lung scan, respectively. Heparinization was instituted, whereupon the patient developed left flank pain and tenderness. Hematocrit fell to 20%.

Urography with tomography demonstrated a well functioning left kidney. The left perirenal fascia was displaced laterally and inferiorly (fig. 4*A*). Gray scale ultrasound examination disclosed a sonolucent fluid collection lateral and inferior to the kidney (figs. 4*C* and 4*D*).

CT scan following contrast infusion demonstrated a homogeneous mass ($\mu = +36$ HU) lying lateral and posterior to the uncompressed well functioning left kidney and confined by the perirenal fascia (fig. 5*A*). Five days later, the absorption coefficient of the hematoma (fig. 5*B*) had decreased from +36 to +20 HU. A second follow-up scan 33 days after the intitial bleed revealed a marked decrease in the size of the perirenal collection (fig. 5*C*), confirmed by a decrease in distension of the left perirenal fascia on tomography (fig. 4*B*). The absorption coefficient of the hematoma had decreased to +16 HU. The patient made an uneventful recovery without treatment.

Case 3

J. B., a 17-year-old white male with biopsy-proven metastatic melanoma, was admitted complaining of acute back and left flank pain following minor trauma. His hemoglobin had dropped from 13 to 8.8 g/100 ml, and the diagnosis of retroperitoneal hematoma was considered. The platelet count, prothrombin time, and partial thromboplastin time were normal. An intravenous pyelogram revealed obliteration of the left psoas margin and of the left renal outline. The intrarenal calcyes and proximal ureter were compressed (fig. 6*A*). Gray scale ultrasound examination and postcontrast CT scan confirmed the presence of a left perirenal hematoma (fig. 6*B*). The patient was treated conservatively and discharged 2 weeks following the episode at which time intravenous pyelography was normal. A follow-up CT scan was not obtained.

Cases 4–6

Three additional female patients had left renal biopsies as part of an evaluation for systemic lupus erythematosis (ages 28 and 46) and Wegener's granulomatosis (age 54). Hematocrits, platelet counts, prothrombin times, and partial thromboplastin times were normal before and after percutaneous renal biopsy. All patients remained asymptomatic after the procedure. In each patient, a CT scan following contrast infusion was obtained within 7 days of the biopsy. In cases 4 and 5 a small lenticular-shaped mass was identified within the perirenal fat posterior to the lower pole of the biopsied kidney (figs. 7*A* and 7*B*). In case 6 a pararenal (retroperitoneal) hematoma was defined adjacent to the paraspinal musculature and extending inferiorly from the lower pole of the left kidney (fig. 7*C*). These hematomas were not of sufficient size to produce clinical symptoms or a drop in hematocrit. Absorption coefficients were +43, +37, and +40 HU, respectively.

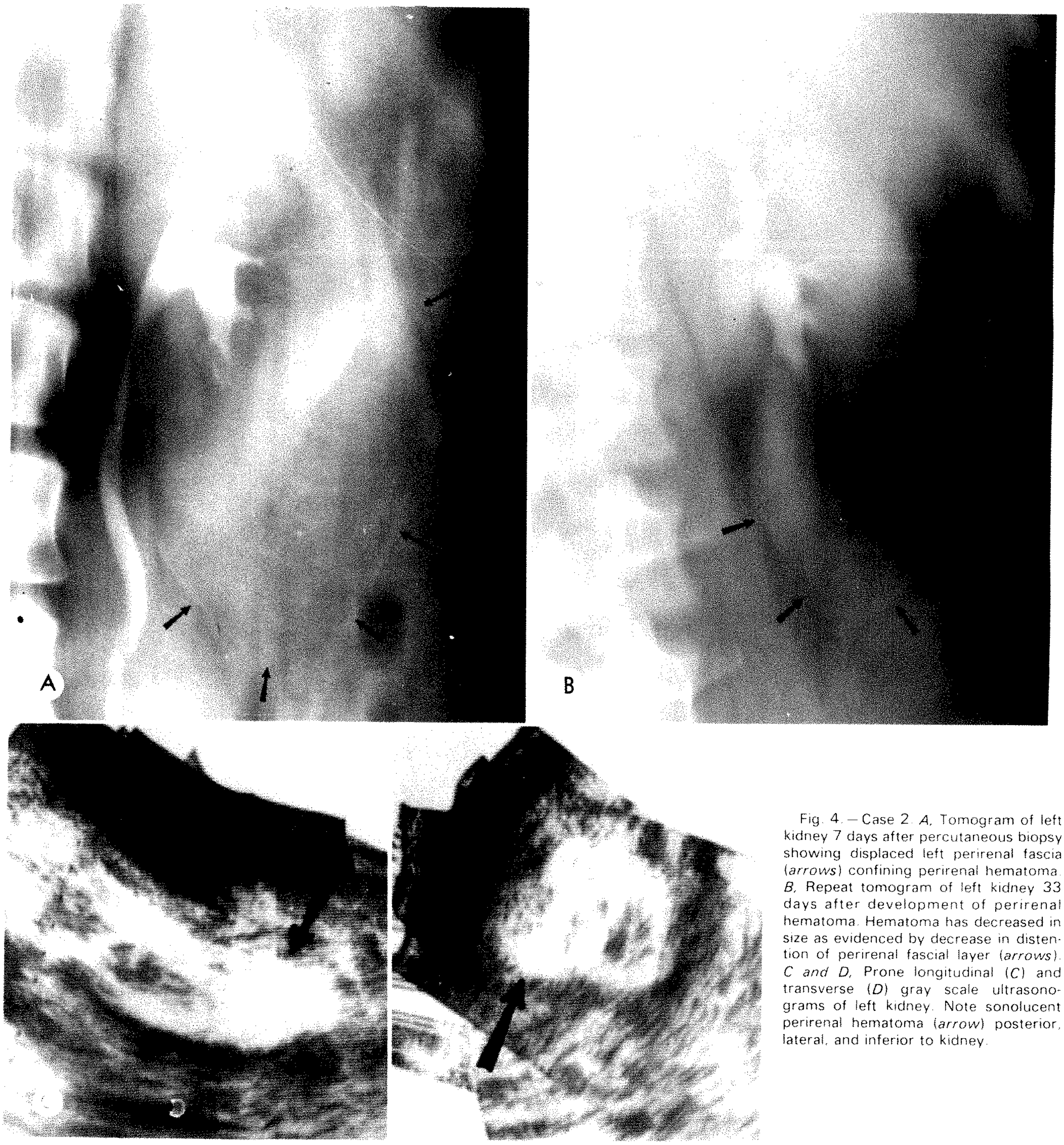

Fig. 4. — Case 2. *A*, Tomogram of left kidney 7 days after percutaneous biopsy showing displaced left perirenal fascia (*arrows*) confining perirenal hematoma. *B*, Repeat tomogram of left kidney 33 days after development of perirenal hematoma. Hematoma has decreased in size as evidenced by decrease in distention of perirenal fascial layer (*arrows*). *C and D*, Prone longitudinal (*C*) and transverse (*D*) gray scale ultrasonograms of left kidney. Note sonolucent perirenal hematoma (*arrow*) posterior, lateral, and inferior to kidney.

Discussion

Meyers et al. [8] have described in detail the fascial layers of the renal capsule and perirenal space as visualized by conventional pyelography, tomography, and angiography and have stressed the importance of distinguishing between subcapsular and perirenal fluid collections. In their review, the subcapsular collections usually compressed renal parenchyma and were often associated with lack of renal function [11]. Angiography demonstrated stretched capsular vessels and a thickened displaced capsular rind, thereby confirming the subcapsular locations of the fluid collections.

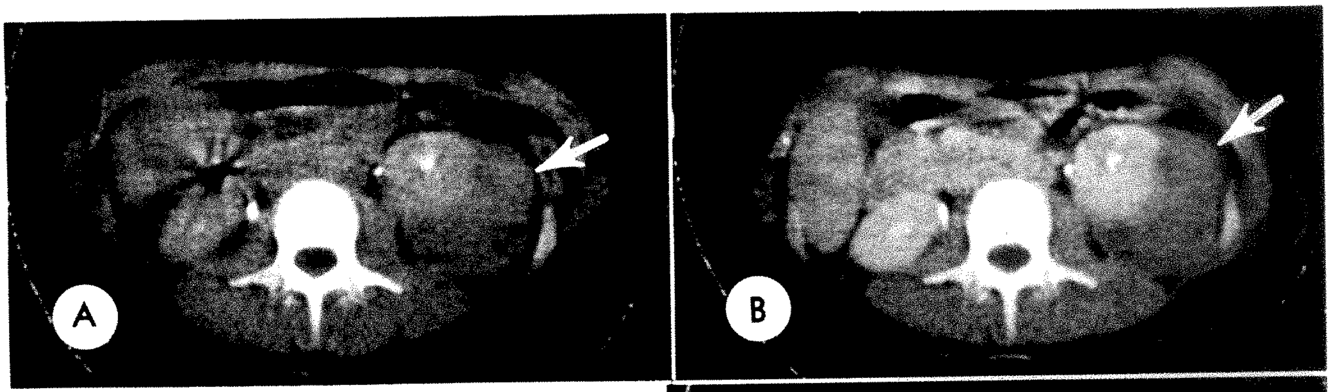

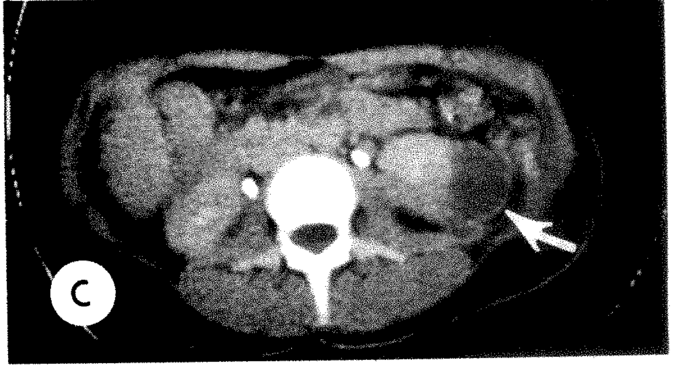

Fig. 5.—Case 2. *A*, CT scan of left kidney after contrast infusion demonstrating large perirenal hematoma (*arrow*) lateral and posterior to kidney. *B*, Repeat scan 5 days later showing decrease in absorption coefficient of hematoma (*arrow*). *C*, Follow-up scan 33 days after bleeding episode showing marked decrease in size of hematoma (*arrow*).

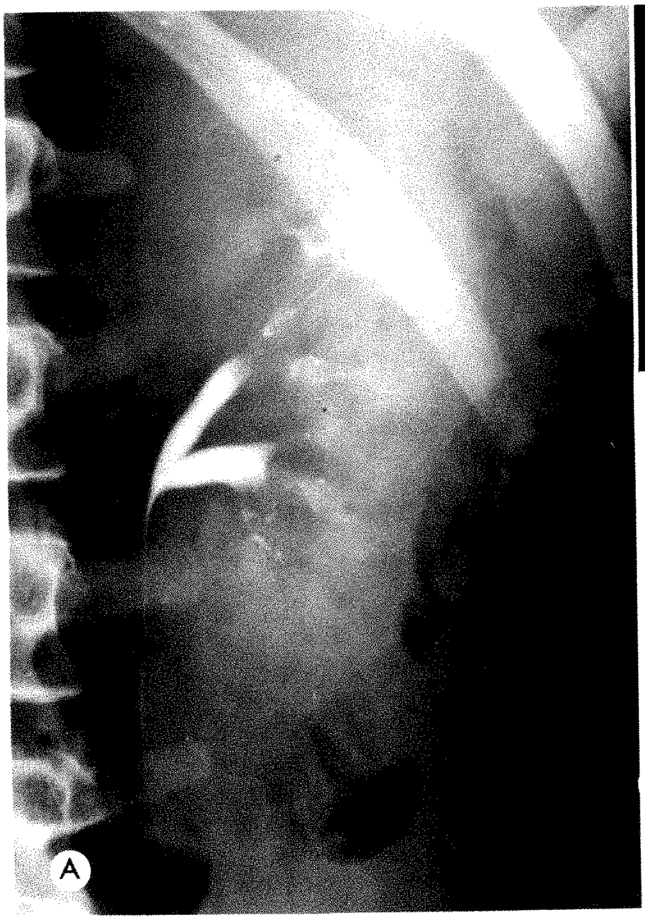

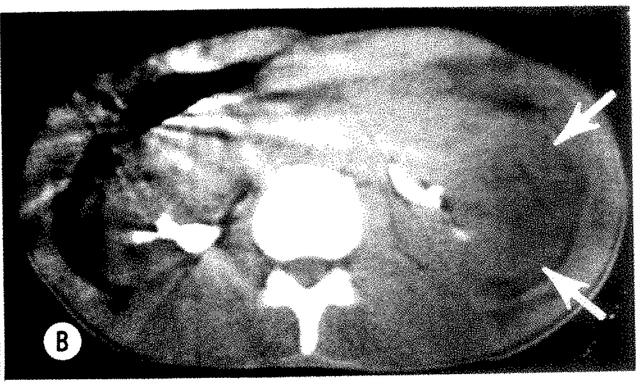

Fig. 6.—Case 3. *A*, Intravenous pyelogram revealing obliteration of left psoas margin and compression of intrarenal calyces and proximal ureter. *B*, CT scan demonstrating left perirenal hematoma (*arrows*) anterior and lateral to left kidney. Note poor definition of left renal margin.

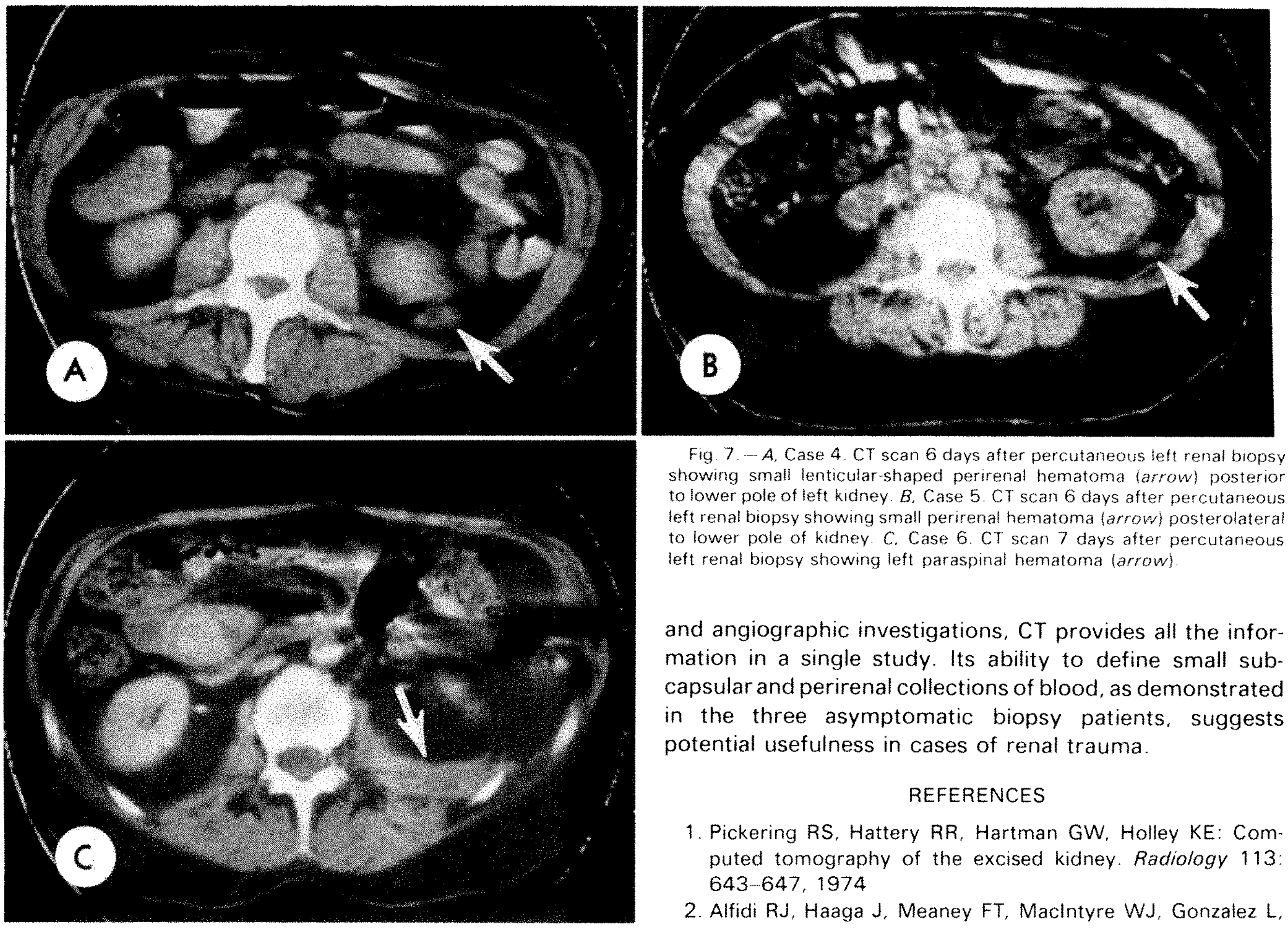

Fig. 7.—*A*, Case 4. CT scan 6 days after percutaneous left renal biopsy showing small lenticular-shaped perirenal hematoma (*arrow*) posterior to lower pole of left kidney. *B*, Case 5. CT scan 6 days after percutaneous left renal biopsy showing small perirenal hematoma (*arrow*) posterolateral to lower pole of kidney. *C*, Case 6. CT scan 7 days after percutaneous left renal biopsy showing left paraspinal hematoma (*arrow*).

In the first of our three symptomatic patients, CT demonstrated renal enlargement associated with poor function and a thickened capsular rind confining a subcapsular hematoma. In addition, a posteriorly located perirenal hematoma was visualized. Both collections were followed toward resolution by serial scans. Conventional tomography, gray scale ultrasound, and angiography confirmed the locations of both collections. The decrease in absorption coefficient of the subcapsular hematoma from +40 to +18 HU within 5 days of the bleeding episode was presumed to indicate liquefaction and disolution of clotted blood.

CT scans of case 2 demonstrated a large perirenal hematoma. The absorption coefficient dropped from +36 to +20 HU in 5 days and on follow-up scans confirmed progression toward resolution. In case 3, the perirenal hematoma secondary to minor trauma was directly visualized by CT scanning. This proved of considerable value in dictating a conservative approach to treatment, since conventional pyelography and tomography had failed to adequately define the location and extent of the bleed.

Thus we feel that CT provides a rapid noninvasive way to evaluate patients for the presence of subcapsular and perirenal bleeding. Although this information can be obtained from a combination of urographic, ultrasonic, and angiographic investigations, CT provides all the information in a single study. Its ability to define small subcapsular and perirenal collections of blood, as demonstrated in the three asymptomatic biopsy patients, suggests potential usefulness in cases of renal trauma.

REFERENCES

1. Pickering RS, Hattery RR, Hartman GW, Holley KE: Computed tomography of the excised kidney. *Radiology* 113: 643–647, 1974
2. Alfidi RJ, Haaga J, Meaney FT, MacIntyre WJ, Gonzalez L, Tarar R, Zelch MG, Boller M, Cook SA, Jelden G: Computed tomography of the thorax and abdomen; a preliminary report. *Radiology* 117:257–264, 1975
3. Sagel S, Stanley RJ, Evens RG: Early clinical experience with motionless whole body computed tomography. *Radiology* 19:321–330, 1976
4. Sheedy PF II, Stephens DH, Hattery RR, Muhm JR, Hartman GW: Computed tomography of the body: initial clinical trial with the EMI prototype. *Am J Roentgenol* 127:23–51, 1976
5. Stanley RJ, Sagel SS, Levitt RG: Computed tomography of the body: early trends in application and accuracy of the method. *Am J Roentgenol* 127:53–67, 1976
6. Stephens DH, Hattery RR, Sheedy PF II: Computed tomography of the abdomen. *Radiology* 119:331–335, 1976
7. Koehler PR, Talner LB, Friedenberg MJ, Kyaw MM: Association of subcapsular hematomas with the nonfunctioning kidney. *Radiology* 106:537–542, 1973
8. Meyers MA, Whalen JP, Evans JA: Diagnosis of perirenal and subcapsular masses: anatomic-radiologic correlation. *Am J Roentgenol* 121:523–538, 1974
9. Capek V, Fojtik F: The significance of selective renal angiography in injuries of the kidney in childhood. *Am J Roentgenol* 90:75–80, 1963
10. Olsson O, Lunderquist A: Angiography in renal trauma. *Acta Radiol* 1:1–23, 1963
11. Pollack HM, Popky G: Spontaneous subcapsular renal hemorrhage: its significance and roentgenographic diagnosis. *J Urol* 108:530–533, 1972

Visualization of the Medullary Rays on Excretory Urography in Experimental Ureteric Obstruction

LAWRENCE R. BIGONGIARI,[1, 2] RONALD M. DAVIS,[1] WILLIAM G. NOVAK,[1] JEFFREY D. WICKS,[1]
EVAN KASS,[3] AND JOHN R. THORNBURY[1]

Excretory urography occasionally delineates striations of alternating density in the renal parenchyma. Experimental observations on a dog model of ureteric obstruction show that the dense striations have the same dynamic alterations as the obstructive nephrogram. They become progressively more dense to a plateau and then fade with relief of obstruction. Previous obstruction is shown to facilitate visualization of the striations presumably by having dilated the tubules. Previous obstructive episode, previous symptoms, or chronic obstruction were present in each of the clinical cases collected which show a similar striation pattern. We conclude that the dense striations represent shadows produced by hyperconcentrated contrast material which has accumulated in dilated collecting ducts or groups of ducts within the medullary rays.

Introduction

Excretory urography during ureteric obstruction occasionally delineates striations of alternating density in the renal parenchyma. A previous report [1] noted that the more radiodense striations correspond in shape, location, orientation, and distribution to the medullary rays. The striated appearance was reproduced by retrograde injection of contrast material into these structures in a cadaver kidney. Similar striations have been visualized in Tamm-Horsfall proteinurea, hypotension, renal vein thrombosis, and infantile polycystic disease. Because these abnormal physiologic states are all characterized by tubular stasis, hyperconcentration of contrast material in dilated ducts of the medullary rays was postulated as the basis of the dense striations.

The medullary rays are bundles of collecting ducts which form in the inner cortex and, as the medullary striations, continue through the medulla to the tip of the papillae. For simplicity we refer to these bundles of collecting ducts as the medullary rays throughout their course. Radiographically, the bundles are visualized as units. These are the structures felt to represent the lucent striations seen arteriographically in renal vein thrombosis as described in a companion paper [2].

An animal model of ureteric obstruction was developed which shows that the striated pattern behaves as an extension of the obstructive nephrogram. Experimentally and clinically, previous obstruction facilitates visualization of the pattern, probably by dilating the tubules in the medullary rays.

Materials and Methods

Dogs weighing 20–40 kg were fasted 24 hr prior to study, anesthetized with sodium pentobarbital, and endotracheally intubated. Studies were made on chronic and acute preparations.

In the chronic preparations, bilateral cutaneous ureterostomies were performed in which a cuff of the bladder was left on the ends of the ureters and sutured to the skin. The dogs were studied no sooner than the second day after surgery. Prior to excretory urography, the ureters were cannulated with no. 8 French infant feeding tubes, and a purse string was sewn around the cannula through the cuff of the bladder. These dogs were subjected to ureteral obstruction and excretory urography every third or fourth day until sacrificed.

In the acute preparations, a midline incision was made and the ureters isolated and severed approximately 10 cm above the bladder. The ureters were then cannulated with feeding tubes secured with a ligature. These dogs were subjected to single episodes of varying degrees of obstruction prior to and during excretory urography and were sacrificed at the end of the day.

In the individual experiments, ureteral obstruction was either complete on one side with partial obstruction on the other, complete on both sides, or partial on both sides. Partially obstructed ureters were either allowed to flow approximately 4–5 drops/min or were uncontrolled because of leakage at the stoma. Excretory urography was performed immediately after obstruction or after up to 2½ hr of preliminary obstruction. Sodium iothalamate (Conray 400) was injected intravenously (75 or 100 ml) and radiographs taken at intervals for up to 6 hr while obstruction was maintained. Arterial blood pressures were monitored in some dogs when possible. Intraureteral pressures were measured by water manometer or pressure transducer, depending on equipment available. Plasma iothalmate concentrations were determined on some animals at intervals by the method of Medzihradsky et al. [3].

The radiographs were reviewed and density of striation pattern graded subjectively as follows: 0 = no visualization; TR = trace, very faint or questionable in part or all of renal parenchyma; I = alternate striation definitely present in part or all of parenchyma; and II = alternate striation prominent throughout entire renal parenchyma. The grading was initially done by a nonradiologist and then reviewed by two radiologists. There was almost entire agreement.

Results

In eight experiments on four chronic preparations, the striation pattern was produced and reproduced at varying degrees of ureteral obstruction with varying duration of

---

Received December 13, 1976; accepted after revision March 28, 1977.

[1] Department of Radiology, University of Michigan Medical Center, Ann Arbor, Michigan 48109.

[2] Present address: Department of Diagnostic Radiology, Kansas University Medical Center, Rainbow Boulevard at 39th Street, Kansas City, Kansas 66103. Address reprint requests to L. R. Bigongiari.

[3] Department of Urology, University of Michigan Medical Center, Ann Arbor, Michigan 48109.

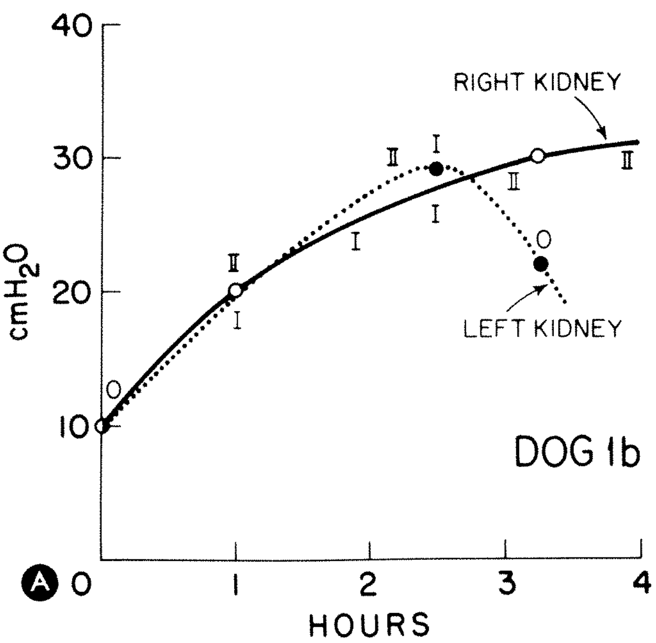

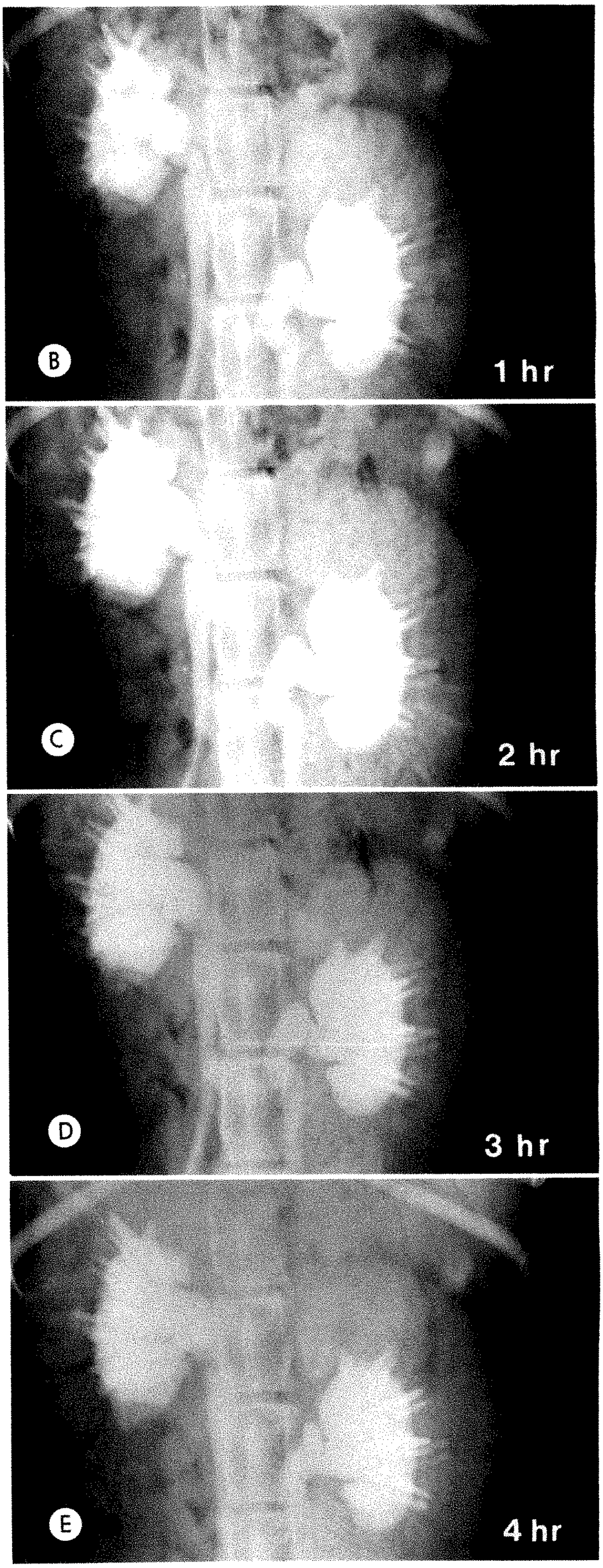

Fig. 1.—*A*, Graph of experiment b on dog 1. Without preliminary obstruction both cannulated ureters were completely obstructed and urographic contrast injected. Striation pattern in right kidney became progressively more dense with time as ureteric pressure rose to plateau. Progression in left kidney was interrupted by leakage which caused pattern to fade and ureteric pressure to fall. *B–E*, Radiographs from experiment 1b at 1, 2, 3, and 4 hr after injection of contrast material showing progression of striation pattern in right kidney and progression and fade in left kidney.

preliminary obstruction. The pattern faded or disappeared with relief of obstruction. When recorded, arterial blood pressure was stable throughout the experiment. The visualized dense striations varied from fine lines tapered peripherally to bands of up to 2–3 mm radiating for varying lengths from the renal papillae toward, but never reaching, the cortex. Results from two experiments are illustrated in figures 1 and 2.

An alternate striation pattern was visualized in one (fig. 3) of seven experiments on acute preparations which had not been subjected to previous percutaneous ureterostomies. Experimental conditions were otherwise identical. The striations were broad and localized to the papillae. Two other acute preparations showed dense papillary opacification but no striation.

The iothalamate excretion curves were parallel in chronic and acute animals (fig. 4).

Discussion

Elkin et al.[4] described and evaluated the "obstructive nephrogram." The affected kidney initially shows faint opacification and then becomes progressively more densely opacified during the study. Brenes et al. [5] and subsequently Elkin [6] concluded that in the obstructed kidney glomerular filtration of contrast is slowed, with little or no tubular excretion. Continued water reabsorption leads to progressive accumulation of contrast in the lumina of the nephrons and collecting ducts. Elkin [6] further states that in experimental animals and in patients, the obstructive nephrogram fades after the relief of obstruction.

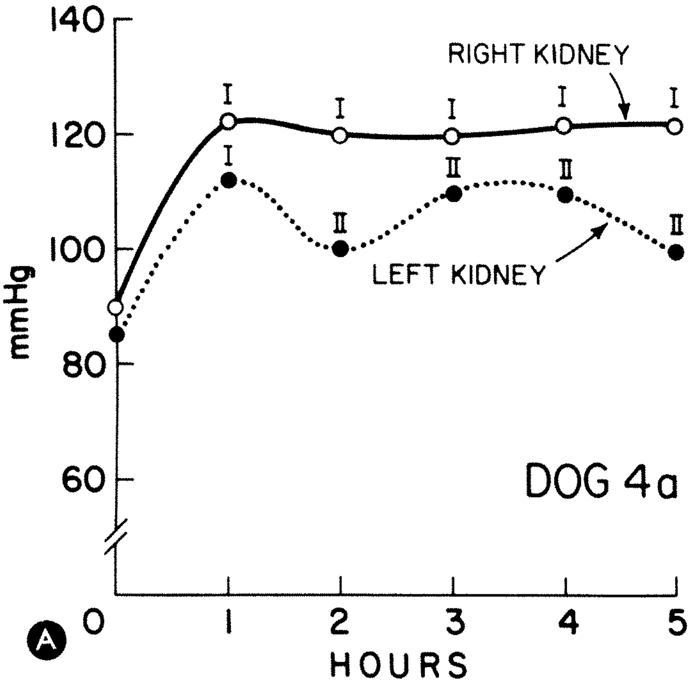

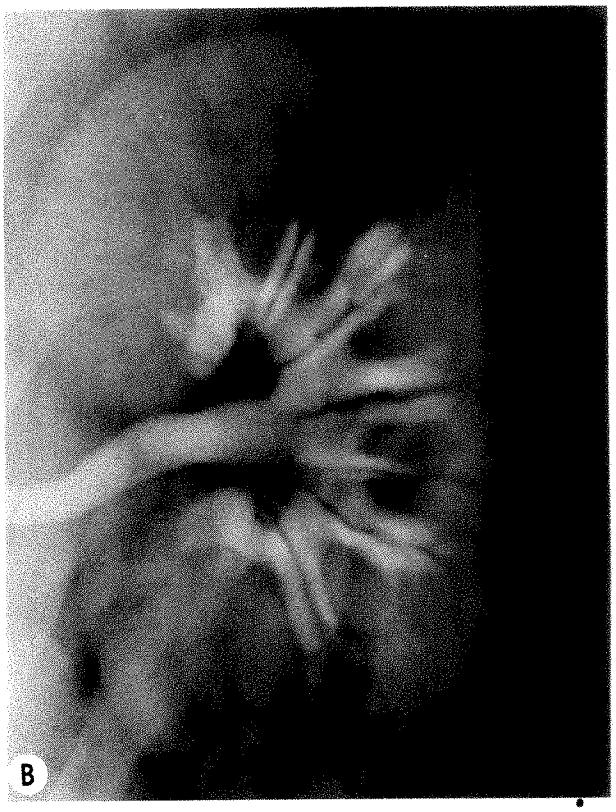

Fig. 2.—*A*, Graph of experiment a on dog 4. Urography performed after 1½ hr of preliminary ureteral obstruction on right and 1 hr on left; ureteral obstruction complete throughout experiment. Parenchymal striations formed and persisted. *B*, Radiograph of left kidney from experiment 4a at 4 hr after injection of urographic contrast demonstrating fine striation.

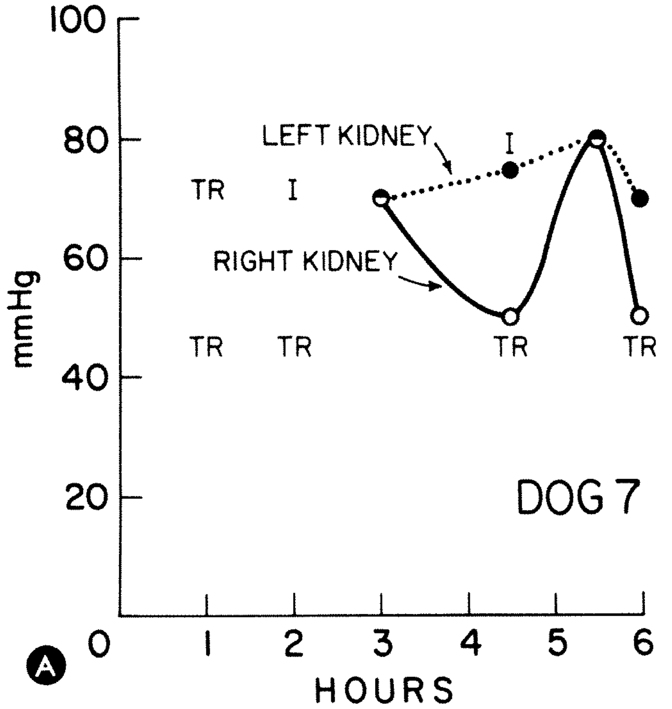

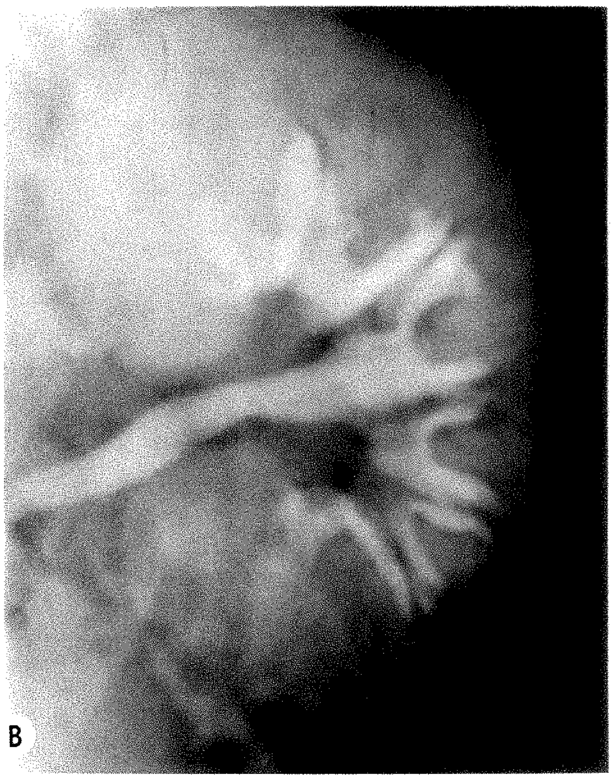

Fig. 3.—Graph of experiment on acute dog 7. Urogram performed after 1½ hr of preliminary obstruction; no pressure data available until 3 hr. Right ureter intermittently completely obstructed because of leakage. Trace papillary striation formed and persisted. Left ureter was allowed to drain at 4–5 drops/min. *B*, Left kidney of acute dog 7 at 2 hr demonstrating broad papillary striation.

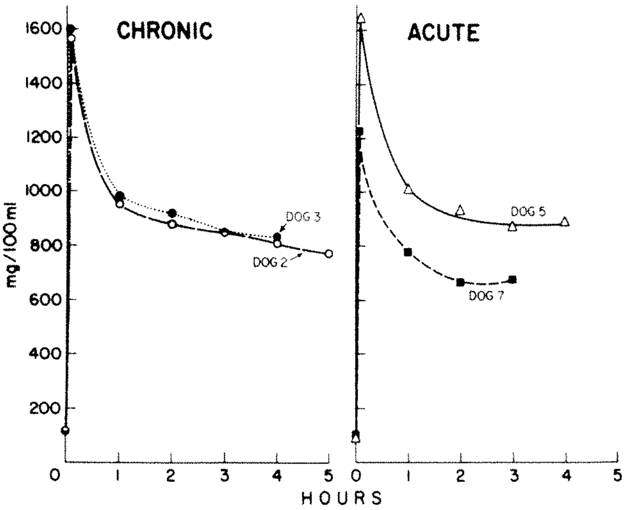

Fig. 4.—Plasma iothalamate excretion curves in chronic and acute preparations. Ureteric obstruction was complete and bilateral in experiments graphed.

In our experimental animals, the behavior of the parenchymal striations parallels that of the obstructive nephrogram. The striations in the distribution and orientation of the medullary rays appear and become more intense to a plateau unless the obstruction is relieved, in which case they fade and disappear (fig. 1). We postulate that the striation is caused by hyperconcentration of contrast by the kidney to the extent of visualization of the bundles of collecting ducts which form the medullary rays, the final conduits by which urine is transported to the renal collecting system. In other words, visualization of the alternate striation pattern is an extension of the obstructive nephrogram. With relief of obstruction, the contents of the medullary rays are washed out into the renal collecting system.

Gottschalk [7] evaluated intrarenal pressures by micropuncture, noting that in the kidney undergoing diuresis (as in excretory urography) resistance to urinary flow is almost exclusively in the collecting ducts. He related this phenomenon to the diminished cross-sectional area available for flow because of the confluence of the collecting ducts as they approach the terminal ducts. The collecting ducts are bundled in the medullary rays. Gottschalk's observation explains the preferential accumulation of contrast material in the medullary rays.

Bretland [8] has postulated that the striated pattern is produced by reflux of nonopacified urine from the renal pelvis into the parenchyma and demonstrated the physical principles by which such an event could occur. We note that the dense striations conform to the anatomy of the medullary rays, stopping short of the renal margin. While this appearance is inconsistent with reflux of unopacified urine into the medullary rays, it is totally consistent with reflux of opacified urine. Bretland's original hypothesis would not explain why we were able to visualize dense striations while the renal pelvis was contrast filled. Since our experimental model does not evaluate pyelotubular reflux, we can draw no conclusions. However, reflux of opacified urine from the pelvis would add to the contrast accumulated in the medullary rays.

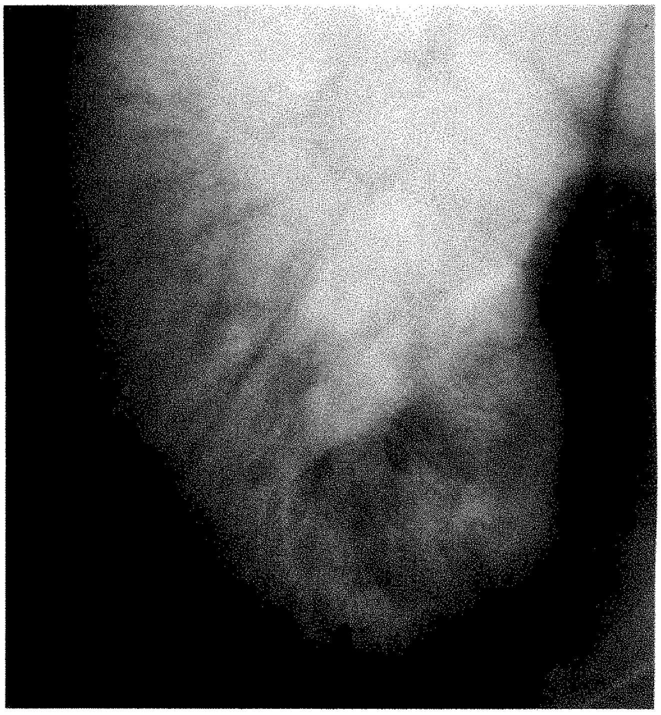

Fig. 5.—Close-up of right lower pole on urogram of 25-year-old male with right ureteral calculus demonstrating parenchymal striation. Acute transient obstruction by stone had been documented 1 year earlier. (Reprinted from [1])

The parallel iothalamate excretion curves in chronic and acute preparations show that removal of contrast material from the plasma was identical in both preparations. This finding is evidence against physiologic variation in contrast handling by the two groups as an explanation for the difference in production of the striated pattern. This observation suggests anatomic difference in the collecting ducts in the kidneys as a more likely explanation. The change would seem due to the urterostomies, probably because of transient obstruction.

Others have noted anatomic change in the tubules of kidneys with ureteral obstruction. Muirhead et al. [9] ligated the ureters of 28 dogs and maintained them for an unspecified period of time by peritoneal dialysis to study the relationship of hydronephrosis and papillary necrosis. Microscopic examination of the kidneys showed generalized dilatation of all tubules in 56% of the animals with dilatation mainly in the collecting tubules and distal segments in 28%. Criteria for dilatation were not specified, nor was it specified whether any tubules were of normal diameter. Edling and Novek [10] noted accumulation of contrast medium in dilated tubules of the medullary rays in their autoradiographic study of the nephrogram in urinary stasis. In their microinjection studies on rats, Lorentz et al. [11] noted "obvious dilation of the tubular lumen" during elevated ureteral pressure.

These observations support and help to explain our observations. The distalmost collecting tubules are bundled in the medullary rays. Intermittent or chronic obstruction facilitates visualization of the linear alternate striation probably by dilating these tubules. The varying widths of the striations (figs. 1 and 2) are interpreted as corresponding to varying degrees of dilation of collecting ducts and/or bundles of collecting ducts. Visualization of striation occurred in only one acutely prepared animal, limited to the papillae (fig. 3). Prior episodes of obstruction or normal anatomic variation in that animal are possible explanations.

The pattern was most dense and reproducible in the chronic preparations which had been submitted to percutaneous ureterostomies. This finding implies that the surgical procedure somehow facilitated visualization of the pattern. However, the faint visualization in an acute preparation without surgery further shows that surgery alone was not the predisposing event. We deduce that the surgical procedure produced a transient partial obstruction of the distal ureter which dilated the collecting ducts in the medullary rays. Such dilation need not be permanent, but may result in increased distensibility of the ducts.

To further evaluate these postulates, a series of clinical cases demonstrating alternate striation on excretory urography was reviewed for incidence of prior obstructive episodes, duration of symptoms prior to study, and chronic obstruction. Among seven cases collected over 3 years, we found four cases of acute ureteric obstruction by stone. In two of these patients there was documentation of previous acute transient obstruction by stone, and the other two patients had prior symptoms at 2 weeks and 2 months, respectively, before ureteric obstruction by stone was demonstrated radiologically. One patient in the series of seven had chronic obstruction by cervical carcinoma. Another had cutaneous ureterostomies similar to our chronic preparations. The remaining patient had chronic obstruction caused by retroperitoneal fibrosis. Therefore, in clinical cases as well, prior or chronic obstruction predisposed to visualization of alternate striation on excretory urography. Figure 5 illustrates the pattern visualized in one of these patients.

The oldest of the seven patients was 28 years and the youngest, 14. Since young patients with a full complement of functioning nephrons are known to produce more intense nephrograms than older patients, our contention that the dense striations are due to hyperconcentration of contrast material is further supported.

Conclusions

From this investigation and review, it seems that two conditions are necessary for the medullary rays to be visualized as an alternate striation pattern in the renal parenchyma on excretory urography. The first is actual dilatation or increased distensibiltiy of the collecting ducts in the medullary rays. The second is tubular stasis to produce hyperconcentration of contrast material in those dilated ducts. Visualization of the pattern in ureteric obstruction implies prior or chronic obstruction.

ACKNOWLEDGMENTS

We are grateful to James Crudup for assistance and technical expertise; to Dr. Paulette Szadaly for assistance, encouragement, and advice; to Patricia J. Dahlstrom for performing the plasma iothalamate assays; and to Chris Malinowski and Janie Supple for preparation of the manuscript.

REFERENCES

1. Bigongiari LR, Patel SK, Appelman H, Thornbury JR: Medullary rays: visualization during excretory urography. *Am J Roentgenol* 125:795–803, 1975
2. Wicks JD, Bigongiari LR, Foley WD, Walter J: Parenchymal striations in renal vein thrombosis: arteriographic demonstration. *Am J Roentgenol* 129:95–98, 1977
3. Medzihradsky F, Dahlstrom PJ, Hunter TB, Thornbury JR, Silver TM: A simple spectrophotometric procedure for the determination of various contrast media in plasma. *Invest Radiol* 10:532–535, 1975
4. Elkin M, Boyarsky S, Martinez J, Kaplan M: Physiology of ureteral obstruction as determined by roentgenologic studies. *Am J Roentgenol* 92:291–301, 1964
5. Brenes LG, Forlano H, Koutouratsas N, Stauffer HM: Mechanism of the nephrographic effect during urinary stasis. *Acta Radiol* [*Diagn*] (Stockh) 4:14–20, 1966
6. Elkin M: Radiology of the urinary tract: some physiological considerations. *Am J Roentgenol* 116:259–270, 1975
7. Gottschalk CW: Micropuncture measurements of intrarenal pressures. *Circ Res* 15, suppl. 1:110–114, 1964
8. Bretland PM: Acute ureteric obstruction–clinical and radiological aspects. *Proc R Soc Med* 67:1215–1217, 1974
9. Muirhead EE, Vanatta J, Grollman A: Papillary necrosis of the kidney. *JAMA* 142:627–631, 1950
10. Edling NPG, Novek J: Autoradiographic studies of the nephrographic effect in urinary stasis. *Invest Radiol* 2: 53–60, 1967
11. Lorentz WB, Lassiter WE, Gottschalk CW: Renal tubular permeability during increased intrarenal pressure. *J Clin Invest* 51:484–492, 1972

Parenchymal Striations in Renal Vein Thrombosis: Arteriographic Demonstration

JEFFREY D. WICKS,[1] LAWRENCE R. BIGONGIARI,[1,2] W. DENNIS FOLEY,[1,3] AND JOSEPH WALTER[1,4]

Arteriographic visualization of parenchymal striation in renal vein thrombosis is reported for the first time. The striations correspond to the location and orientation of the peritubular capillary beds of the renal cortex, which are in linear continuity with the vasa recta of the medulla. Opacification of these vascular structures in a cadaver kidney produced the same striation pattern. One possible physiologic explanation is that renal vein thrombosis causes elevated renal interstitial pressure which slows tubular urine flow. This altered intrarenal state prevents opacification of renal tubular structures while adjacent peritubular vascular structures are opacified, thereby producing a pattern of alternating striation.

While radiographic findings in renal vein thrombosis are well known [1], visualization of a cortical striation pattern on renal arteriography to our knowledge has not been previously described. We report a case in which this pattern was observed as well as the results of an experiment to study the anatomic and possible physiologic bases of the phenomenon.

Case Report

W. S., a 17-year-old white male, was admitted to University of Michigan Hospital in October 1974 for evaluation of left flank and abdominal pain of 2 days' duration associated with nausea and vomiting. Seven months earlier, a routine urinalysis showed 3+ proteinuria. Four months before admission, a normal excretory urogram was obtained at an outside hospital and an open right renal biopsy revealed proliferative glomerulonephritis.

Physical examination was unremarkable except for mild diffuse left lower quadrant tenderness, left flank guarding, and moderate bilateral costovertebral angle tenderness. Blood pressure was 128/80 mm Hg. Urinalysis showed 3+ proteinuria; the sediment contained three white blood cells, no red blood cells, and multiple hyaline casts per high power field. Serum creatinine was 1.2 mg/100 ml and blood urea nitrogen was 18 mg/100 ml.

Chest x-ray was normal. Excretory urography (fig. 1*A*) revealed an enlarged poorly visualized left kidney measuring 17 cm in its long axis. The infundibula were stretched and the pelvis narrow with notching of the proximal left ureter. The right kidney was normal except for an upper pole calyceal diverticulum. Renal venography (fig. 1*B*) demonstrated complete occlusion of the main left renal vein with multiple large intraluminal filling defects considered to represent thrombus. Multiple small collateral veins were visualized draining the renal hilus. The right renal vein was normal. Standard left renal arteriography showed slowed flow with a decreased rate of arterial clearance of contrast and a faint cortical striation insufficient for photographic reproduction. Arteriography at 3X magnification (fig. 1*C*) showed a clear pattern of generalized alternate striation in the visualized parenchyma which developed 6 sec after injection.

A repeat venogram 1 year later revealed extensive recanalization of the left renal vein. Repeat left renal angiography showed no alternate striation pattern.

Materials and Methods

In order to define the anatomy of the alternate striation pattern, contrast material was injected in renal veins of a cadaver kidney. After catheterization of the main renal vein and ligation or clamping of small veins, a 1:4 (vol/vol) solution of Micropaque was hand injected under fluoroscopic control. The injection was stopped when small capsular veins began to leak contrast on the surface of the kidney. Using 2½–3X magnification, radiographs (fig. 2*A*) were obtained with nonscreen film. The specimen was then fixed in formalin and standard histologic sections obtained for light microscopy (figs. 2*B* and 2*C*).

Results

Magnification radiographs of the arteriogram and specimen both demonstrate similar alternating parenchymal striations (fig. 3). The photomicrographs of specimen inner cortex (figs. 2*B* and 2*C*) show the alternating linear arrangement of the renal labyrinth, with peritubular capillaries surrounding the convoluted tubules and the medullary rays, the core of collecting ducts, in the center of the renal lobule. Within the labyrinth are numerous peritubular capillaries and interlobular veins filled with barium. No contrast material is seen within glomeruli, tubules, or medullary rays. Thus the white striations seen on the specimen radiograph represent opacification of the peritubular capillaries.

Discussion

The peritubular capillary bed has been demonstrated by various methods [2–4], and the vascular tubular relationships have been studied in detail [3]. The peritubular capillary bed is linearly contiguous anatomically with the vasa recta of the medulla, forming a vascular bundle between the medullary rays.

The patient's abnormal left renal arteriogram was compared to a normal renal arteriogram from another patient and to the study of his own opposite kidney which had a

---

Received November 29, 1976; accepted after revision March 28, 1977.

[1] Department of Radiology, University of Michigan Medical Center, Ann Arbor, Michigan 48109. Address reprint requests to J. D. Wicks.

[2] Present address: Department of Diagnostic Radiology, Kansas University Medical Center, Rainbow Boulevard at 39th Street, Kansas City, Kansas 66103.

[3] Present address: Department of Radiology, Sir Charles Gairdner Hospital, Perth Medical Center, Shenton Park, Western Australia 6008.

[4] Present address: Department of Radiology, Palo Alto Medical Clinic, Palo Alto, California 94301.

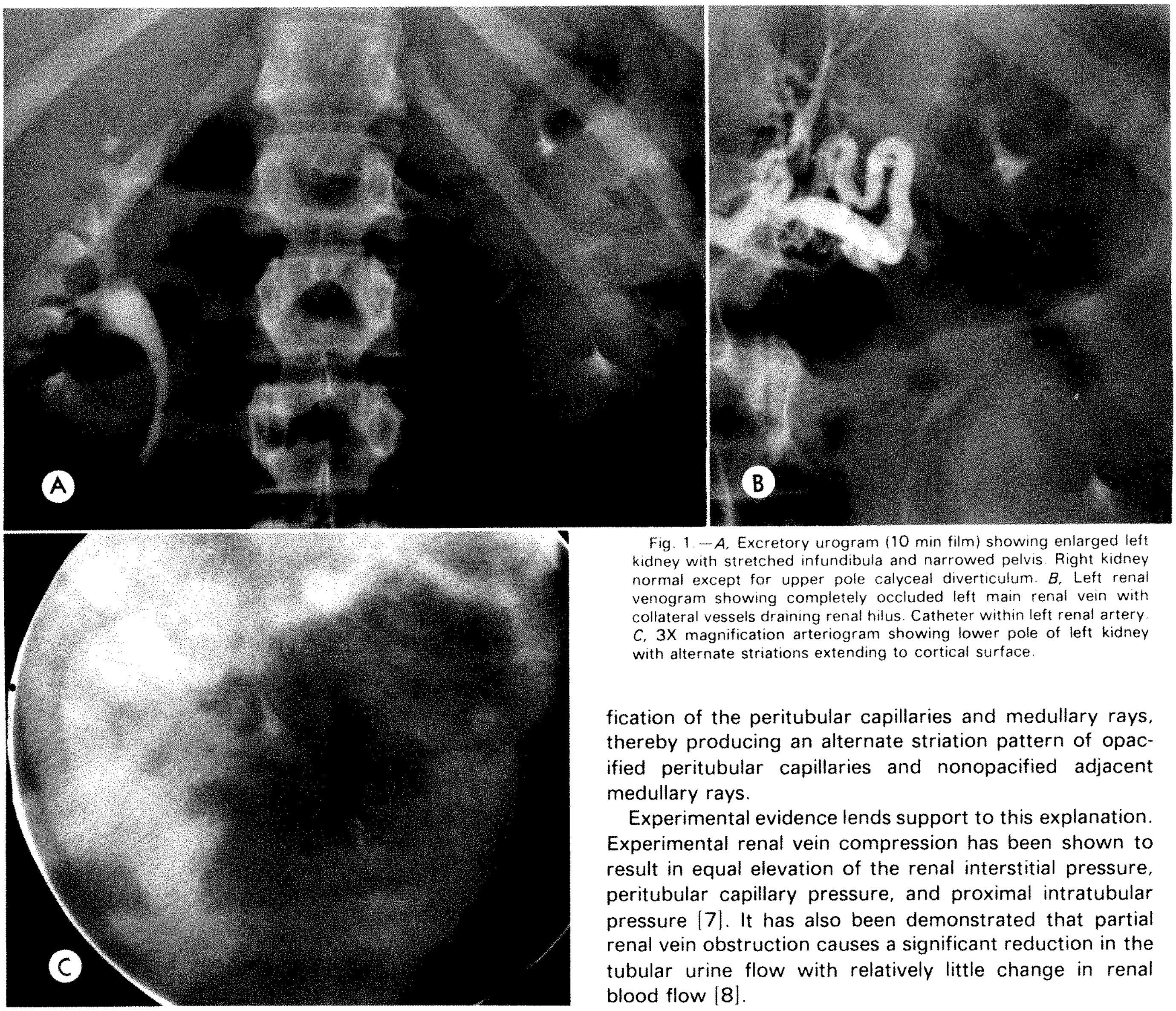

Fig. 1.—*A*, Excretory urogram (10 min film) showing enlarged left kidney with stretched infundibula and narrowed pelvis. Right kidney normal except for upper pole calyceal diverticulum. *B*, Left renal venogram showing completely occluded left main renal vein with collateral vessels draining renal hilus. Catheter within left renal artery. *C*, 3X magnification arteriogram showing lower pole of left kidney with alternate striations extending to cortical surface.

normal renal vein. The angiographic nephrogram results from an initial transient vascular blush followed by the more persistent accumulation of contrast within the renal tubules [5]. The alternate striations in the kidney with renal vein thrombosis occurred about the time of the intrarenal vascular phase of the normal comparison arteriogram and well before the nephrogram phase of both the normal kidney and of the patient's opposite kidney. Thus these stripes are felt to be contrast material within the renal vascular system. A similar pattern has been produced experimentally in dogs during the venous phase of a Thorotrast (not glomerular filtered) renal arteriogram [6].

A possible physiologic explanation for this appearance is that renal vein thrombosis caused elevated renal interstitial pressure resulting in slowed tubular urine flow. The latter prevented the normal, almost simultaneous opacification of the peritubular capillaries and medullary rays, thereby producing an alternate striation pattern of opacified peritubular capillaries and nonopacified adjacent medullary rays.

Experimental evidence lends support to this explanation. Experimental renal vein compression has been shown to result in equal elevation of the renal interstitial pressure, peritubular capillary pressure, and proximal intratubular pressure [7]. It has also been demonstrated that partial renal vein obstruction causes a significant reduction in the tubular urine flow with relatively little change in renal blood flow [8].

Other possible explanations are focal cortical ischemia and lymphatic dilation. Focal cortical ischemia secondary to interlobular artery spasm could produce slowed flow within the peritubular vascular structures, and reduced glomerular filtration, thus delaying the appearance of contrast within the tubular structures. While decrease in caliber, stretching, and separation of the interlobular arteries have been described in experimental complete renal vein occlusion, partial occlusion or slowly developing occlusion may result in dilation and elongation of the interlobular arteries [9]. However, as stated previously, at least in partial occlusion the renal blood flow is relatively unchanged [8].

Dilated lymphatics compressing the adjacent opacified parenchyma could cause an alternate striation pattern. It is known that elevated renal venous pressure causes increased lymph flow [10]. Histologic studies in renal vein thrombosis do demonstrate interstitial edema [11]. How-

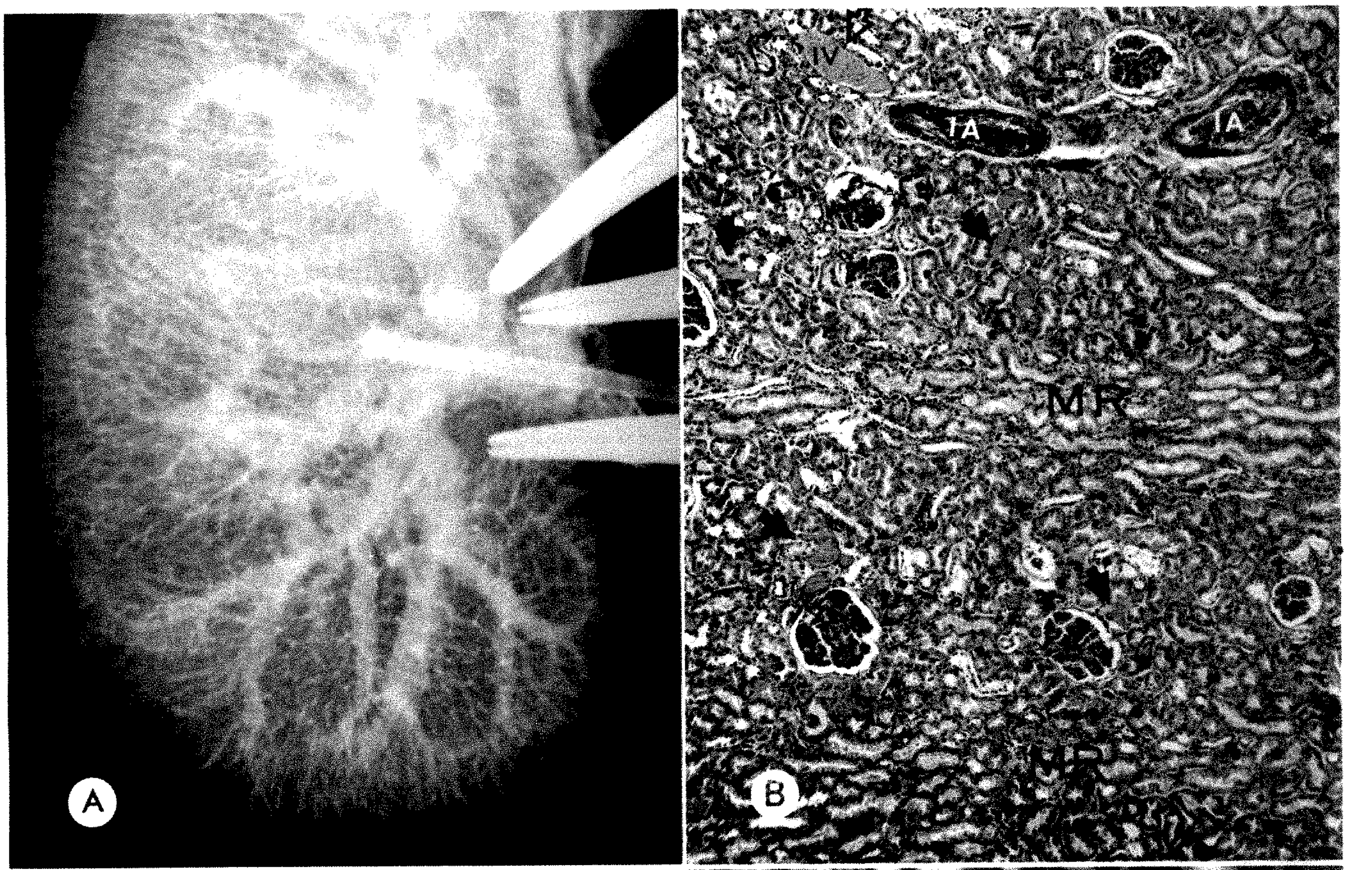

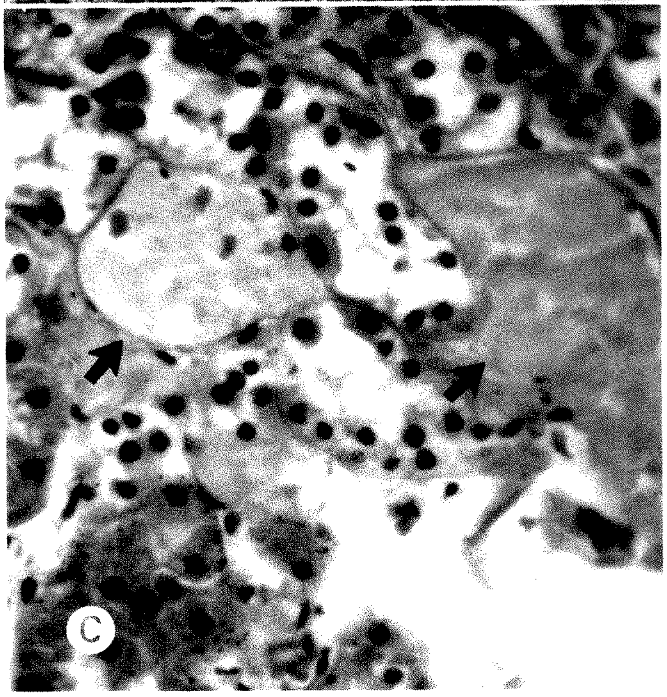

Fig. 2.—Cadaver kidney. *A*, 2½X magnification radiograph after injection of Micropaque into renal vein showing opacified renal venous system and alternating cortical striations. Histologic sections were taken from area of broad striation on lateral margin. *B*, Low power photomicrograph of specimen cortex showing alternating bands formed by medullary rays and peritubular capillaries. Note contrast in the interlobular veins (*open arrow*) and in peritubular capillaries (*arrows*). IV = interlobular vein, IA = interlobular artery, MR = medullary rays. *C*, High power view showing contrast in peritubular capillaries (*arrows*).

ever, it would seem that a higher grade lymphatic obstruction than the already present venous obstruction would be necessary to cause lymphatic dilation sufficient to compress the adjacent tubular and vascular structures.

Alternate striation has been reported on excretory urography in renal vein thrombosis [12]. A previous report from our institution [13] suggested that alternate striation seen on excretory urography in renal vein thrombosis and in other conditions results from hyperconcentration of contrast medium in the medullary rays due to slowed tubular urine flow. In a companion paper [14], we conclude that, at least in ureteric obstruction, the visualized tubules are dilated. As illustrated, the radiodense striations on the urogram stop short of the renal outer parenchymal surface. In contradistinction, the dense striations observed on the arteriogram in this case of renal vein thrombosis extend to the renal margin.

Conclusions

The parenchymal striations visualized in this case are summation shadows of the internal renal architecture. The pattern can be reproduced in a human experimental model by contrast filling of the peritubular capillary beds. We think that the radiopaque component of the similar alternate striation pattern seen on the arteriogram in our case

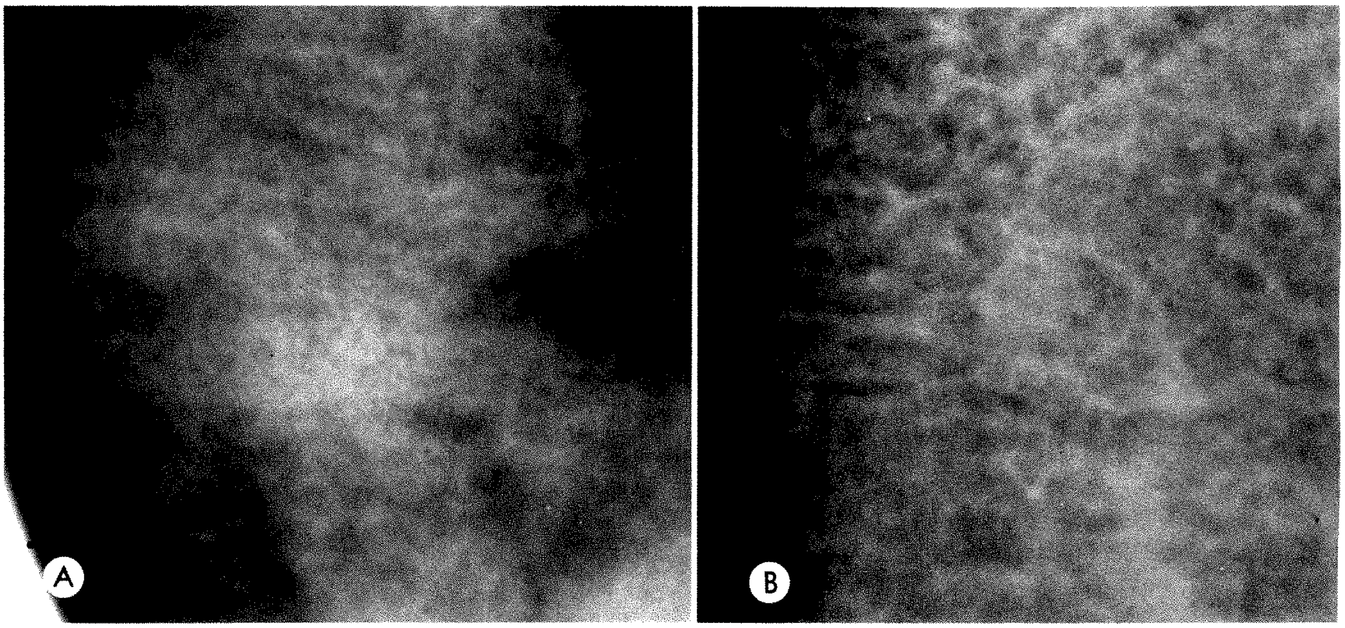

Fig. 3.—*A*, Close-up of 3X magnification arteriogram showing alternating linear striations reaching cortical margin. *B*, Specimen radiograph showing pattern similar to 3*A* but slightly less magnified.

of renal vein thrombosis represents contrast-filled peritubular vascular structures. The radiolucent components of the striated pattern are the bundles of collecting tubules filled with relatively less opacified urine.

ACKNOWLEDGMENTS

We are grateful to Drs. J. R. Thornbury and J. J. Bookstein for critical review; to Dr. W. Fidler, for preparing the histologic sections, and to Chris Malinowski and Linder Markham for typing the manuscript.

REFERENCES

1. Mulhern CB, Arger PH, Miller WT, Chait A: The specificity of renal vein thrombosis. *Am J Roentgenol* 125:291–299, 1975
2. Barclay AE: *Microarteriography*. Oxford, Blackwell, 1951
3. Beeuwkes R III: Efferent vascular patterns and early vascular-tubular relations in the dog kidney. *Am J Physiol* 221:1361–1374, 1971
4. von Kugelgen A, Kuhlo B, Otto KL Jr: Die gefasszrchitectur der niere, in *Zwanglose Abhandlungen aus dem Gebiet du normalen and pathologischen Anatomie*, edited by Bargman W, Doern W, Stuttgart, George Thieme, 1959
5. Edling NPC, Helander CG: Nephrographic effect in renal arteriography. *Acta Radiol* 51:17–24, 1959
6. Bosniak M, Farmelant MH, Bakos C, Hasiotis CA, Williams LF Jr: Experimental in vivo photographic magnification angiography of the canine kidney and bowel. *Invest Radiol* 3:120–127, 1968
7. Gottshalk CW: Micropuncture measurements of intrarenal pressures. *Circ Res* 15, suppl. 1:110–114, 1964
8. Abe Y, Kishimoto T, Yamamoto K, Ueda J: Intrarenal distribution of blood flow during ureteral and venous pressure elevation. *Am J Physiol* 224:746–751, 1973
9. Koehler PR, Bowles WT, McAlister WH: Renal arteriography in experimental renal vein occlusion. *Radiology* 86:851–855, 1966
10. Keyl MJ, Bell RD, Parry WL: Summary of renal lymphatic studies. *J Urol* 109:325–329, 1973
11. Pollak VC, Kanter A, Zaltman S: Renal vein thrombosis. *Postgrad Med* 40:282–286, 1966
12. Coel MN, Talner LB: Obstructive nephrogram due to renal vein thrombosis. *Radiology* 101:573–574, 1971
13. Bigongiari LR, Patel SK, Appelman H, Thornbury JR: Medullary rays: Visualization during excretory urography. *Am J Roentgenol* 125:795–803, 1975
14. Bigongiari LR, Davis R, Novak WG, Wicks JD, Kass E, Thornbury JR: Visualization of the medullary rays on excretory urography in experimental ureteric obstruction. *Am J Roentgenol* 129:89–93, 1977

Transitional Cell Tumors of the Kidney: How Diagnostic is the Angiogram?

STANFORD M. GOLDMAN,[1] CHIEN-HSING MENG,[2] ROBERT I. WHITE,[3] ROGER C. NARAVAL,[4]
STANLEY S. SIEGELMAN,[3] ARTHUR B. DIAMOND,[3, 5] STEVEN L. KAUFMAN,[3] AND DONALD P. HARRINGTON[3]

Angiograms of 51 tests cases including 34 transitional cell carcinomas, eight inflammatory lesions, four hypernephromas, and five miscellaneous disorders were shown to six radiologists for analysis of the angiographic features and specific diagnosis. Overall accuracy was 60% with a false positive rate of 44%. The most common false positive diagnosis occurred with inflammatory lesions (seven of eight). False negative cases were variously called normal, hypernephromas, inflammatory, or other. Vessel encasement (26%), neovascularity (56%), and tumor blush (15%) were recognized far less frequently in the transitional cell tumors of this series than in previous reports in the literature. Further, when hydronephrosis was present, the angiogram was not helpful in determining the etiology. It is concluded that the "classic" angiographic findings associated with this tumor are only moderately reliable since they can be mimicked by other conditions.

Introduction

Preoperative recognition of transitional cell carcinomas of the kidney is extremely important because of the unique operative approach required for their treatment. While radical nephrectomy is considered the definitive surgery for hypernephroma, ureteronephrectomy is the generally accepted treatment for transitional cell carcinomas because of the high incidence of multiple neoplasms.

Recent articles, primarily retrospective, have stressed that a "distinctive angiographic appearance" is associated with this entity [1–5]. In one preoperative study, positive angiographic findings were recognized in 10 of 13 cases [6]. If the angiogram is indeed definitive, then it should be possible to predict with a high degree of certainty which patients require ureteronephrectomy.

This report was prompted by our inability to find the same high percentage of positive angiographic changes even when the diagnosis was quite obvious on the intravenous and/or the retrograde pyelogram. A large series of transitional cell carcinomas of the kidney and ureter was collected and analyzed to reassess the diagnostic value of the angiogram.

Materials and Methods

A total of 51 angiographic studies, including 34 transitional cell carcinomas of the pelvis and/or ureter, were collected from the files of the Sinai Hospital of Baltimore, the Albert Einstein College of Medicine, Johns Hopkins Hospital, and the Greater Baltimore Medical Center over a 6 year period. These cases represented all the transitional cell malignancies for which angiograms were available, as well as a few nonselected "look-a-likes." Representative films from each of the angiograms were selected by one of us (S. M. Goldman). They were then randomized and shown individually to five radiologists with special interest in angiography and/or uroradiology and to one general radiologist in full-time practice at a 500 bed general diagnostic hospital. The participants were asked to choose a diagnosis for each case from among the following: normal, transitional cell carcinoma, hypernephroma, inflammatory, or other. In addition, the five specialists were asked to categorize the angiographic findings without knowledge of the correct diagnosis.

Of the 34 patients with transitional cell carcinomas, 32 had been studied by selective renal angiography, 10 had magnification angiography, and two had epinephrine studies. All 17 cases with lesions other than transitional cell carcinomas were studied by selective renal angiography. There were five magnification studies and four pharmacologically enhanced renal angiograms (one angiotensin, three epinephrine), three inferior vena cavagrams, and two renal venograms performed on these latter patients. The diagnoses of the patients with lesions other than transitional cell carcinoma are shown in table 1.

TABLE 1

Diagnoses in Non-Transitional Cell Patients

Diagnosis	No.
Normal magnified ureteric artery	1
Parapelvic cyst	1
Hypernephromas	4
Lymphoma:	
Reticulum cell sarcoma	1
Lymphosarcoma	1
Inflammatory lesions:	
Ureteritis cystica	1
Blastomycosis	1
Intrarenal abscess	1
Chronic pyelonephritis	3
Chronic pyelonephritis and stone	1
Inflammatory perinephric disease	1
Squamous cell carcinoma	1
Total	17

Received June 11, 1976; accepted after revision March 14, 1977.
Presented at the annual meeting of the American Roentgen Ray Society, Washington, D.C., September 1976.

[1] Department of Radiology, Sinai Hospital of Baltimore, Inc., Belvedere at Greenspring Avenues, Baltimore, Maryland 21215. Address reprint requests to S. M. Goldman.

[2] Deceased. Formerly Department of Radiology, Albert Einstein College of Medicine, 1300 Morris Park Avenue, Bronx, New York 10461.

[3] Department of Radiology, Johns Hopkins Hospital, 601 North Broadway, Baltimore, Maryland 21205.

[4] Department of Radiology, Greater Baltimore Medical Center, 6701 North Charles Street, Towson, Maryland 21204.

[5] Present address: Department of Radiology, Montgomery General Hospital, Olney, Maryland 20832.

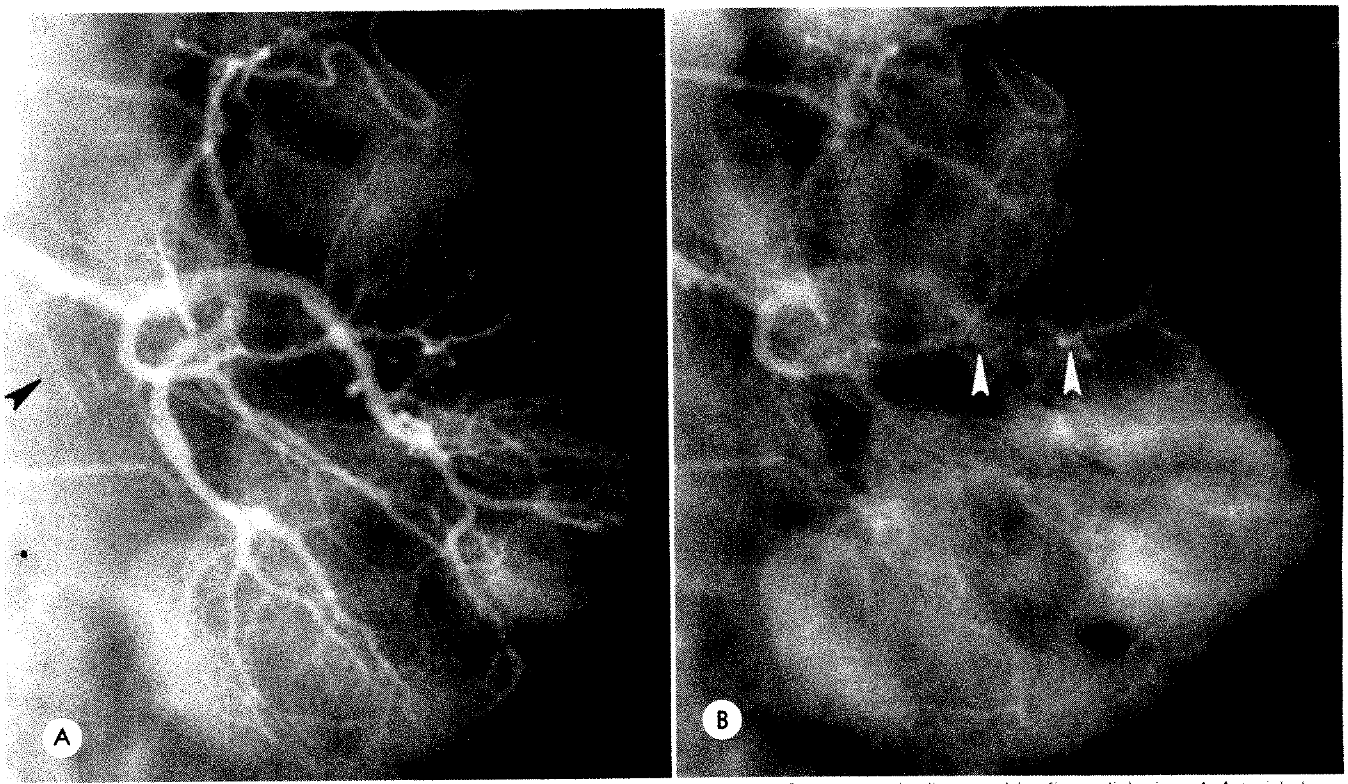

Fig. 1.—Extensive transitional cell carcinoma involving entire upper half of kidney. Case correctly diagnosed by five radiologists. *A*, Arterial phase showing abnormally dilated peripelvic vessels (*arrow*) feeding extensive tumor. *B*, Nephrogram phase showing vessel encased by tumor (*arrows*). Abnormal vessels and poor nephrographic density in superior portion of kidney reflect tumor invasion of renal parenchyma.

Results

Transitional Cell Carcinoma

The overall accuracy of the radiologists was 60% (range, 53%–76%). Interestingly, the general radiologist scored better than one of the full-time angiographers. The false positive rate was 44% (range, 29%–59%) and the false negative rate 40% (range, 24%–47%). The person with the highest accuracy rate also had the highest false positive rate.

The majority of the participants diagnosed 24 of the transitional cell carcinomas correctly (fig. 1) and missed seven (fig. 2). In three cases, opinion was evenly divided: three diagnosed transitional cell carcinomas and three favored other diagnoses.

The types and frequency of the angiographic findings are summarized in table 2. It should be noted that two of the three patients designated as having hydronephrosis were incorrectly diagnosed and placed by the majority into the "other" category.

Non-Transitional Cell Carcinoma

The normal magnified ureteric artery was satisfactorily identified as such by the majority of the radiologists, and the two lymphoma cases were correctly classified as "other." The squamous cell carcinoma was categorized as a transitional cell type, and the parapelvic cyst was placed in each of the five possible categories by at least one participant. Among the hypovascular hypernephromas, one was called a transitional cell cancer by the majority of the observers. In each of the three other cases, three of the six radiologists made the correct pathologic diagnosis, although they were not the same physicians in each instance.

The eight inflammatory lesions in the series provided the greatest challenge. In only one of these was the correct diagnosis made by the majority of the evaluators. Five were called transitional cell carcinomas (figs. 3 and 4), while there was no consensus in the other two cases (fig. 5). Of the four cases in this category with some degree of hydronephrosis, three were called transitional cell carcinomas and one had a variety of diagnoses listed. Two of the inflammatory lesions were thought to have vessel encasement. On seven of the eight angiograms, an enlarged periureteric artery was noted. Neovascularity was seen in six and a blush was present in five.

→

Fig. 2.—Bilateral transitional cell carcinomas of kidney in 35-year-old male. *A and B*, Left kidney with two renal arteries. *A*, Injection of superior renal artery. *B*, Injection of inferior renal artery showing abnormal vasculature (*arrows*) arising from main renal artery and extending superiomedially to supply area in renal pelvis. Correctly diagnosed by three of five radiologists. Angiographic findings equivocal on neovascularity and invasion of parenchyma. *C and D*, Right kidney with obvious mass in renal pelvis but no readily apparent angiographic signs of transitional cell tumor. Correctly diagnosed by one radiologist; two called it normal and two called it other.

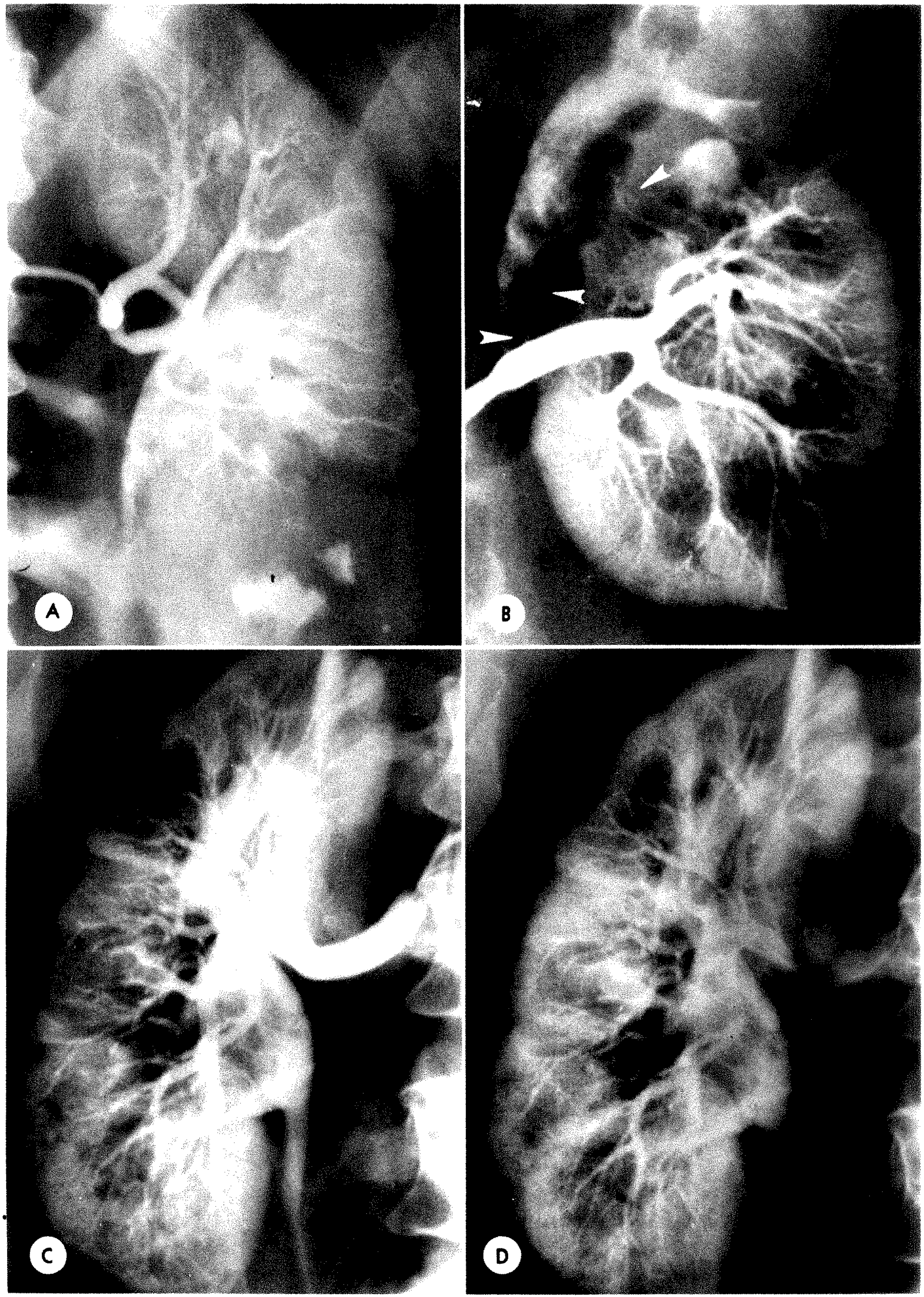
A
B
C
D

TABLE 2

Angiographic Findings in Transitional Cell Carcinoma Patients

Finding	Present	Absent	No Majority Opinion
Neovascularity	19	14	1
Blush	5	28	1
Vessel encasement*	9	21	4
Invasion of renal parenchyma	7	24	3
Hydronephrosis	3	28	3
Enlarged periureteric artery	18	14	2
Other vessels supplying mass	2	31	1
Inflammatory hypervascularization	0	33	1
Arteriovenous shunting	1	33	...
Pooling of contrast	1	33	...

Note. — Majority opinon of six participants on 34 cases.
* Segmental or irregular changes in caliber or contour.

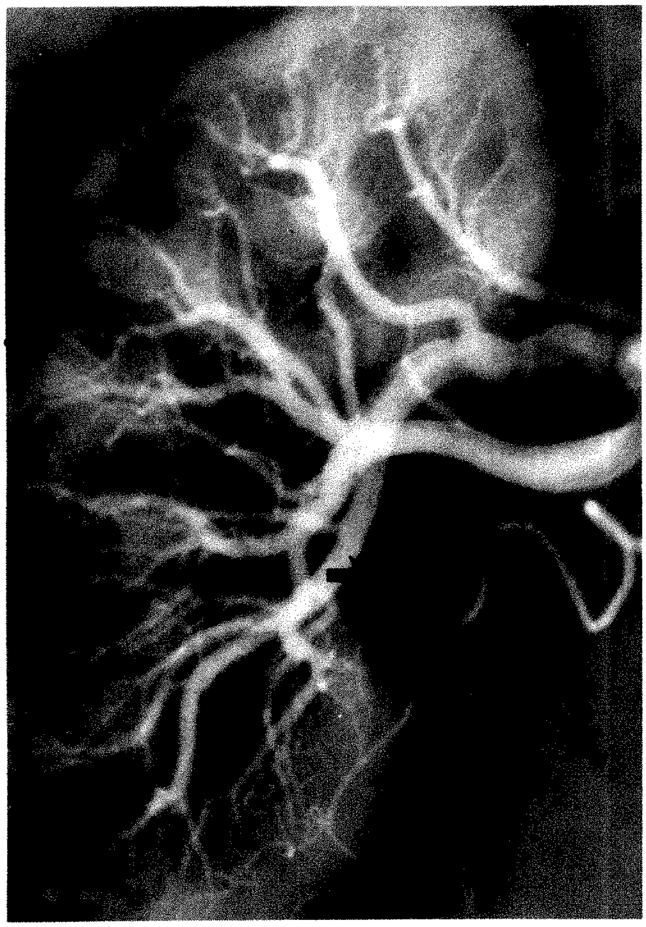

Fig. 3. — Ureteritis cystica (magnification study). Case misdiagnosed as transitional cell carcinoma by five radiologists because of abnormal peripelvic vessels (*arrows*). Notching of ureter, more prominent on renal vein study (not shown), may have added to impression of ureteral tumor.

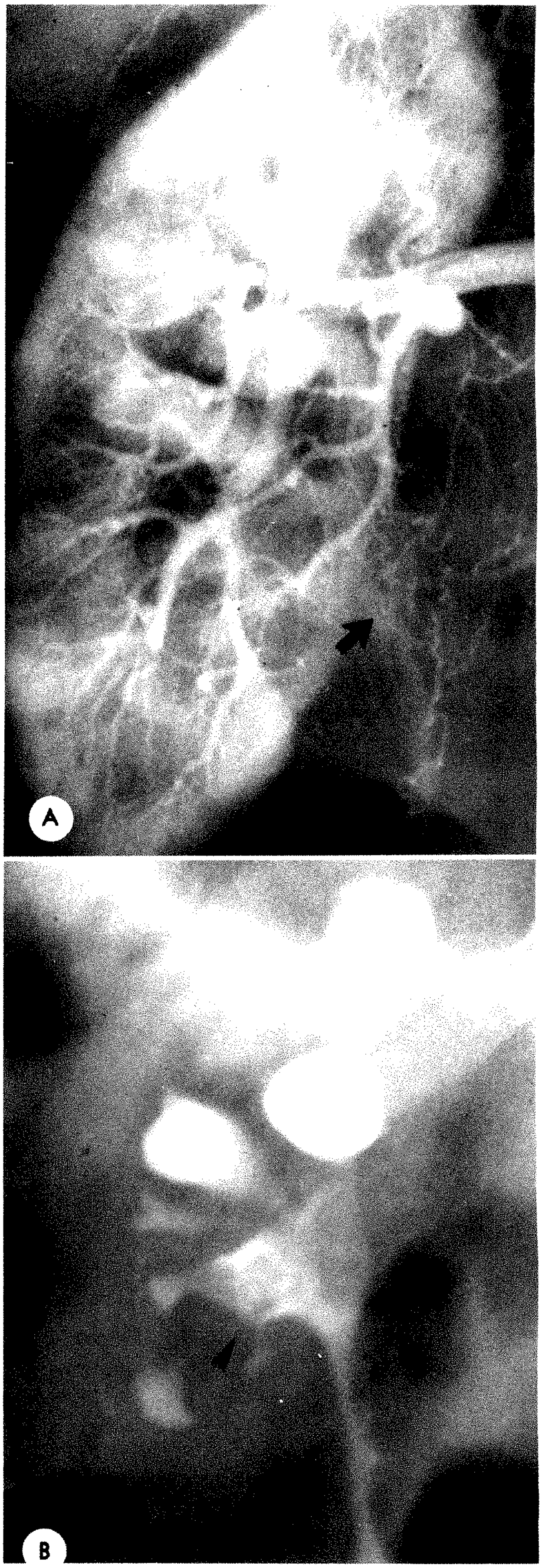

→

Fig. 4. — Four pelvic stones with pyelonephritis. Case correctly diagnosed as inflammatory by one radiologist; three called it transitional cell carcinoma and one called it other. *A*, Renal arteriogram showing enlarged pelviureteric arteries (*arrow*), neovascularity, and possibly blush. *B*, Retrograde pyelogram (not seen by participants) showing stones (*arrows*).

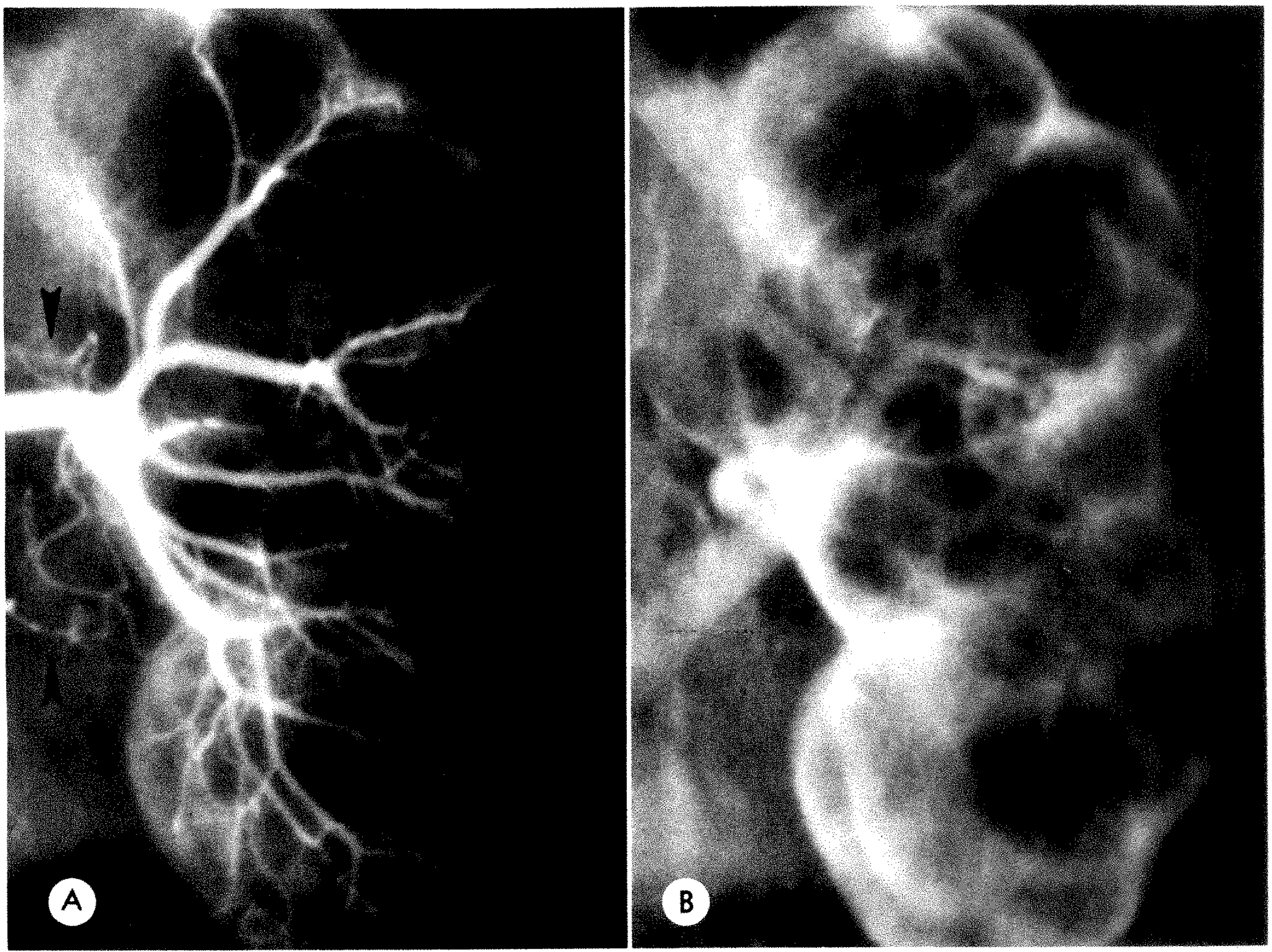

Fig. 5.—Blastomycosis. Case correctly diagnosed as inflammatory by two radiologists; two called it transitional cell carcinoma and one called it other. All recognized angiographic criteria of hydronephrosis but were uncertain of nature of vascularity (*arrows*).

Of the five cases recognized as having hydronephrosis, three of four inflammatory lesions and an obstructing hypernephroma were mistakenly called transitional cell carcinomas.

Discussion

This study was undertaken to determine how frequently certain angiographic findings are seen in patients with transitional cell carcinomas and how helpful these findings are in establishing a correct diagnosis. Table 3 compares the frequency of positive angiographic findings in this study and six other reports. The frequency of tumor blush, neovascularity, vessel encasement, and evidence of invasion of the parenchyma was much lower in the present series compared to other studies. We feel that our results more nearly reflect the true incidence since participants had no knowledge of the correct diagnosis. We do not believe the discrepancy can be explained by differences in tumor population or a difference in definition of the commonly used angiographic terms.

This study fails to support the contention that transitional cell carcinoma can be diagnosed using arteriographic findings alone. Many other entities, particularly inflammatory lesions, have angiographic findings indistinguishable from transitional cell cancer (table 4).

In the preoperative study by Haleem et al. [6], 10 of 13 patients (77%) had positive angiographic findings. Only one of the radiologists in our study approached this degree of diagnostic acumen (76%); he had the highest false positive rate, probably reflecting an overzealous attempt to find transitional cell carcinomas. We believe that the accuracy rate of approximately 60% achieved in this study more nearly reflects the information content of the arteriogram.

The high false positive rate (44%) found in this study reflects the inherent difficulty of angiographically distinguishing several important entities. Overlap between hypovascular hypernephromas and transitional cell carcinomas has already been alluded to in previous communications [1, 4]. More serious, however, is potential

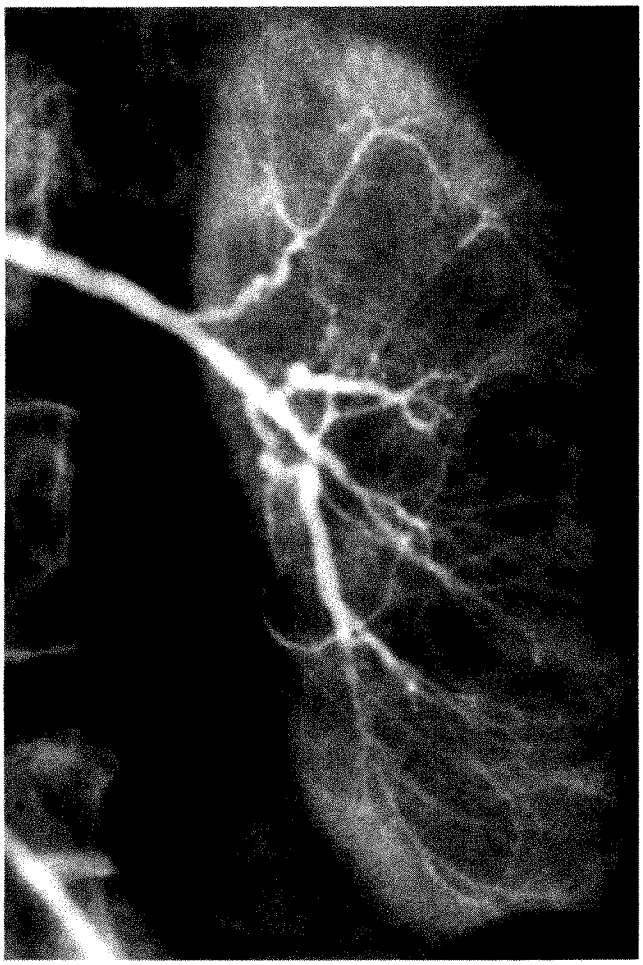

Fig. 6.—Transitional cell carcinoma. Case correctly diagnosed by three radiologists; two called it inflammatory. Single positive angiographic finding recognized by majority was vessel encasement. Participants had difficulty separating transitional cell cancer from inflammation.

TABLE 4

Percentage of Positive Angiographic Findings in Inflammatory Lesions and Transitional Cell Carcinomas

Angiographic Finding	Transitional Cell Carcinomas (N = 22)*	Inflammatory Lesions (N = 8)†
Neovascularity	82	75
Blush	82	71
Vessel encasement	73	25
Invasion of renal parenchyma	...	19
Hydronephrosis	50	50
Enlarged periureteric artery	55	87
Arteriovenous shunting	0	0
Pooling of contrast	...	0

* Data from Rabinowitz et al. [4].
† Present report.

misdiagnosis of an inflammatory lesion as a transitional cell carcinoma, since the wrong type of therapy might be instituted. This fact has not been previously stressed. In our series, seven of the eight inflammatory lesions were incorrectly diagnosed and in five instances were called transitional cell carcinomas. In general, our observers were incapable of separating tumor vasculature from inflammatory vessels (fig. 6). This was also true in the cases in which pharmacoangiography and renal phlebography were available. For example, encasement was noted in two of the infectious processes.

Our study also failed to confirm the observation of Boijsen and Folin [1] that the cause of hydronephrosis could be accurately diagnosed by arteriography. Of the eight cases in which hydronephrosis was recognized angiographically, three of four inflammatory lesions and the one hypernephroma were incorrectly called transitional cell

TABLE 3

Percentage of Positive Angiographic Findings

Angiographic Finding	Present Study (N = 34)	Rabinowitz et al. [4] (N = 22)	Schapira and Mitty [5] (N = 3)	Mitty et al. [3] (N = 3)	Boijsen et al. [1] (N = 10)	Haleem et al. [6] (N = 13)	Lagergren and Ljungvist [2] (N = 9)
Neovascularity	56	82	...	0	60	...	...
Blush	15	82	33	...	60	...	...
Vessel encasement	26	73	66	100	...	...	...
Invasion of renal parenchyma	21	...	33	100	30	39	44
Hydronephrosis	9	50	33	...	50	...	11
Enlarged periureteric artery	53	55	100	100	...	...	...
Other vessels supplying mass	6	...	...	...	...	...	...
Inflammatory hypervascularity	0	...	...	...	...	...	55
Arteriovenous shunting	3	0	0	0	...	...	50*
Pooling of contrast	3	...	...	0	...	...	...

* Seen in three of six cases.

tumors. Of the three transitional cell carcinomas, two were placed in the "other" category. Only one case, a transitional cell cancer, was correctly categorized.

This study did not attempt to establish the accuracy rate when all radiographic modalities are used since this has already been evaluated [6].

In our opinion transitional cell carcinomas of the kidney have a somewhat distinctive angiographic pattern which by itself is only moderately reliable and can be mimicked by other conditions.

ACKNOWLEDGMENTS

We thank Dr. Milton Elkin for helping to find some of the missing cases caused by Dr. Meng's unexpected passing. We also express our appreciation to Mrs. Olga Carr and Mrs. Gloria Cioffi for aid in locating much of the needed material and to Mrs. Marye Baylin for preparation of the manuscript.

ADDENDUM

Since submission of this paper, D. C. Levin et al. (Reticular neovascularity in malignant and inflammatory renal masses. *Radiology* 120:61–68, 1976) have also reported inability to differentiate tumor vascularity from inflammatory lesions when a "reticular neovascularity" is seen on arteriography.

REFERENCES

1. Boijsen E, Folin J: Angiography in carcinoma of the renal pelvis. *Acta Radiol* 56:81–93, 1961
2. Lagergren C, Ljungvist A: The arterial vasculature of renal pelvic carcinomas. *Acta Chir Scand* 130:321–330, 1965
3. Mitty HA, Baron MG, Feller M: Infiltrating carcinoma of the renal pelvis; angiographic features. *Radiology* 92:994–998, 1969
4. Rabinowitz JG, Kinkhabwala M, Himmelfarb E, Robinson T, Becker JA, Bosniak M, Madayag MM: Renal pelvic carcinoma, an angiographic re-evaluation. *Radiology* 102:551–554, 1972
5. Schapira HE, Mitty HA: Tumors of the renal pelvis: clinical review with emphasis on selective angiography. *J Urol* 106: 642–645, 1971
6. Haleem SA, Sprayregen S, Siegelman SS: Preoperative diagnosis of renal carcinoma. *J Urol* 108:695–697, 1972

Sarcoma of the Kidney: Angiographic Features

MASOOD GRANMAYEH,[1] SIDNEY WALLACE,[1] A. FRANK BARRETT,[2] RICHARD FISHER,[3] AND J. H. HESLEP[4]

Sarcomas of the kidney are highly malignant neoplasms. Abnormal vascularity can be detected in almost all types of sarcomas, but arteriovenous shunting, pooling of contrast material, and tumor staining are seldom present. Extension to renal vein and inferior vena cava may occur. While angiographic findings in our seven cases of renal sarcomas were nonspecific, this diagnosis should be considered in a relatively hypovascular neoplasm especially when the capsular arteries contribute considerably to the vascular supply. Nevertheless, statistically the most likely diagnosis of a hypovascular mass is renal cell carcinoma. Angiographic studies do not alter the management of the patient but merely suggest the diagnostic possibility of sarcoma. Angiographic diagnosis of different histologic types of sarcomas is not possible.

The different mesenchymal cells found in the kidney create the potential for various histologic types of sarcoma. Leiomyosarcomas, fibrosarcomas, and liposarcomas are the most frequent malignant renal neoplasms of mesenchymal origin. Rhabdomyosarcomas [1–3], primary osteosarcoma, chondrosarcomas [4–7], malignant neurilemoma [8], and hemangiopericytoma [1] have also been reported. Sarcomas of the kidney are rare, seen in only 0.1% of autopsies [9] and comprising 1.1% of all malignant renal tumors [1, 10, 11].

The presenting features include mass, pain, and hematuria. Pain may be a dull ache due to tumor size, necrosis within the tumor, or passage of a blood clot through the collecting system. Systemic symptoms such as fever, nausea, anemia, and weight loss are not infrequent.

Radiographic investigation has consisted of pyelographic demonstration of a mass with distortion and displacement of the pelvocalyceal system and kidney. We present the angiographic findings in seven patients with a variety of renal sarcomas.

Clinical Material

The series included seven cases from our four institutions. Clinical presentation, age distribution, and angiographic features are summarized in tables 1 and 2. The five females and two males ranged in age from 24–69 years. Three patients had aortography, bilateral selective renal arteriography, and inferior venacavography. The other three underwent aortography and selective renal angiography. In one case study was limited to abdominal aortography. This patient had a nephrectomy in another hospital without angiography and was referred for treatment of recurrent tumor. Intravenous pyelography was the initial examination in all patients.

Illustrative Case Reports

Case 1

M. O., a 69-year-old white female, was seen because of a 5 month history of left upper quadrant pain radiating to the back. She had also been somewhat anorexic with a 5.4 kg weight loss in the previous 3 months. She denied hematuria, frequency, and dysuria. On physical examination, a left upper quadrant mass was found. Laboratory findings were within normal limits.

Intravenous pyelography showed a large soft tissue mass occupying the upper pole of the left kidney. Abdominal aortography and selective left renal arteriography revealed a relatively hypovascular mass with clusters of increased vascularity supplied mainly by the renal artery with some parasitic vessels arising from the lumbar and adrenal arteries. Early arterial phase of selective left renal angiography showed vessels with smooth and irregular encasement as well as amputation. In the late arterial and capillary phase there were multiple areas of tumor staining and pooling of contrast. The zone of transition between tumor and normal kidney was sharp except in one area. No early venous filling was noted (fig. 1). Inferior venacavography was negative.

The surgical specimen obtained at left nephrectomy showed a normal adrenal gland embedded in the mass; the renal vein was patent. Tissue diagnosis was liposarcoma of the kidney.

Case 2

A. S., a 51-year-old white female, presented with intermittent fever, epigastric pain and lower abdominal cramping. The patient did not have hematuria or a palpable mass.

Intravenous pyelography revealed lateral displacement of the left kidney by a large mass. The pelvocalyceal system was dilated because of partial obstruction at the ureteropelvic junction. Abdominal aortography and selective left renal angiography demonstrated a relatively hypovascular tumor supplied by enlarged capsular and pelvic arteries. Selective left renal angiography showed abnormal stretched and tortuous vessels arising from the prominent capsular and pelvic arteries supplying a hypovascular tumor. Occasional arterial encasement was noted. Capillary and venous phases showed neither tumor staining nor pooling of contrast, and no early venous filling (fig. 2). No clear zone of transition between the tumor and normal kidney parenchyma was seen.

Left nephrectomy was performed and an encapsulated tumor arising from the renal capsule and surrounding the kidney was found. Histologic diagnosis was liposarcoma.

Case 3

L. H., a 64-year-old white female, developed gross hematuria

Received December 8, 1976; accepted after revision March 21, 1977.

[1] Department of Diagnostic Radiology, University of Texas System Cancer Center, M. D. Anderson Hospital and Tumor Institute, Houston, Texas 77030. Address reprint requests to M. Granmayeh.

[2] Department of Radiology, Heights Hospital, Houston, Texas 77008.

[3] Department of Radiology, Baylor College of Medicine, Ben Taub Hospital, Houston, Texas 77030.

[4] Department of Radiology, Spohn Hospital, Corpus Christi, Texas 78404.

Am J Roentgenol 129:107–112, July 1977

TABLE 1

Summary of Case Material

Case	Age and Sex	Diagnosis	Hematuria	Palpable Mass	Pain	Systemic Symptoms	Follow-up
M. O.	69, F	Liposarcoma	−	+	+	Anorexia, weight loss	Well 10 months after surgery
A. S.	51, F	Liposarcoma capsular	−	−	+	Intermittent fever	Well 6 years after surgery
J. W.	58, M	Liposarcoma	−	−	+	−	Well 9 months after surgery
L. H.	64, F	Leiomyosarcoma	+	−	+	−	Lost to follow-up after surgery
R. M.	39, M	Leiomyosarcoma*	...	...	...	...	Surgery twice 1 year apart; did not do well, lost to follow-up
B. K.	24, F	Botryoid sarcoma	+	−	−	Malaise, edema	Died immediately after surgery
P. Y.	58, F	Undifferentiated sarcoma	−	+	+	−	Surgery and chemotherapy; died after 8 months with metastatic disease

* Recurrent tumor with metastasis.

TABLE 2

Angiographic Findings

Case	Diagnosis	Tumor Staining	Pooling of Contrast	Encasement of Vessels	Amputation of Vessels	Early Venous Filling	Zone of Transition
M. O. (fig. 1)	Liposarcoma	+	+	+	+	−	±
A. S. (fig. 2)	Liposarcoma	−	−	+	−	−	−
J. W.	Liposarcoma	−	−	+	±	−	−
L. H. (fig. 3)	Leiomyosarcoma	−	−	±	−	−	−
R. M.	Leiomyosarcoma	−	−	+	−	−	−
B. K. (fig. 4)	Botryoid sarcoma	+	+	+	++	−	−
P. Y.	Undifferentiated sarcoma	+	+	+	−	−	−

accompanied by pain in the right flank and right upper quadrant with some frequency of micturition and low grade fever. On physical examination the right flank was tender; no mass was palpated. Laboratory findings were normal except for grossly bloody urine.

Cystoscopy showed a normal bladder and urethra, and intravenous pyelography suggested a mass in the upper pole of the right kidney. Renal angiography revealed a hypovascular mass in the upper pole of the right kidney. This tumor was supplied by prominent stretched inferior adrenal arteries as well as a few intrarenal arterial branches. A few arteries of irregular caliber were seen with no pooling of contrast material or tumor stain. No arteriovenous shunting was seen. The zone of transition was indistinct (fig. 3).

The patient underwent right nephrectomy and adrenalectomy. A lobulated circumscribed nonencapsulated firm mass was obtained which compressed but did not involve the adrenal gland. The tumor extended into the renal vein. Microscopically this was a malignant neoplasm with spindle-shaped cells, primarily muscular, and was considered to be an undifferentiated leiomyosarcoma.

Case 4

B. K., a 24-year-old white female, has recently delivered her third child at approximately 39 weeks gestation without complication. The postpartum course was complicated by persistent bilateral lower extremity edema of mild degree, generalized malaise, and vague lower abdominal discomfort. Because of recurrence of apparent hemorrhagic cystitis, further kidney evaluation was performed.

Intravenous pyelography demonstrsted a space-occupying lesion in the left kidney. Abdominal aortography and selective left renal arteriography revealed a moderately vascular mass with abnormal vessels, pooling of contrast material, and tumor

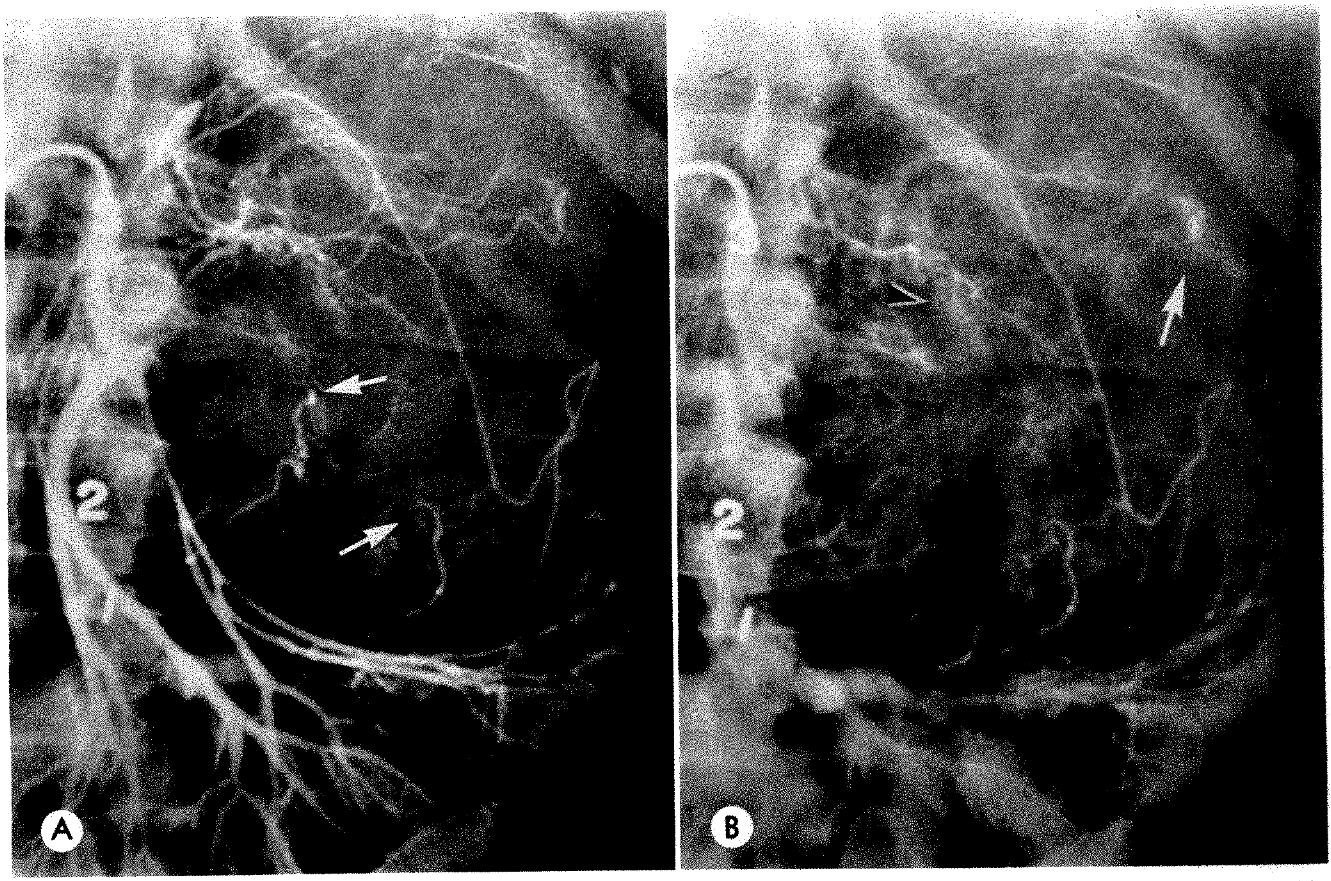

Fig. 1.—Case 1, liposarcoma. *A*, Left renal arteriography, early arterial phase, showing tortuous neoplastic vessels with marginal irregularity arising from intrarenal and adrenal arteries within relatively hypovascular tumor. Note encasement and amputation of vessels (*arrows*). *B*, Late arterial phase showing scattered areas of tumor staining (*arrowhead*) and pooling (*arrow*) of contrast material. No arteriovenous shunting is seen. Kidney is displaced downward with clockwise rotation.

staining. Neoplastic vessels with irregular margins were present and in few areas formed clusters of hypervascularity. Some arteries were encased and amputated. No arteriovenous shunting was demonstrated (fig. 4). Findings suggested renal vein occlusion.

Exploratory laparotomy and biopsy revealed a sarcoma botryoides of the kidney. The postoperative course was complicated by fever; the patient's condition gradually deteriorated and she expired 9 days after surgery. Autopsy revealed direct extension of tumor into both renal veins, the inferior vena cava, and right atrium of the heart.

Discussion

Liposarcoma

In 1958 William and Savage [12] reviewed 29 previously reported cases of liposarcoma of the kidney and in 1973 Lien [13] added two more cases. It is uncertain whether liposarcoma arises from a preexisting benign tumor, a lipoma or angiomyolipoma, or from undifferentiated mesenchymal cells. Lipomas and angiomyolipoma rarely undergo malignant change, and liposarcomas often originate in areas with no fatty tissue such as the renal parenchyma and capsule. This favors the hypothesis that this neoplasm arises from undifferentiated mesenchymal cells [9, 13]. In spite of the renal capsule being composed of smooth muscle and fibrous tissue, all five cases of renal liposarcoma reported by Farrow et al [1] were capsular in orgin.

Angiomyolipomas are frequently multiple and bilateral and found in 50–80% of patients with tuberous sclerosis. The solitary type of angiomyolipoma is more common in middle-aged females without stigmata of tuberous sclerosis. At times the histologic differentiation between angiomyolipoma and liposarcoma is difficult [9, 14]. It has been stated [14–16] that angiomyolipomas independent of tuberous sclerosis do not undergo malignant change even when immature and invasive cells are seen. Ten of 29 cases of renal liposarcoma reviewed by William and Savage [12] had tuberous sclerosis which may indicate that these were angiomyolipomas rather than liposarcomas. None were associated with metastasis or recurrence [1].

Angiographic studies of our three cases with liposarcoma demonstrated relatively hypovascular tumors with subtle and occasional neovascularity, tumor encasement, and amputation. Only in case 1 was pooling of contrast material and tumor staining noted. In one of two cases of liposarcoma reported by Lien [13], angiography was performed but not described in detail.

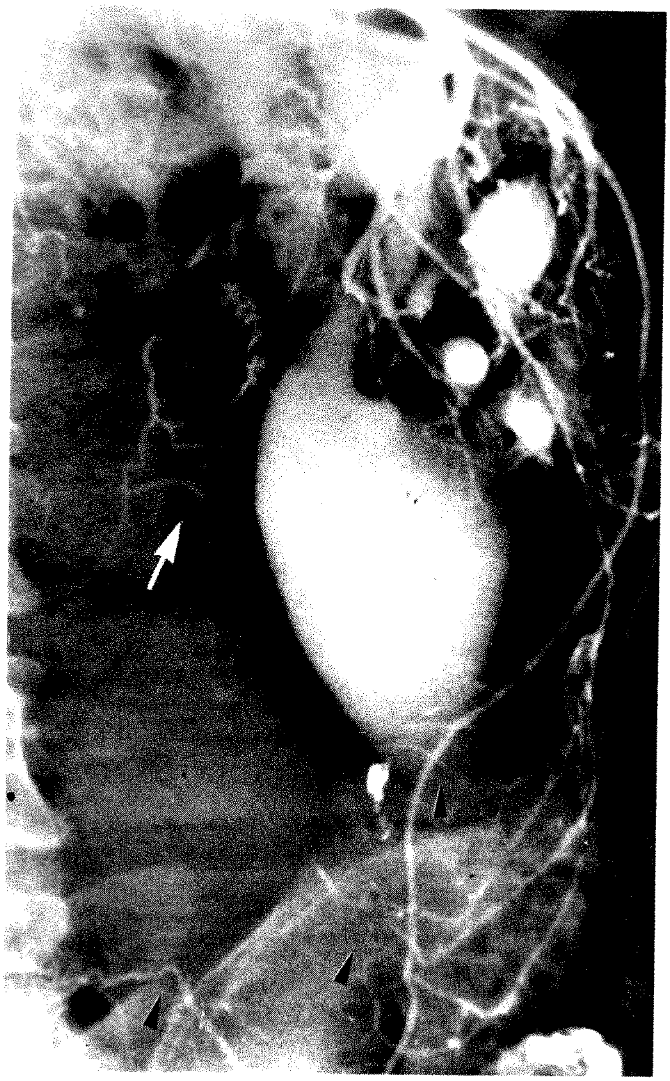

Fig. 2.—Case 2, liposarcoma. Arterial phase of left renal arteriogram showing prominent capsular and pelvic vessels in hypovascular tumor. Fine tortuous irregular vessels arise from prominent capsular (*arrowheads*) and pelvic vessels (*arrow*).

The capsular origin of the liposarcoma in our case 2 was suggested by the enlarged capsular arteries supplying a mass which encircled relatively normal renal parenchyma producing a slight hydronephrosis by partially obstructing the ureteropelvic junction. In contrast, angiomyolipomas are usually hypervascular tumors with small aneurysms, sunburst appearance, and without arteriovenous shunting. Evans and Bosniak [17] described one patient with bilateral malignant angiolipomas which to us were angiographically indistinguishable from the benign variety [17].

Leiomyosarcomas

This neoplasm arises from smooth muscle of the renal capsule, vessels, and pelvocalyceal system. Benign myomata of the kidney are common findings at necropsy, often subcapsular in location. Leiomyosarcomas are the most common sarcomas of the kidney and usually occur after age 40 [18]. However, cases in the neonatal period have been reported [19, 20]. Local recurrence is frequent, particularly if the tumor is not well circumscribed and has extended beyond the kidney. Lungs, liver, and regional lymph nodes are sites of metastasis [9–11].

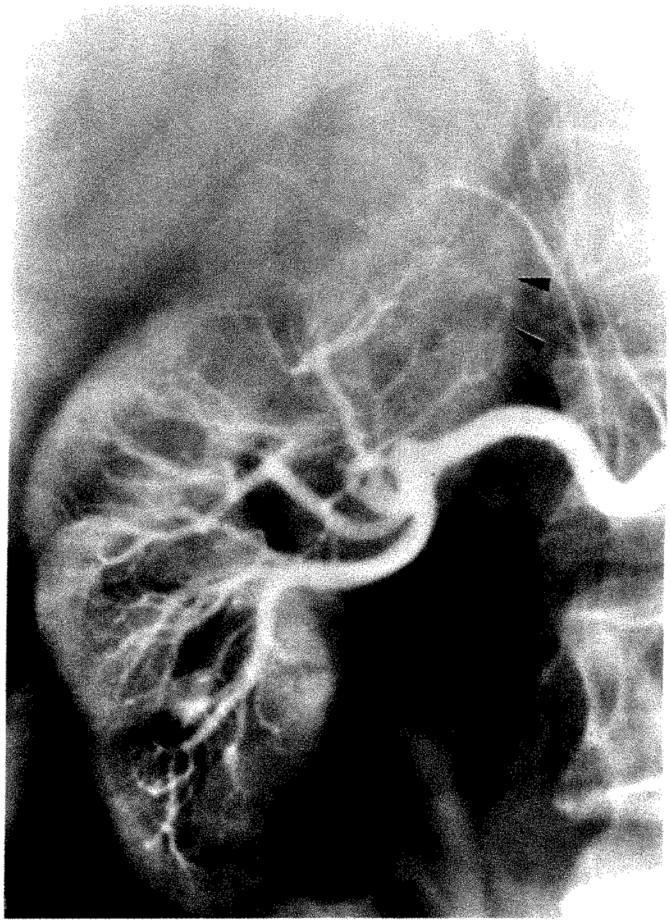

Fig. 3.—Case 3, leiomyosarcoma. Right renal arteriogram showing hypovascular tumor and prominent inferior adrenal arteries. Some vessels are tortuous with irregular margins (*arrowheads*).

Ziter's case of renal leiomyosarcomas [21] exhibited irregular tortuous tumor vessels without pooling of contrast material or arteriovenous shunting. In addition the inferior vena cava was invaded. Angiographic findings in our case 3 are similar to those described by Ziter [21] with sparse neovasculasity. In another of our cases, a recurrent leiomyosarcoma in the renal bed (R. M., tables 1 and 2) numerous abnormal vessels were opacified and encased vessels were present.

Sarcoma Botryoides

This form of rhabdomyosarcoma is a rare tumor and was found in only one of 26 cases reviewed by Farrow et al [1]. This neoplasm may occur in unusual locations where striated muscle is not a normal component, such as the liver, biliary tract, uterus, bronchus, and mediastinum. Because the rhabdomyoblast is frequently found in Wilm's tumor, some feel that a rhabdomyosarcoma is

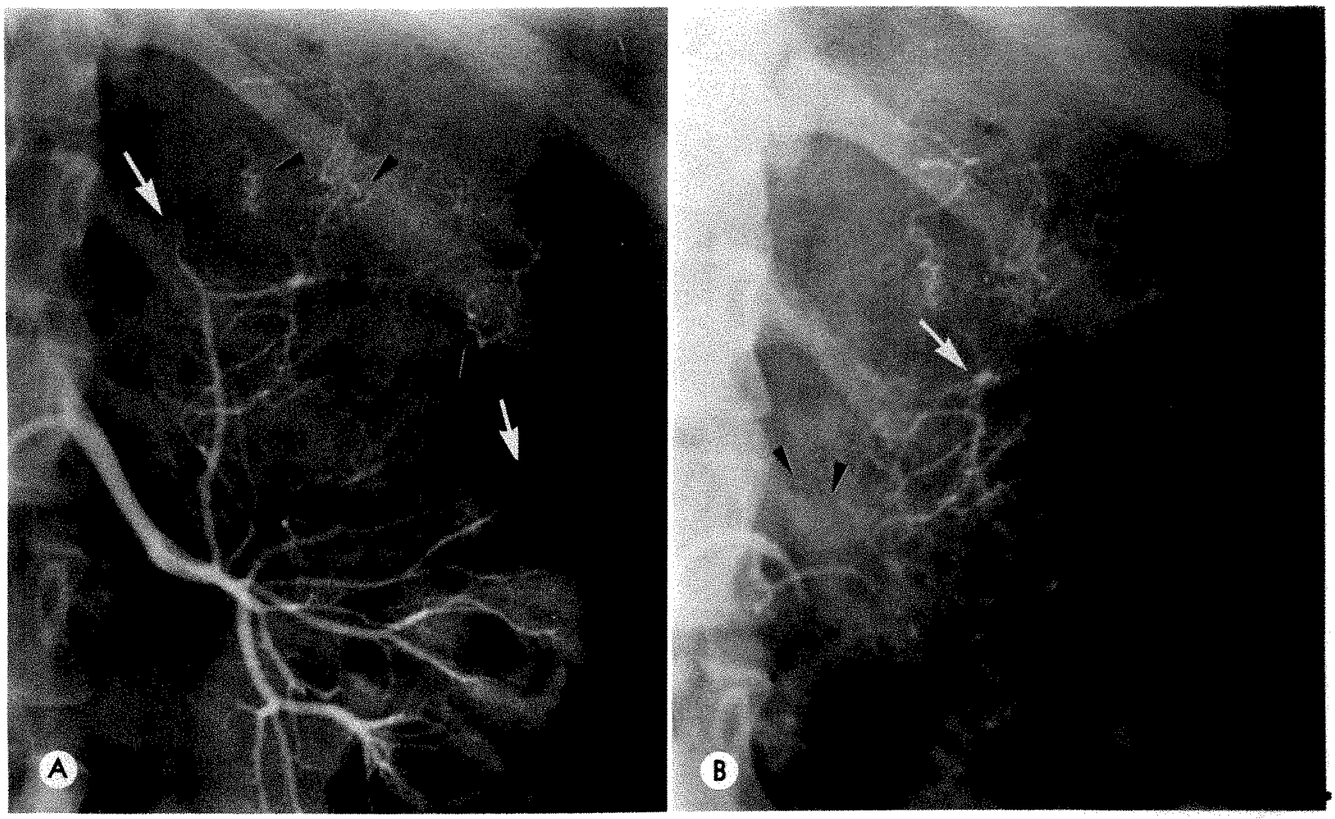

Fig. 4.—Case 4, botryoid sarcoma. *A*, Left renal arteriogram, early arterial phase, showing neoplastic vessels within moderately vascular tumor, clusters of abnormal vessels (*arrowheads*), amputation, and encasement (*arrows*). *B*, Late arterial phase showing delayed circulation with persistent opacification of tumor vessels. Note areas of staining (*arrowheads*) and pooling (*arrow*).

actually a nephroblastoma in which striated muscle cells are dominant [3, 14]. The histogenesis of these tumors in areas devoid of striated muscle is probably from the differentiation of mesoblastic cells [2, 9]. Sarcoma botryoides is a highly malignant neoplasm which carries a poor prognosis as illustrated by case 4.

Angiographic features include moderate neovascularity with arterial encasement, pooling of contrast material, and tumor stain (fig. 4). No other example of the angiographic findings of rhabdomyosarcoma of the kidney, or sarcoma botryoides, could be found in the literature.

Nonsarcomatous Renal Masses

The angiographic picture of a hypovascular mass with occasional vessels of irregular caliber and neovascularity creates the differential diagnosis which includes renal carcinoma, carcinoma of the renal pelvis, metastatic carcinoma to the kidney, renal lymphoma, and masses of infectious origin (tuberculosis, xanthogranulomatous pyelonephritis, and renal abscess).

Renal Carcinoma. Of all malignant renal tumors, 83% are renal carcinomas. According to Watson [22], 16% are hypovascular and 6% avascular. Therefore, renal carcinoma is the most common etiology for a neoplasm with a hypovascular angiographic pattern. When located in the periphery of the kidney, capsular arteries may enlarge but the intrarenal branches usually are the major supplying vessels. However, a hypovascular neoplasm almost entirely nourished by capsular vessels should suggest a capsular sarcoma.

Carcinoma of the renal pelvis. Epithelial neoplasms of the renal pelvis and collecting system with extension into the renal parenchyma are usually infiltrative. Abnormal vessels are few and usually demonstrate encasement of intrarenal arteries and veins, at times resulting in a picture of infarction. This angiographic pattern may be indistinguishable from renal sarcoma.

Metastatic carcinoma to kidney. Angiographic features mimic the pattern seen in the primary neoplasm. Metastases from squamous cell carcinoma and transitional cell carcinoma are likely to be hypovascular. Carcinoma of the lung frequently metastasizes to the kidney and would be an important diagnostic consideration.

Renal lymphoma. Involvement of the kidney is usually a manifestation of a generalized lymphoma. Renal lymphoma may be local but more frequently is diffuse and bilateral. Angiographic study of these infiltrative lesions demonstrates a sparse feathery pattern of abnormal vessels with encasement, amputation, and lack of arborization.

Masses of infectious origin. Subacute and chronic renal absesses, tumefactive xanthogranulomatous pyelonephritis, and tuberculoma all may appear as masses in the kidney. A poor or nonfunctioning kidney with renal stones

(70%) and a history of chronic genitourinary tract infection suggest xanthogranulomatous pyelonephritis. Angiographically these masses show some increased vascularity with abnormal vessels and staining, indistinguishable from sarcomas. Preoperative diagnosis is extremely difficult.

REFERENCES

1. Farrow MG, Harrison EG, Utz DC, ReMine WH: Sarcomas and sarcomatoid and mixed malignant tumors of the kidney in adults. I. *Cancer* 22:545–550, 1968
2. Seabury JC: Renal rhabdomyosarcoma. *JAMA* 201:1043–1044, 1967
3. Harbaugh JT: Botryoid sarcoma of the renal pelvis. A case report. *J Urol* 100:424–426, 1968
4. Chamber A, Carson R: Primary osteogenic sarcoma of the kidney. *Br J Urol* 48:316–317, 1975
5. Soto PJ, Rader ES, Martin J, Gregowicz A: Osteogenic sarcoma of the kidney. Report of a case. *J Urol* 94:532–535, 1965
6. Johnson LA, Ancona VC, Johnson T, Pineda NB: Primary osteogenic sarcoma of the kidney. *J Urol* 104:528–531, 1970
7. Gallagher JC, Winslow DJ, Grossman A: Coexistent chondrosarcoma and transitional cell carcinoma in kidney. *Urology* 3:473–477, 1974
8. Fein RL, Hamm FC: Malignant schwannoma of renal pelvis. A review of the literature and a case report. *J Urol* 94: 356–361, 1968
9. Bennington G, Beckwith J: *Atlas of Tumor Pathology,* section 2, fascicle 12. Washington, D.C., Armed Forces Institute of Pathology, 1975
10. Jenkins JD, Chir M, Anderson CK, Williams RE: Renal sarcoma. *Br J Urol* 43:263–267, 1971
11. Tolia BM, Hajdu SI, Whitmore WF: Leiomyosarcoma of the renal pelvis. *J Urol* 109:974–976, 1973
12. William JP, Savage PT: Liposarcoma of kidney. *Br J Surg* 64:225, 1958
13. Lien WM: Liposarcoma of the kidney. *Postgrad Med J* 49:660–663, 1973
14. Colabawalla BN: Renal hamartoma. *Br J Urol* 44:112–116, 1972
15. Klapproth HJ: Renal angiomyolipoma. *Arch Pathol* 67: 400–411, 1972
16. Perau ML, Gray PT: Mesenchymal hamartomas of kidney. *J Urol* 83:240–261, 1960
17. Evans JA, Bosniak MA: The kidney, in *An Atlas of Tumor Radiology,* Chicago, Year Book Medical Publishers, 1971
18. Gupta OP, Dube MK: Rare primary renal sarcoma. *Br J Urol* 43:546–551, 1971

10. Addison NV, Perch B: Smooth muscle tumors of the kidney. Report of two cases. *Br J Urol* 38:382–387, 1966

20. Weissman MJ, Gaeta JF, Albert DJ: Childhood urogenital sarcoma. *J Surg Oncol* 4:107–116, 1972
21. Ziter FM: Renal leiomyosarcoma. A case report with angiographic finding. *J Urol* 105:776–778, 1971
22. Watson RC: Arteriography in the diagnosis of renal carcinoma. Review of 100 cases. *Radiology* 91:888–897, 1968

Ultrasonic Evaluation of the Obstructed Duplex Kidney

V. J. MASCATELLO,[1, 2] E. H. SMITH,[1] G. F. CARRERA,[1] M. BERGER,[1] AND R. L. TEELE[3]

The problem of a duplex collecting system associated with an obstructed ectopic ureter or ureterocele is common in pediatric urology. Four such patients were studied by gray scale ultrasound which was useful in demonstrating the dilated upper pole collecting system as well as an ectopic ureter and a ureterocele. Although the diagnosis of a nonfunctioning upper pole unit in a duplex kidney is usually suggested by the urogram, ultrasound provides a noninvasive means of confirmation which is independant of function. Further, ultrasound-guided puncture with antegrade pyelography demonstrates the course of the ectopic ureter, thus providing a more complete preoperative evaluation.

Ultrasound has been well established as a reliable method of investigation of the urinary tract [1–3]. Several authors have described the use of renal ultrasonography in children [4–16]. Although the problem of an obstructed nonfunctioning unit in a duplex kidney is a common one in children, only one such patient has been reported [11]. We describe four patients with hydroureteronephrosis of the upper collecting system in a duplex kidney. The role of ultrasound in the evaluation of an ectopic ureter is also discussed.

Materials and Methods

Four patients were studied with commercially available gray scale ultrasound units (Picker Echoview VI or Rohe Rohnar). Serial ultrasonic scans were obtained at intervals of 0.5–1 cm in the longitudinal and transverse planes. Standard 2.25 or 5 MHz 10 cm internally focused transducers were used. Mineral oil was used as an acoustical coupling agent. The two infants studied were well sedated and immobilized prior to examination.

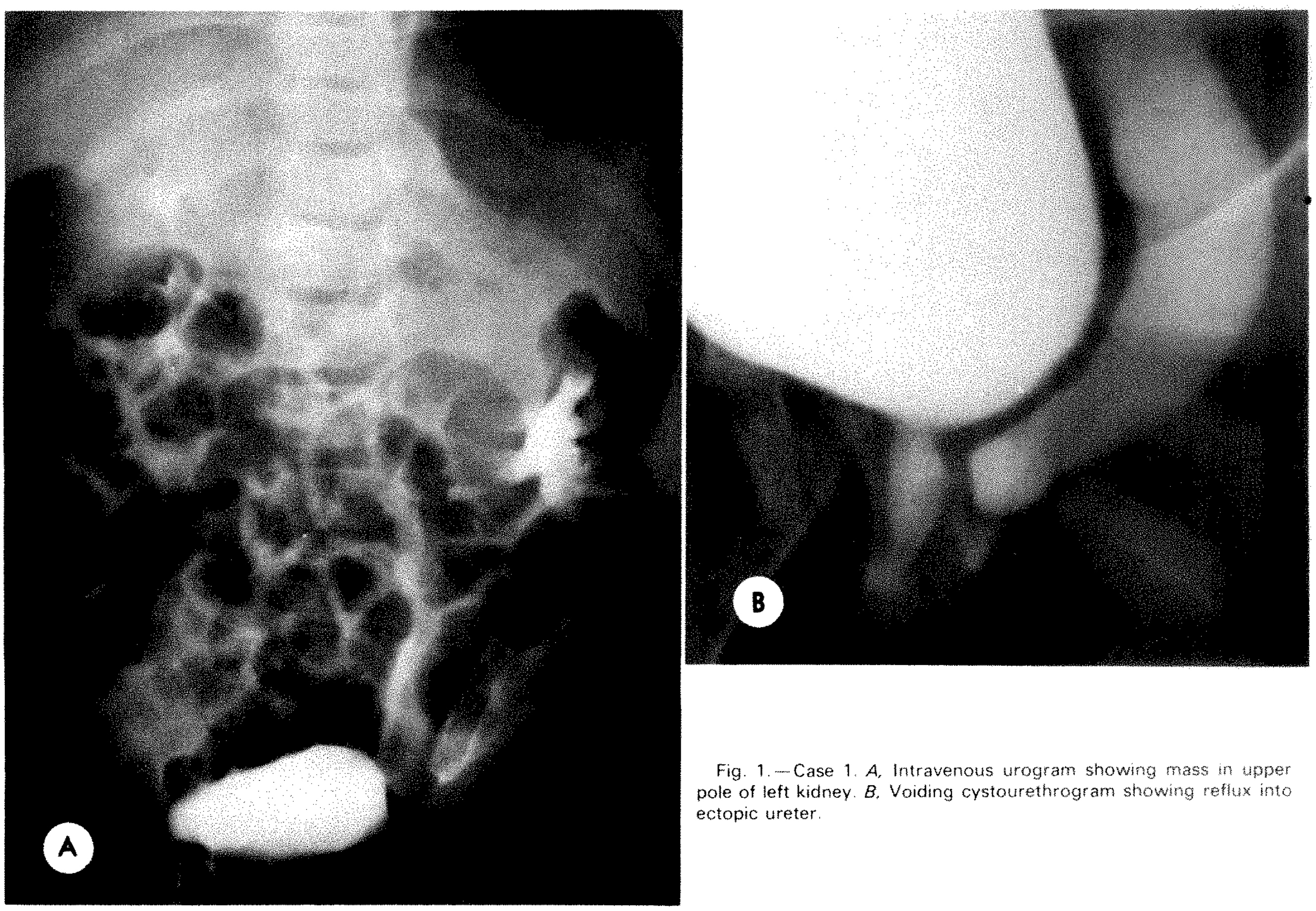

Fig. 1.—Case 1. *A*, Intravenous urogram showing mass in upper pole of left kidney. *B*, Voiding cystourethrogram showing reflux into ectopic ureter.

Received November 9, 1976; accepted after revision April 4, 1977.
This work was supported in part by U. S. Public Health Service grant GM18674.

[1] Department of Radiology, Harvard Medical School and Peter Bent Brigham Hospital, Boston, Massachusetts 02115.

[2] Present address: Department of Radiology, Georgetown University Medical Center, 3800 Reservoir Road, N.W., Washington, D.C. 20007. Address reprint requests to V. J. Mascatello.

[3] Department of Radiology, Children's Hospital Medical Center, 300 Longwood Avenue, Boston, Massachusetts 02115.

Am J Roentgenol **129:113–120, July 1977**

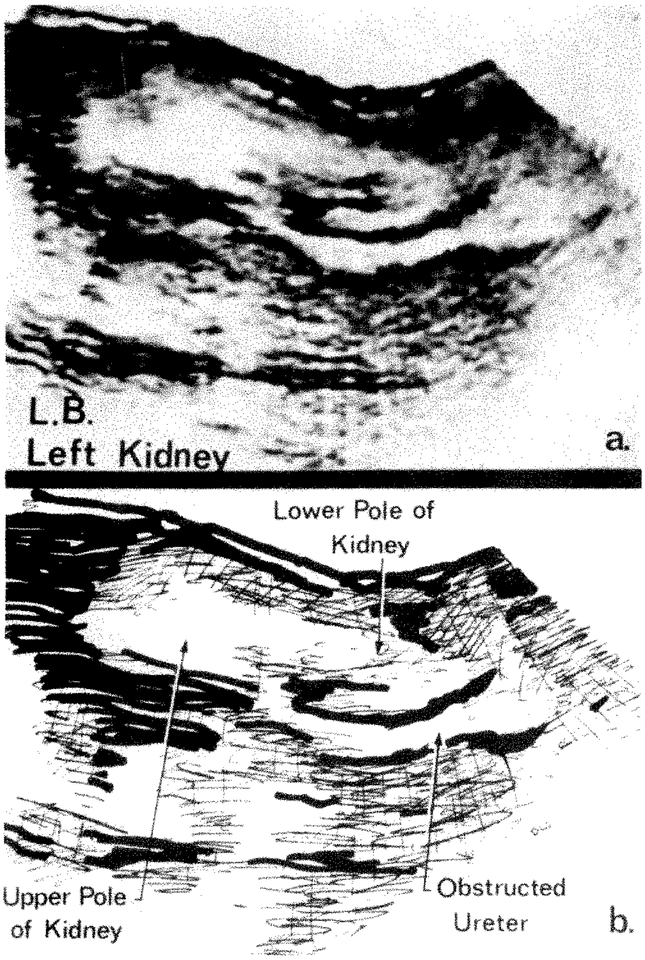

Fig. 2.—Case 1. Longitudinal ultrasound scan with patient prone showing functioning lower pole of kidney and nonfunctioning upper pole unit with dilated obstructed ureter.

Gray scale ultrasound was used to depict the abnormality, while A-mode was added to distinguish between solid and cystic masses.

Case Reports

Case 1

An 18-week-old girl was brought to Children's Hospital Medical Center because of fever and vomitting. Urinalysis was normal; however, urine culture grew more than 100,000 colonies of *Pseudomonas aeruginosa.* Intravenous urography revealed a normal right kidney and a mass in the upper pole of the left kidney (fig. 1*A*). Ultrasonic examination demonstrated normal calyceal echoes in the lower pole of the left kidney and an anechoic mass replacing the upper pole. This mass was continuous with a dilated renal pelvis and ureter (fig. 2). Since the lower pole was normal, the diagnosis of duplication of the renal collecting system with obstruction of the upper pole unit was made.

A voiding cystourethrogram (fig. 1*B*) demonstrated minimal reflux into the upper pole ureter which was obstructed because of ectopic insertion into the internal sphincter of the bladder. The preoperative findings were confirmed at surgery.

Comment. The demonstration of a anechoic mass replacing the upper pole of the kidney in a child should strongly suggest a hydronephrotic collecting system in a duplex kidney. The diagnosis of simple cyst should be made only by exclusion because of its rarity in the pediatric population. The main diagnostic consideration is Wilms's tumor. A careful ultrasonic examination will usually demonstrate internal echoes in this tumor, distinguishing it from localized hydronephrosis. The demonstration of a dilated ureter identifies the site of obstruction as below the ureteropelvic junction.

Case 2

A 14-month-old boy was referred to Children's Hospital Medical Center because of increasing abdominal girth. Physical examination was unremarkable except for an enlarged nontender abdomen. Routine laboratory determinations were normal. Intravenous urography demonstrated severe bilateral hydroureteronephrosis (fig. 3*A*). Voiding cystourethrography and barium enema revealed a mass between the bladder and the rectum (fig. 3*B*). Ultrasonic examination showed a huge mass with multiple septae (fig. 4). These findings, in conjunction with the urogram, were felt to represent an obstructed ectopic ureter in a duplex kidney.

Puncture of the mass was performed through the anterior abdominal wall under ultrasonic guidance; urine was aspirated, contrast injected, and radiographs obtained (fig. 3*C*). The antegrade pyelogram confirmed the nature of the mass and the course of the ureter. At surgery the distal ureter was identifed as an atretic cord posterior to the bladder. Intravenous urography several weeks after the heminephrectomy and subtotal ureterectomy demonstrated regression of the bilateral hydronephrosis.

Comment. More than 50% of abdominal masses in infants are of renal origin [17]. In this child the dilated ectopic ureter acted as a mass which compressed both of the normal ureters.

Case 3

A 4-year-old girl was being treated at Children's Hospital Medical Center with antibiotics for persistent urinary tract infections. Physical examination and routine laboratory determinations were normal. Intravenous urography revealed hypertrophy of the right kidney and pyelonephritic scarring of the left kidney (fig. 5*A*). In addition, there was a mass within the left side of the bladder. Voiding cystourethrography revealed the ureterocele as well as massive reflux into the ureter and collecting system draining the lower pole of the left kidney (figs. 5*B* and 5*C*). Ultrasound clearly demonstrated the ureterocele as a cystic mass (fig. 6). Renal scintigraphy demonstrated that the left kidney was contributing only 5% of the total renal function. At surgery it was found that the parenchyma drained by the normally inserting ureter was destroyed by reflux and infection. Since there was little function remaining, a total nephrectomy was performed rather than a heminephrectomy.

Comment. Since at least 75% of ureteroceles found in children are associated with a duplex kidney [18–24], the urogram should be carefully searched for signs of a duplex kidney. Ultrasonic examination should be obtained if the upper margin of the kidney cannot be identified with certainty at urography.

Case 4

A 27-year-old woman was seen at Peter Bent Brigham Hospital complaining of right flank pain. Her only previous episode of pyelonephritis was at age 14. Physical examination was normal; however, she had a white blood cell count of 14,800 and pyuria.

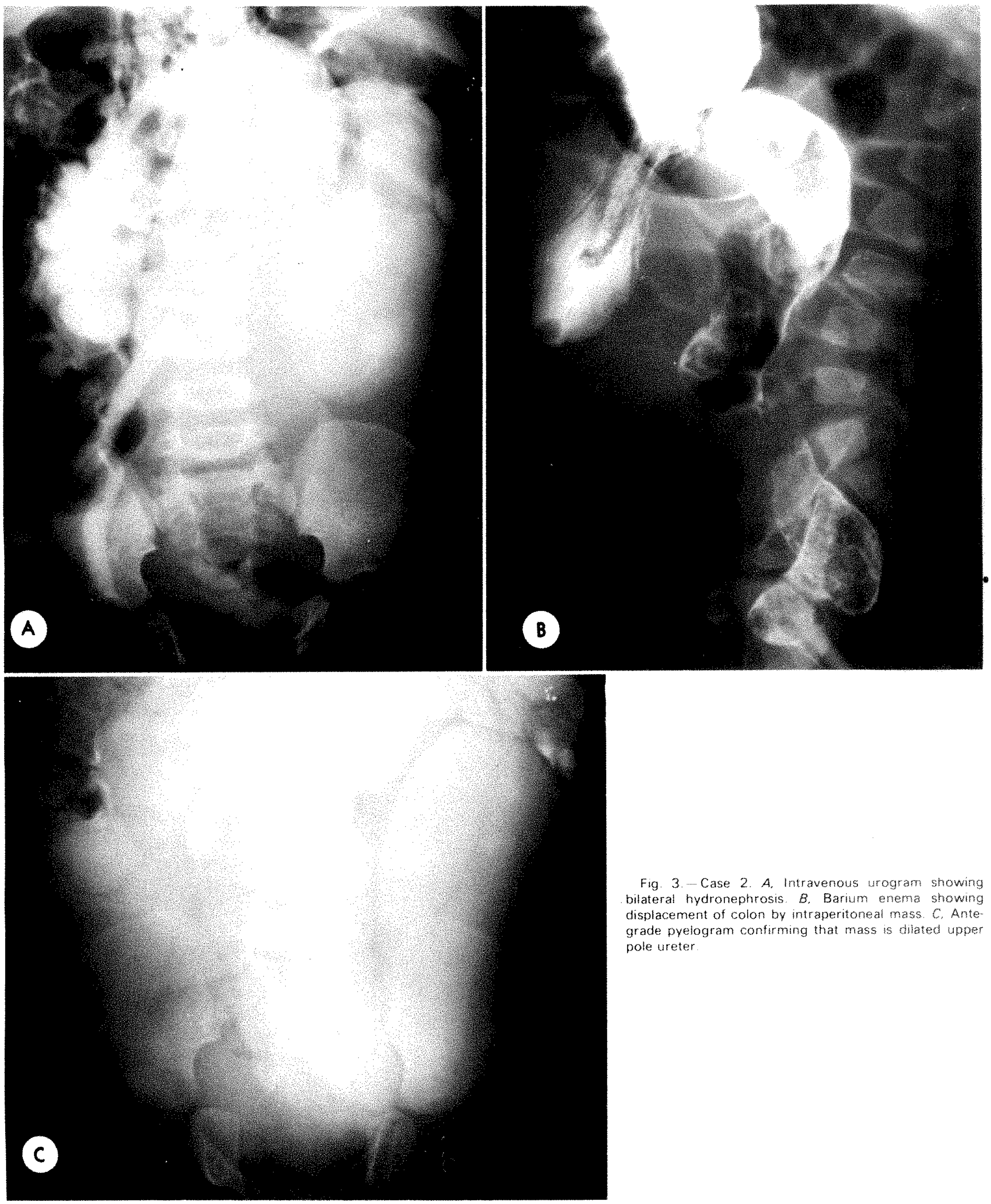

Fig. 3.—Case 2. *A*, Intravenous urogram showing bilateral hydronephrosis. *B*, Barium enema showing displacement of colon by intraperitoneal mass. *C*, Antegrade pyelogram confirming that mass is dilated upper pole ureter.

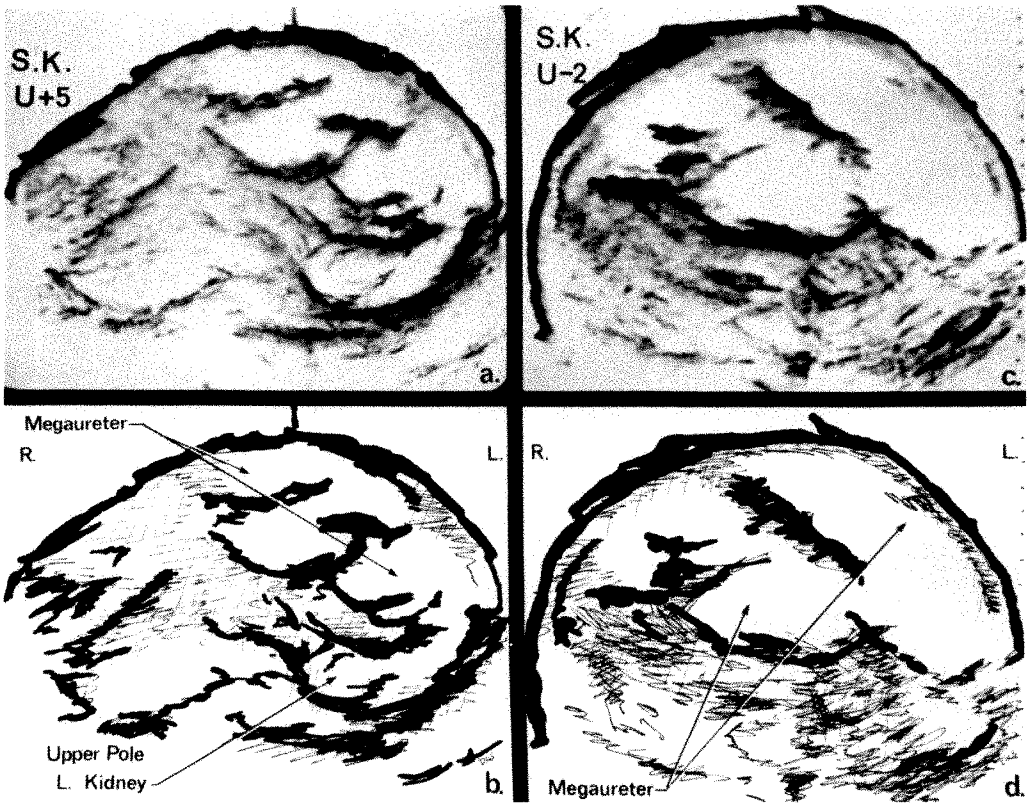

Fig. 4.—Case 2. Transverse ultrasound scans with patient supine showing large multiseptated mass in abdomen.

Intravenous urography demonstrated a normal left kidney (fig. 7*B*). A 4–5 cm mass was recognized in the upper pole of the right kidney. An intravenous urogram 18 months prior to this admission was normal, even in retrospect (fig. 7*A*). A voiding cystourethrogram was normal. Angiography demonstrated a thick-walled avascular mass in the upper pole of the right kidney.

Ultrasonic examination revealed normal calyceal echoes within the lower pole of the right kidney; however, the upper pole was replaced by an anechoic mass (fig. 8). These ultrasonic findings in conjunction with the radiographs suggested the possibility of an obstructed ectopic ureter. The diagnosis was confirmed at surgery, at which time radiographs were obtained following injection of contrast into the ectopic ureter (fig. 7*C*). The exact site of insertion of the ectopic ureter was not determined. It is unclear why the upper pole unit, which was not identified on the previous intravenous urogram, had become so dilated in the intervening 18 months.

Discussion

Duplication of the ureter is the most common major anomaly of the genitourinary system, with an incidence of 1.7% of all autopsies and 2.7%–4.2% of reported urographic series [21–23]. This apparent discrepancy may be explained by the increased morbidity associated with the duplex kidney.

The two ureters of a duplex kidney develop from separate ureteric buds which have grown from a single Wolffian duct [21]. The ureter draining the lower pole enters the bladder at the trigone; the ureter draining the upper pole enters the bladder below this point (fig. 9*A*). Occasionally the upper pole ureter ends ectopically, outside the bladder. In males the ureter ends proximal to the external urinary sphincter, in the vesical neck, prostatic urethra, seminal vesicle, vas deferens, or ejaculatory duct. Therefore, urinary incontinence is not a problem in males. An ectopic ureter is much more common in females, in whom it usually drains into the vesical neck or beyond the sphincter into the urethra, vagina, or uterus (fig. 9*B*). Thus urinary dribbling is a frequent complaint in females with this condition [21].

The upper pole ureter frequently ends in the internal sphincter, as in case 1 (fig. 9*C*), or is associated with a ureterocele, as in case 3 (fig. 9*D*). In either instance the result is usually hydroureteronephrosis of the upper pole system. The renal cortex of the upper pole in these patients is usually a functionless shell of dysplastic tissue [22]. The intravenous urogram is diagnostic in only 50% of the cases because of inadequate contrast excretion by the upper pole [23]. The urogram usually contains only indirect signs suggesting the presence of an obstructed upper pole ureter [21]. These include inferolateral displacement of the lower pole collecting system, poor definition of the upper pole cortex, and tortuosity of the ureter draining the lower pole. Because ultrasound provides a method of imaging the entire duplex kidney (both the functioning and nonfunctioning units), it can exclude extrarenal causes of a displaced collecting system (i.e., neublastoma or adrenal hemorrhage). The demonstration of a duplex kidney in the opposite kidney at ultrasonic examination is a helpful clue to the diagnosis of an obstructed upper pole

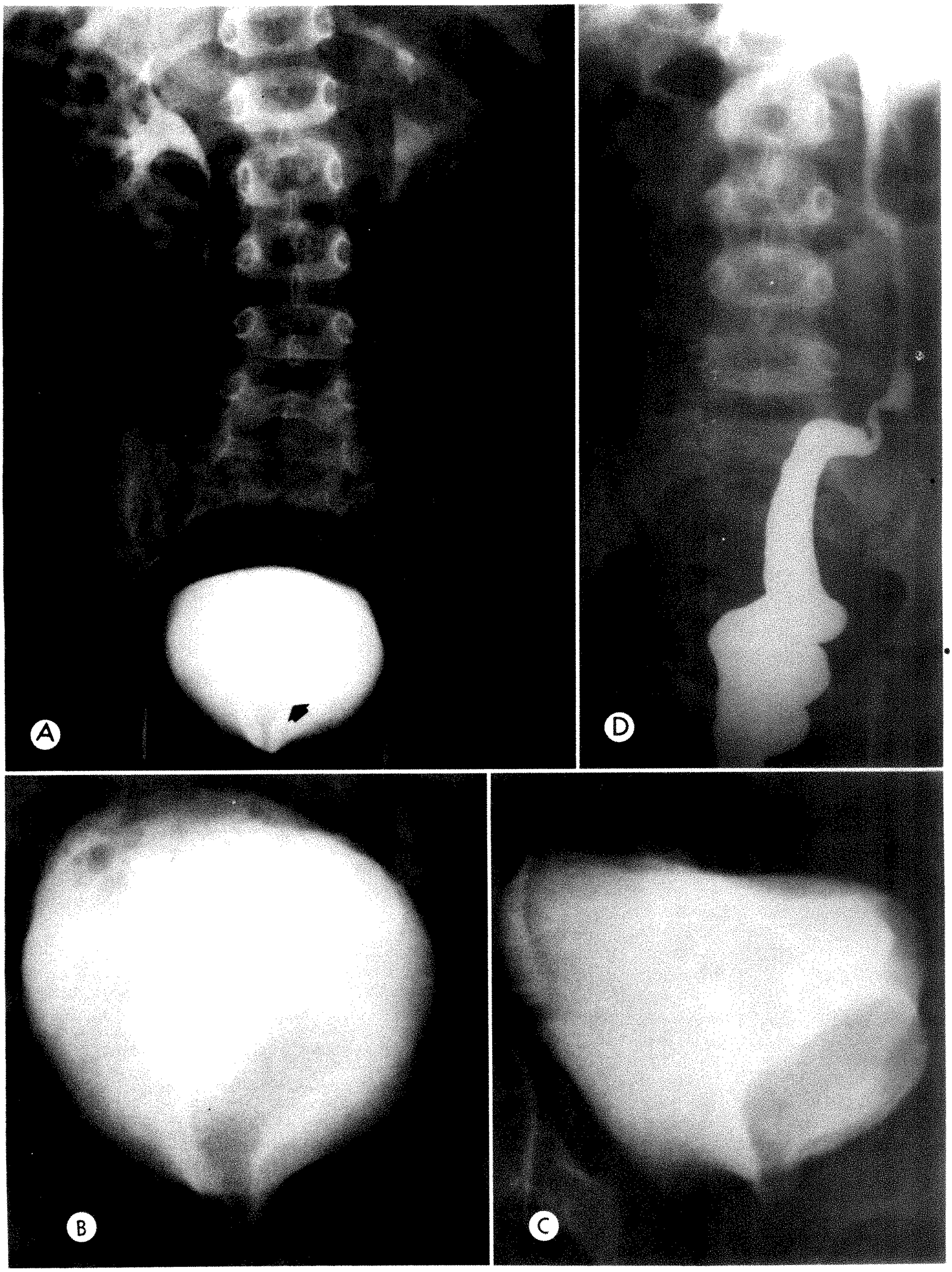

Fig. 5.—Case 3. *A*, Intravenous urogram showing scarring of left kidney and hypertrophy of right kidney. Ureterocele barely visible (*arrow*). *B and C*, Voiding cystourethrograms better showing ureterocele, as well as reflux into lower pole ureter. *D*, Intraoperative film after injection of ureterocele showing course of upper pole ureter.

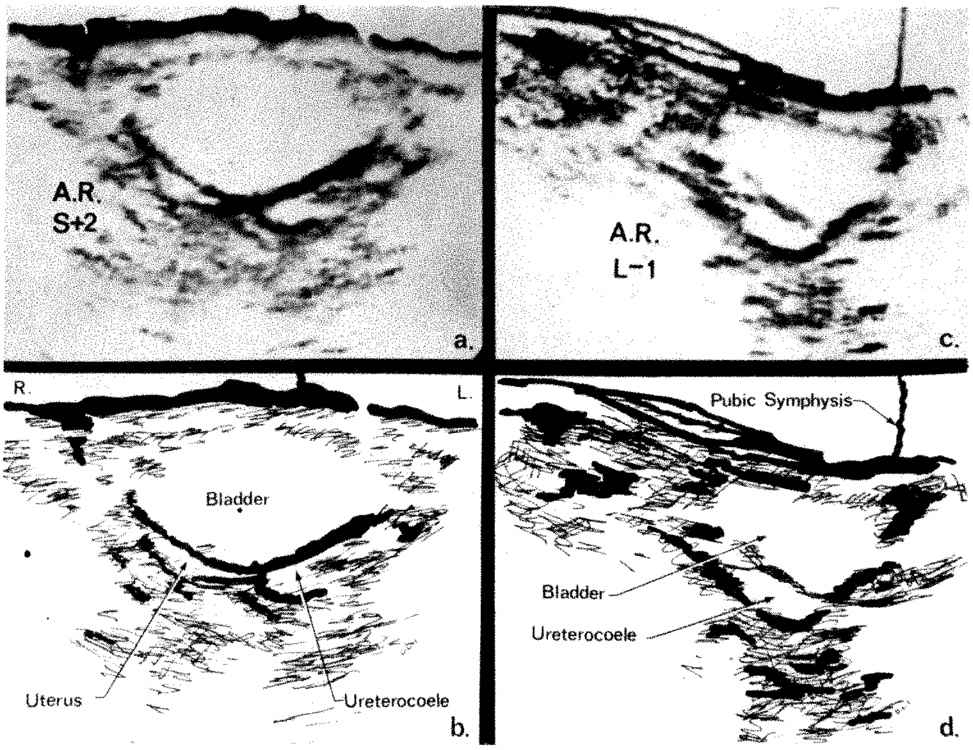

Fig. 6.—Case 3. Ultrasound scans in two projections clearly showing ureterocele.

collecting system, since the duplication is frequently bilateral.

A ureterocele is a cystic dilation of the submucosal segment of the intravesical ureter. In children most ureteroceles are congenital and are associated with a duplex kidney [18–25]. Virtually all of these occur in the ureter draining the upper pole. Significant dilation of the upper pole collecting system and ureter occurs in 85% of these ureteroceles because of a stenotic orifice [23]. Although the ureterocele is usually obvious at urography, ultrasound may help in the occasional difficult case by demonstrating the cystic nature of the ureterocele. Ultrasound clearly identified the ureterocele within the inferior wall of the bladder in case 3. The presence of a cystic mass adjacent to the bladder at ultrasonic examination is nonspecific: the differential diagnosis includes ovarian cyst, bladder diverticulum, hydrosalpinx, and ureterocele.

Antegrade pyelography following puncture of a dilated renal pelvis has been previously described [26]. This method should prove extremely useful in those cases of obstructed ectopic ureter not associated with ureterocele. In these patients the insertion of the ureter can be impossible to ascertain by conventional methods.

Serial radiographs in two projections following the injection of contrast will usually identify the distal end of the ureter. This anatomic information is extremely helpful at surgery. Ultrasound provides a safe effective method which aids in puncture. We used ultrasonically guided puncture and antegrade pyelography successfully in one patient (case 2).

Conclusions

The most common cause of an upper pole renal mass in children is an obstructed nonfunctioning upper pole collecting system in a duplex kidney. Ultrasonic examination can be diagnostic in these individuals since it provides an imaging method independant of renal function. The longitudinal sections are particularly valuable, since they depict on a single section the localized hydronephrosis as well as the normal lower pole calyceal echo pattern. The identification of an upper pole cystic mass which lacks the typical configuration of a simple cyst should raise the question of an obstructed ectopic ureter.

REFERENCES

1. Sanders RC, Bearman S: B-scan ultrasound in the diagnosis of hydronephrosis. *Radiology* 108:375–382, 1973
2. King DS: Renal ultrasonography. *Radiology* 105:633–640, 1972
3. Kyle RF, Deane RF, Morley P, Barnett E: Ultrasonography of the urinary tract. *Br J Urol* 43:709–717, 1971
4. Bearman S, Sanders, RC, Oh KS: B-scan ultrasound in the evaluation of pediatric abdominal masses. *Radiology* 108: 111–117, 1973
5. Hash E: Ultrasound in the investigation of disease of the kidney and the urinary tract in children. *Acta Paediatr Scand* 63:42–48, 1974
6. Von Micsky L, Radkowski MA, Hecker J, Finby N: Optimal diagnosis of renal masses in children by combining and correlating diagnostic features of sonography and radiography. *Am J Roentgenol* 120:438–447, 1974
7. Walls WJ, Roberts FF, Templeton AW: B-scan diagnostic ultrasound in the pediatric patient. *Am J Roentgenol* 120: 431–437, 1974

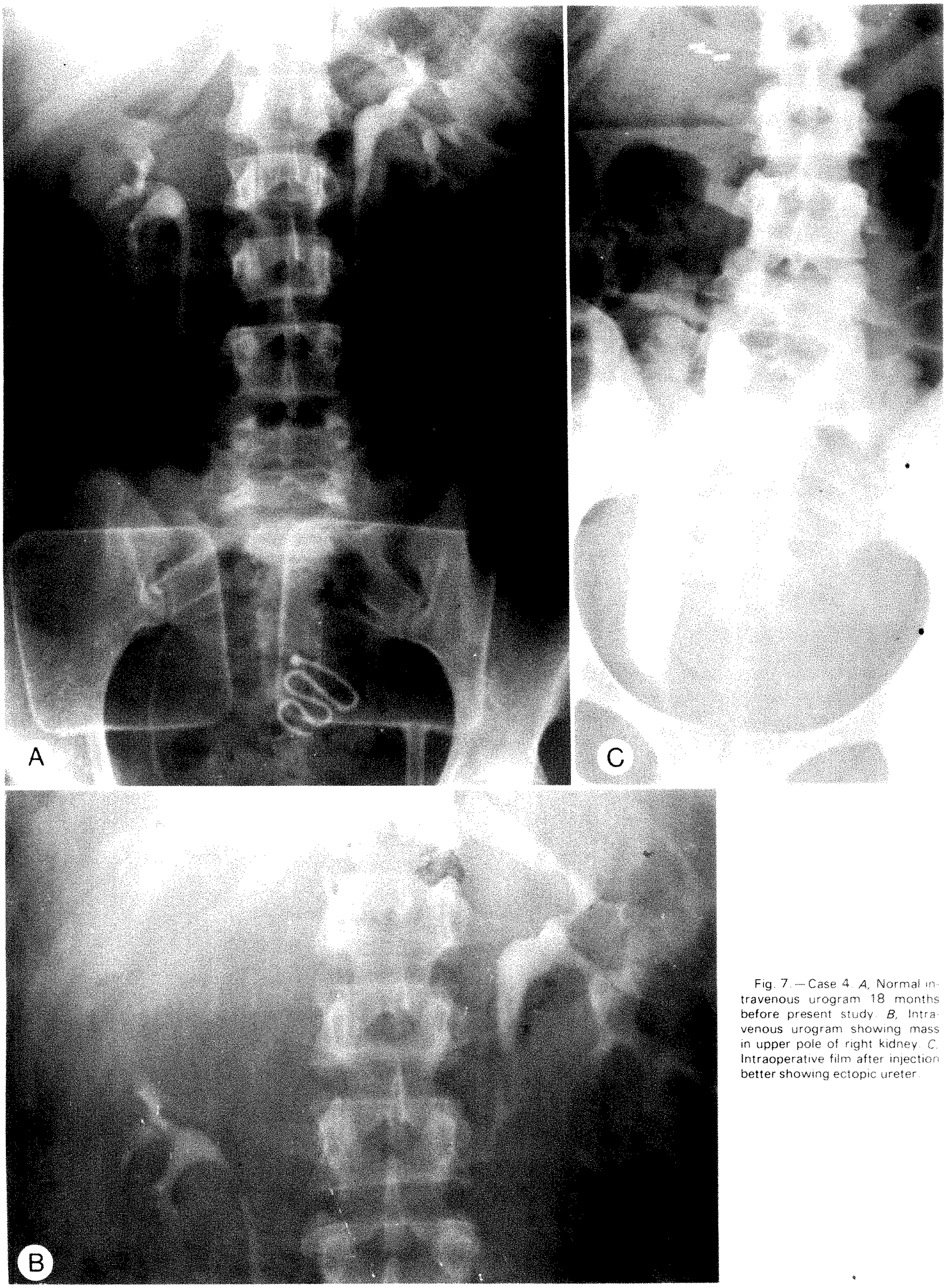

Fig. 7.—Case 4. *A,* Normal intravenous urogram 18 months before present study. *B,* Intravenous urogram showing mass in upper pole of right kidney. *C,* Intraoperative film after injection better showing ectopic ureter.

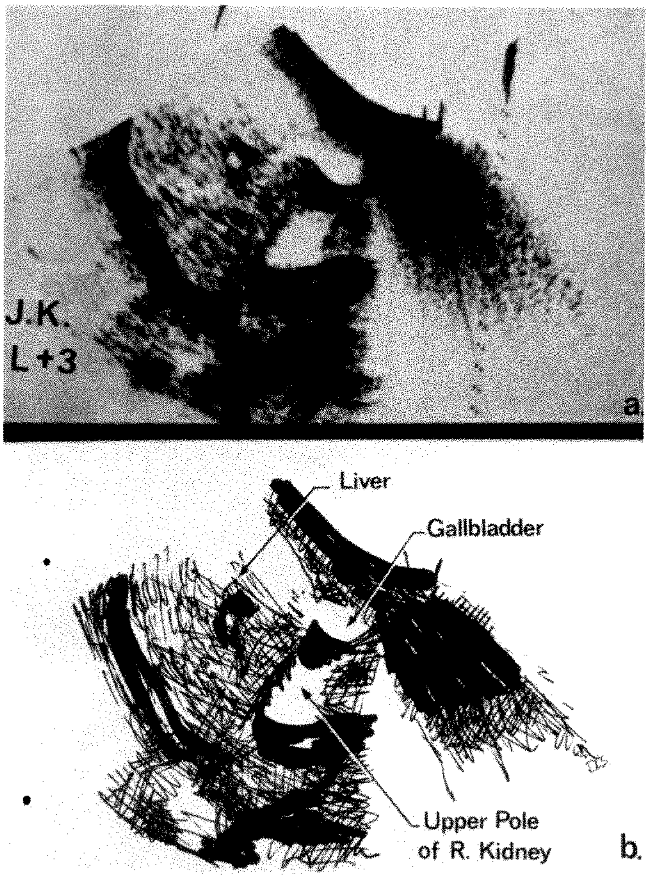

Fig. 8.—Case 4. Ultrasound scan showing anechoic mass in upper pole of right kidney.

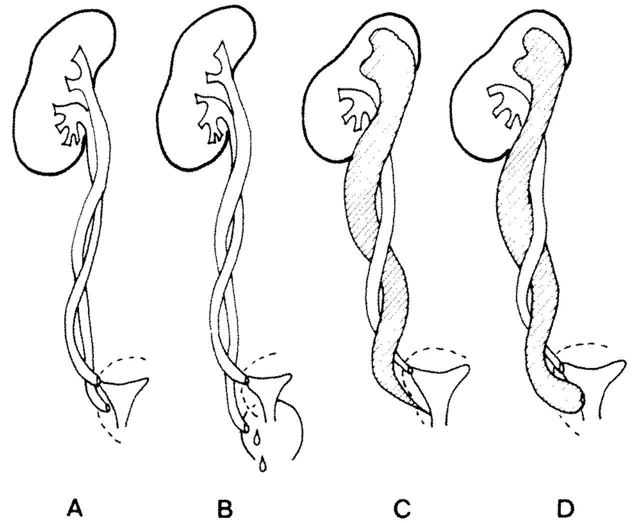

Fig. 9.—Course of ureter of upper pole unit. *A*, Entering bladder inferior to ureter of lower pole unit. Occasionally upper pole ureter ends ectopically. *B*, Ending beyond external sphincta (in females) causing urinary dribbling. *C*, Inserted into urinary bladder sphincter. *D*, Associated with ureterocele.

8. Stuber JL, Leonidas MC, Holden TM: Abdominal ultrasonography in pediatrics. *Am J Dis Child* 129:1096–1101, 1975
9. Lyons EA, Murphy AV, Arneil GC: Sonar and its uses in kidney disease in children. *Arch Dis Child* 37:777–786, 1972
10. Lyons EA, Fleming JE, Arneil GC, Murphy AV, Sweet EM, Donald I: Nephrosonography in infants and children: a new technique. *Br Med J* 2:689–691, 1972
11. Boineau FG, Rothman J, Lewy JE: Nephrosonography in the evaluation of renal failure and masses in infants. *J Pediatr* 87:195–201, 1975
12. Rose JS, Becker JA, Staiano SJ, Compos E: B-mode sonographic evaluation of abdominal masses in the pediatric patient. *Am J Roentgenol* 120:691–698, 1974
13. Goldberg BB, Pollack HH, Capitanio MA, Kirkpatrick JA: Ultrasonography: an aid in the diagnosis of masses in pediatric patients. *Pediatrics* 56:421–428, 1975
14. Goldberg BB, Capitanio MA, Kirkpatrick JA: Ultrasonic evaluation of masses in pediatric patients. *Am J Roentgenol* 116:677–684, 1972
15. Hash E: Ultrasound in the diagnosis of hydronephrosis in infants and children. *J Clin Ultrasound* 2:21–25, 1974
16. Holder TM, Stuber JL, Templeton AW: Sonography as diagnostic aid in the evaluation of abdominal masses in infants and children. *J Pediatr Surg* 7:532–537, 1972
17. Griscom NT: The roentgenology of neonatal abdominal masses. *Am J Roentgenol* 93:447–463, 1965
18. Wiggishoff CC, Kiefer JH: Ureteral ectopia: diagnostic difficulties. *J Urol* 96:671–673, 1966
19. Tanagho EA: Anatomy and management of ureteroceles. *J Urol* 107:720–736, 1972
20. Magg RA: Some observations on the ectopic ureter and ureterocele. *J Urol* 97:1003–1012, 1967
21. Hartman GW, Hodson CJ: The duplex kidney and related abnormalities. *Clin Radiol* 20:387–400, 1969
22. Berdon WE, Baker DH, Becker JA, Uson AC: Ectopic ureterocele. *Radiol Clin North Am* 6:205–214, 1968
23. Uson AC, Lattimer JK, Melicow MM: Ureteroceles in children with emphasis on the frequency of ectopic ureteroceles. *Pediatrics* 27:971–983, 1961
24. Dorst JP, Cussen GH, Silverman FN: Ureteroceles in children with emphasis on the frequency of ectopic ureteroceles. *Radiology* 74:88–89, 1960
25. Barrett DM, Malek RS, Kalalis PP: Problems and solutions in surgical treatment of 100 consecutive ureteral duplications in children. *J Urol* 114:126–130, 1975
26. Sherwood T, Doyle PT, Williams DI: Antegrade pyelography in adults and children. *Proc R Soc Med* 67:1210–1215, 1974

Stereotaxic Instrument for Needle Biopsy of the Mamma

JAN BOLMGREN,[1] BERTIL JACOBSON,[1] AND BJÖRN NORDENSTRÖM[2]

A stereotaxic instrument is described which facilitates percutaneous needle biopsy of the breast for microscopic diagnosis. The instrument consists of an x-ray tube mounted on a hinged arm, pivoting stand, patient table, compression device with film holder and scale system, coordinate-controlled puncture device with separate stand, biopsy instrument, and calculator. The sampling site can be located at a precision within ±1 mm. The instrument can also be used for positioning of metal and dye indicators for guiding surgery and for postoperative identification of excised tumors.

The precise diagnosis of radiographically suspicious, clinically occult lesions of the breast requires microscopic examination. A stereotaxic instrument has been developed which permits location of the sampling site with a precision within ±1 mm. It has also been used for positioning of indicators to serve as guides at surgery and for postoperative identification of an excised tumor.

The instrument consists of an x-ray tube mounted on a hinged arm, pivoting stand, patient table, compression device with film holder and scale system, coordinate controlled puncture device with separate stand, biopsy instrument, and calculator (fig. 1).

Principle

Two stereoradiographs are taken of the breast lesion (fig. 2). The two tube positions P_1 and P_2 form two equal angles α with the normal n to the film plane through the origin O of the scale system. The origin O and the rotation center of the hinged tube arm coincide. Rays from the focus *Fo* form images of the tumor T and a scale system S_x, S_y on a film *Fi*. The film is pressed against the scale system. (In figure 2 the film and scale system are symbolized by one single line.) At exposure with the tube in the two positions, a parallactic displacement is obtained so that the tumor center is imaged on the film with the coordinates x_1 and x_2 and y_{12}, respectively, whereas the two true coordinates are x and y. The magnitude of the parallax depends on the distance z between the tumor center and the film as well as on the tube angle α and the film focus distance r. The following relations hold:

$$x = \frac{r \cdot \sin \alpha \, (x_1 + x_2)}{2r \cdot \sin \alpha - x_1 + x_2}$$

$$y = \frac{2r \cdot \sin \alpha \cdot y_{12}}{2r \cdot \sin \alpha - x_1 + x_2}$$

$$z = \frac{r \cdot \cos \alpha}{r \cdot \sin \alpha + x_2} \left[x_2 - \frac{r \cdot \sin \alpha \, (x_1 + x_2)}{2r \cdot \sin \alpha - x_1 + x_2} \right].$$

Apparatus

The equipment used and the positioning of the patient are shown in figure 1. The x-ray tube with the collimator is mounted on a hinged arm supported by a shaft so that the tube can turn around an axis A_1 and be positioned with inclinations 0°, ±4°, ±10°, ±15°, and ±20° in relation to the normal n through the origin O. The axis A_1 coincides with the film plane and passes through the origin. The shaft is mounted on a pivoting stand supported by a bearing in the footing; the axis of the bearing is displaced 40 mm in the cranial direction relative to the axis A_1.

The pivoting stand permits the x-ray tube, puncture device, and compression device to be turned in a 0°–270° cranial semicircle so that compression and puncture may be performed in any one of the seven standard directions with mutual inclinations of 45° steps. Moreover, the height of the x-ray tube, puncture device, and compression device can be adjusted relative to the patient table by means of an electric motor in order to align an aperture in the compression device in relation to the position of the tumor in the breast.

The patient table is attached to the footing. Part of the table top is replaced by a rubber cloth with a circular hole through which one breast can be brought into the compression device.

The compression device is fixed to the pivoting stand. The adjustable plate of the compression device can be moved manually toward the stationary plate with the film holder. It can be locked at any desired degree of compression. Both plates are supplied with a 50 x 50 mm square aperture.

The puncture device (fig. 3) is supplied with mounting holes and can be attached to the compression device by means of a quick coupling. Also, the puncture device can be mounted on a separate stand for setting of coordinates. The biopsy instrument can be positioned in the three direc-

---

• Received November 3, 1976; accepted after revision March 21, 1977.

This work was supported by grant no. 74-3938 from the Swedish Board for Technical Development.

[1] Department of Medical Engineering, Karolinska Institutet, Stockholm 60, Sweden.

[2] Department of Diagnostic Radiology, Karolinska Sjukhuset, S-104 01 Stockholm 60, Sweden. Address reprint requests to B. Nordenström.

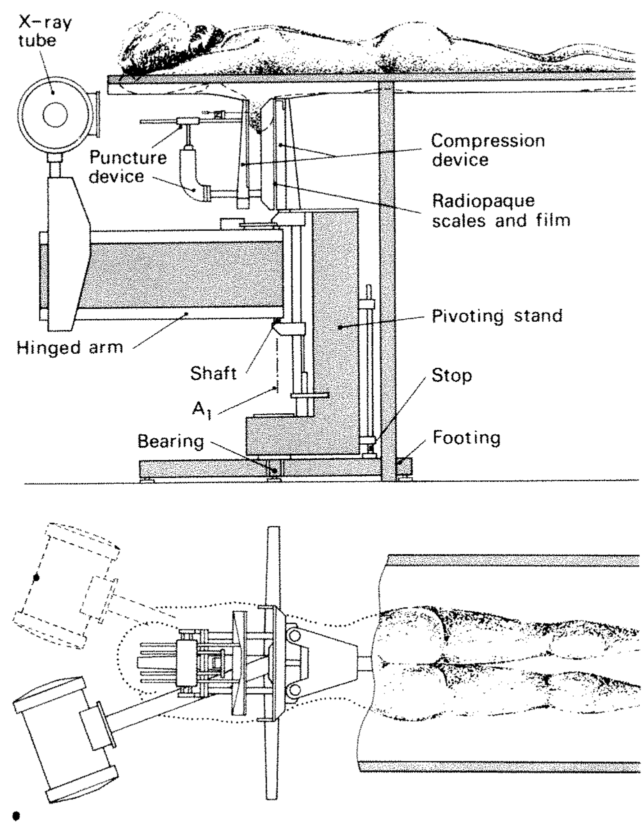

Fig. 1.—Stereotaxic instrument seen from above and from side.

tions x, y, and z by means of a system of guides and stops on the puncture device. The coordinates can be set by means of scales (fig. 3).

The biopsy instrument consists of a 172 mm cannula (outer diameter, 1 mm) and a 205 mm needle with the distal 15 mm shaped as a conical screw. The cannula is fastened to the z-guide of the puncture device by means of a spring-loaded holder. The cannula is supported by a cannula guide in a guide plate that can be pressed against the breast. The cannula guide can be removed for sterilization. The movement of the mounted cannula is restricted to 15 mm by the cannula holder and a stop, which can also be removed for sterilization.

Procedure

Patients with palpable or nonpalpable lesions found at mammography who require further cytological study are selected (fig. 4*A*). The target for the biopsy in the case illustrated is a local accumulation of some small tissue calcifications.

The patient is placed on the examination table with the breast positioned between the compression plates. Positional adjustments are made so that the lesion is projected within the frame of the coordinate system and the apertures in the compression plates. The position is radiographically controlled with the tube in position P_m (fig. 4*B*). Two ±15° radiographs are taken, and the lesion is then projected with a parallactic displacement. The shadow of the aperture of the adjustable compression plate also undergoes a parallactic displacement in the radiograph (fig. 4*C*). The coordinates x_1, x_2, and y_{12} are then determined for the estimated center of the lesion, and the values for x, y, and z are calculated. A corrected z value is obtained by adding the radius of the lesion to z; this makes it possible to sample material from the surface of the lesion during the puncture.

The puncture device with needle and indwelling screw stylet is attached to the stand during the setting of coordinates. The stand has a reference plane corresponding to the origin O. The z-scale rod and the needle are both

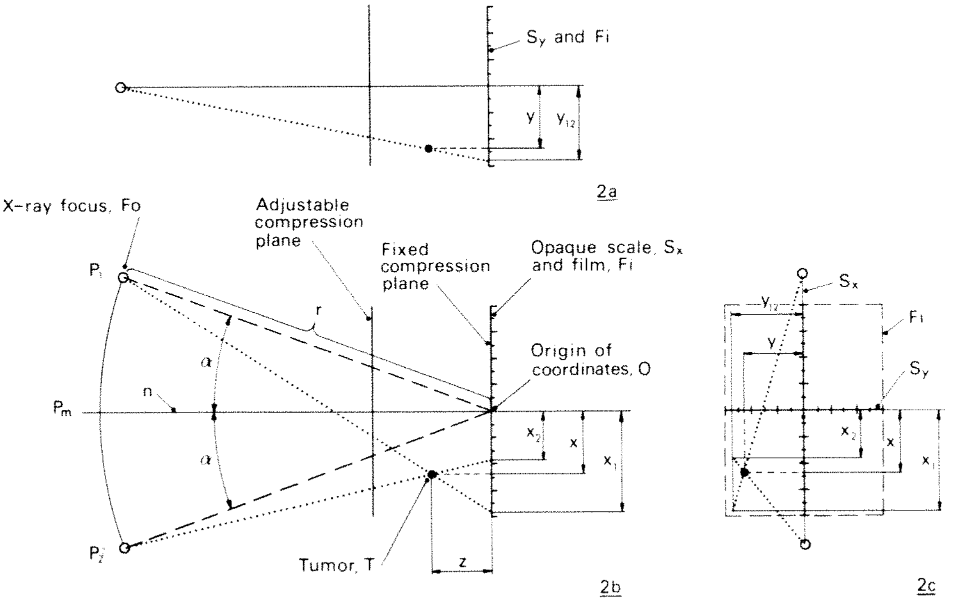

Fig. 2.—Geometry and notations shown in three perpendicular planes.

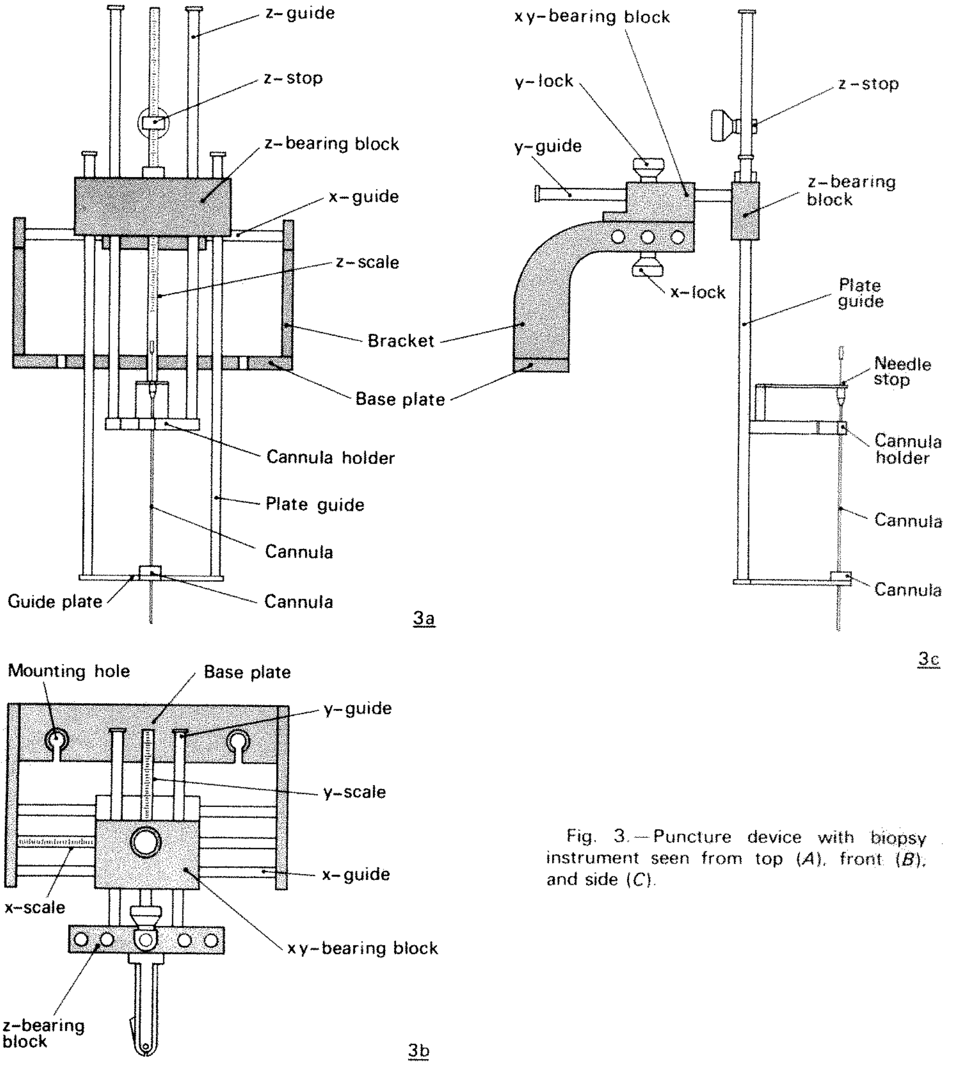

Fig. 3. — Puncture device with biopsy instrument seen from top (*A*), front (*B*), and side (*C*).

aligned so that the needle tip will be positioned exactly at the reference plane when the z reading is zero. The z-scale rod with the attached needle is then pulled back with a distance equal to the corrected z value, and the z-stop is locked. The x and y coordinates are also set and locked.

The puncture device is then attached to the compression device in front of the adjustable compression plate. The skin is washed sterile and local anesthesia applied. The cannula is inserted by means of a slight forward pressure on the z-scale rod and manual rotation of the cannula hub. This prevents axial deviation of the cannula which has an obliquely beveled tip. When the z-stop prevents further forward movement of the cannula, it is positioned with the tip in front of the selected biopsy site (fig. 4*D*).

Sampling is performed in two steps. The screw needle is first rotated clockwise until it stops. The 15 mm long screw tip is then positioned in the tissue in front of the needle tip. A slight forward pressure and rotation is then applied to the cannula hub until the cannula stops. Cell material is retained in the grooves of the screw and protected by the cannula. Any local implantation of material from the screw is thereby prevented when the biopsy instrument is pulled out. A smear is made from the material in the grooves of the screws. The advantage of this sampling technique compared to aspiration biopsy has been described elsewhere [1].

In the case illustrated in figure 4, the material showed the presence of an adenoma. An indirect indication of this diagnosis is also sometimes obtained at the insertion of the biopsy screw; in adenomas the fibrous components partly roll up in the screw grooves which produces considerable mechanical resistance. In malignant lesions the tissue is soft and yields easily.

The stereotaxic instrument has also been used to mark the position of small nonpalpable pathologic processes which are referred for local surgical removal. To facilitate the identification of the lesion for the surgeon, different

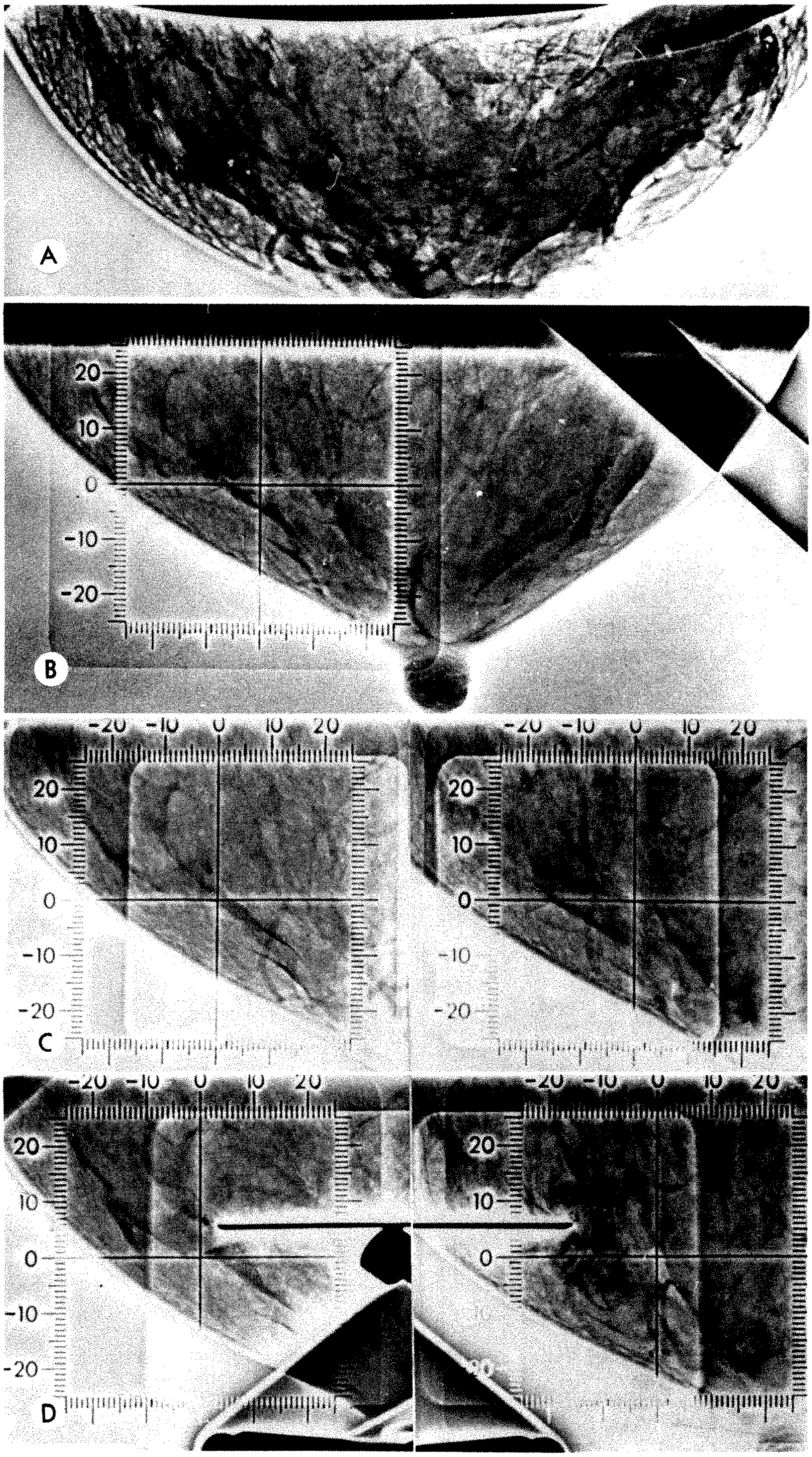
A
B
20
10
0
-10
-20
C
-20 -10 0 10 20
20
10
0
-10
-20
D
-20 -10 0 10 20
20
10
0
-10
-20

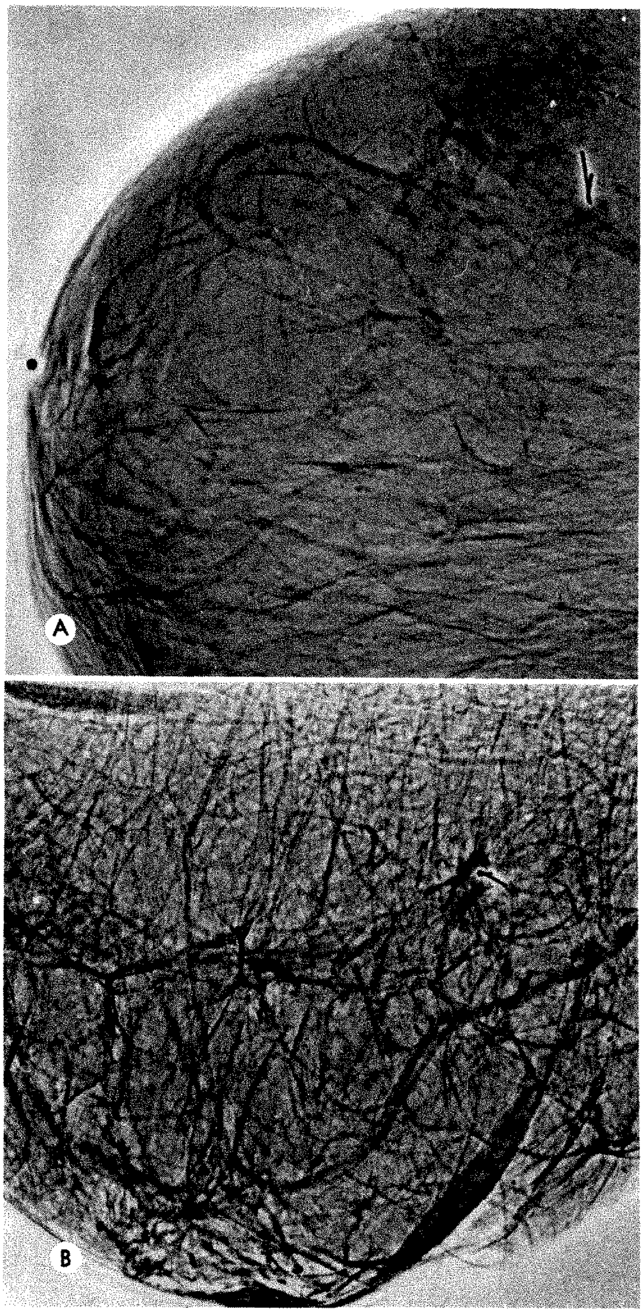

Fig. 5.—Radiopaque indicator consisting of stainless steel suture thread deposited in nonpalpable tumor.

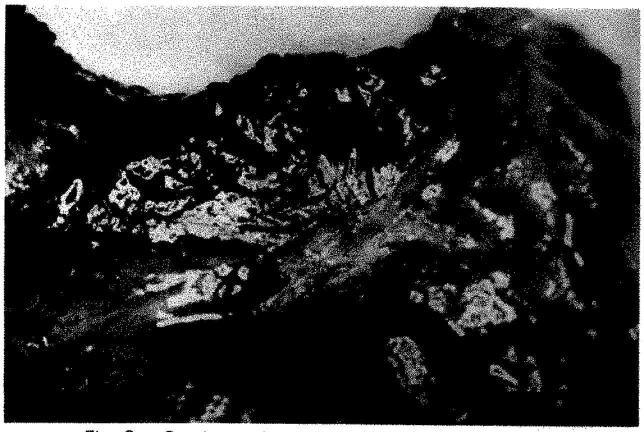

Fig. 6.—Carcinoma located by procedure shown in fig. 5.

radiopaque indicators have been tested. So far the most promising seems to be stainless steel suture threads combined with dye injection. A 1 cm piece of a stainless steel suture thread is inserted into the tip of the biopsy needle and bent over its edge. The needle is then pushed into the puncture canal to the lesion. Upon withdrawal of the needle the suture will remain in the tissue. (If necessary, its position can be visually confirmed by means of two 4° stereo films.) At the withdrawal of the needle, a small amount of a suitable stain such as Indian ink or methylene blue is injected. The puncture canal is then visualized which facilitates the recovery of the lesion for surgery.

Such a suture thread indicator is seen in figure 5. After a local resection the suture thread was found at radiography of the specimen, which made it possible to identify a small carcinoma in the resected tissue (fig. 6).

The instrument described has been found useful in obtaining a correct diagnosis in small nonpalpable breast lesions. This is of particular importance since these tumors, when diagnosed and surgically removed, have a high definite curability. In the first 21 cases with complete follow-up, full agreement was found between cytology and final histology. In three cases of carcinoma, histology was obtained after mastectomy. In 18 cases a local surgical resection was performed: 14 were histologically dysplasias and one fibroadenoma. Three cases were confirmed as containing atypical noncarcinomatous cells.

REFERENCE

1. Nordenström B: New instruments for biopsy. *Radiology* 117:474-475, 1975

←

Fig. 4.—*A*, Local accumulation of small tissue calcifications (*arrow*). *B*, Radiographic control of correct positioning of coordinate system. *C*, Two ± 15° radiographs showing parallactic displacement of calcifications as well as of aperture of compression plate. Center of calcifications are $x_1 = -2$, $x_2 = -13$, and $y_{12} = 6$. *D*, Tip of biopsy cannula close to calcifications shown in two ± 20° radiographs.

Review Article:

Severe Radiation Injuries of the Lung

BERNARD ROSWIT[1] AND DAVID C. WHITE[2]

The lung is a radiosensitive organ whose limited tolerance must be treated with great respect in the radiation management of malignant tumors in the thorax. Severe radiation pneumonopathy can cripple and kill as the outcome of faulty judgment, error, accident, or calculated risk in an effort to control a locally advanced cancer. The clinical and radiologic profile of this unique and challenging syndrome is described and the histopathology and pathogenesis are reviewed. The clinical and technical factors of high risk are discussed, and guidelines for therapeutic management and safer clinical practice are offered.

Introduction

The vast majority of patients who receive radiotherapy for tumors in the chest are effectively treated, for cure or for palliation, with generally subclinical manifestations of radiation changes in the lungs. This review is concerned with the syndrome of severe pneumonopathy, acute exudative or chronic fibrotic, which can cause great suffering, severe disability, and even death. This ominous complication may be the outcome of disrespect for the radiation tolerance of the pulmonary parenchyma, technical errors, individual hypersensitivity, and certain other important factors. The risks are high; the margin for error, small; the penalty to the patient, great.

The onset of severe pneumonopathy is usually insidious, weeks after completion of treatment; yet the final outcome in the individual patient is unpredictable. The alarming acute episode may resolve without significant late residuals, while the late fibrotic phase may arise much later to permanently cripple the lung without early clinical signals of distress.

Although first recognized more than half a century ago, the true nature of this complication and its most effective management are still a challenge to our understanding. This review seems timely and appropriate in view of the trend to escalation of tumor dose and extension of treatment volume in high energy radical therapy of cancer. Further, the developing national crisis in medical liability makes even more compelling a reexamination of the elements of high risk and definition of guidelines for safer practice, using recent advances in radiation biology and radiological technology.

Clinical Profile

The most extraordinary feature of the acute severe exudative syndrome is the long latent period for its clinical expression, even after a gross radiation insult to the lung through high dosage, intensive dose fractionation, or exposure of a relatively large volume of lung tissue. Not until 2–10 weeks after completion of a course of radiation treatment will the patient at risk experience dyspnea, hacking cough, low-grade fever, expectoration of thick white sputum, and a sense of fullness in the chest. This is, more often than not, ascribed to "upper respiratory virus infection." The physical signs may be meager, but dry and moist rales may be heard, and occasionally a friction rub.

Only 7–10 days later will the radiograph reveal the first sign—a diffuse haze in the treatment zone, quickly changing to flocculent patchy infiltrates, then coalescing later to define more precisely the treatment portals in a "straight-edge effect" (figs. 1*A*, 1*B*, and 1*C*). By this time, if the injury has been severe, the clinical signs assume all of the proportions of a fulminating illness with cyanosis, orthopnea, high fever, and intractable cough. Even at this point, the symptoms may be controlled with prompt therapeutic management. However, the lung changes may progress to a chronic fibrotic phase, with increasing pulmonary disability, atelectasis, mediastinal shift, pleuropericardial adhesions, pleural effusion, cor pulmonale, and, finally, death from pulmonary insufficiency (fig. 1*D*). The downward course is complicated by repeated episodes of infection and abcess formation. With less severe injury the patient may become asymptomatic and the fibrotic changes become stabilized 9–12 months after irradiation [1–8].

Not infrequently, the presenting symptoms, signs, and radiographs are misinterpreted. Radiation pneumonopathy may masquerade as infectious pneumonitis, recurrent cancer, lymphangitic spread, or metastasis. Misinterpretation of the complication, mislabled "recurrent cancer," may provoke another course of irradiation, with fatal consequences. By the time the x-ray pattern of the treatment portals becomes clearly manifest, it is almost too late to initiate an attempt at reversal therapy. The consolidation may sometime spread beyond the treatment portals and even be bilateral [9, 10].

Because of severe damage to the pulmonary parenchyma, bronchial tree, and blood vessels, there are profound changes in pulmonary function, reversible and irreversible. There were described in detail in 1956, in a review of five lethal cases from our institution [6]. They include reduction in maximum breathing capacity, pulmonary hypertension, and alveolocapillary block syndrome [4–6, 11, 12].

Presented in part at the annual meeting of the American Radium Society, San Juan, Puerto Rico, May 1975.

[1] Radiation Therapy Center, Veterans Administration Hospital, 130 West Kingsbridge Road, Bronx, New York 10468. Address reprint requests to B. Roswit.

[2] Registry of Radiation Pathology, Armed Forces Institute of Pathology, Washington, D.C. 20305.

Am J Roentgenol 129:127–136, July 1977

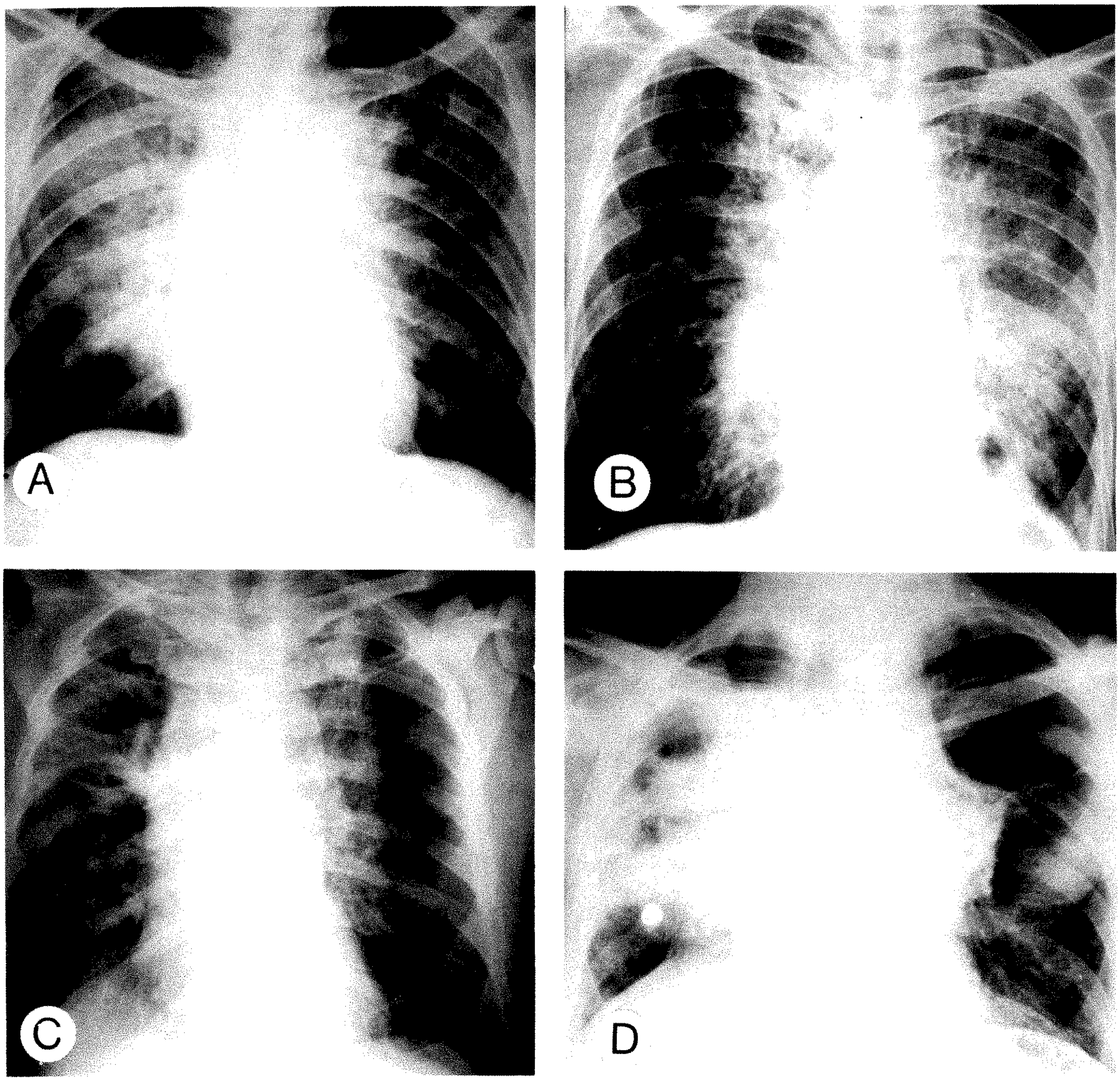

Fig. 1.—*A,* Acute pneumonopathy in patient with inoperable esophageal carcinoma, middle third. Onset was 11 days after completion of rotation therapy using orthovoltage beam (260 kV) to high dose (6,000 rad in 6 weeks); patient died from complication 5 weeks later. *B,* Acute pneumonopathy in patient with anaplastic epidermoid carcinoma resulting after high dose radiotherapy (6,000 rad in 6 weeks) to very large portal using 1 MV resonance generator. Note unusual spread of pathology well beyond well collimated 11 X 14 cm portal. Injury confirmed at autopsy, with typical histologic changes seen remote from irradiated volume. *C,* Acute pneumonopathy in 59-year-old male with bronchial tumor. Onset was 9 days after high dose radiotherapy (6,000 rad in 6 weeks) to large volume (15 X 20 cm) using opposing fields and 1 MV beam. Patient died 10 weeks later. Eradication of tumor and radiation pneumonopathy seen at autopsy. *D,* Severe progressive and disabling fibrosis in 67-year-old male with advanced poorly differentiated epidermoid cancer of right upper lobe and hilar lymph nodes. Radiotherapy given with large portals (22.5 X 21 cm), intensive daily fraction (232 rad), and high total dose (5,972 rad) with cobalt beam (80 cm source-surface distance). (Courtesy of Dr. Flora Mincer, Montefiore Hospital, New York)

There is no consistent correlation between the recognition, duration, and severity of an early radiation pneumonopathy and the occurrence of late delayed pulmonary fibrosis. Progressive pulmonary fibrosis producing a scarred and retracted lung and cor pulmonale may develop seemingly de novo with no clinical evidence of any preexisting acute radiation pneumonopathy.

As with the early pneumonopathy, the volume of lung affected is critical to the outward expressions of the late severe changes (fig. 2). Fibrosis of less than half of a lung will generally be tolerated with little or no discomfort or respiratory difficulty, but it is capable of serving as a nidus for subsequent severe and disabling chronic infectious disease processes (e.g., bronchiectasis

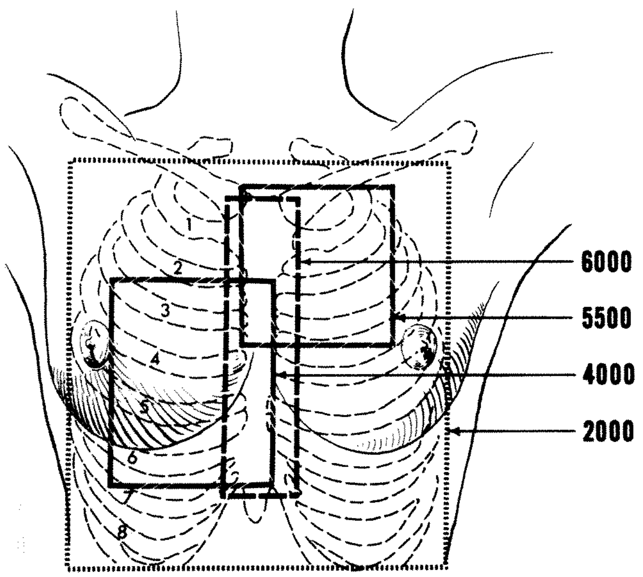

Fig. 2.—Relation between volume of irradiated lung and suggested minimal tolerance dose with 5% risk of injury.

and abcess).

Consideration of the early radiation pneumonopathy would not be complete without taking note of those unpredictable instances where a large proportion of the total lung volume outside the treatment area becomes affected by this degenerative-exudative-regenerative process, in such an overwhelming diffuse fashion that a rapidly debilitative respiratory decrement develops. The pathology usually extends beyond the reported radiation field, thereby suggesting a delayed hypersensitivity immune reaction, as a response to an antigen resulting from intensive irradiation. This antigen may elicit a sensitization of lymphocytes—notably the thymic-derived T cells. The extraordinary latent period for the reaction, the histologic pattern, the involvement of the unirradiated lung, and the response to corticosteroids seem to support this hypothesis.

Corticosteroids produce their effect by suppressing immunity. Kaplan and co-workers [13, 14] observed that the abrupt withdrawal of high dose prednisone during Mopp therapy (Mustargen, Oncovin, procarbazine, and prednisone) can actually activate the acute syndrome in patients previously irradiated by the mantle method. In an immunohistologic study of irradiated rabbit lungs, Dippel et al. [15] indicated that radiation injury in the lung is truly an immunologic reaction. The alveolar manifestations of the rejection phenomena reported by Vaeth and Hagstrom [16] in their analysis of the poor results with human lung transplantation are strikingly analogous to severe radiation pneumonitis.

Histopathology

The earliest histologic responses can develop within days of the initial exposure, although this acute phase generally peaks 1–3 months after the initiation of therapy [17, 18]. Much of the early radiation effect is due to direct damage of the endothelium. The endothelial cells become swollen. This enlargement can be reversible, or the injury may be severe enough to result in cell degeneration and loss of attachment to the capillary basement membrane. Slough of the endothelium is frequently followed by capillary fibrin which forms by the adherence of platelet masses and fibrin thrombosis. The acute endothelial damage results in an abnormal outflow of plasma into the interstitium. At the same time that the functional integrity of the microvasculature is compromised, there is damage to the alveolar epithelium (fig. 3).

Direct radiation effects on mature alveolar lining cells are less evident than the extraordinary enlargement and bizarre configuration of proliferating alveolar lining cells injured during sensitive phases of the reproductive cycle. Multinucleation is common, and the nuclei are usually enlarged approximately in proportion to the increased cell volume. This enlargement of the alveolar lining cells is not exclusive to the radiation response. Similar cytopathology has been observed in a broad spectrum of pulmonary diseases; however, the extreme morphologic transformation with irradiation is rarely encountered in other conditions.

Most of these swollen atypical cells lose the usual tenacious adhesion to the underlying basement membrane and slough, singly or in sheets, from the alveolar surface, abetted by the outpouring of exudate through the septal wall. These detached cells become incorporated into the developing hyaline membrane. An exudate pours from the septal capillaries, accumulates in the interstitium, and penetrates into the alveolus, thereby progressively displacing the functional air volume. The composition of this fluid is variable, but it is protein rich and usually contains abundant fibrin.

Inspiratory efforts compress this trapped exudate into hyaline membranes that consist of amorphous acidophilic layers molded against the alveolar and alveolar duct walls conforming to the cavity contours. Hyaline membrane is one of the characteristics of the early exudative radiation pneumonopathy (fig. 3*A*). However, it is not specific; similar changes are observed in a variety of conditions (e.g., uremia, acute viral and bacterial pneumonias, and after chemical inhalation).

Dissipation or resorption of the exudate is slow even though it may be limited in extent. Damage of the pulmonary lymphatics, whether by direct radiation effects or obstruction of channels from other causes, will retard the elimination of this fluid and lead to relative stagnation within the alveoli and interstitium. In many instances hyaline membrane formation is associated with markedly dilated lymphatic vessels which seem to reflect diminished drainage in a system overburdened by an abnormal accumulation of fluid (fig. 3*B*). Gaseous exchange in the affected lung parenchyma is dramatically diminished. Inspired oxygen fails to reach the alveolar surface because of the exudate and hyaline membrane (fig. 3*C*).

This early response phase includes a mobilization and

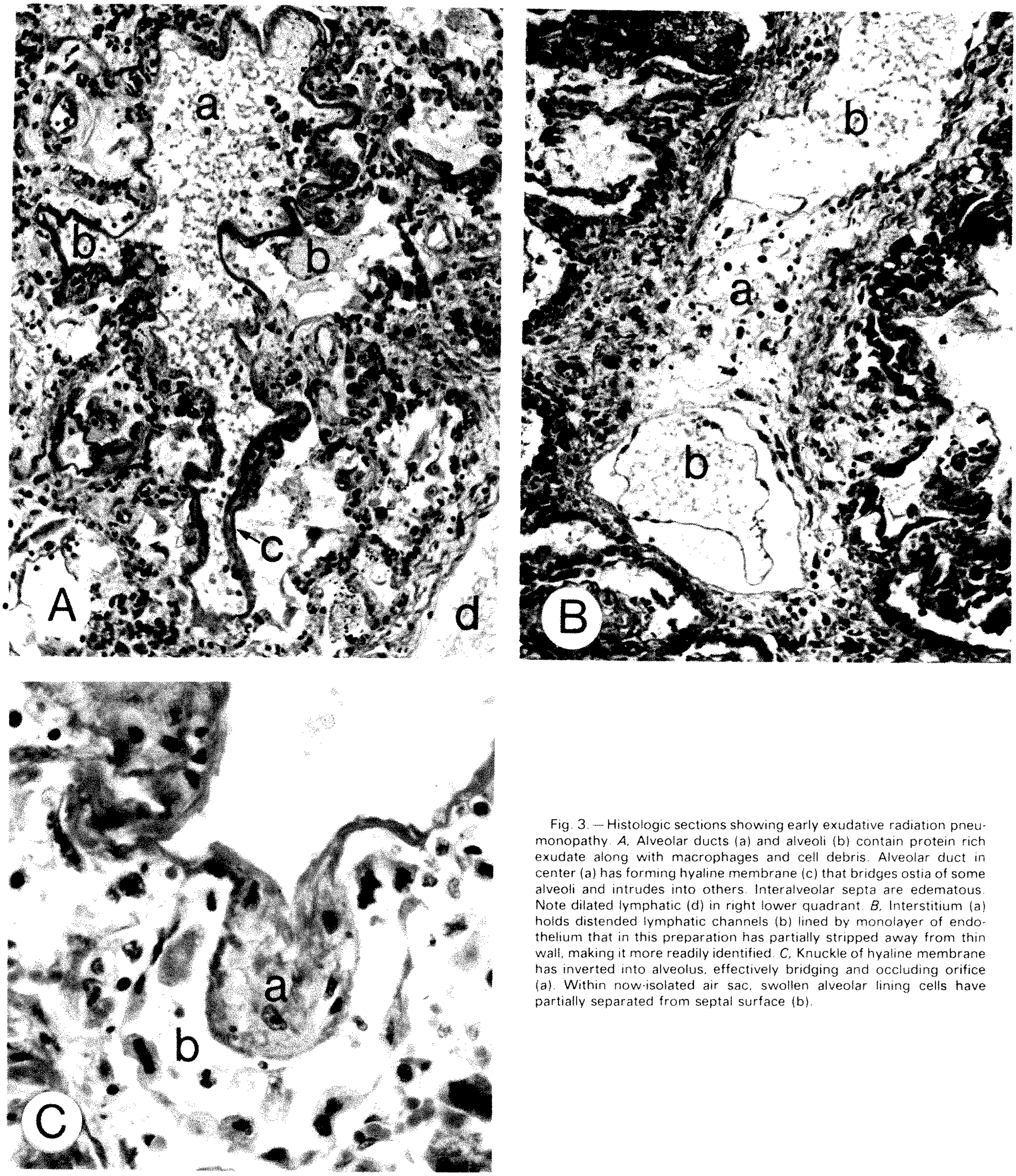

Fig. 3. — Histologic sections showing early exudative radiation pneumonopathy. *A*, Alveolar ducts (a) and alveoli (b) contain protein rich exudate along with macrophages and cell debris. Alveolar duct in center (a) has forming hyaline membrane (c) that bridges ostia of some alveoli and intrudes into others. Interalveolar septa are edematous. Note dilated lymphatic (d) in right lower quadrant. *B*, Interstitium (a) holds distended lymphatic channels (b) lined by monolayer of endothelium that in this preparation has partially stripped away from thin wall, making it more readily identified. *C*, Knuckle of hyaline membrane has inverted into alveolus, effectively bridging and occluding orifice (a). Within now-isolated air sac, swollen alveolar lining cells have partially separated from septal surface (b).

proliferation of the septal cells. While these cells exhibit little phagocytic activity within the interstitium, they become markedly phagocytic as they migrate through the septal wall into the alveolus. They scavenge inspired foreign material and cellular debris and are usually expelled via the air passages. At times they may become so numerous as to completely fill alveolar sacs. In contrast, there is seldom a significant infiltration of inflammatory cells unless viral or bacterial pneumonia intervenes.

At this point in the development of the early exudative

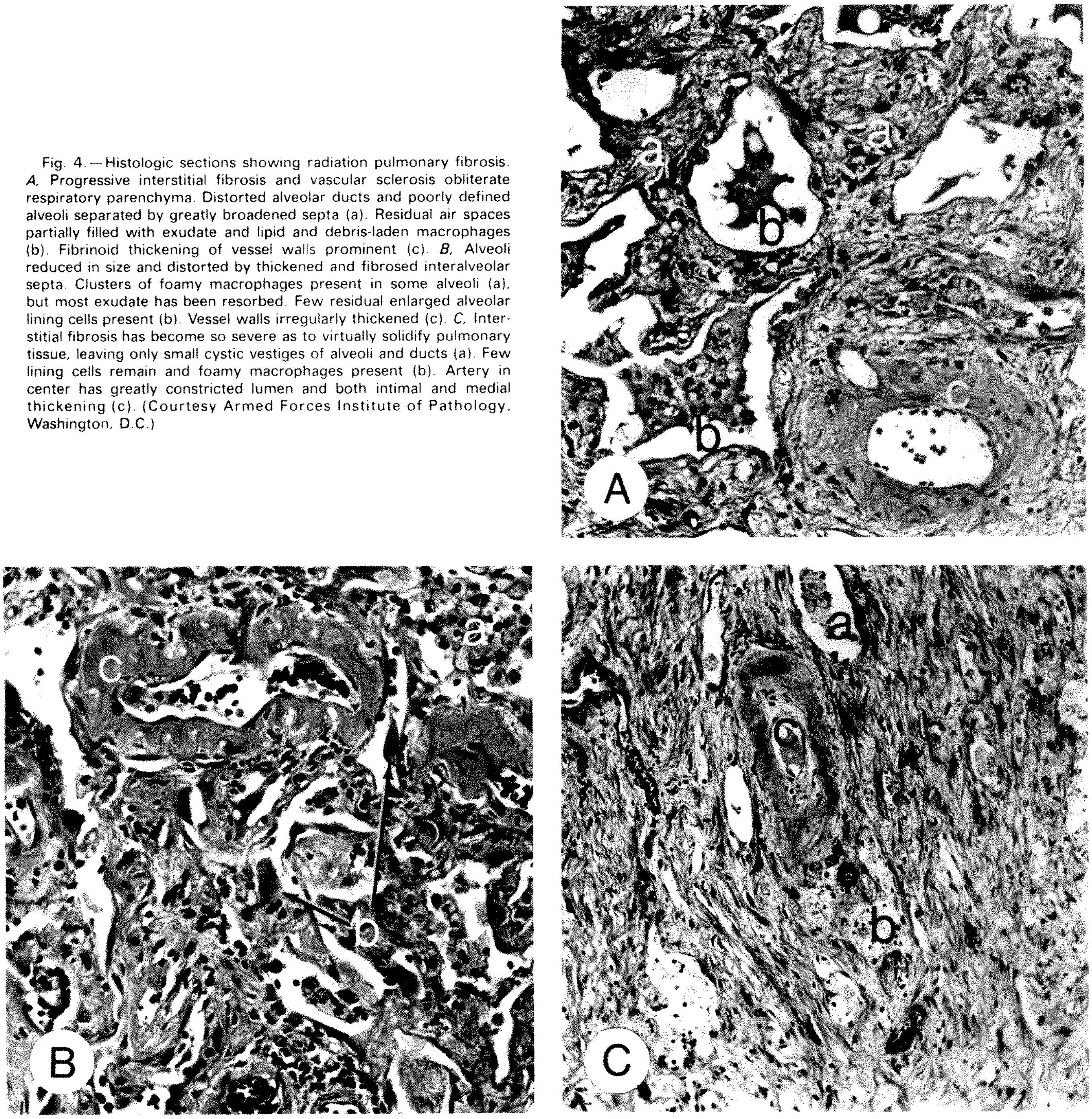

Fig. 4. — Histologic sections showing radiation pulmonary fibrosis. *A*, Progressive interstitial fibrosis and vascular sclerosis obliterate respiratory parenchyma. Distorted alveolar ducts and poorly defined alveoli separated by greatly broadened septa (a). Residual air spaces partially filled with exudate and lipid and debris-laden macrophages (b). Fibrinoid thickening of vessel walls prominent (c). *B*, Alveoli reduced in size and distorted by thickened and fibrosed interalveolar septa. Clusters of foamy macrophages present in some alveoli (a), but most exudate has been resorbed. Few residual enlarged alveolar lining cells present (b). Vessel walls irregularly thickened (c). *C*, Interstitial fibrosis has become so severe as to virtually solidify pulmonary tissue, leaving only small cystic vestiges of alveoli and ducts (a). Few lining cells remain and foamy macrophages present (b). Artery in center has greatly constricted lumen and both intimal and medial thickening (c). (Courtesy Armed Forces Institute of Pathology, Washington, D.C.)

radiation pneumonopathy, the functional decrement is at its maximum and coincides with the acute clinical syndrome. However, all of the tissue changes thus far described are capable of reversal to normal configuration by regeneration and reconstitution.

In clinical practice, most standard therapy procedures involving a limited proportion of total lung volume are followed by full restoration of normal histology. The interstitial and alveolar exudates will be absorbed; the hyaline membrane will be lysed; the abnormal alveolar lining cells will slough and disintegrate with the cell debris phagocytized and removed via the air passages; the epithelium will regenerate; and the microvasculature will revert to normal, reestablishing functional circulation to the parenchyma.

However, in some patients the early tissue response will be severe and prolonged, perhaps because recovery in certain of the innate compensatory and defense mechanisms is deficient or repressed. In our experience intercurrent stress may protract and even amplify this early acute

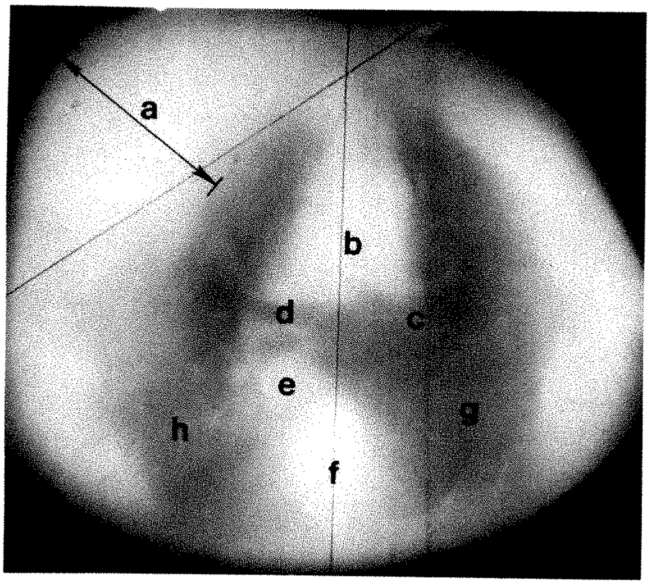

Fig. 5.—Transverse tomogram of 65-year-old woman with massive inoperable carcinoma of left breast and left chest wall (film intended for planning treatment with high energy electron beam). Note tumor volume (a), cardiac shadow (b), right main bronchus (c), left main bronchus (d), aorta (e), thoracic spine (f), right lung (g), and left lung (h).

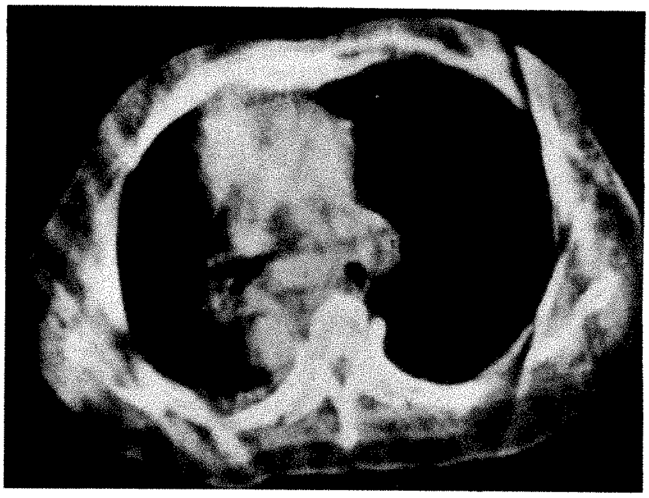

Fig. 6.—CT scan of 60-year-old man with recurrent bronchogenic carcinoma being evaluated for treatment planning. Patient had right lower lobectomy for bronchogenic carcinoma and postoperative ^{60}Co irradiation elsewhere; he received 5,400 rad in 6½ weeks at 13 cm depth through single 11 x 19 portal. Scan revealed large recurrent subcarinal tumor mass associated with x-ray and clinical evidence of esophageal obstruction.

radiation pneumonopathy. For whatever reasons, the longer these early effects persist, the greater is the likelihood that irreversible changes will develop. In the edematous interstitium there will be fibrillar proliferation of collagen strands. The early mural edema of the arterioles and small arteries may be supplanted by randomly distributed and variable subendothelial connective tissue proliferation along with degeneration, usually focal, of the smooth muscle. Fibrinoid necrosis and hyaline alteration may be identified but are usually slow to evolve and are more characteristic of the late phase of radiation injury.

There are two principal lesions characteristic of radiation pulmonary fibrosis. Progressive vascular sclerosis must be considered as primarily responsible for most major lung changes. Progressive interstitial fibrosis, including not only the broadening of the interalveolar septa but thickening of the peribronchial and perivascular regions, the subpleural zone, and the interlobular septa, may be a reaction not only associated with the developing relative ischemia but to altered kinetics of connective tissue proliferation. These two processes are closely interrelated (fig. 4*A*). The area of primary fibrosis is largely confined to the radiation field. However, severe vascular sclerosis will produce secondary parenchymal fibrosis in dependent pulmonary tissue which may extend well beyond the limits of the treatment field. Often these zones of secondary fibrosis halt abruptly at an interlobular septum.

The characteristic pathology of the pulmonary vascular response deserves detailed consideration. There is a reduction of capillaries in the alveolar plexus. Some of these were deleted in the early phase of the radiation response, whereas others have been eliminated by the compression of the progressive fibrosis. Those capillaries remaining are sometimes isolated within a bed of dense collagen. The arterioles and small arteries exhibit the most profound changes and frequently assume prominence in the early stages of pulmonary fibrosis (fig. 4*B*). The vessel walls may be greatly thickened by a fibrinoid degeneration of the media and subendothelial connective tissue proliferation. Later, there is loss of cellular definition in the media with focal replacement and expansion by a hyalinization of the degenerative tissues. These changes will eventually be seen in medium-sized and even larger arteries.

Of considerable diagnostic significance is the variable picture presented by this progressive vascular sclerosis. The different phases of mural thickening are situated randomly along the length of the vessel and are frequently eccentric in cross-sectional location. Thus one microsegment of an artery may be virtually normal in histologic structure, while several microns further on there may be a greatly thickened wall with constricted lumen. This inconsistency of involvement is characteristic of the late radiation-induced vascular changes in all tissues. Diagnostic significance is also ascribed to the presence of clusters of foamy lipid-laden histiocytes in degenerative foci of media and intima.

The progressive scarring steadily destroys the respiratory parenchyma. The residual alveoli show marked variation in size and configuration but with most of them markedly reduced in size. Many will become isolated by the greatly broadened inelastic septa and contain protein-rich substance and foamy macrophages (fig. 4*C*).

In most instances of uncomplicated pulmonary fibrosis, the bronchial and bronchiolar epithelium will remain intact. Intercurrent bacterial invasion, however, can produce a necrotizing bronchitis and bronchiolitis resistant to therapy. The diminished local tissue resistance may preclude

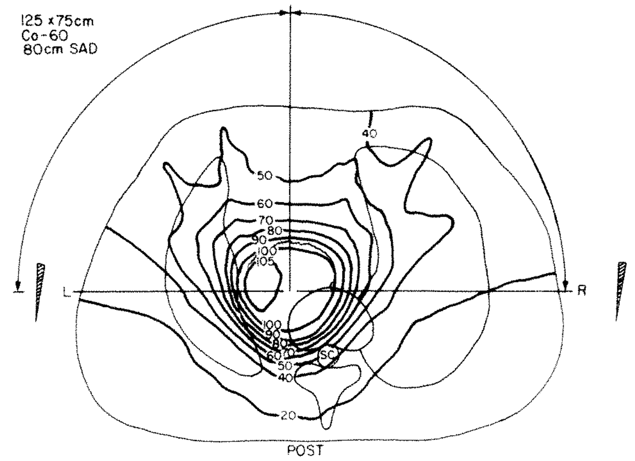

Fig. 7.—Computerized dose distribution corrected for lung heterogeneity for telecobalt, using bilateral 90° arcs with 45° wedges. Additional tumor dose of 5,000 rad in 5½ weeks delivered, with dramatic clinical and objective benefit, while sparing spinal cord and previously treated organs and tissues. (Reprinted with permission from [26])

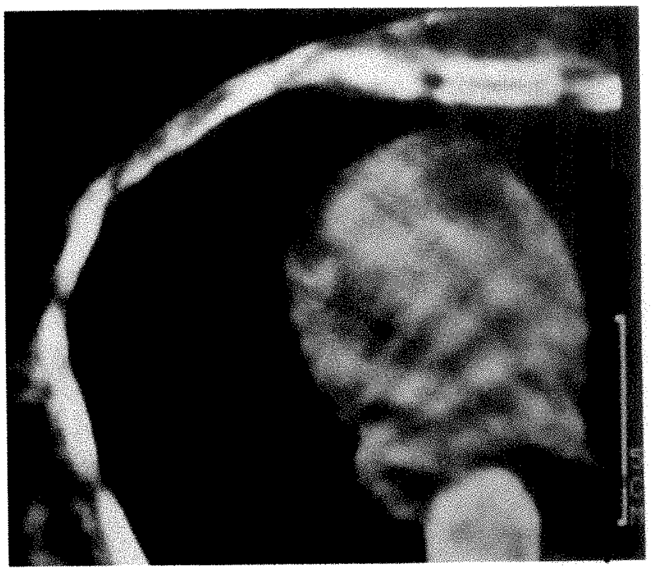

Fig. 8.—CT scan of thorax of 60-year-old woman with chest wall recurrence after bilateral radical mastectomy and postoperative ^{60}Co therapy to internal mammary and supraclavicular areas. Thickness of chest wall and location of underlying lung, heart, and mediastinum defined for planning 8 MeV electron beam therapy.

structural restitution and lead to a continuously smouldering inflammatory condition with a fatal outcome.

Clinical Radiobiology

Total dose of lung tissue, fractionation schedule, exposed lung volume, and individual sensitivity are the most critical factors which can influence the risk of severe radiation injury. Experience indicates that a dose greater than 6,000 rad in 26 fractions in a 5 day per week schedule to a large portion of one lung (more than 50%) is fraught with danger. The larger the irradiated volume, the individual dose fraction, and the cumulative dose, the greater is the risk [19]. The tumor dose must be tailored to the size of the portals. As the tumor volume shrinks, the treatment portals should be progressively reduced and trimmed to spare normal lung (fig. 2).

For treatment of both lungs in patients with disseminated metastases, it is unwise to exceed a total of more than 2,000 rad in 10–13 fractions. In an infant or young child, daily fractions of 140–150 rad and a total of 1,400–1,500 rad represent the limit of lung tolerance [20–22]. Wohl and colleagues [22] recently demonstrated a substantial reduction in lung growth as well as significant impairment of pulmonary function in young children with Wilms's tumor 7–14 years after repeated courses of radiation to the whole lung field.

To overcome this dose limitation in total lung therapy, Mincer and colleagues [23] adopted a moving-strip technique. This allows the irradiation of an entire lung or both lungs by intensive treatment of a narrow segment, shifting the area daily. A total of 85 adult patients with advanced metastatic pulmonary lesions received up to 2,800 rad in 5 weeks. They were significantly benefited, symptomatically and objectively, and pulmonary function improved in most cases as treatment progressed.

For deep-seated neoplasms, especially in large patients, the higher the beam energy, the better the dose distribution and the lesser the hazard of lung injury. For tumors of the breast and chest lesions close to the surface, the electron beam of appropriate energy is preferred to spare the underlying lung parenchyma (fig. 2). Transverse tomography (fig. 5) provides a realistic basis for treatment planning and has been used in our radiation clinic since 1956 [24, 25]. Computed tomography (figs. 6–9) is the ideal tool. Chu [27] found that in one-third of the breast cancer cases, primary disease or chest wall recurrences were best treated with electron beam therapy, which she regards as indispensable for this function. Radiation fibrosis was encountered in only 4% of all her breast cancer patients so treated.

The particular anatomic lung segment harboring the tumor or in the path of the beam plays a significant role in the probability for damage. The lower lung fields, with massive lung volume, are at higher risk than the apical segments. Apical fibrosis is rarely symptomatic, recognized only by the radiologist after completion of the treatment course, especially after breast cancer therapy. The inclusion of the mediastinum or the hilum in the treatment volume in continuity with adjoining lung carries the highest risk [5]. Smith [5] is convinced that damage to the lymphatic outflow tract in this compartment is the most important element in the pathogenesis of the complication.

Most treatment plans for deep-seated chest tumors involve the use of opposed portals. For convenience and economy of setup time in a busy practice, there is a growing tendency to use only one of the portals at each daily session to deliver the prescribed daily tumor dose. Not only is the overlying lung excessively exposed at each session, but the tumor is inhomogeneously irradiated. The larger the thorax, the greater the risk. Wilson and Hall [28]

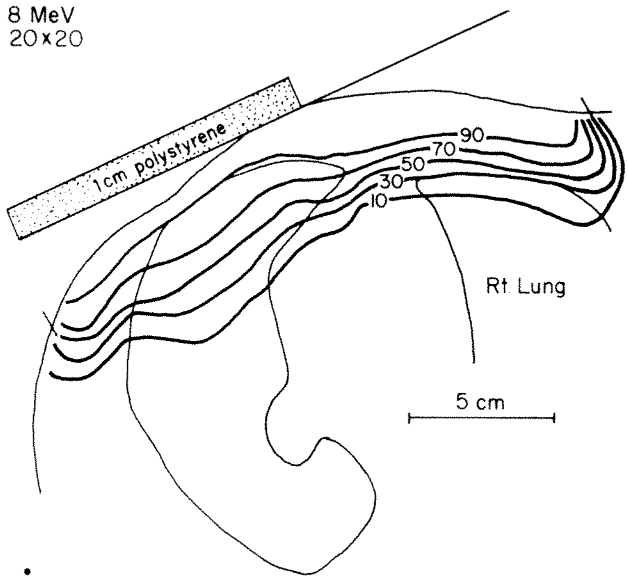

Fig. 9.—Computerized dose distribution documenting uniform dose delivery to chest wall while minimizing radiation to normal lung tissue. Plan incorporates curvature correction, heterogeneity correction, and energy-modifying influence of polystyrene located over thinnest portion of chest wall. (Reprinted with permission from [26])

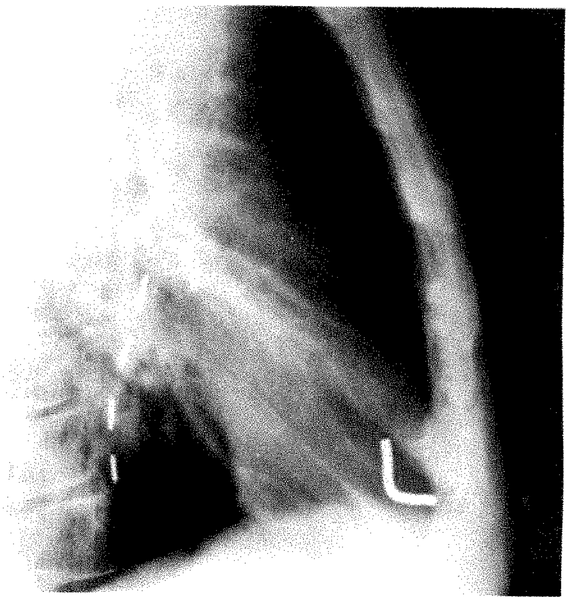

Fig. 10.—Chest radiograph illustrating use of invivo endobronchial dosimeters for precise determination of tissue dose when tumor is encompassed by emphysematous lung. Appropriate corrections for heterogeneity can be accurately determined, minimizing risk of overtreating lung. Dosimeters are radiophotoluminescent glass rods encapsulated in gold shields and inserted in plastic endobronchial catheter during test radiation exposure.

clearly demonstrated the advisability of treating all fields at each therapy session.

• The presence of air-containing lung tissue both in front and behind the tumor permits an increased transmission of radiation to reach the tumor and the contiguous lung [29]. This dose may be significantly higher than the planned dose, calculated from measurement in homogeneous phantoms of unit density [30–32]. It may well be that some cases of severe pulmonary injury, heretofore ascribed to "the individual hypersensitivity of the patient," may be the outcome of failure to give more serious consideration to lung tissue inhomogeneity in treatment planning, and making appropriate corrections. In vivo dosimetry, with miniature radioluminescent detectors, can help materially to improve the accuracy of the calculated dose to the lung, heart, and esophagus, as well as to the tumor (fig. 10). We have used such dosimeters with benefit since 1956 [33].

Kaplan [13] designed a technique of "thin block" radiation for patients with hilar Hodgkin's disease in whom elective whole lung radiation was deemed necessary. Such patients received 1,500 rad to the lungs in 4½ weeks during therapy to the hilum, which receives 4,400 rad in the same period. The risk of radiation injury is thus significantly reduced.

Prescription of the optimum tumor dose is governed principally by consideration of the threshold dose that may result in critical damage to vital organs (e.g., heart, lungs, and spinal cord). Rubin and co-workers [4, 8] advocated the concept of a "tolerance dose" to express the minimal and maximal injurious dose levels acceptable in widely different clinical settings. For example, 4,000 rad is suggested as a minimum tolerance dose (5% risk in 5 years). This is generally acceptable in standard therapy of such relatively favorable lesions as Hodgkin's disease treated with the mantle portal. It obtains under standard conditions such as supervoltage therapy, 1,000 rad per week, and a 5 day per week schedule. In more formidable clinical settings, as in the treatment of carcinoma of the lung, a maximum tolerance dose of 5,500–6,000 rad may need to be seriously considered in return for a chance for improved survival.

When adjuvant chemicals are used, notably actinomycin D, there should be a reduction of the total dose of radiation by at least 10%–15%. In patients with Hodgkin's disease who have received previous chest irradiation, the Stanford University group has eliminated cyclic corticosteroids altogether to minimize the risk of activating a latent radiation injury by steroid withdrawal [13, 14].

The final decision on the dosage regimen will be based upon the training, experience, and judgment of the therapeutic radiologist as well as on recognized standards of reference in the medical literature.

Therapeutic Management

Treatment of the acute exudative reaction must include, above all, the prompt and maintained use of high dose corticosteroid therapy [4–6, 13, 34]. In at least 50% of patients on steroid therapy, one may expect suppression of the acute severe phase, improved exercise tolerance, and x-ray clearance of the pneumonic infiltrates. Withdrawal of steroids must be gradual. Kaplan [13] reported dramatic and almost catastrophic effects of the sudden interruption of steroid therapy.

Corticosteroid therapy may reverse the early acute phase, but fibrosis may continue and, in the worst cases, leads to impaired pulmonary function, cor pulmonale, and, eventually, cardiac failure. Corticosteroids at this stage are no longer of benefit. Antibiotics are often needed in these patients because their lungs are susceptible to frequent attacks by secondary pathogenic invaders.

Immediate and absolute bed rest is of the greatest urgency at the onset of the acute syndrome. In our experience, overexertion and/or overexposure to cold seemed to be responsible for the excitation of an otherwise clinically occult pneumonopathy in several of our patients. Bronchodilators and oxygen therapy are always helpful, but antibiotics are to be used only when the sputum culture is positive for pathogenic organisms.

Prophylactic therapy with cortiocosteroids and other agents has been suggested in hazardous clinical settings, but none have been explored in randomized and controlled studies. Klein et al. [35] described a double-blind study in 116 patients under intensive cobalt therapy, using oxyphenbutazone (Tanderil) as a prophylactic agent. This drug is closely related to another antiinflammatory agent, phenylbutazone (Butazolidon). These workers reported a significant reduction in the frequency and severity of radiation pneumonopathy, without toxic manifestations. Karg [36] reported a similar favorable experience recently in 30 patients who were also given prophylactic treatment with Auxiloson (dexamethasone-21-isonicotinate) in aerosol during radiation exposures ranging from 4,000 to 6,700 rad. If, indeed, the acute exudative reaction becomes more clearly identified in part as an immune response to intensive ionizing radiation, then immunosuppresive agents more effective than cortiocosteroids may be required for prophylactic or therapeutic application in the most appropriate clinical situations.

ACKNOWLEDGMENTS

We express our appreciation to the medical media departments of the Armed Forces Institute of Pathology and the Veterans Administration Hospital, Bronx, and especially to Edward M. Jones, medical artist.

REFERENCES

1. Groover TA, Christie AC, Merritt EA: Intrathoracic changes following roentgen treatment of breast carcinoma. *Am J Roentgenol* 10:471, 1923
2. Hellman S, Kligerman M, Von Essen CF, Scibetta MP: Sequelae of radical radiation for cancer lung. *Radiology* 82:1055-1061, 1961
3. Libshitz HI, Southard ME: Complications of radiation therapy: the thorax. *Semin Roentgenol* 9:41-49, 1974
4. Rubin P, Casarett AW: *Clinical Radiation Pathology*. Philadelphia, Saunders, 1968
5. Smith JC: Radiation pneumonitis: a review. *Am Rev Respir Dis* 87:647-655, 1963
6. Stone DJ, Schwartz MJ, Green RA: Fatal pulmonary insufficiency due to radiation effect upon lungs. *Am J Med* 21: 211-226, 1956
7. Teates D, Cooper G Jr: Some consequences of pulmonary irradiation. A second long term report. *Am J Roentgenol* 96:612-619, 1966
8. Rubin P: Radiographic expression of radiotherapeutic injury: an overview. *Semin Roentgenol* 9:5-13, 1974
9. Bennett DE, Milton RR, Ackerman LV: Bilateral radiation pneumonitis, a complication of radiotherapy of bronchogenic carcinoma: report and analysis of seven cases with autopsy. *Cancer* 23:1001-1018, 1969
10. Smith JC: Radiation pneumonitis: case report of bilateral reaction after unilateral irradiation. *Am Rev Respir Dis* 89: 264-269, 1964
11. Brady LW, Germon PA, Cander L: The effects of radiation therapy on pulmonary function in carcinoma of lung. *Radiology* 85:130-134, 1965
12. Phillips TL, Margolis L: Radiation pathology and the clinical response of lung and esophagus, in *Frontiers in Radiation Therapy and Oncology*, vol 6, edited by Vaeth JM, Baltimore, University Park Press, 1972, pp 254-273
13. Kaplan H: *Hodgkin's Disease*. Cambridge, Mass., Harvard University Press, 1972
14. Castellino RA, Glastein E, Turbow MM, Rosenberg S, Kaplan HS: Latent radiation injury of lungs or heart activated by steroid withdrawal. *Ann Intern Med* 80:593-599, 1974
15. Dippell J, Lissner J, Antaszek C: Untersuchungen zur Pathogenese der Strahlenpenumonitis. *Strahlentherapie* 141:135-140, 1971
16. Veith FJ, Hagstrom JWC: Alveolar manifestations of rejection: an important cause of poor results with human lung transplantation. *Ann Surg* 175:336-348, 1972
17. White DC: *An Atlas of Radiation Histopathology*, U.S. Energy Research Development Administration. Washington, D.C., Government Printing Office, 1975
18. Stetson CG, Boland J: Experimental radiation pneumonitis: radiographic and pathologic correlation. *Cancer* 20: 2170-2183, 1967
19. Evans JC: Time-dose relationship of radiation fibrosis of the lung. *Radiology* 74:104-106, 1960
20. Littman P, Davis LW, Nash J, Tefft M, Borns P, Lepanto P: Hazard of acute radiation pneumonitis in children receiving mediastinal radiation. *Cancer* 33:1520-1525, 1974
21. Margolis IW, Phillips TL: Whole lung irradiation for metastatic tumors. *Radiology* 93:1173-1179, 1969
22. Wohl MEB, Griscom NT, Traggis DG, Jaffee N: Effects of therapeutic irradiation delivered in early childhood upon subsequent lung function. *Pediatrics* 4:507-516, 1975
23. Mincer F, Botstein C, Schwarz G, Zacharopoulos G, McDougall R: Moving strip irradiation in the treatment of extensive neoplastic disease in the chest. *Am J Roentgenol* 108:278-281, 1970
24. Roswit B, Unger SM, Stein J, Malsky SJ, Reid CB: Transverse laminography, the third dimension in body section roentgenography: applications in radiation therapy. *Am J Roentgenol* 81:130-139, 1959
25. Roswit B, Unger SM: Tumor localization with transverse tomography: diagnostic and therapeutic applications. *Radiology* 74:705-720, 1960
26. Laughlin JS, Chu F, Simpson L, Watson RC: Radiation treatment planning. *Cancer* 39, suppl.: 719-278, 1977
27. Chu FCH: The role of electron beam therapy in treatment of breast cancer, in *Frontiers in Radiation Therapy and Oncology*, vol 2, edited by Vaeth JM, Baltimore, University Park Press, 1968, pp 224-237
28. Wilson CS, Hall EJ: On advisability of treating all fields at

each radiotherapy session. *Radiology* 98:419-424, 1971

29. Johns HE, Cunningham JR: Physics of Radiology 3d ed. Springfield, Ill., Thomas, 1969
30. Jacobson LF, Krauer IS: Correction factors for tumor dose in chest cavity due to diminished absorption and scatter in lung tissue. *Radiology* 67:863-876, 1956
31. Holt JG, Laughlin JS: Practical method of obtaining density distribution within patients. *Radiology* 93:161-166, 1969
32. Batho HF: Lung corrections in cobalt 60 beam therapy. *J Can Assoc Radiol* 15:79-83, 1964
33. Roswit B, Malsky SJ, Reid CB, Amato CG, Goebels R: In vivo radiation dosimetry. Review of a 12-year experience. *Radiology* 97:413-424, 1970
34. Moss WT, Haddy FJ, Sweany SK: Some factors altering severity of acute radiation pneumonitis: variation with cortisone, heparin and antibiotics. *Am J Roentgenol* 75:50-54, 1960
35. Klein H, Muller-Fassbender H, Bublath H, Heinze HG: Wirkung von Oxyphenbutazon auf strahlen Pneumonitis beziehungsweise Strahlenfibrose nach Mammakarzinombestrahlung. *Strahlentherapie* 144:421-429, 1972
36. Karg E: Zur Behandlung von Strahlenreaktinonen am Respiration strakt mit Auxiloson. *Strahlentherapie* 142:490-493, 1971

Diagnostic Oncology Case Studies

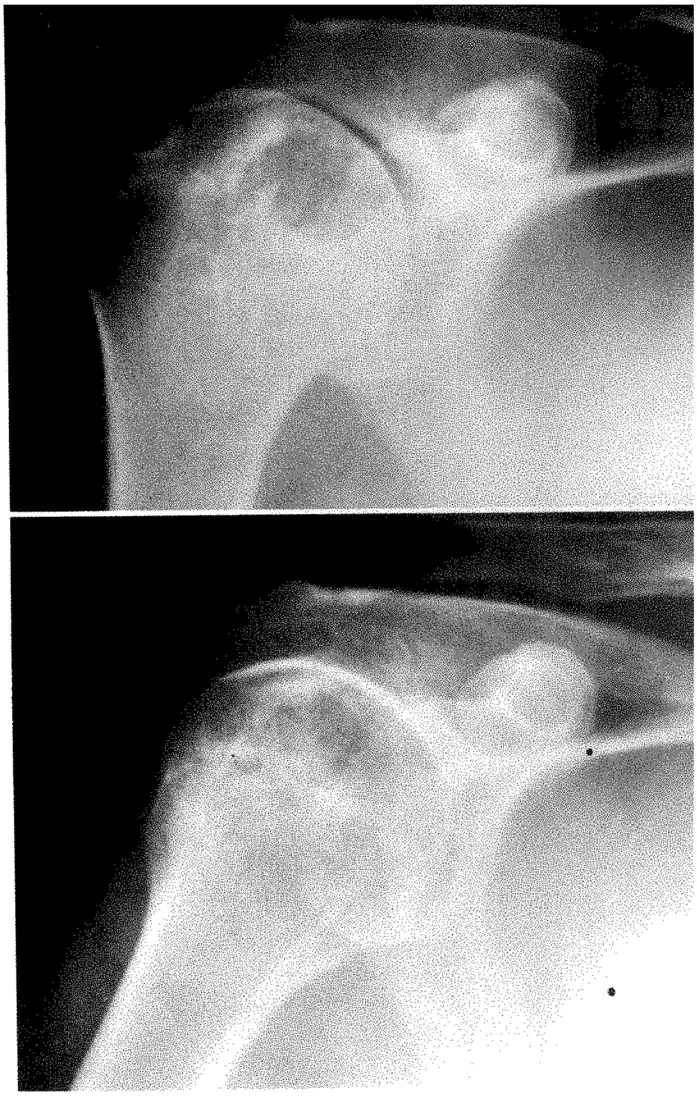

Metastatic Carcinoma Presenting as Shoulder Arthritis

This 53-year-old man complained of gradually increasing pain in his right shoulder after reroofing his house. Subsequently, he had difficulty swimming because of the "arthritis" in his shoulder. There was no family history of gout or rheumatoid arthritis and no prior history of significant bone or joint disease. On the initial study (see above) a lucent area in the proximal humeral epiphysis was noted as well as an incidental finding of a lateral juxtaarticular erosion. The epiphyseal lucency was poorly seen on external rotation view. These findings were interpreted as mild "degenerative arthritis" of the cervical spine and of the right shoulder. Initial treatment consisted of physiotherapy and ultrasound. Pain and range of motion improved initally, but within 3 months progressive soft tissue swelling and diminished range of motion led to a clinical diagnosis of "adhesive capsulitis," and local cortisone injections were begun [1]. Subsequently, the shoulder became more painful, and voluntary range of motion diminished to a point where the patient had to assist his right arm by guiding it with his left.

Clinical examination 1 year after the initial diagnosis of degenerative joint disease revealed marked atrophy of the muscles in the right deltoid region and pain with movement of the right shoulder and elbow. There was no apparent mass or induration of the soft tissues. No other joints were symptomatic.

Repeat radiographs now demonstrated extensive permeative bone destruction involving the right humeral head and shaft, with a pathologic fracture of the greater tuberosity (fig. 1). Lytic lesions were also found in the right scapula and the left eighth rib.

On direct questioning and in retrospect, the patient recalled one episode of gross hematuria 5 months after the shoulder symptoms first began. An excretory urogram therefore was performed which revealed an enlarged left kidney. A left renal angiogram outlined a large hypervascular renal mass (fig. 2). At the conclusion of the selective renal angiogram, the left renal artery was occluded preoperatively

---

This is the third in a bimonthly series of case reports edited by A. Robert Kagan and Richard J. Steckel (Southern California Permanente Medical Group and UCLA Center for the Health Sciences) to present and discuss contemporary problems and procedures in the identification and staging of the more common neoplasms. Case contributed by Alan Fremland, Department of Radiology, Zion Hospital, La Mesa, California 92041.

Am J Roentgenol **129**:137–139, July 1977

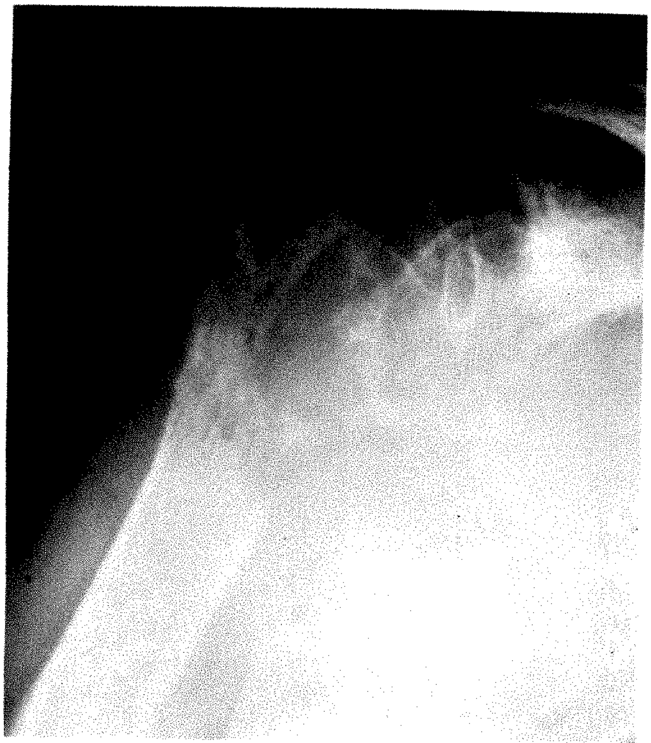

Fig. 1.—Radiograph of right shoulder 1 year later showing extensive destruction of humeral head and shaft (not shown).

by embolization with Gelfoam, followed the next day by a radical nephrectomy [2, 3]. An adenocarcinoma 7.5 cm in diameter was found in the upper pole of the left kidney; regional lymph nodes were negative for tumor. The right humerus was irradiated for palliation, and the patient was placed on systemic therapy consisting of progesterone, cytoxan, methotrexate, and 5-fluorouracil.

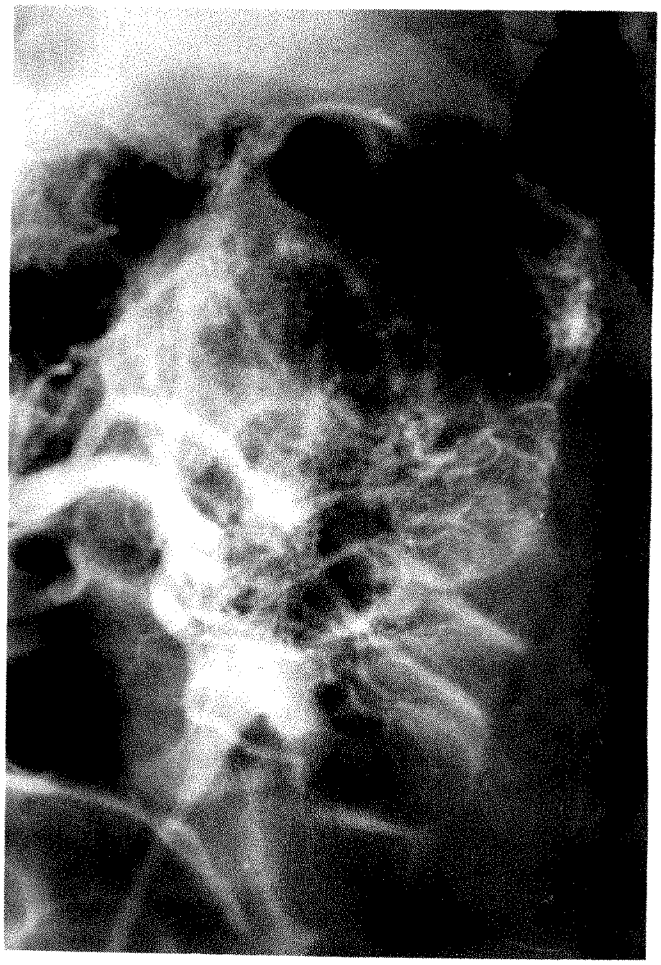

Fig. 2.—Selective left renal arteriogram showing large hypervascular renal mass.

Discussion

Insufficient attention was paid to the significance of an abnormality on the first series of radiographs, and follow-up studies were delayed despite worsening symptoms. Although subchondral lytic areas certainly may occur in degenerative arthritis, they seldom (if ever) do so without further evidence of humeral head deformity, cartilage destruction with joint narrowing, osteophyte formation, or subchondral eburnation. None of these radiographic findings suggesting a severe arthritic process was present. On the other hand, the radiologic differential diagnosis of an epiphyseal lytic defect near a large joint in a middle-aged adult should include degenerative arthritis, rheumatoid or infectious arthritis, gout, villonodular synovitis, myeloma, and a metastatic lesion. In younger individuals, enchondroma, chondroblastoma, and juvenile bone cyst would also be considered.

Benign arthritic or synovial conditions are among the most common illnesses. While bone metastases which mimic benign conditions are less common, a retrospective review of patients with primary and secondary malignant bone tumors often reveals an initial clinical diagnosis of arthritis or bursitis. A major reason for this error in diagnosis is that the clinician relies on initial x-rays which may be interpreted as "benign." Indeed, the initial studies may be regarded as nondiagnostic for tumor even with positive radiologic findings, since a diagnosis of cancer may seem unlikely in a patient with a musculoskeletal complaint and no previous history of a malignancy. In addition, severe musculoskeletal symptoms may occur when 10%–15% of the bone mineral has been destroyed, whereas standard radiographs are only capable of detecting bony destruction in noncortical bone after a 50% or greater reduction in mineral content [4]. Radionuclide bone scans alone are not helpful since they may be interpreted as "positive" *either* with metastases or with inflammatory diseases of the bones and joints [5].

While clearcut signs and symptoms suggesting articular inflammation are often associated with benign bursal and joint disorders, scapulohumeral periarthritis or adhesive capsulitis (frozen shoulder) can be insidious, with an early sensation of stiffness progressing to a severe and painful restriction of shoulder movement [1]. Osteoarthritis of the cervical spine can also cause radicular (segmental) pain in the arm, but local cervical pain or tenderness is often present with this condition [6].

Metastases may become manifest before, simultaneous with, or after the documentation of a primary malignant lesion elsewhere. Whereas the majority of metastases to bone are diagnosed after the primary site has already been identified, bone metastases as the *first* clinical manifestation of a malignant tumor occur most commonly with cancers of the kidney, lung, and pancreas, as well as with lymphomas. The presence of a solid renal mass, with or without hematuria, in conjunction with a lytic bone lesion (sometimes mixed with bone sclerosis) is highly suggestive of metastatic renal carcinoma. Metastasis *to* the kidney from a primary tumor elsewhere can also occur, but this is often a preterminal event associated with a known lung cancer or lymphoma.

Nephrectomy for adenocarcinoma of the kidney in the presence of known metastases is not advocated by everyone. However, of 108 documented cases of metastatic tumor regression after removal of a primary tumor, the most common occurrence was in renal carcinoma (28 patients) followed by melanoma (13 patients) [7]. Palliative nephrectomy is also sometimes justified because of local pain or bleeding [3]. In this patient, nephrectomy with subsequent systemic therapy has not altered the continuing downhill course.

Older patients with persistent unexplained musculoskeletal complaints should have repeated (follow-up) radiographs and, if indicated, correlative bone scans. Tomograms of the affected bone are occasionally helpful, particularly when an abnormality of equivocal significance on conventional radiographic studies is present, as in our patient. Careful correlation of the radiographs, tomograms, *and* bone scans with the clinical and laboratory findings (including blood count, alkaline phosphatase, sedimentation rate, and serum calcium and phosphorus levels) is essential, with repeated studies at regular intervals if the therapeutic response is inadequate or if new symptoms appear. If a bone scan is focally "positive" in an older individual and there are persistent unexplained symptoms (even with negative radiographic studies), a percutaneous or open bone biopsy of the affected area should also be considered [5].

REFERENCES

1. Lundberg BJ: The frozen shoulder. *Acta Orthop Scand* [*Suppl*] 119:1-59, 1969
2. Craven JD: Urologic tract, in *Diagnosis and Staging of Cancer: A Radiologic Approach* edited by Steckel RJ, Kagan AR, Philadelphia, Saunders, 1976, pp 215-243
3. Johnson DE, Kaesler KE, Sammuels ML: Nephrectomy justified in patients with metastatic renal carcinoma? *J Urol* 114: 27-29, 1975
4. Gold RH: Bone and soft tissue, in *Diagnosis and Staging of Cancer: A Radiologic Approach*, edited by Steckel RJ, Kagan AR, Philadelphia, Saunders, 1976, pp 286-312
5. Corcoran RJ, Thrall JH, Kyle RW, Kaminski RJ, Johnson MC: Solitary abnormalities in bone scans of patients with extraosseous malignancies. *Radiology* 121:663-667, 1976
6. Epstein JA, Carras R, Epstein BS, Levine LS: Myelopathy in cervical spondylosis with vertebral subuxation and hyperlordosis. *J Neurosurg* 32:421-426, 1970
7. Sendelar WF, Ketcham AS: Regression of cancer following surgery, in *The Conference on Spontaneous Regression of Cancer*, National Cancer Institute Monograph no. 44, Washington D.C., Government Printing Office, 1976, pp 81-84

Case Reports

Thoracic Wall Invasion Secondary to Pulmonary Aspergillosis: A Complication of Chronic Granulomatous Disease of Childhood

ADELE R. ALTMAN[1]

Extension of lung infection directly into the contiguous thoracic tissues is a well documented complication of actinomycosis and nocardiosis [1]. Less commonly, tuberculosis and, rarely, pyogenic pneumonias may present as chest wall abscesses. Thoracic wall extension of pulmonary aspergillosis is rare, and to my knowledge no previous report has appeared in the American radiologic literature. Radiologists must be aware of the virulence of this fungus when it invades the lung opportunistically in children suffering from chronic granulomatous disease of childhood, a primary immune deficiency disease.

Case Reports

Case 1

T. D., a pale chronically ill 10½-year-old boy, was admitted with an incapacitating painful swelling of the right axilla which extended posteriorly over the chest wall and superiorly into the supraclavicular fossa. His mother affirmed that since age 1 year he suffered from recurring febrile illnesses characterized by pulmonary infections and suppurative adenitis. At age 6 resection of the apical segment of the right upper lobe was performed. Preoperative chest radiographs showed consolidating pneumonia of the apical segment of the right upper lobe associated with hilar adenopathy (fig. 1). The pneumonia had not responded to antimicrobial therapy, including antitubercular drugs. Microscopic examination showed a chronic inflammatory disease of unknown origin.

On initial physical examination, the right upper side of the chest wall was dull to percussion; breath sounds were decreased and bronchial. The left lung sounded normal. The admitting chest radiograph demonstrated dense opacification of the right upper lung field, and the scapula was displaced laterally. The axillary segment of the second rib was eroded and the posterior segment destroyed. The third rib was displaced downward and showed wavy erosion posteriorly (fig. 2*A*). An overpenetrated view confirmed marginal erosion of the body and pedicle of the second thoracic vertebra (fig. 2*B*). The rest of the lung showed chronic postinflammatory changes of the left upper lobe and both lower lung fields, and bilateral hilar adenopathy.

Results of tests for tuberculosis, histoplasmosis, blastomycosis, coccidioidomycosis, and sporotrichosis were negative. Granulocytes showed no reduction of nitroblue tetrazolium dye. The granulocytes ingested staphylococci in normal numbers but were unable to destroy them, establishing the diagnosis of chronic granulomatous disease of childhood.

The axillary abscess was incised and drained. *Aspergillus nidulans* was cultured and was demonstrated in the biopsied tissue using special stains. The patient was treated with amphotericin B and responded well initially. However, 3 months later he was readmitted for excision of a large abscess of the upper lobe of the right lung. Subsequently, a thoracoplasty to close a bronchopleural fistula confirmed osteomyelitis of the second and third ribs and the adjacent vertebral bodies caused by the same fungus.

Case 2

A. M., a febrile irritable 2-year-old boy, was admitted when his mother noted a lump on his right anterior chest wall. For the previous 2 months, he was treated with antibiotics for recurring febrile episodes. He suffered from recurring infections since birth, including pneumonia, tonsillitis, impetigo, otitis media and lymphadenopathy. Physical examination revealed a 2½ x 3 cm oval tender mass fixed to the chest wall adjacent to the right

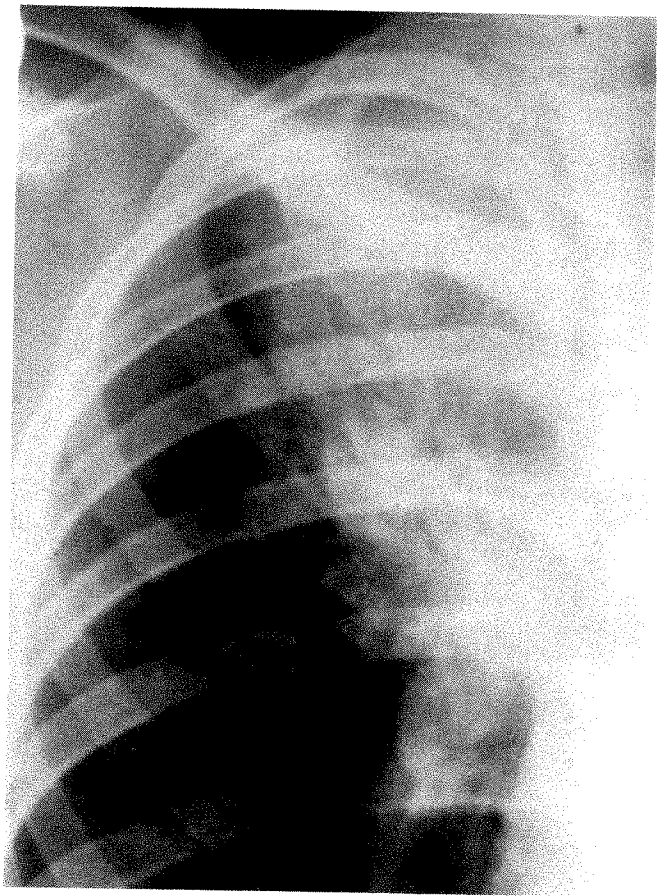

Fig. 1.—Film of right upper lobe showing apical segment pneumonia associated with hilar adenopathy.

Received December 5, 1976; accepted after revision April 6, 1977.

[1] Department of Radiological Sciences, University of Oklahoma Health Sciences Center, P. O. Box 26901, Oklahoma City, Oklahoma 73190.

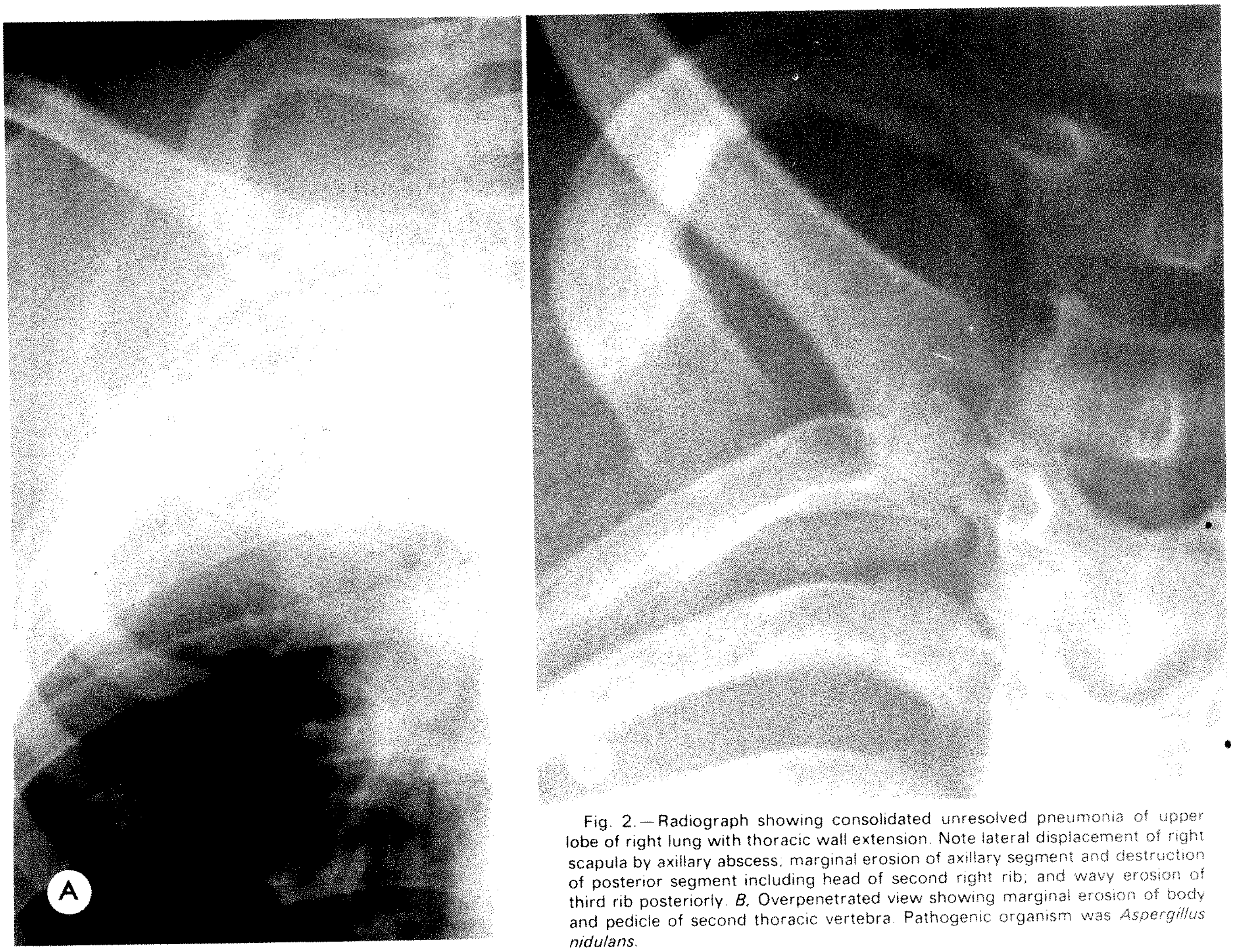

Fig. 2.—Radiograph showing consolidated unresolved pneumonia of upper lobe of right lung with thoracic wall extension. Note lateral displacement of right scapula by axillary abscess, marginal erosion of axillary segment and destruction of posterior segment including head of second right rib; and wavy erosion of third rib posteriorly. *B*, Overpenetrated view showing marginal erosion of body and pedicle of second thoracic vertebra. Pathogenic organism was *Aspergillus nidulans*.

nipple. Another nonmovable mass 1.5 x 2 cm was present in the midepigastrium. Rales were heard in the left posterior lung with scattered rhonchi on the right side.

The chest radiograph showed right upper lobe pneumonia with localized pleural thickening and lytic wavy destruction of the right third rib (fig. 3). Hilar adenopathy and chronic post-inflammatory pulmonary changes were present bilaterally.

Skin test reactions to the usual antigens were negative. A negative nitroblue tetrazolium dye test established the diagnosis of chronic granulomatous disease of childhood. Excisional biopsy of anterior chest wall and abdominal wall masses was performed; *Aspergillus fumigatus* was cultured and was demonstrated in the biopsied tissue.

Discussion

Chronic granulomatous disease of childhood was first described in 1957 by Berendes et al. [2]. It is characterized by recurrent infections which fail to respond to aggressive antimicrobial therapy. Subsequently it was identified as a primary immune deficiency disease in which the patient's granulocytes are unable to destroy ingested bacteria. Immunologic responses are otherwise normal [3].

The disease is transmitted as an X-linked recessive trait, affecting males; rarely, it may be inherited as an autosomal recessive trait. Onset of symptoms occurs early in childhood, with recurrent febrile illnesses consisting of suppurative lymphadenitis, eczematoid dermatitis, visceral abscesses, and osteomyelitis frequently involving the small bones of the hands and feet. Recurring lobar and bronchopneumonias are complicated by empyema, pericarditis, lung abscesses, and massive hilar and mediastinal adenopathy. The pneumonias resolve slowly, frequently leaving one or more masslike residua. Persistent anemia, hepatosplenomegaly, and elevated globulin fractions are the rule.

Aspergillus is a mold common in the human environment but rarely pathogenic to humans. Various species, most commonly *A. fumigatus*, may cause stubborn chronic infections of the ear and lung, although involvement of almost every organ system has been reported [4]. In the lung, aspergillus infection may be limited to the air passages, resulting in an allergic reaction manifested by a Löffler-like syndrome and in development of mucoid plugs. Less commonly, the fungus invades preexisting granulomatous or neoplastic cavities, forming clumped aggregates of

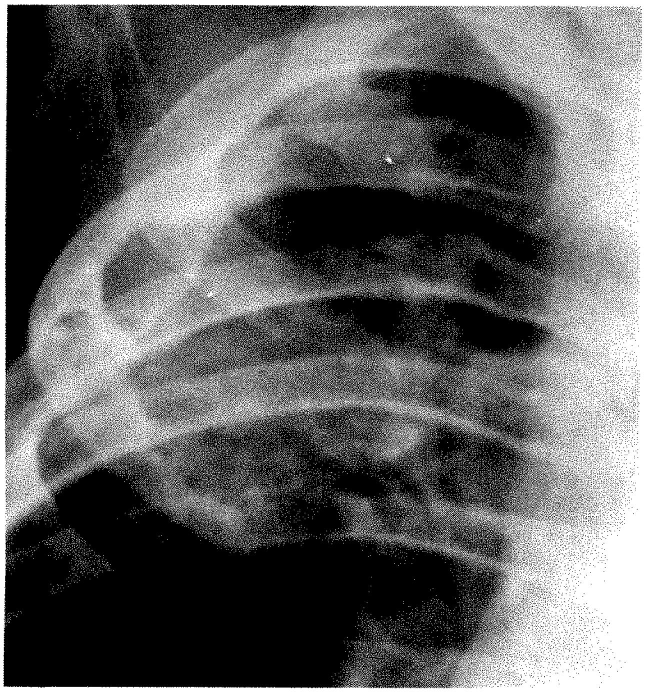

Fig. 3.—Radiograph showing *Aspergillus fumigatus* pneumonia of right upper lobe with pleural involvement and lytic destruction of right third rib.

celluar debris containing mycelia, the "fungus ball" [5, 6].

Rarely, aspergillosis is a fulminating fatal disease, producing disseminated patchy pulmonary infiltrates bilaterally with mediastinal and pericardial involvement [7]. Pulmonary aspergillosis has been reported increasingly in children suffering from debilitating diseases such as leukemia who have been treated with steroids, antibiotics, and chemotherapeutic agents [8].

Invasive pulmonary aspergillosis has been reported in patients afflicted with chronic granulomatous disease of childhood [9–11], but none of those cases had thoracic wall penetration. However, the European clinical literature contains a report [12] in which pulmonary aspergillosis was complicated by osteomyelitis of adjacent posterior ribs and vertebrae and a paraspinal upper thoracic abscess. Although phagocytic function studies of granulocytes were unavailable in 1954, the clinical and autopsy findings suggest that their patient had chronic granulomatous disease of childhood.

In the presence of immune deficiency disease, pulmonary aspergillosis should be considered in the differential diagnosis of consolidating pneumonias which spread across tissue planes into the thoracic wall.

ACKNOWLEDGMENT

I thank Dr. Jean A. Vanhoutte, for permission to include case 2.

REFERENCES

1. Fraser RG, Pare JAP: *Diagnosis of Diseases of the Chest*. Philadelphia, Saunders, 1970
2. Berendes H, Bridges RA, Good RA: A fatal granulomatosus of childhood. The clinical study of a new syndrome. *Minn Med* 40:309–312, 1957
3. Holmes B, Quie PG, Windhorst DB, Good RA: Fatal granulomatous disease of childhood: an inborn abnormality of phagocytic function. *Lancet* 1:1225–1228, 1966
4. Blattner RJ: Pulmonary aspergillosis in children. *J Pediatr* 70:139–141, 1967
5. Zimmerman RA, Miller WT: Pulmonary aspergillosis. *Am J Roentgenol* 109:505–514, 1970
6. Freundlich IM, Israel HL: Pulmonary aspergillosis. *Clin Radiol* 24:248–253, 1973
7. Hunt W, Broders AC, Stinson JC, Carabasi RJ: Primary pulmonary aspergillosis with invasion of the mediastinal contents and lymph nodes. *Am Rev Respir Dis* 83:886–890, 1961
8. Berkel I, Say B, Tinaztepe B: Pulmonary aspergillosis in a child with leukemia. Report of a case and a brief review of the pediatric literature. *N Engl J Med* 269:893–896, 1963
9. Wolfson JJ, Quie PG, Laxdal SD, Good RA: Roentgenologic manifestations in children with a genetic defect of polymorphonuclear leukocyte function. Chronic granulomatous disease of childhood. *Radiology* 91:37–48, 1968
10. Johnston RB, McMurray JS: Chronic familial granulomatosis. Report of five cases and review of the literature. *Am J Dis Child* 114:370–378, 1967
11. Grunberg J, Satge P, Meyer CB, Paupe J, Vialatte J: Nouvelle observation de maladie granulomateuse. Syndrome de Bridge et Good. *Ann Pediatr* 17:560–568, 1970
12. Tobler W, Minder W: Generalisierte chronische Aspergillose beim Kind und ihre Beziehung zur antibiotische Therapie. *Helv Paediatr Acta* 9:209–230, 1954

Calcification in a Paraspinal Malignant Melanoma in a Child

PHILIP STANLEY,[1] STUART E. SIEGEL,[2] AND HART ISAACS[3]

Malignant melanomas are uncommon tumors in childhood, usually arising from the skin. This report documents an intrathoracic malignant melanoma with dumbbell extension into the extradural space appearing radiologically as a calcified paraspinal mass.

Case Report

A 12-year-old white girl was in excellent health until onset of intermittent right subscapular pain. After 3 months she developed right lateral rib cage and flank pain associated with a dry cough and mild dyspnea. A 4.5 kg weight loss occurred during this period. A chest radiograph revealed a large mass, and she was transferred to Childrens Hospital for futher evaluation.

Physical examination revealed a midly tachypneic girl with signs of right pleural effusion. The liver edge was palpable 4 cm below the right costal margin. There was a dilated right pupil without ptosis but no other neurologic abnormalities. Thorough examination of the eyes, skin, and mucosal surfaces failed to reveal any unusual lesions.

Inital laboratory evaluation included a normal hemogram and urinalysis. Serum chemistry studies revealed blood urea nitrogen, 15 mg/100 ml; serum glutamic oxaloacetic transaminase, 34 U; serum glutamic pyruvic transaminase, 15 U; alkaline phosphatase, 116 U; uric acid, 4.9 mg/100 ml; and lactic dehydrogenase, 574 U. Alpha fetoprotein was undetected in the serum. Biochemical analysis of a single voided urine specimen revealed normal levels of vanillylmandelic acid, homovanillic acid, and cysthathionine, but large amounts of 5, 6-dehydroxyindole precursors were detected.

Chest radiograph on admission revealed a calcified mass lying posteriorly in the third right intercostal space and a large right pleural effusion. A small mass in the left lung was also noted (fig. 1). Tomograms revealed a calcified dumbbell tumor at the level of T3 extending into the spinal canal, with erosion of the posterior aspect of the third rib and flattening and separation of the pedicles of T3 and T4 on the right side (fig. 2).

A myelogram demonstrated an extradural mass at this level without obstruction to the flow of Pantopaque (fig. 3). An intravenous urogram and ^{99m}Tc sulphide liver and spleen scans were normal. Primitive large cells suggestive of malignancy were seen in the cell block from the pleural tap.

A right thoracotomy revealed a large mass involving the right upper lobe and adjacent mediastinum with multiple grayish black nodules on the pleura. Biopsies of the mass and several nodules revealed bizarre spindle-shaped cells (fig. 4) containing pigment identified as melanin by Schmorl's bile, Lillie's ferro iron uptake, and indirect aldehyde fuchsin stains. Electron microscopy confirmed the diagnosis of malignant melanoma, demonstrating membrane-bound melanosomes in many of the cells. A section of the fourth rib also contained tumor in the marrow cavity. After surgery, the patient was placed on therapy consisting of dimethyl triazeno imidazole carboxamide (NSC no. 45388) and bacille Calmette Guérin by scarification. She also received a course of radiation therapy to the T3–T4 region.

Despite these therapeutic maneuvers, the disease progessed and the patient died 1 month later. Postmortem examination limited to the thoracic cavity revealed a malignant melanoma in the paraspinal region at T3 extending extradurally into the spinal canal. There was massive tumor involvement of the right pleural space and both lungs. Death was due to complete tumor obstruction of the superior vena cava and massive pulmonary involvement.

Discussion

There has been considerable controversy regarding exact pathologic classification of melanotic tumors in childhood. However, it is agreed that malignant melanoma with lethal potential is rare in prepubertal children [1]. Primary melanocytic lesions usually arise from the skin or retina but can arise from unusual sites. These atypical locations include sympathetic ganglia and meninges [2]. It is probable that in this case the tumor arose from the sympathetic ganglia. However, it is possible that melanoma involving the paravertebral sympathetic ganglia could be metastatic from a leptomeningeal primary not visualized with an autopsy limited to the thorax. There was no evidence of skin, mucosal, or retinal primary tumors on clinical examination. Both histochemical and ultrastructural studies confirmed the diagnosis of malignant melanoma.

Only a few tumors in childhood exhibit nonhomogeneous curvilinear and nodular calcification radiogically and are extradural. Metastatic osteogenic sarcoma may calcify and be paraspinal with extradural extension (P. Stanley and S. E. Siegel, in preparation), but in our patient there was no evidence of a primary tumor. Calcification within meningiomas is not uncommon in adults [3], and extradural menigniomas with dumbbell extension have been described [4] although they are rare in children [5]. Calcification in a paravertebral mass in children is most frequently seen with neuroblastoma and ganglioneuroblastoma; intraspinal extension is not uncommon with these tumors [6, 7]. Calcification in a malignant melanoma is most unusual; there is a single previous report in a 61-year-old woman with metastatic melanoma to the left adrenal from a skin primary [8]. It is of interest that the thoracic sympathetic chain and adrenal medulla are both part of the sympathetic nervous system derived embryologically from the primordial cells of the neural crest, which also give rise to the pigment cells of the integument as well as contributing to the formation of the meninges [2].

The recording of a second case should alert radiologists

Received January 31, 1977; accepted March 17, 1977.

This work was supported in part by grant no. 02649 from the National Institutes of Health.

[1] Department of Radiology, Childrens Hospital of Los Angeles, 4650 Sunset Boulevard, Los Angeles, California 90054. Address reprint requests to P. Stanley.

[2] Department of Pediatrics, Childrens Hospital of Los Angeles, Los Angeles, California 90054.

[3] Department of Pathology, Childrens Hospital of Los Angeles, Los Angeles, California 90054.

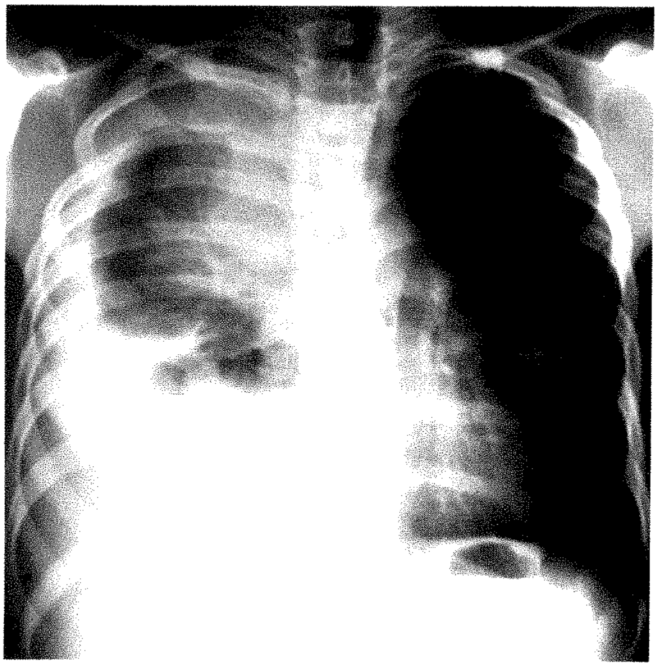

Fig. 1. — Posteroanterior chest film showing large right pleural effusion, mass in left lung, and large right paravertebral mass with calcification.

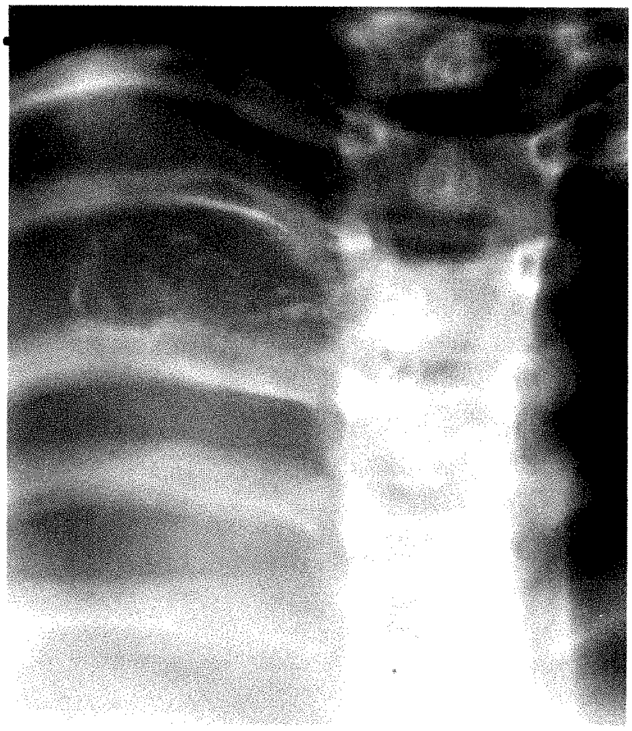

Fig. 2. — Anteroposterior tomogram showing calcified tumor with dumbbell extension into spinal canal.

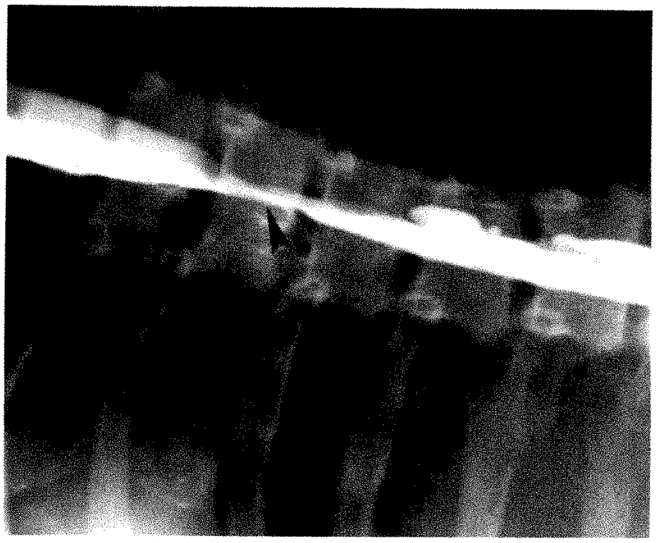

Fig. 3. — Right lateral decubitus view of myelogram showing extradural extent of tumor (*arrow*).

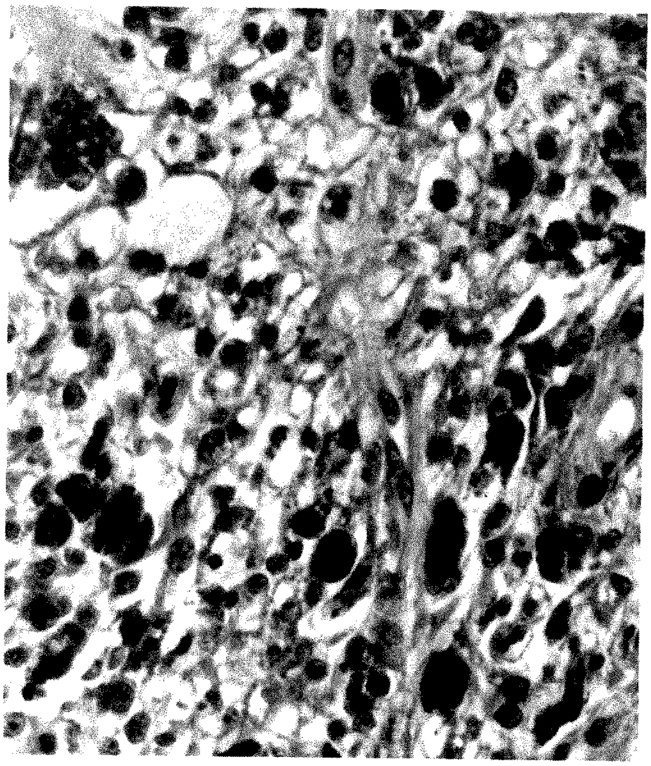

Fig. 4. — Histologic section showing spindle-shaped pleomorphic tumor cells with abundant melanin pigment. H and E, X320.

to include malignant melanomas in the differential diagnosis of calcified tumors arising within the neural crest derivatives. In this situation, examination of the urine for metabolic products is most helpful in reaching the correct diagnosis. The finding of intermediary metabolic products of melanin would indicate the presence of melanotic tumor, whereas raised levels of cathecholamines would suggest a neuroblastoma [9].

REFERENCES

1. Trozak DJ, Rowland WD, Hu F: Metastatic malignant melanoma in prepubertal children. *Pediatrics* 55:191–204, 1975
2. Fu YS, Kaye QI, Lattes R: Primary malignant melanocytic

tumors of the sympathetic ganglia with the ultrastructural study of one. *Cancer* 36:2029–2041, 1975

3. Pear BL, Boyd HR: Roentgenographically visible calification in spinal meningioma. *Am J Roentgenol* 120:32–45, 1974
4. Hallpike JF, Stanley P: A case of extradural spinal meningioma. *J Neurol Neurosurg Psychiatry* 31:195–197, 1968
5. Calogero JA, Moosy J: Extradural spinal meningiomas. *Neurosurgery* 37:442–447, 1972
6. Fagan DJ, Swischuk LE: Dumbbell neuroblastoma or ganglioneuroblastoma of the spinal canal. *Am J Roentgenol* 120:453–460, 1974
7. Kirks DR, Berger PE, Fitz CR, Harwood-Nash DC: Myelography in the evaluation of paravertebral mass lesions in infants and children. *Radiology* 119:603–608, 1976
8. Twersky J, Levin DC: Metastatic melanoma of the adrenal. *Radiology* 116:627–628, 1975
9. Lang WE, Siegel SE, Shaw KNF, Landing BH, Baptista J: Initial urinary cathecholamine metabolites and prognosis in neuroblastoma. Paper presented at the annual meeting of the American Society of Clinical Oncology, Toronto, Ontario, May 1976

Catheter Venography in the Superior Vena Cava Syndrome

W. RICHARD WEBB,[1] GORDON GAMSU, AND BARBARA M. ROHLFING

Superior venacavography is commonly used to evaluate patients with symptoms of superior vena cava obstruction [1–4]. Routinely, iodinated contrast material or radionuclide is injected simultaneously into both antecubital veins, and sequential radiographs or scintigrams of the chest are obtained [1–4]. These methods accurately demonstrate blood flow and collateral pathways [2–5] but may not show the actual site of venous obstruction.

In patients with superior vena cava obstruction and peripherally located collateral pathways, stasis or reversal of blood flow sometimes occurs in the brachiocephalic or subclavian veins. This prevents their complete filling with peripherally injected contrast material or radiopharmaceutical, even though these veins are patent. In such patients, the anatomic point of venous obstruction is not visualized by routine phlebography, and a misdiagnosis of brachiocephalic or subclavian vein obstruction may be made.

A technique of superior venacavography using a percutaneously placed catheter has been described by Amundsen [5]. It is easily performed and allows delineation of vascular anatomy in patients with superior vena cava obstruction, not obtainable by conventional means. The value of the technique is illustrated in this report.

Case Report

A 48-year-old woman was referred for evaluation of a 3 X 5 cm oval mass in the upper lobe of the right lung. Because biopsy of palpable enlarged right supraclavicular nodes revealed poorly differentiated adenocarcinoma, the patient was treated over the next 51 days with 6,000 rad to the right upper lobe and 5,000 rad to the mediastinum. The right upper lobe mass decreased in size following treatment, but the chest radiograph showed volume loss in the right upper lobe and a questionable mediastinal widening (fig. 1). The patient did well until 1 year later when she noted edema of her face, neck, and arms. Physical examination showed some dilatation of chest wall veins, and a tentative diagnosis of superior vena cava obstruction was made.

A radionuclide superior venacavogram was obtained (fig. 2) and interpreted as showing right brachiocephalic and left subclavian vein obstruction. Catheter venography was then performed.

Using the Seldinger technique, a no. 7 French end-hole catheter (U.S. Catheter and Instrument Corp., Glen Falls, N.Y.) was passed into the median basilic vein in the antecubital fossa. Under fluoroscopic control, forceful 5 ml injections of contrast material (Renografin-60, Squibb, Princeton, N.J.) were made. Each injection opacified the vein for a distance of 4–5 cm beyond the catheter tip, and sluggish blood flow allowed excellent visualization of the vessel lumen. Following each injection, the catheter was advanced to the limits of venous opacification and another injection was made; this method ensured that the catheter would not be passed into an abnormal or obstructed segment. Then 30 ml of the same contrast agent was injected with the catheter tip at the junction of the right and left brachiocephalic veins.

Sequential opacification of the left basilic, axillary, subclavian, and brachiocephalic veins disclosed no venous obstruction, narrowing, or intraluminal clot. However, stasis of injected contrast material occurred in the left subclavian vein with slow washout via paravertebral and chest wall collaterals. This appearance at fluoroscopy was identical to that noted on the radionuclide scintigram (fig. 2).

Rapid injection of contrast material with the catheter tip near the superior vena cava accurately located the site of obstruction. An abrupt cutoff of the superior vena cava was noted at its origin (fig. 3*A*). Large paravertebral collaterals reconstituted the azygous system (fig. 3*A* and 3*B*). Internal thoracic collaterals were also well demonstrated.

Discussion

Appropriate surgical or radiation therapy of patients with superior vena cava syndrome requires that the exact site of obstruction be known [5–7]. In most cases, bilateral antecubital phlebography is sufficient to outline vascular anatomy [3, 5, 7]. In some patients, however, peripherally injected contrast material or radionuclide will not fill the subclavian or brachiocephalic veins [3, 5, 8]. This can reflect tumor or clot obstructing the lumen [3, 8], increased intrathoracic pressure [5], or reversal of flow in central veins.

Venous pseudoobstruction is most likely to occur when the central collateral pathways (azygous and right internal thoracic veins) are either obstructed or small, and the majority of blood flow is therefore via lateral thoracic, left internal thoracic, or vertebral branches arising peripherally [8]. If azygous or right internal thoracic veins are predominant, antegrade flow persists within the brachiocephalic and subclavian veins, allowing their opacification following peripheral injection of contrast material.

In patients with superior vena cava syndrome, a catheter technique of venography permits a definition of vascular anatomy not obtainable by usual methods. Fluoroscopic control ensures that the catheter will not be advanced through an abnormal or obstructed segment of vein. This catheter technique should be performed when (1) routine superior venacavography demonstrates obstruction to flow at the level of subclavian or brachiocephalic veins, and (2) therapy requires knowing the exact site of obstruction.

REFERENCES

1. Howard N: Phlebography in superior vena caval obstruction. *Radiology* 81:380–383, 1963

Received January 10, 1977; accepted after revision March 18, 1977.

G. Gamsu is the recipient of training grant GM 01272 from the National Institute of General Medical Sciences.

[1] All authors: Department of Radiology, University of California, San Francisco, California 94143. Address reprint requests to G. Gamsu.

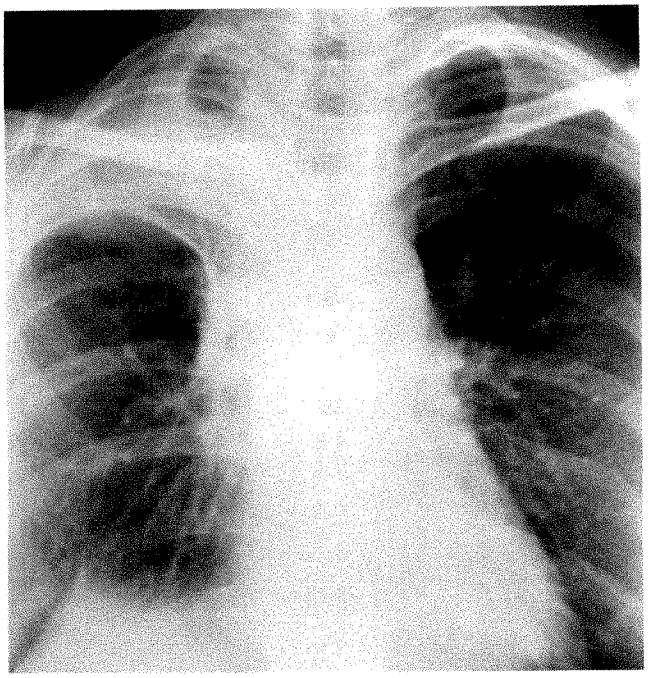

Fig. 1.—Posteroanterior chest radiograph showing volume loss in right upper lobe. Absence of mediastinal shift suggests mediastinal abnormality.

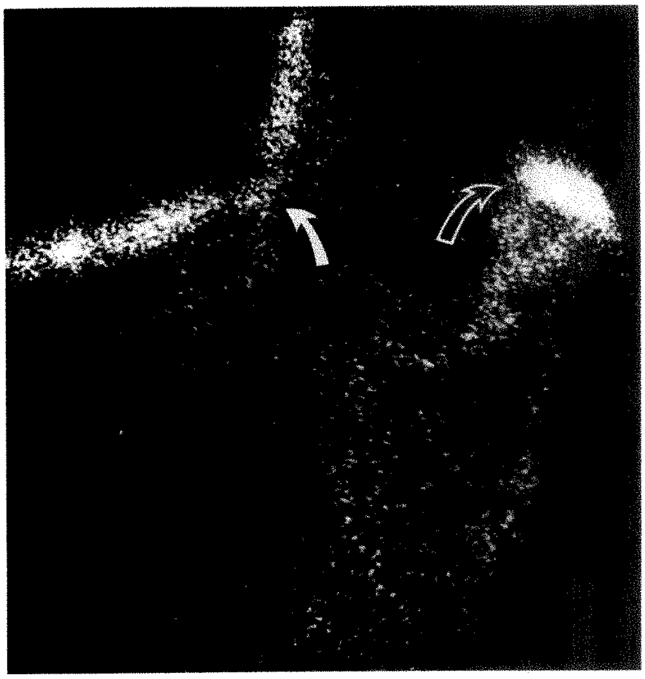

Fig. 2.—Radionuclide superior venacavogram 20 sec after bilateral injection of 5 mCi ^{99m}Tc sulfur colloid. Note apparent obstruction of right brachiocephalic (*solid arrow*) and left subclavian veins (*open arrow*). Retrograde filling of right jugular vein has occurred.

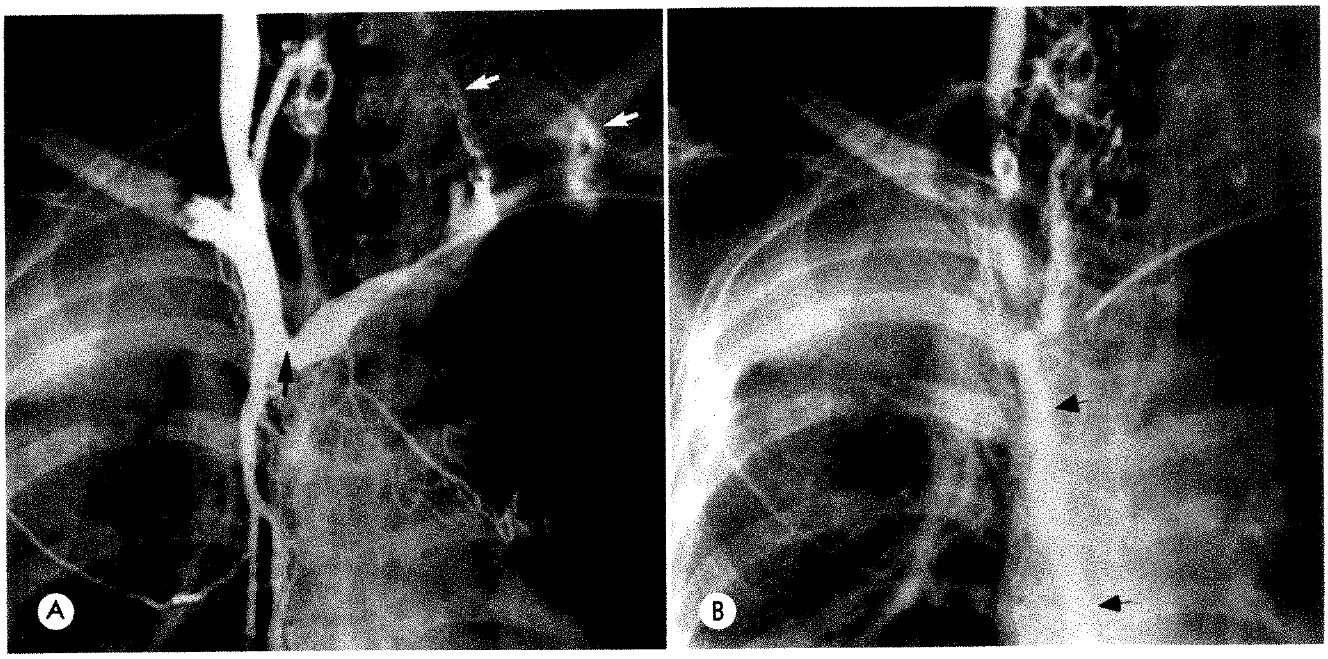

Fig. 3.—Catheter venogram. *A,* Catheter positioned near junction of brachiocephalic veins. Note normal right brachiocephalic vein; obstruction site (*black arrow*) is at origin of superior vena cava. Retrograde flow in left brachiocephalic vein fills paravertebral collaterals (*white arrows*). *B,* Paravertebral collaterals draining via azygous system (*arrows*).

2. Maxfield WS, Meckstroth GR: Technetium-99m superior vena cavography. *Radiology* 92:913–917, 1969
3. Miyamae T: Interpretation of ^{99m} Tc superior vena cavograms and results of studies in 92 patients. *Radiology* 108:339–352, 1973
4. Roswit B, Kaplan G, Jacobson HG: The superior vena cava obstruction syndrome in bronchogenic carcinoma: pathologic physiology and therapeutic management. *Radiology* 61:722–736, 1953
5. Amundsen P: Pulmonary angiography in lung and mediastinal

tumors, in *Angiography*, 2d ed, edited by Abrams HL, Boston, Little, Brown, 1971, pp 539–595

6. Scannell JG: Etiology and surgical approaches in superior vena caval obstruction. *Radiology* 81:378–379, 1963
7. Son YH, Wetzel RA, Wilson WJ: ^{99m}Tc pertechnetate scintiphotography as diagnostic and follow-up aids in major vascular obstruction due to malignant neoplasm. *Radiology* 91:349–357, 1968
8. Okay NH, Bryk D: Collateral pathways in occlusion of the superior vena cava and its tributaries. *Radiology* 92:1493–1498, 1969

Cerebrospinal Fluid Rhinorrhea Demonstrated by Metrizamide CT Cisternography

BURTON P. DRAYER,[1] ROBERT H. WILKINS,[2] MANFRED BOEHNKE,[3] JOSEPH A. HORTON,[1] AND ARTHUR E. ROSENBAUM[1]

Cerebrospinal fluid rhinorrhea is often a difficult diagnostic and therapeutic problem for the physician and a life-threatening situation for the patient. Radionuclide cisternography [1, 2] has become the most widely used method for localization. However, the low resolution character of radioisotopic studies often limits the ability to precisely define the site of leakage [3]. Failure to accurately localize the origin of the leak may require a more extensive exploratory surgical procedure.

Metrizamide (Amipaque; Sterling-Winthrop, Rensselaer, N.Y.), the nonionic water soluble intrathecal myelographic contrast agent, can consistently and accurately delineate the basal subarachnoid cisterns on cranial computed tomography [4]. This report describes a case in which metrizamide CT cisternography proved efficacious for diagnosing the presence and anatomic site of cerebrospinal fluid of rhinorrhea.

Case Report

A 56-year-old woman was admitted with a chief complaint of persistent leakage of fluid from her left nostril. The fluid drainage began 7 years earlier after severe frontal trauma from an automobile accident. It stopped spontaneously 10 months after onset but recurred 4 years later and was treated by a left external ethmoidectomy with fascia lata packing.

The nasal drainage recurred 4 months prior to admission. Neurologic examination was normal with no signs of meningitis. There was near constant drainage of clear fluid which had the chemical characteristics of cerebrospinal fluid.

Pluridirectional tomography revealed an irregularity in the middle two posterior ethmoidal air cells on the left which was not distinguishable from postsurgical reaction. An interruption in the dorsum sella on the left side adjacent to the sphenoid sinus was also noted. Positional attempts to elicit fluid levels were unsuccessful. Radionuclide cisternography confirmed that cerebrospinal fluid leaked into the left nasal passage; however, the site of leakage could not be defined.

In an attempt to better localize the cranial defect associated with the leakage, metrizamide CT cisternography was performed. Metrizamide was introduced into the lumbar subarachnoid space. Prone Trendelenberg CT using a body scanner (EMI 5000) revealed normal metrizamide-filled basal subarachnoid cisterns (fig. 1). Metrizamide also layered in the left nasal passage and could be visualized on a handkerchief placed externally in front of the left external naris (fig. 2*A*). The left sphenoid sinus also contained metrizamide (fig. 2*B*), demarcating the site of leakage (sphenonasal-type cerebrospinal fluid rhinorrhea).

At surgery, an incision was made at the upper gingiva–buccal mucosa junction. Surgical entry, inspection, and muscle packing of the left sphenoid sinus was performed; the exact site of leakage was not definitely determined. After surgery no leakage was observed; however, 2 months later some drainage occurred, but no further diagnostic studies were requested.

Technique

Lumbar puncture is done with the aid of image-intensified fluoroscopy (for needle placement) using a 22 gauge needle with the patient prone on a myelographic tilt table. No premedication or anticonvulsant prophylaxis is necessary. The intrathecal instillation of 6 ml of 190 mg iodine/ml (1.14 g) metrizamide is ascertained by fluoroscopic screening. With the patient erect, the spinal needle is removed, the patient turned prone, and the table tilted into the −60° (Trendelenberg) position. After remaining head down for 60 sec, the patient is returned to the −10° (Trendelenberg) position, placed on a similarly inclined stretcher, and transferred to the CT scanner. During scanning (preferably done with a body scanner or non-water bag head scanner) the patient remains prone or in a knee-chest position to encourage flow of the hyperbaric, radiopaque metrizamide through the cranial defect to enter the sinus and draining nasal (or otic) passage.

Discussion

With the introduction of metrizamide, a water soluble investigational contrast agent is now available to safely study the intracranial subarachnoid spaces. Animal experiments have confirmed the relatively low epileptogenic effect of metrizamide compared to previously used intracranial subarachnoid agents [5]. The decreased toxicity has been obtained by lowering the osmolality and lipid solubility of the contrast material. However, over half of the more than 100 patients studied by metrizamide CT cisternography at our institution had transient adverse reactions of mild to moderate severity. These included headache, nausea, vomiting, and (rarely) short-lived nonfrightening perceptual aberrations [6]. No seizures occurred even without anticonvulsant prophylaxis. Due to the high sensitivity of CT and our immediate intracranial placement technique, low volumes (and concentrations) of metrizamide may be used, thus decreasing the incidence and severity of adverse reactions. The hyperbaric nature of the contrast medium enables facile gravitational movement of the agent to the area of suspected abnormality.

When the location of a cerebrospinal fluid leakage cannot be demonstrated by multidirectional tomography (including positional attempts to detect fluid levels), radionuclide or metrizamide CT cisternography may be neces-

---

Received January 4, 1977; accepted after revision March 23, 1977.

[1] Department of Radiology, University of Pittsburgh School of Medicine, Presbyterian-University Hospital, 230 Lothrop Street, Pittsburgh, Pennsylvania 15261. Address reprint requests to B. P. Drayer.

[2] Department of Neurological Surgery, University of Pittsburgh School of Medicine, Presbyterian-University Hospital, Pittsburgh, Pennsylvania 15261. Present address: Department of Neurological Surgery, Duke University School of Medicine, Durham, North Carolina 27706.

[3] Department of Radiology, Montefiore Hospital, Pittsburgh, Pennsylvania 15213.

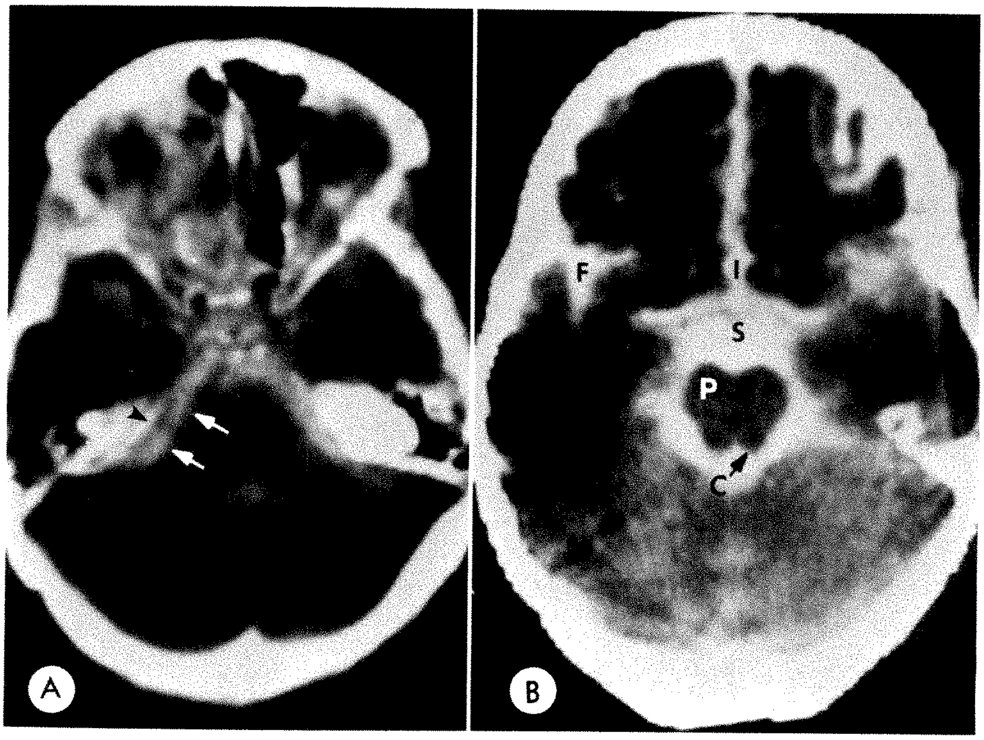

Fig. 1.—*A*, Metrizamide CT cisternography showing cerebellopontine angle cistern (*arrows*) filled with metrizamide and separable from adjacent petrous pyramid (*arrowhead*). *B*, Scan 13 mm cephalad to *A* showing metrizamide completely filling circummesencephalic cisterns and outlining structures such as colliculi (C) and cerebral peduncles (P). Metrizamide-filled suprasellar (S) and interhemispheric (I) cisterns as well as Sylvian fissure (F) seen to advantage.

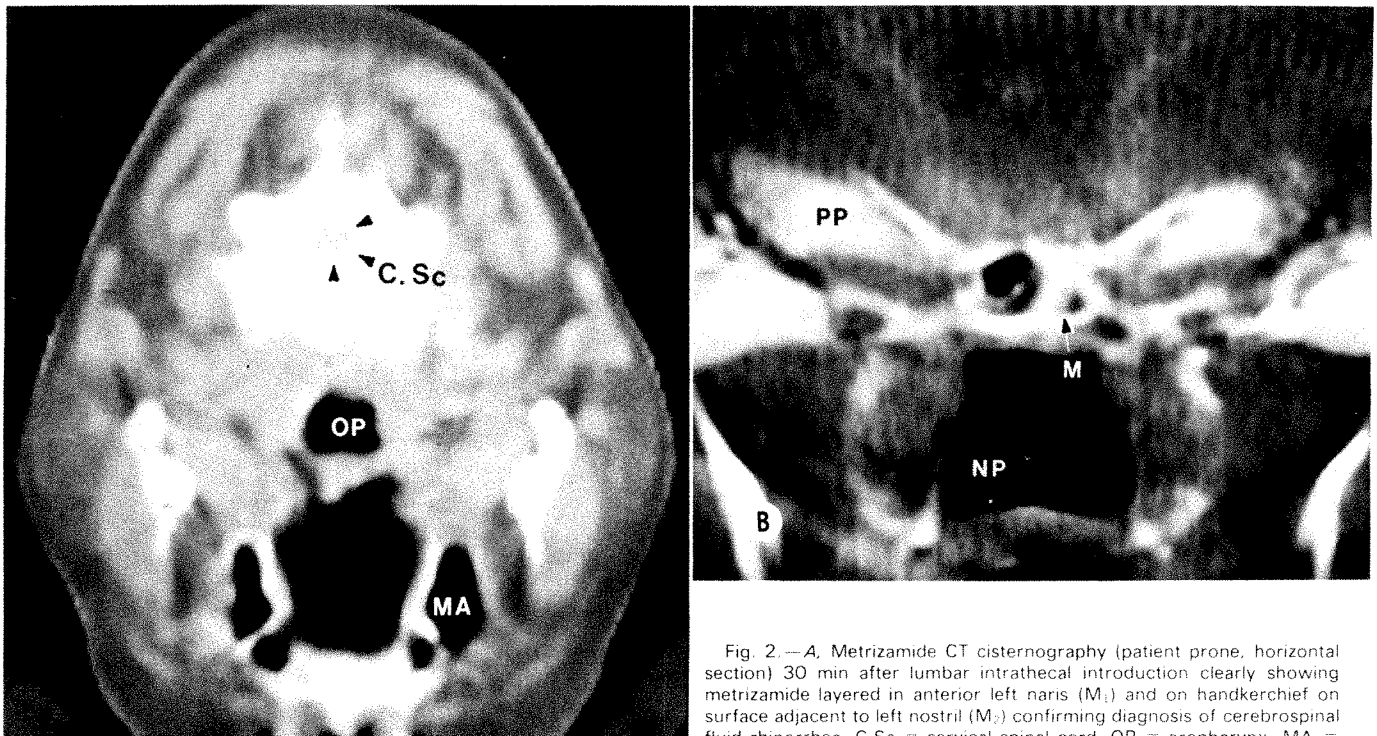

Fig. 2.—*A*, Metrizamide CT cisternography (patient prone, horizontal section) 30 min after lumbar intrathecal introduction clearly showing metrizamide layered in anterior left naris (M_1) and on handkerchief on surface adjacent to left nostril (M_2) confirming diagnosis of cerebrospinal fluid rhinorrhea. C.Sc = cervical spinal cord, OP = oropharynx, MA = maxillary antrum. *B*, Coronal section with patient prone showing metrizamide (M) in left sphenoid sinus localizing site of fluid leakage. NP = nasopharynx, PP = petrous pyramid

sary. Both procedures confirm the presence of an abnormal communication between the intracranial subarachnoid space and the external environment. Adverse reactions are more common with metrizamide; however, if surgical therapy requires precise localization of the defect, metrizamide CT cisternography will be superior to radionuclide cisternography. Water soluble contrast agents have the additional advantage of easier storage and handling than radioisotopes.

Forthcoming CT technology will include improved resolution, accelerated scanning speeds, inclined tables, and additional reconstruction capacities. These improvements, along with development of contrast agents of even lower toxicity, should further enhance the role of intrathecally enhanced CT cisternography as the definitive radiologic study in the evaluation of cerebrospinal fluid rhinorrhea.

REFERENCES

1. Ashburn WL, Harbert Jc, Briner WH, Di Chiro G: Cerebrospinal fluid rhinorrhea studies with the gamma scintillation camera. *J Nucl Med* 9:523–529, 1968
2. Allen MB, Gammal TE, Ihnen M, Cowan MA: Fistula detection in cerebrospinal fluid leakage. *J Neurol Neurosurg Psychiatry* 35:664–668, 1972
3. Oberson R: Radioisotope diagnosis of rhinorrhea. *Radiol Clin Biol* 41:28–35, 1972
4. Drayer BP, Rosenbaum AE: Suprasellar masses on computerized tomography with intrathecal metrizamide. *Lancet* 2:736–737, 1976
5. Metrizamide 1973: Metrizamide, a non-ionic water-soluble contrast medium. *Acta Radiol* [*Suppl*] (Stockh) 335:1–390, 1973
6. Drayer BP, Rosenbaum AE: Amipaque brain penetrance: correlation with adverse reactions and value radiodiagnostically. *Acta Radiol* [*Suppl*] (Stockh). In press, 1977

Inadvertent Intrasplenic Injection of Oily Propyliodone

ETHAN BRAUNSTEIN[1]

Oily propyliodone is a contrast material used commonly in bronchography. In the case described, an attempt was made to demonstrate a bronchopleural fistula by injecting this substance into an empyema cavity. Unfortunately it was injected into the spleen, and then appeared in the liver. Apparently this is the first report of such an occurrence.

Case Report

A 51-year-old Caucasian female alcoholic was admitted to the University of Michigan Medical Center for evaluation of chronic and recurrent chest disease. The patient had a partial left pneumonectomy for cavitary tuberculosis in 1963. A recurrence in February 1976 was treated with rifampin and isoniazid. During her present admission, she had recurrent hemoptysis and spiking fevers, but sputum smears were repeatedly negative for acid-fast bacilli. An empyema cavity was identified on a chest radiograph.

It was decided by the attending surgeon to inject oily propyliodone (Dionosil; Glaxo Labs, London) into the left pleural space to delineate the extent of the empyema space and to determine whether a bronchopleural fistula was present. This was performed without fluoroscopy, and 4 ml of the contrast material were injected inadvertently into the left upper quadrant of the abdomen. The loss of left lung volume and high position of the diaphragm were presumably responsible for misjudging needle placement. Some of the contrast material entered the peritoneal cavity, but much of it was injected directly into the spleen. It apparently entered the portal circulation, for it appeared in the liver on x-rays 20 min after the procedure (figs. 1*A* and 1*B*).

The patient tolerated the procedure well, and there were no untoward effects. Prior to the procedure the hematocrit was 33 and did not change. Liver function tests were abnormal prior to the procedure, presumably due to cirrhosis, but there was no further deterioration afterward. Serum bilirubin went from 5.4 to 5.5, glutamic oxaloacetic transaminase from 539 to 526, lactic dehydrogenase from 204 to 216, and pyruvic transaminase from 383 to 525. This last value was felt to be probably unrelated to the procedure. An abdominal film 24 hr after the procedure demonstrated a redistribution of the intraperitoneal oil and a diminution in the quantity of hepatic oil (fig. 1*C*). No contrast material was seen in the lungs on serveral chest radiographs obtained over a 2 day interval.

The empyema cavity was successfully demonstrated and drained 2 days later. The patient continued to do well 6 weeks after surgery.

Discussion

Complications due to the use of oil-based contrast media have been reported in lymphangiography [1–4] and in hysterosalpingography before the advent of water soluble contrast material [5–8]. Embolic phenomena in the lungs have been reported in both hysterosalpingography and lymphangiography. The stippled appearance of contrast material in the lungs after lymphangiography is well known and generally causes no problems for patients with adequate pulmonary reserve. However, pulmonary infarcts and even cardiovascular collapse have been described in both procedures [4–6].

Hepatic oil embolization has also been described in lymphangiography. It has been postulated that this occurs due to opening of lymphaticovenous anastomoses with direct introduction of oil globules into the venous circulation [1]. A branched arborizing pattern of contrast material has been described in the liver in the early phase, with subsequent dispersal into the venous sinusoids [1, 3]. None of the patients described sustained any ill effects from hepatic embolization. No pathologic changes were seen on liver biopsy of one patient 3 months after lymphangiography [3], and there was no elevation of hepatic enzyme levels.

Particle size of oily propyliodone is generally less than 20 μm in diameter, with an occasional particle up to 100 μm [9]. The liver presumably filters these particles from the portal circulation, preventing their passage to the lungs, thus accounting for the radiographic findings presented here.

ACKNOWLEDGMENT

I thank Dr. William Martel for helpful advice and encouragement.

REFERENCES

1. Bodie J, Linton D: Hepatic oil embolization as a complication of lymphangiography. *Radiology* 99:317–318, 1971
2. Bron K, Baum S, Abrams H: Oil embolism in lymphangiography. *Radiology* 80:194–202, 1963
3. Chavez C, Berrong L, Evers C: Hepatic oil embolism after lymphangiography. *Am J Surg* 110:456–460, 1965
4. Clouse M, Hallgrimsson J, Wenlund D: Complications following lymphangiography with particular reference to pulmonary oil embolism. *Am J Roentgenol* 96:972–978, 1966
5. Henry G, Hunter R: Hysterosalpingography with water soluble medium (Salpix). *Am J Roetgenol* 84:924–928, 1960
6. Ingersoll F, Robbins L: Oil embolism following hysterosalpingography. *Am J Obstet Gynecol* 53:307–311, 1947
7. Shapiro J, Rubenstein B, Jacobson H, Poppel M: Pulmonary oil embolism: a complication of hysterosalpingography. *Am J Roentgenol* 77:1055–1058, 1957
8. Walther O: Frage der Embolie bei Hystersalpingographie mit Lipiodol. *Acta Radiol* (Stockh) 20:457–468, 1939
9. Virtemma P: Dionosil as a contrast agent in microarteriography. *Br J Radiol* 34:441–445, 1961

Received January 24, 1977; accepted after revision March 25, 1977.

[1] Department of Radiology, University of Michigan Medical Center, Ann Arbor, Michigan 48109.

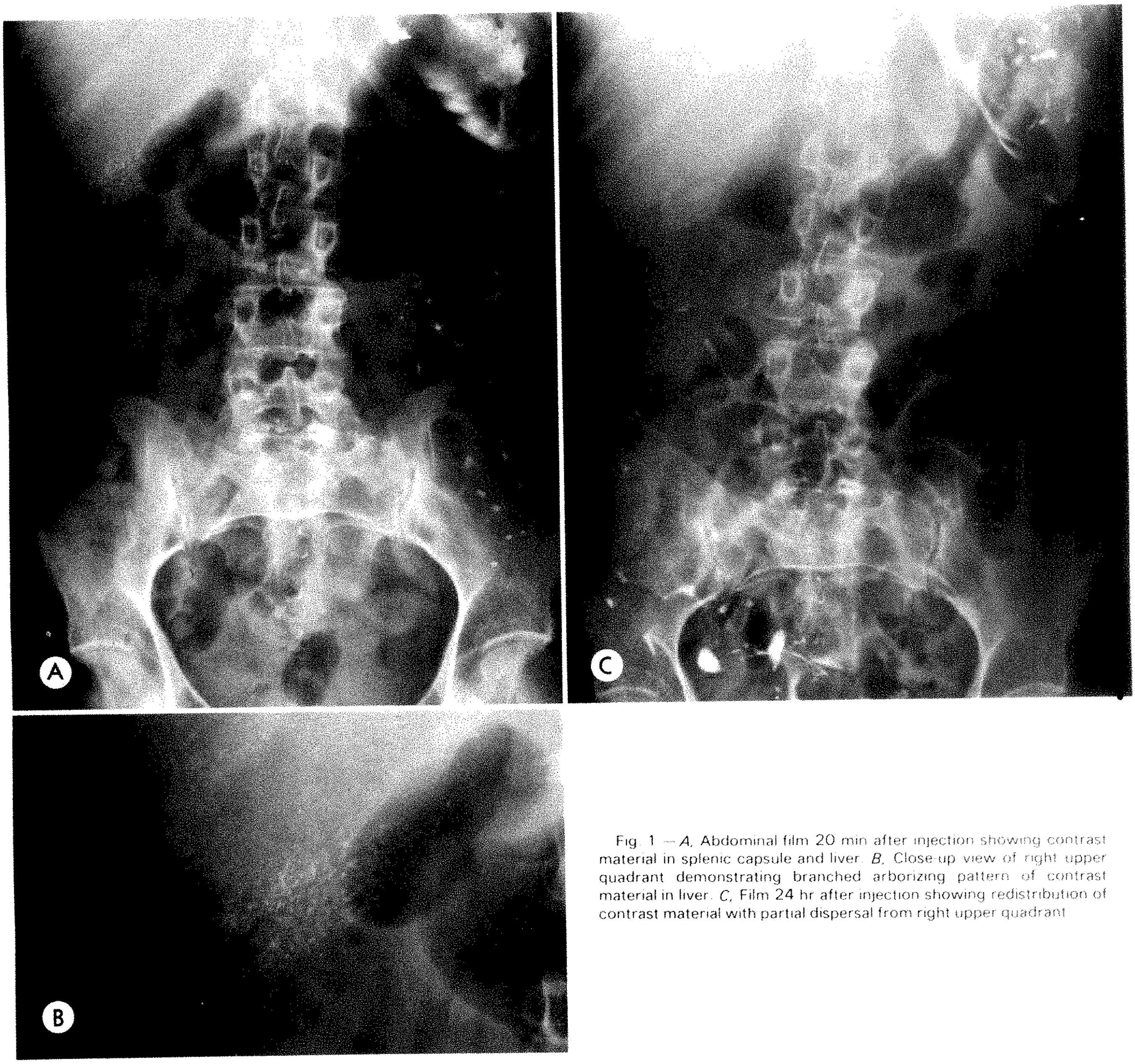

Fig. 1 — *A*, Abdominal film 20 min after injection showing contrast material in splenic capsule and liver. *B*, Close-up view of right upper quadrant demonstrating branched arborizing pattern of contrast material in liver. *C*, Film 24 hr after injection showing redistribution of contrast material with partial dispersal from right upper quadrant.

Absent Arch and Hypoplastic Pedicle: Another Confusing Cervical Spine Anomaly

NANCY A. KIRCHMER[1] AND MOHAMMAD SARWAR[1]

Cervical radiographs often reveal asymptomatic anomalies of the cervical spine. In the clinical setting of neck trauma, however, the less common anomalies may be initially misinterpreted as fractures. It was in such a setting that we recently encountered a previously unreported anomaly: absent neural arch and hypoplastic pedicle at one level with hyperplasia of the corresponding structures of the superjacent verebra. Hadley [1] and others have reported several cases of unilateral absent pedicle, another lesion which falls within the spectrum of congenital unilateral neural arch anomalies.

Case Report

A 21-year-old woman was brought to the emergency room complaining of headache and severe neck pain immediately after a fall down 21 stairs. She denied loss of consciousness. She had pain and tenderness in the posterior occipital region, extending down the cervical midline. There was no focal neurological deficit. Radiographs were initially interpreted as showing fractures of the pedicle, articular facet, and posterior arch of C7 on the left (fig. 1*A*). The patient was placed in Gardner-Wells tongs and cervical traction. Subsequent comparison of the plain films with the body section radiographs revealed an unusual combination of cervical anomalies but no fracture. The right side was normal (fig. 1*E*). On the left, the pedicle and articular facet of C6 appeared larger than normal (fig. 1*F*).Although the pedicle of C7 was quite small, it provided the inferior border of the C6–C7 intervertebral foremen. Frontal body section films revealed the left neural arch of C7 to be absent although that of C6 was hyperplastic (fig. 1*C*). Films through more anterior planes of section revealed a small deformed articular facet of C7 on the left with overgrowth of the ipsilateral facet of C6 (fig. 1*D*). Figure 1*B* illustrates the composite findings observed on both plain and body section radiographs. Tongs and traction were discontinued and the patient was discharged without pain several days later.

Discussion

Normal developmental anatomy of the cervical spine has been well defined [2, 3]. Each vertebral segment develops from six (three paired) chondrification centers; two for the verebral body, two of the costal elements, and one for each side of the neural arch. Outgrowths from each neural arch center become the pedicle, superior and inferior articular processes, transverse process, lamina, and spine. Hence it is not surprising that a spectrum of unilateral neural arch anomalies has emerged with resulting diagnostic confusion. Previously reported cases of unilateral absent pedicle in the cervical spine fall within this spectrum.

Good 45° oblique films of the cervical spine are essential to proper diagnosis. In confusing cases, body section films in both frontal and lateral planes may be necessary. They should be obtained whenever there is doubt about the plain film findings.

REFERENCES

1. Hadley LA: Congenital absence of pedicle from the cervical vertebra. Report of three cases. *Am J Roentgenol* 55:193–197, 1946
2. Epstein BS: *The Spine. A Radiological Text and Atlas*, 3rd ed., Philadelphia, Lea & Febiger, 1969
3. Rothman R, Simeone F: *The Spine*, vol 1, Philadelphia, Saunders, 1975

Received February 3, 1977; accepted March 23, 1977.

[1] Department of Radiology, Division of Neuroradiology, University of Texas Medical Branch, Galveston, Texas 77550. Address reprint requests to M. Sarwar.

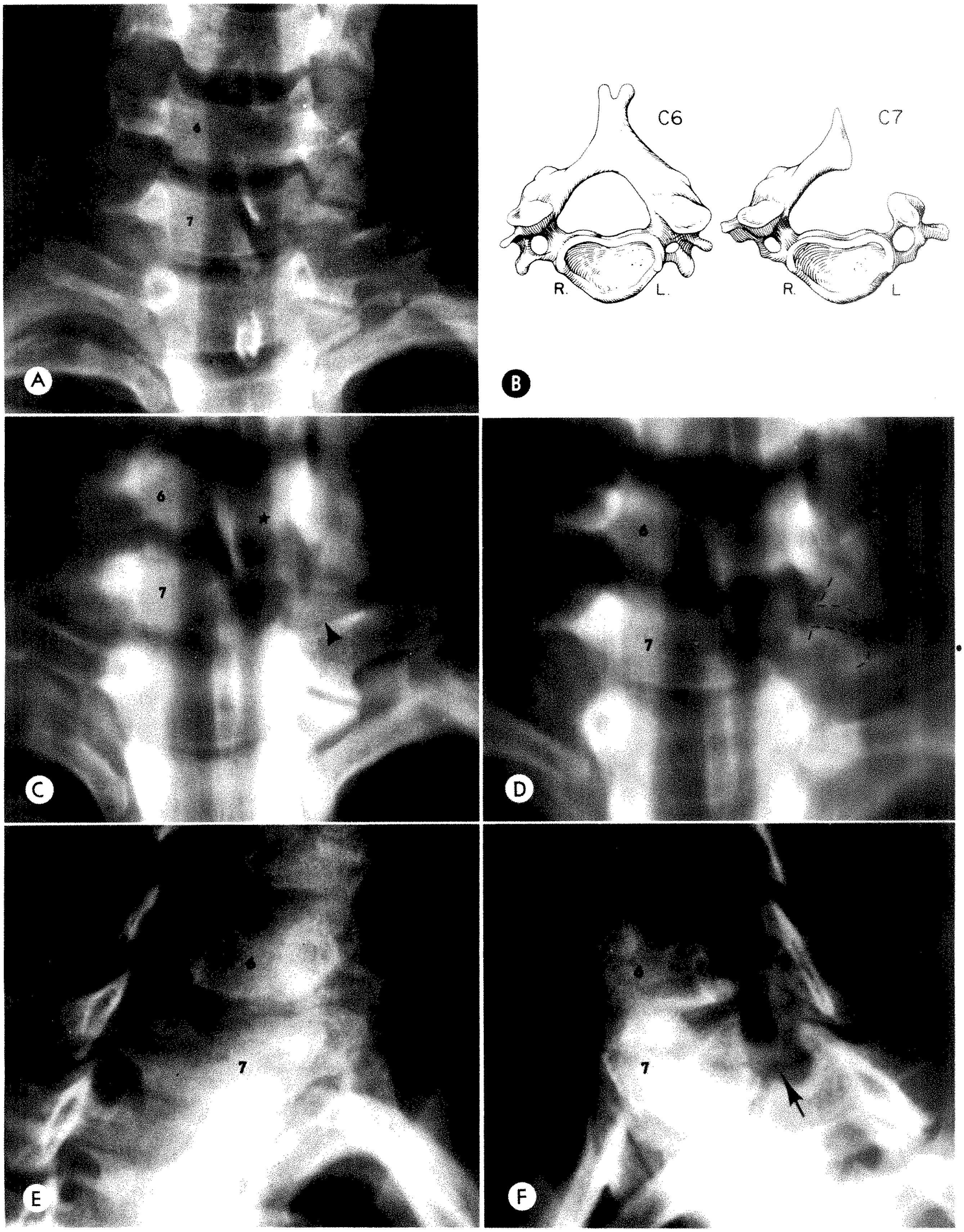

Fig. 1.—*A*, Plain film showing superimposed neural arch anomalies of C6 and C7 leading to erroneous diagnosis of fractures. *B*, Diagram illustrating findings of plain and body section films. *C*, Frontal body section film showing hyperplastic left neural arch of C6 (*asterisk*) and absent neural arch of C7. Left articular facet of C7 is hypoplastic (*arrowhead*). *D*, Retouched film showing hyperplastic left articular process of C6 and hypoplastic articular process of C7. *E* and *F*, Lateral body section radiographs showing normal right side (*E*) and abnormal left side (*F*). Note hypoplastic pedicle of C7 (*arrow*). Pedicle and articular facet of C6 are hyperplastic.

Spurs of the Mandible and Supracondylar Process of the Humerus in Cornelia de Lange Syndrome

JOHN A. CURTIS,[1] A. EDWARD O'HARA,[1] AND GARY G. CARPENTER[2]

While mandibular spurs are a frequent clinical finding in the Cornelia de Lange syndrome, to our knowledge they have not been reported in the radiologic literature. The relative rarity of this syndrome and the apparent specificity of the finding prompted this report. In addition, three of six cases reviewed had a unilateral supracondylar process of the humerus.

Case Report

Baby D., a 2-week-old white male, was transferred from another hospital for evaluation of multiple congenital anomalies. He was the product of an uncomplicated 36 week pregnancy of a 20-year-old with two normal children. Birth weight was 1.5 kg, and Apgar scores were 6 and 8. Physical examination revealed a small dysmature infant in no distress with little spontaneous movement of the extremities, microcephaly, increased space between the nose and upper lip, low set ears, synophrys, flat nasal bridge, cleft palate, grade III/IV harsh systolic murmur, undescended right testis, clinodactyly of the fifth fingers, bilateral simian crease, syndactyly of the second and third toes bilaterally, decreased range of motion at the elbow, low growllike cry, and a palpable midline mandibular spur. Electrocardiogram and laboratory studies were normal. Radiographic findings confirmed the skeletal anomalies including the mandibular spur (fig. 1*A*). Follow-up study at 3 months of age (fig. 1*B*) showed diminution in the prominence of the spur.

Discussion

The Cornelia de Lange syndrome was first described in 1916 by Brachman [1] and more completely defined by Cornelia de Lange in 1933 [2]. Since that time, more than 200 cases have been reported [3]. It is inherited as an autosomal recessive trait [4], occurring in approximately one in every 10,000 live births [5]. Clinically, the syndrome is characterized by mental retardation, dwarfism, hypertrichosis, characteristic facies (including synophrys, short upturned nose with flat bridge, receding chin, thin upper lip, and increased space between the nose and upper lip), characteristic skeletal changes (micromelia, proximally placed thumbs), cutis marmarata and facial cyanosis, and feeble low pitched cry [4, 6, 7].

Frequently associated findings are microbrachycephaly, syndactyly of the second and third toes, clinodactyly of the fifth finger, Kirner deformity, phocomelia, micrognathia, retarded bone age with dysharmonic ossification, short neck, cleft palate, hypoplasia of the long bones, mandibular spurs, gonadal hypoplasia, hypogammaglobulinemia, malrotation, antemongoloid slant, subluxation of the radial head, and simian crease [4, 7, 8].

Although the diagnosis is usually made on physical examination, radiographic changes may be pathognomonic. Kurlander and DeMyer [9] reported the combination of short first metacarpal, hypoplastic middle phalanx of the fifth finger, and deformity of the proximal radial metaphysis with subluxation as probably being specific for the syndrome. They estimate a 50% incidence of this constellation of radiographic signs. A small hard midline spur on the inferior anterior surface of a ridged symphysis mentus is frequently found. Silver [4] reports the incidence of mandibular spurs as high as 100% in some series. Although the mandibular spur is a frequent clinical finding, to our knowledge, it has not been demonstrated radiographically. Furthermore, this finding is apparently pathognomonic of the syndrome.

The mandibular spur has been reported only in infants. We believe that the spur may become incorporated or remodeled into the mandible as the child grows older. This phenomenon is well illustrated by our patient who had a well defined mandibular spur at 3 weeks that became less prominent at 3 months of age. Radiographs of five other proven cases of Cornelia de Lange syndrome (ages 2, 3, 5, 6, and 8 years) showed no evidence of mandibular spur.

The supracondylar process of the humerus is also known as the supracondyloid, supraepitrochlear, epicondylar, and epicondylic process. It is a small horn-shaped bony projection extending obliquely, medially, and downward from the anteromedial surface of the distal humeral shaft approximately 5–7 cm above the medial epicondyle (fig. 2). The process ends in a roughened point at which a dense fibrous band (ligament of Struthers) continues to the medial epicondyle [10]. This fibrous band lies between the tendon of the latissimus dorsi and the coracobrachialis and corresponds to the lower part of the tendon of the vestigial latissimo-condyloideus, a muscle found in climbing mammals [11]. Rarely, this fibrous band may ossify forming a supracondylar foramen, a tunnel which transmits the median nerve and the brachial artery or one of its branches. Usually, the pronator teres muscle has an anomalous insertion from the supracondylar process which also may be the site of insertion of the lower portion of the coracobrachialis muscle [12]. The supracondylar process is found in many reptiles, most marsupials, and some other mammals including cats, lemurs, and American monkeys [12].

The incidence of this finding in the general population ranges from 0.6%–2.7%; it is more common in Europeans and less frequent in Negroes and American Indians [13]. There is some evidence for recessive mode of inheritance. While the spur is usually asymptomatic, it may occasionally present as a mass or be associated with symptoms of median nerve compression and claudication of the brachial

---

Received December 5, 1976; accepted after revision March 1, 1977.

[1] Department of Radiology, Thomas Jefferson University Hospital, 11th and Walnut Streets, Philadelphia, Pennsylvania 19107.

[2] Department of Pediatrics, Thomas Jefferson University Hospital, Philadelphia, Pennsylvania 19107.

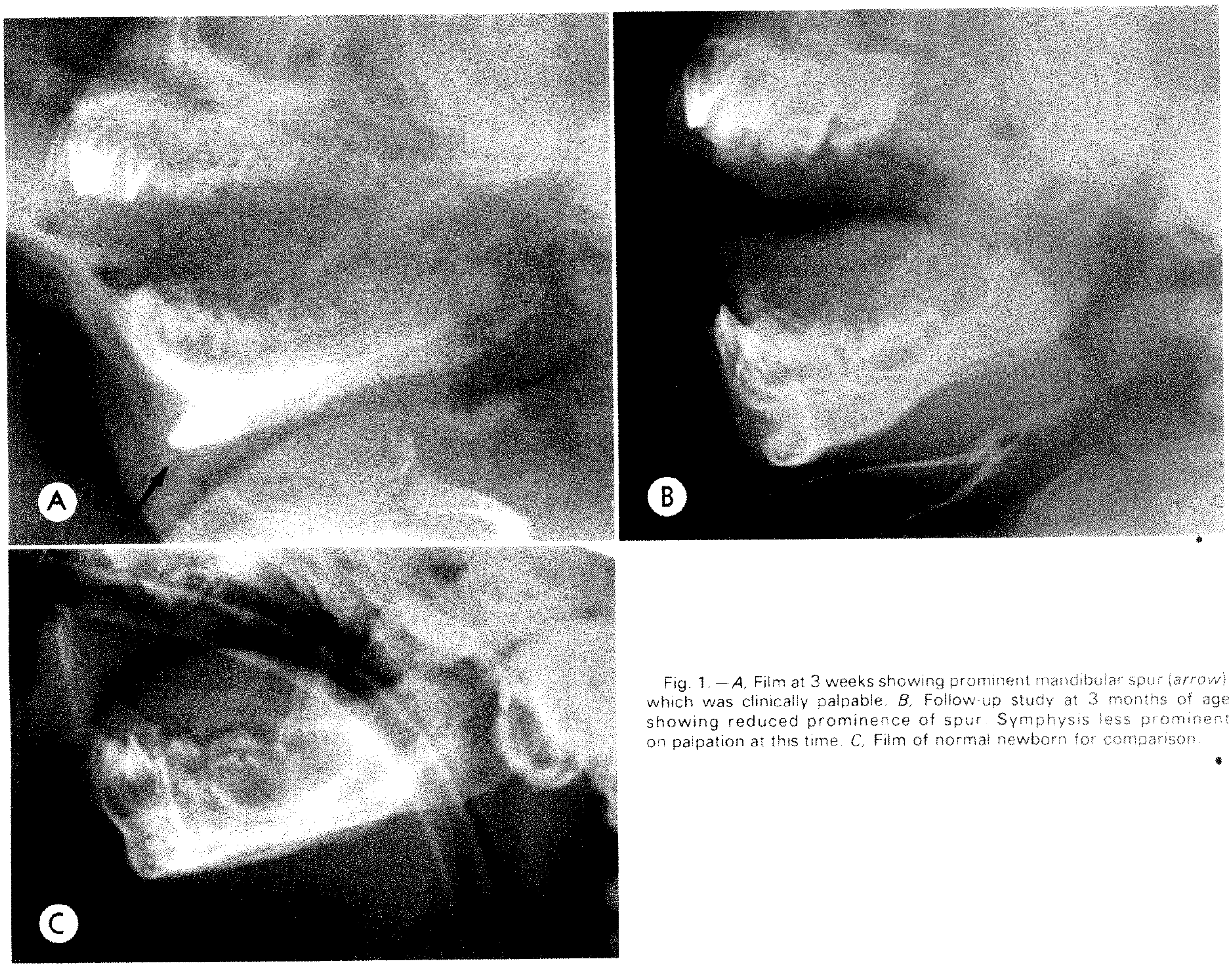

Fig. 1.—*A*, Film at 3 weeks showing prominent mandibular spur (*arrow*) which was clinically palpable. *B*, Follow-up study at 3 months of age showing reduced prominence of spur. Symphysis less prominent on palpation at this time. *C*, Film of normal newborn for comparison.

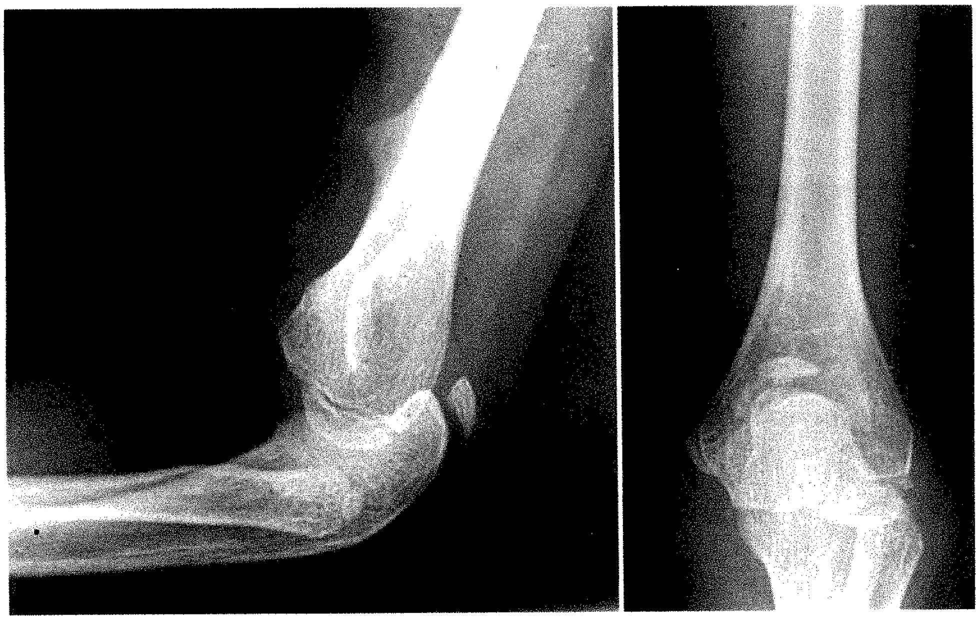

Fig. 2.—Radiographs of another case showing supracondylar process. Note characteristic deformity of proximal radial metaphysis with subluxation of radial head.

artery especially following fracture. The supracondylar process must be distinguished from distal humeral osteochondromas which typically project away from the elbow joint.

A unilateral supracondylar process of the humerus was present in three of six cases of Cornelia de Lange syndrome we reviewed [11]. The high incidence of unilateral supracondylar process of the humerus in the syndrome has recently been emphasized [3]. To our knowledge this anomaly is not associated with any other syndrome.

REFERENCES

1. Brachman W: Ein Fall von symmetrischer Monodaktylie durch Ulnadefekt, mit symmetrischer Flughautibildung in den Ellenbeugen, sowie anderen Abnormalitäten (Zwerghftigkeit Halsrippen, Behaarung). *Jahrb Kinderheilkd* 84: 225–235, 1916
2. de Lange C: Sur un type nouveau de degeneration (typus amstelodamensis). *Arch Med Enfants* 36:713–719, 1933
3. Peters FLM: Radiologic manifestations of the Cornelia de Lange syndrome. *Pediatr Radiol* 3:41–46, 1975
4. Silver HK: The de Lange syndrome: typus amstelodamensis. *Am J Dis Child* 108:523–529, 1964
5. Schuster DS, Johnson SAM: Cutaneous manifestations of Cornelia de Lange syndrome. *Arch Dermatol* 93:702–707, 1966
6. McArthur RG, Edwards JHP: de Lange syndrome: report of 20 cases. *Can Med Assoc J* 96:1185–1198, 1967
7. Ptacek LJ, Opitz JM, Smith DW, Gerritsen J, Warsman HA: The Cornelia de Lange syndrome. *J Pediatr* 63:1000–1020, 1963
8. Lee FA, Kenny FM: Skeletal changes in the Cornelia de Lange syndrome. *Am J Roentgenol* 100:27–39, 1967
9. Kurlander GJ, DeMyer W: Roentgenology of Brachman de Lange syndrome. *Radiology* 88:101–110, 1967
10. Parkinson C: The supracondyloid process. *Radiology* 62: 556–558, 1954
11. Kessel L, Ring M: The supracondylar spur of the humerus. *J Bone Joint Surg* 48:765–766, 1976
12. Bernard LB, McCoy SM: The supracondyloid process. *J Bone Joint Surg* 28:845–846, 1946
13. Newman A: The supracondylar process and its fracture. *Am J Roentgenol* 105:844–849, 1969

Glucagon-producing Islet Cell Tumor of the Pancreas

KYUNG J. CHO,[1] CLYDE W. WILCOX,[2] AND STEWART R. REUTER,[3]

Glucagonoma is the least common type of islet cell tumor of the pancreas [1, 2]. Since McGavran et al. [3] first described a glucagon-secreting pancreatic tumor, a number of cases have been reported; however, the angiographic findings have been described in only five patients [1–5]. Moreover, the characteristic clinical manifestations (glucagonoma syndrome) have not been emphasized in the radiologic literature.

Case Report

A 64-year-old man was admitted to the University of Michigan Medical Center because of a skin rash and a 27.2 kg weight loss in the previous 2 years. He also developed diabetes mellitus 1 year prior to admission, well controlled with 35 units of insulin. Physical examination revealed extensive eczematoid dermatitis involving the trunk, back, groin, neck, and extremities. Vital signs were normal. He had a microcytic, normochromic anemia with hemoglobin, 9.6 g/100 ml; total protein, 4.9 g; and serum albumin, 2.5 g/100 ml.

An upper gastrointestinal barium examination revealed widening of the second portion of the duodenum. Pancreatic angiography demonstrated a large hypervascular mass in the pancreatic head, supplied by dilated pancreaticoduodenal arcades (fig. 1). Many tumor vessels were present. The hepatic and gastroduodenal arteries were displaced, and the superior mesenteric vein was invaded. In the parenchymal phase a relatively well circumscribed homogenous dense tumor stain measured approximately 12.0 cm in diameter. Several well demarcated hypervascular metastases were present in the liver. Blood samples obtained from proximal and distal hepatic veins showed 5,090 and 3,960 pg/ml glucagon, respectively; the inferior vena cava level was 3,090 pg/ml (normal = 50 –100 pg/ml). A skin biopsy revealed necrotizing migratory erythema. A percutaneous needle aspiration biopsy of the pancreatic mass showed carcinoma, compatible with islet cell tumor.

At exploration a large mass was found in the head and uncinate process of the pancreas, invading the superior mesenteric vein. An approximately 95% pancreatectomy was performed with subtotal removal of the tumor. The pancreatic portion of the superior mesenteric vein was resected and the proximal superior mesenteric vein anastomosed to the splenic vein. The histology was islet cell carcinoma. The dermatitis regressed rapidly after resection of the tumor. Three weeks after surgery, the duodenum perforated and an abscess developed in the lesser space which required resection of the duodenum. The patient died of sepsis soon after.

Discussion

The various clinical syndromes caused by functioning islet cell tumors have been well described: hypoglycemia by insulinomas; Zollinger-Ellison syndrome by gastrin-secreting tumors; WDHA syndrome (watery diarrhea, hypokalemia, and achlorhydria) by nonbeta islet cell tumors; and glucagonoma syndrome by alpha cell tumors.

The clinical manifestations of glucagonoma have been thoroughly described in the nonradiologic literature. Mallinson et al. [6] described a glucagonoma syndrome in nine patients that consisted of a typical skin rash (necrolytic migratory erythema), anemia, and diabetes. Of the 14 cases in the literature, including our case, ages ranged from 40 to 69 years (average, 54 years). There were 10 females and four males, a 2.5:1 ratio. Diabetes was present in 12 patients, and all had a skin rash. Nine of the 14 tumors were in the tail of the pancreas and all but two were malignant. The average size was 6.0 cm in diameter (range, 4–12 cm). Hepatic metastases were present in nine patients.

The etiology of the dermatitis is not clear. Becker et al. [7] suggested that it is caused by a defense reaction of the skin to metastatic cells. Mallinson et al. [6] felt that it might be caused by hypoaminoacidemia as a result of excessive catabolism by glucagonemia. The skin rash and diabetes often regress promptly after resection of the tumor.

The angiographic appearance of islet cell tumors in general depends on their size. Small tumors (1–2 cm in diameter) appear as rounded, well circumscribed areas of increased accumulation of contrast material in the late arterial and capillary phases [8, 9]. As they become larger, the supplying arteries dilate and many tumor vessels are seen. The degree of vascularity is generally proportional to the size of the tumor. Vascular displacement may be prominent. Nonfunctioning islet cell tumors are generally large (range, 6–20 cm) when discovered because they produce no syndrome. Typically, they are hypervascular with many pathologic vessels and tumor stain [10].

Since they arise from similar cells, the pancreatic adenomas producing various syndromes should be expected to have similar angiographic appearances. In fact, there is a wide overlapping range of findings in each tumor. The abnormalities seem to correlate better with size of the tumor than with the type of syndrome. The findings in our patient are similar to those in a large nonfunctioning islet cell carcinoma which we recently examined (fig. 2). Except for the presence of liver metastases, which are almost always hypervascular at angiography, islet cell adenomas cannot be distinguished from carcinomas. Danforth et al. [5] recently reported a case of glucagon-secreting tumor which recurred with hepatic metastasis 7 years after total resection of the tumor. Angiographic findings of the recurrent islet cell tumor of their case was similar to our case.

Recently Ingemansson et al. [4] reported a case of glucagon-secreting tumor diagnosed by radioimmunoas-

---

Received January 17, 1977; accepted after revision March 25, 1977.

[1] Department of Radiology, University of Michigan Medical Center, Ann Arbor, Michigan 48109. Address reprint requests to K. J. Cho.

[2] Department of Radiology, Norfolk General Hospital, Norfolk, Virginia 23507.

[3] Department of Radiology, Veterans Administration Hospital, Martinez, California 94553.

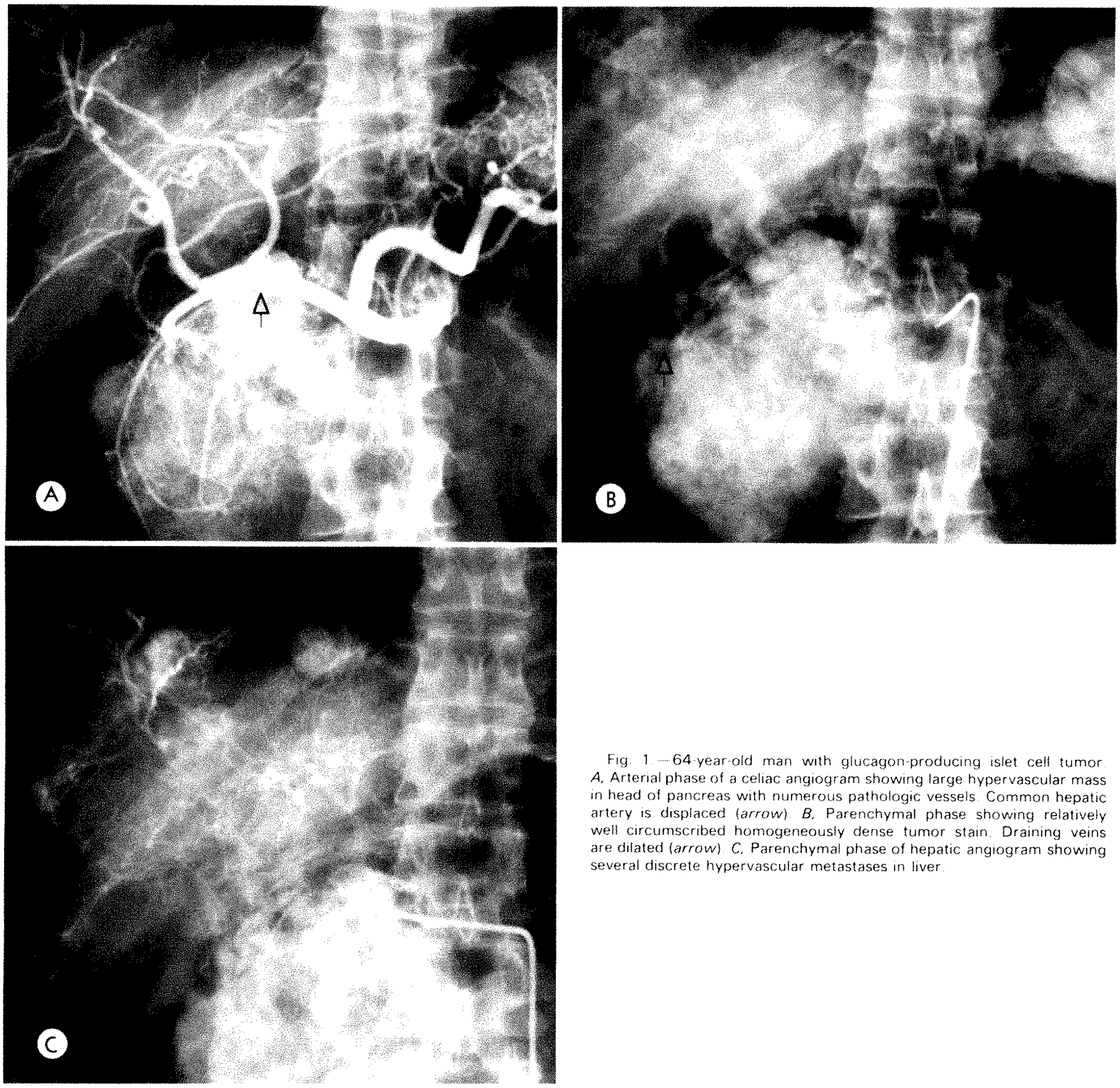

Fig. 1.—64-year-old man with glucagon-producing islet cell tumor. *A,* Arterial phase of a celiac angiogram showing large hypervascular mass in head of pancreas with numerous pathologic vessels. Common hepatic artery is displaced (*arrow*). *B,* Parenchymal phase showing relatively well circumscribed homogeneously dense tumor stain. Draining veins are dilated (*arrow*). *C,* Parenchymal phase of hepatic angiogram showing several discrete hypervascular metastases in liver.

say of blood samples obtained by selective catheterization of the pancreatic veins and also localized by pancreatic angiography. Selective pancreatic vein catheterization and sampling should become an important part of localizing functioning islet cell tumors in patients with normal angiograms or with multiple tumors. The glucagon levels in the blood samples obtained from two different hepatic veins and the inferior vena cava in our case were markedly elevated. The proximal hepatic veins, which appeared to drain the metastases, showed glucagon levels higher than the distal hepatic vein, suggesting hormone secretion by the hepatic metastases.

REFERENCES

1. Auerback RC, Koehler PR: The many faces of islet cell tumors. *Am J Roentgenol* 119:133–140, 1973
2. Scully RE, McNeely BU: Case records of the Massachusetts General Hospital. *N Engl J Med* 292:1117–1123, 1975
3. McGavran MH, Unger RH, ReCant L, Polk HC, Kilo C, Levine ME: A glucagon-secreting alpha-cell carcinoma of the pancreas. *N Engl J Med* 274:1408–1414, 1966
4. Ingemansson S, Lunderquist A, Holst J: Selective catheterization of the pancreatic vein for radioimmunoassay in glucagon-secreting carcinoma of the pancreas. *Radiology* 119:555–556, 1976
5. Danforth DN Jr, Triche T, Doppman JL, Beazley RM, Perrino

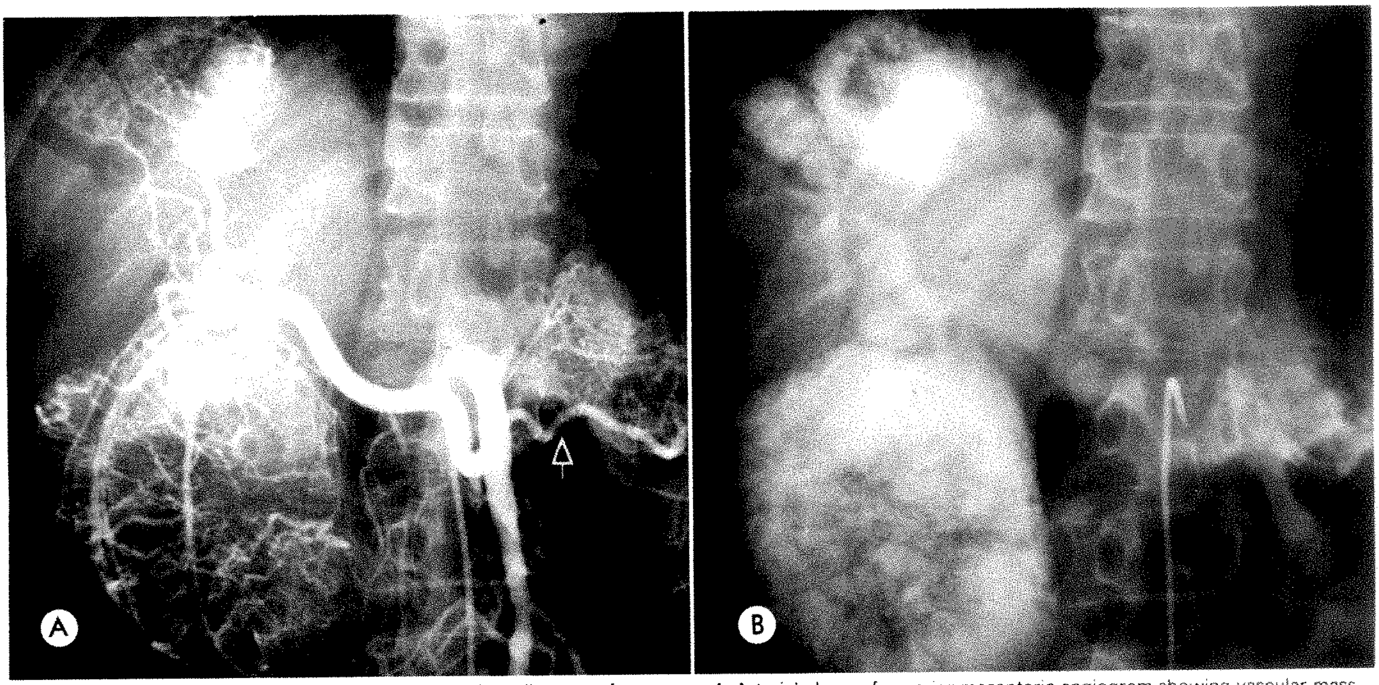

Fig. 2.—57-year-old man with nonfunctioning islet cell tumor of pancreas. *A*, Arterial phase of superior mesenteric angiogram showing vascular mass in tail of pancreas with many pathologic vessels, supplied by enlarged transverse pancreatic artery originating from superior mesenteric artery (*arrow*). Note large vascular metastases in liver supplied by right hepatic artery which also originates from superior mesenteric artery. Left hepatic artery arose from celiac artery (not shown). *B*, Parenchymal phase showing both primary and metastatic tumors with well circumscribed tumor stain. Hepatic metastases have central lucencies, probably representing central necrosis.

PV, ReCant L: Elevated plasma proglucagon-like component with a glucagon-secreting tumor: effect of streptozotocin. *N Engl J Med* 295:242–245, 1976
6. Mallinson CN, Bloom SR, Warin AP, Salmon PR, Cox B: A glucagonoma syndrome. *Lancet* 2:1–5, 1974
7. Becker SW, Kahn D, Rothman S: Cutaneous manifestations of internal malignant tumors. *Arch Dermatol Syph* 45: 1069–1080, 1942
8. Deutsch V, Adar R, Jacob ET, Bank H, Mozes M: Angiographic diagnosis and differential diagnosis of islet cell tumors. *Am J Roentgenol* 119:121–132, 1973
9. Gray RK, Rosch J, Grollman JH Jr: Arteriography in the diagnosis of islet-cell tumors. *Radiology* 97:39–44, 1970
10. Baghery S, Alfidi RJ, Zelch MG: Angiography of nonfunctioning islet cell tumors of the pancreas. *Radiology* 120:57–59, 1976

Multiple Primary Hemangiomas of Bone

CHARLES A. KARLIN[1] AND ANNE C. BROWER[1]

While solitary hemangiomas of bone in the vertebral column or calvarium are not uncommon, their occurrence at other skeletal sites is rare [1-3]. Rarer still are solitary hemangiomas of bone involving multiple skeletal sites [3-6]. We believe this entity differs from diffuse cystic angiomatosis of bone [6, 7].

Case Report

One year before admission, a 38-year-old white male sought medical attention because of numbness in his feet and legs. After extensive evaluation by his local physician, he was told he had "several hemangiomas" involving his bones. During the ensuing year, numbness increased and he developed cold sensations in his feet and legs as well as balance problems while walking. He then developed incontinence of urine and was referred to our institute for further evaluation.

Physical examination on admission was within normal limits except for a firm nontender mass palpated in the area of the right anterior fourth rib. Neurological examination, however, was abnormal. Bilateral hyperesthesia was present from the tenth thoracic level downward, but most pronounced in the L4, L5, and S1 nerve distributions on the right. There was decreased proprioception in the lower extremities and decreased strength in both lower extremities, more so on the right.

The chest radiograph revealed an expansile, lytic, spiculated, destructive lesion involving the anterior portion of the fourth right rib. A similar expansile spiculated lesion involved the proximal posterior left eighth rib. Spine radiographs showed hemangiomatous involvement of the seventh and twelfth thoracic vertebral bodies (figs. 1*A* and 1*B*). Posterior elements of T7, T8, T12, and L5 were also affected. Skull radiographs showed a spiculated "sunburst" lesion characteristic of a hemangioma in the left temporoparietal region (fig. 1*D*). A similar lesion was present in the left ilium, abutting the saccoiliac joint. Radiographs of the extremities, hands, and feet failed to disclose additional abnormalities. All the lesions were interpreted as hemangiomas. However, sarcomatous degeneration was considered in the lesion involving the right fourth anterior rib because of its aggressive appearance with irregular spiculation and cortical destruction (fig. 1*C*).

Pantopaque myelography revealed a high grade extradural block at the seventh thoracic level and a low grade extradural stenosis at the level of T12. Both sites corresponded to the previously indentified hemangiomas of bone at these levels. A ^{99m}Tc pyrophosphate bone scan showed increased radionuclide uptake only in the lesions seen radiographically. All other laboratory studies were within normal limits. No evidence of visceral or soft tissue hemangiomas was found.

The patient underwent surgery for decompression laminectomies at the levels indicated on myelography and for resection of the anterior portion of the right fourth rib. Cross sections of the rib showed changes typical of a hemangioma with bone spiculations radiating from the center (fig. 2*A*). Histologically the rib speciman was interpreted as benign capillary and cavernous hemangioma (fig. 2*B*). No sarcomatous changes were seen. Biopsy specimens from the seventh and twelfth thoracic vertebral levels were also interpreted as capillary and cavernous hemangioma of bone with minimal soft tissue extension.

The expected technical difficulty in surgically removing the hemangiomas causing the cord compression was encountered. Therefore the patient was given appropriate radiation therapy with resultant improvements in symptomatology. To this date he is asymptomatic.

Discussion

Patients with hemangiomatous lesions involving multiple skeletal sites have tended to be lumped into a diagnosis of skeletal angiomatosis [8]. We believe there are two distinct entities within this general diagnosis: (1) diffuse cystic angiomatosis, and (2) multiple primary hemangiomas of bone. Each presents a different clinical course and radiographic picture. The case reported here demonstrates the finding of multiple primary hemangiomas of bone.

Radiographically, diffuse cystic angiomatosis presents as widespread multiple cystic areas of bone destruction [9]. The lesions are usually round or oval and may or may not have well demarcated edges. They are usually situated in the medullary cavity although they can scallop the cortex and may even slighty expand the cortex. Periosteal reaction is not present. Regardless of what bone is involved, the radiographic picture is similar. The striations seen in primary hemangiomas are not present. Pathologic fractures are a common complication.

Multiple primary hemangiomas are seen radiographically as a collection of solitary hemangiomas. Each lesion has a radiographic appearance similar to a solitary hemangioma, and, like the solitary hemangioma, this appearance depends upon the bone involved. For example, primary hemangiomas of the vertebral column are quite common. Though usually a single lesion, two or more vertebral bodies may be involved. Vertical linear streaks or striations represent the classical appearance [10]. Sometimes these striations give a reticulated appearance, as in the involved vertebral bodies of our patient. A primary hemangioma in a flat bone, the skull, or the pelvis has a honeycomblike appearance created by delicate osseous striae or reticulations [10]. If these striations extend from the center of the lesion, a sunburst appearance results [1]. This can be seen both in the pelvis and skull of our patient.

Finally, a primary hemangioma involving the rib often causes a difficult problem in differential diagnosis; the rib is usually markedly expanded, the cortical margin is thinned and distorted, and some areas appear to be destroyed. Bony septa or ridges may extend out perpendicular to axis of the rib simulating a malignant tumor,

---

Received January 31, 1977; accepted after revision April 6, 1977.

[1] Department of Diagnostic Radiology, University of Kansas Medical Center, Rainbow Boulevard at 39th Street, Kansas City, Kansas 66103. Address reprint requests to C. A. Karlin.

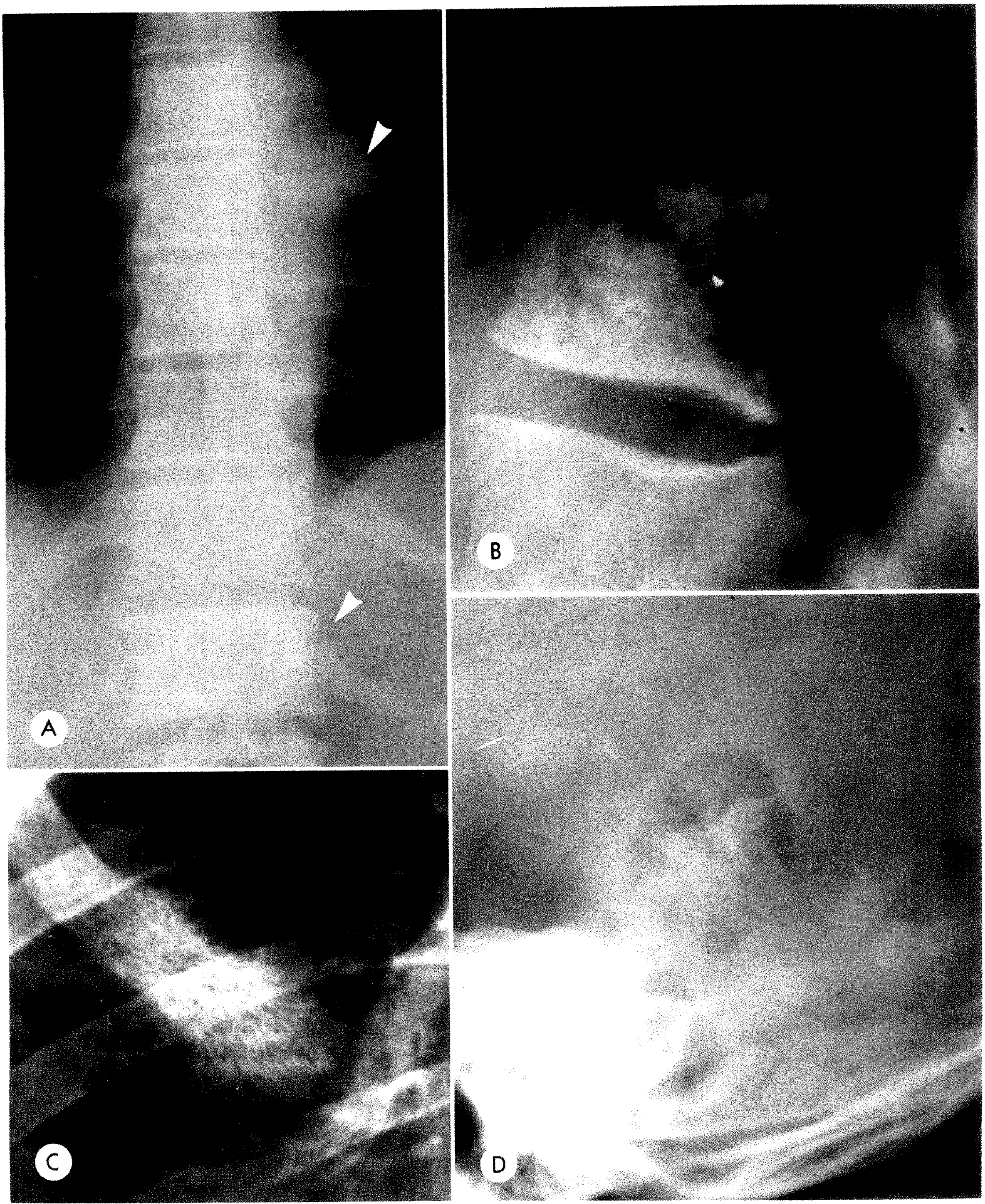

Fig. 1.—*A*, Anteroposterior view of thoracic spine showing hemangiomatous involvement of seventh and twelfth thoracic vertebral bodies as well as posteriomedial aspect of left eight rib (*arrow*). *B*, Coned down view of twelfth thoracic vertebral body showing typical hemangiomatous changes involving body and posterior elements. *C*, Magnification view of anterior right fourth rib. *D*, Coned down view of skull showing characteristic "sunburst" hemangioma in temporal bone

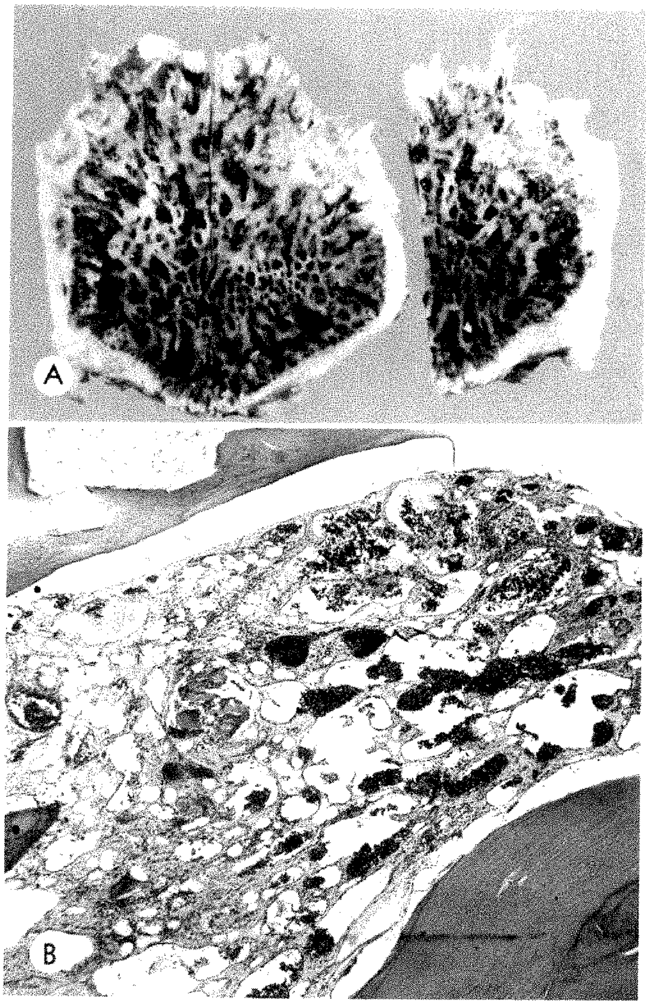

Fig. 2.—*A*, Decalcified section from right fourth rib characteristic of hemangioma involving bone. *B*, Histologic specimen (X40) from surgically resected right fourth rib showing both benign cavernous and capillary hemangiomatous components.

particulary an osteogenic sarcoma [10]. The radiographic appearance of the fourth anterior rib of our patient was so worrisome that an excisional biopsy was done. However, in this particular instance it probably should not have caused concern, knowing that the patient had other primary hemangiomas. Malignant degeneration of a primary hemangioma is not known to occur [2].

The prognosis in diffuse cystic angiomatosis is poor if visceral involvement is present. To date, only 11 cases without extraossous involvement have been reported [7]. The complications in these cases appear to be limited to pathologic fractures. However, the great majority of patients with diffuse cystic angiomatosis will have visceral involvement and their clinical course will depend upon the organ or organs involved. The final outcome is almost always fatal.

A primary hemangioma of bone is often an incidental finding on routine radiography; it does not usually cause a clinical problem and rarely, if ever, causes death. Vertebral hemangiomas have been known to produce a serious neurological problem by compression of the cord through extraosseous extension. Cord compression caused by vertebral involvement with cystic angiomatosis has not been described except secondary to pathologic fracture. Solitary hemangiomas in the jaw have caused severe hemorrhage. Though these are well recognized complications, they are uncommon [3]. Visceral involvement associated with solitary hemangiomas in bone has not been described.

Cases of multiple primary hemangiomas of bone in the recent literature are difficult to find. The few cases described have usually been of multiple hemangiomas involving two or more bones of one extremity [6]. We found only one other case similar to ours. In a study by Unni et al. [3], two of 56 patients with primary hemangiomas of bone had multicentric lesions. One had multiple hemangiomas of several bones in one extremity, but the other had hemangiomas in the pelvis and spine. While our case does demonstrate the complication associated with a vertebral body hemangioma, no other clinical complication has occurred. A search for visceral involvement was made and none was found. His stable clinical course tends to confirm that fact that his disease is self-limiting.

Diffuse cystic angiomatosis and multiple primary hemangiomas of bone do differ both clinically and radiographically. Because of the difference in prognosis, it is important to make a distinction between the two.

REFERENCES

1. Edeiken V, Hodes PJ: *Roentgen Diagnosis of Diseases of Bone*. Baltimore, Williams & Wilkins, 1970
2. Jaffe HL: *Tumors and Tumorous Conditions of Bones and Joints*. Philadelphia, Lea & Febiger, 1958
3. Unni K, Ivins JC, Beabout JW, Dahlin DC: Hemangioma, hemangiopericytoma and hemangioendothelioma (angiosarcoma) of bone. *Cancer* 27:1403–1414, 1971
4. Ackermann AJ, Hart MS: Multiple primary hemangioma of the bones of the extremity. *Am J Roentgenol* 48:47–52, 1942
5. Bucy PC, Capp CS: Primary hemangiomas of bone with special references to roentgenologic diagnosis. *Am J Roentgenol* 23:1–33, 1930
6. Wallis LA, Asch T, Maisel BW: Diffuse skeletal hemangiomatosis: a report of two cases and review of literature. *Am J Med* 37:545–563, 1964
7. Brower AC, Culver JE, Keats TE: Diffuse cystic angiomatosis of bone: report of two cases. *Am J Roentgenol* 118:456–463, 1973
8. Gutierrez RM, Spjut HJ: Skeletal angiomatosis: report of three cases and review of the literature. *Clin Orthop* 85: 82–96, 1972
9. Boyle WJ: Cystic angiomatosis of bone. *J Bone Joint Surg [Br]* 54:626–636, 1972
10. Sherman RS, Wilner D: The roentgen diagnosis of hemangioma of bone. *Am J Roentgenol* 86:1146–1159, 1961.

Technical Note

Keyhole Cone Device for Lateral Magnification Cerebral Angiography

RICHARD L. MANI[1] AND RICHARD C. GROSS[1]

We have developed a new "keyhole" cone device for lateral magnification cerebral angiography. The keyhole lateral projection permits inclusion of the common carotid bifurcation, thereby eliminating the extra filming sequences and contrast injections required to delineate that structure. Magnification radiography has proved to be a valuable technique in the angiographic assessment of extracranial as well as intracranial vascular occlusive disease [1, 2]. In addition, small focal spot magnification provides improved line pair resolution and permits lower patient radiation exposure dose.

Because magnification radiography uses an air gap which produces a higher scatter radiation than conventional radiography, precise coning is imperative to avoid deterioration of the film image. Conventional coning devices cannot be used for magnification "keyhole" lateral projections because they are too long to permit the necessary 23 cm air gap between the head and the film changer and still maintain the required 100 cm target-to-film distance. Through a local vendor, we have developed a prototype lightweight (3 kg) magnification keyhole cone device that, at a target-to-film distance of 100 cm, permits an object-to-film air gap of 17.8–20.5 cm and has a magnification factor of 1.4. This device is interchangeable with larger, conventional keyhole cones. The only caution to potential users relates to the size of the cone base which varies with different models and manufacturers. The device described here has been tested by us in over 400 cerebral arteriograms and has produced films of excellent diagnostic quality. It has been used for anteroposterior magnification as well as lateral projections. The anteroposterior projection is accomplished by elevating the table to the level of the desired air gap. It has been our practice to employ the keyhole cone on all patients suspected of cerebrovascular occlusive disease and appropriate tumor suspects.

The dimensions of the magnification keyhole cone are shown in figure 1. In figure 2 the device is shown in use in a mock angiographic situation, and figure 3 demonstrates the quality of the resulting angiogram.

REFERENCES

1. Baker HL Jr.: The clinical usefulness of magnification cerebral angiography. *Radiology* 98:587–594, 1971
2. Mishkin MM: Direct serial magnification angiography, in *Radiology of the Skull and Brain,* vol 2, edited by Newton TH, Potts DG, St. Louis, Mosby, 1974, pp 973–980

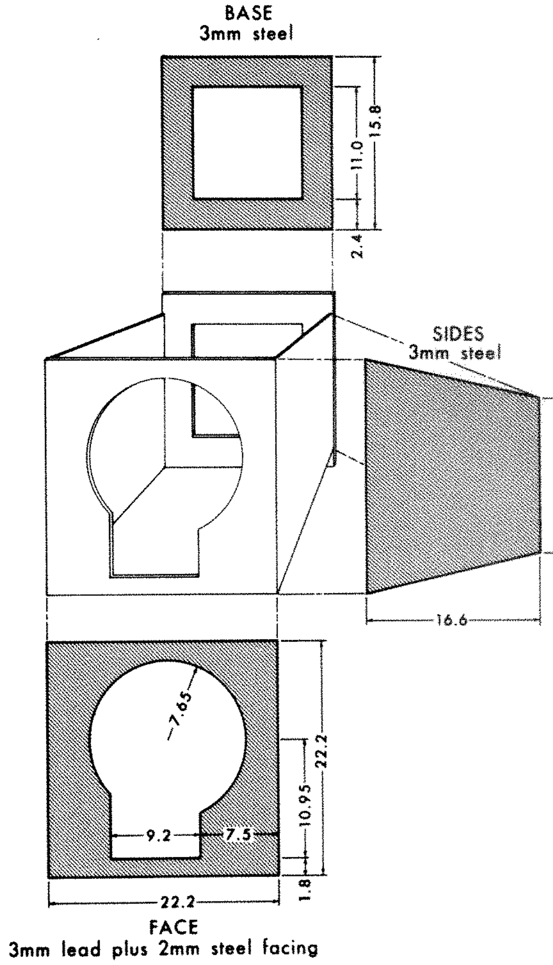

Fig. 1.—Dimensions of keyhole magnification cone. Size of base varies with manufacturer.

Received December 22, 1976; accepted after revision March 18, 1977.

[1] Department of Radiology, University of California School of Medicine, San Francisco, California 94143. Address reprint requests to R. L. Mani.

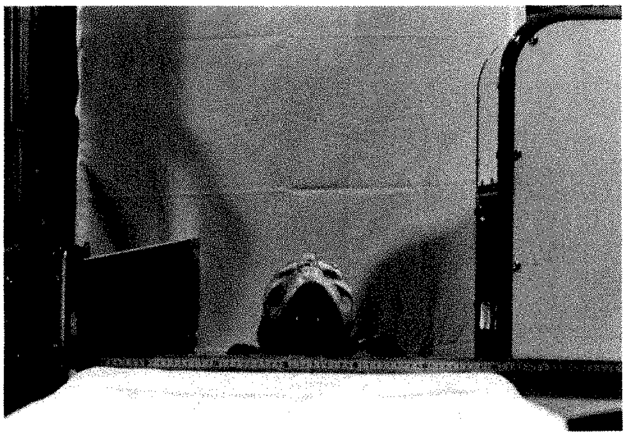

Fig. 2.—Cone in mock angiographic situation. Tube-to-film distance, 100 cm; object-to-film distance, 25 cm.

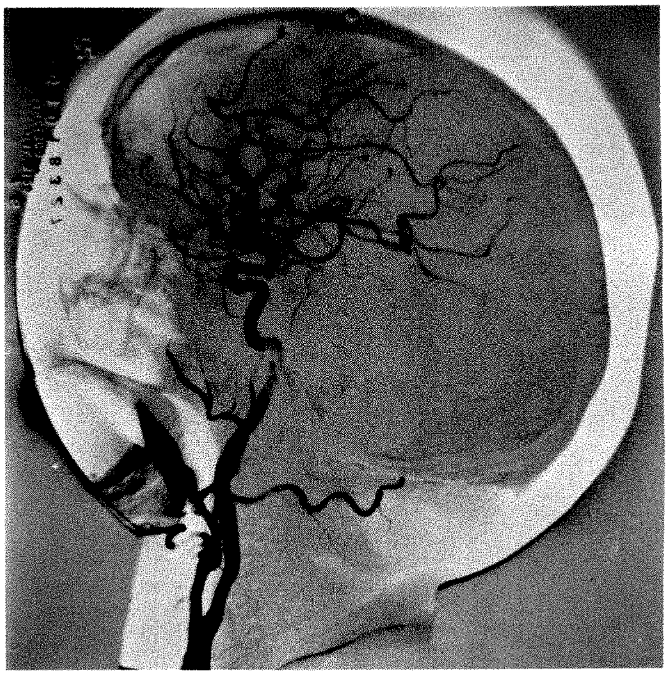

Fig. 3.—Right common carotid arteriogram, lateral projection, using keyhole cone. Magnification factor, 1.4.

Committee Report:

Contrast Media in Diagnostic Radiology: Recommendations for Labels, Package Inserts, and Dosage Determination

WILLIAM H. SHEHADI[1]

Recommendations are made for updating labels, package inserts, and dosage designation. These are based on the experience of the members of the Committee on Safety of Contrast Media of the International Society of Radiology and their collaborators in a prospective survey on adverse reactions to intravascularly administered contrast media. They are considered to be timely and an answer to a long unfilled need. It is felt that these recommendations reflect not only the opinion and concern of the committee but also that of the radiology community at large. These recommendations are of both medical and medicolegal import. Their application is in the best interests of progressive radiology and good patient care.

Revision and updating of labels and package inserts of contrast media used in diagnostic radiology is long overdue [1]. Equally pressing is the need for liberalization of the restrictive dosages stated on package inserts, which are quite at variance with the present day practice of radiology. The package inserts and labels should be frequently reviewed and updated in keeping with changing concepts and technical advances so as to comply with current needs in the practice of radiology.

These needs have been of great concern to the Committee on Safety of Contrast Media of the International Society of Radiology and its collaborators [1]. This concern is shared by officials of the Food and Drug Administration who are involved with the problems of contrast media and their adverse reactions. Concern has also been voiced by many radiologists at the national and international level who are not directly involved in the work of this committee.

Outdated concepts expressed on these labels and package inserts are misleading. The stated dosages are restrictive and unjustified. They place the radiologist and other physicians using contrast media at a serious disadvantage, especially in the medicolegal setting.

With full cognizance of these needs, the chairman appointed a committee consisting of Drs. Ralph Alfidi, Virginia Kanick, Bruce McClennan, Richard Pfister, Derek Stables, John Thornbury, and Homer Twigg to study the problem and make appropriate recommendations. The recommendations are based on the practice of committee members and radiologists participating in a prospective survey of adverse reactions to intravascularly administered contrast media. The dosage range has been retrieved from over 150,000 case reports in our files. These recommendations should become a part of the narrative used on labels and package inserts.

Introduction

The opening paragraph of the package insert should include the following statement:

> All procedures utilizing contrast media carry a definite risk of adverse reactions. While most reactions are minor, life threatening and fatal reactions may occur without warning. The risk/benefit factor should always be carefully evaluated. At all times a fully equipped emergency cart and resuscitation equipment should be readily available, and personnel competent in recognizing and treating reactions of all severity should be on hand.

Expiration Date

The expiration date of contrast media should be a maxium of 5 years from the date of manufacture. The date should be *clearly designated* on the vial or bottle as well as on the outer container and/or box.

Iodine Content

There should be a uniform and clear expression of the iodine content *in miligrams per mililiter* of all contrast media (table 1).

Dose Specification

Tables 2–6 serve as guidelines. These are based on the current practice and experience of radiologists participating in this survey. The dose used should be at the discretion of the radiologist.

In urography (table 3) the usual urographic single bolus dose is 50–100 ml. It is important to note that larger doses do not necessarily cause a greater number of adverse reactions.

In angiography (table 2) the dose administered should reflect both the need to obtain optimal diagnostic information of the organ/system examined and the circumstances under which the examination is performed (i.e., elective or emergency). This should be at the discretion of the radiologist. While these doses represent a cross section of current practice, they are only representative and should not be interpreted as absolute. Medical practice as well as available contrast media are undergoing constant change.

Indications

The following procedures should be added to those

Report of the Committee on Safety of Contrast Media of the International Society of Radiology. W. H. Shehadi, chairman; Ralph Alfidi, Virginia Kanick, Bruce McClennan, Richard Pfister, Derek Stables, John Thornbury, and Homer Twigg. Support was received from the Food and Drug Administration under contract 223-76-3021.

[1] 27 Byram Shore Road, Greenwich, Connecticut 06830.

Am J Roentgenol 129:167–170, July 1977

TABLE 1

Iodine Content of Contrast Media

Contrast Medium	Salt	mg Iodine/ml
Renografin 60%	MGD 52%, NaD 8%	288
Reno M 60%	MGD	282
Conray 280, 60%	MGI	282
Hypaque 60%	MGD	282
Hypaque 50%	NaD	300
Isopaque 280	MgM 60.2%	280
Renografin 76%	MGD	370
Hypaque M 75%	MGD 50%, NaD 25%	385
Conray 400, 66.8%	NaI	400
Cardiografin 85%	MGD	400
Isopaque 440, 82.3%	MGM 7.59%, NaM 1.66%, CaM 0.08%, CaM 0.08%, MgM 0.02%	440
Hypaque 90%	MGD 60%, NaD 25%	462
Reno M Dip 30%	MGD	141
Conray 30%	MGI	141
Hypaque DIU 30%	MGD	141
Hypaque 25%	NaD	150
Cholografin meglumine infusion 10.3%	MGIo	51
Cholografin meglumine 52%	MGIo	260

Note.—Na = sodium, MG = meglumine, Ca = calcium, Mg = magnesium, D = diatrizoate, I = iothalamate, M = metrizoate, Io = iodipamide.

presently listed in the package inserts: (1) renal angiography; and (2) other selective visceral angiography.

Precaution and Preparation

Avoidance of dehydration is one of the most important precautions. There should be no fluid restriction, and normal hydration should be maintained in the routine preparation of patients, particularly in infants and older patients. This applies even more stringently to patients with renal failure, multiple myeloma, or diabetes of long duration [2–5]. However, in an otherwise healthy patient, this does not necessarily preclude withholding fluids for a few hours preceding the examination. Concomitantly, the meal immediately before the examination is withheld to guard against aspiration of gastric contents in case of vomiting.

While pheochromocytoma is not a contraindication, the examination should be performed with caution and at the discretion of the radiologist—with full preparation for any hypertensive crisis that may be precipitated by the procedure. Appropriate blocking agents must be available.

Neither a history of allergy or an adverse reaction to a previous examination utilizing contrast media is a contraindication to a contrast medium examination. In these patients, the incidence of reactions is two and three times, respectively, that of the general population.

TABLE 2

Angiography

Study	Single Dose						Total Dose					
	Low Dose		Average Dose		High Dose		Low Dose		Average Dose		High Dose	
	ml	g I*	ml	g I	ml	g I	ml	g I	ml	g I	ml	g I
Kidney	8	2.96	12	4.44	15	5.55	20	7.4	30	11.1	45	16.65
Liver	20	7.4	35	12.95	50	18.5	70	25.9	120	44.4	225	83.25
Spleen	20	7.4	40	14.8	70	25.9	70	25.9	120	44.4	225	83.25
Celiac artery	30	11.1	45	16.65	60	22.2	80	29.6	120	44.4	225	83.25
Abdominal aorta	30	11.1	45	16.65	60	22.2	80	29.6	150	55.5	225	83.25
Thoracic aorta	40	14.8	50	18.5	60	22.2	90	33.3	150	55.5	225	83.25
Pulmonary artery	30	11.1	50	18.5	60	22.2	100	37.0	150	55.5	200	74.0
Angiocardiography:												
Right heart	35	12.95	45	16.25	60	22.2	90	33.3	120	44.4	225	83.25
Left heart	30	11.1	40	14.8	60	22.2	70	25.9	110	40.7	200	74.0
Coronary arteriography	5	1.85	8	2.96	10	3.7	40	14.8	60	22.2	225	83.25
Cerebral angiography:												
Carotid	8	2.256	10	2.82	12	3.384	30	8.46	40	11.28	100	28.20
Vertebral	6	1.692	8	2.256	10	2.82	12	3.384	24	6.768	30	8.46
Four vessel arch	40	11.28	60	16.92	80	22.56	100	28.2	150	42.3	200	56.4
Peripheral arteriography	20	5.64	50	14.1	80	22.56	120	33.84	180	50.76	240	67.68

Note.—Most frequently used contrast media for all studies except cerebral angiography and peripheral arteriography is Renografin 76%. For the latter two, most frequently used are Reno M 60% and Conray 280 (60%).

*Grams iodine.

TABLE 3

Intravenous Urography

	Low Dose	Average Dose	High Dose
Newborns (0–4.5 kg):			
Volume (ml)	8	10	20
Weight guidelines:			
ml/kg	1–2	4	4
ml/lb	0.5–1	2	2
Iodine content (g):			
Renografin 60%	2.3	2.88	5.76
Reno M 60%, Conray 280 (60%), Hypaque 60%	2.25	2.82	5.64
Hypaque 50%	2.4	3.0	6.0
Children (4.5–45 kg):			
Volume (ml)	15	25–30	50–100
Weight guidelines:			
ml/kg	1	2	2–4
ml/lb	0.5	1	1–2
Iodine content (g):			
Renografin 60%	4.32	7.2–8.64	14.1–28.2
Reno M 60%, Conray 280 (60%), Hypaque 60%	4.23	7.05–8.46	14.1–28.2
Hypaque 50%	4.5	7.5–9.0	15–30
Adults (>45 kg):			
Volume (ml)	50	50–100	100–150
Weight guidelines:			
ml/kg	1	1	1–2
ml/lb	0.5	0.5–0.75	0.75–1
Iodine content (g):			
Renografin 60%	14.4	14.4–28.8	28.8–43.2
Reno M 60%, Conray 280 (60%), Hypaque 60%	14.1	14.1–28.2	28.2–42.3
Hypaque 50%	15.0	15.0–30.0	30.0–45.0
Renografin 76%	18.5	18.5–37.0	37.0–55.5
Conray 400	20.00	20.0–40.0	40.0–60.0

Note.—Single bolus injection.

TABLE 4

Infusion Urography in Adults

	Low Dose	Average Dose	High Dose
Volume (ml)	250	300	450
Weight guidelines:			
ml/kg	2	2	2
ml/lb	1	1	1
Iodine content (g):			
Reno M DIP 30%, Conray 30%, Hypaque DIU 30%	35.25	42.3	63.45
Hypaque 25%	37.5	45.0	67.5

Note.—The average dose of 300 ml is administered in most instances. This examination is utilized more in the adult than in the newborn and pediatric age groups. When utilized in the latter two groups, the total dose administered should be adjusted according to body weight.

TABLE 5

Intravenous Cholangiography Using Cholografin Meglumine 52%

	Low Dose	Average Dose	High Dose
Newborns:*			
Volume (ml)	2	2	5
Iodine content (g)	0.52	0.52	1.3
Children:*			
Volume (ml)	5	5	10
Iodine content (g)	1.3	1.3	2.6
Adolescents (13–18 yr):			
Volume (ml)	10	10–12	15
Iodine content (g)	2.6	2.6–3.12	3.9
Adults (18+ yr):			
Volume (ml)	20	20	40
Iodine content (g)	5.2	5.2	10.4

Note.—Single bolus injection.

*This examination is rarely performed in newborns and children. When indicated, the weight guidelines are 0.3–0.6 ml/kg and 0.15–3 ml/lb.

TABLE 6

Infusion Cholangiography Using Cholografin Meglumine Infusion 10.3%

	Low Dose	Average Dose	High Dose
Adolescents (13–18 yr):			
Volume (ml)	50	75	100
Iodine content (g)	2.55	3.82	5.1
Adults (18+ yr):			
Volume (ml)	100	100	100
Iodine content (g)	5.1	5.1	5.1

Note.—This examination is rarely performed in newborns and children. When used in these age groups, the total dose should be adjusted to the body weight.

Contraindications

Under this heading the following should be deleted: (1) prothrombin time limitations to a contrast medium examination; (2) known hypersensitivity to salts of diatrizoate, salts of iothalamic acid, salts of metrizoic acid, or iodine; (3) presence of hyperthyroidism, tuberculosis (acitve or inactive), or hypertension; and (4) pregnancy. The primary risk in pregnancy is from radiation and not from contrast media. Toxicity of contrast media to the fetus has not been established.

Pretesting

This procedure is not recommended and is of no proven value. There is no known test that can predict who will have a reaction. Pretesting gives a false sense of security

[6–10]. Furthermore, reactions to a pretest dose of contrast media do occur, at times severe enough to be life threatening and even fatal, [6, 8, 11–13].

ACKNOWLEDGMENTS

We express our deep appreciation to the radiologists participating in our prospective survey througn whose collaboration these data became available. Special thanks go to Drs. Arthur Ruskin and John Hazard of the Food and Drug Administration for their encouragement and support.

REFERENCES

1. Shehadi WH, Pfister RC: Report of the Committee on Contrast Media of the International Society of Radiology. *Am J Roentgenol* 122:195–196, 1974
2. Dure-Smith P: Fluid restriction before excretory urography. *Radiology* 118:487–489, 1976
3. Myers GH, Witten DM: Acute renal failure after excretory urography in multiple myeloma. *Am J Roentgenol* 113: •583–588, 1971
4. Talner LB: Urographic contrast media in uremia: physiology and pharmacology. *Radiol Clin North Am* 10:421–432, 1972
5. Diaz-Buxo JA, Wagoner RD, Hattery RR, Palumbo PJ: Acute renal failure after excretory urography in diabetic patients. *Ann Intern Med* 83:155–158, 1975
6. Shehadi WH: Adverse reactions to intravascularly administered contrast media. *Am J Roentgenol* 124:145–152, 1974
7. Shehadi WH, Mishkin MM: Preliminary report of the Committee on Contrast Media of the International Society of Radiology. *Excerpta Medica International Congress Series* no. 338, vol 1, 1973, pp 15–20
8. Shehadi WH: Clinical problems and toxicity of contrast agents. *Am J Roentgenol* 97:762–771, 1966
9. Fischer HW, Doust VL: An evaluation of pretesting in the problem of serious and fatal reactions to excretory urography. *Radiology* 103:497–501, 1972
10. Thomas SF: Drugs: reactions and pretesting. *Radiology* 80:124–126, 1963
11. Payne WW, Morse WH, Raines SL: Fatal reaction following injection of urographic medium; case report. *J Urol* 76: 661–663, 1956
12. Pendergrass EP, Chamberlain GW, Godfrey EW, Burdick ED: Survey of deaths and unfavorable sequelae following administration of contrast media. *Am J Roentgenol* 48: 741–762, 1942
13. Wolfromm R, Dehouve A, Degand F, Wattez E, Lange R, Crehalet A: Les accidents graves par injection intraveineuse de substances iodées pour urographie. *J Radiol Electrol Med Nucl* 47:346-357, 1966

The Federal Government's Impact on Radiology

ROBERT D. MOSELEY, JR.[1] AND OTHA W. LINTON[2]

The areas of involvement by federal agencies which have primary health missions are outlined. The roles of many federal agencies which touch on health peripherally are also discussed.

Legislative and regulatory activities of the federal government have achieved a dominant influence over the future of radiology. This primacy is achieved by the assertion of an all-pervading federal authority or responsibility for nearly all aspects of radiologic practice: technologic improvements, licensure and certification, facilities, materials (drugs and devices), research, personnel management, standards and measures, manpower recruitment, compensation, and professional relationships.

Federal performance standards for existing radiologic equipment have been promulgated during the past few years. The introduction and proliferation of new devices (e.g., computed tomography) have come under federal controls for radiation safety, regional health planning, and cost containment. The distribution of physicians geographically and by specialty is already influenced by federal support for residency programs and has come under stringent review by planning groups.

The multiple roles of the federal government in health care, specifically in radiology, pervade all three constitutional branches. They are found, as well, in those quasiadministrative quasijudicial agencies (e.g., Federal Trade Commission) which regulate much of the nation's commerce.

A half-dozen congressional committees have direct legistative responsibilities in medical economics, health manpower, and radiation safety. Other committees have jurisdiction over matters that have periodic impact on radiologic practice, such as the transportation of radionuclides on scheduled airline flights or standards for chest x-ray examinations of coal miners.

The executive branch is omnipresent in health care. The largest group of regulatory and funding programs is lodged within the Department of Health, Education, and Welfare. Medicare, Medicaid, health manpower, planning research, and drug and device regulation are all major HEW programs. Equally vital are programs such as occupational medicine, workmen's compensation and fair labor practices within the Department of Labor, policies of the Immigration and Naturalization Service for foreign-trained physicians, radiation standard-setting functions of the Department of Commerce through the National Bureau of Standards, and federal subsidies for new technology development from the National Science Foundation.

The federal judiciary is not normally the court of first resort for litigation involving radiologists. Issues such as the tax status of professional corporations and allegations of antitrust violations by medical societies do originate in federal courts. The elasticity of the interstate commerce clause of the Constitution also means that appeals from malpractice actions and enforcement of product safety guarantees in federal legislation may reach federal district or appellate courts.

Under the federal system, much legislation dealing with health requires a partnership in regulation and funding with state and local governments. The health planning programs established by Public Law 93-641 in 1974 are an example. State and local governments and newly created regional agencies are given roles in planning for health facilities. The involved federal health agencies attempt to establish broad guidelines. Actual determinations of policy and choices among contenders for expansion of facilities are made at the local or state level. It is common in federal health legislation to give the states 24 months to enact conforming laws and to provide federal subsidies for state agencies with enforcement responsibilities. A more permissive form of such cooperation resulted from the 1959 Atomic Energy Act. This established the "agreement state" provisions, by which states could assume control of radioactive materials from the Atomic Energy Commission by passing laws acceptable to the AEC. Currently 25 states have chosen to take such responsibility, leaving the Nuclear Regulatory Commission to continue supervision in the rest of the country.

The payment mechanism brings federal pressures on providers of health services, as well as upon state and local governments. Physicians do not have to scale their charges to the 75th percentile of local usual, customary, and regular fees, but that amount is all they will be paid for services to beneficiaries of federal programs. Many health insurance programs are carriers or intermediaries for Medicare. Federal decisions often are adopted by the private plans, both in terms of fee levels recognized and in terms of services covered. For example, last summer just before the Social Security Administration corrected an inadvertent limitation on coverage of head CT scans, several insurance carriers announced their intent to impose a similar limitation.

The federal health purse is too large to be ignored by physicians as individuals or as a group. In 1976, the nation

---

Received February 28, 1977; accepted March 7, 1977.

[1] Department of Radiology, University of New Mexico School of Medicine, Albuquerque, New Mexico 87131. Address reprint requests to R. D. Moseley, Jr.

[2] Governmental Relations, American College of Radiology, Chevy Chase, Maryland 20015.

spent $139.3 billion on all health services and costs, including support for education, research, construction, and the care of millions entitled to health benefits under existing programs, according to Social Security Administration estimates. This represents a 14% increase over the revised estimate of $122.2 billion for 1975. The 1976 estimate works out to a per capita expenditure for health care of $683. The figure for this year includes about $59 billion in public spending, $40 billion in federal funds, and $19 billion from state and local sources.

Besides payments, most federal health programs and regulatory efforts now contain provisions for penalties against physicians who violate their provisions. The legislative demand for strict enforcement and greater penalties is likely to produce action in the Ninety-fifth Congress which began January 1977.

Areas of federal responsibility toward medical care and particularly toward radiology can be categorized under eight broad headings:

1. Reimbursement of physicians and hospitals for services to beneficiaries of various publicly supported health care programs, such as Medicare, Medicaid, Veterans Administration, and Department of Defense health activities.
2. Influence on patterns of practice through health planning activities and stimulation of health maintenance organizations.
3. Influence on the geographic and specialty distributions of physicians through training subsidies to medical school and residency sponsors, and through the National Health Service Corps.
4. A concern for the quality and appropriateness of medical and hospital services delivered to beneficiaries of federal health care programs as manifest in the creation of professional standards review activities, utilization review requirements, and the encouragement of private health care insurers to undertake similar activities.
5. Regulation of drugs, medical devices, and diagnostic products by the Food and Drug Administration to insure safety and efficacy.
6. Support for research in basic and clinical areas and into the socioeconomic milieu of medicine.
7. Support for construction of medical facilities and provision of equipment under successor programs to the Hill-Burton Act within health planning concepts.
8. Regulations and efforts to assure safety of ionizing radiation uses in medicine. These include establishment of standards, licensure of radiation sources, personnel requirements, monitoring of exposures, and radiobiologic investigations.

In all of these areas, the responsibilities and funding of several federal agencies substantially overlap. For example, a recent unpublished study by the American College of Radiology turned up more than 3,000 research projects on ionizing radiation supported by various federal agencies. Much of the support came from the Department of Health, Education, and Welfare through the National Institutes of Health, and from the Food and Drug Administration through the Bureau of Radiological Health. However, other radiation research is sponsored by the Department of Defense, Veterans Administration, National Science Foundation, Energy Research and Development Administration, Environmental Protection Agency, Department of Commerce through the National Bureau of Standards.

On the regulation of radiation sources and uses, there is overlapping jurisdiction among the Nuclear Regulatory Commission, Bureau of Radiological Health, and Environmental Protection Agency. The Environmental Protection Agency claims a broad mandate to advise the president on all matters of federal radiation policy on the basis of its succession to the role of the now defunct Federal Radiation Council. The Bureau of Radiological Health claims jurisdiction over electronic products including x-ray machines under the 1968 Electronic Products Safety Act, and also a general authority over medical radiation uses under sections of the Public Health Service Act. In addition, the FDA's Bureau of Drugs and the new Bureau of Medical Devices and Diagnostic Products also assert responsibilities for manufacture of radiopharmaceuticals and generally for safety and efficacy of all medical devices. Though the Nuclear Regulatory Commission yielded control of the isotopes, it has retained control over licensees in the nonagreement states.

To complicate the radionuclide picture further, the shipment of radioactive materials is the responsibility of the Department of Transportation, where various agencies address problems of air, surface, and water carriers.

To present an overview of the pattern of federal interests in radiology, an outline of organizational responsibilities has been prepared. It is meant to be indicative, rather than inclusive. The interests suggested for each agency are not the only ways in which it may relate to radiology or medicine.

Congress

1. Joint Committee on Atomic Energy authorizes programs of the Nuclear Regulatory Commission and the Energy Research and Development Administration including regulations for uses of isotopes and funding for further development of nuclides (eliminated in Ninety-fifth Congress)
2. Senate Commerce Committee has jurisdiction over electronic products act and its successors, and over transportation of radioactive materials
3. Senate Finance Committee has jurisdiction over federal health programs involving special taxation, such as Medicare and Medicaid
4. Senate Human Resources Committee has jurisdiction through its Subcommittee on Health for those federal health initiatives not based upon special taxation, such as health manpower, medical education, research, and construction
5. House Ways and Means Committee is the point of origin, constitutionally, of all measures dealing with taxes, thus including Medicare and Medicaid, through its Subcommittee on Health
6. House Commerce Committee has broad health jurisdiction through its Subcommittee on Health comparable to 'the Senate Labor and Public Welfare
7. House Education and Labor Committee has jurisdiction over working conditions and some educational activities.

8. Senate and House Committees on Veterans Affairs and on Armed Services have jurisdiction over health care activities for active military personnel, their dependents, and veterans as well as substantial funding for facility construction, support for medical education, and research in government health institutions
9. General Accounting Office is the investigative arm of the Congress, making frequent inquiries into health programs administered by executive branch agencies. GAO reports often serve as a basis for oversight hearings or new legislation
10. Office of Technology Assessment is a research organization which supports the Congress with detailed reports on various national problems, such as the clinical and economic impact of CT scanners on health care
11. Other congressional committees have tangential interests when radiology involves public transportation, product safety, federal budgeting, or other areas seemingly remote from health care

Executive Branch

Department of Health, Education, and Welfare

1. Food and Drug Administration
   - a. Bureau of Radiological Health enforces electronic products act regulating such things as performance of x-ray systems; also has mission under the Public Health Act for education of physicians and other users of ionizing radiation
   - b. Bureau of Drugs has jurisdiction over contrast media and radiopharmaceuticals
   - c. Bureau of Medical Devices and Diagnostic Products enforces a new law extending federal jurisdiction over medical devices similar to classic FDA responsibility for drugs
2. National Institutes of Health
   - a. National Cancer Institute administers the cancer attack program, funds most basic and clinical research on cancer, and supports cancer centers
   - b. National Heart and Lung Institute supports activities devoted to areas indicated by its title, including projects for imaging
   - c. National Institute of General Medical Sciences supports research projects on diagnostic radiology within its biomedical engineering branch and with relatively low priority
   - d. Other categorical institutes
   - e. Division of Research Grants exercises responsibility through its Radiation Study Section and other study sections for peer review screening functions, to receive and review applications for grant and contract support, and to assign to appropriate federal funding agency
3. Health Resources Administration has programs dealing with health statistics, research, facilities, manpower, and planning
4. Health Services Administration has programs dealing with Public Health Service hospitals, Indian health, professional standards review, health maintenance organizations, and National Health Service Corps
5. Social Security Administration
   - a. Bureau of Health Insurance administers Medicare program
   - b. Bureau of Disability Insurance administers federal workmen's compensation and disability programs, including coal miners' black lung disease benefits program prior to 1973 and continuing
6. Social and Rehabilitation Service administers federal portion of state Medicaid programs through Medical Services Administration
7. Office of Education has responsibility for vocational education programs including funding for training of allied health personnel
8. National Institute for Occupational Safety and Health has responsibility for programs in areas indicated by title, including coal miner chest x-ray examination and surveillance of other mining industries
9. National Library of Medicine is the central federal repository of books, magazines, and audiovisual aids dealing with health; also has extensive reference service.

Other Executive Branch Agencies

1. Veterans Administration manages the largest medical care system in the world, providing care to veterans of military service
2. Department of Defense
   - a. Assistant secretary for health and environment plus surgeon general of military services operate health facilities for active military and dependents
   - b. CHAMPUS, program for civilian health providers of services to military and dependents
   - c. Armed Forces Institute of Pathology is the noted repository of disease materials on slides and radiographs; has consultant and teaching facilities, including American Registry of Pathology, Registry of Radiologic Pathology, and Registry of Radiation Pathology
   - d. Armed Forces Radiation Research Institute conducts radiobiological studies
3. Energy Research and Development Administration supports a program of research on radionuclides for medical application
4. Nuclear Regulatory Commission continues to control medical uses of nuclear byproducts in states not having agreements for such regulation; also sets national requirements for health standards of contractors and licensees
5. Department of Transportation, through the Office of Hazardous Materials Operations and Federal Aviation Agency, supervises shipment of radioactive materials and other categories of hazardous materials by common carriers
6. Civil Aeronautics Board approves or denies tariffs governing transportation of hazardous materials, including radiopharmaceuticals, on scheduled airlines
7. Department of Labor has responsibility for working conditions in health occupations
   - a. Occupational Safety and Health Administration has responsibility for worker safety and health programs, including coal miners' black lung disease benefits program
   - b. Wage and Hour Division enforces minimum wage law, overtime provisions
8. Department of Commerce is involved in the importation of x-ray equipment
   - a. National Bureau of Standards performs measurements and develops basic radiation concepts through its Center for Radiation Research
   - b. Bureau of Census works with U.S. Public Health Service National Center for Health Statistics in collection of data about medical care
9. Department of State conducts foreign policy, including science and medical affairs, notably designating U.S. participation in the United Nations Scientific Committee on Effects of Atomic Radiation
10. Department of Justice deals with charges of antitrust violations by physicians and physician organizations under

Sherman Act
   a. Immigration and Naturalization Service sets criteria for admissions of alien physicians and other health workers
   b. Drug Enforcement Administration shares major responsibility for control of illicit drug traffic

11. Federal Trade Commission is an independent agency having some overlap with the Department of Justice in enforcement of fair trade act, including recent alleged violations by medical societies
12. Environmental Protection Agency inherited role of Federal Radiation Council in coordinating federal policy which is carried out through the Office of Radiation Programs. They are attempting to extend mandate beyond one of advising the president
13. National Science Foundation funds research programs and attempts to set national goals for science, including medical science
14. Department of Housing and Urban Development has mortgage guarantee programs which encompass some medical facility construction
15. Civil Service Commission writes job descriptions for individuals working in federal health programs
16. National Aeronautics and Space Administration supports research on life support systems and imaging systems with medical applications
17. Equal Employment Opportunities Commission supervises federal enforcement of fair employment practices, including review of testing and certifying bodies to eliminate racial and ethnic biases

White House

1. Office of Science Advisor was recently revived
2. Office of Management and Budget coordinates and reviews programs and spending levels proposed by the excecutive branch agencies

It can be seen that, well short of the much discussed advent of comprehensive national health insurance, federal agencies already have a pervasive effect upon the practice of medicine and the specialty of radiology. In the recent presidential campaign, both the successful and unsuccessful candidates' platforms included references to efforts to decrease the federal bureaucracy. Would it be too much to hope that we could suggest a good place to start?

An editorial by Moseley and Linton appears in this issue.

Guest Editorials

Therapeutic Value of Thyreocalcitonin

In this issue, Whalen et al. [1] supply conclusive evidence that the administration of synthetic human thyreocalcitonin ameliorates the clinical, radiographic, structural, and biochemical changes in the bones of patients with chronic familial hyperphosphatasemia, a disease which cripples all of its victims and kills most of them before they reach adulthood. Thyreocalcitonin does not cure the condition but controls it, much in the same way that insulin does not cure diabetes mellitus but does control it. The beneficial effect of thyreocalcitonin is the gratifying result of prolonged and painstaking clinical and basic research which has taken place since this disease was first recognized in 1956 by Bakwin and Eiger [2].

The first case [2] was a Puerto Rican girl whose affected sister was later reported [3]. Choremis et al. [4] described an affected 11-year-old Greek boy. Two infantile sisters of Germanic stock were reported by Swoboda [5]. In 1967, Caffey [6] described an affected 6-year-old Jugoslavian boy (necropsy by Mitsudo [7]). Other reported cases included a Portugese Brazilian boy [8], an English infant [9], two Puerto Rican infantile siblings [10], and three juvenile Puerto Rican siblings (one doubtful) [11]. The condition has been variously described as fragile bones with macrocranium, osteoectasia with macrocranium, osteitis deformans juvenilis (Paget's disease), hyperostosis corticalis deformans juvenilis, chronic idiopathic hyperphosphatasemia, osteochalasia desmalis familiaris, and chronic progressive osteopathy with hyperphosphatasia [2-9].

The patient of Wagner and Solomon [12], a Bantu infant in Africa mistakenly reported as an example of hyperostosis corticalis infantilis (Caffey's disease), had all of the major features of chronic familial hyperphosphatasia. Wodehouse et al. [13] described the condition as Paget's disease in a Scottish boy of 5 years. In 1973, Caffey reported an affected premature infant of Anglo-Saxon parentage [14]. Whalen et al. [1] have now added four children, all who appear to be of Central American Indian parentage. Virgil Condon (personal communication) has detected the condition in two infants who appear to be American Indians of Navajo tribe descent at the University of Utah Medical School and Primary Children's Hospital in Salt Lake City.

In this small population of cases, the disease is widely distributed racially and geographically, but with a surprisingly high prevalence in Puerto Ricans and American Indians. The high Puerto Rican incidence may actually represent American Indian incidence because of the rarity of the condition in either blacks of African origin in the United States or blacks native to Africa. Thus physicians responsible for the care of Puerto Rican and American Indian children in particular should be alert in the detection of this disease, especially since effective treatment is now available.

Chronic familial hyperphosphatasia is basically a skeletal disease limited to the membranous elements in growing bones, in which concurrent overproduction and overdestruction occur with accelerated turnover of collagen and minerals. The normal formation of mature Haversian bone is prevented by too rapid destruction of fibrous bone. The growth and formation of endochondral bone is normal [14].

The clinical manifestations have been consistent in all patients. Onset is usually between 3 and 18 months of age. Progressive enlargement of the head due to thickening of the calvarium has been the common initial clinical finding. However, in one infant 10 weeks of age, bowing of the legs preceded enlargement of the head. Bilateral lateral bowing of the thighs (femurs) and ventral bowing of the shanks (tibias) have been conspicuous findings in all of the older children I have seen. Pain, tenderness, and muscular weakness in the extremities and spine cripples most patients; in severe cases, infants have failed to sit up or stand. Some have remained in the supine position permanently until death. In several patients, deficient visual and auditory acuity were present.

Biochemical findings have been abnormal in all patients. The sustained increase in alkaline and acid phophatase activity of the osteogenic type is of primary diagnostic importance. The blood uric acid has been increased in the few patients in which it has been determined. An excessive amount of leucine aminopeptidase was present in the blood of two patients. In all patients tested for tetracycline labeling, the tetracycline was absorbed rapidly and disappeared rapidly. Massive urinary excretion of hydroxyproline and glycine-bound peptides was demonstrated in several patients.

The microscopic changes in the structure of the long bones are described in fine detail in the current report of Whalen et al. [1]. In one necropsy [7], xanthoma elasticum was found in the skin, in the arteries, and in the eyes. Also atherosclerotic changes were found in the heart, arteries, and especially the muscles. It is possible that arterial ischemia is the cause of the pain and profound weakness in the muscles of the spine and extremities.

The radiographic changes in the skull include thickening of the membranous bones in the calvarium often with rounded images of increased density (cotton balls) which increase in number and size with advancing age. The shafts of the long bones are increased in caliber with thickened but rarified cortical walls and failure of normal constrictions at the metaphyseal levels. In older patients there are multiple opaque transverse bands and lines at many levels which raised the question of multiple transverse microfractures; these may be responsible for the pain in the extremities. Gross fractures have developed in many patients, which have suggested osteogenesis imperfecta.

Current incomplete knowledge suggests that the inheritance is autosomal recessive. Karyotypes and chromosomes have been normal in form and number in a few patients. The mother in the family reported by Bakwin and co-workers [2, 3] had radiographic changes in the calvarium similar to Paget's disease, suggesting that latent Paget's disease in a mother may be related to chronic familial hyperphosphatasemia in her offspring.

Although chronic familial hyperphosphatasemia and Paget's disease have several common manifestations, they appear to me to be decisively differentiated by several features. In hyperphosphatasemia, the age at onset is early infancy; the bone lesions are symmetrical and appear to affect the calvarium and every long bone in the body; and mature Haversian bone fails to develop and remains in the immature fibrous stage. Conversely, in Paget's disease onset occurs in the third to fifth decades; the bone lesions are usually focal and asymmetrical; and the lesions develop in normal bone.

The distinctive clinical and radiologic features of chronic familial hyperphosphatasemia have permitted its accurate identification. The work of Whalen et al. [1] now establishes rational, effective therapy.

John Caffey
Childrens Hospital of Pittsburgh
Pittsburgh, Pennsylvania 15213

REFERENCES

1. Whalen JP, Horwith M, Krook L, MacIntyre I, Mena E, Viteri F, Torum B, Nunez EA: Calcitonin treatment in hereditary bone dysplasia with hyperphosphatasemia: a radiographic and histologic study of bone. *Am J Roentgenol* 129:29–35, 1977
2. Bakwin H, Eiger MS: Fragile bones with macrocranium. *J Pediatr* 49:558–564, 1956
3. Bakwin H, Golden A, Fox S: Familial osteoectasia with macrocranium. *Am J Roentgenol* 91:609–617, 1964
4. Choremis C, Yannakos D, Papadatos C, Baroutsou E: Ostetis deformans (Paget's disease) in an 11-year-old boy. *Helv Paediatr Acta* 13:185–188, 1958
5. Swoboda W: Hyperostosis corticalis deformans juvenilis: Ungewöhnliche generalisierte Osteopathie bei zwei Geschwistern. *Helv Paediatr Acta* 13:292–312, 1958
6. Caffey J: *Pediatric X-ray Diagnosis: A Textbook for Students and Practitioners of Pediatrics, Surgery and Radiology*, 5th ed. Chicago, Year Book Medical Publishers, 1967
7. Mitsudo SM: Chronic idiopathic hyperphosphatasemia associated with pseudoxanthoma elasticum. *J Bone Joint Surg* [*Am*] 53:303–314, 1971
8. Fanconi G, et al: Osteochalasia desmalis familiaris. *Helv Paediatr Acta* 19:279–295, 1964
9. Marshall WC, Moncrieff AA: Chronic progressive osteopathy with hyperphosphatasia. *Proc R Soc Med* 955: 238–239, 1962
10. Eyring EJ, Eisenberg E: Congenital hyperphosphatasia: a clinical, pathological and biochemical study of two cases. *J Bone Joint Surg* [*Am*] 50:1099–1117, 1968
11. Thompson RC Jr, Gaull GE, Horwitz S, Schenk RK: Hereditary hyperphosphatasia. Studies of three siblings. *Am J Med* 47:209–219, 1969
12. Wagner JM, Solomon A: Hyperostosis corticalis infantilis (Caffey's disease). *S Afr Med J* 43:754–755, 1969
13. Wodehouse NJY, Fisher MJ, Sigurdsson G, Joplin GE, MacIntyre I: Paget's disease in a 5-year-old: acute response to human calcitonin. *Br Med J* 4:267–268, 1972
14. Caffey J: Familial hyperphosphatasemia with atelia and hypermetabolism of growing membranous bone: review of the clinical, radiographic and chemical features, in *Progress in Pediatric Radiology: Intrinsic Diseases of Bone*, edited by Kaufmann HJ, New York, S. Karger, 1973, pp 438–468

The Federal Crossword Puzzle

Certainly all radiologists are aware that the federal government and its many agencies have programs and policies that affect radiologic practice. However, it is doubtful that most radiologists realize the depth of penetration into the practice of radiology by federal agencies or appreciate the very large number of federal agencies involved.

Our article in this issue outlined the areas of involvement by federal agencies which have primary health missions as well as by many federal agencies which touch on health peripherally but vitally. The crossword puzzle printed here is meant to illustrate dramatically the number of federal agencies and institutions which have an impact on radiology. The fact that they are illustrated as overlapping and at cross purposes is not accidental.

The methods of obtaining information about federal programs and influencing them are well known. The basic references include the *Congressional Directory*, an index of the federal government published each biennium; the *Congressional Record* which reports the daily actions of the Congress; the *Federal Register*, the official publication of the Executive Branch; and the *Commerce Business Daily* which carries announcements about federal contracts.

Far too few radiologists serve on federal advisory committees and task forces which help to set programs and priorities. An even smaller number hold staff positions in health policy roles. The efforts of radiologic organizations and the participation of radiologists must be viewed as essential to the continuing ability of the specialty to perceive and respond to multifaceted federal initiatives. Knowledge may not be strength, but in relation to government involvement in medical care, ignorance cannot be bliss.

Robert D. Moseley, Jr.
University of New Mexico School of Medicine
Albuquerque, New Mexico 87131
Otha W. Linton
American College of Radiology
Chevy Chase, Maryland 20015

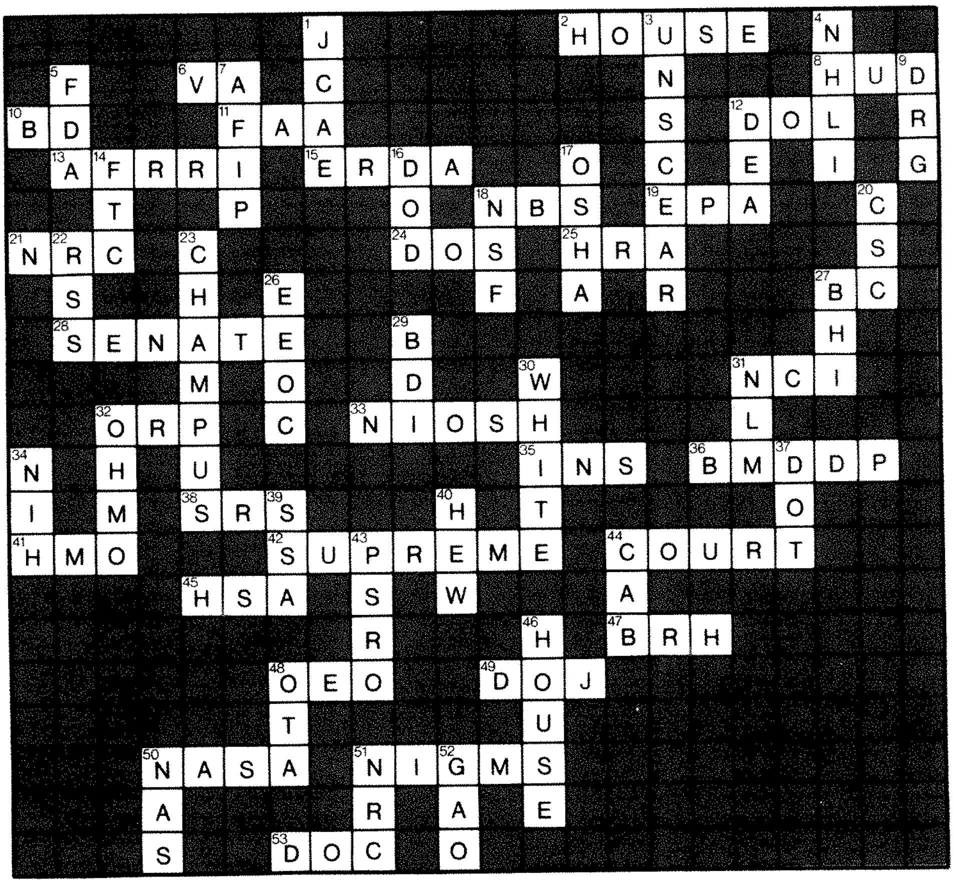

DOWN

1. Joint Committee on Atomic Energy
3. United Nations Scientific Committee on the Effects of Atomic Radiation
4. National Heart and Lung Institute
5. Food and Drug Administration
7. Armed Forces Institute of Pathology
9. Division of Research Grants
12. Drug Enforcement Administration
14. Federal Trade Commission
16. Department of Defense
17. Occupational Safety and Health Administration
18. National Science Foundation
20. Civil Service Commission
22. Radiation Study Section
23. CHAMPUS
26. Equal Employment Opportunity Commission
27. Bureau of Health Insurance
29. Bureau of Disability Insurance
30. and 46. The president's mansion
31. National Library of Medicine
32. Office of Hazardous Materials Operations
34. National Institutes of Health
37. Department of Transportation
39. Social Security Administration
40. Department of Health, Education, and Welfare
43. Professional Standards Review Organization
44. Civil Aeronautics Board
48. Office of Technology Assessment
50. National Academy of Sciences
51. National Research Council (or Nuclear Regulatory Commission)
52. General Accounting Office

ACROSS

2. ____________of Representatives
6. Veterans Administration
8. Department of Housing and Urban Development
10. Bureau of Drugs
11. Federal Aviation Administration
12. Department of Labor
13. Armed Forces Radiation Research Institute
15. Energy Research and Development Administration
18. National Bureau of Standards
19. Environmental Protection Agency
21. Nuclear Regulatory Commission
24. Department of State
25. Health Resources Administration
27. Bureau of the Census
28. World's most exclusive club
31. National Cancer Institute
32. Office of Radiation Programs
33. National Institute of Occupational Safety and Health
35. Immigration and Naturalization Service
36. Bureau of Medical Devices and Diagnostic Products
38. Social and Rehabilitation Service
41. Health Maintenance Organizations
42. and 44. Guardian of the Constitution
45. Health Services Administration
47. Bureau of Radiological Health
48. Office of Economic Opportunity
49. Department of Justice
50. National Aeronautics and Space Administration
51. National Institute of General Medical Sciences
53. Department of Commerce

Preliminary Program
78th Annual Meeting American Roentgen Ray Society

September 27–30, 1977
Sheraton-Boston Hotel

Tuesday, Sept. 27, 10:30 a.m.

Call to order 78th annual meeting: Seymour Fiske Ochsner, New Orleans, Louisiana, president

Installation of President-Elect Harry Z. Mellins, Boston, Massachusetts by Seymour Fiske Ochsner and Charles E. Bickham, Jr., Washington, D.C., chairman, executive council

Presidential Address: Harry Z. Mellins

I. Pediatric Radiology

11 a.m. John Caffey Award Paper to be selected by Society of Pediatric Radiology

11:15 a.m. Chest radiograph diagnoses of PDA in infants. B Burney, WL Smith, EA Franken, JA Smith, EC Klatte, Indianapolis, Indiana

11:30 a.m. Characteristic radiographic findings in left aortic arch with right descending aorta. R Dominguez, KS Oh, LW Young, JP Dorst, Pittsburgh, Pennsylvania

11:45 a.m. Acute chondrolysis complicating slipped capital femoral epiphysis: roentgen diagnosis and differential diagnosis. AB Goldman, R Schneider, W Martel, New York, New York

Noon. CT detection and course of intracranial hematomas in premature infants. CM Rumack, MM McDonald, OP O'Meara, BB Sanders, JC Rudikoff, Denver, Colorado

12:15 p.m. Angiography of extremity masses in children. P Stanley, JH Miller, Los Angeles, California

II. Uroradiology/Sonography

11 a.m. Computed tomography of the adrenal gland. PF Sheedy II, RR Hattery, DH Stephens, B Williamson Jr, RA McLeod, GW Hartman, Rochester, Minnesota

11:15 a.m. Localization of perirenal hematoma. JJ McCort, San Jose, California

11:30 a.m. Radiologic and pathologic findings in replacement lipomatosis. MA Ambos, RB Gordon, MA Bosniak, New York, New York

11:45 a.m. Ultrasonic demonstration of intrarenal anatomy. AT Rosenfield, JH Cook III, KJW Taylor, New Haven, Connecticut

Noon. Sensitivity of ultrasound in detecting urinary tract obstruction. PH Ellenbogen, LB Talner, GR Leopold, FW Scheible, San Diego, California

12:15 p.m. Enhanced ultrasonographic definition of pelvic anatomy by instillation of intraperitoneal fluid. AC Gonzalez, SP Kottle, EP Tuttle, Atlanta, Georgia

III. Cardiovascular Radiology

2 p.m. Pulmonary valve dysplasia: the need for preoperative diagnosis and a comparison to classical valvular pulmonary stenosis. DP Harrington, L Watkins Jr, JS Donahoo, RI White Jr, Baltimore, Maryland

2:15 p.m. Pulmonary artery abnormalities following aorto-right pulmonary artery shunts—angiographic aspects. DC Levin, K Fellows, TA Sos, Boston, Massachusetts

2:30 p.m. Pulmonary atresia versus "type IV truncus": differential by radiographic subtraction. RE Fulton, GD Davis, Rochester, Minnesota

2:45 p.m. Continuing studies with an intravascular blood flow and vascular diameter sensor: radiologic—physiologic correlations. RJ Steckel, A Kolin, RN MacAlpin, H Snow, J Metzger, Los Angeles, California

3 p.m. Cardiomegaly as a cause of nonuniform pulmonary artery perfusion. CF Beckmann, DC Levin, S Ulreich, Boston, Massachusetts

3:15 p.m. The role of "gated" cardiac blood pool studies in evaluation of "stress" Thallium-201 myocardial perfusion studies. JS Soin, RA Boedecker, MA Love, MH Keelan, Milwaukee, Wisconsin

3:30 p.m. Pseudoaneurysm of the left ventricle; plain film and angiocardiographic diagnosis. H Spindola-Franco, N Kronacher, Bronx, New York

3:45 p.m. The incidence of pulmonary embolism in patients with matching unilateral ventilation—perfusion lung scan defects and corresponding pulmonary infiltrates. JA Cavaluzzi, PO Alderson, SL Kaufman, KH Barth, DP Harrington, RI White JR, Baltimore, Maryland

IV. Joint meeting with the Society of Photo-optical Instrumentation Engineers

2 p.m. Effect of fatigue and other physiological factors on observer perception. BG Brogdon, RD Moseley, CA Kelsey, Albuquerque, New Mexico

2:15 p.m. 350 kVp chest radiography: review and comparison with 120 kVp. AV Proto, EJ Lane, Syracuse, New York

2:30 p.m. The influence of computed body tomography on medical decision making: methodology and preliminary results. J Wittenberg, HV Fineberg, EB Black, MK Ikeda, JT Ferrucci Jr, Boston, Massachusetts

2:45 p.m. A comparison of CT scanners with radiographic approach. GA Binder, VM Haughton, CR Wilson, Milwaukee, Wisconsin

3 p.m. Microfocal spot tube mammography. WW Logan, Rochester, New York (three additional papers to be selected by SPIE)

Wednesday, Sept. 28

V. General Session

10:30 a.m. Caldwell Lecture: The conception and development of computed tomography. Godfrey Hounsfield, Hayes, Middlesex, England

11:30 a.m. Announcement of Scientific Exhibit Awards

11:45 a.m. President's Award Paper

Noon. Award Paper, American Society of Neuroradiology

12:15 p.m. Award Paper, Society of Gastrointestinal Radiologists

VI. Chest Radiology

2 p.m. The mediastinal lines: correlation between conventional radiography and CTT. E Kazam, M Heneghan, JP Whalen, New York, New York

2:15 p.m. The radiographic spectrum of pleuropulmonary tularemia. SA Rubin, Little Rock, Arkansas

2:30 p.m. The spectrum of radiographic findings in allergic bronchopulmonary aspergillosis (ABPA). RA Mintzer, LF Rogers, HL Neiman, M Rosenberg, Chicago, Illinois

2:45 p.m. Tuberculosis: the frequency of presentation with unusual radiographic findings. WT Miller, RR MacGregor, Philadelphia, Pennsylvania

3 p.m. A new core-biopsy system for the lung. M Simon, Boston, Massachusetts

3:15 p.m. The earliest roentgenographic features of lung cancer. WE Miller, JR Muhm, DR Sanderson, RS Fontana, Rochester, Minnesota

3:30 p.m. Spectrum of cystic disease of the lung in association with carcinoma. GS Melnick, A Wychulis, E Harmon, B Safirstein, R Dhakhwa, R Maravilla, Newark, New Jersey

3:45 p.m. Alveolar cell carcinoma—two clinical entities with one pathologic diagnosis. WT Miller, J Husted, D Freiman, Philadelphia, Pennsylvania

VII. Neuroradiology

2 p.m. The vertex scan: an important component of cranial computed tomography. SD Wing, AG Osborn, RW Wing, Salt Lake City, Utah

2:15 p.m. The diagnosis of extracerebral fluid collections by computed tomography. SH Cornell, LC Chiu, JH Christie, Iowa City, Iowa

2:30 p.m. The value of computed tomography in management of intracerebral hematoma. B Azar-Kia, S Hempelman, M Fine, Maywood, Illinois

2:45 p.m. The role of computed tomography in the diagnosis and management of cerebral trauma. RA Zimmerman, LT Bilaniuk, D Bruce, C Dolinskas, T Genneralli, Philadelphia, Pennsylvania

3 p.m. Computed tomographic findings in systemic lupus erythematosus. LT Bilaniuk, RA Zimmerman, R Lisak, F Gonzalez, Philadelphia, Pennsylvania

3:15 p.m. The diagnosis of ascending transtentorial herniation by cranial computed tomography. AG Osborn, SD Wing, Salt Lake City, Utah

3:30 p.m. Relative sensitivity of brain scans and computed tomographic (CT) scanning in the detection of nonneoplastic intracranial lesions. RS Manoli, LL Maher, JS Soin, Milwaukee, Wisconsin

Thursday, Sept. 29

VIII. Gastrointestinal Radiology

10:30 a.m. Radiologic diagnosis of splenic vein occlusion. Correlation of angiographic and upper gastrointestinal examinations. KJ Cho, W Martel, Ann Arobr, Michigan

10:45 a.m. Double contrast examination of reflux bile gastritis. SH Ominsky, AA Moss, San Francisco, California

11 a.m. Malposition of the colon in right renal agenesis, ectopia, and anterior nephrectomy. JA Curtis, V Sadhu, RM Steiner, Philadelphia, Pennsylvania

11:15 a.m. Granulomatous colitis and diverticulitis: new observations. MA Meyers, DR Alonso, B Morson, C Bartram, New York, New York

11:30 a.m. The value of the double contrast colon examination in Crohn's disease of the colon and ulcerative colitis. FM Kelvin, TA Oddson, RP Rice, Durham, North Carolina

11:45 a.m. Cancer and chronic ulcerative colitis: can x-ray appearance predict survival patterns? EM James, HC Carlson, Rochester, Minnesota

IX. Abdominal/Osseous Radiology

10:30 a.m. Ultrasound guided fine needle aspiration biopsy of abdominal masses. ML Skolnick, A Dekker, BJ Weinstein, Pittsburgh, Pennsylvania

10:45 a.m. Computed tomography of retrocrural lymphadenopathy. PW Callen, M Korobkin, I Isherwood, San Francisco, California

11 a.m. The use of ultrasound and gallium for diagnosis of abdominal and pelvic abscesses. KJW Taylor, D Sullivan, AT Rosenfield, BD Simonds, New Haven, Connecticut

11:15 a.m. CT detection of intraabdominal abscesses. JR Haaga, TR Havrilla, NE Reich, RJ Alfidi, Cleveland, Ohio

11:30 a.m. Trispiral tomography in the evaluation of carpal injuries. CM Johnson, JW Beabout, Rochester, Minnesota

11:45 a.m. Evaluation of the postoperative lumbar spine with transaxial tomography. FR Murtagh, RM Quencer, MJD Post, Miami, Florida

Noon. Benign tumors of sacrum. J Smith, D Wixon, JJ McSweeney, New York, New York

Noon. Revised radiologic concepts of the Barrett esophagus. AH Robbins, ME Vincent, M Saini, JA Hermos, Boston, Massachusetts

12:15 p.m. Radiographic findings in patients with esophageal involvement by mediastinal granuloma. RL MacCarty, RJ Dukes, CV Strimlan, DE Dines, WS Payne, Rochester, Minnesota

X. Pancreatic/Biliary Radiology

2 p.m. Percutaneous forceps extraction of retained bile duct stones. JP Fotopoulos, JA Caprini, Evanston, Illinois

2:15 p.m. Evaluation of endoscopic retrograde cholangiopancreatography (ERCP) and pancreatic angiography in the diagnosis of pancreatic carcinoma. PC Freeny, TJ Ball, Seattle, Washington

2:30 p.m. A new cholangiographic sign of common bile duct obstruction—isolated opacification of intrahepatic ducts. EB Black, JT Ferrucci, Jr., Boston, Massachusetts

2:45 p.m. Pancreatic gray scale ultrasonography: what to expect. PH Arger, CB Mulhern, JA Bonavita, DM Stauffer, Philadelphia, Pennsylvania

3 p.m. Computed tomography of the gallbladder. TR Havrilla, NE Reich, JR Haaga, RJ Alfidi, A Cooperman, Cleveland, Ohio

3:15 p.m. The "parallel channel" sign of biliary tree enlargement in mild to moderate degrees of obstructive jaundice. MR Conrad, JO Janes, MJ Landay, Dallas, Texas

3:30 p.m. Sonography of the common bile duct—value of the right anterior oblique view. M Behan, E Kazam, New York, New York

3:45 p.m. Patterns of pancreatic carcinoma by real time and gray scale ultrasonography. N Hassani, R Bard, Jamaica, New York

Friday, Sept. 30

XII. Osseous Radiology

10:30 a.m. Multiple levels spinal injuries: the importance of early recognition. L Calenoff, J Chessare, LF Rogers, J Toerge, JS Rosen, Chicago, Illinois

10:45 a.m. Cervical disc vacuum cleft: a useful sign of acute injury. PS Wheeler, Baltimore, Maryland

11 a.m. Significant new observations about cervical spine trauma. MD Miller, JA Gehweiler Jr, S Martinez, OP Charlton, RH Daffner, Durham, North Carolina

11:15 a.m. Conventional and computerized tomography in the assessment of spinal trauma. SLG Rothman, WE Allen III, EL Kier, CC Jaffe, New Haven, Connecticut

11:30 a.m. Clinical assessment of computed tomography for musculoskeletal disorders. JS Wilson, M Korobkin, HK Genant, TM Schumacher, EG Bovill Jr, San Francisco, California

11:45 a.m. The radiographic arthritis survey. JH Mink, RH Gold, R Bluestone, Los Angeles, California

Noon. Evaluation of rheumatoid arthritis and related diseases: a comparison of clinical, scintiphotographic and roentgenographic examination. DL Weissberg, D Resnick, A Taylor, M Becker, N Alazraki, San Diego, California

12:15 p.m. Paravertebral ossification in psoriasis and Reiter's disease. M Sundaram, JT Patton, St. Louis, Missouri

12:15 p.m. The trough line: a roentgenographic sign of posterior dislocation of the shoulder. BC Stufflebam, LF Rogers, S Cisternino, G Kruglic, Chicago, Illinois

XI. Angiography/Head and Neck Radiology

2 p.m. Angiographic demonstration of varicosities of lower intestinal tract: incidence, and clinical significance in review of 700 cirrhotic patients. M Kinkhabwala, A Mousavi, R Adamsons, S Iyer, New York, New York

2:15 p.m. Complications of long-term transbrachial hepatic arterial infusion chemotherapy. ME Clouse, R Ahmed, R Oberfield, J McCaffrey, Boston, Massachusetts

2:30 p.m. Comparison of abdominal ultrasonography with lymphangiography for tumor staging. E Buonocore, PT Wooten, Knoxville, Tennessee

2:45 p.m. Ectopic pregnancy: criteria and accuracy of ultrasonic diagnosis. TL Lawson, Washington, D.C.

3 p.m. Doppler evaluation of extracranial cerebrovascular disease. AB Crummy, P Barriga, WD Turnipseed, C Strother, J Sackett, H Berkoff, F Jarrett, Madison, Wisconsin

3:15 p.m. The myelographic diagnosis of herniated lumbar intervertebral disc: a reappraisal with water soluble contrast medium. SA Kieffer, EF Binet, JV Esguerra, Syracuse, New York

3:30 p.m. The incudo-stapedial joint in health and disease. R Matsubara, H Konrad, WN Hanafee, Los Angeles, California

3:45 p.m. Malignant tumors of the sinuses: radiological, clinical, and pathological evaluation. AL Weber, R Tadmore, PFJ New, KR Davis, KJ Momose, Boston, Massachusetts

XIII. Angiography

10:30 a.m. Informed consent—an audiovisual technique. HH Feigelson, Cincinnati, Ohio

10:45 a.m. High-dose renal pharmacoangiography in the assessment of hypovascular neoplasms. VP Chuang, Lexington, Kentucky

11 a.m. Gastrointestinal angiographic findings in systemic amyloidosis. FM Schroeder, FJ Miller Jr, JA Nelson, RS Rankin, Salt Lake City, Utah

11:15 a.m. Pitfalls of transhepatic portal venography and therapeutic coronary vein occlusions. WC Widrich, AH Robbins, DC Nabseth, WC Johnson, SA Goldstein, Boston, Massachusetts

11:30 a.m. Pelvic fractures with hemorrhage: the effectiveness of angiographic management. TSA Matalon, AC Waltman, CA Athanasoulis, RA Novelline, AJ Greenfield, ML Ezpeleta Jr, Boston, Massachusetts

11:45 a.m. Transcatheter emoblization: complications and prevention with balloon catheters. AJ Greenfield, CA Athanasoulis, AC Waltman, ER LeMoure, ML Ezpeleta Jr, RA Noveline, Boston, Massachusetts

Noon. Occlusion arteriography with a balloon catheter. D Novak, J Weber, Ludwigshafen (Rhein), West Germany

12:15 p.m. Iliac artery fibrodysplasia. JF Walter, JC Stanley, JJ Mehigan, SR Reuter, D Guthaner, Palo Alto, California

Letters

Gas-filled Appendix Dialog

In an article by Lim [1], I am quoted as stating that "a gas-filled appendix is virtually pathognomonic of acute appendicitis if acute abdominal symptoms are also present." Lim reports three cases to show that the presence of gas within the appendix of a patient with acute abdominal symptoms is of no assistance in defining the location and nature of the pathologic process. The clinical and radiologic findings in the three illustrated cases, however, warrant no such conclusion and bear no resemblance to the changes I described and illustrated [2].

In my description of a gas-filled appendix in patients with acute appendicitis [2], it was clearly stated that this finding is likely to occur in the presence of *obstructive appendicitis* when gas produced by gas-forming organisms collects distal to the luminal obstruction. As a result, plain abdominal radiographs may reveal a *persistent localized* collection of gas within the appendix, which is often moderately to markedly distended and *fixed in position;* an upright film may reveal an air-fluid level within the gas-containing appendix. Care was taken to select an *appropriate illustrative example* of such findings in acute appendicitis since it is well documented that simple passive gas filling of a normally located appendix may be observed in the absence of acute appendicitis [2].

Radiologically, the nonpathologic nature of the gas-filled appendix is generally easily determined by observing its transient nature, lack of fixation on multiple views, absence of undue distension, and especially its occurrence in free continuity with a gas-filled cecum; the latter indicates the absence of luminal obstruction which is almost invariably present in acute suppurative appendicitis. These radiologic features of a nonpathologic gas-filled appendix are well illustrated in the cases reported by Lim [1].

In order to appreciate the significance of the sign of a gas-filled appendix in association with acute abdominal symptoms in patients with acute appendicitis, it is essential for the radiologist to apply *correct criteria* in the interpretation of the radiologic findings and obviously correlate these with the clinical features. These should consist of appropriate clinical signs and not simply represent irrelevant abdominal findings, as were present in the cases described by Lim [1].

Norman Joffe
Beth Israel Hospital and Harvard Medical School
Boston, Massachusetts 02115

The statement has been made in the literature, and I have supported it [3, 4], that when the appendix is located at a level lower than the cecum, it does not contain recognizable amounts of air because any amount of air that may be in the appendix escapes into the cecum. Air within the appendix when the appendix is in a lower position than the cecum can be seen only when there is obstruction of the appendiceal lumen. This is a reliable sign indicating obstruction of the appendix and appendicitis. The sign has not been repudiated to my knowledge, and it has been very useful in my experience. It has also been stated that when the appendix is at a level higher than the cecum in any ascending retrocecal or right upper quadrant position, it may normally be filled with gas, a finding which does not imply abnormality and lacks diagnostic significance.

Therefore, the article by Lim [1] offers no useful information and is confusing. In reviewing Lim's cases [1], it is obvious to me from the published radiographs that in each case the appendix extends medially and upward and is at a higher level than the cecum. In this position an appendix may normally fill with gas. This is not an unusual finding and should not be interpreted as indicating pathology of the appendix.

Constantine S. Soter
Northwest Community Hospital
Arlington Heights, Illinois 60005

Reply

Joffe's article [2] is confusing because it cites publications which do not support the description of gas-filled appendix set forth in his letter. For example, the article he cited by Killen and Brooks [5] describes five cases, none meeting his criteria. Air-fluid level was not mentioned for any of the cases. Only a single film of each patient was presented, making it impossible to form an opinion as to the persistent or fixed nature of the appendix. The caliber of the appendix might not satisfy Joffe. Only two of the cases were obstructive appendicitis. Soter would probably consider some of the cases normal because the appendix was located at a higher level than the cecum and the appendix was directed medially and upward.

Consequently, one wonders what are the proper criteria for a pathologic gas-filled appendix. Joffe's illustrations [2, figs. 13*A* and 13*B*] do not help. First, how can one be certain if the gas-containing structure in the right lower quadrant is the appendix? Second, if it is the appendix, how can one be certain whether the appendix is at a level higher or lower than the cecum, since the cecum is not identified? Third, how can one tell from a single examination, if the appendix is fixed, and if multiple views are necessary, how many are required? Fourth, how big must the caliber of the appendix be before it is considered pathologic? (It is of interest to me that the caliber of the appendixes illustrated in figs. 13*A* and 13*B* was not significantly larger than the one Joffe considered normal.)

I am aware of reports and statements that gas-filled appendix may occur in normal individuals. Two major sources quoted by Joffe and Soter are articles by Samuel [6] and Fisher [7]. Samuel [6] documented the presence of gas-filled appendix in normal individuals when the appendix is located at the right upper quadrant only. Fisher [7] depicts a gas-filled appendix in the right lower quadrant (was it at a level lower than the cecum?) which at surgery turned out to be normal. However no clinical details were given. Whether the patient had abdominal symptoms or ileus prior to the radiograph may be relevant.

Although statements have been made that there are cases of identifiable gas-filled appendix in the right lower quadrant in normal individuals, I have not seen adequate documentation of this.

Joffe [2] has stated, "Although a gas-filled appendix may rarely be seen as an incidental finding on plain abdominal radiographs in asymptomatic individuals, its occurence in association with acute abdominal symptoms is virtually diagnostic of acute appendicitis." Until the criteria of gas-filled appendix in a pathologic appendix are more clearly defined, readers will continue to be confused and errors will be made when Joffe's statement is applied.

May Siang Lim
George Washington University School of Medicine
Washington, D.C. 20037

REFERENCES

1. Lim MS: Gas-filled appendix: lack of diagnostic specificity. *Am J Roentgenol* 128:209–210, Feb 1977
2. Joffe N: Radiology of acute appendicitis and its complications. *CRC Crit Rev Clin Radiol Nucl Med* 1:97–160, 1975
3. Soter CS: The use of barium enema in diagnosis of acute appendiceal diseases: a new radiological sign. *Clin Radiol* 19:410–415, 1968
4. Soter CS: The contribution of the radiologist to the diagnosis of acute appendiceal disease. *Med Radiogr Photogr* 45:2–14, 1969
5. Killen DA, Brooks DW Jr: Gas filled appendix: a roentgenographic sign of acute appendicitis. *Ann Surg* 161:474–478, 1965
6. Samuel E: Gas-filled appendix. *Br J Radiol* 30:27–30, 1957
7. Fisher MS: A roentgen sign of gangrenous appendicitis. *Am J Roentgenol* 81:637–639, 1959

Books Received

Receipt of books is acknowledged as a courtesy to the sender. Books of sufficient interest will be reviewed as space permits

The Adult Postoperative Chest. By M. Melamed, F. A. Hipona, C. J. Reynes, W. L. Barker, and S. Paredes. Springfield, Ill.: Thomas, 578 pp., 1977. $31.50

Advanced Exercises in Diagnostic Radiology—Computed Tomography of the Brain, vol. 9. By R. G. Ramsey. Philadelphia: Saunders, 239 pp., 1977. $9.95

Conference on Spontaneous Regression of Cancer, Baltimore, Maryland, May 9 and 10, 1974. Edited by E. F. Lewison. Publication no. NIH 76-1038, Department of Health, Education, and Welfare, 150 pp., 1976. $5.20 (from Superintendent of Documents, Government Printing Office, Washington, D.C. 20402).

Contributions to Nephrology. Vol. 5: **Radiology and the Kidney. Some Present Concepts.** Edited by J. Hodson. Basel: Karger, 85 pp., 1977. $20.50

Cranial Computed Tomography. Edited by W. Lanksch and E. Kazner. Berlin: Springer, 478 pp., 1976. $32

Cysts of the Oral Regions: A Dental Practitioner Handbook. By M. Shear. Bristol: John Wright & Sons, 169 pp., 1976.

Development of Angiography and Cardiovascular Catheterization. By T. Doby. Littleton, Mass.: Publishing Sciences Group, 205 pp., 1976. $18

Gastroenterology, vol. 3, 3d ed. Edited by H. L. Bockus. Philadelphia: Saunders, 1,211 pp., 1976. $38

Gastrointestinal Emergencies, Proceedings of the First International Symposium, Stockholm, Sweden, September 1976. Wenner-Gren Series, vol. 26. Edited by F. R. Bárány and A. Torsoli. Oxford: Pergamon Press, 428 pp., 1977. $30

An Introduction to the Physics of Nuclear Medicine. By P. N. Goodwin and D. V. Rao. Springfield, Ill.: Thomas, 150 pp., 1977.

Percutaneous Transluminal Angioplasty. The Dotter Procedure. By G. J. van Andel. Amsterdam: Excerpta Medica, 179 pp., 1976. $19.25

Pituitary and Parapituitary Tumours Major Problems in Neurology, vol. 6. By J. Hankinson and M. Banna. Philadelphia: Saunders, 217 pp., 1976. $27.50

Radiology of the Alimentary Tract in Infants and Children, Saunders Monographs in Clinical Radiology, vol. 10, 2d ed. By E. B. Singleton, M. L. Wagner, and R. V. Dutton. Philadelphia: Saunders, 461 pp., 1977. $26

Radiology of the Gallbladder and Bile Ducts, Golden's Diagnostic Radiology, section 22. By P. M. Hatfield and R. E. Wise. Baltimore: Williams & Wilkins, 263 pp., 1976. $26.50

The Reston Encyclopedia of Biomedical Engineering Terms. By R. F. Graf and G. J. Whalen. Reston, Va.: Reston Publishing Co., 415 pp., 1977. $29.95

Self-Assessment of Current Knowledge in Nuclear Medicine, 1,012 Multiple Choice Questions and Referenced Answers. By J. B. Selby and G. D. Frey. Flushing, N.Y.: Medical Examination Publishing Co., 213 pp., 1977. $12

Symposium on Pediatric Uroradiology, The Radiologic Clinics of North America, edited by R. L. Lebowitz. Philadelphia: Saunders, 130 pp., April 1977, vol. 15, no. 1. $24 for three issues

Symposium on *Pneumocystic carinii* Infection, Bethesda, Maryland, December 13 and 14, 1973. Edited by J. B. Robbins, V. T. DeVita, Jr., and W. Dutz. National Cancer Institute Monograph 43 (Publication no. NIH 76-930), Department of Health, Education, and Welfare, 223 pp., 1976. $4.75 (from Superintendent of Documents, Government Printing Office, Washington, D.C. 20402).

Textbook of Radiologic Technology, 6th ed. By C. A. Jacobi and D. Q. Paris. St. Louis: Mosby, 559 pp., 1977. $17.50

World Directory of Schools for Medical Assistants, 1973 (bilingual French/English). Geneva: World Health Organization, 112 pp., 1976. $9.60 (ISBN 92 4 05002 2, available through U.N. Bookshop, New York, N.Y., 10017).

1976 Year Book of Cancer. Edited by R. L. Clark, R. W. Cumley, and J. E. McCay. Chicago: Year Book Medical Publishers, 582 pp., 1976. $22.95

Abstracts of Current Literature

Chest

Pulmonary hemorrhage in renal disease: Goodpasture's syndrome and other causes. Schwartz EE, Teplick G, Onesti G, Schwartz AB (Hahnemann Medical College, 230 North Broad Street, Philadelphia, Pennsylvania 19102). *Radiology* 122:39-46, Jan 1977

Nine patients are presented with a combination of recurrent hemoptysis and renal disease. This combination in a young or middle aged man should suggest Goodpasture's syndrome. Other clinical entities may have this presentation. Examples are collagen disease and vasculidtides such as polyarthritis and Wegener's granulomatosis, pulmonary infections such as tuberculosis and necrotizing pneumonia, and coagulopathy which is common in renal failure along with azotemic fluid overload.

The radiographic findings consist of both interstitial and alveolar involvement. Shortly after hemorrhage, confluent alveolar densities are seen. These may be indistinguishable from hypervolemia associated with azotemia and other causes of noncardiogenic pulmonary edema. Repeated bleeding episodes cause the appearance of siderophages in the interstitium with accentuated vascular markings. If bleeding continues over a sufficiently long period, permanent reticular nodular infiltrates develop resembling idiopathic pulmonary hemosiderosis. The changes are generally diffuse, but may also be localized. As opposed to pulmonary venous congestion and edema of left ventricular failure, there is no predilection for perihilar involvment and Kerley B lines or pleural effusion.

As opposed to the previously held belief that hemoptysis heralds Goodpasture's syndrome, it has been the authors' experience and others that there may already be laboratory evidence of kidney involvement.

The combination of recurrent hemoptysis and renal disease in a young or middle aged man should suggest Goodpasture's syndrome. Radiographs in these patients should show evidence of recurrent pulmonary bleeding without other underlying causes. Final diagnosis rests on the demonstration of antiglomerular basement membrane antibodies both in situ and in vitro.

Asher Nov

Complications of percutaneous transthoracic needle aspiration biopsy. Sinner WN (Karolinska Sjukhuset, S-10401 Stockholm, Sweden). *Acta Radiol* [*Diag*] 17:813-828, 1976

The incidence of complications and factors influencing risk of complication are examined in 5,300 needle aspiration biopsies of the lung in 2,726 patients utilizing fine needle aspiration techniques. A pneumothorax was developed by 27.2% of patients which extrapolated to an incidence of 12.9% per puncture: 7.7% of these cases required treatment (exsufflation or chest tube drainage). Factors which correlated positively with occurence of pneumothorax included: deep lesions, multiple punctures, female patient, inflammatory or malignant tumors as contrasted to benign tumors in patients over 50 years of age, emphysema, and inexperienced operator (less than 20 procedures). Eleven percent of patients developed local pulmonary hemorrhage; none required treatment. The incidence of hemoptysis in central lesions was approximately 5% and 2% in peripheral lesions. No treatment was required. In one case as implantation metastasis is assumed to have occured. No tumor spread to the pleural space was observed. Two patients developed empyema and one patient developed a chest wall abscess at the site of an exsufflation needle punctured for treatment of a pneumothorax. Two possible cases of air embolism occurred. Four cases of bilateral pneumothorax occurred. The author recommends that bilateral biopsies not be performed on the same occasion. No treatment was required for two cases of mediastinal emphysema. One patient had bleeding in the chest wall. No treatment was required. There was no mortality in this series.

The diagnostic yield of the authors 5,300 biopsies was as follows: malignant tumor, 46.4%; benign tumor or pseudotumor 9.8%; granuloma, 7.4%; inflammatory lesion, 22.5%; other, 2.8%; and no cytologic diagnosis, 9.3%.

John D. Harley

Survival with inoperable lung cancer. Lanzotti VJ, Thomas DR, Boyle LE, Smith TL, Gehan EA, Samuels ML (Department of Medicine, University of Texas System Cancer Center, 6723 Bertner Avenue, Houston, Texas 77030). *Cancer* 39:303-313, Jan 1977

Regression analysis has been utilized to identify fundamental clinical variables predicting survival of 129 patients with limited but unresectable lung cancer and 187 patients with extensive unresectable lung cancer. Median survival time respectively was 36 and 14 weeks. Within the limited disease group weight loss was the major prognosticator. Within the extensive disease group, symptom status and age were dominant variables. Survival by cell type will be similar within the limited and extensive disease groups reflecting a modest advance in survival for patients with small cell carcinoma of the lung. The study identifies the essential factors which must be considered when analyzing survival as a dependent variable.

Herbert C. Berry

Treatment of hemoptysis by embolization of bronchial arteries. Remy J, Arnaud A, Fardou H, Giraud R, Voisin C (Hopital A. Calmette, 59033 Lille Cedex, France). *Radiology* 122:33-37, Jan 1977

Of 104 patients presented, 49 were treated during massive hemoptysis and 55 after hemoptysis. Arteries to be embolized were selected on the basis of relevant clinical, radiologic, arteriographic, and fiberendoscopic information. Three types of arteries could be embolized: (1) bronchial arteries, (2) nonbronchial systemic arteries penetrating the lung via the triangular ligament, and (3) nonbronchial arteries penetrating the lung via pleural adhesions. The material used was Spongel, fragments measuring 0.5 cm and 1-2 mm thick. The particles were softened in dextrose-saline and injected three to five particles at a time. Enough was injected to obliterate all but a few proximal centimeters of artery. This generally required 20-100 fragments per artery.

Contraindication to this method of treatment was the presence of an anterior spinal artery arising from either a cervical intercostal trunk, an intercostal artery, or an intercostal bronchial trunk.

Complications were most frequently retrosternal burning sensation with dysphagia and mild intercostal pain and fever lasting 2-3 days. In one patient, necrosis of the small bowel was treated by segmental resection. Another patient complained of epigastric pain which resolved after a few hours.

Of the 49 patients treated, hemoptysis was arrested immediately in 41. Of these, six suffered a relapse 2-7 months after the procedure. Of the remaining 35 patients, remission lasted 2-30 months.

Cause of hemoptysis were found to be tuberculosis, bronchiectasis, pneumoconiosis in coal miners, and intracavitary aspergilloma. Treatment of the last is less successful because the blood supply is through the axillary and subclavian arteries, as opposed to bronchial supply in the other entities mentioned.

Asher Nov

Interstitial pneumonia in the immuno-suppressed child. Sbihi A, Lallemand D, Sauvegrain J (J. Sauvegrain, Hopital des Enfants-Malades, 149 rue de Sevres, F 75730, Paris, Cedex 15, France). *J Radiol Electrol Med Nucl* 57:865–871, Dec 1976

The interstitial pneumonia reported by the authors is a very serious disease, with a mortality rate of approximately 40%. The condition affects children who develop immuno-suppression following chemotherapy or radiation therapy for malignant disease. This condition is seen with increasing frequency because of the effectiveness of the administered treatment which has resulted in longer survival of the children. The authors' report is based on 34 cases of acute lymphoblastic leukemia from their own service (treated in 1974 and 1975) as well as other cases which subsequently came to their attention.

In attempting to make a diagnosis the radiologist should retain a high index of suspicion, and should have or search for chest films made before therapy. These serve as a baseline for comparison and are invaluable in evaluating changes observed on subsequent chest radiographs. Changes are predominantly interstitial and may be difficult to evaluate in early stages. There is a progressive thickening of the lung markings presenting a reticular and reticulo-nodular pattern; eventually alveolar involvement occurs with patchy penumonic infiltration. There is accompanying loss of pulmonary function of at least 30%. While these changes may be striking in appearance, they are not necessarily diagnostic and may be produced by other conditions. Leucopenia with a lymphocytic count of 1000/mm^3 is a significant finding. A lung biopsy may be the most significant step in establishing the diagnosis. This helps by demonstrating the structure of the pulmonary parenchyma and the presence of other associated lesions or of a causative microorganism, if any.

William H. Shehadi

Cardiovascular

Systolic thickening and thinning of the septum and posterior wall in patients with coronary artery disease, congestive cardiomyopathy, and atrial septal defect. Corya BC, Rasmussen S, Feigenbaum H, Knoebel SB, Black MJ (Indiana University School of Medicine, 1100 West Michigan Street, Indianapolis, Indiana 46202). *Circulation* 55:109–114, Jan 1977 (By permission American Heart Association)

Echocardiographic septal and posterior wall thicknesses and the percent change with systole were measured in 146 patients with the following diagnoses: acute myocardial infarction (40), chronic coronary artery disease (49), congestive cardiomyopathy (8), atrial septal defect (20), and no cardiac disease (29). Mean diastolic thicknesses for the groups of patients with coronary artery disease and congestive cardiomyopathy were not significantly different from normal although there were abnormal values for individual patients within each group. Mean diastolic thickness of the septum was greater than normal for the group with atrial septal defect ($P < 0.02$). Wall thinning with systole was associated with acute infarction or ischemia ($P < 0.0001$); decreased thickening (less than normal) commonly occurred in patients with acute myocardial infarction, chronic coronary artery disease, and congestive cardiomyopathy. Patients with atrial septal defect had normal thickening with abnormal motion.

Results of this study show that 1) systolic thinning is indicative of an acute event; 2) abnormal changes in systolic wall thickening occur commonly in patients with coronary artery disease or congestive cardiomyopathy; and 3) abnormal wall motion may occur without abnormal wall thickening, as the echoes of patients with atrial septal defect indicate.

Author Abstract

A comparison of real-time, two-dimensional echocardiography and cineangiography in detecting left ventricular asynergy. Kisslo JA, Robertson D, Gilbert BW, Ramm OV, Behar VS (Duke University Medical Center, P. O. Box 3818, Durham, North Carolina 27710). *Circulation* 55:134–141, Jan 1977 (By permission American Heart Association)

Left ventricular wall motion was assessed in 105 consecutive patients both invasively, using biplane cineangiography, and noninvasively, by a real-time, phased-array, two-dimensional echocardiography system. Ventricular wall motion in five anatomic areas of the ventricle (anterolateral, posterolateral, apical, septal, and inferior) was analyzed by both methods in a double-blind manner. Two-dimensional echocardiographic images were deemed adequate for analysis in 82% of the regions (430 of 525). Fifty-five discrepancies were noted in the comparison of the remaining 430 regions.

The reasons for discrepancies in interpretation between the two methods were established for 54 during retrospective review: 33 were due to echocardiography (inadequate target visualization, observer error, or tangential echo views). Fifteen were related to angiography (overlay of silhouettes or observer error), and six were due to other reasons including definition problems or spatial orientation difficulties.

Both real-time, two-dimensional echocardiography and cineangiography have advantages and disadvantages. The techniques used together could provide more complete information concerning ventricular wall movement than is now currently available.

Author Abstract

Nontumorous adrenal hyperfunction: problems in angiographic-clinical correlation. Mitty HA, Gabrilove JL, Nicolis GL (Mount Sinai Hospital, 100th Street and 5th Avenue, New York, New York 10029). *Radiology* 122:89–94, Jan 1977

Forty patients with hyperfunctioning nonneoplastic adrenal glands associated with Cushing's syndrome, congenital adrenal hyperplasia, and aldosteronism were studied. Diagnosis often required combining clinical, laboratory, and angiographic findings. Radiologic studies consisted of preliminary urographic and nephrotomographic examination and venography as a primary angiographic approach. The diagnosis of adrenal hyperplasia using venography is based primarily on adrenal size. Normal adrenal size was defined by McLachlan and Roberts as 7.5 cm^2 (range, 3.8–12.2 cm^2) for the right, and 9 cm^2 (range, 5.7–17 cm^2) for the left. In addition, change in shape, such as increased convexity of the gland borders, and increased separation of intraglandular vessels were also taken into consideration. Diagnosis was possible in only half the patients with Cushing's syndrome, which correlates with the fact that only 50% of the hyperfunctioning adrenals are enlarged when examined pathologically. Two cases of ACTH producing pancreatic tumors causing Cushing's syndrome were also presented. One treatment choice requires localization and removal of the ectopic ACTH producing tumor. Corticalnodular hyperplasia, may cause Cushing's syndrome and must be differentiated from an adenoma. It differs in that it is usually less than 2 cm in nodular size, is bilateral, and often both glands are large. Congenital adrenal hyperplasia is usually associated with significant adrenal enlargement. In this case, clinical and laboratory evaluations are the prime diagnostic methods. Angiography serves to rule out rare virilizing tumor, which may mimic this entity in older children. Primary aldosteronism may be associated with nodular hyperplasia as well as adenoma. Since both are difficult to demonstrate on adrenal venous blood assay, it must be combined with venographic findings for correct diagnosis and therapy. For nodular hyperplasia, medical management is recommended, while a true adenoma should be resected.

Asher Nov

The VA cooperative randomized study of surgery for coronary arterial occlusive disease. II. Subgroup with significant left main lesions. Takaro T, Hultgren HN, Lipton MJ, Detre KM, and participants in study group (V. A. Hospital, Ashville, North Carolina). *Circulation* [Suppl 3] 54:107–117, Dec 1976

Patients with angina pectoris and stenosis of the left main coronary artery had been randomly allocated in 1970–1974 (53 to a medical treatment group and 60 to a surgical treatment group). After follow-up for an average of 2½ years, 36% of the medical group and 20% of the surgical group had died. Relief of angina was better in surgical patients. The prognosis of medically treated patients with left main and right coronary lesions and left ventricular dysfunction is very poor. These patients benefit most from surgery. Graft patency was evaluated 1 year after surgery, when arteriography showed that 69% were open. To assess the risk of the initial angiography, the authors found 284 V.A. patients with lesions of the left main demonstrated by coronary arteriography. Of these five (2%) died within 1 week of that study. There is an increased risk in these patients.

Robert Frech

Prêmature pulmonary valve opening. Wann LS, Weyman AE, Dillon JC, Feigenbaum H (Indiana University School of Medicine, 1100 West Michigan Street, Indianapolis, Indiana 46202). *Circulation* 55:128–133, Jan 1977 (By permission American Heart Association)

Premature opening of the pulmonary valve (opening independent of atrial or ventricular systole) was originally described in a case of sinus of Valsalva rupture into the right atrium. Since that time we have observed five additional cases in which the pulmonary valve opened prematurely. Entities encountered included: 1) constrictive pericarditis; 2) Loeffler's endocarditis; 3) Ebstein's anomaly with tricuspid regurgitation; 4) tricuspid regurgitation following tricuspid valvulectomy, and 5) pulmonary regurgitation accompanied by atrial septal defect. In the first two cases, premature pulmonary valve opening is felt to be due to restriction of diastolic filling of the right ventricle with subsequent early diastolic rise in pressure equalling or exceeding pulmonary artery diastolic pressure. In the latter three cases, the increased volume of blood entering the right ventricle again appeared to result in a rapid rise in initial right ventricular diastolic pressure and to produce premature opening of the pulmonary valve. Premature pulmonary valve opening, therefore, does not appear specific for any particular clinical entity but reflects the relative pressures in the right ventricle and pulmonary artery during diastole.

Author Abstract

Attenuation measurements of whole blood and blood fractions in computed tomography. New PFJ, Aronow S (Massachusetts General Hospital, Boston, Massachusetts). *Radiology* 121:635–640, Dec 1976

By use of computed tomography, intracranial hemorrhages can be diagnosed. Normal blood has a high attenuation in circulation and following extravasation. Attenuation of various whole blood and blood fractions were investigated. The attenuation values of whole blood of various hematocrit levels, protein, iron, hemoglobin, globin, plasma, and calcium were measured with an EMI cranial scanner. It was found that the predominent attenuation was produced by the protein fraction of hemoglobin rather than iron or calcium. At low hemoglobin levels, both circulating and extravasated blood may have the same attenuation as normal brain tissue preventing its discrimination. At very low hemoglobin levels, an intraaxial hemorrhage may appear less dense than brain.

Asher Nov

Two-dimensional echocardiographic assessment of vegetative endocarditis. Gilbert BW, Haney RS, Crawford F, McClelland J, Gallis HA, Johnson ML, Kisslo JA (J. A. Kisslo, Duke University Medical Center, P. O. Box 3818, Durham, North Carolina 27710). *Circulation* 55:346–353, Feb 1977

Real-time, two dimensional echocardiography was used to document the presence and assess the size and location of vegetative lesions of the cardiac valves and chambers in seven patients with bacterial endocarditis. Anatomic correlation (surgical or autopsy) was accurate in all patients. Two-dimensional echocardiography was shown to be of particular value in determining morphologic characteristics of the lesions since this technique provides spatial information concerning moving cardiac structures. Reliable assessment of lesion size and location may, in time, become a valuable method for determining the efficacy of antibiotic therapy. This information may also provide a means for evaluating certain patients for surgical intervention.

Richard Jaffe

Gastrointestinal

The gastrointestinal circulation. Lanciault G, Jacobson ED (University of Texas Medical School, Houston, Texas 77025). *Gastroenterology* 71:851–873, 1976

This extensive review, including 415 references, summarizes research on gastrointestinal circulation with special emphasis on developments of the past 5 years. The authors report that new discoveries in this field relate to the normal structure and function of the gastrointestinal circulation, to its abnormalities and diseases, and to drugs active in the gastrointestinal circulation. Current research in gastric mucosal blood flow utilizing radioisotopes is reviewed. Technical innovations in intestinal circulation have likewise been numerous including angiographic evaluations of mesenteric blood flow and ischemia. The authors evaluate recent investigation of gastric circulation as it relates to gastric secretion and ulcer formation. The physiology and pathophysiology of the intestinal circulation, especially as it relates to ischemia and hemorrhage, are evaluated in detail with emphasis on the use of angiography in the diagnosis, treatment, and investigation of the physiology of intestinal hemorrhage. The authors conclude by presenting a schematic diagram that embodies the major elements regulating gastrointestinal blood flow. These include general cardiovascular function, physical characteristics of blood, neural control, and properties of the blood vessels.

Charles A. Rohrmann, Jr.

Predictive factors and mechanism of arrhythmias and myocardial ischaemic changes in elderly patients during barium enema. Higgins CB, Roeske WR, Karliner JS, O'Rourke R, Berk RN (University of California Medical Center, San Diego, California). *Br J Radiol* 49:1023–1027, Dec 1976

The incidence of significant arrhythmias and ST segment changes during barium enema examination was evaluated by Holter monitoring of 58 unselected patients over the age of 60 years. Forty percent of the group developed new significant arrhythmias of which the most common were frequent and/or multifocal premature ventricular contractions. Seven percent demonstrated ST segment depression. Administration of glucagon did not diminish the incidence of arrhythmias. Predictive factors for ECG abnormalities were advancing age, abnormal prebarium enema ECG, and prebarium enema orthostatic hypotension. Analysis of arrhythmias and response to physiologic maneuvers suggested that the abnormalities were related to increased sympathetic tone which may be intensified by hypovolemia resulting from routine bowel preparation.

Author Abstract

Complications of endoscopic retrograde cholangiopancreatography (ERCP). Bilbao MK, Dotter CT, Lee TG, Katon RM (University of Oregon Health Sciences Center, Portland, Oregon). *Gastroenterology* 70:314–320, 1976

The basis for this report is the result of a postal survey made by the authors in the latter half of 1974. Of 402 United States owners of side-viewing duodenoscopes, 55% responded representing 10,435 endoscopic retrograde cholangiopancreatograms. Procedure failure occurred in 30%, complications in 3%, and death in 0.2%. Of the complications, injection pancreatitis occurred in 94 patients with no deaths. Cholangitic sepsis occurred in 72 patients with eight deaths. Drug reactions occurred in 51 patients with no deaths. Pancreatic sepsis complicating a pseudocyst occurred in 25 patients with five deaths, and instrumental injury occurred in 16 patients with two deaths. Aspiration pneumonia occurred in eight patients, and miscellaneous complications were noted in four patients, no deaths occurring in these groups. Eleven of the 13 fatal cases of sepsis resulted from injecting into a duct obstructed by neoplasm.

Injection pancreatitis developing within 24 hr of the procedure was the most common if not the most serious complication of ERCP. This is reported to be often associated with visible acinar filling of the pancreas. This can be prevented by careful fluoroscopic monitoring of the injections and terminating the injection when side branches are fluoroscopically visualized. Cholangitic sepsis was the second most common complication and most common cause of death. It seldom occurred in the absence of injection into the obstructed common bile duct. Prompt surgical relief of obstruction was generally believed to be the most important preventative measure. Pancreatic sepsis complicating pseudocyst and abscess caused extensive morbidity and a fatality rate of 20%. Again, it was associated with injection into an obstructed duct or cyst. Suggested preventative measures include prophylactic systemic antibiotics, utilization of antibiotics in the contrast agent, avoidance of over-injection of the pancreatic duct, and prompt decompression operation when injection beyond an obstructing process is done. Instrumental injury included three duodenal perforations, one variceal hemorrhage, and 12 intramural injections. Fatalities occurred in one perforation and in the incidence of bleeding varices. Instrumental injury was most common in patients with abnormal anatomy and careful review of the upper gastrointestinal series is suggested to obtain familiarity with the anatomy in advance.

The report concludes that both the success rate and the complication rate for ERCP should improve as experience is increased. Cause and effect relationships are suggested with pancreatic duct injection and acute pancreatitis, injection of an obstructed duct, and cholangitic or pancreatic sepsis, abnormal anatomy and instrumental injury, and inexperience producing a higher complication rate.

Charles A. Rohrmann, Jr.

The pathophysiology and diagnosis of reflux esophagitis. Pope C (Veterans Administration Hospital, Seattle, Washington). *Gastroenterology* 70:445–454, 1976

For the purpose of this review, the author defines reflux esophagitis as being present when there is either a subjective or an objective esophageal response to injury caused by gastroduodenal contents in contact with the esophageal mucosa. Whether a gastroesophageal reflux occurs depends on the integrity of the lower esophageal sphincter (LES). A large number of factors are described as affecting the LES pressure including neural, hormonal, and pharmacological influences, and certain foods. Gastroesophageal reflux is also prevented by flap valve effect at the cardia of the stomach. Information regarding the lower esophageal sphincter in a patient with gastroesophageal reflux provides conclusions which support both the feeling that a weak sphincter can in part allow reflux and that a sphincter can be damaged by reflux. A strong question of cause and effect is therefore introduced. The author makes a careful point of avoiding the association of gastroesophageal reflux and hiatal hernia. The diagnosis of reflux esophagitis can be entirely clinical if the symptoms are well defined. At the present time the best laboratory means is the use of the esophageal pH electrode. Radioisotopic methods may be found to be superior in the future however. Biopsy is stated to be the most sensitive means of determining the effect of reflux on esophageal mucosa but the histologic changes are not useful in predicting symptoms, complications, or the need for therapy. Endoscopy demonstrates evidence of macroscopic damage and barium esophograms show advanced structural abnormalities such as stricture or deep ulcers. The review concludes with 115 references which document the recent developments in the pathophysiology and diagnosis of reflux esophagitis.

Charles A. Rohrmann, Jr.

The radiological demonstration of colorectal polyps undetected by endoscopy. Laufer I, Smith NCW, Mullens JE (McMaster University Medical Centre, Hamilton, Ontario, Canada L8S 4J9). *Gastroenterology* 70:167–170, 1976

In 800 consecutive routine double contrast studies of the colon, 119 polyps were diagnosed radiologically in 78 patients. Of 56 polyps ultimately confirmed by endoscopy or repeat radiology, six were missed at the initial endoscopic examination. Of the six polyps missed on the initial endoscopic examination, five were located just behind a prominent mucosal fold at an area of sharp angulation of the colon. Three were found in the rectum, two at the junction of the descending colon and the sigmoid colon, and one at the splenic flexure. The authors conclude that when a high quality radiologic study of the colon suggests a polypoid lesion which is not confirmed by endoscopy, repeat radiologic study should be undertaken and if again positive, colonoscopy should also be repeated.

Charles A. Rohrmann, Jr.

The radiological findings in Crohn's disease involving the esophagus (in German). Froehlich HI, Huchzermeyer H, Stender H (Institut fuer klinische Radiologie und Abteilung fuer Gastroenterologie und Hepatologie des Departments Innere Medizin, Medizinische Hochschule Hannover, Karl-Wiechert-Allee 9, 3000 Hannover-Kleefeld, Germany). *Fortschr Geb Roentgenstr Nuklearmed* 125:497–500, Dec 1976

The diagnostic difficulties of Crohn's disease involving the esophagus based on the experiences with five patients are discussed.

The radiologic findings of esophageal Crohn's disease are variable but a classification in nonstenosing and stenosing form as used for regional enteritis can also be applied to the esophagus. The nonstenosing form begins with flattened and thickened mucosal folds. Later in the disease, these abnormal folds become increasingly irregular and progress to the typical cobblestone pattern. Peristalsis is absent in these severely involved segments. The stenosing form is more frequent. The stenosis, which exhibits prestenotic dilatation and conic tapering distally, is usually found in the distal esophagus but it occasionally occurs in the midesophagus. The margins of the stenosis are either finely undulated and smooth or irregular with small sacculations. The passage of barium through the stenosis is markedly delayed because of the luminal narrowing and absence of peristalsis in the stenotic region. Skip areas are not encountered in the region of the esophagus. Fistulous tracts arising from the esophagus appear to be rare; only two cases have been described in the literature. Though the described radiologic findings are characteristic, they are not specific of Crohn's disease. The stenosing type cannot be differentiated from esophageal carcinoma or other benign stenoses and the nonstenosing type resembles nonspecific chronic esophagitis such as reflux esophagitis.

Peter F. Winter

Effect of Crohn's disease on colonic diverticula. Berridge FR, Dick AP (Addenbrooke's Hospital, Cambridge, England). *Br J Radiol* 49:926–929, Nov 1976

Fifteen cases in which the same part of the colon has been affected by both diverticular disease and Crohn's disease have been studied. When Crohn's disease affects an area of colon where diverticula are present, radiologic examination may show a diminution in number or disappearance of diverticula with progress of the Crohn's disease. With improvement in the Crohn's disease diverticula may appear.

Author Abstract

Roentgenology of the colon in Crohn's disease. Air contrast studies of the lesions and their development (in English). Brahme F, Fork FT (University of Lund, Allmänna Sjukhuset, Malmoe, Sweden). *Radiologe*, 16:489–496, Oct 1976

Between 1954 and 1973, 201 patients with Crohn's disease underwent air contrast examination of the colon at Malmoe General Hospital. The technique as devised by Welin was employed. These patients had involvement of the ileocecal region (102 patients), of the ileum and more or less extensive parts of the colon (81 patients) or of the colon alone (18 patients). Sixty patients had anorectal changes with (44 cases) or without (16 cases) direct continuity with colonic lesions. The diagnosis was histologically confirmed by examination of surgical specimens in 192 (98.4%) cases and by rectal biopsy in three (1.6%).

According to the authors, air contrast examination of the colon has the following advantages in the diagnosis of Crohn's disease: (1) inflammatory mucosal changes such as submucosal and mucosal edema, ulcerative lesions and inflammatory polyps are shown to good advantage; (2) other changes such as strictures, "pseudodiverticula" and fistulae are very well demonstrated; (3) results are reproducible on follow-up studies because of the strict standardization of the technique; and (4) changes in colonic pliability are well demonstrated, provided that post-evacuation films are included in the procedure.

The technique has the following disadvantages: (1) associated distal ileal changes are less well demonstrated since filling of small bowel loops is deliberately avoided in order not to obscure the sigmoid loops; (2) haustral abnormalities, easily seen on the conventional barium enema, are less apparent in a colon which is fully distended by air; (3) thorough cleansing of the colon is mandatory in air contrast technique and residual fecal matter is more disturbing on air contrast studies compared to "full column" technique. Colonic "parietography", i.e. simultaneous pneumoperitoneum and air insufflation of the colon, was performed in 11 patients in order to determine the thickness of the colonic wall since colonic wall thickening is a characteristic finding of Crohn's disease. Though the desired information could be obtained, this method was abandoned because of patient discomfort during the procedure.

Peter F. Winter

Genitourinary

Calcification in polycystic disease. Kutcher R, Schneider M, Gordon DH (State University Hospital, Box 1208, Brooklyn, New York 11203). *Radiology* 112:77–80, Jan 1977

Two patients with a long history of polycystic disease are presented in whom plain films of the abdomen demonstrate extensive calcifications in kidneys, liver, and spleen. Common signs and symptoms of renal polycystic disease are hypertension, colicky pain, hematuria, urinary tract infection, proteinuria, and flank mass. Common complications are infected cysts and abscess formation, pyelonephritis, cyst rupture, hemorrhage, and ureteric obstruction. The liver may be extensively involved with grossly normal liver function tests. Calcifications took the form of ringlike, curvilinear punctate and irregularly amorphous concretions. Biopsies showed these calcifications to be within the walls of cysts. Califications in kidneys are seen more often in carcinoma, occurring at a rate of approximately 10% of cases as compared to 1%–2% in simple cysts. Similar calcifications have also been described in congenital multicystic kidney, multilocular cysts, hydatid disease, and previous trauma. Areas of calcification in the liver are more common with hydatid cyst, abscess, granuloma, syphilis, and hematoma, as well as malignant disease.

Improved medical management in renal transplantation has increased life expectancy of patients with polycystic disease. The authors believe PCD must be considered in the differential diagnosis of any patient with abdominal calcifications.

Asher Nov

The value of urography following lymphography in malignant diseases. Walker TM, Davies ER, Roylance J (Bristol Royal Infirmary, Bristol, England). *Br J Radiol* 50:93–96, Feb 1977

The need for urography following ascending pedal lymphography in malignant disease has been studied in 298 consecutive patients. Forty percent of the urograms were abnormal. Urographic abnormalities due to the disease being investigated were heralded by abnormal lymphography except in four patients, three with carcinoma of the bladder and one with carcinoma of the cervix. The majority of abnormalities unrelated to the disease being investigated were of no significance. In a small number there was congenital malposition of the kidney so that it fell within the proposed field of treatment. It is concluded that it is unnecessary to do routine urography with every lymphogram. Indications for urography are abnormality or suspected abnormality of the lymphogram, failure to locate the kidneys on plain films and clinical indications such as carcinoma of the bladder or carcinoma of the cervix.

Author Abstract

The less familiar manifestations of schistosomiasis of the urinary tract. Umerah BC (University Teaching Hospital, P.B. Box RW1, Lusaka, Zambia). *Br J Radiol* 50:105–109, Feb 1977

One hundred and fifteen patients with schistosomiasis of the urinary tract were studied. Sixty-five percent of the ureters showed striking deformities, including medial deviation, a straight lumbar course, and in the pelvic segment a bowed appearance with medial and cranial displacement at the vesico-ureteric junction. The appearance, which resembles a "cowhorn," is due to fibrosis in the bladder trigone.

Stasis and dilatation of the upper urinary tract were present in the absence of mechanical obstruction. Strictures were rare (7%), and fluoroscopy during excretory urography confirmed that the changes in the upper urinary tract were due to functional derangement of the ureters and not strictures. Four patterns of bladder calcification are described—the familiar linear rim calcification, an amorphous form, uniform opacity and curvilinear forms.

The diagnosis can be suggested from the postmicturition bladder film which shows a coarse, shaggy or polypoid mucosal pattern in all stages of the disease.

Author Abstract

Delayed opacification in congenital multicystic dysplastic kidney, an important roentgen sign. Cooperman LR (University of California School of Medicine, San Francisco, California). *Radiology* 121:703–705, Dec 1976

Two cases of congenital multicystic dysplastic kidney are presented. A newborn female and a 2-week old male each presented with an abdominal mass. Excretory urograms showed cystic lucencies early in the total body opacification phase. Late films showed persistent calyceal crescents and with further delay, a puddled irregular opacification. These radiographic signs are felt to be typical of unilateral, congenital multicystic kidney. This entity was originally described as a nonfunctioning flank mass, however subsequent reports indicate function. Delayed opacification is thought to be due to tubular reabsorption of water with concentration of contrast material proximal to the distal obstruction in the collecting system and/or ureter. Delayed films up to 24 hr may be highly informative when multicystic kidney is suspected.

The combination of excretory urography and ultrasound examination is felt to be sufficient for evaluation of a flank mass in the newborn and through the first year of life. The use of more aggressive diagnostic procedures, such as retrograde urography, cystoscopy, and angiography, should be reevaluated.

Asher Nov

Ureteroceles vs. pseudoureteroceles in adults: urographic diagnosis. Thornbury JR, Silver TM, Vinson RK (University Hospital, Ann Arbor, Michigan 48109). *Radiology* 122:81–84, Jan 1977

Ureterocele is a cystic dilatation of the distal ureter which protrudes into the bladder. Tanagho defined ureterocele as a congenital cystic dilatation of the submucosal segment of the intravesical ureter. Ureteroceles are usually considered innocuous. Pseudoureteroceles are acquired dilatations of the submucosal portion of the distal ureter. They show asymmetry, moderate to severe obstruction of the upper tract, and evidence of an acquired cause, such as calculus or abnormal bladder mucosal pattern. The halo sign is seen in both ureteroceles and pseudoureteroceles. The authors stress that it is of importance to distinguish between the two, since in their series most pseudoureteroceles were related to malignancy involving the bladder.

Asher Nov

The pear-shaped bladder. Ambos MA, Bosniak MA, Lefleur RS, Madayag MA (New York University Medical Center, 559 First Avenue, New York, New York 10016). *Radiology* 112: 85–88, Jan 1977

The teardrop or pear-shaped bladder was orginally described in cases of pelvic hematoma, either due to trauma or secondary to anticoagulant therapy. Other causes of the pear-shaped bladder are: 1. Pelvic lipomatosis, a condition in which there is deposition of large amounts of adipose tissue mixed with minimal fibrosis and inflammatory action. This is the only process which compresses the bladder bilaterally, but gives increased lucency to the pelvis. 2. Inferior vena cava occlusion due to neoplasm, abdominal sepsis, trauma, extension of lower extremities, thrombi, and idiopathic cases. The diagnosis is suggested if lower extremity edema is present. Urinary bladder distortion is secondary to compression by pelvic venous collaterals and pelvic edema. Definitive diagnosis is made by cavography. 3. Enlarged lymph nodes as seen in lymphoma or, less frequently, leukemia. 4. Lymphocysts. These form after extensive pelvic lymph node dissection. Lymphangiography is diagnostic with pooling of contrast medium in the lymphocysts.

Asher Nov

Short dialysis, middle molecules, and uremia. Nolph KD (University of Missouri Medical Center, Columbia, Missouri). *Ann Intern Med* 86:93-97, Jan 1977

This article provides perspectives on the problem of uremic neuropathy as it is currently seen in patients on chronic dialysis. There are many problems in determing the adequacy of dialysis in the management of a patient with uremia. Dialysis often will improve the neuropathy of chronic renal failure as well as reduce the BUN and creatinine values and correct certain other metabolic derrangements. For a given patient, however, it may be very difficult to determine the optimal dialysis duration. This is in part due to lack of understanding of what specific substances or toxins are being removed by the dialysis procedure. One currently popular concept is that certain "middle molecules" with molecular weights of 500 to 5,000 are the important toxins but the identity of these molecules is not known. Dr. Nolph makes a good case for careful clinical data collection to try to improve upon the empirical pratice of renal dialysis. He clearly points out that there remain major problems to be solved in optimizing the management of patients with chronic renal failure.

David C. Dale
Medicine, University of Washington

Musculoskeletal

Ankle arthrography and ankle distortion (in English). Sanders HWA (Catharina Hospital, Eindohoven, The Netherlands). *Radiol Clin Biol* 46:1–10, Jan 1977

Ankle arthrography was performed in 300 unselected patients with ankle distortion. Using the anterior approach, a mixture of 6 ml 60% Renografin or Conroy 60, 4 ml 1% lidocaine, and 75 IU hyaluronidase was injected until the patient indicated distinct tautness throughout the ankle. After passive and, if possible, active movement of the ankle, three anteroposterior views (neutral, internal, and external rotation) and one lateral view were obtained. The diagnosis of a ligamentous lesion was made if contrast medium was found extraarticularly in the soft tissues or in the tendon sheath of the peroneus muscles. Filling of a medial tendon sheath or of the subtalar articulation was not considered to be of pathologic significance.

In 61% of the patients, a ligamentous lesion was found. The most common lesion was rupture of the anterior talofibular ligament; rutured in 90% of the cases. With a rupture of the anterior talofibular ligament, contrast medium is seen below and ventrolateral to the lateral malleolus, often with extension into the craniomedial direction. With severe ankle distortion, rupture of the anterior talofibular ligament can be associated with a rupture of the calcaneofibular ligament, in which case the tendon sheath of the peroneus muscle is often filled with contrast medium. The posterior talofibular ligament is the strongest lateral ligament and it is only involved with ruptures of the other two lateral ligaments; its rupture cannot be demonstrated arthrographically. With rupture of the anterior tibiofibular ligament, contrast medium is localized anteriorly with craniolateral extension. In the case of a rupture of the anterior tibiofibular ligament, the lateral view usually shows a contrast free zone anterior to the syndesmosis. Rupture of the posterior tibiofibular ligament occurs only in severe ankle injuries, or in combination with other ligamentous lesions or fractures. Tears of the deltoid ligament, which are almost always partial, cause extraarticular contrast localization distally and medially to the medial malleolar tip. It is believed that the deltoid ligament is relatively often involved with rupture of the syndesmosis.

The reliability of the ankle arthrogram approaches 100% if obtained within 5–7 days following the injury. After about a week, the synovial membrane has closed and an ankle ligamentous lesion can no longer be identified by the escape of contrast medium. In 240 cases, additional stress exposures with the ankle in maximum inversion-adduction were obtained and correlated with the ankle arthrograms. Assuming a talar tilt of more than 5% as diagnostic of a lateral ligamentous tear, it was found that the stress examinations were false-positive in 7% and false-negative in 14% of patients with distortion.

In the author's experience, ankle arthrography is a technically simple and quick procedure and has no complications. Arthrographic images are generally interpreted without difficulty. It is suggested that an arthrogram be performed on any ankle distortion of significance, if recognition of a possible ligamentous tear is to be considered important for the treatment and guidance of the patient.

Peter F. Winter

Clinical, radiographic, and pathologic abnormalities in calcium pyrophosphate dihydrate deposition disease (CPPD): pseudogout. Resnick D, Niwayama G, Goergen TG, Utsinger PD, Shapiro RF, Haselwood DH, Wiesner KB (Veterans Administration Hospital, 3350 La Jolla Village Drive, San Diego, California 92161). *Radiology* 122:1-15, Jan 1977

CPPD is a general term for an entity which may be clinically manifested as crystal-induced acute synovitis (pseudogout) and radiographically as chondrocalcinosis. The radiographic appearance of chondrocalcinosis due to calcium pyrophosphate dihydrate crystal deposition is typical and includes heavy punctate and linear calcifications which are often bilateral and symmetrical. The criteria used for the diagnosis of CPPD were: (1) radiographs with typical chondrocalcinosis involving more than one set of joints exclusive of the intervertebral discs; (2) the presence of monoclinic and triclinic crystals aspirated from symptomatic or asymptomatic joints which showed absent or weakly positive birefringence when examined by compensated polarized light microscopy. Of the 85 patients examined, 31 fulfilled both criteria, 48 fulfilled the first criterion, and six, the second. These were divided into a group of definite and two groups of probable CPPD.

The clinical spectrum was divided into six types, the most frequent being type 3, in which there was progressive chronic arthritis with superimposed acute attacks. The joints which were most frequently symptomatic were the knees, hands, wrists, ankles, and subtaylar articulations, and hips. Acute attacks were characterized by sudden onset of pain and swelling of single or multiple joints, particularly the knees, elbows, ankles, and wrists. Attacks usually lasted 1-2 weeks and were occasionally provoked by trauma. Chronic progressive arthritis was most commonly seen in the knees and hips resembling osteoarthritis. Flexion contractions were seen, particularly in the elbows and knees. Joint aspirations revealed intra- and extracellular polymorphonuclear calcium pyrophosphate dihydrate crystals. Serology for rheumatoid factor was negative in 61 patients and weakly positive in one. Articular calcifications were seen in the knees (79%), symphysis pubis (69%), wrists (65%), elbows (54%), and hips (45%). Radiographs of the knees, symphysis pubis, and wrists are the most effective screening test for calcific articular deposits.

The arthropathy was similar to osteoarthritis, in that it showed joint space narrowing, subchondral eburnation, and cyst formation. It differed in several ways. (1) It showed changes uncommonly seen in osteoarthritis at the wrist, elbow, glenohumeral joint. (2) Intraarticular distribution was also unusual, in that it involved the radiocarpal compartment of the wrist and patellofemoral compartment of the knee. (3) Subchondral cyst formation was prominent, resulting in numerous and large radiolucencies. (4) Alterations were frequently severe and progressive, showing collapse and fragmentation with numerous intraarticular bodies. These abnormalities resembled neuropathic arthropathy. (5) Osteophyte formation was variable. There is clinical and radiographic dissociation with symptomatology correlating poorly with the presence, type, and extent of local calcification.

Asher Nov

Septic arthritis: a complication of rheumatoid arthritis. Gelman MI, Ward JR (University of Utah Medical Center, 50 North Medical Drive, Salt Lake City, Utah 84132). *Radiology* 122:17-23, Jan 1977

Fifteen patients with known rheumatoid arthritis are presented. Nine patients had clinical symptoms of septic arthritis for 14 days or less, three for 15-28 days, and five for longer than 1 month. The clinical presentation was usually swelling, while increased heat and redness were less common. In this series, the knee and elbow were the joints most frequently involved. Soft tissue changes, consisting of large joint effusion, adjacent soft tissue swelling, or fat pad edema, were observed on the initial radiographic studies of 13 of the 17 joints examined. Edema of the infrapatellar fat pad seen in rheumatoid arthritis in the acute stage is not commonly observed in chronic or longstanding rheumatoid arthritis; it is frequently associated with complicating bacterial arthritis. Additional signs are asymmetry in soft tissues coupled with information of progressive monarticular swelling and pain. The knee joint lends itself to earlier detection with changes seen in the suprapatellar bursa and infrapatellar fat pad. The ankle joint will at times show changes in the anterior and posterior tibiotalar joint capsule. The authors conclude that although these soft tissue and bony changes should be regarded with suspicion, needle aspiration must be performed for confirmation, identification of organism, and choice of the proper antibiotic.

Asher Nov

Spondylotic fractures. Cyron BM, Hutton WC, Troup JDG (Polytechnic of Central London, 115 New Cavendish Street, London, W1M8JS, England). *J Bone Joint Surg* [*Br*] 58: 462-466, Nov 1976

Long thought to be of a congenital nature, recent data indicates that spondylolysis is an acquired condition. A variety of case reports showing the traumatic nature of this problem have appeared in the radiologic literature within the past few years. These authors propose a specific mechanical etiology of spondylolysis using fresh spine specimens and a simplified two dimensional force analysis study. Forces stressing the posterior elements resulted in fracture deformities of the lamina quite consistent with spondylolysis.

The reason for the high incidence of spondylolysis at L5-S1 is clarified using vector analysis. The authors propose that the mechanical factor in the etiology of spondylolysis is a fatigue failure. Specifically, they mentioned that walking with a heavy backpack could produce an alternating loading stress on the inferior facets causing such a fracture. Apparently, they were referring to the traditional backpacks with shoulder harnesses rather than the more recently designed types which transmit virtually all the weight on the pelvis. They suggested that since the disc is a visco-elastic structure, it may tend to move forward under the action of a continuous vertical shearing force further increasing loading forces on the facets and lamina.

This theory seems to be adequately substantiated at this stage and the original article is recommended.

Gerald R. Smith

Normal "cupid's bow" contour of the lower lumbar vertebrae. Dietz GW, Christensen EE (University of Texas Southwestern Medical School, Dallas, Texas). *Radiology* 121:577-579, Dec 1976

The cortical margin of the inferior end plate in the frontal projection often simulates a Cupid's bow contour aimed cephalad. On the lateral view these parasagittal biconcavities are superimposed and are seen as one concavity in the posterior half of the vertebral body. A review of 200 patients demonstrated this finding in 63.5% of the cases. Males had a higher incidence (72% vs. 55%); blacks had a higher incidence than whites (71% vs. 56%). This finding is seen in L3, L4, and L5. Most frequently this is seen in L4, next at L5, and least at L3.

This contour should not be confused with the findings in sickle cell hemoglobinopathies, osteoporosis, osteomalacia, widespread metastatic tumor, and multiple myeloma. In these last-mentioned significant clinical entities, a biconcave configuration is noted which is more widespread in its distribution or is seen in both the superior and inferior facets.

Asher Nov

Capsular visualization in lipohemarthrosis of the knee. Sacks BA, Rosenthal DI, Hall FM (Beth Israel Hospital, 330 Brookline Ave., Boston, Massachusetts 02115). *Radiology* 122: 31–32, Jan 1977

Lipohemarthrosis (fat and blood) may be seen within the joint when a fracture causes the marrow cavity to communicate with the joint. The radiographic diagnosis of lipohemarthrosis of the knee has been described and is dependent upon fat-fluid level on the horizontal beam radiograph. The authors describe visualization of the capsular wall on routine vertical lateral knee radiographs. This effect is due to joint distension with liquid fat and an adjacent extracapsular fat pad. This effect is similar to seeing bowel wall outlined on both sides by gas on supine abdominal radiographs in the presence of pneumoperitoneum. To further investigate this phenomenon, vertical and horizontal beam lateral radiographs were obtained on cadaver knees following the injection of varying amounts of oil and water. It was found that vertical beam radiographs were less sensitive than horizontals in the diagnosis of lipohemarthrosis. Utilization of both methods was more effective in the suprapatellar region, rather than the infrapatellar region. The authors stress that, though cases of lipohemarthrosis without a recognized fracture have been reported, this sign should alert the radiologist to obtain additional views to confirm a fracture not initially recognized.

Asher Nov

Injuries of the forefoot. Anderson D (University of Tennessee College of Medicine, Memphis, Tennessee 38103). *Clin Orthop* 122:18–27, Jan–Feb 1977

Closed injuries of the forefoot are frequently underdiagnosed because they may be of subtle clinical presentation and because they often occur in motor vehicle accidents in which other injuries to the extremity, head, and trunk are more obvious. Furthermore, radiographic evaluation of the forefoot is frequently inadequate because of underexposure and insufficient views. Tarsometatarsal fracture dislocations may be subtle to diagnose because of their tendency towards spontaneous reduction. The clue to diagnosis may be a fracture of the base of the second metatarsal which is recessed into the tarsus serving as the keystone for foot stability at this level. One should also search for chip fractures of the other metatarsal bases or a compression fracture of the lateral aspect of the cuboid. Fractures of the metatarsals themselves are usually less of a diagnostic problem being seen quite well on the anteroposterior and oblique views. A lateral view, however, is always required to determine the amount of angulation. Dislocations of the metatarsophalangeal joint are easily missed if forefoot x-rays are overexposed. If initially missed, these injuries may go on to produce serious long term complications. Similar dislocations of the interphalangeal joints and fractures of the phalanges require appropriate exposure for radiographic diagnosis.

Frederick A. Matsen III
Orthopedics, University of Washington

Nervous System

Autopsy correlations with computerized tomography: experience with 6,000 CT scans. Jacobs L, Kinkel WR, Heffner RR (Millard Fillmore Hospital, 3 Gates Circle, Buffalo, New York 14209). *Neurology* 26:1111–1118, Dec 1976

In 79 cases the pathologic appearance of the brain was compared to the CT scan performed an average of 9.5 days prior to autopsy. Scans were interpreted by neurologists who were usually supplied with clinical findings and laboratory data. Most scans were performed with a 160 X 160 matrix without contrast enhancement. Pathologic diagnoses included a wide spectrum: six normals, 16 with hydrocephalus, 10 with cortical atrophy, 19 with infarction, 17 with hemorrhage, and 11 with tumor. The overall accuracy rate was 86.2% with no false positives. Eight of 14 cases with brain stem infarction or hemorrhage at autopsy were CT scan negative. The other three false negatives were patients with small, < 1 cm in diameter, metastatic tumor nodules located near the inner table of the skull. The material is illustrated with 12 cases which present the corresponding CT and macroscopic images.

Paul M. Chikos

The limitations of definition of blood vessels with computer intravenous angiography. Bergstrom M, Riding M, Greitz T. (Karolinska sjukhuset, S-10401 Stockholm, Sweden). *Neuroradiology* 11:35–40, May 1976

The ability of an EMI head scanner with a 160 X 160 matrix to detect small caliber contrast-filled structures was studied in vitro. Chambers 2 cm long in a polystyrene phantom varying in diameter from 0.65 mm to 4 mm were filled with contrast varying in concentration from 2 mg to 10 mg of iodine/ml and scanned at 100, 120, 140 kVp for 5, 6½, and 8½ min, respectively. The threshold of detection was 2 mm in diameter for a chamber filled with contrast of 4 mg of iodine/ml concentration. This value agreed with theoretical predictions and the level of iodine concentration is clinically attainable. In this experimental situation, due to the inherent noise in the system no improvement in detection was shown with changes in scanning time or kVp. In the clinical setting the authors expect a higher threshold of visibility due to the inhomogenity of brain, adjacent dense bone, tangential imaging of vessels, and patient motion.

Paul M. Chikos

Radiation exposure in radiographic examinations of the newborn. Wesenberg RL, Rossi RP, Hendee WR (University of Colorado Medical Center, Denver, Colorado). *Radiology* 122: 499–504, Feb 1977

Radiation exposure of the newborn during routine chest and abdominal radiographic examinations has been determined. The exposure has been measured at sites representing the entrance and exit chest, entrance, midline, and exit abdomen, the gonads, and the thyroid. Results of these measurements are reported as a function of kVp and in terms of mR received at the anatomical site per mR output of the generator at 24 in. (61 cm). This reporting procedure facilitates application of the results to exposure estimates under similar conditions at other institutions.

Author Abstract

Comparison of radionuclide scans with computer-assisted tomography in diagnosis of intracranial disease. Clifford JR, Connolly ES, Voorhies RM (1514 Jefferson Highway, New Orleans, Louisiana 70121) *Neurology* 26:1119–1123 Dec 1976

Two hundred eighty-one patients suspected of having intracranial disease were subjected to both radionuclide and CT brain scans. The CT scan yielded more diagnostic information with an error rate of only 1.4%. In 31 patients with brain tumors the CT scan was positive in 30 while the brain scan was positive in 23 cases. In 89 patients with cerebrovascular disease the CT scan was positive in 64 without error while the brain scan was positive in 29 and five were false positives. In 13 patients with degenerative diseases the CT scan was positive in 13 while the brain scan was positive in only one case which was a false positive. In the metabolic and infectious category the CT scan was positive in 14 of 34 while the radionuclide scan was positive in none. In 133 patients in whom both tests were negative, no evidence of CNS disease has been found in 6–18 months of follow-up.

Paul M. Chikos

Diagnosis of progressive multifocal leukoencephalopathy by computed tomography. Carroll BA, Lane B, Norman D, Enzmann D (Stanford University School of Medicine, Stanford, California 94305). *Radiology* 122:137–141, Jan 1977

Three cases of progressive multifocal leukoencephalopathy in whom laboratory, clinical, radiographic, pathologic, and computed tomographic findings are correlated are presented. PML is a subacutely evolving disorder afflicting all parts of the central nervous system. White matter involvement of the cerebral hemispheres is always present. Symptomatology depends on the area of involvement. Progression to coma and death usually occurs 3–6 months following the onset of symptoms.

Pathologic changes consist of enlarged distorted oligodendroglial nuclei containing esosinophilic inclusion bodies associated with enlarged astrocytes with bizarre nuclear configuration found within focal areas of demyelination. Death of oligodendroglia is felt to be responsible for the demyelination. Foci demyelination vary from microscopic to massive. Viral inclusion bodies are considered essential and specific features of PML. The disorder is felt to result from atypical viral infection in a compromised host either by activation of latent papova virus in the brain or dissemination of an extracerebral viral infection. PML is seen in Hodgkin's disease and chronic lymphatic leukemia. PML is less frequent in other lymphomas and leukemias. It has also been found in cases of tuberculosis, renal transplantation with immunosupression, and sarcoidosis.

All diagnostic tests, except for electroencephalogram, are noncontributory and the former is not specific. CT scans reveal low density lesions (10–20 Hounsfield units) of central and convolutional white matter with characteristic scalloped lateral borders. The lesions demonstrate no mass effect or contrast-material enhancement, and do not conform to specific vascular distribution. The main differential diagnosis would be: 1. Cerebral infarctions. These can be distinguished by their superficial location, shape, distribution in vascular territories, frequent contrast-material enhancement, evolution on serial studies, and by the different clinical course. 2. CNS infection. The lesions are often multiple; limitation to the white matter is unusual. When there is progression toward abscess formation, contrast-material enhancement invariably occurs. Mass effect is frequent. Bacterial abscesses are characterized by thin-walled material enhancement, while fungal lesions tend to be thick walled or solid. 3. Other focal demyelinating diseases may appear similar, but differ in their clinical presentation. Such entities as familial leukodystrophy and Schilder's disease do not show the characteristic scalloped occipital lesions of PML. 4. Primary and secondary brain tumors. These usually have a mass effect and show contrast-material enhancement.

The authors believe the CT appearance to be highly specific in the appropriate clinical setting. Recent reports of symptomatic improvement in PML following cytosine arabinoside therapy increase the importance of early diagnosis.

Asher Nov

Automated diagnosis of congenital dislocation of the hip. Endo M, Iinuma TA, Umegaki Y, Tateno Y, Tanaka H, Tsuchiya K (National Institute of Radiological Sciences, Anagawa 4-9-1, Chiba-shi, Japan). *Radiology* 122:25–30, Jan 1977

There is a high incidence of congenital dislocation of the hip among Japanese infants. Early diagnosis entails a radiographic survey which causes exposure of the gonads to radiation and requires a great deal of time. A quantitative method for diagnosis of congenital dislocation of the hip from radiographs was established. It uses one out of nine parameters obtained by geometric measurement of hip radiographs, Uziie's angle, which can be measured from simple anatomic points. This parameter was chosen because of its diagnostic accuracy and was shown to be as accurate as that of the measurement of specialists. This was determined by analysis of ROC (Receiver Operating Characteristics) curve method. Hip radiographs are inverted to the positive photograph of the same size. They are scanned by the raster method and digitized by the photoelectric image input apparatus using a rotating drum, a reflection coefficient of each picture cell (pixel) is punched onto paper tape. Data on the paper tape is converted to magnetic tape. Extraction of contour lines of bone edge is achieved by the wave propagation method developed by Shikano et al. The software necessary to extract Uziie's angle has been developed.

At present, a new method to reduce radiation exposure to the gonads is being developed. This consists of an x-ray pencil beam which is used to track the contour of the hip bones. The computer-controlled beam is generated by collimating rays through a pin hole. This method will enable a completely automated diagnosis with minimal exposure.

Asher Nov

Computed tomographic evaluation of increased intracranial pressure without localizing signs. Weisberg L, Nice CN (Charity Hospital of New Orleans, 1430 Tulane Avenue, New Orleans, Louisiana 70112). *Radiology* 122:133–136, Jan 1977

Twenty-nine alert patients with papilledema and no localizing neurologic signs were evaluated by skull radiography, echoencephalography, electroencephalography, radionuclide imaging, and computed tomography. In eight patients, lesions were demonstrated when ventricular enlargement or abnormal tissue densities were seen. Nineteen patients had normal CT scans, which suggested pseudotumor cerebri; only six of these patients underwent subsequent pneumoencephalography. The authors suggest that in alert patients with papilledema alone, CT can demonstrate ventricular abnormalities and abnormal densities, and assist in the diagnosis of benign intracranial hypertension without pneumoencephalography or angiography.

Asher Nov

Possible adverse effect of methylglucamine diatrizoate compounds on the bowel of newborn infants with meconium ileus. Leonidas JC, Burry VF, Fellows RA, Beatty EC (Children's Mercy Hospital, Missouri). *Radiology* 121:693–696, Dec 1976

Two newborn infants are presented in whom Gastrografin enemas were performed in order to relieve an uncomplicated meconium ileus. The first child underwent three barium enemas of which two were with Gastrografin. Though the child passed pellets of meconium, clinically she showed no improvement. Radiographs on the third day of hospitalization showed irregularity of the colonic gas pattern as well as wide separation of small bowel loops indicative of bowel wall edema and possibly mucosal ulceration. The child continued to deteriorate and died on day 6 of hospitalization. Autopsy revealed fibrinopurulent peritonitis and pseudomembranous enterocolitis of the cecum and ascending colon. There were typical changes of cystic fibrosis in the pancreas and intestine. The second child underwent two barium enemas, one with Gastrografin. Though the child began to pass pellets of meconium, she continued to deteriorate clinically. During surgery a necrotic bowel was resected and reanatomosis was performed. Postoperatively, the patient did poorly and died on the third day of hospitalization.

It has been found in animal experiments that hyperosmolar water soluble contrast media cause inflammatory tissue reactions. Gastrografin has an osmolality of 1,900 mOsm per liter. The authors present these facts and suggest that the use of Gastrografin in meconium ileus should be used with caution. Guidelines for patient selection, number of attempts, and dilution of the contrast require further study.

Asher Nov

Adhesive arachnoiditis following lumbar radiculography with water soluble contrast agents: a clinical report with special reference to metrizamide. Skalpe IO (Ulleval Hospital, Oslo, Norway). *Radiology* 121:647–651, Dec 1976

The goal of this study was to determine possible late sequelae after lumbar radiculography with metrizamide (77 examinations in 73 patients) as compared with methiodal sodium (95 patients) and methylglucamine iocarmate (20 examinations in 18 patients). The rate of adhesive arachnoiditis with the use of methylglucamine iocarmate and metrizamide was very low. Adhesive arachnoiditis following methiodal studies showed a rate of 29% in patients who are not operated on as compared with 48% in those who are. Water soluble contrast agents having a high enough iodine concentration are hypertonic in relation to serum and cerebrospinal fluid. This is thought to be the cause of both acute and late adverse effects of these contrast agents. It has been found that if the osmolality of cerebrospinal fluid can be kept below 500 mOsm/kg of H_2O during lumbar radiculography, adhesive arachnoiditis is unlikely. Metrizamide has the lowest osmolality. It is suggested that metrizamide is a better contrast medium than methylglucamine iocarmate with regard to development of adhesive arachnoiditis.

Asher Nov

Glucagon-aided reduction of intussusception. Fisher JK, Germann DR (St. Luke's Hospital, Wornall Road at 44th Street, Kansas City, Missouri 64111). *Radiology* 122:197–198, Jan 1977

Two cases, a 19-month-old and a 4½-month-old male, in whom a standard barium enema failed to reduce an idiocolic intussusception are presented. In both cases, success was achieved after 0.5 mg of glucagon was injected intramuscularly and a repeat or continued barium enema was performed. Glucagon relaxes smooth muscle, decreases peristalsis, and reduces gastrointestinal spasm by an unknown mechanism. Following administration an effect was noted 5 min later which lasted 30 min. Infrequent side effects are dizziness, vomiting, nausea, dry mouth, weakness, flush, headache, and abdominal stress. Known contraindications are hypoglycemia caused by an insulinoma and catecholamines release by pheochromocytoma. In addition it potentiates warfarin-induced hypothrombinemia when given in high doses. The recommended dosage in the pediatric group ranges from 0.5–1.0 mg. The authors' experience has been to attempt barium enema and, if reduction has not been achieved, to inject glucagon and make a second attempt. There is a consideration that glucagon might be given prior to attempted reductions in intussusception.

Asher Nov

Miscellaneous

Radiography of gynecomastia and other disorders of the male breast. Michels LG, Gold RH, Arndt RD (University of California School of Medicine, Los Angeles, California 90024). *Radiology* 122:117–122, Jan 1977

Twenty-two male mammograms with pathological correlation are reported. The authors stress benign diseases of the male breast. Gynecomastia is defined as abnormal increase in the stromal and ductal components of the male breast. This is to differentiate it from adiposity. Gynecomastia is due to proliferation of stroma in which the features of fibroblasts, hypervascularity, and hyalinization are prominent. True acinar lobules are usually absent. The spectrum of gynecomastia has been termed by Williams, type 1, or florid gynecomastia characterized by intraductal epithelial hyperplasia and a loose cellular stroma. Bannayan and Hajdu found that patients with gynecomastia of up to 4 months duration manifested type 1. Williams's type 2, or quiescent, fibrous gynecomastia is characterized by hyalinized stroma. This type is seen with a gynecomastia for a year or more. Type 1 correlates with what Forman described as a triangular or nondendritic mammographic pattern featuring a retroareolar soft-tissue density with few, if any, radiating extensions. Type 2 correlates with Forman's dendritic pattern, featuring a retroareolar soft-tissue shadow with prominent extensions radiating into the deeper adipose tissues.

Gynecomastia which tended to be bilateral, was usually either pubertal or hormone induced. Unilateral gynecomastia is usually induced by nonhormonal drugs or its idiopathic. Examples of nonhormonal drugs include digitalis, resurpine, ergotomine, diphenylhydantoin, phenothiazine, spironolactone, and thiazide diuretics. Causes of bilateral gynecomastia include exogenous estrogen, embryonal cell carcinoma or choriocarcinoma of the testes, Kleinfeleter's syndrome, adrenal carcinoma, marijuana use, cirrhosis of the liver, and chronic renal dialysis. Other benign conditions included inflammatory diseases, and papillomas which may be solitary or multiple. Gynecomastia may be unilateral, eccentric, and associated with nipple retraction, thus simulating carcinoma. It should be appreciated however that gynecomastia and carcinoma may coexist.

Asher Nov

Effects of therapy on breast calcification. D'Orsi CJ (Harvard Medical School, Boston, Massachusetts 02115). *Br J Radiol* 50:66–67, Jan 1977

A 54-year-old female presented with a stage III adenocarcinoma of the right breast, biopsy proven, and was treated by bilateral adrenalectomy and oophorectomy. External irradiation with adjunct chemotherapy was given and 1 month later mammography was performed showing fine clumped calcification and an irregular density consistent with carcinoma. A benign type of calcification was also present. An additional 2,000 rads was given by an iridium-192 implant. Follow-up mammography, nearly 6 months later, now showed loss of the fine malignant form of calcification and the appearance of a coarse benign form of calcification. The previously noted benign calcification was unchanged. The author speculates whether this unique change represents a mammographic demonstration of treatment effectiveness in calcified malignant breast disease.

T. Noel K. Allan

Transient bacteremia and endocarditis prophylaxis. A review. Everett ED, Hirschmann JV (Infectious Disease Service, P. O. Box 474, Brooke Army Medical Center, Fort Sam Houston, Texas 78234). *Am J Med* 56:61–77, Jan 1977

This excellent review catalogues the many reports on bacteremia after manipulation of the gastrointestinal tract, urinary tract, blood vessels, female pelvic organs and other body tissues. Transient, usually asymptomatic, bacteremia is very common with all kinds of tissue manipulations. The organisms which cause these bacteremias are the same organisms which normally inhabit the surfaces of these tissues. The risk of endocarditis from a transient bacteremia is probably very, very low. Nevertheless, it has become common practice to administer prophylactic antibiotics in certain circumstances. The most widely accepted indications for prophylactic antibiotics are dental manipulations and genitourinary procedures. On the basis of recent experimental studies, dental prophylaxis with penicillin and streptomycin is recommended for patients with abnormal heart valves and the use of ampicillin plus gentamicin is recommended when the same patients undergo genitourinary tract procedures. This article provides some thoughtful opinions as to who should receive antibiotics for a variety of radiographic and other diagnostic procedures.

David C. Dale
Medicine, University of Washington

Suppression of erythroid-colony formation by lymphocytes from patients with aplastic anemia. Hoffman R, Zanjani ED, Lutton JD, Zalusky, R, Wasserman L (Mount Sinai School of Medicine, 100th Street and 5th Avenue, New York, New York 10029). *N Engl J Med* 296:10-13 Jan 6, 1977

Aplastic anemia is a relatively common, rapidly fatal, nonmalignant disease. In most cases the cause for aplastic anemia can never be determined. It has been proposed that many cases of aplastic anemia represent a form of autoimmune disease. This study provides new data to support this possibility. Using recently developed methods to grow colonies of erythroid cells from suspensions of bone marrow, these authors investigated the possibility that serum and lymphocytes from patients with aplastic anemia may suppress bone marrow cell proliferation. In five of seven patients they found substantial suppression of cell growth when lymphocytes from patients with aplastic anemia were added to their cell culture system. The addition of normal lymphocytes had no such effects. Similarly, cell proliferation was not suppressed by the serum of patients or normal individuals. Recently a few patients with aplastic anemia have been treated with immunosuppressive therapies and improved. This data by Hoffman and his colleagues provides some basis for these clinical observations and should stimulate further investigations to determine if aplastic anemia is an autoimmune disease.

David C. Dale
Medicine, University of Washington

Comparison of lymphangiograms and gallium scans in the non-Hodgkin's lymphomas. Cabanillas F, Zornoza J, Haynie TP, Rodriguez V (University of Texas System Cancer Center, M. D. Anderson Hospital, 6723 Bertner, Houston, Texas 77030). *Cancer* 39:85-88, Jan 1977

A total of 92 lymphangiograms and gallium scans were performed in 51 patients with non-Hodgkin's lymphoma both before and after treatment. Of the 40 studies performed prior to treatment, 33 were conclusive. In 85% of the conclusive studies there was agreement in interpretation between the two procedures. Analysis of the 52 procedures after treatment showed agreement in only 56% of the 33 studies that were conclusive. It was found that the lymphangiogram yielded more information than gallium scans on 16 occasions while the gallium scans yielded more information than the lymphangiogram in only five occasions ($p = < .01$). The gallium scan frequently yielded equivocal results especially after treatment. No histologic examination of the tissues was performed to confirm the radiographic findings. The major advantage of the gallium scan appeared to be in the evaluation of disease above the diaphragm and in the mesenteric nodes.

Herbert C. Berry

Scrotal thermography. Gold RH, Ehrlich RM, Samuels B, Dowdy A, Young RT (UCLA Center for the Health Sciences, Los Angeles, California 90024). *Radiology* 122:129-132, Jan 1977

The normal thermographic pattern is characterized by an almost homogeneous emission throughout the scrotum, broken only by a vertical zone of increased emission at the invagination of skin marking the scrotal septum. Scrotal emission averaged 0.78° C (1.4° F) less than that from the outer aspect of the thighs and was never greater than the thigh emission. Emission from each side of the scrotum is never greater than 0.56° C (1° F). An ipsilateral increase in scrotal infrared emission with a difference of at least 2.8° C (5° F) between the normal and abnormal sides was recorded in 15 of 18 patients subsequently found to have an intrascrotal tumor, inflammation, or varicocele. Thermography was unable to distinguish between these disorders. In four patients, a significant increase in heat was found in the absence of positive physical findings. One of these patients had metastasizing seminoma, two patients had feminizing interstitial cell tumors, and one patient had varicocele that resulted in decreased spermatogenesis. Hydroceles tended to produce infrared emission equivalent to or less than that of the contralateral normal side. The authors suggest that lack of diagnostic specificity may be overcome by complimentary use of ultrasound.

Asher Nov

Radiography of hereditary presacral teratoma. Hunt PT, Davidson KC, Ashcraft KW, Holder TM (St. Luke's Hospital, 44th and Wornall Road, Kansas City, Missouri 64111). *Radiology* 122:187-191, Jan 1977

The radiographic findings in 26 patients with familial presacral teratoma at times associated with anorectal stenosis, retrorectal abscess, and vesicoureteral reflux are presented. All patients were examined by conventional radiographs of the sacrum and coccyx, barium enema, excretory urography, and voiding cystourethrography. All but a 3-month-old had sacrococcygeal defects in association with a palpable teratoma. Frontal radiographs, which are more helpful than lateral, show variation from a subtle unilateral sacrococcygeal malformation to a large central sacrococcygeal defect.

There are two significant differential diagnoses. One is anterior meningocele and meningomyelocele which, however, are usually seen in upper sacral segments and with a spina bifida. The second is nonfamilial sacrococcygeal teratomas. These are more common, approximately 60% show visible calcification, are more frequently seen in females, show increasing incidence of malignancy with age, and usually present posterior or inferior to the sacrum and coccyx.

By contrast, the presacral teratoma shows equal sex incidence, low malignancy potential, lack of soft tissue calcification, localization in a presacral position, defects in the sacrococcygeal structures and a familial occurrence.

Pathologic examination of the tumors shows origin from the three germinal layers. The tumors were predominantly cystic. Only one instance of malignant change occurred. The incidence suggests an autosomal dominant inheritance. Because of a low but definite malignant potential, the authors recommend resection of all these tumors and examination of the patient's family.

Asher Nov

Ultrasonics

Ultrasound in the evaluation of adrenal metastases. Forsythe JR, Gosink BB, Leopold GR (Veterans Administration Hospital, 3350 La Jolla, Village Drive, San Diego, California 92161). *J Clin Ultrasound* 5:31-34, Feb 1977

Forsythe et al. have described their experience using ultrasound to detect metastatic tumor to the adrenal glands in 10 patients (five with unilateral metastases and five with bilateral metastases). Six cases had autopsy confirmation. Most cases of adrenal metastases were previously unsuspected. Adrenal metastases were usually large, up to 15 cm in diameter, and displaced the kidney inferiorly, posteriorly, and laterally. This characteristic displacement along with a complete margin between the adrenal mass and the kidney (five of five gray scale scans and three of five bistable scans showed a complete margin) were the important differentiating points in determining the site of origin as the adrenal gland rather than kidney. All gray scale studies displayed considerable internal echoes within the tumor, often with areas of necrosis, while on bistable studies the internal echo characteristics were more difficult to evaluate. The authors suggest gray scale ultrasound B-scanning is a useful part of the workup of patients with bronchogenic carcinoma, since as many as 33% will have adrenal metastases.

John Denny

Nuclear Medicine

Technetium-99m pyridoxylideneglutamate (P.G.) cholescintigraphy. Stadalnik RC, Matolo NM, Jansholt A, Krohn KA, DeNardo GL, Wolfman EF Jr. (Sacramento Medical Center, University of California, Davis, California) *Radiology* 121: 657–661, Dec 1976

The authors evaluated Technetium-99m P.G. for a diagnosis of a variety of hepatobiliary diseases. This new agent is not commercially available and was prepared in the authors' radiopharmacy. Two millicuries of the Technetium-99m P.G. were administered intravenously to normal and nonjaundiced patients and 4–5 mCi to patients with jaundice. Imaging was performed with a standard gamma camera and the patient supine. Images were obtained at 15, 30, and 60 min after injection. Additional images were obtained at 2–6 and 24 hr after injection when obstruction was suspected, or when the biliary system or intestine was not visualized by 1 hr. Each image represented 500,000 counts or 5 min exposure. Less information was accepted if the patients were uncooperative. One hundred eight studies were performed and the studies were grouped according to the final diagnosis as determined by celiotomy and tissue histology (50 patients) or by clinical and laboratory review (31). Twenty-seven normal volunteers completed the study group.

The liver, gallbladder, biliary tract, and gut were well visualized within 30 min of injection in the normal volunteers. Three individuals required repeat study after being on a fat-free diet for 2 hr to visualize the gallbladder. One normal volunteer was subsequently determined to have gallbladder disease.

Similar results were obtained in 19 of 23 normal patient subjects. The remaining four had had previous cholecystectomy. Twenty-two patients had acute and chronic cholecystitis with cystic duct obtruction proved histologically. The gallbladder was not visualized in any of these patients, although the common bile duct and GI tract were visualized. Four patients with nonobstructive cholelithiasis were studied and had normal examinations. Contrast oral cholecystography revealed gallstones in all four. Four patients with incomplete obstruction without jaundice were studied with variable results. In all four patients obstruction was due to extrinsic compression of the common bile duct due to benign disease. Two patients with incomplete obstruction with jaundice were studied and in neither patient was the gallbladder or common bile duct visualized. Colon activity was visualized at 4 and 24 hr, however. Nine patients had complete extrahepatic biliary obstruction, with bilirubins ranging from 1.5 mg to 21 mg percent. The liver was visualized in these patients but in none was the gallbladder, common bile duct, or GI tract seen.

Finally, 17 with jaundice due to hepatocellular disease were studied with bilirubin levels ranging from 1.3 mg to 23 mg percent and the gastrointestinal tract was visualized within 24 hr in all 17 patients indicating patency of the biliary system.

The technique was also compared with other diagnostic tests of biliary patency but the data was insufficient to draw any significant conclusion in most cases. Technetium-99m P.G. cholescintigraphy reliably demonstrated a physiologically normal gallbladder and biliary system. In addition, it appears to be a reliable method of detecting acute cholecystitis with cystic duct obstruction. In the two above situations the test offers a rapid means of evaluating the gallbladder. In addition, complete extrahepatic obstruction can be differentiated from hepatocellular disease in severely jaundiced patients. The test did not, however, reliably differentiate incomplete extrahepatic biliary obstruction from hepatocellular disease. The technique does not reliably detect cholelithiasis.

Thomas Rudd

Radionuclide venography: correlation with contrast venography. Ryo UY, Qazi M, Srikantaswamy S, Pinsky S (Michael Reese Hospital, Chicago, Illinois). *J Nucl Med* 18:11–17, 1977

Radionclide venography (RNV) and contrast venography (CV) were performed in 47 limbs of 35 patients and the findings were compared. Of the 35 patients studied, 31 had clinical signs or symptoms of thrombophlebitis. The performance of RNV and CV was less than 48 hr in all cases.

RNV was performed with the patient supine and two tourniquets on each leg, one above the ankle and the other immediately below the knee. A simultaneous injection of 2 mCi of Technetium 99m MAA albumin was injected into the dorsal vein of each foot. When activity was seen in the calf vein, the ankle tourniquet was released and images of the calf, thigh, and pelvis were obtained using a standard gamma camera. Following this, the knee tourniquets were released and images of the thigh and pelvis were repeated. Finally, both legs were imaged for retained activity and when it was seen the patient was instructed to exercise the legs and repeat views were obtained.

Contrast venography was performed in the standard manner, using the same tourniquet technique and 58 ml of Renografin-60. Each leg was studied individually. After images of the calf were obtained, the tourniquets were released and images of the thigh and pelvis were obtained. Frequently a second injection of contrast medium was required for these latter images.

Sixteen studies were abnormal by both techniques, with the RNV showing at least two of the following abnormalities on all studies: decreased radioactivity in a normal venous channel, abnormal collateral flow, or stasis of radioactivity distal to an obstruction. Retention of radioactivity in the lower leg was an unreliable indicator of the presence of deep venous disease. Three RNV studies showed collateral flow that were interpreted as abnormal, but were demonstrated to be normal branches by contrast venography. Of 28 normal RNV studies, only two were demonstrated to have abnormality by CV. In both cases, CV demonstrated small thrombi attached to the wall of the vein. Overall accuracy of RNV compared to CV was 89%, sensitivity 84%, and specifictiy 93%. RNV represents a simple and reliable technique to detect deep venous disease.

Thomas Rudd

Radiation Oncology

The incidence of radiation pneumonitis as a result of single fraction upper half body irradiation. Prato FS, Kurdyak R, Saibil EA, Carruthers JS, Rider WD, Aspin N (Hospital for Sick Children, 555 University Avenue, Toronto, Ontario M5G1X8, Canada). *Cancer* 39:71–78, Jan 1977

The authors report the incidence of radiation pneumonitis in 43 patients receiving single fraction half body palliative irradiation. The UHB irradiation included the entire body above the umbilicus. Twenty-one of this group of patients also had additional major pulmonary irradiation; 10 mediastinal. The determination of the development of radiation pneumonitis was made in 15 patients from a comparison of radiographs taken before UHB and then 4 or more months after irradiation. In total, of the 15 patients having no major previous pulmonary irradiation, only two developed radiation pneumonitis, both with a dose of 1,000 rads. Of the total group of eight patients having major previous pulmonary irradiation seven developed radiation pneumonitis including several at the 800 rad level. An addendum describes additional clinical material covering a total of approximately 80 patients treated with 800 rads UHB. Three of these patients have developed radiation pneumonitis without having had previous pulmonary irradiation. Caution in the application of this UHB technique is recommended.

Herbert C. Berry

Radiation protection requirements for a whole-body CT scanner. Gross GP, McCullough EC (Mayo Clinic, Rochester, Minnesota 55901). *Radiology* 122:825-826, March 1977

Exposure values for a whole-body CT scanner, obtained from a room protection survey covering one month (119 patients), are reported. It was found that weekly exposures could be expected to be in the range of 350-750 mR/week for a daily load of 12 patients. The h.v.l. of gypsum board, lead, and plate glass at this radiation level was 1.8, 0.020, and 1.3 cm, respectively. The authors suggest that plate glass is not the method of choice for shielding a high-volume body scanner installation unless a large enough lead glass window is not available or cannot be installed in time to meet construction deadlines.

Author Abstract

Therapeutic embolization for intractable chronic bleeding. Higgins CB, Bookstein JJ, Davis GB, Galloway DC, Barr JW (University of California Medical Center, San Diego, California 92103). *Radiology* 122:473-478, Feb 1977

The authors describe the therapeutic embolization of both hypogastric arteries or multiple branches of the hypogastric arteries in five patients with intractable chronic vaginal and/or vesicle bleeding complicating pelvic cancers. Bleeding stopped in three patients and was reduced by 90% and 95% in the other two. One patient had persistent serosanguineous vaginal discharge but no transfusion requirement. Oxycel clot was used in three patients; Gelfoam in two. Two patients had low-grade fevers, two patients had no side effects, and one patient had gluteal pain for 6 hr. The authors describe an additional three patients who have transcatheter embolization of the hypogastric arteries without recurrence of bleeding.

Herbert C. Berry

Solid state radiographic image converters: medical applications. Szepesi Z, Davies DH (Westinghouse Research Laboratories, Pittsburgh, Pennsylvania). *Radiology* 122:817-820, March 1977

Solid state radiographic converter screens have characteristics such as high contrast, high resolution, compact size, light weight, easy handling, moderately high gain, and low price which make them attractive for medical applications. They could be substituted for the image-intensifier tube, the intensifier screen, or the radiographic film. Construction, characteristics, and applications of the radiographic amplifier screen and the radiographic storage screen are discussed along with the advantages of using smaller size film and lower dosages. A promising application for mammography is outlined.

Author Abstract

Sensitivity of radiographic screens to scattered radiation and its relationship to image contrast. Castle JW (Research Laboratories, Eastman Kodak Company, Rochester, New York). *Radiology* 122:805-809, March 1977

For incident x-ray beams of greater than 60 kVp, intensifying screens of rare earth phosphors produced higher radiographic image contrast in the presence of scattered radiation than did screens of calcium tungstate. This was attributed to fundamental energy absorption interaction differences. X-ray absorption is a function of the position of the k-absorption edge of the screen phosphor relative to the x-ray energy spectra of the primary and scattered x-rays. Spectral measurements of x-ray absorption showed that the ratio of primary absorption to scattered absorption is higher for the rare earth screens, causing lower relative sensitivity to the non-information-containing scattered radiation from the radiographic object.

Author Abstract

The role of radiation therapy in localized resectable intestinal non-Hodgkin's lymphoma in children. Nelson DF, Cassady JR, Traggis D, Baez-Giangreco A, Vawter GF, Jaffe N, Filler RM (University of Rochester Medical Center, 601 Elmwood Avenue, Rochester, New York 14642). *Cancer* 39:89-97, Jan 1977

The authors review the role of radiation therapy in 40 children with localized resectable intestinal non-Hodgkin's lymphoma in this retrospective study reviewing data from 1948-1974. Unfavorable prognostic findings at surgery were serosal involvement, presence of tumor at the surgical margins, mesenteric node involvement and the presence of abdominal fluid or blood. Paraaortic nodal involvement or multiple primary foci were universally fatal. No deaths occurred after 15 months and no recurrences occurred after 13 months following diagnosis. Several different treatment groups are described involving surgery alone or combined with chemotherapy and/or irradiation. Overall survival is 40% (16 of 40) with no survivors in the surgery alone group (0 of 4). The authors consider optimal therapy for localized intestinal non-Hodgkin's lymphoma to consist of surgical excision followed by whole abdominal irradiation and multiple agent chemotherapy. They question the routine use of CNS prophylaxis.

Herbert C. Berry

Wide-field resolution in radiography. Klein DJ, Bergeron RT, Bernstein H (University of Southern California School of Medicine, Los Angeles, California). *Radiology* 122:811-815, March 1977

Multiple star test objects were placed so as to record the entire field covered on a 35 X 43-cm (14 X 17-in.) film and radiographed to determine the apparent shape of the focal spot and the directions in which degradation is maximum and minimum. It was found that geometric unsharpness decreases along lines radiating outward from the center of the anode shadow. The small focal spots used in magnification may be anticipated to behave in a similar fashion. It was also shown experimentally that truly lateral resolution is approximately constant over the field. A theoretical explanation for this finding is offered.

Author Abstract

Radiobiology

Radiosensitizing and toxic effects of the 2-nitroimidazole Ro-07-0582 in hypoxic mammalian cells. Moore BA, Palcic B, Skarsgard LD (British Columbia Cancer Foundation, 2656 Heather Street, Vancouver, British Columbia, Canada). *Radiat Res* 67:459-473, 1976

The properties of the electron-affinic 2-nitroimidazole Ro-07-0582 have been examined *in vitro* in two Chinese hamster cell lines, CHO and $CH2B_2$. The drug was found to sensitize hypoxic cells to radiation damage selectively with a high efficiency. At concentrations greater than 10 m*M* the drug has a dose-modifying factor of approximately 3.0 in hypoxic cultures. It does not alter the response of aerobic cells. Pre- or postirradiation treatment of cells with Ro-07-0582 has little, if any, effect. At high cell concentrations, where many sensitizers are ineffective, this compound retains most of its radiosensitizing capability.

Ro-07-0582 is also shown to have a chemotherapeutic potential in that it demonstrates a very selective toxicity for hypoxic cells after a few hours of exposure. It is much less toxic to acrobic cells. This property, while it may serve as a useful complement to the radiosensitizing effect of the drug, suggests that care must be exercised in the clinical application of Ro-07-0582 to avoid possible injury to normal hypoxic tissues in the body.

Author Abstract

Changes in functional vascularity and cell number following x-irradiation of a murine carcinoma. Clement JJ, Song SW, Levitt SH (University of Minnesota Medical School, Minneapolis, Minnesota 55455). *Int J Radiat Oncol Biol Phys* 1: 671–678, July-Aug 1976

Post-irradiation changes in vascular function and cell number in the transplantable SCL carcinoma of A/J mice were examined. Vascular volume/g tumor, as measured by ^{51}Cr-labeled red blood cell dilution, increased within 1 day after 1,000 or 2,000 rad and then decreased. The number of living cells/g tumor, estimated from single-cell preparations, declined to a minimum at day three post-irradiation with 1,000 or 2,000 rad. Calculation of vascularity on a per living cell basis indicated that the vascular volume increased to 197% and 286% of controls 3 days after irradiation with 1,000 and 2,000 rad, respectively. These data indicate that post-irradiation reoxygenation of hypoxic tumor cells may be caused by a decrease in oxygen consuming cells which is greater in magnitude than the corresponding decrease in functional vascularity.

Author Abstract

Time-dose relationships for the cure of an experimental rat tumor with fractionated radiation. Moulder JE, Fischer JJ, Milardo R (J. J. Fischer, Yale University School of Medicine, New Haven, Connecticut 06511). *Int J Radiat Oncol Biol Phys* 1:431–438, March-April 1976

A detailed analysis has been carried out of tumor cure doses for three fractions per week x-ray treatments of an experimental rhabdomyosarcoma in rats. The tumor cure doses rise sharply between 1 and 5 days, have a slight dip at 10 days, and then rise steadily from 10 to 50 days. The 10–50 day portion of the time-dose relationship appears to be linear when plotted on a linear coordinate plot of tumor cure dose versus time; the time-dose relationship is not linear when plotted on log-log coordinates. Because a constant number of fractions/week were used in all fractionation schemes, the relative importance of time and fraction number could not be assessed directly. An analysis of the tumor cure time-dose relationship and the known *in vivo* and *in vitro* characteristics of the tumor cells suggests that there is effective reoxygenation in fractionation schemes longer than 10 days, and that repair of sublethal damage is a more important factor in the increases of the tumor cure dose with fractionation than is repopulation between treatments. A comparison of these tumor cure time-dose relationships with previously published normal tissue tolerance time-dose relationships shows that three fraction/week treatments lasting 5–33 days give no better and often worse results than single doses, but that a three fraction/week treatment lasting 50 days gives dramatically better "therapeutic results."

Author Abstract

Effects of adriamycin on the radiation response of murine hematopoietic stem cells. Hellman S, Hannon E (Harvard Medical School, Boston, Massachusetts 02115). *Radiat Res* 67:162–167, 1976

The effects of adriamycin on radiation response of murine hematopoietic stem cells are studied using the spleen colony technique. Doses of adriamycin causing little cell kill did not affect the radiation survival curve. When dosage sufficient to result in 35% survival (0.8 mg) was given, the shoulder of the radiation survival curve disappeared without any change in the D_0. When tested using divided doses of radiation, repair was not inhibited. Further, the trough seen in controls when the two doses of radiation were separated by 8–12 hr was not seen in the adriamycin-treated group. In fact, with these fractionation schemes survival in the presence of the drug was greater than in its absence.

Author Abstract

Book Reviews

Diagnosis and Staging of Cancer: A Radiologic Approach. By R. J. Steckel and A. R. Kagan. Philadelphia: Saunders, 376 pp., 1976. $25

The book consists of 17 chapters by 18 authors—15 radiologists and three dentists. Each chapter is devoted to the nonhematologic neoplasms of the various anatomical areas with the exception of Hodgkin's disease, non-Hodgkin's lymphoma, and pediatric neoplasms which are treated separately. The authors emphasize the practical solution of various clinical problems encountered in patients with cancer, with particular attention to the use of diagnostic radiology. The basic format is to review the clinical aspects followed by consideration of the role of diagnostic radiology in the detection, differential diagnosis, staging, treatment, and posttreatment evaluation of the patient with cancer.

The book is primarily addressed to physicians who manage cancer patients; thus the radiological emphasis is on "when to" and not "how to" perform or interpret the various radiologic examinations. This aspect of the presentation is a major departure from that found in most texts, and therein lies the primary merit. The examinations are considered in relation to the overall problem and not as individual diagnostic exercises. The proper sequence of examinations, their relationship to one another, the information which can be derived, and the limitations of each are discussed.

It is unfortunate that the authors deliberately chose not to address the problem of cost effectiveness or cost-benefit ratio of the various examinations. In the preface they state "the editors feel it is inappropriate (even if it were feasible) to assign a value to the diagnostic procedures that may affect the quality or duration of human life." This is a commendable attitude when taken in the abstract. However, resources are not limitless, and we must use them with maximum effectiveness. In addition, many studies are uncomfortable and entail a definite, albeit small, risk for the patient. Therefore, cost effectiveness (used to encompass more than economic cost) is of paramount importance.

There are 225 well selected, superbly reproduced, and amply captioned radiographs. The volume is of convenient size, although the glossy paper requires some judicious positioning to avoid glare. The extensive bibliography includes 1,354 citations, 583 of which have a publication date of 1972 or later.

It is unfortunate that the timing of publication was such that the role of computed tomography could be considered only in the central nervous system. Also, there is little information in the chapter on Breast to clarify the current controversy over the potential hazard of radiation-induced neoplasia versus the benefits of mammography.

I would recommend this excellent text to all physicians who care for patients with cancer—radiologists and nonradiologists alike. It should prove to be particularly useful to those in training as well as practitioners who do not have a large experience with cancer patients.

Andrew B. Crummy
University of Wisconsin Medical Center
Madison, Wisconsin 53706

Ultrasonography of the Abdomen. By N. Hassani and R. Bard. New York: Springer-Verlag, 128 pp., 1976. $19.80

This book is a concise presentation of the applications of ultrasound to the study of the upper abdominal organs and the retroperitoneum. It is divided into 10 chapters covering hepatic, splenic, pancreatic, vascular, diaphragmatic, renal, ascites, and retroperitoneal sonography. Obstetrics and gynecology are excluded. An introductory chapter describes the physical principles of ultrasound. The work includes a bibliography of 86 pertinent references and 161 illustrations. Each section is divided into a description of normal anatomy of the area, its examination technique, and commonly encountered pathology.

The book is well illustrated with gray scale ultrasonographs. To my knowledge, it represents the most extensive compilation of gray scale ultrasound to date in book form. All images are of diagnostic quality and reflect excellent scanning technique. Illustrations and legends can be studied without extensive reference to the text. Scans are reproduced by direct photography of the tracings. However, there is little loss of pertinent detail, even in the difficult instance of cinesonogram reproduction.

Hassani and Bard write with clarity and brevity. An impressive amount of clinical ultrasonography is discussed in a short text. The chapters on the liver and pancreas are good summaries of the present advancements in sonographic imaging. The use of vascular landmarks in the study of these organs is clearly and rightfully emphasized. There is a good discussion of splenic lesions. The chapter on renal sonography is one of the most extensive ones, and draws attention to the field of transureteral prostatic ultrasonography. The discussion on radiation therapy planning with the use of ultrasound defers most detail to other more extensive references.

The authors are most successful in highlighting the specific applications of diagnostic ultrasound. The use of sonography for better tissue typing, topographic localizations, assistance in puncture, and serial noninvasive study are all clearly demonstrated. Where detection and differentiation of malignancy is most difficult, the text suffers only those shortcomings which reflect the limitations of ultrasonography itself.

The book will make excellent introductory and reference reading. It can be used to advantage by the beginner as well as the more experienced ultrasonographer. Because of the wealth of principles summarized and the great number of cases illustrated, the work provides enjoyable and valuable reading for anyone concerned with diagnostic ultrasound. A similar work on obstetric and gynecologic ultrasonography is urgently needed, and I would have liked to have seen the present text expanded to include these important fields.

Antonio C. Gonzalez
Woodruff Medical Center
Emory University
Atlanta, Georgia 30303

Graphs and Tables for Use in Radiology. 2d ed. By F. Wachsmann and G. Drexler. Berlin: Springer-Verlag, 240 pp., 1976. $19.70

If only limited library funds are available, this edition of Wachsmann and Drexler's *Graphs and Tables for Use in Radiology* is a must. If one is blessed with adequate library facilities, its references provide an excellent beginning search point for further in-depth reviews. There are more proofing errors than one might have hoped: for example, in the statistical relationship on page 41; the reference to Kelley and Trout on page 79 and the occurrences in matter exposed to 1 R, page 65; the percentage depth dose for 400 cm^2 field 80 cm F.S.D., 6 cm depth (page 111); tissue-air ratio 400 cm^2, 20 cm depth (page 124). The reader is alerted to these oversights by inconsistencies in the table or text, and normal scientific skepticism should prevail. It is to be hoped that the authors will remedy these oversights in this invaluable multinational text.

Peter Wootton
University of Washington
Seattle, Washington 98195

Early Breast Cancer, Its History and Results of Treatment. Experimental Biology and Medicine, vol. 5. By C. M. Mansfield. Basel: Karger, 129 pp., 1976. $23

This book is an excellent review of the mountains of articles (366 references with an author index) published on the treatment of early breast cancer by surgical procedures, radiation, or both. The style is easy to read and the tone is objective. Mansfield is not out to seek and destroy the beliefs of others in order to substitute his own panacea. He concludes that clinical stage I and II breast cancer can be treated in six major ways. He shows that the clinical trials (reviewed in detail) have been unable to construct worthwhile conclusions which would encourage careful selection of patients for more conservative treatment with survival results equal to those of more radical treatment.

I wish Mansfield would have allowed himself more freedom for the types of criticism he proposes for Urban (p. 52), Farrow (p. 58) and Stjernsward (p. 79). In general his criticism is very low pressure and highly appropriate; it is just too scarce. The discussion section is outstanding for clearly elucidating problems such as how inability to determine extent of local or distant spread in early cancer results in the protean difficulties that stem from trying to compare treatments.

Sometimes clinical and pathologic stage I and II became confused in my mind during the many investigations summarized in this book. The importance of 10 year survival should have been stressed more in the lumpectomy and radiotherapy chapter. Few conclusions were submitted in the radiation only chapter. The possibility that an excision biopsy with adequate margins might be curative for some early lesions was not discussed.

A. Robert Kagan
Southern California Permanente Medical Group
Los Angeles, California 90027

Cerebral Radionuclide Angiography. By F. H. DeLand. Philadelphia: Saunders, 309 pp., 1976. $39.75

In 1969, DeLand and Wagner published the *Atlas of Nuclear Medicine,* Volume 1: *Brain.* The present text can be viewed as a logical extension, since it focuses on the dynamic portion of radionuclide evaluation of the brain. The new book is principally an atlas illustrating vertex radionuclide angiography in a variety of conditions.

Since some nuclear medicine units do not perform dynamic studies prior to static brain imaging, a few paragraphs describing the usefulness of the method might have been warranted. (For example, how often are dynamic images useful in establishing a diagnosis?)

The first chapter is a delightful summary of the development of concepts on cerebral blood flow. However, no comment is made as to the response of this circulation to such common stimuli as carotid compression, vasodilators, or carbon dioxide.

The chapter Vascular Embryology consists of just over two text pages and 16 figures on the developing embryo. While useful, the value of this section might have been enhanced if cross reference was made to the chapter on Congenital Diseases so that variations in the arterial and venous supply of the brain could be sequentially discussed. The treatment of Normal Vascular Anatomy is supplemented by frontal cross sections of the skull and brain. These are most striking and suggest an exciting approach to data gathering *if* the appropriate CT or radionuclide scanners were available for widespread clinical use.

The section on Collateral Circulation is largely illuminated by "word flow charts" which show alternate pathways available to the blood flow. Topographical Vascular Anatomy is a chapter which schematically depicts the various areas of the brain in terms of the particular vessel supplying its arterial blood. Frontal cross sections are colored to indicate the degree of detection of ^{99m}Tc from each level by a probe placed over the vertex.

I feel the real "meat" of the book is in the chapter, Vertex Radionuclide Angiography in which the appearance of the vertex view on the cerebral dynamic study is discussed. There is no clear discussion of the anterior view (useful when carotid occlusion is considered) or of the posterior view (of special value when posterior fossa lesions are suspected). The chapter is illustrated by paired contrast angiograms (diagrammatically presented) and radionuclide images.

In the chapters on Trauma and Neoplasms, dynamic studies are supplemented by static images and EEG findings. Occasional anterior cerebral radionuclide angiograms appear without clear prewarning, and at least one posterior dynamic study is present. The chapter on Vascular Diseases is reinforced by a variety of illustrations. The final chapter on Computer Applications is a reasonable approach which could have benefited from a discussion of the use of the procedure in determining cerebral death.

Overall, this book is well thought out and presented and illustrates the vertex radionuclide angiogram to good advantage. It will serve as a valuable reference for both the trainee and practitioner in nuclear medicine as well as for those interested in the central nervous system.

Richard P. Spencer
University of Connecticut Health Center
Farmington, Connecticut 06032

Symposium on Angiography. Edited by E. K. Lang. **Radiologic Clinics of North America,** vol. 14, Philadelphia: Saunders, 227 pp., August 1976

This symposium contains 11 multiauthored chapters covering diverse areas of cardiovascular interest from parathyroid localization to coronary arteriography. Such a wide range of subjects in a 227 page book by 22 coauthors inevitably results in topics of variable quality and interest.

The strength of the symposium is with the chapters on parathyroid localization by John L. Doppman, abdominal visceral venography by Manuel Viamonte, Jr., and angiography of gastrointestinal hemorrhage by Christos A. Athanasoulis and coworkers. Since these chapters reflect the current state of the art, I recommend they be read by all radiologists who have an interest in angiography. The chapters on aortitis and adrenal angiography are excellent reviews with extensive bibliographies.

The reason for including the two chapters on the heart in this short symposium is not clear. The chapter entitled Functional Evaluation of the Heart by Angiocardiography is too brief for the novice and too superficial for the experienced. The chapter on coronary arteriography would seem to fit better in a book solely devoted to coronary angiography.

The illustrations are good, and the text is written in a readable manner. The value of this symposium is that it provides a ready reference for specific areas of angiography with excellent bibliographies for these subjects.

C. J. Tegtmeyer
School of Medicine, University of Virginia
Charlottesville, Virginia 22901

Biological and Environmental Effects of Low-Level Radiation vols. 1 and 2, Proceedings of a Symposium organized by IAEA and WHO, Chicago, November 1975. Vienna: International Atomic Energy Agency, vol. 1, 370 pp., vol. 2, 451 pp., 1976. $51 (Available in U.S. from UNIPUB, Box 433 Murray Hill Station, New York, N.Y. 10016).

An appreciation of the scope of this symposium may be gained from a list of the major topic areas considered: genetic effects, biological effects, theoretical and experimental models, internal exposure, human studies, and risk estimates. A total of 72 papers are distributed among these major subject headings with discussion following each paper. This makes a detailed critique of either individual papers or individual sessions essentially impossible. It can be said that each paper presents information important to a full appreciation of the biological and environmental effects of low level radiation exposure.

For some time, there has been a need for investigators representing the various radiation-related disciplines to discuss low level effects in some detail, with a view to stimulation of further thought and work and perhaps some consideration of the adequacy of present standards for radiation exposure. This is especially true in light of the increasing exposure of populations to radiation and other environmental pollutants which may have either additive or synergistic actions in terms of adverse health effects. Several contributors address this point.

The majority of papers will have continuing value to all concerned with radiation effects and population hazards. The papers dealing with internal exposure and risk estimates should be of special interest to those troubled by present day energy problems as well as the questions posed during deliberations on the advisability of expansion of nuclear electrical generating capacity. The sections on biological effects and human studies plus those dealing with genetics, contain much of interest to the practicing radiologist who must weigh risk versus benefit in his daily activities.

The papers are uniformly well written and illustrated. Several, in languages other than English, have English abstracts which are well prepared and adequately detailed. The editor and editorial staff of the International Atomic Energy Agency should be commended for the speed with which these proceedings appeared in print.

This book deserves thoughtful persual by anyone concerned with research in the area of radiation effects on living systems or by those involved in activities which may result in the application of radiation to man.

Gerald M. Christensen
University of Washington
Seattle, Washington 98195

Advances in Radiation Biology, vol. 5. Edited by J. T. Lett and H. Adler. New York: Academic Press, 277 pp., 1975. $35

This text is the fifth volume in a series on advances in radiobiology. The book is well written and organized and has ample illustrations of good quality. The text discusses in detail the different radiobiologic effects of various types of ionizing radiation. Also described are some of the chemical mechanisms whereby DNA is damaged by ionizing radiation and the effects of radiation modifiers. The development of microdosimetric techniques to aid in the study of the radiobiologic effects is explored.

A most interesting review of the effects of continuous radiation on animal populations is included. Part of this review describes the design of the field studies. Complementary to that review is a discussion of life shortening and premature aging secondary to radiation. These two effects of radiation have been studied extensively in the last 30 years. This discussion provides a historic review and up-to-date information on these effects.

The section on the relationship between the environment and nuclear power stations is most interesting and very informative. Study of this section by professional and lay individuals should help to soothe some of the recent negative public attitudes towards nuclear power. A most useful section reviews the basics of radiotherapy: the four R's known as repair, reoxygenation, redistribution, and regeneration. This discussion provides a good foundation upon which to understand the complexities of radiobiology.

Overall, this text is mainly for the researcher in radiobiology whether he is in the laboratory or in the field. The section discussing the four R's of radiotherapy should be read by radiology (diagnostic and therapeutic) and nuclear medicine residents.

Larry D. Greenfield
City of Hope National Medical Center
Duarte, California 91010

Computed Brain and Orbital Tomography; Technique and Interpretation. By C. F. Gonzales, C. B. Grossman, and E. Palacios. New York: John Wiley & Sons, 276 pp., 1976. $29

This book is the result of the authors' experience with more than 20,000 computed brain tomograms. It is divided into seven major sections: basic physical principles, CT scanning, neuroanatomy, pathologic conditions, radiation therapy, the orbit, and recent developments. The book is presented as an atlas with each case receiving a brief anecdotal explanation.

The authors have addressed the contents to the neophyte in computed tomography by showing easily recognized and commonly occurring pathology. Frequent correlations with other radiographic modalities and occasional pathologic specimens assist the reader's orientation to this new diagnostic tool. The book reads easily and the table of contents and index are helpful guides.

While there is a wealth of interesting and educational cases, there are also some shortcomings. The radiographs are large and well reproduced, but many of the scans are too dark, too small, or show suboptimal technique in demonstrating the desired pathologic findings. Some of the postcontrast injection studies shown would have had more teaching value if the preenhanced study had also been presented. The reader could then develop his own index of suspicion of whom to inject. Finally, and most important, since so many abnormalities in computed tomography look like so many other pathologic findings, it may be misleading to present a case without a differential diagnosis.

This good pictorial overview of computed brain and orbital tomography should appeal to medical students, radiology residents, and neuroclinicians.

Edward V. Grayson
Memorial Hospital
Hollywood, Florida 33021

Radiological Aspects of the Liver and Biliary Tract. X-ray and Radioisotope Diagnosis. By K. Okuda and M. Iio. Tokyo: Igaku Shoin (U.S. distributor, Year Book Medical Publishers). 578 pp., 1976. $79.75

In the preface, Okuda and Iio state their intention to emphasize the gross alterations in structure responsible for abnormal laboratory findings. The major portion of the book is devoted to photographs; technical details of various methods have been abbreviated.

The potential buyer should bear the above caveat in mind. The photographs are, by and large, superb. When viewed as an atlas of Japanese experience in hepatobiliary disease with emphasis particularly on angiography, isotopic imaging, and percutaneous cholangiography, Okuda and Iio succeed. When they depart from their stated goal, they fail. Abbreviated pharmacology, physiology, and technology consume space without providing basic information and would have been better omitted.

The influence of epidemiology is evident. For example, sclerosing cholangitis is not illustrated, a reflection of its rarity in Japan. To overcome regional differences in disease, ample sampling of world literature is provided.

The index is adequate. There is an abundance of typographical and spelling errors. Lack of editing by a person experienced in English usage and idiom is evident and annoying.

While the subtitle of the book seems to preclude discussion of ultrasound, computed tomography is x-ray generated and would appear to be within the scope professed by the authors. I cannot recommend an expenditure of $80 on a text devoted to gross imaging of the hepatobiliary system that includes neither of these modalities.

Solomon S. Schwartz
Hospital of St. Raphael
New Haven, Connecticut 06511

Hormones and Breast Cancer. Edited by M. Namer and C. M. Lalanne. Paris: INSERM, 267 pp., 1976.

This text contains the proceedings of a symposium, Hormones and Breast Cancer, held in Nice, France, May 23 and 24, 1975. The proceedings are divided into these sections: Prognosis of Breast Cancer Hormonodependence, I. Receptors (Hormone), II. Other Methods of Measurement of Hormonodependency; Therapeutic Aspects, I. Castration and Other Surgical Therapeutics, II. Radioimmunological Investigations, III. Hormonal Status of the Post-Menopausal Female; and Workshop on Anti-Hormones.

Presentations are in French or English and most carry summaries in the language opposite to that used in the text. Because of the book's bilingual nature, a good understanding of French is imperative to obtain maximum benefit from the proceedings. A bibliography is included with almost every paper. Illustrations, including some electronmicrographs, are plentiful and of good quality.

The first three papers offer an excellent discussion of the mechanism and role of hormone receptors in general and estrogen receptors in particular—especially in the management of breast cancer. These papers contain particularly clear and concise illustrations which assist the reader in understanding the use of hormone receptors in breast cancer management.

The section on castration and other surgical techniques presents a good discussion of the use of radiation castration in the treatment of breast cancer, although radiation castration is seldom used in the United States. The paper on endocrine surgery reviews different types of endocrine surgery (i.e., oophorectomy), that can be used in managing advanced breast cancer.

A workshop on estrogen antagonists includes interesting papers on Tamoxifen and Nofoxidine in breast cancer management. These papers are especially well done.

Excellent papers on Prolactin and cancer-related antigens in relation to breast cancer are presented in other sections. Many papers discuss laboratory techniques used at particular institutions to measure hormone receptors.

Overall, these proceedings are of value to researchers and physicians, but especially to the surgical, medical, and radiation oncologist involved in management of breast cancer patients.

Larry D. Greenfield
City of Hope National Medical Center
Durate, California 91010

Cerebral Dural Sinuses and Their Tributaries. By J. Browder and H. A. Kaplan. Springfield, Ill.: Thomas, 120 pp., 1976. $14.75

Browder and Kaplan have written a scholarly monograph on an incompletely understood and previously poorly described segment of neuroanatomy. The dural sinuses and contributing venous plexi of 950 fresh autopsy specimens were studied in detail and their anatomy was condensed and illustrated. The authors are world authorities on this subject, having published extensively in the last 5 years on their dissection efforts. They begin by describing briefly the embryology of the dural sinuses. The venous connections and anastomoses with the sinuses are illustrated in chapters 2 and 3, and in the subsequent six chapters the anatomy of each of the major dural sinuses is related in detail. In the final three chapters hindbrain tributaries, hyperplasia of Pacchionian granulations, and cranial emissary veins are discussed.

Overall and internal organization is good. The text is frequently narrative, based on the dissection experiences of the authors. Illustrations are of excellent quality. The cast preparations of the veins and sinuses are especially well done. The paper stock is excellent, contributing to good reproduction of illustrations and print. The book is well annotated.

This monograph is most appropriate for neuroanatomists and neurosurgeons. Neuroradiologists would gain some background information, but unfortunately most of the material described is not germaine to the daily practice of neuroradiology. General radiologists without extensive experience in neuroanatomy or neuroradiology would find little use for this monograph because of its limited scope.

William W. Olmsted
St. Mary's Hospital and Medical Center
San Francisco, California 94117

Roentgenologic Diagnosis, A Complement in Radiology to the Beeson and McDermott *Textbook of Medicine,* 3d ed., 2 vols. By J. G. Teplick and M. E. Haskin. Philadelphia: W. B. Saunders, 1,477 pp., 1976. $60

Excellent illustrations abound in this superb complement to Beeson and McDermott's *Textbook of Medicine.* Designed to follow the text of the parent book, and directed primarily to the radiology resident or the nonradiologist, this book is worth reviewing by radiologists to obtain an overview of certain disease categories. The style and format has not changed from the previous two editions; however, the abundant new references, illustrations, and the addition of computed tomography indicate that the authors are bringing new technologies to the forefront. There are no illustrations of nuclear medicine imaging or ultrasonography, however.

As a review tool and as a starting point to research reference material, this book is excellent. Additionally, it brings into perspective the vast amount of radiographic knowledge which the internal medicine physicians expect radiologists to have at their fingertips.

Of interest is that the two volume complement to the *Textbook of Medicine* has nearly as many pages as the present textbook itself! The vast number of radiographs, approximately 1,900, have demanded this large size. Most illustrations depict classic cases of the disease process under discussion. This format could lead the unwary reader to expect too much from the radiologist who must contend with the inumerable subtle early conditions involved in these disease processes.

Thus, this two volume series is an excellent addition to the medical literature, quite up to date, and of primary interest to the nonradiologist.

Gerald R. Smith
Harborview Medical Center
Seattle, Washington 98104

Testicular Tumors, 2d ed. Edited by D. E. Johnson. Flushing, N.Y.: Medical Examination Publishing Co., 296 pp., 1976. $24

This book is a comprehensive review of the various diagnostic and therapeutic modalities available in the management of testicular neoplasms. The 13 contributors represent various disciplines within the University of Texas System Cancer Center and M. D. Anderson Hospital. Although the emphasis is on diagnostic and therapeutic protocol employed at this institution, the well referenced discussion gives an adequate review of other schools of thought extant in the literature. The text is complete, informative, and quite readable. The chapters entitled Clinical Diagnosis, Laboratory and Radiological Investigations, Testicular Malignancies and the Lymphatic System, and Chemotherapy are particularly well done.

The radiographic illustrations range in quality from adequate to very good, and are generally successful representations of the points the authors seek to illustrate. The photomicrographs of histologic material range from poor to good in quality. Since the book is generally directed toward the clinician involved in the care of these tumors, the photomicrographs could have been more informative if clearly labeled to emphasize the points being made in the text. Furthermore, the micrograph on page 151 is upside down. Other printing and proofing errors have been kept to a minimum with the exception of one misplaced phrase which rendered a whole paragraph illegible.

The publishers have an annoying tendency to place small figures and tables in isolation in the center of a whole page, at times apparently justifying the practice by putting the tables in giant print. One cannot help but get the impression that the combination of several such illustrations on a page would not detract from the quality of the text and would certainly diminish its volume. In summary, this book would be a valuable addition to the library of any urologic surgeon, radiotherapist, diagnostic radiologist, or chemotherapist dealing with the management of these neoplasms.

Mark D. Kiviat
Department of Urology
University of Washington
Seattle, Washington 98195

Radiologic Examination in Orthopaedics: Methods and Techniques. By E. Hapner and H. Ch. Neuli. Baltimore: University Park Press, 199 pp., 1976.

This volume is a collaboration between a Swiss radiologist and an orthopedic surgeon. It essentially describes by means of line drawings, short descriptive paragraphs, and radiographs the basic positioning of the most commonly used orthopedic radiologic examinations, including the entire appendicular skeleton and all the axial skeleton except the skull. Each line drawing demonstrates the position of the anatomic part, the position of the film, and the direction of the central beam. The descriptive written material adjacent to the diagram includes instructions for positioning, film size, and direction of the central ray. The reproduction of the radiographs is of high quality and of adequate size. Contrary to many European texts, the bone in each radiograph is white on a black background, the manner in which most American radiologists are accustomed.

While the authors indicate that the volume is to be used as a ready reference, some of the factors necessary to produce the radiograph, such as the target-film distance, grid or nongrid technique, and type of film, are described in the general technical hints chapter where they are not readily available to the technologist.

There are many areas in which I cannot agree with the authors. Their use of a very thin patient to demonstrate the radiographs is sometimes misleading. Although the entire length of a femur may be presented on a 14 X 17 film, in most adults this results in inadequate technique at one end of the femur due to the large soft tissue difference between the distal thigh and buttocks. Similarly, lateral bending radiographs of the spine on 14 X 17 film to demonstrate the entire spine results in underpenetration of the L4–L5 vertebra which is usually the site of interest.

I was disappointed, since this volume was written by both a radiologist and an orthopedist, that no hints or special techniques were described regarding films through casts and requirements for postreduction films for certain fractures. There are no special requirements listed for radiographs of total joint replacements, particularly the hip and the knee, nor any description of radiographic studies of the postoperative scoliotic spine including Harrington rod fixation. There is no discussion of special care or projections of the injured patient. Among the views not described are detailed studies of the radial head, pillar views of the cervical spine, and tangential views of the scapula for dislocation of the humeral head.

This volume adds little in the way of new information, has only limited value to the office practice of orthopedics or radiology, and adds nothing to the evaluation of modern techniques in orthopedic surgery.

T. W. Staple
MEMRAD Medical Group, Inc.
P. O. Box 1428
Long Beach, California 90801

Urologic Radiology, 2d ed., Golden's Diagnostic Radiology, section 8. By M. L. Sussman and A. Newman. Baltimore: Williams & Wilkins, 517 pp., 1976. $45

Urologic Radiology is another distinguished volume that joins Golden's Diagnostic Radiology series. Sussman and Newman have incorporated many pertinent radiographs into this volume which are reproduced with clarity. Refreshing features are a continuity of style and a logical flow of information that is becoming rare in this era of multiauthored textbooks.

A valuable first chapter describes in detail a variety of imaging techniques used to evaluate the entire urinary tract. Relevant information about excretory urography, radioisotope scanning, abdominal ultrasound, and angiography are concisely discussed. Of particular help are Sussman and Newman's opinions on the relative usefulness of the various techniques and the development of some general guidelines for the appropriate sequence of examinations. This initial integration of the variety of imaging techniques allows the subsequent 19 chapters to be developed in detail, building on this basic imaging knowledge.

Although the chapter headings suggest a traditional organization into basic anatomic and pathologic entities, the interplay between the various imaging techniques applied to a specific problem provides a more useful and stimulating source of information. A typical exquisite example of this approach is chapter 13 which discusses tumors of the kidney. Within this 45 page chapter the authors thoroughly discuss mass lesions of both the renal parenchyma and renal pelvis, including benign cysts and pseudotumors. For example, guidelines are developed for employing ultrasound evaluation of a potential cyst, including the definitive cyst puncture. Isotope scanning is appropriately employed to define functioning renal parenchyma, the hallmark of the "pseudotumor." Angiography is similarly appropriately discussed and illustrated.

This text is useful for the resident learning the fundamentals of uroradiology, for the practicing radiologist encountering a difficult case, or for anyone experienced in one of the imaging techniques who desires to supplement or update his knowledge of complementary techniques.

Curtis H. Northrop
Harborview Medical Center
Seattle, Washington 98104

News

Neuroradiology Seminar

A seminar, Neuroradiology—with Emphasis on CT Scanning and Clinical Practice, will be October 21–23 in Dallas. Sponsor is the Neuroradiology Section of the Radiology Department, University of Texas Health Science Center at Dallas. The seminar will cover all aspects of neuroradiology including CT, angiography, myelography, tomography, and radioisotope scanning. Emphasis will be on practical aspects of evaluating patients with neurological disease. New concepts and technology will also be included as well as clinical and pathologic correlation. Faculty will be members of the departments of Radiology, Neurosurgery, Neurology, and Pathology of the University of Texas Southwestern Medical School. Fee is $175 and the program is approved for 18 hr AMA Category I credit. For additional information write Mary Ryals, Department of Radiology, Parkland Memorial Hospital, 5201 Harry Hines Boulevard, Dallas, Texas 75235.

Ultrasound Preceptor Program

One and two week preceptor programs in ultrasound are being offered by the Section of Diagnostic Ultrasound, Parkland Memorial Hospital, Dallas. The program stresses practical clinical applications of ultrasound, and physicians participate directly in the workup of each case. Registration is limited to one physician per week; technologists will be accepted if sponsored by a physician. Fee is $300 per week and AMA Category I credit is available. More information is available from Mary Starling, Section of Diagnostic Ultrasound, Parkland Memorial Hospital, 5201 Harry Hines Boulevard, Dallas, Texas 75235; telephone (214) 638-1800, ext. 2474.

Pediatric Urinary Tract Symposium

An interdisciplinary symposium on urinary tract disease in infancy and childhood will be November 16–18 in Boston. Focus will be on new developments in the diagnosis and treatment of urologic disease in the young with emphasis on radiology and newer imaging techniques. Sponsor is Tufts University School of Medicine, and the course is aimed at general and pediatric radiologists, urologists, and pediatricians. Among the controversial topics to be discussed during round table discussions are significance and current management of vesicoureteral reflux, lower urinary tract obstruction, and renal cystic disease. Faculty will include D. Baker, S. Bauer, W. Berdon, B. Carter, S. Gellis, B. Girdany, H. Griffiths, T. Griscom, W. Grupe, H. Hendren, J. Hodson, P. Kahn, P. Kelalis, L. King, J. Kissane, R. Lebowitz, W. McAlister, R. McCauley, A. Retik, and A. Schwartz. Tuition is $175; $100 for interns, residents, and fellows. For further information contact Emelie S. Born, Office of Continuing Education, Tufts University School of Medicine, 136 Harrison Avenue, Boston, Massachusetts 02111; telephone (617) 956-6579.

International Neuroradiology Course

An International Course in Advanced Neuroradiology will be March 10 and 11 in Strasbourg, France. The course is organized every 3 years. The 1978 meeting will cover the narrow lumbar canal and recent advances in computed tomography. For information contact Prof. A. Wackenheim, Service de Neuroradiologie, 1, place de l'Hopital, 67005 Strasbourg Cedex, France.

Head and Neck Cancer Meeting

The Northern California Cancer Program and its Head and Neck Demonstration Network will sponsor a national meeting on head and neck cancer, January 11–14, 1978 in San Francisco. The program is designed for the practicing oncologist involved in the care of head and neck cancer patients. Areas covered will include epidemiology, diagnosis, pretreatment evaluation, staging, pretreatment planning, treatment, follow-up, rehabilitation, and supportive care. Emphasis will be on the multidisciplinary approach. The roles of the nurse, oncologist, and members of the rehabilitation team will be stressed in a 1 day session. For information, write Dr. Stephen K. Carter, c/o Northern California Cancer Program Head and Neck Demonstration Network, 14th Avenue and Lake Street, San Francisco, California 94118.

Meeting and Course Review

For reader convenience, a summary of upcoming meetings and courses is provided. Detailed listings of these events appeared in journal issues indicated in parentheses.

Body Imaging Conference, October 8–16, Kauai, Hawaii (March).

Mammographic Training Program, continuing education course, 1 week sessions throughout the year in seven U.S. locations (April).

International Gastrointestinal Cancer Conference, November 6–11, Tel Aviv, Israel (April).

Diagnostic Ultrasound and Medical Imaging, course, August 5–7, Atlanta, Georgia (May).

Medical Oncology Congress, December 4–6, Nice, France (May).

Tumor Ultrasound '77, international symposium, December 5 and 6, London, England (May).

Nuclear Medicine Seminar, August 14–19, Waterville, Maine (May).

Carcino-Embryonic Antigen Symposium, October 7–9, Nice, France (May).

Seminars with Specialists in Diagnostic Radiology, October 27 and 28, San Antonio, Texas (May).

Bermuda Postgraduate Radiology Course, October 24–28 (June).

Southeastern Chapter Society of Nuclear Medicine Annual Meeting, October 12–15, Winston-Salem, North Carolina (June).

Radiology Continuation Course, November 14–18, Minneapolis, Minnesota (June).

Diagnostic Ultrasound in Obstetrics and Gynecology, course, September 8 and 9, Baltimore, Maryland (June).

Advanced Ultrasound of the Abdomen and Obstetrics, course, August 25–27, Lake Buena Vista, Florida (June).

International Annual Meeting, Society of Nuclear Medicine, September 13–16, Groningen, The Netherlands (June).

Radiology Symposium, September 17, Los Angeles, California (June).

Diagnostic Radiology Seminar, September 19–23, Washington, D.C. (June).

Liquid Polibar with Super XL

A Total System

For double-contrast examination of the colon.

Satisfactory results in the double-contrast examination of the colon require special attention to two aspects of the procedure.

First, the barium sulfate formulation. Our Liquid Polibar (56% w/w) is a bubble-free, non-precipitating uniform suspension formulation ... with proper flow and coating characteristics. No blending required and once routines are established, you can rely on its consistency.

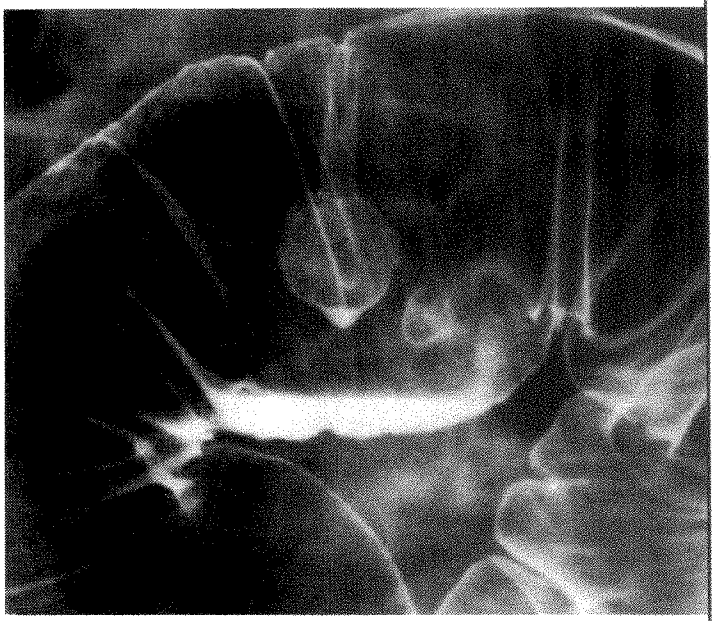

One pedunculated and one smaller sessile polyp at the apex of the sigmond loop.

Film Courtesy of Richard Palmer Gold M.D. Columbia Presb. Medical Center N.Y.

The second concern is with the proper apparatus. The E-Z-EM system is unique in that 1/2″ lumen tubing attached to the enema bag is utilized – for freer, more uniform flow. Miller Air Retention Tip, with or without optional cuff completes the system.

A total system for ease of administration and consistently reliable radiological results. For additional literature, write:

E-Z-EM

7 Portland Ave.
Westbury, New York 11590
(516) 333-8230

© 1/77

International Affiliates: E-Z-EM Rooster B. V., Infirmeriestraat 6-8, Rotterdam 16, Netherlands
E-Z-EM De Mexico, S. A. de C. V., Calz. Azcapotzalco La Villa No 882, Zona Industrial Vallejo, Mexico 16 D. F.

Our commitment to you is now ready to deliver. Synerview.™

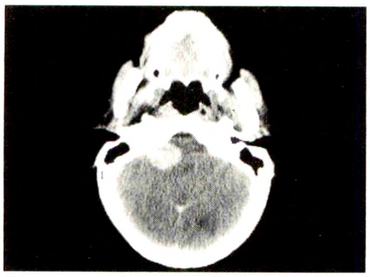
Contrast enhanced coronal section demonstrating a CP angle meningioma. Scan Time: 30 sec. Dose: 3.4 RADS

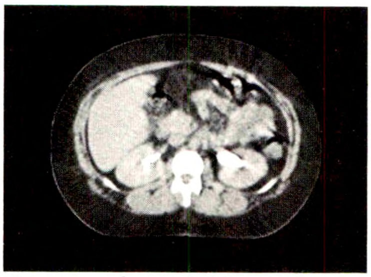
Contrast enhanced abdominal section through liver, kidneys, IVC and aorta. Scan Time: 18 sec. Dose: 4.6 RADS

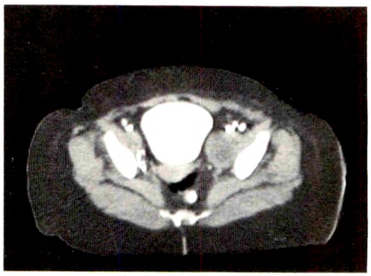
Contrast enhanced pelvic cross section showing a lymphoma. Note the right lateral shift of the bladder. Scan Time: 30 sec. Dose: 6.3 RADS

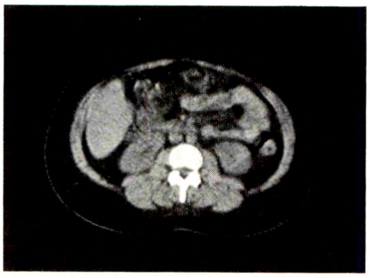
Normal abdominal section demonstrating liver, kidneys, IVC, aorta and duodenum. Scan Time: 18 sec. Dose: 4.6 RADS

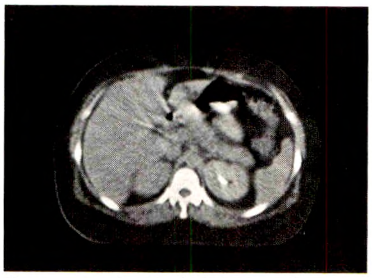
Contrast enhanced abdominal section demonstrating liver, spleen, kidneys, IVC, aorta, SMA and tail of pancreas. Scan Time: 18 sec. Dose: 4.6 RADS

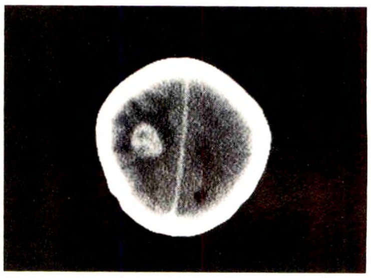
Contrast enhanced right parietal meningioma. Scan Time: 30 sec. Dose: 3.6 RADS

Synerview is a complete computed tomography system available now. It's the result of a promise made fact through Picker's unique human resources.

Using the proven translate/rotate scanning principle, Synerview features whole body and head study capability and is the most cost/effective system available today.

Synerview was a natural evolution for Picker because of our strength in X-ray. And CT is essentially a blend of sophisticated X-ray technology and state-of-the art computer science.

Synerview features that are particularly noteworthly include preselected patient protocols, three field sizes, variable scan speed up to a minimum of 18 seconds, 30-second scan-to-view time, high-resolution data acquisition matrices, imaging stacking, side-by-side images and in-house architectural planning.

In all, Synerview is a product of Picker's corporate commitment to you to manufacture, install, inspect, service and maintain diagnostic visualization systems second to none.

This is another example of Picker's unique human resources benefiting you. It's a result of our expertise in the diagnostic modalities of Computed Tomography, Clinical Laboratory, Nuclear, X-ray, Ultrasound, Therapy, Film Systems and Supplies.

Contact your local Picker representative. Or write Picker Corporation, 595 Miner Road, Cleveland, OH 44143.

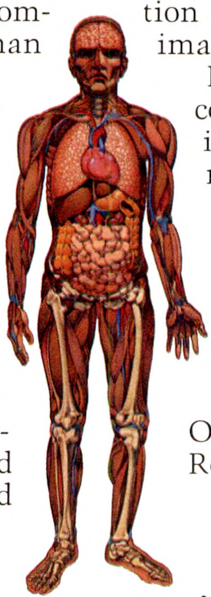

Discover the human resources in Picker's synergy

PICKER®

ONE OF THE C.I.T. COMPANIES

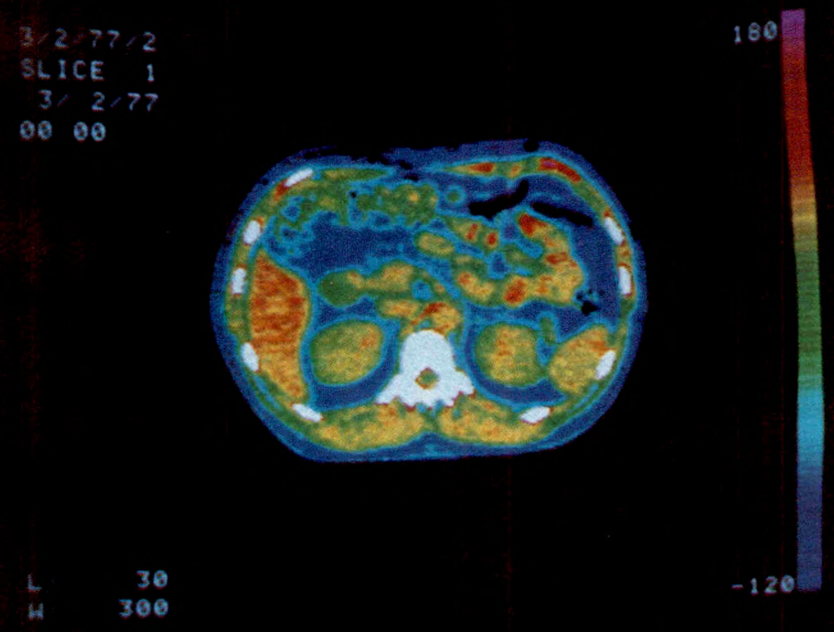
3/2/77/2
SLICE 1
3/ 2/77
00 00
180
-120
L 30
W 300

CHARLES C THOMAS · PUBLISHER

AN INTRODUCTION TO THE PHYSICS OF NUCLEAR MEDICINE *by* **Paul N. Goodwin,** *Albert Einstein College of Medicine, Bronx, New York, and* **Dandamudi V. Rao,** *New Jersey Medical School, Newark.* The prinicples and physics of nuclear medicine are presented in this book in a simple yet comprehensive manner. To aid self-study, problems and multiple-choice questions are included at the end of each chapter. Topics include a review of elementary mathematics, the structure of matter and the nature of radioactivity, nuclear decay processes, the interaction of radiation with matter, scintillation detectors, scanners, gamma cameras and other imaging devices, radionuclides in nuclear medicine, statistics of radiation measurements, radiation safety, and radiation dosimetry. Appendices present an alphabetical list of the elements, conversion factors, physical data for some useful radionuclides, and answers to questions and problems. *'77, 164 pp. (6 3/4 x 9 3/4), 44 il., 4 tables, $18.50*

AN ATLAS OF POLYTOME PNEUMOGRAPHY *by* **Taher El Gammal** *and* **Marshall B. Allen, Jr.,** *both of Medical College of Georgia, Augusta. Assisted by* **Paul Dyken.** This atlas presents a large number of studies which supplement the study of normal anatomy of the cerebrospinal fluid pathways and provide comparison for the identification of abnormal structures. Concentration is on the findings of polytome pneumography but, where possible, correlations are made with angiography, positive contrast ventriculography, and CAT examinations. Relative values of these different examinations are demonstrated. Topics include normal CSF pathways, atrophy, hydrocephalus, intrasellar subarachnoid recess—sellar and suprasellar lesions, and metasellar mass lesions—herniations. *'77, 480 pp. (8 1/2 x 11), 729 il., $39.50*

ELEMENTS OF RADIATION PROTECTION *by* **Ronald V. Scheele** *and* **Jack Wakley,** *both of the Univ. of Virginia School of Medicine, Charlottesville.* The basic ideas and practical aspects of radiation protection are developed by coordinating material from several disciplines. Preliminary chapters deal with atomic structure, ionizing radiations, radioactivity, X-rays and the interaction of radiation with matter. The mechanisms of biological damage and the factors of radiation damage are outlined, as are the acute and long-term biological manifestations of radiation exposure. Technological developments and practical suggestions are presented for reducing the exposure of patients, physicians and technologists in diagnostic radiology, nuclear medicine and radiation therapy. *'75, 112 pp., 15 il., 10 tables, $7.95, paper*

ADMINISTRATION OF A RADIOLOGY DEPARTMENT: Hints for Day-to-Day Operation *by* **Murray L. Janower,** *St. Vincent Hospital, Worcester, Massachusetts.* Various systems which can be applied to the radiology department to insure efficient functioning are presented in this book. In addition to a general overall look at a totally functioning diagnostic radiology department, the various subunits in a department are dissected and discussed in detail. All of these discussions are supplemented by a great deal of statistical data. Specific attention has been given to the methods used in handling patients, the establishment of a quality control program, efficient production of radiological reports, methods of film interpretation, and darkroom operations. *'76, 72 pp., 8 il., 7 tables, $7.50*

ENDOMETRIAL CARCINOMA AND ITS TREATMENT: The Role of Irradiation, Extent of Surgery, and Approach to Chemotherapy *edited by* **Laman A. Gray, Sr.,** *Univ. of Louisville, Louisville, Kentucky. (27 Contributors)* The role of irradiation in the total treatment of endometrial carcinoma is explored, focusing on adjuvant irradiation in the treatment of Stage I adenocarcinoma of the endometrium and on the management of carcinoma involving the cervix and body of the uterus. The extent of surgery and possible new chemotherapeutic approaches are also discussed. The importance of associated and related factors is clarified, and the combinations of modalities of treatment and sequence are detailed. *'77, 240 pp. (6 3/4 x 9 3/4), 17 il., 138 tables, $22.50*

THE PHYSICS OF RADIOLOGY (3rd Ed., 4th Ptg.) *by* **Harold Elford Johns** *and* **John Robert Cunningham,** *both of the Univ. of Toronto, Toronto, Ontario, Canada.* In the Third Edition of this text, the emphasis shifts from 200 kv and caesium 137 radiation toward higher energy radiations. Numerous sections devoted to computer techniques and information dealing with the solid state dosimeter lithium fluoride are included. Other topics include the concepts of kerma, particle fluence and energy fluence. *Radiology* called this book "a valuable addition to the radiological physics literature," and said that "no radiology resident, practicing radiologist, or radiological physicist should be without a copy of this book at hand. It is one of the best texts on the subject available." *'77, 812 pp. (6 1/8 x 9 1/4), 398 il., 92 tables, $25.75*

UROLOGICAL RADIOLOGY OF THE ADULT MALE LOWER URINARY TRACT: Anatomy, Physiology, Pathology and Sequelae, Diagnosis and Management *by* **R. W. McCallum** *and* **V. Colapinto,** *both of St. Michael's Hospital, Toronto, Ontario, Canada.* This monograph outlines the authors' personal experience with over 1000 radiological examinations of the urethra and 240 two-stage urethroplasties. Pre- and postoperative radiological urethrographic examinations and the surgical repair of membranous urethral strictures are detailed. Radiological examinations of the bladder, prostate and urethra are extensively discussed and the literature is reviewed in detail with over 330 references and over 250 original radiographs and illustrations. A description of the neurogenic bladder is provided and a new method of radiological examination of the lower urinary tract in paraplegics is described. *'76, 376 pp. (6 3/4 x 9 3/4), 248 il., 2 tables, $35.50*

"TRAUMA" AND "NO-TRAUMA" OF THE CERVICAL SPINE *edited by* **Kenneth R. Kattan,** *Univ. of Cincinnati College of Medicine, Cincinnati, Ohio. (11 Contributors)* Written with the radiologist, the orthopedic surgeon and the neurosurgeon in mind, this book covers all types of trauma of the cervical spine and the diseases which predispose cervical spine trauma. The chapter on "no-trauma" describes those conditions which resemble trauma. Also presented are methods for viewing cervical spine roentgenograms and how to recognize trauma. Other chapters include the roentgenographic follow-up, the pediatric patient, and trauma in the diseased spine. Anatomy of the cervical spine, mechanism of cervical injury and the technique of roentgen examination are also discussed. *'75, 328 pp., 292 il., $24.50*

Orders with remittance sent, on approval, postpaid

301-327 East Lawrence Avenue • Springfield • Illinois • 62717

We're living up to our reputation...all over your hospital.

General Electric made a commitment, years ago, to develop and market reliable medical systems that would deliver consistently informative diagnostic images.

And we've lived up to that commitment. First in x-ray equipment, and today in an expanded product line. A line that has grown so much that you may not be fully aware of all the areas where we can help you: computed tomography, nuclear imaging, data processing and handling, and radiological capability that matches a broad range of economic as well as diagnostic considerations.

Your GE medical systems representative has the training and know-how to put all this imaging/information capability to work for you. Ask about the systems that match your needs. Some of them are described on the next few pages.

GE
leading the way in diagnostic imaging...
GENERAL ELECTRIC

The power behind the performance

The 120-volt nickel-cadmium battery pack that powers both the AMX™ drive system and x-ray tube was designed by GE. It's backed by a prorated 5-year warranty. The cells store 10,000 mAs at 100 kVp, proportionately more at lower kVp levels. Near-constant potential output during the entire exposure makes the 100 mA rating equivalent to a 150 mA two-pulse generator.

We've improved the most popular system on wheels.

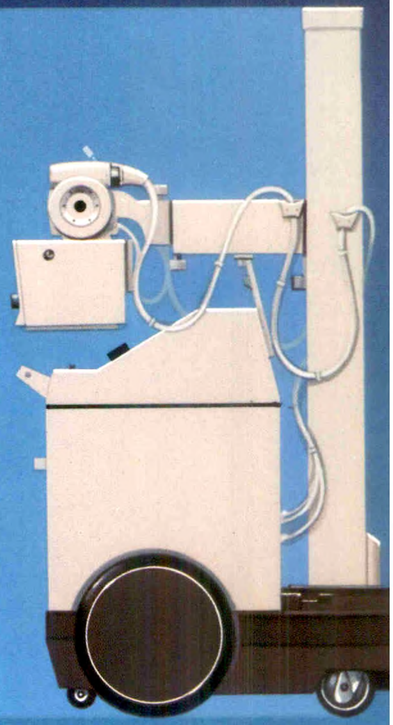

Same sharp AMX images...more ease and durability.

Over 3,000 AMX units are in use today, more than any other mobile system. Excellent imaging is the main reason. Precise kVp setting, plus a 1.0 mm focal spot, provide outstanding film resolution. Now GE adds important new features that make AMX even better.

1. **New heavy-duty casters** roll over rough surfaces with ease.
2. **New recessed wheels** let the AMX slip through narrow doorways, and streamline the equipment's overall appearance.
3. **Extended front bumper** disconnects drive if any obstacle is contacted. Protects both operator and equipment.
4. **Special Drive-Assist** gives you increased torque for climbing inclines up to 6°.
5. **Easy turning and positioning** are provided by a special drive system differential.
6. **New lower profile** easily clears low doorways and elevators. Ideal for older hospitals. Maximum focal spot-to-floor distance of 80 inches has been maintained.
7. **Unique foot-operated column lock** keeps hands free for collimator positioning.
8. **Complete positioning flexibility** and long reach let you solve virtually any positioning problem. Tube unit travels 60 inches vertically, 15 inches horizontally on a telescoping column. Tube angulations: 90° to either side of vertical, 110° up and 10° down. Collimator can be rotated 90°.

The versatile AMX is ideal for emergency room, CCU, pediatric and nursery patient exams . . . anywhere you need mobile imaging. It's also the perfect backup unit during peak periods or power outages. Like all GE equipment, AMX is backed by our commitment to product quality and service. It's our promise that you'll get many years—and many miles—of dependable AMX performance. Your GE representative has all the details plus AMX radiographs for your review. Contact him soon.

General Electric Medical Systems,
Milwaukee, Toronto, Madrid.

GE: leading the way in mobile imaging.

GENERAL ELECTRIC

CHANGEX

Handle more chest studies without handling film.

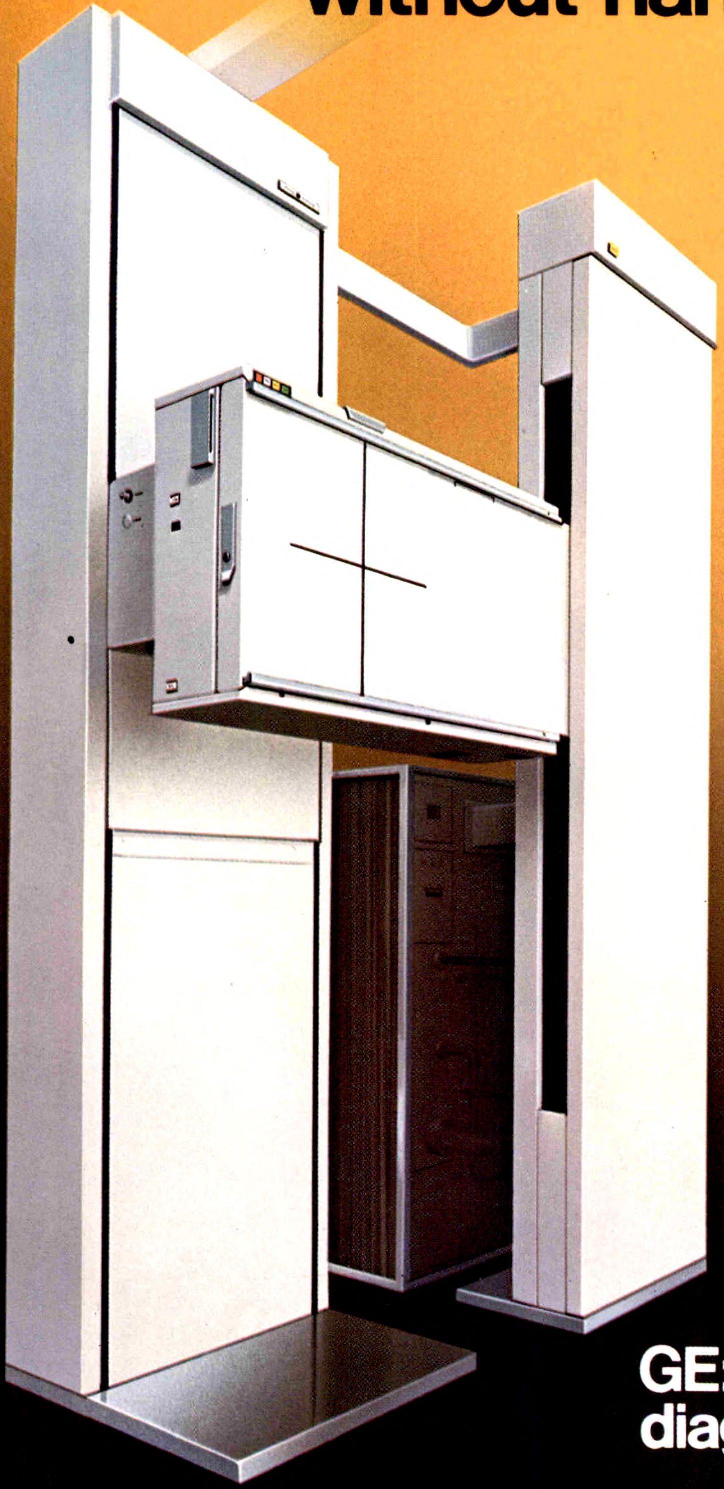

If your department's chest film volume is heavy, Changex system can lighten your load. This compact system—including chest changer, tube support, film transport and Kodak automatic processor—lets the technologist take up to 100 14 x 17 exposures without touching the film or handling individual cassettes.

Inexperienced operators handle Changex with ease. After inserting a loading magazine, the tech just pushes a button to adjust the changer to the patient's height. The x-ray tube moves automatically, maintaining alignment. Inserting the patient's I.D. card advances the film and provides positive patient identification.

Exposed film is transported automatically to the processor, eliminating trips to the darkroom. The technologist is free to concentrate on radiography and to handle more patients.

Film quality is excellent. And the Kodak X-Omat M6A-N processor delivers reliable performance with minimum maintenance. So let Changex increase throughput and reduce film handling. Talk to your GE representative.

General Electric Medical Systems,
Milwaukee, Toronto, Madrid.

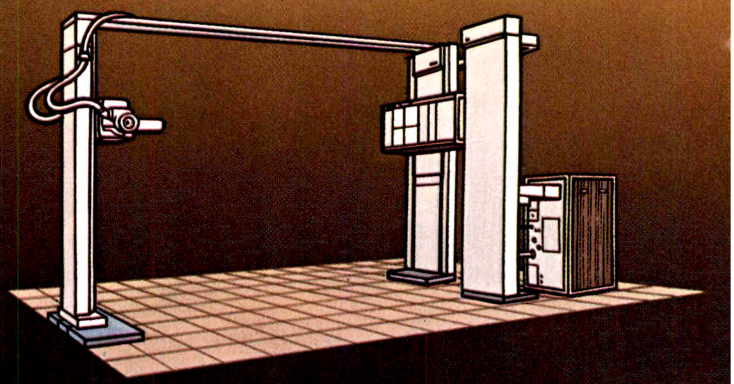

GE: leading the way in diagnostic imaging.

GENERAL ELECTRIC

Low cumulative dose—the total radiation dosage the patient receives in an examination—is directly affected by the number of exposures needed to obtain the necessary diagnostic information. Technologist performance, artifact-caused retakes and amount of tissue imaged may increase the total number of exposures required. MMX puts it all together to minimize cumulative patient dosage:

1. **Positioning is easy and precise** for any breast projection, any size patient; seated or recumbent.
2. **Continuous, close operator/patient contact** enables observation and correction of patient motion prior to exposure.
3. **Fixed 25-inch source-image distance** provides optimum geometry for sharp images.
4. **See-through, anatomically-shaped compressor** helps operator eliminate skin fold-caused artifacts; allows use of collimator light for precise field positioning.
5. **Quantamat™ automatic exposure control** accurately assures consistent diagnostic density.

To help you take full advantage of these low-dosage factors, your GE medical systems representative can provide you with a detailed MMX positioning guide and desktop movie. Contact your GE representative, or write General Electric Medical Systems, P.O. Box 414, Dept. M, Milwaukee, WI 53201.

Another way to look at low dose mammography

MMX

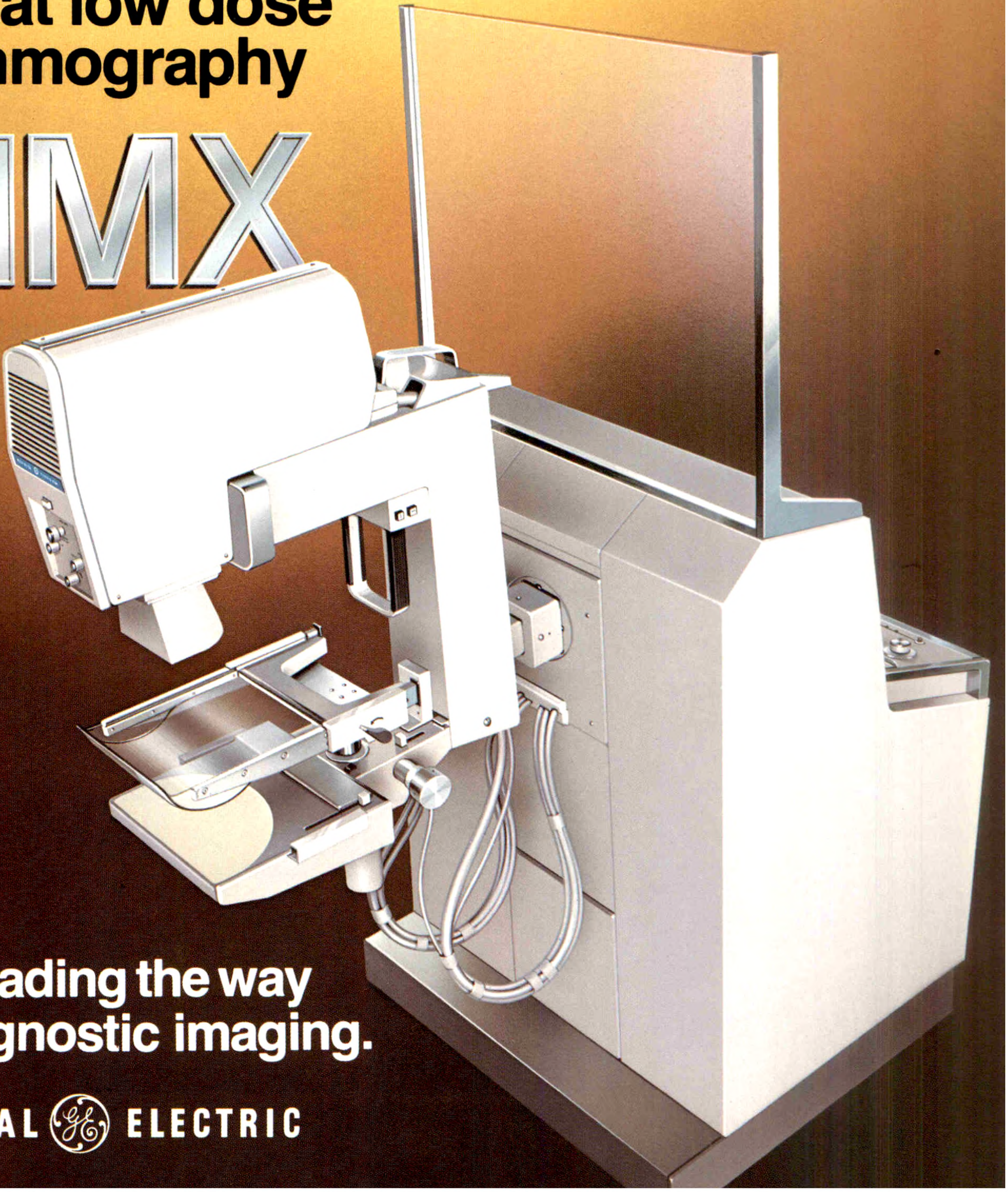

GE: leading the way in diagnostic imaging.

GENERAL ELECTRIC

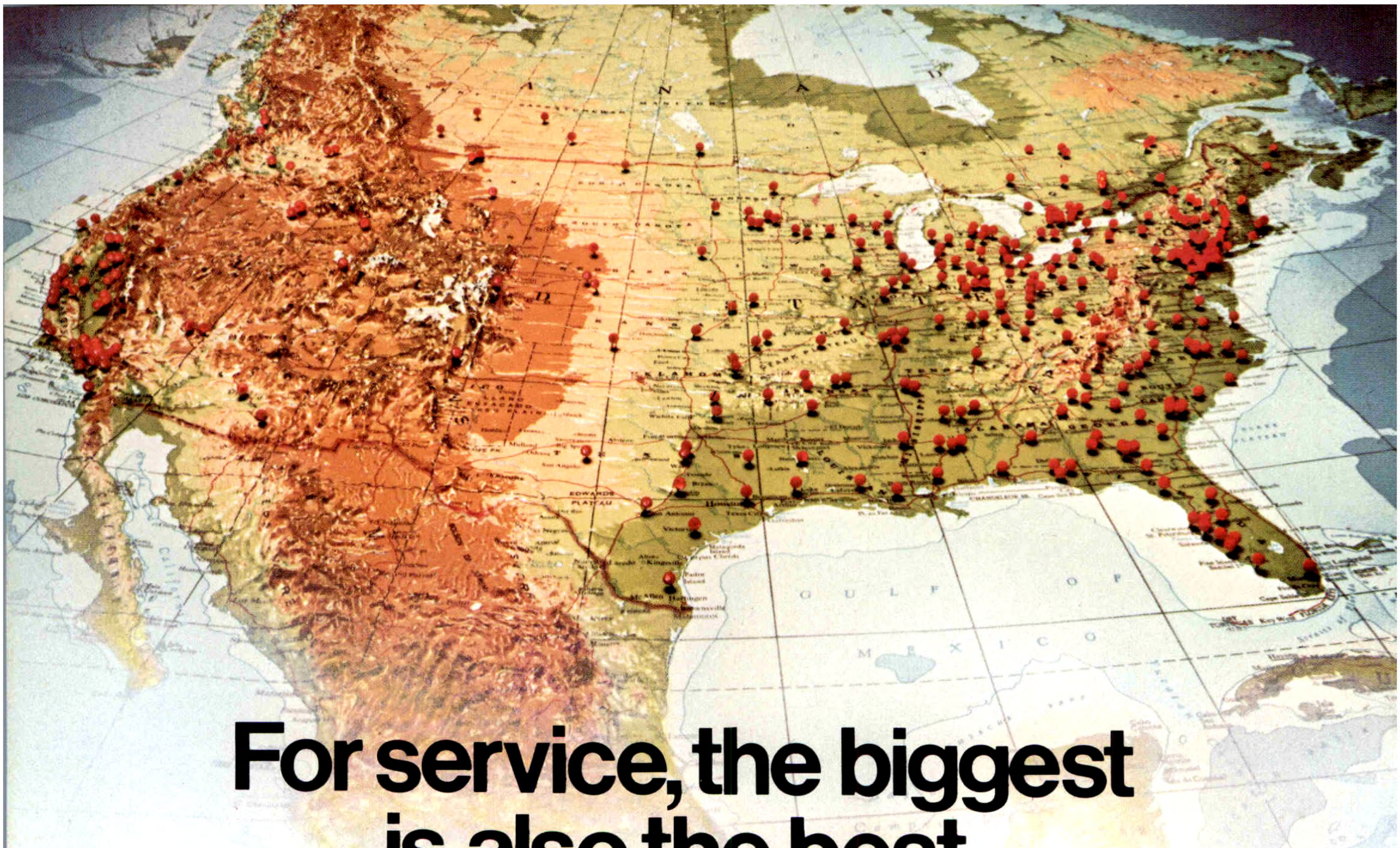

For service, the biggest is also the best.

1,500 people, 100 locations. GE has the largest medical equipment service force in the U.S. Whether you're in a remote rural area or major population center, you get prompt, reliable GE service.

Fully trained and equipped. GE servicemen receive intensive training with experienced service specialists. They're provided with a complete selection of sophisticated tools. And they continuously update their knowledge at GE's multi-million dollar Medical Systems Institute, established in 1971. Plans have now been completed which will double the Institute's size.

Computerized parts supply system links 32 parts depots around the country. With this new system, 95% of needed parts are available in less than 8 hours.

From planning, to installation, to followup service. The serviceman assists GE architectural planners with your room layout. He also helps to "pre-stage" GE systems before delivery. This optional service cuts installation time and cost by at least 50%. The serviceman participates in the actual installation of your system. And he follows up with routine maintenance and 24-hour emergency service.

Planned Maintenance Service. Your department's needs are unique. GE will tailor a PMS program to fit your patient load and exam requirements.

Put the nation's largest, best-trained service force to work for you. Talk to your GE representative.

General Electric Medical Systems
Milwaukee, Toronto, Madrid.

GE: leading the way in service.

GENERAL ELECTRIC

In 1895, Conrad Roentgen relied on Siemens tubes for his pioneering experiments with X-rays.

We've been a pioneer in X-ray systems technology ever since.

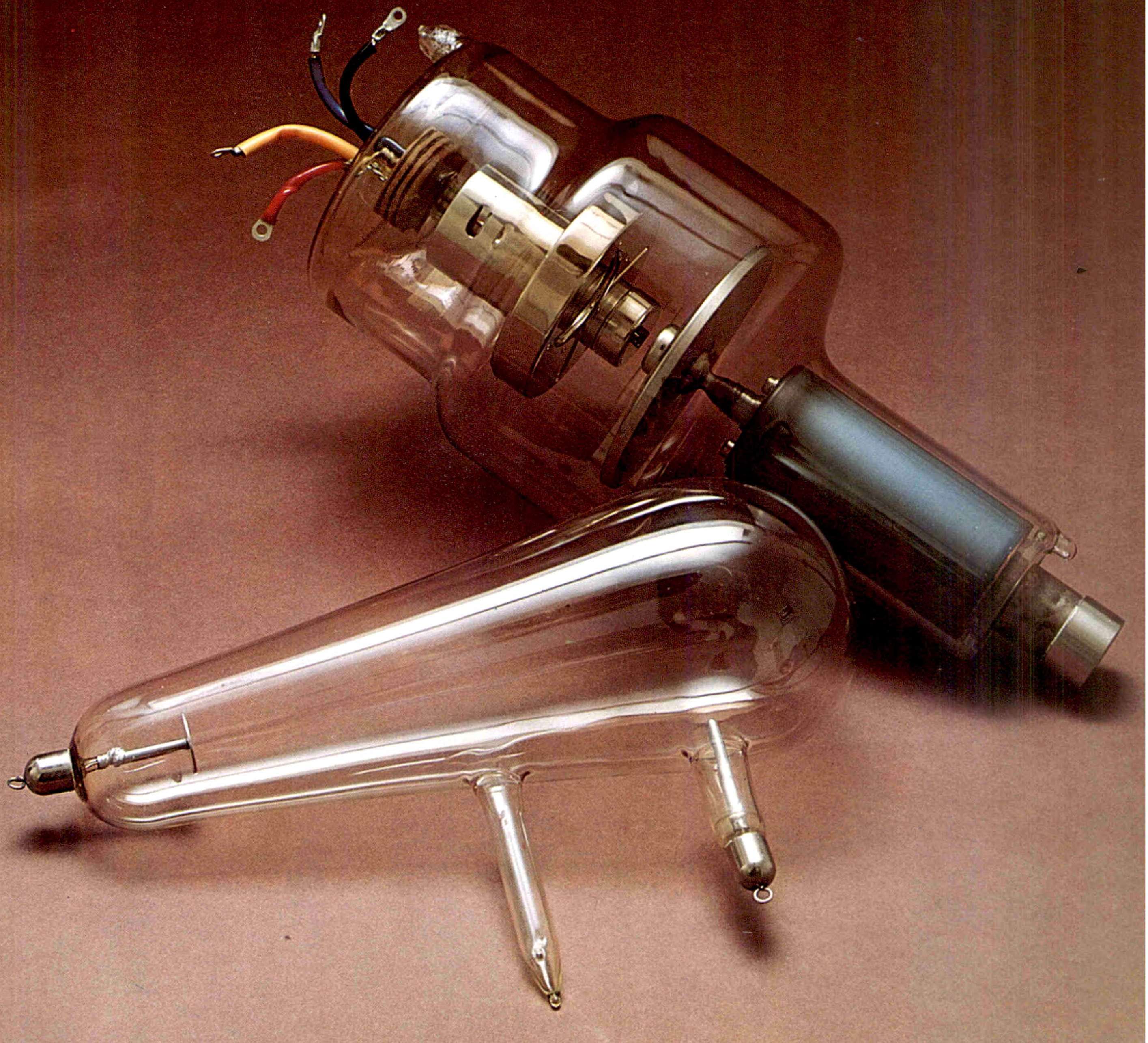

Siemens, the X-ray pioneer

High-capacity 3-phase generators: Today, one in three sold in the U.S. is made by Siemens.

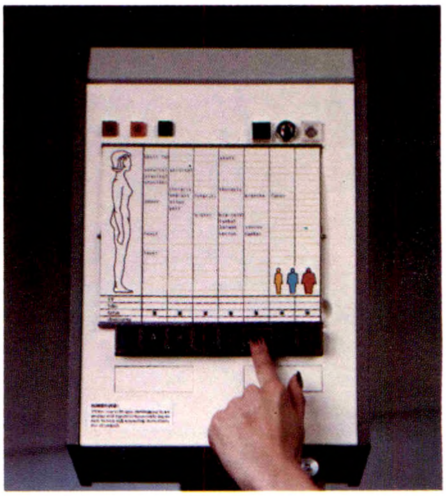

The introduction of high performance, high capacity 3-phase X-ray generators was pioneered in the U.S. by Siemens. Today's most advanced development in this area is represented by our Optimatic series, comprising the Tridoros Optimatic (70 kW), Gigantos Optimatic (100 kW), and Pandoros Optimatic (150 kW). All three generators feature integrated circuit logic techniques and the use of plug-in modules—combinations that provide higher reliability, longer product life, and easier serviceability. The most powerful generator in the series, the Pandoros Optimatic, features unique constant potential output. The high tube current of 2000mA maintains high dose rates, even when x-ray tube voltages are reduced to increase contrast.

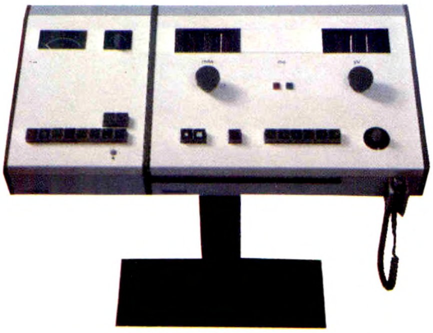

Time Sharing Operation

Another Siemens first was the development of true time sharing generators, whereby one generator is shared by multiple examination units, each operated from a dedicated remote control console.

The time sharing concept provides for more efficient use of generator time, and on-site exposure release. Additional benefits include substantial space and cost savings.

Push-Button Programming

Siemens produced the first commercial X-ray generators featuring single selection programs, to replace manual settings.

For ease of identification, selections are organ-related. And the optimal mA, kV, focal spot and ionization chamber are selected by a single push-button. This development has eliminated the need to consult exposure charts for X-ray settings. And the possibility of error, as well as the need for time-consuming retakes, is greatly reduced.

Both the Siemens Optimatic and Organomatic series of generators feature push-button programming. It is available with either single or three-phase units, and in selected ranges from 25-150 kV and 500-2000 mA.

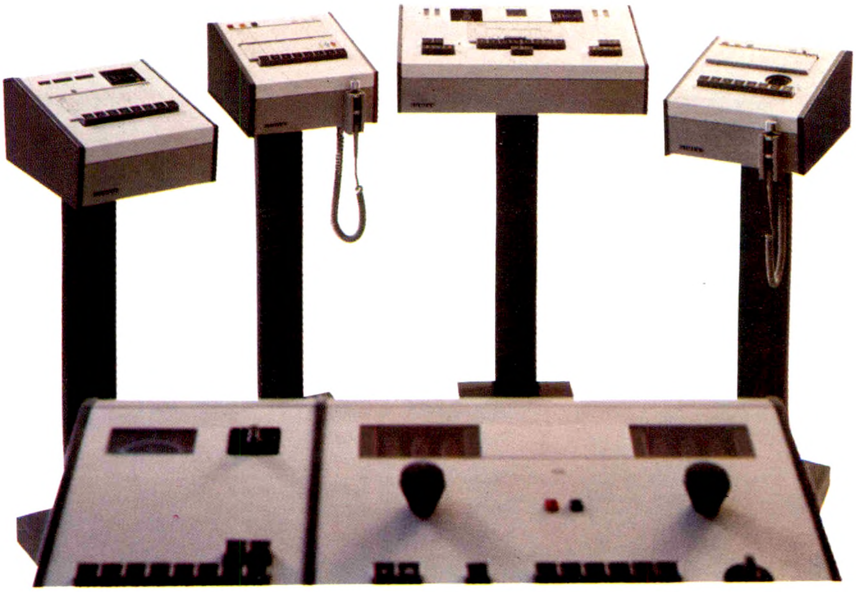

Remote control R/F tables: Today, one in three sold in the U.S. is made by Siemens.

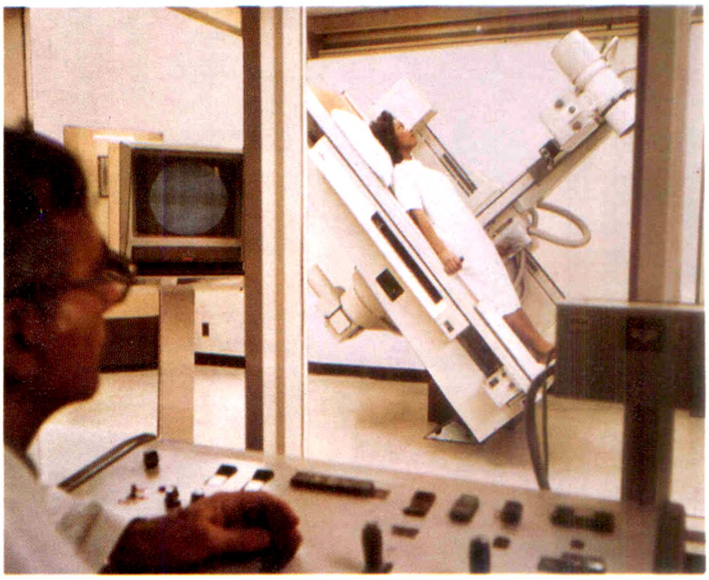

In the 1960's, Siemens introduced the concept of remote control tables—physically separating the clinician from the table and patient. The capability of these tables for automatic patient positioning has contributed to improved procedural control as well as increased patient flow, while responding to the need for increased radiation protection for the operator.

The Siemens Siregraph 2, a 90/90 universal procedure R/F system, features an over-table tube, a fully automatic under-table spotfilm device, an image intensifier television system, and a planigraphic facility. Its capabilities encompass virtually every type of diagnostic examination.

Siregraph 2 is just one in a series of Siemens remote units, comprising a wider choice of general and special purpose R/F systems than is offered by any other manufacturer. To date, Siemens has installed more than 1500 remote systems throughout the world.

A complete heart cath lab: Today, one in three sold in the U.S. is made by Siemens.

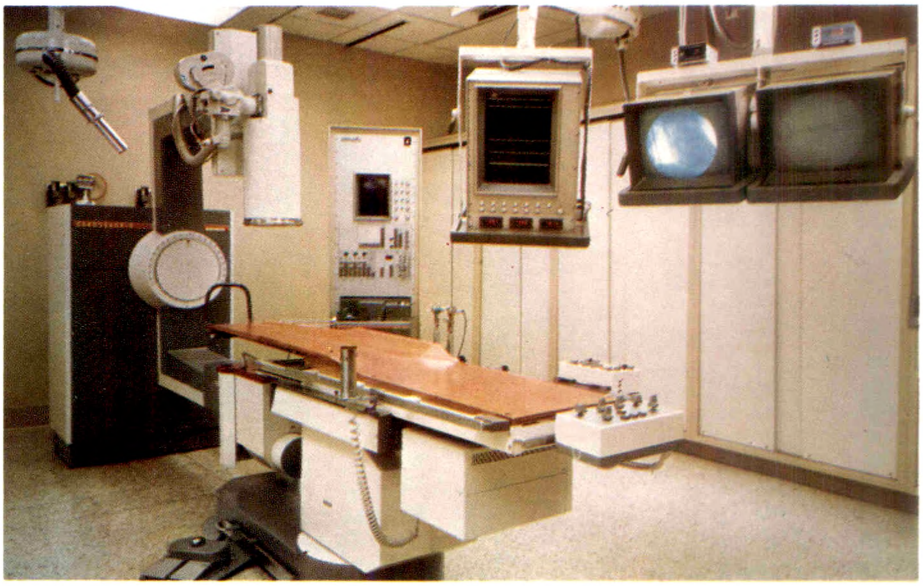

Siemens long experience in x-ray as well as electromedical technology, has led to the development of the first fully integrated heart cath lab system.

The benefits of a single-source cath lab include the assurance of sole-source responsibility for installation and maintenance, together with the functional compatibility of all components in the system.

The primary component, our Cardoskop U X-ray unit, is a dedicated U-arm device with advantages that include the capability for isocentric rotation, mixed oblique projections, improved procedural control, and measureably shorter examination times.

Supporting equipment includes the modularly-designed physiological recording and processing units of the SIEREG System. Its inherent flexibility allows expansion from basic recorders to fully-equipped computer-aided systems.

Siemens, the X-ray pioneer

The tradition continues, with our latest advance – an image intensifier chain having nearly twice the perfomance of present day high resolution systems.

Siemens research in lens, camera, and amplifier technology has led to the development of a radically improved medical television system, called the Videomed H. Unsurpassed in present state-of-the-art, the ultra-high contrast images produced by the Videomed H actually approach the quality of film, thereby facilitating far greater subject discrimination and the capability for more informative diagnosis.

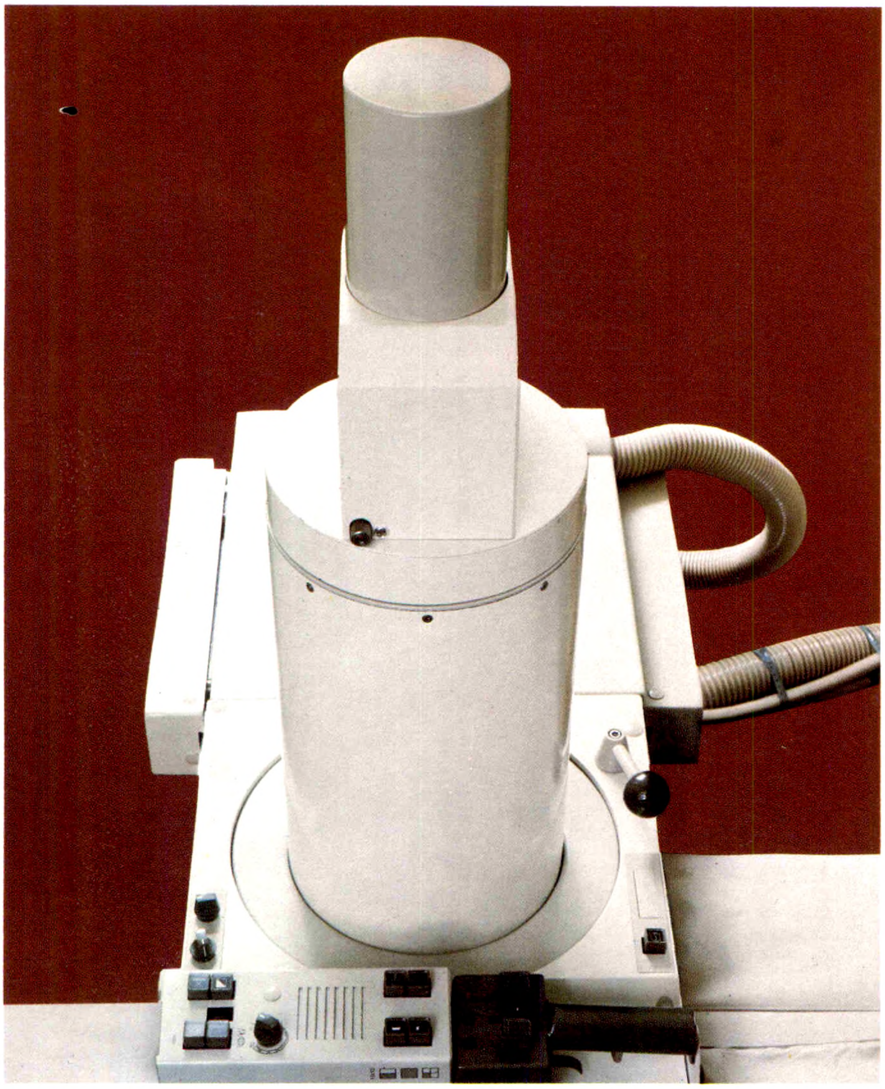

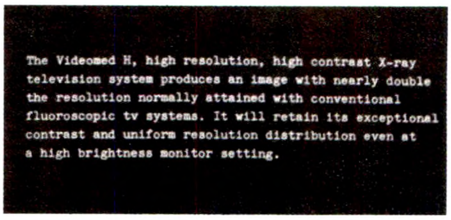

The Videomed H, high resolution, high contrast X-ray television system produces an image with nearly double the resolution normally attained with conventional fluoroscopic tv systems. It will retain its exceptional contrast and uniform resolution distribution even at a high brightness monitor setting.

Actual, unretouched photographs taken with the Videomed H television system (above) and with a present day, high resolution system (below) illustrating the ultra high quality image resolution obtainable with the Videomed H.

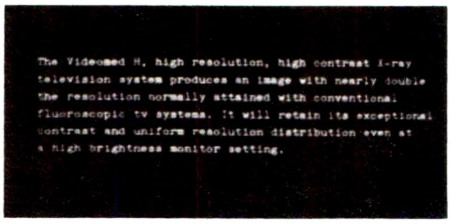

The Videomed H, high resolution, high contrast X-ray television system produces an image with nearly double the resolution normally attained with conventional fluoroscopic tv systems. It will retain its exceptional contrast and uniform resolution distribution even at a high brightness monitor setting.

For details on the Videomed H, or information on other X-ray systems or products, contact your local Siemens representative, or Siemens Corporation Medical Systems Division, 186 Wood Avenue So., Iselin, New Jersey (201) 494-1000. In Canada: Siemens Canada Limited, P.O. Box 7300, Pointe Claire 730-P.Q.

SIEMENS

These are only a few of the people who make our AOT and PUCK filmchangers. Yet, this group alone represents over 250 years of combined experience in x-ray filmchangers.

Many of these men were with us over 25 years ago when we pioneered a unique transport system for the first practical cutfilm changer. Since then, there have been numerous engineering advancements that make our changers the state-of-the-art. Advancements which range from that original transport system to punch card programming to our recent introduction of the Carbon Fiber Reinforced Plastic (CFRP) pressure plate.

Find out what we've done to make angiographic examinations faster, easier, and more accurate than ever before. Write for our brochures which detail the latest innovations in AOT and PUCK cutfilm changers and punch card programming.

Elema-Schonander, Inc., 699 Lively
Boulevard, Elk Grove Village, IL 60007.
(312) 593-6770.

**When a better idea
in film changers
comes along,
it will come from us.**

elema-schonander

Our filmchangers have been working for over 25 years because many of our filmchanger makers have been working with us for over 25 years.

There's one easy way to specify an R/F system tailored exactly to your needs:

It's a Philips' maxim: "Make the system *fit* the customer: don't force the customer to adapt to the system."

That's why Philips' Individualized R/F Systems meet the common needs of all radiologists yet still provide choices that recognize individual techniques, requirements and preferences.

The heart of the Individualized System is the finest 90°/90° universal R/F table on the market: the Diagnost 73.

You can individualize your Diagnost 73 with quality-constructed, easily selected choices – in spot film device/image intensifier combinations, in generators and in fluorographic cameras.

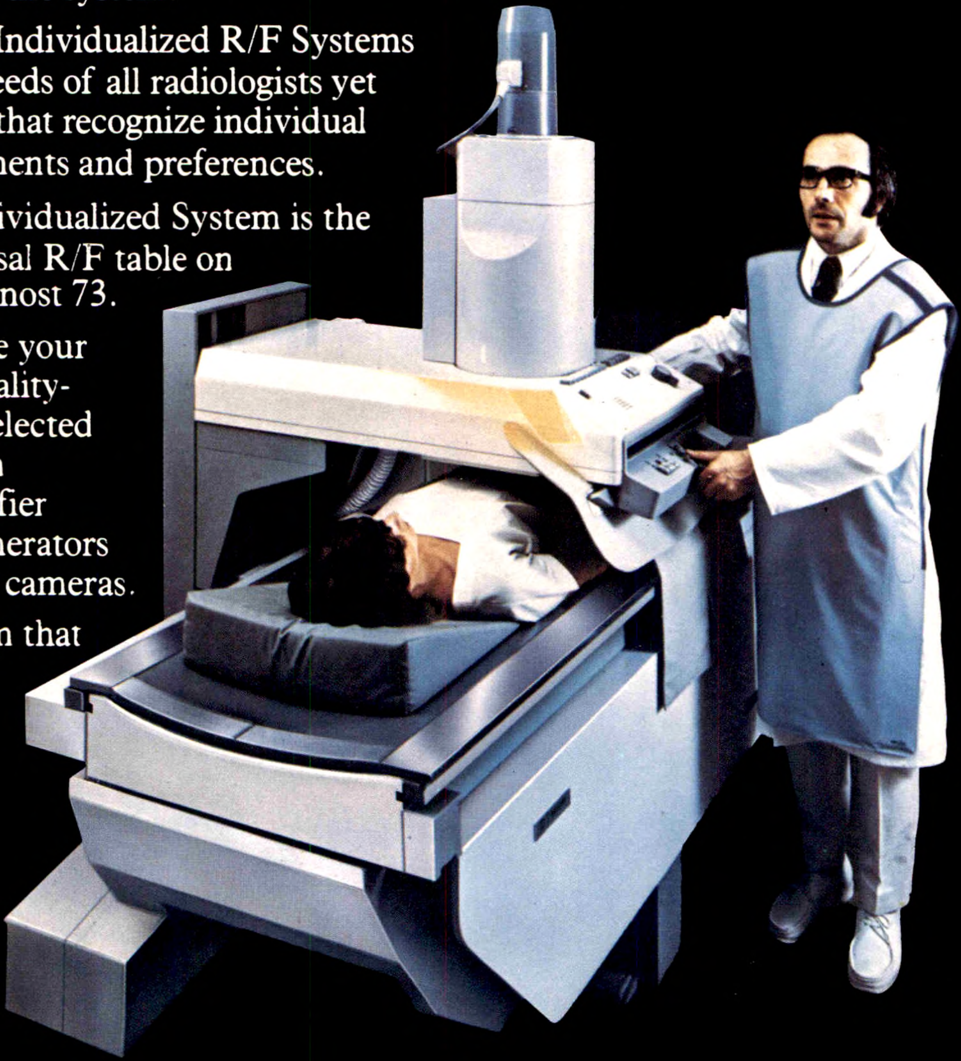

The result is a system that works the way *you* want to work… with optimum diagnostic images every time.

Philips' Individualized R/F Systems: tailored to make your life simpler.

Contact your Philips' representative. Or, call or write:

PHILIPS MEDICAL SYSTEMS, INC.

710 Bridgeport Avenue, Shelton, Conn. 06484

specify Philips

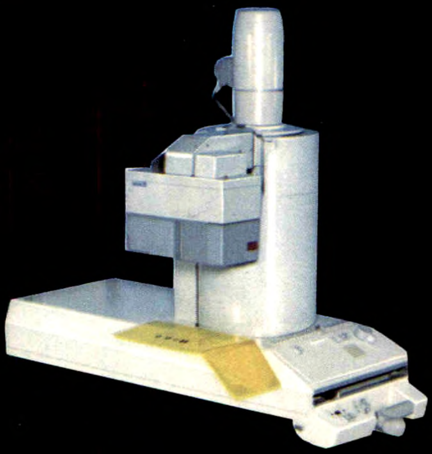

Philips Imaging Systems

Whether you select a 9″ Dual Mode Image Intensifier, a 6″ I.I., or a Philips' exclusive 6″ fiber optic system, you're guaranteed uniform image quality over the entire field. High resolution, high contrast, high conversion factor and high quantum detection efficiency result in optimum image transfer to TV and fluorographic cameras. In short, the best possible diagnost images.

Philips Spot Film Devices

Four spot film devices: choose the one that adapts to your needs and your technique. Fully integrated into the table to eliminate ceiling suspension in most configurations, the spot film device is easily parked to permit tabletop radiography with the Diagnost 73's built-in bucky system and a ceiling suspended X-ray tube.

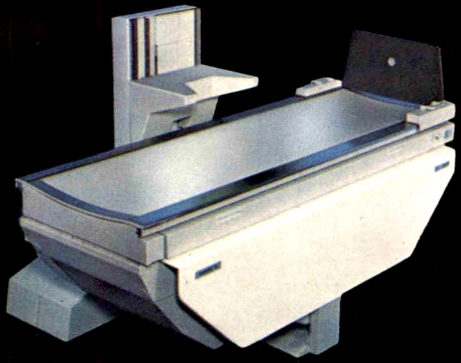

Philips Diagnost 73 Table

The world's finest 90°/90° universal R/F system. A modern table base permits a choice of spot film device/image intensifier combinations. The table features quiet, variable speed tilt motion from upright to 90° Trendelenburg. You can remain in close proximity to the patient and still have an unobstructed view of the TV monitor in any table position.

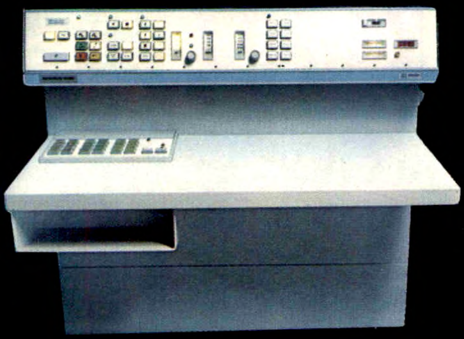

Philips Modular Generators

Designed for flexibility, free technique *and* Anatomically Programmed Radiography (APR). Modular design lets you adapt the generator to *your* needs...with expansion capability to accommodate future requirements.

PHILIPS

PHILIPS®

® TM N.V. Philips of Holland

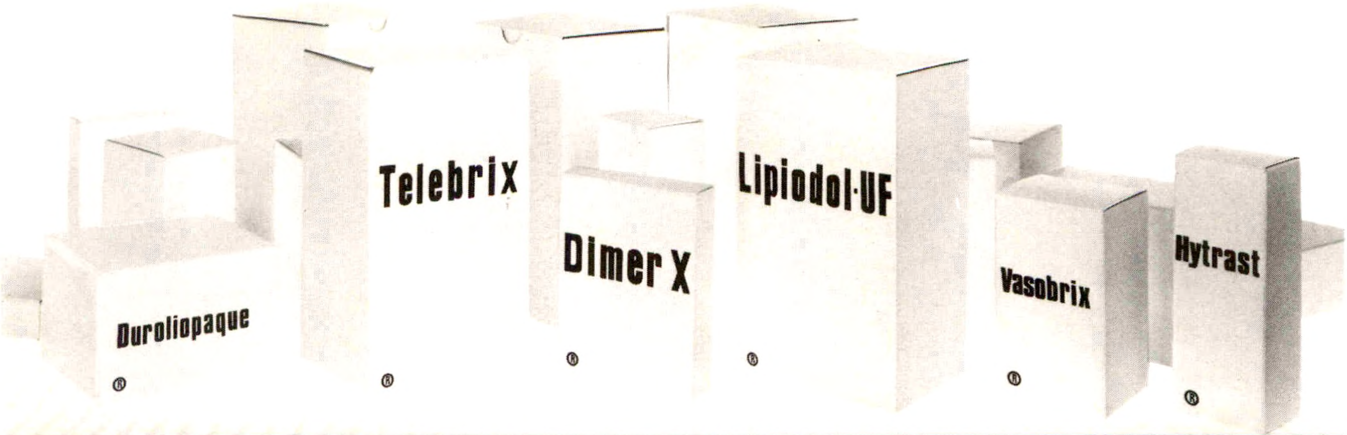

WE MANUFACTURE
contrast
MEDIA
OUR
products
ARE
known
WORLD-WIDE
OUR
name isn't

GUERBET
BETTER CONTRAST MEDIA THROUGH RESEARCH

Laboratoire Guerbet, 16/24, rue Jean-Chaptal
93601 AULNAY-SOUS-BOIS Cedex - FRANCE
Telex : Guerbet 690682

XIV International Congress of Radiology

IN RIO DE JANEIRO, BRAZIL – OCTOBER 23–29, 1977

and South American Tours

Fully Escorted

Tour A FROM LOS ANGELES / $1435.40 Per Person, Double Occupancy Single Supplement $342.00

DEPARTURE OCTOBER, 17 RETURN NOVEMBER 5

LIMA – CUZCO – MACHU PICCHU – RIO DE JANEIRO – IGUASSU FALLS – BUENOS AIRES
DELUXE HOTELS – TRANSFERS – SIGHTSEEING – AIR FARE INCLUDED

Tour B FROM MIAMI / $1220.40 Per Person, Double Occupancy Single Supplement $305.00

DEPARTURE OCTOBER 18 RETURN NOVEMBER 4

LIMA – CUZCO – MACHU PICCHU – RIO DE JANEIRO – IGUASSU FALLS – BUENOS AIRES
DELUXE HOTELS – TRANSFERS – SIGHTSEEING – AIR FARE INCLUDED

Designed for Persons Who Only Wish to Attend the Congress

Tour C FROM NEW YORK / $769.00 Per Person, Double Occupancy Single Supplement $116.00 –AIR FARE INCLUDED

DEPARTING OCTOBER 21, 1977 RETURNING OCTOBER 29, 1977

For brochure containing additional information: AEROLINEAS ARGENTINAS / 545 South Olive Street, Los Angeles, CA 90013

Everything we know about money-saving, time-saving, energy-saving ride sharing programs is yours for the asking.

Free. Our Double Up kit contains facts, figures, ideas, promotional help and other good things you and your company should know about.

I want to know it all. Please send your Double Up kit right away.

Name__________ Title__________
Company__________
Address__________
City__________ State__________ Zip__________

Ad Council

A public service of this magazine, the U.S. Department of Transportation and The Advertising Council.

The Varian Clinac®

Continuing Excellence Makes the Difference

From 4 MV X-ray therapy to high-energy multi-modality therapy, Varian Clinac linear accelerators are meeting the requirements of dynamic radiotherapy departments throughout the world.

Reasons for this widespread acceptance are many. They range from Varian's experience in engineering innovation to manufacturing consistency and worldwide customer support —quality that makes the difference.

When performance and innovation backed by responsive support are your criteria, the choice is clear…
a Varian Clinac. Write or
phone Varian Radiation
Division, 611 Hansen Way,
Palo Alto, CA 94303.
Tel: 415-493-4000.

Clinac 18: The most widely accepted high-energy, multi-modality therapy accelerator in routine standardized production.

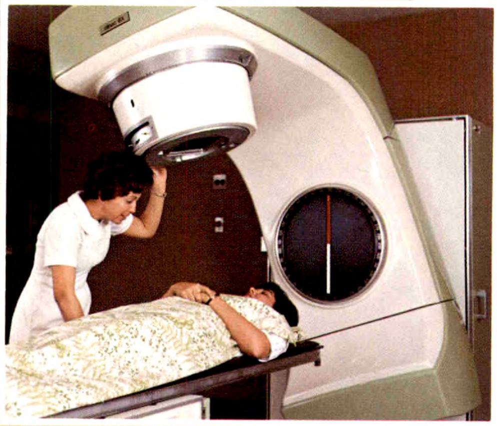

Clinac 6X: The first 360° isocentric non-bent beam standing-wave accelerator producing 6 MV X-rays.

varian

Installations shown—(Above) Clinac 6X and (Center) Clinac 18, Central Arkansas Radiation Therapy Institute, Inc., Little Rock, AR;
(Right) Clinac 4, Sequoia Hospital District, Radiation Oncology Dept., Redwood City, CA.

Customer Support from the Beginning. Varian's extensive service organization provides the expert support necessary for planning and installation. Responsive service from field offices located throughout the world is a Varian trademark.

Built-In Quality. Clinacs are produced by a highly skilled quality-oriented staff at Varian's specialized, modern production facilities in Palo Alto, California.

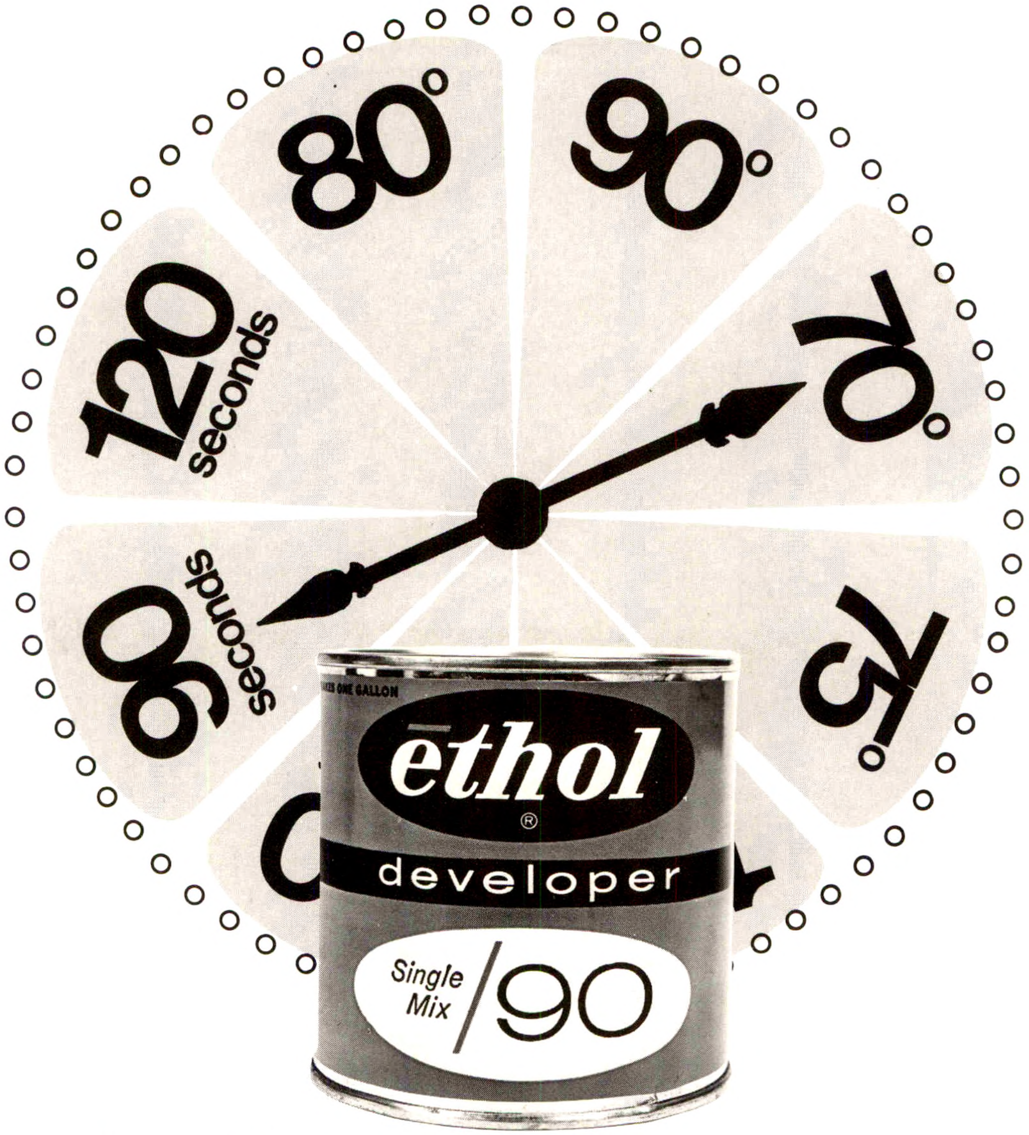

play the numbers game. with ethol 90, you always win.

Ethol 90 is not just another film developer . . . it's the first and original 90-second developer used by leading hospitals the world over and recommended by foremost manufacturers of automatic processors. It is used in an extremely broad range of applications including X-Ray, cineflure, electron microscopy, holography, cardiology and macrophotography.

Do you want to work at 70°, 80°, 90°? Do you want to process for 90, 120 or 180 seconds? Ethol 90 will provide optimum results under all conditions. It is a fine grain, normal contrast, long scale, very rapid working developer. The compensating action in push processing gives a minimum increase in grain, will not block highlights or diminish shadows.

In cineflure film processing radiation factors may be reduced by 50% or more with Ethol 90 and still provide much improved contrast and clearer film base than other developers. Ethol 90 gives a lower tube load, therefore longer life. It works in low gain, borderline image tubes. There is less radiation to doctor and patient and fewer repeat examinations.

Available both powder or liquid form. Replenishers available.
See your X-Ray Supply House or write directly to:

ETHOL CHEMICALS, INC./1808 N. Damen/Chicago, Ill. 60647/(312) 278-1586

ethol®

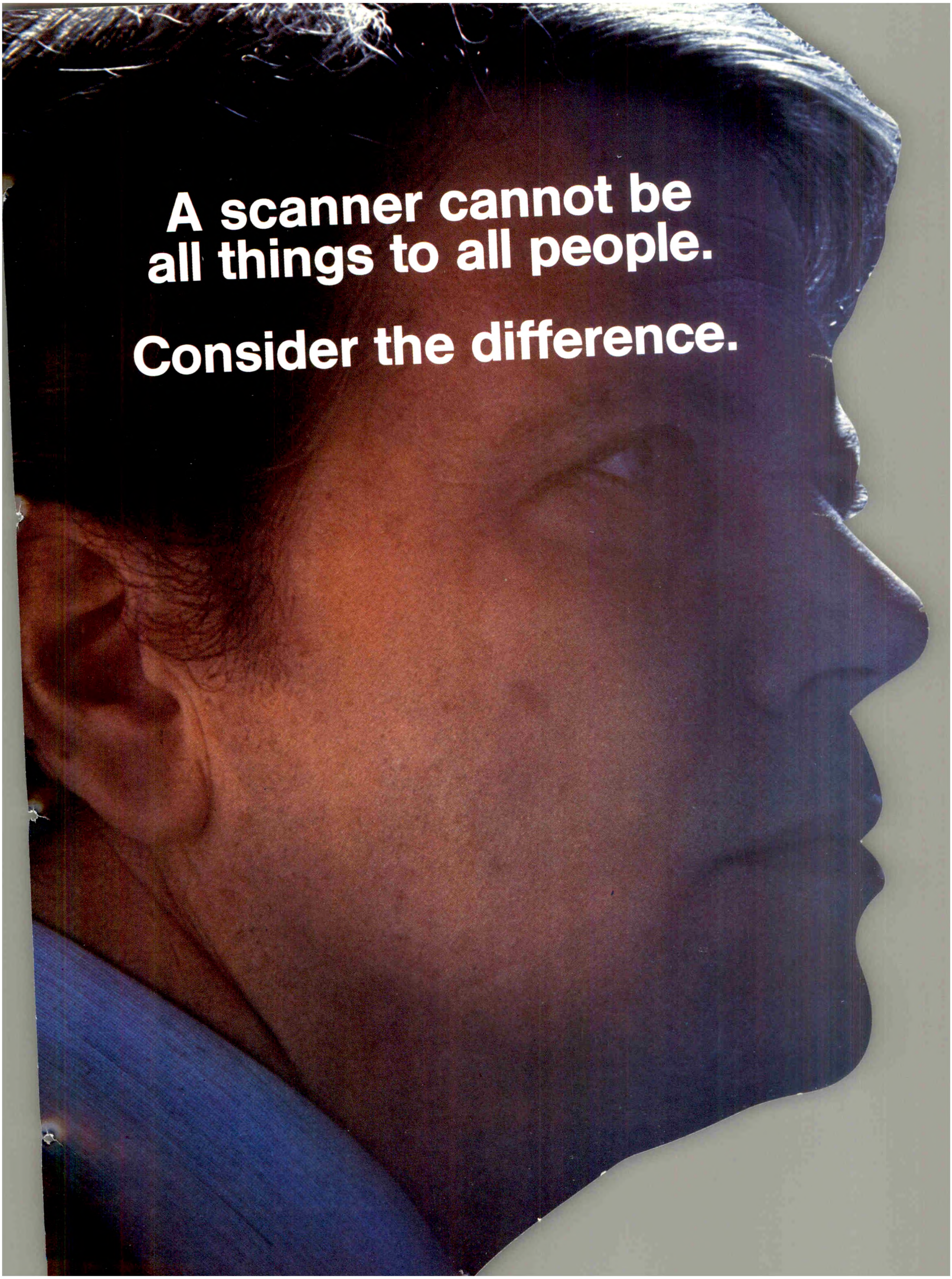
A scanner cannot be all things to all people.
Consider the difference.

Head scans are different than body scans. Successful head scans call for ND 8000, the CT scanner designed for cranial examinations.

CT scanners have advanced the state of the art in diagnostic x-ray to unheard of levels. But, like every new system, care must be taken that scanning systems be evaluated and applied properly.

Scanning systems can be universally good but not necessarily specifically great.

Head and body scans are a classic example. Organ movement, beam geometry, range of attenuation coefficients, radiation quality and reconstruction algorithm are all very significant when applied to head vs. body examinations. Each calls for a different approach.

These considerations, and many others, call for a selection of examination parameters that will create the best possible image at the lowest possible rad dose to the patient.

For head examinations, these parameters are best met with ND 8000 - CGR's new CT head scanner which uses the translation-rotation principle offering maximum flexibility in data collection.

CGR

CGR ND 8000 has been designed specifically for the study of the brain, posterior fossa, neck and orbital cavities. It offers the dual advantage of simultaneously producing superior density resolution and spatial resolution.

The new scanner permits optimum flexibility in choosing parameters. These parameters include :

- A high spatial resolution of 7 lines per centimeter and a high density resolution of 0.2 %. Selection of either of these modes is by pushbutton.
- Irradiation control of 1 to 10 rads to match dosage with specific clinical requirements.
- A fast acquisition time of 20 seconds.
- Detection via Xenon chambers to assure maximum reliability and stability of x-ray radiation measurements.
- Special x-ray tubes with bias control to select optimal x-ray tube focal size.
- A scan gantry with ± 30° tilt for superior slice orientation.
- Additional patient support swivel for ease in positioning.
- Precise centering by laser beam.
- And, of course, complete programs for file management as well as computer assisted image analysis.

ND 8000's reduced scanning time minimizes artifacts caused by patient movement.
In the slow mode, under 360° angulation, the scanner produces 4 times more x-ray photons - approximately 500,000 data samples. Density resolution is 0.2 %. The system has a reconstruction zoom capability equivalent to 512 x 512 points ; a 0.70 mm spatial resolution (FWHM). The smallest volume element is 1.5 mm^3. Reconstruction algorithms are offered for both adults and children. The x-ray tube is bias controlled to permit selection of optimal focal size, providing greater brightness when desired.

D 8000,
e head scanner.
onsider the difference.

ND 8000

ND 8000

ND 8000

ND 8000

ND 8000

ND 8000

ND 8000

ND 8000

Spatial resolution : 7 lines per centimer.
Density resolution : 0.2 % with respect to the density of water.
Selection of one of these 2 modes by pushbutton.

ND 8000 Features

- **Data acquisition for a single slice**
Translation-rotation principle
– 180° in 16 rotation steps of 12°
– 360° in 31 rotation steps of 12°
– Scanning field : 256 mm

- **Gantry tilting : ± 30°**

- **Patient support**
– Vertical and transverse movement under minicomputer regulation.
– Exclusive swivel movement.

- **Accurate centering**
by laser beam.

- **Scanning time**
Standard mode : 180° in 20 seconds.
High resolution mode : 360° in 40 seconds.
Very high resolution mode : 360° in 80 seconds.

- **X-ray tube**
High brightness, 4 kW power dissipated on a focal spot size 7.5 mm in one direction and adjustable from 0.5 to 1.5 mm in the other direction.

- **X-ray stabilization**
Residual system noise well below the unavoidable quantum noise.

- **X-ray filtration**
Optimized for head examinations. Cuts down the artifacts while eliminating unwanted radiation.

- **Detectors**
– 31 Xenon detectors.
– Automatic calibration.
– Efficiency greater than 95 % for 80 KeV x-rays.

- **Collimation**
Motorized positioning of a collimating grid which allows switchover from the density resolution mode to the high spatial resolution mode.

- **Variable scan slice thickness**
3 - 6 - 9 mm.

- **Number of data points**
– 246016 data for 180°.
– 492032 data for 360°.

- **Matrix size**
– 256 x 256 elements.
– Reconstruction zoom capability equivalent to 512 x 512 points.

- **Reconstruction algorithm**
– Selection facilities : High density resolution
High spatial resolution
Adults
Children.
– Patient motion corrected in the image reconstruction program.

- **Reconstruction time**
From 20 to 40 seconds maximum according to the number of data points.

- **Range of x-ray absorption values**
Scale : −1000 corresponds to air, zero to water, +1000 to bone.
– Window level : adjustable in unit steps from −1000 to +1000.
– Window width : adjustable in unit steps from 1 to 512.

- **Image processing**
– Overbrightness.
– Magnification.
– Region of interest.
– Average density value calculation.
– Possibility of displaying the density value of any picture element.

- **Display system**
One or two viewing units allowing image processing independent of acquisition.

- **Image storage**
4 options :
– Floppy disc - 10 image capacity.
– Magnetic tape - 200 image capacity.
– Floppy disc + magnetic tape.
– Big disc unit - 700 images + magnetic tape.

- **Image recording facilities**
4 options :
– Standard camera.
– 105 mm camera.
– Four exposures on 24 x 30 cm x-ray film.
– Electrostatic printer facilitating hard copy documents.

- **Independent diagnostic center (I.D.C.)**
Images with additional administrative and diagnostic information are processed through an independent diagnostic center (I.D.C.).
– a display console
– an electrostatic printer
– a disc unit stores administrative and diagnostic information for retrieval and/or statistical studies.

- **Computer system configuration**
– One 32K MOS memory main computer.
– One 32K MOS specialized processor.
– Temporary storage on a 10 Megabyte magnetic disc.
Optional : a second computer or micro processor integrated into the I.D.C.

CGR

CGR
13 Square Max Hymans
75741 Paris Cedex 15
France - Tél. : 783.50.04

CGR Medical Corporation
2519 Wilkens Avenue
Baltimore, Maryland 21223
USA - (301) 233-2300

CGR Canada Ltee-Ltd.
500 Boulevard de l'Aéroparc
Lachute, Québec, Canada
(514) 562-8806

Help us to help you.

OSHA—the Occupational Safety and Health Act of 1970—benefits everybody. Employers and employees alike.

Today, Red Cross is helping employers all over the country to meet OSHA standards, by training employees in first aid and hazard recognition practices. The result is that, everywhere, factories and other places of business are safer and healthier. Another side benefit: employees trained in first aid are more valuable employees.

Next time you wonder where "all those dollars you gave to the Red Cross" are going—you might consider this: a lot of them are being plowed right back into your business! For information about First Aid Training call your local Red Cross Chapter.

Red Cross. The Good Neighbor.

CHARLES C THOMAS • PUBLISHER

XERORADIOGRAPHY: Uncalcified Breast Masses *by* **John N. Wolfe,** *Hutzel Hospital, Detroit, Michigan.* Information and graphic material are presented which will assist the radiologist in arriving at a reasonable differential diagnosis when confronted with uncalcified breast masses. The order of presentation proceeds from the obvious malignancies characterized by a mass with a well-developed spiculated margin, through the subtler circumscribed carcinomas such as the medullary or colloid variety, to those most difficult ones which do not present a well-defined mass but merely an area of increased density. Benign tumors are also considered in detail. *'77, 208 pp. (8 1/2 x 11), 307 il., $28.00*

THE RENAL UPTAKE OF RADIOACTIVE MERCURY ($^{197}HgCl_2$): Method for Testing the Functional Value of Each Kidney, Technique- Results- and Clinical Application in Urology and Nephrology *edited by* **Claude Raynaud,** *Service Hospitalier Frederic Joliot, Orsay, France. Foreword by* **Pierre Royer.** *(41 Contributors)* Doctor Raynaud and his colleagues introduce and evaluate a new method for study of the relative function of each kidney, namely, the use of ionic mercury uptake. This volume summarizes the results of years of experience with this procedure. Important technical details such as the time after injection at which the measurements are made, the optimum energy levels, corrections for organ depth and the various types of instruments which can be used are critically considered in detail. The major point of this work is that the symmetry of the body, in this case that of the kidneys, can be the basis of important early signs of disease. *'76, 248 pp., 110 il., 47 tables, $22.75*

ANATOMICO-ROENTGENOGRAPHIC STUDIES OF THE SPINE (3rd Ptg.) *by* **Lee A. Hadley,** *Syracuse Memorial Hospital, Syracuse, New York.* Over 900 roentgenographic images are coordinated with actual anatomical conditions in this atlas. Of particular practical interest are the longitudinal follow-up studies of patients. These show the anatomical effect incidental to trauma and resultant changes thereto which were observable upon subsequent examination. These cases were followed for periods varying from five to twenty-six years. The broad scope of study is revealed in the contents which includes development of the spine, disturbances of development, the cervical spine, vertebral arteries, posterior spinal articulations with innervation studies, spinal curvatures, infective spondylitis, tumors and tumorous conditions. *'76, 560 pp. (6 3/4 x 9 3/4), 644 il., $19.75*

A STUDY GUIDE IN NUCLEAR MEDICINE: A Modern Up-to-Date Presentation *compiled and edited by* **Fuad Ashkar, August Miale, Jr.,** *and* **William Smoak,** *all of the Univ. of Miami, Miami, Florida. (22 Contributors)* Comprised of ten sections, this text provides a comprehensive review of nuclear medicine. It will be particularly useful to persons studying for board examinations in nuclear medicine. The articles cover such topics as the interaction of gamma rays with matter, control of radiation exposure to man, basic mathematics of nuclear medicine, electrolytes and body composition, essentials of rectilinear scanning, cardiovascular imaging, and treatment of thyroid disease with radioiodine. Representative illustrated material accompanies the text. *'75, 488 pp., 312 il., 44 tables, cloth-$22.75, paper-$17.50*

Prepaid orders sent postpaid, on approval

301-327 EAST LAWRENCE
SPRINGFIELD • ILLINOIS • 62717

It takes a strong table to be gentle.

Our new Galaxy® II is the strong, silent type.

It's designed to handle heavy x-ray tubes and imaging loads; but more importantly, the punishing patient loads of busy radiology departments become mere routine.

Its most outstanding features are inside. The new internal structures, such as hardened bearing tracks, are the heart of our reliability theme.

But this inner strength now translates into much smoother, quieter movements which provide ease to the operator and less apprehension to the patient.

More room inside assures space for tomorrow's larger, high-heat-capacity x-ray tubes. And, there's fluoroscopic coverage to handle a barium swallow on a 6'2" patient plus greater Bucky coverage and quality improvements in our new Multicon imaging systems. Durable switches have given even more reliability to an already good table resulting in easier operation and longer-life benefits.

Galaxy II, available in 90/90 or 90/15 table versions, can include Flushmount imaging or be equipped with the Multiview front-loading spotfilmer and Multicon Imaging Systems.

This is another example of Picker's unique human resources benefiting you. It's a result of our expertise in the diagnostic modalities of x-ray, ultrasound, nuclear, computed tomography, clinical laboratory, therapy, film systems and supplies. Only Picker has all these resources.

Consult your Picker representative or write Picker Corporation, 595 Miner Road, Cleveland, OH 44143.

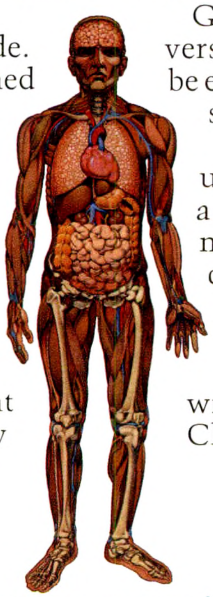

Discover the human resources in Picker's synergy

PICKER®

ONE OF THE C.I.T. COMPANIES

PICKER
STOP
POWER TOP
TILT

Yes... you're a candidate for Heart Attack

You can reduce your risk by

- Not smoking cigarettes,
- Eating foods low in animal fats and cholesterol,
- Reducing if overweight,
- Exercising regularly, moderately,
- Controlling high blood pressure,
- Seeing your doctor regularly,

and by supporting your Heart Association's programs of research, education and community service.

GIVE... so more will live **HEART FUND**

Contributed by the Publisher

INDEX TO ADVERTISERS

Ortho Pharmaceutical Corporation

Calonje Products

C. B. Fleet

The Purdue-Frederick Company

Eastman Kodak Company

E. R. Squibb & Sons, Inc.

Machlett Laboratories

Eastman Kodak Company

E. I. DuPont de Nemours & Co., Inc.

E. R. Squibb & Sons, Inc.

• • •

E-Z-EM Company

Picker Corporation

Charles C Thomas · Publisher

General Electric Company

Siemens Corporation

Elema-Schonander, Inc.

Philips Medical Systems, Inc.

Guerbet Laboratory

Aerolineas Argentinas

Varian Associates

Ethol Chemicals, Inc.

CGR (Paris)

Charles C Thomas · Publisher

Picker Corporation

Hanley Medical Equipment Company

Varian Associates

AMRAD

E-Z-EM Company

Hanley Space Saver X-Ray and Medical Record Cabinets are installed in most hospitals in America.

Top quality and low price is the reason.
5 compartment with doors—$199.50
5 compartment less doors—$171.50
Brochure F.O.B. Factory

AMERICA'S LARGEST DISTRIBUTOR OF X-RAY CABINETS

HANLEY MEDICAL EQUIPMENT CO.
5614 South Grand X-Ray Division St. Louis, Mo. 63111

In reply to advertisers
please mention that you saw
their advertisement in

THE
AMERICAN JOURNAL OF
ROENTGENOLOGY

published monthly for
The American
Roentgen Ray Society
by

CHARLES C THOMAS • PUBLISHER
Springfield, Illinois 62717

Bind Your
Journal Issues
Into Valuable
Vigilant Volumes

Pertinent information you sometimes desperately need is too often in the Journal issue you cannot find. Single copies have a way of getting lost, misplaced or destroyed. It is better for you to let us permanently bind each journal into semi-annual or annual volumes —then your reference source is always complete, organized and instantly at your service. We call them "Vigilant Volumes"; they so carefully store and provide on instant notice so much knowledge of timely value.

The cost per "Vigilant Volume," by official commission from the journal publishers is but $5.95 per volume, permanently hard bound in washable buckram, gold embossed with period dates, journal name and special insignia—plus your name stamped in gold leaf. "Vigilant Volumes" are handsome library additions too, real conversation pieces. These volumes are bound in the authorized colors.

HOW TO ORDER

Simply ship your journal issues to us via parcel post, together with your name, address, AND REMITTANCE, at $5.95 per volume. Within 45 days after receipt, bound volumes will be shipped to you. Price subject to change without notice. Please remit 50¢ per volume for return transportation and handling.

PUBLISHER'S AUTHORIZED
BINDERY SERVICE, Ltd.
(Authorized Binders of All Journals)
4440 W. Roosevelt Rd.
Chicago, Illinois 60624

CT Technology of the Future.

The Varian

Go with the right design from the beginning. Varian's 3-Second Whole-Body CT Scanner anticipates the future in CT Scanning. Varian expertise in high-technology medical systems designed the basic features that continue to pave the way. The fan beam geometry with slip-ring gantry coupler design is fundamental. It permits continuous, smooth rotation of the gantry minimizing mechanical wear. It facilitates multi-rotation scanning and stop-action scans. This was recently demonstrated in stop-action heart studies. And it opens the way for direct up-grade.

The pulsed x-ray source permits such advanced techniques as triggering the x-ray pulses with physiological signals.

The Varian Whole-Body CT Scanner design assures you state-of-the-art scanning today and tomorrow.

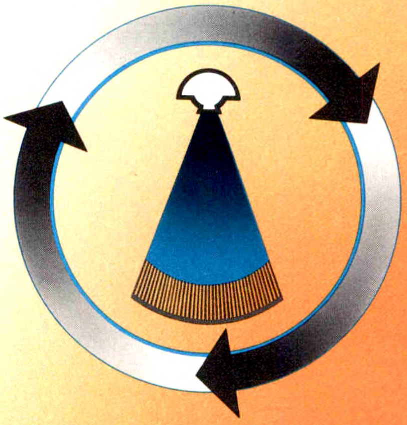

Fan beam design with slip-ring construction permits smooth, non-stop gantry rotation.

Stop-Action Heart Study*

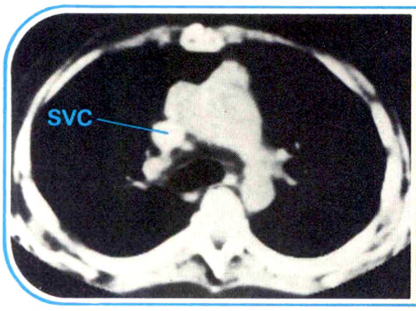

Routine scan of 52-year-old patient during contrast infusion. Only general outline of heart is seen because of cardiac motion. Some contrast, however, can be identified in the superior vena cava (SVC). The right atrium, right ventricle, right ventricular outflow tract, main pulmonary arteries and ascending aorta cannot be distinguished.

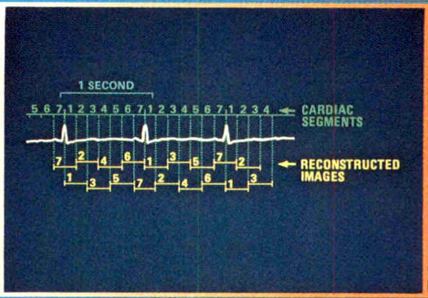

Electrocardiogram obtained during CT heart scan (left). Peak R-R interval for each ECG cycle was divided into 7 equal segments.

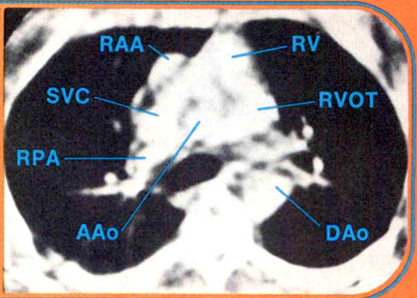

Stop-action heart scan. Data from the routine scan (far left) was used to reconstruct this stop-action image. The right ventricle (RV), the right ventricular outflow tract (RVOT), the descending aorta (DAo), the ascending aorta (AAo), the right pulmonary artery (RPA), the superior vena cava (SVC), and the right atrial appendage (RAA) are now clearly visible.

For complete information, write or call:
Medical Group,
Varian Associates,
611 Hansen Way,
Palo Alto, CA 94303.
Tel: 415-493-4000.

The Varian CT Scanner is supported through a highly skilled, experienced high-technology medical equipment sales and service organization.

Right Now!

CT Scanner

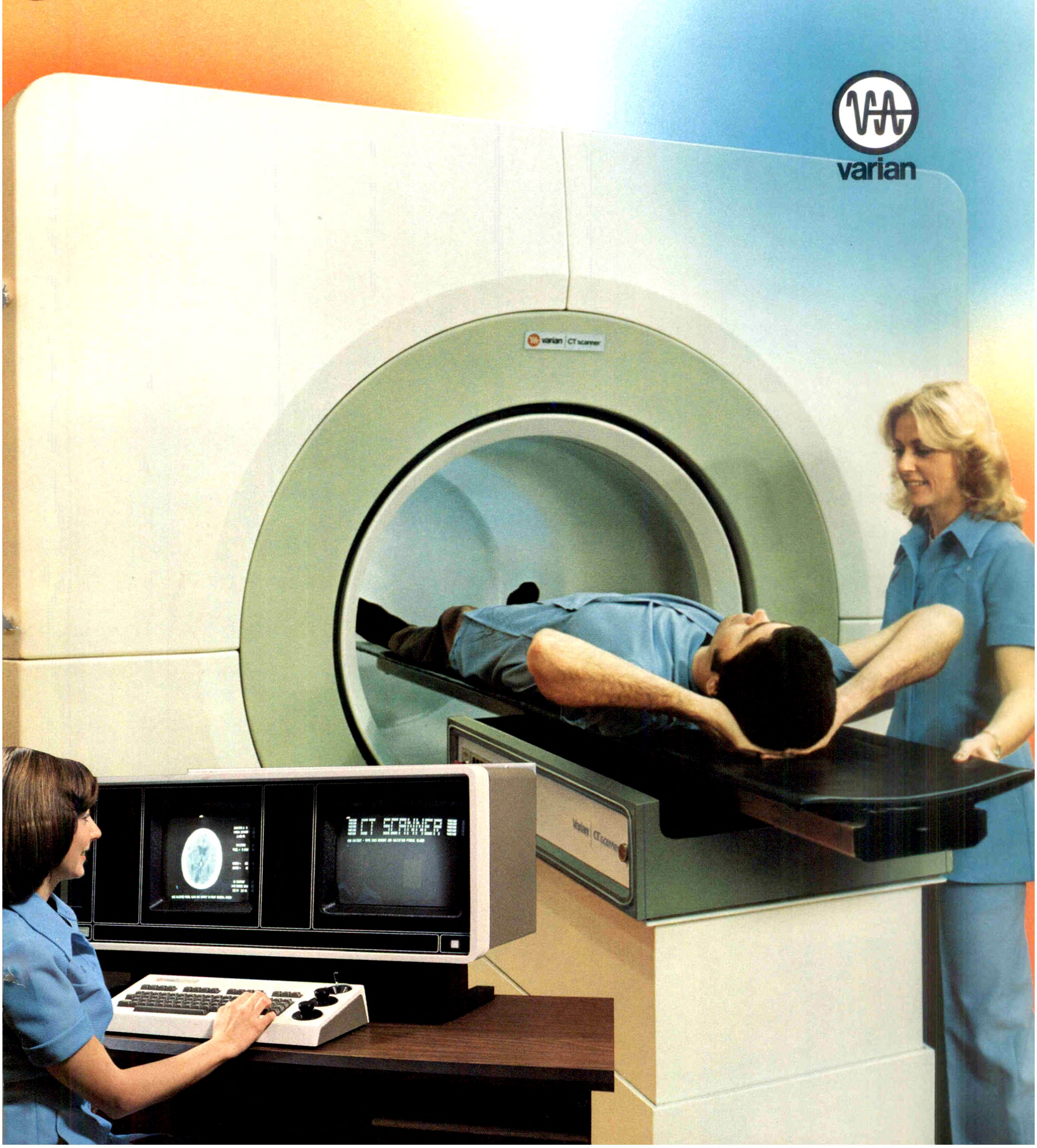

Is there an unhappy Amrad Customer?

Seems unhappy customers abound in the x-ray business. But as far as we know, none of them belong to us. In the little over two years we've been in business, we've now shipped over 500 complete units of a superb space-saving 600-MA, 125 KV x-ray room. You know, the one with that super-slick table, plug-in installation and remote generator control. The one with add-on mammography and tomography capabilities that cost a fraction of any other approach.

And when number 500 went out, we still hadn't heard a whimper. We think a lot of it has to do with our dealer network being so on-their-toes. After all, each of the seventy-five is an independent businessman, too — so they have to be good.

But maybe you should check for yourself. If you ever buy x-ray equipment, send us the coupon below, and we'll send you an unedited list of all the installations we have in our records. Chances are, you'll spot a few colleagues whom you know, and can then find out about this phenomenon in the x-ray business: a manufacturer with no unhappy customers.

Why, you might even want to become a customer yourself!

AMRAD®
AMERICAN RADIOLOGIC
SYSTEMS, Inc.
2055 N. Janice Ave.
Melrose Park, Ill. 60160
(312) 865-2600

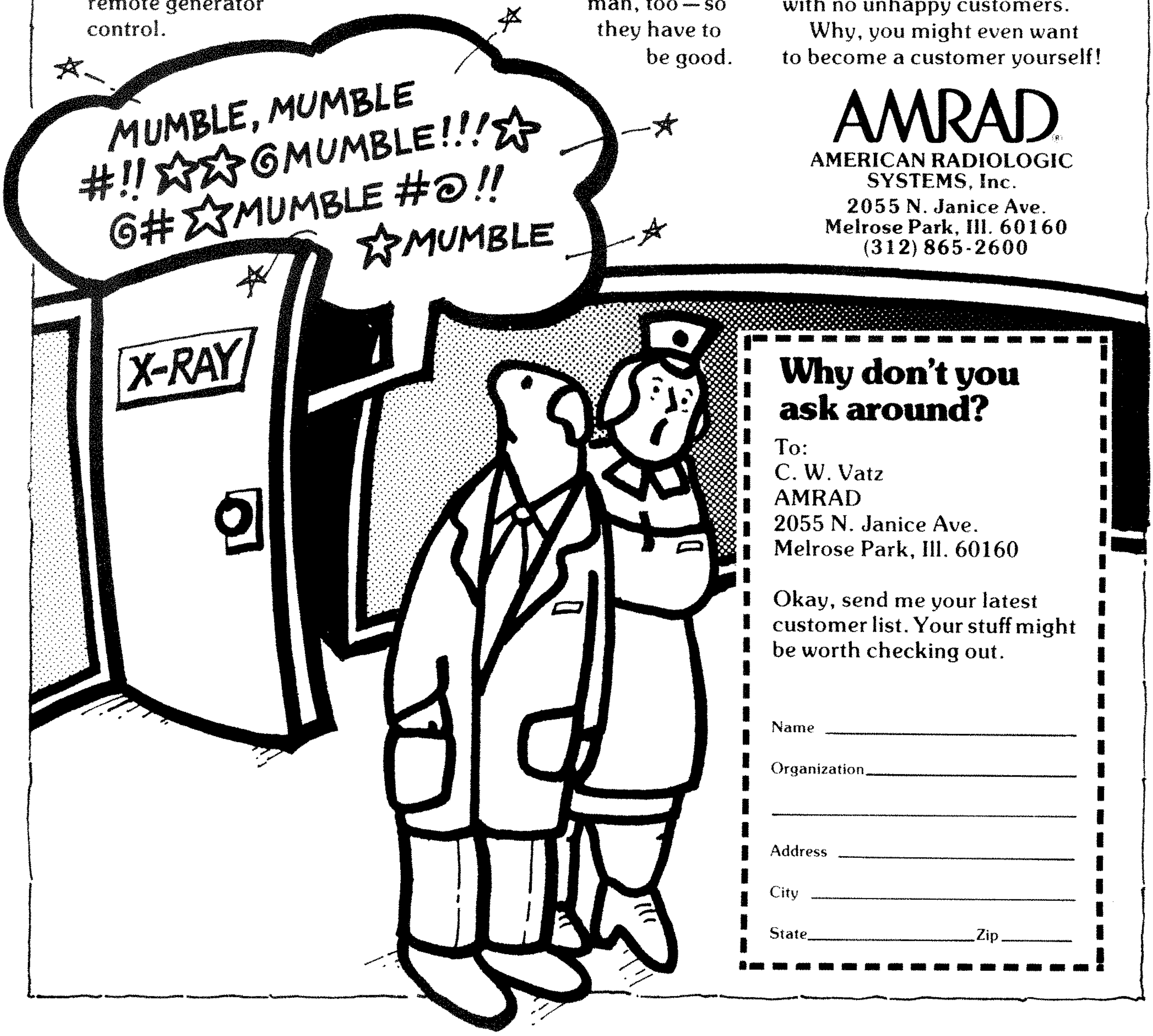
MUMBLE, MUMBLE #!! ☆☆ @MUMBLE!!!☆ @#☆MUMBLE #@!! ☆MUMBLE
X-RAY

Why don't you ask around?

To:
C. W. Vatz
AMRAD
2055 N. Janice Ave.
Melrose Park, Ill. 60160

Okay, send me your latest customer list. Your stuff might be worth checking out.

Name ____________________

Organization ____________________

____

Address ____________________

City ____________________

State ____________ Zip ________

For Double Contrast Stomachs, Use

NEW! E-Z-HD™

High Density with High Fluidity Barium Sulfate for Suspension USP

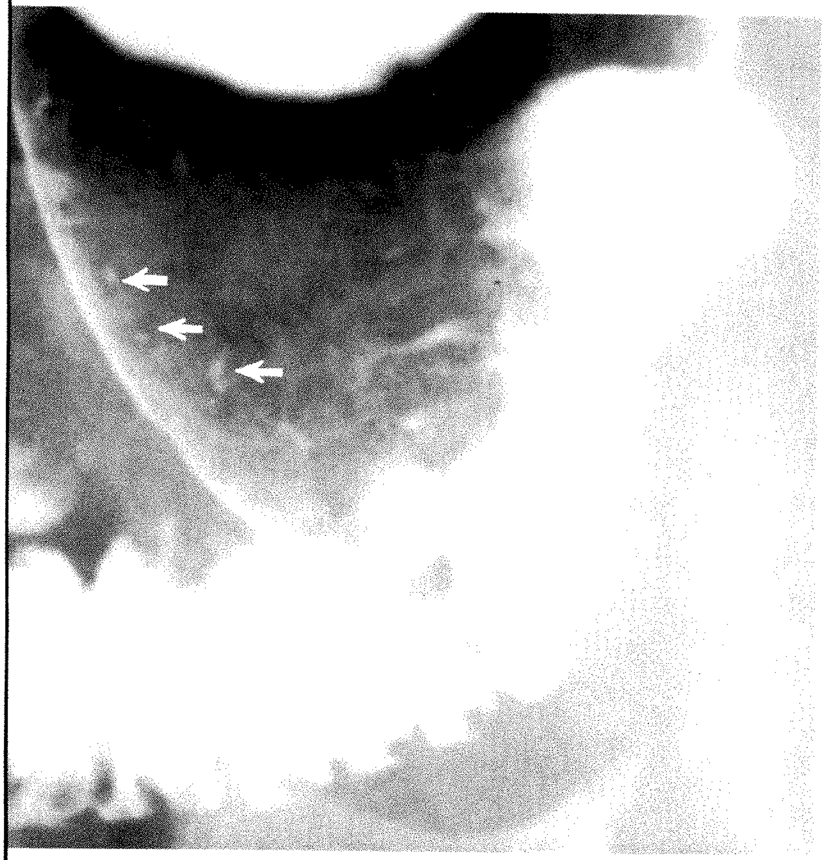

Note the Demonstration of Superficial Erosions

Double contrast radiography appears to offer the potential for significant improvements in diagnostic accuracy.

Double contrast studies of the stomach best demonstrate the surface pattern of the stomach (areae gastricae). This leads to improved detection of superfical erosions and ulcers, malignancies, polyps and other benign tumors, and ulcer scars.

E-Z-HD barium sulfate provides the basic ingredient necessary for good double contrast of the stomach.

The higher the density of the barium suspension, the better the coating, E-Z-HD allows for the highest density suspension of any commercial product on the market today: 85% w/w, 250% w/v. E-Z-HD achieves this density while remaining fluid for ease of administration.

- High density
- High fluidity
- Palatable
- Unit dose convenience.

E-Z-HD – The barium for the double contrast examination of the stomach and duodenum.

Optimal Density & Fluidity for the Modern Double Contrast Examination of the Stomach and Duodenum

Refrences:

David W. Gelfand: The Japanese-Style Double Contrast, Examination of the Stomach, Gastrointest Radiol. 1, 7-17 (1976)

Igor Laufer: The Diagnostic Accuracy of Barium Studies of the Stomach and Duodenum – Correlation with Endoscopy, Radiology 115: 569-573, June 1975

Roscoe E. Miller: The Air Contrast Stomach Examination: an overview. Radiology 117: 743-744 Dec. 1975

E-Z-EM

For Further Information Write:

7 Portland Ave.
Westbury, New York 11590
(516) 333-8230

9/76

American Journal of Roentgenology

Vol. 129 **July 1977** **No. 1**

DIAGNOSTIC IMAGING

Impact of Computed Tomography on Utilization of Cerebral Angiograms. *E. B. Larson, G. S. Omenn, M. T. Margolis, and J. W. Loop* 1
Computed Tomography in Cerebral Hemiatrophy. *C. G. Jacoby, R. T. Go, and F. J. Hahn* 5
Refinements in Chiba Needle Transhepatic Cholangiography. *J. T. Ferrucci, Jr., and J. Wittenberg* 11
CT Demonstration of the Splenic Vein–Pancreatic Relationship: The Pseudodilated Pancreatic Duct. *F. E. Seidelmann, W. N. Cohen, P. J. Bryan, and J. Brown* 17
Retrospective Comparison of Radionuclide Scans and Computed Tomography of the Liver and Pancreas. *R. L. MacCarty, H. W. Wahner, D. H. Stephens, P. F. Sheedy, and R. R. Hattery* 23
Calcitonin Treatment in Hereditary Bone Dysplasia with Hyperphosphatasemia: A Radiographic and Histologic Study of Bone. *J. P. Whalen, M. Horwith, L. Krook, I. MacIntyre, E. Mena, F. Viteri, B. Torun, and E. A. Nunez* 29
Neonatal Mucolipidosis II (I-Cell Disease): Clinical and Radiologic Features in Three Cases. *H. B. Patriquin, P. Kaplan, H. P. Kind, and A. Giedion* 37
Unilateral Locked Facet in Cervical Spine Injuries. *A. T. Scher* 45
Injuries of the Medial Epicondylar Ossification Center of the Humerus. *J. W. Chessare, L. F. Rogers, H. White, and M. O. Tachdjian* 49
Laminar Avulsion in a Cervical Vertebra. *C. V. Cimmino and D. W. Scott, III* 57
Radiographic Manifestations of Bone Metastases from Renal Carcinoma. *G. S. Forbes, R. A. McLeod, and R. R. Hattery* 61
Testicular Venography for Undescended Testes. *M. G. Glickman, R. M. Weiss, and Y. Itzchak* 67
Testicular Venography in the Nonpalpable Testis. *A. B. Diamond, C. H. Meng, M. Kodroff, and S. M. Goldman* 71
Polyarteritis Nodosa and Hepatitis-B Surface Antigen: Role of Angiography in Diagnosis. *R. G. Fisher, D. Y. Graham, M. Granmayeh, and J. G. Trabanino* 77
Computed Tomography in the Diagnosis of Subcapsular and Perirenal Hematoma. *E. G. Schaner, J. E. Balow, and J. L. Doppman* 83
Visualization of the Medullary Rays on Excretory Urography in Experimental Ureteric Obstruction. *L. R. Bigongiari, R. Davis, W. G. Novak, J. D. Wicks, E. Kass, and J. R. Thornbury* 89
Parenchymal Striations in Renal Vein Thrombosis: Arteriographic Demonstration. *J. D. Wicks, L. R. Bigongiari, W. D. Foley, and J. Walter* 95
Transitional Cell Tumors of the Kidney: How Diagnostic is the Angiogram? *S. M. Goldman, C. H. Meng, R. I. White, R. C. Naraval, S. S. Siegelman, A. B. Diamond, S. L. Kaufman, and D. P. Harrington* 99
Sarcoma of the Kidney: Angiographic Features. *M. Granmayeh, S. Wallace, A. F. Barrett, R. Fisher, and J. H. Heslep* 107
Ultrasonic Evaluation of the Obstructed Duplex Kidney. *V. J. Mascatello, E. H. Smith, G. F. Carrera, M. Berger, and R. L. Teele* 113
Stereotaxic Instrument for Needle Biopsy of the Mamma. *J. Bolmgren, B. Jacobson, and B. Nordenström* 121
Severe Radiation Injuries of the Lung. *B. Roswit and D. C. White* 127
Diagnostic Oncology Case Studies: Metastatic Carcinoma Presenting as Shoulder Arthritis. *Contributed by A. Fremland* 137

CASE REPORTS

Thoracic Wall Invasion Secondary to Pulmonary Aspergillosis: A Complication of Chronic Granulomatous Disease of Childhood. *A. R. Altman* 140
Calcification in a Paraspinal Malignant Melanoma in a Child. *P. Stanley, S. E. Siegel, and H. Isaacs* 143
Catheter Venography in the Superior Vena Cava Syndrome. *W. R. Webb, G. Gamsu, and B. M. Rohlfing* 146
Cerebrospinal Fluid Rhinorrhea Demonstrated by Metrizamide CT Cisternography. *B. P. Drayer, R. H. Wilkins, M. Boehnke, J. A. Horton, and A. E. Rosenbaum* 149
Inadvertent Intrasplenic Injection of Oily Propyliodone. *E. Braunstein* 152
Absent Arch and Hypoplastic Pedicle: Another Confusing Cervical Spine Anomaly. *N. A. Kirchmer and M. Sarwar* 154
Spurs of the Mandible and Supracondylar Process of the Humerus in Cornelia de Lange Syndrome. *J. A. Curtis, A. E. O'Hara, and G. G. Carpenter* 156
Glucagon-producing Islet Cell Tumor of the Pancreas. *K. J. Cho, C. W. Wilcox, and S. R. Reuter* 159
Multiple Primary Hemangiomas of Bone. *C. A. Karlin and A. C. Brower* 162

TECHNICAL NOTE

Keyhole Cone Device for Lateral Magnification Cerebral Angiography. *R. L. Mani and R. C. Gross* 165

SPECIAL SECTION

Committee Report: Contrast Media in Diagnostic Radiology: Recommendations for Labels, Package Inserts, and Dosage Determination. *W. H. Shehadi* 167
The Federal Government's Impact on Radiology. *R. D. Moseley, Jr., and O. W. Linton* 171

Guest Editorials:
- **Therapeutic Value of Thyreocalcitonin.** *J. Caffey* 175
- **The Federal Crossword Puzzle.** *R. D. Moseley and O. W. Linton* 176

78th ARRS Meeting Preliminary Program 179
Letters 182
Abstracts of Current Literature 184
Book Reviews 198
News 204

19.12.77

AJR

American
Journal of
Roentgenology

September 1977

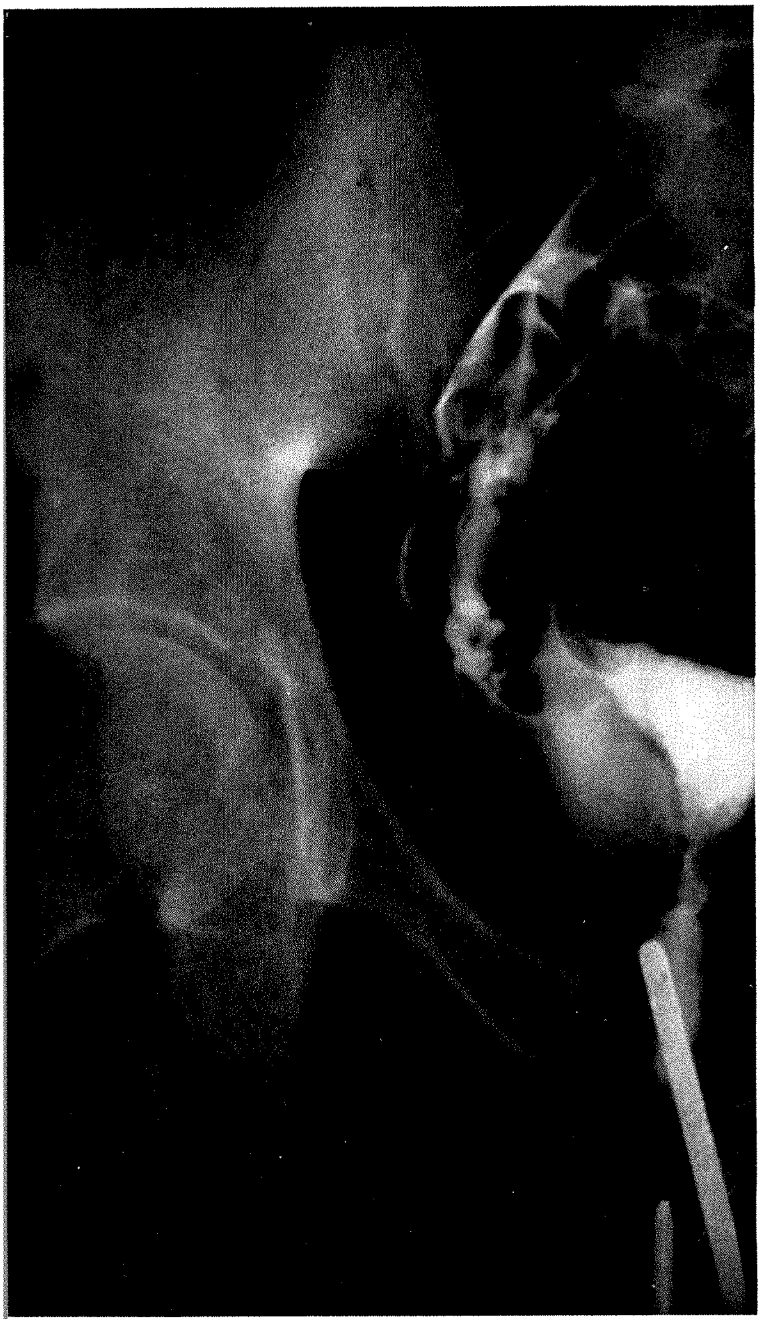

Hysterosalpingogram with Salpix Contrast Medium.

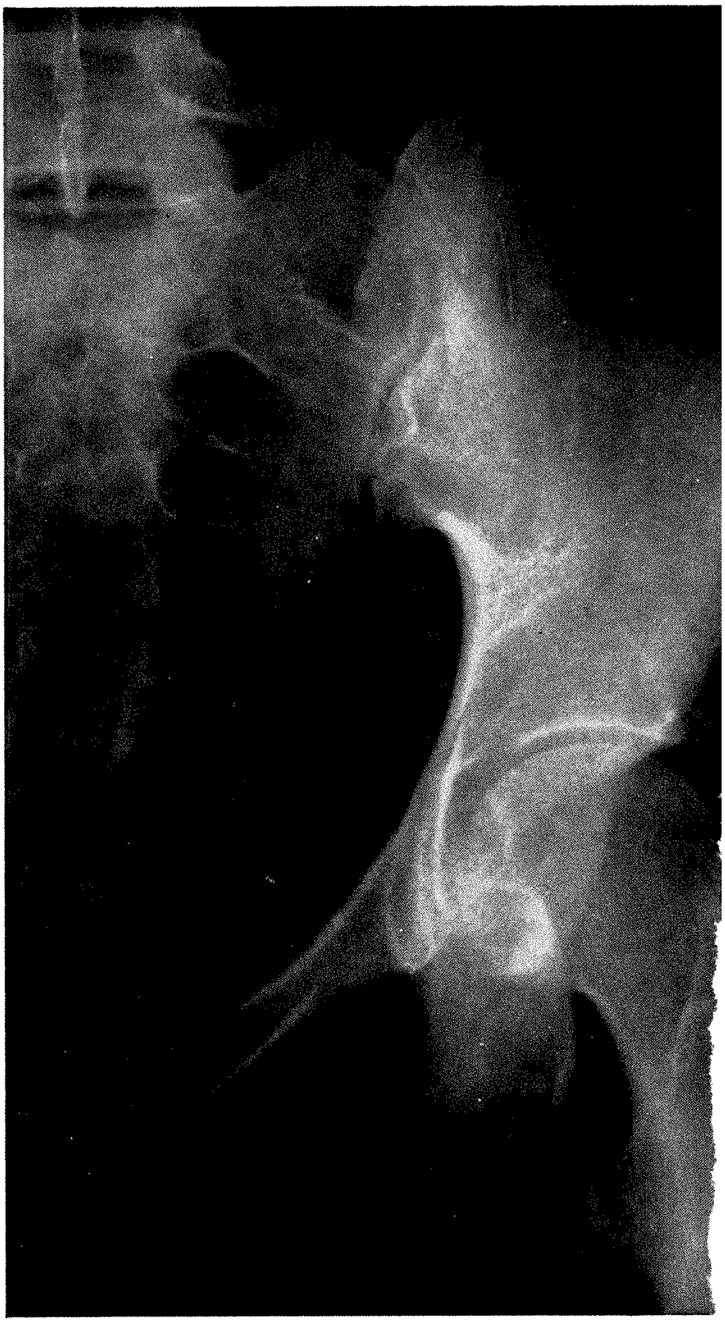

24-hour postinjection x-ray of same patient.

now you see it now you don't

With Salpix as your contrast medium, your gynecologic patient needn't undergo the 24-hour postinjection x-ray usually required with iodized oils. Water-soluble Salpix leaves virtually no irritating radiopaque residue to produce foreign-body reactions, yet it provides the viscosity needed for adequate visualization.

Contraindications: Contraindications to hysterosalpingography include the presence of severe vaginal or cervical infections, existing or recent pelvic infection, marked cervical erosion or endocervicitis, and pregnancy. The procedure is contraindicated during the immediate pre- or post-menstrual phase.

Sensitivity Test: If indicated in the patient's history, an intracutaneous skin test or sublingual absorption observation may be done with 0.1 cc Salpix.

Warning: Not for intravenous use.

© ORTHO PHARMACEUTICAL CORPORATION 1970

Salpix CONTRAST MEDIUM

TRADEMARK

EACH CC CONTAINS:
sodium acetrizoate 0.53 g and
polyvinylpyrrolidone 0.23 g

Ortho

ORTHO PHARMACEUTICAL CORPORATION • RARITAN, NEW JERSEY 08869

Official Journal
American Roentgen Ray Society
American Radium Society

AJR

Including Diagnostic Radiology • Radiation Oncology • Nuclear Medicine Ultrasonography • Related Sciences

Editor Melvin M. Figley

Assistant Editor Rosalind H. Troupin

Editor Emeritus Traian Leucutia

Associate Editors Luther W. Brady • Kenneth L. Krabbenhoft • E. Frederick Lang • Russell H. Morgan

Consulting Editorial Board Kent Ellis • E. Robert Heitzman • Donald L. King • John A. Kirkpatrick, Jr. Eugene C. Klatte • John G. McAfee • Thomas H. Newton Robert G. Parker • Stewart R. Reuter • William B. Seaman • Robert J. Shalek • John Storer • Michel M. Ter-Pogossian • Joseph P. Whalen • David M. Witten

Editorial Staff K. A. Murray, manager • M. B. Wieckowicz, manuscript editor • M. J. Leonard, assistant manuscript editor • C. P. Kaiser, secretary

Published monthly by Charles C Thomas, 301-327 East Lawrence Avenue, Springfield, Illinois 62717. All correspondence, except editorial office business, should be addressed to the publisher. Annual subscription prices: United States and possessions, $40; others, $50; residents in training in U.S., $20 (letter from department required with dates of residency); single copies, $5. Foreign subscription delivery not guaranteed. Undelivered or damaged copies replaced within 60 days of publication; 90 days for foreign subscribers. Allow 90 days for address changes. © 1977 by American Roentgen Ray Society. Second-class postage paid at Springfield, Illinois, and at additional mailing offices. Printed in U.S.A.

American Roentgen Ray Society

OFFICERS 1976–1977

President: Seymour F. Ochsner
President Elect: Harry Z. Mellins
1st Vice-president: E. Frederick Lang
2nd Vice-president: Richard G. Lester
Secretary: James F. Martin
Treasurer: Joseph D. Calhoun

COMMITTEES 1976–1977

Executive Council: S. F. Ochsner, H. Z. Mellins, E. F. Lang, R. G. Lester, J. F. Martin, J. D. Calhoun, M. M. Figley, T. Leucutia, H. C. Carlson, R. A. Alfidi, R. A. Gagliardi, A. E. James, E. Gedgaudas, G. A. Kling, T. F. Leigh, C. B. Holman, R. Buenger, E. C. Klatte, J. P. Tampas, J. L. Gwinn, C. E. Bickham, Jr., chairman

Finance and Budget: R. G. Evens, J. P. Tampas, R. McLelland, J. L. Gwinn, H. G. Carlson

Publications: K. Ellis, F. F. Ruzicka, Jr., E. R. Heitzman, J. V. Rogers, Jr., R. A. Gagliardi, chairman

Editorial Policy: M. M. Figley, E. F. Lang, L. Brady, K. Krabbenhoft, R. Morgan, E. R. Heitzman, J. V. Rogers, K. Ellis, F. F. Ruzicka, Jr., R. A. Gagliardi, chairman

Advisory Committee on Education and Research: G. Wilson, G. W. Hartman, L. F. Rogers, E. Gedgaudas, A. E. James, chairman

Scientific Exhibits: G. Dodd, B. G. Brogdon, R. A. Alfidi, chairman

Constitution and Bylaws: J. H. Walker, W. M. Whitehouse, J. P. Tampas, chairman

American Board of Radiology Representatives: J. F. Roach, R. W. McConnell, S. W. Nelson

Program Committee: S. F. Ochsner, J. F. Martin, C. E. Bickham, Jr., M. M. Figley, R. A. Gagliardi, R. A. Alfidi, E. Gedgaudas, G. A. Kling, A. E. James, H. Z. Mellins, chairman

Instruction Courses: E. Gedgaudas, director; H. O. Peterson, associate director

American College of Radiology Board of Chancellors Representative: W. B. Seaman

Annual Meeting: September 27–30, 1977, Sheraton Hotel, Boston, Massachusetts

Scientific Program: Harry Z. Mellins, president-elect, Peter Bent Brigham Hospital, Boston, Massachusetts

Manager Annual Meeting: George A. Kling, Harper Hospital, Detroit, Michigan

Membership: Charles E. Bickham, Jr., Suburban Hospital, 8600 Old Georgetown Road, Bethesda, Maryland 20014

Business Office: Keith W. Gundlach, comptroller, American College of Radiology, 20 North Wacker Drive, Chicago, Illinois 60606

American Radium Society

OFFICERS 1977–1978

President: Richard H. Jesse
President Elect: Frederick W. George
1st Vice-president: Ivor Fix
2d Vice-president: John Durant
Secretary: Alfred S. Ketcham
Treasurer: Simon Kramer

COMMITTEES 1977–1978

Executive: F. Rutledge, L. W. Brady, R. H. Jesse, F. W. George, I. Fix, J. Durant, S. Kramer, A. S. Ketcham, V. Marcial, chairman

Public Relations: C. Honaker, R. H. Jesse, chairman

Publication: K. L. Krabbenhoft, A. F. Schroeder, G. Seydel, D. Hussey, A. Raventos, L. W. Brady, chairman

Scientific Program: F. George, D. Johnson, M. Boone, P. Chretien, P. J. DiSaia, D. Hussey, R. C. Landgren, C. Perez, S. T. Cantril, R. H. Jesse, chairman

Local Arrangements: J. Helsper, J. J. Romagosa, J. M. Thomson, Jr., A. J. Ballantyne, S. Kramer, S. Ochsner, chairman

Nominating: M. Kligerman, G. Lewis, J. Vaeth, chairman

Constitution and By-Laws: A. S. Glicksman, P. J. DiSaia, K. L. Krabbenhoft, chairman

Janeway Lecture: S. Levitt, L. Davis, A. S. Ketcham, chairman

Audiovisual: C. R. Bogardus, J. Helsper, B. Herrington, L. Bloebaum, C. Honaker, F. George, chairman

Resident Essay: J. T. Phillips, J. Curry, R. Schweitzer, J. T. Wharton, chairman

American Board of Radiology, Representatives: J. J. Stein, R. E. King, N. duV Tapley

American College of Radiology Board of Chancellors Representative: L. W. Brady

American College of Radiology Council Representative: J. del Regato

Editorial Board of AFCOS Newsletter Representative: J. Vaeth

National Council on Radiation Protection and Measurements Liason Representative: L. W. Davis

Annual Meeting: April 26–30, 1978, Marriott Hotel, New Orleans, Louisiana

Scientific Program: R. H. Jesse, M. D. Anderson Hospital, 6723 Bertner Drive, Houston, TX 77030

Local Arrangements: S. Ochsner, 1514 Jefferson Highway, New Orleans, LA 70121

Membership: A. S. Ketcham, secretary, University of Miami School of Medicine, P.O. Box 520875 Biscayne Annex, Miami, Florida 33152

Business Office: N. V. Jordan, c/o R. H. Jesse, M. D. Anderson Hospital and Tumor Institute, 6723 Bertner Avenue, Houston, Texas 77030

Liquid Polibar with Super XL

A Total System

For double-contrast examination of the colon.

Satisfactory results in the double-contrast examination of the colon require special attention to two aspects of the procedure.

First, the barium sulfate formulation. Our Liquid Polibar (56% w/w) is a bubble-free, non-precipitating uniform suspension formulation ... with proper flow and coating characteristics. No blending required and once routines are established, you can rely on its consistency.

The second concern is with the proper apparatus. The E-Z-EM system is unique in that 1/2" lumen tubing attached to the enema bag is utilized – for freer, more uniform flow. Miller Air Retention Tip, with or without optional cuff completes the system.

A total system for ease of administration and consistently reliable radiological results. For additional literature, write:

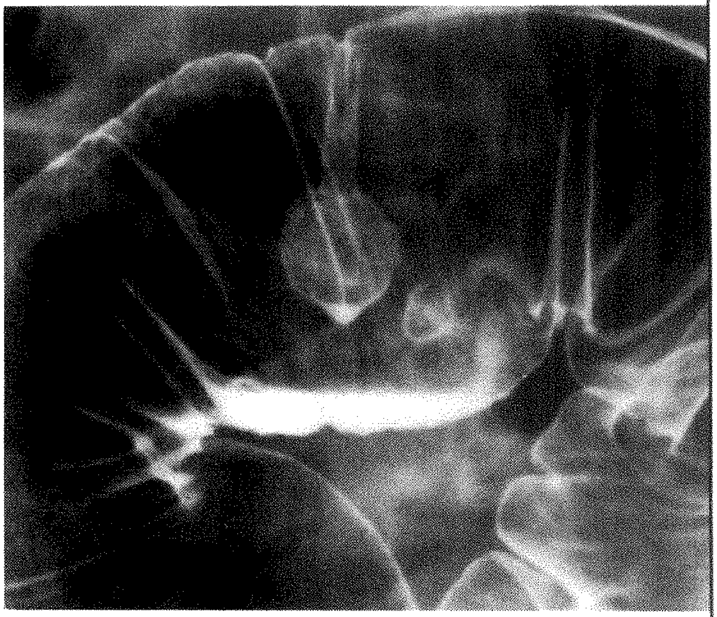

One pedunculated and one smaller sessile polyp at the apex of the sigmond loop.

Film Courtesy of Richard Palmer Gold M.D. Columbia Presb. Medical Center N.Y

E-Z-EM
7 Portland Ave.
Westbury, New York 11590
(516) 333-8230

1/77

International Affiliates: E-Z-EM Rooster B. V., Infirmeriestraat 6-8, Rotterdam 16, Netherlands
E-Z-EM De Mexico, S. A. de C. V., Calz. Azcapotzalco La Villa No 882, Zona Industrial Vallejo, Mexico 16 D. F.

Fleet® Barium Enema Prep Kits: Make us your first choice for fewer retakes.

The greatest defect in colon examinations is in the preparation of the colon.[1]

Fleet® Barium Enema Prep Kits systematize and improve colon prepping because they conform to the recommended method which provides a combination of diet, hydration and proven laxation which stimulates the large and small intestines.[2] The result? Cleaner colons, clearer x-rays and fewer retakes.

All Fleet Prep Kits offer three laxative steps: 1½ oz. of Fleet® Phospho®-Soda followed by four Fleet® Bisacodyl tablets, plus a final cleansing step. Prep Kit 1 offers Fleet® Bisacodyl suppository. Prep Kit 2 offers a large-volume disposable Fleet® Bagenema. And Prep Kit 3 offers our new Fleet® Bisacodyl enema. And all three Prep Kits have easy-to-follow instructions with a choice of flexible time-tables to fit your schedule.

With Fleet Barium Enema Prep Kits, you'll be sure of convenient, dependable, effective colon prepping every time. And that's reason enough to make Fleet Prep Kits your first choice for fewer retakes.

NDC 0132-0211-01
Fleet. Barium Enema Prep Kit 1
CONTENTS: FLEET® PHOSPHO-SODA BUFFERED SALINE LAXATIVE, 1½ FL. OZ. (45 ML.); FLEET® BISACODYL, NF CONTACT LAXATIVE, 4 ENTERIC-COATED TABLETS, 5 MG EA.; FLEET® BISACODYL, NF CONTACT LAXATIVE, 1 SUPPOSITORY, 10 MG.
NDC 0132-0210-01
Fleet. Barium Enema Prep Kit 2
CONTENTS: FLEET® PHOSPHO-SODA BUFFERED SALINE LAXATIVE, 1½ FL. OZ. (45 ML); FLEET® BISACODYL, NF CONTACT LAXATIVE, 4 ENTERIC-COATED TABLETS, 5 MG EA; FLEET® BAGENEMA, 1 UNIT; SOAPSUDS PACKET (1)
NDC 0132-0212-01
Fleet. Barium Enema Prep Kit 3
CONTENTS: FLEET® PHOSPHO-SODA BUFFERED SALINE LAXATIVE, 1½ FL. OZ. (45 ML); FLEET® BISACODYL, NF CONTACT LAXATIVE, 4 ENTERIC-COATED TABLETS, 5 MG EA.; FLEET® READY-TO-USE BISACODYL ENEMA, 10 MG BISACODYL, U.S.P.
Fleet. Phospho-soda buffered saline laxative
Fleet. ready-to-use bisacodyl enema
Comfortip

Fleet Barium Enema Prep Kits
for cleaner colons, clearer x-rays and fewer retakes.

Fleet pharmaceuticals
C.B. Fleet Co., Inc.
Lynchburg, Va. 24505

---

[1] Dr. R.E. Miller, Ad Hoc Committee on Detection of Cancer of the Colon, Detection of Colon Lesions, American College of Radiology, (Chicago, Ill., 1973) p. 76.

[2] Dr. W.R. Eyler, Ibid. pp. 203, 204.

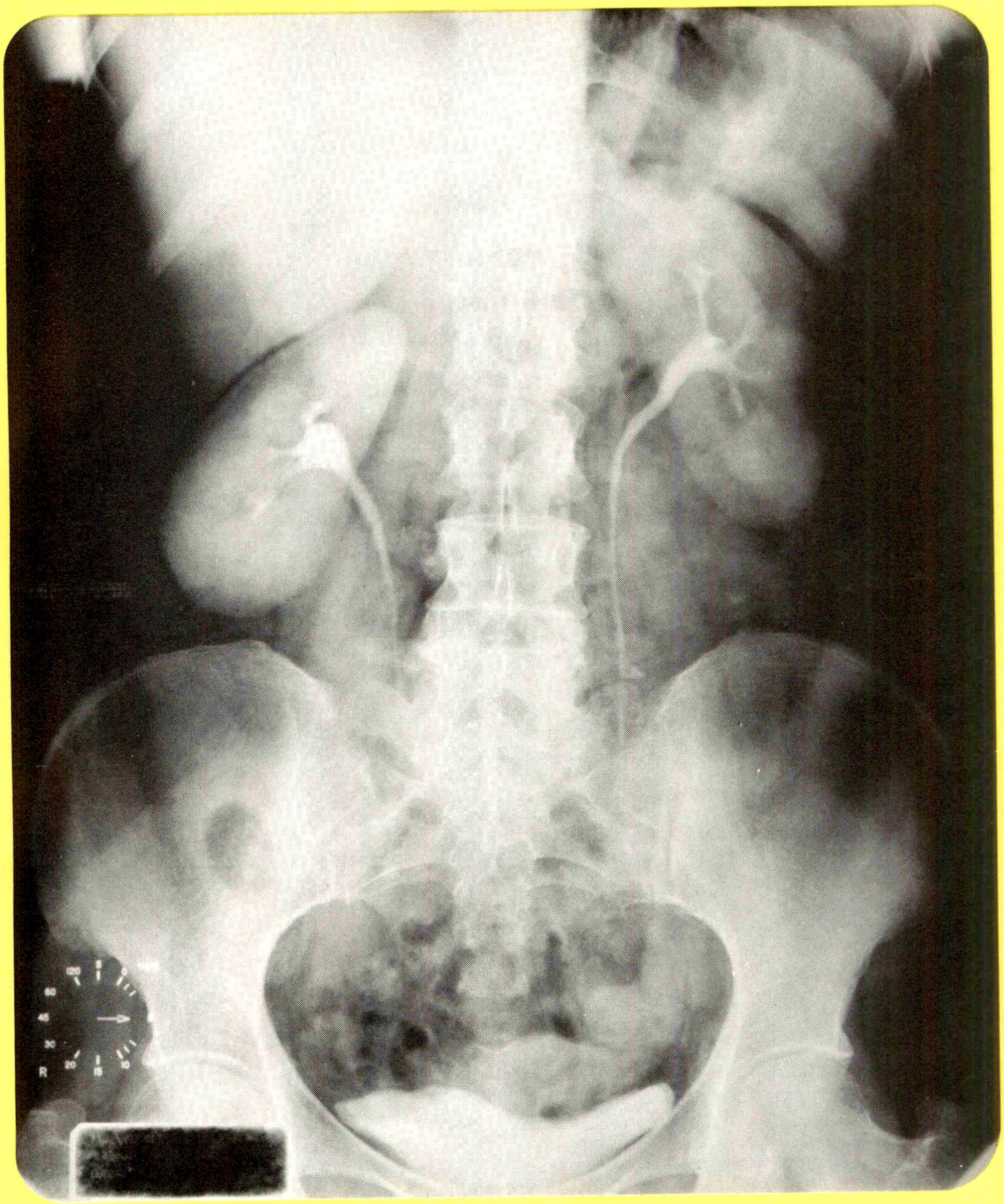

[redacted]

Excellent visualization in intravenous pyelogram 18 hours after administration of 2½ oz. X-PREP Liquid for preradiographic bowel cleansing. (In the files of the Medical Department of The Purdue Frederick Company.)

To prep the bowel for intravenous pyelography

X-PREP® Liquid

(standardized extract of senna fruit)

One step • One dose • One bottle

☐ X-PREP Liquid is designed specifically for preradiographic bowel cleansing—without enemas, suppositories or overhydration.

☐ A single 2½ oz. oral dose is usually all that is required. No residual oil droplets (such as may occur with castor oil).

☐ Pleasant taste meets with high patient acceptance. Ease of administration is appreciated by the patient and nursing staff.

Gray Pharmaceutical Co., Affiliate
The Purdue Frederick Company

© COPYRIGHT 1975, GRAY PHARMACEUTICAL CO./NORWALK, CONN. 06856 A7901 160875

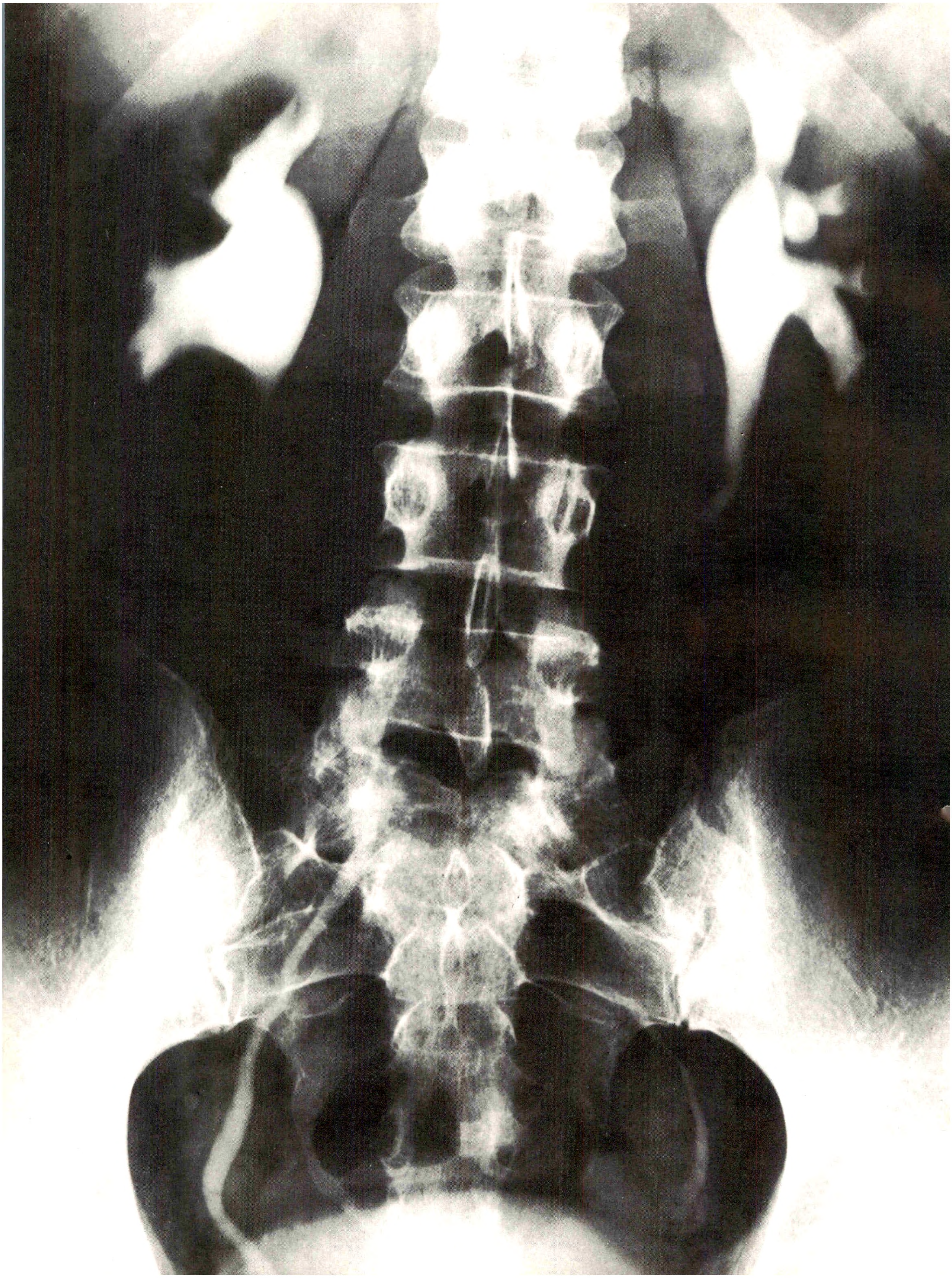

SQUIBB®

The leader in
radiologic
diagnostics

contrast media™

in excretion urography

the reason is clear™

proven diagnostic excellence and rapid visualization

- Rapid concentration of relatively large quantity of medium permits thorough evaluation of urinary tract anatomy.
- Visualization of renal passages may begin as early as 5 minutes after injection.

9 indications

drip infusion pyelography
excretion urography (direct I.V.)
peripheral arteriography
cerebral angiography
venography
splenoportography

operative, T-tube, and
percutaneous transhepatic
cholangiography
arthrography
discography

Renografin®-60

Diatrizoate Meglumine and Diatrizoate Sodium Injection U.S.P.

See next
page for
brief summary.

RENOGRAFIN®-60
Diatrizoate Meglumine and Diatrizoate Sodium Injection U.S.P.

CONTRAINDICATIONS: Contraindicated in persons hypersensitive to salts of diatrizoic acid. **Urography** is contraindicated in patients with anuria. A prothrombin time below 50% and evidence of coagulation defects are contraindications to **percutaneous transhepatic cholangiography** and **splenoportography.** When splenectomy is contraindicated, splenoportography should not be performed since complications of the procedure make splenectomy necessary at times. Significant thrombocytopenia and any condition which may increase the possibility of splenic rupture are contraindications to **splenoportography. Arthrography** is contraindicated if infection is present in or near the joint. **Discography** is contraindicated if there is infection or open injury near the region to be examined.

WARNINGS: A definite risk exists with the use of contrast agents in excretion urography in patients with multiple myeloma. There has been anuria with progressive uremia, renal failure and death. This risk of the procedure in these patients is not a contraindication; however, partial dehydration in preparation for study is not recommended since it may predispose for precipitation of myeloma protein in renal tubules. No therapy, including dialysis, has been successful in reversing this effect. Myeloma should be considered in persons over 40 before undertaking urographic procedures.

In cases of known or suspected pheochromocytoma, if the physician feels that the possible benefits outweigh the considered risks, radiopaque materials should be administered with extreme caution; however, an absolute minimum of material should be injected, the blood pressure should be assessed throughout the procedure, and measures for treating a hypertensive crisis should be available.

Contrast media may promote sickling in homozygous individuals when injected I.V. or intra-arterially. Although a history of sensitivity to iodine *per se* or to other contrast media is not an absolute contraindication, administration of diatrizoate requires extreme caution in such cases. Perform thyroid function tests prior to administration of this preparation since iodine-containing contrast agents may alter the test results. Avoid accidental introduction of this preparation into the subarachnoid space since even small amounts may produce convulsions and possible fatal reactions.

Perform **cerebral angiography** with special caution in extreme age, poor clinical condition, advanced arteriosclerosis, severe arterial hypertension, cardiac decompensation, recent cerebral embolism, or thrombosis. Perform **urography** with extreme caution in persons with severe concomitant hepatic and renal disease.

Usage in Pregnancy: This preparation should be used in pregnant patients only when the physician deems its use essential to the welfare of the patient since safe use during pregnancy has not been established.

PRECAUTIONS: Diagnostic procedures involving use of contrast agents should be performed under the direction of personnel with prerequisite training and a thorough knowledge of the particular procedure. Appropriate facilities should be available for coping with situations which may arise as a result of the procedure and for emergency treatment of severe reactions to the contrast agent itself; competent personnel and emergency facilities should be available for at least 30 to 60 minutes after I.V. administration since delayed reactions have been known to occur. These severe life-threatening reactions suggest hypersensitivity to the contrast agent. A personal or family history of asthma or allergy or a history of a previous reaction to a contrast agent warrants special attention and may predict more accurately than pretesting the likelihood of a reaction although not the type nor severity of the reaction in the individual. The value of any pretest is questionable. The pretest most performed is the slow I.V. injection of 0.5-1.0 ml. of the preparation prior to injection of the full dose; however, the absence of a reaction to the test dose does not preclude the possibility of reaction to the full diagnostic dose. Should the test dose produce an untoward response, the necessity for continuing the examination should be carefully re-evaluated; if deemed essential, examination should proceed with all possible caution. In rare instances, reaction to the test dose may be extremely severe; therefore, close observation and facilities for emergency treatment appear indicated.

Renal toxicity has been reported in a few patients with liver dysfunction who were given oral cholecystographic agents followed by urographic agents; therefore, if known or suspected hepatic or biliary disorder exists, administration of Diatrizoate Meglumine and Diatrizoate Sodium Injection U.S.P. should be postponed following the ingestion of cholecystographic agents. Exercise caution with use of contrast media in severely debilitated patients and in those with marked hypertension. When percutaneous techniques are used, bear in mind the possibility of thrombosis. Consider the functional ability of the kidneys before injecting Diatrizoate Meglumine and Diatrizoate Sodium Injection U.S.P. Contrast agents may interfere with some chemical determinations made on urine specimens; therefore, collect urine before or two or more days after administration of the contrast medium.

In **peripheral arteriography,** hypotension or moderate decreases in blood pressure seem to occur frequently with intra-arterial (brachial) injections; this is transient and usually requires no treatment; monitor blood pressure during the immediate 10 minutes after injection. In **excretion urography,** adequate visualization may be difficult or impossible in uremic patients or others with severely impaired renal function (see Contraindications). Consider the increased osmotic load associated with drip infusion pyelography in presence of congestive heart failure. The diuretic effect of drip infusion pyelography may hinder assessment of residual urine in the bladder. Do not exceed recommended rate (40 ml./min.) of infusion. In **operative and T-tube cholangiography,** inject the contrast agent slowly to prevent extravasation into peritoneal cavity and to minimize reflux flow into pancreatic duct which may result in pancreatic irritation. In **percutaneous transhepatic cholangiography,** aspirate as much of the contrast agent as possible on completion of successful films to reduce possibility of bile leakage and consequent peritonitis. For 24 hours after the procedure carefully and constantly monitor all patients for signs of internal hemorrhage or bile leakage; if these complications are recognized immediately, remedial measures can be instituted promptly with minimal increase in morbidity. Percutaneous transhepatic cholangiography should be reserved for jaundiced patients who are not good candidates for surgery when requisite information has not been obtained with ordinary studies since the procedure is not without risks; attempt the procedure only when competent surgical intervention can be obtained promptly if needed. In **splenoportography,** manipulations which will prolong the time the needle is in the spleen should be avoided since this may contribute to postpuncture bleeding and subcapsular extravasation of the contrast agent. Following splenoportography, closely observe the patient for 24 hours for signs of internal bleeding; patient should lie on his left side for several hours. Leakage of up to 300 ml. of blood from the spleen is apparently not uncommon; fatal hemorrhage has occurred rarely. Blood transfusions and, rarely, splenectomy may be required. In **discography,** postpone the procedure if an infection (including U.R.I. in cervical discography) or open injury is present near the region to be examined to minimize possible introduction of infection. Disk infection has occurred after discography; therefore, care should be taken to preclude contamination and resultant disk infection. Contamination may be introduced into the disk if care is not taken to avoid puncturing the esophagus during cervical discography. If the needle becomes barbed by contact with bone (the two-needle technique helps reduce this hazard), rupture of the disk may occur; this is highly unlikely if the procedure is performed carefully.

ADVERSE REACTIONS: Nausea, vomiting, flushing, or a generalized feeling of warmth are the reactions seen most frequently with intravascular injection. Symptoms which may occur are chills, fever, sweating, headache, dizziness, pallor, weakness, severe retching and choking, wheezing, a rise or fall in blood pressure, facial or conjunctival petechiae, urticaria, pruritus, rash, and other eruptions, edema, cramps, tremors, itching, sneezing, lacrimation, etc. Antihistaminic agents may be of benefit; rarely, such reactions may be severe enough to require discontinuation of dosage. Severe reactions which may require emergency measures (see Precautions) are a possibility and include cardiovascular reaction characterized by peripheral vasodilatation with hypotension and reflex tachycardia, dyspnea, agitation, confusion, and cyanosis progressing to unconsciousness. An allergic-like reaction ranging from rhinitis or angioneurotic edema to laryngeal or bronchial spasm or anaphylactoid shock may occur. Temporary renal shutdown or other nephropathy may occur. Temporary neurologic effects of varying severity have occurred in a few instances particularly in cerebral angiography. There have been a few reports of a burning or stinging sensation or numbness, of venospasm or venous pain, and of partial collapse of the injected vein. Neutropenia or thrombophlebitis may occur.

Adverse reactions as a consequence of **excretion urography** have included cardiac arrest, ventricular fibrillation, anaphylaxis with severe asthmatic reaction, and flushing due to generalized vasodilation. **Cerebral angiography** has caused temporary neurologic complications such as induction of seizures (particularly in patients with convulsive disorders), confusional states or drowsiness, transient paresis, coma, temporary disturbances in vision, or seventh nerve weakness. During **peripheral arteriography,** hemorrhage from puncture site, thrombosis of the vessel, and brachial plexus palsy (following axillary artery injection) have occurred. Complications (in an estimated 4 to 6% of cases) of **percutaneous transhepatic cholangiography** include bile leakage (more likely in presence of complete obstruction due to carcinoma) and biliary peritonitis, gallbladder perforation, internal bleeding, gram-negative bacterial septicemia, and tension pneumothorax from inadvertent puncture of diaphragm and lung. During **splenoportography,** intraperitoneal extravasation of the medium may cause transient diaphragmatic irritation or mild to moderate transient pain which may sometimes be referred to the shoulder, periumbilical region, or other areas; accidental pneumothorax (because of proximity of pleural cavity) may occur. **Arthrography** may induce joint pain or increase existing pain (usually immediate and transient but may be delayed or prolonged up to 24 hours) particularly with large doses and extravasation of medium into soft tissue surrounding the joint. Lipid-like histiocytes have been found in tissue removed following arthrography. The technique of **discography** may be painful particularly when disk pathology exists; pain on injection may also be related to volume of the dose; the nature of the disk pathology or extravasation of the medium may cause referred pain.

Bear in mind the possibility of thrombosis or of other complications due to mechanical trauma when any percutaneous technique is used.

For full information, consult package insert.

HOW SUPPLIED: Renografin-60 (Diatrizoate Meglumine and Diatrizoate Sodium Injection U.S.P.) is a sterile aqueous solution providing 52% diatrizoate meglumine and 8% diatrizoate sodium; the solution contains approximately 29% (288 mg./ml.) bound iodine, 0.32% sodium citrate (buffer), 0.04% edetate disodium (sequestering agent); *the solution contains approximately 3.76 mg. (0.16 mEq.) sodium per ml.* Available in 10, 30, and 50 ml. single-dose vials and in 100 ml. single-dose bottles.

© 1977 E. R. Squibb & Sons, Inc. H657-504

SQUIBB®

contrast media™

SQUIBB HOSPITAL DIVISION
E.R. Squibb & Sons, Inc.
P.O. Box 4000 Princeton, N.J. 08540

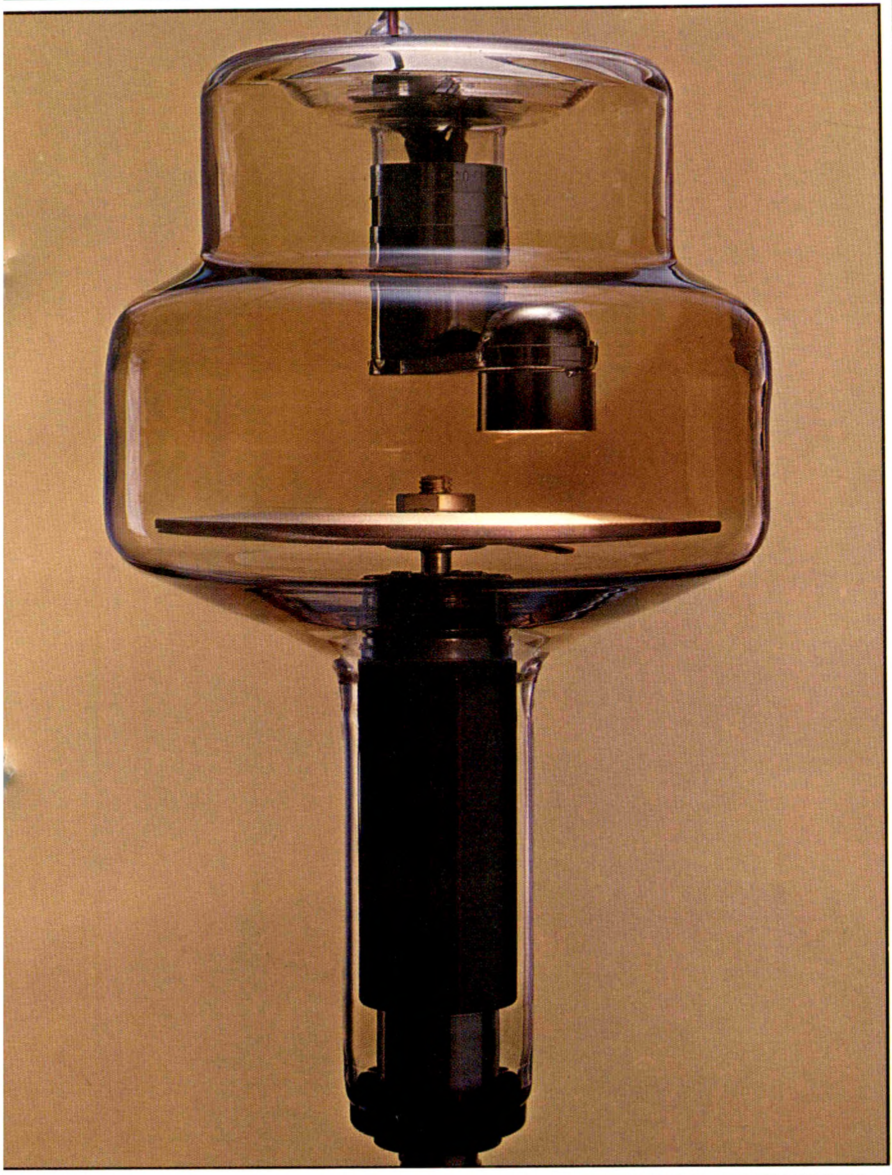

Machlett for high-power angiography

procedure-designed dynamax 78E 15/100 x-ray tube

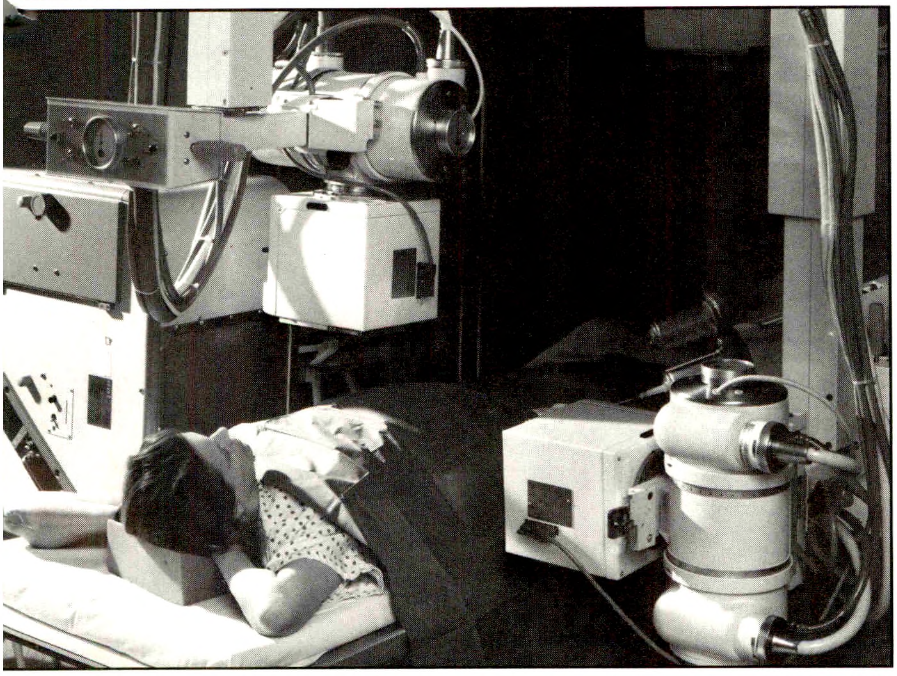

Designed for the exacting techniques of high-power cardiac and abdominal angiography, the Dynamax 78E 15/100 is rated at 100 KW, with the large focus allowing for heavy-duty angiographic factors within the functional range of conventional films and screens.

With the small focus biased, the Dynamax 78E 15/100 will resolve 5.9 line pairs per millimeter at 2-power magnification at 150 mA and 80 kVp.

The Dynamax 78E's high thermal capacity (400kHU) makes it ideally suited for rapid film techniques, providing for high patient volumes and repetitive studies without lengthy cooling periods.

For complete technical information on the Dynamax 78E 15/100, or for consultation relative to its application, contact your x-ray dealer or

MACHLETT

The Machlett Laboratories, Incorporated
1063 Hope St.
Stamford, Connecticut 06907
(203) 348-7511

A Raytheon Company

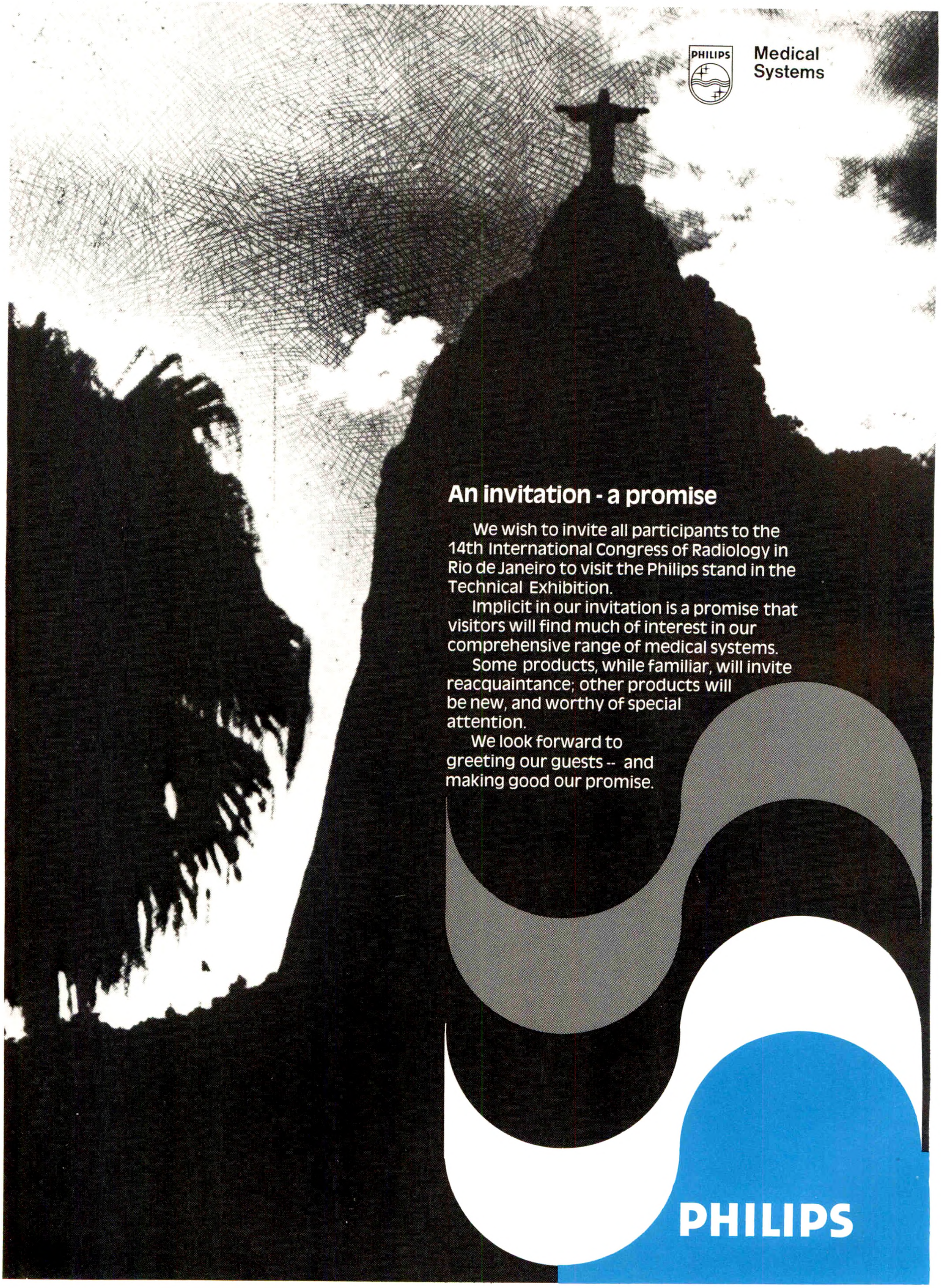

PHILIPS Medical Systems

An invitation - a promise

We wish to invite all participants to the 14th International Congress of Radiology in Rio de Janeiro to visit the Philips stand in the Technical Exhibition.

Implicit in our invitation is a promise that visitors will find much of interest in our comprehensive range of medical systems.

Some products, while familiar, will invite reacquaintance; other products will be new, and worthy of special attention.

We look forward to greeting our guests -- and making good our promise.

PHILIPS

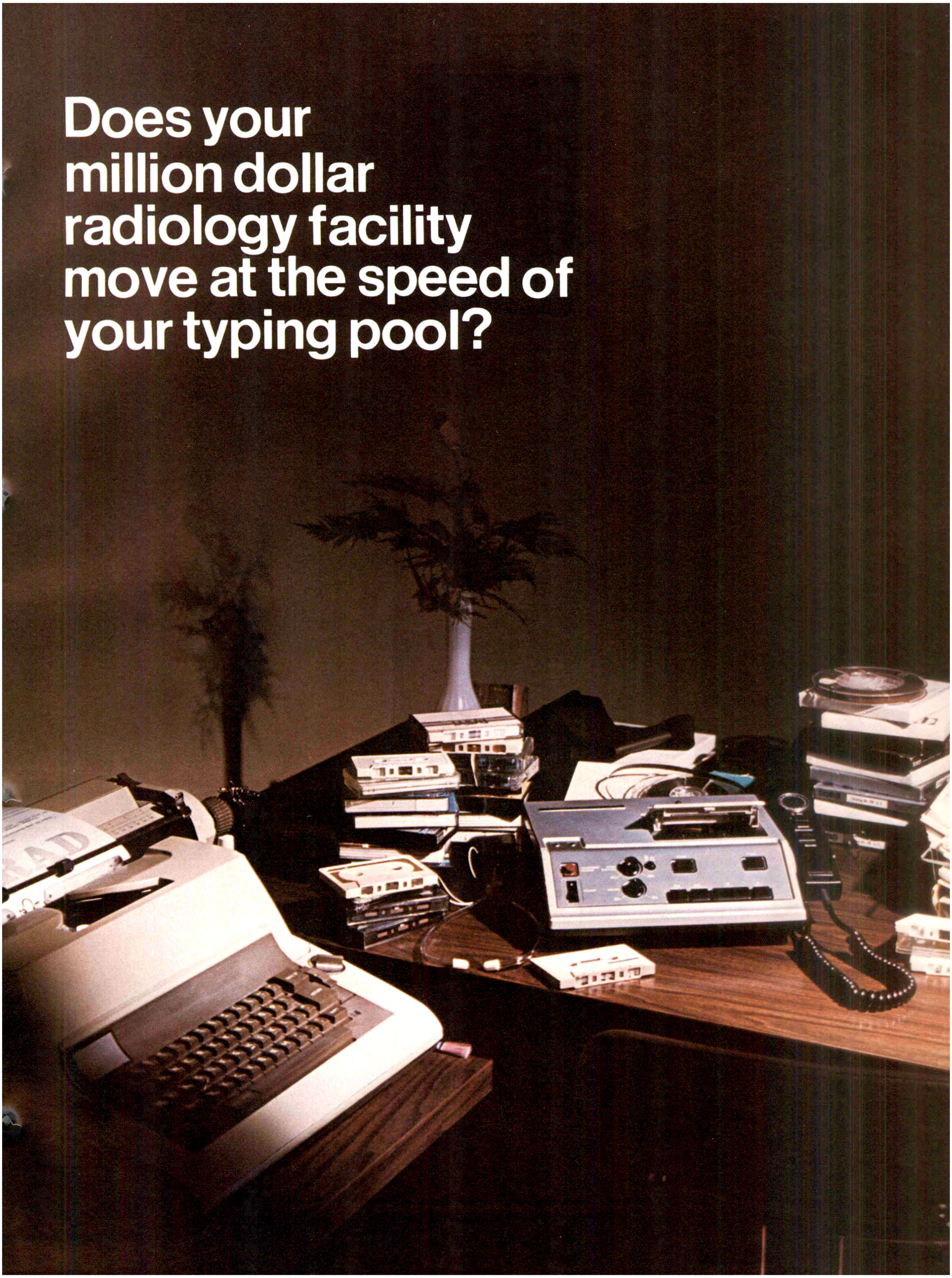
Does your million dollar radiology facility move at the speed of your typing pool?

Meet Siemens SIREP... the reporting system that has a 6,500 word vocabulary, breezes along at 300 wpm, never makes mistakes, never takes time off, never goes on strike, and always remembers to do the billing.

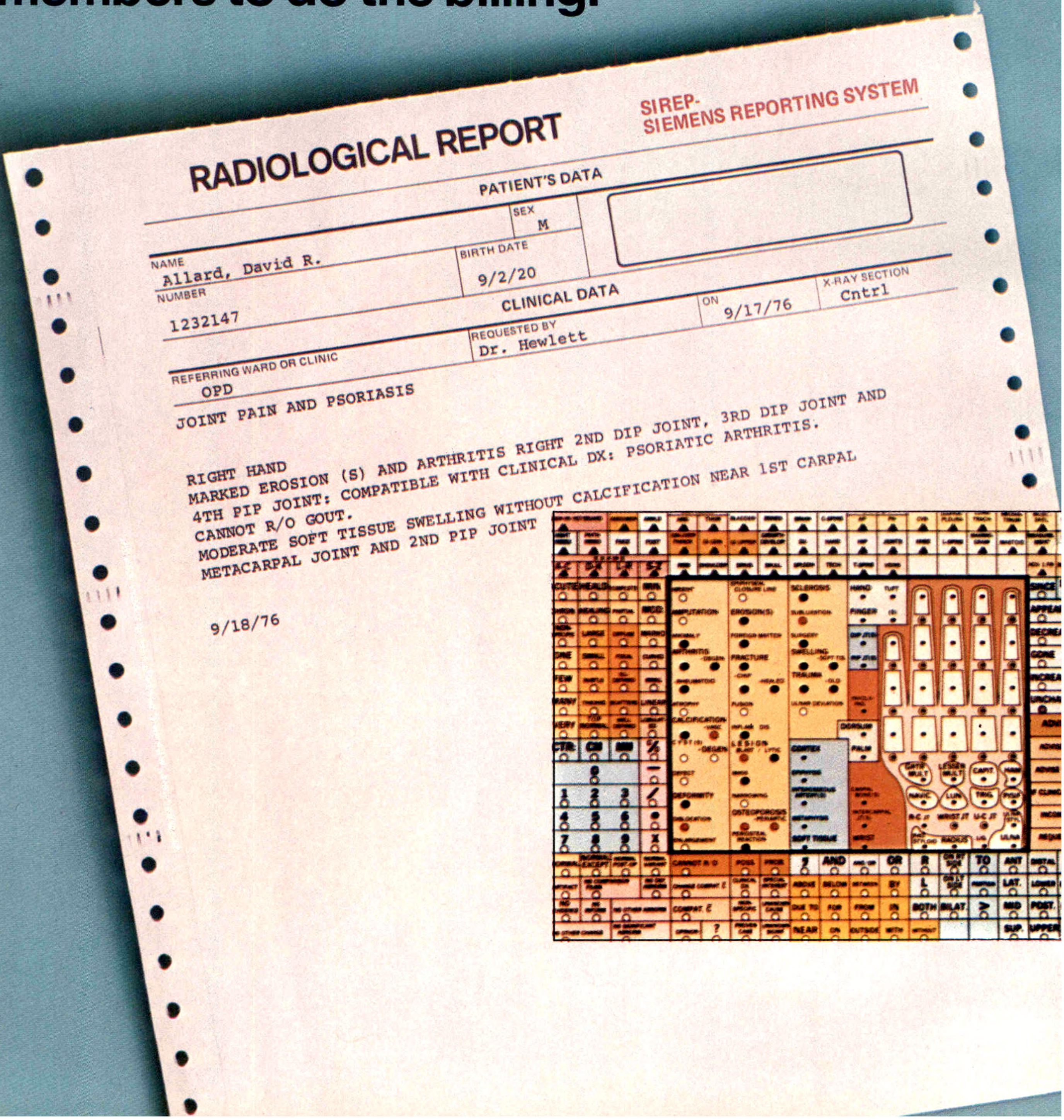

RADIOLOGICAL REPORT

SIREP-
SIEMENS REPORTING SYSTEM

PATIENT'S DATA

SEX M

NAME Allard, David R.

BIRTH DATE 9/2/20

NUMBER 1232147

CLINICAL DATA

ON 9/17/76

X-RAY SECTION Cntrl

REQUESTED BY Dr. Hewlett

REFERRING WARD OR CLINIC OPD

```
JOINT PAIN AND PSORIASIS

RIGHT HAND
MARKED EROSION (S) AND ARTHRITIS RIGHT 2ND DIP JOINT, 3RD DIP JOINT AND
4TH PIP JOINT: COMPATIBLE WITH CLINICAL DX: PSORIATIC ARTHRITIS.
CANNOT R/O GOUT.
MODERATE SOFT TISSUE SWELLING WITHOUT CALCIFICATION NEAR 1ST CARPAL
METACARPAL JOINT AND 2ND PIP JOINT

9/18/76
```

SIREP is the solution to the old problem of dictate and wait.

The radiologist, instead of dictating his findings, simply selects words and phrases from a comprehensive vocabulary of diagnostic, anatomical and pathological terms. Once the report is viewed on a monitor screen and confirmed by the radiologist, SIREP prints out multiple hard copies in a matter of seconds.

To make things even easier, preferred wording for routine reports can be programmed into SIREP's memory-recall bank.

If you're tired of watching your million dollar X-ray department move at the speed of your typing pool, get in touch. We'll send you complete information on SIREP, the system that takes the delays *and expense* out of radiology reporting.

Contact your Siemens representative, or write to Siemens Corporation,
Medical Systems Division,
186 Wood Avenue South, Iselin, N.J. 08830,
(201) 494-1000. In Canada: Siemens
Canada Limited, P.O. Box 7300,
Pointe Claire 730-P.Q.

SIEMENS

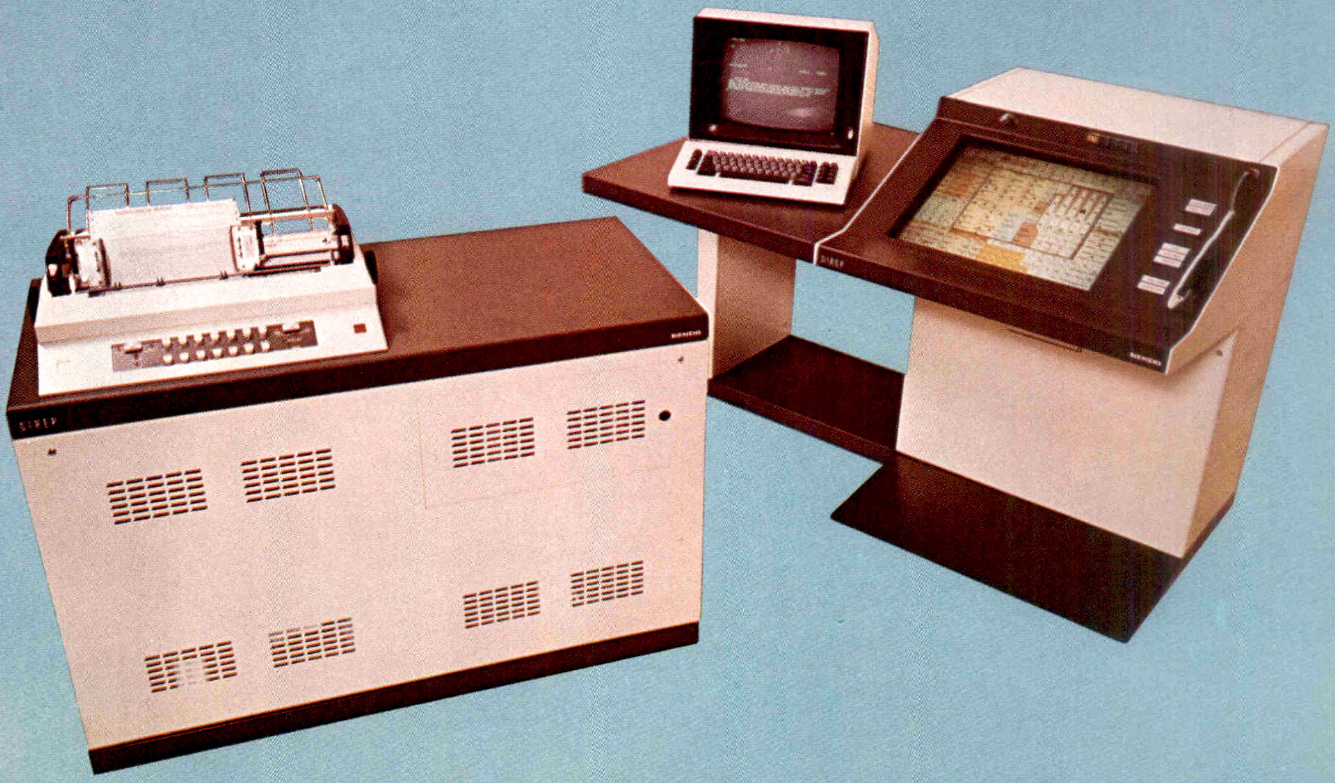

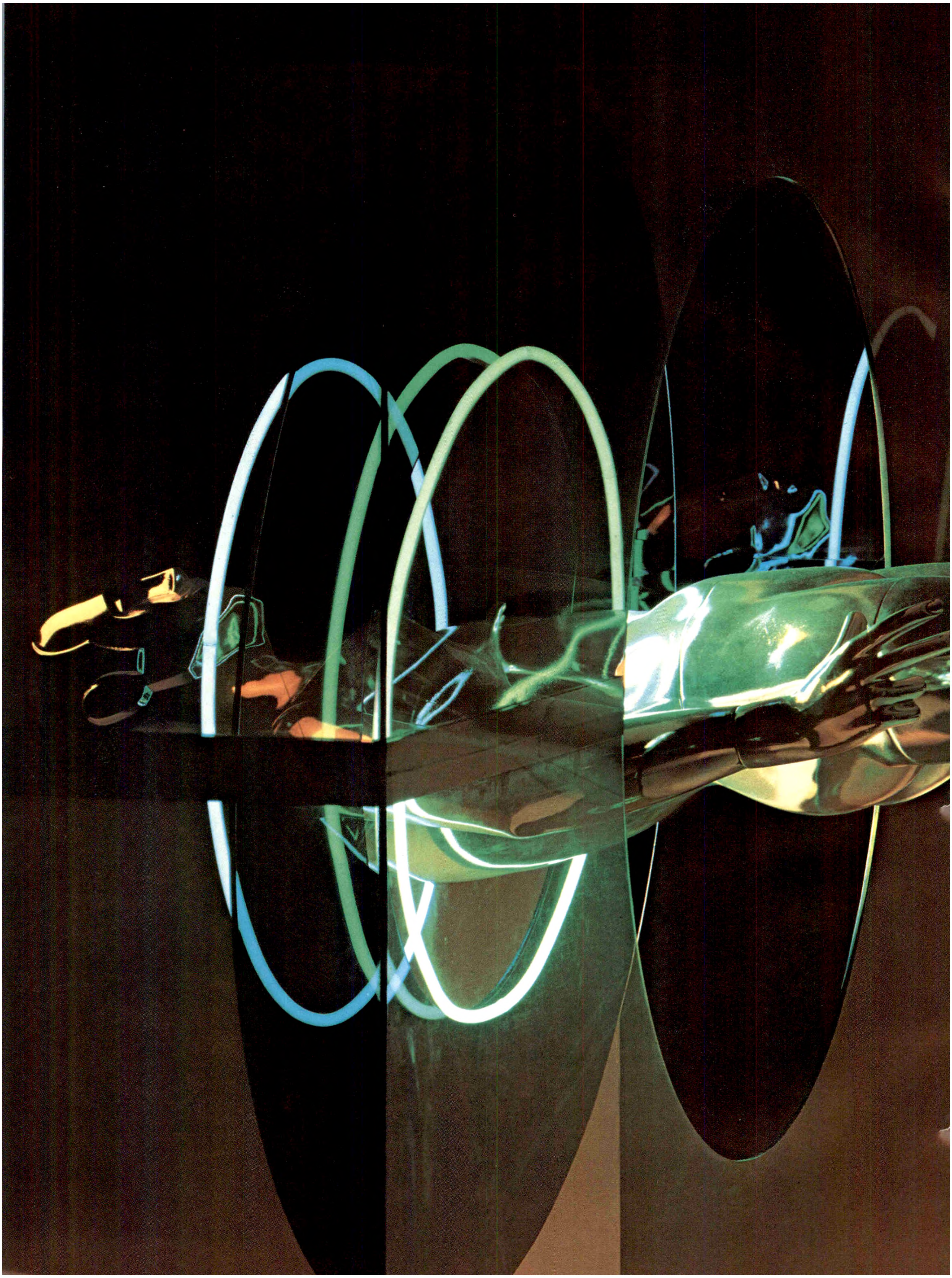

EMI IS BUILDING ON PERFORMANCE...NOT PROMISES; EXPERIENCE...NOT EXPEDIENCY.

If you plan a CT acquisition this year, chances are you'll hear a lot of "generation" talk, engineering specs, promises and claims. But the truth is, when you've examined *all* the facts, no CT company today has more to offer than EMI: proven technology, superior image quality, demonstrated upgradability, dedicated CT service network and a decade of CT experience.

The EMI CT5005 System is—unquestionably—the best, most proven, general diagnostic fast scanner today. Unmatched record of reliability, diagnostic/performance flexibility and dedication to image quality.

EMI-Scans display significantly more clinical data than scans produced on competitive equipment. Exquisite anatomical detail. Optimum spatial and density resolution. Compare.

EMI's record of performance is unequaled in the industry... *more* installations, *more* fast-scan systems, *more* upgrades and *more* patient scans *than all the competition*.

- Over 800 CT systems installed or on order;
- 220 CT5005 fast-scan units in place;
- Over 100 system upgrades completed to date;
- 3 million patient studies on record;
- 10 years of CT experience and know-how.

EMI has the largest, most experienced CT service organization in the world. Over 500 professionals dedicated to customer training, service and support. A nationwide network of highly skilled field service personnel has ready access to local inventories of spare parts to minimize downtime and insure prompt response.

EMI achievements continue to pace the CT industry. *FIRST* CT scanner; *FIRST* fast-scan, general purpose system; *FIRST* upgrade program; *FIRST* trade-in program; *FIRST* redeveloped, low-cost CT system; *FIRST* mobile CT scanner . . . and that's just the *beginning*.

EMI's continuing investment in research and development reflects dedicated responsiveness to the needs of the medical community: image quality, patient safety, operational efficiency and economy.

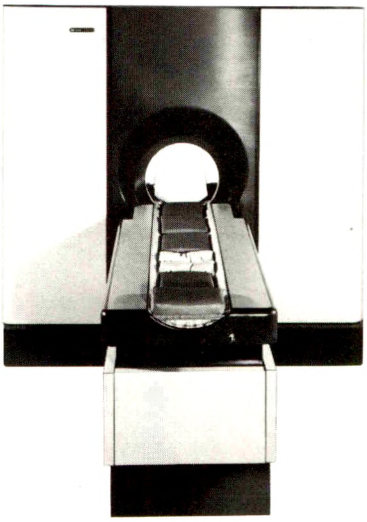

Standard of the Industry.

EMI EMI Medical

EMI Medical Inc, 3605 Woodhead Drive, Northbrook, IL 60062

A member of EMI group. International leader in music, electronics and leisure

in selective coronary arteriography

the reason is clear™

- —excellent image quality
- —"minimal myocardial toxicity"

"... Renografin-76 is eminently suitable as a radiopaque agent for coronary angiography. The film quality was good in every instance, while serious adverse effects were absent in this series of 723 patients." There was a 1% incidence of complications due to the contrast agent (cardiac arrest in 3 and ventricular fibrillation in 5 cases) and a 4% incidence of cardiac complications due to catheterization in this series of patients*

- —eight indications

*Gensini GG, Kelly AE. Reassessment of contrast agent for coronary angiography. Current Therapeutic Research 19: 631-636, 1976

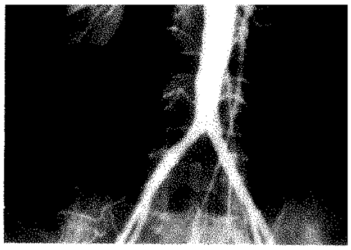
aortography

selective renal arteriography

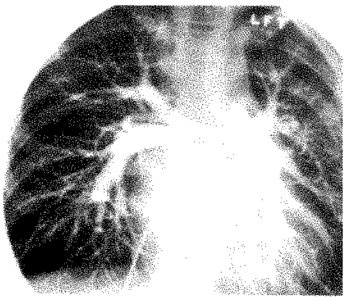
pediatric angiocardiography

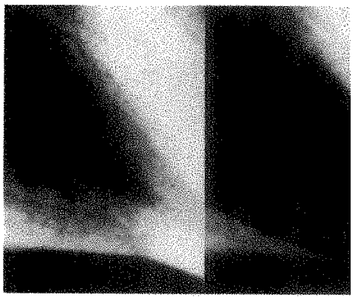
left ventriculography performed following coronary arteriography

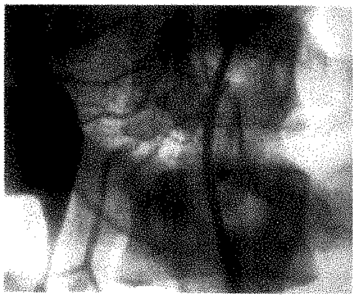
selective visceral arteriography

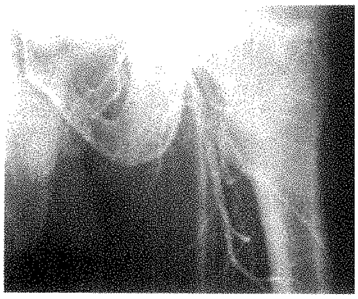
peripheral arteriography

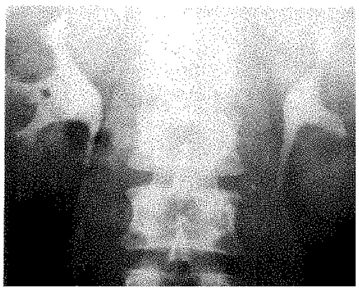
excretion urography

Renografin®-76

Diatrizoate Meglumine and Diatrizoate Sodium Injection U.S.P.

SQUIBB®

contrast media™ The leader in radiologic diagnostics

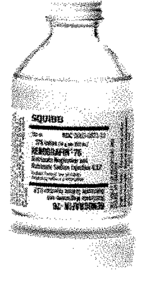

See next page for brief summary.

RENOGRAFIN®-76
Diatrizoate Meglumine and Diatrizoate Sodium Injection U.S.P.

Renografin-76 (Diatrizoate Meglumine and Diatrizoate Sodium Injection U.S.P.) is supplied as a sterile, aqueous solution providing 66% diatrizoate meglumine and 10% diatrizoate sodium with 0.32% sodium citrate as a buffer and 0.04% edetate disodium as a sequestering agent. The solution contains approximately 37% (370 mg./ml.) bound iodine and *approximately 4.48 mg. (0.19 mEq.) sodium per ml.*

CONTRAINDICATIONS: In patients with a hypersensitivity to salts of diatrizoic acid. Urography contraindicated in patients with anuria.

WARNINGS: A definite risk exists with the use of contrast agents in excretion urography in patients with multiple myeloma. There has been anuria with progressive uremia, renal failure and death. This risk of the procedure in these patients is not a contraindication; however, partial dehydration in preparation for study is not recommended since it may predispose for precipitation of myeloma protein in renal tubules. No therapy, including dialysis, has been successful in reversing this effect. Myeloma should be considered in persons over 40 before undertaking urographic procedures.

In cases of known or suspected pheochromocytoma, if the physician feels that the possible benefits outweigh the considered risks, radiopaque materials should be administered with extreme caution; however, an absolute minimum of material should be injected, the blood pressure should be assessed throughout the procedure, and measures for treating a hypertensive crisis should be available.

Contrast media may promote sickling in homozygous individuals when injected I.V. or intra-arterially. Although a history of sensitivity to iodine *per se* or to other contrast media is not an absolute contraindication, administration of diatrizoate requires extreme caution in such cases. Perform thyroid function tests prior to administration of Renografin-76 (Diatrizoate Meglumine and Diatrizoate Sodium Injection U.S.P.) since iodine-containing contrast agents may alter the test results.

Weigh the inherent risks against necessity for performing *angiocardiography* in cyanotic infants and patients with chronic pulmonary emphysema. In *pediatric angiocardiography*, a dose of 10 to 20 ml. may be particularly hazardous in infants weighing less than 7 kg.; this risk is probably significantly increased if these infants have preexisting right heart "strain," right heart failure, and effectively decreased or obliterated pulmonary vascular beds. Perform *urography* with extreme caution in persons with severe concomitant hepatic and renal disease. Perform *selective coronary arteriography* only in selected patients and those in whom expected benefits outweigh the procedural risk. Perform *selective visceral arteriography* with extreme caution in presence of severe generalized atherosclerosis, specifically with plaques or aneurysms at level of iliac or femoral arteries.

Usage in Pregnancy: Use Renografin-76 (Diatrizoate Meglumine and Diatrizoate Sodium Injection U.S.P.) in pregnant patients only when the physician deems its use essential to the welfare of the patient since safe use during pregnancy has not been established.

PRECAUTIONS: Diagnostic procedures involving use of contrast agents should be performed under the direction of personnel with prerequisite training and a thorough knowledge of the particular procedure. Appropriate facilities should be available for coping with situations which may arise as a result of the procedure and for emergency treatment of severe reactions to the contrast agent itself; competent personnel and emergency facilities should be available for at least 30 to 60 minutes after I.V. administration since delayed reactions have been known to occur. These severe life-threatening reactions suggest hypersensitivity to the contrast agent. A personal or family history of asthma or allergy or a history of a previous reaction to a contrast agent warrants special attention and may predict more accurately than pretesting the likelihood of a reaction although not the type nor severity of the reaction in the individual. The value of any pretest is questionable. The pretest most performed is the slow I.V. injection of 0.5 to 1.0 ml. of the preparation prior to injection of the full dose; however, the absence of a reaction to the test dose does not preclude the possibility of reaction to the full diagnostic dose. Should the test dose produce an untoward response, the necessity for continuing the examination should be re-evaluated. If deemed essential, examination should proceed with all possible caution. In rare instances, reaction to the test dose may be extremely severe; therefore, close observation and facilities for emergency treatment are indicated.

Renal toxicity has been reported in a few patients with liver dysfunction who were given oral cholecystographic agents followed by urographic agents; therefore, if known or suspected hepatic or biliary disorder exists, administration of Renografin-76 (Diatrizoate Meglumine and Diatrizoate Sodium Injection U.S.P.) should be postponed following the ingestion of cholecystographic agents. Consider the functional ability of the kidneys before injecting the contrast agent. Use cautiously in severely debilitated patients and in those with marked hypertension. Bear in mind the possibility of thrombosis when using percutaneous techniques. Since contrast agents may interfere with some chemical determinations made on urine specimens, collect urine before or two or more days after administration of the contrast agent.

In *excretion urography*, adequate visualization may be difficult or impossible in uremic patients or others with severely impaired renal function (see Contraindications). In *aortography* repeated intra-aortic injections may be hazardous; this also applies to *pediatric angiocardiography* particularly in infants weighing less than 7 kg. (see Warnings). In *peripheral arteriography* hypotension or moderate decreases in blood pressure seem to occur frequently with intra-arterial (brachial) injections; this is transient and usually requires no treatment. Monitor blood pressure during the immediate 10 minutes after injection. It is recommended that *selective coronary arteriography* not be performed for about 4 weeks after diagnosis of myocardial infarction; mandatory prerequisites to this procedure are experienced personnel, ECG monitoring apparatus, and adequate facilities for immediate resuscitation and cardioversion.

ADVERSE REACTIONS: Nausea, vomiting, flushing, or a generalized feeling of warmth are the reactions seen most frequently with intravascular injection. Symptoms which may occur are chills, fever, sweating, headache, dizziness, pallor, weakness, severe retching and choking, wheezing, a rise or fall in blood pressure, facial or conjunctival petechiae, urticaria, pruritus, rash, and other eruptions, edema, cramps, tremors, itching, sneezing, lacrimation, etc. Antihistaminic agents may be of benefit; rarely, such reactions may be severe enough to require discontinuation of dosage. There have been a few reports of a burning or stinging sensation or numbness of venospasm or venous pain, and of partial collapse of the injected vein. Neutropenia or thrombophlebitis may occur. Severe reactions which may require emergency measures (see Precautions) are a possibility and include cardiovascular reaction characterized by peripheral vasodilatation with hypotension and reflex tachycardia, dyspnea, agitation, confusion and cyanosis progressing to unconsciousness. An allergic-like reaction ranging from rhinitis or angioneurotic edema to laryngeal or bronchial spasm or anaphylactoid shock may occur. Temporary renal shutdown or other nephropathy may occur.

Adverse reactions as a consequence of *excretion urography* include cardiac arrest, ventricular fibrillation, anaphylaxis with severe asthmatic reaction, and flushing due to generalized vasodilatation. Risks of *aortography* procedures include injury to aorta and neighboring organs, pleural puncture, renal damage (including infarction and acute tubular necrosis with oliguria and anuria), accidental selective filling of right renal artery during translumbar procedure in presence of preexistent renal disease, retroperitoneal hemorrhage from translumbar approach, spinal cord injury and pathology associated with syndrome of transverse myelitis, generalized petechiae, and death following hypotension, arrhythmia, and anaphylactoid reactions. In *pediatric angiocardiography*, arrhythmia and death have occurred. During *peripheral arteriography*, hemorrhage from puncture site, thrombosis of the vessel, and brachial plexus palsy (following axillary artery injection) have occurred. During *selective coronary arteriography* and *selective coronary arteriography with left ventriculography*, transient ECG changes (most patients); transient arrhythmias (infrequent); ventricular fibrillation (from manipulation of catheter or administration of medium); hypotension; chest pain; myocardial infarction; transient elevation of creatinine phosphokinase (occurred in about 30% of patients tested); fatalities have been reported; hemorrhage, thrombosis, pseudoaneurysms at puncture site, dislodgment of arteriosclerotic plaques, dissection of coronary vessels, and transient sinus arrest have occurred due to the procedure. Adverse reactions in *selective renal arteriography* include nausea, vomiting, hypotension, hypertension, and post-arteriographic transient elevations in BUN, serum creatinine and glucose. Complications of *selective visceral arteriography* include hematomas, thrombosis, pseudoaneurysms at injection site, dislodgment of arteriosclerotic plaques; other reactions may include urticaria, hypotension, hypertension, and insignificant changes in renal function and liver chemistry tests.

For full prescribing information, consult package insert.

HOW SUPPLIED: Available in 20 ml. and 50 ml. single-dose vials and in 100 ml. and 200 ml. single-dose bottles.

© 1977 E. R. Squibb & Sons, Inc. H627-50

SQUIBB®

contrast media™

SQUIBB HOSPITAL DIVISION
E.R. Squibb & Sons, Inc.
P.O. Box 4000 Princeton, N.J. 08540

Keeping up-to-date with the latest radiologic and diagnostic techniques?

Mosby is...see for yourself.

New Volume III! **CURRENT CONCEPTS IN RADIOLOGY.** *By E. James Potchen, M.D.; with 35 contributors.* Share the knowledge of 35 renowned authorities on topics of practical importance in radiology, nuclear medicine, and radiologic physics in this timely new book. Discussions record current progress in such areas as radionuclide imaging, the radiologic detection of malignant diseases, bone imaging, and thrombus detection. You'll especially want to read four chapters devoted to the use and practices of computed tomography. May, 1977. 472 pp., 487 illus. **Price, $39.50.**

New 3-Volume Set! **NEURORADIOLOGY IN INFANTS AND CHILDREN.** *By Derek C. Harwood-Nash, M.B., Ch.B., F.R.C.P.(C); with the assistance of Charles R. Fitz, M.D.; and 3 contributors.* Unparalleled in scope, this new three-volume set promises to become *the* definitive reference on pediatric neuroradiology. Dr. Harwood-Nash presents in-depth information on: normal anatomy of the skull and spine, their abnormal variations, and pathologic correlations. Other discussions stress such recent diagnostic approaches and techniques as computed tomography, catheter angiography, and ventriculography. Almost 4,000 superb illustrations depict all known disease conditions in children. November, 1976. 1,227 pages plus FM I-XVI in 3 volumes and a 28 page index in each volume, 3,931 illustrations. **Price, $165.00.**

A New Book! **THE MEDIASTINUM: Radiologic Correlations with Anatomy and Pathology.** *By E. Robert Heitzman, Jr., M.D.* This new book provides a foundation for a more analytic and deductive approach to radiological evaluation of the mediastinum. It emphasizes that such an evaluation depends on a thorough understanding of basic principles of anatomy and physiology. The author offers a new anatomical classification of the mediastinum; provides a new radiological classification of the lymph nodes of the mediastinum; and stresses the value of computed tomography in the study of this area. September, 1977. Approx. 384 pp., 598 illus. **About $30.00.**

A New Book! **AN ATLAS OF ENDOSCOPIC RETROGRADE CHOLANGIOPANCREATOGRAPHY.** *By Edward T. Stewart, M.D.; Jack A. Vennes, M.D.; and Joseph E. Geenen, M.D.* This superbly illustrated new atlas provides you with clinical information and technical details of ERCP as it depicts both normal and abnormal conditions of pancreatic ducts and biliary tract. Chapters examine such topics as: indications and contraindications for use of ERCP; normal pancreatogram; neoplasms of the pancrease; and intrahepatic conditions of the biliary tree. October, 1977. Approx. 384 pp., 367 illus. **About $45.00.**

A New Book! **PEDIATRIC ONCOLOGIC RADIOLOGY.** *Edited by Bruce R. Parker, M.D. and Ronald A. Castellino, M.D.* This comprehensive reference examines the importance of radiology in diagnosis and staging of pediatric oncologic diseases. Each chapter discusses clinical aspects and radiographic findings of a particular form of childhood cancer – and concludes with a valuable list of recommended imaging studies. August, 1977. Approx. 500 pp., 523 illus. **About $42.50.**

A New Book! **QUALITY CONTROL IN NUCLEAR MEDICINE: Radiopharmaceuticals, Instrumentation, and In-Vitro Assays.** *Edited by Buck A. Rhodes, Ph.D.; with 62 contributors.* July, 1977. 508 pages plus FM I-XVIII, pages, 7″ × 10″, 293 illustrations. **Price, $39.50.**

ORDER BY PHONE! Call (800) 325-4177 ext. 10. In Missouri call collect – (314) 872-8370 ext. 10. 9 am to 5 pm CDT), Monday through Friday.

A70712

MOSBY

TIMES MIRROR

THE C. V. MOSBY COMPANY
11830 WESTLINE INDUSTRIAL DRIVE
ST. LOUIS, MISSOURI 63141

You can't get Fourth-Generation data out of Third-Generation scanners.

We'd like to tell you why.

In computed tomography, claims about image excellence are escalating as fast as the technology itself.

It's time everyone paused and considered some hard facts:
Fact: All CT images are *not* excellent. Some are not even good.
Fact: Image quality is only as good as the attenuation data collected.
Fact: Data is degraded if detector drift goes uncorrected.
Fact: Data is further degraded if detectors are not utilized efficiently.

At Ohio-Nuclear, we developed both third- and fourth-generation prototype units. We discovered significant differences between these two CT designs and went directly into production of the superior fourth-generation scanner, incorporating our own previously proven unique data handling system.

We now offer those comparative facts to you. Your CT decision should be based on nothing less.

Data stability.
In fourth-generation scanning design, the X-ray source rotates within a stationary arc of fixed detectors, emitting a collimated fan-shaped X-ray beam (source fan) corresponding to the scan field diameter. As this X-ray source fan rotates around the patient, each detector views the X-ray source as it passes through the detector's field of view (detector fan). The detector fan also corresponds to the scan field diameter. For body scanning, field diameter is slightly smaller than the gantry opening. Since a patient does not completely fill the scan field diameter, the X-ray source is seen by each detector, first through the open space not filled by the patient (air), and then through the entire body section being scanned, and finally through air again (Figure 1).

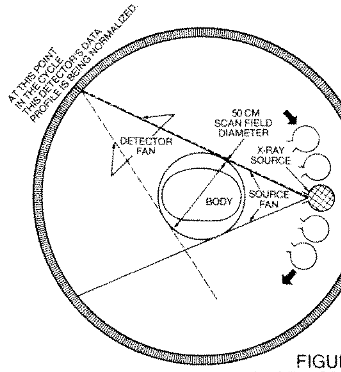

FIGURE 1
FOURTH GENERATION

Since the X-ray source is first viewed through air, each detector has its calibrations based on that known density. Then, after collecting patient data, each detector again views the X-ray source through air to verify calibration.

Via these air calibration values, each individual detector signal chain is monitored (including the crystal, photomultiplier, and analog circuits). Each data profile is then normalized by computer software, so that all patient data from all data profiles, from all scans, is normalized.

Using this system, detector stability is vital only for the duration of an individual scan. Any possible long-term detector drift is therefore not significant. Measured detector gain instability, over the time of a scan, is negligible. This technique of detector calibration and balancing is a *proven technique* which has been used on all previous Delta-Scan systems, and has earned a reputation for outstanding reliability.

Third-generation scanners, by comparison, rotate both the X-ray source and detector array synchronously around the patient (Figure 2).

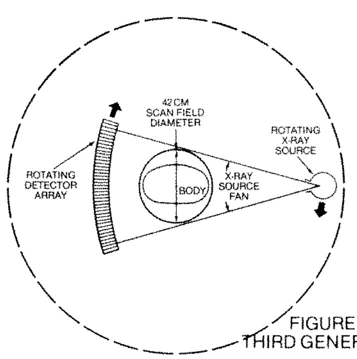

FIGURE 2
THIRD GENERATION

The width of the X-ray source fan also corresponds to the scan field diameter, to accommodate large body cross-sections. A Xenon detector array is used. Because every detector is fixed in a position relative to the source, most detectors view the X-ray beam through the patient without any air or other known-medium calibration. Air calibration of each array member cannot be achieved without removing the patient from the gantry, necessitating "long-term stability" of the more than 300 detectors. Some third-generation scanners attempt to calibrate while the X-ray source is off (between-pulse nulling). This provides a limited calibration, monitoring only post-detector electronics. Drifts of the individual detectors themselves are not accounted for; this may cause CT attenuation numbers to drift.

Data geometry.
In fourth-generation scanners, each detector views the X-ray source and gathers data as the source passes around the patient. In this way, each detector contributes a data profile (or view) through the entire patient cross-section (Figure 3). Failure of several detectors will not cause a localized artifact, or significantly degrade the overall image quality, since all detectors contribute to all areas of each image.

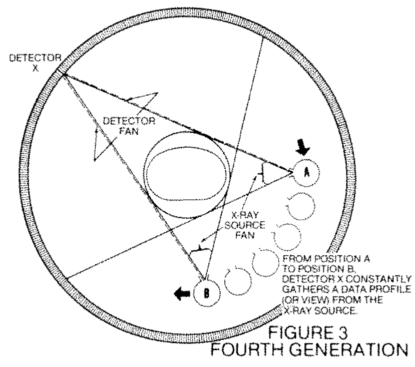

FIGURE 3
FOURTH GENERATION

Also, because the X-ray source is moving relative to each detector, the distance between, and number of data samples collected from each detector need not be fixed. Sampling frequency can be tailored to the scanning mode and quality of resolution desired. The following chart describes the number and spacing of data samples for a head scan with the Delta-Scan 2020.

Scan Time	Number of Samples	Sample Distance
2 sec.	388,800	.5mm
4 sec.	777,600	.25mm
8 sec.	1,555,200	.125mm
16 sec.	3,110,400	.062mm

For additional diagnostic flexibility, the Delta-Scan 2020 also offers three selections of reconstruction matrix, 128, 256, and 512.

In third-generation scanners, by contrast, each detector rotates in the same position relative to the X-ray source. The result may be described as "single beam" data acquisition, where each detector views only one source ray, as opposed to fourth-generation data gathering in the form of a fan of information across the entire patient. Each detector contributes information describing a circular path in the cross-section (Figure 4). Failure of detectors, or inaccuracies in calibration, will result in localized, circular artifacts (Figure 5).

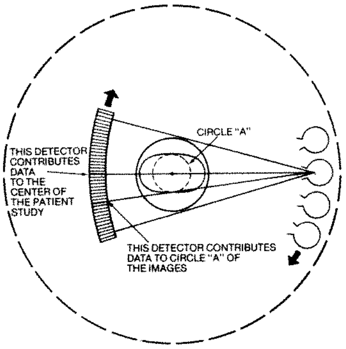
CIRCLE "A"
THIS DETECTOR CONTRIBUTES DATA TO THE CENTER OF THE PATIENT STUDY
THIS DETECTOR CONTRIBUTES DATA TO CIRCLE "A" OF THE IMAGES

FIGURE 4
THIRD GENERATION

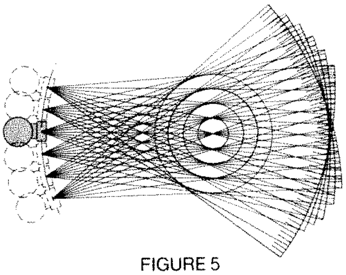

FIGURE 5
THIRD GENERATION

Multiple projections of 9 fan beams showing partial formation of 4 equally spaced concentric circles.

Because the detector array is fixed relative to the source, the distance between and number of data samples per pulse view, is fixed. Increasing the number of pulse views will not increase the number of data circles, which are dictated by detector spacing.

Thus, without increasing the number of detectors within the same arc, it appears that there is no way to improve spatial resolution.

Detector utilization.
In fourth-generation scanners, regardless of the size of the scanned object, every detector in the array collects attenuation data throughout the object being scanned (Figure 3). A selection of scanning fields from 25cm to 50cm is available to suit individual cross-sections and maximize data collection over the field of view. By reducing field size from 50cm to 25cm for head scans, pixel area is reduced by three-fourths, spatial resolution significantly improved, and the entire image matrix utilized efficiently (Figure 6).

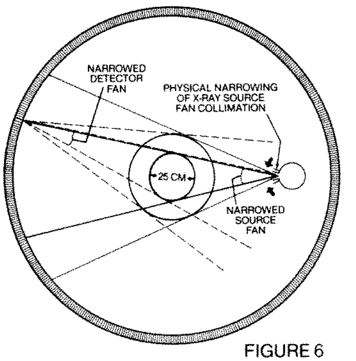

FIGURE 6
FOURTH GENERATION
25 CM SCAN CIRCLE DIAMETER CONFIGURATION

Third-generation scanners, however, utilize their detectors fully only while scanning large bodies (Figure 7). Large numbers of detectors are not utilized when scanning head-sized objects, and contribute no significant or even useful patient information. In a true reconstruction, only a fraction of the total matrix may contain useful information. Computerized image expansion techniques can fill the video display, but cannot change true pixel size or improve spatial resolution.

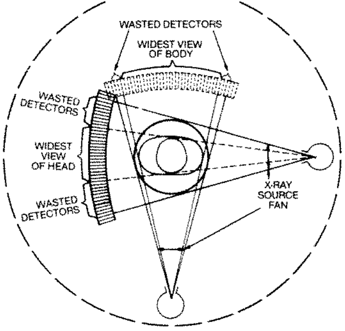

FIGURE 7
THIRD GENERATION

Detector reliability.
The Delta-Scan 2000 Series of fourth-generation scanners utilizes tried and proven scintillation crystal, photomultiplier tube detectors. Each detector is mounted on an immobile frame. By nature of its design, a detector has absolutely nothing to wear out. There is no filament in the photomultiplier tube. Under clinical use, the BGO crystal will never become radiation saturated or decay. Engineers estimate that detectors have an infinite life. They are, however, manufactured under vacuum and, recognizing the possibility that a small number of detectors could prove faulty over the life of the scanner, Ohio-Nuclear designed its detector array so that any defective detector may be individually replaced during normal maintenance.

Conversely, the inherent design of a third-generation rotating detector arc may necessitate removal of the entire detector array for the replacement of a single detector.

Ohio-Nuclear chose to utilize BGO (Bismuth Germanate Oxide) scintillation detectors instead of a Xenon ion chamber because of the scintillator's superior captured photon efficiency (high stopping power), extended dynamic range, and long-term reliability. And, a Xenon detector has only one-fifty thousandth the intrinsic gain of a scintillation photomultiplier detector. Therefore, electronic gain must be introduced to produce a useable signal, which contributes noise to the overall signal. The BGO scintillation crystal photomultiplier detector provides superior gain and dynamic range to insure excellent tissue contrast resolution.

Conclusions.
The fourth-generation Delta-Scan 2000 Series of scanners deliver higher image quality because of the extremely accurate input data quality and because of our unique handling of that data. Furthermore, every detector views the entire patient; thru air, thru the patient, and again thru air. This allows continuous detector calibration, and insures accurate data from every detector on every scan. Total detector utilization across the entire patient (regardless of scanning mode) insures uncompromised image quality at minimal dosages. These are the facts about the data that make up a CT image.

Reproduced above is a fourth-generation Ohio-Nuclear 2-second 512 matrix scan. Let your Ohio-Nuclear representative show you more. Call or write for an immediate response.

ohio-nuclear, inc.
A subsidiary of Technicare Corporation
U.S. — 29100 Aurora Road • Solon, Ohio 44139 Telephone (216) 248-8500
TWX 810 427 2696

PDQ*...

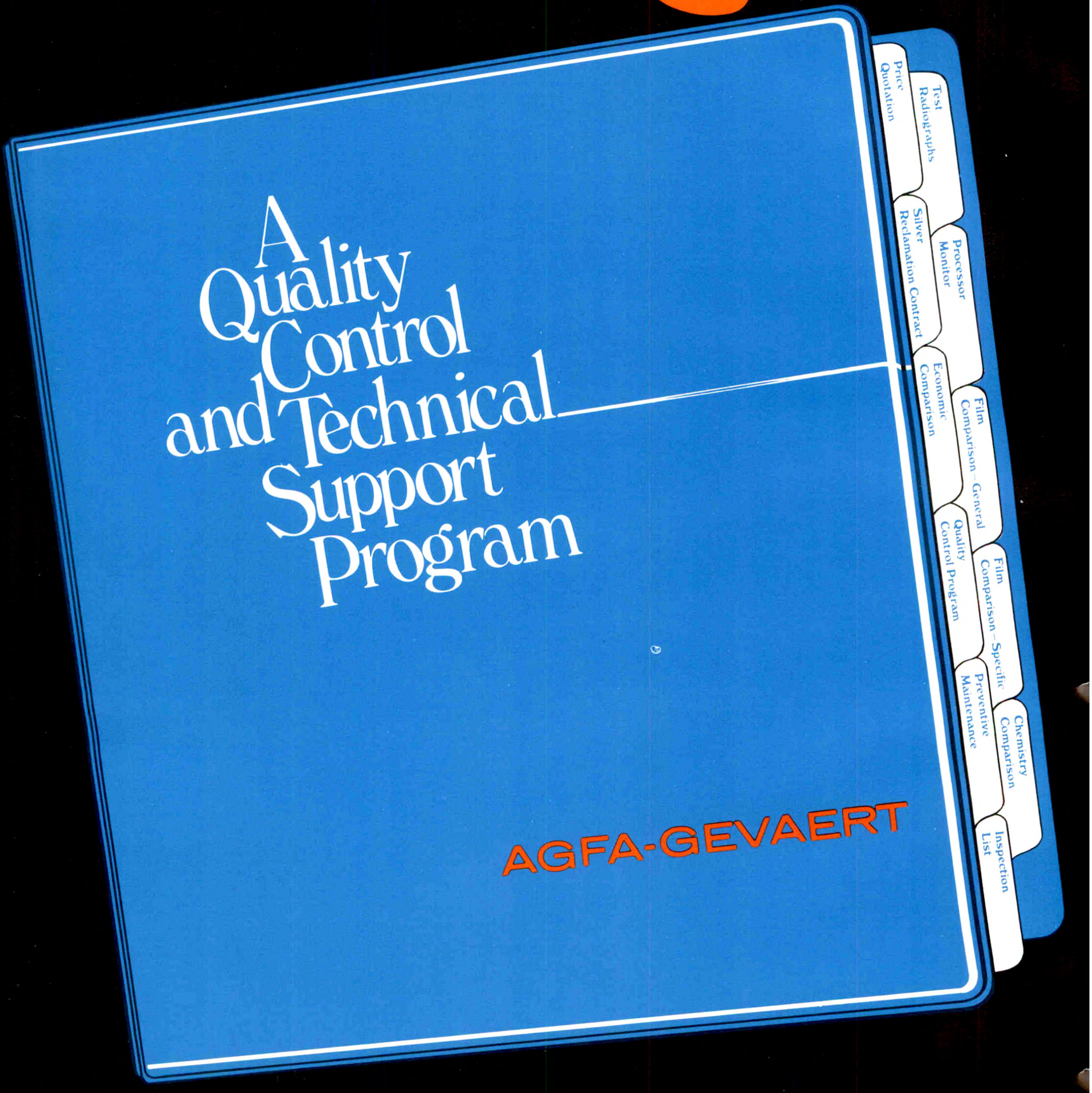

A Quality Control and Technical Support Program

AGFA-GEVAERT

*PDQ... Program for Departmental Quality

It's Not What You Think It Is!

In fact, PDQ really stands for our cost-saving *Program for Departmental Quality,* all provided without cost to Agfa-Gevaert users. It's a continuing program designed and geared to your specific needs, providing the technical security that you need to run your department more efficiently and, at lower cost.

Here's what it covers: film and chemistry, processing, mixing and replenishment, screens and cassettes, illuminators, silver recovery, generating equipment and accessories. Plus a very comprehensive preventative maintenance program. And for your security, it's all outlined in our manual, "A Quality Control and Technical Support Program."

Here's how it works: one of our Agfa-Gevaert PDQ Teams will analyze and evaluate your present systems and procedures, all without cost, of course. You see, our PDQ Teams are a group of experts, each highly skilled in his respective field...x-ray technique, processing, sensitometry, generating equipment and accessories. Together, they'll evaluate the findings, then demonstrate, in writing and through comprehensive comparisons within the manual, those areas where they can effect cost reductions, improve efficiency, and provide better patient care.

More importantly, however, once they've initiated the program, they will continue servicing your needs, providing routine re-evaluations, and suggesting additional cost-saving modifications as they become apparent. Periodic equipment inspections, training, and comprehensive technical data are supplied as a matter of course.

In short, as a user of Agfa-Gevaert film, our PDQ Team will provide you with the technical support that you want, **when you want it!**

PDQ...it's not what you thought it was!

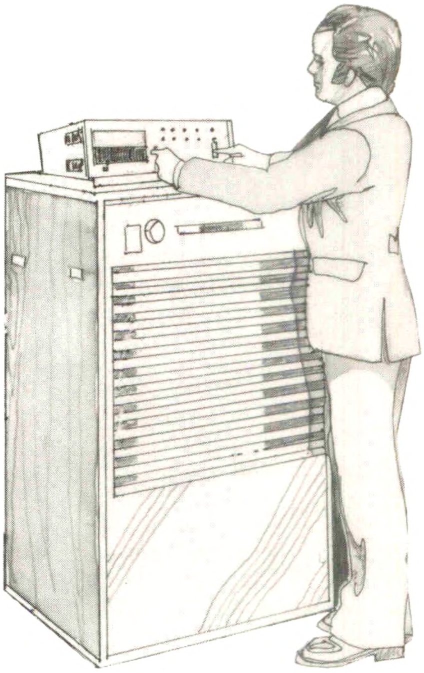

AGFA-GEVAERT

DISTRIBUTED BY: IPCO HOSPITAL SUPPLY CORPORATION
1025 WESTCHESTER AVENUE • WHITE PLAINS, N.Y. 10604 • (914) 682-4500

American Journal of Roentgenology
Guidelines for Authors

The *American Journal of Roentgenology* publishes original and timely contributions to the advancement of radiologic diagnoses and treatment. Although the content is predominantly clinical in origin, laboratory investigations are accepted when their relevance to clinical practice is demonstrable. Material published elsewhere, in substance or illustration, will not be considered. Prior publication of abstracts, however, will not prejudice publication of the complete study. Contributions are reviewed by two outside consultants and are accepted on condition that they are submitted only to this Journal and that they will not be reprinted or translated without consent of the Editor. Statements within an article are the responsibility of the authors and not the Journal or its publisher.

Address all manuscripts and correspondence to the Editor, Dr. Melvin M. Figley, 403 Pacific National Bank Building, 4545 15th Avenue N.E., Seattle, Washington 98105.

Manuscript Form

Manuscripts should be typed double-spaced throughout, including references, tables, and footnotes. Tables, footnotes, and figure legends should be on separate sheets, and a separate title page should be provided. In addition to the original typewritten copy, a duplicate copy complete with figures, tables, and references is required. Authors' names should be on title page only and should not be on figures so that author anonymity can be maintained during the review process.

Figures should be submitted as 13 X 18 cm glossy prints, untrimmed and unmounted. Each should be numbered to correspond with figure legends, and the top should be indicated. Written permission is required for reproduction of previously published figures, and such material must be clearly noted and credited in the manuscript. Specific permission for publication of facial photographs of patients is required. Line illustrations and graphs should be drawn in black ink on white background. Labels on all figures should be of professional quality and sufficiently large to be easily read when reduced in size.

References should be cited in the text by number (e.g., [3, 4]). The bibliography should be arranged in the numerical order that references are cited in the text and typed double-spaced throughout. Data for each reference should be arranged according to the uniform style on bibliographic citations adopted by many biomedical journals. Provide all authors' names and inclusive pages. Abbreviations for titles of medical periodicals should conform to those published in *Index Medicus*. Examples:

1. Miller RE, Chernish SM, Skucas J, Rosenak BD, Rodda BE: Hypotonic roentgenography with glucagon. *Am J Roentgenol* 121:264–274, 1974
2. Boijsen E: Superior mesenteric angiography, in *Angiography,* edited by Abrams H, Boston, Little, Brown, 1971, pp 1091–1119

Organization

Title page. Titles should be brief and specific. Include full names and addresses of all authors and acknowledgment of grant support when appropriate.

Abstract. A description of the purpose, methods, results, and conclusions of the study is required. It should be informative to a reader who has not read the text of the article.

Introduction. Clearly state the purpose of the investigation including necessary background facts.

Materials and methods. Describe the protocol clearly so that an experienced worker can understand what was done. Use standard abbreviations as presented in the *Council of Biology Editors Style Manual,* 3d ed. Metric measurements should be used throughout.

Results. Present results in logical sequence.

Discussion. Interpret the results to lend meaning and importance to the observations. If hypotheses and speculation are included, they must be labeled as such. When results differ from those of previous investigators, an attempt should be made to explain the discrepancy.

References. Only include those references which provide adequate background and present fairly any opposing evidence and concepts. Accuracy of reference data is the responsibility of the author.

Legends. Legends should be brief but should provide sufficient description to interpret the figure.

Special Communications

Case Reports. Concise case reports are accepted if they present unusual experiences that are medically important and educational. Clarity and brevity are essential.

Technical notes. Brief descriptions of new techniques or significant modifications of older ones which are directly applicable to clinical practice will be accepted.

Letters to the Editor. Letters are subject to editing and condensation. Criticism of published articles should be objective and constructive. Letters may also discuss matters of general interest to radiologists.

Proofs and Reprints

Galley proofs will be sent to authors for correction of errors and approval of illustrations. The corrected proof, copy-edited manuscript, and reprint order should be returned to the editorial office within 48 hr of receipt. Failure to adhere to this schedule may mean publication without the author's approval.

1977 Henry H. Janeway Lecture:

Fundamental Mechanisms in Combined Modality Therapy of Cancer

HENRY S. KAPLAN[1]

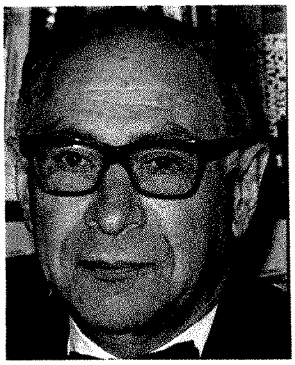

Henry S. Kaplan

In keeping with the multidisciplinary character of the American Radium Society, and in response to the intense interest in combined modality therapy which has emerged in recent years, I have chosen in this Janeway Lecture to examine some of the fundamental mechanisms underlying present and potential approaches to the use of two or more modalities in the treatment of neoplastic disease. Since the subject is far too extensive to be covered definitively in a single lecture, I will highlight a few of its aspects.

Radiosensitizing Treatments Combined with Radiation Therapy

It is important to distinguish conceptually between true radiosensitizing agents and chemotherapeutic agents. The former consist of chemical and other agents which have little or no cytotoxicity for tumor cells when used alone, but which differentially augment the extent of tumor cell killing by a given dose of radiation. In contrast, chemotherapeutic agents have significant anticancer cytotoxicity when used alone. Most of them do not modify the response to ionizing radiation, but may have additive effects when used in combination with radiation therapy. Some compounds, such as actinomycin D, are both radiosensitizers and chemotherapeutic agents.

It is convenient to consider the use of radiosensitizers together with radiation therapy under the four main headings which relate to their fundamental mechanisms of action: (1) chemical agents which substitute for oxygen, (2) halogenated pyrimidine analogs, (3) inhibitors of repair of radiation damage, and (3) chemical agents which confer differential radioprotection on normal tissues.

Electron Affinic Radiosensitizers ("Oxygen Mimics")

The late L. H. Gray [1] generated one of the most plausible and seminal hypotheses in the history of radiobiology when he suggested that, as a result of local disturbances of capillary circulation [2], a significant proportion of cells in a tumor would be likely at any given time to be severely hypoxic and yet remain clonogenic. When irradiated, such cells would be significantly more radioresistant than normally oxygenated tumor cells, and would thus be likely to survive doses capable of eradicating the rest of the tumor, and to repopulate the tumor, thus causing treatment to fail. Several recent critiques of this hypothesis [3-5] suggest that the role of hypoxic clonogenic cells in the relapse of tumors treated with radiation therapy may not be as important as was originally supposed. This may be because most of the initially hypoxic clonogenic cells either lose their clonogenic potential during the course of prolonged hypoxia or the cells become reoxygenated, and thus radiosensitive, during the course of fractionated radiation therapy. Nonetheless, the possibility remains that a small but significant population of neoplasms do fit the Gray model, and would thus be expected to benefit from some form of treatment which circumvents the presence of hypoxic clonogenic cells in the tumor.

The electron affinic chemical radiosensitizers are the latest approach to the hypoxic clonogenic hypothesis, competing with long established approaches such as hyperbaric oxygen and tourniquet anoxia, and the more recent use of high linear energy transfer particulate radiations. It is beyond the scope of this lecture to attempt a critical analysis of the achievements to date of these earlier approaches to the hypoxic clonogenic tumor cell problem. Glassburn et al. [6] have given a comprehensive and scholarly analysis of the worldwide experience to date with hyperbaric oxygen. Their study makes it clear that few of the clinical investigations were randomized clinical trials, that some of the randomized clinical trials were improperly designed with respect to the numbers of fractions of hyperbaric oxygen administered, and that an increase in local tissue injury may have been a significant factor in its use in several studies.

The use of tourniquet hypoxia for the treatment of soft tissue sarcomas and osteogenic sarcomas of the extremities has been carefully studied by Suit and Lindberg [7] and others [8]. Here again, the results on the whole have been disappointing. Local control of these radioresistant tumors under tourniquet hypoxia has required the use of extremely high doses, which have been associated with the occurrence of unacceptable degrees of local tissue injury. Moreover, the high rate of distant metastasis of these tumors has further eroded the net salvage that can be expected from this approach.

Received May 31, 1977; accepted June 8, 1977.
Presented at the annual meeting of the American Radium Society, Las Vegas, April 1977.

[1] Department of Radiology and Cancer Biology Research Laboratory, Stanford University School of Medicine, Stanford, California 94305.

The modern use of beams of fast neutrons, negative pi mesons, and heavy ions offers still another approach to circumventing the hypoxic clonogenic tumor cell problem. Such beams have not been in use sufficiently long to provide definitive evidence concerning their efficacy. However, the high linear energy transfer clinical studies suffer from two inherent disadvantages: the enormous expense and complexity of the apparatus required to generate the beams and the fact that the physical distribution of the particulate radiation is appreciably different from that of conventional photon beams, with the result that observed differences in tumor response cannot necessarily be attributed exclusively to the lower oxygen enhancement ratio of such beams.

Adams et al. [9] argued that the electron affinic radiosensitizers provide the simplest and most unambiguous test of the Gray hypothesis, since their only known effect would be to replace oxygen in hypoxic cells. It is well established that they have no effect on cells that are already well oxygenated, and thus do not increase the overall radiosensitivity of a tumor. Unlike oxygen, they are not metabolized readily in the tissues, and thus would be expected to diffuse for significantly longer distances from the capillaries, permitting them to reach zones of the tumor which are hypoxic and to increase the radiosensitivity of such hypoxic zones toward the level prevailing in the well oxygenated regions.

The earliest oxygen mimics were highly toxic chemical agents such as the nitroxides [10] which could be tested only in bacterial cells. More recently, however, metronidazole (Flagyl) and the Roche compound 7-0582, which are effective sensitizers of mammalian cells in vitro [9, 11] (fig. 1), have become available for clinical investigation. A number of derivatives of these compounds of lesser toxicity are now being synthesized and tested. Although dose-dependent neurotoxicity has been observed with Ro-7-0582 in preliminary clinical trials, significant radiosensitization has been observed in a number of tumors at drug dose levels which are within tolerance limits. These and other aspects of the subject were recently critically reviewed by Fowler et al. [12].

Halogenated Pyrimidine Analogs

The halogenated pyrimidine analogs, synthesized about 25 years ago, were found to have interesting properties which differed dramatically depending on the size of the halogenated atom which replaced the hydrogen at the 5′ carbon in the uracil molecule. Substitution by the smallest of the halogen atoms, fluorine, yielded 5-fluorouracil [13]. This analog, which has been extensively and effectively used as a cancer chemotherapeutic agent, blocks the action of thymidylate synthetase, thus preventing the synthesis of DNA. In contrast, analogs containing the heavier halogen atoms, in particular bromine and iodine, and their deoxyribosides (BUdR and IUdR) are incorporated into DNA to a significant extent in place of thymidine with little or no cytotoxicity until very high levels of substitution have occurred.

Our group at Stanford [14] and a group headed by Waclaw Szybalski [15] independently discovered that cells which had incorporated significant amounts of BUdR or IUdR into their DNA were rendered about threefold more radiosensitive, as measured by an increase in the slope of the dose-survival curve, and that this radiosensitization was independent of the oxygen effect. We then initiated a series of integrated laboratory and clinical investigations aimed at the exploitation of this new approach. BUdR proved to be an effective radiosensitizer of tumors in mice (fig. 2) at dose levels which were well tolerated and relatively nontoxic [16–18]. Kriss and Révész [19] synthesized ^{82}Br-labeled BUdR and demonstrated in rodents that the compound was rapidly dehalogenated after one passage through the liver, making it clear that intraarterial infusion of the radiosensitizer would be required in clinical practice if significant concentrations of the intact compound were to reach the tumor circulation. This approach has been tried in the treatment of cancers of the oral cavity and oropharynx [20], gliomas [21] and more recently osteogenic and soft tissue sarcomas [22].

The hazards and complexities of prolonged intraarterial infusion have had a serious limiting effect on the use of this group of radiosensitizers in other clinical situations. The discovery by Cooper and Greer [23] that 5-diazouracil inhibits the dehalogenation of these compounds suggests that it may now be possible to administer these drugs intravenously in conjunction with 5-diazouracil, thus greatly increasing the scope of clinical investigations of their efficacy.

The halogenated pyrimidine analogs would be expected to yield differential radiosensitization of those tumors in which most of the cells have a shorter mitotic cycle time than that prevailing in the surrounding normal tissues [17, 24]. This situation did not exist in the cancers of the oral cavity selected for our first clinical investigations, since equal or greater radiosensitization was observed in the normal buccal mucosa. This may well have contributed to the failure of combined BUdR infusion and radiotherapy to yield significantly improved results in this region [20]. The cells of gliomas, osteogenic sarcomas, and soft tissue sarcomas would indeed be expected to divide more rapidly, on the average, than their neighboring normal tissue cells. Such tumors remain attractive candidates for the halogenated pyrimidine approach, particularly if these analogs can now be administered intravenously without rapid dehalogenation.

Inhibitors of Repair

Three major types of repair of cellular damage produced by low linear energy transfer ionizing radiation have been extensively studied. Two of these are essentially phenomenologic in character. Recovery from sublethal damage is manifested as a restoration of the "shoulder" of the dose-survival curve over an interval of several hours between two successive fractionated doses [25]. Recovery from potentially lethal damage, an entirely distinct response, is seen as an increase in survival and a decrease in slope of the dose-survival curve if

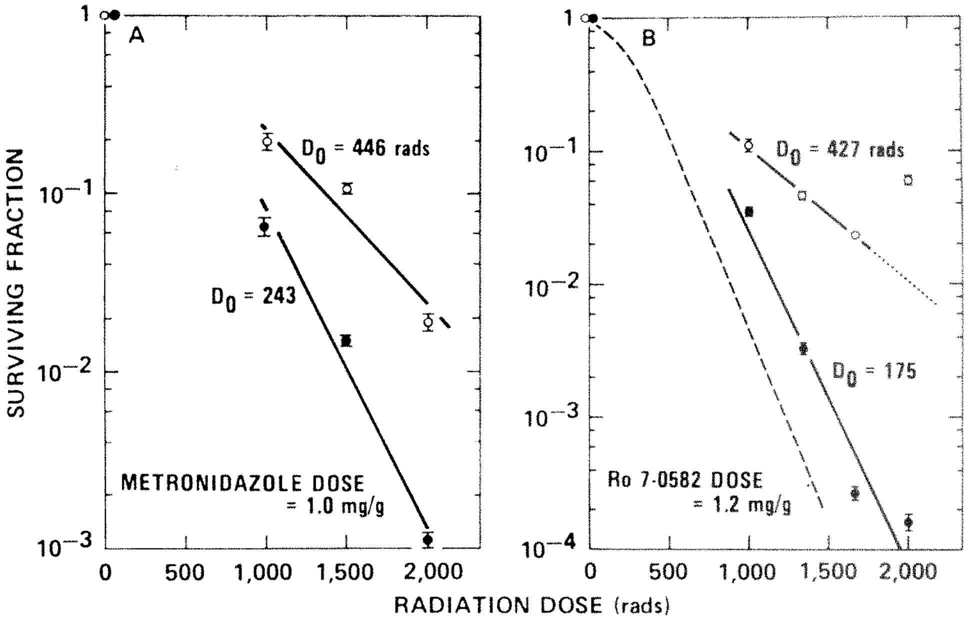

Fig. 1.—Cell survival curves of EMT6 tumors irradiated in mice which were injected with saline (*open circles*) or metronidazole or Ro 7-0582 (*closed circles*) prior to irradiation. *A*, Metronidazole injected 30 min before start of irradiation. *B*, Ro 7-0582 injected 45 min before start of irradiation. Dashed line shows survival curve for well oxygenated EMT6 cells irradiated in vitro. (Reprinted with permission from [11])

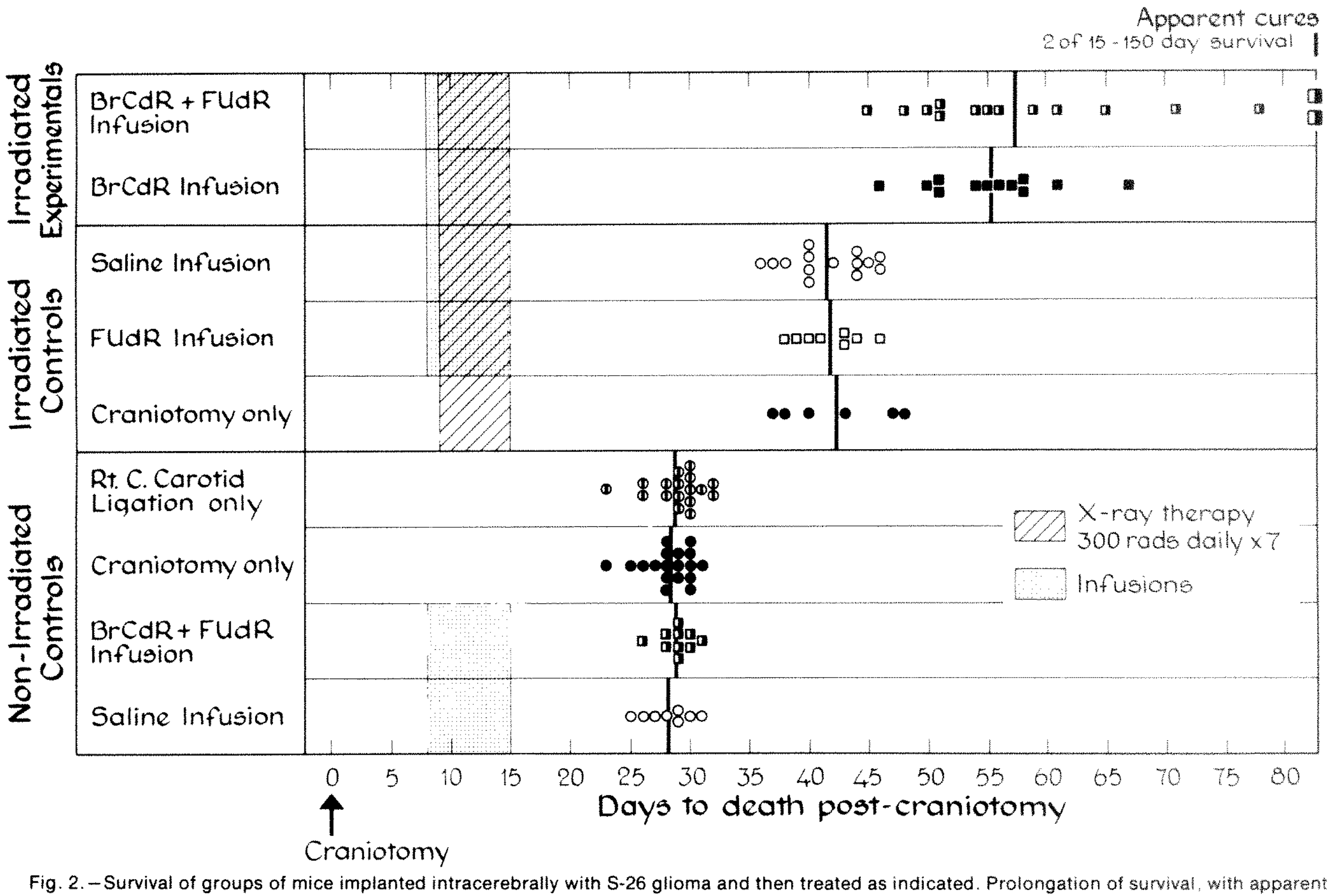

Fig. 2.—Survival of groups of mice implanted intracerebrally with S-26 glioma and then treated as indicated. Prolongation of survival, with apparent cure of two mice, is evident in group treated by infusion of halogenated pyrimidine analog 5-bromodeoxycytidine (BrCdR), with or without adjunctive 5-fluorodeoxyuridine (FUdR), followed by irradiation. BrCdR is known to be converted intracellularly to 5-bromodeoxyuridine (BUdR), then incorporated into cellular DNA. (Reprinted with permission from [16])

cells are permitted to rest in a mitotically inert state for a few hours after irradiation [26, 27]. A third form of repair occurs at the molecular level and involves the enzymatic rejoining of phosphodiester bonds at the site of single strand breaks, but not of double strand breaks, in DNA [28, 29].

Recovery from sublethal damage is essentially similar in normal tissues and in most tumors, and thus not subject to therapeutic exploitation. However, certain experimental tumors, such as osteogenic sarcomas and rhabdomyosarcomas [30], exhibit a very wide shoulder and high quasithreshold dose (D_q), suggesting that their capacity for recovery from sublethal damage may be significantly greater than that of most normal tissues. If so, this would readily explain their apparent radioresistance in treatments involving conventional fractionation, since a daily dose increment of 200 rad would fall in the shoulder region and recovery would occur before the next dose. We recently treated several osteogenic and soft tissue sarcomas with an atypical fractionation regimen involving the use of large dose increments (600–700 rad) to affect the tumor in the exponential region of the dose-survival curve, well beyond the shoulder. Such large dose increments are preceded by intraarterial infusions of BUdR, and are repeated every 5 days for a total of about 4,200–4,500 rad. Adjuvant chemotherapy (high dose methotrexate with leucovorin rescue) is also given in an effort to eradicate pulmonary micrometastases [22]. Preliminary results of this clinical investigation have been quite encouraging (fig. 3). It is likely that other types of tumors also exhibit high D_q values and would thus be more effectively treated with relatively large individual dose increments in an atypical fractionation schedule.

Both recovery from sublethal damage and repair of the single strand breaks in DNA may be inhibited by chemical agents, in particular those which are known to bind to DNA by intercalation. Several such intercalating agents, including quinacrine [31], proflavine [32], and lucanthone [33], have all been shown to sensitize cells when applied at the time of or shortly before irradiation, and to prevent the enzymatic rejoining of single strand breaks (fig. 4). It has therefore been presumed that their radiosensitizing action is attributable to their capacity to inhibit such repair.

The anthracycline antibiotic actinomycin D, which is also an intercalating agent, has been shown to prevent recovery from sublethal damage in split-dose experiments [34] and to increase the slope of the dose-survival curve [35], an effect which again may be attributable to inhibition of repair of single strand breaks. However, the action of this agent is complex, since it is also an actively cytotoxic cancer chemotherapeutic agent which is known to interact in a complementary manner with radiation in relation to cell cycle-dependent survival responses (age-response functions) [36]. Curiously, another anthracycline antibiotic and cancer chemotherapeutic agent, adriamycin, which is also known to bind to DNA and might thus have been expected to inhibit both recovery and repair in a manner similar to actinomycin D, has recently been reported to reduce the width of the shoulder region without affecting split-dose recovery or radiosensitivity [37, 38]. Actinomycin D, which was reported almost 20 years ago [39] to act as a radiosensitizer in children with Wilms's tumor, is the only chemical inhibitor of repair currently in widespread clinical use in conjunction with radiotherapy. However, a clinical trial in progress using lucanthone and radiotherapy has produced favorable preliminary results [33]. My personal feeling is that this group of compounds deserves more attention than they have had to date. They have significant potential as clinical radiosensitizers, since they act only at the time of and immediately following radiation, and could thus be delivered in an intraarterial pulse just prior to irradiation to achieve high concentrations in the tumor. Moreover, since these agents bind to DNA in both resting and mitotically active cells, they are not dependent on DNA synthesis for their incorporation and radiosensitizing action, as are the halogenated pyrimidine analogs.

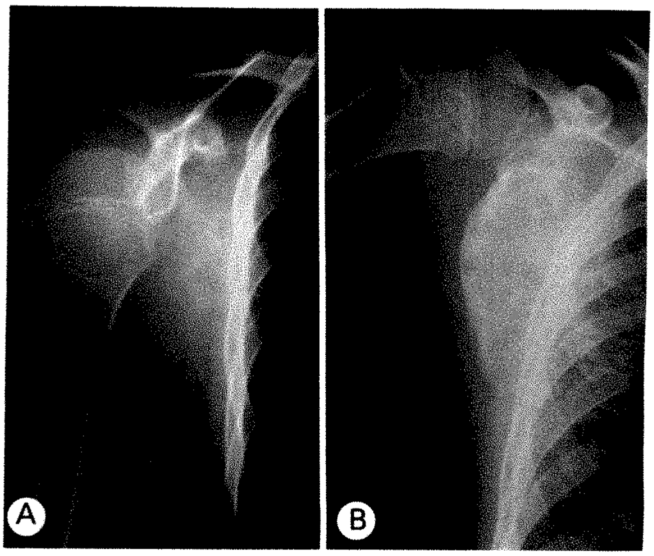

Fig. 3. – Pretreatment (*A*) and 6 months posttreatment (*B*) radiographs of osteogenic sarcoma of right scapula in 11-year-old boy treated with intraarterial infusion of BUdR and paucifractionated high incremental dose radiotherapy. Note increased calcification and partial restoration of bone architecture. (Reprinted with permission from [22])

Differential Chemical Radioprotection

Tourniquet hypoxia, mentioned above as an approach to the problem of hypoxic clonogenic cells in tumors, is necessarily limited in application to the relatively infrequent tumors which arise in the extremities. Chemical agents which confer radioprotection on normal tissues (and on well oxygenated regions in tumors) would not be expected to penetrate efficiently to hypoxic zones, and should thus protect hypoxic tumor cells little if at all. Yuhas and Storer [40] studied such a compound (aminopropylaminoethylphosphorothioate, WR-2721) and demonstrated that it reduced the radiation response of normal tissues, as measured by the LD50/30 in mice, by a factor of 2.60–2.72, whereas it decreased the radiation response of a transplantable tumor by a factor of only 1.14–1.15. More recently, similar differential effects have been demonstrated for normal tissue injury (hair loss) versus the response of autochthonous tumors in situ [41]. This approach has the merit that it could be applied to tumors almost anywhere in the body, since the agent seems to protect all normal tissues, with the possible exception of the central nervous system [42]. However, it

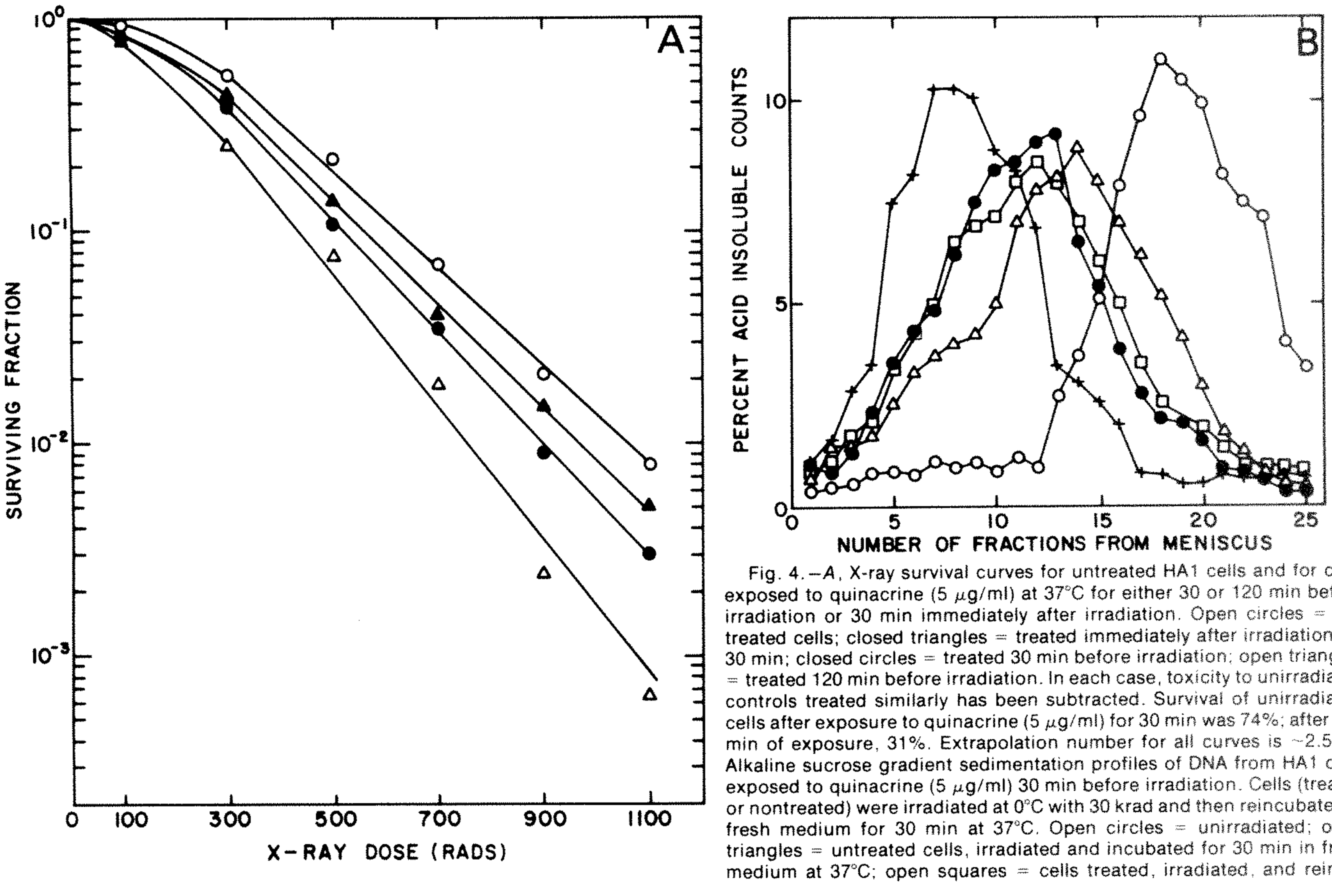

Fig. 4.—*A*, X-ray survival curves for untreated HA1 cells and for cells exposed to quinacrine (5 μg/ml) at 37°C for either 30 or 120 min before irradiation or 30 min immediately after irradiation. Open circles = untreated cells; closed triangles = treated immediately after irradiation for 30 min; closed circles = treated 30 min before irradiation; open triangles = treated 120 min before irradiation. In each case, toxicity to unirradiated controls treated similarly has been subtracted. Survival of unirradiated cells after exposure to quinacrine (5 μg/ml) for 30 min was 74%; after 120 min of exposure, 31%. Extrapolation number for all curves is ~2.5. *B*, Alkaline sucrose gradient sedimentation profiles of DNA from HA1 cells exposed to quinacrine (5 μg/ml) 30 min before irradiation. Cells (treated or nontreated) were irradiated at 0°C with 30 krad and then reincubated in fresh medium for 30 min at 37°C. Open circles = unirradiated; open triangles = untreated cells, irradiated and incubated for 30 min in fresh medium at 37°C; open squares = cells treated, irradiated, and reincubated in fresh medium for 30 min at 37°C; closed circles = cells treated and irradiated but not reincubated; cross = untreated cells, irradiated but not reincubated. (Reprinted with permission from [31])

has the same limitations as all other approaches to the problem of hypoxic clonogenic tumor cells. Extensive radiobiologic and toxicologic studies in animals will be required before the use of this or similar chemical compounds at the clinical level can be undertaken.

Combined Chemotherapy and Radiotherapy

Chemotherapeutic agents and radiation may display independent cytotoxicity, in which case their combined effects on primary tumors or regional metastases may be additive, or they may interact (potentiate, synergize) to yield tumor responses significantly greater than the sum of their individual effects. It is now well recognized that the cytotoxic effects of anticancer agents may be strongly dependent on cell proliferation [43, 44]. Ionizing radiation and the alkylating agents may be lethal for cells at any phase in the cell division cycle, as well as for nonproliferating cells, though some phases of the mitotic cycle are appreciably more sensitive than others [45]. In contrast, other chemotherapeutic agents are cytotoxic only during specific phases of the cell cycle (phase-dependent agents). Elkind and Sakamoto [36] observed that the age-response functions of x-rays and nitrogen mustard were essentially identical. Synchronized cells failed to reveal even additive lethal responses when treated with combinations of x-rays and nitrogen mustard in either sequence. Moreover, fractionation experiments provided no evidence that nitrogen mustard damage interacts appreciably with sublethal x-ray damage. Thus, nitrogen mustard and x-rays seem to have independent cytotoxic effects on cells, and the most that could be expected of their use in combination would be an additive response of the tumor with at least partially nonoverlapping toxic effects on normal tissues.

The results of studies by Elkind and Sakamoto [36] with actinomycin D and x-rays were quite different. Although the age-response pattern at a low dose (1.4 μg/ml) was similar to that of x-rays, the age-response function changed at a higher dose (3.5 μg/ml), with cells becoming resistant not only in late S phase, but also in the G_2 phase of the cell cycle. In fractionation experiments in which actinomycin D was applied at various time intervals after irradiation, survival was consistently lower than would have been expected if the two modalities had acted independently. The potentiation of cell killing observed with x-irradiation followed by actinomycin D seemed to be attributable in part to the fact that the two agents exert their maximal effects on cells at different stages in the cell cycle (age-response complementation).

Another type of potentiation can be imagined which employs pulsed treatment with DNA synthesis inhibitors such as hydroxyurea or mitotic spindle poisons (e.g., colchicine or the *Vinca* alkaloids) to block mitosis, followed by radiation exposure carefully timed to the radiosensitive late G_1/early S phase in the partially synchronized tumor cell population during escape from the block [24]. Though theoretically attractive, this concept cannot currently be implemented because we lack methods to detect the time of escape of tumors from mitotic arrest in vivo. Moreover, there is little or no evidence that the time of escape of tumors would differ appreciably from that of adjacent normal tissues, failing which no differential enhancement of tumor response could be expected.

Chemotherapeutic agents might conceivably enhance the efficacy of radiotherapy by inducing tumor shrinkage [46], thus improving the relative vascularity of the tumor and presumably diminishing the problem posed for radiotherapy by the presence of hypoxic clonogenic cells. This approach has been extensively exploited in clinical investigations, with a few reports of significant improvement in survival [47]. On the whole, however, rather disappointing results have been obtained in the majority of such clinical trials [20, 48, 49].

Steel [50] coined the term "spatial cooperation" to refer to situations in which combined modalities are effective because one agent eradicates foci of neoplasm which have been missed by the other. The most obvious example of this application is the use of adjuvant chemotherapy for the eradication of distant micrometastases in patients in whom surgery or high dose radiotherapy has been used locally to eradicate the primary tumor and perhaps also the regional lymph node metastases. A randomized clinical trial in which patients with Hodgkin's disease were treated with total lymphoid irradiation alone versus total lymphoid irradiation plus adjuvant MOP(P) chemotherapy revealed a highly significant decrease in relapse rate in patients receiving combined treatment, with an improvement in long term survival of patients with stage IIIB disease which approaches statistical significance [51]. Adjuvant combination chemotherapy has also been used following surgery in patients with cancer of the breast [52]. Although postmenopausal women experienced no significant long term decrease in relapse rate, relapses have been diminshed in the premenopausal group, perhaps secondary to hormonal rather than cytotoxic effects of the adjuvant treatment. As chemotherapeutic regimens with greater efficacy against so-called "solid" tumors are developed, it is likely that increasing success will be observed in the eradication of micrometastases in a widening spectrum of neoplasms.

Combined Surgery and Radiotherapy

A comprehensive review of the complex subject of combined surgery and radiotherapy is beyond the scope of this presentation. Three different sequences have been used: (1) radiotherapy followed by surgery (preoperative irradiation); (2) surgery followed by radiotherapy (postoperative irradiation); and (3) surgery both preceded and followed by radiotherapy ("sandwich" technique). Preoperative irradiation may be further subdivided into high and low dose regimens. The results of such studies have been difficult to assess, even in the infrequent instances in which concurrent randomized clinical trials have been performed to compare the combined approach with either irradiation or surgery alone.

Preoperative Irradiation

High doses of radiation have been employed with two rather different purposes. In cancers of the oral cavity and upper air passages, radiation doses of 6,500–7,000 rad have been used in an effort to eradicate the primary lesion; surgery is reserved for patients in whom local recurrences develop. This approach, more appropriately termed radiation therapy and rescue surgery, has been extensively explored by Fletcher and Jesse [53]. More moderate radiation doses, on the order of 5,000 rad, have been used successfully by the same investigators [54] in combination with surgery to decrease metastatic lymph node recurrence rates after neck dissection. However, the same combined regimen has failed to improve survival in patients with cancer of the lung, esophagus, and other sites associated with very high rates of distant metastasis. A general disadvantage of this approach is that surgery is delayed for several weeks and must be optimally timed with respect to radiotherapy to avoid complications such as impairment of wound healing.

Low dose preoperative irradiation has been advocated on radiobiologic grounds by Nias [55], who suggested the use of a single dose of 500 rad delivered on the day of surgery. Although his argument seems valid with respect to the prevention of local recurrences in the operative field, it seems unrealistic to suppose that such preoperative irradiation will also significantly prevent distant metastasis. Although the tumor manipulation which occurs during surgery is undoubtedly a factor contributing to dissemination, it is by no means the most important such factor, as can readily be appreciated by noting the high frequency of distant metastasis prior to biopsy diagnosis in patients with cancers arising in such sites as the lung, breast, ovary, or pancreas. Low dose preoperative irradiation will clearly offer no protection to the patient in whom distant micrometastases are already present; the only potentially useful approaches in such situations are systemic treatments such as adjuvant chemotherapy and/or immunotherapy. However, in the management of neoplasms such as cancer of the rectum, in which a significant proportion of patients die with local postoperative recurrence without distant metastasis [56], low to moderate dose irradiation followed rather promptly by surgery might well be expected to improve survival by decreasing the rate of local recurrence. Clinical evidence in support of this expectation has now emerged from several studies in patients with cancer of the rectum [57].

Postoperative Irradiation

Experience with postoperative irradiation has been replete with seeming paradoxes. There is little doubt that high dose postoperative irradiation of patients with stage II cancer of the ovary, in whom tumor is known to persist in the pelvis following surgery, has substantially increased survival [58]. Yet the same sequence of surgery and "rescue radiotherapy" has yielded disappointing salvage rates in patients with recurrent cancer of the head and neck region.

The use of high dose postoperative irradiation after simple or radical mastectomy in patients with stage II cancer of the breast involves an attempt to apply the above-cited principle of "spatial cooperation," using surgery to deal with the primary tumor and axillary node metastases, and radiation therapy to eradicate local recurrences and metastatic disease in the internal mammary and supraclavicular node chains. Although local recurrence rates are undoubtedly reduced, most reported studies, with some notable recent exceptions [59], fail to reveal any significant beneficial impact on survival.

Surgery with Pre- and Postoperative Irradiation

The so-called sandwich technique has been used principally in patients with stage II seminoma and carcinoma of the testis. While it has yielded excellent results [60], data are not yet available from large scale randomized clinical trials which demonstrate that survival significantly exceeds that attainable with high dose radiotherapy alone. Recently the same concept has begun to find application in the management of pelvic and paraaortic lymph node metastases from other pelvic primary sites (e.g., cervix, prostate, and bladder).

Hyperthermia Combined with Radiotherapy, Chemotherapy, and Ultrasound

Interest in the possibility of using elevated temperatures to destroy tumor cells has waxed and waned for many years. Hyperthermia recently has been studied much more extensively and quantitatively to assess its potential as a single modality and as a sensitizing pretreatment. With rare exceptions [61], hyperthermia alone has been found differentially lethal for transformed or neoplastic cells, relative to its effect on the corresponding normal tissues [62]. Lethality is a function of the temperature and the duration of exposure. It is also now well established that hyperthermia sensitizes cells to the lethal effects of ionizing radiation (fig. 5), as manifested by a significant increase in slope and reduction in D_q of the dose-survival curve in vitro [61, 64–66] and by sharply decreased values for 50% tumor cure probability (TCD_{50}) in vivo [67, 68]. The degree of sensitization is critically dependent on temperature, with enhanced responses beginning to appear at about 41°C and becoming pronounced at 43°C or above.

The effect of hyperthermia on several radiobiologic components of the radiation response has now been carefully studied. Recovery from potentially lethal and sublethal damage was profoundly inhibited [63, 69, 70], with a concomitant reduction in the width of the shoulder region and increase in slope of the dose-survival curve.

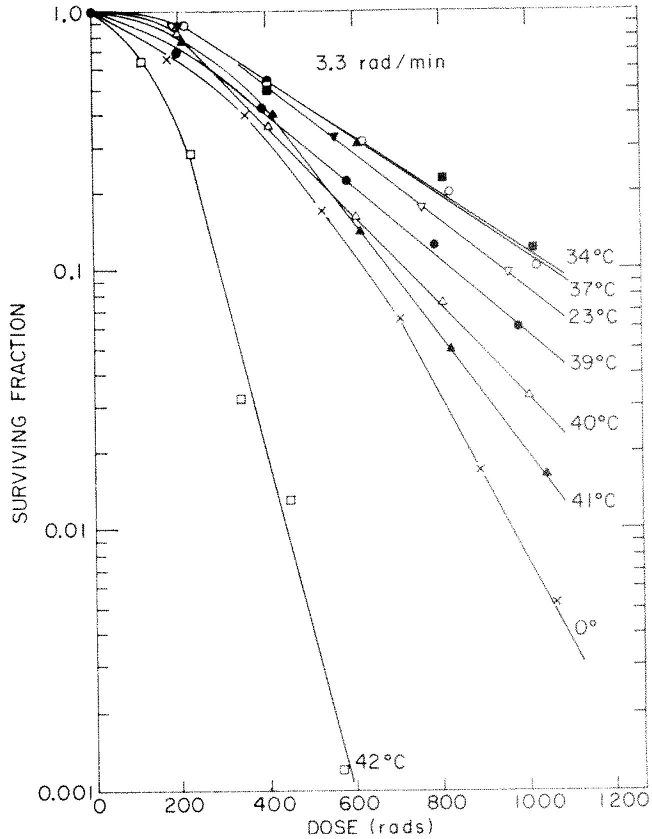

Fig. 5.—Survival of Chinese hamster cells x-irradiated while suspended in DUM-20 at different temperatures (250 kVp, 3.3 rad/min). (Reprinted with permission from [63])

Leith et al. [66] reported a decrease of D_q from 209 to 174, 143, and 87 rad at 37°, 41°, 42°, and 43°C, respectively. Radiosensitization appears to be optimized when the temperature is elevated for a short interval (15 min) before and for a longer interval (45–60 min) after irradiation [70]. The repair of single strand breaks was accelerated, rather than inhibited, at 42°C; however, an increased extent of degradation of radiation-damaged DNA at 42°C was observed [71], which may account for the increased slope of the exponential region of the dose-survival curve of cells exposed to both radiation and significantly elevated temperatures in the 41°–44°C range. Hyperthermia also interferes with mitosis, causing a block in both the S and $G_2 + M$ phases of the cell cycle [72]. Cells seem to be significantly more sensitive to high temperature in certain phases of the cell cycle than in others [73]. Finally, hypoxic cells are considerably more sensitive to the lethal effect of increased temperature than are well oxygenated cells [74]. Hyperthermia reduces the dependence of radiation response on oxygen [75, 76], and would be expected to be helpful in eradication of hypoxic clonogenic tumor cells. Thus the interactions of hyperthermia and ionizing radiation, which are still poorly understood at the molecular level, seem to be extremely complex, involving effects on recovery, effects on the slope of the dose-survival curve, apparent effects on the extent (rather than the rate) of DNA repair, possible complementary effects on age-response functions, and clearly differential effects on hypoxic versus oxic cells resulting in a significant decrease in oxygen enhancement ratio.

The sensitizing effects of hyperthermia are not limited to radiation. Increase of temperature to about 43°C also has been shown to dramatically increase the lethal effect of certain cancer chemotherapeutic agents, notably adriamycin and bleomycin [77, 78] (fig. 6), and the cytotoxic effect of ultrasound [79] (fig. 7). Moreover, it is possible that there may be synergistic interactions between these agents under hyperthermic conditions. The use of hyperthermia in conjunction with radiotherapy, chemotherapy, and/or ultrasound clearly offers exciting new prospects for the treatment of cancer. However, it has also been demonstrated that hyperthermia can decrease the threshold for radiation damage to vital normal tissues such as the spinal cord [80, 81] suggesting that clinical investigations must be approached cautiously. In particular, it will be desirable to assess the susceptibility of normal liver and lung tissue to graded temperatures over various intervals. If their tolerance proves to be at least as good as that of other normal tissues, the possibility of applying hyperthermia combined with adriamycin or ultrasound to the eradication of metastasis in these two major metastatic sites can be seriously entertained.

Although significant advances in the development of microwave, radiofrequency, and ultrasound sources for the induction of hyperthermia have been made in small laboratory animals, the induction of uniform temperatures in the 43°C range in defined volumes of variable shape deep within the human body and the precise monitoring of temperature gradients within such volumes remain formidable technologic problems. I suggest that much of the difficulty could be obviated if hyperthermia were applied directly to the exposed (presumably inoperable) tumor during surgery, and temperatures monitored by thermistor needles implanted at selected sites within the tumor under direct vision. When the desired temperature has been maintained for an appropriate interval, the selected second modality (irradiation, intraarterial infusion of chemotherapeutic agents, or direct application of ultrasound) can also be carried out during surgery. For radiotherapy, this would require ceiling-mounted x-ray apparatus operating in the 250 kVp range, the addition of lead protection to the operating room walls, and the use of highly unorthodox, relatively high single dose increments. If the tumor were in close proximity to vital tissues and organs (e.g., liver, kidney, or gastrointestinal tract), such structures could be displaced by layers of inert material and thus shielded from both the hyperthermia and the irradiation.

If clinically observed sensitization proves to be as striking as that seen experimentally, it would be desirable to administer allopurinol to prevent acute uric acid nephropathy. After tumor regression, it would be quite feasible to continue treatment with external beam megavoltage radiotherapy to dose levels at which a high probability of complete tumor eradication could be expected. Since the total external beam dose would be relatively small, the tolerance of normal tisues for such combined therapy should be better than that following conventional radiotherapy alone. It might also be possible to fractionate such hyperthermic radiation treatments by inducing hyperthermia via wires uniformly implanted through the tumor volume and left in situ for some weeks, after which the wires and the concurrently implanted thermistors could be surgically removed. Exploitation of the full potential of hyperthermic combined modality therapy will clearly require a great deal of ingenuity and a willingness to depart from orthodox methods. However, the potential of this approach seems exciting enough to warrant such measures.

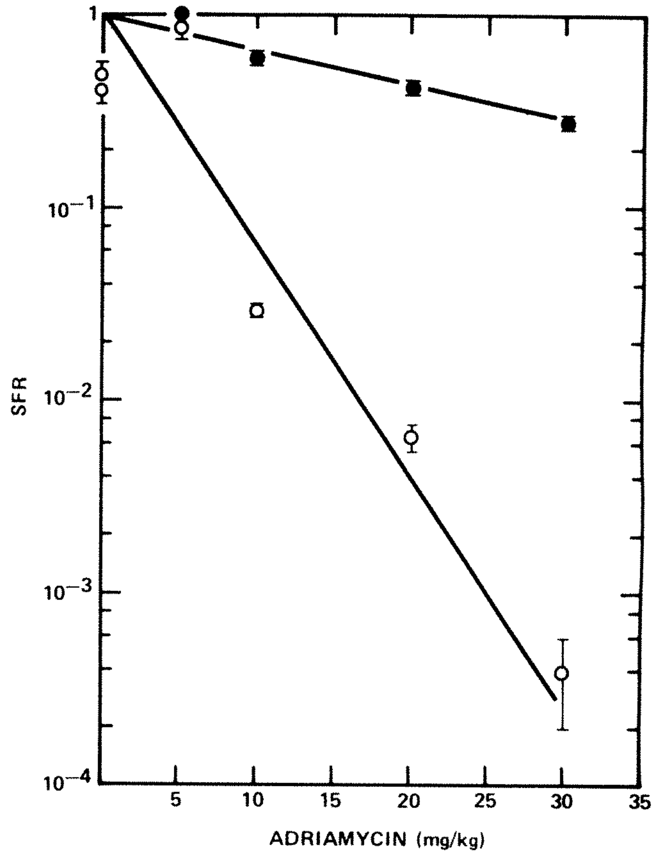

Fig. 6.—Survival (SFR) of EMT-6 tumor cells from tumor-bearing mice treated for 1 hr with indicated concentration of adriamycin while maintained at 37°C (*closed circles*) or at 43°C (*open circles*). (Reprinted with permission from [78])

Adjuvant Immunotherapy after Surgery, Radiotherapy, or Chemotherapy

Nonspecific immunotherapy utilizes adjuvants such as BCG or *C. parvum* to stimulate the macrophages of the host immune system, in the hope that a hyperactive immune system will more effectively carry out tumor surveillance functions, resulting in the inhibition of tumor growth. These treatments are not intended to be given alone; instead, they are aimed at preventing tumor

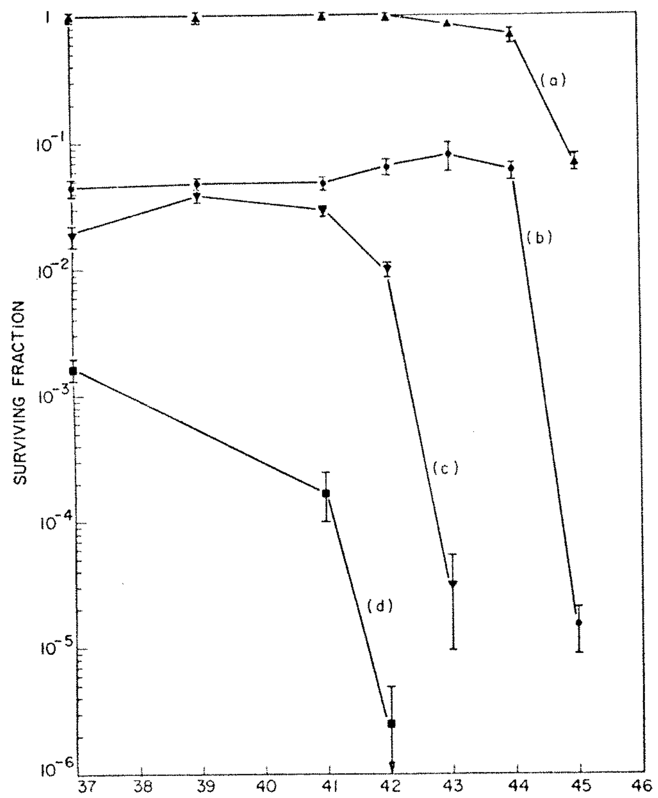

Fig. 7.—Surviving fractions of cells exposed to ultrasound for 30 min at different temperatures and intensities. *a*, heat alone; *b*, 1 W/cm²; *c*, 2 W/cm²; *d*, 2.2 W/cm². (Reprinted with permission from [79])

recurrence in patients whose tumors have been surgically removed or destroyed by irradiation or drugs. Since essentially complete tumor regression has been achieved by such conventional treatments, the effect of immunotherapy can only be assessed in terms of survival and relapse rates. Controversy prevails regarding reported increases of survival in patients with acute leukemia treated with chemotherapy and BCG [82], and in patients with soft tissue or osteogenic sarcomas, malignant melanomas, and other tumors. If there is indeed a real and significant improvement in survival, it would seem to be of small magnitude.

Specific immunotherapy, when developed sufficiently for clinical application, is likely to involve the reinjection into patients of their own peripheral blood lymphocytes sensitized to become cytotoxic "killer" cells by contact, either directly or indirectly via macrophages, with the antigens of their own or similar types of tumor cells. This procedure has been observed to prevent the development of pulmonary micrometastases, and to enhance cure rates, in mice from which previously transplanted "primary" tumors composed of syngeneic Lewis lung carcinoma cells have been surgically removed [83]. Recent studies indicate the feasibility of inducing significant cytotoxicity against lymphoma cells in human peripheral blood lymphocyte subpopulations sensitized in vitro against the same or similar human lymphoma cell lines [84]. However, several problems remain to be worked out in the laboratory before this technique can be introduced at the clinical level.

Conclusions

The current intensification of interest in combined modality approaches stems from our awareness of the limitations which confront any single modality in the management of most patients with cancer. From the analysis presented here, it is clear that rich opportunities lie ahead in combined modality therapies of several types. The intelligent use of these treatments in combination will require an understanding of the underlying mechanisms of their interaction. The assessment of their clinical value will require well designed, carefully conducted randomized clinical trials. One of the most salutary by-products of the emphasis on combined modality therapy is that it is also a strong integrative stimulus which will encourage all physicians who treat cancer, whatever their therapeutic modality, to work together more closely than ever before. From such close cooperation and communication, the cancer patient is bound to benefit, whatever the ultimate merits of combined modality therapy.

REFERENCES

1. Gray LH: Oxygenation in radiotherapy. I. Radiobiological considerations. *Br J Radiol* 30:403-406, 1957
2. Thomlinson RH, Gray LH: The histological structure of some human lung cancers and the possible implications for radiotherapy. *Br J Cancer* 9:539-549, 1955
3. Hall EJ: The oxygen effect—pertinent or irrelevant to clinical radiotherapy? *Br J Radiol* 40:874-875, 1967
4. Kaplan HS: On the relative importance of hypoxic cells for the radiotherapy of human tumours. *Eur J Cancer* 10:275-280, 1974
5. Withers HR: Biological basis for high-LET radiotherapy. *Radiology* 108:131-137, 1973
6. Glassburn JR, Brady LW, Plenk HP: Hyperbaric oxygen in radiation therapy. *Cancer* 39:751-765, 1977
7. Suit HD, Lindberg R: Radiation therapy administered under conditions of tourniquet-induced local tissue anoxia. *Am J Roentgenol* 103:27-37, 1968
8. van den Brenk HAS, Kerr RC, Madigan JP, Cass NM, Richter W: Results from tourniquet anoxia and hyperbaric oxygen techniques combined with megavoltage treatment of sarcomas of bone and soft tissues. *Am J Roentgenol* 96:760-776, 1966
9. Adams GE, Asquith JC, Watts ME: Electron-affinic sensitizers for hypoxic cells irradiated *in vitro* and *in vivo:* current status, in *Advances in Chemical Radiosensitization*, Vienna, International Atomic Energy Agency, 1974, pp 1-12
10. Emmerson PT, Howard-Flanders P: Sensitisation of anoxic bacteria to x-rays by di-*t*-butyl nitroxide and analogues. *Nature* 204:1005-1006, 1964
11. Brown JM: Selective radiosensitization of the hypoxic cells of mouse tumors with the nitroimidazoles metronidazole and Ro 7-0582. *Radiat Res* 64:633-647, 1975
12. Fowler J, Adams G, Denekamp J: Radiosensitizers of hypoxic cells in solid tumors. *Cancer Treat Rev* 3:227-256, 1976
13. Heidelberger C, Chaudhari NK, Danneberg P, Mooren D, Griesbach L, Duschinsky R, Schnitzer RJ, Pleven E, Schei-

ner J: Fluorinated pyrimidines, a new class of tumor-inhibitory compounds. *Nature* 179:663-666, 1957

14. Kaplan HS, Smith KC, Tomlin P: Radiosensitization of *E. coli* by purine and pyrimidine analogues incorporated in deoxyribonucleic acid. *Nature* 190:794-796, 1961
15. Djordjevic B, Szybalski W: Genetics of human cell lines. III. Incorporation of 5-homo- and 5-iododeoxyuridine into the deoxyribonucleic acid of human cells and its effect on radiation sensitivity. *J Exp Med* 112:519-531, 1960
16. Goffinet DR, Brown JM, Bagshaw MA, Kaplan HS: Prolonged carotid arterial radiosensitizer infusion and radiation therapy of mouse gliomas. *Am J Roentgenol* 114:7-15, 1972
17. Kaplan HS: Radiosensitization by the halogenated pyrimidine analogues: laboratory and clinical investigations, in *Radiation Protection and Sensitization*, edited by Moroson HL, Quintiliani M, London, Taylor & Francis, 1970, pp 35-42
18. Maruyama Y, Silini G, Kaplan HS: Studies of the LSA ascites lymphoma of C57BL mice. II. Radiosensitization *in vivo* with 5-bromodeoxycytidine and combined 5-fluorodeoxyuridine and 5-bromodeoxycytidine. *Int J Radiat Biol* 7:453-464, 1963
19. Kriss JP, Révész L: The distribution and fate of bromodeoxyuridine and bromodeoxycytidine in the mouse and rat. *Cancer Res* 22:254-265, 1962
20. Bagshaw MA, Doggett RLS: A clinical study of chemical radiosensitization. *Front Radiat Ther Oncol* 4:164-173, 1969
21. Hoshino T, Sano K: Radiosensitization of malignant brain tumors in bromouridine (thymidine analogue). *Acta Radiol [Ther] (Stockh)* 8:15-26, 1969
22. Goffinet DR, Kaplan HS, Donaldson SS, Bagshaw MA, Wilbur JR: Combined radiosensitizer infusion and irradiation of osteogenic sarcomas. *Radiology* 117:211-214, 1975
23. Cooper GM, Greer S: Irreversible inhibition of dehalogenation of 5-iodouracil by 5-diazouracil and reversible inhibition by 5-cyanouracil. *Cancer Res* 30:2937-2941, 1970
24. Brown JM: Exploitation of kinetic differences between normal and malignant cells. *Radiology* 114:189-197, 1975
25. Elkind MM, Sutton H: Radiation response of mammalian cells grown in culture. I. Repair of x-ray damage in surviving Chinese hamster cells. *Radiat Res* 13:556-593, 1960
26. Hahn GM, Rockwell S, Kallman RF, Gordon LF, Frimdel E: Repair of potentially lethal damage *in vivo* in solid tumor cells after X-irradiation. *Cancer Res* 34:351-354, 1974
27. Phillips RA, Tolmach LJ: Repair of potentially lethal damage in X-irradiated HeLa cells. *Radiat Res* 29:413-432, 1966
28. Kaplan HS: DNA strand scission and loss of viability after x-irradiation of normal and sensitized bacterial cells. *Proc Natl Acad Sci USA* 55:1442-1446, 1966
29. McGrath RA, Williams RW: Reconstruction *in vivo* of irradiated *Escherichia coli* deoxyribonucleic acid: the rejoining of broken pieces. *Nature* 212:534-535, 1966
30. Reinhold HS: Quantitative evaluation of the radiosensitivity of cells of a transplantable rhabdomyosarcoma in the rat. *Eur J Cancer* 2:33-42, 1966
31. Voiculetz N, Smith KC, Kaplan HS: Effect of quinacrine on survival and DNA repair in X-irradiated Chinese hamster cells. *Cancer Res* 34:1038-1044, 1974
32. Kapp DS: Production and repair of x-ray induced strand breaks in DNA: in vitro and vivo studies. Ph.D. thesis, Stanford University, 1970
33. Turner S, Bases RE, Pearlman A, Nobler M, Kabakow B: The adjuvant effect of lucanthone (Miracil D) in clinical radiation therapy. *Radiology* 114:729-731, 1975
34. Elkind MM, Whitmore GF, Alescio T: Actinomycin D: suppression of recovery in x-irradiated mammalian cells. *Science* 143:1454-1457, 1964
35. Bases RE: Modification of the radiation response determined by single-cell technics: actinomycin D. *Cancer Res* 19:1223-1229, 1959
36. Elkind MM, Sakamoto K: Combined effects of x-irradiation and chemotherapeutic drugs (nitrogen mustard and actinomycin D). *Front Radiat Ther Oncol* 4:53-75, 1969
37. Belli JA, Piro AJ: The interaction between radiation and adriamycin damage in mammalian cells. *Cancer Res* 37:1624-1630, 1977
38. Byfield JE, Lynch M, Kulhanian F, Chan PYM: Cellular effects of combined adriamycin and x-irradiation in human tumor cells. *Int J Cancer* 19:194-204, 1977
39. D'Angio GJ: Clinical and biologic studies of actinomycin D and roentgen irradiation. *Am J Roentgenol* 87:106-109, 1962
40. Yuhas JM, Storer JB: Differential chemoprotection of normal and malignant tissues. *J Natl Cancer Inst* 42:331-335, 1969
41. Yuhas JM: Improvement of lung tumor radiotherapy through differential chemoprotection of normal and tumor tissue. *J Natl Cancer Inst* 48:1255-1257, 1972
42. Yuhas JM, Storer JB: Chemoprotection against three modes of radiation death in the mouse. *Int J Radiat Biol* 15:233-238, 1969
43. Hahn GM: Radiotherapy and chemotherapy: some parallels and differences. *Radiology* 114:203-211, 1975
44. Valeriote F, van Putten L: Proliferation-dependent cytotoxicity of anticancer agents: a review. *Cancer Res* 35:2619-2630, 1975
45. Terasima T, Tolmach LJ: Variations in several responses of HeLa cells to x-irradiation during the division cycle. *Biophys J* 3:11-33, 1963
46. Friedman M, Daly JF: Combined irradiation and chemotherapy in the treatment of squamous cell carcinoma of the head and neck. *Am J Roentgenol* 90:246-260, 1963
47. Gollin FF, Ansfield FJ, Brandenburg JH, Ramirez G, Vermund H: Combined therapy in advanced head and neck cancer: a randomized study. *Am J Roentgenol* 114:83-88, 1972
48. Knowlton AH, Percarpio B, Bobrow S, Fischer JJ: Methotrexate and radiation therapy in the treatment of advanced head and neck tumors. *Radiology* 116:709-712, 1975
49. Stefani S, Eells RW, Abbate J: Hydroxyurea and radiotherapy in head and neck cancer. Results of a prospective controlled study in 126 patients. *Radiology* 101:391-396, 1971
50. Steel GG: Mechanisms of action of combined radiotherapy and chemotherapy. Submitted for publication
51. Rosenberg SA, Kaplan HS, Glatstein E, Portlock CS: The role of adjuvant MOPP in the radiation therapy of Hodgkin's disease: a progress report after eight years on the Stanford trials, in *Adjuvant Therapy of Cancer*, Amsterdam, Elsevier/North-Holland Press. In press, 1977
52. Bonadonna G, Brusamolino E, Valagussa P, Rossi A, Burgnatelli L, Brambilla C, DeLena M, Tancini G, Bajetta E, Musumeci R, Veronesi U: Combination chemotherapy as an adjuvant treatment in operable breast cancer. *N Engl J Med* 294:405-410, 1976
53. Fletcher GH, Jesse RH: The contribution of supervoltage roentgenotherapy to the integration of radiation and surgery in head and neck squamous cell carcinomas. *Cancer* 15:566-577, 1962

54. Jesse RH, Fletcher GH: Treatment of the neck in patients with squamous cell carcinoma of the head and neck. *Cancer* 39:868-872, 1977
55. Nias AHW: Radiobiological aspects of pre-operative irradiation. *Br J Radiol* 40:166-169, 1967
56. Morson BC, Bussey HJR: Surgical pathology of rectal cancer in relation to adjuvant radiotherapy. *Br J Radiol* 40:161-165, 1967
57. Kligerman MM: Radiotherapy and rectal cancer. *Cancer* 39:896-900, 1977
58. Fuks Z: External radiotherapy of ovarian cancer: standard approaches and new frontiers. *Semin Oncol* 2:253-266, 1975
59. Høst H: Postoperative radiotherapy in breast cancer. Paper presented at the European Congress of Radiology, Edinburgh, 1975
60. Earle JD, Bagshaw MA, Kaplan HS: Supervoltage radiation therapy of the testicular tumors. *Am J Roentgenol* 117:653-661, 1973
61. Harisiadis L, Hall EJ, Kraljevic U, Borek C: Hyperthermia: biological studies at the cellular level. *Radiology* 117:447-452, 1975
62. Giovanella BC, Stehlin JS, Morgan AC: Selective lethal effect of supranormal temperatures on human neoplastic cells. *Cancer Res* 39:3944-3950, 1976
63. Ben-Hur E, Elkind MM, Bronk BV: Thermally enhanced radioresponse of cultured Chinese hamster cells—inhibition of repair of sublethal damage and enhancement of lethal range. *Radiat Res* 58:38-51, 1974
64. Belli JA, Bonte FJ: Influence of temperature on the radiation response of mammalian cells in tissue culture. *Radiat Res* 18:272-276, 1963
65. Ben-Hur E, Bronk BV, Elkind MM: Thermally enhanced radiosensitivity of cultured Chinese hamster cells. *Nature [New Biol]* 238:209-211, 1972
66. Leith JT, Miller RC, Gerner EW, Boone MLM: Hyperthermic potentiation. Biological aspects and applications to radiation therapy. *Cancer* 39:766-779, 1977
67. Robinson JE, Wizenberg MJ, McCready WA: Radiation and hyperthermal response of normal tissue *in situ*. *Radiology* 113:195-198, 1974
68. Thrall DE, Gillette EL, Dewey WC: Effect of heat and ionizing radiation on normal and neoplastic tissue of the C_3H mouse. *Radiat Res* 63:363-377, 1975
69. Harris JR, Murthy AK, Belli JA: The effect of hyperthermia on the repair of radiation damage in plateau phase cells. *Radiology* 119:227-229, 1976
70. Li GC, Evans RG, Hahn GM: Modification and inhibition of repair of potentially lethal x-ray damage by hyperthermia. *Radiat Res* 67:491-501, 1976
71. Ben-Hur E, Elkind MM: Thermally enhanced radioresponse of cultured Chinese hamster cells: damage and repair of single-stranded DNA and a DNA complex. *Radiat Res* 59:484-495, 1974
72. Kal HB, Hatfield M, Hahn GM: Cell cycle progression of murine sarcoma cells after x-irradiation or heat shock. *Radiology* 117:215-217, 1975
73. Westra A, Dewey WC: Variation in sensitivity to heat shock during the cell cycle of Chinese hamster cells *in vitro*. *Int J Radiat Biol* 19:467-477, 1971
74. Schulman N, Hall EJ: Hyperthermia: its effect on proliferative and plateau phase cell cultures. *Radiology* 113:209-211, 1974
75. Kim SH, Kim JH, Hahn EW: The radiosensitization of hypoxic tumor cells by hyperthermia. *Radiology* 114:727-728, 1975
76. Robinson JE, Wizenberg MJ, McCready WA: Combined hyperthermia and radiation suggest an alternative to heavy particle therapy for reduced oxygen enhancement ratios. *Nature* 251:521-522, 1974
77. Braun J, Hahn GM: Enhanced cell killing by bleomycin and 43° hyperthermia and the inhibition of recovery from potentially lethal damage. *Cancer Res* 35:2921-2927, 1975
78. Hahn GM, Braun J, Har-Kedar I: Thermochemotherapy: synergism between hyperthermia (42-43°) and adriamycin (or bleomycin) in mammalian cell inactivation. *Proc Natl Acad Sci USA* 72:937-940, 1975
79. Li GC, Hahn GM, Tolmach LJ: Cellular inactivation by ultrasound. *Nature* 267:163-165, 1977
80. Goffinet DR, Choi KY, Brown JM: The combined effects of hyperthermia and ionizing radiation on the adult mouse spinal cord. *Radiat Res*. In press, 1977
81. Miller RC, Leith JT, Gerner EW, Veomett RC: Potentiation of radiation myelitis in rats by hyperthermia. *Br J Radiol*. In press, 1977
82. Mathé G, Amiel JL, Schwarzenberg L, Schneider M, Cattan A, Schlumberger JR, Hayat M, de Vassal F: Active immunotherapy for acute lymphoblastic leukemia. *Lancet* 1:697-699, 1969
83. Schechter B, Treves AJ, Feldman M: Specific cytotoxicity *in vitro* in lymphocytes sensitized in culture against tumor cells. *J Natl Cancer Inst* 56:975-979, 1976
84. Treves AJ, Feldman M, Kaplan HS: *In vitro* sensitization of human lymphocytes against histiocytic lymphoma cell lines. I. Primary sensitization of lymphocyte subpopulations. *J Immunol*. In press, 1977

Diagnosis and Evaluation of Retroperitoneal Tumors by Computed Tomography

DAVID H. STEPHENS,[1] PATRICK F. SHEEDY, II, ROBERT R. HATTERY, AND BYRN WILLIAMSON, JR.

Nineteen patients with primary and recurrent retroperitoneal tumors were examined by computed tomography. Correlation between CT and subsequent operative findings was remarkably accurate. CT provided clinically useful information regarding the presence, size, extent, and composition of the tumors and also their effect on adjacent structures. CT is recommended for any patient suspected to have a primary or recurrent retroperitoneal tumor.

The diagnosis of tumors that arise from the retroperitoneal tissues has long been a difficult problem. Conventional radiologic methods usually provide only indirect and imprecise information, even when the tumors attain enormous size. Because of its usual abundant fat and relatively uncomplicated cross-sectional anatomy [1], the retroperitoneal space is especially suitable for examinations by computed tomography (CT). We report the results of our initial experience with CT in the diagnosis and evaluation of primary retroperitoneal tumors and their recurrence.

Subjects and Methods

On reviewing the records of all patients who had abdominal CT during our first 15 months experience with computed body tomography, we found that 19 patients had tumors which originated in the retroperitoneum. At the time of their CT examinations, nine patients had primary retroperitoneal tumors with no prior surgical exploration or established tissue diagnosis. The other 10 patients were evaluated for suspected recurrences of previously resected retroperitoneal neoplasms. All nine of the patients without previously established diagnoses subsequently underwent surgical exploration, and five of the patients with recurrent tumors had subsequent surgery. The interval between CT and surgery in most cases was less than a week and in no case did the interval exceed a month. Thus, relevant operative and gross pathologic information was available for correlation in 14 of the 19 cases.

Twelve of the 19 patients were male. Ages ranged from 2 to 72 years, with half over age 50. The eventual histologic classification of their tumors is listed in table 1. Aside from one lymphatic cyst, all tumors were malignant. Two tumors, designated respectively as undifferentiated round cell neoplasm and mesenchymal sarcoma, could not be classified more specifically.

Not included in this report are lymphomas and metastatic malignancies involving retroperitoneal lymph nodes. Primary tumors of retroperitoneal organs such as pancreas, adrenals, and kidneys as well as tumors that extend into the retroperitoneal space from primary sites in the peritoneal cavity or spine were also excluded.

Two EMI body scanning instruments were used in the CT examinations. With these units, each cross-sectional reconstruction represents 13 mm of tissue thickness and is displayed on a 320 × 320 matrix. All adults in this series were able to suspend respiration during the 20 sec required for each scan.

Conduct of the CT examinations was monitored by a radiologist. In some cases, dilute water-soluble oral contrast material

TABLE 1

Distribution of Retroperitoneal Tumors

Tumor	No. Cases
Leiomyosarcoma:	
Primary	3
Recurrent	4
Liposarcoma, recurrent	2
Fibrous histiocytoma:	
Primary	1
Recurrent	2
Fibrosarcoma, recurrent	1
Hemangiopericytoma, primary	1
Mesenchymal sarcoma, primary	1
Undifferentiated round cell neoplasm, primary	1
Malignant teratoma, primary	1
Paraganglioma, recurrent	1
Lymphatic cyst, primary	1

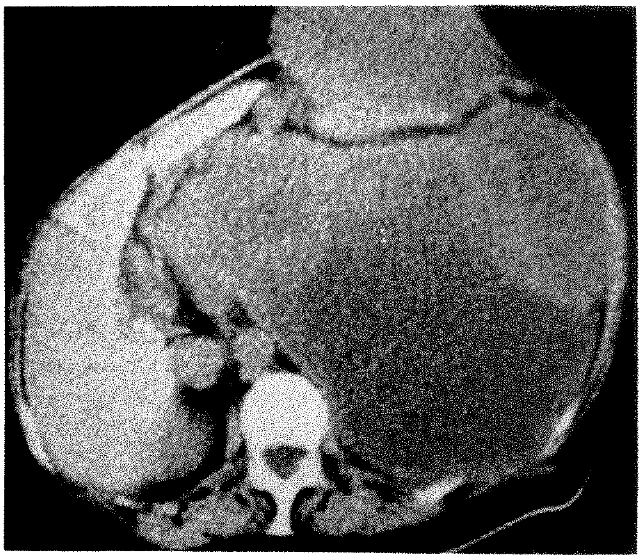

Fig. 1.—Leiomyosarcoma (recurrent). Scan 5 years after resection of retroperitoneal smooth muscle tumor showing huge multiloculated tumor filling large part of abdominal cavity and ventral hernia. Planes between tumor and liver are preserved; there is also plane between mass in hernia and larger intraabdominal mass. Although not completely resectable, tumor was pseudoencapsulated permitting removal of bulk of tumor by blunt dissection. Mass in hernia was separate.

Received April 5, 1977; accepted May 20, 1977.

[1] All authors: Department of Diagnostic Roentgenology, Mayo Clinic and Mayo Foundation, Rochester, Minnesota 55901. Address reprint requests to D. H. Stephens.

Am J Roentgenol **129:395–402, September 1977**

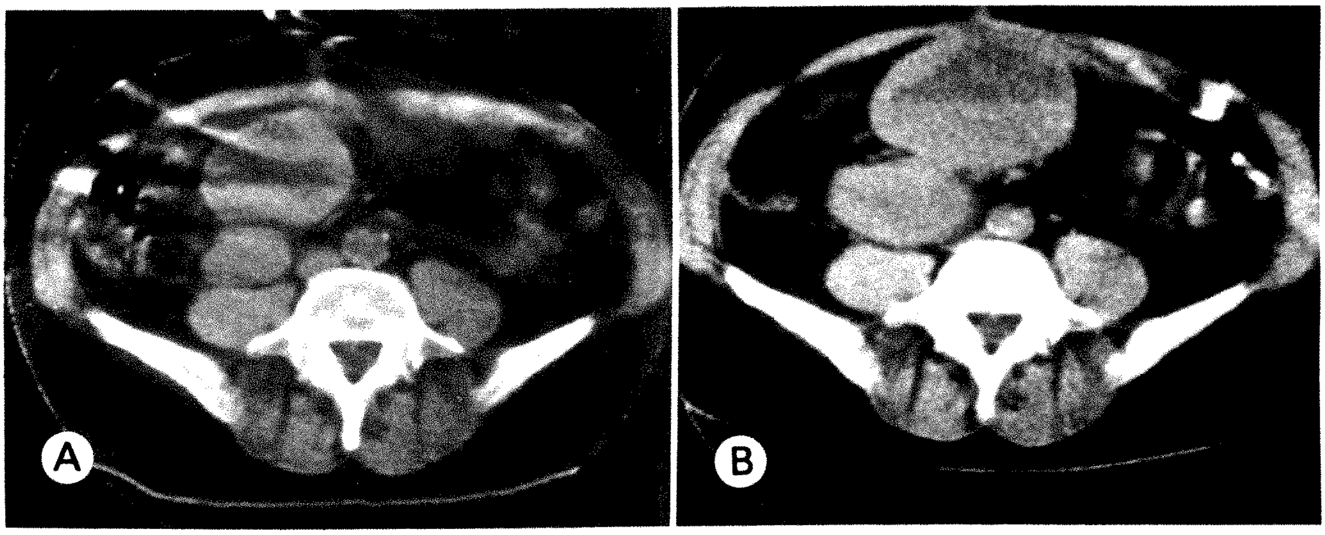

Fig. 2. – Leiomyosarcoma (recurrent). Scans at 6 week interval showing growth of tumor despite chemotherapy. Two tumor masses anterior to right ileopsoas muscle. Note cavitary appearance of larger (anterior) mass with apparent fluid level.

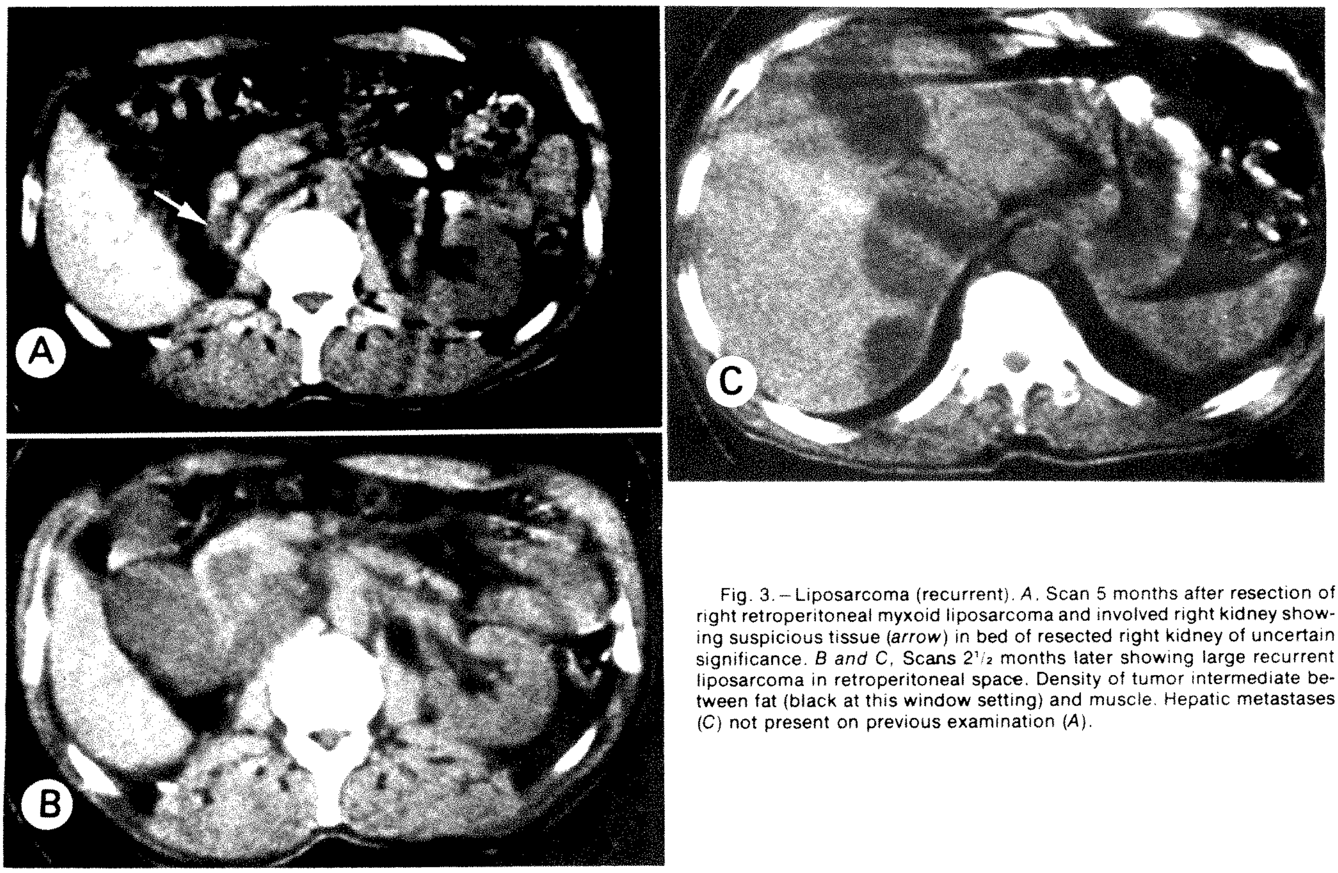

Fig. 3. – Liposarcoma (recurrent). *A*, Scan 5 months after resection of right retroperitoneal myxoid liposarcoma and involved right kidney showing suspicious tissue (*arrow*) in bed of resected right kidney of uncertain significance. *B and C*, Scans 2½ months later showing large recurrent liposarcoma in retroperitoneal space. Density of tumor intermediate between fat (black at this window setting) and muscle. Hepatic metastases (*C*) not present on previous examination (*A*).

was used to opacify the gastrointestinal lumen, and intravenous iodinated contrast material was used to opacify the urinary tract or blood vessels. To take advantage of all the information present on abdominal scans, the images were viewed at a variety of window settings.

Results

In the 14 cases in which surgical exploration followed CT, there was remarkably accurate correlation between the CT findings and the operative and gross pathologic findings. In the patients not subjected to further surgery, CT was valuable as a method of following tumor progression or response to treatment.

Detection

In 18 of the 19 cases, the retroperitoneal neoplasms were obvious on the CT scans. Only the recurrent paraganglioma was not well shown. In that case, disruption

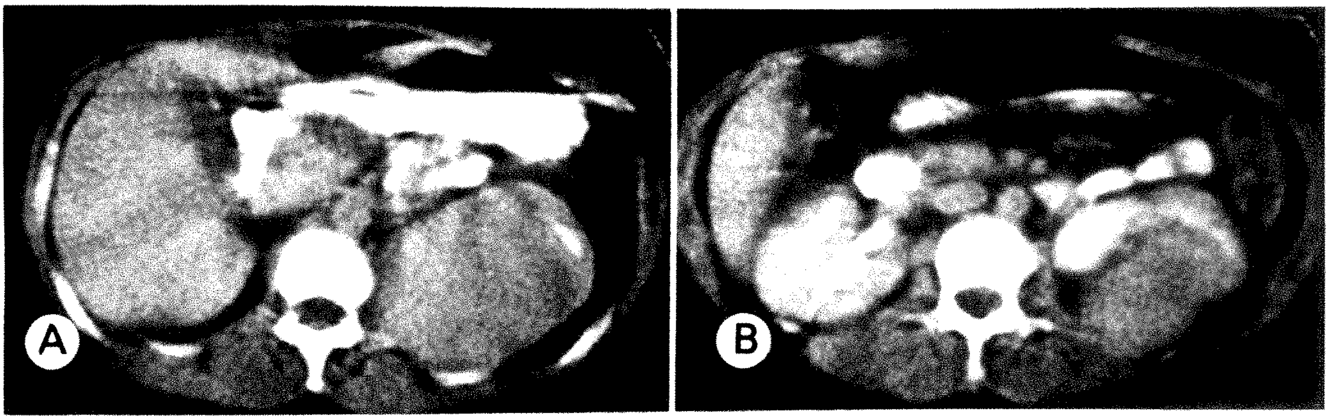

Fig. 4.—Malignant fibrous histiocytoma (recurrent). Scans showing tumor invading left kidney, compressing and distorting opacified renal parenchyma and pyelocalyceal system. Appearance resembles renal carcinoma. Scans made after intravenous and oral contrast administration.

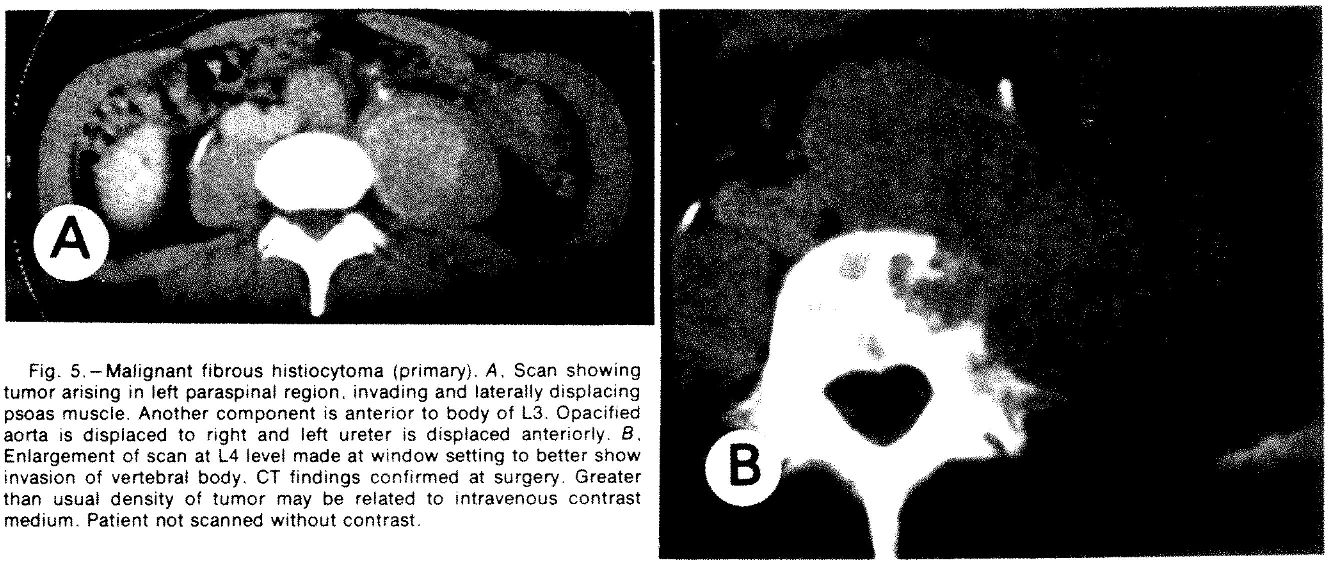

Fig. 5.—Malignant fibrous histiocytoma (primary). *A*, Scan showing tumor arising in left paraspinal region, invading and laterally displacing psoas muscle. Another component is anterior to body of L3. Opacified aorta is displaced to right and left ureter is displaced anteriorly. *B*, Enlargement of scan at L4 level made at window setting to better show invasion of vertebral body. CT findings confirmed at surgery. Greater than usual density of tumor may be related to intravenous contrast medium. Patient not scanned without contrast.

of tissue planes by previous surgery, artifacts emanating from multiple metal clips, and a paucity of retroperitoneal fat made it impossible to detect the mass. The examination was considered indeterminate rather than normal. A 2.5 cm mass was found at surgery. In the other eight cases of tumor recurrence, previous surgical intervention did not significantly interfere with tumor detection.

Size

As is usual with retroperitoneal tumors at the time of their discovery, most of the masses in this series were quite large. Of the 19 tumors, 13 were larger than 10 cm in greatest diameter. At the extreme were enormous tumors, some occupying the greater part of the abdominal cavity and one even protruding beyond (fig. 1).

Because CT accurately displayed the dimensions of the tumors, follow-up examinations were useful to detect changes in size of remaining tumors (figs. 2 and 3). Four of the patients in our series had more than one CT examination.

Location

The location of all the detected tumors was accurately displayed. One tumor that had infiltrated the kidney could not be differentiated by CT findings from a renal carcinoma, but its origin was already known (fig. 4). In another case, previously reported [2], a 5 × 7 cm leiomyosarcoma contiguous with the pancreas but not attached to it was misinterpreted as a pancreatic tumor.

Only five of the 19 tumors were predominately in the paraspinal or posterior pararenal parts of the retroperitoneal space (figs. 4–6). The greater portions of the other 14 tumors were in front of the plane of the spine and psoas muscles. Despite their retroperitoneal origin, many of the tumors projected forward to just beneath the anterior abdominal wall (figs. 1, 2, and 7). One tumor extended through the diaphragm and into the chest (fig. 6). Multiple separate masses, often bilateral, were common among the larger tumors (figs. 1, 2, and 7).

Effect on Adjacent Structures

CT provided important information concerning the effect of tumors on adjacent anatomic structures. Among

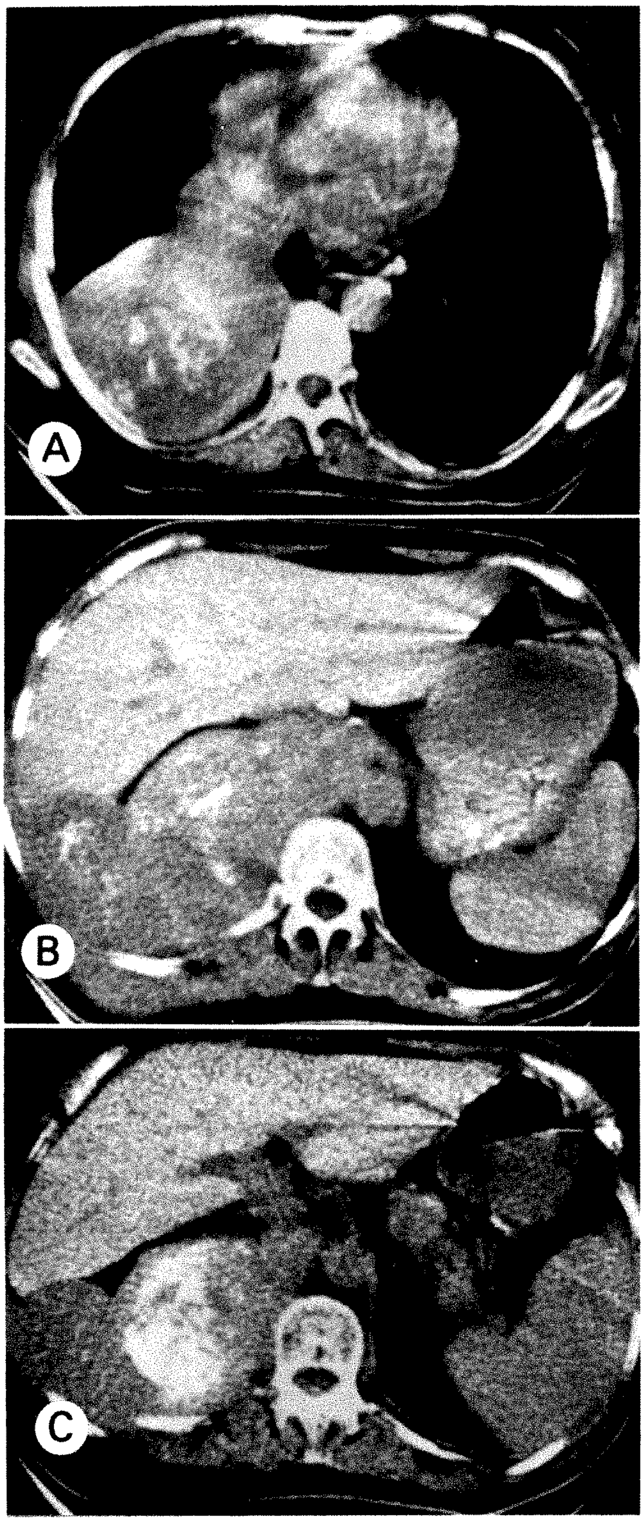

Fig. 6.—Malignant fibrous histiocytoma (recurrent). Scans 3 years after resection of original tumor showing locally aggressive recurrence extending into chest (*A*) and muscles of back (*B*). Note calcification within tumor (*C*).

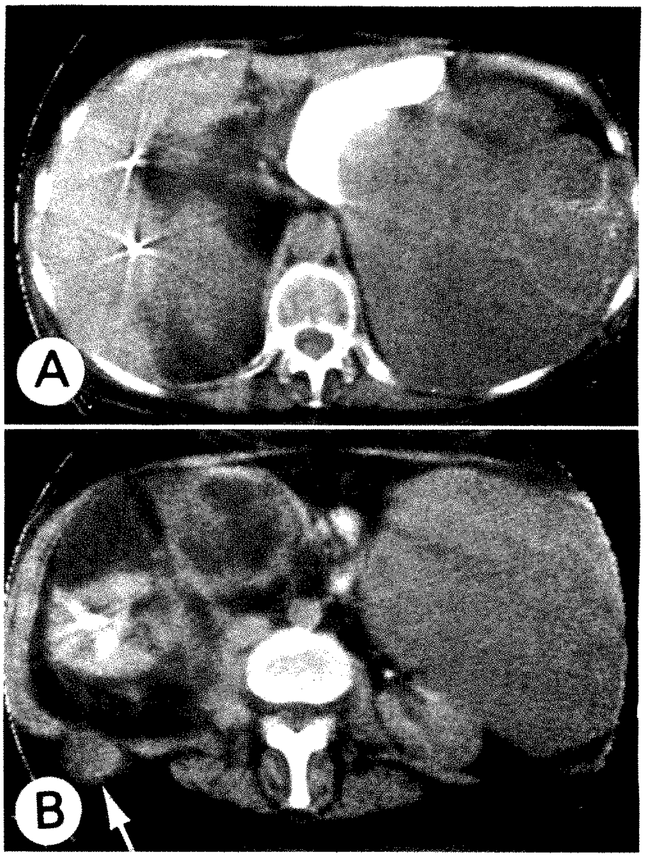

Fig. 7.—Liposarcoma (recurrent). Scans showing huge tumor occupying most of left abdominal cavity and recurrence on right. *A*, Mass compresses and displaces opacified stomach. Circular calcifications in left tumor were not apparent on plain radiographs. Stellate artifacts on right caused by metal clips. *B*, Separate tumor mass in posterior abdominal wall on right (*arrow*).

the 19 cases, virtually all of the abdominal viscera as well as adjacent bone and muscle were seen to be affected by tumor masses. Observed effects included displacement, compression, attachment, and invasion. The relation between a mass and an adjacent structure was most accurately displayed when the plane of their interface was perpendicular to the x-ray beam. When adjacent organs were merely displaced or compressed, CT usually showed the separating tissue planes to be preserved (figs. 1 and 8). These planes were obliterated when tumors became attached (figs. 8 and 9). In several cases tumors were seen to be invading the substance of contiguous structures (figs. 4–6).

Composition

The displayed radiographic densities of the masses provided information about their tissue composition. Central necrosis and tissue degeneration, common among the larger tumors of most types, was seen as diminished central density. This feature was especially prevalent among the leiomyosarcomas, five of which had surgically confirmed cystic degeneration. Evidence of tumor degeneration varied from slight internal diminished density (fig. 8), to obvious cavitation with inhomogeneous contents (fig. 2), to formation of cystic-appear-

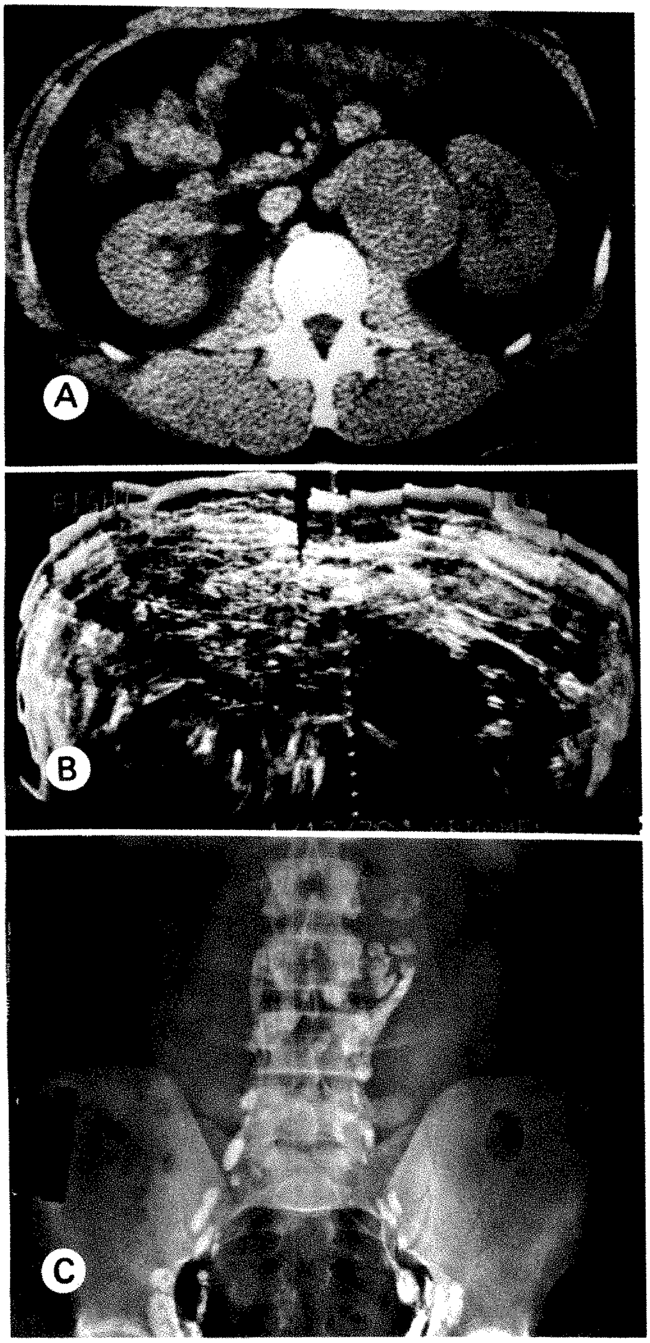

Fig. 8.—Malignant teratoma (primary). *A*, CT scan showing large spherical tumor between aorta and left kidney. Note attachment to aorta, making complete resection impossible. Left kidney laterally displaced but not attached to tumor. Low density components of mass probably represent areas of necrosis subsequently found in removed specimen. *B*, Gray scale ultrasonogram at about same level showing tumor mass. *C*, Lymphogram showing enlarged and distorted nodes in region of tumor but not showing main tumor mass.

ing masses (figs. 1 and 9). Differences in density within a mass were best displayed at narrow window settings (fig. 9).

Despite their origin from adipose tissue, both liposarcomas were of an appreciably greater density than normal retroperitoneal fat and, in fact, were of a slightly greater density than water (figs. 3 and 7). Although the liposarcomas were on the average of slightly lower density than the solid parts of the other sarcomas, their density was no less than the cystic parts of the other tumors.

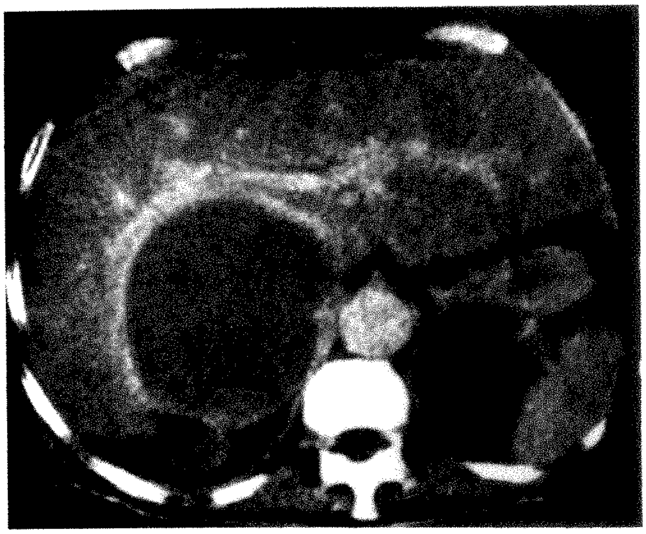

Fig. 9.—Leiomyosarcoma (primary). Scan made after intravenous contrast administration at window settings to display cystic features of tumor. At surgery, large multiloculated tumor could not be separated from undersurface of liver. Note contrast opacification of aorta and intrahepatic vessels.

The solid components of most of the nonlipomatous tumors were about the same density as muscle. One of the fibrous histiocytomas, scanned only with intravenous contrast material, had a density slightly greater than the adjacent muscle (fig. 5). The lesion with the lowest density was the benign cyst, which contained chylous fluid (fig. 10). The only tumors to show calcification were a fibrous histiocytoma (fig. 6) and a liposarcoma (fig. 7).

Metastases

In addition to demonstrating direct extension and metastasis within the retroperitoneal space, CT revealed unsuspected metastatic lesions within the liver (fig. 3*C*) in two cases and outside the abdominal cavity in another (fig. 7*B*).

Comparison with Other Diagnostic Methods

These patients were not subjected to a standard set of diagnostic procedures, but most had at least one other abdominal radiologic examination.

Excretory urography was performed on 12 patients; only one urogram was normal. Seven urograms showed displacement of the kidney or ureter correctly interpreted as caused by an extraurinary mass. On some films, the outline of a soft tissue mass could be seen (fig. 10*A*). Two retroperitoneal masses that had infiltrated or become attached to the kidney could not be distinguished on urography from primary renal tumors. Ureteral obstruction was present in only one case.

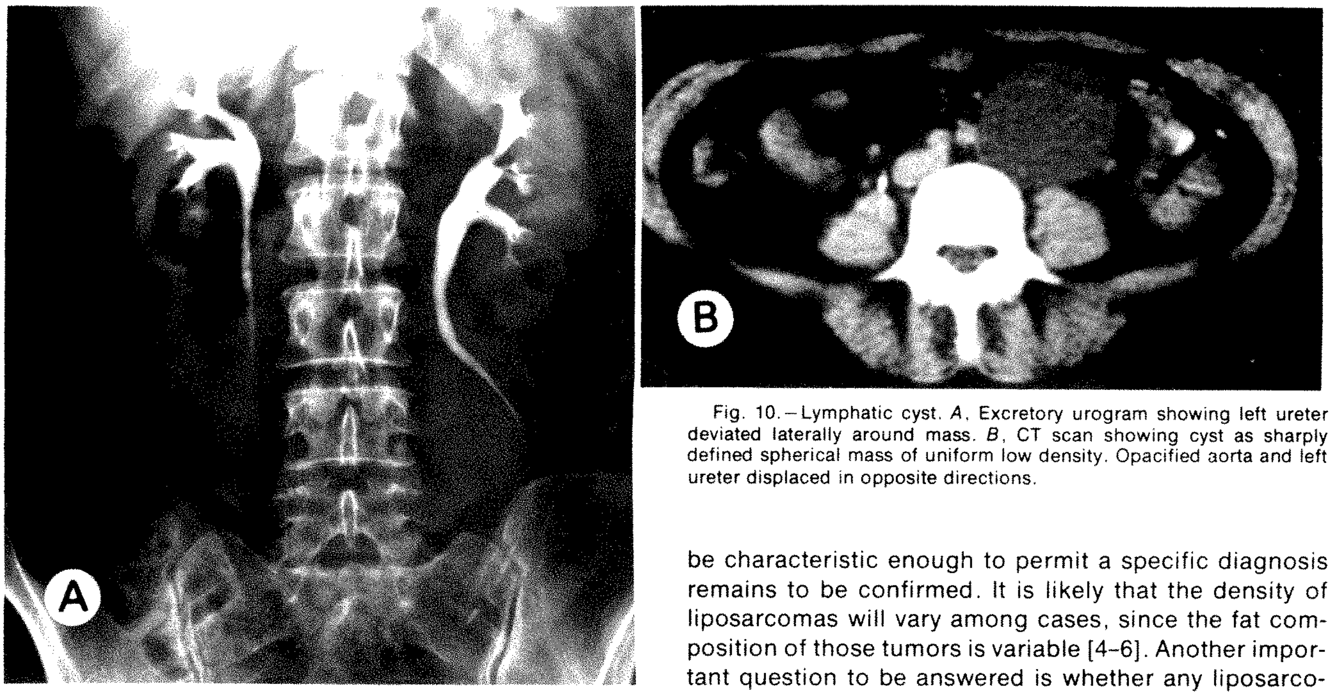

Fig. 10.—Lymphatic cyst. *A*, Excretory urogram showing left ureter deviated laterally around mass. *B*, CT scan showing cyst as sharply defined spherical mass of uniform low density. Opacified aorta and left ureter displaced in opposite directions.

Five patients were examined by ultrasound, and the presence of a mass was identified in all cases. Although ultrasound successfully displayed four of the malignant tumors, the information provided was less precise than that provided by CT, especially with regard to the extent of a lesion and its relation to adjacent structures (fig. 8*B*). The benign cyst was depicted equally well with CT and ultrasound.

Only three patients had angiography, which was usually done less as a diagnostic procedure than to identify the blood supply prior to surgery. One of the leiomyosarcomas was not identified by angiography, but the recurrent paraganglioma that was not clearly shown on CT was identified as a vascular mass by aortography.

The only tumor studied by lymphography was the malignant teratoma. While the lymphogram was clearly abnormal, it did not display the major part of the mass (fig. 8C).

Discussion

Since primary retroperitoneal tumors are uncommon and any series is likely to contain several types of tumors, further experience must be accumulated before many CT findings can be considered characteristic of any one type of tumor. In our series only the benign cyst (fig. 10) had features that clearly set it apart from the other tumors. Among the malignant tumors we found little evidence to permit differentiation of one type from another. Our observations support the reported tendency of leiomyosarcomas to undergo cystic degeneration [3] (figs. 1, 2, and 9), but degeneration was not limited to the smooth muscle sarcomas. Whether the relatively low density of the two liposarcomas in our series (figs. 3 and 7) will prove to be characteristic enough to permit a specific diagnosis remains to be confirmed. It is likely that the density of liposarcomas will vary among cases, since the fat composition of those tumors is variable [4–6]. Another important question to be answered is whether any liposarcomas will be of low enough density to be indistinguishable from normal retroperitoneal fat. Like the two liposarcomas reported here, four others that we have seen in the extremities have been of greater density than normal fat. However, S. Sagel and R. J. Stanley (personal communication) observed one well differentiated liposarcoma in which a large part, though not all, of the tumor was of the same density as normal fat.

Much more common than primary retroperitoneal tumors are neoplasms that involve retroperitoneal lymph nodes: lymphomas and metastatic tumors. While it is not always possible to differentiate these processes from primary retroperitoneal tumors on CT, there are distinguishing features which, together with clinical information, should permit proper interpretation in most cases. Lymph nodes are located along the major abdominal arteries. Lymphomatous paraaortic nodes tend to appear as homogeneous masses that envelop the aorta and vena cava. Metastatically involved nodes may be seen as single or multiple discrete or conglomerate masses in paraaortic or other nodal locations. We have seen very few retroperitoneal metastases that approach the size of the larger primary retroperitoneal tumors. In most cases of both lymphomatous and metastatic retroperitoneal lymphadenopathy, the primary diagnosis will already have been established by the time the retroperitoneal disease is discovered.

Retroperitoneal tumors may resemble primary tumors of organs that they infiltrate (fig. 4). Conversely, primary tumors of retroperitoneal organs such as pancreas and kidney occasionally project into the retroperitoneal space to such an extent that they may resemble retroperitoneal tumors. Usually the bulk of such a mass will remain with the organ of its origin. We have seen one large thrombotic saccular aortic aneurysm that extended to one side and simulated a cavitating tumor [7].

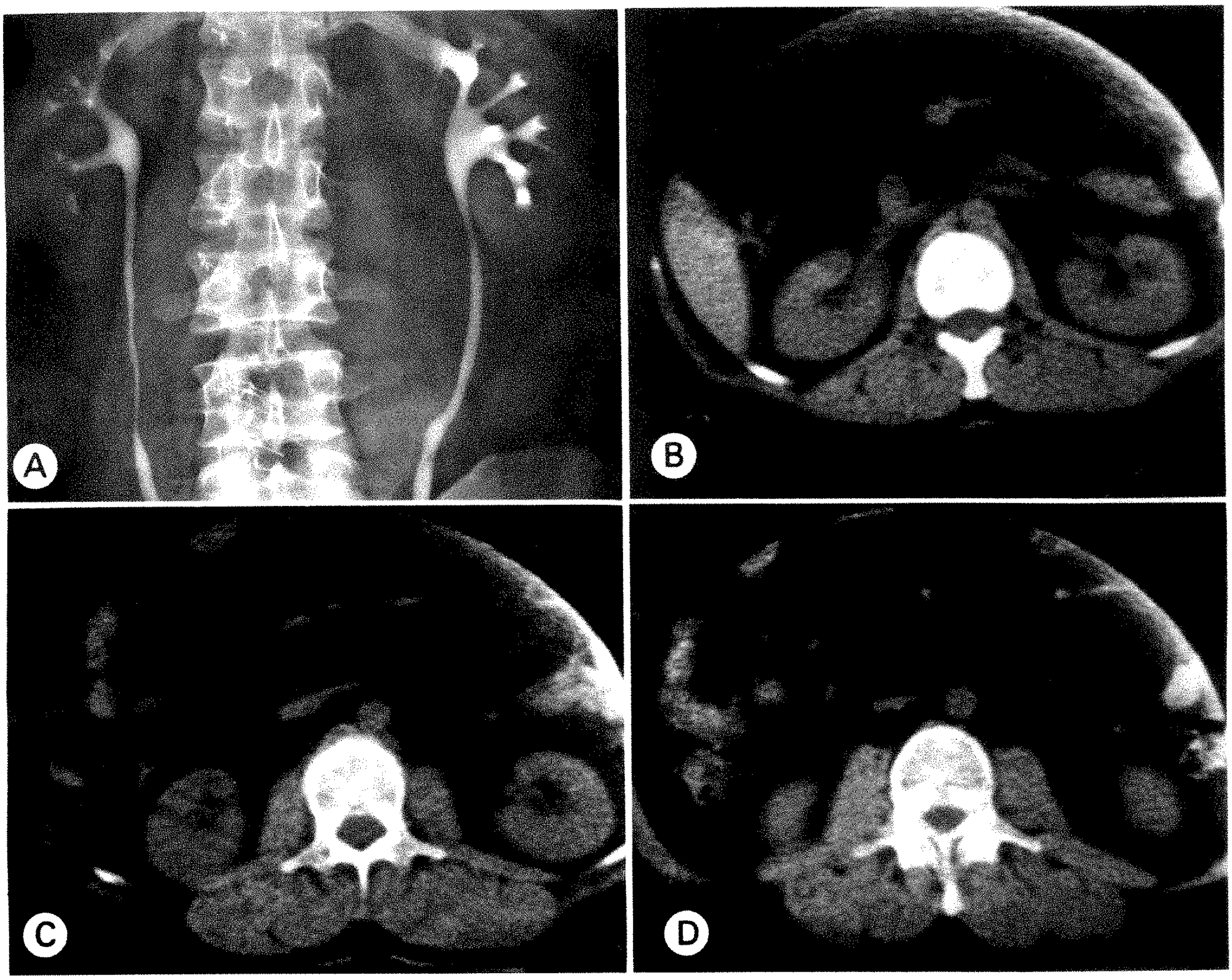

Fig. 11.—Normal variant. *A*, Excretory urogram showing laterally placed left lower kidney and upper ureter, raising question of retroperitoneal mass. *B–D*, CT scans showing deviation of renal axis and upper ureter to be normal variant in patient with abundant retroperitoneal fat.

Other retroperitoneal lesions that might appear similar to tumors on CT are infectious processes such as paraspinal and perinephric abscesses. In these cases, the clinical information will usually be helpful.

Perhaps as important clinically as the detection and differential diagnosis of a retroperitoneal tumor is the exclusion of a suspected tumor. Although primary retroperitoneal tumors are uncommon, they are frequently considered in clinical differential diagnoses. The question of a retroperitoneal mass may also be raised by radiologic findings, such as a soft tissue density on an abdominal radiograph or urographic suggestion of renal or ureteral displacement. In such problems, CT provides an easy and accurate solution (fig. 11).

Conclusions

The results of this review strongly support earlier observations that CT has a major role in the diagnosis of retroperitoneal tumors and their recurrences [7–11]. The clinical usefulness of the information provided by CT is readily apparent. No longer is the lack of an accurate and easily performed diagnostic method a limitation to early detection. Even in cases of advanced tumors, the knowledge provided by CT is invaluable in developing a rational approach to management. Accurate assessment of the extent of a tumor and its relation to adjacent structures is especially important in preoperative surgical planning. Often the extent of a retroperitoneal tumor is more graphically displayed by CT than at surgery. In radiation therapy the advantages of precise localization of a tumor are obvious. For patients receiving chemotherapy or radiation, CT is an excellent method to monitor tumor progression or response.

In summary, CT is an easily accomplished diagnostic method which provides highly accurate and clinically useful information about retroperitoneal tumors. We believe that its use is indicated in any case of suspected primary or recurrent retroperitoneal tumor.

REFERENCES

1. Meyers MA: *Dynamic Radiology of the Abdomen: Normal and Pathologic Anatomy*. New York, Springer, 1976
2. Sheedy PF II, Stephens DH, Hattery RR, MacCarty RL: Computed tomography in the evaluation of patients with suspected carcinoma of the pancreas. Submitted for publication
3. Lumb G: Smooth muscle tumors of the gastrointestinal tract and retroperitoneal tissues presenting as large cystic masses. *J Pathol* 63:139-147, 1951
4. Stout AP: Liposarcoma, the malignant tumor of lipoblasts. *Ann Surg* 119:86-107, 1944
5. Ackerman LV: Tumors of the retroperitoneum, mesentery and peritoneum, in *Atlas of Tumor Pathology*, fascicles 23 and 24, Washington, D.C., Armed Forces Institute of Pathology, 1954
6. Pack GT, Tabak EJ: Collective review: primary retroperitoneal tumors; a study of 120 cases. *Int Abstr Surg* 99:209-231, 313-341, 1954
7. Sheedy PF II, Stephens DH, Hattery RR, Muhm JR, Hartman GW: Computed tomography of the body: initial clinical trial with the EMI prototype. *Am J Roentgenol* 127: 23-51, 1976
8. Alfidi RJ, Haaga JR: Computed body tomography. *Radiol Clin North Am* 14: 563-570, 1976
9. Kreel L: Computerized tomography using the EMI general purpose scanner. *Br J Radiol* 50:2-14, 1977
10. Stanley RJ, Sagel SS, Levitt RG: Computed tomography: early trends in application and accuracy of the method. *Am J Roentgenol* 127: 53-67, 1976
11. Stephens DH, Hattery RR, Sheedy PF II: Computed tomography of the abdomen: early experience with the EMI body scanner. *Radiology* 119:331-335, 1976

Detection of Retroperitoneal Hemorrhage by Computed Tomography

STUART S. SAGEL,[1] MARILYN J. SIEGEL, ROBERT J. STANLEY, AND R. GILBERT JOST

Retroperitoneal hemorrhage can be directly documented by computed tomography. In patients with confusing clinical findings, CT scans may provide a definite diagnoses and direct appropriate therapy. This contention is supported by seven illustrative cases.

Introduction

Hemorrhage into the retroperitoneal space may create a diagnostic dilemma, particularly in the patient without a history of traumatic injury. While clinical evidence may implicate the diagnosis (sudden abdominal pain and development of an abdominal mass in association with a falling hematocrit), often the presentation is less suggestive. The symptoms and signs (vague abdominal pain, thigh pain, low grade fever, hypoactive bowel sounds) may be ambiguous, delayed, or misleading. Conventional radiographic methods used to document retroperitoneal hemorrhage rely greatly upon inferential signs and lack both sensitivity and specificity. Plain abdominal radiographs may demonstrate obscuration of a psoas margin, but slight rotation or minimal spinal scoliosis can cause a similar appearance. About 25% of normal individuals show unequal definition of the psoas borders [1]. Other indirect findings, such as a soft tissue mass, intestinal "ileus" pattern, or displacement or indentation of neighboring organs (kidneys, ureters, stomach, small intestine, or colon), may be visible on plain or contrast radiographs.

Computed tomography is an accurate noninvasive method for directly imaging and discovering disorders of the retroperitoneal space [2, 3] (fig. 1). Sharp delineation of the retroperitoneal structures by surrounding extraperitoneal fat is seen in all but the thinnest patients. Retroperitoneal hemorrhage is detectable on the CT scan as an abnormal soft tissue density, with resultant obscuration, displacement, or compression of normal retroperitoneal structures. Attenuation values within the hematoma are 10–30 EMI units (on a scale of −500 for

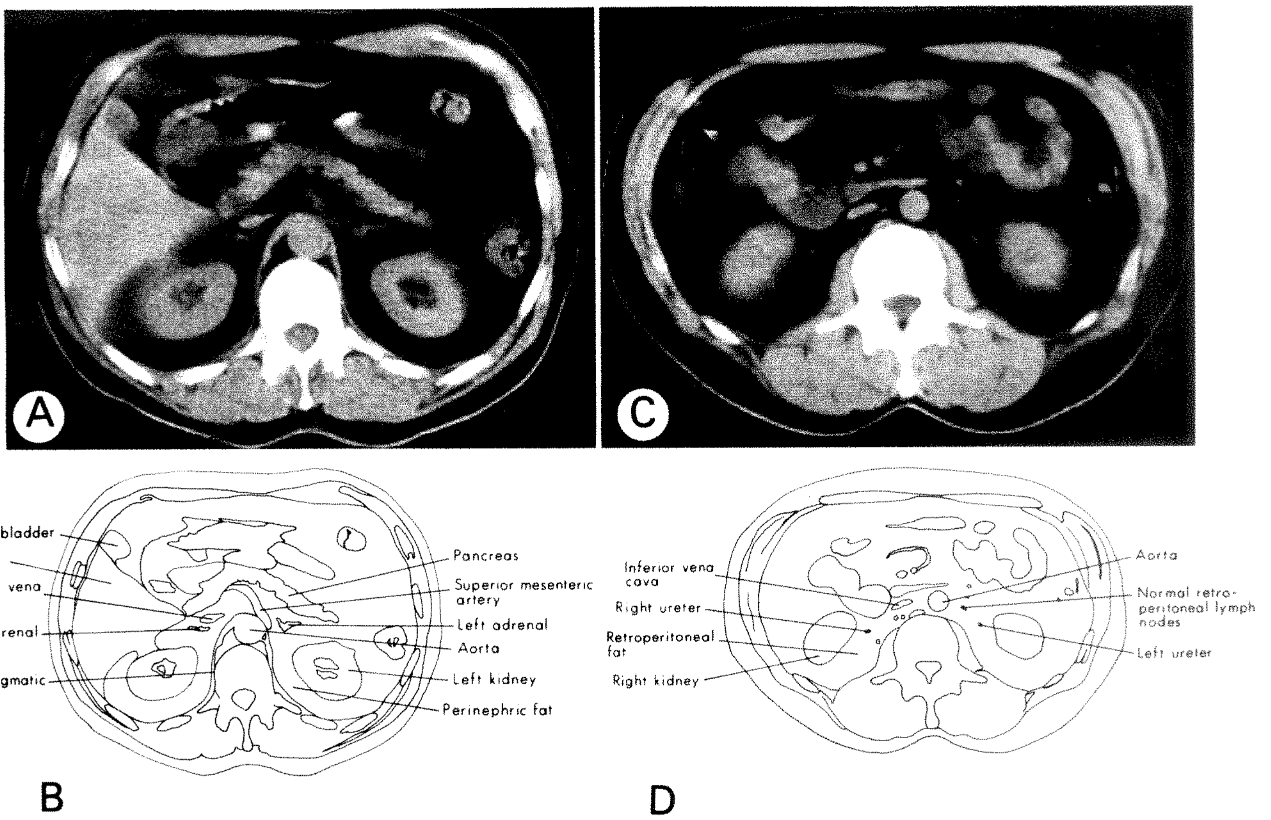

Fig. 1.—*A and B*, CT scan and diagram of normal upper retroperitoneum. *C and D*, CT scan and diagram of normal lower retroperitoneum.

Received March 29, 1977; accepted June 3, 1977.

[1] All authors: Mallinckrodt Institute of Radiology, Washington University School of Medicine, 510 South Kingshighway, St. Louis, Missouri 63110. Address reprints to S. S. Sagel.

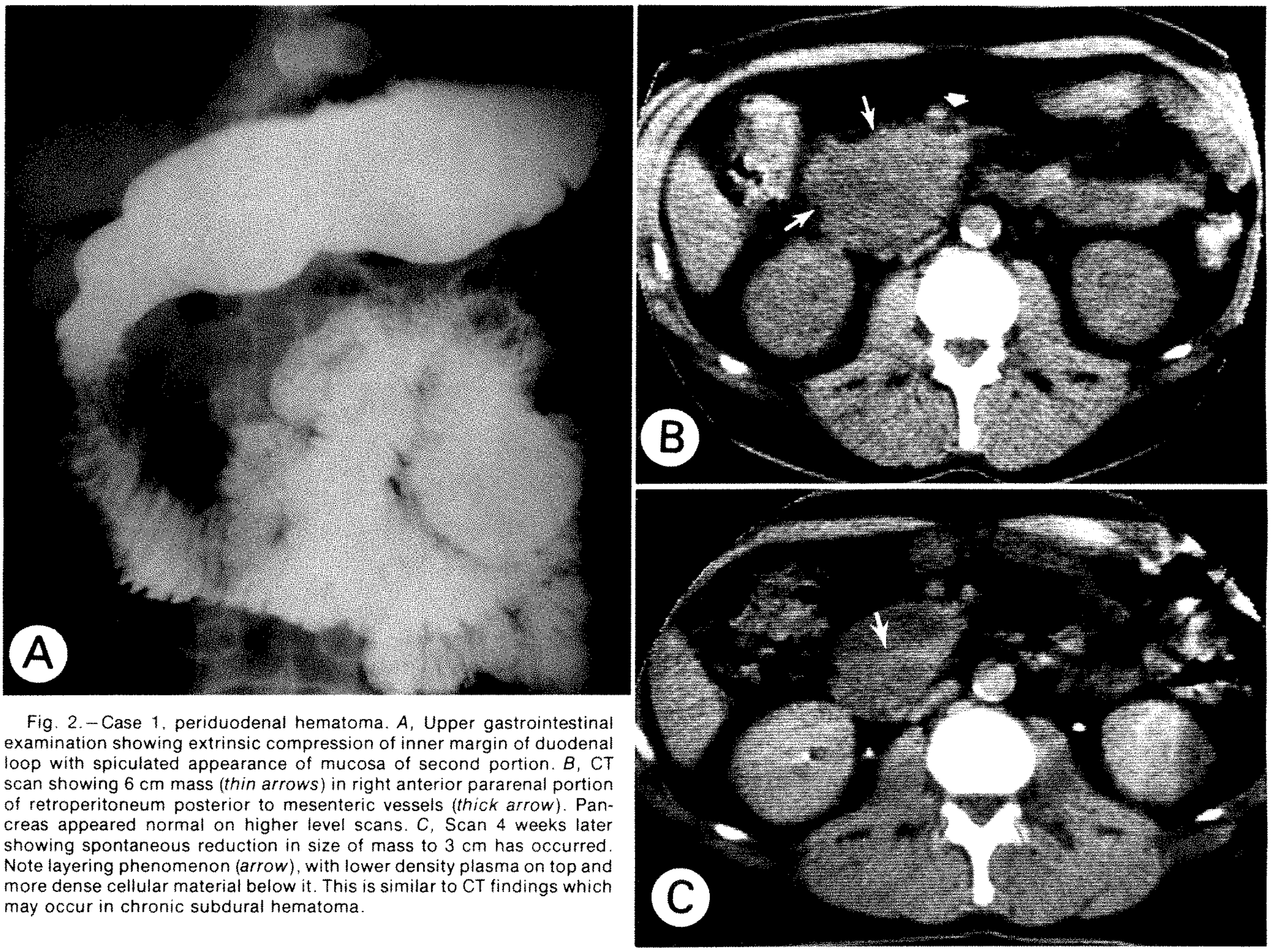

Fig. 2.—Case 1, periduodenal hematoma. *A*, Upper gastrointestinal examination showing extrinsic compression of inner margin of duodenal loop with spiculated appearance of mucosa of second portion. *B*, CT scan showing 6 cm mass (*thin arrows*) in right anterior pararenal portion of retroperitoneum posterior to mesenteric vessels (*thick arrow*). Pancreas appeared normal on higher level scans. *C*, Scan 4 weeks later showing spontaneous reduction in size of mass to 3 cm has occurred. Note layering phenomenon (*arrow*), with lower density plasma on top and more dense cellular material below it. This is similar to CT findings which may occur in chronic subdural hematoma.

air, 0 for water, and +500 for dense cortical bone). The highest values occur in the most acute collections. This paper describes the role of CT scanning in the detection of retroperitoneal hemorrhage.

Case Reports

Case 1

A 46-year-old male alcoholic had low grade fever, mild jaundice, and anemia. No traumatic history was elicited. An upper gastrointestinal series disclosed an abnormal compression of the duodenal loop (fig. 2*A*). A pancreatic mass or peripancreatic hematoma was suspected. CT (fig. 2*B*) demonstrated a large periduodenal hematoma. Clinical improvement ensued without therapy. A repeat CT scan (fig. 2*C*) 4 weeks later demonstrated diminution in the size of the hematoma.

Case 2

An 82-year-old man on Coumadin therapy complained of low back pain. Prothrombin time was 28 sec, with a hematocrit of 26. Spontaneous retroperitoneal bleeding was considered likely. CT examination (fig. 3) demonstrated an unsuspected large abdominal aortic aneurysm with blood extravasating into the retroperitoneum. Surgery disclosed a leaking aneurysm.

Case 3

A 60-year-old man with prior history of diverticulitis had left lower quadrant and left thigh pain for 2 days. Hematocrit was 32. CT scans (fig. 4) demonstrated an abdominal aortic aneurysm and probable retroperitoneal bleeding causing a protuberant left psoas margin. Surgery disclosed a posterior pinhole perforation of the aortic aneurysm that allowed blood to escape into the left psoas muscle, forming a large false aneurysm.

Case 4

A 56-year-old man had vague abdominal pain on the left side and a low grade fever. Excretory urography (fig. 5*A*) disclosed mild left hydronephrosis with persistent narrowing of the left ureter. Retroperitoneal lymphoma (because of clinical history) or a primary ureteral lesion were considered the likely causes. In retrospect, medial deviation of the right ureter can be seen, which should have suggested an aortic aneurysm [4]. CT (figs. 5*B* and 5*C*) demonstrated an aortic aneurysm surrounded by a soft tissue mass. At surgery, a large fibrotic blood clot around the aneurysm was found. It is of interest that the pathologic specimen was initially interpreted (without benefit of all the clinical information) as due to retroperitoneal fibrosis, circumstances quite similar to a recently reported case [2].

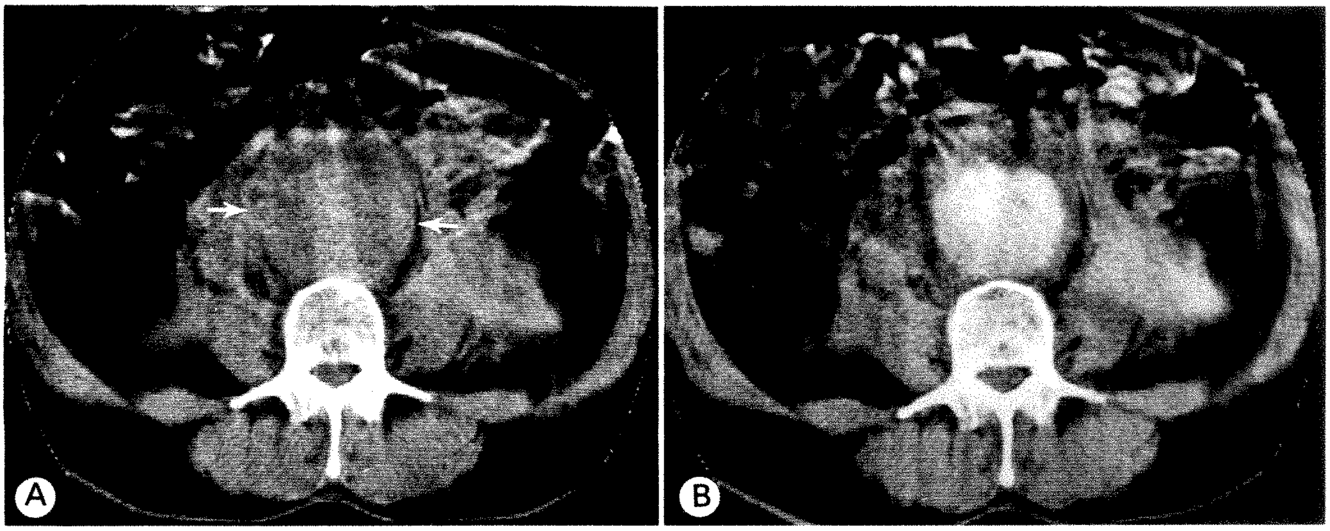

Fig. 3.—Case 2, leaking aortic aneurysm. *A*, CT scan showing 7 cm aneurysm of abdominal aorta (*arrows*). Note obscuration of both lateral psoas margins, more marked on left side. *B*, Scan after intravenous administration of 75 ml of Conray 400 showing suggested enhancement of irregular soft tissue density about left psoas margin. Leaking aortic aneurysm with bilateral retroperitoneal hematomas was considered likely.

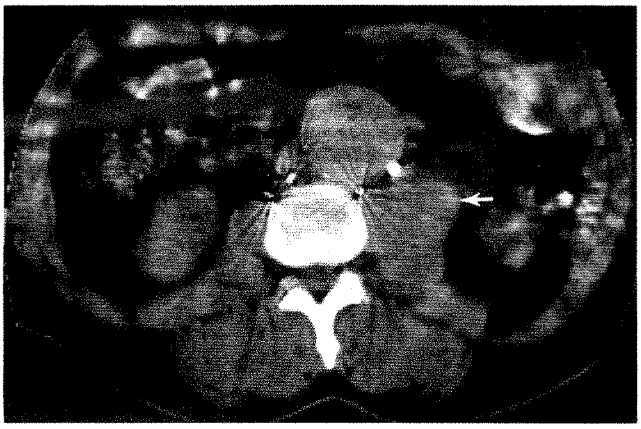

Fig. 4.—Case 3, leaking aortic aneurysm with retroperitoneal hematoma. CT scan showing aneurysm of abdominal aorta, with marked asymmetric lateral bulging of left psoas muscle (*arrow*).

Case 5

A 60-year-old woman on chronic hemodialysis and concomitant heparin therapy developed mild right flank pain. The hematocrit decreased from 36 to 18 in 4 days, and an abdominal mass became palpable on the right side. CT scans (fig. 6) demonstrated a hugh right retroperitoneal mass compatible with a hematoma.

Case 6

A 50-year-old man with diabetes mellitus and suspected Kimmelstiel-Wilson syndrome developed right flank pain 2 days after percutaneous biopsy of the right kidney. Hematocrit fell from 45 to 35. CT (fig. 7) demonstrated a large perinephric hematoma.

Case 7

A 62-year-old man had a supraclavicular lymph node biopsy which revealed adenocarcinoma. Two days after an uneventful ultrasound-controlled percutaneous aspiration of a sonolucent mass in the anterior aspect of the left kidney, CT was performed to exclude a pancreatic carcinoma. The scans (fig. 8) demonstrated incidently a small left perinephric hematoma.

Discussion

Trauma, including of iatrogenic origin, is the most common cause of retroperitoneal hemorrhage. Leakage from an aortic aneurysm and diseases associated with a hemorrhagic diathesis or anticoagulant therapy also may result in retroperitoneal bleeding. Additionally, retroperitoneal hematomas may arise from adrenal or renal disorders, especially neoplastic. Blood loss of a clinically important magnitude from any of these myriad causes frequently can be hidden in the retroperitoneal space. A major diagnostic challenge to both clinician and radiologist can result.

Cases 2 and 3 were not intended to imply that CT is indicated whenever a leaking aortic aneurysm is suspected. Certainly, because of the life threatening nature of ruptured abdominal aortic aneurysm, if the diagnosis is strongly suspected on clinical grounds, the patient should be taken directly to surgery without performing any radiologic studies. However, when the diagnosis is unsuspected or in question, such as in cases 2 and 3, radiologic studies should be performed. While plain abdominal films may suggest the diagnosis [5, 6], they are often inconclusive.

As illustrated by case 5, spontaneous retroperitoneal hemorrhage is a recognized serious complication of anticoagulant therapy, occurring not infrequently in patients undergoing hemodialysis who are receiving Coumadin or heparin [7, 8]. Because the retroperitoneal space may act as a reservoir and conceal large quantities of internal hemorrhage, initially the symptoms are often nonspecific and diagnosis is frequently delayed. Postponement of precise diagnosis may result in irreversible lumbar

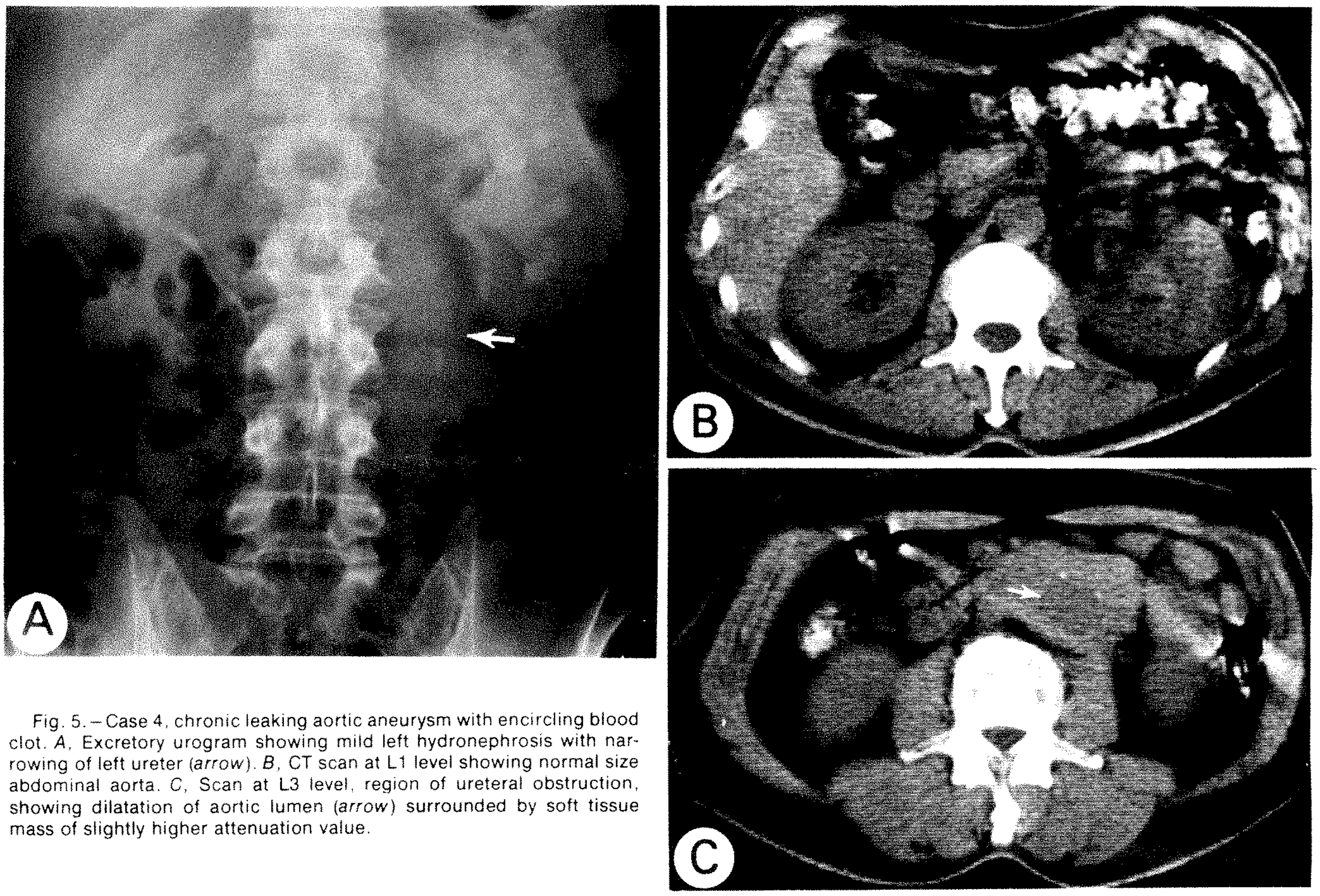

Fig. 5.—Case 4, chronic leaking aortic aneurysm with encircling blood clot. *A*, Excretory urogram showing mild left hydronephrosis with narrowing of left ureter (*arrow*). *B*, CT scan at L1 level showing normal size abdominal aorta. *C*, Scan at L3 level, region of ureteral obstruction, showing dilatation of aortic lumen (*arrow*) surrounded by soft tissue mass of slightly higher attenuation value.

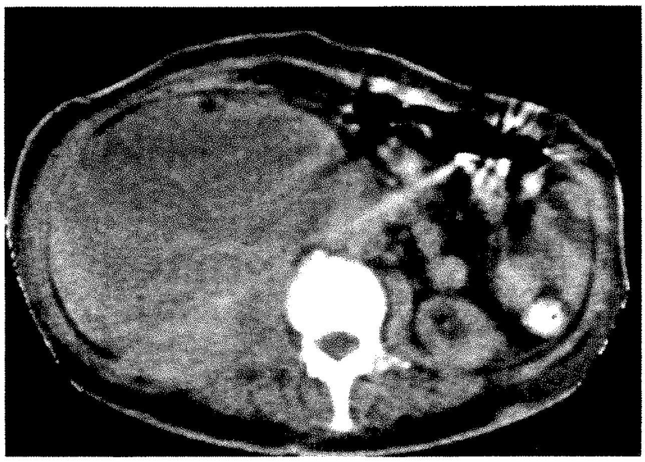

Fig. 6.—Case 5, retroperitoneal hematoma. CT scan showing huge soft tissue mass with attenuation value of 10 EMI units in right side of abdomen obliterating normal renal outline and psoas muscle. Note displacement of bowel loops to left.

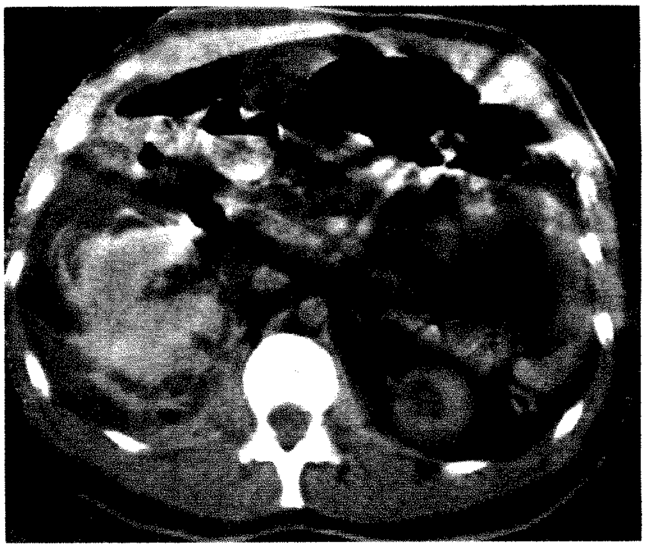

Fig. 7.—Case 6, perinephric hematoma. CT scan showing irregular soft tissue densities surrounding right kidney with infiltration into perinephric fat and toward psoas muscle.

plexus or femoral nerve injury besides the direct consequences of severe internal blood loss [9].

The ability of CT to directly demonstrate hematoma is a distinctive diagnostic advantage. Reliance on indirect signs usually required by conventional radiography is obviated. CT scans can not only detect, quantitate, and localize retroperitoneal hemorrhage, but also may provide an etiologic explanation, thus directing appropriate clinical management. Should a course of watchful waiting be chosen, CT can serve as a noninvasive follow-up method.

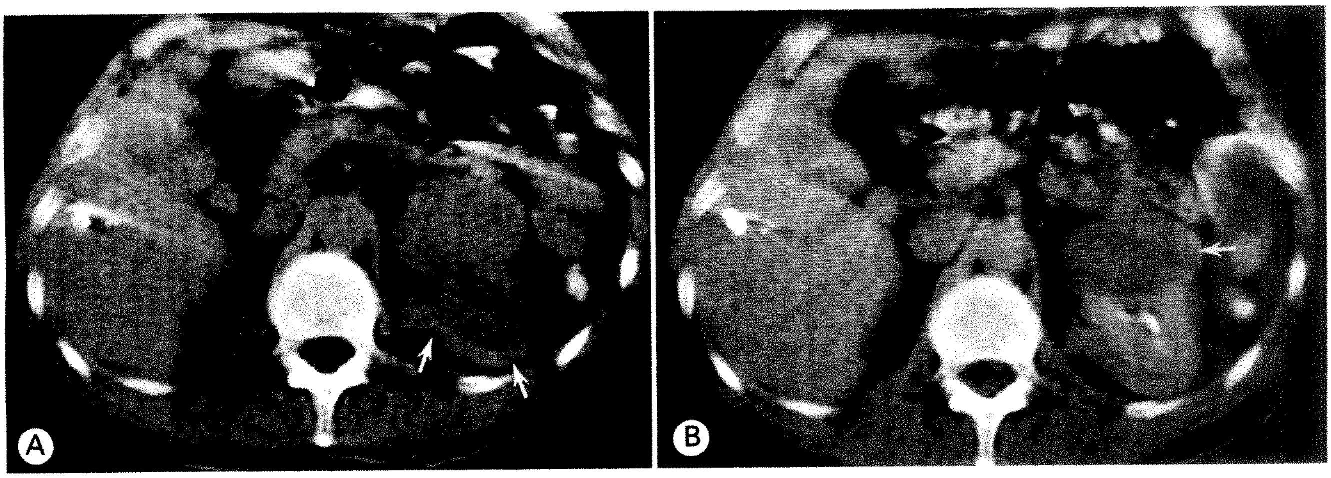

Fig. 8.—Case 7, perinephric hematoma. *A*, CT scan showing small amount of blood (*arrows*) in perinephric space posterior to left kidney. *B*, Scan after intravenous administration of iodinated contrast medium showing enhancement of renal parenchyma without any change in attenuation value of hematoma or cyst projecting off anterior aspect of left kidney (*arrow*).

It is doubtful that CT scans alone are capable of distinguishing retroperitoneal hemorrhage from abscess. Fortunately, the clinical setting customarily permits distinction.

Ultrasound, an alternative diagnostic method capable of directly identifying retroperitoneal pathology [10], was not performed in the illustrated cases, precluding comparative evaluation.

REFERENCES

1. Elkin M, Cohen G: Diagnostic value of the psoas shadow. *Clin Radiol* 13:210–217, 1962
2. Alfidi RJ, Haaga JR: Computed body tomography. *Radiol Clin North Am* 14:563–570, 1976
3. Stanley RJ, Sagel SS, Levitt RG: Computed tomography of the body: early trends in application and accuracy of the method. *Am J Roentgenol* 127:53–67, 1976
4. Peck DR, Bhatt GM, Lowman RM: Traction displacement of the ureter: a sign of aortic aneurysm. *J Urol* 109:983–986, 1973
5. Janower ML: Ruptured arteriosclerotic aneurysms of the abdominal aorta: roentgenographic findings on plain films. *N Engl J Med* 265:12–16, 1961
6. Nichols GB, Schilling PJ: Pseudo-retroperitoneal gas in rupture of aneurysm of abdominal aorta. *Am J Roentgenol* 125:134–137, 1975
7. Coon WW, Willis PW III: Hemorrhagic complications of anticoagulant therapy. *Arch Intern Med* 133:386–392, 1974
8. Milutinovich J, Follette WC, Scribner BH: Spontaneous retroperitoneal bleeding in patients on chronic hemodialysis. *Ann Intern Med* 86:189–192, 1977
9. Chiu WS: The syndrome of retroperitoneal hemorrhage and lumbar plexus neuropathy during anticoagulant therapy. *South Med J* 69:595–599, 1976
10. Kaplan GN, Sanders RC: B-scan ultrasound in the management of patients with occult abdominal hematomas. *J Clin Ultrasound* 1:5–13, 1973

Diagnosis of Urine Extravasation after Renal Transplantation

D. G. SPIGOS,[1] W. TAN,[1] D. G. PAVEL,[1] M. MOZES,[2] O. JONASSON,[2] AND V. CAPEK[1]

Urine extravasation in the early postoperative period after renal transplantation is a serious complication requiring expedient surgical intervention. Whereas clinical and laboratory findings are inconclusive, radiologic diagnostic studies have definite value. Routine ultrasound and radioisotope studies were performed on 111 renal transplant patients. In the eight who developed urine extravasation, ultrasound and/or radioisotope studies identified the extravasation in seven cases. Four of the eight were studied by intravenous pyelography and another two were studied by cystography. All results were positive. We recommend use of radioisotope and ultrasound studies for routine postoperative screening with invasive techniques reserved for inconclusive cases.

While renal transplantation has become an accepted and effective method for treating patients with irreversible renal failure, it also presents diagnostic problems in the immediate and late posttransplantation periods. Urologic complications are reported to be as high as 40% [1]; such complications as urine extravasation and fistulas are reported to occur as infrequently as 0.5% or as commonly as 17% [2, 3].

A urine leak very often is followed by a wound infection, which may lead to loss of graft, generalized sepsis, and ultimately to death of the transplant recipient. Although the reported mortality rate from this complication in the early series of the University of Minnesota was as high as 70% [4], with recent advances in the early diagnosis and correction of the leak, mortality is now negligible although morbidity remains high.

The most common causes of urine extravasation in renal transplantation are defects at the ureteropelvic, ureteroureteric, or ureterovesical anastomoses [5]. The first two types have been associated with a high incidence of urinary fistulas; thus their use is now restricted to only specific cases. Other less common causes of extravasation are infarcts of the kidney, resulting in necrosis of the renal parenchyma [6], and ureteral tip necrosis secondary to a compromise in the blood supply of the ureter [7].

The clinical signs and symptoms of urine extravasation consist of a drop in urine output as well as pain and swelling over the transplant site. The presentation is related to the magnitude of the urinary leak. Whereas with a massive leak, there may be signs and symptoms of peritonitis, with mild extravasation the symptomatology may be largely absent and masked by the effect of high dose steroids [8]. It is often difficult to distinguish the signs and symptoms of urinary extravasation from those of rejection or obstructive uropathy [9]. To aid in the early and definitive diagnosis, radioisotopic and echographic studies of the kidney transplants are performed routinely starting in the early posttransplantation period [10, 11]. Sometimes these methods are augmented with the use of other radiographic diagnostic methods, such as intravenous pyelography, retrograde pyelography, and cystography [12, 13].

Materials and Methods

Among 111 patients who received renal transplants at our institution within the last 4 years, eight developed urine extravasation. There were no deaths encountered in this group of eight patients.

As of 1972, renal transplant recipients at our institution are routinely studied with radioisotopes and ultrasound in their posttransplantation period. A total of 935 isotope scans and 419 echograms were performed on these 111 patients. The isotopes most commonly used are ^{99m}Tc DTPA and ^{131}I Hippuran. Echographic examination is done with a gray scale apparatus with a 2.25 MHz transducer. If there is suspicion of a urologic complication, radiographic studies are also performed. The relative accuracy, usefulness, and correlation of these diagnostic methods are demonstrated in the following four cases.

Illustrative Case Reports

Case 1

A 24-year-old male received a cadaver renal transplant. Ultrasound examination 3 days later showed a perirenal fluid collection (fig. 1*A*); 5 days after transplantation, the radioisotope study showed increased activity in the scrotum consistent with urine extravasation (fig. 1*B*). During exploration, the urine leak was found at the ureteroneocystostomy site. The ureter was reimplanted at a different site, and the patient showed no evidence of urine extravasation in his postoperative period. He underwent nephrectomy 16 days after transplantation because of an episode of acute rejection which did not respond to treatment.

Case 2

A 19-year-old male received a renal transplant. Routine radioisotope study 3 days later raised suspicion of urine extravasation (fig. 2*A*), which was verified by intravenous pyelography (fig. 2*B*). The patient underwent exploratory laparotomies 13 and 17 days after transplant, both failing to reveal the site of extravasation. Despite these negative explorations, an infected urinoma was found when a transplant nephrectomy was performed due to sepsis.

Case 3

A 16-year-old male received a renal transplant; the transplanted ureter was anastomosed to an ileal conduit. Arteriography performed 2 months after transplantation as part of a workup for acute rejection demonstrated an infarct in the upper

---

Received October 5, 1976; accepted after revision May 13, 1977.
Presented at the annual meeting of the American Roentgen Ray Society, Washington, D.C., September 1976.

[1] Department of Radiology, University of Illinois Medical Center, 840 South Wood Street, Chicago, Illinois 60612. Address reprint requests to V. Capek.

[2] Department of Surgery, University of Illinois Medical Center, Chicago, Illinois 60612.

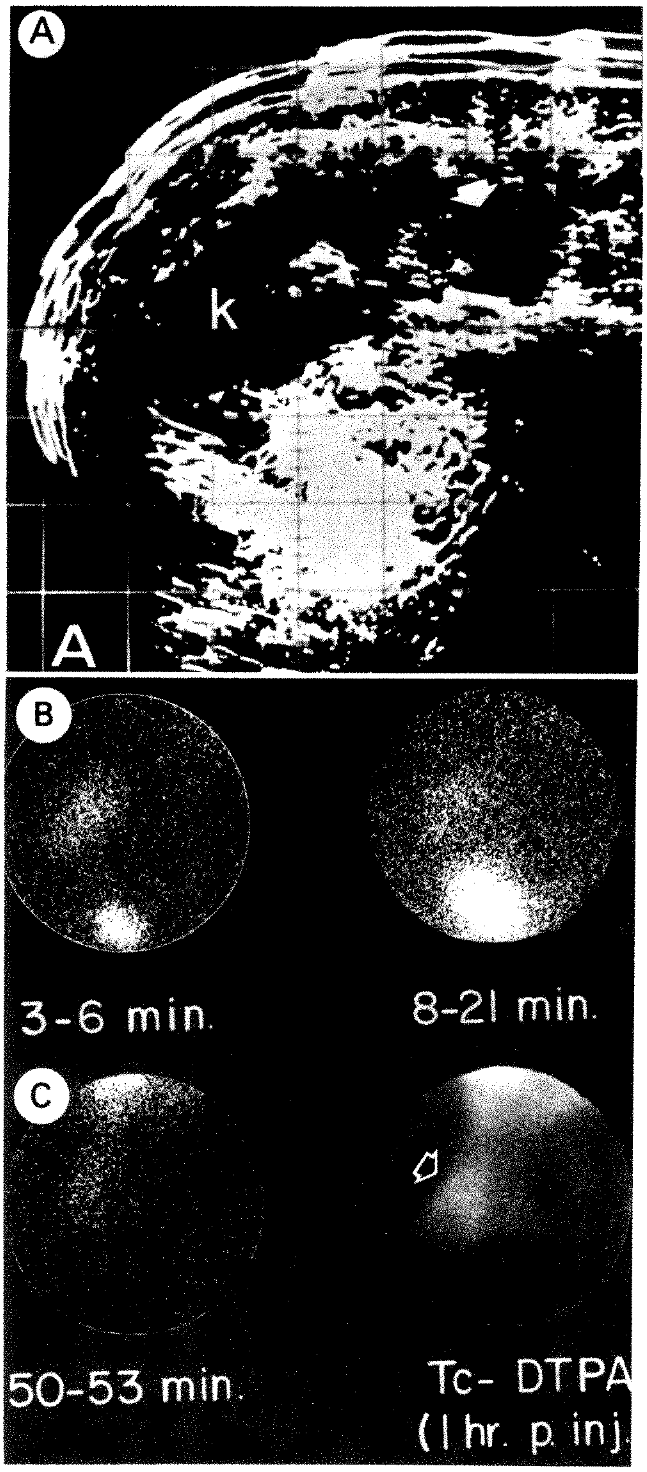

Fig. 1.—Case 1. *A*, Ultrasound scan of renal transplant showing fluid collection medial to kidney (*arrow*). *B*, Hippuran scans without evidence of extravasation. *C*, Delayed Hippuran and ^{99m}Tc DTPA scans over scrotum showing isotope collection (*arrow*) consistent with urine extravasation.

pole of the kidney (figs. 3*A* and *B*). Three days after arteriography, the patient complained of pain over the kidney area and also had a marked drop in urinary output. While urine extravasation was suspected, the isotope and echographic studies were reported as negative (figs. 3*D* and 3*E*). However, loopography identified the urine extravasation (fig. 3*C*). At exploration an infected urinoma was found. A nephrectomy was also performed due to the danger of generalized sepsis. Retrospective analysis of the radioisotope and echographic studies demonstrated the urine leak. The original misinterpretation was due to the presence of the ileal conduit. Because subtle changes in the radioisotope studies and echograms can be easily overlooked, additional radiographic studies should be performed in cases where suspicion of a urine leak exists.

Case 4

A 31-year-old female underwent renal transplantation. One month after transplantation, an elevation of serum creatinine was noted. Ultrasound and radioisotope studies at that time were essentially normal. Renal function did not improve over the next 2 days. Ultrasonography performed as part of a workup for rejection demonstrated a large perirenal fluid collection (fig. 4*A*). Retrograde cystography demonstrated a large extravasation of contrast medium lateral to the transplanted kidney (fig. 4*B*). At exploration a defect was found in the suture line at the dome of the bladder. This was repaired and the patient had an uneventful recovery. This was the only case with a true negative radioisotope study. The ultrasonic examination, despite its nonspecific nature, led to further workup with a cystogram and to an early diagnosis of a urine leak.

Discussion

Routine posttransplantation ultrasound and radioisotope studies are performed on all renal transplant recipients at our institution. Use of one or both diagnostic methods demonstrated seven of eight urine extravasations (table 1).

While ultrasound of the kidney transplant is a sensitive method to demonstrate perirenal fluid collections [11], the differential diagnosis may be difficult when based solely on echographic criteria. Aspiration and biochemical analysis of the fluid may help in differentiating urinoma from other fluid collections such as lymphoceles, hematomas, or abscesses. At times the biochemical differentiation of urine from other body fluid collections (e.g., lymphoceles) may be difficult in a poorly functioning graft because the urea concentration in the urine and serum may be similar. Of the eight patients who developed urine extravasation, six were studied by ultrasound and five of these studies were positive (table 1).

Radioisotope studies are also sensitive in the diagnosis of urine extravasation [10, 12]. They demonstrated urine extravasation in five of seven urine leaks (table 1).

Because isotopic and ultrasound studies can give false positive and false negative results, complete dependence on these tests may be a source of error. In cases where suspicion exists and the echographic and/or isotopic studies are inconclusive, the studies of choice have been intravenous pyelography and/or cystography. Of the eight patients who developed urine extravasation, four were studied by intravenous pyelography, all with positive results. Another two cases were studied by cystography, also with positive results (table 1).

Although intravenous pyelography and cystography are very accurate, we do not recommend their routine use in the follow-up of renal transplants for the following reasons: (1) definite nephrotoxicity is involved in the use of contrast media; (2) in patients undergoing acute tubu-

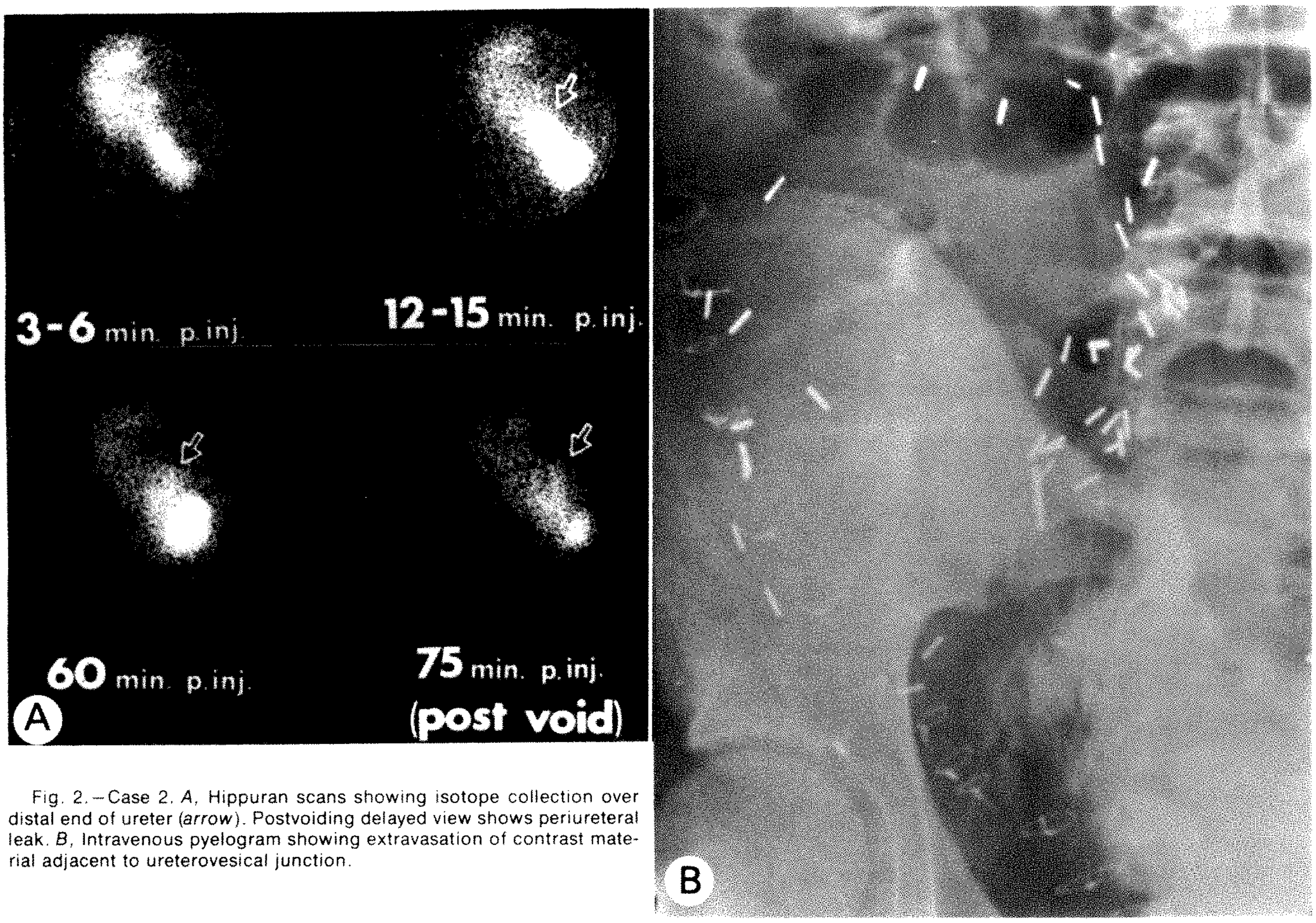

Fig. 2.—Case 2. *A,* Hippuran scans showing isotope collection over distal end of ureter (*arrow*). Postvoiding delayed view shows periureteral leak. *B,* Intravenous pyelogram showing extravasation of contrast material adjacent to ureterovesical junction.

lar necrosis or rejection, the collecting system is poorly visualized; and (3) introduction of a catheter into the bladder of these patients with a compromised immune system may be a source of infection.

Therefore, our practice is to follow the patients closely with the noninvasive techniques of ultrasound and radioisotopic studies and to verify a suspicion of urinary extravasation when necessary by cystography, loopography, and intravenous pyelography. We believe that each of these diagnostic methods alone or combined has a definite role in the early and accurate diagnosis of urine extravasation in kidney transplant recipients.

REFERENCES

1. Ekman H, Bergenta SE, Brunius U, Gelin LE: Urologic complications in renal transplantation. *Scand J Urol Nephrol* 2:40, 1968
2. Leary FJ, Woods JE, Deweerd JH: Urologic problems in renal transplantation. *Arch Surg* 110:1124-1126, 1975
3. Palmer JM, Kountz SK, Swenson RS, Lucas ZJ, Cohn R: Urinary tract morbidity in renal transplantation. *Arch Surg* 98:352-356, 1969
4. Weil R, Simmons RL, Tallent MB, Lillehei RC, Kjellstrand CM, Najarian JS: Prevention of urological complications after kidney transplantation. *Ann Surg* 174:154-160, 1971
5. Starzl TE, Groth CG, Putman CW, Penn I, Halgrimson CG, Flatmark A, Grecelter J, Brettschneider L, Stonington OG: Urological complications in 216 human recipients of renal transplants. *Ann Surg* 1:1-21, 1970
6. Fox M, Tottenham RC: Urinary fistula from segmental infarction in a transplanted kidney: recovery following surgical repair. *Br J Urol* 44:336-338, 1972
7. DeWeerd JH, Woods JE, Leary FJ: The allograft ureter. *J Urol* 109:958-963, 1973
8. Mackinnon KJ, Oliver JA, Morehouse DD, Taguchi Y: Cadaver renal transplantation: emphasis on urological aspects. *J Urol* 99:486-490, 1968
9. Williams G, Birtch AG, Wilson RE, Harrison JH, Murray JE: Urological complications of renal transplantation. *Br J Urol* 42:21-28, 1970
10. Pavel DG, Kahan BD, Quin JL, Bergan JJ, Westerman BR: Multilateral evaluation of renal transplants with radionuclides, in *Dynamic Studies with Radioisotopes in Medicine,* vol 1, Vienna International Atomic Energy Agency, 1974, pp 307-327
11. Spigos DG, Capek V: The role of ultrasound in the diagnosis and therapy of perirenal fluid collection in renal transplantation, in *Ultrasound in Medicine,* vol 2, edited by White K, Barnes R, New York, Plenum Press, 1976, pp 145-156
12. Fletcher EWL, Lecky JW: The radiological demonstration of urological complications in renal transplantation. *Br J Radiol* 49:886-891, 1969
13. Gedgaudas E, White RI, Loken MK: Radiology in renal transplantation. *Radiol Clin North Am* 10:529-544, 1972

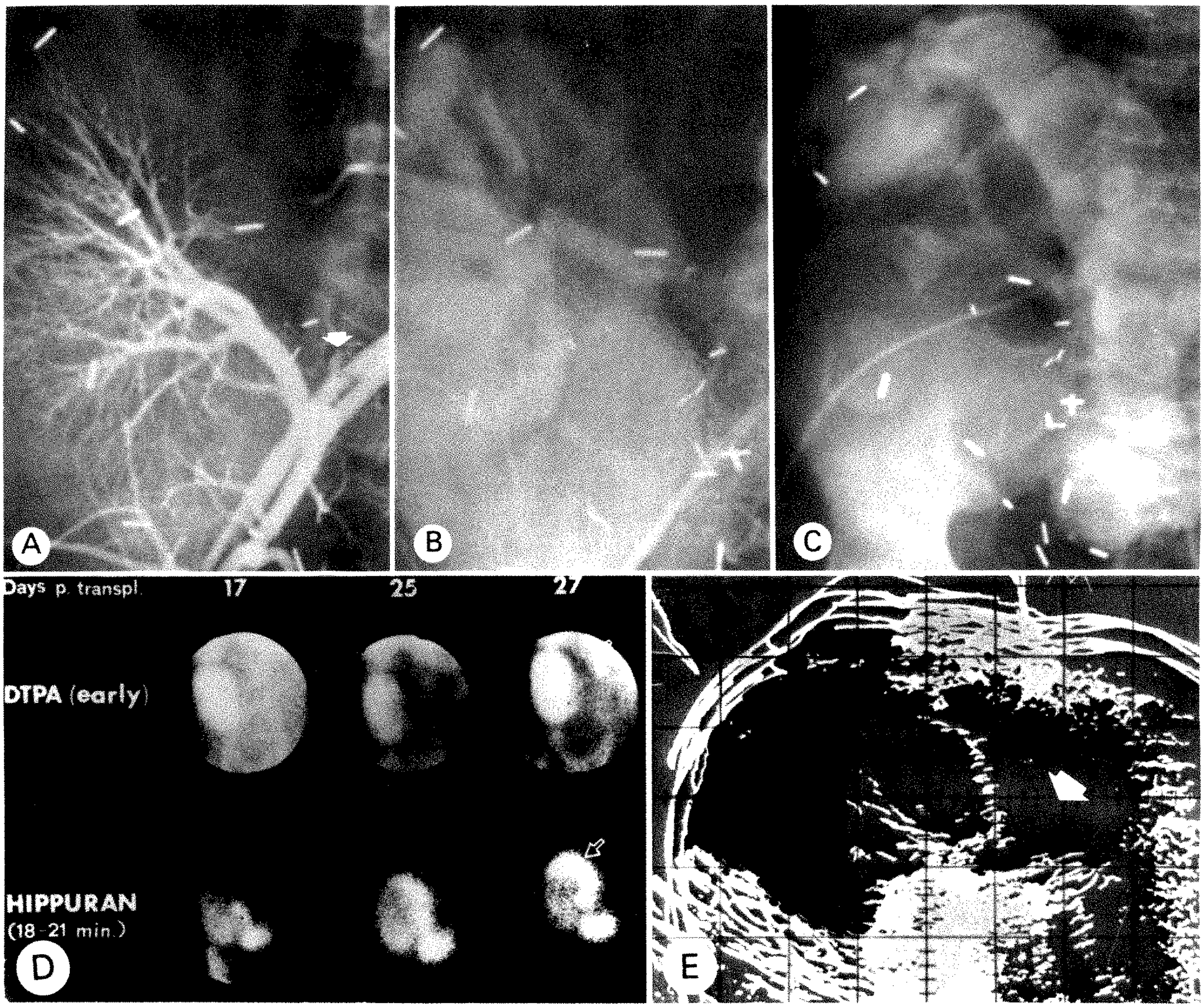

Fig. 3.—Case 3. *A*, Arterial phase of right common iliac arteriogram showing occlusion of artery (*arrow*) of upper pole of kidney. *B*, Late nephrographic phase showing irregular outline of upper pole and triangular radiolucent defect consistent with infarct. *C*, Loopogram showing extravasation of contrast material around kidney. *D*, Serial radioisotope studies showing apparent change in distribution of radioactivity from day 17 to day 27. *E*, Ultrasound scan showing large anechoic area medial to kidney consistent with fluid collection (*arrow*).

Fig. 4.—Case 4. *A*, Ultrasound scan showing large sonolucent areas anterior and lateral (*arrow*) to kidney consistent with perirenal fluid collections. *B*, Cystogram showing large extravasation of contrast material lateral to transplanted kidney.

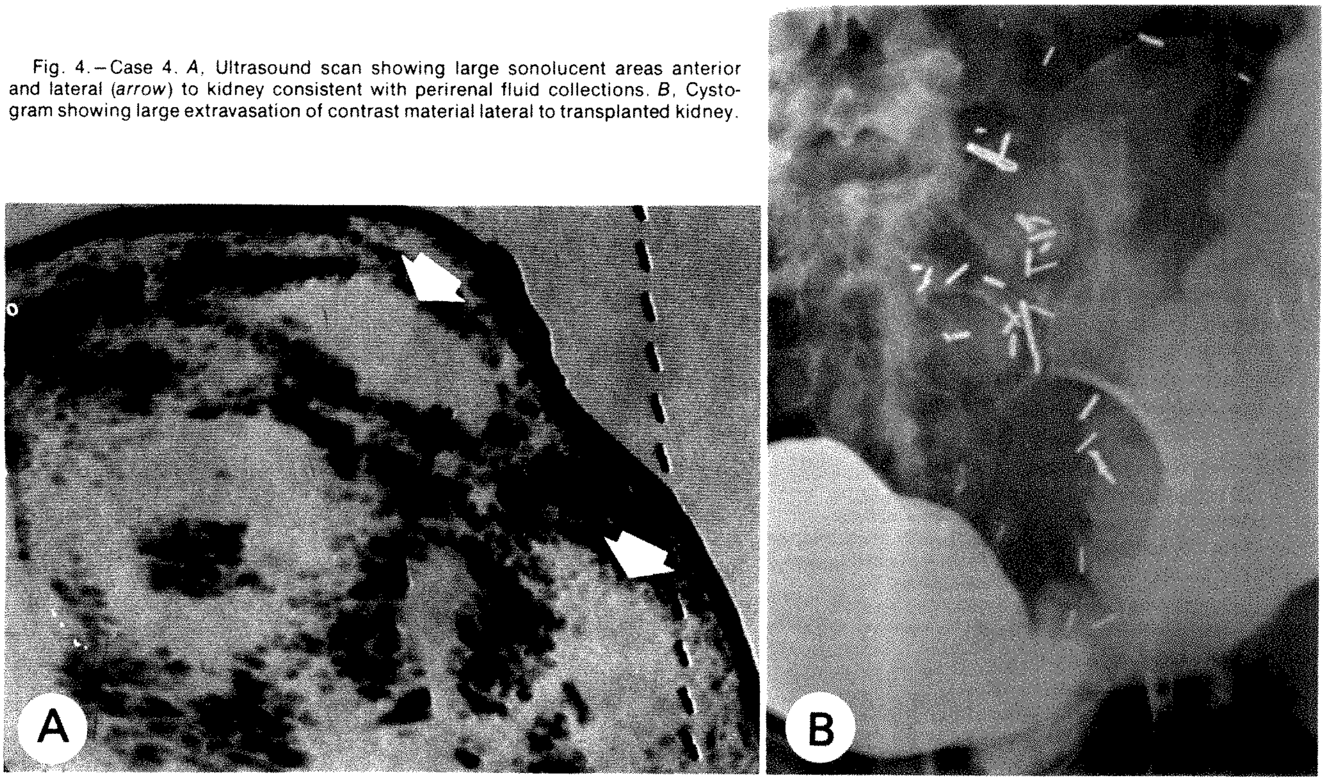

TABLE 1

Summary of Radiologic Findings

Case No.	Age (yr) and Sex	Isotopic Studies	Ultrasound	Intravenous Pyelogram	Cystogram and/or Loopogram	Outcome
1 (fig. 1)	24,M	+	+	...	...	Urine leak found and repaired; kidney resumed good function
2 (fig. 2)	19,M	+	+	+	...	Urine leak not found; sepsis developed. Infected urinoma resulted in nephrectomy
3 (fig. 3)	16,M	−	−	...	+	Infected urinoma found; transplant nephrectomy performed
4 (fig. 4)	31,F	−	+	...	+	Urine leak found and repaired; good function of renal transplant
5	39,F	...	+	...	...	Urine leak found and repaired; recovery of renal function
6	24,F	+	...	+	...	Urine leak found and repaired; good recovery of renal function
7	20,M	+	...	+	...	Urine leak found and repaired; good recovery of renal function
8	16,M	+	+	+	...	Urine leak found and repaired; good recovery of renal function

Fungal Infection of the Urinary Tract: Demonstration by Antegrade Pyelography and Drainage by Percutaneous Nephrostomy

ALAN G. DEMBNER[1] AND RICHARD C. PFISTER[1]

Most fungal infections of the urinary tract involve the drainage structures rather than the kidney parenchyma. They usually occur in patients with diabetes or other chronic debilitating diseases and in the presence of urinary stasis. Conglomeration of fibrillar hyphae results in fungal balls which produce nonopaque filling defects in the renal pelvis, ureter, or bladder. Such fungal ball colonies were demonstrated by percutaneous (antegrade) pyelography in the upper urinary tract in two cases. A percutaneous nephrostomy was performed in one patient to provide drainage of pus in the renal pelvis.

Although uncommon in the past, fungal infections of the urinary tract are apparently increasing in frequency because of more aggressive medical therapy. They should be considered in the differential diagnosis of suspected renal obstruction or inflammation, particularly in debilitated patients. Such patients may have lowered resistance due to underlying neoplasms, diabetes mellitus, chronic disease, immunosuppression, long term wide-spectrum antibiotics, or adrenocorticosteroid treatment. In the pediatric population, patients with chronic granulomatous disease may be predisposed to opportunistic fungal infection.

There are numerous articles dealing with funguria and/or fungemia in which no apparent clinical, radiologic, or pathologic alteration or significant disease is described. This paper is the first to describe two patients with obstructive funguria in which percutaneous pyelography and percutaneous nephrostomy drainage were used.

Case Reports

Case 1

J. C., a 73-year-old diabetic white male, entered the Massachusetts General Hospital with a gangrenous right foot. Laboratory examinations revealed a blood glucose of 1,080 and blood urea nitrogen of 67. The patient underwent amputation below the knee. He had been seen 10 years earlier for urethral stricture of unknown cause with sepsis and decreased renal function. After apparently successful urethroplasty, he was lost to follow-up.

The patient's recent hospital course was complicated over the next several months by recurrent urinary tract infections with urine cultures growing several different bacteria and *Candida albicans*. He was treated with antibiotics specific to the bacteria, but no antifungal agents. Initial excretory urography showed bilateral hydronephrosis. A recurrent urethral stricture was treated with a cystostomy tube.

Late in his hospital course the patient became septic. Nephrotomography showed a small scarred right kidney and persistent hydronephrosis on the opposite side (fig. 1*A*). Since the cause of the unilateral dilatation was not clear, a left percutaneous antegrade pyelogram was performed. It showed moderate ureterectasis without evident obstruction, although filling defects in the distal ureter (fig. 1*B* and 1*C*) and renal pelvis were present (figs. 1*A*-1*C*). The patient died of an acute myocardial infarction 7 days later.

Autopsy showed masses of fibril material in the left kidney and ureter. The material was composed of yeast and pseudohyphae forms of *C. albicans* with fibrin and acute and chronic inflammatory cells (fig. 1*D* and 1*E*). The renal parenchyma was not involved. It is possible that the fungal balls caused intermittent obstruction at the ureterovesical junction and then were molded or fragmented with subsequent passage into the bladder.

Case 2

M. R., an 82-year-old diabetic female, was admitted with complete heart block. Her cardiac status was stabilized, but hospitalization was complicated by deteriorating renal function and fever. Excretory urography demonstrated no opacification of the right kidney. Antegrade pyelography (fig. 2*A*) returned gross pus in which gram stain showed leukocytes and budding pseudohyphae. A percutaneous nephrostomy catheter (no. 12 French) was placed for drainage (fig. 2*B*), and the culture grew pure *C. albicans* (no bacteria). The patient died 2 days later after a cardiac arrest; an autopsy was not obtained.

Discussion

Lundquist [1] cited 17 cases of fungal infections of the urinary tract in the world literature in 1931. Since then other reports have appeared [2-8], and chemotherapy with effective antifungal agents has been stressed [9, 10]. Although various species of fungi have been reported in urinary tract infections, *C. albicans* is the most commonly reported organism, occurring in 57% of all reported cases. It may be found as a normal saprophyte of the skin, intestinal tract, respiratory tract, and external genitalia.

Louria et al. [11] classified systemic *Candida* infections in 95 patients as: (1) disseminated candidiasis, (2) *Candida* endocarditis, and (3) *Candida* meningitis. Lehner [12] believed that renal candidiasis should be a fourth category when he found kidney involvement in 40 of 45 cases of systemic candidiasis. As in case 1, the organism may produce large colonies. These colonies may conglomerate to become fungal "balls" which appear as intraluminal filling defects in radiographic contrast studies of the urinary tract. They have been found most

---

Received February 8, 1977; accepted after revision June 1, 1977.

[1] Department of Radiology, Genitourinary Section, Massachusetts General Hospital and Harvard Medical School, Boston, Massachusetts 02114. Address reprint requests to R. C. Pfister at the Radiology Research Office, Massachusetts General Hospital.

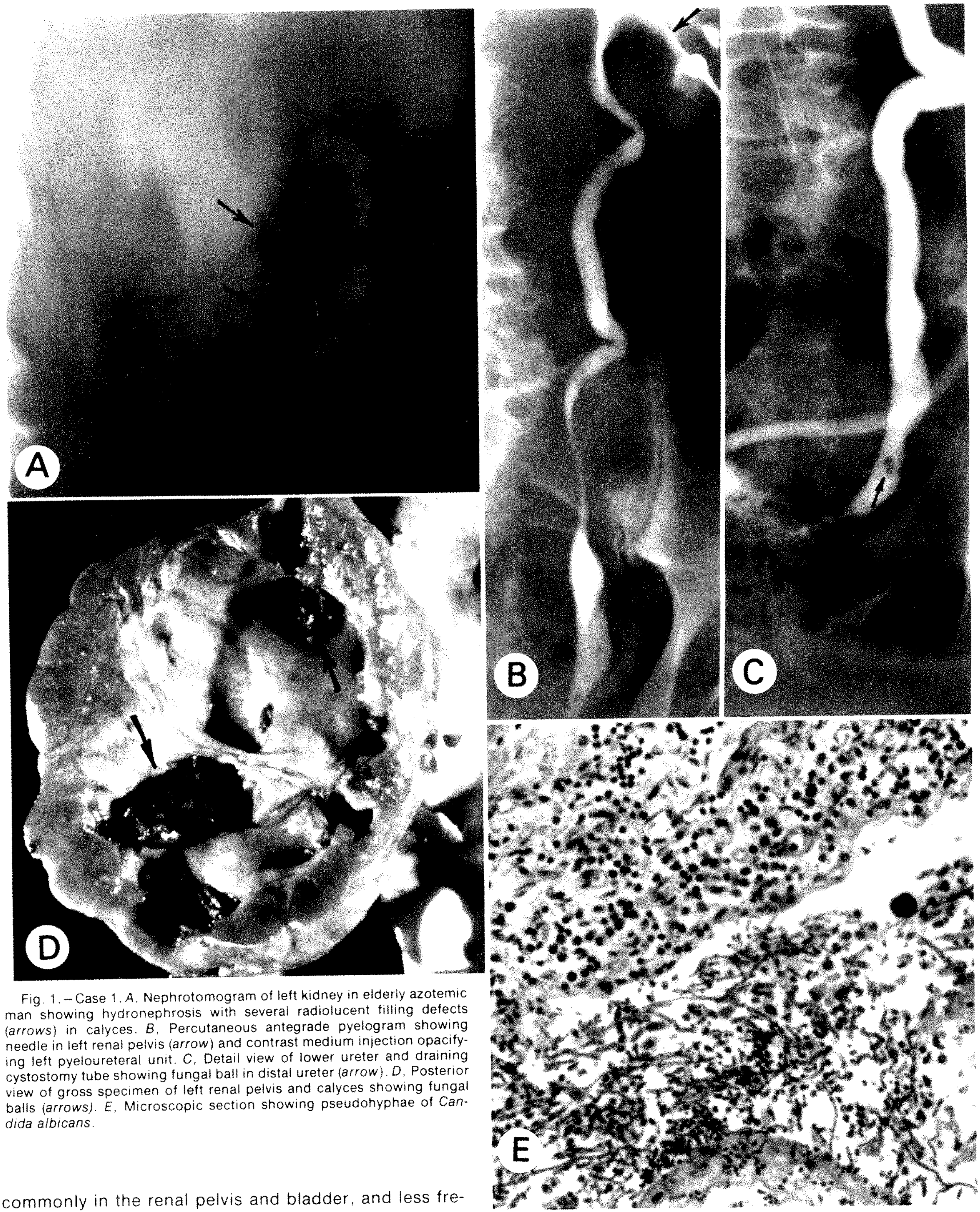

Fig. 1.—Case 1. *A*, Nephrotomogram of left kidney in elderly azotemic man showing hydronephrosis with several radiolucent filling defects (*arrows*) in calyces. *B*, Percutaneous antegrade pyelogram showing needle in left renal pelvis (*arrow*) and contrast medium injection opacifying left pyeloureteral unit. *C*, Detail view of lower ureter and draining cystostomy tube showing fungal ball in distal ureter (*arrow*). *D*, Posterior view of gross specimen of left renal pelvis and calyces showing fungal balls (*arrows*). *E*, Microscopic section showing pseudohyphae of *Candida albicans*.

commonly in the renal pelvis and bladder, and less frequently in the ureter and kidney parenchyma. The radiographic differential diagnosis of these filling defects should include nonopaque calculi, blood clots, neoplasms (usually of uroepithelial origin), sloughed papilla, malacoplakia, and pyeloureteritis cystica [13], as well as fungus balls.

Initially in the evaluation of patients with decreasing

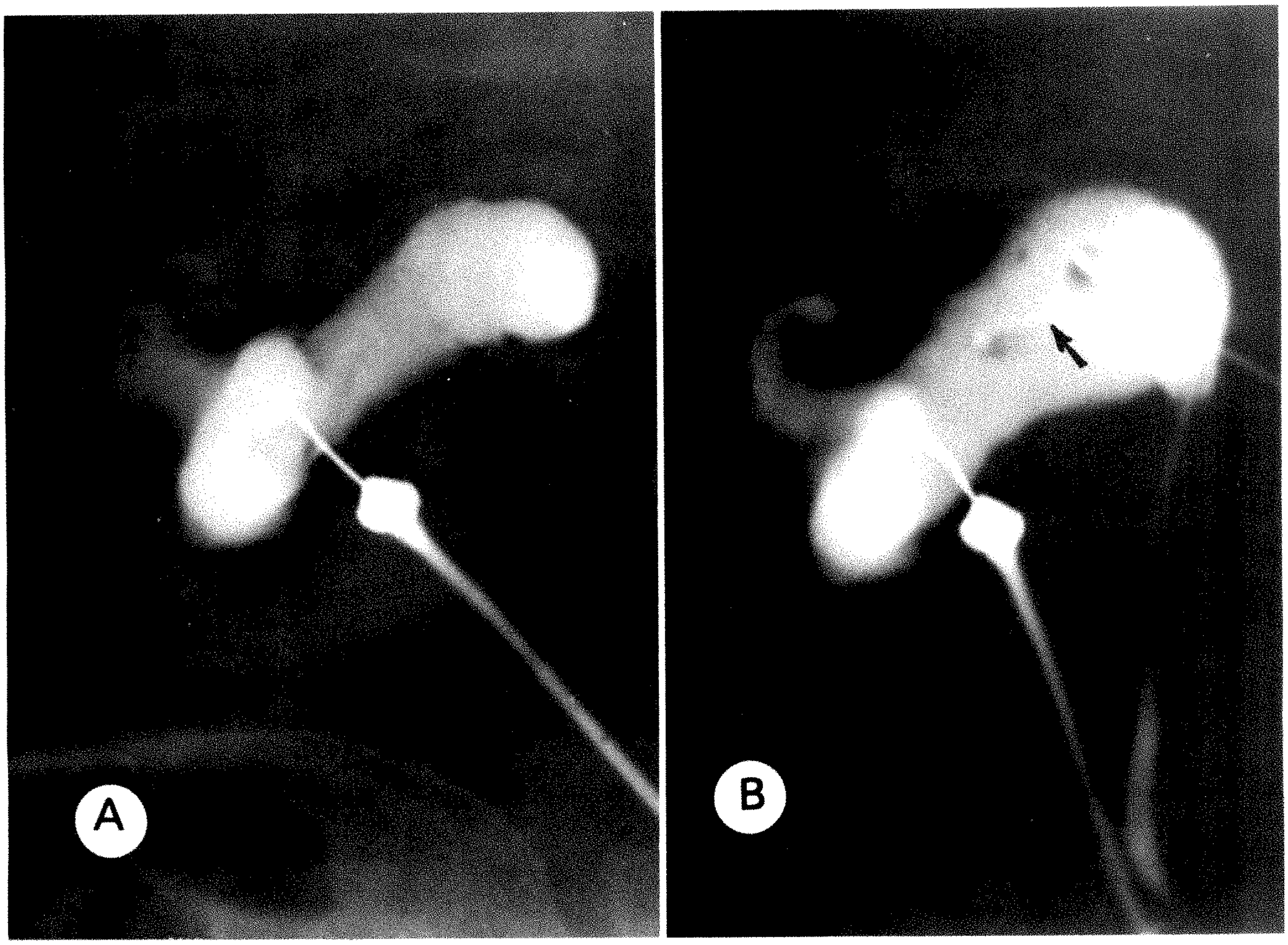

Fig. 2.—Case 2. *A*, Antegrade pyelogram contrast injection showing numerous small lucent filling defects and area of papillary necrosis (*arrow*). Thick creamy pus was returned. *B*, Further opacification showing mild obstruction of ureteropelvic junction and normal ureter. Nephrostomy tube (no. 12 French) placed percutaneously (*arrow*) for drainage.

renal function and fever of unknown origin, excretory urography may show unilaterally or bilaterally decreased visualization or nonvisualization. Further studies are needed to evaluate this problem, including high dose urograms with nephrotomography and retrograde or antegrade pyelography [14] if obstruction or the nature of the filling defects cannot be determined.

Antegrade pyelography is an excellent diagnostic tool because it not only gives visual anatomic information about the nature and site of obstruction, but it also obtains direct material for culture for specific diagnosis. At the same time treatment can be instituted via a percutaneous nephrostomy drainage catheter as in case 2. This is done with local anesthesia and is associated with low morbidity [15].

In our patients and other reported cases of urinary tract fungus balls, diabetes mellitus was a common underlying disease, occurring in 44% of patients. Hurley and Winner [16] provided experimental evidence that primary renal candidiasis is the end stage of initial mild candidemia. The cause of the initial candidemia in diabetics as well as in patients with underlying malignancy or on immunosuppression or steroid therapy has not yet been fully elucidated. Urinary stasis also may be a factor in fungal infections. McDonald and Fagan [17] and Margolin [18] reported fungus balls in patients with stasis secondary to prostatic enlargement and neurogenic bladder. Our patients had hydronephrosis secondary to a previous urethral stricture and ureteropelvic junction obstruction. Sales and Mundy [19] described two patients with chronic pyelonephritis on long term antibiotic therapy with similar *Candida* fungus balls successfully treated with amphotericin B. Such long term antibiotic therapy may change the normal flora sufficiently to promote the growth of *Candida* and increase the chance of fungemia.

The association of radiographic filling defects (usually mobile) in the urinary tract in a compromised host, especially diabetic, with clinical findings of acute or chronic renal failure and stasis should suggest possible urinary tract opportunistic fungal infection. A high index of suspicion in the differential diagnosis with subsequent identification of mycelia in the urinary sediment should lead to appropriate treatment with antifungal agents.

REFERENCES

1. Lundquist CM: On primary mycosis of kidney. *Br J Urol* 3:1–13, 1931
2. Clark RE, Minagi H, Palubinskas AJ: Renal candidiasis. *Radiology* 101:567-572, 1971
3. Boldus RA, Brown RC, Culp, DA: Fungus balls in the renal pelvis. *Radiology* 102:555-557, 1972
4. Gerle RD: Roentgenographic features of primary renal candidiasis. *Am J Roentgenol* 119:731-738, 1973
5. Turner RW: Grigsby TH, Enright JR, Chance HL, Frazier TC, Womack CT, Lang EK: Anuria secondary to mechanical obstruction caused by a *Candida* fungus ball. *J Urol* 109:938-940, 1973
6. Crosse JE, Soderdahl DW, Schamber DT: Renal actinomycosis. *Urology* 7:309-311, 1976
7. Michigan S: Genitourinary fungal infection. *J Urol* 116:390-397, 1976
8. Meyerson DA, Rosenfield AT: Renal aspergillosis: a report of two cases. *J Can Assoc Radiol*. In press
9. Bennett JE: Chemotherapy of systemic mycoses. I. Polyene antibiotics. *N Engl J Med* 290:30-32, 1974
10. Bennett JE: Chemotherapy of systemic mycoses. II. 5-fluorocytosine. *N Engl J Med* 290:320-323, 1974
11. Louria DB, Stiff DP, Bennett B: Disseminated moniliasis in the adult. *Medicine* 41:307-337, 1962
12. Lehner T: Systemic candidiasis and renal involvement. *Lancet* 1:1414–1416, 1964
13. Kamens L: Ureteritis cystica: diagnosis by antegrade pyelography. *Urology* 6:209-211, 1975
14. Sherwood T, Stevenson JJ: Antegrade pyelography: a further look at an old technique. *Br J Radiol* 45:812-820, 1972
15. Pfister RC: A new total system for percutaneous nephrostomy. In preparation
16. Hurley R, Winner HI: Experimental renal moniliasis in the mouse. *J Pathol Bacteriol* 86:75-82, 1963
17. McDonald DF, Fagan CJ: Fungus balls in the urinary tract: case report. *Am J Roentgenol* 114:753-757, 1972
18. Margolin HN: Fungal infections of the urinary tract. *Semin Roentgenol* 6:323-330, 1971
19. Sales JL, Mundy HB: Renal candidiasis: diagnosis and management. *Can J Surg* 16:139-143, 1973

Radiologic Spectrum of Opportunistic Infections of the Upper Gastrointestinal Tract

PATRICIA A. ATHEY,[1,2] HARVEY M. GOLDSTEIN,[1] AND GERALD D. DODD[1]

Clinical findings and barium studies were reviewed in 34 patients with upper gastrointestinal opportunistic infections, including two with gastric involvement. The spectrum of radiologic features is presented with particular attention to early subtle findings such as disturbance of esophageal motility and tiny marginal filling defects. While most cases are due to *Candida albicans*, other organisms may also invade the upper gastrointestinal tract in the debilitated host.

Opportunistic infections are known to occur in the esophagus of debilitated patients. The most commonly recognized clinical situation is invasion by the saprophyte, *Candida albicans*. First described in 1956 [1], sporadic reports of the radiologic findings in esophageal moniliasis are now in the literature [2-7]. We report radiologic experience in 34 patients with opportunistic infections of the upper gastrointestinal tract. These constitute the only large series of cases in the radiologic literature and include two instances of monilial involvement of the stomach, an observation not previously reported in the radiologic literature. The pathogenesis, clinical aspects, and pathologic findings in opportunistic infections of the esophagus are discussed, with emphasis on radiologic features.

Clinical Material

Medical records and barium examinations were reviewed in 34 patients with opportunistic infections of the esophagus and/or stomach seen during the past 4 years. The 21 females and 13 males ranged in age from 5 to 84 years. The major clinical diagnoses, organs involved, and known infecting agents are summarized in table 1. The majority of patients suffered from hematologic disorders, with leukemia the underlying diagnosis in more than half. Most had more than one predisposing factor since virtually all were receiving some form of chemotherapy, corticosteroids, and/or antibiotics. One patient with gastric candidiasis had no known predisposing factors.

Because of the debilitated clinical state of the patients, the diagnosis of opportunistic infection was often based solely on clinical findings and radiologic examination. In only a few patients was an organism actually cultured from the esophagus or stomach near the time of the radiologic examination. In approximately half the patients, *Candida albicans* was cultured from the oropharynx, urine, and/or blood. In two additional patients, there was evidence of a *Klebsiella* infection; in the remainder no organism was documented from any source.

Sixty esophagrams were performed on patients in this series. In one-third, an upper gastrointestinal series was also completed. Repeat examinations were performed to evaluate the status of the esophagus following therapy or because of recurrent infection at a later date. Esophageal involvement was demonstrated radiologically in 33 of the 34 patients. One patient had coexistent esophageal and gastroduodenal candidiasis, while an isolated gastric monilial infection was documented in another.

Radiologic Findings

Esophagus

A large spectrum of radiologic abnormalities may occur with opportunistic esophagitis. Findings may vary from only functional aberrations with no morphologic abnormalities to a grossly ulcerated esophagus which may even progress to stricture formation. Radiologic features appear to reflect the stage or severity of the disease process rather than the infectious etiology.

Abnormal esophageal motility was the most common radiologic finding and was present in all 33 patients with esophagitis. In two patients, abnormal motility was the sole initial finding with no morphologic abnormalities recognized on subsequent examination. The majority of cases demonstrated a slightly dilated, virtually atonic esophagus. In others, a primary peristaltic wave was noted which broke at varying levels in the thoracic esophagus and was followed by a solitary nonperistaltic contraction or multiple segmental contractions. Failure of relaxation of the distal vestibular portion of the esophagus occurred intermittently in one patient.

In most instances the morphologic changes involved the entire thoracic esophagus, although in approximately one-third of the cases, the proximal half was relatively spared even when oropharyngeal manifestations were present. The earliest morphologic abnormalities may be quite subtle and consist of small marginal filling defects which may be mistaken for tiny air bubbles (fig. 1). These tiny marginal irregularities are due to small pseudomembranous plaques. Unless there is a high degree of clinical suspicion, the early stages of esophagitis will not be detected. In fact, several of the esophagrams in our series were originally interpreted as normal.

The most common radiologic abnormality of opportunistic esophagitis is a shaggy marginal contour (fig. 2).

Received March 7, 1977; accepted after revision June 3, 1977.

[1] Department of Diagnostic Radiology, University of Texas System Cancer Center, M. D. Anderson Hospital and Tumor Institute, Houston, Texas 77030. Address reprint requests to H. M. Goldstein.

[2] Present address: Department of Radiology, Hermann Hospital, University of Texas Medical School at Houston, Houston, Texas 77030.

Am J Roentgenol **129:419-424, September 1977**

TABLE 1

Clinical Diagnoses and Infecting Agents

Primary Diagnosis	No. Patients	Organism	
		Positive Culture	Organism Unproven
Leukemia	19	*Candida*, 9; *Klebsiella*, 2	8
Lymphoma	4	*Candida*, 2	2
Testicular carcinoma	2	*Candida*, 2	...
Brain tumor	1	*Candida*	...
Aplastic anemia	1*	*Candida*	...
Malignant histiocytosis	1	*Candida*	...
Atrophic gastritis	1†	*Candida*	...
Lung carcinoma	2	...	2
Colon diverticulitis (postoperative)	1	...	1
Ovarian carcinoma	1	...	1
Myelofibrosis	1	...	1

Note—all patients except one had esophageal involvement.

* Patient had coexistent esophageal and gastroduodenal candidiasis.

† Patient had isolated gastric monilial infection.

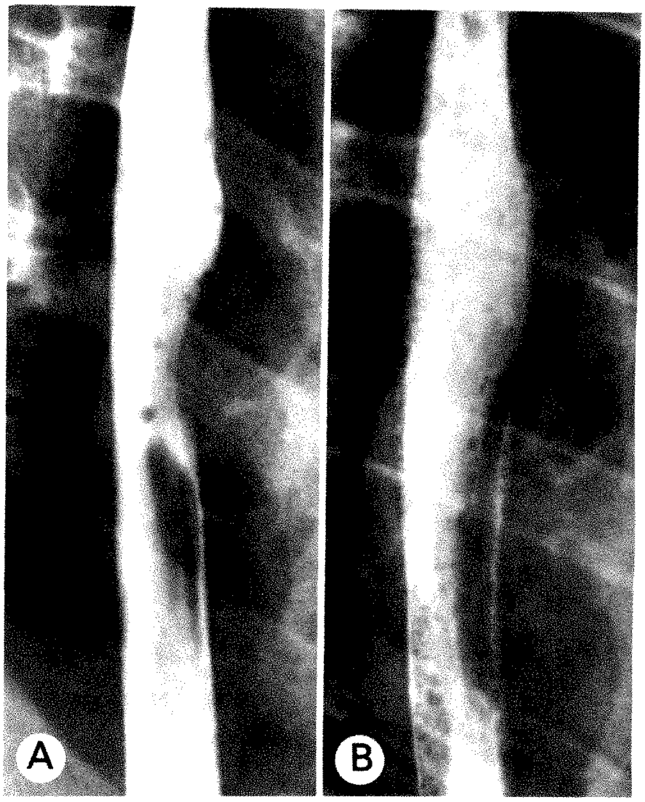

Fig. 1.—*A*, 25-year-old female undergoing chemotherapy for acute leukemia. Esophagram demonstrates tiny marginal filling defects resembling air bubbles. Clinical improvement occurred with therapy for moniliasis. *B*, 26-year-old male on chemotherapy for acute lymphocytic leukemia. Note more advanced esophagitis with marginal filling defects. *Klebsiella* was cultured from blood and at autopsy from esophageal lesions.

This finding has been described previously and was observed in our series. The irregular contour is due primarily to larger pseudomembranous filling defects rather than frank ulcerations, although some superficial ulceration may underlie the membranes at this stage. A "cobblestone" appearance may also be observed [2] or a lacelike pattern due to the inflammatory changes and associated mucosal edema (fig. 3).

Another reflection of the severity of the inflammatory changes may be thickening and irregularity of the mucosal folds which can simulate the appearance of varices (fig. 4). In the more advanced stages, deeper ulcerations may develop which further contribute to the shaggy appearance. A continuing severe inflammatory reaction can lead to frank stricture (fig. 5). This occurred in one patient in our series.

Two patients demonstrated the unusual finding of one or several large nodular filling defects in the esophagus representing "fungus balls" due to candidiasis (fig. 6). The nodules demonstrated no movement at the time of barium examination; in one patient, they were densely adherent to the mucosal surface at endoscopy and autopsy. In the cases with esophageal nodules, the other more typical radiologic findings were lacking. One of these patients had disease confined to the esophagus, while the other also had gastroduodenal involvement.

Stomach

Two cases in this series had monilial infection of the stomach. In one of the patients, the "fungus ball" appearance was noted in the esophagus, stomach, and duodenum. The other patient had isolated gastric involvement. Both cases were similar radiographically with several raised nodular lesions scattered about the stomach. In both, most of the nodules had central ulcerations or depressions giving the target or bull's-eye appearance (fig. 7). The usual differential diagnosis of multiple lesions with this feature includes metastatic melanoma and lymphoma.

Examination of the stomach and duodenum in approximately one-third of the other cases with opportunistic esophagitis yielded no definite findings which could be associated with the infectious process.

Discussion

By far the most common etiologic organism of opportunistic esophagitis is *Candida albicans*, a saprophytic organism that colonizes the skin and mucous membranes. It becomes pathologic when there is a decrease in host resistance. Predisposing factors are many, including malignancy, blood dyscrasia, prolonged use of antibiotics and/or corticosteroids, imperfect immune mechanism, or diabetes [8]. Occasionally there may be no known predisposing factors such as in our patient with atrophic gastritis.

There does not seem to be any age or sex predilection in the development of opportunistic infection of the esophagus. The most common presenting symptoms are dysphagia and/or substernal pain or burning. These symptoms, particularly chest pain, may initially be ascribed to other causes such as heart disease. Oropharyngeal mucous membrane lesions were present in approxi-

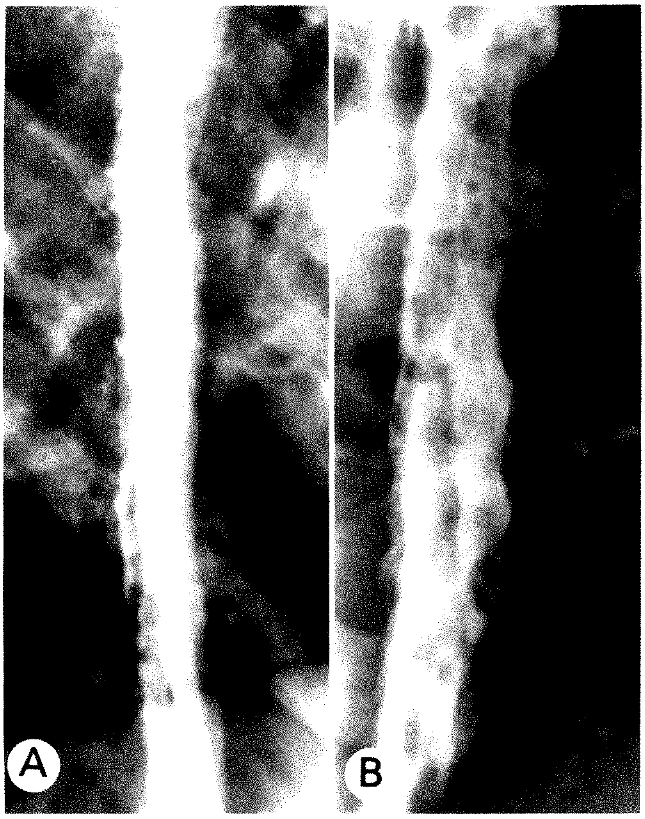

Fig. 2.—*A*, 41-year-old female who developed oral thrush while receiving steroids for brain tumor. Esophagram demonstrates typical shaggy marginal contour and pseudomembranous filling defects. *B*, 36-year-old male with testicular carcinoma who was receiving chemotherapy and antibiotics. Note severe changes of opportunistic esophagitis with irregular contour, pseudomembranes, and thickened folds. *Candida albicans* was cultured from blood.

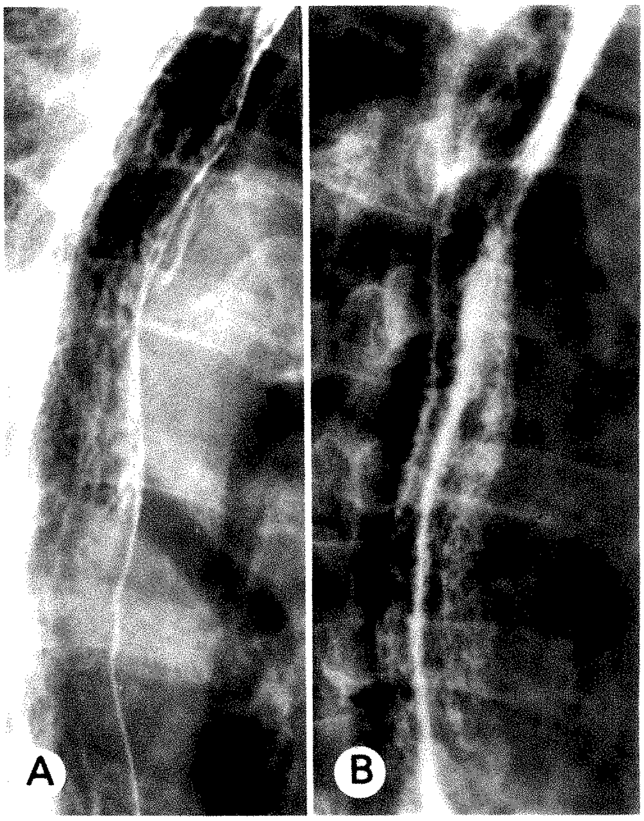

Fig. 3.—*A*, 76-year-old female with myelofibrosis who was receiving chemotherapy and antibiotics. Double contrast esophagram demonstrates "cobblestone" pattern due to mucosal edema. No proof for etiologic agent obtained. *B*, 62-year-old male with chronic myelogenous leukemia. Mucosal views of esophagus demonstrate lacelike pattern. No confirmation of infectious etiology obtained.

mately one-third of the patients. The lesions in the mouth and throat may be attributed to oral thrush, herpetic blisters, or may be nonspecific.

The diagnosis of opportunistic esophagitis is usually made in the appropriate clinical setting when esophageal symptoms are present, particularly in the presence of oropharyngeal findings. Empiric therapy for moniliasis is often begun at this time or delayed for a short time until esophagitis is confirmed by barium study and/or microbiologic techniques. Esophagoscopy was performed in only a few of our patients, including one with gastric candidiasis and another who had coincidental upper gastrointestinal bleeding. Endoscopy is usually not performed in the acute forms of esophagitis because of the theoretical risk of perforation. Most patients in our series were treated orally with Mycostatin. In others, systemic amphotericin B was utilized. Pain was managed with topical anesthetics, although a few patients required narcotics.

The majority of patients recovered from their episodes of esophagitis regardless of whether there was significant regression of the primary disease process. In patients who had repeat barium studies, there was usually some radiologic evidence of improvement to coincide with decreasing clinical symptoms. However, resolution of the radiologic abnormalities ordinarily lags behind clinical recovery. In several instances, the patients died of their primary disease shortly after the development of esophageal candidiasis, but in most instances the esophagitis did not contribute to the patient's clinical deterioration. Three patients were noted to have disseminated systemic candidiasis at autopsy while two others had a gram-negative esophagitis and systemic *Klebsiella* infection.

The radiologic-pathologic correlation is excellent in monilial esophagitis. In addition to the nonspecific inflammatory changes such as superficial ulceration and mural edema, there are scattered cream-colored membranes comprised primarily of fungal colonies and epithelial necrotic debris. The ubiquitous marginal filling defects seen on radiologic examination are caused by these pseudomembranous patches, which become thicker and confluent as the disease progresses. Both superficial and deep ulcerations may occur and produce the typical shaggy appearance of the esophageal contour noted on radiologic examination.

Esophageal intramural pseudodiverticulosis has been associated with the presence of moniliasis. Troupin [9]

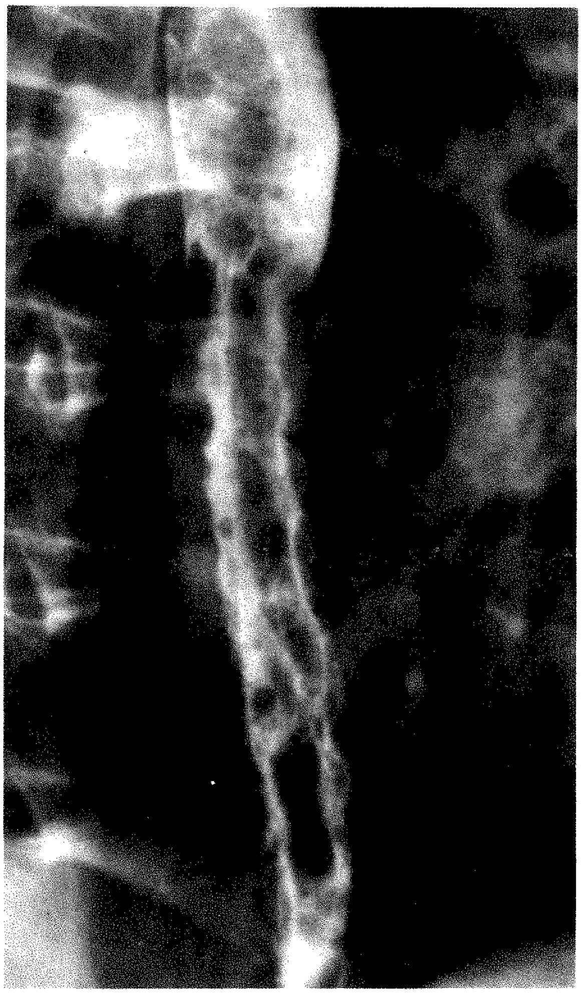

Fig. 4.—36-year-old male with testicular carcinoma on chemotherapy and antibiotics. Esophagram demonstrates grossly thickened and irregular mucosal folds simulating appearance of varices. Positive blood cultures of *Candida albicans* obtained.

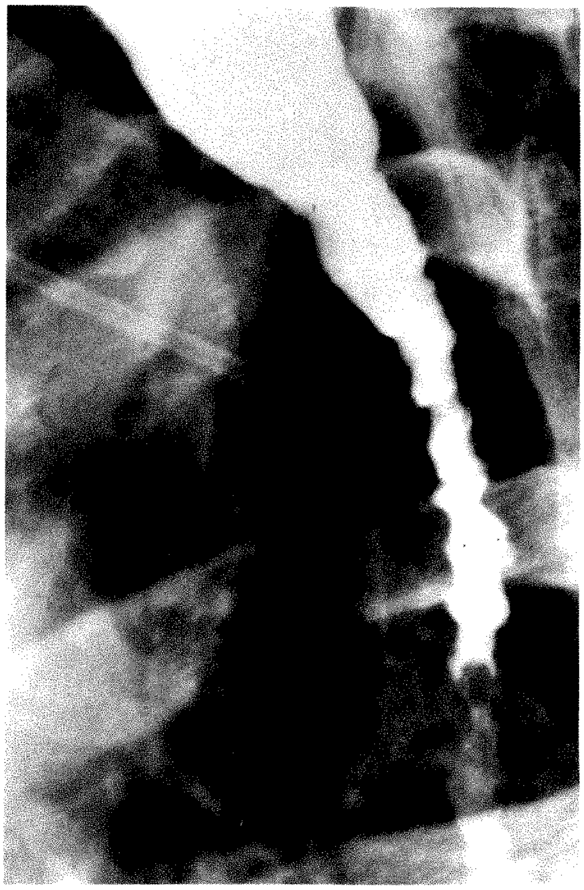

Fig. 5.—28-year-old male with acute leukemia and oral thrush who originally demonstrated typical features of esophageal moniliasis. Repeat esophagram 1 month later demonstrates long corkscrew stricture.

suggested that monilial infection was an etiologic factor in this condition, while others have felt the fungus to be a secondary invader and of no clinical significance in these patients [10]. No instances of intramural pseudodiverticulosis were present in our patient group.

The presence of *Candida albicans* in the stomach has been previously noted primarily in autopsy studies [4]. In a large series of 109 patients with fungal involvement of the gastrointestinal tract [11], 45 demonstrated various lesions associated with gastric candidiasis. Single or multiple ulcerations containing monilia deep in their ulcer beds were the most common lesions. It was not clear in these and other reported cases whether the infection occurred in previously existing ulcers or contributed to the ulcer formation [12]. In addition, there have been reports from Europe of patients with gastric resection and Billroth I anastomoses who developed bezoars composed of mucous material swarming with yeast [13, 14]. Bezoars were not present in our two cases of gastric involvement.

To our knowledge, the two patients with gastric candidiasis in our series are the first reported in the radiologic literature. One patient was a 70-year-old female with aplastic anemia who had nodular filling defects (fungus balls) in the esophagus as well as raised filling defects in the stomach and duodenum. She had positive blood and urine cultures; at autopsy there was evidence of monilial involvement of the liver, spleen, gastrointestinal tract, and genitourinary tract. The other patient, an 84-year-old female with epigastric pain, had none of the known predisposing conditions and was the only such patient in our series. Radiographically, she had several raised filling defects in the stomach. Endoscopically, these were fixed to the mucosa and thought to represent reticulum cell sarcoma [15]. Gastric biopsy and aspirate demonstrated the presence of mycelia. Treatment with Mycostatin and amphotericin B resulted in recovery with return of the radiologic examination to normal. The gastric nodules in both patients demonstrated central ulceration or umbilication. The cases were radiologically indistinguishable from other causes of the target appearance such as melanoma or lymphoma.

Opportunistic infections of the upper gastrointestinal tract are often thought to be synonymous with moni-

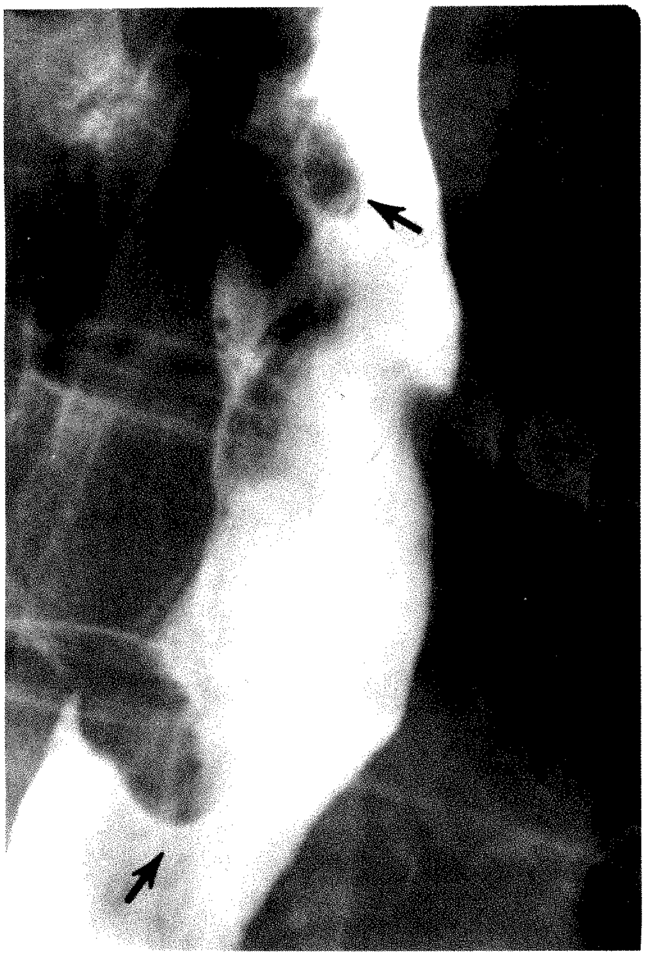

Fig. 6.—70-year-old with aplastic anemia under treatment with steroids. Barium study demonstrates filling defects in esophagus (*arrows*) due to fungus balls. Similar abnormalities present in stomach and duodenum. Disseminated candidiasis found at autopsy.

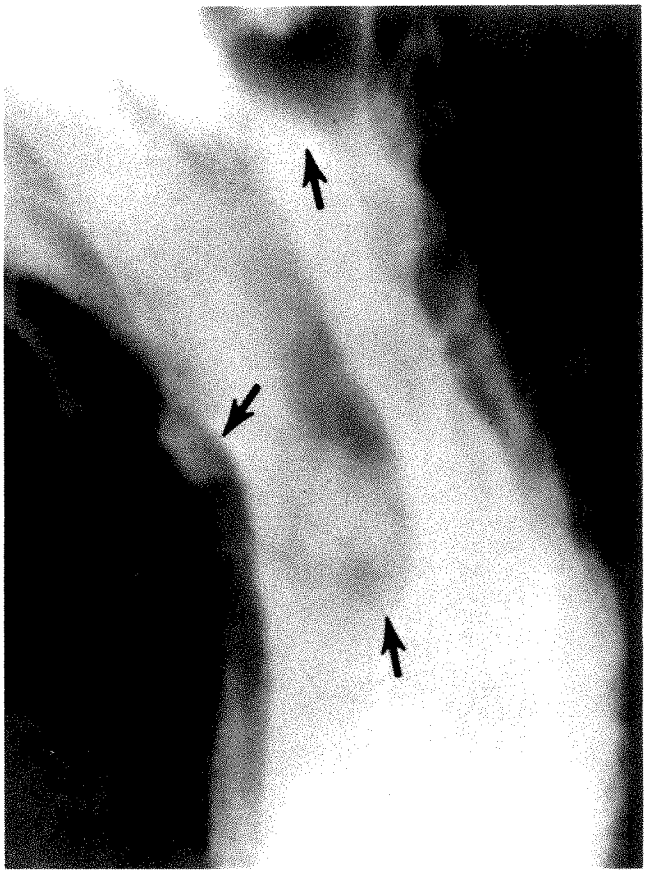

Fig. 7.—84-year-old female with atrophic gastritis but no debilitating illness. Barium examination demonstrates "target" lesions in stomach (*arrows*). Gastric biopsy demonstrated *Candida mycelia*.

liasis. However, several recently reported cases document that other organisms may also be responsible. McManus and Webb [16] reported a case of esophagitis shown to be secondary to *Lactobacillus acidophilus*. Several reports of herpetic esophagitis have also been documented [17-19]. The radiologic features in these cases have been virtually identical with those of esophageal moniliasis. In our patients, there was strong evidence of *Klebsiella* esophagitis in two patients from either pre- or postmortem cultures. These radiologic findings were also indistinguishable from those of patients with candidiasis. In addition, at least four other patients at our institution were found to have herpetic esophagitis at autopsy; unfortunately, esophagrams had not been performed. It is possible that some patients in our series who were presumed to have esophageal moniliasis were infected with other organisms which went unrecognized, particularly if oropharyngeal thrush was absent. A similar question might be raised for other published series. It would appear probable that the true spectrum of organisms responsible for esophagitis in the debilitated patient is often unappreciated.

REFERENCES

1. Andren L, Theander G: Roentgenographic appearances of esophageal moniliasis. *Acta Radiol* [*Diagn*] (Stockh) 46:571-574, 1956
2. Goldberg HI, Dodds WJ: Cobblestone esophagus due to monilial infection. *Am J Roentgenol* 104:608-612, 1968
3. Gonzales G: Esophageal moniliasis. *Am J Roentgenol* 113:233-236, 1971
4. Grieve NWT: Monilial oesophagitis. *Br J Radiol* 37:551-554, 1964
5. Lewicki AM, Moore JP: Esophageal moniliasis. *Am J Roentgenol* 125:218-225, 1975
6. Sheft DJ, Shargo G: Esophageal moniliasis (the spectrum of the disease). *JAMA* 213:1859-1862, 1970
7. Weiss J, Epstein BS: Esophageal moniliasis. *Am J Roentgenol* 88:718-720, 1962
8. Jensen KB, Stenderup A, Thomsen JB, Bichel J: Oesophageal moniliasis in malignant neoplastic disease. *Acta Med Scand* 175:455-459, 1964
9. Troupin RH: Intramural esophageal diverticulosis and moniliasis. *Am J Roentgenol* 104:613-616, 1968
10. Sperling HV, D'Altorio RA: Intramural diverticulosis of the esophagus. *Am J Dig Dis* 18:978-982, 1973
11. Eras P, Goldstein MJ, Sherlock P: *Candida* infection of the gastrointestinal tract. *Medicine* 51:367-379, 1972

12. Mohtashemi H, Davidson FZ: Candidiasis and gastric ulcer. *Am J Dig Dis* 18:915-918, 1973
13. Borg I, Heijkenskjold F, Nilehn B, Wehlin L: Massive growth of yeasts in resected stomach. *Gut* 1:244-249, 1966
14. Pertalla Y, Peltokallio P, Leiviska T, Sipponen J: Yeast bezoar formation following gastric surgery. *Am J Roentgenol* 125:365-373, 1975
15. Nelson RS, Bruni HC, Goldstein HM: Primary gastric candidiasis in uncomprised subjects. *Gastrointest Endosc* 22:92-94, 1975
16. McManus JPA, Webb JN: A yeast-like infection of the esophagus caused by *Lactobacillus acidophilus*. *Gastroenterology* 68:583-586, 1975
17. Berg JW: Esophageal herpes: a complication of cancer therapy. *Cancer* 8:731-740, 1955
18. Meyers C, Durkin MG, Love L: Radiographic findings in herpetic esophagitis. *Radiology* 119:21-22, 1976
19. Weiden PL, Shuffler MD: Herpes esophagitis complicating Hodgkin's disease. *Cancer* 33:1100-1102, 1974

Radiologic Aspects of Beck Gastric Tube in Esophageal Reconstruction

SALEH A. FETOUH,[1] RICHARD H. DAFFNER,[1] R. W. POSTLETHWAIT,[2] AND ROGER C. MILLAR[2]

Over a 28 month period, 19 patients underwent esophageal reconstruction using the Beck tube fashioned from the greater curvature of the stomach. Eighteen had unresectable carcinoma of the esophagus and one had a benign stricture secondary to reflux esophagitis. The degree of palliation was considered good in 13 cases. The surgical aspects of the Beck gastric tube are described and radiologic features in both uncomplicated and complicated cases are illustrated. Early experience with the procedure is encouraging.

A safe method for satisfactory palliation of patients with inoperable carcinoma of the esophagus has not been established, particularly when a complication such as tracheoesophageal fistula is present. The inability to swallow even saliva without aspiration makes the terminal weeks of life intolerable. Plastic tubes, such as the Celestin tube, at times provide some relief. Substernal colon transposition gives excellent palliation but at the cost of excessive morbidity and mortality. In seeking a simpler bypass operation, we are in the process of evaluating a gastric tube. The procedure is also useful for benign conditions such as strictures from reflux esophagitis or lye ingestion, congenital esophageal atresia, and achalasia.

This paper briefly describes the surgical aspects of the Beck gastric tube and discusses its radiologic features in both uncomplicated and complicated situations. The procedure has been in use at Duke University Medical Center and the Veterans Administration Hospital in Durham, North Carolina, for over 2 years.

Case Material

Over a 28 month period, 19 patients have been operated on using the Beck tube esophageal bypass. Eighteen had unresectable carcinoma of the esophagus, five of whom had tracheoesophageal fistulae. One had a benign stricture secondary to reflux esophagitis. There were two postoperative deaths as a result of continued pneumonia and subsequent respiratory failure. None of the gastric tubes became necrotic. Leaks at the cervical anastomosis occurred in seven patients; five closed spontaneously and two required surgery.

The degree of palliation was considered good if the patient was able to take solid foods without difficulty. In this series, 13 patients had good palliation, two had fair palliation requiring a soft or blended diet, two could not be evaluated adequately because of severe medical problems, and two died postoperatively. Most of the patients were started on liquids after 7 days and were taking soft regular food at about 14 days.

Discussion

In 1905, Beck and Carrell [1] demonstrated on an experimental basis that a gastrostomy tube could be constructed from a flap fashioned from the greater curvature of the stomach and brought subcutaneously to the anterior chest wall. In 1912, Jianu [2] used the tubed gastric pedicle to bypass the esophagus in animal and cadaver experiments. However, these attempts were unsuccessful because of inadequacy of blood supply and difficulty in creating sufficient length and mobility of the gastric tube to reach the neck. Further experimental work on dogs was reported in 1944 [3].

In the 1950s the technique of the reversed gastric tube operation was perfected [4–7]. Much of the pioneering work was performed by Gavriliu and Georgescu [5, 6] of Romania. Subsequently, modifications were developed utilizing the gastric tube technique [8–14]. In the 1970s, Heimlich [15, 16] reported his 15 year experience with the reversed gastric tube. He was able to overcome the deficiencies of the Beck-Jianu gastrostomy by augmenting the vascular supply to the greater curvature of the stomach through splenectomy which diverted the entire splenic blood supply to the tube.

In 1975, Gavriliu [17] presented a detailed review of his experience with esophageal replacement in 580 patients, the largest reported series. The early results of our current experience with the Beck tube were reported in 1975 [18].

Surgical Aspects

Originally only patients with tracheoesophageal fistula were selected for this procedure, since they most urgently needed relief. Subsequently patients without fistula but with tracheobronchial invasion, patients with large unresectable tumors, and patients with tumors that regressed after radiation therapy have been included.

Through an abdominal incision, the greater curvature of the stomach is mobilized, preserving the right gastroepiploic vessels. With the aid of a stapler, the greater curvature of the stomach is made to form a gastric tube, based at the antrum (fig. 1). The tube is placed substernally after the neck dissection is complete. The lower part of the cervical esophagus is divided. The proximal end is anastomosed end-to-side to the gastric tube. In some patients the proximal tip of the gastric tube is brought out to the skin surface of the neck as a controlled fistula. This is easily closed as a secondary procedure under local anesthesia.

Received December 27, 1976; accepted after revision April 4, 1977.

[1] Department of Radiology, Duke University Medical Center and Veterans Administration Hospital, Durham, North Carolina 27710. Address reprint requests to R. H. Daffner.

[2] Department of Surgery, Duke University Medical Center and Veterans Administration Hospital, Durham, North Carolina 27710.

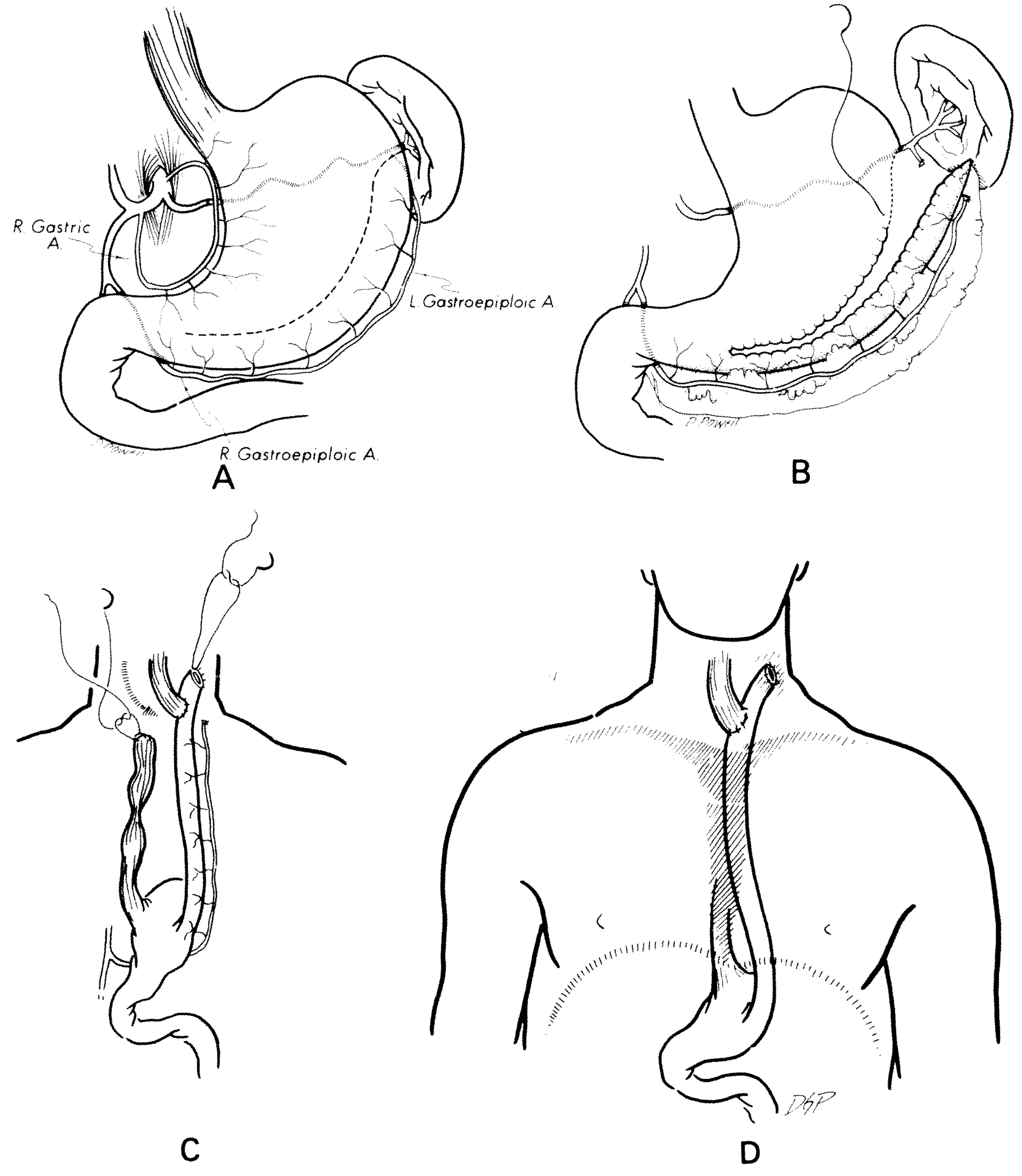

Fig. 1.—Anatomy and surgical technique of Beck gastric tube. *A*, Dotted line indicates incisions along greater curvature. Blood supply to tube is derived from right gastroepiploic vessels. *B*, Appearance of stomach after formation of gastric tube. Note that spleen is left intact. *C* and *D*, Completed tube with controlled fistula which is used in some patients. Note diseased esophagus is left in place.

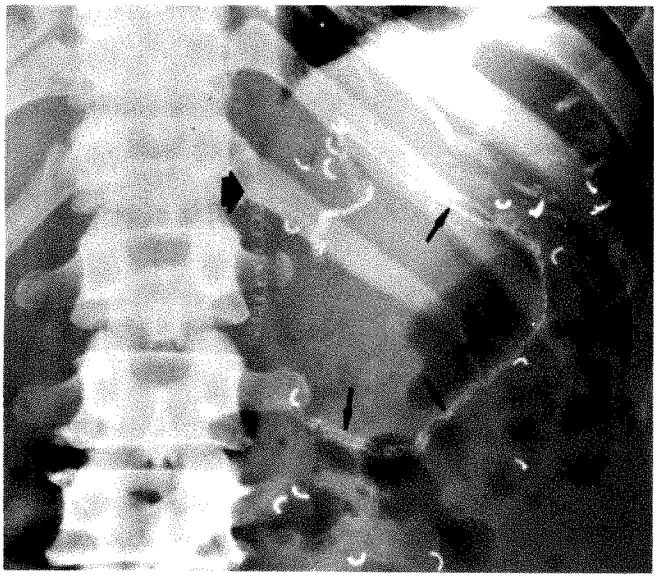

Fig. 2.—Normal plain film appearance of abdomen after Beck tube procedure. Line of staples identifies remnant of greater curvature (*small arrows*). Vertical line of staples identifies position of gastric tube (*large arrow*). Multiple vascular clips are present.

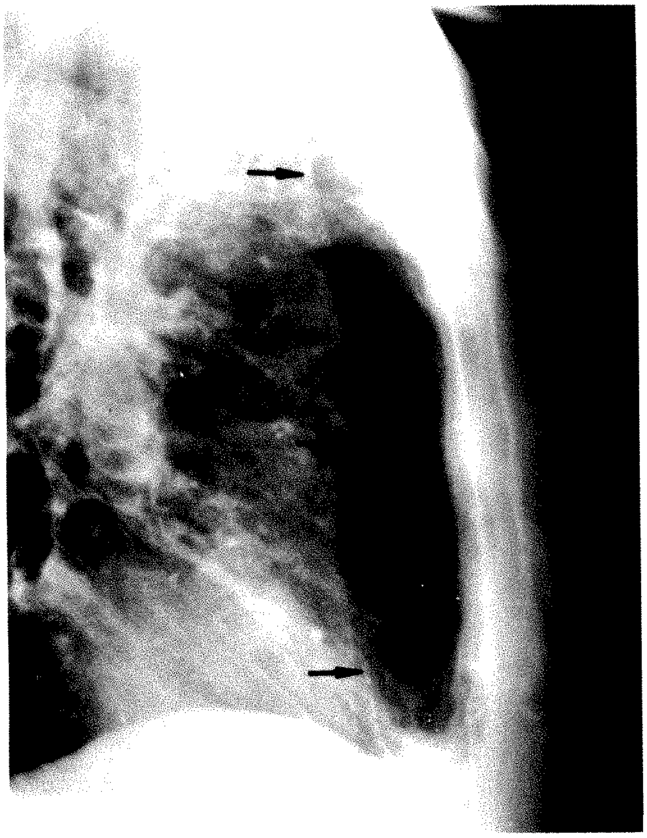

Fig. 3.—Normal appearance of lateral chest after Beck tube procedure. Note substernal lucency and line of staples along its posterior aspect (*arrows*). Position of staple line may vary.

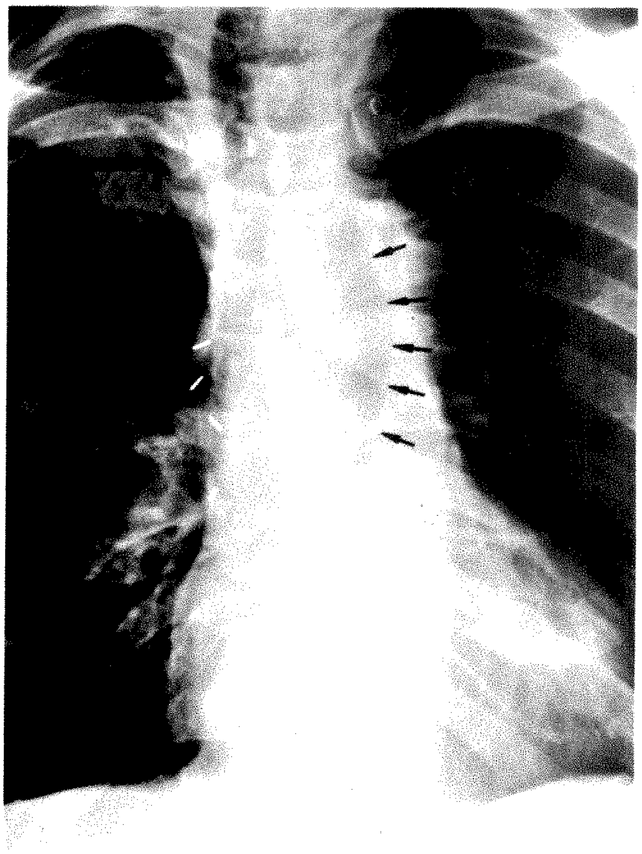

Fig. 4.—Frontal chest film after Beck tube procedure. Paramediastinal gas density representing air within Beck tube is present on left (*arrows*). This may also be located on right side. Multiple metallic clips identify site of prior attempt at resection of carcinomatous esophagus. In this patient trachea deviates to right because of cervical anastomosis of gastric tube in this region.

Radiologic Aspects

Radiologic examination assesses the postoperative morphology of the reconstruction and detects development of early or late complications. On plain films, the staple line along the greater curvature of the stomach will have a characteristic curved appearance in the left upper quadrant of the abdomen (fig. 2). In the chest the staple line along the Beck tube is recognized in the retrosternal tunnel in the lateral view (fig. 3). Another staple line may be seen at the proximal end of the thoracic esophagus on the lateral chest film. Occasionally air is seen in the tube both on the frontal and lateral chest views (figs. 3 and 4).

The first contrast examination is usually performed on the sixth or seventh postoperative day. For this examination we use water soluble contrast medium, looking critically for evidence of leakage at the cervical anastomosis. Contrast material is expected to enter the cutaneous fistula, especially in the recumbent position. This should not be confused with leakage at the cervical anastomosis. Several spot films are taken of the anastomosis in different projections under fluoroscopic control (fig 5).

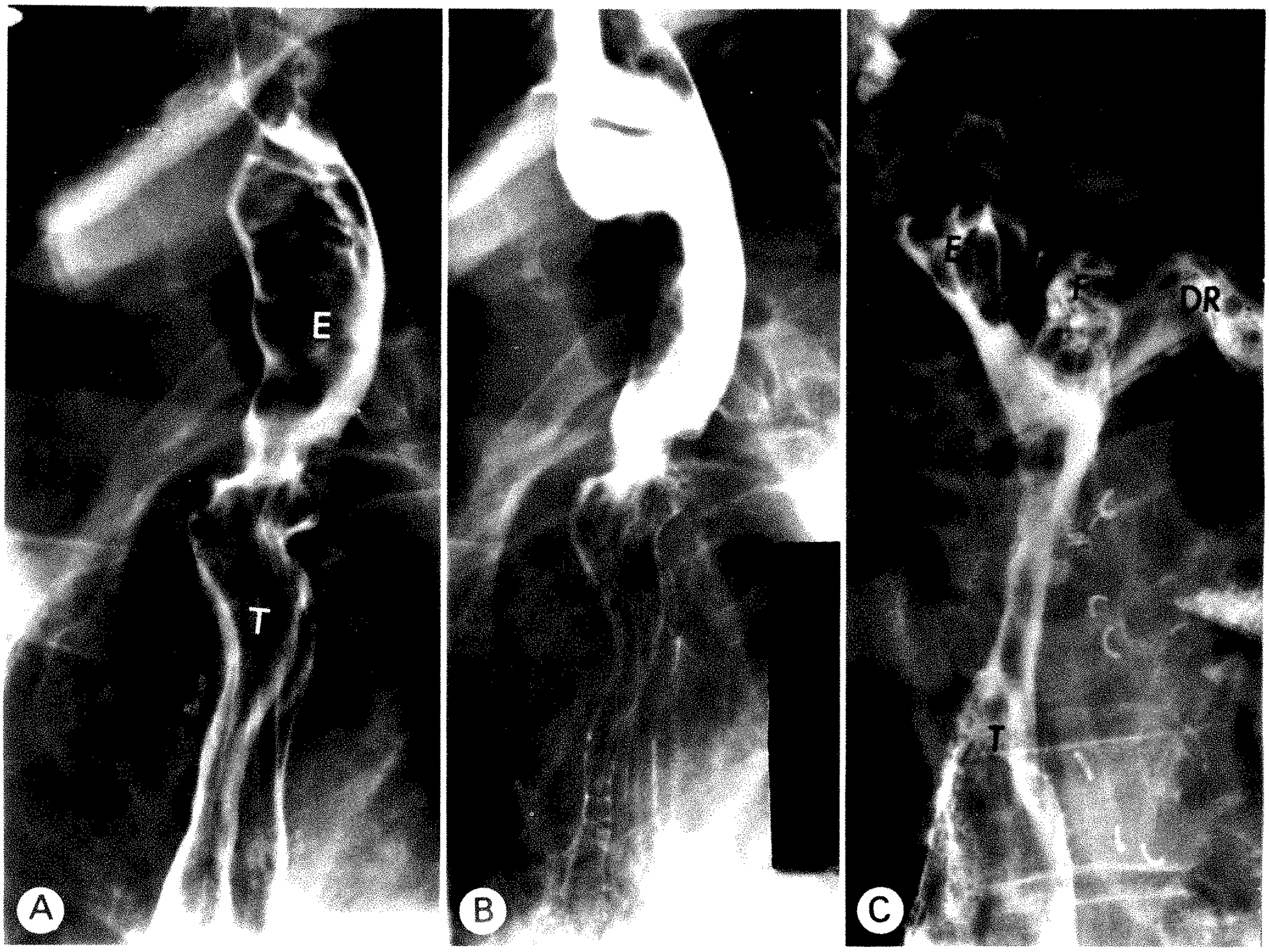

Fig. 5.—Normal postoperative appearance of upper anastomosis. *A and B*, Normal anastomosis without use of cutaneous fistula. Note rugae within gastric tube. *C*, Anastomosis in patient with fistula. Contrast enters fistula. Leakage at anastomosis passes out through Penrose drain. E = proximal esophagus, T = gastric tube, F = cutaneous fistula, DR = drain.

The contrast material should pass readily through the Beck tube to reach the region of the gastric antrum and pylorus. From there it will flow in a retrograde manner to fill the gastric remnant, with occasional reflux into the distal esophagus, as well as antegrade into the duodenum.

Nonfluoroscopic films include the same views of the stomach that would be obtained in a regular upper gastrointestinal examination (fig. 6). The only variation is in obtaining "esophageal" views for which we recommend inclusion of a lateral chest film (fig. 7) for visualization of the Beck tube in its retrosternal position.

No esophageal manometric studies were performed to evaluate the motor function in the gastric tube. Fluoroscopic observations revealed no evidence of peristalsis in the tube which merely acts as a conduit. This is similar to previous experiences with the reversed gastric tube [14, 15].

Complications

The commonest and earliest postoperative complication is leakage at the cervical anastomosis. Unless leakage is suspected clinically, barium is the preferred contrast agent for follow-up evaluation of the integrity of the tube. A baseline barium "esophagogram" is obtained before the patient is discharged from the hospital.

In addition to leakage, other complications were seen radiographically. One patient developed a mediastinal hematoma (fig. 8). Mediastinal drainage was then instituted routinely, and this complication has not been seen again. One patient developed narrowing of the tube at the level of the diaphragm by a band of scar tissue (fig. 9), for which operative division was necessary. Other complications encountered include aspiration pneumonia, pleural effusion, and shock lung.

Other Observations

The need for a procedure less extensive and traumatic than colon interposition is obvious. Eliminating the necessity for splenectomy or mobilization of the tail of the pancreas, as suggested for the reversed gastric tube [15], seems advantageous. Blood supply to the isoperi-

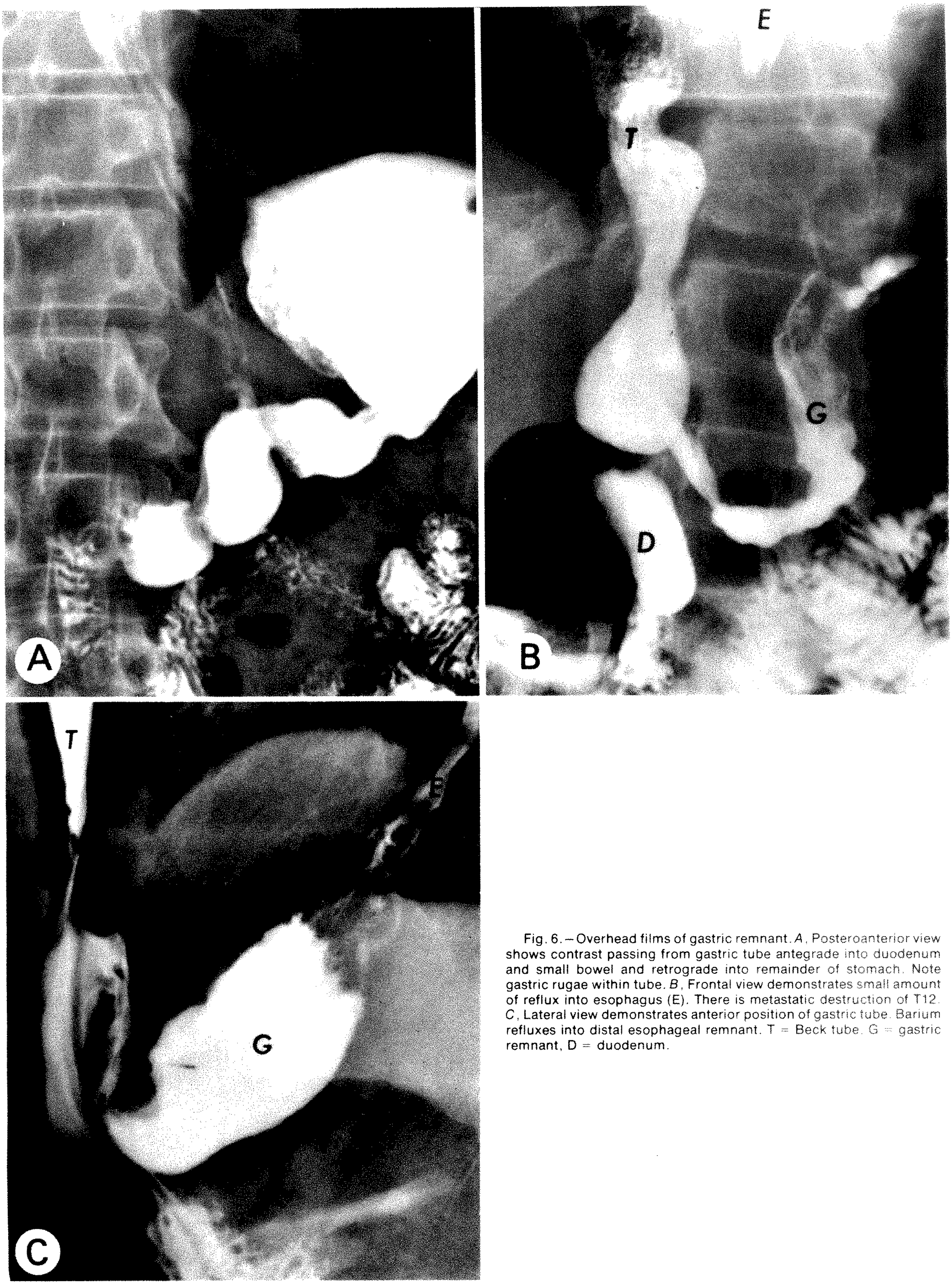

Fig. 6.—Overhead films of gastric remnant. *A*, Posteroanterior view shows contrast passing from gastric tube antegrade into duodenum and small bowel and retrograde into remainder of stomach. Note gastric rugae within tube. *B*, Frontal view demonstrates small amount of reflux into esophagus (E). There is metastatic destruction of T12. *C*, Lateral view demonstrates anterior position of gastric tube. Barium refluxes into distal esophageal remnant. T = Beck tube, G = gastric remnant, D = duodenum.

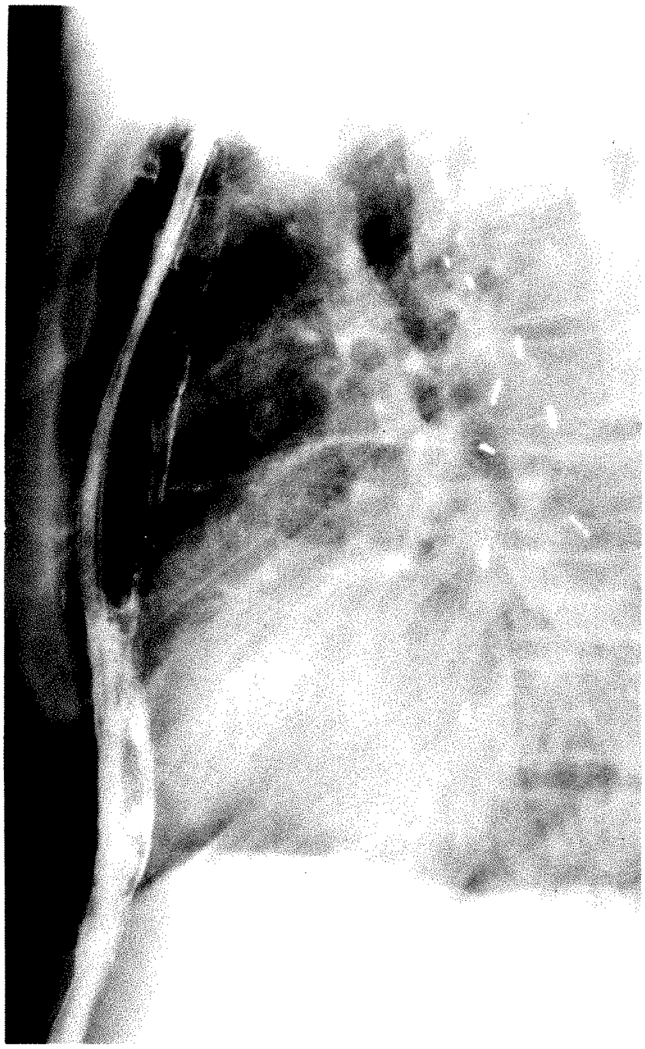

Fig. 7.—Lateral chest view with barium after Beck tube procedure. Stomach tube is present within bypass.

staltic tube had never been a problem. Thoracotomy and its complications are avoided.

With a denervated tube and limited life expectancy, excretion and reflux of acid pepsin should not be a problem. Since the thoracic portion of the esophagus is left in continuity with the gastric remnant to provide drainage, reflux back up to a tracheoesophageal fistula may occur but should be avoided by appropriate positioning. None of our patients complained of reflux esophagitis symptoms.

ACKNOWLEDGMENTS

We express our appreciation to Mrs. Hazel Underwood and Mrs. Faye Brockwell for their efforts in preparation of this manuscript, the staff of Medical Media Production Service of the Veterans Administration Hospital for artwork and excellent photographic assistance, and Dr. Reed Rice for helpful suggestions and critical review.

REFERENCES

1. Beck C, Carrell A: Demonstration of specimens illustrating a method of formation of a pre-thoracic esophagus. *Ill Med J* 7:463, 1905
2. Jianu A: Gastronstime u Oesophagosplastik. *Dtsch Z Chir* 118:383, 1912
3. Swenson O, Magruder TV: Experimental esophagostomy. *Surgery* 15:954-963, 1944
4. Heimlich HJ, Winfield J: The use of a gastric tube to replace or by-pass the esophagus. *Surgery* 37:549-559, 1955
5. Gavriliu D, Georgescu L: Esofagoplastie directa cu material gastric. *Rev Stiintelor Med* 3:33-36, 1951
6. Gavriliu D, Georgescu L: Esofagoplastie viscerala directa. *Chirurgia* 4:104-138, 1955
7. Heimlich HJ: The use of a gastric tube to replace the esophagus as performed by Dr. Dan Gavriliu of Bucharest, Romania. *Surgery* 42:693-695, 1957
8. Sanders GB: Esophageal replacement with reversed gastric tube. *JAMA* 181:944-947, 1962
9. Burrington JD, Stephens CA: Esophageal replacement with gastric tube in infants and children. *J Pediatr Surg* 3:246-252, 1968
10. Glasson MJ, Dey DL, Cohen DH: Esophageal atresia: results of treatment. *Med J Aust* 1:69, 1971
11. Anderson KD, Randolph JG: The gastric tube for esophageal replacement in children. *J Thorac Cardiovasc Surg* 66:333-342, 1973
12. Cohen D: Esophageal reconstruction using a gastric tube. *Aust Paediatr J* 6:22-24, 1970
13. Middleton AW: Esophageal replacement with a gastric tube, in *Proceedings of the Pediatric Surgical Congress*, vol 2, Melbourne, Royal Children's Hospital, 1970, pp 430-435
14. Cohen DH, Middleton AW, Fletcher J: Gastric tube esophagoplasty. *J Pediatr Surg* 9:451-460, 1974
15. Heimlich HJ: Esophagoplasty with reversed gastric tube. Review of fifty-three cases. *Am J Surg* 123:80-92, 1972
16. Heimlich HJ: Reversed gastric tube (RGT) esophagoplasty for failure of colon, jejunum and prosthetic interposition. *Ann Surg* 182:154-160, 1975
17. Gavriliu D: Replacement of the esophagus by a reverse gastric tube. *Curr Probl Surg* 12(10):36-64, 1975
18. Orringer MD, Sloan H: Substernal gastric bypass of the excluded thoracic esophagus for palliation of esophageal carcinoma. *J Thorac Cardiovasc Surg* 70:836-851, 1975

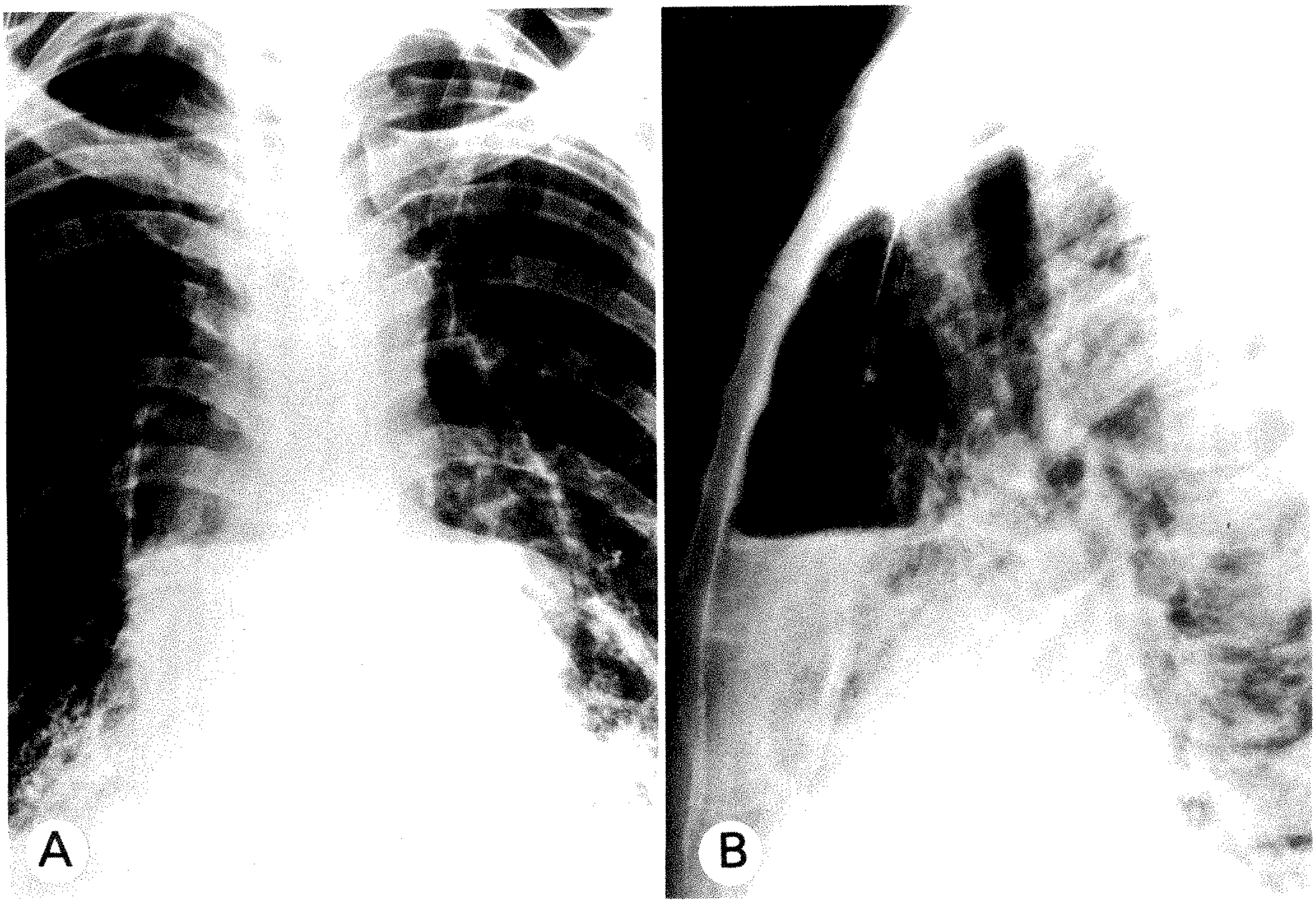

Fig. 8.—Mediastinal hematoma after Beck tube procedure. Frontal (*A*) and lateral (*B*) films demonstrate air-fluid level which was subsequently drained without further recurrence.

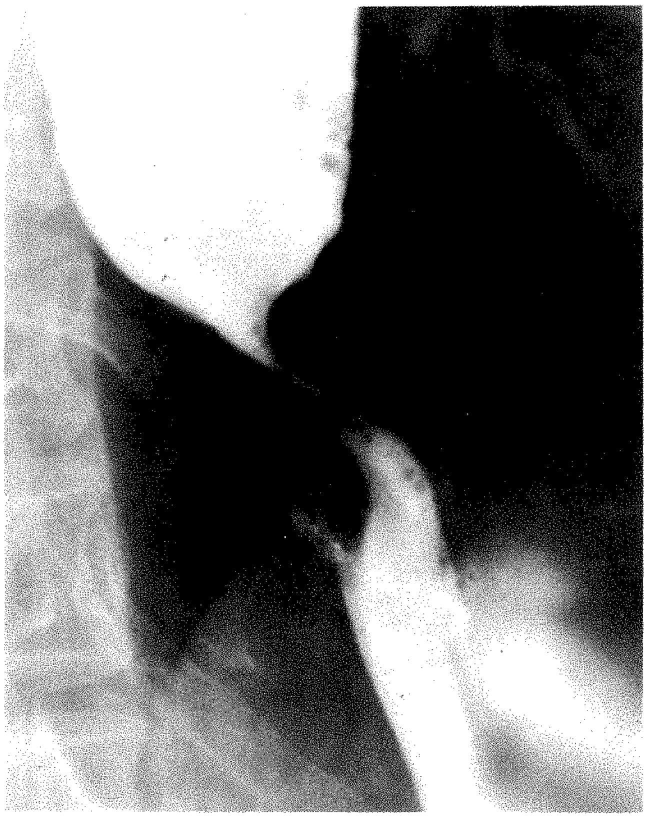

Fig. 9.—Narrowing of gastric tube at distal end. Barium study shows tapered narrowing of gastric tube near its point of passage through diaphragm. Band of scar tissue was found that required operative division.

Air in the Esophagus: A Frequent Radiographic Finding

ANTHONY V. PROTO[1, 2] AND EDWARD J. LANE[1]

While the radiologic literature discusses the presence of air in the esophagus on chest radiographs, this has almost always been reported as a finding associated with other radiologic abnormalities. In a retrospective study, esophageal air was noted on 36% of normal posteroanterior chest radiographs. The radiologic anatomy of the esophagus and the typical locations of air within it are discussed.

The esophagus has received much attention in the radiologic literature, not the least of which has been the observation of air within its lumen on chest radiographs. This finding has almost always been reported in association with other detectable pulmonary parenchymal or mediastinal abnormalities [1-4]. In 1965 Cimmino [5] discussed air in the midesophagus as a normal finding and a possible source of diagnostic error. We too have observed that esophageal air is a frequent radiographic finding. This paper discusses the typical locations in which it is recognized.

Radiologic Anatomy

A knowledge of the surfaces contacted by the lungs in the posterior thorax allows an understanding of the anatomic relationships responsible for visualizing esophageal air. Above the aortic arch, the right and left lungs often make contact immediately anterior to the spine and posterior to the esophagus to form the posterior junction line. More caudally they are separated, not only by the forward arching of the left and right superior intercostal veins [6] but also by the aortic and azygos arches. Consequently, on the posteroanterior chest radiograph the posterior junction line is typically noted to end at about the level of the aortic knob (fig. 1).

Below the azygos and aortic arches, the medial lung surfaces again approach the midline. On the right the lung enters the azygoesophageal recess (fig. 2). On the left, if the descending aorta protrudes sufficiently from the mediastinum, the left lung can intrude itself immediately anterior to the descending aorta (fig. 2) to form the "preaortic interface" [7]. Occasionally the mediastinal anatomy causes the lung in the azygoesophageal recess and preaortic lung to meet to form a true posterior junction line in this area as well (fig. 3).

The most frequently seen posterior junction line is above the aortic knob. The junction line formed below the aortic knob occurs much less commonly. Perhaps for clarity, one might refer to these as the *supraaortic* and *infraaortic* posterior junction lines, respectively. The infraaortic line is not to be confused with the azygoesophageal recess interface and the preaortic interface. These two interfaces form the infraaortic line only if they meet each other. More frequently, however, this is not the case, so that the azygoesophageal recess interface and preaortic interface are individually identified and separated by the intervening mediastinum (figs. 2 and 3).

Air in the esophagus above the azygos and aortic arches will outline the inner right and left esophageal walls. The outer esophageal walls will be outlined by the right and left lungs as they approach each other (figs. 4 and 5*A*).

The supraaortic posterior junction line may or may not

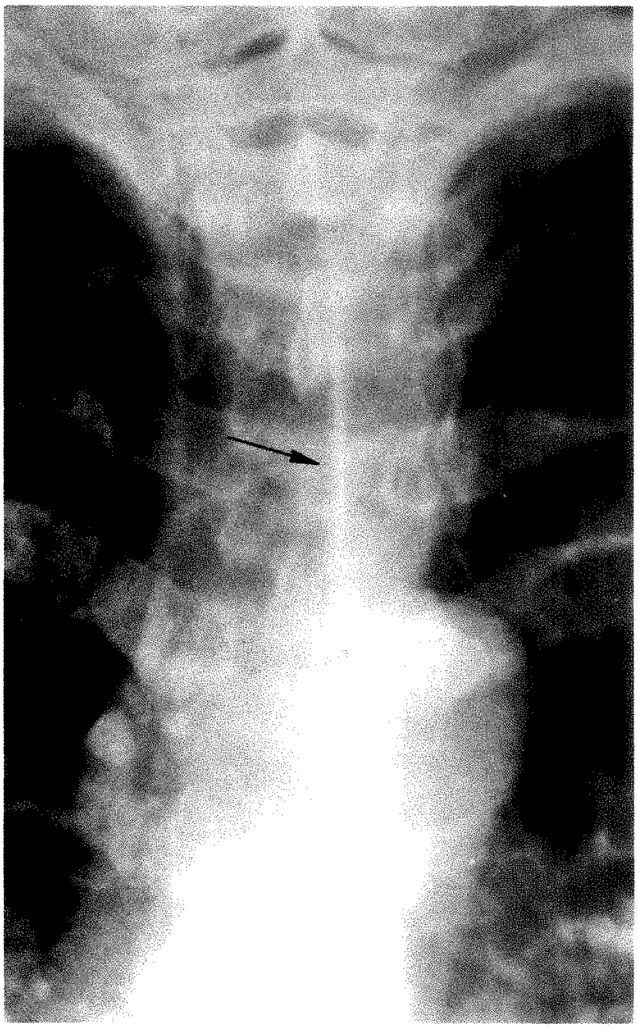

Fig 1.—Posteroanterior chest film showing posterior junction line (*arrow*) typically ending at aortic knob.

Received November 29, 1976; accepted after revision June 1, 1977.
Presented at the annual meeting of the American Roentgen Ray Society, Washington, D.C., September 1976.

[1] Department of Radiology, Upstate Medical Center, 750 East Adams Street, Syracuse, New York 13210. Address reprint requests to E. J. Lane.
[2] Present address: Department of Radiology, Wilford Hall USAF Medical Center, Lackland Air Force Base, Texas 78236.

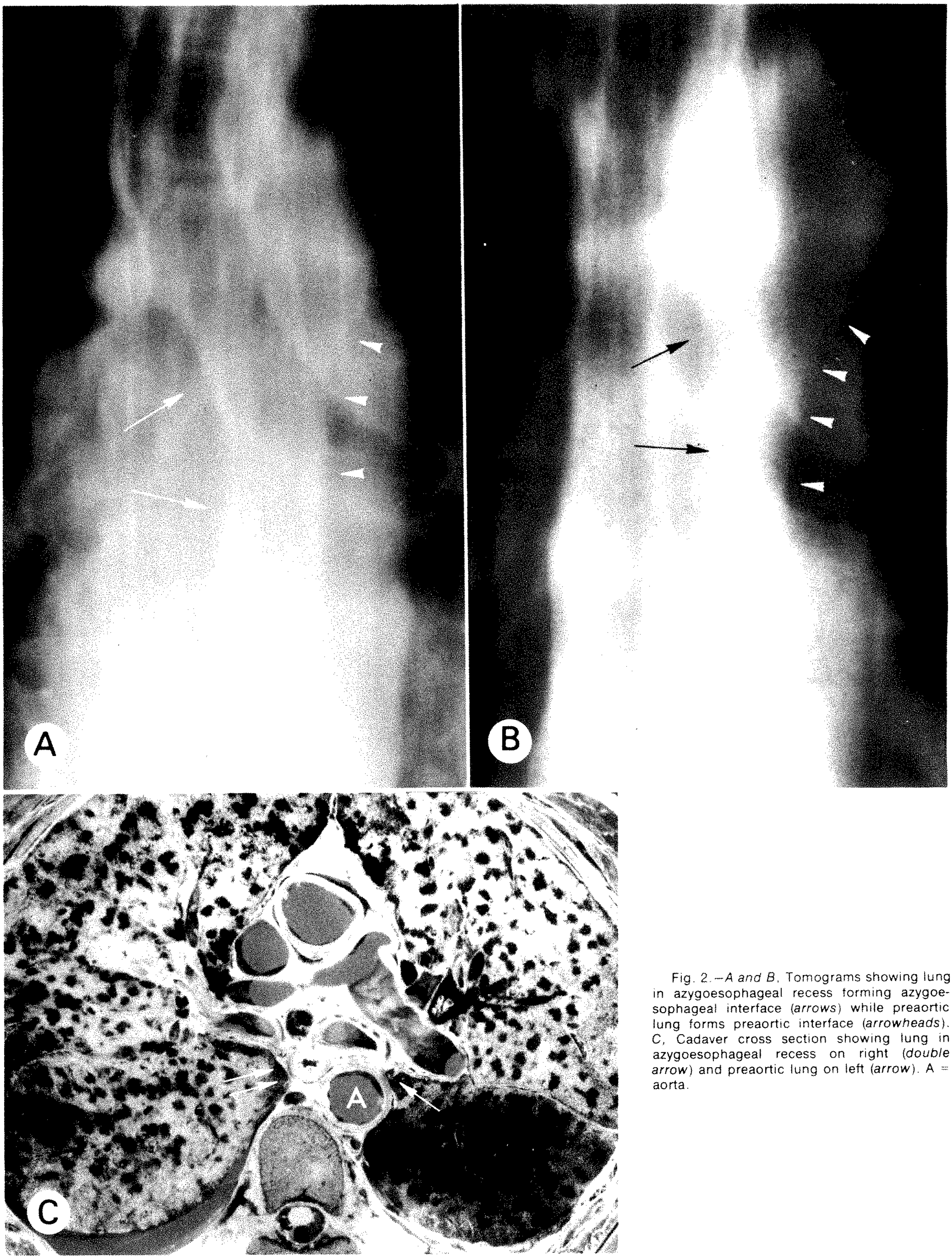

Fig. 2.—*A and B*, Tomograms showing lung in azygoesophageal recess forming azygoesophageal interface (*arrows*) while preaortic lung forms preaortic interface (*arrowheads*). *C*, Cadaver cross section showing lung in azygoesophageal recess on right (*double arrow*) and preaortic lung on left (*arrow*). A = aorta.

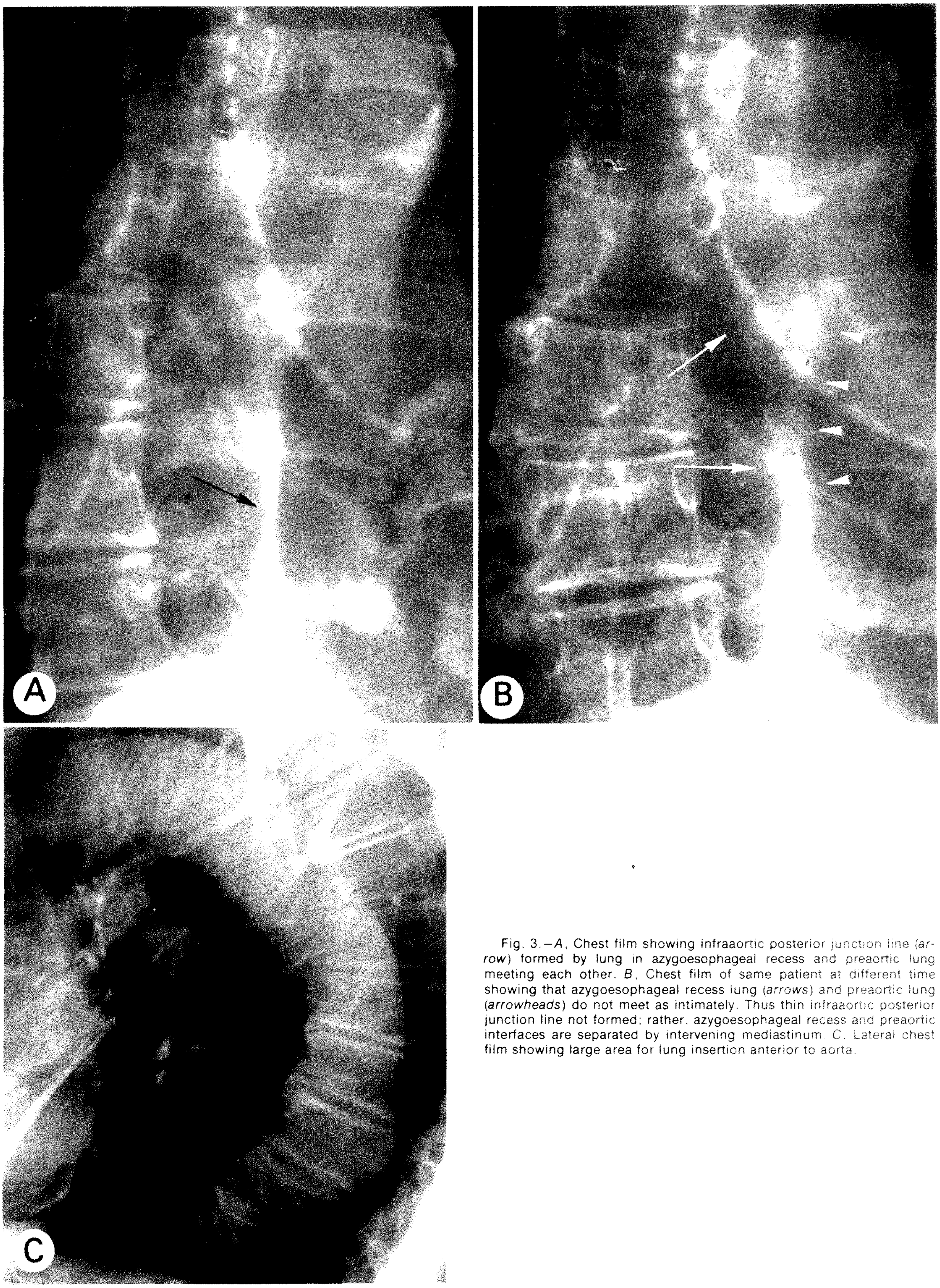

Fig. 3.—*A*, Chest film showing infraaortic posterior junction line (*arrow*) formed by lung in azygoesophageal recess and preaortic lung meeting each other. *B*, Chest film of same patient at different time showing that azygoesophageal recess lung (*arrows*) and preaortic lung (*arrowheads*) do not meet as intimately. Thus thin infraaortic posterior junction line not formed; rather, azygoesophageal recess and preaortic interfaces are separated by intervening mediastinum. *C*, Lateral chest film showing large area for lung insertion anterior to aorta.

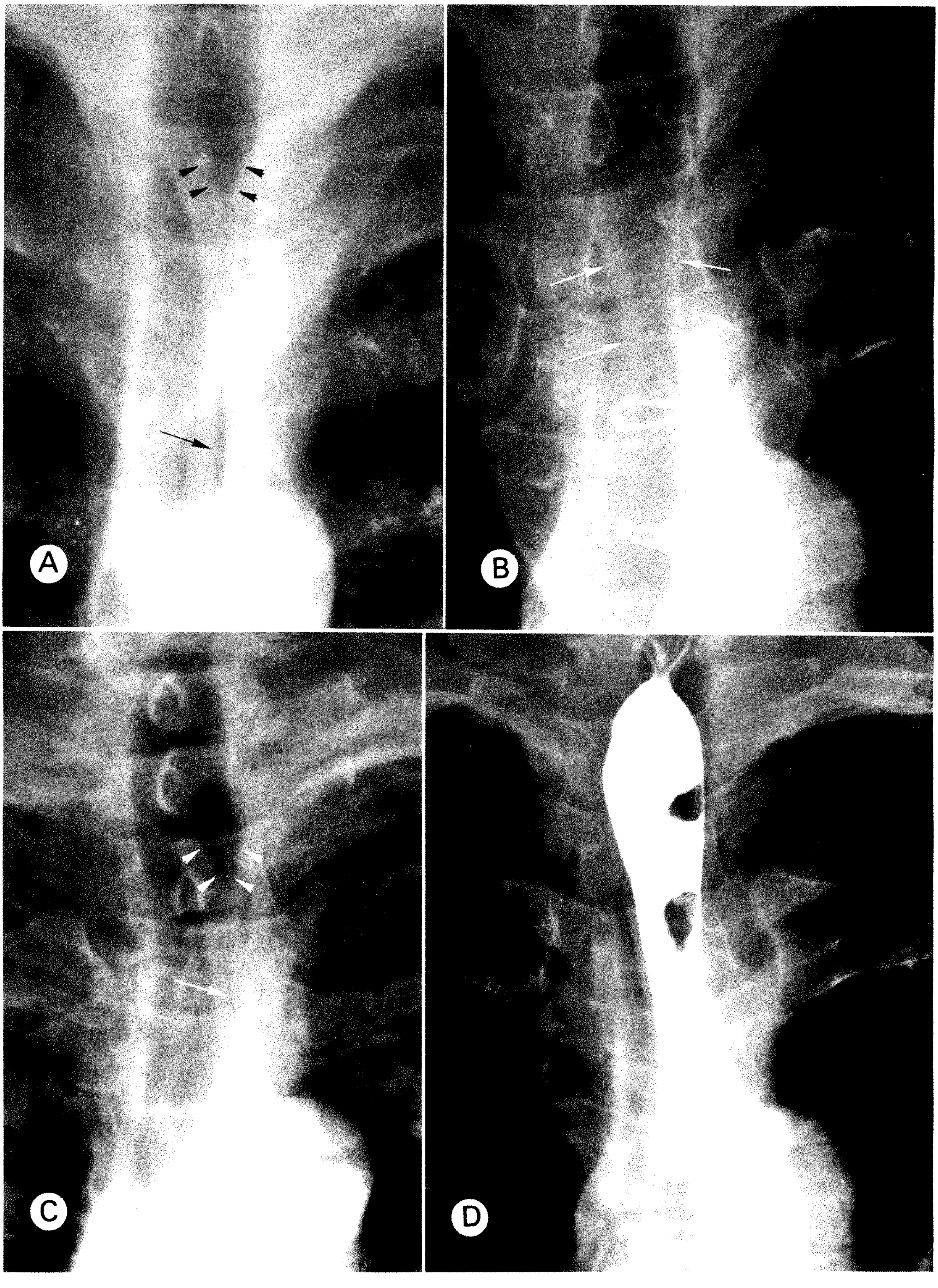
A
B
C
D

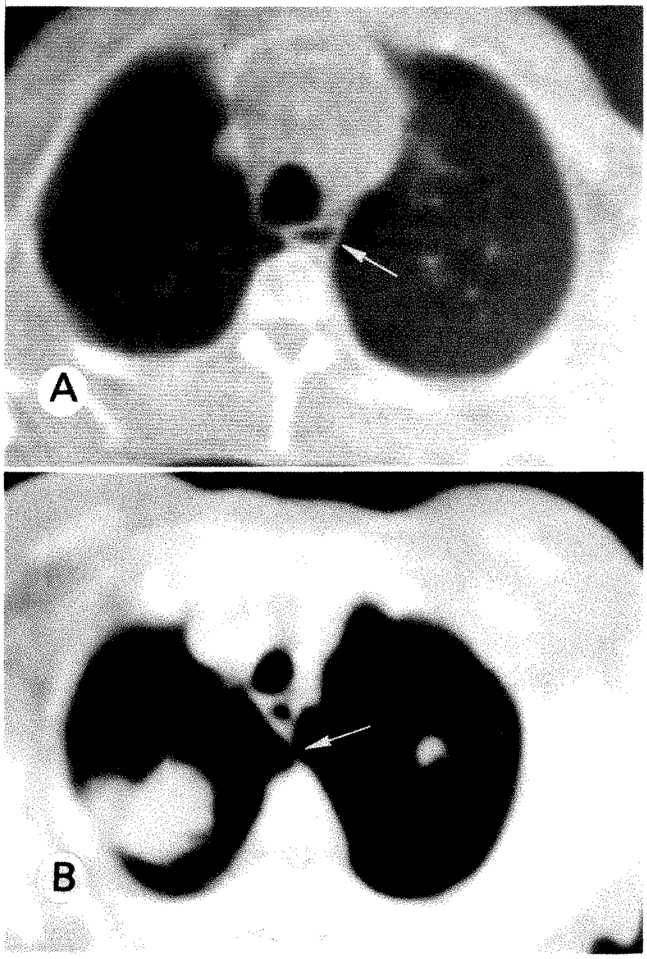

Fig. 5.—*A*, CT scan at most cephalad portion of aortic arch showing transverse anatomy explaining configuration seen in figure 4*B*. Note esophageal air (*arrow*) posterior to trachea and anterior to spine. *B*, CT scan above aortic arch showing both esophageal air and supraaortic posterior junction line (*arrow*).

TABLE 1

Esophageal Air on Normal Chest Radiographs

	No.	%
No esophageal air	128	64
Esophageal air in relation to aortic knob:		
Above	22	11
Medial to	12	6
Immediately below	30	15
Other*	8	4

* In seven air began at aortic knob and extended 8-10 cm caudally. In one air filled almost entire esophagus.

be seen when esophageal air is present (fig. 5), depending upon the depth of the retroesophageal space and the amount of esophageal distention. Visualization of the supraaortic posterior junction line depends on whether the right and left lungs make contact behind the air-filled esophagus.

At the level of the aortic and azygos arches, esophageal air will again outline the inner walls of this viscus. The outer walls will not be outlined, however, since the aortic and azygos arches prevent lung from contacting the left and right esophageal walls, respectively (fig. 6).

Esophageal air below the azygos and aortic arches will outline the inner right and left esophageal walls and will have a typical diamond or triangular-shaped appearance. The outer walls will be outlined on the right by lung in the azygoesophageal recess and on the left by preaortic lung (fig. 7). This is not to say that the azygoesophageal recess and preaortic interfaces always represent the outer boundaries of the right and left esophageal walls when noted on radiographs where no esophageal air is present [7, 8]. Whether they do again depends on the amount of lung intrusion into the mediastinum and the position of the esophagus with respect to the azygoesophageal recess lung and preaortic lung. Air filling of the esophagus will distend this viscus and make its contact with azygoesophageal recess and preaortic lung more probable.

Case Material and Findings

We evaluated 200 consecutive normal and 200 consecutive abnormal adult posteroanterior chest radiographs for (1) absence or (2) presence and location of esophageal air. The only criterion for inclusion was that the mediastinal area was well enough penetrated to be visualized. The chest radiographs were performed at 1.8 m using 120 kVp, 300-600 mA, 1/100-1/60 sec, 1.5 mm focal spot, DuPont Hi-Plus screens, 15:1 grid with 105 lines, and Cronex VI film.

The radiographs were either part of routine physical examinations, films to rule out pneumonia, preoperative studies for nonchest disease, or follow-up films for known chest disease. Tables 1 and 2 show that 36% of normal and about 50% of abnormal chest films demonstrated air in the esophagus.

Esophageal air in both normal and abnormal examinations was present in the following areas in decreasing order of frequency: (1) beginning below the aortic knob and extending 1-4 cm caudad; (2) above the aortic knob; and (3) medial to the aortic knob. The higher incidence of air collection below the aortic knob might be explained by the slight esophageal compression from the crossing left main bronchus [9].

In a small number of both normal and abnormal examinations, air extended below the aortic knob for about 8–10 cm (fig. 8*A*); in one it was recognized in the right anterior oblique projection. One or two in each group had almost entire filling of the esophagus with air (fig. 8*B*).

Air within the esophagus and lung outside of it will

←

Fig. 4.—*A*, Posteroanterior chest film showing esophageal air extending above aortic knob. Note vertical silver of air (*arrow*) immediately above knob and V-shaped air configuration (*arrowheads*) further cephalad. *B*, Chest film in another patient showing esophageal air (*arrows*) distending esophagus to give tubular air configuration above aortic knob. *C* and *D*, Chest films in different patient showing configuration of air and barium in esophagus similar to *A*.

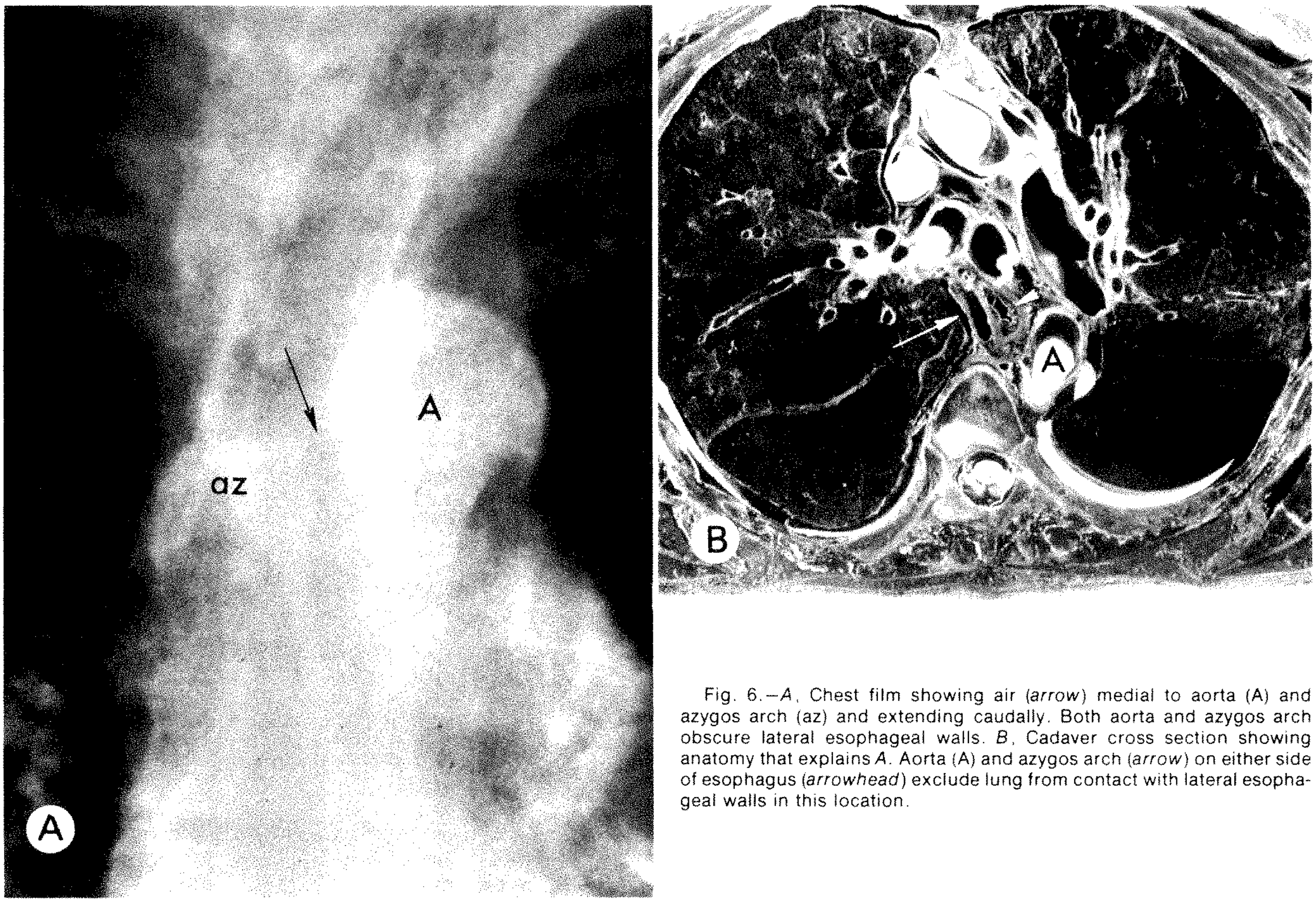

Fig. 6.—*A*, Chest film showing air (*arrow*) medial to aorta (A) and azygos arch (az) and extending caudally. Both aorta and azygos arch obscure lateral esophageal walls. *B*, Cadaver cross section showing anatomy that explains *A*. Aorta (A) and azygos arch (*arrow*) on either side of esophagus (*arrowhead*) exclude lung from contact with lateral esophageal walls in this location.

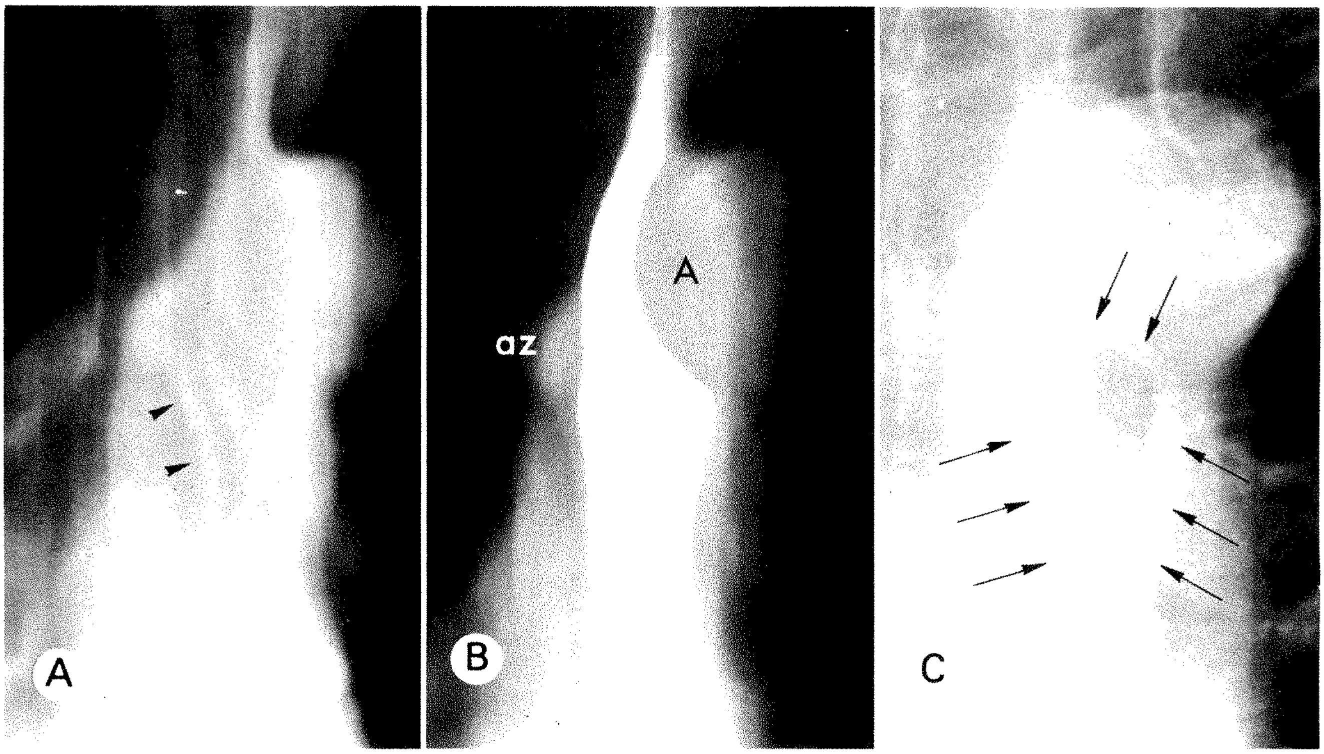

Fig. 7.—*A*, Tomogram showing typical diamond shape of esophageal air below aortic arch. Azygoesophageal recess lung (*arrows*) outlines right outer esophageal wall. Air in esophagus outlines inner right and left esophageal walls. Through midportion of diamond of air, note oblique course of left main bronchus. Esophageal air abutting against bronchus can cause visualization of bronchial wall and apposed esophageal wall as single soft tissue stripe. *B*, Tomogram of barium study in same patient showing azygos arch (az) and aorta (A) causing impressions on esophagus. *C*, Chest film of different patient showing typical triangular appearance (*arrows*) of esophageal air below aortic knob.

TABLE 2

Esophageal Air on Abnormal Chest Radiographs

Abnormality	No Esophageal Air	Esophageal Air in Relation to Aortic Knob			
		Above	Medial to	Immediately Below	Other
Granulomatous disease:					
Lower lobe	4	...	...	1	...
Upper lobe	6	2	1	1	...
Radiation fibrosis	3	1	...	...	...
Cardiomegaly	7	4	...	8	2*
Lower lobe pneumonia	10	5	1	4	...
Scoliosis	2	2	...	1	...
Lower lobe volume loss and/or scar	6	1	1	4	1*
Elevation of right hemidiaphragm	2	...	...	...	...
Cystic fibrosis	1	1	...	...	...
Apical bullae	2	...	2	...	...
Chronic obstructive pulmonary disease	10	1	2	5	...
Pulmonary edema	11	2	...	6	1†
Small effusion	6	2	...	4	...
Postoperative open heart surgery	5	2	2	2	...
Diffuse metastatic disease	2	2	...	5	1†
Diaphragmatic adhesions	3	...	...	...	...
Basilar plate atelectasis	10	2	1	5	1*
Diffuse interstitial scarring	2	...	1	...	...
Combinations of above	9	2	3	4	...
Total no. (%)	101 (50.5)	29 (14.5)	14 (7)	50 (25)	6 (3)

* Air began at aortic knob and extended 8–10 cm caudally.

† Air filled almost entire esophagus

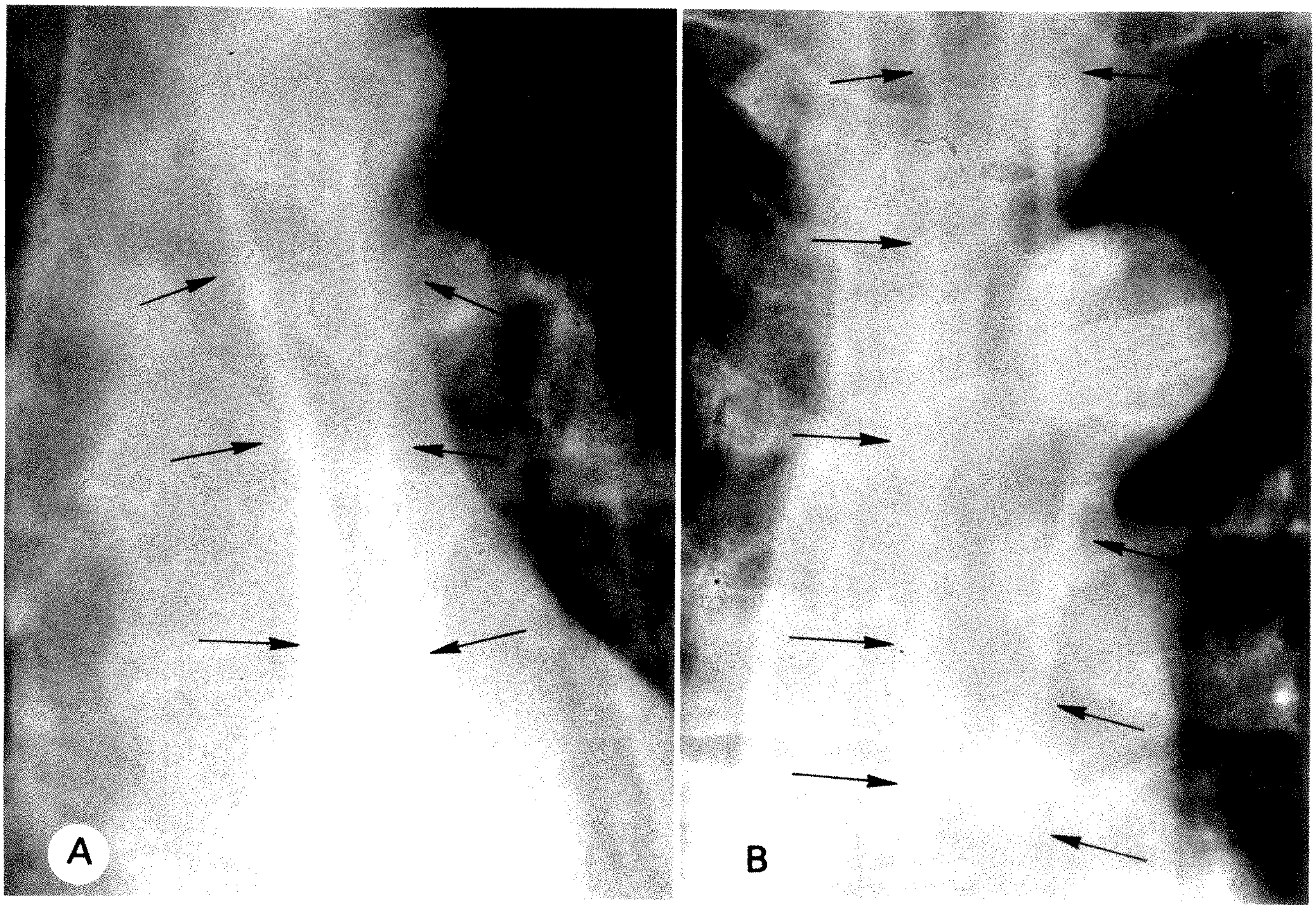

Fig. 8.—*A*, Chest film showing esophageal air (*arrows*) occupying long length of esophagus below aortic knob. *B*, Chest film showing esophageal air (*arrows*) occupying almost entire length of esophagus above and below aortic knob.

cause stripes of soft tissue density to be outlined, as in the illustrations shown. To attribute these stripes to the thickness of the esophageal wall may not always be correct. Differing amounts of periesophageal mediastinal tissue may cause the stripe to vary in thickness. Similarly the x-ray beam may be tangent to the outer and inner esophageal walls at different planes, thereby causing variation in the thickness of the soft tissue stripe. Finally soft tissue stripes are not always observed even when esophageal air is present. This can occur when esophageal air outlines the inner esophageal walls, but when the azygoesophageal recess and preaortic lung have not reached the outer esophageal walls to outline them.

Conclusions

Air in the esophagus is a frequent radiographic finding not only on chest films showing other pulmonary parenchymal or mediastinal abnormalities but on normal examinations as well. The incidence may vary depending on patients studied and radiographic technique used. Knowledge of the typical appearance and locations of esophageal air will undoubtedly contribute to its more frequent recognition, resulting in fewer diagnostic errors and facilitating recognition of disease in and about the esophagus.

REFERENCES

1. Martinez LO: Air in the esophagus as a sign of scleroderma. *J Assoc Can Radiol* 25:234-237, 1974
2. Dinsmore RE, Goodman D, Dreyfuss JR: The air esophagram: a sign of scleroderma involving the esophagus. *Radiology* 87:348-349, 1966
3. Blomquist G, Mahoney PS: Non-collapsing air-filled esophagus in diseases and postoperative chests. *Acta Radiol* 55:32-42, 1961
4. Keats TE, Smith TH: Air esophagogram—a sign of poor respiratory excursion in the neonate. *Am J Roentgenol* 120:300-304, 1974
5. Cimmino CV: A roentgenologic study in mediastinal anatomy afforded by air in the mid-esophagus. *Am J Roentgenol* 94:333-336, 1965
6. Lane EJ, Heitzman ER, Dinn WM: The radiology of the superior intercostal veins. *Radiology* 120:263-267, 1976
7. Heitzman ER, Lane EJ, Hammack DB, Rimmler LJ: Radiological evaluation of the aortic-pulmonic window. *Radiology* 116:513-518, 1975
8. Heitzman ER, Scrivani JV, Martino J, Moro J: The azygos vein and its pleural reflections. I. Normal roentgen anatomy. *Radiology* 101:249-258, 1971
9. Woodburne RT: *Essentials of Human Anatomy*, 5th ed. New York, Oxford University Press, 1973

Hepatic Venography and Wedge Hepatic Vein Pressure Measurements in Diffuse Liver Disease

JOHN A. CAVALUZZI,[1] ROBERT SHEFF,[1] DONALD P. HARRINGTON,[1] STEPHEN L. KAUFMAN,[1]
KLEMENS BARTH,[1] WILLIS C. MADDREY,[2] AND ROBERT I. WHITE, JR.[1]

Ninety patients with chronic diffuse liver disease were evaluated with free hepatic venography, wedge hepatic venography, hepatic vein pressure measurements, and liver biopsy. Free hepatic venograms were normal and minimally pruned in patients with hepatic sarcoidosis and fatty liver due to alcohol, and their biopsies showed little or no fibrosis. Pruning of hepatic vein branches on free hepatic venography correlated well with the corrected wedged hepatic vein pressure and with the degree of fibrosis in patients with alcoholic hepatitis, alcoholic cirrhosis, and postnecrotic cirrhosis. Free hepatic venography correlated better with hemodynamic measurements and fibrosis than did wedge hepatic venography. Free hepatic venography is a reliable predictor of the presence and degree of hepatic fibrosis and may be a useful alternative to liver biopsy in patients with clotting disorders.

Introduction

Angiographic and hemodynamic evaluation of patients with diffuse liver disease and portal hypertension has been used to complement clinical and laboratory appraisal of hepatic disease and to assess the degree of hepatic fibrosis. While less emphasis has been placed on the free hepatic venogram, some investigators state that changes in the hepatic venules on free venography are a sensitive indicator of hepatic fibrosis [1]. The extent of fibrosis and vascular destruction are important prognostic factors.

Our experience with free hepatic venography in 90 patients with several forms of chronic diffuse liver disease provides the basis for this report. We compared free hepatic venograms, wedge hepatic venograms, and hepatic vein wedge pressure measurements with the results of liver biopsies. A subgroup of patients with alcoholic hepatitis was studied before and after 30 days of medical therapy, providing us with the opportunity to compare serial hepatic venography and pressures with serial liver biopsies.

Materials and Methods

From 1972 to 1975, 90 patients with diffuse liver disease were studied. Eleven had fatty livers due to alcohol with biopsies characterized by marked fatty infiltration but no fibrosis. Forty patients with alcoholic cirrhosis had varying manifestations of alcoholism such as ascites, bleeding esophageal varices, and suspected hepatoma. Some were studied as part of a pre- or postshunt evaluation. Their biopsies showed varying degrees of fibrosis, fatty infiltration, and cell necrosis. Serial studies were performed on 32 patients with the clinical syndrome of alcoholic hepatitis with jaundice and an enlarged tender liver [2]. Liver biopsies in these patients were characterized by active cell necrosis in addition to fibrosis. The 32 were part of an ongoing clinical research protocol studying alcoholic hepatitis and were hospitalized in the clinical research center. Studies were performed within the first 10 days of admission and about 30 days after treatment with prednisolone or placebo in a double-blind trial. Finally, the study included three patients with postnecrotic cirrhosis and four patients with hepatic sarcoidosis.

Liver biopsies were interpreted without prior knowledge of venograms or pressures. They were graded numerically according to the amount of fibrosis present and then divided into three groups: mild, moderate, and severe. Free and wedged hepatic venography and pressures were performed by techniques previously described [2, 3]. For pressures and wedged venography, a 6.7 French 80 cm end-hole polyethylene catheter (ID = 1.5 mm, OD = 2.26 mm; Cook Inc., Bloomington, Ind.) was inserted into the femoral vein with the Seldinger technique. Inferior vena caval and right atrial pressures were obtained (Electronics for Medicine Physiologic Recorder, White Plains, N.Y.). A catheter tip deflecting wire was used to engage the main hepatic vein, and the catheter was advanced into the wedge position [2]. The corrected wedged hepatic vein pressure was obtained by subtracting the inferior vena caval pressure at the level of the renal veins from the average of several wedged hepatic vein pressures obtained in different hepatic veins. Normal values for uncorrected and corrected wedge pressures in our laboratory are 10 and 5 mm Hg, respectively. A corrected wedged hepatic vein pressure of 5–10 mm Hg was considered mildly elevated, 10–15 mm Hg moderately elevated, and over 15 mm Hg markedly elevated.

For wedge venography, the end-hole catheter was placed in the wedge position and 8 ml of 76% methylglucamine diatrizoate, heated to body temperature, was injected at a constant flow rate of 2 ml/sec for 4 sec. For free hepatic venography, the end-hole catheter was exchanged for a similar catheter with an end hole and six side holes. Using a deflector system again, the catheter was advanced to the middle of the right hepatic vein. The injection rate for free hepatic venography was 10 ml/sec of 76% methylglucamine diatrizoate for a total of 20 ml. The serial angiographic sequence for both free and wedged hepatic venography was two films per second for 5 sec, then one film per second for 10 sec.

Interpretation of free hepatic venograms was modified using the criteria of Smith et al. [1]: failure to visualize the fifth order branch beyond the injected hepatic vein (zero order) was considered a mild change (fig. 1). A loss of third or fourth order

---

Received February 8, 1977; accepted after revision May 20, 1977.

This work was supported in part by U.S. Public Health Service Training Grant 5-T01HL05970-03 from the National Heart and Lung Institute, and PHS AA 00201-05.

Presented at the annual meeting of the American Roentgen Ray Society, Washington, D.C., September 1976.

[1] Department of Radiology and Radiologic Science, Johns Hopkins Medical Institutions, Baltimore, Maryland 21205. Address reprint requests to R. I. White, Jr.

[2] Department of Medicine, Johns Hopkins Medical Institutions, Baltimore, Maryland 21205.

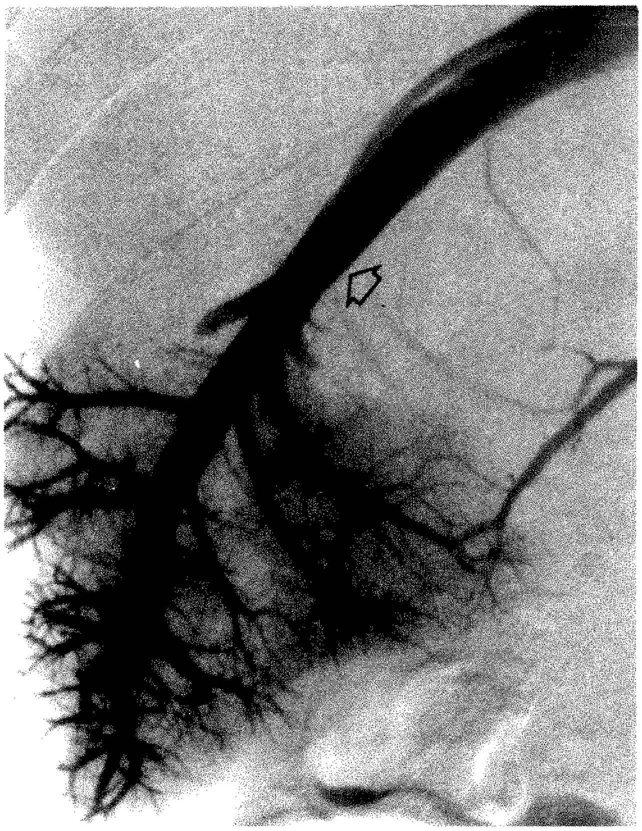

Fig. 1.—Normal free hepatic venogram showing fifth order branches. Zero order branch indicated by arrow. Accessory hepatic vein demonstrated. (Reprinted with permission from [2])

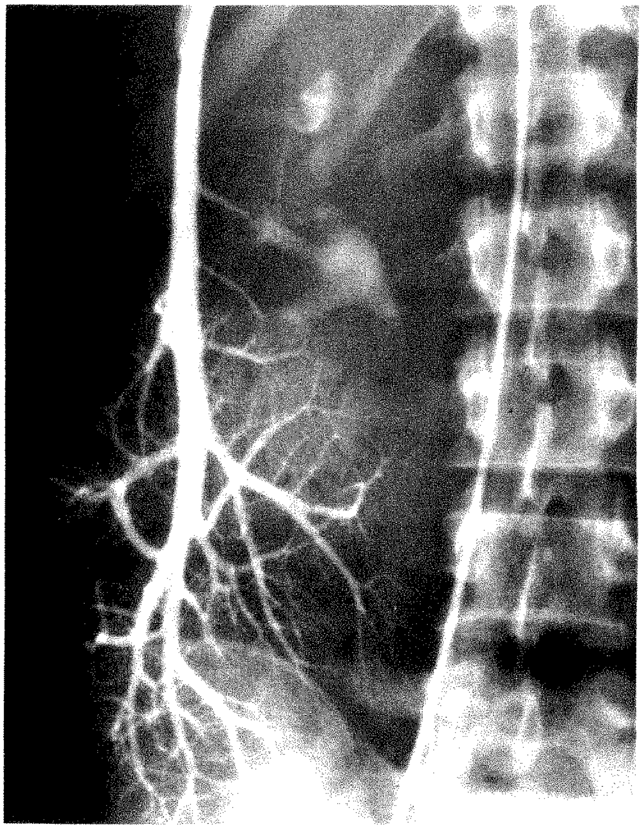

Fig. 2.—Fatty liver. Free hepatic venogram showing normal branching pattern with diffuse hepatomegaly.

branches was considered a moderate change, while loss of first and second order hepatic vein branches constituted a severe change [2]. The wedge venograms were performed and interpreted according to Viamonte's classification. [4].

Results

Alcoholic Liver Disease

Fatty liver. Eleven patients whose biopsies showed pronounced fatty infiltration without cell necrosis or fibrosis were considered to have fatty liver disease. Free hepatic venography showed a normal branching pattern with visualization of fifth order veins. There was stretching of vessels consistent with diffuse hepatomegaly (fig. 2). The corrected hepatic vein wedge pressures were variable but tended to be elevated.

Alcoholic hepatitis. Thirty-two patients had serial free hepatic venograms, wedge hepatic venograms, and hepatic vein pressure measurements before and after 30 days of treatment. Only 20 of the 32 patients had clotting factors sufficient to permit liver biopsies. Patients were divided on the basis of pruning on free hepatic venograms into three groups: mild (10 patients), moderate (16 patients), and severe (six patients).

Patients with mild free venogram changes showed mild to moderate elevation of corrected wedged hepatic vein pressure (9.8 ± 3.5 mm Hg before and 7.5 ± 4.9 mm Hg after therapy). Patients with moderate venographic changes showed moderate to severe elevation of corrected wedged hepatic vein pressure (14.6 ± 4.8 mm Hg before and 13.1 ± 4.0 mm Hg after therapy). Patients with severe pruning of the free hepatic venogram showed severe elevation of corrected wedged hepatic vein pressure (21.8 ± 6.5 mm Hg before and 20.7 ± 5.3 mm Hg after therapy) (fig. 3*A*).

The mean values of corrected wedged hepatic vein pressure measurements were significantly different among the patients with mild, moderate, and severe free hepatic venographic groups ($P < .05$). Within each group, the pressures after therapy did not seem to be significantly different from mean values of the pressures before therapy, and considerable individual variation was present (fig. 3*B*).

Although pressures tended to vary with treatment, the free hepatic venogram classification did not change after 30 days of therapy in any patient; this classification most closely correlated with the extent of fibrosis on serial liver biopsies (fig. 4). However, the wedge hepatic venogram classification changed in seven of the 32 patients and showed less stasis and less portal vein opacification after therapy. Two of the six patients whose initial wedge venograms showed hepatofugal flow reverted to a pattern of hepatopedal flow with mild portal vein stasis

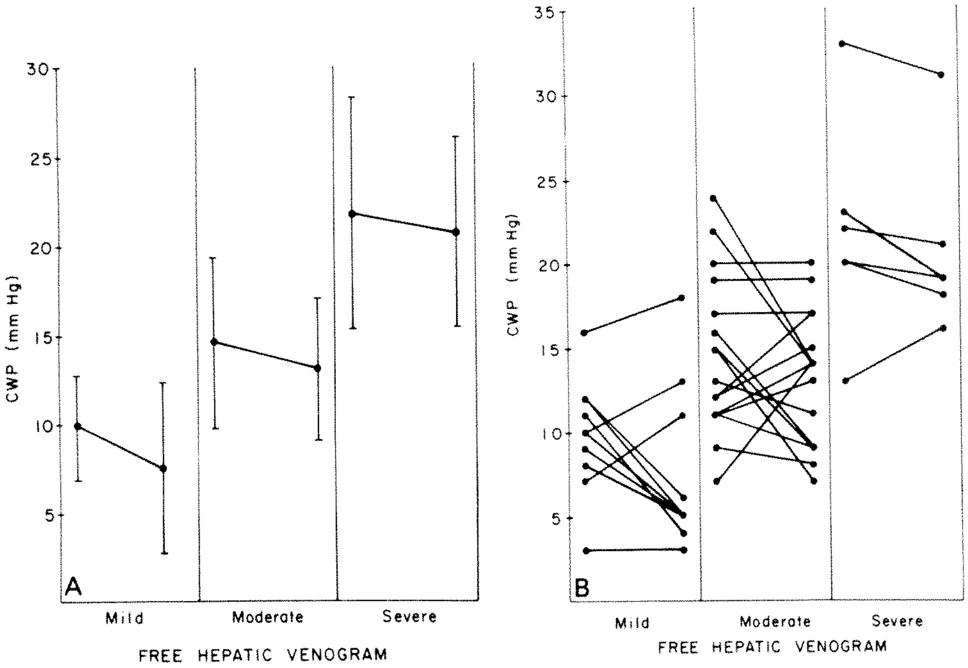

Fig. 3.—Corrected wedge pressure versus free hepatic venogram classification before and after treatment. *A*, Mean and standard deviation of pressures before and after treatment. Patients with mild venographic changes had generally lower pressures than those with severe changes. *B*, Individual serial pressures show scatter and variation within each venographic classification. Mean values of initial corrected wedge pressure were statistically different between mild and moderate venographic groups as well as between moderate and severe venographic groups ($P < .05$).

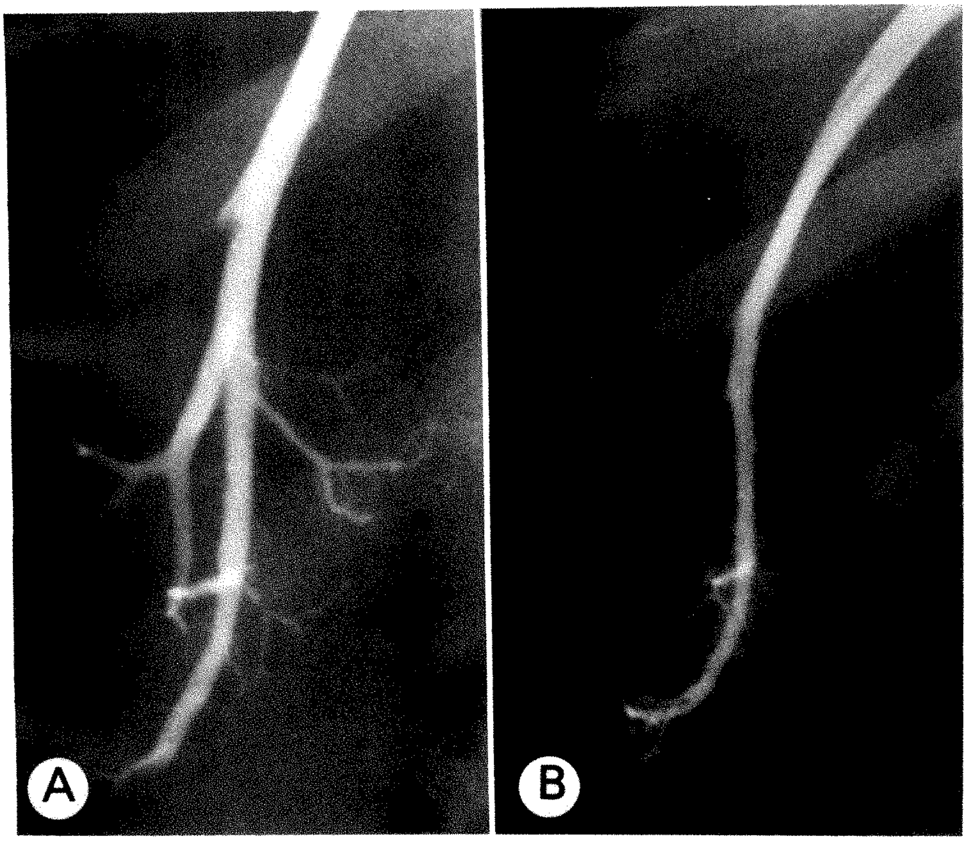

Fig. 4.—Alcoholic hepatitis. Free hepatic venograms before (*A*) and after (*B*) 30 days of medical therapy showing severe pruning with loss of first and second order branches on both studies. Serial liver biopsies showed severe fibrotic changes.

after treatment. The sinusoidal morphology and degree of parenchymal extravasation varied greatly both after treatment and even at different wedged positions on the same day.

Of the 32 patients, 20 had liver biopsies within 48 hr of venography and pressure measurements (fig. 5). In patients whose free venogram showed mild changes, all biopsies showed mild fibrosis except one. In those with

HEPATIC FIBROSIS	Mild	Moderate	Severe
Severe	1	7	4
Moderate	0	8	0
Mild	15	5	0

FREE HEPATIC VENOGRAM

Fig. 5.—Hepatic fibrosis versus free venographic classification. Mild and severe free venographic changes correlated with mild and severe fibrotic changes. Majority of patients with moderate pruning on free hepatic venography had moderate or severe fibrosis by biopsy.

severe free venogram changes, only two patients could be biopsied (each twice), and all four biopsies showed cirrhosis with extensive fibrosis. In the group of patients with moderate free hepatic venogram changes, seven patients had severe fibrosis, eight had moderate fibrosis, and five demonstrated mild fibrosis on their liver biopsies.

Alcoholic cirrhosis. The 40 patients with alcoholic cirrhosis were evaluated because of ascites, encephalopathy, bleeding esophageal varices, suspected hepatoma, or as part of splanchnic-systemic shunt evaluation. Their liver biopsies showed varying degrees of fibrosis. The patterns of wedge and free hepatic venograms were not different from the patients with alcoholic hepatitis. The most extensive fibrosis occurred in patients with severe pruning on free venography.

Sarcoid Liver Disease

Three of the four patients with diffuse sarcoid involvement of the liver were studied serially. The corrected wedge pressure was initially elevated in all patients: minimally in two and moderately in two. Pressures were measured again 6-11 months later; they rose in one patient and remained unchanged in the other two. The free hepatic venograms were either normal (three patients) or showed mild disease (one patient) (fig. 6). Biopsies showed granulomatous involvement and minimal fibrosis.

Postnecrotic Cirrhosis

The three patients with postnecrotic cirrhosis all had elevated corrected hepatic wedge pressures (mean, 16.3 mm Hg). Two of the three patients showed marked pruning of the free hepatic venograms which could not be distinguished from the venograms of patients with severe alcoholic cirrhosis or severe alcoholic hepatitis. The diagnosis of postnecrotic cirrhosis was suggested in one patient by the presence of large extrinsic indentations which represented macronodular regeneration (fig. 7). All biopsies showed severe fibrosis.

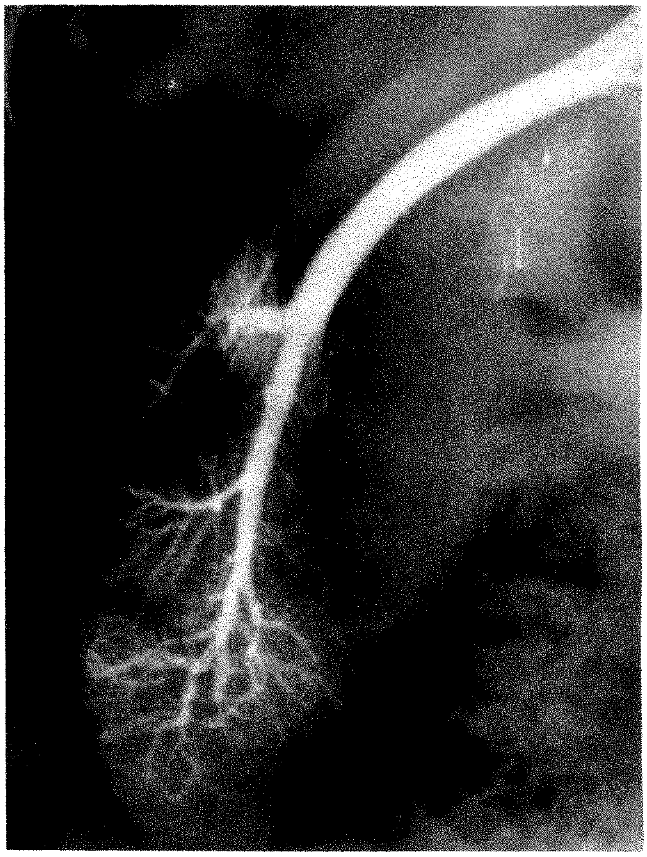

Fig. 6.—Sarcoid liver disease. Free hepatic venogram showing mild changes with loss of fifth order branches.

Discussion

Free hepatic venography was introduced by Rappaport in 1951 [5] and has been systematically used by Smith et al. [1] and Miller et al. [2] to evaluate alcoholic liver disease. These investigators found a positive correlation between the free hepatic venogram and the severity of hepatic fibrosis. Wedge hepatic vein pressure measurements have been found to correlate well with portal pressures in patients with alcoholic liver disease and have largely replaced percutaneous measurements of hepatic and splenic pulp pressures [6-8]. Wedged hepatic vein pressure is corrected for the presence of increased intraabdominal pressure by subtracting the inferior vena caval pressure at the level of the renal veins to obtain the corrected hepatic wedge pressure. In the presence of ascites, free hepatic venous pressure is variable and may reflect the inferior vena caval or right atrial pressure, depending on the severity of the "pinchcock" effect of the diaphragm on the inferior vena cava as it passes through the diaphragmatic hiatus. In general, corrected wedge pressure measurements are useful for documenting the presence of portal hypertension, separating intra- and posthepatic from prehepatic portal hypertension, and assessing the results of portal-sys-

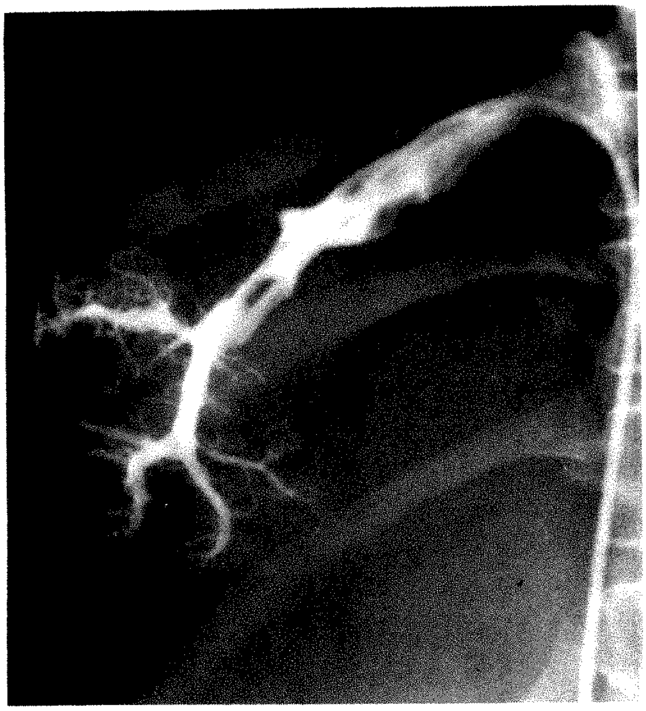

Fig. 7.—Postnecrotic cirrhosis. Free hepatic venogram showing severe pruning with extrinsic indentations representing macronodular regeneration.

temic shunting procedures. Recently, Bookstein et al. [9] evaluated sinusoidal morphology with magnification wedge hepatic venography and found they could predict histology in several forms of portal hypertension.

We systematically compared serial free and wedge hepatic venograms with pressures and liver biopsies. The free hepatic venogram, when graded according to the classification of Miller et al. [2] correlated well with the severity of hepatic fibrosis in patients with alcoholic hepatitis, alcoholic cirrhosis, and postnecrotic cirrhosis. In patients with the syndrome of alcoholic hepatitis, the degree of fibrosis as judged by serial biopsies and serial free hepatic venograms did not change after 30 days of therapy. Pruning of hepatic venules correlated well with the degree of fibrosis in liver biopsies of patients with mild or severe free venographic changes. In the group of patients with moderate free venographic changes, correlation with the degree of fibrosis is less accurate. However, 75% of patients with moderate free venographic changes had moderate or severe fibrosis. Perhaps the disparity can be attributed to the random sampling inherent in any liver biopsy. The free venogram reveals more of the overall pattern of hepatic venous destruction than does an isolated liver biopsy. The lack of fibrosis in patients with alcoholic fatty liver disease correlates with their normal branching pattern on free venography. The elevated pressures reflect the elongation and distortion of the hepatic vascular system along with sinusoidal compression secondary to fatty infiltration and generalized hepatomegaly.

The free hepatic venograms in three patients with postnecrotic cirrhosis could not be distinguished from severe alcoholic cirrhosis or severe alcoholic hepatitis, except in one case by the presence of large regenerating nodules which caused extrinsic indentations upon the injected hepatic vein. The normal or mild free venographic changes in patients with sarcoid liver disease correlated well with the minimal amount of fibrosis seen on biopsy. The elevated pressures seem inconsistent with both the extent of fibrosis and the degree of hepatomegaly. It has been suggested that minute arteriovenous anastomoses may develop within the granulomas, which could result in the transmission of arterial pressure to the portal system [10].

In patients with alcoholic hepatitis, the elevated corrected wedge pressure reflected the severity of free hepatic venographic changes. Great individual variations in pressure changes were noted after treatment (fig. 3*B*). The hepatic wedge pressure is a dynamic variable, reflecting not only sinusoidal resistance but also the hemodynamic status of the patient [11]. Thus it may be affected by cardiac output, plasma volume, the presence of any pulmonary or splanchnic arteriovenous anastomoses, and any acute toxic inflammatory swelling of the liver at the time of the measurement. The corrected hepatic wedge pressures fluctuated without any change in histology in patients with alcoholic hepatitis.

Although changes in the free hepatic venogram remained constant, the wedge hepatic venogram classification changed in seven of 32 patients with alcoholic hepatitis studied serially. Of six patients who initially demonstrated hepatofugal flow, two reverted to hepatopedal flow after therapy, although the free venograms and degree of fibrosis did not change. We used Viamonte's technique of wedge venography [4] and found considerable variation in sinusoidal morphology, both on serial studies and in different locations on the same day. This may represent varying degrees of extravasation within a closed hepatic space in different wedge positions which result in parenchymograms with varying degrees of smudging. Bookstein et al. [9] recently advocated slow hand injections of a smaller volume of contrast material with 0.1 mm focal spot magnification techniques to demonstrate hepatic lobules and venules more clearly. Perhaps with these techniques, histologic correlation with wedge venography might be more apparent. The conventional wedge venogram does demonstrate patency and direction of flow in the portal vein.

We conclude that the free hepatic venogram is a reliable predictor of the degree of hepatic fibrosis in patients with alcoholic liver disease and postnecrotic cirrhosis; it also correlates well with the corrected hepatic wedge pressure in patients with alcoholic hepatitis. The wedge hepatic venogram was useful in establishing the patency and direction of portal venous flow, but not in grading histology. Finally, free hepatic venography and wedged hepatic vein pressure measurements were particularly useful in evaluating patients with diffuse liver disease whose depressed clotting functions may contraindicate liver biopsy (12 of our 32 patients with alcoholic hepatitis).

REFERENCES

1. Smith G, Westgaard T, Bjorn-Hansen R: Hepatic venous angiography in the evaluation of cirrhosis of the liver. *Ann Surg* 173:469–480, 1971
2. Miller FJ, Maddrey WC, Sheff RN, Harrington DP, White RI Jr: Hepatic venographic and hemodynamics in patients with alcoholic hepatitis. *Radiology* 115:313–317, 1975
3. White RI Jr: *Fundamentals of Vascular Radiology*. Philadelphia, Lea & Febiger, 1976
4. Warren WD, Formon JJ, Viamonte M, Zeppa R: Preoperative assessment of portal hypertension. *Ann Surg* 165:999–1012, 1967
5. Rappaport AM: Hepatic venography. *Acta Radiol* 36:165–171, 1951
6. Ruzicka FF Jr, Carillo FJ, D'Alessandro D, Rossi P: The hepatic wedge pressure and venogram vs. the intraparenchymal liver pressure and venogram. *Radiology* 102:253–258, 1972
7. Taylor WJ, Myers JD: Occlusive hepatic venous catheterization in the study of the normal liver, cirrhosis of the liver and non-cirrhotic portal hypertension. *Circulation* 13:369–380, 1956
8. Reynolds TB: The role of hemodynamic measurements in portosystemic shunt surgery. *Arch Surg* 108:276–281, 1974
9. Bookstein JJ, Appleman HD, Walter JF, Foley WD, Turcotte JG, Lambert M: Histologic-venographic correlates in portal hypertension. *Radiology* 116:565–573, 1975
10. Maddrey WC, Johns CJ, Boitnott JK, Iber FL: Sarcoidosis and chronic hepatic disease: a clinical and pathologic study of 20 patients. *Medicine* 49:375–395, 1970
11. Gould L, Shariff M, Zahir M, DiLietu M: Cardiac hemodynamics in alcoholic patients with chronic liver disease and a presystolic gallop. *J Clin Invest* 48:860–868, 1969

"Hot Spot" on Hepatic Scintigraphy and Radionuclide Venacavography

NIHAL S. GOONERATNE,[1, 2] MARIA G. BUSE,[2] JAMES L. QUINN, III[1] and JOHN B. SELBY[3]

Seven patients showing a localized area of increased uptake (hot spot) on ^{99m}Tc sulfur colloid liver scans are described. Four also had dynamic studies. In five patients the hot spot was associated with superior vena caval obstruction, in one it was associated with inferior vena caval obstruction, and in one with a hepatoma. Although a hot spot on static liver images usually indicates superior vena caval obstruction, the addition of radionuclide venacavography is recommended to confirm the diagnosis. A hot spot in the liver area in a radionuclide venogram of the lower limbs suggests inferior vena caval obstruction with collaterals via the liver.

Filling defects are often encountered on ^{99m}Tc sulfur colloid liver scans, while hot spots are less frequently found. The hot spot due to superior vena caval obstruction is classically located anteriorly and medially to the gallbladder fossa [1-4]. Initially this was thought to be a specific finding in superior vena caval obstruction. However, a hot spot on hepatic scintigraphy has been reported in association with liver abscess [5], hepatic hemangioma [6], hepatic hamartoma [7], Budd-Chiari syndrome [8], focal nodular hyperplasia [9], injection of ^{99m}Tc sulfur colloid via a malpositioned catheter [10], hepatic venoocclusive disease [11], and in a patient with a hydatidiform mole without superior vena caval obstruction [12]. Three cases of proven superior vena caval obstruction without a hot spot on the ^{99m}Tc sulfur colloid scan have also been reported [12, 13]. These were attributed to poorly developed collaterals or well developed azygos ascending lumbar deep collaterals [13].

The three most common causes of superior vena caval obstruction are bronchogenic carcinoma, mediastinal tumor and fibrosing mediastinitis (often secondary to histoplasmosis [14] or tuberculosis). The radiographic diagnosis of this condition with contrast venography depends on the demonstration of occlusion of the superior vena cava with multiple collateral venous channels in the chest and abdomen [15]. The contrast study is not without risks. This report describes seven patients who showed hot spots on static hepatic scans, two due to causes not previously reported. The addition of venacavography was found useful in the differential diagnosis.

Materials and Methods

Five patients were seen at Medical University of South Carolina Hospital between 1972 and 1976, one at the Veterans Administration Hospital, and one at Northwestern Memorial Hospital. Hepatic scintigraphy was performed 15-20 min after intravenous administration of 2-8 mCi of ^{99m}Tc sulfur colloid into an arm vein. A scintillation camera (Searle Pho/Gamma 111 HP, Schiller Park, Ill.; or Ohio Nuclear Series 100, Solon, Ohio) equipped with a parallel hole low energy collimator was used for routine static liver images. At a subsequent date, dynamic studies were performed after intravenous administration of 10-15 mCi of high specific activity ^{99m}Tc pertechnetate. Cameras were equipped with a diverging or medium energy collimator. Patient 5 underwent repeat hepatic scintigraphy after injection into a foot vein. Patient 6 had a ^{99m}Tc human albumin microspheres venogram followed by a liver scan on the same day.

Results

Clinical findings are shown in table 1. Diagnoses were confirmed at surgery or autopsy in six patients; patient 7 is alive and inoperable with classical clinical findings of superior vena caval obstruction. In two patients (cases 4 and 5) the entity was not clinically suspected prior to the liver scans. The finding of the hot spots (fig. 1, *A* and *B*) prompted the radionuclide venacavogram (fig. 1, *E–H*) which showed the superior vena caval obstruction.

Case 6 was referred for radionuclide venography to find the source of pulmonary emboli documented on a previous lung scan. Figure 2, *A–D*, shows occlusion of the infrarenal portion of the inferior vena cava with development of multiple collaterals. A hot spot was seen in the right upper quadrant located anteriorly (fig. 2, *D and G*). ^{99m}Tc sulfur colloid was injected into an antecubital vein following the venogram to localize the hot spot to the liver (fig. 2, *E–G*).

Case 3 had clinical and laboratory findings of advanced hepatocellular disease without clinical evidence of superior vena caval obstruction. At autopsy the superior vena cava was patent. In the anterior part of the right lobe corresponding to the region of the hot spot on the liver scan, a vascular mass compressed the liver tissue into a pseudocapsulelike margin. The histologic diagnosis was solitary hepatoma in the right lobe in a postnecrotic cirrhotic liver.

Radionuclide venacavography was not performed in cases 1 and 2 since both showed clinical evidence of superior vena caval obstruction. Case 7 showed clinical evidence of this syndrome, and obstruction of the superior vena cava was shown by radionuclide venacavography.

Discussion

Holmquist and Burdine [3] and later Lee et al. [13] showed that regionally increased radionuclide accumulation in the liver in superior vena caval obstruction is due to collateral circulation of tracer via the umbilical

---

Received February 2, 1977; accepted after revision May 24, 1977.

[1] Division of Nuclear Medicine, McGaw Medical Center of Northwestern University, Chicago, Illinois 60611.

[2] Present address: Division of Nuclear Medicine, Medical University of South Carolina Hospital, 80 Barre Street, Charleston, South Carolina 29401. Address reprint requests to N. S. Gooneratne.

[3] Division of Nuclear Medicine, Veterans Administration Hospital, Charleston, South Carolina 29403.

Am J Roentgenol 129:447-450, September 1977

TABLE 1

Summary of Findings

Case No.	Diagnosis	Clinical Evidence of Vena Caval Obstruction	Vessel Obstructed	Site of Injection	
				Static Image	Dynamic Image
1	Carcinoma of lung	+	SVC	Arm	. . .
2	Carcinoma of lung	+	SVC	Arm	. . .
3	Postnecrotic cirrhosis and hepatoma	−	−	Arm	. . .
4	Carcinoma of lung	−	SVC	Arm	Arm
5 (fig. 1)..........	Carcinoma of lung	−	SVC	Arm, foot	Arm
6 (fig. 2)..........	Renal cell carcinoma	−	IVC	Arm	Foot
7	Carcinoma of lung	+	SVC	Arm	Arm

Note.—All patients showed a hepatic hot spot. In all except case 6, static images were obtained before dynamic. In case 5, a foot injection performed after static and dynamic studies (arm) was negative for a hot spot. SVC = superior vena cava; IVC = inferior vena cava.

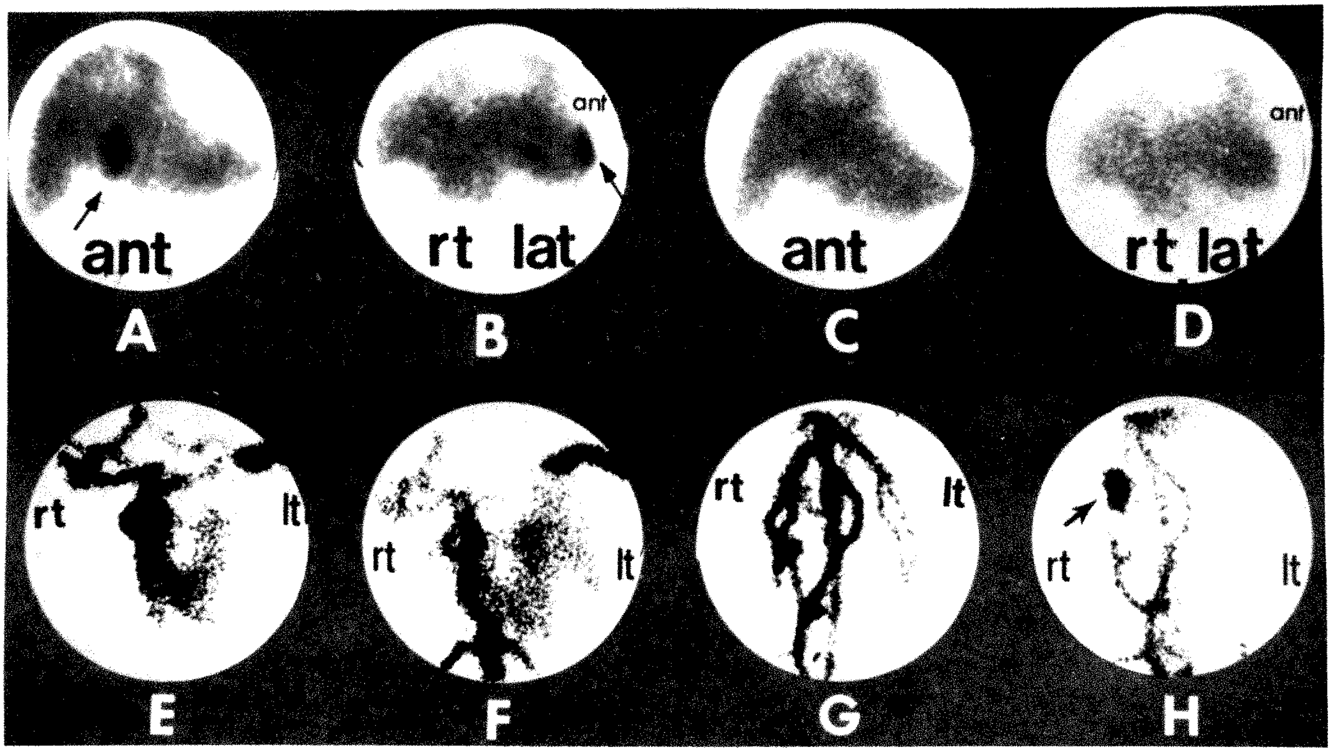

Fig. 1.—Case 5. *A and B*, Anterior and right lateral hepatic scintiscans after intravenous injection of ^{99m}Tc sulfur colloid into arm vein. Note multiple filling defects due to metastases and hot spot (*arrow*). *C and D*, Repeat study after injection into foot vein showing multiple filling defects but no hot spot. *E–H*, Radionuclide venacavogram 48 hr after static liver images (*A and B*) following simultaneous bilateral injection of ^{99m}Tc pertechnetate into antecubital veins. Note collateral channels in chest (*E and F*) and abdomen (*G and H*) and site of hot spot (*arrow*).

vein to the central portion of the liver. The hot spot is observed after intravenous administration of the tracer into an arm vein, but not when injected through a foot vein. Case 5 demonstrates collateral pathways (fig. 1, *E–H*) and the region of the hot spot (fig 1, *H*) as seen on dynamic images (arm injection) and static liver images. (Fig. *1, A and B*). Repeat hepatic scintigraphy after injection in a foot vein on a subsequent date did not show the liver hot spot (fig. 1, *C and D*). These findings confirm the previously reported observations [3, 13].

The hot spot in a routine liver scan following an upper extremity injection is often indicative of superior vena caval obstruction. Similarly, a hot spot seen in the right upper quadrant on radionuclide venography of the lower limbs using the technique of Henkin et al. [16] is evidence of inferior vena caval obstruction with development of collaterals via the liver. Intravenous injection of ^{99m}Tc human albumin microspheres results in deposition of the microspheres in the first capillary bed encountered, usually the lungs. However, in Case 6 it occurred in the liver. Sequential images of the abdomen following an intravenous injection in the foot demonstrated the hot

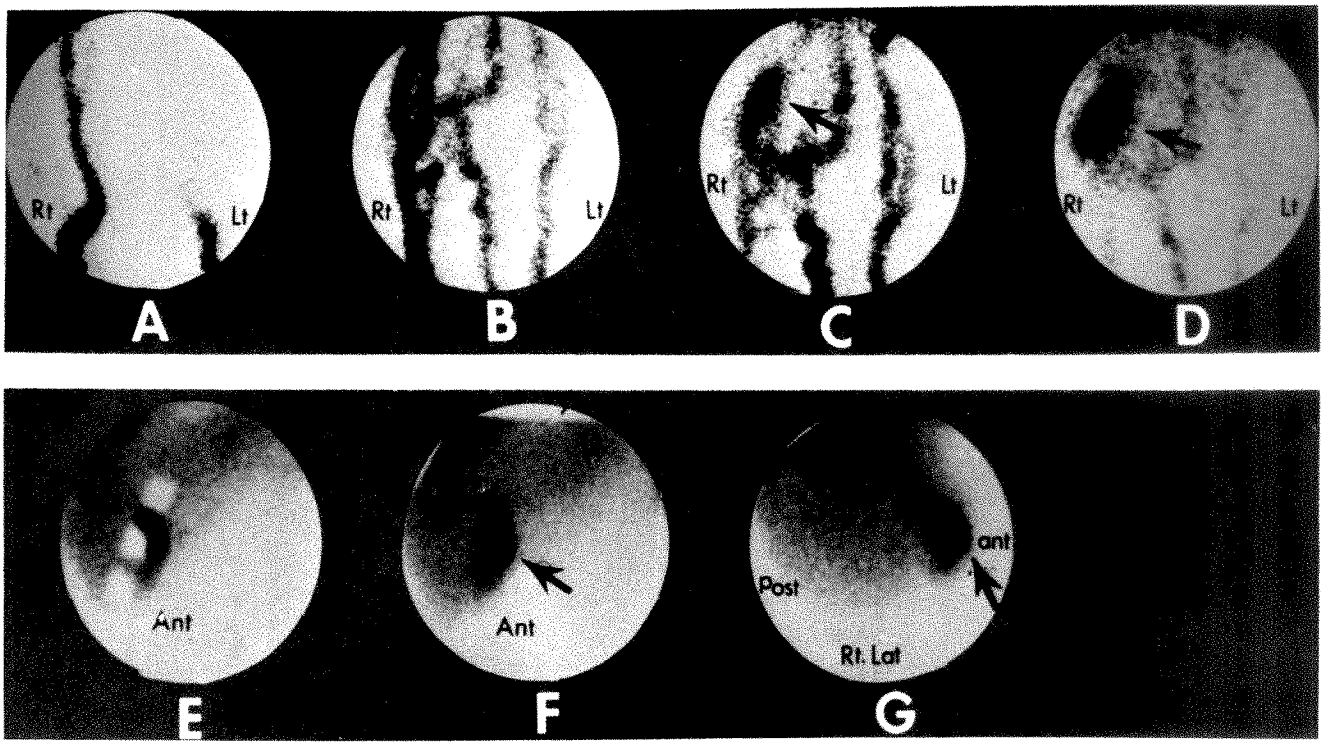

Fig. 2.—Case 6. *A–D*, Radionuclide venogram with ^{99m}Tc human albumin microspheres demonstrating occlusion of common iliacs (*A*) with multiple abdominal collaterals (*B and C*) and hot spot (*arrow, C and D*). *E–G*, Hepatic scintiscans, anterior with costal marker (*E*), anterior (*F*), and right lateral views (*G*), same day as venogram after injection of ^{99m}Tc sulfur colloid into arm vein. Note hot spot (*arrow*) in liver.

spot in the liver (fig. 2, *A–D*) which was confirmed by intravenous injection of ^{99m}Tc sulfur colloid into an arm vein (fig. 2, *E–G*).

Hepatomas are usually seen as cold lesions on ^{99m}Tc sulfur colloid liver scans. The appearance of a hepatoma as a hot spot has not been reported previously. In case 3 the hot spot may have been caused by increased vascularity of the tumor, compression of the liver tissue into a "pseudocapsule," and poor uptake by the rest of the cirrhotic liver, thereby causing the Kuppfer cells in the pseudocapsule to show as a hot spot.

Hot spots on ^{99m}Tc sulfur colloid liver scans are nonspecific, but if located anteriorly and medially to the gallbladder fossa, suggest superior vena caval obstruction. Dynamic images can confirm the diagnosis. In view of the risks inherent in contrast venacavography, and since the morphologic detail provided by radiographic techniques usually is not necessary for appropriate clinical decisions, radionuclide venacavography seems preferable This is particularly true in patients with advanced disease in whom noninvasive radionuclide techniques supply enough information for proper care and treatment. Radionuclide superior venacavography is relatively simple, innocuous, and can be repeated to assess response to treatment. This procedure is warranted when a hot spot is seen on static liver images, even if superior vena caval obstruction is clinically not apparent, and even in the absence of a mass lesion on chest x-ray [17].

The observation of a hot spot in the liver after radionuclide venography of the lower limbs suggests inferior vena caval obstruction. To our knowledge this is the first reported instance of this finding.

ACKNOWLEDGMENT

We gratefully acknowledge the secretarial assistance of Angela Hattaway.

REFERENCES

1. Hughes FA: The value of hepatic scintiangiography and static liver scans in superior vena caval obstruction. *J Nucl Med* 16:626–628, 1975
2. Hopkins GB: Superior vena caval obstruction and increased radiocolloid activity in liver scintiphotos. *J Nucl Med* 14:883, 1973
3. Holmquist DL, Burdine JA: Caval-portal shunting as a cause of a focal increase in radiocolloid uptake in normal livers. *J Nucl Med* 14:348–351, 1973
4. Joyner JT: Abnormal liver scan (radiocolloid "hot spot") associated with superior vena caval obstruction. *J Nucl Med* 13:849–851, 1972
5. Chayes Z, Keonigsberg M, Freeman L: The hot hepatic abscess. *J Nucl Med* 15:305–307, 1974
6. Volpe JA, Johnston GS: "Hot" hepatic hemangioma. A unique radiocolloid-concentrating liver scan lesion. *J Surg Oncol* 2:373–377, 1970
7. Pasquier J, Dorta T: Focal hyperfixation of radiocolloid by the liver. *J Nucl Med* 15:725, 1974
8. Meindok H, Langer B: Liver scan in Budd-Chiari syndrome. *J Nucl Med* 17:365–368, 1976

9. McLoughlin MJ, Colapinto RF, Gilday DL, Hobbs BB, Korobkin MT, McDonald P, Phillips MJ: Focal nodular hyperplasia of the liver. *Radiology* 107:257-263, 1973
10. Helbig HD: Focal iatrogenic increased radiocolloid uptake on liver scan. *J Nucl Med* 14:354-355, 1973
11. Henelin LG, Uszler JM, Sommer DG: Liver scan "hot spot" in hepatic veno occlusive disease. *Radiology* 117:637-638, 1975
12. Hattner RS, Shames DM: Non-specificity of the radiocolloid hepatic "hot spot" for superior vena caval obstruction. *J Nucl Med* 15:1041-1043, 1974
13. Lee KR, Preston DF, Martin NL, Robinson RG: Angiographic documentation of systemic-portal venous shunting as a cause of a liver scan "hot spot" in superior vena caval obstruction. *Am J Roentgenol* 127:637-639, 1976
14. Marshall RJ, Edmundowicz AC, Andrew CE: Chronic obstruction of the superior vena cava due to histoplasmosis. *Circulation* 24:604-609, 1964
15. Okay NH, Bryk D: Collateral pathways in occlusion of the superior vena cava and its tributaries. *Radiology* 92:1493-1498, 1969
16. Henkin RE, Yao JST, Quinn JL, Bergen JJ: Radionuclide venography in lower extremity venous disease. *J Nucl Med* 15:171-175, 1974
17. Kumar B, Coleman RE, McKnight R: Asymptomatic superior vena caval obstruction. *J Nucl Med* 17:853-854, 1976

Doppler Ultrasonic Screening Prior to Venography for Deep Venous Thrombosis

PAUL F. JAQUES,[1] WILLIAM A. RICHEY,[1] CINDY A. ELY,[2] AND GEORGE JOHNSON, JR.[3]

A total of 244 patients were examined using both ultrasonic Doppler technique and conventional venography for deep venous thrombosis. The Doppler examination was 93.8% accurate overall in detecting the condition, with a specificity of 96% and sensitivity of 85.7%. Indications for venography after Doppler evaluation include: (1) a positive or equivocal Doppler examination; and (2) critically ill patients with negative Doppler results where absolute diagnostic accuracy is essential. Had these criteria been followed in this study, 174 normal examinations would have been avoided and only six large vein thrombi (ileofemoral or popliteal) in 244 examinations would have been misdiagnosed.

Clinical diagnosis of deep vein thrombosis is highly fallible [1]. Thus accurate simple diagnostic techniques for this important clinical entity have long been sought. Venography, the principal diagnostic modality for many years, has significant undesirable side effects, including rare life-threatening reactions. Furthermore, venography is expensive in terms of personnel and equipment. Currently available techniques include^{125} I fibrinogen uptake studies, thromboscintography, and the ultrasonic Doppler system. The Doppler examination has proved to be an inexpensive, noninvasive method of evaluating the deep venous system [2, 3] and has been used clinically at our institution for several years. We present data from patients studied during a 2 year period on whom both Doppler and venographic studies of the deep veins of the lower extremities were obtained.

Materials and Methods

A total of 244 limb examinations were performed for suspected deep vein thrombosis by both the ultrasonic Doppler technique and venography between August 1974 and July 1976. The study was sequential but not strictly controlled; examinations were performed by physician request. Doppler examinations were carried out by a nurse technician using a 5.3 MHz ultrasound device (Medsonics BF4A Ultrasound Stethoscope, Mountain View, Calif.) according to the technique of Barnes et al. [4].

An abnormal Doppler examination was reported when there was either no flow in the deep veins or a significant reduction in flow when compared to the same site on the contralateral leg as detected by Doppler probe. Supporting evidence for the abnormality included either a reduction in the phasicity of flow with respiration or in the degree of augmentation to flow achieved by squeezing the calf. When only a reduction in respiratory-dependent phasicity was detected, the Doppler examination was considered equivocal.

Results

The overall results are shown in table 1. Accuracy of the Doppler technique was 93.8% (228 of 244) if the 10 equivocal cases are included as Doppler abnormals. Errors with the Doppler method included nine false negative cases and two false positive (table 2). The sites of the 10 equivocal Doppler examinations are shown in table 3.

Discussion

Venous thrombosis remains an important clinical entity in terms of frequency, local discomfort, late sequellae of venous stasis, and potential for pulmonary embolization [5]. Clinical diagnosis of deep vein thrombosis is at best highly fallible [1], and its treatment is fraught with potential complications [6, 7]. Standard intravenous anticoagulation increases the chance of a hemorrhagic event in a patient by 6.8% with a mortality rate of one per 1,000 [7]. Thus such therapy should not be used for a suspected deep venous thrombosis without firm documentation. In busy community hospitals, strict adherence to this policy would demand an unacceptable venogram case load, not to mention overall patient discomfort, undesirable side effects, and cost. We find the noninvasive bedside Doppler technique a simple rapid screening method.

In studies comparing Doppler with venography, accuracy of the Doppler examinations has ranged from 49% to 93% [8, 9]. Our accuracy rate was 93.8%. The range is in part related to the training and experience of the nurse technician performing the study. After a 1 week training session at the University of Iowa several months prior to this study, the accuracy of our Doppler examinations improved significantly.

The specificity of the Doppler examination was 96.1%; that is, it accurately detected 174 of the 181 normal cases. Sensitivity was 85.7% (54 of the 63 abnormal cases). The probability of a significant (venogram positive) thrombosis being present with a normal Doppler examination was only 5% (nine of 183 examinations; table 1). Furthermore, on the basis of our data, the chance is only one in 30 (3%) that a popliteal or ileofemoral thrombosis will go undetected using Doppler examination alone (six of 183; tables 1 and 2). On the other hand, there is an 11.5% chance (seven of 61 examinations) that a patient with an abnormal or equivocal Dop-

---

Received March 22, 1977; accepted May 20, 1977.

[1] Department of Radiology, University of North Carolina School of Medicine, Chapel Hill, North Carolina 27514. Address reprint requests to P. F. Jaques.

[2] Peripheral Vascular Laboratory, University of North Carolina School of Medicine, Chapel Hill, North Carolina 27514.

[3] Department of Surgery, University of North Carolina School of Medicine, Chapel Hill, North Carolina 27514.

TABLE 1

Overall Results

Doppler Results	Venogram Results		No. Cases
	Positive	Negative	
Abnormal	49	2	51
Equivocal	5	5	10
Normal	9	174	183
Total	63	181	244

TABLE 2

Doppler Error by Site

Most Proximal Site of Error	Doppler Negative Venogram Positive	Doppler Positive Venogram Negative
Ileofemoral	3	1
Popliteal	3	1
Calf	3	0
Total	9	2

TABLE 3

Sites of Equivocal Doppler Examination

Site of Equivocal Examination	Venogram Positive	Venogram Negative
Iliac	5*	0
Femoral	0	2
Popliteal	0	1
Calf	0	2
Total	5	5

* Two thrombus (nonocclusive) and three external compression.

pler examination will have no significant deep venous thrombosis.

Because the false negative rate is so low (3%), we believe that patients with negative Doppler results should generally not undergo venography. Rather, further investigation should be delayed until there is additional clinical indication. In our study, such a policy would have eliminated 174 of 244 venograms performed. In critically ill patients where accuracy of diagnosis is absolutely essential, venography might still be performed despite a normal Doppler examination if clinical suspicion were present.

When Doppler examinations are positive, we feel all patients may benefit from venography. For the false positive cases (11.5%), the risk of unnecessary anticoagulation may be avoided. For the true positive cases, a venogram may define the extent and configuration of the thrombosis as well as provide a rough estimate of its age [10]. In addition, the Doppler technique does not always adequately distinguish between venous thrombosis and extrinsic compression in the more proximal veins, a feature which venography may better define. Patients with equivocal Doppler examinations should also have venography. In our study, five of 10 proved to have significant venous pathology. Indeed all equivocal studies of the iliac veins proved abnormal, two with thrombosis and three with extrinsic compression of iliac veins (table 3).

REFERENCES

1. Haeger K: Problems of acute deep venous thrombosis. *Angiology* 20:219–223, 1969
2. Strandness DE Jr, Sumner DS: Ultrasonic velocity detector in the diagnosis of thrombophlebitis. *Arch Surg* 104:180–183, 1972
3. Yao SJ, Gourmos C, Hobbs JT: Detection of proximal vein thrombosis by Doppler ultrasound flow detection methods. *Lancet* 1:1–4, 1972
4. Barnes RW, Russell HE, Wilson MR: *Doppler Ultrasonic Evaluation of Venous Disease*. Ames, University of Iowa Press, 1975
5. Couch NP: Symposium on phlebothrombosis. *Arch Surg* 104:132–133, 1972
6. Zweifler AJ, Coon WW, Willis PW: Bleeding during oral anticoagulant therapy. *Am Heart J* 71:118–123, 1966
7. Coon WW, Willis PW: Hemorrhagic complications of anticoagulant therapy. *Arch Intern Med* 133:386–392, 1974
8. Milne RM, Gunn AA, Griffiths JMT, Ruckley CV: Postoperative deep venous thrombosis. A comparison of diagnostic techniques. *Lancet* 2:445–447, 1971
9. Evans DS: The early diagnosis of deep vein thrombosis by ultrasound. *Br J Surg* 57:726–728, 1970
10. Lipchik EO, DeWeese JA, Rogoff SM: Serial long-term phlebography after documented lower leg thrombosis. *Radiology* 120:563–566, 1976

The Target Sign: A New Radiologic Sign of Septic Pulmonary Emboli

MELVIN N. ZELEFSKY[1] AND LETTY G. LUTZKER[1]

A new radiographic sign consisting of a pulmonary density suspended in a thin-walled cystic area is described in five patients with hematogenously disseminated infection. A pathogenetic mechanism is suggested to account for this "target sign." The relationship of these findings to pulmonary pneumatoceles is also discussed.

Development of pneumatoceles during the course of suppurative lung disease has long been recognized. Early investigators studying the pathogenesis of these air spaces reported conflicting data and hypotheses regarding the mechanism of their development. Since that time, little additional information has been reported. This paper describes a new radiologic sign that aids in recognition of septic emboli and which may offer further insight into the pathogenesis of pulmonary pneumatoceles.

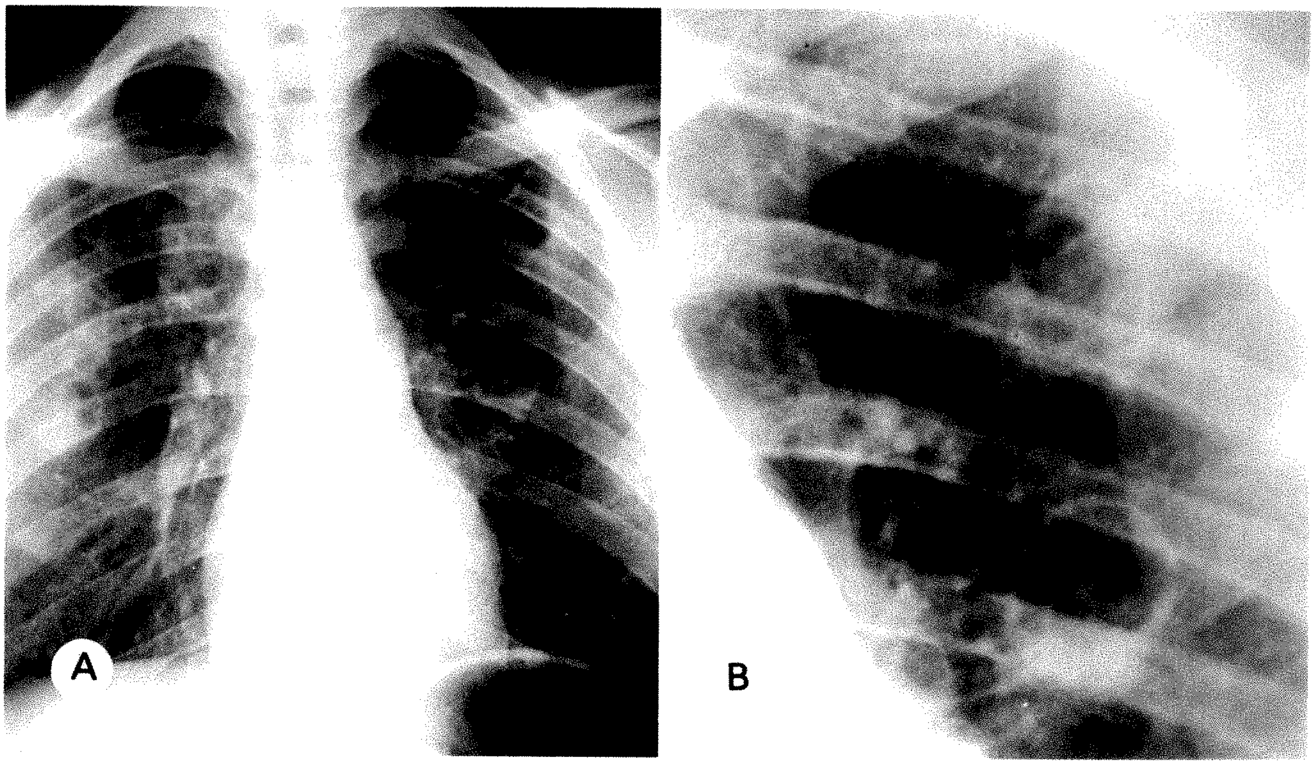

Fig. 1.—Case 1. *A*, Posteroanterior radiograph showing thin-walled cystic areas with central density. *B*, Close-up of left middle lung field.

Case Reports

Case 1

L. B., a 22-year-old addict, had been mainlining (intravenously injecting) cocaine. Two weeks prior to admission, he developed fever and a cough productive of green sputum. Initial blood cultures were positive for *Staphylococcus aureus*. Chest radiographs demonstrated bilateral scattered infiltrates with thin-walled cavities (fig. 1*A*). In one cavity in the left lung, a shallow air-fluid level and a central density, apparently suspended within the cavity, were demonstrated. The density maintained its central position on the shallow apical lordotic projection (fig. 1*B*).

Case 2

F. H., a 37-year-old former heroin addict, was hospitalized with fever and cough productive of sputum containing large numbers of gram-negative rods which on culture proved to be *Klebsiella*. Chest radiographs demonstrated diffuse scattered infiltrates with cavitation (fig. 2*A*). Tomograms of the cavities showed an irregular central nidus (fig. 2*B*).

Case 3

R. D., a 3-year-old child with acute lymphatic leukemia, developed *Escherichia coli* sepsis. Chest radiographs revealed multiple scattered infiltrates which ultimately showed cavitation (fig. 3A) and suspended intracavitary densities (figs. 3*B* and 3*C*). Eventually these densities were eliminated, leaving thin-walled cavities (fig. 3*D*).

Case 4

M. W., a 20-year-old female addict, was transferred to our hospital with a clinical diagnosis of sepsis. Multiple blood cultures were positive for *Staphylococcus aureus*. Physical examination disclosed a murmur over the tricuspid region, consistent with endocarditis of the tricuspid valve. Radiographic examina-

---

Received February 8, 1977; accepted after revision June 3, 1977.

[1] Department of Radiology, Albert Einstein College of Medicine, Bronx, New York 10461. Address reprint requests to M. N. Zelefsky.

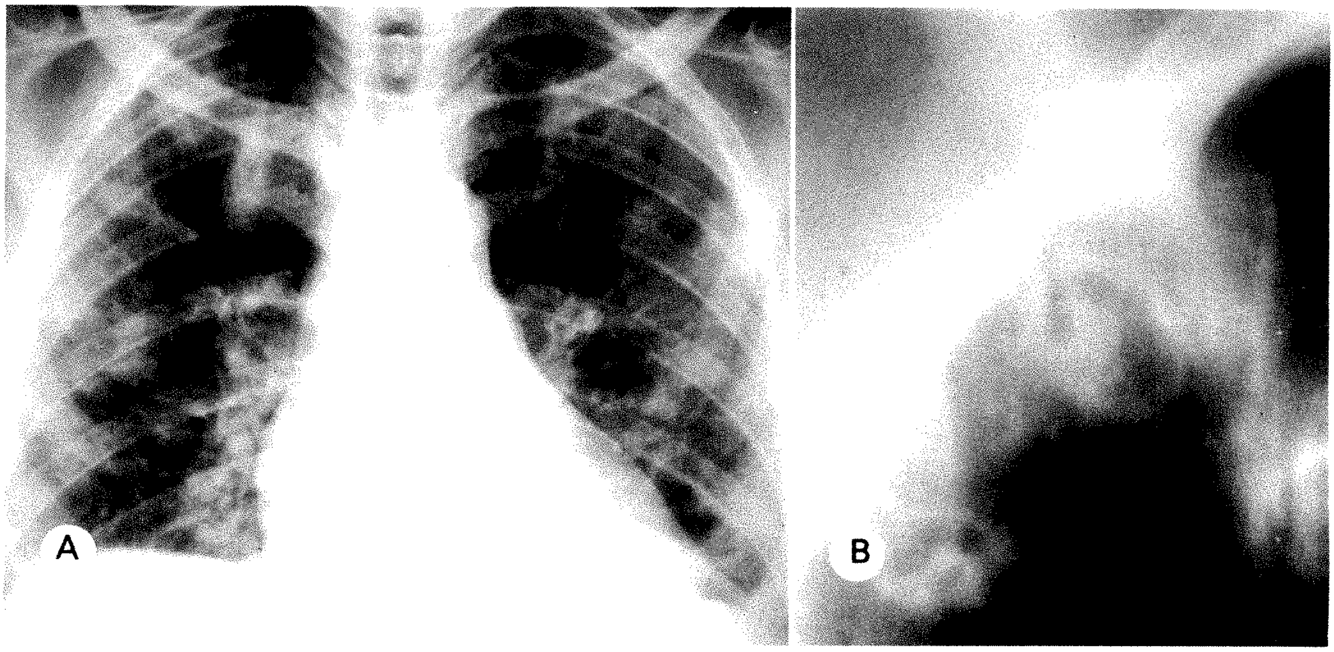

Fig. 2.—Case 2. *A*, Posteroanterior film showing diffusely scattered infiltrates. *B*, Tomogram of right upper lung field.

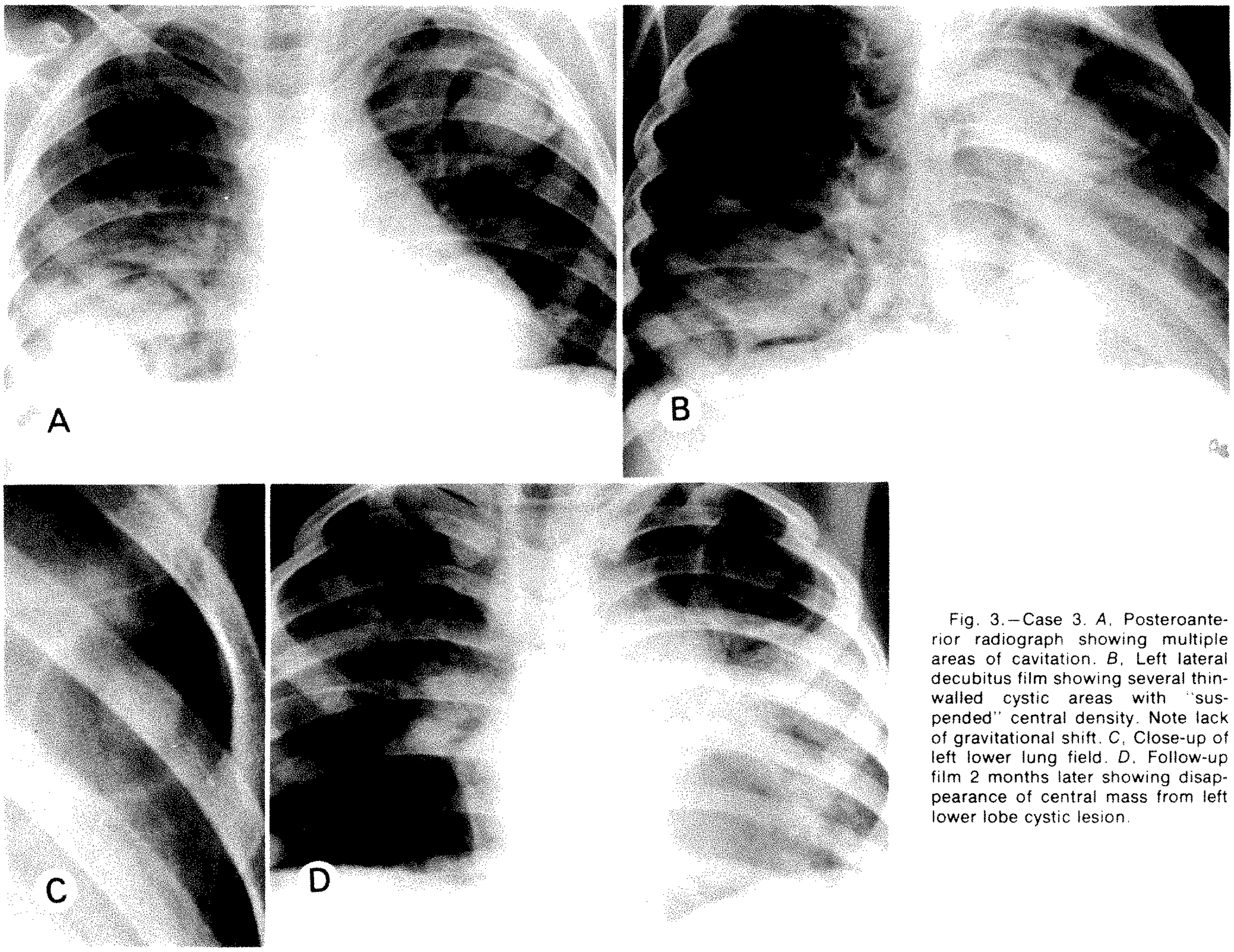

Fig. 3.—Case 3. *A*, Posteroanterior radiograph showing multiple areas of cavitation. *B*, Left lateral decubitus film showing several thin-walled cystic areas with "suspended" central density. Note lack of gravitational shift. *C*, Close-up of left lower lung field. *D*, Follow-up film 2 months later showing disappearance of central mass from left lower lobe cystic lesion.

tion of the chest showed several poorly defined nodular densities in both lung fields. Tomographic examination showed a cavity with an intracavitary density which was not readily appreciated on conventional films.

Discussion

With increased drug abuse. there has been a concomitant increase in the incidence of septic emboli. Perception of a nodular density suspended in a thin-walled hyperlucent cavity may provide a clue to the diagnosis of septic emboli in patients with scattered pulmonary infiltrates. This appearance. the "target sign." has not previously been reported. Our patients all responded to appropriate antibiotic therapy; therefore pathologic proof of the nature of this finding was not available. It is our hypothesis. however. that the central density is a localized nidus of suppuration and that it is surrounded by over-expanded pulmonary lobules.

The mechanism for development of focal overexpansion has been described by Stenkeen and Wolinsky [1]. These investigators induced the development of thin-walled cysts in the lungs of rabbits by infecting them with mycobacteria bovis and partially treating them with isoniazid and streptomycin. Subsequent pathologic studies of the lungs showed thin-walled bullae that could be inflated. but when the inflation pressure was released only the surrounding lung deflated. The walls of the air spaces consisted of compressed septae withoug significant cellular reaction. Their findings were confirmed by Bell [2] and were in keeping with the classical observations of Caffey [3] who noted that pneumatoceles frequently developed in areas of lung where there appeared to be radiologic resolution and that the appearance of pneumatoceles bore no relationship to clinical deterioration.

Stenkeen and Wolinsky [1] postulated that the pneumatocele was the result of edema and infection spreading in the interstitium of the lung adjacent to an area of suppuration. The development of bronchiolar distortion results in a check-valve mechanism causing progressive hyperinflation of the lobule of the lung leading from this bronchiole. In subsequent studies based on pathologic examination of experimentally produced cysts. Yesner et al. [4] postulated that the pneumatocele was the result of hyperinflation of a necrotic cavity associated with a check-valve obstruction of a communicating bronchus.

The target appearance in our cases of septic emboli is hypothesized to be a development of centrifugal spread of edema and inflammation into the surrounding interstitium causing a check-valve bronchiolar obstruction. The infected nidus. fixed at the site of embolization. appears suspended because it is surrounded by the hyperinflated lobules. Eventually there may be sufficient disruption of the interstitium to release the nidus and allow it to be expelled. leaving an empty air space resembling a cyst (case 3).

To date we have observed this sign in five cases of septic embolism. From this experience. we estimate the sign could be found in approximately 10% of such patients. Tomography may show this finding to be even more common.

We have not observed the target sign in other conditions. A fungus ball in patients with *Aspergillus* superinfection may initially mimic the target appearance septic embolism. However. the aspergilloma or fungus ball is usually free within the cavity. as manifested by its gravity-dependent position in decubitus projections. or it may adhere to one wall. It does not appear to be centrally suspended within the cystic space. Tuberculous cavities may also have intracavitary densities. caused by accumulation of casseous material. These are generally gravity dependent. and the cavity walls tend to be thick and sometimes irregular.

REFERENCES

1. Stenkeen W Jr. Wolinsky E: Formation of bullae or cystlike cavities during chemotherapy in rabbits with pulmonary tuberculosis. *Am Rev Tuberc* 75:965-974. 1957
2. Bell J: Experimental pulmonary emphysema. *Am Rev Tuberc* 78:848-861. 1958
3. Caffey J: Regional obstructive pulmonary emphysema in infants and in children. *Am J Dis Child* 60:586-605. 1940
4. Yesner R. Bernstein S. D'Esopo ND: The evolution of bullous cavities in adequately treated experimental pulmonary tuberculosis. *Am Rev Respir Dis* 82:810-823. 1960

A Statistical Description of the Normal Computerized Brain Scan

DAVID F. REESE,[1] PETER C. O'BRIEN, GEORGE W. BEELER, JR., PAUL R. GERDING,
AND CLIFFORD R. ROMME

A total of 100 CT brain scans performed with an EMI head scanner were analyzed in order to define the statistical limits of normal. The statistical parameters are means and standard deviations. Frequency polygons of the attenuation coefficients for each of five brain slices have been constructed. The concept of the water to brain ratio is introduced.

Introduction

The radiologist interprets the computerized tomographic scan (CT scan) by comparing visually the left and the right hemispheres for anatomic symmetry. The entire slice is also compared with a conceptualization of what the observer considers to be normal or abnormal at that particular level. Individual areas of sharply different attenuation are easily seen, but a diffuse increase or decrease in attenuation or subtle differences in one hemisphere compared with the other are difficult to discern.

An analysis of 100 normal CT brain scans provides statistical support for the radiologist's conception of normal or abnormal. Specifically, in analyzing the 100 normal CT brain scans, we computed means for each slice and histograms of the frequency distribution of attenuation coefficients for each slice [1]. In addition, the percentage of cerebrospinal fluid in relation to brain tissue was computed for each slice. By this method, we were able to answer the following questions: What degree of attenuation symmetry should there be between the two hemispheres? What proportion of the volume of a CT brain slice should be brain tissue and what proportion should be cerebrospinal fluid? And what is the mean density of the brain at each level?

Materials and Methods

A total of 100 CT brain scans performed on an EMI head scanner with water bag that were initially regarded by a neuroradiologist as normal were arbitrarily selected from among a series of patients without clinical evidence of a brain abnormality as determined by history and neurologic examination. Most of these patients had such symptoms as headache or dizziness or had histories of ancient trauma, although they had no objective neurologic abnormalities at the time of selection.

The Polaroid prints of these scans were reviewed by a second neuroradiologist, and if he concurred with the initial negative reading, the scans were included in the study. Scans with obvious motion artifacts were excluded. All patients in this study belonged to a patient population with symptoms of sufficient concern to require a CT brain scan and, therefore, cannot be considered as representative of a normal population. (We plan to conduct a similar study involving 100 normal volunteers.)

Statistics will be presented only for the upper five levels in the brain. Slice 1A will not be analyzed because this lowest slice in the cranial vault contains too many artifacts of attenuation caused by an excessive amount of bone in the slice. Also, the algorithm that automatically strips the skull from the brain tissue was frequently unable to negotiate the complex curves generated by the petrous and sphenoid bones.

The five slices are designated as 0, +1, +2, −1, and −2. Slice 0 passes approximately through the pineal gland, and all slices are at a 20° angle to the baseline (fig. 1). A midline drawn by hand through all 500 slices and a computer-generated midline were essentially the same. In the future, the computer-generated midline will be used.

Of the original 100 patients selected for inclusion in the study, one (a child of 7 months) was excluded on the basis of age. A 46-year-old man was found to have brain atrophy and also was excluded. The remaining 98 subjects all had scans at 0 level. This group consisted of 40 males whose ages ranged from 6 to 69 years (mean, 36.30 years) and 58 females ranging from 12 to 70 years (mean, 42.26 years). Eighty subjects had scans at +2 level, 95 at +1 level, 97 at −1 level, and 84 at −2 level. Sixty-six patients had scans taken at all levels.

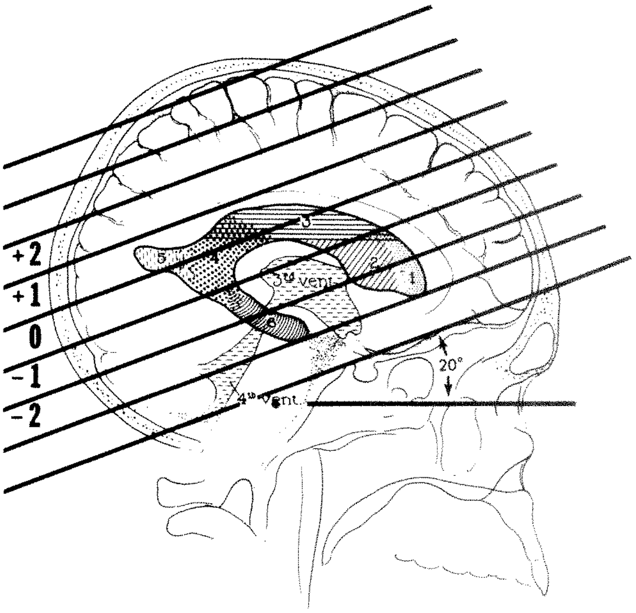

Fig. 1.—Diagram illustrating position of slices. Slice 0 passes approximately through pineal gland or quadrigeminal cisterns (or both). Each slice is analyzed separately because each contains different proportion of cerebrospinal fluid relative to brain.

Received January 20, 1977; accepted after revision May 19, 1977.
Presented at the annual meeting of the American Roentgen Ray Society, Washington, D.C., September 1976.
This work was supported in part by U.S. Public Health Service research grants CB-43982, CA-15902, and NS-52327-B from the National Institutes of Health.

[1] All authors: Mayo Clinic and Mayo Foundation, Rochester, Minnesota 55901. Address reprint requests to D. F. Reese at the Department of Diagnostic Roentgenology.

***Am J Roentgenol* 129:457–462, September 1977**

TABLE 1

Percentiles of Mean Densities in Normal Computerized Brain Scan

	Slice					
	−2 (N = 81)	−1 (N = 95)	0 (N = 98)	+1 (N = 97)	+2 (N = 84)	All (N = 66)
	Total Slice					
Minimum value	13.91	13.69	13.34	13.29	14.15	13.95
Percentiles:						
5	14.85	14.32	13.88	13.83	14.68	14.36
25	16.06	15.31	14.90	14.93	16.16	15.64
50	16.92	16.11	15.59	15.88	17.52	16.36
75	17.73	16.95	16.66	16.96	18.48	17.45
95	20.32	17.86	17.57	17.81	20.18	18.08
Maximum value	21.65	18.21	17.74	19.18	21.25	18.38
	Absolute Difference between Hemispheres					
Percentiles:						
50	0.741	0.418	0.527	0.403	0.402	0.274
75	1.945	0.938	1.004	0.740	0.643	0.508
95	3.103	2.799	2.351	1.638	1.276	0.816
Maximum value	3.904	4.191	2.440	2.221	2.137	1.060

TABLE 2

Percentiles of Percentage Water in Normal Computerized Brain Scan

	Slice					
	−2 (N = 81)	−1 (N = 95)	0 (N = 98)	+1 (N = 97)	+2 (N = 84)	All (N = 66)
	Total Slice					
Minimum value	3.88	3.31	4.97	2.96	0.75	4.85
Percentiles:						
5	5.88	4.61	6.09	4.21	1.31	5.44
25	8.97	6.70	7.37	6.92	3.00	7.56
50	11.73	8.53	9.57	10.28	4.61	9.36
75	15.99	10.97	12.85	14.39	7.37	12.08
95	23.07	14.30	16.68	19.13	12.07	15.10
Maximum value	25.92	19.25	18.44	23.19	18.28	17.87
	Absolute Difference between Hemispheres					
Percentiles:						
50	3.05	1.74	1.81	1.63	1.10	0.98
75	5.70	2.94	3.44	3.83	2.28	1.83
95	12.45	9.01	7.75	7.28	3.77	3.93
Maximum value	22.81	12.61	9.85	10.89	5.89	5.05

Data Analysis

The quantitative description of the CT scan was done in three ways: (1) mean density; (2) percentage water (cerebrospinal fluid); and (3) frequency polygons. In all cases, absorption coefficients of 50 or greater were disregarded because these usually are easily seen by the radiologist and more accurately and easily interpreted visually.

Mean density. For each subject, the mean of all absorption coefficients for each slice was computed. The mean was then computed separately for each hemisphere, and the absolute difference between hemispheres was evaluated. For the 66 patients with scans at all five levels, the data from all slices were pooled and similar statistics computed using the pooled data. The percentiles of the distributions for both sets of statistics were estimated nonparametrically.

Percentage water. In computing percentage water, coefficients from −17 through +10 were arbitrarily defined as representing water (W) and from +11 through +30 as representing brain tissue (B). The percentage water was then defined as $W = W/(W + B) \times 100$ and was computed for the entire slice and separately for each hemisphere.

Frequency polygons. A computer program was written to indicate graphically (via frequency polygons) the distribution of absorption coefficients in each hemisphere. The range of coefficients was divided into 17 class intervals as follows: $-10 \leq x < -5$; $-5 \leq x < 0$; $0 \leq x < 5$; $5 \leq x < 10$; $10 \leq x < 12$; $12 \leq x < 14$; $14 \leq x < 16$; $16 \leq x < 18$; $18 \leq x < 20$; $20 \leq x < 22$; $22 \leq x < 24$; $24 \leq x < 26$; $26 \leq x < 31$; $31 \leq x < 36$; $36 \leq x < 41$; $41 \leq x < 46$; and $46 \leq x < 50$. The frequency polygon is obtained by plotting the percentage frequency observed divided by class interval width for each class interval. Messages are printed out automatically if the proportion of absorption coefficients in any class interval falls outside the normal range for that interval. Limits of normality have been estimated using the observed 2.5 and 97.5 percentiles.

These limits, when displayed graphically, form a "normal envelope" for the frequency polygon. A frequency polygon will

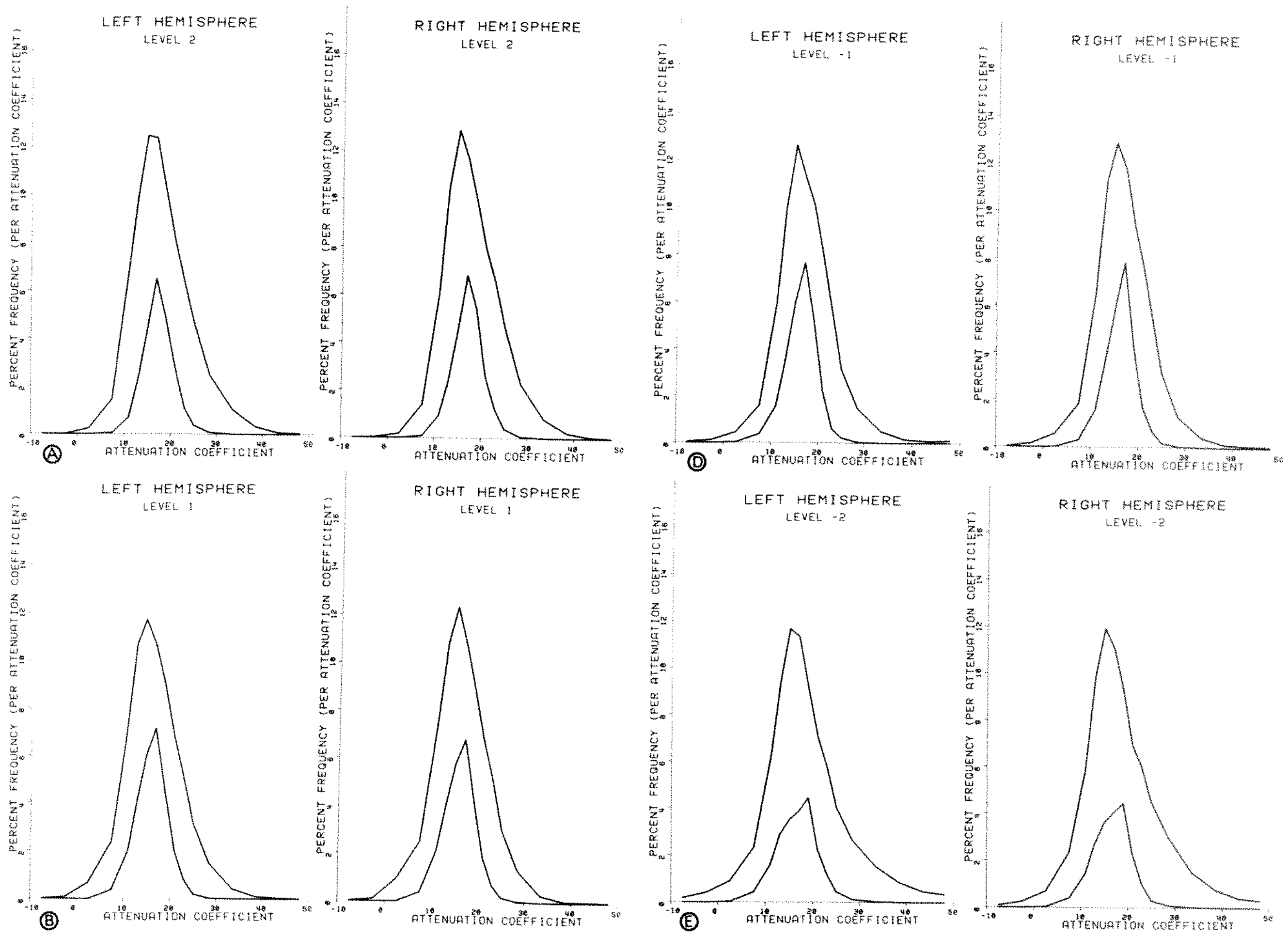

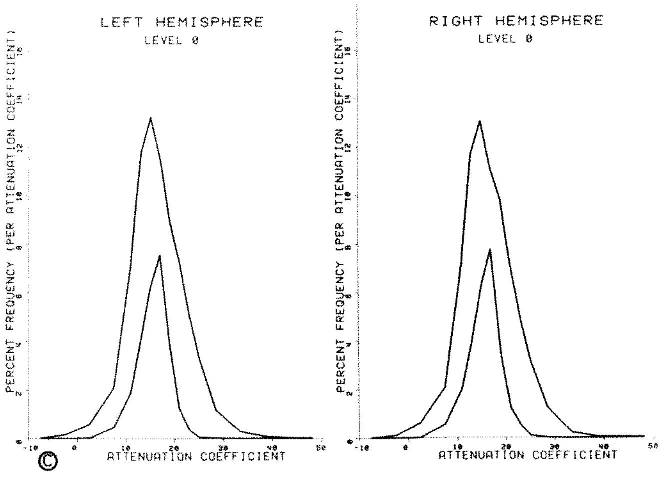

Fig. 2.—Computer-drawn frequency polygons for five standard brain slices. Space between two frequency polygons for each slice level represents normal envelope; frequency of any specific attenuation coefficient at any specified level should fall within this defined space.

fall outside this envelope if and only if one or more of the normal limits are exceeded. Although it is estimated that the normal limits for a given class interval will be exceeded in only 5% of cases (from our "normal" patient population), it is apparent that the normal envelope will be exceeded more frequently. Thus the normal envelope is intended primarily for descriptive purposes. A message is also printed out if the difference in proportions between the left and right hemispheres exceeds the 97.5% limit for any class interval. (Data used to plot the frequency polygons are available from the authors.)

Finally, the relationships of mean density and percentage water to age and sex were studied using regression analysis (data available from authors). Sex differences were tested using analysis of covariance. Based on this analysis, the decision was made to pool the data for males and females in testing for relationships with age. When considering the absolute differences between hemispheres (both for mean density and percentage water), the square root transformation was necessary because of the highly skewed nature of the data.

Results

Summary Statistics

The distributions of the summary statistics are shown in tables 1 and 2. The data are presented in terms of percentiles of the distributions rather than in means and standard deviations because in many cases the data were highly skewed. Of particular significance in these tables are the estimated (nonparametrically) fifth and 95th percentiles. Although the data refer to a patient population, the values define limits that may be useful in classifying future scans.

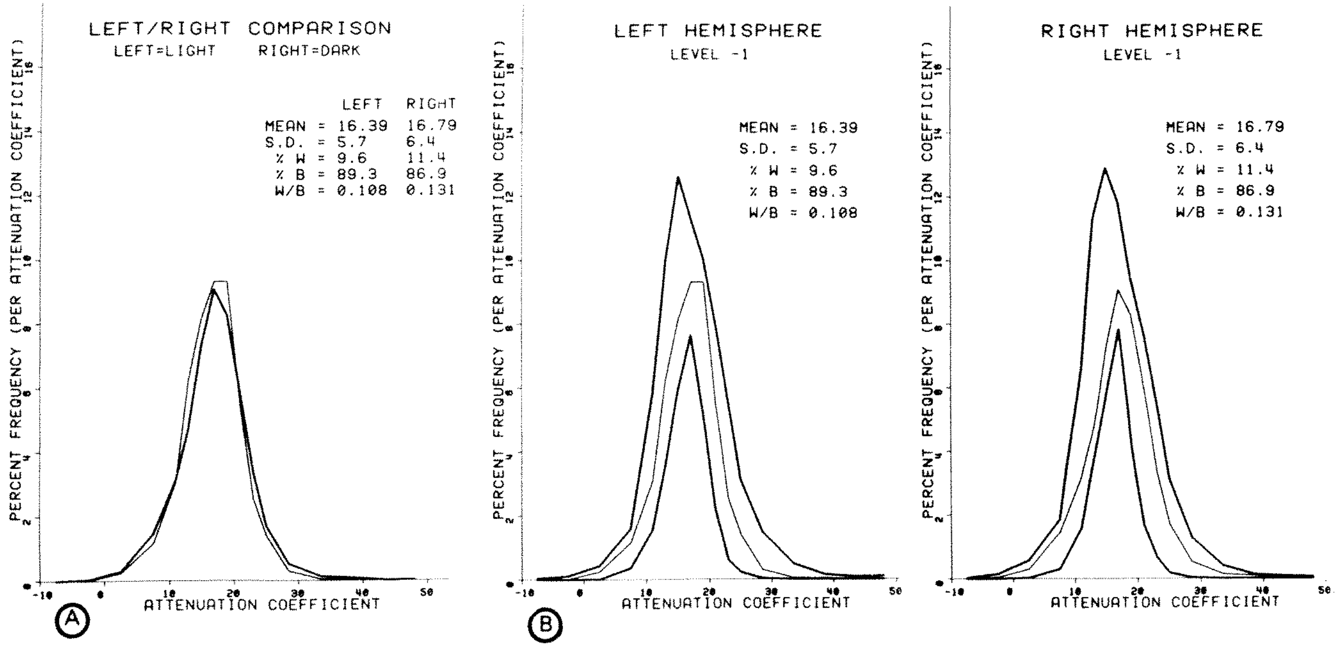

Fig. 3.—*A*, Frequency polygons for normal left and right hemisphere compared with each other. While slight asymmetry is present, no value exceeds absolute difference between hemispheres (table 1). *B*, Same frequency polygons relative to normal envelopes. Hemispheres are normal relative to each other and to population as a whole.

Frequency Polygons

Computer drawn frequency polygons for the five standard brain slices are shown in figure 2. Frequency polygons for normal left and right hemispheres are shown superimposed in fig. 3*A*. The same frequency polygons are displayed relative to normal envelopes in figure 3*B*. Thus computerized programs are available for comparing each hemisphere with its opposite and with a normal population.

In figures 4*A* and 4*B*, the mean attenuation in the right hemisphere is significantly less than in the left hemisphere. Statistics (tables 1 and 2) were normal for the left hemisphere but abnormal for the right hemisphere. Review of the scan (fig. 4*C*) revealed a subtle decrease in the overall attenuation of the right hemisphere. Review of the patient's history revealed that right-sided head trauma had occurred 3 months previously. However, the slices above and below this level were normal, and the patient was neurologically normal at the time of the scan though he complained of headache. Therefore, the significance of the observation is unknown. Nonetheless, a statistical aberration existed, and the radiologist's attention was drawn to an area of potential abnormality.

Percentage Water

The diagnosis of brain atrophy can readily be made by CT scanning, and several methods for measuring the ratio of ventricle to brain have been reported [2]. We report herein a method of measuring the amount of cerebrospinal fluid (water).

By assuming that all attenuation coefficients of 10 or less represent water and all above 10 represent brain, we can estimate the ratio of water to brain in each slice. Table 2 shows the amount of water that might be expected to be found in each of the five slices.

As mentioned previously, of the 100 patients chosen for this study, one man was subsequently excluded because of brain atrophy. Although in this instance the CT brain scan (fig. 5*A*) was interpreted as normal by both radiologists, a pneumoencephalogram (fig. 6) showed a severe cortical atrophy with normal ventricular size and configuration. Review of the history of this 46-year-old patient revealed progressive dementia. However, the abnormality was originally brought to our attention by the statistical analysis: percentage water in the +1 slice was 24%, compared with the upper normal limit of 19.13%. Similarly, mean density for the +1 slice was 13.29, compared with the lower normal limit of 13.83. The two hemispheres were similar (fig. 5*B*) but were outside the normal envelope (fig. 5*C*).

Discussion

The normal CT brain scan can now be described in terms of mean densities and ratios of water to brain. High and low limits of the frequency distribution of the attenuation coefficients have been developed and displayed by frequency polygons. Thus any slice of either hemisphere can be compared with its contralateral fellow or compared with other members of the population using any or all of these statistical descriptions.

We expect that this technique will help in detection and quantitation of such diffuse abnormalities of the brain as edema, atrophy, or certain types of degenerative disease. Because certain information is lost during statistical manipulation, we do not expect this method to improve our detection of such specific lesions as tumors

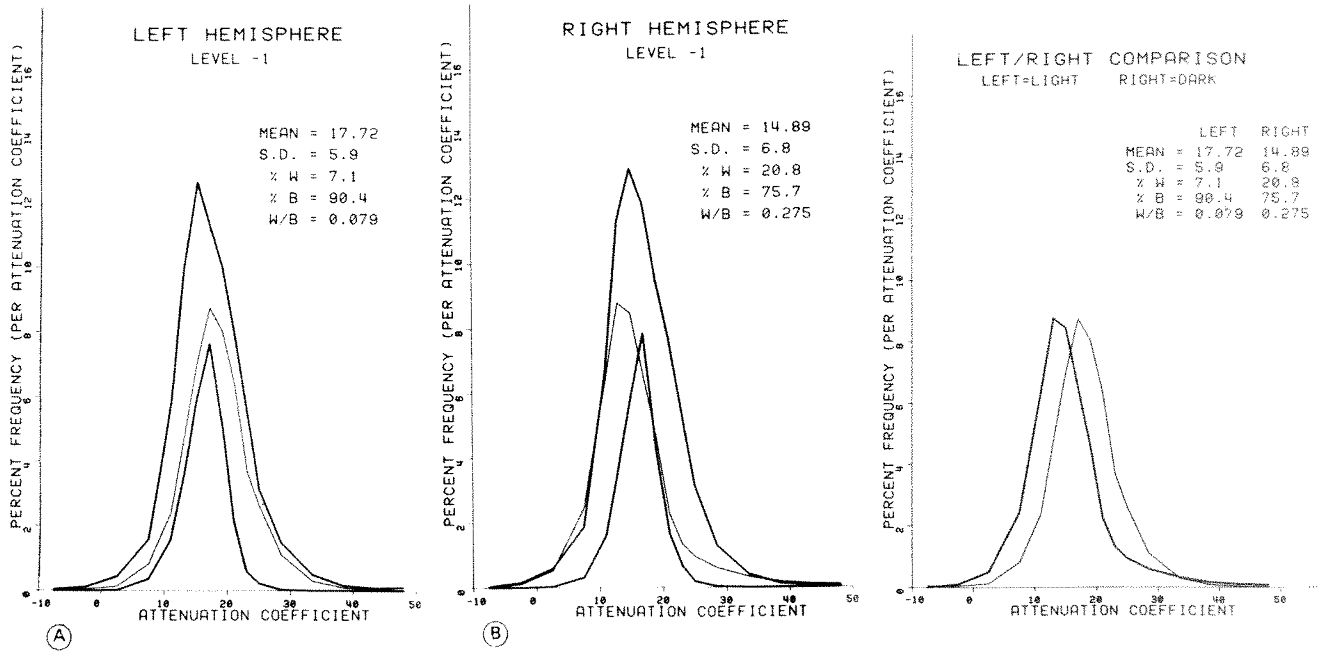

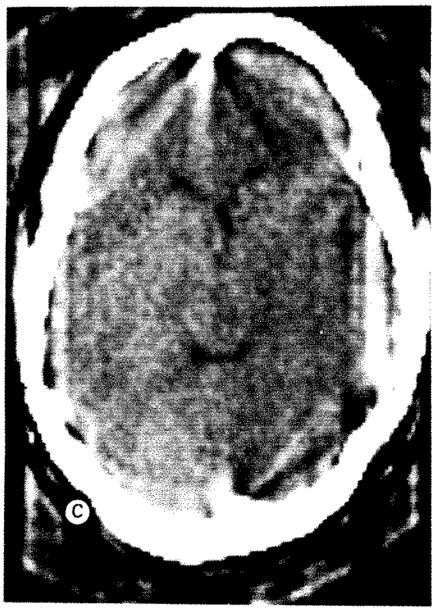

Fig. 4.—*A*, Frequency polygons of left and right hemispheres showing one hemisphere abnormal. *B*, Same frequency polygons relative to those of normal population. Curve for left hemisphere falls completely within normal envelope, whereas curve for right hemisphere is shifted left, indicating abnormally large number of low attenuation coefficients. *C*, Scan showing subtle decrease in overall attenuation of right hemisphere because of motion artifact or possibly because of recent head trauma.

or infarcts. In the future, more sophisticated statistical techniques using volumes obtained from anatomic areas by means of a light-pen may help us detect and analyze tumors and other specific lesions. Changes after the intravenous injection of contrast material also can be quantitated for specific volumes.

New CT head scanners do not use a water bag, and they employ different numeric systems. The statistical description of the normal CT scan as presented in this paper will form a baseline for comparison of present machines to future ones.

Shortcomings of the present study include loss of information because of averaging and motion artifacts which can magnify statistical abnormalities so much that only motion-free scans are worthwhile analyzing. Inferences made from this study depend heavily on the characteristics of our particular head scanner, including dose level and signal-to-noise ratio. In addition, subjects were selected from a patient population. Thus their true health status remains uncertain. They cannot be considered as representative of the general population.

REFERENCES

1. Reese DF, O'Brien PC, Beeler GW Jr, Gerding PR, McCullough EC: An investigation for extracting more information from computerized tomography scans. *Am J Roentgenol* 124:177-185, 1975
2. Huckman MS, Fox J, Topel J: The validity of criteria for the evaluation of cerebral atrophy by computed tomography. *Radiology* 116:85-92, 1975

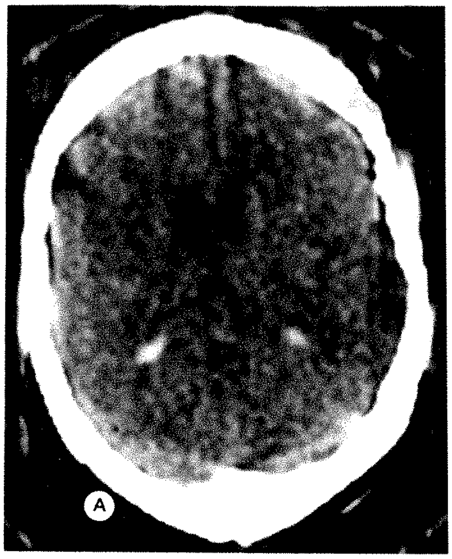

Fig. 5.—*A*, Normal-appearing CT scan. *B*, Left and right hemispheres are symmetric, but percentage water is too high and mean is too low for normality. *C*, Although ventricles were normal in size, frequency polygons show too many low attenuation coefficients. Curves are outside normal envelope.

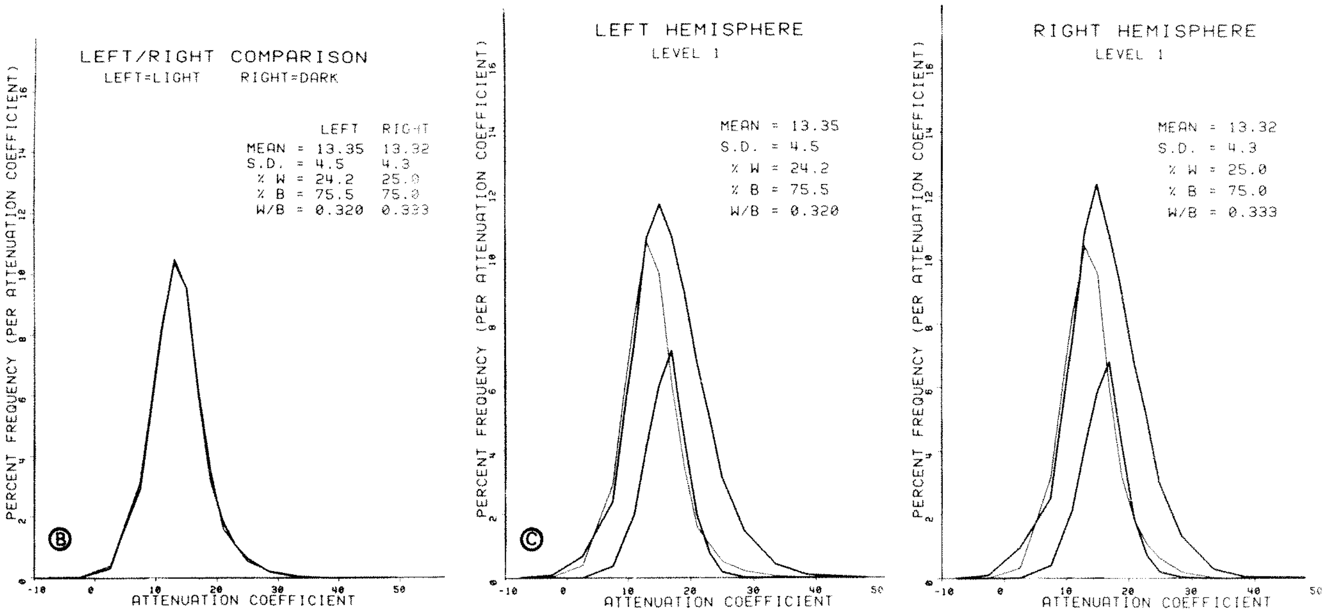

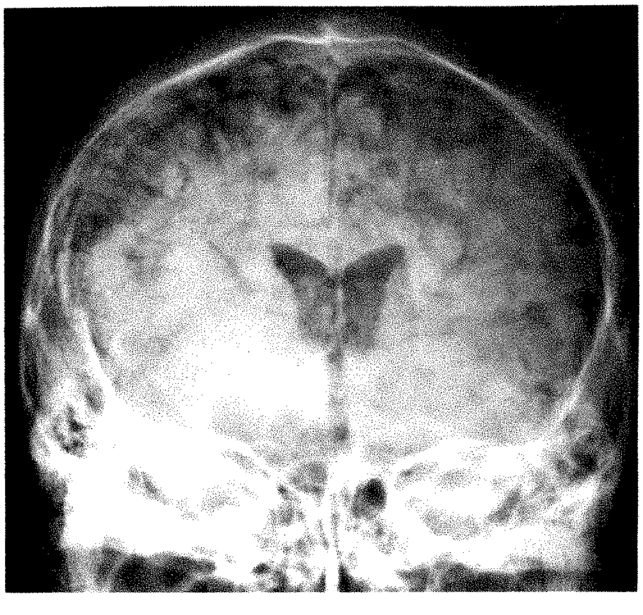

Fig. 6.—Pneumoencephalogram of patient in fig. 5 showing normal ventricular size but diffuse atrophy of cortex. This was demonstrated statistically but not visually on CT scan.

Cerebral Granulomatous Angiitis: Case Report and Literature Review

MICHAEL J FAER,[1] JAY H. MEAD,[2] AND RICHARD D. LYNCH[1]

Granulomatous angiitis is a pathologically distinct central nervous system segmental vasculitis of unknown etiology and pathogenesis which may be indirectly related to herpes zoster infections. The condition primarily affects adults and presents with nonspecific, unexplained progressive neurological dysfunction. The cerebrospinal fluid is often under increased pressure and contains excess protein and white cells, mostly lymphocytes. The necrotizing vasculitis primarily affects the small intracranial arteries and veins and alters vascular permeability, inducing cerebral edema. Angiography demonstrates segmental, diffuse, distal vascular irregularity and narrowing, while computed tomography shows poorly defined, diffuse, non-contrast-enhancing low density areas with or without mass effect. In the appropriate clinical setting, the angiographic and CT findings should be highly suggestive. The possibility of efficacious therapeutic intervention makes early diagnosis important. CT can also be used to monitor therapeutic response.

Granulomatous angiitis is an unusual but distinct pathologic entity of unknown etiology and pathogenesis which primarily involves the central nervous system. Unlike most other causes of cerebral vasculitis, granulomatous angiitis rarely involves the extracerebral vessels and selectively affects the small (less than 200 μm in diameter) leptomeningeal arteries, veins, and occasionally the larger intracranial arteries [1–3]. Since Cravioto and Feigin [1] first defined this necrotizing vasculitis in 1959, only 18 additional cases have been documented in the literature. Granulomatous angiitis has been described as a fatal disease [2], usually diagnosed at autopsy [2, 4]. However, Greco et al. [4] recently reported a biopsy-proven case in a stage I Hodgkin's patient in whom complete clinical and radiologic remission of the Hodgkin's disease and the angiitis was induced by adequate anti-Hodgkin's lymphoma therapy.

This report describes a case of cerebral granulomatous angiitis, reviews the literature, and illustrates and discusses radiographic and CT findings.

Case Report

A 70-year-old white female was hospitalized, unconscious after an unexplained fall in her room. For 4 days prior to admission, relatives noted general disorientation, confusion, and episodes of memory loss. On the night of admission, the patient was arousable only to painful stimuli. Vital signs were stable and examination revealed no focal neurological signs. Lumbar puncture yielded an opening pressure of 148 mm of water, no white blood cells, six red blood cells/mm^3, 188 mg/100 ml of protein, and 77 mg/100 ml of glucose. Cerebrospinal fluid was culture negative.

A radionuclide brain scan, performed during the second hospital day, showed decreased right carotid arterial perfusion and abnormal patchy uptake throughout both cerebral hemispheres. An electroencephalogram revealed nonspecific bilateral dysrhythmia slightly greater on the right. CT of the brain demonstrated bilateral, diffuse, poorly defined non-contrast-enhancing areas of decreased attenuation consistent with diffuse cerebral edema (fig. 1*A*). Intravenous Decadron therapy was begun, and during the next 5 days the patient's mental status gradually improved. On the fifth hospital day, a cerebral angiogram delineated bilateral, diffuse, segmental irregular arterial narrowing without evidence of mass effect, definite site of vascular occlusion, or ancillary angiographic signs of cerebral infarction. The possibility of temporal arteritis was entertained, but the patient's visual acuity, superficial temporal arteries, and erythrocyte sedimentation rate were normal.

Gradually over the next 12 days, the patient's mental and neurological status returned to normal. A repeat radionuclide brain scan was essentially normal except for minimal isotope uptake in the right frontal lobe region. She was discharged on the seventeenth hospital day. She remained stable for 3 weeks before again exhibiting confusion and disorientation. A month after release from the hospital, she was found semicomatose and was readmitted. Examination revealed a blood pressure of 190/110, otherwise stable vital signs, and an unresponsive patient demonstrating decorticate posturing. Lumbar puncture yielded an opening pressure of 320 mm of water. The cerebrospinal fluid contained 500 red blood cells/mm^3, no white blood cells, 91 mg/100 ml of glucose, and 205 mg/100 ml of protein. She was given Decadron and Mannitol, intubated, and hyperventilated to reduce intracranial pressure.

An emergency angiogram delineated a right frontal mass effect and diffuse bilateral segmental arterial narrowing without a definite site of vascular occlusion, neovascularity, or luxury perfusion. Slight inferior displacement of the right posterior cerebral artery suggested uncal herniation (fig. 2). The patient's clinical status stabilized, and a CT scan of the brain was performed (figs. 1*B* and 1*C*). Again, diffuse, bilateral, poorly defined, nonenhancing low density areas were noted, as well as a new right frontal mass effect. No evidence of increased attenuation was demonstrated to suggest recent hemorrhage, basal arachnoiditis, or cerebritis.

Although the exact nature of the patient's neurological dysfunction was uncertain, the clinical impression was irreversible brain damage. The family was informed of the patient's condition, and the decision was made to discontinue Decadron and Mannitol therapy and provide only minimal supportive care. The patient's clinical condition gradually deteriorated, and she expired without regaining consciousness 11 days after readmission.

Received March 15, 1977; accepted after revision May 27, 1977.

The opinions or assertions contained herein are the private views of the authors and are not to be construed as official, nor reflecting the views of the Department of the Army or the Department of Defense.

[1] Department of Radiology, Letterman Army Medical Center, Presidio of San Francisco, California 94129. Address reprint requests to the Technical Publications Editor, Letterman Army Medical Center.

[2] Department of Pathology, Letterman Army Medical Center, Presidio of San Francisco, California 94129.

Am J Roentgenol **129:463–467, September 1977**

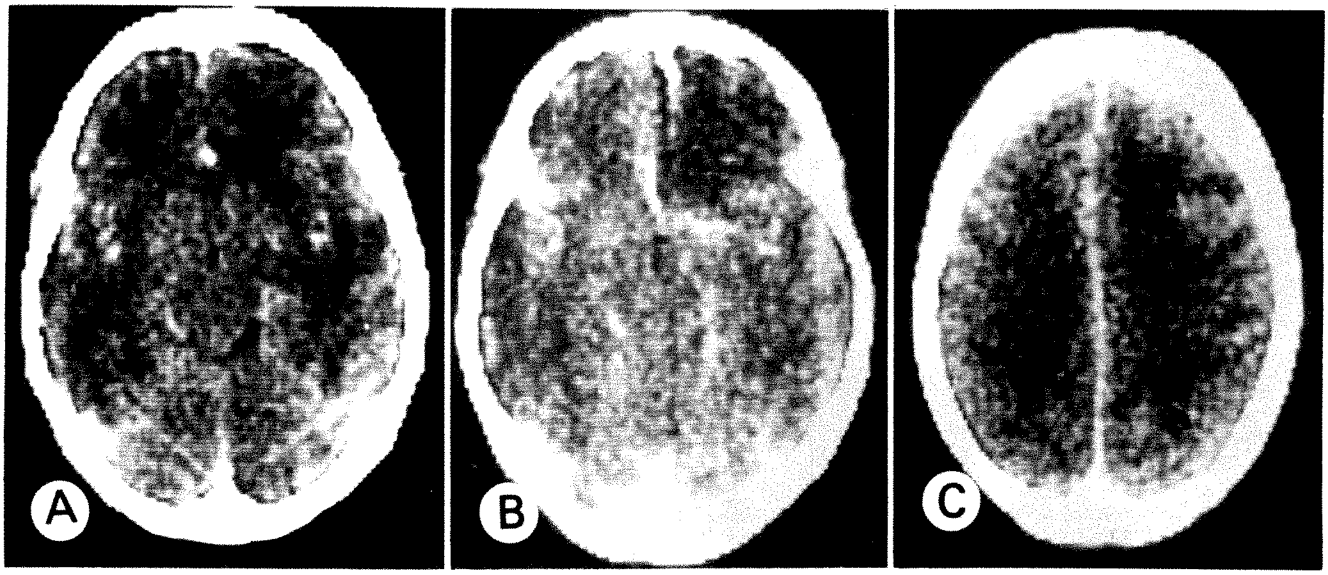

Fig. 1.—*A*, CT scan after administration of contrast material demonstrating diffuse, bilateral, poorly defined low density regions throughout cerebral hemisphere. *B and C*, Postcontrast CT scans 7 weeks later revealing low density area with mass effect shifting midline structures to left. Note high cerebral hemisphere section showing diffuse, poorly defined low density areas with fingerlike extensions into cortical gray matter.

At autopsy the brain weighed 1,325 g. The cerebral hemispheres were diffusely swollen and soft, especially in the right frontal lobe. Asymmetric notching of the right uncus was seen. After fixation and sectioning, several bilateral 1-2 mm punctate cortical gray matter hemorrhages and extensive, predominantly right-sided pontine and midbrain hemorrhages were noted. The ventricles were normal in size and free of blood, and no mass effect was demonstrated (fig. 3*A*).

Microscopic examination revealed a focal pattern of bilateral severe vascular changes involving primarily the small arterioles, venules, and capillaries. The vascular lesions varied from acute stages demonstrating fibrinoid necrosis and infiltration of polymorphonuclear leukocytes, to the more chronic infiltration of lymphocytes, epithelioid-appearing histiocytes, and giant cells resulting in granuloma formation. End-stage vessels were completely sclerosed without perivascular inflammatory infiltrate (fig. 3*B*). The pathologic diagnosis was severe diffuse cerebral granulomatous angiitis. Extracerebral autopsy findings showed no vasculitis.

Discussion

Pathology

The features that make granulomatous angiitis a distinct entity are its predilection for the small intracerebral vessels, focal fibrinoid necrosis, and marked perivascular inflammatory infiltrate [1-5]. Angiitic lesions outside the brain are uncommon (21%) and rarely are severe enough to be clinically manifest [6]. The spectrum of microscopic changes includes: (1) focal fibrinoid necrosis of the vessel wall; and (2) a variable inflammatory infiltrate composed of acute polymorphonuclear leukocytes and chronic lymphocytes, epithelioid-appearing histiocytes, and multinucleated giant cells resulting in granuloma formation. This segmental vasculitis is occasionally associated with parenchymal ischemic or hemorrhagic infarcts either secondary to occlusion of the diseased blood vessels by the vasculitis or by thrombus formation [2, 5].

Granulomatous angiitis can be distinguished from the other vasculitides on the basis of the marked perivascular chronic inflammatory cells, presence of fibrinoid necrosis, and almost exclusive involvement of small intracranial arteries and veins [2, 3, 5]. Periarteritis nodosa, cranial (temporal) arteritis, Takayashu disease, sarcoidosis, and allergic granulomatosis primarily involve larger arteries outside the brain and usually lack venule involvement. Allergic granulomatosis is further excluded by the lack of an atopic history and eosinophilia [7]. Sarcoidosis is the most difficult possibility to exclude, but the presence of marked fibrinoid necrosis and perivascular inflammatory changes and the lack of granulomatous changes elsewhere in the body argue strongly against that diagnosis [2, 4, 6, 8].

Etiology

Although the etiology and pathogenesis of granulomatous angiitis are obscure, herpes zoster virus currently seems the most likely etiologic factor [4, 9]. The correlation of herpes zoster infections, lymphoma, and granulomatous angiitis—all relatively rare conditions—may be more than coincidental [4]. The association of Hodgkin's lymphoma and herpes zoster infections [3], and the syndrome of herpes zoster ophthalmicus complicated by contralateral hemiplegia [4, 5, 10-16] are both well documented. Since a temporal delay of weeks to months is usually present between herpes zoster infection and subsequent development of neurologic symptoms, it is probable that many cases are not recognized [15] and the association may be more common than previously realized [16]. Interestingly, the hemiplegia in most of these patients with the syndrome remits spontaneously, and in

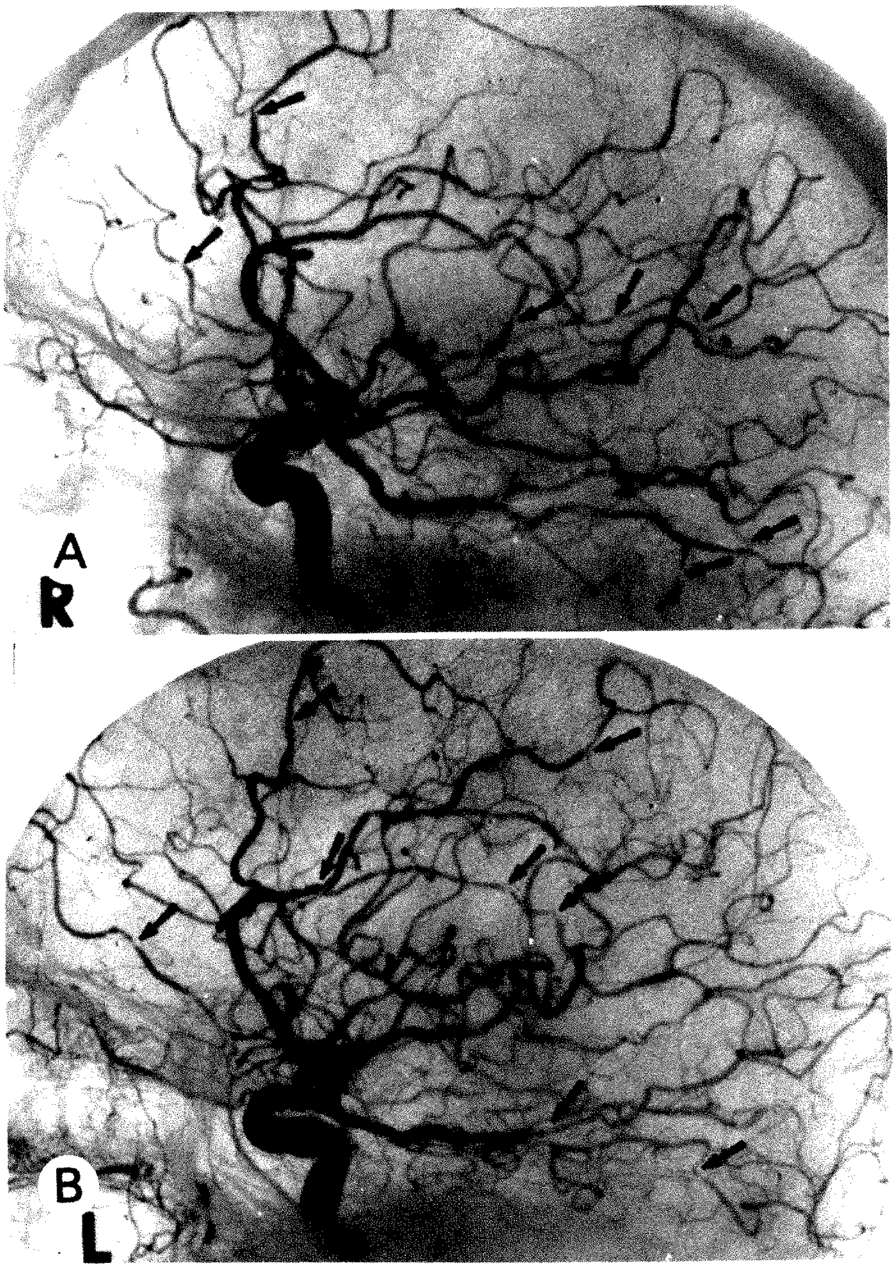

Fig. 2.—Cerebral angiograms showing diffuse irregular segmental arterial narrowing (*arrows*) involving peripheral distribution of anterior, middle, and posterior cerebral arteries. Note asymmetric depression of right posterior cerebral artery.

only a few cases has the pathologic basis for the hemiplegia—the characteristic lesions of granulomatous angiitis—been documented [3, 5, 9].

Postmortem electron microscopic examination has shown intranuclear inclusions in the brain resembling herpes virus particles [17]. To date, only one biopsy of fresh cerebral tissue has been cultured and examined by immunofluorescent electron microscopy techniques [4]. Negative viral studies argue against direct viral involvement in the brain, but do not exclude a viral agent from participating in the pathogenesis. The incorporation of viral nucleic acid within the cellular nucleic acid and the indirect induction of the lesion by an immunologic mechanism seem quite probable [4, 9]. The variable clinical courses following herpes zoster infection suggest either a multifactorial etiology or a single etiology modified by drug therapy and/or other host factors [4, 9]. The pathophysiologic effect of the ischemic necrotizing vasculitis seems to be altered permeability of the vessel wall with consequent outpouring of cells and protein [18] and subsequent cerebral edema.

Clinical Manifestations

To our knowledge, 29 cases of granulomatous angiitis (including our case) have been reported. This condition, which exhibits no definite sex or race predilection, has been found in middle-aged and elderly adults, except for one instance in a 7-year-old boy [16]. The clinical course is usually progressive (93%) with only occasional temporary remissions, and usually results in death (86%) within

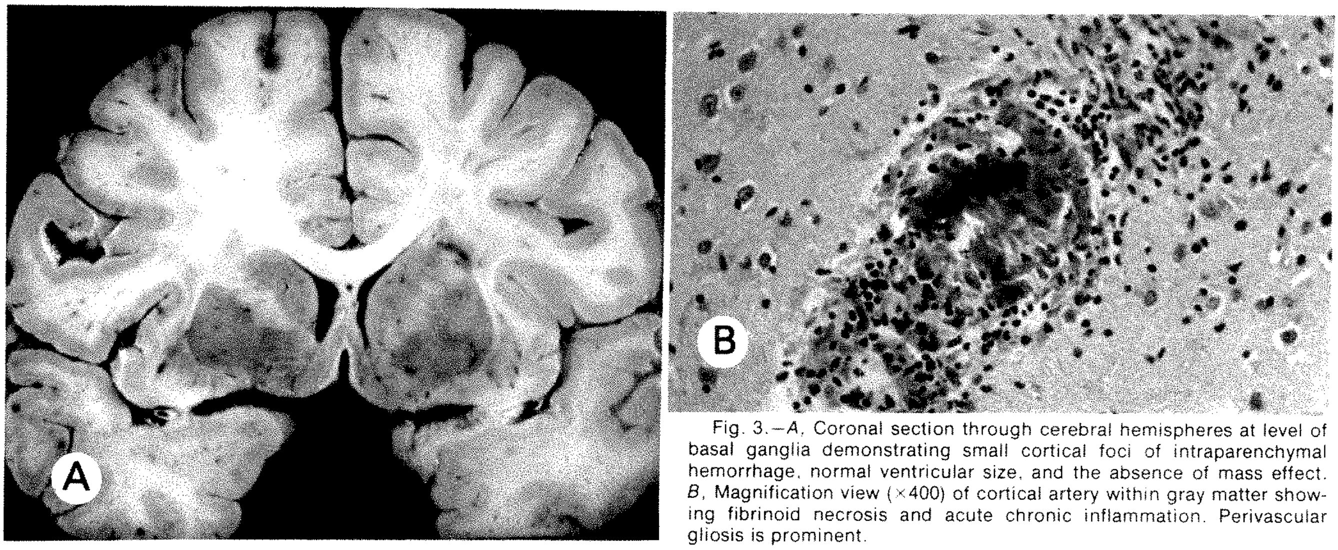

Fig. 3.—*A*, Coronal section through cerebral hemispheres at level of basal ganglia demonstrating small cortical foci of intraparenchymal hemorrhage, normal ventricular size, and the absence of mass effect. *B*, Magnification view (×400) of cortical artery within gray matter showing fibrinoid necrosis and acute chronic inflammation. Perivascular gliosis is prominent.

1 year (68%). Presenting symptoms are most commonly nonspecific disorientation, intellectual deterioration, and impairment of consciousness (69%). Only two cases [5, 6] had presenting features implicating primarily spinal cord involvement. Focal cerebral manifestations were noted in 19 patients. Granulomatous angiitis has been associated with lymphoma on five occasions [3, 4, 19, 20] and temporally related to herpes zoster infections five times [3-5, 9, 16].

Evidence of elevated intracranial pressure was recorded in 12 cases. Of the 23 cases in which the cerebrospinal fluid was analyzed, lymphocytosis was seen in 16, and the protein content was elevated in 17. None of the fluid cultures have been positive for microorganisms.

Diagnosis

Cerebral biopsy was attempted in six cases, but in only three [4, 19, 21] did the biopsy reveal the characteristic lesions of this entity. The low premortem diagnostic accuracy is probably also related to the segmental nature and rarity of the lesion and the relative lack of suggestive, well documented radiographic findings. In the radiologic literature, there is only one case of probable granulomatous angiitis [16]. Unfortunately, this case lacks pathologic confirmation and is atypical in a number of respects [9]. Although not illustrated, three reports [3, 4, 21] described angiographic demonstration of numerous segmental constrictions of the smaller distal intracerebral arteries. To our knowledge, our case is the first illustrated report of CT findings in this entity. Similar CT findings were described by Greco et al. [4], but not illustrated.

We believe that in the proper clinical setting, the angiographic evidence of intracranial, intradural, segmental vasculitis and the CT findings of diffuse, bilateral, poorly defined, non-contrast-enhancing low density areas are highly suggestive and may be specific for granulomatous angiitis. The CT findings are most consistent with cerebral edema and correlate with the proposed pathogenesis and gross pathology of granulomatous angiitis. The postmortem lack of mass effect in our case is probably related to the corticosteroid therapy.

Other neurological processes may produce similar CT findings. Cerebral infarctions most commonly produce patchy unilateral low density lesions on CT which tend to conform to the vascular distribution of the middle and posterior cerebral arteries. Infarctions usually involve both white and gray matter and extend to the cerebral surface in triangular or quadrangular patterns. Infarcts occasionally demonstrate mass effect and may enhance especially 1-4 weeks after clinical onset of symptoms [22-24]. Angiographic findings in cerebral infarction, although not always present, are well known and consist primarily of vessel occlusion, collateral circulation, luxury perfusion, retrograde arterial filling, early draining veins, and venous or dural thrombosis.

Central nervous system infection can present as single or multiple poorly defined low density lesions, located primarily at the junction of the gray and white matter. Granulomatous basal arachnoiditis may result in contrast enhancement of the basal cisterns [25]. When a cerebritis progresses to abscess formation, rimlike contrast enhancement occurs and mass effect is frequently seen [26, 27]. Angiographic findings of mass effect and perivascular blush may be noted, but not the changes of diffuse segmental vasculitis.

Primary and secondary brain tumors can produce focal or multifocal low density areas on CT scans. However, they usually have mass effect, show contrast enhancement, and may have the angiographic findings of tumor neovascularity [27-30].

Progressive multifocal leukoencephalopathy can produce low density nonenhancing lesions. However, they tend to be focal, limited to white matter, have a characteristic scalloped lateral border, and demonstrate no mass effect or angiographic findings [26]. Other demyelinating diseases, such as multiple sclerosis and the leukodystrophies, can produce low density lesions which may or may not be enhanced with contrast on CT scans [27, 28]. However, these also lack angiographic findings.

Segmental intracranial vasculitis can occur with bacterial and tuberculous meningitis but can be differentiated by clinical presentation, CT findings, and laboratory isolation of the pathogenic organism. Cerebral arteritis caused by sarcoid, chemicals, radiation, polyarteritis nodosa, rheumatic arteritis, Wegner's granulomatosis, allergic granulomatous angiitis, hypersensitivity angiitis, and arteritis secondary to methamphetamine can be distinguished by clinical presentation, laboratory findings, and multisystem involvement. Temporal (giant cell) arteritis can be differentiated by extradural and extracranial vascular involvement, markedly elevated erythrocyte sedimentation rate, temporal artery biopsy, and clinical presentation [31].

Therapy

Corticosteroid therapy is often effective in treating herpes zoster infections and cerebral edema. Seven patients with granulomatous angiitis received various forms and dosages of steroid therapy; variable degrees of temporally related clinical improvement were noted [4-9, 17, 19, 21, 32]. In one case [4] the combination of corticosteroid therapy, radiotherapy, and chemotherapy (nitrogen mustard, vincristine, prednisone, and procarbazine) resulted in complete clinical and radiologic remission.

ACKNOWLEDGMENTS

We thank Dr. Jeannette J. Townsend for neuropathologic consultation and Maria Faer and Pat Smith for assistance in manuscript preparation.

REFERENCES

1. Cravioto H, Feigin I: Noninfectious granulomatous angiitis with a predilection for the nervous system. *Neurology* 9:599-609, 1959
2. Nurick S, Blackwood W, Mair WGP: Giant cell granulomatous angiitis of the central nervous system. *Brain* 95:133-142, 1972
3. Rosenblum WI, Hadfield MG: Granulomatous angiitis of the nervous system in cases of herpes zoster and lymphosarcoma. *Neurology* 22:348-354, 1972
4. Greco AF, Kolins J, Rajjoub RK, Barreton HD: Hodgkin's disease and granulomatous angiitis of the central nervous system. *Cancer* 38:2027-2032, 1976
5. Kolodny EH, Rebeiz JJ, Caviness VS Jr, Richardson EP: Granulomatous angiitis of the central nervous system. *Arch Neurol* 19:510-524, 1968
6. Newman W, Wolf A: Non-infectious granulomatous angiitis involving the central nervous system. *Trans Am Neurol Assoc* 77:114-117, 1952
7. Churg J, Strauss L: Allergic granulomatosis, allergic angiitis, and periarteritis nodosa, *Am J Pathol* 27:277-301, 1951
8. Colover J: Sarcoidosis with involvement of the nervous system. *Brain* 71:451-475, 1948
9. Gilbert GJ: Herpes zoster ophthalmicus and delayed contralateral hemiparesis. *JAMA* 229:302-304, 1974
10. Goffinet DR, Glatstein E, Merigan TD: Herpes zoster-varicella infections and lymphoma. *Ann Intern Med* 76:235-240, 1973
11. Acers TE: Herpes zoster ophthalmicus with contralateral hemiplegia. *Arch Ophthalmol* 71:371-376, 1964
12. Anastasopoulos G: Ophthalmic herpes zoster with contralateral hemiplegia. *J Neurol Neurosurg Psychiatry* 21:210-212, 1958
13. Cope S, Jones AT: Hemiplegia complicating ophthalmic zoster. *Lancet* 2:898-899, 1954
14. Hughes WN: Herpes zoster of the right trigeminal nerve with left hemiparesis. *Neurology* 1:167-169, 1951
15. Laws HW: Herpes zoster ophthalmicus complicated by contralateral hemiplegia. *Arch Ophthalmol* 63:273-280, 1960
16. Walter RJ, Gammal TE, Allen MD: Cranial arteritis associated with herpes zoster—case report with angiographic findings. *Radiology* 107:109-110, 1973
17. Reyes MG, Fresco R, Chokroverty S, Salud EQ: Virus-like particles in granulomatous angiitis of the central nervous system. *Neurology* 26:797-799, 1976
18. Hughes JT, Brownell B: Granulomatous giant-celled angiitis of the central nervous system. *Neurology* 16:293-298, 1966
19. Rewcastle NB, Tom MI: Non-infectious granulomatous angiitis of the nervous system associated with Hodgkin's disease. *J Neurol Neurosurg Psychiatry* 25:51-58, 1962
20. Rottino A, Hoffman G: A sarcoid form of encephalitis in a patient with Hodgkin's disease—case report with review of the literature. *J Neuropathol Exp Neurol* 9:103-108, 1950
21. Griffin J, Price DL, Davis L, McKhann GM: Granulomatous angiitis of the central nervous system with aneurysms on multiple cerebral arteries. *Trans Am Neurol Assoc* 98:145-148, 1973
22. Davis KR, Taveras JM, New PFJ, Schur JA, Roberson GH: Cerebral infarction diagnosis by computerized tomography. *Am J Roentgenol* 124:643-660, 1975
23. Wing SD, Norman D, Pollock JA, Newton TH: Contrast medium enhancement of cerebral infarcts in computed tomography. *Radiology* 121:89-92, 1976
24. Yock DH Jr, Marshall WH Jr: Recent ischemic brain infarcts at computed tomography: appearances pre- and postcontrast infusion. *Radiology* 117:599-608, 1975
25. Enzmann D, Norman D, Mani J, Newton TH: Computed tomography of granulomatous basal arachnoiditis. *Radiology* 120:341-344, 1976
26. Carroll BA, Lane B, Norman D, Enzmann D: Diagnosis of progressive multifocal leukoencephalopathy by computed tomography. *Radiology* 122:137-141, 1977
27. Davis DO, Pressman GC: Computerized tomography of the brain. *Radiol Clin North Am* 12:297-313, 1974
28. Baker HL Jr, Campbell JK, Houser OW, Reese DF: Early experience with the EMI scanner for study of the brain. *Radiology* 116:327-333, 1975
29. New PFJ, Scott WR, Schnur JA, David KR, Taveras JM: Computerized axial tomography with the EMI scanner. *Radiology* 110:109-123, 1974
30. New PFJ, Scott WR, Schnur JA, David KR, Taveras JM, Hochberg FH: Computed tomography with the EMI scanner in the diagnosis of primary and metastatic intracranial neoplasms. *Radiology* 114:75-87, 1975
31. Enzmann D, Scott WR: Intracranial involvement of giant-cell arteritis. *Neurology*. In press, 1977
32. Harrison PE: Granulomatous angiitis of the central nervous system: case report and review. *J Neurol Sci* 29:335-341, 1976

Angiography in Vascular Malformations of the Face

G. B. BRADAC,[1] R. S. SIMON,[1] M. BUNTE,[2] AND R. STELLMACH[2]

While angiography has been established as a useful procedure in evaluating vascular malformations of the face, the role of selective catheterization has not been stressed. Five patients with either capillary-cavernous hemangiomas or arteriovenous racemose hemangiomas were selected to illustrate the angiographic features of vascular malformations of the face as well as problems in angiographic evaluation and therapeutic techniques. Angiographic studies were valuable in establishing the extent and type of hemangioma, its blood supply and drainage, and associated intraorbital or intracranial extensions. We believe that selective catheterization is essential in preoperative evaluation of facial hemangiomas, particularly in detecting unsuspected intracranial involvement.

In his study on angiomas of the scalp and face, Dandy [1] stressed the importance of identifying blood supply and the possibility of intracranial extension. Use of cerebral angiography has markedly improved preoperative evaluation. Although the advantages of angiography have already been described [2-6], some aspects have been neglected. We discuss the role of selective catheterization in visualizing blood vessel supply and drainage of malformations in estimating extend and type of angioma, and in evaluating possible additional intracranial malformations.

The pathomorphologic features of the various types of facial vascular malformations are: (1) capillary hemangioma (nevus flammeus) which is present at birth and located commonly in the nuchal region but seldom in the face; (2) immature hemangioma (nevus vasculosus) consisting of dilated capillaries, venules, and arterioles; (3) cavernous hemangioma made up of large vascular spaces composed of veins; and (4) arteriovenous racemose hemangioma (commonly called aneurysm) consisting of hypertrophic arteries in a circumscribed area with dilated draining veins.

Case Reports

Five patients were selected to illustrate the angiographic features of vascular malformations in the face as well as problems in angiographic evaluation.

Case 1

A 26-year-old male suffered from swelling of his left cheek and lower eyelid as well as multiple varicoselike telangiectases of the skin. The left upper lip was livid and infiltrated by a pulsatile angiomatous tumor which had led to a disturbing contortion of the mouth (fig. 1). A left external carotid arteriogram (figs. 2*A* and 2*B*) showed the hemangioma to be mainly supplied by branches of the facial and maxillary arteries. Venous drainage took place via the facial vein, an extraorbital vein continuing into the retromandibular vein, and via the superior ophthalmic vein. An internal carotid arteriogram (figs. 2*C* and 2*D*) demonstrated that the ophthalmic artery also joined in the supply. The angiographic and clinical findings showed this to be a capillary and partly cavernous hemangioma. Treatment was sclerosing followed by excision.

Comment. Angiography demonstrated the extent and type of the hemangioma and revealed an additional blood supply furnished by the internal carotid artery through the ophthalmic artery.

Case 2

A 34-year-old male suffered from hemangioma of the right cheek that had previously been treated by external carotid artery ligation. He was admitted following swelling of the cheek and a

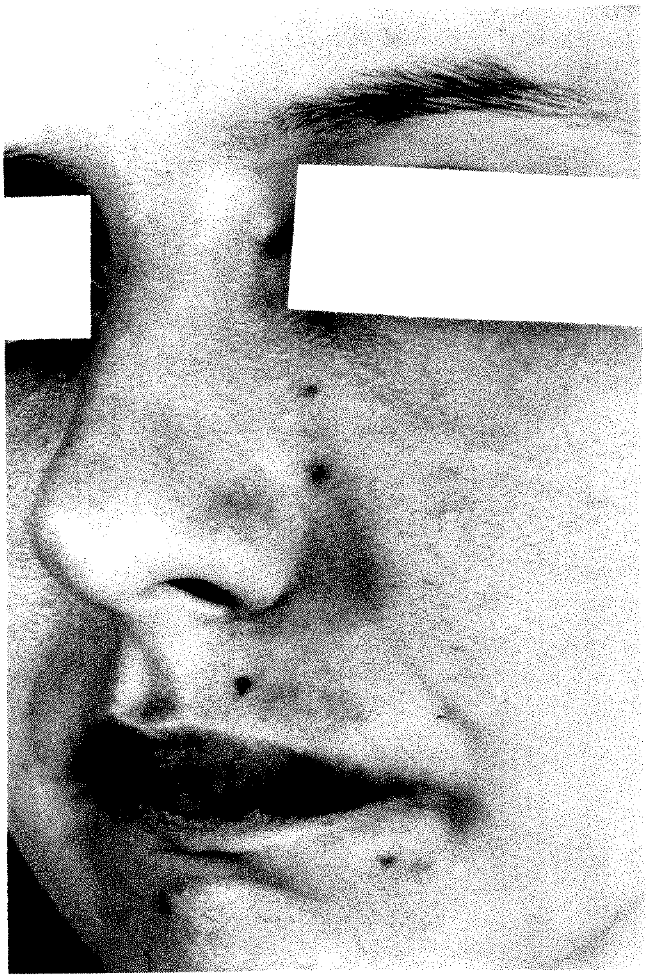

Fig. 1.—Case 1. Angioma of left cheek, lower eyelid, and upper lip.

Received October 28, 1976; accepted after revision April 12, 1977.

[1] Department of Radiology, Section of Neuroradiology, Klinikum Steglitz, Free University of Berlin, Hindenburgdamm 30, 1000 Berlin 45, Germany. Address reprint requests to G. B. Bradac.

[2] Department of Maxillo-Facial Surgery, Klinikum Steglitz, Free University of Berlin, Hindenburgdamm 30, 1000 Berlin 45, Germany.

Am J Roentgenol **129:469–475, September 1977**

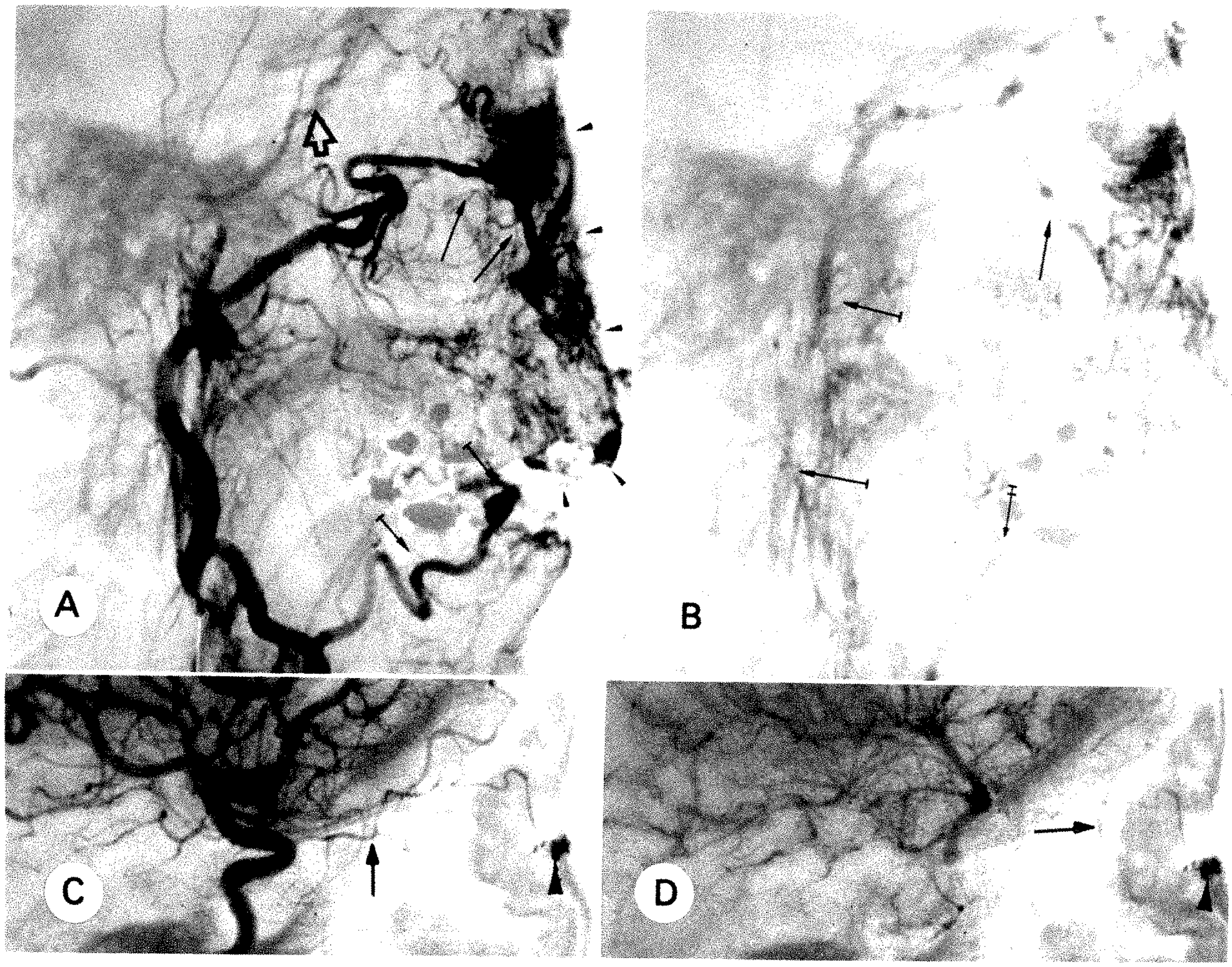

Fig. 2.—Case 1. *A and B,* External carotid arteriogram. *A,* Arterial phase showing angioma (*arrowheads*) primarily supplied by hypertrophied branches of internal maxillary artery, infraorbital artery (*arrows*), branches of temporal artery (*open arrow*), and by facial artery (*hatched arrows*). *B,* Venous phase showing drainage of angioma into superior ophthalmic vein (*arrowhead*), through transverse facial vein (*arrow*) into retromandibular vein (*hatched arrows*), and into facial vein (*double hatched arrow*). *C and D,* Internal carotid arteriogram. *C,* Arterial phase showing ophthalmic artery (*arrow*) partially supplying angioma (*arrowhead*). *D,* Capillary-venous phase showing angioma (*arrowhead*) and choroid blush (*arrow*).

marked exophthalmos with spontaneous hemorrhage from ectatic conjunctival vessels. Ophthalmic bulb motility was limited due to pain. An internal carotid arteriogram disclosed that the ophthalmic artery was largely responsible for the supply of the intra- and extraorbital hemangioma. The hemangioma of the cheek was not visible. Some branches of the ligated external carotid artery were filled retrograde from the internal carotid artery (fig. 3). The hemangioma of the orbit, seen by angiography, was not operated on. By angiographic criteria, the entity was a capillary hemangioma. The hemangioma of the cheek was treated with sclerosing and excision and found to be predominantly cavernous.

Comment. Diagnostic evaluation in this case was made difficult because preoperative angiography had not been performed before the external carotid artery ligation. Supply by the ophthalmic artery probably increased after the external carotid artery ligation. Angiographic demonstration of the hemangioma of the cheek was no longer possible.

Case 3

In this 37-year-old female, a hemangioma of the right upper eyelid had extended frontotemporally for 7 years. She was hospitalized because of additional headaches on the right side and a vascular murmur. A right external carotid arteriogram revealed that a hypertrophied superficial temporal artery was the main supply. Main drainage was through hypertrophied veins located lateral to the orbit and into the retromandibular veins. Partial drainage also occurred via the ophthalmic vein (fig. 4). A right internal carotid arteriogram showed that the hemangioma was also supplied by the ophthalmic artery with an intraorbital extension even though exophthalmos was not present (fig. 4C). At surgery, the malformation was excised and an angiographic diagnosis of arteriovenous racemose hemangioma was confirmed.

Comment. Angiography revealed we were dealing with an arteriovenous racemose hemangioma supplied by the external carotid and ophthalmic arteries. Despite absence of exophthalmos, the angioma extended into the orbit.

Case 4

Since birth, this 5-year-old female had a large livid hemangioma on the forehead, nose, and upper lip (fig. 5). There were no neurologic signs, and sclerosing had been the only treatment. Left external carotid arteriogram disclosed that only the

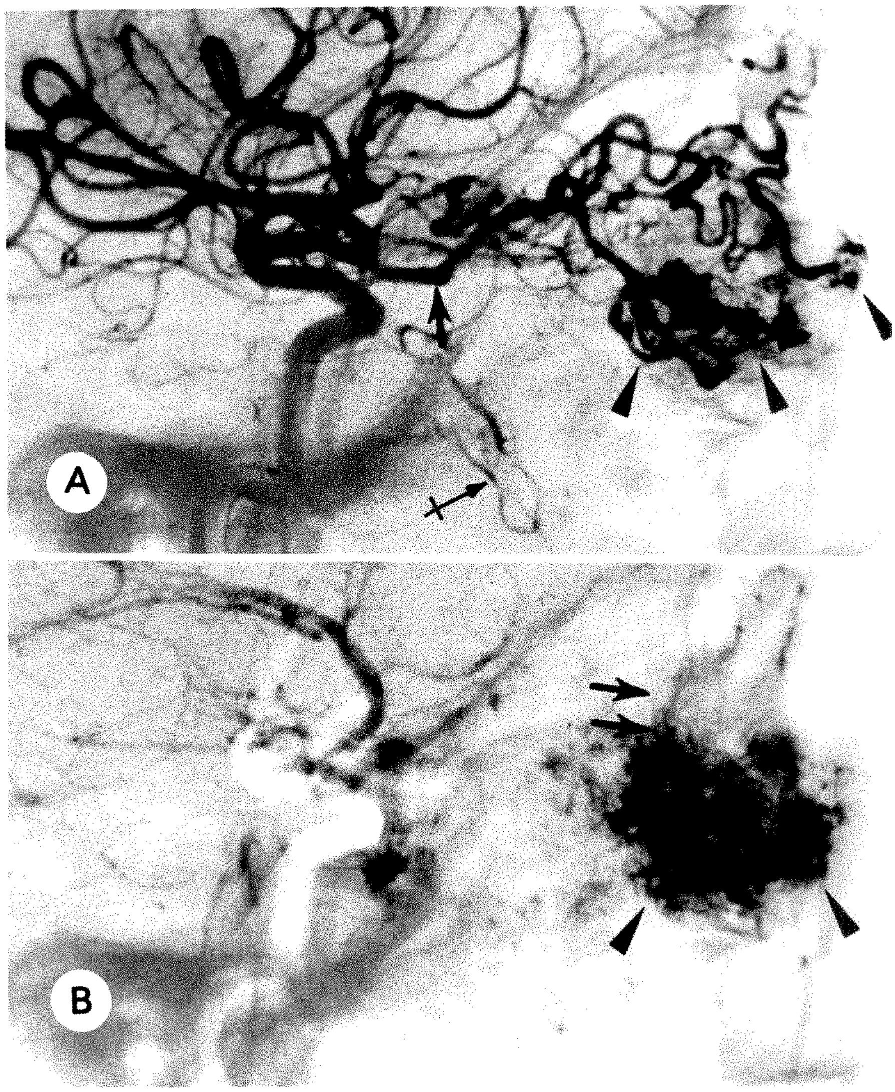

Fig. 3.—Case 2. Angioma of cheek and lower eyelid with intraorbital extension. Internal carotid arteriogram. *A*, Angioma (*arrowheads*) supplied by hypertrophied branches of ophthalmic artery (*arrow*). Note retrograde filling of some branches (*hatched arrow*) of external carotid artery. Vessel already ligated. *B*, Venous phase showing better filling of angioma (*arrowheads*). Note choroid blush (*arrows*).

supraorbital part of the hemangioma was supplied by the facial artery and the superficial temporal artery. While the hemangioma of the cheek was not recognizable, hypertrophied branches of the facial artery were. Drainage occurred from the facial vein and from veins running laterally to the orbit into the retromandibular veins. In addition, there was drainage into the superior ophthalmic vein (fig. 6). A left internal carotid arteriogram showed a normal ophthalmic artery but a large arteriovenous racemose angioma intracranially at the base of the anterior fossa (fig. 6*E*). The right carotid arteriogram was normal. By angiographic criteria, this was a capillary-venous and probably cavernous hemangioma. No therapy was performed at this time for the intracranial malformation.

Comment. Angiography revealed a unilateral supply of this hemangioma, although it reached the midline. Only the superior portion was recognizable. The intracranially located angioma was unexpected because of absence of neurologic signs.

Case 5

A 62-year-old male underwent surgery because of a port wine colored stain on the right cheek. During the previous 2 years, swelling of the left upper jaw developed. When a massive hemorrhage followed a tooth extraction, he was hospitalized. Neurological status was normal. Radiographs showed an evenly limited large oval bone defect corresponding to the tumor site. Because of general vascular sclerosis, selective catheterization was omitted; the catheter tip was positioned in the common carotid artery. Circulation of both the external carotid artery bilaterally and the right internal carotid artery was normal. The left internal carotid arteriogram revealed an arteriovenous angioma intracranially at the base of the anterior fossa (fig. 7). The patient was treated by sclerosing and excision of a capillary-venous and predominantly cavernous hemangioma. The intracranial angioma was not treated.

Comment. Although angiography failed to demonstrate the facial hemangioma, it did demonstrate a second intracranial angioma.

Discussion

Angiography enables differentiation of the following features:

1. In capillary and cavernous hemangiomas, the feeding arteries are seldom dilated. Pathologic vessels may fill during the arterial and/or capillary phases. Occasionally filling may not occur. Capillary and cavernous he-

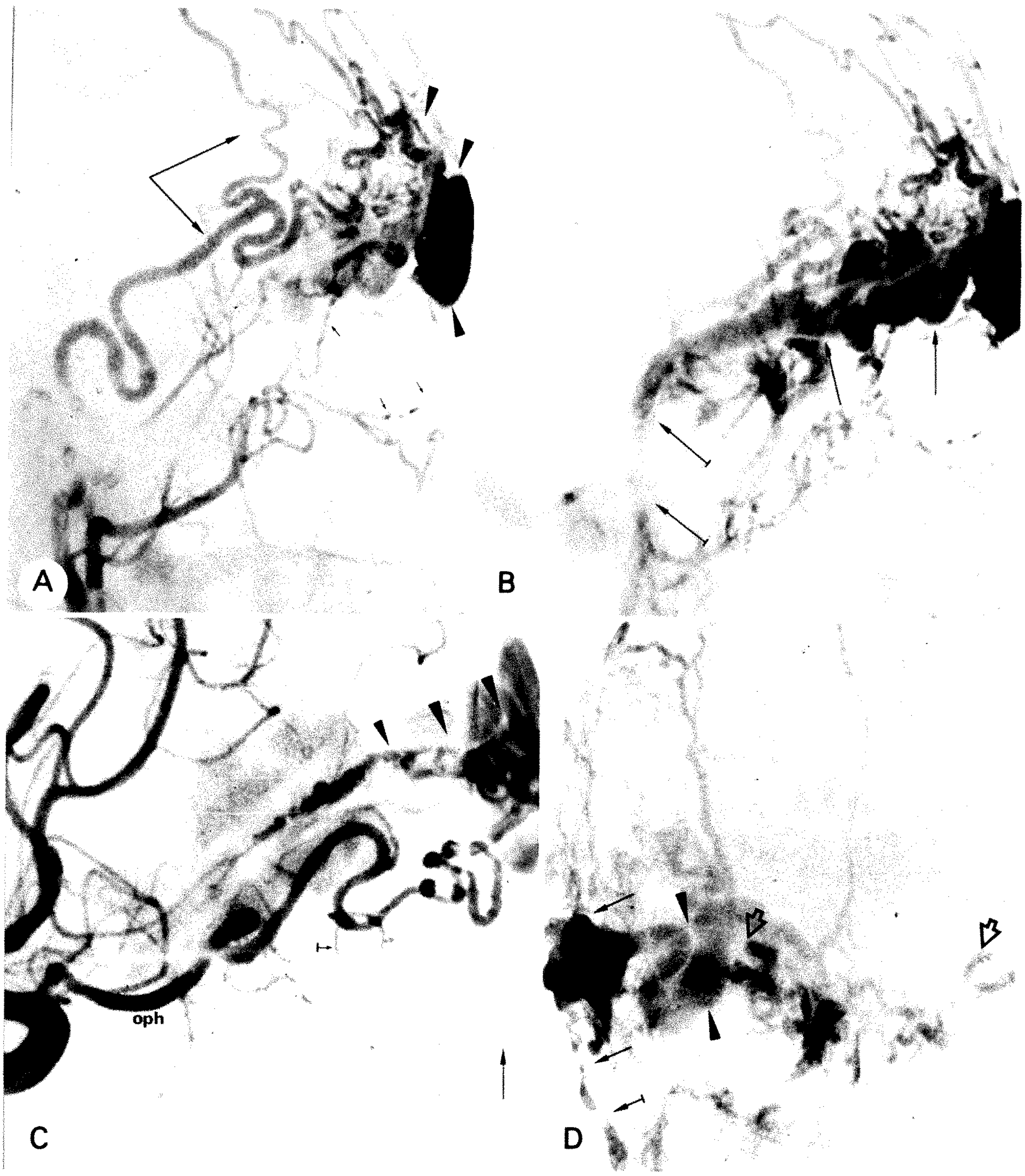

Fig.4.—Case 3. Arteriovenous angioma of orbital and supraorbital region. *A and B*, External carotid arteriogram. *A*, Angioma (*arrowheads*) supplied primarily by hypertrophied branches (*joined arrows*) of superficial temporal artery. Note supply from maxillary artery branches (*small arrows*). *B*, Drainage into hypertrophied frontotemporal vein (*arrows*) flowing into retromandibular vein (*hatched arrows*). Superior ophthalmic vein not visualized. *C*, Internal carotid arteriogram showing angioma supplied by branches of ophthalmic artery (oph). Note intraorbital extension of angioma (*arrowheads*). Branches of ophthalmic artery (*arrow*) in lateral extraorbital region supply portion of angioma. Note choroid blush (*hatched arrow*). *D*, Anteroposterior view of external carotid arteriogram, venous phase. Note drainage of angioma (*arrowheads*) into frontotemporal vein (*arrows*) and retromandibular vein (*hatched arrow*). Angioma drains bilaterally by superior ophthalmic vein (*open arrows*).

mangiomas are often associated; what is commonly seen is the capillary portion, so when the hemangioma is mainly cavernous, it may not be directly visible. Veins fill slowly and are seldom dilated.

2. In arteriovenous racemose hemangiomas, feeding arteries always are hypertrophied; draining veins fill early and are dilated.

Venous drainage in both groups is by extracranial

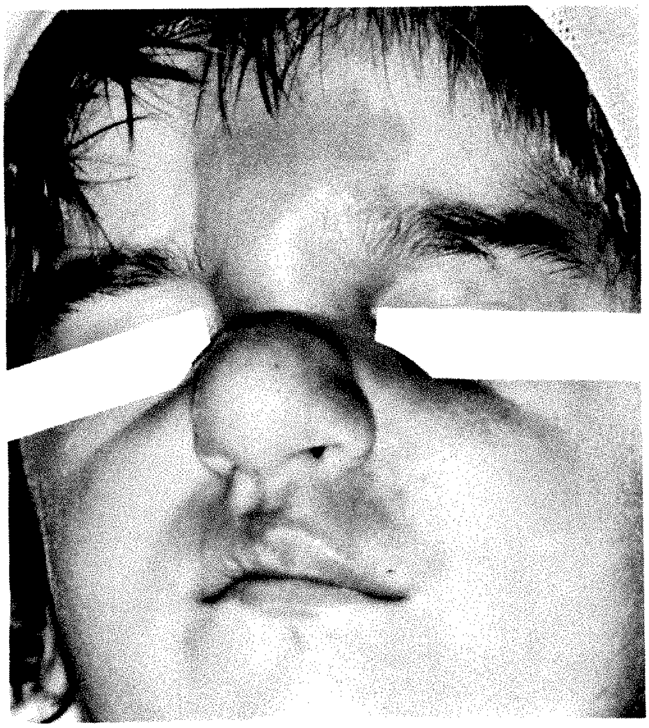

Fig. 5.—Case 4. Angioma of forehead, nose, and upper lip.

veins and often by the superior ophthalmic vein draining into the cavernous sinus. Normally the superior ophthalmic vein is recognizable in external carotid arteriograms [7]; its large size in patients with facial angiomas is probably an adaptation in response to the increased load.

Angiography provides unique information in the following settings. In a hemangioma clinically limited to the face, ophthalmic artery blood supply can sometimes be demonstrated. In cases without clinical exophthalmos, angiography can detect possible intraorbital extension. Finally, an independent second intracranial hemangioma can be detected angiographically.

Occasionally, angiography may fail, such as with case 2 who was examined after external carotid artery ligation. In similar cases studied after external carotid artery ligation, Djindjian et al. [8–10] reported that the malformation was supplied by branches of the subclavian or the vertebral artery. In addition, radiotherapy and injection of sclerosing pharmaceuticals may lead to alterations that make comprehensive angiographic assessment more difficult. Generally, angiography should be performed before therapeutic intervention.

Clinically evident hemangiomas which are not recognizable angiographically are a further diagnostic problem. In one patient (case 5), the surgically confirmed hemangioma could not be demonstrated. Due to the patient's overall sclerotic vascular system, the catheter tip was positioned in the common carotid artery for injection of contrast medium. It remains uncertain whether a superselective filling of the corresponding branches of the external carotid artery would have demonstrated this hemangioma. In case 4, only a small portion of the hemangioma could be demonstrated, although several pathologically hypertrophied arteries could be seen in the external carotid arteriogram. It was assumed that a capillary-venous and probably cavernous hemangioma was present. The possibility of better demonstration after superselective probing of the pathologic vessels as demonstrated by others [10] remains uncertain.

External carotid artery ligation is not adequate treatment. In cases of large angiomas, some branches may fill retrograde. In other cases, blood supply may develop from the ophthalmic artery. In our opinion, initial treatment in capillary and cavernous angiomas should be by direct percutaneous injection of sclerosing solutions. Some authors [11] have reported good results with embolization using Gelfoam following selective angiography. However, this method involves risk, since emboli may enter the internal carotid artery by retrograde flow [8, 9]. We are now studying the use of intraarterially injected sclerosing solutions. Previously we have treated cases of predominantly racemose hemangioma with extirpation. We now believe that embolization with Gelfoam is an appropriate therapeutic technique since emboli follow the predominant flow to the hemangioma, as previously described [8–11].

REFERENCES

1. Dandy WE: Arterio-venous aneurysms of the scalp and face. *Arch Surg* 52:1-32, 1946
2. Bories J, Natali J: Radiologic examination in head and neck localizations of arterio-venous fistulae and congenital aneurysms. *J Cardiovasc Surg* 8:209-215, 1967
3. Brahme F, Jacobson S: Arterio-venous fistulae of face: report of two cases. *Acta Chir Scand* 131:223-225, 1966
4. Thomas ML, Andress MR: Angiography in angiomas of the face. *Am J Roentgenol* 112:332-338, 1971
5. Malan E, Azzolini A: Congenital arterio-venous malformations of face and scalp. *J Cardiovasc Surg* 9:109-140, 1968
6. Stellmach R, Bradac GB, Bunte M, Simon RS: The importance of serial angiography and subtraction for the operative indication in hemangiomas of the facial region. *Dentomaxillofacial Radiol* 2:1-4, 1973
7. Bradac GB, Simon RS, Leonhardt W: The ophthalmic vein in the carotid angiogram. *Neuroradiology* 8:39-47, 1974
8. Djindjian R: Indications, contre indications, accidents, incidents dans l'embolisation de la carotide externe. *J Neuroradiologie* 2:173-200, 1975
9. Djindjian R, Merland J, Theron J: L'arteriographie superselective (A.S.S.) et l'embolisation dans les épitaxis graves. *Ann Otolaryngol Chir Cervicofac* 93:23-33, 1976
10. Merland JJ, Djindjian R: Technique et resultats de l'embolisation des angiomes du territoire carotidien externe. *J Neuroradiologie* 2:201-232, 1975
11. Djindjian R, Cophignon J, Theron J, Merland J, Houdart R: Embolization by superselective arteriography from the femoral route in neuroradiology. Review of 60 cases. *Neuroradiology* 6:20-26, 1973

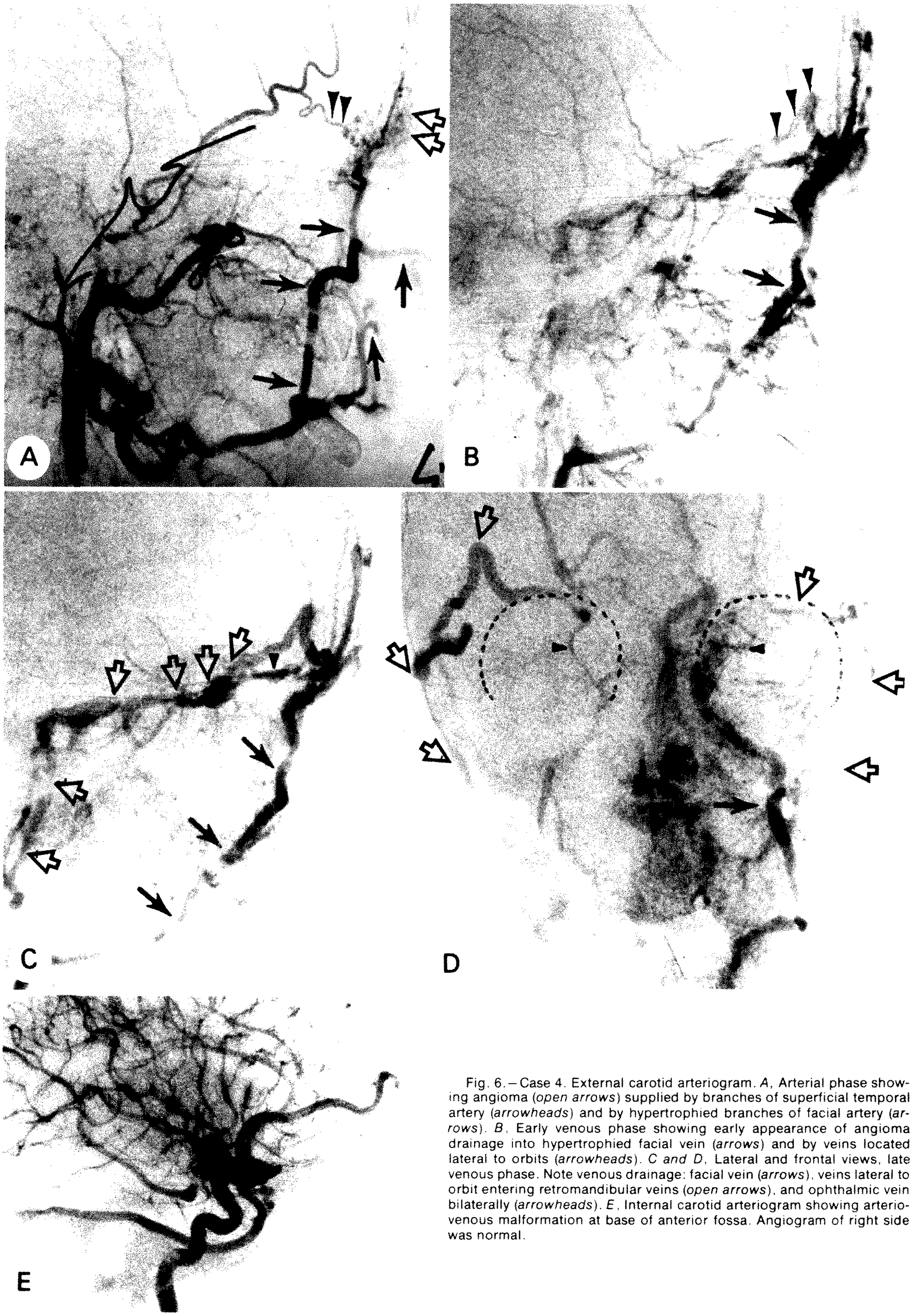

Fig. 6.—Case 4. External carotid arteriogram. *A*, Arterial phase showing angioma (*open arrows*) supplied by branches of superficial temporal artery (*arrowheads*) and by hypertrophied branches of facial artery (*arrows*). *B*, Early venous phase showing early appearance of angioma drainage into hypertrophied facial vein (*arrows*) and by veins located lateral to orbits (*arrowheads*). *C and D*, Lateral and frontal views, late venous phase. Note venous drainage: facial vein (*arrows*), veins lateral to orbit entering retromandibular veins (*open arrows*), and ophthalmic vein bilaterally (*arrowheads*). *E*, Internal carotid arteriogram showing arteriovenous malformation at base of anterior fossa. Angiogram of right side was normal.

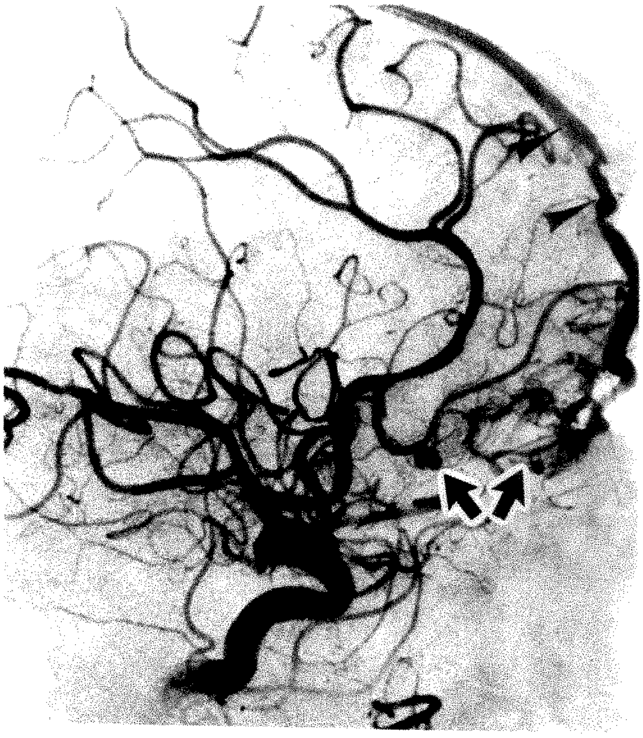

Fig. 7.—Case 5. Angioma of left cheek. Common carotid arteriogram showing arteriovenous angioma at base of anterior fossa (*arrows*) with venous drainage into superior sagittal sinus (*arrowheads*). No pathology was noted in area supplied by external carotid artery.

Angiographic Observations on Chemodectomas of the Head and Neck

STANLEY F. HANDEL,[1] MARK H. MILLER,[1] SIDNEY WALLACE,[1] HELMUTH GOEPFERT,[2] AND RICHARD H. JESSE[2]

Angiographic experience with chemodectomas in 21 patients is reviewed. Arterial supply was identified from the vertebral artery, the internal carotid artery, and branches of the external carotid artery. A striated cephalad extension from a cervical chemodectoma (five patients) is believed to represent arterial supply to tumor in vein. In two patients, internal and external carotid arteriograms did not opacify important arteries originating near the carotid bifurcation. Retrograde filling of sigmoid sinus (four patients), tumor mass in jugular vein (two patients), and arteriovenous shunting (nine patients) were observed during the venous phase. Thorough angiography is essential for evaluation of chemodectomas of the head and neck.

Angiography is essential for the diagnosis and evaluation of chemodectomas (nonchromaffin paragangliomas) of the head and neck. Blood supply, size, and extent of tumor are the critical aspects demonstrable by angiography and are the basis for a successful therapeutic plan. Moreover, other unsuspected primary or metastatic chemodectomas may also be identified, thereby influencing treatment.

In reviewing our angiographic experience with head and neck chemodectomas, we noted several angiographic findings which we believe are helpful in better defining the blood supply of chemodectomas and the presence and extent of venous invasion. We present these findings and stress the need for thorough angiographic study of chemodectomas of the head and neck.

Case Material

Cervicocerebral angiograms of 21 patients with chemodectomas of the head and neck were reviewed retrospectively. This comprised all patients with this diagnosis seen between 1963 and 1976 for whom angiograms were available for review. When possible, all angiogram films were examined, although in some instances only selected teaching file films could be obtained. Unilateral carotid angiograms were obtained in 11 cases, and bilateral carotid angiograms in four patients. Bilateral carotid and unilateral vertebral angiograms were available for five patients, and one patient had unilateral carotid and unilateral vertebral angiography. Repeat angiography after radiation therapy was performed on three patients. Histologic confirmation was obtained in 17 cases. In the other four cases the diagnosis of chemodectoma was presumptive, based on the typical angiographic appearance and location.

Findings

A total of 25 chemodectomas of the head and neck were demonstrated in the 21 patients; four patients had tumors bilaterally. One of these four patients also had a third chemodectoma at the aortic arch. Of the 25 head and neck tumors, seven were at the skull base involving the jugular fossa (glomus jugulare tumors); five were above the carotid bifurcation, but below the skull base (glomus vagale tumors); seven were at the carotid bifurcation (carotid body tumors); and six tumors were not clearly definable as one of the above, since they extended as a single tumor mass from the region of the carotid bifurcation to the jugular fossa. We term these latter tumors confluent cervical chemodectomas. Absence of small glomus tympanicum tumors from our series reflects the referral nature of the hospital from which the bulk of the case material was derived (M. D. Anderson Hospital and Tumor Institute). There were no malignant or metastatic chemodectomas in our series.

In the arterial phase of angiography, the major branches of the external carotid artery (except for the lingual and facial arteries) could be identified in one patient or another as supplying tumor. Of particular interest were three patients in whom important supply originated from the superior thyroid artery (fig. 1). Vertebral artery supply was seen in four of the six patients with vertebral angiograms, and supply from meningeal branches of the internal carotid artery was demonstrable in two instances. In five patients, thin striated cephalad extensions from a lower cervical tumor bulk were seen (fig. 2). We believe that this represents the arterial supply of tumor extending into a vein.

In the venous phase, retrograde filling of the sigmoid sinus was noted in four patients. Nine patients had arteriovenous shunting. Two other patients had a filling defect of tumor seen in the otherwise opacified jugular vein (fig. 3).

Changes in angiographic appearance in three patients after radiotherapy are reported in greater detail separately [1]. The changes included decrease in tumor size, size of supply arteries, venous shunting, and tumor opacification.

Discussion

Numerous reports deal with the value of angiography for chemodectomas [2–10]. Others also stress the need for vertebral angiography on the ipsilateral side of the cervical chemodectoma, and the need for selective external carotid and internal carotid angiography [11–14]. Vascular supply to chemodectomas has been reported

---

Received April 8, 1977; accepted June 3, 1977.

Presented at the annual meeting of the American Society of Neuroradiology, Atlanta, Georgia, May 1976.

[1] Department of Diagnostic Radiology, University of Texas System Cancer Center, M. D. Anderson Hospital and Tumor Institute, 6723 Bertner Avenue, Houston, Texas 77030. Address reprint requests to S. F. Handel.

[2] Department of Surgery, University of Texas System Cancer Center, M. D. Anderson Hospital and Tumor Institute, Houston, Texas 77030.

Am J Roentgenol **129:477-480, September 1977**

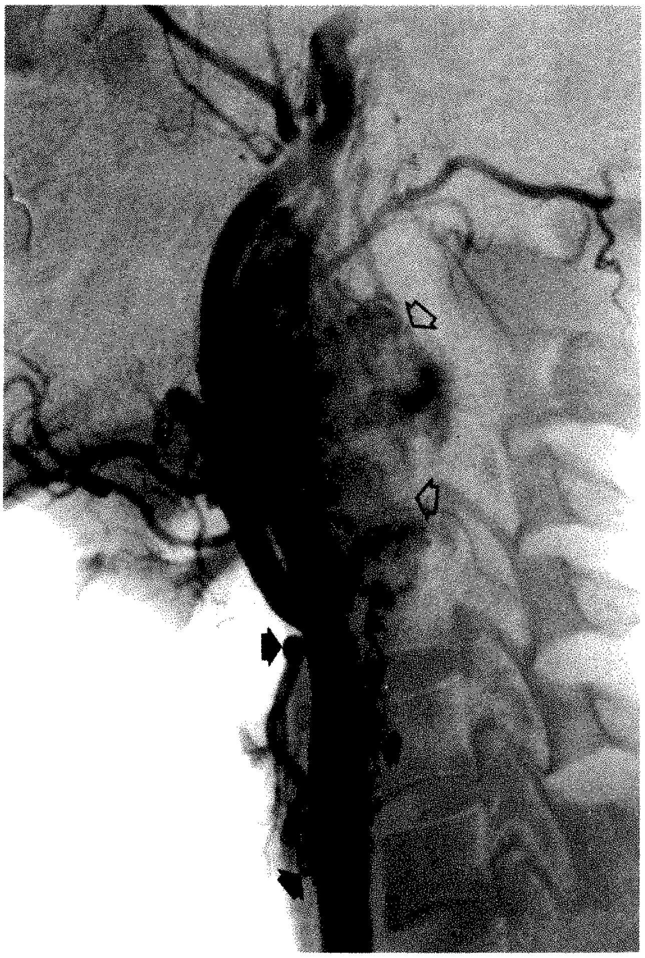

Fig. 1.—Lateral common carotid angiogram showing superior thyroid artery (*closed arrows*) originating just below common carotid bifurcation and supplying high cervical chemodectoma (*open arrows*).

from "multiple small vessels from the external, internal and common carotid arteries" [9]; the ascending pharyngeal and stylomastoid arteries and small branches of the maxillary arteries [13]; posterior auricular artery and small branches of the internal carotid artery [6, 13, 14]; and the vertebral artery [11–14].

Our experience confirms the multiplicity of arterial supply to chemodectomas and the need for thorough cervicocerebral angiography in these patients. Two of our four patients with bilateral tumors were clinically suspected, until undergoing angiography, of having only unilateral tumors. Demonstration of vertebral artery supply in four of our six patients with vertebral angiography similarly demonstrates that unilateral carotid examination is not adequate for assessment of chemodectomas. Moreover, we believe that had more vertebral angiography been performed in our series, additional instances of vertebral artery supply may have been found.

Superior thyroid artery supply to cervical chemodectomas, to our knowledge, has not been reported previously. Awareness of such supply is important, due to the usual origin of the superior thyroid artery from the common carotid artery just proximal to the bifurcation or from the proximal external carotid artery. In such patients, selective internal and external carotid injections may fail to opacify the superior thyroid artery, and thus not demonstrate the extent of tumor and its blood supply. In one of our cases the tumor size was not appreciated with selective artery injections until the catheter was pulled lower into the common carotid artery and the superior thyroid artery visualized. Similarly, we had one patient in whom origin of the ascending pharyngeal artery at the carotid bifurcation necessitated a common carotid injection to demonstrate this important contribution to a glomus jugulare tumor.

Often accurate delineation of the precise arteries supplying a large tumor is difficult due to superimposition, although superselective angiography can eliminate this problem. While thyrocervical or costocervical arterial injections were not performed in any of our cases, examination of these arteries may also be necessary in selected patients.

Extension of various tumors into veins is a common finding at surgery and at postmortem examination. Radiographic evidence of venous extension of tumor was dependent on venography until Kahn [15] described a patient with abnormal vessels within a hypernephroma growing along the renal vein into the inferior vena cava. Subsequently, Ferris et al. [16] and Gregg et al. [17] described patients with hypernephroma, hepatocellular carcinoma and retroperitoneal sarcoma in whom angiography demonstrated a linear striated arterial pattern in the course of a vein. Gregg et al. [17] believed that this was reliable evidence of vascular supply to intravenous neoplasm. Microscopic examination of their pathologic material suggested that the striated vessels were enlarged venous vaso vasorum supplying intravenous extension of tumor.

While we do not have pathologic proof, we believe that the striated vascular pattern extending cephalad along the course of the jugular vein from a cervical tumor in five of our patients represents intravenous extension of chemodectoma. Additionally, striking evidence of venous extension of tumor was seen in two other patients in whom the negative defect of tumor was seen in opacified jugular vein in the venous phase of the angiogram. In neither case was a striated vascular arterial pattern present. This indicates that absence of this striated pattern does not exclude venous invasion. A more indirect angiographic sign of jugular vein involvement is retrograde filling and flow in the sigmoid sinus, as seen in four of our cases. However, this may be due to involvement of the vein either by invasion or simply by compression.

In our series arteriovenous shunting was common, occurring in nine patients (43%). This sign obviously is not an indication of malignancy since none of these patients had malignant chemodectomas. However, presence of direct shunting into intracranial veins and dural sinuses suggests involvement of skull base or meninges and perhaps cerebral blood supply.

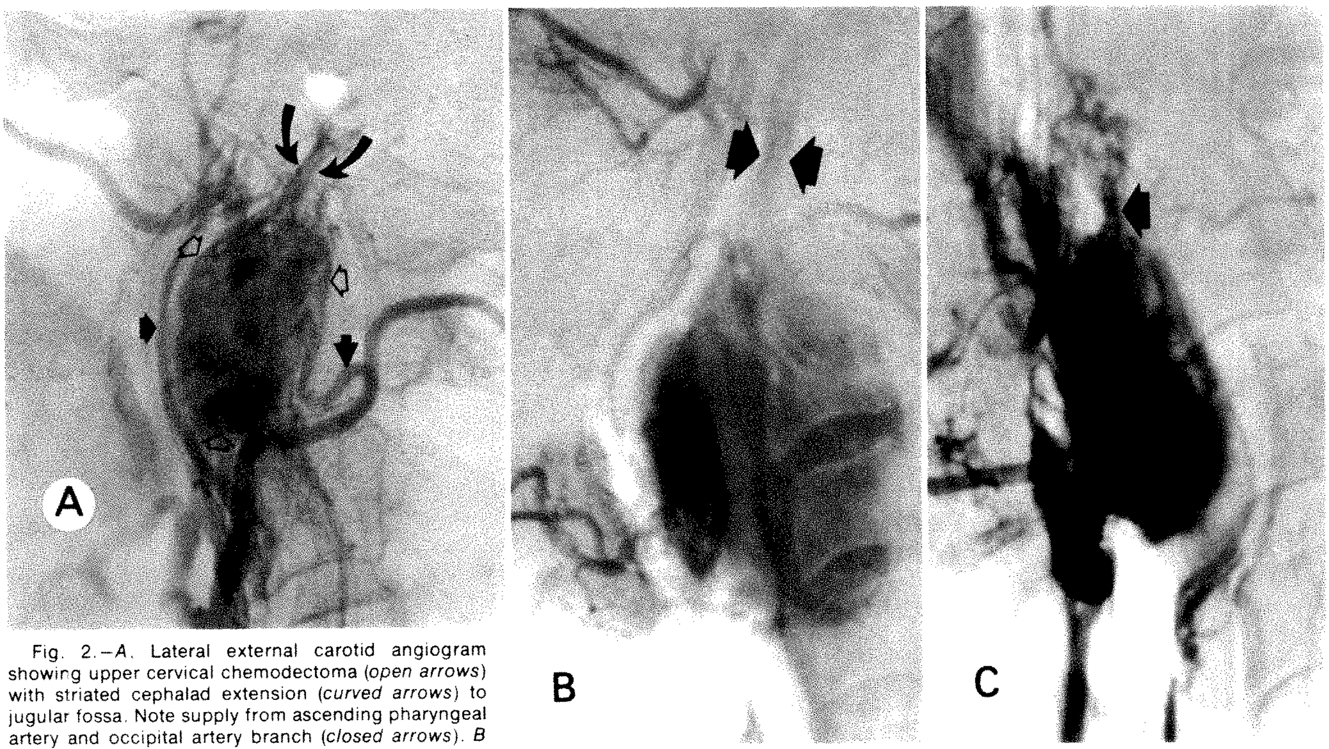

Fig. 2.—*A*. Lateral external carotid angiogram showing upper cervical chemodectoma (*open arrows*) with striated cephalad extension (*curved arrows*) to jugular fossa. Note supply from ascending pharyngeal artery and occipital artery branch (*closed arrows*). *B* and *C*. Lateral external carotid angiograms of two other patients showing striated stain extending upward from cervical tumors (*arrows*).

Fig. 3.—*A*. Venous phase of lateral carotid angiogram showing chemodectoma outlined within partially opacified internal jugular vein. *B*. Lateral internal jugular venogram showing tumor as filling defect in opacified vein. Mass identical in size and position to that seen in venous phase of angiogram (*A*). (Courtesy of Dr. Ken Jensen, St. Joseph's Hospital, Houston, Tex.)

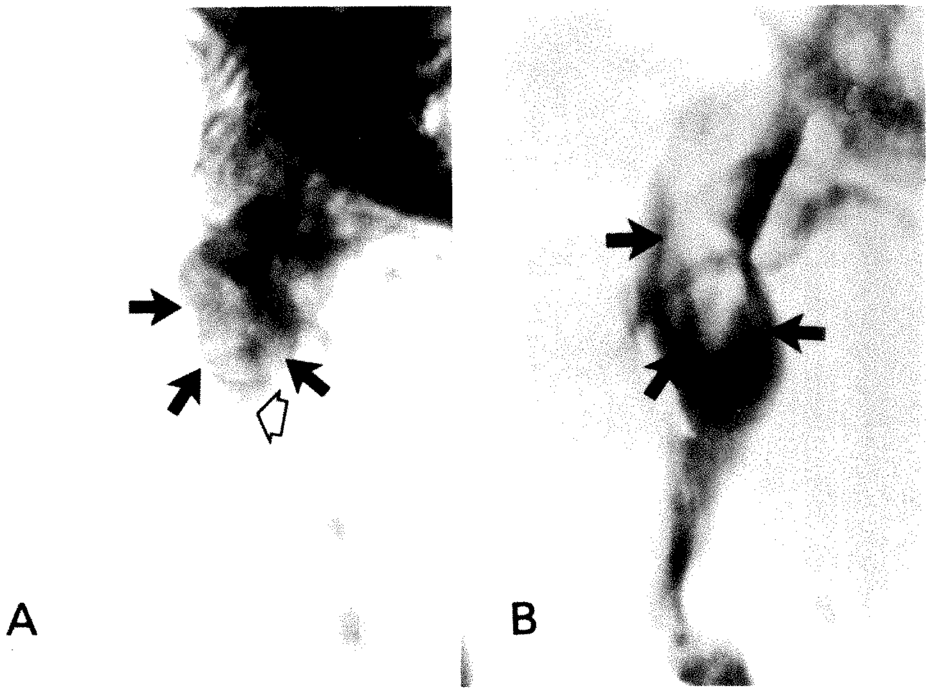

Computed tomography will undoubtedly become an important tool for the diagnosis and evaluation of head and neck chemodectomas. However, for the foreseeable future, angiography remains the most effective method for demonstration of the blood supply to these tumors. Only with thorough angiography, using selective and superselective catheterization techniques, can the location, extent, blood supply, and number of tumors be adequately defined for the surgeon or radiotherapist. Moreover, selective and superselective diagnostic catheter techniques are the prelude to embolization procedures for those patients in whom it is indicated.

REFERENCES

1. Handel SF, Miller MH, Miller LS, Geopfert H, Wallace S: Angiographic changes of head and neck chemodectomas following radiotherapy. *Arch Otolaryngol* 103:87-89, 1977
2. Berrett A: Value of angiography in the management of tumors of the head and neck. *Radiology* 84:1052-1058, 1965
3. Conley JJ: The management of carotid body tumors. *Surg Gynecol Obstet* 117:722-732, 1963
4. Conley JJ, Chusid JG, Schechter MM: Angiography in head and neck surgery. *Arch Surg* 89:609-618, 1964
5. Gehweiler JA, Bender WR: Carotid arteriography in the diagnosis and management of tumors of the carotid body. *Am J Roentgenol* 104:893-898, 1968
6. Jordan CE, Newton TH: Internal carotid artery supply to temporal bone chemodectomas. *Neuroradiology* 8:253-257, 1975
7. Medellin H, Wallace S: Angiography in neoplasms of the head and neck. *Radiol Clin North Am* 8:307-321, 1970
8. Myers EN, Newman J, Kaseff L, Black FO: Glomus jugulare tumor—a radiographic-histologic correlation. *Laryngoscope* 81:1838-1851, 1971
9. Schechter MM, Chusid JG: Chemodectomas of the carotid bifurcation. *Acta Radiol [Diagn] (Stockh)* 5:488-508, 1966
10. Staats EF, Brown RL, Smith RR: Carotid body tumors, benign and malignant. *Laryngoscope* 76:907-916, 1966
11. El Gammal MB: The blood supply of chemodectomas of the head and neck: report of two cases. *Br J Radiol* 44:515-518, 1971
12. Farrell VS, Hawkins TD: Glomus jugulare tumors with special reference to their radiological features. *Br J Surg* 54:789-795, 1975
13. Hawkins TD: Glomus jugulare and carotid body tumors. *Clin Radiol* 12:199-213, 1961
14. Palacios E: Chemodectomas of the head and neck. *Am J Roentgenol* 110:129-140, 1970
15. Kahn PC: The epinephrine effect in selective renal angiography. *Radiology* 85:301-305, 1965
16. Ferris EJ, Bosniak MA, O'Connor JF: An angiographic sign demonstrating extension of renal carcinoma into the renal vein and vena cava. *Am J Roentgenol* 102:384-391, 1968
17. Gregg FP, Goldstein HM, Wallace S, Casey JH: Arteriographic demonstration of intravenous tumor extension. *Am J Roentgenol* 123:100-105, 1975

Metrizamide Myelography

WAYNE R. BOYD[1] AND GEOFFREY A. GARDINER, JR.[1]

Complete myelography using metrizamide and a lumbar puncture is described with special emphasis on the cervical region. Good visualization of the cervical region was obtained in 19 of 20 patients using 10-12 ml and iodine concentrations of 250 mg/ml without special techniques or precautions. Possible explanations of failure to visualize the complete subarachnoid space are discussed.

A new contrast agent for use in positive contrast myelography is currently being investigated. The most commonly used agent now available in the United States is Pantopaque (ethyl iodophenylundecuilate), an oily medium introduced in 1940. Metrizamide, a new water soluble nonionic compound, has been used for several years in Scandinavia with good results. The neurotoxicity and central nervous system irritability are much lower than with previously used water soluble agents [1-4].

One problem in using a water soluble agent has been the lack of adequate cervical and thoracic visualization when the contrast medium is introduced into the lumbar region, preventing a complete myelographic study with one puncture [5]. In preliminary evaluation of metrizamide for use in myelography at our institution, results indicate that an adequate cervical and thoracic myelogram is possible in almost all cases using a lumbar puncture. Excellent to good quality complete myelograms were obtained without sophisticated equipment or unusual techniques (fig. 1).

Materials and Methods

Our series consisted of 45 patients. Only in the last 20 was a concerted attempt made to study the cervical and thoracic regions using a lumbar puncture, because it had been our initial opinion that a satisfactory study could not be obtained.

In the 20 patients in whom complete myelographic examination was attempted with lumbar puncture, a brief neurologic examination was performed before and 24 hr after myelography. Vital signs were taken before and up to 6 hr after myelography. The patient received premedication, usually 0.4 mg atropine and 10 mg Valium intramuscularly. He was placed in a prone position on the x-ray table.

The point of entry was fluoroscopically located; the skin was prepared with tinted aqueous Zephiran and cleaned with an alcohol swab. The area was then draped and a 22 gauge spinal needle was introduced into the subarachnoid space under fluoroscopic control. In most cases the lumbar puncture was performed at the L3-L4 interspace; however, occasionally the L2-L3 and L4-L5 interspaces were used. About 10-12 ml of spinal fluid was withdrawn, and about 10-12 ml (17 ml in one case) of metrizamide (250 mg I/ml) was injected very slowly into the subarachnoid space, usually over a period of at least 3-5 min; then the needle was withdrawn.

Cross-table lateral, oblique, and anteroposterior views of the lumbar subarachnoid space were obtained while the patient was in a nearly upright position. The head of the table was then lowered, and anteroposterior views of the low and midthoracic subarachnoid space were obtained as the contrast material flowed to the cervical region. With the patient's head in a support and extended as much as possible, cross-table lateral, anteroposterior, and oblique views were obtained of the cervical region. The head of the table was elevated and an anteroposterior radiograph of the upper thoracic region was taken. The patient was then requested to remain in an upright or semi-upright position for the next 8 hr.

No special attempts were made to avoid moving the patient. Oblique views were obtained by having the patient turn on one side and then the other. However, excessive motion was avoided to prevent unnecessary mixing and dilution of the contrast material.

Results

Of the 20 cases in our study who underwent complete myelography after lumbar puncture, opacification of the cervical subarachnoid space was graded as excellent (dense opacification) in 13 cases, good (adequate opacification) in six, and poor (borderline or inadequate opacification) in one. In all cases, visualization of the lumbar region was excellent; in all but one case (see below), visualization of the thoracic region was excellent. The studies were reviewed in collaboration and independently and were graded according to the lowest grade given. Visualization qualities of the nerve roots and sleeves, the subarachnoid space, and the spinal cord was used as criteria for grading (figs. 2 and 3).

In the one case of poor cervical visualization, the concentration of contrast material was inadequate because of an abnormally large subarachnoid space. In another patient, several areas of moderately severe stenosis were present in the upper lumbar level. Inadequate visualization of the thoracic canal was presumably due to interrupted flow and increased mixing. After pooling of contrast material, the cervical level was adequately evaluated.

Discussion

There are several advantages in using water soluble contrast agents: (1) better visualization of nerve roots and nerve root sleeves, (2) no need for withdrawal of contrast material after completion of the study, and (3) the ability to use a smaller needle for lumbar puncture. A further advantage of a nonionic compound such as metrizamide is the decreased likelihood of arachnoiditis [4, 6]. One problem has been inadequate cervical and tho-

---

Received December 10, 1976; accepted after revision May 25, 1977.

[1] Department of Radiation Sciences, Loma Linda University School of Medicine, Loma Linda, California 92354. Address reprint requests to W. R. Boyd.

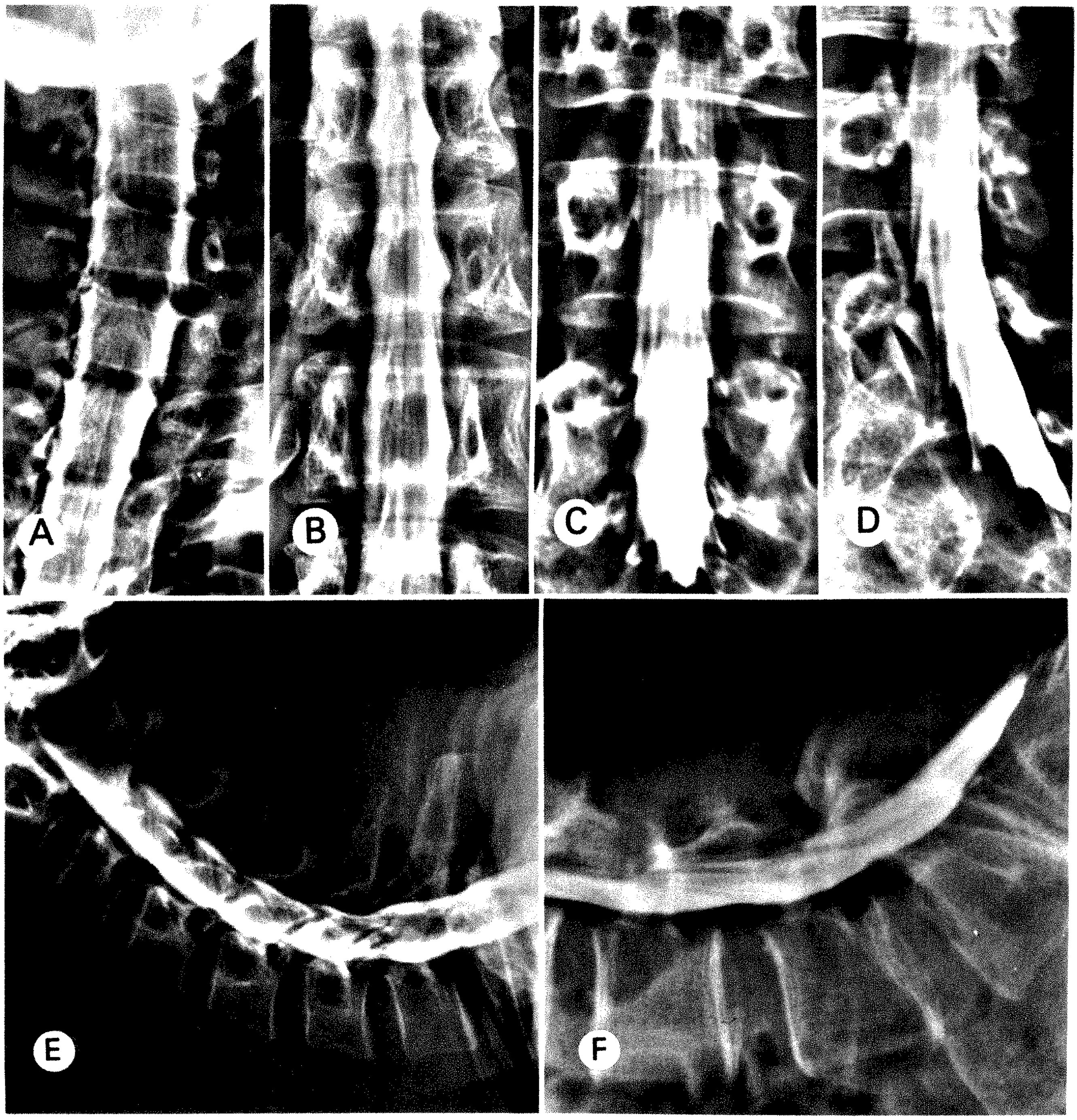

Fig. 1.—Complete myelogram by lumbar injection showing good visualization of lumbar, thoracic, and cervical subarachnoid space.

racic visualization using a lumbar puncture. Punctures at the C1-C2 interspace have been used with good success when a cervical problem was indicated [5, 7]. Specially adapted techniques and equipment have also been tried with varying success, but always at increased cost.

We found that adequate and consistent visualization of the cervical and thoracic canal is possible using metrizamide and lumbar puncture without special equipment or techniques. While the opacity of metrizamide is not as great as Pantopaque, even in the lumbar region, density should not be equated with quality. Visualization of nerve roots and sleeves is usually better with metrizamide.

Several of our earlier attempts at cervical visualization by lumbar puncture were not successful. Using a slow rate of injection of contrast material may have improved visualization in these 20 most recent patients by minimizing turbulence and mixing of the contrast agent with spinal fluid. As evidenced by our one case of poor cervical visualization, the size of the subarachnoid space certainly influences visualization at that level.

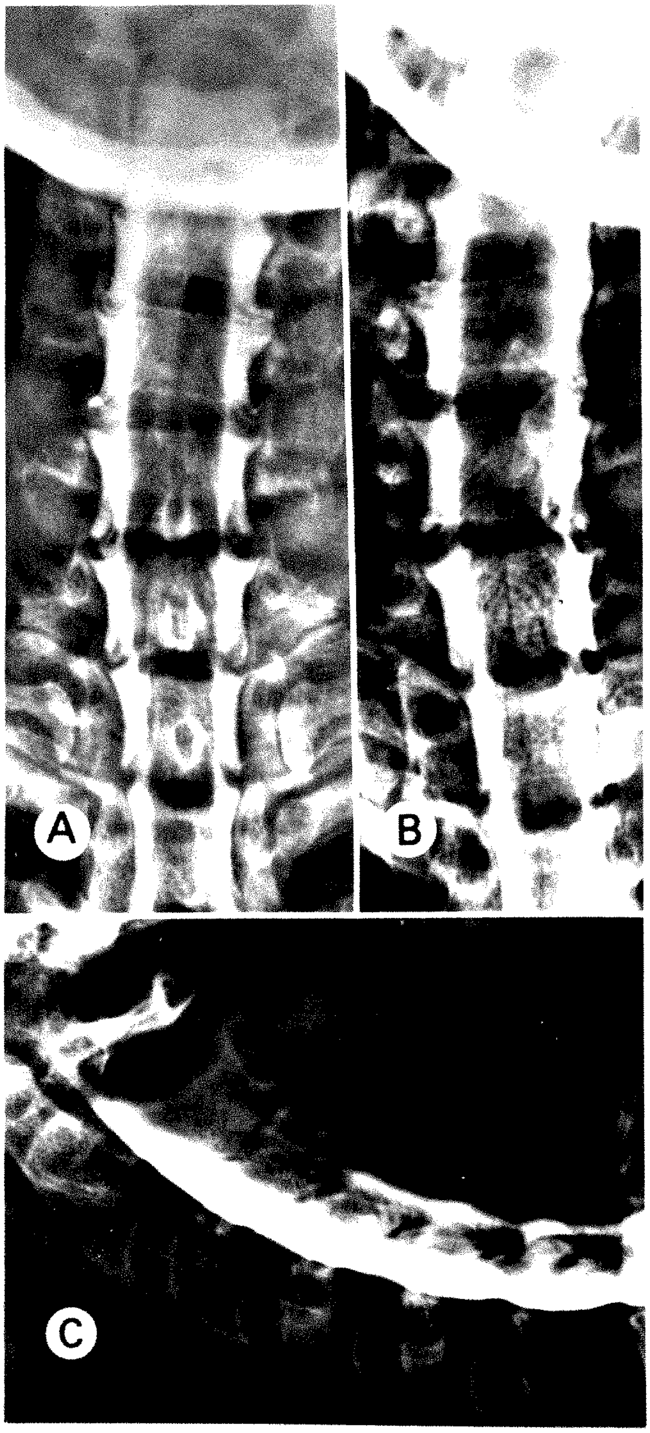

Fig. 2.—Cervical portion of complete myelogram by lumbar approach showing dense opacification.

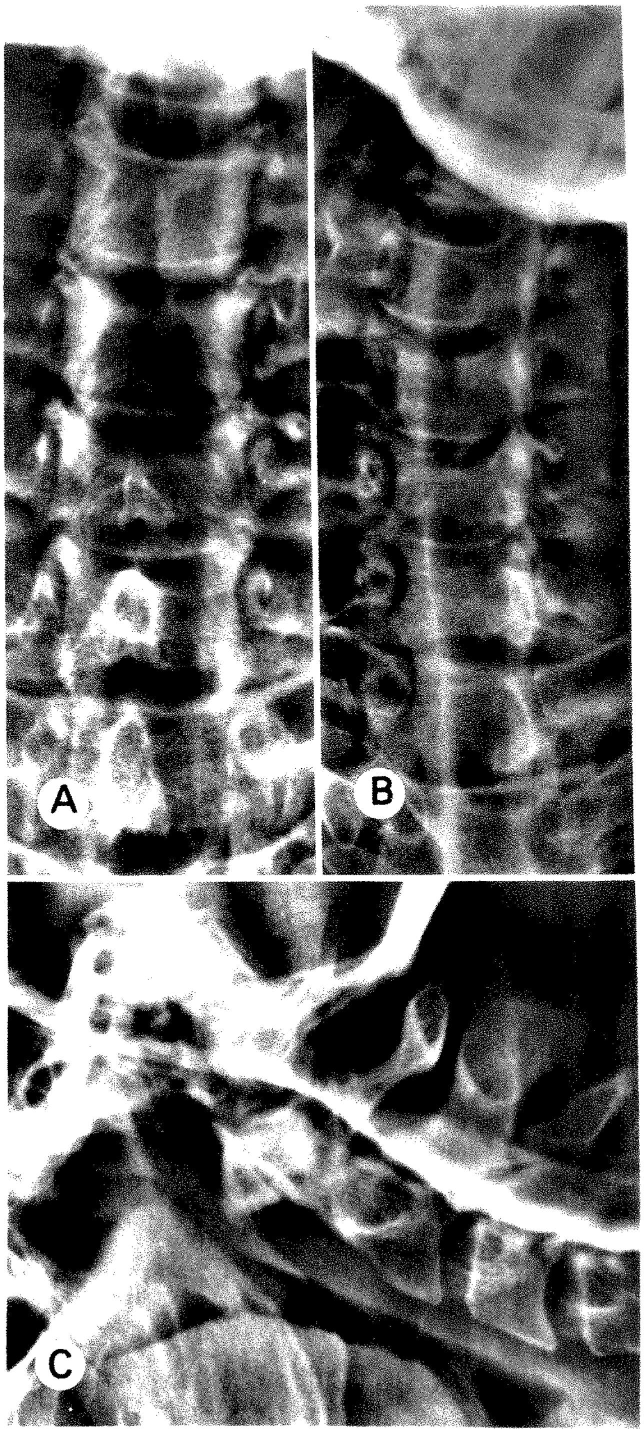

Fig. 3.—Cervical portion of complete myelogram by lumbar approach showing opacity adequate for evaluation.

Since metrizamide is absorbed and excreted by the kidneys, filming delays should be avoided. Because of increased adverse reactions such as vomiting and headaches when metrizamide is taken into the cerebral subarachnoid space, special attention must be taken to avoid spill into the posterior fossa when cervical myelography is performed.

REFERENCES

1. Skalpe IO, Amundsen P: Lumbar radiculography with metrizamide. *Radiology* 115:91-95, 1975
2. Skalpe IO, Torbergsen T, Amundsen P, Presthus J: Lumbar myelography with metrizamide. *Acta Radiol [Suppl]* (Stockh) 335:367-379, 1973

3. Hindmarsh T: Lumbar myelography with meglumine iocarmate and metrizamide. *Acta Radiol [Diagn]* (Stockh) 16:209-222, 1975
4. Ahlgren P: Amipaque myelography: the side effects compared with Dimer X. *Neuroradiology* 9:197-202, 1975
5. Skalpe IO, Amundsen P: Thoracic and cervical myelography with metrizamide: clinical experiences with a water-soluble, non-ionic contrast medium. *Radiology* 116:101-106, 1975
6. Haughton V: Changes of arachnoiditis after metrizamide myelography. Experimental data presented at a Seminar-Workshop on Myelography and the Water Soluble Contrast Medium, Department of Radiology, University of Wisconsin, Madison, March 1976
7. Amundsen P, Skalpe IO: Cervical myelography with a water soluble contrast medium (metrizamide). *Neuroradiology* 8:209-212, 1975

Avulsion of Nerve Rootlets with the Cuatico Needle during Pantopaque Removal after Myelography

G. DOUGLAS HUNGERFORD[1] AND JAMES M. POWERS[2]

Three cases of histologically proven nerve root avulsion during Pantopaque removal with a Cuatico needle are described. While use of such multihole needles poses some risk to patients, we feel the advantages outweigh the disadvantages, particularly when a large volume of Pantopaque has to be removed. To minimize the possibility of nerve root avulsion, we recommend minimal manipulation of the needle and cannula during Pantopaque removal, use of gentle suction, termination of suction and injection of cerebrospinal fluid if pain occurs, and slow withdrawal of the cannula and stylet.

Special needles of several types [1-3], including the Curity cannula (Kendall Research Laboratories, Barrington, Ill.) and Pharmaseal cannula (Pharmaseal, Glendale, Calif.), have been designed to facilitate the removal of iophendylate (Pantopaque) after myelography. The Cuatico needle was the first of these needles, and it is widely used because of the ease and speed with which contrast removal may be accomplished using this design. One instance of nerve rootlet avulsion with the Cuatico needle has been reported [4]; we describe three further cases.

Case Reports

Case 1

J. L. underwent myelography for low back pain, during which 18 ml Pantopaque was introduced at L4-L5. The needle was removed for supine views, and a Cuatico needle was reinserted at L4-L5. Pantopaque removal was difficult and slow from the onset, requiring several slight variations in position of the cannula. Movement of the needle caused severe local pain. Because nerve entrapment was suspected, several milliliters of sterile water was injected and the cannula was carefully removed, causing pain for 5 sec. Filamentous tissue measuring 0.05 × 0.5 cm was seen entering the cannula through one hole and exiting through the adjacent hole. Microscopic examination showed this to be nerve with some attached ganglion cells. There was no subsequent pain or added neurologic deficit.

Case 2

E. S. has a myelogram which showed severe spondylosis in cervical and lumbar regions. The initial lumbar puncture was difficult. The needle was removed for supine views, and a Cuatico needle was later introduced for Pantopaque removal. The needle tip was laterally placed and only half of the 16 ml of dye could be removed. The needle was reinserted in the midline. Because Pantopaque removal was dificult, the cannula was rotated and moved in and out. Suction was applied during some of these maneuvers. The patient developed pain in the right leg and buttock, and removal of the cannula caused pain. A 0.1 × 1.0 cm filament of histologically proven peripheral nerve tissue was firmly embedded in one of the holes of the cannula. There was no subsequent pain or neurologic deficit.

Case 3

C. P. underwent myelography which revealed syringomyelia and a posterior fossa cyst. Pantopaque was trapped in the cyst and only gradually returned to the lumbar sac over the next 3 days, at which time removal was carried out with a Cuatico needle. Removal was difficult and prolonged, requiring two punctures at different levels and manipulation of the needle. When only 2 ml remained, the patient developed pain at the puncture site. Withdrawal of the needle caused sharp local pain for several seconds. A 0.05 × 0.4 cm fragment of peripheral nerve tissue protruded through one hole of the cannula. This tissue consisted of two fascicles of nerve, each 0.025 cm in diameter. There was no subsequent pain or added neurologic deficit.

Discussion

This is apparently the third report of nerve rootlet avulsion during myelography [4, 5] and the second such report involving the Cuatico needle. The Cuatico needle assembly consists of three parts: a regular short-beveled lumbar puncture needle, a solid sharply pointed stylet inserted into the needle shaft, and a separate hollow aspiration cannula. Needles are available in three lengths (6.35, 8.9, and 12.7 cm) and three gauges (17, 18, and 19). The most commonly used needle for adults is 8.9 cm long and 18 gauge. It has a $19^{1}/_{2}$ gauge cannula with nine side holes and a blunt tip. The holes are 0.5 mm in diameter and are arranged in four rows: three rows of two holes and one of three holes. The most proximal hole is about 5 mm from the tip and the most distal hole is 1.4 mm from the tip. The 17 gauge needle uses a cannula with identical holes, but the cannula with the 19 gauge needle has holes 0.36 mm in diameter. When fully inserted, the cannula protrudes 5 mm beyond the tip of the needle.

At the completion of myelography, the cannula is introduced and gently advanced until its hub is locked into the needle hub, or until the tip of the cannula meets the opposite wall of the spinal canal. Pantopaque is then aspirated using gentle suction via a plastic connecting tube. The contrast can frequently be removed without any obstruction or delay. However, one or more of the holes sometimes becomes blocked by arachnoid tissue or nerve rootlets. At this stage the flow of Pantopaque ceases or slows, the examiner immediately becomes

---

Received March 4, 1977; accepted after revision June 3, 1977.

[1] Department of Radiology, Medical University of South Carolina, 80 Barre Street, Charleston, South Carolina 29401. Address reprint requests to G. D. Hungerford.

[2] Department of Neuropathology, Medical University of South Carolina, Charleston, South Carolina 29401.

aware of increased resistance to aspiration, and the patient may complain of pain. Further maneuvers will then be necessary, and sometimes repuncture at a different level will be required. In most cases complete removal of Pantopaque can be achieved in less than 5 min.

The true incidence of nerve rootlet avulsion is difficult to determine. These three cases are the only ones we have encountered in over 200 patients who had Pantopaque removal at our institution using the Cuatico needle; Kennedy and Steinfield [4] reported only one instance in over 450 examinations. This is a conservative estimate, however, since it is possible that nerve rootlets could be avulsed and subsequently fall free in the subarachnoid space, or be caught in tissues along the path of the needle as it was removed and thus remain undetected. We have noted the frequency with which patients complain of brief episodes of pain near the end of the Pantopaque removal. Presumably nerve rootlets are being sucked against the holes of the cannula while this pain is present. It is possible that a careful examination of the cannula in every case after Pantopaque removal with a Cuatico needle would occasionally reveal fragments of nerve tissue.

The avulsion of nerve rootlets did not cause any detectable permanent increase in neurologic deficit, either in our three cases or in the two previously reported. Although pain was associated with this complication, it only lasted for a few seconds.

It is apparent that multihole needles, through which considerable suction may be applied, pose some risk of injury to the patient, and a reappraisal of their use is indicated. While complete removal of Pantopaque with the siphonage technique and a standard short-bevel needle is tedious, it is less likely to cause nerve rootlet avulsion or damage. We believe that the advantages of the Cuatico needle, especially when a large volume of Pantopaque has to be removed, outweigh the potential disadvantages. However, the multihole needles should be used carefully and with close attention to the details of technique which are outlined below.

The common factor in our three cases was difficulty in removing the Pantopaque. Repositioning of the needle and/or cannula together with prolonged suction was used in all instances. In order to minimize the possibility of trapping a nerve rootlet in one of the side holes and subsequently avulsing it, recommendations by Cuatico [6] may be repeated: (1) do not remove the needle while negative pressure is being applied; (2) a few drops of cerebrospinal fluid should be injected through the needle prior to removal; and (3) the needle should be placed in the midline. To these recommendations we would add: (4) the needle and cannula should be manipulated as little as possible during Pantopaque removal; (5) suction should be gentle and applied only when the needle and cannula are stationary; (6) if pain occurs, suction should immediately be stopped and cerebrospinal fluid should be injected through the cannula before manipulating the cannula and/or reapplying suction; and (7) the cannula and the stylet should be withdrawn from the needle slowly to prevent sucking a nerve rootlet against the sharp edge of the needle.

REFERENCES

1. Cuatico W, Gannon W, Samouhos E: A needle designed for myelography. *J Neurosurg* 28:87–88, 1968
2. Chynn KY: Painless myelography: introduction of a new aspiration cannula and review of 541 consecutive studies. *Radiology* 109:361–367, 1973
3. Hinck VC: The myelography needle: a new cannula for aspiration. *Radiology* 120:731–732, 1976
4. Kennedy TF, Steinfeld JR: Nerve rootlet avulsion as a complication of myelography with the Cuatico needle. *Radiology* 119:389, 1976
5. Young DA, Burney RE: Complication of myelography—transection and withdrawal of a nerve filament by the needle. *N Engl J Med* 285:156–157, 1971
6. Cuatico W: Letter. *J Neurosurg* 41:406, 1974

Hand Radiographic Measurements in Growth Hormone Deficiency Before and After Treatment

RAMIRO HERNANDEZ,[1] ANDREW K. POZNANSKI,[1] ROBERT P. KELCH,[2] AND LAWRENCE R. KUHNS[1]

Hand radiographs in 10 male patients (eight white, two black) with isolated growth hormone deficiency were studied before and after treatment. The length of the second metacarpal was the most significantly depressed measurement when considered by chronologic age and responded most to treatment with human growth hormone. All patients had osteoporosis even when evaluated by height age. The bone mass improved with treatment by subperiosteal new bone apposition. Skeletal maturation was retarded with the carpals showing more severe retardation than the tubular bones and responding more dramatically to treatment. The depression in height age and carpal age was very similar, indicating that the carpal age may have the greatest correlation with height. The greater sensitivity of the carpal age deficiency of growth hormone and its greater response to treatment suggest that the carpal age and the phalangeal-metacarpal age should be considered independently during evaluation of skeletal maturation.

Several authors [1-12] have reported the skeletal effects of human growth hormone in children with isolated growth hormone deficiency. Most reported that human growth hormone accelerates skeletal maturation and growth velocity. The increase in height with growth hormone therapy is greater than the increase in skeletal maturation. However, there are some inconsistencies in the literature which stimulated us to evaluate more closely the effects of growth hormone deficiency on maturation and to determine more precisely the effects of therapy. We also wanted to study separately the maturation of the carpals and the tubular bones, since it has been shown that these two areas behave differently in many different disorders [13-15]. We examined bone mineralization more closely, looking specifically at the effects of growth hormone on both the endosteal and periosteal surfaces. The length of the second metacarpal and the width of the epiphyseal plates were also evaluated before and after treatment.

Subjects and Methods

Ten boys (eight white and two black) with isolated growth hormone deficiency were evaluated. All patients had normal adrenocorticotropic hormone reserve and serum thyroxine concentration, and all responded well to human growth hormone administration. Human growth hormone was supplied by the National Pituitary Agency at the University of Maryland and the National Institute of Arthritis and Metabolic Diseases. Radiographs of the hands were obtained before therapy and at yearly intervals.

Table 1 summarizes the clinical data on the patients included in the study. During the first year after diagnosis, the patients received only human growth hormone therapy; no androgens were given. In subsequent years additional hormone therapy was instituted. This study is concerned only with the results of the first year of therapy.

Skeletal maturation of the hands was evaluated by two of us (R. Hernandez and A. Poznanski) by comparison to the Greulich and Pyle atlas [16]. The phalanges and metacarpals were considered separately from the carpals, and a separate bone age was determined for each. The skeletal age was also determined by an experienced bone age reader at the Fels Research Institute who evaluated each bone separately and averaged them.

The length of the second metacarpal was measured using a direct reading Helios caliper and was compared with the standards of Garn et al. [17] for normal white and black populations [18]. The outside diameter T and the medullary diameter M of the midportion of the second metacarpal were measured with a comparator that had a scale with 0.2 mm divisions. The cortical thickness ($C = T - M$) and the percentage of cortical area ($PCA = T^2 - M^2/T^2$) were then calculated. Values of T, M, C, and PCA were compared with the normal standards of Garn et al. [18, 19].

The width of the epiphyseal plate of the phalanges of the second and fourth digits and of the distal radius were measured using the same comparator. Since no normal standards are available for the epiphyseal plate in humans, longitudinal studies of the epiphyseal plate in four normal children from the University School, Ann Arbor, Michigan, were done over a period of 10 years for each child. These measurements were then used as crude standards.

The height age for each of the affected white children was determined using the data of the National Center of Health Statistics Growth Charts of 1976 [20], while the height age of blacks was determined using the standards from Garn et al. [18].

Results

Skeletal Maturation

Skeletal maturation was difficult to assess because of the unusual pattern of maturation in both the phalanges and the carpals and the altered shape of these bones. The phalangeal epiphyseal centers tended to be narrower than normal in four of the nine cases in which they could be evaluated. Also, "ivory epiphyses" (sclerotic dense epiphyses) were seen in five of nine cases. The carpals also had a somewhat unusual appearance. For example, the hamate often had a prominent indentation for the triquetrum. Despite these difficulties, the assessments of the two observers were close with a mean difference of 0.28 years, SD = 0.37, and a maximum difference equal to 1 year. The Fels Research Institute

---

Received March 14, 1977; accepted after revision May 10, 1977.

Presented in part at the annual meeting of the European Society of Pediatric Radiology, Lucerne, Switzerland, May 1977.

[1] Division of Pediatric Radiology, C. S. Mott Children's Hospital, University of Michigan Medical Center, Ann Arbor, Michigan 48109. Address reprint requests to R. Hernandez.

[2] Department of Pediatrics and Communicable Diseases, C. S. Mott Children's Hospital, Ann Arbor, Michigan 48109.

Am J Roentgenol **129:487-492, September 1977**

TABLE 1

Summary of Clinical Data

Case No.	Before Treatment				Growth Velocity after Treatment (cm/yr)
	Age (yr)	Height		Growth Velocity (cm/yr)	
		(cm)	(ft/in)		
1 (W. W.)	21½	126.4	4/1	1.1	6.3
2 (H. D.)	9	101.0	3/4	3.7	7.0
3 (S. R.)	12	128.2	4/2	4.0	8.9
4 (P. J.)	8	102.8	3/4	3.3	8.2
5 (L. D.)	5	87.0	2/10	3.9	8.2
6 (R. M.)	6½	100.2	3/3	4.0	9.5
7 (W. E.)	14½	122.8	4/0	3.8	8.2
8 (S. E.)	7½	110.4	3/7	2.5	9.3
9 (L. C.)	9	108.2	3/7	3.0	11.1
10 (H. L.)	9	101.0	3/4	3.3	10.8

Note.—Treatment consisted of 2 IU of human growth hormone intramuscularly three times per week. Cases 1, 5, and 8 received treatment intermittently, 2 of every 3 months. Cases 1 and 7 received maintenance doses of dessicated thyroid before and during treatment. However, thyroid-stimulating hormone deficiency was never documented. Cases 1 and 6 were black.

evaluations were somewhat higher than ours: mean = +0.46 years, SD = 0.3. Separate plots of the various measurements using bone ages determined by us as well as those obtained at the Fels Research Institute were not significantly different. The plots illustrated here were based on our determinations, since we felt that this may resemble more closely the approach used in most radiologic departments, where bone by bone evaluation is not usually done.

Figure 1 shows the phalangeal-metacarpal (tubular) skeletal age and the carpal skeletal age plotted against the chronologic age. In all of the patients, both skeletal ages were less than chronologic age before treatment. Carpal bone age was more depressed and responded somewhat more dramatically to human growth hormone than the phalangeal-metacarpal age. The carpals were affected in a similar fashion as the tubular bones in cases 1 and 6, both of whom were black. A similar carpal-tubular disharmony was obtained when the Fels bone ages were used, but the differences were slightly smaller.

Second Metacarpal Length and Cortical Measurements

Cortical measurements were obtained using the method of Garn et al. [19] in which the measurements are taken in the midportion of the second metacarpal. The measurements include the outside diameter *T*, the medullary diameter *M*, and the cortical thickness *C*. The length of the second metacarpal *L* was also measured. These measurements were compared to the standards from Garn et al. for whites [17, 19] and blacks [18], and the number of standard deviations from the mean for each of these was computed. The average of these standard deviations was then determined and plotted against chronologic, phalangeal-metacarpal, carpal, and height ages (fig. 2).

In comparing these values with chronologic age, the most affected measurement prior to treatment is the reduced length of the second metacarpal. This measurement also showed more improvement than any other after treatment, increasing from 3.87 to 3.05 SD below normal in 1 year. When the data are considered in respect to skeletal age (either carpal or phalangeal-metacarpal) or height age, the most affected measurement before treatment was cortical thickness.

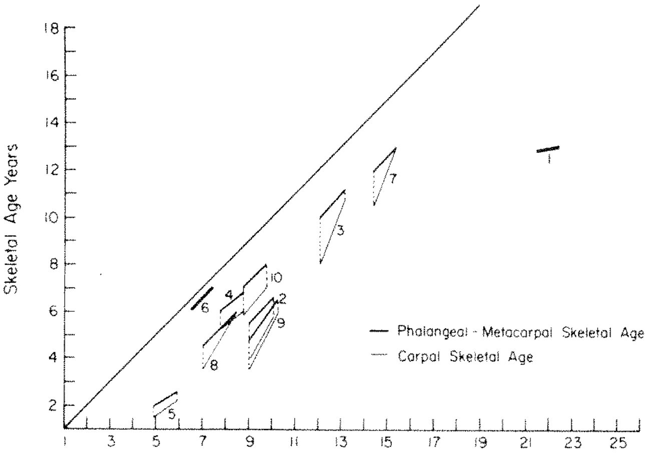

Fig. 1.—Phalangeal-metacarpal and carpal bone age. Average of both observers was used.

It appears that the medullary diameter is relatively normal in these children while the outside diameter *T* is deficient. This is the reason for the small cortical thickness *C*. Most of the gain in cortical thickness with treatment is due to greater increase in subperiosteal apposition rather than endosteal change (slope of *T* is greater than the slope of *M*).

The effects of growth hormone therapy on these measurements in eight white children are plotted according to chronologic age in figure 3. The ratios of the height age to carpal, phalangeal-metacarpal, and chronologic ages are plotted in figure 4. It is apparent that height age and carpal age are the most closely related.

Width of Epiphyseal Plate

The width of the epiphyseal plate of the phalanges and of the distal radius was measured before and after treatment; no significant and consistent increase could be observed. The increase in width of the epiphyseal plates ranged from 0 to 0.8 mm (mean, 0.01). However, this is not significantly different from the changes in width of the epiphyseal plates of the hands of children in the longitudinal study of the University of Michigan, where differences were 0–2.0 mm. One problem in evaluating changes in width of epiphyseal plates is that the irregularity of the plate makes measurements somewhat inaccurate, especially in children with growth hormone deficiency. This irregularity of the epiphyseal plate in such children was described by Rappaport and Rybak [21]. Another problem is that the lack of good normal standards for epiphyseal width makes evaluation difficult.

Discussion

In growth hormone deficiency certain subjective changes are visible on the radiograph. These include the

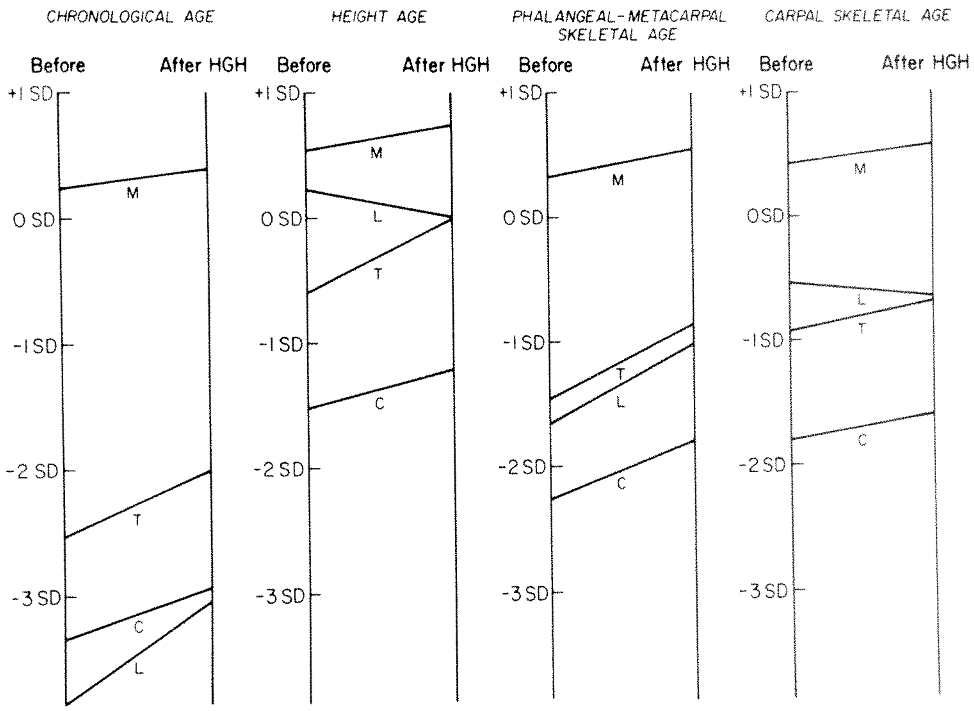

Fig. 2.—Average of standard deviations from means for second metacarpal in 10 patients before and after human growth hormone (HGH) according to chronologic, height, and bone ages. T = outside diameter, M = medullary (inside) diameter, C = cortical thickness, L = length of metacarpal.

very thin slender epiphyses, which are sometimes quite sclerotic and have been called ivory epiphyses [22]. These epiphyses are considerably more common in children with retarded maturation [22]. There are also alterations in the configuration of the carpals, which are more difficult to evaluate. These include unusual early indentations in the hamate.

Both observers found the carpal bone age and phalangeal-metacarpal bone age to be retarded compared to chronologic age. This agrees with the general finding of the delayed skeletal age in this disorder. However, in our series the tubular bone age was less retarded than that of the carpals (fig. 1). This disagrees somewhat with the experience of Tanner et al. [23], who stated that they were similarly affected but did not qualify this with a detailed analysis. The reason for the differences between our data and theirs is unclear, but it may be related to the different methods of bone evaluation. We compared with the Greulich and Pyle atlas [16], while they used the TW2 system [23].

Several authors [2, 6, 11, 12] found that with human growth hormone therapy in patients with growth hormone deficiency, there is an increase in skeletal maturation paralleling the increase in chronologic age. In our experience this was true only of the phalangeal-metacarpal bone age. On the other hand, the carpal age increased more than the chronologic age (fig. 1). This agrees with the findings of Tanner et al. [23], who stated that a catch-up phase occurs in the overall bone age. Thus the carpal age is a more sensitive marker of both the degree of retardation of maturation associated with growth hormone deficiency and of the effects of treatment. Carpal maturation is most closely related to height age; both are similarly affected with treatment, as indicated by the almost constant ratio between them. These data suggest that the carpals should be evaluated separately from the phalangeal-metacarpal centers when evaluating bone age in patients with growth hormone deficiency before and after treatment.

Patients with growth hormone deficiency have a thin bony cortex (*C*) which improves after human growth hormone therapy, whether considered by chronologic, skeletal, or height age (fig. 2). It is most depressed in relation to chronologic age. These data disagree with those of Ferrandez et al. [2] who reported that bone mass was normal if considered in reference to height age. The reason for this difference is not clear and there are not enough data in their paper for comparison.

The gain in cortical thickness is due mainly to an increase in subperiosteal new bone formation (increase in *T*). There is also minimal increase in endosteal resorption (increase in *M*). This effect is most marked in relation to chronologic age. The increase in subperiosteal apposition in our patients was similar to that described by Ferrandez et al. [2]; however, there is a distinct difference among our patients in the response of cortical thickness *C* (tabel 2). This discrepancy must be due to difference in the effect on the medullary surface. We saw minimal further endosteal resorption, while in their cases there must have been significant endosteal apposition.

In a study of adult dogs treated with human growth hormone [24], some endosteal new bone formation occurred as well as subperiosteal apposition similar to that seen in the patients of Ferrandez et al. [2]. It may be that

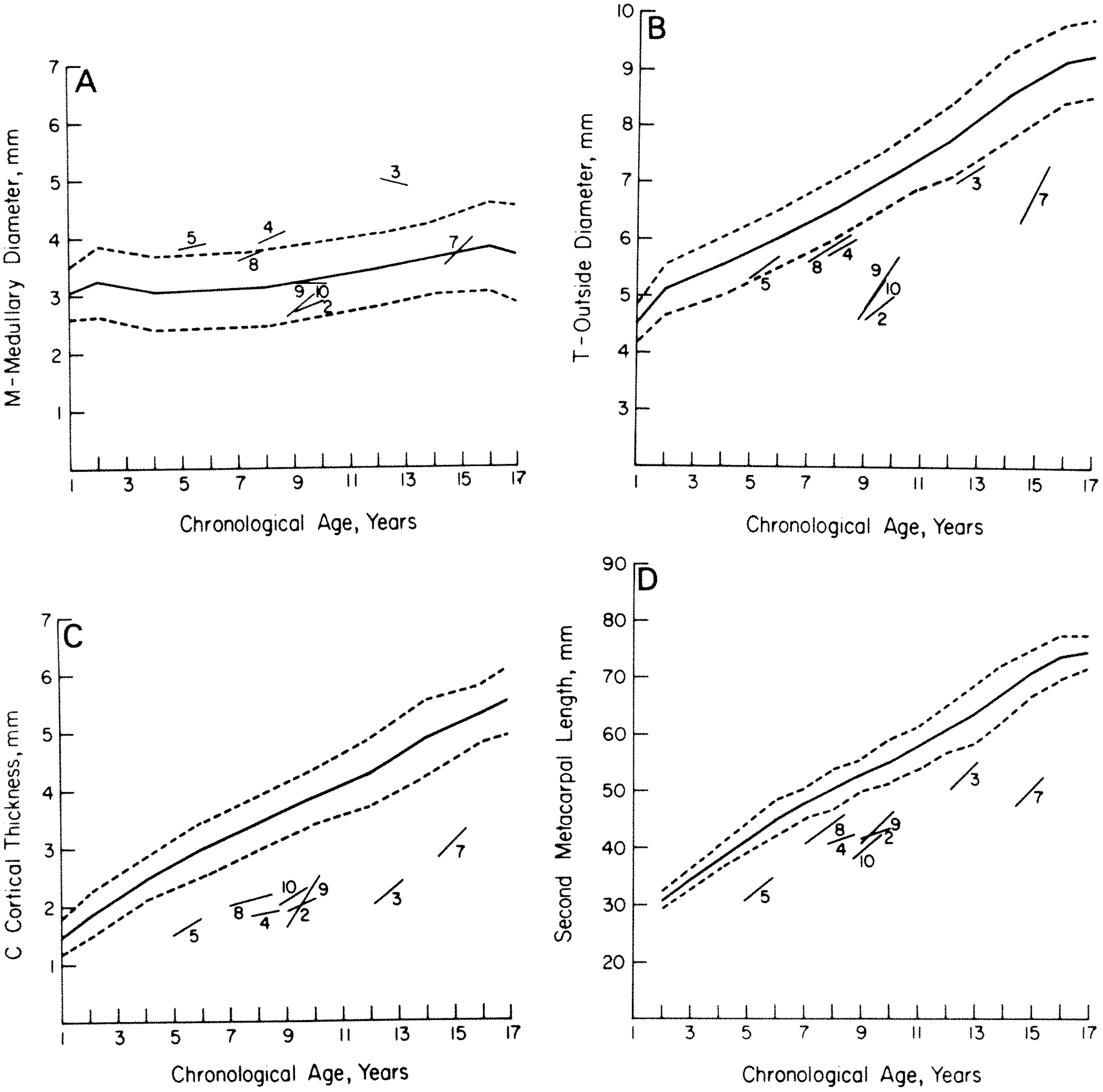

Fig. 3.—Length and cortical measurements of second metacarpal of eight white children before and after therapy according to chronologic age. *A*, Medullary diameter. *B*, Outside diameter. *C*, Cortical thickness. *D*, Length of metacarpal. Solid line = mean; dotted lines = ±1 SD from mean.

these effects are dose related and that a smaller dose, as in our patients, results in primarily subperiosteal new bone formation, while a larger dose causes some endosteal new bone formation.

In animals, the width of the epiphyseal plate is dependent on the amount of growth hormone. Greenspan et al. [25] used the width of the epiphyseal plate of the proximal tibia in the rat as an assay for the hormone. Therefore, it was a surprise that in our patients the epiphyseal plate was not significantly wider after treatment. Increases in width of the epiphyseal plate after treatment with growth hormone have been both illustrated and described [10, 13, 26]. We have seen two patients not included in this series who had a significantly increased width of the epiphyseal plates after treatment with human growth hormone (fig. 5).

While it is difficult to explain the lack of increased width of the epiphyseal plate in our patients, two theories can be postulated. First, most of our patients received only 6 IU/week, while many of the patients of Tanner et al. [23] received more than 20 IU/week. A similarly large dosage was given to the patient with remarkable increase

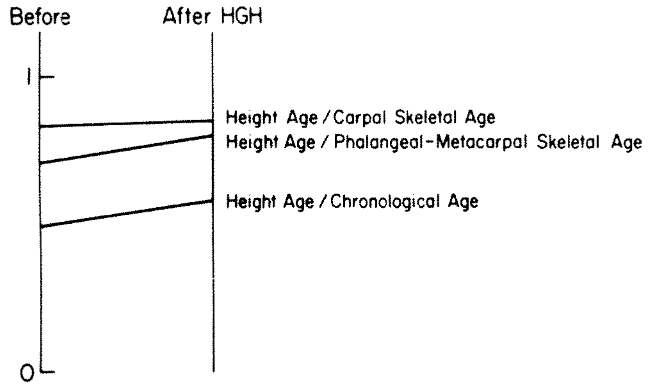

Fig. 4.—Ratios of height age to both bone ages and chronologic age before and after treatment with human growth hormone (HGH).

TABLE 2

Changes in Measurements after Treatment

Measurement	Present Series	Series of Ferrandez et al. [2]
T	+0.51	+0.48
M	+0.16	. . .
C	+0.40	+1.24

Note.—Values represent difference between mean for affected patients and mean of normal population expressed in number of standard deviations from normal.

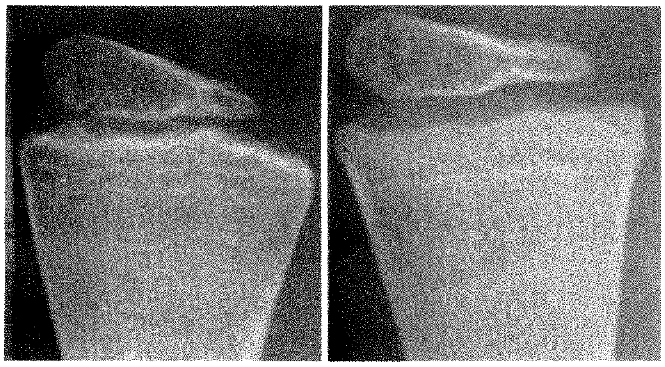

Fig. 5.—Anteroposterior views of distal radius of patient with craniopharyngioma before and after human growth hormone showing significant widening of epiphyseal plate after 4 months of treatment.

in width of the epiphyseal plate illustrated by Poznanski [13]. Since the increase in width of the epiphyseal plate is dose dependent, as evidenced by animal data [25], it may well be that small dosages do not produce this effect radiographically. Further evidence that these changes may be dose dependent is that the dense white metaphyseal bands recently described by Edlin et al. [26] were not present in our patients. The second possibility is that the widening may be transient and could have been missed when the films were taken at 1 year intervals. Rudman et al. [8] and Soyka et al. [11] have shown that the velocity of linear growth accelerates for the first 4–7 months after beginning of treatment and then declines, so that films obtained at 12 months could conceivably have missed this widening.

ACKNOWLEDGMENT

We thank Ms. M. Fischer and Dr. Alex Roche of the Fels Research Institute, Yellow Springs, Ohio, for the evaluation of skeletal maturation in these patients.

REFERENCES

1. Aceto T Jr, Frasier SD, Hayles AB, Meyer-Bahlburg HFL, Parker ML, Munschauer R, Di Chiro G: Collaborative study of the effects of human growth hormone in growth hormone deficiency. I. First year of therapy. *J Clin Endocrinol Metab* 35:483–496, 1972
2. Ferrandez A, Zachmann M, Prader A, Illig R: Isolated growth hormone deficiency in prepubertal children. Influence of human growth hormone on longitudinal growth, adipose tissue, bone mass and bone maturation. *Helv Paediatr Acta* 6:566–576, 1970
3. Goodman HG, Grumbach MM, Kaplan SL: Growth and growth hormone. II. A comparison of isolated growth hormone deficiency and multiple pituitary hormone deficiencies in 35 patients with idiopathic hypopituitary dwarfism. *N Engl J Med* 278:57–68, 1968
4. Kelch RP, Markovs M, Huss J: LH and FSH responsiveness to intravenous gonadotropin-releasing hormone (GnRH) in children with hypothalamic or pituitary disorders: lack of effect of replacement therapy with human growth hormone. *J Clin Endocrinol Metab* 42:1104–1113, 1976
5. Najjar S, Blizzard RM: Current concepts regarding human growth hormone (somatotropin). *Pediatr Clin North Am* 13:437–457, 1966
6. Prader A, Zachmann M, Poley JR, Illig R, Széky J: Long-term treatment with human growth hormone (Raben) in small doses. Evaluation of 18 hypopituitary patients. *Helv Paediatr Acta* 5:423–440, 1967
7. Root A: Growth hormone. *Pediatrics* 36:940–950, 1965
8. Rudman D, Patterson JH, Gibbas DL: Responsiveness of growth hormone-deficient children to human growth hormone. Effect of replacement therapy for one year. *J Clin Invest* 52:1108–1112, 1973
9. Seip M, Trygstad O: Experiences with human growth hormone in pituitary dwarfism. *Acta Paediatr Scand* 55:287–293, 1966
10. Shepard TH II, Waxman S, Bernstein N, Ferrier P: Human growth hormone. II. Further study of its effect on growth in dwarfism. *J Pediatr* 57:363–369, 1960
11. Soyka LF, Bode HH, Crawford JD, Flynn FJ Jr: Effectiveness of long-term human growth hormone therapy for short stature in children with growth hormone deficiency. *J Clin Endocrinol Metab* 30:1–14, 1970
12. Tanner JM, Whitehouse RH: Growth response of 26 children with short stature given human growth hormone. *Br Med J* 2:69–75, 1967
13. Poznanski AK: *The Hand in Radiologic Diagnosis*. Chicago, Saunders, 1974
14. Poznanski AK, Garn SM, Kuhns LR, Sandusky ST: Dysharmonic maturation of the hand in the congenital malformation syndromes. *Am J Phys Anthropol* 35:417–432, 1971
15. Poznanski AK, Garn SM, Kuhns LR, Shaw H: Disharmonic skeletal maturation in the congenital malformation syndromes. *Birth Defects: Orig Art Ser*. In press, 1977
16. Greulich WW, Pyle SI: *Radiographic Atlas of Skeletal Development of the Hand and Wrist*, 2d ed. Stanford, Stanford University Press, 1959
17. Garn SM, Hertzog KP, Poznanski AK, Nagy JM: Metacarpophalangeal length in the evaluation of skeletal malformation. *Radiology* 105:375–381, 1972

18. Garn SM, Miller RL, Larson KE: Metacarpal lengths, cortical diameters and areas from the 10-state nutritional survey including: estimated skeletal weights, weight and stature for whites, blacks, and Mexican-Americans, in *Proceedings of the First Workshop on Bone Morphometry*, edited by Jaworski ZFG, Ottawa, University of Ottawa Press, 1976
19. Garn SM, Poznanski AK, Nagy JM: Bone measurement in the differential diagnosis of osteopenia and osteoporosis. *Radiology* 100:509–518, 1971
20. Hamill PVV, Drizd TA, Johnson CL, Reed RB, Roche AF: *National Center of Health Statistics Growth Charts 1976: Monthly Vital Statistics Reports*. HRA 76-1120, vol 25, no. 3, suppl. 22, 1976
21. Rappaport R, Rybak M: Aspects radiologiques irreguliers des metaphyses des doigts chez des enfants atteints d'insuffisance hypothalamo-hypophysaire. *Arch Fr Pediatr* 26:1135–1144, 1969
22. Kuhns LR, Poznanski AK, Harper HAS, Garn SM: Ivory epiphyses of the hands. *Radiology* 109:643–648, 1973
23. Tanner JM, Whitehouse RH, Marshall WA, Healy MJR, Goldstein H: *Assessment of Skeletal Maturity and Prediction of Adult Height (TW2 Method)*. New York, Academic Press, 1975
24. Harris WH, Heaney RP, Jowsey J, Cockin J, Akins C, Graham J, Weinberg EH: Growth hormone: the effect on skeletal renewal in the adult dog. I. Morphometric studies. *Calcif Tissue Res* 10:1–13, 1972
25. Greenspan FS, Li CH, Simpson ME, Evans HM: Bioassay of hypophyseal growth hormone: the tibia test. *Endocrinology* 45:455–463, 1949
26. Edlin JC, Whitehouse RH, Tanner JM: Relationship of radial metaphyseal band width to stature velocity. *Am J Dis Child* 130:160–163, 1976

Extramedullary Hematopoiesis in Paget's Disease of Bone

SAADOON KADIR,[1] LESTER KALISHER,[1] AND ALAN L. SCHILLER[2]

Two cases of Paget's disease of bone with radiographic manifestation of extramedullary hematopoiesis are described. While extramedullary hematopoiesis usually occurs as a compensatory phenomenon in response to anemia, this was not the case in our patients. We believe pathologic fractures led to extrusion of hematopoietic marrow and resultant tumorous extramedullary hematopoiesis.

Extramedullary hematopoiesis usually occurs in diseases which disrupt the normal functions of blood-forming tissue, to compensate for the increased demands for blood cells [1-7]. In addition, it has been associated with liver disease, infections, sepsis, rickets, hyperparathyroidism, and in other patients without anemia or other obvious hematologic abnormality [2, 3, 5, 6, 8]. The condition has been described in one patient in whom Paget's disease of bone was noted as an incidental finding [9].

We report two patients with Paget's disease of bone in whom extramedullary hematopoiesis was observed. A hypothesis for its etiology in Paget's disease of bone is offered.

Case Reports

Case 1

A 61-year-old man with a 20 year history of Paget's disease of bone was referred because of an abnormal chest radiograph. There was no history of cough, chest pain, hemoptysis, or chest trauma. Dyspnea on exertion had been present for the past 3-4 years. Physical examination of the chest was unremarkable. Radiographs of the chest revealed a large paraspinal mass with fusion of the adjacent vertebral bodies (fig. 1). The hematologic data showed: 3.57 million red blood cells; 34.4% hematocrit with normal red blood cell indexes; 6,500 white blood cells; serum alkaline phosphatase, 112.0 Bodansky units; calcium 10 mg/100 ml; phosphorous, 3.2 mg/100 ml; and uric acid, 8.5 mg/100 ml. At thoracotomy the mass extended from T3-T8. Biopsy confirmed the presence of hyperplastic hematopoietic marrow and Paget's disease of bone.

Case 2

A 66-year-old male with a 30 year history of Paget's disease known to involve the skeleton extensively had gradual onset of painless swelling of the left leg for 2-3 months. There was no history of antecedent trauma. On physical examination there was chronic stasis dermatitis around the ankles with a 4+ pitting edema extending up to the mid thigh.

Pertinent hematologic data were as follows: 4.61 million red blood cells; 38.3% hematocrit with normal red cell indexes; 6,500 white blood cells and a normal differential count; serum alkaline phosphatase, 107 Bodansky units; calcium, 9.5 mg/100 ml; phosphorous, 3.7 mg/100 ml; magnesium, 1 mEq/liter; and uric acid, 9.5 mg/100 ml.

During the workup a pelvic mass was found which displaced the distal left ureter anteromedially and indented the urinary bladder (fig. 2). Angiography showed extrinsic compression of the pelvic vessels with no neovascularity. Polytomography did not reveal any sarcomatous bone changes. Review of chest radiographs taken approximately 14 years ago showed some widening of the paraspinal stripe (fig. 3*A*). Films taken at the present admission showed bilateral paravertebral masses (fig. 3*B*).

Needle biopsy of the pelvic lesion showed mature fatty tissue and hematopoietic elements. However, since osteosarcoma could not be completely excluded, exploration was undertaken. An encapsulated grapefruit-sized mass which seemed to arise from a pedicle deep on the lateral pelvic wall was excised. It extended into the obturator fossa, was adherent to the urinary bladder, and anteriorly to the posterior wall of the left pubic bone. The latter showed evidence of erosion. The diagnosis of fat and hematopoietic elements and Paget's disease of bone was confirmed.

Discussion

While most common sites of extramedullary hematopoiesis are the lymph nodes, liver, and spleen, it has also been seen in a large number of other organs and tissues [2, 6, 7, 10]. In the majority of these cases the condition is diagnosed microscopically; only rarely do patients present with radiographically manifested abnormalities [10].

The mechanism of extramedullary hematopoiesis is still uncertain. Due to its segmental location in the posterior mediastinum, it has been postulated to develop at the branches of the intercostal veins [11, 12]. Another theory is that hypertrophic bone marrow is extruded through the thinned cortices of the proximal ribs [13]. Occurrence in areas remote from the bone marrow may be explained by hematogenous colonization, metaplasia, or reactivation of sites of fetal hematopoiesis [3, 6, 8, 10, 11, 14].

Paget's disease is a chronic bone disorder of unknown etiology characterized by increased bone turnover with formation of abnormal new bone [15-17]. It occurs predominantly in males and may involve almost any bone in the body. The radiologic features have been well characterized [16, 17]. Laboratory data usually show normal serum calcium and phosphorous levels and a markedly elevated serum alkaline phosphatase.

The altered architecture leads to a softening of the bone which commonly results in bowing as well as pathologic fractures [15-17]. These fractures are characteristically incomplete, may occur without external injury, and are seen most frequently during the lytic phase [15]. Once a fracture has occurred, there is rapid spread of the

---

Received March 7, 1977; accepted after revision May 10, 1977.

[1] Department of Radiology, Massachusetts General Hospital and Harvard Medical School, Boston, Massachusetts 02114. Address reprint requests to S. Kadir at Massachusetts General Hospital.

[2] Department of Pathology, Massachusetts General Hospital and Harvard Medical School, Boston, Massachusetts 02114.

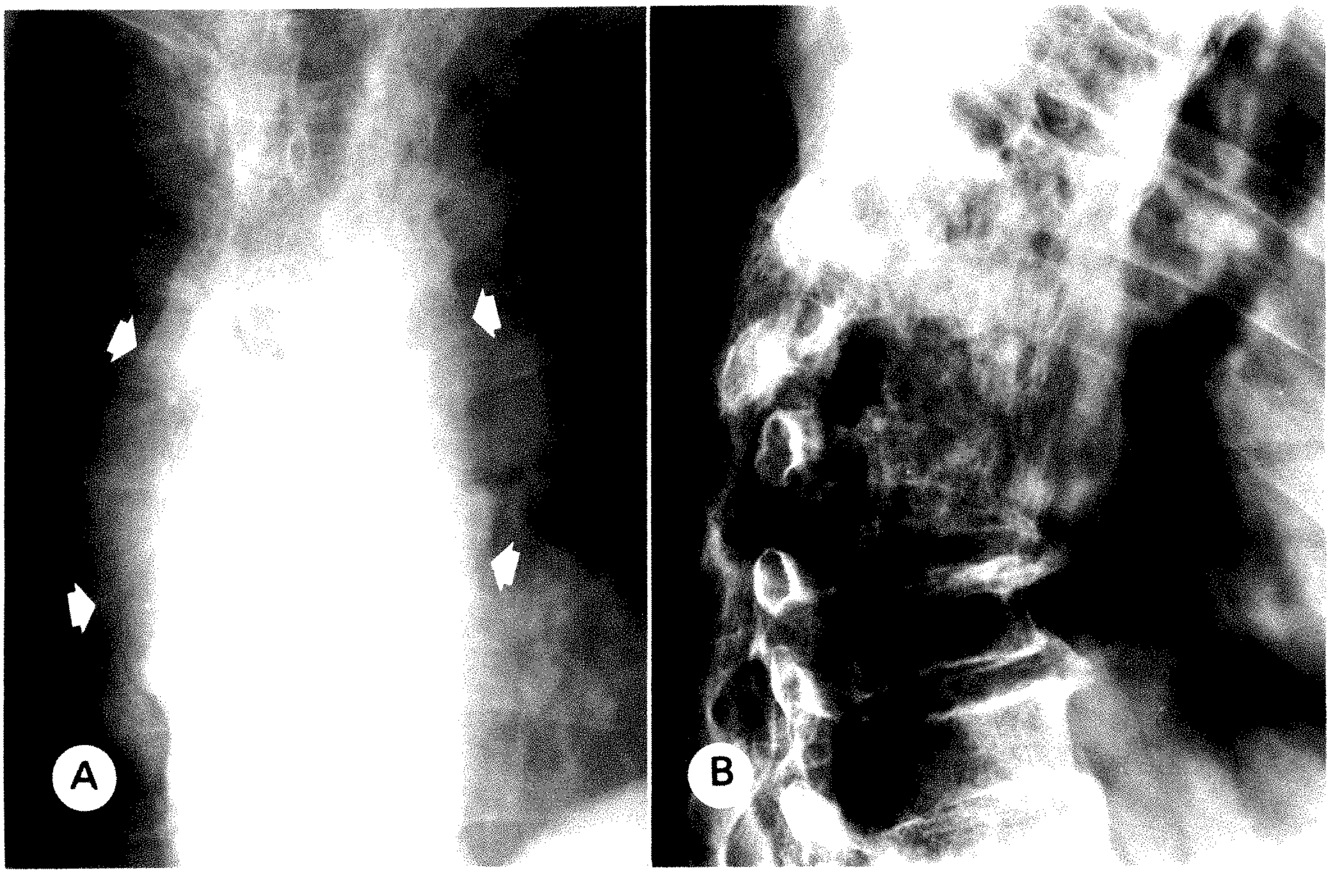

Fig. 1.—Case 1. Anteroposterior (*A*) and lateral (*B*) thoracic spine showing large bilateral paraspinal mass (*arrows*). Note fusion of midthoracic spine. Coarsened trabecular pattern and other stigmata of Paget's disease of bone are seen involving vertebral bodies and ribs.

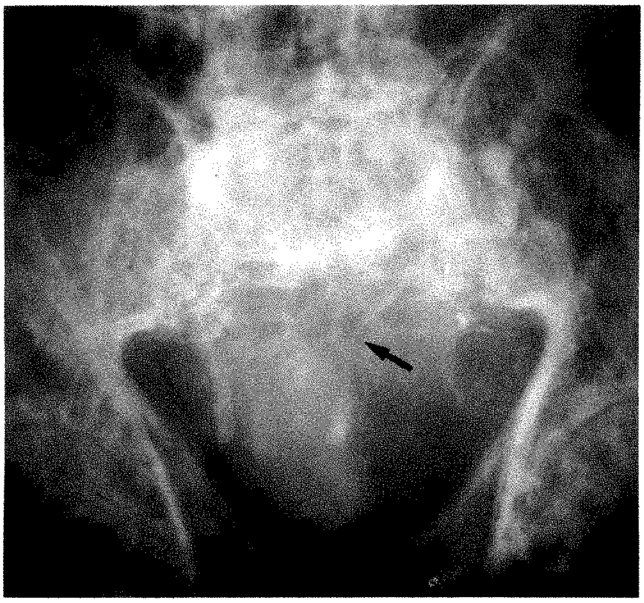

Fig. 2.—Case 2. Intravenous urogram showing anterior and medial displacement of left ureter and medial displacement of bladder by soft tissue mass.

lytic phase [15] which further weakens the structural stability of the bone, making it more prone to subsequent fractures.

Loss of height of vertebral bodies, so commonly seen, may be due to actual compression fractures or represent the effects of prolonged weight bearing upon softened bone [15]. The compression fractures most commonly involve the thoracolumbar spine, and cord compression may occur [15]. Initially, the intervertebral disc spaces are maintained but may be later incorporated into a spinal fusion as the disease progresses (case 1).

Review of the features of Paget's disease of bone offers a further explanation for the occurrence of extramedullary hematopoiesis in our patients. Although the characteristic features for this disease are a thickening of the cortex, the spine and the pelvis are commonly involved by both lytic and reparative phases. Softening of bone and the common occurrence of transverse or pathologic fractures could conceivably result in extrusion of hematopoietic marrow into paraspinal and peripelvic regions, later developing into a locus of active extramedullary hematopoiesis.

Barry [15] reported two patients with Paget's disease and spinal cord symptoms. Radiographs during thoracic myelography in one patient clearly demonstrate the presence of bilateral lobulated paraspinal masses extending from T9–T12. In the second patient, an "extradural tumor" extending from C7 to T3 was found. The histology was interpreted as "vascular adipose tissue." The surgeon's impression was that it represented "an organizing hematoma." Judging from our present experience, these could certainly have represented manifestations of extra-

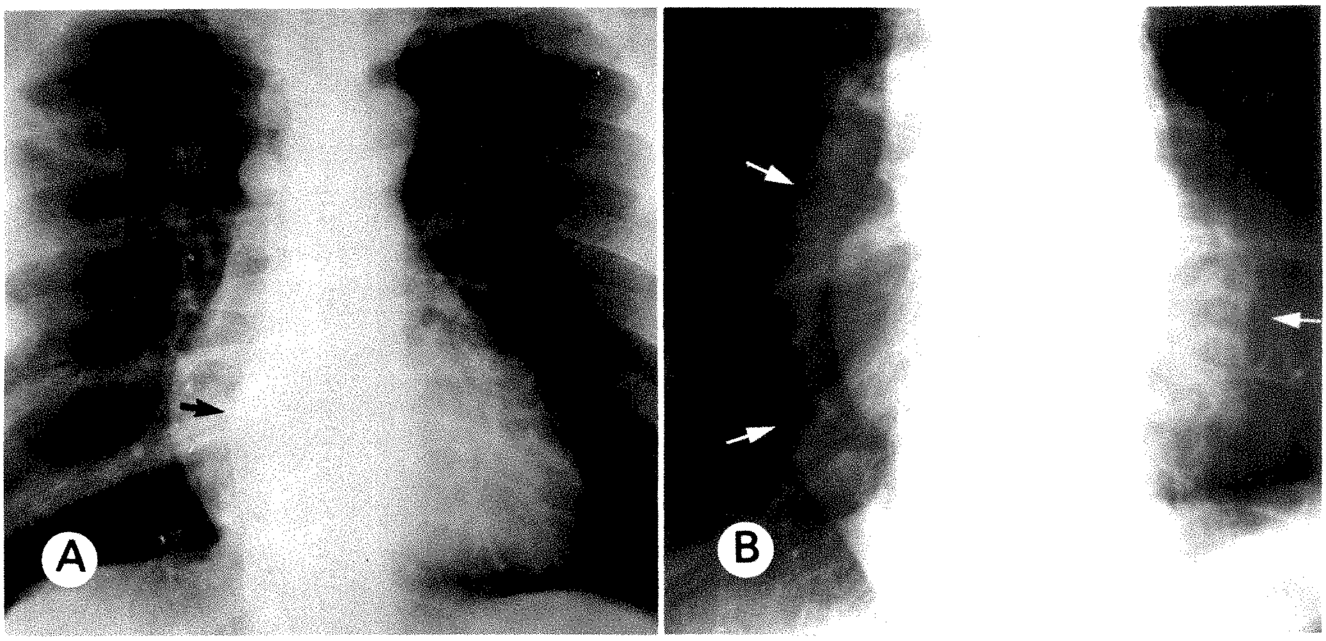

Fig. 3. – Case 2. *A*, Posteroanterior chest film showing widening of right paravertebral line (*arrow*). Right lower ribs show changes of Paget's disease. Note prominent azygos vein. *B*, Detail view of paraspinal area 14 years later showing paraspinal masses bilaterally (*arrows*).

medullary hematopoiesis leading to cord compression. Similarly, the observations made on chest radiographs of our second patient could also be attributed to it. Histologic confirmation at that site is not available.

Usually extramedullary hematopoiesis occurs as a compensatory phenomenon in response to anemia. Although an occasional patient with Paget's disease of bone has severe anemia [17], this was not the case in the previous report of Paget's disease with extramedullary hematopoiesis [9], and it was also not present in our patients.

Extramedullary hematopoiesis has also been reported in the pelvis [3, 10] and in a patient with Paget's disease of bone [9], but the possibility of the Paget's disease as a predisposing factor was not considered. We believe that in our patients with severe long-standing Paget's disease pathologic fractures led to extrusion of hematopoietic marrow and resultant tumorous extramedullary hematopoiesis.

REFERENCES

1. Ross P, Logan W: Roentgen findings in extramedullary hematopoiesis. *Am J Roentgenol* 106:604-613, 1969
2. Jordan HE: Extramedullary erythrocytopoiesis in man. *Arch Pathol* 18:1-21, 1934
3. Blaisdell JL: Extramedullary hematopoiesis in a retroperitoneal tumor. *Arch Pathol* 16:643-648, 1933
4. Korsten J, Grossman H, Winchester PH, Canale VC: Extramedullary hematopoiesis in patients with thalassemia anemia. *Radiology* 95:257-263, 1970
5. Wintrobe MM: Relation of disease of the liver to anemia: type of anemia, response to treatment and relation of type of anemia to histopathologic changes in liver, spleen, and bone marrow. *Arch Intern Med* 57:289-306, 1936
6. Brannan D: Extramedullary hematopoiesis in anemias. *Bull Johns Hopkins Hosp* 41:104-136, 1927
7. Wintrobe MM: *Clinical Hematology*, 6th ed. Philadelphia, Lea & Febiger, 1967
8. Saleeby ER: Heterotopia of bone marrow without apparent cause. *Am J Pathol* 1:69-76, 1925
9. Dodge OG, Evans DMD: Hemopoiesis in a presacral fatty tumour (myelolipoma). *J Pathol* 72:313-317, 1956
10. Lyall A: Massive extramedullary bone marrow formation in case of pernicious anemia. *J Pathol* 41:469-472, 1935
11. Ask-Upmark E: Tumour-simulating intrathoracic heterotopia of bone marrow. *Acta Radiol* 26:425-440, 1945
12. Cone SM: Bone marrow occurring in intercostal veins. *JAMA* 84:1732-1733, 1925
13. Case Records of Massachusetts General Hospital, Case 14-1968. *N Eng J Med* 278:782-791, 1968
14. Knabe K: Über Knochenmarksgewebe in der Nebeniere. *Zentralbl Allg Pathol* 43:57-61, 1928
15. Barry HC: *Paget's Disease of Bone*. Edinburgh, Livingstone, 1969
16. Greenfield GB: *Radiology of Bone Diseases*, 2d ed. Philadelphia, Lippincott, 1975
17. Aegerter E, Kirkpatrick JA: *Orthopedic Diseases*, 3d ed. Philadelphia, Saunders, 1968

Scanning Multiple Slit Assembly: A Practical and Efficient Device to Reduce Scatter

GARY T. BARNES,[1] IVAN A. BREZOVICH,[1, 2] AND DAVID M. WITTEN[1]

A scanning multiple slit assembly consisting of an array of long narrow beam-defining slits coupled with scatter-eliminating slots beneath the patient is a feasible, practical, and efficient method of reducing scatter and increasing contrast and image quality in diagnostic radiology. Measurements of the ratio of scattered-to-primary radiation transmitted by a scanning multiple slit assembly and a conventional high ratio grid under similar conditions showed the relative intensity of scatter transmitted by the slit assembly to be only one-third that of the grid. A noticeable improvement in contrast was obtained using the slit assembly, without increase in patient exposure. The design, construction, and clinical implications of such a scatter-eliminating technique are discussed.

Introduction

The use of a set of moving slits* to reduce secondary radiation in medical radiography was suggested as early as 1903 [1]. The arrangement consisted of one beam-defining fore slit between the x-ray tube and patient and one scatter-eliminating aft slit between the patient and film. The two slits were moved synchronously and scanned the area to be x-rayed. This technique was suggested by the observation that the quality of radiographic images obtained with a small ("coned down") radiation field was substantially better than those obtained with a large field. However, due to the long exposure time required and the successful development of the Bucky diaphragm [2, 3], this method of scatter elimination was not pursued.

In recent years, due to quantification of grid limitations [4-7], the search for better scatter-eliminating devices resumed and resulted in a resurgence of interest in moving slits [8-14]. Only when a device employing a multiplicity of slits was suggested [8, 10-12, 15], along with the availability of high capacity x-ray tubes and fast intensifying screens, did scatter reduction techniques using fore and aft slits become feasible.

In this paper, the performance and important design features of a scanning multiple slit assembly capable of taking 35.6 × 53 cm (14 × 17 inch) radiographs are reported. The principle of the assembly is shown in figure 1. The collimating or fore slits define several long narrow beams of radiation and are aligned and synchronously moved with the scatter-eliminating aft slots.

In using an array of long narrow slits for irradiating a given area of film, a long narrow beam geometry will irradiate a volume with a large surface area. When such a geometry is used, most of the scatter produced will escape and not be incident on the area of the film irradiated by the primary beam, resulting in a small scatter-to-primary ratio. Furthermore, when an array of long narrow irradiated volumes is used and the grid ratio and separation distance of the aft slots are chosen judiciously, very little scatter contribution from neighboring beams will result.

Design of Assembly

Figure 2 shows the scanning multiple slit assembly constructed at the University of Alabama in Birmingham. In its present form, there are 39 beam-defining fore slits located 48.8 cm below the focal spot of the x-ray tube. The fore slit width and spacing between slits are 1.63 mm and 6.50 mm, respectively. The focal spot-to-film distance is 121.9 cm with the tabletop positioned approximately 7.6 cm above the film. This leaves a clearance of roughly 61 cm between the fore slit assembly and tabletop, about equal to that between the bottom of a collimator and tabletop of a conventional arrangement with a 101.6 cm focal spot-to-film distance. The assembly uses a four-way floating tabletop for easy patient positioning.

The scatter-eliminating aft slots actually consist of two sets of slit plates 3 cm apart (fig. 3). The distance between the lower aft plate and the focal spot is 120 cm. The size and spacing of the slits in each plate is determined by the projection of the fore slits onto each of the respective planes. The slit width and spacing in the lower aft plate are 4 mm and 16 mm, respectively. The fore slits and each of the aft plates are mechanically connected by a linkage arm which pivots about the focal spot of the x-ray tube (fig. 3). This eliminates any grid cutoff by the aft slots and maintains alignment of all the plates during the entire scan.

From the point of view of the x-ray technologist, the exposure is made in the same manner as with any conventional unit. After a preset delay, which allows the x-ray tube rotor to reach its operating speed, the scanning motion is initiated by pressing the exposure button. When the slit assembly has moved for about 5 cm and has reached a uniform velocity, it turns on the three-phase generator. A blade attached to the aft slots opens

---

Received January 27, 1977; accepted after revision May 27, 1977.

This work was supported by U.S. Public Health Service research contract N01-CB-53865 from the National Cancer Institute, National Institutes of Health.

[1] Department of Diagnostic Radiology, University of Alabama School of Medicine, Birmingham, Alabama 35233. Address reprint requests to G. T. Barnes.

[2] Present address: Department of Radiation Oncology, University of Alabama School of Medicine, Birmingham, Alabama 35233.

* In the literature the terms slit and slot are often used interchangeably. In this paper a distinction is made. A slit refers to a long narrow cut in a plate about 1.6 mm thick or less, whereas a slot refers to a similar cut in a much thicker piece of material.

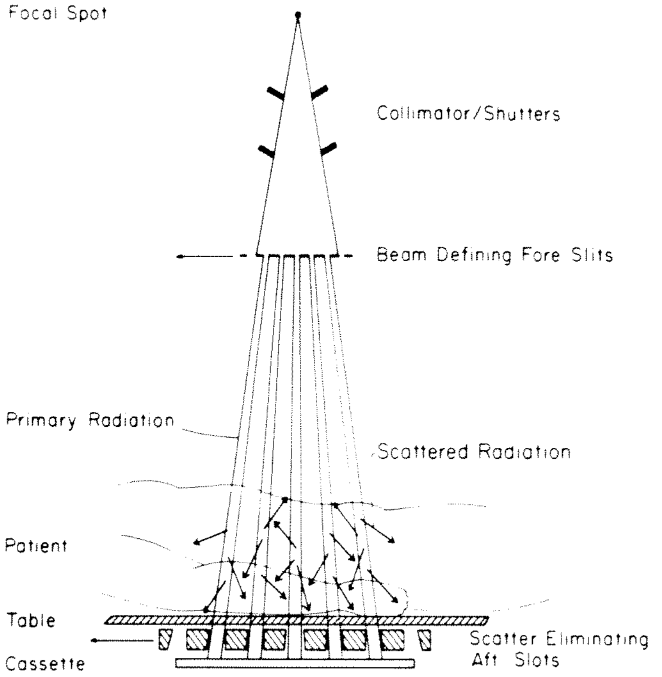

Fig. 1.—Principle of scanning multiple slit assembly.

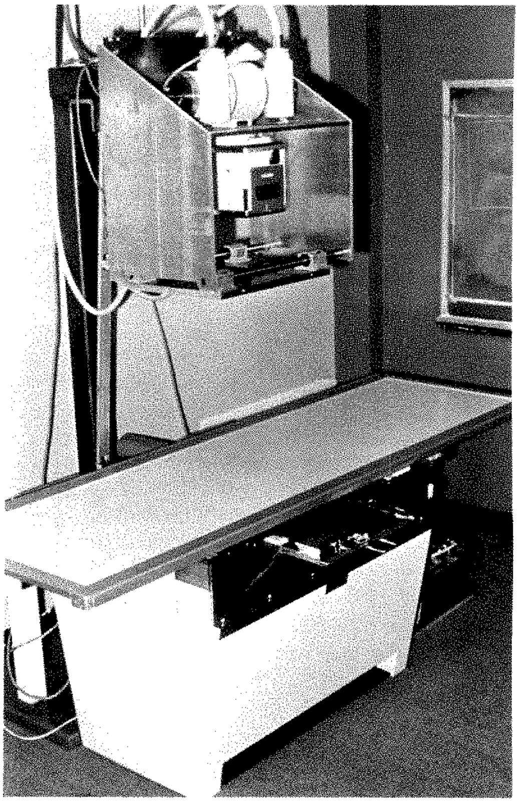

Fig. 2.—Scanning multiple slit assembly. Beam-defining fore slits are beneath collimator and aft slots are between tabletop and Bucky tray. Scanning movement is provided by servomotor coupled by gear belt to aft slot assembly. Fore slits are in turn coupled to aft slots by linkage arm which pivots about focal spot and maintains alignment during scan.

the light path of an optical source-sensor assembly and starts the exposure (fig. 4). After the unit has scanned over a distance of 20 cm (the distance of 10 slit widths plus separation distances in the plane of the lower aft plate), the opening of the light path of a second optical source-sensor assembly terminates the exposure. Immediately thereafter the scanning motion is stopped through regenerative breaking of the drive motor.

The uniformity of scan speed is achieved by a feedback loop in the drive system. A tachometer attached to the drive shaft of the electric motor generates a DC voltage proportional to speed of the motor. This tachometer voltage is fed to the motor control unit which compares it to the voltage of a preselected velocity command signal. The output of the control unit drives the motor in the direction and at a speed so that the difference between the tachometer and command signal vanishes.

The design of the unit discussed here was based on previously reported measurements employing a single fore slit and aft slot [10, 11], which enabled us to calculate the anticipated performance of the scanning multiple slit assembly. Analysis of these measurements indicated that for a given volume to be irradiated and for a given aft slot depth, the relative intensity of scatter will be less for narrower beams placed closer together. This advantage is eventually limited by the loss of primary radiation due to geometric unsharpness of the fore slits at the level of aft slots. This loss is in turn limited by the required design geometry and the focal spot size dictated by exposure time and tube loading considerations.

The relative intensity of scatter will also be less for a given beam width if the scanning beams are further apart and if deeper aft slots are used. However, these means are also limited—the former by exposure time and tube loading considerations, and the latter by the spacing between the tabletop and cassette, which in turn is limited by object magnification and the resultant loss in image sharpness associated with the finite size of the focal spot.

Our scanning multiple slit assembly is a reasonable compromise between these various factors. The fabrication of the components and the actual construction of the device were fairly straightforward. On the basis of our costs for purchased and fabricated components, an estimated price for a production unit including a realistic markup and profit margin is $20,000 (excluding the x-ray tube, high speed starter, collimator, and x-ray generator).

Results

The removal of scatter was measured with a 20 cm thick, 35.6 × 53 cm (14 × 17 inch) Lucite phantom. This was accomplished by placing small lead beam stops centrally on top of the phantom. The radiation emerging beneath the beam stop is due to scatter, while beneath the rest of the phantom it is due to scatter plus primary. X-ray film coupled with fast CaWo$_4$ screens was used as a detector. The resultant film densities were converted to relative exposure values using film sensitometry. To minimize random errors, the results of five runs were averaged. To correct for the systematic experimental error

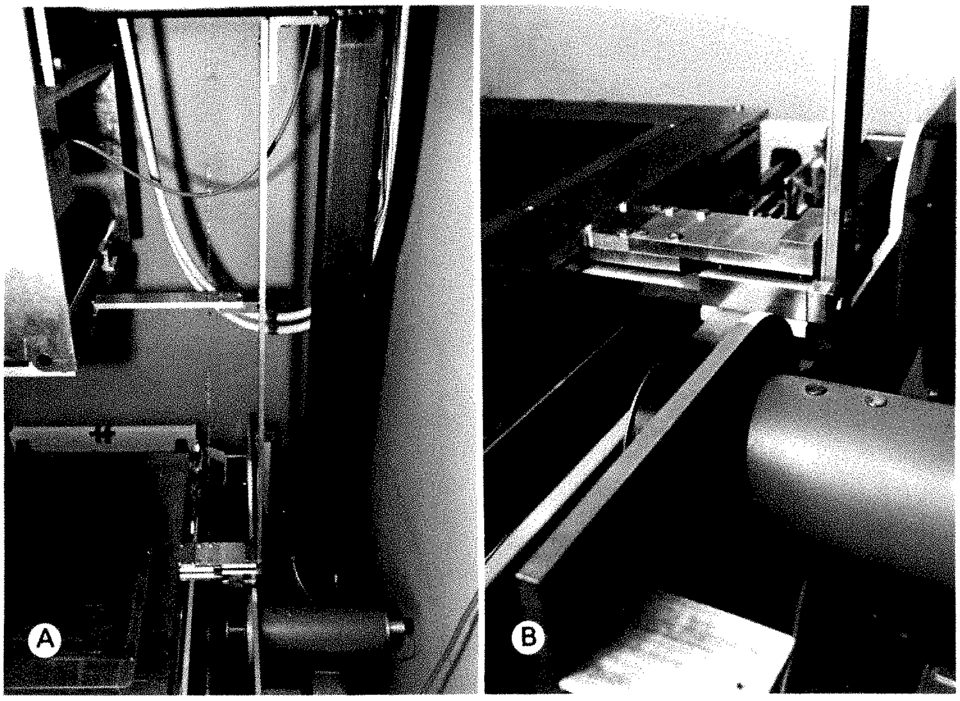

Fig. 3.—*A*, View of scanning multiple slit assembly tabletop removed showing coupling of fore slits and aft slots to linkage arm, design of aft slots, and coupling of drive motor to upper plate of aft assembly. *B*, Close-up view of aft slot assembly showing two plate design and coupling between plates, drive motor, and linkage arm.

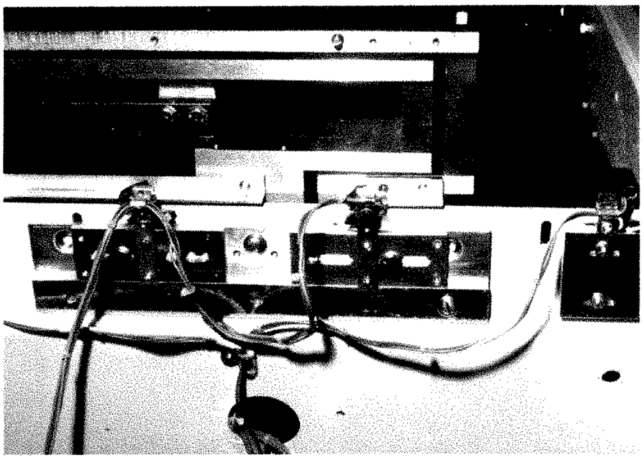

Fig. 4.—*A*, View of aft slot assembly showing (*left to right*) exposure stop, exposure start, and return stop optical source-sensors attached to table base. Attached to aft slot supports (*left to right*) are exposure start/stop blade and return stop blade. During exposure, scanning movement is right to left with scan half-way completed in this picture. After complete scan, assembly is returned to start position.

associated with the perturbation of the radiation field by the beam stop, each run consisted of measurements made with beam stops of various sizes which allowed for a linear regression extrapolation to a zero-size beam stop. Similar measurements were made on a commonly used 12:1 80 line grid positioned in a standard reciprocating Bucky assembly. The lead content of the grid was 570 mg/cm². Both grid and slit assembly were used at 80 kVp (3ϕ). The transmitted ratio of scattered-to-primary radiation with no scatter elimination technique was 8.7 ± 0.6. The ratio for the 12:1 linear grid was 0.92 ± 0.02; and for the scanning multiple slit assembly, 0.29 ± 0.02.

The fraction of primary beam contrast imaged in diagnostic radiology due to the presence of scatter or scatter degradation factor (*SDF*) is given by the equation $SDF = (1 + s/p)^{-1}$, where s/p is the ratio of scattered-to-primary radiation [16]. By substituting in the equation our measurements for the above scattering situation, it can be calculated that 78% of the primary beam contrast is imaged with the scanning multiple slit assembly, whereas only 52% is imaged with the grid. This improvement in contrast will be particularly helpful in perceiving information previously masked by the contrast fluctuations associated with quantum mottle [17, 18].

The improvement in diagnostic quality of the radiographic image achieved by this device at the same x-ray tube kilovoltage and beam quality compared with a standard 12:1 Bucky grid is demonstrated by a clinical example (fig. 5). The subject is an average, moderately obese adult male with an upper abdominal thickness of 25 cm. The improvement in image contrast achieved with this system is most apparent in the clarity of major soft tissue structures and bone detail. The anatomic outline and the soft tissue substance of both the ileopsoas muscles and the kidneys are seen more readily. The margins of the vertebrae and the trabecular pattern of the iliac bones and ribs, which are seen either poorly or not at all on the radiograph made by conventional Bucky technique (fig. 5*A*), are clearly visible on the film made with the multiple slit assembly (fig. 5*B*).

The 1.2 sec exposure time required to produce the radiograph with the scanning multiple slit assembly was dictated by the desire to uniformly scan the subject. Vibrational problems were experienced when faster scan times were attempted. The unit has since been modified to eliminate this problem, and scan times as short as 0.225 sec have been obtained with acceptable scan uniformity. Exposure times much shorter than this are unlikely because of x-ray tube loading limitations. The pres-

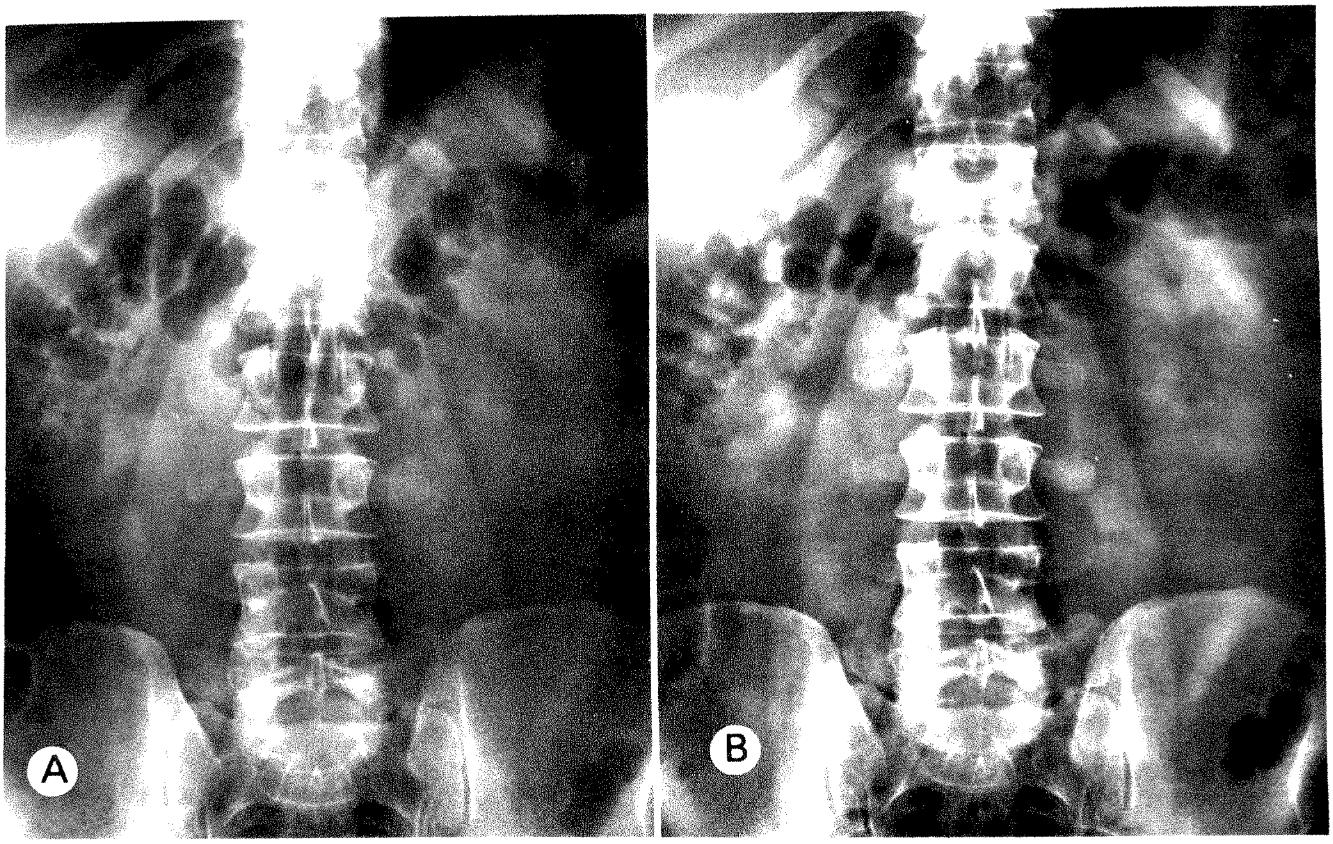

Fig. 5.—Comparison radiographs of single subject using three-phase generators at 94 kVp. *A*, 12:1, 80 line grid using 100 mA at 0.3 sec, 0.3 mm focal spot, 101.6 cm focal spot-to-film distance, 696 mR skin exposure. *B*, Scanning multiple slit assembly using 180 mA at 1.2 sec, 0.6 mm focal spot, 122 cm focal spot-to-film distance, 675 mR skin exposure. Both exposures made with same cassette using moderately fast $CaWO_4$ screens. Films developed in same processor within 15 min of each other. Same technique was used to calibrate kilovoltage and milliamperage of two generators; half-value layers were also closely matched.

ently used x-ray tube allows an exposure for 0.5 sec at 800 mA and 94 kVp on the large focal spot (1.2 mm). Employing 800 mA would allow the film of figure 5*B* to be obtained with an exposure duration slightly under 0.3 sec.

Discussion

When a grid and a scanning multiple slit assembly are compared, the primary and scatter transmission of the two techniques and the amount of scatter emerging determine the relative skin exposure and contrast improvement. The transmission of primary and, more noticeably, scatter by grids increase with x-ray tube kilovoltage [5]; on the other hand, very little kilovoltage dependence is exhibited by the multiple slit assembly. The kilovoltage used to obtain the comparison radiographs was selected so that about the same skin exposure would result. If a lower kilovoltage had been used, less skin exposure would have resulted with the scanning multiple slit assembly than with the grid. At a higher kilovoltage, the skin exposure would have been slightly greater with the multiple slit assembly and would have produced an even more marked improvement in contrast.

Even if the contrast and image quality obtained with a conventional grid are acceptable, an advantage of the scanning multiple slit assembly is that it can be operated at a much higher x-ray tube voltage, yielding images of equivalent quality at a fraction of the radiation exposure. Phantom studies indicate that contrast equivalent to that achieved with the multiple slit assembly may be obtained with a 12:1 grid by using a lower x-ray tube kilovoltage (around 30 kVp lower), but about three times the skin exposure would result.

As pointed out previously [10, 11], the scanning multiple slit assembly can be used to greatest advantage when the beam emerging from the patient is mostly scatter, such as with large film radiographs of the abdomen. An alternative use of such a device would be in mammography, where scatter significantly degrades contrast [19] and conventional grids cannot be used due to poor transmission of low energy x-rays. As in abdominal radiography, the scanning multiple slit assembly could be exploited to produce images of superior quality at the same radiation exposure or equivalent images at substantially less radiation exposure than conventional techniques. Due to its small radiation field size and specialized application, such a unit should be practical for clinical use.

ACKNOWLEDGMENTS

We acknowledge the many helpful discussions with H. Murray Cleare in the early stages of this project, the design contributions and machine shop work of Jerry R. Sewell, the help of Richard B. Gustafson on the generator interface, and the help and suggestions of the service engineering staff, particularly William L. McDanal and Dewey E. Narkates, throughout the development of the project.

REFERENCES

1. Pasche O: Über eine neue Blendenvorrichtung in der Röntgentechnik. *Deutsche Med Wochenschr* 29:266-267, 1903
2. Bucky G: Method and apparatus for projecting roentgen images. U.S. patent no. 1,164,987, December 1915
3. Potter HE: The Bucky diaphragm principle applied to roentgenography. *Am J Roentgenol* 7:292-295, 1920
4. Seemann HE, Splettstosser HR: Some physical characteristics of Potter-Bucky diaphragms. *Radiology* 62:575-583, 1954
5. Seemann HE, Splettstosser HR: The effect of kilovoltage and grid ratio on subject contrast in radiography. *Radiology* 64:572-579, 1955
6. Bonenkamp JG, Boldingh WH: Quality and choice of a Potter Bucky grid. I. A new method for the unambiguous determination of the quality of a grid. *Acta Radiol* 51:479-489, 1959
7. Bonenkamp JG, Boldingh WH: Quality and choice of a Potter Bucky grid. II. Application of the criterion of quality to various types of grids. *Acta Radiol* 52:149-167, 1959
8. Jaffe C, Webster EW: Radiographic contrast improvement by means of slit radiography. *Radiology* 116:631-635, 1975
9. Sashin D, Barnes JO, Ricci JL, Gur D: Electronic moving slit for scatter reduction in diagnostic radiology, in *Proceedings of the Ninth Midyear Topical Symposium of the Health Physics Society*, edited by Carson PL, Hendee WR, Hunt DC, Denver, Colorado, February 1976, pp 787-790
10. Barnes GT, Cleare HM, Brezovich JA: Improvement of contrast and/or reduction of patient exposure in diagnostic radiology by means of a scanning multiple slit assembly, in *Proceedings of the Ninth Midyear Symposium of the Health Physics Society*, edited by Carson PL, Hendee WR, Hunt DC, Denver, Colorado, February 1976, pp 791-795
11. Barnes GT, Cleare HM, Brezovich IA: Reduction of scatter in diagnostic radiology by means of a scanning multiple slit assembly. *Radiology* 120:691-694, 1976
12. Sorenson JA, Nelson JA: Investigations of moving-slit radiography. *Radiology* 120:705-711, 1976
13. Moore R, Korbuly D, Amplatz K: A method to absorb scattered radiation without attenuation of the primary beam. *Radiology* 120:713-717, 1976
14. Eastgate RJ, Siedband MP, Thomason CI, Dewerd LA: Scatter reduction in diagnostic radiology by paired moving slits, in Proceedings of the Fourth International Conference on Medical Physics, Ottawa, Canada, July 1976, *Physics in Canada*, vol 32, 1976, p 1.9
15. Barnes GT, Witten DM: Development and testing of a system to improve x-ray imaging, contrast and sharpness, while retaining the resolution of film. Contract proposal submitted to the National Cancer Institute for research funding proposal no. NCI-CB-53865-33, September 1974
16. Morgan RH: An analysis of the physical factors controlling the diagnostic quality of roentgenographic images. III. Contrast and the intensity distribution function of a roentgen image. *Am J Roentgenol* 55:67-89, 1946
17. Sturm RE, Morgan RH: Screen intensification systems and their limitations. *Am J Roentgenol* 62:617-634, 1949
18. Morgan RH: Threshold visual perception and its relation to photon fluctuation and sine wave response. *Am J Roentgenol* 93:982-997, 1965
19. Barnes GT, Brezovich IA: Contrast—the effect of scatter, in *Breast Carcinoma—The Radiologist's Expanded Role*, edited by Logan WW, New York, John Wiley, in press, 1977

Case Reports

Ulcerative Pseudopolyposis Mimicking Neoplasm Proximal to a Jejunal Obstruction

RONALD L. EISENBERG,[1] MARCUS W. HEDGCOCK,[1] R. BROOKE JEFFREY,[2] AND CAROLYN K. MONTGOMERY[3]

Ulcerative disease has been described proximal to obstructing lesions of the esophagus, stomach, terminal ileum, and colon. We present a case of ulcerative disease proximal to a partially obstructing adhesion of the jejunum and correlate the radiographic and pathologic findings with the prior cases at other sites.

Case Report

A 53-year-old male had a 7 day history of crampy lower abdominal pain with nausea and vomiting. During the week prior to admission he passed flatus intermittently but had no bowel movement. The previous year the patient had experienced 10 similar episodes, with severe cramping abdominal pain lasting from 2 hr to 2 days. The pain remitted after the patient passed large amounts of flatus. He also reported a 27 pound weight loss during that period. Fifteen years prior to admission the patient had undergone umbilical hernia repair.

He had no evidence of melena or hematochezia. Vital signs were within normal limits. Physical examination revealed a soft massively obese abdomen with healed umbilical hernia scar. Bowel sounds were active; there was no tenderness or palpable masses. Laboratory studies showed hematocrit 28.2 and hemoglobin 8.4 mg/100 ml; there were 9,800 white blood cells per high power field with a normal differential count.

Preliminary radiographs revealed a markedly dilated loop of bowel in the left mid abdomen, suggesting possible sigmoid volvulus or internal hernia (fig. 1). A sigmoidoscopy performed to 25 cm demonstrated normal mucosa with negative stool guaiac. Barium enema showed a markedly redundant colon, particularly in the descending and sigmoid portions, but no volvulus or intrinsic bowel lesion. An upper gastrointestinal series with small bowel follow-through revealed an area of marked narrowing in the mid small bowel with dilated bowel proximal to it. The mucosal pattern was abnormal in the dilated region and showed diffuse nodularity extending for 8 cm proximal to the area of narrowing (fig. 2). Distal to the narrowed portion, the small bowel appeared normal. The preoperative diagnosis was lymphoma, adenocarcinoma, or carcinoid. An inflammatory process was not considered in view of the normal terminal ileum and remainder of the small bowel.

At surgery, dense adhesions of the small bowel to a site of the old umbilical hernia incision and herniation of bowel into the abdominal wall were found. Proximal to this, the bowel was dilated and indurated. A ring of small polyps nearly encircled the mucosal lumen at the point of obstruction (fig. 3*A*).

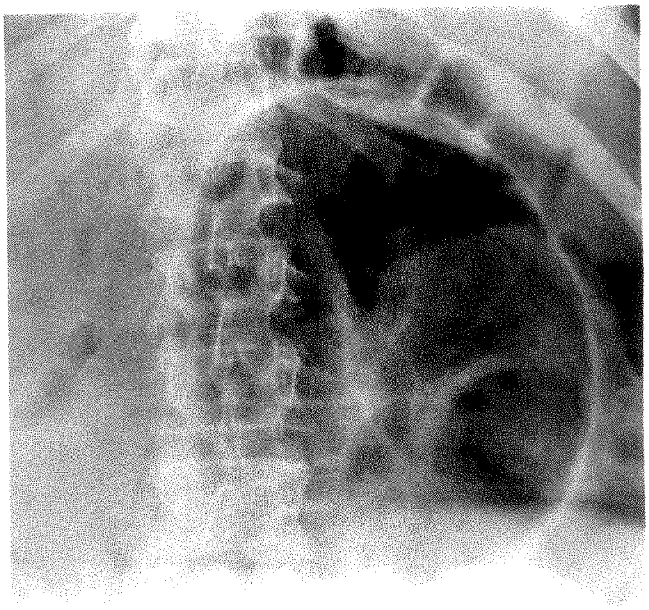

Fig. 1.—Abdominal radiograph demonstrating markedly dilated loop of bowel in midabdomen, suggestive of sigmoid volvulus or internal hernia.

Microscopic examination demonstrated numerous ulcerated inflammatory pseudopolyps at the site of obstruction (fig. 3*B*). The mucosa immediately adjacent to the pseudopolyps was edematous. The muscularis mucosae was hypertrophied and, in the region subadjacent to the polyps, the muscle fibers were splayed and distorted by fibrosis. Mucosal glandlike entrapment was prominent, neural proliferation was absent, and ganglion cells appeared normal. Distal to the point of partial obstruction, the bowel was entirely within normal limits. The patient recovered uneventfully following surgery.

Discussion

Ulcerative lesions of the bowel have been reported proximal to partial or complete obstruction of the lumen. In all these cases, the bowel was normal distal to the obstruction.

Bockus [1] described ulcerative disease in the esophagus proximal to stenotic lesions of the esophagogastric

---

Received February 22, 1977; accepted after revision May 24, 1977.

[1] Department of Radiology, University of California and Veterans Administration Hospital, 4150 Clement Street, San Francisco, California 94121. Address reprint requests to R. L. Eisenberg.

[2] Department of Radiology, University of California School of Medicine, San Francisco, California 94143.

[3] Department of Pathology, University of California and Veterans Administration Hospital, San Francisco, California 94121.

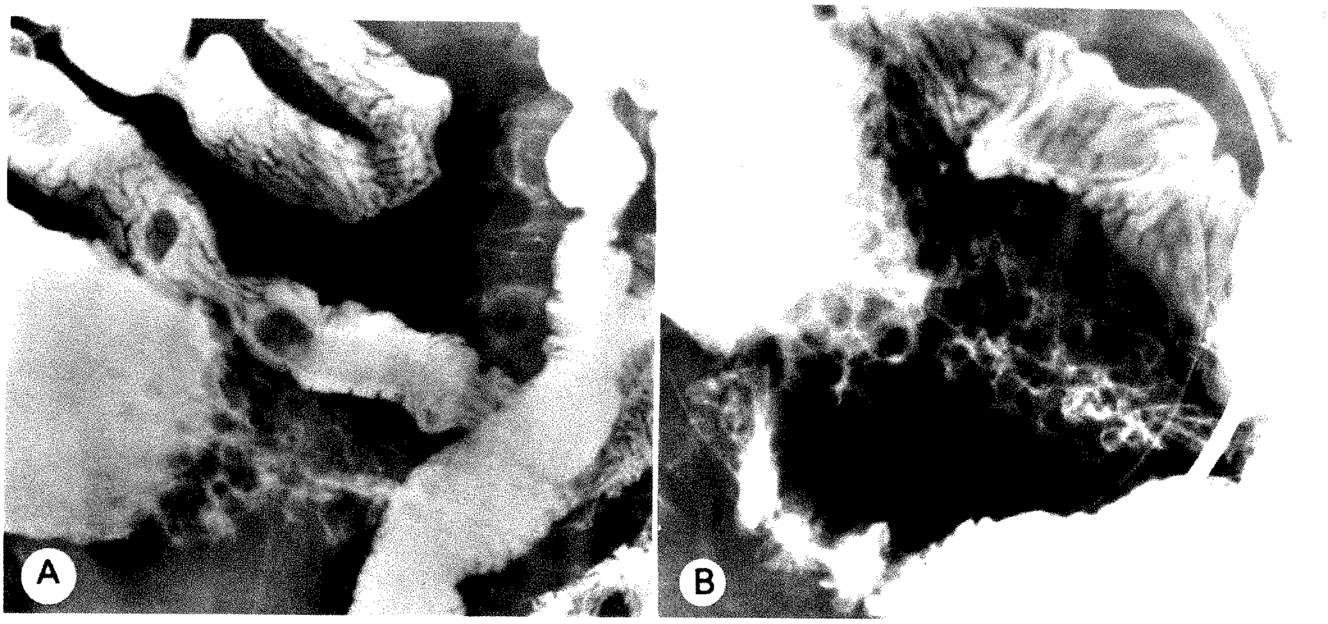

Fig. 2.—Radiographs from small bowel series demonstrating marked nodularity of small bowel proximal to area of partial obstruction.

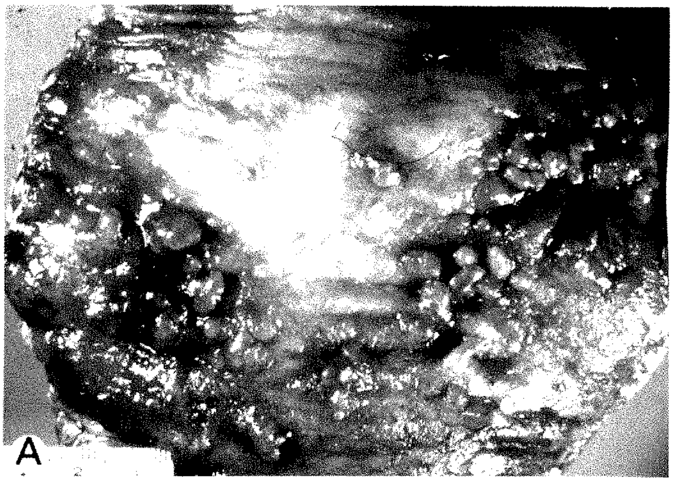

Fig. 3.—*A*, Gross specimen of jejunum demonstrating pseudopolyps proximal to site of obstruction. *B*, Photograph of ulcerated pseudopolyp (×14).

junction and in the stomach proximal to obstructing lesions at the gastric outlet. Ulcerative ileitis proximal to an ileostomy has been attributing to stomal obstruction (ileostomy dysfunction) [2]. A similar entity has been demonstrated proximal to carcinomas of the colon [3–5] with a radiologic and pathologic appearance closely simulating ulcerative colitis, though these patients had no prior history of idiopathic ulcerative colitis. A severe and often fatal colitis has been reported proximal to the functional colonic obstruction of Hirschsprung's disease [6, 7]. An ulcerative colitis has also been seen (in dogs) proximal to experimentally produced colonic obstructions [8].

Our case is the first reported in which ulcerative disease occurred proximal to a partially obstructing lesion of the jejunum. Radiographically, the appearance was somewhat different from ulcerative disease in other portions of the alimentary tract described by previous authors. The most prominent feature in our case was marked nodularity of the mucosa at the distal aspect of the dilated segment. This mimicked a neoplastic process, and a small bowel tumor was the presurgical diagnosis. Discrete ulcerations, reported previously [5],

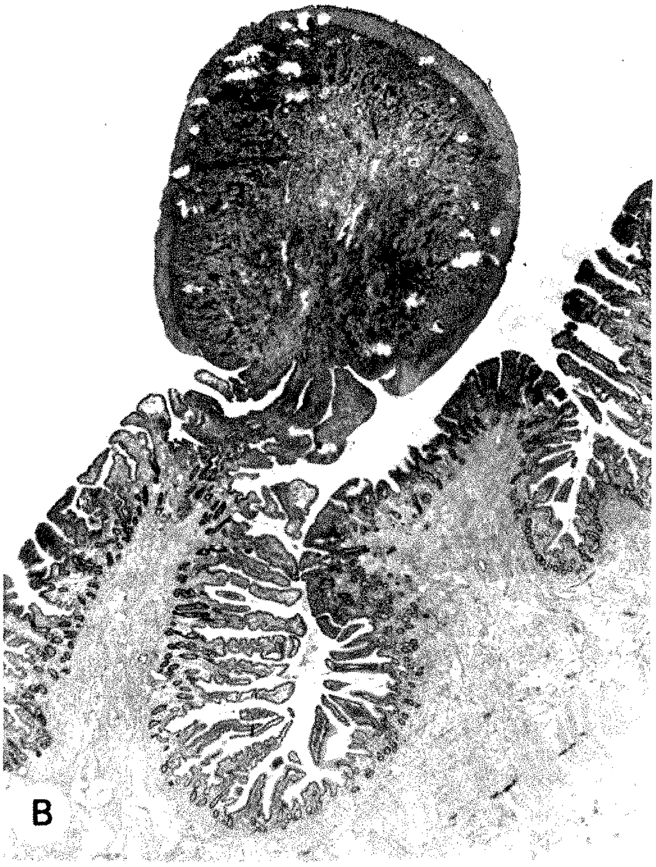

could not be distinguished on radiographs of our patient; no segmentation was evident.

Pathologically, our case closely resembles other reported cases of ulcerative disease proximal to obstructing lesions. Grossly, there was thickened, edematous bowel; the mucosal surface was studded with polypoid excrescenses [2, 5]. Microscopically, ulcerated inflammatory pseudopolyps were seen with hypertrophy of the underlying muscularis mucosae and submucosal fibrosis, all similar to changes seen in inflammatory bowel disease [2, 4, 5]. The pseudopolyps contained numerous chronic inflammatory cells, especially plasma cells, somewhat different from the small amount of cellular infiltrate and marked lack of plasma cells reported by Glotzer et al. [3].

Senturia and Wald [5] have suggested that the pathogenesis of ulcerative disease proximal to obstructing lesions of any segment of bowel appears to be a function of ischemia. Obstructing lesions lead to distention of the bowel with decreased blood flow through the vessels extending from the mesenteric border to the bowel wall. In turn, hypermobility, spasm, and edema of the muscular wall secondary to obstruction add to impairment of the blood supply. Ischemia has its earliest effect upon the mucosa, leading to ulceration predisposing to bacterial infection. Transmural ischemia may result in possible perforation [5]. In our case, the obstructive process was presumably secondary to adhesions with the narrowed segment eventually producing partial obstruction and stasis of bowel contents.

It must be emphasized that ulcerative disease proximal to an obstruction often presents radiographically as marked nodularity with pseudopolyp formation. This may mimic a neoplastic process, especially when seen in the small bowel. Whenever marked nodularity is seen proximal to an obstructing lesion, the possibility of inflammatory disease must be included in the differential diagnosis with lymphoma, carcinoma, and carcinoid.

REFERENCES

1. Bockus HL: *Gastro-enterology*, vol. 1, 2d ed. Philadelphia, Saunders, 1963
2. Fleishner FG, Mandelstam P: Roentgen observations of the ileostomy in patients with idiopathic ulcerative colitis: ileostomy dysfunction. *Radiology* 70:469–479, 1958
3. Glotzer DJ, Roth SI, Welch CE: Colonic ulceration proximal to obstructing carcinoma. *Surgery* 56:950–956, 1964
4. Hurwitz A, Khafif RA: Acute necrotizing colitis proximal to obstructing neoplasms of the colon. *Surg Gynecol Obstet* 111:749–752, 1960
5. Senturia HR, Wald SM: Ulcerative disease of the intestinal tract proximal to partially obstructing lesions: roentgen appearance. *Am J Roentgenol* 99:45–51, 1967
6. Bill AH Jr, Chapman ND: Enterocolitis of Hirschsprung's disease: its natural history and treatment. *Am J Surg* 103:70–74, 1962
7. Hope JW, Borns PF, Berg PK: Roentgenologic manifestations of Hirschsprung's disease in infancy. *Am J Roentgenol* 95:216–229, 1965
8. Glotzer DJ, Pihl BG: Experimental obstructive colitis. *Arch Surg* 92:1–8, 1966

"Backwash Ileitis" with Pseudopolyposis

GEOFFREY A. GARDINER[1]

Inflammatory pseudopolyps in the colon are a common finding in patients with ulcerative colitis. Their prevalence seems to bear a direct relationship to the extent and severity of the disease, but they may be seen in patients with a mild form of ulcerative colitis or even following what historically is the first attack of the disease. However, even when the colitis is severe and produces numerous large pseudopolyps, their occurrence is rare in the ileum.

The pathologic changes of ulcerative colitis frequently extend in a retrograde manner through the ileocecal valve into the ileum. The term "backwash ileitis" has been used to describe this involvement of the small intestine. Backwash ileitis occurs much more frequently when the entire colon is involved, possibly because of the effect of the ulcerative colitis on the ileocecal valve. Despite the prevalence of backwash ileitis, the development of pseudopolyposis or carcinoma in the involved ileum is rare. This is probably due to the milder inflammatory changes usually found in the ileum. At times the inflammation becomes more severe resulting in narrowing and spasm of the ileum which is difficult to distinguish radiologically from Crohn's disease. Occasionally the ulcers penetrate deeply resulting in perforation.

Case Report

A 31-year-old white female had an acute onset of bloody diarrhea at age 17 years. The next year a definitive histologic diagnosis of ulcerative colitis was made. Since then she has had periods of remission and exacerbation, although the longest period of remission lasted only 1½ years.

Two weeks before admission to a local hospital, the patient developed colicky epigastric pain, nausea and vomiting, jaundice, chills, and fever to 38.8°C. On admission the liver was tender and palpable 4-5 cm below the right costal margin. Laboratory work revealed mildly elevated SGOT and SGPT, and alkaline phosphatase of 40 U/liter (normal, 27-75). The stools were 4+ guaiac positive. Sigmoidoscopy revealed multiple polyps; biopsy of one was reported as an "adenomatous polyp of the colon." Barium enema examination showed severe ulcerative colitis with pseudopolyps (fig. 1*A*).

After discharge, the SGOT rose to 235 U (normal, 12-40) and the alkaline phosphatase to 1,515 U/liter. Because of these findings, the patient was referred to our hospital for further study.

Endoscopic retrograde cholangiopancreatography revealed stenosis of both the intra- and extrahepatic bile ducts compatible with sclerosing cholangitis. Barium enema examination showed extensive ulcerative colitis with pseudopolyps involving the entire colon and distal ileum (fig. 1*B*). A total proctocolectomy, including 35 cm of the distal ileum, was performed. Gross examination of the ileum showed multiple polyps as much as 2.3 cm in diameter (fig. 2).

Histologic sections revealed numerous inflammatory cells in the lamina propria and focal aggregates of lymphocytes in the submucosa. The colon had a granular cobblestone appearance with multiple dark brown polyps ranging up to 3.5 cm in diameter. The final diagnosis was "terminal ileum and total colon showing chronic ulcerative inflammation with pseudopolyp and polyp formation." The patient made an uneventful recovery after surgery.

Discussion

Extension of the colitis proximal to the ileocecal valve is a common feature of ulcerative colitis and has been termed backwash ileitis. The reported incidence varies from 1.3% to 39% [1]. Some degree of mucosal ulceration in the ileum has been reported in as many as 75% of cases when the entire colon is involved [2]. Occasionally backwash ileitis occurs when the cecum and ileocecal valve are normal [3].

Radiologic findings of backwash ileitis ordinarily extend only a short distance into the ileum. The ileum is usually not narrowed, the normal mucosal detail is absent, the walls are smooth or slightly uneven, and the ileocecal valve is patulous. If the inflammatory process becomes more severe, the ileum may show irritability, narrowing, and rigidity resembling Crohn's disease.

Dukes [4] described three types of pseudopolyps: (1) polypoid edematous mucosal tags, (2) polyps composed of granulation tissue covered by mucous membrane, and (3) polyps composed of connective tissue covered by a layer of glandular epithelium. Mixed pseudopolyps composed of granulation tissue and intimately mixed mucosal remnants may be the most frequent form [3]. True adenomatous polyps are rarely found.

While inflammatory pseudopolyps in the colon have been reported in over 60% of cases in some series [2, 5], they are rarely encountered in the ileum when it is involved with backwash ileitis. This may be due to the milder inflammatory changes which usually occur in the ileum. "Polypoid islands of mucosa" in the ileum have been described in cases with severe mucosal ulceration [1], and it is well known that inflammatory pseudopolyps in the colon are most numerous where the colitis is most severe and extensive.

Pseudopolyps may occur early in the course of ulcerative colitis. In one group of patients with pseudopolyps, 33% had disease of less than 5 months duration [6]. In a survey of 465 patients with ulcerative colitis, 29.3% were found to have pseudopolyps during a severe first attack

---

Received February 8, 1977; accepted after revision May 5, 1977.

[1] Department of Radiology, Loma Linda University School of Medicine, Loma Linda, California 92354.

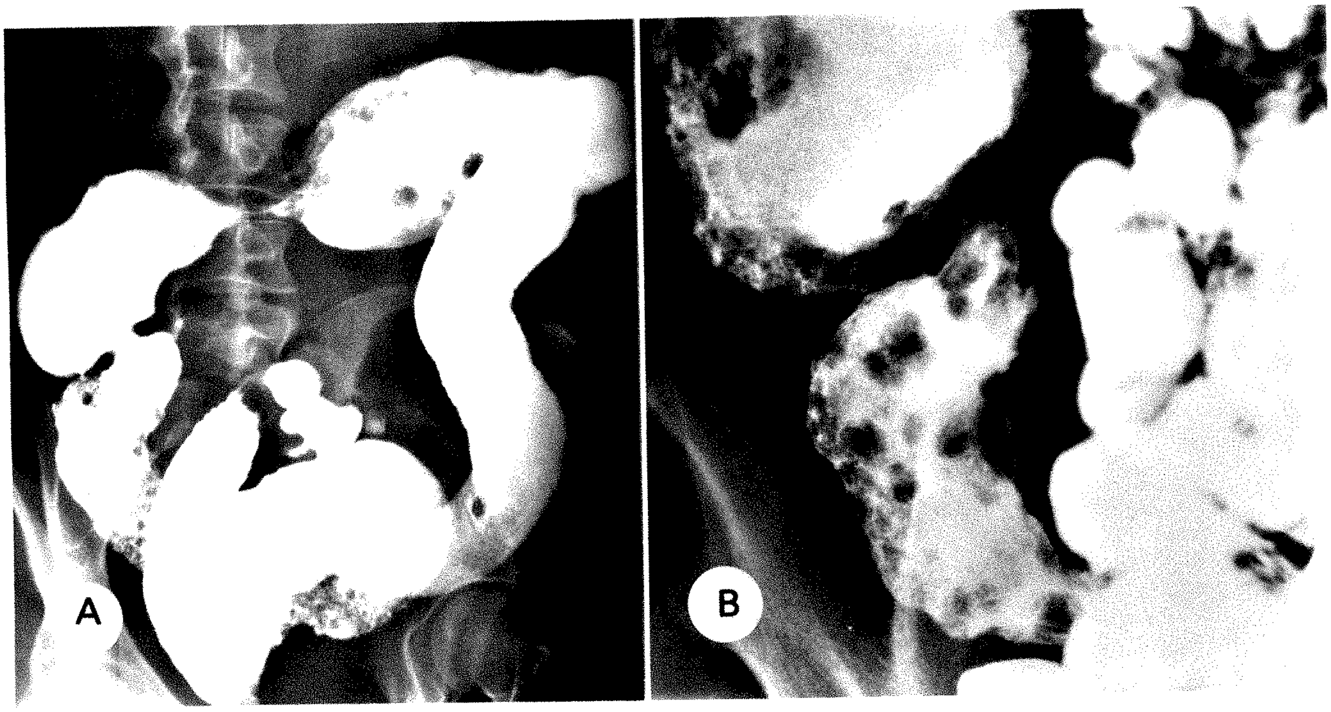

Fig. 1.—*A*, Barium enema study showing advanced changes of ulcerative colitis involving entire colon. Ascending colon is short and ileocecal valve widely patent. There are numerous pseudopolyps. Terminal ileum has nearly same appearance as colon. *B*, Barium study at second admission showing close-up of cecum and ileum. Note severe changes in ileum and many large pseudopolyps.

[7]. Once they have been established, pseudopolyps rarely disappear.

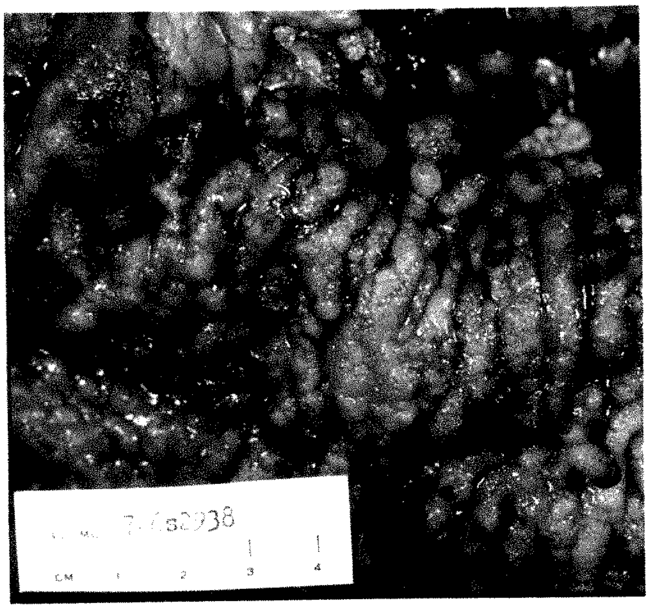

Fig. 2.—Gross specimen of terminal ileum showing large numbers of pseudopolyps.

REFERENCES

1. McCready FJ, Bargen JA, Dockerty MB, Waugh JM: Involvement of the ileum in chronic ulcerative colitis. *N Engl J Med* 240:119-127, 1949
2. Saltzstein SL, Rosenberg BF: Ulcerative colitis of the ileum and regional enteritis of the colon. *Am J Clin Pathol* 40:610-623, 1963
3. Lumb G, Protheroe RHB: Ulcerative colitis. *Gastroenterology* 34:381-405, 1958
4. Dukes CE: Surgical pathology of ulcerative colitis. *Ann R Coll Surg Engl* 14:389-400, 1954
5. Bockus HL, Roth JLA, Buchman E, Kalser M, Staub WR, Finkelstein A, Valdes-Dapena A: Ulcerative colitis. *Gastroenterologia* 86:549-581, 1956
6. Jalan KN, Walker RJ, Sircus W, McManus JPA, Prescott RJ, Card WI: Pseudopolyposis in ulcerative colitis. *Lancet* 2:555-559, 1969
7. de Dombal FT, Watts JM, Watkinson G, Goligher JC: Local complications of ulcerative colitis. *Am J Proctol* 18:198-201, 1967

Mallory-Weiss Syndrome with Esophageal Obstruction Secondary to Adherent Intraluminal Thrombus

MICHAEL J. CURTIN[1] AND FRANCIS D. MILLIGAN[2]

Within the spectrum of emetogenic esophagogastric injuries, the Mallory-Weiss syndrome is a well recognized clinical and pathologic entity [1, 2]. The Mallory-Weiss syndrome is characterized by superficial mucosal lacerations or fissures near the cardioesophageal junction caused by increases in intraluminal and transmural pressure gradients; significant hemorrhage is present in almost all instances. Most lacerations occur in the gastric mucosa or extend across the gastroesophageal junction, but 5%–10% are limited to the esophagus. Gastroscopy with esophagoscopy is the usual and most effective way to establish the diagnosis. This report describes a patient in whom the Mallory-Weiss syndrome with upper gastrointestinal bleeding was radiographically documented. It is the first reported case to present with esophageal obstruction secondary to intraluminal thrombus.

Case Report

E. R., a 30-year-old Negro man, was seen for evaluation of hematemesis. Two days before admission he entered the emergency department complaining of pleuritic chest pain, nausea, vomiting, and periumbilical abdominal pain. The vomiting persisted, and on the day of admission he vomited approximately 100 ml of bright red blood and later some clotted blood. He then complained of severe dysphagia, even for liquids.

Chest and abdominal radiographs were normal. At fluoroscopy a nearly complete obstruction of the distal esophagus was found. There was a conical narrowing of the lumen by an esophageal mass that extended over a segment 6 cm long (figs. 1*A* and 1*B*). An upright lateral radiograph (fig. 1*C*) showed the air-fluid level maintained above the site of obstruction. The surface of this protruding mass was irregular and of varying thickness in its extension longitudinally down the lower one-third of the esophagus. Initially, an intramural lesion with obstruction secondary to hemorrhage and edema was suspected. However, on multiple oblique views no definite double lumen, mucosal stripe, or extraluminal contrast material could be identified.

Esophagoscopy with the Olympus GIF fiberoptic endoscope revealed partial obstruction of the distal esophageal lumen at 35 cm by friable reddish frondlike masses circumferentially adherent to the esophageal mucosa (fig. 2*A*). No definite mucosal tear was identified. Multiple biopsies of these masses revealed only blood clot (thrombus) without evidence of overlying esophageal mucosa.

At repeat endoscopy 1 week after admission, two healing linear mucosal tears were seen in the distal esophagus; biopsies of these areas confirmed the presence of granulation tissue. The previously noted blood clots had disappeared. Just prior to discharge a final esophagogram and endoscopic examination showed a normal esophagus (fig. 2*B*).

Discussion

The spectrum of radiographic abnormalities in emetogenic injuries varies with the degree of esophageal wall damage. The characteristic radiologic findings in Boerhaave's syndrome, which is a full thickness perforation of the distal esophagus, include mediastinal and cervical emphysema, left pleural effusion or hydropneumothorax, and, on contrast studies, usually evidence of transmural perforation [3]. In the Mallory-Weiss syndrome, where there is less esophageal or gastric wall damage, there are generally few radiographic findings. In occasional patients the esophagogram is diagnostic, showing barium trapped in a jagged mucosal tear [4, 5]. More extensive lacerations lead to severe arterial hemorrhage which generally results in massive hematemesis or melena. However, if smooth muscle contraction or clot occludes the mucosal tear, a dissecting intramural hematoma may form [2, 6]. In the esophagus this hematoma usually creates a "double barreled" lumen [2], often well delineated by the "mucosal stripe sign" [7]. In the stomach an intramural hematoma may either circumferentially compress the cardia or merely indent the gastric curvatures as a localized mass.

As demonstrated in this patient, intermediate degrees of gastroesophageal mucosal injury and bleeding may also lead to an intraluminal thrombus without intramural dissection. With partial closure of the mucosal rent and continued slow hemorrhage, large mounds of clot become adherent to the mucosa (fig. 3). The radiographic appearance of such a lesion occurring in the stomach has been described and may mimic a tumor [8]. Dagradi et al. [9], using early endoscopic examination, saw fresh reddish clot occupying the rent in the gastric mucosa in two-thirds of their patients examined within 24 hr of a Mallory-Weiss tear. When the tear involves the esophageal mucosa, the narrow esophageal lumen is more easily compromised by the accumulation of blood clot, and the thrombus may quickly lead to complete or partial obstruction. Other conditions to be considered in the differential diagnosis of an esophageal mucosal lesion include fibrovascular or inflammatory polyp, varices, polypoid carcinoma, and carcinosarcoma.

Received November 30, 1976; accepted after revision May 11, 1977.

[1] Department of Radiology and Radiological Science, Johns Hopkins Medical Institutions, Baltimore, Maryland 21205. Present address: Department of Radiology and Nuclear Medicine, St. Marys Hospital Medical Center, 707 South Mills Street, Madison, Wisconsin 53715. Address reprint requests to M. J. Curtin.

[2] Department of Medicine, Johns Hopkins Medical Institutions, Baltimore, Maryland 21205.

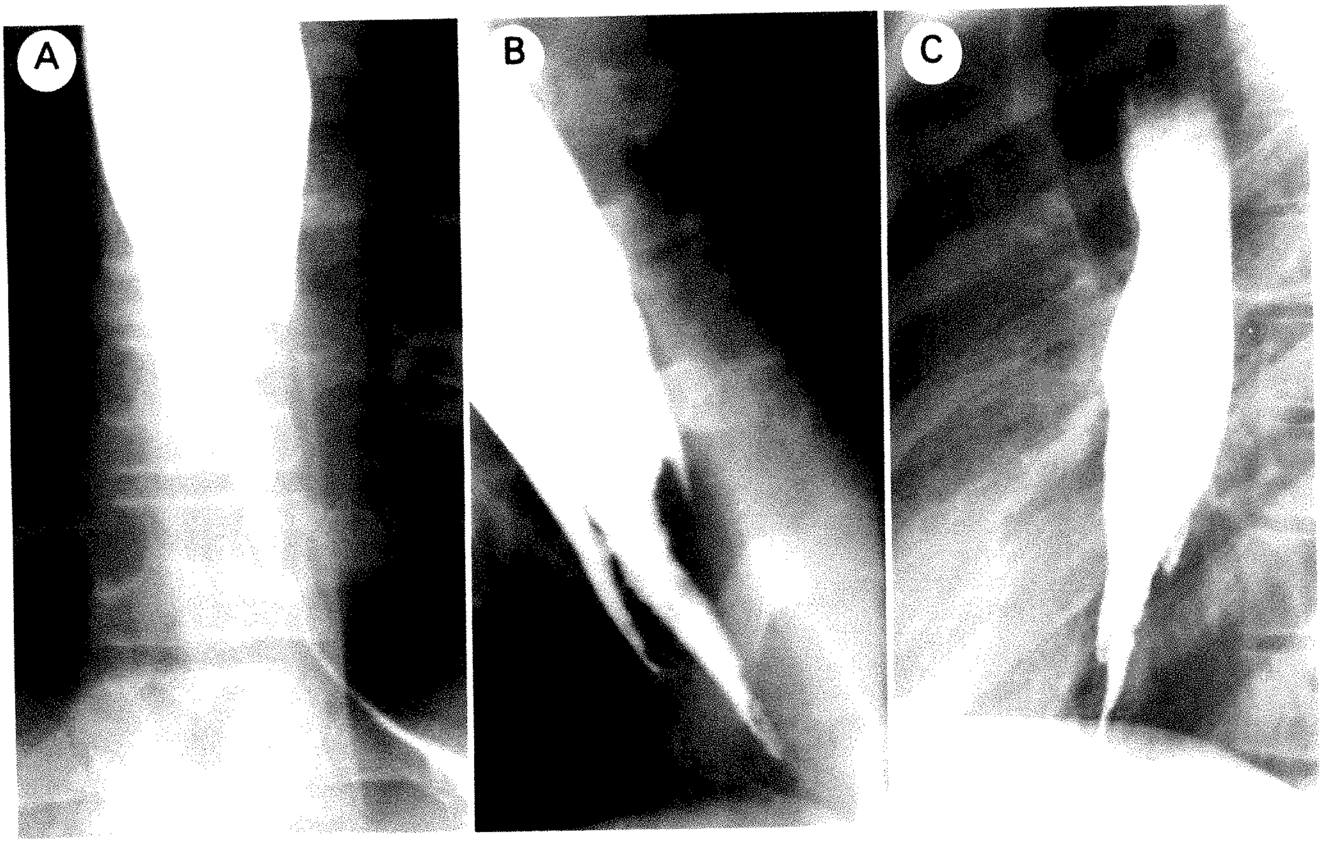

Fig. 1.—*A and B*, Frontal and oblique views of distal esophagus showing near complete obstruction by intraluminal mass of clotted blood. *C*, Detail from upright lateral chest radiograph prior to fluoroscopic placement of Levin tube for removal of barium suspension layered above distal esophageal obstruction.

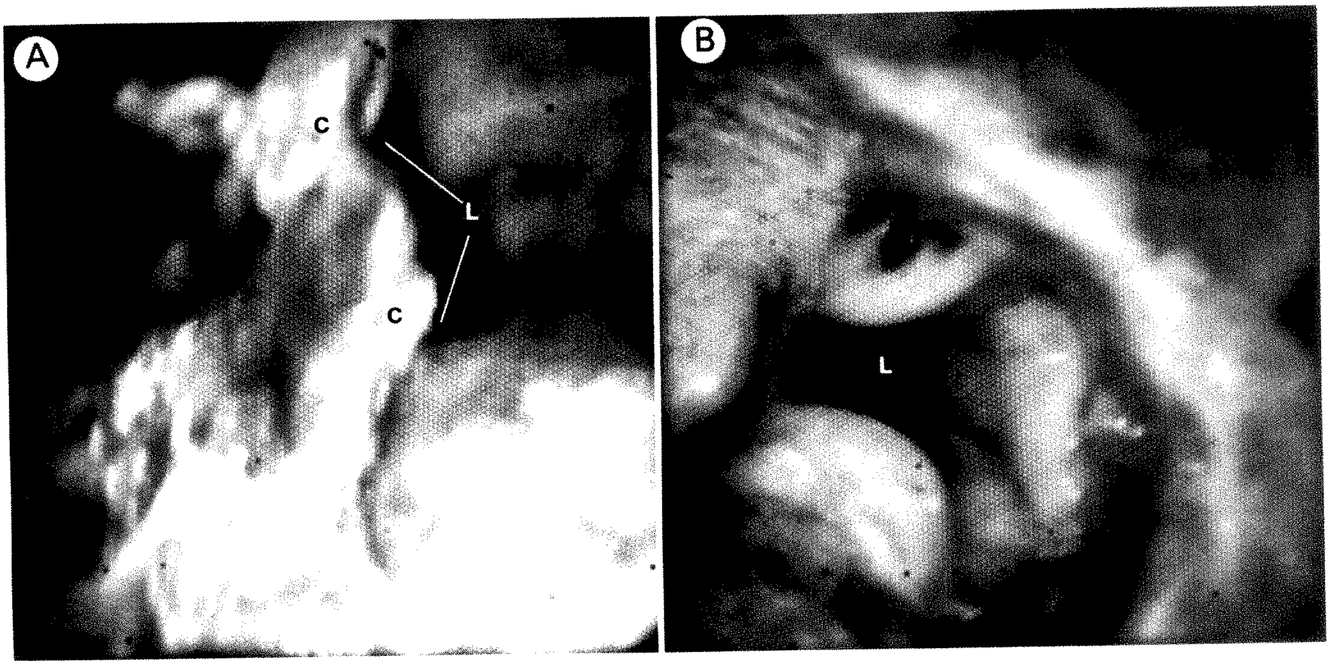

Fig. 2.—*A*, Endoscopic view showing frondlike masses of blood clot (C) obstructing lumen (L) of distal esophagus. *B*, Final endoscopic examination showing normal distal esophageal lumen (L).

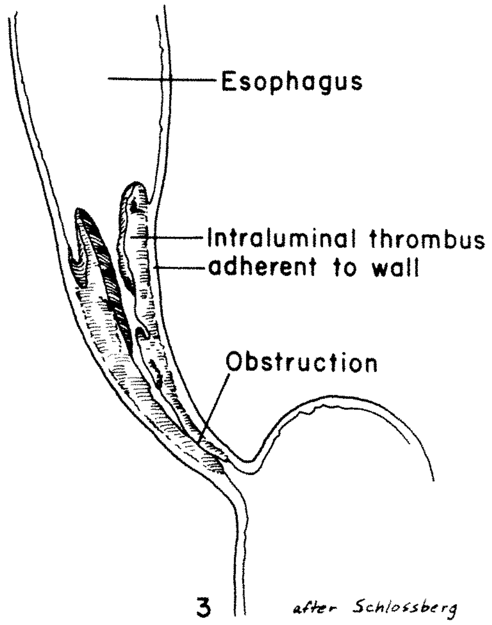

3

Fig. 3.—Gross topographic relationships as reconstructed from radiographs and endoscopic photographs.

In our patient, the combined radiographic and endoscopic findings were suggestive enough of incomplete tear of the esophagus to permit conservative medical therapy. With such treatment, the use of repeated chest radiographs to exclude mediastinal emphysema or pleuritis and sequential esophageal barium studies and endoscopy to assure resolution of the obstructing thrombus and progressive healing of the mucosal rents is necessary.

Perhaps a higher index of suspicion of incomplete esophageal tears in patients with vomiting and minimal to moderate hematemesis will lead to earlier combined radiographic and endoscopic examinations. When an esophageal intraluminal thrombus progresses to partial or complete esophageal obstruction, the possibility of pulmonary aspiration is considerably increased. Earlier diagnosis may help prevent this complication as well as those associated with nasogastric tube passage (e.g., dislodgement of clot with aggravation of bleeding or inadvertent extension of esophageal mucosal tears).

ACKNOWLEDGMENTS

We thank Dr. Martin W. Donner for helpful criticism and Mr. Leon Schlossberg for the medical illustration.

REFERENCES

1. Mallory GK, Weiss S: Hemorrhages from lacerations of the cardiac orifice of the stomach due to vomiting. *Am J Med Sci* 178:506–515, 1929
2. Thompson NW, Ernst CB, Fry WJ: The spectrum of emetogenic injury to the esophagus and stomach. *Am J Surg* 113:13–26, 1967
3. Rogers LF, Puig AW, Dooley BN, Cuello L: Diagnostic considerations in mediastinal emphysema: a pathophysiologic-roentgenologic approach to Boerhaave's syndrome and spontaneous pneumomediastinum. *Am J Roentgenol* 115:495–511, 1972
4. Carr JC: The Mallory-Weiss syndrome. *Clin Radiol* 24:107–112, 1973
5. Butler ML: Radiologic diagnosis of Mallory-Weiss syndrome. *Br J Radiol* 46:553–554, 1973
6. Joffe N, Milan VG: Postemetic dissecting intramural hematoma of the esophagus. *Radiology* 95:379–380, 1970
7. Lowman RM, Goldman R, Stern H: Roentgen aspects of intramural dissection of the esophagus. The mucosal stripe sign. *Radiology* 93:1329–1331, 1969
8. Espiritu CR, Mendoza J, Gratz CJ: Mallory-Weiss syndrome presenting as a gastric tumor. *J Fla Med Assoc* 60:24–25, 1973
9. Dagradi AE, Stempien SJ, Juler G, Broderick J, Wolinski S: The Mallory-Weiss lesion. An endoscopic study of thirty cases. *Gastrointest Endosc* 13:18–19, 1967

Metastatic Melanoma Presenting Clinically as Multiple Colonic Polyps

BARRY A. SACKS,[1] NORMAN JOFFE,[1] AND DONALD A. ANTONIOLI[2]

Metastatic involvement of the gastrointestinal tract secondary to hematogenous spread of malignant melanoma is well documented [1-5]. The small bowel is the most common site of involvement [1-3, 6, 7]; gastric metastases are less common and colonic lesions distinctly rare [1, 2, 4, 8]. Clinical symptoms may include acute or chronic gastrointestinal bleeding, intestinal obstruction secondary to intussusception, anemia, malaise, or weight loss. Pathologically, tumor deposition occurs initially in the submucosa giving rise to intramural plaques or nodules [3, 6, 7]. Subsequent growth may result in bulky intraluminal polypoid lesions which may undergo central ulceration, producing the characteristic "bulls-eye" or "target" lesions seen on radiologic examination [1, 6]. We report a case of metastatic melanoma presenting initially as multiple colonic polyps.

Case Report

G. S., a 53-year-old white female, had intermittent abdominal pain for several months. Physical examination and laboratory data were essentially normal. Air contrast barium enema examination revealed multiple sessile polyps in the region of the splenic and hepatic flexures and in the ascending colon (fig. 1). The findings were confirmed by colonoscopy, at which time two of the polyps were removed and submitted for histologic examination. This surprisingly revealed that the "polyps," which were not visibly pigmented, represented metastatic melanoma (fig. 2). Upper gastrointestinal series and small bowel examination were normal. Reinterrogation of the patient revealed that a hairy nevus had been removed from her back about 20 years earlier, but review of the available histologic specimens confirmed the presence of a benign lesion. Despite thorough clinical examination, no cutaneous or other primary lesions could be detected. Chemotherapy was instituted, but the patient exhibited a progressive deterioration in her clinical course with the development of ascites. Cytologic examination of the ascitic fluid was positive for melanoma cells.

Discussion

Metastases from malignant melanoma may occur many years after presentation of an initial primary lesion. Occasionally, they represent the first evidence of the disease or even occur in the absence of a clinically detectable primary tumor [2, 5]. Gastrointestinal metastases most commonly involve the small bowel and stomach [2, 6, 7], and there is general agreement that the colon is the least common site for the metastases [1-3, 7]. This variation in the incidence at different sites in the alimentary tract may relate to differences in relative blood supplies [2, 6].

The incidence of gastrointestinal metastases is probably much higher than suggested by most antemortem studies [3, 5, 8]. Das Gupta and Brasfield [3] reported only nine clinical cases of confirmed gastrointestinal metastases in more than 1,000 patients with cutaneous melanoma. However, in an autopsy study of 100 cases of metastatic melanoma, they found small bowel metastases in 58, gastric metastases in 26, and colon lesions in 22. The colonic lesions were described in general terms to be polypoid or ulcerative and were often associated with extensive extraintestinal disease in the pelvis. In one patient, a premortem biopsy of a rectal polypoid mass had been found to show metastatic melanoma. Of 18 cases of metastatic melanoma of the small and large bowel reported by Willbanks and Fogelman [5], the colon alone was involved in three; in one of these three the lesions presented as multiple polypoid masses.

The discrepancy between the low incidence of clinically diagnosed gastrointestinal metastases and their relatively high postmortem incidence is presumably related in part to the relatively infrequent occurrence of specific abdominal symptoms during life. Since radiology plays an important role in the initial detection of gastrointestinal metastases, it may also be a reflection of the relative insensitivity of routinely employed radiologic techniques. The more frequent application of careful double contrast studies of the stomach and colon may increase detection of early or small lesions in these areas and aid significantly in reducing the discrepancy between antemortem detection and postmortem incidence.

Our case is of interest in several respects. It reemphasizes the fact that gastrointestinal metastases may represent the initial manifestation of malignant melanoma and that these may occur in the absence of a clinically obvious primary lesion. Moreover, it demonstrates that the colonic metastases may simulate simple polyps both radiologically and endoscopically. According to Willbanks and Fogelman [5], the majority of metastatic polypoid lesions are amelanotic. In our experience the amount of melanin in metastatic lesions is highly variable, even in the same patient. The reason for this variability is not known. In addition, many lesions contain enough pigment granules to be clearly identified microscopically but not on gross examination. For this reason, biopsy and microscopic examination of colonic "polyps" is essential in all patients with a prior history of cutaneous melanoma.

REFERENCES

1. Pomerantz H, Margolin HN: Metastases to the gastrointestinal tract from malignant melanoma. *Am J Roentgenol* 88:712-717, 1962

Received March 17, 1977; accepted after revision May 10, 1977.

[1] Department of Radiology, Beth Israel Hospital, 330 Brookline Avenue, Boston, Massachusetts 02215. Address reprint requests to B. A. Sacks.

[2] Department of Pathology, Beth Israel Hospital, Boston, Massachusetts 02215.

***Am J Roentgenol* 129:511-513, September 1977**

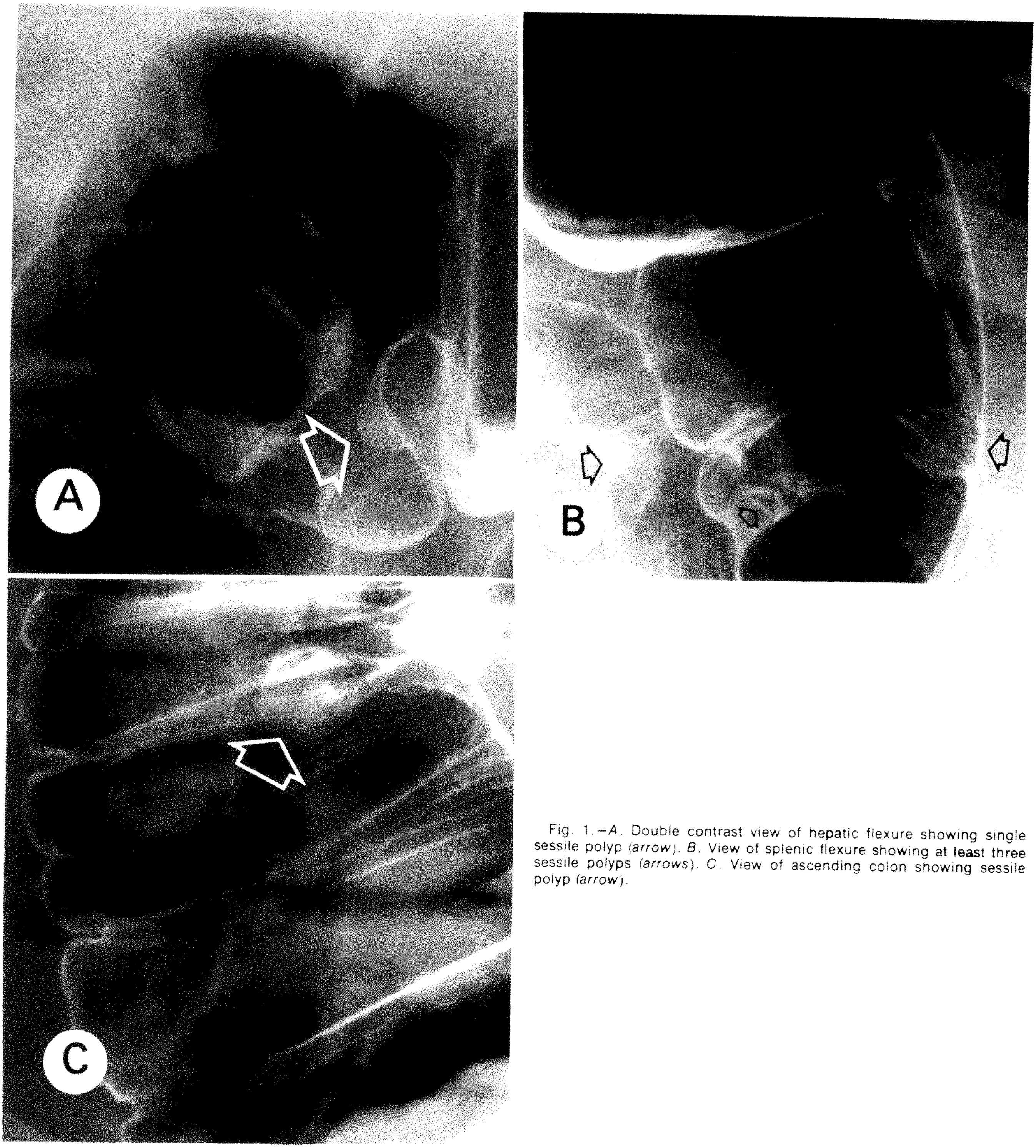

Fig. 1.—*A*. Double contrast view of hepatic flexure showing single sessile polyp (*arrow*). *B*. View of splenic flexure showing at least three sessile polyps (*arrows*). *C*. View of ascending colon showing sessile polyp (*arrow*).

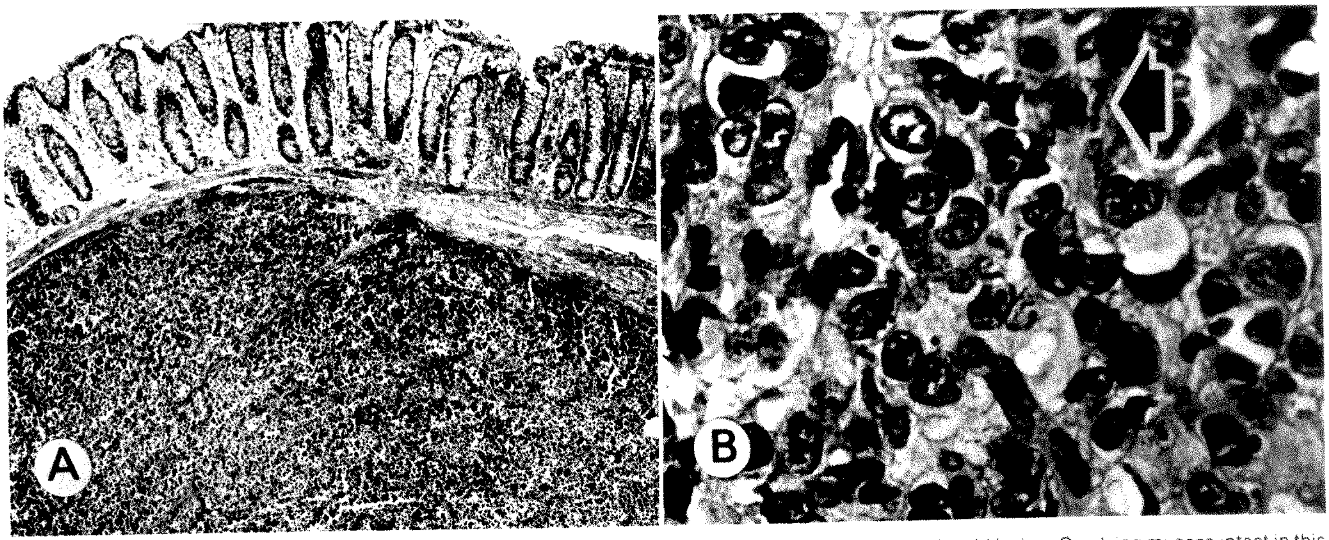

Fig. 2.—*A*. Low power photomicrograph of nodule of melanoma cells filling submucosa in one colonic polypoid lesion. Overlying mucosa intact in this area. H and E stain. ×32. *B*. High power view of malignant melanoma cells showing pleomorphic and hyperchromatic nuclei. Cytoplasm of some cells contains granules of melanin pigment (*arrow*). H and E stain. ×520.

2. Fraser-Moodie A. Hughes RG. Jones SM. Shorey BH. Snape L: Malignant melanoma metastases to the alimentary tract. *Gut* 17:206-209. 1976
3. Das Gupta TK. Brasfield RD: Metastatic melanoma of the gastrointestinal tract. *Arch Surg* 88:969-973. 1964
4. Harris MN: Massive gastrointestinal hemorrhage. *Arch Surg* 88:1049-1051. 1964
5. Willbanks OL. Fogelman MJ: Gastrointestinal melanosarcoma. *Am J Surg* 120:602-606. 1970
6. Meyers MA. McSweeney J: Secondary neoplasms of the bowel. *Radiology* 105:1-11. 1972
7. Willis RA: *The Spread of Tumours in the Human Body*. 3d ed. London. Butterworth. 1973
8. Beckley DE: Alimentary tract metastases from malignant melanoma. *Clin Radiol* 25:385-389. 1974

Bleeding Ileal Varicosity Demonstrated by Transhepatic Portography

MAHESH KINKHABWALA,[1, 2] ALI MOUSAVI,[1] SWAMINATH IYER,[3] AND ROLAND ADAMSONS[4]

Clinical management of a patient with massive gastrointestinal bleeding usually involves the vascular radiologist in two ways [1-5]: (1) precise localization of the bleeding site, and (2) control of the hemorrhage either with drip infusion of a vasoconstrictor pharmacologic drug or by embolization of the bleeding artery. Angiographic localization of the arterial leak from an ulcer bed or a colonic diverticulum is relatively easy, since the pressure head in the injected artery is large and there is also a local vasodilatory effect of the contrast medium on the vessel wall. However, demonstration of venous extravasation in cases of variceal hemorrhage has remained a problem for the angiographer because veins of the gut are usually opacified in the delayed phase of visceral arteriography. Since significant dilution of the contrast material occurs in this phase of angiography, delineation of venous bleeding is difficult. Thus angiographic diagnosis of variceal hemorrhage is usually established by excluding an arterial source of bleeding and visualizing the varices in the late phase of angiography [6]. The technique of percutaneous catheterization of the portal vein and its tributaries enables the angiographer to di-

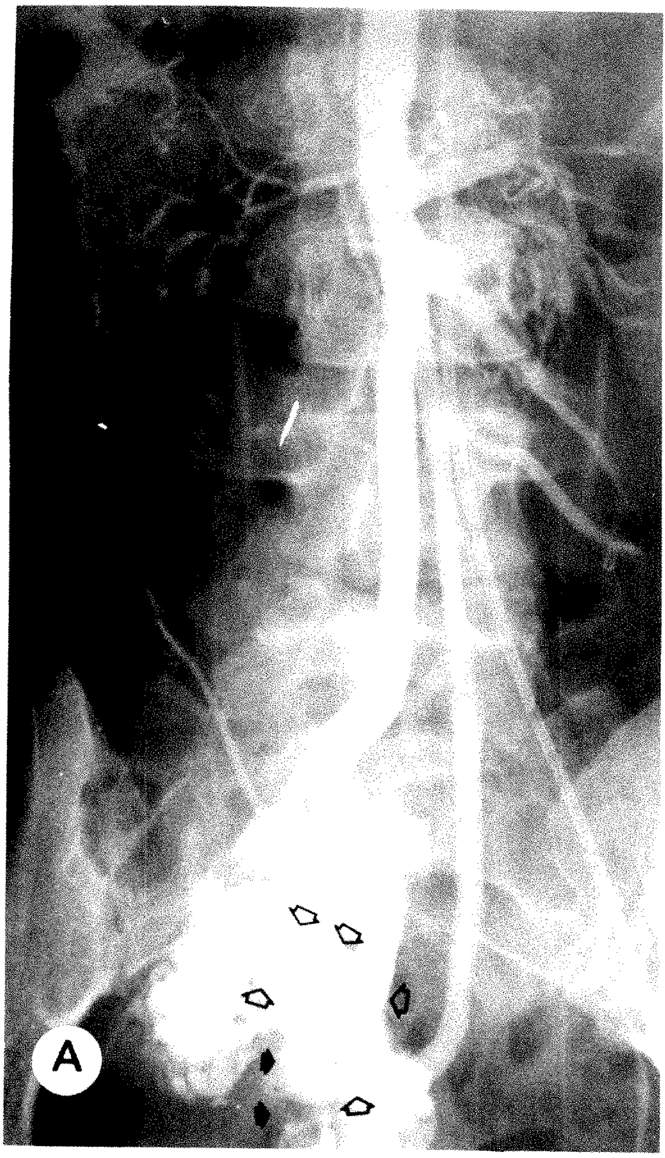

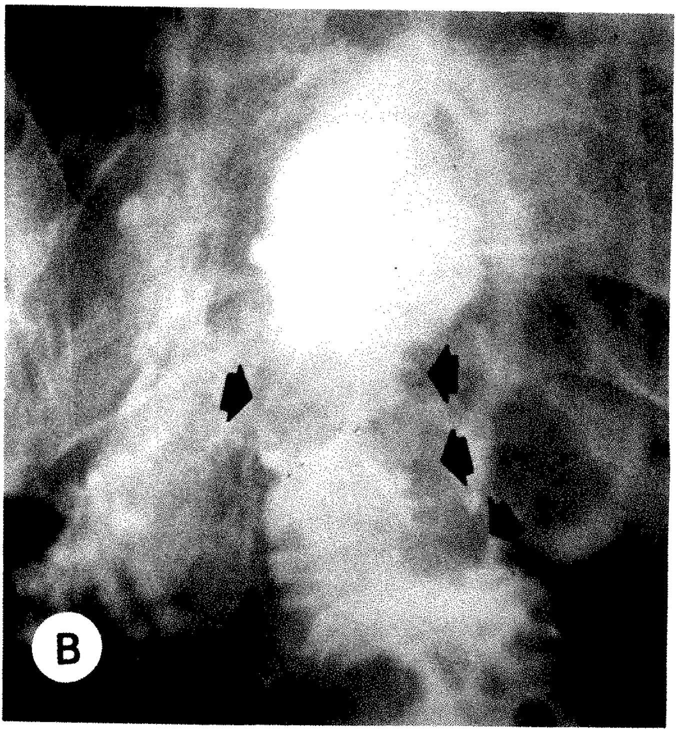

Fig. 1.—*A*, Selective superior mesenteric venogram showing ileal varicosities (*open arrows*) extravasating contrast medium in loop of terminal ileum (*closed arrows*). *B*, Late film of study showing coating of loop of ileum with contrast medium. Filling defects (*arrows*) caused by varicosities in wall of intestine.

Received February 8, 1977; accepted after revision May 18, 1977.

[1] Department of Diagnostic Radiology, State University of New York Downstate Medical Center and Kings County Hospital, Brooklyn, New York 11203.

[2] Present address: Department of Radiology, New York Medical College-Metropolitan Hospital Center, 106th Street and Fifth Avenue, New York, New York 10029. Address reprint requests to M. Kinkhabwala.

[3] Department of Gastroenterology, State University of New York Downstate Medical Center and Kings County Hospital, Brooklyn, New York 11203.

[4] Department of Surgery, State University of New York Downstate Medical Center and Kings County Hospital, Brooklyn, New York 11203.

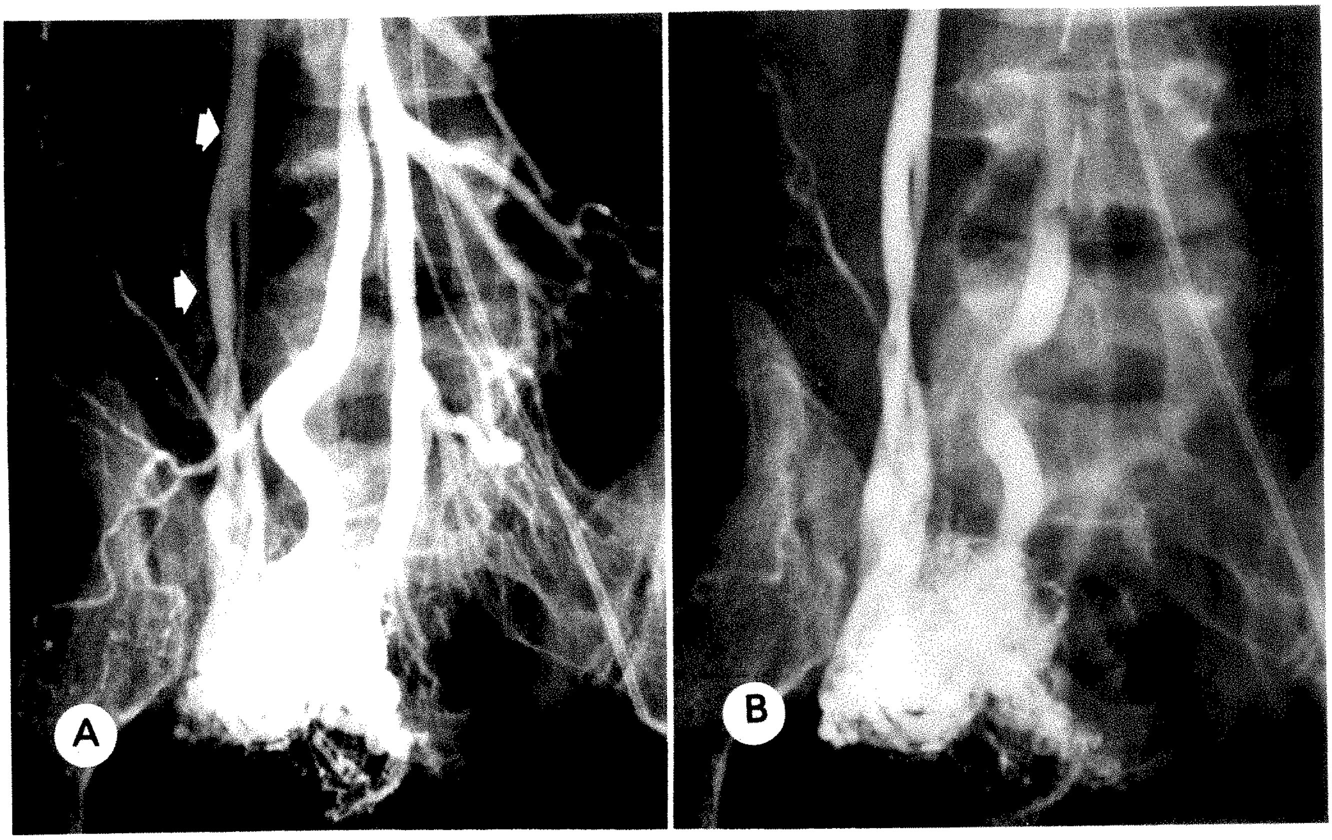

Fig. 2. – Early (*A*) and late (*B*) films of superior mesenteric venogram after pitressin infusion failed to reveal extravasation in ileum. Note intense filling of ovarian vein (*arrows*).

rectly approach the veins of the gastrointestinal tract [7].

We present a case of a middle-aged woman admitted because of massive rectal bleeding. Selective cannulation of the superior mesenteric vein not only revealed large ileal varices but also demonstrated extravasation of the contrast medium in the terminal ileum.

Case Report

A 42-year-old chronic alcoholic female was admitted to Kings County Hospital after 12 hr of rectal bleeding. Physical examination showed a slightly built, pale, conscious female. Liver and spleen were barely palpable below the costal margins. Blood pressure was 90/60; pulse, 120/min; respiration, 30/min. History of right pelvic inflammatory disease was available. Pertinent laboratory data revealed hematocrit of 24; white blood cell count, 8,000; total bilirubin, 1.5 mg/100 ml. Bleeding and clotting times were within normal limits. An emergency colonoscopy revealed massive bleeding gushing from the right side of the colon; however, no definite bleeding site was seen. Nasogastric aspirations were clear of blood.

Selective superior mesenteric arteriography showed no arterial extravasation; however, in the delayed phase large tortuous varicosities were noted in the right lower quadrant of the abdomen. These were interpreted as varicosities of the small intestine. A transhepatic portogram was performed to better delineate these varices and measure the portal pressure. Portal pressure was 37 cm of water (normal, 10 cm). Selective superior mesenteric venography revealed large tortuous ileal varicosities extravasating contrast medium in the terminal small intestine (fig. 1*A*). The delayed film of this study revealed coating of a loop of ileum with the contrast medium due to an active leak from the varicosities (fig. 1*B*).

Pitressin infusion was started in the superior mesenteric artery at a rate of 0.2 U/min to decompress the varicosities. A mesenteric venogram 1 hr later revealed varicosities of ileum; however, no extravasation of the contrast material in the intestine was seen, thus establishing a positive therapeutic effect of vasopressin (fig. 2*A*). More intense filling of the right ovarian vein was observed after start of the infusion, most likely indicating the diversion of blood flow (contrast material) away from the mucosa of the bowel (fig. 2*B*). Portal pressure dropped to 29 cm of water.

The pitressin infusion was continued for 72 hr via an indwelling catheter in the superior mesenteric artery. Rectal bleeding stopped during the infusion; however, after cessation of the infusion she hemorrhaged again rectally. Surgery was performed; marked adhesions between the small intestinal loops and pelvic adnexal structures were found, and 46 cm of terminal ileum containing large varicosities was resected. During surgery, one varix was noted to be actively spurting the blood within the lumen of the gut.

Discussion

Lower gastrointestinal varicosities are thought to be an uncommon source of massive rectal hemorrhage. In patients with active rectal hemorrhage, clinicians and angiographers have usually implicated diverticula and arteriovenous malformations of the right colon, ulcers of the distal duodenum, and tumors of bowel as sources of bleeding [2, 3, 8]. During a clinicopathologic conference of the Massachusetts General Hospital [6], the clinical discussant had not considered intestinal varicosities as a possible source of rectal bleeding, in spite of the patient's long-standing history of portal hypertension. This is most likely due to the clinical misconception that bleeding varices do not extend beyond the duodenum in patients with portal hypertension.

In our review of clinical and radiologic material of 500 cirrhotic patients, we found that 5% were admitted primarily for rectal bleeding even though the majority of these patients also had gastroesophageal varices. Radiologic workup of these patients failed to reveal the more common sources of rectal bleeding, namely, peptic ulcers, anteriovenous malformations, diverticulae, and tumors. However, in these patients ileal and colonic varices or high internal hemorrhoids were delineated at angiography. Thus it would be fair to conclude that they bled from these lower intestinal varicosities. This was especially true in patients who had previous abdominal or pelvic surgery resulting in intestinal adhesions. In our patient the ileal veins were noted to shunt the blood in the ovarian vein, most likely because of adhesions between the ileal loops of the bowel and the pelvic inflammatory disease. Therefore we feel lower intestinal varices should be an important differential diagnostic consideration as a source of rectal hemorrhage in a cirrhotic patient [9, 10].

To the best of our knowledge, this is the first recorded case in which an actual extravasation of the contrast medium from a bleeding venous varicosity of the ileum was observed at angiography. This demonstration was made possible with selective catheterization of the portal vein rather than conventional visceral angiography or splenoportography. Effectiveness of vasopressin infusion in control of variceal hemorrhage was well documented both radiologically and by a recorded drop in the portal pressure.

REFERENCES

1. Baum S. Nusbaum M: The control of gastrointestinal hemorrhage by selective mesenteric arterial infusion of vasopressin. *Radiology* 98:497-505, 1971
2. Baum S, Ward S, Nusbaum M: Stress bleeding from midduodenum: an often unrecognized source of gastro-intestinal hemorrhage. *Radiology* 95:594-602, 1970
3. Casarella WJ, Kanter IE, Seaman WB: Right sided colonic diverticula as a cause of acute rectal hemorrhage. *N Engl J Med* 286:450-453, 1972
4. Goldman ML, Land WC Jr, Bradley EL III, Anderson J: Transcatheter therapeutic embolization in the management of massive upper gastrointestinal bleeding. *Radiology* 120:513-521, 1976
5. Nusbaum M, Baum S, Karoda K, Blakemore WS: Control of portal hypertension by selective mesenteric arterial drug infusion. *Arch Surg* 97:1005-1010, 1968
6. Case records of the Massachusetts General Hospital. *N Engl J Med* 294:385-391, 1976
7. Lunderquist A, Vang J: Transhepatic catheterization and obliteration of the coronary vein in patients with portal hypertension and esophageal varices. *N Engl J Med* 291:646-649, 1974
8. Sheedy PF II, Fulton E, Atwell DT: Angiographic evaluation of patients with chronic gastrointestinal bleeding. *Am J Roentgenol* 123:338-347, 1975
9. Gray RK, Grollman JM Jr: Acute lower gastro-intestinal bleeding secondary to varices of the superior mesenteric venous system: angiographic demonstration. *Radiology* 111:559-562, 1974
10. Hamlyn AN, Morris JS, Lunzer MR, Puritz M: Portal hypertension with varices in unusual sites. *Lancet* 2:1531-1534, 1974

"Hot and Cold" Bone Lesion in Acute Osteomyelitis

CHARLES D. TEATES[1] AND BRIAN R. J. WILLIAMSON[1]

Several authors [1, 2] have recently noted cases of acute osteomyelitis in which areas of diminished activity were seen on bone scans with ^{99m}Tc phosphate compounds. This report describes a patient who also had increased accumulation of ^{67}Ga citrate.

Case Report

A 27-year-old female developed a carbuncle on her left shoulder 3 weeks prior to admission which was treated topically. One week later she developed pain in the right gluteal region followed by fever. Three blood cultures at another hospital (and three at University of Virginia Hospital) were all positive for *Staphylococcal aureus*. In addition she developed staphylococcal pneumonia. She was initially treated with ampicillin but was switched to cephalothin when the organism was found resistant to ampicillin.

On admission to the University Hospital 3 days later, she complained of gluteal pain radiating into the right leg as well as poorly defined lumbar pain. Two small skin pustules were noted. Her temperature was spiking to over 39°C. She was started on nafcillin, later supplemented with rifampin. Pelvic x-rays were normal.

Bone scan with 10.5 mCi of ^{99m}Tc polyphosphate showed the right pelvis to have diminished activity compared to the left (fig. 1). The following day, the patient was injected with 2.3 mCi of ^{67}Ga citrate; 48 hr views showed diffusely increased activity in the region of the right sacroiliac joint and right ilium (figs. 2*A* and 2*B*). A repeat gallium scan 19 days later showed a more diffuse area of increased activity involving the entire right ilium and right acetabulum (figs. 2*C* and 2*D*). While radiographs 1 week after the initial bone scan remained normal, a diffuse destructive pattern in the right ilium and acetabulum was noted 1 month after the initial scan (fig. 3). Bone biopsy was not undertaken. Aspiration from the right hip joint 1 week after admission showed sterile fluid under pressure.

On continued antibiotic therapy, the patient showed gradual clinical improvement over the following months. She has now fully recovered, but radiographs show residua of the osteomye-

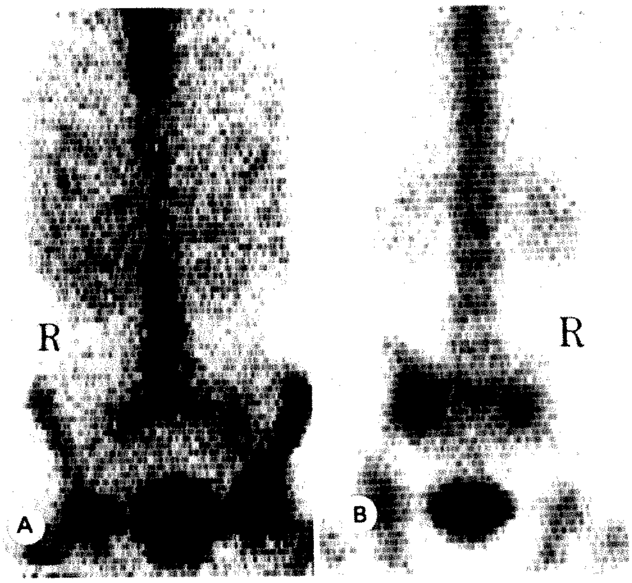

Fig. 1.—Anterior (*A*) and posterior (*B*) body scan 3 hr after injection of 10.5 mCi of ^{99m}Tc polyphosphate. Pelvis is asymmetric with decreased count rates over clinically involved right hemipelvis.

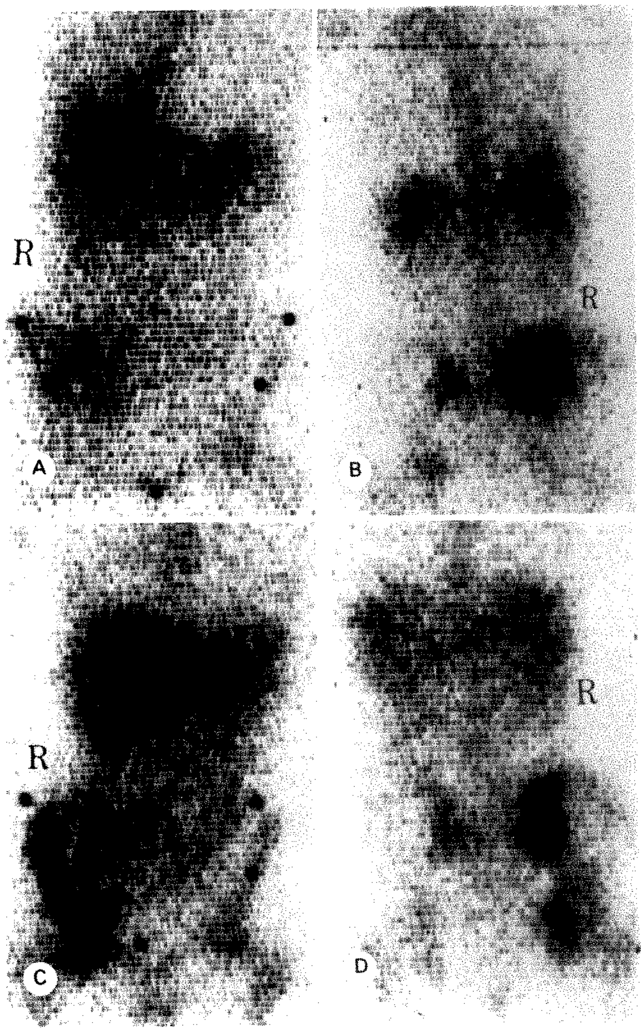

Fig. 2.—Anterior (*A*) and posterior (*B*) body scans 48 hr after injection of 2.3 mCi of ^{67}Ga citrate (injection 1 day after technetium scan). Note abnormal sites of activity in chest in areas of known staphylococcal pneumonia and in right iliac region. Radiographs of pelvis and hips at this time were normal. Repeat anterior (*C*) and posterior (*D*) gallium scans 19 days later showing nearly complete resolution of staphylococcal pneumonia. Diffuse increase in activity in right hemipelvis has now extended into region of acetabulum.

Received December 13, 1976; accepted after revision May 4, 1977.

[1] Division of Nuclear Medicine, Department of Radiology, University of Virginia School of Medicine, Charlottesville, Virginia 22901.

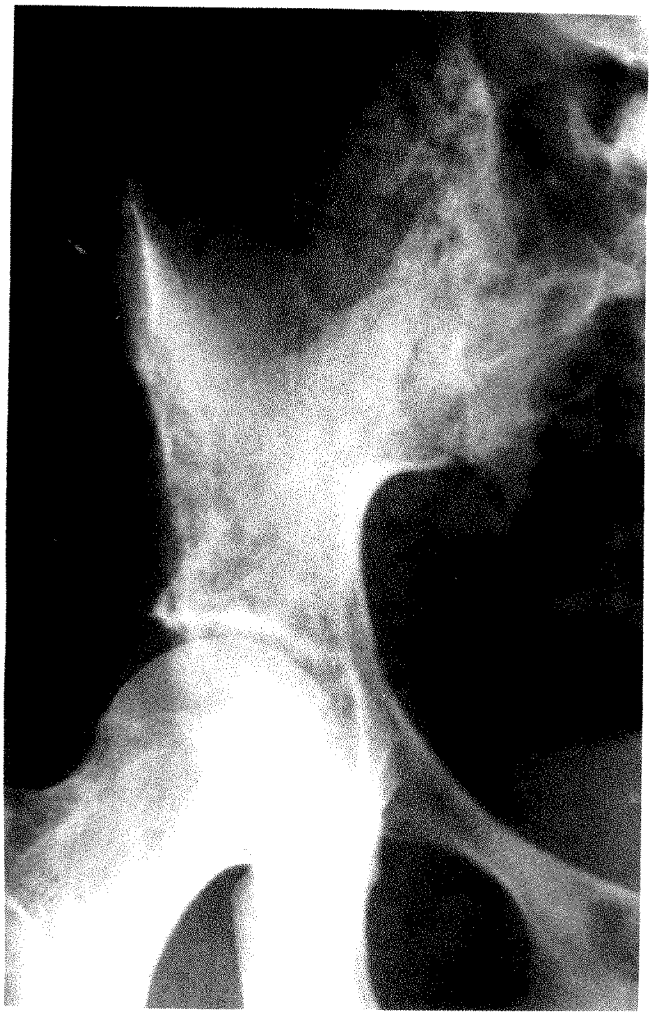

Fig. 3.—Pelvic radiograph 1 month after initial bone scan showing permeative destruction of right ilium, best appreciated above acetabulum. Cecal gas obscures pattern to some extent in ilium.

litis. The right hip joint shows no evidence of a previous septic arthritis.

Discussion

Handmaker and Leonards [1], and later Russin and Staab [2], reported the paradoxic diminished activity on bone scans in the early phase of osteomyelitis. These authors postulate an interference with blood flow to bone by the acute osteomyelitis. They suggest that the bone scan may subsequently become positive because of involvement of the cortex, periosteum, and surrounding soft tissues. The latter structures have a separate blood supply.

Except for biopsy proof, our patient had clinically documented osteomyelitis that showed markedly increased gallium deposition despite the "cold" lesion on bone scan. We are not aware of other reports of this new paradox. There was no clinical evidence of soft tissue involvement, although the patient's initial complaints were of gluteal discomfort which had been present for approximately 2 weeks prior to the bone scan. It is thought that localization of both of these agents requires good blood flow. We cannot explain adequately the differential localization of these radiopharmaceuticals, but we have noted other instances where gallium showed acute osteomyelitis much more dramatically than the ^{99m}Tc phosphate bone scan. As often the case, both scans were abnormal prior to radiographic changes.

In the case presented, the gallium scan more effectively demonstrated acute osteomyelitis. Thus we recommend a gallium scan for detection of osteomyelitis if a routine bone scan is nondiagnostic.

REFERENCES

1. Handmaker H, Leonards R: The bone scan in inflammatory osseous disease. *Semin Nucl Med* 6:95–105, 1976
2. Russin LD, Staab EV: Unusual bone scan findings in acute osteomyelitis: case report. *J Nucl Med* 17:617–619, 1976

An Unusual Scapular Stress Fracture

ANNE C. BROWER,[1] JAMES R. NEFF,[2] AND DAVID A. TILLEMA[2]

Stress or fatigue fractures have been described in many locations, most of them in lower extremities [1-3]. Two different stress fractures have been previously described in the scapula. One involves the coracoid process in trapshooters [4, 5]; the other involves the inferior edge of the glenoid fossa in baseball pitchers [6]. This report describes for the first time a stress fracture of the lateral aspect of the scapula at the attachment of the teres minor in an assembly line worker.

Case Report

A 39-year-old man had right shoulder pain for 3 weeks unrelieved by analgesics and muscle relaxants. There was no preceding injury or trauma to the area. The patient related the pain to his job, which entailed working overhead on an assembly line clamping the tail pipe to the chassis of automobiles. He used his right upper extremity more than his left. His previous history was noncontributory.

Physical examination revealed a normal range of motion of his neck, shoulder, and elbow. Point tenderness was present along the lateral aspect of the right scapula. The pain was exacerbated when he assumed the position used in overhead work.

Radiographs of the right shoulder and scapula showed a linear lucency with localized periosteal reaction along the lateral aspect of the scapula, compatible with a stress fracture (fig. 1*A*). The patient was removed from overhead work and transferred to a different type of job. Radiographs after 2 weeks and then 1 month later showed progressive healing of the area (figs. 1*B* and 1*C*). A follow-up visit 3 months after the initial visit showed the patient to be asymptomatic and the radiographs to be within normal limits (fig. 1*D*).

Discussion

This case presents a hitherto undescribed area for occurrence of a stress fracture: that is, the insertion of

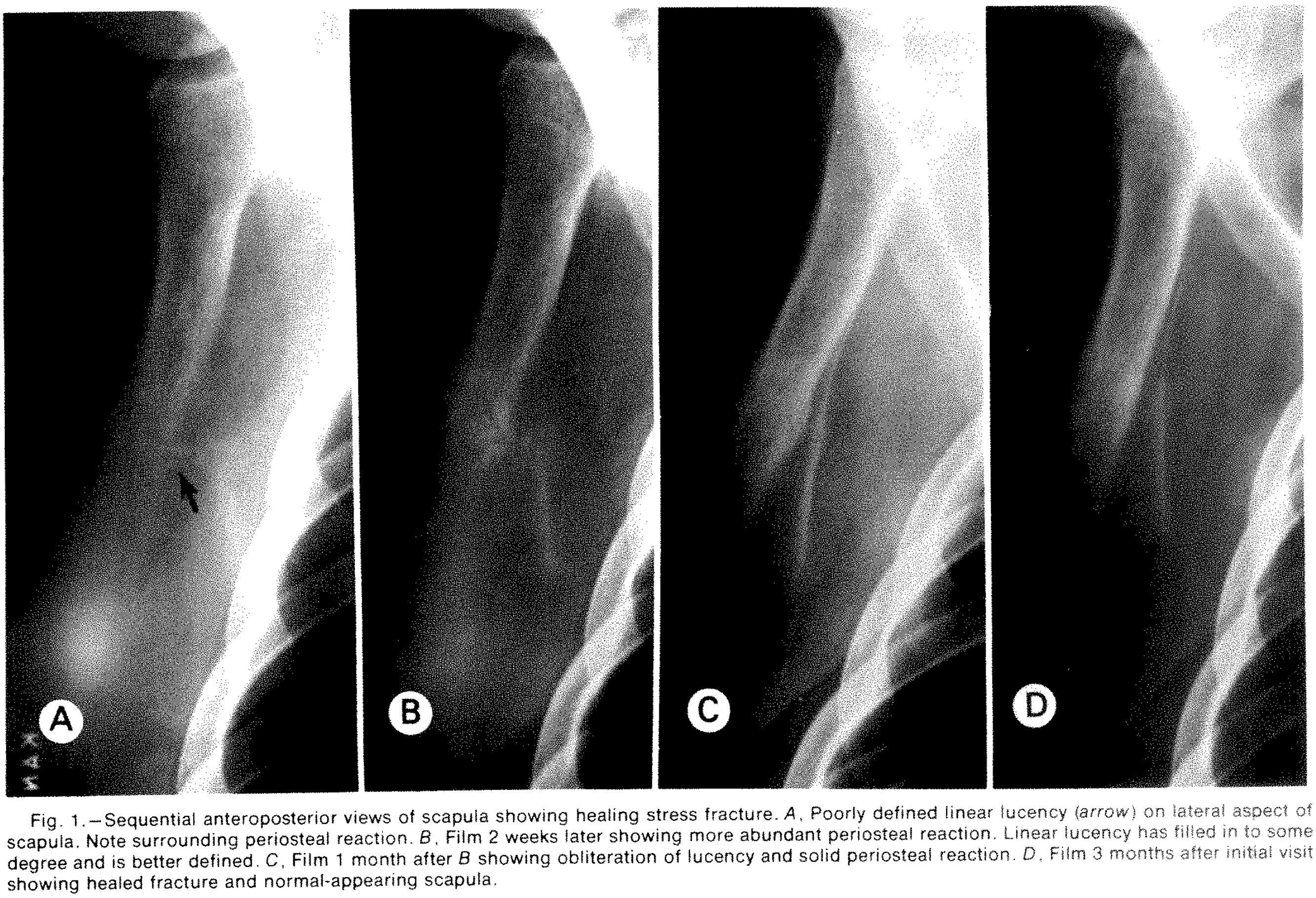

Fig. 1.—Sequential anteroposterior views of scapula showing healing stress fracture. *A*, Poorly defined linear lucency (*arrow*) on lateral aspect of scapula. Note surrounding periosteal reaction. *B*, Film 2 weeks later showing more abundant periosteal reaction. Linear lucency has filled in to some degree and is better defined. *C*, Film 1 month after *B* showing obliteration of lucency and solid periosteal reaction. *D*, Film 3 months after initial visit showing healed fracture and normal-appearing scapula.

Received March 22, 1977; accepted after revision May 20, 1977.

[1] Department of Diagnostic Radiology, University of Kansas Medical Center, Kansas City, Kansas 66103. Present address: Department of Radiology, Medical College of Virginia, MCV Station, Richmond, Virginia 23298. Address reprint requests to A. C. Brower.

[2] Department of Orthopedic Surgery, University of Kansas Medical Center, Kansas City, Kansas 66103.

the teres minor muscle along the lateral border of the scapula. The primary function of the teres minor muscle is to adduct and externally rotate the humerus [7, 8]. This action was brought into repeated use in the patient's overhead work.

The radiographic sequence in this patient is classical for a stress fracture [9, 10]. The first radiograph, taken 3 weeks after initial symptoms, showed maximal osteoclastic resorption with periosteal reinforcement. The second radiograph 2 weeks later demonstrated maximal periosteal reinforcement with healing of the resorptive areas. The radiograph taken 6 weeks after the change in job showed continued improvement; complete healing required at least 3 months.

The proper early recognition of the pathologic process in this patient, despite its unusual location, enabled appropriate treatment with excellent results. Perhaps this particular stress fracture is more common than currently realized. Certainly it should be considered in patients involved in overhead work who complain of shoulder pain.

REFERENCES

1. Morris JM, Blickenstaff LD: *Fatigue Fractures—A Clinical Study*. Springfield, Ill., Thomas, 1967
2. Wilson ES, Katz FN: Stress fractures—an analysis of 250 consecutive cases. *Radiology* 92:481-486, 1969
3. Gilbert RS, Johnson HA: Stress fractures in military recruits—a review of the twelve years' experience. *Milit Med* 131:716-721, 1966
4. Boyer DW Jr: Trapshooter's shoulder: stress fracture of the coracoid process. Case report. *J Bone Joint Surg [Am]* 57:862, 1975
5. Sandrock AR: Another sports fatigue fracture. *Radiology* 117:274, 1975
6. Bennett GE: Shoulder and elbow lesions of the professional baseball pitcher. *JAMA* 117:510-514, 1941
7. Basmajian JV: *Grant's Method of Anatomy*, 8th ed. Baltimore, Williams & Wilkins, 1971
8. Hollinshead WH: *Textbook of Anatomy*, 2d ed. New York, Harper & Row, 1967
9. Johnson LC: Histiogenesis of stress fractures (abstr.). *J Bone Joint Surg [Am]* 45:1542, 1963
10. Sweet DE, Allman RM: RPC of the month from the AFIP. *Radiology* 99:687-695, 1975

Myelosclerosis and Myelofibrosis in Treated Histiocytosis-X

LEE PINCKNEY[1] AND BRUCE R. PARKER[1]

Histiocytosis-X is a disease of unknown origin characterized by widespread histiocytic infiltration of multiple organs including the skeletal system [1]. Myelofibrosis, fibrotic replacement of bone marrow, is rare in childhood. It occurs both as an idiopathic disease and in association with other diseases, commonly leukemia [2]. We describe a case of histiocytosis-X in which myelofibrosis with myelosclerosis and pathologic fractures developed during therapy.

Case Report

A 16-month-old previously healthy black male developed a generalized petechial rash and fever 1 week before admission. The initial physical examination revealed mild splenomegaly and generalized lymphadenopathy. A complete blood count revealed a hematocrit of 16%, a white blood cell count of 6,300/mm^3 (34 polymorphonuclear cells, two bands, and 59 lymphocytes), and a platelet count of 12,000/mm^3. The albumin was 1.7 g/100 ml. Other liver function studies and bleeding parameters were normal. The patient was treated initially with packed red cells, ampicillin, and gentamicin. However, since cultures of the blood, urine, cerebrospinal fluid, throat, and stool were negative, the antibiotics were discontinued. He developed generalized edema and ascites requiring furosemide and albumin. An axillary lymph node biopsy and an iliac crest bone marrow biopsy both demonstrated histiocytic proliferation typical of histiocytosis-X. A liver-spleen scan and radiographic bone survey were normal (figs. *1A* and *2A*).

The patient was treated with prednisone (20 mg daily) and Velban (2-3.5 mg weekly). He required frequent red cell and albumin infusions to control anemia and edema. Unexplained fever continued. After 3 months he was discharged on prednisone (30 mg on alternate days) and Velban (3.0 mg weekly).

The patient was readmitted 3 months later with a hemoglobin of 6.8 g/100 ml, a white blood cell count of 4,200 (58 polymorphonuclear cells, 36 lymphocytes, and six monocytes), and a platelet count of 15,000. There were 14 nucleated red cells per 100 white cells, and mild anisocytosis and poikilocytosis were noted. He was treated with red cells and albumin. A ^{51}Cr red cell survival study indicated a half-life of 8 days (normal, 30 days) and splenic sequestration of red cells. Methotrexate (20 mg/m^2 weekly) and Cytoxan (200 mg/m^2 weekly) were added to the regimen.

During the next 9 months the fever subsided, but the patient required gradually more frequent transfusions and began having respiratory difficulties from an enlarging liver and spleen. The red cell morphology became progressively more abnormal, demonstrating numerous teardrop forms and nucleated red cells. A ^{99m}Tc pyrophosphate bone scan was normal, but an ^{111}In chloride bone marrow scan demonstrated diminished patchy bone marrow uptake with extensive uptake by the enlarged liver and grossly enlarged spleen (fig. 3). A radiographic bone survey demonstrated generalized myelosclerosis.

At splenectomy, a 650 g spleen was removed. Histologic examination revealed extensive extramedullary hematopoiesis, hemosiderosis, and small foci of histiocytes. A concomitant liver biopsy showed similar changes. The platelet count gradually increased to and stabilized at 50,000; requirements for red cell transfusions decreased. The therapeutic regimen of prednisone, Velban, methotrexate, and Cytoxan was maintained. Periodic radiographs revealed progressive bony sclerosis (figs. *1B* and *2B*).

A bone marrow biopsy 19 months after diagnosis and 5 months after splenectomy showed massive fibrosis with occasional foci of histiocytes indicating disease activity (fig. 4). Soon thereafter the patient began limping and complained of pain while walking. Radiographs revealed bilateral pathologic fractures through the sclerotic femoral necks (fig. *1C*). The femoral necks were irradiated (1,500 rad in $1\frac{1}{2}$ weeks), and a cast was applied. Little healing has occurred.

Discussion

The radiographic findings of histiocytosis-X in bone are well described in several recent reviews [3-5]. The most frequent finding is loss of bone density, either as generalized osteoporosis from diffuse marrow infiltration or as sharply marginated focal lesions. Increased bone density is confined to marginal sclerosis around focal lesions usually in the long bones, although healing lesions frequently become sclerotic. A generalized increase in bone density has not previously been reported in histiocytosis-X.

Myelofibrosis in adults has been well described, but it is rarely reported in children [2, 6, 7]. It occurs as an idiopathic disease at all ages. In adults myelofibrosis has been associated with metastatic carcinoma [8], chemical poisoning [9], and chronic infections such as tuberculosis [10]. In children it has been associated with acute myelogenous leukemia [2], and (in a single case) with the McCune-Albright syndrome [11].

The etiology of myelofibrosis is unknown. It may occur as part of the spectrum of myeloproliferative diseases, since fibrous tissue is a normal marrow component [12], or it may be strictly a reaction of marrow to some inciting toxin or drug [13]. Many cases associated with preexistent diseases develop only during drug therapy, as in our patient. However, none of the drugs which this patient received has been previously shown to cause myelofibrosis.

Myelofibrosis and myelosclerosis, while they may occur together, are not the same entity and should not be confused [14]. Sclerosis accompanies myelofibrosis in about half of adult cases and has been reported in only several cases in children [9, 14]. The radiographic find-

---

Received February 28, 1977; accepted after revision May 10, 1977.

[1] Department of Radiology, Children's Hospital and Stanford University Medical Center, Stanford, California 94305. Address reprint requests to B. R. Parker at Stanford Medical Center.

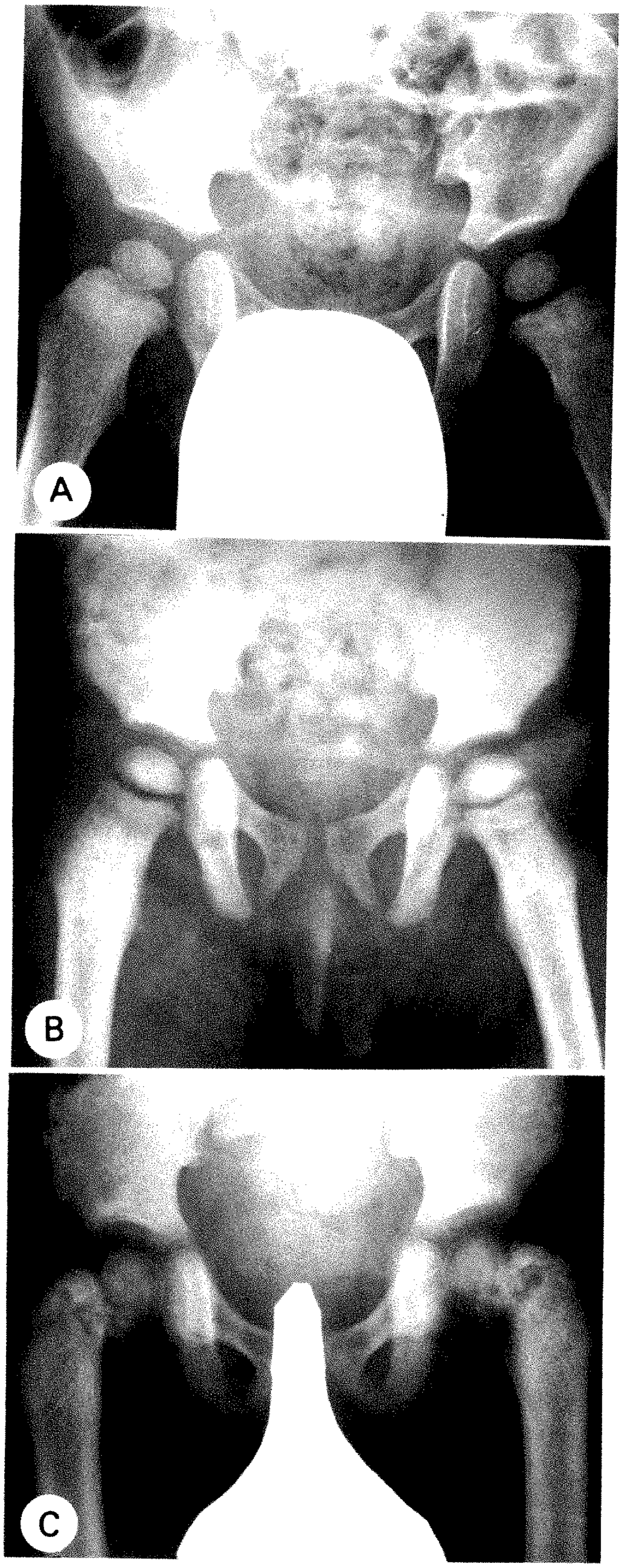

Fig. 1.—*A*, Anteroposterior view of pelvis and hips showing minimal metaphyseal osteoporosis without characteristic lesions of histiocytosis-X. *B*, Film 2 years later showing widened metaphyseal lucent zones, coarsened and thickened trabeculae, and increased overall bony density. Lucency in right iliac crest with sclerotic rim secondary to large bone marrow biopsy and not to underlying disease. *C*, Film 10 months later showing progression of bony sclerosis with bilateral femoral neck fractures resulting in bilateral coxa vara deformities.

←

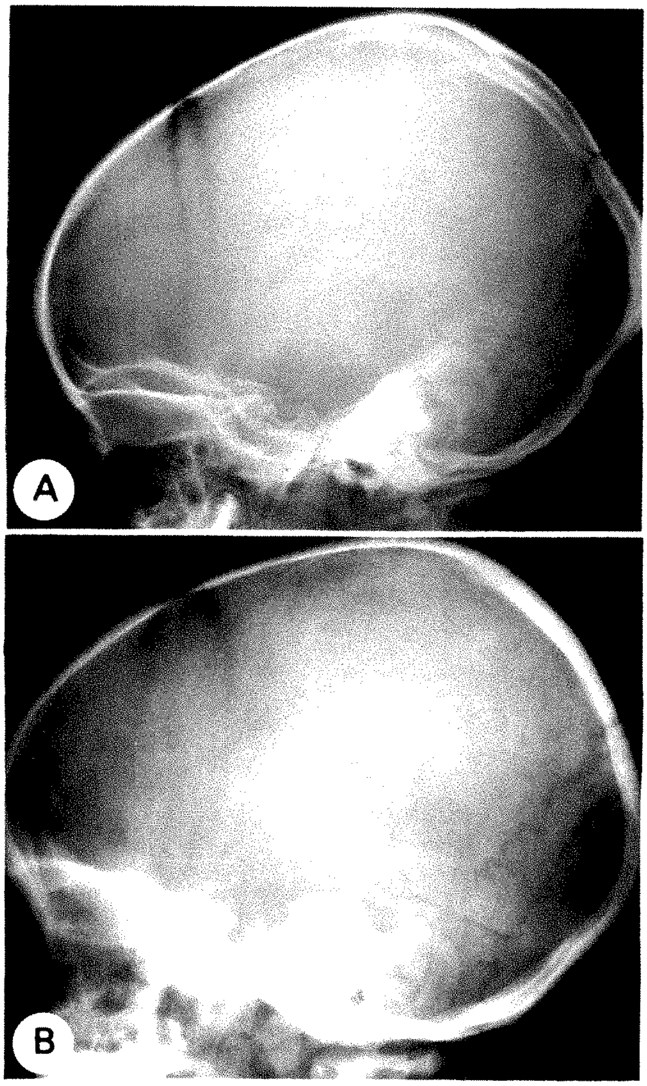

Fig. 2.—*A*, Lateral view of skull showing slight widening of coronal suture with otherwise normal bony calvarium. *B*, Film 2½ years later showing thicker, denser calvarium and markedly increased bony density at base of skull.

ings in myelofibrosis may actually be those of osteoporosis rather than osteosclerosis. Myelosclerosis likewise may occur in response to marrow infiltrations other than fibrotic tissue, as in systemic mastocytosis [15] and the lymphomas, especially Hodgkin's disease [16].

The precise mechanism of myelosclerosis is not known. New calcification is not confined to the sparse network of trabeculae in spongy bone, but is also laid down on the abnormal infiltrating fibrous tissue [13]. This accounts for a radiographic spectrum which includes increased bone density without disruption of trabeculation, increased bone density with blurring or smudging of trabeculation, or markedly increased bone density with obliteration of the medullary cavity. The process may occur unevenly in multiple discrete foci of heavy calcification which, when partially confluent, give a dense mottled appearance. Likewise, certain areas within the marrow space may be more involved, such as the subcortical region beneath vertebral end plates where the spongiosa merges with cortex, resulting in a "rugger jersey" or "sandwich vertebra" appearance.

Usually by the time patients come to medical attention, their visible myelosclerosis (though not necessarily their disease) is stable; documented radiographic progression such as occurred in this case is rare [9, 13].

Pathologic fractures are common in histiocytosis-X but are usually the result of focal lesions. On the other hand, pathologic fractures are rare in idiopathic myelofibrosis, but occur occasionally in cases associated with chemical poisoning [9]. Because our patient did not demonstrate the typical bony changes of histiocytosis-X, we believe his fractures were secondary to the diffuse myelosclerotic process.

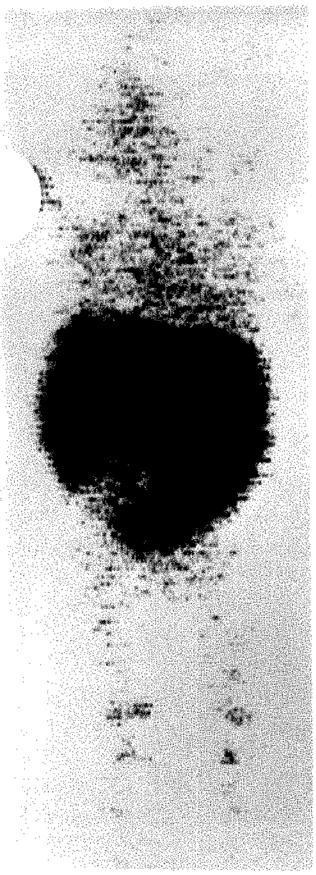

Fig. 3.—Bone marrow scintiscan (anterior projection) performed with ^{111}In showing patchy, irregular, decreased uptake by bone marrow with marked uptake by enlarged liver and massively enlarged spleen.

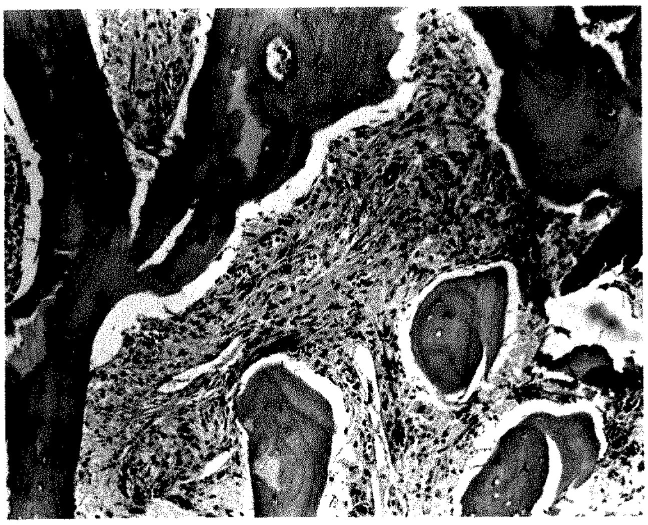

Fig. 4.—Bone marrow biopsy from iliac crest 19 months after start of chemotherapy for histiocytosis-X showing complete replacement of normal marrow elements by fibrous tissue.

REFERENCES

1. Starling KA, Fernbach DJ: Histiocytosis, in *Clinical Pediatric Oncology*, edited by Sutow WW, Vietta TJ, Fernbach DJ, St. Louis, Mosby, 1973, pp 337–358
2. Say B, Berke I: Idiopathic myelofibrosis in an infant. *J Pediatr* 64:580–586, 1964
3. Arcomano JP, Barnett JC, Wunderlich HO: Histiocytosis-X. *Am J Roentgenol* 85:663–679, 1961
4. Ennis JT, Whitehouse G, Ross FGM, Middlemiss JH: The radiology of bone changes in histiocytosis-X. *Clin Radiol* 24:212–220, 1973
5. Kirks DR, Taybi H: Histiocytosis-X, in *Pediatric Oncologic Radiology*, edited by Parker BR, Castellino RA, St. Louis, Mosby, 1977, pp 209–234
6. Boxer LA, Camitta BM, Berenberg W, Fanning JP: Myelofibrosis: myeloid metaplasia in childhood. *Pediatrics* 55:861–865, 1975
7. Tebbi K, Zarkowsky HS, Siegel BA, McAllister WH: Childhood myelofibrosis and osteosclerosis without myeloid metaplasia. *J Pediatr* 84:860–862, 1974
8. Kiely JM, Silverstein MN: Metastatic carcinomas simulating agnogenic myeloid metaplasia and myelofibrosis. *Cancer* 24:1041–1044, 1969
9. Feldman F: Myelosclerosis in agnogenic myeloid metaplasia. *Semin Roentgenol* 9:195–207, 1974
10. Samuelson SM, Killander A, Werner I, Stenkvist B: Myelofibrosis associated with tuberculosis lymphadenitis. *Acta Med Scand* 179:326–335, 1966
11. Shantharaj S, Gilman S, Maurer HS, Rosenthal IM: Hyperthyroidism in an infant with McCune-Albright syndrome: report of a case with myeloid metaplasia. *J Pediatr* 80:275–278, 1972
12. Dameshek W: Some speculation on the myeloproliferative syndromes (editorial). *Blood* 6:372–375, 1951
13. Ward HP, Block MH: The natural history of agnogenic myeloid metaplasia (AMM) and a critical evaluation of its relationship with the myeloproliferative syndrome. *Medicine* 50:357–420, 1971
14. Pettigrew JD, Ward HP: Correlation of radiologic, histologic, and clinical findings in agnogenic myeloid metaplasia. *Radiology* 93:541–548, 1969
15. Jensen WB, Lasser EC: Urticaria pigmentosa associated with widespread sclerosis of the spongiosa of bone. *Radiology* 71:826–832, 1958
16. Pear BL: Skeletal manifestations of the lymphomas and leukemia. *Semin Roentgenol* 9:240–243, 1974

Intrathoracic Desmoid Tumor of the Chest Wall

DAVID L. KLEIN,[1] GORDON GAMSU,[1] AND THOMAS D. GANT[2]

Desmoid tumors are an uncommon form of aggressive fibromatosis. The abdominal wall is the most common site of origin. Extraabdominal desmoid tumors are usually found in the shoulder girdle, chest wall, and lower extremities. Chest wall desmoid tumors have been well described both clinically and pathologically [1, 2], but radiographic documentation has been sparse [3, 4], perhaps because most are extrathoracic and not radiographically apparent.

We recently saw a patient with a large, asymptomatic, intrathoracic, chest wall desmoid tumor. The abnormality was seen only on the chest radiograph. The tumor arose at the site of previous trauma and had grown to a considerable size.

Case Report

A 21-year-old man sustained a severe crushing injury to the left side of his chest in an automobile accident. He did well after treatment with chest tube drainage, tracheostomy, and splenectomy. A chest radiograph 5 weeks after injury (fig. 1*A*) showed considerable chest wall deformity in the form of multiple healing rib fractures and pleural thickening. Clinical follow-up over the next 34 months revealed no pulmonary dysfunction or residual disability. Serial chest radiographs, however, showed an asymptomatic, enlarging, intrathoracic, extrapleural mass at the injury site (fig. 1*B*), which at 34 months measured 9 × 12 cm on the radiograph (fig. 1*C*). Exploratory thoracotomy was undertaken to obtain a tissue diagnosis. Biopsy revealed a desmoid tumor, and the mass was completely excised (fig. 2). The patient returned 6 months after surgery when a 3 cm subcutaneous nodule in the left lower abdominal wall was discovered. This was removed and also proved to be a desmoid tumor.

Discussion

Pathologically viewed, desmoid tumors are grossly circumscribed lesions of firm fibrous consistency arising from the connective tissue sheaths of striated muscle [2]. They characteristically invade surrounding tissues, but do not metastasize. Microscopically, the tumor appears as a well differentiated fibroma, consisting mainly of fibrous tissue with sparse fibroblasts, which distinguish it from malignant fibrosarcoma.

The cause of desmoid tumors is unknown, but both traumatic and hormonal factors have been postulated. Nine of 19 patients with chest wall desmoid tumors reviewed by Weinstein et al. [4] had lesions arising at sites

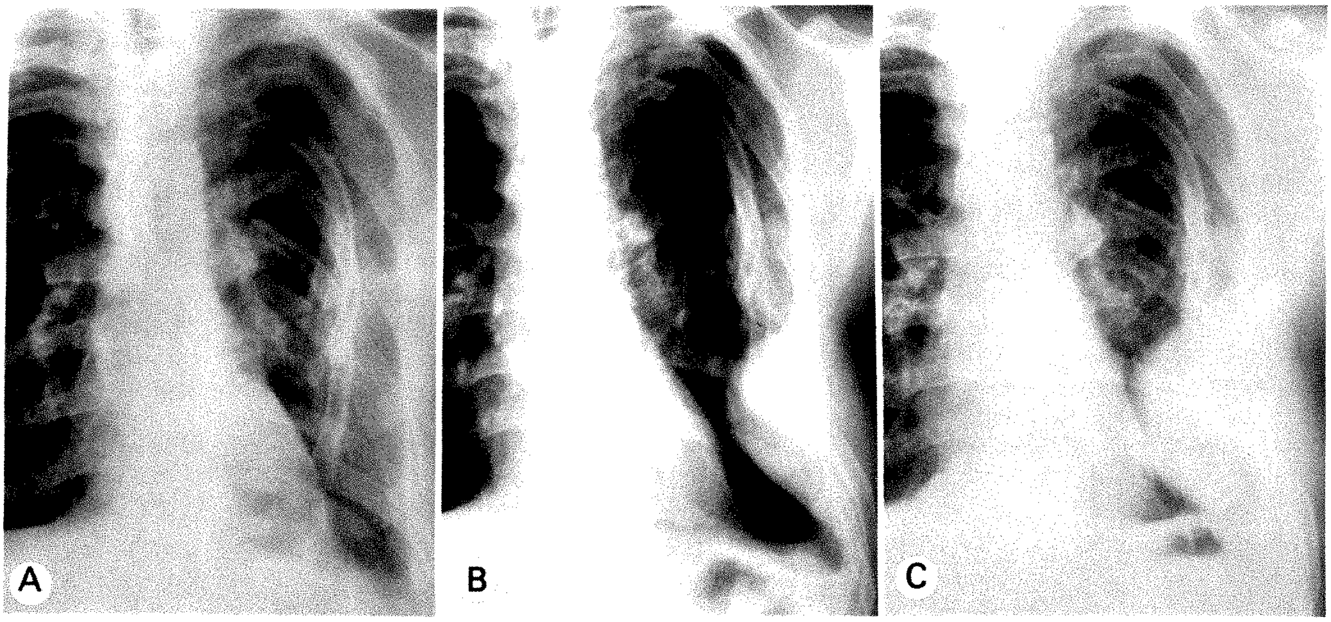

Fig. 1.—*A*, chest film 1 month after injury showing only multiple healing rib fractures and underlying pleural thickening. *B*, Film 19 months after injury showing mass on left side of chest wall extending intrathoracically. *C*, Film 34 months after injury showing further enlargement of chest wall mass.

Received February 28, 1977; accepted after revision May 24, 1977.

G. Gamsu is the recipient of training grant GM 01272 from the National Institute of General Medical Sciences.

[1] Department of Radiology, M-380, University of California School of Medicine, San Francisco, California 94143. Address reprint requests to G. Gamsu.

[2] Department of Surgery, University of California School of Medicine, San Francisco, California 94143.

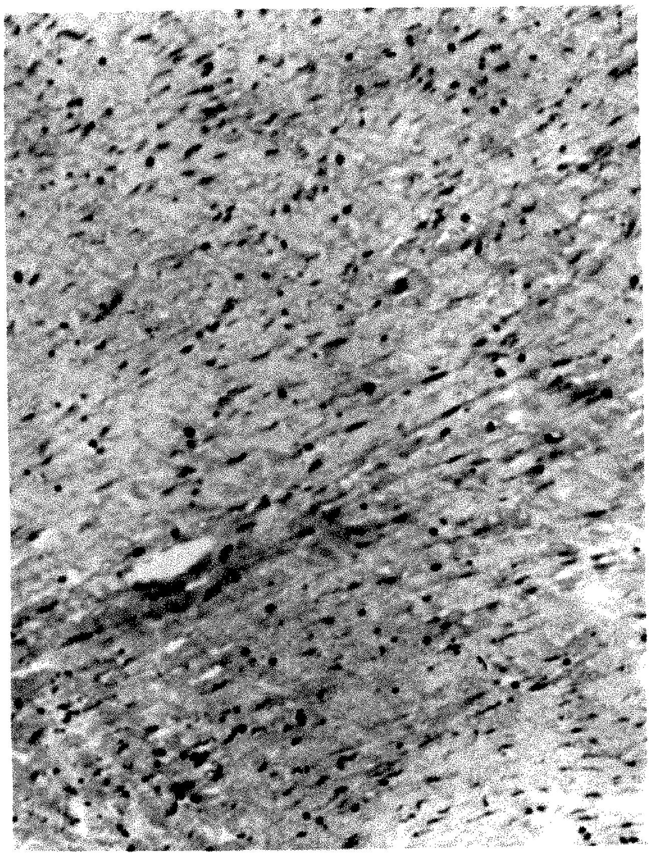

Fig. 2.—Photomicrograph of desmoid tumor showing bundles of well differentiated fibroblasts. Note thin, flattened, pyknotic nuclei. H and E, ×200.

of previous trauma, including surgical scars. In only one of these 19 patients was the tumor an asymptomatic mass discovered radiographically. Das Gupta and coworkers [1] reviewed 72 patients with extraabdominal desmoid tumors, and only two had significant previous local trauma. Although desmoid tumors are more than twice as common in women, there is no definite evidence of a hormonal cause. In an early series of desmoid tumor of the abdominal wall [5], 15 of 17 patients were women; 14 had recently given birth. This led to speculation that either trauma to the abdominal wall or endocrine factors associated with pregnancy might be responsible.

Excision of the tumor is the treatment of choice and may be curative. The invasive tendency of this tumor, however, makes local recurrence a problem, particularly when the lesion is large. The recurrence rate after primary excision varies from 25%–57%. Radiotherapy is sometimes effective and has been advocated for treatment of large or inoperable tumors, or as an alternative to radical surgery [6].

Included in the radiographic differential diagnosis [7] of chest wall soft tissue tumors are malignant soft tissue sarcoma (fibrosarcoma, rhabdomyosarcoma), metastatic disease, and multiple myeloma. The more common benign tumors of the chest wall are desmoid tumor, lipoma, hemangioma, and neural tissue tumors. In our patient, the lengthy clinical course and absence of obvious malignant disease favored diagnosis of a benign lesion. The presence of a slowly growing mass following severe thoracic trauma should cause the radiologist to consider desmoid tumor. Subsequent discovery of a second desmoid tumor at a site unrelated to the first lesion is unusual. We could find only one other report of two desmoid tumors in the same patient, each arising separately and apparently not related to recurrence [8].

REFERENCES

1. Das Gupta TK, Brasfield RD, O'Hara J: Extra-abdominal desmoids: a clinicopathological study. *Ann Surg* 170:109–121, 1969
2. Musgrove JE, McDonald JR: Extra-abdominal desmoid tumors: their differential diagnosis and treatment. *Arch Pathol* 45:513–540, 1948
3. Rosen RS, Kimball W: Extra-abdominal desmoid tumor. *Radiology* 86:534–540, 1966
4. Weinstein EC, Payne WS, Soule EH: Surgical treatment of desmoid tumor of the chest wall. *J Thorac Cardiovasc Surg* 46:242–251, 1963
5. Pack GT, Ehrlich HE: Neoplasms of the anterior abdominal wall with special consideration of desmoid tumors: experience with 391 cases and a collective review of the literature. *Int Abstr Surg* 79:177–198, 1944
6. Hill DR, Newman H, Phillips TL: Radiation therapy of desmoid tumors. *Am J Roentgenol* 117:84–89, 1973
7. Omell GH, Anderson LS, Bramson RT: Chest wall tumors. *Radiol Clin North Am* 11:197–214, 1973
8. Soule EH, Scanlon PW: Fibrosarcoma arising in an extra-abdominal desmoid tumor: report of a case. *Mayo Clin Proc* 37:443–451, 1962

Horseshoe Kidney: Ultrasonic Demonstration

HOWARD J. MINDELL[1] AND EDWARD A. KUPIC[1]

Although horseshoe kidney has been cited as the most common renal fusion anomaly [1], scant reference can be found to its ultrasonic diagnosis. Leopold and Asher [2] demonstrated a bistable ultrasound recording of horseshoe kidney, and Ferrucci [3] noted that ultrasonically, "horseshoe kidney may simulate pancreatic malignancy." However, no gray scale depiction of this potentially misleading finding could be found in the literature [4–10]. We present a case to illustrate the gray scale appearance of this entity and emphasize its misleading potential.

Case Report

A 53-year-old female had a complex medical history, including previous cholecystectomy, sigmoid colon resection for diverticulosis, jejunoileal bypass surgery for obesity, aortomesenteric occlusive vascular disease, gastric ulcer, and psychiatric problems with alcoholism. Surprisingly, however, no prior urographic studies were available. On referral to the Medical Center Hospital of Vermont for undiagnosed abdominal pain, a palpable nonpulsatile firm midabdominal mass 5 cm in diameter was found. SPGT, bilirubin, and amylase levels were normal; alkaline phosphatase was slightly elevated.

Pancreatitis was a strong consideration, and abdominal ultrasound examination was done with an Echoview Picker gray scale system using a 2.25 MHz transducer. An elongate, primarily sonolucent lesion was found extending across the midline about 5 cm above the umbilicus with an anterior central convexity suggesting pancreatic configuration and intimately related posteriorly to the aorta (fig. 1). Selective celiac and superior mesenteric angiography failed to demonstrate any pancreatic abnormality, but an aortic injection revealed a horseshoe kidney with an isthmus bridging lower renal poles at L4-L5. Repeat ultrasound examination facilitated lead marker placement on the lesion in question and an abdominal film confirmed this to be isthmus. Prone sections were unrewarding because the spine shielded the lesion. Endoscopy eventually demonstrated a gastric ulcer as the probable cause of the abdominal pain.

Discussion

Fusion of the nephrogenic blastoma at the fourth fetal week is thought to be the cause of horseshoe kidney [4] and, in addition, prevents usual cephalad renal migration. The horseshoe isthmus is almost invariably across lower poles [1] and typically is caudally located (L4-L5) [9]. The isthmus is characteristically formed by solid renal parenchyma, only rarely by fibrous tissue; Whitehouse [6], in fact, demonstrated a fleshy isthmus in 55 of 59 cases of horseshoe kidney (visible nephrogram across isthmus). It may be anticipated, then, that the isthmus of horseshoe kidney should be recognizable on ultrasound. As a structure best approached anteriorly, however, it may have eluded the attention of renal ultrasonographers using prone sections.

Differential diagnosis may include enlarged pancreas and retroperitoneal lymphadenopathy. The pancreas should appear more cephalad in location; nodes would not be likely to show such smooth lateral extensions as isthmus. Of interest to the ultrasonographer investigat-

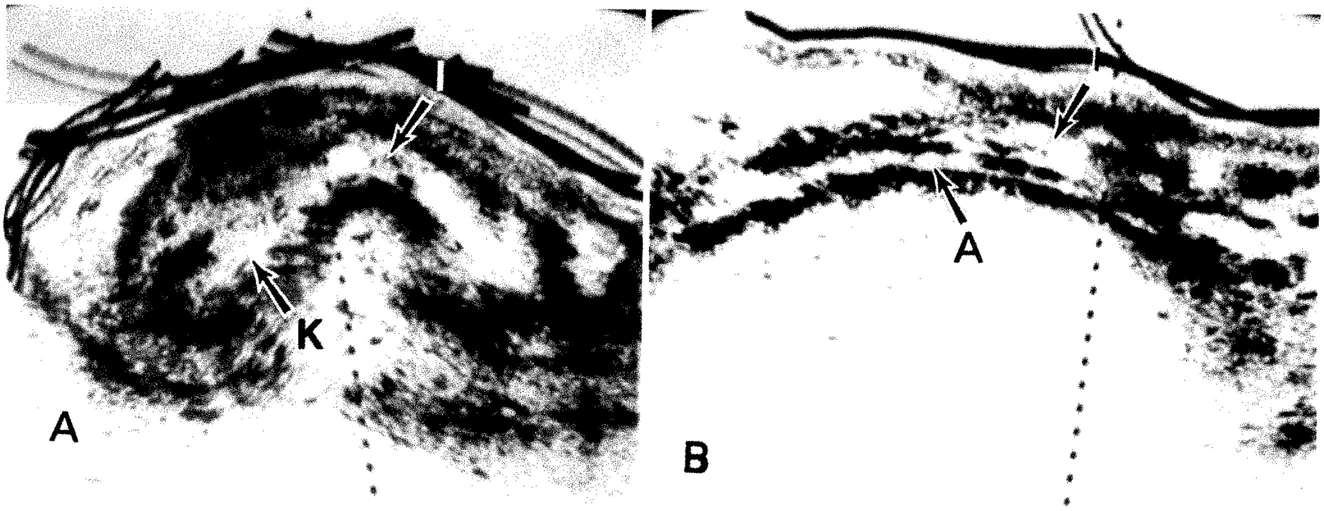

Fig. 1.—*A*, Transverse ultrasound scan 5.0 cm above umbilicus with patient supine showing contiguity of isthmus (I) with right kidney (K). *B*, Longitudinal ultrasound scan 1.0 cm left of midline with patient supine showing intimate relation of isthmus (I) to abdominal aorta (A).

Received February 4, 1977; accepted after revision May 11, 1977.

[1] Department of Radiology, University of Vermont College of Medicine and Medical Center Hospital of Vermont, Burlington, Vermont 05401. Address reprint requests to H. J. Mindell.

ing aortic aneurysm would be the possibility of an associated horseshoe kidney. This combination, reported occasionally [10], requires accurate preoperative documentation for appropriate surgical approach and could lie within the province of diagnostic ultrasound.

ACKNOWLEDGMENT

We thank Thomas Leavitt for performing the ultrasonic studies.

REFERENCES

1. Pitts WR Jr, Muecke ED: Horseshoe kidney: a 40-year experience. *J Urol* 113:743-746, 1975
2. Leopold GR, Asher WM: *Fundamentals of Abdominal and Pelvic Ultrasonography*. Philadelphia, Saunders, 1975
3. Ferrucci JT: Radiology of the pancreas: sonography and ductography. *Radiol Clin North Am* 14:543-561, 1976
4. Segura JW, Kalalis PP, Burke EC: Horseshoe kidney in children. *J Urol* 108:333-336, 1972
5. Pitts WR Jr, Kazam E, Gershowitz M, Muerke EC: A review of 100 renal and perinephric sonograms with anatomic diagnoses. *J Urol* 114:21-26, 1975
6. Whitehouse GH: Some urographic aspects of the horseshoe kidney anomaly— a review of 59 cases. *Clin Radiol* 26:107-114, 1975
7. Freimanis AK, Asher MA: Ultrasonic diagnosis in and about the kidney. *JAMA* 234:1263-1266, 1975
8. Sanders RC: Renal ultrasound. *Radiol Clin North Am* 13:417-434, 1975
9. Shash-Kumar JL, Somers LA, Pilling GP IV, Cresson SL: Wilms' tumor in the horseshoe kidney. *J Pediatr Surg* 9:185-189, 1974
10. Bietz DS, Merendino KA: Abdominal aneurysm and horseshoe kidney—a review. *Ann Surg* 181:333-341, 1975

Technical Notes

A New Subtraction Technique Using Duplicating Film as a Final Print

KAMAL MOJAB,[1] LUIS GARCIA, AND GEORGE TALGE

The purpose of subtraction technique is to eliminate overlying bone images which obscure the vascular pattern in an angiogram. We describe a simple new technique by which subtraction can be obtained using duplicating film for the final print without changing the initial density of contrast medium and radiograph. The vascular pattern remains white with a dark gray background, in contrast to the standard subtraction [1] in which the vascular pattern appears black with a transparent background.

Technique

The materials used include a photographic printer with light source (DuPont Cronex printer), DuPont Cronex subtraction film to make the diapositive or mask, Kodak X-Omat duplicating film to make the print, and a dark room and automatic processor.

First a base film of the area of interest before contrast medium reaches it is selected from the angiographic series. The reverse tone facsimile (mask) of the base film is made by placing a sheet of subtraction film in contact with the base film and exposing it to light through the base film. The exposure time is 2-3 sec with the selector switch of the photographic printer set on subtraction. Then the angiographic film to be subtracted is properly positioned and superimposed over the mask. A sheet of duplicating film with emulsion side down is placed in contact with the mask and angiogram. A print is obtained

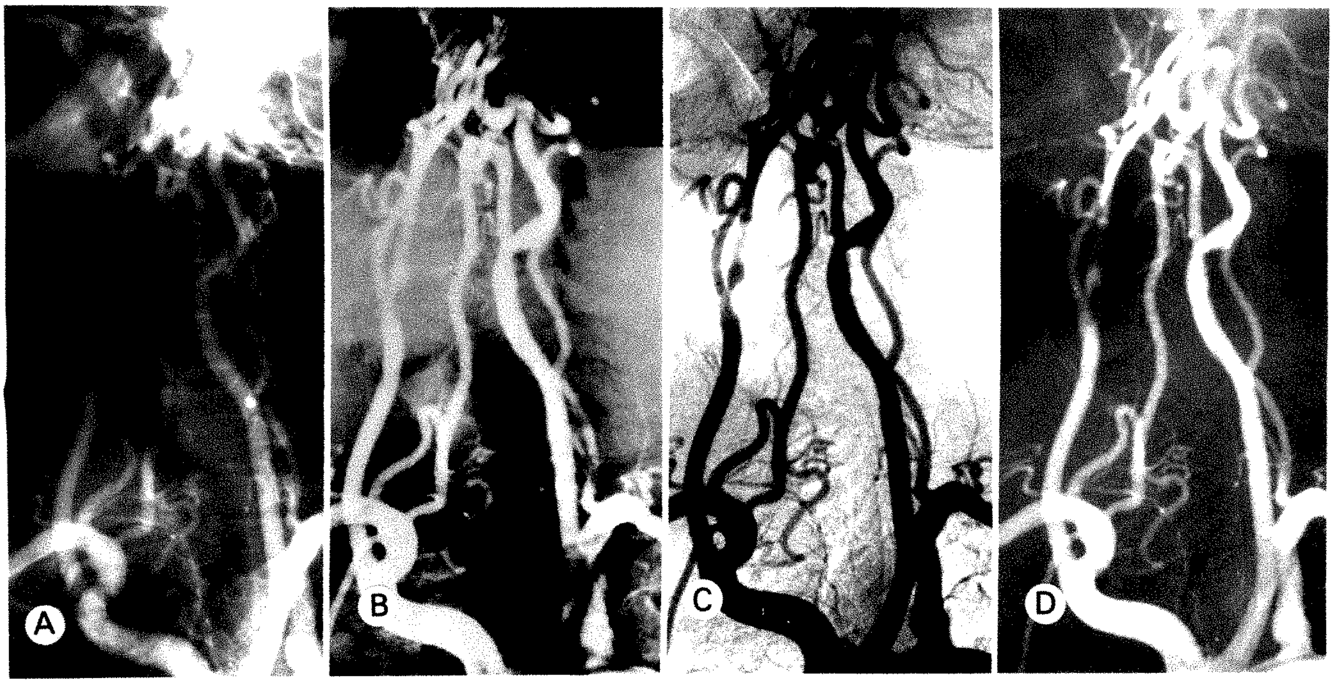

Fig. 1.—Arch aortogram showing arteriosclerosis of brachiocephalic vessels with marked narrowing of common and internal carotid artery bilaterally, more pronounced on left. *A*, Arch aortogram. *B*, Subtraction technique described by Christensen [2]. *C*, Standard subtraction technique of Ziedses des Plants [1]. *D*, Positive subtraction using duplicating film as final print.

Received March 3, 1977; accepted after revision May 24, 1977.

Presented at the annual meeting of the American Roentgen Ray Society, Washington, D.C., September 1976.

[1] All authors: Division of Angiography, Department of Radiology, Cook County Hospital, 1835 West Harrison Street, Chicago, Illinois 60612. Address reprint requests to K. Mojab.

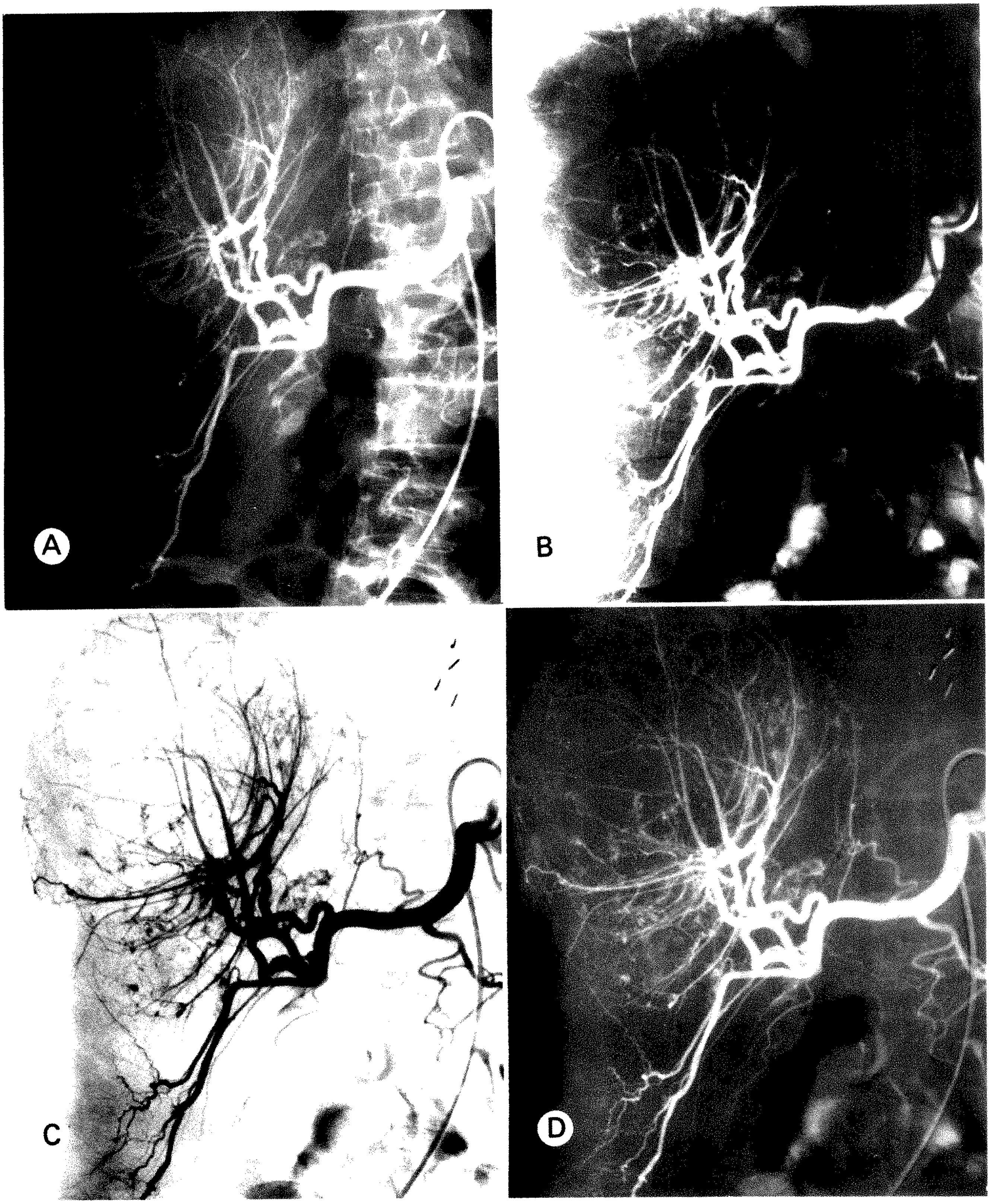

Fig. 2.—Selective hepatic arteriogram showing displacement of intrahepatic branches associated with encasement, puddling, and arteriovenous shunting in patient with adenocarcinoma of stomach metastatic to liver. *A*, Hepatic arteriogram. *B*, Subtraction technique described by Christensen [2]. *C*, Standard subtraction technique of Ziedses des Plantes [1]. *D*, Positive subtraction using duplicating film as final print.

by exposing the combination to light. At this step, the selector switch is set on duplicate. Required exposure time is 2½ min; if the photographic printer is equipped with an intensifying mirror, exposure time is 20 sec.

Discussion

For comparison, the following types of films from aortic arch and brachiocephalic angiography are shown: the angiogram (fig. 1*A*), a subtraction technique described by Christensen [2] (fig. 1*B*), a subtraction technique developed by Ziedses des Plantes [1] (fig. 1*C*), and a positive subtraction by the new technique (fig. 1*D*). Figure 2 shows the same types of films for a hepatic arteriogram.

Positive subtraction using duplicating film for the final print is a simple technique which can be applied to any angiographic procedure without reversing the initial density of the radiograph and contrast medium. This technique is less expensive, more perceptive, and provides better illustrations for publication.

REFERENCES

1. Ziedses des Plantes BG: Application of the roentgenographic subtraction method in neuroradiology. *Acta Radiol [Diagn]* (Stockh) 1:926-966, 1963
2. Christensen EE, Curry TS III, Nunnally J: *An Introduction to the Physics of Diagnostic Radiology*. Philadelphia, Lea & Febiger, 1972

Radiologic Aspects of the New Universal Proximal Femoral Hip Prosthesis

HENRY DRINKER[1] AND JAY C. MALL[2]

This paper describes a new type of hip prosthesis recently developed for use in certain clinical situations which may not require the more extensive total hip arthroplasty. It is being used with increasing frequency at the University of California Medical Center and at numerous hospitals across the United States.

The universal proximal femoral prosthesis is a new design in hemiarthroplasty which appears radiographically much like the familiar cup arthroplasty, but with the femoral stem of a total hip arthroplasty. The device consists of a standard Muller, Aufranc, Charnley, or Moore type femoral stem with either a 22 mm or 32 mm head which articulates with an acetabular component consisting of a high density polyethylene cup enclosed within a metallic cup. Two designs are currently available. In one, the Bateman (3M Surgical Products Division, Fair Lawn, N.J.), the two cups are separate [1]; in the other, the Giliberty (Zimmer USA, Warsaw, Ind.), the cups are molded together [2] (fig. 1). Radiographically, the two types are indistinguishable.

The new prothesis is replacing conventional hemiarthroplasty (Austin-Moore, Thompson) in clinical situations where the femoral head is compromised but the acetabulum is preserved (i.e., femoral neck fracture or avascular necrosis of any etiology). It is thought that this design will prevent premature degeneration and wearing away of the acetabular cartilage that occurs almost invariably with conventional hemiarthroplasty, resulting in a painful hip. An additional advantage is that the operative procedure is shorter and technically less complicated than total hip arthroplasty. At some institutions, it is being used instead of total hip arthroplasty for osteoar-

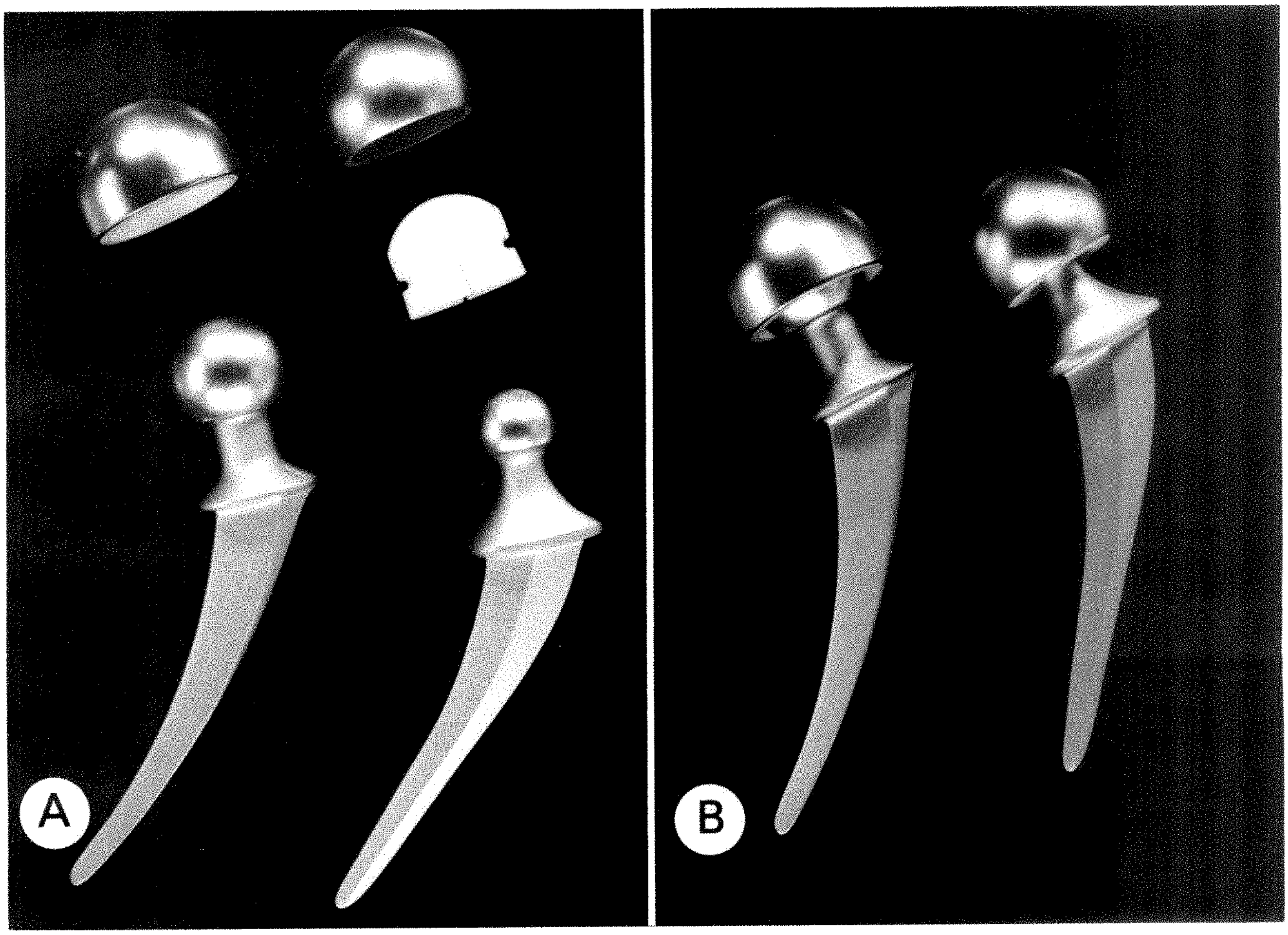

Fig. 1.—Disassembled (*A*) and assembled (*B*) Giliberty (*left*) and Bateman (*right*) variations of universal proximal femoral prosthesis.

Received December 20, 1976; accepted after revision May 3, 1977.

[1] Department of Orthopedics, University of California Medical Center, San Francisco, California 94143.

[2] Department of Radiology, University of California Medical Center, San Francisco, California 94143. Address reprint requests to J. C. Mall.

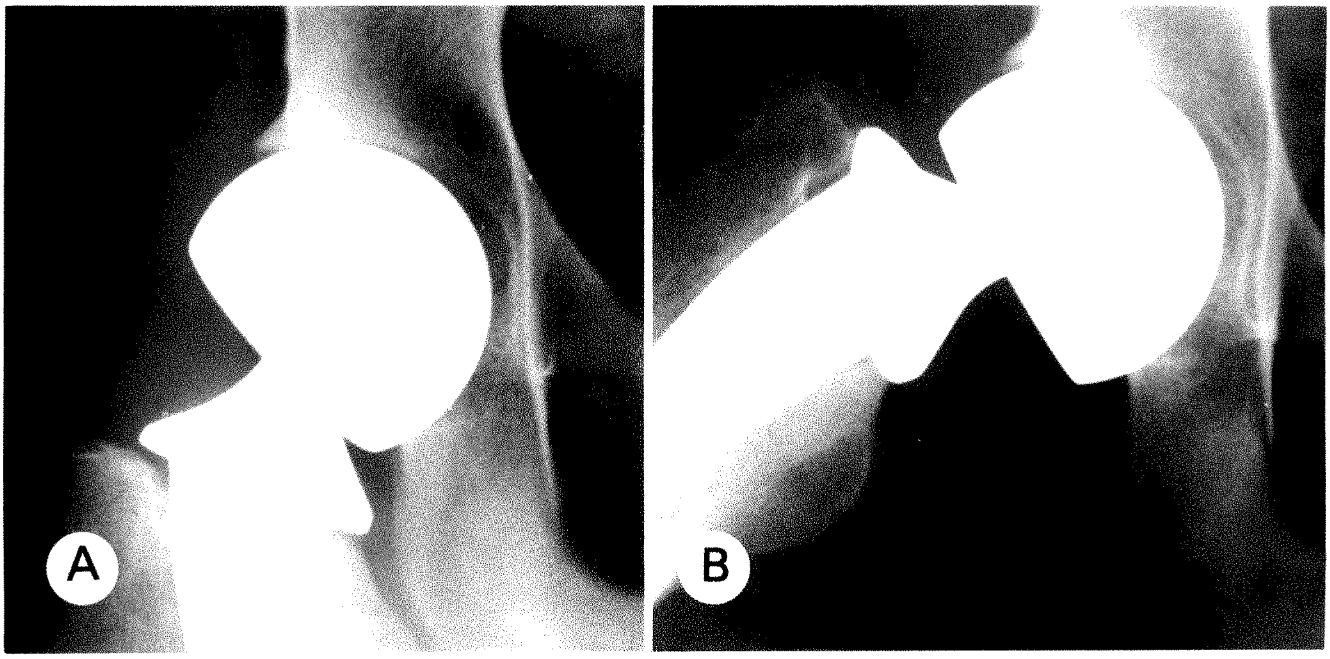

Fig. 2.—Adduction (*A*) and abduction (*B*) views showing preferential motion at articulation of femoral component and cup with minimal motion between cup and acetabulum.

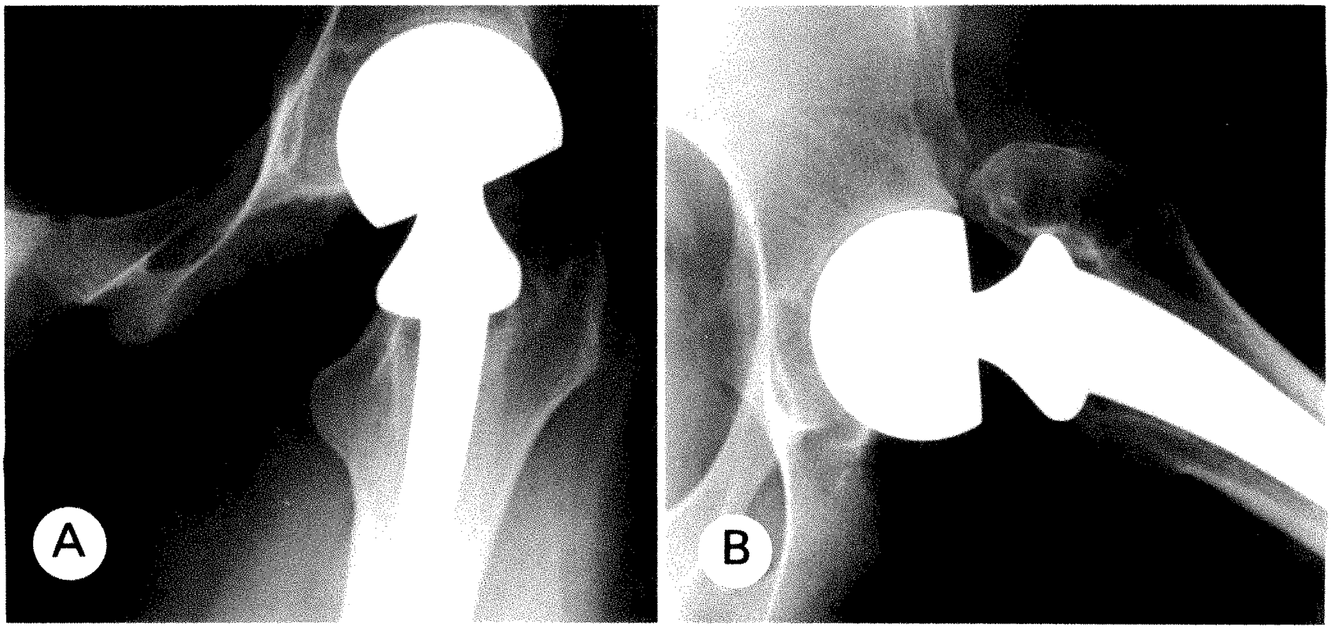

Fig. 3.—Adduction (*A*) and abduction (*B*) views demonstrating motion of cup within acetabulum at extremes of range of motion.

thritis, with a fenestrated Moore type femoral stem to eliminate the need for methylmethacrylate. However, this seems of little benefit since the risks of using methylmethacrylate have proven to be negligible. Problems with the device have been few and include the same complications encountered with conventional hemi- and total arthroplasty (i.e., stem loosening, infection, dislocation, ectopic ossification, etc.).

Mechanically, the device functions as a double compound bearing; the inner bearing is the articulation of the femoral head with the cup, and the outer bearing is the articulation of the cup with the acetabulum itself. The theoretical basis for this design is that relatively more motion is expected to occur at the inner bearing than at the outer, thus sparing the acetabular cartilage (fig. 2). However, movement at the outer bearing may occur at the extremes of the range of motion (fig. 3). Radiographically demonstrable movement at the outer bearing should be considered abnormal if it consistently occurs preferentially to movement at the inner bearing during the range of motion expected from normal activity. Motion studies are required to determine this. In addition, the objective criterion for success of this new design is the radiographic demonstration of maintenance of the acetabular cartilage over time [3].

REFERENCES

1. Bateman J: Single assembly total hip prosthesis—preliminary report. *Orthop Dig* 2:15-22, 1974
2. Giliberty RP: A new concept of a bipolar endoprosthesis. *Orthop Rev* 3:40-45, 1974
3. Drinker H, Murray WR: The universal proximal femoral endoprosthesis—a review of 106 cases. Submitted for publication

Cholecystocholangiography after Cholecystoduodenostomy

JEFFERSON BASTIDAS[1] AND LOUIS M. DelGUERCIO[2]

There are several methods available for diagnosing the jaundiced patient, including the newly popularized endoscopic retrograde cholangiography [1-4] and the revival of percutaneous cholangiography using the "skinny" needle [5-7]. In patients with a previous cholecystoduodenostomy, the biliary tree is also accessible to direct radiographic visualization after transintestinal catheterization of the cystic duct.

Our method is a modification of the steerable catheter system used by Burhenne [8, 9] in the extraction of retained stones. Two patients were evaluated with this technique. However, we feel that the method is readily applicable for diagnosis and possible treatment of a variety of abnormalities of the biliary tree in patients with previous cholecystoduodenostomy.

Technique

Under fluoroscopic control and aided by small injections of contrast material, a gastrointestinal Meditech soft steerable catheter system (Cooper Scientific Corp., Watertown, Mass.) is advanced through the pyloric canal and cholecystoduodenostomy stoma to the cystic duct. Further advancement through the cystic duct is impaired by the spiral valves of Heister. Injection of contrast material at this point results in good opacification of the biliary ducts. Films are then obtained in the conventional

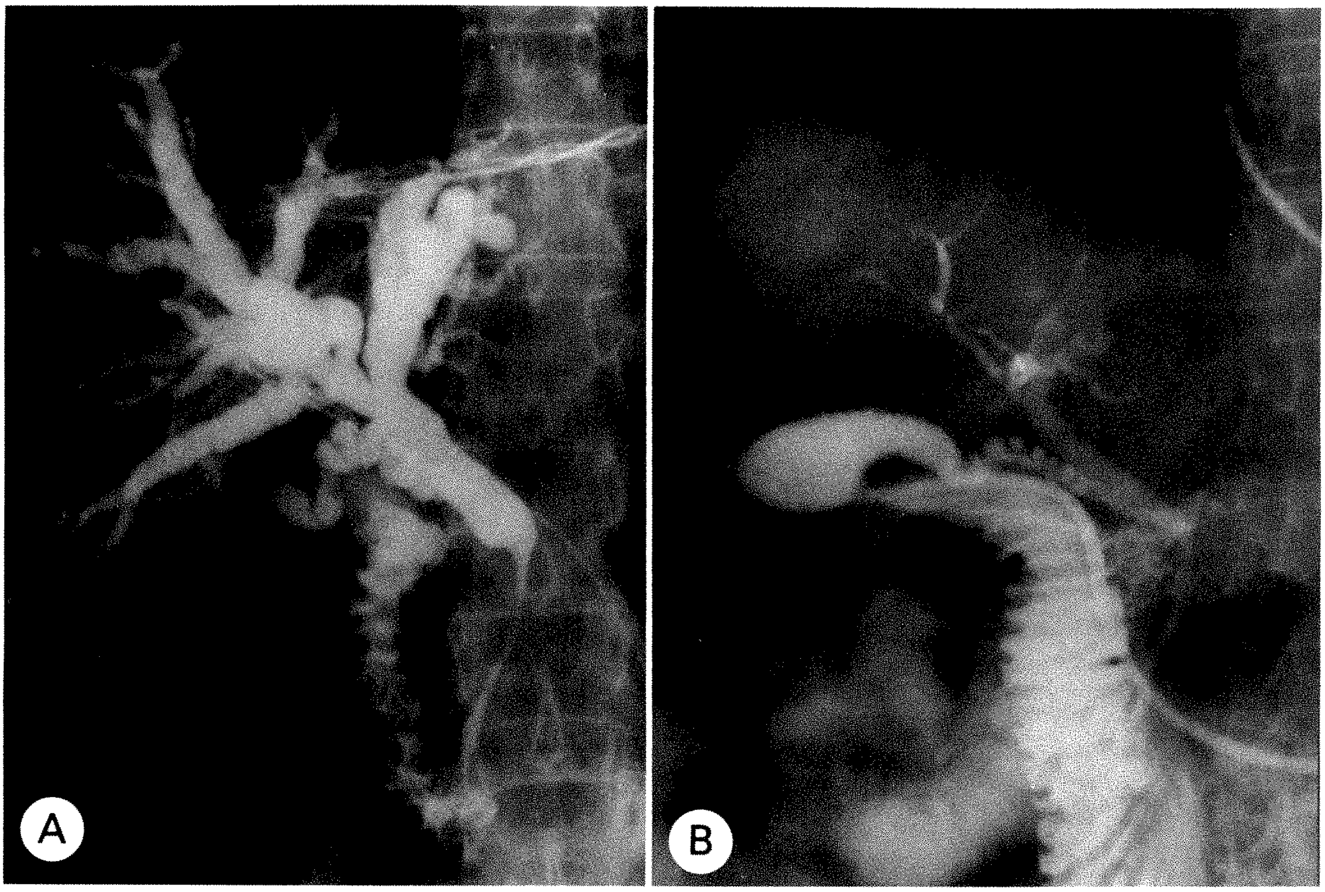

Fig. 1.—Case 1. *A*, Cholangiogram during minilaparotomy showing long stenotic segment of distal common duct, consistent with presumptive diagnosis of carcinoma of head of pancreas. Omental portogram performed at same time was normal. *B*, Transintestinal cholecystocholangiogram 5 months after laparotomy demonstrating normal size of biliary ducts and no evidence of progressive narrowing or obstruction of distal common duct.

Received July 30, 1976; accepted after revision May 11, 1977.

[1] Department of Radiology, Saint Barnabas Medical Center, Old Short Hills Road, Livingston, New Jersey 07039. Address reprint requests to J. Bastidas.

[2] Department of Surgery, Saint Barnabas Medical Center, Livingston, New Jersey 07039.

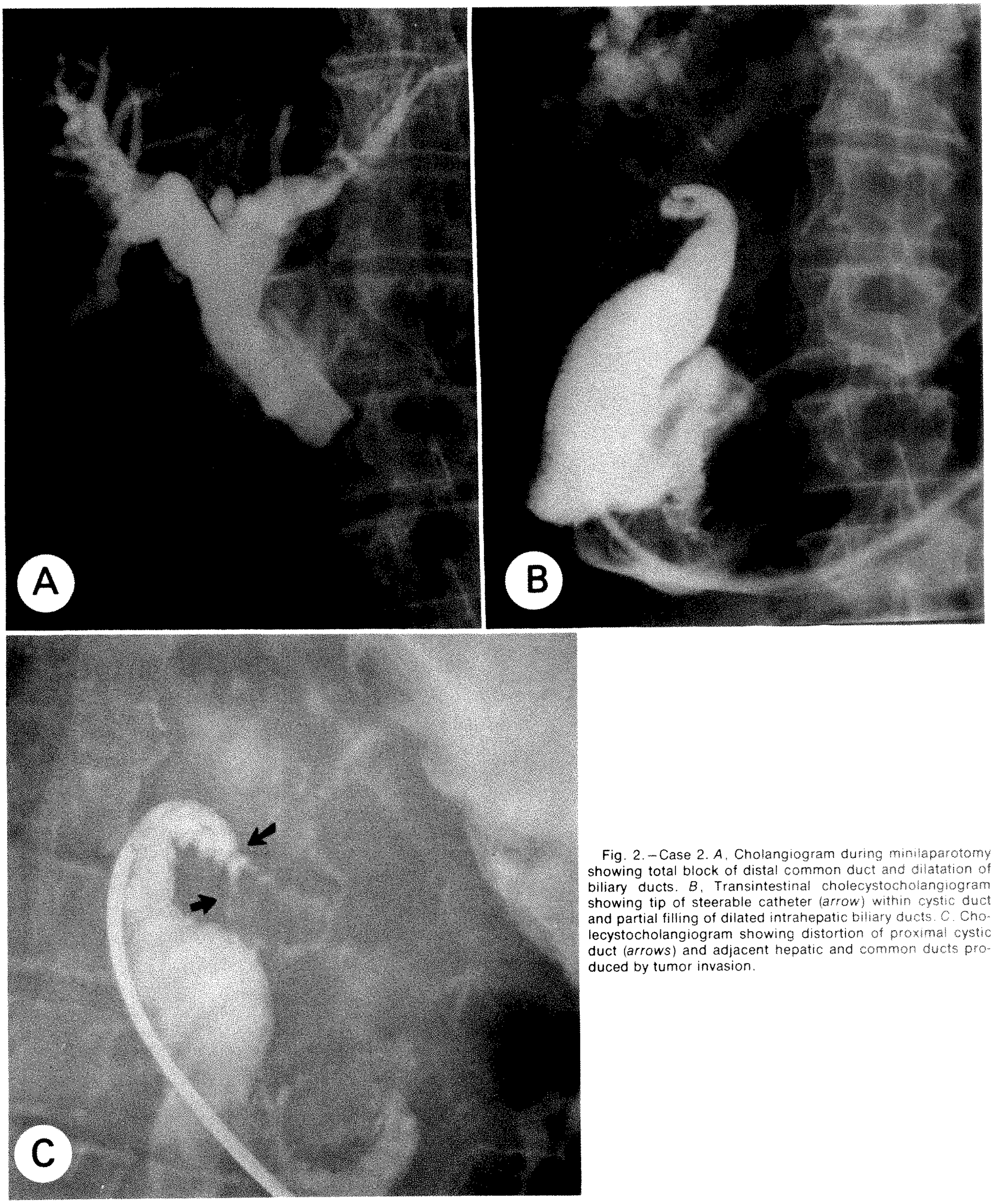

Fig. 2.—Case 2. *A*, Cholangiogram during minilaparotomy showing total block of distal common duct and dilatation of biliary ducts. *B*, Transintestinal cholecystocholangiogram showing tip of steerable catheter (*arrow*) within cystic duct and partial filling of dilated intrahepatic biliary ducts. *C*, Cholecystocholangiogram showing distortion of proximal cystic duct (*arrows*) and adjacent hepatic and common ducts produced by tumor invasion.

manner. The right anterior oblique view with the patient prone facilitates the visualization of the site of the cholecystoduodenostomy.

Case Reports

Case 1

A 66-year-old white female was transferred to Saint Barnabas Medical Center after 2 months of recurrent jaundice. She was treated for hepatitis; the serum bilirubin rose to 14 mg/100 ml and fell to 2 mg/100 ml after steroid therapy. There was no history of blood transfusion or medicines taken. On admission the total bilirubin was 10 mg/100 ml, direct was 7.5 mg/100 ml, and there was borderline alkaline phosphatase elevation.

The patient underwent a minilaparotomy procedure [10, 11]. The operative cholangiogram showed a long stenotic partial obstruction of the distal common duct (fig. 1*A*). The omental portogram was normal.

Exploratory laparotomy 5 days later revealed a huge hard mass of the head of the pancreas extending to the body and tail, encroaching the splenic vessels at the superior border. There was also extension to the superior mesenteric artery, celiac axis, portal vein, and surrounding the vena cava. However, biopsies of the pancreas and a few lymph nodes failed to show neoplasm. A cholecystoduodenostomy was performed, followed by a satisfactory course characterized by gradual reduction of jaundice.

Continuous clinical improvement suggested a benign process rather than carcinoma of the head of the pancreas. Five months later a transintestinal cholecystocholangiogram was performed (fig. 1*B*). The study demonstrated normal-sized intrahepatic biliary radicles and slight improvement of the distal common duct stenosis. At present the patient is alive and well.

Case 2

A 62-year-old male had cecal carcinoma with positive nodes resected. He was admitted 2 years later to Saint Barnabas Medical Center because of painless jaundice with extrahepatic obstruction suggested by liver function tests. Radionuclide liver scan showed a large central defect. Minilaparotomy with operative cholangiography revealed total abrupt obstruction of the distal common biliary duct (fig. 2*A*). Liver biopsy at that time revealed no metastatic disease.

Exploratory laparotomy 2 weeks later demonstrated massive lymph node metastases extending along the root of the superior mesenteric artery beneath the neck of the pancreas and into the porta hepatis, causing obstruction of the distal common duct. The gallbladder was distended. After mobilization of the first portion of the duodenum, a choleocystoduodenostomy was performed.

After transitory improvement the jaundice recurred. For reevaluation of the biliary pathway 5 months later, a transintestinal cholecystocholangiogram was performed. It demonstrated almost total obstruction of the proximal portion of the cystic duct and hepatic duct (figs. 2*B* and 2*C*), consistent with progressive pressure from the known metastatic lymph nodes along the porta hepatis. The patient died 2 months later.

Conclusions

The technique described allows a rapid, sometimes critical evaluation of the status of previously established biliary diversion procedures. It gives excellent radiographic detail of the involved anatomic structures, demonstrates patency of the anastomosis, and, above all, provides a meaningful evaluation of the improvement, progression, or stability of the basic disease process.

REFERENCES

1. Rohrmann CA, Silvis SE, Vennes JA: Evaluation of the endoscopic pancreatogram. *Radiology* 113:297-304, 1974
2. Geisse G, Melson GL, Tedesco FJ, Kelly JJ, Stanley RJ: Stenosing lesions of the biliary tree: evaluation with endoscopic retrograde cholangiography (ERC) and percutaneous transhepatic cholangiography (PTC). *Am J Roentgenol* 123:378-385, 1975
3. Freeny PC, Bilbao MK, Kator RM: "Blind" evaluation of endoscopic retrograde cholangiopancreatography (ERCP) in the diagnosis of pancreatic carcinoma: the "double duct" and other signs. *Radiology* 119:271-274, 1976
4. Menuck L, Amberg J: The bile ducts. *Radiol Clin North Am* 14:499-525, 1976
5. Okuda K, Tanikawa K, Emura T, Kuratomi S, Urabe K, Sumikoshi T, Kanda Y, Fukuyama Y, Muska H, Mori H, Shimokawa Y, Yakushiji F, Matsuura Y: Nonsurgical percutaneous transhepatic cholangiography: diagnostic significance in medical problems of the liver. *Am J Dig Dis* 19:21-36, 1974
6. Redeker AG, Karvountzis GG, Richman RH, Horisawa M: Percutaneous transhepatic cholangiography: an improved technique. *JAMA* 231:386-387, 1975
7. Ferucci JT, Wittenberg J, Sarno RA, Dreyfuss JR: Find needle transhepatic cholangiography: a new approach to obstructive jaundice. *Am J Roentgenol* 127:403-407, 1976
8. Burhenne HJ: Nonoperative retained biliary tract stone extraction: a new roentgenologic technique. *Am J Roentgenol* 117:388-399, 1973
9. Burhenne HJ: Nonoperative roentgenologic instrumentation techniques of the postoperative biliary tract. *Am J Surg* 128:111-117, 1974
10. DelGuercio LRM, Mehta M, Kline R, Kuzmak L, Mattey W: Savings through the direct approach to jaundice. *Am J Surg* 127:157-162, 1974
11. Mehta M, DelGuercio LRM: Minilaparotomy: an integrated procedure for rapid diagnosis in postcholecystectomy biliary tract symptoms. *Ann R Coll Surg Engl* 54:301-305, 1974

Special Lecture:

The Breast Cancer Screening Controversy: A Perspective

MYRON MOSKOWITZ,[1] PETER GARTSIDE,[2] LINDA GARDELLA,[1] IDO DE GROOT,[1] AND DEBORAH GUENTHER[1]

Analysis of the data of the Health Insurance Plan of New York Breast Cancer Screening Study indicates that in patients whose cancers were found by screening, the case fatality rate at all ages is almost half the case fatality rate of controls. The data also strongly suggest that maximal benefit in young women resides in the detection of in situ cancers. Due to relatively low yield of these early lesions, projected 20 year survival in that study may be little different for all women screened compared to controls. We have shown that the yield of these early lesions can be increased by aggressive screening and liberal use of biopsy. Furthermore, where J. C. Bailar has indicated a net gain (or loss) of −4 to +8 lives per 20,000 women using the HIP data, using his method and our data we find a savings of 25-27 lives/20,000 women by 3 year screening to date. These are lives that have been saved by mammography alone.

Controversy over the value of breast cancer screening continues unabated. Caught in the center of this debate are the practicing physicians who desire the best for their patients and the female population, already alarmed at the virtual epidemic of breast cancer. This paper attempts to assess the current risks and benefits of screening by first renalayzing the HIP data and then using the results of a 3 year screening program in Cincinnati.

Magnitude of Risk

In the application of any diagnostic or therapeutic measure in medicine, it is above all required that net benefit exceed expected risk. The magnitude of the risk is somewhat in question, particularly for relatively low levels of radiation [1-3]. If there is a risk, is it within a reasonable range or is it of an unacceptable order of magnitude?

To gain a perspective of risk, if 10,000 women underwent mammography annually for 30 years at 1 rad per year, the estimate of possible breast cancers induced ranges from three to 28, with 1.5-14 of the cases fatal assuming 50% mortality from induced cancers. These estimates are based on extrapolations from high dose data. For a similar population of women who smoke 1-1½ packages of cigarettes per day, 1,000 lung cancers could be expected, and virtually all would die of the disease. Approximately 180 patients would die of accidental deaths. The possible death rate due to breast cancer screening at the levels indicated is a lower risk by a factor of 20 than the current mortality rates involved in therapeutic research projects (assuming a project with a fatality rate of 0.1% per year). Therefore, the overall risk to a population of women age 35 being screened for 30 years is less than the risk of daily living [4] and can be entertained if a reasonable benefit can be expected. Obviously, to minimize risk the dose must be reduced to a minimum acceptable diagnostic level.

Is There a Benefit?

We have previously shown [5] based on a 25 year follow-up of patients with intraductal carcinoma treated by mastectomy that a flat survival curve results after a 20% initial mortality. This suggests that these patients are indeed cured of their disease and will have a normal life expectancy. Urban [6] has reported a 10 year 95% absolute survival rate for 162 patients with minimal breast cancer.

In the Health Insurance Plan study conducted in New York in the early 1960s, approximately 30,000 randomly selected women were offered screening, and a matched group was not screened [7, 8]. Of the 30,000 women to whom screening was offered, 20,000 accepted [7]. The 7-year case fatality rate (per 100) in the control group and study group (including the 10,000 who refused screening and those whose carcinomas were detected outside the screen) is shown in table 1 (S. Shapiro, personal communication).

These data could be interpreted to show benefit only to women over age 50. However, if only those whose cancers were found by screening are included, the results are remarkably different (table 1). These data suggest that if cancers are found by screening, the case fatality rates at all ages can be almost halved.

Can this marked reduction in case fatality rate be explained from data contained in the HIP study itself? If it is assumed that maximal benefit will accrue only to women whose cancers are detected while still in situ, it can be seen that at every age the proportion of in situ cancers is

---

Received November 29, 1976; accepted after revision April 13, 1977.

This study was supported in part by contract no. 1-CN-55310 from the National Cancer Institute and grant DPBC-11 from the American Cancer Society.

Presented at a symposium on Breast Cancer: The Radiologist's Expanded Role, sponsored by Roswell Park Memorial Institute, Buffalo, N.Y., October 1976. Portions also presented at the annual meeting of the Society of Photo-Optical Instrumentation Engineers, Washington, D.C., September 1976. Data reprinted with permission from Logan W (ed): *Breast Carcinoma*, New York, Wiley, 1977, and from *Proceedings of the Society of Photo-Optical Instrumentation Engineers, Application of Optical Instrumentation in Medicine V* (96: 443-452, 1976).

[1] Department of Radiology, University of Cincinnati Medical Center, Cincinnati, Ohio 45267.

[2] Department of Biostatistics, University of Cincinnati Medical Center, Cincinnati, Ohio 45267.

TABLE 1

7 Year Case Fatality Rate

Age at Diagnosis	Study Group			
	Screened and Unscreened	Screened Only*		Control
		Uncorrected	Corrected†	
40–49	42	23	28	40.9
50–59	32	24	30	54
60+	32.6	29	35	40.5

Note.—HIP data (S. Shapiro, personal communication). Values shown are percentages.

* Including only those cancers found by screening.

† Corrected for slight robust health bias factor.

TABLE 2

Percentage of In Situ Cancers

Group	Age 40–49	Age 50–59	Age 60+
Study not screened and interval cases	11	1.3	5.5
Control	12	6	9.1
Study screened	32.3	18.2	11.4

Note.—HIP data.

far greater in patients whose cancers were detected by screening (table 2). The study women who were not screened, or whose cancers were detected as interval cancers, had fewer minimal cancers discovered than the control group. Their case fatality is quite high [9], possibly a function of stage at time of detection [9, 10] (see below). Also, at all ages, the greater the proportion of in situ cancers, the lower the case fatality rate. Therefore, it can be presumed that maximal benefit will accrue to younger women who are (1) screened and (2) in whom early cancer is found.

If this is true, it can be asked why there is no difference in case fatality rate between younger and older screened women in whom proportionately fewer in situ cancers were found (S. Shapiro, personal communication). Although the answer is not completely clear, there are several assumptions that we have made from the beginning of our study which these data tend to support.

1. In older women (over 50), breast tumors are said to be less agressive than in younger premenopausal women. Therefore, case fatality rates, short term monitors, would be less likely to be affected by lack of in situ cancers in older women.
2. Since the mean 20 year survival rate for older women is exceeded by the survival rate of patients after treatment for stage I cancer and stage 0 cancer, the difference in survival between the two is not as critical as for younger women. Therefore, maximum benefit over age 50 will likely accrue to women with both in situ and stage I cancer.
3. In younger women, maximal benefit will accrue to women with in situ and minimal breast cancer.

The arguments advanced for including the survival statistics of the nonscreened study patients with the screened study patients are: (1) lag-lead time bias is avoided or diminished (S. Shapiro, personal communication); (2) self-selection bias is eliminated; (3) screening tends to detect slower growing and smaller lesions and, therefore, the results are biased [7]; and (4) in the HIP study, the general mortality, exclusive of breast cancer mortality, of women who refused screening was higher than those screened. In addition, the general mortality of those screened was lower than the general mortality of the controls. Therefore, it seems that in order to eliminate the effect of this possible bias, the data on the complete study group were combined.

General mortality *exclusive of breast cancer* in the HIP control population (all ages) is 54.3/10,000 patient years [9], while the general mortality in the screened population is 41.5 and in the study-refused group, 77.4. Because these two levels straddle the level in the control population, and because of the disparity in size between the screened and refused screen populations, the net mortality by combining these two populations equals the general mortality of controls. However, *at all ages*, the general mortality difference between control and study-screened is only 24%, while difference in general mortality between control and study-refused is 43%. Thus, in point of fact, the study-screened group resembles much more closely the control population than the control population resembles the refusers. Rather than combine dissimilar populations, it seems to us more logical to correct case fatality rates of the screened population for the slight robust health bias factor which exists (table 1).

It is unlikely that lead time is affected by inclusion of the data from those refusing screening. The unscreened patients in the study group merely have their cancers detected at a later stage of development. Their ultimate survival is not affected by the screening process, *since they were never subjected to it*. Furthermore, the calculation of case fatality rates includes a 1-year allowance for lead time in the screened women (S. Shapiro, personal communication).

Shapiro et al. [10] believe that the overall low apparent incidence rate of breast cancers in the study-refused group is a reflection that women at low risk tend to refuse participation in screening. Yet the data on the women who refused screening reveals the following: (1) 60% of the cancers detected had positive axillary nodes compared to 30% in the screened group [9]; (2) while overall detected incidence is lower in the nonscreened refusers, to date the incidence rate in these women *rises* annually, while it *tends to decline* in women screened all 4 years [10]; and (3) the average annual rise in incidence of breast cancer in the nonscreened refusers is 36.5%, almost three times that in the control population [10].

These observations suggest to us a different set of theories from those already offered by others.

1. Women who refused screening are at no lower risk for breast cancer than those screened.
2. It is likely that the rate of cancer incidence in this subpopulation will continue to rise at an increasing rate. This is because the prevalence was never eliminated, the natural incidence of breast cancer increases with age, and prevalent cancers, initially in situ and minimal, will

continue to make their clinical appearance at such size that they can no longer be ignored. On the other hand, the rate of rise in the control population will tend to stabilize or rise at a predictable rate since these women apparently do take advantage of the medical care available to them. Thus their rate of detection is reasonably predictable.

3. It seems reasonable to assume that these women did not seek medical aid until the cancer was obvious and advanced and are likely to continue to behave in this fashion. Delay in diagnosis may have been a contributing factor in their early death.

These observations, rather than detracting from the need for screening, emphasize the importance of screening to remove as many prevalent cancers as early as possible and the need for increasing the effectiveness of the screen so that the extant cancer pool of in situ and minimal cancer can be significantly reduced before they become invasive. However, excluding the results of these 10,000 refusers does not mean that benefit will necessarily accrue to a whole population of screened women. This is a function of screen efficiency.

To say that screening results are biased and thus invalid because of a predominance of early or small lesions is an exercise in tautology. This is tantamount to saying that the improved survival that comes from screening is biased because curable cancers are found. This reasoning implies that screening would exert its effect by detecting invasive, essentially incurable cancers, which would then be transmuted into curable lesions by the mere fact they have been discovered. The next logical deduction suggested by this reasoning is that there is indeed no form of cancer which is curable, by our current methods, except in women over 50. This is contrary to observed clinical fact, and indeed contrary to the data reported above.

In situ cancer is potentially lethal cancer. As Bailar himself has noted [7] at least 20% of such patients can be expected to die within 7 years of diagnosis. In a 25 year follow-up of 75 patients with intraductal cancer treated by mastectomy, 80% survived [5]. While it is possible that some in situ cancers, particularly in older women, might never become clinically apparent, this is unlikely in 35–50-year-old women whose mean natural life expectancy is 30–40 years, unless the mean duration of the disease is assumed to be longer than 35 years. If the HIP figures of prevalence are accepted as representative, then by conservative calculation the mean duration of carcinoma of the breast approaches 4.3 years. Since the in situ carcinomas found in the HIP study were included in the prevalence data, it can logically be deduced that every minimal or in situ breast cancer will become invasive and, in fact, fatal within the normal projected life span of a 35-year-old woman. By this calculation, 50% of them would be expected to die before they reached 50. If that is correct, there should be little argument that benefits to younger women are maximized by detecting in situ and minimal breast cancer. Until biologic markers are available to indicate which in situ cancer is indolent, it behooves us to regard all such cases as potentially fatal. In our opinion, to do less, in light of current knowledge, is unconscionable.

Reinterpretation of the HIP data, as presented, allows fairly clearcut scientific demonstration that a benefit to screening exists at all ages in women whose cancers are detected by screening. Since this has already been demonstrated by a scientifically controlled study, we believe that these assumptions can be accepted.

Can Benefit Be Increased?

We have, from the inception of the Breast Cancer Demonstration Project in Cincinnati, embarked upon mass screening for breast cancer with the following goals:

1. A maximal effort, by both physical examination and mammography, would be made to detect minimal breast cancer, particularly in younger women. Minimal breast cancer is defined as breast cancer which is either totally in situ; invasive but less than 5 mm in size; intraductal or in situ lobular carcinoma with evidence of less than 10% microinvasion; cystosarcoma phylloides; or tubular carcinoma. This approach requires frequent, often negative biopsies and would be most aggressive during the initial 2 years of screening. Because biopsy is performed on the basis of minimal x-ray and/or physical findings, a high yield of minimal breast cancers results. We firmly believe, within reason, that noncancer biopsies, particularly in younger women, do not represent unnecessary surgery.

At the outset we estimated that approximately 10% of the patients attending our center during the first 2 years of screening would have a biopsy performed, and, overall, approximately 10% of those biopsies performed would yield a carcinoma. These projected rates have been maintained. It is this willingness to accept a high biopsy rate with relatively low yield which differentiates our approach to screening from the standard approach (S. Shapiro, personal communication).

2. Maximal effort would be made to minimize radiation dose. This would be (and was) achieved by relatively high filtration, compression, and restricting the number of images per examination. We aim for two views per breast per examination; only one repeat x-ray of the breast per examination is allowed if the original image is unsatisfactory, unless there are extenuating circumstances.

Insofar as risk is concerned, the skin dose rate per exposure has gone from 7.7 rad in the HIP study [7] to 1.2 rad in our study. The annual average midplane breast dose, including all follow-up and repeat studies, is 1 rad per year in our patients and has been so from the outset of the program.

In the HIP study, the prevalence rate was found to be 2.72 cancers/1,000 [8]. It is very unlikely that point prevalence would be this low for any group of women aged 40 and above. Since point prevalence is an interplay of annual incidence and the duration of the disease, prevalence can be predicted using the formula $P = \Sigma I_j D_j$, where I_j is the incidence rate of the jth age decade, and

D_j is the expected duration for a patient with the disease in the jth age [5]. Assuming a 10–16 year mean duration of breast cancer from in situ to death, the predicted detectable prevalence rate is estimated at 6–10/1,000. The Cincinnati prevalence is 8.9/1,000. It is difficult to conceive that a prevalence rate of 2.7/1,000 could be representative of the true detectable prevalence of breast cancer. This prevalence could be considered detectable prevalence by that screen (i.e., threshold sensitivity), but it is not a reflection of extant detectable prevalence. This is borne out by the large number of incident and interval cancers subsequently found in the screened women in the HIP study (see later).

It is true that extant detectable prevalence will be affected to some degree not only by the natural history of the disease but also by the preexisting health priorities of the women participating in the screening process. Since 54% of the cancers occurring in the HIP control women had positive axillary nodes at the time of detection, a figure which differs significantly ($P < .0002$) from that occurring in the U.S. general nonscreened population at that time, it can be presumed that this prior "skimming" could significantly affect the number of prevalent extant cancers detectable in a population to be newly screened. However, it should not affect the estimate of the total pool of prevalence. Therefore, any estimate of HIP prevalence could be reduced by a correction factor of 13%.

The greater the percentage of in situ cancers present in the initial screening and the larger the prevalence rate, the more likely the screen can be regarded as having lowered threshold sensitivity and dipped into future incidence.

Since the population of women comprising the HIP group was over age 40, and since incidence increases with age, a reasonable detectable prevalence estimate might well be on the order of 800–900/100,000. If that is true, and accepting an annual incidence of 136/100,000 [11], one would expect to find after 4 years 1,258 cancers/100,000 women screened. In fact, in the HIP study group of 20,000 screened women, 1,387 cancers/100,000 were found, based on 132 detected through screening, 91 interval cancers in women who had been screened at least once [11], and 272/100,000 prevalent cancers. Thus the predicted estimate of total cancers present in the duration of the screen is within 10% of the actual number found. This would indicate that missed prevalence will demonstrate itself by subsequent increased incidence.

The results of the Cincinnati study are shown in table 3. It is of interest to compare these results with the HIP data, particularly in the detection of in situ carcinoma where screening can have maximal benefit. Using all modalities, the number of in situ carcinomas in the screened group in the HIP study was 26 (S. Shapiro, personal communication). This is a rate of 129/100,000 patients examined. In the control group, 24 such cancers were found. In the Cincinnati experience, 318 in situ cancers per 100,000 patients were detected, significantly more than the HIP rate ($P < .002$). Using mammography alone, the in situ cancer detection rate for the HIP study was 85/100,000, and by physical examination (including cases detected by physical examination and mammography), the rate was 45/100,000. The corresponding rates in the Cincinnati study were 183/100,000 and 135/100,000, respectively ($P < .05$ for both comparisons).

TABLE 3

Results of Cincinnati Study

	Age				Total
	35–44	45–54	55–64	65+	
No. patients	3,792	3,673	2,019	890	10,374
Cancers detected by mammography only:					
In situ	5	8	4	2	19
In situ plus 10% microinvasion	2	1	1	0	4
Other minimal	1	1	2	2	6
Invasive	2	12	8	4	26
Cancers detected by physical examination:*					
Minimal	1	2	0	2	5
In situ	3	8	3	0	14
Invasive	3	16	15	11	45
Total	17	48	33	21	119
Percentage detected by mammography only:					
Minimal cancers	67	52	70	66	60
Total cancers	59	46	45	38	46

Note.—Data from 3 year screen through June 1976.

* Includes those detected by physical examination plus mammography.

Another method of comparing what is possible today with what was possible then is to compare the number of early cancers found by mammography alone per 100,000 mammograms performed (table 4). In the HIP study, 17 in situ cancers per 64,810 mammograms were detected at all ages, for a rate of 26/100,000 mammograms performed [7]. In the Cincinnati experience overall, 75 in situ carcinomas were found per 100,000 mammograms performed (significantly different at .01 level). While it is not known how many minimal cancers were found in the HIP study, if all minimal carcinomas of the breast in the Cincinnati experience are included, the rate per 100,000 mammograms jumps to 115.

Since concern primarily centers around the younger age group, we compared the Cincinnati yield in the 35–44 age group with the HIP early cancers in the under 50 age group. In Cincinnati, five in situ cancers in 3,792 patients were found by mammography alone, for a rate of 56 per 100,000 mammograms performed. In the HIP study, five minimal breast cancers in 9,880 patients under age 50 were found by mammography alone [9]. Assuming that 3.0 mammograms were done per patient (table 4) [7], the HIP in situ discovery rate by mammography alone is estimated to be 17/100,000 ($P > .05$). If all minimal cancers in the Cincinnati experience are included, the rate jumps to 90/100,000 mammograms.

The Cincinnati data are particularly important in this regard since the philosophical approach to screening has been diametrically opposed to that traditionally performed. We use a highly aggressive approach with generous recommendation for biopsy in order to maximize detection of early prevalent cancers (table 5). As a result

TABLE 4

Mammograms Performed

Group	No. Mammograms	No. Patients	Mammograms per Patient
Cincinnati study:*			
Age 35–44	8,919	3,792	2.35
Age 45–54	9,168	3,673	2.5
Age 55–64	5,151	2,019	2.55
Age 65+	2,006	890	2.25
Total	25,244	10,374	2.43
HIP study	64,810	20,166	3.2

* 3 year screen through June 1976.

TABLE 5

Biopsies Performed

	HIP	Cincinnati
Screening period (yr)	5	2.5
Approximate no. patients ...	20,000	10,400
No. biopsies	644	1,230
Biopsy rate per 100,000 patient years	644	4,730

Note.—Data based on number of patients accepting at least one screen. Cincinnati biopsy rate significantly different from HIP at .0001 level.

TABLE 6

Risks to Age Group 35–44

Approximate No. Patients per Cohort	No. Rad Years, to 30 Years At Risk	Possible Cancers Induced		
		BEIR [1]	WASH 1400 [2]	UNSCEAR [3]
1,900	66	0.75	0.38	0.09
1,900	43	0.49	0.25	0.06
Total induced ..	...	1.24	0.63	0.15
95% confidence limits	...	±2.22	±1.59	±0.77

Note—Data based on 3 year screen to June 1976. To recognize the addition of these estimated induced cancers to spontaneous cancers in a prospective study at the .05 level with 90% assurance, 14.5 million patients would be necessary in each study group.

of this aggressive approach, our prevalence rate to date is 890/100,000 and incidence rate is approximately 60/100,000. In addition, our true positive rate is 95%, remarkably different from the 59% rate of HIP. However, this was achieved at the cost of a high biopsy rate.

Benefit versus Risk to Date

Thus far it has been demonstrated that detection of in situ cancers by screening improves survival in screened patients. Furthermore, detection of these early lesions, even with current methods, has been improved although it has not yet been optimized. How have screening results been affected?

Comparison of Bailar's results using the HIP data [7] and results using his method on the Cincinnati data is intriguing. Bailar [7] calculates that of all cancers detected by mammography alone in the HIP study, only 12 deaths would be averted. He calculates a range of possible cancers induced by the screening from eight to 32, with the number of possible deaths ranging from four to 16 (assuming 50% mortality from induced cancers), for a net benefit of from −4 to +8 lives saved. Substituting the Cincinnati data for the HIP data, and using Bailar's approach for the same size population, approximately 28 deaths could be averted among the cancers found by mammography alone. From 0.75 to 6.6 cancers would be caused by the screening with possibly one to three deaths at 30 years, for a net benefit of 25–27 lives saved (significantly different from HIP at .01 level). The Cincinnati calculations assume 1 rad/year, 5,200 patients screened for 3 years and 5,200 screened for 2 years, adjusted to a rate of 20,000 patients.

Perhaps more to the point are the risks incurred to the age group 35–44 as a result of 3 years of screening to date (table 6). Again, using the method of Bailar, 20% of the patients with in situ carcinomas found by mammography alone would, if not screened, be expected to die, and 40% of the remaining with mammographically detected cancers would be expected to die. Since 264 cancers per 100,000 were found by mammography only, and half of these were in situ, 79 deaths/100,000 would be expected, if not screened. Using the proportion of actual deaths that occurred in the group of mammographically detected in situ in the HIP study to deaths expected (2/14), 68 deaths/100,000 would be averted by this screen. If one subtracts the total number of possible induced cancer deaths calculated by BEIR [1], WASH 1400 [2], or UNSCEAR [3] data (table 6), the net gain thus far for 100,000 patients in the 35–44 age group would be 52, 60, and 66 lives/100,000 examined, respectively.

This maximal benefit is calculated simply on the number of in situ carcinomas detected. It is not based on consideration of the other minimal cancers found either by mammography alone, mammography and physical examination, or physical examination alone. Therefore, this excludes such very early lesions as invasive carcinoma less than 5 mm in size, carcinomas which are 90% intraductal with less than 10% microinvasion demonstrated on multiple sections, tubular carcinoma, and cystosarcoma phylloides.

Presuming the above data are reasonable, it is possible to estimate the benefit/risk based upon the HIP data and alluded to earlier in this paper. For persons under age 50 whose cancers are detected by screening, there is a 44% increase in short term survival, uncorrected by the robust health bias factor. Corrected for the robust health bias factor, this drops to 32%. Since we believe maximum benefit resides in detecting in situ cancers in this age group, it can be projected that long term relative survival will be affected similarly. Thus an estimate of the relatively long term survival from breast cancer that will result from our screening to date can be made.

Normally, the *20 year* relative survival rate is given as 46% [11]. Given the assumptions above, this relative survival should be altered to 61%–66%. Therefore, of the women in the Cincinnati series whose cancers have been detected by *screening* in the 35–44 age group, 67–89 deaths have been averted per 100,000 women screened. Allowing the possible number of breast cancer deaths due to induced cancers by BEIR [1] estimates alone, 51–73 breast cancer deaths have been averted. WASH 1400

[2] risk figures would bring these estimates to 59-81. Approximately 44 were salvaged by mammography alone.

At age 45-54, assuming the HIP age-specific benefit for women whose cancers have been detected by screening, a 44%-55% improvement over relative survival should be expected. Thus 270-324 breast cancer deaths should be averted per 100,000 women screened in this age group to date, 136 by mammography alone. At age 55+, we will assume a 14%-28% improvement in survival. Thus from 991 to 1,133 deaths per 100,000 have been averted, 435 by mammography alone. Therefore, as a result of screening it can be reasonably postulated that if 100,000 women had been screened for 2½ years, from 1,312 to 1,530 cancer deaths would have been averted in each of the age categories.

The importance of detecting minimal and/or in situ cancers can be best appreciated by the following computations. Based on our previous observations [5], we believe that with current treatment methods 80% of patients with in situ and minimal breast cancer can be expected to survive to their normal life span. If we apply the discovery rates of in situ cancer detected by HIP screening, nonscreening, and Cincinnati screening to Cincinnati cancer detection rates, the net person years gained makes an interesting comparison. The figures in table 7 allow for a 5 year lead time for the screened-detected cancers, and no lead time is allowed for nonscreened detected. Furthermore, induced cancer deaths are based upon BEIR estimates [1] for 3 full years of screening and a 40 year life expectancy for patients less than 50 years of age, and 25 year mean life expectancy in the age group 50-65.

Under age 45, the net person years gained over nonscreening per 100,000, using the HIP screen rate, would be 1,986. In the Cincinnati screen to date, from 3,800 person years to 6,878 person years have gained per 100,000. Over the age of 45, the net person years gained increases from 6,172 to 8,729 for the above categories.

TABLE 7

Person Years Gained by Detection of In Situ and/or Minimal Breast Cancers

Group	Age 35-44	Age 45-64
HIP study:		
Control rate	1,728	1,705
Screened rate:		
Gross	4,014	4,263
Net*	1,986	2,477
Cincinnati study:		
In situ cancers:		
Gross	5,908	7,958
Net*	3,880	6,172
Minimal cancers:		
Gross	8,906	10,515
Net*	6,878	8,729

Note. – Rates per 100,000 patients examined. Net rate = gross person years gained minus person years gained without screening (using HIP control rate) minus person years lost as result of induced deaths. HIP detection rates of in situ cancers are shown in table 2.

Conclusions

1. We believe that our data for 3 years of screening to date show a marked benefit from low dose mammographic screening for all ages over 35.
2. We believe these data are replicable because we have done so on two separate cohorts of women.
3. The HIP data demonstrate that there is a population of breast cancer patients for whom benefit of screening is maximal. Unless sufficient numbers of these are found, the net beneficial effect will be too dilute to demonstrate change in survival in the screened population. Our data suggest that this potential benefit has been increased for the population we have screened. We believe this maximization differential is entirely due to the aggressive use of biopsy to diagnose in situ and minimal cancers. We cannot entirely rule out that population bias may be affecting our yield of early cancers.
4. Just as our yield is not necessarily applicable to the screening process, we do not believe that the HIP yield is representative of what can be obtained by aggressively performed mammographic screening.
5. While it is possible to detect a significant number of early lesions by physical examination, at least 59% of the highly curable cancers in younger women in our work would have been missed if physical examination alone were the screening modality.
6. We have now an opportunity by aggressive use of mammography and physical examination to arrest a disease of virtually epidemic proportions.

The responsibility to do so is great on all sides. Those who would destroy the method because it is not being utilized to its fullest potential do incalculable harm. However, an equal burden, if not a greater one, falls upon those who are using the method. It is incumbent upon us to extract the maximum potential from mammography and physical examination if they are to be used as screening tools.

ACKNOWLEDGMENTS

We are deeply indebted to Dr. C. Ralph Buncher for review of our early manuscripts and helpful suggestions; and to Mesdames P. Campbell, S. Cosgrove, B. Brown, and E. Rice for unflagging effort and support.

REFERENCES

1. National Academy of Sciences-National Research Council: *The Effect on Populations of Exposure to Low Levels of Ionizing Radiation*. Report of the Advisory Committee on the Biological Effects of Ionizing Radiation (BEIR report). Washington, D.C., National Academy of Sciences-National Research Council, 1972
2. Nuclear Regulatory Commission, Reactor Safety Study: *An Assessment of Accident Risks in Commercial Nuclear Power Plants*. WASH-1400, NUREG-75/014, Washington, D.C., U.S. Nuclear Regulatory Commission, Appendix 6, G-15, 1975
3. United Nations Scientific Committee on the Effects of Atomic Radiation: *Ionizing Radiation: Levels and Effects*. Vol 2:*Effects*. New York, United Nations, 1972
4. Cardon PV, Dommel WJ, Trumble RR: Injuries to research

subjects. *N Engl J Med* 295:650-654, 1976

5. Moskowitz M, Saenger EL, Gartside PS, Kereiakes JG, Pemmaraju S, Russell P, Gardella L: Benefit versus risk in mammographic screening: one approach. Paper presented at the 8th Annual Conference on Radiation Control, Springfield, Ill., May 1976
6. Urban JA: Changing patterns of breast cancer. *Cancer* 37:111-117, 1976
7. Bailar JC: Mammography: a contrary view. *Ann Intern Med* 84:77-84, 1976
8. Venet L, Strax P, Venet W, Shapiro S: Adequacies and inadequacies of breast examinations by physicians in mass screening. *Cancer* 29:1546-1551, 1971
9. Shapiro S, Strax P, Venet L, Venet W: Changes in five year breast cancer mortality in a breast cancer screening program. *Seventh National Cancer Conference Proceedings:* 663-678, 1973
10. Shapiro S., Goldberg JD, Hutchinson G: Lead time in breast cancer detection and implications for periodicity of screening. *Am J Epidemiol* 100:357-366, 1974
11. Seidman H: *Cancer of the Breast: Statistical and Epidemiological Data*. New York, American Cancer Society, 1972

Guest Editorial

Pulmonary Surfactant Disease States

Although much has appeared in radiologic textbooks regarding primary and secondary lobular disease of the lung [1-3], less attention has been given to diffuse alveolar damage and the surfactant system [4], a vital component of the alveolar surface. Many types of alveolar damage have a similar radiographic appearance, beginning with diffuse homogeneity or very fine nodulation and terminating with an appearance associated with interstitial fibrosis. Because the lung seems to respond in a similar way to a variety of insults of the alveolar lining, it is necessary to thoroughly understand the common features of the histology, histochemistry, and pathophysiology of the alveolar lining. This editorial considers a number of syndromes that relate clinically to a common denominator, aberrations of pulmonary surfactant.

The alveolar wall is a continuous lining of epithelial cells, occasionally interrupted by pores of Kohn, of several distinct cell types (fig. 1) The type 1 pneumocyte is a flattened cell with a smooth contour and small indentations often filled with what has been called hypophase material. The type 2 pneumocyte, a more cuboidal cell, contains numerous osmiophilic inclusion bodies and has numerous microvilli. The irregularities of this cell surface are filled with surfactant.

For some time it has been known that the lung can synthesize fatty acids and incorporate them into phospholipids [5]. These are believed produced and stored as surfactant in the myelinic of lamellar bodies of the type 2 pneumocyte [6]. Surfactant has been shown to be rich in lecithin molecules in which the fatty acids are saturated and 16 carbon atoms long (palmitic acid). Phospholipids with unsaturated fatty acids, or those more than 16 carbon atoms long, constitute only a small fraction of the lipid in surfactant. In lipid films, dipalmitoyl lecithin has a very high collapse resistance which uniquely suits it to the function of lowering the surface tension of the alveolar lining. Phospholipids with the acyl compositions found more universally in mammalian tissues (usually with one polyunsaturated fatty acid) collapse more readily and are therefore unsuitable in the surfactant. As a result of the surfactant compounds, the alveolus is highly resistant to collapse and disruption because of the low surface tensions created [7].

Immediately adjoining the surfactant layer is another called the hypophase, which blends and intermixes with the surfactant. The hypophase is largely composed of mucopolysaccharides whose role in lowering surface tension is insufficiently understood.

Located in the short distance between capillary blood and alveolar air are the capillary endothelial wall, the basement membrane, the alveolar epithelial cells, and the alveolar lining surfactant-hypophase mixture. The composite is only about 1 μm thick but is spread over each of the 70 or so square meters of alveolar surface.

In certain locations the basement membrane is exposed directly to the alveolar gas, indicating that the alveolar lining layer and epithelial cells are discontinuous. In subepithelial spaces, other large nucleated cells called macrophages may work their way into the alveolus. They advance cephalad on the ciliary blanket of the bronchiolar and bronchial cells—the "mucociliary escalator."

The turnover of phospholipids in the lung is extremely rapid. Radioisotope studies have demonstrated a half-life of about 14 hr for the surface-active lecithin [8]. Very likely, the macrophages play a role in its ultimate removal from the lining. These cells contain very active phospholipases and proteases, enzymes that degrade the constituents of surfactant, phospholipids, and protein. Thus the macrophage plays a key role in the homeostatic mechanisms that control the amount of surfactant in the alveolus.

A number of pulmonary disease states occurring in both infants and adults are associated with abnormalities in surfactant. They may resemble one another radiographically.

Neonatal Dysmaturity, Incomplete Development, and Deficiency of Surfactant

The ability of the fetal lung to synthesize dipalmitoyl lecithin increases with gestational age and is probably fully achieved sometime during the third trimester of pregnancy [9]. At birth, surfactant with its high content of dipalmitoyl lecithin is distributed as the alveolar lining layer at the same time air breathing is established. Thereafter, the ability of the lung to retain a residual volume of air depends on the stability of the surfactant system. Moreover, the synthesis and spreading of surfactant molecules probably provides the mechanism for removing extraneous material from the alveolar surface. It is probable that incomplete development of this system and synthesis of dipalmitoyl lecithin is basic to "bronchopulmonary dysmaturity" [10].

Alveoli in a newborn infant with respiratory distress syndrome do not retain air during deflation and collapse to virtually zero volume [9]. Widespread atelectasis occurs along with the replacement of normal surfactant by hyaline membranes [6] having a high mucopolysaccharide content. Extracts from lungs of such infants have abnormally high surface tension [8, 11] and greatly re-

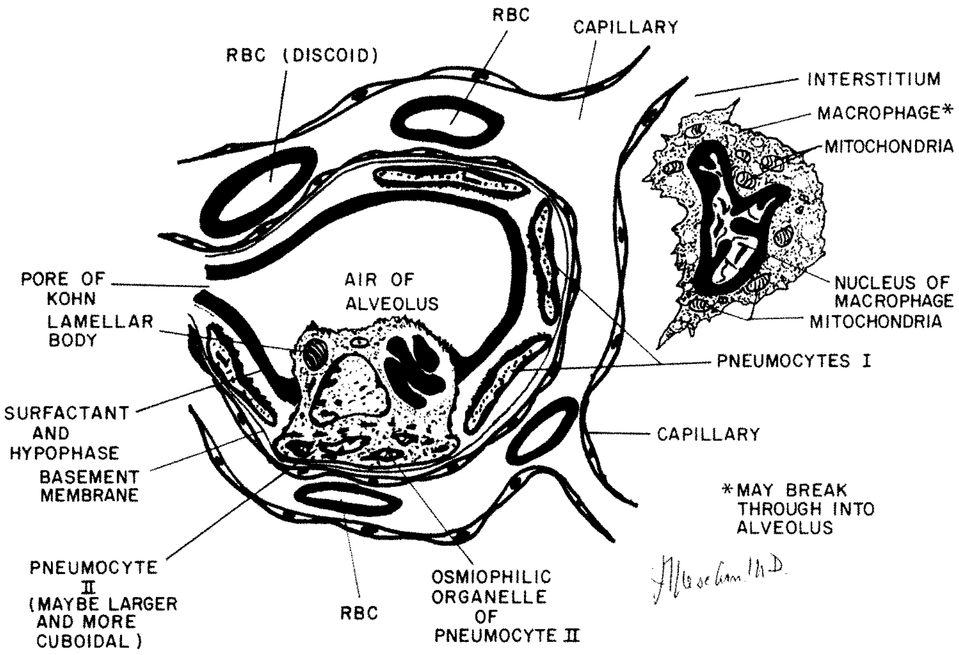

Fig. 1. – Diagram of alveolus showing surfactant-hypophase coating on surface of cellular lining. Cellular constituents of alveolar lining (pneumocytes 1 and 2 and macrophages) also shown. Pneumocyte 2 is protruding beyond surfactant layer into alveolus and may become free in alveolus ultimately to be expectorated.

duced surfactant content. The alveolar lining layer is also discontinuous, disrupted, and dispersed.

In this condition there is an intermixture of three different kinds of alveoli: (1) those that are relatively normal in which surfactants are sufficient; (2) those which are not aerated at all, retain the fetal state, and probably lack surfactant; and (3) those that are aerated, but collapse during exhalation. These alveoli contain insufficient or inactivated surfactants. The ultimate fate of the patient depends on the amount of the first type of alveoli, relative to the second and third types, and its ability to provide sufficient gas exchange. If survival does occur, the introduction of fibrosing alveolitis or bronchopulmonary dysplasia probably progresses in the latter two types of alveoli [8].

Surfactant Deficiency States in Adults

Some evidence suggests that pulmonary embolism depresses the rate of biosynthesis of phospholipids, possibly secondary to local ischemia [6]. It seems reasonable to assume that pulmonary edema dilutes surfactant with deleterious increases of surface tension [12]. It should be noted, however, that the fibrinogen in the edema fluid also may inhibit surfactant function directly. Pulmonary lavage or aspiration of hypo- or hyperosmotic agents may be thought to act in a fashion similar to edema. Other states with suspected but not definitely related reduction of surfactant concentrations are acidosis and acidemia [13] and 15% carbon dioxide atmospheres.

In alveolar proteinosis, there is an overproduction or delayed removal of the alveolar lipids. The high concentration of the non-surface-active lipids and denatured proteins suggests the introduction of foreign components into the surfactant. In this condition as well as in Liebow's desquamative pneumonia [14], there may not be a disorder of synthesis of surfactant, but rather an increase of phospholipid phagocytosis resulting from considerable macrophagic activity.

Agents Known to Disrupt Lining Cells of Alveolus

Damage to the alveolar lining and focal collapse may be associated with extracorporeal circulation and homotransplantation of the lung (in contrast with pulmonary autotransplantation which does not affect the alveolar lining). Aspirated hydrocarbons, prolonged positive-pressure breathing, and a number of cytotoxic agents injure the lining cells: busulfan and cyclophosphamide [15], melphalan used in the treatment of myeloma [16], hexamethonium [17], nitrofurantoin [18, 19] and radiation [4, 20]. Cytoxan [20] and possibly other cytotoxic agents may be included. It is possible that excess alveolar oxygen [20] and hypoxia likewise may lead to a disruption of lining cells, although this is not clearly understood.

Agents of Unknown Effect on Surfactant System [12, 21]

These include such factors as ultrasonic nebulizers, air pollution, and certain pneumonias, especially those involving *Proteus*, *Pseudomonas*, and *Aerobacter* [12]. These particular bacterial groups seem capable of producing phospholipids that have unsaturated or branch-chain acyl groups. These lipids have physicochemical properties that make them unsuitable as surfactant and therefore promote alveolar collapse. The effects of shock, trauma, and transplantation of the lung also may be related by causing the insertion of nonsurfactant lipid [12].

Fortunately other agents in widespread clinical use do not appear to have a deleterious effect on the surfactant system. The anesthetic agents diethyl ether, halothane, and methoxyflurane probably do not alter it [8, 12].

The radiologist confronting radiographs of alveolar disease must acquaint himself with at least the rudiments of hypophase and surfactant biochemistry. Numerous disease syndromes are encountered in daily practice: hyaline membrane disease of the newborn, bronchopulmonary dysplasia, oxygen toxicity, and radiation and drug induced proteinosis. Hopefully, effective therapy of these entities will follow better understanding of the alveolar lining and its properties.

Isadore Meschan
Bowman Gray School of Medicine
Wake Forest University
Winston-Salem, North Carolina 27103

ACKNOWLEDGMENT

I am grateful to Dr. Mosely Waite, Department of Biochemistry, for his critical scientific review and helpful suggestions in the preparation of this editorial.

REFERENCES

1. Fraser RG, Pare JAP: *Diagnosis of Diseases of the Chest: An Integrated Study Based on the Abnormal Roentgenogram.* Philadelphia, Saunders, 1970
2. Heitzman ER: *The Lung: Radiologic-Pathologic Correlations.* St. Louis, Mosby, 1973
3. Meschan I: *Analysis of Roentgen Signs*, vol. 2. Philadelphia, Saunders, 1973
4. Katzenstein ALA, Bloor CM, Liebow AA: Diffuse alveolar damage—the role of oxygen, shock and related factors. A review. *Am J Pathol* 85:210-222, 1976
5. King RJ: The surfactant system of the lung. *Fed Proc* 33:2238-2244, 1974
6. Pariente R: The pulmonary surfactant, in *Pathobiology Annual.* New York, Appleton Century Crofts, 1972, pp 381-403
7. Clements JA: Surface tension in the lungs. *Sci Am* 207:121-130, 1962
8. Scarpelli EM: The "expanding" lung: the pulmonary surfactant system. *Clin Notes Respir Dis* 9:2-16, 1970
9. Avery ME, Wang N, Taeusch H Jr: The lung of the newborn infant. *Sci Am* 228:75-85, 1973
10. Wilson MG, Mikity VG: A new form of respiratory disease in premature infants. *Am J Dis Child* 99:489-499, 1960
11. Scarpelli EM: Pulmonary surfactants and their role in lung disease. *Adv Pediat* 16:177, 1969
12. Greenfield LJ: Symposium on pulmonary problems in surgery: surfactant in surgery. *Surg Clin North Am* 54:979-991, 1974
13. Merritt TA, Farrell PM: Diminished pulmonary lecithin synthesis in acidosis: experimental findings as related to the respiratory distress syndrome. *Pediatrics* 57:22-39, 1976
14. Liebow A: Definition and classification of interstitial pneumonias in human pathology. *Prog Respir Dis* 8:1-33, 1975
15. Kirschner RH, Esterly JR: Pulmonary lesions associated with busulfan therapy of chronic myelogenous leukemia. *Cancer* 27:1074-1080, 1971
16. Codling BW, Chakera TMH: Pulmonary fibrosis following therapy with Melphalan for multiple myeloma. *J Clin Pathol* 25:668-673, 1972
17. Heard BE: Fibrous healing of old iatrogenic pulmonary edema ("hexamethonium lung"). *J Pathol Bacteriol* 83:159-164, 1962
18. Hailey FJ, Glascock HW, Hewitt WF: Pleuropneumonic reactions to nitrofurantoin. *N. Engl J Med* 281:1087-1090, 1969
19. Rosenow EC III: The spectrum of drug-induced pulmonary disease. *Ann Intern Med* 77:977-991, 1972
20. Meschan I, DeArmas CR, Scharyj M: Adult bronchopulmonary dysplasia: the similarity in roentgen and histopathologic appearance between some cases of oxygen toxicity, radiation pneumonitis, and postcytotoxic nonspecific bronchopneumonia. *Radiology* 92:612-615, 1969
21. Riseborough EJ: Fat embolism. *Am Fam Physician* 10(4):80-87, 1974
22. Goerke J: Lung surfactant. *Biochim Biophys ACTA* 344:241-261, 1974

Letters

Optimization of Mammographic Screening Programs

Controversy concerning the National Cancer Institute-American Cancer Society (NCI-ACS) mammographic screening program has centered around estimated radiation risk versus diagnostic benefit for the screened population as a whole. One result of this controversy has been a shift from 35 years to 50 years in the minimum screening age for women examined in the program. The potentially serious consequences of this shift, in terms of possible cancers missed, requires reexamination of the assumption that the probability of finding a cancer is the same for all screenees.

The NCI-ACS trial program was designed to screen women over 35 without regard to patient history. For patients examined in this program, application of the concept of population averaging for risk calculations seems justifiable in light of present radiobiologic knowledge. However, application of the same concept for estimation of potential benefit, in terms of diagnostic yield and, ultimately, reduced mortality, essentially neglects much epidemiologic data concerning breast cancer. To correct this neglect, a screening program for high risk women represents a step in the right direction. However, even this approach fails to utilize epidemiologic data properly. A better approach for any screening program would be to numerically estimate a potential benefit and risk indivudally for each patient—even those examined in mass screening programs. This approach would maximize the ratio of diagnostic yield to potential risk and would also provide additional epidemiologic data for future study. To the practicing clinician, the important question is whether a particular woman should have a mammogram. The answer depends on the potential radiation risk and the potential benefit (i.e., the probability of diagnosing a cancer). The potential radiation risk is presumably dose related and would depend on exposure per examination, retake rate, and number of examinations. Its computation and recording for each patient would encourage efforts to reduce exposures to a minimum consistent with adequate image quality.

In considering potential benefits to an individual patient, it should be noted that previous attempts to identify high and low risk groups for breast cancer [1] have met with equivocal success. Until newer epidemiologic data emerge from the NCI-ACS study and others, it would seem prudent to use present estimates of the risk factors to quantify the probability of finding a cancer in a given individual. Relevant factors include age-specific and familial incidences of breast cancer, menstrual history [2], previous screening history, geographic location [3], and whether the individual was randomly selected from the population (self-selection bias). Current screening data should be analyzed to determine first versus second year detection rates to evaluate the influence of a negative first examination upon the probable outcome of the second one. In assessing breast cancer risk, the roles of thermography and of mammographic parenchymal pattern analysis are controversial and require further clarification.

An aggressive biopsy rate has been shown to improve the detection rate for in situ cancers [4]. This will have considerable impact on overall mortality rates because of the increased survival of those afflicted with in situ disease.

A combination of these and other factors will probably yield a wide range of individual risk/benefit ratios, perhaps differing by a factor of 10 or more. A factor of two is currently given [3] for the over 50 versus the under 50 age group.

An individualized risk/benefit assessment, rather than the current "over 50" approach, would utilize current epidemiologic and dosimetric data more rationally to increase diagnostic yield and reduce the radiation risk for each patient enrolled in a mammographic screening program.

Gregory L. Dubuque
University of Colorado Medical Center
Denver, Colorado 80262

REFERENCES

1. Dunn JE Jr: Epidemiology and possible identification of high risk groups that could develop cancer of the breast. *Cancer* 23:775-780, 1969
2. Staszewiski J: Age at menarche and breast cancer. *J Natl Cancer Inst* 47:935-940, 1971
3. Seidman H: *Cancer of the Breast: Statistical and Epidemiological Data.* New York, American Cancer Society, 1972
4. Moskowitz M, Gartside P, Gardella L, deGroot I, Guenther D: Mammographic screening to date: What have we wrought? *Proceedings of the Society of Photo-optical Instrumentation Engineers, Medicine V* 96:443-452, 1976

SPIE/SPSE Technology Utilization Program
Application of Optical Instrumentation in Medicine VI
September 25-27, 1977

CHAIRMEN: JOEL GRAY[1] AND WILLIAM HENDEE[2]

Sunday, Sept. 25

Noon. Luncheon

1-4:30 p.m. Session I. Laboratory/clinical interface in image evaluation. Robert F. Wagner, chairman, Bureau of Radiological Health, Rockville, Maryland

An overview of some measures of image quality. CE Metz
Critical assessment of imaging parameters and clinical relevance for magnification skeletal radiography. HK Genant
Evaluation of gallbladder imaging by use of radiographic magnification technique. K Doi
A methodology for comparison of radiologic images from different screen/film combinations based on radiologists' subjective judgments. JR Thornbury
Comparison of laboratory and clinical evaluations of mammographic screen/film systems. EA Sickles
Minimum possible exposures in mammography derived from phantom and clinical studies. EP Muntz
Radiologic decision making and physical image properties. HL Kundel
Image noise and smoothing in CT scanning. PM Joseph
Correlation of measured system MTF's with visualization of angiographic information of high predictor value in diagnosis. H Eisenberg
Visual perception limits in angiography. AE Burgess
Controllable parameters of nuclear medicine images. D Patton
Cost-effectiveness considerations in the evaluation of a new technology. BJ McNeil

6-8 p.m. Session II. Sensitometry update. Joel E. Gray, chairman, Radiological Research Laboratories, University of Toronto, Ontario, Canada

Sensitometry in medical imaging. AG Haus, L Marsh, C Vyborny
Sensitometry in computerized tomography. KE Weaver, D Goodenough, E Briefel
A study of some factors influencing film choice for recording nuclear images. DL Lilien, MJ Allen
The D-log E curve and its relationship to lesion contrast and required photon count densities for medical images. FR Whitehead
A new ANSI screen-film-processing sensitometry standard. ET Clarke

8-10 p.m. Session III. Screen film systems and photosensitive materials. Arthur G. Haus, chairman, M.D. Anderson Hospital, Houston, Texas

Equivalent blur of intensifying screens. P Sprawls
Status report. A standard method for determining the efficiency of fluorescent x-ray intensifying screens. RC Placious, ES Moser, RS Holland
Reciprocity law failure in green sensitivity x-ray films. BA Arnold, H Eisenberg, BE Bjarngard
Information content and contrast of rare-earth and calcium tungstate intensifying screens. JW Castle
A free response approach to the measurement and characterization of radiographic observer performance. PC Bunch, JF Hamilton, GK Sanderson, AH Simmons
An analysis of film/screen combinations and patient exposures from *NEXT*. CK Showalter, RE Bunge, RE Gross, ME Seville

Monday, Sept. 26

8:30-10:30 a.m. Session IV. Approaches to equipment service, equipment specification, and performance evaluation. Raymond P. Rossi, chairman, University of Colorado Medical Center, Denver, Colorado

An alternative to vendor-supplied service. WJ Brown, M Randall
Performance evaluation of the falling load technique. PL Rauch, RW Block
Variation of x-ray tube potential as a function of attenuator thickness in automatic kVp variable brightness stabilization fluoroscopy. PJ Lin, RJ Kriz
A systems approach to acceptance testing of diagnostic x-ray equipment. MG Randall, B Horn
Radiologic systems acquisition procedures. T Stone
Developing a new job classification with in-house radiological engineering. C Moler
The effect of electron evaporation on x-ray tube current. IA Brezovich, GT Barnes
An in depth study of fluoroscopic spot film camera systems. R Dobrin, E Beranbaum, A Keegan, L Berkovits, S Rudolph

10:30 a.m.-Noon. Session V. New developments in medical imaging. William R. Hendee, chairman, University of Colorado Medical Center, Denver

A novel proximity x-ray image intensified tube. SP Wang, CD Robbins, CW Bates Jr
Semiquantitative empirical approach to optical transform method for pathological differentiation of human blood cell smears. JHK Yoo
X-ray beam filtration for mammography. M Siedband, RJ Jennings
A digital video acquisition system for extraction of subvisual information in diagnostic medical imaging. MM Frost, HD Fisher, S Nudelman, H Roehrig
Part 1. Design characteristics for an x-ray intensifier-video system for diagnostic radiology. H Roehrig, S. Nudelman, M Capp, MM Frost
Part 2. Psychophysical evaluation of an x-ray intensifier video system for diagnostic radiology correlated with system measures. GW Seeley, H Roehrig, M Capp, MM Frost, S Nudelman
A new radiographic duplicating system. G Zweig, M Stevens

Presented jointly by the Society of Photo-Optical Instrumentation Engineers and the Society of Photographic Scientists and Engineers, immediately preceding and integrated with the 1977 annual meeting of the American Roentgen Ray Society, Sheraton-Boston Hotel, Boston, Massachusetts. Cosponsored by the Bureau of Radiological Health, Department of Health, Education, and Welfare.

[1] Radiological Research Laboratories, University of Toronto, Ontario, Canada.

[2] Division of Radiological Sciences, University of Colorado Medical Center, Denver, Colorado 80220.

Noon. Lunch

1-3:15 p.m. Session VI. Quality control in medical imaging. William S. Properzio, chairman, Bureau of Radiological Health, Rockville, Maryland

Physician requirements for reliability in diagnostic ultrasound. KJW Taylor
Activities of the American Association of Physicists in Medicine and the American Institute of Ultrasound in Medicine in ultrasound instrument performance evaluation. PL Carson
Pulse-echo ultrasonic transducer standardization and quality control. K Erikson
Comparison of ultrasonic beam profiles in water and in attenuating and scattering materials. J Zagzebski, R Banjavic, E Madsen
A proposed recommendation for quality assurance programs for diagnostic radiology facilities. RL Burkhart
Economic analysis of a quality control program. CL Hall
A method of processor control utilizing refrigerated pre-exposed control strips and visual comparative densitometry. DA Page

3:15-5 p.m. Session VII. Performance characteristics of CT scanners. Robert K. Cacak, chairman, University of Colorado Medical Center, Denver
Comparison of translate-rotate and pure rotary CT body scanners. D Boyd, AR Margulis, M Korobkin
Evaluation of several x-ray CT scanners. KE Weaver, DJ Goodenough, DO Davis
Methods for the measurement of exposure from computed tomography. R Jucius
Geometrical limitations of CT scanner resolution. MV Yester, GT Barnes
Detectability in the presence of CT reconstruction noise. KM Hanson
A comparison of the number of rays versus the number of views in reconstruction tomography. RA Schulz
Energy dependence of CT numbers. RA Brooks

Tuesday, Sept. 27

9 a.m.-Noon. Session VIII. Small group sessions on special topics

Noon. Lunch

1-5 p.m. Session IX. Joint session with American Roentgen Ray Society

Effect of fatigue and other physiological factors on observer perception. BG Brogdon, RD Moseley, CA Kelsey
350 kVp chest radiography: review and comparison with 120 kVp. AV Proto, EJ Lane
The influence of computed body tomography on medical decision making: methodology and preliminary results. J Wittenberg, HV Fineberg, EB Black, MK Ikeda, JT Ferrucci Jr
A comparison of CT scanners with radiographic approach. GA Binder, VM Haughton, CR Wilson
Microfocal spot tube mammography. WW Logan
Detection accuracy in chest radiography. J Gray, K Taylor, B Hobbs
Densitometric evaluation of myocardial contrast accumulation. T Sandor, S Paulin, B Sridhar
The objective measurement of image quality in CT and a comparison of computerized and conventional tomography in the assessment of craniofacial anomalies. W Maue-Dickson, M Trefler

Program of the Society for Pediatric Radiology
September 25, 1977
Sheraton-Boston Hotel

Morning

8:00. CT in the diagnosis, treatment, and follow-up of malignant disease in childhood. BJ Reilly

8:15. Radiation dose from computed tomographic body scanning in children: comparison of dose from multiple scanners and its relation to resolving power. RC Brasch, CA Gooding, DP Boyd, M Korobkin

8:30. Wilms's tumor to the heart: clinical and radiographic evaluation. TL Slovis, B Cushing, BJ Reilly, ZA Farooki, AI Philippart, WE Berdon, DH Baker, JO Reed

8:45. Influence of postoperative radiation therapy timing and dose for Wilms's tumor. GJ D'Angio, M Tefft, N Breslow

9:00. The changing radiographic patterns of osteogenic sarcoma. K McCarten, JA Kirkpatrick, N Jaffe

9:15. Pediatric lymphography: performance, interpretation, and accuracy in 193 consecutive children. NR Dunnick, BR Parker, RA Castellino

10:00. Ultrasonic detection of glomerular disease. GW LeQuesne

10:15. Quantitative analysis of pediatric renal function. JM Ash, DL Gilday

10:30. Diagnosis of Potter's syndrome by portable voiding cystourethrography in newborns with respiratory distress due to pulmonary hypoplasia. E Wolf, WE Berdon, DH Baker, HJ Wigger, WA Blanc

10:45. Imperforate vagina with vaginourethral communication. DR Kirks, G Currarino

11.00. Exstrophy of the cloaca (vesicointestinal fissure). F Unger, GF Johnson, W Smith

11:30. Neuhauser Lecture: Neurofibromatosis in children. JF Holt

Afternoon

2:00. Bronchial hemorrhage in cystic fibrosis: results of bronchial artery embolization. KE Fellows, S Schuster, KT Khaw

2:15. Medium chain triglyceride pneumonia. MW Stannard, RM Smith, GW Brumley

2:30. Transdiaphragmatic extension of mediastinal air. PK Kleinman, PW Brill, JP Whalen

2:45. The spontaneous resolution of post-NEC-caused colonic strictures with related clinical/surgical implications. ILD Tonkin, JC Bjelland, TB Hunter, MP Capp, D Jeck, H Firor

3:00. Neonatal intussusception: a report of 12 cases. HB Patriquin, E Afshani, E Effmann, NT Griscom, F Johnson, SS Kramer, K Rapp, BJ Reilly

3:15. Tween-80 enemas in obstructing situations. BP Wood, RW Katzberg

3:45. Tricuspid insufficiency and valvular vegetations in the newborn. HC Bogren, DF Merten, R Ikeda, TA Riemenschneider, GG Janos

4:00. A prospective study of intraventricular hemorrhage in premature newborns using computed tomography. J Burstein, L Papile, R Burstein

4:15. In utero neuroradiologic diagnosis: ultrasound and amniography with postnatal follow-up utilizing computed tomography. PE Berger, JP Kuhn, RW Munschauer

4:30. The radiology of the glycogen storage diseases. JH Miller, P Stanley, GF Gates

4:45. Hypothyroidism in cystinosis. M. Grünebaum, RL Lebowitz

Commercial Exhibitors, American Roentgen Ray Society Meeting

The following exhibitors will have booths at the seventy-eighth annual meeting of the American Roentgen Ray Society in Boston, September 26–30. Firms are listed in alphabetical order with booth numbers and featured products.

Advanced Diagnostic Research Corporation, Tempe, Arizona; 72, 73; ADR real-time scanner

American Science & Engineering, Cambridge, Massachusetts; 108, 109; CT scanner

Americana Corporation, Dallas, Texas; 86; Americana '77 Reference Library

Artronix Inc., St. Louis, Missouri; 62, 63; C.A.T. scanner

Barnes-Hind Pharmaceuticals Inc., Sunnyvale, California; 71; barium

Bar-Ray Products, Inc., Brooklyn, New York; 26, 27; protective aprons, lead-lined products, darkroom accessories

Boehringer Ingelheim Ltd., Elmsford, New York; 84; Torecan (thiethylperiazine), Dulcolax (bisacodyl)

Churchill Livingstone Medical Divison of Longman Inc., New York, New York; 49; second edition, Murray/Jacobson *Radiology of Skeletal Disorders,* three volumes plus fourth supplementary volume

Cook, Inc., Bloomington, Indiana; 41; cardiovascular catheters, guidewires, needles

Cordis Corporation, Miami, Florida; 56; catheter sheath introducer system, specifically designed for percutaneous entry into cardiovascular system without blood loss

Diagnostic Information, Inc., Sunnyvale, California; 60; fluoroscopic imaging system

Du Pont Company, Wilmington, Delaware; 42, 43; medical x-ray films, screens, and film handling equipment

Eastman Kodak Company, Rochester, New York; 50–53; medical x-ray films, processing equipment

EIMAC Division of Varian, Salt Lake City, Utah; 22; diagnostic x-ray tube

Elema-Schonander, Inc., Elk Grove Village, Illinois; 77; AOT and PUCK filmchangers with CFRP pressure plates

EMI Medical Inc., Northbrook, Illinois; 66, 67, 78, 79; CT scanning equipment

Encyclopaedia Britannica, Inc., Chicago, Illinois; 89; *Encyclopaedia Britannica 3, Britannica Junior, Great Books of the Western World,* related products

Eureka X-Ray Tube Co., Chicago, Illinois; 107; x-ray tubes

E-Z-EM Company, Inc., Westbury, New York; 31; barium systems

General Electric Company, Milwaukee, Wisconsin; 14–16, 28–30

Warren H. Green, Inc., St. Louis, Missouri, 92; books

Grune & Stratton, Inc., New York, New York; 55; books and journals

Libin & Associates, Los Angeles, California; 93; Sanyo therapy equipment

Little, Brown and Company Medical Division, Boston, Massachusetts; 85; medical books

Litton Medical Systems, Des Plaines, Illinois, 35–37; advanced Litton 300L ultrasound system

Low X-Ray, White Plains, New York; 54; automatic processor monitor, Chemalert

Machlett Laboratories, Inc., Stamford, Connecticut; 100–103; x-ray tubes and computer systems

Mallinckrodt, Inc., St. Louis, Missouri; 91; complete line of contrast media

Medical Data Services, Richmond, Virginia; 32, 33; Data Base I Reality, custom minicomputer system designed for radiology patient accounting

Medi-Tech Division of Cooper Scientific Corporation, Watertown, Massachusetts; 61; catheters

Medrad, Inc., Pittsburgh, Pennsylvania; 58, 59; Mark IV angiographic injection system

C. V. Mosby Company, St. Louis, Missouri; 64; technical books

Neutron Products, Inc., Dickerson, Maryland; 88; cobalt-60 sources

Ohio-Nuclear, Inc., Solon, Ohio; 68, 69, 80, 81; computed tomography

Pennwalt Medical Products Division, Philadelphia, Pennsylvania; 17; Tomorex™ for curved plane zonography

Pfizer Medical Systems, Columbia, Maryland; 97–99, 111–113; ACTA scanner

Philips Medical Systems, Inc., Shelton, Connecticut; 38–40; diagnostic x-ray equipment

Precise Optics, Bayshore, New York; 90; x-ray image intensifying systems

W. B. Saunders Company, Philadelphia, Pennsylvania; 70; medical books

Siemens Corporation, Iselin, New Jersey; 74–76; SIREP automatic radiologic reporting system and computed tomography display featuring clinical results from SOMATOM whole body scanner and SIRETOM 2000 head scanner

Spectrum X-Ray Corporation, Westville, New Jersey; 104–106

E. R. Squibb & Sons, Inc., Princeton, New Jersey, 82, 83

S & S X-Ray Products, Inc., Brooklyn, New York; 87; x-ray accessory equipment

Charles C Thomas, publisher, Springfield, Illinois; 110; new and standard books in the field; *American Journal of Roentgenology*

Toshiba Medical Systems Division, Toshiba International Corporation, Carson City, California; 24, 25; ultrasound and diagnostic x-ray

USCI, division C. R. Bard, Inc., Billerica, Massachusetts; 57; USCI-Positrol II catheters, stainless steel and Teflon-coated spring guides, percutaneous catheter introducers, stopcocks and manifolds, Kifa products and sterile cardiovascular catheters

Varian Associates, Palo Alto, California; 48; CT scanner

Winthrop Laboratories, New York, New York; 47; Hypaque 25, 50, 75 and Cysto

Williams and Wilkins Company, Baltimore, Maryland; 94; Ledley; *Cross Sectional Anatomy Atlas*; Taveras: *Diagnostic Neuroradiology*; Littleton: *Tomography*; Gottschalk: *Diagnostic Nuclear Medicine*; Hatfield: *Radiology of the Gallbladder and Bile Ducts*; Sussman: *Radiology of the Nose, Paranasal Sinuses and Nasopharynx*; Clouse: *Clinical Lymphography*; Egan: *Technologist Guide to Mammography;* deRoo: *Atlas of Skeletal Age*

Wiley-Medical, John Wiley & Sons, Inc., New York, New York; 65; monographs and journals in radiology including tomography and ultrasound

Xerox Corporation, Pasadena, California; 44–46; Xeroradiography

Abstracts of Current Literature

Chest

Primary adenoid cystic carcinoma (cylindroma) of the trachea. Cleveland RH, Nice CM, Ziskind J (Children's Hospital Medical Center, 300 Longwood Avenue, Boston, Massachusetts 02115). *Radiology* 122:597-600, March 1977

Two cases of adenoid cystic carcinoma of the trachea are presented with a review of the literature. Primary tracheal tumors are rare. Of primary malignant tracheal tumors, adenoid cystic carcinoma accounts for 40% of the cases. Histologically this is a moderately well-differentiated adenocarcinoma with tendency to infiltrate along perineural sheaths, tissue planes, and into bone, often without causing reactive new bone formation. This aggressive infiltration is also manifested by frequent local recurrence. Metastases are seen in approximately 50% of the cases and these are most often to lung, brain, lymph nodes, liver, bone, and skin. Clinical presentation often is mistaken for asthma or chronic bronchitis. This tumor has a predilection for the middle third of the trachea and can at times be distinguished as a soft tissue mass within the tracheal air column. Treatment is either surgery or surgery combined with irradiation.

Asher Nov

Acute inflammation of epiglottitis and supraglottic structures in adults. Schabel SI, Katzberg RW, Burgener FA (Medical University of South Carolina, 80 Barre Street, Charleston, South Carolina 29401). *Radiology* 122:601-604, March 1977

Ten cases of acute epiglottitis in adults are presented. Clinical presentation included: severe sore throat; dyspnea; and stridor with increased secretions and hoarseness. Emergency tracheostomy was necessary in five of 10 patients. Lateral radiographs of the neck with soft tissue technique revealed: (1) swelling of the epiglottis, area of the aryepiglottic folds and arytenoids; (2) narrowing of the airway adjacent to the epiglottis; (3) prevertebral soft tissue swelling; (4) ballooning of the hypopharynx due to obstruction at the glottis; (5) narrowing or obliteration of the valleculae. Chest radiographs were normal in all but one case.

Asher Nov

The right paratracheal stripe. Savoca CJ, Austin JHM, Goldberg HI (University of California, San Francisco, California 94143). *Radiology* 122:295-301, Feb 1977

The right paratracheal stripe (RPS) is seen on posteroanterior chest radiographs as a thin, water-density stripe between the air column of the trachea and the adjacent right lung. The range of width of the right paratracheal stripe in 1,259 normal subjects was 1-4 mm. A stripe width of 5 mm or more is reliable evidence of disease. The differential diagnosis of this finding is lengthy, and best divided into those diseases affecting the trachea; mediastinum; and pleura.

Author Abstract

Fibrosing alveolitis in patients with neurofibromatosis. Webb WR, Goodman PC (University of California School of Medicine, San Francisco, California 94143). *Radiology* 122:289-293, Feb 1977

Fibrosing alveolitis is a manifestation of neurofibromatosis as seen in seven of 70 patients with the disease. This phenomenon was first reported in 1963; 24 cases have been reported since. Fibrosing alveolitis does not appear until later in adulthood. It occurs in 20% of patients over the age of 30 who have neurofibromatosis.

Radiographic findings include linear or small nodular interstitial densities with the linear densities predominating. These changes involve both lungs symmetrically, particularly at the bases. Kerley's B lines are sometimes seen. The second characteristic finding is large upper lobe bullae. The differential diagnosis includes rheumatoid lung, scleroderma, idiopathic fibrosing alveolitis, sarcoidosis, histiocytosis X, idiopathic bullous disease, and tuberous sclerosis. Pulmonary function tests can show obstructive or restrictive lung disease. Pathologic examination reveals alveolar wall thickening progressing to fibrosis and lung destruction. A potential complication of pulmonary fibrosis is scar carcinoma, often an adenocarcinoma.

Asher Nov

Pulmonary alveolar proteinosis: its association with hematologic malignancy and lymphoma. Carnovale R, Zornoza J, Goldman AM, Luna M (University of Texas M. D. Anderson Hospital and Tumor Institute, 6723 Bertner Avenue, Houston, Texas 77030). *Radiology* 122:303-306, Feb 1977

Pulmonary alveolar proteinosis has been described in 177 patients. The association of pulmonary alveolar proteinosis complicating immunologic disease is recognized and has been reported in 13 cases; latest in this series of five patients.

Radiologic manifestations are similar to acute pulmonary edema. An alveolar-filling process is present in a perihilar distribution. Differentiation from pulmonary edema is based on absent pleural effusion and Kerley B lines, normal heart size, and normal pulmonary vein size. The most frequent appearance is symmetric bibasilar infiltrates, but it may present as a unilateral lobar consolidation. Cavitation or pleural effusion are secondary signs of infection, particularly fungal. A clue to the diagnosis is the mildness of symptomatology relative to the striking infiltrates on the chest radiograph. A possible pathogenetic mechanism is unavailability of competent alveolar phagocytes, secondary to profound leukopenia in the hematologic malignancy group. Abnormalities of chest radiographs in cases of hematologic malignancy are often difficult to interpret. The authors point out that pulmonary alveolar proteinosis should be included in a differential diagnosis in these cases.

Asher Nov

Esophageal perforation following the use of the esophageal obturator airway. Scholl DG, Tsai SH (Hennepin County Medical Center, 6th Street and Park Avenue, Minneapolis, Minnesota 55415). *Radiology* 122:315-316, Feb 1977

Both esophageal and pharyngeal perforation have been rare complications of cardiopulmonary resuscitation with use of esophageal obturator airway. Two such cases are reported. In the clinical setting of cardiopulmonary resuscitation, pneumomediastinum, mediastinal widening, pleural effusion, or subcutaneous emphysema should suggest the possibility of injury due to perforation of the esophagus or pharynx. The mechanism is unclear. Further evaluation by esophagraphy is necessary.

Asher Nov

Lung entrapment and infarction by chest tube suction. Stahly TL, Tench WD (Veterans Administration Hospital, 3350 La Jolla Village Drive, San Diego, California 92161). *Radiology* 122:307-309, Feb 1977

Two cases are reported in which thoracentesis with chest tube placement was performed. Aspiration of pulmonary tissue into the chest tube occurred. On the chest radiographs, a progressively well-defined pulmonary infiltrate appeared at the chest tube opening. Entrapment of pulmonary parenchyma and infarction is a complication of thoracentesis. Pulmonary density in the region of the end hole of the chest tube should suggest this possibility.

Asher Nov

Cardiovascular

Suprasternal notch echocardiography: assessment of its clinical utility in pediatric cardiology. Allen HD, Goldberg SJ, Sahn DJ, Ovitt TW, Goldberg BB (University of Arizona Health Sciences Center, Tucson, Arizona). *Circulation* 55:605-612, April 1977 (By permission American Heart Association).

Echocardiographic suprasternal relationships of the transverse aortic arch (TAA), right pulmonary artery (RPA) and left atrium (Y′ LAD) were validated and angiographic-echocardiographic measurement correlations were made for each structure. Normal values were determined with respect to body surface area. In normals, regardless of age or body size, mean dimensional TAA/RPA ratio was 1.2:1 and Y′ LAD equaled the anterior-posterior, or Z axis, left atrial dimension (Z LAD). TAA/RPA ratio was increased in aortic stenosis and tetralogy of Fallot and was decreased in ventricular septal defect, atrial septal defect and pulmonary stenosis. Ratio did not correlate with lesion severity as assessed by cardiac catheterization except in pulmonary stenosis. Discrepant Y′ LAD values (usually increased Y′ LAD and decreased Z LAD) occurred in children with various forms of heart disease. Some had sternal compression but others had normal chests. Children with pectus excavatum showed similar compression.

These findings underscore the need for incorporation of a suprasternal examination into the standard echocardiographic examination of children.

Author Abstract

Cardiac function in total anomalous pulmonary venous return before and after surgery. Matthew R, Thilenius OG, Replogle RL, Arcilla RA, (R. A. Arcilla, 950 East 59th Street, Chicago, Illinois, 60637). *Circulation* 55:361-375, Feb 1977

Of 12 infants with isolated total anomalous pulmonary venous return (TAPVR), cardiac function was restored to normal following surgery in nine. Left atrial size was not found to be critical in the surgical repair of TAPVR. Preoperative left atrial volume was consistently small (53% of predicted) and the normal sized left atrial appendage appeared disproportionately large. Right and left ventricular volume studies were routinely performed.

Four had pulmonary venous obstruction and pulmonary hypertension above systemic pressure; three of these died. The vertical vein was compressed between the left pulmonary artery and bronchus in two cases but this was not observed angiographically. The entrance of the common pulmonary vein into the superior vena cava was atretic in one case, and pulmonary venous opacification was delayed and poor. Drainage was via the portal vein in one patient.

Unobstructed pulmonary venous return was to the left innominate vein (five patients), coronary sinus (two patients), and to the right atrium (one patient).

R. S. Frech

Diagnostic value of retrograde azygography in carcinoma of the esophagus. Morita Y, Shinohara M, Horita S, Sato M, Nakanishi M, Sano F, Nishimura S (Hokkaido University School of Medicine, Hokkaido, Japan). *Jap J Clin Radiol* 22:187-195, Feb 1977

The authors describe their experience with 54 patients on whom retrograde azygography was performed in order to evaluate mediastinal invasion by carcinoma of the esophagus. The findings of azygos venography and operative findings were correlated on these cases and diagnostic value of this method was evaluated. Comparison of retrograde technique and percutaneous rib injection technique was made on 25 patients on whom both methods were utilized. Correlation between operative findings and venographic findings in the evaluation of extraluminal or mediastinal extension of carcinoma was 85.7%. Lateral projection was quite useful for evaluation. Regarding comparison between the antegrade and retrograde studies, antegrade venography usually gave poor visualization of the azygos vein, frequently due to flow defects or to technical difficulties. The authors feel that the retrograde study is much superior to the direct rib injection technique.

Mutsumasa Takahashi

Development of pulmonary arteriovenous shunt after superior vena cava–right pulmonary artery (Glenn) anastomosis. McFaul RC, Tajik AJ, Mair DD, Danielson GK, Seward JB. (A. J. Tajik, Mayo Clinic, Rochester, Minnesota 55901). *Circulation* 55:212-216, Jan 1977

Six to 15 years after the "Glenn" procedure for cyanotic congenital heart disease, right lower lobe pulmonary arteriovenous shunts were found in six patients. On pulmonary arteriograms there were enlarged arteries to the lower lobes. In three children these dilated arteries tapered normally; in another three there were angiomatoid malformations. Pulmonary venous return from this area was not oxygenated. Microscopic examination in one patient showed an increased number of arteries and veins, and the veins were thickened and distended. The shunts are thought to be acquired and a cause of late clinical deterioration and increasing cyanosis.

R. S. Frech

Quantitative evaluation of left ventricular function by radiographic techniques. Reviews of contemporary laboratory methods. Rackley CE (University of Alabama Medical Center, Birmingham, Alabama 35294). *Circulation* 54:980-986, Dec 1976

This is an updated review of angiographic cardiac volume techniques and clinical applications in normals, congenital heart disease, valvular heart disease, idiopathic left ventricular hypertrophy, and coronary artery disease.

R. S. Frech

The role of renin in normal and pathological cardiovascular homeostasis. Griffith lecture. Haber E (Massachusetts General Hospital, Boston, Massachusetts 02114). *Circulation* 54:849-860, Dec 1976

Tigerstedt and Bergman named renin in 1898. They showed that hypertension could be induced in dogs by injecting a crude extract of kidney. During the 1930's Goldblatt's experiments called attention to renal mechanisms of blood pressure control. In 1940 Page and Helmer demonstrated that renin was an enzyme that acted to release the active principle. Renin acts only to cleave a globulin synthesized in the liver, forming angiotensin I, which is in turn cleaved to angiotensin II. Angiotensin II stimulates aldosterone secretion and also produces direct vasoconstriction.

Inhibitor peptides similar to snake venom block the conversion of angiotensin I into angiotensin II. Other peptides inhibit angiotensin II competitively. Upright tilting, sodium depletion, and angiotensin inhibitor peptides stimulate renin secretion.

In a patient with severe right renal artery stenosis a single intravenous dose of inhibitor was administered. A striking drop in blood pressure occurred. Right renal vein renin activity rose to very high levels. The ratio between right and left renal venous renin activity rose from 5.5 to 14.0. (The undesirable hypotension experienced was the result of sodium depletion by diuretics.)

Angiotensin antagonists identify renin-dependent hypertension and are helpful in unilateral renal artery stenosis since renin secretion on the affected side is selectively stimulated.

R. S. Frech

The incidence of congenital anomalies of the coronary arteries in the adult population. Baltaxe HA, Wixson D (University of Nebraska Medical Center, 42d and Dewey Avenue, Omaha, Nebraska 68105). *Radiology* 122:47-52, Jan 1977

A review of 1,000 consecutive coronary angiograms, most of them performed for evaluation of angina pectoris, yielded 9 examples of congenital anomalies of the coronary arteries. In 2 cases the angina may have been due to malposition of the left coronary artery or one of its branches. There were 2 cases of aberrant origin of the circumflex artery from the right coronary artery, 2 cases of aberrant left anterior descending artery, 3 cases in which all three major coronary artery branches arose from the right aortic sinus, and 2 cases of coronary artery fistulas. Malposition of the coronary artery should be considered as a possible cause of angina.

Author Abstract

Leg phlebography: the incidence, nature and modification of undesirable side effects. Bettmann MA, Paulin S (New England Deaconess Hospital, 185 Pilgrim Road, Boston, Massachusetts 02215). *Radiology* 122:101-104, Jan 1977

A prospective study was performed to elucidate the side effects of contrast medium phlebography for the diagnosis of deep vein thrombophlebitis (DVTP). The phlebograms were obtained with the patient in a semi-erect position, with an average dose of 125 ml of contrast medium infused continuously over 7-12 min. Renografin 60, or the same agent diluted to three-quarter strength, was used. The major side effects were pain during the study and a symptom complex resembling DVTP starting 12-36 hours after the study. Both were more common with the standard contrast medium (pain: 59.0% vs. 30.0%; delayed reaction: 24.0% vs. 7.5%), although the percentage of positive studies was unchanged (about 35.0%). Side effects were more frequent and severe than previously thought, but their incidence can readily be lowered.

Author Abstract

Prevalence and characteristics of disproportionate ventricular septal thickening in patients with acquired or congenital heart diseases: echocardiographic and morphologic findings. Maron BJ, Clark CE, Henry WL, Fukuda T, Edwards JE (National Heart, Lung, and Blood Institute, Building 10, Room 7B-15, Bethesda, Maryland 20014). *Circulation* 55:489-496, March 1977 (By permission American Heart Association).

Echocardiographic and necropsy studies were performed in 304 patients with various cardiac diseases. The overall prevalence of disproportionate ventricular septal thickening (septal to free wall ratio ≥ 1.3) was 10%. However, it was related to the type of cardiac lesion. Prevalence was high ($> 20\%$) in pulmonary stenosis or primary pulmonary hypertension, lower ($< 15\%$) in Eisenmenger syndrome or aortic or mitral valvular disease and was not present in atrial or ventricular septal defect. In right ventricular overload, prevalence of disproportionate septal thickening correlated with increasing ventricular systolic pressure.

None of 16 patients with disproportionate septal thickening studied at necropsy showed marked disorientation of cardiac muscle cells in the ventricular septum, characteristic of genetically transmitted asymmetric septal hypertrophy (ASH). Furthermore, disproportionate septal thickening was demonstrated by echocardiography in only one of 59 first degree relatives of patients with disproportionate septal thickening and associated cardiac diseases. Thus, disproportionate ventricular septal thickening associated with other cardiac diseases usually is due to secondary hypertrophy and is not a manifestation of genetically transmitted ASH.

Author Abstract

Echocardiographic observations on the association between mitral valve prolapse and asymmetric septal hypertrophy. Chandraratna PAN, Tolentino AO, Mutucumarana W, Gomez AL (University of Oklahoma Health Sciences Center, P.O. Box 26901, Oklahoma City, Oklahoma 73190). *Circulation* 55:622-626, April 1977 (By permission American Heart Association).

One hundred and ninety consecutive patients with mitral valve prolapse (MVP) were studied by echocardiography. Asymmetric spetal hypertrophy (ASH) was noted in 16 patients. Three patients had syncope which was associated with supraventricular arrhythmias. Three others had episodes of presyncope which were not related to rhythm disturbances. One of the patients with MVP and ASH had a family history of idiopathic hypertrophic subaortic stenosis. The septal thickness ranged from 1.6 to 3.1 cm, mean = 2 cm. The posterior wall thickness ranged from 0.7 to 2.1 cm, mean = 1.0 cm. The ratio of the thickness of the interventricular septum to that of the posterior wall ranged from 1.5 to 2.5, mean = 1.9. The percentage of thickening of the septum in systole was reduced in 13 patients. The excursion of the interventricular septum was reduced in three patients. In nine patients the left ventricular end-systolic dimension was below the lower limit of normal. Percentage fractional shortening of the left ventricle was increased in eight patients. Since MVP predisposes to cardiac arrhythmias which are poorly tolerated in the setting of ventricular hypertrophy and reduced left ventricular compliance, the recognition of this combination of MVP and ASH is of clinical importance.

Author Abstract

The effect of the valsalva maneuver on echocardiographic dimensions in man. Robertson R, Stevens RM, Friesinger GC, Oates JA (Vanderbilt University Hospital, Nashville, Tennessee 37232). *Circulation* 55:596-602, April 1977 (By permission American Heart Association).

Physiologic changes in the circulatory system caused by performing the Valsalva maneuver are blunted or absent in patients with congestive heart failure. Previously there has been no noninvasive method for examining cardiac chamber size during this maneuver. M-mode echocardiography was used to evaluate possible changes in cardiac chamber dimensions in 12 normal subjects (group I) and 15 patients with cardiovascular disease (group II). In group I, the left ventricular end-diastolic dimension decreased 11.2% (±1.5%) and the end-systolic dimension 9.5% (±1.32%), with a fall in stroke volume of 29%. The left atrial (LA) dimension decreased 30%.

In group II, only the response of the LA dimension is reported. There was a diminished response to Valsalva related to the severity of congestive heart failure. Patients in NYHA classes III and IV decreased LA dimension by only 3.8%, significantly less ($P < 0.001$) than those in classes I and II who had essentially normal responses.

Echocardiographically-determined changes in left atrial size in response to the Valsalva maneuver may provide an objective, noninvasive means of evaluating and following patients with suspected or proven congestive heart failure. Possible mechanisms for the changes observed are discussed.

Author Abstract

Gastrointestinal

Gastric bypass for morbid obesity. Cohen WN, Mason EE, Blommers TJ (Upstate Medical Center, Syracuse, New York 13210). *Radiology* 122:609-612, March 1977

Five-hundred patients underwent gastric bypass surgery as treatment for morbid obesity. A gastrojejunostomy is performed, excluding 80%-90% of the stomach without resecting it. Two advantages are gained: (1) sufficient acid-secreting cells are present in the distal segment suppressing the production of gastrin and consequently ulcer formation is avoided; (2) the small proximal stomach limits the amount of food intake. The gastrojejunal stoma is made 12 mm in diameter, thus retarding emptying of the stomach pouch, again limiting the amount of food intake. The gastrojejunostomy is formed close to the ligament of Treitz, leaving both jejunum and ileum for absorption (as opposed to jejuno-ileal bypass).

Preoperative upper gastrointestinal examinations are performed to exclude peptic ulcer disease or hiatal hernia. Immediate complications consist of anastomotic leaks or early obstruction of the gastrojejunostomy. Delayed symptoms may be due to esophagitis, gastritis, or stoma ulceration, such as is seen in conventional Billroth II gastrectomy. A second set of possibilities is excessive narrowing or bezoar formation. A third cause of complications when the patient fails to lose weight is possible enlargement of the gastric pouch. All these possibilities can be investigated radiographically.

Reflux or gas are at times seen in the excluded portion of the stomach and may simulate either an intact stomach on the frontal view or extravasation. This is not clinically significant, unless associated with delayed emptying.

Asher Nov

Varicoid carcinoma of the esophagus. Yates CW, LeVine MA, Jensen KM (St. Joseph Hospital, Houston, Texas 77002). *Radiology* 122:605-608, March 1977

Typically, carcinoma of the esophagus presents with a history of dysphagia and possibly weight loss. Radiographic examination of the esophagus will usually reveal a constricting lesion which can be confirmed by biopsy. Two cases are reported with an atypical appearance and clinical manifestation. Infiltrating submucosal carcinoma of the esophagus may not cause obstruction until late stages. An esophogram will show irregular intraluminal filling defects mimicking varices. These, however remain rigid showing no changes in configuration associated with either position or respiratory maneuvers. On endoscopy they present a pallid white appearance as opposed to a slightly bluish color of varices.

Asher Nov

Splenic flexure carcinoma as a source of hepatic portal venous gas. Gold RP, Seaman WB (Columbia-Presbyterian Medical Center, 622 West 168th Street, New York, New York 10032). *Radiology* 122:329-330, Feb 1977

Most patients with hepatic portal venous gas are seriously ill with some combination of bowel ischemia, distension, and/or necrosis. The authors report a case in which a necrotic splenic flexure carcinoma seeded gas and septic thrombi to the liver.

Author Abstract

Percutaneous fine needle aspiration biopsy of pancreatic and other abdominal masses. Goldstein HM, Zornoza J, Wallace S, Anderson JH, Bree RL, Samuels BI, Lukeman J (University of Texas System Cancer Center, M. D. Anderson Hospital and Tumor Institute, Houston, Texas). *Radiology* 123:319-322, May 1977

The authors describe the use of percutaneous fine needle aspiration biopsy of pancreatic and other abdominal masses in a total of 37 patients. Of the 18 patients with pancreatic masses, a correct or presumptive diagnosis was obtained in 78%. In the group of 19 patients with other than pancreatic masses, cytologic diagnosis was obtained in 18. No complications related to the biopsy technique occurred in either group. Any radiologic or imaging study which localizes and/or outlines the mass may be used as a guideline for the biopsy site. Most biopsies were performed under fluoroscopic control using previous radiologic studies to localize the biopsy site. Success with the fine needle aspiration biopsy technique requires an experienced and skilled cytopathologist.

Herbert C. Berry

Linear and rod-shaped peptic ulcers. Poplack W, Paul RE Jr, Goldsmith M, Matsue H, Bloom S, Moore JP, Norton RA (New England Medical Center, 171 Harrison Avenue, Boston, Massachusetts 02111). *Radiology* 122:317-319, Feb 1977

Rod-shaped peptic ulcers occur both as primary ulcer forms and as a stage in ucler healing. This ulcer morphology had not been described in American literature, but is well known in Japanese literature.

A double-contrast study of the stomach is described in which glucagon, gas-releasing powders, and antifoam agents are utilized. The clue to identifying linear ulcers is abnormality in the mucosal fold pattern. The authors point out that there is no particular clinical manifestation or tendency attributed to this form of linear ulceration.

Asher Nov

Benign ulceration of the cecum. Brodey PH, Hill RP, Baron S (Mt. Zion Hospital and Medical Center, P.O. Box 7921, San Francisco, California 94120). *Radiology* 122:323-327, Feb 1977

Benign nonspecific ulcerations may occur throughout the colon. Of these ulcerations, 50% occur in the cecum and ascending colon in the region of the ileocecal valve. They usually appear singly, but more than one may be present. Size is variable. Location is usually on the antimesenteric wall.

Clinically, patients may present because of acute symptoms similar to those of appendicitis or chronic blood loss, as primary manifestations. Complications include hemorrhage, perforation with peritonitis, or abscess formation and consequent stricture. The cecal appearance on barium enema is variably distorted due to inflammatory reaction. The importance of this entity is that it may present clinically as acute appendicitis and at surgery be mistaken for carcinoma. A possible explanation of these ulcers is the occurence of vascular malformations in the same location. Cecal ulcers should be included in the differential diagnosis of abnormal cecal morphology on barium enema or when bleeding is demonstrated by angiography.

Asher Nov

Angiographic demonstration of intrahepatic arterio-portal anastomoses in hepatocellular carcinoma. Okuda K, Musha H, Yamasaki T, Jinnouchi S, Nagasaki Y, Kubo Y, Shimokawa Y, Nakayama T, Kojiro M, Sakamoto K, Nakashima T (Chiba University Hospital, Chiba 280, Japan). *Radiology* 122:53-58, Jan 1977

Hepatic angiograms of 114 patients with hepatocellular carcinoma (HCC) were studied, particularly changes in the portal vein branches. Arterio-portal shunts of varying sizes, evidenced by opacification of intrahepatic portal branches, were seen in 72 cases (63.2%), with retrograde opacification of the portal vein trunk in 29 (25.4%). At least four types of shunts were found: (*a*) through a tumor thrombus in the portal branch, (*b*) in a retrograde direction via a peripheral tumor nodule, (*c*) through a small tumor invading or amputating an artery, and (*d*) through a tumor located near a major portal vein branch and supplied by a large, coiling artery. Postmortem angiography of the liver in 50 patients with HCC suggests that arterio-portal shunts are the result of the special vasculature in HCC and are highly diagnostic when accompanied by other angiographic changes.

Author Abstract

Genitourinary

Asymmetric renal enlargement in acute glomerulonephritis. Chesney RW, O'Regan S, Kaplan BS, Nogrady MB (S. O'Regan, E-213, Montreal Children's Hospital, 2300 Tupper Street, Montreal, Quebec H3H 1P3, Canada). *Radiology* 122:431-434, Feb 1977

Excretory urograms of 26 patients with a clinical diagnosis of poststreptococcal glomerulonephritis were reviewed. Of these, three patients demonstrated renal asymmetry with a 1.4 cm length difference. Radiologic findings in acute poststreptococcal glomerulonephritis have been described and comprise bilateral nephromegaly, a prolonged nephrogram, and poor concentration of contrast medium.

Unilateral asymmetric renal enlargement is usually due to: (1) acute infection; (2) vascular accident; (3) congenital renal anomalies; (4) obstruction; (5) intrarenal neoplasm.

The longitudinal axis of each kdiney was measured on standard anteroposterior radiographs. Difference in mean length ranged from 0.1 cm to 0.6 cm, the left kidney usually being larger. Asymmetry was considered when there was a difference greater than 1.4 cm.

Unilateral assymmetry was demonstrated in three of 26 cases. In those three, follow-up urography after recovery demonstrated normal kidney size, excretion, pelvic calyceal system, and concentration of contrast medium. One case demonstrated decreasing renal size with the left kidney becoming smaller. The authors conclude that in this setting, asymmetric enlargement does not entail aggressive investigation unless renal asymmetry persists.

Asher Nov

Musculoskeletal

The value of functional examination of the cervical spine in the diagnosis of herniated discs (in German). Distelmaier P (Neurochirurgische Universitaetsklinik, 5300 Bonn-Venusberg, Germany). *Fortschr Geb Roentgenstr Nuklearmed* 126:160-165, Feb 1977

Lateral views of the cervical spine in extreme flexion and extension were obtained in 100 patients prior to surgical fusion. The views were evaluated regarding overall mobility, segmental fixation, segmental instability, and subluxation. The clinical diagnosis in these patients was herniated disc; all patients had failed to respond to conservative therapy. The radiographic findings were compared with discograms, myelograms, and surgical findings.

All 100 patients had one or several surgically documented herniated discs. The herniation was found at the level of an unstable cervical segment in 64 patients, while it was found at a fixed cervical segment in 35. In four patients, the herniated disc was found at the site of subluxation as manifested on the lateral flexion/extension views. In 34 patients, herniated discs were found at different levels, at the site of unstable and fixed segments as well as in functionally normal regions. In 18% of the patients, the flexion/extension views did not contribute to the clarification of the disease process or the localization of the herniated disc. In 26% of the patients, follow-up examinations 1 year later revealed instability of the intervertebral segment just above the fusion.

These results indicate that functional radiographic examination of the cervical spine provides variable information regarding the localization of herniated cervical discs. Examination of the cervical spine in flexion and extension should precede myelography and be performed subsequent to routine cervical spine films in all patients with suspected herniated discs. In addition, functional radiographic examination of the cervical spine can be useful in the postoperative evaluation of these patients.

Peter F. Winter

Massive subperiosteal hemorrhage in neurofibromatosis. Yaghmai I, Tafazoli M (Medical College of Virginia Hospital, MCV Station, Box 728, Richmond, Virginia 23298). *Radiology* 122:439-441, Feb 1977

Neurofibromatosis is seen in association with elephantiasis neuromatosa and overgrowth of abnormal bones, but rarely with subperiosteal hemorrhage. This is a secondary finding after severe or minor trauma to the periosteum, which is abnormally loose from mesodermal dysplasia. The clinical, plain radiographic, and angiographic findings of two cases of massive subperiosteal hemorrhage are presented, and the literature is reviewed.

Author Abstract

Bone imaging after total replacement arthroplasty of the hip joint. A follow-up with different radiopharmaceuticals (in English). Creutzig H (Institut fuer Nuklearmedizin, Medizinische Hochschule Hannover, Postfach 61 01 80, D-3000 Hannover, Federal Republic of Germany). *Eur J Nucl Med* 1:177-180, 1976

To evaluate the role of bone scanning in total hip replacement arthroplasty, bone scans were performed in "risk" patients after unilateral total hip replacement. Eight patients who developed clinical and radiologic signs of periprosthetic infection from 6 months to 2 years after hip replacement were studied every 3 months, and 18 patients with no evidence of complications were examined for 1 year, also at 3 month intervals. Five patients with localized extraosseous infections were also investigated.

Scans were performed 3 hr postinjection of 10 mCi^{99m}Tc-diphosphonate using a scintillation camera or 10-crystal-scanner. For comparison, a bone scan with ^{18}F was performed on each patient once, on a 12.7 cm dual probe rectilinear scanner. Regions of interest were selected over the normal hip, normal femur, prosthetic acetabular cup, and femoral prosthesis. The ratio of activity over the prosthetic acetabular cup to the activity over the normal hip (acetabular uptake ratio) and the ratio of activity over the femoral prosthesis to the activity over the normal femur (femoral uptake ratio) was calculated for each scan.

The average acetabular uptake ratio declines from 3.6 at 3 months after surgery to 2.7 at 6 months, with little change after 6 months. The average femoral uptake ratio decreases from 4.0 at 3 months to 1.6 at 6 months, with slightly further decrease to 1.2 at 9 months. In patients with periprosthetic infection, the uptake ratio always increases from a normal ratio to values between 3 and 5. This increase was seen 1-3 months before clinical and/or radiologic signs became apparent. The scan was always repeated at the time of radiologic evidence of infection; the average uptake ratio of these scans was 9.2.

Four patients with a rise in the uptake ratio to 3.15 developed no signs of infection or loosening on follow-up and the results of their scans are accepted as false-positive. The ^{18}F uptake ratio in normal patients 1 year after surgery or later did not differ from ^{99m}Tc-diphosphonate values. In the cases with infection, the average ^{99m}Tc-diphosphonate uptake ratio was slightly higher than the average ^{18}F uptake ratio, but was not significant. The four patients with false-positive ratios on the ^{99m}Tc-diphosphonate scans had normal ratios on the ^{18}F scans. In the five patients with verified soft tissue infection without osseous involvement, the uptake ratios were elevated on the ^{99m}Tc-diphosphonate scan and, to a lesser degree, on the ^{18}F scan.

The author concludes that the postoperative increase in localization of radioactive tracer in the region of the total hip replacement precludes the diagnostic use of bone scanning during the first few months after surgery. Bone scanning, however, can be very helpful to detect complications which develop 6 months after surgery. The indication for bone scanning after total hip replacement should be the detection of periprosthetic infection or prosthetic loosening in patients with pain following the initial 6 months postsurgery period.

Peter F. Winter

Arteriography in bone tumors. Voegeli E, Euhlinger E (University Hospital, Bern, Switzerland). *Skeletal Radiol* 1:3-14, 1976

The authors have tested the usefulness of arteriography in 100 patients presumed to have bone tumors. Of the 100, 61 lesions proved malignant, 21 benign, and 18 inflammatory. Basic to the technique were: (1) selective arteriography, injecting the contrast as close to the lesion as possible; (2) at least two injections in different projections; and (3) common recourse to subtraction films. Pursued in this manner, arteriography improved diagnostic accuracy in predicting the benign or malignant nature of bone lesions by a factor or approximately 25%. Essential to the diagnosis of malignant bone disease were: (1) vessels irregular in caliber; (2) distortions in the course of vessels; with (3) abrupt angulations in the course of vessels; (4) vascular lakes; and (5) arteriovenous shunts. Hypervascularity, parenchymal strains and early venous drainage without the foregoing were considered nonspecific. It was noteworthy that centrally located lesions and even well vascularized bone tumors failed to be demonstrated arteriographically until the tumor had broken through the bone cortex.

The irregular vascular caliber and associated aneurysmal dilatations central to the recognition of malignant disease by arteriography are attributable to the primitive nature of their vascular channels which often consist of an endothelial layer surrounded by a connective tissue sheath. Such tumor vessels were never observed in the benign or inflammatory bone lesions.

Arteriography was especially valuable in delineating the exact nature and size of soft tissue components of malignant bone tumors. Often tumors proved to be significantly larger by arteriography than could be assessed by routine radiography. In the group of round cell tumors, arteriography revealed the lesions to be as much as one-third larger than was estimated from routine exposures.

Philip J. Hodes

Evaluation of various contrast-agents for improved arthrography. Katzberg RW, Burgener FA, Fischer HW (University of Rochester School of Medicine, Rochester, New York 14642). *Invest Radiol* 11:528, Nov-Dec 1976

In the canine knee joint the monomer methylglucamine iothalamate, the dimer methylglucamine iocarmate, and the nonionic contrast agent metrizamide were examined for use in arthrography. A total of 104 injections were performed with equal iodine concentrations (280-282 mg/ml) and volumes (4 ml) of the three contrast agents. These were evaluated using radiographic comparison and iodine estimations of the joint fluid at various times after injection. Radiographically the dimer was superior, followed by metrizamide and then the monomer. The greatest amount of total iodine within the joint fluid at various times after injection was found with the dimer. Iodine concentrations in the joint fluid were similar for the dimer and metrizamide, both greater than with the monomer.

Author Abstract

Skeletal demineralization and growth retardation in inflammatory bowel disease. Genant HK, Mall JC, Wagonfeld JB, Vander Horst J, Lanzl LH (J. B. Wagonfeld, University of Chicago Hospitals and Clinics, Chicago, Illinois). *Invest Radiol* 11:541, Nov-Dec 1976

Skeletal growth and mineralization in 54 adolescent and adult patients with inflammatory bowel disease have been analyzed comprehensively. Quantitative and qualitative radiologic techniques consisted of conventional roentgenography, photon absorptiometry, and radiographic morphometry. The data are correlated with the type, duration, and severity of disease, and with several modes of therapy. The results indicate that osteopenia and retardation of growth are common in patients with inflammatory bowel disease, particularly in adolescents, in whom the effects of corticosteroids on the skeleton are most deleterious.

Author Abstract

Comparisons between x-ray photodensitometric and gamma-ray absorptiometric findings of bone mineral measurements, and the evidence of their convertibility. Meema HE, Taves DR, Oreopoulos DG (Toronto Western Hospital, Toronto, Canada). *Invest Radiol* 11:550-555, Nov-Dec 1976

Fifty-two bone mineral measurements were made in chronic renal failure patients using two different radiologic techniques concurrently: gamma-ray absorptiometry; and x-ray photodensitometry. Although the sites of measurements of the cortical bone mineral mass in radius were different (distal vs. proximal) and different parameters were determined (in units of gm/cm vs. gm/cm^2), a moderately good correlation was found between measurements by the two techniques ($r = 0.61$, $p < 0.001$). Using external bone width, it was possible to calculate from photodensitometric measurements the bone mass per unit length (gm/cm). This conversion improved the correlation with absorptiometry values considerably ($r = 0.78$, $p < 0.001$). A similar correlation was found between the trabecular bone mass in the distal radius, measured by absorptiometry, and the cortical bone mass in the proximal radius, determined by photodensitometry ($r = 0.79$, $p < 0.001$), the correlation between the cortical and trabecular bone masses by absorptiometry being only slightly higher ($r = 0.84$, $p < 0.001$). The residual variations not explained by the correlations between the absorptiometric and photodensitometric techniques may be largely due to the real differences of bone mineral masses at the two measuring sites and by the inherent methodological errors.

Author Abstract

Arthrography with Amipaque (metrizamide) and other contrast media. A roentgenographic and histologic evaluation in rabbits. Johansen JG, Berner A (Ullevaall Hospital, University of Oslo, Norway). *Invest Radiol* 11:534, Nov-Dec 1976

Arthrography of the knee joint was performed in 30 rabbits for comparison of Amipaque (metrizamide) with Urografin 60% (meglumine-sodium diatrizoate), Isopaque Amin (meglumine-calcium metrizoate), Conray Meglumin 282 (meglumine iothalamate) and Dimer-X (meglumine iocarmate). Films taken at regular intervals show longer contrast duration, and less hydrarthrosis after injection of Amipaque. Minimal focal inflammatory reaction in the synovial membrane is found in many cases when the animals are sacrificed 1 day or 7 days after the injections. No significant difference can be found between the contrast media, and similar changes are also seen after injection of physiologic saline.

Author Abstract

Nervous System

Computed tomography in head trauma. Dublin AB, French BN, Rennick JM (University of California – Davis School of Medicine, Sacramento, California 95817). *Radiology* 122:365-369, Feb 1977

CT was performed on 1,250 patients, 200 of whom had documented head trauma. It is the author's opinion that CT gives rapid specific diagnoses, and in their institution this technique almost completely replaced angiography for acute head trauma. Abnormalities detected included fractures, extracerebral hematomas, intracerebral hematoma and contusion, intraventricular hemorrhage, ventricular enlargement, and brain stem contusion.

Eight fractures were detected of which four were depressed and/or compound. Not only could surgically-correctable fractures be detected, but CT offered the advantage of identifying additional abnormalities such as hematoma or intracranial bone fragments.

Of the extracerebral hematomas detected, 55 were subdural hematomas. The authors describe subdural hematomas as extracerebral collections of fluid whose density is greater than, equal to, or less than that of normal brain tissue. Subdural hematomas may actually increase in density during the first 1-3 days posttrauma. Several patients with postconcussion headaches were seen to have small subdural hematomas on CT. Follow-up showed resolution of the lesions. In these patients, there was no surgical intervention nor was angiography contemplated. Forty-five percent of subdural hematomas are associated with other abnormalities, particularly cerebral contusion and hematoma. This, the authors feel, explains lack of dramatic clinical improvement postevacuation of an extracerebral collection of blood. The volume of a subdural lesion seen on CT is often less than that seen at surgery. Most of these lesions are seen over the cerebral convexity and it is felt that the bony calvaria adds to the overall absorption coefficient, thus decreasing its observed volume. Subdural hematomas are thought to be typically crescent-shaped and to extend over large areas of brain.

Five cases of epidural hematomas were documented; four were supratentorial, one infratentorial. These are usually lenticular in shape and exhibit high density in relation to normal brain tissue.

Of the cases of intracerebral hematoma and contusion, 20 were documented. Sixty percent were associated with other lesions, usually extracerebral collections of blood. Angiography may demonstrate only a mass effect, while CT can differentiate between contusion and hematoma which may be surgically relieved. Judging improvement of intracerebral hematoma should be based on decrease in mass effect and not on CT density. Edema is seen as an area of mass effect with a density other than normal brain tissue. Contusion has a "salt and pepper" appearance due to minute sulci of hemorrhage within normal or edematous brain tissue.

There is early detection of intraventricular hemorrhage permitting earlier ventricular drainage. A third of the survivors may show hydrocephalus, which is either permanent or transient.

Hydrocephalus may be either noncommunicating or communicating, the latter presumably due to blockage of pathways by subarachnoid blood. Though information is incomplete, it appears that communicating hydrocephalus in this setting is transient and a shunt is not required.

Twenty-four cases of brain stem contusion were reported. Of these, 13 had additional surgical lesions such as contusion or edema, subdural hematoma, and intracerebral hematoma. The newly discovered association of surgical lesions may lead to a revision of the concept of "brain stem contusion."

Asher Nov

Lumbar phlebography by catheterization of the lateral sacral and ascending lumbar veins with abdominal compression. Theron J, Houtteville JP, Ammerich H, Alves de Souza A, Adam H, Thurel Cl, Rey A, Houdart R (F-14000 Caen, France). *Neuroradiology* 11:175–182 July 30, 1976

The authors report their experience with 250 lumbar phlebograms performed under local anesthesia in patients with symptoms of disc herniation and negative water soluble lumbar myelograms. To promote complete visualization of the epidural venous plexus, a lateral sacral vein and ascending lumbar vein on opposite sides of the pelvis were selectively catheterized with a 5 French catheter and simultaneously injected while applying pneumatic midline abdominal compression at the level of the iliac crests. Subtracted anteroposterior films were usually sufficient for diagnosis. The normal and pathologic appearance of the epidural venous plexus is well described and illustrated. The diagnosis of disc herniation was based on deformity, displacement, occlusion, and collateral flow involving veins in the anterior epidural space as well as veins exiting the intervertebral foramina. Most of the false negative lumbar myelograms involved disc herniations at the L5-S1 level and lateral herniations at the L3-4 and L4-5 levels. During disc operations the epidural venous plexus at the surgical site is usually ablated. Postoperative lumbar phlebograms should therefore be interpreted with caution and a thorough understanding of the surgery performed.

Paul M. Chikos

Widening of the cervical intervertebral foraman. Schimmel DH, Newton TH, Mani J (University of California School of Medicine, San Francisco, California 94143). *Neuroradiology* 12:3–10, Oct 27, 1976

The authors present seven cases which represent unusual causes of intervertebral foraminal enlargement. In three asymptomatic patients (30-year-old male, 36- and 50-year old females) the cause of foraminal widening was a tortuous vertebral artery. The tortuous vertebral artery caused nonconcentric enlargement of the intervertebral foramen at either the C4-5 or C5-6 level with erosion of the posterior and lateral aspects of the contiguous vertebral body. Nerve root compression by a tortuous vertebral artery has been rarely reported. In a 22-year-old male with a known vascular dysplasia, concentric enlargement of the C5-6 foramen was caused by a lobulated aneurysm of the vertebral artery. These are usually false aneurysms and the result of penetrating trauma or chiropractic manipulation. In two symptomatic cases, foraminal widening without obvious bony destruction was caused by malignant tumor. In one, a 40-year-old male, widening of the C6-7 foramen was caused by metastatic hypernephroma which was hypervascular on angiography. The other malignant tumor was a plasmacytoma which caused concentric enlargement of the C7-T1 foramen in an 82-year-old female. In the last case presented, a 39 year-old-male, the congenital absence of one pedicle of C6 was incidently discovered following trauma and simulated enlargement of the intervertebral foramen. This congenital anomaly is further characterized on spine films by ipsilateral malformation of the lateral mass and transverse process and on myelography by a common dural pouch which transmits two nerve roots. It should be remembered that neurofibroma are the most common cause of intervertebral foraminal enlargement and other infrequent etiologies include meningioma, fibroma, lipoma, and herniated meningocele.

P. M. Chikos

Evaluation of brain and epidural abscesses by computed tomography. Lott T, El Gammal T, Dasilva R, Hanks D, Reynolds J (Medical College of Georgia, Augusta, Georgia 30902). *Radiology* 122:371–376, Feb 1977

Eight cases of brain abscess are presented from a total of 5,000 CT examinations. A single case of epidural abscess is described. The CT appearance of a brain abscess is one of a ring formation with and without contrast enhancement. This is nonspecific in terms of the histology of the lesion. An advantage of CT examination in this setting is that of being able to follow the evolution of an abscess from cerebritis to cavitation and capsule formation. These factors are essential for timing of surgical intervention. Follow-up scans may reveal changes in size of the cavity, resolution, or reaccumulation. It may reveal the presence of multiple abscesses. The authors feel that an epidural abscess may be diagnosed by posterior displacement of the falx from the inner table of the anterior aspect of the skull, suggesting a lesion crossing the midline.

Asher Nov

Pediatric Radiology

Pre-pubertal XY gonadal dysgenesis. Isurgi K, Aso Y, Ishida H, Suzuki T, Kakizoe T, et al. (University of Tokyo Branch Hospital, Mejirodai, Bunkyo-ku, Tokyo 112 Japan). *Pediatrics* 59:569–573, April 1977

Two patients, 7 years and 2 years 10 months, with XY gonadal dysgenesis are presented. Both had nonprogressive virilization of the external genitalia at birth. The 7-year-old patient presented with torsion of a dysgerminoma, and on the opposite side had a gonadoblastoma. Virilization is thought to be due to fetal androgen secretion by the abnormal gonads. In XY gonadal dysgenesis, gonadal tumor development is significantly increased and has been reported occurring in up to 37.5% of patients with this condition. The authors recommend that phenotypical females with XY karyotype should have bilateral prophylactic gonadectomy. Tumor formation is probably related to the hypergonadotropinism, and to predisposition of the intraabdominal gonad in the presence of a Y chromosome.

B. J. Wood

Ductus arteriosus dilatation by prostaglandin E_1 in infants with pulmonary atresia. Heymann MA, Rudolph AM (1403-HSE, University of California, San Francisco, California 94143). *Pediatrics* 59:325-329, March 1977

Infants with pulmonary atresia depend on patency of the ductus arteriosus for survival in the immediate postnatal period. Despite continuing hypoxemia after birth the ductus arteriosus usually constricts, thus reducing pulmonary blood flow. This often occurs while awaiting surgical palliation or correction, leading either to marked deterioration in the infant's condition, or death. In ten infants with pulmonary atresia, we infused prostaglandin E_1 (PGE_1) at a rate of 0.1 μg/kg/min in six and 0.05 μg/kg/min in four into the descending aorta at the orifice of the ductus arteriosus. The ductus arteriosus was effectively dilated; at the narrowest point the diameter, measured in eight infants, almost doubled. In all 10 infants arterial blood Po_2 increased, averaging 24.6 mm/Hg before and 43.7 mm/Hg after the infusion was started. Infusion of PGE_1 directly into the aorta adjacent to the ductus arteriosus avoided the complications of pyrexia, muscular twitching, and excitability which may be related to the effects of prostaglandins on the central nervous system.

Author Abstract

Hypophosphatasia. Kozlowski K, Sutcliffe J, Barylak A, Harrington G, et al. (Royal Alexandra Hospital for Children, Camperdown, Australia). *Pediatr Radio* 5:103-117, 1976

Radiographic analysis of 24 cases of hypophosphatasia (H) from nine pediatric centers was performed. Three cases were of neonatal (lethal), 18 cases of infantile (severe), and three cases were of late (benign) type. Some of the patients were in reality borderline cases between these groups.

In the authors' material all patients showed radiographic signs of the disease. These were divided into diagnostic, characteristic, and suggestive features. All patients had in common generalized (usually irregular) osteoporosis, generalized (usually irregular) metaphyseal changes, craniostenosis (13 of 18 infantile cases) or widened cranial sutures, and often bowing of the long bones. Besides the well known radiographic features of hypophosphatasia were some less well known; (1) spurs of the long bones (Bowdler sign); (2) distal femoral central metaphyseal defects and epiphyseal defects; (3) S-like deformities of the tibiae; (4) abnormal shape of the distal phalanges of the fingers; (5) multiple rib fractures; (6) wedging of the lower thoracic and upper lumbar vertebrae; (7) partial premature fusion of the epiphyses; (8) nephrocalcinosis; (9) loss of lamina dura around the teeth; (10) variation in radiographic appearances of a pair of siblings with lethal form: and, (11) rapid changes in roentgen appearances. In two of the patients (siblings) phosphoethanolamine was undetectable in the urine. The authors doubt if a normal skeletal survey may be present at any stage in any of the three major types of hypophosphatasia.

Author Abstract

Transient tricuspid insufficiency of the newborn: a form of myocardial dysfunction in stressed newborns. Bucciarelli RL, Nelson RM, Egan EA, et al. (Box J-296, University of Florida College of Medicine, Gainesville, Florida). *Pediatrics* 59:330-337, 1977

Fourteen term newborn infants have been recognized as having transient tricuspid insufficiency associated with significant perinatal stress. Five of these underwent cardiac catheterization for presumed congenital heart disease, but had only massive tricuspid valve insufficiency. The other nine infants were diagnosed on the basis of a murmur characteristic of tricuspid valve insufficiency and on other clinical grounds. All had a history of significant perinatal stress in the form of asphyxia with or without hypoglycemia. Frequently, congestive heart failure, persistent cyanosis, and ECG evidence of myocardial ischemia were present. Twelve of the 14 survived, and in each, all cardiac signs and symptoms, including the murmur, spontaneously resolved. The two patients who died had histopathologic evidence of necrosis in the anterior papillary muscle of the tricuspid valve.

The constant features of perinatal stress, ST-T wave abnormalities on the ECG, and spontaneous resolution of the transient tricuspid insufficiency strongly suggest that this syndrome is secondary to a reversible form of myocardial dysfunction, perhaps by affecting papillary muscle specifically. We believe that hypoxia with or without hypoglycemia precipitates the events leading to this clinical syndrome which is distinguishable from other cardiac abnormalities in the newborn by the history, distinctive murmur, and the ECG abnormalities.

Author Abstract

Evaluation of gastro-esophageal reflux surgery in children. Johnson DG, Herbst JJ, Oliveros MA, Stewart DR (Primary Childrens Medical Centre, 320 12th Avenue, Salt Lake City, Utah 84103). *Pediatrics* 59:62-68, Jan 1977

Fifty-five infants and children were treated surgically over a 3-year period for gastroesophageal reflux with complications; 39 were males, 16 were females. The complications included persistent vomiting, vomiting with failure to thrive, esophagitis, stricture and recurrent aspiration pneumonia. With the exception of the ones with marked esophageal strictures, all were treated conservatively for 6 weeks after their referral and evaluation. Only nine patients were operated on before 6 months of age. Other anomalies were present in 25 children, including previous tracheoesophageal fistula in five, mental retardation in eight, trisomy 21 in three, and cardiovascular anomalies in three. The group included several unusual symptoms with rumination syndrome in six, Sandifers syndrome in four, and three with iron deficiency anemia, clubbing, and protein-losing enteropathy. Transabdominal anterior gastropexy was the procedure of choice in most patients. Nissen fundoplication was used for the more complex cases. Good results were obtained in 51 of 55 cases. Evaluation was by barium studies and by esophageal manometry with pH studies. The lower esophageal pressure was not significantly altered by surgery. A fair result was obtained in three patients and this was considered when symptoms were relieved but occasional reflux was recorded on either the esophogram or the pH studies. A poor result was when the patient was not symptom-free or if there was more than occasional reflux or if the previous stricture was not reversed. One patient fell into this category and required additional surgery.

B. J. Wood

Bubbles in hyaline membrane disease: differentiation of three types. Swischuk LE (University of Texas Medical Branch, Galveston, Texas 77550). *Radiology* 122:417-426, Feb 1977

The bubble patterns of chest radiographs in infants with hyaline membrane disease were analyzed for time of appearance and resolution, individual size and shape, general distribution, and behavior during inspiration and expiration. Three bubble types were distinguished. Type I is seen in the acute phase and results from maximal distension of the terminal airways. This gives a finely bubbly appearance creating the false impression of clearing. The radiograph seems to indicate improvement, while clinically the child shows no improvement. The bubbles may relate to positive pressure ventilation but may occur without it. Characteristics are: (1) round, uniform size; (2) usually less than 1.5 mm in diameter; (3) deflate on expiration; (4) may be slightly larger in the lung bases.

Type II almost always occurs as a result of positive pressure assisted ventilation. The air is located in the pulmonary interstitium; not in terminal bronchioles or alveolar ducts. In the early stages the bubbles are: (1) tortuous in configuration radiating from the hilar regions; (2) walls are thicker than Type I and the bubbles are slightly larger, frequently 2 mm in diameter; (3) size is uniform throughout the lung; (4) they do not empty on expiration.

Pulmonary interstitial emphysema produces a stiff lung which does not fill or empty during inspiration and expiration. In addition intrapulmonary tension compresses blood vessels, virtually eliminating pulmonary blood flow.

Type III is seen in the reparative stages. The bubble results from mechanical overdistensions of groups of alveoli in immature and scarred lung. This type of abnormality usually results in children who require prolonged, continuous positive pressure ventilation. Radiographic characteristics of these bubbles include: (1) variable size and definition; (2) relatively thick walls; (3) tendency to empty on expiration. The bubbles may become very large, particularly in the bases.

Asher Nov

Pulmonary pseudocysts in the newborn infant. (University of South Florida, Tampa, Florida 33620). *Pediatrics* 59:199-204. Feb 1977

The occurence of pulmonary pseudocysts is described in premature neonates with hyaline membrane disease receiving continuous distending airways pressure. In four of five, the pseudocyst was preceded by or associated with pulmonary interstitial enphysema, while in the other, it was associated with a pneumothorax. The pseudocyst appeared between 39 hr and 7 days of age. In the three infants where radiographic clearing was documented, spontaneous resolution occurred in 3 days, 5 days, and 3 months. Formation of a pseudocyst is thought to occur when pulmonary interstitial emphysema remains localized beneath the visceral pleura or along fissures.

B. J. Wood

Short rib-polydactyly syndrome type 3. Naumoff P, Young LW, Mazer J, Amortegui AJ (Magee-Womens Hospital, Halket Street and Forbes Avenue, Pittsburgh, Pennsylvania 14213). *Radiology* 122:443-447, Feb 1977

Three infants are described with perinatal death due to asphyxia caused by thoracic narrowing. These plus an additional three cases from the literature present a picture of chondrodysplasia. Radiography is characterized by: (1) shortening of the ribs and severe thoracic narrowing; (2) hypoplastic lungs; (3) short cranial base with sunken nose root, bulging forehead, flattened occiput; (4) abnormal spine; (5) pelvis similar to chondrodysplasia; (6) longitudinal spurs at ends of shortened tubular bones, particularly in femora and tibiae; (7) hexadactyly of either hands and/or feet. A frequently associated visceral anomaly is congenital renal disease. This syndrome is thought to be radiographically similar to but distinct from thanatophoric dwarfism and asphyxiating thoracic dysplasia.

Asher Nov

Miscellaneous

Steroid-dependent asthma treated with inhaled beclomethasone dipropionate. Davies G, Thomas P, Broder I, Mintz S, Silverman F, Leznoff A, Trotman C (Gage Research Institute, University of Toronto, Toronto, Canada). *Ann Intern Med* 86:549-553, May 1977

The efficacy of inhaled beclomethasone was studied in 44 steroid dependent asthmatic patients at the University of Toronto in a carefully controlled double blind trial. In this patient group it was clearly demonstrated that beclomethasone will significantly diminish symptoms and allow patients to markedly reduce prednisone dosages. This form of therapy will also improve pulmonary function as measured by maximum expiratory flow rates. Although beclomethasone therapy leads to little or no suppression of the pituitary-adrenal axis, patients still may have some steroid side effects such as candidiasis in the upper respiratory passages. Overall, 60% of the patients in this study could be withdrawn entirely from prednisone with the use of beclomethasone, indicating that this new form of therapy represents a substantial step forward in the management of patients with asthma.

David C. Dale
Medicine, University of Washington

Successful granulocyte transfusion therapy for gram-negative septicemia. Herzig RH, Herzig GP, Graw RG, Bull MI, Ray KK (Case Western Reserve School of Medicine, 2065 Adelbert Road, Cleveland, Ohio 44106). *N Engl J Med* 296:701-705, March 31, 1977

A randomized clinical trial of granulocyte transfusions for infection in acute leukemia. Alavi J, Root RK, Djerassi I, Evans AE, Gluckman SJ, MacGregor RR, Guerry D, Schreiber AD, Shaw JM, Koch P, Cooper RA (Hospital of the University of Pennsylvania, 3400 Spruce Street, Philadelphia, Pennsylvania 19104). *N Engl J Med* 296:706-711, March 31, 1977

These two important reports give us new information about the utility of granulocyte transfusion therapy for patients with severe granulocytopenia and infections. In the Herzig study, patients with documented gram-negative septicemia were randomized to receive granulocyte transfusions plus antibiotic therapy or antibiotic therapy alone. This study reports a total of 27 patients who experienced 30 episodes of gram-negative septicemia. Herzig and colleagues found that those patients who remained persistently granulocytopenic (severely reduced counts for greater than 10 days) had a grave prognosis with antibiotics alone whereas the comparison group which was given granulocyte transfusions cleared their infections significantly better.

Similar results were also found in the Alavi study. Here patients were randomized; the study included patients with fever but without documented infection. One important observation was that patients with fever and severe granulocytopenia who do not develop a documented infection, with careful blood culture and other microbiological monitoring, are very likely to survive. On the other hand, patients with positive cultures and persistent granulocytopenia are likely to die and the outcome for the infection, at least, is altered by granulocyte transfusions. As pointed out by Boggs in the accompanying editorial, patients who benefit most from granulocyte transfusions are those with the poorest overall prognosis for their underlying leukemic condition and therefore the broad application of granulocyte transfusion support is not necessarily mandated by the studies. Granulocyte transfusion remains, in the eyes of most experts, an experimental method for supportive care.

David C. Dale
Medicine, University of Washington

Failure of specific immunotherapy in fulminant type B hepatitis. Mosely JW (2826 South Hope Street, Los Angeles, California 90007). *Ann Intern Med* 86:272-277, March 1977

Patients with acute viral hepatitis who develop hepatitic encephalopathy have a very poor prognosis. Of those reaching stage IV coma, 80% die because there is no clearly effective therapy. This report of a very carefully conducted, randomized clinical trial of the use of intravenous hepatitis B immune globulin to treat fulminant type B hepatitis, clearly shows that there is no benefit to this form of therapy. In planning the study the investigators prepared a large batch of immune globulin and intended to give enough globulin to reduce the circulating hepatitis B antigen levels. Even when very large doses of the prepared immune globulin were administered, the patient's antigen levels could not be persistently suppressed. Interestingly, the patients did not develop evidence of any antigen-antibody complex disease in response to the antibody infusions except possibly for the development of fever.

This clinical trial should be a model for conducting a controlled study of a new therapy for a relatively rare but very serious medical problem. The problem is an important one, the diagnosis was made with reasonable certainty, the therapy was standardized and regulated, and a substantial number of investigators participated in the study. It was undoubtedly an expensive study; it is unfortunate that it yielded negative results.

David C. Dale
Medicine, University of Washington

Ultrasonics

Ultrasonography in obstructive jaundice. Malini S, Sabel J (Baylor College of Medicine, Texas Medical Center, Houston, Texas) *Radiology* 123:429-433, May 1977

The usefulness of ultrasonography in the preliminary evaluation of obstructive jaundice is described in 35 consecutive patients with icterus. Diagnosis was substantiated by laparotomy, autopsy or liver biopsy. In 23 patients with dilated bile ducts at ultrasonography, obstruction by tumor, stone, or stricture was proven operatively. Obstructive jaundice was differentiated from hepatocellular jaundice in 86% of cases; the site of obstruction was noted to be correct in 85%. The accuracy in the diagnosis of obstructive jaundice was 100% in patients with moderate or severe icterus.

Author Abstract

A simple ultrasonic method for evaluating liver size. Holmes JH, Sundrgren C, Ikle D, Finch J (University of Colorado Medical Center, 4200 East Ninth Avenue North, C277, Denver, Colorado 80262) *J Clin Ultrasound* 5:89-91, April 1977

By measuring the liver area (maximum section) and plotting this against intraabdominal area at the same level, one can calculate tolerance levels for 80% of the population (63 normal patients) with 95% confidence. This provides a simple semi-quantitative index in relating liver size of a specific patient to the normal range. Its use in 14 patients with liver disease was demonstrated.

Author Abstract

Gray scale sonographic anatomy of the pancreas. Ghorashi B, Rector WR (W. R. Rector, General Rose Memorial Hospital, 1050 Clermont Street, Denver, Colorado 80220). *J Clin Ultrasound* 5:25-29, 1977

The normal anatomic relationships and echographic appearance of the normal pancreas are described by Ghorashi and Rector from their experience with over 500 cases using gray scale equipment. As other investigators have recently recommended, the authors emphasize the technique of deep suspended inspiration, multiple views (especially the oblique view) and the single sector scan. Important anatomic land marks that are well described and illustrated include the splenic, superior mesenteric, and portal veins; the superior mesenteric artery; the right renal artery and left renal vein; and, the aorta and vena cava. Using the careful techniques they describe, the authors report they can visualize the normal pancreas in most subjects.

John Denney

Nuclear Medicine

Application of delayed lung imaging following radioaerosol inhalation. Poe ND, Cohen MB, Yanda RL (University of California, Los Angeles, California). *Radiology* 122:739-746, March 1977

Lung scintigraphy following radioaerosol inhalation reveals evidence of airway disease and regions of decreased ventilation. In obstructive pulmonary diseases, aerosol deposition can be so excessive that lung parenchyma is not visualized immediately after radioaerosol administration. Most of the tracer which is deposited is cleared within hours, but the aerosol reaching the alveoli is retained with a half-life in excess of 2 weeks. If imaging is repeated 8-24 hours after inhalation, abnormal bronchi will usually be cleared of tracer, and regional ventilation defects can be visualized.

Author Abstract

Quantitative external counting techniques enabling improved diagnostic and therapeutic decisions in patients with well-differentiated thyroid cancer. Thomas SR, Maxon HR, Kereiakes JG, Saenger EL (Cincinnati General Hospital, Cincinnati, Ohio). *Radiology* 122:731-737, March 1977

A quantitative technique is described which allows the physician to predict more accurately whether a recurrent or metastatic well-differentiated thyroid carcinoma is amenable to radioiodine-131 therapy or is better treated by other means. A calibrated uptake probe and scaler system is used to obtain conjugate view (i.e., diametrically opposed) counting rates for both the whole body and for any areas of abnormal uptake (lesion) at 24, 48 and 72 hours following the administration of 2 mCi ^{131}I. Quantitative calculations accounting for patient attenuation, lesion size, and geometrical factors then provide a determination of the lesion uptake as well as the effective half-life of ^{131}I in the lesion. The radiation dose which would be delivered to the lesion by a given therapeutic amount of ^{131}I may then be calculated to help determine the desirability of ^{131}I treatment. The results of patient studies indicate the potential benefit of such quantitative evaluation.

Author Abstract

New approach to interpretation of technetium-99m pyrophosphate scintigraphy in detection of acute myocardial infarction. Clinical assessment of diagnostic accuracy. Berman DS, Amsterdam EA, Hines HH, Salel AF, Bailey GJ, DeNardo GL, Mason DT. *Am J Cardiol* 39:341-346, March 1977

In the study of 235 patients admitted to the coronary care unit with acute chest pain, the ^{99m}Tc pyrophosphate scintigram was positive in 76 of 81 patients with acute transmural infarction, equivocal in five, and negative in one. The interpretation of the 2+ diffuse pattern of tracer uptake as equivocal rather than positive for acute myocardial infarction renders this technique extremely sensitive and specific for detecting acute myocardial infarction. Of 126 with no evidence of infarction, 87 had negative, 35 equivocal, and four a positive scintigram. Of 18 non-transmural, there were seven positive, nine equivocal, and two negative.

R. S. Frech

Myocardial uptake of technetium-99m stannous pyrophosphate following direct current transthoracic countershock. DiCola VC, Freedman GS, Downing SE, Zaret BL (B. L. Zaret, Yale University School of Medicine, 87 LMP, 333 Cedar Street, New Haven, Connecticut 06510). *Circulation* 54:980-986, Dec 1976

The effect of external direct current countershock upon myocardial scans was studied in dogs. Animals imaged 24 hrs. later had abnormal scintigrams that were indistinguishable from experimental infarction. In three animals, additional areas of radionuclide uptake were seen in overlying noncardiac tissue. There was no reduction in myocardial blood flow. Myocardial necrosis was found in areas of increased radioactivity. The magnitude of these changes increased with larger shock energy.

R. S. Frech

Radiation Oncology

Hypophysectomy in the treatment of disseminated prostate carcinoma. Silverberg GD (Stanford University Medical Center, 300 Pasteur Drive, Stanford, California). *Cancer* 39:1727-1731, April 1977

The author describes 17 patients suffering from pain secondary to disseminated prostate cancer who had hypophysectomy. Patients with hematocrits less than 30% and patients demonstrating evidence of liver involvement did not obtain objective remissions. The mean age of the patients with 68 years; only one patient was refused surgery on the basis of poor operative risk. The average duration of time between the diagnosis of prostate cancer and hypophysectomy was 50 months. The open transsphenoidal microsurgical technique described by Hardy was used in all patients with only minor modification. There were no deaths directly attributable to the surgery and no permanent complications.

Twelve patients showed evidence of remission. Five patients (29%) had both subjective and objective responses. Seven patients (41%) had subjective improvement but no evidence of objective response. Mean durations of response were 11 months and 3.8 months respectively. Overall survival of the patients in this series was 5.7 months.

Herbert C. Berry

Factors in the prognosis of gastric lymphoma. Lim FE, Hartman AS, Tan GC, Cady B, Meissner WA (Lahey Clinic Foundation, 605 Commonwealth Avenue, Boston, Massachusetts). *Cancer* 39:1715-1720, April 1977

Fifty consecutive cases of primary gastric lymphoma were staged by the authors according to TNM categories and then grouped into Stages I-IV based on these categories. The majority of patients had diffuse histiocytic lymphoma (46%) with the next most common histology being well differentiated lymphocytic lymphoma (24%). Of the 50 patients, six had unresectable lesions and underwent laparotomy and biopsy only. The remaining 44 patients in this respective review underwent resections. Postoperative radiotherapy to the site of the primary tumor was given to 25 patients. The authors feel the surgical approach to gastric lymphoma remains paramount as demonstrated by the resectability rate of 88%. They feel attempts should be made to resect all disease without resorting to total gastrectomy if possible in view of the 17% operative mortality rate of total gastrectomy. They feel that postoperative radiotherapy might offer some protection from local recurrence as no apparent isolated local recurrences were found among 15 patients with curative resection who had radiation after operation, while a 10% local recurrence rate was observed among 20 patients with curative resection who did not have radiation after operation. This local recurrence rate is emphasized by the fact that the patients who had irradiation after surgery tended to be those with more advanced disease. They feel that postoperative irradiation should be considered for patients with T3, N1, or N2 lesions, based on their classification. Multiple drug chemotherapy with or without irradiation is suggested in more advanced patients. Survival was related to stage of disease by these authors in range from approximately 90% at 60 months to 5% at 60 months depending on stage.

Herbert C. Berry

Radiotherapy results for nodular sclerosing Hodgkin's disease after clinical staging. Johnson RE, Zimbler H, Berard CW, Herdt J, Brereton HD (Radiation Oncology Branch, National Cancer Institute, Bethesda, Maryland). *Cancer* 39:1439-1444, April 1977

The authors have reviewed their results for radiotherapy of nodular sclerosing Hodgkin's disease after clinical staging not including laparotomy. Only three of 58 consecutive clinical Stage I-III patients initially treated with radiotherapy alone between 1965 and 1969 have died of Hodgkin's disease. Those 46 clinical Stage I or II patients with supradiaphragmatic disease with radiotherapy that included the paraaortic lymph nodes but did not extend below the aortic bifurcation had only one patient in whom subsequent relapse was observed when there was an extension to the iliac lymph nodes. Only three of the 17 patients who relapsed have died, while 13 of 14 surviving relapsers are currently free of disease. Development of extranodal dissemination was observed in only 7% of the patients, indicating to the authors that adjuvant chemotherapy is not warranted in this group of patients. The corrected 10 year survival rates for all 51 Stage I and II patients was 94%. Relapse-free survival for the entire group was 68% at 10 years. The authors feel these results support the omission of a staging laparotomy in clinical Stage I and II patients with supradiaphragmatic presentations of nodular sclerosis Hodgkin's disease.

Herbert C. Berry

Book Reviews

Watson-Jones: Fractures and Joint Injuries, 5th ed. Edited by J. N. Wilson. New York: Churchill Livingstone, 1,372 pp., vols. 1 and 2, 1976. $95

These two volumes constitute a revision of one of the truly classic texts of orthopedic surgery. The revision process was begun by Sir Reginald Watson-Jones and, following his death in 1972, completed by James Noel Wilson of the Royal National Orthopaedic Hospital in London. The first volume is devoted to general topics, including repair of skin, bone and ligaments, associated injuries, radiographic diagnosis, treatment techniques, and fractures in children. Volume 2 groups injuries by region and in addition includes discussions of pathologic fractures and of rehabilitation.

The text is written in a very readable style. The subsections of each chapter are labeled in bold print, greatly enhancing the book's use as a reference source. The illustrations are abundant and include large numbers of radiographs. These are, in general, well produced with only an occasional resort to artificial enhancement. The patient material is extensive, representing almost 50 years of busy orthopedic practice.

The chapter on Clinical and Radiographic Diagnosis revised by Kessel will be of particular interest to radiologists. After an admonition to avoid overreliance on radiographs, one is treated to an interesting collection of radiographic traps. Examples highlight the necessity of appropriate views and proper exposure. After an informative section on the diagnosis of fracture union, the chapter concludes with a haunting photograph of a hand demonstrating extensive radiation dermatitis. It is unfortunate, indeed, that in this otherwise well done chapter, Wilson found it necessary to make a disparaging comment about surgeons in the United States.

Among the weaknesses of this text, one might list the very superficial discussion of arthrography, a technique now well established in the diagnosis of joint pathology. The section of fractures about the hip shows only examples of the Smith-Peterson nail technique. Thus the reader is not exposed to other commonly used methods of internal fixation. The section on fractures in children is quite brief; the standard Salter-Harris classification of epiphyseal injuries is not mentioned.

For the radiologist these volumes may serve as a readily accessible fund of knowledge on orthopedic injuries. They will be a valuable addition to the library of any radiology department seeing a significant volume of adult trauma.

Frederick A. Matsen, III
Department of Orthopedics
University of Washington
Seattle, Washington 98195

Breast Cancer: Its Impact on the Patient, Family, and Community. Frontiers of Radiation Therapy and Oncology, vol. 11. Edited by J. M. Vaeth. Basel: Karger, 214 pp., 1976. $36.75

This book records a symposium of 12 papers and three panel discussions delivered at the San Francisco Cancer Symposium in November 1975. The title suggests a spectrum of topics that seem peripheral to the radiation oncologist, but this volume contains much information of current interest.

Three chapters update and evaluate recent radiotherapy and chemotherapy studies, which are helpful in the current attempts to modify traditional treatment policies. Brady's compact survey of the role of radiation oncology in breast cancer encompasses the lore of radiotherapy knowledge plus a comprehensive and conservative evaluation of new treatment strategies. This contrasts strikingly with DeVita's survey of current accomplishments of chemotherapy in breast cancer. He reviews recent studies demonstrating the high incidence of widespread dissemination of cancer in apparently localized tumors which properly calls for aggressive chemotherapy early in the course of treatment. However, the impact of his thesis is somewhat weakened by portentous and premature statements based on "early findings" and 1 year follow-up. One must await with patience a more responsible analysis based on a 10 year follow-up.

Armentrout's chapter on clinical management of advanced cancer of the breast is a concise, logical discussion of the available treatment options, including manipulation of hormones, together with thoughtful judgments of the value of each. It is a useful chapter for the practicing oncologist.

Three chapters consist of free-wheeling panel discussions of different subjects. They are haphazard and discursive, and fail to impart a logical flow of ideas and information. While I have previously been guilty of organizing similar fruitless panel discussions, I am now reformed. A substantive portion of the book undertakes to discuss the interpersonal relationships between the breast cancer patient on the one hand, and her physicians, nurses, technicians, family, friends, relatives, and clergy plus the professional and semiprofessional mental health onlookers, who have much to say in jargon. This section recalls physicist Failla's aphorism, "More people live off cancer than die from it."

The reader is richly rewarded by an outstanding chapter by Robert Woodson on the Concept of Hospice Care in Terminal Disease. It describes the highly sophisticated, though basic, scientific and artistic system of palliative care developed over the years by Cicely Saunders and her dedicated colleagues. The sensitivity and compassion of the gifted physicians in the three dozen hospices in the United States and Canada is revealed by an exemplary sentence, "What is the dying patient saying when she asks for the time of the day?"

Four types of pain, both single and in combination, are discussed: physical, psychological, social, and spiritual. Tom West's list of specific drugs for each of six types of physical pain will become a reference text for the clinical oncologist. The question of addiction is not an issue in hospice treatment.

Deeply moving is the section on spiritual pain, which differs for each patient according to religious, transracial, or cultural background. The comfort derived from deathbed conversations or confessional with skilled spiritual listeners, whether it be clergymen, Zen master, or guru is only slightly less valuable than drugs.

Despite the varied quality of some chapters, the reader will find much that is useful, original, and often profound.

Milton Friedman
10 Manor Avenue
Greystones, County Wicklow
Ireland

Percutaneous Transluminal Angioplasty: The Dotter Procedure. A Manual for the Radiologist. By G. J. van Andel. Amsterdam: Excerpta Medica, 179 pp., 1976. $19.25

What could be said about "Dotter" transluminal angioplasty that hasn't been said by Dotter? This book answers that question in a clear, concise, easy to read style. To those involved in peripheral vascular radiology, this will read like a novel.

The book is well organized and more comprehensive than the title indicates. It presents a splendid review of the entire field of peripheral arteriosclerosis, providing an excellent review of the following topics: arterial anatomy of the pelvis and lower extremities; pathologic anatomy of arteriosclerosis; pathophysiology of the pelvic and lower extremity circulation; measurement of lower extremity blood pressure; clinical aspects of chronic arterial insufficiency of the pelvis and lower extremities; radiologic diagnosis of atheromatosis of the pelvis and lower extremity arteries; and therapeutic options in chronic arterial insufficiency with justification for conservative, reconstructive, and sympathectomy treatments based on the natural course of atheromatosis. Finally, there is an excellent description of the Dotter procedure and modifications of the technique proposed by others including van Andel.

The procedure is thoroughly reviewed providing perspective as to its application to the problem of lower extremity arteriosclerotic ischemic disease. Clinical results of van Andel and others are reviewed. The material is presented in a straightforward manner which, despite the absence of an index, is easily retrievable. The illustrations are excellent.

The book is recommended to all radiologists to provide the fundamentals necessary to understand the current therapeutic approaches to atherosclerotic vascular disease. Anyone contemplating performance of this procedure would do well to study this manual. It is especially valuable for radiologists, full-time angiographers, vascular surgeons, and general surgeons performing a moderate amount of reconstructive arterial surgery.

Jack L. Eisemann
University of California, Los Angeles
Olive View Medical Center
Van Nuys, California 91405

Symposium on *Pneumocystis carinii* Infection. Edited by J. B. Robbins, V. T. DeVita, Jr., and W. Dutz. DHEW Publication (NIH 76-930), National Cancer Institute Monograph 43. Washington, D.C.: Government Printing Office, 223 pp., 1976. $4.75

This symposium held at Bethesda, Maryland, in December 1973 was sponsored by the National Institute of Child Health and Human Development and the National Cancer Institute. After an introductory historical survey, the book contains 23 scientific papers grouped under three headings: (1) The Organism and the Patient; (2) Clinical Characteristics of the Disease; and (3) Pathology and Therapy. A liberal amount of overlapping of subject material is inevitable but helpful.

European observers first described a plasma cell pneumonia in marasmic infants in the 1920s, identified the suspected etiological agent (discovered by Chagas in 1909) in 1951, and later drew the attention of American scientists in 1957. Subsequently we have become familiar with a second distinctive form of this disease occurring in all ages as a complication of inherited immunodeficiency or, more commonly, of acquired immunodeficiency in patients receiving cytotoxic and immunosuppressive therapy for malignancy, visceral transplants, and other clinical disorders.

Clinical, immunologic, pathologic, and pharmacologic studies are well organized, adequately documented, and are supplemented by reference lists and by informal informative discussions.

Illustrations of the radiographic appearance of pneumocystic infection in the lung are unfortunately restricted and, in many instances, unsatisfactory. A knowledge of the characteristic radiographic findings commonly seen today is assumed. Complex details in a film series illustrating changes in the marasmic infant are lost in the positive type image reproduction; to complete the frustration the accompanying legends are relegated to a remote segment of the text. A presentation of atypical radiographic features using conventional negative film images, and other illustrations dealing with histopathology and immunopathology are more revealing.

An interesting postscript reports the first successful cultivation of *P. carinii* (1975). Failure to culture this organism has limited our ability to study the epidemiology and pathogenesis of pneumocystic infection.

This monograph will have greatest appeal to the microbiologist and the clinician attending the immunodeficient patient. For the radiologist it will have limited value as a reference work.

Maurice J. Blocklyn
Crozer Chester Medical Center
Chester, Pennsylvania 19013

Cysts of the Oral Regions. By M. Shear. Bristol: John Wright & Sons, 170 pp., 1976. £ 4.5

This volume is the 23d of 24 in the series *Dental Practitioner Handbooks* edited by Donald D. Derrick. The relatively small monograph has a linen cover and 170 pages including a bibliography and cross references. There are 108 figures including tables. Twenty-two of the figures are radiographs of generally good quality. There are more than 200 references, many of which are recent.

Shear has attempted to bring current views on cystic changes of the jaws into one compact volume. He includes clinical data, radiologic features, pathogenesis, pathology, and a brief comment on treatment.

The material is well organized and begins with a 3 page chapter on historic aspects. He describes and illustrates the pathology with halftone microscopic reproductions. Much of the material is taken from his own material, including 750 jaw cysts over a 15 year period.

The radiologic descriptions are lucid and easy to follow. Line drawings are sometimes used to emphasize a point. Shear uses conventional radiography and does not refer to use of panoramic radiographic techniques. He suggests the latter for examining mucocele of the antrum.

The material is well covered, but not in too much detail. The usual cysts that an oral surgeon will see in practice are discussed, but Shear has made no attempt at long differential diagnoses or specialized views. This material is aimed at the practicing oral surgeon and would be useful to the radiologist who works in conjunction with oral surgeons. It will make a handy reference, but there has been no attempt to be encyclopedic.

David L. Berens
50 High Street
Buffalo, New York 14203

Contributions to Nephrology. vol. 5: **Radiology and the Kidney, Some Present Concepts.** Edited by C. J. Hodson. Basel: Karger, 86 pp., 1977. $20.50

This soft-cover book contains a wealth of information concerning the basic concepts of uroradiology as well as a brief overview of how a sophisticated exam of the urinary tract is performed and evaluated by the radiologist. It is intended as a brief introduction of the subject for nephrologists of areas of renal disease with which they are most concerned and are liable to require radiographic examination and consultation. The book in its present form is also a good review for the practicing radiologist who performs and monitors intravenous urograms and is interested in this technique as an individualized examination. It is also good background material for radiology residents on which to build their knowledge.

The book is written in three sections by three different contributors who are authorities in uroradiology. The divisions include a well described section on fundamental concepts of urography which covers a broad range of disease states and the radiological procedures used to evaluate them. There is a section on diseases of the renal parenchyma including a discussion on the normal morphology of the kidney. The third section deals with the urography of renal failure. The photographs of x-rays are of good quality and depict the points being presented. A number of line drawings are included in the second section in place of radiographs to outline numerous disease states. These are adequate to portray the necessary information, but it would have been nice to have seen x-ray examples. It was also necessary to flip pages back and forth between the text and the line figures to see what was being described, which was distracting.

The minimal length of the book also required that topics be abbreviated and condensed, although they were generally well covered. It is unfortunate that there was not room to elaborate further on the material which would have made the work of more value as a reference book.

With the possible exception of the cost of this volume being slightly high for a small soft-cover book, it is in general an excellent collection of information about the radiology of the urinary tract and would make a worthwhile addition to one's medical library.

Ronald D. Harris
Scripps Clinic Medical Institutions
La Jolla, California 92037

An Introduction to the Physics of Nuclear Medicine. By P. N. Goodwin and D. V. Rao. Springfield, Ill.: Thomas, 150 pp., 1977

Goodwin and Rao have succeeded well in their task of designing a basic physics book for technicians and physicians entering the field of nuclear medicine. Brevity and clarity are outstanding features of all chapters. There is no material which is not essential, and it is adequate for board or registry preparation.

Twelve short chapters cover basic mathematics, basic nuclear physics, reaction of radiation safety and dosimetry. The first chapter on math review would probably have to be supplemented liberally for beginning technician students, and other chapters are rather skeletal in coverage; but generally the brevity of the book is a strong point. The index is adequate and a short appendix of radionuclides will be useful.

William A. Wilcox
Minneapolis Radiology Associates
Minneapolis, Minnesota 55422

NEWS

San Diego Course

The San Diego Postgraduate Radiology Course will be October 3-6 at Vacation Village. Recent concepts in subdivisions of diagnostic radiology will be reviewed including computed tomography of the head and body. Fee is $250; 20 hr AMA Category I credit is available. For information and registration, write Nomi Feldman, Box 750, La Jolla, California 92038.

Neuroradiology and CT

Neuroradiology and CT Scanning for the Practicing Radiologist is a seminar scheduled for October 21-23 at the Fairmont Hotel, Dallas. Sponsor is the Neuroradiology Section, University of Texas Health Science Center at Dallas. All aspects of neuroradiology will be covered including CT, angiography, myelography, tomography, and radioisotope scanning, with clinical and pathologic correlation. Guest faculty will be: F. R. Brahme and R. Livingston, both University of California, San Diego; and N. E. Leeds, Albert Einstein College of Medicine. Staff faculty will be members of the Departments of Radiology, Neurosurgery, Neurology, and Pathology from the sponsoring school. Fee is $200 and the program will carry 18 hr AMA Category I credit. Information is avaiable from M. Ryals, Department of Radiology, Parkland Memorial Hospital, 5201 Harry Hines Boulevard, Dallas, Texas 75235.

Arthrography Workshop

An Arthrography Course and Workshop is scheduled for December 15-17 at the Hospital for Special Surgery, New York City. Registration is $200 and is limited to 60 participants; 16 hr AMA Category I credit is available. For information, write R. H. Freiberger, director, Department of Radiology, Hospital for Special Surgery, 535 East 70th Street, New York, New York 10021.

CT, Ultrasound, and X-ray

Computed Tomography, Ultasound, and X-ray—An Integrated Approach, is the title of a problem-oriented course offered January 16-20 at the Fairmont Hotel, San Francisco. Sponsors are Radiology Research and Education Foundation and Extended Programs in Medical Education, University of California, San Francisco. Following a series of comprehensive lectures on different imaging approaches to specific clinical problems, a panel of experts will discuss and formulate ways to integrate the modalities in a rational and efficient diagnostic plan. Although emphasis will be on computed tomography, a review of nuclear medicine, angiography, and conventional radiologic approaches will also be presented. Clinical topics will include: jaundice, pancreatic, hepatic, renal, and adrenal masses, abdominal abscess, retroperitoneal lymphadenopathy, brain tumor, spine and disc disease, bone and soft tissue masses, ischemic heart disease, pulmonary embolism, mediastinal mass, and thyroid nodule. Faculty with fields of expertise are: computed tomography—R. J. Alfidi, Cleveland Clinic; S. S. Sagel, Washington University; M. Korobkin and D. Norman, both University of California, San Francisco; L. M. Zatz, Palo Alto Veterans Administration Hospital; nuclear medicine—A. Gottschalk, Yale University; P. B. Hoffer, University of California, San Francisco; ultrasound—G. Leopold, University of California, San Diego; R. A. Filly, University of California, San Francisco; W. F. Sample, University of California, Los Angeles; angiography—J. J. Bookstein, University of California, San Diego; H. Goldstein, M. D. Anderson Hospital and Tumor Institute; S. R. Reuter, University of California, Davis; R. A. Castellino, Stanford University; T. H. Newton and H. C. Redman, both University of California, San Francisco. Course fee is $300; $200 for residents and interns with letter of verification. Category I credit is available from the AMA and California Medical Association. For information, contact Extended Programs in Medical Education, University of California, Room 569-U, San Francisco, California 94143; telephone (415) 666-4251.

New England Nuclear Medicine Meet

The thirteenth annual meeting of the New England Chapter of the Society of Nuclear Medicine will be October 22 and 23 at the Copley Plaza Hotel, Boston. The course will include updated cardiac material on ^{201}thallium heart studies, gated studies, and infarct imaging. Also included will be radionuclide evaluation of patients suspected of pulmonary emboli, and bone scan pattern recognition. Participants include E. Fordham, B. L. Holman, C. D. Maynard, H. W. Strauss, and S. Treves. For information, write W. D. Kaplan, Division of Nuclear Medicine, Sidney Farber Cancer Institute, 44 Binney Street, Boston, Massachusetts 02115.

Angiography Courses

Two consecutive angiography courses are being sponsored by the Harvard Medical School, October 7-9 and 10-13 at the Copley Plaza Hotel, Boston. Part I Coronary Circulation, the Myocardium, and Adult Heart Disease, is designed primarily for radiologists and cardiologists who participate in, intend to perform, or wish to remain abreast of coronary arteriographic studies, ventriculography, and cardiovascular radiology. This section will emphasize application of conventional radiologic studies, echocardiography, and nuclear imaging techniques to the diagnosis of heart disease as well as technical aspects of coronary arteriography and ventriculography, contrast agents, complications of these techniques, and grading and effect of coronary artery stenosis. Each day, eight combined refresher course-seminars will supplement the formal program. There will also be equipment displays and demonstrations. Fee for part I is $200; $140 for residents or fellows. Combined fees for parts I and II are $400; $275 for residents and fellows.

Part II is Angiography for the Practitioner. This course is designed for radiologists who perform or intend to perform angiographic studies. It will define the present state of the art and emphasize practical considerations. The field will be explored in depth with a daily combination of courses, seminars, film reading panels, and lectures. Sixteen 45 min refresher course-seminars will assess: equipment; complications and prevention; splenic, pancreatic, and hepatic arteriography; detection of gastrointestinal bleeding; physiologic monitoring; technology of intravascular hemostasis; renal arteriography and trauma; peripheral arteriography and venography; pediatric angiography; ultrasound of the abdomen; and thoracic and abdominal aorotography. Fee for part II alone is $250; $175 for residents and fellows.

Part I carries 19 hr AMA Category I credit, while part II carries 23 hr. For additional information, write H. L. Abrams, Department of Radiology, Harvard Medical School, 25 Shattuck Street, Boston, Massachusetts 02115.

Stress Management Symposia

Two consecutive 1 day symposia on stress will be October 1 and 2 at the Sheraton Palace Hotel in San Francisco. Sponsors are the University of California Schools of Dentistry, Medicine, Nursing, and Pharmacy in conjunction with the Institute for the Study of Human Knowledge. The first symposium is Stress Management; the second is Approaches to Stress. Chairmen are H. Selye, R. Ornstein, and C. Swencionsis. Continuing education credit is available. For information contact University of California, Continuing Education in Health Sciences, 1308 Third Avenue, San Francisco, California 94143; telephone, (415) 666-2894.

Chest Disease Course

Chest Disease: 1977—An Interdisciplinary Approach with Emphasis on Radiology is a course slated for October 17-21 at the Copley Plaza Hotel, Boston. Sponsor is the Harvard Medical School. This intensive 5 day multidisciplinary course is designed for radiologists, chest physicians, internists, thoracic surgeons, and others. There will be a daily review of radiologically oriented topics with emphasis on clinical-radiologic-pathologic correlations. Other subjects include bacterial diseases of the lung, pulmonary tuberculosis, pulmonary hemodynamics, respiratory distress, and lung cancer. Course fee is $300; $200 for residents and fellows. Thirty-one hours AMA Category I credit is available. For information, contact P. G. Herman, Department of Radiology, Harvard Medical School, 25 Shattuck Street, Boston, Massachusetts 02115.

Clinical Nuclear Medicine

A postgraduate course, Clinical Nuclear Medicine: 1977, will be October 27-29 at Dunfey's Parker House Hotel, Boston. Sponsor is Harvard Medical School. The 2½ day course is designed for those practicing nuclear medicine and will offer three morning sessions of didactic material and two afternoon workshops. Topics will include bone imaging, practical cardiac examinations, and critical review of recent clinical developments in nuclear medicine. The course carries 17 hr Category I AMA credit; fee is $175, $125 for residents and fellows. Additional information is available from W. D. Kaplan, Department of Radiology, Peter Bent Brigham Hospital, 721 Huntington Avenue, Boston, Massachusetts 02115.

University of Miami Seminars

Seven consecutive radiology seminars have been scheduled by the University of Miami between January and March 1978. Titles, locations, and details are:

1. January 13-17, Third Annual Seminar, Problems in Pediatric Radiology, Sonesta Beach Hotel and Tennis Club, Key Biscayne. Fee $185; $100 for residents and fellows.
2. January 17-20, Postconvention Seminar in Pediatric Radiology, Radiographic-Pathologic Correlation of Pediatric Diseases, Colony Beach and Tennis Resort, Longboat Key, Sarasota. Fee, $100. (For information on 1 and 2, contact H. A. Wexler, Department of Radiology, University of Miami School of Medicine, P. O. Box 520875, Biscayne Annex, Miami 33152.)
3. March 4-7, Eighth Annual Radiological Special Procedures Seminar, Konover Hotel, Miami Beach. Fee $250; $120 for residents and fellows.
4. March 7-11, Sixteenth Annual Clinical Radiology Seminar, Controversies in Radiology, Konover Hotel, Miami Beach. Fee $215; $105 residents and fellows.
5. March 12-15, Second Annual Seminar, Practical Aspects of Computed Tomography, Konover Hotel. Fee $150; $75 residents and fellows.
6. March 15-18, Practical Aspects of Ultrasonography, Konover Hotel. Fee $200; $100 residents and fellows.
7. March 17-20, Postconvention Seminar Bahamian Cruise (Nassau). Fee $50 (cruise fee to be determined).

For information on courses 3-5 and 7, contact Mrs. L. R. Kelley, Department of Radiology, University of Miami School of Medicine, P. O. Box 520875, Biscayne Annex, Miami 33152. For details on course 6, contact Mrs. J. K. Allen, Department of Nuclear Medicine, Division of Ultrasound, Mount Sinai Medical Center, 4300 Alton Road, Miami Beach 33140.

Osteopathic Radiology Courses

Three courses are being sponsored by the American Osteopathic College of Radiology: 50th Annual Clinical Assembly, October 2-6, Los Angeles; Fifth Annual Refresher Course, January 19-21, Chicago; and Ninth Regional Conference, April 6-8, Orlando, Florida. Tentative topic of the Orlando conference is Radiology of Bones and Joints. For details, contact M. K. Willman, 800 West Jefferson, Kirksville, Missouri 63501.

Beth Israel Courses

Three postgraduate courses have been announced by Beth Israel Medical Center in New York City. The first, Diagnosis, Treatment, and Rehabilitation of Carcinoma of the Oral Cavity and Related Structures, will be October 26. This course is designed for physicians, dentists, dental hygenists, nurses, and paraprofessionals and will emphasize recognition of premalignant and malignant conditions of the oral cavity (soft tissue and bone) and treatment and rehabilitation. Faculty includes M. Nussbaum and C. E. Barr. Cosponsor is the American Cancer Society. There is no fee, and accreditation is available.

On November 16, Recent Advances in the Diagnosis and Management of Cancer of the Prostate will be presented. This course will discuss recent advances in laboratory evaluation of patients with carcinoma of the prostate and discuss the value of lymphangiography and staging pelvic lymphadenectomy. The role of radiation therapy in the management of carcinoma of the prostate and endocrine therapy will also be presented as well as interstitial therapy, chemotherapy, and radical surgery. The course carries AMA Category I credit. Faculty will be L. A. Orkin and J. Vogel.

Urological Trauma will be a 1 day course in January (date to be determined). This course will present a comprehensive review of current diagnosis and therapeutic practices in urological trauma. Clinical, radiologic, and therapeutic principles involved in injury to the urinary tract will be discussed.

Information for all courses is available from B. R. Lawrence, Postgraduate Education Office, Beth Israel Medical Center, 10 Nathan D. Perlman Place, New York, New York 10003; telephone, (212) 420-2851.

Radiopharmaceutical Application

G. D. Searle & Co. has submitted a new drug application to the Food and Drug Administration. The drug, ^{131}I-19-iodocholesterol, may be used in nuclear medicine to detect various adrenal diseases such as Cushings Disease, hyperaldosteronism, and adrenal adenoma. The new drug application is the first submitted by Searle for an in vivo-administered radiopharmaceutical, and covers results generated in multicenter clinical trials.

Las Vegas Angiography Course

A fourth postgraduate course, Advances in Angiography: Integrating Angiography with the New Imaging Modalities, Technical, Clinical and Equipment Advances, will be January 19-21 at the MGM Grand Hotel Las Vegas. Sponsors are Shadyside Hospital of Pittsburgh and the University of Pittsburgh School of Medicine. The course is designed for radiologists, cardiologists, and others involved in cardiovascular procedures. The format will feature both general and tutorial sessions. General sessions will include new developments, advances in interventional techniques, comparison multiimaging, and specific general vascular and cardiovascular topics. Fee is $150. Additional information is available from Shadyside Hospital, Radiology Seminar, Department of Radiology, 5230 Centre Avenue, Pittsburgh, Pennsylvania 15232.

Infectious Diseases Symposium

The Third International Symposium on Infectious Diseases is scheduled for October 31-November 2 in Guadalajara, Mexico. Sponsors are the University Autónoma of Guadalajara and the Mexican Association of Infectious Diseases. For information, contact Educación Continuada, U A G, Montevideo no. 3331, Acueducto Providencia, Guadalajara, Jaliso, México.

Nuclear Medicine and Biology Congress

The Second International Congress of the World Federation of Nuclear Medicine and Biology has been scheduled for September 18-21, 1978, at the Washington (D.C.) Hilton Hotel. Scientific symposia will concentrate on medical and health physics; instrumentation; radiochemistry; radiopharmaceuticals; data analysis; radioassays; biochemical and physiologic measurements in vivo; and bone, joint, cardiovascular, endocrine, metabolic, pulmonary, and renal disorders in adults and children. The education program will consist of two premeeting courses, and there will be teaching sessions during the meeting. Morning activities will feature a plenary session and small group discussions, while afternoons will be devoted to contributed papers, poster sessions, panels, and minisymposia. For additional information and call-for-papers, write H. N. Wagner, Jr., WFNMB Second International Congress, 1629 K Street, N.W., Suite 700, Washington, D.C. 20006.

Meeting and Course Review

For reader convenience, a summary of upcoming meetings and courses is provided. Detailed listings of these events appeared in journal issues indicated in parentheses.

Body Imaging Conference, October 8-16, Kauai, Hawaii (August).

Mammographic Training Program, continuing education course, 1 week sessions throughout the year in seven U.S. locations (April).

International Gastrointestinal Cancer Conference, November 6-11, Tel Aviv, Israel (April).

Medical Oncology Congress, December 4-6, Nice, France (May).

Tumor Ultrasound '77, international symposium, December 5 and 6, London, England (May).

Carcino-Embryonic Antigen Symposium, October 7-9, Nice, France (May).

Seminars with Specialists in Diagnostic Radiology, October 27 and 28, San Antonio, Texas (May).

Bermuda Postgraduate Radiology Course, October 24-28 (June).

Southeastern Chapter Society of Nuclear Medicine Annual Meeting, October 12-15, Winston-Salem, North Carolina (June).

Radiology Continuation Course, November 14-18, Minneapolis, Minnesota (June).

Neuroradiology—with Emphasis on CT Scanning and Clinical Practice, seminar, October 21-23, Dallas, Texas (July).

Ultrasound Preceptor Program, continuing one and two week programs, Dallas, Texas (July).

Pediatric Urinary Tract Symposium, November 16-18, Boston, Massachusetts (July).

Head and Neck Cancer Meeting, January 11-14, 1978, San Francisco, California (July).

International Course in Advanced Neuroradiology, March 10 and 11 Strasbourg, France (July).

Ultrasound Postgraduate Course, two sessions, January 2-March 10, and April 3-June 9, Winston-Salem, North Carolina (August).

Ultrasound Series, two sessions, October 3-7, and December 12-16, Baltimore, Maryland (August).

Aspen Uroradiology Seminar, February 19-24, Colorado (August).

Cancer of Bladder and Prostate, conference, November 4 and 5, Louisville, Kentucky (August).

Computed Body Tomography Course, January 30-February 2, San Diego, California (August).

Radiologic Societies

International Societies

Fleischner Society. Secretary, E. Robert Heitzman, State University of New York Upstate Medical Center, Syracuse NY 13210

Inter-American College of Radiology. Secretary, Gaston Morillo, Department of Radiology, Jackson Memorial Hospital, 1611 NW 12th Avenue, Miami FL 33136.

XIV International Congress of Radiology, Oct 23–29, 1977, Rio de Janeiro. Secretary-General, O. J. Machado, Sociedade Brasileira de Radiologia, Av. Churchill, 97-5° and ZC-39, 20,000, Rio de Janeiro, Brazil.

International Skeletal Society. Secretary-Treasurer, Jack Edeiken, Radiology Dept, Thomas Jefferson University Hospital, 11th and Walnut Sts, Philadelphia PA 19107.

International Society of Radiology. Hon. Secretary-Treasurer, W. A. Fuchs, Department of Diagnostic Radiology, University Hospital, Inselspital, CH-3010 Bern, Switzerland.

U.S. National Societies

American Association of Physicists in Medicine. Secretary, John Wright, Radiology Department, Geisinger Medical Center, Danville PA 17821.

American Board of Radiology. Secretary, C. Allen Good, Kahler East, Rochester MN 55901.

American College of Radiology. Executive Director, William C. Stronach, 20 N. Wacker Drive, Chicago IL 60606.

American Institute of Ultrasound in Medicine. Executive Secretary, Donna LaMaster, PO Box 25065, Oklahoma City OK 73125.

American Nuclear Society. Program Chairman, Ted D. Tarr, U.S. Energy Research and Development Administration, Mail Station A-436 Office of Assistant Administrator for Nuclear Energy, Washington DC 20545.

American Osteopathic College of Radiology. 1977 Program Chairman, George O. Faerber, 1087 Dennison Avenue, Columbus OH 43201. Annual Meeting: Oct17-21, 1976, New Orleans LA.

American Radium Society. Secretary, A. S. Ketcham, University of Miami School of Medicine, P.O. Box 520875 Biscayne Annex, Miami, FL 33152. 1978 Annual Meeting: Marriott Hotel, New Orleans, LA, April 26–30.

American Roentgen Ray Society. Secretary, James Franklin Martin, 300 S. Hawthorne Rd., Winston-Salem NC 27103. Annual Meetings: 1977, Sheraton Hotel, Boston MA, Sept 27–30; 1979, Sheraton Centre, Toronto, Candada, March 24–30; 1980 MGM Grand Hotel, Las Vegas, Nevada, April 19–25; 1981, San Francisco Hilton, California, March 21–27; 1982, New Orleans Hilton, Louisiana, April 24–30.

American Society of Neuroradiology. Secretary, Arthur E. Rosenbaum, University of Pittsburgh School of Medicine, Pittsburgh PA 15261.

American Society of Therapeutic Radiologists. Secretary, W. J. Taylor, Mason Clinic, 1100 9th Avenue, Seattle WA 98101.

American Thermographic Society. Executive Director, Mrs. N. M. Oldfield, P. O. Box 2055, Gaithersburg, MD 20760. President, G. D. Dodd, M.D. Anderson Hospital, Houston, TX 77030.

Association of University Radiologists. Secretary-Treasurer, J. E. Whitley, Bowman Gray School of Medicine, Winston-Salem, NC 27103.

Health Physics Society. Executive Secretary, Richard J. Burk, Jr., 4720 Montgomery Lane, Bethesda MD 20014.

National Medical Association. Secretary, E. Mapp, Episcopal Hospital, Philadelphia, PA 19148.

North American Society of Cardiac Radiology. Secretary-Treasurer, Erik Carlsson, University of California, San Francisco CA 94143.

Radiation Research Society. Executive Director, Richard J. Burk, Jr., 4720 Montgomery Lane, Bethesda MD 20014.

Radiological Society of North America, Inc. Secretary, Theodore A. Tristan, Fifteenth Floor, One MONY Plaza, Syracuse NY 13202. Annual Meeting: 1977, Nov 27–Dec 2; 1978, Nov 26–Dec 1, all Chicago; 1979, Nov 25–30, Atlanta, GA; 1980, Nov 16–21, Dallas, TX.

Section on Radiology, American Medical Association. Secretary, Antolin Raventos, Dept. of Radiology, School of Medicine, University of California, Davis.

Society of Cardiovascular Radiology. Secretary-Treasurer, W. J. Casarella, Columbia-Presbyterian Medical Center, New York, NY 10032. Annual Meeting: 1978, Fairmont Hotel, New Orleans, LA, Feb 19–23.

Society of Gastro-Intestinal Radiologists. Secretary-Treasurer, Walter Whitehouse, Dept of Radiology, University of Michigan, Ann Arbor MI 48104.

Society of Nuclear Medicine. President, 475 Park Avenue S, New York NY 10016.

Society for Pediatric Radiology. Secretary-Treasurer, N. Thorne Griscom, Children's Hospital Medical Center, 300 Longwood Ave., Boston MA 02115.

Society of Uroradiology. Secretary-Treasurer, Howard M. Pollack, Dept of Radiology, Episcopal Hospital, Front St at Lehigh Ave, Philadelphia PA 19125.

U.S. State and Local Societies

Alabama

Alabama Academy of Radiology. Secretary-Treasurer, J. L. Wayland, 401 West College St, Florence, AL 35630.

Section of Radiology, National Medical Association. Secretary, Ivy Brooks, Dept of Radiology, Veterans Administration Hospital, PO Box 511, Tuskegee AL 36083.

Southern Radiological Conference. Secretary-Treasurer, J. W. Maxwell, PO Box 2144, Mobile AL 36601.

Alaska

Alaska Radiological Society. Chapter ACR. Secretary-Treasurer, John J. Kottra, 3200 Providence Ave. Anchorage AK 99504.

Arkansas

Arkansas Chapter of ACR. Secretary-Treasurer, Richard Seibold, Jr., Wadley Hospital, Texarkana AR 75501.

Arizona

Arizona Radiological Society. Chapter of ACR. Secretary, Irwin M. Freundlich, 1501 N Campbell Ave, Dept of Radiology, Tucson AZ 85724.

California

California Radiological Society, California Chapter of ACR. Executive Secretary, J. Michael Allen, 1225 8th St. Suite 590, Sacramento CA 95814.

East Bay Radiological Society. Secretary-Treasurer, Norman P. Moscow, 33 Oakvale Ave, Berkeley CA 94705.

Los Angeles Radiological Society. Secretary, A. Franklin Turner, LAC/USC Medical Center, Box 778, Los Angeles CA 90033.

Northern California Radiological Society. Secretary-Treasurer, Jan C. Buhl, 7733 Bahama Ct. Fair Oaks CA 95628

Northern California Radiotherapy Association. Secretary-Treasurer, John D. Earle, Stanford Medical Center, Stanford CA 94305.

Orange County Radiological Society. R. Lawrence Argue, 100 E Valencia Mesa Dr, Fullerton CA 93632.

Radiological Society of Southern California. Secretary-Treasurer, Duane Eugene Blickenstaff, La Jolla Radiology Medical Group, Inc. 7849 Fay Ave, La Jolla CA 92037.

Redwood Empire Radiological Society. Secretary, Hal B. Peterson, 357 Perkins St, Sonoma CA 95476.

San Diego Radiological Society. President, Donald J. Fleischli, 7849 Fay Ave, La Jolla CA 92037.

San Francisco Radiological Society. Secretary-Treasurer, Philip A. Brodey, Dept of Radiology, Mount Zion Hospital and Medical Center, San Francisco CA 94115.

South Bay Radiological Society. Secretary, R. T. Filipi, 14105 Okanogan Dr., Saratoga, CA 95070.

South Coast Radiological Society Chapter of ACR. Secretary-Treasurer, Brian R. Schnier, Dept of Radiology, Cottage Hospital, Pueblo at Bath, Santa Barbara CA 93105.

Southern California Radiation Therapy Society. Secretary-Treasurer, Jerome Stuhlborg, 514 N Prospect, Redondo Beach CA 90277.

Western Neuroradiological Society. Secretary-Treasurer, R. A. Kramer, Palo Alto Medical Clinic, 300 Homer Ave, Palo Alto, CA 94301.

Colorado

Colorado Radiological Society, Chapter of ACR. Secretary, John Pettigrew, 2215 N Cascade, Colorado Springs CO 80907.

Rocky Mountain Radiological Society. Secretary-Treasurer, J. M. Grogan, 4200 E 9th Ave, Denver CO 80206.

Connecticut

Connecticut Valley Radiologic Society. Secretary-Treasurer, Gerald N. LaPierre, 759 Chestnut St, Springfield MA 01107.

Radiological Society of Connecticut, Inc. Secretary, Gerald L. Baker, 85 Jefferson St, Hartford CN 06106.

Delaware

Delaware Chapter of ACR. Secretary, Ekkehard S. Schubert, Wilmington Medical Center, PO Box 1951, Wilmington DE 19899.

District of Columbia

Section on Radiology, Medical Society of the District of Columbia. Secretary-Treasurer, Albert M. Zelna, 21 Masters St, Potomac MD 20854.

Florida

The Florida Radiological Society, Chapter of ACR. Secretary, John T. Johnson, P.O. Box 2075, Sanford FL 32771.

The Florida West Coast Radiological Society, Inc. Secretary-Treasurer, M. Silbiger, 1 Davis Blvd, Suite 103, Tampa, FL 33606.

Greater Miami Radiological Society. Secretary, Kenneth D. Keusch, 6201 S.W. 112th St., Miami FL 33156.

North Florida Radiological Society. Secretary, Charles E. Bender, 1430 16th Ave S, Jacksonville Beach FL 32250.

Northeast Florida Radiological Society. Secretary, O. L. Jeter Jr, Orange Park Community Hospital, Orange Park, FL 32073.

Georgia

Atlanta Radiological Society. Secretary-Treasurer, James H. Larose, Dept of Nuclear Medicine, South Fulton Hospital, East Point GA 30344.

Georgia Radiological Society, Chapter of ACR. Secretary, T. Vanderzalm, Medical College of Georgia, Augusta, GA 30902.

Hawaii

Hawaii Radiological Society, Chapter of ACR. Secretary-Treasurer, N. T. Ikemoto, 1350 Ala Moana Blvd, #2007, Honolulu, HI 96814.

Illinois

Chicago Radiological Society, Division of the Illinois Radiological Society, Chapter of ACR. Secretary-Treasurer, Harold J. Lasky, 55 E Washington St, Suite 1735, Chicago IL 60602.

Illinois Radiological Society, Inc., Chapter of ACR. Secretary, Robert D. Dooley, Hinsdale Medical Center, Hinsdale IL 60521.

Indiana

Indiana Roentgen Society of ACR. Secretary, R. F. Fox, Duemling Clinic, 2828 Fairfield Ave, Fort Wayne, IN 46807.

Tri-State Radiological Society. Secretary, Thomas Harmon, St. Mary's Hospital, Evansville IN 47750.

Iowa

Iowa Radiological Society, Chapter of ACR. Secretary-Treasurer, Dale L. Roberson, 1948 First Ave NE, Cedar Rapids IA 52402.

Kansas

Kansas Radiological Society, Chapter of ACR. Secretary-Treasurer, Ralph H. Baehr, 310 Medical Arts Bldg, Topeka KA 66604.

Kentucky

Bluegrass Radiological Society. Secretary-Treasurer, James King, 3313 Overbrook Dr, Lexington KY 40504.

Kentucky Chapter of ACR. Secretary-Treasurer, John Hummel, Jr., Kentucky Baptist Hospital, Louisville KY 40204.

Louisiana

Ark-La-Tex Radiological Society. Secretary, Erich K. Lang, Confederate Memorial Medical Center, LSU School of Medicine, Shreveport LA 71101.

Louisiana Radiological Society, Chapter ACR. Secretary-Treasurer, Stover L. Smith, 250 Vincent Ave, Metairie LA 70005.

Secton on Radiology, Southern Medical Association. Secretary, Michael Sullivan, 1514 Jefferson Highway, New Orleans LA 70121.

Maine

Maine Radiological Society, Chapter of ACR. Secretary-Treasurer, Peter E. Giustra, Dept of Radiology, Penobscot Bay Medical Center, Rockland ME 04841.

Maryland

Maryland Radiological Society, Chapter of ACR. Secretary, S. M. Goldman, Sinai Hospital of Baltimore, Belvedere at Greenspring Avenues, Baltimore, MD 21215.

Massachusetts

Massachusetts Radiological Society, Chapter of ACR. Secretary, Alan H. Robbins, 150 S. Huntington Ave., Boston MA 02130.

New England Roentgen Ray Society. Secretary, Melvin E. Clouse, 185 Pilgrim Rd, Boston MA 02115.

Northeastern Society for Radiation Oncology. Secretary, C. C. Wang, Massachusetts General Hospital, Boston MA 02114.

Michigan

Michigan Radiological Society, Chapter of ACR. Secretary-Treasurer, Francis P. Shea, Bon Secours Hospital, 468 Cadieux, Grosse Pointe MI 48230.

Michigan Society of Therapeutic Radiologists. Secretary-Treasurer, William T. Knapp, St. Mary's Hospital, 830 S Jefferson, Saginaw MI 48601.

Minnesota

Minnesota Radiological Society, Chapter of ACR. Secretary-Treasurer, J. B. Marta, 125 W. College Ave, St. Paul, MN 55102.

Missouri

Greater Kansas City Radiological Society. President-Secretary, R. W. Lambie, Suite 108 Doctors Bldg West, 701 E 63d, Kansas City MO 64110.

Greater St. Louis Society of Radiologists. Secretary-Treasurer, William B. Hutchinson, 2821 Ballas Rd, St. Louis MO 63131.

Missouri Radiological Society, Chapter of ACR. Secretary-Treasurer, E. M. Herman, 701 E. 63rd St., Kansas City, MO 64110.

Mississippi

Mississippi Radiological Society, Chapter of ACR. Secretary-Treasurer, James B. Barlow, 514B E Woodrow Wilson, Jackson MS 39216.

Montana

Montana Radiological Society. Secretary-Treasurer, E. Drouillard, St. Patrick Hospital, Missoula, MT 59801.

Nebraska

Nebraska Chapter of ACR. Secretary-Treasurer, W. H. Northwall, Good Samaritan Hospital, Kearney, NB 68847.

New Hampshire

New Hampshire Chapter of ACR. Secretary-Treasurer, Edward P. Kane, Claremont General Hospital, Claremont NH 03743.

New Jersey

Radiological Society of New Jersey, Chapter of ACR. Secretary, Milton Gallant, 2424 Morris Ave, Union NJ 07083.

New Mexico

New Mexico Society of Radiologists, Chapter of ACR. Secretary, W. M. Jordan, 1100 Central Ave SE, Albuquerque NM 87106.

New York

Bronx Radiological Society, New York State, Chapter of ACR. Secretary-Treasurer, Leon J. Corbin, 1369 Rosendale Ave, Bronx NY 10472.

The Brooklyn Radiological Society. Secretary-Treasurer, E. Arida, 450 4th Ave, Brooklyn, NY 11215.

Buffalo Radiological Society. Secretary, Jerald P. Kuhn, 9267 Jennings Rd, Eden NY 14057.

Central New York Radiological Society. E. Mark Levinsohn, Radiology Dept, Upstate Medical Center, 750 E Adams St, Syracuse NY 13210.

Kings County Radiological Society. Secretary, Melvin Moore, 7815 Bay Parkway, Brooklyn NY 11214.

Long Island Radiological Society. Secretary, A. Trachtenberg, 117 Mt. Grey Road, Setauket, NY 11733.

Mid-Hudson Radiological Society. Secretary-Treasurer, William D. Stiehm, 37 Flower Hill Rd, Poughkeepsie NY 12603.

New York Roentgen Society. Secretary-Treasurer, Thomas C. Beneventano, 111 E 210th St, Bronx NY 10467.

New York State Chapter of ACR. Secretary-Treasurer, Albert F. Keegan, 6 Secor Dr, Port Washington NY 11050.

Northeastern New York Radiological Society. Secretary, Donald R. Morton, Dept of Radiology, St. Claire's Hospital, Schenectady NY 12304.

Rochester Roentgen Ray Society. Secretary-Treasurer, R. Hainen, 4 Sugarwood Drive, Rochester, NY 14534.

Westchester County Radiological Society. Secretary, Leonard Cutler, 16 Guion Pl, New Rochelle NY 10802.

Nevada

Nevada Radiological Society, Chapter of ACR. Secretary, Charles F. Veverka, Carson Tahoe Hospital, Carson City NV 89701.

North Carolina

Catawba Valley Radiological Society. Secretary, J. N. Owsley, 18 13th Ave. NE, Hickory NC 28601.

North Carolina Chapter of ACR. Secretary-Treasurer, M. A. Jones, Durham County Hospital, Durham, NC 27705.

Southeastern Chapter Society of Nuclear Medicine. Secretary, V. J. Sodd, University of Cincinnati Medical Center, Cincinnati, OH 45267. Annual Meeting: 1977, Oct 12–15, Hyatt House and Benton Convention and Civic Center, Winston-Salem, N.C.

North Dakota

North Dakota Radiological Society, Chapter of ACR. Secretary, H. C. Walker Jr., PO Box 624, Devils Lake, ND 58301.

Ohio

Cleveland Radiological Society. Secretary-Treasurer, John B. McCoy, Elyria Medical Arts Bldg, Suite 12, Elyria OH 44035.

Greater Cincinnati Radiological Society. Secretary-Treasurer, C. D. Eversole, 722 Scott St, Covington, KY 41011.

Northwestern Ohio Radiological Society. Secretary, Gerald Marsa, 3939 Monroe St, Toledo OH 43606.

Ohio State Radiological Society, Chapter of ACR. Secretary, W. Howland, Aultman Hospital, 2600 Sixth St, S.W., Canton, OH 44710.

Oklahoma

Northwestern Oklahoma Radiological Society. Secretary, William L. Lavendusky, 100 Center Plaza Suite C, Tulsa OK 74119.

Oklahoma State Radiological Society, Chapter of ACR. Secretary, Bob G. Eaton, 2508 Stillmeadow Rd, Edmond OK 73034.

Oregon

Oregon State Radiological Society, Chapter of ACR. Secretary-Treasurer, Ray F. Friedman, 3324 SW 44th St, Portland OR 97221.

Pennsylvania

Pennsylvania Radiological Society. Secretary, Joseph A. Marasco, Jr., St. Francis Hospital, Pittsburgh PA 15201.

Philadelphia Roentgen Ray Society. Secretary, Marvin E. Haskin, 230 N Broad St, Philadelphia PA 19102.

Pittsburgh Roentgen Society. Secretary, Ronald J. Clearfield, Citizens General Hospital, 651 Fourth Ave, New Kensington PA 15068.

Rhode Island

Radiological Society of Rhode Island, Chapter of ACR. Secretary, Stefan Frater, Rhode Island Hospital, Providence RI 02902.

South Carolina

South Carolina Radiological Society, Chapter of ACR. Secretary, George W. Brunson, 4315 Woodleigh Rd, Columbia SC 29206.

Tennessee

Memphis Roentgen Society. Secretary-Treasurer, D. Randolph Ramey, Baptist Memorial Hospital, 899 Madison Ave, Memphis TN 38140.

Tennessee Radiological Society, Chapter of ACR. Secretary-Treasurer, Jerry W. Grise, Methodist Hospital, 1265 Union Ave, Memphis TN 38104.

Texas

Central Texas Radiology Society. Secretary-Treasurer, E. Jerome Schoolar, Scott and White Clinic, Temple TX 76501.

Dallas-Fort Worth Radiological Society. Secretary-Treasurer, J. H. Arndt, P.O. Box 26592, Dallas, TX 75226.

Houston Radiological Society. Secretary, Thomas S. Harle, 103 Jesse H. Jones Library Bldg, Texas Medical Center, Houston TX 77030.

Louisiana-Texas Gulf Coast Radiological Society. Secretary-Treasurer, B. A. King, Jr., PO Box 3008, Port Arthur TX 77640.

San Antonion Civilian Military Radiological Society. Secretary, Jose Maria Chao, Diagnostic Clinic, San Antonio TX.

Texas Radiological Society, Chapter of ACR. Secretary-Treasurer, Donald N. Dysart, Scott and White Clinic, Temple TX 76501.

Vermont

Vermont Radiological Society, Chapter of ACR. Secretary, Peter Dietrich, Medical Center Hospital of Vermont, Burlington VT 05401

Virginia

Mid-Shenandoah Valley Radiological Society. Secretary, Kenneth L. Dwyer, King's Daughters Hospital, Staunton VA 24401.

Richmond Radiological Society. Secretary, Melvin Vinik, 9504 Carterwood Rd, Richmond VA 23229.

Virginia Chapter of ACR. Secretary-Treasurer, Charles P. Winkler, 3500 Kensington Ave Suite 2–A, Richmond VA 23221.

Washington

Pacific Northwest Radiological Society. Secretary-Treasurer, Kenneth D. Moores, 1118 9th Ave, Seattle WA 98101.

Washington State Radiological Society, Chapter of ACR. Secretary-Treasurer, Donald J. Hesch, 3216 NE 45th Pl, Seattle WA 98105.

West Virginia

West Virginia Radiological Society, Chapter of ACR. Secretary-Treasurer, Andrew W. Goodwin II, 200 Medical Arts Bldg., Charleston WV 25301.

Wisconsin

Milwaukee Roentgen Ray Society. Vice President, Thomas C. Lipscomb, 1004 N 10th St, Milwaukee WI 53233.

Society of Nuclear Medicine, Central Chapter. G. J. Weir, Jr., Marshfield Clinic, Marshfield, WI 54449. Fall meeting: Oct. 1, 2, 1977, Radionuclides and Endocrinology/Metabolism.

Wisconsin Radiological Society, Chapter of ACR. Secretary-Treasurer, June Unger, Wood VA Hospital, Wood WI 53193.

Wisconsin Society of Therapeutic Radiologists. Secretary, M. Greenberg, Milwaukee County General Hospital, 8700 W Wisconsin Ave, Milwaukee WI 53222.

Wyoming

Wyoming Radiological Society, Chapter of ACR. Secretary, Thomas E. Hettinger, 1609 E 19th St, Cheyenne WY.

Canada

Canadian Association of Radiologists. Honorary Secretary, C. Germain Beauregard, Suite 806 1440 St., Catherine St W, Montreal, Quebec, Canada H3G 1R8.

Edmonton and District Radiological Society. Secretary, B. Caplan, 12320 103rd Ave, Edmonton, Alberta T5N ORZ, Canada.

Toronto Radiological Society. Secretary, H. Shulman, Sunnybrook Hospital, 2075 Bayview Avenue, Toronto, Ontario, Canada.

Central and South America

Asociacion Costarricense de Radiologia. Secretary, F. A. Arguedas Haug, Apartado 8-5340, San Jose, Costa Rica.

Colegio Brasileiro de Radiologia. Secretary-General L. C. C. Teixeira, 01311 Avenida Paulista, 491, 13th Floor, cj. 132, São Paulo, Brazil.

Sociedad Childena de Radiologia. Secretary, Manuel Neira, Casilla 13426, Santiago, Chile.

Sociedad Colombiana de Radiologia. Secretary-General, Gustavo Sanchez Sanchez, Bogota, Colombia.

Sociedad de Radiologia del Atlantico. Secretary, Raul Fernandez, Calle 40 #41-110, Baranquilla, Colombia.

Sociedad de Radiogia. Radiotherapéutica y Medicine Nuclear de Rosario. Secretary-General Marcela Muñoz, Santa Fe 1798, Rosario, Argentina.

Europe

Bavarian-American Radiologic Society. Secretary, Stuart A. O'Byrne, Radiology Service, Stuttgart, West Germany, 5th General Hospital, APO NY 09154.

British Institute of Radiology. Honorary Secretaries, D. H. Trapnell, P.N.T. Wells, 32 Welbeck St, London, W1M/7PG, England.

Cekoslovenská Radiologická Spolećnost. Secretary, Jaromir Kolar Radiological Clinic, Parha 2, Unemocnice 2, Czechoslovakia.

Danish Radiological Society. Secretary General, Johannes Praestholm, Radiological Department I, Bispebjerg Hospital, DK-2400, Copenhagen NV.

Deutsch Röntgengesellschaft. President, Wolfgang Frik, Dept of Radiology, Techn Univ Aachen, D-5100 Aachen, Goethestrasse 27/29, West Germany.

European Society of Paediatric Radiology. Permanent Secretary, C. Fauré, Service de Radiologie, Hôpital des Enfants Malades, 149, rue de Sèveres—75730 Paris Cedex 15, France.

Faculty of Radiologists (of Ireland). Honorary Secretary, M. Ryan, Faculty of Radiologists, Royal College of Surgeons in Ireland, Stephen's Green, Dublin 2, Ireland. Annual meeting and scientific symposium: Oct 7, 8, 1977.

The Hospital Physicists' Association. Honorary Secretary R. F. Mould, Westminster Hospital, Physics Department, Page St. Wing, London SW1P2AR, England.

Norsk Forening for Medicinsk Radiologi. General Secretary, Arnulf Skjennald, Ullevål sykehus, Oslo, Norway.

Nederlandse Vereniging voor Radiologie. Secretary, H. E. Schütte, Department of Radiology, Elizabeth Gasthuis, Haarlem, Netherlands.

Royal College of Radiologists. Secretary, P. D. Thomson, 28 Portland Pl, London, W1N4DE, England.

Scandinavian Radiological Society. Secretary-General, C-E. Unnérus, Havsvindsv. 5C., 02120 Esbo 12 (Hagalund-Tapiola) Finland.

Schweizerische Gesellschaft für Radiologie und Nuklearmedizin. Societe Suisse de Radiologie et de Medecine Nucleaire. Secretary, Gustav A. Schoch, 7 Gellerstrasse, CH—4052 Basel, Switzerland.

Sociedad Española de Radiologia y Electrologia Médicas y de Medicina Nuclear. Secretary-General, Pilar Gallar Barberá, Villanueva, Madrid 1, Spain.

Societá Italiana di Radiologia Medica e Medicina Nucleare. Administrative Secretary, R. Dall'Acqua, Ospedale Mauriziano, 10128, Torino, Italy.

Sociéte Française de Radiologie Médicale, Médecine Nucléaire et Electrologie. Secretary-General, J. Sauvegrain, Hôpital des Enfants-Malades, 149 Rue de Sèvres, 75730 Paris Cedex 15, France. Annual Meeting: 1977, Nov 15–18, Centre International de Paris.

Société Francaise de Neuroradiologie. Secretary-General, R. Djindjian, 16, rue de l'Université 75, Paris 7°, France.

Svensk Förening för Medicinsk Radiologi. Secretary, Hans Ringertz, Department of Pediatric Radiology, Karolinska Sjukhuset, S–104 01 Stockholm, Sweden.

Africa

Association of Radiologists of West Africa. Honorary Secretary, A. A. Obisen, Department of Radiology, University College Hospital, Ibadan, Nigeria.

Radiological Society of South Africa. Secretary, Dr. A. Visser, PO Box 8850, Johannesburg, South Africa.

South African International Radiological Congress. Director, Dr. Paul Sneider, PO Box 4878, Johannesburg, South Africa. Durban Annual Congress: Oct 1978, International and National Congress.

Near East and Asia

Bengal Radiological Association. Honorary Secretary, B. Chatterji, 262 Rash Behari Ave, Calcutta 700019, India.

Indian Radiological Association. Honorary General Secretary, S. P. Aggarwal, 10–B Kasturba Ghandi Marg, New Delhi 110001, India.

Indonesian Radiological Society. Secretary, Gani Iljas Sasmitaatmadja, Radiology Department, Faculty of Medicine, University of Indonesia. Salemba 6, Jakarta, Indonesia.

Iranian Radiological Society. Secretary Majid Rooholamini, PO Box 14–1151.

Philippine College of Radiology. Secretary-Treasurer, Antonio Chavez, Box 1284, Commercial Center, Makati, Rizal, D–708, Philippines.

Radiological Society of Thailand. Secretary, Dusdee Prabbasawat, Department of Radiology, Siriraj Hospital Faculty of Medicine, Mahidol University, Bangkok 7, Thailand.

Royal Australasian College of Radiologists. Honorary Secretary, T. P. Loneragan, 45 Macquarie St, Sydney NSW 2000, Australia. Annual Meeting: Sept 16–20, 1977, Gold Coast via Brisbane.

American Journal of Roentgenology

Please enter my subscription as follows:

Beginning with ____________, ____________.
month year

Name ____

Street Address ______________________________________

City and State ______________________ Zip Code ____________

My specialty is ______________________

Send gift subscription for ____________ years to:

Beginning with ____________, ____________.
month year

Name ____

Address ____

City and State ______________________ Zip Code ____________

Specialty: ______________________

Enclosed is $ ____________

Subscription rates are: $40 for the United States and possessions; others, $50; residents in training in U.S., $20 (letter required from institution).

Please send this form and remittance to: Charles C Thomas, Publisher, 301-327 East Lawrence Avenue, Springfield, Illinois 62717

Special Subscription Rate for Residents

At the 1976 meeting of the American Roentgen Ray Society, a special $20 subscription fee to this journal was approved for radiology residents training in U.S. institutions. To obtain this special rate, residents should accompany their applications and checks with a letter from their department chairmen certifying they are residents in approved training programs. All subscriptions should be sent to Charles C Thomas, publisher, 301-327 East Lawrence Avenue, Springfield, Illinois 62717.

This rate is intended to help the beginning resident start a library of significant literature early in his career. The rate represents a substantial subsidy by the society, and it is hoped that residents will take advantage of a program intended to enhance their educational experience. Some departments have indicated plans to provide a journal subscription as an additional benefit for their residents. With the new low rate, this would appear to be a very feasible program. The special price is limited to the period of resident training.

The *American Journal of Roentgenology* is pleased to offer this significant educational subsidy and would be gratified if every resident in this country were to take advantage of it.

Raymond A. Gagliardi
Chairman, Publications Committee

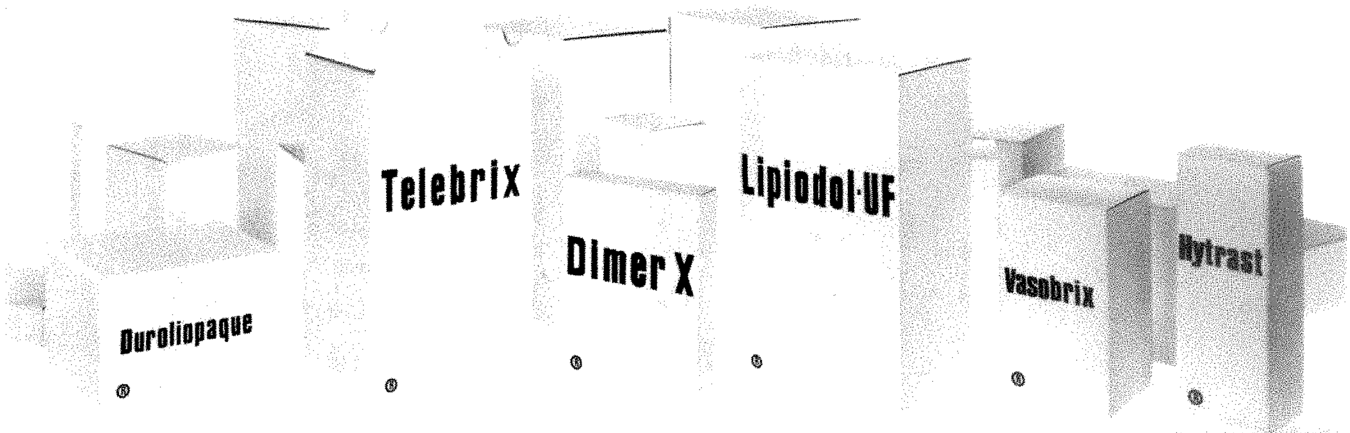

WE MANUFACTURE

contrast

MEDIA

OUR

products

ARE

known

WORLD-WIDE

OUR

name isn't

GUERBET

BETTER CONTRAST MEDIA THROUGH RESEARCH

Laboratoire Guerbet, 16/24, rue Jean-Chaptal
93601 AULNAY-SOUS-BOIS Cedex - FRANCE
Telex : Guerbet 690682

Next time you think a CT salesman is playing games...

Ask him to play 20 Questions.

Consider these 20 key questions before you select a CT system:	GE					
	YES	NO	YES	NO	YES	NO
1. Are images consistently free of streak artifacts caused by motion (voluntary and involuntary), without the need for water bags or bean bags?	✓					
2. Are the "sample images" taken from a BRH compliant unit?	✓					
3. Is the scanner a production model—not a prototype—so it's eligible for third party reimbursement?	✓					
4. Does the scanner comply with the Medical Devices Act?	✓					
5. Are fast-scan production models now at clinical sites for visitations?	✓					
6. Does x-ray photon capture exceed 85%, to preclude needless patient radiation exposure?	✓					
7. Are nationwide service and engineering available?	✓					
8. Are future upgrades possible via software?	✓					
9. Is comprehensive financing offered *directly* through the manufacturer?	✓					
10. Does system reliability provide clinical availability on the order of 95%?	✓					
11. Can viewing and reconstruction occur simultaneously?	✓					
12. Is detector life sufficient to avoid regular detector replacement and resultant increased operating cost?	✓					
13. Is the system safe? Has it obviously been designed with patient and operator safety in mind?	✓					
14. Is average installation time 3 weeks or less?	✓					
15. Is complete in-service training provided at no extra cost?	✓					
16. Do head scans show clear bone/brain interface without "undershooting?"	✓					
17. Is a planned maintenance service contract available?	✓					
18. Does the manufacturer have a long-standing reputation in medical systems—to understand departmental and hospital needs?	✓					
19. Are such basic features as tilting gantry, auto technic determination, external and internal alignment lights and 60 cm gantry aperture provided?	✓					
20. Does the system include other desirable features such as complete diagnostics, coronal and saggital reconstruction, multiformat camera, 200 slice disc drive and variable slice thickness?	✓					
TOTAL	20	0				

General Electric Medical Systems, Milwaukee, Toronto, Madrid.

GENERAL ELECTRIC

PET-TV
from Diagnostic Information, Inc.

Diagnostic Information knows that there are two major requirements in fluoroscopy: a high quality fluoroscopic image and lower x-ray dose rates. Our new PET-TV gives you both. It gives you superb quality diagnostic images at a very low dose. With a properly filtered x-ray beam, the dose rate at the table top averages around 1.5 R/min. for adult patients.

The new PET-TV system benefits from our original breakthrough in image intensifiers: The Panel Electron Tube. This revolutionary PET-intensifier makes better use of the available x-ray photons, just as it does in the PET-Scope. We developed our PET-TV by adding a high quality TV system with a SIT tube in the TV camera.

The SIT tube is not an untried novelty; it's the tube used in Apollo space missions, selected for its outstanding reliability and low-light performance.

The PET system gives you clear, low-lag and low-noise images at low-dose levels. And you still retain the option of direct viewing.

The system adapts to most any spot film device; it's light, maneuverable, compact, and generally requires no overhead suspension. It's just what you—and your patients—deserve.

write or phone. We'll be glad to supply the details.

Diagnostic Information Incorporated
246 Sobrante Way, Sunnyvale,
California 94086.
Phone: (408) 736-3500.

Diagnostic Information Incorporated

See the PET-TV
at ARRS booth 60.

They deserve a lower dosage.

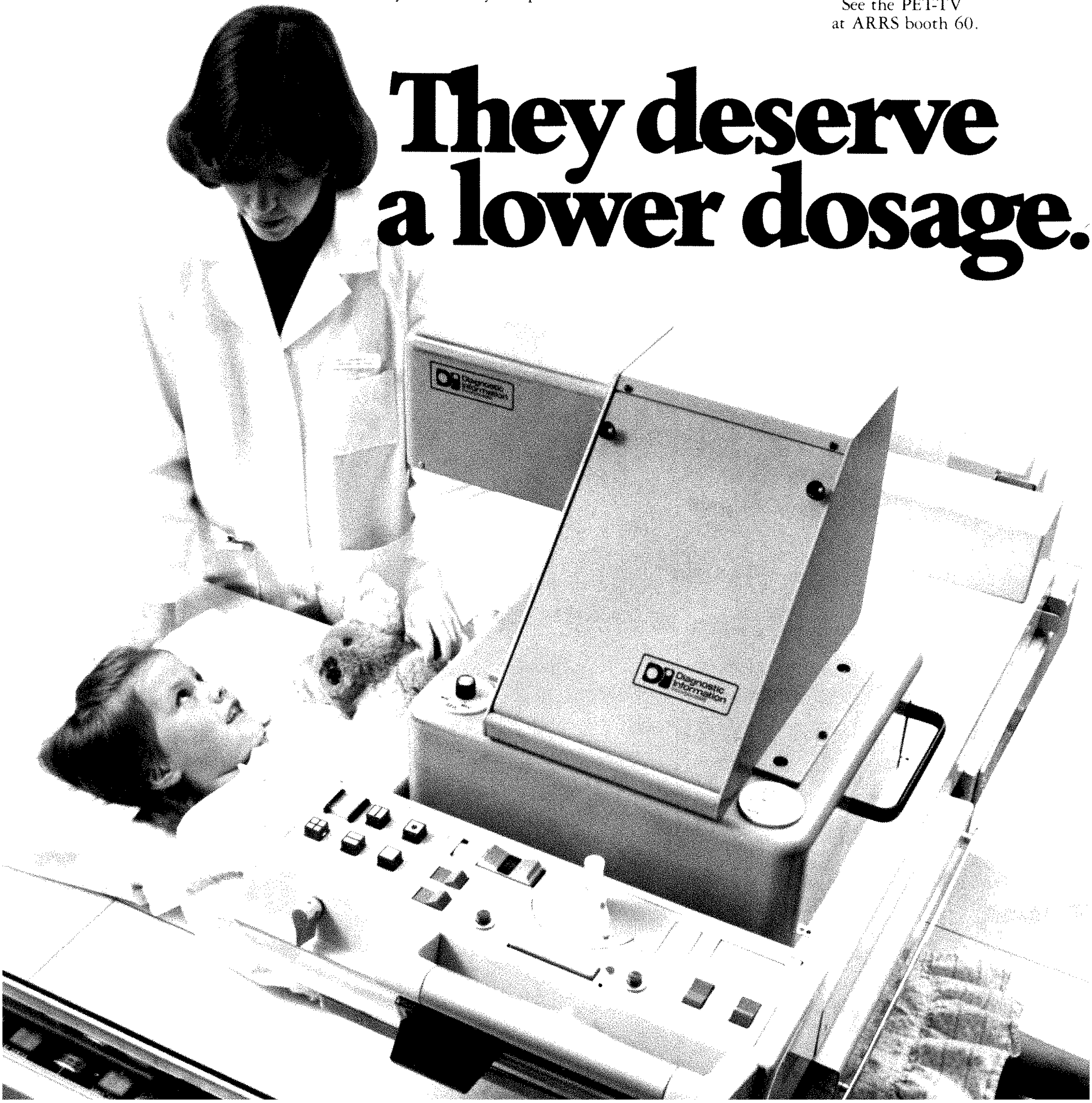

CHARLES C THOMAS • PUBLISHER

XERORADIOGRAPHY: Uncalcified Breast Masses *by* **John N. Wolfe,** *Hutzel Hospital, Detroit, Michigan.* Information and graphic material are presented which will assist the radiologist in arriving at a reasonable differential diagnosis when confronted with uncalcified breast masses. The order of presentation proceeds from the obvious malignancies characterized by a mass with a well-developed spiculated margin, through the subtler circumscribed carcinomas such as the medullary or colloid variety, to those most difficult ones which do not present a well-defined mass but merely an area of increased density. Benign tumors are also considered in detail. This section illustrates the classic types of pathology followed by examples of variations. Medical students, radiology residents and practicing radiologists who have, at some time in their career, encountered problems in the differential diagnosis of breast tumors will find this volume to be an invaluable supplement to standard mammography texts. *'77, 208 pp. (8 1/2 x 11), 307 il., $28.00*

AN ATLAS OF POLYTOME PNEUMOGRAPHY *by* **Taher El Gammal** *and* **Marshall B. Allen, Jr.,** *both of Medical College of Georgia, Augusta. Assisted by* **Paul Dyken.** This atlas presents a large number of studies which supplement the study of normal anatomy of the cerebrospinal fluid pathways, and provides comparison for the identification of abnormal structures. Concentration is on the findings of polytome pneumography but, where possible, correlations are made with angiography, positive contrast ventriculography, and CAT examinations. Relative values of these different examinations are demonstrated. *'77, 480 pp. (8 1/2 x 11), 729 il., $39.50*

NON-INVASIVE METHODS IN CARDIOLOGY *edited by* **Samuel Zoneraich,** *State Univ. of New York, Stony Brook. (25 Contributors)* In emphasizing bedside cardiology, this book presents a comprehensive and current review of the basic concepts, physiologic correlates, necessary equipment and practical interpretation of non-invasive techniques. Such topics as phonocardiography, systolic time intervals, nuclear cardiology, congenital heart disease, and echocardiography are discussed. With numerous photographs, tracings, illustrations and bibliographic references, this volume will interest the practicing physician, medical student, intern and resident. *'75, 596 pp. (6 3/4 x 9 3/4), 396 il., 18 tables, $35.50*

INDICATIONS AND ALTERNATIVES IN X-RAY DIAGNOSIS: A Guide to the Effective Employment of Roentgenologic Studies in the Solution of Diagnostic Problems (2nd Ed.) *by* **Melvyn H. Schreiber,** *Univ. of Texas Medical Branch, Galveston.* This illustrated volume describes and depicts the various kinds of roentgenologic examinations available for the unravelling of diagnostic problems. It is divided into chapters based on organ systems, with common abnormalities illustrated. The emphasis is on providing the reader with a thorough background in the uses to which ordinary and special x-ray studies may be put, with alternatives presented when the indicated examinations cannot be performed or when more than one kind of examination is available for the solution of a specific problem. Indications and contraindications are carefully defined. *'74, 192 pp., 98 il., $11.50, paper*

KINESIOLOGY: Of the Human Body Under Normal and Pathological Conditions (5th Ptg.) *by* **Arthur Steindler,** *State Univ. of Iowa, Iowa City.* This comprehensive study of the mechanics of joint function covers general kinetics, the trunk and spine, the extremities, and the gait. The author emphasizes the clinical significance and practical applications of kinetic findings. *The Journal of Bone and Joint Surgery* said, "No physician or educator who deals with the musculoskeletal system can consider his library complete without this brilliant treatise." *'77, 736 pp. (6 1/2 x 10), 655 il., $24.50*

UROLOGICAL RADIOLOGY OF THE ADULT MALE LOWER URINARY TRACT: Anatomy, Physiology, Pathology and Sequelae, Diagnosis and Management *by* **R. W. McCallum** *and* **V. Colapinto,** *both of St. Michael's Hospital, Toronto, Ontario, Canada.* This monograph outlines the authors' personal experience with over 1000 radiological examinations of the urethra and 240 two-stage urethroplasties. Pre- and postoperative radiological urethrographic examinations and the surgical repair of membranous urethral strictures are detailed. Radiological examinations of the bladder, prostate and urethra are extensively discussed and the literature is reviewed in detail with over 330 references and over 250 original radiographs and illustrations. A description of the neurogenic bladder is provided and a new method of radiological examination of the lower urinary tract in paraplegics is described. *'76, 376 pp. (6 3/4 x 9 3/4), 248 il., 2 tables, $35.50*

THE BASIC PHYSICS OF RADIATION THERAPY (2nd Ed.) *by* **Joseph Selman,** *Univ. of Texas, Austin.* This new Second Edition has been completely updated. All obsolete material has been eliminated and several chapters have been rearranged. The general format, however, remains essentially unchanged. A separate section has been added to cover electron beam therapy and a new chapter has been introduced to deal with the growing interest in radiotherapy with heavy particles. Chapters covering radionuclides have been reworked and made more comprehensive, as has the section on radiation protection. Major emphases remain in such areas as simple mathematics; basic physical concepts; radiation quality, exposure and dosage; therapy planning; new modalities; and radium and radionuclide therapy. Also included are discussions of radiobiology and health physics. *'76, 768 pp., 356 il., 66 tables, $25.75*

PALEOPATHOLOGICAL DIAGNOSIS AND INTERPRETATION: Bone Diseases in Ancient Human Populations *by* **R. Ted Steinbock,** *Harvard Medical School, Boston. Foreword by* **T. Dale Stewart.** The author provides a systematic approach for diagnosing bone lesions in excavated skeletal series and interpreting the significance of such diseases in ancient human populations. Chapters discuss the biology and gross anatomy of normal bone to aid in understanding the bond changes produced by pathological conditions. The major traumatic, infectious, nutritional, metabolic, degenerative and neoplastic diseases of bone are also covered. A special section is devoted to establishing nutritional deficiency as the cause of peculiar lesions found in large numbers of excavated crania. *'76, 440 pp., 274 il., 16 tables, $22.75*

Orders with remittance sent, on approval, postpaid

301-327 East Lawrence Avenue • Springfield • Illinois • 62717

Announcing New

The Clinac® 20 is here–providing new treatment power for today's and tomorrow's radiotherapy techniques. From Varian–leading producer of advanced radiotherapy accelerators.

Clinac 20 treatment power results from innovation in accelerator guide technology and full use of subsystems refined by more than three years of experience.

The Clinac 20 delivers precise high-energy x-rays at 15 MV, and electrons with energies ranging from 6 to 20 MeV at isocenter.

The Clinac 20 is in production–backed by the most experienced factory and field support organization in radiotherapy today.

Write or call Varian Associates, Medical Group,
611 Hansen Way, Palo Alto, CA 94303.
Tel: 415-493-4000.

varian

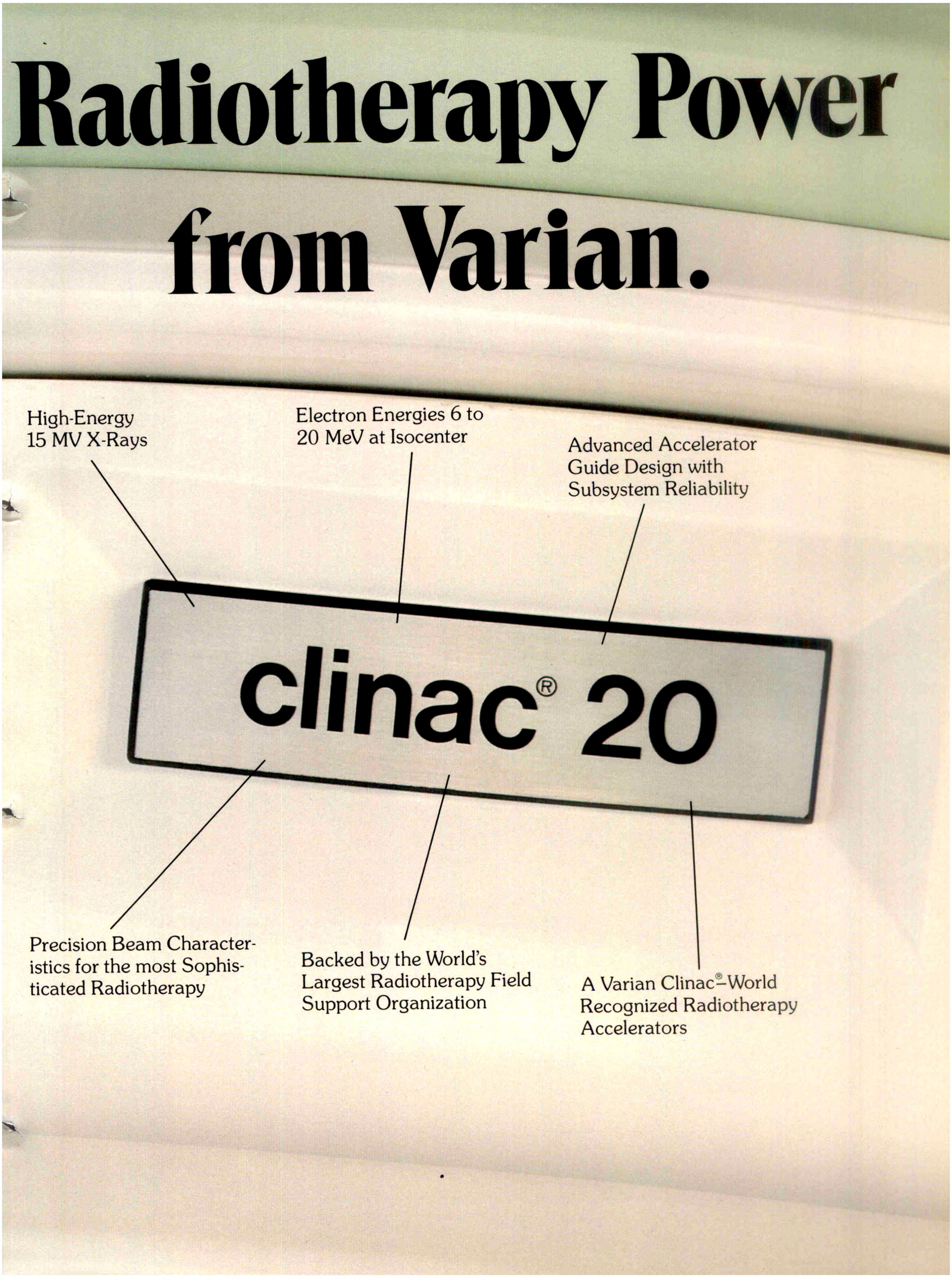

Radiotherapy Power from Varian.

High-Energy
15 MV X-Rays

Electron Energies 6 to
20 MeV at Isocenter

Advanced Accelerator
Guide Design with
Subsystem Reliability

Precision Beam Characteristics for the most Sophisticated Radiotherapy

Backed by the World's
Largest Radiotherapy Field
Support Organization

A Varian Clinac®–World
Recognized Radiotherapy
Accelerators

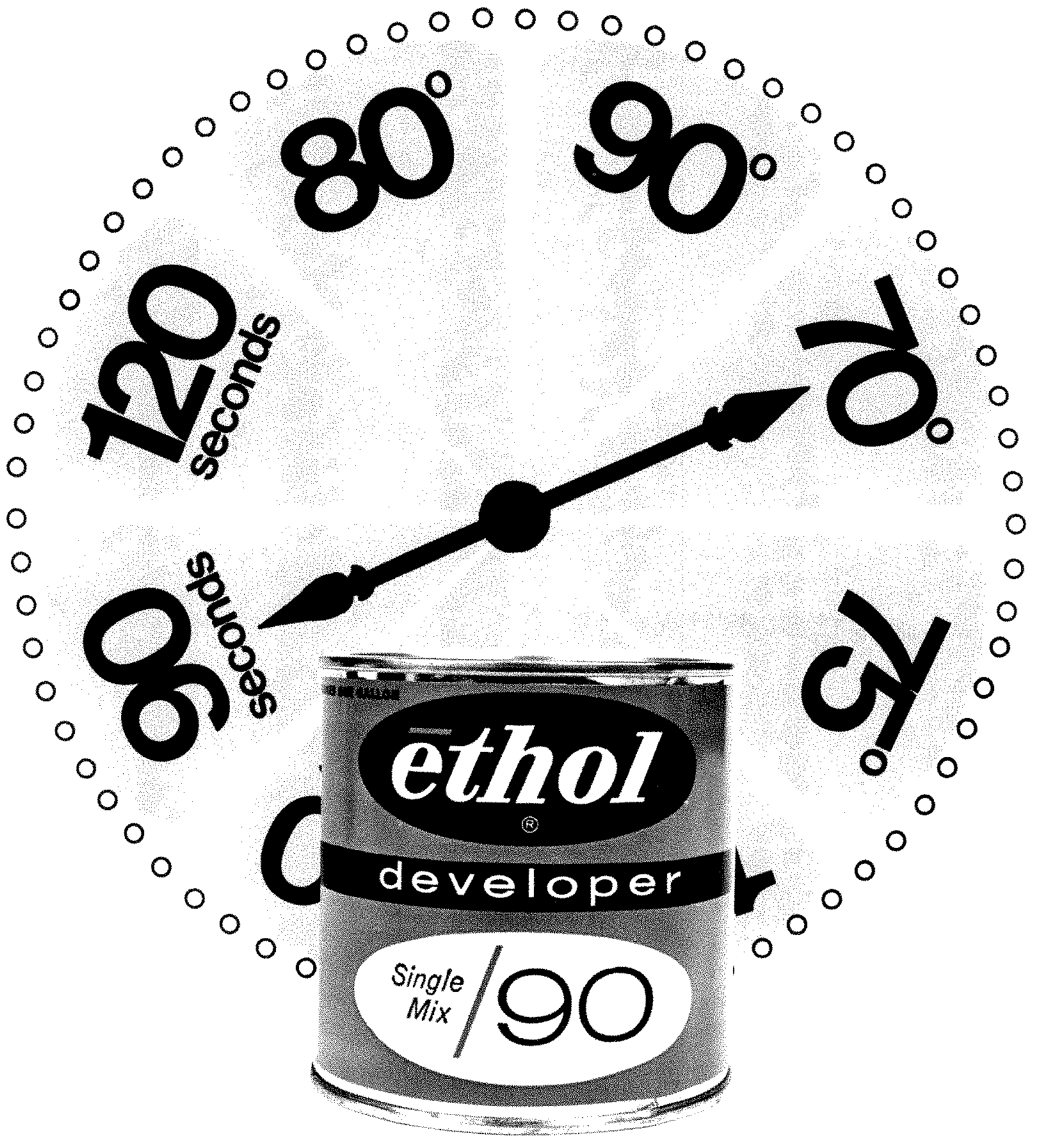

play the numbers game. with ethol 90, you always win.

Ethol 90 is not just another film developer . . . it's the first and original 90-second developer used by leading hospitals the world over and recommended by foremost manufacturers of automatic processors. It is used in an extremely broad range of applications including X-Ray, cineflure, electron microscopy, holography, cardiology and macrophotography.

Do you want to work at 70°, 80°, 90°? Do you want to process for 90, 120 or 180 seconds? Ethol 90 will provide optimum results under all conditions. It is a fine grain, normal contrast, long scale, very rapid working developer. The compensating action in push processing gives a minimum increase in grain, will not block highlights or diminish shadows.

In cineflure film processing radiation factors may be reduced by 50% or more with Ethol 90 and still provide much improved contrast and clearer film base than other developers. Ethol 90 gives a lower tube load, therefore longer life. It works in low gain, borderline image tubes. There is less radiation to doctor and patient and fewer repeat examinations.

Available both powder or liquid form. Replenishers available.
See your X-Ray Supply House or write directly to:

ETHOL CHEMICALS, INC./1808 N. Damen/Chicago, Ill. 60647/(312) 278-1586

ethol

We're living up to our reputation...all over your hospital.

General Electric made a commitment, years ago, to develop and market reliable medical systems that would deliver consistently informative diagnostic images.

And we've lived up to that commitment. First in x-ray equipment, and today in an expanded product line. A line that has grown so much that you may not be fully aware of all the areas where we can help you: computed tomography, nuclear imaging, data processing and handling, and radiological capability that matches a broad range of economic as well as diagnostic considerations.

Your GE medical systems representative has the training and know-how to put all this imaging/information capability to work for you. Ask about the systems that match your needs. Some of them are described on the next few pages.

GE
leading the way in diagnostic imaging...
GENERAL ELECTRIC

The table/spotfilmer of

RFX

1. **Lower dose fluoroscopy** is made practical by the 6:1 ratio fluoroscopic grid. A big improvement over traditional "compromise" 8:1 or 10:1 ratios.
2. **High kVp spotfilms are now practical** with the 12:1 ratio of the 103 line criss-cross grids for greater control over film quality. Now even double contrast studies become routine at traditional table bucky kilovoltages.

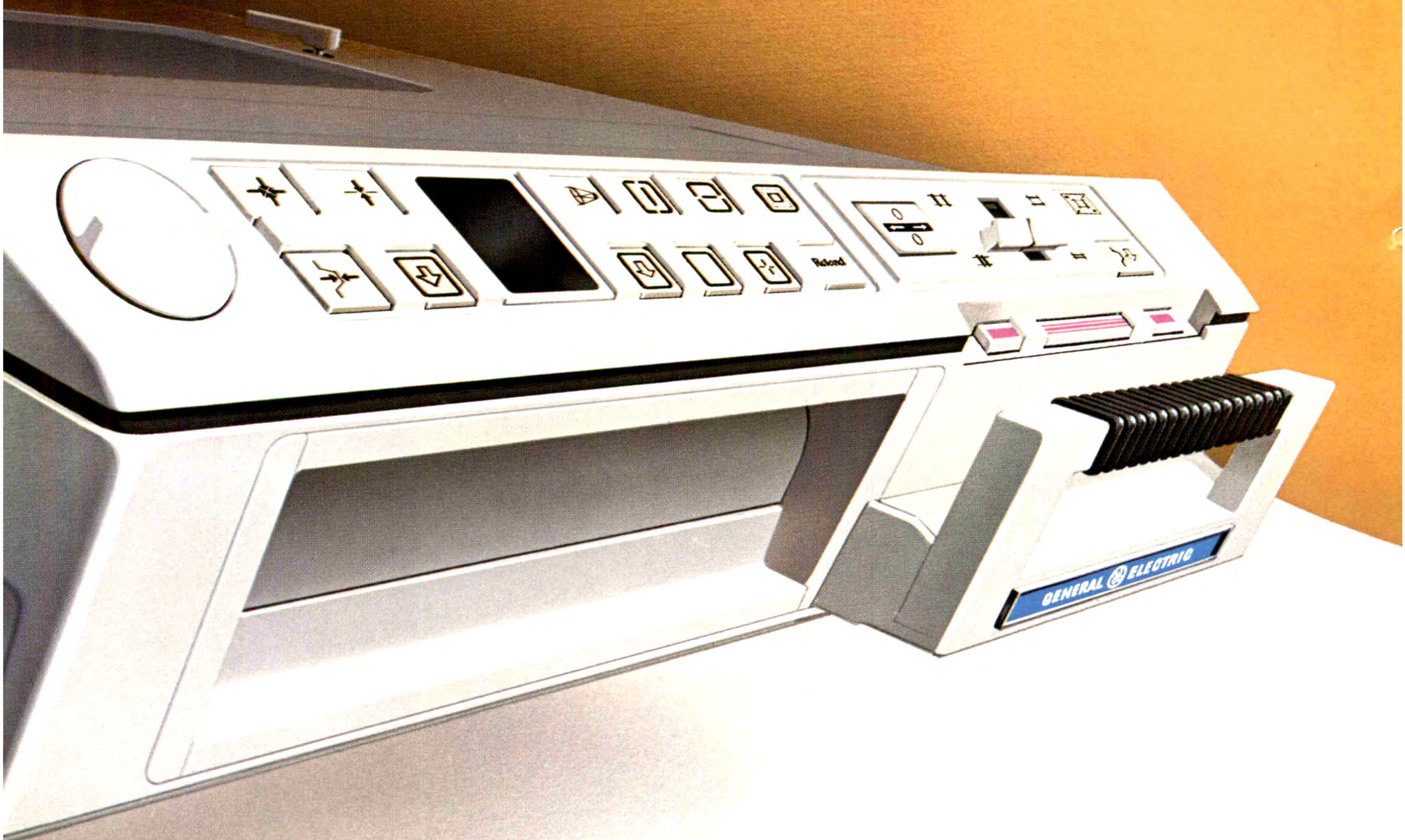

3. **RFX spotfilmer puts total control at your fingertips**—gloves or no gloves.
   - The motorized compression cone control is right up front where you can put your finger on it fast.
   - Coordinated collimator controls are a finger's reach from the positioning handle. Fast-acting collimator blades are servo-positioned.
   - Two-step, prepare-expose switch is positioned for easy left or right hand use and may be used for exposure-delay when held in the first step.
   - The patient positioning control is located adjacent to collimator controls and provides immediate table top response.
   - No more spot counting for the technologist. After the last exposure, cassette moves automatically to the loading position and the RELOAD light signals for a fresh cassette.
   - Positioning ease is provided by a longitudinal power assist with unique direct interactive response.
   - Mini-spot formatting for 6 on 1 or 9 on 1 arthrograms is available.

the future is available today.

4. **Spotfilm exposure starts .75 second after the cassette is called for.** With no shock-induced vibration effect.
5. **Rapid sequence spotfilms are now possible.** Automatic advance with sequence anticipation logic reduces the interval between exposures to approximately .5 second for studies such as cervical esophograms and voiding cystourethrograms.
6. **Front and rear cassette loading** lets you use front loading port when working alone, rear loading port for higher productivity when working with an assistant or when doing myelography.
7. **Masking is automatic with format selection** —no longer must masks and cones be moved into place to achieve a new film format. Full-field fluoroscopy through the compression cone is possible; masking is independent of the cone.
8. **The table angulates smoothly, with soft start and stop,** and full speed of 4½ degrees per second. RFX Thirty angulates to 30° Trendelenburg; RFX Ninety is a full Trendelenburg unit. Choice of 4-way or flat 2-way table top.
9. **The table is designed to take the day-in, day-out abuse** of heavy workloads. Smoothly contoured surfaces clean up easily; controls are sealed for protection against barium spills.
10. **Maxiray™ 100 tube meets the demands of today's procedure schedules;** features forced oil circulation cooling.
11. **Automatic exposure control** is provided by the RFX's thin profile Quantamat™ ion chambers; you get consistent film density from study-to-study.

Get the complete RFX story from your GE representative.
General Electric Medical Systems,
Milwaukee, Toronto, Madrid.

RFX:
why consider
anything
less?

GENERAL ELECTRIC

User-Selectable Constant Load generators from GE let you effectively match kW output to technic.

Up to 40% shorter exposure time plus longer tube life... compared with falling load.

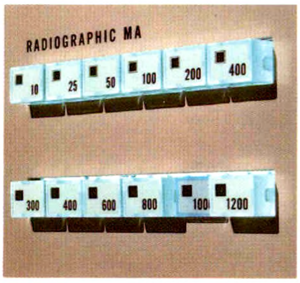

It just makes good economic sense to get all the kW performance you pay for in a generator. From full-rated maximum power down to conservative mA levels, you should be able to exercise your professional judgment in selecting optimum technic for each and every procedure. This is the basis of GE's User-Selectable Constant Load concept.

Consider the facts: The alternative, falling load or "falling kW" generators, in theory begin each exposure at the full rated maximum load. This load then begins to fall off from the initial peak during the exposure. In the latest falling load designs, there is no provision for user control of the initial load applied to the x-ray tube. The installing serviceman adjusts for only one kW setting for the large focal spot and another for the small focal spot*.

At a constant 80 kVp, a tube and generator rated as "100 kW" would have a performance curve like this, in theory:

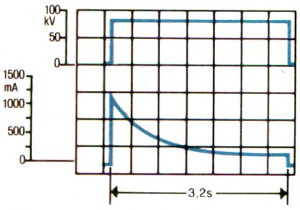

Continuously falling load with constant voltage and falling tube current

However, falling load generators are routinely installed with de-rated initial loads of 85% of rated tube kW, or lower. So, using the constant 80 kVp example, the load curve for a falling load generator would look more like this, in actual practice:

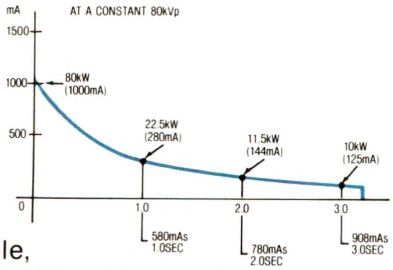

Note that a 1.0 second exposure yields only 580 mAs, even though it started at 1000 mA. In contrast, a GE generator set at 1000 mA will deliver 600 mAs in only 0.6 seconds. In this example, User-Selectable Constant Load is more than 40% faster than falling load.

Using the same example, but assuming that a 1.0 second exposure time is permissible, then a user-selected 600 mA tube load is all that is really needed.

There is no reason to subject the x-ray tube anode to the excessive thermal shock of the full rated maximum load when 600 mA will do the job. Statistically longer tube life will result.

Detail-intensive exams: Falling load applied to the small focal spot also extends exposure times for "detail-intensive" examinations. The technologist—equipped with a falling load generator and faced with a detail requirement that's coupled with a motion-stopping problem—may be forced to use the large focal spot much more often than professional judgment dictates.

Automatic Exposure Control: AEC in falling load generators also results in longer exposure times because of reduced initial load and reduced average power.

Motion-stopping spotfilms: Spotfilming using GE constant load provides the short exposure times you require. Gall bladder spotfilms at lower kVp levels—even using a grid—are practical with constant load. They are "cleaned up" like your table bucky films.

GE User-Selectable Constant Load generators enable you to optimize the power requirements for any technic; any patient situation. That's one of the reasons for GE's worldwide reputation for designing and building dependable high-performance generators. Your GE representative has the facts.

General Electric Medical Systems,
Milwaukee, Toronto, Madrid.

leading the way in diagnostic imaging.

GENERAL ELECTRIC

---

*Constant load settings are routinely provided for tomography and for a breathing technic at low mA only.

COMPUTED TOMOGRAPHY, ULTRASOUND AND X-RAY
AN INTEGRATED APPROACH

January 16-20, 1978

Fairmont Hotel
San Francisco

This problem-oriented course will review the major clinical topics for which more than one useful modality is available to the practicing radiologist. Following a series of comprehensive didactic lectures on the different imaging approaches to each specific clinical problem, a panel of experts will discuss and formulate ways to integrate these modalities into a rational and efficient diagnostic plan. Although the emphasis of this course will be on computed tomography and diagnostic ultrasound, a review of the nuclear medicine, angiographic, and conventional radiologic approaches to each clinical topic will be presented.

THE CLINICAL TOPICS TO BE REVIEWED INCLUDE

Jaundice
Pancreatic mass
Hepatic mass (es)
Renal mass
Adrenal mass
Abdominal abscess
Retroperitoneal Lymphadenopathy

Brain Tumor
Spine and Disc disease
Bone and Soft Tissue masses
Ischemic Heart disease
Pulmonary embolism
Mediastinal mass
Thyroid nodule

This program is presented by the Radiology Research and Education Foundation and Extended Programs in Medical Education, University of California School of Medicine, San Francisco, California. It is acceptable for Category I credit towards the certificate in Continuing Education for the California Medical Association and the American Medical Association.

For further information please contact: Extended Programs in Medical Education University of California, Room 569-U, San Francisco, California 94143 or call (415) 666-4251.

Fee: $300.00 includes hardbound publication of the proceedings
$200.00 residents and interns with letter of verification.

Easier Viewing...faster...

with the NEW S&S MODULAR MOBILE ILLUMINATOR SYSTEM

Here is a unique mobile viewing system that has been designed to provide the best features suggested by Radiologists.

It is most attractive with a formica top that will be an asset in any decor. It can be adjusted to suit individual preferences. The base is strongly constructed and superior to any other base previously available.

Three console styles available.

Bases for all widths 4 to 8 bank wide.
Consoles 19" wide, 24" high, 16" deep.
Top is 1¼" thick, 24" wide.

S. & S. X-RAY PRODUCTS INC.

The Complete Line of X-Ray Accessories

Accessory Catalog on request.
SOLD BY LOCAL X-RAY DEALERS

87-93 JAY STREET, BROOKLYN, N.Y. 11201
Telephone: 212-852-6900

THE DEPARTMENT OF RADIOLOGY
UNIVERSITY OF MINNESOTA

announces

Fortieth Annual Course

SPECIAL IMAGING IN RADIOLOGY

November 14-18, 1977

A five-day comprehensive review
for practicing radiologists,
including

- **Computerized Tomography**
- **Nuclear Radiology**
- **Ultrasound**
- **Mammography**

An authoritative faculty

For further information contact:

Continuing Medical Education
c/o Annual Radiology Course
Box 293 Mayo Memorial Bldg.
University of Minnesota
Minneapolis, Minnesota 55455
Telephone (612) 373-8012

Equal Educational Opportunity

CT Technology of the Future..

The Varian

Go with the right design from the beginning. Varian's 3-Second Whole-Body CT Scanner anticipates the future in CT Scanning. Varian expertise in high-technology medical systems designed the basic features that continue to pave the way. The fan beam geometry with slip-ring gantry coupler design is fundamental. It permits continuous, smooth rotation of the gantry minimizing mechanical wear. It facilitates multi-rotation scanning and stop-action scans. This was recently demonstrated in stop-action heart studies. And it opens the way for direct up-grade.

The pulsed x-ray source permits such advanced techniques as triggering the x-ray pulses with physiological signals.

The Varian Whole-Body CT Scanner design assures you state-of-the-art scanning today and tomorrow.

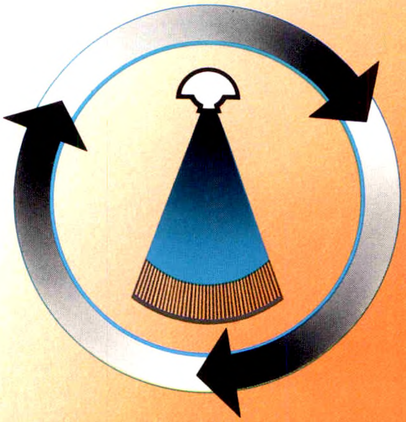

Fan beam design with slip-ring construction permits smooth, non-stop gantry rotation.

Stop-Action Heart Study*

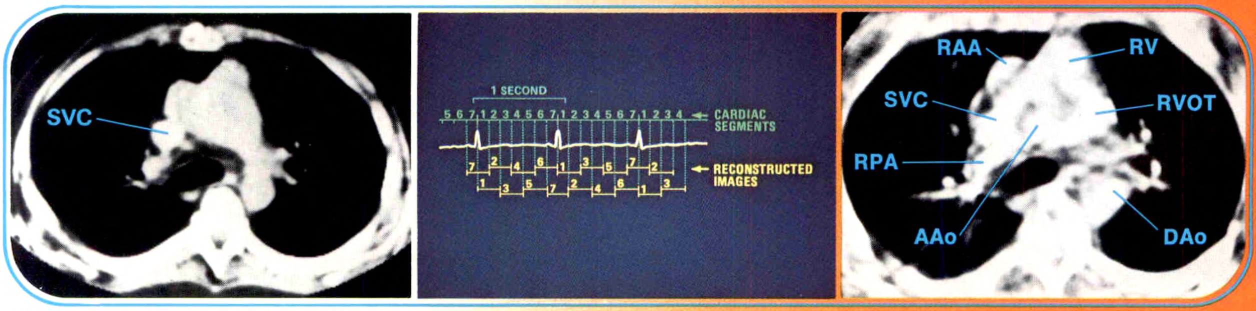

Routine scan of 52-year-old patient during contrast infusion. Only general outline of heart is seen because of cardiac motion. Some contrast, however, can be identified in the superior vena cava (SVC). The right atrium, right ventricle, right ventricular outflow tract, main pulmonary arteries and ascending aorta cannot be distinguished.

Electrocardiogram obtained during CT heart scan (left). Peak R-R interval for each ECG cycle was divided into 7 equal segments.

Stop-action heart scan. Data from the routine scan (far left) was used to reconstruct this stop-action image. The right ventricle (RV), the right ventricular outflow tract (RVOT), the descending aorta (DAo), the ascending aorta (AAo), the right pulmonary artery (RPA), the superior vena cava (SVC), and the right atrial appendage (RAA) are now clearly visible.

For complete information,
write or call:
Medical Group,
Varian Associates,
611 Hansen Way,
Palo Alto, CA 94303.
Tel: 415-493-4000.

The Varian CT Scanner is supported through a highly skilled, experienced high-technology medical equipment sales and service organization.

Right Now!
CT Scanner

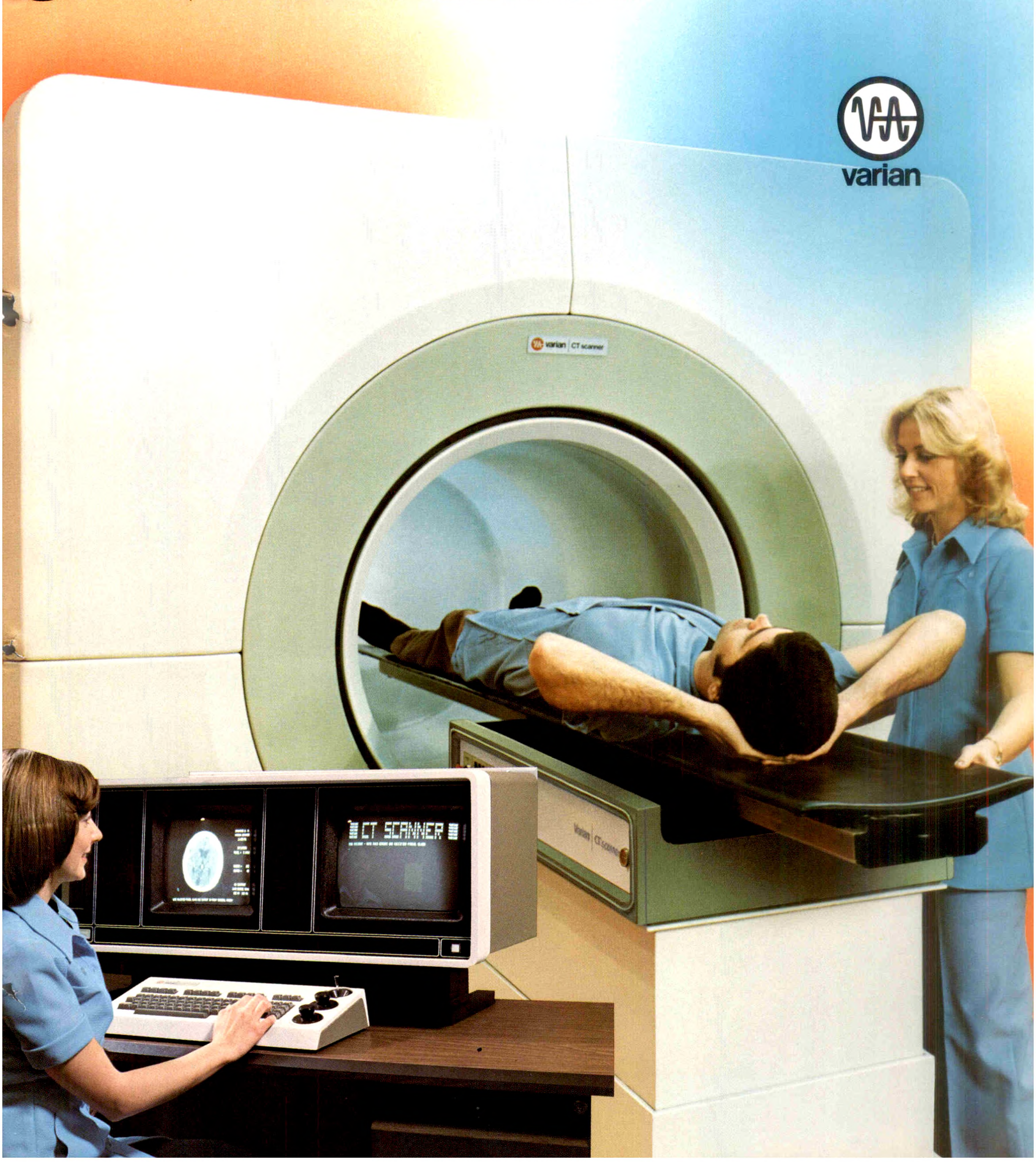

Your decision to buy a CT scanner is an important one...and an expensive one

Before you decide on a CT system...

The New

0200 FS

Whole Body CT System

Pfizer
MEDICAL SYSTEMS, INC.
A SUBSIDIARY OF PFIZER INC.
9052 Old Annapolis Road
Columbia, MD 21045

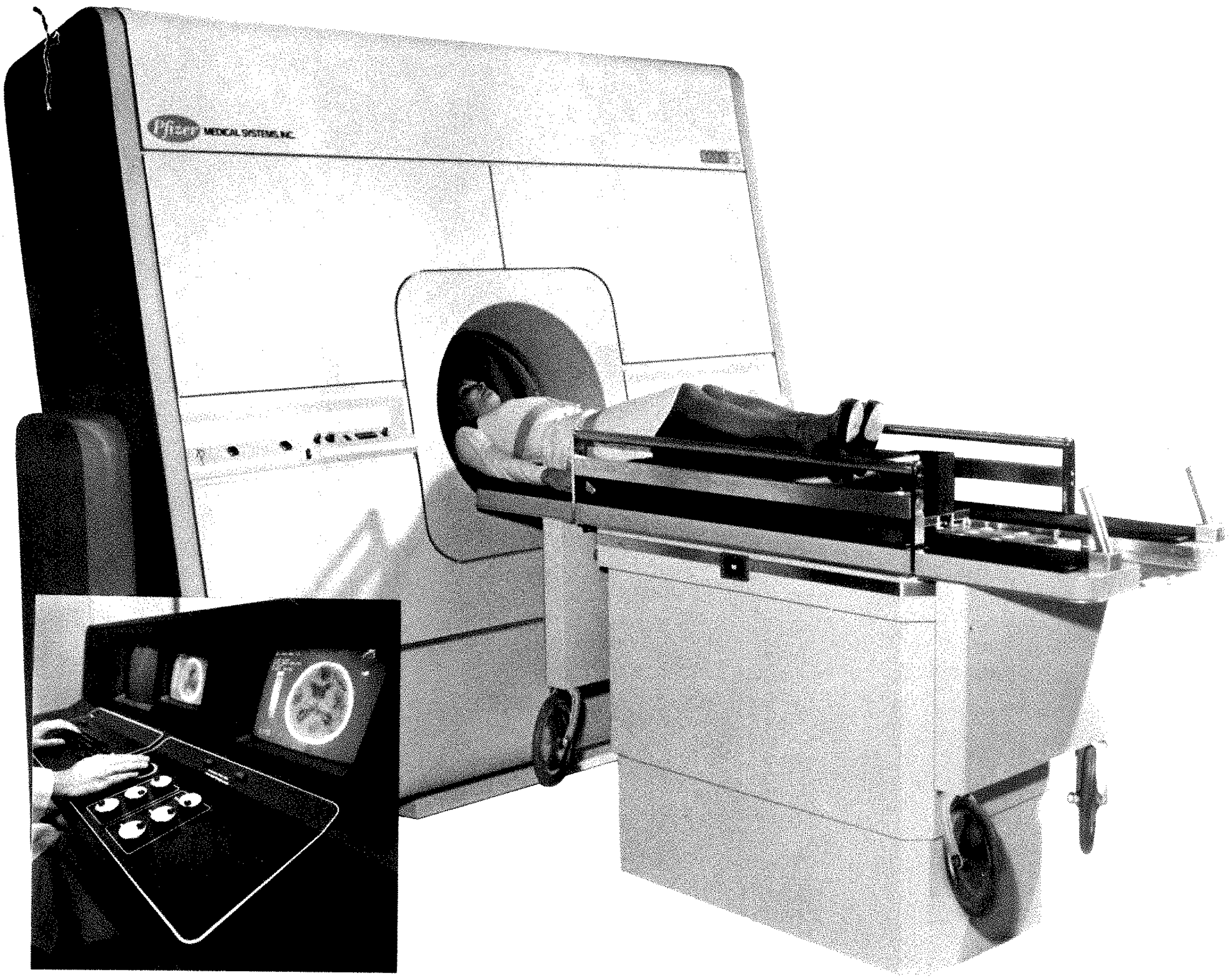

Instant Image Reconstruction

0200FS images are reconstructed immediately upon completion of the patient scan. A scan can be completed in as little as 20 seconds – and displayed seconds later – allowing immediate diagnosis and maximum patient throughput.

Mobile Patient Handling System

The 0200FS offers a unique mobile patient bed system which allows patient preparation and positioning outside the scanning room. This multiple bed system assures optimum safety and comfort for the patient, and offers a particularly efficient means for maximizing patient throughput.

Diagnostic Flexibility

The 0200FS is a whole body CT system designed to optimize scan quality as well as diagnostic flexibility. This advanced system features flexibility in: slice thickness (5-13mm), dosage (according to diagnostic requirements), and matrix size (160, 256, 320).

Software Capability

The 0200FS standard software offers advanced capabilities in image manipulation. The trackball cursor may be used to delineate regions of interest for measurement, magnification and statistical analyses. These features, coupled with multiplanar reconstructions, computer printouts, and area histograms, make the 0200FS the system which offers the most advanced image manipulation capability available.

Designed Modularity

The 0200FS system has been designed to keep your installation in pace with the state of the art. Our modular construction helps assure that your scanner will always be technologically up to date

Established Record of Service

Service is provided by a worldwide network of dedicated, experienced service engineers – each capable of total system maintenance. Throughout the many dozens of ACTA-Scanner installations, this service force has established an enviable record for 1976 of more than 96% uptime.

The New
0200FS
Whole Body CT System

Pfizer
MEDICAL SYSTEMS, INC.
A SUBSIDIARY OF PFIZER INC.
9052 Old Annapolis Road
Columbia, MD 21045

For this cost...

$740,000

Ohio Nuclear Delta Scan 2020
(Or to upgrade a Delta Scan 50,
the total cost is $792,500.)

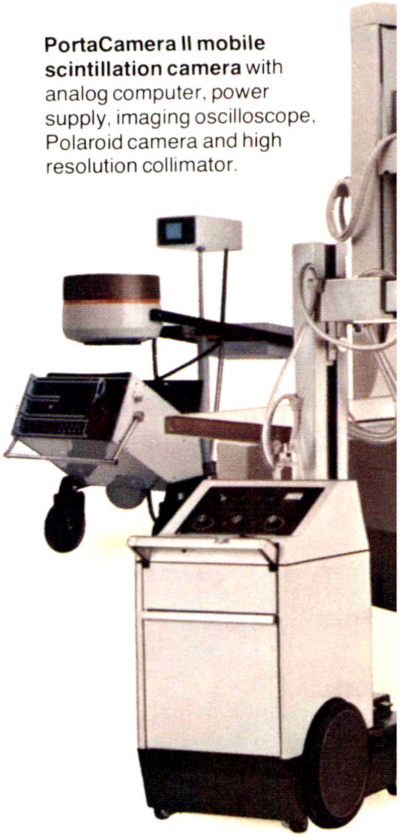

PortaCamera II mobile scintillation camera with analog computer, power supply, imaging oscilloscope, Polaroid camera and high resolution collimator.

AMX II auto/mobile x-ray system, with batteries.

...why not get all this?

If you want 360° rotate only fast-scan CT, you could order the system shown at the far left. Or—for about the same cost—get a GE Fast-Scan™ CT/T plus all the other equipment shown here.

For nearly three-quarters of a million dollars, your hospital deserves a lot more than just CT. And if you're like most hospitals, you need more than CT.

You may also need a versatile radiographic/tomographic system like our RT Table. And a sharp-imaging mobile unit like the AMX. You may need a compact, easy-to-use film viewer. And maybe your nuclear department needs a reliable, portable scintillation unit like PortaCamera II. With a full-line medical equipment manufacturer like GE, you can meet all those needs at a realistic price.

So if you're about to invest in CT, consider the extra value you get with GE. Contact your General Electric representative, or call our CT Marketing Manager, 414/544-3189.

GE Medical Systems, Milwaukee, Toronto, Madrid.

GENERAL ELECTRIC

RT Table radiographic/ tomographic system with MST 625 three-phase generator.

CT/T Fast-Scan system with 5-second scans, excellent images, up to 4 head studies/hour throughput, complete diagnostics package, variable slice thickness and the lowest reported skin dose of any CT system.

Fluoroline Slimline 4-over-4 Illuminator with panoramic mounting, line cord, standard switches and table.

Full year service contract on all GE equipment shown here (include only if you're considering upgrading a currently-on-order Delta Scan 50 to a Delta Scan 2020).

CHARLES C THOMAS • PUBLISHER

ENDOMETRIAL CARCINOMA AND ITS TREATMENT: The Role of Irradiation, Extent of Surgery, and Approach to Chemotherapy *edited by* **Laman A. Gray, Sr.,** *Univ. of Louisville, Louisville, Kentucky. (27 Contributors)* The role of irradiation in the total treatment of endometrial carcinoma is explored, focusing on adjuvant irradiation in the treatment of Stage I adenocarcinoma of the endometrium and on the management of carcinoma involving the cervix and body of the uterus. The extent of surgery and possible new chemotherapeutic approaches are also discussed. The importance of associated and related factors is clarified, and the combinations of modalities of treatment and sequence are detailed. '77, *240 pp. (6 3/4 x 9 3/4), 17 il., 138 tables, $22.50*

ANATOMICO-ROENTGENOGRAPHIC STUDIES OF THE SPINE (3rd Ptg.) *by* **Lee A. Hadley,** *Syracuse Memorial Hospital, Syracuse, New York.* "The work is beautifully illustrated with excellent roentgenograms and photographs. The volume is a tribute to a devoted investigator's experience with the spine, accumulated over 30-odd years. His attempt to coordinate the roentgenographic image with the actual anatomical condition of the structure is successfully achieved." Thus said the *Journal of the American Medical Association* in its review of this book. The broad scope of study in the text is revealed in the contents which includes development of the spine, vertebral arteries, posterior spinal articulations with innervation studies, spinal curvatures, infective spondylitis, tumors and tumorous conditions. '76, *560 pp. (6 3/4 x 9 3/4), 644 il., $19.75*

THE RENAL UPTAKE OF RADIOACTIVE MERCURY ($^{197}HgCl_2$): Method for Testing the Functional Value of Each Kidney, Technique- Results- and Clinical Application in Urology and Nephrology *edited by* **Claude Raynaud,** *Service Hospitalier Frederic Joliot, Orsay, France. Foreword by* **Pierre Royer.** *(41 Contributors)* Doctor Raynaud and his colleagues introduce and evaluate a new method for study of the relative function of each kidney, namely, the use of ionic mercury uptake. This volume summarizes the results of years of experience with this procedure. Important technical details such as the time after injection at which the measurements are made, the optimum energy levels, corrections for organ depth and the various types of instruments which can be used are critically considered in detail. The major point of this work is that the symmetry of the body, in this case that of the kidneys, can be the basis of important early signs of disease. '76, *248 pp., 110 il., 47 tables, $22.75*

THE HAND ATLAS *by* **Moulton K. Johnson** *and* **Myles J. Cohen,** *both of UCLA, Los Angeles.* This atlas illustrates the anatomy of the hand, layer by layer, beginning with the skin and ending with x-ray studies of the bones. Photographs of dissections of unembalmed specimens provide realistic illustrations, all of which are approximately life-size or larger. To demonstrate their potential size, the major spaces of the hand have been injected with radiopaque contrast media. With few exceptions, the anatomical structures illustrated are as the authors have found them and as the surgeon may expect to find them. Topics include the distal volar forearm, palm, thumb, fingers, radial side of the hand, dorsum of the hand, spaces of the hand, and wrist mechanics. '75, *108 pp. (8 1/2 x 11), 121 il. (8 in color), $22.00*

Prepaid orders sent postpaid, on approval

301-327 EAST LAWRENCE
SPRINGFIELD • ILLINOIS • 62717

Help us to help you.

OSHA—the Occupational Safety and Health Act of 1970—benefits everybody. Employers and employees alike.

Today, Red Cross is helping employers all over the country to meet OSHA standards, by training employees in first aid and hazard recognition practices. The result is that, everywhere, factories and other places of business are safer and healthier. Another side benefit: employees trained in first aid are more valuable employees.

Next time you wonder where "all those dollars you gave to the Red Cross" are going—you might consider this: a lot of them are being plowed right back into your business! For information about First Aid Training call your local Red Cross Chapter.

Red Cross.
The Good
Neighbor.

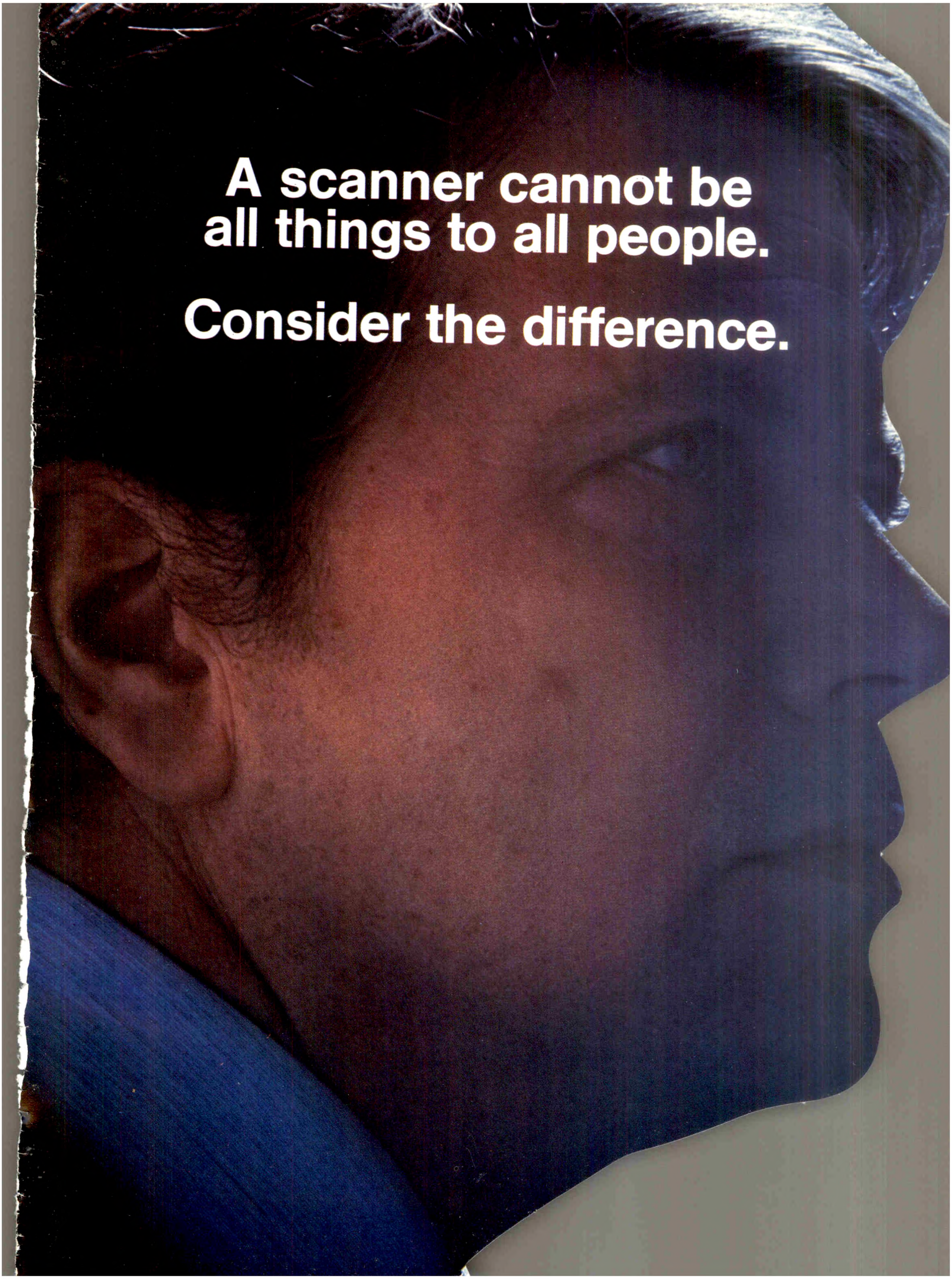
A scanner cannot be all things to all people.
Consider the difference.

Head scans are different than body scans. Successful head scans call for ND 8000, the CT scanner designed for cranial examinations.

CT scanners have advanced the state of the art in diagnostic x-ray to unheard of levels. But, like every new system, care must be taken that scanning systems be evaluated and applied properly.

Scanning systems can be universally good but not necessarily specifically great.

Head and body scans are a classic example. Organ movement, beam geometry, range of attenuation coefficients, radiation quality and reconstruction algorithm are all very significant when applied to head vs. body examinations. Each calls for a different approach.

These considerations, and many others, call for a selection of examination parameters that will create the best possible image at the lowest possible rad dose to the patient.

For head examinations, these parameters are best met with ND 8000 - CGR's new CT head scanner which uses the translation-rotation principle offering maximum flexibility in data collection.

CGR

CGR ND 8000 has been designed specifically for the study of the brain, posterior fossa, neck and orbital cavities. It offers the dual advantage of simultaneously producing superior density resolution and spatial resolution.

The new scanner permits optimum flexibility in choosing parameters. These parameters include :
- A high spatial resolution of 7 lines per centimeter and a high density resolution of 0.2 %. Selection of either of these modes is by pushbutton.
- Irradiation control of 1 to 10 rads to match dosage with specific clinical requirements.
- A fast acquisition time of 20 seconds.
- Detection via Xenon chambers to assure maximum reliability and stability of x-ray radiation measurements.
- Special x-ray tubes with bias control to select optimal x-ray tube focal size.
- A scan gantry with ± 30° tilt for superior slice orientation.
- Additional patient support swivel for ease in positioning.
- Precise centering by laser beam.
- And, of course, complete programs for file management as well as computer assisted image analysis.

ND 8000's reduced scanning time minimizes artifacts caused by patient movement.
In the slow mode, under 360° angulation, the scanner produces 4 times more x-ray photons - approximately 500,000 data samples. Density resolution is 0.2 %. The system has a reconstruction zoom capability equivalent to 512 x 512 points ; a 0.70 mm spatial resolution (FWHM). The smallest volume element is 1.5 mm^3. Reconstruction algorithms are offered for both adults and children. The x-ray tube is bias controlled to permit selection of optimal focal size, providing greater brightness when desired.

D 8000,
e head scanner.
onsider the difference.

ND 8000

ND 8000

ND 8000

ND 8000

ND 8000

ND 8000

ND 8000

ND 8000

Spatial resolution : 7 lines per centimer.
Density resolution : 0.2 % with respect to the density of water.
Selection of one of these 2 modes by pushbutton.

ND 8000 Features

- **Data acquisition for a single slice**

Translation-rotation principle
- 180° in 16 rotation steps of 12°
- 360° in 31 rotation steps of 12°
- Scanning field : 256 mm

- **Gantry tilting : ± 30°**

- **Patient support**

- Vertical and transverse movement under mini-computer regulation.
- Exclusive swivel movement.

- **Accurate centering**

by laser beam.

- **Scanning time**

Standard mode : 180° in 20 seconds.
High resolution mode : 360° in 40 seconds.
Very high resolution mode : 360° in 80 seconds.

- **X-ray tube**

High brightness, 4 kW power dissipated on a focal spot size 7.5 mm in one direction and adjustable from 0.5 to 1.5 mm in the other direction.

- **X-ray stabilization**

Residual system noise well below the unavoidable quantum noise.

- **X-ray filtration**

Optimized for head examinations. Cuts down the artifacts while eliminating unwanted radiation.

- **Detectors**

- 31 Xenon detectors.
- Automatic calibration.
- Efficiency greater than 95 % for 80 KeV x-rays.

- **Collimation**

Motorized positioning of a collimating grid which allows switchover from the density resolution mode to the high spatial resolution mode.

- **Variable scan slice thickness**

3 - 6 - 9 mm.

- **Number of data points**

- 246016 data for 180°.
- 492032 data for 360°.

- **Matrix size**

- 256 x 256 elements.
- Reconstruction zoom capability equivalent to 512 x 512 points.

- **Reconstruction algorithm**

- Selection facilities : High density resolution
  High spatial resolution
  Adults
  Children.
- Patient motion corrected in the image reconstruction program.

- **Reconstruction time**

From 20 to 40 seconds maximum according to the number of data points.

- **Range of x-ray absorption values**

Scale : −1000 corresponds to air, zero to water, +1000 to bone.
- Window level : adjustable in unit steps from −1000 to +1000.
- Window width : adjustable in unit steps from 1 to 512.

- **Image processing**

- Overbrightness.
- Magnification.
- Region of interest.
- Average density value calculation.
- Possibility of displaying the density value of any picture element.

- **Display system**

One or two viewing units allowing image processing independent of acquisition.

- **Image storage**

4 options :
- Floppy disc - 10 image capacity.
- Magnetic tape - 200 image capacity.
- Floppy disc + magnetic tape.
- Big disc unit - 700 images + magnetic tape.

- **Image recording facilities**

4 options :
- Standard camera.
- 105 mm camera.
- Four exposures on 24 x 30 cm x-ray film.
- Electrostatic printer facilitating hard copy documents.

- **Independent diagnostic center (I.D.C.)**

Images with additional administrative and diagnostic information are processed through an independent diagnostic center (I.D.C.).
- a display console
- an electrostatic printer
- a disc unit stores administrative and diagnostic information for retrieval and/or statistical studies.

- **Computer system configuration**

- One 32K MOS memory main computer.
- One 32K MOS specialized processor.
- Temporary storage on a 10 Megabyte magnetic disc.

Optional : a second computer or micro processor integrated into the I.D.C.

CGR

CGR
13 Square Max Hymans
75741 Paris Cedex 15
France - Tél. : 783.50.04

CGR Medical Corporation
2519 Wilkens Avenue
Baltimore, Maryland 21223
USA - (301) 233-2300

CGR Canada Ltee-Ltd.
500 Boulevard de l'Aéroparc
Lachute, Québec, Canada
(514) 562-8806

After 25 years of constantly improving our film transport system to make 6 exposures per second practical,

and sharpening resolution to produce the very clearest possible image in angiograms,

there's still one thing today's Schonander AOT-R won't do for you...

Stop working.

It would seem that a good high speed cut sheet film changer is doing its job when it produces clear diagnostic information.

But to Schonander, a film changer isn't doing its job unless it's doing its job for you... constantly and without interruption.

So, the AOT-R cut sheet film changer is built to be reliable.

Not just because you can count on its exclusive pressure plates to give you angiograms with superb image quality. Or a film transport system that operates perfectly at all exposure rates, including 6 exposures per second.

Or even because of AOT-R conveniences like a loading magazine and receiving cassette on the same side of the changer. Or the fact that it's economical, and doesn't waste film.

These are things that people working with our cut sheet film changers have come to rely on and expect from an innovative, research-oriented company that helped pioneer rapid serial angiography.

When it comes right down to the bottom line, radiologists who wanted a good film changer, wanted the AOT. Not just because of the name behind it. Or because over 12,000 AOT's have been installed over the last 25 years. Or because the AOT-R does what's required.

But simply, because it works.

For more information, write or call Elema-Schonander, Inc., 699 Lively Boulevard, Elk Grove Village, IL. 60007. (312) 593-6770. Or contact your local x-ray equipment distributor.

elema-schonander

**When a better idea
in film changers comes along,
it will come from us.**

INDEX TO ADVERTISERS

In Order of Appearance

Ortho Pharmaceutical Corporation
E-Z-EM Company
C. B. Fleet
The Purdue—Frederick Company
E. R. Squibb & Sons, Inc.
Machlett Laboratories
Philips Medical Systems (Eindhoven)
Siemens Corporation
EMI Medical, Inc.
E. R. Squibb & Sons, Inc.
C. V. Mosby
Ohio Nuclear
Low X-Ray

• •

Guerbet Laboratory
General Electric Company
Diagnostic Information
Charles C Thomas • Publisher
Varian Associates
Ethol Chemicals, Inc.
General Electric Company
University of California (San Francisco)
S & S X-Ray
University of Minnesota
Varian Associates
Pfizer Medical Systems
General Electric Company
Charles C Thomas • Publisher
CGR (Paris)
Elema-Schonander, Inc.
Hanley Medical Equipment Company
Philips Medical Systems, Inc.
E-Z-EM Company
Liebel-Flarsheim Company

Hanley Space Saver X-Ray and Medical Record Cabinets are installed in most hospitals in America.

Top quality and low price is the reason.
5 compartment with doors—$199.50
5 compartment less doors—$171.50
Brochure F.O.B. Factory

AMERICA'S LARGEST DISTRIBUTOR OF X-RAY CABINETS

HANLEY MEDICAL EQUIPMENT CO.
5614 South Grand X-Ray Division St. Louis, Mo. 63111

In reply to advertisers
please mention that you saw
their advertisement in

THE
AMERICAN JOURNAL OF
ROENTGENOLOGY

published monthly for
The American
Roentgen Ray Society
by
CHARLES C THOMAS • PUBLISHER
Springfield, Illinois 62717

"How many people do you know who have been cured of cancer?"
Flip Wilson,
National Crusade Chairman

Almost everybody knows someone who has died of cancer. But the fact is about two million living Americans have been cured. Not only cured but leading active, normal lives. Another fact is millions more could be.

By getting to the doctor in time. By availing themselves of the most effective treatments today. By advances made through cancer research. Research made possible with the help of the American Cancer Society.

To save more people, the American Cancer Society needs more money. So, please, give. We want to wipe out cancer in your lifetime.

American Cancer Society
This space contributed by the publisher.

There's one easy way to specify an R/F system tailored exactly to your needs:

It's a Philips' maxim: "Make the system fit the customer: don't force the customer to adapt to the system."

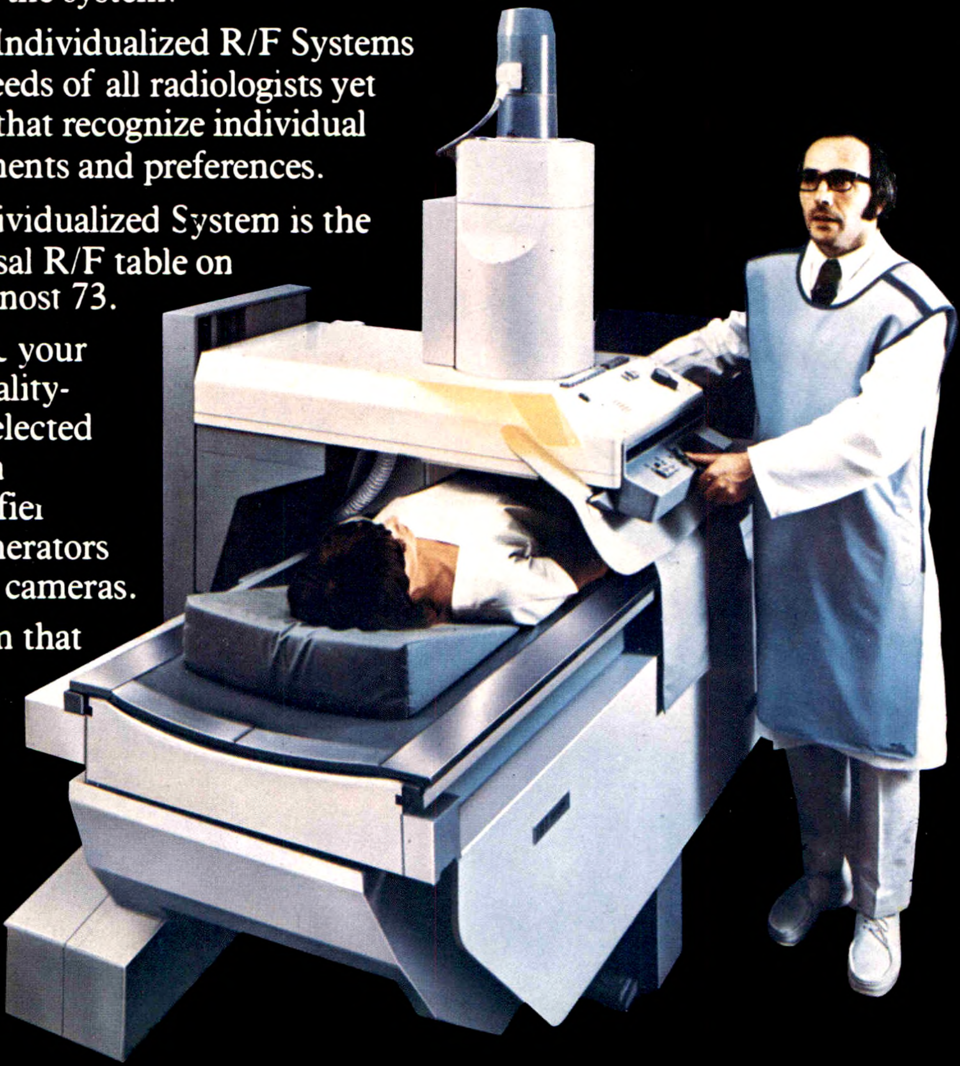

That's why Philips' Individualized R/F Systems meet the common needs of all radiologists yet still provide choices that recognize individual techniques, requirements and preferences.

The heart of the Individualized System is the finest 90°/90° universal R/F table on the market: the Diagnost 73.

You can individualize your Diagnost 73 with quality-constructed, easily selected choices – in spot film device/image intensifier combinations, in generators and in fluorographic cameras.

The result is a system that works the way *you* want to work… with optimum diagnostic images every time.

Philips' Individualized R/F Systems: tailored to make your life simpler.

Contact your Philips' representative. Or, call or write:

PHILIPS MEDICAL SYSTEMS, INC.

710 Bridgeport Avenue, Shelton, Conn. 06484

specify Philips

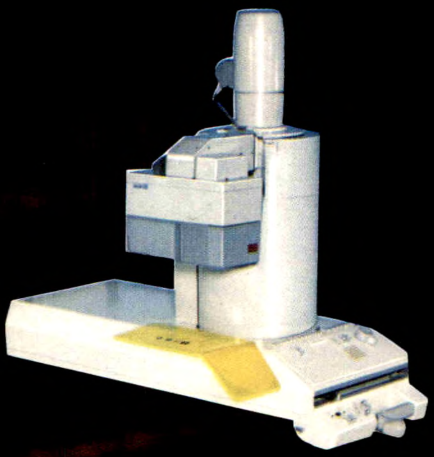

Philips Imaging Systems

Whether you select a 9″ Dual Mode Image Intensifier, a 6 I.I., or a Philips' exclusive 6″ fiber optic system, you're guaranteed uniform image quality over the entire field. High resolution, high contrast, high conversion factor and high quantum detection efficiency result in optimum image transfer to TV and fluorographic cameras. In short, the best possible diagnost images.

Philips Spot Film Devices

Four spot film devices. choose the one that adapts to your needs and your technique. Fully integrated into the table to eliminate ceiling suspension in most configurations, the spot film device is easily parked to permit tabletop radiography with the Diagnost 73's built-in bucky system and a ceiling suspended X ray tube

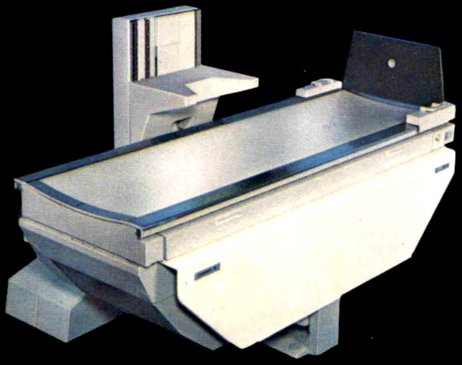

Philips Diagnost 73 Table

The world's finest 90° 90° universal R F system. A modern table base permits a choice of spot film device image intensifier combinations. The table features quiet, variable speed tilt motion from upright to 90° Trendelenburg. You can remain in close proximity to the patient and still have an unobstructed view of the TV monitor in any table position.

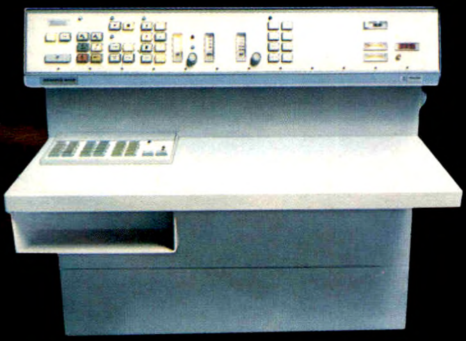

Philips Modular Generators

Designed for flexibility, free technique *and* Anatomically Programmed Radiography (APR). Modular design lets you adapt the generator to *your* needs…with expansion capability to accommodate future requirements.

PHILIPS®

® TM N.V. Philips of Holland

For Double Contrast Stomachs, Use

NEW! **E-Z-HD**™

High Density with High Fluidity
Barium Sulfate for Suspension USP

Note the Demonstration of Superficial Erosions

Double contrast radiography appears to offer the potential for significant improvements in diagnostic accuracy.

Double contrast studies of the stomach best demonstrate the surface pattern of the stomach (areae gastricae). This leads to improved detection of superfical erosions and ulcers, malignancies, polyps and other benign tumors, and ulcer scars.

E-Z-HD barium sulfate provides the basic ingredient necessary for good double contrast of the stomach.

The higher the density of the barium suspension, the better the coating, E-Z-HD allows for the highest density suspension of any commercial product on the market today: 85% w/w, 250% w/v. E-Z-HD achieves this density while remaining fluid for ease of administration.

- High density
- High fluidity
- Palatable
- Unit dose convenience.

E-Z-HD – The barium for the double contrast examination of the stomach and duodenum.

Optimal Density & Fluidity for the Modern Double Contrast Examination of the Stomach and Duodenum

Refrences:

David W. Gelfand: The Japanese-Style Double Contrast, Examination of the Stomach, Gastrointest Radiol. 1, 7-17 (1976)

Igor Laufer: The Diagnostic Accuracy of Barium Studies of the Stomach and Duodenum – Correlation with Endoscopy, Radiology 115: 569-573, June 1975

Roscoe E. Miller: The Air Contrast Stomach Examination: an overview. Radiology 117: 743-744 Dec. 1975

E-Z-EM

For Further Information Write:

7 Portland Ave.
Westbury, New York 11590
(516) 333-8230

9/76

why...

should you consider Tomographic capabilities for your head radiography?

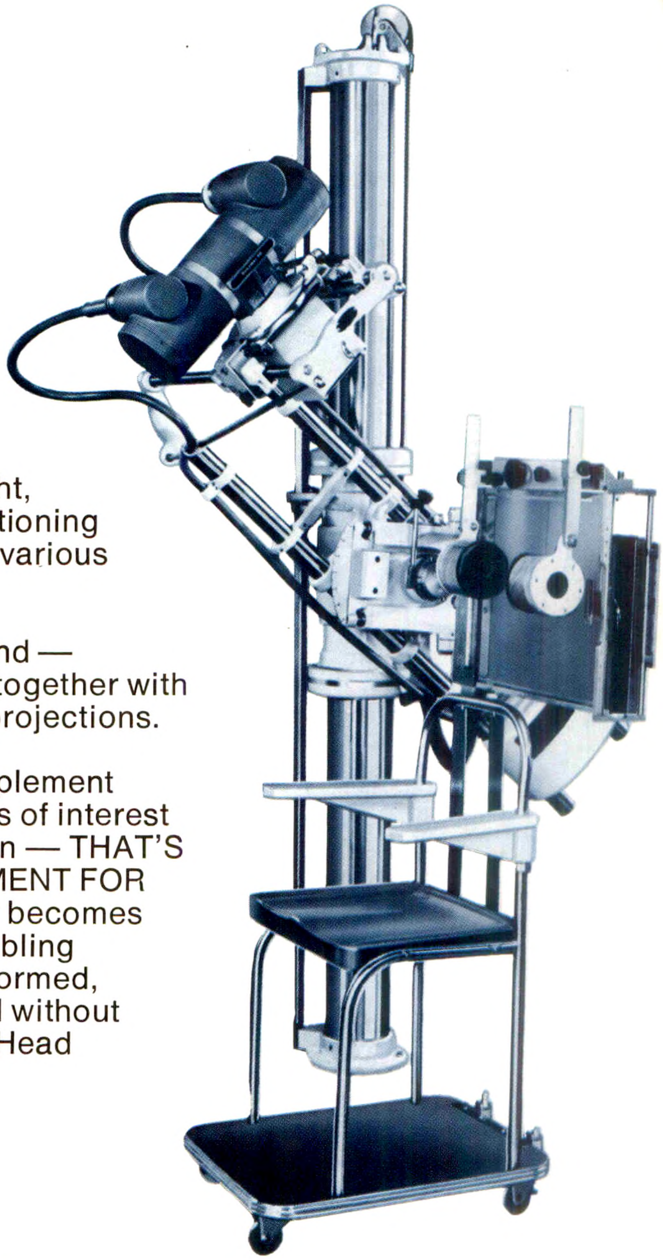

Because the head is a complex structure that contains the skull, brain and organs of sight, hearing, taste and smell, accurate patient positioning and x-ray tube angulation are a "must" for the various projections required in head radiography.

The Franklin Head Stand is dedicated to this end — providing accurate positioning and alignment together with patient comfort even during the most difficult projections.

Tomographic studies can often be used to supplement conventional radiographs when specific planes of interest must be analyzed for diagnostic interpretation — THAT'S WHY WE OFFER A TOMOGRAPHIC ATTACHMENT FOR THE FRANKLIN HEAD STAND. This accessory becomes an integral part of the Franklin Head Stand enabling supplementary tomographic studies to be performed, with the patient either sitting or recumbent and without compromising the positioning flexibility of the Head Stand for conventional radiography.

why not...

supplement your head radiography capabilities by specifying the Franklin Radiographic Head Stand equipped for Tomography?

For additional information contact your local x-ray equipment supplier or:
Liebel-Flarsheim Company,
Division of Sybron Corporation,
111 E. Amity Road,
Cincinnati, Ohio 45215 U.S.A.
(513) 761-2700

SYBRON | Liebel-Flarsheim

American Journal of Roentgenology

l. 129 September 1977 No. 3

Janeway Lecture: Fundamental Mechanisms in Combined Modality Therapy of Cancer. *H. S. Kaplan* 383

DIAGNOSTIC IMAGING

Diagnosis and Evaluation of Retroperitoneal Tumors by Computed Tomography. *D. H. Stephens, P. F. Sheedy, II, R. R. Hattery, and B. Williamson, Jr.* 395
Detection of Retroperitoneal Hemorrhage by Computed Tomography. *S. S. Sagel, M. J. Siegel, R. J. Stanley, and R. G. Jost* 403
Diagnosis of Urine Extravasation after Renal Transplantation. *D. G. Spigos, W. Tan, D. G. Pavel, M. Mozes, O. Jonasson, and V. Capek* 409
Fungal Infection of the Urinary Tract: Demonstration by Antegrade Pyelography and Drainage by Percutaneous Nephrostomy. *A. G. Dembner and R. C. Pfister* 415
Radiologic Spectrum of Opportunistic Infections of the Upper Gastrointestinal Tract. *P. A. Athey, H. M. Goldstein, and G. D. Dodd* 419
Radiologic Aspects of Beck Gastric Tube in Esophageal Reconstruction. *S. A. Fetouh, R. H. Daffner, R. W. Postlethwait, and R. C. Millar* 425
Air in the Esophagus: A Frequent Radiographic Finding. *A. V. Proto and E. J. Lane* 433
Hepatic Venography and Wedge Hepatic Vein Pressure Measurements in Diffuse Liver Disease. *J. A. Cavaluzzi, R. Sheff, D. P. Harrington, S. L. Kaufman, K. Barth, W. C. Maddrey, and R. I. White, Jr.* 441
"Hot Spot" on Hepatic Scintigraphy and Radionuclide Venacavography. *N. S. Gooneratne, M. G. Buse, J.L. Quinn, III, and J. B. Selby* 447
Doppler Ultrasonic Screening Prior to Venography for Deep Venous Thrombosis. *P. F. Jaques, W. A. Richey, C. A. Ely, and G. Johnson, Jr.* 451
The Target Sign: A New Radiologic Sign of Septic Pulmonary Emboli. *M. N. Zelefsky and L. G. Lutzker* 453
A Statistical Description of the Normal Computerized Brain Scan. *D. F. Reese, P. C. O'Brien, G. W. Beeler, Jr., P. R. Gerding, and C. R. Romme* 457
Cerebral Granulomatous Angiitis: Case Report and Literature Review. *M. J. Faer, J. H. Mead, and R. D. Lynch* 463
Angiography in Vascular Malformations of the Face. *G. B. Bradac, R. S. Simon, M. Bunte, and R. Stellmach* 469
Angiographic Observations on Chemodectomas of the Head and Neck. *S. F. Handel, M. H. Miller, S. Wallace, H. Goepfert, and R. H. Jesse* 477
Metrizamide Myelography. *W. R. Boyd and G. A. Gardiner, Jr.* 481
Avulsion of Nerve Rootlets with the Cuatico Needle during Pantopaque Removal after Myelography. *G. D. Hungerford and J. M. Powers* 485
Hand Radiographic Measurements in Growth Hormone Deficiency Before and After Treatment. *R. Hernandez, A. K. Poznanski, R. P. Kelch, and L. R. Kuhns* 487
Extramedullary Hematopoiesis in Paget's Disease of Bone. *S. Kadir, L. Kalisher, and A. L. Schiller* 493

RADIATION PHYSICS

Scanning Multiple Slit Assembly: A Practical and Efficient Device to Reduce Scatter. *G. T. Barnes, I. A. Brezovich, and D. M. Witten* 497

CASE REPORTS

Ulcerative Pseudopolyposis Mimicking Neoplasm Proximal to a Jejunal Obstruction. *R. L. Eisenberg, M. W. Hedgcock, R. B. Jeffrey, and C. K. Montgomery* 503
"Backwash Ileitis" with Pseudopolyposis. *G. A. Gardiner* 506
Mallory-Weiss Syndrome with Esophageal Obstruction Secondary to Adherent Intraluminal Thrombus. *M. J. Curtin and F. D. Milligan* 508
Metastatic Melanoma Presenting Clinically as Multiple Colonic Polyps. *B. A. Sacks, N. Joffe, and D. A. Antonioli* 511
Bleeding Ileal Varicosity Demonstrated by Transhepatic Portography. *M. Kinkhabwala, A. Mousavi, S. Iyer, and R. Adamsons* 514
"Hot and Cold" Bone Lesion in Acute Osteomyelitis. *C. D. Teates and B. R. J. Williamson* 517
An Unusual Scapular Stress Fracture. *A. C. Brower, J. R. Neff, and D. A. Tillema* 519
Myelosclerosis and Myelofibrosis in Treated Histiocytosis-X. *L. Pinckney and B. R. Parker* 521
Intrathoracic Desmoid Tumor of the Chest Wall. *D. L. Klein, G. Gamsu, and T. D. Gant* 524
Horseshoe Kidney: Ultrasonic Demonstration. *H. J. Mindell and E. A. Kupic* 526

TECHNICAL NOTES

A New Subtraction Technique Using Duplicating Film as a Final Print. *K. Mojab, L. Garcia, and G. Talge* 528
Radiologic Aspects of the New Universal Proximal Femoral Hip Prosthesis. *H. Drinker and J. C. Mall* 531
Cholecystocholangiography after Cholecystoduodenostomy. *J. Bastidas and L. M. DelGuercio* 534

SPECIAL LECTURE: **The Breast Cancer Screening Controversy: A Perspective.** *M. Moskowitz, P. Gartside, L. Gardella, I. de Groot, and D. Guenther* 537

Guest Editorial: Pulmonary Surfactant Disease States. *I. Meschan* 545
Letters 548
Program of 1977 SPIE/SPSE Meeting 549
Program of 1977 Society for Pediatric Radiology Meeting 551
ARRS Meeting Commercial Exhibitors 552
Abstracts of Current Literature 553
Book Reviews 564
News 567
Radiologic Societies 570

27-3-78

AJR

American
Journal of
Roentgenology

December 1977

UNIVERSITY COLLEGE OF
LIBRARY

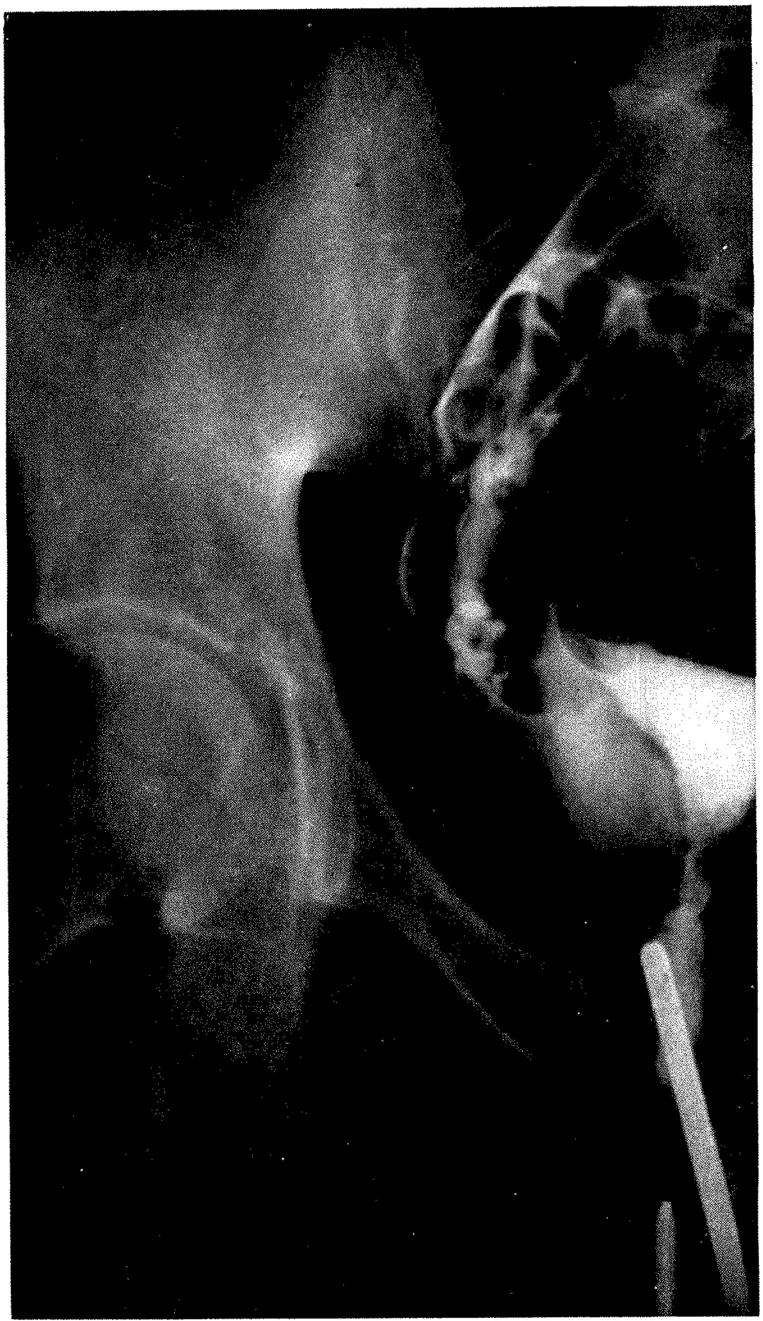

Hysterosalpingogram with Salpix Contrast Medium.

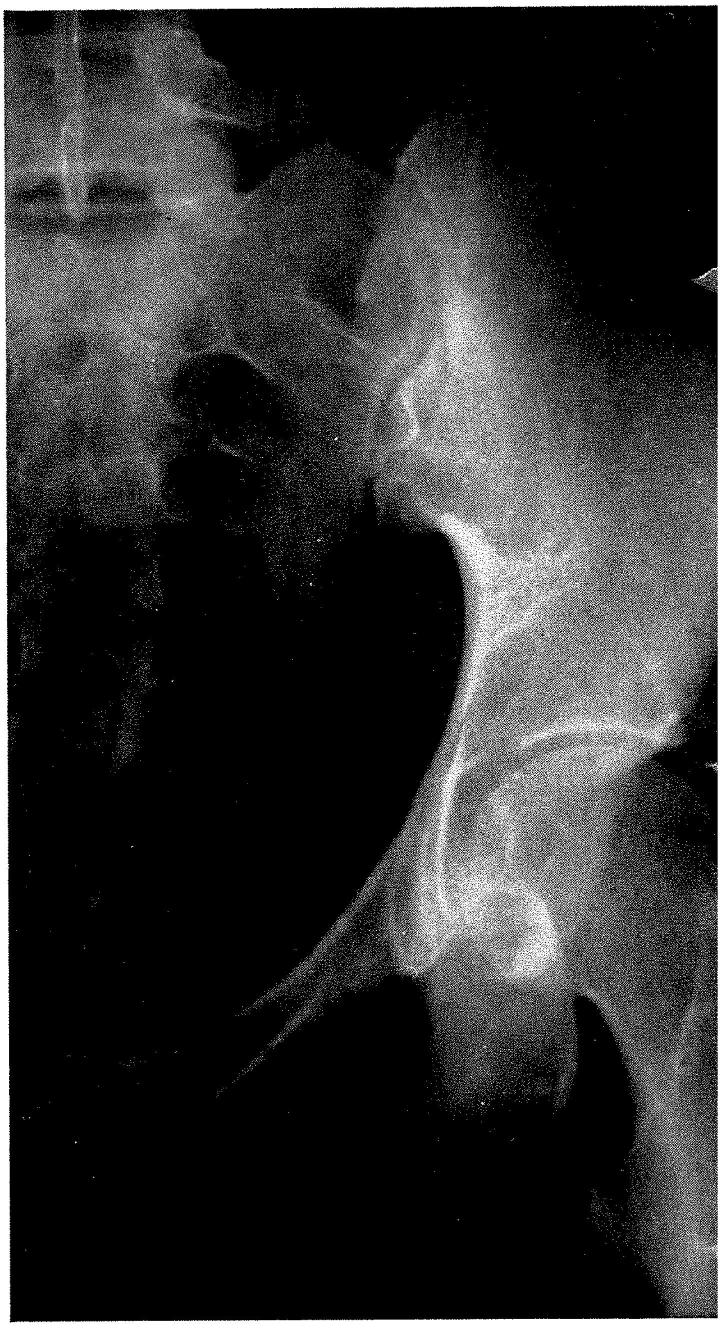

24-hour postinjection x-ray of same patient.

now you see it

now you don't

With Salpix as your contrast medium, your gynecologic patient needn't undergo the 24-hour postinjection x-ray usually required with iodized oils. Water-soluble Salpix leaves virtually no irritating radiopaque residue to produce foreign-body reactions, yet it provides the viscosity needed for adequate visualization.

Contraindications: Contraindications to hysterosalpingography include the presence of severe vaginal or cervical infections, existing or recent pelvic infection, marked cervical erosion or endocervicitis, and pregnancy. The procedure is contraindicated during the immediate pre- or post-menstrual phase.
Sensitivity Test: If indicated in the patient's history, an intracutaneous skin test or sublingual absorption observation may be done with 0.1 cc Salpix.
Warning: Not for intravenous use.

© ORTHO PHARMACEUTICAL CORPORATION 1970

Salpix CONTRAST MEDIUM
TRADEMARK

EACH CC CONTAINS:
sodium acetrizoate 0.53 g and
polyvinylpyrrolidone 0.23 g

Ortho

ORTHO PHARMACEUTICAL CORPORATION • RARITAN, NEW JERSEY 08869

Official Journal
American Roentgen Ray Society
American Radium Society

AJR

Including Diagnostic Radiology • Radiation Oncology • Nuclear Medicine Ultrasonography • Related Sciences

Editor Melvin M. Figley

Assistant Editor Rosalind H. Troupin

Associate Editors Luther W. Brady • Kenneth L. Krabbenhoft • E. Frederick Lang • Russell H. Morgan

Consulting Editorial Board Kent Ellis • E. Robert Heitzman • Donald L. King • John A. Kirkpatrick, Jr. Eugene C. Klatte • John G. McAfee • Thomas H. Newton Robert G. Parker • Stewart R. Reuter • William B. Seaman • Robert J. Shalek • John Storer • Michel M. Ter-Pogossian • Joseph P. Whalen • David M. Witten

Editorial Staff K. A. Murray, manager • M. B. Wieckowicz, manuscript editor • M. J. Leonard, assistant manuscript editor • C. P. Kaiser, secretary

Published monthly by Charles C Thomas, 301–327 East Lawrence Avenue, Springfield, Illinois 62717. All correspondence, except editorial office business, should be addressed to the publisher. Annual subscription prices: United States and possessions, $40; others, $50; residents in training in U.S., $20 (letter from department required with dates of residency); single copies, $5. Foreign subscription delivery not guaranteed. Undelivered or damaged copies replaced within 60 days of publication; 90 days for foreign subscribers. Allow 90 days for address changes. © 1977 by American Roentgen Ray Society. Second-class postage paid at Springfield, Illinois, and at additional mailing offices. Printed in U.S.A.

American Roentgen Ray Society

OFFICERS 1977-1978

President: Harry Z. Mellins
President Elect: Paul A. Rimenschneider
1st Vice-president: Joseph D. Calhoun
2nd Vice-president: Charles E. Bickham, Jr.
Secretary: James F. Martin
Treasurer: Harley C. Carlson

COMMITTEES 1977-1978

Executive Council: H. Z. Mellins, P. A. Riemenschneider, J. D. Calhoun, C. E. Bickham, Jr., J. F. Martin, H. C. Carlson, M. M. Figley, R. G. Evens, B. G. Brogdon, R. A. Gagliardi, E. Gedgaudas, G. A. Kling, T. F. Leigh, S. F. Ochsner, J. F. Wiot, R. E. Buenger, E. C. Klatte, J. P. Tampas, J. L. Gwinn, Chairman

Finance and Budget: A. E. James, E. C. Klatte, R. McLelland, J. P. Tampas, R. G. Evens, Chairman

Publications: M. P. Cap., K. Ellis, F. F. Ruzicka, Jr., E. R. Heitzman, R. A. Gagliardi, chairman

Editorial Policy: M. M. Figley, E. F. Lang, R. H. Troupin, E. R. Heitzman, K. Ellis, F. F. Ruzicka, Jr., M. P. Capp, R. A. Gagliardi, chairman

Advisory Committee on Education and Research: J. E. Youker, G. Wilson, G. W. Hartman, L. F. Rogers, E. Gedgaudas, chairman

Scientific Exhibits: T. C. Beneventano, G. Dodd, B. G. Brogdon, chairman

Constitution and Bylaws: J. H. Walker, W. M. Whitehouse, J. P. Tampas, chairman

American Board of Radiology Representatives: J. F. Roach, R. W. McConnell, S. W. Nelson

Program Committee: H. Z. Mellins, J. F. Martin, J. L. Gwinn, M. M. Figley, R. A. Gagliardi, B. G. Brogdon, E. Gedgaudas, G. A. Kling, P. Riemenschneider, chairman

Instruction Courses: E. Gedgaudas, director; G. W. Hartman, associate director

American College of Radiology Board of Chancellors Representative: W. B. Seaman

Annual Meeting: March 27-30, 1979. Sheraton Centre, Toronto. Canada

Scientific Program: P. A. Riemenschneider, president-elect, Cottage Hospital, Santa Barbara, California 93105

Manager Annual Meeting: George A. Kling, Harper Hospital, Detroit, Michigan

Membership: John L. Gwinn, 4650 Sunset Blvd., Los Angeles, California 90027

Business Office: Keith W. Gundlach, comptroller, American College of Radiology, 20 North Wacker Drive, Chicago, Illinois 60606

American Radium Society

OFFICERS 1977-1978

President: Richard H. Jesse
President Elect: Frederick W. George
1st Vice-president: Ivor Fix
2d Vice-president: John Durant
Secretary: Alfred S. Ketcham
Treasurer: Simon Kramer

COMMITTEES 1977-1978

Executive: F. Rutledge, L. W. Brady, R. H. Jesse, F. W. George, I. Fix, J. Durant, S. Kramer, A. S. Ketcham, V. Marcial, chairman

Public Relations: C. Honaker, R. H. Jesse, chairman

Publication: K. L. Krabbenhoft, A. F. Schroeder, G. Seydel, D. Hussey, A. Raventos, L. W. Brady, chairman

Scientific Program: F. George, D. Johnson, M. Boone, P. Chretien, P. J. DiSaia, D. Hussey, R. C. Landgren, C. Perez, S. T. Cantril, R. H. Jesse, chairman

Local Arrangements: J. Helsper, J. J. Romagosa, J. M. Thomson, Jr., A. J. Ballantyne, S. Kramer, S. Ochsner, chairman

Nominating: M. Kligerman, G. Lewis, J. Vaeth, chairman

Constitution and By-Laws: A. S. Glicksman, P. J. DiSaia, K. L. Krabbenhoft, chairman

Janeway Lecture: S. Levitt, L. Davis, A. S. Ketcham, chairman

Audiovisual: C. R. Bogardus, J. Helsper, B. Herrington, L. Bloebaum, C. Honaker, F. George, chairman

Resident Essay: J. T. Phillips, J. Curry, R. Schweitzer, J. T. Wharton, chairman

American Board of Radiology, Representatives: J. J. Stein, R. E. King, N. duV Tapley

American College of Radiology Board of Chancellors Representative: L. W. Brady

American College of Radiology Council Representative: J. del Regato

Editorial Board of AFCOS Newsletter Representative: J. Vaeth

National Council on Radiation Protection and Measurements Liason Representative: L. W. Davis

Annual Meeting: April 26-30, 1978, Marriott Hotel, New Orleans, Louisiana

Scientific Program: R. H. Jesse, M. D. Anderson Hospital, 6723 Bertner Drive, Houston, TX 77030

Local Arrangements: S. Ochsner, 1514 Jefferson Highway, New Orleans, LA 70121

Membership: A. S. Ketcham, secretary, University of Miami School of Medicine, P.O. Box 520875 Biscayne Annex, Miami, Florida 33152

Business Office: N. V. Jordan, c/o R. H. Jesse, M. D. Anderson Hospital and Tumor Institute, 6723 Bertner Avenue, Houston, Texas 77030

TV or not TV?
That is no longer the question; the replay's the thing.

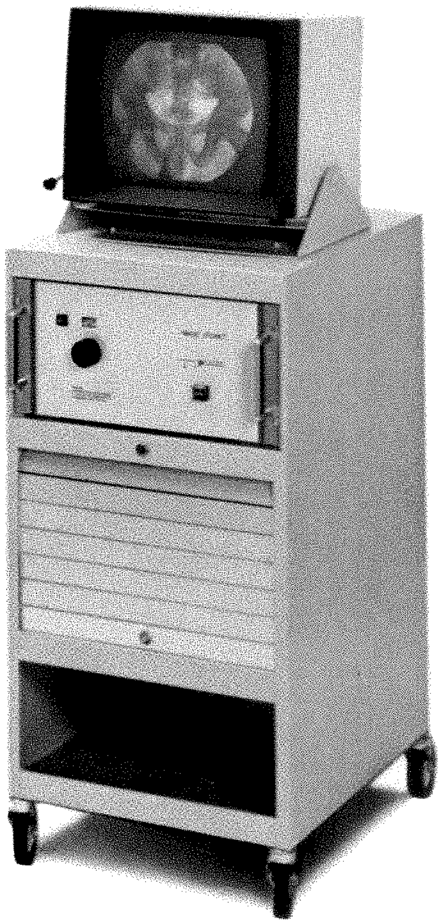

The Siemens fluoroscopy system — Siremobil® plus Image Store® recorder — gives you new mobility, utility and safety in the O.R.

The Image Store® recorder with TV monitor and camera attachment.

Now you can concentrate on fluoroscopy in the operating room, with less worry about excessive exposure. The new Siemens system combines our highly mobile Siremobil image intensifier, for real-time fluoroscopic imaging, with the Image Store video disc recorder for instant TV replay.

Siremobil itself lowers radiation exposure through automatic dose control and a two-pulse generator that delivers higher energy for a shorter duration.

The combined Siremobil/Image Store system can provide a radiation reduction of up to 30—40 fold. Live fluoroscopy time is substantially reduced with the use of the Image Store's hold, recall and instant replay features. And the system retains all the basic advantages of the Siremobil regarding mobility, positioning, and asepsis in the operating environment.

For the complete picture, write or call
Siemens Corporation, Medical Systems Division,
186 Wood Avenue
South, Iselin,
New Jersey 08830
(201) 494-1000. In Canada:
Siemens Canada Limited,
P.O. Box 7300,
Pointe Claire 730-P.Q.

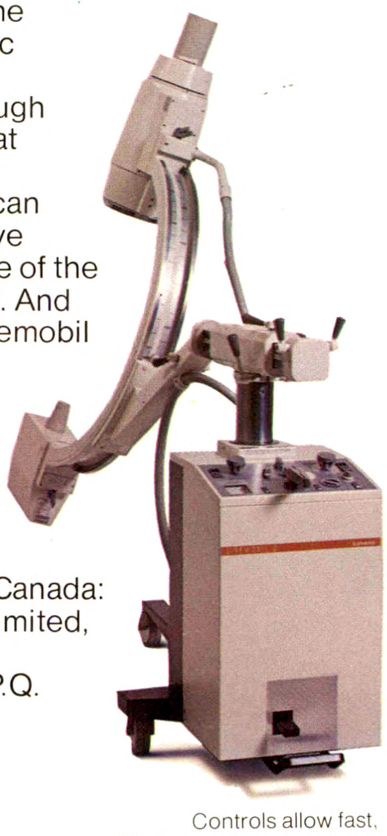

Controls allow fast, effortless movement of unit and C-arm in any direction.

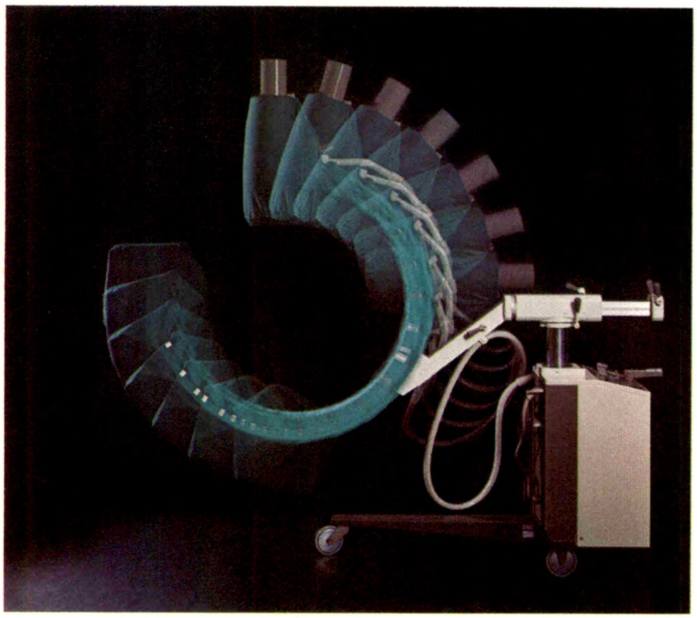

The Siremobil C-arm fluoroscopic unit maintains full mobility while draped for asepsis.

SIEMENS

Clean & Clear

Clean bowel means clear picture. X-PREP Liquid is designed specifically for preradiographic bowel cleansing—without enemas, suppositories, or overhydration.

Good-to-excellent visualization is usually obtained with a single, simple dose.* No residual oil droplets (as is often the case with castor oil) obscure the picture.

Pleasant taste of X-PREP Liquid meets with high patient acceptance.* Simplicity and ease of administration are appreciated by the patient at home, by the nursing staff at the hospital.

*References available on request.

One step · One dose · One bottle

X-PREP Liquid

(standardized extract of senna fruit)

To prep the bowel for radiography

Gray Pharmaceutical Co., Affiliate
The Purdue Frederick Company

©COPYRIGHT 1971, GRAY PHARMACEUTICAL CO./NORWALK, CONN. 06856 B6374 124473

Litton opens the era of fast,

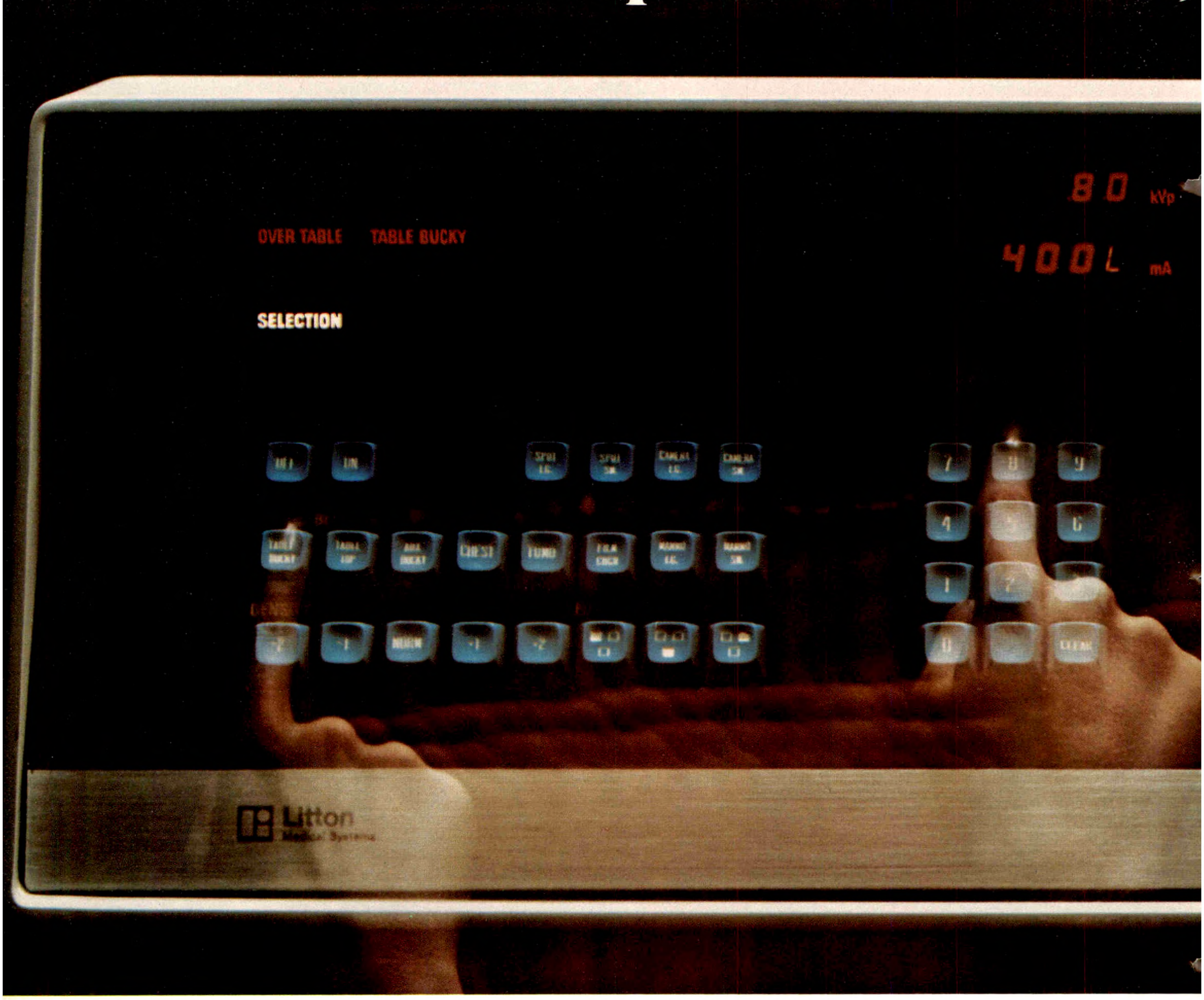

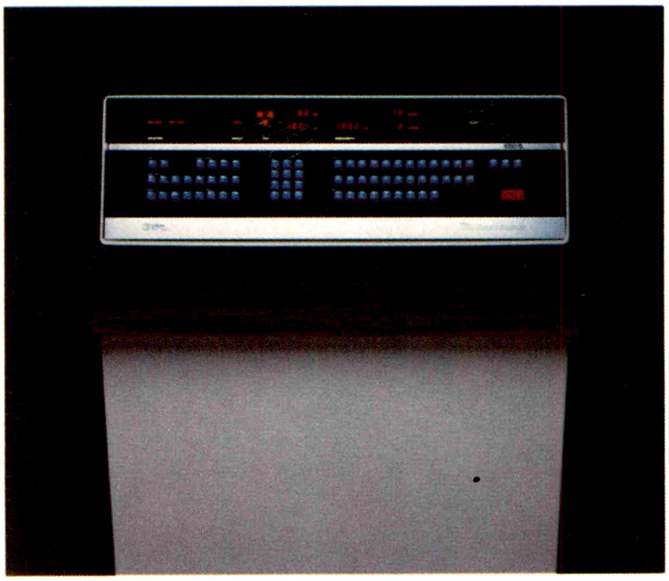

Speed without haste...fast new linear-sequence generators from Litton use the latest in computer-logic to accelerate radiological procedures.

Parameter selection is now a simple left-to-right sequence. Each parameter chosen is displayed in sharp, readable displays on the console of the Litton 650S single-phase generator, shown above.

The Litton 650S is the first of a new generation, designed to help the operator work rapidly but with an absolute minimum of error-caused retakes. All technique and display function "decoding" is accomplished by solid-state computer logic, assuring consistent repeatability.

linear-sequence generators

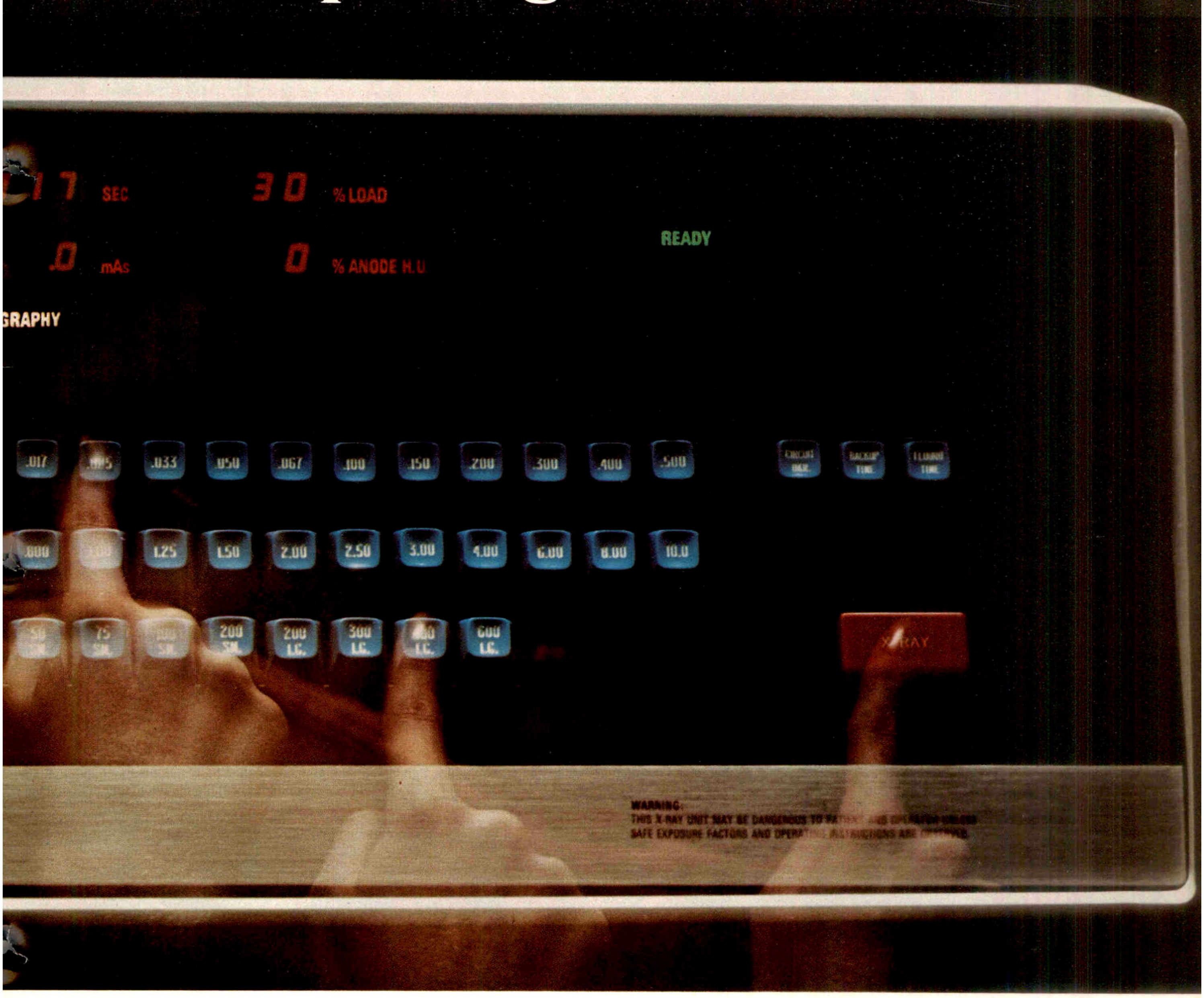

Versatile, too! Use the Litton 650S for general radiographic and fluoroscopic procedures as well as for specialized mammographic and tomographic examinations. May also be used with rapid film changer radiography.

A companion generator, the new Litton 1050T three-phase, incorporates many of the same features and innovations. For instance, both generators have optional Automatic Exposure Control and Forced Extinction Termination to assure repetitive densities down to millisecond exposure times. Both sport handsome, low-profile consoles with separable control panels.

Enter the new era of fast, efficient linear-sequence generators.

Your Litton representative can show you how. Or, write today for a comprehensive brochure.

Litton
Medical Systems
515 E. Touhy Avenue, Des Plaines, Illinois 60018

Technology, resources, people committed to mankind's better health.

TONY
RAG

KODAK'S RARE EARTH IMAGING. IT CAN BE COMMON PRACTICE.

The rare earth phosphors in Kodak Lanex screens absorb more x-rays—more energy—to achieve twice the speed of fast calcium tungstate screens. Image quality is similar, but exposure time, milliamperage, or kilovoltage can be reduced. As a result, you can handle both your regular and special examinations routinely. And you can get more efficient use from your present exposure equipment.

Specifically, Kodak Lanex screens absorb about 60% of the x-ray quanta that exit from a patient. Whereas, fast calcium tungstate screens absorb about 40%.

While Lanex screens absorb more x-rays, they also convert more of the absorbed energy into usable light. This dual efficiency enables Lanex screens, with Kodak ortho G film, to provide image quality similar to fast calcium tungstate screens, with Kodak X-Omat RP film, but at twice the speed.

And that means you can use shorter exposure times to minimize the effects of voluntary or involuntary motion in geriatric or pediatric patients.

Or you can reduce kilovoltage to obtain increased subject contrast in angiographic or tomographic examinations.

Or you can use lower milliamperage settings for a smaller focal spot for improved geometric sharpness.

Or you can distribute your work load to utilize low-powered or portable units.

With Kodak rare earth imaging products, the opportunities are many.

Ask your Kodak Technical Sales Representative about them. Or contact your medical x-ray products dealer. Or write:
Eastman Kodak Company,
Department 740-B, Rochester,
New York 14650.

TURNING ENERGY INTO IMAGES

Kodak

RADIOGRAPHY • COMPUTERIZED TOMOGRAPHY
ULTRASOUND • NUCLEAR MEDICINE • THERMOGRAPHY

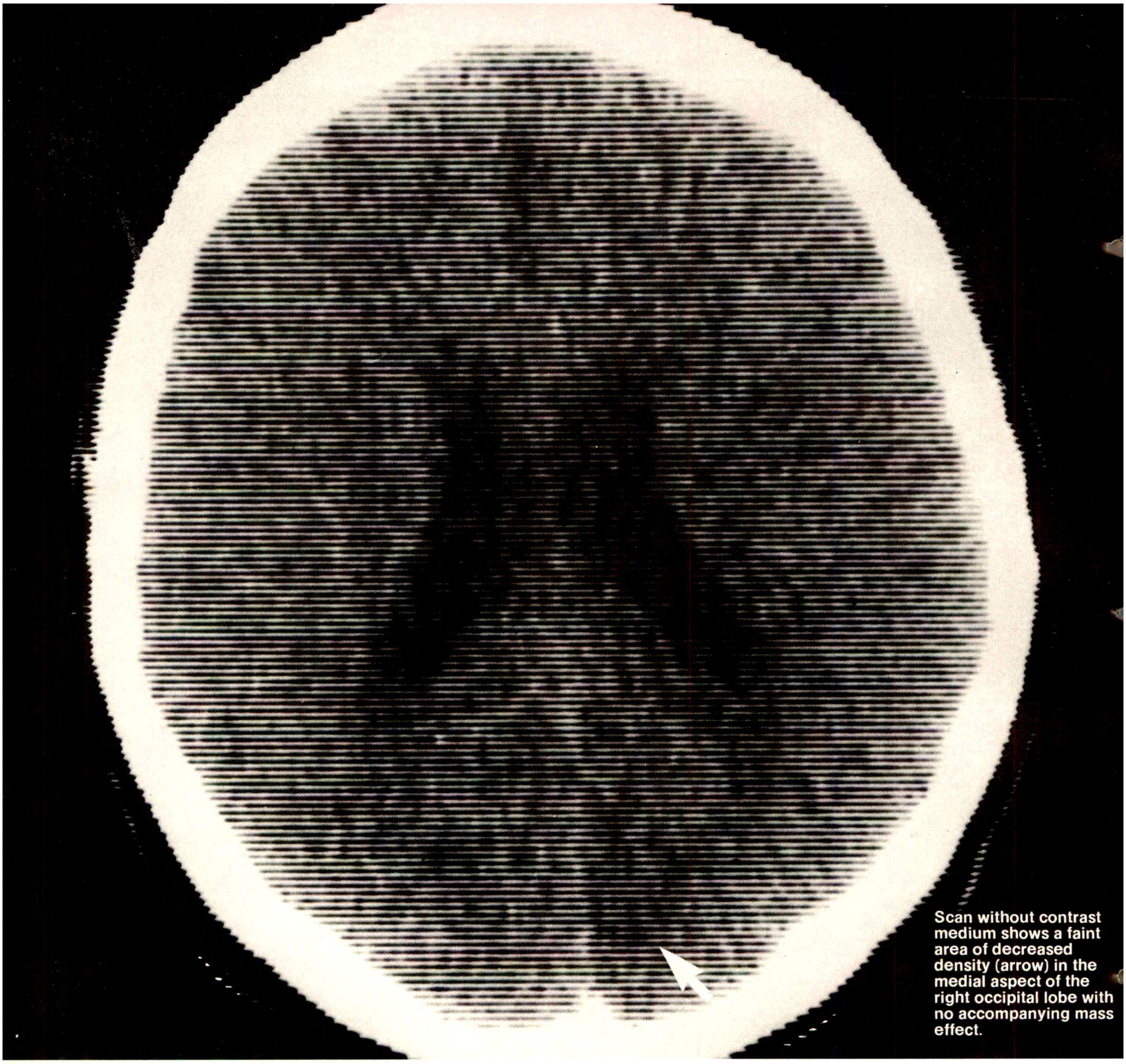

Scan without contrast medium shows a faint area of decreased density (arrow) in the medial aspect of the right occipital lobe with no accompanying mass effect.

Use of this contrast medium to enhance CT brain scans "revealed both an increased detectability and an improved pathologic differentiation of many lesions."*

—**Identifies** lesions not seen on plain CT scans.

—**More specifically defines** nature, size and behavior of wide variety of lesions visualized on plain CT scans.

—**Aids in detection** of aneurysms, arteriovenous malformations, sites of active infection, and in diagnosis of other intracranial pathology.

—**Rules out** the presence of tumor in suspicious areas which may otherwise not have been satisfactorily visualized.

*Davis KR: Massachusetts General Hospital, Boston, MA. Personal communication.

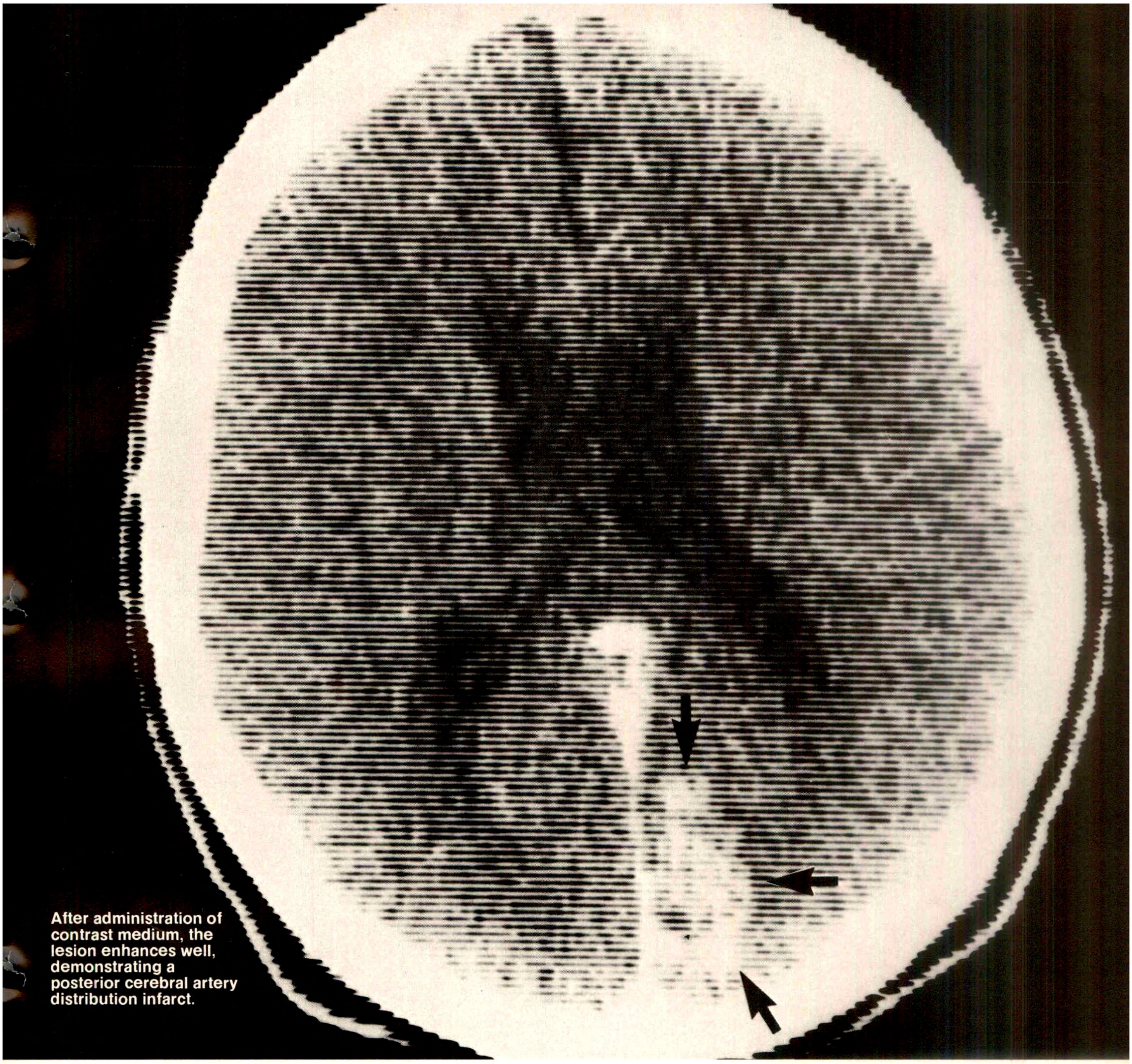

After administration of contrast medium, the lesion enhances well, demonstrating a posterior cerebral artery distribution infarct.

Reno-M-DIP®

Diatrizoate Meglumine Injection USP 30%

for enhanced CT scanning of the brain

The leader in
radiologic
diagnostics

SQUIBB®
contrast media™

See next page for brief summary.

Reno-M-DIP®
Diatrizoate Meglumine
Injection USP 30%

for enhanced CT scanning of the brain

Reno-M-DIP (Diatrizoate Meglumine Injection USP) for drip infusion provides a sterile, aqueous solution of 30% diatrizoate meglumine which contains approximately 14% (42.3 g per 300 ml) bound iodine and 0.04% edetate disodium (sequestering agent). *The solution contains approximately 0.054 mg (0.002 mEq) sodium per ml (16.2 mg/300 ml).*

CONTRAINDICATIONS: Contraindicated in patients hypersensitive to salts of diatrizoic acid and in patients with anuria.

WARNINGS: A definite risk exists in the use of I.V. contrast agents in patients with multiple myeloma. There has been anuria with progressive uremia, renal failure and death. This risk of the procedure in these patients is not a contraindication; however, partial dehydration in preparation for study is not recommended since it may predispose to precipitation of myeloma protein in renal tubules. No therapy, including dialysis, has been successful in reversing this effect. Myeloma should be considered in persons over 40 before I.V. administration of a contrast agent.

In cases of known or suspected pheochromocytoma, if the physician feels that the possible benefits outweigh the considered risks, radiopaque materials should be administered with extreme caution; however, an absolute minimum of material should be injected, the blood pressure should be assessed throughout the procedure, and measures for treating a hypertensive crisis should be available.

Contrast media may promote sickling in homozygous individuals when injected I.V. or intra-arterially. Use diatrizoate meglumine with extreme caution in persons with severe concomitant hepatic and renal disease. Perform thyroid function tests prior to administration of diatrizoate meglumine since iodine-containing contrast agents may alter the test results. Although a history of sensitivity to iodine *per se* or to other contrast media is not an absolute contraindication, administration of diatrizoate meglumine requires extreme caution in such cases.

PRECAUTIONS: Diagnostic procedures involving use of contrast agents should be performed under the direction of personnel with prerequisite training and a thorough knowledge of the particular procedure (see ADVERSE REACTIONS). Severe life-threatening reactions suggest hypersensitivity to the contrast agent. A personal or family history of asthma or allergy or a history of a previous reaction to a contrast agent warrants special attention and may predict more accurately than pretesting the likelihood of a reaction although not the type nor severity of the reaction in the individual. The value of any pretest is questionable. The pretest most performed is the slow I.V. injection of 0.5 to 1.0 ml of the preparation prior to injection of the full dose; however, the absence of a reaction to the test dose does not preclude the possibility of reaction to the full diagnostic dose. Should the test dose produce an untoward response, the necessity for continuing the examination should be carefully re-evaluated; if deemed essential, examination should proceed with all possible caution. In rare instances, reaction to the test dose may be extremely severe; therefore, close observation and facilities for emergency treatment appear indicated.

Do not exceed recommended rate of infusion. Renal toxicity has been reported in a few patients with liver dysfunction who were given oral cholecystographic agents followed by urographic agents; therefore, if known or suspected hepatic or biliary disorder exists, diagnostic infusion studies should be postponed following the recent ingestion of cholecystographic agents. The diuretic effect of the drip infusion procedure may hinder an assessment of residual urine in the bladder. Consider the functional ability of the kidneys before injecting diatrizoate meglumine. Adequate visualization may be difficult or impossible in uremic patients or others with severely impaired renal function. Contrast agents may interfere with some chemical determinations made on urine specimens; therefore, collect urine before or two or more days after administration of the contrast medium.

Usage in Pregnancy: This preparation should be used in pregnant patients only when the physician deems its use essential to the welfare of the patient since safe use during pregnancy has not been established.

ADVERSE REACTIONS: Adverse reactions accompanying I.V. use of iodine-containing contrast agents are usually mild and transient although severe and life-threatening reactions (including fatalities) have occurred. Because severe reactions to the procedure and/or to the contrast agent are possible, appropriate emergency facilities and well-trained personnel should be available and should remain available for 30 to 60 minutes following the procedure to treat the reaction since severe delayed reactions have been known to occur.

Reactions most frequently encountered with contrast agents by drip infusion are nausea and urticaria. Chills, metallic taste, vomiting, dizziness, a rise or fall in blood pressure, itching, flushing, or generalized feeling of warmth, sneezing, etc. may occur and, rarely, may be severe enough to require discontinuation of dosage. Severe reactions which may require emergency measures include cardiovascular reaction characterized by peripheral vasodilatation with hypotension and reflex tachycardia, dyspnea, confusion, and cyanosis progressing to unconsciousness. An allergic-like reaction ranging from rhinitis or angioneurotic edema to laryngeal or bronchial spasm or anaphylactoid shock may occur. Temporary renal shutdown or other nephropathy may occur. Although local tissue tolerance to diatrizoate meglumine is usually good, I.V. injection of the medium in a more concentrated formulation has produced a few instances of a burning or stinging sensation and of venospasm or venous pain.

For full prescribing information, consult package insert.

HOW SUPPLIED: Available in single-dose bottles of 300 ml.

The leader in
radiologic
diagnostics

SQUIBB®
contrast media™

©1977 E. R. Squibb & Sons, Inc. H657-503

THERASIM 750

UNIVERSAL SIMULATOR

for use with Cobalt Teletherapy
Units, Linear Accelerators and
Brachytherapy.
Now available – ASK US!

**Atomic Energy
of Canada Limited**

Commercial Products

P.O. Box 6300, Ottawa, Canada, K2A 3W3
Tel. 613/592-2790 • Cable Nemota • Telex 053-4162

77.8M

Computerized Litton 300L

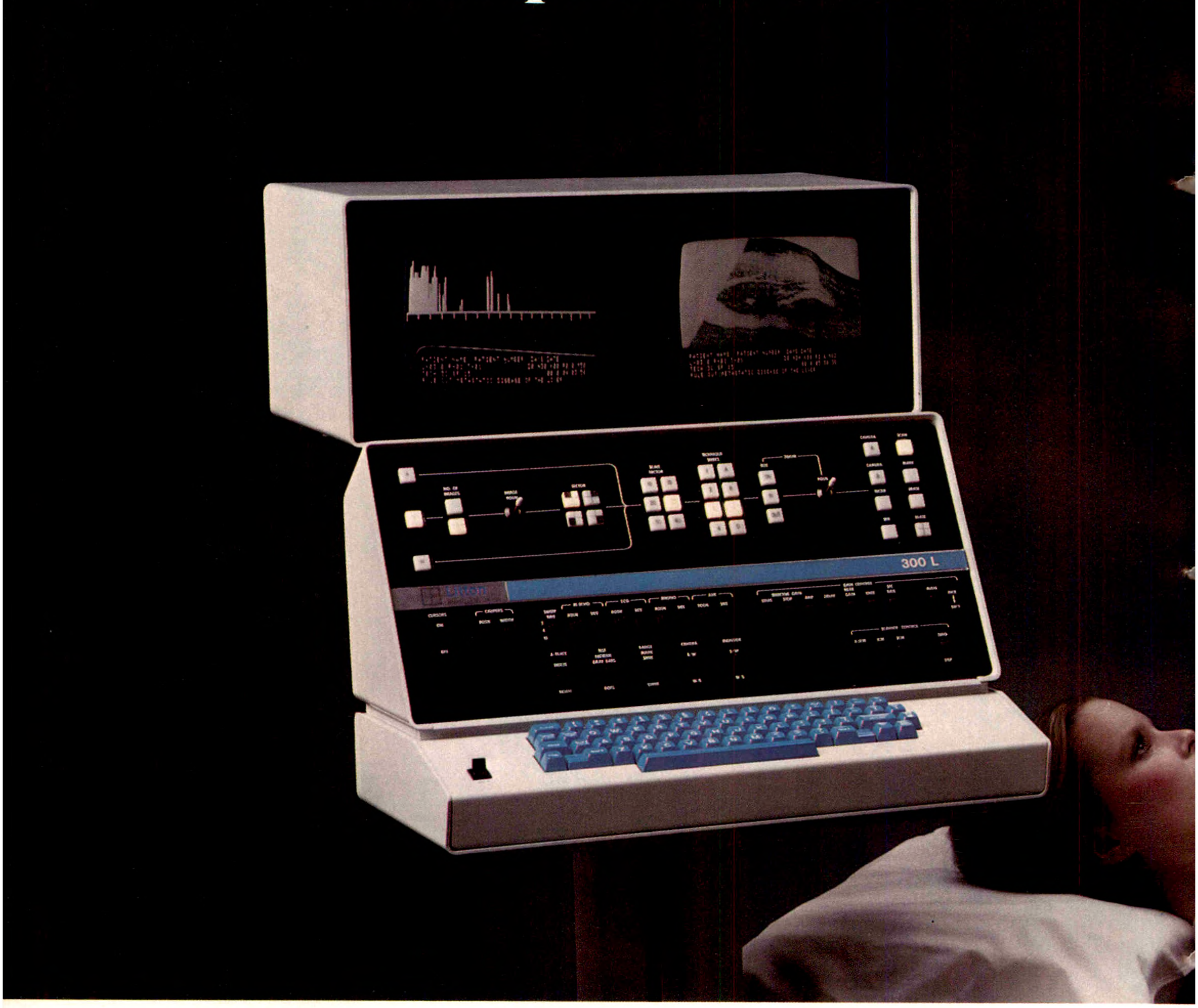

Until now, ultrasound as a diagnostic tool has been viewed as a beautiful idea...attractive for many reasons, with great potential for expanding your diagnostic capabilities...but still more of an art than a science.

Now the new Litton 300L computerized tri-mode ultrasound system has transformed this idea into beautiful reality.

The Litton 300L computer permits the operator to select more processing procedures, automatically enhances the data and improves accuracy of distance measurements. The number of controls needed has been reduced and total patient processing simplified.

No elaborate set-up time. Faster patient thruput.

Modular and mobile. Control console and twin TV monitors can be individually positioned for optimum viewing ease. In fact, the compact modularity of the Litton 300L is what makes it so beautiful.

Clinical usefulness improves, reproducibility of images is enhanced and serial examinations can be accurately done by the Litton 300L. Zoom circuitry lets the operator visualize an area of interest without loss of reference.

If you have been considering ultrasound but wanted more science and less art, let the new Litton 300L show you the perfect marriage: human-engineered ultrasound with computer assistance.

Ask your Litton representative or write for a comprehensive brochure.

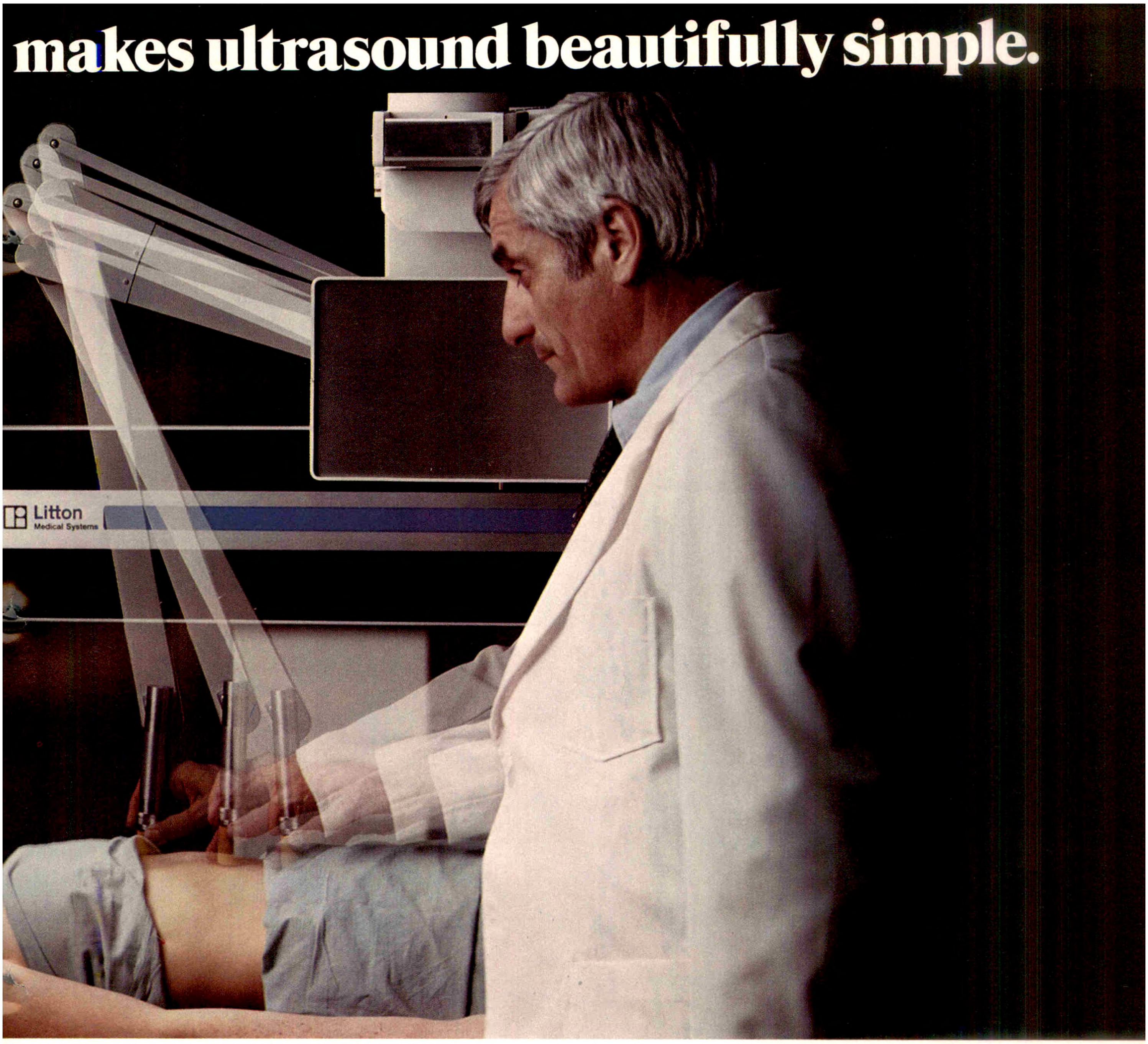

Litton
Medical Systems
515 E. Touhy Avenue, Des Plaines, Illinois 60018

Technology, resources, people
committed to mankind's better health.

Your Pyne rep now carries two top-line products that give superior results.

Now Pyne offers you a new **two-product system** that gives you the ultimate in x-ray results. To top-quality Fuji Film we've added the distribution of Kyokko Intensifying Screens. Together, they're an unbeatable team!

Fuji's still your Number 1 film value for its exceptional contrast, low fog level, and latitude. But Kyokko Intensifying Screens, made by world-famous Dai Nippon Toryo Co., Ltd., let you achieve high-speed without compromise to superior resolution. Result: you get outstanding x-ray results with minimum exposure times. (Kyokko offers both high-speed and medium-speed screens.)

Play both these aces, and you've got a winning hand.

KYOKKO

FUJI FILM
X-RAY

Distributed throughout the U.S. by:

PYNE X-RAY CORPORATION

NEW YORK
20 North Avenue
Larchmont, New York 10538
(914) 834-4567

CHICAGO
1211 West Norwood Avenue
Itasca, Illinois 60143
(312) 773-3360

LOS ANGELES
3637 San Fernando Road
Glendale, California 91204
(213) 240-0280

For Double Contrast Stomachs, Use

NEW! E-Z-HD™

High Density with High Fluidity Barium Sulfate for Suspension USP

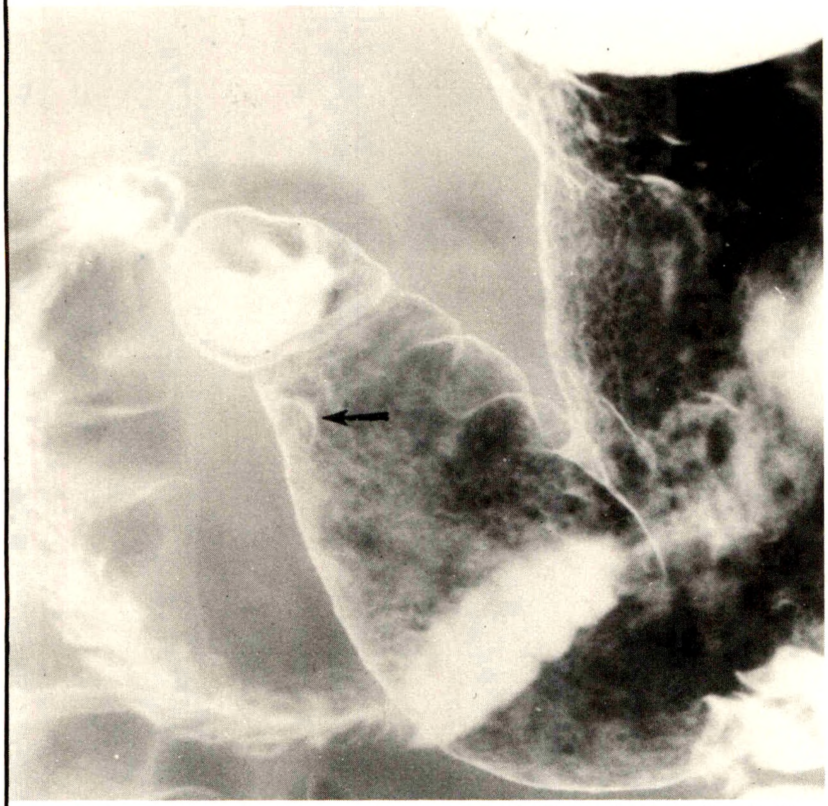

NOTE THE ANTRAL POLYP (ARROW) AND THE LACELIKE AREAE GASTRICAE IN THE BODY OF THE STOMACH.
Film, courtesy of Robert E. Koehler, M.D. Washington University, Dep't. of Radiology, St. Louis, Missouri.

Double contrast radiography appears to offer the potential for significant improvements in diagnostic accuracy.

Double contrast studies of the stomach best demonstrate the surface pattern of the stomach (areae gastricae). This leads to improved detection of superfical erosions and ulcers, malignancies, polyps and other benign tumors, and ulcer scars.

E-Z-HD barium sulfate provides the basic ingredient necessary for good double contrast of the stomach.

The higher the density of the barium suspension, the better the coating, E-Z-HD allows for the highest density suspension of any commercial product on the market today: 85% w/w, 250% w/v. E-Z-HD achieves this density while remaining fluid for ease of administration.

- High density
- High fluidity
- Palatable
- Unit dose convenience.

E-Z-HD – The barium for the double contrast examination of the stomach and duodenum.

Optimal Density & Fluidity for the Modern Double Contrast Examination of the Stomach and Duodenum

Refrences:

David W. Gelfand: The Japanese-Style Double Contrast, Examination of the Stomach, Gastrointest Radiol. 1, 7-17 (1976)

Igor Laufer: The Diagnostic Accuracy of Barium Studies of the Stomach and Duodenum – Correlation with Endoscopy, Radiology 115: 569-573, June 1975

Roscoe E. Miller: The Air Contrast Stomach Examination: an overview. Radiology 117: 743-744 Dec. 1975

E-Z-EM

For Further Information Write:

7 Portland Ave.
Westbury, New York 11590
(516) 333-8230

9/77

PDQ*...

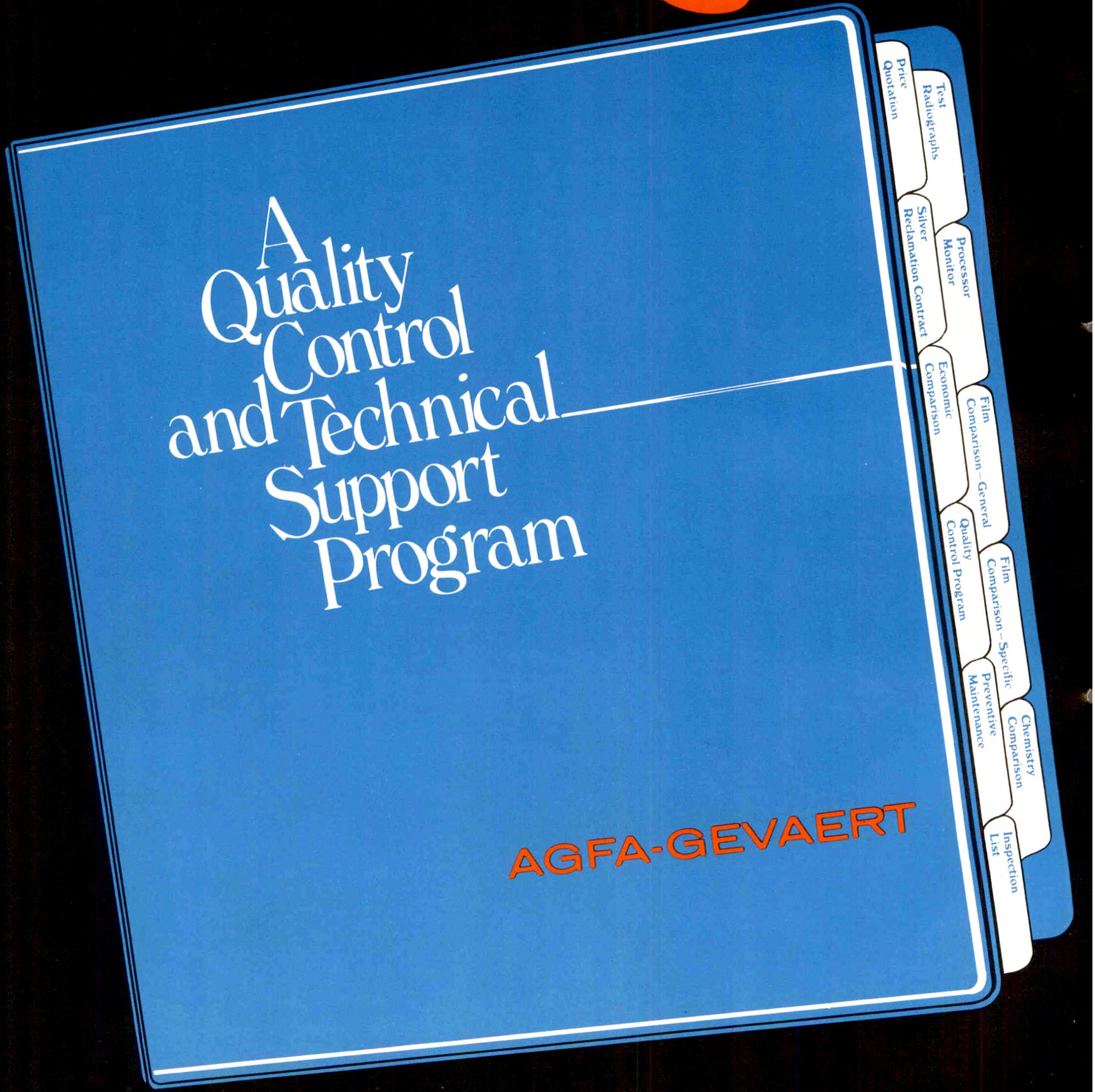

A Quality Control and Technical Support Program

AGFA-GEVAERT

*PDQ . . . Program for Departmental Quality

It's Not What You Think It Is!

In fact, PDQ really stands for our cost-saving *Program for Departmental Quality,* all provided without cost to Agfa-Gevaert users. It's a continuing program designed and geared to your specific needs, providing the technical security that you need to run your department more efficiently and, at lower cost.

Here's what it covers: film and chemistry, processing, mixing and replenishment, screens and cassettes, illuminators, silver recovery, generating equipment and accessories. Plus a very comprehensive preventative maintenance program. And for your security, it's all outlined in our manual, "A Quality Control and Technical Support Program."

Here's how it works: one of our Agfa-Gevaert PDQ Teams will analyze and evaluate your present systems and procedures, all without cost, of course. You see, our PDQ Teams are a group of experts, each highly skilled in his respective field...x-ray technique, processing, sensitometry, generating equipment and accessories. Together, they'll evaluate the findings, then demonstrate, in writing and through comprehensive comparisons within the manual, those areas where they can effect cost reductions, improve efficiency, and provide better patient care.

More importantly, however, once they've initiated the program, they will continue servicing your needs, providing routine re-evaluations, and suggesting additional cost-saving modifications as they become apparent. Periodic equipment inspections, training, and comprehensive technical data are supplied as a matter of course.

In short, as a user of Agfa-Gevaert film, our PDQ Team will provide you with the technical support that you want, **when you want it!**

PDQ...it's not what you thought it was!

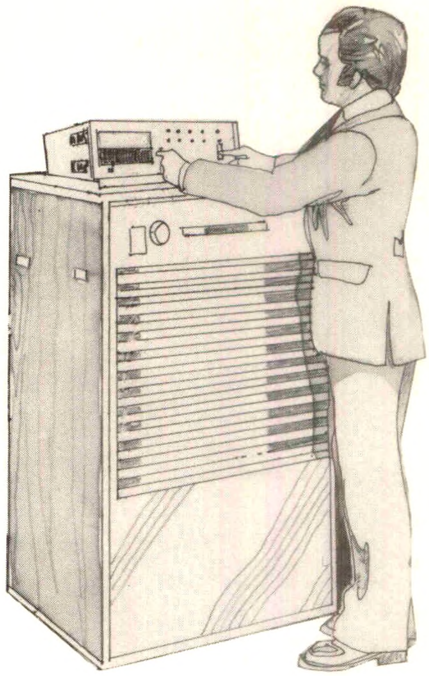

AGFA-GEVAERT

DISTRIBUTED BY: IPCO HOSPITAL SUPPLY CORPORATION
1025 WESTCHESTER AVENUE • WHITE PLAINS, N.Y. 10604 • (914) 682-4500

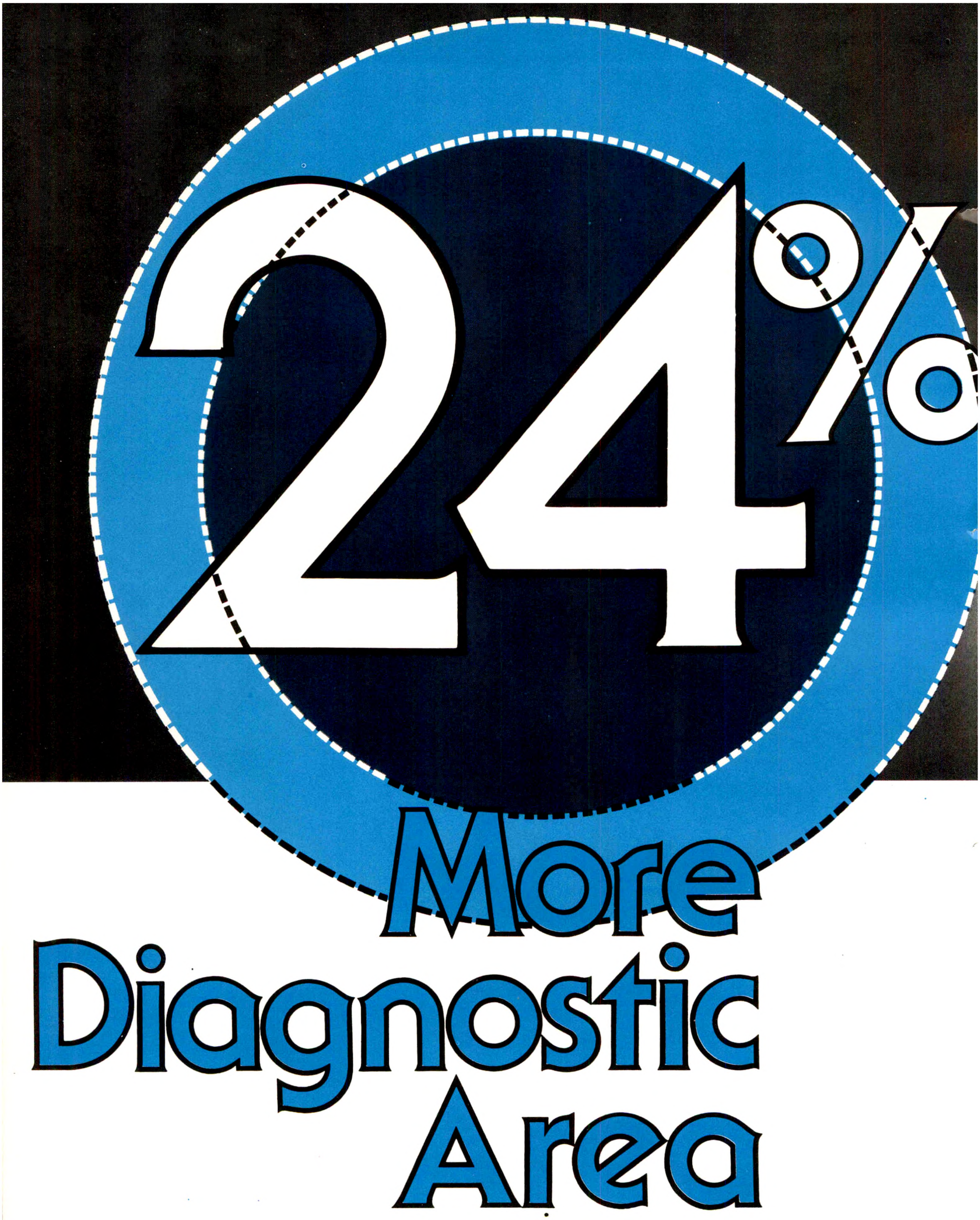
24%
More
Diagnostic
Area

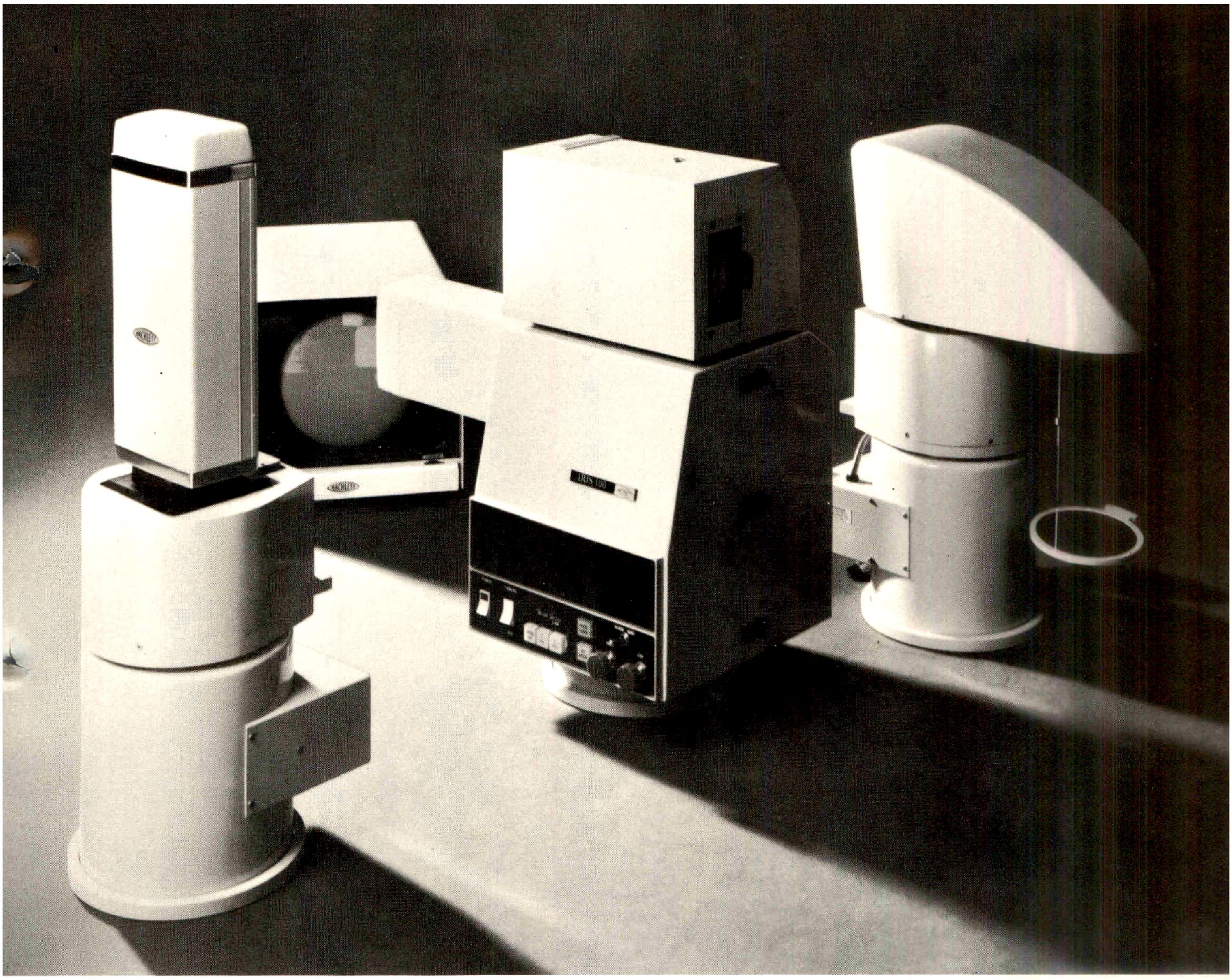

With the new Machlett 17 cm Image Intensifying Systems

***DYNAVISION-17 for TV viewing**
***DYNAVIEW-17 for mirror viewing**
***IRIS 100-17 for combined TV viewing and 100 mm spot filming**

That's nearly one-fourth more anatomy than you see with 6 inch (15 cm) input systems. Think of the added usefulness for your diagnostic R/F equipment.

The heart of each of the systems is the new Machlett Dynascope 17 cm cesium iodide image tube. It gives excellent resolution, increased contrast and improved gain. Available in single or dual field.

For modernizing older equipment or equipping new rooms contact your Machlett x-ray equipment supplier or your Machlett representative.

MACHLETT **The Machlett Laboratories, Incorporated**
1063 Hope Street
Stamford, Connecticut 06907
(203) 348-7511

A Raytheon Company

Du Pont's Quality Control Hospital Center cut

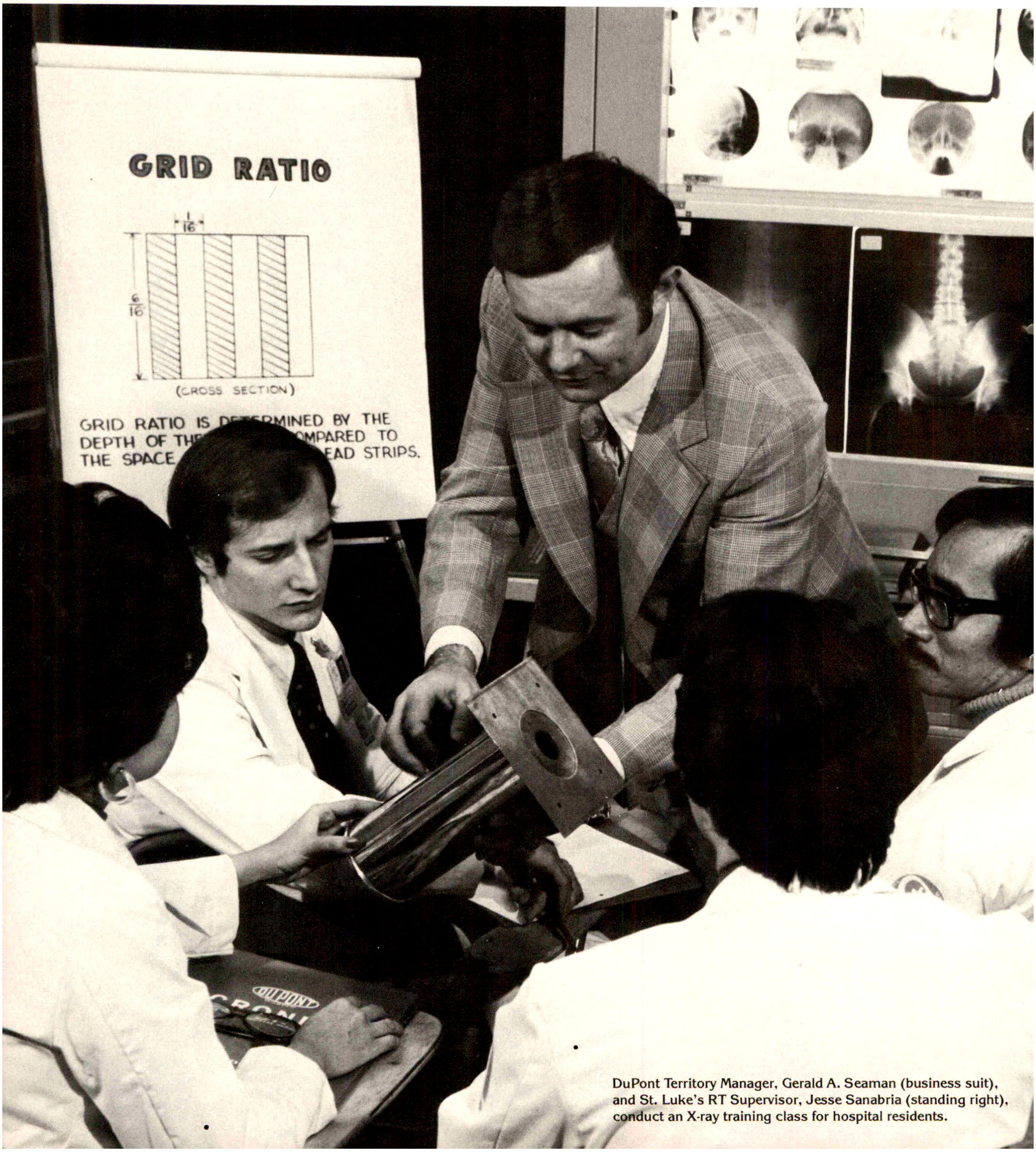
GRID RATIO
1/16
6/16
(CROSS SECTION)
GRID RATIO IS DETERMINED BY THE DEPTH OF THE … COMPARED TO THE SPACE … LEAD STRIPS.
DU PONT
CRONEX

DuPont Territory Manager, Gerald A. Seaman (business suit), and St. Luke's RT Supervisor, Jesse Sanabria (standing right), conduct an X-ray training class for hospital residents.

Program helps St. Luke's X-ray repeat rate to 3%.

"Living teaching aids," like Du Pont's Gerald Seaman, help technicians, residents and supervisors improve X-ray quality and department efficiency.

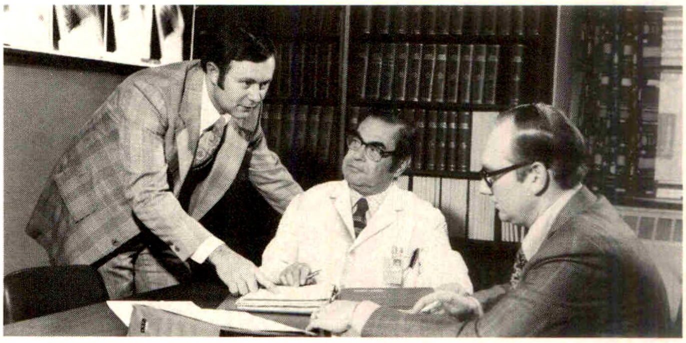

Left to right: Gerald A. Seaman, DuPont Territory Manager; Nathaniel Finby, M.D., Director of Radiology at St. Luke's, and Alexander Ziss, St. Luke's Administrative Director of Radiology.

A team of hospital and DuPont professionals reduced the X-ray examination repeat rate from 10% to 3% in just three months at St. Luke's Hospital Center, New York City. This reduction helped St. Luke's stay within a reduced film budget.

That's one of the features of DuPont's Quality Control Program: to train people to deliver high-quality radiographs efficiently.

As Nathaniel Finby, M.D., Director of Radiology at St. Luke's, says, "DuPont offers more than just film. DuPont representatives serve as 'living teaching aids,' training my staff to turn out better radiographs, more efficiently. This approach is helping my people do a better job."

St. Luke's staff of 135 identifies and solves problems faster now. Mark Suffin, Technical Administrator at the Hospital, coordinated the successful Quality Control Program. He reports that employee morale is high and a new team spirit has evolved.

This is all part of DuPont's commitment...personal involvement to help improve patient care and reduce costs.

Personal Involvement: The key to extra quality in radiologic systems.

DU PONT

REG US PAT & TM OFF

American Journal of Roentgenology
Guidelines for Authors

The *American Journal of Roentgenology* publishes original and timely contributions to the advancement of radiologic diagnoses and treatment. Although the content is predominantly clinical in origin, laboratory investigations are accepted when their relevance to clinical practice is demonstrable. Material published elsewhere, in substance or illustration, will not be considered. Prior publication of abstracts, however, will not prejudice publication of the complete study. Contributions are reviewed by two outside consultants and are accepted on condition that they are submitted only to this Journal and that they will not be reprinted or translated without consent of the Editor. Statements within an article are the responsibility of the authors and not the Journal or its publisher.

Address all manuscripts and correspondence to the Editor, Dr. Melvin M. Figley, 403 Pacific National Bank Building, 4545 15th Avenue N.E., Seattle, Washington 98105.

Manuscript Form

Manuscripts should be typed double-spaced throughout, including references, tables, and footnotes. Tables, footnotes, and figure legends should be on separate sheets, and a separate title page should be provided. In addition to the original typewritten copy, a duplicate copy complete with figures, tables, and references is required. Authors' names should be on title page only and should not be on figures so that author anonymity can be maintained during the review process.

Figures should be submitted as 13 X 18 cm glossy prints, untrimmed and unmounted. Each should be numbered to correspond with figure legends, and the top should be indicated. Written permission is required for reproduction of previously published figures, and such material must be clearly noted and credited in the manuscript. Specific permission for publication of facial photographs of patients is required. Line illustrations and graphs should be drawn in black ink on white background. Labels on all figures should be of professional quality and sufficiently large to be easily read when reduced in size.

References should be cited in the text by number (e.g., [3, 4]). The bibliography should be arranged in the numerical order that references are cited in the text and typed double-spaced throughout. Data for each reference should be arranged according to the uniform style on bibliographic citations adopted by many biomedical journals. Provide all authors' names and inclusive pages. Abbreviations for titles of medical periodicals should conform to those published in *Index Medicus*. Examples:

1. Miller RE, Chernish SM, Skucas J, Rosenak BD, Rodda BE: Hypotonic roentgenography with glucagon. *Am J Roentgenol* 121:264–274, 1974
2. Boijsen E: Superior mesenteric angiography, in *Angiography*, edited by Abrams H, Boston, Little, Brown, 1971, pp 1091–1119

Organization

Title page. Titles should be brief and specific. Include full names and addresses of all authors and acknowledgment of grant support when appropriate.

Abstract. A description of the purpose, methods, results, and conclusions of the study is required. It should be informative to a reader who has not read the text of the article.

Introduction. Clearly state the purpose of the investigation including necessary background facts.

Materials and methods. Describe the protocol clearly so that an experienced worker can understand what was done. Use standard abbreviations as presented in the *Council of Biology Editors Style Manual,* 3d ed. Metric measurements should be used throughout.

Results. Present results in logical sequence.

Discussion. Interpret the results to lend meaning and importance to the observations. If hypotheses and speculation are included, they must be labeled as such. When results differ from those of previous investigators, an attempt should be made to explain the discrepancy.

References. Only include those references which provide adequate background and present fairly any opposing evidence and concepts. Accuracy of reference data is the responsibility of the author.

Legends. Legends should be brief but should provide sufficient description to interpret the figure.

Special Communications

Case Reports. Concise case reports are accepted if they present unusual experiences that are medically important and educational. Clarity and brevity are essential.

Technical notes. Brief descriptions of new techniques or significant modifications of older ones which are directly applicable to clinical practice will be accepted.

Letters to the Editor. Letters are subject to editing and condensation. Criticism of published articles should be objective and constructive. Letters may also discuss matters of general interest to radiologists.

Proofs and Reprints

Galley proofs will be sent to authors for correction of errors and approval of illustrations. The corrected proof, copy-edited manuscript, and reprint order should be returned to the editorial office within 48 hr of receipt. Failure to adhere to this schedule may mean publication without the author's approval.

ARS Presidential Address:

Cancer of the Breast: A Time for Caution

LUTHER W. BRADY[1]

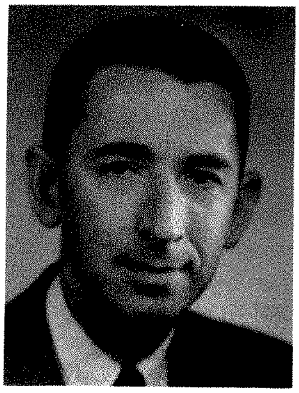

L. W. Brady

Cancer of the breast accounts for 26% of all malignancies in the female and for 20% of all deaths due to cancer in women. In 1977, the American Cancer Society anticipates that 89,000 new cases of breast cancer will be diagnosed, and 33,700 deaths will be attributed to the disease. These estimates are based upon data from the National Cancer Institute's Third National Survey (1969–1971) [1].

Breast cancer is a major clinical problem in that, although most patients present with localized or regional disease, more than half die with disseminated disease. Prior concepts, upon which treatment has been based, conceived the disease as a localized process gradually spreading from a single focus in one breast, involving contiguous breast tissue, then lymph nodes, and finally spreading to distant sites. For more than 75 years this has been the basis of surgical treatment. But surgical thinking is rapidly changing. Limited operations for selected cancers, a new view of the role of radiation therapy in conjunction with surgical procedures, and the tentative reliance on adjuvant chemotherapy have become accepted in the best surgical circles.

These changing concepts offer great promise for optimum management of the patient with breast cancer. But, unfortunately, many of the important factors influencing prognosis have been omitted in the public debate over the efficacy of one treatment technique over another. We must eliminate chauvinism about our specialties and determine how we can best coordinate surgery, radiation therapy, and chemotherapy to optimize treatment. Therapeutic goals include cure of the patient, acceptable cosmetic effect, and good functional result. These must remain paramount in our thinking.

Well established factors influencing prognosis must be considered in the selection of any treatment program. For cancer of the breast these include: size of the tumor; location of the tumor in the breast; pathologic staging and nodal status; histologic tumor typing; grading of tumor; description of cellular reaction; type of surgery performed; description of any adjuvant therapy (radiation therapy, chemotherapy, immunotherapy); absolute 10 year survival rates; statement of local/regional recurrence rate; and description of cosmetic and functional result. These eleven factors must be weighed in the final selection of a treatment program for each patient.

Surgical techniques should be chosen with these factors in mind, considering the maximum potential for cure consonant with the fewest complications. Radiation therapy should be applied with carefully established criteria. Chemotherapy, now an important mode of adjuvant treatment, must be used in patients where the risk of disseminated disease is high.

Each of the treatment techniques has major potentials. The surgical procedure in appropriately selected patients may be all that is required for control of disease. Radiation therapy to the chest wall and regional lymph nodes in the postoperative period can prevent local and regional occurrence. Chemotherapy, when combined with appropriate surgery and/or radiation therapy, improves local control of the disease process and favorably influences metastatic spread. It is possible that chemotherapy may eventually eliminate surgical treatment of some cancers, or at least reduce the amount of tissue that must be removed or definitively irradiated.

Some contemporary concerns by those dealing with breast cancer relate to the role of mammography, the type of workup and selection of patients for various treatment programs, the choice of appropriate surgery, the role for radiation therapy, the role for chemotherapy, and the influence of these treatment technqiues on immunocompetence and tumor induction.

Mammography

There is no question that mammographic examinations allow earlier diagnosis of breast cancer, thus permitting more effective treatment with improved survival for the earliest cases. In the work from the 27 American Cancer Society/National Cancer Institute Breast Cancer Detection Demonstration Projects, 1,171 unsuspected cancers were found in 260,000 mammographic studies [2]. If mammography had not been used, these breast cancers would not have been detected as early. There was no evidence of axillary nodal involvement in 79% of

---

Presented at the annual meeting of the American Radium Society, Las Vegas, Nevada, April 1977.

[1] Department of Radiation Therapy and Nuclear Medicine, Hahnemann Medical College and Hospital of Philadelphia, 230 North Broad Street, Philadelphia, Pennsylvania 19102.

detected cases; thus these represent early, highly curable tumors.

For cancers detected by mammography alone, 5 year survival rates of up to 95% have been reported [3]. In spite of the major controversy over the proper role for this diagnostic technique, the following represent generally selected criteria for mammographic examinations.

Guidelines developed by the National Cancer Institute/American Cancer Society/American College of Radiology advise annual screening for all women over the age of 50, since in this group, benefits clearly outweigh any minimal long term risk from radiation.

For women aged 35-50, mammography should be offered to those at high risk to develop breast cancer. Ten indications in this age group are: chronic cystic mastitis, with or without pain; lumps and thickening in the breast; nipple discharge or other nipple abnormalities; personal history of breast cancer; familial history of breast cancer (maternal, paternal, or sisters); early onset of menstruation; no previous pregnancy; first full-term pregnancy at age 30 or older; breast surgery scheduled for diagnostic purposes; and fear of breast cancer that requires the reassurance of a negative examination.

It is estimated that 80% of women between the ages of 35 and 50 will belong to at least one of these groups. The remaining women in the 35-50 age group and those under 35 without particular breast problems should be taught the proper technique of breast self-examination and urged to perform it regularly every month.

Because breast cancer is so serious a problem and mammography so valuable a clinical diagnostic aid, contradictory judgments about the hazards of mammography based on fragmentary, tentative, or inconclusive data should be avoided. An unsuspected cancer, successfully treated, is a medical triumph.

Pretreatment Workup

Appropriate workup for a patient with cancer of the breast includes chest films, biochemical profile, complete blood count, and radionuclide liver and bone scans all done within the context of a careful, complete history and physical examination. It seems appropriate to recommend that "lumpectomy" be carried out, the diagnosis of cancer established, and a metastatic workup performed prior to the choice of treatment. Unfortunately, this is not done with regularity.

Data accumulated from the National Cancer Institute breast cancer epidemiologic studies indicate that most patients do not have appropriate workup prior to the selection of treatment. Table 1 indicates the type of workup in a group of patients reviewed. In 24% of the patients, a chest radiograph was not performed before mastectomy, and more than 80% had no metastatic workup prior to mastectomy.

Table 2 demonstrates an important change in distribution of cases from 1970 to 1976: a greater proportion of patients with earlier disease were seen in 1976. This improvement is related to a higher level of diagnostic sensitivity among practicing physicians and to greater utilization of diagnostic screening techniques.

TABLE 1

Baseline Workup for Extent of Disease

Workup	Percentage
Chest x-ray before mastectomy	76
Metastatic bone survey or bone scan:	
Prior to surgery	10
After surgery	15
Before other treatment	3
Not performed or recorded	72

Note.—Unpublished data from National Cancer Institute breast cancer epidemiologic studies.

TABLE 2

Change in Presenting Stage

Stage at Initial Presentation	Percentage	
	1970	1976
O	2	5
I	25	54
II	45	29
III	28	12

Note.—Unpublished data from National Cancer Institute breast cancer epidemiologic studies.

Surgery

The modern surgical approach to breast cancer is based upon the following precepts:

1. Breast tissue surrounding a localized breast cancer is no more a threat than the tissue in the opposite breast.
2. Breast cancer may disseminate before it is clinically apparent in as many as 50% of patients. Recent data from bone scanning indicate that this incidence increases with increasing tumor size in the breast, with axillary node involvement, as well as with advancing stage [4].
3. Many women now wish to consider various treatment options and may even select one which is stated as having greater risk.

To decrease the complications from radical mastectomy, more conservative resections are currently being carried out. The classical Halstead radical mastectomy is no longer performed, and the number of patients having the standard radical mastectomy is declining. More patients now have modified radical mastectomy, simple mastectomy, or total mastectomy than as recently as 1970. The extent of this change is shown in table 3. This has been motivated by a desire to diminish the incidence of surgical complications and in the hope that the end result of the surgical technique would not be compromised.

In a recent study by Robinson et al. [5], modified radical mastectomy was shown not to compromise the potential for cure in carefully selected patients compared to previous data using radical mastectomy (table 4). However, the histopathologic information provided by radical mastectomy is important in planning further treatment. Axillary lymph node metastasis and the level of nodal involvement are important criteria in selecting patients

TABLE 3

Type of Mastectomy

Type	Percentage	
	1970 (N = 179)	1976 (N = 48)
Radical	51	25
Modified radical	16	57
Total	18	5
Partial	3	6
No surgery	5	5
No data	7	2

Note.—Unpublished data from National Cancer Institute breast cancer epidemiologic studies.

TABLE 4

Survival at 5 Years

	Total Group	Type of Mastectomy	
		Modified Radical	Radical
No. patients	541	205	336
Mean age (years)	59.0	62.3	57.0
Positive axillary nodes (%)	38.4	31.2	42.9
5 year survival (%):			
Negative axillary nodes	85.2 (94.3)	84.0 (96.0)	86.0 (94.0)
Positive axillary nodes	66.1 (71.4)	66.0 (75.0)	66.0 (70.0)
Total	77.9 (86.4)	78.2 (88.9)	77.6 (83.3)

Note.—Data from the Mayo Clinic, 1965–1968 [5]. Numbers in parentheses represent relative survival.

for various postoperative treatment programs. In addition, the surgical procedure removes the major portion of the tumor and gives information on the cell type. The role of surgery in the treatment of patients with carcinoma of the breast is well established and makes significant contributions to overall patient management.

Radiation Therapy

Local chest wall recurrence as well as regional axillary, supraclavicular, and internal mammary nodal recurrences occur after all forms of primary surgical management of breast cancer. The frequency of the different types of recurrence has been established in large surgical series. Postoperative irradiation of patients at risk can prevent local and regional recurrence and provide important clinical and emotional reassurance for the patient. Furthermore, data recently available (H. Host, personal communication) indicate that postoperative irradiation also has an important influence on improving disease-free survival (fig. 1).

Radiation therapy in the management of the patient with breast cancer makes four contributions:

1. As definitive treatment for patients with clinical T1, T2, N0 lesions. Numerous studies [6–10] establish the fact that 5 year survivals in the range of 90% or better can be achieved by definitively administered radiation as the primary means of management of patients with small tumors limited to the breast.

2. For postoperative control of local and regional recurrence. This has a beneficial influence on survival [9; H. Host, personal communication]. Indications for postoperative radiation therapy to the peripheral lymphatics include: outer quadrant lesions with positive axillary nodes; small inner or central quadrant lesions with negative axillary nodes; and outer, inner, or central quadrant lesions without grave signs (which indicate poor prognosis) and with less than 20% positive axillary nodes. Indications for postoperative irradiation to the chest wall in addition to the peripheral lymphatic areas include: 20% or more positive axillary lymph nodes; breast mass greater than 2 cm; central or inner quadrant mass with positive axillary nodes; multiple foci of invasive cancer; vascular, perineural, or lymphatic invasion; and grave signs, including fixation of tumor to pectoral fascia and skin fixation, edema, or erythema.

3. As preoperative management in selected cases. Patients with inflammatory carcinoma and stage III carcinoma may benefit from preoperative irradiation as an alternative to definitive radiotherapy or definitive primary surgery.

4. For palliation of symptoms due to brain metastases, bone metastases, lung metastases, superior vena caval obstruction due to metastases, spinal cord epidural metastatic disease, liver metastases, and others.

Chemotherapy

The current strategy for use of adjuvant chemotherapy for patients with T1, T2, N1 (stage II) lesions of the breast primarily involves prolonged, intensive, intermittent chemotherapy following primary treatment. The rationale is based upon the clinical demonstration of successful chemotherapy in other tumor sites (e.g., solid tumors in childhood, acute leukemia, osteosarcoma, Hodgkin's disease, etc.). The following ongoing clinical trials under the aegis of the National Cancer Institute illustrate this principle [11]: Greenspan's combination of antimetabolites; alkylating agents with corticosteroids and androgens; the Cooper regimen of five drugs; the Cytoxan-methotrexate-5-fluorouracil programs; various studies on L-phenylalanine mustard under the National Surgical Adjuvant Breast Program; and the ECOG programs. The Milan study using CMF is another example [12].

The potential of these approaches has barely been realized. Breast cancer is a chronic heterogeneous disease, and the yield of clinical trials of necessity will take considerable time for evaluation. Overall strategy should be based upon careful application of increasing knowledge, recognizing that early trends are important, but that premature alterations of plans may be counterproductive in the long run. The pressure of widely publicized, premature conclusions is almost irresistable, but the scientific community, the public, and Congress must always be aware of the necessity to proceed in a deliberate manner.

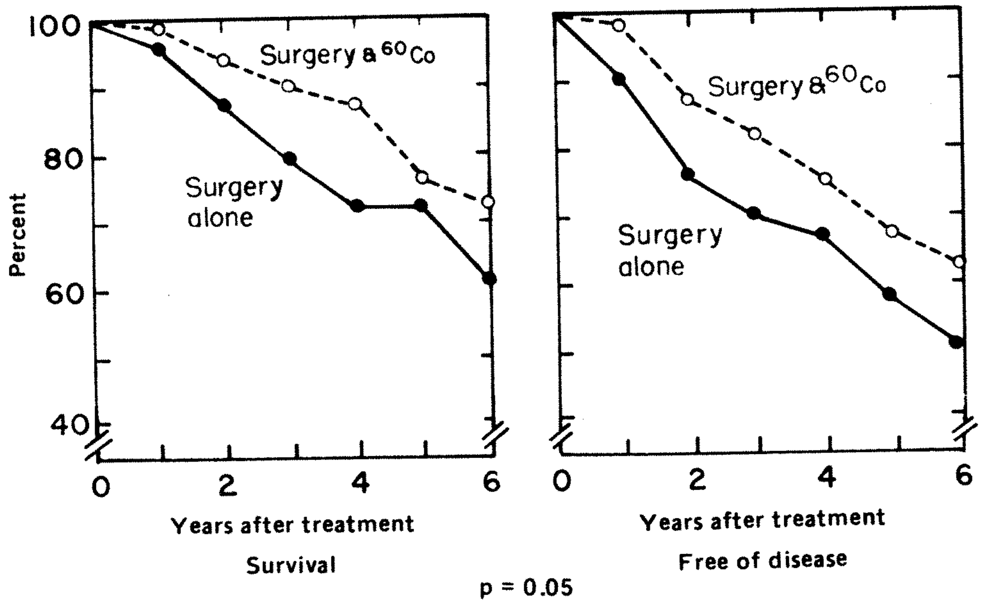

Fig. 1. – Effect of postoperative irradiation on disease-free survival. Stage II mammary carcinoma, ^{60}Co trial, axillary nodes histologically positive. (Reprinted with permission from Brady LW, Fletcher GH, Levitt SH: Cancer of the breast: the role of radiation therapy after mastectomy. *Cancer* 39:2868-2874, 1977)

Although new concepts of chemotherapy may bring great benefit to patients afflicted with breast cancer, cautious interpretation of results must prevail at this time. The first National Surgical Adjuvant Breast Program trial indicated that there was no overall benefit from the utilization of thiotepa in patients with negative axillary nodes regardless of menopausal status (H. Host, personal communication). However, there was a presumed treatment effect in premenopausal patients with four or more positive nodes. In this particular group of patients, the 10 year experience indicates improved survival. Thiotepa was administered in short-term fashion and immediately related to the surgical procedure. Postmenopausal patients, however, derived no benefit regardless of the nodal status.

Current clinical chemotherapy trials are directed toward stage II patients. Recent evaluation of the L-Pam study [13] revealed an overall benefit at 2 years, most marked in patients 49 years of age or less, premenopausal, and with three or more positive axillary nodes. This study established that single adjuvant chemotherapy was safe and feasible. In the Milan trial [12] using Cytoxan, methotrexate, and 5-fluorouracil in patients with stage II disease, significant treatment benefits seem limited to premenopausal patients especially in the category of one to three or more positive axillary nodes. These effects were not noted in patients who were postmenopausal. The lack of effect in postmenopausal patients suggests the need for concomitant additive hormonal therapy and/or longer treatment. The effect in the premenopausal patients may be due in part to chemical castration, as confirmed by studies in premenopausal patients with recurrence done at the Mayo Clinic and by the Cancer Acute Leukemia Group B (unpublished data).

Data from the various clinical trials using chemotherapy as an adjuvant to surgery in stage II breast cancer indicate the agents do delay recurrence in some patients, most strikingly in those who are premenopausal. It will not be clear for some time which current program is superior. A large number of patients will be necessary because of the multiple issues of prognosis involved. Yet because definitive results for each trial are not available immediately, long term analyses must proceed concomitantly with the introduction of each new clinical trial.

The major value of systemically administered chemotherapy is to deal with patients who have high risk of distant disseminated disease. However, in this same group of patients, there is also a large tumor cell burden. Therefore, the integration of chemotherapy in other multidiscipline treatment programs is of importance for a major effect on the tumor in all locations.

Chemotherapeutic agents suppress the immune response, damage normal tissue, and may themselves cause cancer. As Constanza [14] has pointed out, they may be of greater harm than benefit. For these reasons, patients with more advanced disease have generally been the subjects of clinical trials. Even so, cancer chemotherapy is one of the major accomplishments of modern medicine.

Conclusions

For patients with cancer of the breast, specific factors influencing prognosis have been identified and must be stated when treatment results are assessed. There is good evidence that the mammographic study is a valuable asset in early diagnosis and that surgical management is useful for both staging and cure.

Radiation therapy is valuable for local and regional control and for relapse-free survival. In selecting radiation therapy, it must be remembered that criteria for selection of patients are important, that irradiated volumes and dosages are critical, and that long term risks are minimal.

Patients at risk for recurrent disease will benefit from adjuvant chemotherapy, although criteria for selection of cases are important. In addition, techniques, dosages, and length of treatment are critical. Long term risks of such treatment are real but probably small.

With both radiation therapy and adjuvant chemotherapy, the criteria for selection of patients are similar.

Public debate as to the efficacy of one treatment technique versus another in the management of the patient with breast cancer contributes little to progress and may in fact be harmful. Integration of multidisciplinary techniques may contribute more to the ultimate outcome of this disease than any single treatment modality alone. Patients at high risk may require all techniques to deal with their major tumor cell burden.

Breast cancer represents a major clinical problem. Much has been done to identify factors of importance in anticipating ultimate outcome. Integration of these prognostic factors as well as those that are only now being observed into major treatment programs may optimize selection of the most appropriate treatment. Only by a modulated multidisciplinary approach can the cure rate for breast cancer be significantly advanced.

REFERENCES

1. American Cancer Society: Cancer Facts and Figures. New York, American Cancer Society, 1977
2. Dodd DG: Present status of thermography, ultrasound and mammography in breast cancer detection. *Cancer* 39:2796–2805, 1977
3. Update on mammography. *American College of Radiology Bulletin,* vol 32, no. 10, October 1976
4. Brady LW, Croll MN: Clinical uses of bone scanning. *Skel Radiol* 1:161–167, 1977
5. Robinson GN, can Heerden JA, Payne WS, Taylor WF, Gaffey TA: The primary surgical treatment of carcinoma of the breast: a changing trend toward modified radical mastectomy. *Mayo Clin Proc* 51:433–442, 1976
6. Weber E, Hellman S: Radiation as primary treatment for local control of breast carcinoma. *JAMA* 234:608–611, 1975
7. Prosnitz LR, Goldenberg IS, Packard RA, Levene MB, Harris J, Hellman S, Wallner PE, Brady LW, Mansfield CM, Kramer S: Radiation therapy as initial treatment for early stage cancer of the breast without mastectomy. *Cancer* 39:917–923, 1977
8. Pierquin B, Baillet F, Wilson JF: Radiation therapy in the management of primary breast cancer. *Am J Roentgenol* 127:645–648, 1976
9. de Schryver A: The Stockholm breast cancer trial: preliminary report of a randomized study concerning the value of preoperative or post-operative radiotherapy in operable disease. *Int J Radiat Oncol Biol Phys* 1:601–609, 1976
10. Wallner PE, Brady LW, Loughead J, Matsumoto T, Antoniades J, Prasasvinichai S, Glassburn JR, Asbell SO, Damsker JI: Subtotal mastectomy and radiation therapy in the definitive management of localized breast malignancy. *Am J Roentgenol* 127:505–507, 1976
11. Fisher B, Montague E, Redmond C, Barton B, Borland D, Fisher ER, Deutsch M, Schwarz G, Margolese R, Donegan W, Volk H, Konvolinka C, Gardner B, Cohn I Jr, Lesnick G, Cruz AB, Lawrence W, Nealon T, Butcher H, Lawton R: Comparison of radical mastectomy with alternative treatments for primary breast cancer: a first report of results from a prospective randomized clinical trial. *Cancer* 39:2827–2839, 1977
12. Bonadonna G, Rossi A, Valagussa P, Bonfi A, Veronesi U: The CMF program for operable breast cancer with positive axillary nodes: updated analysis on the disease-free interval, site of relapse and drug tolerance. *Cancer* 39:2904–2915, 1977
13. Fisher B: L-phenylanaline mustard (L-Pam) in the management of primary breast cancer: an update of earlier findings and a comparison of those utilizing L-Pam plus 5-fluorouracil (5-Fu). *Cancer* 39:2883–2903, 1977
14. Constanza ME: The problem of breast cancer prophylaxis. *N Engl J Med* 293:1095–1097, 1975

Gray Scale Ultrasonography of the Gallbladder: An Evaluation of Accuracy and Report of Additional Ultrasound Signs

JOSEPH C. ANDERSON[1] AND ROGER K. HARNED[1]

Ultrasound examinations of 76 patients with suspected gallbladder disease were compared with radiographic, surgical, and pathologic findings to determine the accuracy of the ultrasound examinations. In 13 of the 76, the gallbladder was not visualized by ultrasound. Diagnosis of the presence or absence of gallstones was correctly made by ultrasound in 56 of 63 visualized gallbladders, for an accuracy rate of 89%. A high proportion of nonvisualized gallbladders (10 of 13) contained gallstones. Previously unreported ultrasound findings of a stone impacted in the proximal cystic duct and findings of a collection of bile in the lesser sac associated with cholelithiasis and choledocholithiasis are illustrated.

Several reports on the value of ultrasound in the diagnosis of gallbladder disease have appeared [1–7] (table 1). Early reports indicated a large number of gallbladders were nonvisualized by ultrasound, and a high false negative rate was encountered. The accuracy rate has increased with improved technique and equipment with B-scan gray scale capability [5–9]. Expanded criteria [4] for diagnosis of gallstones have also aided in reducing the number of cases which are indeterminate by ultrasound examination. Our experience with ultrasonic evaluation of the gallbladder was reviewed to assess the accuracy of the examination. Two ultrasound findings related to gallbladder disease which have not been reported previously are illustrated.

Subjects and Methods

Seventy-six patients suspected of gallbladder disease were examined by B-mode gray scale ultrasound at our institution. Indications for examination included suspected cholecystitis, nonvisualized gallbladder by oral cholecystography, palpable right upper quadrant mass, suspected right upper quadrant mass by radiography, and jaundice of unknown etiology. Radiographs and medical records were reviewed to determine the radiographic, laboratory, surgical, and pathologic findings to correlate with the ultrasound findings. The criteria considered as conclusive evidence of the presence or absence of cholelithiasis were surgical or pathologic examination of the gallbladder, or conclusive oral or intravenous cholecystography.

Ultrasound studies were performed with a Picker Echoview 5 ultrasound scanner with EDC gray scale. The highest ultrasound frequency that allowed sufficient depth penetration for visualization of the gallbladder was used in order to obtain the best possible resolution. Transducer frequencies were 2.25, 3.5, and 5.0 MHz. Patients were examined in the supine and sitting positions with suspended respiration. Closely spaced transverse and longitudinal sections through the gallbladder were obtained. The majority of patients were fasting for at least 12 hr prior to the examination.

Ultrasound findings were classified as negative for calculi, cholelithiasis, or nonvisualization. Surgical proof of diagnosis was available in 30 cases. Conclusive oral or intravenous cholecystography was considered as proof in 30 and 15 cases, respectively. Autopsy proof was available in one case.

Results

Criterion for a gallbladder negative for calculi was identification of a smoothly marginated echo-free zone in the right upper quadrant, posterior and medial to the right lobe of the liver, with a shape characteristic of the gallbladder.

The classical findings of cholelithiasis were the presence of high amplitude echoes from the lumen of the gallbladder usually associated with an acoustic shadow distant to the calculus. Movement of the echo complex to the dependent portion of the gallbladder with change in position of the patient was used as additional evidence of cholelithiasis. Occasionally with very small calculi the only ultrasound finding was irregularity of the contour of the posterior wall of the gallbladder. A linear, horizontally distributed collection of floating calculi was present in one case. In another patient, gas containing calculi presented as strong echoes from the nondependent portion of the gallbladder.

Low level echoes from within the gallbladder without acoustical shadowing and with sluggish motion on change of position of the patient were found in two cases which had viscous bile or biliary "sludge." Findings of a calculus impacted in the proximal cystic duct

TABLE 1

Accuracy of Ultrasound for Detection of Cholelithiasis

Reference	No. Cases	Gallbladder		Accuracy in Visualized Gallbladders (%)
		Visualized	Not Visualized	
Hublitz et al. [1]	12	11	1	. . .
Goldberg et al. [2]	195	114	81	72
Doust and Maklad [3]	50	45	5	80
Crow et al. [4]	50	46	4	100
Arnon and Rosenquist [5]	123	121	2	90
Leopold et al. [6]	75	69	6	91
Lawson [7]	81	61	20	95
Present report	76	63	13	89

Received April 27, 1977; accepted after revision August 16, 1977.

[1] Department of Radiology, University of Nebraska Medical Center, 42nd and Dewey Avenue, Omaha, Nebraska 68105. Address reprint requests to J. C. Anderson.

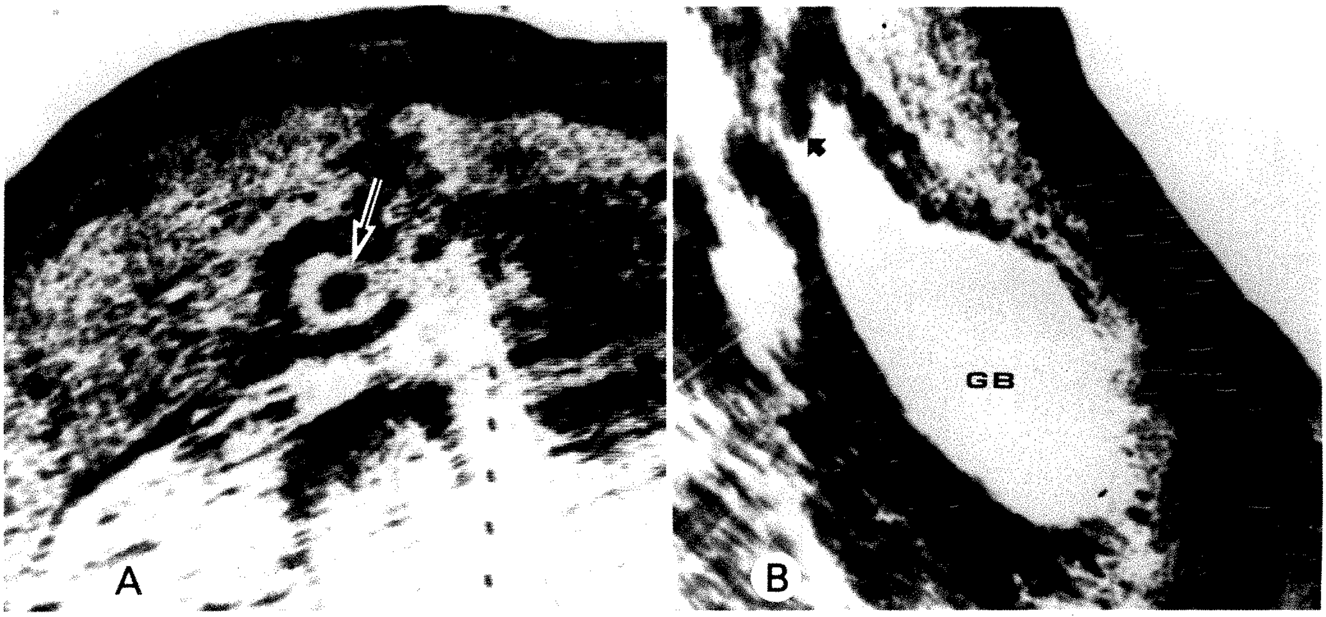

Fig. 1.—Case 1. Gallbladder calculus with stone impacted in proximal cystic duct. *A*, Transverse scan through cystic duct region showing calculus (C) causing target-shaped echo pattern. *B*, Longitudinal scan with patient in sitting position showing calculus (*arrow*) in nondependent region of gallbladder (GB).

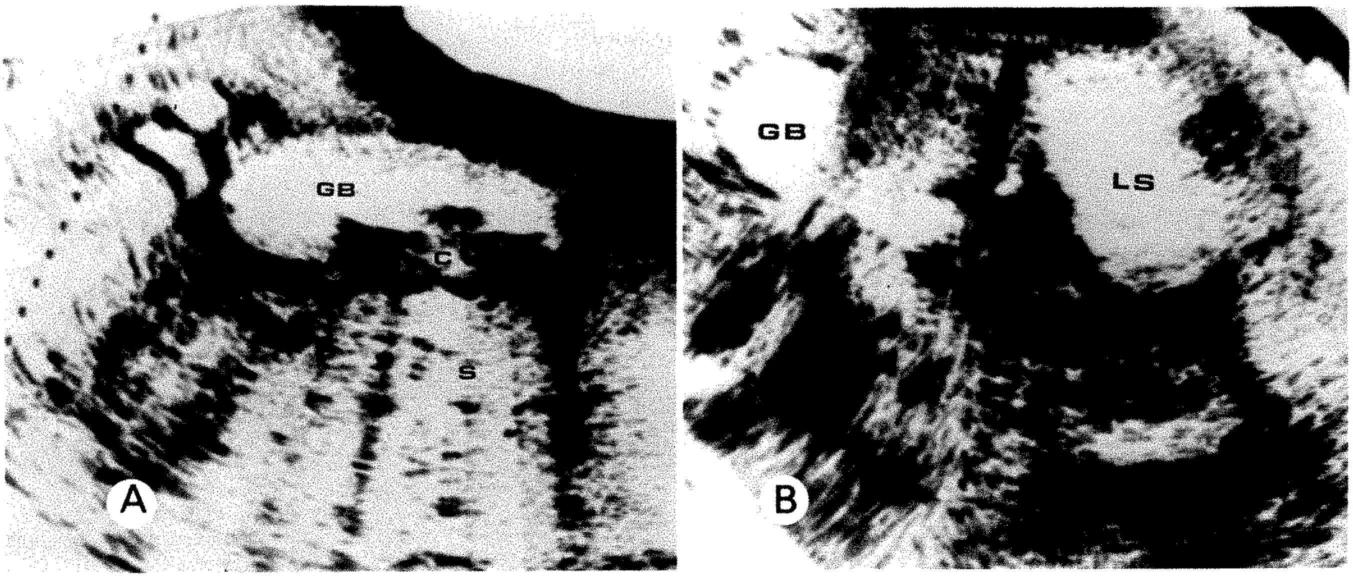

Fig. 2.—Case 2. Cholelithiasis with associated collection of bile in lesser sac. *A*, Longitudinal scan showing calculi (C) in dependent portion of gallbladder (GB). Note shadowing (S) posterior to calculi. *B*, Transverse scan showing echo-free mass in left upper quadrant secondary to collection of bile in lesser sac (LS).

and bile collection in the lesser peritoneal sac were also noted (see later).

The gallbladder was classified as nonvisualized if a structure characteristic of the gallbladder shape could not be definitely identified. Cases which showed only right upper quadrant echoes with acoustic shadows and no positive identification of the gallbladder were included in the nonvisualized group.

Of 76 cases with known diagnoses from conclusive radiographic, surgical, or pathologic findings, 40 had gallbladders without calculi and 36 had cholelithiasis. The gallbladder was visualized by ultrasound in 63 cases and was correctly diagnosed in 56, for an overall accuracy of 89%. When the gallbladder was visualized, the sensitivity of ultrasound in detection of gallstones among the total number of proved cases of cholelithiasis was 81% (21 of 26). Of 37 cases proved negative for calculi, 35 had negative ultrasound results, for a specificity of 95%.

Ultrasound studies were positive for calculi in two cases which were proved negative for cholelithiasis. One of the errors was misinterpretation of viscous bile as multiple small calculi. We have been able to differentiate this entity from cholelithiasis in subsequent cases. The other error resulted from dilated loops of bowel secondary to closed loop obstruction in the right upper quadrant. Of the five cases in which ultrasound yielded false negative findings, two had numerous tiny calculi and one had a 5 mm solitary calculus in a large gallbladder. The remaining two were observer errors: one was cholelithiasis in retrospect, and the other a 3 × 2 × 1 cm calculus (no apparent reason for the error). Total errors were seven in 63 visualized cases.

Of the 13 cases nonvisualized by ultrasound, 10 were found to have cholelithiasis. At surgery the gallbladder was usually contracted or filled with calculi.

Case Reports

Case 1

A 57-year-old woman was referred to our institution for treatment of carcinoma of the breast with metastasis to the chest wall. She developed a painful mass in the right upper quadrant of the abdomen 1 week before admission. An ultrasound scan of the right upper quadrant showed the palpable mass to be the gallbladder. On transverse scan of the gallbladder neck, a target-shaped echo pattern was seen. The outer dense rim of echoes was interpreted as the gallbladder, the middle echo-free zone was thought to represent bile, and the central echo-dense region was believed to represent a calculus impacted in the cystic duct (fig. 1). The gallbladder was mildly enlarged. Cholecystectomy revealed cholelithiasis with a calculus obstructing the proximal cystic duct.

Case 2

A 50-year-old mentally retarded woman was admitted with a temperature of 39.5°C and complaints of abdominal and left shoulder pain progressive over 24 hr. Physical examination revealed abdominal tenderness and guarding with distention and tympany. Radiographs of the abdomen showed multiple loops of dilated large and small bowel consistent with paralytic ileus. There was radiographic evidence of a right upper quadrant mass. An ultrasound scan showed the gallbladder to be dilated with classical findings of multiple gallstones. Further scanning of the upper abdomen showed an echo-free zone 7 cm in diameter in the left upper quadrant which was thought to represent a fluid-filled mass (fig. 2). This finding persisted following emptying of the stomach by nasogastric intubation.

Surgical examination showed cholelithiasis and chronic cholecystitis. The left upper abdomen was explored, and on entering the lesser sac a large collection of infected bile was found and drained. A calculus was present in the common duct; however, the site of biliary leak was never identified. The location and size of the echo-free zone on the ultrasound examination corresponded well with the lesser sac collection of bile.

Discussion

The usefulness of ultrasonic evaluation of the gallbladder has been reported [1, 6, 8]. It has become an accepted mode of examination in patients with suspected acute cholecystitis and in patients with nonvisualized gallbladder by oral cholecystogram. The overall accuracy rate in our series compares well with findings of others [4–7]. Since the rather high number of nonvisualized gallbladders may be secondary to the nonfasting state, we now perform such examinations with the patient in a fasting state. We recommend that ultrasound examination of the gallbladder be performed as a supplement to the nonvisualized cholecystogram and as the initial study when the likelihood of successful radiographic study is small.

A frequent error in ultrasonic examination of the gallbladder has been failure to recognize calculi when present in the cystic duct. In case 1, a target-shaped echo pattern in the region of the proximal cystic duct is reported as a helpful finding in detection of a cystic duct calculus. Additional pathology indirectly related to gallbladder disease is occasionally identified on the ultrasound scan. In case 2 ultrasound was helpful in leading the surgeon to a collection of extravasated bile in the lesser sac.

REFERENCES

1. Hublitz UF, Kahn PC, Sell LA: Cholecystosonography: an approach to the nonvisualized gallbladder. *Radiology* 103:645–649, 1972
2. Goldberg BB, Harris K, Broocker W: Ultrasonic and radiographic cholecystography. *Radiology* 111:405–409, 1974
3. Doust BD, Maklad NF: Ultrasonic B-mode examination of the gallbladder. *Radiology* 110:643–647, 1974
4. Crow HC, Bartrum RJ, Foote SR: Expanded criteria for the ultrasonic diagnosis of gallstones. *J Clin Ultrasound* 4:289–292, 1976
5. Arnon S, Rosenquist CJ: Gray scale cholecystosonography: an evaluation of accuracy. *Am J Roentgenol* 127:817–818, 1976
6. Leopold GR, Amberg J, Gosink BB, Mittelstaedt C: Gray scale ultrasonic cholecystography: a comparison with conventional radiographic techniques. *Radiology* 121:445–448, 1976
7. Lawson TL: Gray scale cholecystosonography: diagnostic criteria and accuracy. *Radiology* 122:247–251, 1977
8. Gosink BB, Leopold GR: Ultrasound and the gallbladder. *Semin Roentgenol* 11:185–189, 1976
9. Leopold GR, Sokoloff J: Ultrasound scanning in the diagnosis of biliary disease. *Surg Clin N Am* 53:1043–1052, 1973

Accuracy of Biliary Duct Ultrasound: Comparison with Cholangiography

HARVEY L. NEIMAN[1] AND RICHARD A. MINTZER[1]

Thirty patients were studied by diagnostic ultrasound and percutaneous transhepatic or surgical cholangiography to evaluate diagnostic accuracy in differentiating obstructive from nonobstructive hepatobiliary disease. Correct recognition of biliary duct caliber was accomplished by ultrasound in 86% of cases, and was most accurate (89%) in patients with dilated intrahepatic biliary radicals. Diagnostic ultrasound is sufficiently accurate to be a useful screening tool for determining the caliber of the biliary duct system and, on this basis, obstructive from nonobstructive hepatobiliary disease.

Several reports in the literature show that the gallbladder, common bile duct, and intrahepatic biliary ducts can be visualized by ultrasound, but none compare the relative accuracy of the modality with a standard [1-5]. The introduction of Chiba needle percutaneous transhepatic cholangiography has enabled comparison of ultrasound observations with in vivo anatomic information.

Subjects and Methods

Twenty-five patients were studied by both diagnostic ultrasound and Chiba needle percutaneous transhepatic cholangiography. An additional five patients were studied with diagnostic ultrasound and operative cholangiography. These 30 represent all patients who had undergone both diagnostic ultrasound and cholangiographic examination during a 6 month period in 1976. All patients with obstruction were surgically proven. Many of the nonobstructed cases were also surgically proven; however, several had overwhelming clinical evidence of nonobstructive disease. For the most part these cases proved to be examples of hepatitis.

Ultrasound studies were performed on a Picker Echoview 8A gray scale system using a 2.25 MHz 19 mm diameter, 10 cm internal focus transducer. Images were recorded with a Dunn camera. Chiba needle cholangiography was performed by the techniques described by Okuda et al. [6].

Results

The diagnostic accuracy of ultrasound compared to cholangiography is indicated in table 1. Ultrasound demonstrated dilatation of the common bile duct or intrahepatic biliary radicals in 16 of 18 patients; all were ultimately shown to have obstructive jaundice by percutaneous transhepatic cholangiography (fig. 1). In patients with nondilated ducts, ultrasound was accurate in nine of 11 patients. In a twelfth, the ultrasound study was nondiagnostic because of excessive amounts of gas. The intrahepatic biliary radicals were the most accurate marker of obstructive jaundice, since their ultrasound status correlated with the ultimate diagnosis in 89% of cases. The common bile duct was convincingly identified in approximately 65% of cases. In the two patients with obstructive jaundice and a normal ultrasound study, the percutaneous transhepatic cholangiogram demonstrated only minimal dilatation of the intrahepatic biliary radicals and common bile duct.

The degree of confidence was also assessed; diagnoses were judged as possible, probable, and definite. In 71% of the cases the diagnosis was reported as definite. In the remaining correct diagnoses, a degree of uncertainty was added to the final report.

Dilated intrahepatic biliary radicals are seen as straight or curved, single or branched tubular structures. These are best visualized in longitudinal, single pass, breath-holding sections of the liver from the midline to 4-5 cm to the right (fig. 2). Not infrequently, the ducts were also seen to advantage in the left lobe on transverse scans (fig. 3).

The accuracy of ultrasound in evaluating the cause of biliary obstruction was also investigated. In three cases the area of the pancreatic bed could not be seen because of gas, despite multiple attempts on different days. Of the remaining 15 cases, the etiology was identified in 11 and not suggested in four. In patients ultimately shown by intraoperative cholangiography or percutaneous transhepatic cholangiography to have nonobstructive jaundice, the diagnosis was primarily alcoholic or infectious hepatitis.

Discussion

Our analysis confirms the observation that biliary duct dilatation can be confidently recognized by ultrasound. The status of the intrahepatic biliary radicals is more easily assessed than the size of the common bile duct. While it would seem that the differentiation of biliary ducts from hepatic vessels would be a problem, this is not a major concern in patients with obstruction.

Correct description of biliary duct caliber was achieved by ultrasound in 89% of cases with dilated ducts and

TABLE 1

Diagnostic Accuracy in Recognizing Dilated Ducts

Technique	Dilated Ducts	Nondilated Ducts
Ultrasound	16/18*	9/12†
Percutaneous transhepatic cholangiography	18/18	5/7‡
Operative cholangiography	0	5/5

* Two false negative.
† Two false positive and one failure.
‡ Two failures.

Received October 8, 1976; accepted after revision August 12, 1977.
Presented at the annual meeting of the American Roentgen Ray Society, Washington, D.C., September 1976.

[1] Department of Radiology, McGaw Medical Center of Northwestern University, 303 East Chicago Avenue, Chicago, Illinois 60611. Address reprint requests to H. L. Neiman.

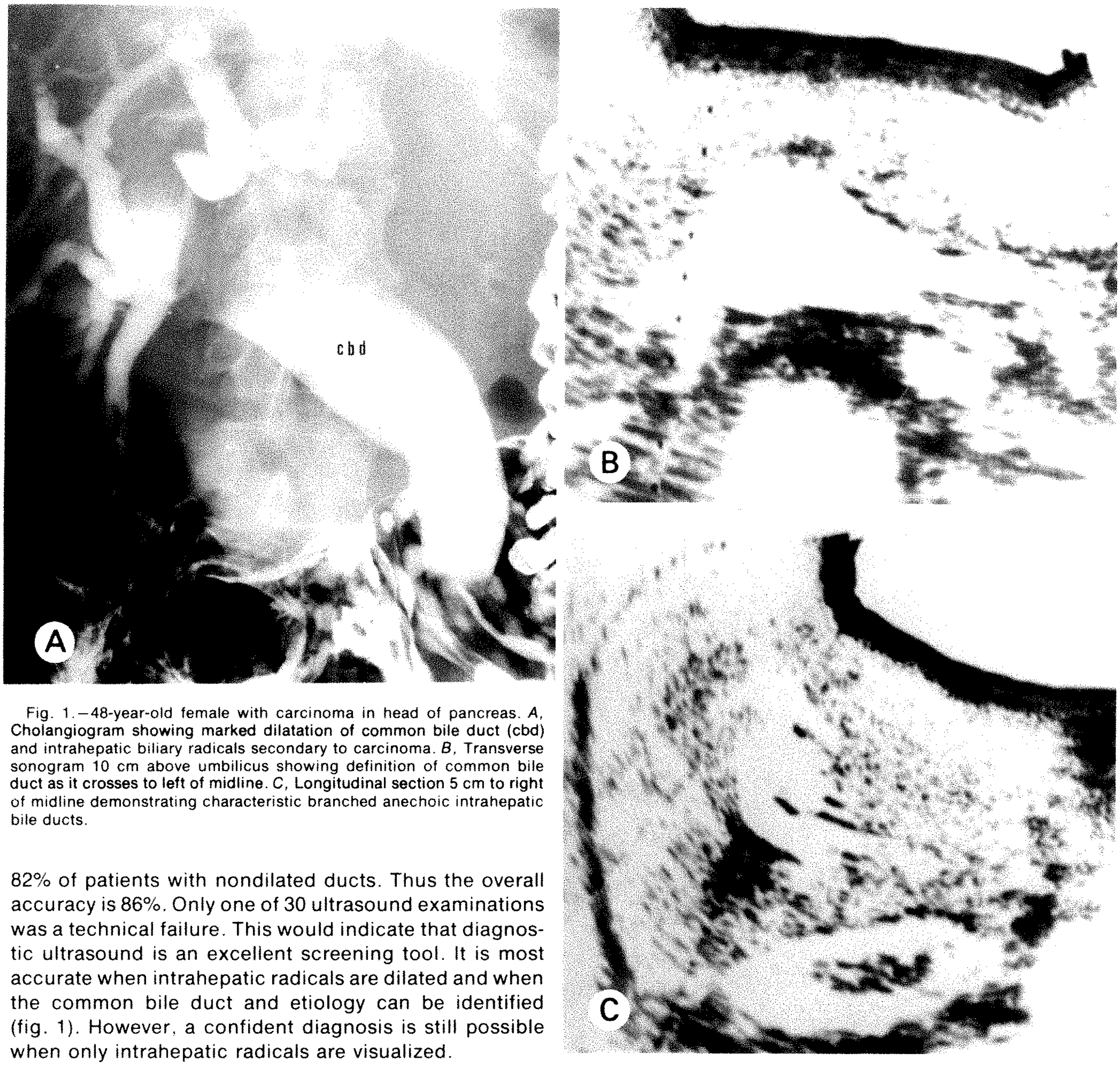

Fig. 1.—48-year-old female with carcinoma in head of pancreas. *A*, Cholangiogram showing marked dilatation of common bile duct (cbd) and intrahepatic biliary radicals secondary to carcinoma. *B*, Transverse sonogram 10 cm above umbilicus showing definition of common bile duct as it crosses to left of midline. *C*, Longitudinal section 5 cm to right of midline demonstrating characteristic branched anechoic intrahepatic bile ducts.

82% of patients with nondilated ducts. Thus the overall accuracy is 86%. Only one of 30 ultrasound examinations was a technical failure. This would indicate that diagnostic ultrasound is an excellent screening tool. It is most accurate when intrahepatic radicals are dilated and when the common bile duct and etiology can be identified (fig. 1). However, a confident diagnosis is still possible when only intrahepatic radicals are visualized.

The etiology of the obstruction is not as easily diagnosed by ultrasound. In those cases where the pancreatic bed was not obscured by gas, the etiology of the obstruction was suggested in 73% of cases (fig. 4). This is less ($\chi = 9.76$, $P < .05$) than the 84% diagnosed by Walls et al. [7] in their review of pancreatic ultrasound.

Chiba needle percutaneous transhepatic cholangiography has proved to be a highly accurate and relatively safe means of studying the biliary system [3]. Nevertheless, percutaneous cholangiography is not without risk, and ultrasound offers a useful and safe screening alternative, although less accurate than cholangiography ($\chi^2 = 4.89$, $P < .05$). It is the procedure of choice before cholangiography. An additional benefit of ultrasound not available with percutaneous transhepatic cholangiography is its ability to assess the presence of both ascites and metastatic foci in the liver, thus aiding in the staging of neoplastic lesions.

REFERENCES

1. Doust BD, Maklad NF: Ultrasonic B-mode examination of the gallbladder. *Radiology* 110:643-647, 1974
2. Goldberg BB, Harris K, Brocker W: Ultrasonic and radiographic cholecystography. *Radiology* 111:405-409, 1974
3. Reid MH: Visualization of the bile ducts using focused ultrasound. *Radiology* 118:155-158, 1976
4. Stone LB, Ferrucci JT Jr, Warshaw AL, Wittenberg J, Slutsky M: Gray scale ultrasound diagnosis of obstructive biliary disease. *Am J Roentgenol* 125:47-50, 1975
5. Taylor KJW, Carpenter DA, McCready VR: Ultrasound and scintigraphy in the differential diagnosis of obstructive

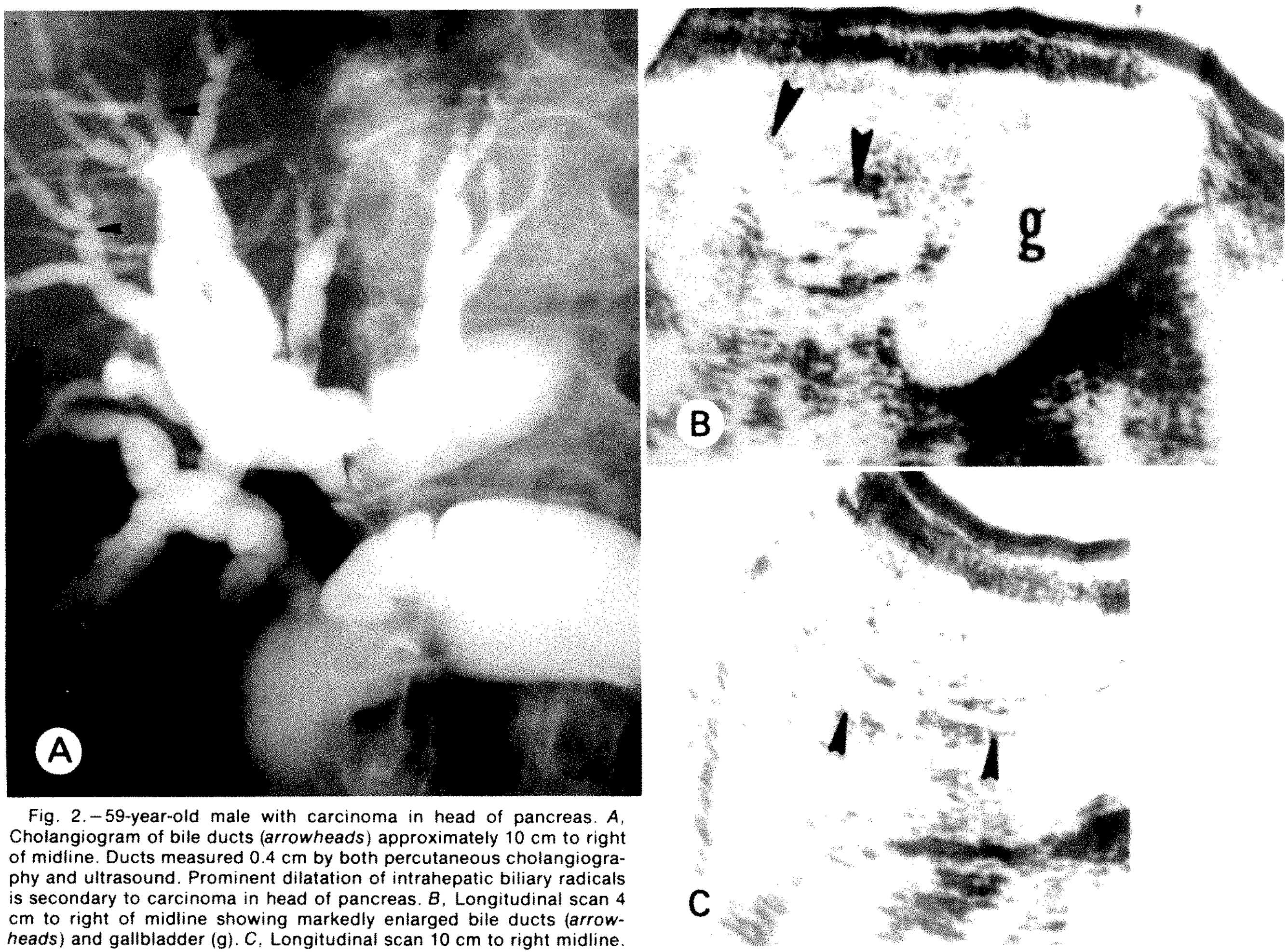

Fig. 2.—59-year-old male with carcinoma in head of pancreas. *A*, Cholangiogram of bile ducts (*arrowheads*) approximately 10 cm to right of midline. Ducts measured 0.4 cm by both percutaneous cholangiography and ultrasound. Prominent dilatation of intrahepatic biliary radicals is secondary to carcinoma in head of pancreas. *B*, Longitudinal scan 4 cm to right of midline showing markedly enlarged bile ducts (*arrowheads*) and gallbladder (g). *C*, Longitudinal scan 10 cm to right midline. Bile ducts remain visible and correlate with ducts in same location in *A*.

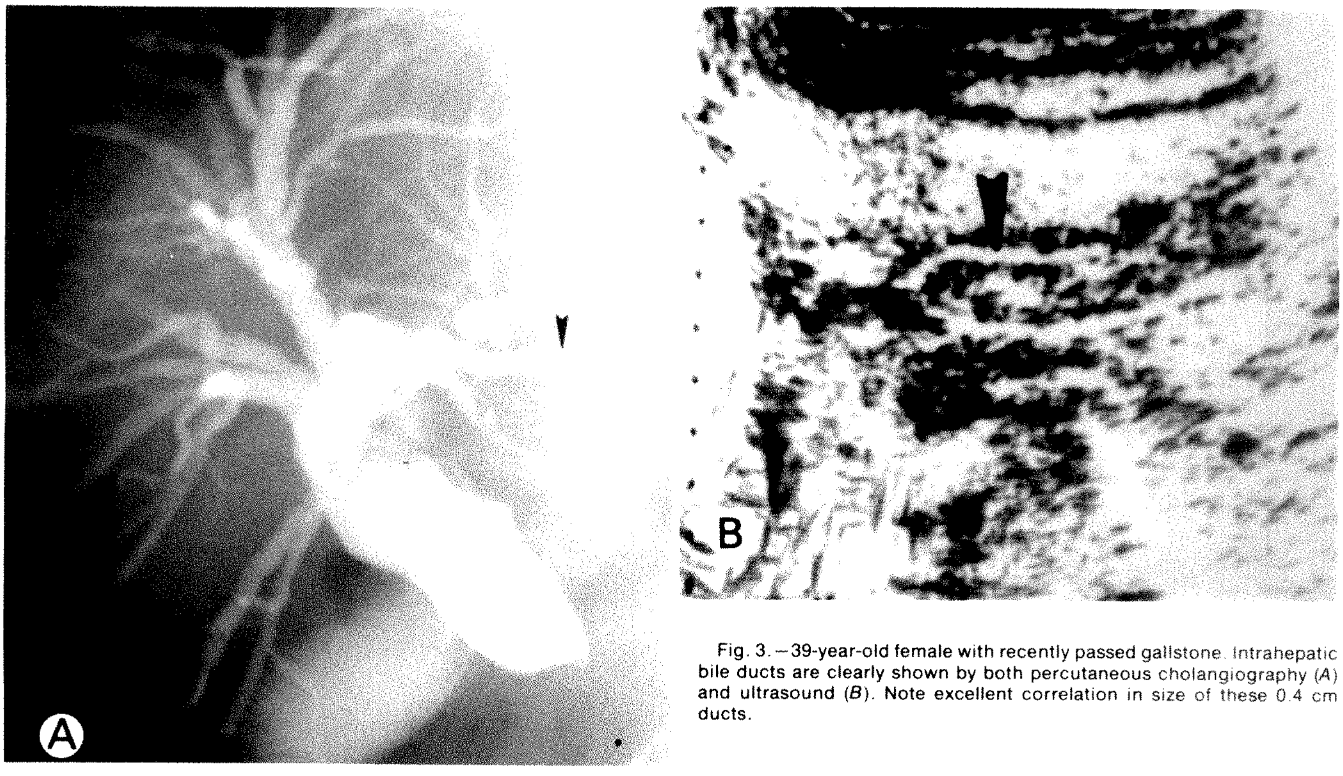

Fig. 3.—39-year-old female with recently passed gallstone. Intrahepatic bile ducts are clearly shown by both percutaneous cholangiography (*A*) and ultrasound (*B*). Note excellent correlation in size of these 0.4 cm ducts.

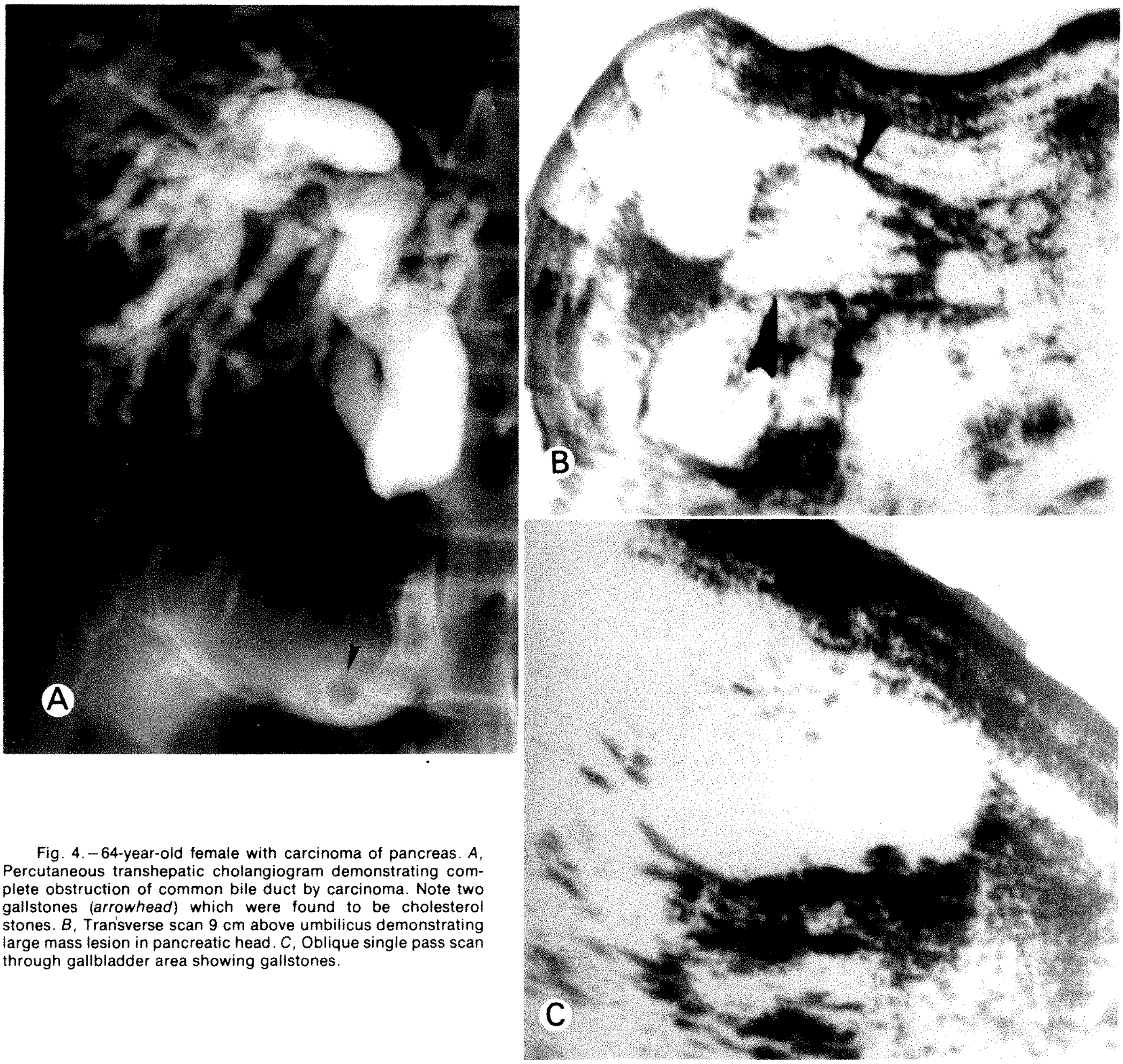

Fig. 4.—64-year-old female with carcinoma of pancreas. *A*, Percutaneous transhepatic cholangiogram demonstrating complete obstruction of common bile duct by carcinoma. Note two gallstones (*arrowhead*) which were found to be cholesterol stones. *B*, Transverse scan 9 cm above umbilicus demonstrating large mass lesion in pancreatic head. *C*, Oblique single pass scan through gallbladder area showing gallstones.

jaundice. *J Clin Ultrasound* 2:105–116, 1974

6. Okuda K, Tanikawa K, Emura T, Kuratomi S, Jinnouchi S, Urade K, Sumikoshi T, Kanda Y, Fukuyama Y, Musha H, Mori H, Shimokawa Y, Yakushaiji F, Matsuura Y: Nonsurgical percutaneous transhepatic cholangiography—diagnostic significance in medical problems of the liver. *Am J Dig Dis* 19:21-36, 1974
7. Walls WJ, Gonzalez G, Martin NL, Templeton AW: B-Scan ultrasound evaluation of the pancreas. *Radiology* 114:127–134, 1975

Gray Scale Echographic Patterns of Hepatic Metastatic Disease

WILLIAM SCHEIBLE,[1] BARBARA B. GOSINK, AND GEORGE R. LEOPOLD

Abnormal gray scale hepatic echograms in 76 patients with known or suspected metastatic disease were reviewed. A varied echographic pattern was found, with the gray scale appearances falling into three identifiable categories (dense, lucent, and bulls-eye) and a fourth group difficult to characterize. Prior chemotherapy seemed to have little consistent effect on echographic patterns. A pattern of dense lesions was associated in a large percentage of cases with adenocarcinoma. Carcinoma of the colon commonly produced this appearance. The remaining echographic patterns showed little correlation with specific primary sites or cell types.

With the advent of gray scale equipment, the liver parenchyma is now more easily evaluated by ultrasound. The utility of this technique in cases of obstructive jaundice and diffuse parenchymal disease has been well documented [1, 2]. Its ability to determine the nature of defects on isotope scans is well known [3, 4]. The method has proven useful in following the therapeutic response of both primary and secondary hepatic tumors [5, 6]. The delineation of metastatic malignancy within the liver has also been described in the literature, with most reports suggesting that liver metastases present a relatively sonolucent appearance on gray scale echography [1, 5, 7]. Other studies indicate that a spectrum of echographic patterns exists [8, 9]. Our experience to date shows that in addition to a sonolucent pattern, other echographic appearances secondary to metastatic disease can also be defined. Furthermore, our results indicate that metastatic adenocarcinoma of the colon usually produces a relatively specific and identifiable echographic pattern. Given this information, the ultrasonographer can occasionally aid in directing the diagnostic approach to an otherwise unknown primary site.

Subjects and Methods

We reviewed 76 cases with abnormal gray scale hepatic echograms due to known or suspected metastatic disease. Of these patients, 47 (62%) had histologically verified metastases, either by open or percutaneous liver biopsy (21 cases) or by autopsy examination (26 cases). In 29 others with known primary tumors and clearly abnormal echograms, the pathologic proof of liver metastases is yet to be established. Most of these patients (24 of 29) have correlative radioisotope liver-spleen scans that confirm parenchymal abnormality.

All patients were supine during examination; multiple longitudinal and transverse scans were obtained at about 2 cm intervals. When necessary, scans in the left lateral decubitus position were also performed for better visualization of the liver parenchyma. Generally, a single-pass parasagittal scan during deep inspiration was the most reliable means of depicting hepatic parenchyma. All scans were obtained using commercially available gray scale equipment, utilizing either a 3.5 or 2.25 MHz transducer. Gain settings were adjusted so that echoes from normal liver parenchyma were clearly identified (fig. 1). Recording was performed using either Polaroid film, x-ray film, or heat-sensitive paper.

Results

Three basic patterns of parenchymal abnormality were readily identified. We classified them as dense, lucent, and bulls-eye. A fourth category is composed of cases which do not fit easily into these groups. Generally, these patients showed a mixture of one or more of the above echographic patterns, diffusely inhomogeneous echoes, and/or a large mass otherwise difficult to characterize.

The most common echographic pattern was that of single or multiple echodense foci within the liver parenchyma (fig. 2). These lesions are readily separable from the less echogenic surrounding parenchyma and may coalesce into lobular masses. Whether single or multiple, the lesions tend to be large, usually over 4 cm in diameter. In our series, 28 patients (37%) displayed this pattern (table 1). Of these 28 patients, 20 had primary adenocarcinoma of the colon, by far the most common primary lesion in our series. It is of interest that of the 24 cases of adenocarcinoma of the colon, 20 demonstrated this appearance of large dense metastases; 17 of these patients had not received chemotherapy. In two patients with adenocarcinoma of the colon, a central lucent area was present within a large dense metastasis. This lucency was presumably secondary to tumor necrosis. One of these patients had received chemotherapy; the other had not been treated.

The echogenicity of colon metastases has previously been noted in a review of bistable patterns of metastatic neoplasm [10]. In our series, with the exception of one case of epidermoid carcinoma of the lung and another of metastatic leiomyosarcoma, only adenocarcinoma yielded this dense pattern. In addition to colorectal primary lesions, we identified echodense metastatic lesions in four patients with biopsy-proven adenocarcinoma. The site of the primary lesion was thought to be from the gastrointestinal tract, although it has not been definitely identified. One patient with this pattern had primary breast carcinoma and presented with several small sharply marginated echodense foci (fig. 3). This latter pattern appears quite distinct from the larger, less sharply marginated lesions of metastatic adenocarcinoma of the colon (c.f. figs. 2 and 3).

A second common manifestation of hepatic metastases is that of a well defined sonolucent area entirely

---

Received March 18, 1977; accepted July 27, 1977.

[1] All authors: Department of Radiology, University of California Medical Center, 225 West Dickinson Street, San Diego, California 92103, and Veterans Administration Hospital, La Jolla, California. Address reprint requests to W. Scheible at University of California Medical Center.

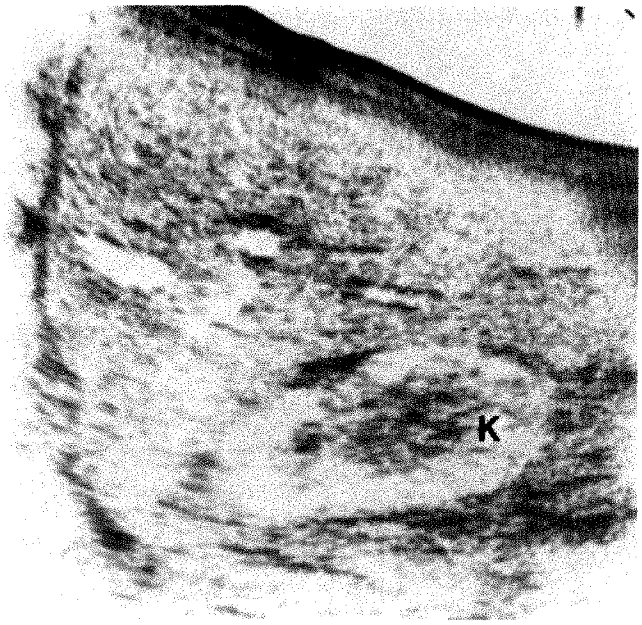

Fig. 1.—Longitudinal sector scan showing normal gray scale appearance of liver parenchyma, essentially homogeneous with interspersed vascular markings. K = kidney

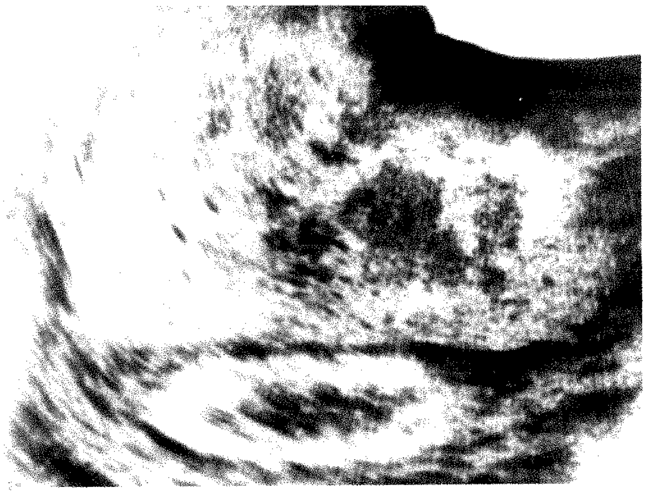

Fig. 2.—Several dense lesions in right lobe of liver, metastatic from colon. Note marked enlargement and deformity of liver. No prior therapy.

TABLE 1
Echographic Patterns

Primary Lesion	No. Cases	Echographic Pattern			
		Dense	Lucent	Bulls-eye	Other
Colon	24	20	1	1	2
Stomach	5	...	1	...	4
Duodenum/ampulla	2	...	1	...	1
Adenocarcinoma (probable gastrointestinal tract)	5	4	1	...	...
Pancreas	2	...	2	...	...
Breast	2	1	1	...	...
Carcinoid	1	...	...	1	...
Lung:					
Epidermoid	4	1	...	1	2
Oat cell	7	...	...	4	3
Large cell	1	...	...	1	...
Adenocarcinoma	4	1	1	...	2
Nasopharynx (epidermoid	1	...	...	1	...
Thyroid (medullary)	1	...	...	1	...
Renal (squamous)	1	...	...	1	...
Prostate	1	...	...	...	1
Testis (embryonal cell)	2	...	...	...	2
Melanoma	4	...	1	1	2
Lymphoma:					
Hodgkin's	1	...	...	...	1
Non-Hodgkin's	3	...	2	...	1
Sarcoma:					
Leiomyosarcoma	2	1	1	...	...
Alveolar soft part	1	...	...	1	...
Schwannoma variant	1	...	1	...	...
Undifferentiated anaplastic carcinoma	1	...	1	...	...
Total	76	28	14	13	21

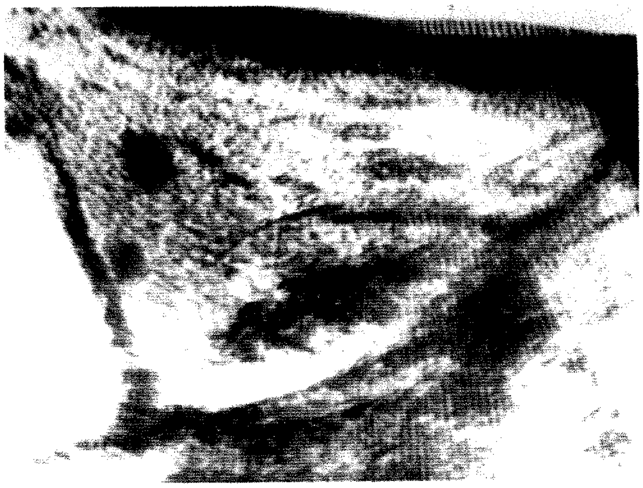

Fig. 3.—Longitudinal scan showing two separate dense foci near diaphragm representing metastatic breast carcinoma. Patient also has right pleural effusion.

surrounded by normal liver parenchyma (fig. 4). This pattern has been described in several previous reports [1, 5, 7]. Typically, fine low-level echoes are noted within these lesions, indicating their solid nature. In our series, 14 patients (18%) showed this appearance, but there was no correlation with a predominant tissue type (table 1). It is of interest that both lymphoma (four cases) and melanoma (three of four cases) exhibited either this pattern exclusively or as part of a mixed appearance.

Bulls-eye lesions are those in which a dense central focus is surrounded by a more lucent periphery (fig. 5), which in turn is readily separable from the adjacent liver parenchyma. Thirteen patients (17%) had this pattern. We noted this feature in association with a wide spectrum of primary lesions (table 1). Four cases of oat cell carcinoma of the lung gave this appearance.

Finally, 21 of 76 patients (28%) representing a diverse group of primary tumors do not readily fall into one of the

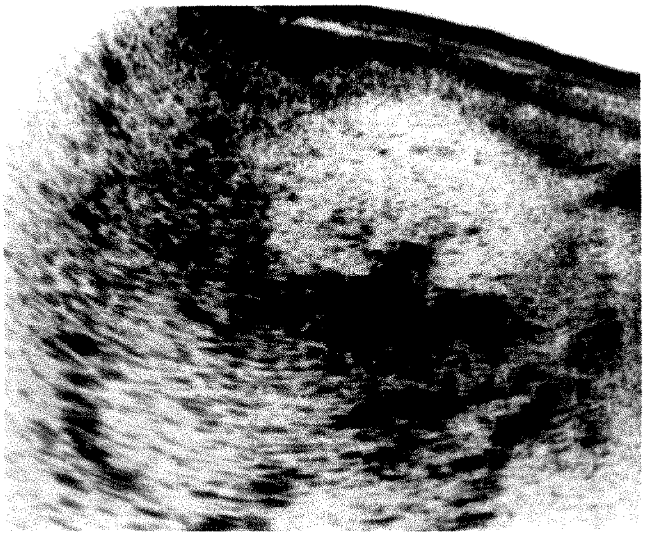

Fig. 4.—Large lucent focus in anterior portion of right lobe of liver. Primary site was adenocarcinoma of lung.

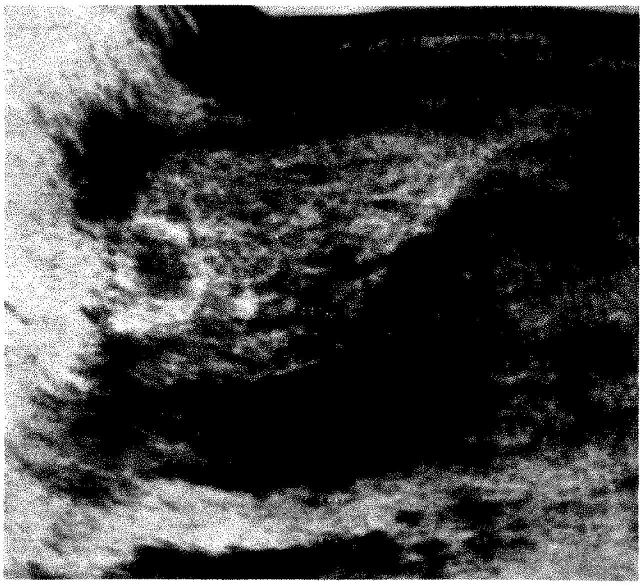

Fig. 5.—Bulls-eye lesion adjacent to diaphragm in patient with metastatic oat cell carcinoma of lung.

above subgroups (table 1). A mixed pattern (fig. 6), seen in eight cases, encompasses those instances in which at least two of the previously described gray scale patterns were present simultaneously. Diffuse inhomogeneity (fig. 7) characterizes those livers whose echographic pattern is clearly abnormal, with multiple coarse, dense, and/or lucent areas, but without a dominant pattern of focal lesions. Five patients exhibited this appearance. Finally, eight patients showed one or more poorly defined masses with a variable and often bizarre echo pattern not easily characterized (fig. 8). Four of the eight had received chemotherapy prior to ultrasound examination; perhaps this relatively disordered appearance is a manifestation of patient response to therapy.

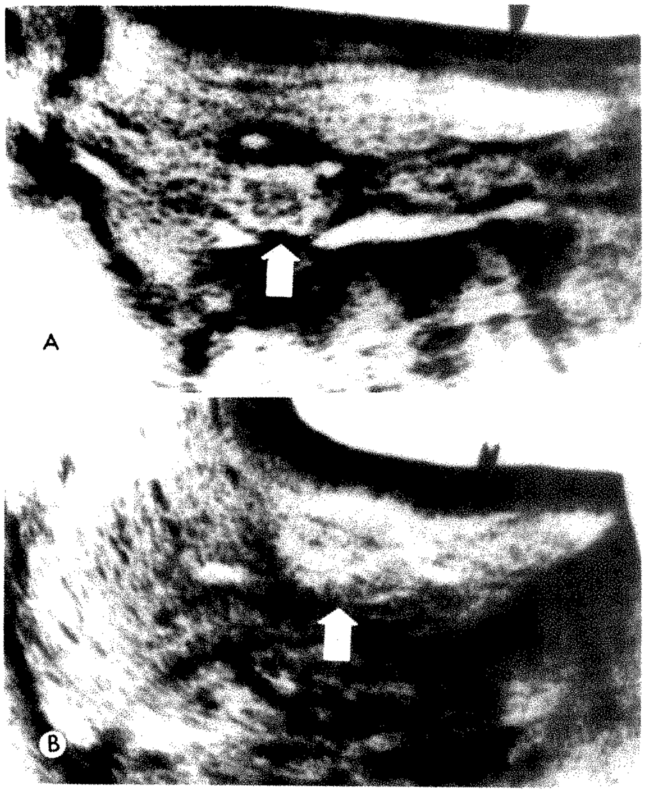

Fig. 6.—*A*, Mixed pattern manifested by bulls-eye lesion in caudate lobe (*arrow*). *B*, Sonolucent deposit in anterior aspect of right lobe (*arrow*). Melanoma was primary lesion.

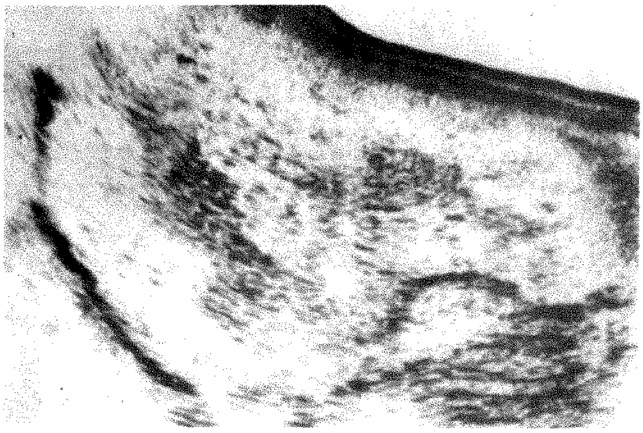

Fig. 7.—Diffuse inhomogeneous pattern in metastatic oat cell carcinoma of lung. Liver is enlarged.

In addition to these definable abnormalities of hepatic parenchyma, it should be noted that many patients exhibited gross enlargement and/or contour irregularities of the liver. These features also should be looked for as additional clues to possible metastatic disease.

Discussion

It is clear that metastatic disease to the liver presents a varied gray scale echographic appearance. A review of the gross and microscopic pathologic material available on many of our patients failed to explain why these

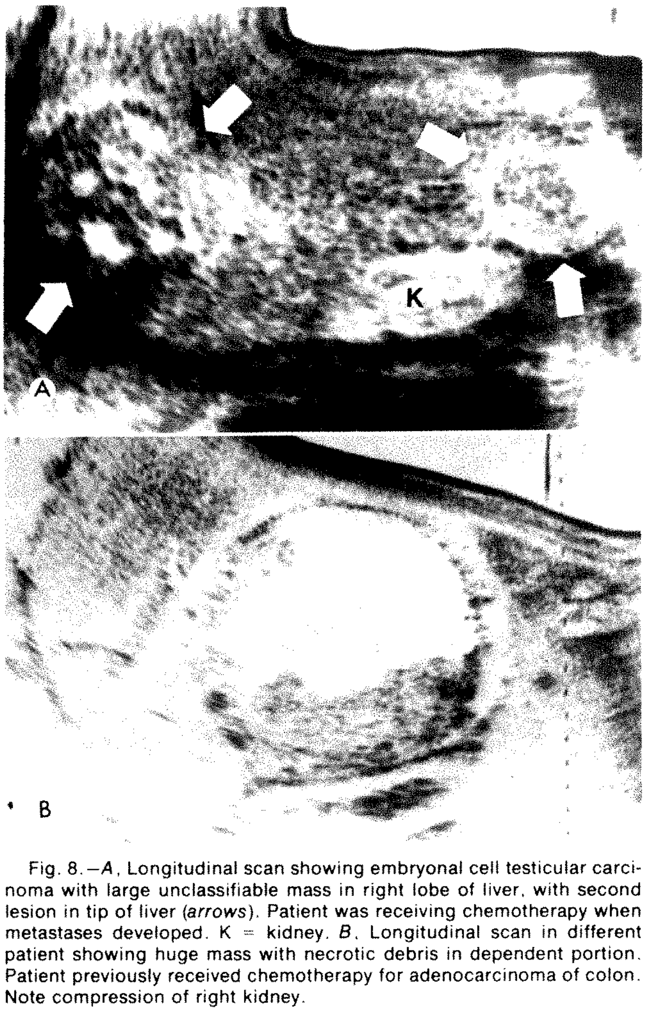

Fig. 8.—*A*, Longitudinal scan showing embryonal cell testicular carcinoma with large unclassifiable mass in right lobe of liver, with second lesion in tip of liver (*arrows*). Patient was receiving chemotherapy when metastases developed. K = kidney. *B*, Longitudinal scan in different patient showing huge mass with necrotic debris in dependent portion. Patient previously received chemotherapy for adenocarcinoma of colon. Note compression of right kidney.

varying echo patterns exist. The most consistent pattern in our series, that of primary colonic tumors producing dense metastases, is illustrative. Histologic material was available in nine cases. Mucin production by the metastatic deposits ranged from scant to exuberant and was independent of prior chemotherapy. Likewise, the degree of necrosis was highly variable. All the dense metastatic colon deposits had relatively well developed fibrous tissue, perhaps relating to their echographic appearance. However, several noncolon primary lesions with a spectrum of echographic patterns also had this feature.

Tumor necrosis would seem a plausible explanation for the appearance of sonolucent lesions, but was not a consistent feature in these cases. In fact, some purely lucent lesions had a minimal amount of histologic tumor necrosis. The wide variety of primary sites suggests that there may not be a common histologic basis for this appearance.

Dilated, congested hepatic sinusoids are often described around focal metastatic deposits, and initially it was theorized that this could explain the bulls-eye appearance. This did not seem to be the case, and no common histologic finding could be detected that would account for this metastatic pattern.

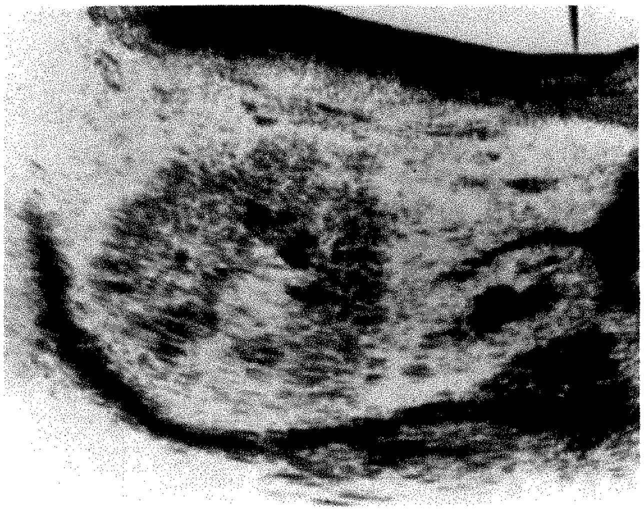

Fig. 9.—Large dense metastasis with presumed central necrosis in patient receiving chemotherapy for adenocarcinoma of colon.

Finally, although ultrasound is clearly of value in following the therapeutic response of metastatic disease in an individual patient, the course of treated hepatic metastatic disease is extremely variable and consequently so are the echographic features. The phenomenon observed most frequently following chemotherapy was the development of central lucency within a dense lesion, evidently due to tumor necrosis (fig. 9). Also, as noted above, large and poorly defined lesions were seen in several cases treated prior to ultrasound examination.

With regard to specificity, it would seem that adenocarcinoma of the colon generally produces a dense lesion. Moreover, 26 of 45 primary adenocarcinoma metastases gave a dense pattern. Conversely, the dense appearance in all but two of 28 instances was correlated with a primary adenocarcinoma. Though the series included only four cases each of melanoma and lymphoma, both resulted in discrete metastatic lesions with either a sonolucent or bulls-eye appearance or a mixture of the two patterns.

Although this review indicates little apparent specificity regarding primary sites and the echographic features of their liver metastases, perhaps further experience may enable the ultrasonographer to better direct the search for primary malignancy. In addition, pattern recognition could conceivably aid in predicting responsiveness of metastatic disease to planned therapy. Precise correlation between tumor histology and gray scale patterns awaits large numbers of cases.

REFERENCES

1. Taylor KJW, Carpenter DA, Hill CR, McCready VR: Gray scale ultrasound imaging: the anatomy and pathology of the liver. *Radiology* 119:415-423, 1976
2. Perlmutter GS, Goldberg BB: Ultrasonic evaluation of the common bile duct. *J Clin Ultrasound* 4:107-111, 1976

3. Garrett WJ, Kossoff G, Uren RF, Carpenter DA: Grey scale ultrasonic investigations of focal defects on ^{99m}Tc sulphur colloid liver scanning. *Radiology* 119:425–428, 1976
4. Taylor KJW, Sullivan D, Rosenfield AT, Gottschalk A: Grey scale ultrasound and isotope scanning: complimentary techniques for imaging the liver. *Am J Roentgenol* 128:277–281, 1977
5. Taylor KJW, Carpenter DA, McCready VR: Grey scale echography in the diagnosis of intrahepatic disease. *J Clin Ultrasound* 1:284–287, 1973
6. Gilby ED, Taylor KJW: Ultrasound monitoring of hepatic metastases during chemotherapy. *Br Med J* 1:371–373, 1975
7. Carlsen EN: Liver, gallbladder, and spleen. *Radiol Clin North Am* 13:543–556, 1975
8. McArdle CR: Ultrasonic diagnosis of liver metastases. *J Clin Ultrasound* 4:265–268, 1976
9. Green B, Bree RL, Goldstein HM, Stanley C: Gray scale ultrasound evaluation of hepatic neoplasms: patterns and correlations. *Radiology* 124:203–208, 1977
10. Melki G: Ultrasonic patterns of tumors of the liver. *J Clin Ultrasound* 1:306–314, 1973

Isodense Masses on CT: Differentiation by Gray Scale Ultrasonography

PATRICK J. BRYAN[1] AND W. MARTIN DINN[1]

Alterations in echo patterns enable isodense structures and lesions to be clearly identifiable by gray scale ultrasonography when they are not distinguishable by computed tomography (CT). In certain clinical situations this capability is a distinct advantage of ultrasound over CT. Findings in three cases with abnormalities visualized by ultrasound, but not by CT, are presented. In addition, a cadaver was scanned with CT and ultrasound and then sectioned in corresponding transverse planes for anatomic correlation.

Computed tomography (CT), a major breakthrough in diagnostic radiology, offers several advantages over conventional radiographic images. These include the production of cross-sectional images without superimposition of structures and the ability to differentiate tissues of only slightly different radiographic density (linear attenuation coefficients). However, there is a limit to the ability of CT to differentiate structures of closely similar attenuation coefficients, and it is generally accepted that 0.5% represents that limit with present equipment [1].

We have encountered several instances in which anatomic structures or lesions could not be visualized on CT scans, whereas they were clearly delineated on ultrasonography. In each case the anatomic structure or lesion was isodense with surrounding tissue, rendering it invisible on the CT scan even with narrow window settings. CT scans were performed on a Delta Scanner 50 (Ohio Nuclear, Solon, Ohio) at a scanning time of 2 min 43 sec. Ultrasound scans were performed with Unirad Sono II and III (Unirad, Denver, Colo.).

Case Reports

Case 1

J. T., a woman with Burkitt's lymphoma, was shown on a CT study to have a large pelvic mass due to ovarian lymphoma (fig. 1*A*). The uterus could be seen indenting the bladder but could not be differentiated from the contiguous ovarian tumor. The Hounsfield number of the uterus was identical to that of the tumor. A sonogram (fig. 1*B*) clearly delineated the uterus and the homogeneous ovarian tumor posterior to it.

Case 2

R. B., a 54-year-old male, had metastatic seminoma of the testis. CT showed extensive periaortic adenopathy with effacement of the abdominal aorta (fig. 2*A*). Sonography clearly demonstrated the aorta surrounded by the enlarged nodes (fig. 2*B*).

Case 3

A very thin patient with chronic pancreatitis had a CT study. There was very little retroperitoneal fat, and the body of the pancreas could not be visualized even after injection of intravenous contrast medium (fig. 3*A*). Sonography oultlined the pancreas quite clearly (fig. 3*B*).

Cadaver Study

A cadaver was scanned with CT and ultrasound and then sectioned in corresponding transverse planes for anatomic correlation. Multiple metastases were present in the liver (fig. 4*A*). These could not be appreciated on the CT scans (fig. 4*B*) since they were isodense with the liver. However, they were clearly obvious on the sonogram (fig. 4*C*). In the same cadaver the gallbladder was also indistinguishable on the CT scans due

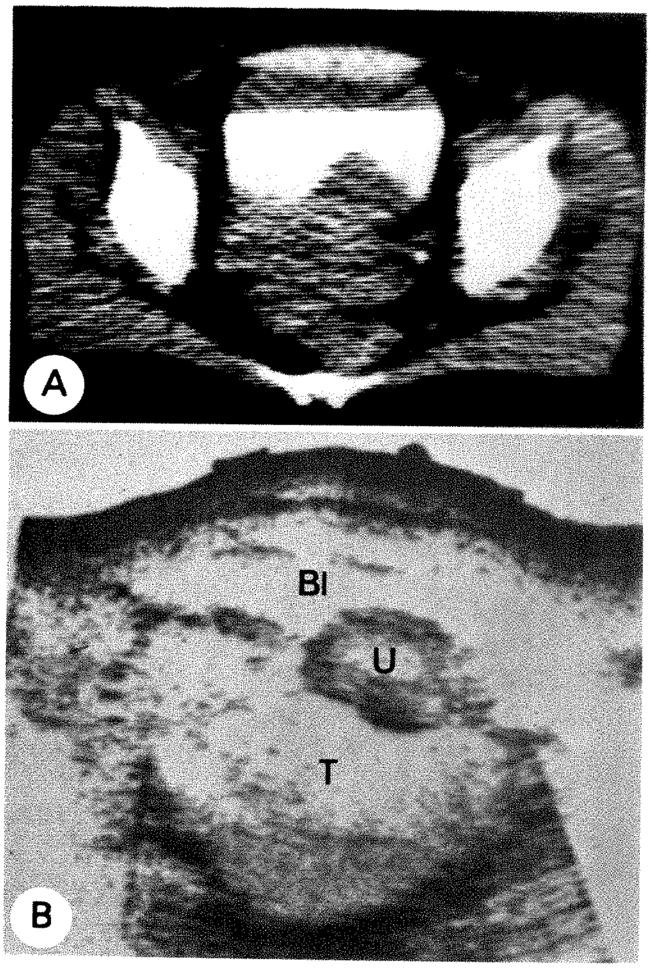

Fig. 1.—Case 1. *A*, CT scan showing pelvic mass posterior to bladder. Uterus indents bladder posteriorly but cannot be distinguished from mass. Fluid level in bladder is due to contrast-laden urine posteriorly and unopacified urine anteriorly. *B*, Transverse sonogram showing uterus (U) clearly delineated from bladder (Bl) in front and tumor (T) behind.

Received December 17, 1976; accepted after revision August 18, 1977.

[1] Department of Radiology, State University of New York Upstate Medical Center, 750 East Adams Street, Syracuse, New York 13210. Address reprint requests to P. J. Bryan.

Am J Roentgenol **129 : 989–992, December 1977**

UNIVERSITY COLLEGE OF MEDICINE
LIBRARY

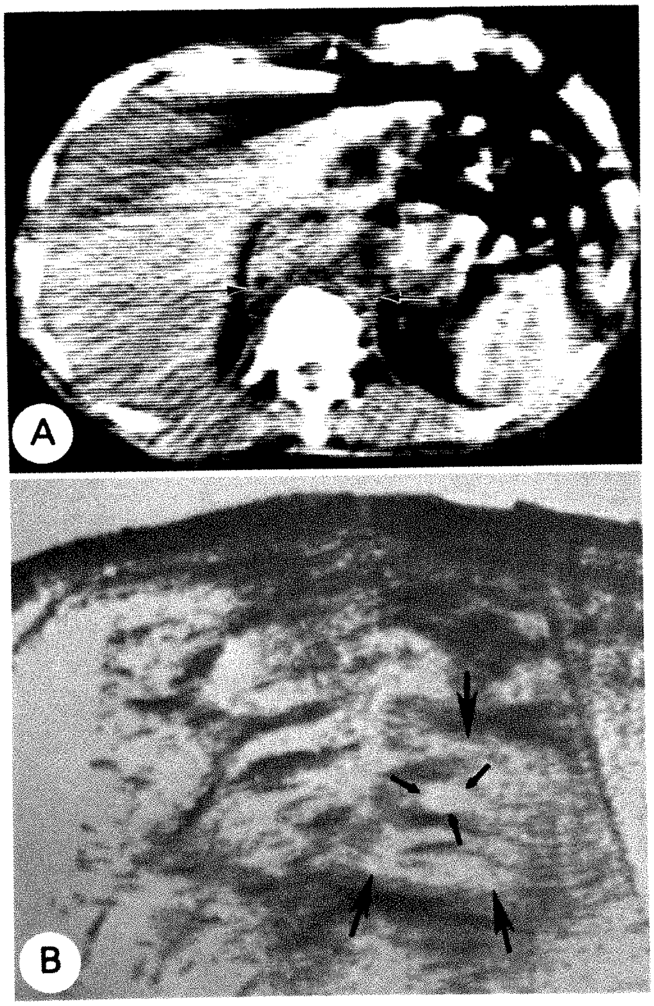

Fig. 2.—Case 2. *A*, CT scan of upper abdomen showing periaortic adenopathy splaying crura of diaphragm (*arrows*). Aorta is not visualized among surrounding nodes. *B*, Transverse sonogram showing aorta (*small arrows*) clearly distinguishable from surrounding adenopathy (*large arrows*).

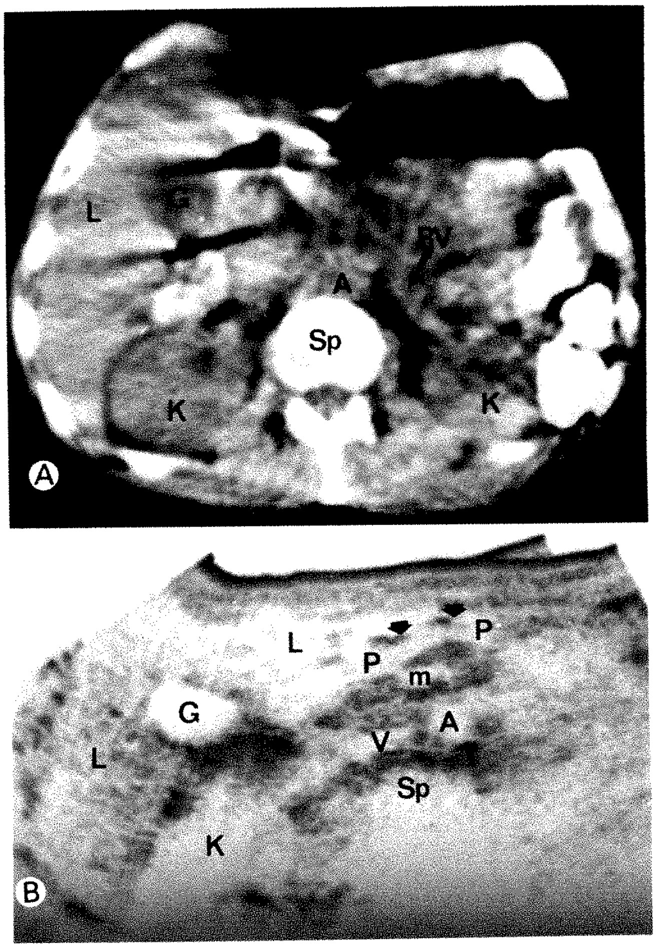

Fig. 3.—Case 3. *A*, CT scan showing lack of visualization of body of pancreas even after injection of intravenous contrast medium. *B*, Sonogram clearly outlining body of pancreas (P). *Arrows* indicate anterior margin of pancreas. A = aorta, V = inferior vena cava, Sp = spine, m = superior mesenteric artery, L = liver, G = gallbladder, K = kidney, RV = left renal vein.

to isodensity with the liver (fig. 5*B*), but it was very obvious on the sonogram (fig. 5*C*).

Discussion

In computed tomography, structures are differentiated by variations in the linear attenuation coefficients (radiographic density) of tissues. At the kilovoltage levels used in CT scanning, the linear attenuation coefficient is due mainly to the Compton effect which is related to electron density (and thus to mass density). Sonography, on the other hand, detects mismatches of acoustic impedance of tissues to produce echoes [2]. Acoustic impedance is the product of density and velocity; thus an acoustic mismatch will occur if the velocity of sound in two tissues differs, even if their density is identical. Sound velocity does vary in biologic tissues [2], and there is evidence that it is greatest in soft tissues with high collagen content [3]. Collagen has high elasticity, which increases sound velocity and hence acoustic impedance [3]. Collagen is thought to be the main source of internal echoes which give a characteristic and distinctive appearance to various body organs on gray scale sonography [3-5]. Whereas the boundaries of organs or of masses are larger than a wavelength and act as specular reflectors of ultrasound, weak internal echoes arise largely from diffuse and variable reflectors which are smaller than or equal to a wavelength.

The internal echo pattern of pathologic lesions is frequently different from adjacent normal tissue. Liver metastases usually have fewer and weaker internal echoes than normal liver, although they may occasionally be more echogenic [6]. Lymphomatous tissue typically appears very homogeneous with very low-level internal echoes (fig. 1*B*), and a correct histologic diagnosis can frequently be suggested on the basis of its sonographic appearance. When fluid is isodense with adjacent tissue, it is very easily distinguished by sonography since it is completely homogeneous with no reflecting interfaces and thus appears as an echofree structure [7] (fig. 4*D*).

We have often noted obscuration of the aorta on CT

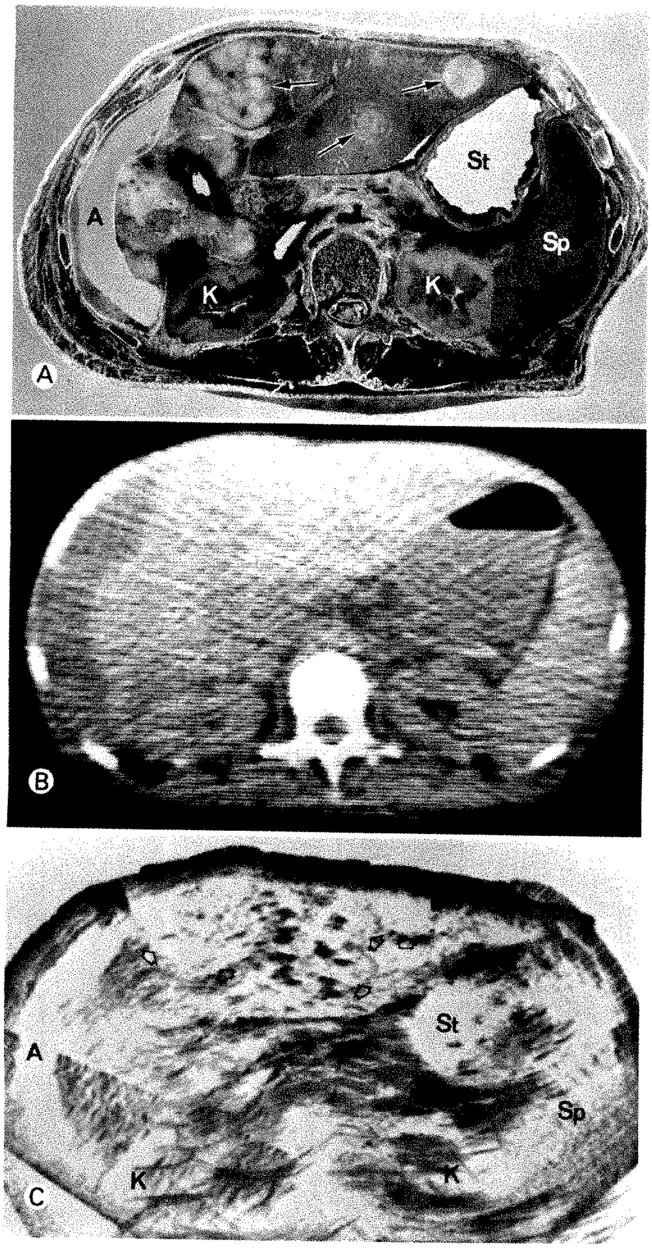

Fig. 4.—*A*, Transverse section of cadaver revealing multiple metastases in liver (*arrows*) and ascites. *B*, CT scan of intact cadaver showing no evidence of liver metastases. *C*, Transverse sonogram of intact cadaver clearly showing liver metastases (*arrows*). Sp = spleen, St = stomach, K = kidney, A = ascites.

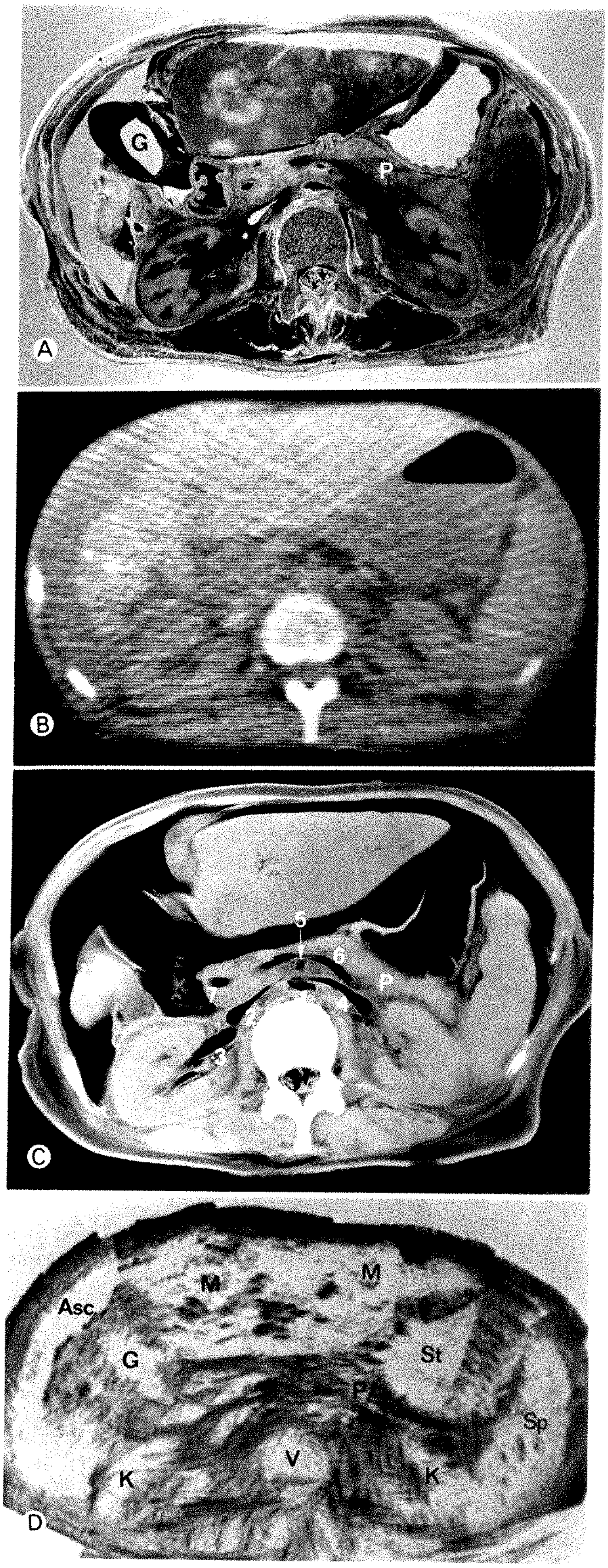

→

Fig. 5.—*A*, Section of cadaver showing gallbladder (G) and liver metastases. *B*, CT scan. Gallbladder cannot be differentiated since bile was of similar density to liver. Note calcification in metastasis in right lobe. *C*, Radiograph of cadaver section taken at 25 kV. Metastases can scarcely be appreciated due to isodensity with liver. Calcification in right lobe is seen. Note vascular anatomy seen on this 13 mm thick section. 1 = aorta, 2 = inferior vena cava, 3 = left renal vein, 4 = right renal vein, 5 = superior mesenteric artery, 6 = splenic vein, 7 = common bile duct, P = pancreas. *D*, Sonogram at same level showing gallbladder (G) as fluid-filled structure and liver metastases (M). P = pancreas, K = kidney, St = stomach, Sp = spleen, V = vertebra, Asc = ascitic fluid.

images by periaortic nodes; this has been described as a characteristic feature of periaortic adenopathy [8, 9]. Obscuration is caused by the close similarity of the linear attenuation coefficient of the aorta and that of the surrounding tumor. The aorta can be imaged if the patient is scanned while intravenous contrast material is injected. The aorta becomes denser than the surrounding adenopathy, but it approaches isodensity again a few minutes after the end of the injection due to diffusion of contrast into the extracellular fluid [10]. However, visualization of the aorta is not usually necessary to make the diagnosis of periaortic adenopathy, since the irregular contour of the enlarged lymph nodes distinguishes them from aortic aneurysm. Gray scale sonography nearly always distinguishes the aorta from surrounding adenopathy in these cases (fig. 2).

Patient movement is a potential cause of loss of resolution on CT because of averaging effects and the production of artifacts [11]. Overall patient motion, respiratory motion, peristalsis, and cardiovascular motion are all contributory. Of these the most important and troublesome is respiratory motion. However, respiratory motion should be minimal in paraaortic adenopathy, and it should not be a factor in the case of a large pelvic tumor (case 1, fig. 1). The question of motion does not, of course, arise in the cadaver study (figs. 4 and 5); thus the nonvisualization of the metastases and of the gallbladder can be attributed entirely to isodensity.

Lesions or structures which are not identifiable on CT because of isodensity may become visible after injection of intravenous contrast material. Isodense liver metastases usually become visible after contrast enhancement. However contrast enhancement may occasionally render a previously visible lesion isodense, so unenhanced as well as enhanced studies may be necessary in some situations [12]. However, repeating scans with contrast enhancement doubles the radiation exposure and introduces the risks associated with intravenous contrast. Moreover, it seldom helps in the case of a nonvisualized pancreas in a thin person (fig. 5). Such lean individuals usually provide the best sonographic images, and for that reason we recommend ultrasonography as the method of choice for imaging the pancreas in such patients.

Future improvement in contrast resolution of CT may result from energy-selective reconstructions which analyze the entire energy spectrum of the x-ray beam, rather than assuming a single average energy as done at present [13]. This would specifically examine the portion of the overall attenuation which is due to photoelectric absorption, and thus detect tissues with different effective atomic numbers. Even with this refinement, however, it is likely that isodensity will still be a problem in some cases.

Application of computers to signal processing in ultrasound along with high resolution, high frequency transducers will almost certainly further improve tissue differentiation by sonography. In the near future computerized ultrasound equipment will probably allow quantification of velocity, attenuation, scattering, and of alterations in the latter two and in internal echo patterns with varying frequencies [14, 15]. Tissue characterization, as distinct from mere visualization, may then become a possibility.

REFERENCES

1. Bassano DA, Chamberlain CC, Mozley JM, Kieffer SA: Physical performance and dosimetric characteristics of the Delta-Scan 50 whole body/brain scanner. *Radiology* 123:455-462, 1977
2. Wells PNT: *Physical Principles of Ultrasonic Diagnosis.* New York, Academic Press, 1969
3. Fields S, Dunn F: Correlation of echographic visualizability of tissue with biological composition and physiological state. *J Acoust Soc Am* 45:809-812, 1973
4. Calderon C, Vilkomerson D, Megrich R, Etzold KF, Kinsley B, Haskin M: Differences in the attentuation of ultrasound by normal, benign, and malignant breast tissue. *J Clin Ultrasound* 4:249-254, 1976
5. Lemons RA, Quate C: Acoustic microscopy: biomedical applications. *Science* 188:905-911, 1975
6. Taylor KJW, Carpenter DA, Hill CR, McCready VR: Gray scale ultrasound imaging: the anatomy and pathology of the liver. *Radiology* 119:415-423, 1976
7. Dinn WM, Bryan PJ, Brown J, Kieffer SA: Anatomic correlation of computed tomography and gray scale ultrasonography of the abdomen. Exhibit presented at the annual meeting of the American Roentgen Ray Society, Washington, D.C., September 1976
8. Sheedy PF II, Stephens DH, Hattery RR, Mahon JR, Hartman GW: Computed tomography of the body: initial clinical trial with the EMI prototype. *Am J Roentgenol* 127:23-51, 1976
9. Stanley RJ, Sagel SS, Levitt RG: Computed tomography of the body: early trends in application and accuracy of the method. *Am J Roentgenol* 127:53-67, 1976
10. Kormano M, Dean PB: Extravascular contrast material: the major component of contrast enhancement. *Radiology* 121:379-382, 1976
11. Alfidi RJ, MacIntyre WJ, Haaga JH: The effects of biological motion on CT resolution. *Am J Roentgenol* 127:11-15, 1976
12. Bryan PJ, Dinn WM, Grossman ZD, Wistow BW, McAfee JG, Kieffer SA: Correlation of computed tomography, grayscale ultrasonography, and radionuclide imaging of the liver. *Radiology* 124:387-393, 1977
13. Alvarez RR, Macovski A: Energy-selective reconstructions in x-ray computerized tomography. *Phys Med Biol* 21:733-744, 1976
14. Lele PP, Mansfield AB, Murphy AI, Namery J, Senapati N: Tissue characterization by ultrasonic frequency-dependent attenuation and scattering: ultrasonic tissue characterization, in *Proceedings of the 1st International Symposium on Ultrasonic Tissue Characterization*, Washington, D.C., National Bureau of Standards, 1976, pp 167-196
15. Waag RC, Lerner RM, Gramiak R: Swept-frequency ultrasonic determination of tissue macrostructure: ultrasonic tissue characterization, in *Proceedings of the 1st International Symposium on Ultrasonic Tissue Characterization*, Washington, D.C., National Bureau of Standards, 1976, pp 213-228

Myelolipoma of the Adrenal: Two Cases with Ultrasound and CT Findings

MICHAEL BEHAN,[1] ERIC C. MARTIN,[1, 2] EDWARD C. MUECKE,[3] AND ELIAS KAZAM[1]

Myelolipoma of the adrenal gland is a rare tumor composed of varying proportions of fat and bone marrow elements. In about half of the reported cases with radiologic findings the mass was radiolucent, indicating the presence of fat; the remainder were of soft tissue density or calcified. Arteriography is of limited value in diagnosis, since myelolipomas are typically avascular. With the advent of gray scale ultrasound and computed tomography (CT), fat can be detected in lesions which do not appear radiolucent on radiographs. Two cases of myelolipoma are reported in which ultrasound showed a markedly echogenic mass, an appearance characteristic of lipomatous tumors. In the second case, the mass was of soft tissue density on radiographs, markedly echogenic on sonogram, and definitively fatty on CT scan. Ultrasound and CT are valuable techniques for making a preoperative diagnosis of this tumor.

The presence of bone marrow cells in an adrenal lipoma was first described by Gierke in 1905 [1]. Oberling introduced the term myelolipoma in 1929 to describe such tumors [2]. Many earlier descriptions of adrenal lipomas are now thought to represent myelolipomas.

Fewer than 200 myelolipomas have been recorded in the world literature, of which 95% are only descriptions of pathology. In 1957 the first surgical removal of a myelolipoma was reported [3]. Since then, 10 other surgically proven cases have been reported [4–13], and two more were illustrated in radiologic textbooks [14, 15]. About 50% of these lesions appeared radiolucent on radiographs. Without this sign, a presurgical diagnosis would not be possible. We report how ultrasound and CT facilitated the preoperative diagnosis in two patients with adrenal myelolipoma.

Case Reports

Case 1

A 47-year-old female with no relevant history had flank pain and fever for 6 weeks. On physical examination there was moderate obesity and a large right flank mass, thought to be renal. The hemoglobin was 10.4 g/100 ml and the erythrocyte sedimentation rate, 76 mm/hr. Urinalysis demonstrated pyuria but no hematuria. No organism was isolated from the urine. Intravenous urography and nephrotomography showed a radiolucent suprarenal mass 11 cm in diameter displacing the right kidney inferiorly.

Sonography showed a mass 10.5 cm in diameter posterior to the right lobe of the liver, compressing the upper pole of the right kidney (fig. 1*A*). The lesion was markedly echogenic, a finding characteristic of lipomatous tissue. Angiography of the right renal artery with epinephrine showed a suprarenal mass of fat density compressing the adrenal medially. Branches of the inferior adrenal artery were draped around the inferior and medial margins of the mass. There was neither neovascularity nor blush (fig. 1*B*).

Surgery was performed through a thoracolumbar incision, and a smooth firm mass with a yellowish surface was dissected free of the kidney. It was removed in its entirety and the kidney was preserved. Both bone marrow and fat elements were seen within the tumor on histologic examination, typical of a myelolipoma.

Case 2

A 55-year-old man had dysuria for 3 months. He had had a myocardial infarction 3 years earlier. The only positive laboratory finding was microscopic hematuria. Intravenous urography showed a left suprarenal mass of soft tissue density about 5 cm in diameter displacing the kidney inferiorly. There were bilateral adrenal calcifications and irregular calcification in the lateral margin of the mass (fig. 2*A*). The right adrenal calcification was confined to the gland, and there were no associated masses to suggest a myelolipoma. Aortography and selective left renal arteriography confirmed that the mass was extrarenal, most probably adrenal. Neither neovascularity nor blush was seen (fig. 2*B*).

Sonography showed a very echogenic left suprarenal mass displacing the kidney inferiorly and indenting its superomedial aspect. The mass had poorly defined margins since it blended with retroperitoneal fat which had similar acoustic properties (fig. 2*E*). CT examination with intravenous contrast medium showed a 5 × 6 cm fatty left suprarenal mass displacing the tail of the pancreas anteriorly and the left kidney inferiorly. There were flecks of calcium in the periphery of the mass continuous with the left adrenal calcification (figs. 2*C* and 2*D*).

At surgery a 6 cm mass was removed; on sectioning it was fatty with scattered areas of hemorrhage. There was a thin rim of adrenal tissue which was partially calcified. Histologically it was a myelolipoma.

Discussion

We reviewed the radiologic findings in 14 patients with myelolipoma [4–15] including our two patients. All patients had evidence of a mass above the kidney on barium studies, intravenous urography, or plain radiography. In seven instances the mass was radiolucent; however, in one case the initial radiolucency changed to soft tissue density at a subsequent examination. Three patients had bilateral adrenal calcifications. In two of these the mass was also calcified. In one instance the mass alone was heavily calcified. In most patients on whom it was performed, intravenous urography demonstrated a suprarenal rather than renal mass.

Angiography was performed on nine patients. In seven

Received May 23, 1977; accepted after revision August 16, 1977.

[1] Department of Radiology, New York Hospital-Cornell Medical Center, 525 East 68th Street, New York, New York 10021. Address reprint requests to M. Behan.

[2] Present address: Department of Radiology, State University of New York Downstate Medical Center, Brooklyn, New York 11203.

[3] Department of Surgery, New York Hospital-Cornell Medical Center, New York, New York 10021.

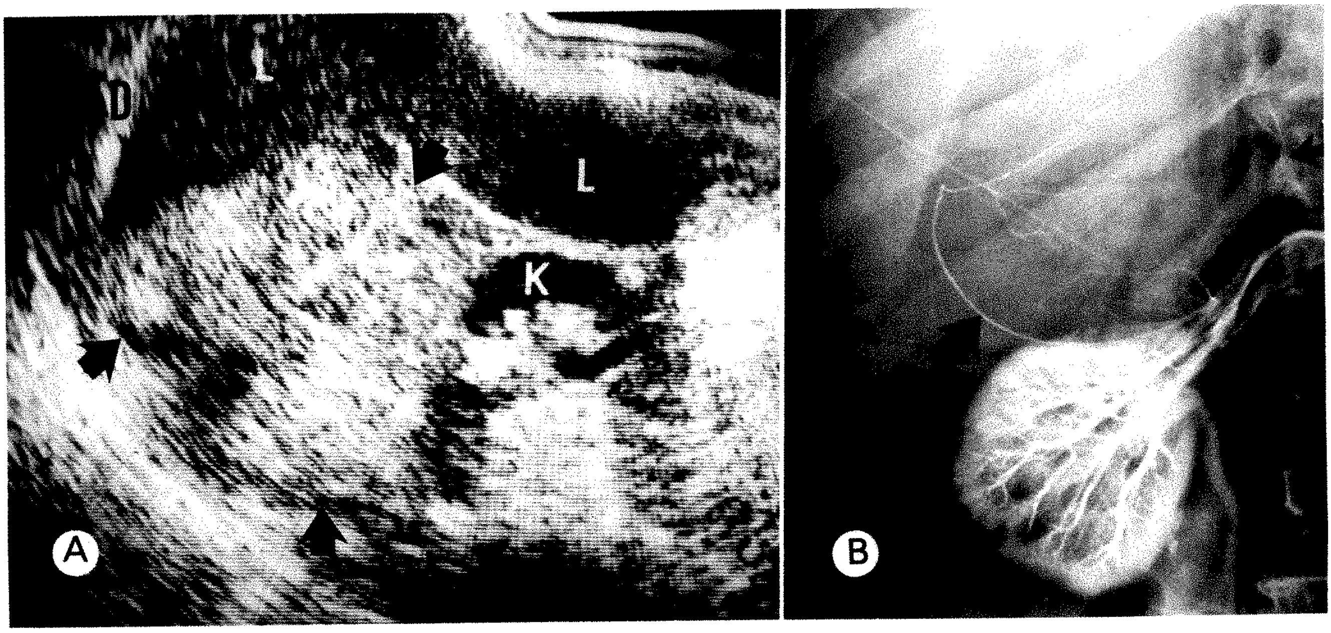

Fig. 1.—Case 1. *A*, Sagittal sonogram of right upper quadrant showing markedly echogenic lobulated mass (*arrows*) displacing right kidney (K) inferiorly and indenting posteroinferior aspect of right hepatic lobe (L). D = diaphragm. *B*, Selective right renal arteriogram showing radiolucent mass above right kidney displacing it inferiorly. Branches of inferior adrenal artery (*arrows*) are draped around mass.

of these an avascular mass was demonstrated with the adrenal vessels draped around the lesion. A faint blush was seen within the mass in one instance [14], and in another patient a small arteriovenous malformation was noted at the periphery of the tumor [10]. Adrenal venography in two cases showed displacement of veins around the tumor but no evidence of encasement.

The only previous report of sonographic findings merely described a solid mass [12]. In our two patients, ultrasound showed that the tumors were markedly echogenic (figs. 1*A* and 2*E*). This is an appearance which we have found characteristic of lipomatous masses [16]. However, it is not definitively diagnostic, since other tumors may occasionally be very echogenic. In case 1 the mass was so different in acoustic properties from adjacent renal parenchyma that continuity of its contours with those of the kidney could not be ascertained. Therefore, the mass could not be localized definitively as intrarenal or extrarenal by sonography. In both cases the mass could be overlooked on a cursory examination because of its acoustic similarity to adjacent retroperitoneal fat.

In case 2, CT showed a hypovascular, predominantly fatty mass contiguous to the left adrenal (figs. 2*C* and 2*D*). The rim, which contained a thin layer of adrenal tissue, was irregularly calcified.

Myelolipomata are rare tumors. In a series of 4,074 consecutive autopsies, an incidence of 0.8% was noted [11]. The majority of reported lesions were small tumors (a few millimeters in diameter) found incidentally at autopsy [17]. Larger lesions may become symptomatic, usually causing pain and leading to surgical intervention. Most surgical specimens have weighed several hundred grams.

The etiology of myelolipomas is not known. It is suggested that they are caused by metaplasia of mesenchymal stem cells, which are the precursors of both adrenal and myeloid tissues [4]. Myeloid transformation in the adrenals has been produced in rats after subcutaneous injection of anterior pituitary extract and methyl testosterone. These changes appeared in the adrenal cortex (zona glomerulosa and fasciculata) but not in the medulla [18]. Chronic infection and trauma have also been proposed as causative factors [5]. Three of eight patients in one series dying of burn injuries had myeloid cells in the adrenal cortex [19]. Anemia has also been suggested as a possible stimulus. Hemopoietic activity in the adrenal gland may occur in children as a secondary response to chronic anemia, although such activity is rare in adults [5]. Although the tumors are generally regarded as nonfunctioning, nine patients in Plaut's series of 100 [17] had various endocrine dysfunctions.

In the same series [17], pathologic examination showed a range of appearances from almost entirely lipomatous to almost entirely myeloid. The findings in our two patients suggest that fat within such a tumor can be recognized by its marked echogenicity on the sonogram, even if it is of soft tissue density radiologically (case 2). This must then be verified by CT, since the sonographic appearance is characteristic but not pathognomonic of lipomatous masses. Thus sonography and CT are more sensitive than conventional radiography to the presence of fat within the mass. However, a preoperative diagnosis with these two methods may not be possible where myeloid elements or hemorrhage predominate, or if the lesion is heavily calcified.

The differential diagnosis of fatty tumors in the suprarenal area includes retroperitoneal lipoma and liposarcoma or a renal angiomyolipoma protruding from the upper

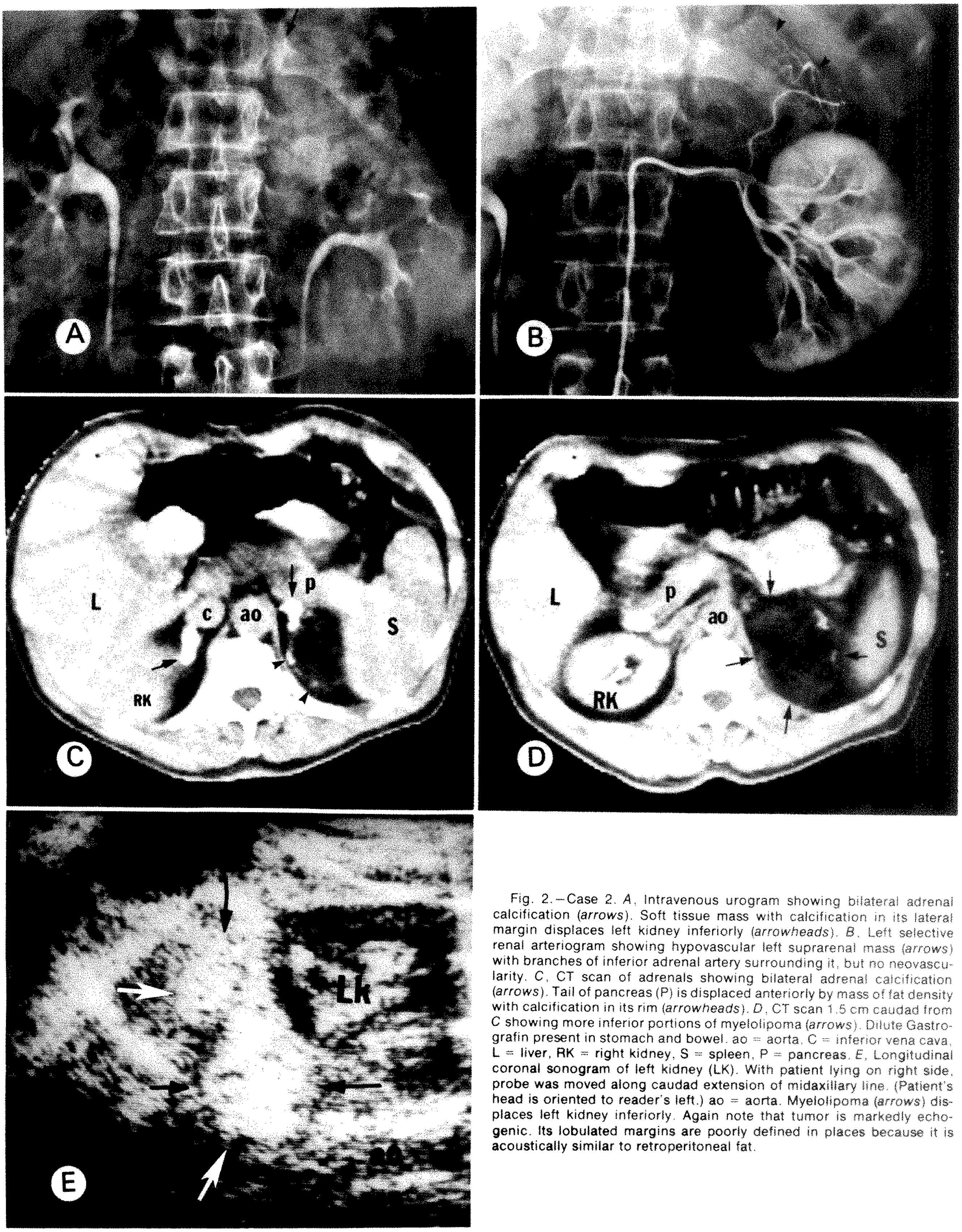

Fig. 2.—Case 2. *A*, Intravenous urogram showing bilateral adrenal calcification (*arrows*). Soft tissue mass with calcification in its lateral margin displaces left kidney inferiorly (*arrowheads*). *B*, Left selective renal arteriogram showing hypovascular left suprarenal mass (*arrows*) with branches of inferior adrenal artery surrounding it, but no neovascularity. *C*, CT scan of adrenals showing bilateral adrenal calcification (*arrows*). Tail of pancreas (P) is displaced anteriorly by mass of fat density with calcification in its rim (*arrowheads*). *D*, CT scan 1.5 cm caudad from *C* showing more inferior portions of myelolipoma (*arrows*). Dilute Gastrografin present in stomach and bowel. ao = aorta, C = inferior vena cava, L = liver, RK = right kidney, S = spleen, P = pancreas. *E*, Longitudinal coronal sonogram of left kidney (LK). With patient lying on right side, probe was moved along caudad extension of midaxillary line. (Patient's head is oriented to reader's left.) ao = aorta. Myelolipoma (*arrows*) displaces left kidney inferiorly. Again note that tumor is markedly echogenic. Its lobulated margins are poorly defined in places because it is acoustically similar to retroperitoneal fat.

pole. Angiography is useful for localizing the mass to the adrenal rather than to the kidney. Myelolipomas and retroperitoneal lipomatous tumors are typically avascular, whereas angiomyolipomas are vascular. The vascularity may be assessed either by CT or angiography.

In conclusion, ultrasound and CT can greatly facilitate the correct preoperative diagnosis of myelolipoma of the adrenal. Angiography continues to be of value in localizing the tumor and demonstrating its blood supply.

REFERENCES

1. Gierke E: Über Knochenmarksgwebe in der Nebenniere. *Zeiglers Beitr Pathol Anat* 7, suppl.:311-324, 1905
2. Oberling C: Les formations myelolipomateuses. *Bull Assoc Fr Etude Cancer* 18:234-246, 1929
3. Dykman J, Freedman D: Myelolipoma of the adrenal with clinical features and surgical excision. *J Mt Sinai Hosp NY* 24:793-796, 1957
4. Figueroa G, Tedeschi L: Myelolipoma of the adrenal gland. *Bost Med Q* 2:34-37, 1966
5. Dean G: Myelolipoma of the adrenal gland. *Scott Med J* 16:513-518, 1971
6. Parsons L, Thompson JE: Symptomatic myelolipoma of the adrenal gland. *N Engl J Med* 26:12-15, 1959
7. Whittaker LD: Myelolipoma of the adrenal gland. *Arch Surg* 97:628-631, 1968
8. Newman PH, Silen W: Myelolipoma of the adrenal gland. *Arch Surg* 97:637-639, 1968
9. Engelking RC, Esparza XI, Velasco DJ, Maldonado E: Myelolipoma of the adrenal gland and kidney adenocarcinoma. *J Urol* 98:419-421, 1967
10. Tulcinsky DB, Deutsch V, Bubis JJ: Myelolipoma of the adrenal gland. *Br J Surg* 57:465-467, 1970
11. Olsson CA, Krane RJ, Klugo RC, Selikowitz SM: Adrenal myelolipoma. *Surgery* 73:665-670, 1973
12. Gee WF, Chikos PM, Greaves JP, Ikemoto N, Tremann JH: Adrenal myelolipoma. *Urology* 5:562-566, 1975
13. Rubin HB, Hirose F, Benfield JR: Myelolipoma of the adrenal gland. *Am J Surg* 130:354-358, 1975
14. Kahn PC: Adrenal angiography, in *Angiography*, 2d ed, edited by Abrams HL, Boston, Little, Brown, 1971, p 938
15. Bosniak MA, Siegelman SS, Evans JA: *The Adrenal, Retroperitoneum and Lower Urinary Tract.* Chicago, Year Book Medical Publishers, 1976
16. Kazam E, Behan M: The echographic appearance of fat. In preparation
17. Plaut A: Myelolipoma in the adrenal cortex. *Am J Pathol* 34:487-515, 1958
18. Selye H, Stone H: Hormonally-induced transformation of adrenal into myeloid tissue. *Am J Pathol* 26:211-233, 1950
19. Delarue J, Montsaingeon A: Metaplaises myeloides dans la cortico suprarenale des brûles. *Compt Rend Soc Biol* 144:777-778, 1950

Ultrasound-guided Drainage of Fluid-containing Masses Using Angiographic Catheterization Techniques

JOHN GRØNVALL,[1] SVEN GRØNVALL, AND VIKTOR HEGEDÜS

A new method combining experience of ultrasonic diagnostic and puncture technique with the use of existing angiographic tools is described. Using this method, intraabdominal fluid-containing mass lesions were drained for diagnostic and therapeutic purposes. In three patients, severe life-threatening lesions were successfully diagnosed and treated solely by this method. In one other case the method greatly facilitated major surgery. The importance of integration of diagnostic radiology and ultrasound is stressed.

Ultrasound-guided puncture of cystic mass lesions has been successfully used during the last few years [1-4]. This technique has been of value in obtaining samples of intraabdominal accumulations of fluid for histologic, bacteriologic, and biochemical analyses. Therapeutic emptying of pancreatic cysts and perinephric abscesses was also reported [2, 5]. In our experience, a similar technique can also be used to establish permanent drainage of intraabdominal lesions containing fluid of various types (serous fluid or pus), thus in some cases making surgical intervention unnecessary. In addition, the intracavitary catheter can be used for contrast studies and for instillation of various medications.

Materials and Methods

In the ultrasound section of our department during the past year, 24 diagnostic punctures of intraabdominal cavities (13 cysts and 11 abscesses) were performed. In four of these cases, drainage was carried out according to the technique described below.

After ultrasonic verification of the site of the lesion, bistable ultrasonic equipment with a transducer for percutaneous puncture was prepared [3, 4]. Figure 1 shows the necessary instruments. After thorough antiseptic treatment of the skin and using sterilized oil, ultrasonically controlled percutaneous puncture of the lesion was performed. For lesions near the surface, an angiographic needle was used; for deeper lesions, equipment usually used for percutaneous transhepatic cholangiography (Surgimed, Ølstykke, Denmark) was chosen.

Specimens for bacteriologic, histologic, and enzymatic analyses were withdrawn through the puncturing instrument. Then a guide wire (William Cook Europe, Søborg, Denmark) normally used at angiography was inserted through the puncturing in-

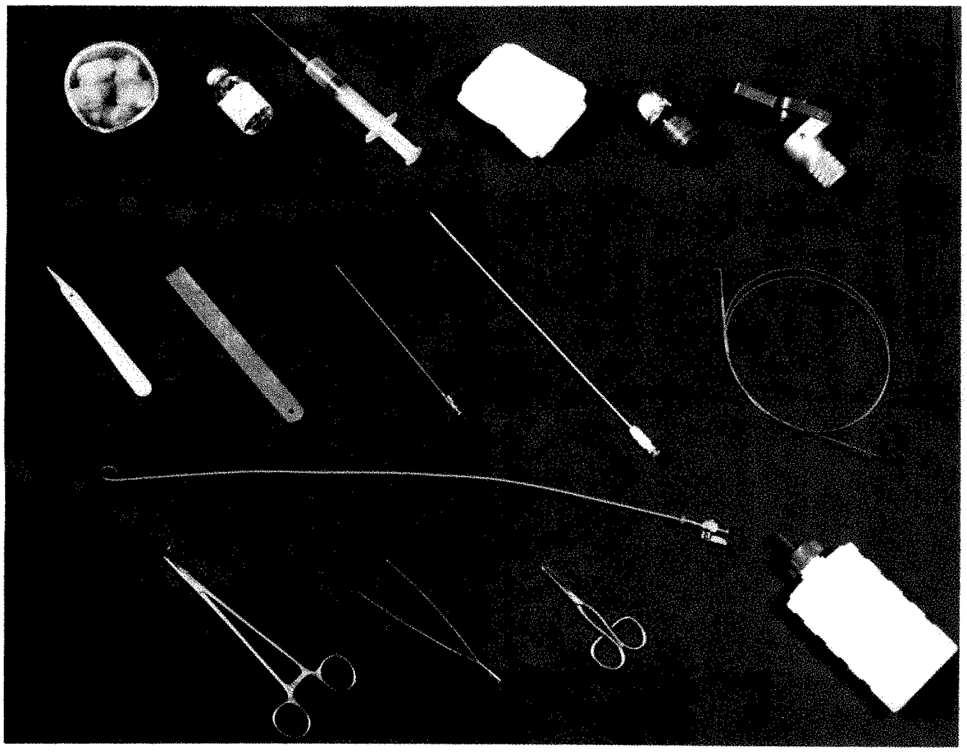

Fig. 1.—Instruments for ultrasound-guided drainage of fluid-containing lesions: iodine, local anesthesia, syringe, sterilized oil, sterilized ultrasound transducer for percutaneous puncture, knife, ruler, needle, percutaneous transhepatic cholangiography set, guide wire, pigtail catheter with side holes, suturing facilities, pincet, scissors, suction bottle.

Received May 5, 1977; accepted after revision August 16, 1977.
This work was supported by a grant from the Statens Videnskabelige Forskningsfond, Denmark.

[1] All authors: Department of Diagnostic Radiology, Glostrup University Hospital, Copenhagen, DK-2900 Glostrup, Denmark. Address reprint requests to V. Hegedüs.

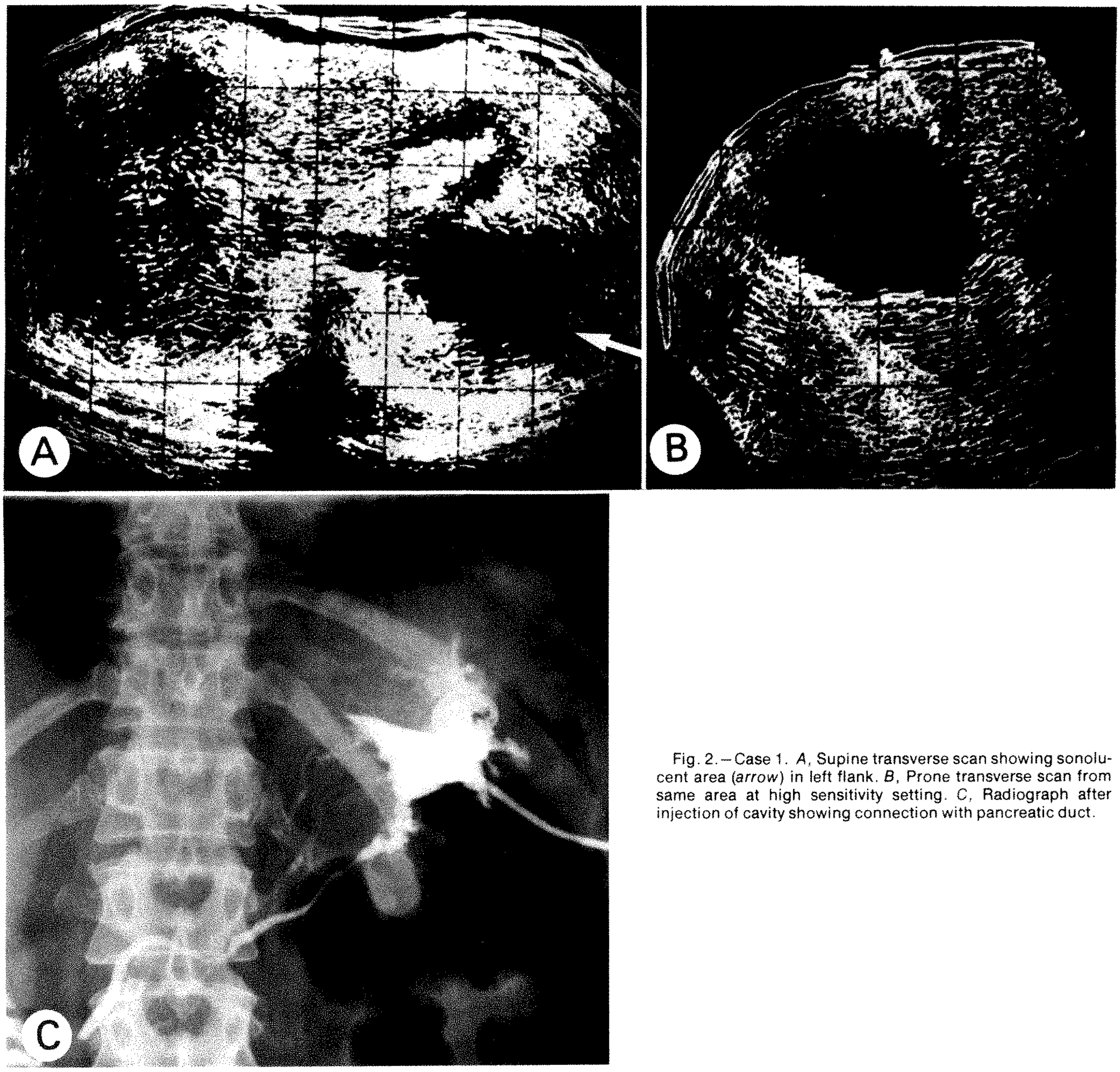

Fig. 2.—Case 1. *A*, Supine transverse scan showing sonolucent area (*arrow*) in left flank. *B*, Prone transverse scan from same area at high sensitivity setting. *C*, Radiograph after injection of cavity showing connection with pancreatic duct.

strument. To avoid intracavitary traumatic lesions, J-shaped soft-end guide wires were used, and the necessary length from the surface to the lesion was measured on the ultrasonic image. Guided by the wire, a pigtail angiography catheter (William Cook Europe, Søborg, Denmark) was placed in the cavity for draining purposes. The drain was then sutured to the skin and connected to a suction bottle. The cavities were delineated radiographically using injection of water soluble contrast medium through the draining catheter. The diagnostic and therapeutic results of this technique in four case reports are reported.

Case Reports

Case 1

A 46-year-old woman with a 3 year history of duodenal ulcer was admitted three times in 2 years for fever and severe abdominal and left thoracic pain. At each admission, a cystic process adjacent to the tail of the pancreas was diagnosed. During the first admission, a pancreatic cyst verified at surgery was drained. At the second admission, a percutaneous ultrasound-guided needle puncture of the cyst was performed; 250 ml of brown fluid containing pancreatic enzymes was aspirated. However, the cyst refilled rapidly. Although adjudged earlier as technically difficult, a second operation was performed resulting in marsupialization of the cyst.

At the third admission, surgery was definitely contraindicated. Therefore an ultrasound-guided percutaneous puncture was performed and 50 ml purulent fluid was aspirated. Total drainage of the thick fluid was not possible. Therefore permanent drainage was established according to the technique described (figs. 2*A* and 2*B*). The patient tolerated the procedure without discomfort.

Immediately afterward, radiographic investigation of the cavity was made (fig. 2*C*). After the appropriate bacteriologic verifi-

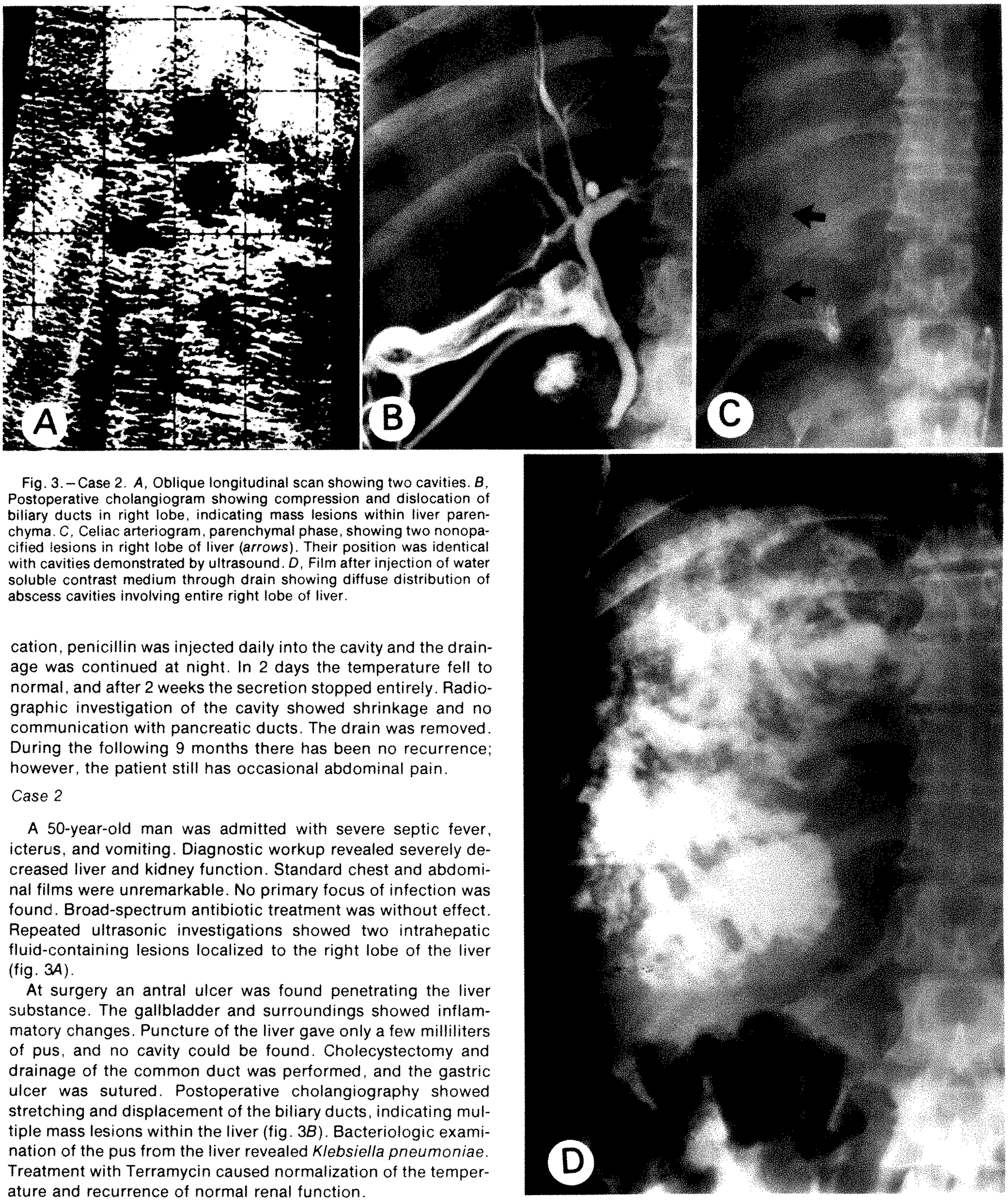

Fig. 3.—Case 2. *A*, Oblique longitudinal scan showing two cavities. *B*, Postoperative cholangiogram showing compression and dislocation of biliary ducts in right lobe, indicating mass lesions within liver parenchyma. *C*, Celiac arteriogram, parenchymal phase, showing two nonopacified lesions in right lobe of liver (*arrows*). Their position was identical with cavities demonstrated by ultrasound. *D*, Film after injection of water soluble contrast medium through drain showing diffuse distribution of abscess cavities involving entire right lobe of liver.

cation, penicillin was injected daily into the cavity and the drainage was continued at night. In 2 days the temperature fell to normal, and after 2 weeks the secretion stopped entirely. Radiographic investigation of the cavity showed shrinkage and no communication with pancreatic ducts. The drain was removed. During the following 9 months there has been no recurrence; however, the patient still has occasional abdominal pain.

Case 2

A 50-year-old man was admitted with severe septic fever, icterus, and vomiting. Diagnostic workup revealed severely decreased liver and kidney function. Standard chest and abdominal films were unremarkable. No primary focus of infection was found. Broad-spectrum antibiotic treatment was without effect. Repeated ultrasonic investigations showed two intrahepatic fluid-containing lesions localized to the right lobe of the liver (fig. 3*A*).

At surgery an antral ulcer was found penetrating the liver substance. The gallbladder and surroundings showed inflammatory changes. Puncture of the liver gave only a few milliliters of pus, and no cavity could be found. Cholecystectomy and drainage of the common duct was performed, and the gastric ulcer was sutured. Postoperative cholangiography showed stretching and displacement of the biliary ducts, indicating multiple mass lesions within the liver (fig. 3*B*). Bacteriologic examination of the pus from the liver revealed *Klebsiella pneumoniae*. Treatment with Terramycin caused normalization of the temperature and recurrence of normal renal function.

A few weeks later the earlier symptoms recurred. Celiac arteriography showed diffuse liver enlargement and severe peripherial resistance to the arterial and portal flow. In addition, two irregular cavities identical to the ones found by ultrasound in the right lobe of the liver were verified (fig. 3*C*). An ultrasound-guided percutaneous permanent drainage of the cavities was established according to the technique described. Specimens from the drained pus showed anaerobic infection. Radiographic investigation with contrast material injected through the catheter showed a huge irregular cavity affecting the entire right lobe of the liver without connection to the biliary ducts (fig. 3*D*). Due

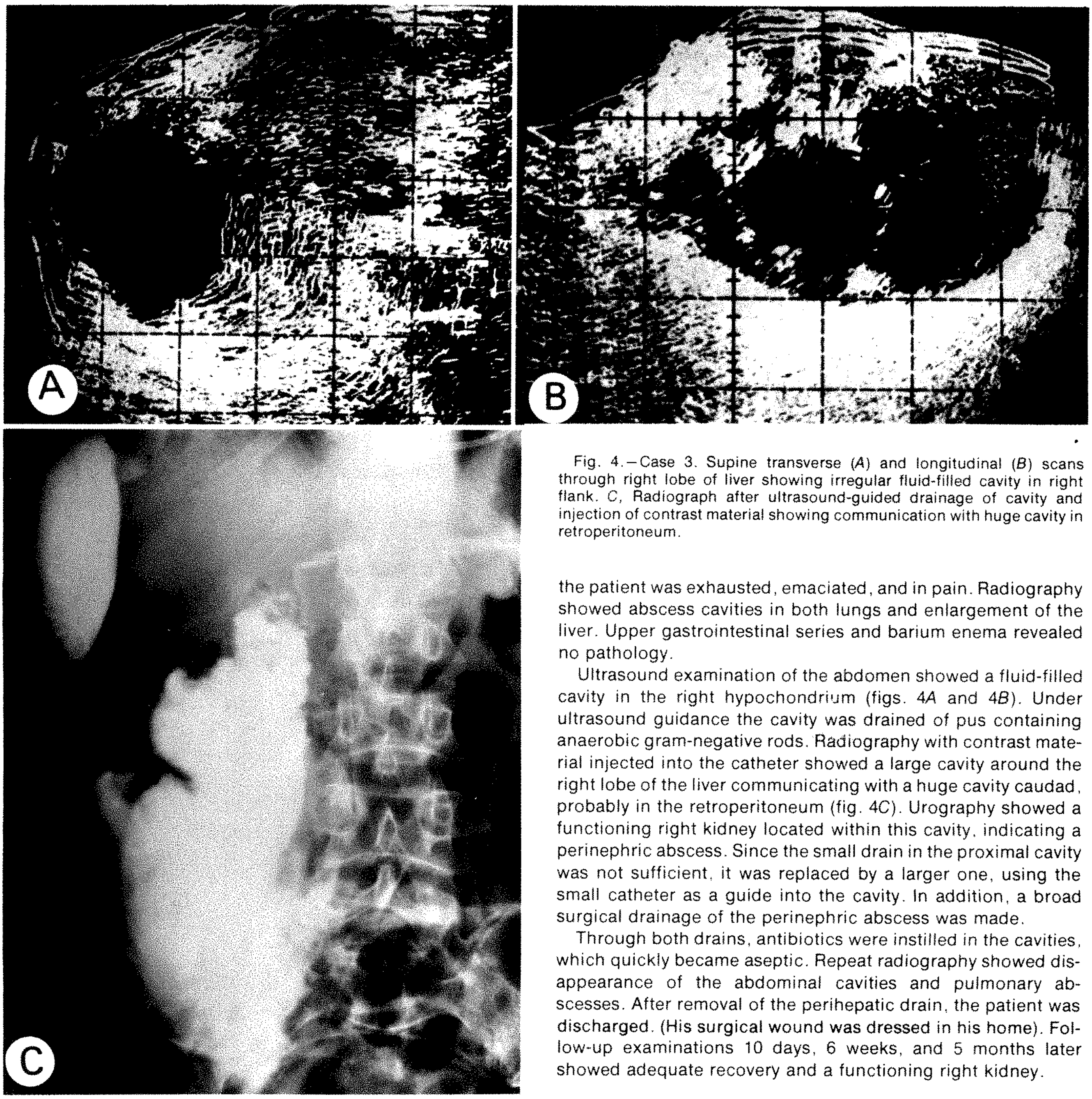

Fig. 4.—Case 3. Supine transverse (*A*) and longitudinal (*B*) scans through right lobe of liver showing irregular fluid-filled cavity in right flank. *C*, Radiograph after ultrasound-guided drainage of cavity and injection of contrast material showing communication with huge cavity in retroperitoneum.

to appropriate antibiotic treatment and drainage of 800–1,000 ml of pus daily for 7 days, the output diminished successively and the patient returned to normal.

After 3 weeks, radiography showed total shrinkage of the cavity, and the drain was removed. During 1 month of convalescence, several ultrasonic examinations revealed no mass lesions, and laboratory values showed diminishing liver abnormalities. The patient subsequently returned to work and is completely recovered.

Case 3

A 62-year-old man with duodenal ulcer for several years and advancing polyarthritis the last 25 years was admitted because of the changing character of his epigastric pains. At admission the patient was exhausted, emaciated, and in pain. Radiography showed abscess cavities in both lungs and enlargement of the liver. Upper gastrointestinal series and barium enema revealed no pathology.

Ultrasound examination of the abdomen showed a fluid-filled cavity in the right hypochondrium (figs. 4*A* and 4*B*). Under ultrasound guidance the cavity was drained of pus containing anaerobic gram-negative rods. Radiography with contrast material injected into the catheter showed a large cavity around the right lobe of the liver communicating with a huge cavity caudad, probably in the retroperitoneum (fig. 4*C*). Urography showed a functioning right kidney located within this cavity, indicating a perinephric abscess. Since the small drain in the proximal cavity was not sufficient, it was replaced by a larger one, using the small catheter as a guide into the cavity. In addition, a broad surgical drainage of the perinephric abscess was made.

Through both drains, antibiotics were instilled in the cavities, which quickly became aseptic. Repeat radiography showed disappearance of the abdominal cavities and pulmonary abscesses. After removal of the perihepatic drain, the patient was discharged. (His surgical wound was dressed in his home). Follow-up examinations 10 days, 6 weeks, and 5 months later showed adequate recovery and a functioning right kidney.

Case 4

A 41-year-old male was admitted because of fever, back pain, increase of abdominal girth, and exhaustion. He had undergone surgery $2^{1}/_{2}$ years earlier for carcinoma of the descending colon. Admission abdominal films showed a large round mass lesion in the middle of the abdomen.

Ultrasound showed one large and many smaller fluid-containing cystic mass lesions (fig. 5*A*). Ultrasound-guided drainage according to the technique described evacuated primarily 500 ml of brownish turbid fluid, which resembled the contents of a pancreatic cyst. Despite adequate drainage, expansion of the abdomen recurred a few days later. Repeat ultrasound revealed increased size of other cysts, and a second drain was inserted. Radiography with contrast material injected into the catheter showed filling of multiple interconnecting cavities (figs. 5*B* and

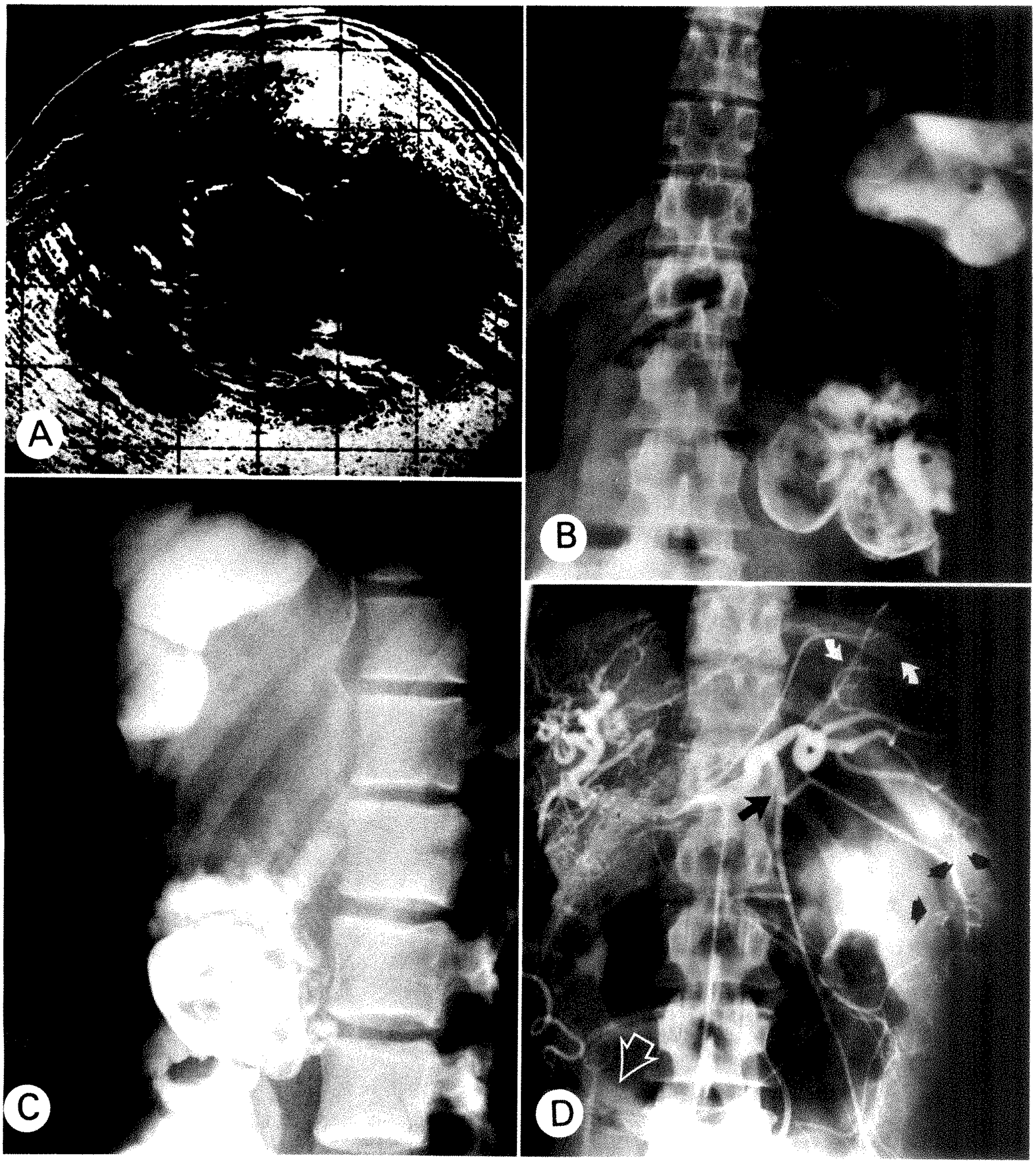

Fig. 5.—Case 4. *A*, Supine transverse scan at umbilical level showing large cystic multiloculated mass lesion. *B* and *C*, Frontal and lateral radiographs after second ultrasound-guided drainage showing complex system of intercommunicating cavities. *D*, Celiac arteriogram showing large artery (*black arrow*) and some small stretched arteries (*white arrows*) arising from splenic artery. Right branch of large artery communicates with gastroepiploic artery (*open arrow*), while left branch at its peripheral portion divides into small tumor arteries (*short arrows*).

5*C*). Bacteriologic, histologic, and chemical examination of the drained fluids showed no pancreatic enzymes and no evidence of malignant or inflammatory cells.

Because of large volumes of fluid produced through the drains for 3 weeks, it was felt that surgery was necessary. Preoperative angiography of the celiac axis and the superior mesenteric artery showed multiple areas of neoplastic vascularity (fig. 5*D*). At surgery, a large complex of thick-walled cysts was found. After careful dissection the splenic artery was ligated, and the complex was easily released from the greater curvature of the stomach and lifted out en bloc. At the site demonstrated by angiography, carcinomatous tissue involved the mesocolon. Pathologic examination showed a highly differentiated adenocarcinoma in all the specimens, probably metastatic from the colonic tumor. All the cysts had adenomatous walls with excreting capacity. The postoperative course was uneventful, and the patient is now undergoing cancer chemotherapy.

Discussion

Percutaneous ultrasound-guided puncture of intraabdominal organs is a well known procedure [1, 2, 4–6]. Emptying of kidney and pancreatic cysts using percutaneous needle technique has also been described. However, because some lesions, have fluid-producing properties, one puncture will usually serve only as a diagnostic tool. The technique described here combines and develops the ultrasonic puncturing technique and the experience gained through the use of angiography. None of our patients had any discomfort during the procedures. The drainage procedures took only minutes under local anesthesia. Furthermore, in cases 1–3 the technique was the treatment of choice and avoided the risks of surgery. The drainage technique was life saving, especially in cases 1 and 2, since surgical intervention was tried and had failed. Particularly for patients in very poor condition, this technique is an easily performed alternative to surgery. We therefore stress the importance of this integration of ultrasonic and angiographic technique, emphasizing the advantages of their coexistence within one department [7].

REFERENCES

1. Smith EH, Bartrum RJ: Ultrasonically guided percutaneous aspiration of abscesses. *Am J Roentgenol* 122:308–312, 1974
2. Hancke S, Pedersen JF: Percutaneous puncture of pancreatic cysts guided by ultrasound. *Surg Gynecol Obstet* 142:551–552, 1976
3. Holm HH, Kristensen JK, Rasmussen SN, Northeved A, Barlebo H: Ultrasound as a guide in percutaneous puncture technique. *Ultrasonics* 10:83–86, 1972
4. Holm HH, Pedersen JF, Kristensen JK, Rasmussen SN, Hancke S, Jensen F: Ultrasonically guided percutaneous puncture. *Radiol Clin North Am* 13:493–503, 1975
5. Melvin RC, Sanders RC, Mascardo AD: Perinephric abscess aspiration using ultrasound guidance. *Am J Roentgenol* 128:459–464, 1977
6. Holm HH, Kristensen JK, Rasmussen SN, Pedersen JF, Hancke S: *Abdominal Ultrasound*. Copenhagen, Munksgaard, 1976
7. Cimmino CV, King DL: The general radiologist and ultrasound (editorial). *Am J Roentgenol* 127:867, 1976

Gray Scale Ultrasound Evaluation of Popliteal Artery Aneurysms

TERRY M. SILVER,[1] RONALD L. WASHBURN,[1] JAMES C. STANLEY,[2] AND WILLIAM S. GROSS[2]

Gray scale B-scan ultrasonography is accurate in identifying and assessing morphologic features of popliteal artery aneurysms. Eight patients with suspected popliteal aneurysms had 12 aneurysms demonstrated by ultrasonography, including two not visualized by arteriography due to proximal occlusive disease and three covert aneurysms opposite a contralateral palpable popliteal mass. Half the patients had bilateral aneurysms demonstrated by ultrasonography.

Popliteal artery ultrasonography is useful to: (1) evaluate suspected aneurysms in patients who cannot or should not be subjected to invasive arteriographic studies or operation; (2) confirm or refute equivocal diagnoses of aneurysms generated by arteriographic studies or physical examination; (3) defect contralateral clinically covert aneurysms or small aneurysms in patients with generalized extrapopliteal aneurysmal disease; (4) delineate the extent of intraaneurysmal thrombus and determine exact aneurysm size in all dimensions; and (5) define a thrombosed aneurysm or one not opacified because of limited contrast material passing through proximally obstructed arteries. The latter two uses of ultrasonography represent significant advantages over arteriography.

Although the popliteal arteries are the most common sites of peripheral arterial aneurysms [1], their detection often goes unrecognized until complications evolve. Early diagnosis is important in management of these aneurysms, since surgical therapy prior to development of complications offers the greatest benefit to patients. In our experience popliteal artery ultrasonography has proved useful in accurate identification of aneurysms and assessment of their anatomic-morphologic features. This report establishes the value of the procedure in the diagnosis and management of suspected popliteal artery aneurysms.

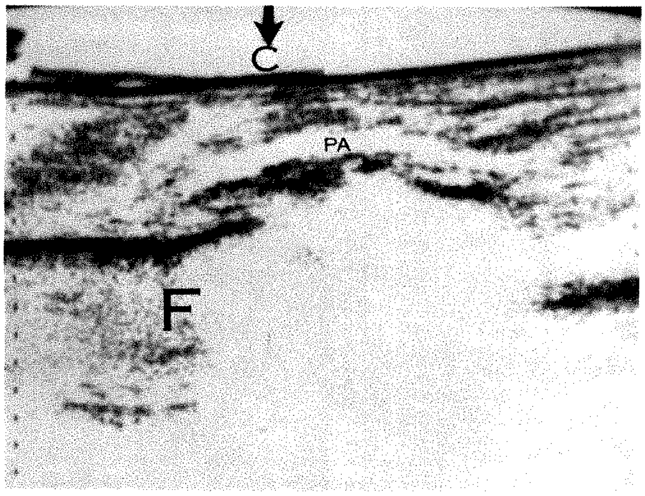

Fig. 1.—Longitudinal B-scan through posterior aspect of popliteal fossa showing normal caliber popliteal artery (PA). (Head to left.) F = femur, C = popliteal crease.

Materials and Methods

The popliteal fossae of eight white male patients (50-83 years of age) with suspected popliteal artery aneurysms were studied by ultrasound. Seven of these patients also were studied by arteriography. All patients had clinical, laboratory, or radio-

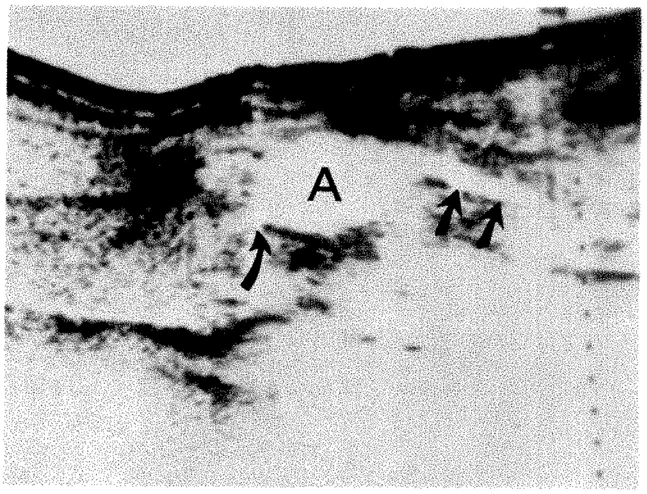

Fig. 2.—Case 2. Longitudinal scan of popliteal artery aneurysm (A) showing continuity of cystic mass with proximal (*curved arrow*) and distal (*paired arrows*) popliteal artery, establishing diagnosis of aneurysm. (Head to left.) Aneurysm on contralateral side was also documented sonographically.

TABLE 1

Physical, Sonographic, Arteriographic, and Surgical Findings

Case No.	Age and Sex	Clinically Palpable Mass		Sonography		Arteriography		Surgery	
		Right	Left	Right	Left	Right	Left	Right	Left
1	........76,M	+	–	+	+	–	–*	+	–
2	........50,M	+	–	+	+	+	–†	+	+‡
3	........50,M	–	–	+	+	+	–*	+	–
4	........67,M	+	–	+	–	+	–	+	–
5	........70,M	–	–	+	–	+	–	–	–
6	........63,M	+	–	+	–	+	–	–	–
7	........56,M	–	+	+	+	–	+†	+‡	–
8	........83,M	–	+	–	+	...	...	–	–

Note.—All patients except cases 1 and 8 had aortoiliac aneurysm confirmed by arteriography or surgery.

* Occluded proximal arteries.

† Bypass graft visualized around excluded aneurysm.

‡ Prior surgical diagnosis.

Received June 14, 1977; accepted August 10, 1977.

[1] Department of Radiology, Section of Ultrasound, University of Michigan Medical School, University Hospital, Ann Arbor, Michigan 48109. Address reprint requests to T. M. Silver.

[2] Department of Surgery, University of Michigan Medical School, University Hospital, Ann Arbor, Michigan 48109.

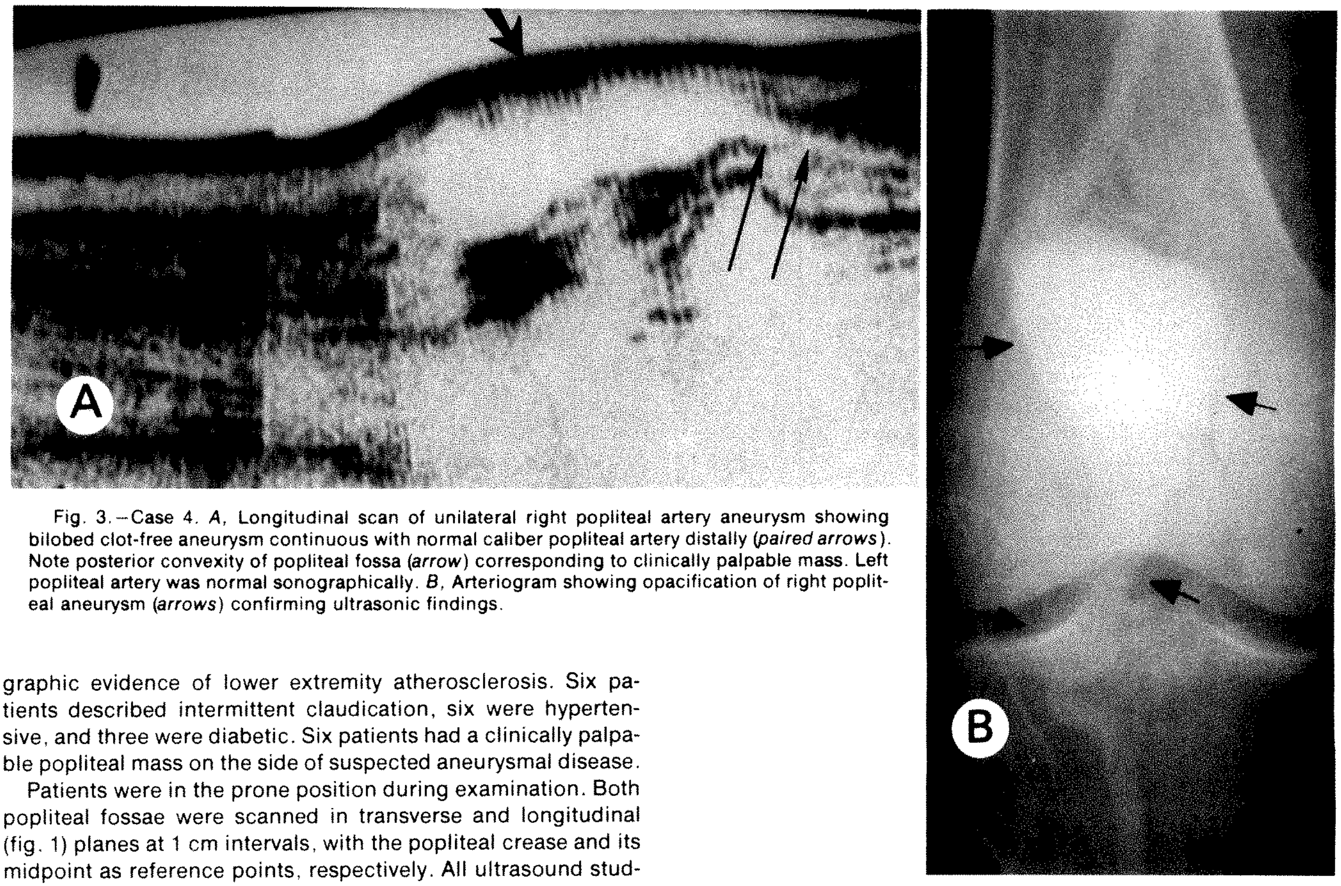

Fig. 3.—Case 4. *A*, Longitudinal scan of unilateral right popliteal artery aneurysm showing bilobed clot-free aneurysm continuous with normal caliber popliteal artery distally (*paired arrows*). Note posterior convexity of popliteal fossa (*arrow*) corresponding to clinically palpable mass. Left popliteal artery was normal sonographically. *B*, Arteriogram showing opacification of right popliteal aneurysm (*arrows*) confirming ultrasonic findings.

graphic evidence of lower extremity atherosclerosis. Six patients described intermittent claudication, six were hypertensive, and three were diabetic. Six patients had a clinically palpable popliteal mass on the side of suspected aneurysmal disease.

Patients were in the prone position during examination. Both popliteal fossae were scanned in transverse and longitudinal (fig. 1) planes at 1 cm intervals, with the popliteal crease and its midpoint as reference points, respectively. All ultrasound studies were performed with a commercially available gray scale ultrasound unit using a 3.5 MHz and/or 5.0 MHz internally focused transducer. Popliteal fossae were coated with mineral oil to eliminate air between the transducer and skin. The images were permanently recorded on Polaroid film. Sonolucent areas on gray tone displays were verified and examined by A-mode for pulsatile characteristics.

Results

In the eight patients, 12 popliteal artery aneurysms were demonstrated by ultrasonography (fig. 2; table 1). The ultrasound study confirmed the presence of popliteal artery aneurysms in all six patients with unilateral palpable popliteal fossa masses (fig. 3*A*). In three of these patients the contralateral popliteal artery was also found by ultrasound to be aneurysmal. In the two remaining patients without clinically palpable popliteal masses, one had ultrasound evidence of bilateral aneurysms and the other a unilateral aneurysm. Thus bilateral popliteal artery aneurysms were observed in half the patients. Among unilateral lesions, all but one were on the right side.

Precise measurement of popliteal artery aneurysm size was possible in each instance by ultrasonography. Anteroposterior diameters were 1.5–4.0 cm; transverse diameters, 1.75–5.5 cm; and length, 3.0–9.0 cm. Intraaneurysmal clot was demonstrated in nine of the 12 aneurysms (figs. 4*B* and 4*C*).

Arteriography confirmed the presence of six popliteal aneurysms. Two aneurysms were not demonstrated arteriographically because proximal occlusive disease prevented adequate accumulation of contrast within the diseased popliteal vessel (fig. 5*C*). Similarly, one aneurysm which was thrombosed (fig. 5*A*) and two others previously excluded surgically were also not visualized on arteriography. A final patient with a unilateral popliteal aneurysm was not subjected to arteriography. Six popliteal artery aneurysms were confirmed surgically, including three demonstrated preoperatively by arteriography (fig. 3*B*).

Discussion

Popliteal artery aneurysms are most often encountered in male patients in the sixth and seventh decades of life. These lesions are second only to abdominal aortic aneurysms in frequency. Popliteal aneurysms are bilateral in about half the cases, and a similar frequency of extrapopliteal aneurysms exists (six of our eight patients) [1,2]. Most important among the latter are aortoiliac aneurysms, affecting as many as two-thirds of the patients (six of our eight cases) [2]. Arteriosclerosis has proven to be the underlying cause of nearly all popliteal artery aneurysms currently encountered [1].

Clinical manifestations of popliteal artery aneurysms are invariably related to complications. Acute ischemia of the distal extremity associated with aneurysmal thrombosis or distal thromboembolization is the most common complication. Aneurysm expansion with impingement on adjacent neural structures or compression of venous

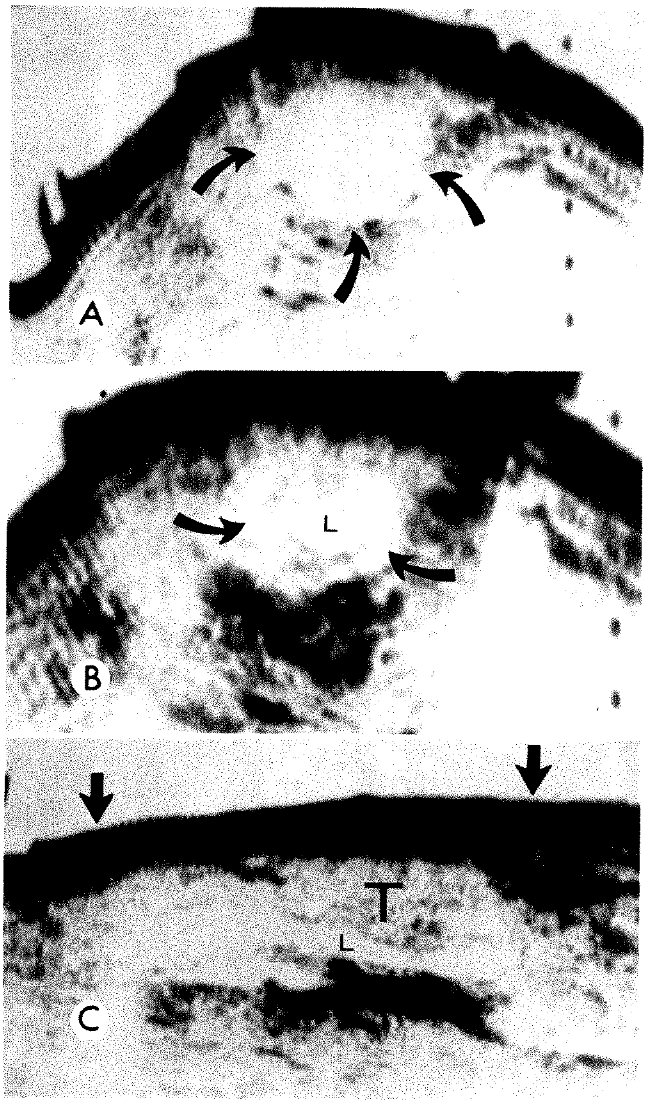

Fig. 4.—Case 1. *A and B*, B-scan transverse sections through right popliteal artery aneurysm at low and high gain settings. At low gain setting (*A*) outer wall (*arrows*) of aneurysm is seen better, while circumferential cuff of clot (*arrows*) around luminal channel (L) is best seen at high gain setting (*B*). *C*, Longitudinal scan of right popliteal fossa showing length of aneurysm (*between arrows*) and extensive intraaneurysmal thrombus (T) surrounding thin fluid-filled luminal channel (L).

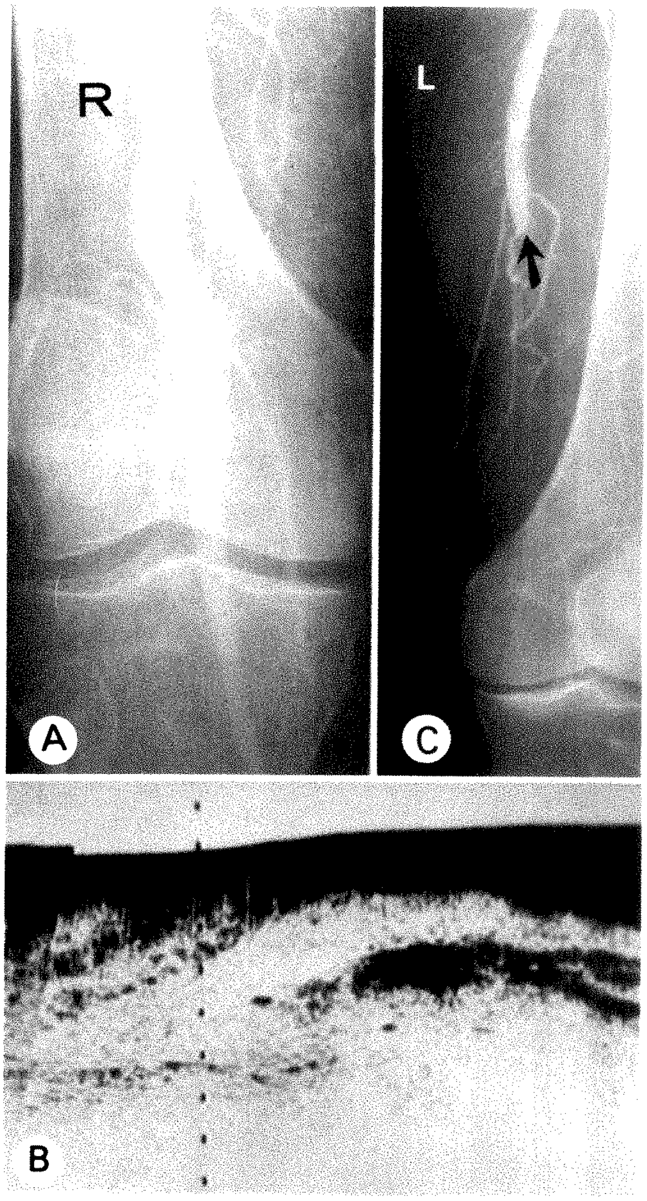

Fig. 5.—Case 1. *A*, Arteriogram showing gradual narrowing of right popliteal artery lumen distally but no opacification of aneurysm. *B*, Sonogram of left popliteal fossa showing aneurysmal dilatation of popliteal artery, with intraluminal echoes due to clot. Lesion was not palpable and was clinically unsuspected. *C*, Arteriogram showing occlusion of left superficial femoral artery (*arrow*) preventing demonstration of left popliteal artery and aneurysm.

channels may cause discomfort and edema of the distal extremity. Rupture is a less common complication of popliteal artery aneurysms, occurring in about 5% of cases [1]. The exact incidence of popliteal artery aneurysms and the frequency with which complications occur remain poorly defined, although noninvasive studies such as B-scan ultrasonography may provide a better definition of the former.

Ultrasound evaluation of suspected popliteal artery aneurysms avoids some of the uncertainties of physical examination and provides easily reproducible objective data. An important advantage of ultrasonography over arteriography is its capacity to define the outer wall of the aneurysm and thus establish more accurate size measurements (fig. 4*A*). In addition, the presence and location of thrombus within an aneurysm can be directly visualized by B-scan ultrasound, facilitating diagnosis (figs. 4*B* and 4*C*). Clinical implications of the latter relative to potential distal embolization and an increased incidence of rupture may not be considered if arteriographic studies alone are used. Caution must be exercised in the performance of the ultrasound study to ensure that scans perpendicular to the long axis of the aneurysm are obtained, or the diameter may be erroneously overestimated.

Ultrasonography of the popliteal fossa can differentiate popliteal aneurysms from popliteal cysts [3] or neoplasms [4] which may also present as palpable masses. The presence of a popliteal artery aneurysm is firmly established when sonograms demonstrate continuity between the proximal or distal popliteal artery and the mass (fig. 2), or when pulsations of the mass are documented [5, 6]. In addition, ultrasound is useful to sequentially document progression in the diameter of a dilated popliteal artery in a patient known to have either contralateral popliteal aneurysmal disease or distant aneurysms [7]. Furthermore, ultrasonography may prove useful as a screening procedure to detect popliteal and other peripheral aneurysms [8].

Ultrasonography is an accurate, noninvasive, reproducible, painless, and easily performed study that may be used effectively in diagnosing and planning the management of patients with popliteal artery aneurysms. Our experience indicates that popliteal artery ultrasonography is useful to: (1) confirm or refute equivocal diagnoses of aneurysms generated by arteriographic studies or physical examination; (2) define thrombosed aneurysms or aneurysms not opacified because of limited contrast material passing through proximally obstructed arteries; (3) detect contralateral clinically covert aneurysms; (4) detect asymptomatic small aneurysms in patients with generalized extrapopliteal aneurysmal disease; (5) assess the extent of intraaneurysmal thrombus and exact aneurysm size in all dimensions; and (6) evaluate borderline dilated popliteal arteries or aneurysms in patients who cannot and should not be subjected to invasive arteriographic studies or surgery.

REFERENCES

1. Wychulis AR, Spittell JA, Wallace RB: Popliteal aneurysms. *Surgery* 68:942–952, 1970
2. Dent TL, Lindenauer, SM, Ernst CB, Fry WJ: Multiple arteriosclerotic arterial aneurysms. *Arch Surg* 105:338–344, 1972
3. Moore CP, Sarti DA, Louie JS: Ultrasonographic demonstration of popliteal cysts in rheumatoid arthritis. *Arthritis Rheum* 18:577–580, 1975
4. Scott WW, Scott PP, Sanders RC: B-scan ultrasound in the diagnosis of popliteal aneurysms. *Surgery* 81:436–441, 1977
5. Sarti DA, Louie JS, Lindstrom RR, Nies K, London J: Ultrasonic diagnosis of a popliteal artery aneurysm. *Radiology* 121:707–708, 1976
6. Carpenter JR, Hattery RR, Hunder GG, Bryan RS, McLeod RA: Ultrasound evaluation of the popliteal space. Comparison with arthrography and physical examination. *Mayo Clin Proc* 51:498–503, 1976
7. Collins GJ, Rich NM, Phillips J, Hobson RW, Andersen CA: Ultrasound diagnosis of popliteal arterial aneurysms. *Am Surg* 42:853–858, 1976
8. Davis RP, Neiman HL, Yao JST, Bergan JJ: Ultrasound scan in diagnosis of peripheral aneurysms. *Arch Surg* 112:55–58, 1977

Pitfalls in the Angiographic Management of Hemorrhage: Hemodynamic Considerations

ERNEST J. RING,[1] JUAN A. OLEAGA,[1] DAVID FREIMAN,[1] JAMES W. HUSTED,[1] ARTHUR C. WALTMAN, JR.,[2] AND STANLEY BAUM[1]

Selective arterial infusions of vasopressin have often been successful in controlling arterial bleeding. When bleeding occurs in an area with a dual blood supply through a vascular arcade, situations may arise which can compromise angiographic management. These include: (1) artifacts caused by pressure injections of contrast material inaccurately depicting the usual distribution of blood flow in the arcade; (2) catheter-induced vasospasm altering the flow dynamics through the arcade; (3) vasopressin-induced constriction of the proximal portion of an arcade changing the origin of blood flow to the distal arcade; and (4) proximal occlusion of one limb of an arcade permitting continuation of bleeding through collateral channels. When angiographic techniques fail to control bleeding because of these circumstances, hemostasis may be achieved by treating both limbs of the vascular arcade.

The role of angiography in the management of acute hemorrhage is established. Numerous reports have documented high success rates controlling bleeding from diverse etiologies using selective infusions of posterior pituitary extract to constrict bleeding vessels [1-4] and emboli [5, 6] or inflated balloon catheters [7] to occlude bleeding arteries. However, despite increasing sophistication with the application of these techniques, therapeutic failures still persist [8, 9].

We review the complex hemodynamics which may occur when bleeding originates from a branch of a vascular arcade. The direction of blood flow through such an arcade is readily reversible; this may permit circumstances which complicate the angiographic examination and in some cases prevent successful transcatheter therapy.

Case Material and Findings

Angiographic examinations performed on 134 patients with acute arterial bleeding and demonstrable extravasation treated by transcatheter techniques were reviewed. The technique of the examination has been described previously [10]. Of the 134 patients, 101 were treated with posterior pituitary extract infusion, 26 with selective arterial embolization, four with balloon occlusions, and three with a combination of embolization and posterior pituitary extract infusion.

In 37 patients the bleeding occurred in an area which derived its blood supply from a vascular arcade formed by two separate major vessels. These 37 angiographic examinations were evaluated to identify any complications or artifacts that could be attributed to the variability of blood flow associated with this anatomic arrangement.

The bidirectional potential of flow through the arcades was apparent in 18 of 37 cases. In 10 of 18, the initial attempt at transcatheter therapy was unsuccessful. In each instance a modification of therapy was required to diminish blood flow to the actual bleeding branch: vasopressin infusion into both limbs of the arcade, five cases; reduction of vasopressin dose to decrease proximal constriction, one case; embolization of both limbs of an arcade, two cases; balloon occlusion of both limbs of an arcade, one case; and balloon occlusion of one limb of an arcade with embolization of the other limb, one case. In two additional cases bleeding was not controlled and only in retrospect was the failure related to artifacts of flow in the vascular arcade. It is likely that had these been recognized, appropriate alterations in therapy might have controlled the bleeding. In the remaining six cases, the artifacts did not affect management but illustrate potential difficulties that can complicate angiographic therapy.

The artifacts of flow demonstrated in the 18 cases were: (1) artifacts caused by pressure injections of contrast material, six cases; (2) reversal of flow caused by catheter-induced vasospasm, four cases; (3) proximal constriction and changes in flow dynamics caused by vasopressin infusions, four cases; and (4) collaterals around an embolic or balloon occlusion, four cases.

Analysis of Flow Artifacts

The term vascular arcade describes an arterial blood supply derived from two separate major vessels that can communicate through a wide anastomosis capable of permitting blood to flow in either direction. The term is used here to include any vascular communication that can readily accept blood flow from a second major vessel. Examples of vascular arcades that may be significant in the angiographic management of bleeding include: (1) middle colic artery–left colic artery anastomosis at the splenic flexure of the colon; (2) inferior pancreaticoduodenal–superior pancreaticoduodenal arterial arcades in the duodenum; (3) right gastric–left gastric arterial arcade along the lesser curvature of the stomach; (4) left gastroepiploic–right gastroepiploic arterial communications along the greater curvature of the stomach; and (5)

Received April 13, 1977; accepted after revision August 23, 1977.
This work was supported in part by U.S. Public Health Service grant AM-19453-01 from the National Institute of Arthritis and Metabolic Disease.

[1] Department of Radiology, Hospital of the University of Pennsylvania, Philadelphia, Pennsylvania 19104. Address reprint requests to E. J. Ring.

[2] Department of Radiology, Massachusetts General Hospital, Boston, Massachusetts 02114.

Am J Roentgenol **129:1007-1013, December 1977**

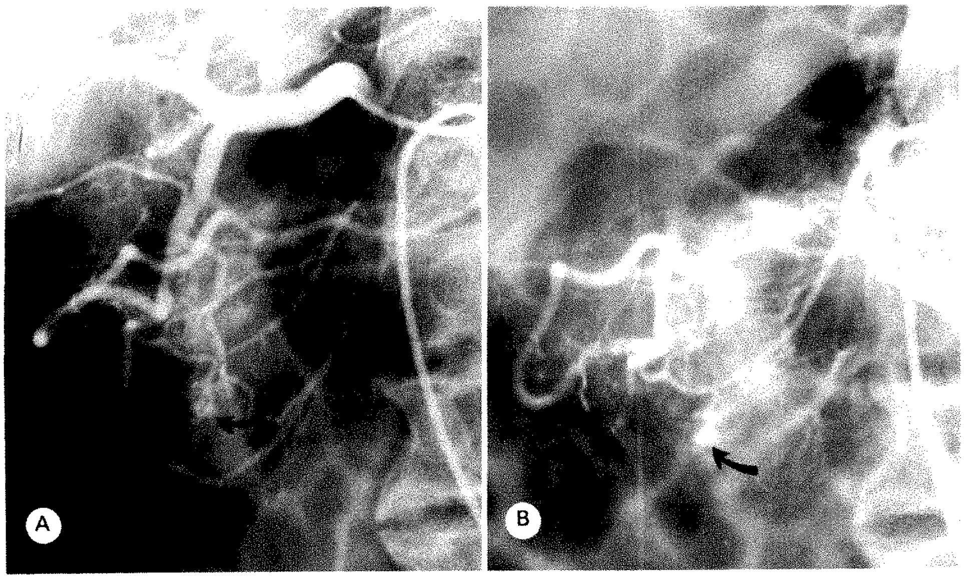

Fig. 1.—Bleeding duodenal ulcer. *A*, Injection into hepatic artery demonstrating extravasation from small duodenal branch (*arrow*). *B*, Injection into inferior pancreaticoduodenal artery demonstrating same branch as well as extravasation (*arrow*). Infusions into both limbs of arterial arcade may be necessary because of difficulty determining which vessel actually supplies bleeding point.

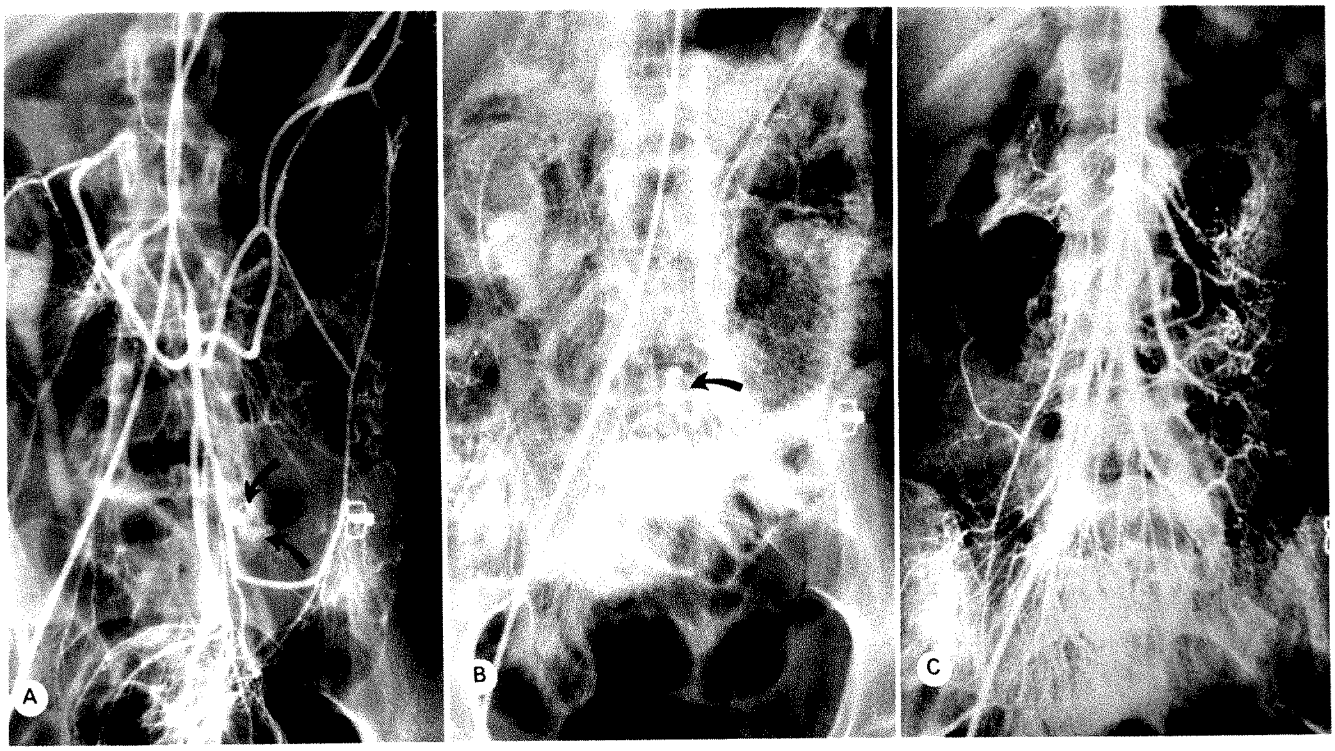

Fig. 2.—Arteriograms showing bleeding from midtransverse colon in patient with granulomatous colitis. *A*, Inferior mesenteric arteriogram performed with catheter partially obstructing origin of vessel. Entire colonic blood supply is opacified and extravasation is demonstrated in midtransverse colon (*arrows*). *B*, Catheter in superior mesenteric artery. Middle colic artery and bleeding point are opacified. *C*, Infusion of vasopressin begun into superior mesenteric artery to control bleeding of middle colic artery. Repeat superior mesenteric arteriogram performed 20 min after infusion of vasoconstrictor shows constriction of middle colic artery and no further extravasation.

transpelvic communications between the right and left internal iliac arteries.

Pressure Injections of Contrast Material

Pressure injections of contrast material into one limb of a vascular arcade may temporarily alter flow dynamics through the arcade. Selective arterial injections into each vessel supplying the arcade may show an overlap of blood flow which cannot exist physiologically but is created by the force of the injection (fig. 1). Similarly, injections through a catheter partially obstructing the origin of a vessel can greatly exaggerate the distribution of the injected vessel (fig. 2). When a bleeding point is demonstrated in this fashion, the arteriogram can erroneously

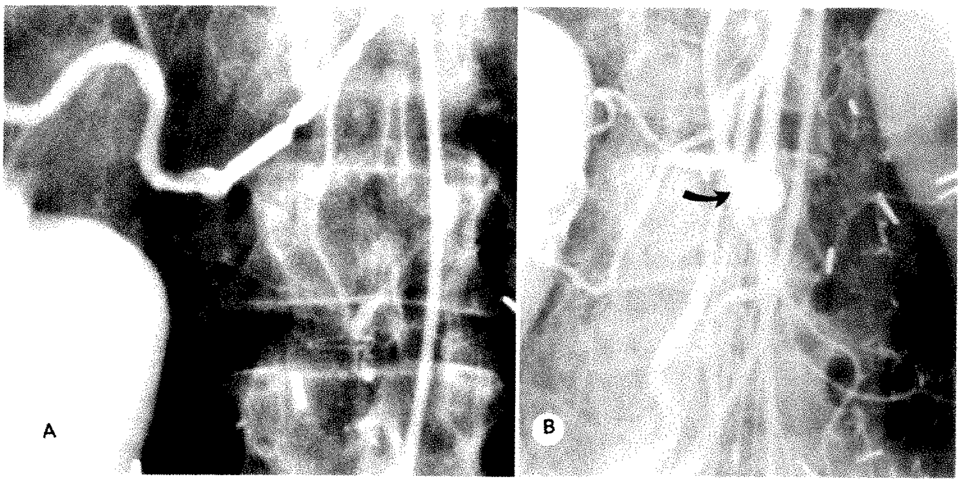

Fig. 3.—Arteriograms of bleeding duodenal ulcer. *A*, Hepatic arteriogram demonstrating extensive spasm in common hepatic artery induced by catheterization. Note lack of flow into gastroduodenal artery. *B*, Superior mesenteric arteriogram showing entire pancreaticoduodenal arcade and bleeding point (*arrow*) supplied by branches from superior mesenteric artery.

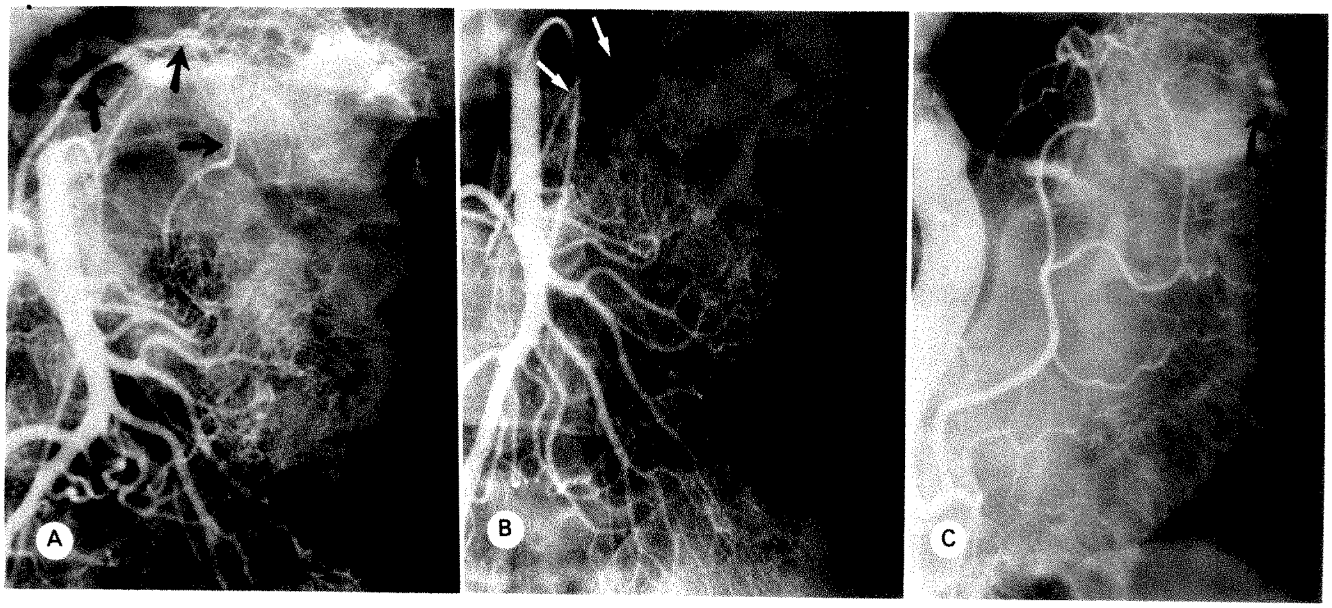

Fig. 4.—Arteriograms showing bleeding diverticulum of splenic flexure. *A*, Superior mesenteric arteriogram showing filling of middle colic artery (*arrows*) and bleeding point in proximal portion of descending colon (*curved arrow*). *B*, Repeat arteriogram 20 min after infusion of vasopressin showing intense constriction of middle colic artery (*arrows*). There is no filling of arcade to splenic flexure. *C*, Second catheter introduced into inferior mesenteric artery while infusion continues in superior mesenteric artery. Arcade is opacified at splenic flexure to point of intense constriction in middle colic artery. Bleeding point now receives blood supply from inferior mesenteric limb of arcade (*arrow*). On posttherapy arteriograms, region of arcade supplying bleeding point appeared constricted when vasopressin was infused into inferior mesenteric artery.

suggest that the bleeding branch is supplied by the injected limb of the arcade, when in fact it derives its blood supply from a second, noninjected anastomatic vessel.

Since posterior pituitary extract infusions are injected at low rates which do not alter flow patterns in the same manner as the pressure injections, the distribution of the vasoconstrictor through the arcade is not necessarily the same as the contrast material depicted by the arteriogram. On the basis of a selective angiogram it may be difficult to anticipate which branches of the arcade are actually supplied by the injected vessel and which branches will receive the pituitary extract infusion. In addition, if the bleeding branch were artifactually opacified by the initial pressure injection of contrast material and a repeat angiographic examination is performed to determine the effect of the infusion, the distribution of the injected branch may again be exaggerated and show continued extravasation. This angiographic appearance suggests a primary failure of the extract to constrict the bleeding branch when in fact the medication was never delivered to the bleeding point. In this setting, delivery of the vasoconstrictor to all branches of a vascular arcade can be assured only if a second catheter is introduced through the other femoral artery and both limbs of the arcade are infused.

Catheter-induced Vasospasm

Even when an initial arteriogram accurately localizes the bleeding branch to the injected limb of the arcade, this flow pattern may only be transient. When catheters

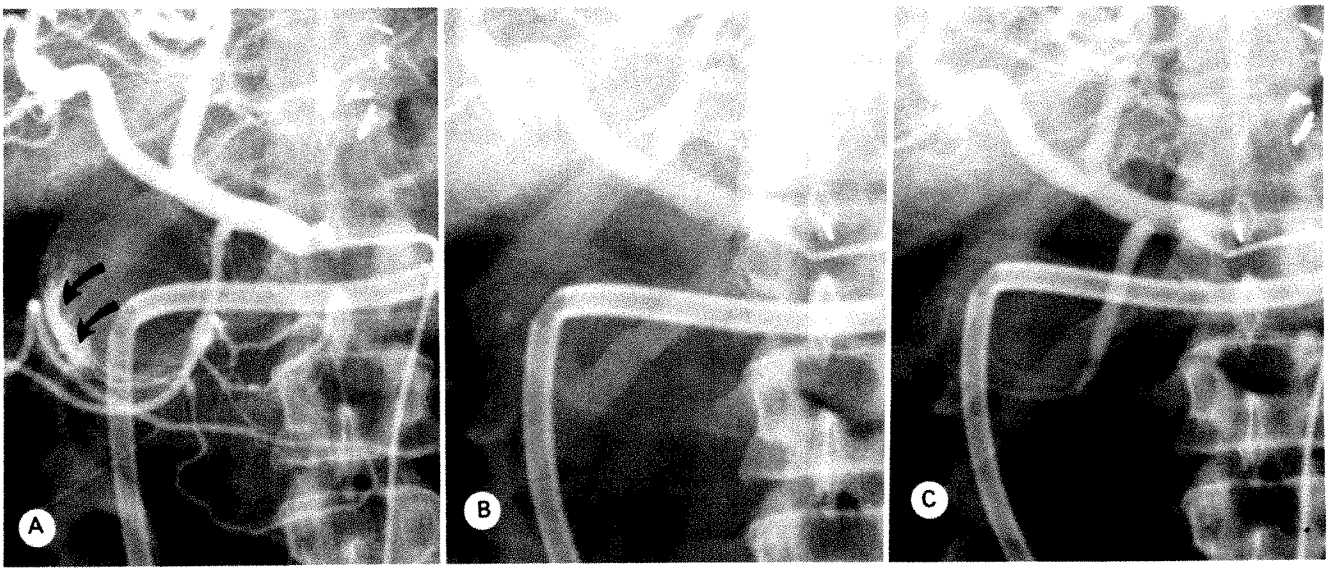

Fig. 5.—Bleeding duodenal ulcer. *A*, Selective hepatic arteriogram showing massive extravasation from branch of gastroduodenal artery (*arrows*). *B*, Repeat arteriogram showing opacification of only origin of gastroduodenal artery; nasogastric aspirate continued to show bright red blood. Vasopressin infused 20 min at 0.2 U/min. *C*, Repeat arteriogram after infusion rate reduced to 0.1 U/min for additional 20 min. Constriction of gastroduodenal artery is now decreased so that filling of portion of arcade supplying bleeding point occurs. Constriction is evident in right gastroepiploic artery (*arrow*). When infusion decreased, nasogastric aspirate cleared.

and guide wires are being manipulated in one limb of an arcade to attempt subselective catheterization, vasospasm may develop proximally. The resulting increased vascular resistance can cause flow in the arcade to reverse so that the bleeding point receives its blood supply from the other limb of the arcade. When this occurs, the vascoconstrictor must then be infused into the alternate blood supply in order to reach the bleeding branch. The vasospasm is usually temporary; when it resolves blood flow can revert to its original direction. This may again alter the distribution of the vasoconstrictor so that bleeding recurs.

It is relatively common for arterial spasm to develop in the common hepatic artery during subselective catheterization of the gastroduodenal artery. When this occurs, flow through the pancreatic arcades reverses and the bleeding point can temporarily derive its blood supply from branches of the superior mesenteric artery (fig. 3). To avoid this we now prefer to attempt treatment of bleeding duodenal ulcers with vasopressin infusions directly into the hepatic artery and do not attempt to place catheters selectively in the gastroduodenal artery. This has been shown to be safe since there is now considerable evidence to indicate that hepatic arterial infusions of posterior pituitary extract do not decrease hepatic arterial blood flow [11].

Vasopressin Infusions

The constricting effect of posterior pituitary extract is thought to begin peripherally and progress centrally with increasing dosage [12]. Therefore, it seems unlikely that collateral vessels play a role when vasopressin fails to control bleeding in a region supplied by end arteries, such as in the small bowel, since the entire vascular bed is perfused by the vasoconstrictor. However, when the bleeding branch receives its blood supply from a vascular arcade, the infusion of vasopressin into one limb of the arcade can produce enough proximal constriction of the main arcade that flow distal to the point of constriction reverses (fig. 4). A bleeding branch which originally derived its blood supply from the infused limb of the arcade but is distal to the area of intense constriction after the infusion will then receive blood flow from the noninfused limb. Since the vasopressin does not reach the bleeding branch, the hemorrhage will not be controlled.

Reducing the rate of the infusion may diminish the degree of constriction of the proximal segment of the arcade and allow the vasopressin to reach branches further distal in the arcade (fig. 5). Attempts to titrate the effect of the extract in this fashion, however, are unpredictable. Infusions through separate catheters into each limb of the arcade will promote constriction of the entire arcade and assure delivery of the vasoconstrictor to the bleeding branch (fig. 6).

Whenever intraarterial infusions of vasopressin are utilized to control bleeding, care must be given to avoid excessive ischemia. When a single vessel is infused with the extract, the intensity of vasoconstriction is evaluated by performing an arteriogram 15–20 min after start of the infusion and comparing the changes in the appearance of the vasculature with that of the preinfusion arterial injection. If the posttherapy arteriogram shows evidence of delayed or prolonged forward flow through the capillary and venous phases or there is beading of the most proximal branches of the vessel infused, the dose of the vasoconstrictor should be reduced by 50%. Another arteriogram is then performed after an additional 15–20 min to evaluate the effect of the new dose of the vasoconstrictor. There is considerable clinical experience to indi-

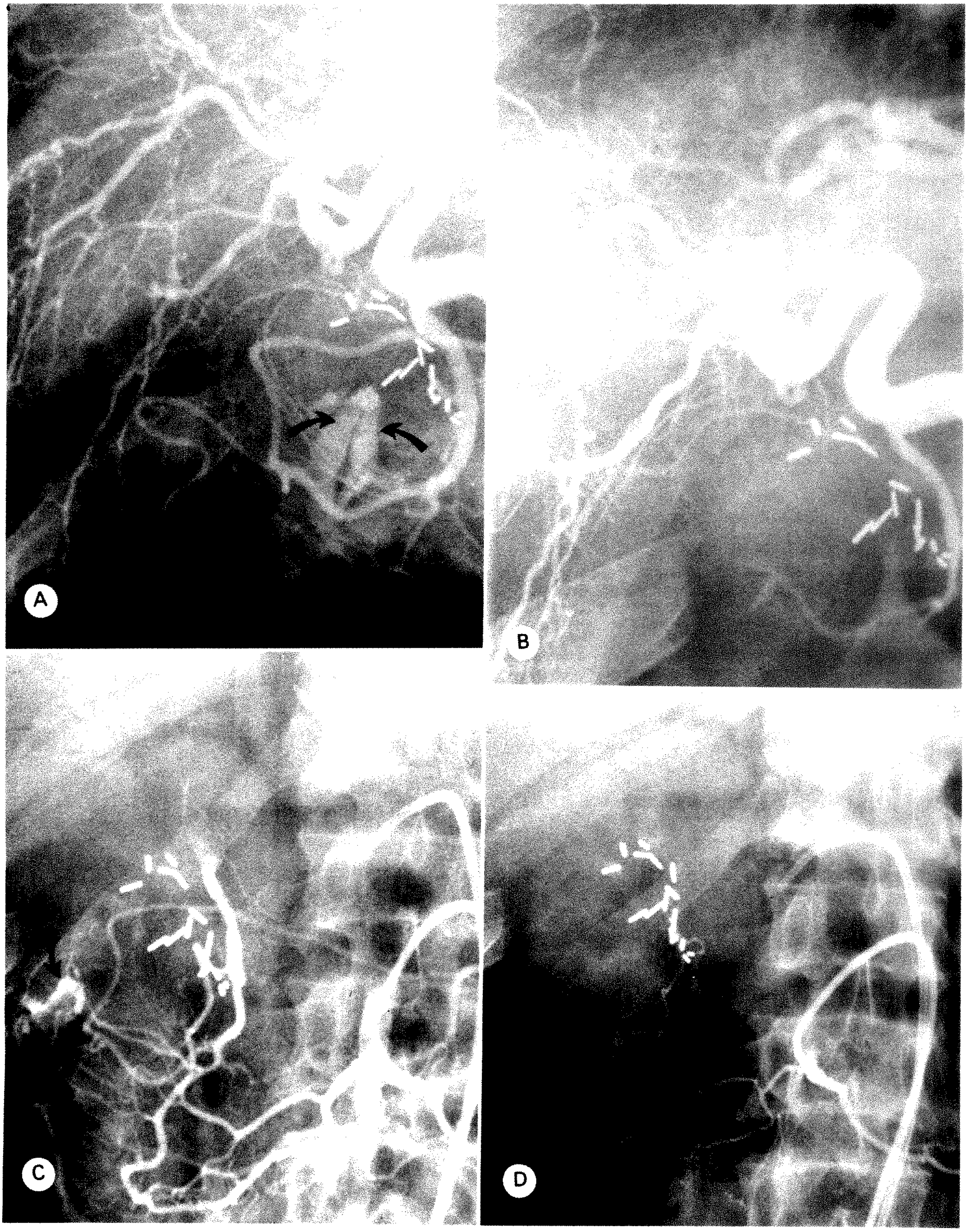

Fig. 6.—Arteriograms of bleeding duodenal ulcer. *A*, Selective hepatic arteriogram showing extravasation from branch of gastroduodenal artery (*arrows*). *B*, Repeat hepatic arteriogram 20 min after infusion of vasopressin at 0.2 U/min. Note prominent constriction of gastroduodenal artery and no extravasation. *C*, Second catheter was introduced through left femoral artery into inferior pancreaticoduodenal artery to control continued bleeding. Filling of bleeding branch and continued extravasation (*arrow*) occurred despite hepatic infusion of vasopressin. *D*, Repeat inferior pancreaticoduodenal arteriogram after vasopressin was infused at 0.1 U/min through both catheters. All branches of pancreatic arcades are constricted and no additional extravasation occurred.

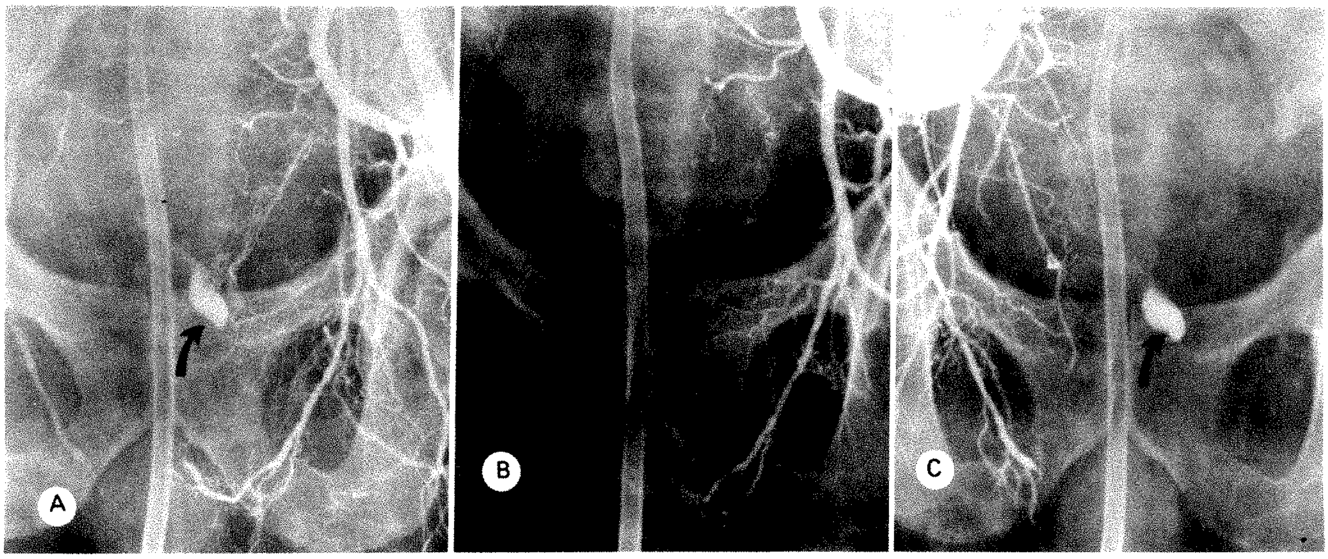

Fig. 7.—Bleeding following transurethral resection of prostate. *A*, Selective left internal iliac arteriogram demonstrating extravasation in region of prostatic bed (*arrow*). *B*, Repeat arteriogram after embolization of internal iliac artery with autologous clot. Bleeding branch is occluded (*arrow*). *C*, Injection of contrast through right internal iliac artery demonstrating filling of bleeding branch through transpelvic arcade and extravasation into prostatic bed (*arrow*). Embolization successfully controlled bleeding.

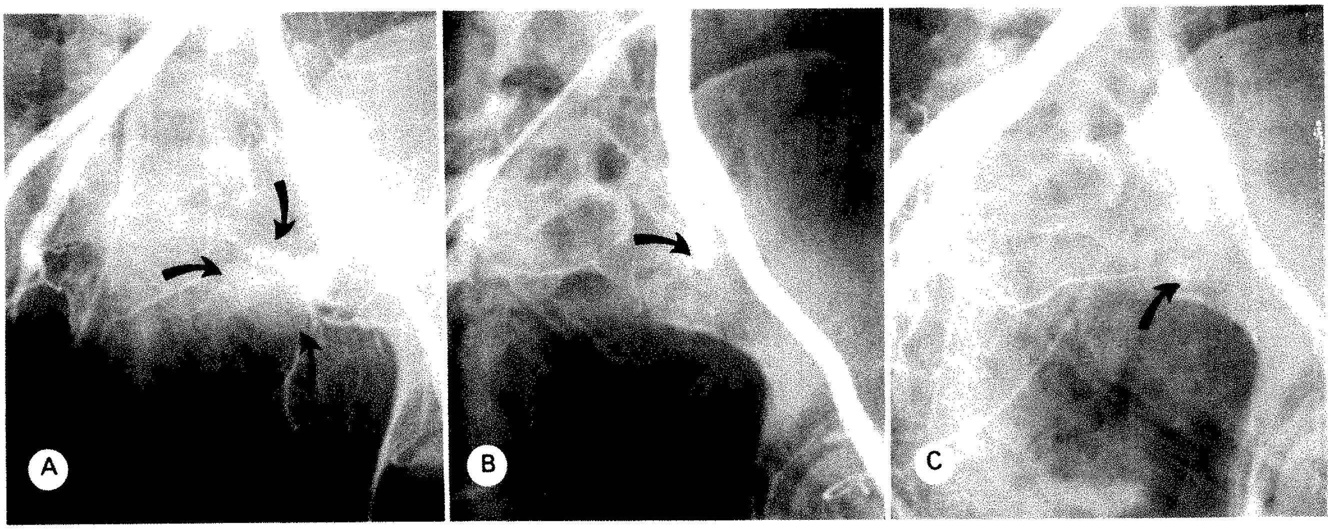

Fig. 8.—Massive vaginal bleeding secondary to cervical carcinoma. *A*, Pelvic aortogram demonstrating massive extravasation from left internal iliac artery (*arrows*). *B*, No. 2 Fogerty catheter inserted through catheter in internal iliac artery and inflated with contrast material (*arrow*). Injection through angiographic catheter demonstrates complete obstruction of flow in internal iliac artery. *C*, Contrast injected into second catheter in right internal iliac artery. Transpelvic collaterals supply bleeding point (*arrow*). Bleeding was controlled completely by inflation of additional Fogerty catheter at origin of right internal iliac artery.

cate that an infusion rate of 0.2 U/min will effectively control bleeding without risking ischemia in the majority of cases [1].

When both limbs of a vascular arcade are receiving vasopressin infusions, the degree of constriction of the entire arcade is similarly evaluated by separate arterial injections into each vessel being infused. Because each infusion adds to systemic levels of the vasoconstrictor, the effect of the two infusions is partially additive. In our patients, infusion rates of 0.1–0.15 U/min were employed in each limb of the arcades. In no case was there clinical or angiographic evidence of tissue ischemia.

The patient's fluid and electrolyte balance must be monitored throughout the infusion because of the antidiuretic hormone effect of vasopressin. Water retention and hyponatremia may occur, but these are generally adequately managed with diuretics and saline replacement.

Collateral Flow around Embolic Occlusion

The development of collateral flow beyond a proximal mechanical obstruction may be rapid [13]. Current techniques of arterial embolization using autologous clots

[5], Gelfoam [6], and injected coiled wires [14] promote occlusion of medium-sized vessels corresponding to the size of the embolic material. This usually accomplishes control of bleeding since the pressure within a distal bleeding vessel is considerably lowered after direct flow is obstructed even if the bleeding branch fills through collateral vessels. However, the development of massive bleeding through collateral channels following embolization has been documented [6] (fig. 7). When embolization is used therapeutically, all potential collateral pathways must be sequentially examined to detect alternate blood supply to a bleeding branch. In addition, should delayed rebleeding develop after embolization, repeat arteriography is necessary to evaluate newly developed collateral sources for the bleeding. These collateral vessels must then be occluded to obtain permanent hemostasis.

A balloon catheter inflated in the origin of a vessel is hemodynamically similiar to a proximal occlusion by an embolus. Collateral flow can result in alternate supply of the bleeding point (fig. 8). An injection through a second catheter may be necessary to demonstrate potential collaterals while the balloon is inflated. If a second source of blood supply to the bleeding branch is demonstrated, this must also be occluded.

Conclusions

To avoid failures of transcatheter treatment of acute bleeding originating in areas supplied by more than one artery, special care must be given. Repeat angiography should always be performed 15-20 min after beginning the infusion of a vasoconstrictor. The repeat injection should be performed using the same rate and volume as the original arteriogram. This angiogram should be analyzed to confirm that the bleeding branch is well visualized and that there is no further extravasation.

If the bleeding branch is not visualized or there is evidence of continued bleeding, a hemodynamic artifact should be suspected. A second catheter should be introduced through the other femoral artery and injections made to fill the alternate blood supply to the arcade. If the other limb of the arcade fills the bleeding branch and there is extravasation from that branch, vasopressin should be infused into both limbs of the arcade. Posttherapy arteriograms in each limb of the arcade are necessary to confirm that the bleeding has stopped and that excessive ischemia will not result.

REFERENCES

1. Athanasoulis CA, Waltman AC, Novellin RA: Angiography, its contribution to the emergency management of gastrointestinal hemorrhage. *Radiol Clin North Am* 14:265-280, 1976
2. Conn HO, Ramsby GR, Storer EK: Selective intraarterial vasopressin in the treatment of upper gastrointestinal hemorrhage. *Gastroenterology* 63:634-645, 1972
3. Rosch J, Gray RK, Grollman JH,. Ross G, Steckel RJ, Weiner M: Selective arterial drug infusions in the treatment of acute gastrointestinal bleeding. *Gastroenterology* 59:341-345, 1970
4. Ring EJ, Athanasoulis CA, Waltman AC, Margolies MN, Baum S: Arteriographic management of hemorrhage following pelvic fracture. *Radiology* 109:65-70, 1973
5. Bookstein JJ, Cholsta EM, Foley D, Walter JF: Transcatheter hemostasis of gastrointestinal bleeding using modified autogenous clot. *Radiology* 113:277-285, 1974
6. Reuter RS, Chuang VP, Bree RL: Selective arterial embolization for control of massive upper gastrointestinal bleeding. *Am J Roentgenol* 125:119-126, 1975
7. Wholey MH, Stockdale R, Hung TK: A percutaneous balloon catheter for the immediate control of hemorrhage. *Radiology* 95:65-71, 1970
8. Conn HO, Ramsby GR, Storer EH, Mutchnick MG, Joshi PH, Phillips MM, Cohen GA, Fields GN, Petroski D: Intraarterial vasopressin in the treatment of upper gastrointestinal hemorrhage: a prospective controlled clinical trial. *Gastroenterology* 68:211-221, 1975
9. Athanasoulis CA, Baum S, Waltman AC, Ring EJ, Imbembo A, Salm TJV: Control of acute gastric mucosal hemorrhage. *N Engl J Med* 290:597-603, 1974
10. Baum S, Athanasoulis CA, Waltman AC, Ring EJ: Angiographic diagnosis and control of gastrointestinal bleeding, in *Advances in Surgery*, vol 7, edited by Welch C, Chicago, Year Book Medical Publishers, 1973, pp 149-198
11. Barr JW, Lakin RC, Rosch J: Vasopressin and hepatic artery: Effect of selective celiac infusion of vasopressin on the hepatic artery flow. *Invest Radiol* 10:200-205, 1975
12. Baum S, Nusbaum M: The control of gastrointestinal hemorrhage by selective mesenteric arterial infusion of vasopressin. *Radiology* 98:497-505, 1971
13. Rosch J, Dotter CT, Brown MJ: Selective arterial embolization. A new method for control of acute gastrointestinal bleeding. *Radiology* 102:303-306, 1972
14. Gianturco C, Anderson JH, Wallace S: Mechanical devices for arterial occlusion. *Am J Roentgenol* 124:428-435, 1975

Angiography of Pancreatic Arteriovenuos Malformation

VINCENT P. CHUANG,[1] CALIXTO M. PULMANO,[1] JOSEPH F. WALTER,[2, 3] AND KYUNG J. CHO[2]

Three cases of pancreatic arteriovenous malformation are presented. This entity is known to be a part of Osler-Weber-Rendu disease. However, asymptomatic pancreatic arteriovenous malformation also occurs. The angiographic features are specific and consist of dilated and tortuous feeding arteries, racemose intrapancreatic vascular network, and early filling veins. Massive gastrointestinal hemorrhage is a frequent complication. The importance of preoperative localization of the lesion and postoperative confirmation of complete resection by angiography is stressed.

Pancreatic arteriovenous malformation is a very rare entity; it is known to be frequently associated with Osler-Weber-Rendu disease [1, 2], although it can be an isolated finding [1, 3]. It may be asymptomatic, but sometimes causes massive gastrointestinal hemorrhage. The following three cases illustrate the clinical spectrum of this entity and their characteristic angiographic features.

Case Reports

Case 1: Asymptomatic

A 63-year-old female underwent surgery for mucinous adenocarcinoma of the rectum at which time the uterus and upper vagina were resected with the rectum due to local tumor extension. There was no history of hemorrhagic tendency, mucocutaneous telangiectasia, nor chronic pancreatitis. She had no clinical signs or symptoms of recurrence during a 3 year follow-up. However, serum carcinoembryonic antigen levels were markedly elevated: 1,943 and 540 ng/ml on two occasions. A liver and spleen scan and liver function tests were normal.

Visceral angiography was performed to search for occult metastasis. The celiac and superior mesenteric arteriograms showed no abnormality of liver, spleen, and intestine. The entire pancreas was extremely hypervascular. A racemose vascular network appeared in 1 sec, followed by a dense pancreatic stain and several early draining veins (fig. 1). Within 6 sec, the entire pancreatic stain had cleared. The portal vein was normal and there was no hepatofugal flow. The angiographic features were thought to be typical of an arteriovenous malformation that was probably an incidental finding, unrelated to the previous rectal malignancy and elevated carcinoembryonic antigen level. Three months later, the carcinoembryonic antigen level rose to 6,590 ng/ml.

An exploratory laparotomy 5 months after angiography revealed liver metastasis from rectal adenocarcinoma. Prominent venous lakes were seen on the surface of the pancreas. The pancreatic parenchyma appeared normal on close inspection and palpation. A biopsy was deliberately not done. The patient has been treated with chemotherapy for 6 months and is clinically stable.

Case 2: Massive Gastrointestinal Hemorrhage

A 7-month-old boy was admitted with a 4-month history of recurrent hematemasis and melena. He had no mucocutaneous stigmata nor family history of hereditary hemorrhagic telangiectasia. Upper gastrointestinal series with small bowel follow-through, barium enema, sigmoidoscopy, and gastroendoscopy were all unremarkable. Bilirubin and amylase were normal.

Celiac, superior mesenteric, splenic, and gastroduodenal arteriography revealed a diffuse arteriovenous malformation of the pancreas, duodenum, and jejunum (fig. 2). Multiple operations were required to control upper gastrointestinal hemorrhage in which the second, third, and fourth portions of the duodenum, proximal jejunum, and a wedge of stomach were resected. The histopathologic examination showed diffuse arteriovenous malformation in all the excised specimens. He had no recurrent bleeding during a 2 year follow-up.

Case 3: Osler-Weber-Rendu Disease

A 56-year-old male with known Osler-Weber-Rendu disease was admitted for massive hematemasis and melena. He had a history of recurrent epistaxis and chronic alcoholism. Physical examination revealed mucous telangiectases of the lips and numerous spider angiomata of the face. Endoscopy demonstrated bleeding esophageal varices.

Arteriography showed dilated dorsal and transverse pancreatic arteries which led to an extensive racemose vascular network in the body and tail of the pancreas. The splenic vein was opacified in $1^1/_2$ sec (fig. 3A). A dense vascular stain of the body and tail appeared at 2–5 sec, but disappeared by 7 sec (3 sec after the end of contrast injection) (fig. 3B). The inferior mesenteric and short gastric veins were opacified, indicating a hepatofugal portal flow secondary to hyperkinetic portal hypertension. The pancreatic head was also involved, but to a lesser extent. Variceal bleeding was transiently controlled by intraarterial vasopressin infusion.

Because of recurrent hemorrhage, an exploratory celiotomy was performed. Initial inspection failed to reveal any pancreatic abnormality. Since varices were present at the splenic hilus, the spleen was resected. An intraoperative celiac arteriogram using a previously placed celiac artery catheter showed persistence of the pancreatic arteriovenous malformation. The portal pressure was 33 mm Hg; portal venous flow, 760 ml/min; cardiac output, 8.4 liter/min. The body and tail of the pancreas were resected. After pancreatic resection, the portal pressure dropped to 13 mm Hg. The portal venous flow was 720 ml/min and cardiac output, 4.9 liter/min. Liver biopsy was performed. Histopathologic examination revealed diffuse arteriovenous malformation and slight focal chronic pancreatitis in the body and tail of the pancreas, chronic passive congestion of the spleen, and early mixed micro- and macronodular cirrhosis of the liver. Postoperatively the patient developed recurrent intraabdominal hemorrhage complicated by multisystem failure. He expired 2 weeks later.

Discussion

The three cases described demonstrate the spectrum of pancreatic arteriovenous malformation. The pancreatic arteriovenous malformation in case 3 is known to

---

Received May 2, 1977; accepted after revision July 28, 1977.

[1] Department of Diagnostic Radiology, University of Kentucky Medical Center, Lexington, Kentucky 40506. Address reprint requests to V. P. Chuang.

[2] Department of Radiology, University of Michigan Medical Center, Ann Arbor, Michigan 48105.

[3] Present address: Palo Alto Medical Clinic, Palo Alto, California 94301.

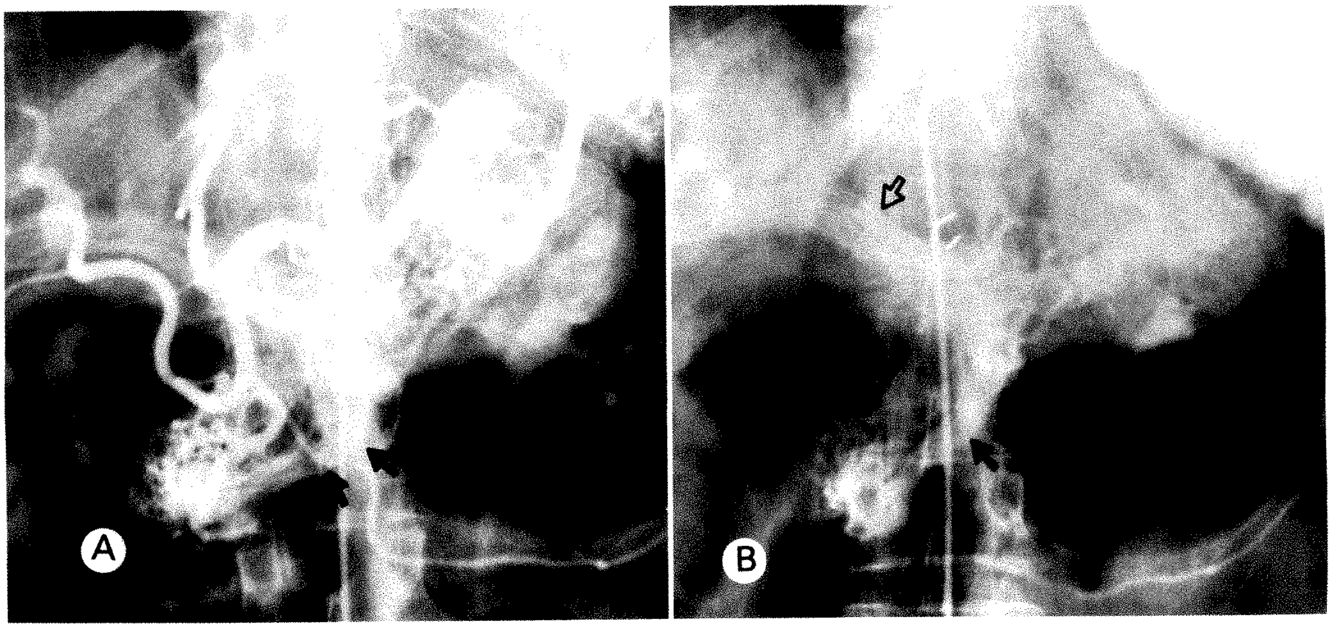

Fig. 1.—Case 1, asymptomatic. *A*, Celiac arteriogram at 1.5 sec showing racemose vascular network of entire pancreas and early draining vein (*arrows*). *B*, At 5 sec, most of pancreatic stain has cleared. Prominent pancreatic vein (*closed arrows*) and portal vein (*open arrow*) are still opacified. At celiotomy, pancreas appeared normal except for prominent draining veins on pancreatic surface.

be a part of the visceral angiodysplasia of hereditary hemorrhagic telangiectasis (Osler-Weber-Rendu disease). Lande et al. [2] speculated that loss of the regulatory sphincteric mechanism of the arteriolar-capillary junction in this entity results in unrestricted overflow of the arterial blood into the capillaries and venules, producing an arteriovenous shunt. Eventually, marked dilatation, elongation, and tortuosity of arterioles, capillaries, and venules occur. In case 1, the arteriovenous malformation was an isolated abnormality and the patient was asymptomatic. In case 2, the malformation involved both the pancreas and intestinal tract, but there were no mucocutaneous stigmata of Osler-Weber-Rendu disease. The presence of pancreatic arteriovenous malformation as a distinct entity without Osler-Weber-Rendu disease has been described by Grannis et al. [3]. It is possible that this is a forme fruste of the disease.

The angiographic features of pancreatic arteriovenous malformation consist of dilated and tortuous feeding arteries, racemose intrapancreatic vascular network, and early filling veins. The racemose vascular network causes a transient dense pancreatic stain. The early filling veins appear as early as the midarterial phase. Another important feature is the early clearance of the pancreatic stain and the arteriovenous malformation complex. In cases 1 and 3, the pancreatic stain completely cleared by 6 and 7 sec, respectively. In case 2, the pancreatic stain persisted slightly longer, perhaps because of the associated intestinal lesions. The angiographic features of arteriovenous malformations are quite specific and compare very well with corrosion casts of injected pathologic specimens [4].

The angiographic differential diagnosis includes pancreatitis and certain hypervascular neoplasms. In recurrent pancreatitis, particularly with acute exacerbation, the pancreas may become quite hypervascular, and a dense stain is occasionally present [5]. However, the pancreatic stain is usually seen in the parenchymal phase. Although the draining veins may be densely opacified, they are not dilated and do not appear as early as in arteriovenous malformation. Roe et al. [6] reported a case of acute pancreatitis which had marked hypervascularity, arteriovenous shunting, and early portal venous filling. We also observed similar findings in a patient with recurrent pancreatitis. In these cases, the clinical history of pancreatitis should clarify the issue. Hypervascular pancreatic neoplasms include cystadenoma, islet cell adenomas, rare carcinomas, and metastases. These tumors frequently stain densely in the venous phase, and enlarged feeding arteries and early draining veins are absent. Overall, the unique feature of the arteriovenous malformation lies in its hyperkinetic nature which distinguishes it from all other pancreatic lesions.

Of various pancreatic diseases which cause massive gastrointestinal hemorrhage, pancreatic arteriovenous malformation is the least common [7]. The malformation may cause gastrointestinal hemorrhage via bleeding directly into the pancreatic duct and subsequently into the duodenum. When associated with intestinal mucosal arteriovenous malformations (case 2), direct intestinal hemorrhage can occur. Finally, the hyperkinetic portal hypertension resulting from an arteriovenous malformation may cause variceal bleeding (case 3) [8].

Angiography has become an important method in both diagnosis and treatment of gastrointestinal hemorrhage. In pancreatic arteriovenous malformation the arterio-

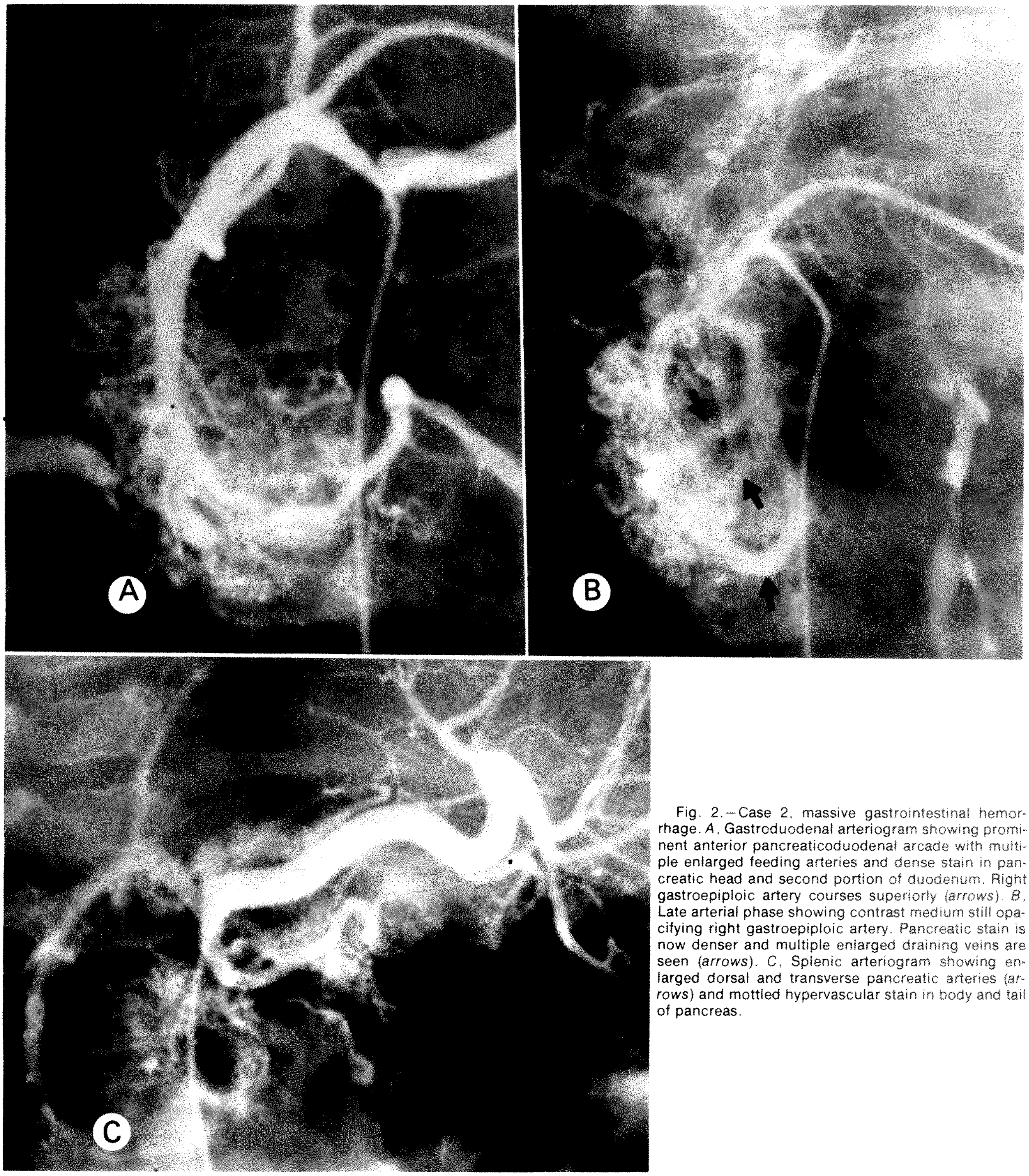

Fig. 2.—Case 2, massive gastrointestinal hemorrhage. *A*, Gastroduodenal arteriogram showing prominent anterior pancreaticoduodenal arcade with multiple enlarged feeding arteries and dense stain in pancreatic head and second portion of duodenum. Right gastroepiploic artery courses superiorly (*arrows*). *B*, Late arterial phase showing contrast medium still opacifying right gastroepiploic artery. Pancreatic stain is now denser and multiple enlarged draining veins are seen (*arrows*). *C*, Splenic arteriogram showing enlarged dorsal and transverse pancreatic arteries (*arrows*) and mottled hypervascular stain in body and tail of pancreas.

gram establishes not only a firm diagnosis, but also the extent of the lesion and the degree of its hyperkinetic nature. Angiographic mapping is a valuable aid for successful surgical resection. Massive bleeding in case 2 was successfully controlled after total resection of the entire lesion in several operations. Though the lesion in case 3 was demonstrated clearly at angiography, the pancreas appeared normal even to close inspection. The surgeon resected the pancreas only after confirmation of the lesion by intraoperative arteriography and demon-

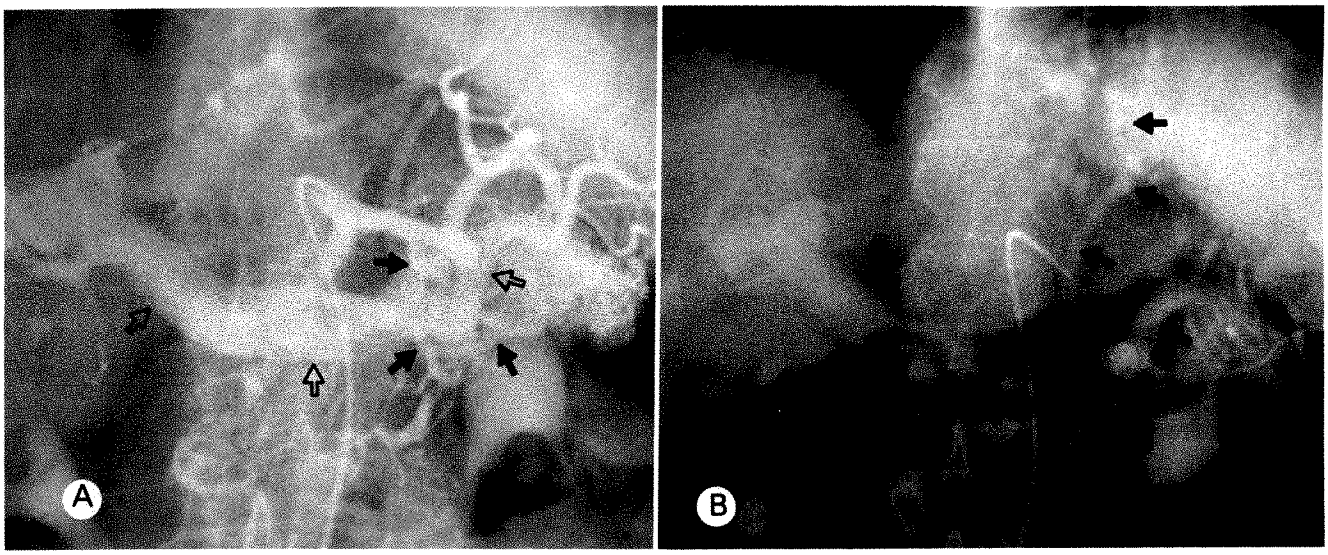

Fig. 3.—Case 3, Osler-Weber-Rendu disease. *A*, Splenic arteriogram showing enlarged dorsal and transverse pancreatic arteries (*closed arrows*), dense racemose vascular network in tail of pancreas, and early opacified splenic and portal veins (*open arrows*). *B*, Film 3 sec after contrast medium injection showing clearance of pancreatic stain. In addition to splenic and portal veins (*open arrows*), short gastric vein with multiple gastric and esophageal varices (*closed arrows*) and inferior mesenteric veins (*wide arrow*) are opacified, indicative of hyperkinetic hypertension.

stration of a significantly elevated portal venous pressure. Postoperative angiography will be useful to insure complete resection of the lesion.

REFERENCES

1. Halpern M, Turner AF, Citron BP: Hereditary hemorrhagic telangiectasia: an angiographic study of abdominal visceral angiodysplasias associated with gastrointestinal hemorrhage. *Radiology* 90:1143-1149, 1968
2. Lande A, Bedford A, Schechter LS: The spectrum of angiographic findings in Osler-Weber-Rendu disease. *Angiology* 27:223-240, 1976
3. Grannis FW, Foulk WT, Miller WE, Payne WS: Diagnosis and management of an arteriovenous fistula of pancreas and duodenum. *Mayo Clin Proc* 48:780-782, 1973
4. Hales RM: Multiple small arteriovenous fistulae of the lungs. *Am J Pathol* 32:927-943, 1956
5. Reuter SR, Redman HC: Inflammatory disease of the pancreas, in *Gastrointestinal Angiography*, Philadelphia, Saunders, 1972, pp 202-212
6. Roe M, Greenough WG: Marked hypervascularity and arteriovenous shunting in acute pancreatitis. *Radiology* 113:47-48, 1974
7. Walter JF, Chuang VP, Bookstein JJ, Reuter SR, Cho KJ, Pulmano CM: Arteriography of massive abdominal hemorrhage secondary to pancreatic disease. *Radiology* 124:337-342, 1977
8. Viamonte M, Warren WD, Fomon JJ: Liver panangiography in the assessment of portal hypertension. *Radiol Clin North Am* 8:147-167, 1970

Pulmonary Angiography for Pulmonary Emboli: Rational Selection of Oblique Views

A. S. GOMES,[1, 2] J. H. GROLLMAN, JR.,[1] AND J. MINK[1]

In the performance of pulmonary arteriography, the anteroposterior projection may be insufficient for the diagnosis of pulmonary embolism, and additional views, usually oblique, are required. Of 57 positive pulmonary arteriograms which were reviewed, additional views were necessary in 26 cases. The efficacy of the additional views in each case was assessed with regard to the demonstration of the segmental arteries of the various lobes of the lung. Following an inconclusive anteroposterior injection, the best visualization of the arteries of the right lung can generally be obtained with an injection made in the right posterior oblique projection. Similarly, following an inconclusive anteroposterior injection, the left posterior oblique or lateral view is recommended for optimal visualization of the pulmonary vasculature of the left lung.

Pulmonary arteriography is the most specific test for the detection of pulmonary emboli [1, 2]. Angiography is indicated in the evaluation of patients suspected of having pulmonary emboli when the perfusion lung scan or ventilation-perfusion scans are rendered inconclusive due to the presence of parenchymal or pleural disease. The frequent necessity for definitive diagnosis by pulmonary arteriography is well documented [2-5].

In performing pulmonary arteriogrphy, it is customary to begin with an injection in the anteroposterior projection. If the initial projection is inconclusive, additional views are needed [2, 3, 6]. However, there is scant information regarding the frequency of inconclusive anteroposterior views and which additional views should be selected to optimally visualize the vasculature in the various segments of the lung [3].

This paper analyzes these problems based on a systematic review of 57 positive pulmonary arteriograms. The number of cases in which views in addition to the anteroposterior projection were required for diagnosis is noted, and the efficacy of the selective views in each case is assessed.

Materials and Methods

All 57 positive arteriograms were performed at UCLA Center for the Health Sciences from 1968-1976. The majority were performed transfemorally using a pulmonary artery-seeking catheter [7, 8]. The anteroposterior injections were performed with the catheter tip positioned in the main pulmonary artery in patients with a mean pulmonary artery pressure of 40 mm Hg or less. In those with mean pulmonary artery pressures greater than 40 mm Hg, and thus evidence of underlying prior cardiopulmonary disease [9, 10], the anteroposterior injection was performed with the catheter tip in the right or left pulmonary artery (eight cases). The initial injection was performed in the anteroposterior projection in all but one case. The main pulmonary artery injections were performed with the patient supine and in deep inspiration using 60 ml of 76% Renografin at a rate of 35-40 ml/sec. The oblique views (30°-45°) were usually performed using 40 ml of contrast at a rate of 20 ml/sec injected selectively into the right or left pulmonary artery. Film sequences were three films per second for 3 sec followed by one film per second for 3 sec, with exposure times of 20-50 msec. When lung scans were available, they were used to help determine which lung should be evaluated initially and later which segments.

Since there had been no systematic approach for the selection of oblique views during this period, the choice varied with the angiographer. Therefore, particularly in the right lung, in one patient a right posterior oblique view may have been selected to visualize the basilar segments, while in another the left posterior oblique view may have been selected to evaluate pathology in the same area.

Each study was first viewed in the anteroposterior projection. The area of positivity or question was localized; subsequently the oblique view was evaluated to determine whether it provided improved visualization of the vessels in the area of question. Every study was viewed separately by each of us; when disagreement occurred, majority ruled. The only criteria for diagnosis of the presence of an embolus were (1) an intraluminal filling defect or (2) an occluded vessel.

Results

In our series the anteroposterior projection was diagnostic in 31 of the 57 cases. In 16 of the 31 cases it was the only projection obtained. In the 15 remaining, the oblique views were obtained because the angiographer was unsure of the diagnosis. Nevertheless, in our review the emboli were clearly defined in the anteroposterior projection.

There were 26 cases where the anteroposterior view

TABLE 1

Right Lung: Projections Diagnostic for Pulmonary Embolus

Site of Embolus	No. Cases	Diagnostic Projection			
		Anteroposterior	Right Posterior Oblique	Left Posterior Oblique	Lateral
Main right pulmonary artery	5	4	...	1	...
Right upper lobe	19	12	4	1	2
Right middle lobe	3	3	...	...	...
Right lower lobe	28	15	8	4	1

Note.—Anteroposterior view was performed first in all cases.

Received April 5, 1977; accepted after revision August 19, 1977.

[1] Department of Radiology, UCLA School of Medicine, Center for the Health Sciences, Los Angeles, California 90024. Address reprint requests to J. H. Grollman, Jr.

[2] Present address: Department of Radiology, University of Minnesota Hospitals, Minneapolis, Minnesota 55455.

Am J Roentgenol **129:1019-1025, December 1977**

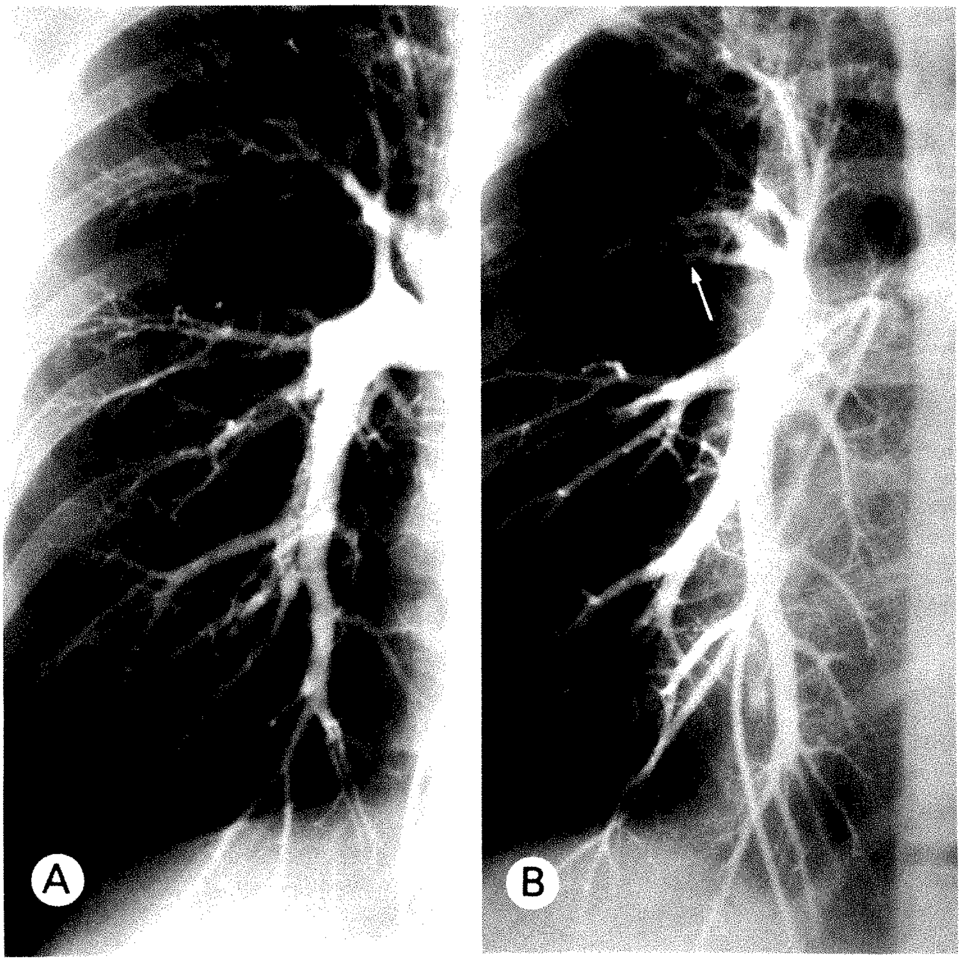

Fig. 1.—Embolus in anterior segmental artery, right upper lobe. *A*, Anteroposterior view of right lung showing only some avascularity above minor fissure. *B*, Right posterior oblique view clearly showing site of embolus (*arrow*). Note that vessels to basilar segments are widely separated on this view.

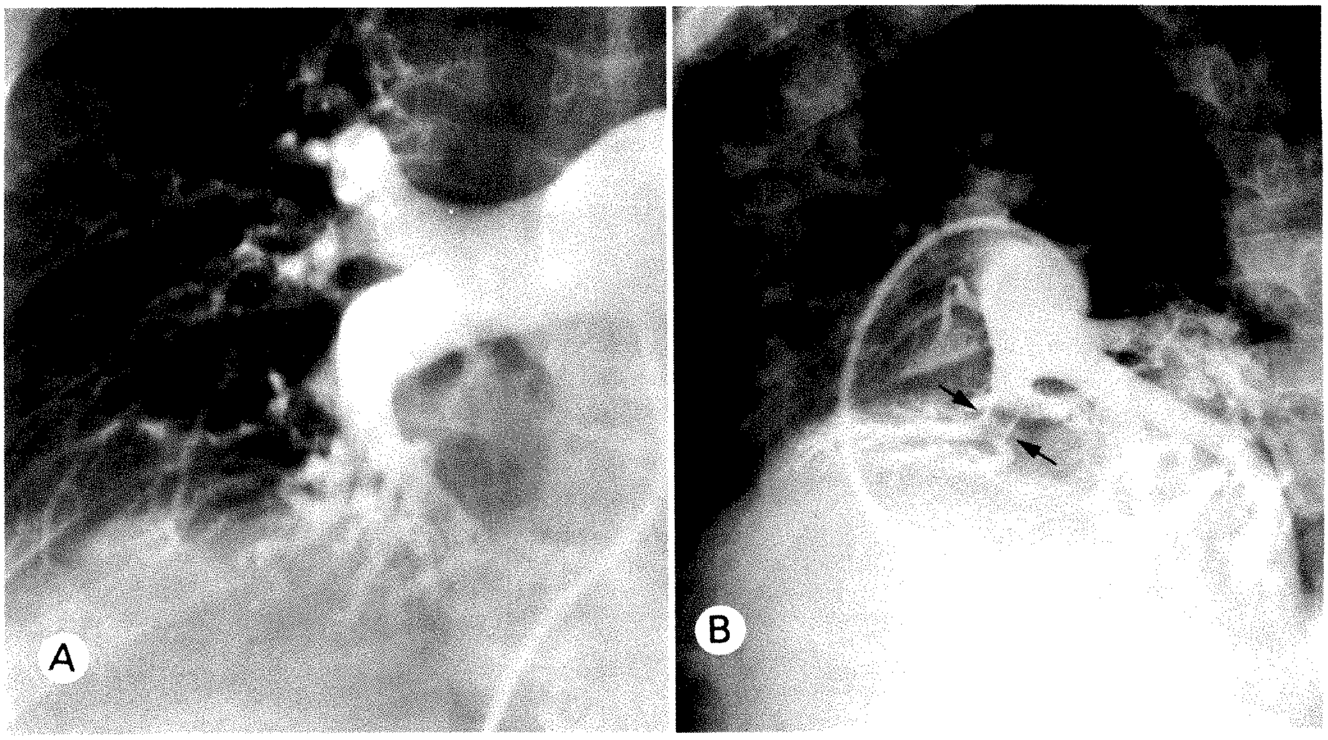

Fig. 2.—Embolus in lateral basal segmental artery, right lower lobe. *A*, Anteroposterior view, main pulmonary artery injection, showing crowding of vessels and slowed flow in right base. Equivocal defects are seen in branches to lateral basal and medial basal segmental arteries. *B*, Right posterior oblique view, selective right lower lobe injection, clearly showing lateral basal artery embolus (*arrows*).

TABLE 2

Left Lung: Projections Diagnostic for Pulmonary Embolus

Site of Embolus	No. Cases	Diagnostic Projection			
		Anteroposterior	Right Posterior Oblique	Left Posterior Oblique	Lateral
Main left pulmonary artery	1	1	...	...	...
Left upper lobe	9	6	...	3	...
Lingula	4	1	...	3	...
Left lower lobe	24	13	1	6	4

Note.—Anteroposterior view was performed first in all cases.

was suspicious but not diagnostic; additional views, oblique or lateral, were used to confirm the diagnosis. Review of the arteriograms with respect to the localization and visualization of emboli in the various lobes revealed the following findings.

Right Lung (Table 1)

In four of the five cases with an embolus in the main right pulmonary artery, the anteroposterior view clearly showed the embolus. In the fifth case, both selective right and left posterior oblique views of the right pulmonary artery were performed. The embolus was seen only on the left view, presumably due to foreshortening of the main pulmonary artery in the right oblique.

In 12 of the 19 cases with an embolus in the right upper lobe, the anteroposterior view was diagnostic. The right posterior oblique view after an equivocal anteroposterior injection was diagnostic in four cases (fig. 1). A lateral projection in one of these patients showed the embolus, but less well than the right posterior oblique. The anteroposterior projection was diagnostic in all three cases of embolus in the right middle lobe.

Of 28 cases of embolus in the right lower lobe, the anteroposterior view was inconclusive in 13. A selective right posterior oblique view was diagnostic in eight of these (fig. 2). The vessels to the four basilar segments were well laid out in all but two of the eight cases. In these two cases there was severe atelectasis with effusion, and the vessels to the posterior basal and medial basal segments were poorly seen due to their displacement toward the spine. There were two other cases with severe basilar atelectasis and one with mild atelectasis, yet in these cases the basilar segmental vessels were still well seen.

The left posterior oblique confirmed four of the 13 cases of right lower lobe pulmonary emboli that were not diagnosed by the anteroposterior view. In three of these there was no significant atelectasis, and the vessels to all four basilar segments were well seen. In the one case with severe atelectasis, the vessels to the medial basal and posterior basal segments were poorly seen, but the embolus in the vessel in the lateral segment was detected.

In two of the 15 cases where the anteroposterior view was diagnostic, left posterior oblique injections were also made. In one case with no atelectasis, all four segmental branches (although projected over the spine) were seen, as was the clot in the lateral basal segmental artery. In the other case, with severe interstitial lung disease and decreased volume, the vessels were again projected over the spine, and medial basal segmental artery clot was not seen.

Emboli occurred in the artery to the superior segment of the right lower lobe in two cases. These were confirmed on a selective right pulmonary artery injection performed in the lateral projection in one case without atelectasis, and with a right posterior oblique injection in one case with severe atelectasis.

Left Lung (Table 2)

In the one case of embolus in the main left pulmonary artery, the anteroposterior view was diagnostic. In six of the nine cases of embolus in the left upper lobe, the anteroposterior view was diagnostic. In the other three cases, the embolus was shown in the left posterior oblique projection. In three of the four cases of embolus in the lingula, the left posterior oblique injection, following the anteroposterior injection, confirmed the diagnosis. One of these had moderate left lower lobe atelectasis and effusion.

The anteroposterior view showed the embolus in 13 of 24 cases with an embolus in the left lower lobe. In two of these, additional views were obtained even though the emboli were well seen in the anteroposterior injection. In one, the right posterior oblique projection showed poor visualization of the left lower lobe vessels. In the other the left posterior oblique view showed the embolus well.

On the left posterior oblique view, used for confirmation in six cases of left lower lobe embolus, the vessels to the basilar segments were well seen despite severe atelectasis in four. The right posterior oblique view was selected once with poor visualization of the basilar segmental vessels because of severe atelectasis. In four cases the lateral view was diagnostic: two with posterior basal clot and two with lateral basal clot. In one of these latter cases there was severe atelectasis, and the lateral view was diagnostic when both the anteroposterior and left posterior oblique were not.

Discussion

Since many patients undergoing pulmonary arteriography are acutely ill, it is imperative that angiography be performed quickly and efficiently. The large number of cases in which the anteroposterior view alone was inconclusive, necessitating additional views for diagnosis, underscores the need for additional views and the need for a rational approach to the selection of additional projections.

Most emboli are multiple and tend to lodge in the lower lobes, with slightly greater frequency in the right lung [2]. There is usually no difficulty visualizing the anterior basal and lateral basal segmental arteries of the lower lobes. However, the medial basal and posterior basal segmental arteries are frequently difficult to visualize, particularly when there is significant atelectasis or effusion. With loss of lung volume, these vessels crowd

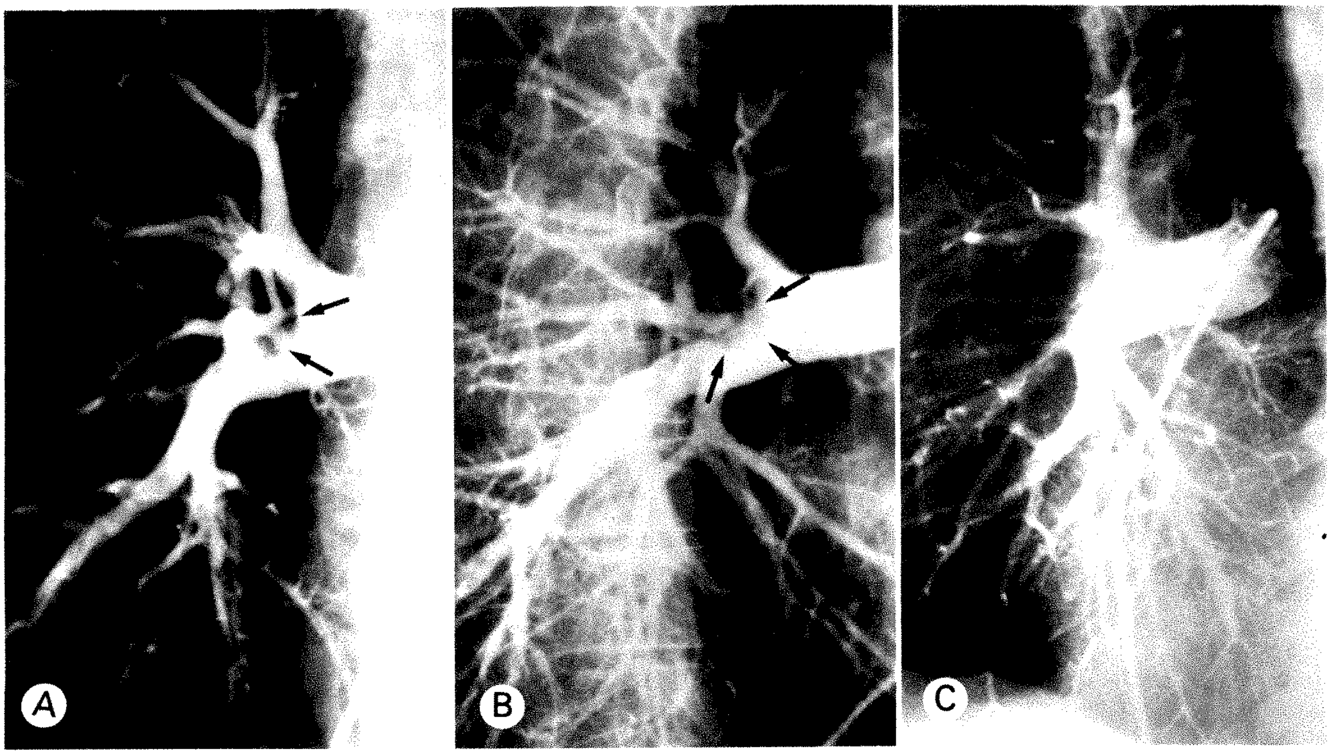

Fig. 3.—Embolus to proximal right pulmonary artery. *A*, Anteroposterior view, main pulmonary artery injection, showing suspicious area (*arrows*). *B*, Left posterior oblique view showing embolus (*arrows*). *C*, Right posterior oblique view with embolus not seen. Note that with well expanded lungs, right lower lobe vessels are well seen in both oblique projections.

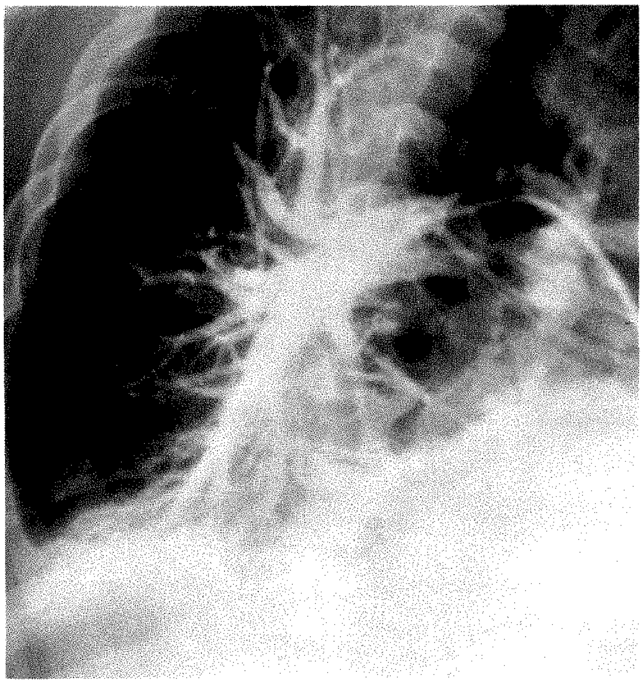

Fig. 4.—Left posterior oblique view, selective right pulmonary artery injection, in patient with right lower lobe atelectasis and effusion. Note marked crowding of vessels with displacement toward spine and poor visualization of basilar segmental arteries (cf. fig. 3*B* in which there is good expansion of lung).

medially toward the spine (fig 2*A*). Further, the left lateral basal segmental arteries can be difficult to evaluate in the presence of left lower lobe atelectasis.

Our findings in cases of right lower lobe pulmonary emboli indicate that, in the well expanded lung, visualization of the four basilar segmental arteries can be obtained in the anteroposterior and right or left posterior oblique views (fig. 3). However, in the presence of atelectasis and concomitant loss of volume in the right lower lobe, it is our impression that the right posterior oblique view allows the greatest opportunity for visualization of the segmental arteries to the medial and posterior basal segments (figs. 2*B* and 4). After the anteroposterior view, the right posterior oblique view afforded the best opportunity for visualization of the right upper lobe segmental artery lesions. The anteroposterior view sufficed in our cases with right middle lobe emboli.

In the evaluation of the left lower lobe, our data favor the use of the left posterior oblique view when the anteroposterior view is inconclusive. The left posterior oblique view was diagnostic both in cases with well expanded lungs and in the presence of severe atelectasis (fig. 5). The lateral view was useful in four cases. Although it is likely that in well expanded lungs optimal visualization of the lateral, medial, and posterior basal segments could be obtained in the right posterior oblique projection [3], in the presence of atelectasis the left posterior oblique view is preferable. Further, since all

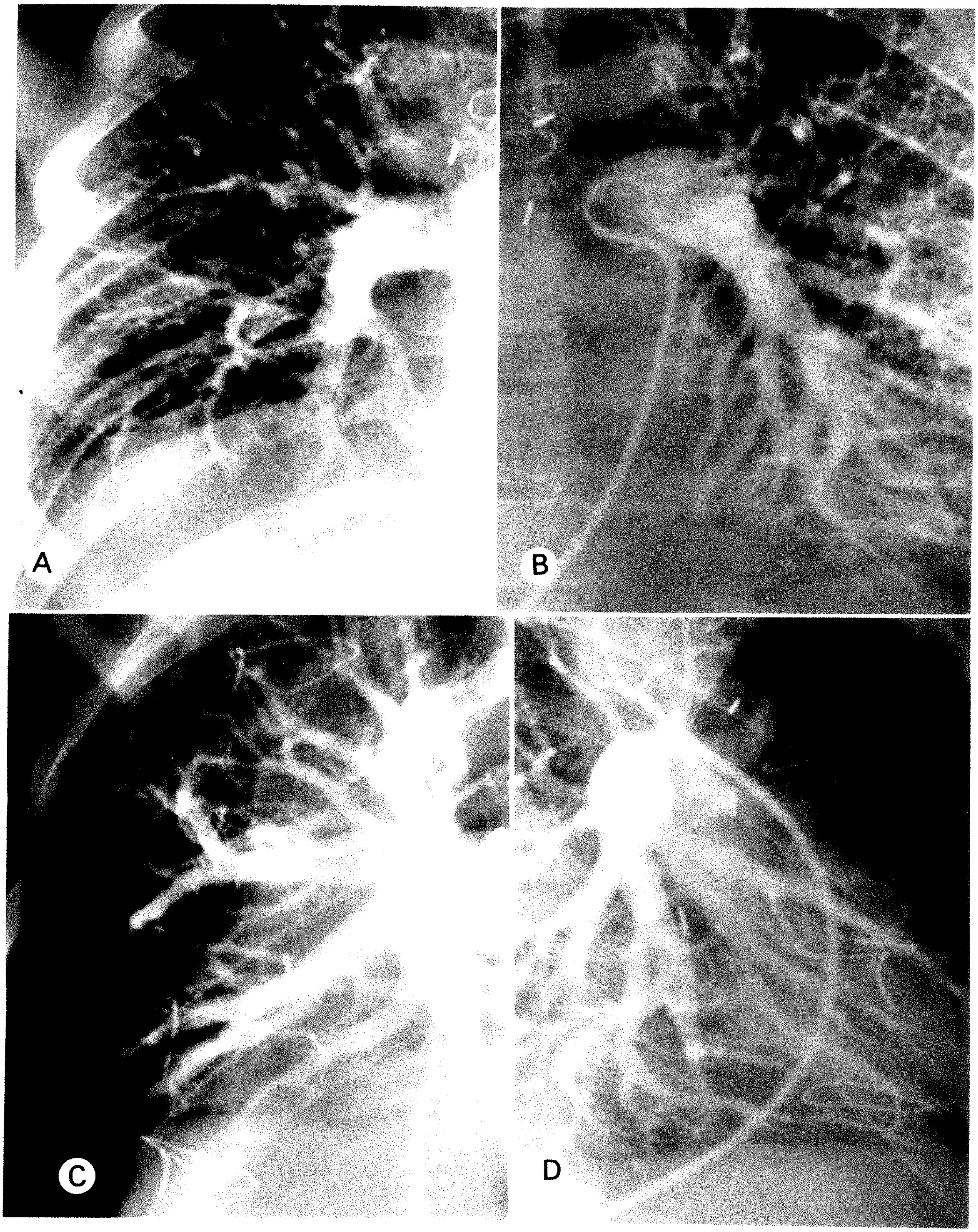

Fig. 5. – Follow-up arteriogram (previous embolus right lower lobe) in patient with mild atelectasis of both lower lobes. *A* and *B*, Anteroposterior view, midphase of main pulmonary artery injection, showing loss of volume in both lower lobes. *C*, Right posterior oblique projection of right pulmonary artery clearly showing segmental vessels of right lower lobe. *D*, Left posterior oblique view, left pulmonary artery injection, showing vessels to lower lobe well laid out despite atelectasis.

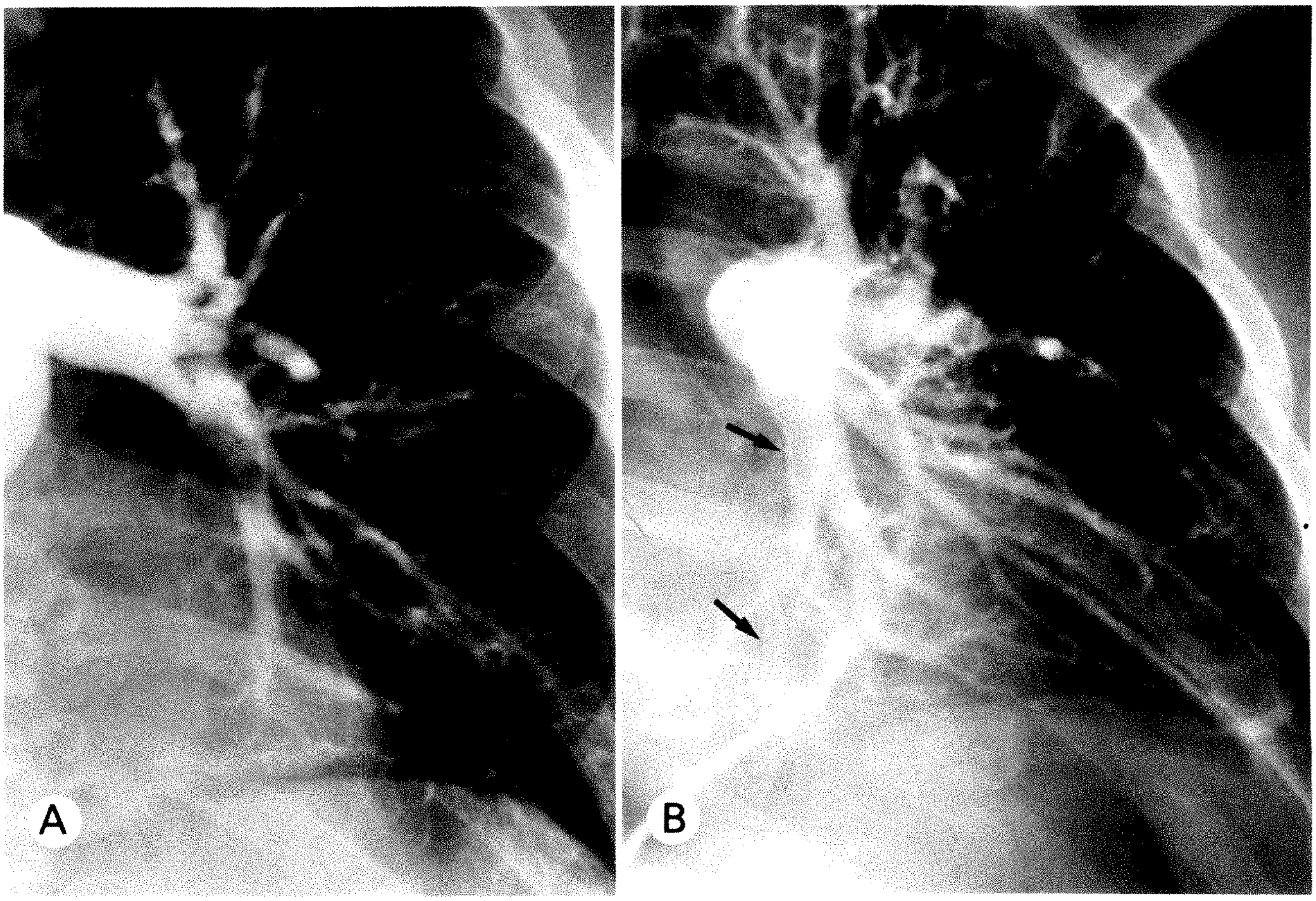

Fig. 6.—Left pulmonary emboli. *A*, Anteroposterior projection, main pulmonary artery injection, clearly showing multiple filling defects in left pulmonary artery. *B*, Left posterior oblique view better showing full extent of posterior basal segmental artery clot (*arrows*).

of our cases of lingula emboli were visualized on the left posterior oblique projection, that projection appears to be the oblique view of choice for evaluating the segmental arteries of the left lower lung field (fig. 6).

In our experience the left posterior oblique view should also be used if the anteroposterior view is inconclusive in cases with left upper lobe emboli (fig. 7). With regard to visualization of the very proximal left pulmonary artery, we found the anteroposterior view to be satisfactory in our single case and did not encounter the need for a right posterior oblique view as described by others [6, 11]. However, if necessary, the right posterior oblique view would visualize this area, avoiding the foreshortening present in the left posterior oblique and anteroposterior projections.

Therefore, we conclude that in pulmonary arteriograms where the injection in the anteroposterior projection is inconclusive, additional projections, usually oblique, may be diagnostic. From our data, it is not possible to conclusively compare the right and left posterior oblique projections for a given lung, since in the majority of our patients both oblique views were not obtained; nor would it be proper to perform such a comparative study unless it were done with simultaneous biplane filming. However, it is our impression that the best visualization of the arteries of the right lung can generally be obtained with an injection made in the right posterior oblique projection. Similarly, following an inconclusive anteroposterior injection, the left posterior oblique or lateral view is recommended for optimal visualization of the pulmonary vasculature of the left lung. However, the angiographer should be willing to individualize. If these views do not provide adequate information, additional views such as the lateral, superselective, and (in well expanded lungs) the opposite oblique should be performed if necessary.

REFERENCES

1. Dalen JE, Brooks HL, Johnson LW, Meister SG, Szucs MM, Dexter L: Pulmonary angiography in acute pulmonary embolism: indications, techniques, and results in 367 patients. *Am Heart J* 81:175-185, 1971
2. Kelley JM, Elliott LP: The radiologic evaluation of the patient with suspected pulmonary thromboembolic disease. *Med Clin North Am* 59:3-36, 1975
3. Johnson BA, James AE, White RI Jr: Oblique and selective pulmonary angiography in the diagnosis of pulmonary embolism. *Am J Roentgenol* 118:801-808, 1973
4. Wagner HN Jr, Strauss HW: Radioactive tracers in the differential diagnosis of pulmonary embolism. *Prog Cardiovasc Dis* 17:271-282, 1975

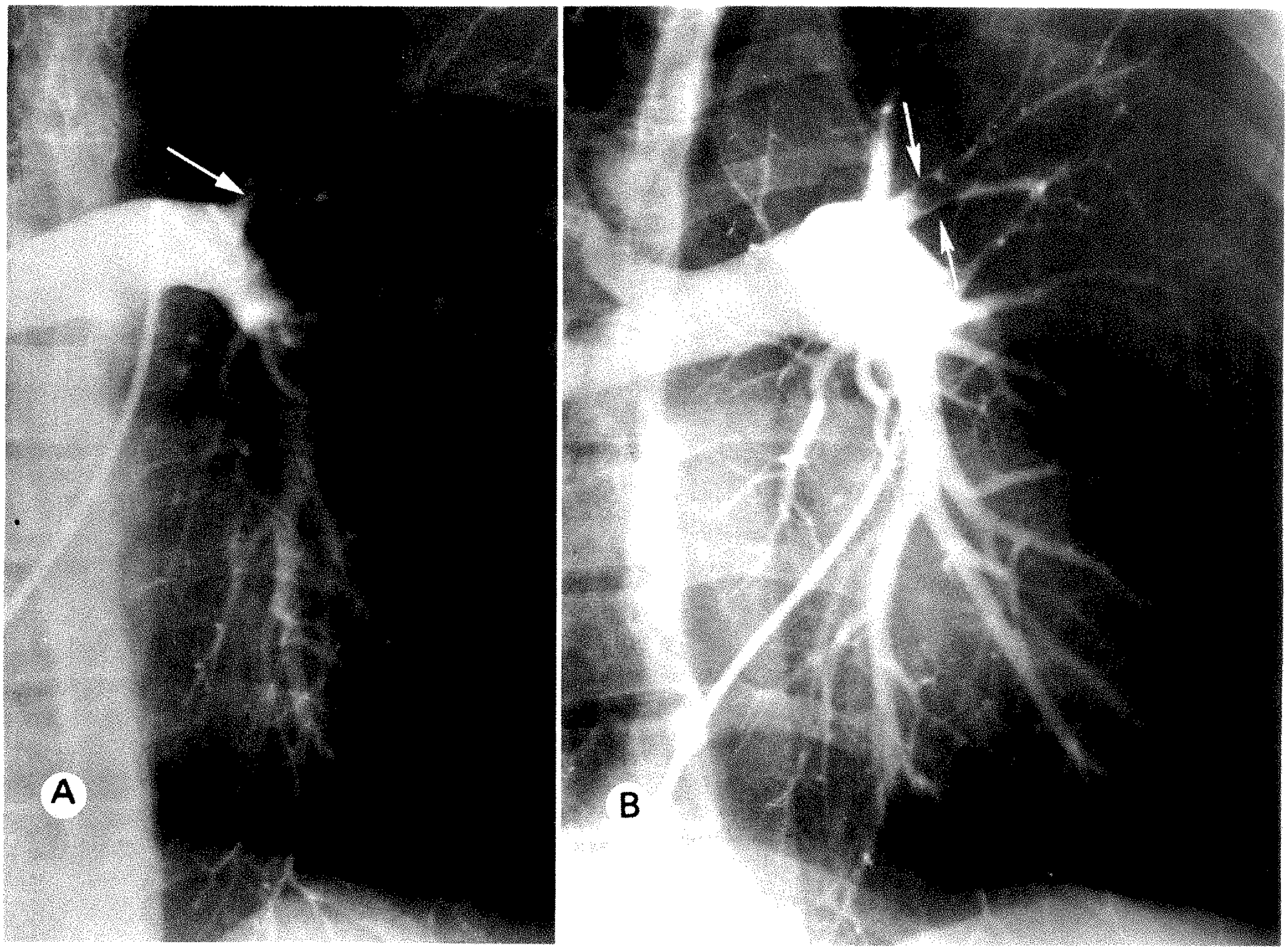

Fig. 7.—Embolus to anterior segmental artery, left upper lobe. Anteroposterior (*A*) and left posterior oblique (*B*) views clearly showing embolus (*arrows*). Note improved visualization of segmental arteries to left lower lobe in *B*.

5. Moser KM, Guisan M, Cuomo A, Ashburn WL: Differentiation of pulmonary vascular from parenchymal diseases by ventilation/perfusion scintiphotography. *Ann Intern Med* 75:597-605, 1971
6. Ranniger K: Pulmonary arteriography: a simple method for demonstration of clinically significant pulmonary emboli. *Am J Roentgenol* 106:558-562, 1969
7. Grollman JH Jr, Gypes MT, Helmer E: Transfemoral selective bilateral pulmonary arteriography with a pulmonary-artery-seeking catheter. *Radiology* 96:202-204, 1970
8. Stein MA, Winter J, Grollman JH Jr: The value of the pulmonary-artery-seeking catheter in percutaneous selective pulmonary arteriography. *Radiology* 114:299-304, 1975
9. McIntyre KM, Sasahara AA: Hemodynamic and ventricular responses to pulmonary embolism. *Prog Cardiovasc Dis* 3:175-190, 1974
10. Miller GAH, Sutton GC: Acute massive pulmonary embolism. Clinical and hemodynamic findings in 23 patients studied by cardiac catheterization and pulmonary arteriography. *Br Heart J* 32:518-523, 1970
11. Chait A, Summers D, Krasnow N, Wechsler BM: Observations on the fate of large pulmonary emboli. *Am J Roentgenol* 100:364-373, 1967

A Radiographic Study of Congenital Pulmonary Atresia with Ventricular Septal Defect

BENIGNO SOTO,[1] ALBERT D. PACIFICO,[2] RODRIGO F. LUNA,[1] AND L. M. BARGERON, JR.[3]

A radiographic analysis of 66 patients with congenital pulmonary atresia and ventricular septal defect was made to determine the frequency and variability of the (1) atrioventricular and ventriculoarterial relation, (2) source of pulmonary blood flow, and (3) pulmonary arterial anatomy.

Of the 66 patients, 63 had situs solitus and 62 had atrioventricular concordance; the aorta arose from the right ventricle in six, left ventricle in six, and biventricularly in 54. Pulmonary arteries were present and confluent in 41 patients, nonconfluent in five, absent in 15, and in five patients a mixed distribution to selected areas of each lung existed. In almost half of those in whom pulmonary arteries were present, the source of pulmonary blood flow was from systemic arteries (bronchials) originating from the upper descending thoracic aorta. In some, these collaterals obscured detection of pulmonary arteries when conventional anteroposterior views of the aortogram were made. The use of semiaxial craniocaudal projections and/or selective angiography were required for proper definition.

Chest radiographs were correlated with angiographic details and did not permit differentiation of the various subsets of congenital pulmonary atresia from each other nor from classical tetralogy of Fallot. Abnormal central vessels were identified in 31 patients suggesting this diagnosis. The right or left pulmonary artery identified by angiography was not detected on the plain chest film in about half of the group. Angiograms of the intra- and extracardiac details of this group of malformations are presented, correlated with plain chest films, and their surgical implications discussed.

The phrase congenital pulmonary atresia with ventricular septal defect describes a group of cardiac malformations which are characterized by (1) absence of direct anatomic continuity of the pulmonary arteries with the heart, (2) varying degrees of atresia or agenesis of the main and distal pulmonary arteries, and (3) varying sources of pulmonary blood flow [1-6]. We present a radiographic analysis of 66 patients with this malformation each having two atria, and two atrioventricular valves emptying into two respective and well developed ventricles. Patients with truncus arteriosus types I-III were excluded [7]. This report describes the angiographically determined frequency of the following anatomic variations: (1) visceroatrial situs, (2) atrioventricular relation, (3) origin of aorta, (4) presence and distribution of the pulmonary arteries, and (5) sources of pulmonary blood flow. A correlative analysis of features identified on the plain chest films is presented.

Definition of Terms

Patients with these congenital cardiac defects may be classified, using embryologic and pathologic considerations, into a variety of categories: tetralogy of Fallot with congenital pulmonary atresia, end-stage tetralogy of Fallot, transposition of the great arteries, double outlet right or left ventricle, and corrected transpositon—each with pulmonary atresia. However, the separation into these subsets often cannot be made by usual angiographic and surgical methods, because it is not always possible to determine the ventricle from which the main pulmonary artery would have arisen were it not atretic. In addition, it is usually of no clinical importance to make this differentiation.

The surgical problem in each of these malformations is similar and consists of reestablishing ventriculopulmonary artery continuity with a valved external conduit. This usually involves closing the source of pulmonary blood flow and closing the ventricular septal defect so that the aorta arises from the systemic ventricle. When there is valvular pulmonary atresia, a main pulmonary artery segment, and normally related great arteries, an outflow tract patch may be used in place of a valved external conduit. The cardiac radiologist must define the presence and distribution of pulmonary arteries, the source of pulmonary flow, the location of the aorta with respect to each ventricle, and the ventricular septal defect. The origin of the atretic pulmonary artery bears little clinical significance.

Therefore, we prefer to classify these malformations under the heading of congenital pulmonary atresia with ventricular septal defect. The three major divisions are (1) bilateral presence of pulmonary arteries, further delineated as confluence or nonconfluence of left and right pulmonary arteries; (2) bilateral absence of pulmonary arteries (truncus arteriosus type IV); and (3) mixed types. Further definition is made of the situs of the viscerae and atria, atrioventricular relation, position and origin of the aorta, and position and size of the ventricular septal defect. This classification is similar to that of Edwards and McGoon [1].

When the pulmonary arteries are present and confluent, the entity has been called pseudotruncus arteriosus. The majority of these cases have a biventricular origin of the aorta, and the morphology of the right

---

Received February 3, 1977; accepted after revision August 23, 1977.

[1] Department of Diagnostic Radiology, University of Alabama School of Medicine, 619 South 19th Street, Birmingham, Alabama 35294. Address reprint requests to B. Soto.

[2] Department of Surgery, University of Alabama School of Medicine, Birmingham, Alabama 35294.

[3] Department of Pediatrics, University of Alabama School of Medicine, Birmingham, Alabama 35294.

ventricle is similar to that found in the tetralogy of Fallot. This has been described as tetralogy with congenital pulomonary atresia or as end-stage tetralogy of Fallot. When the aorta is further dextroposed, originating entirely from the right ventricle, the entity has been called transposition of the great arteries with congenital pulmonary atresia [8]. However, the angiographer, and sometimes the surgeon, cannot be certain that had the main pulmonary artery been connected with the heart it would have arisen from the left ventricle. It may have arisen from the right ventricle, in which case the entity might be called double-outlet right ventricle with pulmonary atresia [9]. Similarly, if the aorta arises entirely from the left ventricle, the entity may be described as double-outlet left ventricle with pulmonary atresia or simply as ventricular septal defect with pulmonary atresia. These considerations and the surgical limitations make us believe it reasonable to group these cardiac malformations under the heading of congenital pulmonary atresia with ventricular septal defect, although we recognize the variety of terms indicated above are preferred by others.

Patients with congenital pulmonary atresia with ventricular septal defect may have positional anomalies of the heart, abnormal visceroatrial situs, and abnormal atrioventricular connections. When atrioventricular discordance is present, the phrase corrected transposition with pulmonary atresia is sometimes preferred, since corrected transposition is a malformation characterized by atrioventricular discordance and a discordant ventriculoarterial relation. We prefer to describe this malformation as congenital pulmonary atresia with ventricular septal defect, and atrioventricular discordance as origin of the aorta from the right ventricle.

The pulmonary arterial system is the usual anatomic arterial tree which supplies blood to the alveolar capillaries within the lungs. It is formed by main pulmonary artery, right and left pulmonary arteries, and their lobar, segmental, and subsegmental branches. In some patients part of this usual anatomic sequence may be absent. Right and left pulmonary arteries are seen angiographically as gently curved structures, concave toward the midline, extending downward and outward from each hilum. The descriptive terms "palm leaf" or "comma" have been used for these configurations [10, 11]. The left and right pulmonary arteries may not join together (nonconfluent) or they may be connected by a confluence. This confluence may or may not join a partially developed main pulmonary trunk.

The source of pulmonary blood flow may be a ductus arteriosus, well developed bronchial collateral arteries, a coronary-pulmonary fistula, a collateral artery from the innominate artery, a surgically created systemic pulmonary arterial shunt, or large bronchial collaterals. In some patients well developed bronchial collateral arteries join the pulmonary arteries in the hilum, while in others these extend within each lung to form a second and separate well developed intrapulmonary arterial tree. These vessels, which originate from the upper descending thoracic aorta, usually have a spiral coiled pattern and may have areas of stenosis along their course.

TABLE 1

Angiographic Findings

Finding	Confluent Pulmonary Arteries	Absent Pulmonary Arteries*	Nonconfluent Pulmonary Arteries	Mixed
Situs:				
Solitus	39 (95.1)	15 (100.0)	5	4
Inversus	2 (4.9)	0	0	1
Atrioventricular connections:				
Concordant	40 (97.0)	14 (93.3)	4	4
Discordant	1 (2.4)	1 (6.7)	1	1
Origin of the aorta:				
Biventricular	31 (75.6)	13 (87.0)	4	3
Right ventricle	4 (9.8)	2 (13.0)	1	0
Left ventricle	6 (14.6)	0	0	0
Systemic-pulmonary connections:				
Patent ductus arteriosus	13 (32.0)	0	1	2
Large systemic arteries	19 (46.0)	14 (93.0)	3	1
Small systemic arteries	1 (2.0)	1 (6.7)	0	0
Surgically created shunts	8 (20.0)	0	1	2

Note.—Numbers in parentheses are percentages.

* Truncus arteriosus type IV.

TABLE 2

Radiographic Findings

Finding	Confluent Pulmonary Arteries	Absent Pulmonary Arteries*	Nonconfluent Pulmonary Arteries	Mixed
Heart size:				
Normal	35	10	5	5
Enlarged	6	5	0	0
Aortic arch:				
Right	13	9	3	1
Left	28	6	2	4
Pulmonary artery:				
Right	20	2	3	1
Left	15	2	1	0
Lobar and segmental branches	17	2	1	1
Collateral circulation	24	10	4	0
Abnormal central vessels:				
Right	15	7	3	0
Left	11	12	2	1

* Truncus arteriosus type IV.

Whether these arteries are truly enlarged bronchial arteries or other systemic arteries is a matter of controversy [12, 13].

When there is absence of the true anatomic pulmonary arterial tree, the arterial supply to the lung is solely from these bronchial collateral arteries and the condition is called truncus arteriosus type IV, as described by Collett and Edwards [7]. Some patients have varying combinations of pulmonary arterial pattern called the mixed type. This usually consists of a pulmonary arterial system to one or more lobes and a separate systemic arterial supply to the remaining lobes.

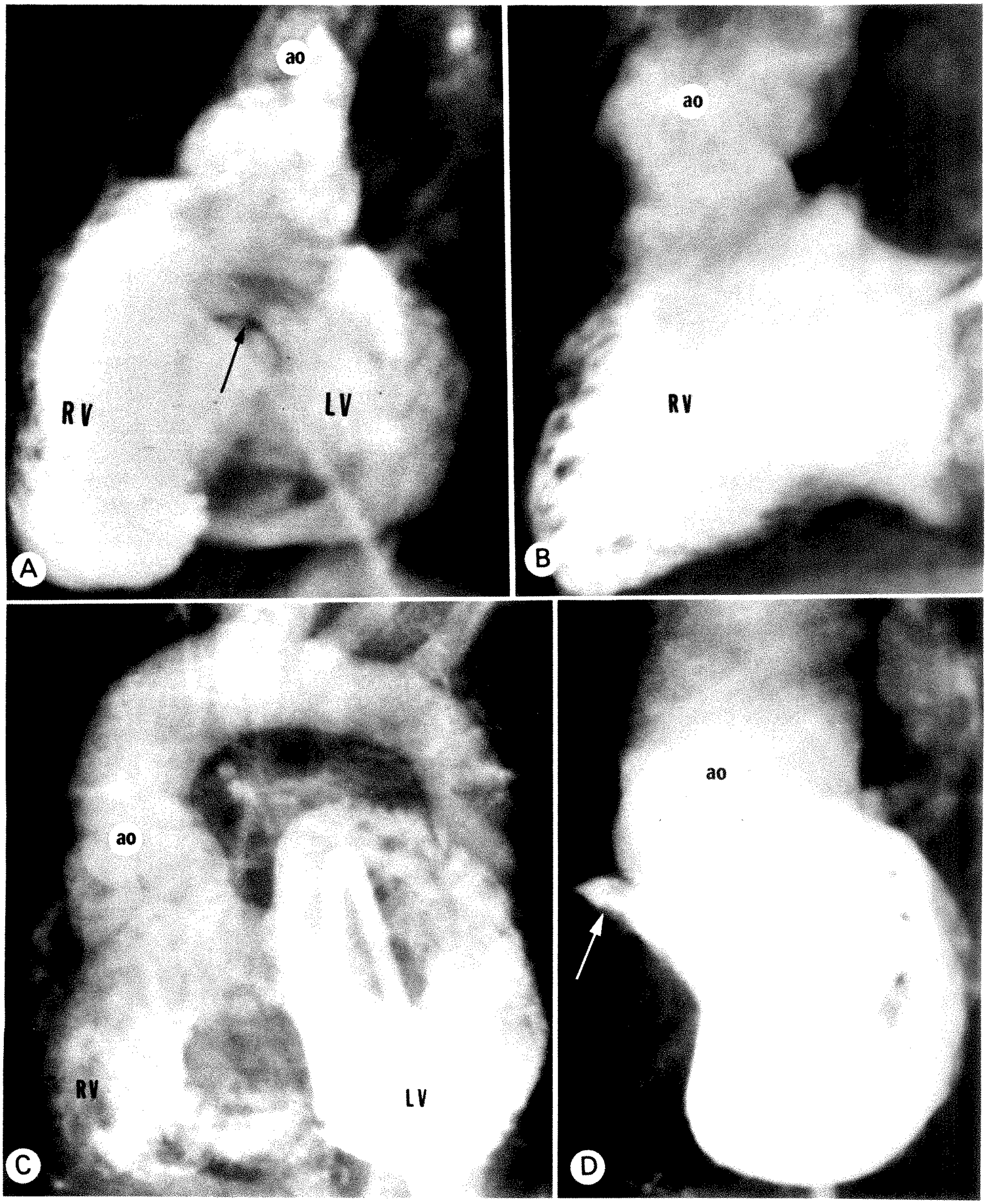

Fig. 1.—Origin of aorta. *A*, Right ventricular angiogram, lateral view, showing aorta originating equally from both ventricles. Note large ventricular septal defect (*arrow*). *B*, Right ventricular origin of aorta. *C*, Right ventricular origin of aorta in patient with situs inversus and discordant atrioventricular relation. *D*, Left ventricular origin of aorta. Note ventricular septal defect (*arrow*).

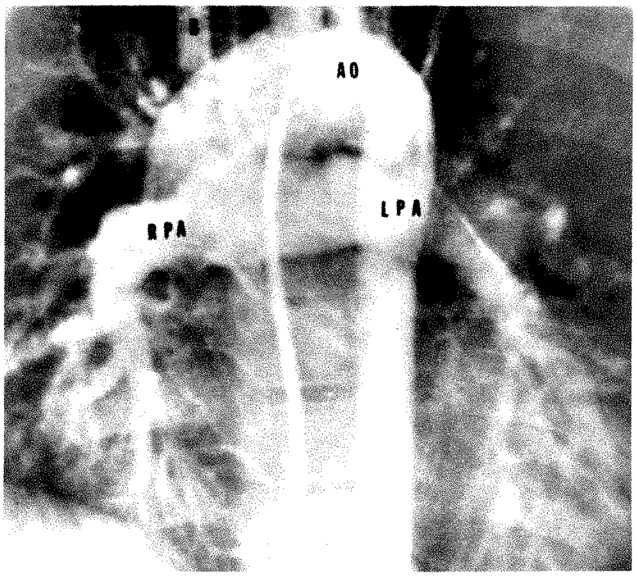

Fig. 2.—Aortogram showing pulmonary arterial system in patient with confluent pulmonary arteries and right Blalock-Taussig shunt. Tip of catheter is in aortic arch (AO). Right (RPA) and left (LPA) pulmonary arteries are opacified through Blalock anastomosis (B). Pulmonary arteries have usual "palm leaf" configuration.

Subjects and Methods

A total of 66 patients with congenital pulmonary atresia and ventricular septal defect who had complete radiographic studies made at the University of Alabama in Birmingham were selected for this study. Patients with truncus arteriosus types I-III were arbitrarily excluded. Patients ranged in age from 2 days to 47 years; there were 34 males and 32 females. Of the 66, 41 had confluent pulmonary arteries, 15 truncus arteriosus type IV, five had nonconfluent pulmonary arteries, and five had the mixed type.

The angiographic study consisted of a right ventricular angiogram, aortogram after injection of contrast media into the upper descending thoracic aorta, and, in some cases, films made from selective injection of vessels originating from the upper descending thoracic aorta. More recently, the craniocaudal semiaxial projection has been used to improve identification of the pulmonary arteries. These angiograms were obtained on large film series (roll film, Elema-Schonander changer) and 35 mm cine.

The segmental approach for the diagnosis of congenital heart disease was followed [4]. Definition of the (1) situs of the viscerae and atria, (2) atrioventricular connection, and (3) ventricular-great artery relation were made for each patient based upon angiography. Chest films were examined with particular attention to heart size, position of the aortic arch, and identification of the right and left pulmonary arteries and their branches. Abnormal blood vessels in the hilum of the lungs were identified and later correlated with angiographic studies. Indentation in the opacified esophagus has been found useful as an indicator of large bronchial arteries, but was not evaluated in this study.

Results

The angiographic details are listed in table 1. The findings recognized from analysis of the chest radiographs are described in table 2. Heart size was considered enlarged if the cardiothoracic ratio was greater than 0.56.

Surgery was performed on 48 of the 66 patients and consisted of corrective procedures in 29, systemic-pulmonary artery shunts in 12, and exploratory thoracotomy alone in seven. Surgically correlatable information on intracardiac and pulmonary artery anatomy was therefore available in only 29 of the 66 patients.

Confluent Pulmonary Arteries

Confluent pulmonary arteries was the most frequent type of congenital pulmonary atresia in this series (41 patients). There were 25 females and 16 males, ranging in age from 2 days to 34 years. The visceroatrial situs was solitus in all but two patients, and the atrioventricular relation was concordant in all but one.

Angiographic studies. The origin of the aorta in the 41 patients was biventricular in 31, from the left ventricle in six, and from the right ventricle in four (fig. 1). The source of pulmonary blood flow was the bronchial collateral arteries arising from the descending thoracic aorta in 20 patients, a patent ductus arteriosus in 13, and solely a surgically created systemic-pulmonary artery shunt in eight. In some cases the presence of the pulmonary arterial system was easily demonstrated soon after injection of contrast material into the aorta (fig. 2). However, when the source of pulmonary blood flow is bronchial collateral arteries arising from the descending thoracic aorta, demonstration of the pulmonary arterial system may be difficult and may require selective catheterization of each of these vessels [14, 15] (fig. 3). Simple aortography in this patient (fig. 3) did not demonstrate a pulmonary arterial system; without the use of selective arteriography of each collateral vessel, a diagnosis of truncus arteriosus type IV would have been incorrectly made.

More recently we have found improved radiographic separation of the pulmonary confluence from the systemic collateral arteries with the use of semiaxial craniocaudal projections (fig. 4.). The angiographic details of the intra- and extracardiac anatomy were verified at the time of corrective surgery in 29 of these 41 patients.

Chest films. The heart size was normal on chest films in 35 patients (85%) and the main pulmonary artery segment was concave or absent in 31 (75%). The right and left pulmonary arteries were identified only in about half of the cases (table 2). The peripheral vessels were decreased and/or of normal caliber in the same proportion of cases, but no evidence of increased vascularity was found in this series. On lateral views, the shadow of the right and left pulmonary arteries was visualized in 30 of 36 patients (83%) (fig. 5). The majority of patients in whom pulmonary arteries were not identified on the plain chest film, but were identified angiographically, were infants.

Peripheral collateral circulation commonly observed in cyanotic patients with reduced pulmonary blood flow was identified in 24 patients of this group. This term was used by Campbell and Gardner [11] to describe vascular markings which do not appear related to the comma shape of the normal pulmonary artery. These markings are dense vascular shadows high in the mediastinum and nodular hilar structures with abnormal branching in the

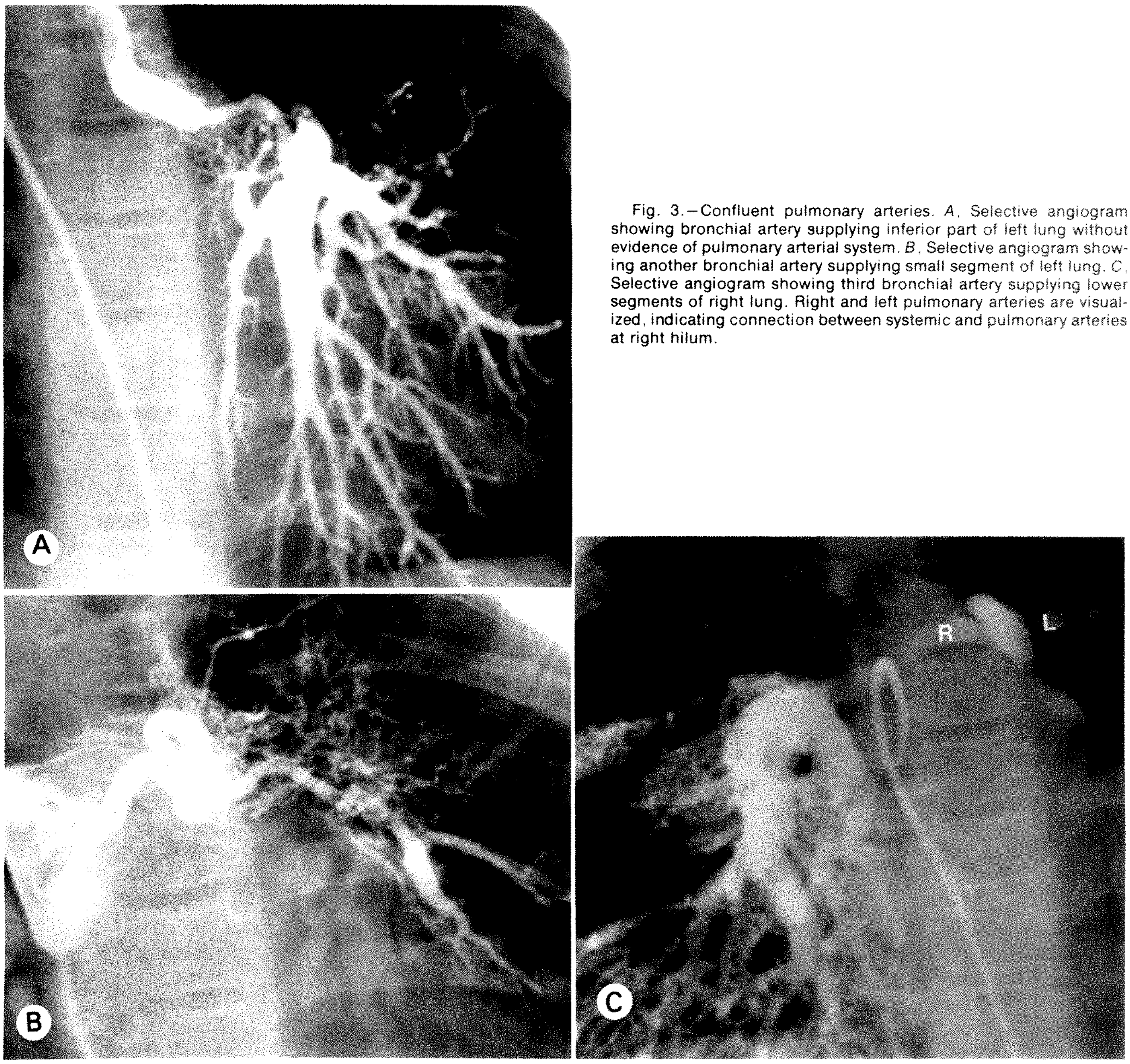

Fig. 3.—Confluent pulmonary arteries. *A*, Selective angiogram showing bronchial artery supplying inferior part of left lung without evidence of pulmonary arterial system. *B*, Selective angiogram showing another bronchial artery supplying small segment of left lung. *C*, Selective angiogram showing third bronchial artery supplying lower segments of right lung. Right and left pulmonary arteries are visualized, indicating connection between systemic and pulmonary arteries at right hilum.

lung field, and are radiographic evidence of collateral circulation, most probably bronchial arteries.

The aortic arch was on the right side in 13 patients (32%), a frequency similar to that previously reported for patients with this malformation [6]. Unusual vascular markings were identified in the hilum in 15 of the 41 patients in this group. The angiograms indicated that these vessels were abnormal systemic connections arising from the upper descending thoracic aorta (fig. 6). They were identified more frequently in the right (37%) than left hilum (27%), which differs from the results of Jefferson et al. [13], who reported an equal distribution. Our angiographic studies identified these abnormal hilar vessels in four additional patients, although this was not suspected from the plain chest radiograph. The association of normal heart size, right aortic arch, concave pulmonary segment, and decreased pulmonary vascularity are the most important chest film findings in these patients and are not significantly different from classical tetralogy of Fallot.

Absence of Pulmonary Arteries (Truncus Arteriosus Type IV)

The absence of pulmonary arteries was the second most common subset in this series, present in 15 of the 66 patients (22%). There were nine males and six females, ranging in age from 2 to 26 years.

Angiographic studies. Situs solitus with a concordant atrioventricular relation was found in 14 patients; one patient had a discordant relation. The origin of the aorta was biventricular in 13 patients and from the right ventricle in two (fig. 7).

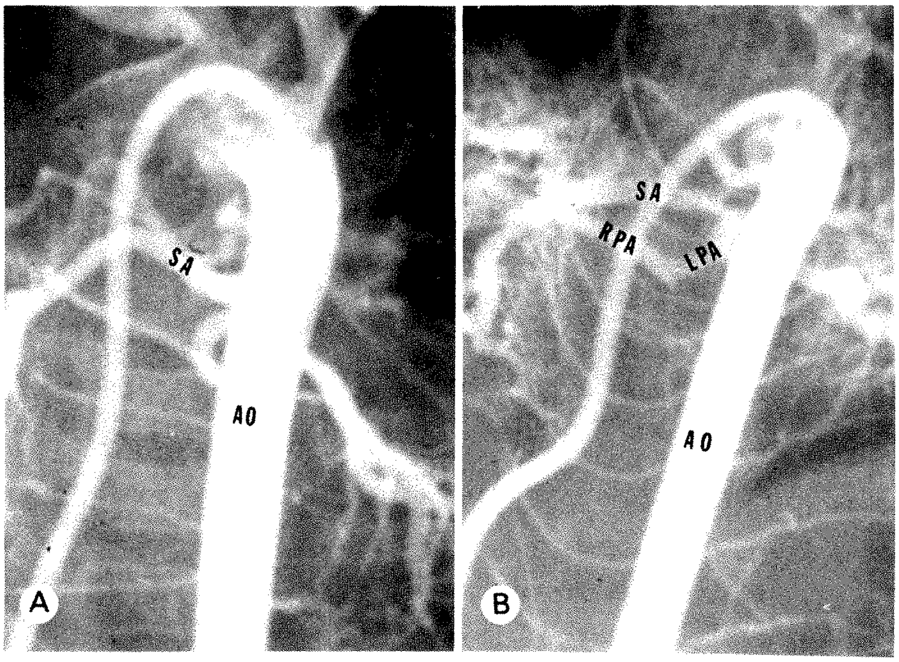

Fig. 4.—Aortogram in patient with confluent pulmonary arteries. *A*, Anteroposterior view showing systemic arteries (SA) originating from upper descending aorta (Ao) and supplying both lungs. Pulmonary arterial system not evident because of superimposition of systemic branches. *B*, Semiaxial craniocaudal view of same patient showing separation of systemic arteries (SA) above, and right (RPA) and left (LPA) pulmonary arteries below.

The diagnosis of truncus arteriosus type IV in these patients rests upon the absence of an identifiable pulmonary artery. The source of pulmonary blood flow is solely bronchial arteries originating from the descending thoracic aorta. This must be differentiated from patients who have the same source of pulmonary blood flow, but who in addition have a true and separate pulmonary arterial system, as discussed above. The importance of this differentiation is clear, since surgical correction is possible only when a true pulmonary arterial system is present. Four of these 14 patients underwent exploratory thoracotomy, but a pulmonary artery could not be found in any, verifying the angiographic diagnosis.

Chest films. Ten patients had normal sized hearts and five had cardiomegaly on chest radiography (fig. 8). The main pulmonary artery segment was absent in 13 patients, reduced from normal in one, and normal in another. Enlarged systemic arteries in the latter two patients were shown by angiography to account for this misinterpretation of the plain films. Peripheral vessels were of small caliber in each case, and peripheral collateral circulation was identified in 10 patients.

The posteroanterior film chest more frequently demonstrated abnormal hilar vessels in patients with absent pulmonary arteries, but these films were not significantly different from those of patients with confluent pulmonary arteries when the whole group is considered. However, absence of pulmonary artery branches was more clearly demonstrated in the lateral projection (fig. 8), as emphasized by Vix and Klatte [16].

Nonconfluence of Pulmonary Arteries

There were five patients who had nonconfluence of pulmonary arteries. All were male, ranging in age from 2 months to 13 years.

Angiographic studies. Situs solitus was present in all five patients; the atrioventricular relation was concordant in four patients and discordant in one. The aorta had a biventricular origin in four patients and arose from the right ventricle in one. The source of pulmonary blood flow was bronchial collateral arteries in each patient (fig. 9). Corrective surgery performed in one patient verified the angiographically determined anatomy. Systemic–pulmonary artery shunts were made in three patients, confirming the presence of a nonconfluent pulmonary artery.

Chest films. The heart size was normal in all five (fig. 10). Although the main pulmonary artery was absent in each patient, large bronchial collateral arteries were responsible for the incorrect identification of a pulmonary artery segment, reported as normal in two and diminished in three patients. The right pulmonary artery was identified in three patients and the left pulmonary artery in one. The peripheral vessels were of small caliber in four cases and normal in one. Peripheral collateral circulation was uniformly present. Abnormal hilar vessels were identified on the right in three patients and on the left in two. These findings were similar to those found by analysis of the plain chest films of patients with confluent pulmonary arteries and also those with absent pulmonary arteries; thus they were not helpful in differentiating these entities.

Mixed Type

Five patients had the mixed type of congenital pulmonary atresia with ventricular septal defect. There were four males and one female, ranging in age from 3 days to 47 years.

Angiographic studies. Situs solitus was present in four patients and situs inversus totalis in one. Four patients

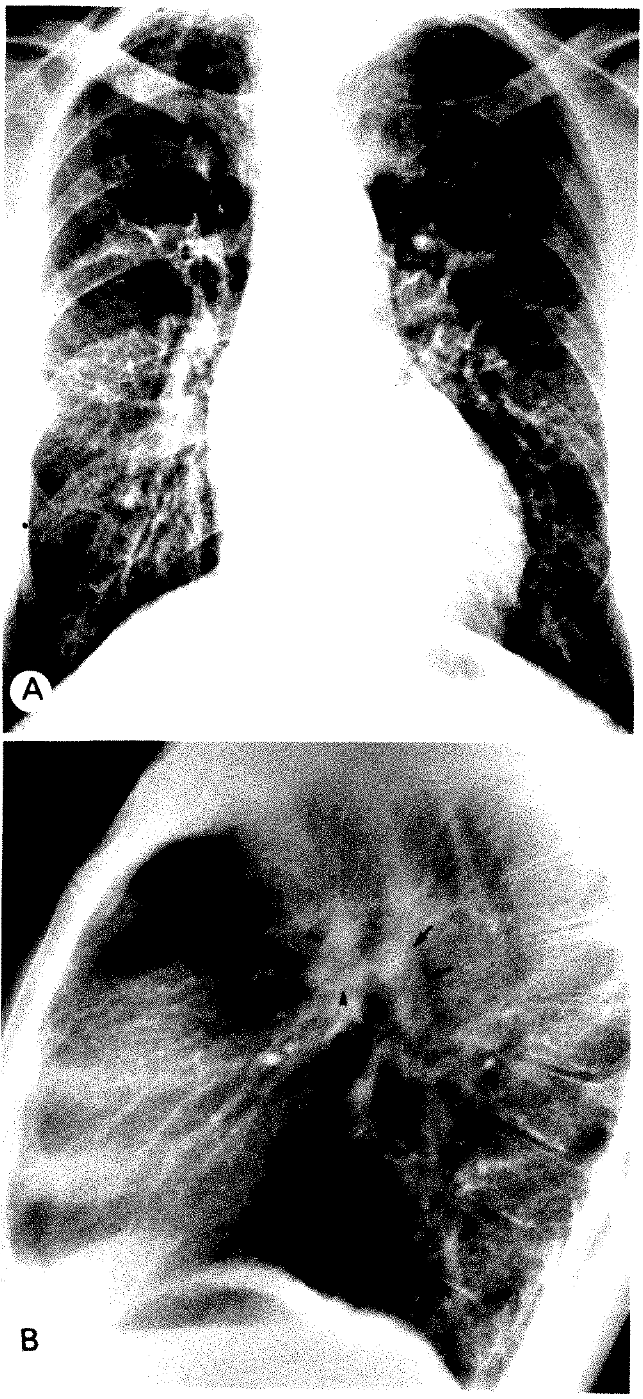

Fig. 5.—Chest radiographs in posteroanterior (*A*) and lateral (*B*) views showing congenital pulmonary atresia, ventricular septal defect, and confluent pulmonary arteries. Normal-sized heart and diminished pulmonary vascularity are prominent features. Note right (*arrowheads*) and left (*arrows*) pulmonary arteries. Signs of peripheral collateral circulation are seen in lower segments.

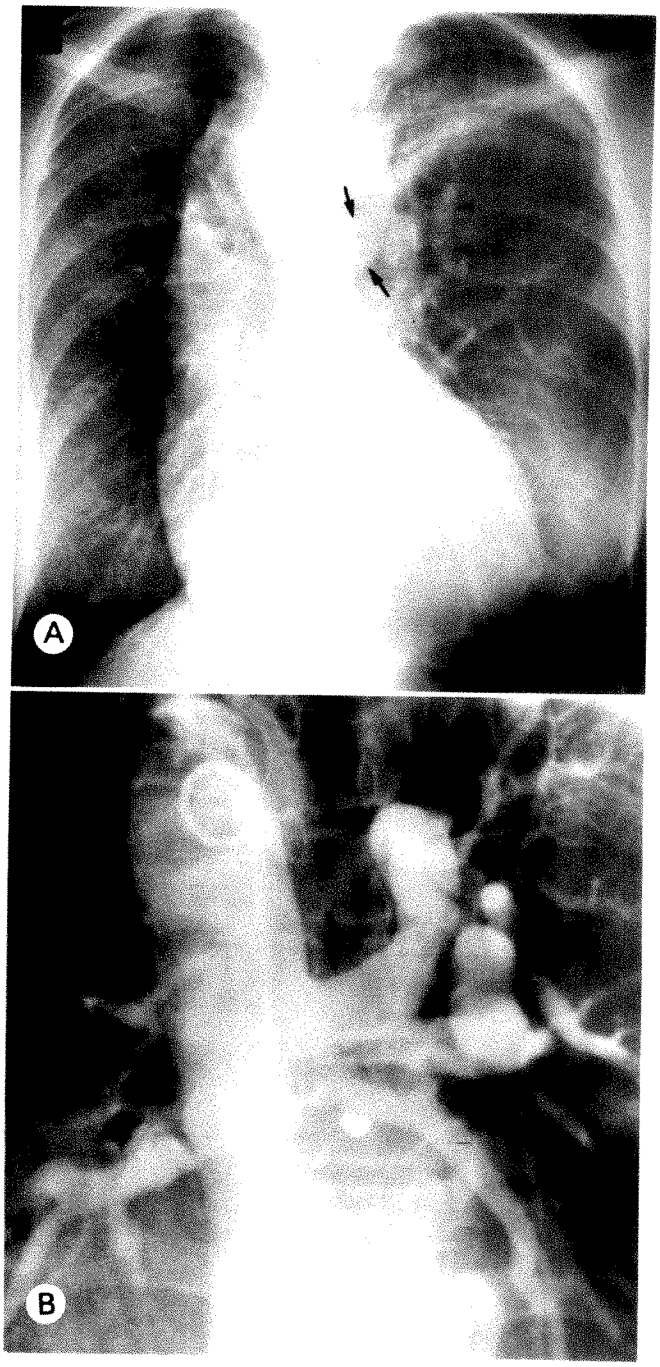

Fig. 6.—*A*, Posteroanterior chest film of patient with confluent pulmonary arteries showing diminished peripheral pulmonary vascularity and large abnormal vascular shadows at left hilum (*arrows*) and more peripherally (*arrowheads*). Abnormal vessel is in higher position than pulmonary artery, indicating collateral vessel. *B*, Angiogram of same patient showing that abnormal vessel (*arrow*) is systemic artery supplying left lung and originating from descending thoracic aorta. Right and left pulmonary arteries were demonstrated in later frames.

had a concordant atrioventricular relation and one, a discordant connection. The source of pulmonary blood flow was in part a patent ductus arteriosus in two patients, a surgically created systemic-pulmonary artery shunt in two, and solely large bronchial arteries in one. Each patient had some segments of either lung supplied by a pulmonary arterial system and other segments supplied solely by bronchial arteries (fig. 11).

Chest films. Heart size on the chest radiographs was normal in all five cases. The pulmonary artery segment

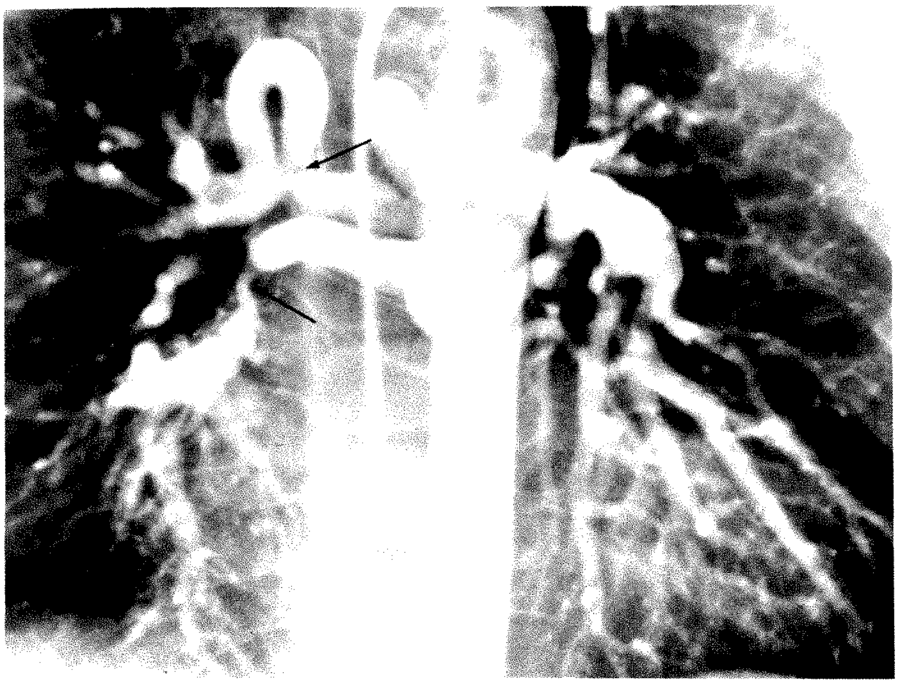

Fig. 7.—Aortogram, anteroposterior projection, showing systemic circulation of lungs in patient with absent pulmonary arteries (truncus arteriosus type IV). Tip of catheter is at upper descending aorta. Two systemic arteries supply right and left lungs, respectively. Notice tortuosity of these channels and areas of stenosis (*arrows*) following classical "spiral" coiled course.

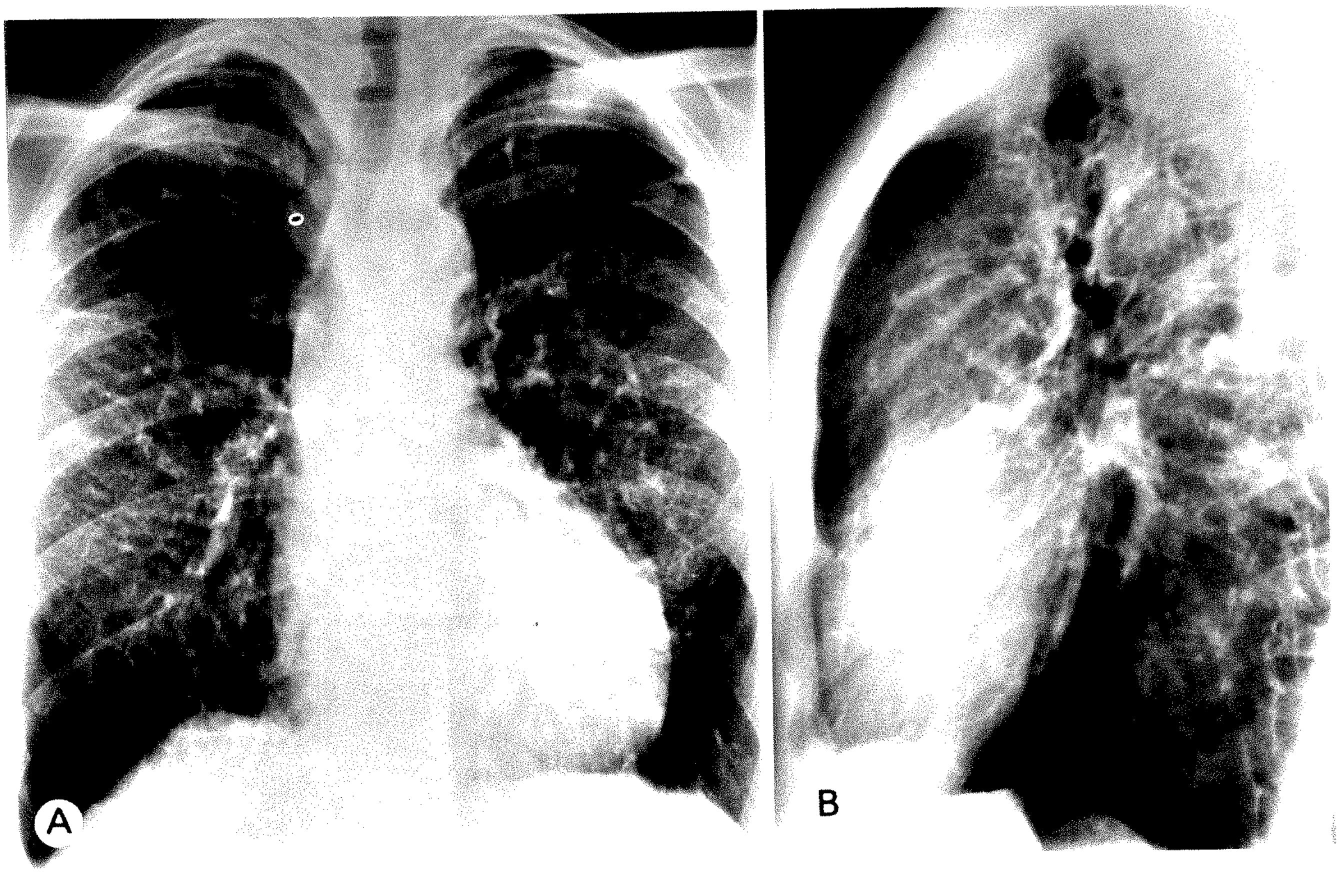

Fig. 8.—Posteroanterior (*A*) and lateral (*B*) chest films of patient with absent pulmonary arteries (truncus arteriosus type IV). Right and left branches of main pulmonary artery are not visualized.

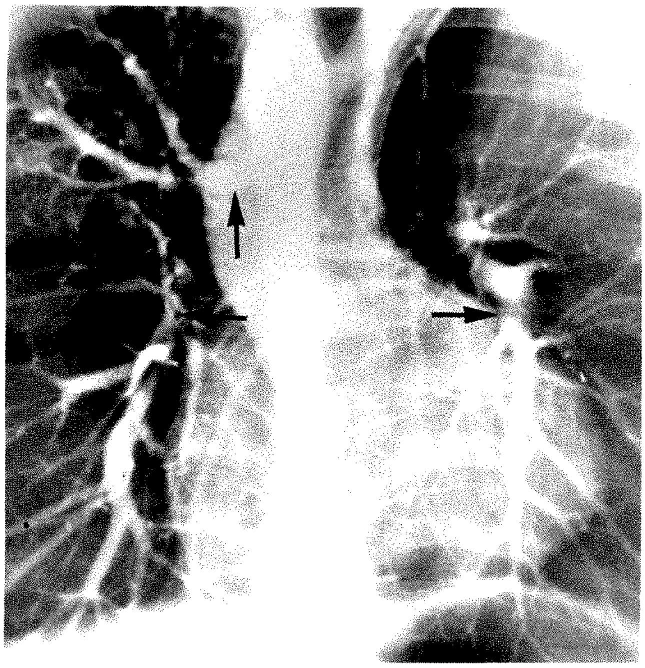

Fig. 9.—Aortogram of patient with nonconfluent right and left pulmonary arteries showing several small bronchial arteries supplying right and left lungs. In addition, large bronchial artery supplies right upper lobe (*vertical arrow*). Vessels outlined by horizontal arrows have angiographic appearance of pulmonary arteries. These two vessels are not confluent and their proximal parts are within hilum of each lung.

was absent in three patients and indeterminate in two. Peripheral pulmonary vascularity was diminished in four patients and normal in one. Peripheral collateral circulation was absent in each patient, and abnormal hilar vessels were identified in only one patient. Analysis of the chest films in this group does not demonstrate any unique characteristics which permit differentiation from other subsets of these malformations.

Discussion

The major challenge to the cardiac radiologist studying patients with congenital pulmonary atresia is to provide precise knowledge of the absence or presence, size, and distribution (confluent central, nonconfluent central, or peripheral) of the left and right pulmonary arteries. This information allows the surgeon to decide whether palliative or corrective surgery is possible and/or advisable. In those cases without pulmonary arteries, surgery is not possible. Pulmonary arteries were present and confluent in 41 of the 66 patients (62%), nonconfluent in five (8%), absent in 15 (23%); in five (8%) a mixed distribution existed.

Aortography in the conventional anteroposterior view showed systemic arteries (bronchial) originating from the upper descending thoracic aorta supplying both lungs in 24 of 51 patients (47%) in whom pulmonary arteries were identified. It is this subset of patients with congenital pulmonary atresia with ventricular septal defect who require special attention by the cardiac radiologist. The presence of pulmonary arteries may not be identified without either selective angiograms of the bronchial arteries or a semiaxial craniocaudal view to separate the overlapping pulmonary artery from the bronchial collateral arteries (figs. 3 and 4). Since lack of identification of pulmonary arteries deems the patient inoperable, either of these specialized angiographic methods should be used when pulmonary arteries are not readily identified by conventional aortography.

The decision for or against surgery also requires the following details which must be defined angiographically: (1) atrioventricular relations; (2) presence, position, and anatomy of both a right and left ventricle and their respective atrioventricular valves; (3) position and origin of the aorta; (4) location, size, and number of ventricular septal defects; (5) absence or presence, size, and distribution (confluent central, nonconfluent central, or peripheral) of the left and right pulmonary arteries; and (6) source of pulmonary blood flow.

Situs solitus of the viscera and atria occurred in 95% of this series, and the atrioventricular relation was concordant in 94%. There was biventricular origin of the aorta in 72%; it arose completely from the right ventricle in 9% and from the left ventricle in 9%. Corrective surgery was performed in 29 of the 66 patients; in each case the angiographic definition of right ventricular and central pulmonary artery anatomy was verified. The right ventricle had an underdeveloped or absent infundibulum, with either atresia of the pulmonary valve or main pulmonary artery. The ventricular septal defect was single, large, and located either in the typical position found in classic tetralogy of Fallot or slightly more anteriorly, as often found in truncus arteriosus types I and II.

When the aorta originates both from the left and right ventricle so that it overrides the ventricular septal defect, the anatomy of the right ventricle is similar to that of tetralogy of Fallot. The infundibulum is absent or severely underdeveloped and the cephalad margin of the ventricular septal defect is formed by the aortic valve leaflets. The aorta is large and aorticmitral valve continuity is ususally present (fig. 1A).

When the aorta originates entirely from the right ventricle, the appearance of the right ventricle is similar to normal. The infundibulum is usually well developed and there is discontinuity between the aortic valve and the atrioventricular values. The ventricular septal defect is usually located more anteriorly than in classical tetralogy of Fallot. The left ventricle is a posterior chamber with no outlet except for the ventricular septal defect (fig. 1B).

When the aorta originates from the morphologic left ventricle, the angiographic appearance of the left ventricle is similar to that of the normal heart. The ventricular septal defect is almost always located in the anterior interventricular septum in the left ventricular outflow tract (fig. 1*D*).

When atrioventricular discordance is associated with pulmonary atresia, the intracardiac angiographic anatomy is similar to that of corrected transposition if the aorta arises from the right ventricle (fig. 1*C*). When the aorta arises from the left ventricle and there is atrioventricular discordance, the angiographic anatomy is similar to that in isolated ventricular inversion.

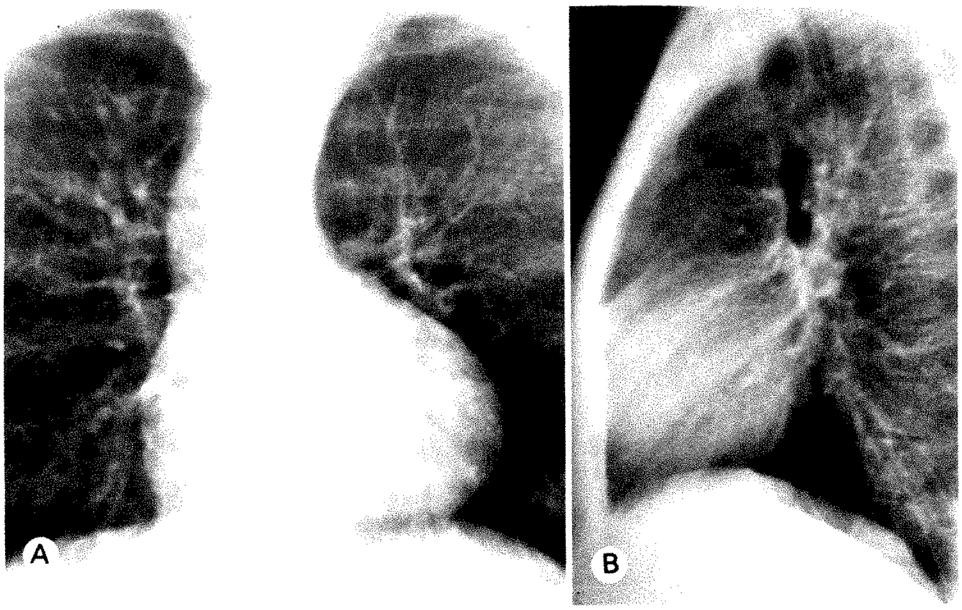

Fig. 10.—Posteroanterior (*A*) and lateral (*B*) chest films of child with nonconfluent right and left pulmonary arteries showing slightly enlarged heart with upturned apex and right aortic arch. Large vascular shadow is seen in right suprahilar region, indicating presence of abnormal vessel. Right and left pulmonary arteries not identified in *B*.

The plain chest radiograph does not permit differentiation of the various subsets of congenital pulmonary atresia with ventricular septal defect from each other or from classical tetralogy of Fallot. These types of malformations may be suspected when a heart of normal size is associated with a concave or absent pulmonary artery segment, reduced peripheral pulmonary vascularity, and, in some cases, the presence of unilateral or bilateral abnormal hilar vessels.

REFERENCES

1. Edwards JE, McGoon DC: Absence of anatomic origin from the heart of pulmonary arterial supply. *Circulation* 47:393–398, 1973
2. Kirklin JW, Pacifico AD: Surgical treatment of congenital heart disease, in *The Heart*, edited by Hurst JW, New York, McGraw-Hill, 1974, pp 758–761
3. Pacifico AD, Kirklin JW, Bargeron LM Jr, Soto B: Surgical treatment of common arterial trunk with pseudotruncus arteriosus. *Circulation* 49, suppl. 2:II 20–II 26, 1974
4. Shinebourne EA, Macartney FJ, Anderson RH: Sequential chamber localization: logical approach to diagnosis in congenital heart disease. *Br Heart J* 38:327–340, 1976
5. Kirklin JW: Surgical treatment of patients with absence of direct anatomic continuity between pulmonary arterial system and the heart and ventricular septal defects, in *Heart Disease in Infancy*, edited by Barratt-Boyes BG, Newtze JN, Harris EA, Baltimore, Williams & Wilkins, 1973, pp 211–220
6. Somerville J: Management of pulmonary atresia. *Br Heart J* 32:641–651, 1970
7. Collett RW, Edwards JE: Persistent truncus arteriosus: a classification according to anatomic types. *Surg Clin North Am* 29:1245–1270, 1949

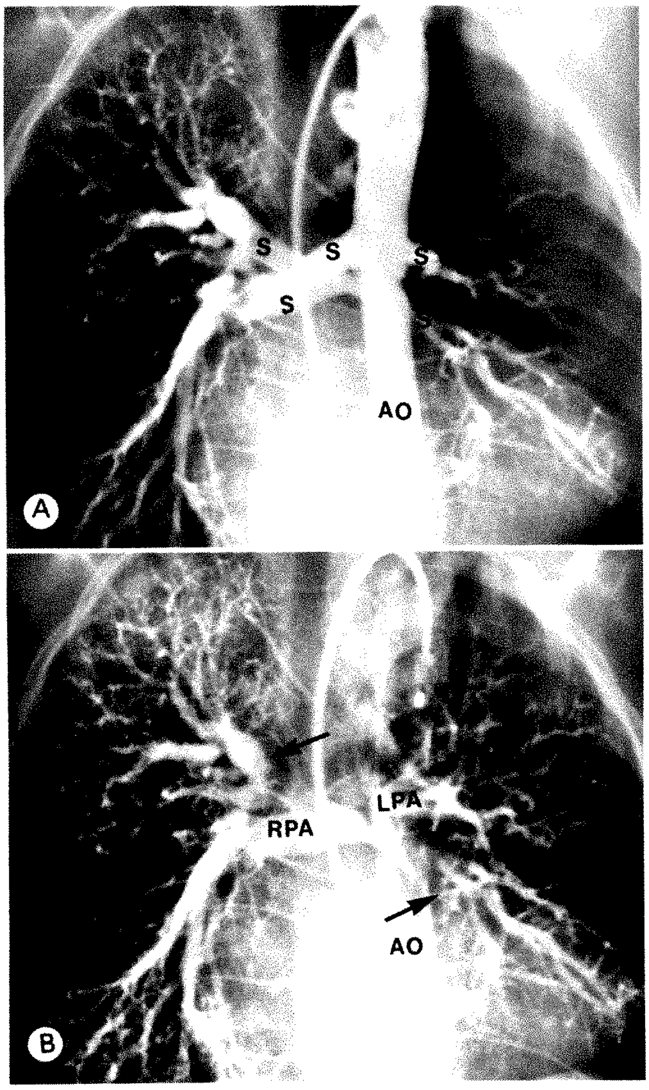

←

Fig. 11.—Aortogram in patient with mixed type. Early (*A*) and late (*B*) phase showing systemic bronchial arteries (S) originating from descending aorta providing circulation to right and left lungs. Right (RPA) and left (LPA) pulmonary arteries, not seen in *A*, are well visualized in *B*. Right upper lobe and left lower lobe are supplied solely by bronchial arteries (*arrows*).

8. Marcelletti C, Mair DD, McGoon DC, Wallace RB, Danielson GK: Complete repair of transposition of the great arteries with pulmonary atresia. *J Thorac Cardiovasc Surg* 72:215–220, 1976
9. Baker WP, Kelminson LL, Turner WM Jr, Blount SG Jr: Absence of pulmonic valve associated with double-outlet right ventricle. *Circulation* 36:452, 1967
10. Proceedings of the annual meeting of the Netherlands' Society of Radiology, April 1971. *Radiol Clin Biol* 42:169–176, 1973
11. Campbell M, Gardner F: Radiographic features of enlarged bronchial arteries. *Br Heart J* 12:183–200, 1950
12. Klinkhamer AC: Angiography in candidates for total correction of persistent truncus arteriosus or pseudotruncus arteriosus. *Radiol Clin Biol* 42:169–176, 1973
13. Jefferson K, Rees S, Somerville J: Systemic arterial supply to the lungs in pulmonary atresia and its relation to pulmonary artery development. *Br Heart J* 34:418–427, 1972
14. Chesler E, Beck W, Schrire V: Selective catheterization of pulmonary or bronchial arteries in the preoperative assessment of pseudotruncus arteriosus and truncus arteriosus, type IV. *Am J Cardiol* 26:20–24, 1970
15. Levin DC, Baltaxe HA, Goldbert HP, Engle MA, Ebert PA, Sos TA, Levin AR: The importance of selective angiography of systemic arterial supply to the lungs in planning surgical correction of pseudotruncus arteriosus. *Am J Roentgenol* 121:606–613, 1974
16. Vix VA, Klatte EC: The lateral chest radiograph in diagnosis of hilar and mediastinal masses. *Radiology* 96:307–316, 1970

Contrast Medium Reactions Correlated with Time of Day

JEROME J. CUNNINGHAM[1]

Dynamic physiologic and psychological changes occur in patients awaiting excretory urography. A total of 2,000 patients were studied to see if rates of reaction to urographic contrast materials are influenced by the time of day such injections are given. Examinations performed between 7:00 A.M. and 2:00 P.M. were evaluated. The data suggest that reactions to radiographic contrast medium occur randomly and that a "safe" or "safer" time of day cannot be defined.

There are at least two reasons to speculate that the rate of adverse reactions to urographic contrast medium might vary with the time of day such injections are given. First, studies of circadian rhythms in man and higher primates have shown that endogenous antiinflammatory steroid levels fall steeply after reaching a high plasma value at approximately 6:00 A.M. [1-3]. If there is a positive link between contrast reactions and steroid levels, as proposed by some [4], it is not unreasonable to speculate that early morning urographic studies might be "safer" than those performed later in the day when endogenous steroid production is reduced.

Lalli [5] has attempted to associate high levels of anxiety with adverse contrast medium reactions. Patients awaiting urography are awakened early because of normal hospital activities. They are deprived of food and water for varying intervals, and most are aware that an unpleasant examination is imminent. Measures taken to provide informed consent may be applied either as verbal explanations or the signing of forms. All of these mechanisms can reasonably be expected to provoke anxiety which increases as time lapses. If these speculations concerning anxiety are correct, an early morning urogram might also be "safer" than one performed later in the day when anxiety levels have risen.

In order to ascertain whether the rate of reactions during urography is influenced by the time of the injection, we studied a group of unselected patients.

Subjects and Methods

Over a 1 year period, 2,000 consecutive adult patients having urography were observed for adverse reactions to contrast medium. The presence or absence of a reaction was recorded on a form which also required notation of the time of day the injection was given. Resident physicians giving the injections were unaware of the aim of the study, and the forms were submitted anonymously to insure a candid evaluation.

Hospital patients and outpatients were assigned random appointments. Each patient had been given laxatives the evening before, and the patients had no food or liquids from midnight unless there was a contraindication to the preparation such as renal failure, diabetes, hyperuricemia, or hyperproteinuric states. Physicians giving the injections were instructed to pleasantly tell the patient that an injection would be given which would allow the kidneys to become visible on the subsequent radiographs. Most patients were told prior to the injection that a warm feeling or unpleasant taste might occur. Otherwise, there was no formal conversation except that any question a patient might ask was honestly answered.

The dose of contrast medium given was 1.1 ml/kg of meglumine diatrizoate rounded to the nearest 50 ml if renal function was normal; 2.2 ml/kg was injected if the serum creatinine was elevated. All injections were given as a bolus over 1-2 min. A check sheet was completed on each patient indicating no reaction, one or more subjective reactions (severe nausea, retching, faintness without change in pulse or blood pressure, panic, nervousness), or one or more objective reactions (hives, change in pulse or blood pressure, facial edema, respiratory muscle spasm, sneezing, nasal congestion).

Results and Discussion

Examinations performed between 7:00 AM and 2:00 P.M. were evaluated. Of the 2,000 cases, 118 were excluded because of an injection after 2:00 P.M., illegible reporting, or insufficient data. In my opinion the study group reflects a reasonable sample of the patients that might undergo urography in a busy hospital radiology department over a 1 year period, and the time interval selected is a reasonable estimation of the average working day for urographic procedures.

The correlation of reaction rates with time of day is shown in table 1. The overall reaction rate was 7%, of which most were subjective problems requiring no therapy. There were no life-threatening complications, and the most vigorous treatment used was the injection of antihistamines or small doses of dilute epinephrine to reduce facial edema or bronchospasm.

Statistical analysis of the reaction rates as related to time of day showed a completely random distribution. For example, when time of day was correlated with combined objective/subjective reaction rates including two apparent aberrant values of 9.1% and 11.2%, the *P* value was .5737. This calculation indicates a high probability that rates of reaction are independent of time. Additionally, there was no correlation with subjective reactions alone and time of day, objective reactions alone and time of day, sex of the patient, or clinical indication for the examination. Age distribution was totally random, with approximately 25 patients in each of the decades between ages 20 and 70.

This study suggests that given a sample population of moderate size operating within a restricted time frame, there is no particularly "safe" time period in the course

---

Received January 17, 1977; accepted after revision July 1, 1977.

[1] Department of Radiology, Bowman Gray School of Medicine, Winston-Salem, North Carolina 27103.

TABLE 1

Reactions by Time of Day

Time Injection Given	No. Patients	Reactions			Reaction Rate (%)
		Subjective	Objective	Total	
7:00-7:59 AM	222	9	3	12	5.4
8:00-8:59 AM	339	26	5	31	9.1
9:00-9:59 AM	504	26	7	33	6.5
10:00-10:59 AM	398	19	8	27	6.8
11:00-11:59 AM	282	13	5	18	6.4
12:00-12:59 PM	89	8	2	10	11.2
1:00-1:59 PM	48	3	0	3	6.2
Total	1882	104 (5.5%)	30 (1.6%)	134 (7.1%)	...

of an average working day when reaction rates to urographic contrast medium are perceptibly lower.

ACKNOWLEDGMENT

I thank Dr. David Groves for performing the statistical analyses.

REFERENCES

1. Faiman C, Winter JS: Diurnal cycles in plasma FSH, testosterone and cortisol in men. *J Clin Endocrinol Metab* 33:186-192, 1971
2. Rose RM, Kreuz LE, Holaday JW, Sulak KJ, Johnson CE: Diurnal variation of plasma testosterone and cortisol. *J Endocrinol* 54:177-178, 1972
3. Michael RP, Setchell KDR, Plant TM: Diurnal changes in plasma testosterone and studies on plasma corticosteroids in non-anesthetized male rhesus monkeys. *J Endocrinol* 63:325-335, 1974
4. *Proceedings of the National Uroradiological Conference.* Chicago, American College of Radiology, 1974.
5. Lalli AF: Urographic contrast media reactions and anxiety. *Radiology* 112:267-271, 1974

Accuracy of Bipedal Lymphography in Hodgkin's Disease

MICHAEL THOMAS KADEMIAN[1] AND GEORGE W. WIRTANEN[1]

Bipedal lymphography was used as part of the initial staging evaluation of 145 patients with Hodgkin's disease. Histologic correlation was available in 131 patients. The accuracy of interpretation was 95%. A review of other large series confirms that at least 85%-90% accuracy can be expected. Reasons for false positive and false negative interpretations are discussed.

Bipedal lymphography is routinely used in the evaluation of patients with the diagnosis of Hodgkin's disease. Despite the common use of this procedure, there have been relatively few reports on the accuracy of interpretation in large series. This report evaluates the accuracy of interpretation of bipedal lymphography in 131 patients with surgical histologic correlation. A summary of results in other large series is included.

Subjects and Methods

Since 1970, 145 patients with the diagnosis of previously untreated Hodgkin's disease have undergone bipedal lymphographic examination. All patients later underwent exploratory staging laparotomy. Because inappropriate node sampling occurred in 14 patients, only 131 could be evaluated for the accuracy of lymphographic interpretation.

All lymphograms were bipedal, using marker FDC Blue no. 1, cannulation with 30 gauge needles, with hair-clip stabilization, a gravity injection system, and Ethiodol, usually 4-5 ml unilaterally. This amount was sufficient to result in thoracic duct and mediastinal and supraclavicular node opacification. Vascular phase films followed the procedure, and nodal phase films were usually taken the following day or at 72 hr for procedures done with an intervening weekend.

The criteria for positive interpretation in Hodgkin's disease have been extensively described [1-4]. Characteristic findings include lacunar defects seen as punched out, rounded, small or large filling defects in the nodes which result in the characteristic accentuated reticular pattern. Absence of nodal opacification may indicate complete replacement by malignancy. Abnormal displacement of lymphatic vessels, collateralization on vascular phase films, or persistence of contrast material in lymphatic vessels on 24 hr radiographs may be present with Hodgkin's disease.

Lymphograms were interpreted as positive or negative for malignancy, with no equivocal category. Studies thought to be abnormal due to inflammatory or other benign conditions were so described. Similarly, studies thought to represent changes consistent with Hodgkin's disease were interpreted positive for malignancy. Only the interpretations positive for malignancy were considered positive; all others were considered negative.

Results

Although 145 patients had bipedal lymphography as part of the initial evaluation of the extent of their Hodgkin's disease, only 131 are available for histological correlation. Fourteen patients were excluded because surgeons failed to biopsy nodes which were positive radiographically. The incidence of surgical failure to biopsy microscopically involved nodes in negative lymphograms is indeterminate.

In 30 patients the lymphogram was interpreted as positive. Histologic examination revealed the presence of Hodgkin's disease in 26 of these patients, for an accuracy rate of 87%.

The remaining 101 studies were interpreted as negative. Of these 101, 98 were histologically confirmed to have no involvement with Hodgkin's disease, an accuracy rate of 97%. The correct interpretation was made in 124 of 131 patients, for an overall accuracy rate of 95%.

The radiographs and histologic specimens were reviewed in all patients in whom discrepancies occurred between the lymphographic interpretation and histologic findings. In two of the four false positive cases the lymphogram was interpreted as positive in the periaortic nodes. Histologic review showed reactive hyperplasia in these nodes. This histologic finding was thought compatible with the radiographically positive appearance of the lymph nodes. The lymph nodes in the third false positive case were normal histologically, and on retrospective review the radiographs were thought to show no evidence of lymphomatous involvement in opacified lymph nodes. The original interpretation was considered in error. Histologic sections of the fourth false positive case could not be located for review. In the three false negative interpretations, histologic review showed only small microscopic foci in periaortic nodes, too small to be detected by lymphography.

In four additional patients, positive celiac lymph nodes were obtained surgically, although the lymphogram was interpreted as negative. These nodes did not contain contrast or demonstrate changes consistent with post-lymphographic effect, and had not been opacified radiographically. They were all at the level of the celiac axis and were superior to nodes visualized with the bipedal study. These four studies were not considered false negatives since lymphographic evaluation was not possible because they were not visualized. The inability to opacify celiac nodes is an intrinsic limitation of the procedure.

Received June 8, 1977; accepted after revision August 16, 1977.

This investigation was supported in part by National Cancer Institute grant no. 5 PO1 CA 19278-01 to the Wisconsin Clinical Cancer Center; American Cancer Society Clinical Fellowship no. 4054 to M. T. Kademian; and the Ladish Foundation.

[1] Division of Radiation Oncology, Department of Human Oncology, University of Wisconsin Center for Health Sciences, 1300 University Avenue, Madison, Wisconsin 53706. Address reprint requests to G. W. Wirtanen.

Am J Roentgenol **129:1041-1042, December 1977**

TABLE 1

Accuracy of Lymphographic Interpretation in Hodgkin's Disease

Reference	Institution	No. with Histology	Equivocal	Lymphangiographic Interpretation				Overall Accuracy	
				Positive		Negative		No.	%
				No.	%	No.	%		
Castellino et al. [1]	Stanford	166	0	41/55	76	111/111	100	152/166	92
Glees et al. [2]	Royal Marsden	47	2	18/24	75	19/21	90	37/45	82
Martire [3]	Baltimore Cancer Center	60	0	13/22	59	38/38	100	51/60	85
Hellman [5]	Harvard	144	73*	25/31	81	38/40	95	63/71	89
Kaplan et al. [6]	Stanford	271	48	61/81	76	137/142	96	198/223	89
Banfi et al. [7]	NCI, Milan	104	2	29/29	100	70/73	96	99/102	97
Gamble et al. [8]	M. D. Anderson	. . .	. . .	134/139	96	. . .	. . .	. . .	. . .
Present report	Univ. Wisconsin	131	0	26/30	87	98/101	97	124/131	95

* Presumably.

Discussion

The radiographic criteria for positive interpretation have been described [1-4]. In this study, such criteria were employed, and an overall accuracy of interpretation of 95% was obtained. Survey of other large series confirms that accuracy of interpretation ranges from 82%–97% (table 1).

In this series seven lymphograms were incorrectly interpreted. In two of the false positive studies, benign changes were seen which were thought to explain the positive appearance of lymph nodes on lymphography. Castellino et al. [1] have shown that false positive lymphographic interpretations are usually secondary to nonspecific reactive changes in the lymph nodes such as fibrosis, sinus histiocytosis, reactive follicular hyperplasia, or amorphous hyaline deposition. The three false negative interpretations occurred in patients in whom Hodgkin's disease involvement of nodes was microscopic and too small to be detected lymphographically.

This study and other large series confirm that an accuracy rate of at least 90% can be expected. Of equal importance in staging of patients with Hodgkin's disease is the correct biopsy of nodes which have been interpreted as positive on lymphography. In this series, 14 patients (10%) had inappropriate nodes sampled, as confirmed by postoperative films. In the series of Castellino et al. [1], 13 of 179 cases had inappropriate node sampling at the time of laparotomy. One of the purposes of lymphography in Hodgkin's disease has been to provide surgeons with the information necessary for directed excisional node biopsy. To reduce the frequency of inappropriate node sampling, intraoperative radiography should be used.

Specimen radiography of lymph nodes interpreted as positive but negative histologically may suggest nodes for further sectioning which occasionally demonstrate a focus of Hodgkin's disease. ^{67}Ga scanning and computed tomography may provide significant clinical information in areas in which nodes do not opacify.

In summary, the accuracy of lymphographic interpretation in Hodgkin's disease approximates 90%. Surgical-radiographic correlation is essential. False positive interpretations occur with benign reactive changes. False negative studies are infrequent, except in early microscopic nodal involvement with Hodgkin's disease.

REFERENCES

1. Castellino RA, Billingham M, Dorfman RG: Lymphographic accuracy in Hodgkin's disease and malignant lymphoma with a note on the reactive lymph node as the cause of most false-positive lymphograms. *Invest Radiol* 9:155-164, 1974
2. Glees JP, Gazet JC, MacDonald JS, Peckham MJ: The accuracy of lymphography in Hodgkin's disease. *Clin Radiol* 25:5-11, 1974
3. Martire JR: Histologic correlation of lymphograms in Hodgkin's disease: an evaluation of diagnostic criteria. *South Med J* 67:1317-1321, 1974
4. Viamonte M: Current status of lymphography. *JAMA* 222:1299-1301, 1972
5. Hellman S: Current studies in Hodgkin's disease, what laparotomy has wrought. *N Engl J Med* 290:894-898, 1974
6. Kaplan HS, Dorfman RF, Nelsen TS, Rosenberg SA: Staging laparotomy and splenectomy in Hodgkin's disease: analysis of indications and patterns of involvement in 285 consecutive, unselected patients. *Natl Cancer Inst Monogr* 36:291-301, 1973
7. Banfi A, Lattuada A, Musumeci R: Lymphography and laparotomy in Hodgkin's disease: their prognostic value and relevance in the therapeutic program, in *Radiology, Proceedings of the 13th International Congress of Radiology*, vol 2, edited by Gomez-Lopez J, Bonmati J, Amsterdam, Excerpta Medica, 1974, pp 11-16
8. Gamble JF, Fuller LM, Martin RG, Sullivan MP, Jing BS, Butler JJ, Schullenberger CC: Influence of staging celiotomy in localized presentation of Hodgkin's disease. *Cancer* 35:817-825, 1975

Primary Chylopericardium: The Role of Lymphangiography

THOMAS E. GALLANT,[1] ROBERT J. HUNZIKER,[1] AND THOMAS C. GIBSON[2]

Primary chylopericardium is often a benign asymptomatic disease, but patients with associated mediastinal lymphatic tumors may develop cardiac tamponade. Lymphangiography demonstrates mediastinal lymphatic abnormalities in these high risk patients on whom subtotal pericardiectomy and thoracic duct ligation should be performed. Since such tumors have been found in half of reported cases and because extrathoracic lymphangiomas may coexist, lymphangiography with skeletal survey is recommended in all cases. These conclusions are based on a review of 31 published cases and an additional case of our own. Lymphangiographic findings were available in 17 of these patients.

Chylopericardium is a rare cause of an enlarged cardiac silhouette; a literature review yielded only 38 cases [1–15]. Each case was carefully scrutinized for laboratory or clinical data suggesting underlying disease processes. Patients in whom chylopericardium was associated with surgery, inflammation, radiation, nonlymphatic tumor, or chylothorax were eliminated from the analysis. On that basis we were able to define 31 cases of primary chylopericardium, and we report an additional case with special reference to the lymphangiographic findings.

Case Report

A 19-year-old white female was admitted for evaluation of cardiomegaly noted on a nursing school entrance chest radiograph. The patient was otherwise healthy and entirely asymptomatic. No significant environmental exposures were known, and

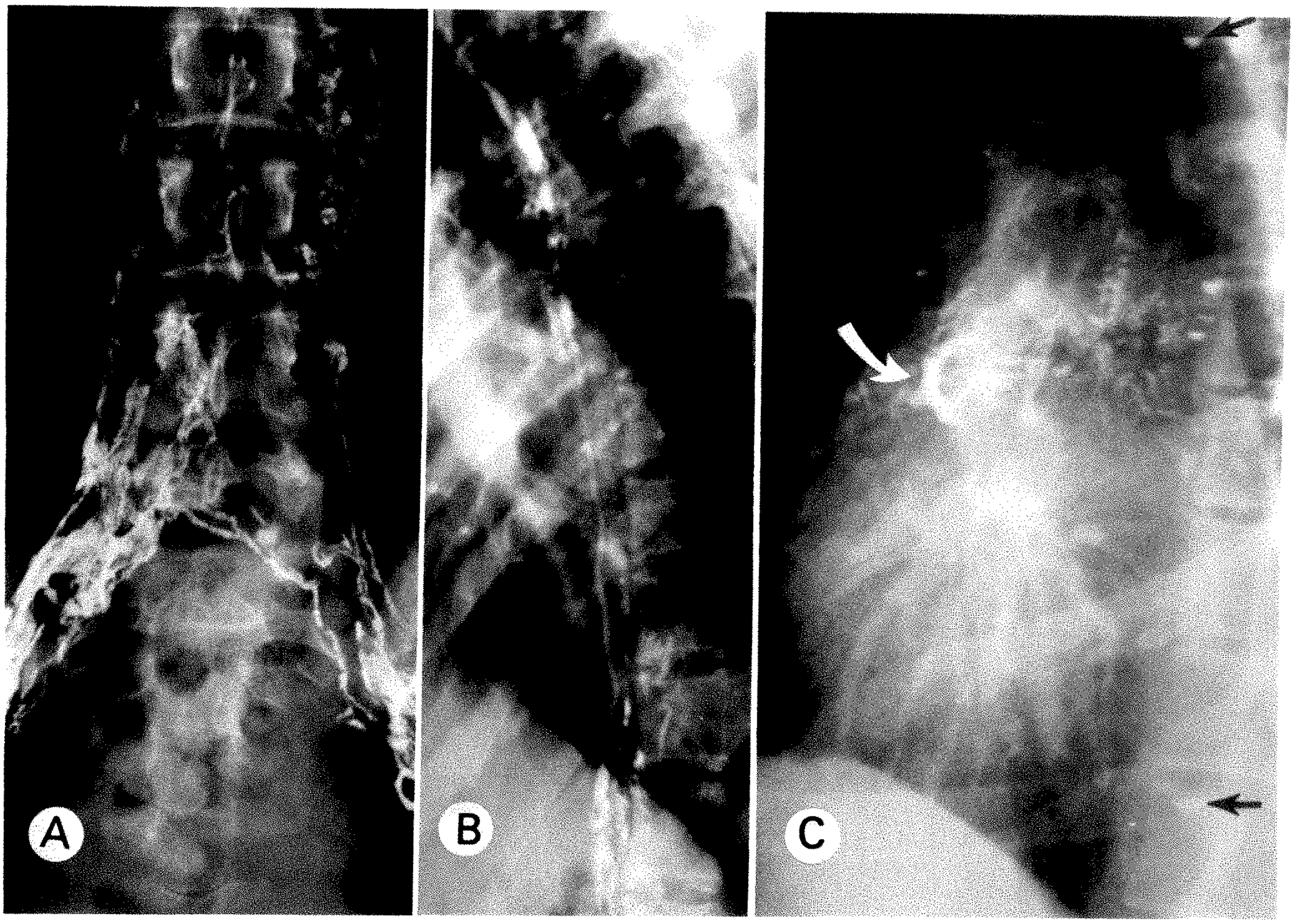

Fig. 1.—Anteroposterior abdominal film (*A*) and lateral chest film (*B*) during lymphatic injection showing multiple mildly ectatic lymph channels. *C*, Oblique chest film 5 hr after injection showing large plexus of abnormal lymphatics in upper mediastinum (*white arrow*) and contrast-lymph fluid levels (*black arrows*) posteriorly.

Received March 7, 1977; accepted after revision July 28, 1977.

[1] Department of Radiology, University of Vermont College of Medicine and Medical Center Hospital of Vermont, Mary Fletcher Unit, Burlington, Vermont 05401. Address reprint requests to T. E. Gallant.

[2] Department of Medicine, University of Vermont College of Medicine and Medical Center Hospital of Vermont, Burlington, Vermont 05401.

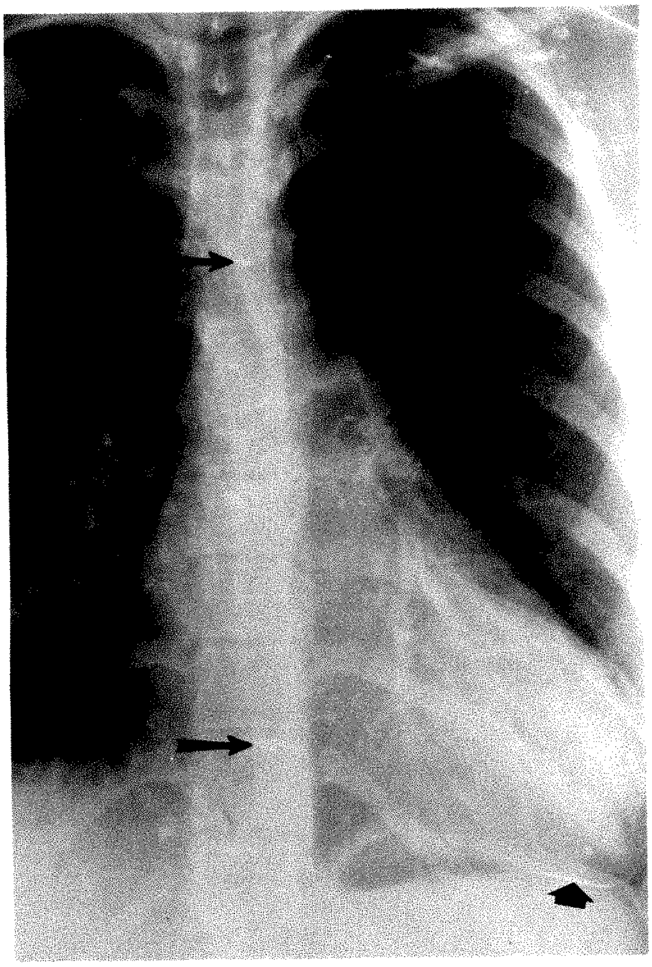

Fig. 2.—Posteroanterior chest film 24 hr after injection showing pooled contrast material in pericardium (*short arrow*). Dilated posterior lymphatics remain filled (*long arrows*).

the review of systems was negative except for an episode of acute epiglottitis requiring tracheostomy at age 4. Recovery from that illness was prompt and without complication.

Physical examination revealed a blood pressure of 110/70 and an S4 gallop, but no evidence of elevated venous pressure or pulsus paradoxicus. There was no peripheral edema and the patient was afebrile. She was not anergic and an intermediate strength PPD was negative. An electrocardiogram showed nonspecific T-wave flattening. The chest radiograph showed only cardiomegaly.

Thyroid function tests, Westergren sedimentation rate, antinuclear antibody screen, lupus cell preparation, rheumatoid factor, and syphilis serology were all normal. An echocardiogram showed a large pericardial effusion. Percutaneous pericardiocentesis yielded 250 ml of chylous fluid with a white blood cell count of 6,400/ml, 96% of which were lymphocytes. The aspirate contained 118 mg/100 ml of cholesterol, 6.7 mg/100 ml of total protein, and 112 mg/100 ml of glucose. Titers of antinuclear antibody and rheumatoid factor were normal in the fluid. No bacteria or mycobacteria were seen on smears of the aspirate, and cultures were sterile.

Bipedal lymphangiography, performed 3 days after pericardiocentesis, showed irregularly ectatic paraaortic, abdominal, and thoracic lymphatic channels (figs. 1*A* and 1*B*). A large plexus of abnormal lymphatics were opacified in the upper mediastinum at 5 hr (fig. 1*C*). Contrast pooled in the pericardium on upright radiographs taken at the completion of lymphatic injection and 24 hr later (fig. 2). Paratracheal and perihilar nodes were also opacified but appeared normal. When diagnostic studies were completed, the patient was discharged. During careful follow-up (10 months), she has remained asymptomatic. No surgery is planned unless clinical evidence of deterioration is found.

TABLE 1

Clinical and Surgical Findings

	No.	%
Sex:		
Male	18	56
Female	14	44
Symptoms:		
None	14	44
Dyspnea	13	41
Cough	4	12
Edema	2	6
Surgical findings:		
Normal	10 (2)*	31
Lymphangiectasis	11 (2)*	34
Lymphatic tumor	6 (2)	19
Pericardial thickening	2 (1)	6
No data	3	9

Note.—Patients ranged in age from 1 day to 62 years. Numbers in parentheses are patients with tamponade.

* One of the two had tamponade only after pericardiocentesis.

TABLE 2

Lymphangiographic findings

Finding	No.	%
Normal	6	35
Thoracic duct obstruction	4	24
Lymphangiectasia	8	47
Pericardial pooling	4	24
Extrathoracic lymphatic abnormalities	4	24

Note.—Data on 17 patients who underwent lymphangiography.

Discussion

Primary chylopericardium is an uncommon cause of pericardial effusion; it has been associated with abnormal thoracic lymphatics in over half of the reported cases. Clinical and surgical findings are summarized in table 1. Several mechanisms have been proposed to explain the development of chylous effusions. Most secondary effusions are caused by interruption of the thoracic duct by surgery, inflammation, or nonlymphatic tumor. Normal lymphatic valves prevent chylous reflux into the pericardial plexus even after ligation of the thoracic duct proximal to the pericardial tributaries, unless concurrent superior vena caval ligation prevents collateral flow [16, 17]. Valvular incompetence in otherwise normal lymphatics could permit chyle to reflux into the pericardium. Blunt chest trauma may rupture lymphatic valves, as it ruptures bronchi, by precipitously elevating intrathoracic pressure.

Most primary chylous pericardial effusions result from retrograde flow through abnormal lymphatics into the rich pericardial plexus. Such abnormal lymphatic channels may represent small lymphangiomas, or they may be a part of larger lymphatic tumors [2]. Distinctions between true neoplasms and lymphatic malformations are often not clear-cut [18, 19]. Small collections of ectatic vessels were found more commonly in reported cases than were larger tumors.

Radiographically manifest masses have not been found in reported cases of primary chylopericardium. The lymphatic tumors and malformations were small and obscured by adjacent mediastinal structures, as noted by Pachter and Lattes [18] in their review of mediastinal lymphatic tumors. Most of the tumors were found in the posterior mediastinum.

Rectilinear scanning of the chest at 6 and 24 hr after oral administration of ^{131}I-triolein showed nuclide pooling in the mediastina of three patients. False negative results were obtained in one patient who was scanned at 6 hr only [15]. Scanning gives little detailed information about underlying abnormalities and has not demonstrated extrathoracic lymphangiomas.

It is clear that the true morphology of the lymphatic lesions is best demonstrated by lymphangiography. Thoracic lymphangiectasis was demonstrated in eight of 17 patients who underwent lymphangiography, and four showed pericardial contrast pooling. Extrathoracic lymphatic abnormalities were found in four patients (table 2). Primary chylopericardium may be associated with generalized lymphangiomatosis in adults, but children with multifocal disease have not had pericardial involvement [19–21]. A skeletal survey is recommended to rule out associated bony lesions in adults, and lymphangiography is useful to assess the extent of local and systemic involvement [20, 22].

It is important to note that demonstrable abnormalities of thoracic lymphatic vessels were present in four of five patients who presented with cardiac tamponade and in one of two patients who developed tamponade after pericardiocentesis. Tamponade was absent in 12 other patients with demonstrable thoracic lymphatic abnormalities. In patients with mediastinal lymphatic abnormalities, subtotal pericardiectomy and proximal thoracic duct ligation are recommended to avoid tamponade. Intractable chylothorax may develop if pericardial drainage is not accompanied by ductal ligation. Repeat surgery is then necessary, and two fatalities have been reported [2, 7].

REFERENCES

1. Groves LK, Effler DB: Primary chylopericardium. *N Engl J Med* 250:520–523, 1954
2. Dunn RP: Primary chylopericardium: a review of the literature and an illustrated case. *Am Heart J* 89:369–377, 1975
3. Jenner RE, Oo HLA: Isolated chylopericardium due to mediastinal lymphangiomatous hamartoma. *Thorax* 30:113–117, 1975
4. Servelle M, Letvitcharov P, Andrieux JB, Zafari I, Jabbour J, Harnaez E, Thiollet J: Le chylopericarde: mechanisme de production. *Ann Chir Thorac Cardiovasc* 11:211–216, 1972
5. Longeais Y, Feuillu J, Kerdiles Y, Helou JY, Thomet J, Coutel Y, Ferrand B: Une observation de chylopericarde: problemes diagnostiques et therapeutiques. *Ann Chir Thorac Cardiovasc* 11:231–238, 1972
6. Ketelers JY, Dupuis C, Soots G, Lerche E, Dubar P: Le chylopericarde (à propos d'une observation). *Ann Chir Thorac Cardiovasc* 11:228–229, 1972
7. Conso JF, Binet JP, Langlois J, Planche C, Belloy A, Domart A, Modai J: Chylopericarde isolé, à propos d'une cas: révue des cas publiés. *Ann Chir Thorac Cardiovasc* 11:217–222, 1972
8. Patney NL: Primary massive chylopericardium. *J Indian Med Assoc* 62:318–321, 1974
9. Warembourg H, Ribet M, Pauchant M, Macquet V, Tonnel-Levy M, Ducloux G: Le chylopericarde isolé. *Lille Med* 20:672–677, 1975
10. Delaney A, Daicoff GR, Hess PJ, Victorica B: Chylopericardium with cardiac tamponade after cardiovascular surgery in two patients. *Chest* 69:381–383, 1976
11. Lee CY, DiLoreto PC, Kim S: Isolated primary chylopericardium in pregnancy. *Obstet Gynecol* 43:586–591, 1974
12. Jacob T, DeLeval M, Stark J, Waterston DJ: Chylopericardium as a complication of aortopulmonary shunt. *Arch Surg* 108:870–871, 1974
13. Flejou Y, Despres JP, Guay JM: Observation de chylopericarde isolé: à propos d'une cas chez un nourrison, revue de la littérature. *Arch Mal Coeur* 67:611–618, 1974
14. Motoji T, Hiramori K, Nagara H, Mori K, Kondo M, Hashimoto A, Hirosawa K, Hiekata T, Matsumoto Y: Primary isolated chylopericardium. *Respir Circ* (Tokyo) 23:447–451, 1975
15. Savran SV, Ratshin RA, Shirley JH, Naguwa SM, Goodman L: Idiopathic chylopericardium: ^{131}I-triolein scan for noninvasive diagnosis. *Ann Intern Med* 82:663–665, 1975
16. Weidner WA, Steiner RM: Roentgenographic demonstration of intrapulmonary and pleural lymphatics during lymphangiography. *Radiology* 100:533–539, 1971
17. Cha EM, Sirijintakarn P: Anatomic variation of the thoracic duct and visualization of mediastinal lymph nodes: a lymphographic study. *Radiology* 119:45–48, 1976
18. Pachter MR, Lattes R: Mesenchymal tumors of the mediastinum. III. Tumors of lymph vascular origin. *Cancer* 16:108–117, 1963
19. Kittredge RD, Finby N: The many facets of lymphangioma. *Am J Roentgenol* 95:56–66, 1965
20. Goldstein MR, Benchimol A, Cornell W, Long DR: Chylopericardium with multiple lymphangioma of bone. *N Engl J Med* 280:1034–1037, 1969
21. Berberich FR, Bernstein ID, Ochs HD, Schaller RT: Lymphangiomatosis with chylothorax. *J Pediatr* 87:941–943, 1975
22. Collard M, Fievez M, Godart S, Toussaint JP: The contribution of lymphangiography in the study of diffuse lymphangiomatosis: report of a case with anatomic observations. *Am J Roentgenol* 102:466–470, 1968

Ether-dissolved Ethiodol for Lymphangiography: An Experimental Study

K. JONSSON,[1, 2] J. H. ANDERSON,[3] B. OSBORNE,[4] and S. WALLACE[1]

In order to decrease administration time, the viscosity of Ethiodol was reduced by mixing it with ether; this mixture was evaluated in lymphangiography of dogs. The ether-Ethiodol solution was injected into a cannulated lymph vessel of one hind limb and compared to pure Ethiodol in the other. For the ether-Ethiodol solution, the time required for complete injection was 10-30 min in most cases compared to 60-105 min for Ethiodol alone. The radiographic appearance of the lymph vessels and nodes appeared similar on both sides, and follow-up lymphangiograms in two animals after 1 and 3 weeks showed no difference from the original study. Microscopic examination of the opacified lymph nodes on both sides revealed no histologic differences. The technique has potential clinical application.

Introduction

Lymphangiography is a tedious procedure for the patient, often requiring 1-1.5 hr or more after lymphatic cannulation for the contrast medium to fill the pelvic and retroperitoneal lymph vessels. If pressure is used to increase the injection rate of contrast medium, lymph vessels may rupture, especially in the inguinal and iliac regions.

Different methods have been used to increase the rate of injection of Ethiodol without increasing the pressure of injection. The most common technique is to decrease the viscosity of the contrast medium by heating it to body temperature before injection [1]. Pharmacologic agents have also been used. Cumarin (5,6-benzo-α-pyron) mixed with Ethiodol dilates the lymph vessels and allows for an increase in the injection rate [2].

Diethyl ether has been mixed with oil-based contrast medium to reduce viscosity, thereby decreasing the time for contrast administration for lymphangiography [3, 4]. The injection time for lymphangiography in patients (6-10 ml in each extremity) was reported to be 5-10 min [3]. No complications were noted, other than a slight burning sensation along the leg during injection. No information on the morphologic effects of the ether-oil mixture on the lymph vessels or nodes was reported.

This report presents our experience with ether-dissolved Ethiodol for pedal lymphangiography in dogs, including information relating to histologic changes.

Materials and Methods

Twenty-two mongrel dogs weighing 17-25 kg underwent lymphangiography. The animals were anesthetized with intravenous pentobarbital sodium (30 mg/kg). Patent blue was injected in the interdigital spaces of both hind paws. A sterile cutdown procedure was used to isolate and cannulate a pedal lymph vessel. A mixture of Ethiodol and ethyl ether (Mallinckrodt, St. Louis, Mo.) was injected into the cannulated lymph vessel of one leg, while Ethiodol alone (3.25 ml) was injected into the contralateral cannulated lymph vessel. The ether-Ethiodol solution was made immediately before the start of the injection by carefully mixing in a sterile beaker 0.75 ml of ether via a sterile 1 ml glass tuberculin syringe to 2.5 ml of Ethiodol. The mixture was then quickly drawn into a 5 ml sterile glass syringe.

Injections were made using 0.91 kg weight on the barrel of the glass syringe supported on a stand. Identical syringes, catheters, and needles were used bilaterally, and the injections were started at the same time. In five animals, anteroposterior films of the lower limbs, pelvis, and abdomen were obtained at 2 and/or 5, 10, 15, 20, 25, and 30 min after the start of injection, then at 15 min intervals until the injection of contrast medium was completed on both sides. In 17 animals, similar films were obtained every 15 min for 1.5-2 hr after the start of injection.

Thirteen animals were sacrificed in order to obtain histologic evaluation of the opacified lymph nodes. Three animals were sacrificed 2-4 hr after completion of the contrast medium injection. The remaining dogs were sacrificed after 1 day (one animal), 2 days (two), 3 days (one), 5 days (two), 7 days (one), 18 days (one), and 21 days (two). Prior to the sacrifice, repeat bilateral lymphangiography with Ethiodol only was performed in two animals 7 and 21 days, respectively, after the first examination.

The lymph nodes of the sacrificed animals were located in the popliteal fossa, in the pelvis, and at the level of the aortic bifurcation. After dissection, the lymph nodes were bisected and fixed in formalin; after processing, slides were stained with hematoxylin and eosin. Slides were coded, examined, and described microscopically without prior knowledge of the individual protocol. The lymph nodes from similar locations on either side of the same dog were then compared. The degree of acute inflammation and accumulation of plasma cells was graded on a scale of 1-3. The appearance of vacuoles, the presence or absence of giant cells, and the formation of granulomas were noted.

Results

The time required for the injection of the solution of ether and Ethiodol was 10-30 min in all animals (fig. 1 *A*), except in three where it was 60-75 min. The corresponding injection time for Ethiodol alone was 60-105 min in all animals, except in one animal where it was 30 min. With few exceptions a completed injection resulted

---

Received June 9, 1977; accepted after revision September 2, 1977.

J. H. Anderson is the recipient of Research Career Development Award 5-K04-CA00083-02 RAD from the National Cancer Institute.

[1] Department of Diagnostic Radiology, University of Texas System Cancer Center, M. D. Anderson Hospital and Tumor Institute, Houston, Texas 77030.

[2] Present address: Department of Diagnostic Radiology, General Hospital, 214 01 Malmö, Sweden.

[3] Section of Experimental Diagnostic Radiology, University of Texas System Cancer Center, M. D. Anderson Hospital and Tumor Institute, 6723 Bertner Avenue, Houston, Texas 77025. Address reprint requests to J. H. Anderson.

[4] Department of Pathology, University of Texas System Cancer Center, M. D. Anderson Hospital and Tumor Institute, Houston, Texas 77025.

Am J Roentgenol **129:1047-1050, December 1977**

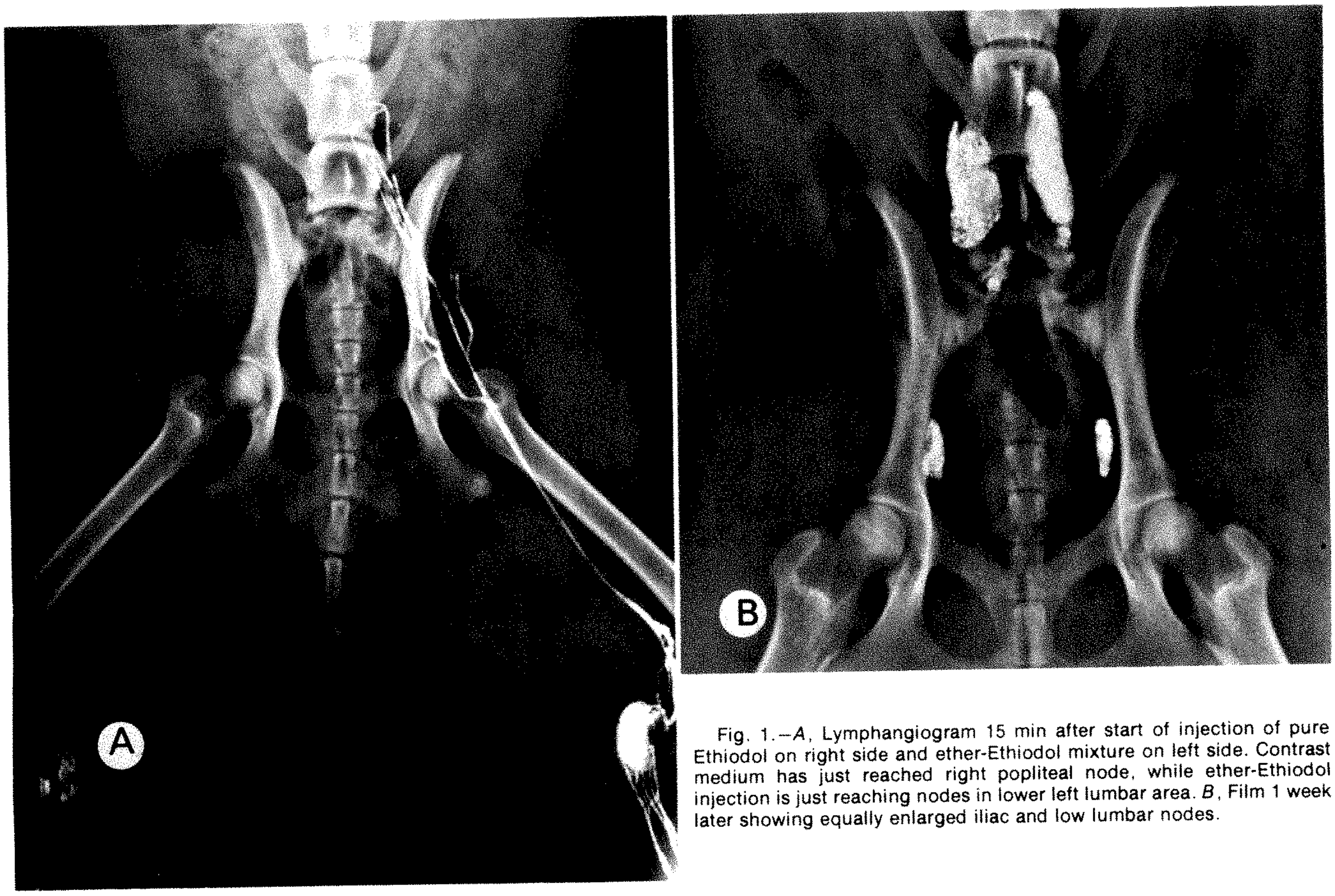

Fig. 1.—*A*, Lymphangiogram 15 min after start of injection of pure Ethiodol on right side and ether-Ethiodol mixture on left side. Contrast medium has just reached right popliteal node, while ether-Ethiodol injection is just reaching nodes in lower left lumbar area. *B*, Film 1 week later showing equally enlarged iliac and low lumbar nodes.

in opacification of the lymph nodes at the aortic bifurcation. There was no extravasation of contrast medium during injection.

The radiographic appearance of the lymph vessels and nodes was the same whether Ethiodol alone or the ether-Ethiodol mixture was used. Follow-up radiographs prior to sacrifice showed no difference in opacification of the nodes when the two sides were compared. In all animals where late films were obtained, enlargement of the opacified lymph nodes was evident (fig. 1*B*). This was most likely related to inflammatory response in the paws and lymph nodes due to the cutdown or the presence of contrast material. Repeat lymphangiography in two animals 7 and 21 days after the primary examination showed no difference in filling or radiographic appearance of lymph vessels or nodes (fig. 2).

The histologic examination of the lymph nodes showed no difference between the sides where pure Ethiodol and the combination of ether and Ethiodol were used. A reaction to the contrast medium was seen in all specimens sacrificed 2 days or more after the lymphangiography. Epithelioid histiocytic granulomas were seen in six specimens from three dogs evenly distributed between nodes from the sides receiving Ethiodol and those receiving the ether-Ethiodol mixture. The granulomas appeared to be part of the relatively late stage of reaction to contrast medium. Initially, there was an infiltrate of polymorphonuclear leukocytes and plasma cells, followed by the formation of giant cells at the periphery of the vacuoles containing media. In some of the nodes from dogs sacrificed 2–3 weeks after injection, there were occasionally more organized epithelioid histiocytic granulomas surrounding these vacuoles.

Discussion

Decreasing the administration time of contrast medium in lymphangiography has been accomplished by using pharmacologic agents which dilate the lymph vessels. Collard [2] mixed contrast medium with Cumarin in order to dilate the lymph vessels, reducing injection time from 3 to 1 hr. Ratkevich et al. [4] investigated the reduction of the viscosity of oily contrast media by means of heating or mixing with ether. In the range of 10°–50°C, an increase in temperature of 5°C results in the same reduction in viscosity as would occur by increasing the volume 2% by the addition of ether. However, a sophisticated injection pump is required to heat the contrast medium.

Ether has been used intravenously without adverse effects. Boely [5] used ether mixed with serum in 14 patients with chronic leg ulcers due to thromboplebitis, arteriosclerosis, or trauma. A solution of 6% ether was infused intravenously and, as a result, the pain from the

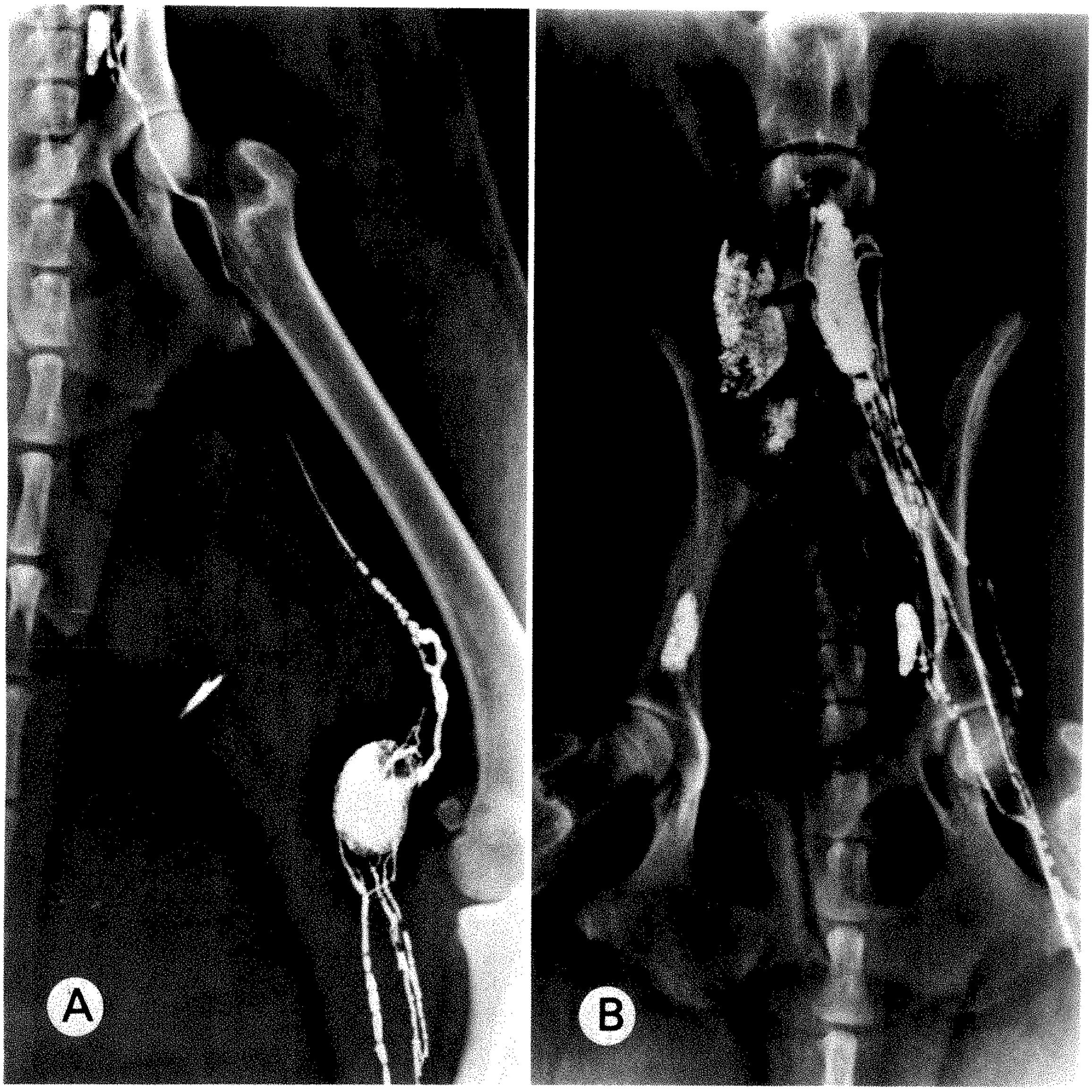

Fig. 2.—*A*, Repeat lymphangiography on left side showing lymph vessels of limb almost identical to primary study (fig. 1). *B*, Repeat lymphangiography at pelvic and lower lumbar level.

ulcers diminished considerably and healing was initiated. It was presumed that the dramatic effect was due to augmented capillary circulation.

Popov [3] used 2-3 ml of ether per 8 ml of oily contrast medium (iodlipol) for lymphangiography. The same ratio of ether and Ethiodol was used in our study. This proportion of ether reduced viscosity and, with three exceptions, resulted in an injection time of 10-30 min. It is difficult to explain the longer injection time in three animals which was similar to the contralateral side with pure Ethiodol. The time of preparation of the solution of ether-Ethiodol may be critical. To prevent evaporation of ether, this is now done immediately prior to injection. The barrel may have stuck or jammed against the wall of the syringe, giving a prolonged injection time.

Radiographically, no adverse side effects could be attributed to the pure Ethiodol or the ether-Ethiodol solution. The follow-up radiographs of the lymph nodes showed no abnormalities other than enlargement, which occurred with both contrast agents. In the two animals where follow-up lymphangiography was performed, the appearance of the lymph vessels was the same as at the primary examination (fig. 2). Even the valves of the lymph vessels appeared the same. Sclerosing or other adverse effects on the lymph vessels could not be established radiographically. There is no doubt that some of the ether immediately diffused through the walls of the lymph vessels, since ether vapor was noted in the expired air of the animals within 5 min after the start of injection.

Since histologic examination of the lymph nodes could not establish any difference between the two sides, no histologic change related to the ether was apparent. The study suggests that there were no apparent adverse effects due to the use of Ethiodol mixed with ether. The method allows a considerably shorter injection time due to the reduced viscosity of the contrast medium. Popov [3] reported "slight burning pain" accompanying the use of the ether-Ethiodol mixture. This could not be evaluated in our animal study.

All dogs developed bilateral edema of the hind paws. In view of its equal occurrence with both Ethiodol and ether-Ethiodol, it presumably was due to the surgical procedure or local wound infection. The edema was still present bilaterally even after 3 weeks. Evaluation of any irritating effect of ether-Ethiodol on the lymphatic vessels in the production of edema was thus difficult.

This technique seems to have potential clinical application in reducing the time for lymphangiography. Such application should involve carefully planned clinical trials with constant patient monitoring. As with all procedures involving ether, precaution against open flames and sparks should be taken to avoid accidents relating to the flammability and explosiveness of the agent.

REFERENCES

1. Viamonte M: Advances in lymphangio-adenography. *Acta Radiol [Diagn]* (Stockh) 2:394–400, 1964
2. Collard M: Radiologische Studie über die Wirkung von Pharmaka auf die Lymphgefässe der unteren Extremitäten. *Fortschr Geb Roentgenstr Nuklearmed* 115:643–649, 1971
3. Popov VI: The use of ether-dissolved iodlipol in direct lymphography. *Vestn Rentgenol Radiol* 41:75–77, 1966
4. Ratkevich GI, Bogoslovskaya EP, Evseenko LS, Lantsberg IA, Kutsovskaya FA: The effect of viscosity of the oil preparations in lymphography. *Vestn Rentgenol Radiol* 44:63–66, 1969
5. Boely C: L'ether intraveineux dans les troubles vasculaires. *Presse Med* 68:50, 1960

Left Adrenal Neuroblastoma with Normal-appearing Urogram

JACK O. HALLER,[1] WALTER E. BERDON,[2] DAVID H. BAKER,[2] AND E. GEORGE KASSNER[1]

Adrenal neuroblastomas are usually diagnosed by intravenous urography because of the displacement of the kidney or distortion of its contour. This report describes five children with left adrenal neuroblastoma where the mass was purely anterior to the kidney and produced displacement vectors similar to tumors in the body or tail of the pancreas.

Neuroblastomas arising in the adrenal gland produce a characteristic mass effect on the kidney: lateral and/or inferior displacement, outward tilt of the renal axis, and flattening of the upper pole [1]. In the past few years we have seen five children with left adrenal neuroblastomas in whom none of these signs were evident on the intravenous urogram.

Case Material and Findings

The clinical and radiographic features are summarized in table 1. All patients were asymptomatic. Four children had palpable abdominal masses, discovered during routine physical examinations. Case 2 had intravenous urography during the investigation of lymphadenopathy; an abdominal mass was not palpated. Three years earlier she had been treated for an orbital rhabdomyosarcoma with apparent cure. The urinary VMA was elevated in cases 1 and 3, but normal in cases 2 and 4.

In three cases plain radiographs showed calcifications overlying the left kidney. In cases 4 and 5, the calcifications extended below the kidney. In case 2 tomograms in the left posterior oblique projection showed a few calcifications lateral to the renal contour.

In all cases frontal films of the intravenous urogram showed that the axis, position, and contour of the ipsilateral kidney were normal (figs. 1-3); in case 5 the kidney appeared flattened by an anteroposterior mass effect (fig. 4). In case 3, tomograms in the frontal projection showed a mass anterior to the kidney (fig. *2B*). Lateral

TABLE 1

Clinical and Radiographic Features

Case No.	Sex and Age (years)	Clinical Features	Calcifications	Abnormalities on Intravenous Urography	Mass Effects on Gastrointestinal Tract	Sonographic Diagnosis
1 . . .	F, 1/9	Asymptomatic mass	None	Posterior displacement	Indentation of stomach; draping of small bowel*	Solid mass with posterior displacement and flattening of kidney
2 . . .	F, 4	Lymphadenopathy; no palpable mass (previous orbital rhabdomyosarcoma)	Overlying upper pole of kidney	None†	Draping of small bowel*	Cyst (study of excised specimen)
3 . . .	M, 1 1/2	Asymptomatic mass	None	None (tomograms showed mass anterior to kidney)	Indentation of stomach; draping of small bowel	Mesenteric cyst versus accessory spleen
4 . . .	M, 3	Asymptomatic mass	Overlying lower pole of kidney and left lower quadrant	Slight medial deviation of upper ureter	Indentation of stomach; medial displacement of duodenojejunal junction; draping of small bowel; anterior displacement of colon	. . .
5 . . .	F, 2/3	Asymptomatic mass	Overlying lower pole of kidney and left lower quadrant	Anteroposterior flattening and posterior displacement of kidney (lateral view)	Draping of small bowel	. . .

Note.—Cases 1 and 2 from Downstate Medical Center; cases 3-5 from Babies Hospital.
* Plain radiographs only.
† Aortogram and anteroposterior view of left renal arteriogram showed normal kidney; adrenal branches not visualized.

Received April 28, 1977; accepted after revision August 10, 1977.

[1] Department of Radiology, State University of New York Downstate Medical Center, 450 Clarkson Avenue, Brooklyn, New York 11203. Address reprint requests to J. O. Haller.

[2] Department of Radiology, Babies Hospital, New York, New York 10032.

Am J Roentgenol **129:1051-1055, December 1977**

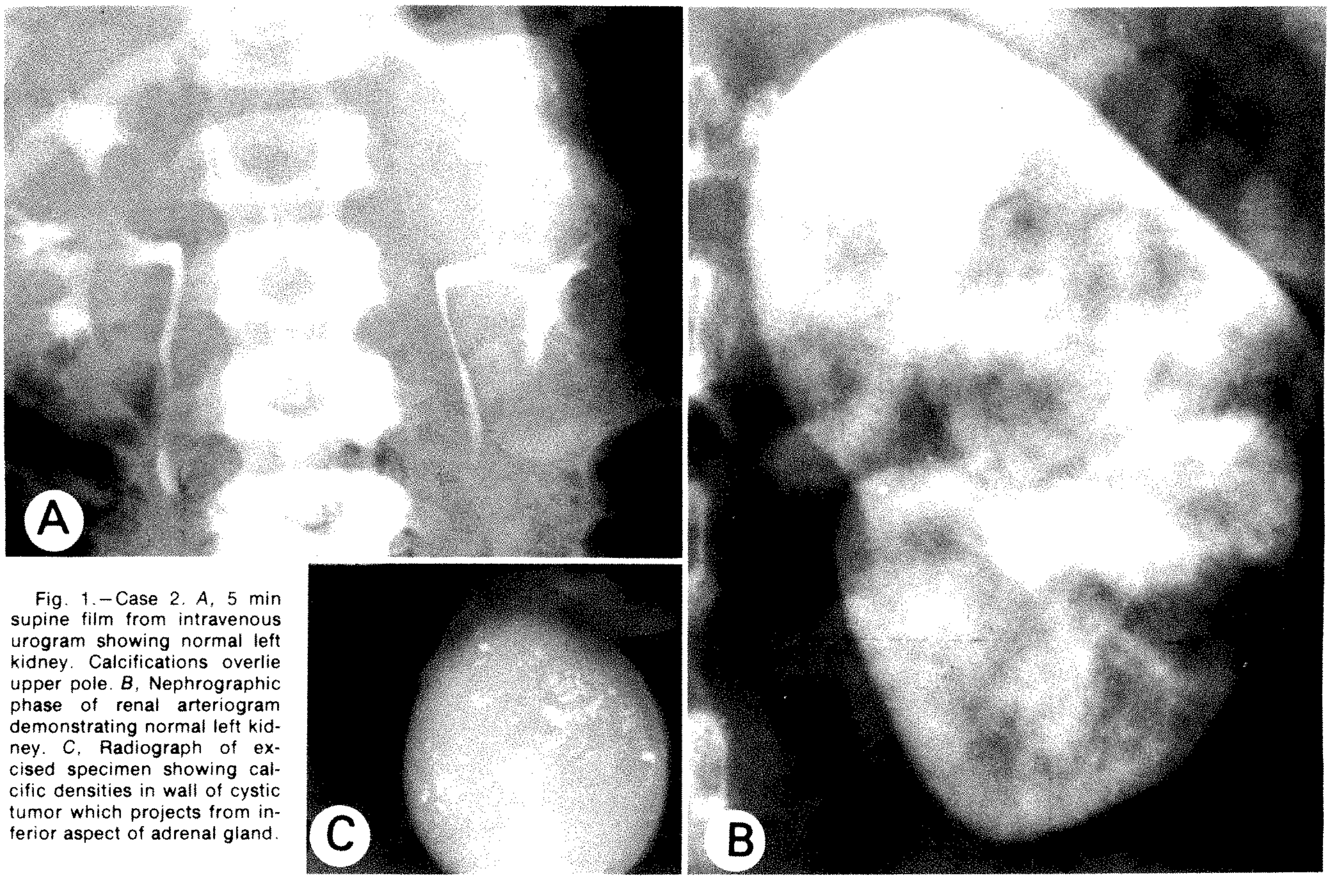

Fig. 1.—Case 2. *A*, 5 min supine film from intravenous urogram showing normal left kidney. Calcifications overlie upper pole. *B*, Nephrographic phase of renal arteriogram demonstrating normal left kidney. *C*, Radiograph of excised specimen showing calcific densities in wall of cystic tumor which projects from inferior aspect of adrenal gland.

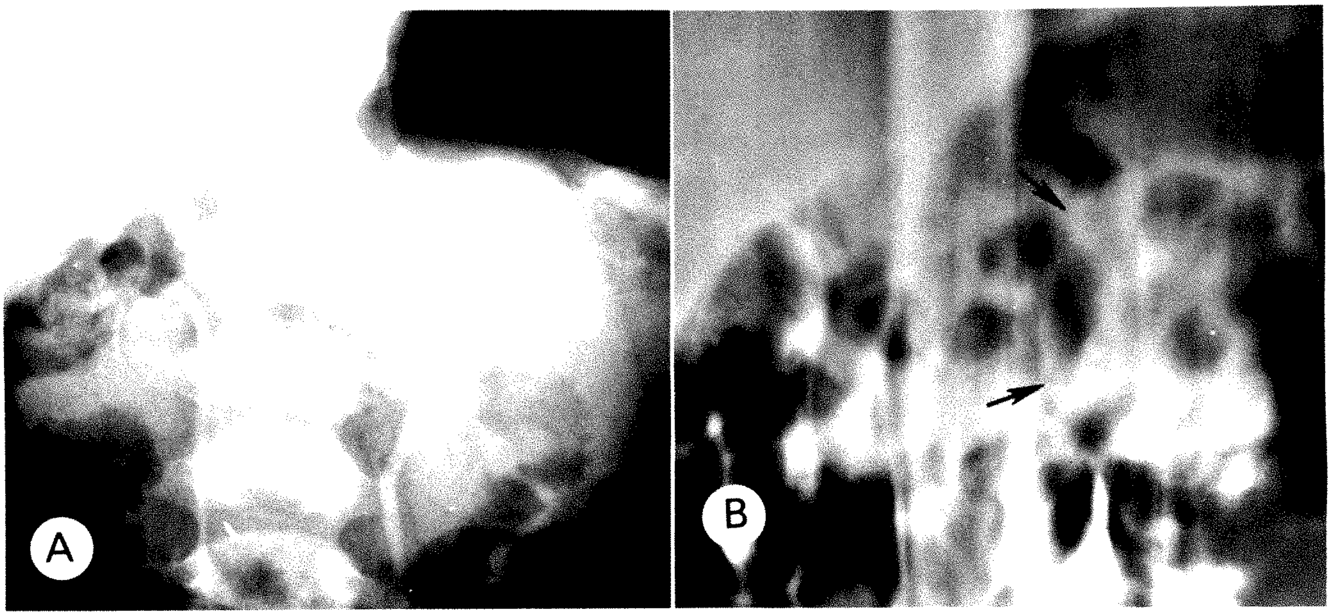

Fig. 2.—Case 3. *A*, Supine film from intravenous urogram showing normally contoured left kidney and displacement of stomach and small bowel. *B*, Frontal tomogram anterior to left kidney showing round mass with smooth contour (*arrows*).

views were obtained in each case. The ipsilateral kidney was displaced posteriorly in cases 4 and 5. Oblique projections in cases 2 and 4 showed no abnormality of renal axis or position.

In each case plain films and barium studies showed a mass effect on the gastrointestinal tract (table 1; figs. 2*A*, 3*B*, 3*C*, and 4). Arteriography was done only in case 2 (fig. 1*B*). No abnormality was detected on the aortogram

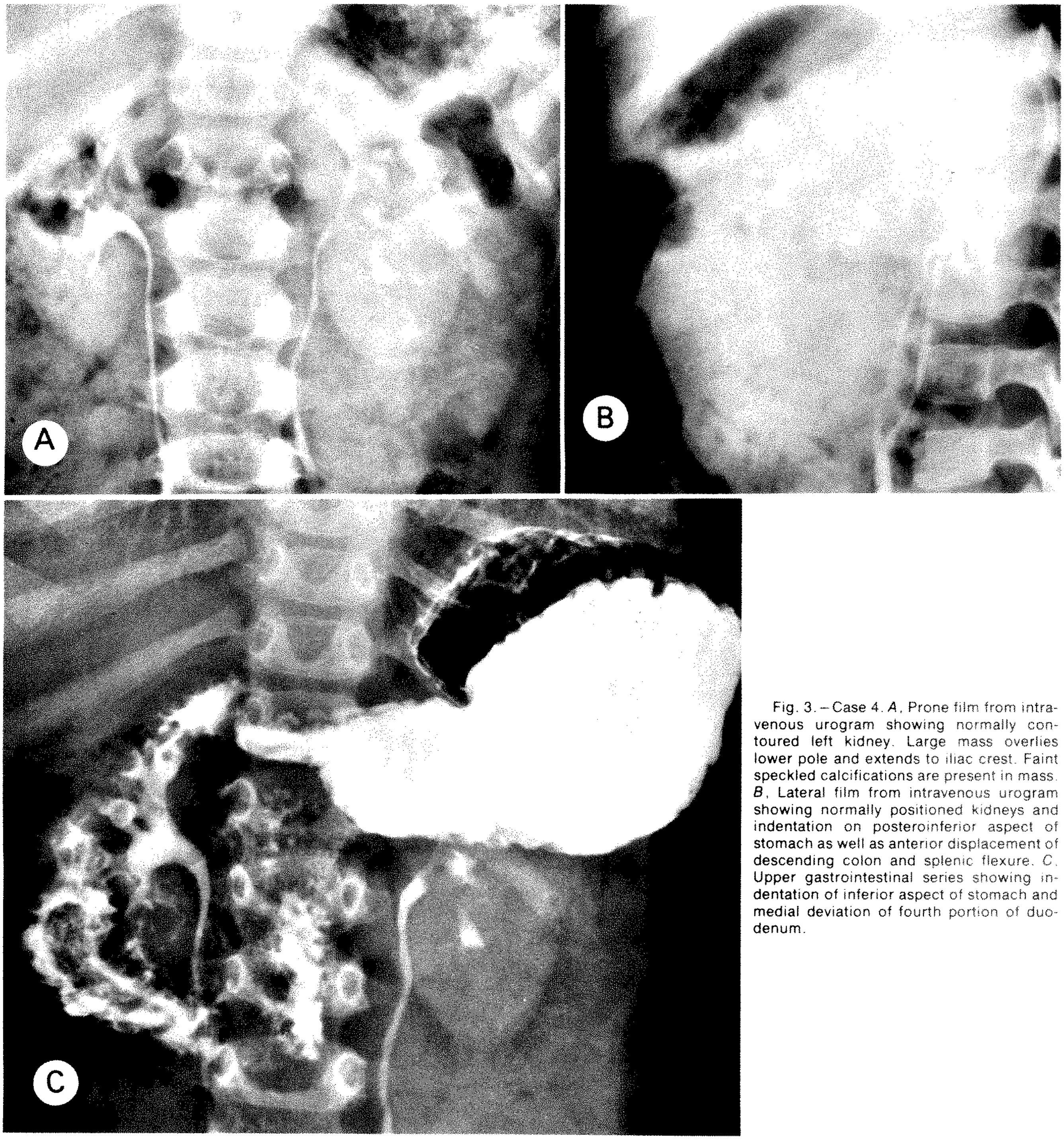

Fig. 3.—Case 4. *A*, Prone film from intravenous urogram showing normally contoured left kidney. Large mass overlies lower pole and extends to iliac crest. Faint speckled calcifications are present in mass. *B*, Lateral film from intravenous urogram showing normally positioned kidneys and indentation on posteroinferior aspect of stomach as well as anterior displacement of descending colon and splenic flexure. *C*, Upper gastrointestinal series showing indentation of inferior aspect of stomach and medial deviation of fourth portion of duodenum.

and left renal arteriogram. Sonograms demonstrated a mass anterior to the kidney in two cases; the acoustical features were thought to be consistent with a solid tumor in case 1 and a cyst in case 3. Preoperative sonograms were not obtained in the other three patients. Scans of the resected specimen in case 3 showed a thick-walled cyst with strong reflections from calcifications in its wall.

In each case the diagnosis of adrenal neuroblastoma was confirmed at surgery. In case 1–3 the tumor was confined to the adrenal gland (stage I). In case 4 there were metastases to ipsilateral paraaortic lymph nodes (stage II). In case 5 there were metastases to paraaortic and celiac axis lymph nodes, liver, and bone marrow (stage IVS).

Discussion

The left adrenal gland is predominantly *suprarenal*, but adrenal tissue extends medial and anterior to the kidney.

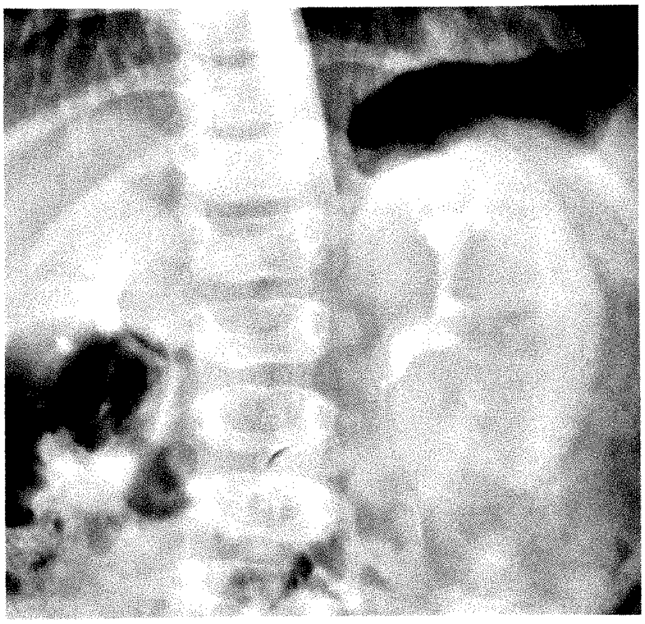

Fig. 4.—Case 5. Prone film from intravenous urogram showing flattening of left kidney; position and axis of kidney are normal. Lateral projection showed posterior displacement and anteroposterior flattening of kidney. Faint calcifications are seen overlying lower half of kidney.

Bulky adrenal masses usually push the kidney down and outward and flatten the contour of its upper pole. Other common mass effects are separation of the kidney and spleen and indentation of the posterior aspect of the stomach [2] (fig. 5*A*). Adrenal tumors arising in the anteroinferior portion of the gland may grow anteriorly with displacement vectors similar to tumors in the body and tail of the pancreas (fig. 5*B*) [3; J. P. Whalen, personal communication]. In such cases there may be radiographic mass effects on the gastrointestinal tract: (1) displacement of the small bowel, splenic flexure, and/or duodenojejunal junction (figs. 3*B* and 3*C*); (2) indentation of the posterior and inferior aspects of the stomach (fig. 5*B*); and (3) anterior displacement of splenic flexure and proximal descending colon (fig. 3*C*). Since the tumors are within the perirenal fascia, the kidney may appear flattened on the frontal projection (fig. 4). Flattening and posterior displacement of the kidney may also be evident on sonograms or lateral radiographs (fig. 3*C*).

Gastrointestinal complaints and "negative" VMA studies are relatively frequent in children with neuroblastoma. A child with an abdominal mass whose intravenous urogram is "negative" may undergo an extensive fruitless investigation of the gastrointestinal tract. The diagnosis of adrenal neuroblastoma should be strongly considered even if the mass is anterior to the left kidney, particularly if there is posterior displacement of the kidney. Our experience has shown that the intimate relationship of the tumor to the subjacent kidney may not be evident on the frontal films of the intravenous urogram, but careful study of lateral and oblique projections may reveal subtle mass effects. Nephrotomography (including cuts anterior to the kidney) and barium studies of the upper and lower gastrointestinal tract may be needed to complete the vector analysis. Mesenteric and retroduodenal metastases can often be detected on the upper gastrointestinal series, particularly if the supine cross-table lateral projection is used [4]. Sonography is a helpful adjunct to the vector analysis, since flattening and posterior displacement of the ipsilateral kidney may not be clearly shown on conventional radiographic studies. However, it should be appreciated that some neuroblas-

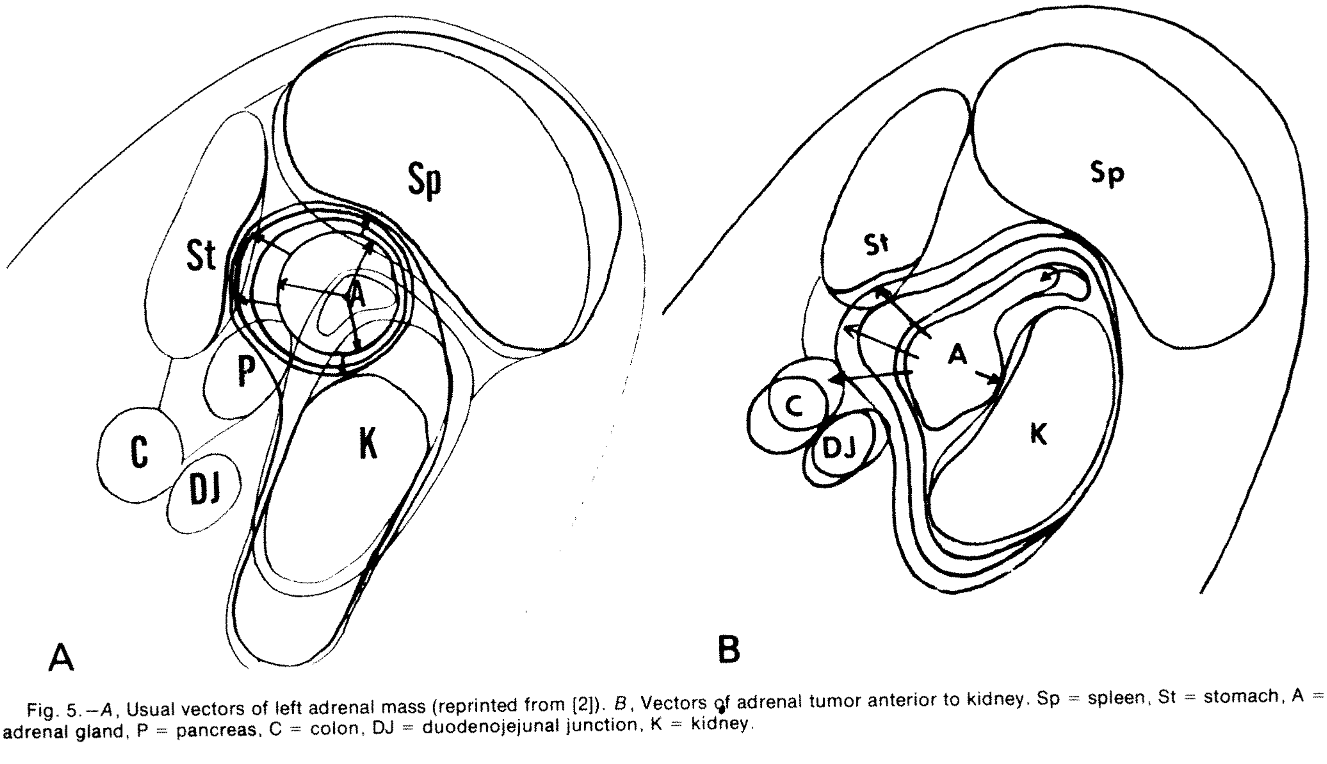

Fig. 5.—*A*, Usual vectors of left adrenal mass (reprinted from [2]). *B*, Vectors of adrenal tumor anterior to kidney. Sp = spleen, St = stomach, A = adrenal gland, P = pancreas, C = colon, DJ = duodenojejunal junction, K = kidney.

tomas are relatively anechoic, which may lead to the erroneous diagnosis of a benign cyst [5].

REFERENCES

1. Silverman FN: The urinary tract, in *Pediatric X-ray Diagnosis*, 6th ed, edited by Caffey J, New York, Yearbook Medical Publishers, 1973, pp 751-818
2. Whalen JP, Evans JA, Shanser J: Vector principle in the differential diagnosis of abdominal masses: the left upper quadrant. *Am J Roentgenol* 113:104-118, 1971
3. Whalen JP: *Radiology of the Abdomen*. Philadelphia, Lea & Febiger, 1976
4. Sorabella P, Berdon WE, Baker DH: The right angle upper gastrointestinal series in the diagnosis and staging of neuroblastoma. *Am J Roentgenol* 120:573-582, 1974
5. Green WM, King DL, Casarella WJ: A reappraisal of sonolucent renal masses. *Radiology* 121:163-171, 1976

Acute Appendicitis with Abscess Simulating Carcinoma of the Sigmoid

JAMES M. HALLS[1] AND HARVEY I. MEYERS[1]

Acute appendicitis with abscess often produces a distinctive extrinsic pressure deformity of the cecum. If the abscess is large or disseminated, other parts of the gastrointestinal tract may be secondarily involved. Abscesses usually produce extrinsic compression defects with benign radiologic characteristics, but occasionally the lesions may simulate malignant disease. Even careful evaluation of the clinical symptoms and signs may not be helpful in the differentiation of benign from malignant disease. Three examples of atypical acute appendicitis are described in patients with clinical and radiologic findings strongly suggestive of malignant disease.

The diagnosis of acute appendicitis is usually made clinically but in patients with atypical symptoms it is sometimes necessary to use radiologic techniques. In acute appendicitis with abscess, a characteristic extrinsic pressure deformity of the tip or medial wall of the cecum is sometimes seen, but changes may not be confined to this site. Difficulty in radiologic interpretation may arise if the abscess deforms segments of the large bowel distant from the cecum. We report three cases of acute appendicitis with abscess, in which the atypical radiographic findings suggested malignant disease.

Case Reports

Case 1

W. W., a 56-year-old male, was referred to the Los Angeles County-University of Southern California Medical Center for treatment of rectal carcinoma. He had a 2 day history of vague epigastric pain and had noted some bright red rectal bleeding. The abdomen was mildly distended with slight guarding in the right lower quadrant. Rectal examination revealed a nontender 4 × 2 cm anterior mass. The stools were 3+ for occult blood, but there were no signs of parasites or ova. Hematocrit was 43%; white blood cell count, 11,200.

Barium enema examination showed complete obstruction to the retrograde flow of barium just above the rectosigmoid junction (fig. 1*A*). A successful enema examination the next day showed an irregular stricture about 5 cm long at the rectosigmoid junction. The stricture had a sharp proximal margin suggestive of carcinoma. The mucosa of this region appeared to be destroyed (fig. 1*B*). At surgery a periappendiceal abscess was found extending down to involve the rectosigmoid junction.

Case 2

D. V., a 56-year-old diabetic female, had diarrhea about 10 times a day for 5 days prior to admission.There was no rectal bleeding or weight loss, and the patient had been well until the present illness. The abdomen was soft and no tenderness could be elicited. On rectal and sigmoidoscopic examination, a firm circumferential lesion was noted at about 10 cm. There was no evidence of parasites or ova in the stools, and tests for occult blood were negative. White blood cell count was 5,200.

Barium enema examination demonstrated a short irregular narrowing at the rectosigmoid junction, and a small quantity of barium leaked into the presacral soft tissues (fig. 2). At surgery, an inflammatory mass involving the appendix, terminal ileum, and distal sigmoid colon was found. Microscopy revealed acute and chronic inflammation with acute appendicitis.

Case 3

W. B., a 28-year-old male, had intermittent crampy abdominal pain for 5 months. There was a sudden onset of crampy left lower quadrant pain with diarrhea 2 days before admission. The left lower abdomen was tender; temperature was 38.7°C. White blood cell count was 16,000 with 86% neutrophils. Sigmoidoscopy showed a firm constricting lesion in the distal sigmoid

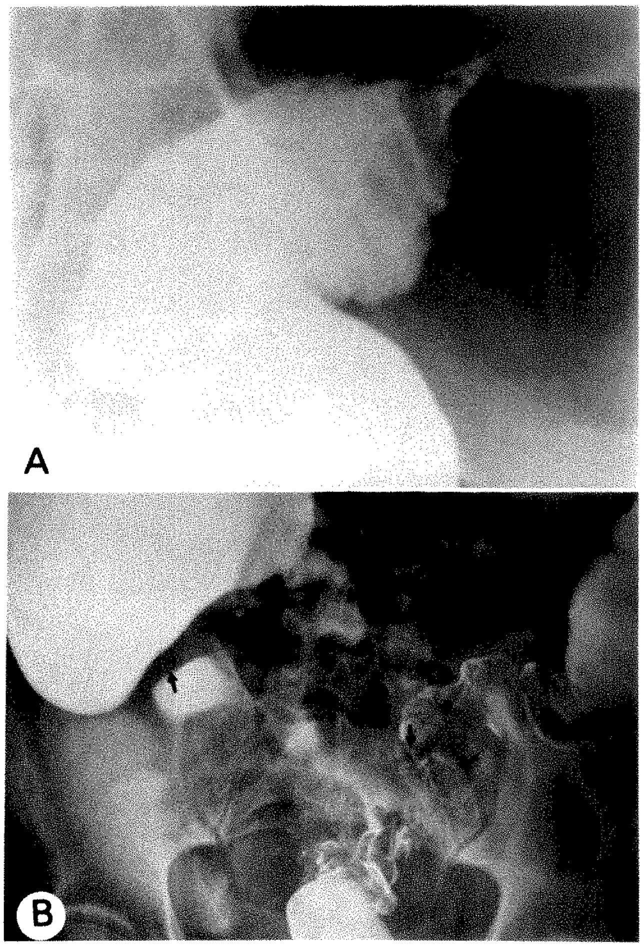

Fig. 1.—Case 1. *A*, Barium enema examination showing stricture at rectosigmoid junction with complete obstruction to retrograde flow of barium. *B*, Examination 1 day later showing irregular narrowing just above rectosigmoid junction with abrupt proximal margin. Extrinsic pressure defect of cecum also demonstrated.

Received March 8, 1977; accepted after revision August 23, 1977.

[1] Department of Radiology, Los Angeles County-University of Southern California Medical Center, 1200 North State Street, Los Angeles, California 90033. Address reprint requests to J. M. Halls.

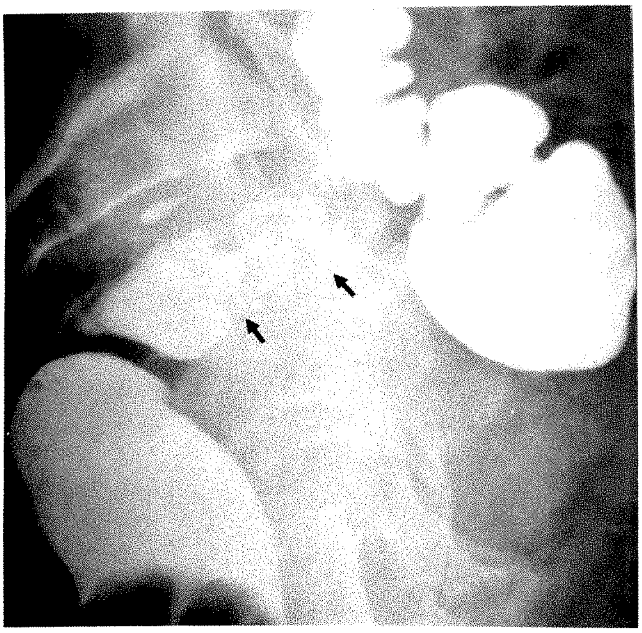

Fig. 2.—Case 2. Barium enema examination showing short segment of irregular narrowing at rectosigmoid junction. Small amount of barium has leaked into presacral space.

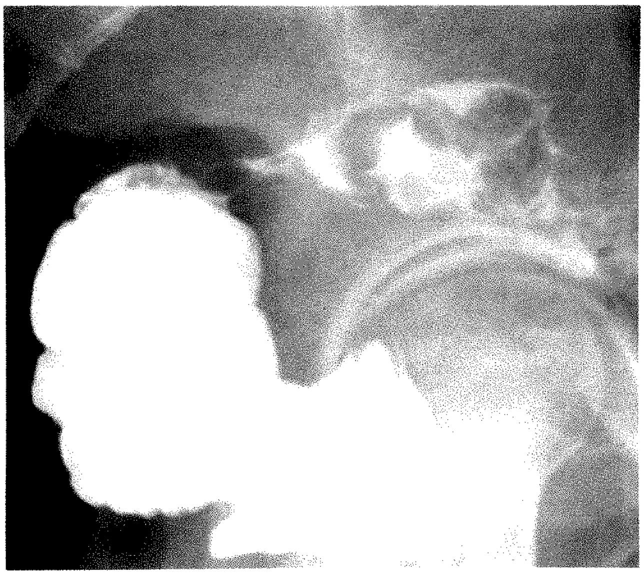

Fig. 3.—Case 3. Barium enema examination, lateral view, showing irregular stricture in distal sigmoid colon.

colon with some nodularity and friability of the mucosa. There were no parasites or ova in the feces.

Barium enema examination showed a 12 cm segment of irregular narrowing just above the rectosigmoid junction with preserved mucosa in the proximal two-thirds; however, there was apparently mucosal destruction in the distal one-third (fig. 3). There were no diverticula in the region, and because of the patient's age diverticulitis was believed unlikely. The preservation of some of the mucosa and the absence of ulceration also ruled out Crohn's disease. Scirrhous carcinoma of the colon or metastatic disease seemed to be likely causes.

At surgery a 3 × 3 cm inflammatory mass was found involving the appendix, terminal ileum, and distal sigmoid colon. Frozen sections revealed acute and chronic inflammation. The mass and the appendix were removed.

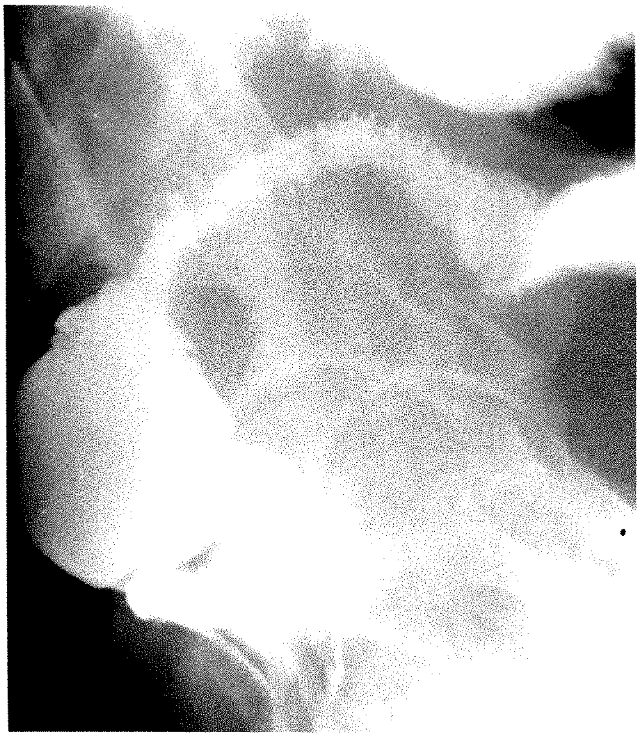

Fig. 4.—Pelvic abscess producing characteristic deformity of rectosigmoid. Note displacement, distensibility, and transverse ridging of intact mucosa.

Discussion

Acute appendicitis with abscess occasionally masquerades as malignant disease, particularly if the soft tissue mass displaces and deforms bowel at a site other than the cecum. Meyers and Oliphant [1] reported three cases of ascending retrocecal appendicitis in which inflammatory changes were noted at unusual sites in the cecum and ascending colon. In two there was a masslike infiltration of the proximal ascending colon. A radiologic diagnosis of primary carcinoma of the colon was made in one case, and extraperitoneal lymphoma was thought to be the cause of the changes in the second.

Mayson and Rosenthal [2] described the radiologic findings in delayed diagnosis of appendicitis in three soldiers involved in the Vietnam war. In one case there was a smooth curvilinear extrinsic compression defect of the medial wall of the cecum. An oblique view of the sigmoid showed a short segment of narrowing with irregularities along its inferior border.

Joffee [3] discussed uncommon radiologic findings associated with acute perforative appendicitis. He described a case in which the sigmoid was indented by a walled-off abscess producing radiologic changes simulating a primary submucosal lesion of the colon. He stressed the need for careful correlation of the radiologic findings with the history and clinical signs.

Phillips [4] described an area of constriction 2-12 cm long confined to the sigmoid colon in patients with tuboovarian abscess. The majority of these lesions were larger than 5 cm and were always associated with an intact mucosa. However, in one example the constricted region had an abrupt proximal margin suggesting a neoplasm.

Our cases had atypical histories; radiologic studies were performed as part of the overall investigation of unidentified intraabdominal disease. All three cases had circumferential lesions just beyond the rectosigmoid junction on both rectal and sigmoidoscopic examination, and strictures of varying lengths were demonstrated by barium enema examination. In case 1, there was complete obstruction to the retrograde flow of barium initially, but a successful study was possible the next day. It is interesting that case 1 was referred from an outside hospital for treatment of rectal carcinoma.

All three sigmoid strictures were unlike the smooth tapered deformities more commonly seen secondary to pelvic abscess (fig. 4). The strictures had shoulder deformities and an abnormal mucosal pattern much more suggestive of primary malignant disease. Even correlation of the radiographic findings with clinical symptoms and signs was not helpful, and all three patients underwent surgery with a preoperative diagnosis of carcinoma.

These examples illustrate a rare but real difficulty in differentiating the deformity produced by appendiceal abscess from primary malignant disease of the colon. All of our cases showed nonfilling of the appendix with cecal deformity of varying degree. These appearances although not fully appreciated at the time, were the only clues to suggest the correct diagnosis of benign inflammatory disease.

ACKNOWLEDGMENT

We appreciate the assistance of Marie Andrianos in the preparation of this manuscript.

REFERENCES

1. Meyers MA, Oliphant M: Ascending retrocecal appendicitis. *Radiology* 110:295-299, 1974
2. Mayson PB, Rosenthal SJ: Roentgen findings in delayed diagnosis of appendicitis. *Am J Roentgenol* 103:347-350, 1968
3. Joffe N: Some uncommon roentgenologic findings associated with acute perforative appendicitis. *Radiology* 110:301-305, 1974
4. Phillips JC: A spectrum of radiologic abnormalities due to tubo-ovarian abscess. *Radiology* 110:307-311, 1974

Ultrasonography in Tumors Arising from the Spine and Bony Pelvis

LUIS ALONSO deSANTOS[1] AND HARVEY M. GOLDSTEIN[1]

Gray scale ultrasonography is a useful tool in evaluating pelvic and abdominal soft tissue masses that may be associated with bony neoplasms. Four patients are described: two with giant cell tumors, one with Ewing's sarcoma, and one with a sacrococcygeal teratoma. Ultrasound is especially helpful in assessing the extent of disease, treatment planning, and in following the results of therapy.

Gray scale ultrasound has been used successfully in the evaluation of various neoplastic conditions arising in abdominal and pelvic structures. However, its use in the evaluation of abdominal and pelvic soft tissue components of musculoskeletal tumors has not been discussed.

A number of musculoskeletal tumors frequently have soft tissue components associated with the bony abnormality. When these tumors originate in the skeleton in proximity to the abdomen and pelvis, a soft tissue mass associated with them may extend into these cavities. Our experience indicates that ultrasound may be extremely useful in evaluating the presence and extent of the extraosseous components as well as assessing the therapeutic response.

Materials and Methods

Ultrasound studies were performed in the usual manner with commercially available gray scale ultrasound equipment (Sonograph 3, Unirad Corporation, Denver, Colo.). Both 2.25 and 3.5 mHz transducers were used depending on patient size and the area examined. Recording was made on 70 mm film.

Case Reports

Case 1

A 22-month-old female was referred for evaluation and treatment of a malignant sacrococcygeal teratoma previously diagnosed on open biopsy. A pelvic mass was palpable on rectal examination. An intravenous urogram and retrograde cystogram demonstrated anterior displacement of the urinary bladder with an intact sacrum (fig. 1*A*). Gray scale ultrasound examination confirmed the presence of a solid retrovesical pelvic mass (fig. 1*B*).

The patient was started on combination chemotherapy. Approximately 1 month later, a repeat ultrasound examination showed marked decrease in the size of the mass (fig. 1*C*). Intravenous urogram revealed the urinary bladder had returned to normal location (fig. 1*D*). The patient was continued on chemotherapy but developed pulmonary metastases.

Case 2

A 27-year-old female presented with a 1 month history of progressive right abdominal discomfort and numbness of the right leg. Radiologic examination revealed a destructive lesion involving the right iliac crest, and the diagnosis after biopsy was giant cell tumor with considerable aneurysmal bone cyst components.

Intravenous urogram showed a large soft tissue mass originating from the superior portion of the right iliac crest with medial displacement of the lower right ureter (fig. 2*A*). Barium studies also showed displacement of the small bowel and ascending colon. Sonography revealed a large solid mass extending anteriorly from the right ilium into the right abdomen (fig. 2*B*).

After therapeutic occlusion of the right internal iliac artery, the pain subsided. Repeat radiologic examination 2 months later revealed no change in the size of the mass, but increased calcification in its periphery was noted. Similarly, ultrasonography revealed no change from the previous study. Currently the patient remains asymptomatic.

Case 3

A 26-year-old female was referred for a destructive lesion of the right side of the fifth lumbar vertebral body. A bone biopsy revealed a giant cell tumor. A complete excision of L5 with placement of a tibial graft was performed.

Two years after surgery the patient developed a complete spinal block at L4, and at decompressive laminectomy there was evidence of tumor recurrence. Subsequent local radiotherapy and systemic chemotherapy was administered, but the tumor continued to grow. Intravenous urogram demonstrated a right abdominal mass with medial displacement of the ureter, elevation of the right kidney, and mild calyceal dilatation (fig. 3*A*). Gray scale ultrasonography confirmed the huge mass in the right abdomen extending up from the pelvis to the subhepatic area (fig. 3*B* and 3*C*).

Despite chemotherapy, ultrasound study 2 months later demonstrated no change in the size or characteristics of the mass. When last seen the patient had developed metastatic disease to the lungs.

Case 4

A 14-year-old boy was referred for a destructive lesion of the left iliac crest. Bone biopsy revealed Ewing's sarcoma. Intravenous urogram revealed marked displacement of the urinary bladder towards the right as well as medial displacement of the left ureter (fig. 4*A*). Gray scale ultrasound confirmed the large mass extending from the iliac crest to above the umbilicus. The bulk of the mass was intrapelvic and intraabdominal; however, an extrapelvic mass component was also demonstrated (fig. 4*B*).

The patient is currently being treated with chemotherapy and local radiotherapy.

Discussion

A review of the literature yielded only a few reports of the use of ultrasound in the evaluation of masses related

---

Received June 14, 1977; accepted August 10, 1977.

[1] Department of Diagnostic Radiology, University of Texas System Cancer Center, M. D. Anderson Hospital and Tumor Institute, 6723 Bertner Avenue, Houston, Texas 77030. Address reprint requests to H. M. Goldstein.

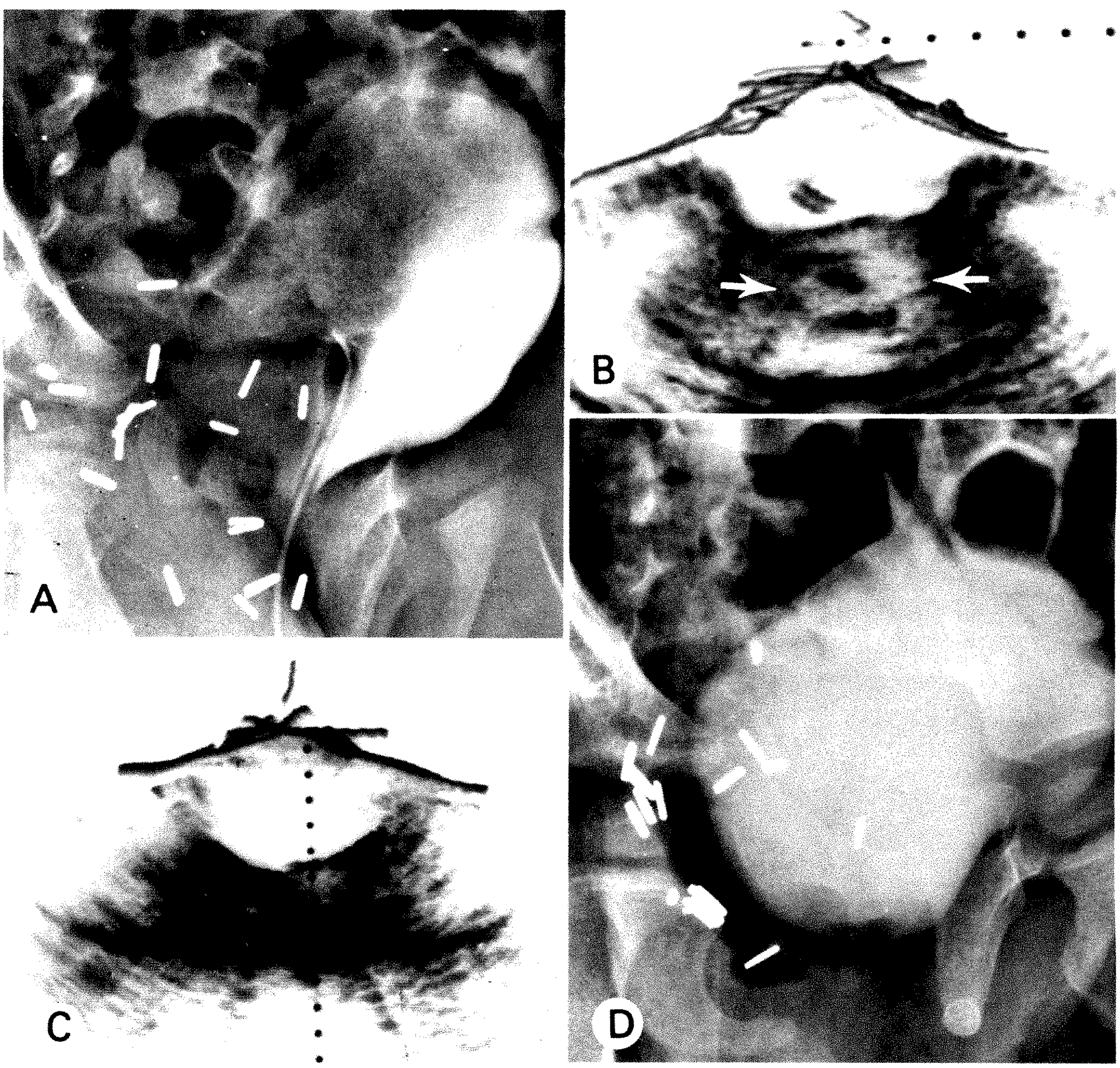

Fig. 1.—22-month-old female with sacrococcygeal teratoma. *A*, Oblique cystogram demonstrating elevation and anterior displacement of bladder by large mass. *B*, Transverse pelvic sonogram revealing 5 cm solid mass posterior to bladder (*arrows*). Note catheter in bladder. *C*, Posttreatment sonogram 1 month later showing almost complete resolution of retrovesical mass. *D*, Comparable oblique view of bladder during repeat intravenous urogram showing no mass effect.

to the musculoskeletal system. These were primarily aneurysms and rheumatoid cysts located in the popliteal fossa area [1-3]. We were unable to locate any reports of the use of ultrasound in the evaluation of the extraosseous component of skeletal neoplasms.

The neoplasms described here are among the more common ones to have a significant extraosseous mass component. Displacement of the rectum and bladder in patients with sacrococcygeal teratoma is secondary to the presence of a soft tissue mass seen in virtually all these lesions [4, 5]. The true incidence of a soft tissue component in giant cell tumors is not known, but a significant percentage do have considerable extraosseous mass, especially when the tumor arises in the pelvic region. This may be due in part to the thinner cortex of the pelvic bones and/or to the more aggressive biologic behavior that this tumor often exhibits when it involves the pelvic girdle. Because of the permeative nature of Ewing's sarcoma, an extraosseous component is seen in over 90% of cases [6]. The extent of the soft tissue mass may be difficult to evaluate, and frequently the extent is larger than expected by conventional radiology [7].

For proper staging, as much specific anatomic infor-

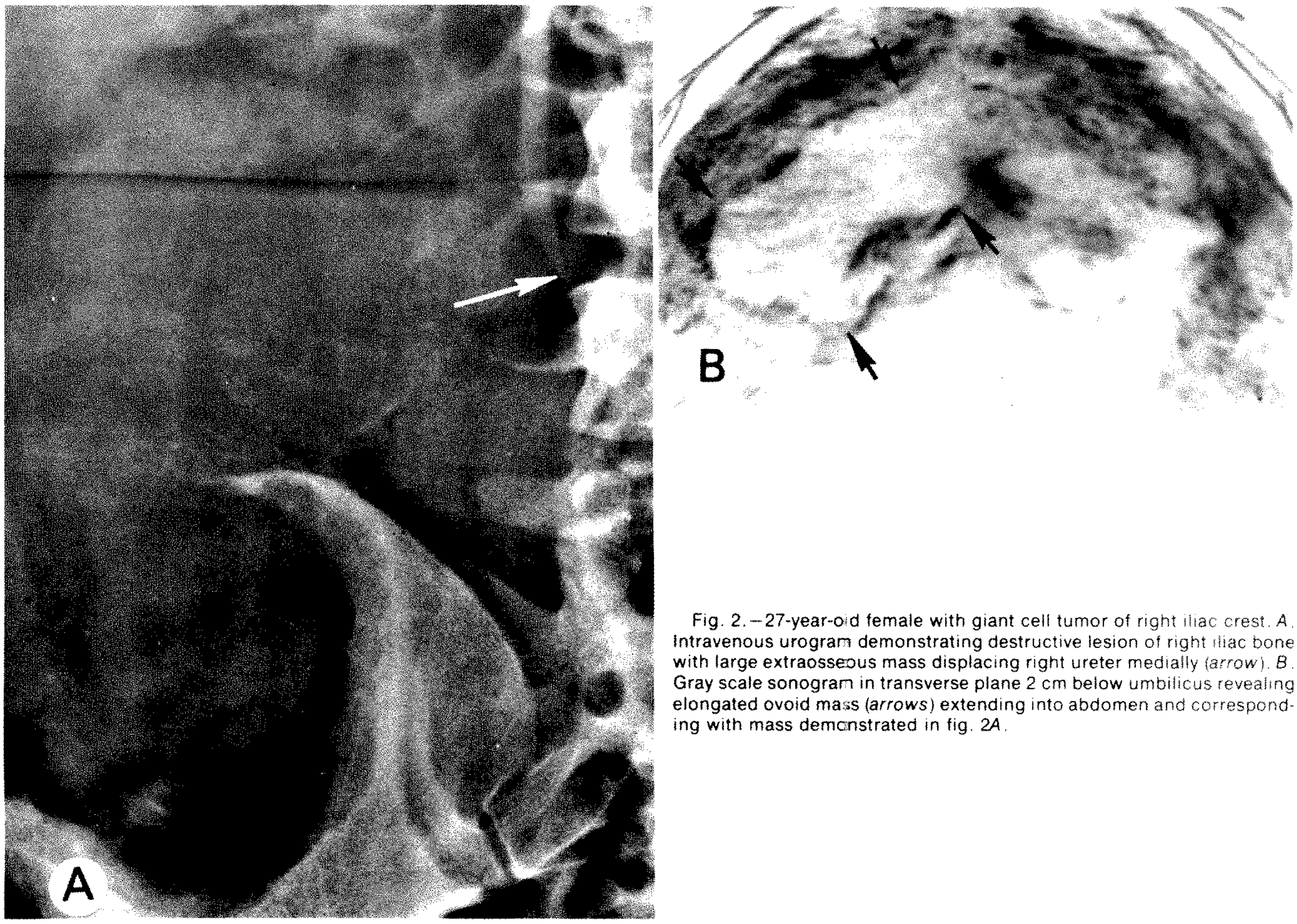

Fig. 2.—27-year-old female with giant cell tumor of right iliac crest. *A*, Intravenous urogram demonstrating destructive lesion of right iliac bone with large extraosseous mass displacing right ureter medially (*arrow*). *B*, Gray scale sonogram in transverse plane 2 cm below umbilicus revealing elongated ovoid mass (*arrows*) extending into abdomen and corresponding with mass demonstrated in fig. 2*A*.

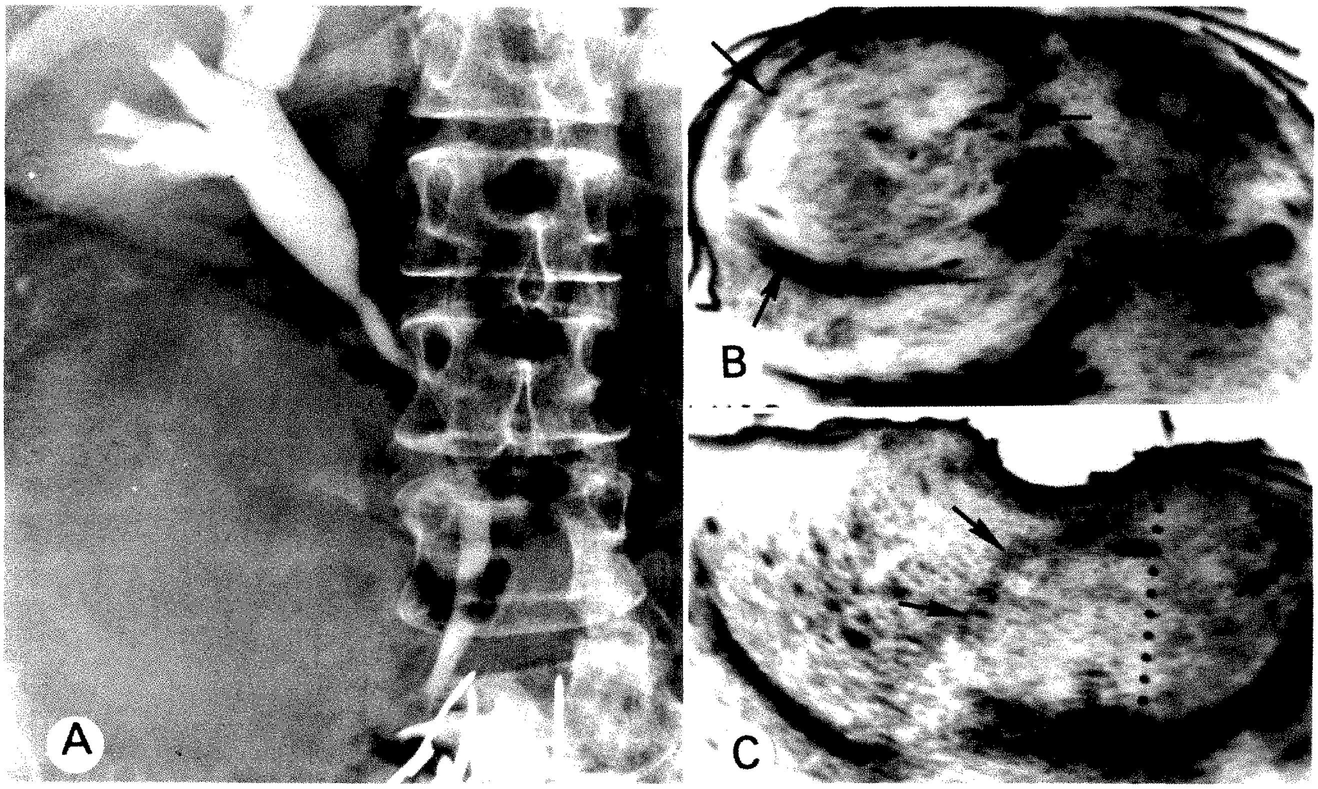

Fig. 3.—26-year-old female with giant cell tumor of fifth lumbar vertebra. *A*, Intravenous urogram demonstrating destructive bony changes and large soft tissue mass. Note upward rotation of kidney and marked medial displacement of right ureter. *B*, Transverse scan 1 cm below umbilicus defining large intraabdominal solid mass on right (*arrows*). *C*, Longitudinal scan 8 cm to right of midline demonstrating large mass extending to right hepatic margin. Interface at mass-liver junction (*arrows*) indicates extrahepatic location of mass.

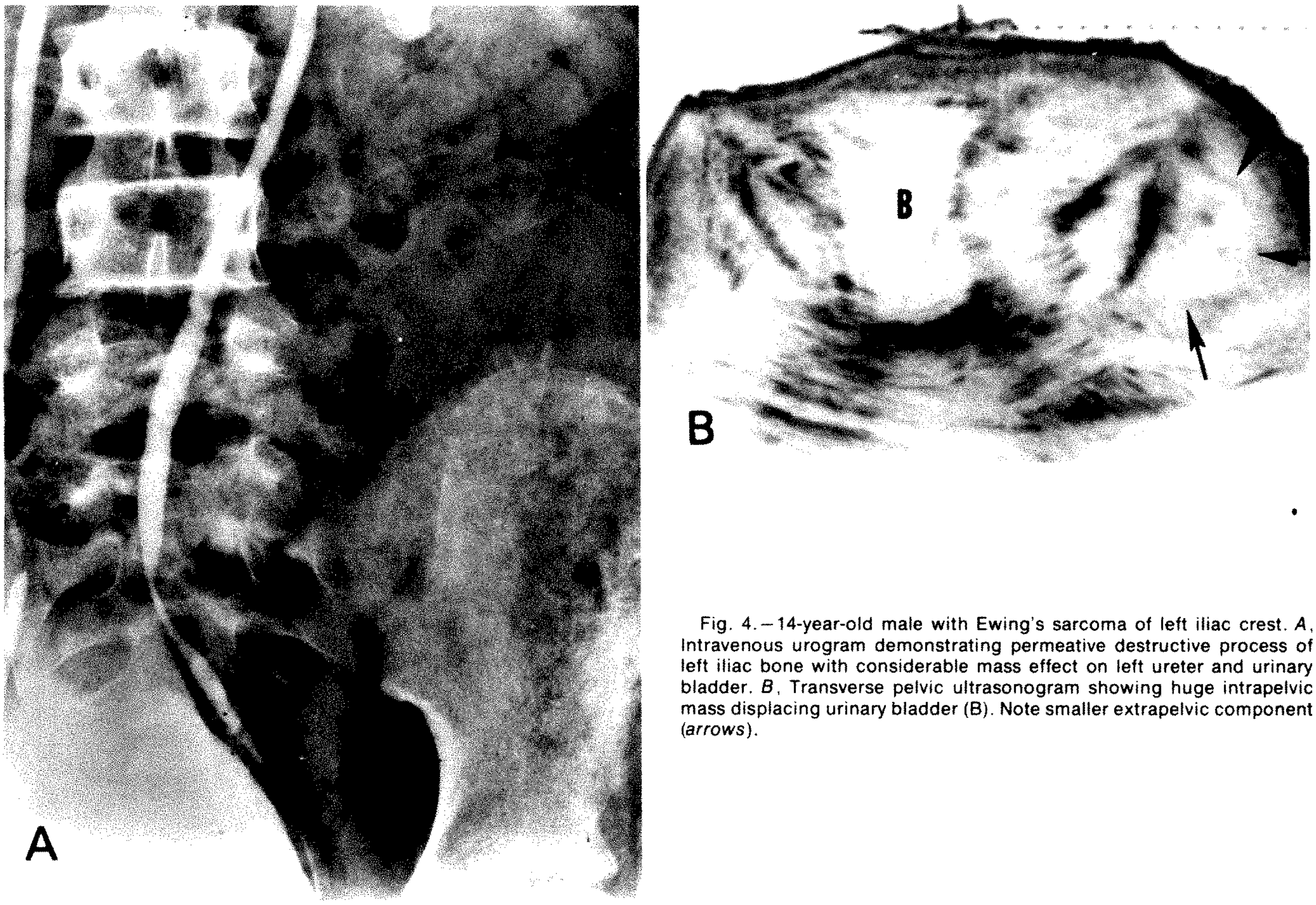

Fig. 4.—14-year-old male with Ewing's sarcoma of left iliac crest. *A*, Intravenous urogram demonstrating permeative destructive process of left iliac bone with considerable mass effect on left ureter and urinary bladder. *B*, Transverse pelvic ultrasonogram showing huge intrapelvic mass displacing urinary bladder (B). Note smaller extrapelvic component (*arrows*).

mation as possible about the primary bone process is desirable. Accurate determination of the boundaries of a tumor in relation to adjacent organs is essential if surgery is contemplated, since the approach will change depending on the anatomic relations. Extent of the mass in the anteroposterior diameter may be difficult to assess by conventional radiology alone. Ultrasound scanning provides information regarding the retroperitoneal versus intraperitoneal location and extent of a soft tissue mass. If radiotherapy comprises part of the treatment plan, sonography also becomes useful in defining all three dimensions of the mass so that adequate portals and penetration can be calculated. Finally, regardless of the type of cancer therapy used, ultrasonography is a rapid and accurate method of following the size and character of a mass in conjunction with treatment.

REFERENCES

1. Campbell S, Pryse-Davis J, Coltart TM, Seller MJ, Singer JD: Ultrasound in the diagnosis of spina bifida. *Lancet* 1:1065–1068, 1975
2. McDonald DG, Leopold RG: Ultrasound B-scanning in the differentiation of Baker's cyst and thrombophlebitis. *Br J Radiol* 45:729-732, 1972
3. Sarti DA, Louie JS, Lindstron RR, Nies K, London J: Ultrasonic diagnosis of popliteal artery aneurysms. *Radiology* 121:707-708, 1976
4. Eklof O: Roentgenologic findings in sacrococcygeal teratoma. *Acta Radiol* 3:41-48, 1965
5. Vaughan VC, McKay RJ: *Nelson Textbook of Pediatrics.* Philadelphia, Saunders, 1975
6. Lichtenstein L: *Bone Tumors.* St. Louis, Mosby, 1972
7. Jaffe HL: *Tumors and Tumorous Conditions of the Bones and Joints.* Philadelphia, Lea & Febiger, 1961

Radiographic Diagnosis of Acute Peroneal Tendon Dislocation

CHARLES C. CHURCH[1]

Acute dislocation of the peroneal tendons at the ankle is accompanied, in a significant proportion of cases, by a characteristic small shelllike avulsion fracture of the lateral malleolus, rendering the lesion diagnosable radiographically. This small fracture is usually best seen on internal rotation oblique or occasionally on anteroposterior films of the ankle. It is seen as a bone flake only a few millimeters thick but often 1 cm or more in vertical diameter lying adjacent to the posterolateral surface of the lateral malleolus. It is an infrequent injury, now usually the result of a ski accident. Failure to recognize and treat the lesion can result in chronic disability.

Traumatic dislocation of the peroneal tendons at the ankle is an infrequent but not rare injury, now most often the result of a skiing accident. The frequency of occurrence in skiing appears to be about 0.5% of all injuries [1]. Other forms of trauma, particularly associated with soccer and ice skating, have accounted for many of the reported cases of acute peroneal tendon dislocation, especially prior to the current surge in popularity of skiing.

Although this lesion has been discussed in European and American medical and surgical literature, it has not been described in the radiologic literature. Further, an informal survey of radiologists, even in areas where skiing is popular, reveals a general lack of familiarity with this lesion. Many cases can be diagnosed radiographically, and failure to treat the injury early and adequately often results in chronic disability.

Peroneal tendon dislocation was apparently first described by Monteggia (cited in [2]) in a ballet dancer. Since that description, sporadic reports have appeared in both European and North American literature, numbering well in excess of 100 cases.

Anatomy and Mechanism of Injury

The peroneus longus and brevus muscles lie in the lateral compartment of the leg, originating from the lateral aspect of the upper two-thirds of the fibular shaft as well as the intermuscular septum between the anterior and posterior compartments. Both muscles become tendons before reaching the level of the ankle joint; their tendons run behind the lateral malleolus in the peroneal groove on the posterolateral aspect of the fibula. On reaching the inferior extremity of the groove, the peroneus brevus tendon passes anteriorly and inferiorly to insert on the base of the fifth metatarsal, while the peroneus longus tendon runs obliquely across the plantar aspect of the foot to insert into the medial cuneiform and the base of the first metatarsal. Behind the lateral malleolus, the tendons have a common sheath. These tendons are normally prevented from springing forward around the lateral aspect of the malleolus by the superior peroneal retinaculum, which is a thickening of the fascial layer passing posteriorly from the posterolateral ridge of the fibula to the periosteum of the calcaneus. The tendon sheaths, superior retinaculum, and posterior surface of the fibula then, in effect, form a tunnel for the tendons of the peroneus longus and brevus (figs. 1 and 2). In some individuals the peroneal tendon groove may be quite shallow, which may predispose to the tendon dislocation.

The injury appears to result from violent passive dorsiflexion of the foot, usually occurring during a forward fall. A strong reflex contraction of the peroneal muscles is then thought to occur, causing the peroneal tendons to move forward in bowstring fashion, tearing away the periosteum from the lateral aspect of the fibula to which the superior retinaculum is attached. The avulsed periosteum often carries with it a flake of fibular cortex [1]. The tendons thus may come to rest lateral to the malleolus. The retinaculum is reportedly never torn [1, 3], the periosteum and/or cortex of the fibula being the point of greatest weakness. Eversion (or possibly even inversion) of the foot during dorsiflexion is probably also important in the production of this lesion, although the contribution of these additional forces, if any, is still in dispute [2, 3].

Case Reports

Case 1

A 34-year-old female apparently sustained a dorsiflexion, eversion ankle injury while skiing. Pain and swelling were localized to the region of the lateral malleolus, and she was unable to continue skiing. Subtle, well localized crepitation could be palpated over the lateral malleolus, and the patient could feel a "snap" or "pop" in the same region on dorsiflexion of the foot.

Radiography of the ankle (fig. 3) revealed a thin flake of bone slightly longer than 2 cm in its superoinferior dimension avulsed from and lying adjacent to the lateral aspect of the lateral malleolus. At surgery, the diagnosis of peroneal tendon dislocation was confirmed. The retinacular mechanism was repaired after deepening the groove of the peroneal tendons. Clinical result was excellent.

Case 2

A 20-year-old female sustained a dorsiflexion and (eversion?) injury while skiing. Peroneal tendon dislocation was diagnosed in the orthopedic department. Ankle x-rays revealed no evidence of fracture. Conservative treatment by closed reduction

---

Received January 17, 1977; accepted after revision July 25, 1977.

[1] Department of Radiology, University of Washington, Seattle, Washington 98195. Present address: Department of Radiology, Toledo Hospital, 2142 North Cove Boulevard, Toledo, Ohio 43606.

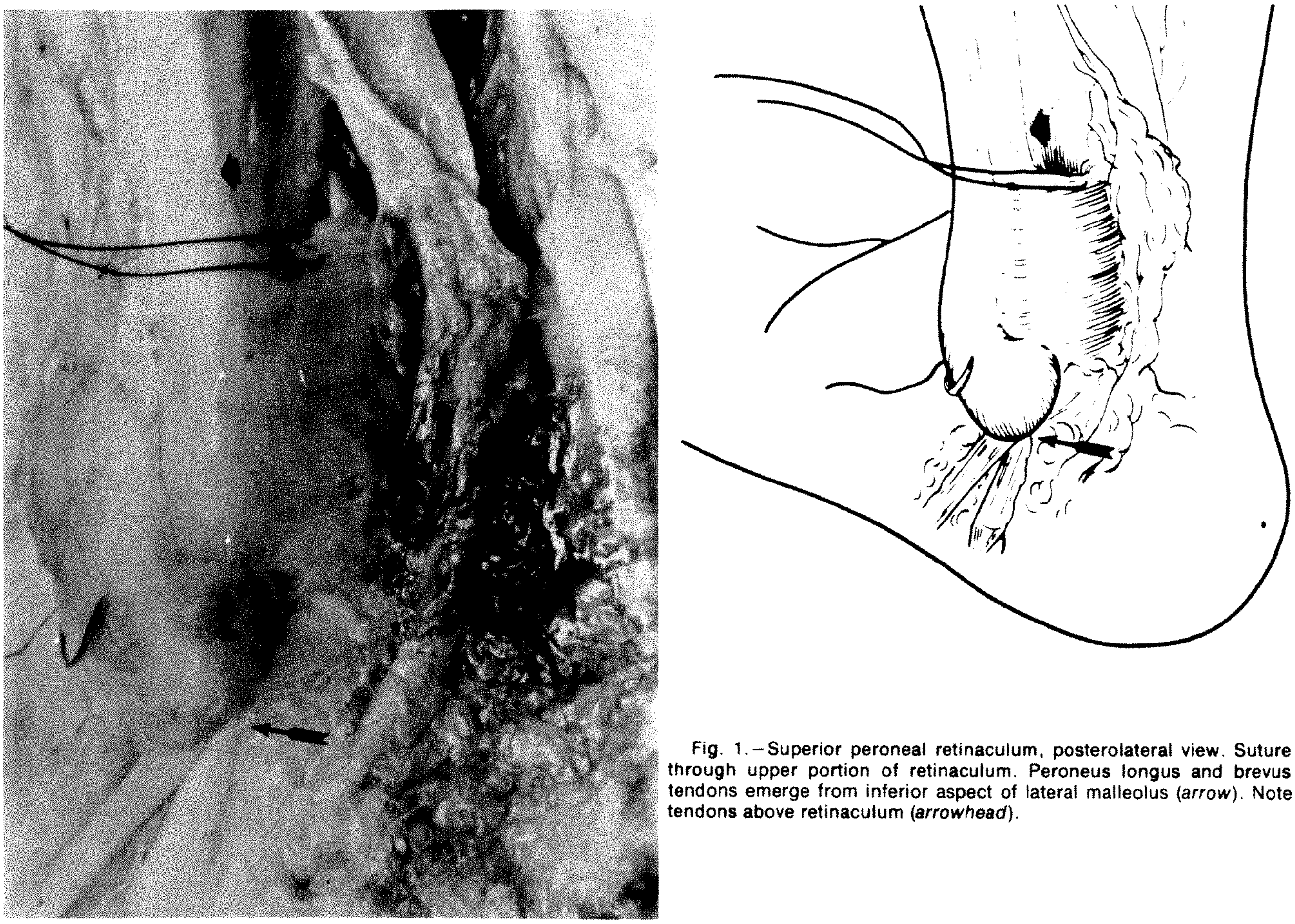

Fig. 1.—Superior peroneal retinaculum, posterolateral view. Suture through upper portion of retinaculum. Peroneus longus and brevus tendons emerge from inferior aspect of lateral malleolus (*arrow*). Note tendons above retinaculum (*arrowhead*).

and immobilization in plaster failed to prevent repeated dislocations while still in plaster, probably in part because of the patient's refusal to remain nonweightbearing. At surgery the periosteum to which the retinaculum is attached was sutured back to the lateral malleolus from which it had been avulsed.

Case 3

A 20-year-old female sustained an injury to her left ankle while skiing. The injury resulted in pain over the lateral malleolus, and she was unable to continue skiing. At the emergency department ankle x-rays revealed a very thin flake of bone lying along the posterolateral border of the lateral malleolus. She was referred to the orthopedic clinic with a diagnosis of ankle sprain. There a diagnosis of peroneal tendon dislocation was made and confirmed clinically.

Case 4

A 19-year-old male sustained an ankle injury while skiing. X-rays revealed a small flake fracture as in cases 1 and 3 (fig. 4). The condition was diagnosed as ankle sprain and treated with a plaster cast for 6 weeks. After removal of the cast, he had continued disability due to repeated painful dislocation of the peroneal tendons. The patient was ultimately referred to another physician who diagnosed peroneal tendon dislocation. Surgery confirmed avulsion of the anterior end of the superior peroneal retinaculum with a small cortical avulsion fracture.

Case 5

A 20-year-old male slipped on a stairway which resulted in dorsiflexion of his right ankle. No fracture was seen on x-rays of the ankle. The injury was diagnosed as a ligamentous strain and treated with a plaster cast. At his first examination out of plaster, the peroneal tendons could be felt to dislocate with dorsiflexion and eversion of the foot. Peroneal tendon dislocation was confirmed and treated surgically. Surgical findings were similar to those described in case 2.

Case 6

An 18-year-old female sustained a dorsiflexion ankle injury in a fall from a skateboard. Peroneal tendons were felt to dislocate on physical examination, and no evidence of fracture was noted on x-ray. Peroneal tendon dislocation was confirmed and treated surgically. The surgical findings were similar to cases 2 and 5.

Discussion

The radiographic diagnosis of peroneal tendon dislocation depends upon recognition of the thin cortical fracture, which is usually seen adjacent to the lateral malleolus on both internal rotation oblique and anteroposterior projections. These fractures are considered pathognomonic [1], occurring in 15% of cases in some

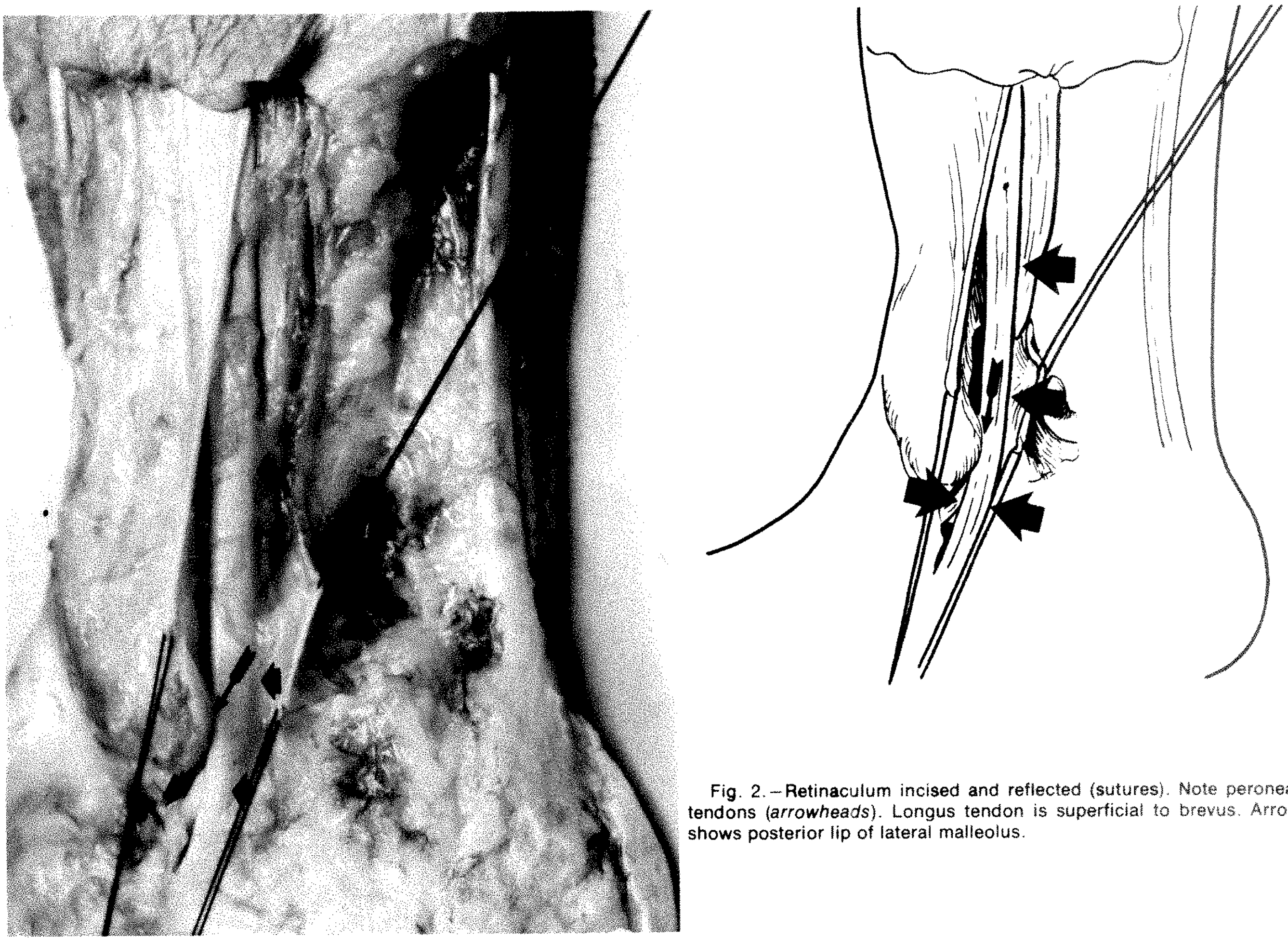

Fig. 2.—Retinaculum incised and reflected (sutures). Note peroneal tendons (*arrowheads*). Longus tendon is superficial to brevus. Arrow shows posterior lip of lateral malleolus.

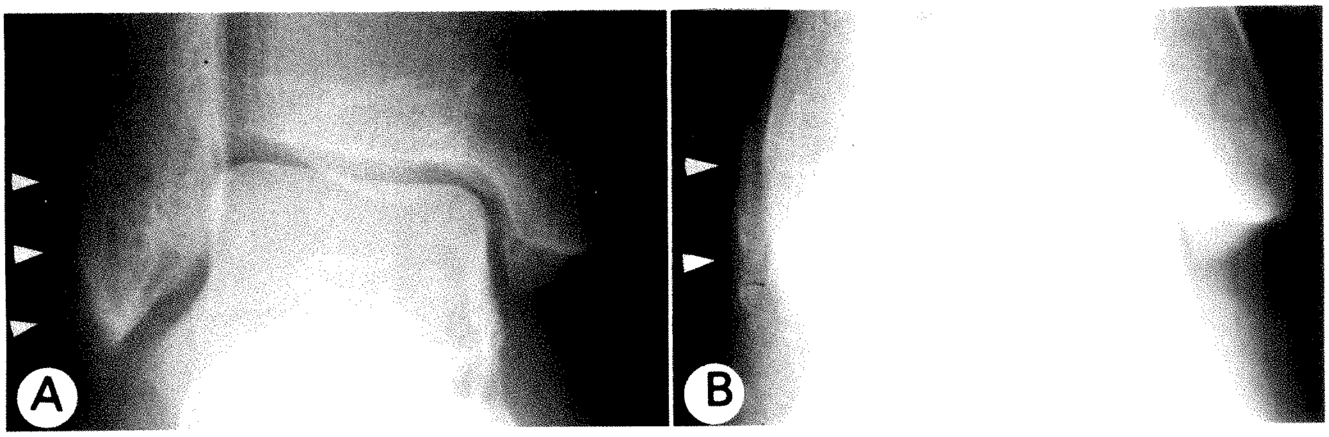

Fig. 3.—Case 1. *A*, Anteroposterior radiograph showing flake fracture from lateral aspect of lateral malleolus (*arrows*). *B*, Film enhanced for soft tissue detail.

series [4] to 50% in others [1]. Three of our six cases had fractures. The absence of a fracture may make diagnosis more difficult, perhaps partly explaining the discrepancy in these percentages.

Clinical diagnosis requires a high index of suspicion, particularly because spontaneous reduction is common and considerable swelling may be present. Clinical signs are swelling and tenderness localized to the posterolateral aspect of the lateral malleolus with intense pain in this region caused by eversion against resistance. The tendons can be felt to dislocate or move with forcible dorsiflexion and eversion of the foot [1, 4].

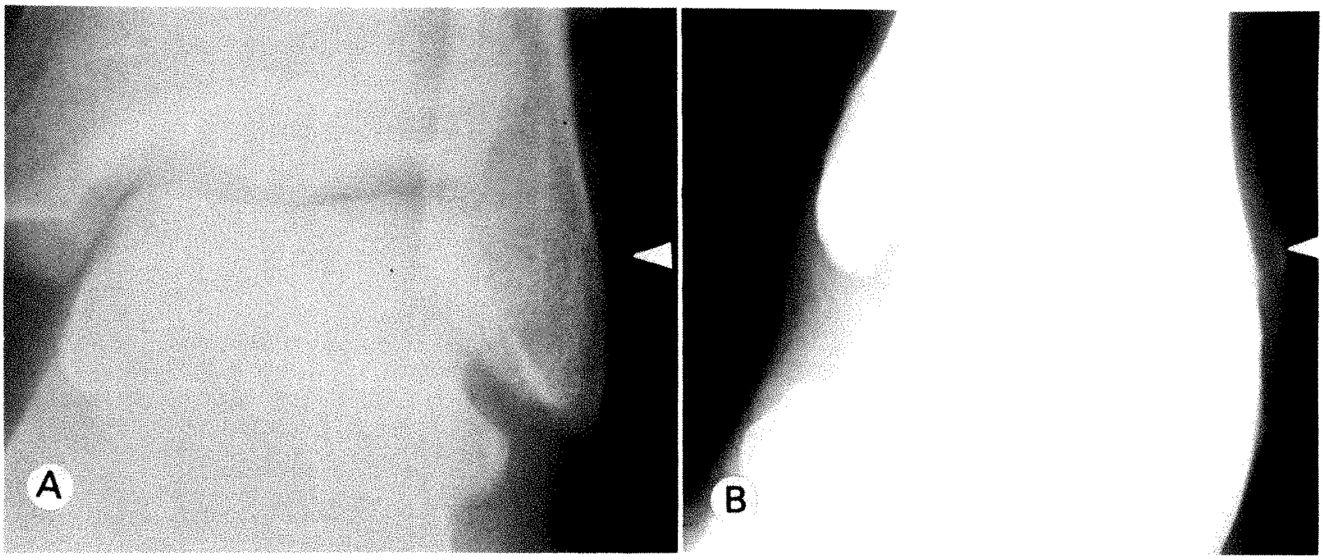

Fig. 4.—*A*, Anteroposterior film showing extremely thin fracture fragment slightly more dense than soft tissues (*arrows*). *B*, Film enhanced for soft tissue detail.

Proper treatment of this injury is still somewhat controversial. There are advocates of both conservative treatment and of open repair, but it is widely agreed that mere strapping of the ankle is insufficient and predisposes to chronic recurrent dislocation.

ACKNOWLEDGMENTS

I acknowledge the member of my family, Sue Carol Church, whose injury prompted this report; and Drs. J. E. Stewart and S. T. Hanson, Jr., who treated two of these cases.

REFERENCES

1. Earle AD, Moritz JR, Tapper EM: Dislocation of the peroneal tendons at the ankle: an analysis of 25 ski injuries. *Northwest Med* 71:108–110, 1972
2. Stover CM, Bryan DR: Traumatic dislocation of peroneal tendons. *Am J Surg* 103:180–186, 1962
3. Eckert WR, Davis EA: Acute rupture of the peroneal retinaculum. *J Bone Joint Surg [Am]* 58:670–673, 1976
4. Jonasch E: Traumatische Peroneussehnen-Luxation. *Munch Med Wochenschr* 109:2320–2321, 1967

Subchondral Pseudocysts in Rheumatoid Arthritis

CHARLES RENNELL,[1] FRANK MAINZER,[2] CARTER V. MULTZ,[1] AND HARRY K. GENANT[2]

Subchondral cyst formation (geode) is a not uncommon manifestation of rheumatoid arthritis which may at times impede correct radiologic interpretation. Four patients with rheumatoid arthritis who demonstrated striking subarticular cystic erosive disease are described. These cases emphasize the nature and appearance of this interesting finding.

Subchondral pseudocysts (geodes) in patients with rheumatoid arthritis may produce radiographic findings that are easily mistaken for other diseases, particularly gout. Our European colleagues have been aware of this possibility for many years [1-7], and a few reports have appeared in the nonradiologic American literature [7-11]. In a recent study of arthritic hips, Resnick et al. [12] described subchondral lucencies in 10 of 13 patients with rheumatoid arthritis or its variants and correlated the pathologic and radiographic findings. Other joints of patients with rheumatoid arthritis may be involved similarly, and this involvement deserves emphasis. The following cases describe similar lesions in the hand, wrist, foot, and knee.

Case Reports

Case 1

A 35-year-old Spanish-American man presented with a 3-year history of polyarthralgia and soft tissue nodules around the wrists and elbows. Laboratory studies revealed: sedimentation rate, 36; calcium, 9.5 mg/100 ml; phosphorus, 3.6 mg/100 ml; RA latex fixation, 1:640; uric acid, 5.6 mg/100 ml. Radiographs of the feet demonstrated cystic lesions without cartilage loss (fig. 1*A*). Bones and joints of the hands were normal. Soft tissue nodules were demonstrated at the elbows. Biopsy of the cystic lesion in the distal portion of the fifth right metatarsal revealed necrosis and collagenous tissue consistent with that of rheumatoid pannus (fig. 1*B*).

Case 2

A 50-year-old Caucasian woman had a 6 year history of rheumatoid arthritis, primarily involving the hands and wrists. In the month preceding examination, the symptoms had increased to involve the feet, knees, and shoulders. On examination, bilateral joint tenderness with swelling involved multiple joints. Laboratory studies revealed: antinuclear antibody (ANA) negative; RA latex fixation, 1:80; uric acid, normal. Sedimentation rate was 45-65 mm/hr. Radiographs of the hands and feet showed multiple cystic erosions with minimal cartilage narrowing and demineralization (fig. 2). A biopsy of the cystic lesion in the distal left radius revealed findings consistent with those of rheumatoid nodule.

Case 3

A 48-year-old Caucasian man (previously reported as "rheumatoid nodulosis" [11]) was examined because of multiple nodules over the dorsal surfaces of the hands, feet, elbows, and Achilles tendons. Physical examination revealed multiple nontender subcutaneous nodules 0.5-1 cm in size over the dorsum of the feet, hands, and elbows. Joint effusion or articular synovial thickening was not evident. Laboratory findings included: RA latex fixation, 1:2,560; sensitized sheep cell titer, 1:2,048; ANA, negative; sedimentation rate, 25 mm/hr; serum uric acid, 6.8 mg/100 ml.

Radiographs of the hands (fig. 3) and feet showed striking soft tissue nodularity and large subchondral cystlike lesions that involved primarily the wrist and metacarpophalangeal joints. Only minimal periarticular erosive disease and mild narrowing of the joint space were noted. No periarticular, fusiform, soft tissue swelling was present. Moderate osteoporosis without periarticular accentuation was identified.

A subcutaneous nodule was excised from the left middle finger for biopsy. Histologic findings were consistent with rheumatoid nodule.

Case 4

A 59-year-old Caucasian man had progressive arthritis involving the hands, wrists, elbows, and knees for 19 years. In 1973, recurrent effusion of the olecranon bursa and painful soft tissue nodules required bursal excision and removal of the nodules at the elbow. The histologic appearance was consistent with that of rheumatoid nodule. Since 1974, recurrent effusions of the elbow, shoulder, and knee have required repeated aspiration. Laboratory studies revealed: calcium, 9.9 mg/100 ml; phosphorus, 3.8 mg/100 ml; uric acid, 6.6 mg/100 ml; RA latex fixation, "positive." A radiograph of the right knee showed multiple large cysts in the subarticular regions of the distal femur and proximal tibia (fig. 4).

Discussion

The term geode has been applied in the European literature to describe large subchondral lucencies which appear cystic radiographically. Histologic examination, however, demonstrates no evidence of an epithelial lining as seen in true cysts. Magyar et al. [6] and Resnick et al. [12] have shown that geodes represent invasion of bone by pannus at the chondro-osseous margin or by synovial fluid at the surfaces of weakened cartilage. They usually communicate with the joint and may represent a means of decompression of a joint under increased pressure. The largest lesions are in joints that are under greatest pressure (e.g., the knee) [3, 4]. They also tend to develop in patients who maintain physical activity, resulting in increased pressure in the joints [2]. Pannus may invade subchondral bone without extending over the cartilage, resulting in cysts without narrowing of the joint space [12]. Other investigators [11, 13] have theorized that true intraosseous rheumatoid nodules may develop in situ in the subarticular regions as a part of a systemic vasculitis.

Received May 5, 1977; accepted after revision September 2, 1977.

[1] Department of Radiology, Valley Medical Center, San Jose, California 95128.

[2] Department of Radiology, University of California, San Francisco, California 94143. Address reprint requests to H. K. Genant.

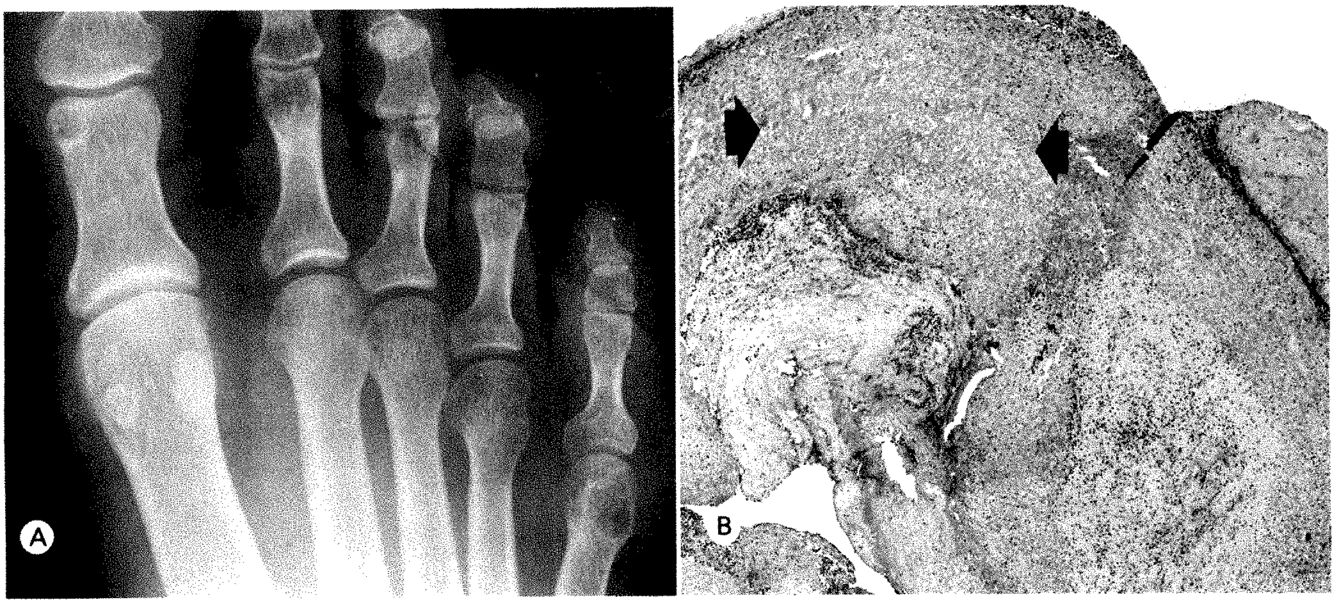

Fig. 1.—Case 1. *A*, Anteroposterior radiograph of right forefoot showing cystlike erosions involving right fifth metatarsal head and first interphalangeal joint. Note mild soft tissue swelling without cartilage loss. *B*, Low power view of histologic section of biopsy from fifth metatarsal head. Area of fibrinoid necrosis (*arrows*) is surrounded by collagenous tissue containing histiocytes, lymphocytes, and scattered polymorphonuclear leukocytes, consistent with rheumatoid pannus.

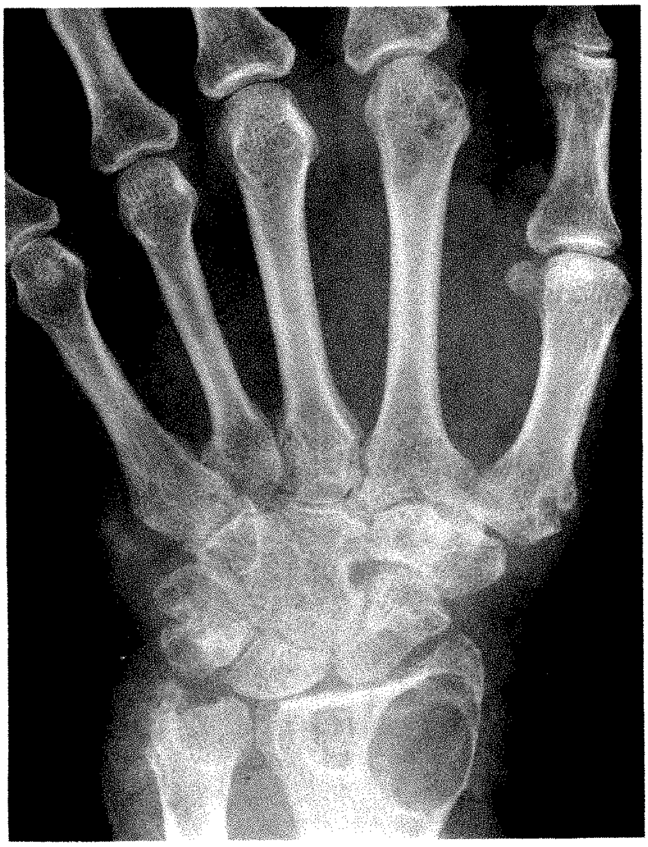

Fig. 2.—Case 2. Radiograph of left wrist showing large geode of distal radius associated with loss of cartilage and ulnar drift at radiocarpal articulation. Minor erosive changes are present.

When patients with rheumatoid arthritis present with soft tissue masses and cystlike bone lesions, the radiographic appearance may be misinterpreted as that of gout. Usually a careful evaluation of the soft tissue masses and of the distribution of the bony abnormality permit the proper diagnosis. Gouty tophi are well circumscribed and may contain calcific deposits. The rheumatoid soft tissue masses do not calcify, and their margins are not as well circumscribed. The masses tend to merge with the normal soft tissues. A definite tendency to symmetrical distribution is noted in abnormalities of the bones and joints. In the early stages, when soft tissue masses are the primary abnormality, they are difficult to differentiate from gout. By the time frank subchondral geodes appear, the symmetrical distribution of the underlying arthritis is quite typical of rheumatoid arthritis.

Ginsberg et al. [11] suggest that presence of soft tissue rheumatoid nodules and cystic bone lesions combined with minimal synovitis or erosive articular diseases represents a distinctive variant of rheumatoid disease which they term rheumatoid nodulosis. In some patients with rheumatoid arthritis the cystic lesions may be predominant, whereas in others the cartilaginous destruction predominates. In all likelihood these conditions represent the two ends of a spectrum within the variable manifestations of rheumatoid arthritis.

REFERENCES

1. Kersley GD, Gibson HJ, Desmarais MHL: Nodule formation in rheumatic disease. *Ann Rheum Dis* 5:141–152, 1946

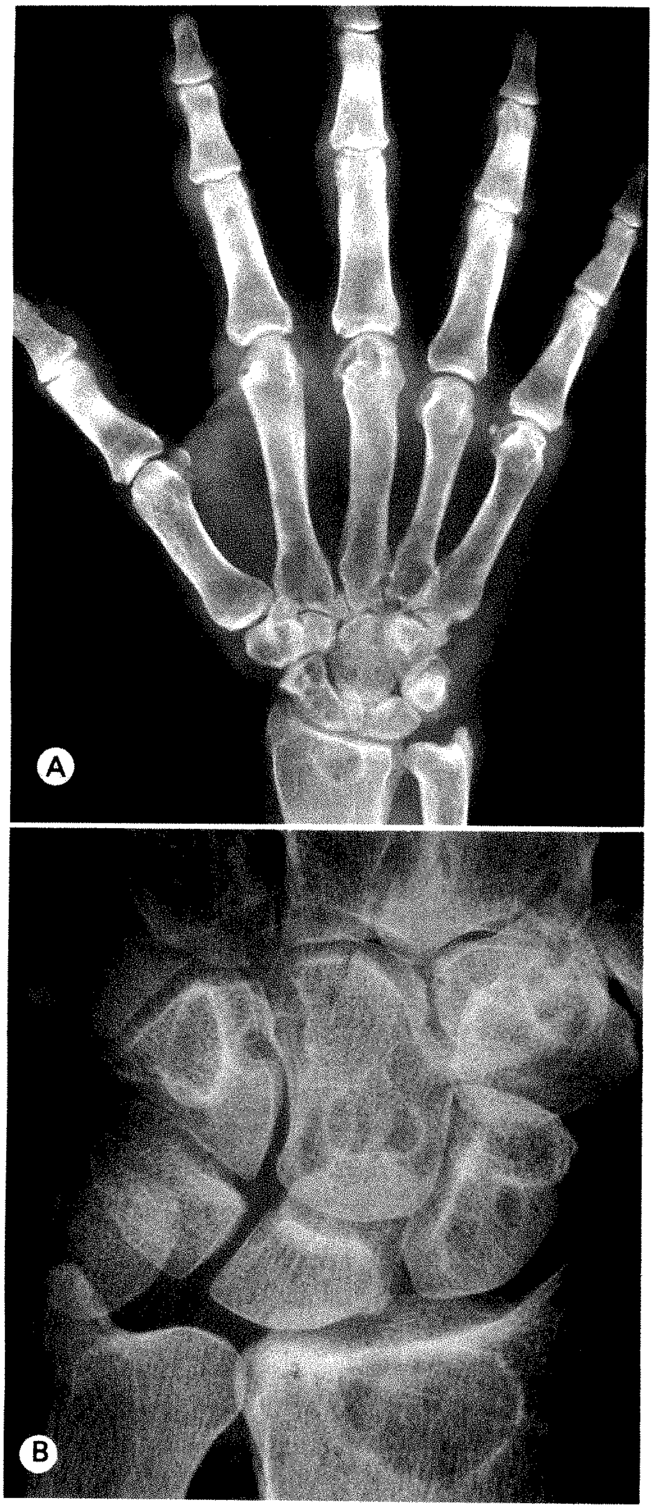

Fig. 3.—Case 3. *A*, Right hand and wrist. Nodular soft tissue swellings are result of rheumatoid nodules. Multiple cystic erosions involve predominantly wrist and metacarpophalangeal joints. *B*, Left wrist containing large nodule in distal radius and numerous smaller cystlike erosions in carpus.

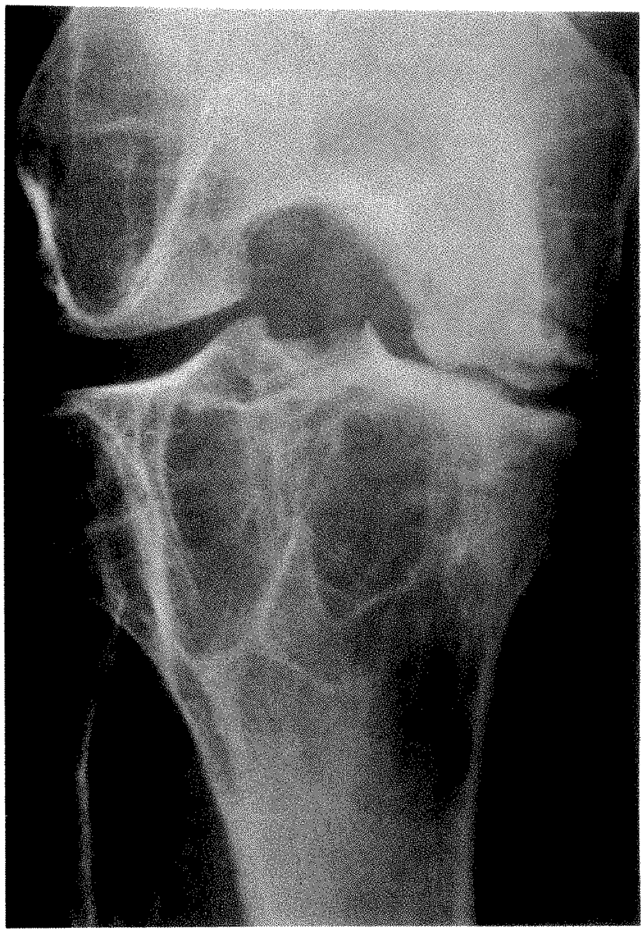

Fig. 4.—Case 4. Radiograph demonstrating reactive sclerosis and loss of cartilage of medial compartment of right knee. Striking cystic erosions involve subchondral bone of proximal tibia and distal femoral condyles.

2. Castillo, BA, el Sallab RA, Scott JT: Physical activity, cystic erosions, and osteoporosis in rheumatoid arthritis. *Ann Rheum Dis* 24:522-527, 1965
3. Jayson MI, Rubenstein D, Dixon AS: Intra-articular pressure and rheumatoid geodes (bone "cysts"). *Ann Rheum Dis* 29:496-502, 1970
4. Jayson MI, Dixon AS, Yeoman P: Unusual geodes ("bone cysts") in rheumatoid arthritis. *Ann Rheum Dis* 31:174-178, 1972
5. Magyar E, Talerman A, Fehér M, Wouters HW: Giant bone cysts in rheumatic arthritis. *J Bone Joint Surg [Br]* 56:121-129, 1974
6. Magyar E, Talerman A, Fehér M, Wouters HW: The pathogenesis of the subchondral pseudocysts in rheumatoid arthritis. *Clin Orthop* 100:341-344, 1974
7. Bywaters EG: The early radiological signs of rheumatoid arthritis. *Bull Rheum Dis* 11:231-234, 1960
8. Lowney ED, Simons HM: "Rheumatoid" nodules of the skin; their significance as an isolated finding. *Arch Dermatol* 88:853-858, 1963
9. Watt TL, Baumann RR: Pseudoxanthomatous rheumatoid nodules. *Arch Dermatol* 95:156-160, 1967

10. Ganda OP, Caplan HI: Rheumatoid disease without involvement. *JAMA* 228:338-339, 1974
11. Ginsberg MH, Genant HK, Yü TF, McCarty DJ: Rheumatoid nodulosis: an unusual variant of rheumatoid disease. *Arthritis Rheum* 18:49-58, 1975
12. Resnick D, Niwayama G, Coutts RD: Subchondral cysts (geodes) in arthritic disorders: pathologic and radiographic appearance of the hip joint. *Am J Roentgenol* 128:799-806, 1977
13. Kersley GD, Ross FG, Fowles SJ, Johnson C: Tomography in arthritis of the small joints. *Ann Rheum Dis* 23:280-287, 1964

Angiographic Features of Osteosarcoma

ISSA YAGHMAI[1]

Arteriography was carried out in 64 cases of pathologically confirmed osteosarcoma to evaluate the angiographic features of this lesion. This investigation proved that a variety of angioarchitectures exist in osteosarcomas, mainly related to the histologic type of tissue as well as the degree of differentiation of a tumor. Fibroblastic and chondroblastic osteosarcomas proved to be less vascular than the osteoblastic type, while the most differentiated tumor appeared to be the least vascular. This technique proved useful in choosing the proper site, or sites, for biopsy as well as for determining the intra- and extraosseous extension of the tumor. Instances were also encountered in which it was of assistance in differentiating osteosarcoma from pathologically similar bone lesions.

The accurate diagnosis of osteosarcoma is often dependent on a careful correlation of its radiographic and pathologic features. However, in some instances the pathologist is hard pressed to adequately differentiate between a benign bone lesion and osteosarcoma. Unfortunately, this difficulty is not peculiar to pathologists, but often extends to radiologists as well [1-7]. There are some traumatic, inflammatory, and neoplastic bone lesions which represent radiographic and histopathologic patterns similar to osteosarcoma. Since osteosarcomas tragically involve the young age group and can require mutilating surgery, any contribution toward confirming or disproving the diagnosis should be of value, provided such an investigation causes little or no harm to the patient. Arteriography has proven to be a significant aid in diagnosing an osteosarcoma in doubtful cases.

Materials and Methods

Arteriography was performed without mortality or significant morbidity in 64 cases of pathologically confirmed osteosarcoma. This material was selected from a series of patients seen during the last 10 years at Tadj-Pahlavi Hospital, Teheran, Iran, and the Medical College of Virginia Hospitals, Richmond, Virginia. Initially, arteriography was carried out in typical cases of different radiographic varieties of osteosarcomas, but subsequently was done only in atypical or questionable cases. The average patient age was 16 years (range 10-26 years). Secondary osteosarcomas were not included in this series.

All patients were studied by a percutaneous arterial needle or catheter injection of contrast medium. In the majority of osteosarcomas of the extremities, direct puncture was the procedure of choice. A manual injection of 20-40 ml of contrast material (Hypaque 50% or Renografin 60%), depending on the size and location of the lesion as well as the age of the patient, was sufficient for excellent visualization of the angioarchitecture of osteosarcomas. Radiographs were obtained with a rapid film changer, using at least 2 films/sec for 4 sec, then one film every 1-2 sec for 16 sec. All cases were studied in two planes; biplane arteriography will save time and limit the dosage of contrast material.

Subtraction technique is extremely valuable in bone angiography, where visualization of the intraosseous vascular pattern is essential. In cases of osteolytic osteosarcoma, the vascular network associated with the lesion is readily visible, disclosing abnormal vessels, displaced vessels, arteriovenous shunting, and areas of abnormal tissue staining. In cases of sclerotic osteosarcoma, these findings are more difficult to appreciate because of obscuration by increased bony density. Subtraction can be done in the usual fashion, or by modified technique using the most informative film in arterial phase as a mask to subtract the most informative venous phase film. The final subtraction film shows arteries in white and veins in black against a gray background (fig. 1*C*). The anatomic relation between arteries and veins is shown on a single film, and can be especially advantageous in correlating normal and abnormal arteriovenous relationships.

Results

The 64 cases in the present series fell into three categories on the basis of plain radiographic appearance: osteolytic, 14; sclerotic, eight; and mixed osteosarcoma, 42. However, all three types share all or most of the following angiographic findings [8-23].

The arterial blood supply to the tumor was always derived from the arteries of the surrounding soft tissues rather than from the diaphyseal nutrient artery. This may be partly due to the fact that the majority of the tumors were in advanced stages and extended beyond the normal bone limits. The caliber of supplying arteries was usually large, but they were never invaded by the tumor. Displacement of the artery was seen in the majority of these cases due to the mass effect. The second and third order branches commonly showed evidence of encroachment, direct invasion, or complete obstruction (figs. 2 and 3).

Neovascularity and hypervascularity were present in all instances, demonstrating pathologic vessels of variable size and shape. The contrast material stayed much longer in the pathologic vessels than in normal ones, perhaps because of the lack of elasticity of the vessel walls. In osteolytic and mixed osteosarcomas, the vascular network of the tumor was often easily seen on arteriograms and, because of superimposition of arteries, gave a reticular pattern to the lesion. In cases of sclerotic osteosarcomas, however, the arteries arising from soft tissue surround the periphery of the tumor, giving rise to numerous arterial branches radiating toward the center of the tumor. The veins follow a similar course. In other words, the sunburst periosteal reaction is seen around the arteries and veins supplying the sclerotic osteosarcoma (figs. 2*B* and 2*C*).

Early venous drainage occurred in 86% of the cases

Received February 28, 1977; accepted after revision July 28, 1977.

[1] Department of Radiology, Virginia Commonwealth University, Medical College of Virginia, MCV Station Box 728, Richmond, Virginia 23298.

Am J Roentgenol **129:1073-1081, December 1977**

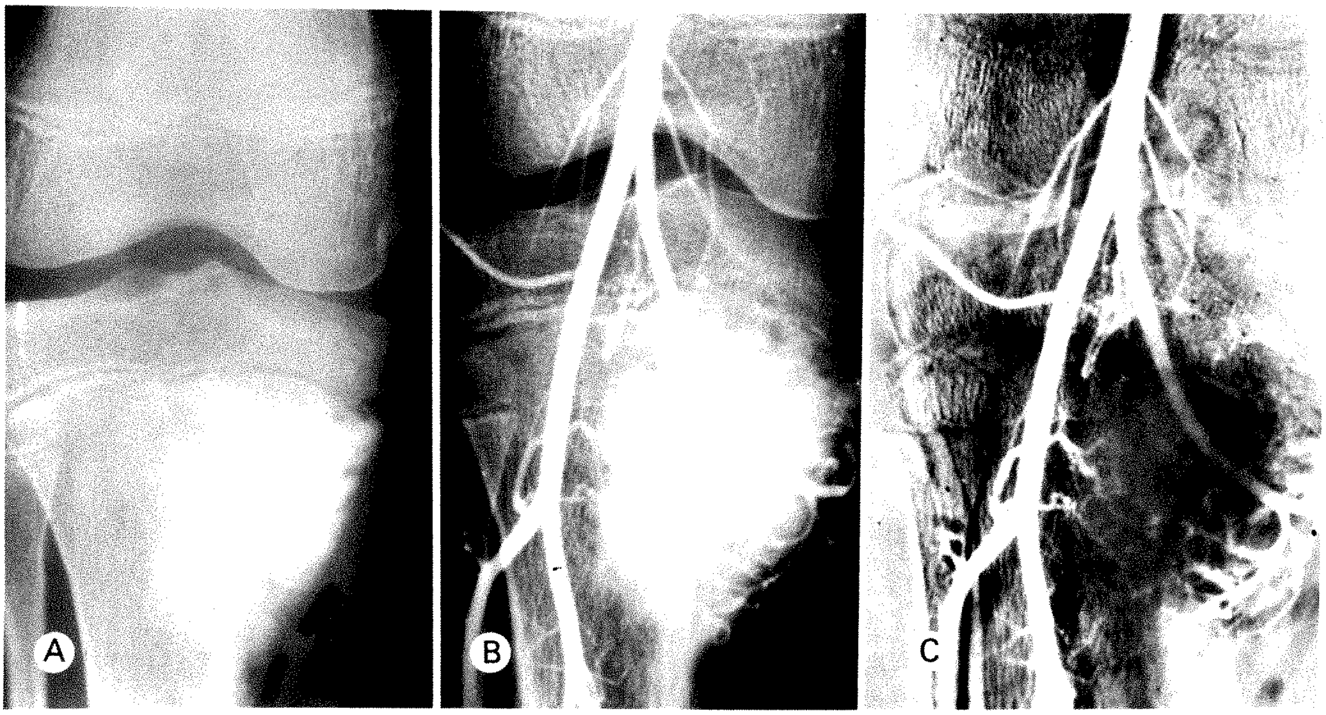

Fig. 1.—Sclerotic osteosarcoma involving medial aspect of metaphysis of proximal right tibia in 13-year-old male. *A*, Anteroposterior view of right knee revealing typical sclerotic osteosarcoma with amorphous density. *B*, Angiogram proving presence of hypervascularity and abnormal arteries around lesion. *C*, Modified subtraction film revealing arteries in white, veins in black, and tumor stain in gray.

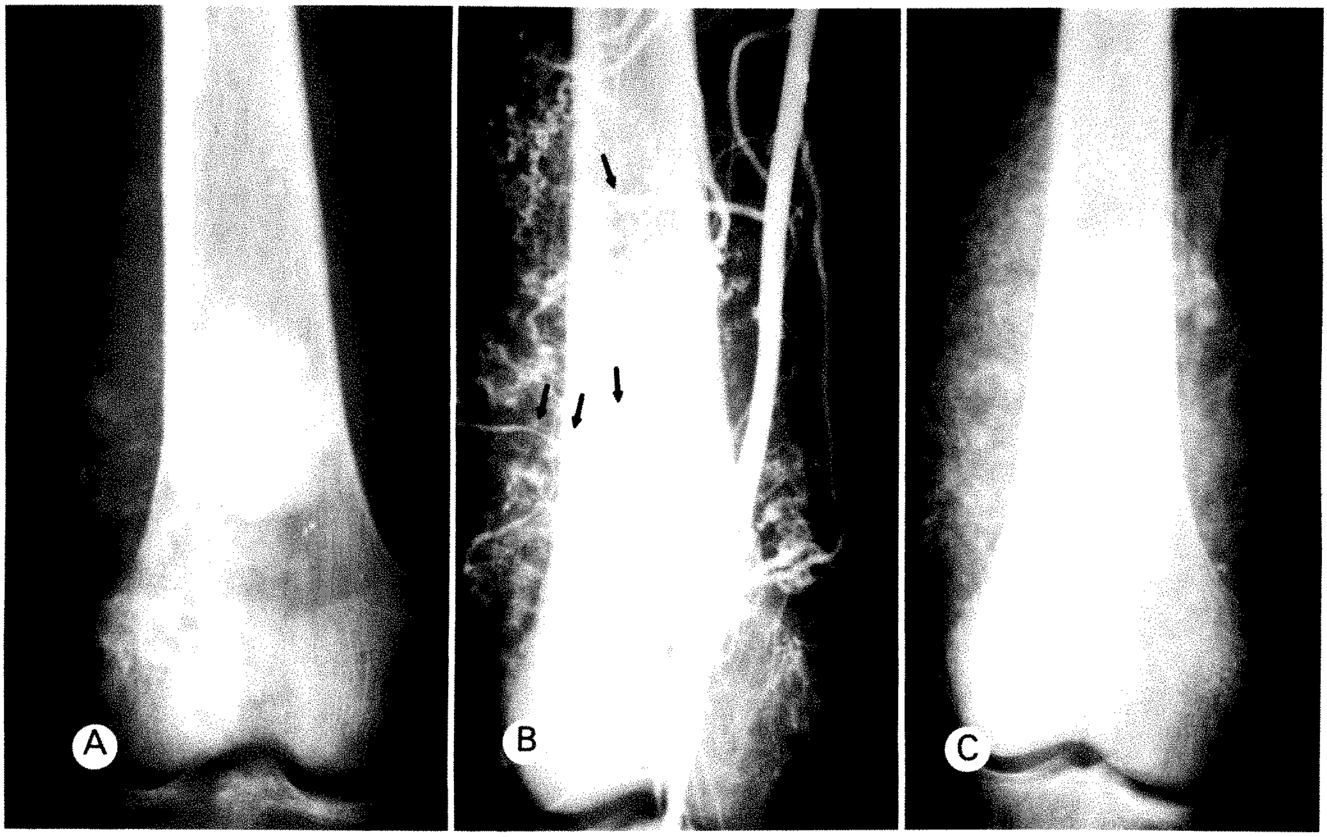

Fig. 2.—Mixed osteosarcoma involving distal femur in 15-year-old male. *A*, Plain anteroposterior view of right femur showing soft tissue ossification adjacent to bony lesion involving distal right femur. *B*, Arteriogram revealing considerable hypervascularity, abnormal vessels, encasement and obstruction of several second and third degree arteries in early arterial phase (*arrows*). *C*, Venous phase showing heavy tumor stain and exact soft tissue confines of tumor, as well as abnormal veins around tumor.

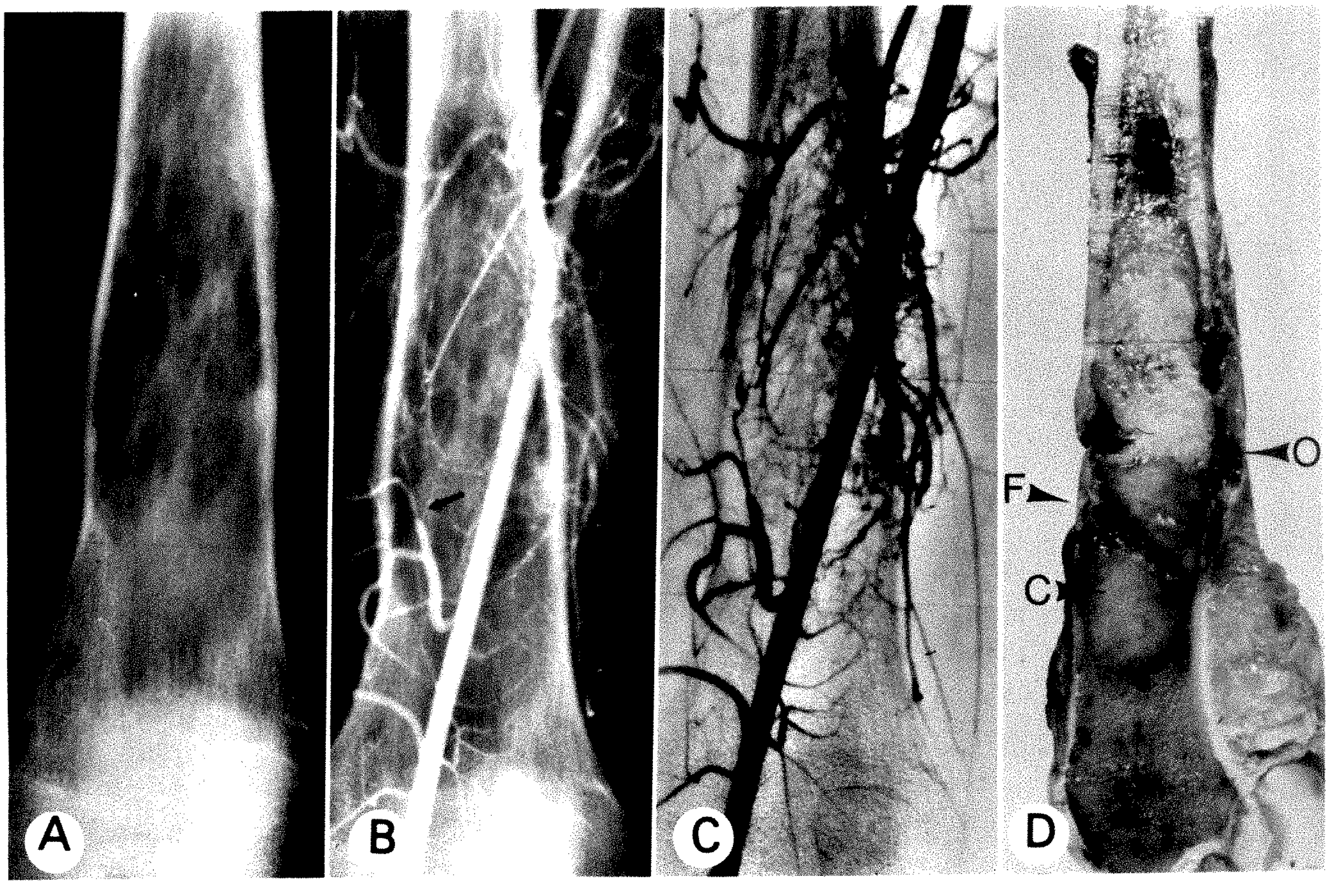

Fig. 3.—Fibroblastic and chondroblastic osteosarcoma involving lower one-third of right femur in 19-year-old female. *A*, Anteroposterior view of femur showing radiolucent lesion with thinning of cortex and minimal periosteal reaction. Tumor was diagnosed as benign lesion (probably fibrous dysplasia) radiographically. *B and C*, Arteriograms showing moderate vascularity and pathologic vessels, especially in upper part of tumor. Encasement of second and third degree arteries was highly suggestive of malignancy (*arrows*). Biopsy of lower medial part of tumor was diagnosed as fibrosarcoma. *D*, Postsurgical pathologic specimen showing three types of tissues: majority is chondroid and fibroid tissue (C, F) and only small area of osteoid tissue (O). Tumor classified as osteosarcoma.

and was primarily the result of rapid circulation through the tumor. Frank arteriovenous shunting was present in 16% of cases.

Tumor stain was related to the degree of vascularity of the osteosarcoma. It was evident from the angiograms that all osteosarcomas were more vascular than the surrounding soft tissues. Several of the tumors were markedly heterogeneous in their vascularity and tumor stain; some regions contained a myriad of wide vessels in an irregular reticular pattern, and other areas had sparser and narrower vessels.

In 19 cases of the present series, nonuniform angioarchitecture within the tumor was noted, with little or no vascularity in a part of the tumor. The cause of these changes was related to hematoma in four cases; necrosis, nine cases; fracture, three cases; and the presence of chondroblastic and well differentiated fibroblastic tissue, three cases (figs. 3*B* and 3*C*).

The pathologic vessels and staining were best seen on subtraction films, particularly in sclerotic osteosarcomas (figs. 1*C* and 4*C*). The draining veins were usually dilated. They showed evidence of displacement, direct invasion of the wall, or intraluminal extension of tumor. These findings were responsible for obstruction of major veins in 22% of the cases. The presence of venous lakes was a distinct finding in the majority of osteolytic and mixed osteosarcoma. They were not detectable in osteoblastic tumors of this series.

In 98% of the cases, the osteosarcoma had extended well beyond the confines of the host bone to involve the adjacent soft tissues. The tumor stain was a highly reliable criterion for determining the extraosseous and intraosseous extent of the tumor.

Discussion

The difficulty in the pathologic interpretation of osteosarcoma results from the great variability which exists in the histopathology of these lesions. Most pathologists indicate two essential criteria for the diagnosis of an osteosarcoma: (1) the presence of sarcomatous stroma and (2) the direct formation of osteoid and bone within the tumor [1–7]. On this basis, osteosarcomas fall into four different groups: (1) osteoblastic, (2) telangiectatic, (3) chondroblastic, and (4) fibroblastic, depending on the predominate histologic pattern.

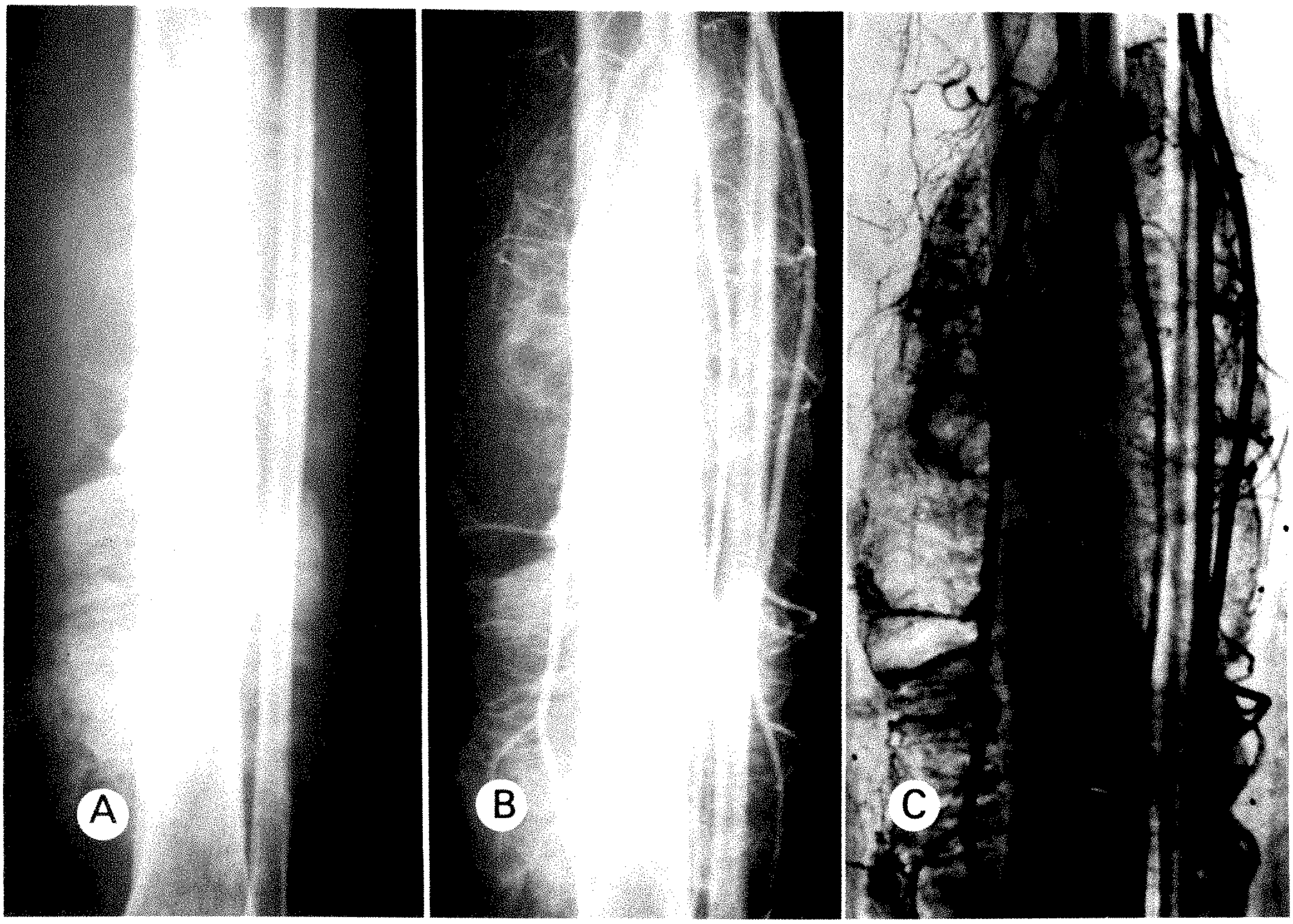

Fig. 4.—Sclerotic osteosarcoma involving shaft of left tibia in 18-year-old male with typical sunburst periosteal reaction (*A*). *B and C*, Arteriograms revealing hypervascularity and abnormal vessels in tumor area. Tumor vessels arise from surrounding soft tissue and extend into tumor mainly perpendicular, via radiolucent area between elements of sunburst periosteal reaction. These findings are best seen in subtraction film (*C*).

Histopathologic studies of the blood vessels of malignant bone neoplasms by Lagergren et al. [24] revealed that osteoblastic tissues are the most vascular part of any osteosarcoma. Osteoblastic osteosarcomas in our experience, regardless of their plain radiographic findings (sclerotic, osteolytic, or mixed), appeared highly vascular. The histopathologic variability of osteosarcoma creates a spectrum of angioarchitecture, although a careful correlation of histology and angiography proved that all osteosarcomas were more vascular than surrounding soft tissues. In our series, 95% of cases were classified as highly vascular tumors, regardless of their plain radiographic appearance.

Some authors [25] believe that sclerotic bone neoplasms are less vascular than osteolytic or mixed tumors, although our experience with subtraction films showed sclerotic osteosarcomas are hypervascular. Sclerotic osteosarcomas in our series were diagnosed as osteoblastic osteosarcomas histopathologically. Their plain radiographic features were typical and presented two different radiographic patterns. One group had amorphous dense sclerosis on plain radiographs and moderate vascularity associated with light tumor stain on angiography (fig. 1); the second group, more commonly seen, presented considerable sunburst periosteal reaction (fig. 4), within which was seen a special type of circulation typical of this type of osteosarcoma. There was no evidence of tumor necrosis or hematoma in sclerotic osteosarcomas.

Osteolytic and mixed osteosarcomas were noted in 56 cases. Histopathologically these lesions were diagnosed as osteoblastic osteosarcoma in 51 cases, presenting all or most of the angiographic features of osteosarcoma. Two cases were classified as telangiectatic osteosarcoma, two as fibroblastic osteosarcoma, and one as fibrochondroblastic osteosarcoma.

Telangiectatic osteosarcoma appeared to be the most vascular and presented numerous vessels with aneurysmal dilatation in the tumor area. Considerable tumor necrosis, noted in both cases, clinically presented very rapid growth as well as poor prognosis. Both of our patients had diffuse lung and liver metastases at the time of angiography.

Fibroblastic and chondroblastic osteosarcomas created more diagnostic difficulty than the others. On plain radiographs especially, these osteosarcomas usually stimulated benign bone lesions such as benign osteoblastoma, fibrous dysplasia, enchondroma, or infection.

We believe the plain radiographic findings in these cases are related to the proportions of chondroid, fibroid, or osteoid tissue. For example, if a lesion contains more chondroid tissue, plain radiographic findings will be similar to intramedullary or cortical chondrosarcoma (fig. 3*A*); or, in case of fibrous tissue, it may occasionally demonstrate sequestration as seen in fibrosarcoma and osteomyelitis.

The angiographic features of lesions of chondroid or fibroid tissue also are not typical and appeared to be the least vascular osteosarcomas. Therefore, the degree of vascularity of a chondroblastic or fibroblastic osteosarcoma is dependent on the percentage of the tumor occupied by chondroid or fibroid tissue, and the degree of their cell differentiation. These types of tumors usually present a heterogeneous angioarchitecture (fig. 2).

The highly vascular part of a heterogeneous osteosarcoma corresponded to the less differentiated areas, from which cells or cell aggregates might easily be carried to the lungs. Angiography will not only detect the vascularity of the tumor and its extension into the medullary channel or soft tissue, but afford the opportunity to choose the best site, or sites, for biopsy.

Differential Diagnosis

Due to the variety of radiographic features which exist in osteosarcomas, from purely osteolytic to amorphous sclerotic, the radiologist must differentiate osteosarcoma from numerous bone lesions. Similarly, the presence of a variety of cells (e.g., osteoblastic, fibroblastic, mesenchymal, synovial, and giant cells in a tumor), as well as histopathologic similarities to several other malignant and benign bone lesions, makes differentiation difficult for the pathologist as well. There are several bone lesions for which histologic differentiation from osteosarcoma is impossible; such lesions can usually be distinguished by a combination of plain radiographic and histopathological findings. However, benign conditions such as stress fracture, exuberant callous formation, myositis ossificans, benign osteoblastoma, and osteomyelitis occasionally have been confused both histologically and radiographically with osteosarcoma. In these instances, angiography can provide useful radiologic information to prevent unnecessary surgery.

Callous formation in the early stage, especially associated with stress fractures or in cases with exuberant callous formation, occasionally has been diagnosed as osteosarcoma. Amputations as a result of such histopathologic and radiographic misinterpretations are well known in most institutions. In doubtful situations, we find angiography of great value in solving the problem. The absence of hypervascularity and a nearly normal arteriogram in callous formation can easily differentiate it from osteosarcoma (fig. 5*B*).

Benign osteoblastoma, a rare bone lesion, is another lesion that simulates osteosarcoma. Our experience with arteriography in benign osteoblastoma is limited to one case and is obviously inconclusive. Angiography in that case revealed mild hypervascularity and neovascularity without encasement, encroachment of second and third degree arteries, tumor stain, or abnormal veins (fig. 6*B*). Absence of soft tissue extension was a significant finding in this tumor.

Myositis ossificans circumscripta is another tumorlike lesion with some radiographic and histopathologic similarities to osteosarcoma. In the active stage, which usually starts about 2 weeks after trauma and continues for 6–10 weeks, this lesion appears as a soft tissue mass with scattered foci of new bone formation and periosteal reaction of adjacent bone. Histopathologically, these lesions frequently have been interpreted as osteosarcoma. Angiography at this stage shows some degree of hypervascularity, depending on the age and degree of maturation of the lesion, and lacks all other angiographic findings of osteosarcoma (fig. 7*B*) [26]. Early and late stages of myositis ossificans circumscripta usually are diagnosed by plain radiography or histopathology. Therefore, there is no indication for angiography.

Osteomyelitis is a common lesion which may simulate osteosarcoma. In radiographs of its active phase, it mimics round cell tumors more than osteosarcoma. In the subacute and chronic stages, it can simulate osteosarcoma radiographically, as well as pathologically. The angiographic features of osteomyelitis change according to the stage of the disease. In the acute phase there is evidence of hypervascularity and neovascularity, although this gradually diminishes to normal vascularity in the chronic stage (fig. 8*B*). In all stages of the disease, the angiographic findings lack all other features of osteosarcoma. Soft tissue extension in the active stage is commonly seen and therefore should not be mistaken for malignancy.

Malignant bone lesions which simulate osteosarcoma radiographically and histopathologically are fibrosarcoma, chondrosarcoma, and parosteal sarcoma. Arteriography is of no help in differentiating fibrosarcoma or chondrosarcoma from osteosarcoma; however, it is important in the differentiation of parosteal sarcoma from osteosarcoma. Parosteal sarcoma shows substantial new bone formation, but only minimal (if any) increase in vascularity (fig. 9*B*). These highly differentiated tumors usually do not have a poorly differentiated malignant or vascular component; however, Jaffe [5] distinguishes two types of parosteal osteosarcoma, one of which has a more malignant course. When angiography reveals a highly vascular region in a parosteal sarcoma, it is probably of this more malignant type.

Conclusions

From the material presented, together with data collected from the literature, the following facts concerning osteosarcoma seem to be established.

1. The arterial supply of an advanced osteosarcoma is

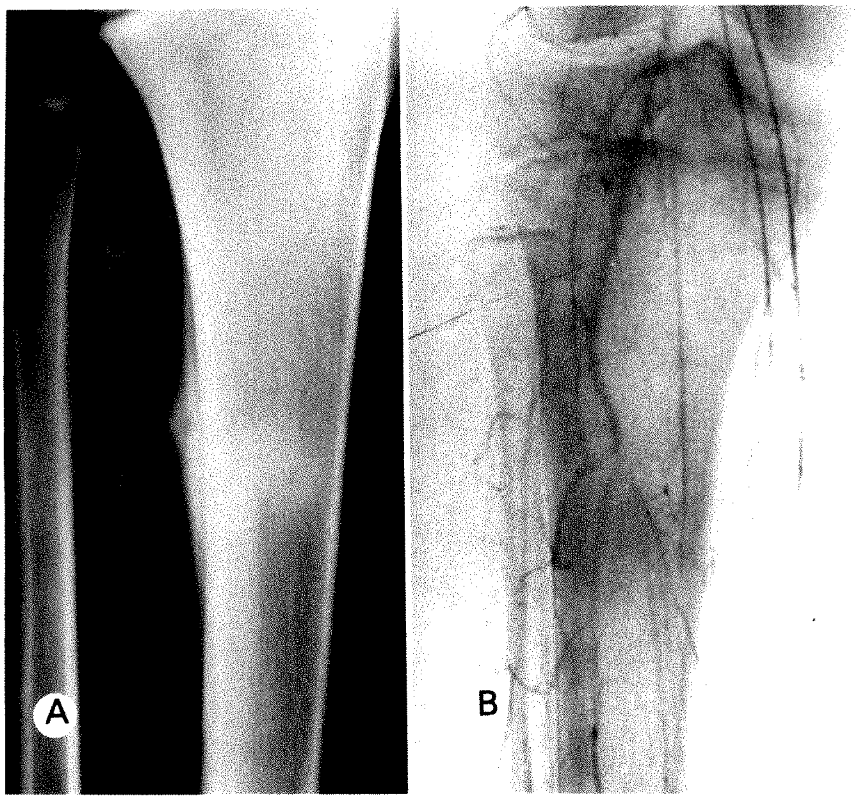

Fig. 5.—Stress fracture involving tibia in 13-year-old female. *A*, Tomogram showing lamellated periosteal reaction with intraosseous bony density and lucency. Osteoid osteoma was considered. *B*, Angiogram showing normal vascularity.

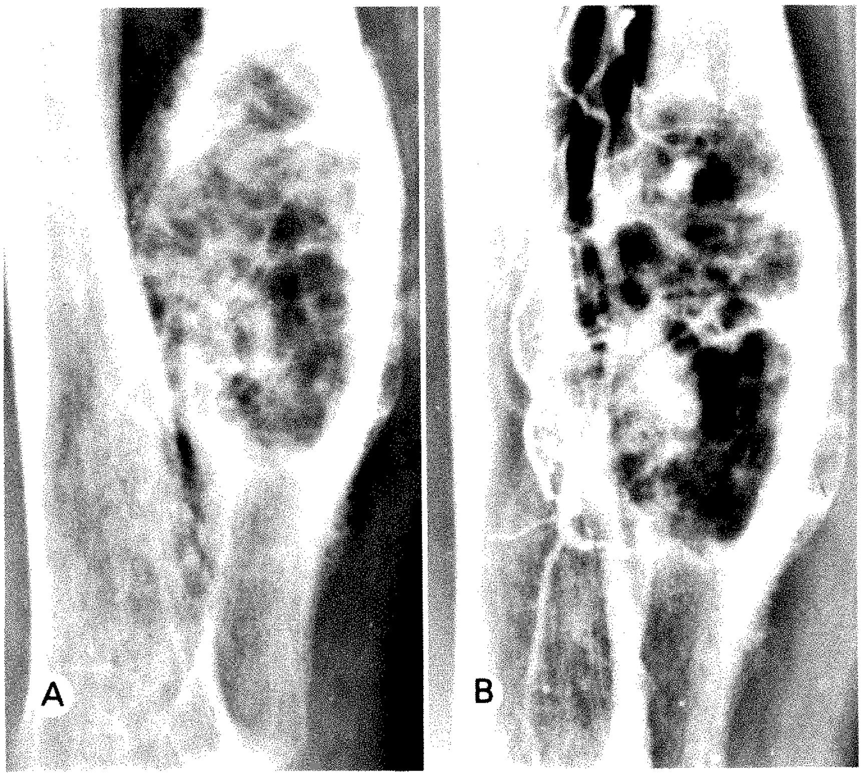

Fig. 6.—Benign osteoblastoma involving lower one-third of ulna in 27-year-old male. *A*, Anteroposterior view of forearm showing well defined, expansile, lobulated radiolucent lesion with minimal periosteal reaction. Lesion was diagnosed as benign bone lesion; however, biopsy was reported as osteosarcoma. *B*, Angiogram showing mild hypervascularity and stain. Absence of soft tissue extension or vessel encasement suggested benign neoplasm. En bloc resection of lesion was recommended and showed benign osteoblastoma.

primarily from the soft tissue surrounding the lesion; diaphyseal nutrient arteries did not contribute significant blood supply.

2. Osteosarcomas, regardless of their plain radiographic appearance, are hypervascular. Osteoblastic tissue in an osteosarcoma is more vascular than the chondroblastic part.

3. The degree of vascularity has a direct relationship

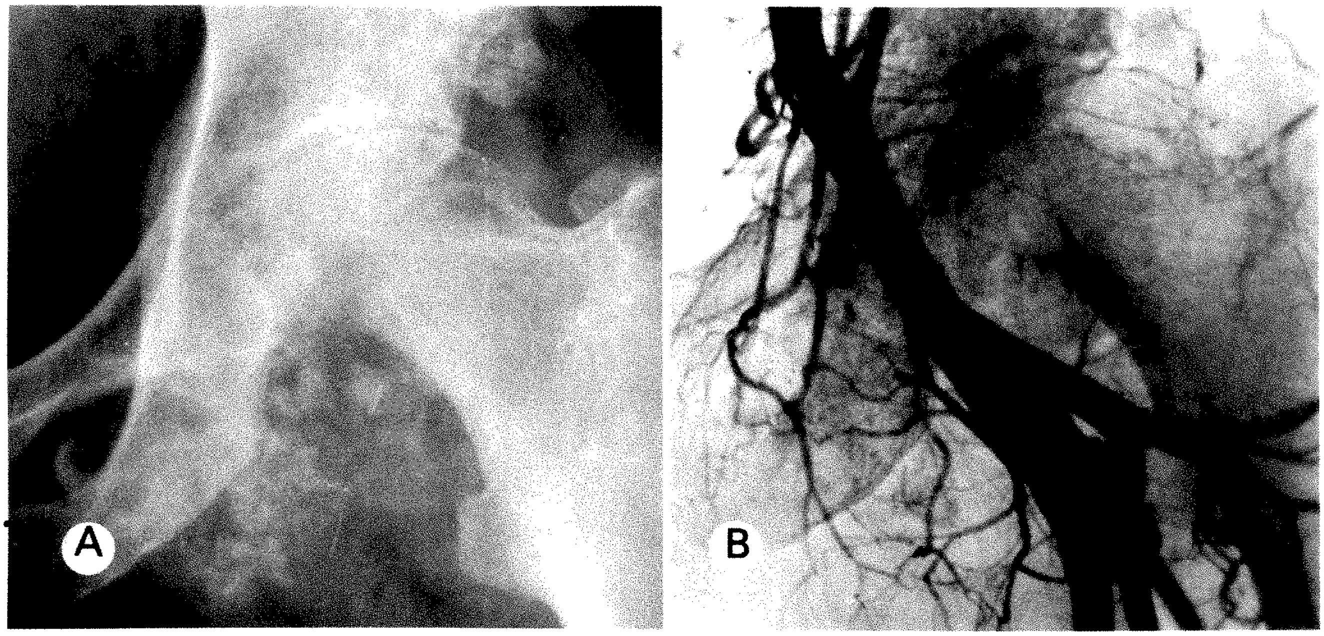

Fig. 7.—Myositis ossificans involving left hip in 29-year-old male. *A*, Anteroposterior view of left hip revealing destructive lesion involving lower margin of femoral head, associated with scattered osseous densities in surrounding soft tissue, suggestive of fast growing bone-forming lesion. *B*, Arteriogram showing displaced femoral artery and its branches, with a few small caliber vessels typical of myositis ossificans in healing stage.

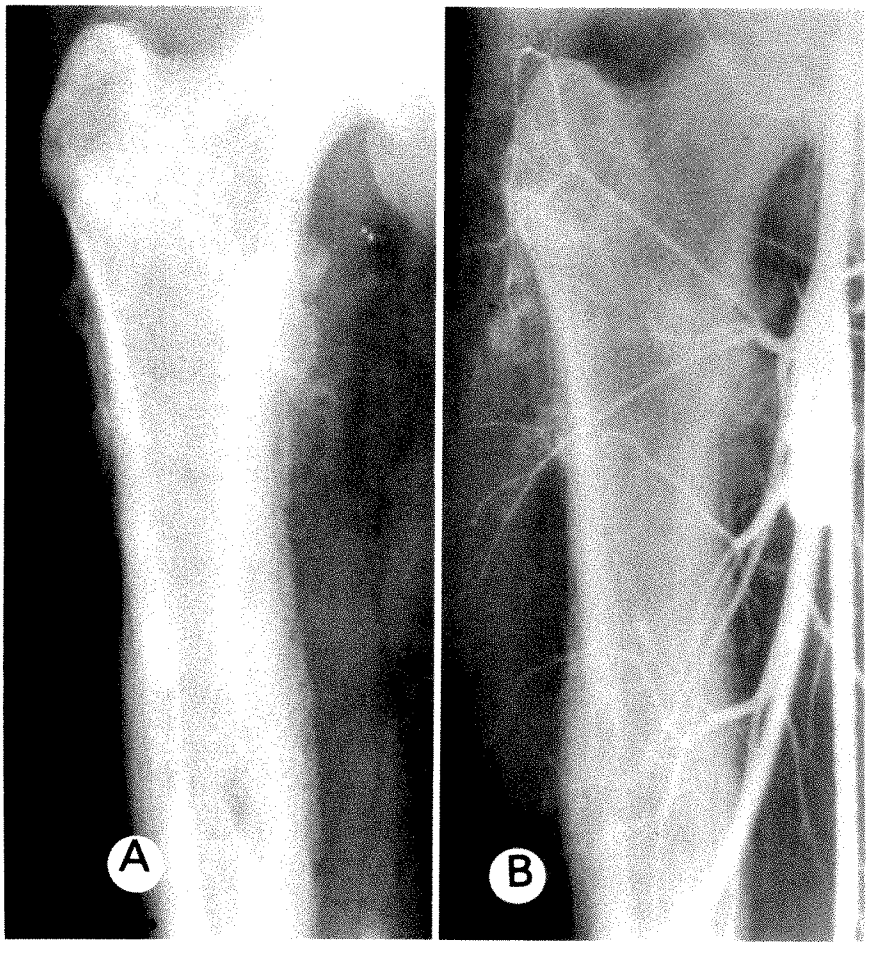

Fig. 8.—Subacute osteomyelitis involving upper shaft of right femur in 17-year-old male. *A*, Plain radiograph showing lamellated periosteal reaction and scattered bony density in soft tissue adjacent to lesion. Radiologic diagnosis was rapidly growing bone lesion; however, differentiation from inflammatory lesion was difficult. *B*, Arteriogram revealing normal vascularity.

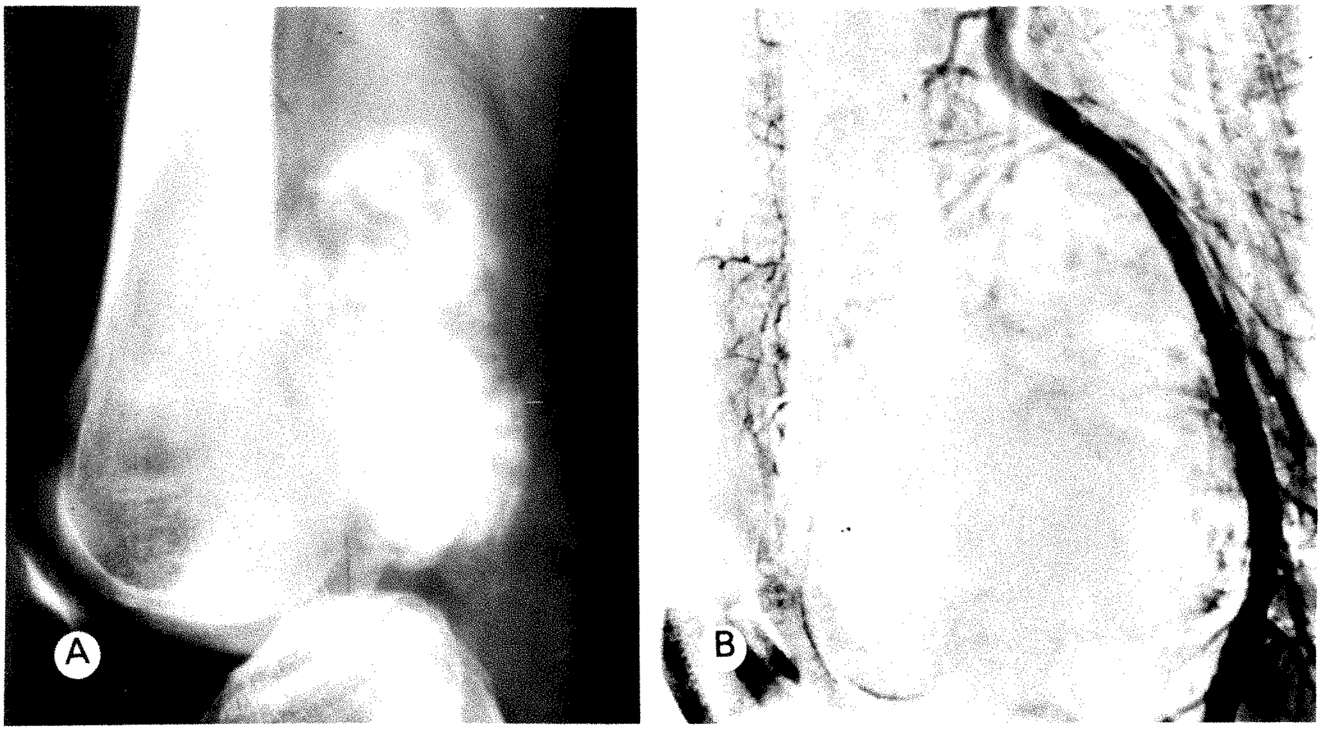

Fig. 9.—Parosteal sarcoma (juxtacortical osteosarcoma) of distal end of right femur in 42-year-old male with previous history of slow growing mass in same area for previous 4 years. *A*, Plain lateral view of distal right femur revealing sclerotic mass arising from periosteum of distal femur with amorphous density and areas of radiolucency typical for parosteal sarcoma. *B*, Subtraction film of arteriogram in early arterial phase showing only displacement of vessels by tumor with no definite evidence of abnormal vessels or stain.

to the differentiation of the cells. Well differentiated zones are less vascular. The best example of this type lesion is parosteal sarcoma.

4. Angiography will demonstrate the angioarchitecture of an osteosarcoma and delineate its intramedullary and extraosseous extent. This information will guide in the selection of the proper site for biopsy.

5. In cases of chondroblastic or fibroblastic osteosarcoma, a single biopsy is not sufficient for a definite diagnosis. In these instances, a biopsy from the most vascular and least vascular part may be the only way to reach a definite diagnosis and establish the degree of malignancy of the lesion.

6. Angiography is helpful to differentiate osteosarcoma from histopathologically similar benign bone lesions such as healing fracture, myositis ossificans, benign osteoblastoma, and osteomyelitis. Therefore, it should be used in doubtful cases before performing radical surgery.

REFERENCES

1. Ackerman LV: Extraosseous localized nonneoplastic bone and cartilage formation (so-called myositis ossificans): clinical and pathological confusion with malignant neoplasms. *J Bone Joint Surg [Am]* 40:279-298, 1958
2. Aegertar EE, Kirkpatrick JA Jr: *Orthopedic Diseases. Physiology, Pathology, Radiology*, 3d ed. Philadelphia, Saunders, 1968
3. Dahlin DC: *Bone Tumors. Special Aspects and Data on 3987 Cases*, 2d ed. Springfield, Ill., Thomas, 1967
4. Edeiken J, Hodes FJ: *Roentgen Diagnosis of Disease of Bone*, 2d ed. Baltimore, Williams & Wilkins, 1958
5. Jaffe HL: *Tumors and Tumorous Conditions of the Bones and Joints*. Philadelphia, Lea & Febiger, 1958
6. Norman A, Dorfman H: Juxtacortical circumscribed myositis ossificans: evaluation and radiologic features. *Radiology* 96:301-306, 1970
7. Shanoff LB, Spira M, Hardy SB: Myositis ossificans: evaluation to osteogenic sarcoma. Report of a histologically verified case. *Am J Surg* 113:537-541, 1967
8. Baciu C, Brosteau G, Stanciuleseu P, Balenty PV: The value of arteriography in the differential diagnosis of bone tumors. *Lyon Chir* 59:206-212, 1963
9. Brondolo W, Scopeta AM: Angiographic pictures in primary bone tumors of extremities. *Arch Ostop* 14:925-932, 1959
10. Brunelli B: Arteriography in the diagnosis of bone tumors of the limbs. *Panminerva Med* 2:180-187, 1960
11. Cockshott WP, Evans KT: The place of soft tissue arteriography. *Br J Radiol* 37:367-375, 1964
12. Dos Santos R: Arteriography in bone tumors. *J Bone Joint Surg [Br]* 32:17-29, 1950
13. Halpern M, Freiberger RH: Arteriography as a diagnostic procedure in bone disease. *Radiol Clin North Am* 8:277-288, 1970
14. Hudson TM, Haas G, Enneking WF, Hawkins IF Jr: Angiography in the management of musculoskeletal tumors. *Surg Gynecol Obstet* 141:11-21, 1975
15. Imura S, Shimantzo D: Arteriography in bone tumors. *Surg Ther* (Osaka) 16:11-16, 1957
16. Inclan A: The possibilities of roentgenographic study of the arterial circulation in the early diagnosis of bone malignancy. *J Bone Joint Surg* 24:259-269, 1942

17. Lasser EC, Schobinger von Schowinger R: Arteriography in bone tumors. A preliminary report. *NY State J Med* 55:3425–3430, 1955
18. Margulis AR, Murphy TO: Arteriography in neoplasms of extremities. *Am J Roentgenol* 80:330–339, 1958
19. Mucchi L, Columella F: Arteriography in diseases of bone. *J Fac Radiol* 3:135–146, 1951
20. Sakai N: Angiographic study of bone tumors. Indications for the decision of surgery, with special reference to the hindquarter amputation. *J Jpn Orthop Assoc* 41:65–80, 1967
21. Strickland B: The value of arteriography in the diagnosis of bone tumours. *Br J Radiol* 32:795–813, 1959
22. Voegell E, Uehlinger E: Arteriography in bone tumors. *Skeletal Radiol* 1:3–14, 1976
23. Yaghmai I, Shamsa AZ, Shariat S, Afshari R: Value of arteriography in the diagnosis of benign and malignant bone lesions. *Cancer* 27:1135–1147, 1971
24. Lagergren C, Lindbom A, Soderberg G: The blood vessels of osteogenic sarcoma (histologic, angiographic and microangiographic studies). *Acta Radiol* 55:161–176, 1961
25. Schobinger R: The arteriographic picture of metastatic bone disease. *Cancer* 11:1264–1268, 1958
26. Yaghmai I: Myositis ossificans: diagnostic value of arteriography. *Am J Roentgenol* 128:811–816, 1977

Occurrence of Lung Granulomas in Patients with Stage I Sarcoidosis

YALE ROSEN,[1] JUDITH K. AMOROSA,[2] SANGGIU MOON,[3] JEFFREY COHEN,[2] AND HAROLD A. LYONS[4]

Granulomas were found in the lungs of 21 consecutive patients with stage I sarcoidosis who underwent open lung biopsy. The extent of granulomatous disease and fibrosis was significantly less ($P < .05$) than seen in open lung biopsies from larger groups of patients with stage II and stage III sarcoidosis. The results of this study support what had previously been widely suspected: that is, if sufficient lung tissue is studied microscopically, granulomas will be found in the lungs of all patients having sarcoidosis with mediastinal lymphadenopathy but no radiographically demonstrable lung abnormalities.

Although the impression is widely held that granulomatous lung lesions probably occur in all patients with sarcoidosis whose chest radiographs show mediastinal lymphadenopathy but no pulmonary lesions (stage I), this has not been well documented. In 1967 Scadding [1] stated "It may well be that in nearly all cases of BHL [bilateral hilar lymphadenopathy] some sarcoid tubercles are actually present at some time in the lungs; the proportion could be determined by biopsy procedures in a large series which would be unjustifiable." Bacharach [2] stated that "the extent of parenchymal granulomatous involvement can be gauged only roughly on roentgenographic examination. The asymptomatic patient demonstrating only hilar lymph nodes will usually, at thoracotomy, be found to have considerable parenchymal involvement." Several previous reports [3-8], mostly of small numbers of patients studied by various lung biopsy procedures, indicate a high incidence of lung granulomas in stage I disease (table 1).

Materials and Methods

Consecutive open lung biopsies from 21 patients with the clinical diagnosis of stage I sarcoidosis were studied. Open lung biopsy in patients with stage I sarcoidosis is not a routine procedure at our institution. Of the 21 biopsy specimens, 15 were obtained as part of a triple biopsy study [9] in which patients with the clinical diagnosis of sarcoidosis underwent biopsy of scalene and mediastinal lymph nodes in addition to open lung biopsy. The aim of that study was to determine which tissues provided the highest yield of granulomas. Patients were considered to have stage I disease if the prebiopsy chest radiograph demonstrated mediastinal lymphadenopathy but no pulmonary parenchymal lesions (fig. 1). Stage II included patients exhibiting mediastinal lymphadenopathy and lung infiltrates, and stage III, lung infiltrates only.

Most biopsy specimens were obtained from the lingula of the left lung. With few exceptions these consisted of single fragments of tissue 0.5–3.5 cm in greatest dimension (average, 2.1 cm). Microscopic sections were routinely stained with hematoxylin and eosin, the Ziehl-Nielssen stain for acid-fast bacilli, and the PAS and Gomori methenamine silver stains for fungi. No microorganisms were demonstrated. Cultures of the lung biopsy specimens for mycobacteria in 13 cases and for fungi in 12 cases were all negative. Mediastinal lymph node biopsies were available from 20 patients. All showed nonnecrotizing granulomas with negative stains for acid-fast bacteria and fungi. Only two patients had Kveim tests; each was positive.

All microscopic slides were initially viewed through a dissecting microscope in order to estimate the extent of granulomatous involvement of the lung parenchyma. The extent of parenchymal granulomas was designated as minimal if only a few granulomas were present; 1+ if the granulomas occupied less than one-third of the area of the biopsy specimen; 2+, one- to two-thirds of the area; 3+, more than two thirds of the area.

Standard radiographic techniques were used regardless of the stage of the disease. No magnification radiographs were taken. The prebiopsy chest films of 10 patients were available for review. Posteroanterior and lateral views taken with 120–140 kV technique were available in all 10 cases. Two radiologists independently evaluated the lung fields from the 10 study patients and 10 normal controls. In all cases the mediastinum was first blocked out by a strip of black film. Complete agreement that the lung fields were negative was reached by both observers on all of the study and control films. Nine of the 10 study patients had bilateral mediastinal lymphadenopathy. Eight patients had right paratracheal adenopathy; five, left paratracheal; nine, right hilar; and all 10, left hilar adenopathy. In the remaining 11 cases only the original radiographic reports were available.

Results

Nonnecrotizing granulomas were found in the lung biopsy specimens of all 21 patients (table 2; fig. 2). In 17 cases (81%) the granulomas occupied less than one-third of the area of the biopsy specimen (1+), and in seven cases the extent was considered minimal. In table 2 the lung findings in patients with stage I disease are compared with a large group of open lung biopsies from patients with stage II and stage III sarcoidosis that we studied. As expected, the difference in percentage of patients with minimal granulomatous disease in stage I compared to stages II and III combined is significant ($P <$ .05). Similarly the difference between the percentage of patients with less than one-third parenchymal involvement (minimal and 1+) in stage I compared to stages II

Received April 1, 1977; accepted after revision August 18, 1977.

This work was supported in part by U.S. Public Health Service grant 16651.

[1] Department of Pathology, Kings County Hospital Center and State University of New York Downstate Medical Center, 451 Clarkson Avenue, Brooklyn, New York 11203. Address reprint requests to Y. Rosen.

[2] Department of Radiology, Kings County Hospital Center and State University of New York Downstate Medical Center, Brooklyn, New York 11203.

[3] Department of Pathology, Lutheran Medical Center, Brooklyn, New York 11203.

[4] Department of Medicine, Pulmonary Disease Division, Kings County Hospital Center and State University of New York Downstate Medical Center, Brooklyn, New York 11203.

TABLE 1

Results of Lung Biopsy in Stage I Sarcoidosis

Reference	No. Patients	Lung Biopsy Procedure	No. (%) with Lung Granulomas
Young et al. [3]	4	Open	4 (100)
Reid and Lorriman [4]	2	Open	1 (50)
Young et al. [5]	10	Needle	6 (60)
Koerner et al. [6]	8	Transbronchial	6 (75)
Khan et al. [7]	7	Transbronchial	6 (86)
Koontz et al. [8]	20	Transbronchial	11 (55)

TABLE 2

Extent of Lung Granulomas in Relation to Radiographic Findings

Radiographic Finding	Minimal	1+	2+	3+	Total
Stage I	7	10	3	1	21
Stage II	3	19	16	12	50
Stage III	3	9	6	6	24

Note.—Minimal = only a few granulomas in entire biopsy specimen; 1+, granulomas occupy less than one-third of area of biopsy specimen; 2+, granulomas occupy one- to two-thirds of area of biopsy specimen; 3+, granulomas occupy more than two-thirds of area of biopsy specimen.

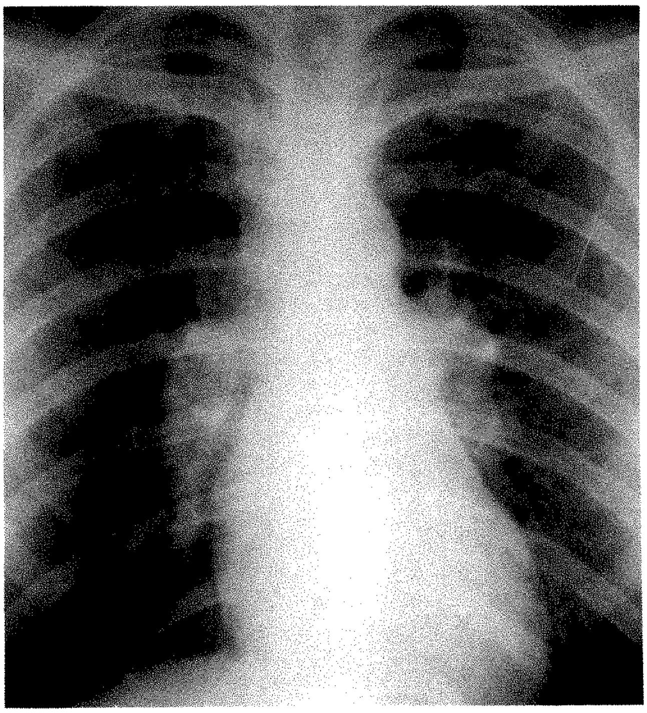

Fig. 1.—Posteroanterior chest film showing unremarkable lung fields and bilateral hilar and right paratracheal adenopathy.

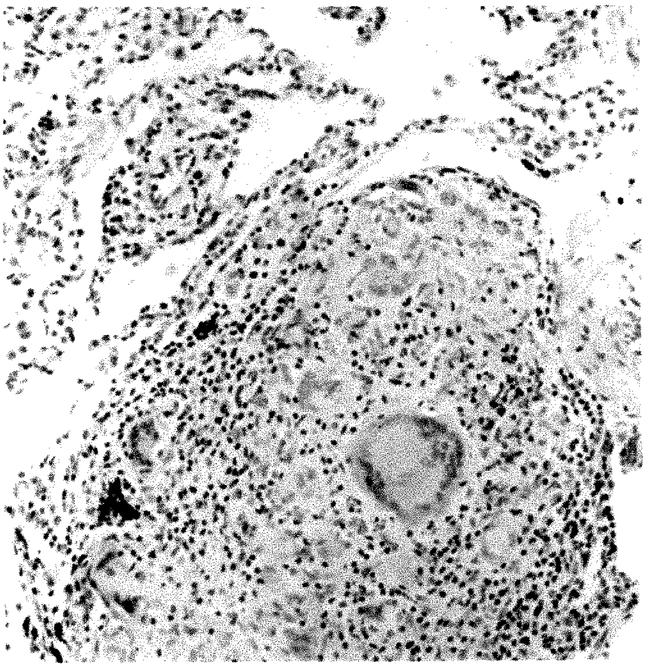

Fig. 2.—Open lung biopsy from same patient as figure 1 showing nonnecrotizing granulomas and nongranulomatous interstitial inflammation. H and E, ×100.

and III combined is significant ($P < .05$). The differences between the figures for stages II and III are not significant.

Fibrosis was present in eight (38%) of the stage I biopsies. This is in contrast to the presence of fibrosis in 62% of 107 open lung biopsies which we examined from patients with stage II and stage III sarcoidosis. The difference is significant ($P = .05$). Of the eight stage I biopsies in which fibrosis was found, five were considered focal and mild, and one case each was focal and moderate, diffuse and mild, and diffuse and severe.

Discussion

We documented the occurrence of pulmonary granulomas in 100% of 21 patients with stage I sarcoidosis. As might be expected because of the absence of radiographic lung abnormalities, the extent of parenchymal granulomatous disease and fibrosis is less in this group than in patients having stage II and stage III disease.

From the data presented in table 2, it would be tempting to conclude that granulomatous disease of the lungs is not likely to be radiographically demonstrable if the granulomas occupy less than one-third of the volume of the lung parenchyma. This conclusion is not warranted, since we cannot assume that the biopsy specimen is representative. The finding of minimal and 1+ granulomatous disease in about half of the patients with stage II and stage III disease indicates that a significant number of these biopsies are indeed not representative of the extent of disease throughout the lungs.

Our results indicate that when a sufficiently large volume of tissue is available for study, the incidence of lung granulomas is 100% in patients with sarcoidosis having radiographically demonstrable mediastinal lymphadenopathy without lung abnormalities. The largest previous study of lung biopsy in stage I sarcoidosis involved a group of 20 patients studied by transbronchial biopsy [8]. The relatively low incidence of lung granulomas in that series (55%) compared to 100% in our open lung biopsy series can be attributed to the comparatively small size of transbronchial biopsy specimens.

REFERENCES

1. Scadding JG: *Sarcoidosis.* London, Eyre & Spottiswoode, 1967
2. Bacharach T: Sarcoidosis: a clinical review of 11 cases. *Am Rev Respir Dis* 84:12-16, 1961
3. Young RC, Carr C, Shelton TG, Mann M, Terrin A, Laurey JR, Harden KA: Sarcoidosis: relationship between changes in lung structure and function. *Am Rev Respir Dis* 95:224-238, 1967
4. Reid L, Lorriman G: Lung biopsy in sarcoidosis. *Br J Dis Chest* 54:321-334, 1960
5. Young RL, Lordon RE, Krumholz RA, Harkleroad LE, Branam GE, Weg JG: Pulmonary sarcoidosis. I. Pathophysiologic correlations. *Am Rev Respir Dis* 97:997-1008, 1968
6. Koerner SK, Sakowitz AJ, Appelman RI, Becker NH, Schoenbaum SW: Transbronchial lung biopsy for the diagnosis of sarcoidosis. *N Engl J Med* 293:268-270, 1975
7. Khan MA, Corona F, Masson RG, Whitcomb ME: Transbronchial lung biopsy for sarcoidosis (letter). *N Engl J Med* 295:225, 1976
8. Koontz CH, Joyner LR, Nelson RA: Transbronchial lung biopsy via the fiberoptic bronchoscope in sarcoidosis. *Ann Intern Med* 85:64-66, 1976
9. Addrizzo JR, Minkowitz S, Lyons HA: Triple biopsy in the diagnosis of sarcoidosis, in *Proceedings of the Fifth International Sarcoidosis Conference,* Prague, University of Karlova, 1971, pp 476-479

Diagnostic Oncology Case Studies

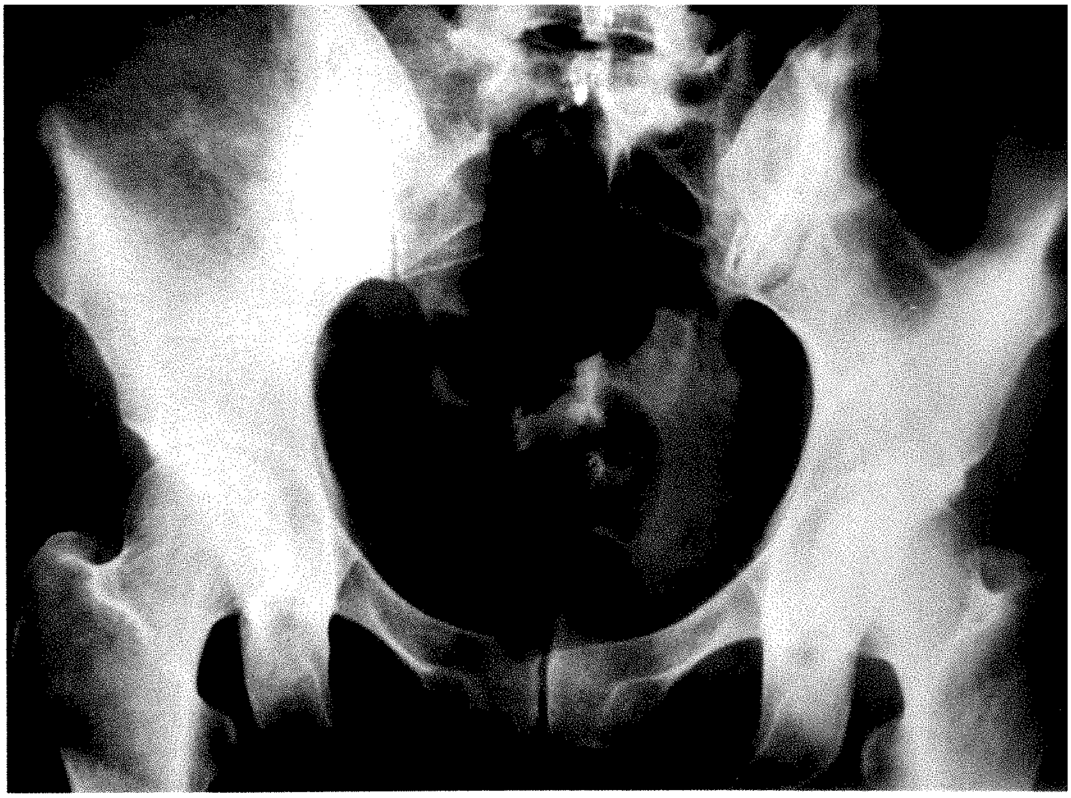

Chronic Sciatic Pain in a Young Woman with Sclerosis of the Iliac Bone

At 28 years of age this woman first noted intermittent shooting pain and numbness in her right calf, which responded to conservative treatment for suspected chronic lumbosacral strain with possible disc herniation. Plain radiographic studies of the pelvis and lumbosacral spine were negative.

At age 31, severe right gluteal pain developed with radiation to the anterior thigh, leg, and foot. These symptoms recurred intermittently for a year, at which time the pain became constant and was associated with a mild foot drop, as well as numbness and tingling over the plantar and dorsal aspects of the right foot and the anterolateral right leg. The pain was made worse by bending and coughing. The past history included a severe lower back injury and a concussion at the age of 14 years.

Physical examination demonstrated a limp favoring the right leg, with a foot drop, as well as hypesthesia and dysesthesia over the anterolateral aspect of the right leg and the dorsal and plantar aspects of the foot. Decreased sensation to pinprick was also noted over the right thigh, and there was tenderness to light palpation in the right buttock with restricted right leg raising. Right ankle reflex was absent, and there was the suspicion of a firm mass deep to the right gluteal musculature. The lumbar myelogram showed a small midline impression on the ventral aspect of the dura at the L3–L4 level. An electromyogram demonstrated a reduced number of functioning motor units in the right anterotibial and gastrocnemius muscle groups. The neurological impression was an L5–S1 radiculopathy of undetermined cause.

Radiographs of the lumbar spine and the pelvis (see above) revealed severe and widespread sclerosis of the right ilium which had been noted 1 year earlier but attributed to "osteitis condensans ilii." Within 2 months, periosteal new bone formation in the soft tissues adjacent to the right pelvic brim was detected in addition to the previously noted sclerosis (fig. 1*A*). A right pelvic soft tissue mass was also demonstrated (figs. 1*B* and 1*C*). Computed tomography confirmed a large right gluteal and pelvic soft tissue mass, with sclerosis of the right ileum and the sacrum (fig. 2).

The right gluteal mass was biopsied surgically, revealing an anaplastic tumor which infiltrated widely into the adjacent soft tissues. The sciatic nerve was not identified at the time of open biopsy. A poorly differentiated chondrosarcoma, chondroblastic osteosarcoma, or a mesenchymal chondrosarcoma were submitted as pathologic differential diagnoses. Although metastatic workup was negative, a hemipelvectomy was not considered because of the degree of anaplasia and the medial extent of the mass, which crossed the sacroiliac joint. Radiation therapy was recommended only if the tumor responded first to intensive chemotherapy [1]. Accordingly, the patient

---

This is one of a bimonthly series of case reports prepared by A. Robert Kagan and Richard J. Steckel (Southern California Permanente Medical Group and UCLA Comprehensive Cancer Center) to present and discuss contemporary problems and procedures in the identification and staging of the more common neoplasms. Case contributed by Richard Kalinowski, Department of Radiology, Southern California Permanente Medical Group, Los Angeles, California 90027.

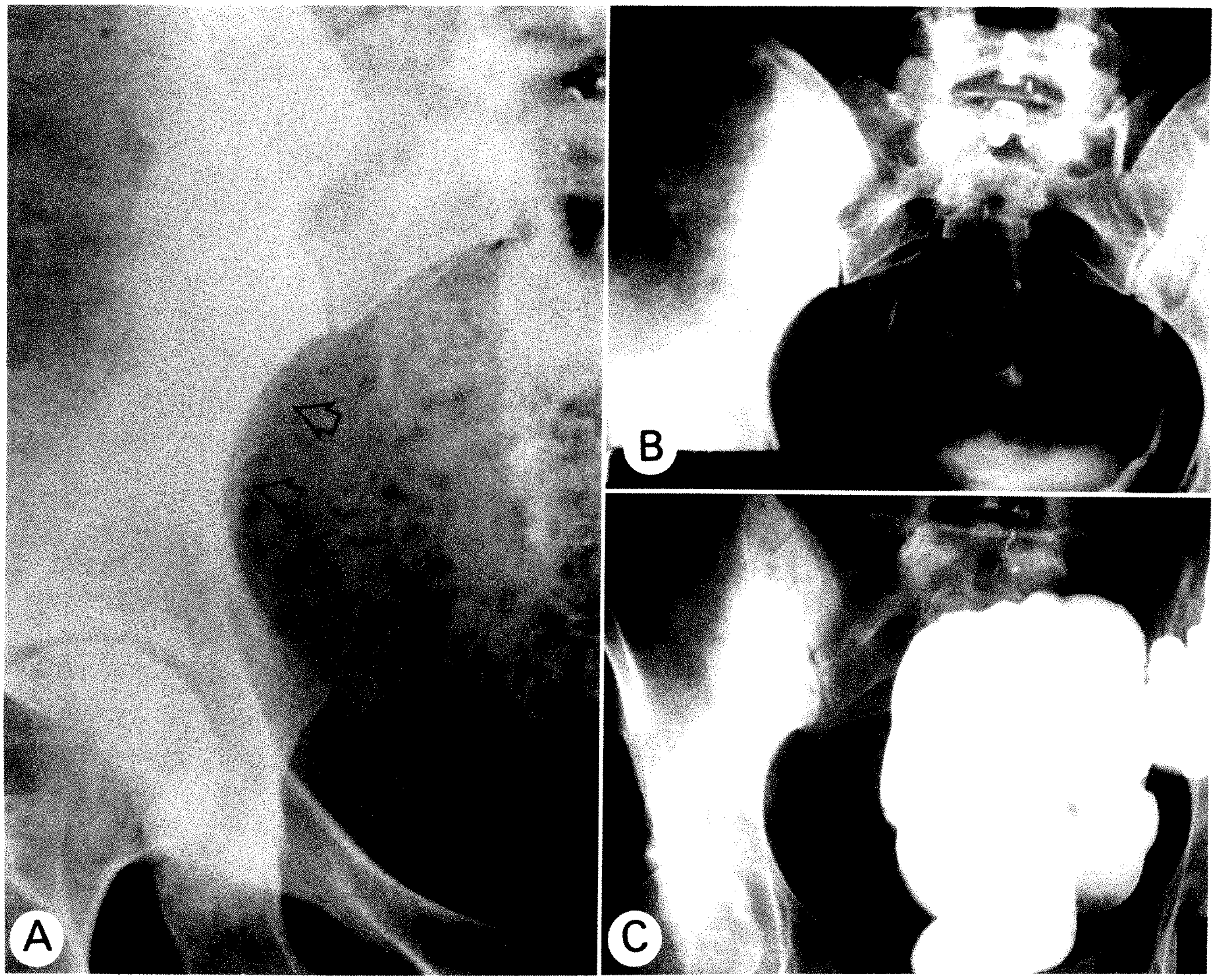

Fig. 1.—*A*, Periosteal elevation on medial margin of right iliac bone, inferior to sacroiliac joint (*arrows*). *B and C*, Right pelvic soft tissue mass displacing ureter and rectum medially.

was placed on high-dose intravenous methotrexate with Citrovorum rescue [2]. Unfortunately, local pain became worse and the mass remained large. Prompt pain relief in the pelvis was obtained with a thoracic cordotomy. Widespread metastases have recently developed in other bones.

Discussion

Although pain radiating down the anterior and posterior thigh may be caused by various diseases, including inflammatory conditions involving the iliac or the pubic bones, sciatic pain associated with an intrinsic bone tumor is unusual. Pain from a primary bone tumor is often localized, but a sciaticalike syndrome is occasionally associated with widespread bone metastases which include the pelvic areas. Other causes of sciatic or of anterior thigh pain include, of course, external pressure impinging upon the lumbar nerve roots (as in disc herniations), or upon the cauda equina, the lumbosacral plexus, or the sciatic or femoral nerves. Intrinsic neural tumors should also be considered for completeness, but they are unusual and are therefore rarely suspected preoperatively. Neoplastic or inflammatory conditions involving the sacroiliac joints and the retroperitoneal or pelvic soft tissues, including the lymph nodes and the iliopsoas muscle, may also lead to neural syndromes in the lower extremities.

On a clinical basis, disc disease would be the most likely cause of sciatic pain in a young woman, especially with a past history of back trauma. However, radiation of pain to the anterior thigh is inconsistent with L5-S1 root involvement and should raise the possibility of another lesion. The mistaken assumption of osteitis condensans ilii on recent radiographic studies dissuaded her physicians from considering a malignancy. Approximately 95% of all cases of sciatic pain (from L4-L5 and L5-S1 root compression) are indeed attributable to lumbar intervertebral discs, spondylolisthesis, or occasionally to benign sacroiliac disease. Nonneoplastic conditions which may also cause pain and localized sclerosis of the

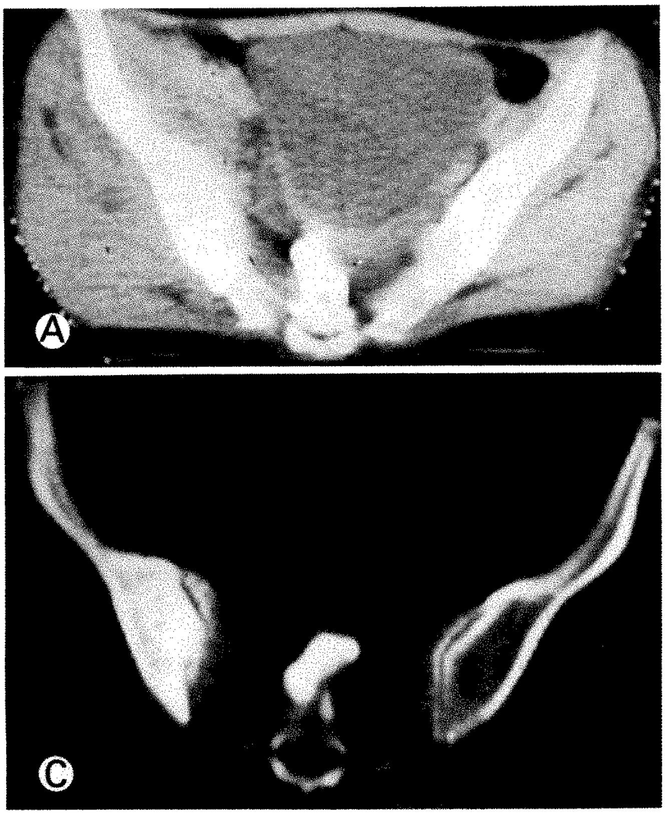

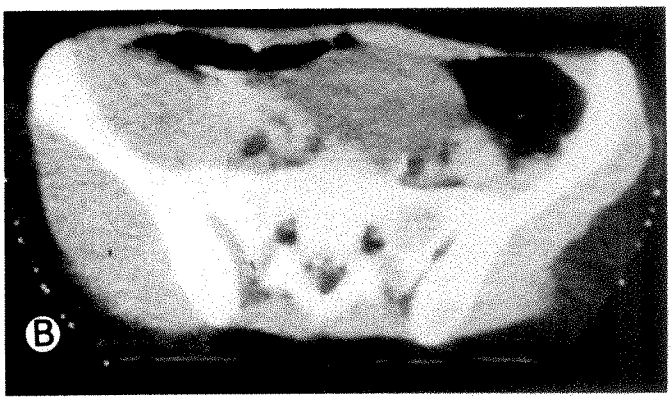

Fig. 2.—CT scans showing large right pelvic mass displacing bladder to left and extending into soft tissue planes of right buttock (*A and B*). Tumor-induced sclerosis involved right wing of sacrum (*B*) as well as right iliac bone (emphasized through use of different window setting in *C*).

iliac bone include granulomatous or septic arthritis, colitis, osteomylitis, Reiters syndrome, psoriatic arthritis, and Marie-Strumpell spondylitis.

Part of the delay in diagnosis may have been caused by an initial failure to recognize neoplastic periosteal elevation, which may be subtle when associated with flat bones [3]. However, the relatively rapid development of unilateral sclerosis of the iliac bone, with broad and diffuse involvement lateral to the sacroiliac joint, is inconsistent with the diagnosis of osteitis condensans ilii. The latter condition is common in young (usually parous) women, is usually bilateral, and is localized to the juxtaarticular region of the ileum. The present patient is somewhat older than the average for osteosarcoma (without Paget's disease) and is younger than average for chondrosarcoma. Nevertheless, the pelvis is a favored site for the latter tumor. Extraskeletal chondrosarcomas and osteosarcomas have been reported. This pelvic tumor could conceivably have been extraskeletal in origin, but the prognosis would have been the same [4, 5].

Hemipelvectomy is not helpful in an osteo- or chondrosarcoma which invades the symphysis pubis or which directly adjoins or crosses the sacroiliac joint [6-8]. Therefore, the use of the CT scan to delineate the soft tissue and bony extent of this tumor helped to prevent a radical approach which would have been futile. The use of CT scans to elucidate persistent and unexplained severe neuromuscular problems, as well as known masses in the pelvic region, may complement standard radiographic examinations including myelography. Gray scale ultrasound may also provide complementary information in some patients, especially in distinguishing solid from cystic pelvic masses. However, ultrasound is of no value in assessing bone or periosteal involvement, and "shadowing" of underlying soft tissues by osseous structures may sometimes occur.

REFERENCES

1. Beck JC, Wara WM, Bovill EG Jr, Phillips TL: The role of radiation therapy in the treatment of osteosarcoma. *Radiology* 120:163-165, 1976
2. Jaffe N, Traggis D, Cassady JR, Filler RM, Watts H, Frei E: Multidisciplinary treatment for macrometastatic osteogenic sarcoma. *Br Med J* 2:1039-1941, 1976
3. Gold RJ: Bone and soft tissue, in *Diagnosis and Staging of Cancer: A Radiologic Approach*, edited by Steckel RJ, Kagan AR, Philadelphia, Saunders, 1976, pp 286-312
4. Spjut HJ, Dorfman HD, Fechner RE, Ackerman LV: *Tumors of Bone and Cartilage*. Washington, D.C., Armed Forces Institute of Pathology Fascicle, 1971
5. Allan CJ, Soule EK: Osteogenic sarcoma of the somatic soft tissues. *Cancer* 27:1121-1133, 1971
6. Marcove RC, Mike V, Hutter RVP, Huvos AG, Shoji H, Miller TR, Kosloff R: Chondrosarcoma of the pelvis and upper end of the femur. *J Bone Joint Surg [Am]* 54:561-572, 1972
7. McKenna RJ, Schwinn CP, Soong KY, Higinbotham NL: Sarcomata of the osteogenic series (osteosarcoma, fibrosarcoma, chondrosarcoma, parosteal osteogenic sarcoma, and sarcomata arising in abnormal bone): an analysis of 552 cases. *J Bone Joint Surg [Am]* 48:1-26, 1966
8. Marcove RC, Mike V, Hajek JV, Levin AG, Hutter RVP: Osteogenic sarcoma in childhood. *NY State J Med* 71:885-859, 1971

Preliminary Results Using Twice-a-day Fractionation in the Radiotherapeutic Management of Advanced Cancers of the Head and Neck

SAMUEL JAMPOLIS,[1] GUDRUN PIPARD,[1, 2] JEAN-CLAUDE HORIOT,[1] MICHEL BOLLA,[1] AND CHRISTIAN LE DORZE[1]

Twenty-four cases of advanced T4 cancers of the head and neck were treated using a twice-a-day treatment fractionation delivering a 1,200 rad weekly tumor dose and 7,000 rad total tumor dose in 5½–6 weeks. Acute normal mucosal reactions and skin reactions were plotted weekly and corresponded to reactions observed when delivering 1,000 rad per week in five treatment sessions. Chronic problems have been limited to severe neck fibrosis appearing in three of five patients who underwent a planned neck dissection 6 weeks after the completion of radiotherapy. Local control was observed in 14 of 23 patients (61%) and regional control in 22 of 23 patients (96%).

During the past 30 years the clinical practice of radiotherapy has evolved considerably. However, the generally accepted scheme of fractionation has remained relatively fixed at four to six treatment sessions per week and one session per day. This treatment fractionation, although acceptable to radiotherapists and patients, may not be the most optimal with respect to the cellular kinetics and radiosensitivity of the proliferating tumor system. The considerable clinical experience which has accumulated regarding the local and regional control achievable with a well planned radiotherapeutic program has also defined a group of locally advanced tumors that show uniformly disappointing results with conventional radiotherapy dose and fractionation schemes. For this reason a radiotherapeutic schedule involving twice-a-day fractionation for advanced T4 (M. D. Anderson Hospital staging system [1]) cancers of the head and neck region was begun in January 1975 at the Centre Georges-François Leclerc, Dijon, France. Patients were chosen for this study when the probability of local control was estimated at less than 20%.

The theoretical reasons to support this treatment approach have been previously explained [2] and will be briefly reviewed.

1. The redistribution of surviving cells into a more sensitive phase of the cell cycle, which take place in the interval between dose fractions, can result in a differential sensitization of the malignant tissue relative to the nonproliferating tissues (e.g., spinal cord, fibrovascular tissue, and cartilage).

2. That portion of the tumor system which is the most sensitive to irradiation (e.g., cells without capacity to repair sublethal damage) will be killed with a low dose of irradiation. The surviving cells can then redistribute into a more radiosensitive phase of the cell cycle and allow for the same proportional killing effect to recur with the second fractionated dose. By giving multiple daily fractions, a protracted treatment regimen is avoided, thereby decreasing the problem of tumor repopulation. This would otherwise have reduced the therapeutic gain if only one low dose fraction per day had been given over a protracted period of time to arrive at the desired total tumor dose.

3. Allowing 6–8 hr between fractions permits maximum repair of sublethal damage [3, 4] and gives the surviving malignant cells a potentially greater time to move into the radiosensitive phases of the cell cycle.

4. By delivering multiple daily fractions, the overall treatment time can be shortened while maintaining an acceptable normal tissue tolerance. In advanced cancers the total tumor dose is delivered in a shorter period of time, which may result in an additional benefit in achieving local tumor control.

Materials and Methods

From January 1975 to March 1976, 24 patients with advanced T4 cancers of the head and neck (tables 1 and 2) received the twice-a-day fractionation. All treatment sessions were spaced 6–8 hr apart with a 16 hr interval overnight. The treatment was given 5 days per week and extended over a period of 5 weeks and 4 days to 6 weeks (depending on the total tumor dose). The first four patients received a weekly tumor dose of 1,250 rad; the remainder received 1,200 rad. A total tumor dose of either 6,960 rad or 7,200 rad was delivered to all patients. Every treatment field was irradiated at each session using portal arrangements planned according to the techniques outlined by Fletcher [1]. The general treatment plan used opposing ^{60}Co fields to deliver a tumor dose of 4,800 rad. Depending on the tumor regression observed at that time, field reductions and different energy combinations were then employed for the remainder of the treatment. Patients initially staged N2A, N2B, N3A, and N3B (M. D. Anderson Hospital nodal classification system [1]) were scheduled to have a modified or radical neck dissection 6 weeks after completion of irradiation.

All patients have had follow-up examinations in our department of radiotherapy.

Results

Twenty-four patients were studied for acute normal mucosal reactions by plotting on a weekly basis the reaction observed in the mucosa across the faucial arch. The first four patients who received 1,250 rad weekly tumor dose experienced mucosal reactions more severe

---

Received May 18, 1977; accepted August 9, 1977.

[1] Division of Therapeutic Radiology, Centre Georges-François Leclerc, Dijon, France.

[2] Present address: Hôpital Cantonal de Genève, Genève, Switzerland.

TABLE 1

Primary Sites of Involvement

Site	No. Cases
Base of tongue	10
Tonsillar fossa	4
Oral tongue	3
Nasopharynx	1
Supraglottic larynx	2
Pyriform sinus	1
Floor of mouth	1
Pharyngeal walls	2

TABLE 2

Clinical Stage

Stage	No. Cases
NO	5
N1	4
N2A	5
N2B	1
N3A	2
N3B	7

Note.—All patients were T4.

than would be expected using conventional irradiation at 1,000 rad per week [5]. As a result of this clinical observation, the weekly tumor dose was reduced to 1,200 rad; no further problems were encountered with acute normal mucosal reactions during the treatment. The general distribution of mucosal reactions (fig. 1) showed that a majority of patients developed a minimal to moderate erythema between 1,200 rad and 2,400 rad, a studded mucositis between 3,600 rad and 4,800 rad, and in one-half of the patients a confluent mucositis between 6,000 rad and 7,200 rad. Of the 24 patients, 23 completed their irradiation as planned without experiencing undue difficulty. One patient required hospitalization and a feeding gastrostomy in order to complete the irradiation treatment. The clinical finding of a moist desquamation in the skin was infrequently observed, and when it appeared, it usually occurred at the junction of the lateral and anterior fields. The only chronic complication observed has been marked neck fibrosis appearing in three of the five patients who underwent a neck dissection 6 weeks after completion of irradiation.

Tumor regression was estimated weekly by one of us (either S. Jampolis or J.-C. Horiot) to determine if a correlation existed between tumor regression during treatment and subsequent local control (fig. 2). Although no statistical relationship could be established, of the nine local failures six occurred with an estimated tumor regression of 80% or less at the end of treatment. The 14 patients with local control all had an estimated tumor regression of 80% or greater, with nine of the 14 having almost complete regression of the tumor (90% or more) at the end of treatment. It should be noted that when a tumor regression of 80% or greater was achieved at the end of treatment, the local control was 74% (14 of 19 patients) in contrast to the overall local control rate of 61% (14 of 23 patients). All patients have been followed for a minimum of 13 months with only five followed for less than 18 months. As can be seen from table 3, seven of the nine cases of persistent or recurrent disease have appeared by 1 year in our series, while all four cases of persistent or residual disease treated in the M. D. Anderson Hospital series [2] appeared during the same period of observation.

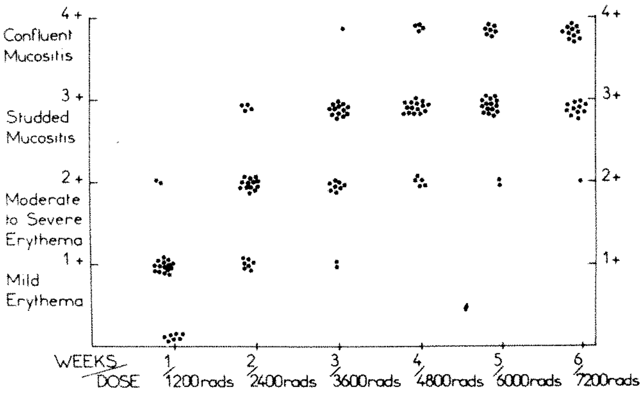

Fig. 1.—Mucosal reactions during treatment (24 cases).

Regional control within the neck was excellent; only one of 23 patients had recurrent or persistent disease. This failure occurred in the posterior spinal chain of lymph nodes in a patient staged N3B in whom a neck dissection was not performed after irradiation.

In spite of the high local and regional control, only nine of the patients are alive without evidence of disease. Four other patients, two with local and regional control, have distant metastases. The other two have local failure, regional control, and no evidence of distant metastases.

Discussion

A twice-a-day fractionation treatment program has been routinely employed at the Centre Georges-François Leclerc for the past 2 years. The radiobiologic principles which helped establish the clinical basis for this fractionation scheme have been indirectly supported by the increased local and regional tumor control observed in this series. The tolerance of the normal tissues to this accelerated fractionation and the relative absence of long-range complications have been encouraging. In view of the preliminary increased local and regional control rates in this group of advanced T4 cancers of the head and neck, the justification for further investigation of this treatment approach appears established. Because of the high incidence of distant metastases observed in these cases, a second pilot study was begun in March 1976 to evaluate whether the addition of prophylactic intensive multiple drug chemotherapy after multifraction irradiation will aid in preventing distant metastases. These results will be discussed in a future communication.

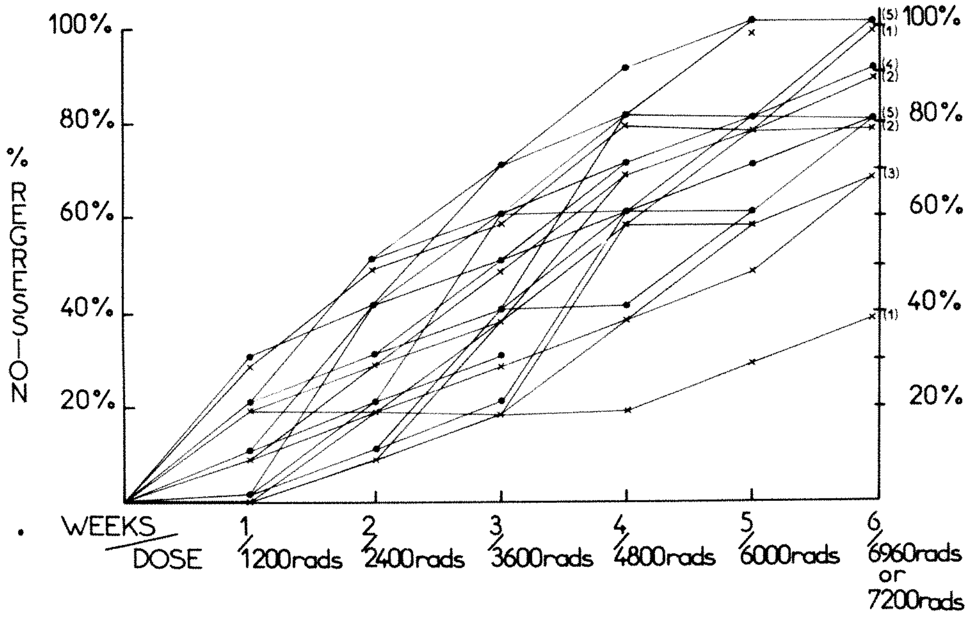

Fig. 2.—Tumor regression during treatment (23 cases). Closed circles = control at primary site; crosses = failure at primary site.

TABLE 3

Cumulative Recurrence Rates

	Shukovsky et al. [2]*	Present Report†
No. patients	19	23
Recurrence:		
Residual	1	2
6 months	2 (11)	5 (22)
12 months	4 (21)	7 (30)
18 months	4 (21)	9 (39)

Note.—Numbers in parentheses are percentages.

* M. D. Anderson Hospital (July 1973–July 1974): twice-a-day fractionation; 1,100–1,200 rad/week; 6,000–7,500 rad in 5–6½ weeks. Stage distribution: T3, six patients; T4, 11 patients; massive postoperative recurrence, three patients. One patient excluded because of insufficient dose.

† Centre Georges-François Leclerc (January 1975–March 1976): twice-a-day fractionation; 1,200–1,250 rad/week; 6,960–7,200 rad in 5½–6 weeks. One patient excluded because of insufficient information at time of death; no evidence of disease at last examination performed 1 month before death.

REFERENCES

1. Fletcher GH: *Textbook of Radiotherapy,* 2d ed. Philadelphia, Lea & Febiger, 1973
2. Shukovsky LJ, Fletcher GH, Montague ED, Withers HR: Experience with twice-a-day fractionation in clinical radiotherapy. *Am J Roentgenol* 126:155–162, 1976
3. Withers HR: Recovery and repopulation *in vivo* by mouse skin epithelial cells during fractionated irradiation. *Radiat Res* 32:227–239, 1967
4. Withers HR, Elkind MM: Radiosensitivity and fractionation response of crypt cells of mouse jejunem. *Radiat Res* 38:598–613, 1969
5. Fletcher GH, MacComb WS: *Radiation Therapy in the Management of Cancer of the Oral Cavity and Oropharynx.* Springfield, Ill., Thomas, 1962

Evaluation of Radiation Therapy for Bone Metastases: Pain Relief and Quality of Life

HARVEY A. GILBERT,[1] A. ROBERT KAGAN,[1] HERMAN NUSSBAUM,[1] AROOR R. RAO,[1] JOEL SATZMAN,[2] PAUL CHAN,[1] BRENT ALLEN,[2] AND ALAN FORSYTHE[3]

The records of 158 patients irradiated for bone metastases were reviewed to evaluate the effectiveness of pain relief and to judge the effect of treatment on overall quality of life. Within 3 months 73% of the sites treated had pain relief, with 55%–65% having sustained relief up to 1 year or death. Of patients surviving more than 3 months, 63% maintained a satisfactory quality of life and were able to take care of most personal needs. The median survival of all patients was 1 year from initial treatment for bone metastasis. Radiation dose and the primary tumor site do not seem to be significant prognostic factors for initial pain relief or quality of life.

Few patients with metastatic bony involvement have a normal life. While immediate pain relief afforded by localized irradiation is important, the overall quality of life is equally significant. We analyzed the records of all patients treated in our department for bone metastases between 1970 and 1973 to determine the effectiveness of pain relief at 3 months and at 1 year and also to judge the effect of treatment on quality of life.

Subjects and Methods

The records of 158 patients irradiated for bone metastasis were reviewed; 38 patients did not live 3 months. The primary sites responsible for metastasis included: breast, 68; lung, 27; prostate, 16; and other, 47 (seven kidney, three lymphoma, three gastrointestinal, three gynecologic, three sarcoma, 14 myeloma, one liver, three head and neck, one thyroid, one melanoma, and eight unknown). Mean age of the 158 patients was 57 years (range, 11–88 years). Mean age by site was: breast, 54 years; lung, 59 years; prostate, 66 years; and other, 56 years.

The majority of these patients (92%) have died; those living have been followed for more than 2 years. Patients were treated by wide field radiation therapy directed at the metastatic site with three different treatment schemes. During the first 2 years all patients were treated by a protracted course of 3,000 rad in 3 weeks to 4,000 rad in 4 weeks. Beginning in 1972 all patients were treated by either 2,000 rad in five fractions or 1,300 rad in two fractions with or without a repeat course 3 weeks later. Most patients were treated with megavoltage equipment. Opposed fields were most commonly employed. The confirmation of bone metastasis was both by radionuclide scan and radiograph. Biopsy was seldom used except for the "solitary" metastasis. Systemic therapy of some type was always administered to patients with lymphoma and those with breast and prostate tumors. Systemic treatment was not always given to patients with other solid tumors.

Patients were scored for pain relief every 3 months. An average of two bony sites per patient were treated by radiation.

Quality of life was defined at two levels. Level 1 was defined as ability to take care of most personal needs (Karnofsky 70%–100%). At level 2, a patient required major help in self care (Karnofsky 0%–70%). Quality of life was defined as good if most of the patient's life, measured from treatment of the first bone metastasis, was in level 1. The presence of debilitating skeletal pain was associated with level 2, in which the patient either spent most of the time in bed or ambulated infrequently with aid. Therefore the Karnofsky level is a useful index to measure the quality of life in a patient who has been treated for metastatic bony disease.

Results

Median survival from first treated bone metastasis was 12 months (table 1), and median survival from first symptoms of bone metastasis was 14 months. Surprisingly, the median survival from the first visceral metastasis was 11 months, indicating that in this select population visceral metastasis did not adversely affect survival. Of the 158 patients, 38 lived less than 3 months after radiation therapy and were excluded from further evaluation (10 breast patients, 17 lung patients, one prostate patient, and 10 other).

Of 187 evaluated sites in the remaining 120 patients, 137 (73%) achieved an initial local pain-free status at 3 months. Pain relief was sustained up to 1 year or until death before 1 year for 103 sites (55%). Patients dying before 1 year contributed 24 of these 103 sites. At 50 sites (27%), pain relief was never achieved. Pain relapsed at 34 sites that had been rendered initially pain free. These are considered failures for the 1 year evaluation.

The percentage of sustained pain relief (up to 1 year or until death) was similar whether the primary site was breast, lung, prostate, or other. It was our impression that lesions of the extremities were more resistant to pain relief. Pain relief tended to occur more often in nonweight-bearing and nonlytic areas (not statistically significant). No apparent advantage of one irradiation dose-time relationship over another was obvious. This could not be correlated to site treated or type of metastasis.

Quality of life was good (level 1) in 63% of the 120 patients (table 2). These patients achieved a relatively pain-free status wherein they could ambulate and remain

---

Received May 2, 1977; accepted after revision August 12, 1977.

Computing assistance was obtained from the UCLA Health Sciences computing facility supported by special resources grant RR-3 from the National Institutes of Health.

[1] Department of Radiation Therapy, Southern California Permanente Medical Center, Los Angeles, California 90027. Address reprint requests to H. A. Gilbert.

[2] Department of Orthopedics, Southern California Kaiser Permanente Medical Center, Los Angeles, California 90027.

[3] Health Sciences Computing Facility, University of California, Los Angeles, California 90024.

TABLE 1

Survival by Primary Site

Primary Site	No. Patients	Median Survival (months) From First Visceral Metastasis	Median Survival (months) From First Treated Bony Metastasis	Patients Surviving Less than 3 Months (%)
Breast	68	15	15	15
Lung	27	3	3	63
Prostate	16	11	16	6
Other	47	9	9	21
Total	158	11	12	24

TABLE 2

Overall Quality of Life

Primary Site	No. Patients	Karnofsky Level 1 More than Half of Remaining Life (%)
Breast	58	59
Lung	10	70
Prostate	15	76
Other	37	66
Total	120*	63

* 38 patients who survived less than 3 months were excluded from analysis.

free of the depressing effects of analgesics and systemic chemotherapy.

Patterns of Metastasis

Metastasis was clinically localized only to bone in 65% of our patients. The quality of life and pain-free status was little influenced by the presence of visceral metastasis in this series. It is of clinical importance that patients with bone metastasis often have multiple sites of involvement.

Serious Complications

Twenty-nine patients developed serious complications such as cord compression and pathologic hip fracture. Both complications ranged from 26% for breast to 6% for prostate cancer patients. Of the 29, 25 had predominantly lytic disease.

Twelve patients had pathologic femur fractures. Major lessons learned from these patients were:

1. Patients with large lytic lesions involving major portions of the cortex in weight-bearing bone should undergo prophylactic pinning prior to irradiation.
2. Patients with predominantly lytic disease who are treated without prophylactic pinning should be reevaluated radiographically at 3 month intervals after treatment. When pain relief was achieved by irradiation alone, the interval before subsequent fracture was 6 months or greater.
3. For patients with lytic femur disease, x-rays of the entire femur should be routine. In two patients fractures occurred unexpectedly in the mid or distal femur just below an irradiated field.

Fourteen patients developed a spinal cord compression syndrome. Observations concerning patients at high risk for epidural spinal cord compression are:

1. Unilateral painful radicular pain (thoracic or lumbar) preceded eventual motor paralysis in most cases.
2. In several patients, neurologic compression developed above a previously irradiated vertebra treated for bone pain. Careful observation and a high index of suspicion for neurologic involvement may have suggested larger radiation portals at the time of initial treatment or an earlier diagnosis of treatment failure.
3. Electromyograms were useful for predicting spinal cord compression from metastatic vertebral disease. In 10 patients with vertebral metastasis who had pathologic denervation potentials of the paraspinous muscles, partial myelographic blocks were found. While preliminary, these data are noteworthy since paraplegia is obviously a catastrophic complication. A negative electromyogram is helpful in ruling out significant neurologic involvement, but a positive test is *not* diagnostic of its presence.

Discussion

It is incorrect to assume that a patient referred to the radiation therapy department with bone metastasis will have a short life expectancy. Furthermore, in our series, associated visceral metastasis did not significantly affect the median survival of 14 months. Within our clinical groups, patients with cancer of the lung have a much shorter median survival. Radiation therapy is effective in the long term management of localized bony metastatic disease. Pathologic fractures in the extremities and cord compression must be avoided.

Extended radiation fields are unnecessary; judicious local field irradiation appears to be sufficient. Neither the dose-time relationship nor the primary site seemed to affect pain relief or the quality of life.

Allen et al. [1] achieved 80% pain relief using 500–1,700 ret. Jensen and Roesdahl [2] noted 60% pain relief with 500–700 rad; however, nearly one-half of their patients died within 4 months. Vargha et al. [3] reported 90% pain relief at 400–800 rad. We agree with Varga et al. [3] that prolonged courses of irradiation for the palliation of bony metastasis is wasteful. An evaluation of single doses of 800 rad is underway. However, our series showed that if patients live long enough, relapse from 6 months to 1 year can result in serious complications. We believe that routine reevaluation and follow-up of patients functioning at level 1 is crucial. Patients with lytic disease, radicular pain, and metastasis to the femurs seem to be at high risk for serious complications (fracture, cord compression, etc.).

We realize that in evaluating the problem of pain relief, factors such as the placebo effect, the effect of chemotherapy, hormones, and analgesic medicines, and the difficult psychosocial environment of the cancer patient significantly complicate the reproducibility of this type of investigation from center to center.

REFERENCES

1. Allen KL, Johnson TW, Hibbs GG: Effective bone palliation as related to various treatment regimens. *Cancer* 37:984–987, 1976
2. Jensen NH, Roesdahl K: Single-dose irradiation of bone metastases. *Acta Radiol Ther* 15:337–339, 1976
3. Vargha ZO, Glicksman AS, Boland J: Single-dose radiation therapy in the palliation of metastatic disease. *Radiology* 93:1181–1184, 1969

Case Reports

Peripelvic Renal Pseudocyst due to Obstruction

ZORAN L. BARBARIC[1] AND IRWIN N. FRANK[2]

Peripelvic masses displacing the collecting system within the kidney have various origins. Although they are usually benign, an occasional malignant lesion is encountered. Therefore, further radiologic evaluation is required. We describe a patient with two peripelvic masses which disappeared when bilateral urinary tract obstruction was relieved.

Case Report

A 70-year-old male was seen with a 5 week history of recurrent left flank pain. Excretory urography confirmed the presence of a radiopaque left ureteral calculus about 5 mm in diameter located at the level of L5 causing mild obstruction. In addition a 5 cm mass in the left kidney distorted the pelvocalyceal system (fig. 1*A*). This mass was radiolucent on nephrotomography. The right kidney appeared normal at this time, except for a 2 mm calculus in the lower pole calyx (fig. 1*D*). Microhematuria and left costovertebral angle tenderness was present. Ultrasound evaluation of the mass performed 6 days later was "suggestive of a cyst."

The patient remained free of symptoms for 10 days; he then experienced sudden onset of right flank discomfort. Repeat excretory urography revealed that he had passed the left ureteral calculus and that the previously noted peripelvic mass was moderately smaller (fig. 1*B*). However, the right pelvocalyceal system now appeared similar to that seen on the left side, with a definite mass lesion distorting the right renal pelvis and infundibulum (fig. 1*E*). The right ureter was dilated to the ureterovesical junction suggesting obstruction. The radiopaque calculus previously seen in the right kidney was no longer present. It was suspected that the calculus had recently passed and that there was residual edema at the right ureterovesical junction. The patient remained free of symptoms, and a follow-up excretory urogram 10 weeks later appeared normal (figs. 1*C* and 1*F*). There was no residual distortion of the pelvocalyceal system and no evidence of obstruction.

Discussion

Benign masses of various types are known to cause pelvocalyceal distortion. Some represent exaggerated normal renal tissue (e.g., septum of Bertin, lobar dysmorphism, and focal hypertrophy) [1-4]. Vascular impression [5], infarct [6], intrarenal hematomas [7, 8], renal artery aneurysm, and circumscribed fibrolipomatosis [9] may also produce this type of calyceal distortion. Extramedullary hematopoiesis [10] occurs rarely as a cause of this radiologic finding. Peripelvic cystic masses which distort the pelvocalyceal system include cortical cysts, true pelvic cysts [11], and peripelvic diverticula [12]. To this group of peripelvic masses we add peripelvic renal pseudocyst due to urinary tract obstruction.

There are only two possible explanations concerning the etiology of the described mass. The most likely cause is loculated extravasated urine due to increased pressure within the collecting system during the obstruction [13]. Extravasation had to occur prior to urography and stopped once the pressure in the two systems was equalized. The only other conceivable, but much less likely, explanation is that the mass effect represented a loculated collection of lymph due to a ruptured lymphatic channel, unable to accomodate the increased lymph output of the obstructed kidney.

Whatever the cause, this loculated collection of fluid differs from cystic peripelvic masses in several respects. Most important, the collection spontaneously disappears over a period of several weeks after the obstruction is relieved. Both the peripelvic cyst and the peripelvic diverticulum have a flattened epithelial lining, while the pseudocystic collection of urine is walled off by sinusoidal fat, renal pelvis, and the sinusoidal part of the renal capsule.

The clinical significance of this finding is that the peripelvic urine collection due to obstruction could be mistaken for a mass lesion, and the patient could be subjected to an extensive radiologic workup or even exploratory surgery. However, the only requisite for these patients is a follow-up excretory urogram a few weeks after the obstruction has been relieved. The mass should be smaller or absent by that time, and further urologic/radiologic workup is not indicated. Should the peripelvic mass lesion remain unchanged in this time interval, further investigations should be performed to determine whether a neoplasm is present.

REFERENCES

1. King MC, Fridenberg RM, Tena LB: Normal renal parenchyma simulating tumor. *Radiology* 91:217-222, 1968
2. Lopez FA: Renal pseudotumors. *Am J Roentgenol* 109:172-184, 1970
3. Charghi A, Dessureault P, Drouin G, Gautheir GE, Perras P,

---

Received June 9, 1977; accepted after revision August 12, 1977.

[1] Department of Radiology, University of Rochester School of Medicine and Dentistry, Strong Memorial Hospital, Rochester, New York 14642. Address reprint requests to Z. L. Barbaric.

[2] Department of Surgery, University of Rochester School of Medicine and Dentistry, Strong Memorial Hospital, Rochester, New York 14642.

Am J Roentgenol 129:1097-1098, December 1977

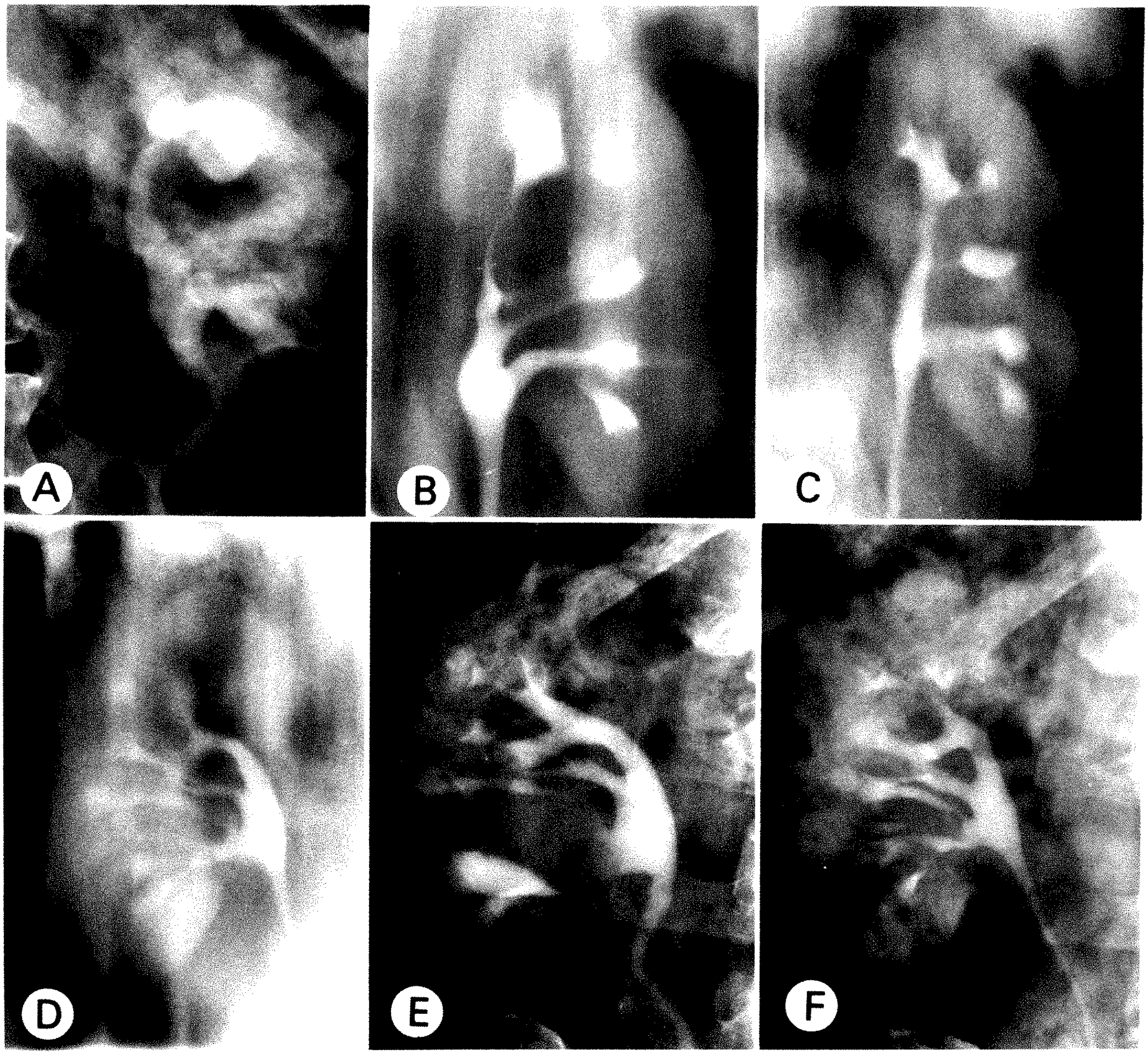

Fig. 1.—Excretory urography. *A–C*, Left kidney. *A*, First examination showing moderate obstruction at left midureter with mild hydronephrosis and hydroureter. Radiolucent peripelvic mass displaces and distorts upper and middle infundibulum. *B*, Examination 10 days later showing left ureter no longer obstructed. Mass is somewhat smaller. *C*, Examination 2½ months later showing complete disappearance of left renal mass. No obstruction is identified. *D–F*, Right kidney. *D*, First examination showing normal kidney; however, there is extrarenal pelvis. *E*, Examination 10 days later showing moderate obstruction of right ureter. Newly formed mass effect distorts middle and lower infundibulum. *F*, Examination 2½ months later showing disappearance of peripelvic mass after relief of obstruction.

Roy P, Charbonneau J: Malposition of a renal lobe (lobar dysmorphism): a condition simulating renal tumor. *J Urol* 105:326–329, 1971

4. Felson B, Moskowitz M: Renal pseudotumors: The regenerated nodule and other lumps, bumps, and dromedary humps. *Am J Roentgenol* 107:720–729, 1969
5. Kyaw MM, Newman H: Renal pseudotumors due to ectopic accessory renal arteries: the angiographic diagnosis. *Am J Roentgenol* 113:443–447, 1971
6. Ranniger K, Abrams E, Bordent A: Pseudotumor resulting from a fresh renal infarct. *Radiology* 92:343–344, 1969
7. Sukthomya C, Levin B: Pseudotumors of kidney secondary to anticoagulant therapy. *Radiology* 88:701–703, 1967
8. Klinger ME, Tanenbaum B, Elguezabal A: Pseudo-tumors of the kidney secondary to anticoagulant therapy. *J Urol* 106:507–511, 1971
9. Olsson O, Weiland PO: Renal fibrolipomatosis. *Acta Radiologica [Diagn]* (Stockh) 1:1061–1070, 1963
10. Redlin L, Francis RS, Orlando MM: Renal abnormalities in agnogenic myeloid metaplasia. *Radiology* 121:605–608, 1976
11. Deliveliotis A, Kavadis CHR: Parapelvic cysts of the kidney: report of seven cases. *Br J Urol* 41:386–393, 1969
12. Williams G, Blandy JP, Tresidder GC: Communicating cysts and diverticula of the renal pelvis. *Br J Urol* 41:163–170, 1969
13. Olsson O: Frequency of backflow in acute renal colic. *Acta Radiol [Diagn]* (Stockh) 12:469–480, 1972

Contralateral Renal Herniation after Nephrectomy: A Cause of Pseudo-Crossed Renal Ectopia

KYUNG J. CHO,[1] JOSEPH F. WALTER,[2] AND JOHN W. KONNAK[3]

Crossed renal ectopia is an uncommon anomaly, generally congenital [1]. Rarely, crossed renal ectopia may be acquired due to contralateral displacement of a kidney by a large retroperitoneal mass. This was termed pseudo-crossed renal ectopia by Greenspan and Bryk [2]. We report an unusual case of acquired crossed renal ectopia of the remaining kidney after a radical thoracoabdominal nephrectomy for renal cell carcinoma.

Case Report

A 36-year-old obese woman weighing 166 kg had a left radical nephrectomy for hypernephroma. Periaortic node dissection, splenectomy, and adrenalectomy were also performed by the thoracoabdominal approach. An intravenous pyelogram and renal arteriogram done at a local hospital had demonstrated a large vascular mass in the upper pole of the left kidney. The right kidney was normal. Hemoglobin was 15 g/100 ml; hematocrit, 47%; and creatinine, 0.8 mg/100 ml. The hypernephroma was confined to the kidney. The postoperative course was complicated by wound infection and dehiscence which gradually healed by granulation. The patient did well until 7 months after surgery, when she experienced sudden sharp pain in her left flank. Physical examination revealed evidence of bowel herniation into a left thoracoabdominal incisional hernia sac.

She was readmitted to the hospital 2 years later because of Pickwickian syndrome and left flank pain. The serum creatinine was 2 mg/100 ml. Urinalysis showed proteinuria with 3 g of protein in a 24 hr collection. The right kidney was not visualized on an intravenous pyelogram with nephrotomograms. Since a neoplasm of the remaining kidney was suspected, an aortogram and renal arteriogram were performed, demonstrating that the right kidney and much of the small intestine was displaced into the left upper quadrant through a large incisional hernia (fig. 1). An inferior venacavogram and right renal venogram showed displacement and torsion of the right renal vein (fig. 2). There was a 5 mm Hg pressure gradient between the renal vein and the inferior vena cava, presumably secondary to the torsion. It was thought that the proteinuria and mildly elevated creatinine were caused by the partially obstructed renal vein. Because of the patient's pulmonary problems and massive obesity, surgical correction of the renal herniation was not attempted.

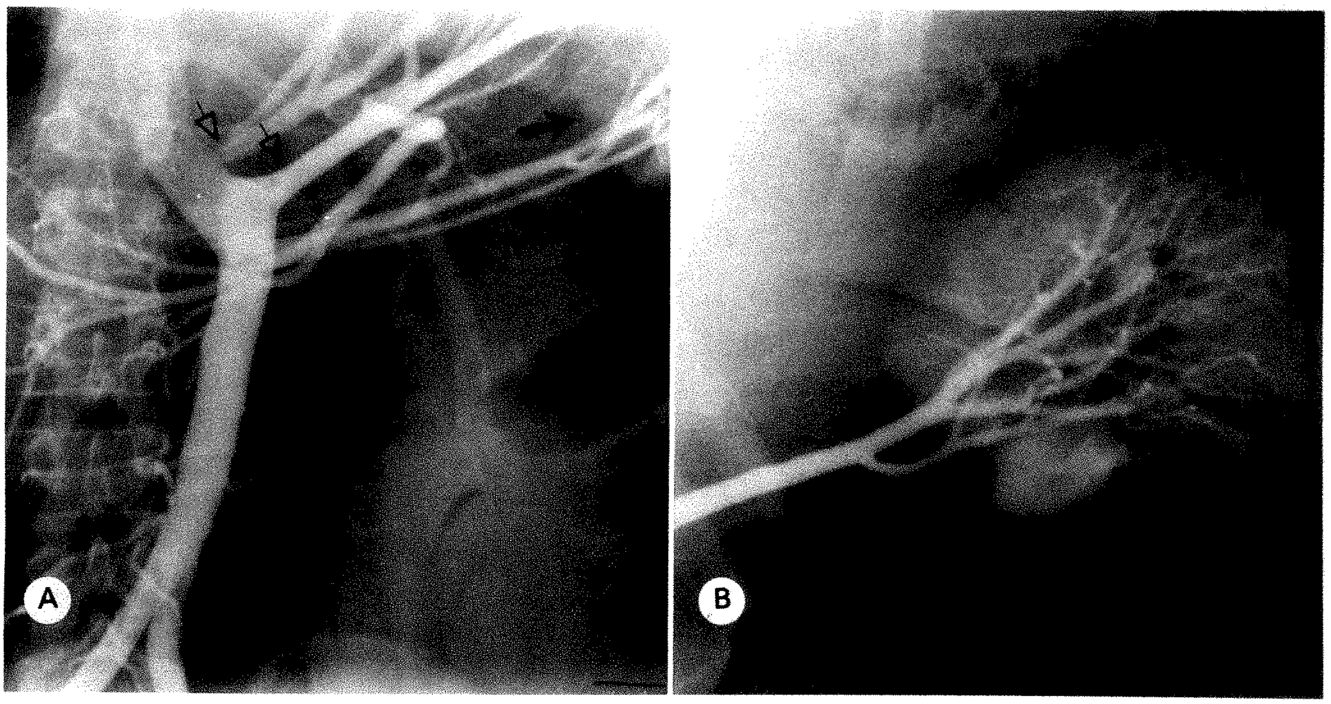

Fig. 1.—*A*, Abdominal aortogram showing aorta displaced to left by herniation of upper abdominal viscera (*open arrows*). Note two right renal arteries stretched across midline to right kidney in left flank incisional hernia (*arrow*). *B*, Selective injection into larger of two right renal arteries demonstrating normal-appearing right kidney lying lateral to left rib cage.

Received May 23, 1977; accepted after revision August 12, 1977.

[1] Department of Radiology, University of Michigan Medical Center, Ann Arbor, Michigan 48109. Address reprint requests to K. J. Cho.

[2] Department of Radiology, Palo Alto Medical Clinic, Palo Alto, California 94301.

[3] Department of Urology, University of Michigan Medical Center, Ann Arbor, Michigan 48109.

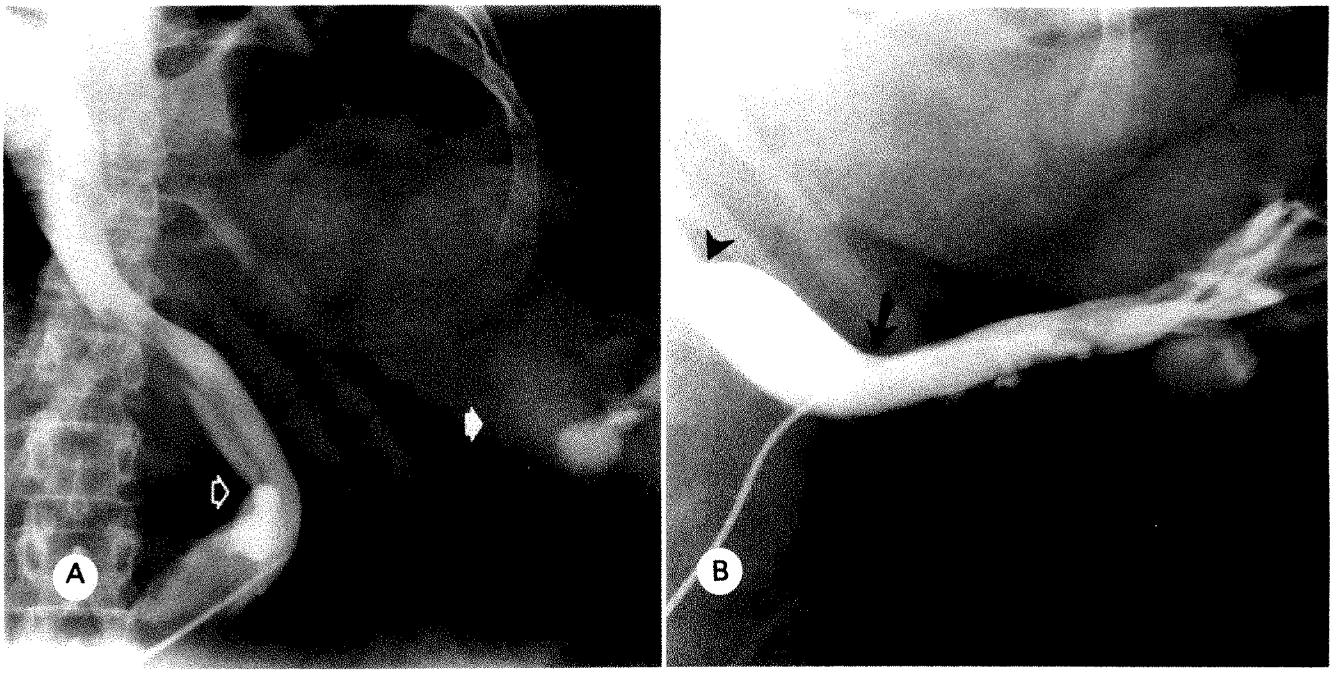

Fig. 2.—*A*, Inferior venacavogram showing displaced and twisted inferior vena cava (*open arrow*). Right kidney is herniated through bed of resected left tenth rib (*arrow*). *B*, Right renal venogram revealing patent renal vein. Mild torsion is present at origin of right renal vein (*arrow*) and inferior vena cava (*arrowhead*).

Discussion

Both intraperitoneal and retroperitoneal masses have been known to displace a kidney across the spine into the opposite side of the abdomen [2-4]. Greenspan and Bryk [2], reporting a case of pseudo-crossed renal ectopia produced by a large retroperitoneal cyst, found 35 reports of such cases. Herniation usually occurs following an operation on the kidney, and the kidney is generally displaced into an ipsilateral hernia sac [5]. In our case the kidney was displaced contralaterally across the spine into the left flank hernia sac. This unusual type of renal displacement was attributed to the patient's massive obesity and large incisional hernia into which both bowel and kidney had herniated.

The angiographic study in our patient was helpful in demonstrating why the kidney was not seen; it had herniated outside the abdomen and was not included on the nephrotomograms. Also, the establishment of a pressure gradient between the renal vein and inferior vena cava offered a possible explanation for the proteinuria and elevated creatinine.

The kidney may move in all directions, even medially across the spine, with or without previous surgery [6]. Thus the entire abdomen should be searched when a routine pyelogram fails to show the kidney in the expected location.

REFERENCES

1. Emmett JL, Witten DM: *Clinical Urography*. Philadelphia, Saunders, 1971
2. Greenspan A, Bryk D: Pseudo-crossed renal ectopia. *J Can Assoc Radiol* 24:321-322, 1973
3. Woesner ME, Lang DW, Selvaggi FP: Contralateral displacement of the kidney by solitary renal cyst. *Am J Roentgenol* 116:766-772, 1972
4. Forde WJ, Ostrolenk DG, Finby N: Renal displacement associated with enlargement of spleen. *Am J Roentgenol* 84:889-897, 1960
5. Ney C, Friedenberg RM: *Radiographic Atlas of the Genitourinary System*. Philadelphia, Lippincott, 1966
6. Prather GC: Medial ptosis of the kidney. A new renal syndrome. *N Engl J Med* 238:253-257, 1948

Gray Scale Ultrasonography in Retroperitoneal Lymphangiomyomatosis

J. WALSH,[1] K. J. W. TAYLOR, AND A. T. ROSENFIELD

Lymphangiomyomatosis is a rare tumorlike condition characterized by smooth muscle proliferation involving major lymphatic trunks in the mediastinum and retroperitoneum, lymph nodes in these areas, and lymphatics, bronchi, and vessels in the lung. Mass lesions of the mediastinum or retroperitoneum are usually difficult to demonstrate radiographically [1]. We describe ultrasound findings in a case of lymphangiomyomatosis. Such findings have not previously been reported to our knowledge.

Case Report

•G. G., a 24-year-old white female, noted abdominal swelling in December 1973. Her gynecologist found ascites without abdominal masses. A lymphangiogram demonstrated obstruction in multiple iliac and paraaortic areas with saccular lymphatic dilatation (fig. 1). A chest radiograph showed increased reticular markings at the lung bases.

At exploratory laparotomy 5 liters of chylous peritoneal fluid was withdrawn. In the retroperitoneum overlying the aorta, a nonresectable diffuse soft saccular mass extended from the retroduodenal space to the right common iliac area. Biopsy of the sac wall and nodes at the root of the mesentery disclosed lymphangiomyomata. Treatment with medium chain triglycerides and low fat diet resulted in continued absence of ascites.

In December 1975, the patient developed sudden dyspnea on exertion. On admission to Yale-New Haven Hospital 3 months later, physical examination showed a right pleural effusion and abdominal distention. Chest radiography revealed diffuse interstitial disease, a normal heart, and a right hydropneumothorax (fig. 2). An excretory urogram showed displacement of both ureters laterally and anteriorly. The bladder was displaced anteriorly and to the left (fig. 3). Transverse gray scale ultrasound scans disclosed multiple large cystic lesions, some with low level internal echoes, which extended anteriorly to the abdominal wall (fig. 4*A*). A longitudinal scan demonstrated cystic lesions extending from the true pelvis to the liver (fig. 4*B*). The patient was treated with right thoracostomy and tube drainage and a fat-free diet.

Discussion

Lymphangiomyomatosis is an uncommon myoproliferative disorder confined to women of reproductive age. The disease may be localized to the mediastinum or retroperitoneum or occur as a diffuse form with multifocal involvement of lymphatic channels, lymph nodes, and the pulmonary parenchyma. Thoracic manifestations include pneumothorax, chylous effusion, and "honeycombed" lung. Abdominal involvement may be signaled by chyloperitoneum.

Pathologically, the lymphangiomyoma consists of one or more nodules of tumorlike proliferation of smooth muscle fascicles, divided from each other by lymph channels [2]. The smooth muscle meshwork involves the

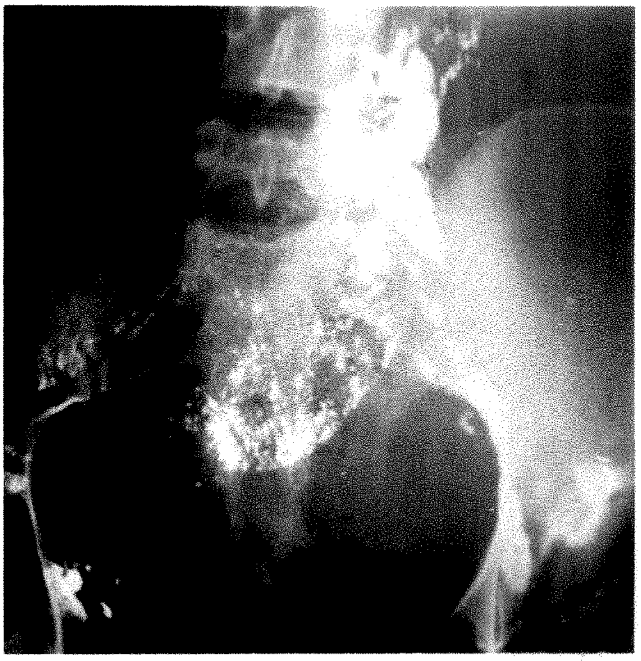

Fig. 1.—24 hr lymphangiogram follow-up film showing saccular lymphatic dilatation.

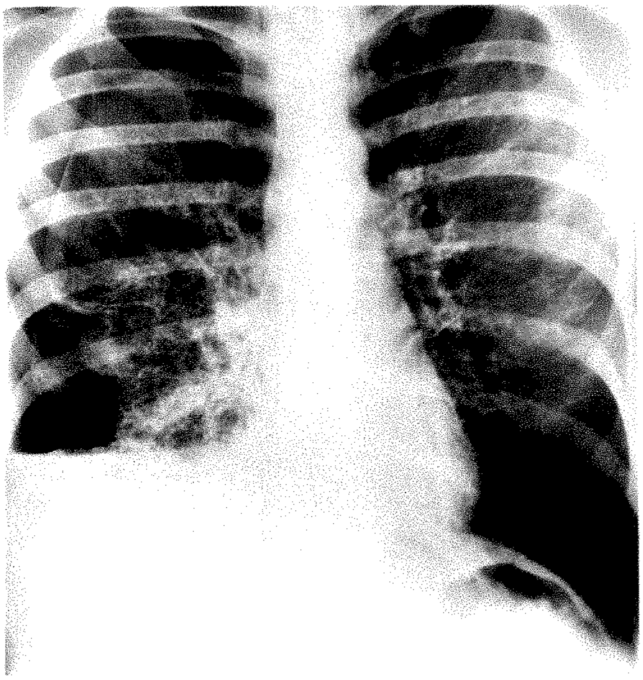

Fig. 2.—Chest film showing diffuse bilateral interstitial parenchymal process. Note large right hydropneumothorax.

Received December 22, 1976; accepted after revision June 29, 1977.

[1] All authors: Department of Diagnostic Radiology, Yale University School of Medicine, 333 Cedar Street, New Haven, Connecticut 06510. Address reprint requests to K. J. W. Taylor.

walls of preexisting lymphatic channels and replaces the sinusoids of lymph nodes. Lymphatic obstruction leads to distended collateral vessels and small and large lymph cysts.

The mediastinal and retroperitoneal masses which are part of this disease are usually relatively small [3]. However, in two of the six cases reported by Cornog and Enterline [1], large cystic retroperitoneal masses were present. Our patient is similar in exhibiting multiple large cystic abdominal masses.

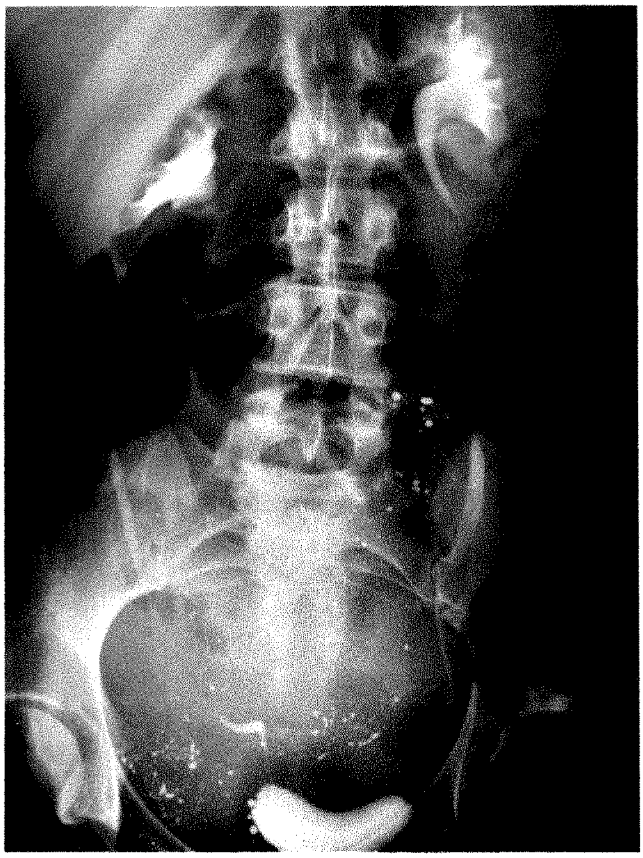

Fig. 3.—Excretory urogram showing lateral deviation of upper ureters and lower left ureter and medial deviation of distal right ureter and bladder. There is residual contrast within pelvis from previous lymphangiogram.

Gray scale ultrasound is ideally suited for the diagnosis of retroperitoneal lymphangiomyomatosis. Cystic structures of varying size lying along the course of the abdominal aorta and inferior vena cava are characteristic and easily demonstrated. The cyst walls are thick and often continuous with the walls of nearby cysts giving a septated appearance. Low level echoes may be seen within the cysts, presumably due to cellular debris.

The ultrasound differential diagnosis of diffuse cystic abdominal lesions should include ovarian cystadenomatous masses and cystic lymphangiomatosis. A serous or mucinous cystadenoma of the ovary is characteristically a multilocular cyst arising in the pelvis. Cystic lymphangiomas (cystic hygromas) are benign tumors composed of multiple large dilated cystic spaces lined by endothelial cells and separated by intervening connective tissue stroma. Developmental defects in lymphatics are thought to create obstruction and lymph accumulation. Abdominal cystic lymphangiomatosis may present an ultrasound pattern similar to that of lymphangiomyomatosis [4]. However, correlation of the clinical history and characteristic chest radiograph with abdominal ultrasound will confirm the diagnosis of lymphangiomyomatosis.

REFERENCES

1. Cornog JL Jr, Enterline HT: Lymphangiomyoma: a benign lesion of chyliferous lymphatics synonymous with lymphangiopericytoma. *Cancer* 19:1909-1930, 1966
2. Wolff M: Lymphangiomyoma: clinicopathologic study and ultrastructural confirmation of the histogenesis. *Cancer* 31:988-1007, 1973
3. Miller WT, Cornog JL Jr, Sullivan MA: Lymphangiomyomatosis: a clinical-roentgenologic-pathologic syndrome. *Am J Roentgenol* 111:565-572, 1971
4. McQuown DS, Fishbein MC, Moran ET, Hoffman RB: Abdominal cystic lymphangiomatosis: report of a case involving the liver and spleen and illustration of two cases with origin in the greater omentum and root of the mesentery. *J Clin Ultrasound* 3:291-296, 1975

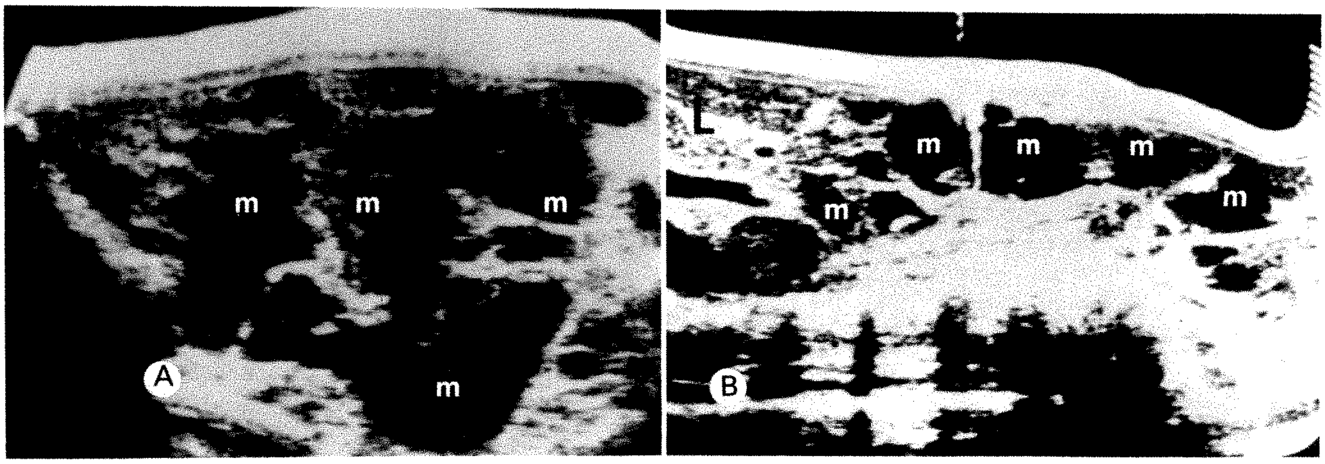

Fig. 4.—*A*, Transverse sonogram of true pelvis showing multiple cystic masses. *B*, Longitudinal parasaggital section through liver (L) at level of inferior vena cava showing multiple masses (m) extending from interior portion of liver to true pelvis. Note thick septae between masses. Some masses are sonolucent while others have low level echoes within them.

Diffuse Interstitial Calcification of the Lungs in Chronic Renal Failure Mimicking Pulmonary Edema

HOSSEIN FIROOZNIA,[1] ROCHELLE PUDLOWSKI, CORNELIA GOLIMBU, MAHVESH RAFII,
AND DOROTHY McCAULEY

With growing use of long term hemodialysis and increasing life span of uremic patients, complications of chronic renal failure are being encountered with increasing frequency [1-4]. These include renal osteodystrophy and soft tissue calcifications (cutaneous, occular, arterial, periarticular, and visceral). Affected viscera often include stomach, kidney, lung, and heart. Although most complications are well known, pulmonary calcification is often not recognized [2, 5-7]. Consequently, the clinical and radiographic manifestations of this lesion may be mistakenly ascribed to pulmonary edema or pneumonia [2, 5, 6, 8]. Pulmonary calcification, when extensive, can be a significant factor in the death of uremic patients [1, 2, 6, 8]. We report a case that was diagnosed as pulmonary edema; however, an autopsy documented lethal pulmonary calcification. The importance of accurate recognition of this serious complication is stressed because pulmonary calcification is potentially reversible [4, 8, 9].

Case Report

A 42-year-old male was diagnosed by renal biopsy as having severe glomerulonephritis. He had hypertension, anemia, secondary hyperparathyroidism, and cardiomegaly at age 39. In spite of hemodialysis, hypertension remained refractory, and a bilateral nephrectomy was performed. The patient improved considerably and returned to work for about 3 years while on maintenance hemodialysis. For 6 months prior to the final hospitalization, symptoms of gradually deteriorating heart failure developed, and he noted increasing dyspnea, orthopnea, and a chronic nonproductive cough. These proved unresponsive to treatment including hemodialysis. During the previous 3 years of hemodialysis, chest radiographs had revealed cardiomegaly and occasional instances of hypervolemia and pulmonary edema but the latter two always cleared after hemodialysis. About 12 weeks prior to admission (fig. 1), increased interstitial markings developed in the lower parts of the lungs which were diagnosed as interstitial pulmonary edema. These remained unchanged for the entire 3 month period.

On admission, cardiac arrythmia and paroxysmal noctural dyspnea were noted. The patient's cardiorespiratory status steadily deteriorated and he succumbed with cardiac arrest. Representative pre- and postdialysis chemistries were: BUN, 130/70; creatinine, 16/8; calcium, 7.8/7.9; and phosphorus, 12/6. Skeletal x-rays revealed prominent subperiosteal resorption of the digits and other bones and other findings indicative of secondary hyperparathyroidism.

At autopsy the lungs weighed 1,100 g each and were very rigid. Microscopy revealed extensive calcification of alveolar septae as well as the walls of many small vessels. No alveolar exudates, interstitial edema, or infiltrates were present (fig. 1C). Calcification of the myocardium and severe hyperplasia of the parathyroid glands were also noted.

Discussion

Metastatic pulmonary calcification is calcification of the lungs in the presence of conditions associated with an abnormality of calcium metabolism without prior tissue damage [5, 6, 10-12]. This differs from: (1) idiopathic calcinosis [13] wherein there is no abnormality of calcium metabolism; (2) calciphylaxis [14] which needs prior tissue sensitization; and (3) dystrophic calcification in which calcification occurs in damaged tissues. The leading causes of metastatic calcification are chronic renal failure [1, 6, 11, 12, 15], destructive bone diseases [5, 10], and parathyroid tumors [5]. Less frequently, hypervitaminosis D [15], phosphate and steriod therapy for the treatment of hypercalcemia [10], and, experimentally, parathyroid extracts [16] have caused metastatic calcification.

The overall incidence of metastatic pulmonary calcification is low. In one study [5], only 13 of 7,221 postmortem examinations revealed this finding. However, this condition is a common complication of chronic renal failure. It occurs in 50% or more of renal patients with metastatic soft tissue calcification [15]. The lung calcification is usually sparse and seen only on histologic examination [7], although occasionally it is extensive [1, 2, 6, 8, 17]. The lung is the organ most commonly affected by metastatic calcification [6]. In most reported cases, as in our patient, granular and linear calcification of the basement membrane of the alveolar septae and calcification of the walls of the bronchi and small pulmonary arteries and veins occur [1, 2, 5, 8]. Occasionally extensive interstitial fibrosis may also be present [2, 5, 18]. The alveoli may be dilated and contain air [18] or may be filled with extensive hyalinized fibrous tissue or calcification to form a solid mass [6, 18].

In extensive metastatic pulmonary calcification, diffusion capacity is decreased and severe alveolar-capillary block may occur because of involvement of the alveolar septae [2, 6, 11]. The patient may present with respiratory insufficiency without right heart failure [6], with a chest radiograph suggesting pulmonary edema [1, 2, 6, 11] or pneumonia [2, 6, 12]. Pulmonary edema due to cardiac failure may be mimicked by concomitant rales and peripheral edema [2]. Some patients with this condition also have myocardial calcification which may be exten-

---

Received February 3, 1977; accepted after revision August 16, 1977.

[1] All authors: Department of Radiology, New York University Medical Center, 560 First Avenue, New York, New York 10016. Address reprint requests to H. Firooznia.

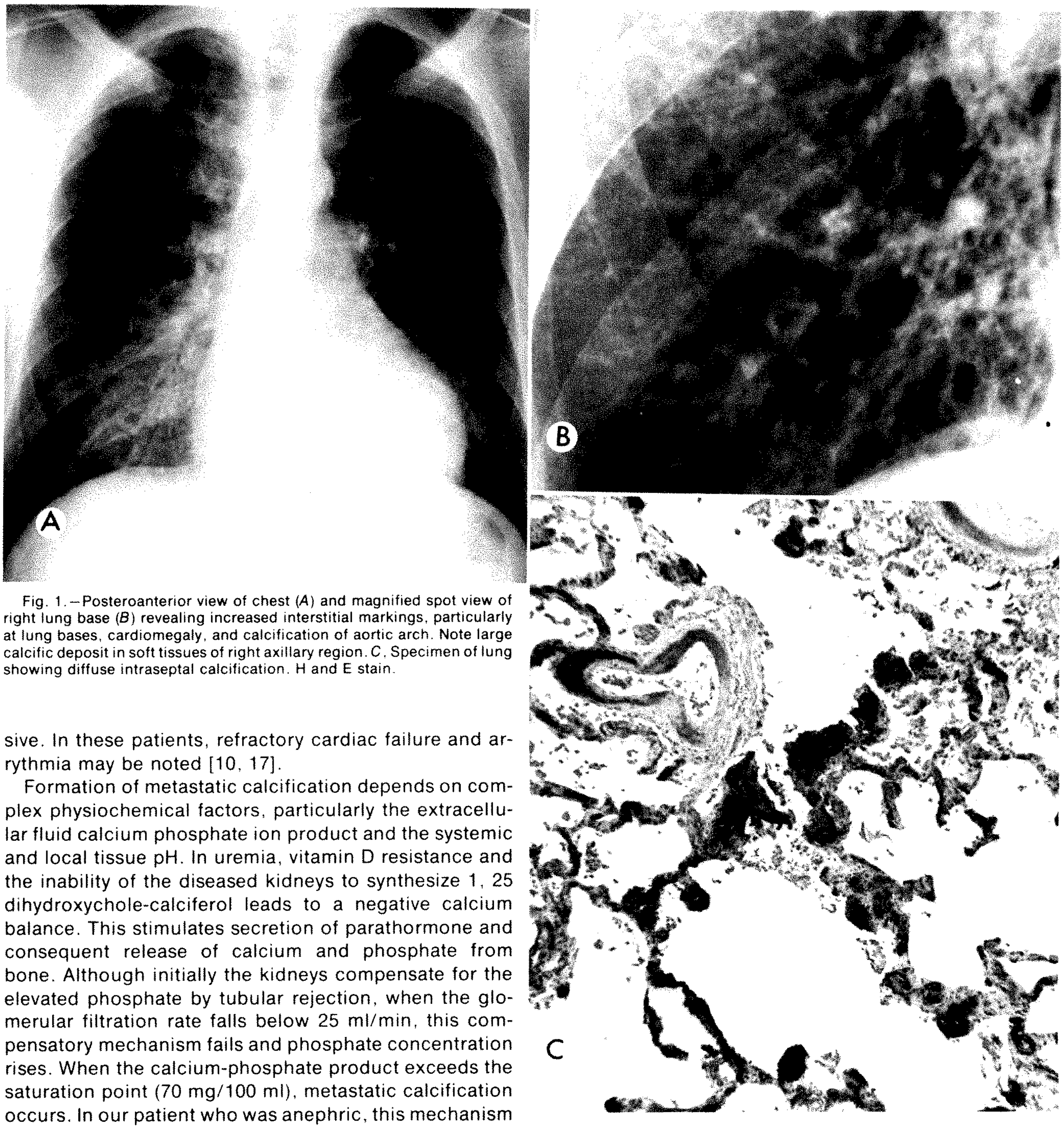

Fig. 1.—Posteroanterior view of chest (*A*) and magnified spot view of right lung base (*B*) revealing increased interstitial markings, particularly at lung bases, cardiomegaly, and calcification of aortic arch. Note large calcific deposit in soft tissues of right axillary region. *C*, Specimen of lung showing diffuse intraseptal calcification. H and E stain.

sive. In these patients, refractory cardiac failure and arrythmia may be noted [10, 17].

Formation of metastatic calcification depends on complex physiochemical factors, particularly the extracellular fluid calcium phosphate ion product and the systemic and local tissue pH. In uremia, vitamin D resistance and the inability of the diseased kidneys to synthesize 1, 25 dihydroxychole-calciferol leads to a negative calcium balance. This stimulates secretion of parathormone and consequent release of calcium and phosphate from bone. Although initially the kidneys compensate for the elevated phosphate by tubular rejection, when the glomerular filtration rate falls below 25 ml/min, this compensatory mechanism fails and phosphate concentration rises. When the calcium-phosphate product exceeds the saturation point (70 mg/100 ml), metastatic calcification occurs. In our patient who was anephric, this mechanism was felt responsible for metastatic pulmonary calcification.

The predilection of certain viscera (lung, kidney, and stomach) to calcification is probably due to loss of free hydrogen ions which creates the local alkaline milieu necessary for calcification. In dialysis patients, it has been postulated that acidosis in the interdialytic interval leaches calcium from bone which is then deposited in soft tissues during the postdialysis alkalosis [6, 11]. Generally, metastatic calcification develops over long periods of time [6], although it can occur in a few weeks [1, 5]. In dialysis patients, it is usually related to the length of survival of the patient receiving dialysis, but it also may be seen in nondialyzed patients, or occasionally in uremic patients without a high ion product [1, 5, 6, 19].

Radiographically, metastatic pulmonary calcification may manifest a spectrum of changes. In most reported cases, unilateral or bilateral patchy to confluent infiltrates mimick pneumonia [2, 5]. A pattern resembling pulmonary edema also has been observed [1, 2, 6, 8]. The calcification is usually very fine and sometimes very diffuse [6], although two patients, one with bilateral wedge-shaped areas of calcification [1] and another with a focal nodular form [18], have been reported. Radiographic diagnosis of diffuse pulmonary calcification is seldom made prior to death [2, 5, 6, 8]. Only rarely have definite punctate calcifications within the pulmonary opacities been identified on chest films [1, 2, 11], probably because of the very fine and diffuse nature of the intraseptal calcifications [2, 6]. According to Rubin and Siegelman [7], the difficulty in recognizing calcification may also be due to confusing opacities produced by associated cardiorenal complications.

The chest x-rays in our patient had an unchanging interstitial pulmonary edema pattern for a 3 month interval which did not clear with dialysis, and no diagnosis of diffuse pulmonary calcification was made. The findings in our patient are similar to other reported cases [2, 6]. Metastatic pulmonary calcification may resemble an intraalveolar process [2, 6], although interstitial calcification is the dominant finding pathologically. The difficulty in differentiating primarily interstitial diffuse calcification from alveolar disease of water density was noted by Felson [20]. Tomograms, grid films, and scanning of the lungs with bone-seeking radionuclides may be helpful [1, 21]. Computed tomography of the lungs may also eventually prove useful.

The possibility of pulmonary calcification should be considered in uremic patients if pulmonary infiltrates develop that resemble pneumonia and/or pulmonary edema and if these fail to respond to hemodialysis and other measures [2]. Appropriate treatment may reverse the course of this potentially lethal complication [4, 8, 9, 17, 18]. Because calcification may occur even with normal or low levels of serum calcium, control of serum phosphate is often critical in the management and reversal of pulmonary calcification. This is achieved by frequent dialysis, strict control of dietary phosphates, and use of phosphate-binding oral antacids [2, 4]. Prevention of hypercalcemia and control of blood pH are also important [1, 4, 18]. In patients with poorly controlled secondary hyperparathyroidism, more frequent dialysis [4], renal transplantation, or parathyroidectomy have been found effective. In autonomous tertiary hyperparathyroidism, early parathyroidectomy may reverse pulmonary calcification [4, 9].

REFERENCES

1. McLachlan MSF, Wallace M, Sene Viratne C: Pulmonary calcification in renal failure: a report of 3 cases. *Br J Radiol* 124:544–556, 1968
2. Mootz JR, Sagel SS, Roberts TH: Roentgenographic manifestations of pulmonary calcifications. *Radiology* 107:55–60, 1973
3. Pendras JP: Parathyroid disease in long term maintenance hemodialysis. *Arch Intern Med* 124:312–321, 1969
4. Rubini ME, Coburn JW, Massry SG, Shinaberger JH: Renal osteodystrophy: some therapeutic considerations relative to long term dialysis and transplantation. *Arch Intern Med* 124:663–669, 1969
5. Kaltreider HB, Barum GL, Bogaty G, McCoy MD, Tucker M: So-called "metastatic" calcification of the lung. *Am J Med* 46:188–196, 1969
6. Neff M, Yalcin S, Gupta S, Berger H: Extensive metastatic calcification of the lung in an azotemic patient. *Am J Med* 56:103–109, 1974
7. Rubin EH, Siegelman SS: *The Lungs in Systemic Diseases.* Springfield, Ill., Thomas, 1969
8. Davidson RC, Pendras VP: Calcium related cardio-respiratory death in chronic hemodialysis. *Trans Am Soc Artif Intern Organs* 13:36–40, 1967
9. Lawton RL, Gulesserian HP, Rossi NP: Surgical problems in patients on maintenance dialysis. *Arch Surg* 97:283–290, 1968
10. Fierer JA, Wagner BM, Strebel RF: Metastatic calcification of the myocardium. *Am J Cardiol* 26:423–426, 1970
11. Parfitt AM: Soft tissue calcification in uremia. *Arch Intern Med* 124:544–556, 1969
12. Boner G, Jacob ET, Perzner S, Jungmann A: Diffuse calcification of lungs in a patient on maintenance hemodialysis. *Isr J Med Sci* 7:1182–1187, 1971
13. Brunson JG, Gall EA: *Concepts of Disease.* New York, MacMillan, 1971
14. Selye H, Berczi I: The present status of calciphylaxis and calcergy. *Clin Orthop* 69:28–52, 1970
15. Mulligan RM: Metastatic calcification. *Arch Pathol* 43:177–230, 1947
16. Cooke CR, Myland JW: Pathological calcification of the lungs following the intravenous administration of calcium. *Am J Med* 29:363–368, 1960
17. Terman DS, Alfrey AC, Hammond WS, Donndelinger T, Ogden DA, Holmes JH: Cardiac calcification in uremia: a clinical, biochemical and pathologic study. *Am J Med* 50:744–755, 1971
18. Smith JC, Stanton LW, Kramer NC, Parrish AE: Nodular pulmonary calcification in renal failure: report of a case. *Am Rev Respir Dis* 100:723–728, 1969
19. Parfitt AM, Massry SG, Winfield AC, DePalma JR, Gordon A: Disordered calcium and phosphorus metabolism during maintenance hemodialysis. *Am J Med* 51:319–330, 1971
20. Felson B: Thoracic calcifications. *Dis Chest* 46:300, 1969
21. McLaughlin AF: Uptake of ^{99m}Tc bone-scanning agent by lungs with metastatic calcification: a case report. *J Nucl Med* 16:322–323, 1975

Massive Esophageal Hemorrhage in Leukemia

PHILLIP H. STRATEMEIER[1]

The esophagus is commonly involved in patients with leukemia. Inflammatory mucosal alterations frequently occur secondary to opportunistic *Candida albicans* infection. Other lesions reported include submucosal masses, strictures, and submucosal hemorrhage [1-4]. Spontaneous massive esophageal hemorrhage has not been reported in the radiologic literature, and minimally in other medical literature [5].

Case Report

This was the third admission for a 65-year-old white male who presented 6 months earlier with anemia. A preleukemic state was diagnosed, and he was placed on vincristine and prednisone. Frequent episodes of epistaxis occurred during the following 5 months which required multiple transfusions with packed red blood cells. One month prior to this admission he was admitted for extensive soft tissue petechiae. His hemoglobin was 10g/dl with a platelet count below 10,000. White blood cell count was 2,600 with 9% blasts. A diagnosis of myelomonocytic leukemia was then made.

He presented on the current admission with a 2 day history of acute hematemesis and hematochezia. He was treated with packed red blood cells and platelets, and the bleeding stopped. One week later he complained of dysphagia and inability to swallow liquids or solids. A barium esophagram demonstrated a large irregular intraluminal filling defect, with almost complete obstruction (figs. 1*A* and 1*B*). This defect was thought to be a large intraluminal blood clot. Massive hematesis recurred with bright red blood per rectum, and the patient expired the following day.

Autopsy findings showed petechiae and ecchymoses involving the soft tissue areas, and multiple internal organs correlating with the hemorrhagic diathesis. Necrotic mucosa was present in the upper gastrointestinal tract, particularly the esophagus. In addition there was a large intraluminal clot throughout the length of the esophagus corresponding to the radiographic appearance (fig. 1*C*). There were leukemic infiltrates in all organs and much of the soft tissue. Death was attributed to exsanguination, secondary to acute myelomonocytic leukemia.

Discussion

Minor amounts of esophageal hemorrhage in leukemia have been previously described in the radiologic literature, usually associated with a *Candida albicans* esophagitis [1, 3]. Prolla and Kirsner [6] described three mechanisms accounting for hemorrhage. Esophagitis secondary to *Candida albicans* is frequently present in patients with altered immune response and patients on steroid therapy. A thick adherent membrane forms with extension of the mycelia through the esophageal wall. This is followed by sloughing of the membrane leaving a denuded and ulcerated mucosa. While this mucosa often bleeds, massive hemorrhage is not characteristic. Our patient had no fungal infection at postmortem examination.

A second mechanism is the development of an agranulocytic and pseudomembraneous esophagitis consisting of a membrane composed of necrotic debris, fibrin, and bacterial colonies. This bacterial overgrowth is related to a granulocytopenia. As in fungal esophagitis, mucosal bleeding is usually minor.

The third mechanism is the development of disseminated petechiae and ecchymoses generally involving the lamina propia. This may lead to mucosal necrosis and ulceration and ultimately result in perforation into the esophageal lumen. Massive bleeding has been described by Givler [5], but it is not a common occurrence. This third pathogenesis may also occur in any patient having a hemorrhagic diathesis or in those patients on anticoagulant therapy [7-9]. In addition, necrotic mucosa due to any of the three mechanisms is susceptible to laceration from intubation or violent regurgitation.

The radiographic appearance of an intraluminal filling defect must be differentiated from mucosal lesions that cause ulceration and nodularity. An example is the cobblestone appearance of *Candida albicans* esophagitis that may also occur in patients receiving steroid therapy or in patients who have a depressed immune response from other causes [1, 3, 4]. Submucosal masses such as hematomas may appear identical to a clot when the overlying mucosa is necrotic, although when the mucosa is intact, they have smooth margins and generally persist longer than an intraluminal clot [5]. Mural nodules of leukemic cells can develop, particularly in chronic lymphocytic leukemia and less often with chronic myelogenous leukemia [2, 6]. These nodules can become necrotic and bleed into the submucosal space also causing large filling defects on barium studies.

In summary, patients with leukemia may develop massive spontaneous intraluminal esophageal hemorrhage as a result of a bleeding diathesis. A similar pathogenesis may occur in patients receiving anticoagulant therapy and those with other bleeding disorders. Lesser degrees of hemorrhage can result from esophagitis, particularly due to *Candida albicans*, from submucosal masses, or from mural involvement by leukemic nodules.

REFERENCES

1. Weiss T, Epstein B: Esophageal moniliasis. *Am J Roentgenol* 88 : 718-720, 1962
2. Gildenhorn HL, Fahey JL, Solomon RD: Functional esophageal obstruction due to leukemic infiltration. *Am J Roentgenol* 88 : 736-740, 1962

Received April 25, 1977; accepted July 26, 1977.

[1] Department of Diagnostic Radiology, University of Arizona Health Sciences Center, Tucson, Arizona 85724. Present address: Department of Radiology, Oak Knoll Hospital, Naval Regional Medical Center, Oakland, California 94627.

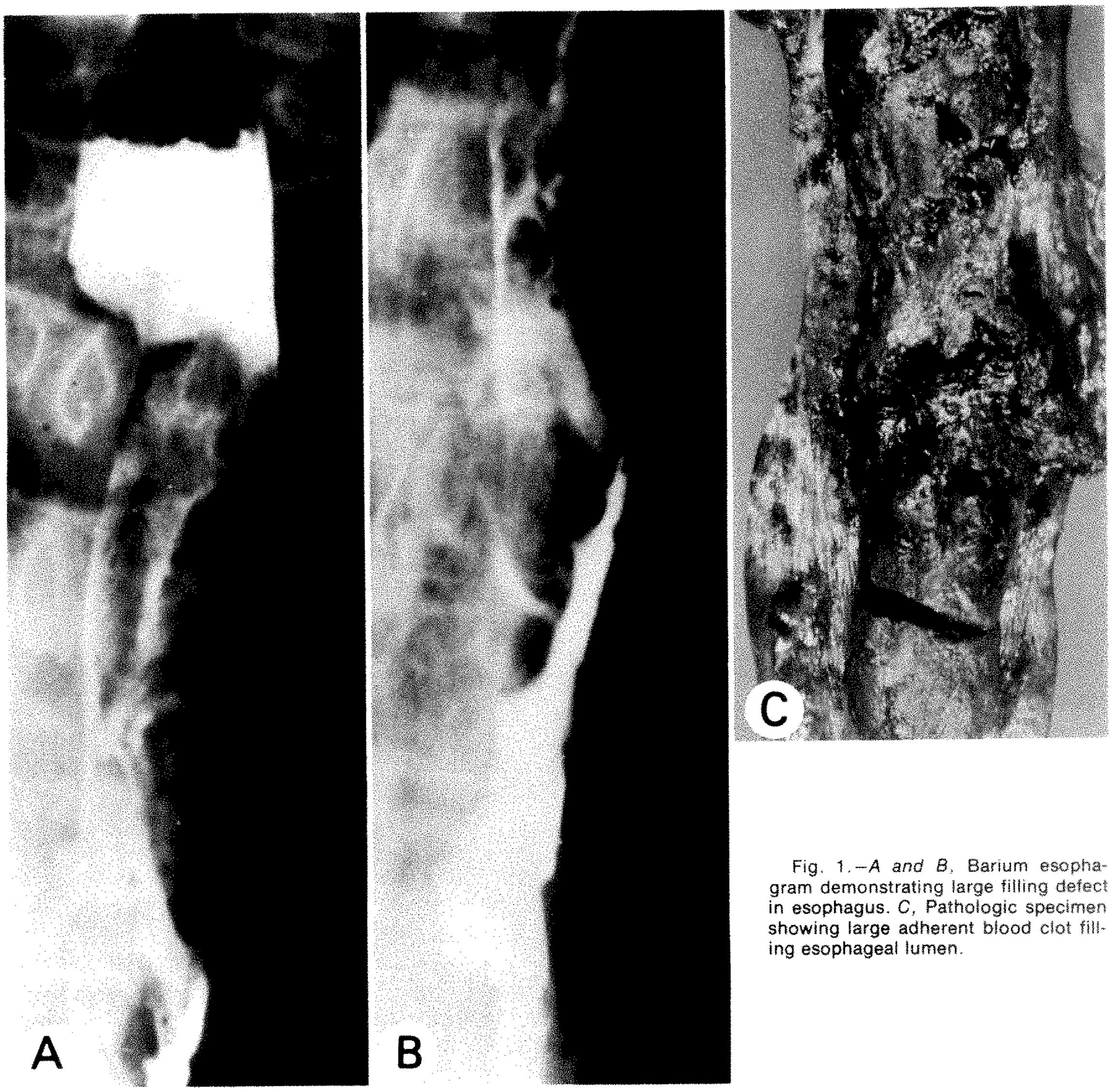

Fig. 1.—*A and B*, Barium esophagram demonstrating large filling defect in esophagus. *C*, Pathologic specimen showing large adherent blood clot filling esophageal lumen.

3. Goldberg HI, Dodds WJ: Cobblestone esophagus due to monilial infection. *Am J Roentgenol* 104 : 608–612, 1968
4. Pochedly C, Reichman I, Irwin GAL: Constrictive esophagitis due to *Candida albicans* in acute childhood leukemia. *J Pediatr* 80 : 892–893, 1972
5. Givler RL: Esophageal lesions in leukemia and lymphoma. *Am J Dig Dis* 15 : 31–36, 1970
6. Prolla JC, Kirsner JB: The gastrointestinal lesions and complications of the leukemias. *Ann Intern Med* 61 : 1084–1103, 1964
7. Lien JWK, Dufresne LR, Daly DS: Intramural esophageal bleeding in a hemodialysis patient. *Can Med Assoc J* 111 : 1230–1231, 1974
8. Chen P, Lebowitz R, Lewicki AM: Spontaneous hematoma of the esophagus. *Radiology* 100 : 281–282, 1971
9. Andress M: Submucosal hematoma of the oesophagus due to anticoagulant therapy. *Acta Radiol* [*Diagn*] (Stockh) 11 : 216–219, 1971

Lymph Node Calcification in Hodgkin's Disease after Chemotherapy

MARGARET BERTRAND,[1] JAMES T. T. CHEN,[1] AND HERMAN I. LIBSHITZ[1,2]

Calcification of mediastinal lymph nodes after radiation therapy in Hodgkin's disease has been well documented in the radiologic literature [1-8]. We have not found mention of similar findings after chemotherapy. We report two patients with calcification of anterior mediastinal nodes, one of whom also had calcification of a paraaortic node.

Case Reports

Case 1

E. G., a 31-year-old black female, had stage III mixed cellularity Hodgkin's disease. At the time of initial diagnosis, chest films revealed marked anterior mediastinal, hilar, and paratracheal adenopathy (figs. 1*A* and 1*B*). After five cycles of MOPP chemotherapy (nitrogen mustard, oncovine, prednisone, procarbazine), the patient underwent complete remission including disappearance of lymphadenopathy in the chest. Peripheral disease recurred after 18 months.

For the next 3½ years the patient had numerous courses of chemotherapy with a variety of agents including BCNU, vinblastine sulfate, cytoxan, prednisone, procarbazine and chlorambucil. During this interval the Hodgkin's disease was fairly well controlled and intrathoracic nodal enlargement never returned. However, in the interim the patient developed calcification within several anterior mediastinal lymph nodes (figs. 1*C* and 1*D*). Additionally, at this time an abdominal radiograph revealed calcification in the region of a paraaortic lymph node (fig. 2*B*) which had not been present at diagnosis (fig. 2*A*). When last seen, 5½ years after diagnosis, the patient's illness was complicated by pancytopenia and recurrent pulmonary infections.

Case 2

A. R., a 25-year-old white male, was seen 4 years after stage IVB Hodgkin's disease had been diagnosed elsewhere. Historically, a six cycle course of MOPP therapy had produced a remission. The patient did well for 2 years at which time he developed a lesion in a lumbar vertebral body for which he received local radiation therapy. Vinblastine sulfate and lateral chlorambucil were given.

On initial examination at our institution the patient had splenomegaly and peripheral lymphadenopathy. Over the next 9 months the patient, who was not a reliable clinic attender, had intermittent chemotherapy which included vincristine, procarbazine, chlorambucil, and prednisone. The patient developed diffuse pulmonary disease after 8 months of chemotherapy at our center, and was admitted for evaluation. Opportunistic infections were ruled out by appropriate clinical tests. Discharge diagnosis was presumed parenchymal Hodgkin's disease. The patient was then lost to follow-up.

Initially this patient's chest radiograph suggested punctate calcifications in the anterior mediastinal nodes. After several months of additional chemotherapy at our center, these calcifications progressed to an appearance very similar to that of case 1.

Discussion

Calcification in Hodgkin's disease of previously involved intrathoracic lymph nodes after radiation therapy has been described in several series and in sporadic case reports over the last 15 years. Wyman and Weber [1] reported nine cases of intrathoracic nodal calcification following radiation therapy. No correlation between amount of radiation therapy and degree of calcification could be established. The calcification was noted from 1 to 14 years after completion of therapy. The timing of the first appearance of the calcification could not be accurately assessed because interval chest radiographs were not available in several cases.

Brereton and Johnson [2] reported a prospective study of 164 patients with Hodgkin's disease who received radiation to the mediastinum. Four of these patients developed calcification in nodes. Each of these four had disease in the areas that subsequently calcified. The calcifications appeared 1-5 years after therapy. Three of the four patients remained free of disease for intervals ranging from 6 to 8 years after initial treatment.

Nodal calcification in patients with Hodgkin's disease in extrathoracic locations has also been seen. Calcification has been reported after radiation therapy in lymph nodes of the pelvis, abdomen, and supraclavicular and axillary regions [3, 9]. Paraaortic nodal calcification was noted in our case 1 after chemotherapy alone. A single occurrence of spontaneous calcification in retroperitoneal Hodgkin's disease has been reported [10].

Fifteen cases of tumor calcification after therapy for a variety of malignancies were reported from the M. D. Anderson Hospital several years ago [3]. Of these, two were shown to have calcification following chemotherapy alone. Neither of these represented Hodgkin's disease; one patient had reticulum cell sarcoma, and the other, embryonal cell carcinoma of the testis.

It has been postulated that calcification occurring after therapy represents dystrophic calcification deposited in response to local changes in degenerating tumor tissue (necrosis, hemorrhage, fibrosis). Such has been the finding in the reported cases that underwent histologic examination [3, 9].

Although our two patients developed other pulmonary involvement with Hodgkin's disease, they did not develop evidence of recurrent disease (enlargement) of the calcified nodes. This is in keeping with the suggestion

---

Received June 3, 1977; accepted after revision August 16, 1977.

[1] Department of Radiology, Duke University Medical Center, Durham, North Carolina 27705. Address reprint requests to M. Bertrand.

[2] Present address: Department of Diagnostic Radiology, University of Texas System Cancer Center, M. D. Anderson Hospital and Tumor Institute, Houston, Texas 77030.

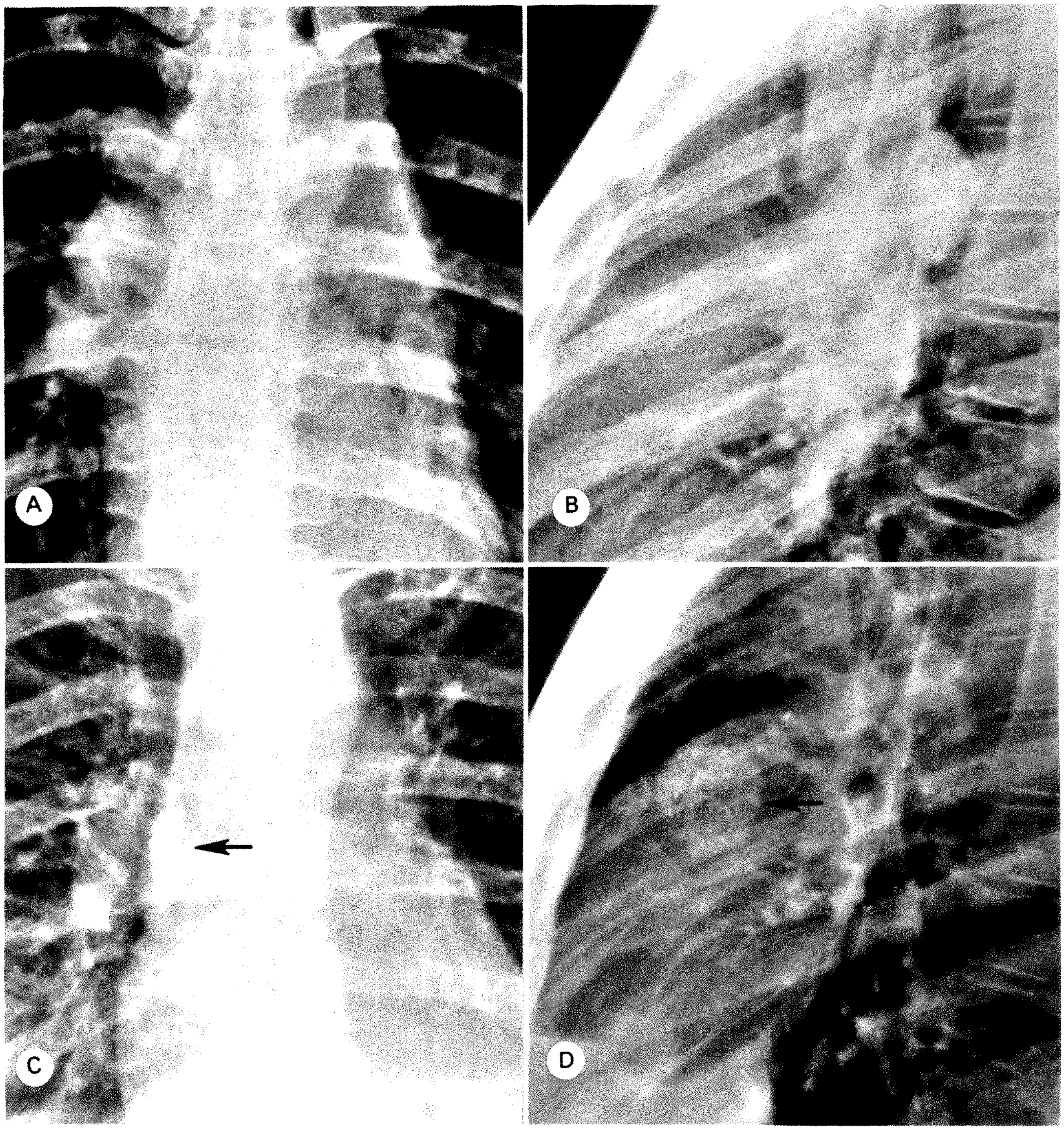

Fig. 1.—Case 1. Pretreatment posteroanterior (*A*) and lateral (*B*) chest films showing nodal masses and Hodgkin's disease in mediastinal and hilar areas. *C and D*, Similar views 6 years after chemotherapy showing nodal calcifications (*arrows*) in anterior mediastinum.

by Brereton and Johnson [2] that calcification of nodes represents a favorable local response.

The radiographic features of the anterior mediastinal nodal calcification of our two cases are similar to those reported for intrathoracic nodal calcification after radiation therapy. The pattern of calcification is not specific. Early in the course it tends to be punctate. Later it can become more dense as the nodes coalesce and shrink [4]. In addition to posttherapy intrathoracic nodal calcification, the differential diagnosis of intrathoracic nodal calcification includes sarcoidosis, hamartoma, silicosis, tuberculosis, histoplasmosis, coccidioiodomycosis, and berylliosis.

REFERENCES

1. Wyman SM, Weber AL: Calcification in intrathoracic nodes in Hodgkin's disease in the chest. *Radiology* 93:1021–1024,

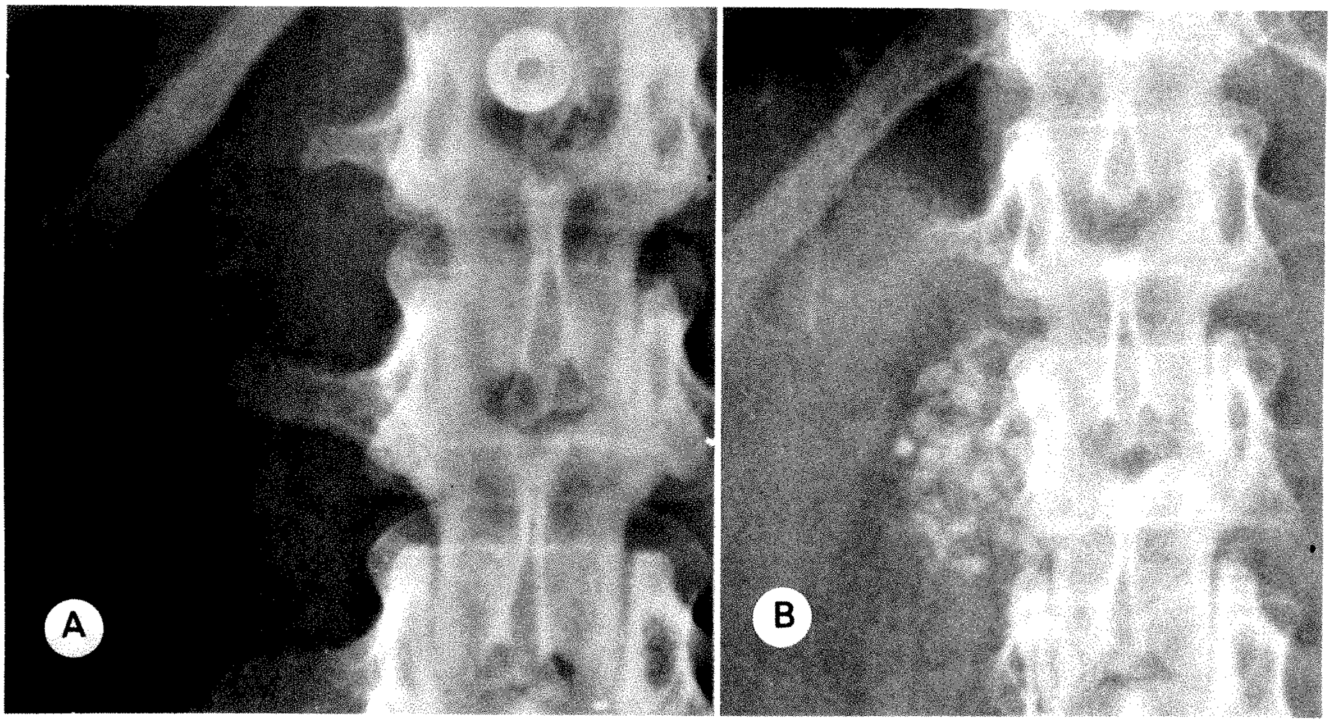

Fig. 2.—Case 1. *A*, Pretreatment abdominal film. *B*, Similar view after chemotherapy showing calcification in paraaortic node.

1969

2. Brereton HD, Johnson RE: Calcification in mediastinal lymph nodes after radiation therapy of Hodgkin's disease. *Radiology* 112:705-707, 1974
3. Dolan PA: Tumor calcification following therapy. *Am J Roentgenol* 89:166-274, 1973
4. Strickland B: Intra-thoracic Hodgkin's disease. II. Peripheral manifestations of Hodgkin's. *Br J Radiol* 40:930-938, 1967
5. Whitfield AGW, Jones EL: Lymph node calcification in Hodgkin's disease. *Clin Radiol* 21:259-260, 1960
6. Grebell FS, Lyons AR: Case reports: a further case of lymph node calcification in Hodgkin's disease following radiotherapy. *Br J Radiol* 44:720-723, 1971
7. Buraczewski J, Dziukowa J, Zomer J: Calcification in lymphogranulomatosis. *Fortschr Geb Roentgenstr Nuklearmed* 117:28-33, 1972
8. Libshitz HI, Southard ME: Complications of radiation therapy: the thorax. *Semin Roentgenol* 9:41-49, 1974
9. McLennan TW, Castellino RA: Calcification in pelvic lymph nodes containing Hodgkin's disease following radiotherapy. *Radiology* 115:87-89, 1975
10. Case records of the Massachusetts General Hospital. *N Engl J Med* 254:1139-1141, 1956

Localization of ^{67}Ga Citrate in a Mycotic Aneurysm

JOHN A. MICHAL, III,[1] AND R. EDWARD COLEMAN[1]

Many recent reports have demonstrated that ^{67}Ga citrate imaging is an accurate method of detecting occult inflammatory processes [1-4]. Gallium-67 imaging is particularly useful in a patient with a strong clinical suspicion of an abscess which cannot be confirmed by routine clinical and radiologic procedures [1]. Abnormal accumulation has been reported in several types of inflammatory processes [1-5]. We recently studied a patient with a mycotic aneurysm and an abnormal ^{67}Ga scan. To our knowledge, this has not been previously reported.

Case Report

A 39-year-old white man was admitted for evaluation of right hip pain. History included progressive familial parkinsonism, intermittent low back pain, gout, and weight loss (31.75 kg in the previous year). He was admitted to another hospital with fever and exacerbation of chronic right hip pain radiating into the thigh after an uncomfortable automobile ride. On admission to the outside hospital, his white blood cell count and sedimentation rate were elevated. A chest radiograph was normal. He was treated with muscle relaxants for 3 days.

Since no decrease in hip pain was noted, the patient was transferred to the University of Utah Medical Center. Physical examination revealed a diaphoretic obese male with a slight tachycardia and a temperature of 39.4°C. The lungs were clear to percussion and auscultation, and the heart was normal. Tenderness in the right lower quadrant was noted, but no mass could be palpated. Neurologic examination revealed an intention tremor but no neurologic deficit in the extremities. Laboratory data again demonstrated a leukocytosis and an elevated sedimentation rate. Chest radiography revealed bilateral upper lobe infiltrates. Blood cultures grew *Streptococcus viridans*. Intravenous penicillin G was administered with prompt defervescence, clearance of lung infiltrates, and elimination of bacteremia. Lumbar spine radiographs demonstrated degenerative disease with narrowed disc spaces at multiple levels. An intravenous pyelogram was normal except for a right pelvic mass indenting the bladder. Barium enema examination confirmed the right pelvic mass.

The right hip pain and lower abdominal tenderness persisted.

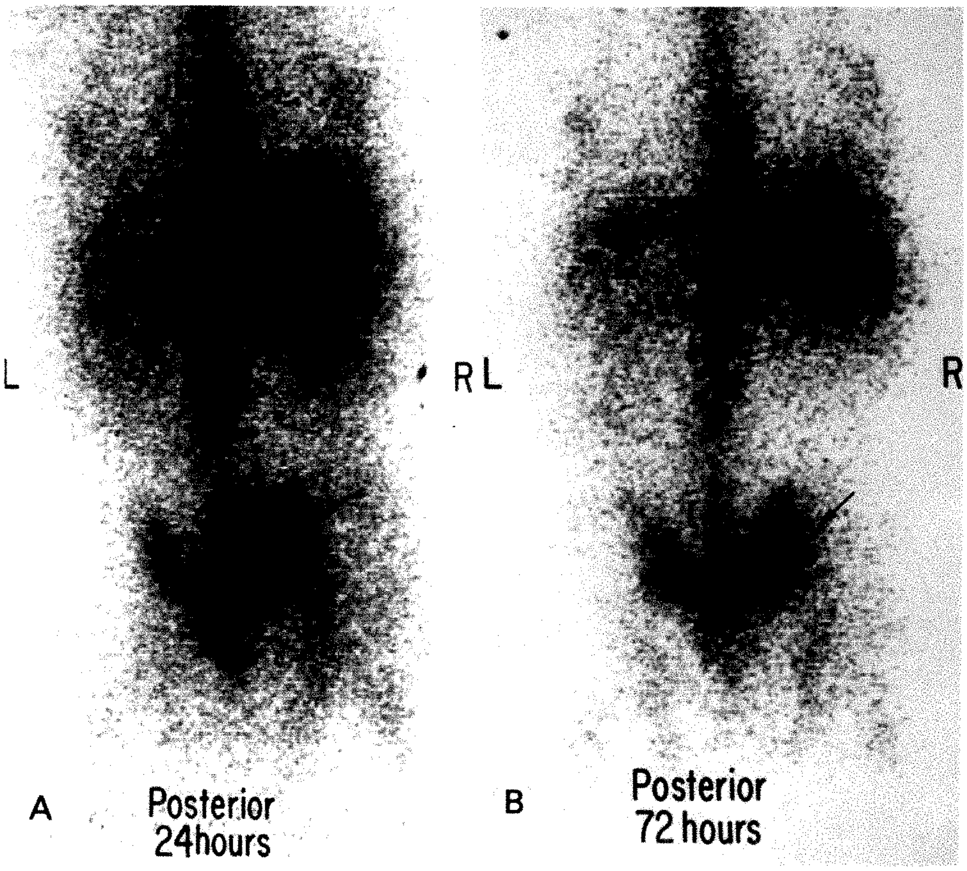

Fig. 1.—Gallium-67 scans showing persistent abnormal activity (*arrows*) at 24 and 72 hr in right pelvic area.

Received April 27, 1977; accepted after revision August 3, 1977.

[1] Department of Radiology, University of Utah Medical Center, Salt Lake City, Utah 84132. Address reprint requests to R. E. Coleman.

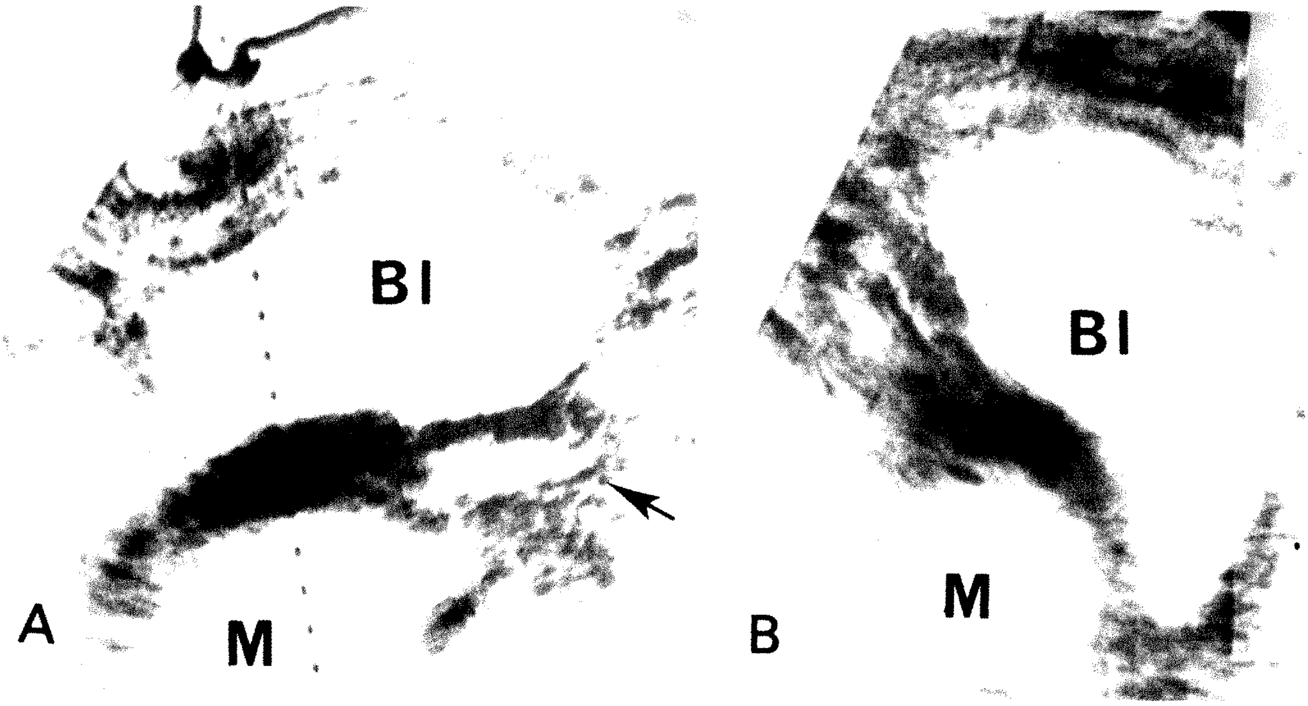

Fig. 2.—Ultrasound of pelvic region in sagittal plane 2 cm right of midline (*A*) and in transverse plane 2 cm above symphysis pubis (*B*) showing 5 cm sonolucent mass (M) behind bladder (Bl) and indenting right posterior aspect of bladder. Note tubular structure (*arrow*) between bladder and mass in *A*, thought to represent right iliac artery.

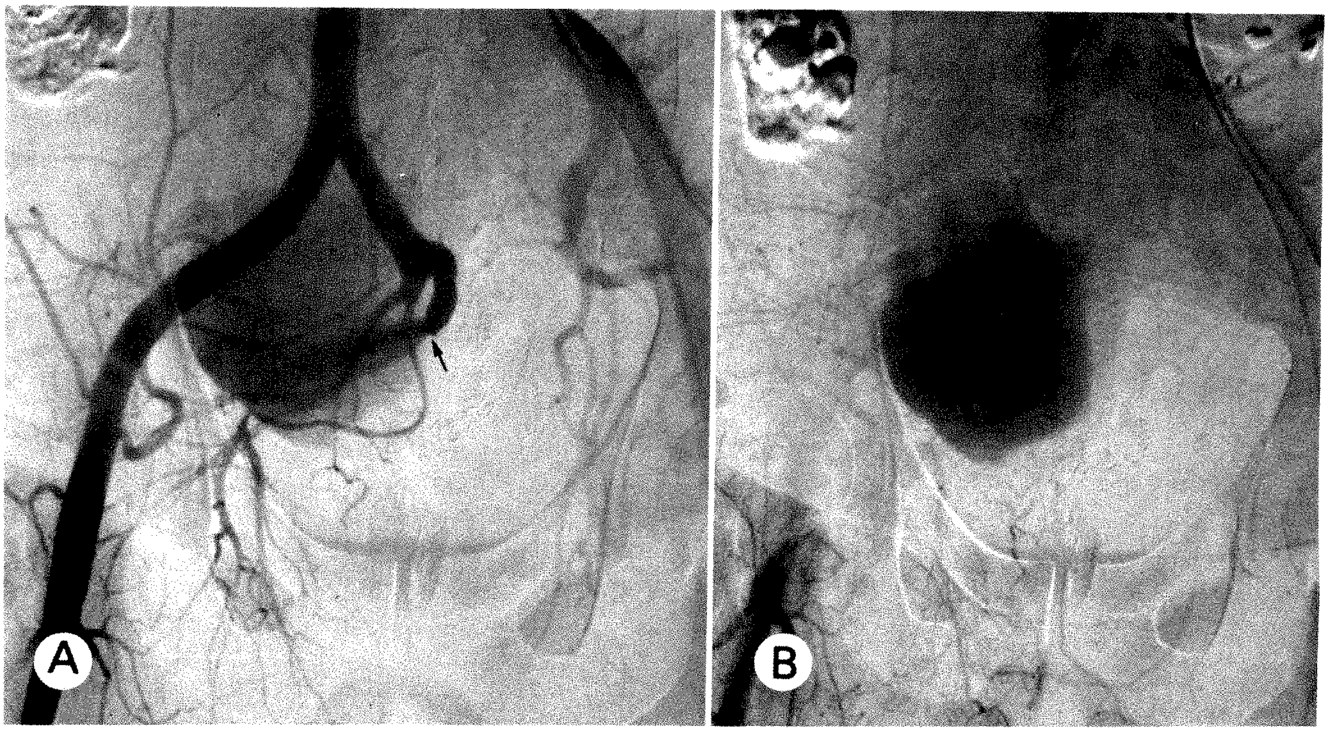

Fig. 3.—Iliac angiogram. Subtraction films of arterial phase (*A*) and late arterial phase (*B*) demonstrating contrast filling large aneurysm of major branch of right hypogastric artery (*arrow*) in *A*, with residual contrast in aneurysm in *B*.

A ^{67}Ga citrate scan was performed to determine whether an intraabdominal abscess was present, since the source of bacteremia had not been identified. Subacute bacterial endocarditis was considered but felt unlikely since the patient had no heart murmur, splenomegaly, or evidence of peripheral emboli. Abnormal ^{67}Ga accumulation was noted in the right posterior pelvis on scans obtained 24, 48, and 72 hr after injection (fig. 1). Ultrasound revealed the mass to be sonolucent without the internal echos typical of an abscess (fig. 2). Arteriography revealed a 6 cm round aneurysm of a large branch of the right internal iliac artery with rapid pulsatile flow (fig. 3).

At surgery, the aneurysm was identified and the feeding and draining vessels ligated. A biopsy of the aneurysm revealed a mixture of dense scar tissue with hyalinized thrombus material and granulation tissue. Pathologically it was considered to be a mycotic aneurysm. Cultures of the aneurysm were negative since the patient had been on intravenous penicillin for 12 days. The postoperative course was uncomplicated, and the patient was discharged well and free of pain.

Discussion

Gallium-67 citrate has been used in patients with sepsis of undetermined origin and in patients with medical and surgical diseases [1-5]. Imaging with ^{67}Ga citrate has been an accurate method of localizing deep abscesses in a wide variety of patients. Although abnormal accumulation can be associated with either an inflammatory process or tumor, this lack of specificity is generally not a problem.

In the patient reported here, the ^{67}Ga citrate scan demonstrated an abnormal area of accumulation in the region of the fluid-containing mass noted on ultrasound. This was subsequently demonstrated to be a mycotic aneurysm. A previous study has suggested that ^{67}Ga scanning may be beneficial in demonstrating infected heart valves in patients with suspected bacterial endocarditis [6], but another study did not find this approach to be useful [1]. We were unable to find any previous report of ^{67}Ga scanning in patients with mycotic aneurysms. In a patient with a suspected mycotic aneurysm, the combination of ultrasound and ^{67}Ga scanning may be beneficial.

REFERENCES

1. Kumar B, Coleman RE, Alderson PO: Role of 67-gallium imaging in the evaluation of patients with suspected inflammatory lesions. *Arch Surg* 110:1237–1242, 1975
2. Silva J, Harvey WE: Detection of infections with gallium-67 and scintigraphic imaging. *J Infect Dis* 130:125–131, 1974
3. Littenberg RL, Taketa RM, Alazraki NP, Halpern SE, Ashburn WL: Gallium 67 for localization of septic lesions. *Ann Intern Med* 79:403–406, 1973
4. Blair DC, Carroll M, Silva J, Fekety FR: Localization of infectious processes with gallium citrate Ga67. *JAMA* 230:82–84, 1974
5. Kumar B, Coleman RE: Significance of delayed ^{67}Ga localization in the kidneys. *J Nucl Med* 17:872–875, 1976
6. Wiseman J, Rouleau J, Rigo P, Strauss HW, Pitt B: Gallium-67 myocardial imaging for the detection of bacterial endocarditis. *Radiology* 120:135–138, 1976

Exostosis after Iliac Bone Marrow Biopsy

WILLIAM A. MURPHY[1]

Recently, Gilsanz and Grunebaum [1] described a posterior-superior iliac spine lytic lesion in children as a result of marrow biopsy. An exostosis may also develop at the site of an iliac trephine bone marrow biopsy.

Case Reports

Case 1

An 18-year-old woman with known systemic lupus erythematosis was admitted to Barnes Hospital for evaluation of thrombocytopenia. Because a sternal aspirate was not diagnostic, a trephine bone marrow biopsy of the right iliac crest was performed. Increased numbers of megakaryocytes were found, and the final diagnosis was idiopathic thrombocytopenia.

Detail (fig. 1) from a plain film of the abdomen 2½ years after biopsy demonstrated a bony exostosis at the previous biopsy site, characterized by a lucent core, by otherwise uniform radiodensity, and by sharp margins with a smooth transition into normal ilium.

Case 2

A 73-year-old woman was evaluated for gastrointestinal bleeding and anemia. During the workup, a trephine bone marrow biopsy of the right iliac crest was performed. Final diagnosis was iron deficiency anemia due to multiple benign colonic polyps.

Detail (fig. 2*A*) from a plain film of the abdomen 4 years later demonstrated a bony exostosis at the previous biopsy site with characteristics similar to case 1, but with less mineralization. After a fall 18 months later, the patient complained of persistent right hip pain. A radiograph at that time showed a fracture at the base of the exostosis (fig. 2*B*), with additional periosteal reaction along the lateral margin of the ilium.

Discussion

The exostosis which may develop after iliac bone marrow biopsy results from the local trauma of that diagnostic procedure. A small hematoma probably develops as marrow elements leak into the soft tissues. If blood simply collects in the adjacent soft tissues, then the exostosis probably develops by ossification of the hematoma in a manner similar to the development of myositis ossificans. If, however, the periosteum is elevated or stimulated by a combination of the procedure and its accompanying hemorrhage, then periosteal reaction plays a role in formation of the exostosis.

In the two cases presented here, a lucent core or central defect is a characteristic observation. I believe this reflects removal or displacement of a periosteal plug by the trephine needle. If so, then the central deficiency suggests that periosteal reaction helps to determine the form of the exostosis. If the biopsy is transiliac, periosteum may also be stimulated on the intrapelvic surface (fig. 2).

Early stages of healing may be seen several weeks after biopsy and may remain for many years. Although the incidence of occurrence is uncertain, it is not common, even in this referral medical center.

Postbiopsy exostosis can be differentiated from myositis ossificans due to closed trauma and from dystrophic calcification due to avulsed ligaments by the lucent core or central defect. It can be differentiated from the iliac horns of the nail-patella syndrome by location, appearance, and bilaterality [2].

As illustrated in case 2, prominence of the postbiopsy exostosis may subject it to fracture. Recognition of its origin will preclude further investigation, expense, and radiation exposure.

REFERENCES

1. Gilsanz V, Grunebaum M: Radiographic appearance of iliac marrow biopsy sites. *Am J Roentgenol* 128:597–598, 1977
2. Fong EE: "Iliac horns" (symmetrical bilateral central posterior iliac processes): a case report. *Radiology* 47:517–518, 1946

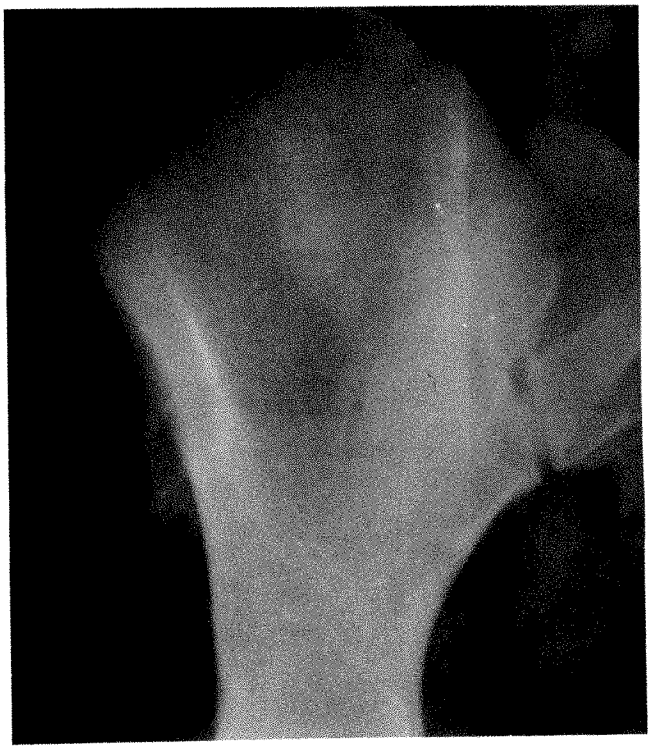

Fig. 1.—Case 1. Postbiopsy exostosis characterized by lucent core.

Received May 19, 1977; accepted after revision August 9, 1977.

[1] Mallinckrodt Institute of Radiology, Washington University School of Medicine, 510 South Kingshighway Boulevard, St. Louis, Missouri 63110.

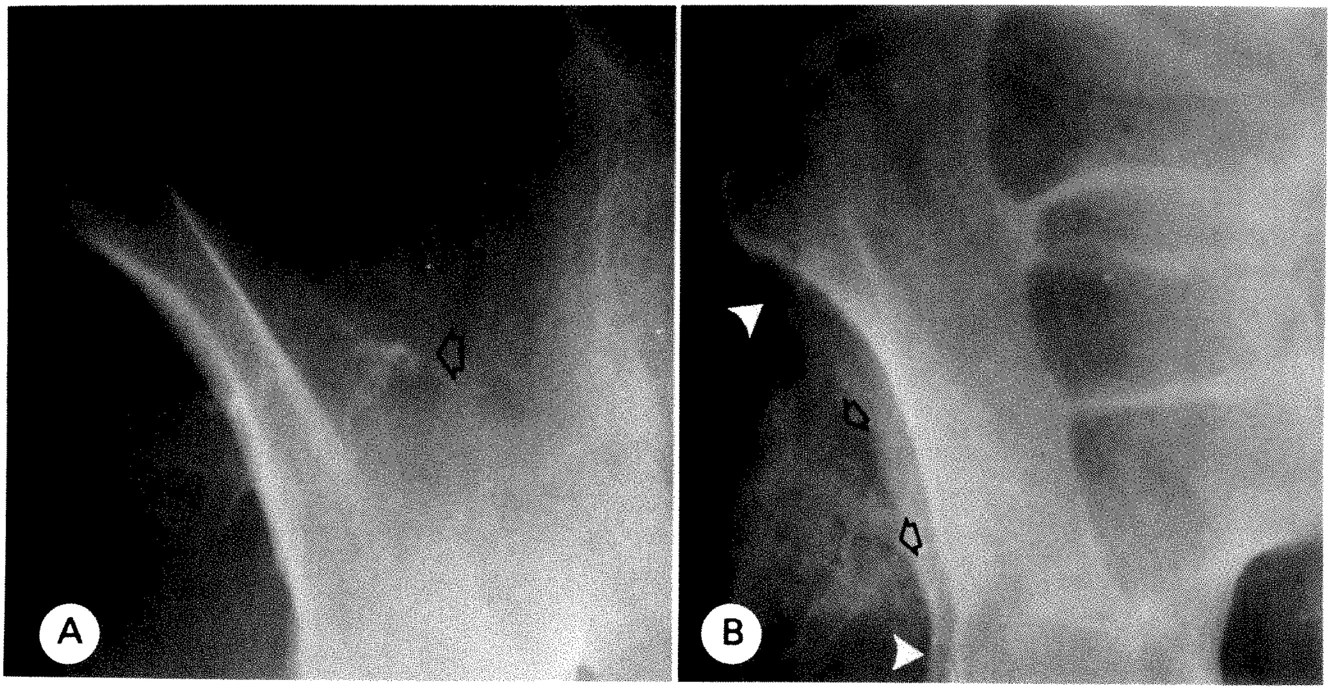

Fig. 2.—Case 2. *A*, Film 4 years after biopsy showing smooth, homogeneous exostosis still with central defect at apex, possibly due to absence of plug of periosteum. Transiliac biopsy stimulated intrapelvic periosteal reaction (*arrow*). *B*, Film 5½ years after biopsy showing periosteal exostosis fractured at base (*arrows*) and new periosteal reaction (*arrowheads*) along lateral iliac cortex.

Pathologic Fracture in an Unusual Case of Gout

JOHN BURNHAM,[1, 2] KEITH FRAKER,[1] AND HOWARD STEINBACH[3]

While descriptions of gout antedate the birth of Christ, portions of this disease remain incompletely explored. We discuss three unusual aspects of gout encountered in a patient seen at the Santa Clara Valley Medical Center: (1) increased incidence of gout in Filipinos, (2) spinal and sacroiliac involvement with gout, and (3) pathologic pelvic fracture due to gout. We believe this is the first documented description of gout as the cause of a pathologic fracture.

Case Report

S. N., a 70-year-old Filipino woman, was admitted complaining of inability to walk for 2 weeks following a minor fall at home. Over the previous 10 years she had noted the gradual onset of pain, swelling, and loss of motion in the metacarpo- and metatarsophalangeal joints, knees, shoulders, wrists, and elbows. She had experienced occasional erythema and heat in these joints (especially the metacarpo- and metatarsophalangeal joints) but no incapacitating arthritic episodes. During the 5 years prior to admission she developed subcutaneous nodules located over the elbows, left shoulder, hands, feet, knees, and wrists.

Family history was positive for "rheumatism" but not for gout. Medical history was remarkable for hypertension. Medications included indomethacin, phenylbutazone, and corticosteroids for arthritis, and hydrochlorothiazide for hypertension.

Initial physical examination revealed large hard nodules about the metacarpophalangeal joints and over the extensor surfaces of the elbows. There was boggy synovial thickening over several metacarpophalangeal joints, over the proximal interphalangeal joints of the first and second fingers, the wrists, knees, and right shoulder. Enlargement of abdominal organs was not noted. There was exquisite tenderness on pelvic compression.

Laboratory findings included hematocrit, 28%; sedimentation rate, 94; uric acid, 12 mg/100 ml; fluorescent antinuclear antibody, negative; rheumatoid factor by tube, positive at 1:80 (borderline); fasting blood sugar, normal; VDRL, negative; alkaline phosphatase, 124 (normal under 85); creatinine, 3.1 mg/100 ml; blood urea nitrogen, 68 mg/100 ml.

Radiography of the left foot revealed large, sharply demarcated erosions of the metatarsophalangeal joints of the great and second toes with adjacent tophi. There was extensive erosion of the tarsal bones of the foot (fig. 1*A*). The lumbar spine film showed preservation of the intervertebral discs and sclerotic-rimmed cystlike destructive lesions adjacent to the discs in all lumbar vertebral bodies. These cystic lesions predominated at the anterosuperior aspects of the vertebral bodies. In addition, loss of definition and destructive areas with discrete margins were noted in the posterior articulations at the L4-L5 and L5-S1 levels (fig. 1*B*).

Pelvic radiography revealed bilaterally symmetric sacroiliac disease with sclerotic-rimmed lucent erosions which involved both surfaces of the sacroiliac joints and the adjacent surfaces of the sacrum and ilium above the true joints. A fracture extended through the right sacroiliac lesion to the iliac crest. There was a lytic destructive lesion of the pubic bones adjacent to the symphysis which extended toward the left. A pathologic fracture traversed the left superior and inferior pubic rami (fig. 2).

The preliminary diagnosis of gout was confirmed when aspirate from the subcutaneous nodules of the forearms and left pubic lesion revealed numerous needle-shaped crystals polarizing as monosodium urate. The patient was treated with allopurinol, colchicine, and dietary protein restriction, and the serum uric acid level declined. The patient was discharged 1 month later and subsequently lost to follow-up.

Discussion

This case presented several unusual aspects of gout. First, our patient was Filipino, one of the South Pacific races reported to have an increased incidence of hyperuricemia and gout. While scattered reports of elevated serum uric acid levels with or without associated gout exist for several other South Pacific racial groups (including the New Zealand Maoris [1], Australian Aborigines [2], and Mariana Islanders [3]), more extensive research has been done with the Filipinos. Findings indicate that hyperuricemia and gout occur mainly in Filipinos residing outside their native islands [4-6]. Healey et al. [4], who tested several hundred male Filipinos living in various Philippine provinces, found no statistical elevation of serum uric acid levels nor increased incidence of gout. In contrast, serum uric acid levels and frequency of gout in Filipino populations living in Hawaii [6] and Washington [4] were significantly elevated over control populations from these same areas.

Healey et al. [4] speculated that some aspect of the new environment—most likely the increased purine load on American diets—uncovered an underlying genetic defect in many Filipino males. In testing this hypothesis, he found that four of 13 Filipino males with normal serum uric acid levels did not increase their urinary uric acid excretion following a dietary purine load, while all 10 normal Caucasian controls did [7]. This renal uric acid retention corresponded to that seen in gouty patients with normal serum uric acid levels and suggested a basis for increased hyperuricemia and gout in Filipinos living outside their native islands. While most of the foregoing work involved Filipino men, similar increases in serum uric acid levels and gout have been documented in Filipino women [6].

Received March 31, 1977; accepted after revision July 22, 1977.

[1] Department of Radiology, Santa Clara Valley Medical Center, 751 South Bascom Avenue, San Jose, California 95128. Address reprint requests to K. Fraker.

[2] Present address: 132 A Nimshew Stage, Chico, California 95926.

[3] 4141 Geary Boulevard, San Francisco, California 94118.

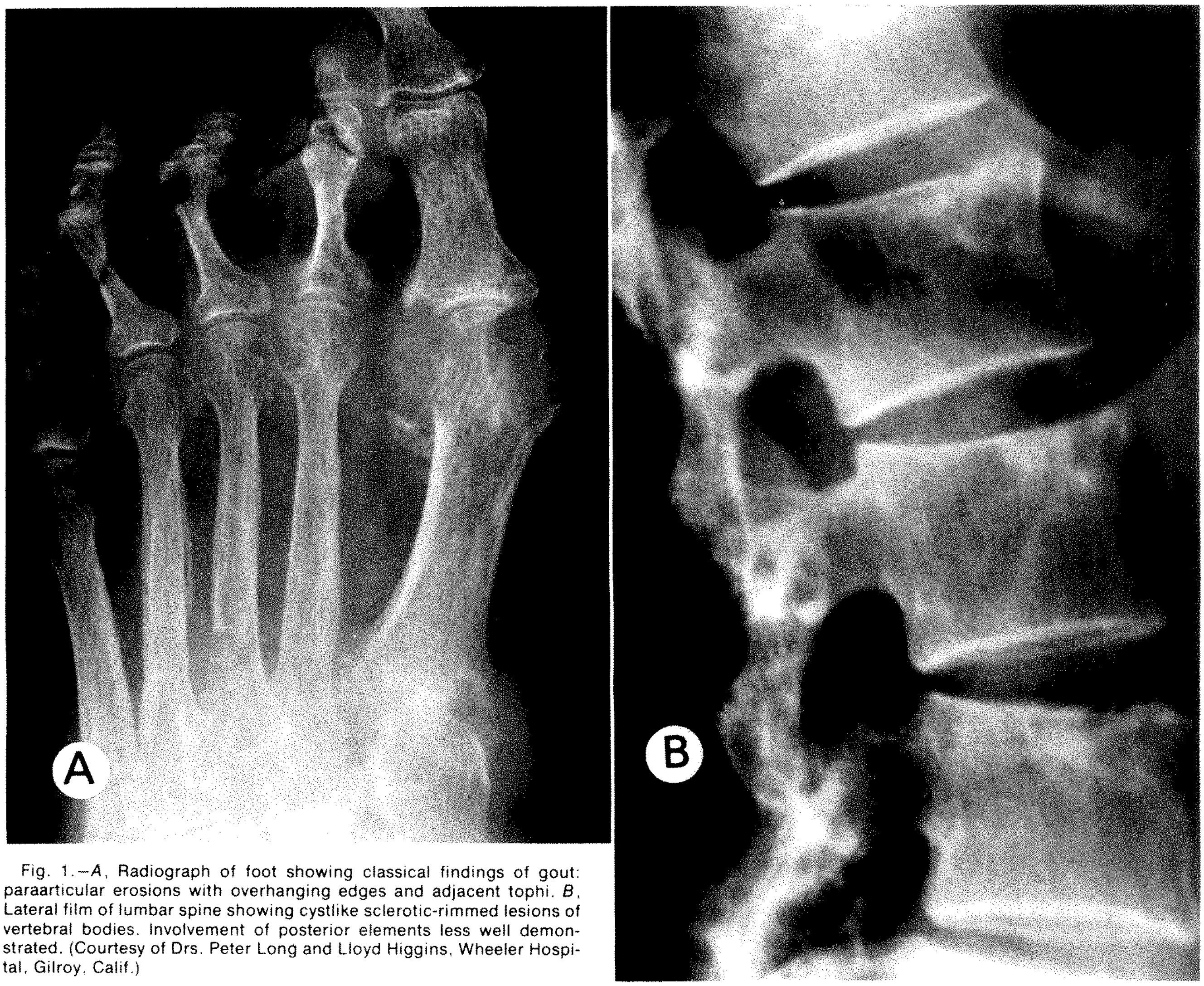

Fig. 1.—*A*, Radiograph of foot showing classical findings of gout: paraarticular erosions with overhanging edges and adjacent tophi. *B*, Lateral film of lumbar spine showing cystlike sclerotic-rimmed lesions of vertebral bodies. Involvement of posterior elements less well demonstrated. (Courtesy of Drs. Peter Long and Lloyd Higgins, Wheeler Hospital, Gilroy, Calif.)

Second, our patient exhibited an unusual distribution and severity of bone and joint involvement with gout. Formerly considered rare, sacroiliac involvement may occur in up to 17% of patients with long-standing gout [8, 9]. Alarcon-Segovia et al. [8], in a study of 143 essentially untreated patients with gout, found radiologically detectable sacroiliac abnormalities in 24 (16.8%). Of these, 23 showed marginal sclerosis and 15 showed focal osteoporosis and sclerotic-rimmed erosions like those seen in our case. Patients who showed sacroiliac changes usually had a longer history of gout and more rapidly progressive disease than did those without sacroiliac abnormalities. Severe sacroiliac gout has also been described in conjunction with hemoglobinopathy E and hypersplenism in two Malayan aborigines [10].

Although gout is included in the differential diagnosis of low back pain, and despite the frequency of low back pain complaints among gouty patients [11], there are few reports of spinal involvement with gout. Isolated case reports of spinal changes due to gout include: (1) odontoid erosion associated with cervical disc-space narrowing [12]; (2) subluxation of the first cervical vertebra [13]; (3) paraplegia as a complication of gout [14, 15]; and (4) gouty involvement of the posterior articulations in the lower lumbar spine [16]. Prominent unilateral calcific thoracic lipping on the right side has also been observed in gouty patients, although the roles of associated diseases such as osteoarthritis, diabetes, and diffuse idiopathic skeletal hyperostosis (DISH) have not been elucidated [11, 17, 18].

Forrester and Nesson [19] stress the fact that gout is the rarest cause of sacroiliitis. Also, the use of aspirin in patients with sacroiliac pain may give a falsely positive elevation of the uric acid level and therefore complicate the diagnosis. They noted that when gout involves the lumbosacral spine, the radiographic changes are identical to the peripheral joint findings: soft tissue tophi, boney erosions with sclerotic margins, and splayed or overhanging edges. The striking case they showed had lumbar spine and sacroiliac gout with bony changes similar to those seen in our patient.

The pathologic bases of the changes seen in the lum-

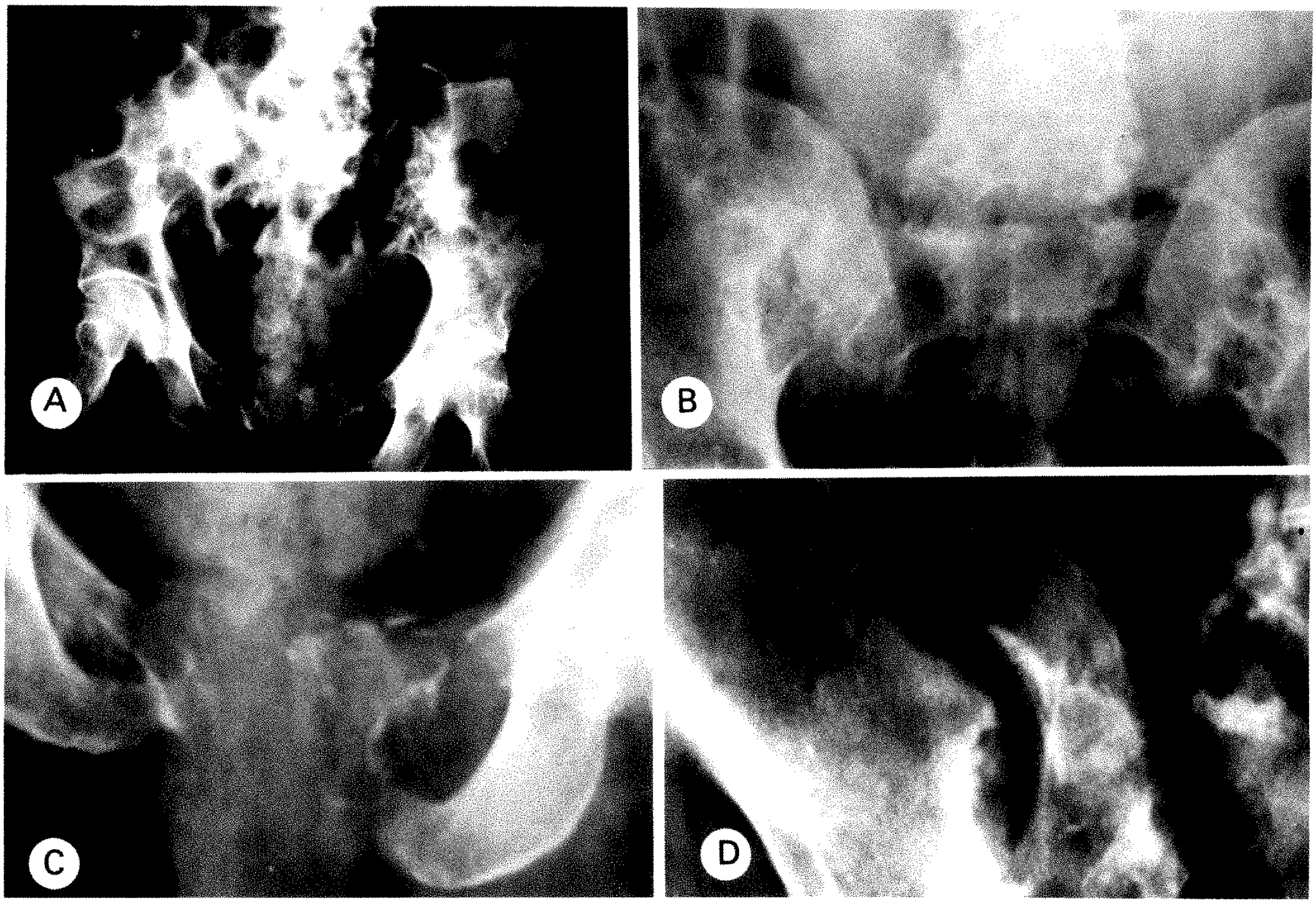

Fig. 2.—*A*, Full view of pelvis showing cystlike erosions of both sacroiliac joints and pubic area with pathologic fractures through right ilium and left pubic rami. (Courtesy of Drs. Peter Long and Lloyd Higgins, Wheeler Hospital, Gilroy, Calif.) *B*, Coned view of sacroiliac joint destruction. *C*, Coned view of left pubis showing destructive lesion and pathologic fractures through both pubic rami. *D*, Coned view of right ilium about 3 weeks later showing widened fracture.

bar spine of our patient were best described by Lichtenstein et al. [20] and Hall and Selin [16] in their postmortem evaluations of patients with gout. Lichtenstein et al. [20] found chalky deposits of urates within the lumbar intervertebral discs as well as in the contiguous spongy bone of the vertebral bodies in a 56-year-old male with extensive long-standing gout. The discs and vertebrae were otherwise unaltered. They showed no radiographs of this area, although similar spinal changes were suggested by the lumbar radiographs of our patient. The poor definition and sclerotic-margined destructive lesions of the lower lumbar posterior articulations and apophyses seen in our patient were similar to the pathologic description of a patient suffering from gout examined by Hall and Selin [16]. They found extensive urate deposits in the capsules and ligaments over the articular cartilage at the L4-L5 and L5-S1 levels posteriorly without disc invasion.

Finally, we know of no other documented cases of pathologic fracture due to gout. Lichtenstein et al. [20] described a right femoral neck fracture which occurred during a hypertensive-encephalopathic seizure in a patient suffering from gout. Nonunion of the fracture occurred, though no underlying radiographic lesion was demonstrated at the fracture site. Months later, at autopsy, extensive urate deposits were found on the fibrous tissues at the fracture site, though no adjacent bony involvement with gout was described. This deposition probably represented simple urate precipitation at the site of trauma. This phenomenon is known to occur in gout.

Our patient sustained minor trauma with resultant fracture to her left pubic rami and a second fracture extending from her right sacroiliac lesion through the right ilium. Biopsy at the pubic fracture site confirmed the underlying gouty pathology.

REFERENCES

1. Prior IAM, Rose B, Harvey H, Davidson F: Hyperuricemia gout and diabetic abnormality in Polynesian people. *Lancet* 1:333-338, 1966
2. Emerson BT, Douglas W, Doherty R, Feigl P: Serum urate concentrations in the Australian Aboriginal. *Ann Rheum Dis* 28:150-156, 1969

3. Burch TA, O'Brien W, Need R, Kurland L: Hyperuricemia and gout in the Mariana Islands. *Ann Rheum Dis* 25:114-116, 1966
4. Healey LA, Skeith J, Decker J, Bayani-Sioson PS: Hyperuricemia in Filipinos: interaction of heredity and environment. *Am J Hum Genet* 19:81-85, 1967
5. Fisher HW: The diseases of Filipino men. *Hawaii Med J* 18:252, 1959
6. Steuerman J, Farias A: Hyperuricemia in Filipinos. *Hawaii Med J* 20:151-153, 1960
7. Healey LA, Bayani-Sioson PS: A defect in the renal excretion of uric acid in Filipinos. *Arthritis Rheum* 14:721-726, 1971
8. Alarcon-Segovia D, Cetina J, Diaz-Jouanen E: Sacroiliac joints in primary gout: clinical and roentgenographic study of 143 patients. *Am J Roentgenol* 118:438-443, 1973
9. Malawista SE: Seegmiller J, Hathaway B, Sokoloff L: Sacroiliac gout. *JAMA* 194:954-956, 1965
10. Burns-Cox C, Lambeth J, MacLean R: Sacroiliac gout associated with hemoglobin E and hypersplenism. *Radiology* 95:413-416, 1970
11. Tkach S: Gouty arthritis of the spine. *Clin Orthop* 71:81-86, 1970
12. Vinstein AL, Cockerill E: Involvement of the spine in gout. *Radiology* 103:311-312, 1972
13. Kersley G, Mandel L, Jeffrey M: Gout: an unusual case with softening and subluxation of the first cervical vertebra and splenomegaly. *Ann Rheum Dis* 9:282-303, 1950
14. Kosskoff Y, Morris L, Lubic L: Paraplegia as a complication of gout. *JAMA* 152:37-38, 1953
15. Litvak J, Briney W: Extradural spinal deposition of urates producing paraplegia: a case report. *J Neurosurg* 39:656-658, 1973
16. Hall J, Selin G: Spinal involvement in gout. *J Bone Joint Surg* 42:341-343, 1960
17. Rosenquist R, Small C, Deeb P: Unusual manifestations of gout. *Arch Pathol* 68:1-10, 1959
18. Resnick D, Shaul S, Robins J: Diffuse idiopathic skeletal hyperostosis (DISH): Forestier's disease with extraspinal manifestations. *Radiology* 115:513-524, 1975
19. Forrester DM, Nesson JW: *The Radiology of Joint Disease*. Philadelphia, Saunders, 1973
20. Lichtenstein L, Scott H, Levin M: Pathologic changes in gout: survey of 11 necropsied cases. *Am J Pathol* 32:871-895, 1956

Mondini Defect: A Variant

PETER M. SOM,[1] MANSHO T. KHILNANI, SAMUEL L. BERANBAUM, AND BERNARD S. WOLF

In recent years, the advent of polytomography has made possible substantial advances in the understanding of the anatomy of inner ear abnormalities. Prior to utilization of the polytome, amost all information was limited to pathologic examination of several large collections of temporal bones, notably the Ibsen-Mackeprang and the Toynbee and Mygind collections [1, 2]. Further attention was focused on the inner ear as a result of the experience gained from the effects of thalidomide administration. This paper reviews the variety and scope of abnormalities of the cochlea and includes an illustrative case.

Case Report

A 52-year-old white male had sudden hearing loss 2 months before examination. He stated that he developed extreme dizziness 2 days after a prolonged jet flight. This was accompanied by a sudden loss of hearing in the left ear. He had no tinnitus, nausea, or vomiting.

Hearing tests revealed a profound sensory neural hearing loss in the left ear. In the right ear, there was normal hearing at 500-1,000 Hz, mild to moderate gradual sloping high frequency sensory neural hearing loss at 1,000-4,000 Hz, and a profound sensory neural hearing loss from 4,000-8,000 Hz. Thus the patient had a profound sensory neural hearing loss on the left side and high frequency hearing loss on the right side.

Polytomography of the temporal bones was performed in the anteroposterior, semiaxial, and lateral projections (figs. 1-3). The chief features were a normal cochlear basal turn, but with a common cloaca for the middle and apical cochlear turns on the left (Mondini abnormality). A normal cochlea was demonstrated on the right. The semicircular canals were normal bilaterally. The internal auditory canal was narrow on the left, and the crista falciformis divided the canal into two equal compartments. The right internal auditory canal was normal. The carotid canal was slightly more anterior than normal on the left but was not laterally displaced. The jugular fossa was dominant on the right. The vestibular aqueducts were normal bilaterally. A diagram of the abnormalities in this case compared to a normal temporal bone is shown in figure 4.

Discussion

On the basis of histopathologic examinations, four major pathologic patterns of congenital cochlear abnormalities have been described [3]. In 1863, E. M. Michel (cited in [4]) described a defect characterized by a total lack of development of the inner ear structures. This malformation can affect the entire petrous portion of the temporal bone or only the labyrinthine region. It can present as isolated spaces within the petrous bone without differentiation into identifiable inner ear components. The external and middle ears are usually anatomically normal. This defect can be diagnosed radiographically.

In 1791, C. Mondini (cited in [4, 5]) described a malformation of the cochlea consisting of a partial aplasia resulting in 1-1½ coils instead of the normal 2½-2¾ cochlear coils, with the middle and apical coils sharing a common cloaca. Embryologically there is an interruption in the development of the cochlea at about the sixth week of gestation when the cochlea is only a short curved tube consisting essentially of only a basal coil. The degree of development of the neurosensory structures in such cases varies widely. When sensory epithelium is present, there is usually some hearing function. However, when the sensory epithelium is only partially formed or absent, hearing is proportionally affected. The semicircular canals and vestibule may be normal. The endolymphatic duct has been described as markedly dilated. Mondini did not describe any abnormality of the internal auditory canal. Although the opposite ear may appear normal radiographically, there is almost always some histopathologic abnormality.

In 1892, A. Scheibe (cited in [4]) described a variety of deafness in which the bony otic capsule is fully formed. However, the saccule and cochlear duct are rudimentary, usually represented by mounds of undifferentiated cells. The entire organ of Corti is abortive. This is considered the most common inherited congenital form of deafness. Some residual low frequency hearing may be present, and a response to amplification techniques is sometimes obtained. No radiographic abnormality is demonstrable.

In 1904, G. Alexander (cited in [4]) described deafness due to aplasia of the membranous cochlear duct. The defect appears to affect primarily the neural receptor cells of the basal coil of the cochlea. This results in a high frequency hearing loss which can respond to amplification aids of the remaining low frequency hearing. This anomaly presents no radiographic findings. Thus of the four classically described abnormalities of the cochlea, only the Michel and Mondini types can be recognized radiographically.

As a result of the increasing use of polytomography, it has become evident that some congenital malformations of the inner ear do not fit into the classical descriptions of the Mondini and Michel malformations [2, 6, 7]. For example, Valvassori et al. [6] reported a series of cochleas that were obviously reduced in caliber rather than showing a reduction in the number of coils. All of these cases had markedly reduced cochlear function. Jensen [2] described a series of cases that had enlargement of

---

Received May 19, 1977; accepted after revision August 16, 1977.

[1] All authors: Department of Radiology, Mount Sinai Hospital, 100th Street and Fifth Avenue, New York, New York 10029. Address reprint requests to P. M. Som.

Am J Roentgenol 129:1120-1122, December 1977

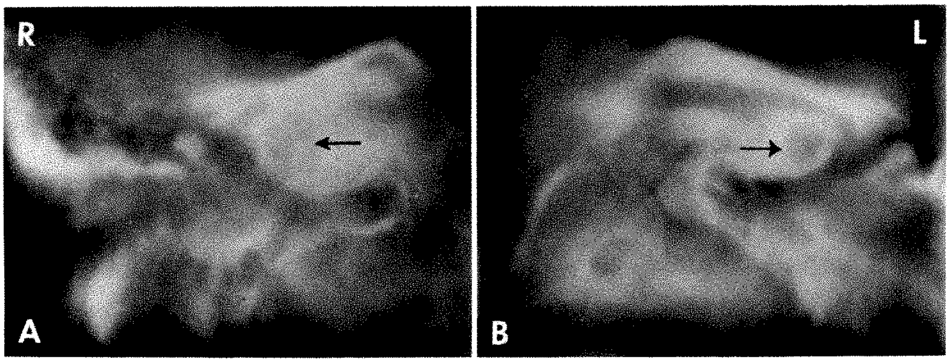

Fig. 1 – Anteroposterior tomogram. *A*, Right side showing cochlea normal both in size and number of turns (*arrow*). Beneath chochlea, hypotympanum extends more medially than usual. On other sections, promontory on this side was normal. *B*, Left side showing common cloaca (*arrow*) for middle and apical cochlear turns. Hypotympanum is enlarged, as on right side. Promontory (curved bone outlining inferior lateral margin of cloaca) is smaller than on normal right side.

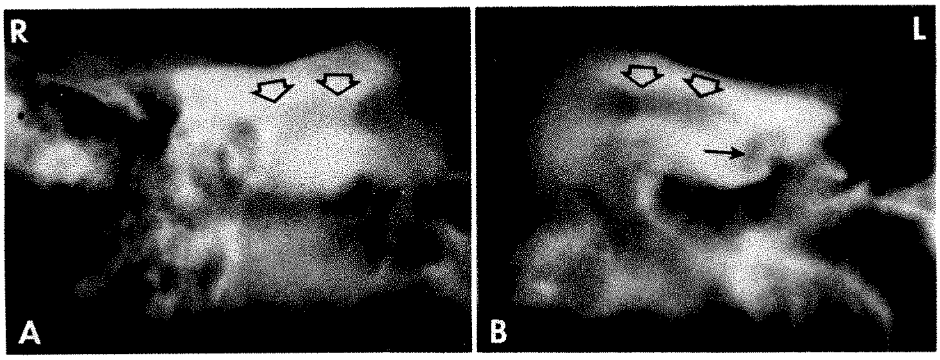

Fig. 2. – Anteroposterior tomogram. *A*, Right side showing normal internal auditory canal (upper margin outlined by open arrows). Measurements 5 and 10 mm from lamina cribosa were 6 and 5 mm, respectively. *B*, Left side showing narrow internal auditory canal (upper margin outlined by open arrows). Measurements 5 and 10 mm from lamina cribosa were each 3 mm. Small promontory outlines lateral margin of basal turn (*small arrow*).

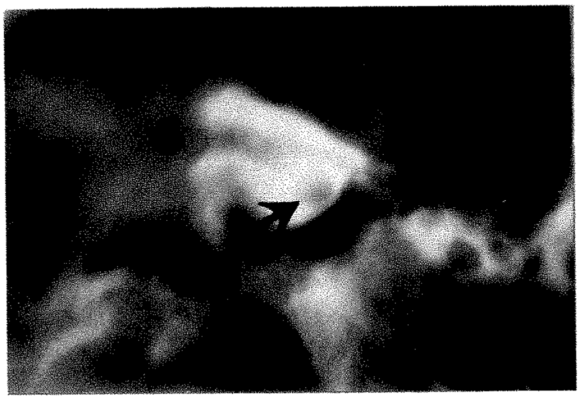

Fig. 3. – Semiaxial tomogram, left side, showing common cloaca (*arrow*) of middle and apical cochlear turns.

the bony inner ear structures with slightly irregular margins. All the cochlear turns were present; however, the lamina spiralis was irregularly thickened and identification of individual cochlear turns difficult. There were some associated neurosensory abnormalities. However, Jensen also pointed out that minor alterations in the caliber of the cochlea, as long as the number of turns is normal and there is no major reduction in their lumen, should be considered carefully before being called radiographically abnormal. In other words, minor alterations in size may represent normal variants [8].

Cochlear aplasia is a well documented cochlear malformation. It may or may not have an associated narrow or atretic internal auditory canal. Extensive anomalies of the remaining labyrinth are usually present [9]. Cochlear aplasia may be considered an anatomic subdivision of the Michel type of malformation. Cochlear dysplasia is a malformation in which there is development of a solitary cochlea cavity with no cochlear remnants within the cavity. Specifically, no basal turn is present in contrast to the classical Mondini type of abnormality.

The variety of cochlear malformations demonstrable by current radiologic techniques reinforces the concept that malformations are best described in purely anatomic terms, rather than denoting them with eponyms. It should be emphasized that, with the exception of the more extreme cases of cochlear aplasia, there is poor correlation between the osseous radiographic changes and vestibular function and hearing.

Our case illustrates a developmental anomaly involving primarily the inner ear structures and, to a lesser degree, the middle ear cavity. The cochlear changes are those described by Mondini. The associated internal auditory canal changes, not described by Mondini, point out the need to describe the findings anatomically rather than to try and fit them into a particular syndrome. This patient had a minor middle ear developmental anomaly of an enlarged hypotympanum in association with the inner ear anomalies of the cochlea and internal auditory canal. This association of middle and inner ear developmental anomalies has been noted previously, but considered to be rare except in cases caused by thalidomide. Polytomography is revealing these abnormalities to be more common than the sparse reports previously noted in the radiologic literature.

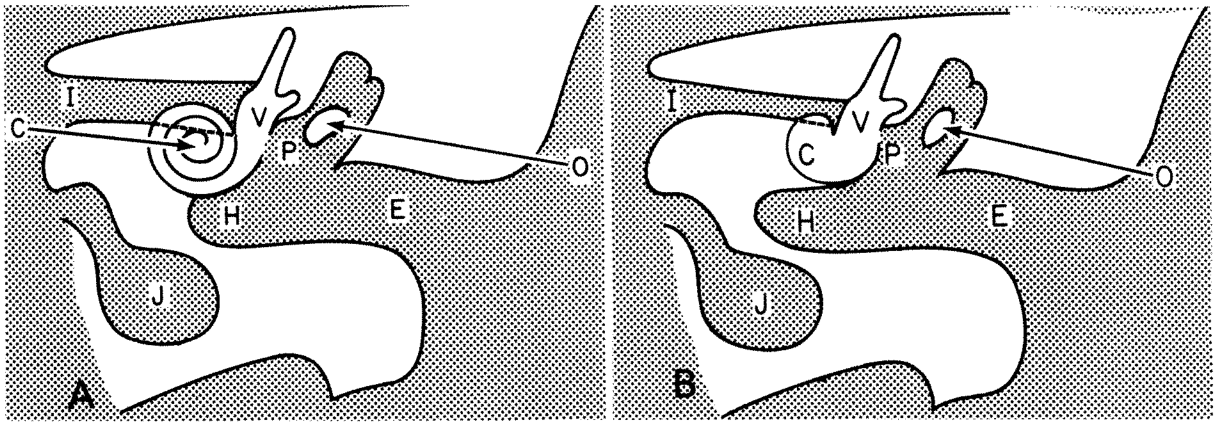

Fig. 4.—*A*, Diagrammatic representation of "thick" anteroposterior temporal bone section showing normal configuration. I = internal auditory canal; J = jugular fossa; V = vestibule; E = external auditory canal; O = ossicles; H = hypotympanum; P = promontory; C = cochlea. *B*, Diagrammatic representation of abnormalities of current case showing narrow internal auditory canal (I), larger than normal hypotympanum (H) extending more medially underneath promontory (P), slightly smaller curve of promontory, and smaller cochlea (C) with basal turn and common cloaca for remaining turns. J = normal jugular fossa; V = vestibule with normal semicircular canals; E = external auditory canal; O = ossicles.

ACKNOWLEDGMENT

We thank Dr. A. Kumar for his case material.

REFERENCES

1. Jensen, J: Malformations of the inner ear in deaf children. *Acta Radiol [Suppl]* (Stockh) 286:27-35, 1969
2. Jensen J: Congenital anomalies of the inner ear. *Radiol Clin North Am* 12:473-482, 1974
3. Ormerad FC: The pathology of congenital deafness. *J Laryngol Otol* 74:919-950, 1960
4. Paparella MM, Shumrick DA: *Otolaryngology,* vol 2. Philadelphia, Saunders, 1973
5. Jensen J, Rovsing H: *Fundamentals of Ear Tomography.* Springfield, Ill., Thomas, 1971
6. Valvassori G, Nauton R, Lindsay J: Inner ear anomalies: clinical and histopathological considerations. *Ann Otol* 78:929-938, 1969
7. Nauton R, Valvassori G: Inner ear anomalies: their association with atresia. *Laryngoscope* 78:1041-1049, 1968
8. Reisner K: Tomography in inner and middle ear malformations. *Radiology* 92:11-20, 1969
9. Jensen J, Rovsing H: Tomography in congenital malformations of the middle ear. *Radiology* 90:268-275, 1968

Technical Notes

A Method of Reducing Cost in CT Systems That Employ Floppy Discs

LAURENCE D. CROMWELL,[1] WILLIAM E. MOORE,[1] DOUGLAS SCHUMACHER,[1] AND ALY SALAM[2]

Certain characteristics of the newer EMI CT units present both convenience and challenges to the user. First, the EMI CT-1010 dedicated head unit comes with a highly desirable option, the diagnostic display console. Information is transferred from the computer system disc to a floppy disc in the console. The console can then function as an independent unit. Second, the slice thickness is 8 mm rather than 13 mm. This means that six scans (12 slices) are now used rather than four scans (eight slices). If contrast enhancement is used in addition, the minimum examination per patient will require 24 slices. Presently, eight slices may be stored on one side of a floppy disc. Thus, with contrast enhancement, three floppy discs are required per patient. At a cost of $5 each and at a very nominal figure of 2,000 patients per year, the cost to the user in terms of just floppy discs is $30,000. The problem will be even more acute when the 320 × 320 matrix is available, since this will require storage of four times the amount of information as the current 160 × 160 matrix. This means that only two slices in the 320 format may be stored on one side of a floppy disc. In an effort to minimize cost and also storage space of floppy discs, we have written information on the reverse side of "one-sided" floppies, thus creating "flippies."

Technique

The standard floppy disc, as purchased from EMI (fig. 1), consists of a paper-protected round magnetic disc about the size of a 45 rpm record. The oval reading window is slightly outward of the round localizing window. The localizing window is asymmetrically located; therefore, if the floppy disc is turned over, the localizing is in a different position relative to the sensing device in the diagnostic display console.

There is an easy solution to this dilemma, using only a paper punch. A symmetrically placed hole is made the same amount off-center through both sides of the protective paper, but not through the magnetic disc itself (fig. 1*B*). Thus, a "flippy" is created from a floppy. Figure 1*C* demonstrates the reverse side of the flippy and how it is placed in the diagnostic display console. Note that the flippy disc is entirely symmetrical. All that remains is initialization of the disc, which is easily accomplished in the EMI system by erasing both sides of the flippy.

Results

We have used this method to convert floppy discs to two-sided use very successfully since April 1977. During that time, no migration of the magnetic field from one side of the flippy to the other has been detected. Two methods were used to determine this. Test patterns were placed on both sides of the flippy discs, and the discs were checked for any sign of cross-talk. If any occurred, it was below the discriminator settings of the diagnostic display console. We also inspected the discs with Magnasee (Burroughs Computer Corp.), a compound designed to visualize any magnetic field on a floppy disc. Again, no migration was observed. Although we cannot make any statements about long term stability of the discs, there is no reason to expect migration to occur. It should be noted that the storage surface of the flippy disc is not damaged during the hole-punching process, since the round localizing window is located inward of the oval reading window.

The storage of the information is in a much more convenient format. The nonenhanced slices can be put on one side and the enhanced cuts of the same level on the other. In addition, the amount of storage space and the number of floppies per person has been decreased from three to two. On a routine examination with and without contrast, three sides are required, thus previously three floppy discs. With the flippies, scans are recorded on both sides of one disc and the first side of the second. At a modest rate of 2,000 patients per year, our cost for floppy discs alone decrease from $30,000 to $20,000. The savings should be even greater once the 320 × 320 matrix becomes available.

We believe that users and vendors of equipment should cooperate in achieving cost containment which may ultimately be passed on as savings to the general public. Our simple technique doubles information storage capacity. This is extremely cost-effective and will be applicable to a wide number of users once retrofits are installed on the current first generation EMI scanners.

Received June 20, 1977; accepted after revision August 16, 1977.
This work was supported in part by grant no. TO1-CA-05198 from the National Institutes of Health.

[1] Department of Radiology, University of Washington, Seattle, Washington 98195. Address reprint requests to L. D. Cromwell.

[2] Field Engineering, EMI Medical Inc., Atlanta, Georgia 30336.

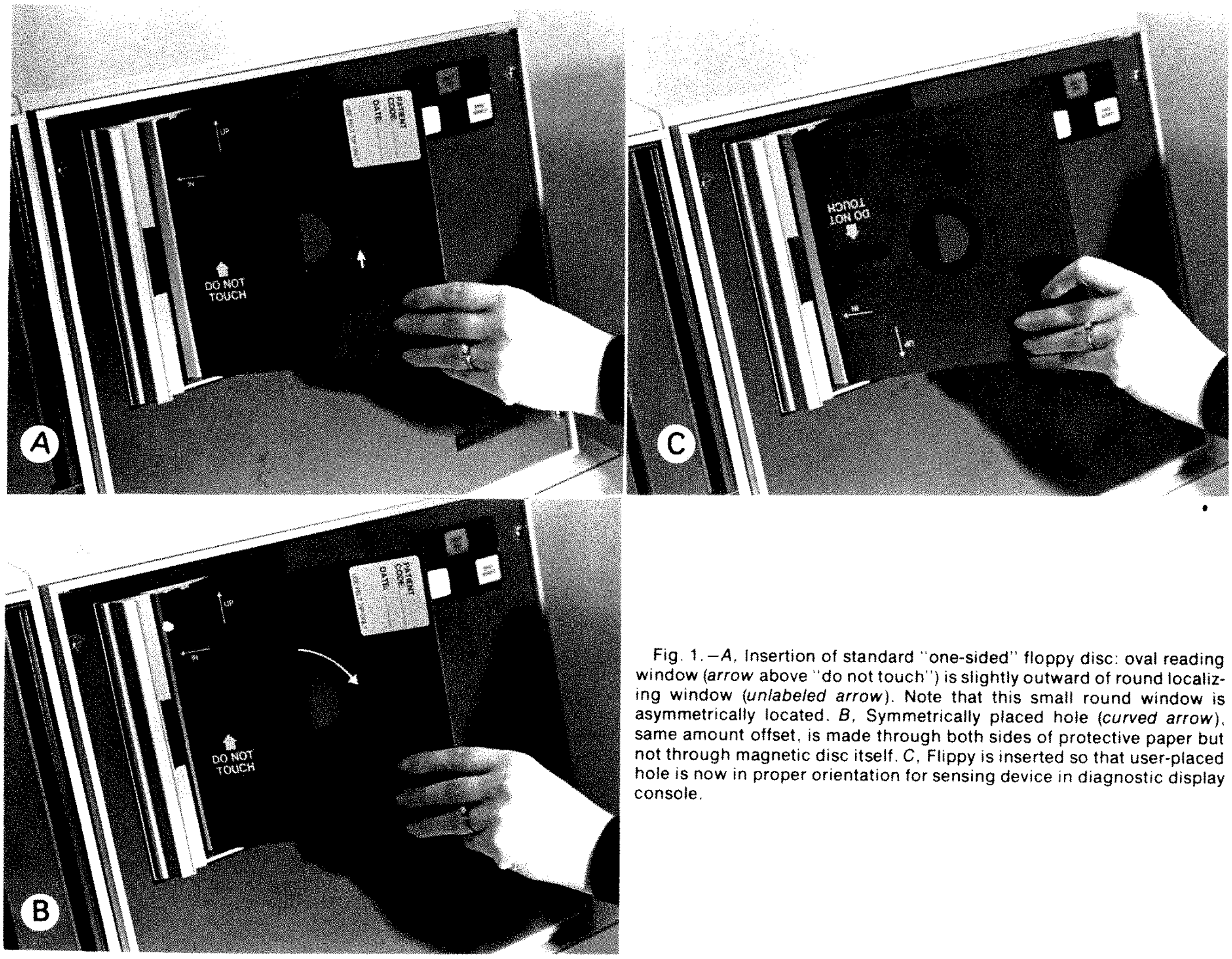

Fig. 1.—*A*, Insertion of standard "one-sided" floppy disc: oval reading window (*arrow* above "do not touch") is slightly outward of round localizing window (*unlabeled arrow*). Note that this small round window is asymmetrically located. *B*, Symmetrically placed hole (*curved arrow*), same amount offset, is made through both sides of protective paper but not through magnetic disc itself. *C*, Flippy is inserted so that user-placed hole is now in proper orientation for sensing device in diagnostic display console.

Information storage and retrieval will soon become a major problem with the availability of the 320 × 320 matrix. High density floppy discs are presently on the market, and EMI is working on adapting them to the diagnostic display console. The procedure described here should be applicable to the new floppy discs as well.

An alternative method to punching the holes and creating flippies would be to purchase compatible double-sized floppy discs from a manufacturer. However, the cost of these discs is substantially higher than the single-sided floppies. The cost can be reduced somewhat if they are purchased with the assistance of EMI. The higher cost of the double-sided floppy discs covers additional testing by the manufacturer in order to guarantee them. Due to high quality control, this testing is usually superfluous, and one-sided floppies can generally be made into two-sided flippies by the method described.

ACKNOWLEDGMENT

We thank Debbie Burch for technical assistance.

A Wedge Filter for Craniocervical Angiography

LAURENCE D. CROMWELL,[1, 2] CHARLES W. KERBER,[1,3] AND WILLIAM R. VERMEERE[1]

Wedge filters have been routinely used in radiation therapy [1-3], but with few exceptions their value has not been optimally exploited in diagnostic radiology. The first mention of a compensatory filter to diminish the intensity of a portion of the radiation beam was discussed by Pfahler in 1906 [4]. A few additional reports describe the introduction of various materials into the radiation beam which modify the clinical radiograph [5-9]. The principle of a wedge filter is readily adapted to produce radiographs of more uniform density, particularly when the areas of interest vary in thickness. This report shows the techniques and advantages of using an easily manufactured polycarbonate wedge for cerebral and arch angiography.

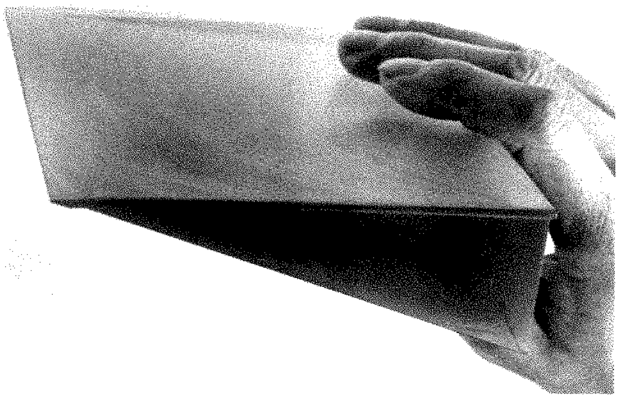

Fig. 1 – Resin wedge filter.

Technique

An easily constructed wedge filter can be made in a plexiglass mold of Lexan (General Electric) and a commercially available resin (Fiberlay, Seattle, Wash.). The resin contains a catalyst which hardens overnight, and the mold becomes an integral part of the finished wedge filter. The 20° wedge filter is 5 cm high and 13.5 cm long and wide (fig. 1). The construction cost should be less than $50. The device mounts on the base plate of the collimator which is attached in the usual manner to a radiographic tube housing having 0.3 and 1.0 mm focal spots.

The wedge filter is routinely used for arch arteriography, with the thick part of the wedge oriented in the cephalad direction. The filter is also routinely used when either an oblique or lateral view of the head and neck is obtained, with the thick part of the wedge superimposed on the thin part of the patient.

For arch arteriography, the focal-film distance is 100 cm, and the tube is angled caudally 20°. The head is turned routinely to the right and the patient placed in a 15° right posterior oblique position. The exposures are made

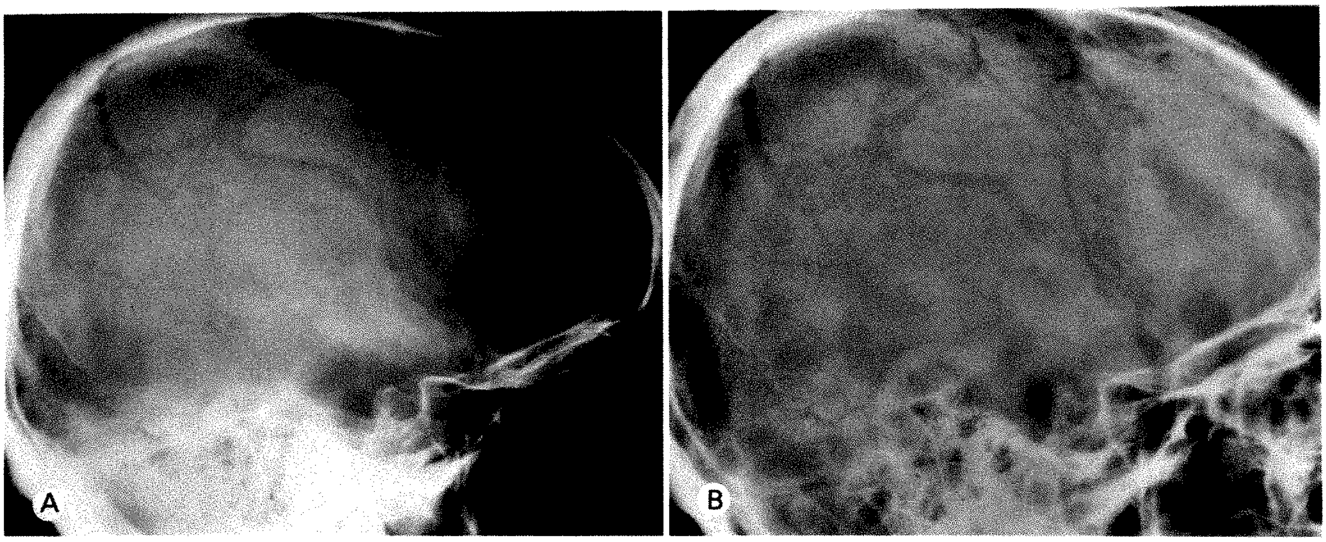

Fig. 2. – Lateral view of head. *A*, Standard film exposure without wedge filter. *B*, Exposure with wedge filter showing more uniform densities throughout image.

Received February 3, 1977; accepted after revision July 14, 1977.

[1] Department of Diagnostic Radiology, University of Oregon Health Sciences Center, Portland, Oregon 97201.

[2] Present address: Department of Diagnostic Radiology, University of Washington Health Sciences Center, Seattle, Washington 98195. Address reprint requests to L. D. Cromwell.

[3] Present address: Department of Diagnostic Radiology, University of Pittsburgh School of Medicine, Pittsburgh, Pennsylvania 15261.

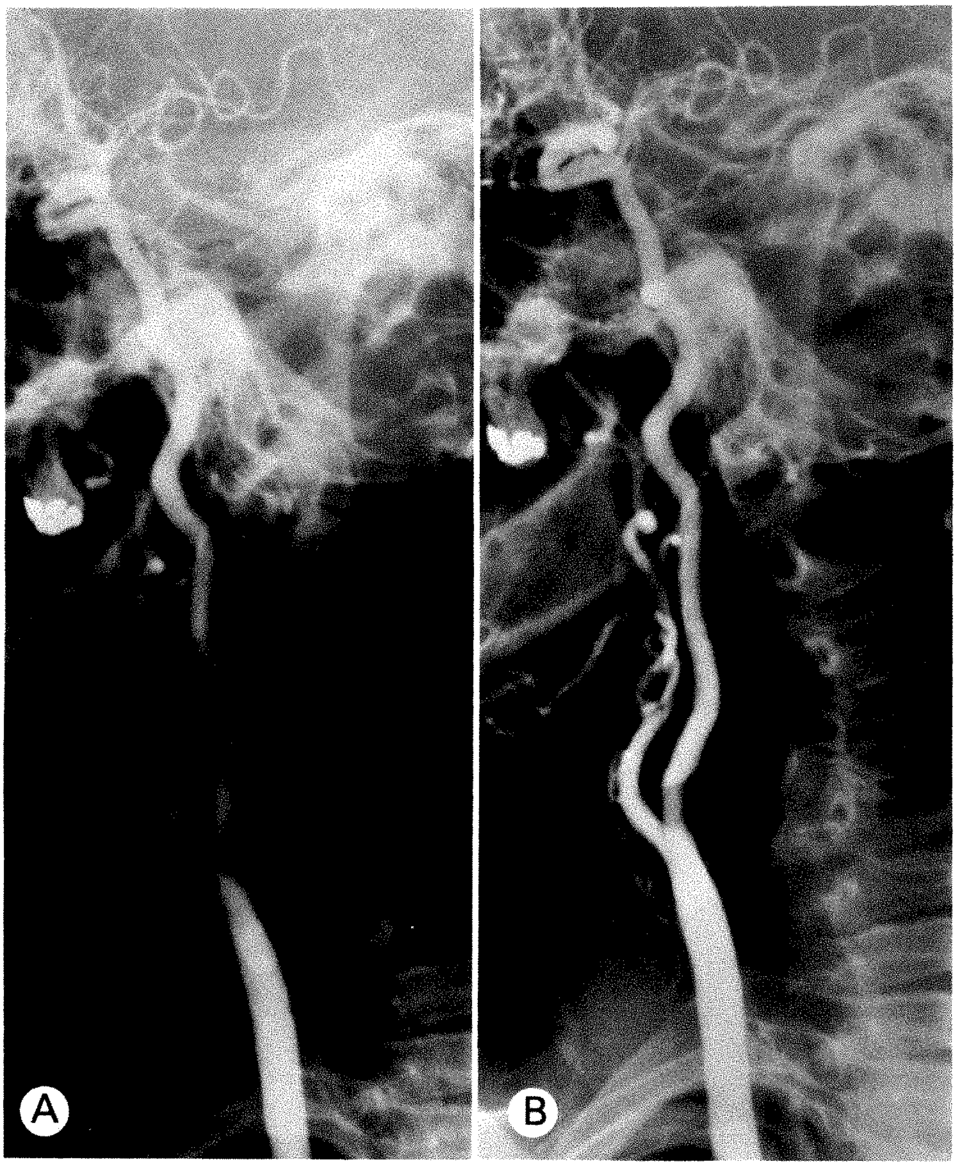

Fig. 3.—Oblique view of carotid arteriogram. *A*, Standard exposure without wedge filter. *B*, Exposure with wedge filter.

TABLE 1

Radiation For One Exposure With and Without Wedge Filter

View and Site	Without Filter (mR)	With Filter (mR)
Arch:		
Sternal notch	542.5 ± 61.9	357.5 ± 5
Thyroid	537.5 ± 32	237.5 ± 9.6
Angle of mandible	542.5 ± 45.8	200. ± 11.6
Sella	390 ± 35.6	127.5 ± 5
Oblique:		
Thyroid	272.5 ± 17.1	71.3 ± 4.8
Angle of mandible	285 ± 17.3	122.5 ± 5
Outer orbit	130 ± 26.5	102.5 ± 22.2
Sella	177.5 ± 20.6	127.5 ± 5
Lateral:		
Thyroid	212 ± 25	56.3 ± 4.8
Orbit	150 ± 11.6	30 ± 4.1
Sella	230 ± 8.2	56.3 ± 2.5
Cranium	215 ± 10	55 ± 5.8

Note.—All exposures are mean of four determinations. Error analysis is 1 SD.

at 83 kVp, 100 mA, and 0.025 sec. Kodak RPR film and High Plus screens are used. The oblique and lateral views are obtained at 85 and 100 cm, respectively, using 65 kVp and 180 mA. The times for the oblique and lateral views are 0.08 and 0.10 sec, respectively. The voltage is lowered to 63 kVp if the wedge filter is not used. Processing is done with a Kodak Industrial "B" processor and DuPont chemicals. The processor is slowed to a 3 min cycle.

Measurements of exposure to various sites were made with the torso and head portion of an average-man phantom and thermoluminescent dosimeters (TLD-100) with the above techniques.

Results

The use of a wedge filter in arch aortography provides a radiographic image of more uniform density. Lateral and oblique views of the head and facial structures demonstrate enhanced soft tissue detail (figs. 2 and 3). Measurements indicate that the beam modification results in reduction of patient exposure (table 1). In addition to its effectiveness, the filter is low in cost, approximately $50.

ACKNOWLEDGMENT

We express our appreciation to Elwood Tramm (Longview, Wash.) for making the original wedge filter.

REFERENCES

1. Groom AC: The design of wedge filters for x-ray therapy. *Br J Radiol* 24:676-681, 1951
2. Tranter FW: The design of wedge filters for use with a 4-Mev linear accelerator. *Br J Radiol* 30:329-330, 1957
3. Tulley TJ: Wedge filters for use with a 100-curie cobalt 60 teletherapy unit. *Br J Radiol* 29:227-229, 1956
4. Pfahler GE: Transaction of the American Roentgen Ray Society, 1906, p 217
5. Fuchs AW: Radiography of the entire body, employing one film and single exposure. *Radiogr Clin Photog* 10:9-14, 1934
6. Vaughn CE, Weaver RT, Adamson DL: Roentgenographic visualization of placenta utilizing plastic filter. *Can Med Assoc J* 46:314-321, 1942
7. Carbajal R, Alcantara R: Iodine wedge filter for roentgenographic use. *Radiology* 61:243-245, 1953
8. Freedman ML, Matteson SR: A collimator for reduced radiation dose with improved visualization of soft tissues. *Radiology* 118:226-228, 1976
9. Barbaric ZL, Paris BS: The application of the wedge aluminum filter in excretory urography. *Radiology* 122:263, 1977

Special Lecture:

Roles for Radiologists in Tomorrow's Medical Care System

RUSSELL H. MORGAN[1]

During the past 100 years, advances in science and technology, including the disciplines of medicine, have created a society of incredible complexity. Unfortunately, a social stability has not evolved to match this complexity. Hence the social order is frequently threatened, and the public repeatedly voices concern for the future of many of its institutions, including the health care system. The challenge to medicine, in its response to this concern, is the development of new models which will provide quality health care at reasonable cost and equitable accessibility. This will be difficult and can be done only if medicine itself makes a major commitment to it. Radiologists can exert a critical influence. In recent years, radiology has become the very center of the health care system. Its leaders therefore are in an unusual position to play a vital part in formulating the changes needed to improve tomorrow's health care. This will be a new role for many radiologists. Let us hope they can rise to the challenge.

It is difficult to predict what the medical care system will be a few years from now. Many forces, including political, social, economic, as well as professional, are at work, some to promote change, others to maintain the status quo. To me the future medical care system and what role the radiologist will play in it are far from certain.

Currently much unrest exists in many branches of society regarding the health services received. Complaints of the inaccessibility of physicians, the high cost of care, and the insensitivity of the medical profession to the basic needs of the people are heard repeatedly. And yet, there perhaps has never been a period in history when medical progress has been greater than in the last 50 years, nor have we had a better understanding of man's illnesses, their diagnosis and treatment. Why then does this unrest exist? What has gone wrong? It would seem that we should be living in a medical paradise rather than in a setting in which the political and social forces are increasingly directed against our profession.

The answers to these questions can perhaps be found, at least in part, in the priorities which the medical profession has set for itself. Although it has been completely unplanned, there can be no question that these priorities have been centered almost exclusively on activities which can be classified as reductionistic; that is, on activities which seek an understanding of man and his diseases by the study of smaller and smaller components of the human body. There has been preciously little interest in holistic processes in which an understanding is sought to the problems of man as an individual and as a participant in an increasingly complex society. Perhaps this is as it should be. Perhaps mankind's holistic problems should be left to the social and political scientists. However, because so much disease is inextricably entwined with how man deals with his surroundings, I doubt the wisdom of this premise. If the public, and especially the political leaders who speak for it, are to regard our profession with increasing respect and benevolence, we must increase our attention to the ills of the whole man and his relation to the ecosystems which surround him. I do not mean to imply that the reductionistic pursuits and practices of medicine should be lessened. Rather, we should also turn our attention to the problems which require holistic solutions. How do we go about this?

If we examine the social structure of today, we find that devotion to reductionism is by no means limited to medicine. Indeed, the entire scientific and technological world has long been singularly reductionistic in its objectives. Hence, it might be well to take a look at the manner in which science and technology generally have created problems before we prescribe solutions for what ails the medical care system.

Problems of Technological Progress

There is no question that scientific knowledge on all fronts has expanded during the past century with astonishing rapidity. With it has come a never-ending array of technological creations that influence every phase of our lives. In the process, society has become incredibly complex.

Unfortunately, society has not developed a stability to match this complexity, and, as a consequence, a disturbing anxiety has developed which, if not corrected, may lead ultimately to social chaos and even to the end of our civilization. In saying this, I do not wish to be an alarmist. Rather, I wish to call attention to what seem to be unmistakable signs forecasting trouble ahead. If appropriate action is taken, possibly this trouble can be avoided.

Social stability in the face of technological complexity should be an attainable goal, but it will take a great deal of effort. Interestingly, it has been achieved by a number of biologic species. To illustrate this, let me quote from an address by Lord Eric Ashby [1] at the convocation of the Johns Hopkins University at its centennial celebration. He was speaking of biologic species which had

---

Presented at the James Picker Foundation Symposium on The Radiologist in Society: Prospects and Problems for the 1980s, Key Biscayne, Florida, April 1977.

[1] University Professor of Medicine, Johns Hopkins University, Baltimore, Maryland 21205.

attained social stability in the face of great technological complexity, using the termite colony as an example.

> The social life of a termite colony is astonishingly complex. But over the millennia of evolution, there has developed in the colony a stability to match the complexity. To put it [crassly], social life in a termite colony is stable because its citizens are genetically coded to serve the community. They have no option but to cooperate. Their genes oblige them to be loyal. In the course of evolution, social patterns which lack stability may well have arisen, but natural selection took its toll; these patterns sunk without a trace.
>
> This balance of complexity and stability is characteristic of all natural ecosystems. It is characteristic, too, of primitive human societies where constraints and taboos, with ruthless sanctions for infringing them, imposed on the *community* [emphasis mine] something akin to the genetic coding imposed on a colony of termites. But [recent] man-made ecosystems seem to have run into an evolutionary trap. Societies of high technology have evolved a marvelous complexity without a corresponding evolution of stability. City dwellers, particularly, are locked in interdependence without any force to keep them loyal except their own consent. The delicately balanced mechanisms of a great city have no built-in gyroscope to guarantee that they are kept in balance. They can be snarled by physical or by human fault. Over the hazards of physical breakdown we can be reasonably optimistic; a technological fault like a power failure may cause temporary confusion, but there are very impressive checks and balances to minimize such faults and research is going on vigorously all the time . . . to produce fail-safe systems. Over the hazards of human breakdown we have no such grounds for optimism. The risks are getting worse, not better, and less is being done [it seems] to search for remedies. A few men on strike in the [sanitation] or garbage [collection] services; a handful of urban guerillas kidnapping and planting bombs; gangs of frustrated teenagers bent on mugging and arson; in short, any group which – for good or bad – rejects the obligations for symbiosis in an urban community, is weakening the cement which holds the community together.
>
> The dysfunction between complexity and stability in industrial nations has arisen because the consumer-appetite of the public (as each person trys to optimize his own welfare, along the lines of classical political economics) has steered evolution into ever greater complexities in production, in communication and in transport. But the consumer-appetite has put no corresponding pressure upon the evolution of stability to match this complexity. A consequence of this is that social and political institutions have been allowed to become obsolescent in a way in which industrial institutions have not. To remedy this dysfunction we need to revise political systems [in particular to invent new ways for participation]; we need new formulae for international understanding especially between the nations which own raw materials and the nations which need them; we need ethical gyroscopes to keep in balance the knife-edge stability of our technological societies.
>
> But who are to be the selectors for social values? There seem to be only two ways to stabilize the complex society of human beings. One is despotism; the other is consensus. In the west, we reject despotism as a stabilizer. So we have to find new social and political techniques to achieve consensus.

Lord Ashby carried his solution to the problem no further, but it is evident that if society is to develop a stable social system by consensus, its members must exercise a level of selflessness and discipline not heretofore attained by any human society in modern times. On this ground, the achievement of a stable society in the face of the incredibly complex technological ambience we have created for ourselves seems rather remote. Nevertheless, we must try.

I do not wish to imply that technology is wholly responsible for the problems besetting our social system. What I wish to make clear, however, is that technological progress during the past century has made us terrifyingly vulnerable to social breakdown. Few recognize and appreciate the extent to which we have become dependent on the continuing operation of technical support systems of an incredibly complex nature. Consequently, we must reexamine our priorities, and, where necessary, reorder them so that from now on, efforts promoting the development of social stability may go hand-in-hand with those directed toward technological progress.

Proposed Solutions

It is evident that the years ahead will require of our political system leadership of great wisdom and courage. Where can these attributes be found? How can we bring the individuals who have them into positions of influence? I do not know the answer to these questions, but on the assumption that there is some relationship between wisdom and intelligence, it is noteworthy that we are not now making very good use of our intellectual resources in the attainment of social stability. For many years, the brightest members of society have been following careers in medicine. Yet there is without doubt no profession which has designed its educational system so effectively to isolate its members from societal leadership as has medicine. Medical curricula are almost devoid of material which will assist the physician in taking a significant role in addressing social problems. This is a shame because physicians, as a group, have through the ages been courageous citizens who exhibit a level of compassion unequalled by most other professionals.

There can be little question that if we are to use our human resources well in creating a stable society, we must begin to broaden the perspective of tomorrow's physicians. It is not enough that they be educated in the ever-increasing scientific complexities of their profession; they must also be given the tools by which they may gain a soundly based understanding of the political, economic, and cultural forces which affect the social order. From this, they hopefully may begin to play a part in molding the forces for social stability in a manner commensurate with their role in promoting scientific and technological progress. To do this, changes in medical school curricula will be needed. The single-track science curriculum, typical of many medical schools, is anachronistic and must be modified. If our society is to survive, the physician of tomorrow must be more than a repository of the latest scientific information. He or she must be in a position to contribute fully as much to the evolution of a stable society as to the advancement of scientific medicine.

How can this be done? The answer may lie in the recognition that studies in the holistic sciences are as essential a part of the medical curriculum as studies that are reductionistic. Although it should be self-evident, man is more than a composite of organs, cells, enzyme systems, genes, and molecules. He is a whole being and a component of a complex series of what Odum [2] calls supraindividual systems including populations, cultures and ecosystems. From an examination of today's medical curricula, it appears that medical educators and scientists are abysmally ignorant of the importance of holism in the training of physicians. As a consequence, the current medical care system rests on but "half a science of man" and will continue to do so until our sights are broadened.

What are these holistic studies of which I speak? At Cambridge [3], the list includes archaeology, philosophy, social and political science, history of art, and Greek history. Other subjects, perhaps more closely related to medicine, are anthropology, ecology, and public health. Ecology is particularly important because it is just emerging as an integrative discipline, "focusing attention on man as *a part of*, rather than *apart from* [emphasis mine], his natural surroundings" [2]. I dare say that in another 10–15 years, more and more educators will be "discovering" that ecology is an essential part of the training of the complete physician.

If the perspectives of medical educators are broadened and medical curricula are appropriately altered, will the physicians of tomorrow be able to cope with the difficulties which currently beset the medical care system? Perhaps not. The curricular changes suggested here will be helpful, but major revision in the attitudes of both physicians and of the public will be needed as well. As already pointed out, it is essential that the selfish motivation that today pervades much of society, including the medical profession, gives way to attitudes of selflessness and self-discipline; concern for human rights must be accompanied by concern for human responsibilities. These changes will be difficult to achieve. Unlike the members of a termite colony, humans are not genetically coded to be loyal to the principles of selflessness, discipline, and responsibility. Indeed, it seems that most of the time the reverse is true. Most individuals and population groups (corporations, labor unions, nations, and the like) appear to seek goals that, if achieved, will benefit only those setting the goals.

Can these attitudes be changed? I do not know; it is difficult to be optimistic, but an effort must be made. There could not be a more appropriate group to make a beginning than the members of the health professions.

Roles of Radiologists

I shall not dwell long on the role radiologists should play in providing the best possible care to the patients referred to them and in providing maximum support to the internists, surgeons, pediatricians, and other physicians who depend upon them for diagnostic and therapeutic assistance. Such a role is taken for granted. Nor shall I comment on the increasingly important place of radiologists as teachers of medicine. Radiology has become an essential educational instrument in recent years, and it may be expected that radiologists will be called upon more and more to share teaching responsibilities at all levels (medical students, residents, and physicians seeking continuing education). These roles are also well understood. What I shall speak to now are some roles which are rather new and hence not recognized.

The place of radiology in American medicine has grown at an extraordinary rate from the time the x-ray was discovered by Roentgen in 1895. Interestingly, this growth has been almost entirely reductionistic in character. The primary force that has motivated most of the technological advances in medical radiology has been the quest for more and more diagnostic information: information which will permit recognition of finer and finer details of the pathologic processes in patients undergoing radiologic examination. Such problems as the radiation doses delivered to patients or the design of equipment that lowers medical costs, both largely holistic in character, have for the most part been given a much lower priority.

For instance, attempts to reduce medical costs by the development of less expensive radiologic equipment have until now been almost totally set aside by the search for more and more diagnostic information. To illustrate this, I need only point out that equipment costs which would have been regarded as little short of prohibitive two decades ago are today accepted without a murmur. Each year the quest for more diagnostic information goes on and leads to technological innovations of ever increasing complexity and cost. It is almost as if we were blinded by our success to the point where we find it impossible to imagine that society may not place the same values as we do on limitless technological progress. It is doubtful that this situation will prevail much longer. There is a growing realization that the value of technological progress in radiology, when measured in terms of morbidity and mortality, may be disappointingly small [4]. The principal beneficiaries of this progress have been our medical and surgical colleagues whose diagnostic skills have been sharpened by it. While this is important, is its value sufficient to justify the rapidly escalating costs it imposes? The answer is not clear.

We are beginning to see the intrusion of state and local regulatory agencies in determinations of where and when radiographic and fluoroscopic equipment can be purchased. Unless we radiologists begin to recognize that a balance must be struck between technological advancement and other societal priorities, we are in for serious trouble. The technological revolution through which we are living may be creating unacceptable distortions in the social and economic fabric of our times, and we had better be aware of them. The problem is particularly troublesome in medicine because cost-benefit relationships are extremely difficult to assess. In other walks of life, it is usually easier to assign priorities to acquisition of goods and services. On the other hand, good health is quite properly regarded as an invaluable asset, and most doctors as well as patients find it difficult to draw the line in deciding what can be afforded.

Difficult as it may be, the enormous rise in the cost of medical care demands that a major effort be made to establish boundary conditions on what constitutes good medical care. Recent studies suggest that there is substantial overuse of radiologic and laboratory services in medical practice. This is perhaps not surprising because few, if any, constraints have been placed on the number of services physicians in training (who provide much of the health care) are permitted to order. This, together with malpractice problems, makes it hard to set reasonable limits on what should be done.

Here is where radiologists have a major responsibility. Sitting as they do at the very center of the health care process, radiologists, in cooperation with other health professionals, have an obligation to participate actively in the development of models of health care which not only are of high professional quality but are available at reasonable cost. The acceptance of radiologists in this role may come slowly at first. Many health professionals in other disciplines consider radiology a major cause of many of the problems besetting the health care system. They are unsure of radiologists' priorities and motivations. Many resent the monopolistic privileges radiologists enjoy in hospitals. In the academic sphere, their respect for the research of many radiologists is low. Yet radiologists have an enormous opportunity to show that these allegations are for the most part untrue if they become actively involved in the planning and development of the improvements needed in the health care system.

Radiologists should also take the lead in developing methods by which radiologic services can be delivered at lower cost. A good starting point is a cooperative effort with x-ray manufacturers to reduce when possible the complexity of modern radiographic equipment. Is it necessary that every laboratory in a hospital radiology department be equipped with a 1,000 mA 3-phase unit? Must every hospital have a CT scanner? I hardly think so.

Radiologists should also become increasingly involved in the planning and allocation of the radiologic resources of his or her community (as distinct from institution). Such involvement is essential to overcome costly duplication of resources. How many radiologists are actively engaged in communitywide planning of radiologic facilities to assure maximum service at minimum cost? The number must be small, and yet what a superb opportunity to work with health systems agencies and hospital services cost review commissions in improving the cost-effectiveness of services. In this process, radiologists may often be required to bury self-interest, but the benefits can be great.

In addition to their role in controlling costs, do radiologists have a large part to play in providing the leadership needed to achieve stability within our society? I think they do. I am delighted that more and more radiologists are becoming medical school deans. It shows that an increasing number of radiologists are willing to assume responsible positions where the rewards are principally the satisfaction of helping one's colleagues. Moreover, it is good training for the next step, namely, the assumption of responsibility for some part in the drive for social stability in the face of rapid technological progress. Radiologists are well suited for this role if they will accept the challenge. Let us hope that many will respond.

It is evident that radiologists can and should play exciting roles in the years ahead, not only within the reductionistic activities of their specialty and profession, but in a variety of holistic endeavors which could be of great benefit to the medical care system and the society which it serves. For most of us, these will be new roles, requiring levels of selflessness, discipline, and responsibility to which we may be unaccustomed. Nevertheless, the personal satisfaction to be gained by responding to this challenge can, I believe, be limitless.

REFERENCES

1. Ashby E: Toward prophecy as a science. *Johns Hopkins Magazine* 27:72-76, 1976
2. Odum EP: The emergence of ecology as a new integrative discipline. *Science* 195:1289-1293, 1977
3. Ellis JR: Human values in medical education. Philadelphia, Society for Health and Human Values, 1976
4. Knowles JH: The responsibility of the individual. *Daedalus* 106:57-80, 1977

Guest Editorial

On Maps and Comparing Cross-sectional Imaging Methods

Comparison between computed tomography (CT) and ultrasound imaging is essential and inevitable. In a few preliminary reports, diagnostic accuracy for each has been assessed after a sequence of side-by-side patient examinations. Additional factors, such as the cost per examination, radiation dosage (or absence of ionizing radiation exposure), interpretive reliability, and bedside (portable) versus laboratory usage, have also been considered in this context. For the most part, however, such studies have been partisan, either as a result of the orientation of the investigators or because of technical disparities in the available instrumentation. Such gross biases are relatively easy to recognize, and presumably they can be corrected readily with an appropriate experimental design.

Nevertheless, there is an insidious and basic flaw in the simple comparative approach which limits its general usefulness. The flaw is the implicit but incorrect assumption that both methods provide the same anatomic information. This problem is addressed specifically by Bryan and Dinn [1] in this issue and is of the greatest importance in understanding the practical uses of the two techniques.

The medical imaging process is one of mapping the anatomy of a body region. In practice, the map which we obtain is quite incomplete. This limitation was put forcefully (although in a much broader context) by the semanticist Korzybski in his aphorism, "The map is not the territory" [2]. The essence of this discussion is that ultrasound imaging and CT scanning are two entirely different types of maps, not just alternate means of displaying the same information.

CT is an extension of traditional photon imaging with film. Images are maps of mass attenuation, which result from the interaction of the photon stream and the target medium at an atomic level. In the photoelectric energy range, mass attenuation is due principally to the atomic number of the constituent atoms, while in the Compton range it is related to electron density (and, indirectly, the mass density of the region). Conventional radiographic images are quite insensitive to these variables, hence the classical "four densities" of standard radiography. CT is a more precise method of retrieving the information content of the photon beam which traverses a tissue region, resulting in a continuum of densities which spans the gas-to-bone spectrum.

Ultrasound wave propagation is influenced by the elastic properties of the target medium. Phonon (as distinct from photon) interactions in biologic tissues are particularly complex and are not fully described. However, the interactions occur at a macromolecular level of organization and depend on both the composition of the material and physical structure of the target region. The ability to sense and display structural changes within an otherwise uniform material is, in fact, a unique feature of elastic wave methods. For simplicity, ultrasound images of a tissue region may be thought of as a map of the distribution and state of the macrostructural supporting elements (chiefly collagenous) which are present.

Some predictions of the most effective clinical uses of ultrasound and CT can be made through an appreciation of the type of mapping which each performs. CT is most helpful in distinguishing fields with different atomic composition, such as in separating a transudate from hemorrhage (high iron content), in grading the fat content of an organ, or in revealing calcifications. In the diagnosis of abdominal conditions, such situations are relatively infrequent. Since the atomic makeup of the viscera remains relatively uniform despite a variety of gross pathologic changes, CT may have some utility in showing the end result of the process (i.e., an enlarged or shrunken organ or a distorted organ margin). However, it will not often provide specific information about the histopathologic nature of the disease. This is the "isodense" situation common in CT imaging, which is discussed by Bryan and Dinn [1].

The method of visualization with ultrasound is quite different. Since elasticity depends on both composition and structure, focal or diffuse pathology related to the basic processes of edema, dehydration, and cellular infiltration (including fibrosis and neoplastic replacement) will each alter the appearance of an organ in a characteristic way. A practical example of the influence of structure on elasticity imaging is the present ability of ultrasound to distinguish the renal cortex and pyramids as separate tissue regions. These regions are identical in atomic composition and appear as such on CT scans.

Little is known about organ elasticity, although there is sufficient rationale for further basic research. Present evidence suggests that ultrasound imaging has the capability for pathologic specificity in diagnosis. The specificity for atomic composition which is the hallmark of CT is not relevent pathologically, although it may be exploited eventually as tissue-specific contrast agents are devised.

CT can trace its ancestry to the mathematical problem in reconstructing a region from line integral projections, which was reported by Radon in an obscure Leipzig journal in 1917 [3]. Reconstruction methods were reported in the radioastronomy literature by Bracewell [4] and others beginning in the mid 1950s. Since the introduction of CT, there has been a concerted industrial development of body scanning devices which has already passed through several instrumentation "generations" during the past 2 years. The implementation of a CT scanner involves a sophisticated technology, but the physical foundation is familiar to radiologists as a simple extension of well known radiographic imaging concepts.

World War I sonar echoranging is a likely paternal candidate for ultrasound imaging. Medical usage was initiated by the works of Wild and Reid [5] in the early 1950s. However, only in the past 2 years has technically satisfactory instrumentation been available. Some two decades of clinical use of primitive, low performance instrumentation, a large majority of technically untutored practitioners, and a general absence of scientific foundation have all conspired to place ultrasound imaging in the category of a promising but still mysterious, empirically substantiated art form.

There are few body scanning CT systems in use, though the principles should be evident to all radiologists. There are many ultrasound imaging systems in use, but few centers where their operation is treated scientifically. Bryan and Dinn [1] deserve credit for elucidating an aspect of the science of ultrasound imaging for the practitioner. We may hope that further such work will lead to a truly unbiased means of assessing the individual merits of our two newest body imaging techniques.

Jason C. Birnholz
Harvard Medical School
Boston, Massachusetts 02115

REFERENCES

1. Bryan PJ, Dinn WM: Isodense masses on CT: differentiation by gray scale ultrasonography. *Am J Roentgenol* 129:989-992, 1977
2. Korzybski A: *Science and Sanity.* Lakeville, Conn. International Non Aristotelian Library, 1948
3. Radon J: Über die Bestimmung von Funktionen durch ihre integralverte langs gewisser Manningfaltigkerten. *Ber Saechs Akad Wiss* [*Math-Phys*] (Leipzig) 69:262-277, 1917
4. Bracewell RN: Strip integration in radio astronomy. *Aust J Phys* 9:198-217, 1956
5. Wild JJ, Reid JM: Application of echoranging techniques to the determination of structure of biological tissues. *Science* 115:226-230, 1952

From Earlier Pages . . .

For us, who have grown up with radiology as a recognized specialty, firm in its place among the medical sciences, it is sometimes difficult to realize that at one time x-ray examination was not available. Even so, medicine was expanding rapidly in that unlit state. Roentgen's discovery came 50 years after the development of surgical anesthesia[*] and 5 years after aseptic ritual and rubber gloves had become essential for surgical procedures.[†] It was almost simultaneous with the appearance of ice cream cones,[‡] corn flakes,[§] and the first kiss presented in movies made for public consumption![‖]

As we all know, word of the discovery spread very rapidly, and many fertile minds contrived useful and bizarre plans for exploiting the new source of information. But it is not generally appreciated how soon the traditional uses for x-ray examination became established. In July 1896, 7 months AD (after discovery) and only 6 months AA (after announcement), surprisingly modern use of radiography in diagnosis and postoperative control was reported in an English journal [4]. Much of the contemporaneous writing concerned itself with the physics and technology of the science, or with the discovery and localization of opaque foreign bodies. In contrast, this report, appearing in the first volume of this journal, describes the use of radiography in (1) confirming a clinical diagnosis and (2) controlling the subsequent treatment. The absence of a tone of wonder in the description of the events shows this means of examination had found its proper place in the mind of this surgeon: he sought and obtained information of the type and essential quality of that required today.

The surgeon was Albert E. Morison, and he says, "R.L. aged sixteen, consulted me on June 16th., 1896, complaining of weakness of the arm and pain at the back of the elbow on movement. He gave the following history: — On January 19th, while walking, he tripped in a cart rut and fell on the tip of his right elbow. Two hours after he went to a doctor, who told him the bone was broken and set it, applying splints . . . . As it still continued weak and painful, on February 3rd he went to a bone setter, and he applied strapping to the limb.

"Present State. — The posterior part of the upper arm is very much smaller than the opposite arm, owing to atrophy of the triceps . . . and he is unable to straighten his forearm on the upper arm by about 25° . . . [fig. 1].

"Operation. — The limb was previously thoroughly purified and made aseptic.

"July 23rd: Chloroform having been administered, an elastic bandage was applied to the arm high up to make it avascular . . . . The olecranon was next fixed between the finger and thumb, and a thin slice removed to give a raw osseous surface. The upper end of the ulna was treated in a similar manner. The two ends of bone were then drilled obliquely, and two strands of thin silver wire passed through the holes, and on being tightened the two surfaces of bone came into good apposition. The cavity of the joint was washed out with weak corrosive lotion, and the skin wound closed with silk sutures, two sutures of the same material being passed through the

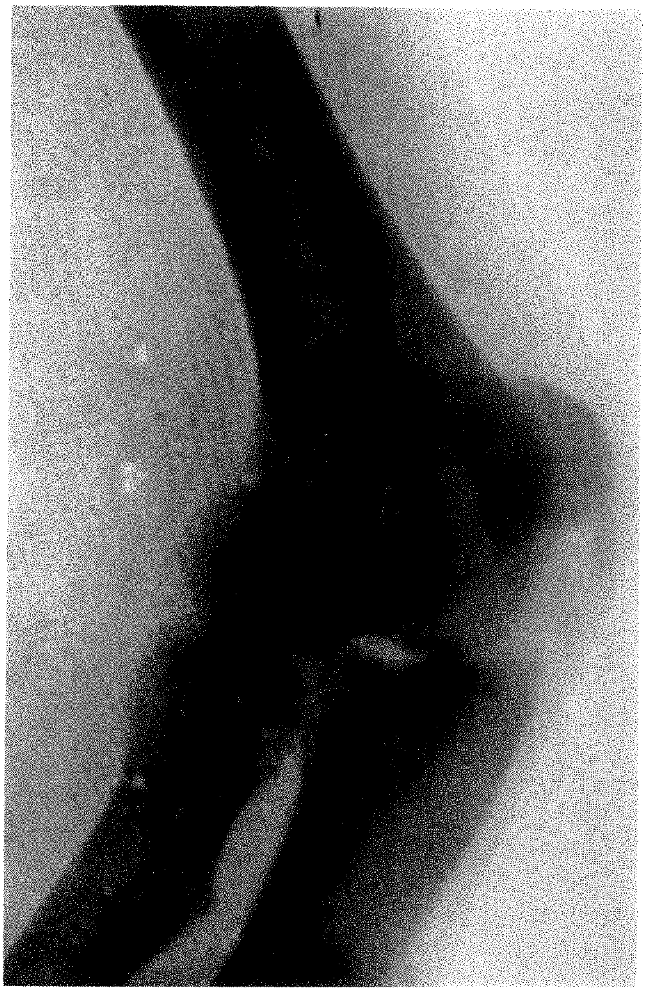

Fig. 1

This is the first in a series of historical vignettes from E. Frederick Lang. He has kindly consented to search the dusty archives of this and other journals for glimpses of the radiologic past to help freshen our perspectives of radiology today.

[*] Although many drugs, including alcohol, had long been used as soporifics in operations, ether was used for the first time publicly by Morton in 1846, and chloroform anesthesia began in 1847 [1].

[†] Ernst von Bergmann in Berlin in 1891 established the present standardized procedures for asepsis in 1886 after introducing steam sterilization in surgery. William S. Halsted had introduced rubber gloves in 1890 [1].

[‡] Ice cream cones were introduced by Italo Marcioni, in New Jersey, in 1896 and he patented his mould on December 13, 1903 [2].

[§] Cornflakes were introduced in 1898 by William K. Kellogg in Battle Creek, Michigan [2].

[‖] The Edison Company filmed a scene from a popular stage play in 1896, showing John Rice and May Irwin kissing [3].

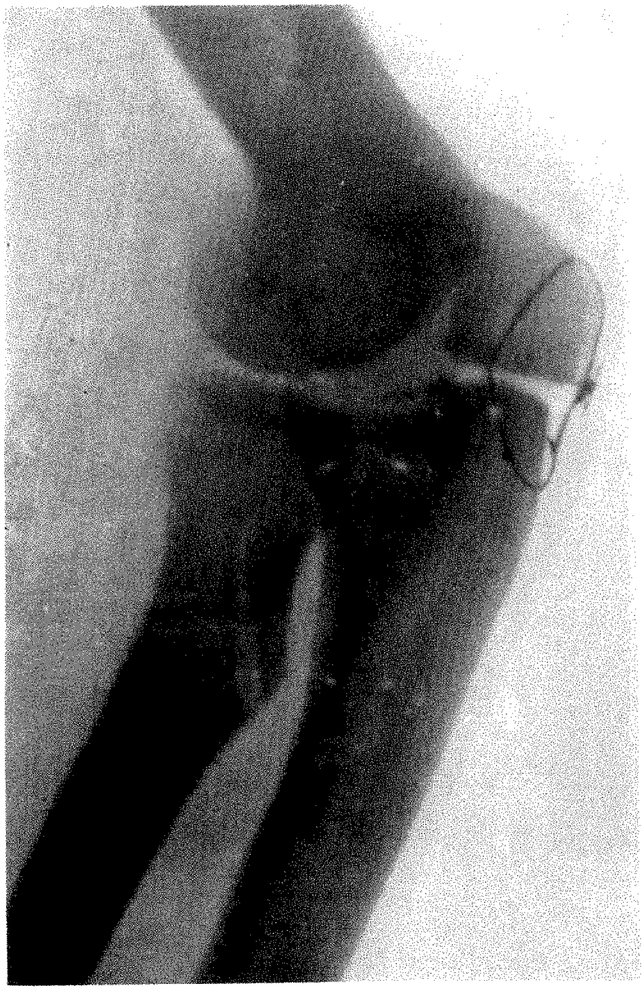

Fig. 2

periosteum. Antiseptic dressings were applied, and the arm bandaged to a straight anterior splint.

"Progress and After-Treatment.—Except for sickness continuing eighteen hours patient had no inconvenience. The highest temperature was 99.6 on the evening after the operation, and the patient was allowed up on the second day.

"August 1st: Wound dressed, skin sutures removed, passive movement commenced.

"7th: Can get the arm almost to a right angle. Splint removed and a sling used . . . .

"14th: Union is apparently perfectly firm, there being no lateral movement to be obtained between the fragments. Flexion is gradually increased each day until complete.

"September 24th: Movement is apparently perfect, though the arm is still weak, and there is still atrophy of the triceps . . . . Patient was sent to Messrs. Brady and Martin, of Newcastle-on-Tyne, to have the arm skiagraphed. The skiagram [fig. 2] shows that there is still a slight space between the fragments. A point of interest is whether this space is filled in with fibrous tissue or with cartilaginous matrix which will eventually become bone. I am indebted to Messrs. Brady and Martin for the excellent skiagrams which illustrate the case. Figure 1 was taken on July 10th, before, and Figure 2 on September 24th, two months after the operation."

The radiographers, Brady and Martin, were well known makers of scientific and surgical instruments, and in the issue from which this report is taken they offer their new catalogue covering apparatus for chemistry, bacteriology, heat, hydrostatics, light, electricity and magnetism, Roentgen photography, pneumatics, sound, mechanics and meteorology, and pure chemicals and reagents. Equipment for producing x-rays was readily available from many such instrument makers, and from opticians and dealers in photographic and electrical equipment. Some offered to make the exposures, as did Brady and Martin, and at that time there were no restrictions covering production or use of Roentgen's rays.

Although the technique for these x-rays is not provided, and given the interests of 80 years ago this information was almost de rigueur, the fact that the extremity was a region small enough to be easily examined contributed to the quality of the examination. Further follow-up on this patient is not available, but the progress so far leaves little to be desired, from the point of view of either the course of healing or the radiographic information about it.

E. Frederick Lang
Harper Hospital
Detroit, Michigan 48201

REFERENCES

1. Garrison FH: *An Introduction to the History of Medicine,* 4th ed. Philadelphia, Saunders, 1929
2. Robertson P: *The Book of Firsts.* New York, Potter, 1974
3. Solomon SJ: *The Film Idea.* New York, Harcourt Brace Jovanovich, 1972
4. Morison AE: Skiagrams of fracture of the olecranon treated by suturing with wire. *Arch Clin Skiagraphy* 1:25-27, 1896

Letters

Renal Cyst Puncture

A recent paper by Erich Lang [1] makes reference on page 726 to a brief article of mine published in the *Journal of Urology* [2]. Lang's statement has no basis in any data presented in that paper. It may be that Lang is referring to the questionnaire that was answered here and returned to him, describing a patient with an infected benign renal cyst diagnosed by percutaneous puncture, who had an associated perinephric abscess. We were not entirely certain that the perinephric abscess postdated the puncture, but included it in our reply to him as our one complication. However, this patient did have intravenous urography and nephrotomography beforehand, contrary to Lang's statement, and, in addition, did not have a nephrectomy, but simply drainage.

Howard J. Mindell
Medical Center Hospital of Vermont
Burlington, Vermont 05401

REFERENCES

1. Lang EK: Renal cyst puncture and aspiration: a survey of complications. *Am J Roentgenol* 128:723-727, 1977
2. Mindell HJ: Percutaneous renal cyst puncture: unusual results in two cases. *J Urol* 114:332-336, 1975

Faceted Air Bubbles

A frequently aired anecdote concerns a well known Scottish radiologist arguing with and failing to convince a surgeon that some filling defects in the common bile duct demonstrated during T tube cholangiography were stones and not air bubbles. The radiologist finally wrote in his report, "There are a number of faceted air bubbles." The punchline relies on the fact that it is axiomatic in most radiologists' minds that if such filling defects have facets they cannot be air bubbles, which are always spherical. This axiom was shattered when we recently observed air temporarily trapped in a rather large duodenal bulb. The air bubbles assumed a hexagonal shape which could be confused with facets (fig. 1).

Low surface tension is required for bubbles to form. In this case there must, fortuitously, have been the right mixture of air and fluid, presumably gastric juices and water from the barium solution, so that bubbles formed when the mixture was squirted through the duodenal channel. It is easy to reproduce the appearance shown in the photograph by squirting a soap solution into water—many of the bubbles so formed will be hexagonal. I have not been able to reproduce this appearance using a pure solution of Barosperse 30%.

Soap bubbles have been used as an analogue computer [1], on the basis that soap film when stretched between two points will, on reaching the equilibrium, be minimized to form the shortest distance between the two points. Air bubbles will usually form spheres, the smallest possible surface area for a given volume. When air bubbles of equal size come into contact, they form a hexagonal shape (as in a honeycomb, which starts as a soft wax cylinder). Over 100 years ago Joseph Plateau (cited in [2]) described the geometric properties of bubbles. He noted that when three film surfaces meet along a line, they make an angle of 120°. Our photograph clearly shows 120° intersections and three surfaces meeting at a line. In projection these appear as three lines meeting at a point. Since only three surfaces meeting along a line are required to make the 120° angles, theoretically this appearance could be produced by only three air bubbles.

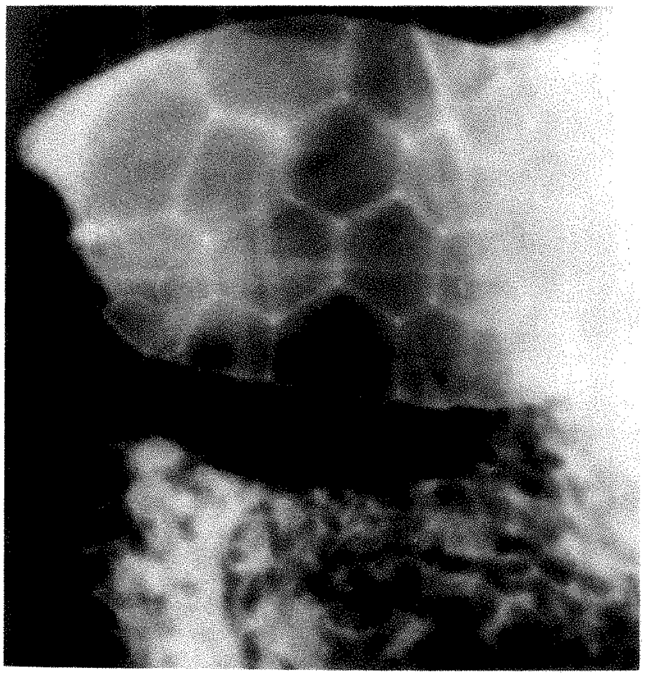
Fig. 1

So it seems that we must now drop this little anecdote that drove home what we thought was a fundamental truth. It can presumably be modified to hold true that if the filling defects are single or separate and have facets, they must be stones. But such modifications kill the punchline.

ACKNOWLEDGMENT

I thank Dr. Edward Dana for bringing this case to my attention.

Peter Dure-Smith
University of California (Irvine) Medical Center
Orange, California 92668

REFERENCES

1. Isenberg C: The soap film: an analogue computer. *Am Sci* 64:514-518, 1976
2. Bragg WL, Nye JF: A dynamic model of a crystal structure. *Proc R Soc Lond* [*A*] 190:474, 1947

Editor's Comment

This is a very provocative picture. Why are the bubbles so uniform in size? Do they pack the entire volume of the duodenum? If so, how many surfaces do they have? Eighteen? If that many, where are their images?

MMF

Intraarterial Lidocaine

We support the recommendation by Guthaner et al. [1] of the combination of lidocaine with 60% meglumine iothalomate (1 mg/ml) for peripheral arteriography. We too have used this technique for 2 years (approximately 1,000 patients) and are amazed at the reduction of the pain level and the elimination of the need for general anesthesia during peripheral arteriography. A subsequent report by Gordon and Westcott [2] recommended a similar technique, but using 2 mg lidocaine/ml contrast (60% meglumine diatrizoate). We have been satisfied with the results of the 1 mg/ml mixture, but the heavier premedication as used by Guthaner et al. is probably important.

A recent report by Widrich et al. [3] recommends injection of 2% lidocaine immediately prior to contrast injection with similar improvement of pain control. It is of interest that prior injection of procaine was originally described 25 years ago [4]. Although we have not subjected this technique to a controlled trial, our initial experience led us to discard prior injection of lidocaine in favor of the combination which, with the same dose, seemed to result in better pain control. The technique of Widrich et al. [3], which involves five injections of contrast medium to study the abdomen and lower extremities, results in excessive lidocaine dosages (sometimes to just subtoxic levels).

The lidocaine-contrast mixture is also useful for other "painful" studies, such as pelvic arteriography and upper extremity arteriography. It is of particular value in the study of surgically placed arteriovenous shunts for dialysis, since the arterial injection is especially painful. However, dilution of the contrast media to approximately 30% strength is desirable. One note of caution: lidocaine should not be used when injecting close to the cephalic vessels, such as in the proximal subclavian artery. On two occasions during subclavian arteriography with the catheter tip 1–2 cm beyond the origin of the vertebral artery, the patients noted dizziness and scintillating scotomata. The study demonstrated retrograde reflux of contrast into the vertebral artery, and presumably the lidocaine produced the neurologic phenomena.

J. H. Grollman, Jr.
UCLA Center for the Health Sciences
Los Angeles, California 90024

Ronald J. O'Reilly
St. Mary's Medical Center
Long Beach, California 90801

REFERENCES

1. Guthaner DF, Silverman JF, Hayden WG, Wexler L: Intraarterial analgesia in peripheral arteriography. *Am J Roentgenol* 128:737–739, 1977
2. Gordon IJ, Westcott JL: Intra-arterial lidocaine: an effective analgesic for peripheral angiography. *Radiology* 124:43–45, 1977
3. Widrich WC, Singer RJ, Robbins AH: The use of intra-arterial lidocaine to control pain due to aortofemoral arteriography. *Radiology* 124:37–41, 1977
4. Goodwin WE, Walter RC: Intra-aortic procaine injection in aortography. *Angiology* 4:410–412, 1953

High kVp Chest Radiography

Christensen et al. [1] recently studied the effect of kilovoltage (kVp) on detectability of pulmonary nodules and discussed the relationship between radiographic beam energy and quality of the radiographic image. They point out that although the increase in kilovoltage decreases the contrast between intrapulmonary structures and the surrounding normal lung tissue, it also decreases much more strikingly the contrast between bones and adjacent normal lung tissue. The net effect is easier visualization of intrapulmonary structures due to less obscuration by the overlying ribs. We would like to reemphasize an additional critical factor discussed by Dyke et al. [2] but overlooked by Christensen et al. [1]. This critical factor is also overlooked in the standard textbooks on radiologic physics [3–6] except the monograph by Seeman [7].

On a radiograph, a nodule casts a shadow the optical density of which differs from that of the surrounding tissue by

$$\Delta D = 0.43\,\gamma\,\Delta x\,\Delta\mu, \tag{1}$$

where ΔD is optical density, γ is the film contrast (slope of the characteristic curve), Δx is the thickness of the nodule, and $\Delta\mu$ is the difference in linear attenuation coefficient between the nodule and the surrounding lung tissue. Dyke et al. [2] rewrote the above expression as

$$\Delta x = \frac{2.3\,\Delta D}{\gamma\Delta\mu}. \tag{2}$$

If ΔD is set equal to the smallest change in optical density the eye can detect, then Δx is the thinnest detectable nodule or, as Dyke et al. [2] named it, the depth resolution. At present, no theoretical formula exists for the smallest ΔD value the eye can detect [8]. However, ΔD will depend on the amplitude of the radiographic mottle and thus the radiation quality and the film-screen combination; it is expected that different film-screen combinations will have optimum imaging ability at different kVp values. The ΔD value also depends on the size of the shadow, the sharpness of its boundaries, obscuring shadows, and viewing distance of the observers [8].

When an appropriate film-screen combination is used, the eye will be able to detect density variations close to 0.03. Keeping equation (2) in mind, the conclusion of Christensen et al. [1] can be restated as follows: as kilovoltage increases, $\Delta\mu$ between a pulmonary nodule and normal lung tissue decreases, resulting in a decrease in depth resolution; however, $\Delta\mu$ between bone and normal lung tissue decreases more strikingly, and the dependence of ΔD on obscuring shadows is removed or Δx decreases. The combination of these two effects results in a net decrease in Δx.

As stated in many textbooks on radiologic physics, Christensen et al. [1] assume that the film contrast (γ) is essentially constant over the useful range of the characteristic curve. It is not, and as pointed out by Dyke et al. [2], γ versus optical density is a bell-shaped curve. For radiographic films, γ peaks at optical densities close to 1.5 and decreases rapidly for adjacent densities. At low kilovoltage, large areas of the chest radiograph are either under- or overexposed. In addition to obscuration by the overlying ribs, the amplitude of γ is far from its maximum value, and the depth resolution is large or poor over a large area of the film. As the kilovoltage is increased, obscuration of overlying ribs is reduced, large areas of the film have a density close to 1.5, the amplitude of γ is close to maximum, and the depth resolution is better than at low kilovoltage over a large area of the film. Therefore, pulmonary nodules will be visualized more easily at a higher kilovoltage, a fact that has been corroborated by Christensen et al. [1]. However, the reason for enhanced visibility of pulmonary nodules is more than a lessening of obscuration from shadows of overlying ribs. Large areas of the film are exposed at densities in which γ is close to maximum; therefore large areas of the film will have greater depth resolution to detect smaller nodules.

Marshall E. Bein
Peter Spiegler
Leo G. Rigler
UCLA Center for the Health Sciences
Los Angeles, California 90024

REFERENCES

1. Christensen EE, Dietz GW, Murry RC, Moore JG, Stokely EM: Effect of kilovoltage on detectability of pulmonary nodules in a chest phantom. *Am J Roentgenol* 128:789–793, 1977
2. Dyke WP, Barbour JP, Charbonnier FM: Depth resolution: a mechanism by which high kilovoltage improves visibility in chest films. *Radiology* 117:159–164, 1975
3. Ter-Pogossian MM: *The Physical Aspect of Diagnostic Radiology.* New York, Harper & Row, 1967
4. Johns HE, Cunningham JR: *The Physics of Radiology*, 3d ed. Springfield, Ill., Thomas, 1969
5. Hendee RE: *Medical Radiation Physics.* Chicago, Year Book Medical Publishers, 1970
6. Christensen EE, Curry TS III, Nunnally J: *An Introduction to the Physics of Diagnostic Radiology*. Philadelphia, Lea & Febiger, 1973
7. Seeman HE: *Physical and Photographic Principles of Medical Radiography.* New York, John Wiley & Sons, 1958
8. Halmshaw R: *Physics of Industrial Radiology.* New York, American Elsevier, 1966

Reply

We did not elaborate on the reasons for the somewhat increased visibility of nodules with the higher kilovoltage techniques, except to mention that interference is reduced. Bein and colleagues correctly describe one of the more important reasons. However, we have a general objection to the term depth resolution coined by Dyke et al. and the assumption that it is a new concept. Equation (1) of Bein et al. is from the definition of film γ:

$$\gamma = \frac{\Delta D}{\Delta(\log E)},$$

where Δ (log relative exposure) may be given as $2.3/\Delta x \Delta \mu$ for adjacent film areas. The derivative of the generally sigmoid-shaped H and D curve is, indeed, somewhat bell shaped. However, texts (references 3 and 6 above) specifically mention the problem of recording a broad range of densities, the reduction of contrast of structures near the heel and toe of the H and D curve in such an instance, and discuss kilovoltage as a method of reducing the range of densities which must be recorded. Average gradient is mentioned in separate context as being convenient for other purposes. We feel that the effect on radiographic contrast (a well known term) of recording structures at different densities is generally understood. Rearranging a familiar formula and coining a new term seems superfluous.

Robert Murry
University of Texas Health Science Center
Dallas, Texas 75235

An Unfinished Phantasy

Reporting of films is one of the many new-found talents of the computer. Soon, the machine will be taught to interpret the difference in numbers its sensors perceive. Not only will it print the results in varying shades of color, it will point out a gamut of diagnostic possibilities based on clinical input.

Fortunately for me, for us, a human intermediary is still necessary. However, the length of our radiologic survival is inversely proportional to the quality and quantity of information we put into the machine. A little dragging of the feet will see me to the conclusion of my medical career. Will my younger colleagues grow bored talking to their computers or rather to a worldwide series of computers making instantaneous and correct diagnoses?

Most of our errors are those of omission; the machine does not omit. When we are tired, we see less; the machine is never too tired to see. Our psyches, ambient light, an overheard word distract us from a differential density. The machine has no ego, it is blind to all but its sensors; it is deaf, it will not be distracted.

In our future departments of diagnostic imaging, our computers, provided with clinical data, will indicate and schedule the test to be done. The nursing station will be notified of necessary preparation and will automatically receive appropriate medication. The patient will be summoned and tested by the machine. Diagnosis and proposed therapy will be made by the machine. Indeed, nothing short of surgery (really?) is beyond the machine.

What shall become of us? I will steal away to my hoary sanctuary and survive on reminiscences of diagnoses past. I will recall the day when reports were the creative product of a human mind and not the numbered regurgitation of a machine. I will cherish the memory of typing errors such as "calcific erotic stenosis" or "the patient was prepped and raped in the usual manner." Such errors are the result of human fallibility or subliminal desire. I know the machine does not suffer from human fallibility. I have no knowledge concerning its desires.

Solomon S. Schwartz
Hospital of St. Raphael
New Haven, Connecticut 06511

Report of 1977 American Radium Society Meeting

The American Radium Society held its fifty-ninth annual meeting, April 24–28, 1977, in Las Vegas, Nevada. The central focus of the meeting was set forth by the Janeway Lecture, Fundamental Mechanisms in Combined Modality Therapy of Cancer, delivered by Henry S. Kaplan. He underlined how best to integrate the multiple treatment techniques available in the management of cancer and what might be expected to improve the outlook for cancer patients in the future.

From this keynote, the current management of malignant tumors of the gastrointestinal tract was addressed with review of clinical-pathologic bases for rational therapeutic approaches to gastrointestinal malignancies including stomach, pancreas, and colorectal carcinoma. Results of current therapeutic techniques were evaluated. Utilization of pre- and postoperative radiation therapy along with adjuvant chemotherapy was identified as the emphasis for future evaluation.

A multidisciplinary panel addressed the problem of appropriate management technique for small round cell tumors of bone including diagnosis and treatment of multiple myeloma, Ewing's sarcoma, and histiocytic lymphoma involving bone. The diagnostic characteristics of the diseases along with appropriate surgical management with radiotherapy and chemotherapy were discussed. Appropriate management for multiple myeloma relies primarily on precise diagnosis and systemically administered chemotherapy, with radiotherapy serving as an adjuvant for palliation of symptomatic bony areas of involvement. Ewing's sarcoma responds best with combined techniques of appropriate diagnosis along with radiotherapy and systemically administered chemotherapy. Histiocytic lymphoma involving bone requires a precise diagnosis, with radiotherapy and systemic chemotherapy given as primary means of management.

The impact of surgical staging on management of pelvic malignancy was reviewed with emphasis on pretreatment surgical exploration for staging in carcinoma of the cervix, carcinoma of the endometrium, and ovarian cancer. Renewed interest in surgical staging has resulted from pilot studies carried out under the aegis of the gynecologic oncology group evaluating the distribution of pelvic and periaortic lymph node involvement with cervical cancer, endometrial cancer, ovarian cancer, and sarcoma of the uterus. These findings are changing the concepts of pathophysiology of pelvic malignancy. From pretreatment surgical exploration, early cancer may now be more realistically defined and the true effects of drugs and/or radiation for these patients may be sought without confusion based on clinical staging hazards. Similarly, for more advanced cases, the disease may be more suitably defined for drug or new combination study. Treatment techniques directed toward combinations of surgery, more aggressive radiotherapy, and chemotherapy need to be explored in order to evaluate their efficacy.

Malignancy induces an immunologic reaction often late, inadequate, and sometimes inappropriate. In general, patients whose immune system is intact following cancer therapy have a better prognosis than patients lacking an intact immune response. Whether this relationship is cause and effect or simply a reflection of a generalized disorder associated with malignancy is unclear. However, it is known that nutritional status, patient age, and type of treatment influence immunologic responsiveness. The variability in biomarkers in clinical cancer, nutritional status, and surgical, chemotherapeutic, and radiotherapeutic treatment requires a broad exchange among many investigators in order to assess appropriately the effects of those agents on immunocompetence.

Treatment of head and neck cancer was said to necessitate the integration of multimodal treatment techniques if maximum potential of cure is to be achieved with a minimum of complications.

Survival in breast cancer is influenced by the size of the primary tumor, presence of axillary metastases, menopausal status of the patient, and possibly by variable histologic features. The disease tends to pursue a long natural history with local recurrences following treatment tending to occur early. The influence of local recurrences on survival has not been precisely defined. Because of the number of variables influencing survival, local recurrence, time, and extent of distant metastases, it is extremely difficult to assess new therapeutic approaches. The Presidential Address identified the need for caution in evaluating the outcome as a consequence of various treatment techniques because of the long natural history of the disease process. To report end results of treatment identifying the efficacy of one treatment over another at the end of 3 years is inappropriate in this disease process. In early cancer of the breast, equally good results can be obtained either by definitive radiotherapy or definitive surgery. In the former, however, cosmesis and function are preserved, whereas in the latter the patient is subjected to various complications as a consequence of treatment plus the loss of the breast. Utilization of postoperative radiation therapy after modified radical mastectomy or radical mastectomy has now been carefully defined indicating its use in those individuals who are at risk for regional and local recurrence. Data indicate that combined treatment has a significant influence on survival. Preliminary results also seem to indicate that adjuvant chemotherapy used in conjunction with radical mastectomy has an impact on premenopausal women but no significant impact on postmenopausal women.

Radiation therapy and surgery used independently in treatment have been associated with the cure of numerous malignant tumors. More recently, chemotherapeutic agents alone have produced apparent cures in some malignancies including gestational choriocarcinoma, childhood acute lymphocytic leukemia, and advanced Hodgkin's disease. There is historic precedent for the combination of radiation and chemotherapy as adjuvant treatment to surgery in the cure of Wilms's tumor and childhood sarcomas. Interest in the use of combined modalities has increased with promising results in Hodgkin's disease patients who have systemic symptoms, adult soft tissue sarcomas, and cancers of the rectosigmoid, breast, and testicle. However, results of these preliminary studies must be viewed with extreme caution regarding the eventual impact on the natural history of these diseases and the potential long term deleterious effects that may ensue from such treatment combinations. It is clear from review of some of these studies that both the radiation and medical oncologist must have a better understanding of the other's specialty with regard to philosophy, rationale, language, technique, and complications. The radiation oncologist and the surgeon must be familiar with the proper study sequence in the screening and development of new agents, the pharmacology of antineoplastic agents, drug-x-ray interactions, and the long term sequelae of drug administration including the risk of second tumor induction. Similarly, the medical oncologist must have knowledge of surgical techniques as well as radiation therapy techniques along with basic biologic principles involved in treatment.

To have greater impact on cancer, all oncologists must clearly improve their capabilities independently as well as jointly. Although the goal of all oncologists is to increase the cure of malignant diseases, each must retain an independent identity because of the inherent complexities of each field and the difficulty for a single individual to master each and to possess expertise in all. Nevertheless, oncologists must continually strive to increase mutual understanding and cooperation among the fields in order to maximize the ultimate effort.

Society officers during the 1977 meeting were: Luther W. Brady, president; Richard H. Jesse, president-elect; Morton M. Kligerman, first vice-president; George C. Lewis, second vice-president; Alfred S. Ketcham, secretary; Frederick W. George, treasurer; Felix Rutledge, Victor Marcial, and Jerome M. Vaeth, members of the executive committee.

Three major decisions were reached by the society. After 3 years of study, the society unanimously endorsed the retention of its name, American Radium Society. It was felt that this would relate appropriately to its historic precedence and also continue to represent the oldest multidisciplinary scientific cancer society in the United States. Second, the society unanimously endorsed the concept of publication of its papers in three journals: *Cancer*, *International Journal of Radiation Oncology*, and the *American Journal of Roentgenology*. Finally, the society elected to initiate a program of refresher courses to begin it its sixtieth annual meeting, April 26–30, 1978, at the Marriott Hotel in New Orleans.

Officers elected for 1977–1978 were: Richard H. Jesse, president; Frederick W. George, president-elect; Ivor Fix, first vice-president; John Durant, second vice-president; Simon Kramer, treasurer; and Felix Rutledge, Luther W. Brady, and Victor Marcial, members of the executive committee.

Luther W. Brady
Chairman, Publications Committee
American Radium Society

AJR Reviewers and Abstractors, 1977

The journal acknowledges with special pleasure the work of the following individuals in reviewing manuscripts, selecting and writing abstracts of the literature, and preparing book reviews. The quality of the journal is directly dependent on these valuable contributions. The editors and editorial staff are most sincerely appreciative.

D. Adams
R. P. Ainsworth
A. Alavi
R. J. Alfidi
T. N. K. Allan
D. Allen
P. W. Anderson
C. A. Athanasoulis
H.L. Atkins
S. P. Axelbaum
R. Baker
H. Baltaxe
M. Baron
R. J. Bartram, Jr.
J. Bassingwaite
R. Bauman
W. J. Bean
J. A. Becker
M. Becker
J. Bentson
D. L. Berens
R. M. Berk
H. Berry
J. Blackman
N. Blank
D. M. Blaufox
M. J. Blocklyn
J. J. Bookstein
M. L. M. Boone
S. Borden
M. Bosniak
W. Boswell
L. W. Brady
R. L. Bree
B. A. Brill
R. C. Brown
J. B. Buchanan
R. E. Buenger
H. Burko
J. Butler
M. A. Capitanio
T. Carlile
H. Carlson
E. Carlsson
S. Carter
W. J. Casarella
A. Chait
A. A. Chambers
C. H. J. Chang
W. H. Chapman
C. Chesnut
P. Chikos
K. Cho
E. E. Christensen
G. M. Christensen
V. Chuang
J. L. Clements, Jr.
W. P. Cockshott
G. C. Coggs
C. Cole-Beuglot
W. G. Connor
L. Cromwell
A. Crummy
J. J. Cunningham
D. C. Dale
A. J. Davidson
K. Davis
M. Deck
J. Denny
R. Dinsmore
K. T. Dockray
G. D. Dodd
M. Donner
J. Doppman
B. Doust
J. S. Dunbar
P. Dure-Smith
W. Eckelman
J. Edeiken
J. L. Eisemann
L. Elliot
K. Ellis
J. Eltringham
R. G. Evens
K. Fellows
A. H. Felman
J. Fennessy
J. T. Ferrucci
D. C. Figge
R. A. Filly
R. A. Flom
E. Fordham
D. M. Forrester
E. A. Franken
R. Fraser
R. Frech
R. Freiberger
A. K. Freimanis
G. D. Frey
R. M. Friedenberg
G. W. Friedland
M. Friedman
P. Friedman
D. E. Fuller
T. O. Gabrielson
G. Gamsu
G. Gates
H. K. Genant
J. P. Geraci
A. Gerdes
D. Gilday
M. Glickman
R. H. Gold
B. B. Goldberg
H. Goldberg
H. S. Goldman
M. L. Goldman
H. M. Goldstein
L. R. Goodman
A. C. Gonzalez
A. F. Govoni
B. B. Gosink
C. B. Graham
R. Gramiak
E. V. Grayson
R. Greene
L. D. Greenfield
R. J. Griep
T. W. Griffin
N. T. Griscom
J. H. Grollman
J. E. Hall
J. M. Halls
G.E. Hanks
T. Hanks
J. Harley
D. Harrington
G. B. Harris
R. D. Harris
W. Harvey-Smith
D. Harwood-Nash
R. R. Hattery
V. Haughton
D. Heimbach
E. R. Heitzman
S. Hellman
F. Hendrickson
F. Hipona
P. J. Hodes
L. B. Holman
R. A. Holmes
M. Huckman
G. A. Irwin
K. L. Jackson
H. Jacobson
R. Jaffe
M. Janower
P. S. Jensen
M. L. Johnson
P. M. Johnson
D. Jones
M. Judkins
A. R. Kagan
J. J. Karo
J. Kaye
W. A. Kelly
F. M. Kelvin
J. G. Kereiakes
S. A. Kieffer
L. E. Kier
F. C. Killien
D. L. King
J. A. Kirkpatrick
D. R. Kirks
M. D. Kiviat
E. C. Klatte
P. R. Koehler
M. Korobkin
J. F. Kotalik
K. L. Krabbenhoft
A. F. Lalli
B. Lane
E. F. Lang
M. S. Lapayowker
E. C. Lasser
P. Lauber
J. S. Laughlin
R. L. Lebowitz
T. G. Lee
R. Leighton
J. C. Leonidas
G. R. Leopold
J. R. LePage
D. C. Levin
S. H. Levitt
T. K. Lewellen
J. Li
J. W. Loop
T. Lyons
N. F. Maklad
A. Maravilla
M. T. Margolis
R. H. Marshak
W. Martel
J. E. Martin
L. O. Martinez
F. A. Matson
R. Mazess
J. G. McAfee
B. L. McClennan
J. J. McCort
R. McClelland
D. S. McQuown
M. J. Meagher
B. P. Menanteau
S. W. Miller
R. R. Million
R. Moe
D. Moody
R. H. Morgan
R. D. Moseley, Jr.
P. Moskowitz
A. Moss
W. T. Moss
J. Muhm
T. P. Naidich
H. L. Neiman
W. B. Nelp
S. W. Nelson
T. H. Newton
C. Nice
D. Norman
C. H. Northrop
A. Nov
S. B. Novy
A. E. Oestreich
W. W. Olmsted
R. E. O'Mara
S. Order
B. Parker
R. G. Parker
A. G. Peck
C. A. Perez
R. C. Pfister
D. J. Phillips
L. A. Phillips
T. L. Phillips
N. D. Poe
H. M. Pollack
D. G. Potts
A. K. Poznanski
J. A. Purdy
J. Rabinowitz
J. N. Rasey
D. F. Reese
B. J. Reilly
D. Resnick
S. R. Reuter
H. Ricketts
R. Robinson
L. F. Rogers
C. Rohrmann
F. D. Rollo
M. A. Rosenberg
T. Rudd
C. Rumbaugh
F. Ruzicka
J. Sackett
S. Sagel
W. F. Sample
R. C. Sanders
E. N. Sargent
G. T. Scanlon
H. M. Schreiber
R. Schultz
S. S. Schwartz
R. Scott
B. H. Scribner
W. B. Seaman
R. Shalek
J. Shapiro
M. Shaub
P. K. F. Sheedy
W. H. Shehadi
M. E. Siegel
S. S. Siegelman
T. M. Silver
P. Simpkin
E. B. Singleton
L. M. Skolnick
E. H. Smith
G. Smith
J. Smith
W. M. Smoak
T. Sos
R. Soulen
R. P. Spencer
L. Squire
D. P. Stables
R. J. Stanley
T. W. Staple
W. B. Steel
E. A. Stevens
G. M. Stevens
J. K. Stevenson
J. Storer
R. Strand
M. Takahashi
L. B. Talner
R. N. Taxin
H. Taybi
K. J. W. Taylor
W. J. Taylor
C. J. Tegtmeyer
A. W. Templeton
F. Templeton
M. M. Ter-Pogossian
F. D. Thomas
J. R. Thornbury
J. M. Tishler
S. Treves
M. Viamonte
V. Vix
S. Wallace
W. J. Walls
J. Walter
A. C. Waltman
B. N. Weissman
L. Wexler
J. P. Whalen
R. I. White
W. Widrich
L. M. Wiegenstein
W. A. Wilcox
R. H. Wilkinson
J. E. Williams
F. Winsberg
P. F. Winter
J. Wiot
H. Withers
D. Witten
M. J. Wizenberg
B. S. Wolf
J. N. Wolfe
A. H. Wolson
B. J. Wood
P. Wootton
R. Worsnop
J. Youker
L. W. Young
H. Yune
F. Zboralski
C. J. Zylak

Abstracts of Current Literature

Chest

Computed tomography of the mediastinum. Goldwin RL, Heitzman ER, Proto AV (SUNY Upstate Medical Center, Syracuse, New York 13210). *Radiology* 124:235-241, July 1977

Ninety-one scans of the mediastinum were reviewed. These were compared with a mediastinal scan done on a fresh cadaver and anatomic transverse preparations which were radiographed. The left subclavian artery, subclavian veins, trachea, esophagus, aortic arch, pulmonary arteries, and pulmonary veins were consistently identifiable. Based on these anatomic landmarks the authors suggest that mediastinal computed tomography may be of value in: (1) locating lesions which are obscured by the mediastinum; (2) determining tissue density of mediastinal lesions; (3) diagnosing mediastinal widening caused by fatty infiltration or prominent great vessels; (4) additional investigation of abnormal plain film findings of the mediastinum; and (5) determining extent and localization of mediastinal tumors.

Asher Nov

Radiology of airway foreign bodies in children. Reed MH (Children's Health Science Center, Winnipeg, Manitoba, Canada). *J Can Assoc Radiol* 28:111-118, June 1977

The author describes his experience with 91 children with airway foreign bodies seen in a 9 year period. Ages ranged from 9 months to 13 years. In 50 cases, the foreign body was in the right bronchial tree, in 30 cases on the left, in five in the larynx and trachea, and in the remaining six cases the foreign body was bilateral.

Ten patients had radiopaque foreign bodies, six being metal, two egg shells, one bone fragment, and one sunflower seed. Apart from the actual foreign body, no other radiographic abnormalities were seen in any of these patients. In the other 81 patients in whom the actual foreign body was not visible radiographically, the foreign body was unilateral in 74 and bilateral or in the region of the carina in seven. In 51 cases (nonopaque foreign bodies) frontal and lateral chest radiographs were abnormal, and in 33 of these cases there was hyperlucency of the involved lung, unilateral atelectasis in 11, unilateral consolidation in six and bilateral over inflation in one.

The remaining 23 of the 74 patients with radiolucent foreign bodies had normal conventional chest radiographs. Thirteen patients in this group had additional abnormalities demonstrated by other methods.

The author strongly recommends that chest fluoroscopy or posteroanterior chest radiographs in expiration be obtained where the diagnosis is in doubt.

Jack M. Tishler

Radiological changes in the chest in malignant trophoblastic disease. Ang AH, Chan WF (University of Malaya, Kuala Lumpur, Malaya). *Australas Radiol* 20:333-337, Dec 1976

Malignant trophoblastic neoplasia is more common in Africa and the Far East than in Western countries. In this series, the incidence in Malaysia is reported to be 1 in 980 hospital deliveries. Of 22 patients with malignant trophoblastic disease reviewed from 1969 to 1975, 18 were found to have intrathoracic metastases on radiologic examination of the chest. Clinical presentation in these 18 patients was with pulmonary symptoms in 10, cerebral in one, combined pulmonary and cerebral in one, and gynecologic in three. The remaining three were asymptomatic, their pulmonary metastases being discovered in the course of routine follow-up for recent molar pregnancy.

Histologic confirmation was available for the three patients presenting with gynecologic symptoms and an additional five patients with evidence of pelvic disease. In the remaining 10 patients, the diagnosis was made on the history of recent pregnancy (molar in eight), urinary gonadotrophin assays, and abnormal chest x-rays.

The high incidence of intrathoracic spread necessitates an awareness of the radiographic findings. These were variable, the most common appearance being discrete intrapulmonary nodules which occurred in 15 of 18 patients. The lesions (multiple in 10) were well circumscribed and measured 0.5-20 cm. Cavitation was noted in one patient. Other findings included pleural effusion in two, hilar mass in one, confluent shadows in two, and miliary mottling in one. Other radiologic findings, although not incident in this series, include pulmonary hypertension, pulmonary infarction, paramediastinal mass, and pulmonary calcification.

Because of potentially successful treatment with chemotherapy, even in widespread disease, the diagnosis of trophoblastic disease should be considered whenever these radiologic appearances are encountered in the young female patient.

John Branson

Cardiovascular

Angiographic determination of arterial patency after percutaneous catheterization in infants and small children. Hurwitz RA, Franken EA, Girod DA, Smith JA, Smith WL (Indiana University School of Medicine, Indianapolis, Indiana 46202). *Circulation* 56:102-105, July 1977

The femoral artery was examined 6 months or more after percutaneous catheterization for left heart study. During the study period, 48 of 118 children having repeat arterial catheterization were examined from the opposite leg. Cineangiograms of the iliac area showed occlusion of the previously catheterized femoral artery in four of the 48. All four with blockage were asymptomatic and possessed good pedal pulses, while two had decreased femoral pulsations. It is concluded that 3%-8% of patients weighing less than 25 kg have arterial occlusion after catheterization. During a 10 year experience the authors found no evidence of tissue damage in patients undergoing percutaneous arterial catheterization. Though distal pulses have been weak in some patients, leg function and motion were good, capillary filling was adequate, and by the day following catheterization most pulses were palpable. No patient had surgical embolectomy prior to this investigation.

R. S. Frech

Correlation of coronary arteriograms and left ventriculograms with postmortem studies. Hutchins GM, Bulkley BH, Ridolfi RL, Griffith LSC, Lohr FT, Piasio MA (Johns Hopkins Medical Institutions, Baltimore, Maryland 21205). *Circulation* 56:32-37, July 1977

Coronary arteriograms and left ventriculograms were compared with myocardial pathology in 28 patients. Premortem decreased or absent segmental wall motion frequently did not indicate a myocardial lesion. Differences in ventriculographic and pathologic assessments were found in 52% of the segments. Good wall motion meant normal myocardium, but normal myocardium did not always have normal motion. Scar caused reduced wall motion, but reduced wall motion did not necessarily mean scar. Poorly moving but morphologically normal segments were found: (1) adjacent to segments with infarcts; (2) in the distribution of critically narrowed coronary arteries; or (3) in hearts with valvular heart disease and myocardial hypertrophy.

R. S. Frech

Anomalies of the systemic venous return. Tuma S, Samanek M, Voriskova M, Benesova D, Prazsky F, Huein B (Cardiopulmonary Laboratory, University Hospital, Vuvalu 84, Prague 5, Motol, Czechoslovakia). *Pediatr Radiol* 5:193-197, 1977

Anomalies in the course and drainage of systemic veins, in particular the inferior vena cava, markedly complicate or even prevent cardiac catheterization and some surgical procedures. Such anomalies have been observed in 32 of 1,266 children subjected to catheterization and angiocardiography i.e. 2.5%. Severe anomalies of a superior vena cava were observed in six children, one of them having an associated anomaly of an inferior vena cava. Anomalies of the inferior vena cava were observed in 27 children. The latter included persistent paired development of the inferior vena cava, aplasia of suprarenal portion with azygos or hemiazygos continuation, its persistence at the side of the cardiac apex, and combination of these findings. In 19 of the children with an anomaly of the inferior vena cava there was a visceral situs indeterminatus associated, often with severe congenital heart disease and with a large intracardiac shunt (e.g. transposition of the great arteries and stenosis or atresia of the pulmonary artery). Suspicions of such combinations of visceral situs indeterminatus with anomalies of the inferior vena cava and severe congenital heart disease can be suspected on plain chest films, but the diagnosis can be definitely determined only by angiocardiography.

Author Abstract

Surgical correction in infancy to reduce mortality in transposition of the great arteries. Kawabori I, Guntheroth WG, Morgan BC, Mohri H, Dillard DH (University of Washington School of Medicine, Seattle, Washington 98195). *Pediatrics* 60:83-85, July 1977

The high mortality for infants with transposition of the great vessels has been significantly reduced since surgical and balloon atrial septostomy. The authors believe a further reduction in mortality is possible by early interatrial baffle procedure. Experience with total repair of uncomplicated transposition of the great vessels in 12 patients, 3 days to 6 months of age, with hypoxia or intractable congestive heart failure is reported. Surgery was performed under deep hypothermia. All infants without adequate atrial communication had a previous balloon septostomy. Operation was successful in 10 of the 12 patients, and the survivors have been followed for 1 month to 8 years: average 4 years. Early surgical repair, between 3 and 6 months of age, is advocated.

B. J. Wood

Clinicopathologic correlations de subitaneis mortibus. XXIII. Rheumatoid arthritis and ankylosing spondylitis. James TN (University of Alabama Medical Center, Birmingham, Alabama 35294). *Circulation* 55:669-677, April 1977

The conduction system of the heart was examined at necropsy in two cases of rheumatoid arthritis and one of ankylosing spondylitis. The sinus node, the atrioventricular node, and His bundle had degenerative disease.

Initial appearance of almost any feature of rheumatoid heart disease is characteristically late in the clinical course of the arthritis. Pericarditis, valvulitis, coronary arteritis, and heart block are the more familiar changes. Additional complications are myocardial infarction from vasculitis and focal fibrosis and degeneration of all parts of the heart including the conduction system. More degeneration was found in the conduction system than could be accounted for on the basis of either a vascular lesion or pericarditis. Since the sinus node is organized in the collagen framework, and the atrioventricular node and His bundle are either bordered or surrounded by collagen, one is tempted to relate this proximity to the degenerative changes. In one patient atrial fibrillation was attributable to virtual total destruction of the sinus node. Given the extensive destruction of the atrioventricular node and His bundle in these three hearts, it is surprising that more patients with rheumatoid arthritis do not have failure of atrioventricular conduction.

R. S. Frech

Intrarenal collateral circulation in the pediatric patient. Kirks DR, Fitz CR, Korobkin M (Children's Medical Center, 1935 Amelia Street, Dallas, Texas 75235). *Pediatr Radiol* 5:154-159, March 1977

Both extrarenal and intrarenal collateral circulation may be seen in pediatric patients with segmental renal artery stenosis. Angiography and renal vein sampling should be part of the radiologic investigation of unexplained hypertension. Since stenotic lesions in infants and children are usually due to fibromuscular dysplasia and are usually intrarenal, intrarenal collateral circulation would be anticipated. The presence of intrarenal collateral is indicative of significant segmental renal artery stenosis.

B. J. Wood

Cranial and caudal angulation for coronary angiography revisited. Sos TA, Baltaxe HA (New York Hospital, Cornell Medical College, 525 East 68th Street, New York, New York 10021). *Circulation* 56:119-123, July 1977

Projections utilizing cranial and caudal angulation of the x-ray tube in various obliquities have been described recently for coronary angiography and left ventriculography. These views provide improved visualization of the proximal branches of the left coronary artery, the region of the crux of the right coronary artery, and the left ventricle.

R. Frech

The assessment of mitral stenosis and prosthetic mitral valve obstruction, using the posterior aortic wall echocardiogram. Strunk BL, London EJ, Fitzgerald J, Popp RL, Barry WH (W. H. Barry, Stanford University School of Medicine, Stanford, California 94305). *Circulation* 55:885-891, June 1977

The posterior aortic wall echocardiogram approximates the left atrial volume curve for filling and emptying. Normal left atrial emptying occurs in three distinct phases: early rapid emptying phase, middle conduit phase, and late atrial systolic phase. An atrial emptying index is described for patients in normal sinus rhythm and atrial fibrillation for use in assessing the severity of mitral stenosis and detection of prosthetic mitral valve obstruction. Patients with mitral stenosis have a characteristic pattern of slow left atrial emptying in early diastole, with loss of the conduit phase in middiastole. The atrial emptying index was significantly related to mitral valve area, and therefore, provides a useful noninvasive tool for quantitating the degree of mitral stenosis. In the same group of patients there was not a significant correlation between the mitral valve E-F slope and the mitral valve area index.

Determination of the emptying index also proved useful in the evaluation of patients with prosthetic mitral valve obstruction, and in documenting improvement in left atrial emptying after mitral valve surgery.

Richard B. Jaffe

Arteriography of the traumatized hand. Experience in 150 Cases. Blonstein A, Doyon D, Harry G (D. Doyon, Département de Radiologie, C.H.U. de Bicetre, 78 rue de General-Leclerc, F 94270, Le Kremlin-Bicetre, France). *J Radiol Electrol Med Nucl* 58:93-102, 1977

Arteriography of the hand is a simple and safe procedure which readily provides information about the status, distribution, and functional activity of the traumatized hand, both pre-

and postoperatively. The examination is usually performed as an emergency procedure following trauma to the hand which has sustained crushing injuries, thermal or chemical burns. Preoperatively it is essential to determine the anatomy and distribution of the vessels, extent of injury to the vessels, and their functional activity. Postoperatively, arteriography will determine the results of the vascular surgery and repair of the hand.

The main blood supply of the hand is from the radial and ulnar arteries. The interosseous arteries can play an important role when there is a leison or malformation of either of the two arteries. In about 5% of cases there is an artery of the median nerve which goes to the second palmer space.

Arteriography is best performed under local anesthesia, preferably by brachial plexus block. Thus the patient remains conscious and alert and is able to cooperate. The vessel of choice for the injection of the contrast medium is the brachial artery. When this is not accessible, the axillary or femoral artery may be used, the latter after catheterization by the Seldinger technique. Heparnization is accomplished by administration of 0.5 mg heparin per kg body weight. To avoid spasm of the vessel 10 mg papaverine is injected, followed by injection of 9-12 ml of contrast medium in 3 sec. This dose may be repeated but a total of no more than 50 ml should be administered. Films are made at 1 sec intervals for 5 sec at the completion of the injection. Radiographic magnification is recommended.

At the completion of the examination, the artery should be compressed at the site of the needle puncture for 5 min. Though infrequent, arterial spasm can be a disturbing complication interfering with the successful performance of the examination. This may occur when anesthesia is inadequate, in the young where the artery is of small caliber, and when technical difficulties are experienced in entering the artery with a needle or catheter. Pathologic findings encountered include: (1) severed arteries; (2) interruption of the function of the artery resulting in decrease or loss of blood supply to the area supplied by the vessel; (3) delayed circulation due to disease of the blood vessel; (4) arteriovenous shunts with early flow of blood into the venous circulation. In this series of 150 cases, conditions for which the examination was performed were soft tissue injuries, amputations, thrombosis, grafts, burns, and transplants.

William H. Shehadi

Gastrointestinal

Aperistalsis and esophagitis. Simeone JF, Burrell M, Toffler R, Smith GJW (Yale University School of Medicine, New Haven, Connecticut). *Radiology* 123:9-14, April 1977

Aperistalsis of the esophagus was demonstrated in six patients with esophagitis. This was observed in reflux, caustic, and infectious esophagitis, and has occurred both as a transient phenomenon with no further sequelae, and as the initial manifestation of involvement in patients who subsequently suffered stricture. Based on biopsy and autopsy specimens in two cases, a possible mechanism of aperistalsis related to the damage to neurons in Auerbach's plexus is postulated. The presence of aperistalsis has been the first significant clue to esophageal inflammation in several cases.

Author Abstract

The columnar-lined esophagus: analysis of 26 cases. Robbins AH, Hermos JA, Schimmel EM, Friedlander DM, Messian RA (Veterans Administration Hospital, Boston, Massachusetts). *Radiology* 123:1-7, April 1977

In 1950, Barrett described an esophageal ulcer associated with columnar epithelium. This was interpreted as representing gastric mucosa. Twenty-six patients are presented. All had oral barium examinations, esophagogastroscopy, and cytologic examination of the esophagus. Clinical presentations were: dysphagia, weight loss, hematemesis, hiatal hernia or previous hiatal hernia repair, heartburn, regurgitation, and heartburn and/or regurgitation. Radiologic features were: hiatal hernia, reflux, distal esophageal stricture, midesophageal stricture, mucosal abnormality, and esophageal ulcer. Histology included: villus-like folds or projections into the lumen, columnar epithelial cells with apical mucus secretory granules, goblet cells similar to those in the intestine, and mucosal glands with both mucous and goblet cells.

The authors believe their findings indicate that Barrett's esophagus is usually due to gastroesophageal reflux causing replacement of the normal squamous epithelium by columnar epithelium. The columnar epithelium is characteristically without parietal cells. Antireflux treatment in these patients will generally reverse the epithelial stricture. They therefore suggest that Barrett's esophagus, rather than representing ectopic gastric mucosa, is a part of the spectrum of reflux esophagitis.

Asher Nov

Radiological findings in Yersinia ileitis. Ekberg O, Sjoström B, Brahme F (University of Lund, Malmö General Hospital, Malmö, Sweden). *Radiology* 123:15-19, April 1977

This article is based on 51 small bowel examinations from 25 patients who underwent laparotomy and appendectomy. Surgical diagnosis was acute terminal ileitis. Bacteriologic and serologic tests were positive for Yersinia enterocolitica.

Bacteriology: *Yersinia enterocolitica* (Pasteurella X) is a gram negative rod. It is closely related to *Yersinia pseudotuberculosis* and *Yersinia pestis*. There are several serotypes which are pathogenic in man. The diagnosis is made by culture from appendix or fecal material, or serological testing. This incidence in this particular medical center is 5.6% of all patients treated for suspected appendicitis and 70% of patients in whom, at laparotomy, acute regional ileitis was observed.

Clinical features: acute gastroenteritis, fever, vomiting, diarrhea, right iliac fossa tenderness within 24 hr, erythema nodosum and/or peripheral arthritis may develop during the second week. Resolution generally takes place within 3 weeks. Neither recurrence, chronicity, or late complications are known.

Radiologic findings: three distinct features are described. These depend on the state of the disease. Transition between these forms is insidious. Abnormalities are confined to the distal 10-20 cm of the ileum. The nodular stage is seen within 3 weeks. Numerous round uniform mural nodules, ranging in size up to 1 cm are noted. Ileal wall thickening is noted and is expressed by increased distance between loops and between the ileum and the colon. Neither strictures nor ulcers were demonstrated. The diffuse edematous stage is seen during the fourth to fifth week. There is effacement of the normal mucosal fold pattern with moderate dilatation of the lumen. The stage of resolution is seen between weeks 5-8. Both small nodules and edmatous bowel are present: both show resolution and decrease in size. Abnormal findings generally disappear within 10 weeks.

The treatment of Crohn's disease and acute benign ileitis as caused by Yersinia are markedly different. Combined bacteriology, serology, and radiologic examination can establish the correct diagnosis.

Asher Nov

Pancreatic pseudocyst of the mediastinum. Kirchner SG, Heller RM, Smith C (Vanderbilt University Hospital, Nashville, Tennessee 37232). *Radiology* 123:37-42, April 1977

Two case reports and the findings of 15 additional reported cases are reviewed. Radiologic findings consisted of posterior mediastinal mass as the most common location. Route of access is generally via the aortic or esophageal hiatus. Other possibilities are via the foramen of Morgagni or diaphragmatic erosion. A mass in that location characteristically produces an anterior and lateral displacement of the lower esophagus and stomach. Other findings are pleural effusion and, at times, pancreatic calcifications. The most common etiology in adults is pancreatitis secondary to alcoholism. In children, trauma is the major cause.

Asher Nov

Accuracy of computed tomography of the liver and biliary tract. Levitt RG, Sagel SS, Stanley RJ, Jost RG (Mallinckrodt Institute of Radiology, Washington University School of Medicine, 150 South Kingshighway, St. Louis, Missouri 63110). *Radiology* 124:123-238, July 1977

Two hundred sixty-six CT scans were reviewed. Of these 212 were performed specifically to investigate liver and biliary tract, 54 were an investigation of other abdominal organs. Normal liver is found to have the uniform density with attenuation values of +40 to +70 Hounsfield units. Benign, malignant, and metastatic neoplasms are seen as low density lesions with attenuation values of 10-20 Hounsfield units. Hepatic cysts present as low density lesions with attenuation value close to water. Abscesses are visualized as low density area in the liver having attenuation values between cyst and neoplasms. Hematomas appear as low density lesion with attenuation values similar to abscesses showing a crescentic or lobulated appearance. Clinical history may aid in the diagnosis. Hepatocellular disease cannot be detected on CT scans unless the disease is advanced and causes change in size or shape of the liver, a uniform increase in attenuation such as in fatty infiltration, or increased attenuation such as in hemochromatosis. Diagnosis of obstructive jaundice can be made based on findings of dilated intrahepatic and/or extrahepatic biliary tract, seen as linear or circular structures with an attenuation value close to water and radiating peripherally from the hilus of the liver. Cause of obstruction may often be demonstrated. These include enlarged gallbladder, metastases to porta hepatis, common bile duct calculi, and carcinoma of the pancreatic head. Nonobstructive jaundice generally shows a normal appearing liver and biliary tract.

Asher Nov

Fusion anomalies of the pancreatic ductal system: differentiation from pathologic states. Belber JP, Bill K (Veterans Administration Hospital, 150 Muir Road, Martinez, California 94553). *Radiology* 122:637-642, March 1977

The embryologic development of the pancreas consists of two small ventral and caudate buds which fuse early and a second larger dorsal and cephalad bud. The ventral bud rotates and comes to lie in a dorsal position and more caudal than the dorsal bud. The ventral bud duct is the main duct emptying at the papilla of Vater, while the duct of the dorsal bud comprises the main duct of the neck, body, and tail of the pancreas. The main dorsal bud duct between point of fusion with the ventral bud duct and duodenum may either disappear, empty into the duodenum, not empty into the duodenum, or form the major source of drainage into the duodenum. The two ventral buds, if they do not unite, may each empty separately into the duodenum. If the left ventral bud does not fuse or rotate it may form an annular pancreas. A variation which may be confused with real pathology is lack of fusion between the dorsal and ventral pancreatic ducts, a variation seen in 5.5%-10% postmortem injection studies. In these cases retrograde injection of contrast material into the pancreatic duct through the papilla of Vater will fill only a small section. The question arises whether this is foreshortened by disease or due to lack of fusion. When foreshortening is due to developmental anomaly, a normal arborization pattern will be evident. On the other hand, if this is due to pathology, the normal branching pattern will not be seen.

When a small ductal system is identified emptying into both the papilla of Vater and the minor papilla, though this system is confined to the head, it indicates that ductal fusion has taken place and suggests obstruction of the dorsal pancreatic duct. The point of fusion may show a relative narrowing and should not be confused with pathology when normal branching pattern and normal ductal diameter is seen proximally.

Asher Nov

Rectal wall bleeding – an overlooked source of massive lower gastrointestinal hemorrhage. Thomson TG, Gold RE, Grace DM, Passi RB (University of Western Ontario, London, Ontario, Canada). *J Can Assoc Radiol* 28:142-145, June 1977

The authors describe their experience with two cases of massive gastrointestinal bleeding from the rectum. Both cases had previous normal sigmoidoscopic examinations. The authors emphasize the importance of including the entire rectum on the film during the angiographic examination so that this rather uncommon but important source of intestinal bleeding is not overlooked.

Jack M. Tishler

Genitourinary

Upper calyx reno-vascular obstruction in children: Fraley's syndrome. Benz G, Willich E (Universitats-Kinderklinik, Im Neuenheumer Feld 150, D-6900 Heidelberg 1, Federal Republic of Germany). *Pediatr Radiol* 5:213-218, 1977

Intrarenal vascular obstruction of the upper calcyceal infundibulum has been distinguished by Fraley as an entity separate from an asymptomatic vascular impression. Clinically, this form of intrarenal vascular obstruction presents as nephralgia or hematuria. This infundibular obstruction is caused by normal renal vessels, usually the upper segmental artery: radiologically, the vessels produce a constant well-defined filling defect in the infundibulum at IVP, and, the upper calyx group is distended and shows delay in emptying. We found this condition in 14 children from 1968-1975. Control studies showed no progression in the radiologic findings, even over a long period. In one of our cases angiography was indicated to exclude tumor or cyst; in another case, surgery was necessary. Complications are urinary tract infection or stone formation. Therefore, children with Fraley's syndrome require regular clinical examination.

Author Abstract

Evaluation of bronchospasm during excretory urography. Littner MR, Rosenfield AT, Ulreich S, Putman CE (Yale University School of Medicine, New Haven, Connecticut). *Radiology* 124:17-21, July 1977

Fifty-seven patients underwent excretory urography and were compared with eight healthy subjects who were injected intravenously with 100 ml of 5% saline. Maximal expiratory flow volume, partial expiratory flow volume, forced expiratory volume in 1 sec curves were all plotted for each subject both before injection and at 3, 10, and 20 min postinjection. Each patient provided history concerning smoking, hay fever, asthma, drug reaction, hives, food, and contrast media. Contrast was administered as 100 ml of sodium diatrizoate as a bolus or a rapid infusion of 200 ml of methylglucamine (66%) and sodium (10%) diatrizoate combination.

All 57 patients receiving contrast showed a significant decrease peak expiratory flow (PF), forced expiratory flow in 1 sec (FEV_1), and maximal expiratory flow volume, 40% (MEF 40%) as compared to preinjection studies. The 25 patients with a history of allergy had a significantly decreased PF, FEV_1, and MEF40% as compared to the 32 other patients. This was noted at the 3 min study and showed no significant difference at the 10 and 20 min. The subgroups of allergies did not show any significant differences. Control subjects showed various degrees of flushing which may be attributed to the hypertonicity of the solution but showed no difference in pre- and postinjection pulmonary studies.

This study indicates a direct and documented result of contrast material injection. It also documents no change as caused by anxiety and pain caused by injection. No subjects with previous history of allergy were clearly documented to be at a greater risk.

Asher Nov

Phlebography, urography, and lymphography in the diagnosis of metastases from testicular tumors. Lien HH, Kolbenstvedt A (Norwegian Radium Hospital, Oslo, Norway). *Acta Radiol [Diagn]* 18:177-185, March 1977

The value of pedal lymphography, urography, and phlebography of the inferior vena cava, left renal vein, and left testicular veins in the search for retroperitoneal metastases was investigated in 120 patients with testicular tumors. The number of patients with demonstrated retroperitoneal metastases was as follows: lymphography for the foot, 34; cavography, 28; urography 20; phlebography of left renal and testicular veins, 31; all examinations combined, 39. Thirty-five of the 39 patients with radiologic evidence of retroperitoneal metastases had two or more positive examiantions. Of four patients with only one positive examination, two had abnormal cavography, and two had only abnormal left testicular vein phlebography. The authors emphasize the value of left renal and testicular vein phlebography as an adjunct to pedal lymphography which remains the most sensitive of these radiographic modalities, and cite the simplicity and safety of the technique.

J. D. Harley

Urinoma. McInerney D, Jones A, Roylance J (United Bristol Hospitals, Bristol, England). *Clin Radiol* 28:345-351, May 1977

The clinical and radiological features of five patients who developed a urinoma are described and these are reviewed with cases previously reported in the literature, a total of 90 patients. Urinoma, a rare condition, is a mass formed by encapsulated extravasated urine. It may follow closed renal injury, surgery, or obstruction. The essential factors are continued renal function, rupture of the collecting system and distal obstruction. The extravasated urine is localized within the perirenal fascia and stimulates an intense fibrous reaction which forms a thick wall.

Early diagnosis is important for successful treatment. The clinical features include malaise, vague abdominal pain, weight loss, and a palpable mass. Plain films usually reveal a mass with loss of the retroperitoneal landmarks. High-dose excretion urography usually shows renal displacement, hydronephrosis, and extravasation of contrast medium into the urinoma. Should renal function be inadequate for diagnosis, renal puncture, preceded by ultrasound examination, is the investigation of choice. The anatomy of the perirenal space is discussed with an account of cadaver experiments to simulate rupture and subsequent extravasation.

T. Noel K. Allan

Musculoskeletal

Radiologic diagnosis of loosening and infection in hip prosthesis. Dussalt RG, Goldman AB, Ghelman B (Hospital for Special Surgery, New York, New York). *J Can Assoc Radiol* 28:119-123, June 1977

The authors report their experience with 39 patients with hip prostheses presenting with pain and subsequently requiring surgical intervention. Plain films of the affected hip demonstrated the following changes associated with loosening and/or infection: (1) a lucent line greater than 2 mm between opaque cement and bone, 16 of 18 patients; (2) widening of a lucent line in serial films, 7 of 7 patients; (3) fracture through the cement, 1 patient; (4) abnormal motion of the prosthesis in serial film, 3 patients; and (5) periosteal new bone formation, 15 patients.

Hip arthrography demonstrated: (1) extension of contrast material between cement and bone or between prosthesis and bone, 19 of 21 patients (absence did not exclude loosening); and (2) contrast filling of paraarticular cavities were seen in five, all subsequently shown to be infected protheses. Hip aspiration and culture was diagnostic in 60% of the authors' cases in whom infected prostheses were subsequently demonstrated.

The authors conclude that the distinction between infection and loosening without infection cannot be readily established on plain films alone. A lucent line greater than 2 mm between the opaque cement and bone, and laminated periosteal new bone formation suggested infection as did contrast filling of the paraarticular cavities on arthrograms. Arthrography in addition to hip aspiration for culture, although not definitive, correlated reasonably well with subsequent surgical findings.

J. M. Tishler

Hip joint restoration in juvenile rheumatoid arthritis. Bernstein B, Forrester D, Singsen B, King KK, Kornreich H, Hanson V (Childrens Hospital of Los Angeles, P101 Box 54700, Los Angeles, California 90054). *Arthritis Rheum* 20:1099-1104, June 1977

Six children with long standing juvenile rheumatoid arthritis and radiologic evidence of severe hip joint damage were found 6 months to 5 years afterward to have radiographic evidence of significant joint space widening and remodeling of articular surfaces. Hip function had improved in all children. Restoration of the cartilage can occur when the disease activity is controlled if associated with continued ambulation.

Author Abstract

Plant thorn synovitis. Sugarman M, Stobie DG, Quismorio FP, Terry R, Hanson V (University of Southern California, School of Medicine, 2025 Zonal Avenue, Los Angeles, California 90033). *Arthritis Rheum* 20:1125-1128, June 1977

Five children with inflammatory monoarthritis due to penetration of the joint by plant thorns mimicked the clinical and radiographic picture of juvenile rheumatoid arthritis. Chronic low grade inflammation resulted in epiphyseal overgrowth and synovial proliferation. Biopsy of the synovium demonstrated granulomatous synovitis.

D. M. Forrester

Ununited fracture of the hook of the hamate. Carter PR, Eateon RG, Littler JW (Roosevelt Hospital, 3600 Gaston Avenue, Dallas, Texas), *Bone Joint Surg* [Am] 59:583-588, July 1977

Patients having localized pain over the hamate following trauma are prime suspects for a fracture of the hook of the hamate. Unfortunately this injury is difficult to visualize with routine films. Even carpal-tunnel views often fail to show this fracture acutely because the patient is in a painful condition and cannot extend his wrist sufficiently to obtain an optional radiograph. This unusual fracture may not be rare, rather rarely demonstrated. In the acute situation, lateral tomograms may be required. If the fracture is immobilized promptly it normally heals, however if not immobilized some of these fractures become chronically painful and require careful surgical removal of the ununited segment of the fracture. Surgical excision permits early return of function, especially in athletes and laborers who must be able to grip hard objects very firmly.

Gerald R. Smith

Bone scanning in the evaluation of exercise-related stress injuries. Wilcox JR Jr, Moniot AL, Green JP (Naval Regional Medical Center, San Diego, California). *Radiology* 123:699-703, June 1977

Bone scintigraphy was used to evaluate 34 patients with the physical findings and history of stress fracture of the lower extremity. Of the 34, 21 had abnormal studies, 11 involving the femoral neck, 9 the tibia, and 1 the femur. All of these had abnormal scintiscans prior to or at the time of the appearance of radiographic changes. Of the 9 with abnormal tibial studies, radiographic changes never evolved in 3. No false negatives were found among the 13 with normal scintiscans.

Author Abstract

Ewing's tumour of rib. Branson J (St. Vincent's Hospital, Sydney, Australia). *Australas Radiol* 20:341-345, Dec 1976

The series consists of four cases of Ewing's tumor of the rib. All patients were in their second decade, three males and one female. All patients presented with the typical clinical features of localized chest pain of several months duration and in two cases with tenderness and swelling. In all cases the plain chest x-ray demonstrated a soft tissue mass which was intrathoracic but extrapulmonary, and in three cases this mass was very large. The rib lesions were not always well defined unless well penetrated films of the ribs were taken. When this was done the radiologic changes seen were those of lytic bone destruction and periosteal new bone formation. In no case was the so-called typical "onion skin" appearance demonstrated. The author stresses that well penetrated radiographs should be made and that the presence of an intrathoracic extrapulmonary mass associated with the typical bone features in a person of the appropriate age should be enough to alert the physician to consider the diagnosis of Ewing's tumor.

T. J. Hanks

The radiology of the hip joints and pelvis in cerebral palsy. Griffiths GJ, Evans KT, Roberts GM, Lloyd KN (Welsh National School of Medicine, Cardiff, Wales). *Clin Radiol* 28:187-191, March 1977

The radiologic appearances found in the pelvis and hip joints in 79 patients with cerebral palsy, aged 5-16 years, were studied. These findings were correlated with the clinical severity and distribution of the disease. Subluxation of the hip joints was found in 14% and dislocation in an additional 6%. Spasticity was the predominant neuromuscular handicap in 69 of 79 cases (88%). The acetabular angle and femoral neck shaft angle were related to the degree of migration of the femoral head. The acetabular angle, iliac angle, iliac index, and femoral neck shaft angle were all significantly increased in the deranged group. In the dislocated group, the mean neck-shaft angle was 154°. When the degree of spasticity was asymmetrical, there was a striking relationship between the laterality of the spasticity and the laterality of the deranged hip, pelvic obliquity, and increased acetabular angle. A typical teardrop-shaped femoral head was seen in 48%, spina bifida occulta in 3.8%. No ectopic calcification or ossification of soft tissue was noted. An awareness that these children are at risk from subluxation and dislocation of the hip and the importance of early diagnosis and treatment are emphasized.

Author Abstract

Fracture of the hook of the hamate in athletes. Star HH, Job FW, Boyes JH, Ashworth CR, (2300 South Hope Street, Los Angeles, California 90007), *J Bone Joint Surg* [Am] 59:575-582, July 1977

In a series of 20 cases of fracture of the hook of the hamate in athletes, the authors have concluded that the injury occurs when direct trauma hits the hook of the hamate. They doubt that the injury is a ligamentous or tendon stress. This type of fracture should be suspected in athletes such as baseball and tennis players and golfers who complain of persistent pain over palmar aspect of the wrist. The carpal tunnel view properly performed helps establish the diagnosis. The fractured hook should be removed since removal eliminates symptoms and decreases the likelihood of subsequent rupture of the flexor tendons. Excellent radiographs and line drawings clarify the radiologic and surgical approach to this problem.

Gerald R. Smith

Nervous System

Intracranial infections: investigation by computerized axial tomography. Claveria LE, du Boulay GH, Moseley IF (National Hospital, Queen Square, London WC1N 3BG, England) *Neuroradiology* 12:59-71, Nov 1976

The authors report their experience in 51 patients with proven intracranial infections who were studied with a 160 × 160 matrix EMI scanner. The diagnosis and localization of cerebral abscess was correct in 24 of 26 cases (92%). Most abscesses could be characterized as low density areas which showed smooth uniform capsular visualization after contrast enhancement, surrounding cerebral edema, and relatively small mass effect. Contrast enhancement was observed as early as the second day after the onset of neurological symptoms and usually disappeared after successful surgical drainage. Small abscesses and granulomas showed homogenous contrast enhancement of the entire lesion. The typical appearance of a brain abscess was closely mimicked by cystic gliomas and metastatic tumor. However, these lesions tended to have higher CT density, a more irregular capsule, and more marked mass effect. Some infarcts also show peripheral contrast enhancement. Again this enhancement was not as regular in contour or as uniform in thickness as the typical abscess. Five patients with herpes encephalitis demonstrated extensive low density lesions in the temporal lobes (bilateral in one case) without contrast enhancement or mass effect. In two of these cases the internal capsule was also involved and both had profound hemiplegia. In seven cases with generalized encephalitis and 12 with meningitis, all had normal CT scans except for one patient with tuberculous meningitis who had hydrocephalus.

Paul M. Chikos

Usefulness of coronal sections in computed tomography of the head. Takahashi M, Tamakawa Y, Odani R, Nakano Y, Arii H, Shindo M (Akita University School of Medicine, Akita, Japan). *Nippon Acta Radiol* 37:531-539, June 1977

Using the ACTA Scanner 0100 equipped with a tilting gantry and a computer program requiring no water bag, coronal sections were obtained in addition to transverse axial sections in the diagnosis of intracranial and facial diseases. The neck was hyperextended in prone and supine positions and the central x-ray was directed perpendicularly to the orbitomeatal line. Special immobilization devices were introduced in order to obtain good immobilization and hyperextension of the neck. Coronal sections were useful in 35 of 65 examinations and the value of this technique was demonstrated in central cerebral tumors, high convexity tumors, and tumors adjacent to and involving the skull base. Lesions of the orbits and paranasal sinuses were evaluated with this technique to good advantage. This technique was indispensable in the evaluation of intracranial and facial diseases.

Mutsumasa Takahashi

Cerebral abscess with special reference to the angiographic changes. Nielsen H, Halaburt H (Rigshospitalet, DK-2100, Copenhagen, Denmark). *Neuroradiology* 12:73-78, Nov 1976

The authors report their experience with 40 patients in whom angiography was performed preoperatively and a cerebral abscess identified at surgery. All abscesses were supratentoral and most often in a frontal location (37.2%). The angiogram was abnormal in all but one case. Common angiographic findings included: displaced arteries in 38 cases (95%), segmental arterial constriction in 33 (82.5%), avascular radiolucent area in 33 (82.5%) and displaced veins in 30 (75%). In 19 cases (47.5%) a definite abscess capsule was identified and the specific diagnosis of abscess made. The capsule was defined as a hypervascular blush which appears in the capillary phase, persists into the late venous phase, and was often best seen on the subtracted lateral view. This blush was attributed to vascular proliferation superimposed on compressed vessels at the periphery of the abscess. Capsule formation was identified in nine of 18 (50%) cases studied within the first 10 days of clinical symptoms and did not appear to occur more frequently with a longer duration of clinical symptoms.

Paul M. Chikos

Diagnosis of intrasellar cisternal herniation (empty sella) by computer assisted tomography. Bajraktari X, Bergstrom M, Brismar K, Goulatia R, Greite T, Grepe A (Karolinska Sjukhuset 5-10401, Stockholm, Sweden). *J Computer Assisted Tomography* 1:105-116, Jan 1977

Twenty-six cases of "empty-sella" syndrome proven by pneumoencephalography were examined by CT techniques. The CT scan was sometimes helpful but results indicated that the potential of CT in revealing intrasellar cisternal herniation is limited.

Michael J. Meagher

Computer assisted tomography in 90 cases of exophthalmos. Salvolini U, Menichelli F, Pasquini U (Ospedale Civile Umberto 1°, Ancona, Italy). *J Computer Assisted Tomography* 1:81-100, Jan 1977

The first 90 cases of proptosis examined by CT in the authors' institution are presented. Forty-seven tumor and 43 nontumor lesions are shown in an "atlas" type format. Reproduction quality is quite good, with clear definition of the lateral rectus musculature.

Michael J. Meagher

Dynamic positron emission tomography for study of cerebral hemodynamics in a cross section of the head using positron-emitting 68 Ga-EDTA and 77 Kr. Yamamoto Y, Thompson C, Meyer E, Robertson J, Feindel W (Montreal Neurological Institute, Quebec H3A 2B4, Canada). *J Computer Assisted Tomography* 1:43-56, Jan 1977

Emission tomographic studies on 120 patients with various forms of intracranial pathology are reviewed. The patients were scanned with a positron detecting ring device. Radiopharmaceuticals used were 68-EDTA for transit time and uptake studies; 77 Kr for quantitation of regional cerebral blood flow, producing whole body exposures of 60-120 mrads and 4-8 mrads respectively. Scans of patients with arteriovenous malformations, intracranial tumors, and cerebrovascular occlusive disease showed that useful information can be gained from this technique, although current resolution capability is marginal (3 cm at full width, half maximum).

Michael J. Meagher

Variation with time of the attenuation values of intracranial hematomas. Bergstrom M, Ericson K, Levander B, Svenson P, Larson S (Karolinska Sjukhuset, 5-10401, Stockholm, Sweden). *J Computer Assisted Tomography* 1:57-63, Jan 1977

Fourteen cases of intra and extraaxial intracranial hematomas were examined. Six cases were either subdural or epidural, eight were intracerebral. Various densities (20-60 Hounsfield units) were observed within the hematomas and closely approximated values obtained by direct measurement of the clot density at surgery. A monoexponential function was developed which describes the decrease in density seen with time in both types of hematomas. The authors suggest that the high attenuation values of fresh hematomas are due to clot retraction.

Michael J. Meagher

Ring blush associated with intracerebral hematoma. Zimmerman RD, Leeds NE, Naidich TP (Albert Einstein College of Medicine, Bronx, New York 10461). *Radiology* 122:707-711, March 1977

Seven patients with intracerebral hematoma are presented in whom the transitory phenomenon of a ring blush was seen. The ring blush is seen on contrast-enhanced CT scans from 6 days to 6 weeks postictus. The ring measures 3-6 mm in width and is localized to the periphery of the lesion. Clear-cut correlation was not seen in either angiography, radionuclide brain images, surgery, or pathology. A ring blush was previously reported in primary and metastatic neoplasms, infarction, abscess, and is to be viewed as a nonspecific finding. Proposed mechanism for this phenomena are: (1) limited hypervascularity in surrounding granulation tissue; (2) extravasation of contrast material due to blood brain barrier breakdown; and (3) loss of autoregulation with luxury perfusion. A ring blush is to be interpreted within the context of the total clinical picture, a definitive diagnosis being made only if serial scans are done over an adequate interval of time. A ring blush due to intracerebral hematoma will continue to diminish in size and decrease in attenuation until it eventually disappears. As opposed to the situation in neoplasm or infection, the ring blush of hematoma is usually present at a stage when a mass effect is no longer seen.

Asher Nov

Dense intracranial epidermoid tumors. Braun IR, Naidich TP, Leeds NE, Koslow M, Zimmerman HM, Chase NE (Montefiore Hospital, 111 East 210 Street, Bronx, New York 10467. *Radiology* 122:717-719, March 1977

Epidermoid tumors may appear as sharply marginated, dense lesions measuring 80-120 Hounsfield units on noncontrast CT scans rather than as the homogeneously lucent lesions measuring −8 to +32 Hounsfield units previously described. The characteristic density range and the lack of contrast enhancement distinguish dense epidermoid tumors from other lesions.

Author Abstract

Pediatric Radiology

Infantile hepatic hemangioendotheliomas associated with hemihypertrophy. Wood BP, Putman TC, Chacko AK (University of Rochester Medical Center, 601 Elmwood Avenue, Rochester, New York 14642). *Pediatr Radiol* 5:242-245, 1977

An infant presented with congenital hemihypertrophy, hepatomegaly, and a low thoracic paraspinal mass. Liver scan showed multiple defects in the uptake of radioisotope. Surgical exploration revealed multiple infantile hemangioendotheliomas of the liver and a paraspinal hemangioendothelioma. In review of 69 reported cases of this entity in the liver and viscera, there has been no previous note of hemihypertrophy associated with this abnormality.

Author Abstract

Metatropic dwarfism and its variants. Kozlowski K, Morris L, Reinwein H, Sprague P, Tamaela LA (Royal Alexandra Hospital for Children, Sydney, Australia). *Australas Radiol* 20:367-385, Dec 1976

Metatropic dwarfism is a rare type of bone dysplasia which occasionally has a fatal outcome. The disease was separated from the group of "unclassified" congenital bone disorders by Maroteaux, Spranger, and Wiedemann in 1966 on the basis of six personal cases and 12 cases previously published under erroneous titles such as achondroplasia or Morquio's disease. Since 1966 about 20 patients have been reported under the diagnosis of metatropic dwarfism.

The authors comprehensively review the condition and suggest that not all of the 12 cases published prior to the original Maroteaux paper can be categorized as metatropic dwarfism with certainty, and similarly not all of those patients reported since as metatropic dwarfism have shown the same symptoms as patients in Maroteaux's description.

The authors report six cases of metatropic dwarfism or its variants, four of which are the first Australian cases, and one of which is the first Indonesian case. They note that long term observations in severe neonatal dysplasias are now to be expected because of improving postnatal care and suggest that when the radiographic diagnosis of a bone dysplasia is unknown or uncertain, long term observation, familial studies, microscopic, ultrastructural, and biochemical studies of cartilage may aid in a more accurate diagnosis.

T. J. Hanks

The arteriographic manifestations of Takayasu's arteritis in children. Goldin RL, Perri G, Cremin BJ (Groote Schuur Hospital Observatory, Cape Town, South Africa). *Pediatr Radiol* 5:224-230, 1977

Eighteen children, 4-13 years of age, were seen at the University of Cape Town Teaching Hospitals from 1967 to 1976 and diagnosed as Takayasu's arteritis by aortography. There were 10 females and eight males. Clinical manifestations ranged from minor ischemia to severe hypertension and congestive heart failure. On aortography, there may be tortuosity, stenosis, aneurysm formation, obstruction, or irregularity of the wall. Findings were commonest in the abdominal aorta, then in the descending aorta. Aortitis associated with main branch lesions at the same level was the most common finding but branch lesions did occur without associated aortic lesions. Stenotic lesions occurred commonly, particularly renal artery stenosis associated with hypertension. Occlusion was common in branches but rare in the aorta itself. Aneurysms were seen in all segments of the aorta except the arch. Emphasis is placed on total aortography in assessment of these patients.

B. J. Wood

Radiographic findings in early onset neonatal group B streptococcal septicemia. Leonidas JC, Hall RT, Beatty EC, Fellows RA (Boston Floating Hospital, 171 Harrison Avenue, Boston Massachusetts 02111.) *Pediatrics* 59:1006-1011, 1977

Chest roentgenograms obtained in the first 2 days of life of 67 infants with respiratory distress were reviewed to determine whether the radiographic features of group B streptococcal septicemia were diagnostic or distinctive. The retrospective review contained 24 infants with proven and 14 with suspected septicemia, as well as 29 patients with other causes of respiratory distress. The films were reviewed in random order by two pediatric radiologists without their prior knowledge of clinical or laboratory data. Typical radiographic appearance of pneumonia was present in only 10 of the 24 proven and two of the 14 suspected cases of group B streptococcal sepsis. The radiographic pattern of respiratory distress syndrome was just as common among these patients. The most prominent associated radiographic feature of infants with proven septicemia was cardiomegaly which was significantly increased when compared with infants who had other causes of respiratory distress ($P < .001$). X-ray recognition of neonatal group B streptococcal septicemia is limited because of superimposition of roentgen patterns probably related to associated disorders.

Author Abstract

Urinary tract anomalies in neonates with spontaneous pneumothorax and/or pneumomediastinum. Bashour BN, Balfe JW (Hospital for Sick Children, 555 University Avenue, Toronto, Ontario M5G 1X8, Canada). *Pediatrics* 59:1048-1049, 1977

All cases of spontaneous pneumothorax and/or pneumomediastinum, and of congenital urinary tract anomalies among 6,236 neonates between 1961-1967 were reviewed. Eighty-seven infants fell into these categories. Bilateral renal agenesis cases were excluded as were infants who had had resuscitation or assisted ventilation. Thirty-eight infants had lung rupture only, 40 had urinary tract anomalies only, and nine had both. This association of lung rupture and urinary tract anomaly is highly significant. All nine infants having both died from respiratory failure within the first 24 hr. Renal anomalies were: infantile polycystic kidneys, three; posterior urethral valves, two; hypoplasia of the kidney, two; multicystic kidney, one; and dysplasia, one.

B. J. Wood

Bronchopulmonary dysplasia in premature infants. Oppermann HC, Wille L, Bleyl U, Obladen M (Rontgenabteilung, Universitats-Kinderklinik, im Neuenheimer Feld 150, D-6900 Heidelberg 1, Federal Republic of Germany) *Pediatr Radiol* 5:137-141, March 1977

In a group of 70 premature and newborn infants treated with artificial ventilation, 24.3% developed bronchopulmonary dysplasia (BPD). Only in a very few cases did the typical radiologic stages, as described by Northway, succeed each other in a chronological order. It is impossible to differentiate BPD stage I or II from RDS stage III and IV without a knowledge of the clinical course and of the duration of artificial ventilation. The lower the gestational age, the more severe and earlier do the radiologic and histologic changes occur. The radiologic differential diagnosis of BPD includes Wilson-Mikity syndrome, congenital pulmonary lymphangiectasia, neonatal tuberculosis, cystic fibrosis, and Hamman-Rich syndrome.

Author Abstract

Radiographic features of fucosidosis. Lee FA, Donnell GN, Gwinn JL (Childrens Hospital, P.O. Box 54700, Los Angeles, California 90054). *Pediatr Radiol* 5:204-208, 1977

Fucosidosis is an uncommonly recognized lysosomal storage disease which presents with psychomotor deterioration and which progresses in some cases to death. The roentgenographic findings in five boys from three families are described. Skeletal abnormalities of a dysostosis multiplex nature are present and though not diagnostic should direct the clinician to perform appropriate biochemical and tissue assay studies to establish the diagnosis.

Author Abstract

Intractable diarrhea in a boy with vasoactive intestinal peptide-producing ganglioneuroblastoma. Jansen-Goemans A, Engelhardt J (Zuiderziekenhuis, Groeneveld 15, Rotterdam 24, The Netherlands). *Pediatrics* 59:710-716, May 1977

A 1-year-old boy had intractable diarrhea and symptoms of the watery-diarrhea-hypokalemia-achlorhydria (WDHA) syndrome, a well-known entity in adults. Resection of a ganglioneuroblastoma situated in the neck caused prompt relief of symptoms. The ganglioneuroblastoma in this instance contained the enterohormone vasoactive intestinal peptide (VIP); blood levels of this peptide were elevated preoperatively. After tumor resection, the VIP level returned to normal and the diarrhea ceased on the day of the operation. The genesis of the diarrhea in relation to the production of polypeptides from neuroendocrine origin is discussed (APUD-cell concept). VIP may be the mediator in the WDHA syndrome in ganglioneuroblastoma.

Author Abstract

Miscellaneous

Single view negataive mode xeromammography: an approach to reduce radiation exposure in breast cancer screening. Buchanan JB, Jager RM (University of Louisville School of Medicine, Louisville, Kentucky 40201). *Radiology* 123:63-68, April 1977

Xeromammograms of 60 patients detected as having breast cancer out of 10,000 asymptomatic women and 100 patients out of 3,000 symptomatic women were reviewed. Three radiologists reviewed a single view: mediolateral negative mode xeromammogram or craniocaudad view. These were rated as:

(1) no evidence of breast cancer; (2) strong evidence of breast cancer; (3) equivocal, necessitating an additional view.

Of the 60 asymptomatic patients with biopsy proven cancer, 59 patients could have been diagnosed using the mediolateral view only. A single case necessitated the additional craniocaudal view. Of the 100 symptomatic patients, 99 could have been diagnosed using the mediolateral view only. Using the craniocaudal view, 55 of the 60 patients could have been diagnosed; and 91 of the 100 symptomatic patients. Skin radiation exposure measured in rads: positive mode—mediolateral view, 0.95; craniocaudal view, 0.90; both views, 1.85. Negative mode measured: mediolateral view, 0.77; craniocaudal view, 0.72; both views, 1.49. Current dose of radiation is 2-5 rads to the skin. Using single view negative mode xeromammography the dose can be decreased from 1.85 rads to 0.77 rads.

This single, mediolateral, negative mode xeromammograph having both diagnostic accuracy and low dosage is recommended as a screening modality. In cases of questionable diagnosis an additional view should be obtained. It is stressed that data is as yet limited but appears promising.

Asher Nov

Lymphography in malignant ovarian tumors (in German). Kwasny R, Fuchs WA (Institut fuer Diagnostische Radiologie der Universitaet Bern, Inselspital, 3010 Bern, Switzerland). *Fortschr Geb Roentgenstr Nuklearmed* 126:564–566, June 1977

Lymphography was performed in 81 patients with malignant ovarian tumors. The diagnosis of nodal metastasis was made when solitary or multiple, well demarcated filling defects of at least 1 cm in diameter with destruction of the peripheral sinuses were encountered in the regional lymph nodes (paraaortic lymph nodes at the level of L2-3 and external iliac lymph nodes) and when obstruction of lymphatic circulation due to malignant infiltration was evident. In 22 (21%) patients, lymphography was abnormal for tumor; in five (17%) of 30 patients with stage I disease (tumor confined to the ovaries, uni- or bilaterally); in four (21%) of 19 patients with stage II disease (tumor in one or both ovaries with pelvic extension); in four (19%) of 21 patients with stage III disease (tumor in one or both ovaries with intraperitoneal metastasis outside the pelvis); and in nine (82%) of 11 patients with stage IV disease (tumor in one or both ovaries with distant metastasis). The paraaortic lymph nodes at the level of L2-3 were involved in eight (36%) patients, the iliac lymph nodes in five (24%), and both the paraaortic and iliac lymph nodes in nine (40%). The location of the lymphatic metastasis was independent of the different clinical stages. Lymphographic evidence of metastatic involvement of the inguinal lymph nodes was not observed.

Peter F. Winter

Persistence of contrast medium in lymph nodes as a prognostic criterion in Hodgkin's disease (in German). Roxin T, Leahu S, Bujar H (Institutul de Medicina Interna, N. Gh. Lupu, Sos. Stefan cel Mare, 19-21, 72202 Bukarest, Romania). *Fortschr Geb Roentgenstr Nuklearmed* 126:567-570, June 1977

Following lymphography in 104 patients with Hodgkin's disease, the persistence of retained lipiodol in the inguinal and retroperitoneal lymph nodes was observed on follow-up radiographs obtained at regular intervals. In patients with normal lymphograms, an amount of contrast medium sufficient for interpretation remained in the external iliac nodes for an average period of 12 months, in the superior paraaortic nodes for an average of 8 months, and in the inguinal, common iliac, and inferior paraaortic nodes for an average of 4 months. In patients with abnormal lymphograms, the average time of retained contrast medium was prolonged; in external iliac nodes the period was 18 months; in superior paraaortic nodes, 10 months; in inguinal nodes, 8 months; and in common iliac and inferior paraaortic nodes, 6 months.

In the abnormal lymph nodes, the persistence of contrast medium related to histologic type: in patients with lymphocyte predominence or nodular sclerosing type of Hodgkin's disease, the average period was 12 months, while in patients with lymphocyte depletion type, the average period was 6 months. In patients with mixed cellularity type, the persistence of contrast medium varied considerably, with an average of 10 months. In addition, the persistence of contrast medium depended on the lymphographic findings: lymph nodes with lacunar defects retained the contrast medium for a longer period, occasionally up to 36 months, whereas lymph nodes with a reticular pattern of filling defects lost contrast medium more rapidly.

Peter F. Winter

Nuclear Medicine

Radioisotopic study of the adrenal glands using ^{131}I-19-iodocholesterol. Troncone L, Galli G, Salvo D, Barbarino A, Bonomo L (Catholic University of Sacred Heart, Rome, Italy) *Br J Radiol* 50:340-349, May 1977.

Scintigraphy of the adrenal gland with ^{131}-I-19-iodocholesterol has recently been added to radiologic techniques in adrenal imaging and has been used successfully to demonstrate anatomic and functional disorders of the adrenals in a variety of clinical situations. A review of the authors' experience stresses the diagnostic value of this method. Radiologic findings and results of scintillation imaging are complementary: their comparison improves and clarifies indications for scintigraphy. Hyperadrenal cortical diseases always gave satisfactory scintigrams, the most interesting results being obtained in adrenal cortical hyperplasia and unilateral hyperfunctioning adenomas. In these cases the evaluation of the response to stimulation or suppression tests was very useful. Scintigraphy was less valuable in demonstrating malignant and nonmalignant tumours.

Author Abstract

Cardiac localization of ^{99m}Tc-(Sn)-pyrophosphate following irradiation of the chest. Soin JS, Cox JD, Youker JE, Swartz HM (Medical College of Wisconsin, Milwaukee, Wisconsin). *Radiology* 124:165-168, July 1977

Seventy patients referred from radiation therapy for bone imaging were evaluated for cardiac uptake of the bone imaging agent. This group was further subdivided into 32 patients who had left hemithorax radiation and 38 patients who did not. These patients were compared to a randomly selected group of 70 nonirradiated patients. All patients were given 15mCi of ^{99m}Tc-(Sn)-pyrophosphate and imaged with an Anger type gamma camera, using a whole body table. In most patients, close-up anterior and left lateral views of the chest were obtained. Cardiac uptake was graded from 0 to 3 depending on the amount of uptake relative to overlying ribs. Sixty percent of the patients with prior left hemithorax irradiation had uptake. Only 12% of the 38 patients who received radiation therapy to other areas of the body showed cardiac uptake. Nine percent of the randomly selected nonirradiated group showed uptake. The cardiac uptake was generally diffuse and appeared to increase as a function of time postirradiation. The mechanism of cardiac localization of pyrophosphate following radiation therapy is undetermined at present. The pathologic and clinical significance is also uncertain. When interpreting pyrophosphate cardiac images for the possibility of acute infarction, prior radiation therapy should be considered in the differential diagnosis of a positive study.

Thomas G. Rudd

Gallium-67 citrate imaging in Hodgkin's disease: final report of cooperative group. Johnston GS, Go MF, Benua RS, Larson SM, Andrews GA, Hubner KF (National Institutes of Health, Bethesda, Maryland). *J Nucl Med* 18:692-698, 1977

An interinstitutional study to assess the value of ^{67}Ga imaging in Hodgkin's disease is reported: 248 untreated, and 420 treated patients were studied. All patients were given approximately 50 μCi of ^{67}Ga per kg body weight. Images were made at 48 or 72 hr. All studies were done with a rectilinear scanner using a single window set for 160 to 320 KeV. Eighty-eight percent of the untreated and 56% of the treated patients had abnormal images. Tumor histology had little effect on the incidence of abnormal scans except for the lymphocyte-predominant type which gave a significantly lower percentage of abnormal scans before and after treatment. The sensitivity for detecting tumor at individual sites was considerably lower, averaging about 60%. Again, the incidence of abnormal scans was much lower in the treated group, regardless of whether they received chemotherapy or radiation therapy. The false positive rate in patients with surgically explored sites was about 6%. In addition, a small number of nonmalignant lesions showed a positive scan.

Abnormal scan findings were found in up to 26% of sites in which disease was unsuspected before the scan was performed. Of sites where disease was subsequently proven to exist, the scan detected unsuspected disease 13% of the time. As expected, the gallium scan had the highest incidence of abnormality in the neck and thorax (80%-90%), and the lowest incidence in the abdomen and inguinal-femoral regions (48%). Tumor size was an important limitation. No lesions less than 1 cm in size were detected by gallium imaging. The reliability of detection increased linearly with lesion size up to 5 cm in diameter. Lesions larger than 5 cm tended to have a lower incidence of abnormality by gallium imaging, presumably due to impaired blood supply to the larger lesions. Gallium imaging and lymphangiography had approximately equal sensitivity and specificity for detecting intraabdominal disease.

A significant number of asymptomatic patients were demonstrated to have abnormal gallium scans during routine follow-up. The application of routine gallium imaging to the follow-up of treated patients deserves additional scrutiny.

Thomas G. Rudd

A clinical comparison of Xe-127 and Xe-133 for ventilation studies. Atkins HL, Susskind H, Klopper JF, Ansari AN, Richards P, Fairchild RG (Brookhaven National Laboratory, Upton, New York 11973). *J Nucl Med* 18:653-659, 1977

Xenon-133 and xenon-127 were compared by performing ventilation studies with both radionuclides in 19 patients with a variety of lung diseases. Assessment of the counting rate over the chest, relative to the radioactivity in the lungs, permitted the evaluation of each isotope in terms of usable photons detected by a scintillation camera with a large field of view and appropriate collimation. A greater photon yield was obtained with Xe-127. Markedly improved resolution was shown by measurement of a line phantom, but was not apparent on subjective appraisal of scintiphotos except in the washout phase. Xenon-127 appears to be preferable to Xe-133 because of the higher counting rates, lower patient radiation dose, and longer shelf life. In addition, a prior perfusion study using a TC-99m radiopharmaceutical does not affect the quality of a Xe-127 ventilation study. The use of Xe-127 therefore permits the selection for ventilation studies of only those patients with suspected pulmonary embolism, and eliminates unnecessary radiation exposure. A further improvement in image quality obtained with Xe-127 should be possible with certain modifications of the scintillation camera that would permit use of the 375-keV photopeak along with the 172- and 203-keV gamma energies. Charcoal traps designed for Xe-133 will require additional shielding and longer storage time when used for Xe-127. Xenon-127, however, might be used again after appropriate processing.

Author Abstract

Location and size of acute transmural myocardial infarction estimated from thallium-201 scintiscans. A clinicopathological study. Wackers FJT, Becker AE, Samson G, Busemann Sokole E, Van Der Schoot JB, Vet AJTM, Lie K, Durrer D, Wellens H (Yale University School of Medicine, New Haven, Connecticut 06510). *Circulation* 56:72-78, July 1977

A clinicopathologic study was performed in 23 patients who died from acute transmural myocardial infarction. They had been studied with electrocardiograms and thallium-201 scans during the acute phase. There was agreement in 91% of the studies between scintigraphic and postmortem location of infarction in 70% between the ECG and postmortem findings. It was concluded that thallium scintigraphy provided more precise location of infarction than the ECG and that the size of the scintigraphically abnormal area reflected the extent of necrotic myocardium.

R. S. Frech

Scintigraphic evaluation of lymphoma: a comparative study of ^{67}Ga-citrate and ^{111}In-bleomycin. Bekerman C, Moran EM, Hoffer PB, Hendrix RW, Gottschalk A (E. M. Moran, University of Chicago, Chicago, Illinois). *Radiology* 123:687-694, June 1977

Sequential whole-body scans with both ^{67}Ga-citrate and ^{111}In-bleomycin were performed for 14 patients undergoing staging for Hodgkin's disease or other lymphomas. A comparison of these scans gave a sensitivity in detecting the pathologically-proved tumor sites of 84% for ^{67}Ga-citrate and only 56% for ^{111}In-bleomycin. In 12 patients, the gallium scan demonstrated the lesions more clearly; in the others, the uptake of the two radionuclides was equal. In no case was a clinically diagnosed or histologically proved lesion identified by ^{111}In-bleomycin that was not also demonstrated by ^{67}Ga-citrate. ^{111}In-bleomycin does not complement the ^{67}Ga-citrate scan in the scintigraphic evaluation of lymphomas.

Author Abstract

Diagnosis of angiotensinogenic hypertension: the complementary roles of renal scintigraphy and the saralasin infusion test. McAfee JG, Thomas FD, Grossman Z, Streeten DHP, Dailey E, Gagne G (SUNY Upstate Medical Center, Syracuse, New York 13210). *J Nucl Med* 18:669-675, 1977

A recently developed 1-day screening procedure for angiotensinogenic ("high-renin") hypertension is based on (A) a fall in blood pressure in response to intravenous infusion of the angiotensin antagonist, saralasin (P-113), and (B) peripheral venous renin assays by radioimmunoassay, in a sodium-depleted state. Out of 700 hypertensive patients screened by these tests, 160 had renal imaging performed with technetium-99m glucoheptonate and iodine-131 Hippuran. The P-113 infusion test proved superior to peripheral venous renin assays for the detection of angiotensinogenic hypertension. Positive infusion tests correlated well with renal vein renin assays. Frequently, however, both these tests were positive with bilateral renal disease and/or malignant hypertension. While renal imaging proved valuable in indicating which patients had a unilateral abnormality, it frequently could not distinguish unilateral renovascular disease from unilateral parenchymal disease unrelated to angiotensinogenic hypertension. Twenty-five patients in this series had arteriographic renal artery stenosis, of whom 3 had false negative P-113 infusion tests, 9 had negative peripheral renin assays, and 3 had no imaging abnormalities. This study indicates that scintigraphy is a useful procedure for the investigation of hypertensive patients when the initial P-113 infusion test is positive, or discordant with other findings. By imaging, angiotensinogenic hypertension due to bilateral renal disease can be distinguished from unilateral renovascular disease, and the site of the ischemic renal tissue can usually be identified.

Author Abstract

Scintigraphic patterns of gallium-67 uptake in the breast. Kim YC, Brown ML, Thrall JH (University of Michigan Medical Center, Ann Arbor, Michigan). *Radiology* 124:169–175, July 1977

A review of 542 consecutive whole body Ga-67 citrate scans obtained over a 30 month period were analyzed to determine the presence of increased tracer concentration in the breast. The dose of gallium was 50 μCi per kg of body weight and images were obtained 48 to 72 hr after injection. All studies were performed with a dual probe rectilinear scanner, using a window setting of 80 to 440 KeV.

Of 542 patients, 32 demonstrated significant breast uptake. There were 31 women and one man in the group. Three patients had abnormal scans secondary to pathologic lesions in the breast, including one primary adenocarcinoma, and one patient with histiocytic lymphoma involving the breast. These three patients had asymmetric breast uptake. The remaining 29 patients all had symmetric breast uptake which fell into three basic patterns: (1) the "doughnut" pattern in which the peripheral breast activity was greater than the subareolar region; (2) the "subareolar" pattern in which subareolar localization was greater than in the periphery; and (3) "diffuse" pattern in which activity was uniform throughout the breast. The doughnut pattern tended to be associated with hyperprolactinemia and was seen in postpartum patients and patients in chronic renal failure. The subareolar pattern was seen in 15 patients, and was associated with the administration of estrogen containing compounds. In addition, three patients not on estrogen therapy but taking drugs which included meprobamate, reserpine, and compazine, had this pattern. The diffuse pattern was seen in five obese individuals on no medication and in an additional four patients who were taking a variety of medications. The degree and the type of breast uptake of Ga-67 citrate depends on the underlying stimulus. Asymmetric breast uptake should raise the suspicion of a significant pathologic lesion.

Thomas G. Rudd

Radiation Oncology

The role of radiotherapy in treatment of inoperable lung cancer. Berry RJ, Laing AH (Middlesex Hospital Medical School, London W1P 7PN, England). *Int J Radiat Oncol Biol-Phys* 2:433–439, May–June 1977

The results of the second Oxford lung cancer trial involving 148 patients in the "mandatory treatment arm" are presented. Inoperable patients were assigned randomly and prospectively to one of three treatment groups: radiotherapy, 48; procarbazine continuous chemotherapy, 49; or intermittent quadruple chemotherapy, 51 (Mustargen, Velban, Natulan, Prednisone). Only six patients were symptom-free on entry. There was no difference in survival among the three groups (12% 1 year survival, median survival 125 days). Radiotherapy was completed as planned in 79% (38/48) versus 42% (21/49) and 50% (26/51) in the single and multiple drug groups, respectively. The primary tumor became smaller in 44%, 24%, and 39% respectively. Troublesome symptoms were not controlled until death in 50%, 65%, and 45%, respectively. Doses of irradiation were 4,000 rads/25Rx/25 days (<150 cm two fields) and 3,500 rads/20Rx/25 days (>150 cm two fields).

The authors feel that when assessed both by survival and quality of remaining life, the best treatment for the majority of inoperable bronchus cancers is no specific anticancer therapy based on the results of this and the earlier Oxford trial. The exceptions are in small cell cancer bronchus patients, small "curable" primaries of other cell types, and in palliation of SVC syndrome, hemoptysis, and possible osseous metastases.

Herbert C. Berry

Results of cobalt therapy of carcinoma of the larynx. Ghilezan N (Institut Oncologique de Cluj-Naposa, Roumania). *J Radiol Electrol Med Nucl* 58:353–358, May 1977

Cancer of the larynx offers the radiation therapist the most gratifying results for cure and long term survival. The superficial location of this organ renders it readily accessible to radiation therapy. Furthermore it is readily accessible to direct laryngoscopic examination. Thus the location and extent of the tumor can be determined before starting radiation therapy, and, later, the tissue reaction and the extent of tumor regression can be observed during the course of treatment. A total of 116 patients with carcinoma of the larynx were treated with cobalt 60. The location of the carcinoma was supraglottic in 75 cases (65%) and glottic in 41 (35%). Patient age ranged from 33 to 78 years with the greatest number between 51 and 60. Supraglottic tumors occurred predominantly in the young while glottic tumors were in patients over 50 years of age.

Laryngeal cancer is almost exclusively a disease of the male. Of the 116 patients in this series 113 were males. In every patient the clinical and radiologic diagnosis of laryngeal carcinoma was confirmed by biopsy. Treatment dose varied between 5,500 and 7,000 rads, delivered through two apposing lateral fields during a 30–40 day period. The field size varied between 20 and 50 cm^2 (4×5, 5×6, 4×7, 6×8) depending on the size and location of the tumor. The treatment was well tolerated and was not interrupted by radiation reaction. Minor reactions, consisting of epithelitis, dysphagia, and dysphonia occurred in some cases but required no treatment. In a few cases of severe reactions, antibiotics, steroids, and a high protein semiliquid diet were administered. Five patients developed postradiation edema which required tracheotomy, four of whom have survived 5 years.

The overall 3 and 5 year survival are 60% and 53%, respectively. The five year survival for glottic carcinoma is 63% and for supraglottic carcinoma, 48%. The results are determined by the size and degree of extension of the disease. If the tumor can no longer be seen on direct laryngoscopy the patient has a 92% chance of obtaining a cure. If the tumor can still be seen at the end of the treatment then the chances of cure are 26%.

William H. Shehadi

Radiotherapy of intra-oral carcinoma. Shigematsu Y (Osaka University Medical School, Osaka, Japan). *Nippon Acta Radiol* 37:261–285, March 1977

Review of 460 cases of intraoral carcinoma treated with radiotherapy are reported. Discussions center on treatment technique, rationale and prognosis, dealing with carcinoma of the tongue, floor of the mouth, and gingiva. The radiotherapy technique for these tumors cannot be standardized and should be varied depending upon the site, stage, control rate, functional defects, and complication. The author has considerable difficulty in deciding whether one should use prophylactic radiation to the neck for possible cervical metastasis. Clinical trials have been proposed for hyperbaric oxygen radiotherapy for carcinoma of the tongue, brachytherapy with ^{192}Ir thin-wire-technique and combined radiotherapy and chemotherapeutic agent.

Mutsumasa Takahashi

Hodgkin's disease: an evaluation of staging laparotomy in 82 patients. Roberts SY, Roeser HP, Kynaston B, Whitaker SV, Hocker GA, Battersby AC (Queensland Radium Institute, Australia). *Australas Radiol* 20:314–320, 1976.

The findings of staging laparotomies in 82 patients with Hodgkin's disease are presented. Subdiaphragmatic disease was discovered in 30 patients, the spleen being the most common site of involvement (26 patients). Staging was advanced in 23 patients and reduced in three, with consequent changes in the treatment plan of these patients. In an additional four patients, treatment was altered by the distribution of the subdiaphragmatic disease, discovered without any change in stage. Lymphangiography was found to be an unreliable staging procedure, largely due to the frequent presence of disease in areas outside the lymphangiographic field, such as spleen, mesenteric, and celiac nodes, rather than to inaccuracy of the procedure itself.

Correlation of laparatomy findings with presenting sites of disease failed to identify any patient group which, on clinical grounds, had a low probability of abdominal involvement and might thus be spared a laparotomy. No patient died as a result of the operation. Postoperative morbidity (three major, eight minor complications) was considered acceptable in view of the value of the information obtained.

F. W. de Wilde

Clinical experience with Californium-252 (first report). Tsuya A, Kaneta K, Onai Y, Irifune T, Tomura T (Cancer Institute Hospital, Tokyo, Japan). *Nippon Acta Radiol* 37:238-248, March 1977

The authors report on application of ^{252}Cf small sources to 10 patients with recurrent or residual malignant tumors. Neutron doses from 500-2,800 rads with an average of 1,300 rads were given to the tumor bed. The treatment was given with ^{252}Cf needles or by surface molds. The initial results for radioresistant tumors were encouraging with diminution of tumor size, but the observation period was too short for final conclusion. Representative cases treated with this technique were detailed. The authors also attempted to establish a method for effective and safe handling of ^{252}Cf small sources to reduce exposure to radiotherapists.

Mutsumasa Takahashi

Cesiumtherapy of breast cancer. A five-year report on 400 consecutive patients. Spitalier J, Brandone H, Ayme Y, Amalric R, Santamaria F, Seigle J (Cancer Institute, B.P. 156, Marseilles, F 13273 Cedex 02, France). *Int J Radiat Oncol Biol Phy* 2:231-235, March-April 1977

The authors review their results of 400 consecutive patients treated with primary telecesiumtherapy for breast carcinoma between 1960 and 1970. One hundred sixty-nine of patients were N_0, 231 were N_1, 85 patients were T_1, 210 T_2, and 104 T_3. The entire breast was treated to a dose of 6,000 rads over 6 weeks with an additional 2,000 rad in 2-week boost. N_0 cancers also received 6,000 rads in 6 weeks to the axilla and N_1 cancers received 7,000 rads in 7 weeks. Of the patients, 39% had no radiation sequelae or only pigmentation. More important radiation sequelae were noted in only two patients (1%). Two hundred seventy-six patients (69%) survived for 5 years, 219 of this group of 276 retained their breasts and were apparently alive and cured at 5 years. Overall 5 year survival rates appeared to be better for patients with preirradiation wedge resection (86.8%) versus those without preirradiation wedge resection (57%). There was a 50% chance of obtaining cure with postirradiation mastectomy in those patients with local failures according to the authors.

Herbert C. Berry

The therapeutic implications of splenic involvement in stage IIIA Hodgkin's disease. Levi JA, Wiernik PH (National Cancer Institute, Baltimore Cancer Research Center, University of Maryland Hospital, 22 South Greene Street, Baltimore, Maryland 21201). *Cancer* 39:2158-2165, May 1977

A comparative analysis was undertaken of 13 pathologically staged IIIA Hodgkin's disease patients whose abdominal disease was localized to the spleen (III$_{s}$A); 17 IIIA patients with spleen and abdominal lymph node involvement (III$_{s+n+}$A) and 44 stage IIA patients. Three groups were treated with either extended field irradiation alone or limited field followed by MOPP chemotherapy. Relapse rates after irradiation alone were 17% for the III$_{s}$A patients; 63% for the III$_{s+n+}$A patients and 25% for the stage IIA patients. With the addition of chemotherapy no relapses occurred among the III$_{s}$A and III$_{s+n+}$A patients while 13% of the stage IIA patients relapsed. The most common sites of relapse for the III$_{s+n+}$A patients were extralymphatic (60%) while no extralymphatic relapses have occurred among the IIA patients ($p < .02$). The authors feel that combined irradiation and chemotherapy should be considered for stage III$_{s+n+}$A Hodgkin's disease patients when extensive intraabdominal involvement cannot be covered by initial radiation ports.

Herbert C. Berry

Radiation therapy of cancer of the digestive tract. Feremans WP (Clinique Longchamps, Avenue W. Churchill 235, 1180 Bruxelles, Belgium). *J Bel Radiol* 59:439-445, Sept-Oct 1976

Surgery has been the accepted method of treatment of carcinoma of the digestive tract—pancreas, stomach, colon, rectum. Yet despite the advances made in surgical technique there has been no improvement in the survival rate during the past 30 years. By comparison, significant improvement has been obtained, with extended survival rates, through the use of radiation therapy combined with surgery. In selected cases further improvement is obtained through the added use of chemotherapy, using 5-flurouacil. High energy radiation therapy, from a cobalt source, linear accelerator, or betatron, may be administered preoperatively, postoperatively, or alone, exclusive of surgery or any other modality.

The author comments on the variations in the dosages, techniques, and the time interval between surgery and radiation therapy. The dose varies between 2,500 and 5,000 rads delivered to the tumor, 750 rads weekly dose for cobalt and 1,000 rads for betatron. In postoperative radiation therapy the same weekly dose is administered as in preoperative treatment, but the total dose is 5,500-6,500 rads. When radiation therapy is the only method of treatment the total dose is 6,000-7,000 rads when cobalt is used and 6,000-8,000 rads when betatron is used.

Based on his experience and that of others quoted from the literature the author is of the opinion that radiation therapy, with or without chemotherapy, when combined with surgery, gives better results with improved survival rate than when surgery is used alone. Radiation therapy as the only method of treatment is indicated in: (1) small noninfiltrating rectal carcinoma, using contact therapy or interstitial radiation with radium or iridium implants; (2) when the initial preoperative course of radiation therapy has resulted in a cure, with complete tumor sterilization, thus eliminating the necessity of surgery; (3) when the general condition of the patient, or the size and extent of the tumor do not permit surgical intervention.

In carcinoma of the pancreas, while no cure is obtained, both subjective and objective improvement take place. In inoperable carcinoma of the stomach a 1 year survival is frequently observed and in isolated cases 2 and 3 year survival occur. In rectal carcinoma, up to 80% 5-year survival has been observed in cases of well defined polypoid tumors, and up to 3 year survival in ulcerating carcinoma without extension to the anal canal.

William H. Shehadi

Physics

Factors affecting the use of quantitative information from a CT scanner. McCullough EC (Mayo Clinic, Rochester, Minnesota 55901). *Radiology* 124:99-107, July 1977

Computed tomography can be used quantitatively in a variety of ways in both diagnosis and therapy. However, the successful use of CT numbers depends on the appreciation of several features of CT scanning, including the diagnostic viewer. It is also possible to employ the quantitative output of a CT scanner to improve the accuracy of isodose curve computations for photon (or electron beam) radiotherapy. A quality-control program is mandatory for anyone wishing to use CT numbers for this purpose.

Author Abstract

An inaccuracy in computed tomography: the energy dependence of CT values. Zatz LM, Alvarez RE (Veterans Administration Hospital, 3801 Miranda Avenue, Palo Alto, California 94304). *Radiology* 124:91-97, July 1977

The CT values of a variety of materials were studied in an EMI and a Syntex head scanner. The presence of bone-simulating rings changed the CT values despite the use of constant length water paths and software corrections. Errors due to beam hardening in CT scanning are discussed. These errors could be of significance, particularly in quantitative studies. The changes in CT values with kV setting of the scanner are used to illustrate their energy dependence and the peculiarities of the scaling system introduced by EMI. The difficulty in specifying a standard scale or unit for CT scanner is discussed.

Author Abstract

Compton radiography. I. Our approach and the current status in the world. Okuyama S, Mishina H, Sera K, Fukuda H, Shishido F, Matsuzawa T (Research Institute for Tuberculosis and Cancer, Tohoku Universiti, Sendai, Japan). *Nippon Acta Radiol* 37:256-260, March 1977

The authors report techniques of obtaining tomographic images with Compton ray scatters when an object is irradiated with a collimated beam of monochromatic gamma ray. When a slice of an object is irradiated with collimated beam of gamma ray, Compton rays are scattered at right angles to the incident beam. The Compton ray is imaged by using a scintillation camera. The image obtained is a tomographic image of the tissue or object irradiated with the thin collimated gamma ray beam. The authors experimentally obtained tomographic images of various objects. Magnification and stereopsis will be possible with improvement of the method.

Mutsumasa Takahashi

Analysis of the dense lesion at computed tomography with dual kVp scans. Marshall WH, Easter W, Zatz LM (Stanford University School of Medicine, Stanford, California 94305). *Radiology* 124:87-89, July 1977

By scanning the brain first at 100 and then at 140 kVp one can distinguish, in vivo, between blood and calcium or iodine solutions. The higher atomic number of calcium or iodine causes their CT values to decrease significantly while blood shows no significant change. This principle was applied to eight patients with hemorrhages, calcified lesions, or iodine-contrast augmented lesions. Hemorrhages showed no significant change with change in kVp, while the lesions containing calcium or iodine showed a highly significant change. This is a useful maneuver for determining the nature of a high density lesion.

Author Abstract

Radiobiology

Estimation of population doses from stomach mass screening, 1975. Hashizume T, Kato Y, Maruyama T, Kamata R, Urahashi S (National Institute of Radiological Sciences and Nihon University, Tokyo, Japan). *Nippon Acta Radiol* 37:578-589, June 1977

Mass x-ray survey of stomach diseases has been performed in Japan on a large scale because the incidence of carcinoma of the stomach is considerbly higher than that found in other countries. It has been suggested that mass surveys may be associated with high exposure doses to the gonads and bone marrow. The authors attempted to estimate radiation dose from such mass survey on the basis of nation-wide radiological survey.

The number of such examinations in the nation was estimated to be 2.38 million for males and 1.74 million for females, for a total of 4.12 million. The gonad doses were estimated to be 10.4 mrad per examination for males and 150 mrad per examination for females when measured using an ionization chamber on a tissue equivalent phantom. In addition, bone marrow doses for such examination was estimated to be 450 mrad for males and 390 mrad for females. The genetically significant dose was 0.15 mrad per person per year and per capita mean marrow dose was 16.5 mrad per person per year, while the leukemia significant dose was 14.5 mrad per person per year. These exposures should be kept in mind and serious consideration should be given in order to minimize exposure doses.

Matsumasa Takahashi

Book Reviews

Diagnostic Radiology in Paediatrics. Postgraduate Paediatrics Series. By I. R. S. Gordon and F. G. M. Ross. London: Butterworths, 384 pp., 1977. $49.95

This attractive volume is a survey of pediatric radiology, emphasizing radiographic findings and their relationship to the analysis of anatomical problems in the child. The book contains six chapters of the major body systems (skeletal, cardiovascular, respiratory, gastrointestinal, urinary, and central nervous system) and three additional chapters on skeletal dysplasias, tumors of bone, and measurements in pediatric radiology.

A very conscious effort to be brief allows the authors to present a panorama of pediatric radiology in 365 pages. Differential diagnosis, clinical findings, and an extensive bibliography have been pared to the bare minimum. The information in the text is important, succinct, and handsomely presented, with large pages and small type. The illustrations are carefully chosen, nicely reproduced with classic examples, and accompanied by helpful line drawings and diagrams. Major radiographic findings are stressed, together with a mention of less important or inconstant features. People interested in detail may be disappointed in the omissions or in the brevity of the discussion of each disease, but a fine overview of the subject has been substituted.

The resulting volume is convenient in size, attractively presented, and highly readible with excellent illustrations. It is a fine volume to leaf through just for the fun of it. I enthusiastically recommend this volume for students of pediatric radiology and for professionals in other pediatric subspecialities. A person desiring greater discussion, clinical findings, and differential diagnoses may use the references to expand their inquiry into any particular disease.

Spencer Borden, IV
Massachusetts General Hospital
Boston, Massachusetts 02114

Computerized Tomography with the General Purpose Scanner. By L. Kreel. Amsterdam: Excerpta Medica, 320 (2 × 2) slides, 45 pp., 1977. $288

This interesting series of slides forms a general survey of CT and can be used as an introduction to the field as well as for teaching purposes and review. The accompanying pamphlet has two formats. The first segment is a general description of the topics included, starting from the skull and brain and technical matters and proceeding through the chest and abdomen. The second segment is a specific legend to each slide with line drawings depicting the pathology or the pertinent details. My overall impression of this series is favorable. The format is basic enough to be used by a wide variety of viewers, including technicians and radiologists as well as other personnel interested in the overall capabilities of CT units. Most slides were of excellent detail.

The organization of the slides is somewhat cumbersome, since all must be inverted with the slide number placed in the lower left corner for viewing. Approximately every tenth slide also requires further adjustment for normal orientation. This problem would occur only once provided the user does not change the storage slide trays.

I found the line drawings to be helpful; however, more specific labeling of the arrows would be useful. One line drawing was out of sequence with the numbered slide (no. 79). During the original review of the slides one must be careful to clarify these small problems.

Overall, the slide series and descriptions are educational, well sequenced, and clearly designed to orient the radiologist and others to the value and uses of CT head and body scanners.

Gerald R. Smith
Harborview Medical Center
Seattle, Washington 98104

Endometrial Carcinoma and Its Treatment: The Role of Irradiation, Extent of Surgery, and Approach to Chemotherapy. Edited by L. A. Gray. Springfield, Ill.: Thomas, 225 pp., 1977. $22.50

This volume represents a collection of papers presented during a 2 day symposium on endometrial carcinoma at Louisville, Kentucky, November 1975. Gray, himself a distinguished authority and author in gynecologic oncology, has organized and summarized the presentations in a most effective manner. The author index represents an outstanding and unusual assemblage of authoritative opinion on this subject. The reports from the major cancer centers are current and impressive. The opinions are often diverse; each subject is dealt with effectively and extensively. Although the book represents a profile of current treatment approaches in endometrial carcinoma, of particular value is the wealth of background information and data provided by the authors in support of their management results. This is certainly the most exhaustive treatment of the subject ever presented in a single volume.

The book deals almost exclusively with the treatment of endometrial cancer; accordingly, and rather regretfully, the exciting and controversial epidemiologic aspects of endometrial carcinoma, including the role of exogenous estrogens, are touched upon only briefly. Nor should one look for consensus in treatment programs. This is not the purpose of the volume. The information for the most part is available in the existing literature, but to date has not been as effectively presented in a single volume. It is a welcome addition to the library of any clinician significantly involved in the treatment of endometrial carcinoma.

David C. Figge
Gynecologic Oncology
University Hospital
Seattle, Washington 98195

The Basic Physics of Radiation Therapy, By J. Selman. Springfield, Ill.: Thomas, 742 pp., 1976. $25.75

This book is principally directed at residents in radiotherapy but might equally well serve to teach physics to radiotherapy technicians. Practicing radictherapists might benefit from it as a basic reivew, though it is not quite suitable as a reference source.

In 17 chapters—each complete in its own right—all aspects of physical principles underlying radiation therapy are covered in a comprehensive and comprehensible manner, generally without sacrificing accuracy for simplicity. As appropriate in a book for clinicians, emphasis is placed on radiation dosage, teletherapy with high energy units and linear accelerators, implant therapy with radium, radon, and artificial radionuclides, surface therapy with beta particles, and radiation protection. Therapeutic application of radioisotopes is also included, with the introductory chapter on Radioactivity and Nuclear Physics particularly well written. The use of heavy particles (high-LET radiation) in radiation therapy is briefly discussed, sufficient to inform the interested reader about this modality. As usual in books on radiation physics, the chapter on radiobiology is weak and incomplete.

This book is readable, the mathematical prerequisites are minimal, and the price is reasonable. It is recommended as a basic text on the physics of radiation therapy.

Peter F. Winter
Lahey Clinic Foundation
Boston, Massachusetts 02215

Appareil Pulmonaire et Médiastin. I. Generalités. Séméiologie. Pathologie du Mediastin. (The Lungs and Mediastinum. I. General Considerations, Signs of Lung Disease, and Pathology of the Mediastinum). By V. Bismuth, M. Bléry, J. Rémy, J. Caron, and M. Coulomb. (Part 1 of vol. 4 of *Traité de Radiodiagnostic*). Paris: Masson, 512 pp., 1977.

This book forms the first half of one of the 20 volumes of the major French language compendium of diagnostic radiology, *Traité de Radiodiagnostic*. Authors are from France and nearby countries. Taking the current book as an example, however, it is evident that the information covered is worldwide.

General Considerations includes a review of anatomy and physiology of the thoracic respiratory tract, radiologic technique, and modalities (including CT and nuclear medicine), radiographic anatomy, and artifacts. This worthwhile review is slowed by a surfeit of abbreviations in chapter 2 (pulmonary function) and a complete breakdown of the numbering of references in chapter 4. Pretesting for reaction to contrast material is unfortunately recommended. Otherwise this section is of comfortable length, with excellent diagrams (the shape of the great fissures on an illustration based on D'Hour's 1934 treatise was particularly useful; p. 8). The radiographic reproduction is excellent throughout the book (but the process used erases the density differences which ought to be shown between overexposed, well exposed, and underexposed films; figs. I—96, 97). The bibliography has extensive up-to-date as well as classic references from the French, English, American, and, occasionally, German literature.

Signs of Lung Disease is a compact complete overview of radiographic signs. Mainly it reviews information from the major English language texts. Disagreements between the masters of chest radiology are thereby discussed. Patterns of pulmonary volume loss and the range of silhouette signs are nicely covered. Acute pneumococcal pneumonia in the child is unfortunately not included as a cuase of round pulmonary density.

Pathology of the Mediastinum includes the gem of the book, Rémy's introduction to radiologic anatomy and signs of the mediastinum, including interfaces. His treatment of radiology of the thymus is the most complete and valuable of the individual pathology treatments. (Primary disease of the heart, great vessels, and esophagus are covered in other volumes of the *Traité*.).

In summary, this work will be chiefly of interest to the radiologist who reads French but not English. However, all radiologists could benefit from the mediastinum sections, and from attention to the many superb radiographic reproductions.

Alan E. Oestreich
University of Missouri
Columbia, Missouri 65201

Radiation Protection for Medical and Allied Health Personnel. NCR Report no. 48. Washington, D.C.: National Council on Radiation Protection and Measurements, 72 pp., 1976. $4.50

NCRP Report no. 48 is designed to be used by employees of a hospital or research laboratory in which radiation may be used. Administrators and supervisory personnel will find the report helpful in alerting them to areas where possible hazards may exist. The report conveys information about radiation protection for individuals identified as allied health personnel (including technologists, nurses, orderlies, secretaries, janitors, etc.). In this report the radiation sources, uses, and facilities considered include those associated with diagnostic radiology, radiation therapy, nuclear medicine, radioactive materials, and research laboratories. The report singles out the requirement of the services of a radiation protection supervisor, either on a full-time or part-time basis depending on the size of the institution, and defines the responsibilities of the supervisor.

Sections 3-7 (which include x-ray department, radioactive nuclides, laboratories, the morgue, and disposal of radioactive waste) discuss both general and specific situations in simple terms. For example, pertinent guidelines are provided for diagnostic radiology personnel who receive the greatest exposure while performing fluoroscopy, angiography, and other special studies. Guidelines are given for personnel attending patients being treated with sealed sources and patients who have received millicurie amounts of radionuclides. Rules governing laboratories where radioactive material is used are given in section 5 and include a brief discussion concerning the handling of experimental animals containing radioactive material. Section 6 provides some simple guidelines for the handling of patients who have died after receiving a therapeutic dose of a radionuclide. The disposal of radioactive waste (solid, liquid, and gaseous) is discussed in section 7. In sections 3-7, the reader is referred to other NCRP reports which provide more detailed instructions on the same subject.

The appendices include useful general information on exposure rates from secondary radiation to persons manually restraining patients during radiographic procedures; appropriate caution signs required in areas where significant amounts of radiation or radioactive materials may be found; appropriate exposure rates around the bed of a patient containing 100 mg of radium; and emergency procedures to be followed in the event of spills, loss of a sealed source, rupture of a sealed source, and in the case of a major calamity involving fire, earthquake, or a massive spill. The final appendix contains a glossary of terms useful to allied health personnel.

This report provides some useful teaching material and guidelines and answers many questions which allied health personnel may have concerning exposure to radiation.

James G. Kereiakes
University of Cincinnati College of Medicine
Cincinnati, Ohio

Structural Shielding Design and Evaluation for Medical Use of X-rays and Gamma Rays of Energies Up to 10 MeV.

NCRP Report no. 49. Washington, D.C.: National Council on Radiation Protection and Measurements, 126 pp., 1976. $3.50

NCRP Report no. 49, which supercedes NCRP Report no. 34, is concerned with structural shielding design and evaluation for medical installations utilizing x-rays and gamma rays of energies up to 10 MeV. The report is mainly intended for radiologic physicists, radiologists, and regulatory personnel specialized in radiation protection. Sections should be of interest also to architects, hospital administrators, and others concerned with the planning of new radiation facilities.

The concept of maximum permissible dose equivalent as expressed by the NCRP (i.e., the maximum dose equivalent that persons shall be allowed to receive in a stated period of time) has been used as the basis for the recommendations in this report. The introduction recommends that the shielding be designed by a qualified expert and that the final shielding drawings and specifications be reviewed by a qualified expert and by the pertinent federal, state, or local agency (if applicable) before construction is begun. Recent availability of new data used to calculate the shielding in radiation facilities has resulted in revision from previous recommendations of some of the shielding requirement tables given in Appendix C. However, installations designed before the publication of this report and meeting the requirements of the Appendix C shielding tables in NCRP Report no. 34 need not be reevaluated.

The appendix on Computation of Barrier Requirements provides new examples on the use of the basic principles of shielding design. In addition, a new table has been included which lists the detailed assumptions made in the computation of secondary barrier requirements for typical radiation installations. Minimum shielding requirement tables given in Appendix C include new data for an 8 MV therapy installation. Appendix D contains figures providing attenuation in lead, concrete, and in certain cases iron for various energies of x- and gamma rays. Appendix E contains architectural and equipment information to be supplied to the qualified expert for use in shielding design. An adjunct to the report presenting full-sized reproductions of the curves for barrier requirements is an innovation for the NCRP. In summary, this report provides a valuable reference source to those actively involved in structural shielding design and evaluation.

James G. Kereiakes
University of Cincinnati College of Medicine
Cincinnati, Ohio

Current Concepts in Radiology, vol. 3. Edited by E. J. Potchen. St. Louis: Mosby, 453 pp., 1977. $39.50

In his preface, Potchen states that he will attempt to provide a bridge between what is in current journal publications and the more formalized textbooks in the field. The book includes information about older technologies, such as chest x-ray studies and bone radiology, as well as the newer technologies of computed tomography and nuclear medicine. However, diagnostic ultrasound is not covered.

The text is organized into 17 chapters with related material together. Four chapters are devoted to CT. Some of this information might be more helpful to those already working with CT scanning (e.g., chap. 5: Alternative Display Formats for Computed Tomography).

The chapter on breast cancer detection provides an introduction to radiologic evaluation of breast cancer. Also, the chapters on nuclear imaging are very good as are those involving bone and chest radiography. Metabolic considerations in Bone Disease by Whalen et al. was excellent, with radiographic and pathologic illustrations as well as flow charts of superb quality. This chapter covers an area seen often in radiographic practice, and residents in radiology would do well to read this.

The chapter on Comparative Radiology: Dysplasias of the Canine Forelimb, might be of interest to a few radiologists, but I feel that perhaps a chapter on current concepts in diagnostic ultrasound or other areas of diagnostic radiology would have been more beneficial.

The content organization and quality of illustrations are, on the whole, very good. The book does attempt to bridge current literature and traditional texts, and can be recommended.

Stanley B. Novy
1615 St. Joseph Professional Building
Houston, Texas 77002

Radiologic Diagnosis of Renal Parenchymal Disease. Saunders Monographs in Clinical Radiology, vol. 11. By A. J. Davidson. Philadelphia: Saunders, 317 pp., 1977. $24.50

This monograph in the Clinical Radiology series deals with the upper urinary tract. Davidson confines the text to his primary topic of renal parenchymal disease and only where appropriate discusses diseases in the surrounding structures, or in the lower urinary tract, when a part of the disease process affects the kidneys. The text is well written and for the most part is clear and understandable. The book is printed on good quality paper, and the illustrations are sharp with the abnormalities easily identifiable.

The chapters are determined by the differential diagnoses of a particular urographic appearance of the kidneys. These constitute diagnostic sets which are, therefore, dependent on similarities in renal size, contour, and uni- or bilaterality of the disease process. Where appropriate, other modalities such as arteriography and ultrasound are used to help illustrate and amplify the urographic findings and aid in the diagnosis of parenchymal disease.

Each disease process is discussed within each section. Included are clinical presentation, radiologic features, as well as histopathologic descriptions which allow for insight into why and how the anatomic changes in the kidneys occur. This method lumps many different pathologic processes which have as an end result a similar renal morphology into a given diagnostic set. The method can be an effective educational tool, especially for those in learning situations, such as residency programs. However, as a result of grouping many diseases together, some redundancy exists since many diseases will fit into several different categories. At times this is somewhat confusing. Tables are used at the end of the chapters to help summarize the abnormal findings for the different disorders.

Concise chapters on both the history and physiology of urography are also neatly presented. In addition, the technical aspects of performing urograms in normal patients, as well as in those with renal failure, are discussed. There is a worthwhile introductory section on renal anatomy and embryology, but, unfortunately, very little discussion or illustration of congenital renal anomalies. A separate chapter on the modern approach to renal mass lesions is included. It is too bad that the newness of computed tomography when the book was written limited the description of this valuable technique to only a few examples.

This book is moderately priced and an excellent addition to the reference library of practicing physicians in radiology, nephrology, and urology. I also feel that it is a worthwhile reference book for residents in both radiology and urology which will help them to categorize renal disease radiographically and clinically.

Ronald D. Harris
Scripps Clinic Medical Institutions
La Jolla, California 92037

Pituitary and Parapituitary Tumors. Major Problems in Neurology, vol. 6. By J. Hankinson and M. Banna. Philadelphia: Saunders, 217 pp., 1976. $27.50

Lesions in and about the sellar region often present problems in diagnosis and definitive therapy. This book is divided into chapters related to specific areas of expertise. The initial sections are devoted to anatomy and pathophysiology. In order to keep the material within a reasonable volume, there has been some sacrifice of detail in clinical presentation, particularly differential diagnosis.

The aspects of diagnosis and endocrine management of pituitary dysfunction have been formulated well and make an excellent guide in a rapidly changing and expanding field. Likewise, neuroopthalmology receives critical coverage essential to definitive diagnosis. The radiologic section is well illustrated with a broad spectrum analysis of the varying lesions. More emphasis on tomography would seem indicated. The advancing technology of CT scanning almost makes it impossible to keep current in print. Fortunately the surgical and radiotherapy chapters have not digressed into the "best or preferred" method of treatment. Each author adequately reviews the present-day concepts of therapy. It would have been helpful if the book had contained a summary chapter or table of salient features of all the lesions with respect to their differential diagnoses and management.

This monograph offers a good statistical review of all the lesions of the sellar region. It has an adequate bibliography for reference and is a worthwhile book for a wide range of physicians.

William A. Kelly
Neurological Surgery
University Hospital
Seattle, Washington 98195

Books Received

Receipt of books is acknowledged as a courtesy to the sender. Books that appear of sufficient interest will be reviewed as space permits.

Quality Control in Nuclear Medicine. Radiopharmaceuticals, Instrumentation, and In Vitro Assays. Edited by B. A. Rhodes. St. Louis: Mosby, 508 pp., 1977. $39.50

Reconstruction Tomography in Diagnostic and Nuclear Medicine. Edited by M. M. Ter-Pogossian, M. E. Phelps, G. L. Brownell, J. R. Cox, Jr., D. O. Davis, and R. G. Evens. Baltimore: University Park Press, 573 pp., 1977. $65

Cancer Management. Edited by W. Lawrence, Jr., and J. J. Terz. New York: Grune & Stratton, 566 pp., 1977. $38.50

Radiation Protection in Dentistry. Manual on Radiation Protection in Hospitals and General Practice, vol. 4. By K. Koren and A. H. Wuehrmann. Geneva: World Health Organization, 52 pp., 1977. $4 (ISBN 92 4 154041 9, available in U.S. from Q Corp., 49 Sheridan Ave., Albany, N.Y. 12210)

Radiographic Contrast Agents. Edited by R. E. Miller and J. Skucas. Baltimore: University Park Press, 515 pp., 1977. $29.50

Therapeutic Radiology. Continuing Education Review. 418 Essay Questions and Referenced Answers. By J. A. Stryker and J. A. Clement. Flushing, N.Y.: Medical Examination Publishing, 183 pp., 1977. $12

Experimental Neuroonkologie (in German). By D. Schreiber and W. Jänisch. Leipzig: Johann Ambrosius Barth, 198 pp., 1974. 29,60 DDR M

Radiology and Injury in Sport. By J. W. Bowerman. New York: Appleton-Century-Crofts, 330 pp., 1977. $26.50

Cancer, Diagnosis, Treatment, and Prognosis, 5th ed. By J. A. del Regato and H. J. Spjut. St. Louis: Mosby, 1,013 pp., 1977. $51.50

The Physical Principles of Diagnostic Radiology. By P. Sprawls, Jr. Baltimore: University Park Press, 365 pp., 1977. $24.50

The Urinary Tract. Advanced Exercises in Diagnostic Radiology, vol. 10. By A. Walsh and J. G. McNulty. Philadelphia: Saunders, 104 pp., 1977. $6.95

Radiation Protection Design Guidelines for 0.1–100 MeV Particle Accelerator Facilities. NCRP Report no. 51. Washington, D.C.: National Council on Radiation Protection and Measurements, 159 pp., 1977. $5

Clinical Radiobiology. By W. Duncan and A. H. W. Nias. Edinburgh: Churchill Livingstone, 226 pp., 1977. $22.50

Doppler Ultrasonic Evaluation of Venous Disease. By R. W. Barnes, H. E. Russell, and M. R. Wilson. **Doppler Ultrasonic Assessment of Peripheral Arterial Disease** and **Doppler Ultrasonic Evaluation of Cerebrovascular Disease,** both by R. W. Barnes and M. R. Wilson. All part of a programmed audiovisual set with texts and tapes. Iowa City: University of Iowa, texts 251 pp., 296 pp., and 196 pp, respectively, 1976

Review of NCRP Radiation Dose Limit for Embryo and Fetus in Occupationally Exposed Women. NCRP Report no. 53. Washington, D.C.: National Council on Radiation Protection and Measurements, 42 pp., 1977. $3.50

News

Radiology of Neoplastic Diseases

The Radiology Department of Duke University Medical Center has scheduled its sixth annual tutorial postgraduate course on Radiology of Neoplastic Diseases for April 3-7 in Durham, North Carolina. Course emphasis will be on personalized, tutorial type of teaching by recognized authorities with ample time for discussion. All facets of neoplastic disease will be covered including diagnostic techniques. A detailed abstract book with references will be provided. Guest faculty will be: G. D. Dodd, Houston, Texas; K. R. Maravilla, Dallas, Texas; and G. D. Potter, New York City. Other faculty will be from Duke University Medical Center. The course carries 27 hr AMA Category I credit. Inquiries should be directed to the program director, Robert McLelland, Radiology, Box 3808, Duke University Medical Center, Durham, North Carolina 27710; telephone (919) 684-4397.

Nuclear Medicine Symposium

Nuclear Medicine 1978 is the title of a symposium organized by Albert Einstein College of Medicine and scheduled for April 3-6 at the Waldorf Astoria Hotel in New York City. The course carries 22 hr AMA Category I credit; fee is $225 ($110 for residents and technologists). Topics will include basic concepts of nuclear medicine including instrumentation, thyroid studies, cardiovascular, kidney and bone imaging, thrombosis detection, radioimmunoassay, and complementary techniques including ultrasound and computed tomography. For information, contact M. H. Stromer, program administrator, Nuclear Medicine Symposium, Albert Einstein College of Medicine, 1300 Morris Park Avenue, Bronx, New York 10461; phone, (212) 379-3165.

International Computed Tomography Symposium

An International Symposium and Course on computed tomography will be March 19-24 in Miami Beach, Florida, under the direction of J. M. Taveras and P. F. J. New. The symposium will provide an opportunity for exchange of information and identification of priorities in CT research. A comprehensive series of presentations is planned for the structured course; a physics program will also be included. To have a paper considered for presentation, submit a 100-200 word abstract to J. M. Taveras, Department of Radiology, Massachusetts General Hospital, Boston, Massachusetts 02114. General information is available from S. Lincoln also at Massachusetts General Hospital. The program will carry AMA Category I credit. Fees are $160 for physicians and $60 for others.

Department Management Seminar

New York University's School of Continuing Education has announced dates for a new 3 day seminar, Managing the Department. Cities and dates are: Houston, January 23-25; San Francisco, March 20-22; Chicago, May 24-26; and Toronto, June 7-9. The seminar will cover managing as a full-time job; organizing for performance; defining organizational relationships; delegating authority; and other management-related topics. Seminar leader Patrick Kimball is a member of the business faculty at Pace University. For information contact H. E. Kaplan, Information Services Manager, New York Conference Management Center, 360 Lexington Avenue, New York City 10017; telephone (212) 953-7262.

Practical Neuroradiology

Practical Neuroradiology is the title of the 14th Annual Radiology Postgraduate Seminar sponsored by the Radiology Department, Medical College of Virginia, and scheduled for March 5-9 in Williamsburg. For information contact E. Blanchard, Department of Continuing Medical Education, Medical College of Virginia, MCV Station, Richmond, Virginia 23298.

Spring Roentgen Conference

The sixth annual Spring Roentgen Conference of the New Orleans Radiology Society will be April 20-22 at the Marriott Hotel in New Orleans. The meeting will be divided into two separate sessions; registrants may attend one or both. April 20 will be devoted to abdominal imaging with nuclear medicine, ultrasound, and computed tomography. April 21 and 22 will cover aspects of general diagnostic radiology. The program will carry 18 hr AMA Category I credit and is cosponsored by the American College of Radiology. For additional information, write New Orleans Radiology Society, P. O. Box 19024, New Orleans, Louisiana 70179.

Pediatric and Newborn Seminar

A seminar on Pediatric and Newborn Radiology will be February 5-10 at the Given Institute of Pathobiology in Aspen, Colorado. The postgraduate seminar is designed specifically for radiologists, pediatricians, and neonatologists. During the five morning sessions, approaches to radiographic interpretation of newborn and pediatric diseases and syndromes grouped by body systems will be discussed. Guest speakers will include: J. Gwinn, Childrens Hospital of Los Angeles; E. A. Franken, Jr., James Whitcomb Riley Hospital for Children, Indianapolis; D. Altman, Variety Childrens Hospital, Miami; C. Gooding, University of California, San Francisco; L. E. Swischuk, University of Texas, Galveston. The seminar will carry 20 hr AMA Category I credit. Fee is $175. For additional information, contact the Office of Postgraduate Medical Education, University of Colorado School of Medicine, 4200 East Ninth Avenue, Denver, Colorado 80262; phone (303) 394-5241.

Big Sky Radiology Conference

The Big Sky, Montana, Radiology Conference at the Huntley Lodge will be February 9-11. The conference is designed for continuing education in diagnostic radiology and radiation oncology. The format will be a combination of didactic lectures, workshops, and a self-study series. Cosponsor is the American College of Radiology. Faculty will include: P. R. Almond and E. Montague, both M.D. Anderson Hospital, Houston; R. Fraser, University of Alabama; T. H. Newton, University of California, San Francisco; L. E. Swischuk, University of Texas, Galveston; and members of the Columbus Hospital staff in Great Falls, Montana. The conference carries 14 hr AMA Category I credit. Fees are $110, $50 for residents (with letter from program director). For additional information, contact V. B. Graves, Columbus Hospital, Great Falls, Montana 59401.

Legal Aspects of Radiology

The schools of Medicine and Law of Vanderbilt University will sponsor a symposium on the Legal Aspects of Radiology and the Radiological Sciences, April 19-21. Experts from the fields of law, radiology, and legal medicine will discuss medical malpractice, courtroom procedures, partnerships and contracts, informed consent, legislation, insurance, and countersuit. For more information, contact A. E. James, Jr., Department of Radiology, Vanderbilt University School of Medicine, Nashville, Tennessee 37232.

Aspen Radiology Conference

The eighth annual Aspen Radiology Conference is scheduled for February 26-March 3 at the Aspen Institute for Humanistic Studies. This conference, sponsored by Beth Israel Hospital, Denver, is designed for practicing radiologists and other physicians interested in diagnostic radiology, computed tomography, nuclear radiology, and ultrasound. Independent refresher courses will be offered in diagnostic radiology of the chest, gastrointestinal, and genitourinary tracts; nuclear radiology of thrombotic diseases, neural, pulmonary, and cardiac systems; diagnostic ultrasound of cardiac, ob/gyn, abdomen, and retroperitoneum. Two days will be devoted to CT scanning of the abdomen and head and comparison of this modality to others. The conference carries 25 hr AMA Category I credit. For additional information, contact Aspen Radiology Conference, Beth Israel Hospital, West 17th Avenue and Lowell Boulevard, Denver, Colorado 80204; phone (303) 825-2190, extension 354.

Automation of Administrative Systems

New York University's School of Continuing Education has announced dates and locations of a new seminar, Automation of Administrative Systems. This 3 day seminar covers background, economics, and benefits of automation, automation and its impact on the organization, major areas of concern, and other topics. Locations and dates are: New York, February 13-15 and Chicago, April 24-26. Seminar leader is R. M. Bloomfield, president of Marshall, Roberts & Co., management consultants. For additional information, contact H. E. Kaplan, Information Services Manager, New York Conference and Management Center, 360 Lexington Avenue, New York 10017; phone (212) 953-7262.

Meeting and Course Review

For reader convenience, a summary of upcoming meetings and courses is provided. Detailed listings of these events appeared in journal issues indicated in parentheses.

Mammographic Training Program, continuing education course, 1 week sessions throughout the year in seven U.S. locations (April).

International Course in Advanced Neuroradiology, March 10 and 11, Strasbourg, France (July).

Ultrasound Postgraduate Course, two sessions, January 9-March 3, and April 3-June 9, Winston-Salem, North Carolina (August).

Aspen Uroradiology Seminar, February 19-24, Colorado (August).

Computed Body Tomography Course, January 30-February 2, San Diego (August).

CT, Ultrasound, and X-ray, course, January 16-20, San Francisco (September).

University of Miami Seminars, seven consecutive seminars, January-March 1978, Florida (September).

Osteopathic Radiology Courses, January 19-21, Chicago, and April 6-8, Orlando, Florida (September).

Las Vegas Angiography Course, January 19-21 (September).

Computerized Tomography Society, seminar, February 25 and 26, Washington, D.C. (October).

Skeletal and GI Meeting, postgraduate course, January 30-February 2, Mexico City (October).

Texas Preceptor Programs, four continuing 1 and 2 week programs, Dallas (October).

XI Neuroradiological Symposium, June 4-10, Wiesbaden, Germany (October).

Diagnostic Nuclear Imaging, course, March 4 and 5, San Francisco (October).

Emergency Room Radiology, course, May 10-12, San Francisco (October).

Medical Instrumentation Meeting, March 28-April 1, Washington, D.C. (October).

Midwinter Conference, January 27-29, Los Angeles (November).

Fleischner Society Symposium, February 27-March 1, San Diego (November).

Pancreas, Liver, and Biliary Tract Symposium, January 6 and 7, Seattle (November).

Diagnostic Radiology Seminar, February 2-4, Dallas (November).

Angiography Course, February 20-23, New Orleans (November).

Puerto Rico Diagnostic Course, February 6-10 (November).

Utah Diagnostic Course, January 28-February 4, Snowbird (November).

Computed Tomography Meeting, December 27-30, Disney World, Florida (November).

Gastrointestinal Refresher Course, February 16-18, San Diego (November).

Radiopharmacology Symposium, May 21-24, Innsbruck, Austria (November).

American Journal of Roentgenology

Please enter my subscription as follows:

Beginning with ____________, __________.
month year

Name ____

Street Address ____

City and State ______________________ Zip Code ______________

My specialty is ______________________

Send gift subscription for __________ years to:

Beginning with ____________, __________.
month year

Name ____

Address ____

City and State ______________________ Zip Code ______________

Specialty: ______________________

Enclosed is $ __________

Subscription rates are: $40 for the United States and possessions; others, $50; residents in training in U.S., $20 (letter required from institution).

Please send this form and remittance to: Charles C Thomas, Publisher, 301-327 East Lawrence Avenue, Springfield, Illinois 62717

Special Subscription Rate for Residents

At the 1976 meeting of the American Roentgen Ray Society, a special $20 subscription fee to this journal was approved for radiology residents training in U.S. institutions. To obtain this special rate, residents should accompany their applications and checks with a letter from their department chairmen certifying they are residents in approved training programs. All subscriptions should be sent to Charles C Thomas, publisher, 301-327 East Lawrence Avenue, Springfield, Illinois 62717.

This rate is intended to help the beginning resident start a library of significant literature early in his career. The rate represents a substantial subsidy by the society, and it is hoped that residents will take advantage of a program intended to enhance their educational experience. Some departments have indicated plans to provide a journal subscription as an additional benefit for their residents. With the new low rate, this would appear to be a very feasible program. The special price is limited to the period of resident training.

The *American Journal of Roentgenology* is pleased to offer this significant educational subsidy and would be gratified if every resident in this country were to take advantage of it.

Raymond A. Gagliardi
Chairman, Publications Committee

Author Index Volume 129

Index key: b = book review, c = case report, e = editorial, l = letter, o = obituary, t = technical note

Adamsons R, see Kinkhabwala M
Ahmed R, see Clouse ME
Alagratnam D, see Asokan S
Alavi A, see Dolinskas CA
Alavi SM: *Advanced exercises in diagnostic radiology: computed tomography of the brain* (b), 960
Ali MV, see Shenoy SS
Allen B, see Gilbert HA
Allen RW: Informed consent for urography? (l), 358
Altman AR: Thoracic wall invasion secondary to pulmonary aspergillosis: a complication of chronic granulomatous disease of childhood (c), 140
Ambos MA, Bosniak MA, Madayag MA, Lefleur RS: Infiltrating neoplasms of the kidney, 859
———, see Bosniak MA
Amendola MA, Ostrum BJ: Diagnosis of isodense subdural hematomas by computed tomography, 693
Amorosa JK, see Rosen Y
Amplatz K, see Castaneda-Zuniga WR
Anderson JC, Harned RK: Gray scale ultrasonography of the gallbladder: an evaluation of accuracy and report of additional ultrasound signs, 975
Anderson JH, Wallace S, Gianturco C: Transcatheter intravascular coil occlusion of experimental arteriovenous fistulas, 795
———, see Jonsson K
Antonioli DA, see Sacks BA
Armbuster TG, Slivka J, Resnick D, Georgen TG, Weisman M, Master R: Extraarticular manifestations of septic arthritis of the glenohumeral joint, 667
Asokan S, Alagratnam D, Eftaha M, Radhakrishnan J, Lim LT, Teresi M: Ultrasonography of a mediastinal pseudocyst (c), 923
Athanasoulis CA, see Baum S
Athey PA, Goldstein HM, Dodd GD: Radiologic spectrum of opportunistic infections of the upper gastrointestinal tract, 419
Austin JHM: *The adult postoperative chest* (b), 773
Aviad Y, see Weinstein D
Azizi F, see Rosenthal DI

Baker DA, see Morin ME
Baker DH, see Haller JO
Balow JE, see Schaner EG
Bance DA, see Berry RJ
———, see Goodhead DT
Bank WO, see Chestnut JS
Barash PG, see McLoud TC
Barbaric ZL, Frank IN: Peripelvic renal pseudocyst due to obstruction, 1097
Bargeron LM Jr, see Soto B
Barnes DWH, see Berry RJ
Barnes GT, Brezovich IA, Witten DM: Scanning multiple slit assembly: a practical and efficient device to reduce scatter, 497
Barnes LE, see Dubois PJ
Barrett AF, see Granmayeh M
Barth K, see Cavaluzzi JA
Bastidas J, DelGuercio LM: Cholecystocholangiography after cholecystoduodenostomy (t), 534
Baum S, Athanasoulis CA, Waltman AC, Galdabini J, Schapiro RH, Warshaw AL, Ottinger LW: Angiodysplasia of the right colon: a cause of gastrointestinal bleeding, 789
———, see Ring EJ
Bean WJ: *Practical echocardiology* (b), 960
Beckmann CF, Levin DC, Ulreich S: Cardiomegaly as a cause of nonuniform pulmonary artery perfusion, 661
Beeler GW Jr, see Reese DF
Behan M, Martin EC, Muecke EC, Kazam E: Myelolipoma of the adrenal: two cases with ultrasound and CT findings, 993
Bein ME, Spiegler P, Rigler LG: High kVp chest radiography (l), 1139
Beranbaum SL, see Som PM
Berdon WE, see Haller JO
Berens DL: *Cysts of the oral regions* (b), 565
Berger M, see Mascatello VJ
Berkow AE, Salo BC: The kinky chest tube: a sign of entrapment following median sternotomy, 883
Bernardino ME, Zimmerman RD, Citrin CM, Davis DO: Scleral thickening: a CT sign of orbital pseudotumor, 703
Berry RJ, Bance DA, Barnes DWH, Cox R, Goodhead DT, Sansom JM, Thacker J: High energy fast neutrons from the Harwell variable energy cyclotron. II. Biologic studies in mammalian systems, 717
———, see Goodhead DT
Bertrand M, Chen JTT, Libshitz HI: Lymph node calcification in Hodgkin's disease after chemotherapy, 1108
Beydoun MT, see Goldstein HM
Bhave DG, see Kelsey CA
Bigongiari LR, Davis R, Novak WG, Wicks JD, Kass E, Thornbury JR: Visualization of the medullary rays on excretory urography in experimental ureteric obstruction, 89
———, see Wicks JD
Bilaniuk LT, see Dolinskas CA
Birnholz JC: On maps and comparing cross-sectional imaging methods (e), 1133
Blieden LC, Schneeweiss A, Deutsch V, Neufeld HN: Anomalous venous connection from the left atrium to the cardinal venous system: "levoatriocardinal vein" (c), 937
Blocklyn MJ: *Symposium on* Pneumocystis carinii *infection* (b), 565
Boehnke M, see Drayer BP
Bolla M, see Jampolis S
Bolmgren J, Jacobson B, Nordenström B: Stereotaxic instrument for needle biopsy of the mamma, 121
Bookstein JJ, Davis GB: Intravenous versus intraarterial vasopressin (l), 947
Borden S IV: *Diagnostic radiology in paediatrics* (b), 1156
Bosniak MA, Ambos MA, Madayag MA, Lefleur RS, Casarella WJ: Epinephrine-enhanced renal angiography in renal mass lesions: is it worth performing?, 647
———, see Ambos MA
Bowen A III: *Symposium on pediatric uroradiology. Radiology clinics of North America* (b), 773
Bowie JD, see Rochester D
Boyd WR, Gardiner GA Jr: Metrizamide myelography, 481
Bradac GB, Simon RS, Bunte M, Stellmach R: Angiography in vascular malformations of the face, 469
Brady LW: Cancer of the breast: a time for caution, 969
———: Report of 1977 American Radium Society meeting,
Brandly J, see Moncada R
Braunstein EM: Inadvertent intrasplenic injection of oily propyliodine (c), 152
———, Martel W: Voluntary glenohumeral dislocation, 911
Brezovich IA, see Barnes GT
Brogdon BG, see Kelsey CA
Brower AC, Neff JR, Tillema DA: An unusual scapular stress fracture (c), 519
———, see Hart KZ
———, see Karlin CA
Brown J, see Seidelmann FE
Bruneau RJ, see Wandtke J
Bryan PJ, Dinn WM: Isodense masses on CT: differentiation by gray scale ultrasonography, 989
———, see Seidelmann FE
Buchler DA, see Kademian MT
Bunte M, see Bradac GB
Burnett LL, see Bush WH Jr
Burnham J, Fraker K, Steinbach H: Pathologic fracture in an unusual case of gout, 1116
Buse MG, see Gooneratne NS
Bush WH Jr, Burnett LL, Gibbons RP: Needle tract seeding of renal cell carcinoma (c), 725

Cacciarelli AA: Posterior widening of the S1-S2 interspace in children: a normal varient of sacral development, 305
Caffey J: Therapeutic value of thyreocalcitonin (e), 175
Callen PW, Korobkin M, Isherwood I: Computed tomographic evaluation of the retrocrural prevertebral space, 907

Callipari F, see Preisman RA
Capek V, see Spigos DG
Capp MP, see Tonkin IL
Cardoso M, see Moncada R
Carpenter GG, see Curtis JA
Carrera GF, see Mascatello VJ
Carroll B: Pulmonary hypoplasia and pleural effusions associated with fetal death in utero: ultrasonic findings (c), 749
Casarella WJ, see Bosniak MA
Castaneda-Zuniga WR, Hammerschmidt DE, Sanchez R, Amplatz K: Nonsurgical splenectomy, 805
Cavaluzzi JA, Sheff R, Harrington DP, Kaufman SL, Barth K, Maddrey WC, White RI Jr: Hepatic venography and wedge hepatic vein pressure measurements in diffuse liver disease, 411
Chameides L, see Gordon IJ
Chan P, see Gilbert HA
Chandler HL, see Rosenthal DI
Chapman WH: *Urological radiology of the adult male lower urinary tract: anatomy, physiology, pathology and sequelae, diagnosis and management* (b), 377
Charbonnier FM: Kilovoltage and lung nodule detectability (l), 759
Chatterton BE: Progressive abnormalities in the brain scan in adrenal leukodystrophy (c), 939
Chen JTT, see Bertrand M
Chessare JW, Rogers LF, White H, Tachdjian MO: Injuries of the medial epicondylar ossification center of the humerus, 49
Chestnut JS, Bank WO, Deeb ZL, Horton JA: Hypnotic anesthesia for cerebral angiography (t), 751
Cho KJ, Wilcox CW, Reuter SR: Glucagon-producing islet cell tumor of the pancreas (c), 159
———, Walter JF, Konnak JW: Contralateral renal herniation after nephrectomy: a cause of pseudo-crossed renal ectopia, 1099
———, see Chuang VP
———, see McCormick TL
Christensen GM: *Biological and environmental effects of low-level radiation* (b), 200
Chuang VP, Pulmano CM, Walter JF, Cho KJ: Angiography of pancreatic arteriovenous malformation, 1015
Church CC: Radiographic diagnosis of acute peroneal tendon dislocation, 1065
Cimmino CV, Scott DW III: Laminar avulsion in a cervical vertebra, 57
Citrin CM, see Bernardino ME
Clark TM, see O'Reilly GV
Cleveland RH, Fellows KE, Lebowitz RL: Notching of the ureter and renal pelvis in children, 837
———, see Gilsanz V
Clouse ME, Ahmed R, Ryan RB, Oberfield RA, McCaffrey JA: Complications of long term transbrachial hepatic arterial infusion chemotherapy, 799
Clouser M, see Libshitz HI
Cohen J, see Rosen Y
Cohen WN, see Seidelmann FE
Coleman RE, see Michal JA III
Colodny AH, see Griscom NT
Cook JH III, Rosenfield AT, Taylor KJW: Ultrasonic demonstration of intrarenal anatomy, 831
Cossrow JI, Curtis JA, Edeiken J: Enophthalmos simulating orbital emphysema (c), 728
Coulam CM: *Cranial computerized tomography* (b), 772
Cox R, see Berry RJ
Cromwell LD: *Diagnostic neuroradiology* (b), 377
———, Kerber C, Margolis MT: Selective carotid angiography in the diagnosis of orbital hemangiopericytoma: report of two cases (c), 730
———, Kerber CW, Vermeere WR: A wedge filter for craniocervical angiography, 1125
———, Moore WE, Schumacher D, Salam A: A method of reducing cost in CT systems that employ floppy discs, 1123
Cronin TG Jr, see Del Fava RL
Crum CP, see O'Reilly GV
Crummy AB: *Diagnosis and staging of cancer: a radiologic approach* (b), 198
Culham JAG, see Freedom RM
Culver GJ, see Shenoy SS
Cunningham JJ: Contrast medium reactions correlated with time of day, 1039
Currarino G, Kirks DR: Lateral widening of epiphyseal plates in knees of children with bowed legs, 309
———, see Kirks DR
Curtin MJ, Milligan FD: Mallory-Weiss syndrome with esophageal obstruction secondary to adherent intraluminal thrombus (c), 508
Curtis JA, O'Hara AE, Carpenter GG: Spurs of the mandible and supracondylar process of the humerus in Cornelia de Lange syndrome (c), 156
———, Sadhu V, Steiner RM: Malposition of the colon in right renal agenesis, ectopia, and anterior nephrectomy, 845
———, see Cossrow JI

Daffner RH, Whitfield PW: Recurrent ganglion cyst: the value of preoperative ganglionography (c), 345
———, see Fetouh SA
Dalinka MK: A simple aid to the performance of shoulder arthrography (t), 942
Danley R, see Moncada R
DaSilva O, see Stadalnik RC
Davies R, see Stadalnik RC
Davis DO, see Bernardino ME
Davis GB, see Bookstein JJ
Davis M, see Schreiber MH
Davis R, see Bigongiari LR
Deeb ZL, see Chestnut JS
DeGroot I, see Moskowitz M
Dekker W, see Op den Orth JO
Del Fava RL, Cronin TG Jr: Typhlitis complicating leukemia in an adult: barium enema findings (c), 347
DelGuercio LM, see Bastidas J
Dembner AG, Pfister RC: Fungal infection of the urinary tract: demonstration by antegrade pyelography and drainage by percutaneous nephrostomy, 415
deSantos LA, Goldstein HM: Ultrasonography in tumors arising from the spine and bony pelvis, 1061
DeSmet AA, Kramer D, Martel W: The metal-cement interface in total hip prosthesis, 279
Deutsch V, see Blieden LC
Dewanjee MK, see Kahn PC
Diamond AB, Meng CH, Kodroff M, Goldman SM: Testicular venography in the nonpalpable testis, 71
———, see Goldman SM
Dinn WM, see Bryan PJ
Dinsmore RE, see Miller SW
Dodd GD, see Athey PA
———, see Goldstein HM
Dolinskas CA, Bilaniuk LT, Zimmerman RA, Kuhl DE: Computed tomography of intracerebral hematomas. I. Transmission CT observations on hematoma resolution, 681
———, Bilaniuk LT, Zimmerman RA, Kuhl DE, Alavi A: Computed tomography of intracerebral hematomas. II. Radionuclide and transmission CT studies of the perihematoma region, 689
Doppman JL, see Schaner EG
Drayer BP, Wilkins RH, Boehnke M, Horton JA, Rosenbaum AE: Cerebrospinal fluid rhinorrhea demonstrated by metrizamide CT cisternography (c), 149
Drinker H, Mall JC: Radiologic aspects of the new universal proximal femoral hip prosthesis (t), 531
Dubois PJ, Orr DP, Meyers EN, Barnes LE: Undifferentiated parotid carcinoma with osteoblastic metastases (c), 744
Duchesneau PM, see Weinstein MA
Dubuque GL: Optimization of mammographic screening programs (l), 548
Dunnick NR, Parker BR, Castellino RA: Pediatric lymphography: performance, interpretation, and accuracy in 193 consecutive children, 639
Dure-Smith P: Faceted air bubbles (l), 1137

Edeiken J, see Cossrow JI
Eftaha M, see Asokan S
Ehrlich I, Kricun ME, Gonzalez CF: EMI scan density of methyl methacrylate (t), 351
Eisemann JL: *Percutaneous transluminal angioplasty: the Dotter procedure. A manual for the radiologist* (b), 565
Eisenberg H, see Levin DC
Eisenberg RL, Hedgcock MW, Jeffrey RB, Montgomery CK: Ulcerative pseudopolyposis mimicking neoplasm proximal to a jejunal obstruction (c), 503
Ekelund L: Radiologic findings in renal amyloidosis, 851
Eto RT, see Stanley P
Evens RG, Rujanavech N, Mikhael MA: Utilization, reliability, and cost effectiveness of cranial computed tomography in evaluating pseudotumor cerebri, 263

Faer MJ, Mead JH, Lynch RD: Cerebral granulomatous angiitis: case report and literature review, 463
Fagan CJ: Antepartum diagnosis of con-

joined twins by ultrasonography (c), 921
Feigin DS, Siegelman SS, Theros EG, King FM: Nonmalignant lymphoid disorders of the chest, 221
Fellows KE, see Cleveland RH
Felman AH, Frias JL: The trichorhinophalangeal syndrome: study of 16 patients in one family, 631
Ferrucci JT Jr, Wittenberg J: Refinements in Chiba needle transhepatic cholangiography, 11
Fetouh SA, Daffner RH, Postlethwait RW, Millar RC: Radiologic aspects of Beck gastric tube in esophageal reconstruction, 425
Fierstien SB, see McDaniel MM
Figge DC: *Endometrial carcinoma and its treatment: the role of irradiation, extent of surgery, and approach to chemotherapy* (b), 1156
Firooznia H, Pudlowski R, Golimbu C, Rafii M, McCauley D: Diffuse interstitial calcification of the lungs in chronic renal failure mimicking pulmonary edema, 1103
Fishbone G, Nunez D Jr, Leon R, Paz G, Isturiz P, McLoughlin C: Massive splenic infarction in sickle cell-hemoglobin C disease: angiographic findings, 927
Fisher RG, see Granmayeh M
______, Graham DY, Granmayeh M, Trabanino JG: Polyarteritis nodosa and hepatitis-B surface antigen: role of angiography in diagnosis, 77
Foley WD, see Wicks JD
Forbes GS, McLeod RA, Hattery RR: Radiographic manifestations of bone metastases from renal carcinoma, 61
Forsythe A, see Gilbert HA
Fraker K, see Burnham J
Frank IN, see Barbaric ZL
Frankl G: Breast cancer controversy continues (l), 758
Freedom RM, Culham JAG, Rowe RD: Angiocardiography of subaortic obstruction in infancy, 813
Freiman D, see Ring EJ
Fremland A: Diagnostic oncology case studies: mestastatic carcinoma presenting as shoulder arthritis, 137
Frias JL, see Felman AH
Friedman AK: Breast cancer controversy continues (l), 758
Friedman M: *Breast cancer: its impact on the patient, family, and community* (b), 564
Fulkerson JP, Ozonoff MB: Multiple symmetrical fractures of bone of unresolved etiology, 313

Galdabini J, see Baum S
Gallant TE, Hunziker RJ, Gibson TC: Primary chylopericardium: the role of lymphangiography, 1043
Gamsu G, see Klein DL
______, see Webb WR
Gant TD, see Klein DL
Garcia L, see Mojab K
Gardella L, see Moskowitz M
Gardiner GA Jr: "Backwash ileitis" with pseudopolyposis (c), 506
______, see Boyd WR
Gartside P, see Moskowitz M
Gates GF, see Stanley P
Genant HK, see Rennel C
Gerding PR, see Reese DF
Gerson ES, Gerzof SG, Robbins AH: CT confirmation of pelvic lipomatosis: two cases (c), 338
Gerzof SG, see Gerson ES
Gianturco C, see Anderson JH
Gibbons RP, see Bush WH Jr
Gibson TC, see Gallant TE
Giedion A, see Patriquin HB
Gilbert HA, Kagan AR, Nussbaum H, Rao AR, Satzman J, Chan P, Allen B, Forsythe A: Evaluation of radiation therapy for bone metastases: pain relief and quality of life, 1095
Gildersleeve S, Kuhns LR: An abdominal belt to encourage full inspiration in children during tomography (t), 354
Gilsanz V, Cleveland RH, Wilkinson RH: Aseptic necrosis: a complication of dislocation of the metacarpophalangeal joint (c), 737
Gilula LA, see Murphy WA
Glickman MG, Weiss RM, Itzchak Y: Testicular venography for undescended testes, 67
Gloyna RE, Zornoza J, Goldstein HM: Primary ulcerative carcinoma of the esophagus, 599
Go RT, see Jacoby CG
Goepfert H, see Handel SF
Goergen TG, see Armbuster TG
Gold RH: *Mammography: techniques–diagnosis–differential diagnosis–results* (b), 957
______, see Hansen GC
Goldman SM, Meng CH, White RI, Naraval RC, Siegelman SS, Diamond AB, Kaufman SL, Harrington DP: Transitional cell tumors of the kidney: how diagnostic is the angiogram?, 99
______, see Diamond AB
Goldstein HM, Beydoun MT, Dodd GD: Radiologic spectrum of melanoma metastatic to the gastrointestinal tract, 605
______, see Athey PA
______, see deSantos LA
______, see Gloyna RE
______, see Katragadda CS
______, see Zornoza J
Goldstein RA, see Rohatgi PK
Golimbu C, see Firooznia H
Gomes AS, Grollman JH Jr, Mink J: Pulmonary angiography for pulmonary emboli: rational selection of oblique views, 1019
Gonzalez AC: *Ultrasonography of the abdomen* (b) 198
Gonzalez CF, see Ehrlich I
Goodhead DT, Berry RJ, Bance DA, Gray P, Stedeford JBH: High energy fast neutrons from the Harwell variable energy cyclotron, 709
______, see Berry RJ
Goodman PC, Minagi H, Thomas AN: Radiographic appearance of the chest after pleural space reduction procedures: construction of a pleural tent and phrenoplasty, 229
Gooneratne NS, Buse MG, Quinn JL III, Selby JB: "Hot spot" on hepatic scintigraphy and radionuclide venacavography, 447
Gordon DH: Intravenous versus intraarterial vasopressin (l), 947
Gordon IJ, Shah BL, Hardman DR, Chameides L: Giant dural supratentorial arteriovenous malformation (c), 734
Gosink BB, see Scheible W
Gouliamos AD, Johnsrude IS, Jackson DC: Pulmonary vein avulsion (c), 331
Govoni AF: *Manuale di ecotomografia* (b), 378
Graham DY, see Fisher RG
Granmayeh M, Wallace S, Barrett AF, Fisher R, Heslep JH: Sarcoma of the kidney: angiographic features, 107
______, see Fisher RG
Gray P, see Goodhead DT
Grayson EV: *Computed brain and orbital tomography: technique and interpretation* (b), 201
Green B, see Katragadda CS
Greenfield LD: *Advances in radiation biology* (b), 200
______: *Hormones and breast cancer* (b), 201
______: *Tumour localization with radioactive agents* (b), 959
Griscom NT, Hargreaves HK, Schwartz MZ, Reddish JM, Colodny AH: Huge splenic cyst in a newborn: comparison with 10 cases in later childhood and adolescence, 889
Grollman JH Jr, O'Reilly RJ: Intraarterial lidocaine (l), 1138
______, Straede PD: Rotating platform for ascending phlebography (t), 941
______, see Gomes AS
Grønvall J, Grønvall S, Hegedüs V: Ultrasound-guided drainage of abscesses using angiographic catheterization techniques, 997
Grønvall S, see Grønvall J
Gross RC, see Mani RL
Gross WS, see Silver TM
Grünebaum M, Lebowitz RL: Hypothyroidism in cystinosis, 629
Guenther D, see Moskowitz M
Guest JA, Malangoni MA, Holden RW, Yaw PB: Peripheral arterial embolism of multiple pellets after shotgun injury to an extremity (c), 933

Haber K, see Hunter TB
Hahn FJ, see Jacoby CG
Hallberg J, see Kelsey CA
Haller JO, Berdon WE, Baker DH, Kassner EG: Left adrenal neuroblastoma with normal-appearing urogram, 1051
Halls JM, Meyers HI: Acute appendicitis with abscess simulating carcinoma of the sigmoid, 1057
Halpern SE, see Preisman RA
Hammerschmidt DE, see Castaneda-Zuniga WR
Han SY, Witten DM: Diffuse calcification of the breast in chronic renal failure (c), 341
Handel SF, Miller MH, Wallace S, Goepfert H, Jesse RH: Angiographic observations on chemodectomas of the head and neck, 477

Hansen GC, Gold RH: Central depression of multiple vertebral end-plates: a "pathognomonic" sign of sickle hemoglobinopathy in Gaucher's disease (c), 343

———, Weisenburger T: Diagnostic oncology case studies: testicular seminoma with an abdominal mass, 707

Hardman DR, see Gordon IJ

Hargreaves HK, see Griscom NT

Harned RK, see Anderson JC

Harolds JA, see Lorenzo RL

Harrington DP, see Cavaluzzi JA

———, see Goldman SM

Harris RD: *Contributions to nephrology, vol. 5: radiology and the kidney, some present concepts* (b), 566

Harris RD: *Radiologic diagnosis of renal parenchymal disease* (b), 1158

Hart KZ, Brower AC: Unilateral hypertrophy of multiple pedicles (c), 739

Harvey-Smith W: *Lung disease, state of the art, 1975-1976* (b), 959

Hattery RR, see Forbes GS

———, see MacCarty RL

———, see Stephens DH

Hedgcock MW, see Eisenberg RL

Hegedüs V, see Grønvall J

Heller RM, Kirchner SG, O'Neill JA: Perforation of the pharynx in the newborn: a look-alike for esophageal atresia (c), 335

Herlinger H, Laufer I: *Gastroenterology. vol. 3: liver, gallbladder, bile ducts, and pancreas,* 3d ed (b), 961

Hernandez R, Poznanski AK, Kelch RP, Kuhns LR: Hand radiographic measurements in growth hormone deficiency before and after treatment, 487

Heslep JH, see Granmayeh M

Hessel SJ: Perspectives on benefit-cost analysis in medical care (e), 753

Holden RW, see Guest JA

Horiot JC, see Jampolis S

Horton JA, see Chestnut JS

———, see Drayer BP

Horwith M, see Whalen JP

House AJS, Thomson KR: Evaluation of a new transthoracic needle for biopsy of benign and malignant lung lesions, 215

Hungerford GD, Powers JM: Avulsion of nerve rootlets with the Cuatico needle during Pantopaque removal after myelography, 485

Hunter TB, Haber K: Sonographic diagnosis of a wandering spleen (c), 925

Hunziker RJ, see Gallant TE

Husted JW, see Ring EJ

Hutson D, see Viamonte M Jr

Irwin GAL: *Roentgen diagnosis of bones, a self-teaching manual* (b), 377

Isaacs H, see Stanley P

Isherwood I, see Callen PW

Isturiz P, see Fishbone G

Itai Y: Gastric polyps or erosions? (l), 358

Itzchak Y, see Glickman MG

Iyer S, see Kinkhabwala M

Jackson DC, Gouliamos AD

Jacobs RP, see Webb WR

Jacobson B, see Bolmgren J

Jacoby CG, Go RT, Hahn FJ: Computed tomography in cerebral hemiatrophy, 5

Jaffe RB: *Echocardiography* (b), 957

Jampolis S, Pipard G, Horiot JC, Bolla M, Le Dorze C: Preliminary results using twice-a-day fractionation in the radiotherapeutic management of advanced cancer of the head and neck, 1091

Jander HP, Laws HL, Kogutt MS, Mihas AA: Emergency embolization in blunt hepatic trauma, 249

Jaques PF, Richey WA, Ely CA, Johnson G Jr: Doppler ultrasonic screening prior to venography for deep venous thrombosis, 451

Jeans WD: Pneumothorax and renal cyst puncture (l), 947

Jeffrey RB, see Eisenberg RL

Jesse RH, see Handel SF

Jing B-S, see Lindell MM Jr

Joffe N: Gas-filled appendix dialog (l), 182

———, see Sacks BA

Johnson G Jr, see Jaques PF

Johnsrude IS, see Gouliamos AD

Jonasson O, see Spigos DG

Jonsson K, Anderson JH, Osborne B, Wallace S: Ether-dissolved ethiodol for lymphangiography: an experimental study, 1047

Jost RG, see Sagel SS

Kademian MT, Buchler DA, Wirtanen GW: Bipedal lymphangiography in malignancies of the uterine corpus, 903

———, Wirtanen GW: Accuracy of bipedal lymphography in Hodgkin's disease, 1041

Kadir S, Kalisher L, Schiller AL: Extramedullary hematopoiesis in Paget's disease of bone, 493

Kagan AR: *Early breast cancer, its history and results of treatment* (b), 199

———, see Gilbert HA, Fremland A, Hansen GC, Kalinowski R

Kahn PC, Milunsky C, Dewanjee MK, Rudders RA: The place of ^{57}Co-bleomycin scanning in the evaluation of tumors, 267

Kalinowski R: Diagnostic oncology case studies: chronic sciatic pain in a young woman with sclerosis of the iliac bone, 1087

Kalisher L, see Kadir S

———, see Toombs BD

Kaplan HS: Fundamental mechanisms in combined modality therapy of cancer, 383

Kaplan P, see Patriquin HB

Karlin CA, Brower AC: Multiple primary hemangiomas of bone (c), 162

Kappelman NB, see Rosenfield AT

Kass E, see Bigongiari LR

Kassner EG, see Haller JO

Katragadda CS, Goldstein HM, Green B: Gray scale ultrasonography of calcified liver metastases, 591

Kattan KR: Backward "displacement" of the spinolaminal line at C2: a normal variation, 289

Katzen BT, see Rubin BE

Kaufman AS, Kuhns LR: The lateral decubitus view: an aid in evaluating poorly defined pulmonary densities in children, 885

Kaufman SL, see Cavaluzzi JA

———, see Goldman SM

Kay CJ: *Self-assessment of current knowledge in nuclear medicine: 1,012 multiple choice questions and referenced answers* (b), 774

Kazam E, see Behan M

Keats TE, see Tonkin IL

Kelch RP, see Hernandez R

Kelly WA: *Pituitary and parapituitary tumors* (b), 1159

Kelsey CA, Moseley RD, Brogdon BG, Bhave DG, Hallberg J: Effect of size and position on chest lesion detection, 205

Kelvin FM: *Radiology of the gallbladder and bile ducts. Section 22, Golden's diagnostic radiology* (b), 957

Kerber CW, see Cromwell LD

Kereiakes JG: *Radiation protection for medical and allied health personnel* (b), 1157

———. *Structural shielding design and evaluation for medical use of x-ray and gamma rays of energies up to 10 MeV* (b), 1158

Khilnani MT, see Som PM

Kieffer SA, see Weinberger G

Kimura K, see Moncada R

Kind HP, see Patriquin HB

King FM, see Feigin DS

Kinkhabwala M, Mousavi A, Iyer S, Adamsons R: Bleeding ileal varicosity demonstrated by transhepatic portography (c), 514

Kirchmer NA, Sarwar M: Absent arch and hypoplastic pedicle: another confusing cervical spine anomaly (c), 154

Kirchner SG, see Heller RM

Kirks DR, Currarino G: Imperforate vagina with vaginourethral communication, 623

———, see Currarino G

Kiviat MD: *Testicular tumors* (b), 202

Klein DL, Gamsu G, Gant TD: Intrathoracic desmoid tumor of the chest wall (c), 524

Kodroff M, see Diamond AB

Kogutt MS, see Jander HP

Konnak JW, see Cho KJ

Korobkin M, see Callen PW

Kramer D, see DeSmet AA

Kraus JF, see Stadalnik RC

Kricun ME, see Ehrlich I

Krook L, see Whalen JP

Kuhl DE, see Dolinskas CA

Kuhns LR: *Radiology of the alimentary tract in infants and children* (b), 772

———, see Gildersleeve S

———, see Hernandez R

———, see Kaufman AS

Kunzmann A, see Rochester D

Kupic EA, see Mindell HJ

Lane EJ, see Proto AV

Lang EK: Complications of renal cyst puncture (l), 948

Lang EF: From earlier pages, 1135

——: Traian Leucutia, 1892–1977 (o), 945
Lantieri R, see Schwartz EE
Larson EB, Omenn GS, Margolis MT, Loop JW: Impact of computed tomography on utilization of cerebral angiograms, 1
Laufer I, see Herlinger H
Laws HL, see Jander HP
Lebowitz RL, see Cleveland RH
——, see Grünebaum M
Le Dorze C, see Jampolis S
Lee K, see Tsukamoto Y
Lee KR, Robinson RG, Neff JR: Demonstration of a false aneurysm of the extremity by dynamic radionuclide scintigraphy (c), 931
Lefleur RS, see Ambos MA
——, see Bosniak MA
Leon R, see Fishbone G
Leopold GR, see Scheible W
Le Page J, see Viamonte M Jr
Levin B, see Rochester D
Levin DC, Eisenberg H, Wilson R: Arteriography in the evaluation of pancreatic pseudocysts, 243
——, see Beckmann CF
Libshitz HI, Clouser M, Zornoza J, Osborne BM: Radiographic findings of immunoblastic lymphadenopathy and related immunoblastic proliferations, 875
——, see Bertrand M
Lim LT, see Asokan S
Lim MS: Gas-filled appendix dialog (l), 182
Lindell MM Jr, Jing B-S, Wallace S: Laryngeal tuberculosis, 677
Linton OW, see Moseley RD Jr
Loke J, see Putman CE
Loop JW, see Larson EB
Lorenzo RL, Harolds JA: The use of prone films for suspected bowel obstruction in infants and children, 617
Luna RF, see Soto B
Lutzker LG, see Zelefsky MN
Lynch RD, see Faer MJ
Lyons HA, see Rosen Y

MacCarty RL, Wahner HW, Stephens DH, Sheedy PF, Hattery RR: Retrospective comparison of radionuclide scans and computed tomography of the liver and pancreas, 23
MacIntyre I, see Whalen JP
Madayag MA, see Ambos MA
——, see Bosniak MA
Maddrey WC, see Cavaluzzi JA
Mainzer F, see Rennel C
Malangoni MA, see Guest JA
Mall JC, see Drinker H
Mani RL: Aortofemoral graft catheterization (l), 759
——, Gross RC: Keyhole cone device for lateral magnification cerebral angiography (t), 165
Maravilla A: *Radiology of the abdomen: anatomic basis* (b), 379
Margolis MT, see Cromwell LD
——, see Larson EB
Marsan RE, see Unger EL
Martel W, see Braunstein EM
——, see DeSmet AA
Martin EC, see Behan M
Mascatello VJ, Smith EH, Carrera GF, Berger M, Teele RL: Ultrasonic evaluation of the obstructed duplex kidney, 113
Mason DT, see Stadlanik RC
Master R, see Armbuster TG
Matsen FA III: *Watson-Jones: fractures and joint injuries* (b), 564
Matthay RA, see Putman CE
Maturi RA, see Miller SW
McCaffrey JA, see Clouse ME
McCauley D, see Firooznia H
McCormick TL, Cho KJ: Angiographic findings in renal amyloidosis, 855
McDaniel MM, Fierstien SB: An aid to C1–C2 percutaneous puncture (t), 353
McLeod RA, see Forbes GS
McLoud TC, Barash PG, Ravin CE: PEEP: Radiographic features and associated complications, 209
McLoughlin C, see Fishbone G
Mead JH, see Faer MJ
Mena E, see Whalen JP
Menanteau BP: *Paleopathological diagnosis and interpretation: bone diseases in ancient human populations* (b), 379
Meng CH, see Diamond AB
——, see Goldman SM
Meschan I: Pulmonary surfactant disease states (e), 545
Meyers EN, see Dubois PJ
Meyers HI, see Halls JM
Michal JA III, Coleman RE: Localization of ^{67}Ga citrate in a mycotic aneurysm, 1111
Mihas AA, see Jander HP
Mikhael MA, see Evens RG
Millar RC, see Fetouh SA
Miller MH, see Handel SF
Miller SW, Dinsmore RE, Wittenberg J, Maturi RA, Powell WJ Jr: Right and left ventricular volumes and wall measurements: determination by computed tomography in arrested canine hearts, 257
——, see Stanley P
Milligan FD, see Curtin MJ
Milunsky C, see Kahn PC
Minagi H, see Goodman PC
Mindell HJ: Renal cyst puncture (l), 1137
——, Kupic EA: Horseshoe kidney: ultrasonic demonstration (c), 526
Mink J, see Gomes AS
Mintzer RA, see Neiman HL
Mojab K, Garcia L, Talge G: A new subtraction technique using duplicating film as a final print (t), 528
Moncada R, Cardoso M, Danley R, Rodriguez J, Kimura K, Pickleman J, Brandly J: Acute cholecystitis: 137 patients studied by infusion tomography of the gallbladder, 583
——, Cardoso M, Danley R, Rodriguez J, Kimura K, Pickleman J, Brandly J: Infusion tomography of the gallbladder: mechanism of gallbladder wall opacification in experimental acute cholecystitis, 587
Montgomery CK, see Eisenberg RL
Moon S, see Rosen Y
Moore WE, see Cromwell LD
Morgan RH: Roles for radiologists in tomorrow's medical care system, 1129
Morin ME, Baker DA: Lymphocele: a complication of surgical staging of carcinoma of the prostate (c), 333
Moseley RD Jr, Linton OW: The federal government's impact on radiology, 171
——, Linton OW: The federal crossword puzzle (e), 176
——, see Kelsey CA
Moskowitz M, Gartside P, Gardella L, DeGroot I, Guenther D: Special lecture. The breast cancer screening controversy: a perspective, 537
Mousavi A, see Kinkhabwala M
Mozes M, see Spigos DG
Muecke EC, see Behan M
Multz CV, see Rennel C
Murphy WA: Exostosis after iliac bone marrow biopsy, 1114
——, Siegel MJ, Gilula LA: Arthrography in the diagnosis of unexplained chronic hip pain with regional osteopenia, 283
Murry R: High kVp chest radiography (l), 1139

Naraval RC, see Goldman SM
Neff JR, see Brower AC
——, see Lee KR
Neiman HL, Mintzer RA: Accuracy of biliary duct ultrasound: comparison with cholangiography, 979
Neufeld HN, see Blieden LC
Newton D: Clearance of radioactive tantalum from the human lung after accidental inhalation, 327
Nishitani H, see Tsukamoto Y
Niwayama G, see Resnick D
Nordenström B, see Bolmgren J
Northrop CH: *Urologic radiology* (b), 203
Novak WG, see Bigongiari LR
Novy SB: *Current concepts in radiology* (b), 1158
Nunez D Jr, see Fishbone G
Nunez EA, see Whalen JP
Nussbaum H, see Gilbert HA

Oberfield RA, see Clouse ME
O'Brien PC, see Reese DF
Ochsner S: Informed consent for urography? (l), 359
Oestreich AE: *Appareil pulmonaire et médiastin. I. Generalités. Séméiologie. Pathologie du médiastin* (b), 1157
O'Hara AE, see Curtis JA
Okawa T, see Tsukamoto Y
Oleaga JA, see Ring EJ
Olmsted WW: *Cerebral dural sinuses and their tributaries* (b), 202
Omenn GS, see Larson EB
O'Neill JA, see Heller RM
Onitsuka H, see Tsukamoto Y
Op den Orth JO, Dekker WW: Gastric polyps or erosions? (l), 357
O'Reilly GV, Clark TM, Crum CP: Skeletal involvement in mycosis fungoides (c), 741
O'Reilly RJ, see Grollman JH Jr
Orr DP, see Dubois PJ
Osborne BM, see Jonsson K
——, see Libshitz HI

Oshiumi Y, see Tsukamoto Y
Ostrum BJ, see Amendola MA
Ottinger LW, see Baum S
Ozonoff MB, see Fulkerson JP

Pacifico AD, see Soto B
Parker BR, see Dunnick NR
———, see Pinckney L
Parker FB, see Weinberger G
Patel SK: *The adrenal retroperitoneum and lower urinary tract. Atlas of tumor radiology* (b), 773
Patriquin HB, Kaplan P, Kind HP, Giedion A: Neonatal mucolipidosis II (I-cell disease): clinical and radiologic features in three cases, 37
Pavel DG, see Spigos DG
Paz G, see Fishbone G
Pereiras R, see Viamonte M Jr
Pfister RC, see Dembner AG
Phillips HE, see Shauffer IA
Pickleman J, see Moncada R
Pinckney L, Parker BR: Myelosclerosis and myelofibrosis in treated histiocytosis-x (c), 521
Pipard G, see Jampolis S
Polishuk WZ, see Weinstein D
Postlethwait RW, see Fetouh SA
Powell WJ Jr, see Miller SW
Powers JM, see Hungerford GD
Poznanski AK, see Hernandez R
Preisman RA, Halpern SE, Shishido R, Waltz T, Callipari F, Reit R: Uptake of ^{131}I by a papillary meningioma (c), 349
Present AJ: E. Dale Trout, 1901-1977 (o), 363
Proto AV, Lane EJ: Air in the esophagus: a frequent radiographic finding, 433
Pudlowski R, see Firooznia H
Pulmano CM, see Chuang VP
Putman CE, Loke J, Matthay RA, Ravin CE: Radiographic manifestations of acute smoke inhalation, 865

Quinn JL III, see Gooneratne NS

Radhakrishnan J, see Asokan S
Rafii M, see Firooznia H
Randall PA, see Weinberger G
Rao AR, see Gilbert HA
Ravin CE, see McLoud TC
———, see Putman CE
Reba RC, see Rohatgi PK
Reddish JM, see Griscom NT
Reese DF, O'Brien PC, Beeler GW Jr, Gerding PR, Romme CR: A statistical description of the normal computerized brain scan, 457
Reid L: The lung: its growth and remodeling in health and disease, 777
Reit R, see Preisan RA
Rennel C, Mainzer F, Multz CV, Genant HK: Subchondral pseudocysts in rheumatoid arthritis, 1069
Resnick D, Niwayama G: On the nature and significance of bony proliferation in "rheumatoid variant" disorders, 275
———, see Armbuster TG
Reuter SR, see Cho KJ
Reimenschneider PA: Hickey lecture. Radiology manpower update, 1976: shortage or surfeit?, 575
Richey WA, see Jaques PF
Rigler LG, see Bein ME
Ring EJ, Oleaga JA, Freiman D, Husted JW, Waltman AC Jr, Baum S: Pitfalls in the angiographic management of hemorrhage: hemodynamic considerations, 1007
Robbins AH, see Gerson ES
Robinson RG, see Lee KR
Rochester D, Levin B, Bowie JD, Kunzmann A: Ultrasonic appearance of the Krukenberg tumor (c), 919
Rodriguez J, see Moncada R
Rogers LF, see Chessare JW
Rohatgi PK, Simon DB, Goldstein RA, Reba RC: Strontium-87m lung scans in pulmonary aspergillosis, 879
Rohlfing BM, see Webb WR
Rohrmann CA Jr: *Radiological atlas of common diseases of the small bowel* (b), 379
Romme CR, see Reese DF
Rosen Y, Amorosa JK, Moon S, Cohen J, Lyons HA: Occurrence of lung granulomas in patients with stage I sarcoidosis, 1083
Rosenbaum AE, see Drayer BP
Rosenfield AT, Siegel NJ, Kappelman NB, Taylor KJW: Gray scale ultrasonography in medullary cystic disease of the kidney and congenital hepatic fibrosis with tubular ectasia: new observations, 297
———, see Cook JH III
———, see Walsh J
Rosenthal DI, Chandler HL, Azizi F, Schneider PB: Uptake of bone imaging agents by diffuse pulmonary metastatic calcification, 871
Roswit B, White DC: Severe radiation injuries of the lung, 127
Rowe RD, see Freedom RM
Rubin BE, Katzen BT: Selective hepatic artery embolization to control massive hepatic hemorrhage after trauma, 253
Rudd TG: *Scintillation camera lung imaging. An anatomic atlas and guide* (b), 378
Rudders RA, see Kahn PC
Rujanavech N, see Evens RG
Russell E, see Viamonte M Jr
Ryan RB, see Clouse ME

Sacks BA, Joffe N, Antonioli DA: Metastatic melanoma presenting clinically as multiple colonic polyps (c), 511
Sadhu V, see Curtis JA
Sagel SS, Siegel MJ, Stanley RJ, Jost RG: Detection of retroperitoneal hemorrhage by computed tomography, 403
Salam A, see Cromwell LD
Salo BC, see Berkow AE
Sanchez R, see Castaneda-Zuniga WR
Sanders RC: Complications of renal cyst puncture (I), 947
Sansom JM, see Berry RJ
Sarwar M, Swischuk LE: Bilateral internal auditory canal enlargement due to dural ectasia in neurofibromatosis (c), 935
———, see Kirchmer NA
Satzman J, see Gilbert HA
Schaner EG, Balow JE, Doppman JL: Computed tomography in the diagnosis of subcapsular and perirenal hematoma, 83
Schapiro RH, see Baum S
Scheible W, Gosink BB, Leopold GR: Gray scale echographic patterns of hepatic metastatic disease, 983
Scher AT: Unilateral locked facet in cervical spine injuries, 45
Schiller AL, see Kadir S
Schneeweiss A, see Bleiden LC
Schneider PB, see Rosenthal DI
Schreiber MH, Davis M: Intraluminal diverticulum of the esophagus, 595
Schumacher D, see Cromwell LD
Schwartz EE, Lantieri R, Teplick JG: Erosion of the inferior aspect of the clavicle in secondary hyperparathyroidism, 291
Schwartz MZ, see Griscom NT
Schwartz SS: *Radiological aspects of the liver and biliary tract. X-ray and radioisotope diagnosis* (b), 201
———: An unfinished phantasy (I), 1139
Scott DW III, see Cimmino CV
Seidelmann FE, Cohen WN, Bryan PJ, Brown J: CT demonstration of the splenic vein-pancreatic relationship: the pseudodilated pancreatic duct, 17
Selby JB, see Gooneratne NS
Sequeira J, see Shauffer IA
Seydel HG: *Conference on spontaneous regression of cancer* (b), 774
Shah BL, see Gordon IJ
Shauffer IA, Phillips HE, Sequeira J: The jet phenomenon: a manifestation of esophageal web (c), 747
Sheedy PF II, see MacCarty RL
———, see Stephens DH
Sheff R, see Cavaluzzi JA
Shehadi WH: Committee report: contrast media in diagnostic radiology: recommendations for labels, package inserts, and dosage determination, 167
Shenoy SS, Culver GJ, Ali MV: Intraluminal duodenal diverticulum: diagnosis during endoscopic pancreatography (c), 929
Shishido R, see Preisman RA
Siegel MJ, see Sagel SS
———, see Murphy WA
Siegel NJ, see Rosenfield AT
Siegel SE, see Stanley P
Siegelman SS, see Feigin DS
———, see Goldman SM
Silver TM, Washburn RL, Stanley JC, Gross WS: Gray scale ultrasound evaluation of popliteal artery aneurysms, 1003
———, Thornbury JR: Pneumothorax and renal cyst puncture (I), 947
Simon DB, see Rohatgi PK
Simon RS, see Bradac GB
Simpson LD, see Stewart JR
Skucas J, see Wandtke J
Slivka J, see Armbuster TG
Smith EH, see Mascatello VJ
Smith GR: *Roentgenologic diagnosis* (b), 202
———: *Computerized tomography with the general purpose scanner* (b), 1156

Smith JA, see Tucker TT
Smith WL, see Tucker TT
Som PM, Khilnani MT, Beranbaum BL, Wolf BS: Mondini defect: a variant, 1120
Soter CS: Gas-filled appendix dialog (l), 182
Soto B, Pacifico AD, Luna RF, Bargeron LM Jr: A radiographic study of congenital pulmonary atresia with ventricular septal defect, 1027
Spataro R, see Wandtke J
Spencer RP: *Cerebral radionuclide angiography* (b), 199
Spiegler P, see Bein ME
Spigos DG, Tan W, Pavel DG, Mozes M, Jonasson O, Capek V: Diagnosis of urine extravasation after renal transplantation, 409
Stadalnik RC, Vera Z, DaSilva O, Davies R, Kraus JF, Mason DT: Electrocardiographic response to intravenous urography: prospective evaluation of 275 patients, 825
Stanley JC, see Silver TM
Stanley P, Gates GF, Eto RT, Miller SW: Hepatic cavernous hemangiomas and hemangioendotheliomas in infancy, 317
______, Siegel SE, Isaacs H: Calcification in a paraspinal malignant melanoma in a child (c), 143
Stanley RJ, see Sagel SS
Staple TW: *Radiologic examination in orthopaedics: methods and techniques* (b), 203
Steckel RJ, see Fremland A, Hansen GC, Kalinowski R
Stedeford JBH, see Goodhead DT
Steinbach JBH, see Burnham J
Steiner RM, see Curtis JA
Stellmach R, see Bradac GB
Stephens DH, Sheedy PF II, Hattery RR, Williamson B Jr: Diagnosis and evaluation of retroperitoneal tumors by computed tomography, 395
______, see MacCarty RL
Stewart JR, Simpson LD: Computed tomography and the quality of radiation therapy (e), 943
Straede PD, see Grollman JH Jr
Stratemeier PH: Massive esophageal hemorrhage in leukemia, 1106
Swischuk LE, see Sarwar M

Tachdjian MO, see Chessare JW
Talge G, see Mojab K
Tan W, see Spigos DG
Taylor KJW, see Cook JH III
______, see Rosenfield AT
______, see Walsh J
Teates CD, Williamson BRJ: "Hot and cold" bone lesion in acute osteomyelitis (c), 517
Teele RL, see Mascatello VJ
Tegtmeyer CJ: *Symposium on angiography* (b), 200
Teplick JG, see Schwartz EE
Teresi M, see Asokan S
Thacker J, see Berry RJ
Theros EG, see Feigin DS
Thomas AN, see Goodman PC
Thomson KR, see House AJS
Thornbury JR, see Bigongiari LR
______, see Silver TM
Tillema DA, see Brower AC
Tonkin IL, Keats TE, Capp MP: Radiographic isolation of the inferior vena cava, 657
Toombs BD, Kalisher L: Metastatic disease to the breast: clinical, pathologic, and radiographic features, 673
Torun B, see Whalen JP
Trabanino JG, see Fisher RG
Tsukamoto Y, Nishitani H, Oshiumi Y, Okawa T: Spontaneous disappearance of gastric polyps: report of four cases, 893
______, Onitsuka H, Lee K: Radiologic aspects of diffuse idiopathic skeletal hyperostosis in the spine, 913
Tucker TT, Smith WL, Smith JA: Fluid-filled cystic adenomatoid malformation, 323

Ulreich S, see Beckmann CF
Unger EL, Marsan RE: Ruptured aneurysm 20 years after surgery for coarctation of the aorta (c), 329

Vera Z, see Stadalnik RC
Vermeere WR, see Cromwell LD
Viamonte M Jr, Pereiras R, Russell E, Le Page J, Hutson D: Transhepatic obliteration of gastroesophageal varices: results in acute and nonacute bleeders, 237
Viteri F, see Whalen JP

Wahner HW, see MacCarty RL
Wallace S, see Anderson JH
______, see Granmayeh M
______, see Handel SF
______, see Jonsson K
______, see Lindell MM Jr
Walsh J, Taylor KJW, Rosenfield AT: Gray scale ultrasonography in retroperitoneal lymphangiomyomatosis, 1101
Walter JF, see Wicks JD
______, see Cho KJ
______, see Chuang VP
Waltman AC Jr, see Baum S
______, see Ring EJ
Waltz T, see Preisman RA
Wandtke J, Skucas J, Spataro R, Bruneau RJ: Pneumatosis intestinalis as a complication of jejunoileal bypass, 601
Warshaw AL, see Baum S
Washburn RL, see Silver TM
Webb WR, Gamsu G, Rohlfing BM: Catheter venography in the superior vena cava syndrome (c), 146
______, Jacobs RP: Transpleural abdominal systemic artery—pulmonary artery anastomosis in patients with chronic pulmonary infection, 233
Weinberger G, Randall PA, Parker FB, Kieffer SA: Involvement of an aberrant right subclavian artery in dissection of the thoracic aorta: diagnostic and therapeutic implications, 653
Weinstein CE, see Weinstein MA
Weinstein D, Aviad Y, Polishuk WZ: Hysterography before and after myomectomy, 899
Weinstein MA, Duchesneau PM, Weinstein CE: Computed angiotomography, 699
Weisenburger T, see Hansen GC
Weisman M, see Armbuster TG
Weiss RM, see Glickman MG
Whalen JP, Horwith M, Krook L, MacIntyre I, Mena E, Viteri F, Torun B, Nunez EA: Calcitonin treatment in hereditary bone dysplasia with hyperphosphatasemia: a radiographic and histologic study of bone, 29
White DC, see Roswit B
White H, see Chessare JW
White RI Jr: Aortofemoral graft catheterization (l), 759
______, see Cavaluzzi JA
______, see Goldman SM
Whitfield PW, see Daffner RH
Wicks JD, Bigongiari LR, Foley WD, Walter J: Parenchymal striations in renal vein thrombosis: arteriographic demonstration, 95
______, see Bigongiari LR
Wilcox CW, see Cho KJ
Wilcox WA: *An introduction to the physics of nuclear medicine* (b), 566
______, *Radiologic science: workbook and laboratory manual* (b), 960
Wilkins RH, see Drayer BP
Wilkinson RH: *Fairbank's atlas of general affections of the skeleton* (b), 378
______, see Gilsanz V
Williamson B Jr, see Stephens DH
Williamson BRJ, see Teates CD
Wilson R, see Levin DC
Winter PF: *The basic physics of radiation therapy* (b), 1157
Wirtanen GW, see Kademian MT
Witten DM, see Barnes GT
______, see Han SY
Wittenberg J, see Ferrucci JT Jr
______, see Miller SW
Wolf BS, see Som PM
Wootton P: *Graphs and tables for use in radiology* (b), 199

Yaghmai I: Angiographic features of osteosarcoma, 1073
Yaw PB, see Guest JA

Zelefsky MN, Lutzker LG: The target sign: a new radiologic sign of septic pulmonary emboli, 453
Zimmerman RA, see Dolinskas CA
Zimmerman RD, see Bernardino ME
Zornoza J, Goldstein HM: Cavitating metastases of the small intestine, 613
______, see Gloyna RE
______, see Libshitz HI

Subject Index Volume 129

Index key: a = abstract, b = book review, c = case report, e = editorial,
l = letter, o = obituary, t = technical note

The majority of the subjects in the Journal can be classified readily as a disease entity, a diagnostic procedure or a treatment method. These can be brought together rationally in their application to some body part or region. Accordingly, the basic organization of this index is anatomic and, to the extent possible and convenient, entries are listed under a body part or region. Entities that affect more than one body part or diseases, procedures, or methods for which there are numerous titles are given independent listing as well. Other subjects not readily referenced anatomically are listed alphabetically. Original articles, abstracts of literature, book reviews, and editorials are indexed. News items and books received are not listed. A given entry will be listed at least once, often twice, and occasionally three times. For brevity, titles of articles and abstracts are often permuted.

Abdomen, see also pelvis and specific organs and diseases
  CT evaluation of retrocrural prevertebral space, 907
  CT of retroperitoneal tumors, 395
  Radiology of the abdomen: anatomic basis (b), 378
  Ultrasonography of the abdomen (b), 198
  Ultrasound guided drainage of abscesses, 997
  Visualization of lateral edge of liver in ascites (a), 764
Abscess, see also organs and regions
  Acute appendicitis with, simulating carcinoma, 1057
  Cerebral, angiographic changes (a), 1148
  Ultrasound guided drainage of, 997
Accelerators, see therapeutic radiology, apparatus
Achalasia, see stomach
Acinus, see lungs
Acrocephalosyndactyly, see bones, fingers, skull
ACTA scanner, see computed tomography
Actinomycosis, see also organ
  Actinomycin-D, local recurrence of breast cancer irradiated with and without (a), 955
Addison's disease, see adrenals
Adenoma, see under individual organs and regions
Adrenals
  The adrenal, retroperitoneum and lower urinary tract. Atlas of tumor radiology (b), 773
  Left, neuroblastoma, 1051
  Myelolipoma of, ultrasound and CT, 993
  Nontumorous hyperfunction (a), 185
  Progressive abnormalities in brain scan in leukodystrophy (c), 939
  Radioisotopic study of (a), 1151
  Ultrasound in metastases (a), 194
Agammaglobulinemia, see gamma globulins
Aganglionosis, see colon
Alzheimer's disease, see brain
American Journal of Roentgenology, reviewers and abstractors, 1977, 1142
American Radium Society, report of 1977 meeting, 1140
American Roentgen Ray Society
  Commercial exhibitors, 1977 meeting, 552
  Local activities, 1977 meeting, 360
  Scientific program, 1977 meeting, 179
Amipaque, ventriculography with (a), 953
Amyloidosis
  Angiographic findings in renal, 855
  Radiologic findings in renal, 851
Anastamoses, see arteries
Anemia, see also sickle cell disease
  Suppression of erythroid-colony formation by lymphocytes from patients with aplastic (a), 194
Aneurysm, see also under individual arteries, aorta, heart
  Asymptomatic left ventricular (a), 763
  False, of extremity by dynamic radionuclide scintigraphy (c), 931
  Gray scale ultrasound evaluation of popliteal artery, 1003
  Localization of ^{67}Ga citrate in mycotic (c), 1111
  20 years after surgery for coarctation (c), 329
Anger camera, see radionuclide imaging
Angina pectoris, see heart
Angiocardiography, see coronary arteries, heart
Angiography, see also diseases and organs
  Symposium on angiography (b), 200
Angiography, complications
  Aortofemoral graft catheterization (l), 759
  Cardiovascular arterial patency, in infants and small children (a), 1143
  Complications of long term hepatic arterial chemotherapy, 799
  Postangiographic care of femoral puncture site (a), 762
  Subintimal injection as complication of abdominal (a), 950
Angiography, technique
  Arteriography of traumatized hand (a), 1144
  Cranial and caudal angulation for coronary (a), 1144
  Cryodynamic hand, in Raynaud's syndrome (a), 950
  Intraarterial lidocaine (l), 1138
  Intravascular coil occlusion of arteriovenous fistulas, 795
  Intravenous versus intraarterial vasopressin (l), 947
  Management of hemorrhage, 1007
  Nonsurgical splenectomy, 805
  Pharmacoangiography of bone and soft-tissue tumors (a), 372
  Pulmonary, for emboli, 1019
  Wedge filter for craniocervical (t), 1125
Angioma, see also individual organs
  Angiodysplasia of right colon, 789
Angiotensin
  Diagnosis of, renal scintigraphy and saralasin infusion (a), 1152
Angitis, see arteritis
Ankle
  Arthrography and distortion (a), 189
  Peroneal tendon dislocation, 1065
  Pseudotibiotalar slant (a), 766
  Role of lateral malleolus in displaced fractures of (a), 371
Anticoagulants, see blood
Antrum, see stomach
Aorta
  Aberrant right subclavian artery in dissection of thoracic, 653
  Aneurysm 20 years after surgery for coarctation (c), 329
Aortic valve, see heart
Aortography, see aorta
Appendix
  Acute with abscess simulating carcinoma, 1057
  Gas-filled (l), 182
Aqueduct of Sylvius, see brain
Aqueduct, vestibular, see ear
Arachnoid, see also cisterns, meninges
  Arachnoiditis following lumbar radiculography with metrizamide (a), 193
  Spontaneous, normal-pressure cerebrospinal fluid fistulas in middle fossa (a), 767
Arnold-Chiari malformation, see brain
Arteries, see also angiography; specific blood vessels; organs and regions; thrombosis
  Aberrant right subclavian, in dissection of thoracic aorta, 653
  Angiography of testicular (a), 949
  Complications of long term hepatic chemotherapy, 799
  Early femoral atherosclerosis in hyperlipoproteinemia (a), 365
  Embolization of external carotid (a), 949
  Gray scale ultrasound evaluation of popliteal aneurysms, 1003
  Percutaneous transluminal angioplasty: the Dotter procedure. A manual for the radiologist (b), 565
  Peripheral embolism of multiple pellets (c), 933
  Polyarteritis nodosa and hepatitis-B surface antigen, 77
  Takayasu's arteritis in children (a), 1150
  Transpleural systemic-pulmonary anastomosis in chronic pulmonary infection, 233
Arteriosclerosis, see also under specific blood vessels
  Regression and progression of early femoral, in hyperlipoproteinemic patients (a), 365
Arteritis
  Cerebral granulomatous, 463
  Polyarteritis nodosa and hepatitis-B surface antigen, 77
  Takayasu's, in children (a), 1150
Arteriovenous malformations
  Angiography of pancreatic, 1015
  Angiography in vascular of face, 469
  Giant dural supratentorial (c), 734
  Intravascular coil occlusion, 795
Arthritis, see also individual joints and spine
  Calcium pyrophosphate dihydrate deposition disease (a), 190
  Chalky joint effusion (a), 766
  Diabetic osteoarthropathy (a), 370
  Metastatic carcinoma presenting as shoulder, 137
  Multiple joint involvement with villonodular synovitis (a), 766
  Plant thorn synovitis (a), 1147
  Septic, of glenohumeral joint, 667
Arthritis, rheumatoid
  Bony proliferation in "variant" disorders, 275
  Clinicopathologic correlations (a), 1144
  Hip joint restoration in juvenile (a), 1147
  Septic (a), 190
  Subchondral pseudocysts, 1069
Arthrography, see also under specific joints
  Aid to performance of shoulder (t), 942

  Amipaque (metrizamide) and other contrast media, in rabbits (a), 558
  Ankle (a), 189
  Evaluation of contrast agents for (a), 558
  In unexplained chronic hip pain, 283
Ascites, visualization of lateral edge of liver in (a), 764
Aseptic necrosis, see bone or part
Aspergillosis, see also organ
  Strontium-87m lung scans in pulmonary, 879
  Thoracic wall invasion secondary to pulmonary (c), 140
Astrocytoma, see brain neoplasms; glioma
Atlas and axis, see spine
Atomic bomb and atomic energy, see radiation
Atrial septal defect, see heart, congenital abnormalities
Atrium, see heart
Auditory canal, see ear
Azygos vein
  Retrograde azygography in carcinoma of esophagus (a), 554

Bacteremia
  Granulocyte transfusion for gram-negative septicemia (a), 561
  Transient, and endocarditis prophylaxis (a), 193
Basal cell nevus syndrome, see bones
Bile ducts, see also gallbladder
  Accuracy of CT of liver and biliary tract (a), 1146
  Biliary tract size and drainage time: comparison of endoscopic and intravenous cholangiography (a), 369
  Cholecystocholangiography after cholecystoduodenostomy (t), 534
  Comparison of biliary duct ultrasound and cholangiography, 979
  Gastroenterology. Vol. 3: liver, gallbladder, bile ducts and pancreas (b), 961
  Noncalculous obstruction (a), 367
  Radiological aspects of the liver and biliary tract. X-ray and radioisotope diagnosis (b), 201
  Radiology of the gallbladder and bile ducts (b), 957
  Technetium-99m pyridoxylideneglutamate cholescintigraphy (a), 195
  Ultrasonography in obstructive jaundice (a), 562
Biopsy, see also under specific organs
  Complications of percutaneous transthoracic needle (a), 184
  Needle for, of lung lesions, 215
  Percutaneous fine needle aspiration (a), 556
  Postirradiation in prostatic cancer (a), 376
  Septicemia as complication of percutaneous liver (a), 764
  Stereotaxic needle, of mamma, 121
Bladder, see also urinary tract; urography
  Pear-shaped (a), 189
  Pelvic phlebography for cancer of urinary, and prostate (a), 369
Bleomycin
  ^{57}Co, in evaluation of tumors, 267
  Scintigraphic evaluation of lymphoma, comparative study (a), 1152
Bone, see also under individual bones and diseases
  Comparisons between x-ray photodensitometric and gamma-ray absorptiometric findings of bone mineral (a), 558
  Demineralization and growth retardation in inflammatory bowel disease (a), 558
  Exostosis after iliac marrow biopsy (c), 1114
  Hand measurements in growth hormone deficiency, 487
  Multiple symmetrical fractures, 313
  Pharmacoangiography of, and soft-tissue tumors (a), 372
  Watson-Jones: fractures and joint injuries (b), 564
Bone, diseases
  Abnormalities in relatives with Marfan syndrome (a), 949
  Extramedullary hematopoiesis in Paget's disease, 493
  Fairbank's atlas of general affections of the skeleton (b), 378
  Massive subperiosteal hemorrhage in neurofibromatosis (a), 557
  Metatropic dwarfism and variants (a), 1149
  Myelosclerosis and myelofibrosis in histiocytosis-X (c), 521
  Neonatal mucolipidosis II (I-cell disease), 37
  Paleopathological diagnosis and interpretation: bone disease in ancient human populations (b), 379
  Precocious onset of Paget's disease (a), 558
  Prepubertal XY gonadal dysgenesis (a), 559
  Radiographic features of fucosidosis (a), 1150
  Radiographic and radioisotope scanning in detection of Paget's disease (a), 371
  Radiologic aspects of diffuse idiopathic hyperostosis in spine, 913
  Roentgen diagnosis of bones, a self-teaching manual (b), 379
  Short rib-polydactyly syndrome (a), 561
  Spurs of mandible in Cornelia de Lange syndrome (c), 156
  Trichorhinophalangeal syndrome, 631
Bone, infection
  "Hot and cold" lesion in acute osteomyelitis (c), 517
Bone, metabolic abnormalities
  Erosion of clavicle in secondary hyperparathyroidism, 291
  Hereditary dysplasia, calcitonin treatment, 29
  Hypophosphatasia (a), 560
  Hypothyroidism in cystinosis, 629
  Morphometry and osteopenia in spinal osteoporosis (a), 770
  Pathologic fracture in gout (c), 1116
  Renal osteodystrophy in childhood (a), 952
  ^{99m}Tc pyrophosphate scans in hyperparathyroidism (a), 374
  ^{99m}Tc Sn-pyrophosphate in parathyroid disease (a), 374
  Therapeutic value of thyreocalcitonin (e), 175
  Xeroradiography of hand in renal osteodystrophy (a), 371
Bone, neoplasm
  Arteriography in tumors (a), 557
  Angiography of osteosarcoma, 1073
  Chronic sciatic pain with sclerosis of iliac bone, 1087
  Ewing's tumor of rib (a), 1148
  Metastases from renal carcinoma, 61
  Metastatic carcinoma presenting as shoulder arthritis, 137
  Multiple primary hemangiomas of (c), 162
  Parotid carcinoma with osteoblastic metastases (c), 744
  Primary malignant fibrous histiocytoma (a), 951
  Radiation therapy for metastases, 1095
  Radionuclide skeletal survey for pediatric neoplasms (a), 771
  Skeletal involvement in mycosis fungoides (c), 741
  Thermographic, radionuclide, and radiographic detection of metastases (a), 766
  Ultrasonography in tumors arising from spine and pelvis, 1061
Bone, radionuclide imaging
  "Hot and cold" lesion in acute osteomyelitis (c), 517
  Imaging after arthroplasty of hip joint (a), 557
  Radionuclide skeletal survey for pediatric neoplasms (a), 771
  Scanning in evaluation of exercise-related stress injuries (a), 1147
  ^{99m}Tc pyrophosphate scans in hyperparathyroidism (a), 374
  ^{99m}Tc Sn-pyrophosphate in parathyroid disease (a), 374
  Thermographic, radionuclide, and radiographic detection of metastases (a), 766
Book reviews
  The adrenal, retroperitoneum and lower urinary tract. Atlas of tumor radiology, 773
  The adult postoperative chest, 773
  Advanced exercises in diagnostic radiology: CT of the brain, 960
  Advances in radiation biology, 200
  The basic physics of radiation therapy, 1157
  Biological and environmental effects of low-level radiation, 200
  Breast cancer: its impact on the patient, family, and community, 564
  Cerebral dural sinuses and their tributaries, 202
  Cerebral radionuclide angiography, 199
  Computed brain and orbital tomography technique and interpretation, 201
  Conference on spontaneous regression of cancer, 774
  Contributions to nephrology, 566
  Cranial computerized tomography, 772
  CT with the general purpose scanner, 1156
  Current concepts in radiology, 1158
  Cysts of the oral regions, 565
  Diagnosis and staging of cancer: a radiologic approach, 198
  Diagnostic neuroradiology, 377
  Diagnostic radiology, in paediatrics, 1156
  Early breast cancer, its history and results of treatment, 199
  Echocardiography, 957
  Endometrial carcinoma and its treatment: the role of irradiation, extent of surgery, and approach to chemotherapy, 1156
  Fairbank's atlas of general affections of the skeleton, 378
  Gastroenterology. Vol. 3: liver, gallbladder, bile ducts, and pancreas, 961
  Graphs and tables for use in radiology, 199
  Hormones and breast cancer, 201
  Introduction to the physics of nuclear medicine, 566
  Lung disease. State of the art, 1975-1976, 959
  The lungs and mediastinum. I. General considerations, signs of lung disease, and pathology of the mediastinum, 1157
  Mammography: technique-diagnosis-differential diagnosis-results, 957
  Manuale di ecotomografia, 378
  Paleopathological diagnosis and interpretation: bone disease in ancient human populations, 379
  Pituitary and parapituitary tumours. Major problems in neurology, vol. 6, 1159
  Practical echocardiology, 960
  Radiation protection for medical and allied health personnel, 1157
  Radiologic diagnosis of renal parenchymal disease, 1158
  Radiologic examination in orthopaedics: methods and techniques, 203
  Radiologic science: workbook and laboratory manual, 960
  Radiological aspects of the liver and biliary tract. X-ray and

radioisotope diagnosis, 201
  Radiological atlas of common disease of the small bowel, 379
  Radiology of the abdomen: anatomic basis, 378
  Radiology of the alimentary tract in infants and children, 772
  Radiology of the gallbladder and bile ducts, 957
  Roentgen diagnosis of bones, a self-teaching manual, 379
  Roentgenologic diagnosis, 202
  Scintillation camera lung imaging. An anatomic atlas and guide, 377
  Self-assessment of current knowledge in nuclear medicine: 1,012 multiple choice questions and referenced answers, 774
  Structural shielding design and evaluation for medical use of x-rays and gamma rays of energies up to 10 MeV, 1158
  Symposium on angiography, 200
  Symposium on pediatric uroradiology. Radiologic clinics of North America, 773
  Symposium on Pneumocystic carinii infection, 565
  Testicular tumors, 202
  Tumor localization with radioactive agents, 959
  Ultrasonography of the abdomen, 198
  Urologic radiology, 203
  Urological radiology of the adult male lower urinary tract: anatomy, physiology, pathology and sequelae, diagnosis and management, 379
  Watson-Jones: fractures and joint injuries, 564
Bowel, see colon; intestine; gastrointestinal tract
Brachytherapy, see therapeutic radiology
Brain, see also computed tomography, cranial; cerebral angiography; cisterns, subarachnoid; meninges; sella turcica
  Cerebral abscess: angiographic changes (a), 1148
  Cerebral dural sinuses and their tributaries (b), 202
  Cerebral granulomatous angiitis, 463
  Dynamic positron emission tomography for study of cerebral hemodynamics (a), 1149
  Giant dural supratentorial arteriovenous malformation (c), 734
  Intraoperative localization of bone fragments using ultrasound (a), 769
  Progressive abnormalities in scans in adrenal leukodystrophy (c), 939
  Rhinorrhea, ventricular radiopharmaceutical stasis, and hydrocephalus (a), 372
  Ventriculography with Amipaque (a), 953
Brain, angiography
  Abscess (a), 1148
  Cerebral radionuclide angiography (b), 199
  Clinical comparison of contrast agents (a), 372
  Hypnotic anesthesia (t), 751
Brain, computed tomography
  Advanced exercises in diagnostic radiology: CT of brain (b), 960
  Of ancient Egyptian brain (a), 372
  Angiotomography, 699
  Autopsy correlations (a), 191
  Cerebral hemiatrophy, 5
  Cerebrum in multiple sclerosis (a), 767
  Comparison of radionuclide scans, intracranial disease (a), 191
  Computed brain and orbital tomography: technique and interpretation (b), 201
  Coronal sections of head (a), 1148
  Cost effectiveness in pseudotumor cerebri, 263
  Degenerative diseases (a), 766
  Dense intracranial epidermoid tumors (a), 1149
  Descending transtentorial herniation (a), 768
  Epidural abscesses (a), 559
  Evaluation of increased intracranial pressure (a), 192
  Head trauma (a), 558
  Impact on utilization of cerebral angiograms, 1
  Intracerebral hematoma resolution, 681
  Intracranial infections (a), 1148
  Intrasellar cisternal herniation (a), 1149
  Isodense subdural hematomas, 693
  Multifocal leukoencephalopathy (a), 953
  Neurologic disorders of children (a), 954
  Progressive multifocal leukoencephalopathy (a), 192
  Radionuclide studies and, of perihematoma region, 689
  Ring blush associated with intracerebral hematoma (a), 1149
  Scintigraphy with ^{99m}Tc pertechnetate and, in tumors (a), 953
  Statistical description of normal, 457
  Time variation of attenuation values of intracranial hematomas (a), 1149
  Volume of fluid-filled cavities (a), 954
  White and gray matter differentiated (a), 768
Brain, infarction
  Scanning in occlusion of posterior cerebral arteries (a), 771
Brain, neoplasm
  Dense epidermoid tumors (a), 1149
  Epidural abscesses by CT (a), 1149
  Palliative radiation therapy for metastatic (a), 375
  Uptake of ^{131}I by papillary meningioma (c), 349
Brain, radionuclide imaging
  Cerebral radionuclide angiography (b), 199
  Cerebrovascular disease in childhood (a), 769
  Comparative evaluation of ^{99m}Tc, ^{99m}TcO4, and ^{99m}Tc DTPA as imaging agents (a), 770
  Comparison of, with CT of intracranial disease (a), 191
  CT and, of perihematoma region, 689
  Progressive abnormalities in, in adrenal leukodystrophy (c), 939
  Scintigraphy with ^{99m}Tc pertechnetate and CT in cerebral tumors (a), 953
Breast, see also mammography
  Cancer, its impact on the patient, family and community (b), 564
  Diffuse calcification of, in chronic renal failure, 341
  Scintigraphic patterns of ^{67}Ga uptake in (a), 1153
Breast, neoplasm, diagnosis, see also mammography
  Cancer controversy continues (1), 758
  Carcinoma (a), 956
  Mammography: technique-diagnosis-differential diagnosis-results (b), 957
  Metastatic disease to, 673
  Optimization of screening programs (1), 548
  Radiography of gynecomastia and male breast (a), 193
  Screening controversy (special lecture), 537
  Single view negative xeromammography (a), 1150
  Stereotaxic needle biopsy of mamma, 121
  Thermography, mammography, and clinical examination (a), 373
Breast neoplasm, therapy
  Brachial edema after treatment of carcinoma (a), 762
  Cancer of (ARS presidential address), 696
  Cesiumtherapy (a), 1154
  Early breast cancer, its history and results of treatment (b), 199
  Effects of therapy on calcification (a), 193
  Hormones and breast cancer (b), 201
  Local recurrence of (a), 955
  Prognosis of young women with (a), 771
Bronchi, see also lungs
  Lung, growth and remodeling, 777
Bursa, see specific joints

Calcification, see specific organs, regions, and diseases
Californium, clinical experience with (a), 1154
Cancer, see neoplasms; therapeutic radiology; radiobiology; under organs, regions, individual neoplasms
Carotid artery, see arteries; brain; angiography
Carpus, see wrist
Cathartics, see colon
Cauda equina, see spinal cord
Cavography, see venae cavae
Cecum, see colon
Cephalhematoma, see skull
Cephalometry, see skull
Cerebellopontine angle, see brain
Cerebral angiography, see brain; angiography
Cerebral palsy, see body parts
Cervix, see uterus
Cesium, see therapeutic radiology
Chemodectoma, see also organ, region
  Angiographic observations on, of head and neck, 477
Chemotherapy, see individual drugs
Cholangiography, see also bile ducts; gallbladder
  Biliary tract size and drainage time: comparison of endoscopic and intravenous (a), 369
  Cholecystocholangiography after cholecystoduodenostomy (t), 534
  Complications of endoscopic retrograde (a), 187
  Noncalculous biliary duct obstruction (a), 367
  Oral antidiabetic agents and excretion of intravenous biliary contrast media (a), 367
  Refinements in transhepatic, 11
Cholecystography, see cholangiography; gallbladder
Choledochal cyst, see bile ducts
Cholografin, see cholangiography; Iodipamide
Chondroblastoma, see bone, neoplasms
Chondroma, see organ
Chondromalacia, see specific joint
Chondromatosis, see specific joint
Chondrosarcoma, see bone, neoplasm
Chordoma, see spine
Choroid plexus, see brain
Clavicle, erosion of, in secondary hyperparathyroidism, 291
Cobalt, see therapeutic radiology
Co-bleomycin, see also radionuclide imaging; organ
  ^{57}Co-bleomycin in tumor evaluation, 267
Colitis, "backwash ileitis" with pseudopolyposis (c), 506
Collimators, see radiography, apparatus; therapeutic radiology, apparatus

Colon, see also gastrointestinal tract; colitis
  Acute appendicitis with abscess simulating carcinoma of sigmoid, 1057
  Angiodysplasia of right, bleeding cause, 789
  Benign ulceration of cecum (a), 556
  Colorectal polyps (a), 187
  Crohn's disease and colonic diverticula (a), 188
  Crohn's disease (a), 188
  Effect of methylglucamine compounds on, in newborns (a), 192
  Glucagon-aided reduction of intussusception (a), 193
  Human rectal mucosa: changes caused by laxatives (a), 763
  Malposition of, in right renal agenesis, ectopia, and anterior nephrectomy, 845
  Metastatic melanoma presenting as multiple polyps (c), 511
  Myocardial ischemic changes during barium enema (a), 186
  Prone films for obstruction in children, 617
  Radiation therapy in intestinal non-Hodgkin's lymphoma (a), 196
  Splenic flexure carcinoma, source of hepatic portal venous gas (a), 556
  Treatment of diverticular hemorrhage (a), 764
  Typhlitis complicating leukemia (c), 347
Colonoscopy, see endoscopy
Computed tomography
  Analysis of dense lesion with dual scans (a), 1155
  Automated measurements of mean density (a), 953
  Correction for collimator width in reconstructive (a), 955
  Cost reduction (t), 1123
  CT with the general purpose scanner (b), 1156
  Definition of blood vessels (a), 191
  Density of methyl methacrylate (t), 351
  Inaccuracy (a), 1155
  Isodense masses, differentiation by gray scale ultrasonography, 989
  Maps and cross-sectional imaging (e), 1133
  Measurements of whole blood and blood fractions (a), 186
  National Academy of Sciences recommendations, 760
  Parathyroid localization (a), 949
  Quantitative information from a scanner (a), 1154
  Radiation protection (a), 196
  Radiation therapy and quality of (e), 943
Computed tomography, abdominal
  Abdominal in subcapsular and perirenal hematoma, 83
  Lipomatosis (c), 338
  Liver and biliary tract (a), 1146
  Liver and pancreas, isotope and, 23
  Myelolipoma of adrenal, ultrasound and, 993
  Renal space occupying lesions (a), 765
  Retrocrural prevertebral space, 907
  Retroperitoneal hemorrhage, 403
  Retroperitoneal tumors, 395
  Splenic vein-pancreatic relationship, 17
  Testicular seminoma with abdominal mass, 707
Computed tomography, cranial
  Advanced exercises in diagnostic radiology: CT of brain (b), 960
  Of ancient Egyptian brain (a), 372
  Angiotomography, 699
  Autopsy correlations with (a), 191
  Cerebral hemiatrophy, 5
  Cerebrum in multiple sclerosis (a), 767
  Computed brain and orbital tomography: technique and interpretation (b), 201
  Coronal sections in head (a), 1148
  Cost effectiveness in pseudotumor cerebri, 263
  Cranial computed tomography (b), 772
  CSF rhinorrhea by metrizamide cisternography (c), 149
  Degenerative diseases of brain (a), 766
  Dense intracranial epidermoid tumors (a), 1149
  Descending transtentorial herniation (a), 768
  Evaluation of brain and epidural abscesses (a), 559
  Head trauma (a), 558
  Impact on use of cerebral angiograms, 1
  Increased intracranial pressure (a), 192
  Intracerebral hematoma resolution, 681
  Intracranial infections (a), 1148
  Intrasellar cisternal herniation (a), 1149
  Isodense subdural hematomas, 693
  Multifocal leukoencephalopathy (a), 953
  Neurologic disorders of children (a), 954
  Pituitary adenomas (a), 372
  Progressive multifocal leukoencephalopathy (a), 192
  Radionuclide scans and, with intracranial disease (a), 191
  Radionuclide studies of perihematoma region, 689
  Ring blush associated with intracerebral hematoma (a), 1149
  Statistical description of normal brain scan, 457
  Time variation of attenuation values of intracranial hematomas (a), 1149
  Volume of fluid-filled cavities (a), 954
  White and gray matter differentiated (a), 768
Computed tomography, orbital
  Exophthalmos (a), 1149
  Orbit (a), 952
  Scleral thickening, sign of orbital pseudotumor, 703
  Unilateral endocrine exophthalmos (a), 767
Computed tomography, thoracic
  Mediastinum (a), 1143
  Right and left ventricular volumes and wall measurements, 257
Contrast media, see also individual media
  Antibody activity in sera of patients suffering reaction (a), 373
  Arthrography agents (a), 558
  Bronchospasm during excretory urography (a), 1146
  Cardiac conduction abnormalities, coronary arteriography, in dogs (a), 366
  Comparison of agents in cerebral angiography (a), 372
  Effect of methylglucamine compounds on bowel of newborns (a), 192
  Excretion of sodium tyropanoate and sodium ipodate in dogs (a), 368
  Perfluoroctylbromide in gastroenterography (a), 369
  Reactions correlated with time of day, 1039
  Recommendations for labels, package inserts, and dosage, 167
Coronary angiography, see coronary arteries
Coronary arteries
  Arterial occlusive disease, significant left main lesions (a), 186
  Arteriograms and left ventriculograms compared with postmortem studies (a), 1143
  Cardiac conduction abnormalities due to coronary arteriography, in dogs (a), 366
  Chronic congestive heart failure (a), 365
  Congenital anomalies, indicence (a), 555
  Interventricular septal motion with left anterior descending artery lesions (a), 365
  Myocardial infarction with normal arteriogram (a), 949
  In persistent truncus arteriosus (a), 366
Corpus callosum, see brain
Cost analysis, see economics
Cowper's duct, see urethra
Craniopharyngioma, see brain, neoplasm
Crohn's disease, see also organ
  Colon (a), 188
  Colonic diverticula (a), 188
  Esophagus (a), 187
  Growth and prognosis after surgery in children (a), 954
Cyclotron, see therapeutic radiology, apparatus
Cystic fibrosis, see mucoviscidosis
Cystography, see bladder
Cystourethrography, see bladder; urethra
Cysts, see under organs and regions

Dacryocystography, see lacrimal gland
Deafness, see ear
Desmoid tumor, see organ
Diphosphonate, see under organs and regions
Diverticulitis, see colon
Diverticulum, see organ
Doppler ultrasound, see ultrasound
Dosimetry, see radiation measurement; radiography
Ductus arteriosus, see heart, congenital abnormalities
Duodenum, see also gastrointestinal tract; intestine; peptic ulcer
  Intraluminal diverticulum: endoscopic pancreatography (c), 929
Dural sinuses, see also brain
  Cerebral dural sinuses and their tributaries (b), 202
Dura mater, see meninges
Dwarfism, metatropic, and its variants (a), 1149

Ear
  Auditory canal enlargement, dural ectasia in neurofibromatosis (c), 935
  Auditory canal enlargement in neurofibromatosis without acoustic neuroma (a), 954
  Mondini defect (c), 1120
Echinococcus, see under organs and regions
Echocardiography, see heart; ultrasound
Economics, medical
  Benefit-cost analysis (e), 753
  Cost reduction in CT systems (t), 1123
Editorials
  Computed tomography and the quality of radiation therapy, 943
  Federal crossword puzzle, 176
  Image presentation: how can it be improved?, 355
  On maps and comparing cross-sectional imaging methods, 1133
  Perspectives on benefit-cost analysis in medical care, 753
  Pulmonary surfactant disease states, 545
  Therapeutic value of thyreocalcitonin, 175

- Effusion, see under region
- Ehlers-Danlos syndrome (a), 951
- Elbow, injuries of medial epicondylar ossification center, 49
- Electron beam therapy, see therapeutic radiology
- Electronic imaging, see diagnostic radiology; radiography
- Embolism, see also thrombosis
  - Peripheral artery, of multiple pellets (c), 933
  - Pulmonary angiography for, 1019
  - Target sign of septic pulmonary, 453
- Embolism, therapeutic
  - Angiographic management of hemorrhage, 1007
  - Arterial, for hemorrhage following hip arthoplasty (a), 951
  - Control of massive hepatic hemorrhage, 253
  - Emergency, in hepatic trauma, 249
  - External carotid artery (a), 949
  - Intravascular coil occlusion of experimental arteriovenous fistulas, 795
  - Nonsurgical splenectomy, 805
  - Therapeutic, for chronic bleeding (a), 196
  - Transhepatic obliteration of gastroesophageal varices, 237
  - Treatment of diverticular hemorrhage (a), 764
  - Treatment of hemoptysis (a), 184
- Emission tomography, dynamic positron, for study of cerebral hemodynamics (a), 1149
- Embolization, see thrombosis
- Endoscopy
  - Complications of, retrograde cholangiopancreatography (a), 187
  - Intraluminal duodenal diverticulum (c), 929
  - Undetected colorectal polyps (a), 187
  - Varices by fibre-optic (a), 763
- Enteritis, see intestine
- Enterocolitis, see colon; intestine
- Ependymona, see brain, neoplasm
- Epidermoids, see skull; brain
- Epiglottis
  - Acute, in adults (a), 553
  - Enlarged (a), 954
- Esophagus, see also stomach
  - Air, 433
  - Aperistalsis and esophagitis (a), 1145
  - Beck gastric tube, 425
  - Columnar-lined (a), 1145
  - Crohn's disease (a), 187
  - Gastroesophageal reflux surgery in children (a), 560
  - Hemorrhage in leukemia (c), 1106
  - Intraluminal distension (a), 764
  - Intraluminal diverticulum, 595
  - Jet phenomenon (c), 747
  - Mallory-Weiss syndrome (c), 508
  - Multiple adenomatous neoplasms (a), 763
  - Perforation due to obturator airway (a), 553
  - Perforation of pharynx, look-alike for atresia (c), 335
  - Primary ulcerative carcinoma, 599
  - Reflux (a), 187
  - Retrograde azygography in carcinoma of (a), 554
  - Rheumatoid (a), 951
  - Transhepatic obliteration of gastroesophageal varices, 237
  - Varices by fibre-optic endoscopy (a), 763
  - Varices treated with percutaneous obliteration of gastric coronary vein (a), 365
  - Varicoid carcinoma (a), 556
- Exophthalmos, see eye; orbit
- Eye, CT in exophthalmos (a), 1149
- Exostosis, see bone
- Extremities, see fingers; hand; under names of bones and joints

- Face fractures, angiography in vascular malformations, 469
- Falx cerebri, see meninges
- Femur, avascular necrosis (a), 952
- Fetus, see also pregnancy; radiation, injurious effects; radiobiology
  - Antepartum diagnosis of conjoined twins by ultrasonography (c), 921
  - Gray scale measurement of biparietal diameter (a), 769
  - Pulmonary hypoplasia and pleural effusions with fetal death in utero: ultrasonic findings (c), 749
- Fibrosis, see organs and regions
- Filters, see radiography, apparatus; therapeutic radiology, apparatus
- Fingers, see also hand
  - Aseptic necrosis of metacarpophalangeal joint (c), 737
  - Gamekeeper's thumb (a), 951
- Fistula, see organs
- Fontanelle, see skull
- Foot, injuries (a), 191
- Foreign bodies, see organ or part
- Fossa, pituitary, see sella turcica
- Fractionation, see dosimetry; radiobiology; therapeutic radiology
- Fractures, see individual bones
- Fucosidosis, radiographic features (a), 1150

- Gallbladder, see also bile ducts; cholangiography
  - Acute cholecystitis, 583
  - Cholecystocholangiography after cholecystoduodenostomy (t), 534
  - Excretion of sodium tyropanoate and sodium ipodate in dogs (a), 368
  - Gastroenterology. Vol. 3: liver, gallbladder, bile ducts, and pancreas (b), 961
  - Gray scale ultrasonography, 975
  - Radiology of the gallbladder and bile ducts (b), 957
  - ^{99m}Tc pyridoxylideneglutamate cholescintigraphy (a), 195
  - Wall opacification in infusion tomography, 587
- Gallium, see also radionuclide imaging; organs and regions
  - Lymphangiograms and, in non-Hodgkin's lymphomas (a), 194
  - Mycotic aneurysm (c), 1111
  - Scintigraphic evaluation of lymphoma, comparative study (a), 1152
  - Scintigraphic patterns of uptake in breast (a), 1153
- Ganglion, recurrent cyst (c), 345
- Gastrointestinal tract
  - Caustic burns (a), 368
  - Circulation (a), 186
  - Crohn's disease in children (a), 954
  - Ehlers-Danlos syndrome (a), 951
  - Faceted air bubbles (l), 1137
  - Metastatic melanoma, 605
  - Opportunistic infections, 419
  - Perfluoroctylbromide as contrast medium (a), 369
  - Radiation therapy (a), 1154
  - Radiology of the alimentary tract in infants and children (b), 772
- Gelfoam, see embolism
- Genitourinary tract, see urinary tract; urography; individual organ
- Giant cell tumor, see organ
- Glioblastoma, see brain, neoplasm
- Glioma, see brain, neoplasm
- Glucagon, in reduction of intussusception (a), 193
- Goiter, see thyroid
- Gonadoblastoma, see ovary
- Gout, see also bone, metabolic abnormalities
  - Pathologic fracture (c), 1116
- Granuloma, see organ
- Graves's disease, see thyroid
- Gynecology, see ovary; pregnancy; uterus

- Hand, see also fingers
  - Angiography in Raynaud's syndrome (a), 950
  - Arteriography (a), 1144
  - Aseptic necrosis of metacarpophalangeal joint (c), 737
  - Metacarpophalangeal joints (a), 766
  - Normal and abnormal images (a), 770
  - Radiographic measurements in growth hormone deficiency, 487
- Heart, see also coronary arteries
  - Abnormalities in relatives with Marfan syndrome (a), 949
  - Asymptomatic left ventricular aneurysm (a), 763
  - Chronic congestive failure in coronary artery disease (a), 365
  - Correlation of arteriograms, left ventriculograms, and postmortem studies (a), 1143
  - Electrocardiographic response to intravenous urography, 825
  - Evaluation of myocardial function with ^{201}Tl scintimetry (a), 375
  - Fluoroscope-generated electromagnetic interference in pacemaker (a), 365
  - Myocardial ischemic changes during barium enema (a), 186
  - Premature pulmonary valve opening (a), 186
  - Primary chylopericardium: role of lymphangiography, 1043
  - Quantitative evaluation of left ventricular function by radiographic techniques (a), 554
  - Rheumatoid arthritis and ankylosing spondylitis (a), 1144
  - Right and left ventricular volumes and wall measurements by CT, 257
  - Significance of left atrial wall calcification (a), 366
  - Surgery for arterial occlusive disease, group with significant left main lesions (a), 186
  - Transient tricuspid insufficiency of newborn (a), 560
- Heart, congenital abnormalities
  - Angiocardiography of subaortic obstruction in infancy, 813
  - Anomalous pulmonary venous connection of left lung with intact atrial septum (a), 762
  - Congenital pulmonary atresia with ventricular septal defect, 1027
  - Coronary arterial origin in persistent truncus arteriosus (a), 366
  - Development of pulmonary arteriovenous shunt after superior vena cava-right pulmonary artery anastomosis (a), 554
  - Ductus arteriosus dilatation by prostaglandin E_1 in infants with pulmonary atresia (a), 560

  Echocardiographic detection of intracardiac right-to-left shunts (a), 373
  Function in anomalous pulmonary venous return (a), 554
  Surgical correction of transposition of great arteries (a), 1144
  Venous connection from left atrium to cardinal venous system (c), 937
  Ventricular septal thickening (a), 535
Heart, radionuclide imaging
  Acute transmural myocardial infarction estimated from ^{201}Tl scintiscans (a), 1152
  Cardiac ventricular function by radioisotopic technics (a), 955
  Clinical features, myocardial infarction with normal arteriogram (a), 949
  Differentiation of transiently ischemic from infarcted myocardium by serial imaging (a), 763
  Early diagnosis of myocardial infarction in the dog (a), 770
  Gated cardiac blood pool scans in ischemic and congestive cardiomyopathy (a), 950
  Interpretation of ^{99m}Tc pyrophosphate scintigraphy in myocardial infarction (a), 562
  Localization by ^{99m}Tc-(Sn)-pyrophosphate following irradiation (a), 1151
  Myocardial function with ^{201}Tl scintimetry (a), 375
  Myocardial uptake of ^{99m}Tc stannous pyrophosphate following transthoracic countershock (a), 562
Heart, ultrasound
  Detection of intracardiac right-to-left shunts (a), 373
  Disproportionate ventricular septal thickening (a), 555
  Echocardiography (b), 957
  Effects of valsalva maneuver (a), 555
  Interventricular septal motion with left anterior descending coronary artery lesions (a), 365
  Mitral stenosis and prosthetic mitral valve obstruction (a), 1144
  Mitral valve prolapse and asymmetric septal hypertrophy (a), 555
  Practical echocardiology (b), 960
  Real-time, two-dimensional echocardiography and cineangiography in left ventricular asynergy (a), 185
  Suprasternal notch, in pediatrics (a), 554
  Systolic thickening and thinning of septum and posterior wall (a), 185
Hemangioendothelioma, see organ or region
Hemangiopericytoma, see organ or region
Hemihypertrophy, see organ or region
Hemorrhage, see under organs, and systems
Hepatoma, see liver
Hip
  Arterial embolization for hemorrhage following arthroplasty (a), 951
  Arthrography in unexplained chronic pain, 283
  Avascular necrosis of head of femur (a), 952
  Bone imaging after total replacement arthroplasty (a), 557
  Cerebral palsy (a), 1148
  Diagnosis of congenital dislocation (a), 192
  Joint restoration in juvenile rheumatoid arthritis (a), 1147
  Loosening and infection in prosthesis (a), 1147
  Metal-cement interface in total prostheses, 279
  Radiologic aspects of universal proximal femoral prosthesis (c), 531
Histiocytosis X, myelosclerosis and myelofibrosis in treated (c), 521
Hodgkin's'disease, see also lymphoma
  Accuracy of lymphography, 1041
  ^{67}Ga citrate imaging (a), 1151
  Lymph node calcification after chemotherapy (c), 1108
  Persistence of lymphographic contrast medium (a), 1151
  Radiotherapy for nodular sclerosing (a), 563
  Significance of histopathology for laparotomy-negative stage I and stage II patients (a), 955
  Staging laparotomy (a), 1153
  Therapeutic implications of splenic involvement (a), 1154
Humerus
  From earlier pages, 1135
  Injuries of medial epicondylar ossification center, 49
Hyaline membrane disease, see respiratory distress syndrome
Hyperinsulinism, see pancreas
Hyperparathyroidism, see parathyroid
Hypertension, see also specific organs, renal hypertension
  Diagnosis (a), 1152
Hypothalamus, see brain
Hypotonic duodenography, see duodenum
Hysterography, see uterus
Hysterosalpingography, see uterus

Ileocecal valve, see colon
Ileum, see intestines
Ilium, see also pelvis
  Chronic sciatic pain, 1087
  Exostosis after bone marrow biopsy (c), 1114
Imaging, see computed tomography; radiography; radionuclide imaging; thermography; ultrasound
Immunology, see gamma globulins; radioimmunoassay; therapeutic radiology
In-bleomycin, see also radionuclide imaging and organs
  Scintigraphic evaluation of lymphoma, ^{67}Ga-citrate and (a), 1152
Instruction, see education
Intervertebral disc, see spine
Intestine, see also appendix; duodenum; gastrointestinal tract
  "Backwash ileitis" with pseudopolyposis (c), 506
  Bleeding ileal varicosity demonstrated by transhepatic portography (c), 514
  Cavitating metastases, 613
  Growth and prognosis after surgery for Crohn's disease in children (c), 954
  Intractable diarrhea with vasoactive peptide-producing ganglioneuroblastoma (a), 1150
  Pneumatosis, complication of jejunoileal bypass, 601
  Prone films for bowel obstruction in children, 617
  Radiological atlas of common disease of the small bowel (b), 379
  Radiological findings in Yersinia ileitis (a), 1145
  Ulcerative pseudopolyposis mimicking neoplasm (c), 503
Ischium, see pelvis
Islands of Langerhans, see pancreas

Jaundice, see bile ducts; gallbladder; liver
Jaws, cysts of the oral regions (b), 565
Jejunum, see intestine
Joints, see also individual joints, arthritis
  Abnormalities in calcium pyrophosphate dihydrate deposition disease (a), 190
  Bony proliferation in "rheumatoid variant" disorders, 275
  Involvement with pigmented villonodular synovitis (a), 766
  Plant thorn synovitis (a), 1147
  Roentgenologic picture of diabetic osteoarthropathy (a), 370
  Subchondral pseudocysts in rheumatoid arthritis, 1069

Keloids, see skin
Kidney, see also urinary tract; urography; renal angiography
  Acute rejection in homotransplantation (a), 370
  Angiographic findings in amyloidosis, 855
  Asymmetric enlargement in acute glomerulonephritis (a), 556
  Calcification in polycystic disease (a), 188
  Computed tomography in subcapsular and perirenal hematoma, 83
  Contralateral herniation after nephrectomy: pseudo-crossed renal ectopia (c), 1099
  Contributions to nephrology (b), 566
  CT evaluation of renal space occupying lesions (a), 765
  Determination of extraction fraction by double-tracer method (a), 374
  Long-term follow-up of patients with renal failure (a), 766
  Malposition of colon in right agenesis, ectopia, and anterior nephrectomy, 845
  Notching of ureter and pelvis in children, 837
  Opacification in congenital multicystic dysplastic (a), 188
  Parenchymal striations, vein thrombosis, 95
  Radiologic diagnosis of renal parenchymal disease (b), 1158
  Radiologic findings in amyloidosis, 851
  Redistribution of blood flow (a), 765
  Short dialysis, middle molecules, and uremia (a), 189
  Ultrasonic evaluation of obstructed duplex, 113
  Upper calyx obstruction in children (a), 1146
  Urinoma (a), 1147
  Urographic visualization of multicystic (a), 369
Kidney, angiography
  Acute rejection in homotransplantation (a), 370
  Epinephrine-enhanced, in mass lesions, 647
  Findings in amyloidosis, 855
  Infiltrating neoplasms, 859
  Redistribution of blood flow by contrast media (a), 765
  Sarcoma, 107
  Transitional cell tumors, 99
Kidney, cysts
  Complications of puncture (1), 947
  Cyst puncture (1), 1137
  Lymphoma simulating adult polycystic disease (a), 765
  Peripelvic pseudo, due to obstruction (c), 1097
  Pneumothorax and cyst puncture (1), 947
Kidney, neoplasm
  Bone metastases, 61
  Epinephrine-enhanced angiography, 647
  Infiltrating, 859
  Lymphoma simulating adult polycystic disease (a), 765
  Needle tract seeding (c), 725
  Sarcoma, 107
  Sonography of thrombosis of inferior vena cava in tumors (a), 768

  - Transitional cell carcinoma, 99; (a), 765
  - Ultrasonic characterization (a), 769
- Kidney, radionuclide imaging, function and serum calcium effect on visualization with bone scans (a), 770
- Kidney, transplantation
  - Acute rejection (a), 370
  - Urine extravasation after, 409
- Kidney, ultrasound
  - Characterization of solid lesions (a), 769
  - Horseshoe (c), 526
  - Intrarenal anatomy, 831
  - Medullary cystic disease and congenital hepatic fibrosis, 297
  - Obstructed duplex kidney, 113
  - Thrombosis of inferior vena cava in tumors (a), 768
- Knee, see also semilunar cartilages
  - Capsular visualization in lipohemarthrosis (a), 191
  - Lesions (a), 952
  - Vascular injuries associated with dislocation (a), 371
  - Widening of epiphyseal plates in bowed legs, 309

- Larsen's syndrome, see bone; face; joints
- Larynx
  - Airway foreign bodies in children (a), 1143
  - Cobalt therapy of carcinoma (a), 1153
  - Enlarged epiglottis (a), 954
  - Laryngeal tuberculosis, 677
- Lectures
  - Hickey, radiology manpower update, 575
  - Janeway, fundamental mechanisms in combined modality therapy of cancer, 383
  - Neuhauser, lung: its growth and remodeling in health and disease, 777
- Leiomyoma, see organ
- Letters, see subject
- Leucutia, Traian (o), 945
- Leukemia
  - Massive esophageal hemorrhage (c), 1106
  - Randomized clinical trial of granulocyte transfusions for infection (a), 561
  - Typhlitis complicating (c), 347
- Liposarcoma, see organs
- Liver, see also bile ducts; blood
  - Anomalies of intrahepatic portal venous system (a), 763
  - Cavernous hemangiomas and hemangioendotheliomas in infancy, 317
  - Complications of long term arterial chemotherapy, 799
  - Gastroenterology. Vol. 3: liver, gallbladder, bile ducts, and pancreas (b), 961
  - Immunotherapy in fulminant type B hepatitis (a), 561
  - Infantile hemangioendotheliomas associated with hemihypertrophy (a), 1149
  - Infusion tomography in fluid containing masses (a), 950
  - Multiple hepatitis viruses (a), 368
  - Radiological aspects of the liver and biliary tract. X-ray and radioisotope diagnosis (b), 201
  - Roentgenographically visible fatty, in cystic fibrosis (a), 954
  - Septicemia as complication of percutaneous biopsy (a), 764
- Liver, angiography
  - Adenomas and focal nodular hyperplasia in women on oral contraceptives (a), 375
  - Angiogaphic abnormalities in partial Budd-Chiari syndrome (a), 762
  - Arterio-portal anastomoses in hepatocellular carcinoma (a), 556
  - Embolization to control massive hemorrhage, 253
  - Emergency embolization in hepatic trauma, 249
- Liver, computed tomography
  - Accuracy (a), 1146
  - Comparison of isotope and CT, pancreas and, 23
- Liver, radionuclide imaging
  - Comparison of isotope and CT scans in pancreas and, 23
  - "Hot spot" on scintigraphy and venacavography in vena caval obstruction, 447
- Liver, ultrasound
  - Calcified metastases, 591
  - Evaluating size (a), 562
  - Gray scale patterns of metastatic disease, 983
  - Medullary cystic disease of kidney and congenital hepatic fibrosis, 297
  - And spleen in lymphomas (a), 769
- Lungs, see also pleura; respiratory distress syndrome
  - Abdominal belt for inspiration in children during tomography (t), 354
  - The adult postoperative chest (b), 773
  - Airway foreign bodies in children (a), 1143
  - Angiography for emboli, 1019
  - Calcification in chronic renal failure mimicking edema (c), 1103
  - Chest after pleural space reduction, 229
  - Clearance of radioactive tantalum after accidental inhalation, 327
  - Complications of percutaneous transthoracic needle aspiration biopsy (a), 184
  - Effect of size and position on lesion detection, 205
  - Growth and remodeling, 777
  - Hypoplasia and pleural effusions with fetal death in utero (c), 749
  - Kilovoltage and nodule detectability (1), 759
  - Kinky chest tube, sign of entrapment following median sternotomy, 883
  - Lateral decubitus view, 885
  - Lung disease. State of the art, 1975-1976 (b), 959
  - The lungs and mediastinum. I. General considerations, signs of lung disease, and pathology of the mediastinum (b), 1157
  - Needle for biopsy of lesions, 215
  - PEEP: radiographic features and complications, 209
  - Radiation pneumonitis from single fraction upper half body irradiation (a), 195
  - Radiographic manifestations of acute smoke inhalation, 865
  - Severe radiation injuries, 127
  - ^{87m}Sr scans in aspergillosis, 879
  - Surfactant disease states (e), 545
  - Uptake of bone imaging agents by diffuse pulmonary metastatic calcification, 871
  - Vein avulsion (c), 331
- Lungs, diseases
  - Alveolar proteinosis with hematologic malignancy and lymphoma (a), 553
  - Anomalous venous connection of left, with intact atrial septum (a), 762
  - Bronchopulmonary dysplasia in premature infants (a), 1150
  - Bubbles in hyaline membrane (a), 560
  - Entrapment and infarction by chest tube suction (a), 553
  - Fibrosing alveolitis in neurofibromatosis (a), 553
  - Fluid-filled cystic adenomatoid malformation, 323
  - Hemorrhage in renal disease: Goodpasture's syndrome (a), 184
  - Nonmalignant lymphoid disorders, 221
  - Primary adenoid cystic carcinoma of trachea (a), 553
  - Pseudocysts in newborn infant (a), 561
  - Pseudosequestration (a), 365
  - Radiographic findings of immunoblastic lymphadenopathy, 875
  - Steroid-dependent asthma treated with inhaled beclomethasone dipropionate (a), 561
  - Target sign of septic pulmonary emboli, 453
  - Treatment of hemoptysis by embolization (a), 184
- Lungs, edema; calcification in chronic renal failure (c), 1103
- Lungs, infection
  - Findings in neonatal group B streptococcal septicemia (a), 1150
  - Interstitial pneumonia in (a), 185
  - Occurrence of granulomas in patients with stage I sarcoidosis, 1083
  - Symposium on Pneumocystis carinii infection (b), 565
  - Thoracic wall invasion secondary to aspergillosis (c), 140
  - Transpleural systemic artery-pulmonary artery anastomosis, 233
- Lungs, neoplasm
  - Primary adenoid cystic carcinoma of trachea (a), 553
  - Radiotherapy in treatment of inoperable cancer (a), 1153
  - Survival with inoperable cancer (a), 184
  - Thoracic metastasis in malignant melanoma (a), 762
  - Trophoblastic disease (a), 1143
- Lungs, radionuclide imaging
  - Cardiomegaly as cause of nonuniform pulmonary perfusion, 661
  - Clinical comparison of ^{127}Xe and ^{133}Xe (a), 1152
  - Delayed imaging following radioaerosol inhalation (a), 562
  - Experimental ischemic lesions after inhalation of diffusible radioaerosol (a), 374
  - Scintigraphic assessment of arterial involvement in aortitis syndrome (a), 955
  - Scintillation, 377
  - ^{87m}Sr lung scans in aspergillosis, 879
  - Uptake of bone imaging agents by diffuse metastatic calcification, 871
- Lupus erythematosis, aseptic necrosis of wrist (a), 766
- Lymph nodes, see also Hodgkin's disease; lymphography; lymphoma
  - Calcification after chemotherapy (c), 1108
  - Radiographic findings of immunoblastic lymphadenopathy, 875
- Lymphangiography, see lymphography
- Lymphangioleiomyomatosis, gray scale ultrasonography in retroperitoneal (c), 1101
- Lymphography
  - Accuracy in Hodgkin's disease, 1041
  - Ether-dissolved ethiodol for lymphangiography, 1047
  - Gallium scans and, in non-Hodgkin's lymphomas (a), 194
  - Lymphocele: complication of surgical staging of carcinoma of prostate (c), 333
  - Malignancies of uterine corpus, 903
  - Patterns of malignant lymphoma (a), 949
  - Pediatric, 639
  - Persistence of contrast medium as prognostic criterion in Hodg-

  kin's disease (a), 1151
  Phlebography, urography, and, in diagnosis of metastasis from testicular tumors (a), 1147
  Primary chylopericardium, 1043
  Urography after, in malignant disease (a), 188
Lymphoma, see also Hodgkin's disease
  Early lymphographic pattern of malignant (a), 949
  Factors in prognosis of gastric (a), 563
  Lymphangiograms and gallium scans in non-Hodgkin's (a), 194
  Radiographic findings of immunoblastic lymphadenopathy and related immunoblastic proliferations, 875
  Renal, simulating adult polycycstic disease (a), 765
  Scintigraphic evaluation, comparative study (a), 1152
  Ultrasonography of liver and spleen in (a), 769
Lymphoma, non-Hodgkins's, radiation therapy in intestinal (a), 196

Macroradiography, see radiography
Mammography, see also breast, neoplasm
  Breast cancer screening controversy, 537
  Optimization of screening programs (1), 548
  Radiography of gynecomastia and male breast (a), 193
  Single view negative mode xeromammography (a), 1150
  Technique--diagnosis--differential diagnosis--results (b), 957
  Thermography, mammography, and clinical examination (a), 373
Marfan's syndrome, abnormalities in relatives (a), 949
Mediastinum
  Air in esophagus, 433
  CT of (a), 1143
  CT evaluation of retrocrural prevertebral space, 907
  Kinky chest tube: sign of entrapment following median sternotomy, 883
  The lungs and mediastinum. I. General considerations, signs of lung disease, and pathology of the mediastinum (b), 1157
  Pancreatic pseudocyst (a), 1145
  Right paratracheal stripe (a), 553
  Ultrasonography of pseudocyst (c), 923
Medulla oblongata, see brain
Medullary sponge kidney, see kidney
Megacolon, see colon
Megalencephaly, see brain
Meglumine iodipamide, see iodipamide and iodoxamate
Melanoma, see also organs
  Calcification in paraspinal, in a child (c), 143
  Metastatic, presenting as multiple colonic polyps (c), 511
  Metastatic to gastrointestinal tract, 605
  Thoracic metastasis in malignant (a), 762
Meninges, see also arachnoid
  CSF rhinorrhea by metrizamide CT cisternography (c), 149
  Spontaneous, normal-pressure cerebrospinal fluid fistulas in middle fossa (a), 767
Meningioma, see brain
Meningomyelocele, see spinal cord
Menisci, see semilunar cartilages
Metaphyses, see bone
Metrizamide
  Arachnoiditis following lumbar radiculography (a), 193
  Myelography, 481
Microangiography, see angiography
Mitral valve, see heart
Moyamoya disease, see arteries
Mucocele, see organ
Mucolipidosis, see bone, diseases
Mucopolysaccharidosis, see bone
Mucoviscidosis, see also organ
  Roentgenographically visible fatty liver in cystic fibrosis (a), 954
Mushroom worker's disease, see lungs, diseases
Mycosis fungoides, skeletal involvement (c), 741
Myelography
  Aid to C1-C2 percutaneous puncture (t), 353
  Avulsion of nerve rootlets with Cuatico needle during Pantopaque removal, 485
  Metrizamide, 481
Myelomeningocele, see spinal cord
Myelopathy, see spinal cord
Myocardium, see heart
Myoglobinuria, see kidneys

Navicular bone, see wrist
Necrotizing enterocolitis, see colitis
Neck
  Angiographic observations on chemodectomas of head and, 477
  Twice-a-day fractionation radiotherapeutic management of cancer of head and, 1091
Neoplasm, see also radiobiology; therapeutic radiology; organs, regions, and individual neoplasms
  ^{57}Co-bleomycin scanning in evaluation of tumors, 267
  Conference on spontaneous regression of cancer (b), 774
  Diagnosis and staging of cancer: a radiologic approach (b), 198
  Fundamental mechanisms in combined modality therapy of cancer, 383
  Radiotherapy of intra-oral carcinoma (a), 1153
  Tumor localization with radioactive agents (b), 959
  Twice-a-day fractionation radiotherapeutic management of cancer of head and neck, 1091
Nervous system, see organ
Neuroblastoma, see organ
Neurofibromatosis
  Internal auditory canal enlargement without acoustic neuroma (a), 954
  Massive subperiosteal hemorrhage in (a), 557
Neuroradiology, see also brain; nerves; spinal cord
  Diagnostic neuroradiology (b), 377
Neutrons
  High energy fast, from Harwell variable energy cyclotron. I. Physical characteristics, 709; II. Biologic studies in mammalian systems, 717
Nuclear medicine, see also radionuclide imaging; radionuclides; and under diseases, organs, and regions
  Self-assessment of current knowledge in nuclear medicine: 1,012 multiple choice questions and referenced answers (b), 774
Nuclides, see radionuclides; under individual radionuclides

Obituaries
  Leucutia, Traian, 945
  Trout, E. Dale, 363
Observer performance, see radiographs, interpretation
Obstetrics, see pregnancy; uterus
Occlusion, see thrombosis; embolism
Oculoauriculovertebral syndrome, see ear; eyes; spine
Oligodendroglioma, see brain, neoplasm
Oral cavity, radiotherapy of carcinoma (a), 1153
Orbit
  Angiography of hemangiopericytoma (c), 730
  Computed brain and orbital tomography, 201
  CT in exophthalmos (a), 1149
  CT of, using thin sections (a), 952
  Enophthalmos simulating emphysema (c), 728
  Radiation therapy for exophthalmos (a), 376
  Scleral thickening: CT sign of pseudotumor, 703
  Teratoma in newborn (a), 954
  Unilateral endocrine exophthalmos (a), 767
Ossicles, auditory, see ear
Osteoarthritis, see arthritis; under joints
Osteodystrophy, see bone, metabolic abnormalities
Osteomyelitis, see bone, infection
Osteoporosis, see bone metabolic abnormalities
Osteosarcoma, see bone, neoplasm
Osteotomy, see bone
Ostium primum defect, see heart, congenital abnormalities
Otolaryngology, see ear
Ovary
  Lymphography in malignant tumors (a), 1151
  Postoperative pelvic irradiation of stage II carcinoma (a), 956
  Ultrasonic appearance of Krukenberg tumor (c), 919
Oxygen, hyperbaric, as radiotherapeutic adjuvant in advanced cancer of uterine cervix (a), 376

Paget's disease
  Extramedullary hematopoiesis in, 493
  Precocious onset of (a), 371
  Radiography and radioisotope scanning in (a), 371
Pacemakers, see heart
Pancreas
  Angiography of arteriovenous malformation, 1015
  Anomalies of ductal system (a), 1146
  Arteriography in pseudocysts, 243
  Comparison of isotope and CT scans of liver and, 23
  Complications of endoscopic retrograde cholangiopancreatography (a), 187
  CT of splenic vein relationship to, 17
  Gastroenterology. Vol. 3: liver, gallbladder, bile ducts, and pancreas (b), 961
  Glucagon-producing islet cell tumor of (c), 159
  Gray scale sonographic anatomy of (a), 562
  Percutaneous fine needle aspiration biopsy of (a), 556
  Pseudocyst of mediastinum (a), 1145
  Significance of ductal obstruction in differential diagnosis (a), 369
  Ultrasonography of mediastinal pseudocyst (c), 923
Pancreatitis, see pancreas
Papillary necrosis, see kidneys
Paraganglioma, see brain, neoplasm
Parathyroid
  CT for localization (a), 949
  Erosion of clavicle in secondary hyperparathyroidism, 291

  ^{99m}Tc Sn-pyrophosphate and bone image changes in disease of (a), 374
Parietal bone, see skull
Parotid gland, carcinoma with osteoblastic metastases (c), 744
Patella, see knee
Pediatric radiology, see specific procedures and diseases
Pelvis, see also specific pelvic bones and organs
  Chronic sciatic pain with sclerosis of iliac bone, 1087
  CT of lipomatosis (c), 338
  Gray scale patterns in male (a), 769
  Hip joints and, in cerebral palsy (a), 1148
  Ultrasonography in tumors from spine and bony, 1061
Peptic ulcer, linear and rod-shaped (a), 556
Periostitis, see bone
Peritoneum, practolol (a), 764
Pharynx, perforation of, look-alike for esophageal atresia (c), 335
Phlebography, see venography
Phocomelia, see fingers; other extremities
Pituitary gland
  CT in adenomas (a), 372
  Hypophysectomy in treatment of disseminated prostate carcinoma (a), 562
  Pituitary and parapituitary tumors. Major problems in neurology, vol. 6 (b), 1159
  Treatment of Cushing's disease by irradiation (a), 375
Platyspondyly, see spine
Pleura, pulmonary hypoplasia and effusion of, with fetal death in utero (c), 749
Pneumocystis carinii, see also lungs
  Symposium on *Pneumocystis carinii* infection (b), 565
Pneumatosis intestinalis, see intestine
Pneumoencephalography, see brain
Pneumomediastinum, see also mediastinum
  Urinary tract anomalies in neonates with spontaneous pneumothorax (a), 1150
Pneumothorax, see also pleura
  Renal cyst puncture and (1), 947
  Urinary tract anomalies in neonates with spontaneous (a), 1150
Popliteal artery, see arteries
Polydactyly, see bone
Polyphosphate, see under organs and regions
Polyps, see organ
Porencephaly, see brain
Pregnancy, see also fetus; radiation, injurious effects; radiobiology
  Antepartum diagnosis of conjoined twins by ultrasonography (c), 921
Prostate
  Appraisal of postirradiation biopsy in cancer (a), 376
  Hypophysectomy in treatment of disseminated carcinoma (a), 562
  Lymphocele: complication of surgical staging of carcinoma (c), 333
  Pelvic phlebography through profundal dorsal vein of penis for cancer of urinary bladder and (a), 369
Prune belly syndrome, see abdomen; urinary tract
Pseudolymphoma, see lymphoma
Pseudotruncus arteriosus, see heart
Pubis, see pelvis
Pulmonary arteries, see also heart
  Angiography for emboli, 1019
  Growth and remodeling of lung in health and disease, 777
  Scintigraphic assessment of arterial involvement in aortitis syndrome (a), 955
Pulmonary atresia, see heart, congenital abnormalities
Pulmonary valve, see heart
Pulseless disease, see arteries
Pyelography, see urography
Pylorus, see stomach
Pyrophosphate, see organ

Radiation
  Biological and environmental effects of low-level radiation (b), 200
Radiation, injurious effects, see also therapeutic radiology, complications
  Cardiac localization of ^{99m}Tc-(Sn)-pyrophosphate following irradiation (a), 1151
  Radiation pneumonitis from single fraction upper half body irradiation (a), 377
  Severe, of lung, 127
  Summary statement from workshop on late effects of irradiation to head and neck in infancy and childhood, 761
  Therapy for cervical carcinoma (a), 956
Radiation, measurement, see radiography, exposures in diagnostic procedures
Radiation, physics
  The basic physics of radiation therapy (b), 1157
  Graphs and tables for use in radiology (b), 199
  Introduction to the physics of nuclear medicine (b), 566
Radiation, protection
  Radiation protection for medical and allied health personnel (b), 1157
  Structural shielding design and evaluation for medical use of x-rays and gamma rays of energies up to 10 MeV (b), 1158
  Whole-body CT scanner (a), 196
Radiation, therapy, see therapeutic radiology
Radiculography, see myelography
Radiobiology, see also neoplasm; radiation, injurious effects; under specific diseases, organs, and regions
  Advances in radiation biology (b), 200
  Biological and environmental effects of low-level radiation (b), 200
  Effects of adriamycin on response of murine hematopoietic stem cells (a), 197
  High energy fast neutrons from variable energy cyclotron. II. Biologic studies in mammalian systems, 717
  Mechanisms in combined modality therapy of cancer, 383
  Radiosensitizing effects in hypoxic mammalian cells (a), 196
  Time-dose relationships for cure of rat tumor with fractionated radiation (a), 197
  Vascularity and cell number following x-irradiation of murine carcinoma (a), 197
Radiographs, interpretation
  Current concepts in radiology (b), 1158
  Diagnostic radiology in paediatrics (b), 1156
  Effect of size and position on chest lesion detection, 205
  Illusory biplane images (a), 768
  Kilovoltage and lung nodule detectability (1), 759
  Roentgenologic diagnosis (b), 202
  Unfinished phantasy (1), 1139
Radiography, see also specific organs and procedures
  Abdominal belt to encourage inspiration in children during lung tomography (t), 354
  Aid to performance of shoulder arthrography (t), 942
  Compton (a), 1155
  From earlier pages, 1135
  High kVp chest (1), 1138
  Image presentation (c), 355
  Kilovoltage and lung nodule detectability (1), 759
  Lateral decubitus view: aid in evaluating pulmonary densities in children, 885
  Prone films for bowel obstruction in children, 617
  Radiologic examination in orthopaedics: methods and techniques (b), 203
  Radiologic science: workbook and laboratory manual (b), 960
  Subtraction technique using duplicating film as final print (t), 528
Radiography, apparatus
  Cone for lateral magnification cerebral angiography (t), 165
  Fluoroscopic time on TV monitor (a), 373
  Resolution in wide field radiography (a), 196
  Rotating platform for ascending phlebography (t), 941
  Scanning multiple slit assembly, 497
  Sensitivity of screens to scattered radiation (a), 196
  Solid state image converters (a), 196
  Wedge filter for craniocervical angiography (t), 1125
Radiography, complications
  Contrast medium reactions correlated with time of day, 1039
  Evaluation of bronchospasm during excretory urography (a), 1146
Radiography, exposures in diagnostic procedures
  Estimation of population doses from stomach mass screening, 1975 (a), 1155
  Radiation exposure in radiography of newborn (a), 191
Radiology, practice
  Benefit-cost analysis (e), 753
  Federal crossword puzzle (e), 176
  Federal government's impact on radiology, 171
  Image presentation (e), 355
  Informed consent for urography? (1), 358
  Radiology manpower update, 1976, 575
  Roles from radiologists in tomorrow's medical care system, 1129
Radionuclide imaging, see also under organ
  Comparison of isotope and CT scans of liver and pancreas, 23
  False aneurysm of extremity by dynamic scintigraphy (c), 931
  Imaging experimental pulmonary ischemic lesions after inhalation of diffusible radioaerosol (a), 374
  Tumor localization with radioactive agents (b), 959
Radionuclides, therapy, see also therapeutic radiology
  Clinical experience with ^{252}Cf (a), 1154
Radiosensitivity, see also radiobiology
  Effects of adriamycin on radiation response of murine hematopoietic stem cells (a), 197
  Effects of 2-nitroimidazole Ro-07-0582 in hypoxic mammalian cells (a), 196
Raynaud's syndrome, cryodynamic hand angiography in (a), 950

Rectum
  Human mucosa: changes caused by laxatives (a), 763
  Wall bleeding (a), 1146
Reflux, see stomach; ureters
Relative biological effectiveness, see radiobiology
Renal angiography, see kidney, angiography; renal arteries
Renal arteries, see also kidney
  Intrarenal collateral circulation in stenosis (a), 1144
Renal hypertension
  Diagnosis of angiotensinogenic hypertension, scintigraphy and saralasin infusion (a), 1152
  Intrarenal collateral circulation (a), 1144
  Role of renin in normal and pathologic cardiovascular hemostasis (a), 554
Renal failure, see kidney
Reporting, see radiographs, interpretation
Respiratory distress syndrome
  Bronchopulmonary dysplasia in premature infants (a), 1150
  Pulmonary findings in neonatal group B streptococcal septicemia (a), 1150
Respiratory tract, see individual organs
Retroperitoneum
  The adrenal retroperitoneum and lower urinary tract. Atlas of tumor radiology (b), 773
  CT of hemorrhage, 403
  CT of tumors, 395
  Gray scale ultrasonography in lymphangiomyomatosis (c), 1101
Rheumatoid arthritis, see arthritis, rheumatoid
Ribs, Ewing's tumor of (a), 1148
Roentgenograms, see radiographs; radiography

Sarcoidosis, occurrence of lung granulomas in patients with stage I, 1083
Sarcoma, see specific organ
Sacrum, see also pelvis
  Hereditary presacral teratoma (a), 194
  Normal widening of S1-S2 interspace in children, 305
  Pathologic fracture in gout (c), 1116
Scanner, see computed tomography; radionuclide imaging
Scapula, stress fracture (c), 519
Scintigraphy, see radionuclide imaging
Scleroderma, chalky joint effusion (a), 766
Screens, see radiography, apparatus
Scrotum, thermography (a), 194
Sella turcica, intrasellar cisternal herniation by computed tomography (a), 1149
Semilunar cartilages, see also knee
  Lesions of menisci (a), 952.
Shields, see radiation, protection
Shoulder
  Arthrography (t), 942
  Rotator cuff tear on routine radiographs (a), 370
  Septic arthritis of glenohumeral joint, 667
  Voluntary glenohumeral dislocation, 911
Sickle cell disease
  Central depression of multiple vertebral end-plates like sickle hemoglobinopathy in Gaucher's disease (c), 343
  Massive splenic infarction in (c), 927
Sigmoid, see colon
Skeleton, see bone
Skull
  Internal auditory canal enlargement due to dural ectasia in neurofibromatosis (c), 935
  Uncommon sphenoidal fractures and their sequelae (a), 372
Small bowel, see intestine; gastrointestinal tract
Smoke, radiographic manifestations of acute inhalation, 865
Society for Pediatric Radiology, scientific program, 1977 meeting, 551
Society of Photographic Scientists and Engineers, scientific program, 1977 meeting, 549
Society of Photo-Optical Instrumentation Engineers, scientific program, 1977 meeting, 549
Soft tissues, pharmacoangiography of bone and tumors of (a), 372
Sphenoid sinus, see sinuses, paranasal
Spinal cord, see also arachnoid; meninges; myelography
  Avulsion of nerve rootlets with Cuatico needle during Pantopaque removal, 485
  Metrizamide myelography, 481
Spine, see also atlas and axis; sacroiliac joint
  Absent arch and hypoplastic pedicle (c), 154
  Anatomic variations of seventh cervical vertebra simulating fracture (a), 952
  Avulsion of laminae, 57
  Central depression of multiple vertebral end-plates like sickle hemoglobinopathy in Gaucher's disease (c), 343
  "Cupid's bow" contour of lower lumbar vertebrae (a), 190
  Herniated discs (a), 557
  Locked facet in cervical injuries, 45
  Neurological degenerative diseases (a), 768
  Normal backward "displacement" of spinolaminal line at C2, 289
  Radiologic aspects of diffuse idiopathic hyperostosis, 913
  Reactive sclerosis of pedicle and spondylosis (a), 371
  Spondylotic fractures (a), 190
  Thoracolumbar injuries (a), 766
  Ultrasonography in tumors arising from, and bony pelvis, 1061
  Unilateral hypertrophy of multiple pedicles (c), 739
  Widening of cervical intervertebral foramen (a), 559
Spleen
  Huge cyst in newborn, 889
  Injection of oily propyliodone (a), 152
  Massive infarction in sickle cell-hemoglobin C disease (c), 927
  Nonsurgical splenectomy, 805
  Sonographic diagnosis of wandering (c), 925
  Ultrasonography of liver and, in lymphomas (a), 769
Spondylitis, see spine; arthritis
Staphylococci, see specific organ
Stomach, see also gastrointestinal tract; peptic ulcer
  Benign lymphoid hyperplasia of antrum (a), 367
  Damage caused by acid ingestion (a), 368
  Estimation of population doses from mass screening (a), 1155
  Gastric bypass for morbid obesity (a), 555
  Linear and rod-shaped peptic ulcers (a), 556
  Polyps or erosions? (l), 357
  Prognosis of gastric lymphoma (a), 563
  Spontaneous disappearance of polyps, 893
Streptococci, see specific organ
Subaortic stenosis, see heart, congenital abnormalities
Subtraction, see radiography
Sutures, see skull
Syndactyly, see fingers
Syndrome, see by name
Synostosis, see skull
Synovitis, see arthritis

Takayasu's arteritis, see arteritis
Talus, see ankle
Tantalum, clearance of radioactive from human lung after inhalation, 327
Tarsus, see foot
Technetium, see also radionuclide imaging; organs
Tendon, see part; joint
Terotoma, see organ or region
Testis
  Angiography (a), 949
  Phlebography, urography, and lymphography in diagnosis of metastases from (a), 1147
  Seminoma with abdominal mass, 707
  Testicular tumors (b), 202
  Venography in nonpalpable, 71
  Venography for undescended, 67
Tetralogy of Fallot, see heart, congenital abnormalities
Thallium, see also radionuclide imaging; organs
  Acute transmural myocardial infarction (a), 1152
  201 imaging and gated cardiac blood pool scans in cardiomyopathy (a), 950
Therapeutic radiology, see also dosimetry; radiations, injurious effects; radiobiology; and names of diseases, organs, and regions
  The basic physics of radiation therapy (b), 1157
  Cesium therapy of breast cancer (a), 1154
  Cobalt therapy of carcinoma of larynx (a), 1153
  CT and quality of therapy (e), 943
  Intraoral carcinoma (a), 1153
  Therapy for bone metastases, 1095
  Treatment of inoperable lung cancer (a), 1153
Therapeutic radiology, apparatus
  High energy fast neutrons from variable energy cyclotron. I. physical characteristics, 709; II. Biologic studies in mammalian systems, 717
Therapeutic radiology, complications
  Brachial edema after treatment of mammary carcinoma (a), 762
  Cardiac localization of ^{99m}Tc-(Sn)-pyrophosphate (a), 1151
  Cervical carcinoma (a), 956
  Injuries of lung, 127
  Pneumonitis from single fraction upper half body irradiation (a), 195
Therapeutic radiology, technique
  ^{252}Cf (a), 1154
  Twice-a-day fractionation management of cancer of head and neck, 1091
  Ultrasonic evaluation of ports (a), 373
Thermography
  Radionuclide, radiographic, and, detection of bone metastases (a), 766
  Scrotal (a), 194
Thorax, see also specific organs and regions

  - The adult postoperative chest (b), 773
  - Chest after pleural space reduction, 229
  - Intrathoracic desmoid tumor of chest wall (c), 524
  - Short rib-polydactyly syndrome (a), 561
  - Wall invasion secondary to pulmonary aspergillosis (c), 140
- Thromboembolism, see embolism; thrombosis
- Thrombosis, see also embolism
  - Cardiovascular arterial patency after percutaneous catheterization in infants and small children (a), 1143
  - Doppler ultrasonic screening and venography for deep venous, 451
  - Pedal venous pressure: detecting deep vein (a), 762
- Thumb, see fingers
- Thyroid
  - Hypothyroidism in cystinosis, 629
  - Improving decisions in well differentiated cancer (a), 562
  - Summary from workshop on late effects of irradiation to head and neck in infancy and childhood, 716
- Tomography, see organs and specific types
- Trachea, primary adenoid cystic carcinoma (cylindroma) (a), 553
- Transposition of great vessels, see heart, congenital abnormalities
- Treatment planning, see therapeutic radiology
- Tricuspid valve, see heart
- Trisomy, see Down's syndrome
- Trophoblastic disease, see organ or part
- Trout, E. Dale (o), 363
- Truncus arteriosus, see heart, congenital abnormalities
- Tuberculosis, see also under organ

- Ulcers, see peptic ulcer and under organ
- Ultrasound, see also under organs and regions
  - Comparison of cross-sectional imaging (e), 1133
  - Evaluating liver size (a), 562
  - Gallbladder, 975
  - Gray scale patterns of pelvic disease in the male (a), 769
  - Isodense masses on CT: differentiation by gray scale, 989
  - Manuale di ecotomografia (b), 378
  - Radiation therapy ports (a), 373
  - Tumors arising from spine and bony pelvis, 1061
  - Ultrasonography of the abdomen (b), 198
- Ureter
  - Blind buds (a), 955
  - Excretory urography in experimental obstruction, 89
  - Notching of, and renal pelvis in children, 837
  - Ureteroceles vs. pseudoureteroceles in adults (a), 189
- Urinary tract, see also specific urinary organs
  - The adrenal, retroperitoneum, and lower urinary tract. Atlas of tumor radiology (b), 773
  - Anomalies in neonates with spontaneous pneumothorax and/or pneumomediastinum (a), 1150
  - Fungal infection, pyelography and percutaneous nephrostomy, 415
  - Gray scale patterns of pelvic disease in the male (a), 769
  - Imperforate vagina with vaginourethral communication, 623
  - Schistosomiasis (a), 188
  - Symposium on pediatric uroradiology. Radiologic clinics of North America (b), 773
  - Urine extravasation after renal transplantation, 409
  - Urinoma (a), 1147
  - Urologic radiology (b), 203
  - Urological radiology of the adult male lower urinary tract: anatomy, physiology, pathology and sequelae, diagnosis and management (b), 379
- Urography
  - After lymphography in malignant disease (a), 188
  - Bronchospasm during excretory (a), 1146
  - Electrocardiographic response to intravenous, 825
  - Excretory in experimental ureteric obstruction, 89
- Uterus, neoplasm; see also pregnancy
  - Combined therapy for endometrial carcinoma (a), 376
  - Complications after radiation therapy (a), 956
  - Endometrial carcinoma and its treatment: the role of irradiation, extent of surgery, and approach to chemotherapy (b), 1156
  - Hyperbaric oxygen as radiotherapeutic adjuvant (a), 376
  - Hysterography before and after myomectomy, 899
  - Lymphangiography in, corpus, 903
  - Postoperative radiotherapy of cervical cancer (a), 771

- Vagina, imperforate with vaginourethral communication, 623
- Vagotomy, see gastrointestinal tract
- Valsalva sinus, see aorta
- Valves, see organs
- Varices, see also esophagus
  - Bleeding ileal varicosity demonstrated by portography (c), 514
  - Esophageal by fibre-optic endoscopy (a), 763
  - Esophageal treated with percutaneous obliteration (a), 365
  - Transhepatic obliteration of gastrointestinal, 237
- Vascular sling, see pulmonary arteries
- Vasopressin, intravenous versus intraarterial (l), 947
- Veins, see also angiography; embolism; arteriovenous malformations; portal vein; thrombosis; organs and regions
  - Angiographic abnormalities in partial Budd-Chiari syndrome (a), 762
  - Anomalies of intrahepatic portal system in hepatic fibrosis (a), 763
  - Connection from left atrium to cardinal system (c), 937
  - CT splenic, pancreatic relationship, 17
  - Doppler ultrasonic screening and venography for deep thrombosis, 451
  - Parenchymal striations in renal, thrombosis, 95
  - Pulmonary avulsion (c), 331
  - Screening for detection of deep, thrombosis (a), 762
  - Transhepatic obliteration of gastroesophageal varices, 237
- Venae cavae
  - Anomalies of systemic venous return (a), 1144
  - Catheter venography in superior, syndrome (c), 146
  - "Hot spot" on hepatic scintigraphy and radionuclide venacavography in, obstruction, 447
  - Nonmalignant venographic abnormalities of inferior (a), 366
  - Radiographic isolation of inferior, 657
  - Sonography of thrombosis of inferior in renal tumors (a), 768
- Venography, see also veins, organs, and regions
  - Brachial edema after treatment of mammary carcinoma, phlebography (a), 762
  - Leg phlebography, side effects (a), 555
  - Lumbar phlebography by catheterization (a), 559
  - Pelvic phlebography through profundal dorsal vein of penis for cancer of urinary bladder and prostate (a), 369
  - Radionuclide venography, correlation with contrast venography (a), 195
  - Rotating platform for ascending phlebography (t), 941
- Ventricles, see brain; heart
- Ventricular septal defect, see heart, congenital abnormalities
- Ventriculography, see brain; heart
- Vertebrae, see spine
- Vesicoureteral reflux, see ureter
- Volvulus, see specific organ

- WDHA syndrome, intractable diarrhea with vasoactive intestinal peptide-producing ganglioneuroblastoma (a), 1150
- Wilms's tumor, see kidney
- Wolf syndrome, see bone
- Wrist
  - Aseptic necrosis in systemic lupus erythematosus (a), 766
  - Fracture of hook of hamate (a), 1148
  - Ununited fracture of hook of hamate (a), 1147
- Xenon, comparison of 127 and 133 for ventillation studies (a), 1152
- X-rays, see radiology; dosimetry; radiation; radiography; therapeutic radiology; and under diseases, organs, and regions

Official Journal
American Roentgen Ray Society
American Radium Society

Volume 129

AJR

Including Diagnostic Radiology • Radiation Oncology • Nuclear Medicine Ultrasonography • Related Sciences

Editor Melvin M. Figley

Assistant Editor Rosalind H. Troupin

Associate Editors Luther W. Brady • Kenneth L. Krabbenhoft • E. Frederick Lang • Russell H. Morgan

Consulting Editorial Board Kent Ellis • E. Robert Heitzman • Donald L. King • John A. Kirkpatrick, Jr. Eugene C. Klatte • John G. McAfee • Thomas H. Newton Robert G. Parker • Stewart R. Reuter • William B. Seaman • Robert J. Shalek • John Storer • Michel M. Ter-Pogossian • Joseph P. Whalen • David M. Witten

Editorial Staff K. A. Murray, manager • M. B. Wieckowicz, manuscript editor • M. J. Leonard, assistant manuscript editor • C. P. Kaiser, secretary

Published monthly by Charles C Thomas, 301-327 East Lawrence Avenue, Springfield, Illinois 62717. All correspondence, except editorial office business, should be addressed to the publisher. Annual subscription prices: United States and possessions, $40; others, $50; residents in training in U.S., $20 (letter from department required with dates of residency); single copies, $5. Foreign subscription delivery not guaranteed. Undelivered or damaged copies replaced within 60 days of publication; 90 days for foreign subscribers. Allow 90 days for address changes. © 1977 by American Roentgen Ray Society. Second-class postage paid at Springfield, Illinois, and at additional mailing offices. Printed in U.S.A.

American Roentgen Ray Society

OFFICERS 1977-1978

President: Harry Z. Mellins
President Elect: Paul A. Rimenschneider
1st Vice-president: Joseph D. Calhoun
2nd Vice-president: Charles E. Bickham, Jr.
Secretary: James F. Martin
Treasurer: Harley C. Carlson

COMMITTEES 1977-1978

Executive Council: H. Z. Mellins, P. A. Riemenschneider, J. D. Calhoun, C. E. Bickham, Jr., J. F. Martin, H. C. Carlson, M. M. Figley, R. G. Evens, B. G. Brogdon, R. A. Gagliardi, E. Gedgaudas, G. A. Kling, T. F. Leigh, S. F. Ochsner, J. F. Wiot, R. E. Buenger, E. C. Klatte, J. P. Tampas, J. L. Gwinn, Chairman

Finance and Budget: A. E. James, E. C. Klatte, R. McLelland, J. P. Tampas, R. G. Evens, Chairman

Publications: M. P. Cap., K. Ellis, F. F. Ruzicka, Jr., E. R. Heitzman, R. A. Gagliardi, chairman

Editorial Policy: M. M. Figley, E. F. Lang, R. H. Troupin, E. R. Heitzman, K. Ellis, F. F. Ruzicka, Jr., M. P. Capp, R. A. Gagliardi, chairman

Advisory Committee on Education and Research: J. E. Youker, G. Wilson, G. W. Hartman, L. F. Rogers, E. Gedgaudas, chairman

Scientific Exhibits: T. C. Beneventano, G. Dodd, B. G. Brogdon, chairman

Constitution and Bylaws: J. H. Walker, W. M. Whitehouse, J. P. Tampas, chairman

American Board of Radiology Representatives: J. F. Roach, R. W. McConnell, S. W. Nelson

Program Committee: H. Z. Mellins, J. F. Martin, J. L. Gwinn, M. M. Figley, R. A. Gagliardi, B. G. Brogdon, E. Gedgaudas, G. A. Kling, P. Riemenschneider, chairman

Instruction Courses: E. Gedgaudas, director; G. W. Hartman, associate director

American College of Radiology Board of Chancellors Representative: W. B. Seaman

Annual Meeting: March 27-30, 1979. Sheraton Centre, Toronto. Canada

Scientific Program: P. A. Riemenschneider, president-elect, Cottage Hospital, Santa Barbara, California 93105

Manager Annual Meeting: George A. Kling, Harper Hospital, Detroit, Michigan

Membership: John L. Gwinn, 4650 Sunset Blvd., Los Angeles, California 90027

Business Office: Keith W. Gundlach, comptroller, American College of Radiology, 20 North Wacker Drive, Chicago, Illinois 60606

American Radium Society

OFFICERS 1977-1978

President: Richard H. Jesse
President Elect: Frederick W. George
1st Vice-president: Ivor Fix
2d Vice-president: John Durant
Secretary: Alfred S. Ketcham
Treasurer: Simon Kramer

COMMITTEES 1977-1978

Executive: F. Rutledge, L. W. Brady, R. H. Jesse, F. W. George, I. Fix, J. Durant, S. Kramer, A. S. Ketcham, V. Marcial, chairman

Public Relations: C. Honaker, R. H. Jesse, chairman

Publication: K. L. Krabbenhoft, A. F. Schroeder, G. Seydel, D. Hussey, A. Raventos, L. W. Brady, chairman

Scientific Program: F. George, D. Johnson, M. Boone, P. Chretien, P. J. DiSaia, D. Hussey, R. C. Landgren, C. Perez, S. T. Cantril, R. H. Jesse, chairman

Local Arrangements: J. Helsper, J. J. Romagosa, J. M. Thomson, Jr., A. J. Ballantyne, S. Kramer, S. Ochsner, chairman

Nominating: M. Kligerman, G. Lewis, J. Vaeth, chairman

Constitution and By-Laws: A. S. Glicksman, P. J. DiSaia, K. L. Krabbenhoft, chairman

Janeway Lecture: S. Levitt, L. Davis, A. S. Ketcham, chairman

Audiovisual: C. R. Bogardus, J. Helsper, B. Herrington, L. Bloebaum, C. Honaker, F. George, chairman

Resident Essay: J. T. Phillips, J. Curry, R. Schweitzer, J. T. Wharton, chairman

American Board of Radiology, Representatives: J. J. Stein, R. E. King, N. duV Tapley

American College of Radiology Board of Chancellors Representative: L. W. Brady

American College of Radiology Council Representative: J. del Regato

Editorial Board of AFCOS Newsletter Representative: J. Vaeth

National Council on Radiation Protection and Measurements Liason Representative: L. W. Davis

Annual Meeting: April 26-30, 1978, Marriott Hotel, New Orleans, Louisiana

Scientific Program: R. H. Jesse, M. D. Anderson Hospital, 6723 Bertner Drive, Houston, TX 77030

Local Arrangements: S. Ochsner, 1514 Jefferson Highway, New Orleans, LA 70121

Membership: A. S. Ketcham, secretary, University of Miami School of Medicine, P.O. Box 520875 Biscayne Annex, Miami, Florida 33152

Business Office: N. V. Jordan, c/o R. H. Jesse, M. D. Anderson Hospital and Tumor Institute, 6723 Bertner Avenue, Houston, Texas 77030

Vol. 129 **July 1977** **No. 1**

DIAGNOSTIC IMAGING

Impact of Computed Tomography on Utilization of Cerebral Angiograms. *E. B. Larson, G. S. Omenn, M. T. Margolis, and J. W. Loop* 1

Computed Tomography in Cerebral Hemiatrophy. *C. G. Jacoby, R. T. Go, and F. J. Hahn* 5

Refinements in Chiba Needle Transhepatic Cholangiography. *J. T. Ferrucci, Jr., and J. Wittenberg* 11

CT Demonstration of the Splenic Vein–Pancreatic Relationship: The Pseudodilated Pancreatic Duct. *F. E. Seidelmann, W. N. Cohen, P. J. Bryan, and J. Brown* 17

Retrospective Comparison of Radionuclide Scans and Computed Tomography of the Liver and Pancreas. *R. L. MacCarty, H. W. Wahner, D. H. Stephens, P. F. Sheedy, and R. R. Hattery* 23

Calcitonin Treatment in Hereditary Bone Dysplasia with Hyperphosphatasemia: A Radiographic and Histologic Study of Bone. *J. P. Whalen, M. Horwith, L. Krook, I. MacIntyre, E. Mena, F. Viteri, B. Torun, and E. A. Nunez* 29

Neonatal Mucolipidosis II (I-Cell Disease): Clinical and Radiologic Features in Three Cases. *H. B. Patriquin, P. Kaplan, H. P. Kind, and A. Giedion* 37

Unilateral Locked Facet in Cervical Spine Injuries. *A. T. Scher* 45

Injuries of the Medial Epicondylar Ossification Center of the Humerus. *J. W. Chessare, L. F. Rogers, H. White, and M. O. Tachdjian* 49

Laminar Avulsion in a Cervical Vertebra. *C. V. Cimmino and D. W. Scott, III* 57

Radiographic Manifestations of Bone Metastases from Renal Carcinoma. *G. S. Forbes, R. A. McLeod, and R. R. Hattery* 61

Testicular Venography for Undescended Testes. *M. G. Glickman, R. M. Weiss, and Y. Itzchak* 67

Testicular Venography in the Nonpalpable Testis. *A. B. Diamond, C. H. Meng, M. Kodroff, and S. M. Goldman* 71

Polyarteritis Nodosa and Hepatitis-B Surface Antigen: Role of Angiography in Diagnosis. *R. G. Fisher, D. Y. Graham, M. Granmayeh, and J. G. Trabanino* 77

Computed Tomography in the Diagnosis of Subcapsular and Perirenal Hematoma. *E. G. Schaner, J. E. Balow, and J. L. Doppman* 83

Visualization of the Medullary Rays on Excretory Urography in Experimental Ureteric Obstruction. *L. R. Bigongiari, R. Davis, W. G. Novak, J. D. Wicks, E. Kass, and J. R. Thornbury* 89

Parenchymal Striations in Renal Vein Thrombosis: Arteriographic Demonstration. *J. D. Wicks, L. R. Bigongiari, W. D. Foley, and J. Walter* 95

Transitional Cell Tumors of the Kidney: How Diagnostic is the Angiogram? *S. M. Goldman, C. H. Meng, R. I. White, R. C. Naraval, S. S. Siegelman, A. B. Diamond, S. L. Kaufman, and D. P. Harrington* 99

Sarcoma of the Kidney: Angiographic Features. *M. Granmayeh, S. Wallace, A. F. Barrett, R. Fisher, and J. H. Heslep* 107

Ultrasonic Evaluation of the Obstructed Duplex Kidney. *V. J. Mascatello, E. H. Smith, G. F. Carrera, M. Berger, and R. L. Teele* 113

Stereotaxic Instrument for Needle Biopsy of the Mamma. *J. Bolmgren, B. Jacobson, and B. Nordenström* 121

Severe Radiation Injuries of the Lung. *B. Roswit and D. C. White* 127

Diagnostic Oncology Case Studies: Metastatic Carcinoma Presenting as Shoulder Arthritis. *Contributed by A. Fremland* 137

CASE REPORTS

Thoracic Wall Invasion Secondary to Pulmonary Aspergillosis: A Complication of Chronic Granulomatous Disease of Childhood. *A. R. Altman* 140

Calcification in a Paraspinal Malignant Melanoma in a Child. *P. Stanley, S. E. Siegel, and H. Isaacs* 143

Catheter Venography in the Superior Vena Cava Syndrome. *W. R. Webb, G. Gamsu, and B. M. Rohlfing* 146

Cerebrospinal Fluid Rhinorrhea Demonstrated by Metrizamide CT Cisternography. *B. P. Drayer, R. H. Wilkins, M. Boehnke, J. A. Horton, and A. E. Rosenbaum* 149

Inadvertent Intrasplenic Injection of Oily Propyliodone. *E. Braunstein* 152

Absent Arch and Hypoplastic Pedicle: Another Confusing Cervical Spine Anomaly. *N. A. Kirchmer and M. Sarwar* 154

Spurs of the Mandible and Supracondylar Process of the Humerus in Cornelia de Lange Syndrome. *J. A. Curtis, A. E. O'Hara, and G. G. Carpenter* 156

Glucagon-producing Islet Cell Tumor of the Pancreas. *K. J. Cho, C. W. Wilcox, and S. R. Reuter* 159

Multiple Primary Hemangiomas of Bone. *C. A. Karlin and A. C. Brower* 162

TECHNICAL NOTE

Keyhole Cone Device for Lateral Magnification Cerebral Angiography. *R. L. Mani and R. C. Gross* 165

SPECIAL SECTION

Committee Report: Contrast Media in Diagnostic Radiology: Recommendations for Labels, Package Inserts, and Dosage Determination. *W. H. Shehadi* 167

The Federal Government's Impact on Radiology. *R. D. Moseley, Jr., and O. W. Linton* 171

Guest Editorials:
- **Therapeutic Value of Thyreocalcitonin.** *J. Caffey* 175
- **The Federal Crossword Puzzle.** *R. D. Moseley and O. W. Linton* 176

78th ARRS Meeting Preliminary Program 179

Letters 182

Abstracts of Current Literature 184

Book Reviews 198

News 204

Vol. 129 August 1977 No. 2

DIAGNOSTIC IMAGING

Effect of Size and Position on Chest Lesion Detection. *C. A. Kelsey, R. D. Moseley, B. G. Brogdon, D. G. Bhave, and J. Hallberg* 205

PEEP: Radiographic Features and Associated Complications. *T. C. McLoud, P. G. Barash, and C. E. Ravin* 209

Evaluation of a New Transthoracic Needle for Biopsy of Benign and Malignant Lung Lesions. *A. J. S. House and K. R. Thomson* 215

Nonmalignant Lymphoid Disorders of the Chest. *D. S. Feigin, S. S. Siegelman, E. G. Theros, and F. M. King* 221

Radiographic Appearance of the Chest after Pleural Space Reduction Procedures: Construction of a Pleural Tent and Phrenoplasty. *P. C. Goodman, H. Minagi, and A. N. Thomas* 229

Transpleural Abdominal Systemic Artery-Pulmonary Artery Anastomosis in Patients with Chronic Pulmonary Infection. *W. R. Webb and R. P. Jacobs* 233

Transhepatic Obliteration of Gastroesophageal Varices: Results in Acute and Nonacute Bleeders. *M. Viamonte, Jr., R. Pereiras, E. Russell, J. LePage, and D. Hutson* 237

Arteriography in the Evaluation of Pancreatic Pseudocysts. *D. C. Levin, H. Eisenberg, and R. Wilson* 243

Emergency Embolization in Blunt Hepatic Trauma. *H. P. Jander, H. L. Laws, M. S. Kogutt, and A. A. Mihas* 249

Selective Hepatic Artery Embolization to Control Massive Hepatic Hemorrhage after Trauma. *B. E. Rubin and B. T. Katzen* 253

Right and Left Ventricular Volumes and Wall Measurements: Determination by Computed Tomography in Arrested Canine Hearts. *S. W. Miller, R. E. Dinsmore, J. Wittenberg, R. A. Maturi, and W. J. Powell, Jr.* 257

Utilization, Reliability, and Cost Effectiveness of Cranial Computed Tomography in Evaluating Pseudotumor Cerebri. *R. G. Evens, N. Rujanavech, and M. A. Mikhael* 263

The Place of ^{57}Co-Bleomycin Scanning in the Evaluation of Tumors. *P. C. Kahn, C. Milunsky, M. K. Dewanjee, and R. A. Rudders* 267

On the Nature and Significance of Bony Proliferation in "Rheumatoid Variant" Disorders. *D. Resnick and G. Niwayama* 275

The Metal-Cement Interface in Total Hip Prostheses. *A. A. DeSmet, D. Kramer, and W. Martel* 279

Arthrography in the Diagnosis of Unexplained Chronic Hip Pain with Regional Osteopenia. *W. A. Murphy, M. J. Siegel, and L. A. Gilula* 283

Backward "Displacement" of the Spinolaminal Line at C2: A Normal Variation. *K. R. Kattan* 289

Erosion of the Inferior Aspect of the Clavicle in Secondary Hyperparathyroidism. *E. E. Schwartz, R. Lantieri, and J. G. Teplick* 291

PEDIATRIC RADIOLOGY

Gray Scale Ultrasonography in Medullary Cystic Disease of the Kidney and Congenital Hepatic Fibrosis with Tubular Ectasia: New Observations. *A. T. Rosenfield, N. J. Siegel, N. B. Kappelman, and K. J. W. Taylor* 297

Posterior Widening of the S1-S2 Interspace in Children: A Normal Variant of Sacral Development. *A. A. Cacciarelli* 305

Lateral Widening of Epiphyseal Plates in Knees of Children with Bowed Legs. *G. Currarino and D. R. Kirks* 309

Multiple Symmetrical Fractures of Bone of Unresolved Etiology. *J. P. Fulkerson and M. B. Ozonoff* 313

Hepatic Cavernous Hemangiomas and Hemangioendotheliomas in Infancy. *P. Stanley, G. F. Gates, R. T. Eto, and S. W. Miller* 317

Fluid-Filled Cystic Adenomatoid Malformation. *T. T. Tucker, W. L. Smith, and J. A. Smith* 323

RADIOLOGIC PHYSICS

Clearance of Radioactive Tantalum from the Human Lung after Accidental Inhalation. *D. Newton* 327

CASE REPORTS

Ruptured Aneurysm 20 Years after Surgery for Coarctation of the Aorta. *E. L. Unger and R. E. Marsan* 329

Pulmonary Vein Avulsion. *A. D. Gouliamos, I. S. Johnsrude, and D. C. Jackson* 331

Lymphocele: A Complication of Surgical Staging of Carcinoma of the Prostate. *M. E. Morin and D. A. Baker* 333

Perforation of the Pharynx in the Newborn: A Near Look-Alike for Esophageal Atresia. *R. M. Heller, S. G. Kirchner, and J. A. O'Neill* 335

CT Confirmation of Pelvic Lipomatosis: Two Cases. *E. S. Gerson, S. G. Gerzof, and A. H. Robbins* 338

Diffuse Calcification of the Breast in Chronic Renal Failure. *S. Y. Han and D. M. Witten* 341

Central Depression of Multiple Vertebral End-plates: A "Pathognomonic" Sign of Sickle Hemoglobinopathy in Gaucher's Disease. *G. C. Hansen and R. H. Gold* 343

Recurrent Ganglion Cyst: The Value of Preoperative Ganglionography. *R. H. Daffner and P. W. Whitfield* 345

Typhlitis Complicating Leukemia in an Adult: Barium Enema Findings. *R. L. Del Fava and T. G. Cronin, Jr.* 347

Uptake of ^{131}I by a Papillary Meningioma. *R. A. Preisman, S. E. Halpern, R. Shishido, T. Waltz, F. Callipari, and R. Reit* 349

TECHNICAL NOTES

EMI Scan Density of Methyl Methacrylate. *I. Ehrlich, M. E. Kricun, and C. F. Gonzalez* 351

An Aid to C1-C2 Percutaneous Puncture. *M. M. McDaniel and S. B. Fierstien* 353

An Abdominal Belt to Encourage Full Inspiration in Children during Tomography. *S. Gildersleeve and L. R. Kuhns* 354

Editorial: Image Presentation: How Can It Be Improved? *J. W. Loop* 355

Letters 357

1977 American Roentgen Ray Society Local

Memorial 363

Abstracts of Current Literature 365

Book Reviews 377

News 380

Vol. 129 September 1977 No. 3

Janeway Lecture: Fundamental Mechanisms in Combined Modality Therapy of Cancer. *H. S. Kaplan* 383

DIAGNOSTIC IMAGING

Diagnosis and Evaluation of Retroperitoneal Tumors by Computed Tomography. *D. H. Stephens, P. F. Sheedy, II, R. R. Hattery, and B. Williamson, Jr.* 395

Detection of Retroperitoneal Hemorrhage by Computed Tomography. *S. S. Sagel, M. J. Siegel, R. J. Stanley, and R. G. Jost* 403

Diagnosis of Urine Extravasation after Renal Transplantation. *D. G. Spigos, W. Tan, D. G. Pavel, M. Mozes, O. Jonasson, and V. Capek* 409

Fungal Infection of the Urinary Tract: Demonstration by Antegrade Pyelography and Drainage by Percutaneous Nephrostomy. *A. G. Dembner and R. C. Pfister* 415

Radiologic Spectrum of Opportunistic Infections of the Upper Gastrointestinal Tract. *P. A. Athey, H. M. Goldstein, and G. D. Dodd* 419

Radiologic Aspects of Beck Gastric Tube in Esophageal Reconstruction. *S. A. Fetouh, R. H. Daffner, R. W. Postlethwait, and R. C. Millar* 425

Air in the Esophagus: A Frequent Radiographic Finding. *A. V. Proto and E. J. Lane* 433

Hepatic Venography and Wedge Hepatic Vein Pressure Measurements in Diffuse Liver Disease. *J. A. Cavaluzzi, R. Sheff, D. P. Harrington, S. L. Kaufman, K. Barth, W. C. Maddrey, and R. I. White, Jr.* 441

"Hot Spot" on Hepatic Scintigraphy and Radionuclide Venacavography. *N. S. Gooneratne, M. G. Buse, J.L. Quinn, III, and J. B. Selby* 447

Doppler Ultrasonic Screening Prior to Venography for Deep Venous Thrombosis. *P. F. Jaques, W. A. Richey, C. A. Ely, and G. Johnson, Jr.* 451

The Target Sign: A New Radiologic Sign of Septic Pulmonary Emboli. *M. N. Zelefsky and L. G. Lutzker* 453

A Statistical Description of the Normal Computerized Brain Scan. *D. F. Reese, P. C. O'Brien, G. W. Beeler, Jr., P. R. Gerding, and C. R. Romme* 457

Cerebral Granulomatous Angiitis: Case Report and Literature Review. *M. J. Faer, J. H. Mead, and R. D. Lynch* 463

Angiography in Vascular Malformations of the Face. *G. B. Bradac, R. S. Simon, M. Bunte, and R. Stellmach* 469

Angiographic Observations on Chemodectomas of the Head and Neck. *S. F. Handel, M. H. Miller, S. Wallace, H. Goepfert, and R. H. Jesse* 477

Metrizamide Myelography. *W. R. Boyd and G. A. Gardiner, Jr.* 481

Avulsion of Nerve Rootlets with the Cuatico Needle during Pantopaque Removal after Myelography. *G. D. Hungerford and J. M. Powers* 485

Hand Radiographic Measurements in Growth Hormone Deficiency Before and After Treatment. *R. Hernandez, A. K. Poznanski, R. P. Kelch, and L. R. Kuhns* 487

Extramedullary Hematopoiesis in Paget's Disease of Bone. *S. Kadir, L. Kalisher, and A. L. Schiller* 493

RADIATION PHYSICS

Scanning Multiple Slit Assembly: A Practical and Efficient Device to Reduce Scatter. *G. T. Barnes, I. A. Brezovich, and D. M. Witten* 497

CASE REPORTS

Ulcerative Pseudopolyposis Mimicking Neoplasm Proximal to a Jejunal Obstruction. *R. L. Eisenberg, M. W. Hedgcock, R. B. Jeffrey, and C. K. Montgomery* 503

"Backwash Ileitis" with Pseudopolyposis. *G. A. Gardiner* 506

Mallory-Weiss Syndrome with Esophageal Obstruction Secondary to Adherent Intraluminal Thrombus. *M. J. Curtin and F. D. Milligan* 508

Metastatic Melanoma Presenting Clinically as Multiple Colonic Polyps. *B. A. Sacks, N. Joffe, and D. A. Antonioli* 511

Bleeding Ileal Varicosity Demonstrated by Transhepatic Portography. *M. Kinkhabwala, A. Mousavi, S. Iyer, and R. Adamsons* 514

"Hot and Cold" Bone Lesion in Acute Osteomyelitis. *C. D. Teates and B. R. J. Williamson* 517

An Unusual Scapular Stress Fracture. *A. C. Brower, J. R. Neff, and D. A. Tillema* 519

Myelosclerosis and Myelofibrosis in Treated Histiocytosis-X. *L. Pinckney and B. R. Parker* 521

Intrathoracic Desmoid Tumor of the Chest Wall. *D. L. Klein, G. Gamsu, and T. D. Gant* 524

Horseshoe Kidney: Ultrasonic Demonstration. *H. J. Mindell and E. A. Kupic* 526

TECHNICAL NOTES

A New Subtraction Technique Using Duplicating Film as a Final Print. *K. Mojab, L. Garcia, and G. Talge* 528

Radiologic Aspects of the New Universal Proximal Femoral Hip Prosthesis. *H. Drinker and J. C. Mall* 531

Cholecystocholangiography after Cholecystoduodenostomy. *J. Bastidas and L. M. DelGuercio* 534

SPECIAL LECTURE: **The Breast Cancer Screening Controversy: A Perspective.** *M. Moskowitz, P. Gartside, L. Gardella, I. de Groot, and D. Guenther* 537

Guest Editorial: Pulmonary Surfactant Disease States. *I. Meschan* 545

Letters 548

Program of 1977 SPIE/SPSE Meeting 549

Program of 1977 Society for Pediatric Radiology Meeting 551

ARRS Meeting Commercial Exhibitors 552

Abstracts of Current Literature 553

Book Reviews 564

News 567

Radiologic Societies 570

Vol. 129 October 1977 No. 4

DIAGNOSTIC IMAGING

Hickey Lecture: Radiology Manpower Update, 1976: Shortage or Surfeit? *P. A. Riemenschneider* 575

Acute Cholecystitis: 137 Patients Studied by Infusion Tomography of the Gallbladder. *R. Moncada, M. Cardoso, R. Danley, J. Rodriguez, K. Kimura, J. Pickleman, and J. Brandly* 583

Infusion Tomography of the Gallbladder: Mechanism of Gallbladder Wall Opacification in Experimental Acute Cholecystitis. *R. Moncada, M. Cardoso, R. Danley, J. Rodriguez, K. Kimura, J. Pickleman, and J. Brandly* 587

Gray Scale Ultrasonography of Calcified Liver Metastases. *C. S. Katragadda, H. M. Goldstein, and B. Green* 591

Intraluminal Diverticulum of the Esophagus. *M. H. Schreiber and M. Davis* 595

Primary Ulcerative Carcinoma of the Esophagus. *R. E. Gloyna, J. Zornoza, and H. M. Goldstein* 599

Pneumatosis Intestinalis as a Complication of Jejunoileal Bypass. *J. Wandtke, J. Skucas, R. Spataro, and R. J. Bruneau* 601

Radiologic Spectrum of Melanoma Metastatic to the Gastrointestinal Tract. *H. M. Goldstein, M. T. Beydoun, and G. D. Dodd* 605

Cavitating Metastases of the Small Intestine. *J. Zornoza and H. M. Goldstein* 613

The Use of Prone Films for Suspected Bowel Obstruction in Infants and Children. *R. L. Lorenzo and J. A. Harolds* 617

Imperforate Vagina with Vaginourethral Communication. *D. R. Kirks and G. Currarino* 623

Hypothyroidism in Cystinosis. *M. Grünebaum and R. L. Lebowitz* 629

The Trichorhinophalangeal Syndrome: Study of 16 Patients in One Family. *A. H. Felman and J. L. Frias* 631

Pediatric Lymphography: Performance, Interpretation, and Accuracy in 193 Consecutive Children. *N. R. Dunnick, B. R. Parker, and R. A. Castellino* 639

Epinephrine-enhanced Renal Angiography in Renal Mass Lesions: Is It Worth Performing? *M. A. Bosniak, M. A. Ambos, M. A. Madayag, R. S. Lefleur, and W. J. Casarella* 647

Involvement of an Aberrant Right Subclavian Artery in Dissection of the Thoracic Aorta: Diagnostic and Therapeutic Implications. *G. Weinberger, P. A. Randall, F. B. Parker, and S. A. Kieffer* 653

Radiographic Isolation of the Inferior Vena Cava. *I. L. Tonkin, T. E. Keats, and M. P. Capp* 657

Cardiomegaly as a Cause of Nonuniform Pulmonary Artery Perfusion. *C. F. Beckmann, D. C. Levin, and S. Ulreich* 661

Extraarticular Manifestations of Septic Arthritis of the Glenohumeral Joint. *T. G. Armbuster, J. Slivka, D. Resnick, T. G. Goergen, M. Weisman, and R. Master* 667

Metastatic Disease to the Breast: Clinical, Pathologic, and Radiographic Features. *B. D. Toombs and L. Kalisher* 673

Laryngeal Tuberculosis. *M. M. Lindell, Jr., B.-S. Jing, and S. Wallace* 677

Computed Tomography of Intracerebral Hematomas. I. Transmission CT Observations on Hematoma Resolution. *C. A. Dolinskas, L. T. Bilaniuk, R. A. Zimmerman, and D. E. Kuhl* 681

Computed Tomography of Intracerebral Hematomas. II. Radionuclide and Transmission CT Studies of the Perihematoma Region. *C. A. Dolinskas, L. T. Bilaniuk, R. A. Zimmerman, D. E. Kuhl, and A. Alavi* 689

Diagnosis of Isodense Subdural Hematomas by Computed Tomography. *M. A. Amendola and B. J. Ostrum* 693

Computed Angiotomography. *M. A. Weinstein, P. M. Duchesneau, and C. E. Weinstein* 699

Scleral Thickening: A CT Sign of Orbital Pseudotumor. *M. E. Bernardino, R. D. Zimmerman, C. M. Citrin, and D. O. Davis* 703

Diagnostic Oncology Case Studies: Testicular Seminoma with an Abdominal Mass. *Contributed by G. C. Hansen and T. Weisenburger* 707

RADIATION PHYSICS

High Energy Fast Neutrons from the Harwell Variable Energy Cyclotron. I. Physical Characteristics. *D. T. Goodhead, R. J. Berry, D. A. Bance, P. Gray, and J. B. H. Stedeford* 709

High Energy Fast Neutrons from the Harwell Variable Energy Cyclotron. II. Biologic Studies in Mammalian Systems. *R. J. Berry, D. A. Bance, D. W. H. Barnes, R. Cox, D. T. Goodhead, J. M. Sansom, and J. Thacker* 717

CASE REPORTS

Needle Tract Seeding of Renal Cell Carcinoma. *W. H. Bush, Jr., L. L. Burnett, and R. P. Gibbons* 725

Enophthalmos Simulating Orbital Emphysema. *J. I. Cossrow, J. A. Curtis, and J. Edeiken* 728

Selective Carotid Angiography in the Diagnosis of Orbital Hemangiopericytoma: Report of Two Cases. *L. D. Cromwell, C. Kerber, and M. T. Margolis* 730

Giant Dural Supratentorial Arteriovenous Malformation. *I. J. Gordon, B. L. Shah, D. R. Hardman, and L. Chameides* 734

Aseptic Necrosis: A Complication of Dislocation of the Metacarpophalangeal Joint. *V. Gilsanz, R. H. Cleveland, and R. H. Wilkinson* 737

Unilateral Hypertrophy of Multiple Pedicles. *K. Z. Hart and A. C. Brower* 739

Skeletal Involvement in Mycosis Fungoides. *G. V. O'Reilly, T. M. Clark, and C. P. Crum* 741

Undifferentiated Parotid Carcinoma with Osteoblastic Metastases. *P. J. Dubois, D. P. Orr, E. N. Meyers, and L. E. Barnes* 744

The Jet Phenomenon: A Manifestation of Esophageal Web. *I. A. Shauffer, H. E. Phillips, and J. Sequeira* 747

Pulmonary Hypoplasia and Pleural Effusions Associated with Fetal Death In Utero: Ultrasonic Findings. *B. Carroll* 749

TECHNICAL NOTE

Hypnotic Anesthesia for Cerebral Angiography. *J. S. Chestnut, W. O. Bank, Z. L. Deeb, and J. A. Horton* 751

Guest Editorial: Perspectives on Benefit-Cost Analysis in Medical Care. *S. J. Hessel* 753

Letters 758

National Academy of Sciences CT Recommendations 760

National Cancer Institute Report on Irradiation-related Thyroid Cancer 761

Abstracts of Current Literature 762

Book Reviews 772

News 775

Vol. 129 November 1977 No. 5

DIAGNOSTIC IMAGING

Neuhauser Lecture: The Lung: Its Growth and Remodeling in Health and Disease. *L. Reid* 777

Angiodysplasia of the Right Colon: A Cause of Gastrointestinal Bleeding. *S. Baum, C. A. Athanasoulis, A. C. Waltman, J. Galdabini, R. H. Schapiro, A. L. Warshaw, and L. W. Ottinger* 789

Transcatheter Intravascular Coil Occlusion of Experimental Arteriovenous Fistulas. *J. H. Anderson, S. Wallace, and C. Gianturco* 795

Complications of Long Term Transbrachial Hepatic Arterial Infusion Chemotherapy. *M. E. Clouse, R. Ahmed, R. B. Ryan, R. A. Oberfield, and J. A. McCaffrey* 799

Nonsurgical Splenectomy. *W. R. Castaneda-Zuniga, D. E. Hammerschmidt, R. Sanchez, and K. Amplatz* 805

Angiocardiography of Subaortic Obstruction in Infancy. *R. M. Freedom, J. A. G. Culham, and R. D. Rowe* 813

Electrocardiographic Response to Intravenous Urography: Prospective Evaluation of 275 Patients. *R. C. Stadalnik, Z. Vera, O. DaSilva, R. Davies, J. F. Kraus, and D. T. Mason* 825

Ultrasonic Demonstration of Intrarenal Anatomy. *J. H. Cook, III, A. T. Rosenfield, and K. J. W. Taylor* 831

Notching of the Ureter and Renal Pelvis in Children. *R. H. Cleveland, K. E. Fellows, and R. L. Lebowitz* 837

Malposition of the Colon in Right Renal Agenesis, Ectopia, and Anterior Nephrectomy. *J. A. Curtis, V. Sadhu, and R. M. Steiner* 845

Radiologic Findings in Renal Amyloidosis. *L. Ekelund* 851

Angiographic Findings in Renal Amyloidosis. *T. L. McCormick and K. J. Cho* 855

Infiltrating Neoplasms of the Kidney. *M. A. Ambos, M. A. Bosniak, M. A. Madayag, and R. S. Lefleur* 859

Radiographic Manifestations of Acute Smoke Inhalation. *C. E. Putman, J. Loke, R. A. Matthay, and C. E. Ravin* 865

Uptake of Bone Imaging Agents by Diffuse Pulmonary Metastatic Calcification. *D. I. Rosenthal, H. L. Chandler, F. Azizi, and P. B. Schneider* 871

Radiographic Findings of Immunoblastic Lyphadenopathy and Related Immunoblastic Proliferations. *H. I. Libshitz, M. Clouser, J. Zornoza, and B. M. Osborne* 875

Strontium-87m Lung Scans in Pulmonary Aspergillosis. *P. K. Rohatgi, D. B. Simon, R. A. Goldstein, and R. C. Reba* 879

The Kinky Chest Tube: A Sign of Entrapment Following Median Sternotomy. *A. E. Berkow and B. C. Salo* 883

The Lateral Decubitus View: An Aid in Evaluating Poorly Defined Pulmonary Densities in Children. *A. S. Kaufman and L. R. Kuhns* 885

Huge Splenic Cyst in a Newborn: Comparison with 10 Cases in Later Childhood and Adolescence. *N. T. Griscom, H. K. Hargreaves, M. Z. Schwartz, J. M. Reddish, and A. H. Colodny* 889

Spontaneous Disappearance of Gastric Polyps: Report of Four Cases. *Y. Tsukamoto, H. Nishitani, Y. Oshiumi, and T. Okawa* 893

Hysterography Before and After Myomectomy. *D. Weinstein, Y. Aviad, and W. Z. Polishuk* 899

Bipedal Lymphangiography in Malignancies of the Uterine Corpus. *M. T. Kademian, D. A. Buchler, and G. W. Wirtanen* 903

Computed Tomographic Evaluation of the Retrocrural Prevertebral Space. *P. W. Callen, M. Korobkin, and I. Isherwood* 907

Voluntary Glenohumeral Dislocation. *E. M. Braunstein and W. Martel* 911

Radiologic Aspects of Diffuse Idiopathic Skeletal Hyperostosis in the Spine. *Y. Tsukamoto, H. Onitsuka, and K. Lee* 913

CASE REPORTS

Ultrasonic Appearance of the Krukenberg Tumor. *D. Rochester, B. Levin, J. D. Bowie, and A. Kunzmann* 919

Antepartum Diagnosis of Conjoined Twins by Ultrasonography. *C. J. Fagan* 921

Ultrasonography of a Mediastinal Pseudocyst. *S. Asokan, D. Alagratnam, M. Eftaha, J. Radhakrishnan, L. T. Lim, and M. Teresi* 923

Sonographic Diagnosis of a Wandering Spleen. *T. B. Hunter and K. Haber* 925

Massive Splenic Infarction in Sickle Cell–Hemoglobin C Disease: Angiographic Findings. *G. Fishbone, D. Nunez, Jr., R. Leon, G. Paz, P. Isturiz, and C. McLoughlin* 927

Intraluminal Duodenal Diverticulum: Diagnosis during Endoscopic Pancreatography. *S. S. Shenoy, G. J. Culver, and M. V. Ali* 929

Demonstration of a False Aneurysm of the Extremity by Dynamic Radionuclide Scintigraphy. *K. R. Lee, R. G. Robinson, and J. R. Neff* 931

Peripheral Arterial Embolism of Multiple Pellets after Shotgun Injury to an Extremity. *J. A. Guest, M. A. Malangoni, R. W. Holden, and P. B. Yaw* 933

Bilateral Internal Auditory Canal Enlargement due to Dural Ectasia in Neurofibromatosis. *M. Sarwar and L. E. Swischuk* 935

Anomalous Venous Connection from the Left Atrium to the Cardinal Venous System: "Levoatriocardinal Vein." *L. C. Blieden, A. Schneeweiss, V. Deutsch, and H. N. Neufeld* 937

Progressive Abnormalities in the Brain Scan in Adrenal Leukodystrophy. *B. E. Chatterton* 939

TECHNICAL NOTES

Rotating Platform for Ascending Phlebography. *J. H. Grollman, Jr., and P. D. Straede* 941

A Simple Aid to the Performance of Shoulder Arthrography. *M. K. Dalinka* 942

Guest Editorial: Computed Tomography and the Quality of Radiation Therapy. *J. R. Stewart and L. D. Simpson* 943

Memorial: Traian Leucutia 945

Letters 947

Abstracts of Current Literature 949

Book Reviews 957

News 963

Radiologic Societies 965

Vol. 129 December 1977 No. 6

ARS Presidential Address: Cancer of the Breast: A Time for Caution. *L. W. Brady* 969

DIAGNOSTIC IMAGING

Gray Scale Ultrasonography of the Gallbladder: An Evaluation of Accuracy and Report of Additional Ultrasound Signs. *J. C. Anderson and R. K. Harned* 975

Accuracy of Biliary Duct Ultrasound: Comparison with Cholangiography. *H. L. Neiman and R. A. Mintzer* 979

Gray Scale Echographic Patterns of Hepatic Metastatic Disease. *W. Scheible, B. B. Gosink, and G. R. Leopold* 983

Isodense Masses on CT: Differentiation by Gray Scale Ultrasonography. *P. J. Bryan and W. M. Dinn* 989

Myelolipoma of the Adrenal: Two Cases with Ultrasound and CT Findings. *M. Behan, E. C. Martin, E. C. Muecke, and E. Kazam* 993

Ultrasound-guided Drainage of Fluid-containing Masses Using Angiographic Catheterization Techniques. *J. Grønvall, S. Grønvall, and V. Hegedüs* 997

Gray Scale Ultrasound Evaluation of Popliteal Artery Aneurysms. *T. M. Silver, R. L. Washburn, J. C. Stanley, and W. S. Gross* 1003

Pitfalls in the Angiographic Management of Hemorrhage: Hemodynamic Considerations. *E. J. Ring, J. A. Oleaga, D. Freiman, J. W. Husted, A. C. Waltman, Jr., and S. Baum* 1007

Angiography of Pancreatic Arteriovenous Malformation. *V. P. Chuang, C. M. Pulmano, J. F. Walter, and K. J. Cho* 1015

Pulmonary Angiography for Pulmonary Emboli: Rational Selection of Oblique Views. *A. S. Gomes, J. H. Grollman, Jr., and J. Mink* 1019

A Radiographic Study of Congenital Pulmonary Atresia with Ventricular Septal Defect. *B. Soto, A. D. Pacifico, R. F. Luna, and L. M. Bargeron, Jr.* 1027

Contrast Medium Reactions Correlated with Time of Day. *J. J. Cunningham* 1039

Accuracy of Bipedal Lymphography in Hodgkin's Disease. *M. T. Kademian and G. W. Wirtanen* 1041

Primary Chylopericardium: The Role of Lymphangiography. *T. E. Gallant, R. J. Hunziker, and T. C. Gibson* 1043

Ether-dissolved Ethiodol for Lymphangiography: An Experimental Study. *K. Jonsson, J. H. Anderson, B. Osborne, and S. Wallace* 1047

Left Adrenal Neuroblastoma with Normal-appearing Urogram. *J. O. Haller, W. E. Berdon, D. H. Baker, and E. G. Kassner* 1051

Acute Appendicitis with Abscess Simulating Carcinoma of the Sigmoid. *J. M. Halls and H. I. Meyers* 1057

Ultrasonography in Tumors Arising from the Spine and Bony Pelvis. *L. A. deSantos and H. M. Goldstein* 1061

Radiographic Diagnosis of Acute Peroneal Tendon Dislocation. *C. C. Church* 1065

Subchondral Pseudocysts in Rheumatoid Arthritis. *C. Rennell, F. Mainzer, C. V. Multz, and H. K. Genant* 1069

Angiographic Features of Osteosarcoma. *I. Yaghmai* 1073

Occurrence of Lung Granulomas in Patients with Stage I Sarcoidosis. *Y. Rosen, J. K. Amorosa, S. Moon, J. Cohen, and H. A. Lyons* 1083

Diagnostic Oncology Case Studies: Chronic Sciatic Pain in a Young Woman with Sclerosis of the Iliac Bone. *Contributed by R. Kalinowski* 1087

RADIATION ONCOLOGY

Preliminary Results Using Twice-a-day Fractionation in the Radiotherapeutic Management of Advanced Cancers of the Head and Neck. *S. Jampolis, G. Pipard, J.-C. Horiot, M. Bolla, and C. Le Dorze* 1091

Evaluation of Radiation Therapy for Bone Metastases: Pain Relief and Quality of Life. *H. A. Gilbert, A. R. Kagan, H. Nussbaum, A. R. Rao, J. Satzman, P. Chan, B. Allen, and A. Forsythe* 1095

CASE REPORTS

Peripelvic Renal Pseudocyst due to Obstruction. *Z. L. Barbaric and I. N. Frank* 1097

Contralateral Renal Herniation after Nephrectomy: A Cause of Pseudo-Crossed Renal Ectopia. *K. J. Cho, J. F. Walter, and J. W. Konnak* 1099

Gray Scale Ultrasonography in Retroperitoneal Lymphangiomyomatosis. *J. Walsh, K. J. W. Taylor, A. T. Rosenfield* 1101

Diffuse Interstitial Calcification of the Lungs in Chronic Renal Failure Mimicking Pulmonary Edema. *H. Firooznia, R. Pudlowski, C. Golimbu, M. Rafii, and D. McCauley* 1103

Massive Esophageal Hemorrhage in Leukemia. *P. H. Stratemeier* 1106

Lymph Node Calcification in Hodgkin's Disease after Chemotherapy. *M. Bertrand, J. T. T. Chen, and H. I. Libshitz* 1108

Localization of ^{67}Ga Citrate in a Mycotic Aneurysm. *J. A. Michal, III, and R. E. Coleman* 1111

Exostosis after Iliac Bone Marrow Biopsy. *W. A. Murphy* 1114

Pathologic Fracture in an Unusual Case of Gout. *J. Burnham, K. Fraker, and H. Steinbach* 1116

Mondini Defect: A Variant. *P. M. Som, M. T. Khilnani, S. L. Beranbaum, and B. S. Wolf* 1120

TECHNICAL NOTES

A Method of Reducing Cost in CT Systems That Employ Floppy Discs. *L. D. Cromwell, W. E. Moore, D. Schumacher, and A. Salam* 1123

A Wedge Filter for Craniocervical Angiography. *L. D. Cromwell, C. W. Kerber, and W. R. Vermeere* 1125

SPECIAL LECTURE: Roles for Radiologists in Tomorrow's Medical Care System. *R. H. Morgan* 1129

Guest Editorial: On Maps and Comparing Cross-sectional Imaging Methods. *J. C. Birnholz* 1133

From Earlier Pages 1135

Letters 1137

Report of 1977 ARS Meeting 1140

AJR Reviewers and Abstractors, 1977 1142

Abstracts of Current Literature 1143

Book Reviews 1156

News 1160

Index to Volume 129 1163

We help you help.

An employee of yours has a house fire, a disabled parent, an emergency of any kind.

That's just when Red Cross—America's Good Neighbor—steps in to lend a hand. Because helping people is what we're all about.

You could say all this helps your company, too.

Because easing people over life's rough spots makes them easier in their minds. And no one has to tell you how important that is on the job.

So help Red Cross any way you can.

When you help us, it helps your people.

And when you help your people, you help yourself.

A Public Service of This Magazine & The Advertising Council Ad Council

Red Cross. The Good Neighbor.

Yes... you're a candidate for Heart Attack

You can reduce your risk by

- Not smoking cigarettes,
- Eating foods low in animal fats and cholesterol,
- Reducing if overweight,
- Exercising regularly, moderately,
- Controlling high blood pressure,
- Seeing your doctor regularly,

and by supporting your Heart Association's programs of research, education and community service.

GIVE... so more will live HEART FUND

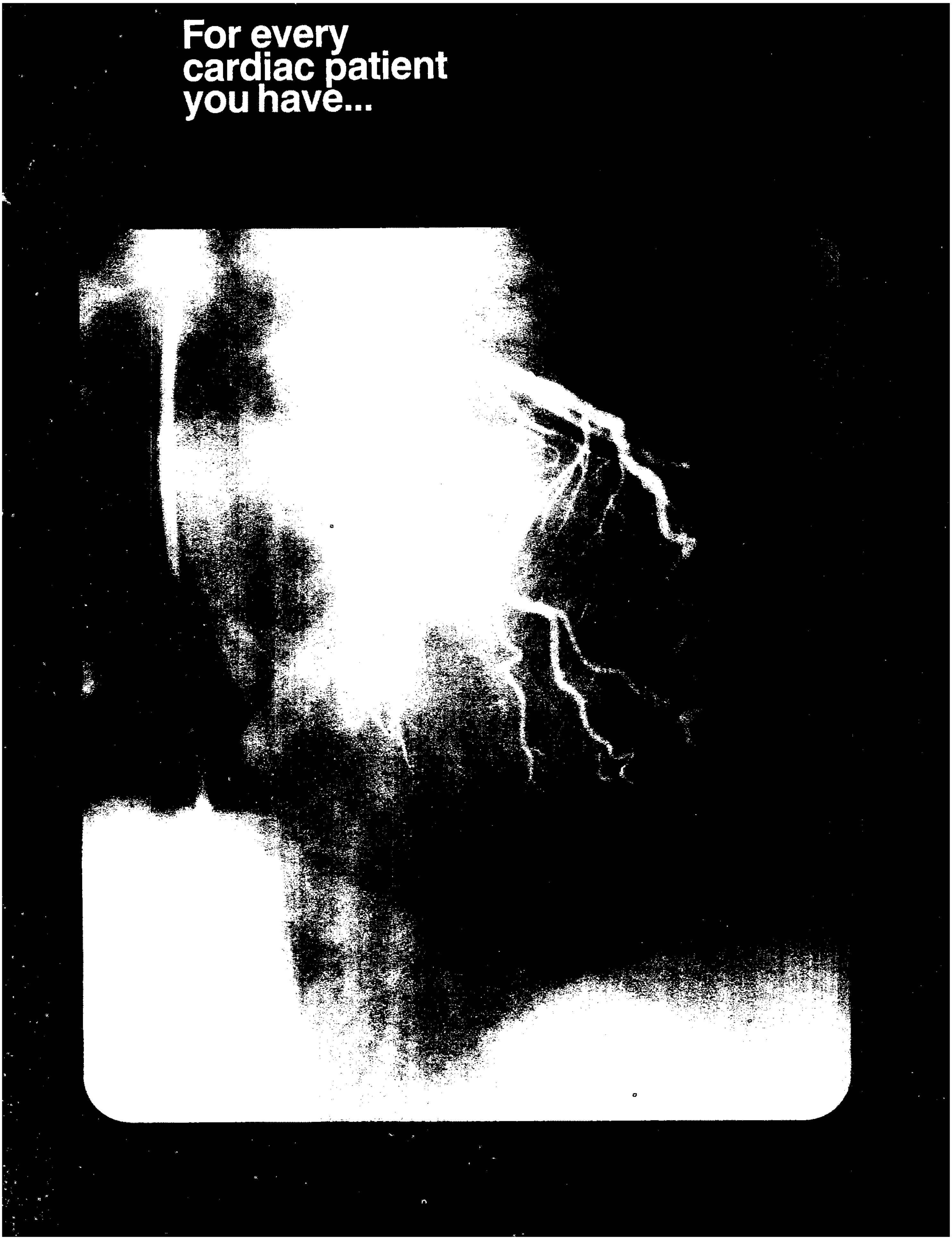

For every
cardiac patient
you have...

Computerized X-ray Generator Guarantees Optimum Technique for Every Exposure!

PHILIPS **Optimus** M200:

the ultimate clinical application of computer technology

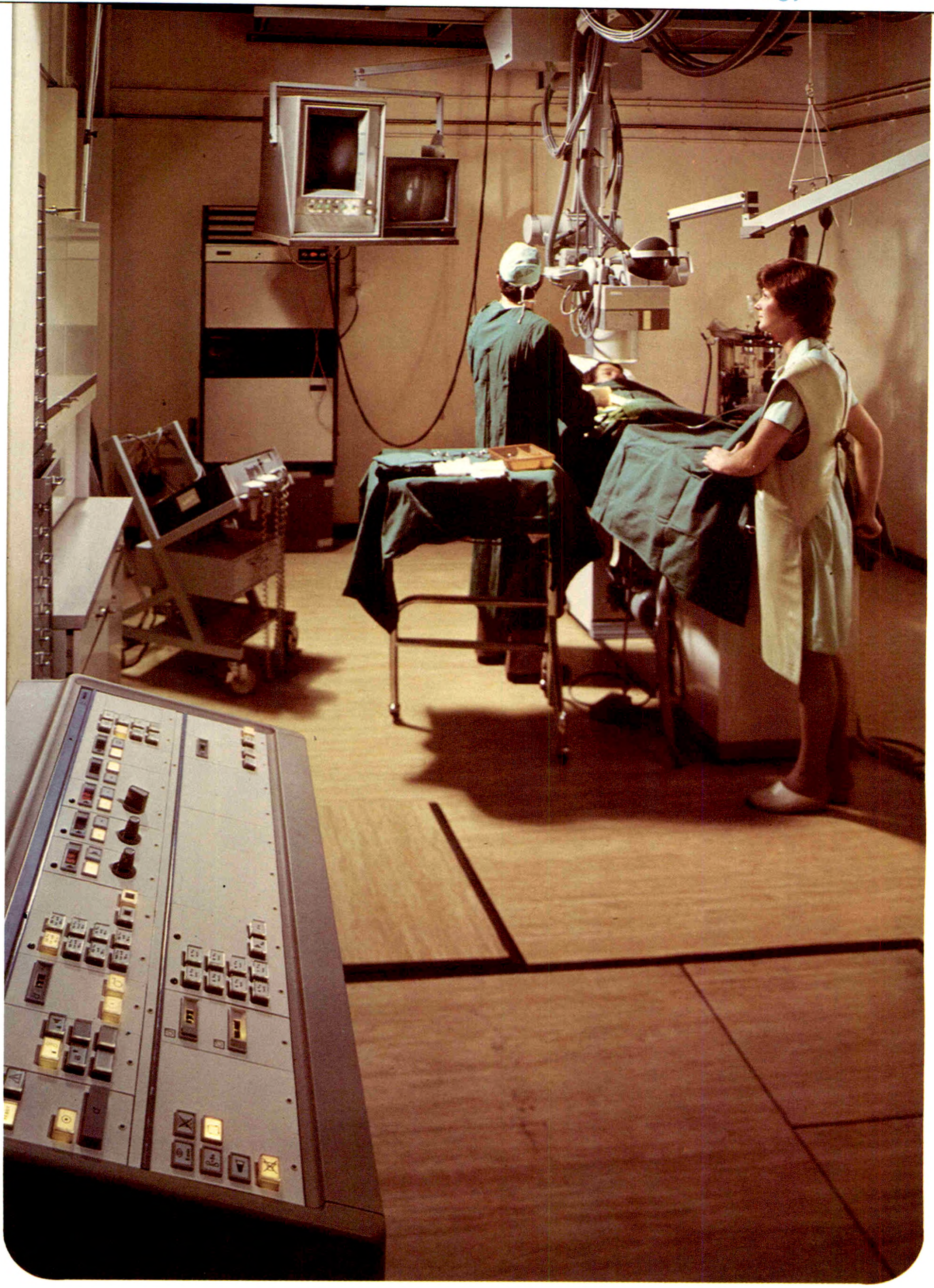

PHILIPS®

® TM N.V. Philips of Holland

The Computer: Medical Language, Medical Results

Consider computer technology completely dedicated to cardiovascular diagnostics...micro-circuitry that thinks and operates in your language according to your parameters and your procedure needs. Consider technology advanced to a degree that guarantees the perfect exposure for every run on every patient, regardless of age, size or weight. *This* is the OPTIMUS.

Full automation makes such accuracy simple for you. A range of programs covering every examination technique is built into the generator at installation. You select the medical parameters for each program. For examination, simply turn on the generator and press one button for the program you want. The OPTIMUS does the rest.

Patient Measuring Shots: Your Instant Preview

Automatically (in 5 milliseconds), the OPTIMUS measures the absorption characteristics of the patient and then the computer selects the exact factors for an ideal exposure. Factors are selected in discrete mA/kV steps. Your technique is always the highest mA and the lowest kV.

In a fraction of a second, all other technical parameters are calculated and set by the generator. You're insured perfect results before the cine run starts. The measuring shots can be engaged at any time to determine optimum technique for any projection.

Measuring shots drastically reduce the radiation dose required by less automated systems to determine technique factors. In the time equivalent to one cine frame, you know exactly what the results will be.

Procedure interruptions due to factor adjustment or "trial and error test shots"are eliminated. You and the technician devote minimum attention to technique selection and maximum attention to your patient.

A New Standard of Image Quality

The OPTIMUS' high output permits short exposures with low tube tensions. As a result, images are rich in contrast and detail. Low kV lets you visualize extremely small vessels with unprecedented ease. And not only are geometric unsharpness and motion unsharpness both minimized, but the OPTIMUS automatically weighs one against the other in selecting the technique which optimizes image quality.

From Maximum to Minimum Instantly

The OPTIMUS' secondary tetrode system switches exposures on and off *and also regulates the kVp level.* Now it's possible to change technique from maximum to minimum instantly. This is the same basic concept Philips' cine pulse has used successfully for the past twenty years!

Full Generator Use

More than any other system on the market, the OPTIMUS gives you the *full* capability of a generator. Over 100 hospitals throughout the world are enjoying that OPTIMUS capability right now! It's the product of all Philips' experience in both generators and computer technology...the logical result of progress from Philips' cine pulse to automated Modular Generators to Anatomically Programmed Radiography. The OPTIMUS: it's the most logical choice for you, too.

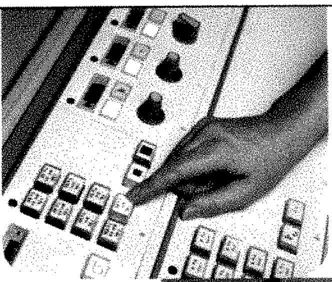

Press one button for optimum technique for every exposure.

A built-in memory lets you change technique and return to the initial program with no operator changes – for every patient!

Secondary tetrodes – another first from Philips . . . 20 years ago!

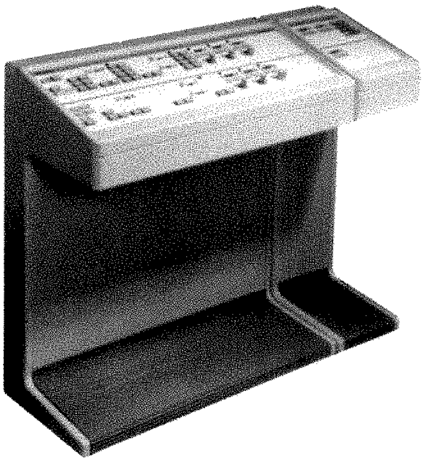

The OPTIMUS: computerized because it does a job only a computer can do!

For more information, contact
your Philips' representative.
Or, call or write:

PHILIPS MEDICAL SYSTEMS, INC.
710 Bridgeport Avenue, Shelton, Conn. 06484

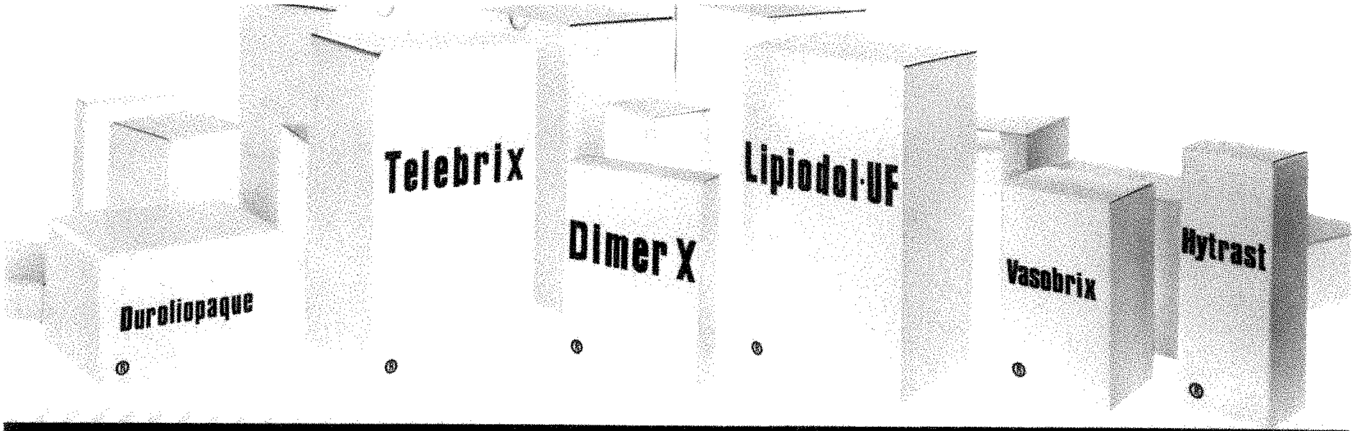

WE MANUFACTURE

contrast

MEDIA

OUR

products

ARE

known

WORLD-WIDE

OUR

name isn't

GUERBET

BETTER CONTRAST MEDIA THROUGH RESEARCH

Laboratoire Guerbet, 16/24, rue Jean-Chaptal
93601 AULNAY-SOUS-BOIS Cedex - FRANCE
Telex : Guerbet 690682

To all other manufacturers of 105° tables, our apologies.

Sorry, gentlemen. No matter how good other tilt-tables are, no matter how much they cost, this table has simply been better thought-out.

You see, we started from scratch to build a 15° Trendelenberg table that's the radiologist's dream, without forgetting the technologist. With a pivot point relocated to lower the top to where it should be for patient, radiologist and technologist comfort. With a built-in mini-computer that monitors movements and cushions the patient from rapid stops and starts. With a sophisticated input/feedback control of the fluoroscopic staging that virtually eliminates inertia—it feels as if you're moving a 3-ounce wand.

There's no obstruction behind the spot-film device—allowing you many new techniques such as cross-table radiography during fluoroscopy, or even a fluoroscopic exam of a litter patient. The full-floating top literally doubles fluoroscopic coverage.

Then this super fluoroscopic table turns into the ideal radiographic table. With a 32-inch table-top height. With a manual four-way floating top that allows patient positioning without physical contact. With a table-top-to-film distance less than many non-tilt tables. And with that mini-computer, constantly monitoring, reminding and helping with procedures.

Write direct or phone your Amrad dealer. Let him show you what we've got to apologize for.

This one obsoletes 'em all.

AMRAD®

The common-sense people in x-ray.

Amrad Incorporated, 2020 North Janice Avenue,
Melrose Park, Illinois 60160 (312) 865-2600

Synerviews.

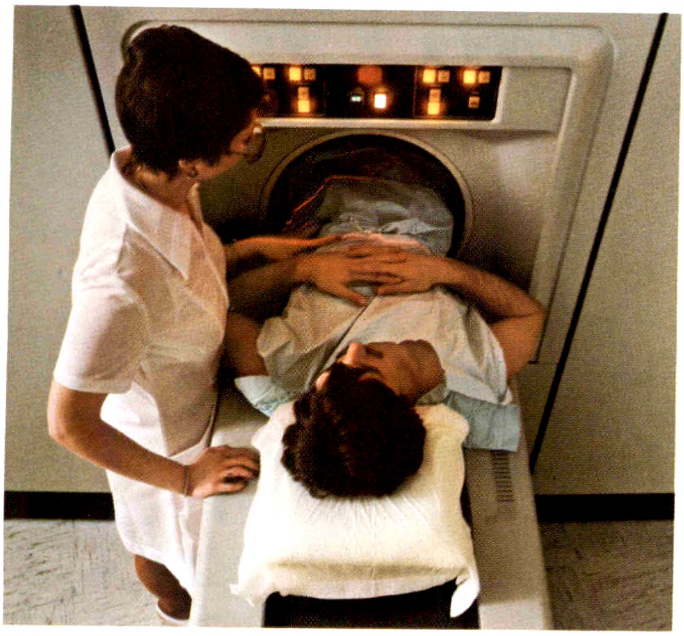

Synerview™ by Picker now enables you to view consistently high quality images with reliability in computed tomography.

Synerview is a complete CT system providing visualization of head and body cross-sections. Using the proven translate/rotate scanning principle, it is designed to provide the most desirable cost/benefit relationship.

Some outstanding viewing features include, black-and-white image viewing of gray-scale display, color image viewing of color-spectrum display, interactive keyboard for display control and image selection, function switches for special image manipulations, horizontal/vertical cursor manipulation control and much more.

Some overall Synerview highlights include preselected patient protocols, three field sizes, variable scan speed from 12-60 seconds, 30-second scan processing time, high-resolution data acquisition matrices, imaging stacking, side-by-side images and in-house architectural planning.

In all, Synerview is a Picker corporate commitment to manufacture, supply and service diagnostic visualization systems second to none.

This is another example of Picker's unique human resources benefiting you. It's a result of our expertise in the diagnostic modalities of Computed Tomography, X-ray, Ultrasound, Nuclear, Clinical Laboratory. Therapy, Film Systems and Supplies. Only Picker has all these resources.

Contact your local Picker representative. Or write Picker Corporation, 595 Miner Road, Cleveland, OH 44143.

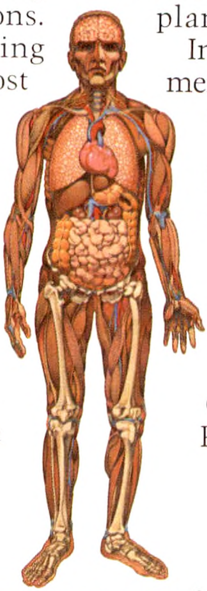

Discover the human resources in Picker's synergy

PICKER®

ONE OF THE C.I.T. COMPANIES

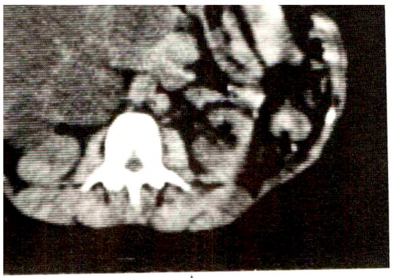

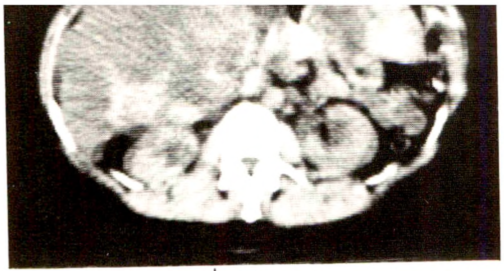

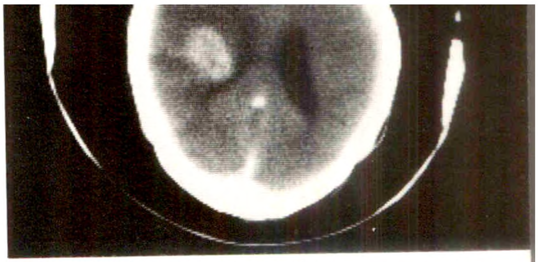

Contrast enhanced metastasis.
30 Sec. 3.4 RADS.

↕ Polycystic liver. 18 Sec. 4.6 RADS. ↕

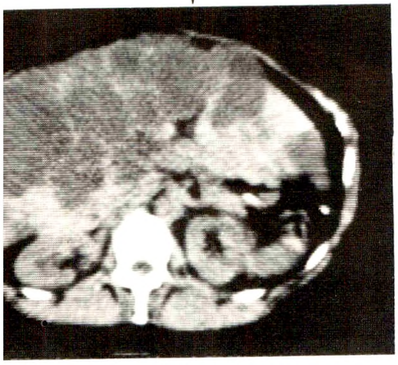

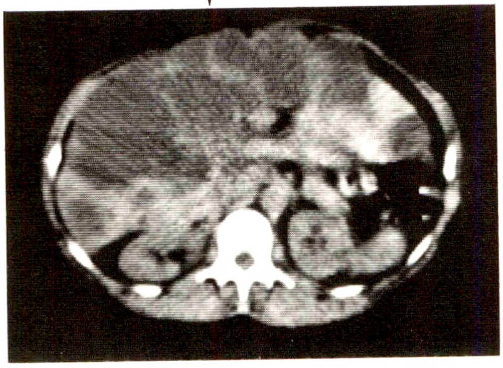

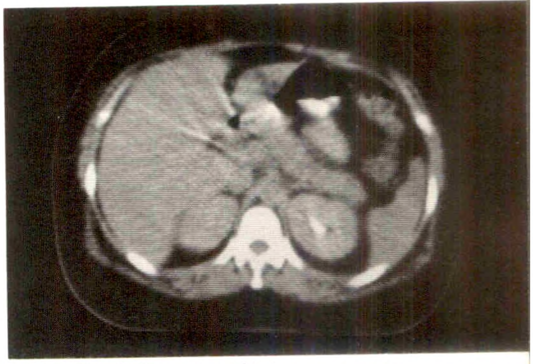

Abdominal slice visualizing pancreas.
18 Sec. 4.2 RADS.

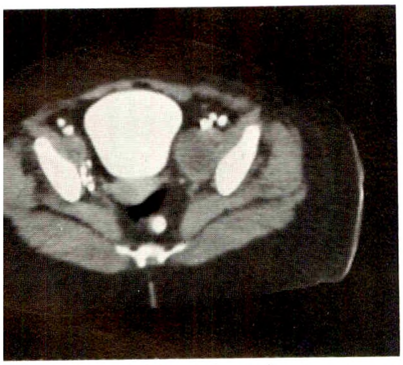

rast enhanced lymph nodes;
phoma. 30 Sec. 6.3 RADS.

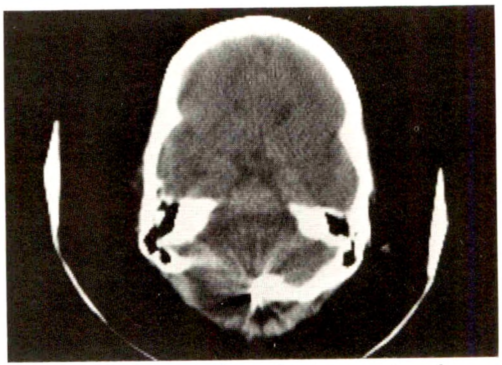

Supraorbitomeatal plane demonstrating the
Pentagon. 30 Sec. 3.4 RADS.

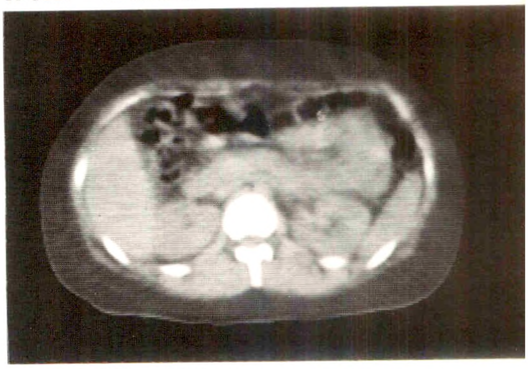

Normal abdominal section.
18 Sec. 4.2 RADS.

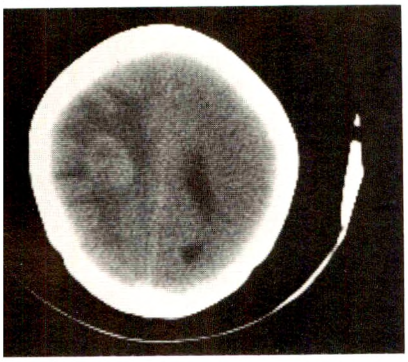

astasis.
ec. 3.4 RADS.

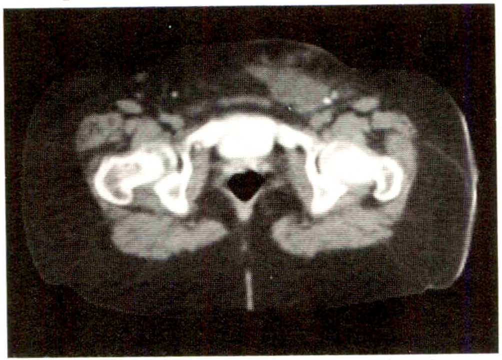

Contrast filled bladder and femoral heads.
30 Sec. 6.3 RADS.

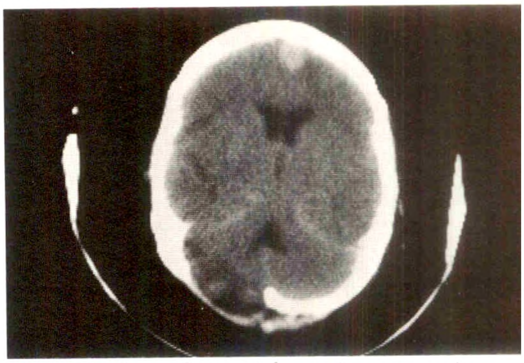

Contrast enhanced tentorial margin; metastasis.
30 Sec. 3.4 RADS.

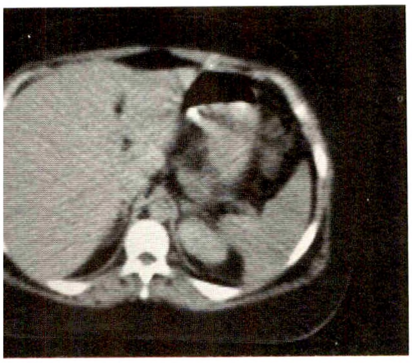

operitoneal structures

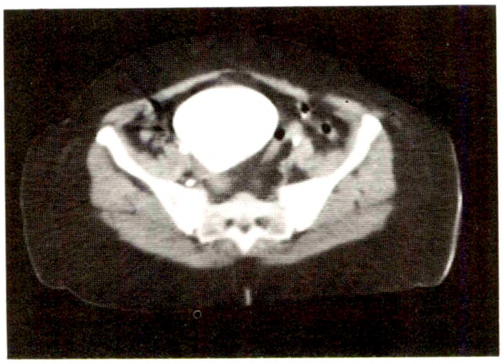

Pelvic vessels and nodes.

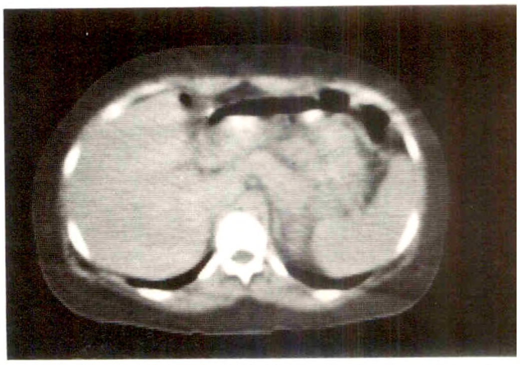

Normal pancreas and SMA.

Breast Cancer: earlier warning system

Futility and frustration beset the physician confronted with breast cancer. For the last 35 years, the survival rate has not significantly changed despite intensive educational programs aimed at earlier detection, and improvement in treatment techniques.

What is the outlook? We know the key to reducing mortality from breast cancer is in the *earliest possible* diagnosis. The stage at which breast cancer is detected is *crucial* to the outcome of treatment. By the time a lump is discovered through BSE or clinical examination, critical time may have been lost.

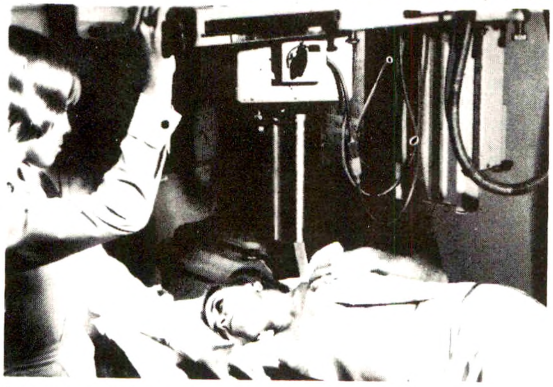

Mammography

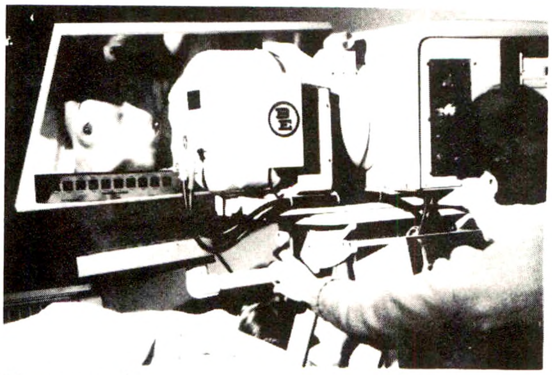

Thermography

And we *do* have the means to achieve earlier diagnosis. We do have an *earlier* warning system. Mammography and thermography can detect breast cancer *before* a lump is discernible by palpation. To demonstrate that it is practical and feasible to detect breast cancer earlier by using these modalities, the American Cancer Society and the National Cancer Institute are funding a network of breast cancer demonstration projects. Supported by grants of $2-million from the ACS and $4-million from the NCI, 20 such centers are expected to be operative across the country by the end of the year. Each will screen at no charge, approximately 5,000 women annually, in what is considered to be the ideal detection program—to include clinical examination, mammography and thermography. Each of these detection methods contributes independently to the detection of breast cancer, and none can be dispensed with in the search for early disease.

At present we cannot prevent breast cancer, but the potential for saving more lives is immense. The five-year survival rate surges dramatically from 53% when axillary nodes are positive, to approximately 85% when the disease is localized, to nearly 100% for in-situ cancer.

We have an earlier warning system. Let's use it.

® **american cancer society**

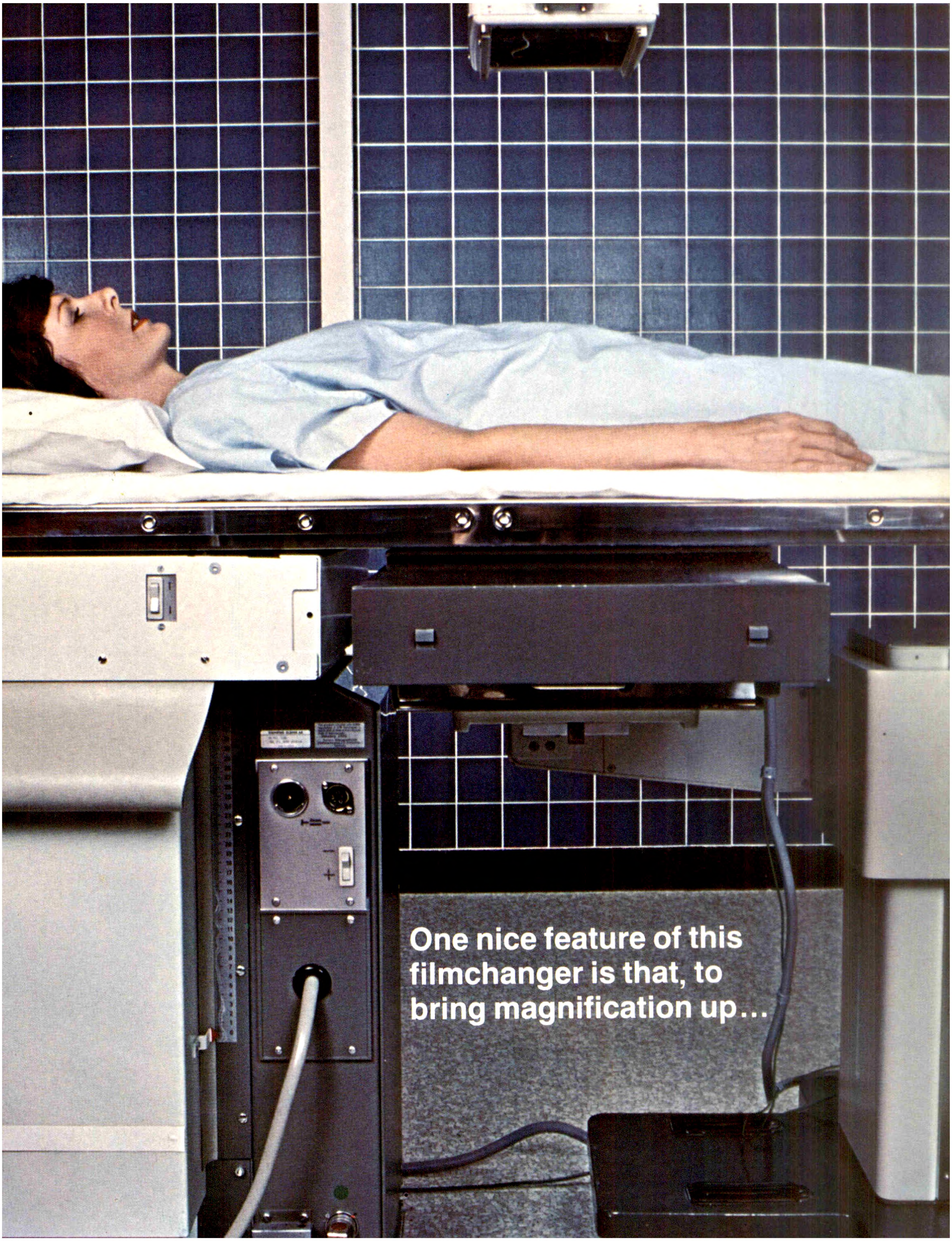

One nice feature of this filmchanger is that, to bring magnification up…

...you simply bring the PUCK down.

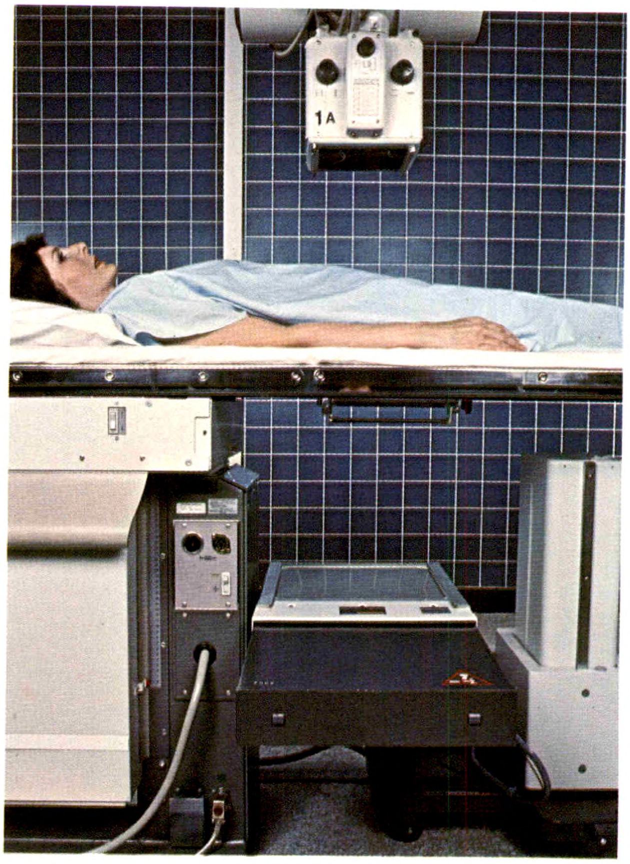

The Puck is quite a remarkable cutfilm changer. It's economical, it's mobile and it's compact—only 6¾ inches thick. Yet, it produces superb image quality for abdominal, peripheral, thoracic and cerebral angiography. With up to 3 exp/sec and with 20 film capacity. With patient identification and sequential numbering of each film.

But, that's just the beginning.

An available stand allows Puck to travel 400mm (approx. 16") vertically and to be tilted for frontal and lateral projections. By lowering Puck while it's under a table without vertical adjustment, you can select up to approximately 2:1 magnification. With a vertically adjustable table the range of magnification is increased.

No other rapid filmchanger offers this advantage.

In addition to magnification, Puck offers very low x-ray attenuation and perfect screen/film contact. Our new CFRP front plate makes this possible. This unique Carbon Fiber Reinforced Plastic plate makes no compromise between x-ray attenuation and screen/film contact. Together with today's micro-focus tubes and rare earth screens, the CFRP lends itself very well to the magnification capabilities of Puck.

And no other compact changer offers this advantage.

In addition to compact size, increased magnification, and the CFRP plate, Puck offers the convenience and accuracy of punch card programming. Punch card programming allows you to pre-determine the number of films in a series, and to split a magazine load on two or more runs. The card can also correlate the filmchanger with the injector and control the movements of a programmed table. In biplane, only one punch card is necessary to operate frontal and lateral changers, and they can be programmed for alternate or simultaneous exposures.

Puck is available in two models to fit film sizes of 35 x 35cm or 24 x 30cm. See how Puck can fit into your special procedure room.

For detailed information about Puck cutfilm changers and stands, write Elema-Schonander, Inc. 699 Lively Blvd., Elk Grove Village. IL. 60007. Or call (312) 593-6770.

When a better idea in filmchangers comes along, it will come from us.

elema-schonander

We're living up to our reputation...all over your hospital.

General Electric made a commitment, years ago, to develop and market reliable medical systems that would deliver consistently informative diagnostic images.

And we've lived up to that commitment. First in x-ray equipment, and today in an expanded product line. A line that has grown so much that you may not be fully aware of all the areas where we can help you: computed tomography, nuclear imaging, data processing and handling, and radiological capability that matches a broad range of economic as well as diagnostic considerations.

Your GE medical systems representative has the training and know-how to put all this imaging/information capability to work for you. Ask about the systems that match your needs. Some of them are described on the next few pages.

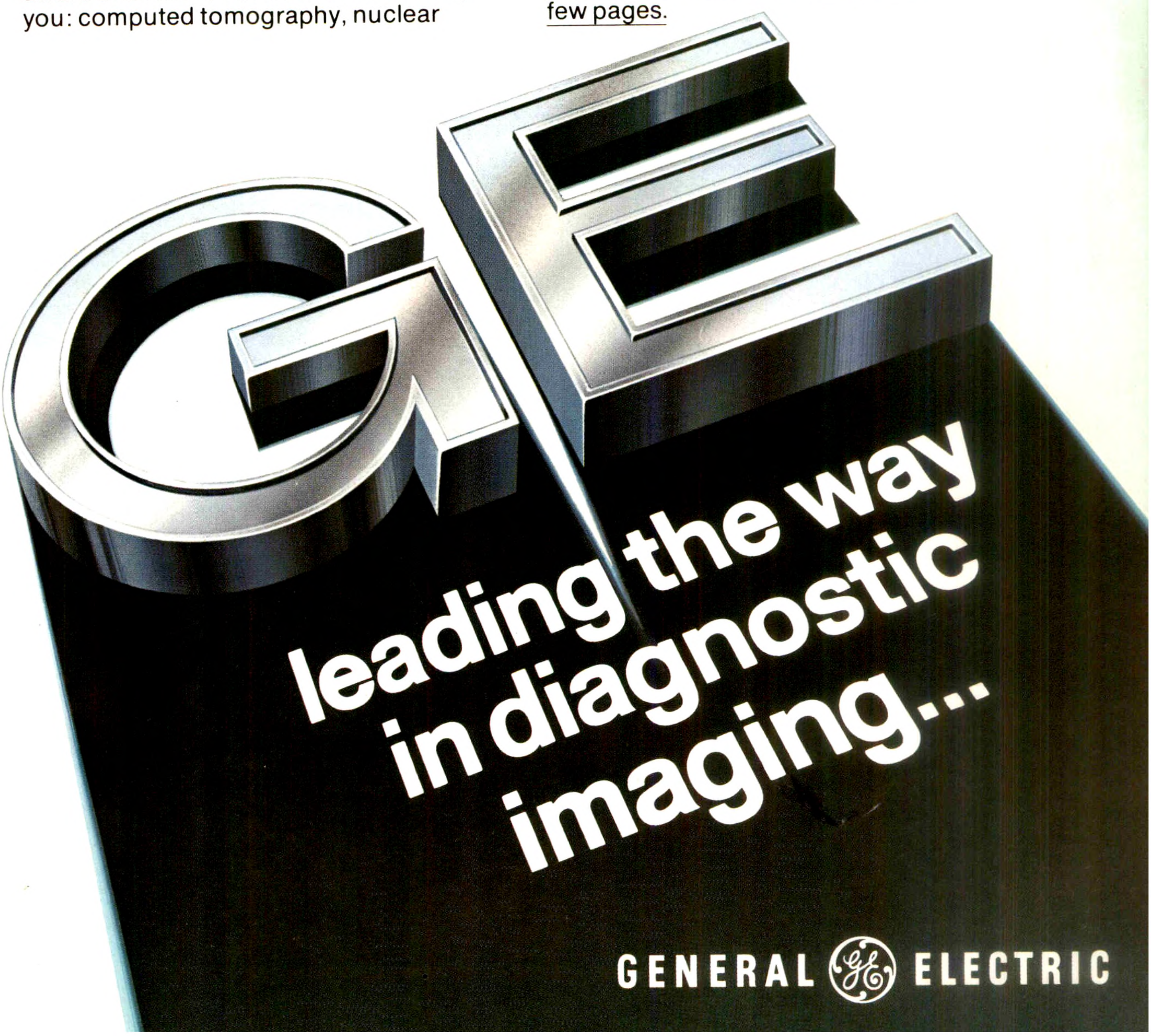

GENERAL ELECTRIC

The table/spotfilmer of

RFX

1. **Lower dose fluoroscopy** is made practical by the 6:1 ratio fluoroscopic grid. A big improvement over traditional "compromise" 8:1 or 10:1 ratios.
2. **High kVp spotfilms are now practical** with the 12:1 ratio of the 103 line criss-cross grids for greater control over film quality. Now even double contrast studies become routine at traditional table bucky kilovoltages.

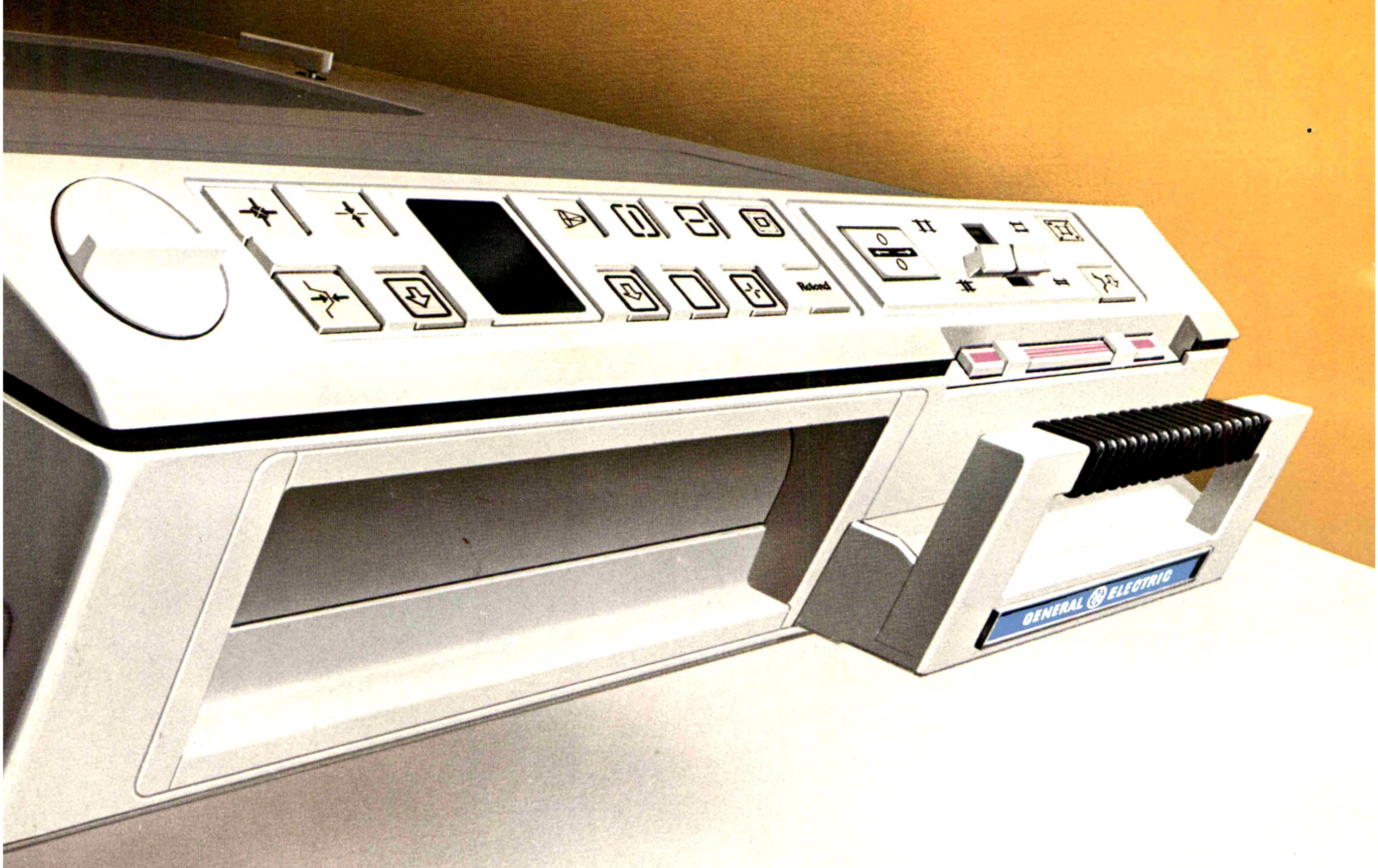

3. **RFX spotfilmer puts total control at your fingertips**—gloves or no gloves.
   - The motorized compression cone control is right up front where you can put your finger on it fast.
   - Coordinated collimator controls are a finger's reach from the positioning handle. Fast-acting collimator blades are servo-positioned.
   - Two-step, prepare-expose switch is positioned for easy left or right hand use and may be used for exposure-delay when held in the first step.
   - The patient positioning control is located adjacent to collimator controls and provides immediate table top response.
   - No more spot counting for the technologist. After the last exposure, cassette moves automatically to the loading position and the RELOAD light signals for a fresh cassette.
   - Positioning ease is provided by a longitudinal power assist with unique direct interactive response.
   - Mini-spot formatting for 6 on 1 or 9 on 1 arthrograms is available.

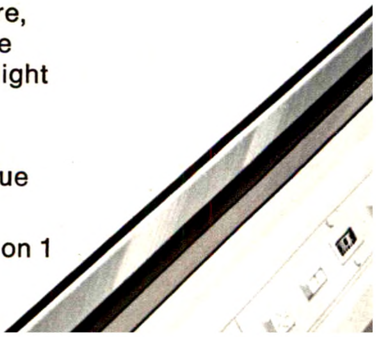

the future is available today.

4. **Spotfilm exposure starts .75 second after the cassette is called for.** With no shock-induced vibration effect.
5. **Rapid sequence spotfilms are now possible.** Automatic advance with sequence anticipation logic reduces the interval between exposures to approximately .5 second for studies such as cervical esophograms and voiding cystourethrograms.
6. **Front and rear cassette loading** lets you use front loading port when working alone, rear loading port for higher productivity when working with an assistant or when doing myelography.
7. **Masking is automatic with format selection**—no longer must masks and cones be moved into place to achieve a new film format. Full-field fluoroscopy through the compression cone is possible; masking is independent of the cone.
8. **e table angulates smoothly, with soft**
art and stop, and full speed of 4½
grees per second. RFX Thirty angulates
30° Trendelenburg; RFX Ninety is a full
endelenburg unit. Choice of 4-way or flat
vay table top.
9. **e table is designed to take the day-in,**
y-out abuse of heavy workloads.
noothly contoured surfaces clean up
sily; controls are sealed for protection
ainst barium spills.
10. **axiray™ 100 tube meets the demands of**
day's procedure schedules; features
rced oil circulation cooling.
11. **itomatic exposure control** is provided
the RFX's thin profile Quantamat™ ion
ambers; you get consistent film density
om study-to-study.

et the complete RFX story from your GE
presentative.
neral Electric Medical Systems,
lwaukee, Toronto, Madrid.

RFX: why consider anything less?

GENERAL ELECTRIC

User-Selectable Constant Load generators from GE let you effectively match kW output to technic.

Up to 40% shorter exposure time plus longer tube life... compared with falling load.

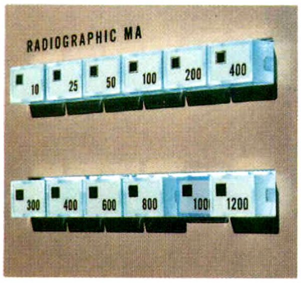

It just makes good economic sense to get all the kW performance you pay for in a generator. From full-rated maximum power down to conservative mA levels, you should be able to exercise your professional judgment in selecting optimum technic for each and every procedure. This is the basis of GE's User-Selectable Constant Load concept.

Consider the facts: The alternative, falling load or "falling kW" generators, in theory begin each exposure at the full rated maximum load. This load then begins to fall off from the initial peak during the exposure. In the latest falling load designs, there is no provision for user control of the initial load applied to the x-ray tube. The installing serviceman adjusts for only one kW setting for the large focal spot and another for the small focal spot*.

At a constant 80 kVp, a tube and generator rated as "100 kW" would have a performance curve like this, in theory:

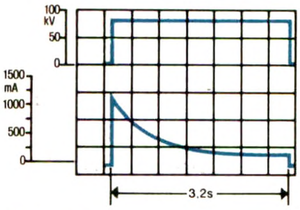

Continuously falling load with constant voltage and falling tube current

However, falling load generators are routinely installed with de-rated initial loads of 85% of rated tube kW, or lower. So, using the constant 80 kVp example, the load curve for a falling load generator would look more like this, in actual practice:

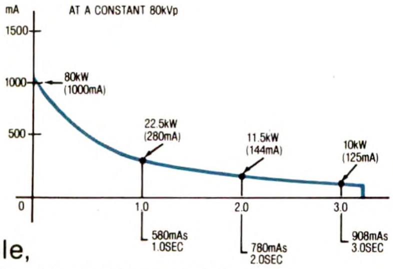

Note that a 1.0 second exposure yields only 580 mAs, even though it started at 1000 mA. In contrast, a GE generator set at 1000 mA will deliver 600 mAs in only 0.6 seconds. In this example, User-Selectable Constant Load is more than 40% faster than falling load.

Using the same example, but assuming that a 1.0 second exposure time is permissible, then a user-selected 600 mA tube load is all that is really needed.

There is no reason to subject the x-ray tube anode to the excessive thermal shock of the full rated maximum load when 600 mA will do the job. Statistically longer tube life will result.

Detail-intensive exams: Falling load applied to the small focal spot also extends exposure times for "detail-intensive" examinations. The technologist—equipped with a falling load generator and faced with a detail requirement that's coupled with a motion-stopping problem—may be forced to use the large focal spot much more often than professional judgment dictates.

Automatic Exposure Control: AEC in falling load generators also results in longer exposure times because of reduced initial load and reduced average power.

Motion-stopping spotfilms: Spotfilming using GE constant load provides the short exposure times you require. Gall bladder spotfilms at lower kVp levels—even using a grid—are practical with constant load. They are "cleaned up" like your table bucky films.

GE User-Selectable Constant Load generators enable you to optimize the power requirements for any technic; any patient situation. That's one of the reasons for GE's worldwide reputation for designing and building dependable high-performance generators. Your GE representative has the facts.

General Electric Medical Systems,
Milwaukee, Toronto, Madrid.

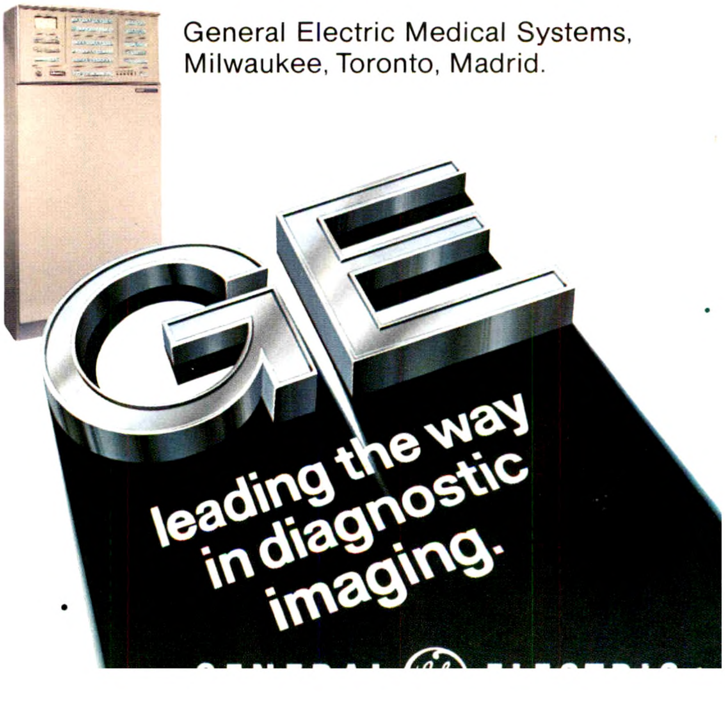

---

*Constant load settings are routinely provided for tomography and for a breathing technic at low mA only.

Maybe your business needs some new partners

We suggest that you form an alliance with the arts...that your company actively support now some form of the visual or performing arts.

There are vital humanistic reasons for this. All in life is not competition and striving for affluence. And there are sound business reasons for such support. For example: the design industry would be without vitality were there no modern art museums; the fashion industry uninspired without the great collections of textile artistry; and the advertising business very uncreative without the theater, art, and the world of music to draw upon. In fact, all business and industry need the arts.

Your support can be monetary, of course. You know of the financial crisis in the "labor intensive" field of the arts, and corporate gifts are essential. But there are many other kinds of gifts.

Your support can be the use of a display window to promote a local repertory company. Or the volunteering of interested employees' time, with their "time off" your contribution. There are many ways your company can help, and they're listed in a booklet which we hope you'll send for.

Start being a patron today! The arts deserve and need your support. And your new partnership will be a thoroughly enjoyable experience.

- -

Support the Arts

Business Committee for the Arts, Inc.
1700 Broadway, New York, N.Y. 10019

Gentlemen:
Please send your booklet "126 Ways To Support the Arts."

Name ______________________________

Address ______________________________

City ______________ State ________ Zip ________

Film after film after film after film.
Rapido® M-7A.

Picker has proven its leadership in Cassetteless Radiography—and saved space in the process.

Consider our Rapido M-7A* System: Requires less space, increases productivity, cuts costs, minimizes patient radiation. And, it provides even higher quality work than conventional systems.

Additionally the Automatic Exposure Control (A.E.C.) system designed for the Rapido provides optimal radiographic film densities—consistently.

To increase throughput and reduce operator fatigue, the Rapido incorporates four 75-film-capacity load magazines (14x17", 17x14", 11x14", 10x12"). This translates into a saving of 2,000 pounds (907 kg) of cassettes that don't have to be loaded, transported or unloaded.

Other key features: Push-button film-size selection for automatic centering of each size in the exposure area... unique patient identification with a 3x5" card eliminating ID work in the darkroom. And, a four-way floating table top which offers 50" longitudinal and 12" of transverse motion.

This is another example of Picker's unique human resources benefiting you. It's a result of our expertise in the diagnostic modalities of x-ray, ultrasound, nuclear, computed tomography, clinical laboratory, therapy, film systems and supplies. Only Picker has all these resources.

Consult your Picker representative or write Picker Corporation, 595 Miner Road, Cleveland, OH 44143.

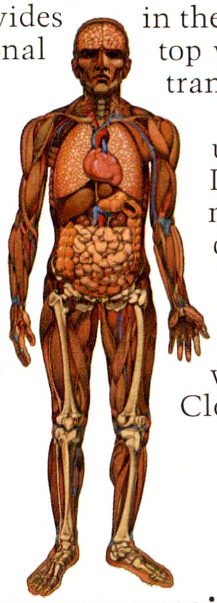

Discover the human resources in Picker's synergy

PICKER®
ONE OF THE C.I.T. COMPANIES

*Used in union with the Kodak® RP® X-Omat® M-7A processor which are registered trademarks of Eastman Kodak Co., Rochester, N.Y.

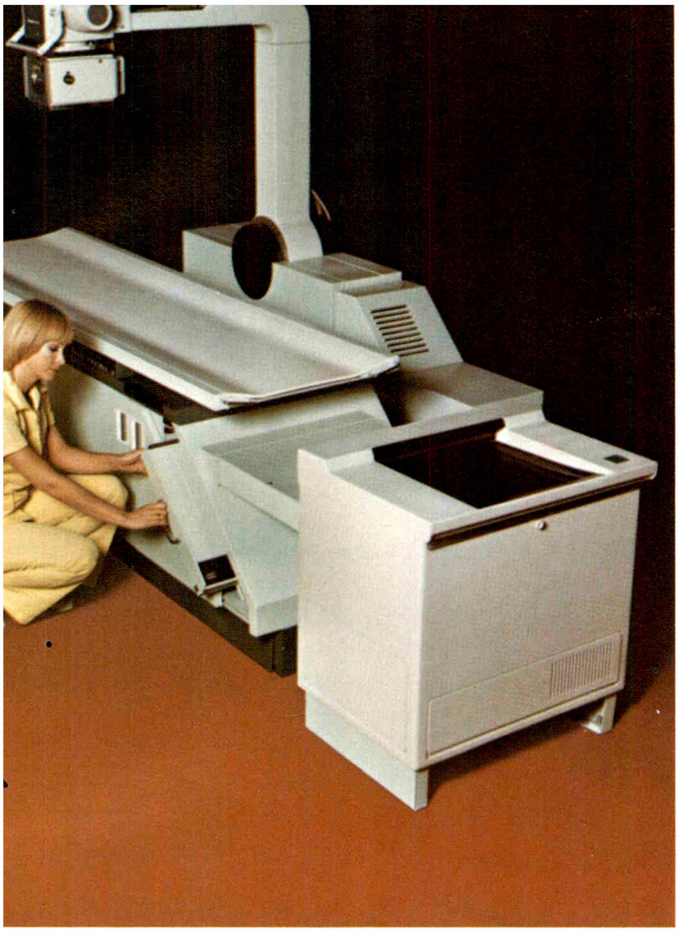

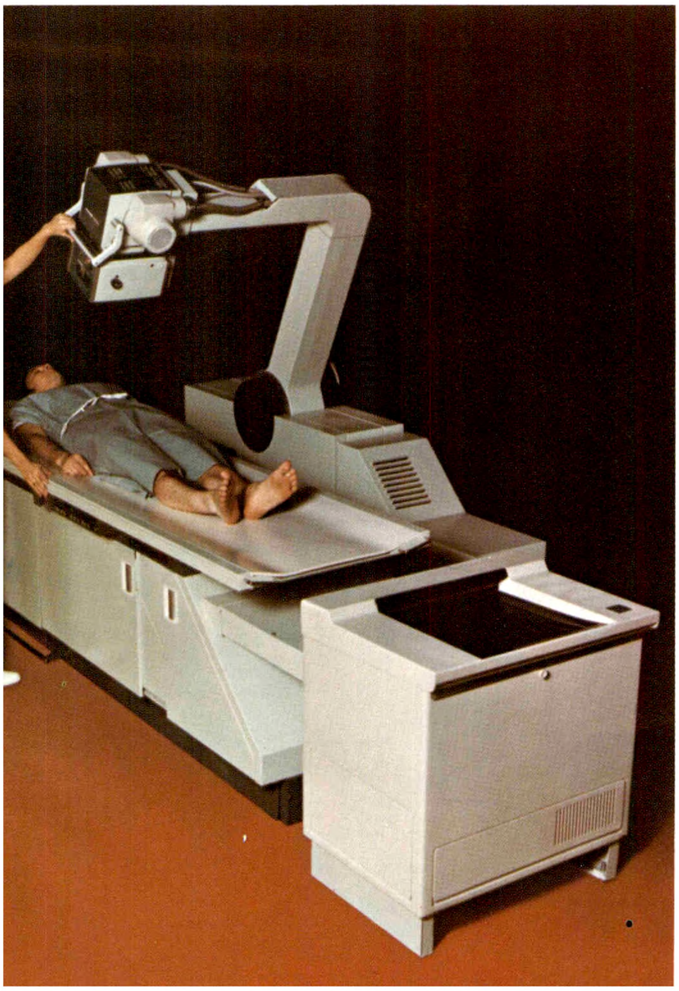

OUR LAURA HAS A LEARNING PROBLEM. BUT SHE'S DOING FINE IN SCHOOL.

"Not long ago, if a child had a learning problem, everybody just sort of gave up. I'm glad our Laura wasn't growing up back then."

"Today we know that even children with severe handicaps can learn much more than people used to realize."

"Through special education, Laura is really getting a lot out of school. Just as important, she is getting along well with other children. She's leading a pretty normal, happy life."

If you have a child with any kind of handicap (physical, mental or emotional) who is not getting the special education he needs, we have free information that can help. Just fill in this coupon.

CLOSER LOOK, BOX 1492
WASHINGTON, D.C. 20013

Name

Address

City State Zip

Handicap or Problem

CLOSER LOOK
(a free service of the U.S. Office of Education,
Department of Health, Education & Welfare)

Liquid Polibar with Super XL

A Total System

For double-contrast examination of the colon.

Satisfactory results in the double-contrast examination of the colon require special attention to two aspects of the procedure.

First, the barium sulfate formulation. Our Liquid Polibar (56% w/w) is a bubble-free, non-precipitating uniform suspension formulation ... with proper flow and coating characteristics. No blending required and once routines are established, you can rely on its consistency.

The second concern is with the proper apparatus. The E-Z-EM system is unique in that 1/2″ lumen tubing attached to the enema bag is utilized – for freer, more uniform flow. Miller Air Retention Tip, with or without optional cuff completes the system.

A total system for ease of administration and consistently reliable radiological results. For additional literature, write:

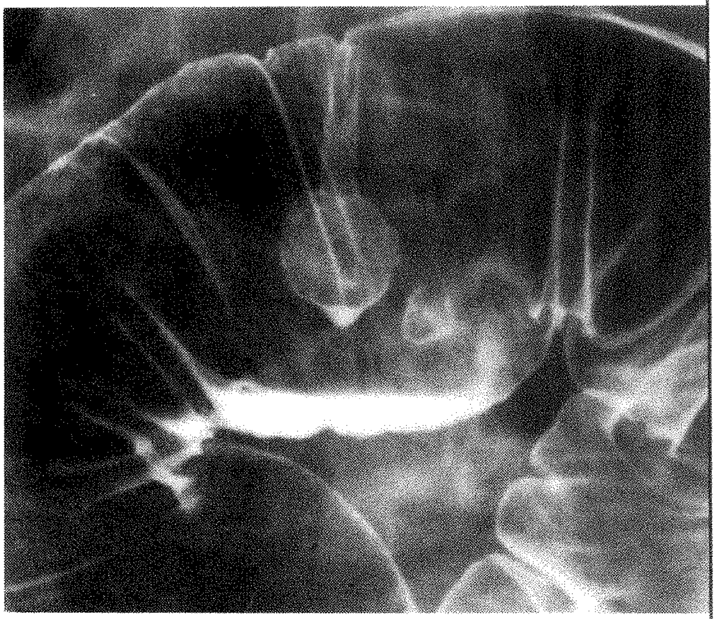

One pedunculated and one smaller sessile polyp at the apex of the sigmond loop.

Film Courtesy of Richard Palmer Gold M.D. Columbia Presb. Medical Center N.Y.

E-Z-EM

7 Portland Ave.
Westbury, New York 11590
(516) 333-8230

1/77

International Affiliates: E-Z-EM Rooster B. V., Infirmeriestraat 6-8, Rotterdam 16, Netherlands

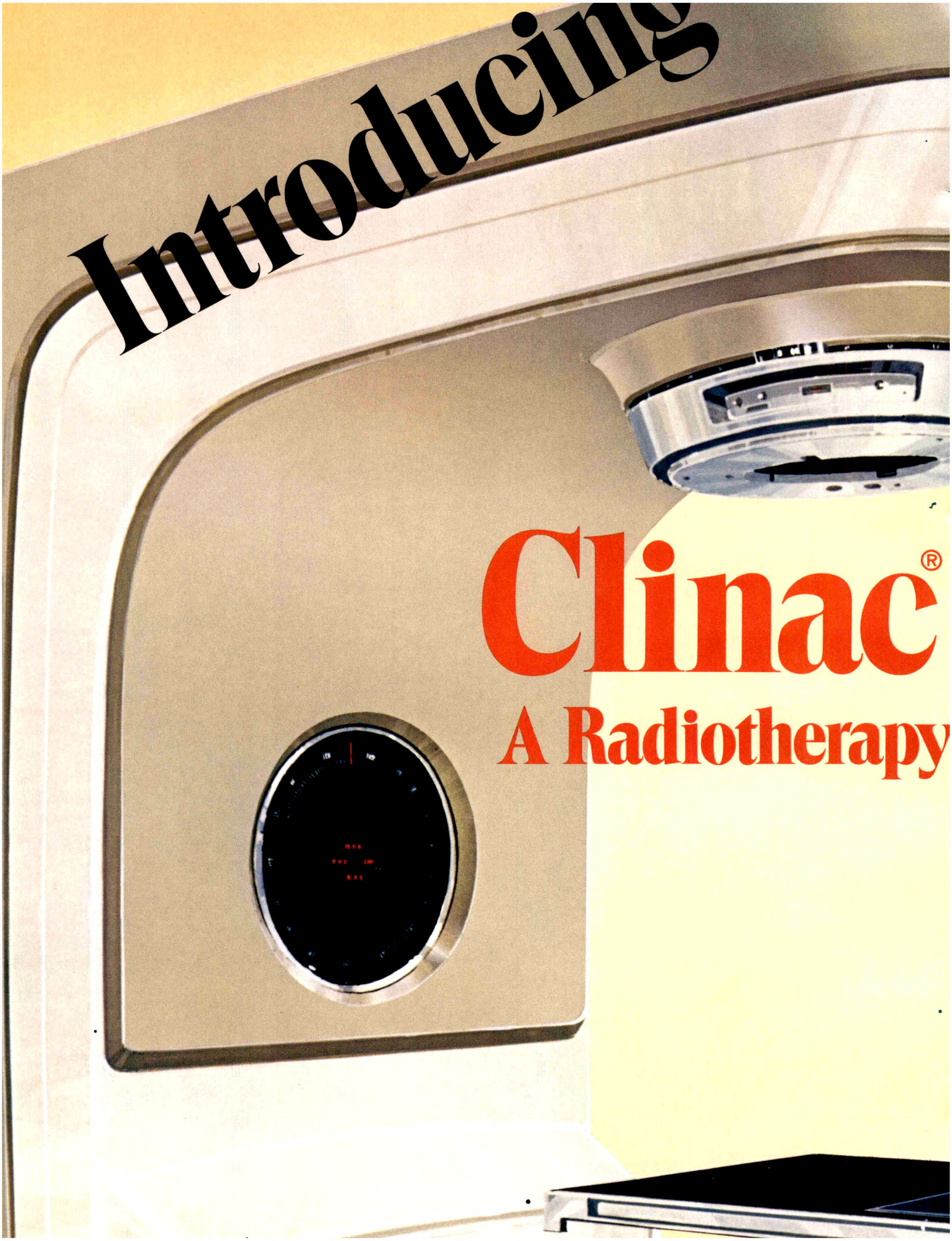
Introducing
Clinac®
A Radiotherapy

The Clinac 6/100 Medical Linear Accelerator is a first in low-energy radiotherapy equipment. A product of Varian advanced accelerator technology, its fully rotational 100 cm source-to-axis distance, 6 MV straight-through beam eliminates the need for complex beam-bending systems. The result is a precise, stable treatment beam.

An important evolution in the low-energy Clinac line, the Clinac 6/100 has the most advanced features including dual dosimetry, gantry-mounted digital display, and automation compatibility.

A bold new design based on proven performance, the Clinac 6/100 uses key subsystem designs perfected and proven reliable through nine years of clinical experience in the highly successful Clinac 4.

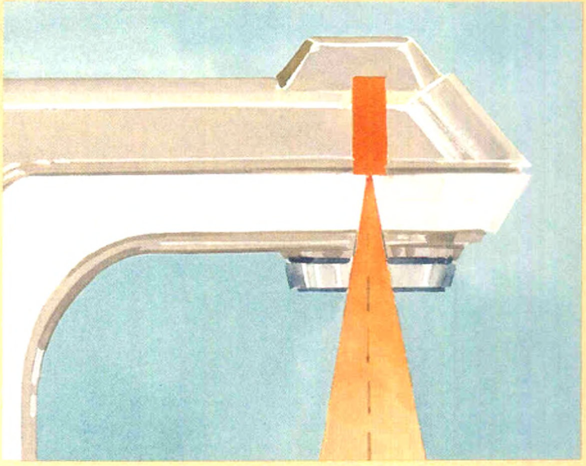

As with all Clinacs, the Varian Clinac 6/100 is backed by the world's largest linear accelerator field service organization. Write or call today for full details.
Medical Group, Varian Associates,
611 Hansen Way, Palo Alto, CA 94303.
Tel: (415) 493-4000.

6/100

ccelerator First!

varian

COMPUTED TOMOGRAPHY, ULTRASOUND AND X-RAY:

An Integrated Approach

January 16-20, 1978

Fairmont Hotel
San Francisco

This problem-oriented course will review the major clinical topics for which more than one useful imaging modality is available to the practicing radiologist. Following a series of comprehensive didactic lectures on the different imaging approaches to each specific clinical problem, a panel of experts will discuss and formulate ways to integrate these modalities into a rational and efficient diagnostic plan. Although the emphasis of this course will be on computed tomography and diagnostic ultrasound, a review of the nuclear medicine, angiographic, and conventional radiologic approaches to each clinical topic will be presented.

THE CLINICAL TOPICS TO BE REVIEWED INCLUDE:

- Jaundice
- Pancreatic Mass
- Hepatic Mass (es)
- Renal Mass
- Adrenal Mass
- Abdominal Abscess
- Thyroid Nodule
- Brain Tumor
- Spine and Disc Disease
- Bone and Soft Tissue Masses
- Ischemic Heart Disease
- Pulmonary Embolism
- Mediastinal Mass
- Retroperitoneal Lymphadenopathy

This program is presented by the Radiology Research and Education Foundation and Extended Programs in Medical Education, University of California School of Medicine, San Francisco, California. It is acceptable for Category I credit towards the certificate in Continuing Education for the California Medical Association and the American Medical Association.

For further information please contact: Extended Programs in Medical Education, University of California, Room 569-U, San Francisco, California 94143 or call (415) 666-4251.

Fee:
$300.00 includes hardbound publication of the proceedings
$200.00 residents and interns with letter of verification

• PERCUTANEOUS ANGIOGRAPHY •

S. Swamy
Michael Reese Medical Center
Chicago

Lewis Irwin Segal
Louis A. Weiss Memorial Hospital
Chicago

S. Mouli
Foster-McGaw Medical Center
Chicago

A new dimension is added to the practice of angiography with the publication of this comprehensive volume. In-depth clarification is offered to all diagnostic radiologists of the basic techniques of angiography, the problems encountered and the limitations of the technique. The authors use a systematic approach to their topic throughout the book, employing numerous sketches to further elucidate critical points. With the additional aid of over 1300 roentgenographic illustrations, they have emphasized salient physiological subjects, and have presented the gross histological architecture of lesions and their meaningful angiographic representation.

The text is divided into three sections: *Basics, Techniques,* and *Patterns.* The first section carefully covers the roles of the patient, the doctor and the equipment. It also deals with the programming of standard studies, including suggestions for such details as catheter curves, wire, amount of contrast and rate of filming.

The second section — *Techniques* — describes specific angiographic methods. The anatomical aspects are presented in an entirely new way which makes them more useful as well as more interesting. Physiological points with regard to hemodynamics are discussed, as are accepted pharmacological agents and their practical applications. The rationale for the technique is thoroughly explained and a special recipe section is wholly devoted to the systematic study of disease processes in their entirety.

The final portion of the text explores patterns in angiography. The authors, relying on their extensive experience with the technique, have classified the patterns according to pathology rather than anatomy. This classification is based on available examples with special reference to common patterns. It will give the reader a broad logical background which will aid in establishing a proper diagnosis. A voluminous bibliography with over 1500 references follows the text.
'77, 848 pp. (8 1/2 x 11), 1455 il., $80.00

Orders with remittance sent, on approval, postpaid

CHARLES C THOMAS • PUBLISHER

301-327 East Lawrence Avenue • Springfield • Illinois • 62717

S & S MV112 MOTORIZED VIEWER

Featuring MAGAZINE LOADING INSTANT RANDOM ACCESS

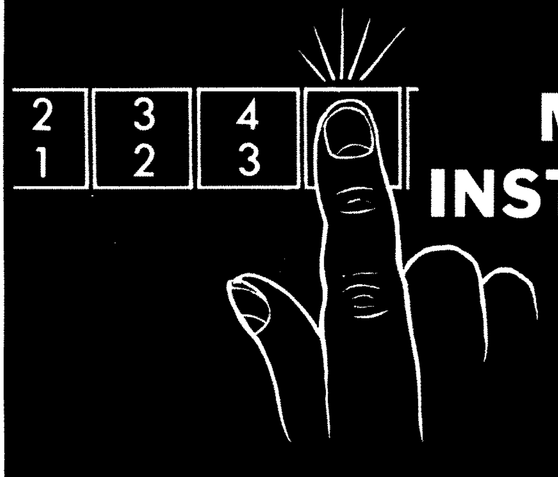

★ 112 FILM CAPACITY

★ VIEW ANY FILM IN 12 SECONDS OR LESS.

★ MAGAZINE EASILY REMOVED; EASILY INSERTED.

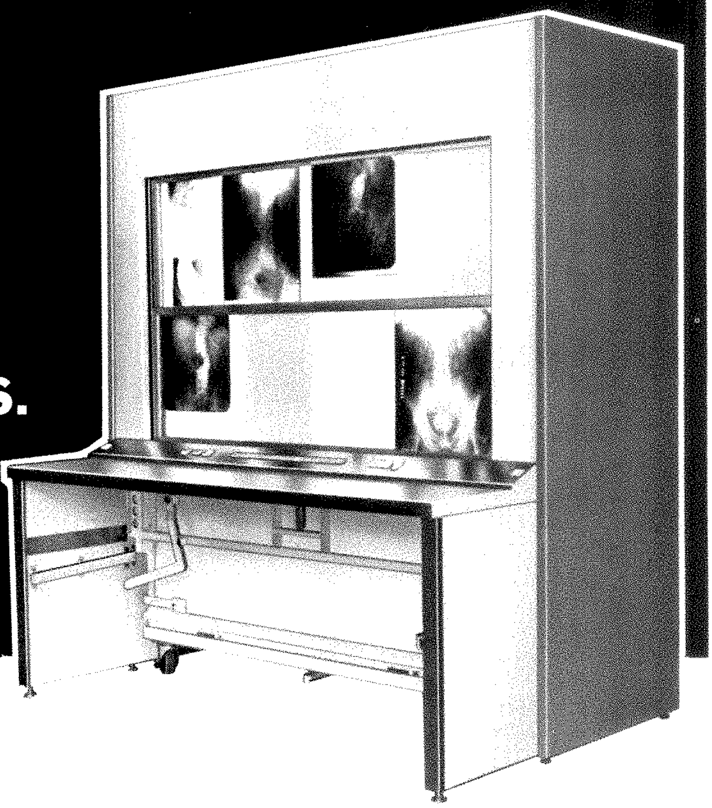

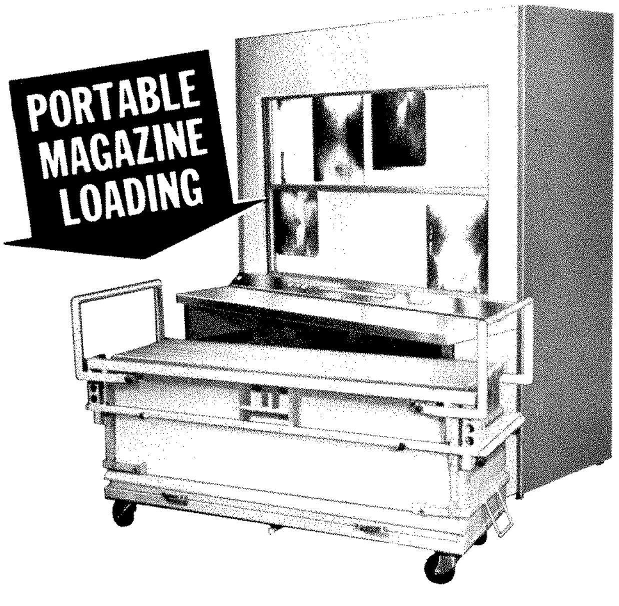

FEATURES:

- **Complete random access.** Numbered push buttons locate each frame in upper or lower position, as you prefer for viewing.
- 28 Plexiglas frames, 4 films wide, 112 film capacity. Viewed 4 over 4.
- Push button individual or master control of lights for each viewing area. Dividers between viewing areas. No light spillover.
- Viewing panels and stored films in a **portable magazine that can be rolled from machine to machine.** Ball-bearing casters and convenient flip-up/fold down handles on each end of the magazine for easy stand-up movement.
- Unobstructed leg area under shelf permits comfortable seating and close viewing.
- Improved mechanism includes built-in safety features, automatic overload protection to minimize any possibility of damage. Magazine is locked into machine when in use. All solid state controls.

S.&S.

MANUFACTURED BY:
S. & S. X-RAY PRODUCTS INC.
87-93 JAY STREET, BROOKLYN, N.Y. 11201
Telephone: 212-852-6900

Manufactured in USA by **S & S**, who have made more motorized viewers than any one else in the world. Sold by local X-Ray dealers backed up by **S & S** parts inventories and experience.

SOME OF THE MANY S. & S. ACCESSORIES SOLD BY YOUR LOCAL X-RAY DEALER

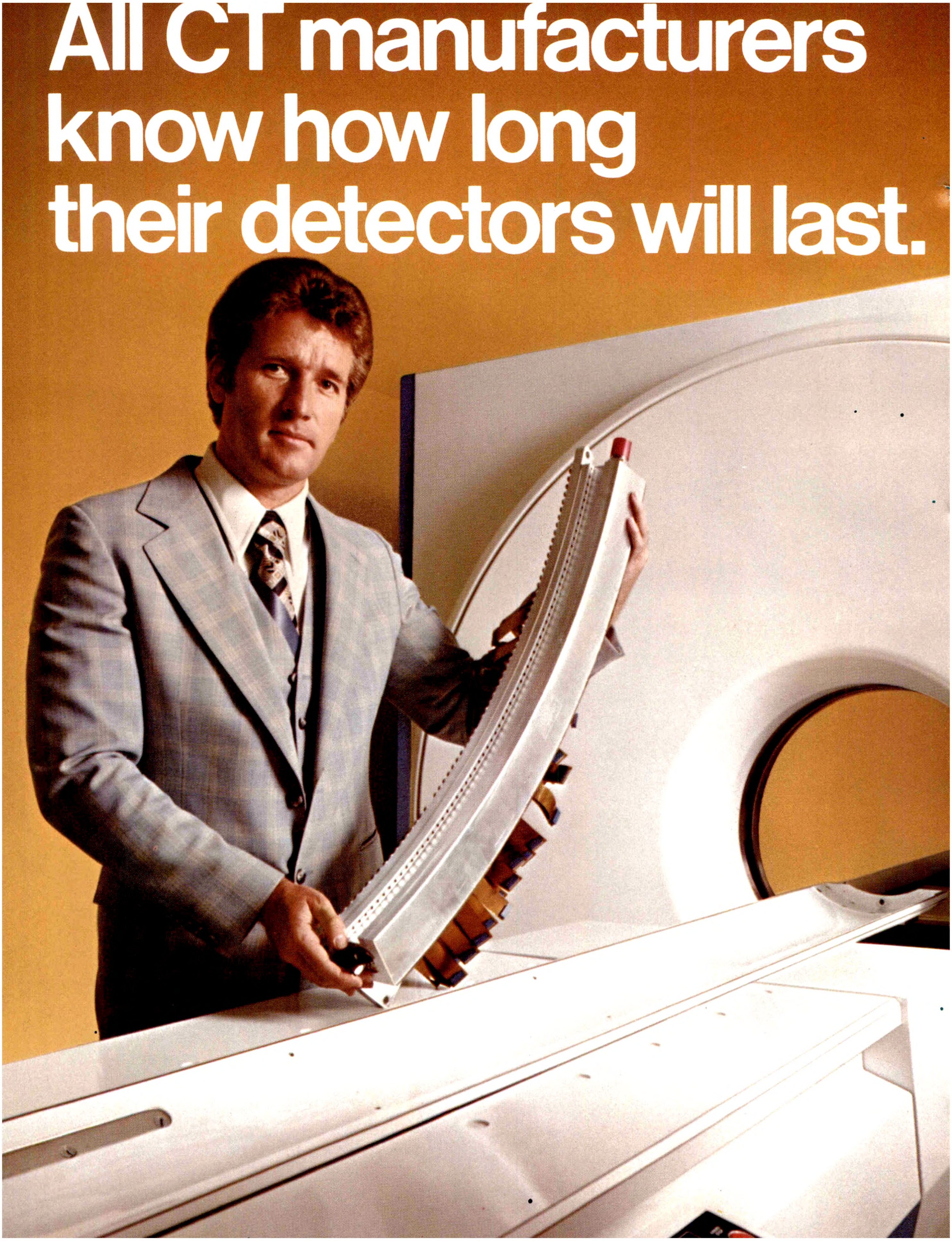
All CT manufacturers know how long their detectors will last.

Only General Electric gives you a 5-year warranty.

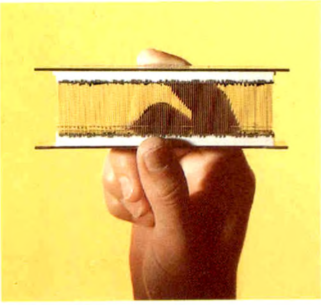

This X-1 detector segment illustrates how tungsten plates which form the detector cells are mounted in a precision-milled matrix for dimensional stability. As the detector rotates, these plates are always aligned with the beam. The xenon gas volume within the single-chamber housing is common to each of the cells, providing detector uniformity.

Most CT manufacturers offer only a 1-year detector warranty. We're so sure of our CT/T system detector, we back it for a full 5 years.

Some manufacturers seem to avoid the topic of anticipated detector life. But GE makes this straightforward promise: if your CT/T detector fails for any reason within 5 years of installation, we'll repair or replace it... absolutely free.

GE can make this kind of commitment because we've designed our detector to provide years of exceptional performance. And we've proven that performance at actual clinical sites.

So when you're comparing CT systems, ask about anticipated detector life and its impact on operating expense. You can't afford not to.

For more information on our warranty and CT/T, contact your GE representative.

General Electric Medical Systems,
Milwaukee, Toronto, Madrid.

GENERAL ELECTRIC

CHARLES C THOMAS • PUBLISHER

AN INTRODUCTION TO THE PHYSICS OF NUCLEAR MEDICINE *by* **Paul N. Goodwin,** *Albert Einstein College of Medicine, Bronx, New York, and* **Dandamudi V. Rao,** *New Jersey Medical School, Newark.* The principles and physics of nuclear medicine are presented by this book in a simple yet comprehensive manner. To aid self-study, problems and multiple choice questions are included at the end of each chapter. Topics include a review of elementary mathematics, the structure of matter, the nature of radioactivity, nuclear decay processes, scintillation detectors, scanners, gamma cameras and other imaging devices, radionuclides in nuclear medicine, statistics of radiation measurements, radiation safety, and radiation dosimetry. Appendices present a list of the elements, conversion factors, and physical data for some radionuclides. *'77, 164 pp. (6 3/4 x 9 3/4), 44 il., 4 tables, $18.50*

UROLOGICAL RADIOLOGY OF THE ADULT MALE LOWER URINARY TRACT: Anatomy, Physiology, Pathology and Sequelae, Diagnosis and Management *by* **R. W. McCallum** *and* **V. Colapinto,** *both of St. Michael's Hospital, Toronto, Ontario, Canada.* This comprehensive, well-organized monograph of the adult male lower urinary tract stresses radiological diagnostic procedures and relates detailed descriptions of the anatomy, physiology, etiology and pathology of the bladder, prostate and urethra. Radiological examinations of the bladder, prostate and urethra are extensively discussed and the literature is reviewed in detail with over 330 references and 250 original radiographs and illustrations. A new method of radiological examination of the lower urinary tract in paraplegics is described. *'76, 376 pp. (6 3/4 x 9 3/4), 248 il., 2 tables, $35.50*

AN ATLAS OF POLYTOME PNEUMOGRAPHY *by* **Taher El Gammal** *and* **Marshall B. Allen, Jr.,** *both of Medical College of Georgia, Augusta. Assisted by* **Paul Dyken.** This atlas presents a large number of studies which supplement the study of normal anatomy of the cerebrospinal fluid pathways, and provides comparison for the identification of abnormal structures. Concentration is on the findings of polytome pneumography but, where possible, correlations are made with angiography, positive contrast ventriculography, and CAT examinations. Relative values of these different examinations are demonstrated. Topics include normal CSF pathways, atrophy, hydrocephalus, intrasellar subarachnoid recess—sellar and suprasellar mass lesions—herniations. *'77, 480 pp. (8 1/2 x 11), 729 il., $39.50*

ANATOMICO-ROENTGENOGRAPHIC STUDIES OF THE SPINE (3rd Ptg.) *by* **Lee A. Hadley,** *Syracuse Memorial Hospital, Syracuse, New York.* Over 900 roentgenographic images are coordinated with actual anatomical conditions in this atlas. Of particular interest are the longitudinal follow-up studies of patients showing the anatomical effect incidental to trauma and resultant observable changes. The broad scope of study is revealed in the contents which include development of the spine, disturbances of development, the cervical spine, vertebral arteries, posterior spinal articulations with innervation studies, spinal curvatures, infective spondylitis, tumors and tumorous conditions. This atlas will be indispensable to neurologists, neurosurgeons, and osteopathic physicians. *'76, 560 pp. (6 3/4 x 9 3/4), 644 il., $19.75*

THE FUNDAMENTALS OF X-RAY AND RADIUM PHYSICS (6th Ed.) *by* **Joseph Selman,** *Tyler Junior College, Tyler, Texas.* Now in its Sixth Edition, this classic volume has again been revised and enlarged to accommodate a constantly changing field. The development of new types of intensifying screens, both as modifications of existing phosphors and in the form of completely new rare earth phosphors, is discussed in great detail. Also receiving special attention is the advent of a practical 350-kV unit for chest radiography using a field emission tube, the Bureau of Radiological Health report on population exposure to x rays in radiography, and the proposed new International System of Units (SI). This book has proven to be eminently useful to student and graduate technologists, teachers, and radiology residents. *'77, 600 pp., 296 il., 29 tables, $18.75*

THE ADULT POSTOPERATIVE CHEST *by* **Myron Melamed; Florencio A. Hipona,** *Harvard Medical School, Boston;* **Carlos J. Reynes,** *Loyola Univ., Maywood, Illinois;* **Walter L. Barker,** *Univ. of Illinois, Chicago; and* **Santiago Paredes,** *Boston Univ. School of Medicine, Boston. Foreword by* **Hiram T. Langston.** This study of adult pulmonary and cardiovascular radiography after surgery systematically assesses the extraneous factors imposed upon x-ray film by the surgical act. The book offers an atlas against which problem pictures can be compared for quick identification. Brief comments about behavior of the pleura, lung redistribution and postoperative function are included. The cardiovascular section covers the postsurgical status of congenital and acquired lesions. *'77, 396 pp., 578 il., 1 table, $31.50*

ENDOMETRIAL CARCINOMA AND ITS TREATMENT: The Role of Irradiation, Extent of Surgery, and Approach to Chemotherapy *edited by* **Laman A. Gray, Sr.,** *Univ. of Louisville, Louisville, Kentucky. (27 Contributors)* The role of irradiation in the total treatment of endometrial carcinoma is explored, focusing on adjuvant irradiation in the treatment of Stage I adenocarcinoma of the endometrium and on the management of carcinoma involving the cervix and body of the uterus. The extent of surgery and possible new chemotherapeutic approaches are also discussed. The importance of associated and related factors is clarified, and the combinations of modalities of treatment and sequence are detailed. The data assembled here is unprecedentedly detailed; the opinions expressed are authoritative. *'77, 240 pp. (6 3/4 x 9 3/4), 17 il., 138 tables, $22.50*

THE RENAL UPTAKE OF RADIOACTIVE MERCURY ($^{197}HgCl_2$): Method for Testing the Functional Value of Each Kidney, Technique-Results- and Clinical Application in Urology and Nephrology *edited by* **Claude Raynaud,** *Service Hospitalier Frederic Joliot, Orsay, France. Foreword by* **Pierre Royer.** *(41 Contributors)* The first chapters of this text describe several techniques of uptake measurement along with simplified systems of external counting, scanners or gamma cameras, and specific problems associated with the deep position of the kidney or Hg metabolism. The rest of the book discusses the normal values of Hg renal uptake and the results obtained in patients. The major point of this work is that, in the case of the kidneys, symmetry of the body can be the basis of early signs of disease. *'76, 248 pp., 110 il., 47 tables, $22.75*

Orders with remittance sent, on approval, postpaid

301-327 East Lawrence Avenue • Springfield • Illinois • 62717

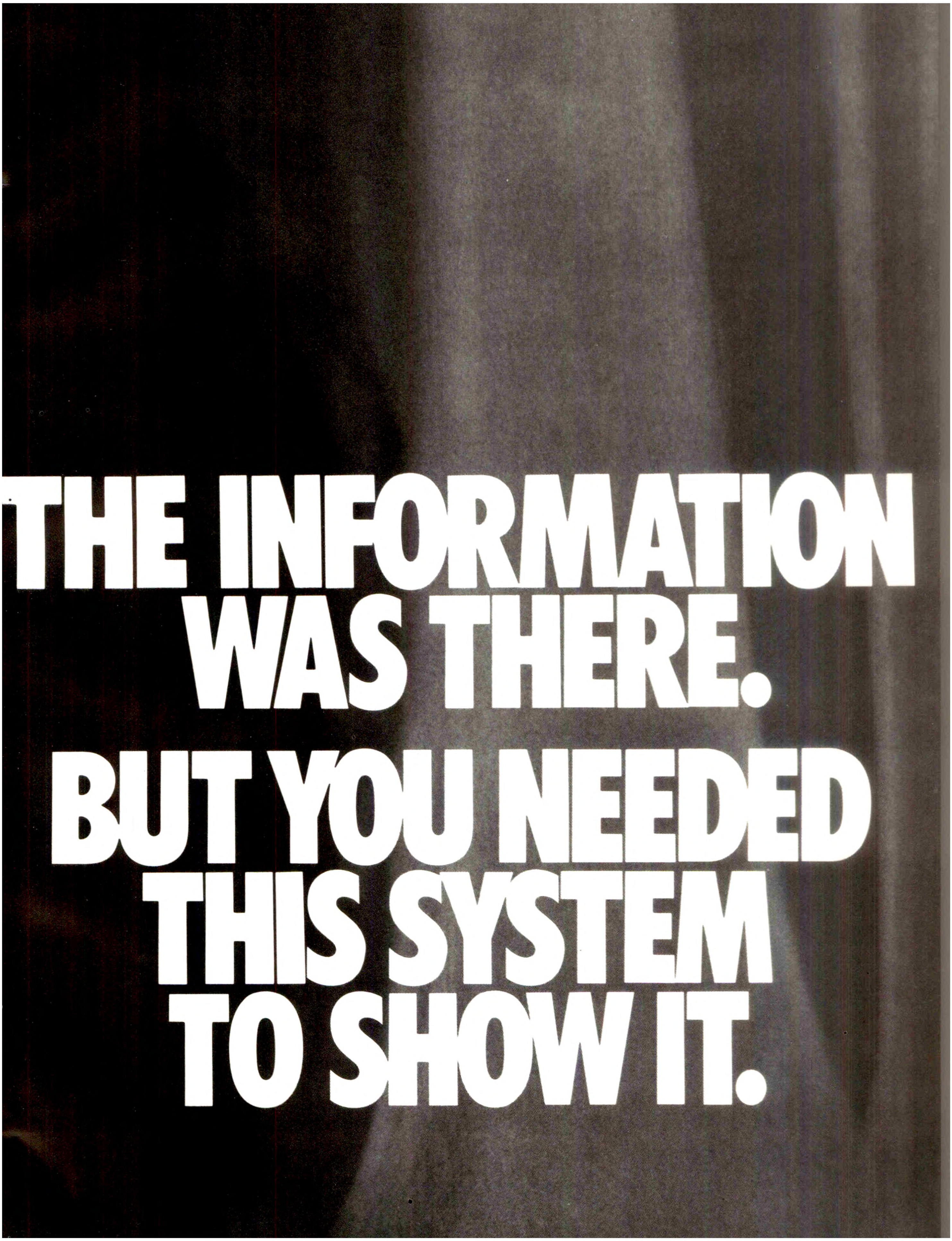

THE INFORMATION
WAS THERE.
BUT YOU NEEDED
THIS SYSTEM
TO SHOW IT.

Direct magnification with the RSI Magnigraphic System provides more diagnostic information.

Adult patient whose chronic leg ulceration presented a question of underlying osteomyelitis. Conventional radiograph (A) demonstrates thick periosteal new bone along shaft of tibia with overlying soft-tissue ulceration. Magnification radiograph (B) demonstrates fine, spiculated periosteal new bone formation not visible on conventional radiograph, extending into adjacent soft tissue. The slightly rotated magnification view indicates an evolving process and supports a diagnosis of active osteomyelitis.

Technique on (A)	Technique on (B)
60 kV	60 kV
600 mA	3 mA
.5 seconds	1 second
40" SID	24" SID
Non-screen film technique	Rare earth film/ screen technique

The RSI Magnigraphic System

- reveals pathology beyond the imaging capability of conventional contact radiography
- brings to light subtle and minute anatomic changes
- resolves marginal, equivocal and nonspecific findings
- substantially reduces quantum mottle and increases resolution in magnification radiography using rare earth film/screen combinations

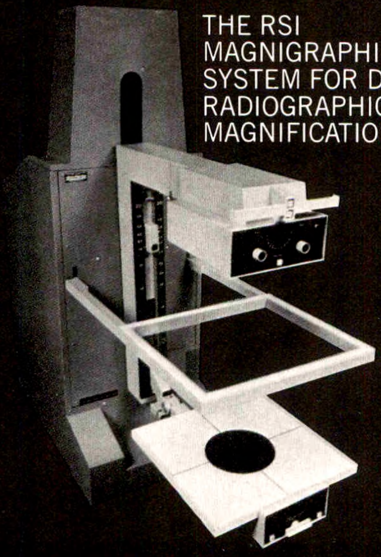

THE RSI
MAGNIGRAPHIC
SYSTEM FOR DIRECT
RADIOGRAPHIC
MAGNIFICATION

LIFT FLAP AND SEE THE DE

DIRECT MA
WITH T
MAGNIGRA
MADE THE

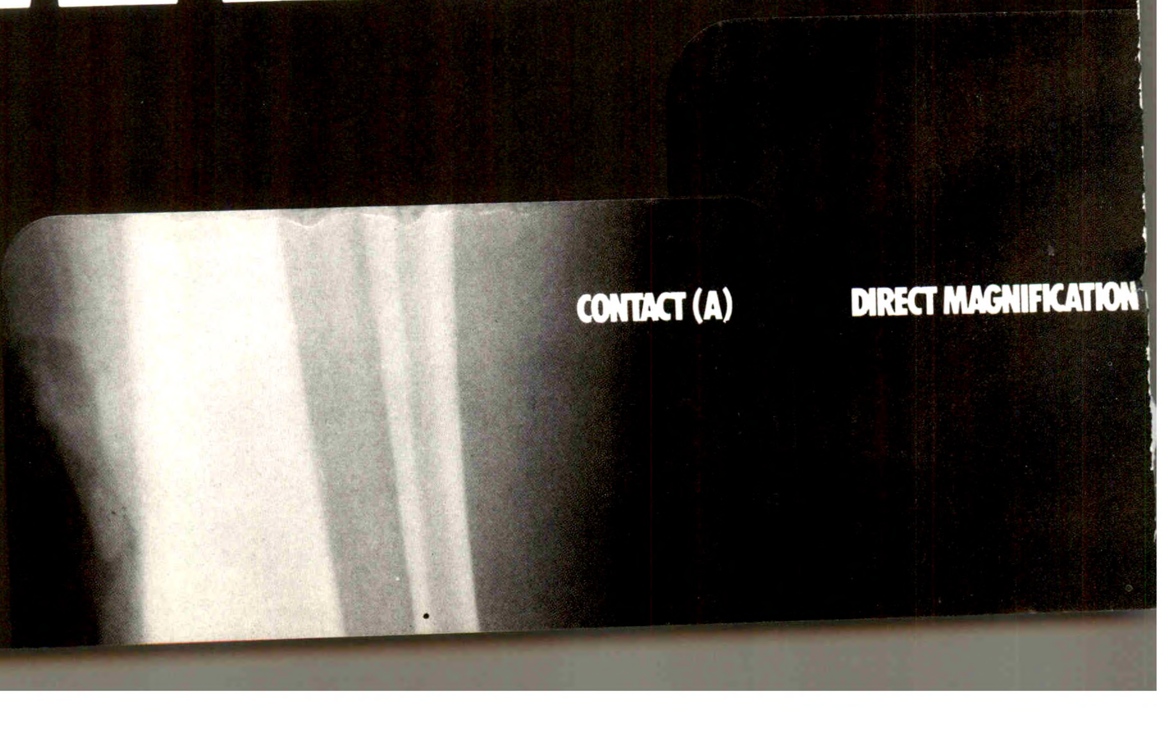

FROM A NEW C

VALUE OF DIRECT MAGNIFICATION IN 215 EXAMI

DISORDER	NO. OF CASES	NOT HELPF
ARTHRITIS	39	23
METABOLIC	32	25
**INFECTION*	*31*	*7*
TRAUMA	17	54
NEOPLASM	86	36
OTHER	10	40
TOTAL	215	30

†GENANT HK, *ET AL: RADIO*

THE RADIOLOGIC SCIENCES

WAS ESS

MAKING TH

45% OF

LINICAL STUDY:[†]

NATIONS CLASSIFIED BY PATHOLOGICAL DIAGNOSIS[†]

UL(%)	HELPFUL (%)	ESSENTIAL (%)
	72	5
	50	25
	48	*45*
	46	0
	56	8
	60	0
	56	14

LOGY 123: 47-55, APRIL 1977

NC. MAGNIGRAPHIC SYSTEM
ENTIAL TO
S DIAGNOSIS[*]
THE TIME.

GNIFICATION
THE RSI
PHIC SYSTEM
DIFFERENCE!

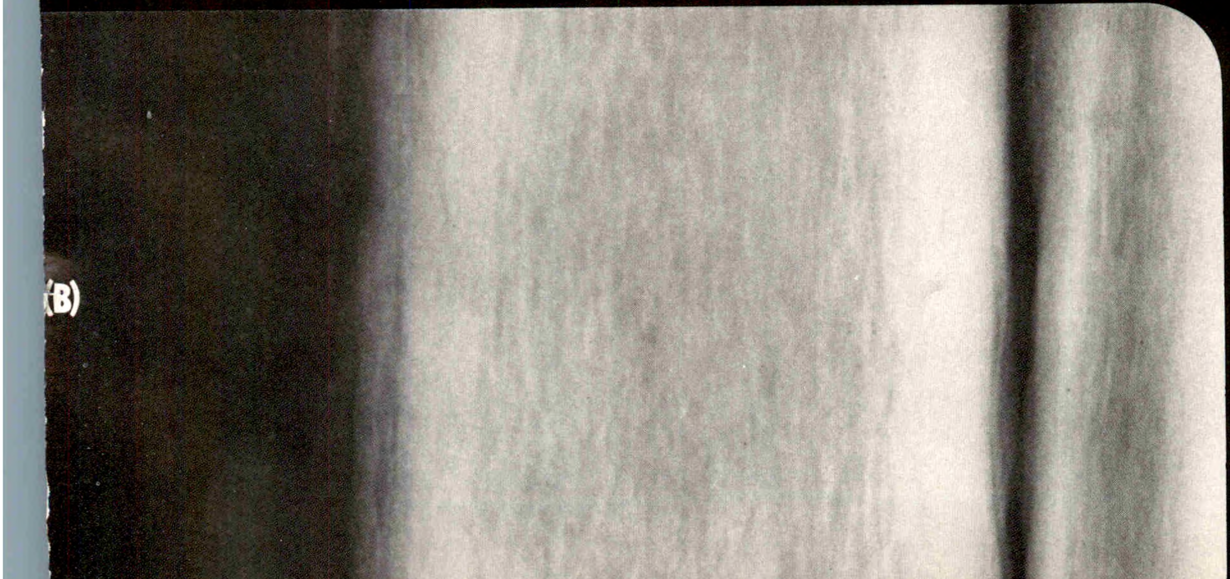

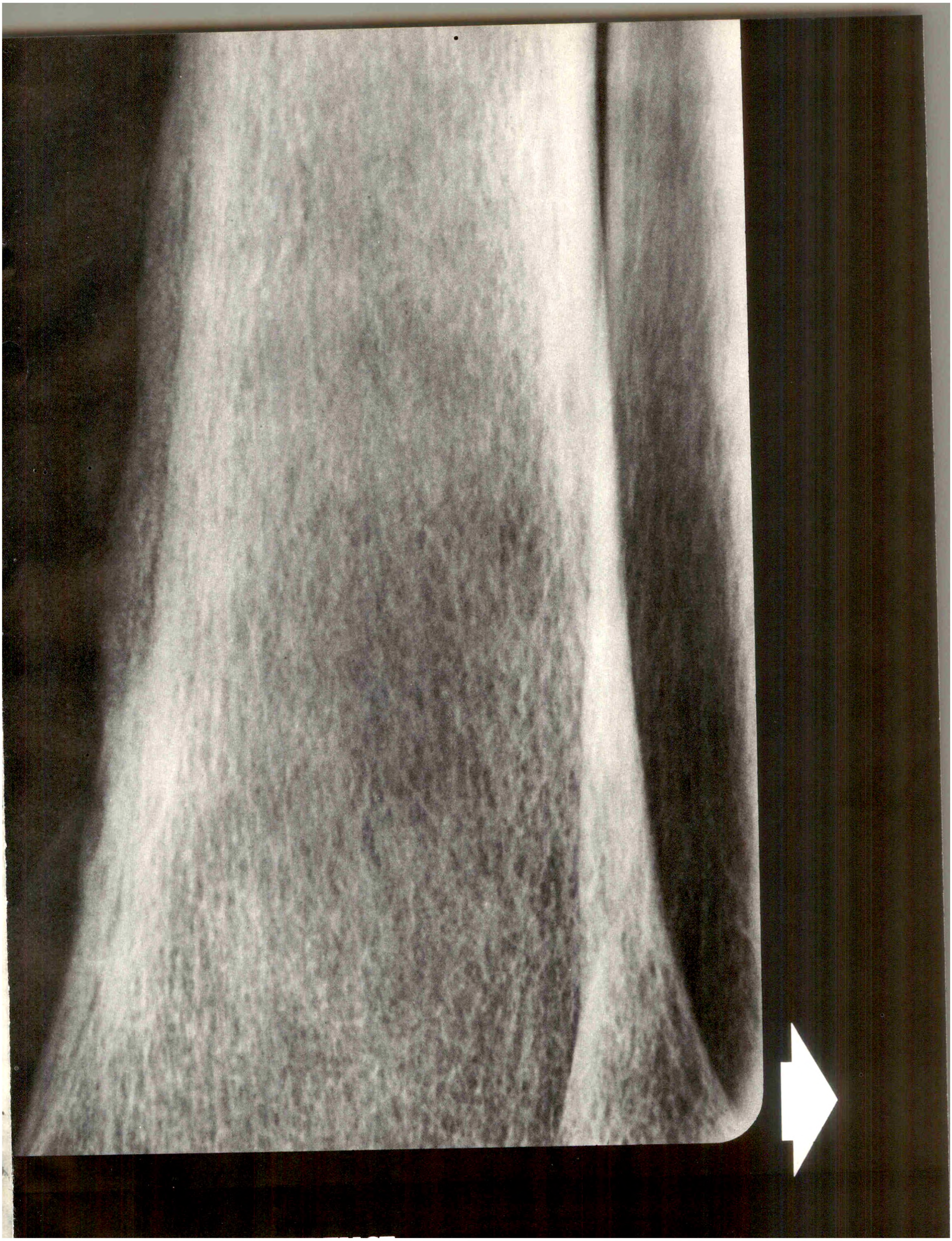

THE RSI MAGNIGRAPHIC SYSTEM: THE FIRST FULLY INTEGRATED SYSTEM FOR DIRECT MAGNIFICATION

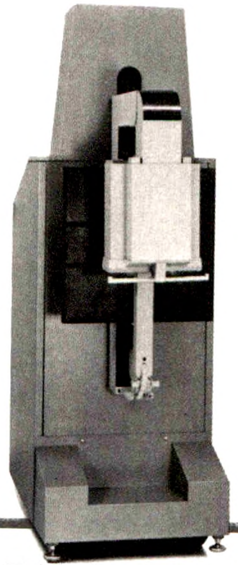

Produces images of extremely high resolution, excellent contrast and minimum noise

An increasing number of investigators are demonstrating that the RSI Magnigraphic System produces diagnostic images of exceptionally high resolution, excellent contrast and minimum quantum mottle—especially when used with ultra high speed rare earth film/screen combinations.

Clinical assessment of 215 skeletal x-ray examinations—85 of thin body parts and 130 of thick parts—demonstrated that direct magnification performed with the RSI Magnigraphic System was *helpful* in reaching a diagnosis in 56% of the cases and *essential* in 14%. Moreover, in evaluating arthritic, metabolic and infectious bone disorders, direct magnification with the RSI System was helpful in more than half of the cases, and was considered essential in close to one quarter.*

*Genant HK, *et al: Radiology 123*: 47-55, April 1977

Wide range of clinical applications

The RSI Magnigraphic System has the potential to improve detection, diagnosis and serial assessment in a wide variety of clinical conditions. These include:

☐ detection of metabolic, neoplastic and infectious bone disease. For example, the RSI System makes it possible to detect early periosteal and cortical changes caused by breakthrough of bone tumor into soft tissue.

☐ assessment of subtle resorptive changes within the joint in early rheumatoid arthritis

☐ identification of tiny metaphyseal chip fractures often not evident on routine radiographs

☐ assessment of patients with facial trauma before plastic surgery, as well as baseline preoperative evaluations before orthopedic procedures

The ideal focal spot

Instead of the helical filament of conventional x-ray tubes, the electron gun of the RSI Magnigraphic System employs a smooth, solid, circular cathode which permits precise focusing of the electron stream down to the desired focal spot size. The result is a "nominal" focal spot diameter of 0.09 mm, considerably smaller than the smallest focal spot of conventional tubes.

In contrast to conventional tubes which suffer significant loss of quality at the cathode end of the film, the electron optics and 45° target angle of the RSI Magnigraphic System maintain essentially uniform image quality over the entire image plane.

The target angle of the anode has been set at 45° to maintain the circular beam symmetry and virtually eliminate the heel effect. There is no double peaking and essentially no off-focus radiation. The result is an image source of near-perfect characteristics for direct magnification—an image source capable of providing high-resolution, high-contrast radiographs of greatly enhanced diagnostic value.

For complete clinical and technical information on the RSI Magnigraphic System, write to Radiologic Sciences Inc., 2920 Coronado Drive, Santa Clara, CA 95051. Or telephone 408-247-5180

RADIOLOGIC SCIENCES INC.
A SUBSIDIARY OF PFIZER INC.
SANTA CLARA CA 95051

ELECTRON GUN OF RSI MAGNIGRAPHIC SYSTEM

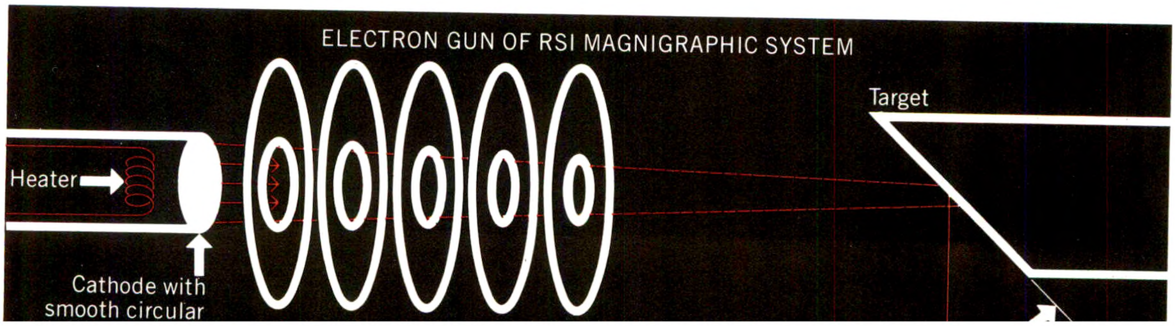

INDEX TO ADVERTISERS

In Order of Appearance

Ortho Pharmaceutical Corporation
Siemens Corporation
The Purdue-Frederick Company
Litton Medical Systems
Eastman Kodak Company
E. R. Squibb & Sons, Inc.
Atomic Energy of Canada
Litton Medical Systems
Pyne X-Ray Corporation
E-Z-EM Company
Low X-Ray
Machlett Laboratories
E. I. DuPont de Nemours & Co., Inc.

• • •

Philips Medical Systems
Guerbet Laboratory
AMRAD
Picker Corporation
Elema-Schonander, Inc.
General Electric Company
Picker Corporation
E-Z-EM Company
Varian Associates
University of California (San Francisco)
Charles C Thomas • Publisher
S & S X-Ray
General Electric Company
Charles C Thomas • Publisher
Radiologic Sciences, Inc.
Hanley Medical Equipment Company
Picker Corporation
Medi-Tech, Inc.
Artronix, Inc.

Hanley Space Saver X-Ray and Medical Record Cabinets are installed in most hospitals in America.

Top quality and low price is the reason.
5 compartment with doors—$199.50
5 compartment less doors—$171.50
Brochure F.O.B. Factory

AMERICA'S LARGEST DISTRIBUTOR OF X-RAY CABINETS

HANLEY MEDICAL EQUIPMENT CO.
5614 South Grand X-Ray Division St. Louis, Mo. 63111

In reply to advertisers
please mention that you saw
their advertisement in

THE
AMERICAN JOURNAL OF
ROENTGENOLOGY

published monthly for
The American
Roentgen Ray Society
by

CHARLES C THOMAS • PUBLISHER
Springfield, Illinois 62717

A Public Service of This Magazine
& The Advertising Council

Ad Council

Some-body needs you.

**Red Cross.
The Good
Neighbor**

It takes a strong table to be gentle.

Our new Galaxy® II is the strong, silent type.

It's designed to handle heavy x-ray tubes and imaging loads; but more importantly, the punishing patient loads of busy radiology departments become mere routine.

Its most outstanding features are inside. The new internal structures, such as hardened bearing tracks, are the heart of our reliability theme.

But this inner strength now translates into much smoother, quieter movements which provide ease to the operator and less apprehension to the patient.

More room inside assures space for tomorrow's larger, high-heat-capacity x-ray tubes. And, there's fluoroscopic coverage to handle a barium swallow on a 6'2" patient plus greater Bucky coverage and quality improvements in our new Multicon imaging systems. Durable switches have given even more reliability to an already good table resulting in easier operation and longer-life benefits.

Galaxy II, available in 90/90 or 90/15 table versions, can include Flushmount imaging or be equipped with the Multiview front-loading spotfilmer and Multicon Imaging Systems.

This is another example of Picker's unique human resources benefiting you. It's a result of our expertise in the diagnostic modalities of x-ray, ultrasound, nuclear, computed tomography, clinical laboratory, therapy, film systems and supplies. Only Picker has all these resources.

Consult your Picker representative or write Picker Corporation, 595 Miner Road, Cleveland, OH 44143.

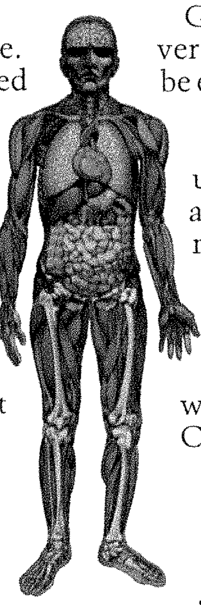

Discover the human resources in Picker'synergy

PICKER®
ONE OF THE C.I.T. COMPANIES

See Picker at RSNA

PICKER
STOP
POWER TOP
TILT

THE SOFT·STEERABLE CATHETER SYSTEM FOR NON-OPERATIVE REMOVAL OF RETAINED BILIARY STONES VIA THE BURHENNE TECHNIQUE*

CONCEPT

Using the Burhenne technique and the MEDI-TECH steerable catheter, a significant number of non-operative removals of retained biliary stones have been achieved with consistent success.*

The safe, simple procedure, developed by Dr. H. Joachim Burhenne, is performed as a follow-up to cholecystectomy, after it has been determined, by a postoperative cholangiogram, that there are retained stones. The procedure is performed, at least four weeks after surgery, by removing the T-tube and advancing the MEDI-TECH Soft Steerable Catheter through the remaining T-tube tract.

Unique maneuverability of the soft-steerable catheter tip permits the physician to dislodge, manipulate and reposition the stone(s). Contrast media is injected through the Luer-Lock and the Open Lumen of the MEDI-TECH catheter to enhance visualization. Then, with the stone in desired position, a wire basket or snare is passed through the Tuohy-Borst fitting and the open lumen to the site. When the stone is secured, the entire assembly is withdrawn. Although the soft-tip provides sufficient torque for this procedure, patient discomfort is minimal and no anesthesia or pre-medication is used.

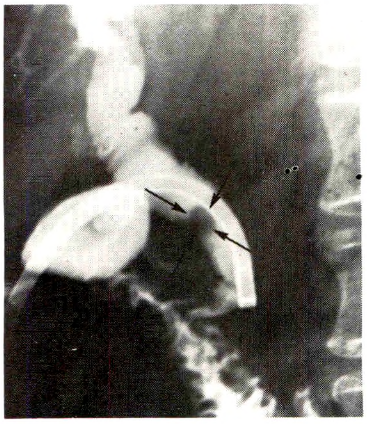

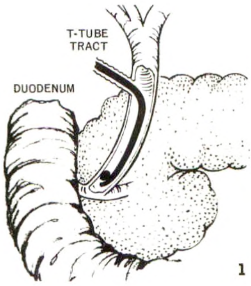

1

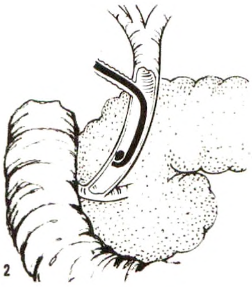

2

3

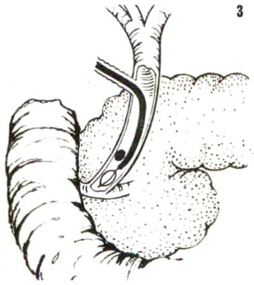

4

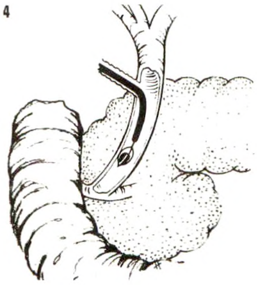

*REFERENCE

Burhenne, H. J., The Technique of Biliary Duct Stone Extraction, RADIOLOGY, 113:567-572, December 1974.

AN X-RAY CINE FILM of the Burhenne procedure is available. Please contact MEDI-TECH to arrange a viewing of the film and to obtain copies of reference articles plus complete information on the MEDI-TECH/BURHENNE Biliary Catheter System.

THE COMPLETE BILIARY CATHETER SYSTEM includes the MEDI-TECH Remote Control Handle, Special Biliary Catheters and Wire Stone Removal Baskets.

ALSO

the same MEDI-TECH Control Handle is used with a variety of other catheters and special accessories to perform a broad range of vascular, bronchial, GI and other procedures described in MEDI-TECH literature.

MEDI TECH®
DIVISION
Cooper Scientific Corporation

372 MAIN STREET, WATERTOWN, MASS. 02172
(617) 923-1720

MEDI-TECH
Division of Cooper Scientific Corporation
372 Main Street, Watertown, Mass. 02172

☐ Please send me complete information and prices on the Soft-Steerable Biliary Catheter System.
☐ We would be interested in viewing the X-Ray Film.

Name__________ Dept.__________
Hosp.__________
Address__________
City__________ State__________ Zip__________
Phone__________ (   ) Area Code

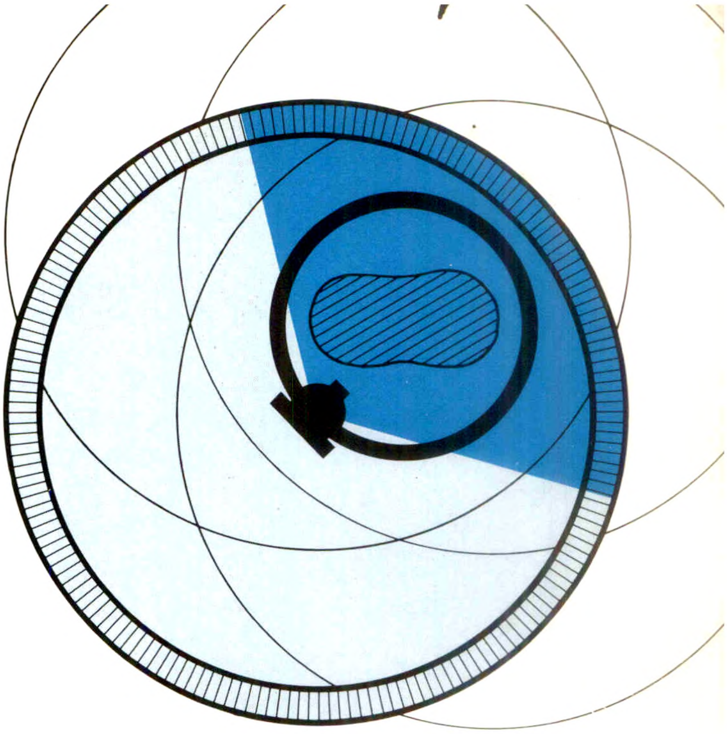

THE NEW GEOMETRY FOR WHOLE BODY CT IMAGING

HE NEW CT-SCAN GEOMETRY IS A CONTINUOUSLY OTATING SYSTEM WITH A CONCENTRIC X-RAY SOURCE ND AN ECCENTRIC DETECTOR RING TRANSLATING ROUND THE PATIENT.

SIMPLE, RELIABLE AND VERY FAST.
EXCELLENT CLINICAL SENSITIVITY AT A LOW COST.

TAKE THE ADVANTAGES OF THE:

- CONTINUOUS ROTATING FAN BEAM
- ROTATE/TRANSLATE GEOMETRY
- CIRCULAR, STATIONARY DETECTOR ARRAY

COMBINED, THEY REPRESENT THE OPTIMAL GEOMETRY FOR VERY FAST, WHOLE BODY CT IMAGING.

For more information on this unique system, visit Artronix at the Radiological Society of North America Meeting in Chicago (Booth 3213), or contact:

rtronix, Inc.
314 Hanley Industrial Court
. Louis, Missouri 63144
14) 968-4740

artronix
INCORPORATED

American Journal of Roentgenology

Vol. 129 **December 1977** **No. 6**

ARS Presidential Address: Cancer of the Breast: A Time for Caution. *L. W. Brady* 969

DIAGNOSTIC IMAGING

Gray Scale Ultrasonography of the Gallbladder: An Evaluation of Accuracy and Report of Additional Ultrasound Signs. *J. C. Anderson and R. K. Harned* 975
Accuracy of Biliary Duct Ultrasound: Comparison with Cholangiography. *H. L. Neiman and R. A. Mintzer* 979
Gray Scale Echographic Patterns of Hepatic Metastatic Disease. *W. Scheible, B. B. Gosink, and G. R. Leopold* 983
Isodense Masses on CT: Differentiation by Gray Scale Ultrasonography. *P. J. Bryan and W. M. Dinn* 989
Myelolipoma of the Adrenal: Two Cases with Ultrasound and CT Findings. *M. Behan, E. C. Martin, E. C. Muecke, and E. Kazam* 993
Ultrasound-guided Drainage of Fluid-containing Masses Using Angiographic Catheterization Techniques. *J. Grønvall, S. Grønvall, and V. Hegedüs* 997
Gray Scale Ultrasound Evaluation of Popliteal Artery Aneurysms. *T. M. Silver, R. L. Washburn, J. C. Stanley, and W. S. Gross* 1003
Pitfalls in the Angiographic Management of Hemorrhage: Hemodynamic Considerations. *E. J. Ring, J. A. Oleaga, D. Freiman, J. W. Husted, A. C. Waltman, Jr., and S. Baum* 1007
Angiography of Pancreatic Arteriovenous Malformation. *V. P. Chuang, C. M. Pulmano, J. F. Walter, and K. J. Cho* 1015
Pulmonary Angiography for Pulmonary Emboli: Rational Selection of Oblique Views. *A. S. Gomes, J. H. Grollman, Jr., and J. Mink* 1019
A Radiographic Study of Congenital Pulmonary Atresia with Ventricular Septal Defect. *B. Soto, A. D. Pacifico, R. F. Luna, and L. M. Bargeron, Jr.* 1027
Contrast Medium Reactions Correlated with Time of Day. *J. J. Cunningham* 1039
Accuracy of Bipedal Lymphography in Hodgkin's Disease. *M. T. Kademian and G. W. Wirtanen* 1041
Primary Chylopericardium: The Role of Lymphangiography. *T. E. Gallant, R. J. Hunziker, and T. C. Gibson* 1043
Ether-dissolved Ethiodol for Lymphangiography: An Experimental Study. *K. Jonsson, J. H. Anderson, B. Osborne, and S. Wallace* 1047
Left Adrenal Neuroblastoma with Normal-appearing Urogram. *J. O. Haller, W. E. Berdon, D. H. Baker, and E. G. Kassner* 1051
Acute Appendicitis with Abscess Simulating Carcinoma of the Sigmoid. *J. M. Halls and H. I. Meyers* 1057
Ultrasonography in Tumors Arising from the Spine and Bony Pelvis. *L. A. deSantos and H. M. Goldstein* 1061
Radiographic Diagnosis of Acute Peroneal Tendon Dislocation. *C. C. Church* 1065
Subchondral Pseudocysts in Rheumatoid Arthritis. *C. Rennell, F. Mainzer, C. V. Multz, and H. K. Genant* 1069
Angiographic Features of Osteosarcoma. *I. Yaghmai* 1073
Occurrence of Lung Granulomas in Patients with Stage I Sarcoidosis. *Y. Rosen, J. K. Amorosa, S. Moon, J. Cohen, and H. A. Lyons* 1083
Diagnostic Oncology Case Studies: Chronic Sciatic Pain in a Young Woman with Sclerosis of the Iliac Bone. *Contributed by R. Kalinowski* 1087

RADIATION ONCOLOGY

Preliminary Results Using Twice-a-day Fractionation in the Radiotherapeutic Management of Advanced Cancers of the Head and Neck. *S. Jampolis, G. Pipard, J.-C. Horiot, M. Bolla, and C. Le Dorze* 1091
Evaluation of Radiation Therapy for Bone Metastases: Pain Relief and Quality of Life. *H. A. Gilbert, A. R. Kagan, H. Nussbaum, A. R. Rao, J. Satzman, P. Chan, B. Allen, and A. Forsythe* 1095

CASE REPORTS

Peripelvic Renal Pseudocyst due to Obstruction. *Z. L. Barbaric and I. N. Frank* 1097
Contralateral Renal Herniation after Nephrectomy: A Cause of Pseudo-Crossed Renal Ectopia. *K. J. Cho, J. F. Walter, and J. W. Konnak* 1099
Gray Scale Ultrasonography in Retroperitoneal Lymphangiomyomatosis. *J. Walsh, K. J. W. Taylor, A. T. Rosenfield* 1101
Diffuse Interstitial Calcification of the Lungs in Chronic Renal Failure Mimicking Pulmonary Edema. *H. Firooznia, R. Pudlowski, C. Golimbu, M. Rafii, and D. McCauley* 1103
Massive Esophageal Hemorrhage in Leukemia. *P. H. Stratemeier* 1106
Lymph Node Calcification in Hodgkin's Disease after Chemotherapy. *M. Bertrand, J. T. T. Chen, and H. I. Libshitz* 1108
Localization of ^{67}Ga Citrate in a Mycotic Aneurysm. *J. A. Michal, III, and R. E. Coleman* 1111
Exostosis after Iliac Bone Marrow Biopsy. *W. A. Murphy* 1114
Pathologic Fracture in an Unusual Case of Gout. *J. Burnham, K. Fraker, and H. Steinbach* 1116
Mondini Defect: A Variant. *P. M. Som, M. T. Khilnani, S. L. Beranbaum, and B. S. Wolf* 1120

TECHNICAL NOTES

A Method of Reducing Cost in CT Systems That Employ Floppy Discs. *L. D. Cromwell, W. E. Moore, D. Schumacher, and A. Salam* 1123
A Wedge Filter for Craniocervical Angiography. *L. D. Cromwell, C. W. Kerber, and W. R. Vermeere* 1125

SPECIAL LECTURE: Roles for Radiologists in Tomorrow's Medical Care System. *R. H. Morgan* 1129

Guest Editorial: On Maps and Comparing Cross-sectional Imaging Methods. *J. C. Birnholz* 1133
From Earlier Pages 1135
Letters 1137
Report of 1977 ARS Meeting 1140

AJR Reviewers and Abstractors, 1977 1142
Abstracts of Current Literature 1143
Book Reviews 1156
News 1160
Index to Volume 129 1163